



QIR

THE 15th INTERNATIONAL CONFERENCE on QIR

(Quality in Research)

PROCEEDING

ISSN: 1411-1484

in conjunction with:



6th IEEE International
Conference on Advanced
Logistics and Transport
(ICALT 2017)



International Conference in
Saving Energy in Refrigeration and
Air Conditioning (ICSERA)



International Conference on
Dwelling Form I-DWELL

3rd Binnual Meeting on Bioprocess Engineering



2nd International Symposium on Biomedical Engineering

Organized by:



UNIVERSITAS
INDONESIA

FACULTY OF
ENGINEERING

Co-Hosted by:



UNIVERSITAS UDAYANA
FAKULTAS TEKNIK



POLITEKNIK
NEGERI BALI

*The Westin Resort
Nusa Dua, Bali*
24-27 July 2017



PREFACE

WELCOME FROM THE RECTOR OF UNIVERSITAS INDONESIA

It is both a pleasure and honor for me to welcome you all to the 15th International Conference on QiR (Quality in Research) 2017 in Nusa Dua, Bali, Indonesia.

Universitas Indonesia strives to be one of the leading research universities and the most outstanding academic institution in the world. UI is distinctive among research universities in its commitment to the academic invention and research activities through various scientific programs. QiR 2017 is our main academic conference in the field of engineering and technology which has been successfully held for the last two decades. It is our hope that this world class scientific program would showcase our scientists and researchers achievements and provide forums for scientific exchanges in their respective fields.



The theme this year of 'Science, Technology and Innovation for Sustainable World', is very relevant with the fact that the globalization today results in very competitive atmosphere in all aspects. However, this flourishing competition should consider the harmony and balance between human needs and the environment quality for creating favorable sustainable future. Scientists and researchers, hand in hand with industrial experts are creating and developing new sustainable technologies that enable us to make products and services more efficient, design better buildings, produce safer cars, keep people healthier and building smarter cities.

I extend my sincere thanks to the Faculty of Engineering Universitas Indonesia, supporting parties and institutions for their participation and contributions in QiR 2017. I would also thank our colleagues from Universitas Udayana and Politeknik Negeri Bali for their gracious support and hospitality. Additionally, I extend a hearty thank you to the members of the organizing committees for dedicating their valuable time so that each one of us enjoys an exceptional conference program over the next several days. May we have a successful, stimulating, fruitful and rewarding conference.

Prof. Dr. Ir. Muhammad Anis, M.Met.

Rector

Universitas Indonesia



PREFACE

WELCOME FROM THE DEAN OF FACULTY OF ENGINEERING UNIVERSITAS INDONESIA

Welcome to the 15th International Conference on QiR (Quality in Research) 2017. The Faculty of Engineering Universitas Indonesia is delighted to host our flagship international academic event this year back in Bali, Indonesia. This two-day, biennial conference is presented together with our co-hosts Universitas Udayana and Politeknik Negeri Bali with the hope that this would be able to provide an international media for exchange of the knowledge, experience and research as well as the review of progress and discussion on the state of the art and future trend of prospective collaboration and networking in broad field of science, technology and innovation.



The main theme for this year conference, “Science, Technology and Innovation for Sustainable World” is consistent with the mission of our faculty to be a leading institution with the initiatives that responds to local, national and global societal needs. In that context, the Faculty of Engineering Universitas Indonesia is performing state-of-the arts research and development in engineering and architecture areas which results in technology and innovation which contribute to sustainable development at both national and global level. QiR 2017 provides platforms and forums to disseminate our scientific achievements and exchange information with our counterparts from Indonesia and all over the world. This event will allow for further research and education collaborations between Universitas Indonesia and its partners worldwide.

I would like to express my deepest appreciation to our sponsors, supported parties and various contributors for their never ending supports of this conference. I would also like to convey my gratitude to all of our distinguished speakers for making the time to share their knowledge with us. To our fellow researchers and/or practitioners from Indonesia and overseas, welcome and enjoy your stay in this Nusa Dua, Bali. I would also like to invite all participants in expressing our appreciation to all members of the QiR 2017 organizing committee for their hard work in making this conference success.

Prof. Dr. Ir. Dedi Priadi, DEA
Dean Faculty of Engineering
Universitas Indonesia



PREFACE

WELCOME FROM THE QIR 2017 ORGANIZING COMMITTEE

On behalf of the organizing committee, it is a great pleasure for us to welcome you to the 15th International Conference on Quality in Research (QIR) 2017 to be held in Bali, Indonesia on July, 24 – 27, 2017. This biennial event is co-organized with the Faculty of Engineering Universitas Udayana and Politeknik Negeri Bali.



The main theme for this year conference is “Science, Technology and Innovation for Sustainable World”. Under this theme the conference focuses on the innovative research and contribution in science and technology toward achieving sustainable world. In line with this theme, it is our utmost pleasure to hold the QIR 2017 in conjunction with the 6th IEEE-International Conference on Advanced Logistics and Transport (ICALT), the 2nd International Symposium on Biomedical Engineering (ISBE 2017), International Conference in Saving Energy in Refrigeration and Air Conditioning (ICSERA) and the 3rd Biannual Meeting on Bioprocess Engineering.

The QIR 2017 brings together national and international academicians, researchers, executives, government, industrial and business officials, practitioners and leaders to present and discuss a vast range of engineering, architectural designs and community development based on green and smart technology. It is our hope and aim that this conference would be able to provide an international media for exchange of the knowledge, experience and research as well as the review of progress and discussion on the state of the art and future trend of prospective collaboration and networking in broad field of science, technology and innovation. Furthermore, QIR 2017 benefits industry sector, since it would create a close contact between and among the audiences. The audiences mostly come from different job and activities: therefore this is a great potential and opportunity to meet each other, creating fruitful discussions and broaden business relationship.

QIR has been growing, since its first event two decades ago, into our flagship academic event with international reputation. This year, we have received almost 1000 submissions from more than 26 countries. Along with our events in conjunction, more than 500 oral and poster presentations is scheduled with expected 700 participants gather in the event.

On behalf of QIR 2017 committee, we would like to thank all of our speakers, participants, contributors, partners and professional associations for their generous contributions. We also would like to acknowledge the support from our International Advisory Board members and distinguished reviewers. Last but not least, a special thanks to our local co-organizer, Universitas Udayana and Politeknik Negeri Bali.

We wish all of you a productive and rewarding conference, also a pleasant and memorable stay in Nusa Dua, Bali, Indonesia.

Thank you and we hope to see you again in QIR 2019.

Ardiyansyah, Ph.D.

General Chair of QIR 2017 Organizing Committee



CONFERENCE ORGANIZER

ADVISOR

- Prof. Prof. Dr. Ir. Dedi Priadi, DEA.,
- Dr. Ir. Muhamad Asvial, M.Eng.
- Ir. Hendri DS Budiono, M.Eng
- Dr. Badrul Munir, ST., M.Eng.Sc
- Jos Istiyanto, S.T., M.T., Ph.D.
- Dr. Ir. Wiwik Rahayu, DEA.
- Prof. Dr. Akhmad Herman Yuwono, M.Phil., Eng.

GENERAL CHAIR

Ardiyansyah, PhD., Universitas Indonesia

CO-CHAIR

Dr. Eny Kusrini, Universitas Indonesia

INTERNATIONAL ADVISORY BOARD

- Prof. Muhammad Anis, Universitas Indonesia
- Prof. Rosari Saleh, Universitas Indonesia
- Prof. Dedi Priadi, Universitas Indonesia
- Prof. Hiroshi Murase, Nagoya University, Japan
- Prof. Manabu Tanaka, Director of JWRI
- Prof. Kazuhiro Ito, Professor at JWRI
- Assoc. Prof. Yosuke Kawahito, Associate Professor at JWRI
- Prof. Afshin Ghajar, Oklahoma State University
- Prof. Josaphat Tetuko Sri Sumantyo, Chiba University
- Prof. Pega Hrnjak, University of Illinois at Urbana Champaign
- Prof. Greet Vanden Berghe, KU Leuven
- Prof. Joong Kee Lee, KIST, Korea
- Prof. Pekka Leviäkangas, University of Oulu
- Prof. Marie-Anne Guerry, Vrije Universiteit Brussel
- Prof. Rainer Leisten, University of Duisburg Essen
- Prof. Hamid Ullah – Universiti Teknologi Brunei

STEERING COMMITTEE

- Dr. Tri Tjahjono, Universitas Indonesia
- Prof. Yulianto S. Nugroho, Universitas Indonesia
- Prof. Benyamin K., Universitas Indonesia
- Prof. Winarto, Universitas Indonesia
- Dr. Ing. Dalhar Susanto, Universitas Indonesia
- Prof. Widodo Wahyu Purwanto, Universitas Indonesia
- Prof. Isti Surjandari Prajitno, Universitas Indonesia
- Prof. Suardana, Universitas Udayana
- I Made Rajendra, M.Eng, Politeknik Negeri Bali

SCIENTIFIC PUBLICATION PARTNER

- Dr. Nyoman Suwartha
- Dr. Mohammed Ali Berawi

TECHNICAL PROGRAM COMMITTEE

- Dr. Cindy Rianti Priadi
- Sugeng Supriadi, Ph.D
- Dr. Basari
- Chairul Hudaya, Ph.D
- Wahyuaji N. Putra, MT
- Dr.-Ing. Yulia Nurliani Lukito



CONFERENCE ORGANIZER

- Dr. Bambang Heru Susanto
- Komarudin, Ph.D
- I Dewa Gede Ary Subagia, PhD
- Dr. Wayan Nata Septiadi
- Dr. I Nyoman Suamir

Secretariat and Registration

Herra Astasusmini, SE
Agnes Sagita Nauli, S.I.A.
Indah Sari Dewi

Treasurer

- Evy Surpiningsih, S.Pd., MM
- Nuri Nugraini, Amd

Programme and Protocol

Tikka Anggraeni, M.Si.

Design and Documentation

- Rengga Wibisono, S.Sos.
- Muhammad Badi

Web and Information System

- I Gede Dharma Nugraha, S.T., M.T.
- Boma Anantasatya Adhi, ST., M.T.
- Ruki Harwahyu, S.T., M.T., M.Eng.
- Ardiansyah, ST., M.Eng.
- Gunawan Heri Saputra, Amd

Exhibition and Sponsorship

- Dr. Ir. Nahry., MT.
- Dr. Adi Surjosatyo, M.Eng.
- Dr. Muhammad Suryanegara
- Kemas Ridwan Kurniawan, ST., MSc., PhD.
- Dr. Tania Surya Utami, S.T., M.T.
- Ir. Erlinda Muslim, MEE.

Venue and Facilities

- Jumiardi, S.Ars
- Hadi Mulyadi

Meal

- Yunita Dewi Hapsari
- Indri Feriani

Conference Organizing Committee :
Faculty of Engineering Universitas Indonesia
Dekanat Building 3th Floor Kampus UI, Depok 16424, Indonesia
Phone : +62-21- 7863503, Fax : +62-21 - 7270050
Email : qir@eng.ui.ac.id,
Website : <http://qir.eng.ui.ac.id>
www.eng.ui.ac.id



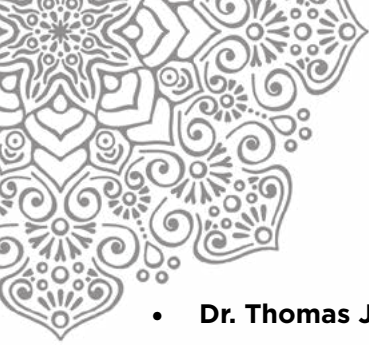
REVIEWER

Agung Saragih, *Universitas Indonesia, Indonesia*
Agus Pamitran, *Universitas Indonesia, Indonesia*
Ahmad Gamal, *Universitas Indonesia, Indonesia*
Akhmad Hidayatno, *Universitas Indonesia, Indonesia*
Akhmad Herman Yuwono, *Universitas Indonesia, Indonesia*
Andi Rustandi, *Universitas Indonesia, Indonesia*
Andyka Kusuma, *Universitas Indonesia, Indonesia*
Anne Zulfia Syahril, *Universitas Indonesia, Indonesia*
Ardiyansyah Ardiyansyah, *Universitas Indonesia, Indonesia*
Ayomi Dita, *Universitas Indonesia, Indonesia*
Badrul Munir, *Universitas Indonesia, Indonesia*
Cindyrianti Priadi, *Universitas Indonesia, Indonesia*
Deni Ferdian, *Universitas Indonesia, Indonesia*
Djoko M Hartanto, *Universitas Indonesia, Indonesia*
Donanta Dhaneswara, *Universitas Indonesia, Indonesia*
Dwi Marta Nurjaya, *Universitas Indonesia, Indonesia*
Dwinanti Rika, *Universitas Indonesia, Indonesia*
Dwita Sutjningsih, *Universitas Indonesia, Indonesia*
Ellen Tangkudung, *Universitas Indonesia, Indonesia*
Eny Kusrini, *Universitas Indonesia, Indonesia*
Erly Bahsan, *Universitas Indonesia, Indonesia*
Ghiska Ramahdita, *Universitas Indonesia, Indonesia*
Gs Boedi Andari, *Universitas Indonesia, Indonesia*
Herr Soeryantono, *Universitas Indonesia, Indonesia*
Heru Purnomo, *Universitas Indonesia, Indonesia*
Imam Jauhari Maknun, *Universitas Indonesia, Indonesia*
Jachrizal Soemabrata, *Universitas Indonesia, Indonesia*
Jaka Fajar Fatriansyah, *Universitas Indonesia, Indonesia*
Jessica Sjah, *Universitas Indonesia, Indonesia*
Kemas Ridwan Kurniawan, *Universitas Indonesia, Indonesia*
Komarudin Komarudin, *Universitas Indonesia, Indonesia*
Maya Arlini Puspasari, *Universitas Indonesia, Indonesia*
Misri Gozan, *Universitas Indonesia, Indonesia*
Mohammed Ali Berawi, *Universitas Indonesia, Indonesia*
Muhamad Sahlan, *Universitas Indonesia, Indonesia*
Muhammad Arif, *Universitas Indonesia, Indonesia*
Muhammad Ibadurrohman, *Universitas Indonesia, Indonesia*
Nahry Yusuf, *Universitas Indonesia, Indonesia*
Nofrijon Sofyan, *Universitas Indonesia, Indonesia*
Nuraziz Handika, *Universitas Indonesia, Indonesia*
Nyoman Suwartha, *Universitas Indonesia, Indonesia*
Paramita Atmodiwirjo, *Universitas Indonesia, Indonesia*
Radon Dhelika, *Universitas Indonesia, Indonesia*
Riko I Made, *Universitas Indonesia, Indonesia*
Romadhani Ardi, *Universitas Indonesia, Indonesia*
Sigit Hadiwardoyo, *Universitas Indonesia, Indonesia*
Sotya Astuningsih, *Universitas Indonesia, Indonesia*
Sri Harjanto, *Universitas Indonesia, Indonesia*
Sugeng Supriadi, *Universitas Indonesia, Indonesia*
Sunaryo Sunaryo, *Universitas Indonesia, Indonesia*
T, Ilyas, *Universitas Indonesia, Indonesia*
Tjandra Setiadi, *Universitas Indonesia, Indonesia*
Toha Saleh, *Universitas Indonesia, Indonesia*
Tri Tjahjono, *Universitas Indonesia, Indonesia*
Triatno Yudo Harjoko, *Universitas Indonesia, Indonesia*
Vika Rizkia, *Universitas Indonesia, Indonesia*
Wahyuaji Narottama Putra, *Universitas Indonesia, Indonesia*



REVIEWER

Wardhana Sasangka, *Universitas Indonesia, Indonesia*
Widjaja Martokusumo, *Universitas Indonesia, Indonesia*
Widjojo Prakoso, *Universitas Indonesia, Indonesia*
Widodowahyu Purwanto, *Universitas Indonesia, Indonesia*
Winarto, *Universitas Indonesia, Indonesia*
Wiratni Budhijanto, *Universitas Indonesia, Indonesia*
Yandi Andri Yatmo, *Universitas Indonesia, Indonesia*
Yudan Whulanza, *Universitas Indonesia, Indonesia*
Yudha Pratesa, *Universitas Indonesia, Indonesia*
Yulianto Snugroho, *Universitas Indonesia, Indonesia*
Yulianurliani Lukito, *Universitas Indonesia, Indonesia*
Zulkarnain Zulkarnain, *Universitas Indonesia, Indonesia*
Abdul Halim, *Universitas Indonesia, Indonesia*
Abdul Muis, *Universitas Indonesia, Indonesia*
Ajib Setyo Arifin, *Universitas Indonesia, Indonesia*
Alfan Presekal, *Universitas Indonesia, Indonesia*
Arief Udhiarto, *Universitas Indonesia, Indonesia*
Basari Basari, *Universitas Indonesia, Indonesia*
Catur Apriono, *Universitas Indonesia, Indonesia*
ChairulHudaya, *Universitas Indonesia, Indonesia*
Diyatul Husna, *Universitas Indonesia, Indonesia*
Eko Tjipto Rahardjo, *Universitas Indonesia, Indonesia*
Filbert Hilman Juwono, *Universitas Indonesia, Indonesia*
Fitri Yuli Zulkifli, *Universitas Indonesia, Indonesia*
Gunawan Wibisono, *Universitas Indonesia, Indonesia*
Muhamad Asvial, *Universitas Indonesia, Indonesia*
Muhammad Salman, *Universitas Indonesia, Indonesia*
Muhammad Suryanegara, *Universitas Indonesia, Indonesia*
Prima Dewi Purnamasari, *Universitas Indonesia, Indonesia*
Purnomo Sidi Priambodo, *Universitas Indonesia, Indonesia*
Ruki Harwahyu, *Universitas Indonesia, Indonesia*
Taufiq Alif Kurniawan, *Universitas Indonesia, Indonesia*
Tomy Abuzairi, *Universitas Indonesia, Indonesia*
Achmad Munir, *Bandung Institute of Technology, Indonesia*
Denny Setiawan, *Ministry of Communication and Informatics, Indonesia*
Faiz Husnayain, *Ajou University, Indonesia*
Fauzan Hanif Jufri, *Ajou University, Indonesia*
Hana Baili, *Centrale Supelec, Indonesia*
Hugeng Hugeng, *Multimedia Nusantara University, Indonesia*
Mudrik Alaydrus, *Mercu Buana University, Indonesia*
Ratno Nuryadi, *Agency for Assessment and Application of Technology (BPPT), Indonesia*
Sri Purwiyanti, *Lampung University, Indonesia*
Victor Widiputra, *Ajou University, Indonesia*
Yohandri Yohandri, *Padang State University, Indonesia*
Yoyok Dwi Setyo Pambudi, *National Nuclear Energy Agency (BATAN), Indonesia*
Aji Nur Widyanto, *Universität Duisburg-Essen, Indonesia*
Boma Anantasatya Adhi, *Waseda University, Indonesia*
Budi Sudiarto, *Universität Duisburg-Essen, Indonesia*
Dwi Riana Aryani, *Seoul National University of Science & Technology, Indonesia*
Faiz Husnayain, *Ajou University, Indonesia*
Fauzan Hanif Jufri, *Ajou University, Indonesia*
Kazuyuki Saito, *Chiba University, Indonesia*
Muhammad Firdaus Lubis, *Korea Institute of Science and Technology, Indonesia*
NaufanRaharya, *The University of Sydney, Indonesia*
Victor Widiputra, *Ajou University, Indonesia*



KEYNOTE SPEAKER

- **Dr. Thomas J. Goldsby** | Ohio State University, USA.
- **Prof. Jackie Yi-Ru Ying** | Institute of Bioengineering and Nanotechnology in Singapore
- **Prof. Dr. Drs. Benyamin Kusumoputro, MSc.** | Universitas Indonesia, Indonesia

INVITED SPEAKER

- **Dr. Bambang Trigunaryah, Ph.D., PMP.** | King Fahd University of Petroleum and Minerals, KSA
- **Prof. Dr. rer. nat. habil Uwe Lahl** | Technische Universitat Darmstadt (TUD), Germany
- **Dr. Guillermo Rein** | Imperial College London, United Kingdom
- **Prof. Jae Dong Chung, B.S., M.S., Ph.D** | Sejong University, South Korea
- **Prof. Dr. Yifan CHEN, FIET, SMIEEE** | University of Waikato, New Zealand
- **Prof. Dr.-Ing Ir. Kalamullah Ramli, M.Eng.** | Universitas Indonesia, Indonesia
- **Prof. Dr. Ir. H.J. (Erik) Heeres** | University of Groningen, Netherland
- **Prof. Nishikawa Hiroshi** | Joining and Welding Research Institute Osaka University, Japan
- **Ashok K. Das, B.Arch., M.A., M.Arch., Ph.D** | University of Hawai'i Manoa, USA
- **Professor Margaret Petty** | Queensland University of Technology, Australia
- **Professor Kousuke Hiromori** | Tohoku University, Japan
- **Professor Masafumi Yohda** | Tokyo University of Agriculture and Technology, Japan
- **Dr. Mark Harrison** | Queensland University of Technology, Australia
- **Prof. Joe da Costa** | The University of Queensland, Australia
- **Dr. Volkan Degirmenci** | University of Warwick, United Kingdom
- **Prof. Marie-Anne Guerry** | Vrije Universiteit Brussel, Belgia
- **Prof. Pekka Leviakangas** | University of Oulu, Finland
- **Peter Simmonds** | ASHRAE Instructor



ACKNOWLEDGEMENT

The 15th International Conference on QIR (Quality in Research) Organizing Committee wishes to express its gratitude and appreciation to :

Prof. Dr. Ir. Muhammad Anis M.Met., Rector of Universitas Indonesia for consenting to be the guest of honour

All invited speakers session, moderators and conference speakers, for their participation.
 All conference Sponsors, Supporters, Exhibitors and advertisers for their generous support.
 All participants and others who have in one way or another contributed towards the success of this conference.

PLATINUM SPONSOR



SILVER SPONSOR



SUPPORTED BY





KEYNOTE SPEAKER

Thomas Goldsby
Ohio State University

Dr. Thomas J. Goldsby is a Harry T. Mangurian, Jr. Foundation Professor in Business and Professor of Logistics at The Ohio State University. He holds a B.S. in Business Administration from the University of Evansville, M.B.A. from the University of Kentucky, and Ph.D. in Marketing and Logistics from Michigan State University. He is the Co-Editor-in-Chief of the Journal of Business Logistics and former Editor of Transportation Journal. He serves as Associate Director of the Center for Operational Excellence (COE), a Research Fellow of the National Center for the Middle Market, and a research associate of the Global Supply Chain Forum, all housed at Ohio State's Fisher College of Business.



His research interests include logistics strategy, supply chain integration, and the theory and practice of lean and agile supply chain strategies. He has published more than 50 articles in academic and is the co-author of five books and is a proud recipient of: the Best Paper Award at the Transportation Journal (2012-2013), Bernard J. LaLonde Award at the Journal of Business Logistics (2007), and has twice received the Accenture Award for best paper published in the International Journal of Logistics Management (1998 and 2002). Dr. Goldsby has received recognition for excellence in teaching at Iowa State University, The Ohio State University, and The University of Kentucky.

Jackie Yi-Ru Ying
Institute of Bioengineering and Nanotechnology in Singapore

Prof. Jackie Yi-Ru Ying was born in Taipei in 1966. She earned a B.Eng. degree, graduating summa cum laude from Cooper Union in 1987. She then attended Princeton University, receiving her MA in 1988 and her PhD in 1991, both in chemical engineering. She spent a year as a Humboldt Fellow at the Institute for New Materials in Saarbrücken and researched nanocrystalline materials with Herbert Gleiter. Prof. Ying became a professor in the Department of Chemical Engineering at the Massachusetts Institute of Technology (MIT) in 1992. She was made a full professor in 2001; at 35 she was one of MIT's youngest full professors. She returned to Singapore in 2003 to serve as the first executive director of the Institute of Bioengineering and Nanotechnology, a division of the Agency for Science, Technology and Research (A*STAR). Her research concerns the biomedical and catalytic applications of nanostructured systems and materials.



She was elected to the Singapore Women's Hall of Fame in 2014. She was one of the recipients of the inaugural 2015 Mustafa Prize awarded by the Mustafa Science and Technology Foundation. She was also awarded the "Top Scientific Achievement" award for "her great scientific and technological contributions and achievements to the synthesis of well-designed advanced nanostructured materials and systems, nanostructured biomaterials and miniaturised biosystems for various interesting applications".



KEYNOTE SPEAKER

Benyamin Kusumoputro

Universitas Indonesia

Prof. Dr. Drs. Benyamin Kusumoputro, MSc is a Professor in Computer Intelligence in the Electrical Engineering Department, Faculty of Engineering Universitas Indonesia. He was born in Bandung on November 17th, 1957. He graduated from Bandung Institute of Technology in 1981 with a Bachelor Degree in Physics and was awarded a Master of Engineering Science in Optoelectronics and Laser Applications from Universitas Indonesia, and a Doctoral degree in Engineering from Electrical and Electronics Engineering Department, Bio- sensors, Tokyo Institute of Technology, Tokyo, Japan in 1993. His interest area of research includes: Development of Computational Intelligence and Methodology for Artificial Senses.



He is a member of Institute of Electrical Engineering of Japan (IEEJ), International Society for Optical Engineering (SPIE), International Association of Science and Technology for Development (IASTED), and World Scientific and Engineering Academy and Society (WSEAS). Some of the awards he has received are: Bronze Medal of Civil Servant, Government of Indonesia, 2005; University Research Achievement, Universitas Indonesia in 2005; and representing Universitas Indonesia in the National Outstanding Lecture Competition in 2016.

INVITED SPEAKER

Uwe Lahl

Technische Universität Darmstadt (TUD)

Prof. Uwe Lahl was born on 20 March 1951. Prof. Uwe Lahl holds a doctorate (Dr.rer. nat.) and a professorial degree (PD, Habilitation). Since April 2014, he is Head of the Ministry of Transportation of the German federal state of Baden-Württemberg. Before, he was manager at the BZL Kommunikation und Projektsteuerung GmbH (2009 - 2014) and Head of the Directorate General for Environmental Health, Air Pollution Control, Safety of Installations and Transport, Chemical Safety at the Federal Ministry for the Environment, Nature Conservation and Nuclear Safety (2000-2009).



Since 2008, he is, too, associated Professor at Technical University of Darmstadt. In 2010, he started teaching at the University of Indonesia at the Faculty of Engineering in the Department of Environmental Engineering and became adjunct Professor at the University of Indonesia in 2011.



INVITED SPEAKER

Bambang Trigunarsyah

King Fahd University of Petroleum and Minerals

Dr. Bambang Trigunarsyah is an Associate Professor in the Construction Engineering and Management Department, King Fahd University of Petroleum and Minerals (KFUPM), Dhahran, Saudi Arabia. He earned his BSc in Engineering (Civil) from Colorado School of Mines in the USA, a Master degree in Civil Engineering (Construction Management) from the University of Indonesia, and a PhD in Engineering Project Management from the University of Melbourne, Australia. Dr. Bambang Trigunarsyah research interests are in the area of: Construction management and economic, Constructability and operability of infrastructure project, Knowledge management in project based organization, Post-disaster reconstruction project management, Quality management in construction, and Infrastructure project delivery and infrastructure asset management.

Previously, Dr. Bambang Trigunarsyah was an Associate Professor and the Course Leaders for Master of Project Management and Master of Infrastructure Management in the School of Civil Engineering and Built Environment, Queensland University of Technology (QUT), Australia, from 2007 to 2013. He continues his association with QUT as an Adjunct Associate Professor. Dr. Bambang Trigunarsyah was the Head of the Civil Engineering Department at Universitas Indonesia (2004-2006) and an Associate Professor in Construction Project Management. Dr. Bambang Trigunarsyah started his full time tenure at Universitas Indonesia in 2001, following the completion of his PhD study from the University of Melbourne, Australia



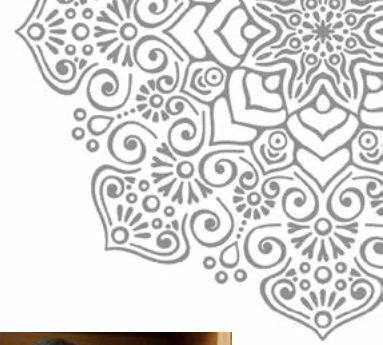
Guillermo Rein

Imperial College London

Dr. Guillermo Rein studied Mechanical Engineering at University of California at Berkeley (MSc 2003, PhD 2005) and before then was at ICAI Universidad Pontificia Comillas (Ingeniero Industrial, 1999). Dr. Rein is editor in Thermal Energy at the Department of Mechanical Engineering of Imperial College and Editor-in Chief of the Journal Fire Technology. His research is centered on heat transfer, combustion and fire science.

Over the last 15 years, he has been best known in three areas: 1) how polymers and wood ignite and how to avoid it; 2) how engineers can design better structures that resist fires; and 3) how wildfires spread in the forest and how to manage them. Dr. Guillermo Rein is known in the building sector for changing the way UK fire engineers design modern infrastructure. His work has been recognized internationally with a number of research awards (e.g. Lund Award, Wildfire Early Career Award, Hinshelwood Prize, and Distinguished Paper in the Combustion Symposium). Dr. Guillermo Rein has been featured in several international media (e.g. Financial Times, BBC Radio, and New York Times) for his expertise.





INVITED SPEAKER

Jae Dong Chung

Sejong University



Prof. Jae Dong Chung received his Bachelor of Science in 1990 from Seoul National University and continued on to finished his Master of Science in 1992 and Ph.D in August 1996 from the same university. He is currently a Professor at the Department of Mechanical Engineering, Sejong University Korea. His research fields include (1) thermal energy storage and transport; (2) Refrigeration Driven by Low Temperature Energy Sources: Desiccant Cooling, Adsorption Cooling; (3) Phase Change; (4) Nano-scale Heat Transfer.

In 2016, Prof. Jae Dong Chung received the Best Paper Award by Minister of Land, Infrastructure and Transport. He was also awarded as Outstanding Academic Award by Society of Air Air-conditioning and Refrigerating Engineers of Korea in 2014, and also Best Paper Award by Minister of Ministry of Trade Industry and Energy in 2014. Prof Jae Dong Chung also joined professional association i.e. The Korean Society of Mechanical Engineering, Thermal Division as an Director of General Affairs since 2009 until present, Chairperson of the division of Low Temperature Facilities Engineering in SAREK, Vice president of B1 commission of IIR from 2015 until present, International Journal of Air-Conditioning and Refrigeration as an Editor from 2009 until present, Journal of Mechanical Science and Technology as an Associate Editor from 2008 until present and so forth.

Yifan Chen

University of Waikato



Dr. Yifan Chen is a Professor of Engineering and the Associate Dean of External Engagement for the Faculty of Science and Engineering and the Faculty of Computing and Mathematical Sciences in the University of Waikato, Hamilton, New Zealand. His current research interests include electromagnetic medical imaging and diagnosis, transient communication with application to healthcare, touchable communication and computation with application to targeted drug delivery and contrast-enhanced medical imaging, fundamentals and applications of nanoscale and molecular communications, and channel modelling for next-generation wireless systems and networks.

He is the Coordinator of the European FP7 “CoNHealth” project on intelligent medical ICT, an elected Working Group Co-leader of the European COST Action TD1301 “MiMed” project on microwave medical imaging, an Advisory Committee Member of the European Horizon 2020 “CIRCLE” project on molecular communications, a Voting Member of the IEEE Standards Development Working Group 1906.1 on nanoscale and molecular communications, an Editor for IEEE ComSoc Best Readings in Nanoscale Communication Networks and IEEE Access Special Section in Nano-antennas, Nano-transceivers, and Nano-networks/Communications, and a Vice Chair of the IEEE Nano-scale, Molecular and Quantum Networking Emerging Technical Subcommittee. He is a Fellow of IET and a Senior Member of IEEE.



INVITED SPEAKER

Kalamullah Ramli

Universitas Indonesia

Prof. Kalamullah Ramli is a Professor in Computer Engineering since July 1, 2009. He finished his Master in Telecommunication Engineering at University of Wollongong, NSW, Australia, in 1997. He then continued his Doktorarbeit on Computer Networks in year 2000 at Universitaet Duisburg-Essen, NRW, Germany, and obtained his Dr.-Ing. in year 2003. His research interests include embedded system, network and information security, computer and communications, and intelligent transportation system. Prof. Kalamullah Ramli was the Director General of Post and ICT Operations of the Ministry of Communication and Information Technology (2013 - 2016). Prof. Kalamullah Ramli has many collaboration work between universities from German, Italy and Malaysia. One of his collaboration received an "AsiaLink" grant from the European Comission between 2005 - 2007 to deliver an initiative named "Improving Mobility of Student between Europe and ASEAN" which resulted in a prototype model of Credit Transfer System Platform between ASEAN and Europe. Based on this experience he was elected as one of the speaker on ASAIHL Conference on December 2008 in Jakarta. This ASAIHL is managed by ASEAN Universities to implement a platform for Credit Transfer System between Universities in ASEAN.



H.J. (Erik) Heeres

University of Groningen

Prof. Dr. Ir. H.J. Heeres was born in 1963. He graduated in 1990 from the University of Groningen, with a thesis on the development of novel homogeneous lanthanide catalysts for the conversion of unsaturated hydrocarbons. Afterwards, he performed a post-doctoral research at the University of Oxford, in the group of J.M. Brown on asymmetric catalysis from 1990 to 1991. In 1995 he graduated from Technical University Twente in Chemical Engineering and achieved a Master Degree. From 1991 to 1999, he was employed at Shell Research, in Amsterdam and Pernis, and worked on a range of applied catalysis topics. He joined the chemical reaction engineering department of the University of Groningen, in 1999, as an assistant professor. Four years later, he was appointed full professor in green chemical reaction engineering. His research interest concerns on the development of efficient catalytic technology for acid- and metal-based catalytic biomass conversions, with an emphasis on biofuels (catalytic pyrolysis, pyrolysis oil upgrading), platform chemicals (levulinic acid, hydroxymethylfurfural) and performance materials from biomass (starch modifications). The group is actively involved in national and international consortia (for example, the European Union 6th framework project Biocoup) dealing with catalytic pyrolysis oil upgrading. Prof. Dr. Ir. H.J. Heeres is the (co-) author of 185 papers in international peer reviewed journals (h-index 44) and 12 patents in the field of applied catalysis and chemical reaction engineering. Heeres is also a member of the KoninklijkeHollandscheMaatschappij der Wetenschappen and an associate editor of the Journal of fuel processing technology.





INVITED SPEAKER

Nishikawa Hiroshi

Joining and Welding Research Institute Osaka University

Nishikawa Hiroshi was born at Japan in 1973. He is an Associate Professor at Joining Welding Research Institute, Osaka University from 2007 until present. Nishikawa Hiroshi finished his Bachelor Engineering in 1997 at Department of Welding and Production Engineering, Osaka University and continued to finish his Master of Engineering in 1999 at Department of Adaptive Machine Systems, Graduate School of Engineering, Osaka University. On 2002, he achieved his Doctoral of Engineering from the same university.



Ashok K. Das

University of Hawai'i Manoa

Ashok K. Das, Ph.D received his Bachelor of Architecture from the School of Planning and Architecture, New Delhi India in 1996. He continued to finish his master degree in Environmental Planning and Management at Kansas State University, Manhattan and received his Master of Art and Master of Architecture in 2001. In 2008, he started pursuing his doctoral degree in Urban Planning at University of California, Los Angeles. His research interests revolve broadly around issues of urban poverty in developing countries, primarily in South and Southeast Asia. His current research areas are: (1) community participation and empowerment, (2) slum upgrading, basic services and low-income housing, (3) integrated community-based microfinance for urban poverty alleviation, (4) local planning and governance for disaster preparedness and risk education, and (5) the role of civil society and NGOs in urban planning and development. Currently Ashok is an Assistant Professor at the Department of Urban and Regional Planning, University of Hawai'i. He is also an Affiliate Faculty at the Center for Southeast Asian Studies at the same university. Since 2009, Ashok has been involved with the Cleanopolis Energy System India Private Limited (CESIPL) as an Adviser. He was invited as an expert to a discussion on "Rural-urban linkages and drivers of inequality in Asia" in May 2017 with representatives, directors and vice presidents of the Ford Foundation to explore ways for its global philanthropic mission to transcend the rural-urban dichotomy.





INVITED SPEAKER

Margaret Petty

Queensland University of Technology

Prof. Margaret Maile Petty studied Art History at the University of Oregon, Eugene to obtain her Bachelor of Art with Summa Cum Laude in 2000. After graduation, she continued her study for a Master Degree at The Bard Graduate Center, New York City and obtained her Master of Art in 2002. Before she received her Doctoral Degree in Architectural History at Victoria University of Wellington in 2016, she took the doctoral course work and qualifying exams at The Bard Graduate Center, New York City in 2005. Currently she



is Professor and Head of the School of Design in the Creative Industries Faculty at Queensland University of Technology, Australia. Her research broadly investigates the discourse, production, and consumption practices of the modern built environment, with a particular focus on artificial lighting and interiors. She has published broadly in academic journals such as the JSAH, Journal of Design History, Home Cultures, Interiors, and PLAT and is co-editor of *Cities of Light: Two Hundred Years of Urban Illumination* (Routledge, 2015), as well as *Architectures of Display: Department Stores and Modern Retail* (Ashgate, 2017). She is co-founder and member of the Advisory Board of DesignCo, Society of Architectural Historians (SAH), Society of Architectural Historians of Australia and New Zealand (SAHANZ) and International Committee on the History of Technology (ICHOTEC).

Kousuke Hiromori

Tohoku University

Kousuke Hiromori is a Ph.D candidate in the Department of Chemical Engineering, Tohoku University. He was awarded a Bachelor of Science and Master of Science both from Chemical Engineering, Tohoku University. His Thesis topic is: Recovery of Vitamin E from Rice Bran Deodorizer Distillate Using Ion-Exchange Resins.

Kousuke Hiromori has also won ICRBO 2016 Best Poster Presentation Award and Incentive Student Award of the Society of Chemical Engineers' Japan in 2017. His list of publication includes: "Novel simple process for tocopherols selective recovery from vegetable oils by adsorption and desorption with an anion-exchange resin (published in *Food Chemistry*, 2016), Development of Novel Process for Efficiently Separating and Purifying Tocotrienols (published in *Japan Society for Food Engineering Journal*, 2016).



INVITED SPEAKER

Masafumi Yohda

Tokyo University of Agriculture and Technology

Professor Masafumi Yohda received his Bachelor Degree in 1982 from The University of Tokyo and continued to finished his Master Degree in 1984 and Ph.D. in 1987 from the same university. He is a Professor at Department of Biotechnology and Life Science, Tokyo University of Agriculture and Technology from 2003 until now.



Currently, he serves as the Vice Dean of Institute of Global Innovation Research, Tokyo University of Agriculture and Technology. His research interests including Biochemistry, Molecular Biology, Biophysics, System Engineering and Environmental Science. In 1999, Professor Masafumi Yohda was rewarded for the excellent paper award of Journal of Bioscience and Bio Engineering. He joins many professional memberships such as The Japanese Biochemical Society as a Councilor, Protein Society of Japan as a Director, The Society of Biotechnology as a Director, Manager of East Japan Branch, The Chem-Bio Informatics Society as Director.

Mark Harrison

Queensland University of Technology

Dr. Mark Harrison obtained an undergraduate degree in biochemistry from the University of Queensland in 1992. He completed his PhD (2001) at the University of Queensland, researching the molecular mechanisms by which cells transport, store, and detoxify essential metal ions. He then undertook post-doctoral work at Newcastle University (Newcastle-upon-Tyne, UK) researching the biological chemistry of metalloproteins and their role in essential metal ion homeostasis. Dr. Mark Harrison returned to Australia in 2003 and was awarded a 3 year Queensland State Government Smart State Fellowship in 2004 to produce enzymes in a model plant. The development of this technology in sugarcane was a key part of the \$3.8 million research collaboration between Syngenta, one of the world's largest integrated agribusiness companies, and QUT.



Dr. Mark Harrison is a biochemist with extensive basic, applied, and commercial research experience. He is a Senior Research Fellow and foundation member of the QUT Centre for Tropical Crops and Biocommodities (<https://www.qut.edu.au/research/our-research/institutes-centres-and-research-groups/centre-for-tropical-crops-and-biocommodities>). Dr. Mark Harrison also provides consulting services to the Australian food and bio-industrial sector. Research in his group is focused on the conversion of agricultural wastes and residues into more valuable food, feed, fibre, fine chemical, and fuel products, (<https://research.qut.edu.au/biorefining/>).

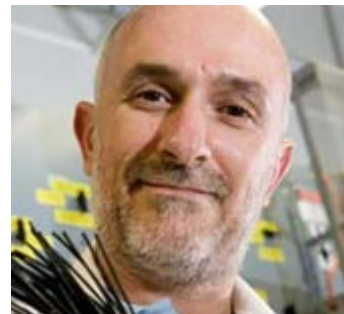


INVITED SPEAKER

Joe da Costa

The University of Queensland

Prof. Joe da Costa is an Australian Research Council (ARC) Future Fellow and a Professor in the School of Chemical Engineering at the University of Queensland, Brisbane Australia. He is also the Director of the FIM2Lab - Functional Interfacial Materials and Membranes Laboratory. Prof. Joe da Costa has over 30 years working experience in industrial, consultancy and academic roles in Brazil, England, and Australia. Currently, he leads several research projects in the area of H₂, CO₂, O₂, ethanol separation and desalination using inorganic membranes and membrane reactors, in addition to catalysts for wastewater processing. Prof. Joe da Costa has over 250 international publications including 13 book chapters, and he is an editorial board member of Nature's Scientific Report open source journal. Also, he held a prominent leadership position as a member of the Independent Scientific Panel advising the Queensland Government on underground coal gasification, and a member of the International Panel of Experts assessing the Brazilian programs of Centers of Excellence. His work has been cited over 6800 times, and his h-index is 44. He is a Chartered Professional Engineer in the Colleges of Mechanical Engineering and Chemical Engineering of the Institution of Engineers Australia.



Volkan Degirmenci

University of Warwick

Dr Volkan Degirmenci is an Assistant Professor in School of Engineering in the University of Warwick, UK. Dr. Degirmenci obtained his PhD in Chemical Engineering from Middle East Technical University, Ankara, Turkey, in 2007. Then he joined to the Molecular Heterogeneous Catalysis research group at Eindhoven University of Technology, Netherlands as a postdoctoral fellow in 2008. Next he moved to UK to the Queen's University Belfast in 2012 where he was promoted to Assistant Professor in Chemical Engineering.



Recently he joined the School of Engineering at University of Warwick in 2015. The research interests of Dr. Degirmenci are in the field of heterogeneous catalysis and reactor design with a focus on microporous and mesoporous materials. The topics of his recent research are directed towards the development of sustainable processes for biomass conversion, in-situ spectroscopy for the understanding of the reaction mechanisms and structure-activity relations in heterogeneous catalysis.



INVITED SPEAKER

Marie-Anne Guerry

Vrije Universiteit Brussel

Prof. Marie-Anne Guerry pursues her Doctoral Degree in mathematical sciences on 1985 at Vrije Universiteit Brussel and received her PhD in 1992. At the moment, Prof. Marie-Anne Guerry is a Professor at the Department of Business Technology and Operations, Vrije Universiteit Brussel since 2012. Her research expertise are Markov modeling, manpower planning and career studies.



Prof. Marie-Anne Guerry is an active reviewer for Linear Algebra and its Application, Elsevier (since 2009), British Journal of Applied Science & Technology (since 2013), Applied Mathematical Modelling, Elsevier (since 2013), TOP Journal of Operations Research, Springer Publishing Company (since 2014), Central European Journal of Operations Research, Springer Publishing Company (since 2014), Applied Stochastic Models in Business and Industry, John Wiley & Sons (since 2014), Personnel Review, Emerald (since 2015) and many more.

Pekka Leviakangas

University of Oulu

Prof. Pekka Leviakangas (born in 1962, PhD in technology) has several experiences as an expert in civil service, business and research. He is currently the Principal Scientist at VTT Technical Research Centre of Finland Ltd. In 2012-2016 he acted as Associate Professor at Curtin University in the School of Built Environment, Programme Director of the Australasian Centre for Building Information Modelling and Research Professor at University of Oulu in industrial engineering and management. His previous positions include Chief Research Scientist, Team Leader and Customer Manager at VTT, Vice-President of Jaakko Pöyry Group subsidiary (JP-Transplan), Corporate Analyst of Finnish Railways (VR-Group Ltd), R&D Manager of Finnish National Road Administration's South-eastern region, and private consultant. He was an adjunct professor of Tampere University of Technology in the department of Logistics and Business Information for 2008-2014. His own research covers innovation management, value analysis, impact analysis, service sciences, project finance, investment, financial and socio-economic analysis, restructuring issues and new technology deployment. His primary research area has been on transport sector, but his activities have extended to other fields such as bioeconomy, climate change, meteorology, education, construction and infrastructure management.





INVITED SPEAKER

Peter Simmonds

ASHRAE Instructors

Peter Simmonds is managing director/principal of Building and Systems Analytics LLC. Peter has been involved in the design and operation of tall, supertall and megatall buildings around the world for more than 30 years. An ASHRAE member since 1989, Peter has twice chaired Technical Committee 9.12 Tall Buildings, and is a member of TC 2.1 Thermal Comfort and Human Physiology, and TC 7.5 Smart Building Systems. He also serves on the Standards Committee and is Secretary of the College of Fellows.

Peter has authored or coauthored more than 60 technical papers, articles and books. Most recently, he was the author of the new ASHRAE Design Guide for Tall, Supertall and Megatall Building Systems (2015). He was also a co-author of the ASHRAE/REHVA Active and Passive Beam Application Design Guide (2014).

He has one Bachelor of Science degree in Mechanical Engineering and another in Research and Development from Reading Technical College in England; a Master's degree from Hogere Technische School, Den Bosch, The Netherlands; and a Ph.D. from Technical University of Delft, The Netherlands.





PROGRAM AT GLANCE

Date : 24 - 27 July 2017
Location : BICC the Westin, Nusa Dua, Bali.

The Arrangement of the QIR 2017 Conference can be seen at the table below

Date	Time	Program	
24 July	03.00-05.00 p.m	Registration and Welcome Cocktails	
25 July	Full Day	Exhibition	
	08.30-10.15 am	Opening Ceremony	
	10.15-10.30 am	Coffee break	
	10.30-11.15 am	Plenary Lecture 1 Prof. Benyamin Kusumoputro	
	11.15-12.00 pm	Plenary Lecture 2: Prof. Thomas Goldsby	
	01.00-03.00 pm	Parallel Session	Each parallel session will be started with presentation by Invited Speakers
		03.00-03.30 pm	
	03.30-06.00 pm	Parallel Session	
	06.00-07.00 pm	Poster Session Day 1	
	07.00-09.00 pm	Banquette Dinner	
	26 July	Full Day	Exhibition
08.30-10.00 am		Parallel Session	Each parallel session will be started with presentation by Invited Speakers
		10.00-10.30 am	
10.30-12.00 pm		Parallel Session	
12.00-01.00 pm		Lunch	Poster Session Day 2
		01.00-02.00 pm	
01.00-03.00 pm		Parallel Session	
03.00-03.30 pm		Coffee break	
07.00-09.00 pm		Dinner and Closing Ceremony	
27 July		08.00am-08.00 pm	Social Tour



QIR

*The Westin Resort
Nusa Dua, Bali*
24-27 July 2017

SYMPOSIUM A

**International Symposium on
Civil and Environmental
Engineering**





The 15th International Conference Quality In Research (QIR) 2017

DEVELOPMENT OF INTEGRATED MANAGEMENT SYSTEM BETWEEN QUALITY MANAGEMENT SYSTEM AND OCCUPATIONAL HEALTH AND SAFETY MANAGEMENT SYSTEM IN MINISTRY OF PUBLIC WORK AND PUBLIC HOUSING – A CONCEPTUAL FRAMEWORK

RINGGY MASUIN¹, YUSUF LATIEF², T. YURI ZAGLOEL³, LENI SAGITA⁴

¹*Doctoral Program Student Civil Department Faculty of Engineering University of Indonesia*

²*Professor, Civil Department Faculty of Engineering University of Indonesia*

³*Professor, Industrial Engineering Department Faculty of Engineering University of Indonesia*

⁴*Lecturer, Civil Engineering Department Faculty of Engineering University of Indonesia*

ABSTRACT

This paper reviews the literature on integrated management system (IMS) between quality management system and occupational health and safety management system. The term integrated management system is clarified as it is typically applied to integrated risk, integrated process, and integrated audit in order to achieve orderly construction. The objective of the present study is to analyze the evolution of IMS research, presenting its contributions and gaps in the IMS scope. The analysis was conducted through a theoretical framework of IMS. Some clarification in terms of integrated risk, integrated process and integrated audit of engineering and its theoretical developments. Methodology used in this paper is comprehensive literature review of integrated management system between quality management system and occupational health and safety management system to influence performance of integrated risk, integrated process and integrated audit of quality and safety system in orderly construction. This paper piloting project in time phase of activities In Ministry of Public Work and Public Housing as a core activities. Results of this study shows conceptual framework for development of integrated management system between Quality Management System and Occupational Health and Safety Management System. All management systems were used Deming Cycle (PDCA) theory and have common feature. In this study, author found that Fayol Theory based on activities management can develop management system into integrated management system. Based on activities in System Engineering Phase, authors found that life cycle system in construction are the best system suited in Integrated Management System between Quality Management System and Occupational Health and Safety Management System as the state-of-the-art of this research. This integrated management system was piloting in Ministry of Public Works and Housing Provision that application of independent system management. Implementation of integrated management system assumes can achieve orderly construction with less of rework, less risk of accident, and risk of waste. It is suggested the gaps found in this paper are explored in future studies.

Keywords: Integrated Audit, Integrated Management System, Integrated Process, Integrated Risk



1. INTRODUCTION

Economic globalization and the intensification of competitiveness has led many organizations to adopt management tools that enable them to obtain high-quality products and processes without harming employees' life quality. (Simon, Honore Petnji Yaya et al. 2014). In construction management the discussion on quality management system problems, health and safety management system and environment are generally not discussed simultaneously. The quality management system and health and safety management system and environment are still done separately and are still done independently, whereas in reality these two systems interact and have the same process through the PDCA cycle (Beckmerhagen et al., 2003; Labodova, 2004; Zeng et al., 2007; Karapetrovic and Casadesús, 2009; Oliveira, 2013; Abad et al., 2014). About 80% of the activities of the quality management system, safety and environmental management are common to every management system (Jørgensen, 2008).

An Integrated Management System (IMS) is a construction to avoid duplication of tasks that aims to take advantage from the elements common of two or more separate systems, putting them to work together in a single and more efficient IMS (Beckmerhagen et al., 2003; Labodova, 2004; Zeng et al., 2007; Karapetrovic and Casadesús, 2009; Oliveira, 2013; Abad et al., 2014). Organizations often operate in turbulent environments characterized by intense competitiveness, constant technological progress, new market requirements, and scarce natural resources. This scenario imposes the constant need for change in the operation and organization management. The integration of certifiable management systems is an effective alternative to integrated standard and risk management as strategic decision (Octavian, 2016; Hoyle et.al, 2009; Oprean et.al, 2006). The proposed subject was integration process, integration risk, integration audit and system information

At the last decade, several approaches to IMS have being studied, such as evaluation of motivations, benefits and drawbacks of integration (see i.e. Simon et al. 2012; Bernardo et al. 2015; Gianni and Gotzamani, 2015), characterization of the integration levels (Bernardo et al. 2012; Abad et al. 2014), integration of audits (Karapetrovic and Willborn, 2000; Bernardo et al. 2010; Simon et al. 2011), integration strategy (Zeng et al. 2007; Savino and Batbaatar, 2015) and models and guidelines for the integration process (Domingues et al. 2016; Oliveira, 2013).

2. INTEGRATED MANAGEMENT SYSTEM APPROACH

Both scholarly literature and the practical activities of organizations, indicate two dominant approaches to identification and description of the management process. One of these was developed by H. Fayol and other by E.W. Deming. H. Fayol identified five managerial function constituting the management process. These are: organization, planning, coordination, control and command. In accordance with the spirit of Fayol's theory, the key managerial functions include: planning, organization, command, control and coordination. Of course, this basic set of managerial functions can be combined with other elements such as knowledge management, information management, decision making, etc. In Fayol's approach, several factors result in the integrative character of the management process. E.W Deming's proposal constitute an interesting supplement to H. Fayol's theory. While Fayol concentrated generally on managerial activities in their entirety, Deming stressed the never ending cyclical nature of such activities. Over the last decade,



management systems standards have become more aligned. This alignment is characterized by a common base that supports the structure of management system: the PDCA cycle (Plan, Do, Check, Act) of continual improvement (Bernardo et al. 2015; Oliveira, 2013; Zeng et al. 2007).

3. EVALUATION OF QMS AND OHSAS IN MINISTRY OF PUBLIC WORKS AND PUBLIC HOUSING

In fact, Ministry of Public Works and Public Housing implemented Quality Management System (QMS) and Occupational Health and Safety Management System (OHSAS) independently. Evaluation used survey to 37 project sampling (average 1 project per province) from 340 project (average 10 project per province). Evaluation divided into 6 regions including: Sumatera, Java, Kalimantan, Sulawesi, Bali / NTB, and Papua. The sampling project is divided into 4 project categories consisting of Bina Marga (BM) project, Water Resources (SDA), Cipta Karya (CK), and Housing (Pera). The results evaluation of QMS shown in figure 1.

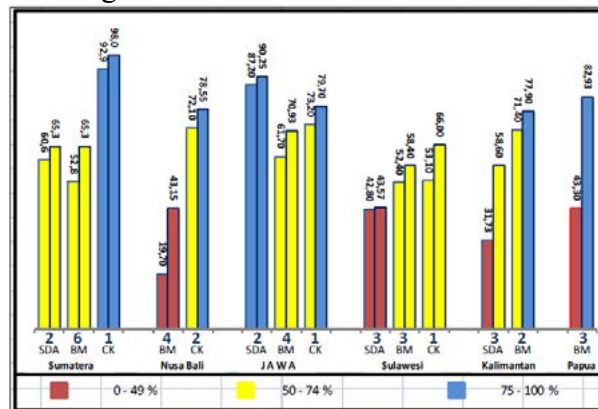


Figure 1 The Results of QMS in 2015 (Executive Summary Ministry of PUPR, 2015)

Figure 1 explained that all construction projects in Ministry of Public Works and Public Housing already implemented QMS (50 -74% or yellow block) but not based on QMS regulation. It is expected to achieve the best results and international standards that can meet the needs and expectations of service users and even beyond it (beyond the expectation) and improve the performance of service providers.

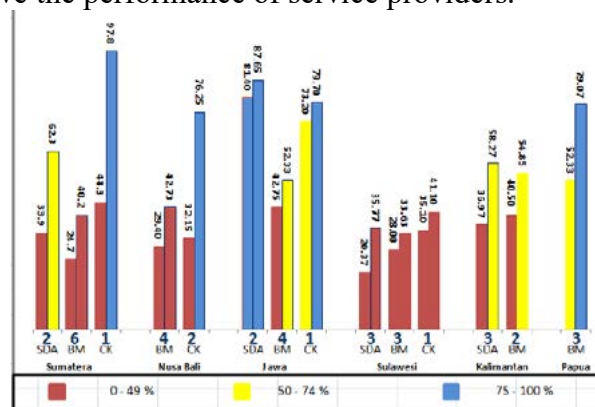
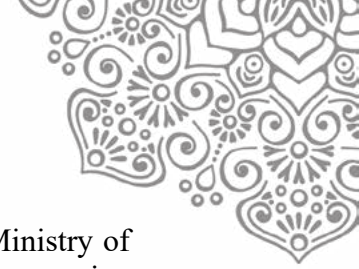


Figure 2 The Results of OHSMS at 37 Construction Projects in 2015

Source: Executive Summary Ministry of Public Works and Public Housing, 2015



The results evaluation of health and safety shown in figure 2 explored that Ministry of Public Works and Public Housing have “unsaved activities/red blocks” (implementation range was 0 – 49%)” for health and safety.

Figure 1 and Figure 2 expressed that QMS is done their process activity independently with OHSAS, evaluate their audit independently, documenting the process independently and have different regulation. Figure 2 explored several cases of occupational accidents in Indonesia have shown a significant impact both on the side of corporate performance decline, causing delay projects, cost overrun, and humanitarian aspects. For both results in Figure 1 and Figure 2, only Directorate General of The Housing Provision that hasn’t implemented quality management system and occupational safety and health management system.

4. STATE-OF-THE-ART

Evaluation of system management implementation in Ministry of Public Works and Public Housing, shown in figure 1 and figure 2 that QMS and OHSAS independently in single system probably have the same risk of rework and risk of accident that can causes time-consuming in order to achieve orderly construction. In fact, doing construction is almost always deal with QMS and OHSAS in same time in same activities. Those process of activity are manage shape into knowledge management as shown in the figure 3 as the state-of-the-art of this paper.

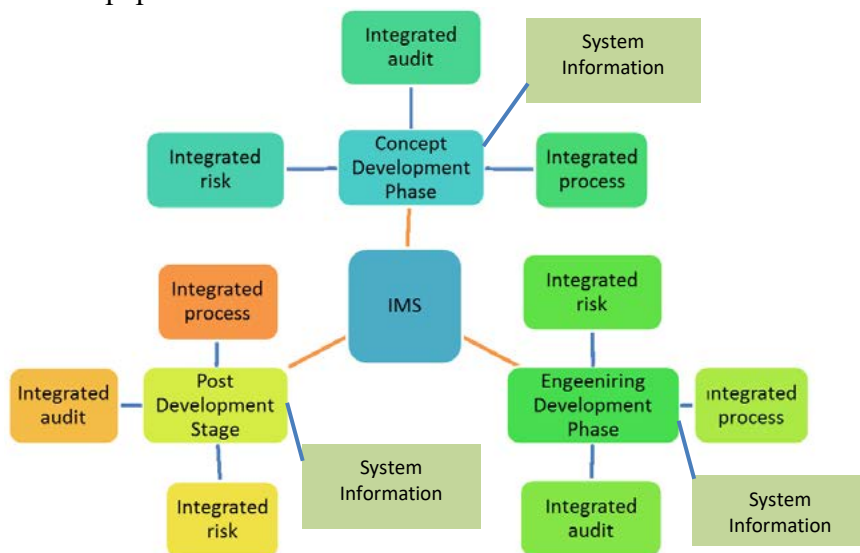
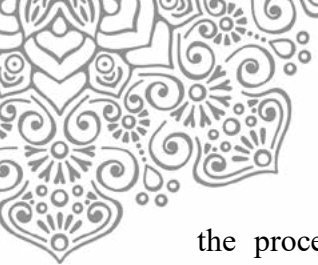


Figure 3 State-Of-The-Art (Author Own Research)

Integration process used in construction is linier system engineering such as concept development phase, development phase, and post development phase (Kossiakof, 2011; Benjamin, 2015). Organizations need to evaluate quality, health and safety risk. They require risk evaluation within organization which control in the highest risk item (Chad et.al, 2015; Bogdul et.al, 2015). **Integrated risk management as the second level has the role to play in making the public service more effective. It contributes to better program management** (Office of the Auditor General of Canada, 2003). The third elements of integration is integration audit. Integration audit can only be conducted when



the process within organization are integrated (Chad et.al, 2015; Bogdul et.al, 2015; opincaru et.al., 2004). Implementation of integration management system is depend to system information (Trols, 2015), stakeholders and resource management (Nunhes et.al, 2015; Nunhes et.al, 2016). Process for achieving orderly construction in Figure 3 (concept development phase, engineering development phase, post development phase) have various variable as in table 1.

**Table 1 Variable used in Each System Engineering System Phase
 (Concept Development, Engineering Development, Post Development)
 (Author Review based on Literature Review in Table 2)**

Variable X1. Integrated Process	X1.1 Work Breakdown Structure	X.1.1.1 Scope	Variable X3. Integrated Audit	X.3.1 Audit Plan	X.3.1.1 Context of the organization
		X.1.1.2 Normative references			X.3.1.2 Leadership
		X.1.1.3 Terms and definition			X.3.1.3 Planning
		X.1.1.4 Context of the organization			X.3.1.4 Support
		X.1.1.5 Leadership			X.3.1.5 Operation
	X.1.2 Business Process	X.3.1.6 Performance evaluation			
	X.1.2.1 Plan Activities	X.3.1.7 Improvement			
	X.1.2.2 Flow Activities	X.3.2 Audit team			
	X.1.3 Support Process	X.1.3.1 Support resources		X.3.3 Audit Appraisal	
		X.1.3.2 Support activities		X.3.4 Audit Schedule & checklist	
		X.1.3.3 Flow Support Activities			
	X.1.4 Operation process	X.1.4.1 Operation process		Variable X4. System Information	X.4.1 IT Plan/Procedure
X.1.4.2 Flow operation activities		X.4.1.2 Normative references			
X.1.5 performance evaluation	X.1.5.1 Analysis of performance	X.4.1.3 Terms and definition			
	X.1.5.2 Performance evaluation	X.4.1.4 Context of the organization			
X.1.6 improvement	X.1.6.1 Process control	X.4.1.5 Leadership			
	X.1.6.2 improvement	X.4.1.6 Planning			
Variable X2. Integrated Risk	X.2.1 Identify Risk	X.2.1.1 Scope	X.4.1.7 Support		
		X.2.1.2 Normative references	X.4.1.8 Operation		
		X.2.1.3 Terms and definition	X.4.1.9 Performance evaluation		
		X.2.1.4 Context of the organization	X.4.1.10 Improvement		
		X.2.1.5 Leadership	X.4.2 Software & hardware		
	X.2.2 Analysis Risk	X.2.2.1 Planning	X.4.3 Data		
		X.2.2.2 Support	X.4.4 Flow Communication		
		X.2.2.3 Operation			
	X.2.3 Evaluation Risk	X.2.3.1 Evaluation			
		X.2.3.2 Performance evaluation			
X.2.4 Control Risk	X.2.4.1 Control risk				
	X.2.4.2 Improvement				

Variables are work breakdown structure, business process, support process, operation process, performance evaluation and improvement for integration process variable (Thaís Vieira Nunhes, et.al, 2017; Maria Gianni and Katerina Gotzamani, 2015; Merce Bernardo, 2014, Mercè Bernardo, 2015; Alexandra Simon, Juan Jose Tarí, Jose F. Molina-Azorín, 2015; Calcedo et.al, 2015; Mercè Bernardo, Marti Casadesus, Stanislas Karapetrovic, Inaki Heras, 2009). Identify risk, analysis risk, evaluation risk, and control risk for integrated risk variable (Merce Bernardo et.al, 2015; Yarahmadi et.al, 2015; Alexandra Simon, 2012; Alena Labadova, 2004; Beatrix Barafort, et.al, 2016; T.Karzkozka et.al, 2017). Audit plan, audit team, audit appraisal, and audit schedule and checklist for integrated audit (Sendil Mourougan, 2015; Cristinel Roncea, 2016; Merce Bernardo et.al., 2010; Simon, Merce Bernardo et.al, 2015; Merce Bernardo et.al, 2011; Ajay D Jewalikar, Dr. Abhijeet Shelke, 2016; Alexandra Simon, et. al., 2011; Zoé Hoy and Andrea Foley, 2015; Richard Roessler and Hannes Schlieter, 2015; Alexandra Simon et.al, 2012; Alexandra Simon et.al, 2012). Through an information technology management system, it can provide added value to the organization as a whole such as IT plan/procedures, software & hardware, data, and flow communication for system information (Iveta Mezinaska et.al., 2015; Florida Veljanoska and Majlinda Axhiu, 2015; Dorin Maier et.al, 2015). That is explored from table 2.



Table 2 State-of-the-Art

No	Features Author	Deming Cycle	H. Fayol cycle	Core Activities	System Information	Stakeholder Management	Integrated Risk	Integrated process	Integrated audits	Government Focus	Employee Focus	Results
1.	Chairini, 2017	✓		✓			✓				✓	Majority of risk in production is nonconformance product, untrained employee and less of awareness.
2.	Rebelo, 2017	✓		✓			✓				✓	Integrated Management System can reduce hazard in doing business.
3.	Nunhes, Ferreira Motta et al. 2016	✓		✓		✓					✓	Identify research gaps in the scope of IMS.
4.	Nunhes, Motta Barbosa et al. 2016	✓		✓		✓		✓			✓	The results indicated the most integrated elements are the high management responsibility, work instructions, control of documents and records, internal communication and structure and accountability
5.	Merce Bernardo, 2016	✓		✓		✓			✓		✓	Findings state of the art for future research, especially data for lack analysis of studies approaching IMS and performance
6.	El MorrChristo, 2016	✓			✓			✓				Less risk of death in IT e-Health
7.	Truls Löfstedt, 2015	✓			✓			✓			✓	IMS is a devices and systems that managers use to ensure that the behaviors and decisions of their employees are consistent with the organization's objectives and strategies and documented in an IT
8.	Abrahamsson, Isaksson et al. 2010			✓		✓		✓			✓	Results show that there are advantages in integration, but that the scope and level of integration often is limited.
9.	Manzanera et al, 2014	✓						✓		✓		Dividing the design process in other sectors as well as strategies that can be generalized to the government applicable
10.	Veljanoska, 2013	✓			✓			✓			✓	IT used to capture integrated management system transaction, support system, decision making system.



No	Features Author	Deming Cycle	H. Fayol cycle	Common feature	System information	Stakeholder Management	Integrated Risk	Integrated process	Integrated audits	Government Focus	Employee Focus	Results
11.	Simon et.al, 2012	✓						✓			✓	Explored evolution of integrated management system, benefit and difficulties and implemented IMS in chemical firms
12.	Raisiene, 2011			✓		✓		✓			✓	Seeing the potential advantages and weaknesses IMS for organizations that seek to optimize the management processes
13.	M. Sokovic, D. Pavletic, K. Kern Pipan, 2010	✓									✓	Advantage organizations to know the challenges and constraints of the organization in carrying out the integration of the system / standard. If these challenges are not detected early will cause delays organization.
14.	Asif, de Bruijn et al. 2009	✓		✓		✓		✓			✓	IMS implementation can be facilitated through enablers such as securing senior management's full support, addressing strategic planning, allocating and prioritizing resources, establishing goals, targets and milestones, involvement of end-users in the design and implementation phase, support of IMS experts, fostering a culture of teamwork, and through employees' training.
15.	Gapp, Fisher et al. 2008										✓	The findings show the importance of technical factors approach (visible) and philosophy (invisible) than cultural 5S management framework using Kaizen
16.	Badreddine, Romdhane et al. 2009	✓						✓			✓	Integrating to achieve satisfaction at the level of correspondence, coordination and integration
17.	Alena Labodová, 2004	✓					✓	✓			✓	The implementation of integrated management system based on risk analysis on greenfield.
18.	Present research	✓		✓	✓	✓	✓	✓	✓	✓		Advantage organizations to know the challenges and obstacles in the organization in implementing integration of systems / standards to achieve orderly construction

Source: Author own research, 2017



Table 2 explored the journey of in integrated management systems in academic review that Integrated Management System consist of integration process, integration risk, integration audit, and system information. Variable explore in Table 1 which is integrated process, integrated risk, integrated audit, and system information are review in table 2. Table 2 describe that previous studies about integrated management systems concerned in contractor's view or employee's view to achieve continuous improvement with high quality product without harming employees life. In fact, the present of government in standardized the integrated management system is very important and not have been studied. This studies concerned in government view (Ministry of Public Work and Public Housing) to achieve orderly construction with less risk of rework, less risk of accident and less risk of waste in orderly time phase construction. This variable assumes can reduce risk of rework and risk of accident that can causes time-consuming in order to achieve orderly construction.

5. CONCEPTUAL FRAMEWORK

80% of activities in QMS and OHSAS have the same activities (Jørgensen, 2008). All process is combined in integrated process. All management system process used PDCA cycle or we used to know as Deming cycle. This basic approach has common requirements in each steps of the PDCA cycle for the multiple standards. These common requirements of management systems can be met by common procedures or process. This is a fundamental truth in the path to integrated management system standards (Thaís Vieira Nunhes, et.al, 2017; Maria Gianni and Katerina Gotzamani, 2015; Merce Bernardo, 2014, Mercè Bernardo, 2015; Alexandra Simon, Juan Jose Tari, Jose F. Molina-Azorín, 2015; Calcedo et.al, 2015; Mercè Bernardo, Marti Casadesus, Stanislas Karapetrovic, Inaki Heras, 2009; Merce Bernardo et.al, 2015; Yarahmadi et.al, 2015; Alexandra Simon, 2012; Alena Labadova, 2004; Beatrix Barafort, et.al, 2016; T.Karzkozka et.al, 2017; Sendil Mourougan, 2015; Cristinel Roncea, 2016; Merce Bernardo et.al., 2010; Simon, Merce Bernardo et.al, 2015; Merce Bernardo et.al, 2011; Ajay D Jewalikar et.al., 2016; Alexandra Simon, et. al., 2011; Zoé Hoy and Andrea Foley, 2015; Richard Roessler and Hannes Schlieter, 2015; Alexandra Simon et.al, 2012; Alexandra Simon et.al, 2012; Iveta Mezinska et.al., 2015; Florida Veljanoska and Majlinda Axhiu, 2015; Dorin Maier et.al, 2015).

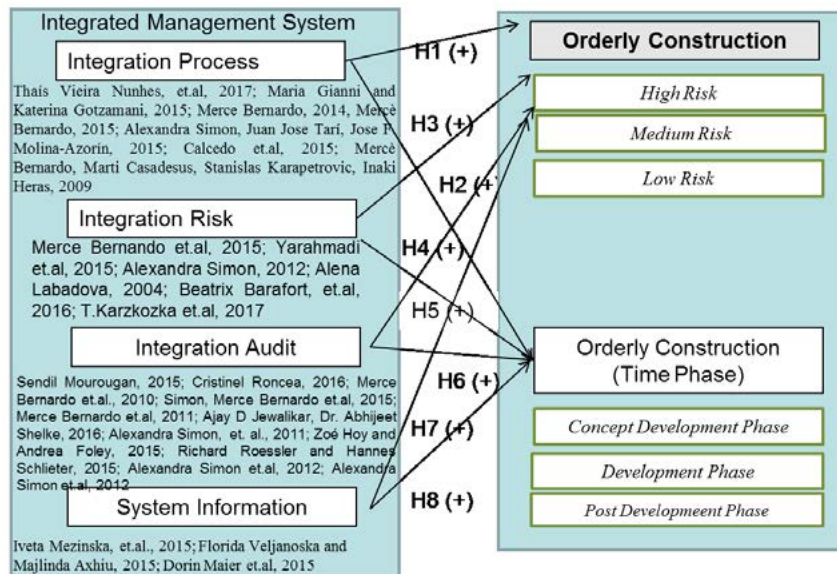
That common requirement, procedures and process is summarized in knowledge management such as **integration process** (Thaís Vieira Nunhes, et.al, 2017; Maria Gianni and Katerina Gotzamani, 2015; Merce Bernardo, 2014, Mercè Bernardo, 2015; Alexandra Simon, Juan Jose Tari, Jose F. Molina-Azorín, 2015; Calcedo et.al, 2015; Mercè Bernardo, Marti Casadesus, Stanislas Karapetrovic, Inaki Heras, 2009), **integrated risk** (Merce Bernardo et.al, 2015; Yarahmadi et.al, 2015; Alexandra Simon, 2012; Alena Labadova, 2004; Beatrix Barafort, et.al, 2016; T.Karzkozka et.al, 2017), **integrated audit** (Sendil Mourougan, 2015; Cristinel Roncea, 2016; Merce Bernardo et.al., 2010; Simon, Merce Bernardo et.al, 2015; Merce Bernardo et.al, 2011; Ajay D Jewalikar, Dr. Abhijeet Shelke, 2016; Alexandra Simon, et. al., 2011; Zoé Hoy and Andrea Foley, 2015; Richard Roessler and Hannes Schlieter, 2015; Alexandra Simon et.al, 2012; Alexandra Simon et.al, 2012). **That variables are formed into an integrated management system.**

Integrated management systems (IMS) also requires an information technology management system (Iveta Mezinska, Inga Lapin et al., 2015; Florida Veljanoska and



Majlinda Axhiu, 2015; Dorin Maier et.al, 2015). The implementation of IMS assumes to be orderly construction with less risk of rework, less risk of accident and less risk of waste in orderly time phase construction (concept of development, engineering development, post development) as illustrated in the conceptual framework in Figure 4.

Figure 4 the Conceptual Framework (Author Own Research)



This conceptual framework will examine the relationships among the integration process, the integration risk, the integration audit and the system information with the elements of the Orderly Construction’s block. To prove this concept, each relationship can be formed as a hypothesis as shown below:

- H1: The integration process has a positive impact on risk reduction
- H2: The integration process has a positive impact on achieving orderly construction
- H3: The integration risk has a positive impact on risk reduction
- H4: The integration risk has a positive impact on achieving orderly construction
- H5: The integration audit has a positive impact on risk reduction
- H6: The integration audit has a positive impact on achieving orderly construction
- H7: The System information has a positive impact on risk reduction
- H8: The System information has a positive impact on achieving orderly construction

Later those hypothesis will be tested through the next survey asking the opinions from the experts related.

6. CONCLUDING REMARKS

This paper is a comprehensive literature review of quality management system and occupational health/safety management system to form an integrated management system (IMS). The IMS aims to improve the performance of construction process by integrating process and audit of quality/safety system. Results of this study found the conceptual framework the integrated management system between Quality Management System and Occupational Health /Safety Management System.



7. REFERENCES

- Abrahamsson, S., et al. (2010). Integrated management systems: advantages, problems and possibilities. 13th Toulon-Verona Conference.
- Asif, M., et al. (2009). "Process embedded design of integrated management systems." International Journal of Quality & Reliability Management 26(3): 261-282.
- Badreddine, A., et al. (2009). A new process-based approach for implementing an integrated management system: quality, security, environment. Proceedings of the International MultiConference of Engineers and Computer Scientists.
- Bugdol, et.al., 2015, integrated Management System, Springer, Poland
- De Oliveira, O. J. (2013). "Guidelines for the integration of certifiable management systems in industrial companies." Journal of cleaner production 57: 124-133.
- El MorrChristo, Ginsburg Liane, Nam Victor (Seungree), Susan Woollard, Bojay Hensen, IT integration and Patient Safety the case of a software tool, ELSEVIER, Science Direct, Procedia Computer Science 98 (2016) 534 – 539
- Florida Veljanoska, Majlinda Axhiu, Information Systems as support to corporate management, Management Information Systems Vol. 8, 4/2013
- Gapp, R., et al. (2008). "Implementing 5S within a Japanese context: an integrated management system." Management Decision 46(4): 565-579.
- Hoyle, D., (2009), ISO 9000 Quality Systems Handbook, sixth edition, Butterworth Heinemann/Elsevier Ltd Great Britain
- Holdsworth, Rodger, 2016, Practical applications approach to design, development and implementation of an integrated management system, Elsevier
- Kymal, et.al., 2015, Integrated Management System, ASQ quality press, Milwaukee Wisconsin
- Manzanera, et.al., 2014, Design of an integrated management system (IMS) in a government-run medical evaluation organisation, The TQM Journal
- Nunhes, T. V., et al. (2016). "Evolution of integrated management systems research on the Journal of Cleaner Production: Identification of contributions and gaps in the literature." Journal of cleaner production 139: 1234-1244.
- Nunhes, T. V., et al. (2016). "Identification and analysis of the elements and functions integrable in integrated management systems." Journal of cleaner production.
- Octavia, Andrei, Risk Management and Quality Management an Integrate Approach, Economy Transdisciplinarity Cognition, 2016
- Popescu, S.G., Petruş, A.A., Metode de analiză a riscului în managementul proiectului, Calitatea acces la succes, Journal, Vol.13, No.127/April, p. 8-14
- Raisiene, A. G. (2011). "Advantages and limitations of integrated management system: the theoretical viewpoint." Socialines Technologijos 1(1).
- Saleh Binobaid, Mohammed Almeziny, Ip-Shing Fan, Using an integrated information system to reduce interruptions and the number of non-relevant contacts in the inpatient pharmacy at tertiary hospital, www.sciencedirect.com, 2015
- Simon, A., et al. (2014). "Can integration difficulties affect innovation and satisfaction?" Industrial Management & Data Systems 114(2): 183-202.
- Simon, A. Karapetrovic, S. and Casadesus, M (2012) Evolution of Integrated Management System in Spanish Firms. Journal of Cleaner Production, 23 (2012), 8-19



- Simon, A. Karapetrovic, S. and Casadesus, M (2012). Difficulties and benefits of integrated management systems . *Industrial Management and Data Systems*, 112 (5), 828-846.
- Simon, A. Bernando, M, Karapetrovic, S and Casadesus, M (2012). Implementing integrated management system in chemical firms. *total Quality Management & Business Excellence*.
- Simon, A. Bernando, M, Karapetrovic, S and Casadesus, M. (2011) Integration of standardized environmental and quality management systems audits. *Journal of Cleaner Production*, 19 (17-18), 2057-2065.
- Truls Löfstedt, 2015, Exploring Integrated Management Systems - Challenges and Potential in Relation in IT Governance, Conference Paper
- Yang, Heechun, 2016, Impact of time management for IT services management, Science Direct
- Zutshi, A. and A. S. Sohal (2005). "Integrated management system: the experiences of three Australian organisations." *Journal of Manufacturing Technology Management* 16(2): 211-232.
- Zeng, S., et al. (2007). "A synergetic model for implementing an integrated management system: an empirical study in China." *Journal of cleaner production* 15(18): 1760-1767.
- Zeng, S., et al. (2008). "Towards occupational health and safety systems in the construction industry of China." *Safety science* 46(8): 1155-1168.



CUSTOMER SATISFACTION OF FEEDER TRANSIT OF TRANSJAKARTA CORRIDOR PULO GADUNG – DUKUH ATAS 2, JAKARTA: STRUCTURAL EQUATION MODELING ANALYSIS

Jachrizal Sumabrata¹, Samuel Edy Mataram Simanjuntak², Jachryandestama³

¹Centre for Sustainable Infrastructure Development FTUI, rjs@eng.ui.ac.id

²Civil Engineering, Faculty of Engineering, University of Indonesia, Depok 16424, Indonesia

³Institute of Transport and Logistics Studies, University of Sydney

ABSTRACT

PT. Transportasi Jakarta, supervised by Government of DKI Jakarta, tries to improve Transjakarta BRT services for its customers. To support the BRT system, PT. Transportasi Jakarta provides Transjakarta feeder buses that operate to transporting passengers outside Transjakarta bus lanes to Transjakarta bus stops. Along with Transjakarta feeder buses, private owned public transports are also used as feeders of Transjakarta despite their condition. Private owned public transport has begun aging, and its service quality has been decreasing. Moreover, customer satisfaction is crucial because it influences consumers' decision to use public transport. PLS-SEM (Partial Least Square- Structural Equation Modeling) analysis conducted to determine customer satisfaction to quality of service. The studies are limited to feeder transport users in the corridors 4 (Pulo Gadung - Dukuh Atas 2). The results are that Transjakarta feeder bus users are very satisfied with the service and transport facilities variable. On the other hand, private owned medium size bus transport (Metro Mini) users are very satisfied with the information and technology variables mainly on the availability of public transport information while private owned small bus transport (Mikrolet) users are very satisfied with the safe and security variable mainly on security in carrying passenger goods.

Keywords: Service quality, passengers' satisfaction, SEM (Structural Equation Modeling), Transjakarta Feeder Transit.

1. INTRODUCTION

The high use of private transport will lead to problems such as congestion (Peter Newman, 1999; Prabhat Shrivastava, 2006). By increasing the public to use public transport as Transjakarta feeder, it will be more effective and efficient transportation system in general. The existence of the feeder transit is very important because appropriately implemented feeder transit can increase the number of public transport users particularly from along the routes area (Yannis Tyrinopoulos, 2008). Nowadays, Public transport users are decreasing because of unpleasant services because feeder transit of Transjakarta has become old and worn. Passengers who used to rely on public transport will move to use private vehicles which are more secure and comfortable. If there is no improvement, then service quality will decrease while user complaints will increase which affect the satisfaction level of public transport users.

The concept of quality has been extensively applied to public transport as it covers so many diverse topics such as comfort and safety inside the vehicle, journey times and even the convenience of the service and the existence of supporting infrastructure (Litman, 2008;



Hensher et al., 2003; Hensher and Houghton, E., 2004, de Oña, de Oña, Eboli & Mazzulla, 2013). Furthermore, consumer satisfaction is important to the service providers of transportation (Laura. & Mazulla. 2007; Laura & Mazulla, 2011; Harifah, 2014; Mouwen, 2015), companies or organizations in transport should be able to find ways to improve customer satisfaction (De Borger, 2002).

Some authors proposed A structural equation modeling (SEM) in public transport (Bamberg and Schmidt 1998; Fillone et al. 2005). Specifically, SEM was adopted for describing customer satisfaction in public transport services (Andreassen 1995; Karlaftis et al. 2001; Eboli and Mazzulla 2012). Structural equation modeling was applied to measure passengers' satisfaction with public city transport services and to verify how much some service characteristics could influence the perceived quality (de Oña, de Oña, Eboli and Mazzulla, 2013 and Antonucci, L. et al., 2014). Authors claim that factors affecting customer satisfaction with public city transport can be grouped into latent variables consisting service organization, safety and reliability, human resources and comfort and cleanliness.

Therefore, this study analyzes the factors in determining users' satisfaction of feeder transit of Transjakarta by quantifying its factors and identify the most important factors influencing customer satisfaction with feeder transit of Transjakarta as an integral part of mass transit.

2. METHODS

The data are obtained by distributing a questionnaire containing a number of statements regarding the quality of feeder transit services of Transjakarta on the bus stop along corridor 4 Pulo Gadung - Dukuh Atas 2 as shown in figure 1. The questionnaires were distributed to 211 respondents who are in Transjakarta bus stop where previously used public transportation including the private owned medium bus (metromini and kopaja) and private owned small bus (mikrolet and angkot) to get to the bus stop.

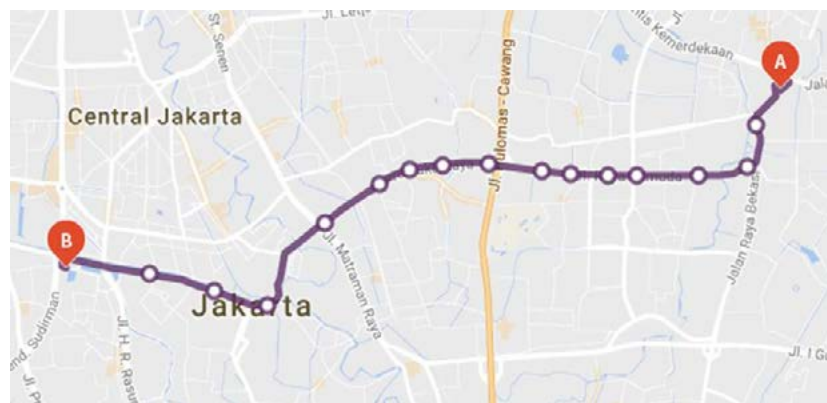


Figure 1. Bus stop on corridor 4, Pulo Gadung (A) – Dukuh Atas 2(B)

This research explores the relationship between global customer satisfaction (i.e., passenger satisfaction about overall service) and service quality attributes, based on needs and expectations expressed by the customers of public transport services.

The model that used are the relationship between customer satisfaction and service quality variables as shown in the figure 2.

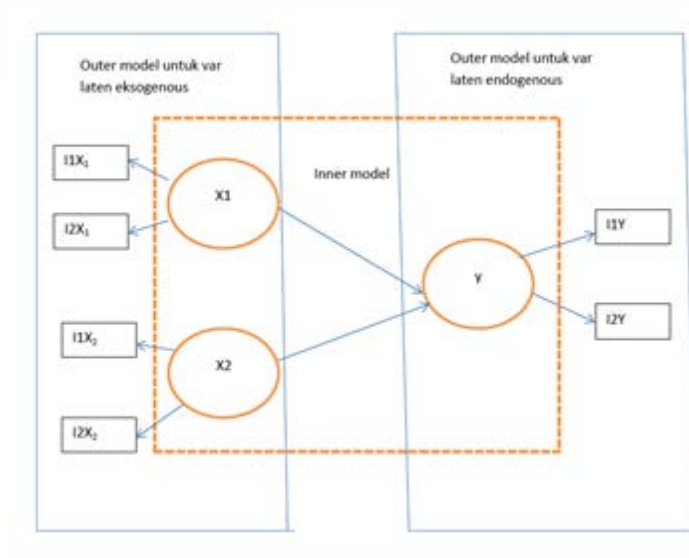


Figure 2. Research Model

Data were analyzed using SEM-PLS. First, the data must be processed using descriptive analysis to describe the characteristics of the respondent. Then for the model analysis of research conducted with SmartPLS version 2.0 software. SmartPLS Software is one of the tools to do model forms Partial Least Square (PLS), which is part of the Structural Equation Modeling (SEM) based variants that can simultaneously perform testing measurement model and structural model at a time (Wong K. K., 2013).

SEM PLS consists of three components, namely the structural model, the measurement model and the weighting scheme (Bacon, 1999; Hwang, 2010; Wong, 2011; Monecke & Leisch, 2012). The third part is a characteristic of SEM with PLS. The model will be described as shown in figure 3.

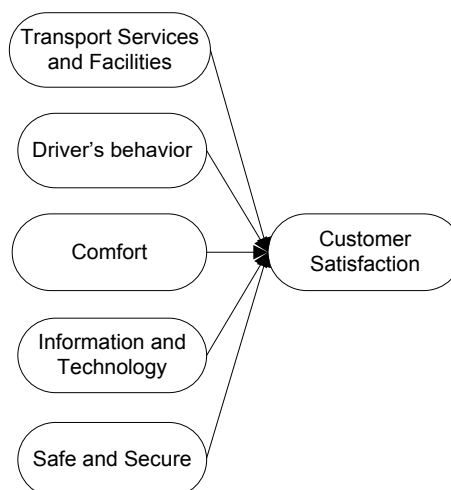


Figure 3, Model SEM-PLS



SEM using PLS models only allow the relationship between variables that recursive (same direction) only. It is similar to the path analysis (path analysis) model but is not the same as the SEM based covariance that also allows non-recursive (reciprocal) relationship.

In the structural model, which is also known as inner model, all the latent variables by connected one to another based on the theory of substance. The latent variables are divided into two, namely the exogenous and endogenous. Exogenous latent variables are the cause variables or variables without preceded by other variables with arrows leading to the other variables (endogenous latent variables).

Measurement model, which is also known as outer model, connecting all manifest variables or indicators with latent variables. Within the framework of PLS, the manifest variables can only be associated with one latent variable. All manifest variables that associated with the latent variable are referred to as a 'block'. Thus, each latent variable has a variable block manifest. A block must contain at least one indicator. A block associated with latent variables can be reflective (manifest variables as indicators that are affected by the same concepts and underlying) or formative (indicators that make or cause changes in latent variables)

Partial Least Square (PLS) as the family regression based method that introduced by Herman (Wold, 1985) to review the creation and development models and methods for the social sciences with a prediction oriented approach. PLS has assumptions of freely distributed research data, meaning that the research data do not refer to any particular distribution. PLS is an alternative method of SEM that can be used to solve relationship problem between the complex variables, but the small data sample size between 30 and 100, considering that SEM has 100 of a data sample size.

SEM with PLS is to predict and develop theories. It is different with SEM based covariance that use to test and confirm existing theories. Furthermore, PLS-SEM was also used to predict endogenous latent variables or to identify main variables if the research is exploratory research or extension of an existing structural theory.

3. RESULTS AND DISCUSSION

Descriptive analysis conducted on 211 respondents' data of Transjakarta feeder bus transit users as shown on table 1.

Table 1 Respondent Data of Transjakarta Feeder Transit User

Variables	Percent	Variables	Percent
Gender		Trip Origin	
Male	61 %	House	79 %
Female	39 %	School	7 %
Age		Office	18 %
> 40 years	4 %	Shopping Centre	3 %
30 – 39 years	14 %	MD	1 %
20 – 29 years	52 %	Relatives	15 %
< 20 years	30 %	Others	0 %
Variables	Percent	Variables	Percent



Occupation		Trip Purpose	
Priv. employees	37 %	Feeder Transit	
Housewife	3 %	Work	37 %
Student	44 %	School	39 %
Gov. Employees	4 %	Shop	9 %
TNI /POLRI	1 %	Treatment	1 %
Entrepreneur	3 %	Visit Relatives	9 %
Unemployed	7 %	Others	5 %
Others	1 %		
Formal Education		Travel Time To the Bus Stop	
Junior High School	3 %	< 5 minutes	23 %
High School	62 %	5 – 10 minutes	51 %
Undergraduate	32 %	> 10 minutes	27 %
Postgraduate	3 %		
Type of Feeder Transit			
Bus feeder	17 % (operated by PT Transjakarta)		
KWK	8 % (informal small size bus)		
Mikrolet	36 % (informal small size bus)		
Kopaja	13 % (informal medium size bus)		
Metromini	26 % (informal medium size bus)		

The PLS SEM analysis conducted to determine the relationship between the variables of service quality and customer satisfaction according to the research model. The model for each three types of bus using SEM with PLS approach are as follows:

a. Feeder Bus of Transjakarta

This model uses a sample of 36 respondents which has five main measurement dimensions that were used as the measuring tool of satisfaction. By using Structural Equation Modeling (SEM) approach Partial Least Squares (PLS), the test and analysis results of bus feeder Transjakarta model is shown in table2:

Table 2 Coefficient table Between Transjakarta Bus Feeder Construct

Code	Exogenous Variables	T Statistics ((O/STERR))	Code	Manifest Variables	Loading Factor
A -> SATISFACTION	Transport Services and Facilities	6.4123	a1	neat and maintained vehicles	0.7896
			a3	seats with ample leg room	0.7696
			a4	clean windows	0.7467
			a5	space for luggage	0.7058
			a7	vehicle not broke down	0.6883
			a2	clean seats	0.6261
Code	Exogenous Variables	T Statistics ((O/STERR))	Code	Manifest Variables	Loading Factor



C -> SATISFACTION	Comfort	5.4728	c7	easy moved to other transport	0.8526
			c8	bus stop location	0.7096
			c9	cheap and affordable fares	0.7072
			c3	temperature	0.6539
			c1	operate time	0.5409
			c5	other passenger behavior	0.5246
E -> SATISFACTION	Safe and Secure	2.9824	e2	emergency door	0.8175
			e1	feel safe and secure during trip	0.8123
			e4	feel safe carrying goods	0.7504
D -> SATISFACTION	Information and Technology	2.3769	d3	fares information	0.9345
			d4	information service complaints	0.8544
B -> SATISFACTION	Driver's Behavior	0.2815	b2	dress neatly	0.9112
			b4	give attention	0.8108
			b1	drive carefully	0.7986
			b3	friendliness	0.6346

Table 2 shows it each path coefficient and loading factor on the satisfaction variable with the transport services of feeder bus of Transjakarta, and facilities variable is felt best when compared to other satisfaction parameters that have been tested.

b. Medium size bus

This model uses a sample of 83 respondents with five main measurement dimensions which are used as the measuring tool of satisfaction. Test and analysis results of bus feeder Transjakarta model as shown in Table 3 :

Table 3 Coefficient table Between Medium Size Bus Construct

Code	Exogenous Variables	T Statistics (O/STERR)	Code	Manifest Variables	Loading Factor
D -> SATISFACTION	Information and Technology	3.8647	d2	availability	0.7842
			d4	information service complaints	0.7452
			d3	fares information	0.6775
			d1	route trip information	0.6586
A -> SATISFACTION	Transport Services and Facilities	1.9608	a1	neat and maintained vehicles	0.8001
			a2	clean seats	0.782
			a4	clean windows	0.6006
			a3	seats with ample leg room	0.5413
B -> SATISFACTION	Driver's Behavior	1.7254	b3	friendliness	0.8675
			b4	give attention	0.8405
			b2	dress neatly	0.57
			b1	drive carefully	0.513
C -> SATISFACTION	Comfort	1.1662	c3	temperature	0.829
			c4	smell	0.6381
			c2	ease of carrying goods	0.6305
			c1	operate time	0.5867
			c9	cheap and affordable fares	0.584
			c7	easy moved to other transport	0.5679
E -> SATISFACTION	Safe and Secure	0.5946	c5	other passenger behavior	0.4998
			e2	emergency door	0.8032
			e4	feel safe carrying goods	0.7845
			e3	provide first aid	0.642
			e1	feel safe and secure during trip	0.6057



Table 3 shows each path coefficient and loading factor on the variable satisfaction. For medium-size bus transportation, satisfaction to information and technology felt best when compared to other satisfaction parameters that have been tested. In the satisfaction variable with the information and technology, respondents feel that the availability of public transport is felt most well demonstrated by the greatest loading factor among other manifest variables that make the latent variable of information and technology.

c. Small size bus

This model uses a sample of 92 respondents with five main measurement dimensions which are used as the measuring tool of satisfaction. By using Structural Equation Modeling (SEM) approach Partial Least Squares (PLS), test and analysis results of bus feeder Transjakarta model as shown in Table 4:

Table 4. Coefficient table Between Small Size Bus Construct

Code	Exogenous Variables	T Statistics (O/STERR)	Code	Manifest Variables	Loading Factor
E -> SATISFACTION	Safe and Secure	4.6267	e4	feel safe carrying goods	0.8337
			e1	feel safe and secure during trip	0.7901
			e2	emergency door	0.6857
			e3	provide first aid	0.5881
B -> SATISFACTION	Driver's Behavior	2.0889	b3	friendliness	0.8287
			b2	dress neatly	0.7994
			b4	give attention	0.7445
			b1	drive carefully	0.719
A -> SATISFACTION	Transport Services and Facilities	1.0314	a4	clean windows	0.7796
			a2	clean seats	0.7704
			a1	neat and maintained vehicles	0.6979
			a3	seats with ample leg room	0.6385
			a7	vehicle not broke down	0.5555
			a5	space for luggage	0.5489
D -> SATISFACTION	Information and Technology	0.7074	d2	availability	0.8631
			d3	fares information	0.7361
			d4	information service complaints	0.725
			d1	route trip information	0.7026
C -> SATISFACTION	Comfort	0.4862	c6	No overcrowded	0.7633
			c5	other passenger behavior	0.7371
			c2	ease of carrying goods	0.7154
			c3	temperature	0.6832
			c7	easy to moved to other transport	0.6741
			c4	smell	0.6735
			c8	bus stop location	0.624
			c9	cheap and affordable fares	0.5977
			c1	operate time	0.5266

Table 4 shows each path coefficient and loading factor on the variable satisfaction. For the small size bus type, satisfaction with the safe and secure variable is felt best when compared to other satisfaction parameters that have been tested. Within the safe and secure variable, respondents felt that their safety when carrying goods in public transport is felt most,



demonstrated by its greatest loading factor among other manifest variables that make up the latent variable E

4. CONCLUSION

Through the research results obtained, then the conclusions can be drawn from this research are:

1. It can be concluded that the factor that customer are most satisfied for Transjakarta feeder transit, are as follows:
 - a. Feeder Bus Transjakarta
Transjakarta users show that they are very satisfied with the transport services and facilities compared with the other satisfaction parameters. In quality service variables which are considered the best is vehicle neat and well maintained.
 - b. Private owned medium size bus
Medium size bus users show that they are very satisfied with information and technology variable compared with the other satisfaction parameters. In quality service variables which are considered the best is the information about the availability of the vehicle.
 - c. Private owned small size bus
Small size bus users show that they are very satisfied with safe and secure variable compared with the other satisfaction parameters. In quality service variables which are considered the best is feel safe carrying goods.
2. Factors that customer are least satisfaction with the quality of service for Transjakarta feeder transit are:
 - a. Feeder Bus Transjakarta
The level of customer satisfaction with service quality variables of bus feeder Transjakarta is the variable of the driver's behavior. Respondents perceived that friendliness is the lowest among other driver's behavior indicator.
 - b. Private owned medium size bus
The level of customer satisfaction with service quality variables of medium size bus is the safe and secure variable. Respondents perceived that feel safe and secure during the trip is the lowest among other safe and secure indicator.
 - c. Private owned small size bus
The level of customer satisfaction with service quality variables of small size bus is the comfort variable. Respondents perceived that operational time is the lowest among other comfort indicators.

The recommendation that can be given to the feeder transit of Transjakarta operator and further researches are:

1. Feeder Bus Transjakarta
The lowest factor of the driver's behavior is friendliness. This type of vehicle has to set the standard procedure operational about how to interact with passengers.
2. Private owned medium size bus
The lowest factor within safe and secure factors is safe and secure feeling during the trip. It can be noted that public transportations commit numerous violations such as embark and/or disembark of passengers regardless of bus stops, unmaintained bus condition, and the drivers often violate the rules of traffic. Suggestion that should be considered by the transport operator is the



car must pass roadworthiness and consider replacing vehicles that conditions are not roadworthy.

3. Private owned small size bus

The lowest factor amongst comfort factors is operational time. Having no setting for operational schedule made passengers unable to know the operational schedule certainly. Adjustment to operational schedule should be made so that passenger know when using public transport.

5. REFERENCES

1. Andreassen, T.W., (1995), (Dis)satisfaction with public services: The case of public transportation, *Journal of Services Marketing* 9, pp 30–41.
2. Antonucci, L., Crocetta, C., d'Ovidio, F.D., Ernesto T., (2014), Passenger satisfaction: A multi-group analysis, *Quality and Quantity*, 48(1), pp 337-345.
3. Bacon, L. D., (1999), Using LISREL and PLS to Measure Customer Satisfaction, *Sawtooth Software Conference Proceedings*, Feb 2-5, pp 305-306.
4. Bamberg, S., Schmidt P., (1998), Changing Travel-Mode Choice as Rational Choice: Results from a Longitudinal Intervention Study, *Rationality and Society*, 10(2), pp 223-252.
5. De Borger, B. C., (2002), Public transit performance: what does one learn from frontier studies?, *Transport Reviews*, 22(1), pp 1–38.
6. de Oña, J., de Oña, R., Eboli L., Mazzulla, G., (2013), Perceived service quality in bustransit service: A structural equation approach, *Transport Policy*, 29, pp 219-226.
7. Fillone, A. M., C. M. Montalbo, N. C. Tiglao, (2005), Assessing urban travel: A structural equations modeling (SEM) approach, *Proceedings of the Eastern Asia Society for Transportation Studies* 5, pp 1050-1064.
8. Harifah, Mohd. Noor, Na'asah, Nasrudin., and Foo, Jurry, (2014), Determinants of Customer Satisfaction of Service Quality: City Bus Service in Kota Kinabalu, Malaysia, *Procedia - Social and Behavioral Sciences* 153, pp 595-605.
9. Hensher, D.A., Houghton, E., (2004), Performance-based quality contracts for the bus sector: delivering social and commercial value for money, *Transportation Research Part B* 38, pp 123-146.
10. Hensher, D.A., Stanley, J., (2003), Performance-based quality contracts in bus service provision. *Transportation Research Part A* 37, pp 519-538.
11. Hwang, H. M., (2010), A comparative study on parameter recovery of three approaches to structural equation modeling, *Journal of Marketing Research*, 47, pp 699-712.
12. Karlaftis, M. G., J. Golias, E. Papadimitriou, (2001), Transit quality as an integrated traffic management strategy: Measuring perceived service. *Journal of Public Transportation* 4 (1), pp 27-44
13. Ken Kwong-Kay Wong, (2013), Partial Least Squares Structural Equation Modeling (PLS-SEM) Techniques Using SmartPLS, *Marketing Bulletin*, Technical Note 1, pp 1-32.



14. Laura Eboli, Gabriella Mazzulla, (2007), Service Quality Attributes Affecting Customer Satisfaction for Bus Transit, *Journal of Public Transportation*, Vol. 10, No.3, pp 21-34
15. Laura Eboli, Gabriella Mazzulla, (2011), A methodology for evaluating transit service quality based on subjective and objective measures from the passenger's point of view, *Transport Policy*, 17, pp 172–181.
16. Laura Eboli, Gabriella Mazzulla, (2012), Structural Equation Modelling for Analysing Passengers, 15th meeting of the EURO Working Group on Transportation, Paris, *Procedia - Social and Behavioral Sciences* 54, pp. 96-106.
17. Litman, T., (2008), Valuing transit service quality improvements, *Journal of Public Transportation* 11(2), pp 43-64
18. Monecke, A., Leisch F., (2012), SEM PLS: Structural Equation Modelling Using Partial Least Square. *Journal of Statistic Software*, pp 1-32.
19. Mouwen A., (2015), Drivers of Customer Satisfaction with Public Transport Services, *Transportation Research: Part A, Policy And Practice* (78), pp 1-20.
20. Peter Newman, J. Kenworthy, (1999). *Sustainability and Cities: Overcoming Automobile Dependence*, Washington DC, Island Press.
21. Prabhat Shrivastava, M. O., (2006), A model for development of optimized feeder routes and coordinated, *Transport Policy*, pp,413-425.
22. Wold, H., (1985), *Encyclopedia of Statistical Sciences*. In S. K. Johnson, *Partial Least Squares*, New York, John Wiley & Sons, Ltd., (pp. 581-591
23. Wong, K., (2011), Review of the book *Handbook of Partial Least Squares: Concepts, Methods and Applications*, by V. Esposito Vinzi, W.W. Chin, J. Henseler & H. Wang (Eds)., *International Journal of Business Science & Applied Management*, 6(2), pp 52-54.
24. Yannis Tyrinopoulos, C. A., (2008), Public transit user satisfaction: Variability and policy implications, *Transport Policy*, pp 260-272.



MAPPING OF THE SUB-SIAK WATERSHED BASED ON REMOTE SENSING AND SIMULATION OF ITS PERFORMANCES BASED ON THE SWAT

SANDHYAVITRI Ari ¹⁾, FAUZI Manyuk ²⁾, SUTIKNO Sigit ³⁾, FAJRI Mardan ⁴⁾*,
IQBAL Muhammad ⁵⁾

^{1,2,3,4,5} Civil Engineering Department, University of Riau, Pekanbaru, 28293, Indonesia

*ari.sandhyavitri@lecturer.unri.ac.id

ABSTRACT

One of the deepest and important rivers in Indonesia was Siak River. The objectives of this study were to develop watershed map of sub-Siak using remote sensing (RS) Landsat ETM+ (Enhanced Thematic Mapper) images data 2002, 2007, 2012, and simulate 4 indicators performance of the existing sub-Siak watershed, Riau, Indonesia based on 2 scenarios; (i) an existing condition in 2012, and (ii) projection the condition after conservation schemes. The simulated conservation schemes may include replanting bushes and arid areas with the local vegetation such as Waru (*Hibiscus tiliaceus*), and Kayu Ara (*Ficus sp*). After conducting the simulations, it was revealed that the watershed indicators performance encompassing; (i) the percentage of vegetation coverage areas (PPV) will be better, (ii) percentage of critical land areas (PLK) will decrease, (iii) water flow regime coefficient (KRA) will improve, and (iv) annual flow coefficients (KAT) become better. The hydrological models of this watershed were developed using the Soil and Water Assessment Tool (SWAT). The hydrological model of this watershed is acceptable as the determination coefficient (R^2) was $0.50 > 0.4$ and NS was $0.5 > 0.36$. Hence, it proves that RS data were useful to develop time series maps concerning the change of the sub-Siak watershed coverage areas in 2002, 2007, 2012, identified the magnitude of land use changes, and the SWAT may simulate the hydrological model of the watershed.

Keywords: Landsat, Remote Sensing, Watershed Performances, Land Use Change, SWAT, Simulation, Conservation

1. INTRODUCTION

In 2015, the Ministry of Public Work Department, Indonesia stated that the Siak watershed, Riau Province, Indonesia was classified as a critical one. This was based on the fact that a decreasing in the quality and quantity of the Siak river water (Ministry of Public Work, Indonesia, 2015). Before the 1980s, the Siak river water depth was about 20-30 meters with the total length was 672 km and width of 50-75 m (Yesi Gusriani, 2012). This river was considered as the deepest river in Indonesia. In 2015, the riverbed depth was limited to remain 8-13 meters (Yesi Gusriani, 2012, Fatimah Ratna Sari and Denny Zulkaidi, 2014). This indicates that this watershed health performance was at the risks (Asdak, C., 1995). Hence, there is a need to develop the sub-Siak watershed map based on remote sensing, and investigate its performances based on the Soil and Water Assessment Tool (SWAT), which is currently relatively rarely applied in Indonesian cases (Asdak, C., 1995; Ari Sandhyavitri, et al, 2015).



Large scale plantation activities within the area of Siak watershed have converted the existing vast forested lands to become plantation areas (especially these area allocated to the development of palm oil plantation area), settlement/residential areas, farming and agricultural ones. These activities were assumed to reduce the existing watershed performances (Ari Sandhyavitri, et all, 2015).

2. METHODOLOGY/ EXPERIMENTAL

2.1 WATERSHED PARAMETERS EVALUATION PERFORMANCES

There are 4 main watershed parameter performances was evaluated in this paper. This is based on based the Minister of Forestry of the Republic of Indonesia Decree, Number: P. 61 / Menhut II / 2014 concerning A Guideline for Monitoring and Evaluation of Watershed (The Minister of Forestry of the Republic of Indonesia Decree, 2014).

This decree highlights four main parameters in order to evaluate the watershed performances encompassing; (i) the percentage of critical land areas, (ii) the percentage of vegetation coverage areas, (iii) water flow regime Coefficient (KRA), and (iv) annual of water flow coefficient. The valuation parameters can be seen in table 1 below:

Table 1. Evaluation Criteria for Watershed Performances.

CRITERIA	SUB- CRITERIA	PARAMETERS
A. Land Area	Percentage of critical land areas (PLK)	$PKL = \frac{\text{Critical Land Area}}{\text{Watershed Area}} \times 100\%$(1)
	Percentage of vegetation coverage areas (PPV)	$PPV = \frac{\text{vegetation coverage areas}}{\text{Watershed Area}} \times 100\%$(2)
B. Quality and Quantity (Water Managem ent)	Water flow regime Coefficients (KRA)	$KRA = \frac{Q_{\max}}{Q_{\min}} \times 100\%$(3) Q = rate of flow (m3/second)
	Annual flow coefficients (KAT)	$KAT = \frac{Q_{\text{annually}}}{P_{\text{annually}}} \times 100\%$(4) Q = rate of flow (m3/second) P = annual precipitation thickness

2.2 RESEARCH LOCATION

The research was conducted in the sub-Siak watershed, Rau, Indonesia. The automatic water level record (AWLR) station was located in Pantai Cermin village, Kampar District with the geographical location of 00 ° 35 '24 "latitude and 101 ° 11' 46" East (Figure 1 and 2). Data of the AWLR was obtained from the Pantai Cermin Station 2001 to 2012. The climatic data including precipitation was obtained from <http://globalweather.tamu.edu/>. The existing land cover data was obtained from the Watershed Management Board (BPDAS, 2012).

3. RESULTS AND DISCUSSION

3.1 MAPPING OF SUB-SIAK WATERSHED BASED ON REMOTE SENSING (RS)

The RS images data were obtained from the NOAA satellite of Landsat ETM+ (Enhanced Thematic Mapper) with 30 m spatial resolution for 2002, 2007 and 2012 images.



Supervised classification method and images interpretation techniques were then applied in obtaining the land use map of this watershed.

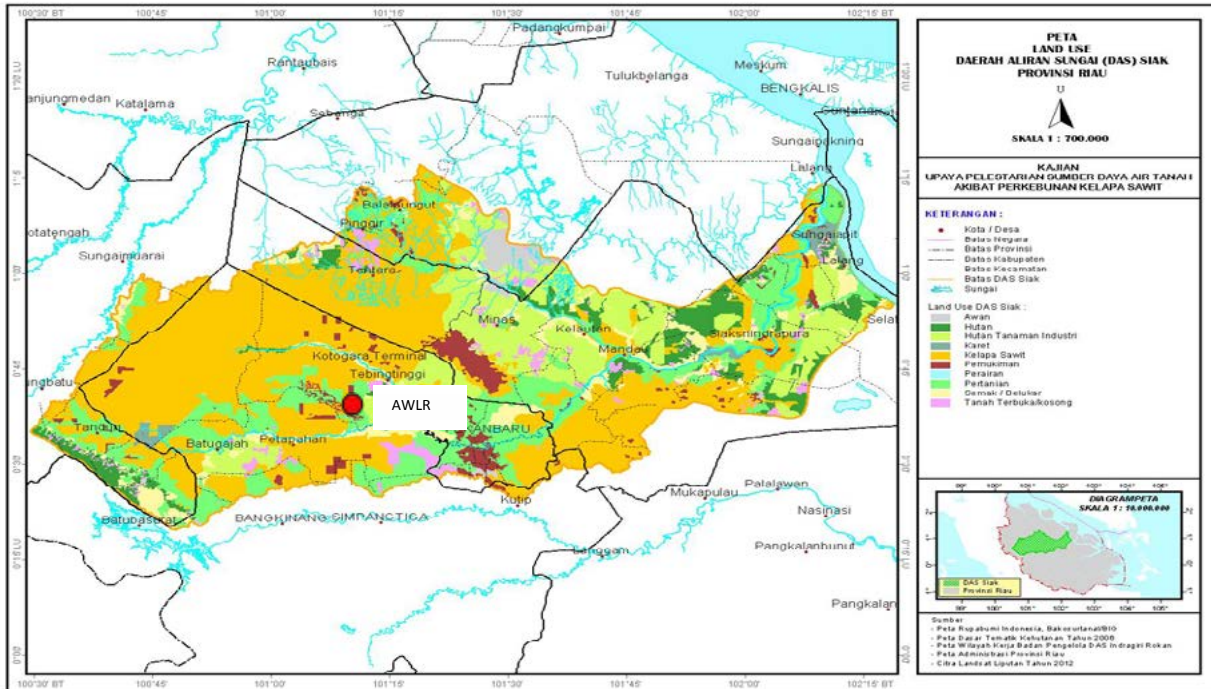


Figure 1. The location of the automatic water level record (AWLR) station was at Pantai Cermin, sub-Siak Watershed, Riau Province, Indonesia

In order to obtain the topographic data, this research used the ASTER GDEM (Global Digital Elevation Model) with a resolution of 30 m. It may be downloaded from <http://gdem.ersdac.jspacesystems.or.jp/>. A spatial map of the sub-Siak watershed was the developed based on Geographic Information System (GIS) (Figure 2).

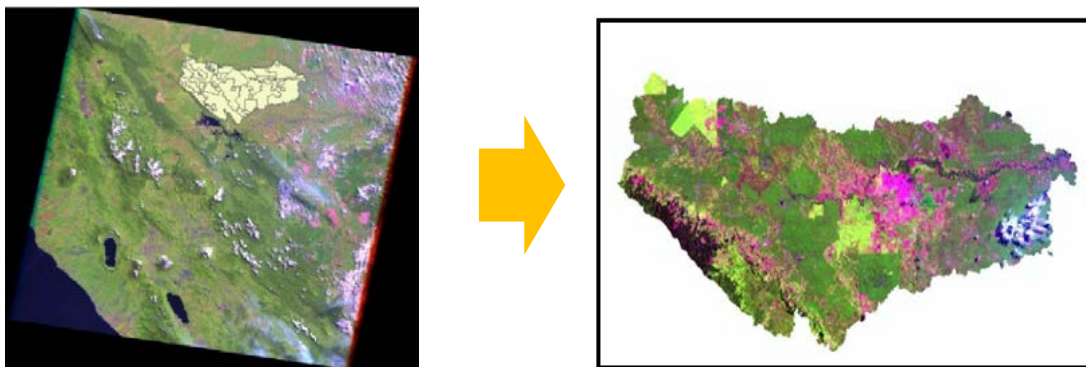
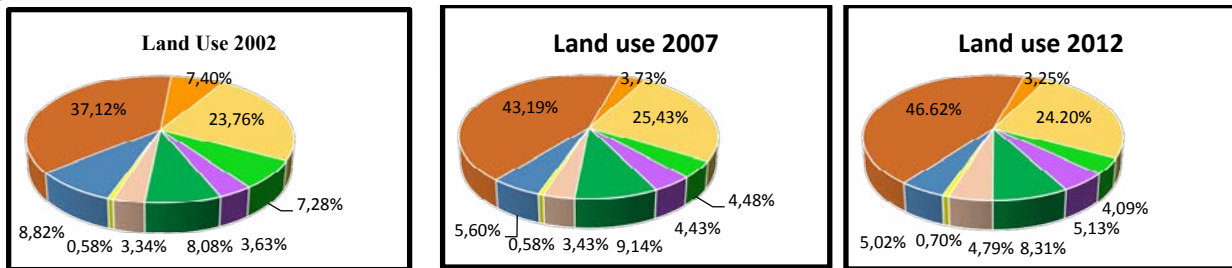


Figure 2. Interpretation of satellite image of sub-Siak Watershed using GIS.

Multispectral Classification criteria were applied to classify the existing land use change in the period of 2002, 2007 and 2012. Supervised classification methods (maximum classification, MLC) and normalized difference vegetation index (NDVI) were then used to produce spatial watershed area.



Notes:
Tropical forest, Industrial forest, Rubber plant, Oil palm plantation, Settlement, water bodies, Agriculture, Bushes and shrubs, Arid area

Figure 3. Land use change (%), 2002, 2007, 2012.

There was a trend that the sub-Siak watershed land use has been fluctuating during the period of 2002, 2007, and 2012. The significant land coverage area was dominated by oil palm plantation (46%), agriculture (24%), and Bushes and shrubs (8%).

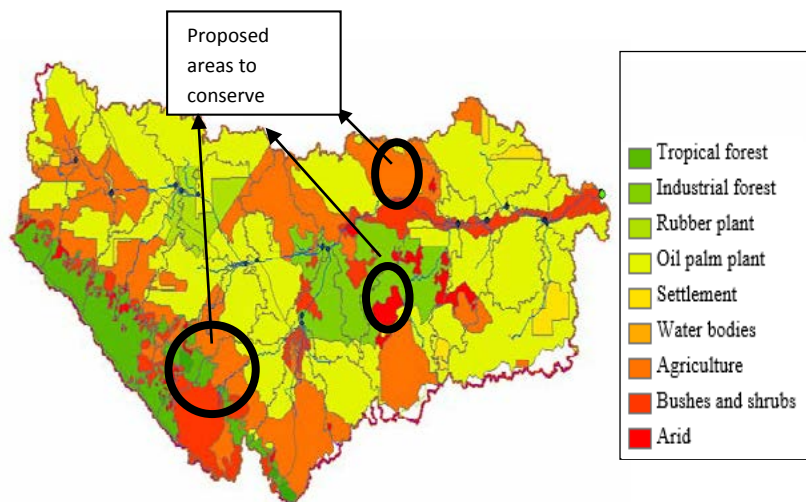


Figure 4. The existing land use of the sub-Siak watershed in 2012 (Scenario 1):

The north and south parts of this sub-Siak watershed (in the circles) are proposed to be conserved, as there are numbers of critical areas scattered within these locations. These conservation areas encompass sub districts of Kampar, Rokan Hulu and Bengkalis (Figure 4).

Table 2 Land use data of sub-Siak watershed, in 2012

Land use	Percentage	Area (ha)
Tropical forest	7.16 %	12186.32
Industrial forest	7.31 %	12441.62
Rubber plant	2.30 %	3914.6
Oil palm plant	46.62 %	79347.24
Settlement	1.99 %	3386.98
Water bodies	0.01 %	17.02
Agriculture	24.20 %	41188.4
Bushes and shrubs	8.19 %	13939.38
Arid	2.22 %	3778.44
Total		12186.52



The critical land in this study was mainly consisted of bushes and arid areas (13,939 ha + 3,778 ha = 17,717 ha). These critical areas were then planted with Waru (*Hibiscus tiliaceus rubra*) or Red Cottonwood, and Kayu Ara (*Ficus sp*). These vegetation were very common to find around the river banks in the sub-Siak watershed (Figure 5).



Figure 5. Waru (*Hibiscus tiliaceus rubra*) and Kayu Ara (*Ficus sp*).

It is acknowledged that there are several soil and water simulation models may examine the impacts of different land use practices on the water watershed areas, including the Soil and Water Assessment Tool (Neitsch SL, et all. 2005).

The Soil and Water Assessment Tool (SWAT) is one of water assessment tools that is capable of simulating the impacts of land management practices on the watershed, and measuring sedimentation process over time (Arnold, J.G., R. Srinivasan, R.S. Muttiah, and J.R. Williams. 1998; Neitsch SL, et all. 2005). The SWAT is one of the widely used tools for modeling agricultural and mixed land uses within a watershed (Migliaccio, K.W., and P. Srivastava, 2007).

Table 2 showed that in 2012 the oil palm plantation area covers 79,006 ha (>46% of the watershed total areas of 17,020 ha). The remaining primary tropical forest area was 12,118 ha (7%). The total bushes and arid areas were 18,092 ha (10.63%) and these last areas were classified as a critical land. This critical area is then simulated to be conserved and planted with the local vegetation, for example Waru (*Hibiscus tiliaceus*), and Kayu Ara (*Ficus sp*). Then, the Soil and Water Assessment Tool (SWAT) applied to simulate the hydrological model of this sub-Siak watershed (Neitsch SL, et all. 2005, Migliaccio, K.W., and P. Srivastava, 2007).

3.2 SIMULATION WATERSHED PERFORMANCE

Simulation is focused on the development of hydrology model of the existing watershed condition in 2012 (scenario 1), and after conservation scenario has been applied (scenario 2). The conservation scenario 2 would be implemented in the scrubs and arid areas (critical land areas) (Figure 3). The watershed map was developed using remote sensing data obtained from the extraction of Landsat satellite images data, which have a spatial resolution of 30 m. Supervised classification method and image interpretation techniques were then applied in obtaining the land use map of 2012.

The following watershed indicators performance were presented as follow:

1. Percentage of vegetation coverage areas (PPV). It was identified that the total



vegetation coverage areas in 2012 were 121,829 ha and the total watershed area was 170,200 ha. The percentage of vegetation coverage areas was calculated based on the total vegetation area (121.829 ha) divided by the total watershed area (170.200 ha) = 71,6%. After simulating of scenario 2 and implementation of conservation scheme, it was revealed that the percentage of vegetation coverage areas becomes 124,286/170,200 = 73 %. Based on the Minister of Forestry of the Republic of Indonesia Decree, Number: P. 61 / Menhut II / 2014, this value was classified as a fairly watershed condition (The Minister of Forestry of the Republic of Indonesia Decree, 2014). Hence there is no attention required to manage the watershed based on the parameter of vegetation coverage area for both scenario 1 and 2.

2. Percentage of critical land cover performance (PLK). The percentage of the existing critical land (Scenario 1) was as the following calculation. $PKL = \text{Critical Land Area} / \text{Watershed Area} \times 100\% = (13,939 + 3,778) / 170,200 \times 100\% = 10.41\%$. After implementing conservation scheme (Scenario 2), the scrubs and arid land areas were decreased to become 9,989 ha and 1,221 ha respectively. The percentage of the critical lands cover would decline from 10.41% to 6.47% (<10%). This 6.47% figure means that there is no attention required as the watershed critical level is considered low. This scenario 2 result was better than that scenario 1 result.

3. Water flow regime coefficient (KRA). This is obtained from the ratio of the maximum flow rate (Q_{maks}) with a minimum flow rate (Q_{min}) of the watershed. Q_{maks} Value of sub-Siak watershed in 2012 was $191.52 \text{ m}^3 / \text{sec}$, while Q_{min} is $13.14 \text{ m}^3 / \text{sec}$. Then the KRA value of sub-Siak watershed in 2012 was $191.52 / 13.14 = 14.58$.

However, in the period of 2002-2012 the KRA coefficient was relatively fluctuated, the condition of KRA was considered very good as $KRA < 20$ (very low) except in 2003, the condition was dropped to 31. This was because of in 2003 there was a period of long dry season condition caused by the El-Nino effect. The KRA are dynamic functions of various hydrology parameters including global weather conditions such as rainfall, temperature, humidity and wind speed. $KRA < 20$ means that the watershed may capture most of the rainwater into its soil, or the infiltration rate was relatively high and the rainwater runoff was relatively low (Hambali, R. 2008).

4. Annual Water flow Coefficient (KAT). This parameter was obtained from the comparison between the annual river water flows (Q) with the precipitation thickness (P). The annual water flow (Q) was obtained from the data observation of the discharge of water volume and it is divided by the total area of this watershed. The result was then converted into units of mm. while the value of precipitation (P) was taken from <http://globalweather.tamu.edu/>. The existing of Q value of water discharge in 2012 was 1398.27 mm, and P value was 3117.64 mm. The annual flow coefficient was 0.45. After simulating conservation, it was identified that the water flow $Q = 1390.36$ and the value of $P = 3117.64$. Then the annual flow coefficient was $1390.35 / 3117.64 = 0.44 (< 0.45)$. This scenario 2 result was better than that in the scenario 1.

3.3 THE HYDROLOGICAL SIMULATION MODEL USING SWAT

In order to yield the acceptable output of the hydrological model, the analyses have been applied in 4 stage such as; GIS processing, the configuration of input files in SWAT, model run, and last but not least conducting a reading out-put. Obviously, this stages required several iterations in order to yield optimum results complying with the output parameter standards (R^2 dan NS) (Table 3 and 4). These results also need to be validated.



The statistical methods used to validate the model by calculating the coefficient of determination (R^2) and the Nash - Sutcliffe efficiency model (NS) as presented in equations of (1) and (2).

$$R^2 = \frac{[\sum_{i=1}^n (Q_{obs} - \bar{Q}_{obs})(Q_{cal} - \bar{Q}_{cal})]^2}{\sum_{i=1}^n (Q_{obs} - \bar{Q}_{obs})^2 \sum_{i=1}^n (Q_{cal} - \bar{Q}_{cal})^2} \dots\dots\dots(1)$$

$$NS = 1 - \frac{\sum_{i=1}^n (Q_{obs} - Q_{cal})^2}{\sum_{i=1}^n (Q_{obs} - \bar{Q}_{obs})^2} \dots\dots\dots(2)$$

Which are:

Q_{obs} = rate of flow observation ($m^3/second$),

Q_{cal} = simulated rate of flow obtained from the SWAT ($m^3/second$),

\bar{Q}_{obs} = an average rate of flow observation ($m^3/second$),

\bar{Q}_{cal} = an average simulated rate of flow obtained from the SWAT ($m^3/second$).

Determination coefficient criteria (R^2) were defined as the following table.

Table 3. Criteria of Determination coefficient

R² Value	Interpretation
$0,7 < R^2 < 1,0$	High impacts
$0,4 < R^2 < 0,7$	Medium impacts
$0,2 < R^2 < 0,4$	Low impacts
$R^2 < 0,2$	No impacts

(Source: Hambali, 2008)

Motovilov, Y.G., Gottschalk, L., Engeland, K. & Rodhe, A. 1999, recommended *Nash-Sutcliffe Efficiency (NSE)* as the following table.

Table 4. *Nash-Sutcliffe Efficiency (NSE) criteria*

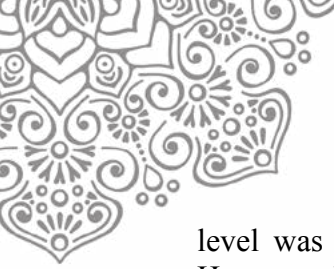
NSE	Interpretation
$NSE > 0,75$	Good
$0,36 < NSE < 0,75$	Moderate
$NSE < 0,36$	Low

(Source : Motovilov, Y.G., Gottschalk, L., Engeland, K. & Rodhe, A. 1999)

Scenario 1. The Watershed Existing Condition

The SWAT simulation has been applied to the existing condition of watershed (scenario 1) using 5 main input data, such as; (i) the digital elevation data (DEM) which were obtained from the satellite data (<http://gdem.ersdac.jspacesystems.or.jp/>), (ii) land use data, and (iii) soil classification data (obtained from the Watershed Management Board, BPDAS, 2012), (iv) water level data 2012 (obtained from AWRL in Pantai Cermin station, Sub-Siak River, Riau, Indonesia), and (v) global weather data including precipitation data 2012 (<http://globalweather.tamu.edu/>).

The hydrograph results of scenario 1 were presented in figure 6. This hydrograph shows that the fluctuation of water level was a function of rain fall. During the period of rain season in January to April, and October to December showed a trend that the river water



level was relatively higher compared to the dry season period (May to September). However, in this case the global climate change and El-Nino effect were not put into an account in this scenario.

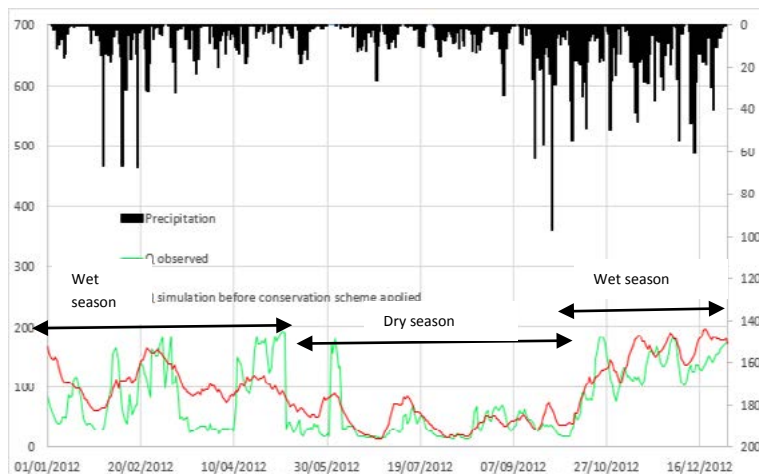


Figure 6. Hydrograph model for the year 2012 developed using the SWAT

Based the SWAT simulation, it was identified that the determination coefficient (R^2) of this model was $0.59 > 0.4$ and NS was $0.5 > 0.36$. Thus this hydrological model for this watershed in 2012 was considered acceptable (Neitsch SL, et all. 2005; R. Rosso, A. Peano, I. Becchi and G. A. Bemporad, 1994).

Scenario 2. After Conservation

Based the SWAT simulation, after conservation, it was revealed that the determination coefficient (R^2) was $0.50 > 0.4$ and NS was $0.5 > 0.36$. Thus this hydrological model for this watershed was also considered acceptable (Figure 7).

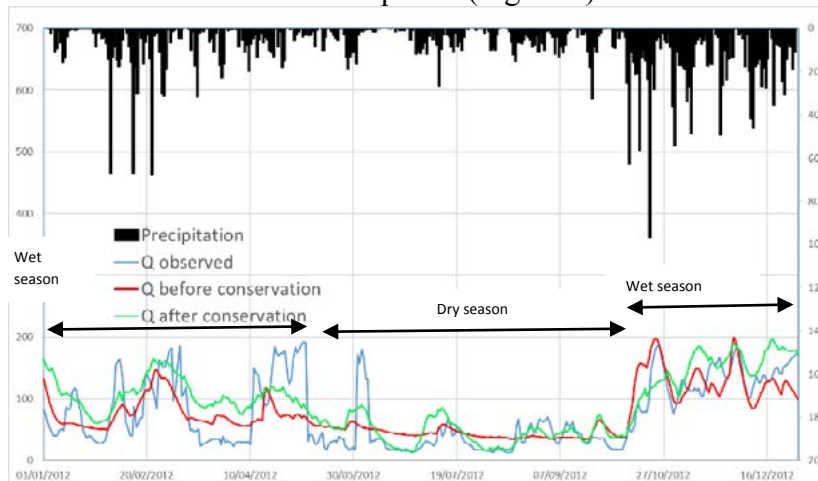


Figure 7. Comparison of 3 hydrographs based on Q observation, and 2 models after calibration

It was identified that, the simulated hydrograph (before and after conservation) were relatively smooth compared to the real conditions as, these simulations take into account statistic approaches which accommodate a certain level of errors (Neitsch SL, et all. 2005;



D. C. Garen and D. S. Moore, 2005). The water balance parameters were calculated using the curve number method (D. C. Garen and D. S. Moore, 2005) for the surface runoff. The Hargreaves method (G. Hargreaves and Z. A. Samani, 1985) was used for the potential evapotranspiration process.

This study utilized 24 input parameters in the SWAT simulation in order to maintain their less complexity in the calculation process (G. Hargreaves and Z. A. Samani, 1985). These 24 input data have yield R^2 and NS values of > 0.4 and 0.36 respectively which are considered acceptable. Hence, the hydrological model for this watershed is considered valid. After 9 times of iterations process using SWAT, some of the final input data and their fitted values were presented as follow; R_CN2.mgt (SCS runoff curve number) fitted value=54.005, V_ALPHA_BF.gw (Baseflow alpha factor) = 0.989, V_GW_DELAY.gw (Groundwater delay)= 164.646, V_REVAPMN.gw (Threshold depth of water in the shallow aquifer required for return flow to occur)= 614.213, V_CH_L1.sub (Longest tributary channel length in subbasin) = 0.218, and V_OV_N.hru (Manning's "n" value for overland flow)=1.415.

4. CONCLUSION

The remote sensing data from the Landsat ETM+ have yield land cover maps of the sub-Siak watershed for 2002, 2007 and 2012. Based on the watershed existing condition, it was identified that PLK value was 10,41%, the percentage of vegetation coverage areas (PPV) 71,6%, KRA was 14,58 and KAT= 0,45. After an application of the conservation scheme the condition of the watershed including PLK improve by 37%, PPV 2%, KRA 60%, and KAT 2%. These values show that the overall watershed performances in scenario 2 were better than those in scenario 1. The hydrograph simulation model for this watershed was also considered acceptable as the determination coefficient (R^2) was $0.50 > 0.4$ and NS was $0.5 > 0.36$.

5. ACKNOWLEDGEMENT

We would like to thank the Civil Engineering Faculty, Universitas Riau and Research and Development Board (Balitbangda), Riau Province, Indonesia for technically facilitating this research study.

6. REFERENCES

- A. Saltelli, E. M. Scott, K. Chan and S. Marian, 2000, Sensitivity Analysis, John Wiley & Sons Ltd., Chichester.
- Ari Sandhyavitri, et all, 2015. The Changes of Land Use Pattern Affect to the Availability of Water Resources in Siak Watershed, Riau Province, Indonesia, Proceeding of the 14th International Conference on QIR (Quality in Research), Lombok, Indonesia, 10-13 August 2015, ISSN 1411-1284, 208-213.
- Arnold, J.G., R. Srinivasan, R.S. Muttiah, and J.R. Williams. 1998. Large area hydrologic modeling and assessment Part I: Model Development. Journal of the American Water Resources Association, 34(1): 73-89.
- Asdak, C., 1995, Hydrology and Watershed Management (Hidrologi dan Pengelolaan Daerah Aliran Sungai). Yogyakarta : Gadjah Mada University Press, 25-40.
- ASTER GDEM (Global Digital Elevation Model) with a resolution of 30 m. It may be



- downloaded from <http://gdem.ersdac.jspacesystems.or.jp/> and <http://www.jspacesystems.or.jp/ersdac/GDEM/E/4.html>
- BPDAS, 2012, Siak Watershed Land Cover, Riau, Indonesia, 2-012.
- D. C. Garen and D. S. Moore, 2005, Curve Number Hydrology in Water Quality Modeling: Uses, Abuses, and Future Directions, *Journal of the American Water Resources Association*, Vol. 41, No. 2, pp. 377-388
- Fatimah Ratna Sari and Denny Zulkaidi, 2014. Managing Zonation Principles for Developing River Area (Prinsip Pengaturan Zonasi Untuk Pengembangan Kawasan Tepi Sungai), *Studi Kasus: Sungai Siak, Kota Pekanbaru*, *Jurnal Perencanaan Wilayah dan Kota*, Vol. 2, No. 2, Sekolah Arsitektur, Perencanaan dan Pengembangan Kebijakan ITB, 211-219.
- G. Hargreaves and Z. A. Samani, 1985, Reference Crop Evapotranspiration from Temperature,” *Applied Engineering in Agriculture*, Vol. 1, No. 2, pp. 96-99
- Hambali, R. 2008. Water Potential Analyses using Mock Model (Analisis Ketersediaan Air dengan Model Mock). *Bahan Ajar*. Yogyakarta: Universitas Gadjah Mada
- Migliaccio, K.W., and P. Srivastava, 2007. Hydrologic components of watershed-scale models. *Transactions of the ASAE*, 50(5): 1695-1703.
- Ministry of Public Work, Indonesia, 2015, Siak River Condition Deteriorating (Kondisi Sungai Siak Makin Memprihatinkan), Available at [GoRiau.com](http://www.goriau.com/berita/siak/kondisi-sungai-siak-makin-m), <<http://www.goriau.com/berita/siak/kondisi-sungai-siak-makin-m>, 1-2.
- Motovilov, Y.G., Gottschalk, L., Engeland, K. & Rodhe, A. 1999. Validation of a Distributed Hydrological Model Against Spatial Observations. *Elsevier Agricultural and Forest Meteorology*. 98 : 257-277.
- Neitsch SL, et all. 2005. Soil and Water Assessment Tool, Theoretical Documentation Version 2005. Grassland Soil and Water Research Laboratory, Agricultural Research Service, Blackland Research Center- Texas Agricultural Experiment Station. USA.
- R. Rosso, A. Peano, I. Becchi and G. A. Bemporad, 1994, An Introduction to Spatially Distributed Modelling of Basin Response,” *Water Resources Publications*, Highland Ranch, pp. 3-30.
- The Minister of Forestry of the Republic of Indonesia Decree, 2014, Number: P. 61 / Menhut II / 2014 concerning A Guideline for Monitoring and Evaluation of Watershed. 7-15
- Yesi Gusriani, 2012, A Strategy for Managing of Water Pollution in Siak Watershed (Strategi Pengendalian Pencemaran Daerah Aliran Sungai (Das) Siak), Kabupaten Siak, Program Studi Ilmu Administrasi Negara FISIP Universitas Riau, Pekanbaru, 2-3.



GROUNDWATER POTENTIAL MODELLING IN CENTRAL LAMPUNG USING RESISTIVITY METER METHOD (GEOELECTRIC METHOD) (Case Studi in Bumi Ratu Nuban District Central Lampung)

Eva Rolia¹, Dwita Sutjiningsih², Herr Suryantono³

¹Doctoral Program Student CivilEngineering Departement Faculty of Engineering University of Indonesia, Depok 16424, Indonesia. Email : roliaeva@yahoo.com

²CivilEngineering Departement Faculty of Engineering University of Indonesia, Depok 16424, Indonesia. Email : dwita@eng.ui.ac.id

³CivilEngineering Departement Faculty of Engineering University of Indonesia, Depok 16424, Indonesia. Email : herr.soeryantono@ui.ac.id

ABSTRACT

Water plays a central and critical role in the life of every living creature. Thus, the presence of the groundwater should be administered properly both in its quality and quantity to fulfill the human demand. Groundwater consuming tends to increase along with the population growth rate, therefore planning and wise groundwater consuming is required to preserve and protect the water resources in the District of Bumi Ratu Nuban Central Lampung regency. The groundwater research was conducted using Geoelectric tool with Schlumberger configuration.

This study is aimed to determine groundwater movement pattern, describe recharge and discharge groundwater zone to govern groundwater conservation. But, the main points carried out in this research are to know the layer type of rock and the presence of groundwater aquifers using the Geoelectric tool Schlumberger configuration and to conduct the modeling using Ip2Win software in Bumi Ratu Nuban district areas; Bumi Rahrjo, Bumi Rahayu and Tulung Kakan with the measurement in 13 spots. Schlumberger configuration was used in this research due to its accuracy to measure under surface conditions vertically based on the resistivity value of rocks.

The study reveals that resistivity value of rocks in Bumi Ratu Nuban districts is dominated by the value between 100 -5000 Ω m. It can be assumed that thick layers of rock in this area are sand and gravel aquifers. The aquifer in this area is phreatic aquifer with the thickness of at least 3.53 m and maximum of 74.95 m. The good potential aquifer was found in Tulung Kakan and Bumi Rahrjo villages. The rock layers dominated in the study area are clay, sand, sand argillaceous and sandy loam.

Keyword : *Geoelectric, Groundwater*

1. INTRODUCTION

National Geological Agency states that Lampung province has 9 groundwater basins; 4 basins across the provinces, 3 basins across districts/towns, and two basins in one of the districts. Overall, the groundwater in Lampung Province has a potential of 2335.91 million m^3 / year for free ground water and pressure ground water to 1123 million m^3 / year. The problem that often arises in the ground water drilling process is to obtain potential ground water both in quality and quantity.

Thus, the availability of groundwater maps is very important. Based on this map, the groundwater conditions, ranging from patterns and flows, stored places, and the time-to-time amount can be easily known or even more efficiently predicted. By knowing the map of groundwater, it is relatively easy to determine the zoning of recharge and discharge areas to establish the type of business or activities which can be done on it, the right way to do



conservation attempts, restriction of uptake, and how wise and prudent in use. In the framework of sustainable development, it is necessary to conduct groundwater zoning, not only to meet the Sustainable Development Goals, but also the environmental awareness and economic principles of justice between generations, to fulfil the demand of present and future generations.

Bumi Ratu Nuban is a district located in the southern part of Central Lampung, which borders directly with Pesawaran District. Bumi Ratu Nuban district consists of 10 villages, with bounded area of 65.14 km² and the population of 30,000.

Guoliang Cao (2015) assessed the variable rate recharge areas in North China by connecting the groundwater balance model on the basis of monthly meteorology data, irrigation and soil moisture monitoring data. The method used is to integrate groundwater unsaturated flow model MODFLOW. The model results show the effect of thickening the unsaturated zone in the recharge area. Thickening of the unsaturated zone can result in an average reduction of up to 70% on clay.

Liang Xiuyu (2012) covered the dynamics of groundwater by estimating groundwater recharge time with the numerical solution of the equation, because the percolation in recharge-discharge areas cannot be measured in real terms. The method used was monitoring wells for 100 days to estimate the recharged parameters by rainfall and evapotranspiration, which is then simulated with numerical equations using MODFLOW.

The concept of groundwater basin rests on the stratigraphy and lithology of the rocks in a region. In the groundwater theory, it is known that both the magnitude and direction of groundwater movement can be calculated with the aid of the flownet concept. By knowing the flownet shape of a region the recharge and discharge area can be determined (Jacob, 2012). This research are to know the layer type of rock and the presence of groundwater aquifers using the Geoelectric tool Schlumberger configuration and to conduct the modeling using Ip2Win software in Bumi Ratu Nuban

In this study the stratigraphy and lithology of the rocks are determined based on measurements of geoelectric. Geoelectric method utilizes electrical resistance properties of the rocks, which are influenced by values such as metallic and non-metallic mineral content, the content of electrolytes (salts), water content, porosity rock, rock permeability, texture / compactness of rocks, as well as temperature (Todd, 1980). Hence, the detection of the presence of groundwater aquifers is required, particularly in the district of Bumi Ratu Nuban Central Lampung regency by using geoelectric Schlumberger configuration. Geoelectric data were processed by software IP2Win to determine the lithology of rocks in the study area and the location of the depth of the aquifer. The Software IP2Win data processing results only display pictures of rock layers, while the groundwater flow pattern treated with SIP2D and MODFLOW will be done in future studies.

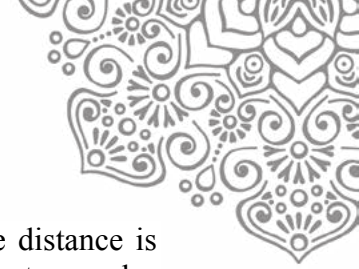
2. METHODOLOGY

2.1 Data Collection Method

The method used in collecting the data is geoelectric resistivity sounding with Schlumberger configuration. The tools used in this research are:

- a. Geoelectric (Resistivity Meter) Naniura type equipped with two current electrodes, two potential electrodes, two wire rolls of current electrode, two wire rolls of potential electrodes, accumulator, and a hammer to plant electrode.
- b. GPS

This configuration is used to determine variations in vertical resistivity value. This configuration uses four electrodes; two electrodes for current flow and the other two electrodes for potential flow. Potential electrode spacing is altered along 0.5 m, 5 m and 10



m. Potential electrode is less likely to be changed despite the current electrode distance is always changing. In this study, the electrode currents spread of at least 150 meters and a maximum of 200 meters, depending on the field conditions. This measurement is performed in four villages, with 13-point soundings with the aim to obtain sufficient information for analysis, modeling and interpretation of the data.

Several things required for measuring the ground water aquifer resistivity using geoelectric comprise of:

- a. The distance between two current electrodes (AB)
This distance is varied to obtain the picture of each layer. The farther the distance between the current electrode, the deeper the geoelectric device can detect the groundwater aquifer underneath.
- b. The distance between two potential electrodes (MN).
- c. Electric current (I) injected in to the ground
- d. The potential difference (ΔV) between two potential electrodes.
- e. From AB and MN can be obtained geometry correction factor (K),

$$K = \pi \frac{(L^2 - l^2)}{l} \quad (1)$$

where $L = \frac{AB}{2}$; $l = \frac{MN}{2}$

2.2 Data Processing

The data obtained from measurements in the field are a large current (I) and the potential difference (V) carried out in the calculations to determine the price of the apparent resistivity ρ_a , which is the product of the geometry factor K with potential and current comparison. The formulation is shown as follows:

$$\rho_a = k \frac{\Delta V}{I} \quad (2)$$

Having obtained the value of pseudo resistivity, 1D modeling is then made to get the value of the actual resistivity. The software used for the data processing of 1D and 2D is Ipi2Win. The data input in this software is the apparent resistivity and distance between the current electrode (AB / 2). The relationship graph between apparent and actual resistivity formed from IP2Win data processing will produce a picture of the type of rock layers and the rock thickness with numbers of corrections or less than 5%. If it is more than 5%, then the graphic depiction is repeated.

Geoelectrical sounding data can be calculated and analyzed digitally by using IP2Win Software. IP2 Win software can analyze induced polarization data with some electrode Schlumberger configuration. IP2Win is software for analyzing geoelectrical data from one or more VES (Vertical Electrical Sounding) points. Using IP2 Win includes some steps. The first step in using IP Win is data input, the second step is data error correction, the next step is adding data point, and the last step is cross section creation. Data input can be done directly from field data (sounding data consist of AB/2, V, I, and K) or indirect field data (sounding data consist of AB/2 and Rho).



3. RESULT AND DISCUSSION

3.1 Map of Research Location

Geoelectric measurements conducted at 13 observation points. Coordinates x, y and elevation z obtained from measurements using GPS.

Table 1. Geoelectric Measurement Point

Village	Measuring Point	Locations	Elevation (MSL)
Sidowaras	1	Residential	+64 m
	2	Residential	+ 66 m
	11	Residential	+ 90 m
	12	Residential	+ 90 m
Bumi Rahayu	4	Oil Palm Plantation	+70 m
	5	Chicken Farm	+60 m
Bumi Raharjo	10	Residential	+ 66 m
	8	Residential	+ 68 m
	9	Residential	+ 67 m
	13	Residential	+ 69 m
Tulung Kakan	3	Cassava Plantation	+67 m
	6	Residential	+ 64 m
	7	Pemukiman Warga	+ 65 m

The picture below shows 13 measuring point in the Bumi Ratu Nuban District. The area having the highest elevation is Sidowaras village, points 11 and 12 with a height of 90 m above sea level. The area having the lowest elevation measurement point is Bumi Rahayu, whose measurement spot is behind the chicken farm, with a height of 60 m above sea level.



Figure 1. Geoelectric Measurement Map in the Bumi Ratu Nuban district Central Lampung

Based on the results of geoelectric estimation and measurement of water level, then obtained a description of the type of rock layers, aquifer type and depth of the aquifer in the research area which can be described as follows:



3.2 Groundwater Aquifer Characteristics of Sidowaras Village

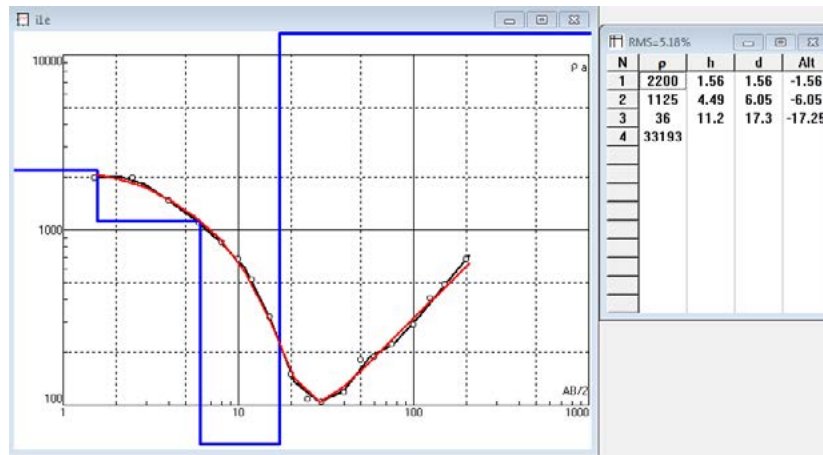


Figure 2. Graph of resistivity value at the measurement point 1

The picture above is a graph of the actual type of resistivity that has been processed, and the samples were taken at the measuring point 1. The measurement at measuring point one is at Sidowaras village in residential areas, with the coordinates $X = 05^{\circ}03'238''$ and $Y = 105^{\circ}14'385''$ and elevation of 64 m above sea level. There are three layers of rock ; the layer surface, sand, and clay. Sand was detected at a depth of 1.56 to 6.05 m, so that the thickness of the sand layer is 6.05 m. Clay of impermeable layer which is at a depth of 6.05 m - 17.3 m from ground level. The sand is a type of aquifer layer that is able to carry and store water because it is permeable. It is seen that the resistance value type is 1125 Ω m, classified as a layer of sand with a range of $102 - 5 \times 10^3 \Omega$ m.

There were 4 measurement points taken in Sidowaras village, and the depth aquifer layout was obtained as in the table below:

Table 2. Characteristics of Aquifer Sidowaras Village

No.	Measuring Point	Coordinates		The Depth of The Aquifer From Ground Surface (m)	The Thickness of The Aquifer (m)	Types of Aquifers	Error (%)
		X	Y				
1.	1	$05^{\circ}03'238''$	$105^{\circ}14'385''$	-1,56 s.d -6,05	4,49	Phreatic	5,18
2.	2	$05^{\circ}03'012''$	$105^{\circ}14'323''$	-0,832 s.d -3,75	3,582	Phreatic	4,04
3.	11	$05^{\circ}02'925''$	$105^{\circ}13'855''$	-1,01 s.d -24,4	23,43	Phreatic	4,40
4.	12	$05^{\circ}02'833''$	$105^{\circ}13'945''$	-0,832 s.d -3,95	4,782	Bebas	4,01

From the above table it is shown that the aquifer type in Sidowaras village (measuring point 1, 2, 11, 12) is a phreatic aquifer with little groundwater potential. The thickness of the layer of groundwater aquifers containing less than 5 m is just below the measuring point 11 with the adequate thickness of aquifer. The average rate on the data processing error was 4.40%. Rock layer indicated as groundwater is a layer of sand or gravel that are permeable, and underneath the aquifer in the form of clay layer that is impermeable. From the results of measurement and data processing in the four points in Sidowaras village, it can be concluded that the ground water in the area is less potential and it can be found at a maximum depth of -30 m above the ground (phreatic aquifers).



3.2 Groundwater Aquifer Characteristics of Kampung Bumi Rahayu

Here will be displayed a graph for the actual resistivity of measuring point 4:

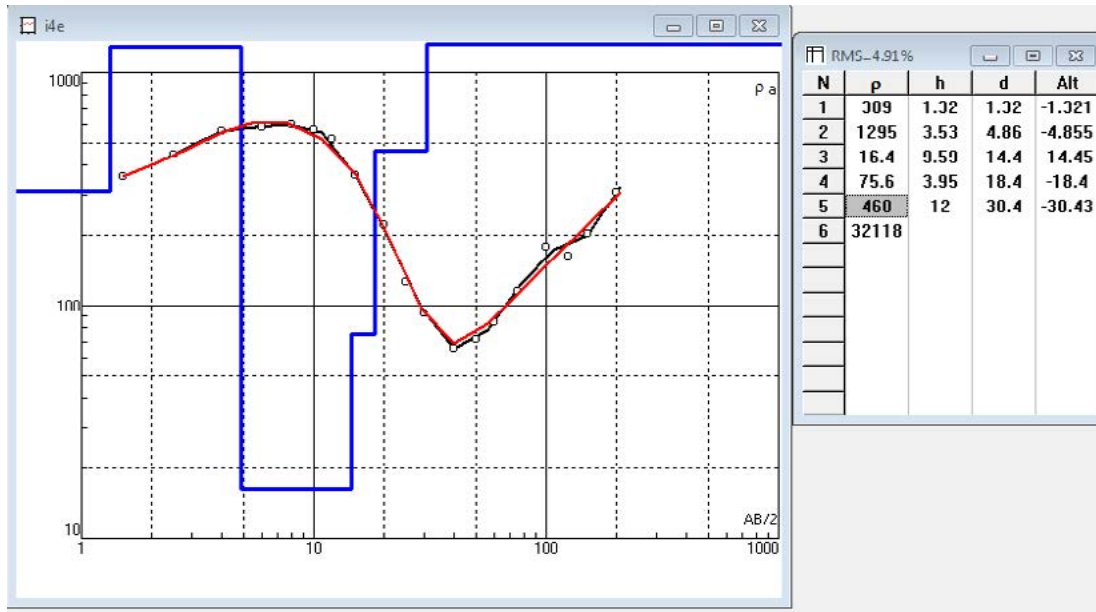


Figure 3. Point 4 Measurement of Actual Resistivity Value

Point 4 measurement was done in front of the chicken farm in residential areas of Bumi Rahayu village, with $X = 05^{\circ}04'464''$ and $Y = 105^{\circ}14'345''$ as well as the elevation of 70 m above sea level. Rock layers lying in this research area are sand (permeable layer), clay (impermeable layer), and sandy loam (semi-permeable layer). The lowest resistivity value was 16.4 Ωm indicated as a layer of silt. A layer of clay is not an aquifer, this layer can absorb water, but cannot remove the water. The maximum depth that can be detected from the data processing is 30.4 m above the ground. There are two types of aquifers lying in this area; phreatic aquifer located at a depth of 1.32 m - 4.86 m from ground level, and semi confined aquifer at a depth of 18.4 m - 30.4 m. The error rate on data processing was 4.91%.

Table 3. Aquifer Characteristics of the Bumi Rahayu Village

No.	Measuring Point	Coordinates		The Depth of The Aquifer From Ground Surface (m)	The Thickness of The Aquifer (m)	Types of Aquifers	Error (%)
		X	Y				
1.	4	$05^{\circ}04'464''$	$105^{\circ}14'345''$	-1,32 s.d -4,86	3,53	Phreatic	4,91
				-18,4 s.d -30,4	12,0	Semi Confined	
2.	5	$05^{\circ}04'597''$	$105^{\circ}14'265''$	-0,75 s.d -4,73	3,98	Phreatic	3,43

Aquifer types in Bumi Rahayu village are phreatic and semi confined aquifers. It is called phreatic aquifer because the location is above the local ground water aquifer depth level of 1.5 m. Geoelectric measurement was conducted in July 2016 during the dry season. Potential groundwater aquifer is not good because the maximum thickness of 3.98 meters. At the measuring point 4 there were found two types of aquifers, phreatic and semi confined aquifers. At the measuring point 5 only 1 phreatic aquifer layer was found. The average rate on a data processing error was 4.17%. This is acceptable because the value of the error rate is below 5%. The maximum depth read on the data processing in Bumi Rahayu village was \pm 30 meters. This is possible because the maximum cable distance when measuring was only



200m. The limitations for excavation in the measuring process on the land were the power cables, population density and the severity of ground surface as the pavement. It was impossible for us to plug in electrical electrodes into the ground, so that the maximum stretch of cable could not be reached.

3.3 Groundwater Aquifer Characteristics of Bumi Raharjo Village

The data processing of Bumi Raharjo village, measuring point 8, is extracted as follows:

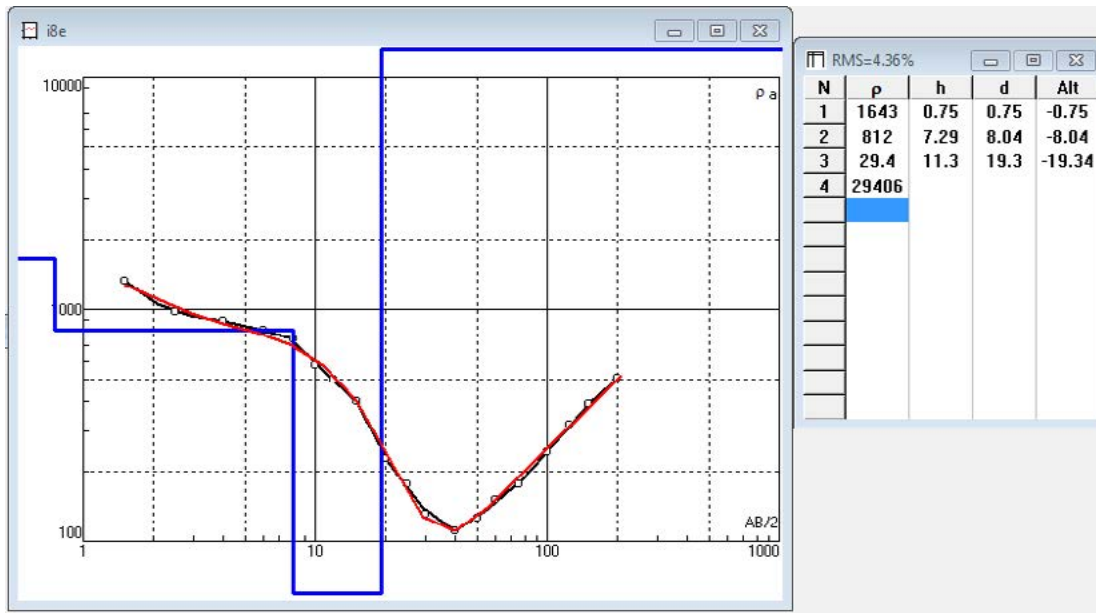


Figure 4. Point 8 Measurement of Actual Resistivity Value

Point 8 measurement was located in a residential area of Bumi Raharjo village, with $X = 05^{\circ}05'248''$ and $Y = 105^{\circ}14'150''$ as well as the elevation of 68 m above sea level. The stretch of the maximum current cable was 200 meters. The rock layers were detected up to 19.3 m and a data processing error rate was 4.36%. This data can be used as the value of the error rate was below 5%. Constituent layers of rock were composed of sand and clay, detected from the actual reading resistivity value. There was a layer of sand with resistivity value of 812 Ωm , and clay 29.4 Ωm . Geoelectric measurements in Bumi Raharjo village performed at 4 measuring points are presented in the table below.

Table 4. The Aquifer Characteristics of Bumi Raharjo Village

No.	Measuring Point	Coordinates		The Depth of The Aquifer From Ground Surface (m)	The Thickness of The Aquifer (m)	Types of Aquifers	Error (%)
		X	Y				
1.	8	$05^{\circ}05'248''$	$105^{\circ}14'150''$	-0,75 s.d -8,04	7,29	Phreatic	4,36
2.	9	$05^{\circ}05'237''$	$105^{\circ}13'925''$	-0,75 s.d -75,7	74,95	Phreatic	4,44
3.	10	$05^{\circ}05'559''$	$105^{\circ}13'625''$	-0,5 s.d -5,91	5,41	Phreatic	4,17
4.	13	$05^{\circ}04'033''$	$105^{\circ}57'145''$	-1,02 s.d -53,8	52,78	Phreatic	3,60

The average error rate on a 4 point measurement carried out in Bumi Raharjo was 4.15%. The results of data processing can be accepted because the value of error is below 5%. The



aquifer type in this area is phreatic aquifer located above the ground water level of 1.5 meters. The potential groundwater aquifer is quite large because the thickness of the aquifer in this area reaches ± 75 m. Groundwater is easy to obtain in this area so that it can be said that Bumi Raharjo is a potential groundwater because of its promising availability. At a depth of -0.5 meters, shallow ground water has already been found. The aquifer layer type in this region is a layer of sand and gravel.

3.4 Groundwater Aquifer Characteristics of Tulung Kakan Village

Geoelectric measurements in Tulung Kakan Village were performed at 3 measuring points ; point 3, 6, and 7. Being displayed is the actual resistivity measuring point 3:

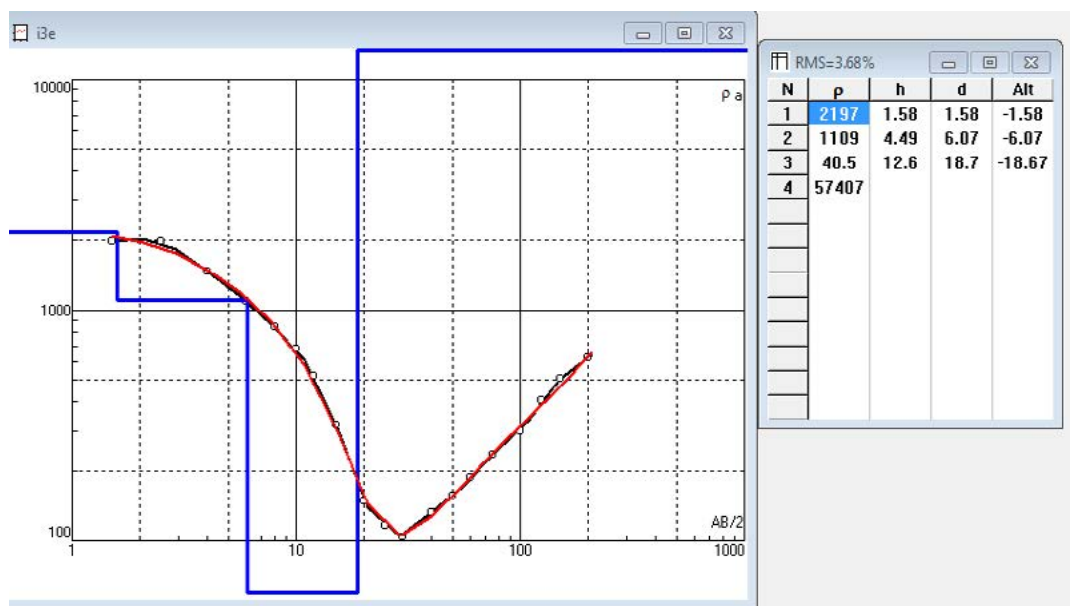


Figure 5. Point 3 Measurement of Actual Resistivity Value

The measurement in measuring point 3 was located in front of Sido Bangun security post in residential areas Tulung Kakan Bumi Ratu Nuban, with X = 05°03'885 "and Y = 105°12'019" as well as the elevation of 67 m above sea level. A layer of sand aquifer with resistivity value $> 1000 \Omega\text{m}$ was located at a depth of ± 1.5 meters. The type of aquifer is phreatic because it is located above or equal to the local ground water table. The error rate measurement and data processing was 3.68%. The rock layers that dominate in this area are sand and argillaceous sand. The aquifer type formed in Tulung Kakan village is shown in the table below:



Table 5. Aquifer Characteristics of Tulung Kakan Village

No.	Measuring Point	Coordinates		The Depth of The Aquifer From Ground Surface (m)	The Thickness of The Aquifer (m)	Types of Aquifers	Error (%)
		X	Y				
1.	3	05 ⁰ 03'885"	105 ⁰ 12'019"	-1,58 s.d -6,07	4,49	Bebas	3,68
2.	6	05 ⁰ 04'401"	105 ⁰ 13'034"	-0,50 s.d -21,7	21,2	Bebas	3,57
3.	7	05 ⁰ 03'964"	105 ⁰ 12'124"	-0,5 s.d -38,7	38,3	Bebas	4,57

The three measurement points in Tulung Kakan village were identified as a phreatic aquifer of sand layer. The location of aquifers is above the local water level at a depth of 1.2 meters from the ground. Potential groundwater in this area is quite good because the thickness of the aquifer reaches \pm 38 meters. The average error rate of data processing with IP2Win was 3.94%. This data can be used for data processing error rate is less than 5%. Aquifer layer of sand is interpreted based on the value of resistivity between 100 to 5000 Ω m.

Of the four villages and 13 points of measurements made in the District of Bumi Ratu Nuban, it reveals that the Bumi Raharjo and Tulung Kakan villages have an aquifer with better potential compared to Sidowaras and Bumi Rahayu villages. Measuring point 9 and 13 have a thickness of the aquifer to more than 50 meters. Aquifer layer in this area is a layer of sand and is generally a type of phreatic aquifer. Rock layers making up on the study area are in the form of sand, loam, sandy loam or sand argillaceous.

Geoelectric method can be used as a device to identify the type of rock layers that exist in the study area based on the value of the electrical resistivity. For further research, it is inevitable to conduct data processing with multiple software such as GMS, MODFLOW, and Geostudio to determine groundwater recharge and discharge areas. Thus, the recharge and discharge areas zoning can be applied so that soil water conservation awareness and actions can be implemented optimally.

4. CONCLUSION

From the research results of geoelectric measurements conducted in the District of Bumi Ratu Nuban as many as 13 measurement points, with the longest current electrode span 200 meters, it can be concluded that:

- Rock layers formed in the research areas are identified as a layer of clay rocks, sand, sandy loam, sand argillaceous while bedrock at a depth that further undetected for a maximum electrode stretch only 200 meters, and maximum readings of actual resistivity \pm 75 meters.
- Type of aquifer layers identified as aquifer layer of sand is phreatic because it is located on the face of the local groundwater. The result of the measurement of ground water level of wells population is 1.2 m to 1.5 m above the ground.
- The minimum thickness of the aquifer is 3.53 m at Bumi Rahayu village, while the thickest layer of the aquifer in Bumi Raharjo with 74.95 meters thick.
- Aquifers with good potential are in Tulung Kakan and Bumi Raharjo as the thickness of the aquifer reaches 74.95 meters. Potential aquifers in Bumi Rahayu and Sidowaras are not good because the average thickness of the aquifer that is very thin which is between 3 m to 5 m.



5. ACKNOWLEDGEMENT

The authors thanks to Kemeristek Dikti and LPDP for scholarship in order the completion of doctoral studies at University of Indonesia, National Geological Agency states that Lampung Province, Dr. Muh. Sarkowi, Diah Indriana Kusumastuti, Ph.D., Ahmad Zakaria, Ph.D., (My Lecture at Lampung University), Muhammadiyah University of Metro Lampung, Dr. RR. Dwinanti Martanti (University of Indonesia)

6. REFERENCES

- Aad, G., et al. (2010). "Charged-particle multiplicities in pp interactions at measured with the ATLAS detector at the LHC." *Physics Letters B* **688**(1): 21-42.
- Abdel-Raouf, O. and M. Mesalam (2016). "Implementation of magnetic, gravity and resistivity data in identifying groundwater occurrences in El Qaa Plain area, Southern Sinai, Egypt." *Journal of Asian Earth Sciences* **128**: 1-26.
- Al-Khafaji, W. M. S. and H. A. Z. Al-Dabbagh (2016). "Visualizing geoelectric–Hydrogeological parameters of Fadak farm at Najaf Ashraf by using 2D spatial interpolation methods." *NRIAG Journal of Astronomy and Geophysics*.
- Anomohanran, O. (2015). "Hydrogeophysical and hydrogeological investigations of groundwater resources in Delta Central, Nigeria." *Journal of Taibah University for Science* **9**(1): 57-68.
- Bear, J. (2012). *Hydraulics of groundwater*, Courier Corporation.
- Chow, V. T., et al. (1988). *Applied hydrology*.
- Domenico, P. A. (1972). "Concepts and models in groundwater hydrology."
- Freeze, R. A. and J. A. Cherry (1979). *Groundwater*.
- Kodoatie, R. J. (2012). "Tata Ruang Airtanah."
- Mohamaden, M., et al. (2016). "Application of electrical resistivity method for groundwater exploration at the Moghra area, Western Desert, Egypt." *The Egyptian Journal of Aquatic Research* **42**(3): 261-268.
- Prawati, E. and E. Rolia "Pengaruh Pemompaan Sumur Bor Terhadap Perubahan Muka Air Tanah."
- Rolia, E. (2001). *Penggunaan Metode Geolistrik Untuk Mendeteksi Keberadaan Air Tanah*. Jurnal Tapak. Universitas Muhammadiyah Metro
- Rolia, E. (2002). *Studi Air Tanah Di Daerah Pesisir Teluk Lampung Dengan Metode Geolistrik*, Skripsi. Universitas Lampung. Bandar Lampung.
- Todd, D. K. and L. W. Mays (1980). "Groundwater hydrology."



15th International Conference on Quality in Research (QiR 2017)

Dry Dams Performance on Consecutive Rainfall During Rainy Season at Upper Ciliwung Watershed

Evi Anggraheni^a, Dwita Sutjiningsih^a, Airlangga Mardjono^b and Teuku Iskandar^c

^a*Civil Engineering Department, Universitas Indonesia, Depok, 16424, Indonesia*

^b*Indonesian commission on Large Dam (Inacold), Jakarta, Indonesia*

^c*Ciliwung-Cisadane River Basin Agency, Jakarta, Indonesia*

ABSTRACT

Jakarta is the capitol of Indonesia which located at the downstream part of Ciliwung. Flooding is a most natural hazard at Jakarta, almost every years its occur at Jakarta. Many infrastructure and researches have been done to decrease risk of flooding. Ciawi and Sukamahi Dams is one of the structural method proposed by government to decrease the peak flood through the retention capacity. That Dams will be constructed with the dry dam type which contain without gates or [turbines](#). Bottom outlet combine with the spillway was design for Ciawi and Sukamahi dam. Dry dam is designed to hold an excess water in times of flooding and allow water to move freely in normal conditions, in the future, its can be used to sediment and water quality control also. The concept is considered a long-term and permanent flood mitigation strategy. Benefit of this dam High maintenance is required especially after the event of a flood to remove debris and sediment deposits. Dry dam inundation area must be control strictly because when the area is not properly control, its will be occupying by habitant. Win Tr 20 has been chosen as the hydrological model that will represent the Upper Ciliwung watershed behavior. The production function of its model adopt the Soil Conservation Service Curve Number as we called SCS-CN. Consecutive rainfall will be applied by the rainfall distribution on the WIN TR 20. Flood routine with consecutive rainfall compute using level pool routine combine with spillway and bottom outlet. The objective of this study is to analyze the dry dam performance when the consecutive rainfall occurs during rainy season. The initial idea from this dry dam is to prolong the time lack before flood arrived in Jakarta to give sufficient time for evacuation. First Result from simulation with single design rainfall show that the Ciawi and Sukamahi increase the time lack of flood peak into downstream.

Keywords: Flooding; Dry Dam; Consecutive Rainfall; Flood Routine and Time Lack



1. INTRODUCTION

Jakarta is the capitol of Indonesia, its located between 5°19'12" to 6°23'54" south and 106°22'42" to 106°58'18" east latitude with the average elevation about 7 MSL (Mean Sea Level). Area of Jakarta around 664 km², with the population 9.6 million people in 2.2 million households in 2010 (Abidin, 2001). As a capitol of Indonesia, center of administration, economic and governance located at Jakarta. Since the rapid economic growth, population is growing and development at Jakarta is expanding around the city. Ciliwung River is one of 13 rivers which through into Jakarta and the most affected river to Jakarta. The length of the main stream of this river is almost 120 km, with the river basin covering an area of 400 km². Ciliwung river flows across Bogor City, Bogor, Depok, South Jakarta and East Jakarta. Its upstream located in the border of Bogor and Cianjur (Gunung Gede-Pangrango and Puncak). According to (Bhakti, 2015), Ciliwung watershed is one of critical watershed in Indonesia. The river is regarded as the worst affected rivers than other rivers flowing in Jakarta. Aside of that, the shape Ciliwung basin from upstream to Katulampa weir areas have dendritic shapes. This form characterizes that the increase in the flow with decreased flow during floods have equal duration, while the downstream direction has parallel shape (elongated) and narrowing. With this shape, the headwaters has an important role, the contribution of runoff from this area is quite large. If the physical conditions, especially land-use, changes, it will lead to changes in the amount of flooding or runoff. (Siti Murniningsih, 2016).

Flooding is the natural hazard that occur each year at Jakarta. The biggest flood in the last three centuries on 2007 inundated about 40 % of the city, killed 80 people and forced about 340.000 to flee (Brinkman, 2008). Many research and infrastructure have been developed to decrease the flooding risk, however its not effective yet to solve the flood problem at Jakarta. Recently, the government propose to build two dry dam at the upper Ciliwung Watershed named Ciawi and Sukamahi Dams. Both of them will build in order to reduce the peak flow and increase the peak flood time into Jakarta. Ciawi and Sukamahi are the first dry dams in Indonesia. Dry dam is designed to hold an excess water in times of flooding and allow water to move freely in normal conditions, in the future, its can be used to sediment and water quality control also. The concept is considered a long-term and permanent flood mitigation strategy. (Lempérière, 2006).

The objective of this study is to analyze the dry dam performance when the consecutive rainfall occurs during rainy season. The initial idea from this dry dam is to prolong the time lack before flood arrived in Jakarta to give sufficient time for evacuation. First Result from simulation with single design rainfall show that the Ciawi and Sukamahi increase the time lack of flood peak into downstream.

The first simulation has been done by single design rainfall for 50 years return period and 100 year return period. Second simulation using consecutive rainfall base on the rainfall event on February 2007. Drainage area is delineated by Arc.GIS 10.1 software base on digital elevation model (DEM) map which is generated from contour data at scale 1:25.000.



2. METHODOLOGY

2.1. Study Area and Rainfall Data

Ciliwung river is flowing from Gunung Gede Pangrango into Java Sea at North Jakarta. The Upper Ciliwung delineate from Gede Pangrango until Katulampa Weir at Bogor City. The area from its watershed about 150 km² and length 25 km. Ciawi Dam located at the meeting point of Cisarua, Ciawi and Ciliwung Hulu Rivers. Sukamahi Dam located at Cisukabirus River. Upper Ciliwung Watershed affected by 3 rainfall station, Gadog, Cilember and Gunungmas. The discretization of ciliwung watershed based on Ciawi and Sukamahi Dam can be show at the following figure.

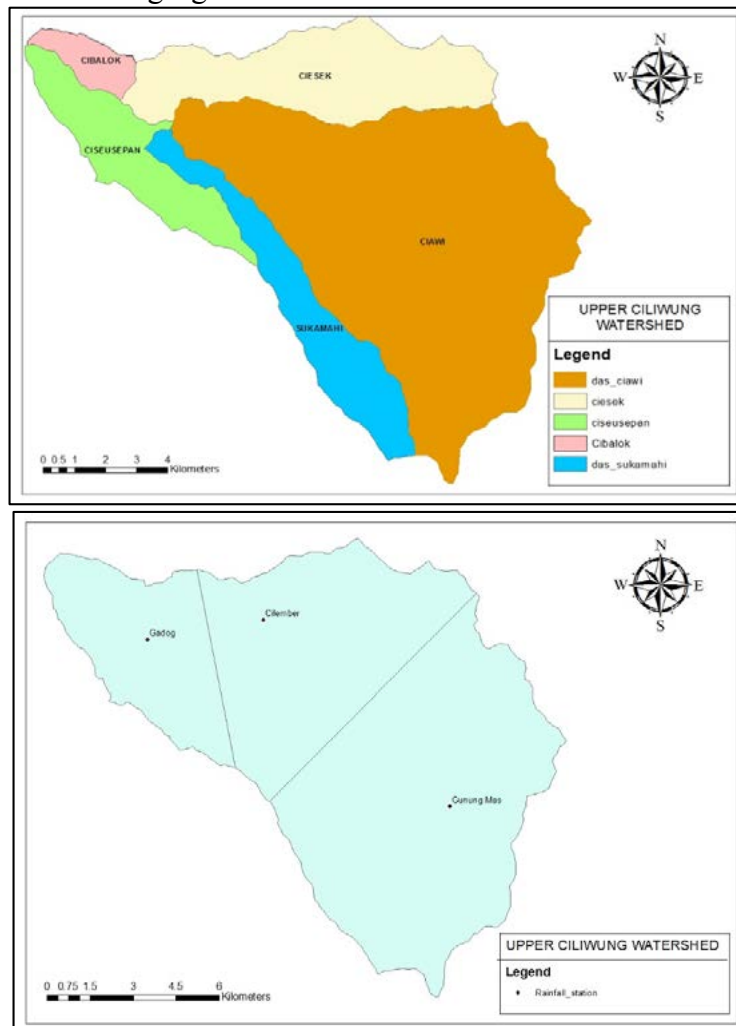


Figure 1a. Upper Ciliwung Discretization, 1b. Rainfall Station

Design rainfall in this study is using log pearson type III. This method considers to statistical parameters, mean, standard deviation and skewness, and is a most flexible and reliable method. It is nothing more but an analysis process and is comparatively complicated than others. (Lee, 2005). This research using 14 years data set from 2003 until 2016 from 3 station with rainfall area using thiessen polygon (Figure 1b.). Rainfall data set can be seen from the table 1.



Table 1. Rainfall Data at Upper Ciliwung Watershed

No	Years	Rainfall Stations			Rainfall Data
		Gadog	Cilember	Gunung Mas	
	Percentage	26.7	47.13	76.92	1
		0.18	0.31	0.51	1
1	2003	161	110	118	123
2	2004	97	70	78	79
3	2005	112	101	157	132
4	2006	72	66	127	98
5	2007	144	108	156	139
6	2008	158	135	105	124
7	2009	125	122	152	138
8	2010	145	131	106	121
9	2011	97	95	115	106
10	2012	113	78	80	85
11	2013	145	131	120	128
12	2014	150	75	120	111
13	2015	110	131	56	89
14	2016	78	87	90	87

2.2. SCS-CN Model

The computation of effective rainfall (production) is performed on each sub watershed by using the Soil Conservation Service - Curve Number (SCS-CN) function. SCS-CN model was developed by USDA (United States Department of Agriculture) by adopting the watershed characteristic. Curve number (CN) value estimated for each sub watershed depend on 3 parameters: land use or land cover, soil characteristic and 5 days antecedent rainfall. It assumes that the flood flow are essentially composed of surface runoff water or at least responding runoff processed. The hypothesis of the SCS-CN method is about the ratios of the two actual potential quantities are equal as the following equation (Chow, 1988):

$$\frac{F_a}{S} = \frac{P_a}{P - I_a}$$

From the continuity principle:

$$P = P_e + I_a + F_a$$

By study of result from many experimental watersheds, an empirical relation was developed thus the equation of SCS-CN:

$$P_e = \frac{(P - I_a)^2}{P - I_a + S} \text{ where as } I_a = 0.2S$$

$$P_e = \frac{(P - 0.2S)^2}{P + 0.8S}$$

The evolution of the runoff coefficient as follows:



$$C_t = \frac{(P_t - 0.2S)}{(P_t + 0.8S)} \left(2 - \frac{(P_t + 0.2S)}{(P_t + 0.8S)} \right)$$

Where C_t is the runoff coefficient and P_t is the total rainfall amount in millimeter at time (t), S is the retention capacity of catchment area in mm. In the following equation the runoff coefficient called as the parameter CN, and parameter CN is called “Curve Number”, the value of CN is between 0 and 100,

$$S = 25.4 \left(\frac{1000}{CN} - 10 \right).$$

The Custom of CN data used to be standard Cover Description using assumptions on the Land Use Detail.

2.3. Hydrological Model Win-TR 20

TR 20 was first developed by the USDA (United States Department of Agriculture) in 1973 and then refined into Win TR 20 by the same institution in 1992. Win TR 20 is a surface water hydrological model that can simulate the amount of flooding spatially within the scale of river basin. This model can be used to analyze the current river basin conditions or simulate the impact of changes in land use in the river basins to adopt the principle of work of the SCS-CN models. Direct runoff / flood by rain hypothetical or real rainy conditions. (Evi Anggraheni, 2016).

WinTR20 represents the watershed as a system of sub-areas and reaches. Sub-areas are the separate individual drainage areas that generate the hydrographs that feed into the upstream end of a stream reach. “Stream Reaches” represent the main flow paths that the hydrographs are routed through. They can accommodate one of two forms of routing: Storage Routing (lakes, dams, wetlands, etc.) or Reach Routing (stream or river channels) (NRCS, 2015).

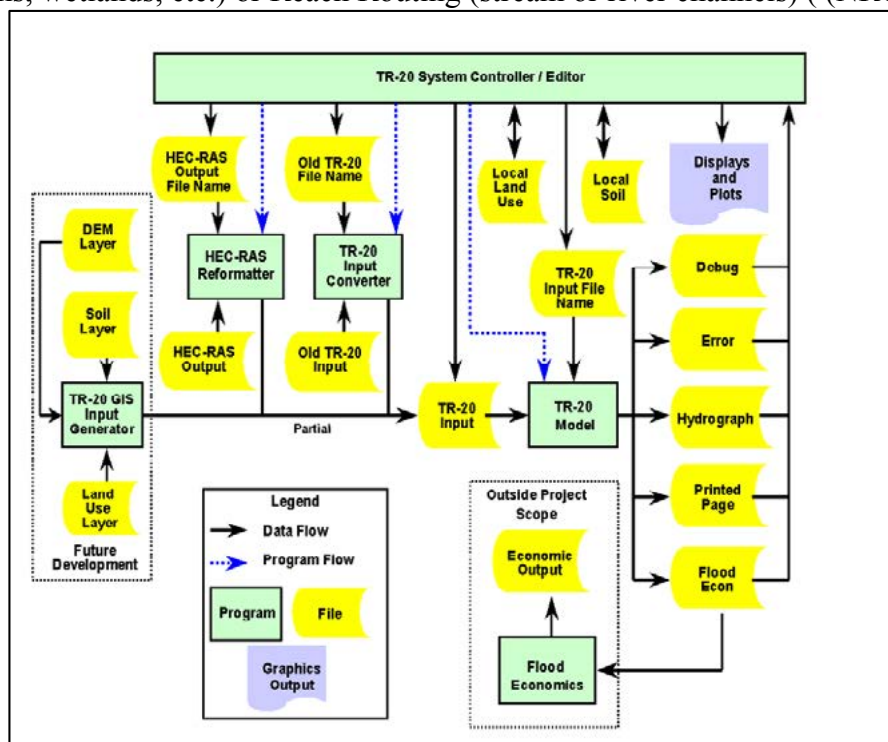
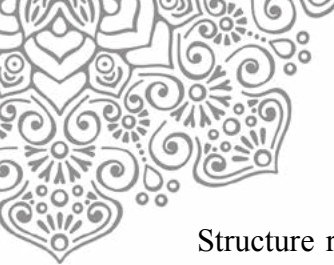


Figure 2. Win TR 20 Procedure



Structure routine on WIN TR 20 based on the level pool routine method and the channel routine based on Muskinggum method.

3. RESULTS AND DISCUSSION

3.1. Upper Ciliwung Watershed Characteristic

More than 30% land cover at Upper Ciliwung watershed is a buildup area (See Figure 3). In order to compute using Win TR 20, we divide the Upper Ciliwung Watershed into 5 sub watershed (figure 1a). Sub Area and reaches parameter are presented at the table 2 below.

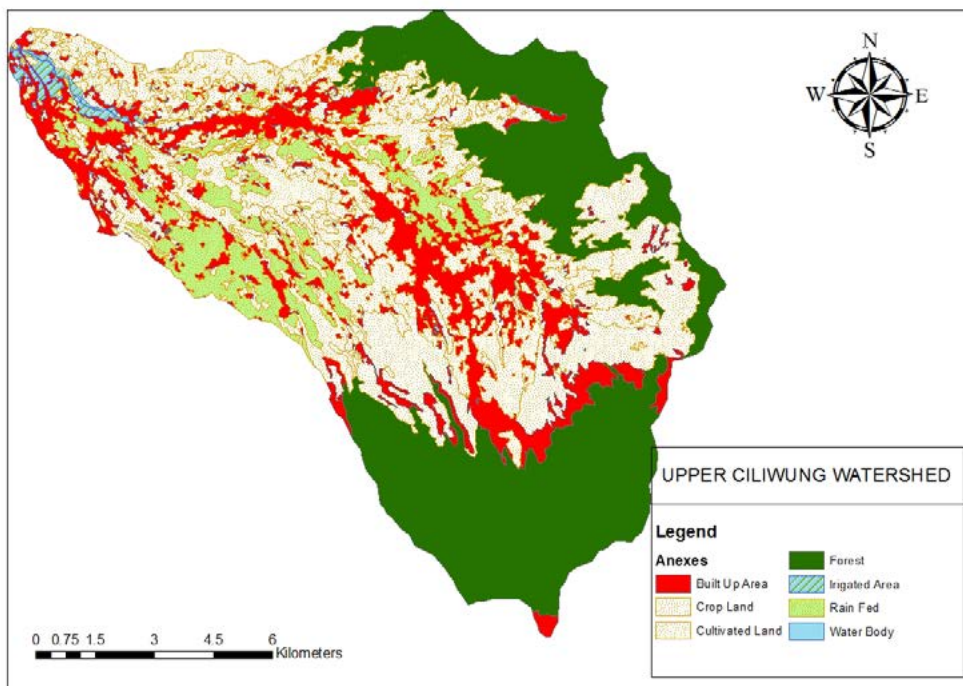


Figure 3. Land Cover at Upper Ciliwung Watershed

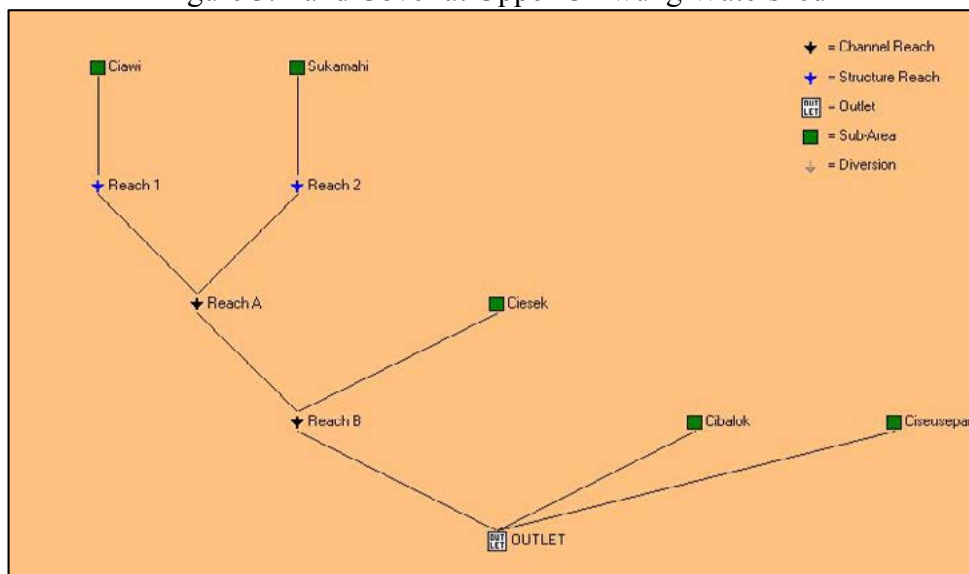


Figure 4. Win TR 20 Schematic



Table 2a Sub Area Parameter

Watershed	A (km ²)	Length (km)	L (m)	Slope	TC (minutes)	Tc (hr)	CN
Ciawi	87.7	19.67	19670	0.05	125.07	2.08	83
Sukamahi	16.90	14.20	14200	0.05	97.32	1.62	70
Ciesek	27.04	12.50	12500	0.17	54.76	0.91	83
Cibalok	4.40	2.50	2500	1.15	7.64	0.13	86
Ciseusepan	14.82	9.20	9200	0.32	34.02	0.57	83

Table 2b Reach Parameter

Reach Parameters	Reach A	Reach B	Reach 1	Reach 2
Receiving Reach	Reach 1	Reach 1	Reach 2	Outlet
Reach Type	Structure	Structure	Channel	Channel
Reach Length (m)	-	-	2600	4300

3.2. Simulation Results

First simulation discharge result based on the single design rainfall data recorded from 3 station using thiessen polygon method. This simulation using 50 years return period and 100 year return period with the rainfall value 155 mm and 161 mm. This simulation neglecting the antecedent rainfall condition. Maximum discharge from 50 years return period about 595 m³/s at the upstream of Ciawi Dam and 582 m³/s at the downstream, 97 m³/s and 91 m³/s at the upstream and downstream Sukamahi Dam and 909 m³/s at Katulampa Weir or the outlet (Figure 5a, 5b and 5c)

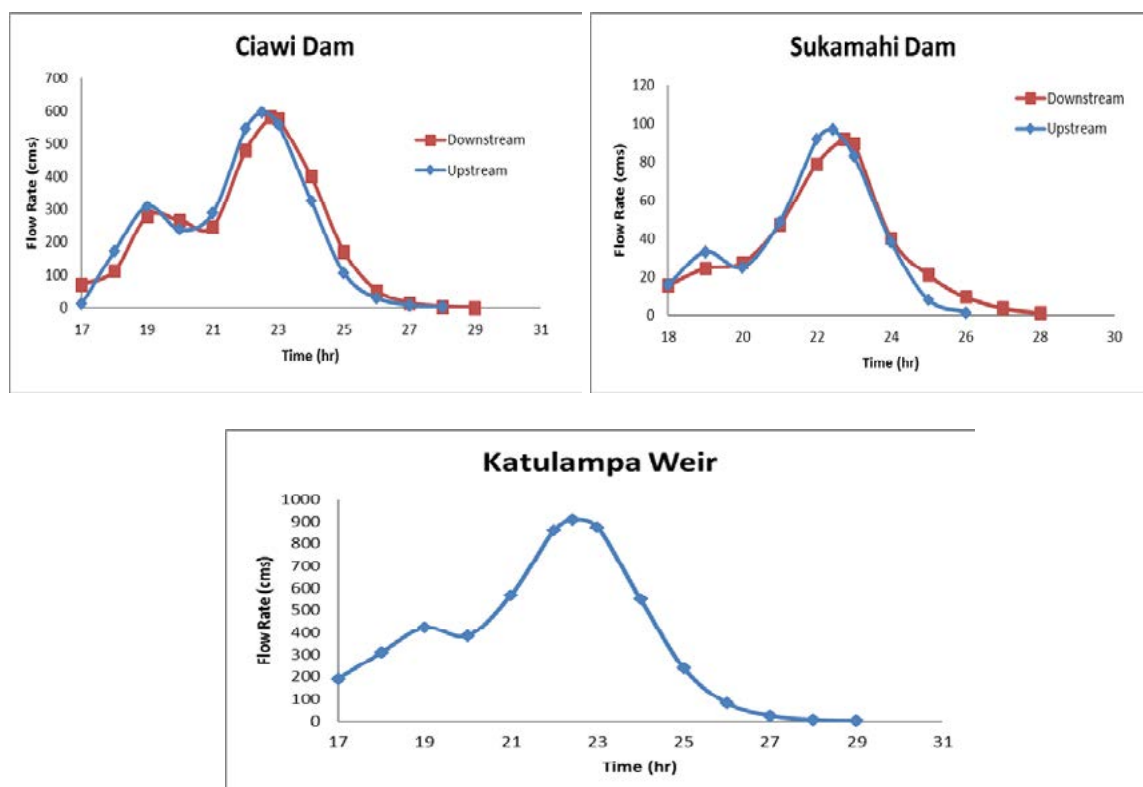


Figure 5a. Ciawi Hydrograph, 5b. Sukamahi Hydrograph and 5c. Katulampa Hydrograph



Second simulation using real rainfall data on February 2007 (biggest flood). On January 2007 there are 3 days that have big consecutive rainfall about 156 mm, 144 and 110 mm. Antecedent Moisture Condition (AMC) has been used also for this simulation based on the real condition. First day using AMC I (mean dry condition), second day AMC II (Normal Condition) and third day using AMC III (saturated condition). Hydrograph for the three location can be seen on the following figure (Figure 6a, 6b and 6c)

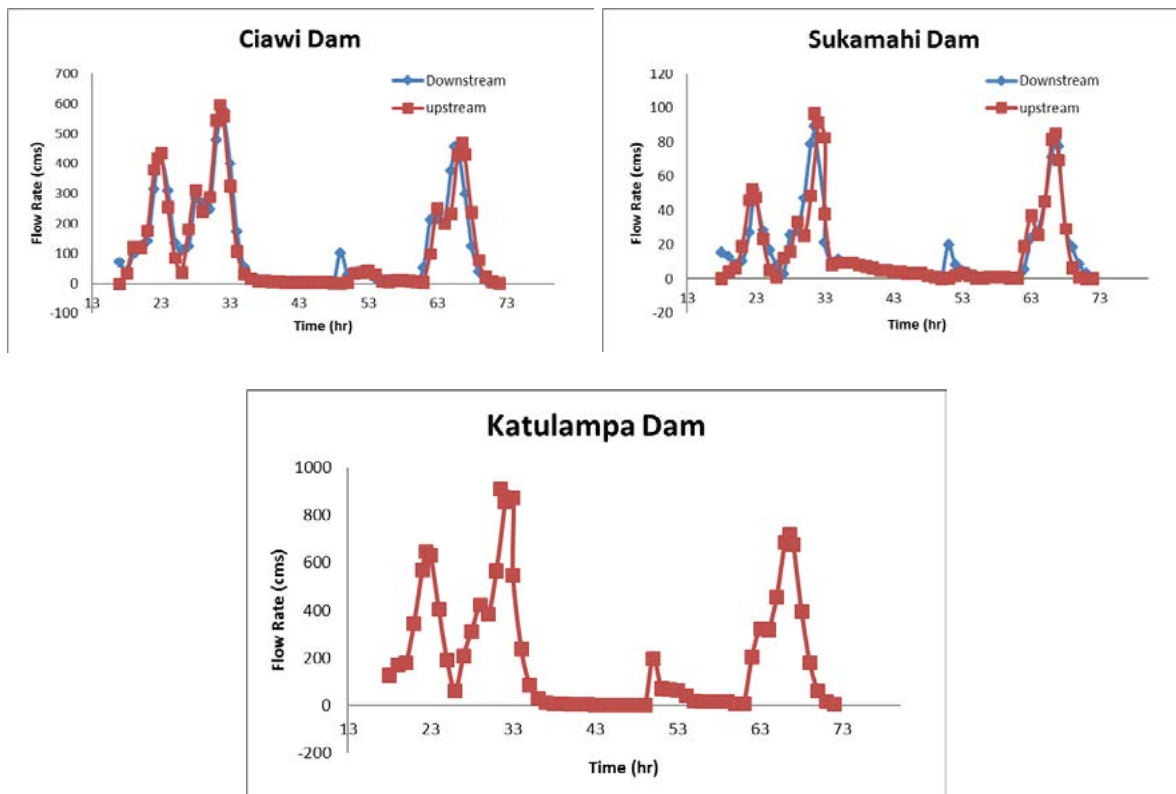


Figure 6a. Consecutive Rainfall at Ciawi, 6b. Sukamahi, 6c. Katulampa

4. CONCLUSION

The result shown that the magnitude discharge between upstream and downstream at Ciawi Dam seem small either at Sukamahi Dam. Sukamahi Dam reduce 5% and Ciawi reduce 2% peak discharge. However, the peak time at Ciawi prolong until 20 minutes and Sukamahi more 10 minutes than Ciawi. Storage effect at Sukamahi seem more effective than Ciawi because the catchment area of Sukamahi is smaller than Ciawi.

Second simulation shown that the discharge from the consecutive rainfall produce three peak discharge. First rainfall approximately with the 50-year rainfall value however we use AMC 1 (dry condition) so the peak discharge was decrease than the first simulation. Rainfall that occur during the AMC 1 will fill the soil storage first before flowing to be surface runoff. Due to that condition the discharge at the first day decrease than the first simulation. However, at the third day when the rainfall is small (smaller than 2 year return period), the



discharge still rises up. That condition is caused by the simulation of AMC III. At the third days, the soil is already saturated so almost all rainfall became the surface runoff. Further research is still needed to find the optimum model to decrease the peak discharge and to hold the exceed rainfall longer than before at the upper Ciliwung Watershed. Integration the several technologies still possible to applied at that location.

5. ACKNOWLEDGEMENT

Acknowledgements are addressed to Cecilia Ratna, Novi Susanti as well as to the staff in the Hydraulics, Hydrology and River Laboratory, and the Environmental Engineering Laboratory, Civil Engineering Department, Faculty of Engineering, Universitas Indonesia, for their contribution in conducting field surveys, data processing, and computation using the WinTR-20 application

6. REFERENCES

- Abidin, H. D. (2001). Land subsidence of Jakarta (Indonesia) and Its Geodetic Monitoring System. *Natural Hazard Vol 23*, 365-387.
- Bhakti, W. Y. (2015). *Prediksi Laju Erosi Potensial dan Laju Timbulan Sampah Potensial pada Luasan Penutup Lahan Kedap Air (Studi Kasus DAS Ciliwung) Berbasis Sistem Informasi Geografis (SIG)*. Depok: Universitas Indonesia.
- Brinkman, J. a. (2008). *Jakarta Flood Hazard Mapping Framework*. Jakarta.
- Chow, V. t. (1988). *Applied Hydrology*. Mc Grown Hill.
- Evi Anggraheni, a. D. (2016). Effectiveness Of Hypotetic Retention Ponds Simulation on The Integrated Flood Management System. *International Conference of Asosiation of Indonesian Hydraulic Engineer*.
- Lee, C.-Y. (2005). Application of Rainfall Frequency Analysis on Studying Rainfall Distribution Characteristics of Chia-Nan Plain Area in Southern Taiwan. *Journal of Crop, Environment & Bioinformatics*.
- Lempérière, F. (2006). The role of dams in the XXI century, Achieving a Sustainable Development Terget. *Hydropower and Dams*.
- NRCS, U. (2015). *Hydrology Model Basic Tutorial*.
- Siti Murniningsih, a. E. (2016). Identification the effect of spatial land use variability using GIS at The Upstream Ciliwung Watershed. *ARPN Journal of Engineering and Applied Sciences*.



15th International Conference on Quality in Research (QiR 2017)

Analysis of Retrofit on School Building with Shear Wall and Steel Bracing

Fauzan^{a1}, Febrin A. I.^b, Farizzi A. S.^c, Yogi I. R.^d, Zev A. J.^e

^{a,b}Lecturer at Department of Civil Engineering, Andalas University, Padang City, 25163, Indonesia

^cConstruction Engineer at PT Total Bangun Persada, 11440, Indonesia

^dEnginner Staff at PT Waskita Karya, 13340, Indonesia

^eStudent at Department of Civil Engineering, Andalas University, Padang City, 25163, Indonesia

ABSTRACT

The earthquake on 30 September 2009 with 7,6 magnitude occurred in West Sumatera and it caused the damage to both physical public facilities and infrastructures. The education sectors suffered from structural damage to the school buildings. In order to establish of the new Indonesian Seismic Code, SNI 03-1726-2012, it will affect to the performance of structures which was built before the establishment of the new seismic code, in which the building may not be adequate to withstand the working loads. In this study, the performance and strucutral strength of a two-story RC school building (SMAN 3 Batusangkar) designed using previous seismic code (SNI 03-1726-2002) and it was constructed before 2009, was evaluated based on the new seismic code. The result of evaluation on the SMAN 3 Batusangkar building shows that the building can not resist the working loads applied to the structure, especially the earthquakae loads, so the building structure needs to be retrofitted. Two retrofitted methods of the building were proposed in this study, they are using shear wall and steel bracing systems, which installed on the building frame with different locations. The addition of shear wall and steel bracing are very effective in strengthening the building structure, where the load-bearing capacity of the structure increased significantly and the building is able to resist all working loads.

Keywords: Earthquake, Retrofit, Shear Wall, Steel Bracing, School Building.

* Corresponding author.

E-mail address: fauzanrn@yahoo.com



1. INTRODUCTION

In recent years, some parts of Indonesia experienced large earthquakes. It started from Aceh on December 26, 2004, Nias and Mentawai on March and April 2005, Bengkulu on September 12 and 13, 2007, and the last earthquake in Pariaman on September 30, 2009. After the earthquake on September 30, 2009, the education sector suffered from structural damage of the school buildings. The 2132 classrooms were heavily damaged, 1335 were moderately damaged, and 1144 were minor damaged [1]. Schools area is strategic target as the dissemination of disaster information center. Therefore, as a disaster risk reduction efforts of schools in Indonesia, the government of Indonesia throughs the National Agency for Disaster Management (BNPB), Ministry of Public Works, and Ministry of Education and Culture make a program called SAFE school.

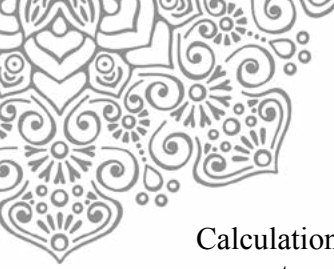
Based on a history of the earthquakes that occurred in recent years, it is known that the earthquake has peak ground acceleration (PGA) greater than the PGA that has been set in the earthquake map in SNI 03-1726-2002 Code [2]. So, this code is not applicable with current condition. The government through BSNI (Indonesian National Standardization Agency) has established a new seismic code, SNI 03-1726-2012, Earthquake Resilience Planning Standards for Structural Building and Non-Building [3]. Therefore, an evaluation or assessment of the existing building designed using the old seismic code, including school building, should be done based on the new seismic code.

2. EVALUATION OF THE EXISTING BUILDING

In this study, the performance and structural strength of a school public building in West Sumatera, Senior High School (SMAN) 3 Batusangkar Building, was evaluated. The school was two-story RC building, which is designed using previous seismic code (SNI 03-1726-2002) and constructed before 2009, so it is necessary to evaluate based on the new seismic code. The details of building are described in the Figure 1 and Table 1.

Table 1 Details of The SMAN 3 Batusangkar Building

Structural Elements	Properties
Beam size	B1 (30 cm x 65 cm)
	B2 (25 cm x 40 cm)
	B3 (25 cm x 30 cm)
	B4 (30 cm x 40 cm)
Column size	K1 (30 cm x 40 cm)
	K2 (30 cm x 30 cm)
Slab thickness	12 cm
Total height of frame	7.2 m
Number of column	56
Compressive strength of concrete	K-225 ($f'_c = 18.675$ MPa)
Yield strength of reinforcement (f_y)	320 MPa
Plan area	52.5 m x 10 m



Calculation and structural analysis are applied by a three-dimensional structure made of a computer program, ETABS 9.7.1 [4]. The loads are taken into account included the dead load/ weight of its own building, live, and seismic load. An analysis of the seismic load used dynamic analysis based on SNI 03-1726-2012 Code. The minimum load for design of buildings and other structures code, SNI 1727-2013 Code, was used to calculate the working loads [5]. The dynamic analysis used seismic response spectrum design for Batusangkar City, as seen in the Figure 2 (source: <http://puskim.pu.go.id>, application design spectra of Indonesia 2011) [6].

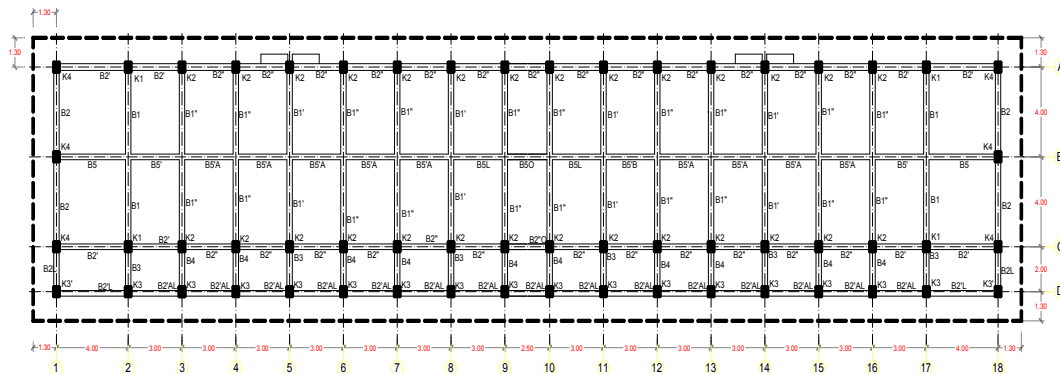
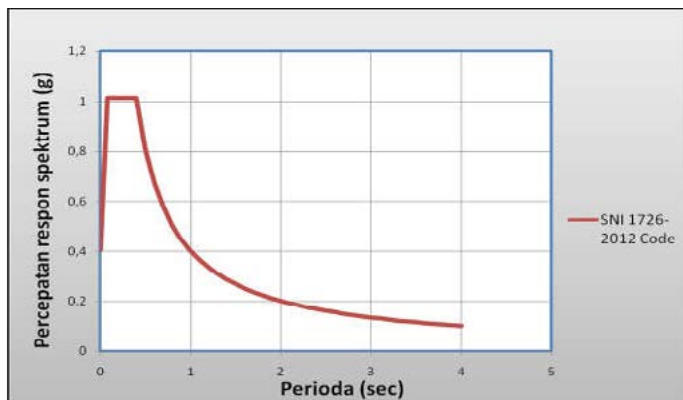


Figure 1 Perspective and plan of the school building



Variable	Value
PGA (g)	0.602
Ss (g)	1.398
S1 (g)	0.600
CRs	1.906
CR1	0.955

Figure 2 Response spectrum graph for Batusangkar City based on SNI 1732-2012



2.1. The Flexural Capacity of Existing Columns

Figure 3 shows the P-M interaction diagram for columns of the building structure. It can be seen in the figure, there are several points of axial forces and bending moments exceed the interaction diagram, this means that the capacity of column is not strong enough to resist the working loads.

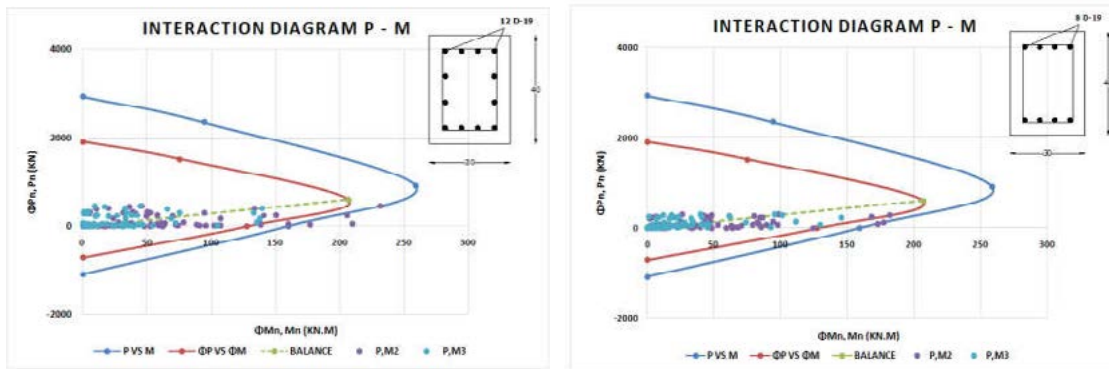


Figure 3 Interaction diagram of the existing column

2.2. The Shear Capacity of Existing Columns

Table 2 shows the shear capacity of the columns. As seen in the table, the shear capacity of column K1 is sufficient, nominal shear is higher than the ultimate shear (V_u). However, the shear capacity of both columns K2 (1st and 2nd floors) could not meet the requirement.

Table 2 Column shear capacity of the existing structure

Story	Code	Shear Reinforcement Installed		V_u (ETABS) (kN)	ϕV_n (kN)	Explanation ($V_u \leq \phi V_n$)
		Diameter (mm)	Space (mm)			
1 st Floor	K1 30/40	10	200	67,15	103,99	OK
	K2 30/30	10	200	71,25	55,71	NOT OK
2 nd Floor	K2 30/30	10	200	60,4	55,71	NOT OK

2.3. Inter Story Drift (SNI 03-1726-2012 Code)

Table 3 Inter story drift of the existing structure

Story	H (m)	UX (m)	Drift X (m)	X Dir. (m)	a	$s \leq a$	UY (m)	Drift Y (m)	Y Dir. (m)	a	$s \leq a$
2	3.6	0.2096	0.1819	0.3032	0.04154	NOT OK	0.0474	0.025	0.041667	0.04154	NOT OK
1	3.6	0.0277	0.0277	0.0462	0.04154	NOT OK	0.0224	0.0224	0.037333	0.04154	OK



Table 3 shows the value of inter story drift in x and y-directions. From the table, it can be seen that maximum of the story drift for x and y-direction are 0.3032 m and 0.04167 m, respectively. These values are less than the allowable inter story drift of 0.04154 m. Based on the above analysis result of the existing building by using the new Indonesian seismic code, it can be said that the SMAN 3 Batusangkar building structure is not capable to resist the working loads.

3. RECOMMENDATION OF THE RETROFITTING

3.1. Retrofitting of Structures

Retrofitting is a method to increase the resistant capacity of structure. A seismic retrofit provides existing structures with more resistance to seismic activity due to earthquakes. Retrofitting techniques can be classified as local and global retrofitting. Local retrofitting is the maintenance of local deficiencies in building like crushing of columns, flexure and shear failure of beams, columns and shear walls, also rebuilding infill masonry. Global retrofitting is maintenance of global deficiencies in building like plan and vertical irregularities. The global retrofit includes the addition of shear wall and steel bracing [7]. In this study, there are two retrofitted systems, shear wall and steel bracing systems which was analysed. The systems were attached on the building frames with different locations.

3.1.1. Retrofitted with Shear Wall

Shear wall system is one of the most commonly used lateral-load resisting systems in multi-story buildings. Shear wall has very high in-plane stiffness and strength which can be used to simultaneously resist large horizontal loads and support gravity loads [8]. The proposed thickness of shear wall is 25 cm with compressive strength of concrete (f_c') is 25 Mpa. The yield strength of the D-16 mm longitudinal reinforcement is 390 MPa. The yield strength of the D-10 mm transversal reinforcement is 240 MPa. Specification detail of the shear wall in the retrofitted structure can be seen in the Figure 4.

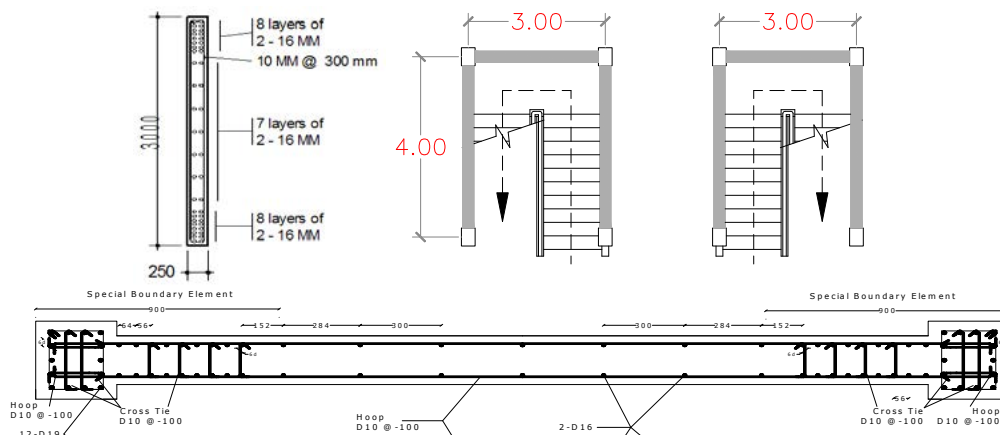


Figure 4 Specification detail of shear wall

Four different locations that added to the shear wall system on the building were modelled, as shown in Figure 6:



- Model A, shear wall attached on a core area of stairs in the 1st floor (Figure 6a)
- Model B, shear wall attached on a core area of stairs in the 1st and 2nd floors (Figure 6b)
- Model C, shear wall attached on a corner area of the building in the 1st floor (Figure 6c)
- Model D, shear wall attached on a corner area of the building in the 1st and 2nd floors (Figure 6d)

3.1.2. Retrofitted with Steel Bracing

Bracing system is one of structural system which forms an integral part of the frame. Bracing is efficient because the diagonals work in axial stress and therefore it is called for minimum member sizes in providing the stiffness and strength against horizontal shear [9]. In this study, steel bracing with the V-inverted was selected to retrofit the existing structure. Based on the results of bracing designed calculations (with input parameters: yield strength of 390 MPa, ultimate strength of 520 MPa and elastic modulus of 200.000 MPa), IWF profile with dimension of 250.250.9.14 provides enough lateral stiffness and stability. The specification detail of the steel bracing can be seen in Figure 5.

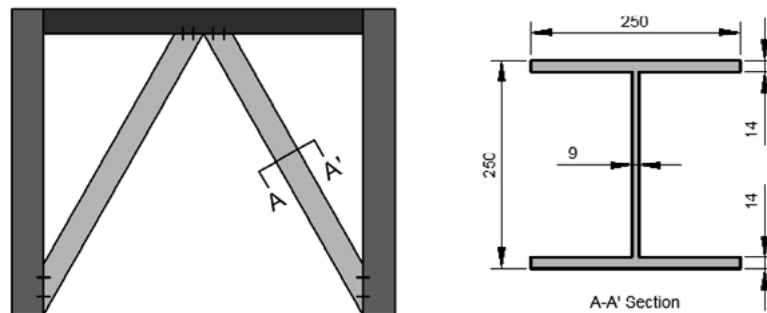
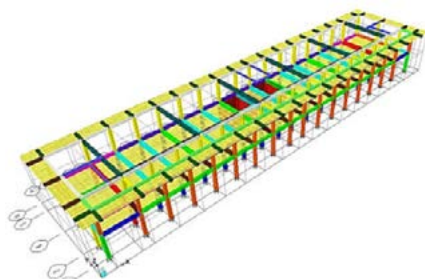


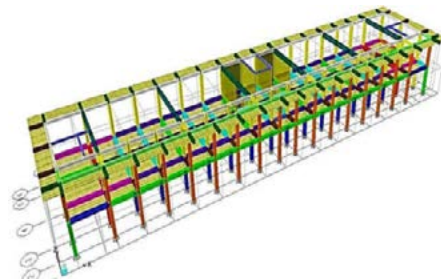
Figure 5 Specification detail of steel bracing

Four different locations that added to the steel bracing system on the building were modelled, as shown in Figure 6:

- Model E, the bracing attached on X direction both front and rear on 1st floor (Figure 6e)
- Model F, the bracing attached in corners area X and Y directions (L shape) on 1st floor and 2nd floors (Figure 6f)
- Model G, the bracing attached in X and Y directions (U shape) on 1st and 2nd floors (Figure 6g)
- Model H, the bracing attached in Y direction and central part of the building in X direction on 1st and 2nd floors (Figure 6h)



(a) Model A



(b) Model B

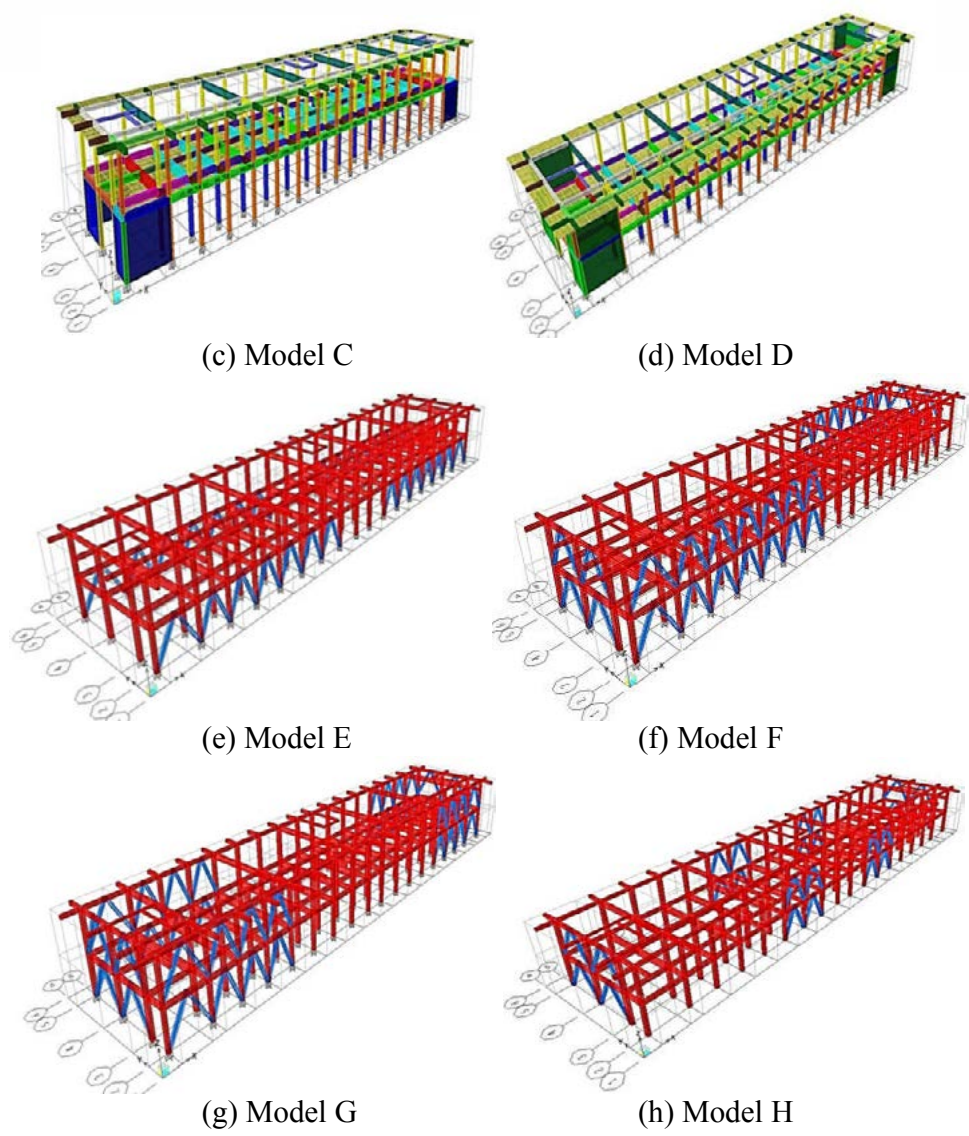


Figure 6 The 3-D modeling of retrofitted structures

3.2. Analysis of Retrofitted Structures

Structural analysis using ETABS v9.7.1 was carried out for all models. From the eight retrofitted building models analyzed, the result of interstory drift shows that the four models (Models A,C,E, and H) do not meet requirement based on new seismic code, SNI 1726-2012, where the story drift exceeds the allowable drift, as shown in Table 4. Therefore, there are four models recommended for retrofitting structures: models B and D using shear wall system and models E and H using steel bracing system. The comparison for recommended models of the retrofitted building are discussed below.



Table 4 Interstory drift of all retrofitted model

Model	Story	H (m)	UX (m)	Drift X (m)	s X Dir. (m)	a	s ≤ a	UY (m)	Drift Y (m)	s Y Dir. (m)	a	s ≤ a
A	2	3.6	0.0279	0.0255	0.0850	0.054	NOT OK	0.0217	0.014	0.0450	0.054	OK
	1	3.6	0.0024	0.0024	0.0080	0.054	OK	0.0079	0.0079	0.0263	0.054	OK
B	2	3.6	0.0081	0.0059	0.0197	0.054	OK	0.0182	0.012	0.0387	0.054	OK
	1	3.6	0.0022	0.0022	0.0073	0.054	OK	0.0066	0.0066	0.022	0.054	OK
C	2	3.6	0.0234	0.0225	0.0750	0.054	NOT OK	0.0164	0.012	0.0397	0.054	OK
	1	3.6	0.0009	0.0009	0.0030	0.054	OK	0.0045	0.0009	0.015	0.054	OK
D	2	3.6	0.0149	0.0141	0.047	0.054	OK	0.0169	0.012	0.041	0.054	OK
	1	3.6	0.0008	0.0008	0.0027	0.054	OK	0.0046	0.0046	0.0153	0.054	OK
E	2	3.6	0.0232	0.023	0.0767	0.054	NOT OK	0.021	0.012	0.04	0.054	OK
	1	3.6	0.0002	0.0002	0.0007	0.054	OK	0.0089	0.0089	0.0297	0.054	OK
F	2	3.6	0.016	0.016	0.0533	0.054	OK	0.012	0.0095	0.0317	0.054	OK
	1	3.6	0.0001	0.0001	0.0000	0.054	OK	0.0021	0.0021	0.007	0.054	OK
G	2	3.6	0.0162	0.0162	0.054	0.054	OK	0.012	0.0098	0.0327	0.054	OK
	1	3.6	0.0001	0.0001	0.0000	0.054	OK	0.0021	0.0021	0.007	0.054	OK
H	2	3.6	0.026	0.0238	0.0793	0.054	NOT OK	0.021	0.0138	0.046	0.054	OK
	1	3.6	0.0022	0.0022	0.0073	0.054	OK	0.0076	0.0076	0.0253	0.054	OK

3.3. The Location Point of Columns and Beams to Compared the Structural Response
The location point of columns and beams to compare structural response can be seen in Figure 7. The positions are taken from one interior beam and another one interior column of the center of each floor.

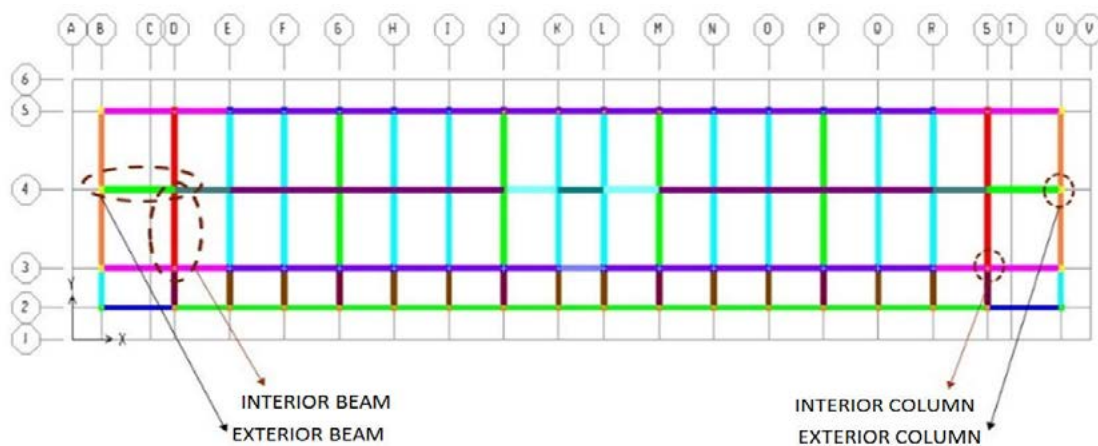


Figure 7 Location point of columns and beams to compare the structural response



4. RESULTS AND DISCUSSION

4.1. The Internal Force in Beams

The comparison of shear force on the beam between existing and retrofitted building is shown in Table 5. From the table, it can be seen that the building using steel bracing and shear wall have smaller value than the existing structure. The retrofitting provides great rigidity to the structure, so it reduces the shear force in the structure by around 90%. Table 6 shows a comparison of bending moment on the beam. As seen in the table, the bending moment of the beam was also reduced up to 70% due to the present of shear wall and steel bracing in the building.

Table 5 Comparison of shear force in the beam between existing and retrofitted structures

Location of View	Story	Shear Force (kg)				
		Existing	Model B	Model D	Model F	Model G
The Interior Beam	1	20684	17732	14746	15423	15615
	2	3337	2553	1906	1867	1791
The Exterior Beam	1	6649	4298	3152	3560	4025
	2	376	248	248	219	242

Table 6 Comparison of bending moment in the beam between existing and retrofitted structures

Location of View	Story	Bending Moment (kg.m)				
		Existing	Model B	Model D	Model F	Model G
The Interior Beam	1	19018	17226	14046	15773	16223
	2	5347	2469	1409	1199	1121
The Exterior Beam	1	5092	3822	2815	3421	3797
	2	258	131	127	119	125

4.2. The Internal Force in Columns

The comparison of internal force in the columns (axial, shear, and bending moment) between existing and retrofitted buildings can be seen in Tables 7, 8, and 9, respectively. It can be seen from Table 7, the axial force on Models B and D were lower around 20 – 35% than existing building, however, on Models F and G, were higher around 32 – 35% than existing building.

From Table 8, shear force in the retrofitted structures were smaller than the existing structure. The percentage of reduction that occurs in the shear force of the columns are around 90 – 95%. This is mainly due to the retrofit can resist the lateral loads, especially the earthquake load.

Adding the shear wall and steel bracing systems on the building structure can reduce bending moment. The percentage of bending moment reduction around 95% compared to the existing structure, as seen in the Table 9.



Table 7 Comparison of axial force in the columns between the existing and the retrofitted structures

Location of View	Story	Axial Force (kN)				
		Existing	Model B	Model D	Model F	Model G
The Interior Column	1	76,6	29,89	16,53	121,8	123,63
	2	24,86	10,97	6,22	9,46	8,61
The Exterior Column	1	61,16	4,37	57,16	64,62	64,87
	2	17,55	0,89	0,56	12,14	12,15

Table 8 Comparison of shear force in the columns between the existing and the retrofitted structures

Location of View	Story	Shear Force (kN)				
		Existing	Model B	Model D	Model F	Model G
The Interior Column	1	68,91	2,77	0,68	0,61	0,73
	2	22,09	9,83	8,65	0,51	0,6
The Exterior Column	1	77,53	24,71	3,26	14,62	14,93
	2	6,83	6,18	0,74	3,16	3,52

Table 9 Comparison of bending moment in the columns between the existing and the retrofitted structures

Location of View	Story	Bending Moment (kN.m)				
		Existing	Model B	Model D	Model F	Model G
The Interior Column	1	134,86	8,44	4,22	3,27	4,04
	2	38,78	19,28	17,57	0,87	1,04
The Exterior Column	1	145,25	28,1	1,79	17,61	17,65
	2	40,47	38,8	22,07	20,26	20,21

4.3. Displacement

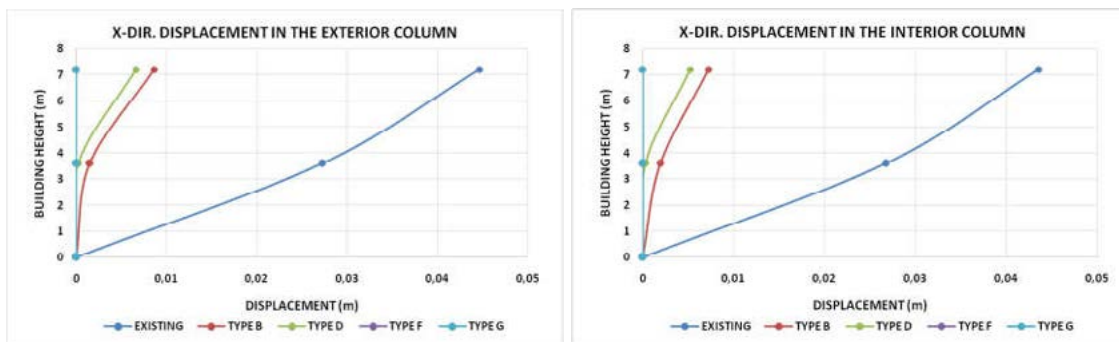


Figure 8 Comparison of X-dir. displacement between existing and retrofitted structures

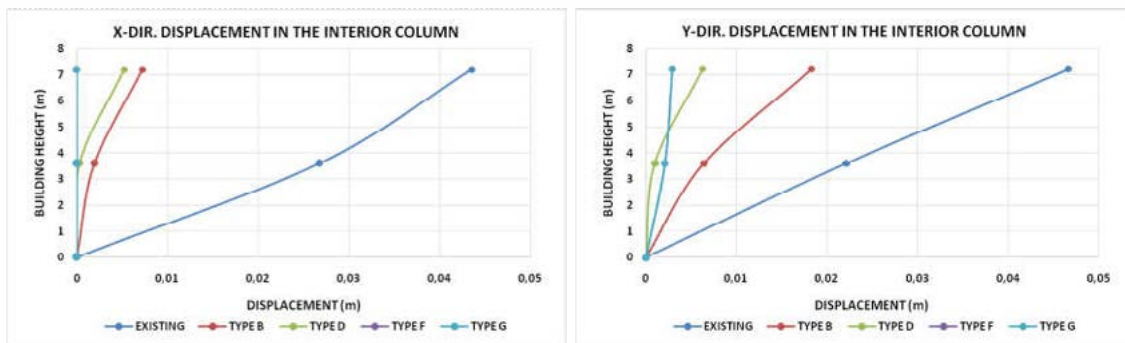
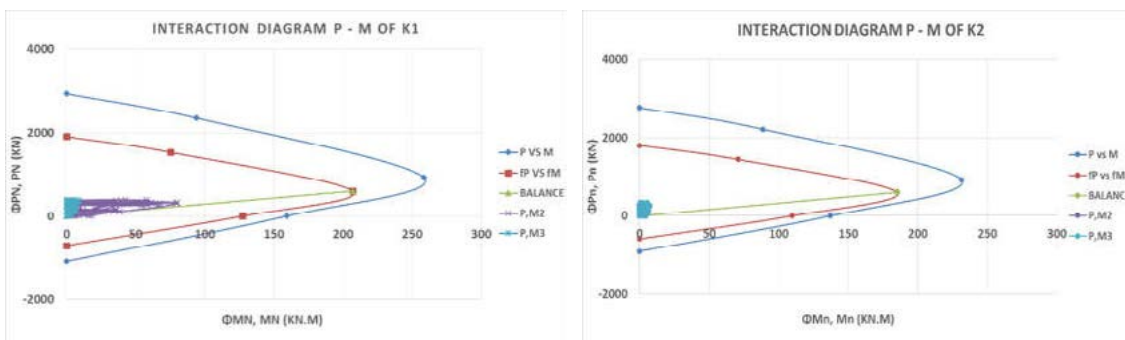


Figure 9 Comparison of Y-dir. displacement between existing and retrofitted structures

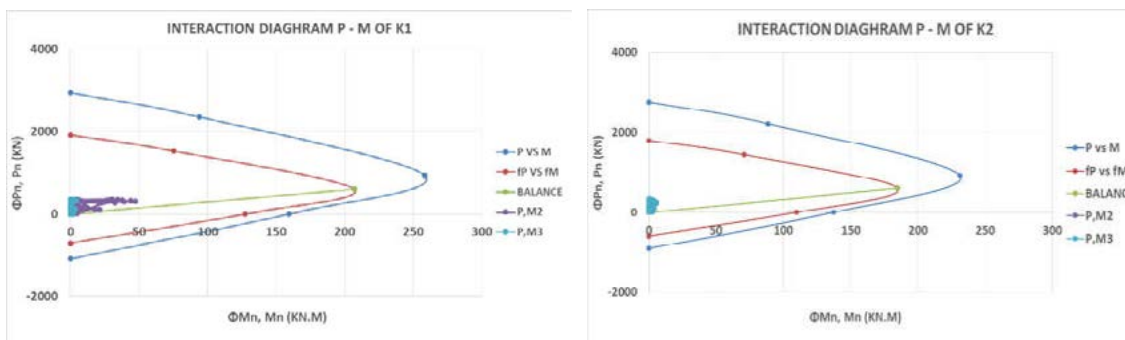
Comparison of X and Y direction displacements in interior and exterior columns between existing and retrofitted structures can be seen in Figures 8 and 9. As seen in the figures, the displacement of the exterior column in x and y direction in retrofitted structure was reduced around 99% of the existing structure.

4.4. Interaction Diagram of The Columns After Retrofitting

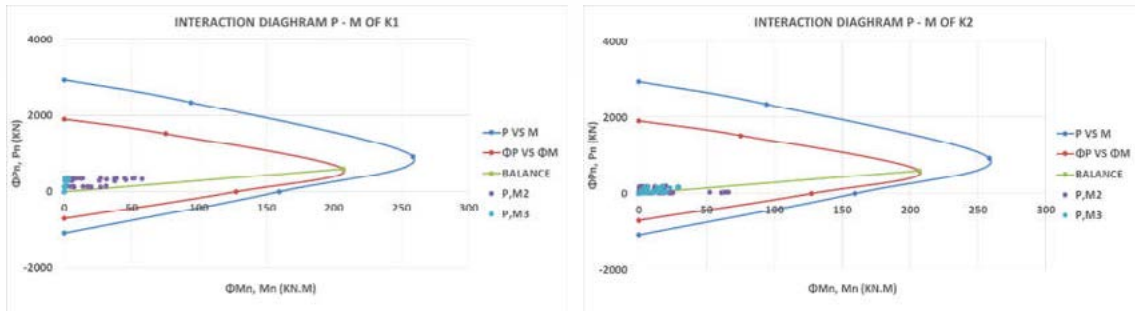
Figure 10 shows the P-M interaction diagram of column on the four models of retrofitted building structures. From the figure, it can be seen that the axial forces and bending moments for all models are not exceeded the interaction diagram, that means the capacity of column is strong enough to resist the working loads.



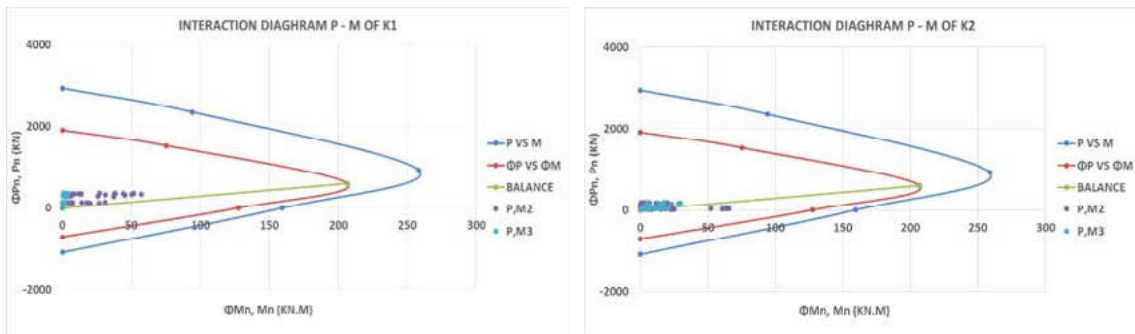
(a) Model B



(b) Model D



(c) Model F



(d) Model G

Figure 10 Interaction diagram of columns in the retrofitted structures

4.5. Cost and Volume of The Work

Table 10 shows the comparison of the cost of retrofitted building for the four retrofitted building models which analyzed by Unit Price of Work of Batusangkar City, 2017 [10]. The table shows that the use of shear wall has cost minimum Rp. 253.044.039,- (Model B), whereas the use of steel bracing required lower cost, particularly of Model F, which amounted Rp. 192.125.000,-.

Table 10 Comparison of the retrofit structure cost

Retrofit Method (1)	Volume (2)	Unit Price (3)	Cost of Material (4) = 2 x 3
Model B (Shear Wall)	39,6 m ³	Rp. 6.390.001/ m ³	Rp. 253.044.039,-
Model D (Shear Wall)	50,4 m ³	Rp. 6.390.001/ m ³	Rp. 322.056.050,-
Model F (Steel Bracing)	15370 kg	Rp. 12.500,-/ kg	Rp. 192.125.000,-
Model G (Steel Bracing)	17291 kg	Rp. 12.500,-/ kg	Rp. 216.140.000,-

From the above cost comparison, the steel bracing system installed on corners area X and Y directions (L shape) on the 1st floor of the building (Model F) is more economical and more effective in the ease of implementation than the shear wall system.



5. CONCLUSION

From the above structural analysis, it can be concluded that:

- (i) The building of SMA N 3 Batusangkar is unable to resist the working loads based on the evaluation of the feasibility structure which analyzed using SNI 1726-2012. The structure should be retrofitted.
- (ii) Retrofitted of the building by adding steel bracing and shear wall systems are very effective for reducing the displacement by 60-99% and the internal force by 10-95% compared to the existing structure.
- (iii) Models B and D which used shear wall system, and models F and G used steel bracing system can be applied in the retrofitted school building to reduce the internal force and displacement due to the working loads.
- (iv) Retrofitted using steel bracing system is more economical and easier to be installed than the shear wall, so the method of retrofit using steel bracing models F and G are very recommended for strengthening the structure of SMA N 3 Batusangkar, which it can also be applied to other typical school buildings.

6. REFERENCES

- [1] Disaster of Management Coordination Board of West Sumatra, (2009), The Map of Total Damage Public Facilities caused Earthquake in West Sumatra, Indonesia.
- [2] National Standardization Agency of Indonesia, (2002), Design Standard of Earthquake Resistance for Buildings, SNI 03-1726-2002, Jakarta, Indonesia.
- [3] National Standardization Agency of Indonesia, (2012), Design Method of Earthquake Resistance for Buildings and Other Structures, SNI 1726-2012, Jakarta, Indonesia.
- [4] Computers and Structures, Inc., (2005), Manual ETABS (Integrated Building Design Software). California, USA.
- [5] National Standardization Agency of Indonesia, (2003), Minimum load for the design of buildings and other structures, Jakarta, Indonesia.
- [6] http://puskim.pu.go.id/Aplikasi/desain_spektra_indonesia_2011/
- [7] Central Public Works Department and Indian Building Congress, (2007), Handbook on Seismic Retrofit of Buildings. Association Indian Institute Technology.
- [8] S., Anshuman, et al., (2011), Solution of Shear Wall Location in Multi-Story Building. IJSCE vol. 2 no. 2. Civil Engineering Group, BITS Pilani, India.
- [9] M., Adhitya, et al., (2015), Study on Effective Bracing Systems for High Rise Steel Structures. SSRG-IJCE vol. 2 issue 2. Civil Engineering East West Institute of Technology, Bangalore-91, India.
- [10] Central Public Works Department of Batusangkar City, (2017), Work Unit Price Triwulan I 2017, Indonesia.



THE RELATIONSHIP BETWEEN SPECIFIC LAND USE CATEGORIES AND IMPERVIOUSNESS FOR PREDICTING THE IMPACT OF EXCESSIVE LAND DEVELOPMENT IN URBAN AREA AT SEMARANG, CENTRAL JAVA

Dwita Sutjiningsih^a, Yosef Prihanto^b

^a*Department of Civil Engineering, Faculty of Engineering, Universitas Indonesia, Depok 16424, Indonesia*

^b*Environmental Science Programme, School of Postgraduate, Universitas Indonesia, Jakarta Pusat 10430, Indonesia*

ABSTRACT

Most researchers agree that imperviousness is the key predictive variable in simulation and empirical models used to estimate the stream quality as response variable. Therefore, the decision in selecting the imperviousness estimation method is crucial. This study aims at testing the accuracy of land use and population density methods to estimate the directly connected impervious area (DCIA) of subwatershed for predicting the impact of land development especially the flood discharge in a moderately urbanized city. The DCIA consists of rooftops and road network and elaborated based on nine land use categories on administrative- and watershed-based area in Semarang, Central Java. The digitized World View Satellite Imagery 2012 combined with in-situ observation by Geospatial Information Agency in 2013 and repeated in 2016 are used for calibration purposes. In predicting flood discharge, the land use method shows accurate results in all four cases, while the population density method shows somewhat overestimated results, especially in the area dominated by green open space, agricultural, and industrial area as well. In cases where direct measurement is impossible due to time and money constraints, the land use method is more accountable than population density method in accurately predicting the DCIA in the watershed.

Keywords: DCIA (Directly Connected Impervious Area); Imperviousness; Land use method; Population density method; Semarang.

1. INTRODUCTION

As claimed by numerous researchers, the difficulty in maintaining urban stream quality in facing the development in the watersheds is underlined by the strong relationship between imperviousness and stream quality. Researchers agree that the percentage of impervious cover on the watersheds, which represents the imperviousness in Reformulated Impervious Cover Model (ICM) and in most simulations and empirical models as well, is the key predictive variable used to estimate the stream quality as response variable (Schueler, 2009). According to former work of Schueler (1995), imperviousness consists of two primary components, namely the rooftops and the transport system. He cited the report based on actual measurement in 1994 at City of Olympia, Washington, that traditional zoning has strongly emphasized and regulated the rooftops and largely neglected the transport component, despite transport-related imperviousness consisting of 63 to 70% of total imperviousness at the site in 11 residential, multifamily and commercial areas.

Center for Watershed Protection (2003) studies indicate that the size of one-hundred-year floods can potentially double in watersheds with impervious cover levels greater than 20 to



30%. The study of Canters et al. (2006) shows that mapping of impervious surface distribution using remote-sensing data produced substantially different estimates of discharge than traditional approaches based on expert judgment of average imperviousness for different types of urban land use. Said (2014) described that based on its degree of imperviousness an urbanized watershed is composed of Directly Connected Impervious Area (DCIA), Non-Directly Connected Impervious Area (NDCIA), and Pervious Area (PA). From DCIA runoff flows directly into the drainage system, while from NDCIA runoff may pass through a PA before it reaches the drainage system. The sum of DCIA and NDCIA is equal to Total Impervious Area (TIA).

Although in most urbanized watersheds the impervious cover is the dominant factor, it is really difficult to estimate its amount. Kelly and McGinnis (2002) stated that the decision on selecting method for estimating the degree of imperviousness should consider the three basic attributes, namely: relatively accurate, easy to do, and easy to derive the required information. Other important considerations are available time, skill and funding, required accuracy, and ability to predict future imperviousness. In general, there are four methods commonly used in the watershed, namely direct measurement, based on specific land use categories, based on road density, and based on population density. Direct measurement is the most accurate method, but it is also the most expensive one, while the last method is the cheapest but least accurate method. The majority of researchers has the opinion that land use method is the best compromise of accuracy and cost. Referring to Lee and Heany's (2003) suggestion, the impact on stream quality as response variable should be estimated using DCIA as key predictive variable; however, the required data/information as well as the availability of funds and skilled workers to estimate the DCIA in the watershed is in general very limited.

This study aims at testing the accuracy of two selected methods, namely the land use method and the population density method in estimating the DCIA of subwatershed in predicting the impact of land development, especially in terms of flood discharge in a moderately urbanized city. The DCIA is an impervious area with a direct hydraulic connection to the drainage system or a water body via continuous paved surfaces, gutters/drain pipes, and/or conventional conveyance structures (Holyoke Community College, 2011). In this study, DCIA is defined as part of the district and/or subwatershed consisted of rooftops and road network as commonly found in urban areas elsewhere in the developing countries. The calibration of estimated DCIA used the digitized digital data derived from interpretation of World View Satellite Imagery 2012 combined with in-situ observation by Geospatial Information Agency in 2013, and repeated in 2016.

Semarang consists of 16 Districts (Kecamatan), where the eastern part of the city is more densely populated in comparison to the western part. Nine land use categories are applied on each district, as well as on eleven subwatersheds covering the whole area of the city. Only four subwatersheds (Banjir Kanal Timur, Bringin, Plumbon and Silandak) are fully located in the city and therefore further elaborated. The assessment of the results is based on the coefficient of determination (R^2) and the Nash Sutcliffe Efficiency (NSE) criteria.

2. METHODOLOGY/EXPERIMENT

The computation procedure consists of three steps:

The First Step: derivation and calibration of the relation between DCIA and total land use area dominated by impervious cover through elaboration of administrative-based



(district/kecamatan) land use data and also the relation between percentage of DCIA and the population density data. Land use area dominated by impervious cover comprises of well-organized residential area, unorganized residential area, industrial area, public/social facilities, and commercial & services area.

The Second Step: computation of Curve Number (CN) values through elaboration of watershed-based approach land use data needed for computing the flood discharge using WinTR-20 application. Estimation of DCIA in the subwatershed is based on the assumption that the relation between DCIA and total land use area dominated by impervious cover, as well as the relation between percentage of DCIA and the population density data, which has been derived in the first step, are also valid in the subwatershed area. The CN value for individual land use type refers to the USDA (1989).

The Third Step: simulation of flood discharge in each subwatershed using hydrology model basic WinTR-20 version 3.10 developed by USDA-NRCS (2015). The subwatersheds characteristics covering area and time of concentration are elaborated based on the information from topographical map (RBI and BIG map), while the delineation of the subwatershed boundary referred to the information from Ministry of Public Works & Human Settlements. The land cover is interpreted from satellite imagery in 2012. The amount of rainfall intensity and its distribution is hypothetical.

2.1. Size of datasets

Semarang is a moderately urbanized city, which consists of 16 Districts (Kecamatan) namely Banyumanik, Candisari, Gajahmungkur, Gayamsari, Genuk, Gunungpati, Mijen, Ngaliyan, Pedurungan, Semarang Barat, Semarang Selatan, Semarang Tengah, Semarang Timur, Semarang Utara, Tembalang, and Tugu. The eastern part of the city is more densely populated in comparison to the western part.

The area of each district is measured based on digital administrative map of Semarang, in the document of Semarang City Spatial Planning 2010-2030 published by Regional Development Planning Agency (Bappeda) of Semarang. The data of districts, villages, population as well as the number of households are retrieved from “Semarang dalam Angka 2014” published by Central Bureau of Statistics (BPS) of Semarang City (See Table 1).

Nine land use categories are applied on each district. Detailed information of land use distribution as presented in Figure 1 is processed based on digital data derived from interpretation of World View Satellite Imagery 2012, combined with in-situ observation by Geospatial Information Agency in 2013, and repeated in 2016.

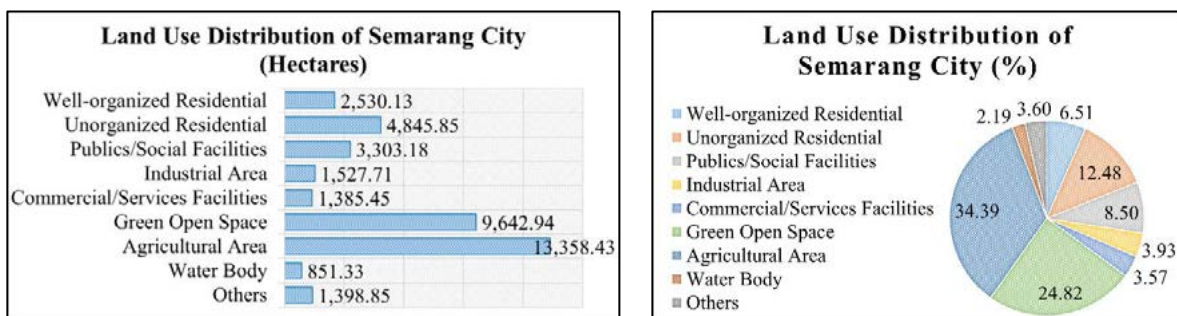


Figure 1. Land Use Distribution of Semarang City.



Table 1. Description of Administrative Region of Semarang City.

Nr.	District (Kecamatan)	District Area (Hectares)	Number of Villages	Number of Households	Population (Persons)	Population Density (Persons per Hectare)
1	Banyumanik	3,093	11	37,110	131,404	42
2	Candisari	661	7	19,840	79,646	120
3	Gajahmungkur	941	8	15,126	63,660	68
4	Gayamsari	643	7	19,715	73,850	115
5	Genuk	2,746	13	25,506	95,218	35
6	Gunungpati	6,151	16	22,040	77,333	13
7	Mijen	5,382	14	17,934	59,425	11
8	Ngaliyan	4,489	10	45,023	124,195	28
9	Pedurungan	2,200	12	45,828	178,544	81
10	Semarang Barat	2,360	16	44,281	158,510	67
11	Semarang Selatan	615	10	22,266	79,952	130
12	Semarang Tengah	535	15	20,783	70,727	132
13	Semarang Timur	562	10	21,836	78,019	139
14	Semarang Utara	1,243	9	32,285	128,134	103
15	Tembalang	4,145	12	45,235	154,697	37
16	Tugu	3,078	7	8,733	31,592	10
Total		38,844	177	443,541	1,584,906	71 (Average)

The same categories of land use are also applied on eleven (Babon, Banjir Kanal Barat, Banjir Kanal Timur, Barat, Blorong, Bringin, Plumbon, Silandak, Tengah, Timur, and Tugu) subwatersheds covering the whole area of the city (See Table 2). Further elaboration are conducted only on four subwatersheds (Banjir Kanal Timur (BKT), Bringin, Plumbon and Silandak), which are fully located in the city.

Table 2. Distribution of Subwatersheds Area in the District of Semarang City.

Nr.	District (Kecamatan)	Subwatersheds in the Districts (Hectares)										
		Babon	BKB	BKT*	Barat	Blorong	Bringin*	Plumbon*	Silandak*	Tengah	Timur	Tugu
1	Banyumanik	1,960	954	284	-	-	-	-	-	-	-	-
2	Candisari	-	18	663	-	-	-	-	-	4	-	-
3	Gajahmungkur	-	-	2	-	-	-	-	-	-	-	-
4	Gayamsari	-	-	19	-	-	-	-	-	-	646	-
5	Genuk	-	-	2	-	-	-	-	-	-	2,822	-
6	Gunungpati	-	6,360	-	-	-	-	-	-	-	-	-
7	Mijen	-	1,735	-	-	1,394	994	1,443	2	-	-	-
8	Ngaliyan	-	311	-	155	6,00	2,116	813	767	-	-	472
9	Pedurungan	-	-	117	-	-	-	-	-	-	2,202	-
10	S.Barat	-	232	-	1,918	-	-	-	129	-	-	-
11	S.Selatan	-	69	181	-	-	-	-	-	386	-	-
12	S.Tengah	-	2	-	-	-	-	-	-	552	-	-
13	S.Timur	-	-	60	-	-	-	-	-	520	1	-
14	S.Utara	-	10	13	-	-	-	-	-	1,156	-	-
15	Tembalang	2,300	-	1,988	-	-	-	-	-	-	-	-
16	Tugu	-	-	-	452	-	31	39	106	-	-	2,438
Total Area		4,260	9,691	3,329	2,525	1,400	3,141	2,295	1,004	2,618	5,671	2,910

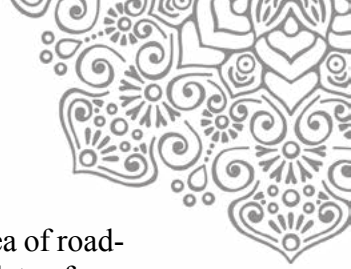
* Subwatersheds fully located in Semarang City.

2.2. Determination of directly connected impervious area (DCIA)

Referring to the birdview from Google Map and in-situ observation in Semarang City, most of rooftops and road-network are directly connected into the drainage system, as is commonly found in urban areas in the developing countries. Therefore, the DCIA in Semarang City is determined based on recognized rooftops and road-network.

2.2.1. DCIA in Semarang City

Roof area is obtained through the calculation of digital data of roof mapping from Ministry of Public Works in 2011. It was improved based on SPOT 5 satellite imagery interpretation



of 2014 record based on 1: 25,000 scale information. Computation of length and area of road-network is based on mathematical approach using digital road-network data from topographical map (RBI map 1:25,000). The results are improved based on World View satellite imagery interpretation recorded in 2012, and in-situ observation in 2013, and combined with the data in the document of Semarang City Spatial Planning Year 2010-2030 published by Public Works Service of Semarang City. The distribution of rooftops and road-network area in Semarang City as presented on Table 3 shows the DCIA in the district as sum of rooftops and road-network area in each district.

Table 3. Distribution of Rooftops and Road-network Area (DCIA) in Semarang City.

Nr.	District (Kecamatan)	Rooftops Area		Road-network Area		Rooftops & Road-network Area (DCIA)	
		(Hectares)	(%)	(Hectares)	(%)	(Hectares)	(%)
1.	Banyumanik	503.82	16.29	135.81	4.39	639.63	20.68
2.	Candisari	199.07	30.10	60.40	9.13	259.47	39.24
3.	Gajahmungkur	196.48	20.87	72.79	7.73	269.27	28.60
4.	Gayamsari	151.91	23.61	58.71	9.12	210.62	32.73
5.	Genuk	422.37	15.38	109.15	3.98	531.52	19.36
6.	Gunungpati	272.69	4.43	95.08	1.55	367.77	5.98
7.	Mijen	308.29	5.73	93.61	1.74	401.91	7.47
8.	Ngaliyan	810.49	18.05	145.71	3.25	956.20	21.30
9.	Pedurungan	451.61	20.53	150.64	6.85	602.25	27.38
10.	Semarang Barat	555.27	23.53	170.15	7.21	725.42	30.74
11.	Semarang Selatan	214.37	34.87	63.64	10.35	278.01	45.22
12.	Semarang Tengah	212.12	39.63	55.87	10.44	267.99	50.06
13.	Semarang Timur	183.78	32.72	58.56	10.43	242.35	43.15
14.	Semarang Utara	291.37	23.44	106.22	8.55	397.59	31.99
15.	Tembalang	463.85	11.19	139.86	3.37	603.71	14.56
16.	Tugu	134.39	4.37	22.10	0.72	156.49	5.08
Semarang City		5,371.89	13.83	1,538.30	3.96	6,910.19	17.79

2.2.2. Application of Land Use Method in the Subwatershed

The relation between measured land use area dominated by impervious cover in the district (X) and measured DCIA in the district (Y) is presented on Figure 2a, whereas Figure 2b presents the calibration result to test its validity. The result shows that the R² (=0.8141) of the line of perfect agreement indicates that the estimated DCIA in the district is acceptable.

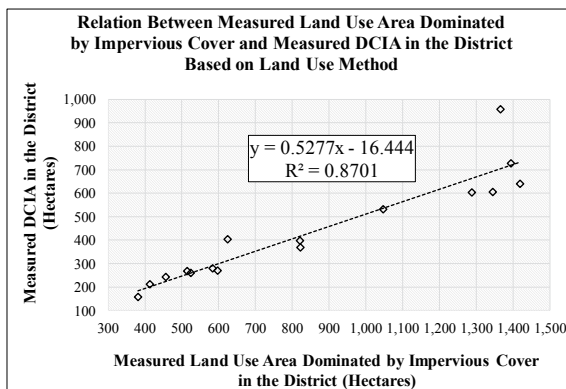


Figure 2a.

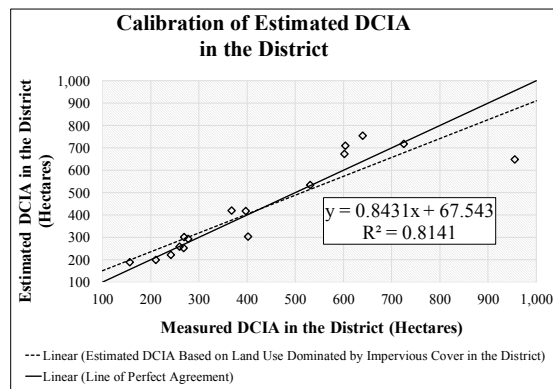


Figure 2b.

Figure 2. (a) Relation Between Measured Land Use Area Dominated by Impervious Cover and Measured DCIA in the District Based on Land Use Method; (b) Calibration of Estimated DCIA in the District.



Hence, the equation that will be used for estimating the DCIA in the subwatershed is,

$$Y = 0.5277 X - 16.444 ; R^2 = 0.8701 \quad (1)$$

by taking into account the weighted average of the district-areas contained within the subwatershed.

2.2.3. Application of Population Density Method in the Subwatershed

The similar procedure as above is applied. Figure 3a present the relation between population density in the district (X) and percentage of measured DCIA in the district (Y). The calibration result presented on Figure 3b shows that the line of perfect agreement ($R^2 = 0.887$) indicates that the estimated percentage of DCIA in the district is acceptable.

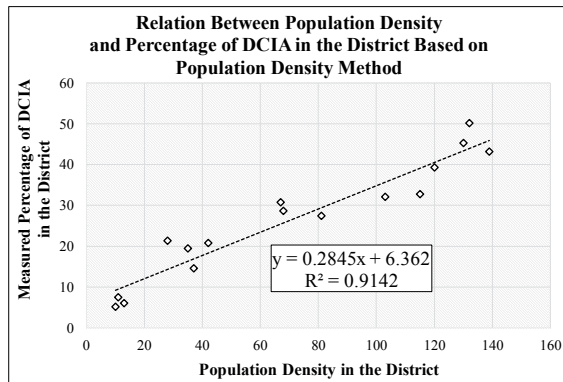


Figure 3a.

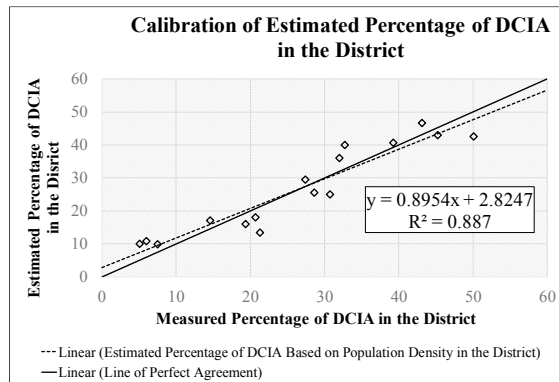


Figure 3b.

Figure 3. (a) Relation Between Population Density and Percentage of DCIA in the District Based on Population Density Method; (b) Calibration of Estimated Percentage of DCIA in the District.

Hence, the equation that will be used for estimating the DCIA in the subwatershed is,

$$Y = 0.2845 X + 6.362 ; R^2 = 0.9142 \quad (2)$$

by taking into account the weighted average of the district-areas contained within the subwatershed.

3. RESULTS AND DISCUSSION

Land use maps of four subwatersheds fully located in the city are based on information from topographical map, while the delineation of subwatershed boundary is referring to the information from Ministry of Public Works & Human Settlements. The land cover is interpreted from Satellite Imagery in 2012. Table 4 presents the land use distribution and Figure 4 shows the land use map of four subwatersheds. Table 5 presents the weighted factors needed to convert the DCIA from district-based into subwatershed-based.

Table 4. Land Use Distribution in Banjir Kanal Timur, Silandak, Bringin and Plumbon Subwatersheds in Semarang City.

Nr.	Land Use	Banjir Kanal Timur		Silandak		Bringin		Plumbon	
		Area (Ha)	%	Area (Ha)	%	Area (Ha)	%	Area (Ha)	%
1	Well-organized Residential	527.32	15.84	85.21	8.48	137.71	4.39	57.09	2.49
2	Unorganized Residential	682.51	20.50	154.62	15.38	177.59	5.66	127.84	5.57
3	Industrial Area	24.31	0.73	172.96	17.21	71.09	2.26	5.94	0.26
4	Publics/Social Facilities	456.16	13.70	144.80	14.41	128.81	4.10	55.72	2.43
5	Commercial & Services Area	191.25	5.74	26.36	2.62	23.01	0.73	26.21	1.14



Nr.	Land Use	Banjir Kanal Timur		Silandak		Bringin		Plumbon	
		Area (Ha)	%	Area (Ha)	%	Area (Ha)	%	Area (Ha)	%
6	Green Open Space	631.00	18.95	200.23	19.92	999.16	31.82	489.15	21.31
7	Agricultural Area	610.47	18.33	121.65	12.10	1,458.41	46.45	1,427.93	62.22
8	Water Body	39.89	1.20	15.66	1.56	26.24	0.84	12.97	0.57
9	Others	167.09	5.02	83.52	8.31	117.98	3.76	92.14	4.01
	Total	3,330.00	100.00	1,005.00	100.00	3,140.00	100.00	2,295.00	100.00

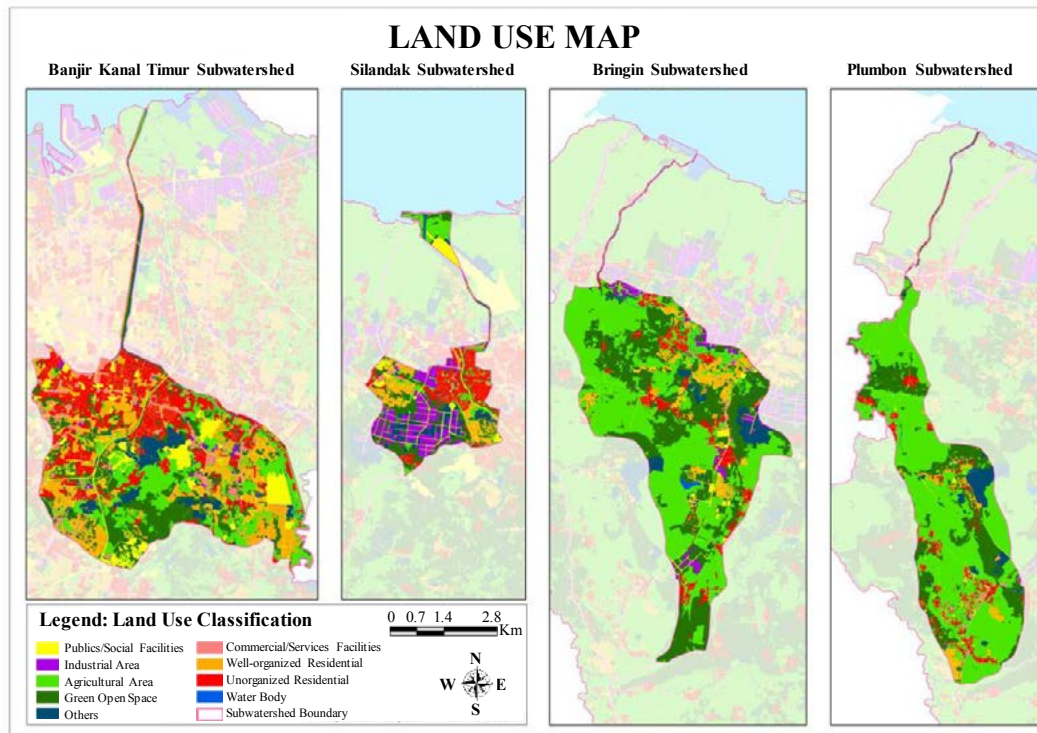


Figure 4. Land Use Maps of Banjir Kanal Timur, Silandak, Bringin and Plumbon Subwatersheds.

Table 5. Distribution of Weighted Factor for Banjir Kanal Timur, Silandak, Bringin and Plumbon Subwatersheds in Semarang City.

Nr.	Distric (Kecamatan)	Banjir Kanal Timur		Silandak		Bringin		Plumbon	
		Area (Ha)	%	Area (Ha)	%	Area (Ha)	%	Area (Ha)	%
1	Banyumanik	284	8.53	-	-	-	-	-	-
2	Candisari	663	19.92	-	-	-	-	-	-
3	Gajahmungkur	2	0.06	-	-	-	-	-	-
4	Gayamsari	19	0.57	-	-	-	-	-	-
5	Genuk	2	0.06	-	-	-	-	-	-
6	Gunungpati	-	-	-	-	-	-	-	-
7	Mijen	-	-	2	0.20	994	31.65	1,443	62.88
8	Ngaliyan	-	-	767	76.39	2,116	67.37	813	35.42
9	Pedurungan	117	3.51	-	-	-	-	-	-
10	Semarang Barat	-	-	129	12.85	-	-	-	-
11	Semarang Selatan	181	5.44	-	-	-	-	-	-
12	Semarang Tengah	1	-	-	-	-	-	-	-
13	Semarang Timur	60	1.80	-	-	-	-	-	-
14	Semarang Utara	13	0.39	-	-	-	-	-	-
15	Tembalang	1,988	59.72	-	-	-	-	-	-
16	Tugu	-	-	106	10.56	31	0.99	39	1.70
	Total	3,330	100.00	1,005	100.00	3,140	100.00	2,295	100.00



The proportion of DCIA of each subwatershed based on Land Use Method is computed using equation (1) in combination with the data from Table (4) and (5). The result is presented in Figure 5a. Meanwhile, Figure 5b presents the result using Population Density Method, which has been computed using equation (2) in combination with the data from Table (1) and (5).

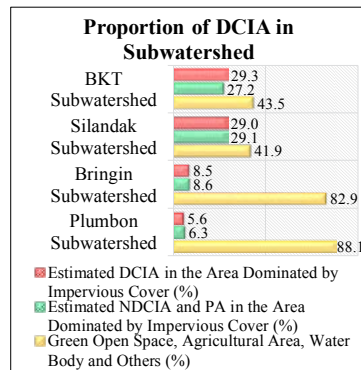


Figure 5a.

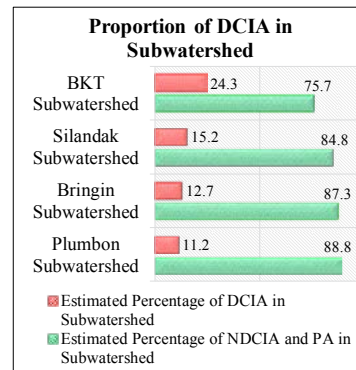


Figure 5b.

Figure 5. Proportion of Estimated DCIA in Subwatersheds (a) Based on Land Use Method; (b) Based on Population Density Method.

The two methods show similar tendency, where BKT has the highest percentage of DCIA, followed by Silandak, Bringin and Plumbon. A significant difference is present in Silandak, where the estimated value using Population Density Method is far less than the estimated value using Land Use Method. The most probable cause is the type of land use, where Silandak is dominated by industrial area with low population density, while BKT is dominated by residential area with relative high population density. Another interesting fact is that these four subwatersheds can be grouped into two categories based on its land uses distribution, namely urbanized (BKT and Silandak) and less-urbanized (Bringin and Plumbon) subwatersheds.

The scenarios for flood hydrograph simulation use hypothetical rainfall intensity 100 mm/day with hypothetical distribution starts at noon and lasting in 3 hours (60%; 20%; 20%). Table 6 summarizes the required information for flood discharge simulation using WinTR-20.

Table 6. Input Data for Flood Discharge Simulation Using WinTR-20.

Subwatershed	Area (Hectares)	Time of Concentration T_c (Hours)	Weighted CN Value		
			Direct Measurement Method (Observed)	Land Use Method (Estimated 1)	Population Density Method (Estimated 2)
Banjir Kanal Timur	3,330	2.24	79.75	79.02	83.62
Silandak	1,005	1.28	79.24	78.69	81.89
Bringin	3,140	3.19	72.52	72.11	81.42
Plumbon	2,295	3.39	73.12	73.14	81.13

The simulation results are presented in Figures 6a and 6b as flood hydrographs. Table 7 summarizes the comparison of main parameters, which consisted of peak discharge (Q_p), time to peak (T_p) and flood duration (T_B). To be noted that index-1 is used for measured/observed value, whereas index-2 for estimated value based on Land Use Method, and index-3 for estimated value based on Population Density Method.

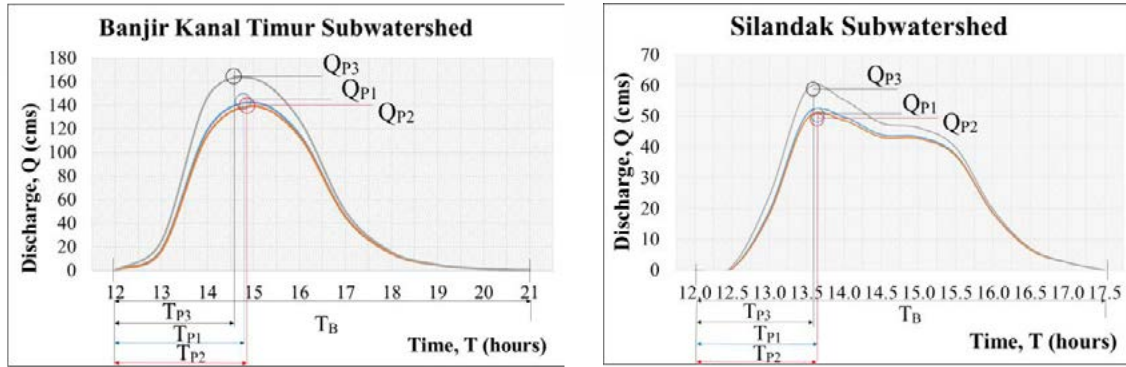


Figure 6a. Flood Hydrograph Simulation in Urbanized Banjir Kanal Timur and Silandak Subwatersheds.

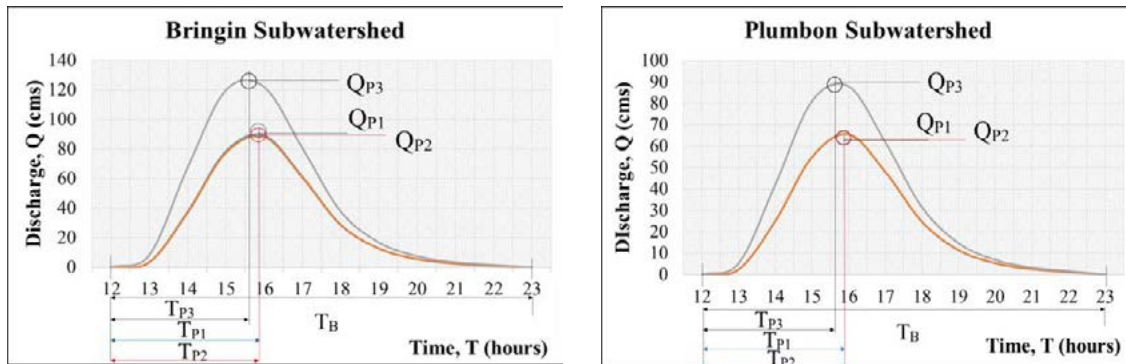


Figure 6b. Flood Hydrograph Simulation in Less-Urbanized Bringin and Plumbon Subwatersheds.

Table 7. Flood Discharge Simulation Results in Four Subwatersheds at Semarang City.

Subwatershed	Peak Discharge (cms)			Time to Peak (hours)			Flood Duration (hours)		
	Q _{P1}	Q _{P2}	Q _{P3}	T _{P1}	T _{P2}	T _{P3}	T _{B1}	T _{B2}	T _{B3}
Banjir Kanal Timur	143.0	139.50	167.30	2.76	2.77	2.57	9.00	9.00	9.00
Silandak	53.30	51.80	60.70	1.68	1.68	1.64	6.00	6.00	6.00
Bringin	90.90	89.30	128.30	3.75	3.75	3.62	11.00	11.00	11.00
Plumbon	65.90	65.90	90.30	3.95	3.95	3.62	11.00	11.00	11.00

As depicted in Figure 6 and Table 7, the differences of simulated peak discharge (Q_{P2}) and time to peak (T_{P2}) based on Land Use Method with the observed/measured values (Q_{P1} and T_{P1}) are infinitesimal. However, the simulation results based on Population Density Method (Q_{P3} and T_{P3}) give quite meaningful differences from the observed/measured values (Q_{P1} and T_{P1}), especially on less-urbanized subwatersheds such as Bringin and Plumbon. There is no difference of flood duration (T_B) between the two methods (T_{B2} and T_{B3}) with the observed value (T_{B1}), since flood duration is more dependent on the size of the watershed and rainfall intensity. Table 8 summarizes the accuracy of both methods in predicting the flood hydrographs using the coefficient of determination (R^2) and using the Nash Sutcliffe Efficiency (NSE) criteria.



Table 8. Degree of Accuracy of the Simulation Results Using Land Use Method and Population Density Method.

Subwatershed	Coefficient of Determination (R ²)		Nash Sutcliffe Efficiency (NSE)	
	Land Use Method	Population Density Method	Land Use Method	Population Density Method
Banjir Kanal Timur	0.9999	0.9962	0.9985	0.9525
Silandak	0.9998	0.9977	0.9988	0.9695
Bringin	1.0000	0.9856	0.9998	0.6396
Plumbon	1.0000	0.9851	1.0000	0.7163

Based on the Coefficient of Determination (R²) and Nash Sutcliffe Efficiency (NSE) criteria, the Land Use Method shows consistent results for all four subwatersheds, with R² and NSE values close to 1.0, whereas the Population Density Method is only accurate for subwatersheds with high and uniform level of urbanization, such as in Banjir Kanal Timur and Silandak. In subwatersheds dominated by green open space and agricultural area, the results using population density method are somewhat overestimated, as depicted by the NSE values in Bringin and Plumbon. Nevertheless, the results of both methods are still acceptable and in line with the statement by Lee and Heany (2003), where the Land Use Method is proved to be more accurate than the Population Density Method in predicting flood discharge in all four subwatersheds.

4. CONCLUSION

The results show that both methods are acceptable, where the Land Use Method proved to be more accurate than the Population Density Method in predicting flood discharge in all four subwatersheds. However, based on Nash Sutcliffe Efficiency (NSE) criteria, the Land Use Method is more appropriate for estimating the DCIA in urbanized subwatersheds like Banjir Kanal Timur and Silandak, since the predicted flood discharge in less-urbanized area (Bringin and Plumbon) the Population Density Method results in higher flood discharge compare to the simulation using Direct Measurement Method. Therefore, in case of lack of resources for direct measurement of DCIA, the Land Use Method is proven to be more reliable for estimating the DCIA.

5. ACKNOWLEDGEMENT

The authors would like to thank all parties for their support in all or parts of the works. Special thanks goes to the Management of Geospatial Information Agency (*Badan Informasi Geospasial*), who provided us with all the required maps and data and to the staffs who graciously provided us with land use analysis of Semarang. We would like to thank the anonymous reviewers for their useful comments as well.

6. REFERENCES

- Badan Informasi Geospasial (BIG). Geospatial Information Agency of the Republic of Indonesia.
- Canters, F., Chormanski, J., Van de Voorde, T., and Batelaan, O., (2006), Effects of different methods for estimating impervious surface cover on runoff estimation at catchment level. *In: Proceedings of 7th International Symposium on Spatial Accuracy Assessment in Natural Resources and Environmental Sciences 2006*, Lisbon, 5th-7th July, Portugal.



- Gerald, K., Rimpiläinen, U-M., and Salminen, O., (2013), How does imperviousness develop and affect runoff generation in an urbanizing watershed? *Fennia* 191: 2, pp. 143–159. ISSN 1798-5617.
- Holyoke Community College, (2011), EPA Region 1 MS4 Stormwater General Permits and LID Training Clinic: Tools and Methodologies for Tracking/Reducing Impervious Cover, Horsley Witten Group, Inc., Holyoke, MA, USA.
- Kelly, F., and McGinnis, S., (2002), Estimating Impervious Cover and Its Impact on Water Resources, A Technical Report for the Upper Delaware Watershed Management Project May 2002, North Jersey Resource Conservation and Development, Annandale, NJ.
- Lee, J.G., and Heaney, J.P., (2003), Estimation of Urban Imperviousness and its Impacts on Storm Water Systems, *Journal of Water Resources Planning and Management*, 129(5), pp. 419-426.
- Said, A., (2014), Generalized Method for Estimating Variability in Directly Connected Imperviousness Area, *Global Journal of Engineering Science and Research Management*, 1(8), pp. 65-79.
- Schueler, T.R., (1995), Site planning for urban stream protection, Chapter 2: The Importance of Imperviousness, Metropolitan Washington Council of Governments, Washington, DC.
- Schueler, T.R., Fraley-McNeal, L., and Capiella, K. (2009), “Is Impervious Cover Still Important? Review of Recent Research”, *Journal of Hydrologic Engineering*, Vol. 14, No. 4, pp. 309-315, April 1, 2009.
- USDA, (1989), Engineering Hydrology Training Series, Module 104. Soil Conservation Service.
- USDA-NRCS, (2015). WinTR-20 version 3.10.



Reliability of Smoothed Particles Hydrodynamics Method in Simulating 3D Fluid Flow Towards Conservation of Mass and Energy (Simulated on Constriction in a Vertical Pipe)

Betania Caesariratih Lydiana, Dwinanti Rika M, Herr Soeryantono
Departemen Teknik Sipil, Fakultas Teknik, Depok, Indonesia

E-mail : betania.caesar@gmail.com

ABSTRACT

Numerical method of modelling flow of surface water is currently evolving towards particle-based method as an alternative to grid-based method due to the difficulties and limitations of the grid based methods in simulating high velocity impact (HVI) phenomena as free surfaces, moving material interfaces, deformable boundary and large deformation based on (Liu & Liu, 2003). Particle-based method is still developing and is nearly in its mature stage, hence reliability testing is needed. The purpose of this study is to evaluate the ability of the Smoothed Particles Hydrodynamics method in simulating a 3-dimensional fluid flow through constriction of a vertical pipe. Examination of this method is done by reviewing the results based on the Conservation of Mass and Conservation of Energy. The simulations are done by using visual basic for excel as the program platform. The model used in this simulation is a square-vertical pipe with a constriction segment right in the middle of it. The scenarios on these simulations are varied by the number of particles and the value of rest density. The results from these simulations are, the value of velocity generally increases while the value of pressure decreases in the constriction segment, so that the principles of the Conservation of Energy have been fulfilled, despite in some scenarios the pressure value is altered in some segments of the constriction. The percentage difference between the particle's density with the rest density value still fluctuates even though the value of rest density has been varied. The set of particles visually expand on higher value of rest density, and is visually dense on the lower value of rest density. The results show that the Conservation of Mass has not yet been completely fulfilled. Overall, the results from some of the simulations are not stable because of the ability of the program platform. Therefore, in general, the results show that the simulation still has to be improved due to the incapability of the program platform that is not stable in doing simulation of fluid flow phenomenon. But on the other hand SPH method is able to simulate three-dimensional fluid flow through constriction of vertical pipe.

Keywords: *Smoothed Particle Hydrodynamics; 3-dimension simulation; fluid flow simulation; constriction; vertical pipe*

1. INTRODUCTION

Numerical modelling of hydraulic flow phenomenon often encountered problems due to the unfixed domain. The common methods of numerical modelling that are used today are the Finite Difference and Finite Element Method. With these methods, nodes are the discretization form. A set of nodes forms a grid within the limits fixed domain. So as to model hydraulic flow phenomenon, these methods are less precise because some phenomenon has an unfixed domain boundary in space and time. Therefore, in the field of hydraulics, other methods with the potential to model that kind of phenomenon, are needed. We see potential in the Smoothed Particles Hydrodynamics (SPH) method,



because the result of its numerical computation is more effective, accurate and stable in solving partial differential equation in every possible boundary condition (Liu & Liu, 2010). SPH method was developed by Gingold and Monaghan (1977) and Lucy (1977). In the early days of its development, this method was used for modelling in the astrophysics field, but then was developed to model a free-surface flow by (Monaghan, 1994) (Gomez-Gesteira, et al., 2010).

SPH method assume the flow of fluid as a bunch of particles, and each particle is equipped with node. Nodes in this method are also a discretization form. Nodes are not fixed by space so it can move along by the movement of the particles. Each node is equipped with smoothing kernels that has an ability to interpolate the value of the variable reviews of other surrounding particles. Character of nodes on this method indicate that modelling is no longer restricted to a fixed space form. So the model's domain with this method does not have to be fixed according to time and space, then this method has the potential to model the hydraulic flow phenomenon.

Nowadays lot of fluid flow model is done by the SPH method, but it's only simulating the flow without reviewing its hydraulic characteristics. Thus, the purpose of this study is to examine the ability of the SPH method in simulating a 3-dimensional fluid flow through constriction of vertical pipe. The examination will be done by using parameters such as Law of Conservation of Mass and Energy. Variables review from this simulation results; velocity, density, and pressure.

2. METHODOLOGY

In this research, model of the phenomenon was simulated by Visual Basic for excel. Governing equation in fluid flow consists of 3 fundamental conservation laws, conservation of mass, energy, and momentum (Liu & Liu, 2003). From conservation of mass we know that mass of system should be constant, and flowrate of a flow should also be constant. From the conservation of energy, we know the relationship between velocity and pressure (Potter, et al., 2012).

Fluid flow can be modelled using a differential equation form of fluid motion with the Navier-Stokes equations, which is one of the governing equations of fluid flow. This model can be applied only on an isotropic, homogeneous and incompressible fluid flow (Potter, et al., 2012). Navier-Stokes equations in the Lagrangian formulation is as follows,

$$\rho \frac{\partial u}{\partial t} = -\nabla p + \mu \nabla \cdot (\nabla u) + f \quad (1)$$

on the left side of the equation, $\left(\frac{\partial u}{\partial t}\right)$ shows the change of velocity against time, the acceleration. On the right side shows a total force consisting of internal forces and external forces. Then by the equation, the value of the acceleration can be determined as follows,

$$a_i = \frac{f_{pressure} + f_{viscosity} + f_{gravity} + f_{Surface Tension} + f_{Buoyancy}}{\rho} \quad (2)$$



SPH formulation is derived by discretizing the Navier-stokes equations spatially, leading to a set of ordinary differential equations with respect to time (Liu & Liu, 2003). SPH method is a numerical method with node as a discretization form on each particle reviews. Nodes along with particles in the domain model can move freely in space and time. Each particle has its own entities value. Entities own a value of mass (m_i), velocity (u_i), forces (F_i), position (r_i), density (ρ_i), and pressure (p_i). Basically, this method is an interpolation method to approximate values and derivatives of continuous field quantities by using discrete sample points (Vijaykumar, 2012). The interpolation equation for various quantities observed using the SPH method is as follows,

$$A_s(r) = \sum_j A_j \frac{m_j}{\rho_j} W(r - r_j, h) \quad (3)$$

Where $A_s(r)$ is the value of the quantity to be determined. j is a symbol for surrounding particles. m_j is the mass of the particle j , ρ_j is the density of j particles, and $W(r - r_j, h)$ is a smoothing kernels with r_j indicates the position of the particle j , and A_j is the j 's value of quantity A . Each particle is equipped with Smoothing Kernels as a boundary for interpolating value of quantities among particles. The uses of kernels are divided into three types of kernels, the default kernel, pressure kernel and viscosity kernel. For default kernel, we use Poly6 kernel types, and it's used for all equation except for internal forces equation. For pressure equation, we use spiky kernel and for viscosity equation, we use viscosity kernel (Kelager, 2006).

Particle's mass is a constant that has been identified in the beginning, but particle's density is a continuous variable that has to be recomputed during the particle's movement (Kelager, 2006). By the general SPH equation we can see that density take a big role on it. The density equation used is as follows,

$$\rho_i = \sum_j m_j W(r_i - r_j, h) \quad (4)$$

The force due to the pressure can be set using the formulation of the ideal gas law. But for fluid, the equation must be modified by adding the value of the pressure in a state of calm, in order to show the internal cohesion and has a constant density (Desbrun & Gascuel, 1996), so that the formulation is,

$$p = k(\rho - \rho_o) \quad (5)$$

According to the Navier-Stokes equations, the particle's acceleration can be computed by knowing the internal forces and external forces. Internal forces consist of pressure and viscosity forces,

$$f_i^{viscosity} = \frac{\mu}{\rho_i} \sum_j (u_j - u_i) m_j \frac{45}{2\pi h^6} (h - \|r\|) \quad (6)$$

$$f_i^{pressure} = - \sum_{j \neq i} \left(\frac{p_i + p_j}{2\rho_j} \right) m_j \left(- \frac{45}{\pi h^6} \frac{r}{\|r\|} (h - \|r\|)^2 \right) \quad (7)$$

By the suggestion from (Muller, et al., 2003), this pressure equation will result a more stable value of pressure forces because it symmetrized the interpolation by calculate the arithmetic mean of the pressures of interacting particles. External forces consist of gravity and surface tension forces,



$$f_i^{gravity} = \rho_i g \quad (8)$$

$$f_i^{surface} = -\sigma \frac{n_i}{\|n_i\|} \left(\sum_j \frac{m_j}{\rho_j} \left(-\frac{945}{32\pi h^9} (h^2 - \|r\|^2)(3h^2 - 7\|r\|^2) \right) \right) \quad (9)$$

Sum of these internal and external forces then will be divided by density value to determine the acceleration of each particle. We use Leapfrog Scheme for calculate the time integration. The leap interval is $1/2 \Delta t$. Structural integration is implicit Euler, the equation is as follows,

$$r_{t+\Delta t} = r_t + \Delta t u_{t+1/2\Delta t} \quad (10)$$

$$u_t \approx \frac{u_{t-1/2\Delta t} + u_{t+1/2\Delta t}}{2} \quad (11)$$

Model of this simulation uses a constriction pipe form as a boundary container. Boundary container is made as a restriction of fluid flow, so that when the fluid particles collides or touch the boundary, there will be a collision momentum that effects the position and velocity of the fluid particle. The responsive process to the collision is called collision handling. Collision handling processes are divided into two, namely the collision detection and collision response. Collision detection is a detection process that occurs collision on the particle. Meanwhile, collision response is the handling of information obtained from the collision detection. The position and speed that have been modified as a result of the collision is formulated as follows,

$$r_i = r_i + dn \quad (12)$$

$$u_i = u_i - \left(1 + cr \frac{d}{\Delta t \|u_i\|} \right) (u_i \cdot n) \quad (13)$$

Model domain form is one of the physical parameter. The model used in this simulation is a square-vertical pipe with a constriction segment right in the middle of it,

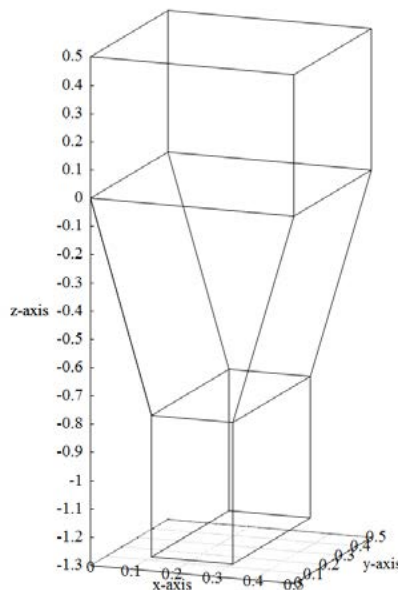


Figure 1. Model Domain



Initial condition of this model should be identified in the beginning. Amount, initial position, and initial velocity of particle are the initial condition and it depend on the scenario. Some water properties are also needed. Water properties that we need are as follows,

- Density (ρ_0) : 998.29 kg/m³
- Viscosity : 3.5 (1.003 x 10⁻³) Pa.s
- Surface Tension : 0.0728 N/m
- Gas Stiffnes : 3 J

3. RESULT AND DISCUSSION

This research uses 12 scenarios that varies by the number of particles and the value of rest density. At first, we just use 4 scenarios that was varied only by the number of particles, but the result showed that the value of density and pressure was not stable. So we assume that if we vary the value of rest density, it will result a more stable value of density and pressure. So the scenarios became like this,

Table 1. Scenarios

Scenario	Number of Particle	Value of Rest Density
1	800	<i>Rest density:</i> 998.29 kg/m ³
2	1200	
3	1800	
4	2100	
1a	800	<i>Rest density:</i> 200 kg/m ³
2a	1200	
3a	1800	
4a	2100	
1b	800	<i>Rest density:</i> 1500 kg/m ³
2b	1200	
3b	1800	
4b	2100	

The results of all simulations are presented in a flow-path diagram for velocity, density, pressure and energy value. From these flow-path we can see the change in the property's value as follow,

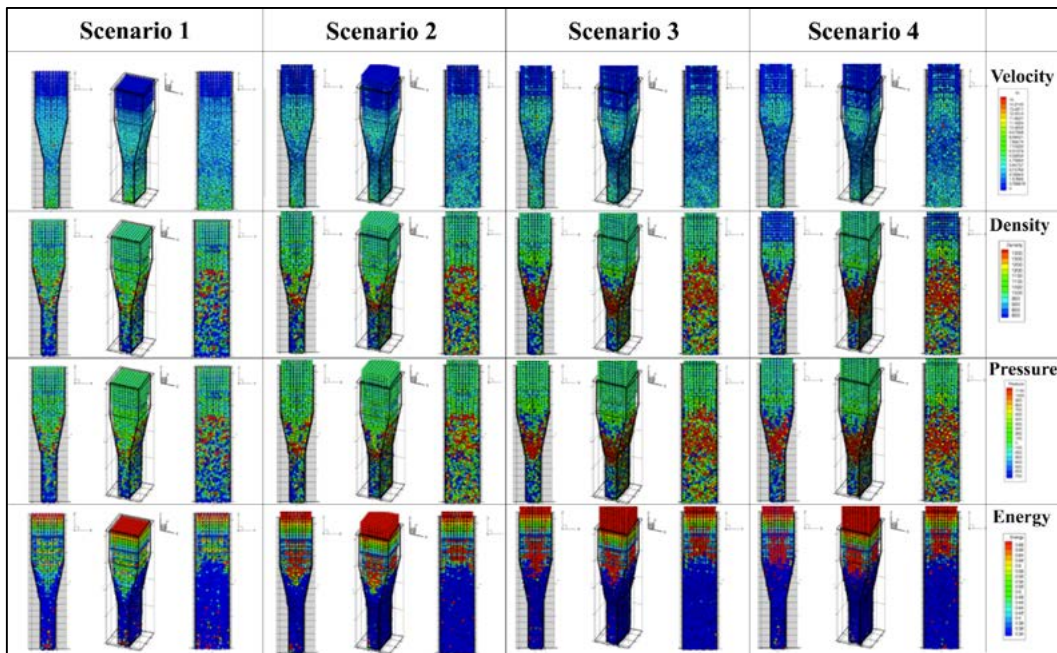


Figure 2. Scenario 1 – 4 Flow-path

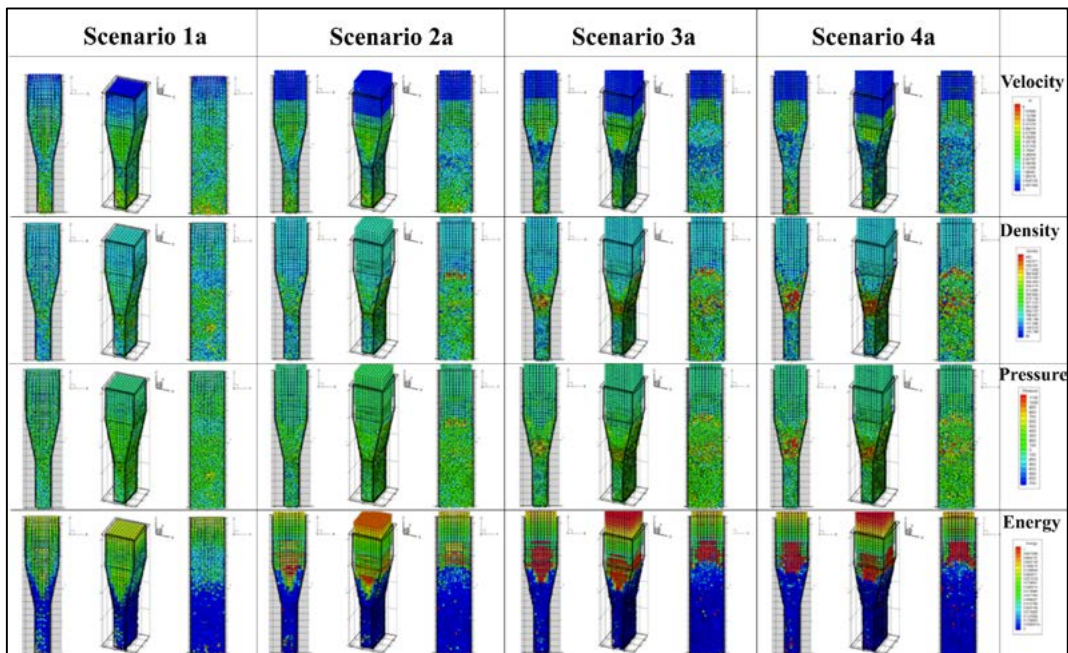


Figure 3. Scenario 1a – 4a Flow-path

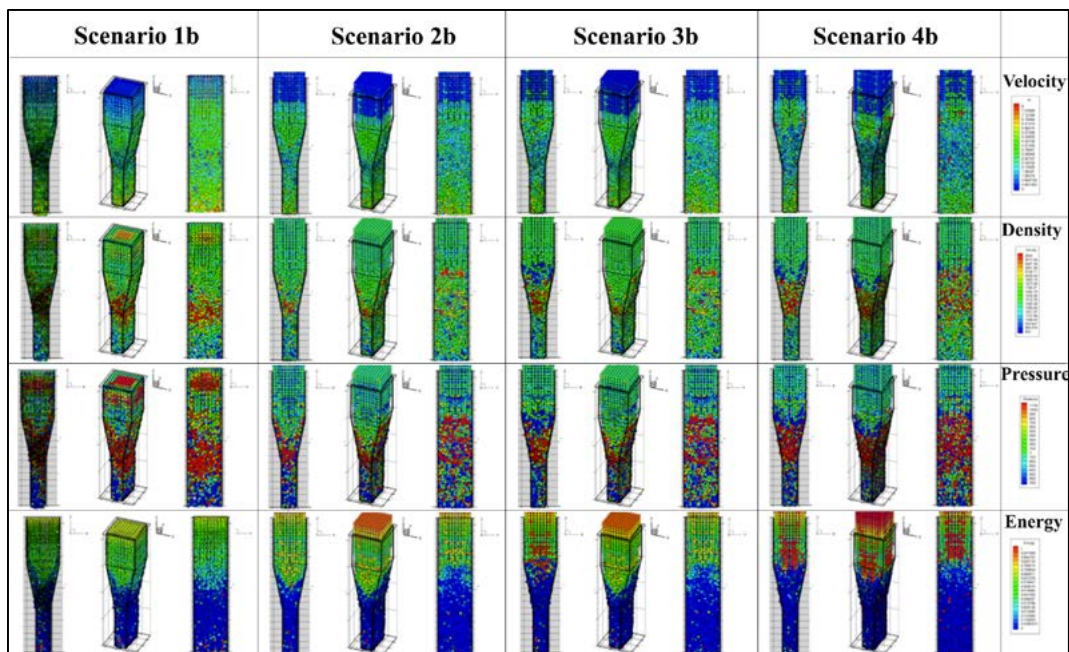


Figure 4. Scenario 1b-4b Flow-path

Velocity value was reviewed in every t (time) and we observed the change on every observable segment. The average of velocity value in every scenario generally increases on every part. On the second part of the pipe (constriction part), velocity value of the particles that hit the boundary, were decreased. However, on the third part (after constriction part) the velocity value was increased again. The reduction of this value was occurred by the insistence of the boundary and particles. To fulfil the continuity equation, every part of the pipe should have a constant value of flowrate, so we compute the average flowrate of the particles in every part. The result is, not every scenario has a constant value of flowrate in every part, but the difference is not significant. Flowrate value looks more stable on the scenarios that use 998.29 kg/m^3 as the rest density value.

In every scenario, the density value still is not stable. Percentage of the differences are quite diverse, ranging from 0.04% until 100%. The difference percentage increase in the scenario that use more amount of particles than the less one. By the average density value on every observable segment, we compute the average mass of every particle. The result is the average mass value is not much different from the values that was identified in the beginning.

The movement of particles still looks like balls. Some of the particles are accelerated to every direction randomly. On the constriction part, particles were insistence and cause a big increment on pressure value in every scenario. Pressure increment also occurred by the increment of density on that part. Generally, the average pressure value was decrease on every observable segment. Pressure and density value were act the same because of their relationship is linear. Bernoulli equation almost fulfilled because generally, the average value of pressure decrease while the average value of velocity increase. But in some scenarios, pressure value was irrelevance. In 2100 particles scenario, pressure value increase significantly on the constriction part. From figure 1 – figure 3, we can see that the colour on constriction part is red (high pressure), but after that part, the colour change significantly to blue (low pressure). The increment of



pressure and density value on constriction part indicated that the particles are in a compressible condition, however it was not what we expected.

From all scenarios, the differences of the simulation can be seen on the particles movement visualization. Example of the movement can be seen on this figure,

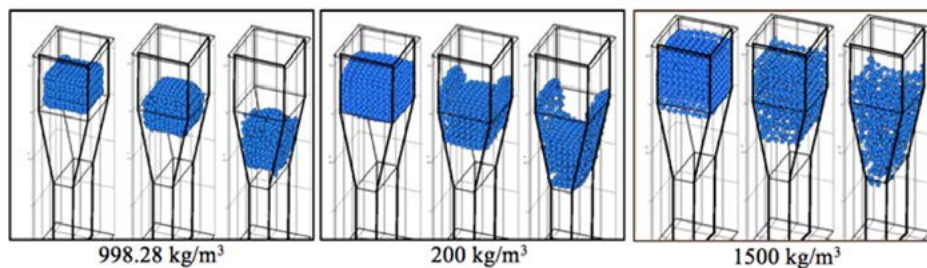


Figure 5. Particles movement ($t = 0.2, 0.3, 0.4$)

Particle's movement on the normal density (998.29 kg/m^3) simulation, visually looks like there're tugged and form like a ball then collectively move downward. The lower density (200 kg/m^3) simulation, visually looks like the particles on the boundary side stuck on it while the others are moving downward. Then, the higher density (1500 kg/m^3) simulation, visually looks like every particle are move apart each other then move downward. Particles on the normal density simulations looks more cohesive than the others. Particles on the lower density looks stick to the boundary. And particles on the higher density looks very loose.

4. CONCLUSION

SPH Method has potential in simulating a hydraulics phenomenon, not only visually capable, but also from the quantity properties. Conservation of mass and energy can be used as parameters for testing its reliability. Variable reviews on this research are; density, mass, pressure, velocity, flowrate, and energy. Flow phenomenon used on this research is a 3D fluid flow through constriction of vertical pipe. This 3 dimensional fluid flow simulation conclude as follow,

- Generally, average value of velocity increase on every part of the pipe. The increment of this value is influenced by the gravity force and the pressure forces by its neighbouring particles. Velocity value increase along the decrement of pipe's cross-sectional area, so this proves the conservation of mass.
- Average value of density still not really stable. The differences between its density and the rest density on the observable segment is not significant. Density and pressure value will always behave the same because of the relationship between them is linear. The largest density and pressure value occurred on the constriction part and on the boundary. Different value of rest density effects the simulation results visually.
- Generally, the average value of pressure decreased, but on the constriction part, its value increased because of the insistence of each particles and boundary. While the average velocity value increased, the average pressure value decreased. It has fulfilled the principle of the conservation of energy despite in some scenarios the pressure value altered in some segments of the constriction.
- Energy value on this research still does not result an appropriate value. The energy value is still not stable on every part.



The main problem on this research is the density value is not stable. Density value affects the pressure value, so maybe the equation of density still has to be improved.

5. ACKNOWLEDGEMENT

the authors would like to thank Evi Anggraheni and Dwita Sutjningsih for their support on this paper.

6. REFERENCES

- Desbrun, M. & Gascuel, M.-P., 1996. Smoothed Particles: A new paradigm for animating highly deformable bodies. *iMAGIS - GRAVIR / IMAG*.
- Gomez-Gesteira, M. et al., 2010. Foreword: SPH for free-surface flows. *Journal of Hydraulic Research*.
- Kelager, M., 2006. *Lagrangian Fluid Dynamics Using Smoothed Particle Hydrodynamics*, Denmark: DIKU.
- Liu, G. R. & Liu, M. B., 2003. *Smoothed Particle Hydrodynamics : a meshfree particle method*. Singapore: World Scientific Publishing Co. Pte. Ltd.
- Liu, M. & Liu, G., 2010. Smoothed Particle Hydrodynamics (SPH): an Overview and Recent Developments. *Arch Comput Methods Eng*, February, Volume 17, p. 52.
- Monaghan, J., 1994. Simulating Free Surface Flows with SPH. *Journal of Computational Physics*, pp. 399-406.
- Muller, M., Charypar, D. & Gross, M., 2003. Particle-Based Fluid Simulation for Interactive Applications. *SIGGRAPH Symposium on Computer Animation* , p. 7.
- Potter, M. C., Wiggert, D. C. & Ramadan, B. H., 2012. *Mechanics of Fluids*. Stamford(CT): Cengage Learning.
- Vijaykumar, A., 2012. *Smoothed Particle Hydrodynamics Simulation for Continuous Casting*, Stockholm: KTH SCI.



EROSION AND TRANSPORT RATES OF SEDIMENTS AT DEGRADED COASTAL WATERS IN BEDONO VILLAGE, SAYUNG DEMAK, CENTRAL JAVA

Max Rudolf Muskananfolal*, Haeruddin¹, Pujiono Wahyu Purnomo¹, Bambang Sulardiono¹

¹*Department of Aquatic Resources, Faculty of Fisheries and Marine Science, Universitas Diponegoro, Tembalang, Semarang 50277, Indonesia*

ABSTRACT

Bedono village, which lies at the coast of Demak Northern Java, is characterized by a number of rivers, estuaries with important habitats such as mangroves, and silty-clay coasts. The village has experienced severe degradations in terms of erosion and coastline changes as well as damages of houses, buildings, roads, tambaks (fishponds), and mangroves. This condition has affected the social and economic lives of local people as well as the environmental ecosystem in the area. Therefore, it is crucial to enforce coastal development and management of the affected area to restore its quality. This study is aimed to investigate erosion patterns and transport rates of sediments as a basis for coastal development and management. The study was conducted in December 2016 to represent west rainy season.

Sediment transport and erosion rates were examined using data of current velocity and grain size of surface sediments. Current velocity were measured using a current meter fixed at 100 cm above seabed during high tides. Current speeds were recorded every hour during one tidal cycle at day time. Surface sediment samples were taken using a Van Veen grab for further analysis of mean grain size distribution and sediment textures in the laboratory.

The results show that friction velocities range from 0.547 cm s⁻¹ to 1.641 cm s⁻¹ at stations 1, 2 and 3. Bed shear stresses range between 0.12 N m⁻² and 0.27 N m⁻² at stations 1, 2, 3. Bed load sediment transport rates range between 0.164 g cm⁻¹s⁻¹ and 4.419 g cm⁻¹s⁻¹ and suspended load transport rates range between 0.015 g cm⁻¹s⁻¹ and 32.045 g cm⁻¹s⁻¹ in December west rainy season. Sediment textures in the study area are dominated by clay fractions followed by fine sands.

Keywords: Erosion and transport rates of sediments, coastal waters, Bedono Sayung Demak

*Corresponding author's email: maxmuskananfolal@yahoo.com



1. INTRODUCTION

Bedono village at Sayung sub-district Demak regency is a coastal village which is directly influenced by the processes in the sea as well as in mainland (Dahuri *et al.*, 1996). The main characteristic of this coastal ecosystem is influenced by the dynamics of sea causing the region to be more vulnerable to erosion and deposition of sediments due to the interactions between these two constricting characteristics (Pinet, 1992; Muskananfolo *et al.*, 2016).

Researches conducted in the coastal region of Demak reveal that the western part of Demak; Bedono and Timbulsloko villages, has experienced heavy degradation. Ecological effects, among others, include loosing of mangroves, damage of fishponds (tambaks) and changes in biodiversity in the surrounding waters and estuaries (Rositasari *et al.*, 2010; Putri *et al.*, 2014; Adinugroho, 2015).

Extensive erosion occurred in Bedono village is assumed to be caused by stronger effects from the seaside through changes in hydrooceanographic conditions and increase in sea level. These effects fluctuate depending on the seasons and will be intensified by anthropogenic influences from inhabitants activities in mainland. On the other hand, increase in sea level can lead to negative effects of erosion (Wirakusumah & Lubis, 2002; Inter-governmental Panel on Climate Change, 2007). Increase in sea level in Semarang area has reached 39 cm since year 1950 (Wirakusumah & Lubis, 2002; Anindya *et al.*, 2006; Suripin, 2002).

The investigation of sediment transport in marine environment is concerned mainly with: determination of the direct of net sediment transport; estimation of sediment transport rates; and identifying the location of accretional or erosional conditions. Approaches based upon empirical equations for transport rates, related to tidally-and wave-induced near bed shear stresses have shown to be variable (Owen & Thorn, 1978; Middleton & Southard, 1984; Pattiaratchi & Collins, 1985).

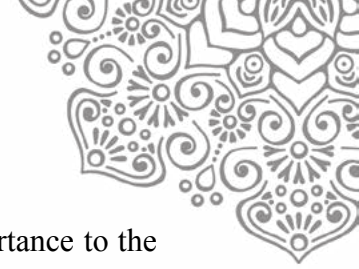
Sediment transport rates can be calculated using data of current velocities and grain sizes of sediments (Heathersaw & Hammond, 1979; Pau & Hammer, 2013). In this respect, numerous studies have examined the profile of current velocity within 1 or 2 m above the sea bed in areas of fully turbulent tidal currents (Sternberg, 1966; Nece & Smith, 1970, Amos *et al.*, 2010). These studies have verified that under conditions of natural conditions of natural stability and steady flow, the velocity profile close to a hydraulically rough bed can be represented by the von Karman- Prandtl equation:

$$U = U_*/k \ln Z/Z_0 \quad (1)$$

Where U_* is the friction velocity that equals $\sqrt{\tau_0/\rho}$, where τ_0 is the shearing stress on the sea bed, k which is the roughness length equals 0.4 and Z_0 is the roughness length.

The present study applies the above technique to the microtidal coast of Bedono Coastal waters to measure velocity profiles at 100 cm above the sea bed; estimate sediment transport rates; and forecast the stability of the sea bed on the basis of the relationship between bed shear stress and grain size of the bed sediments.

Bedono Waters was selected for this study because it has experienced severe damaged due to waves actions and coastal erosion in Northern Coast of Java. The area functions as fishing ponds/Tambaks, tourisms, place for living for local people. Therefore, the aims of the study are to analyze the velocity profiles patterns and grain size distribution around Bedono Village, to estimate the rates of sediment transport around coastal waters of Bedono, and to



predict sea bed stability of the study area. The information is of paramount importance to the re-suspension of fine-grained sediments into the water column.

This information will be useful for local authorities and interested people in deciding the suitability of the area for specific developments. The information can also be used in the estimation of sediment transport rates (from seaward) into the coastal regions of Bedono.

2. METHODOLOGY

2.1 Data Collection

The study was conducted in December 2016 at Coastal waters of Bedono, Demak to represent rainy season where waves are high. There are 3 stations for measuring current velocities and sediment grain size distribution: station 1, which is located at the middle of water channel, station 2 near mangrove forest (East) and station 3 near the old cemetery (West). This location is one of the main stream where water from Java sea (North) flows into Bedono region (South) during high tide and water from Bedono region (South) flows out into open Java Sea (North). There is an old cemetery located at west site; while the East site is covered by heavily populated mangrove forests. These two sites also function as the two main tourism sites in Bedono area where visitors come not only from Central Java, but also from other provinces. Water depth during high tide is 2-3 metres.

This area is considered to represent topographical and environmental settings of Bedono Village where incoming high tide water flow into Bedono area and outgoing low tide water flow out of Bedono area to open Java sea.

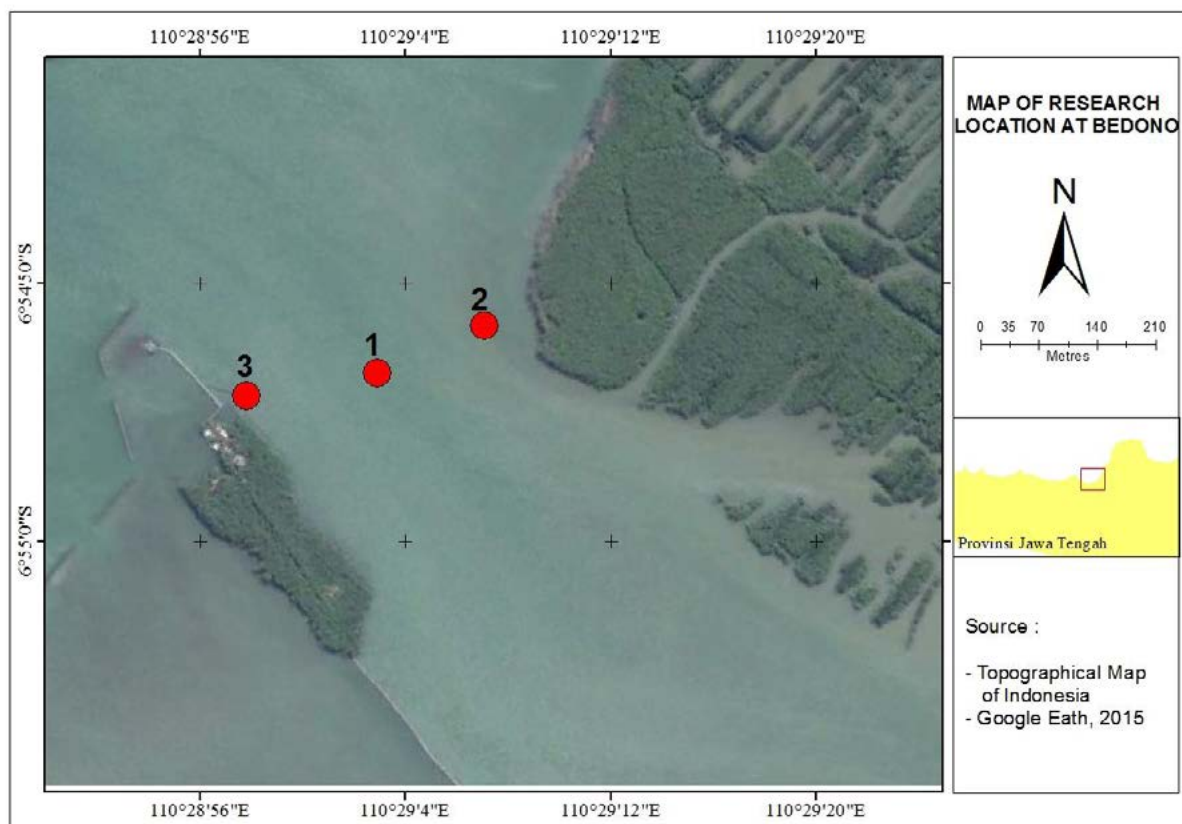


Figure 1 Study area at Bedono Waters, Demak



Primary data collections consisted of the measurements of currents velocity, collection of the surface sediment samples, visual observations of wave characteristics, measurement of seawater temperature and salinity.

2.2. Currents Measurements

Currents velocity measurement over one tidal cycle was undertaken at 100 cm above sea bed, using one current meter. The currentmeter was dropped from a boat which was connected with a cable. The current velocity was measured (recorded) every hour during one tidal cycle from 08.00 am to 16.00 pm (WIT). By applying the ‘Quadratic Stress Law’ (Sternberg, 1972) to the obtained data, bed shear stress (τ_0) and friction velocity (U_*) can be calculated. It has been shown experimentally (Sternberg, 1966) that in a turbulent flow the boundary shear stress is proportional to the fluid density and the square of the mean velocity:

$$\tau_0 \propto \rho U_z^2 \quad (2)$$

or introducing a proportionality coefficient:

$$\tau_0 = C_D \rho U_z^2 \quad (3)$$

Where C_D is the drag coefficient relating to the mean velocity near the seabed to the force exerted by the fluid per unit area of the bed. If the velocity is measured at a standard distance from the bed (generally 100 cm in oceanographic research) then equation (3) becomes:

$$\tau_0 = C_{100} \rho U_{100}^2 \quad (4)$$

or, in terms of the friction velocity:

$$U_* = C_{100}^{1/2} U_{100} \quad (5)$$

Investigations in the laboratory (Nikuradse, 1933) and in the sea (Sternberg, 1968) have revealed that for hydrodynamically rough flows the drag coefficient assumes a constant value related to the bed configurations. Hence, given a representative value of C_{100} the boundary shear stress can be estimated from a single measurement of mean velocity within the boundary layer.

The results of Sternberg (1972) indicate that for naturally sorted sand sediment textures an estimate of boundary shear stress (τ_0) from measurements of U_{100} is best obtain from the following equation:

$$\tau_0 = (3 \times 10^{-3}) \rho U_{100}^2 \quad (6)$$

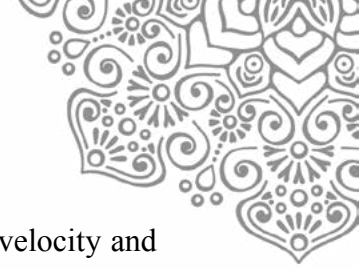
or, in terms of friction velocity:

$$U_* = 5.47 \times 10^{-2} U_{100} \quad (7)$$

The data obtained in the present investigation is applied to equation (6) and (7) to estimate the shear stress exerted on the bed and shear velocity of the flow. By knowing the shear stress operating on the seabed, then it is possible to predict sediment movements.

2.3. Grain Size Measurements

Nine samples of surface sediments were collected during the field data collections. Sediment samples were collected using a Van Veen grab sampler. The samples were then analysed for their grain size distribution in the laboratory (McManus, 1988). To estimate sediment stability



in the study area, the data on mean grain size were then compared with friction velocity and discussed (Miller *et al.*, 1977).

2.4. Sediment Transport Rates

The rate of sediment transport is the mass of sediment that is moved over a given distance in a set time. This sort of information is required, for instance, when breakwaters, jetties and groins are to be built to prevent the loss of beach sand. Sediment transport rates are usually calculated as bedload (q_b) and suspended load (q_s).

Experiment findings and theoretical considerations have shown that the rate of bedload transport is proportional to the cube of the shear velocity (Dyer, 1970; Dyer, 1986):

$$q_b \propto U_*^3 \quad (8)$$

For the transport of suspended load, Dyer (1980) showed that it is related to shear velocity as follows:

$$q_s \propto U_*^7 \quad (9)$$

3. RESULTS AND DISCUSSION

3.1. Current Velocity Profiles

The measurements of current velocity profiles, friction velocity and bed shear stress are presented in Table 1.

Table 1 Current velocity profiles at study area, Bedono

No	Local Time (WIT)	Station 1 110,484 BT / 6,9149 LS			Station 2 110,483 BT / 6,9135 LS			Station 3 110,483 BT / 6,9151 LS		
		Current Velocity at 100 cm above seabed ($m s^{-1}$)	τ_0 (Nm^{-2})	U^* ($cm s^{-1}$)	Current Velocity at 100 cm above seabed ($m s^{-1}$)	τ_0 (Nm^{-2})	U^* ($cm s^{-1}$)	Current Velocity at 100 cm above seabed ($m s^{-1}$)	τ_0 (Nm^{-2})	U^* ($cm s^{-1}$)
1	08.00	0.3	0.27	1.641	0.2	0.12	1.094	0.2	0.12	1.094
2	09.00	0.3	0.27	1.641	0.2	0.12	1.094	0.2	0.12	1.094
3	10.00	0.2	0.12	1.094	0.3	0.27	1.641	0.3	0.27	1.641
4	11.00	0.2	0.12	1.094	0.2	0.12	1.094	0.3	0.27	1.641
5	12.00	0.2	0.12	1.094	0.2	0.12	1.094	0.1	0.03	0.547
6	13.00	0.2	0.12	1.094	0.2	0.12	1.094	0.2	0.12	1.094
7	14.00	0.2	0.12	1.094	0.2	0.12	1.094	0.1	0.03	0.547
8	15.00	0.1	0.03	0.547	0.1	0.03	0.547	0.2	0.12	1.094
9	16.00	0.2	0.12	1.094	0.2	0.12	1.094	0.1	0.03	0.547

The results in Table 1 show that current velocities at 100 cm above seabed at the study area range from 0.1 $m s^{-1}$ to 0.3 $m s^{-1}$. Current velocities are higher during the onset of high tide, become relatively stable at full tide at noon, and decrease towards low tide in the afternoon. These conditions correspond with and influence friction velocity and bed shear stress occurring at the sea bed.



For the logarithmic profiles, friction velocity (U_*) increases with an increase in water depth. U_* reaches a maximum at the beginning and peak of the high water, it then decreases and stable during full high tide, and gradually decreases towards the end of the low water period. Friction velocities range from 0.547 cm s^{-1} to 1.641 cm s^{-1} at station 1, 2 and 3. Bed shear stresses range from 0.12 N m^{-2} to 0.27 N m^{-2} at station 1, 2, 3. These conditions indicate that the bed shear stress exerted on the sea bed is higher enough to move sediment grains during the period of high tide. Therefore, there is a net transport of suspended sediments from the sea towards coastal region of Bedono during high tide while there is a seaward transport of suspended sediments from coastal coastal and mangrove areas of Bedono to open sea. This means that in December the sea surface condition was hydrodynamically rougher. These findings verified the fact that mean grain size of surface sediments was coarser in higher energy areas especially the site close to mangrove trees which was supported by findings of Middleton & Southard, (1984); Dyer, (1986); Amos *et al.*, (2010).

3.2. Sediment grain size distribution

The results obtained from the analysis of sediment textures and grain size distribution are presented in Table 2.

Table 2 Sediment grain size distribution in the study area, Bedono Demak

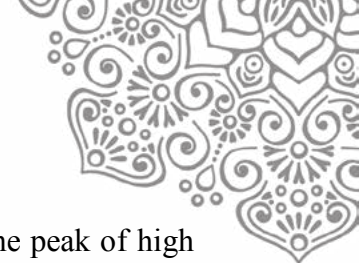
Station	Fine Sand (%)	Silt (%)	Clay (%)
1	33,44	0,19	66,37
2	52,08	0,08	47,84
3	11,52	0,04	88,44

The results in Table 2 shows that sediment texture distribution consists of fine sand, silt and clay. Sediments in station 1 is dominated by clay (66.37%); station 2 is dominated by fine sands (52.08%); and station 3 is dominated by clay (88.44%). These patterns indicate that hydrodynamically station 1 and 3 are relatively low energy areas, while station 2 is a higher energy area. This is because location of station 2 is more open to the sea, while station 1 and 3 are protected from wave actions by breakwaters at the front of these two stations. These findings on low energy and high energy regions with grain size distributions were supported by the research results of Dyer (1986), Middleton & Southard (1984) that finer grain size sediments represent low energy and coarser sediment grains represent higher energy regions.

3.3. Sediment Transport Rates

The rate of sediment transport is the mass of sediment that is moved over a given distance in a set time. This sort of information is required, for instance, when breakwaters, jetties and groins are to be built to prevent the loss of beach sand.

The obtained results by applying friction velocities data to equations (8) and (9), shows that bed load sediment transport ranges between $0.164 \text{ g cm}^{-1}\text{s}^{-1}$ and $4.419 \text{ g cm}^{-1}\text{s}^{-1}$ and suspended load transport ranges between $0.015 \text{ g cm}^{-1}\text{s}^{-1}$ and $32.045 \text{ g cm}^{-1}\text{s}^{-1}$ in December. The estimated friction velocities from velocity measurements in the present investigation indicated that at the beginning of the flow (high water) the shear stress is not



strong enough to move the grains at the seabed. The movement occurs near the peak of high water where current velocity is sufficient to produce high shear stress at the seabed.

The mean diameter of bottom sediments range from 2 μm to 94 μm in December west rainy season. The threshold friction velocity required to move these grain are 0.8 cm s^{-1} to 1 cm s^{-1} respectively (Miller *et al.*, 1977). Finer grain size obtained in station 1 and 3 samples may be due to the influence of high river discharges during rainy season where a great amount of sediment budget enter the sea and it may also be due to calm weather conditions occurring at the time of field data collections as calm water condition (less energy) allows finer sediment to sink (Dyer, 1970; Pinet, 1992; Amos *et al.*, 2010).

4. CONCLUSION

Friction velocities at coastal waters of Bedono range from 0.547 cm s^{-1} to 1.641 cm s^{-1} at station 1, 2 and 3. Bed shear stresses range from 0.12 N m^{-2} to 0.27 N m^{-2} at station 1, 2, 3.

The mean diameter of bottom sediments range from 5 μm to 125 μm . The threshold friction velocity required to move these grain are from 0.8 cm s^{-1} to 1 cm s^{-1} respectively.

The condition of surface sediment at the sea bed around the coast of Bedono waters are relatively stable during the beginning of the high tide. With an increase in water level, this condition changes to be unstable (incipient motions of sand grains start to occur) where bed shear stress increases to a level where it is sufficient to cause sediment movement.

It is concluded generally that the transport rates of bed load sediment is relatively low. However, it seems that during rough sea conditions (peak of western monsoon) the transport rates of sediment is higher. This may be amplified by sediments carried by river discharges during west monsoon rainy seasons.

5. ACKNOWLEDGEMENT

This study was funded by PNBPN UNDIP 2016. We would like to thank Jumsar, Irman and Marius for field data collection. We also thank Prof. Dr. Ir. Sahala Hutabarat, M.Sc. and Prof. Dr. Ir. Agus Hartoko, M.Sc. for their suggestions and comments given at the earlier version of this paper.

6. REFERENCES

- Adinugroho, M. (2015), Correlation of Heavy Metal Concentration Pb and Cd with Fish Larvae Distribution in Semarang Bay. MSi Thesis of MSDP Study Program, Faculty of Fisheries and Marine Science, Universitas Diponegoro Semarang, 197 pp.
- Anindya, W., Hartoko, A., Suripin, (2006), Study of Sealevel Rise as a Base for Rob Problem Solving in Coastal Region of Semarang City, *Jurnal Pasir Laut*, Vol. 1, No.2, Januari 2006, pp. 31-42
- Amos, C.L., Umgiesser, G; Ferrarin, C., Thompson, C.E.L., Whitehouse, R.J.S., Sutherland, T.F., Bergamasco, A., (2010), The erosion rates of cohesive sediments in Venice lagoon, Italy, *Continental Shelf Research* 30, pp. 859–870.
- Dahuri, R., Rais, J., Ginting, S.P., Sitepu, M.J., (1996), *Integrated Coastal and Ocean Resource Management*, PT Pradnya Paramita. Jakarta.
- Dyer, K.R., (1970), Current velocity profiles in a tidal channel, *Geophysical Journal of the Royal Astronomical Society*, 22, pp. 153 -161
- Dyer, K.R., (1980), Velocity profiles over a rippled bed and the threshold of movement of sand, *Estuarine and coastal marine science*, 10, pp. 181-199.



- Dyer, K.R.,(1986). Coastal and estuarine sediment dynamics, John Wiley & Sons, Inc.,342 pp.
- Heathershaw, A.D., Hammond, F.D.C.,(1979), Offshore sediment movement and its relation to observed tidal current and wave data.Swansea Bay (SKER) project, topic report: 6. Inst. Oceanogr. Sci. Rep. No. 92
- IPCC.,(2007), Mitigation of Climate Change. Working Group III Contribution to the Fourth Assessment, Report of the Intergovernmental Panel on Climate Change.
- McManus, J.,(1988), Grain size determination and interpretation, In: Techniques in Sedimentology (Turker, M., ed.), Blackwell Scientific Publication, Oxford, pp.63-85.
- Middleton, G.V., Southard, J.B.,(1984), Mechanics of sediment movement.The Society of Economic Paleontologists and Mineralogists, Tulsa, Oklahoma, 401 pp.
- Miller, M.C., McCave, L.N., Komar, P.D.,(1977). Threshold of sediment motion under unidirectional currents, *Sedimentology*, 6, pp.303 - 314.
- Muskananfolo, M.R., Purnomo, W.P., Sulardiono,B.,(2016),Rehabilitation Model of Degraded Coastal Area in Bedono Village for Conservation and It's Utilization .**Research Report, Universitas Diponegoro Semarang, 43 pp.**
- Nece, R.E., Smith, J.D.,(1970), Proc. A.S.C.E., 96:WW2, 335 pp.
- Nikuradse, J. (1933), Laws of flow in rough pipes,Natl. Advisory Comm. Aeronautics Tech. Mem.1292 (translation from German, 1950).
- Owen, M.W., Thorn, M.F.,(1978), Effect of waves on sand transport by currents.Proc. 16thCoastal Eng. Conf., pp. 1675-1687.
- Pau, M., Hammer,Ø., (2013),Sediment mapping and long-term monitoring of currents and sedimentfluxes in pockmarks in the Oslofjord, Norway, *Marine Geology*, pp. 262 – 273.
- Pattiaratchi, C.B., Collins, M.B.,(1985), Sand transport under the combined influence of waves and tidal currents: an assessment of available formulae, *Marine Geology*, 67, pp.83-100.
- Pinet, P.R.,(1992), *Oceanography, An introduction to the planet oceanus*, West Publishing Company, New York, 570 pp.
- Putri, M.P; Supriharyono, Muskananfolo, M.R., (2014),Hydro-oceanographic Characteristics and Participation Rate of Society in Reducing Coastal Damages at Bedono Village, Sayung Sub-district, Demak Regency. *Journal of Aquatic Resources Management*, Volume 3, Nomor 4, Year 2014, pp. 225 - 234
- Rositasari, R., Witasari, Y., Lestari, M. Puspitasari, Surinati, D.,(2010),An Analysis of SemarangCoastal Environment Based on the Characteristics of Sediments, Oceanography, Heavy Metals Contaminats and Toxicity. Progress Report of Activities Phase 1, Insentive Program for LIPI Researcher 2010. Oceanography Research Center, Indonesia Institute of Sciences, 49 pp.
- Sternberg, R.W., (1966), Boundary layer observations in a tidal current.*J. Geophys. Res.*, 71, pp. 2175-2178.
- Sternberg, R.W.,(1968), Friction factors in tidal channels with differing bed roughness. *Mar. Geol.*, 6, pp. 243-260.
- Sternberg, R.W.,(1972), Predicting Initial Motion and Bedload Transport of Sediment Particles in the Shallow Marine Environments. In:Shelf Sediment Transport, Process and Pattern (Swift, D.J.P., Duane, D.B. and Pilkay, O.H., eds.). Dowden, Hutchinson and Ross, pp. 61 – 82.
- Suripin (2002), Conservation of soil and water resources. Publisher: Andi, Yogyakarta.
- Wirakusumah, A. D., Lubis,(2002),The anticipation of the impacts of Global Warming towards Investment and DevelopmentOpportunities,National Seminar on the Influence of Global Warming towards the Coast and the small Islands in terms of Sea Level Rise and Flooding, Jakarta.



EFFECTIVENESS OF HORIZONTAL DRAIN FOR SLOPE STABILITY OF COAL MINING, CASE STUDY OF SLOPE FAILURE IN TAMBANG GUNTUR, SOUTH KALIMANTAN

Yulian Firmana Arifin^a, Setyo Mulyo Kurniawan^b, Ellyn Normelani^c

^{a c} *University of Lambung Mangkurat, Banjarbaru 70714, Indonesia*
^b *Coal Mine Manager, PT. Utami Jaya Mulya, Banjarbaru 70714, Indonesia*

Abstract

Slope failure occurred in Tambang Guntur PT. Borneo Indobara in Tanah Bumbu, South Kalimantan results in not only technical problems but also a financial problem. The mining operation was terminated. An investigation was conducted to determine the cause of the landslide and obtain methods to prevent further landslides. This study focused on the inquiry into the slope failure occurred in the location mentioned above. Several boreholes were performed to determine detail sub-soil layers and soil properties especially the shear strength of soils. A piezometer was installed and used to obtain the pore-water pressure data located close to the landslide. Additional data such as rainfall data and topography data is also used. A calculation using computer program was also used to model and obtain the safety factor of the slope. The result shows that the landslide occurred due to extremely high rainfall and extended period of rain. A horizontal drain was installed to reduce pore-water pressure as a method of slope stabilization. This paper presents and discusses the effectiveness of the horizontal drain in the field to stabilize the slope.

Keywords: landslide; coal mine; horizontal drain; rainfall; slope stability

1. INTRODUCTION

Landslide is a disaster that resulted not only damage to infrastructure but also casualties. Djamal (2002) reported that from 1990 to 2002 more than 800 slope failure occurred in Indonesia that claimed more than 1000 dead and hundreds injured. It also results in damage to more than 500 infrastructure and dozens of kilometers of roads. In 2016, National Disaster Management Authority of Indonesia (BNPB) reported that there were 625 incidents of landslides in Indonesia (BNPB, 2016). The landslides occurred not only on natural slopes that are close to public property but also in the excavation work for example in open pit mines.

Tambang Guntur is active block coal exploitation in the district of Tanah Bumbu, South Kalimantan. Mining activities have been carried out by the open pit mine system with a ladder on each slope. Although the slopes of the pit have been designed very well with a safety factor of more than 1.3, landslide with a diameter of approximately 30 meters, and 20 meters high occurred (Figure 1.a). The landslide coincided with the very high rainfall. Seepage of 700 ml/s was observed close to the first landslide. After a month, at the same location, a larger landslide with a diameter up to 60 meters and a height of 30 meters happened (Figure 1.b).

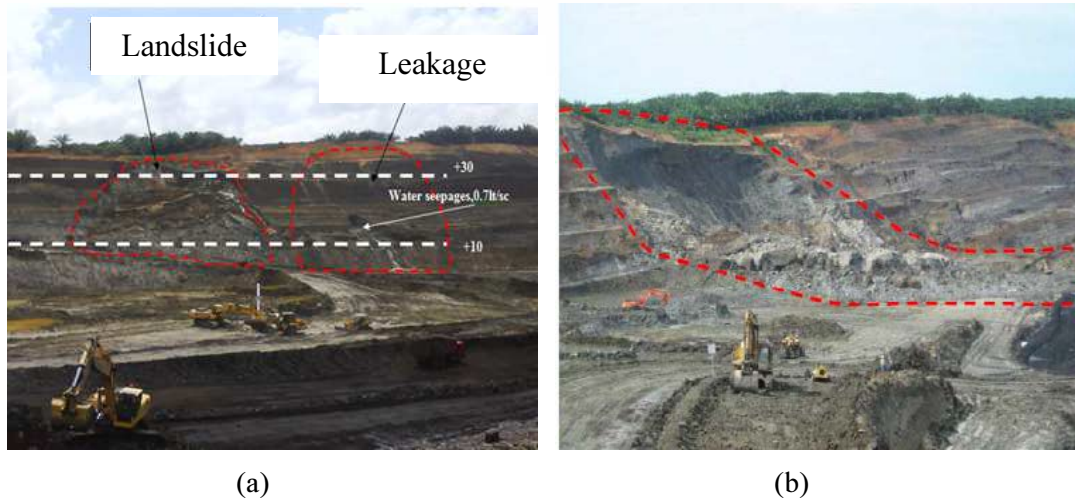


Figure 1. Slope failure at Tambang Guntur (a) first landslide, and (b) further landslide

In Indonesia, many slope failures coincided with or followed an extremely high rainfall (Djamal, 2002; Apip et al., 2010; Hirnawan, 2010; Liao, 2010; Arifin, 2010; Prayuda, 2012; Sumaryono, 2014; Zakaria, 2015). In other countries, some studies have also presented the effect of rainfall on landslides. For example, Singapore (Rahardjo et al., 2002; Rahardjo et al., 2003), Malaysia (Ng et al., 2015; Ismail et al., 2016), Thailand (Kanjankul et al., 2016), and Philippine (Orense, 2004). During periods of rain, water infiltrates into the soil to raise the water table, increase the pore-water pressure, and subsequently enhance the risk of landslides. According to Rahardjo et al. (2002), prolonged heavy rain destroyed matric suction that plays a significant role in the stability of earthworks.

One method commonly used to decrease the ground water level on the slopes is the use of horizontal drain that is defined as holes drilled into a cut slope or embankment and equipped with a perforated metal or slotted plastic liner (Royster, 1980). Some studies have been done to examine the effectiveness of horizontal drain application (Rahardjo et al., 2003; Carrol et al., 2011; Jude et al., 2014; Ng et al., 2015; Ismail et al., 2016; Mukhlisin and Aziz, 2016). The effectiveness of the horizontal drainage system is affected by the location, length and spacing, soil properties, and slope geometry (Ismail et al., 2016). Horizontal drains should be placed as low as possible in the slope for lowering the water table since horizontal drains located in the upper regions of the slope are unnecessary in the long term (Rahardjo et al., 2003). By mean parametric study, Ismail et al. (2016) concluded that horizontal drains might effectively decrease the groundwater level for cut slopes with high groundwater level by installing it sufficiently deep into the slope to intercept the groundwater from the fractured rock. Ng et al. (2015) and Ismail et al. (2016) suggested that the use of geophysical resistivity to identify the best location and the length of the horizontal drain by analyzing the delineation of high water content zone and the possible seepage flow path. Jude et al. (2014) used value-engineering analysis to define the inclination of slope and horizontal drain material.

Due to the successful design and utilization of horizontal drain in slope stabilization are often governed by local experience, the information about the application in the field yet required. This paper presents the effectiveness of horizontal drain use at Tambang



Guntur Mine in Tanah Bumbu District, South Kalimantan. The effectiveness is described regarding the increase in slope factor of safety as compared to the element of security for the case without horizontal drains.

2. SOIL INVESTIGATION AND INSTRUMENTATION

The study of subsoil and sampling was conducted using a drilling machine Jakro 200 types of wireline systems with penetration capability of 200 m. The points of the drill locations are shown in Figure 2. Soil as a result of drilling with a diameter of 89 mm was placed in core boxes, for example as illustrated in figure 3(a). Samples were taken at intervals of 5 m and adjusted to rock lithology before being sent to the laboratory.

The pore-water pressure was measured using a vibrating wire piezometer. The piezometer was installed at a depth of 47 m in BH12 after the core drilling process has been completed. The drilling and installation were conducted in Desember 2013 to respond to the seepage on the slopes. The pore water pressure reading was carried out efficiently on 1st January 2014. The data was collected daily. Figure 3(b) shows the photo of the pore-water pressure measurement in the field.

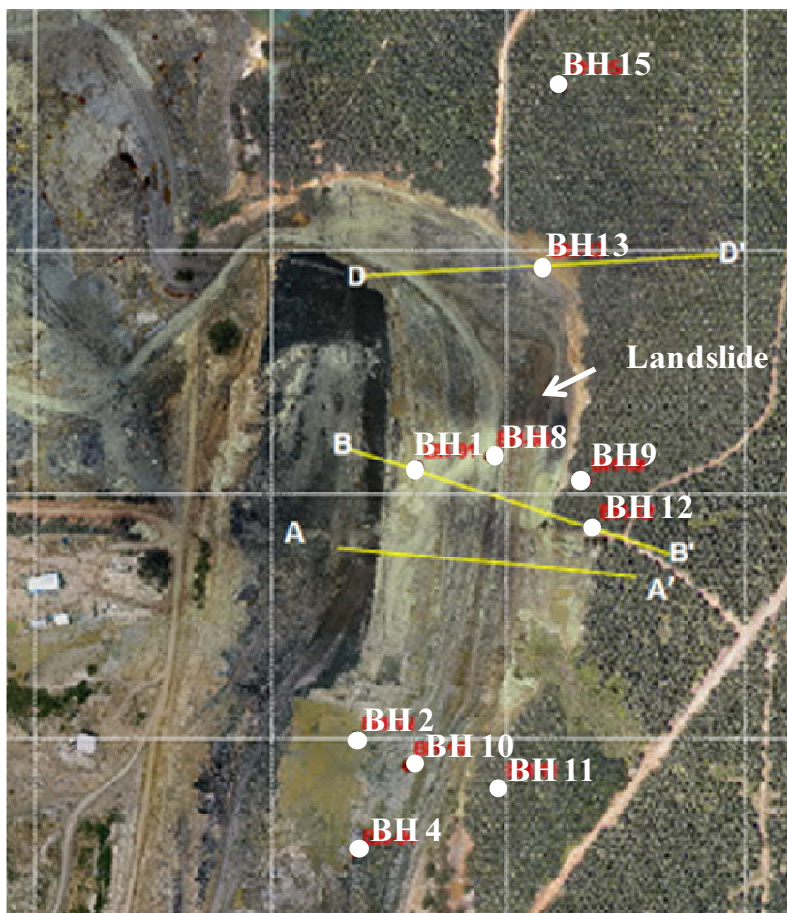


Figure 2. Bore hole locations



Figure 3. (a) Example of core box, and (b) pore-water pressure measurement

The research was focused on bore holes BH1, BH8, BH9, and BH12, and a cross-section B-B because it is the nearest location to the first landslide (Figure 4). As shown in the figure, BH8 has a depth of 60 m placed approximately 15 m over the toe, and BH12 has 77-m deep with an inclination of 40° placed in the top of the slope. Figure 4 also shows the surface of the slope before and after the landslide occurred. Before landslide, the ground surface has a slope of 40°. The landslide changed the slope to be 21°.

Based on the borehole profiles, it was determined that the soil being studied was eight layers of mudstone namely ms-1 to ms-8 (Figure 4). The volumetric weight of the material and unconfined compression test (UCT) results vary from 21.00 to 23.06 kN/m³ and from 0.18 to 0.87 MPa, respectively. The mudstone was brittle and easily broken. By strength, the material is classified as very low strength rock (Deere and Miller, 1966) or fragile (Brown, 1981; Marinatos and Hoek, 2000).

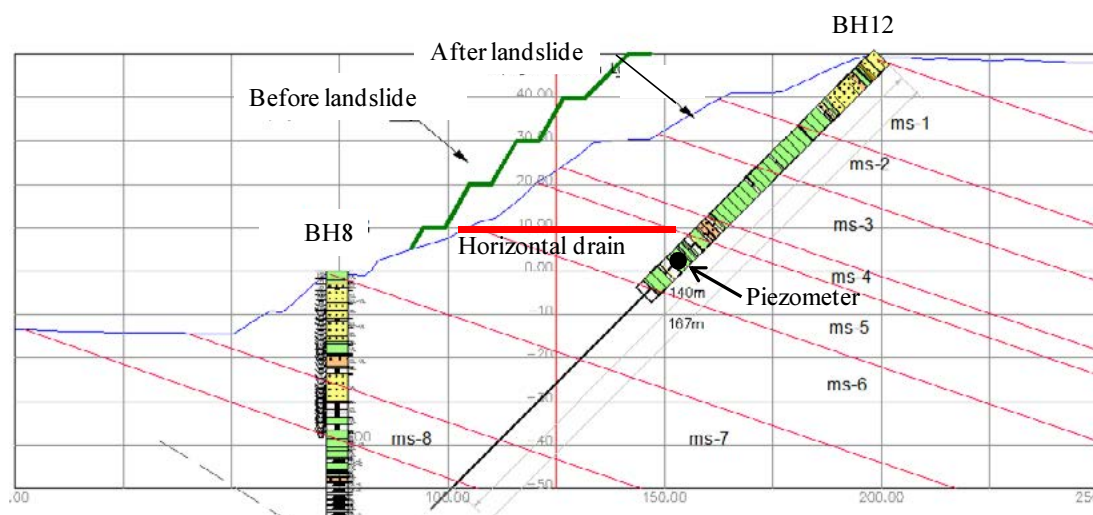


Figure 4. Cross section B-B



3. HORIZONTAL DRAIN INSTALLATION

On June 1st 2014, a horizontal drain was installed to reduce pore-water pressure in the slope at the bottom of the slopes. Drilling horizontally was carried out to a length of 50 m using the crawler drill-type with a maximum capacity of 100 m. Figure 5(a) shows horizontal drilling process. As shown in the figure, a little water flows out of the borehole. The problems faced during the drilling process were stuck rod, water loss, rain, and puddles. A perforated galvanized pipe was installed in the hole after drilling has been completed. Immediately after the pipe was installed, the water flows through the pipe as shown in Figure 5(b). The debit was measured manually using a plastic bucket and a stopwatch. The highest debit recorded after pipe installation reaches 1200 ml/s.

4. RAINFALL EFFECT ON PORE-WATER PRESSURE IN THE SLOPE

Figure 6 shows pore-water pressure and rainfall data at monitoring period March and April 2014. As shown in Figure 6(a), the pore-water pressure data is almost constant at 112 kPa with a slight change in response to rainfall condition. For examples, on 1 and 14 March, the pore-water pressure increased to reach pressures of 121 and 115 kPa in response to rainfall of 50 and 37 mm/day, respectively. It appears that the pore water pressure increases due to rainfall higher than 30 mm/day. In addition, the pore water pressures are controlled by relatively high existing groundwater level and seepage that occurs on the slopes. In April, pore-water pressure rose to 120 kPa to respond four days rain with maximum rainfall of 50 mm/day. It resulted in a landslide on 10 April 2014 with a diameter of 30 m and 20-m high as shown in Figure 1(a). After the landslide, pore-water pressure decreased gradually. A Similar trend occurred in May that larger landslide coincided with extremely long and high rainfall on 13 Mei 2014.



Figure 5. (a) Horizontal drilling process, and (b) installation of the perforated galvanized pipe

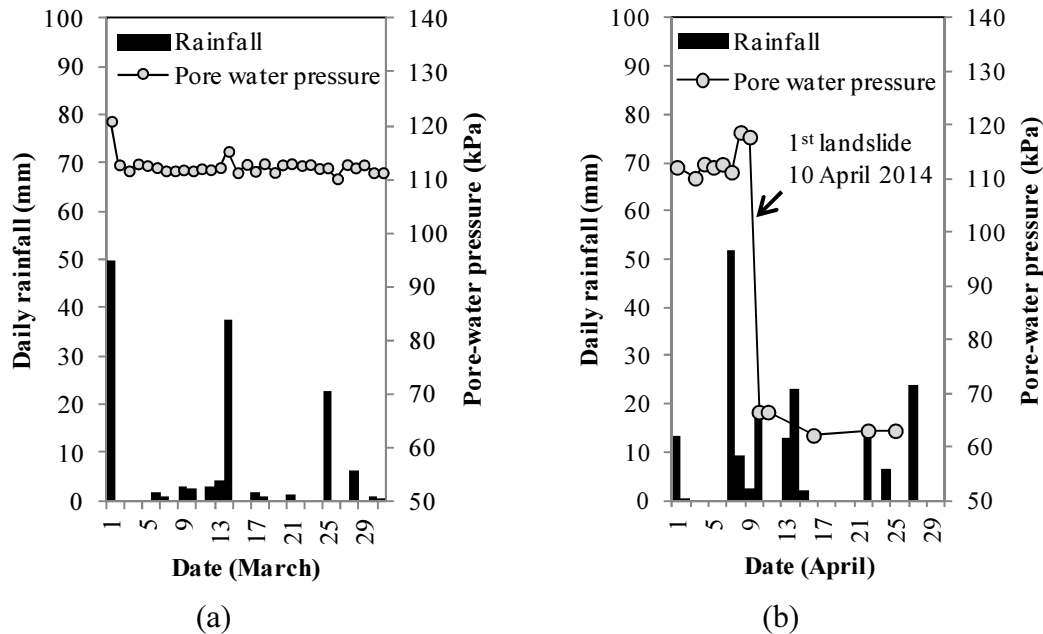


Figure 6. Pore-water pressure reading and rainfall data (a) monitoring period: 1-31 March 2014, and (b) monitoring period: 1-30 April 2014

Figure 7 shows a 9-month data set of average rainfall and pore-water pressure. The figure also shows the times of events (i.e., landslides and installation of the horizontal drain). From January to March, pore-water pressure increased from 105 to 112 kPa. In April and May when the landslide occurred, the pore-water pressure decreased to 74 and 71 kPa, respectively. It was because of the water flowed out through fracture and slide surface formed by the landslide. In June, the horizontal drain was installed. Increase in pore-water pressure in response to high rainfall and extended period of rain in July has not ever resulted in the landslide. This was one proof of the effectiveness of horizontal drain to prevent a landslide. Pore-water pressure decreased in August and September in response to rainfall and the use of the horizontal drain.

5. EFFECT OF HORIZONTAL DRAIN ON SAFETY FACTOR OF SLOPE

Another way to observe the effectiveness of horizontal drain on slope stability is to consider the factor of safety. The slope stability analysis was performed using the limit equilibrium slope stability software (i.e., Slide). Several simplifications were made to analyze slope safety factors. (1) The slopes with the soil layers were modeled with the features present in the Slide software. (2) The horizontal drainage hole was not directly applied to the model. (3) the changes in pore water pressure due to horizontal drain were converted to the height of ground water level (GWL) in the slope. (4) Only slope safety factors were obtained from this calculation.

Figure 8 is an example of slope stability analysis performed in this study at the condition before the first landslide. Based on computation result, a safety factor of slope on March with the pore-water pressure of 112 kPa converted to the ground water level of 11.4 m under ground surface was very close to 1 (i.e., 1.058). In the field, a landslide occurred.

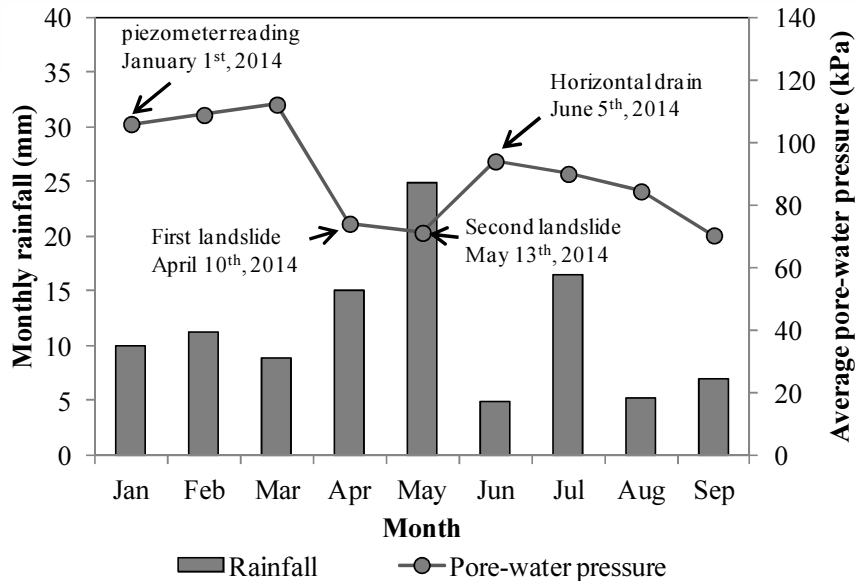


Figure 7. Average rainfall and pore-water pressure from Jan-Sep 2014

In July where the horizontal drain has been installed, the safety factor of slopes with an inclination of 20° and pore-water pressure of 90 kPa (i.e., GWL of 13.18 m) was 1.3. The safety factor increased by decreasing pore-water pressure in August and September. For long-term mining exploitation, deeper excavation is planned to a depth of 65 m. Stability of slope with a depth of 65 m, the inclination of 20° , and pore-water pressure of 120 kPa (i.e., assumed as the highest pore-water pressure occurred in the slope) was conducted using Slide. The safety factor obtained was 1.0. Higher safety factor (i.e., >1.3) can be reached by maintaining the pore-water pressure at a maximum of 70 kPa. The result reveals that another horizontal drain at the location as low as possible in the slope should be installed to increase the stability of the slope.

Besides height of ground water level, pore-water pressure influences the shear strength of the rock. Positive pore-water pressure results in decreasing the shear strength of saturated rock (Mesri et al., 1972). Its variation affects alteration in the stresses and the behavior of rock and soil thus triggering rupture and deformation of the crust (Mohammed, 1997). The cohesive and frictional properties of rock mass were significantly reduced from drained to the undrained condition. Since horizontal drain that allows water to flow out from rock mass can be equated with the drained condition, its presence in the slope will maintain the shear strength of rock mass forming the slope.

Mudstone which is dominant in the slope being studied is another reason of landslide due to its sensitivity to water absorption and desorption. The strength of mudstone decreases significantly when it is in contact with water (Lee et al., 2007). Jiang et al. (2014) found that rapid crack growth occurred in the first 72 hours of water infiltration. Moreover, the presence of discontinuity in mudstone as shown in Figure 3 provides channels for water to intrude the mudstone. The longer time mudstone in contact with water, the wider its crack and cause a new fracture in the material. In the field, high pore-water pressure drives water to penetrate into the discontinuity of mudstone. The decrease in shear strength of mudstone due to in contact with water was not considered in safety factor calculation using Slide.

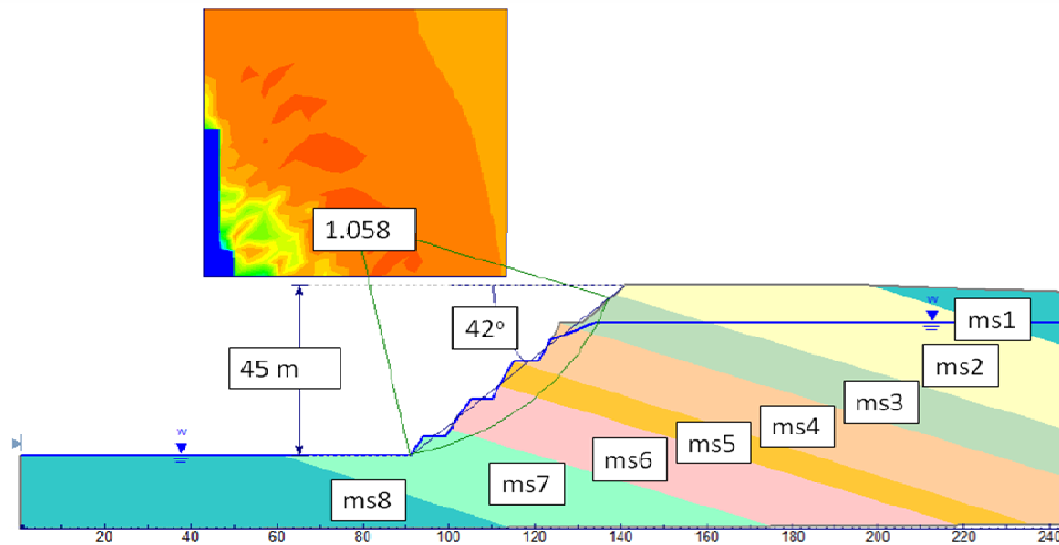


Figure 8. A model using the limit equilibrium slope stability software.

6. CONCLUSION

The effectiveness of horizontal drain for slope stability of coal mining has been analyzed using pore-water pressure data in the field and computer program. The landslide at Tambang Guntur coincided with or followed not only extremely high rainfall but also an extended period of rain. The horizontal drain installed in the slope has been successful to reduce the pore-water pressure that is highly influenced by rainfall. In the field, increase in pore-water pressure in response to high rainfall and extended period of rain during the term of study has not ever resulted in a landslide.

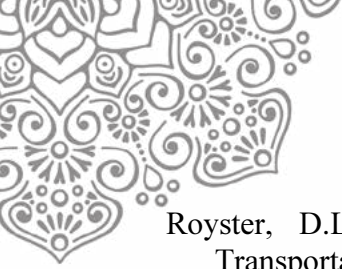
The safety factor of slope obtained using a computer analysis increases by decreasing the pore-water pressure. For long-term mining exploitation, another horizontal drain located as low as possible in the slope is required.

7. REFERENCES

- Apip, Takara, K., Yamashiki, Y., Ibrahim, A.B., Sassa, K., (2010), A geotechnical-hydrological approach for defining critical rainfall-induced shallow landslides and warning system at large scale, *J. SE Asian Appl. Geol.*, Vol. 2(3), pp. 185–194.
- Arifin, Y.F., (2010), Investigation of potential erosion in Loksado, Hulu Sungai Selatan, South Kalimantan, *In: Proceeding of Seminar Nasional Teknik Sipil VI, Institut Teknologi Sepuluh Nopember Surabaya (in Bahasa)*
- BNPB (Badan Nasional Penanggulangan Bencana), (2016), <http://dibi.bnpb.go.id/>
- Brown, E.T., (1981), Rock characterization, testing and monitoring—ISRM suggested methods. Pergamon, Oxford, pp. 171–183.
- Carrol, R.W.H., Pohll, G., Reeves, D.M., Badger, T., (2011) Approach to developing design guidelines for horizontal drain placement to improve slope stability, *Conference of MODFLOW and More 2011: Integrated Hydrologic Modeling.*
- Deere, D.U., Miller, R.P., (1966) Engineering classification and index properties of rock. Technical Report No. AFWL-TR-65-116, University of Illinois, Illinois.



- Djamil, H., (2002), Landslide disaster occurred from 1990-2002 in Indonesia, *In: Proceeding of International Congress Interpraevent 2002 in the Pacific Rim-Matsumoto, Japan, Vol.2*, pp. 619-628.
- Hirawan, F., (2010), Slope Instability Zoning Mapping of Landslide Hazardous Area for the Stabilization System, FIG Congress 2010, Facing the Challenges – Building the Capacity, Sydney, Australia, 11-16 April 2010.
- Ismail, M.A.M., Ng. S.M., Abustan, I., (2016), Parametric Study of Horizontal Drains for Slope Stability Measure: A Case Study in Putrajaya, Malaysia, *KSCE Journal of Civil Engineering*, pp.1-6.
- Jiang, Q., Cui, J., Feng, X., Jiang, Y., (2014), Application of computerized tomographic scanning to the study of water-induced weakening of mudstone, *Bull Eng Geol Environ*, 73. pp. 1293-1201.
- Jude, T.M.H., Afshar, N.R., Selaman, O.S., Taib, S.N.L., (2014), Application of value engineering in slope stabilization. *International Journal of Innovative Research in Advanced Engineering*, Vol. 1(10), pp. 211-216.
- Kanjanakul C, Chub-uppakarn, T., Chalermyanont, T., (2016), Rainfall thresholds for landslide early warning system in Nakhon Si Thammarat. *Arab J Geosci*, 9. pp. 584-595.
- Lee, D.H., Lin, H.M., Wu, J.H., (2007), The basic properties of mudstone slope in Southwestern Taiwan. *Journal GeoEng* 2(3), pp. 81–95.
- Liao, Z., Hong, Y., Wang, J., Fukuoka, H., Sassa, K., Karnawati, D., Fathani, F., (2010) Prototyping an experimental early warning system for rainfall-induced landslides in Indonesia using satellite remote sensing and geospatial datasets, *landslides*, Vol. 7(3), pp. 317–324.
- Marinos, P., Hoek, E., (2000) GSI: a geologically friendly tool for rock mass strength estimation. *In: Proceedings of the GeoEng 2000 at the international conference on geotechnical and geological engineering*, Melbourne, Technomic publishers, Lancaster, pp. 1422–1446.
- Mesri, G., Jones, R.A., Adachi, K., (1972) Influence of pore water pressure on the engineering properties of rock, *Annual Report, Advanced Research Project Agency (ARPA)*.
- Mohammed, M.M., (1997) Effect of groundwater on stability of rock and soil slopes, *Master Thesis, Department of Mining and Metallurgical Engineering, McGill University*.
- Mukhlisin, H., Aziz, N.A.B.A., (2016), Study of horizontal drain effect on slope stability. *Journal geological society of India*. Vol. 87. pp. 483-490.
- Ng, S.M., Ismail, M.A.M., Abustan, I., (2015), A Preliminary Study of Continuous Discharge Flow from Horizontal Drains using 3-Dimensional Resistivity Model, *KSCE Journal of Civil Engineering*, Vol. 19(6), pp.1865-1869.
- Orense, R.P., (2004), Slope Failure Triggered by Heavy Rainfall. *Philippine Engineering Journal*. Vol. 25(2), pp. 73-90.
- Prayuda, D.D., (2012) Temporal and spacial analysis of extreme rainfall on the slope area of Mt. Merapi, *Civil Engineering Forum*, Vol.21(3), pp.1285-1290.
- Rahardjo, H., Hritzuk, K.J., Leong, E.C., Rezaur, R.B., (2003) Effectiveness of horizontal drains for slope stability, *Engineering Geology*, 69, pp. 295-308.
- Rahardjo, H., Leong, E.C., Rezaur, R.B., (2002) Studies of rainfall-induced slope failures. *Proceedings of the National Seminar, Slope 2002*. 27-April 2002. Bandung, Indonesia. pp.15–29.



- Royster, D.L. (1980) Horizontal drains and horizontal drilling: an overview. Transportation Research Record.
- Sumaryono, Arifianti, Y., Triana, Y.D., Ika, W., Irawan. W., Suantika, G., (2014) The Application of Landslide Inventory Data Base of Indonesia (LIDIA) For Supporting Landslide Susceptibility Mapping in Cianjur Regency, West Java, Indonesia, GSTF International Journal of Geological Sciences (JGS)Vol.1 No.2.
- Zakaria, Z., Hirnawan, F., Widayati, S., (2015) Rain and Earthquake-Induced Landslides in West Java, Indonesia, Case Study in Subang Area Near the Baribis Fault, with Implications for an Early Warning System. In: Lollino G. et al. (eds) Engineering Geology for Society and Territory - Volume 2. Springer.



EFFECTS OF VEGETATION DISTRIBUTION ON EXPERIMENTAL MICRO-DRAINAGE CHANNEL

Robby Yussac Tallar^a, Erick Wijaya^a, Reinaldo^a and Jian-Ping Suen^b

^a*Universitas Kristen Maranatha, Jln. Surya Sumantri No. 65, Bandung 40641*

^b*National Cheng Kung University, No. 1 University Road, Tainan 701, Taiwan R.O.C*

ABSTRACT

Waterbodies are facing a diversity of threats in many parts of the world. To restore and preserve waterbodies environments, it is necessary to implement eco-hydraulics concept design into waterbody restoration projects. Eco-hydraulics is an integrated approach that deals with natural ecosystems as well as environmental impacts and mitigation measures. It incorporates species-habitat relationships and interactions of ecological and biological aspects within waterbodies. Physical habitat components including vegetation in the bed channel are considered affected the characteristics of flows in micro-drainage channels. Therefore, this paper aims to evaluate the characteristics of flows in vegetated micro-drainage channel with different scenarios. A laboratory study to explore the effect of vegetation in terms of roughness of vegetation on the hydraulics of flow in 8 m length x 40 cm width a rectangular channel is presented. The study consists of an extensive set of rectangular flume experiments for flows with certain slope and gravel bed with Sirih Gading (*Epipremnum aureum*) as selected flexible vegetation both submerged and unsubmerged. Two types of vegetation distribution patterns were set up to observe the hydraulic parameters and characteristics of flows in channels such the flow-resistance due to vegetation. Parameters affecting flow-resistance due to vegetation for both scenarios are discussed, compared and results are summarized and presented. The relationships dependencies of hydraulic parameters are presented. The results shown that the flow-resistance due to non-uniformly distributed vegetation pattern ($\lambda = 167.56$) is higher than uniformly distributed vegetation pattern ($\lambda = 38.24$). We also compared experiments with the two forms of vegetation distribution methods to control experiments without vegetation. For further research, the changes type of vegetation, position and others can be investigated. Hence, the study can be improved by checking the water quality within. Analysis and comparisons with rigid vegetation has also should be investigated with the present experimental work on flexible vegetation.

Keywords: Eco-hydraulics; Flow-resistance; Hydraulic parameters; Micro-drainage; Vegetation distribution



1. INTRODUCTION

Waterbodies are facing a diversity of threats in many parts of the world (Acreman, et. al., 1993; Djuangsih, 1993; Boothby, 1997; Zhao, et al., 2010; Ye, et. al., 2013). Human activity plays a determining role in the formation of the waterbody environments (Niemi et.al., 2007; Wang et.al., 2010). To restore and preserve waterbodies environments, it is necessary to implement eco-hydraulics concept design into waterbody restoration projects (Skute et.al., 2008; Tallar, R.Y and Suen, J.P., 2015). This concept links the disciplines of hydraulics with many aspects such as aquatic ecology, water engineering, river engineering and other aspects. Basically, eco-hydraulics is an integrated approach that deals with natural ecosystems as well as environmental impacts and mitigation measures (Putra et.al., 2008). The core concept of eco-hydraulics is to detain and/or retain water flow as long as possible and to reduce the velocity flowing in waterbodies. It also incorporates species-habitat relationships and interactions of ecological and biological aspects within waterbodies. In term of channel system, physical habitat components including vegetation in the bed channel are considered affected the characteristics of flows in micro-drainage channels. Therefore, this paper aims to evaluate the characteristics of flows in vegetated micro-drainage channel with different scenarios.

2. METHODOLOGY/ EXPERIMENTAL

2.1. Hydraulic Model

A length 8m x width 40cm x height 60cm, rectangular flume with glass on the lateral sides was used for this experiment. Certain slope has been set up with a schematic physical model to run different scenarios of simulation (Fig. 1 and 2).

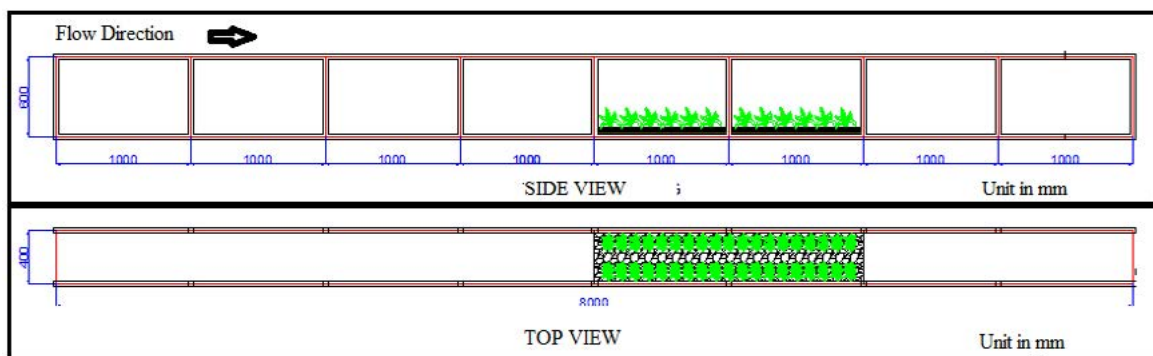


Figure 1 Schematic Design of Physical Model

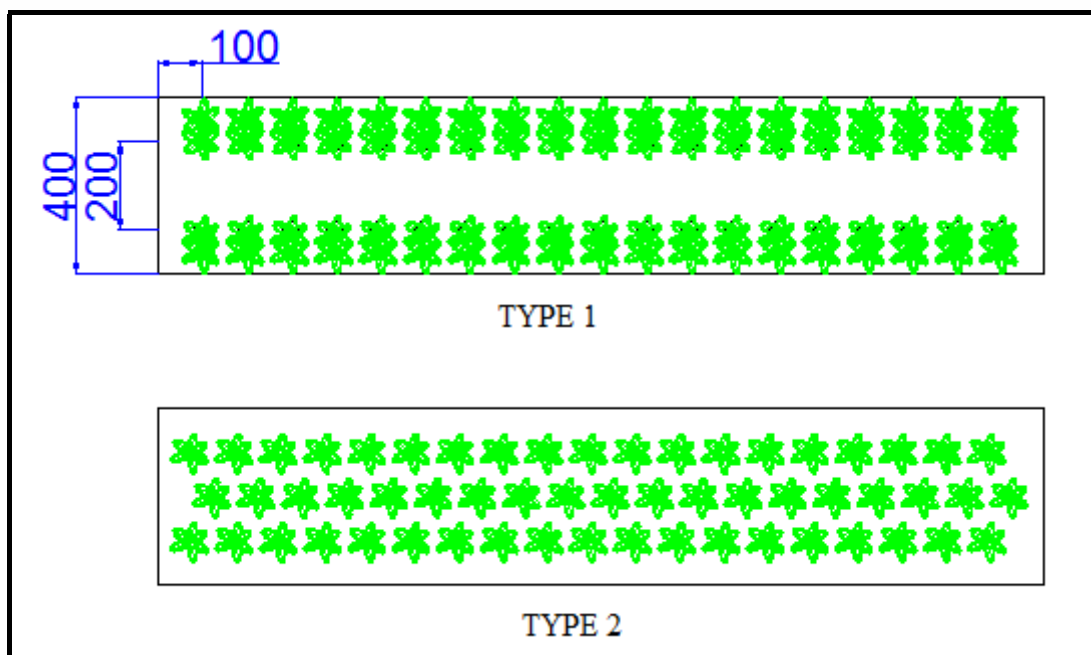


Figure 2 Two Types Patterns of Distribution of Vegetation

2.2. Simulation Scenario

This research was conducted several scenarios with several constraints. Based on previous results study, it is indicated that flow-resistance in vegetated micro-drainage channel will be affected if the discharge above 20% and below 60% of Q_{max} , therefore we set the scenarios as follow in Table 1.

Table 1 Simulation Scenario of the Study

Discharge	Distribution Pattern 1	Distribution Pattern 2
30% of Q_{max}	Scenario 1	Scenario 4
40% of Q_{max}	Scenario 2	Scenario 5
50% of Q_{max}	Scenario 3	Scenario 6

3. RESULTS AND DISCUSSION

The study consists of an extensive set of rectangular flume experiments for flows with certain slope and gravel bed with Sirih Gading (*Epipremnum aureum*) as selected flexible vegetation both submerged and unsubmerged (Figure 3). Two types of vegetation distribution patterns were set up to observe the hydraulic parameters and characteristics of flows in channels such the flow-resistance due to vegetation (Figure 4).



Figure 3 Sirih Gading (*Epipremnum aureum*)



Figure 4 Two types of vegetation distribution patterns

The analysis includes flow velocity both two types of vegetation distribution patterns and the result can be seen on Figure 5. The percentage of difference can be seen on Table 2.

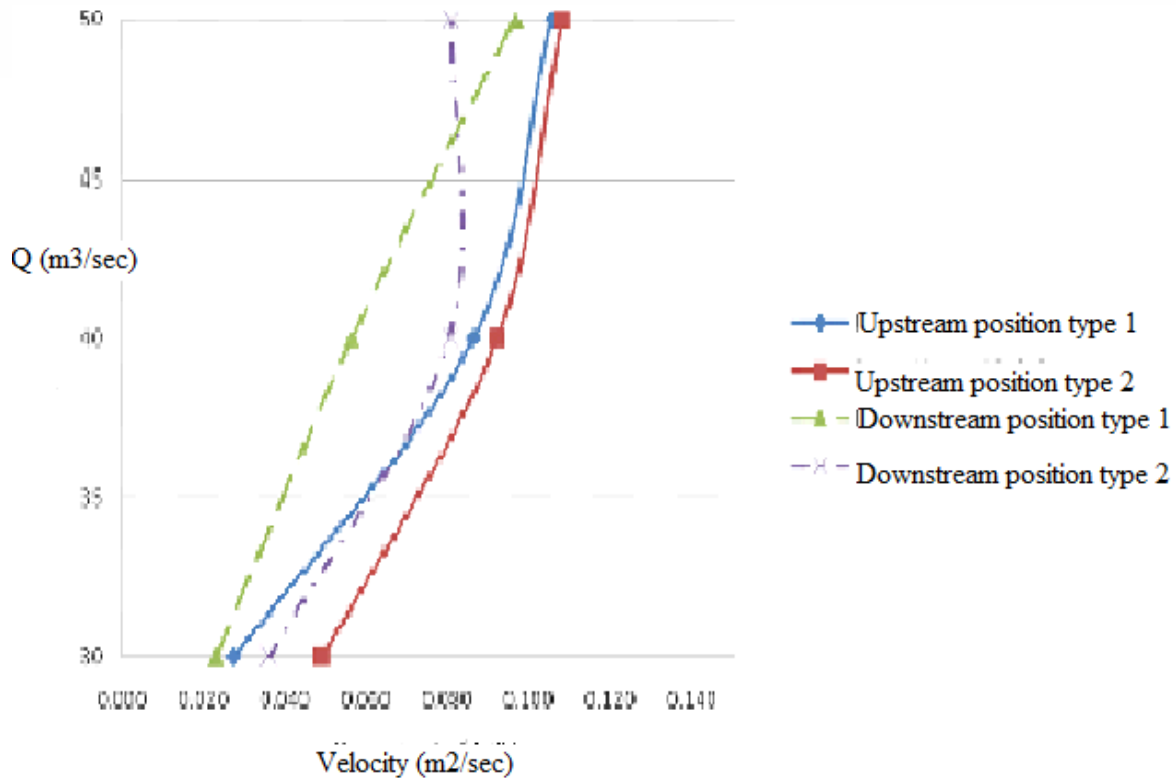


Figure 5. Comparison Flow Velocity of Pattern 1 and Pattern 2 (upstream and downstream position)

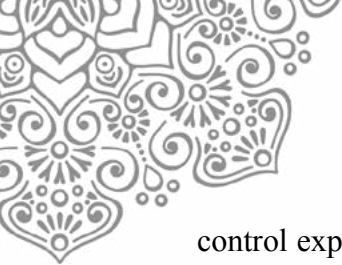
Table 2 % Difference Pattern 1 and Pattern 2

Q	% Difference	
	Type 1	Type 2
30%	15,44	27,22
40%	20,63	16,87
50%	10,43	12,59

Then, calculating the flow-resistance due to distribution of vegetation pattern by using Equation 1.

$$\lambda = \frac{4 \cdot A_P}{a_x \cdot a_y} \cdot C_w \quad (1)$$

The results shown that the flow-resistance due to non-uniformly distributed vegetation pattern ($\lambda = 167.56$) is higher than uniformly distributed vegetation pattern ($\lambda = 38.24$). We also compared experiments with the two forms of vegetation distribution methods to



control experiments without vegetation. Reduced velocity due to vegetation occurred in the experimental flume.

4. CONCLUSION

The present study focuses on straight simple vegetated rectangular channel with slightly slope. Based on the study, it is indicated that vegetation distribution in micro-drainage channels contributed in the effects of characteristics of flows which consisted of the hydraulic parameters (discharge, depth, Manning's coefficient) and flow-resistance. Vegetation is a very important factor and plays an important role in lining of water courses. Vegetation in micro-drainage channel retards the flow of water by causing a loss of energy through turbulence and by exerting additional drag forces. For further research, the changes type of vegetation, position and others can be investigated. Hence, the study can be improved by checking the water quality within. Analysis and comparisons with rigid vegetation has also should be investigated with the present experimental work on flexible vegetation.

5. ACKNOWLEDGEMENT

The authors gratefully acknowledge the research supported in part by Universitas Kristen Maranatha, Indonesia and in part by Ecological Water Resources Management Laboratory, Hydraulic and Ocean Engineering Department, National Cheng Kung University, Taiwan R.O.C

6. REFERENCES

- Acreman, M. C., J. R. Meigh & K. J. Sene (1993) Modelling the decline in water level of Lake Toba, Indonesia. *Advances in Water Resources*, 16, 207-222.
- Boothby, J. (1997) Pond conservation: towards a delineation of pondscape. *Aquatic Conservation: Marine and Freshwater Ecosystems*, 7, 127-132.
- Djuangsih, N. (1993) Understanding the state of river basin management from an environmental toxicology perspective: an example from water pollution at Citarum river basin, West Java, Indonesia. *Science of the Total Environment*, 134, Supplement 1, 283-292.
- Niemi, G. J., J. R. Kelly & N. P. Danz (2007) Environmental indicators for the coastal region of the north American great lakes: Introduction and prospectus. *Journal of Great Lakes Research*, 33, 1-12.
- Putra, S. S., C. Hassan, Djudi & H. Suryatmojo (2013) Reservoir Saboworks Solutions in Limboto Lake Sedimentations, Northern Sulawesi, Indonesia. *Procedia Environmental Sciences*, 17, 230-239.
- Škute, A., D. Gruberts, J. Soms & J. Paidere (2008) Ecological and hydrological functions of the biggest natural floodplain in Latvia. *Ecohydrology & Hydrobiology*, 8, 291-306.
- Tallar, R. Y & J. P. Suen (2015) Aquaculture Water Quality Index: a low-cost index to accelerate aquaculture development in Indonesia. *Aquaculture International*, 1-18.
- Wang, J., L. Zhu, Y. Wang, J. Ju, M. Xie & G. Daut (2010) Comparisons between the chemical compositions of lake water, inflowing river water, and lake sediment in Nam Co, central Tibetan Plateau, China and their controlling mechanisms. *Journal of Great Lakes Research*, 36, 587-595.
- Ye, X. C., Q. Zhang, J. Liu, X. H. Li & C. Y. Xu (2013) Distinguishing the relative impacts of climate change and human activities on variation of streamflow in the Poyang Lake catchment, China. *Journal of Hydrology*, 494, 83-95.
- Zhao, Y., Z. Yang & Y. Li (2010) Investigation of water pollution in Baiyangdian Lake, China. *Procedia Environmental Sciences*, 2, 737-748.



ANALYSIS OF FLOOD EMERGENCY RESPONSE INSTRUMENT IN INDONESIA

Toha Saleh^{1,a}

¹*Civil Engineering Department, Faculty of Engineering, Universitas Indonesia, Indonesia*

^a*toha@eng.ui.ac.id*

ABSTRACT

One of measures to reduce the flood impact in Indonesia has been done by flood emergency response action plan. The action plan is generated from decision making process assisted by instrument such computer models which have capability in producing scenarios and decision to be taken. This research is conducted to identify how the written procedures (delivered by international and national agencies) related to flood emergency response, being accommodated by those (computer) models. By using qualitative analysis, the element procedures of an effective flood emergency response model have been reviewed. The result shows that the detailed information such human and material resources, facilities information, and warning time-lag, have not been properly and entirely accommodated by the (computer) model. Highlights are also given to propose more effective instrument to improve the management of flood crisis.

Keywords: *flood emergency response, flood management, computer model*

1. INTRODUCTION

In the last decade (2003-2012), about 42% of natural disasters are caused by flood hazards, killing more than 50.000 people and causing over 180 million US\$ of damage [1]. Asia was the most affected continent, where Indonesia contributed to more than 70 times flood events, more than 5 million affected, and about US\$ 5 billion damages.

Specifically for Jakarta, the capital of Indonesia who suffered from flood almost every year, it is recorded that in 2007, the flood inundated about 70 percent of the Jakarta's area. It killed at least 57 people and sent about 450,000 fleeing their homes. The flood paralyzed the centre of Indonesia's economy for several days and businesses claimed to lose about US\$1 billion [2]. In 2011, flood caused severe flooding in several neighborhoods with a 50-centimeter-deep flood that submerged the main road and caused up to US\$ 1 million damages [3]. In 2013, the floods killed at least 20 people and sent at least 33,502 fleeing their houses as reported by the National Disaster Mitigation Agency (BNPB) [4]. The fact that there are losses and casualties in every flood event, indicate the level of flood measures still not in a good manner.

In reduce and avoid the numerous damages, loss, or even casualties resulted from a flood disaster, the management of such event should be done, and this can be done by providing the local authorities, and also the community, with flood crisis management models as decision support tools. However, decision support tools really depend on the information as the input. The questions are: how this tool (such computer model) can give an accurate result? What kind of information should be placed and recognized to produce a better suggestion or alternative of decision? Based on what parameters the information is collected and listed? Therefore, it is necessary to assess the structure of parameter used in the computer model whether those models have accommodated the principle and procedures which have been written in flood emergency response management strategy and policy.

By analyzing and recognizing parameters that should be considered in such tool(s), it is expected to produce more effective flood management models in supporting the formulation of management plans and best alternative for flood emergency response.



2. METHODOLOGY

Many decision support made by utilizing computer models as the tool, or known as Decision Support Systems (DSS). DSS is defined as computer-based tools having interactive, graphical, and modeling characteristics to address specific problems and assist individuals in their study and search for a solution to their management problems [5].

DSS have evolved from a simple model-oriented systems to advanced multi-function entities. DSS provides varying analysis without much programming effort and is usually directed towards non-technical users/managers. The first important aspect of DSS is that they provide information which are used in the decision making process. The emphasis here is not on the quantity of information, but rather the quality. There are multiple factors that qualify information as having good quality (such as timeliness, relevant, accurateness, consistency, unbiased, etc.) but the important consideration factor is how information is used in order to attain a certain goal [6].

In the context of flood management, the Flood Emergency Planning introduced by World Meteorological Organization (WMO) addressed some steps that have to be taken in order to gain better management and decision making process [7]. Those steps are illustrated as follows:

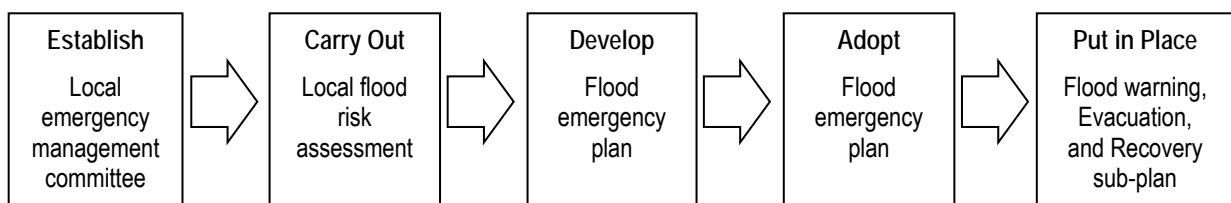


Figure 1. Flood Emergency Planning (WMO, 2006; adapted from ARMCANZ, 2000)

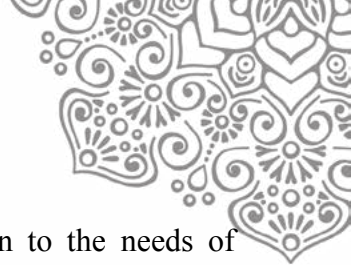
Flood emergency response can be defined as the implementation of pre-planned activities during flooding to reduce the adverse impacts to the population and material values and infrastructure at risk. [8].

A Flood Emergency Plan (FEP) outlines the roles and responsibilities of all parties to be involved, actions to be taken, coordination arrangements and communication channels to be used prior to, during and after a flood event. The purpose of planning for flood emergencies is to reduce the risk to health and life and the damage caused by flooding. Local plans should describe how flood hazard threats are identified. Specifically, the plan should include:

- Areas likely to flood and the extent and depth of flooding
- Frequency of occurrence (both historical and predicted or probable)
- Magnitude and intensity duration, seasonal pattern, speed of onset
- Location of critical infrastructure at risk
- Spatial extent (either around the known location of the hazard or as an estimate for non-localized hazards)
- The location of flood defense resources (equipment, sandbags, etc.)
- Traffic and evacuation routes and corridors
- Warning mechanisms

It is expected that in the development of the concept model, has to involve the improvement of information sharing and collaborative decision-making at different levels of scale (shared, common community, department), and between the main actors in the diagnostic process of the threats and intervention on the ground. It will introduce a complete system including a method and a tool to compile and organize all relevant information on floods and useful for crisis planning.

The output of this study is a concept model that can assist the simulation of flood crisis management, together with alternatives measures for decision support based on integrated flood management planning and principles. The model must be able to simulate several alternatives and



scenarios in selected case, as well as providing good and relevant information to the needs of decision-making process. The actual problem solving and application in the field will be a separate constituent in selecting alternatives generated by the model. The methodology in comparing the models is based on OSIRIS-Model approach.

3. RESULTS AND DISCUSSION

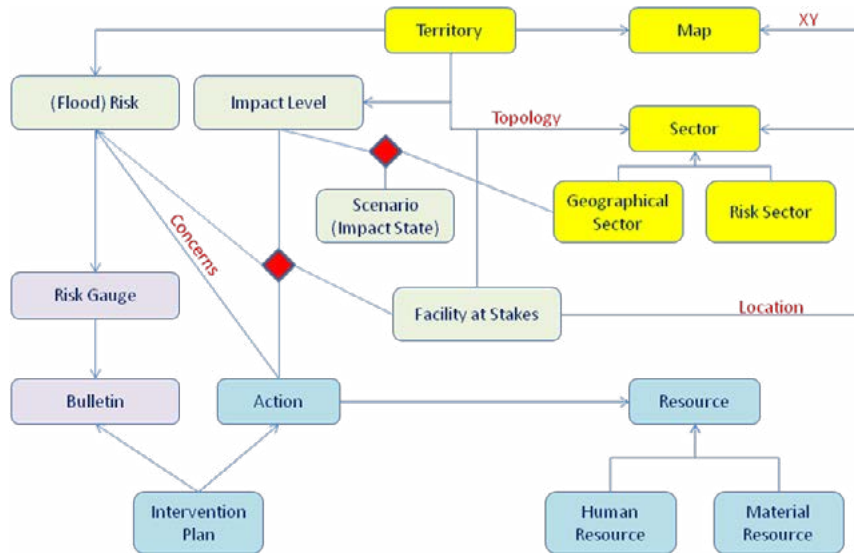


Figure 2. OSIRIS simplified data model in UML

The result shows that the detailed information such human and material resources, facilities information, and warning time-lag, have not been properly and entirely accommodated in the (computer) model.



Figure 3. Interaction Platform of OSIRIS-Flood (Shows the results)

Simple comparative analysis between applications of some decision support tools is conducted to gain better understanding of the characteristics of each tool, the principle, the method, as well as the objective and purpose of each tool.



The comparison of the tools is limited only to those tools which used for disaster management with focus on flood disaster management tools.

Name and Info of DSS	Origin	Objective and Purpose	Method and Function
HAZUS (Hazards US)	US, 2003	Estimating potential losses from earthquake, floods, and hurricanes	GIS technology; to estimate physical, economic, and social impacts of disasters
SAHANA-FOSS	Srilanka, 2004	Provide a set of modular, web-based disaster management applications	Synchronization between multiple instances, allowing for responders or district offices to capture data on victims in the field
UN-SPIDER	2006	Focus on the need to ensure access to and use of such solutions during all phases of the disaster management cycle, including the risk reduction phase	Integrated communication
FLOODSITE	UK, 2008	Tool for risk information on flood event to the investment and economic values	Communication and dissemination
OSIRIS Flood	France, 2005	Tool for the preparation and management of flood crisis (provide flood-operational solutions) for local officials	Set of procedure to follow to compile and organize all relevant information on floods and useful for crisis planning: sources of data for forecasting, flood maps and scenarios, and vulnerability issues, action plans and procedures to be provided to limit the damage, human and material resources available
INASAFE	Indonesia, 2011	Produces realistic natural hazard impact scenarios for better planning, preparedness and response activities.	Combines one exposure layer (e.g. location of buildings) with one hazard scenario (e.g. flooding footprint) and returns a spatial impact layer along with textual statistical summary and action questions.
CEDD	Spain, 2006	DSS tool for flood mapping	Fuzzy Logic; Interact and synchronize stakeholders in flood management in order to follow mapping result.

Specific for Indonesia case, InaSAFE is free software that produces realistic natural hazard impact scenarios for better planning, preparedness and response activities. It provides a simple but rigorous way to combine data from scientists, local governments and communities to provide insights into the likely impacts of future disaster events. However, there was a lack of human and material resources, facilities information, and warning time-lag considered in the model.

As for the parameters considered in the concept model, based on various type of tools and references, it can be tabulated as below

Table 1. Matrix of variables in flood emergency response

Variable	Activity/Description	Data	Model which represents
Location	Location identification	Map	All
	Geo reference (connection to GIS)	Geo-spatial referencing	Haz, OS, UNS
		Zoning/sector	Haz, OS, UNS
Hydrological	Generate hydrological data	General data	All; exc. UNS



information	Information of flood	Flood status	All
		Flood scale	All
	Report	Bulletin (past records)	OS, InaS
Infrastructure at stakes	Identify the stakes and location	Land use info	OS, UNS, SF, InaS
		Position and level of exposure	OS, SF, InaS
	Identify the impact	Number of occupants	OS, SF, InaS
Resources	Resources identification	Human resources	OS, InaS
		Material and equipment resources	OS
	Access to resources	Accessibility info	OS
		Organization (PIC)	OS
Scenario for action	Assess the possibility scenario	Classification	OS, InaS, Haz
	Action plan generation	Data support	OS, InaS
	Regulation support	Regulation for action	OS, SF
Communication and plan	Flow of communication	Flow of information	All
		Institutional/stakeholder	OS, UNS, InaS

4. CONCLUSION

This assessment has concluded some points:

- Mapping is the most important step but has to be done manually
- Data requirement of each steps has to be adjusted in order to keep track for each iteration
- The detailed information for human resources data is more complicated (to obtain)
- Variation of stakes identified in the location still need to be validated
- The selection of flood states is the key issue in generating the preference graphs
- Some obstacles related to the language justification and translation

DSS are there to facilitate a manager in making operational decisions, but the ultimate burden of responsibility lies with the manager. Managers can sometimes be over-optimistic in their expectations of a DSS and develop a unrealistic reliance on the system (Power, C.J; *Caveat Emperor*).

The effective operation of the total floodplain management process is determined by how well the various agencies are coordinated as they perform their individual tasks and how well they communicate with other stakeholders in the basin.

5. ACKNOWLEDMENT

The wirtter would like to thank to Prof. Jean-Louis Batoz, Dr. Gilles Morel and Dr. Dwita for their guide throughout the study and providing adequate references.

6. REFERENCES

- 1 EM-DAT IDD, 2013. ([http://www.emdat.be/result-disaster-profiles?disgroup= natural&dis_type=Flood &period=2003\\$2012](http://www.emdat.be/result-disaster-profiles?disgroup= natural&dis_type=Flood &period=2003$2012))
- 2 BAPPENAS, 2007. The Jakarta Flood Report. (<http://bappenas.go.id>)
- 3 Indonesia's Urban Studies, 2011. (<http://indonesiaurbanstudies.blogspot.com/2011/02/jakarta-annual-flooding-in-february.html>)
- 4 National Disaster Mitigation Agency (BNPB), 2013. www.bnpb.go.id
- 5 Loucks, D.P., and J.R. daCosta, (editors), 1991, Decision support systems: Water Resources Planning. Springer-Verlag, Berlin, Germany.
- 6 Sauter, V, Louw, R.E, 2002, Decision Support Systems, University of Missouri St. Louis
- 7 WMO, 2006. adapted from ARMCANZ, 2000
- 8 WMO, 2011. IFM Tools Series No.11, World Meteorological Organization



- 9 G. Morel, F. Hissel, 2010. ***OSIRIS-inondation: a support tool for local flood crisis planning and management.*** Colloque SHF : «risques inondation en Ile de France», Paris, 24-25 mars 2010.
- 10 APFM (Associated Programme on Flood Management), 2011. Integrated Flood Management Tools Series: Flood Emergency Planning.
- 11 Jonkman, S.N., Bockarjovab, M., Kokc, M., Bernardinid, P., May 2008. **Integrated hydrodynamic and economic Modelling of flood damage in the Netherlands.** Ecological Economics 66 (1), 77-90.
- 12 Marnix van der Vat, et.al. 2004. ***Methodology for Decision Support Systems for Flood Event Management***, Floodsite Project Report
- 13 OPPENHEIM, Nobert, 1980, ***Applied Models in Urban and Regional Analysis***, Prentice-Hall Inc., Englewood Cliffs, New Jersey.
- 14 **OSIRIS-Inondation Guideline**, 2008
- 15 Qi, Honghai, Altinakar, M.S., Ying, X., Wang, S.S.Y, 2005. **Risk and Uncertainty Analysis in Flood Hazard Management Using GIS and Remote Sensing Technology.** In: Proceeding of American Water Resources Association Annual Conference, Seattle, Nov 2005.
- 16 Taliercio, G., 2010. **Flood Crisis Management in the Meuse Basin:** General framework of strategies, methods, tools and technologies used at different territorial scales and by different stakeholders, AMICE Flood – EPAMA.
- 17 Saleh, T., Orientilize, M., Rasul, R., 2008. ***Policy Study on Public Participation in Flood Control Infrastructure and Facility Management.*** Quality in Research Conference 2009, Universitas Indonesia.
- 18 Simonovic, S.P., 2002, **A Spatial Fuzzy Compromise Programming for Management of Natural Disasters**, ICLR Research Paper Series, No. 24.
- 19 Government of Indonesia, 2007. Disaster Management Law (UU No.24 tahun 2007) tentang Penanggulangan Bencana (Pasal. 48 – 50)



MEASUREMENT OF TOLL ROAD SERVICE QUALITY (TRSQ) USING STRUCTURAL EQUATION MODEL APPROACH

Herry T. Zuna^a, Adani T. Zafira^a, Muhammad Ismail H. Sadjidullah^{a*}

^a*Indonesia Toll Road Authority, Indonesia*

ABSTRACT

Better service is an essential prerequisite for customers' satisfaction. As a service, toll road applied Minimum Service Standard (SPM) to achieve the level of service expected by users. Understanding which of the attributes preferred by users becomes necessary. Toll Road Service Quality (TRSQ) model is the modification of SERVQUAL model that perceived toll road services from users' perspective. It consists of seven attributes namely information, accessibility, reliability, mobility, security, rest areas, and responsiveness. This study aimed to measure TRSQ model using Structural Equation Model (SEM) with Partial Least Square (PLS). Results suggest the correlation of service attributes in TRSQ model and users' satisfaction. Out of 11 toll roads being surveyed, accessibility has the greatest impact on users' satisfaction and deemed to be the most important aspect on toll road services.

Keywords: Structural Equation Model; Toll Road Service Quality; User Satisfaction; Toll Road

1. INTRODUCTION

In order to intensify economic growth and mobility, toll road as one of the provision of infrastructures plays a significant role to intensify economic growth and mobility. Toll road gives alternative route to users, travel time savings and efficient distribution to achieve economic equity across the nation (Zuna et al, 2015). Toll road is distinguished from non-toll road by the service it grants. The implementation of tariffs in toll roads equals with the services given to users. Therefore, by paying the fees, expectation rises in their perception.

To meet user expectation, Minimum Service Standard (SPM) is applied for toll roads in Indonesia to maintain the quality of the services. However, the provided level of services sometimes fails to fulfill user's expectation (Zeithaml et al., 1990). This problem happens because the government misses to deliver user expectations into the operational service standard. The fact that service quality of toll road used in Indonesia is not yet affected by user perception adds the gap between user's expectation and services that provided. This situation occurs because toll roads do not have a competitive market. Despite of the dissatisfaction, Zuna et al. (2016) said users will continue to use toll roads in needs for mobilization.

It is known that the concepts of service quality and service satisfaction have been considered in management activities (Mosahab et al., 2010). Customer satisfaction holds an important effect to measure company's accomplishment. It is necessary to determine the



attributes of toll road service quality and how it influences users by understanding their satisfaction standard.

Toll Road Service Quality

Toll roads are seen as goods because of the tangible nature of the roads. However, toll roads can also be considered as services because of the better services it gives to users than non-toll roads (Zuna, et al, 2015). The service includes faster route, safer environment, shorter travel time, and comfortable surrounding throughout the journey. Those will be alternated to the fees users have to pay in accordance with the Indonesia Ministry of Public Works and Housing's Decree Number 16/PRT/M/2014, concerning toll road minimum standards.

Bateson (1995) remarked that service quality has unique characteristics; intangibility, heterogeneity, inseparability and perishability, which makes it difficult to measure. Customer's expectations and perceptions could be used to measure service quality (Ebollu and Mazzulla, 2008). Service quality is formed from customers' points of view and perception of a service (Heide and John, 1992). Kotler (1995) described customer satisfaction as a comparison between expected service and perceived service. The perspectives of both the provider and the receiver have to be included in every research on service quality (Czepiel, 1990).

The SERVQUAL model established by (Parasuraman et al., 1988) proposes to qualify a service based on five distinct dimensions: reliability, responsiveness, assurance, empathy, and tangibles. The SERVQUAL instrument consists of 22 statements assesses the gap between customers' expectations of the service and their perception of the 6 actual service received. SERVQUAL has been designed to be applicable in an extensive spectrum of services and the format could be adapted to fit specific needs (Parasuraman et al., 1988). Despite being criticized as imperfect model, it remains the most widely applied measure of service quality (Sivadas and Baker-Prewitt, 2000). Ladhari (2009) stated that to receive reliable and valid results when using the SERVQUAL model to measure service quality was choosing the right dimensions that fit into specific service being measured. Customer's expectation as well as their perceptions takes a roll in which best way to measure service quality in service sector (Shahin, 2005).

Zuna et al. (2016) created Toll Road Service Quality (TRSQ) developed from the combination of SERVQUAL and SPM. The data were obtained and analyzed using the ANN approach. TRSQ considers SERVQUAL dimensions, but also considers the physical aspects addressed by SPM. TRSQ has seven dimensions: accessibility, reliability, mobility, safety and security, rest areas, and responsiveness.

Structural Equation Model

Structural Equation Model (SEM) is a statistical modeling technique which is widely used in the behavioral sciences (Hox and Bechger, 2007). When dealing with relations between constructs such as satisfaction, role ambiguity, or attitude, SEM is likely to be the methodology of choice (Monecke and Leisch, 2012). SEM offers advantages over some familiar methods and provides a general framework for linear modeling since it is designed for working with multiple related equations simultaneously. Special cases of SEM are regression, canonical correlation, confirmatory factor analysis, and repeated measures analysis of variance (Kline, 1998).



There are only two types of variables in SEM exogenous or endogenous. An exogenous variable has path arrows pointing outwards and none leading to it. Meanwhile, an endogenous variable has at least one path leading to it and represents the effects of other variables. SEM has several distinct approaches based on its function such as Covariance-based SEM (CB-SEM), Partial Least Squares (PLS), Generalized Structured Component Analysis (GSCA), and Nonlinear Universal Structural Relational Modeling (NEUSREL). CB-SEM uses software packages such as AMOS, EQS, LISREL and MPlus. PLS, which focuses on the analysis of variance, can be carried out using PLS-Graph, VisualPLS, SmartPLS, WarpPLS, as well as the PLS module in the “r” statistical software package. While GSCA is implemented through VisualGSCA or a web-based application called GeSCA. NEUSREL’s Causal Analytics software has been used for NEUSREL approach (Wong, 2013).

PLS is a soft modeling approach to SEM with no assumptions about data distribution, unlike CB-SEM where it aims at reproducing the same covariance matrix (Vinzi et al., 2010). Hence, PLS-SEM can be a better option rather than CB-SEM when the similar situations are encountered (Bacon, 1999). SmartPLS is a stand alone software specialized for PLS path models. The model is specified via drag and drop by drawing the structural model for the latent variables and by assigning the indicators to the latent variables (Monecke and Leisch, 2012).

2. METHODOLOGY/ EXPERIMENTAL

This study is based on questionnaires of the customer satisfaction survey at 2013 gathered by Indonesia Toll Road Authority (BPJT). The data were obtained from 11 toll roads in Java which varies from urban/rural toll roads and operated by government/private sector. The data from questionnaires combined with Toll Road Service Quality (TRSQ) model are used as an approach for modelling the service quality that explained the relationship between satisfaction and expectation from toll roads user perspective.

Toll Road Service Quality Modelling:

As described above, TRSQ model is used as a model that can explain the correlation between expectation and perspective from toll road user based on research from Zuna, et al., (2016). TRSQ model is a combination of SERVQUAL model and service dimension in Toll Road Minimum Standards (SPM) that has 7 dimensions such as information, accessibility, reliability, mobility, safety and security, rest area, and responsiveness.

Partial Least Squares-Structural Equation Modelling:

Structural Equation Modelling (SEM) with Partial Least Squares (PLS) approach is used to estimate causal relationship in path models that involve latent variables and its manifest. PLS is used to estimate the connection between 7 dimensions from TRSQ and 33 manifest variables from questionnaires. With PLS modelling, those variables and dimensions are created to two steps of calculations as a model like a picture below.

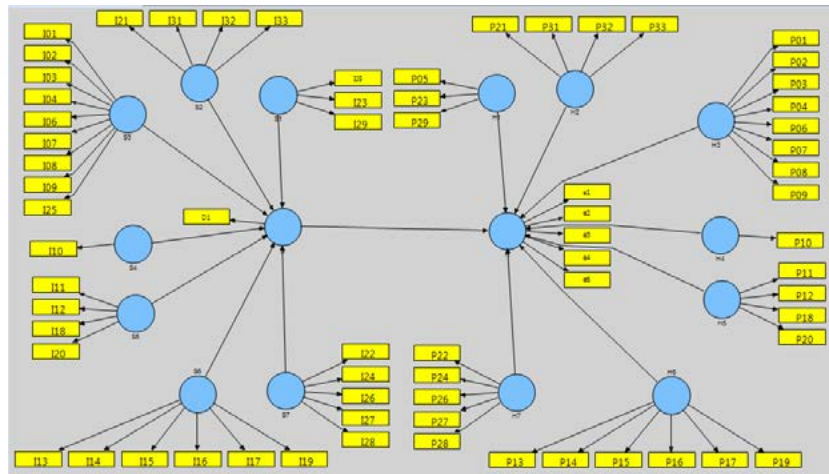


Figure 1 SEM – PLS Modelling with TRSQ Dimensions

The 7 TRSQ dimensions serve as a reflective construct for satisfaction and hope. For PLS modelling to be able to calculate the models, satisfaction variable use D1 as an input unit and hope variable used variable from E1 to E5 in which value had been switched to the opposite for each variable to create a models with equal level of value to analysis.

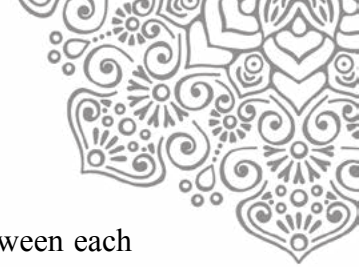
Table 1 Endogenous variables and its indicator

Code	Endogenous Variable	Code	Indicator
S	Satisfaction	D1	level of satisfaction
		e1	Accident caused by road condition
		e2	Accident caused by other toll road user
H	Hope	e3	Crime events when using the road
		e4	The easiness to get fare information, entrance and exit toll road access, or helpline access
		e5	illegal charge, including illegal towing along the toll road

3. RESULTS AND DISCUSSION

SEM PLS Model Analysis: The statistical software application Smart PLS 2.0 is used to analyze the correlation between satisfaction and hope factors that being tested. PLS uses a two steps process to evaluate 11 PLS models. The PLS path model evaluation steps consist of:

- Measurement model (Outer model)
Model evaluation with PLS Algorithm to determine manifest and construct's reliability and validity.
- Structural model (Inner Model)



Model evaluation with Bootstrapping process to estimate correlation between each endogenous variables.

The steps that is taken into consideration are meant to evaluate reliability and validity of measurements indicator, and henceforth estimate the relationship between satisfaction and hope from toll road user's perspective.

Measurement model (Outer model)

First step that we analyze is the models with PLS Algorithm to get loading factor scoring from each manifests. After each running process, we reduce the number of manifests variables that receive score less than 0.5. Thus, this means if they have less than 50% capability to explain their own construct variables. After reducing manifests variable with loading factor selection, we analyze the models with other criteria for validity and reliability test.

For Average Variance Extracted (AVE), composite reliability, R² and cronbachs alpha, the results from its analysis are shown in the table below:

Table 2 Validity and reliability test results

Toll Road Sample Number	Indicator	AVE	Composite Reliability	R Square	Cronbachs Alpha
1	H	1	1	0.5227	1
	S	1	1	0.0536	1
2	H	1	1	0.1948	1
	S	1	1	0.0645	1
3	H	1	1	0.8008	1
	S	1	1	0.2147	1
4	H	1	1	0.5184	1
	S	1	1	0.0143	1
5	H	1	1	0.3361	1
	S	1	1	0.0544	1
6	H	1	1	0.3332	1
	S	1	1	0.1184	1
7	H	0.6106	0.8623	0.3584	0.7888
	S	1	1	0.2036	1
8	H	0.6168	0.7507	0.628	0.665
	S	1	1	0.2446	1
9	H	1	1	0.4362	1
	S	1	1	0.0943	1
10	H	0.5764	0.8009	0.7205	0.7595
	S	1	1	0.3985	1
11	H	1	1	0.5325	1
	S	1	1	0.0677	1



From validity and reliability test with PLS Algorithm, 11 toll roads that had been tested show insignificant result of R^2 test for satisfaction variable from toll road samples number 1, 2, 4, 5, 9, and 11. The results reflect the correlation between satisfaction and its TRSQ models have less than 10% capability to explain. Meanwhile, other validity and reliability test results such as AVE, cronbach alpha, and composite reliability had already passed the limits to be considered as a valid and reliable variables.

Structural model (Inner model)

For inner model, correlation between each construct that form endogenous indicator is shown in the table below:

Table 3 Inner model test results

No.	Toll Road Sample	Most Significance TRSQ Satisfaction	Most Significance Manifest for Satisfaction	Most Significance TRSQ Hope	Most Significance Manifest for Hope
1	Jakarta – Bogor – Ciawi (Jagorawi)	S3 (Reliability)	I01 (Comfort while driving along the toll roads)	H2 (Accessibility)	P32 (Officer honesty when transacting substation)
2	Jakarta – Tangerang (Janger)	S4 (Mobility)	I10 (Smoothness / no barriers / no jams when driving road toll)	H1 (Information)	P05 (The position and location of signs / traffic information boards)
3	Semarang Seksi A, B, C	S3 (Reliability)	I06 (The number and quality of ornamental plants along the side and median road)	H2 (Accessibility)	P33 (Quality of service personnel substation)
4	Jakarta – Cikampek (Japek)	S4 (Mobility)	I10 (Smoothness / no barriers / no jams when driving road toll)	H5 (Safety & Security)	P11 (The level of safety (number of accidents) while driving along the motorway)
5	Serpong – Pondok Aren (BSD)	S3 (Reliability)	I01 (Comfort while driving along the toll roads)	H3 (Reliability)	P07 (The number and size of trees on the side of the highway as a shade)
6	Tangerang – Merak (Merak)	S2 (Accessibility)	I33 (Quality of service personnel substation)	H5 (Safety & Security)	P20 (Security at the resting place of crime)
7	Cikampek – Purwakarta – Padalarang (Cipularang)	S2 (Accessibility)	I32 (Officer honesty when transacting substation)	H2 (Accessibility)	P32 (Officer honesty when transacting substation)



No.	Toll Road Sample	Most Significance TRSQ Satisfaction	Most Significance Manifest for Satisfaction	Most Significance TRSQ Hope	Most Significance Manifest for Hope
8	Padalarang – Cileunyi (Padaleunyi)	S6 (Rest Area)	I15 (The quality and availability of parking at a rest area)	H1 (Information)	P05 (The position and location of signs / traffic information boards)
9	Palimanan – Plumbon – Kanci (Palikanci)	S3 (Reliability)	I07 (The number and size of trees on the side of the highway as a shade)	H6 (Rest Area)	P15 (The quality and availability of parking at a rest area)
10	Kanci – Penjagaan	S2 (Accessibility)	I32 (Officer honesty when transacting substation)	H5 (Safety & Security)	P18 (Rest area without charges)
11	Surabaya – Gempol (Surgem)	S2 (Accessibility)	I33 (Quality of service personnel substation)	H6 (Rest Area)	P15 (The quality and availability of parking at a rest area)

From 11 toll roads that had been modelled, there are 4 toll roads, on each with reliability (S3) and accessibility (S2), serve as dominant satisfaction indicator. This indicates reliability and accessibility as a general factor that explains satisfaction from TRSQ model. However, there are 3 toll roads each with accessibility (H2) and safety and security (H5), serve as dominant hope indicator, which means as a representative for user toll roads expectation. For accessibility that got chosen as a main indicator for satisfaction and hope, it explains that from 11 toll road samples, mainly from toll roads samples that tested have been able to answer their user's expectation for accessibility indicator. Meanwhile, for 33 manifests variables each from 7 TRSQ dimensions, there are 2 toll roads each with officer honesty when transacting (I32), comfort while driving along the toll road (I01), and quality of service personnel substation (I33) as manifest with the biggest factor that got chosen by majority of toll road samples for satisfaction. As for variable of hope, 2 toll roads each got officer honesty when transacting (P32), the position and location of signs / traffic information boards (P05), and the quality and availability of parking at a rest area (P15) got picked as a manifest variable with biggest loading factor comes from a most significance TRSQ dimensions for hope. With several similarities between manifest that got picked for satisfaction and hope, variable officer honesty when transacting (32) comes as an manifest with highest loading factor.

4. CONCLUSION

TRSQ is a reliable tool to describe performance of toll road operator from users perspective. The results from PLS modelling with TRSQ shows correlation between satisfaction and expectation from toll road users. Based on this correlation, accessibility appear to be the most significant dimension for both users satisfaction and expectation.



Meanwhile, officer honesty in transaction indicates the highest loading factor among other manifests in general. However, this study results in low value of R square on 6 out of 11 toll road samples. It is caused by the use of SEM method with PLS approach to process non parametric data. This approach is done to match the questionnaire data obtained and get the size of the relationship between the variables tested (the value of statistical test results) and the picture of the relationship between the variables indicated by the arrows in the SEM model that was analyzed. The disadvantages of the method used in this study is the lack of matching questionnaire form with the desired model so that some adjustments to the variables are used. This implies that the model needs another type of based on SEM assumption to accommodate each variable's indicators.

5. ACKNOWLEDGEMENT

The authors would like to thank the Indonesia Toll Road Authority (BPJT), the Ministry of Public Works and Housing, for supporting our study by providing primary data from their survey on 2013.

6. REFERENCES

- Anon., 2014. *Peraturan Menteri PU No. 16 Tahun 2014 Tentang Standar Pelayanan Minimum (SPM) Jalan Tol*. s.l.:Kementerian Pekerjaan Umum.
- Bacon, L. D., 1999. *Using LISREL and PLS to Measure Customer Satisfaction*. La Jolla, California, Sawtooth Software Conference Proceedings.
- Bateson, 1995. SERVQUAL: Review, Critique, Research Agenda. *European Journal of Marketing*, 30(1), pp. 8-32.
- Bhakar, S. S., Bhakar, S., Bhakar, S. & Sharma, G., n.d. The Impact Of Co-Branding on Customer Evaluation of Brand Extension.
- Czepiel, J. A., 1990. Service Encounters and Service Relationships: Implications for Research. *Journal of Business Research*, Volume 20, pp. 13-21.
- Ebolli, L. & Mazzulla, G., 2008. Willingness to Pay of Public Transport Users for Improvement in Service Quality. *European Transport*, Volume 38, pp. 107-118.
- Heide, J. & John, G., 1992. Do Norms Matter in Marketing Relationships?. *Journal of Marketing*, Volume 56, pp. 32-44.
- Hox, J. J. & Bechger, T. M., 2007. An Introduction to Structural Equation Modeling. *Family Science Review*, Volume 11, pp. 354-373.
- Kline, R. B., 1998. *Principles and Practice of Structural Equation Modeling*. New York: The Guilford Press.
- Kotler, P., 1995. *Marketing Management*. Jakarta: Erlangga [in Bahasa].
- Ladhari, R., 2009. A Review of Twenty Years of SERVQUAL Research. *International Journal of Quality and Service Sciences*, 1(2), pp. 172-198.
- Monecke, A. & Leisch, F., 2012. semPLS: Structural Equation Modeling Using Partial Least Squares. *Journal of Statistical Software*, 48(3).
- Mosahab, R., Mahamad, O. & Ramayah, T., 2010. Service Quality, Customer Satisfaction and Loyalty: A Test of Mediation. *International Business Research*, 3(4).



- Parasuraman, A., Zeithaml, V. A. & Berry, L. L., 1988. SERVQUAL: A Multiple-Item Scale for Measuring Consumer Perceptions of Service Quality. *Journal of Retailing*, 64(1).
- Ringle, C. M., Sarstedt, M. & Mooi, E. A., 2010. Response-Based Segmentation Using Finite Mixture Partial Least Squares Theoretical Foundations and an Application to American Customer Satisfaction Index Data. Issue In Data Mining, *Annals of Information Systems: R/ Stahlbock et al*, pp. 19-49.
- Ringle, C. M., Sarstedt, M. & Schlittgen, R., n.d. Finite Mixture and Genetic Algorithm Segmentation in Partial Least Squares Path Modeling: Identification of Multiple Segments in Complex Path Models.
- Shahin, A., 2005. *SERVQUAL and Model of Service Quality Gaps: A Framework for Determining and Prioritizing Critical Factors in Delivering Quality Services*. Iran: Department of Management, University of Isfahan.
- Sihombing, L. B., n.d. Toll Road Infrastructure Development in Indonesia: A System Dynamics Perspective.
- Sivadas, E. & Baker-Prewitt, J. L., 2000. An Examination of the Relationship Between Service Quality, Customer Satisfaction and Store Loyalty. *International Journal of Retail and Distribution Management*, 28(2), pp. 73-82.
- Vinzi, V. E., Trinchera, L. & Amato, S., 2010. *PLS Path Modeling: From Foundations to Recent Developments and Open Issues for Model Assessment and Improvement..* Berlin, Germany: Springer Berlin Heidelberg.
- Wong, K. K.-K., 2013. Partial Least Squares Structural Equation Modeling (PLS-SEM) Techniques Using SmartPLS. *Marketing Bulletin*, 24(1).
- Zeithaml, V. A., Parasuraman, A. & Berry, L. L., 1990. *Delivering Quality Service: Balancing Customer Perceptions and Expectations*. New York: Free Press.
- Zuna, H. T., Hadiwardoyo, S. P. & Rahadian, H., 2015. Analyzing Service Quality of Toll Road and Its Relation with Customer Satisfaction in Indonesia using Multivariate Analysis. *Quality in Research*.
- Zuna, H. T., Hadiwardoyo, S. P. & Rahadian, H., 2016. Developing a Model of Toll Road Service Quality using an Artificial Neural Network Approach. *International Journal of Technology*, Volume 4, pp. 562-570.



EFFECT OF PLANTS VETIVERA ZIZANIOIDES (AKAR WANGI) ON PERFORMANCE OF FIELD PLANT SUBSURFACE CONSTRUCTED WETLANDS -MULTILAYER FILTRATION WITH VERTICAL FLOW

Ariani Dwi Astuti *)
Muhammad Lindu *)
Ramadhani Yanidar *)
Maria Manda Kleden *)
ariani_da@trisakti.ac.id

*)Department of Environmental Engineering, FALTL, Trisakti University, Jakarta

ABSTRACT

Canteen wastewater contains high-organic content that have to be treated before being discharged and not contaminating the water stream. Most of Senior High Schools in DKI Jakarta do not have canteen wastewater treatment plant. Nowadays there are more than 172 Senior High Schools in DKI Jakarta. A subsurface constructed wetland (SCW) field plants were designed, implemented and operated at a Senior High School, in Jakarta Selatan. The type of SCW was multilayer filtration (MLF) type with vertical flow and have successfully been used for the treatment of a real canteen wastewater. The SCW-MLF field plants was operated at a hydrolic load of 6.9 m³/day and the organic loading rate was 1.43-8.3 kg BOD/day. The SCW-MLF field plants units were planted with *Vetivera zizanioides*. Monitoring and evaluation of the performance of the units were carried out through regular physico-chemical of the inlet and outlet wastewater. The results indicated significant removals of different pollutants in SCW-MLF in terms of COD, BOD, TKN, TP and oil and grease. The removal efficiencies of COD, BOD, TKN, and TP were 70.5%, 75%, 62.6%, and 54.3%. The COD and BOD organic loading at SCW-MLF were 917.08 – 4.126,84 kg COD/Ha/day and 309.78 – 850.73 kg BOD/Ha/day. In order to study the influence of vegetation in TN and TP removal processes, a pilot unit multilayer filtration (MLF) was operated with the same surface hydrolic loading. The removal efficiencies of COD, BOD, TKN, and TP were 41.9%, 51.4%, 19.8%, and 36.6% in MLF. The SCW-MLF proved to be more efficient than MLF not only in COD, BOD, oil and grease removals but also for TKN, TP because of the vegetation. In conclusion SCW-MLF is proved to be effective for canteen wastewater treatment due to its function as a garden and high quality effluent that complied with Ministry of Environment and Forestry's Standard for wastewater Nr. P.68/2016 for COD, BOD, and TKN.

Keywords: Multilayer Filtration, Organic loading, Removal Efficiency, Subsurface Constructed Wetlands, Vegetation

1. INTRODUCTION

In Jakarta, there are more than 176 Senior High School and Vocational School, but most of them do not have a wastewater treatment plant (WWTP), wastewater generated directly discharged into receiving water bodies. Wastewater produced by the schools not only wastewater from toilets or bathrooms but also from the canteen/cafeteria. Canteen wastewater contains high-organic content that have to be treated before being discharged.

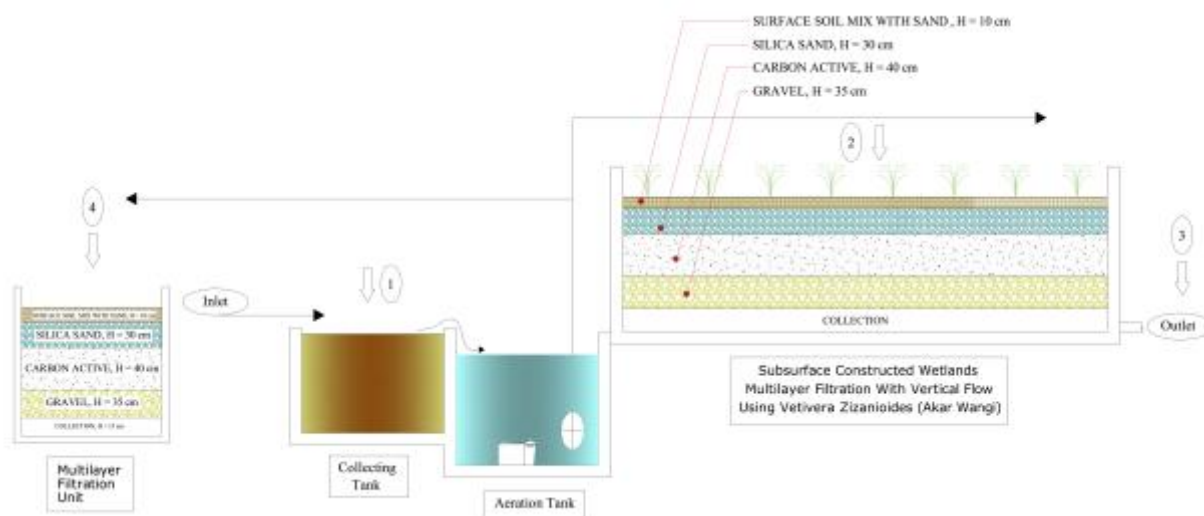


Constructed wetland is planned or controlled system which has been designed and constructed using natural processes that involve vegetation, media, and microorganisms to treat wastewater (Mengzhi, 2009). Constructed Wetlands are widely used as advanced treatment of wastewater, in various countries to treat domestic and non-domestic wastewater, but not for canteen wastewater treatment that containing high concentrations of organic compound. Some researches in constructed wetlands conducted to process wastewater containing low concentrations of heavy metals and do not use multilayer filtration. Vertical wetlands treated domestic wastewater achieved 99% COD removal (Tanner et al. 2012). Therefore, it is necessary to study the canteen wastewater treatment by combining biofilter and constructed wetlands that are expected to be a canteen wastewater treatment alternative which is simple because it does not require complicated technology, it is cheaper in terms of cost of manufacture and operation as well as maintenance, and more natural (US EPA, 2000). *Vetiveria zizanioides* can reduce dissolved P by 99% after three weeks and 74% N dissolved after five weeks. This study was carried out to evaluate the potential of *Vetiveria zizanioides* in subsurface constructed wetland multilayer filtration (SCW-MLF) vertical flow treated high-organic wastewater. The performance of planted subsurface constructed wetland Multilayer Filtration (SCW-MLF) versus unplanted Multilayer Filtration (MLF) was evaluated. Based on the performance data, removal rate constants were calculated dan the growth of *Vetiveria zizanioides* were measured. The study aims to document for the first time that *Vetiveria zizanioides* can be used in constructed wetland multilayer filtration systems for the treatment of high-organic wastewater.

2. METHODOLOGY/ EXPERIMENTAL

2.1. Experimental Setup

The wastewater treatment unit was located at a Senior High School in Jakarta Selatan and consisted of collecting tank (0.75 m x 0.84 m x 0.55 m) and aeration tank (1.5 m x 0.84 m x 0.7 m) as preliminary treatment process, then flowed in parallel to biofilter tank (Multilayer filtration-MLF) and subsurface constructed wetland multilayer filtration type vertical flow (SCW-MLF) for advanced treatment (Figure 1).



1, 2, 3 and 4 : point of sampling

Figure 1. Scheme of SCW-MLF and MLF Units



Due to topography of the site and water distribution, the facility was equipped with pump. The depth of the reactor also being adjusted to surface water level and the depth of existing drainage system. The SCW-MLF (15 m x 0.84 m x 1.05 m) with *Vetivera Zizanioides* unit was designed with vertical flow type and has detention time of 17.76 hours. SCW-MLF and Multilayer filtration-MLF is designed with the same surface loading rate.

2.3 Water analysis

Water samples were collected from sampling point and analysis was performed immediately for dissolved oxygen (DO) and pH. Chemical oxygen demand (COD), total Kjeldal nitrogen (TKN), and total phosphorus (TP) were determined according to the Standard Methods (APHA, 1998). Removal efficiency was calculated by the percentage of deduction in concentration for each pollutant as follows: removal efficiency = $(1 - C_{eff}/C_{inf}) \times 100\%$, where C_{inf} and C_{eff} the influent and effluent concentrations in mg/L. Environmental physical factor such as temperature and humidity also has been measured.

2.4 Area Contants

Area contants were calculated according to Moshiri (1993)

$$A = \frac{Q \times \ln \frac{C_i}{C_e}}{K} \dots\dots\dots(1)$$

A = Areaconstructed wetland (m^2); Q = flowrate influent (m^3/day); C_e = concentration of effluent (mg/L); C_i = concentration of influent (mg/L); K = Area contants (m/day).

Organic loading rate (kg/Ha/day) were calculated as below:

$$\text{Organic loading rate} = \left[\frac{(C_i - C_e) \text{ mg/L} \times 1000}{10^6} \right] \times \frac{Q}{A} \dots\dots\dots(2)$$

3. RESULTS AND DISCUSSION

3.1 Subsurface Constructed Wetland Multilayers Filtration with *Vetivera Zizanioides* Unit (SCW-MLF)

The result of study on SCW-MLF vertical flow with *Vetivera Zizanioides* in order to treat COD, BOD, TKN, and TP in canteen’s wastewater is shown in Figure 2, and 3.

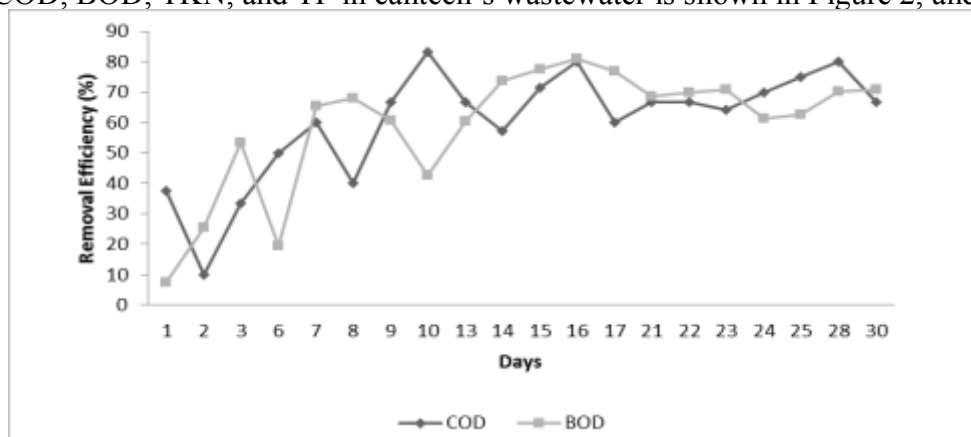


Figure 2. Removal Efficiency of COD and BOD in SCW-MLF

Based on Figure 2, SCW-MLF vertical flow with *Vetivera Zizanioides* has effectively removed COD and BOD parameter. The removal efficiency of COD treatment in steady state was 64.29% - 80%. The SCW-MLF type vertical flow with *Vetivera Zizanioides*



has organic loading rate as much as 971.08 - 4126.84 kg COD/Ha/day. The research result showed that COD concentration of effluent was 83 mg/L and complied with the quality standard of domestic wastewater Nr. P.68/2016 according to the Ministry of Environment and Forestry. The standard of COD concentration is 100 mg/L.

Based on observation and water analysis, plant has quite significant effect in reducing BOD as indicated by laboratory analysis result on day-30 on which the effluent standard was 30 mg/L and thus complied with the regulation requirement. The highest BOD concentration in outlet was on day-2 at 382.55 mg/L and the lowest was 26 mg/L on day-30. Based on the graph, BOD treatment efficiency at steady state was 61.2% - 70.8%. During high concentration on day-24 at 225 mg/L, treatment efficiency was 61.2%, while on low concentration at 94 mg/L the efficiency was 70.8%. The SCW-MLF type vertical flow with *Vetivera Zizanioides* has organic loading rates as much as 309.78 – 850.73 kg BOD/Ha/Day, this results much higher compared to organic loading rate of CW for Domestic wastewater according to Moshiri (1993) 150 kg BOD/Ha/Day. Result of analysis of TP and TKN on outlet of SCW-MLF type vertical flow with *Vetivera Zizanioides* shown in Figure 3.

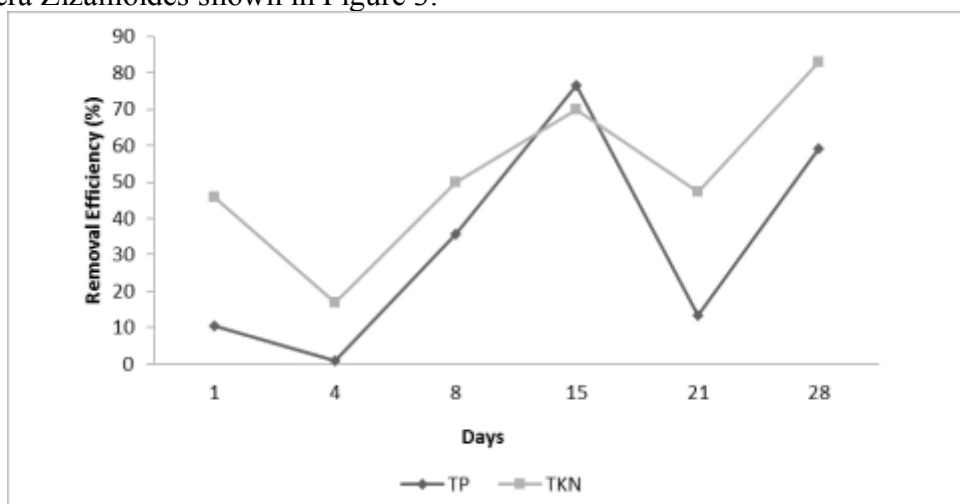
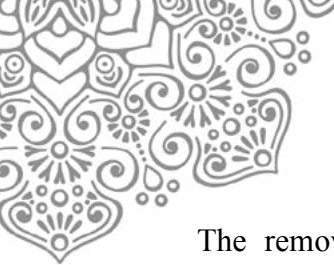


Figure 3. Removal Efficiency of TP and TKN in SCW-MLF

The removal efficiency of TP on SCW-MLF vertical flow with *Vetivera Zizanioides* was 45.71% - 76.54%, while the removal efficiency of TKN was 10.37% - 77.13%. This result indicates that the unit is effective in reducing the two parameters and in line with research conducted by Zheng *et al.* in China (1997) that *Vetivera Zizanioides* can be used to treat high concentration of dissolved N and P in a eutrophicated river, removal efficiency of dissolved P reached to 99% after three weeks and 74% of dissolved N after five weeks. This shows that SCW-MLF vertical flow with *Vetivera Zizanioides* is very effective in the removal of these two organic matters. The plant has the ability to reduce TKN and TP parameter in wastewater and use TKN and TP as nutrient for its growth and reproduction. TKN and TP substance in SCW-MLF was transformed into organic and inorganic matter by microorganism through decomposition and synthesis process.

The removal of TP in SCW-MLF vertical flow with *Vetivera Zizanioides* was possible due to soil adsorption, plant absorption and removal by microorganism living in the roots and stem. Phosphate was converted into orthophosphate and was able to be absorbed by the plant. Transformation process was affected by environment's abiotic factors; sunlight, air medium and biotic factors such as microbes and plant.



The removal of nitrogen concentration in SCW-MLF vertical flow with *Vetivera Zizanioides* was possible due to ammonification which followed by nitrification, assimilation, fixation and denitrification processes. Nitrogen fixation is conversion of nitrogen in gas form into organic nitrogen by certain microorganism with nitrogenase enzyme. The reaction can take place in aerobic and anaerobic condition by bacteria. Nitrogen fixation occurred in water surface, sedimentation, plant rhizosphere and leaves surface as well as stem. Nitrogen assimilation is the process on which plant assimilate the nitrogen. Plant reduce inorganic nitrogen into organic nitrogen that will be used by plant tissue. Plant use a large amount of nitrogen during growth phase.

The dissolved oxygen on outlet of the treatment unit was 3.02 - 3.36 mg O₂/L which indicates the process was aerobic. The measurement of pH of SCW-MLF outlet with *Vetivera zizanioides* was 6.5 - 7.6 which shows that the average pH condition is optimum and is a supporting factor in bacterial growth.

Organic loading rates of phosphate was 0.66 – 17.08 kg/Ha/day or 0.24 - 6.15 ton/Ha/year, while organic loading rates of nitrogen removed was 3.09 - 60.18 kg/Ha/day or 1.12 – 21.66 ton P/Ha/year. Several authors mentioned that *Vetivera zizanioides* has the potential to remove 54 Ton P/Ha/year and 102 ton N/Ha/year. Chang et al. (2012) treated domestic wastewater using *Typha orientalis* and *Arundo donax* var. *versicolor* and has mean mass removal of rate 44.3 gr/m²/day or 443 kg/Ha/day for COD; 1.27 gr/m²/day or 12.7 kg/Ha/day for TN; 0.39 gr/m²/day or 3.9 kg/Ha/day for TP.

3.2 Multilayers Filtration Unit (MLF)

The objective of treatment using MLF was to evaluate the effectiveness of *Vetivera Zizanioides* on SCW-MLF vertical flow with *Vetivera zizanioides*. The MLF unit is designed at the same setting and layer without any plant. Attached growth process is also known as biofilter method in which microbes mass grow attached to the medium. The medium used in MLF unit is similar those in SCW-MLF vertical flow with *Vetivera Zizanioides*.

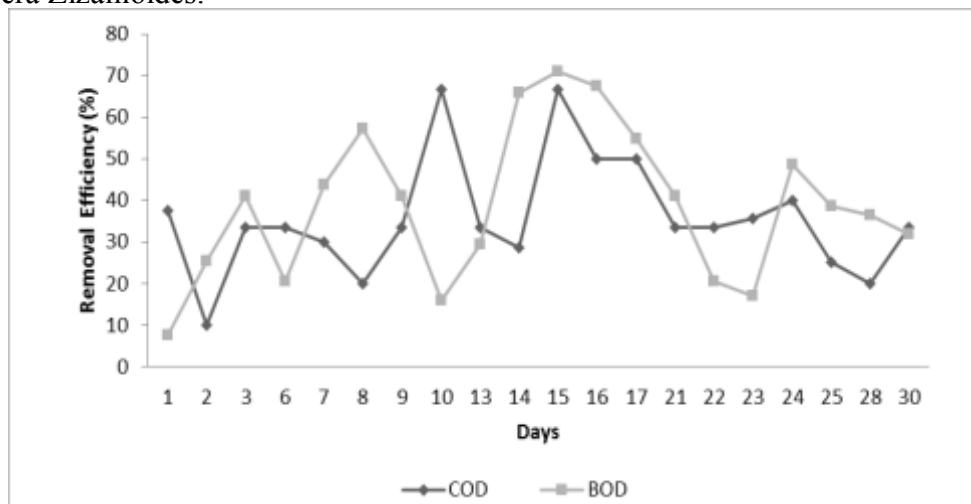


Figure 4. Removal Efficiency of COD and BOD in MLF

Based on Figure 4, COD concentration removal in MLF unit at steady state (day-21 – day-30) was 20% - 40% which indicate that there was biological treatment occurred in this unit eventhough with lower efficiency compare to that of SCW-MLF vertical flow with *Vetivera Zizanioides*. The removal efficiency of this unit has declining trend due to the high input loading. COD concentration of MLF outlet in steady state was 749 – 166



mg/L. The standard required by the regulation of Ministry of Environment and Forestry Nr. P.68/2016 which is 100 mg/L. The figure also pointed out that BOD concentration removal in MLF unit at steady state (day-21 – day-30) was 15% - 48.51%. Concentration of MLF BOD outlet at steady state was 181 - 62 mg/L. This concentration is higher than regulation which is 30 mg/L. This MLF unit has COD organic loading rate as much as 9.24 - 545.41 kgBOD/Ha/day.

Removal efficiency of TP concentration in MLF was 0.56% - 41.08%, while removal efficiency of TKN was 2.56% - 33.33% as can be seen in Figure 6. Treatment efficiency in MLF unit was fluctuated with a declining trend and lower when compared to SCW-MLF type vertical flow with *Vetivera zizanioides*. Dissolved oxygen rate of 3.69 - 4.02 mg O₂/L indicates that the process was in aerobic flow condition. The measurement of pH was 6.7 – 7.3 shows that average pH condition is optimum pH and a supporting factor in bacterial growth.

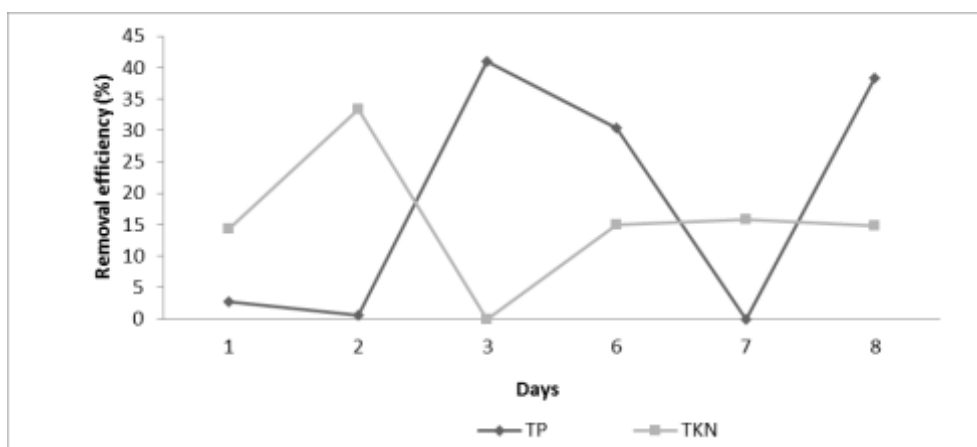


Figure 5. Removal Efficiency of TP and TKN in MLF

3.3 Effect of *Vetivera Zizanioides* to the Efficiency of Canteen Wastewater Treatment

The removal of COD in SCW-MLF vertical flow with *Vetivera Zizanioides* unit was 69.24% - 80%, while MLF unit without plant was 20% - 40.7%. The BOD removal in SCW-MLF vertical flow with *Vetivera Zizanioides* unit was 61.2% - 70.8% while MLF unit without plant was 15% - 48.51%. The comparison of COD between aeration tank outlet, outlet of SCW-MLF vertical flow with *Vetivera Zizanioides* unit and outlet of MLF unit without plant is shown in Figure 6.

On the first week, effluent concentration on each unit for both COD and BOD parameter was almost in the same level, however the difference was significant after that period. Treatment efficiency on SCW-MLF vertical flow with *Vetivera Zizanioides* increased linear with the growth of plant. According to Vymazal (2010), Abou-elela et al. (2013) vertical flow SCW results high removal efficiency of TP, TN and NH₄-N. The higher the plant and the more leaves growth, the roots also growth and thus plant ability to absorb organic material was higher. Furthermore, the deeper and spread out the roots were, the microorganism around the roots were more abundant. These increased the removal efficiency of SCW-MLF vertical flow with *Vetivera zizanioides*. SCW-MLF were affected by medium, the roots of *Vetivera zizanioides* and microorganism living in both medium, while MLF unit affected only by 2 factors, the medium and microorganism living in it. That is the explanation why microorganism



capacity in MLF unit was less effective compared to SCW-MLF with *Vetivera Zizanioides* unit. The result was similar with the analysis of Negisa *et al.* (2014) on oil palm industry. *Vetivera zizanioides* was able to remove COD on low concentration Palm Oil Mill Effluent (POME) by 94% and 39% at high concentration POME. *Vetivera Zizanioides* was able to remove BOD by 90% at minimum concentration POME and 60% at maximum concentration POME, while control set (without plant) was only able to remove 15% of BOD.

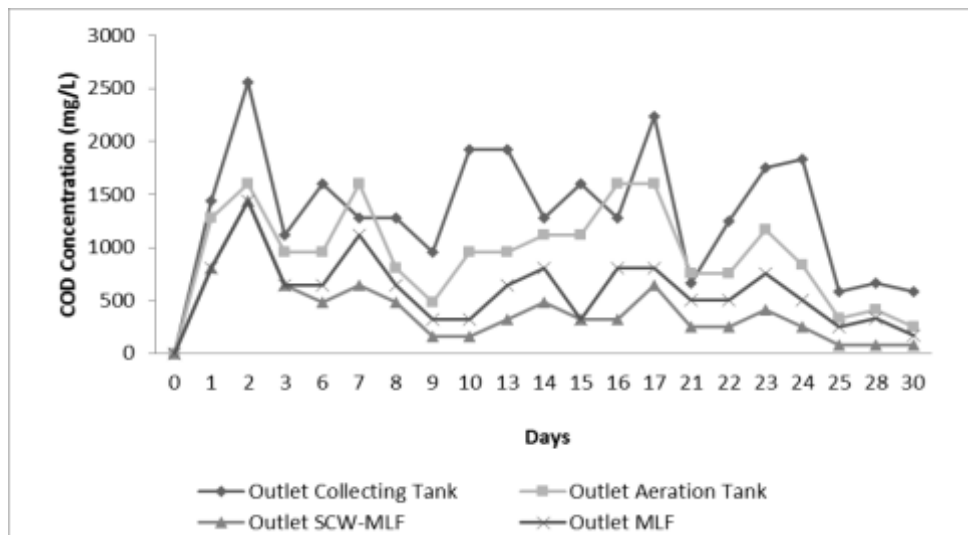


Figure 6. COD Concentration in Outlet Units

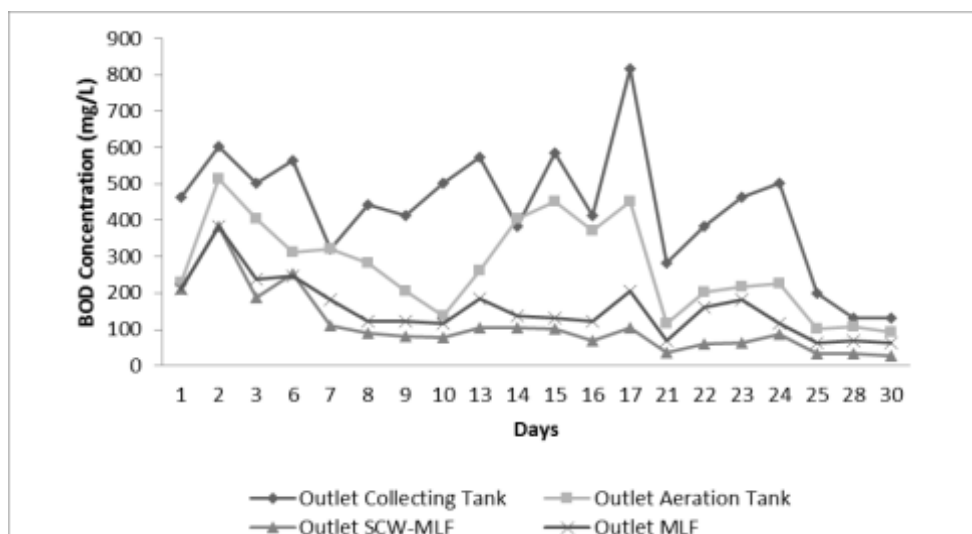


Figure 7. BOD Concentration in Outlet Units

Removal efficiency of TP in SCW-MLF vertical flow with *Vetivera Zizanioides* was 45.71% - 76.54%, while removal on MLF unit without plant was 0.56% - 41.08%. Removal efficiency of TKN with *Vetivera Zizanioides* unit was 10.37% - 77.13% while MLF unit without plant was 2.56% - 33.33%. The graph compared TP and TKN parameter in aeration tank outlet, in outlet of SCW-MLF vertical flow with *Vetivera Zizanioides* and outlet of MLF without plant is shown in Figure 8 and 9.

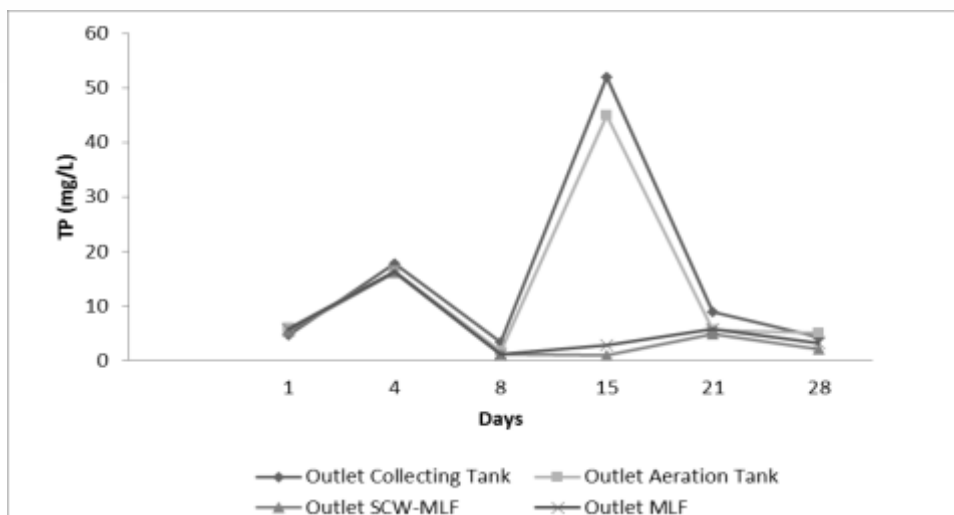


Figure 8. TP Concentration in Outlet Units

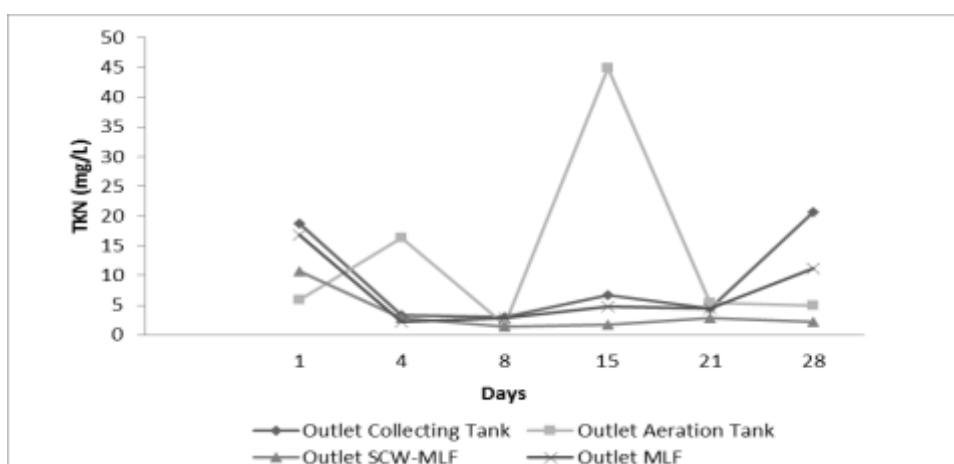


Figure 9. TKN Concentration in Outlet Units

TKN removal on SCW-MLF unit was possible due to ammonification which followed by nitrification, assimilation and fixation processes. In MLF unit, only ammonification and nitrification process occurred because assimilation process can only be done where plant existed. It caused the removal efficiency of SCW-MLF is higher compared to MLF. Plant use biomass from microorganism metabolism into N, P, CO₂, H₂O and simple organic compound to provide nutrient for its growth and reproduction. The biomass surplus will be cultivated in roots. Aerobic microorganism uses the remaining carbon, phosphate and nitrogen to form new cells and convert some of them into energy. Oxygen function as electron acceptor during oxidation of organic material and the reaction will stop when oxygen was no longer available. Plant has an important role in reducing pollutant : organic matter, nitrogen and phosphorus (Gikas & Tsihrantzis 2012). This results is similar with research by Hoang et al. (2011) with *Sesbania sesban* and Konnerup et al. (2008) with *Canna* and *Heliconia*. There are four function/benefit of plant; as filter for suspended solid material, growth medium of microorganism, root supply oxygen into the medium and maintain substrate (Tchobanoglous, 1987, Brix, 1993 in Moshiri, 1993).



In this study, indication of growth and reproduction of *Vetivera Zizanioides* were height and growth of new shoots. The average plant height after acclimatization (during planting) was 60.5 cm. Height of plant was measured for 30 days during research period. In addition, *Vetivera zizanioides* also remove the odor and vector that usually lived in wastewater or stagnant water such as mosquito, flies, etc. Further more, *Vetivera Zizanioides* in canteen wastewater treatment unit give a beautiful landscape view. Area contants in each unit were calculated and compared to area contants according to Moshiri (1993) as can be seen in Table 2.

Table 2. Area Contants at SCW-MLF and MLF

No.	Parameter	K of SCW-MLF (m/day)	K of MLF (m/day)	K of Moshiri (m/day)
1.	COD	0,568 – 0,887	0,1229 – 0,284	0,055 – 0,16
2.	BOD	0,55 – 0,78	0,009 – 0,320	0,027 – 0,18
3.	TKN	0,35 – 0,98	0,09	0,033 – 0,55
4.	TP	0,08 – 0,79	0,09 – 0,20	0,027 – 0,033

Two-sided t test was used to detect any significant differences on the mean with and without plants of different parameter and pollutant removal efficiencies of the two units, with $p < 0.05$ defined that there is significant difference in SCW-MLF with plants compare to MLF without plants, t calculation more than t table as can be seen at Table 3.

Table 3. T-Test Results

No.	Parameter	T calculation	T Table
1.	COD	6.166	1.729
2.	BOD	5.172	1.729
3.	TKN	2.417	2.015
4.	TAPI	2.358	2.015
5.	Oil and Grease	2.471	2.015

4. CONCLUSION

SCW-MLF vertical flow with *Vetivera Zizanioides* unit is effectively reduced concentrations of COD, BOD, TP, TKN in the canteen wastewater compared to those in MLF. SCW-MLF were affected by medium in multylayer, the roots of *Vetivera zizanioides* and microorganism living in both medium, while MLF unit affected only by 2 factors, the medium and microorganism living in it. SCW-MLF can be an alternative canteen wastewater treatment that is low cost in operational and give a beautiful landscape view. Besides no odors or insects were detected during the operation of SCW-MLF.

5. ACKNOWLEDGEMENT

This work was supported by grants from Directorate for Research and Community Services Directorate General of Strengthening Research and Development Ministry for Research, Technology and Higher Education In accordance with the Agreement Assignment Implementation Research Grant Nr. 003 / SP2H / LT / DRPM / III / 2016 and Nr. 214 / SP2H / LT / DRPM / III / 2016, February 17th, 2016 and March 10th, 2016.



6. REFERENCES

- Abou-elela, S.I. et al., (2013). Municipal wastewater treatment in horizontal and vertical flows constructed wetlands. *Ecological Engineering*, 61, pp.460–468. Available at: <http://dx.doi.org/10.1016/j.ecoleng.2013.10.010>.
- APHA, (2012), Standard Methods For The Examination of Water and Wastewater, American Public Health Association, American Water Works Association, Water Environment Federation, Washington DC, United State of America.
- Chan Y.J., Chong M.F., Law C.L., Hassell D.G., (2009), *Chemical Engineering Journal*, Volume 155, pp. 1–18.
- Chang, J. et al., (2012). Treatment performance of integrated vertical-flow constructed wetland plots for domestic wastewater. *Ecological Engineering*, 44, pp.152–159. Available at: <http://dx.doi.org/10.1016/j.ecoleng.2012.03.019>.
- Crites, R., Tchobanoglaus, G., (1998), *Small and Decentralized Wastewater Management Systems : Wetlands and Aquatic Treatment Systems*, Mc Graw-Hill, Singapore.
- Gikas, G.D. & Tsihrintzis, V.A., (2012). Short communication A small-size vertical flow constructed wetland for on-site treatment of household wastewater. *Ecological Engineering*, 44, pp.337–343. Available at <http://dx.doi.org/10.1016/j.ecoleng.2012.04.016>.
- Hoang, T. et al., 2011. Treatment of high-strength wastewater in tropical constructed wetlands planted with *Sesbania sesban* : Horizontal subsurface flow versus vertical downflow. *Ecological Engineering*, 37(5), pp.711–720. Available at: <http://dx.doi.org/10.1016/j.ecoleng.2010.07.030>.
- Konnerup, D., Koottatep, T. & Brix, H., 2008. Treatment of domestic wastewater in tropical , subsurface flow constructed wetlands planted with *Canna* and *Heliconia*. , 5, pp.248–257.
- Moshiri, G.A., (1993), *Constructed Wetland for Water Quality Improvement*, Lewis Publishers, London.
- Ministry of Environment and Forestry’s Regulation for domestic wastewater standard Nr. P.68/2016
- Negisa et al., (2014), Phytoremediation Potential of Vetiver System Technology for Improving the Quality of Palm Oil Mill Effluent. Hindawi Publishing Corporation *Advances in Materials Science and Engineering*. Volume 2014, Article ID 683579, 10 pages <http://dx.doi.org/10.1155/2014/683579>
- Tanner, C.C. et al., 2012. Constructed wetlands and denitrifying bioreactors for on-site and decentralised wastewater treatment: Comparison of five alternative configurations. *Ecological Engineering*, 42, pp.112–123. Available at: <http://dx.doi.org/10.1016/j.ecoleng.2012.01.022>.
- US-EPA, 2000. *Constructed Wetland Treatment for Municipal Wastewater*. United States Environmental Protection Agency, EPA/625/R-99/010. Office of Research and Development, Cincinnati.
- Vymazal, J., (2010), *Constructed Wetlands for Wastewater Treatment*. Water 2010, Volume 2, pp. 530-549, www.mdpi.com/journal/water



Identification of Country Standard Measureable Influence Indicators on Construction Project Duration Performance in Indonesia

Basuki Anondho,¹; Ayomi Dita Rarasati²; Yusuf Latief³; Khrisna Mochtar,⁴

Abstract:

The duration of construction project implies a complex interaction with various aspects that affect or influence the duration itself. Developing a descriptive model to determine those dominant influence variables should give an alternative option on duration prediction models and provide convenience to understand the practical purpose. This practical purpose needs a measureable indicator factor that commonly provides such like official country statistical data. Since there are lot of country statistical data, identifying measureable indicators become important as dominant influence indicators on construction project duration. The current research describes step by step identifying dominant influence external factors in building construction project in Jakarta, Indonesia. The process started with literature selection to identify factors influence the performance of construction industry. The output of literature study was followed by exploratory phase to analyzing the output of questionnaire based on the literature study. Exploratory phase reduce and grouping factors by identifying dominant factors so it accommodates the practical purpose. The next phase was confirmatory by analyzing dominant factors in an integrated relation system. At this phase, the floor area and number of story are included in the system using Partial Least Square – Structural Equation Modelling (PLS-SEM). The results show that the rates of exchange currency value, interest, inflation, GDP, absorb of new technology, labor availability, materials price are the dominant indicators out of 12 origin indicators.

Keywords:

Measureable Indicators, Factors Analysis, PLS-SEM, Influence Variable, Project Duration

Introduction

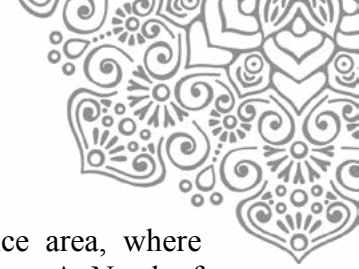
There is no doubt that duration prediction is a one of key success factors since it becomes the base of budgeting, planning, implementation, monitoring and even for litigation purposes (Skitmore et al. 2003). Construction project duration prediction is one of several key factors to be considered before starting the project. It determines the success or fail of a construction project (Nguyen et al. 2013). Therefore, developing a supporting model for construction project duration prediction is the first and essential step in a project construction. The duration of construction project implies a complex interaction with various aspects that affect or influence each other. A descriptive model that can determine the dominant variables should provide variation on the developed prediction models and provide convenience to understand the practical purpose (Dursun and Stoy, 2012). Several previous studies have already identified this problem as construction productivity factors that affect the overall company performance and

¹ Ph.D Candidate at Universitas Indonesia, Jakarta, Lecturer at Tarumanagara University, Jakarta.

² Lecturer at Construction and Project Management Postgraduate Program, Department of Civil Engineering Universitas Indonesia.

³ Professor at Construction and Project Management Postgraduate Program, Department of Civil Engineering Universitas Indonesia.

⁴ Lecturer at Construction and Project Management Postgraduate Program Department of Civil Engineering Universitas Indonesia, Professor at Department of Civil Engineering Institut Teknologi Indonesia.



country development (El-gohary et al, 2014). The problem is for a difference area, where uncertainty occurs; there will be a difference construction project performance. A Need of prevalent influence factors or indicators becomes one of the solutions for duration estimation.

The study carried out by Chan et al, (2004) show that there are five major group of latent independent variables influence the project success, including duration prediction. The result identifies 6 external factors influenced the project performance, which are: Economic environment, Social environment, Political environment, Physical environment, Industrial environment and Technology advanced. The research was aimed at conducting a review on literature for identifies critical success factors on construction project. This descriptive research conducted by using seven major journals and one of the outputs is external environment that has several factors. *Dai et al (2009)* was also conducted a qualitative research to identify several latent variables that influenced human resource productivity by using analysis factor method. Some identify latent factors were: Tool equipment which represents technology, Project management and human resource qualification. Political risks, Economic risks, Adequacy of funding also represent of economic, Constructability and Pioneering represent of technology are some influence external factors (*Hwang, 2013*). A further study on external factors by Anondho et al (2014) was conducted by using questioner with factors analysis and structural equation model method to indicate dominant country standard measureable indicators. The choice of country standard measureable indicators is to meets difference area requisite. Those summarize of previous research shows that external latent variables could be divided into 3 main influenced variables which are: Economic, Human Resource and Technology. Base on this concept, indicators identify by search on BPS tables related to those variables.

The different between this research with the previous one is that this research add floor area and number of storeys as internal factors in the integrated system, corresponding to some researcher recommendation as describe below. Both methods were used for reducing indicator and accommodating the latent variables. Starting with literature study on 38 journals as descriptive indicators and variables identification of other previous researches. The resume of the study was used as questions on the questioner. Those previous research approaches on construction duration prediction have some notes as side conclusions. Kumaraswamy and Chan (1995) state that the construction duration also depends on technical parameters such as the total gross floor area and the number of storey in a building. Several researches based on Bromilow's BTC duration estimation formula, also found that the speed of construction tends to decrease when gross floor area decreases and/or the number of floor levels increases (Love et al. 2005). A repetition research in Germany, conducted by Dursun et al, (2012), state that the research analyses indicated gross external floor area is relating to the construction of the building for describing construction duration.

This paper describe a propose development model to accommodate both influence external factors and technical internal parameters such as the total gross floor area and the number of storey in a single frame of partial least square method to identify dominant and useful factors on duration estimation. The result of factors identification and reducing makes number of an influence factors less for practical use on estimating project duration purpose, especially for Indonesia as a developing county.

Methodology

Based on previous study stated above, a systematic step is planned as a methodology of the present research. It started with literature study to indicate at least the latent variables as main



variables. Furthermore, those identified latent variables are broken down into factors or indicators contained in the official statistics agency, which generally provided by the local government. By doing this, an indicator has a specific measure for a certain area.

Base on those indicators, a questioner is being constructed and distribute to estimator, site manager or project manager as respondent in several construction projects. Input questioners processed by factor analysis to reduce indicators and grouping new latent variables as identification dominant indicators.

Factors analysis result processed in an integrated model with floor are and number of storeys, internal factors as recommended, in partial least square method as the last stage of indicators identification. Detail of the methodology shown in figure 1.

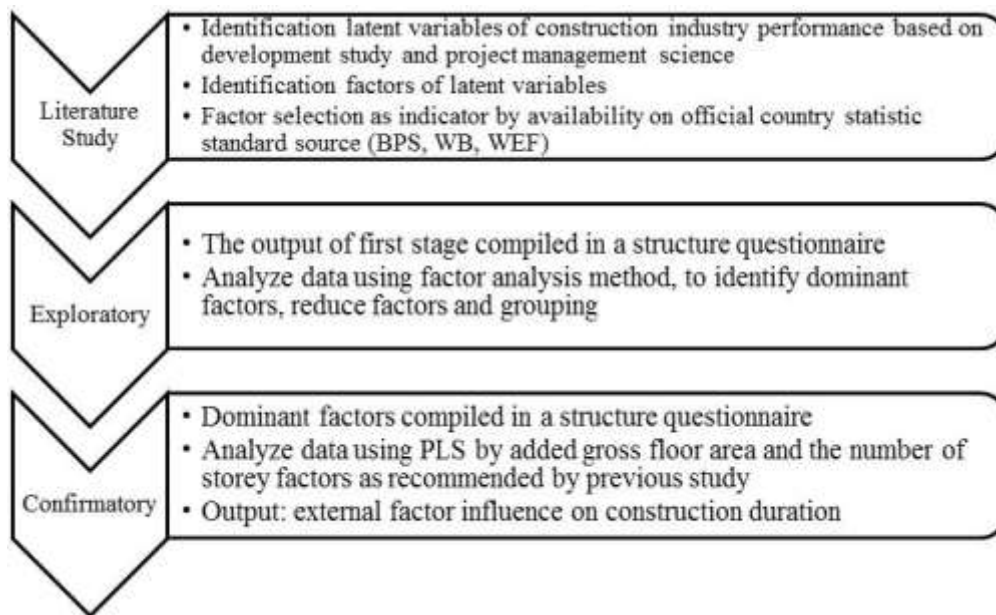
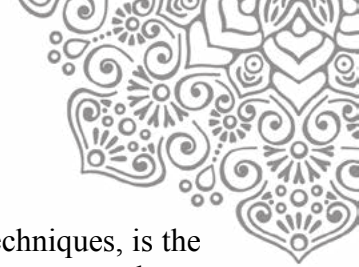


Figure 1: Identification step to reduce and select dominant indicator

Step 1: The goal of literature selection is to integrate and summarize what is known in an area. A review pulls together and synthesizes different results. It collects what is known up to a point in time and indicates the direction for future research (Neuman, 2006). It starts with identification main group or latent variables that influence the performance or duration of construction project derive on development study. Next, literature selection is to breakdown each latent variable into factor based on previous study in journals. Last literature identification is matching each factor with indicator provide by official institution which transform them into measurable indicator.

Step 2: Factor analysis is being used in exploratory to practical used purpose. Factor analysis is a multivariate technique and the primary advantage of multivariate techniques is their ability to accommodate multiple variables in an attempt to understand the complex relationships not possible with univariate and bivariate methods. Dominant factors, grouping and factor reduction, can be achieved by identify the separate dimensions of the structure and then determine the extent to which variable is explained by each dimension. Once these dimensions and the explanation of each variable are determined, the two primary uses for factor analysis- summarization and data reduction can be achieved. Data reduction can be achieved by calculating score for each underlying dimension and substituting them for the original variables



(Hair et al., 1998). The starting point in factor analysis, as with other statistical techniques, is the research problem. The general purpose of factor analytic techniques is to find a way to condense (summarize) the information contained in a number of original variables into a smaller set of new composite dimensions or variates (factors) with a minimum loss of information, to search for and define the fundamental constructs or dimensions assumed to underlie the original variables.

Step 3: The aim of using partial least square based structural equation modeling (PLS-SEM) is to predicting or develops a theory (Sarwono et al, 2015). Structural equation modeling based on Partial Least Square is used to predict and develop a theory as research goals. It different from structural equation modeling based on covariant. Covariant base is used to test an existing theory. In this research, confirmatory is the main purpose on indicators and variables produced by step 2 in an integrated model. The benefit of using PLS-SEM it doesn't need normality and a large amount of data. Since construction project data naturally has a few amounts in a particular area, using PLS SEM is a proper method to multivariate analyzes. Another advantage of SEM-PLS method, it accommodate both formative and reflective at the same time so the construction duration depends on both technical parameters and external influence factors include in a one system.

Results and Discussion

Step 1: Literature Study Identification

According to Budiono (2009), factors that affect the growth of a country are economic factors that influenced the investment in construction, quality of human resources, and the level of used technology. It is similar with above previous researches summarize. The search on BPS data gives 12 standard measureable indicators identified in this first part which grouped in three latent variables which are: Inflation(A1), Materials price index(A2), Gross domestic product(A3), Exchange rate(A4) and Interest rate(A5) on Economics latent variable, Labor availability rate(B1), Works experience rate(B2), Education level rate(B3), Health human indeks (B4) on Human Resource latent variable and New technology availability(C1), Absorb of new technology rate(C2) and Innovation rate(C3) on Technology latent variable . Those 3 latent variables group is also derived from literature study, including several economics development text books. The 12 indicators become a question in the questioner that distributed to certain respondents with range of qualification between estimators to project manager.

Step 2: Exploratory (Reduce and Dominant Factors Identification)

	Component		
	1	2	
A4	.885	.140	Exchange currency value
A5	.861	.180	Interest rate
A1	.801	.324	Inflation rate
A3	.794	.347	GDP rate
B3	.564	.231	Education rate
C2	.563	.531	Absorb of new technology rate
B1	.351	.734	labor availability rate
A2	.074	.691	Materials price rate
B2	.200	.674	Labor Experience rate
C1	.436	.506	New technology availability

Figure 2: SPSS® v.20 Factors Analysis output



Identify dominant variables analysis using analysis factor reduces 12 indicator into 10 dominant selected indicators and grouping into 2 exploratory variable groups

The output of factors analysis using SPSS[®] program version 20 tool grouping indicators into 2 groups with certain indicators each which are:

- Group 1 consists of: Exchange rate (A4), Interest rate (A5), Influence rate (A1), GDP (A3), Level of education rate (B3), Absorb new technology index (C2) in decline loading factor order as dominant factors.
- Group 2 consist of: Labor availability index (B1), Materials price rate (A2), Labor experience rate (B2) and Avaibility new technology index (C1) also in decline loading factor order as dominant factors.

It gives 2 major influence variables with several measurable Country Standard influence indicators each. Each group could be used as factor influence on duration performance of construction project separately. The reduce of indicators and variables groups through factor analysis technique has successfully explore interdependent factors covariant which eliminate some factors with less loading factor and grouping in similar factors dimension. It well recommended as appropriate tools to determine number of latent variables and identify limited dominant influence factor.

Step 3: Confirmatory (Dominant Factors Identification in Integrated Model)

Build the partial least square model in this research, started by modeling each condition as stated. There are three main group stated:

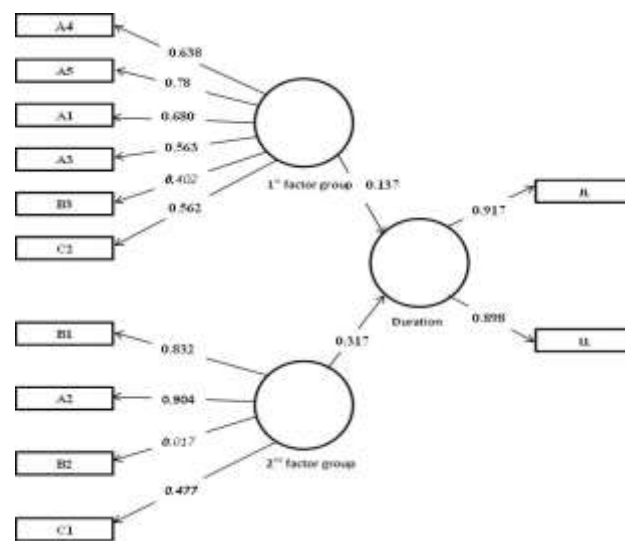


Figure 3: Output of PLS program on factors influence on duration

1. Relation between duration with latent variables
The first step, identify that duration is influenced by 2 group of latent variables as research output. This output is derived from factor analysis.
2. Relation between duration with technical parameter
Several previous research recommend that gross floor area and number of storey factor need to be consider as influence factor on construction project duration. Figure 3 show the represent of the recommendation.
3. Relation between latent variables with its indicators.



Factor analysis in the first step reduces factors and identifies dominant factors and grouping them in several latent group variables. It means that certain latent variables influenced by some indicators.

The next step is merging all components above to integrated external indicators, latent variables and external technical parameter factors as confirmatory. Identification Indicators on construction project duration by applying result factor analyzes data on this PLS model and run the program provide an output that has opportunity to reduce another factor and identify dominant factors in an integrated system. The result of partial least square analysis drops another three factors since those has loading factor less than 0.5. Those three are: B3 (education rate), B2 (Labor experience rate), and C1 (new technology viability) as seen in figure 3. Reducing some factors give researcher an opportunity to choose several method on duration prediction.

Conclusion

This step by step approach in identifying influence and dominant Country Standard Indicator quite successfully reduce 2 indicators and clustering the rest in same category indicators in a group. Further analysis by PLS with involving floor area and number of storey reduce another 3 indicators in an integrated system. The result remains 7 out of 12 indicators divided into 2 groups, which are:

Group I: Exchange rate (A4), Interest rate (A5), Influence rate (A1), GDP (A3), , Absorb new technology index (C2)

Group II: Labor availability index (B1), Materials price rate (A2).

On the basis of the work above, it is shown that factors identification through factors analysis exploratory, followed by least square analysis as confirmatory orderly, has reduced factors in a more systematic way.

Those 2 dimension groups show that duration of certain building construction project influenced by either group I or group 2. By knowing this, a duration estimate method could be improved by considering those 2 groups. This is another gain of the research in addition to reduce number of influence factors for practice purpose.

However, developing more basic factors as the input variables is still possible, since a various country development rate indicators is available for further research to explore. Number of respondent is another alternative to develop an incisive research.

Reference

- Anondho, Basuki; Soeleiman, Lydiawati (2014). *Identifikasi Faktor Pengaruh Terukur Terhadap Durasi Probabilistik Proyek Konstruksi Di Jakarta*. Jakarta: Hibah Bersaing DIKTI.
- Boediono. (2009). *Ekonomi Indonesia, Mau ke Mana?*. Jakarta : Kepustakaan Populer Gramedia.
- Chan, Albert P. C; Scott, David; Chan, Ada P. L. (). *“Factors Affecting the Success of a Construction Project”*. 2004, ASCE/Februari
- Dai, Jiukun; Goodrum, Paul M; Maloney, William F; dan Srinivasan, Cidambi. (2009). *“Latent Structures of the Factors Affecting Construction Labor Productivity”*. ASCE: Journal of Construction Engineering and Management, Vol. 135, No. 5.



- Dursun, Onur and Stoy, Christian: “*Determinants of construction duration for building projects in Germany*”; Engineering, Construction and Architectural Management Vol. 19 No. 4, 2012
- El-Gohary, Khaled Mahmoud, M.Eng; and Aziz, Remon Fayek, Ph.D. “*Factors Influencing Construction Labor Productivity in Egypt*”, Journal of Management in Engineering @ ASCE; January/February 2014.
- Hair Jr, Joseph F; Anderson’ Rolph E; Tatham’ Ronalf L; Black, William C. “*Multivariate Data Analysis*”, Prentice-Hall, New Jersey, USA,1998.
- Hwang, Bon-Gang; and E-Sin Janicia Lim; 2013; “Critical Success Factors for Key Project Players and Objectives: Case Study of Singapore”
- Jonathan Sarwono; Umi Narimawati: “*Membuat Skripsi, Tesis dan Disertasi dengan Partial Least Square SEM (PLS-SEM)*”;Penerbit Andi; Yogyakarta; 2015.
- Kumaraswamy and Chan (1995), *A study of the factors affecting construction durations in Hong Kong*; Construction Management and Economics
- Neuman, William Lawrence. *Social Research Methods: Qualitative and Quantitative Approaches* 6th ed. 2006. Pearson Education Inc: USA.
- Nguyen, Long D.; Phan, Duc H.; and Tang, Llewellyn C. M.: “*Simulating Construction Duration for Multistory Buildings with Controlling Activities*”; Journal Of Construction Engineering And Management © ASCE / August 2013.
- Peter E. D. Love; Raymond Y. C. Tse; and David J. Edwards; *Time-cost relationships in Australian Building Construction Projects*; Journal Of Construction Engineering And Management © Asce / February 2005.
- Skitmore, R.M. and Ng, S.T. (2003) *Forecast Models for Actual Construction Time and Cost. Building and Environment 8(8)*; QUT e print; Elsevier



15th International Conference on Quality in Research (QIR 2017)

**AN ASSESSMENT ON SUSTAINABILITY OF THE RAILWAY – AIRPORT LINK
AS AN ALTERNATIVE MODE OF TRANSPORTATION
TO RADIN INTEN II AIRPORT**

Ika Kustiani
Amril Ma'ruf Siregar

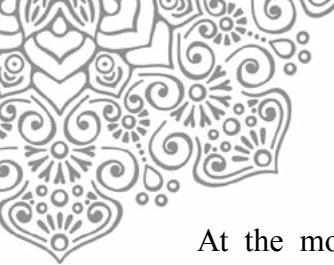
Abstract

The rapid economic development in the Province of Lampung is indicated by, among other things, the increase of air transportation mode users. The data shows that for the last four years, the number of passengers of the Radin Inten II Airport increased by 52% and the number of cargos increased by 257%. To support these demand, cost-effective and efficient transportation systems are vital, therefore the government has recently completed the construction of the Radin Inten II Airport expansion. Moreover, currently the government is planning to build a link between the airport facilities with railway transportation mode. This link provides additional alternative of transportation to airport. This research was carried out to assess the future demand for railway transportation mode to airport and to measure how this can achieve financial, environmental and social performance for sustainability. The assessment methods were utilizing dynamic, purposive and random sampling method to review the opinion of stakeholders of transportation system to airport. Stakeholders' opinion survey also reviewed a set of physical and managerial interventions that could potentially be implemented to improve the performance and sustainability of the railway transportation system. These interventions were drawn from suggestions made by experts in transportation system. The review of these proposed interventions was executed by integrating the results from a stakeholders' opinion survey with a Triple Bottom Line (TBL) sustainability framework. The integration of these two methods was designed to identify an alternative solution that was not only robust but also preferred by the stakeholders of railway and airport transportation system. The results showed that the physical changes that required large capital cost were less desirable and the managerial changes that give private company a greater authority were less favourable by all stakeholders.

Keywords: Transportation mode; Sampling method; Stakeholders opinion survey; physical and managerial interventions; Triple Bottom Line sustainability framework;

I. INTRODUCTION

Based on the data provided by the Province of Lampung Department of Transport, there are significant increase of the number of passengers at Radin Intan II Airport by 58% from 2010 to 2014 as well as the number of cargo by 257%. The airport provides services for domestic flights as well as embarkation flights for hajj pilgrims and overseas Indonesian workers. Currently, the airport serves for about 25 arrival and 25 departure flights a day from major cities in Indonesia. From January to September 2016, the average passenger that arrived were 2,455 per day and the number of passengers that departed were 2,521 per day. The airport operates 14 hours a day and peak hour is at 17 to 18 o'clock with 8 flights. Airport is one of transport nodes that play an important role in intermodal transportation systems, in particular among air, road and railway modes. To improve airport operational service, it needs to be supported by reliable and quality public transportation. The challenge to provide a better, faster cheaper and safe public transportation becomes more important along with the dynamics development of the region.



At the moment, the only access to the airport from Bandar Lampung Central Business District is through Trans Sumatra Highway. On average travel time is 45 minutes for private cars and taxis. Longer time is needed for Airport Bus. Every year, the travel time is increasing since the number of vehicles are increasing. This problem is exacerbated by the prediction of potentially high increase in the number of airport passengers in the future. It can be predicted that the current transportation mode to access the airport can no longer supports the demand. Therefore, an alternative mode of transportation is urgently needed to shorten the travel time from and to the airport. Fortunately, the airport location is close to railway track and utilizing it is one of possible options to effectively and efficiently transport people in mass from and to the airport.

Railway services has many advantages compare to other forms of transportation mode such as: enable to transport people in mass, lower/affordable cost, lower pollutant emission, lower land requirement, comfortable, safe, and free from traffic. There are some criteria that govern the type, size or class of a train station such as: operation facilities, number of tracks, supporting facilities, frequency of traffics, number of passengers and goods, revenues, and level of service (safety, security, reliability, comfort, easiness and equality). Based on those criteria, an airport train is considered as a short distance type railway service in which the distance is between 10 to 100 kilometers or the time travel is between half to three hours. In general, a high frequency or a short headway type of trains are needed with a maximum headway of 10 to 15 minutes or minimum there are 4 trains in one hour.

The current Branti Railway Station is classified as a small station and operates as longsideing and transfer station. At the moment, the railway provides services to transport passengers in short distance from Tanjung Karang to Kotabumi and medium distance from Tanjung Karang to Kertapati. The railway runs 2 return trains for economy and executive classes for medium distance and 1 return trains for short distance. The railway also provides services for transporting goods such as coals, pulp and others. The travel speed for passengers' trains are 36 – 52 km per hour and for goods carriages are 25 – 40 km per hour.



Figure 1. Airport – Train Station Link Concept

Based on the previous assessment, there are some problems exist in developing a mass rapid transportation system from Tanjung Karang CBD to the airport via railway. The nearest train station to the airport (Branti) is about 1.3 kilometers. Therefore, it is needed to relocate the current location of Branti Station to enable it to be operated as an airport train station. It is planned that a skybridge will be constructed to connect the train station with the airport terminal as can be seen from Figure 1. In addition to that, a double track railway is a must as



well as separation of track for passengers and goods. Improvements of facilities at Tanjung Karang and Labuhan Ratu Stations to support airport train station operation are also needed. For Indonesia Railway Authority, pioneering airport train to provide transportation services that accommodate passengers' mobility from one transportation mode to another in mass and in accordance to passengers' preferences is the challenge that must be done as soon as possible. Therefore, studies were required to understand the factors that influence users to switch to rail service as well as factors that influence the sustainability of the Railway – Airport Link. This study was conducted to find out the characteristics of passengers of each transportation mode to airport (taxi, private cars, and Trans Lampung bus), the number of passengers that might switching to train; and the technical and managerial intervention alternatives that favourable to stakeholders.

II. METHODOLOGY

2.1. Opinion survey

According to Abernethy, Jinapala, and Makin (2001) the objectives of measuring and quantifying stakeholders opinions are to:

1. Assist users to exert some influence on policies that affect their lives and economies,
2. Assist project planners in identifying the project components that are most likely to satisfy the concerns of affected users,
3. Provide a balanced view of alternative strategies and estimate differences of opinion between stakeholders, and
4. Provide a means of continuing mixed (quantitative and qualitative) evaluation of peoples' reaction to the impact of a project.

Among different stakeholders of transportation projects, users are the most fundamental. Opinion survey of the people most affected by transportation project is aimed to capture opinion and discourse on the current level of service, expectation of future service levels and willingness to bear the consequences of possible upgrades to service levels and/or infrastructure. It is very important to increase local support, co-operation, and benefit.

Abernethy, Jinapala and Makin (2001) explained aspects to be considered when gathering the opinion of people are: technique/methodology, preparation of questionnaires, and analysis of findings. Reported works on opinion surveys generally used a quantitative design with a questionnaire method. It is widely uses since it is an easy, quick and economical method; and reliable and capable of analysing large sample size subsets containing variations of possible determinant factors such as age, gender, or income. In designing the questionnaire, the following should be considered carefully:

1. As short as possible: based on a brief interview via 10 to 15 questions/statements,
2. Should be in written/spoken in the local language,
3. Consider the respondents might have low education level.

In general, the users' perceptions that need to be taken into account are:

1. Service delivery (operational): adequacy/sufficiency, reliability/predictability, tractability/convenience/flexibility, equity;
2. Asset/infrastructure condition (maintenance): railway, station, train
3. Economic aspect: fare
4. Environmental aspect: air quality and green corridors
5. Management aspect: effectiveness and efficiency of the services

2.2. Travel Fare

Travel fare is the most important aspect in choosing a mode of transportation. If the fare to be paid is considered too expensive, people tend to choose cheaper alternatives. However,



when there is no choice, they are forced to use this mode of transportation. Basically, fare are determined based on the following aspects: users, operator and regulator (government). In determining train service fee, it is needed to compare the ability to pay (ATP) and the willingness to pay (WTP) of train users to pay a sum of money for services provided. The value of ATP and WTP also affect the frequency of using the facility.

When the fare are determined based on ATP and WTP, user aspect is the subject who determine the amount of fare applied. The fare applied follows the following principles:

1. The fare applied cannot exceed the ATP of target communities. When the fare applied is higher than ATP, government intervention in the form of subsidy (direct or cross-subsidy) or other government supports are needed to obtain a fare that equal to ATP.
2. Since the WTP is the function of level of service of public transportation, the opportunity to increase fare still exists by increasing performance of service.
3. In case that fare applied is far below the ATP and WTP, there is flexibility in the calculation or application of the new fare.

Basically, ATP is transportation budget to travel intensity ratio. It measure the ability of public to pay the service provided based on ideal income. There are two type of ATP that are general ATP and ATP based on occupation, however both can be calculated using household budget method. ATP is influenced by income, travel frequency, estimation on daily transportation cost, and other costs.

WTP can be defined as the average amount of money that passengers willing to incur as a payment for service received. It is affected by several factors such as: quantity and quality of service, purpose of utilization and users' income. One method to analyse WTP for train services is based on users' perception on fare and service of the public transport such as: expected rates, service priority expected, and willingness to pay more for improved safety.

2.3. The Triple Bottom Line Sustainability

Sakthivadivel et al. (1999) stated that performance assessment is an integral part of performance-oriented management. It can be used to measure the general health of a system, the impact of interventions and to diagnose the constraint threats and institutional strengths. The most popular type of performance assessment is a measurement on sustainability performance. The triple bottom line (TBL) sustainability performance is a concept proposed by John Elkington in 1995. The TBL is an expanded spectrum of values and criteria for measuring organisational (and societal) success that takes into account ecological and social performance in addition to financial performance. Because of its goal of sustainability, the TBL is famously described as 'people, planet, and profit'.

To measure sustainability in a complex system, a structured approach is appropriate to identify the main issues of concern for stakeholders, or the objectives relating to sustainability, and it then should address these objectives using selected indicators and performance measures. Sustainability criteria and incators for transportation infrastructure from various research from 2000-2013 are summarized in Table 1. From these research the framework indicators of sustainable infrastructure development for this study were developed. The study employed three sustainability criteria and two facilitating criteria that can be further break down into 40 indicators.



Table 1. Sustainability Criteria and Indicators for Transportation Infrastructure from Previous Research

Sustainability Criteria and Indicators		Author					Facilitating Criteria and Indicators		Author					
Social Criteria (People):		1	2	3	4	5	Technology Criteria		1	2	3	4	5	
1.	Public safety (including traffic accidents level)	X	X	X	X	X	1.	Capacity of infrastructure (supply)	X	-	-	-	X	
2.	Public security (traffic disruption level)	-	X	X	X	X	2.	Quality of infrastructure	-	-	-	-	X	
3.	Public health	X	X	X	-	X	3.	Technology and design of infrastructure	-	-	X	-	-	
4.	Public welfare (including savings from other transportation mode)	-	-	-	-	X	4.	Levels of service (performance)	X	X	X	-	X	
5.	Equity / fairness	-	X	-	X	-	5.	Integration of infrastructure (transportation mode)	-	-	-	-	X	
6.	Facilities for the disabled and elderly	-	X	X	X	X	6.	Ability to cope with population / private vehicle / road network growth and diversification of transportation mode	-	X	X	-	X	
7.	Access to public services	X	-	-	X	X			-	-	-	-	-	-
8.	Social interaction and social access	-	-	-	-	-	7.	Facilities for pedestrians and non-motorcycle vehicle / bike	-	-	X	-	X	
9.	Tradition/cultural protection	-	X	-	-	-			-	-	-	-	-	-
10.	Behaviour of community as user (as an effect of education & skill rate)	-	X	X	-	X			-	-	-	-	-	-
Environmental Criteria (Planet):		1	2	3	4	5	Governance Criteria:		1	2	3	4	5	
1.	Air pollution (ambient air quality)	X	X	X	X	X	1.	Regulation and institution	X	-	-	-	-	
2.	Land pollution (including waste) & land degradation (e.g. permanent puddle and flood)	-	-	X	X	X	2.	Cooperation with other institutions	-	-	-	-	X	
3.	Noise pollution	-	X	X	X	X	3.	Budget for R & D	X	X	X	-	X	
4.	Water resources / ground water pollution	X	X	X	-	X	4.	Conformity with the spatial planning & land use control	-	X	X	-	X	
5.	Use of energy (fuel consumption and efficiency of movement / mobility)	X	X	X	X	X			5.	Quality of human resources	-	-	X	-
6.	Use of renewable energy / efficiency of natural resources	-	X	-	X	X	6.	Community / users participation	X	X	X	X	-	
7.	Disruption to landscape / conversion rate of land (land use)	X	X	-	X	X	7.	Law enforcement / sanctions / control / call center	X	-	X	-	X	
9.	Green area and ecological network (hubs, nodes, corridors)	-	-	-	-	X								
10.	Protection of wildlife / habitat / biodiversity	-	X	X	X	-								
Economic Criteria (Profit):		1	2	3	4	5								
1.	Cost of infrastructure (capital & MOM)	X	X	X	X	X								
2.	Revenue from trip / service / users fee (willingness to pay)	X	X	X	X	X								
3.	Local government revenue (savings on O&M on other transportation mode, revenue per capita)	-	X	-	-	-								
4.	Locals & regional economic opportunities (creation of jobs, absorption of labor) and effect on Gross Regional Domestic Product	-	X	-	-	X								
5.	Supporting growth center / investment development (business, education, industrial, etc.)	X	X	-	-	X								
6.	Increase land value	-	-	-	-	X								

Note: 1 (Sahely, *et al.*, 2005); 2 (Litman and Burwell, 2006); 3 (Tamin, 2007); 4 (Haghenas dan Vaziri, 2012), 5 (Kusbimanto, 2013)

III. RESULTS AND DISCUSSION

Opinion surveys conducted for this study consist of three different surveys that were two users' opinion survey and one key stakeholders' opinion survey. As a result, each survey required different respondents and methodologies; however, the stages were typical that are: defining the population of concern, specifying sampling frame, specifying sampling method, developing questionnaires, conducting field surveys, analysing and interpreting data.

3.1. Users' opinion survey

1. Measuring interest on train service to airport

Passengers' opinion survey was carried out through questionnaires to gather information about passengers' interest on choosing airport train service, and origin and destination of passengers. The survey method utilized **Random Sampling** and the number of respondents was calculated based on Slovin equation as follow: $n = N / (1 + N e^2)$. Where: n = minimum



number of samples, N = number of passengers per day, and e = prediction on passengers' increase.

Based on the data, the average number of passengers per day in 2016 was 2,448. It was predicted that the rate of passengers' increase of 5% per year applied following the rate of Sukarno – Hatta Airport. As a result of the equation above, the minimum number of samples needed is 345 per day.

Opinion survey on airport passengers' interest in using train service to access airport was conducted on Thursday, Friday and Saturday in the month of September 2016 against 450 respondents. From 441 valid respondents, 61% of respondents comes from Bandar Lampung and 74% said interested to choose train service.

Based on the number of passengers in the Year 1998 to 2015, a polynomial regression graphs was drawn to predict the number of passengers in 10 and 20 years (Year 2026 and 2036). Based on the graph, it can be predicted that in the Year 2026: the number of passenger from Bandar Lampung would be 378 passengers and 280 of them would prefer to use train to transport from Bandar Lampung. The number is becoming more striking in the Year 2066. The number of passengers from Bandar Lampung would become 1,704 per day and 1,200 of them would choose train to transport to the airport.

2. Measuring the Ability to Pay (ATP) and the Willingness to Pay (WTP)

The questionnaires survey utilized a **Dynamic Method** in which the respondent was chosen based on incidental sampling (anytime and anywhere) as long as they fulfil the requirements as a sample of a population (Amirin, 2011). Respondents were passengers of three different type of transportation mode that exist in the airport at the moment that were: bus, private car and taxi. The number of respondent was 350 passengers that consist of 151 private cars, 148 taxi, and 51 taxi. The responds gathered from the survey was analysed using multiple regression with SPSS. With 95% of confidence level, the value of R^2 for formula obtained was 0.72. The questionnaires were designed in four sections as follow:

a. Characteristics of passengers:

It consists of 12 questions that addressed to find out the characteristics of airport passengers at Radin Inten II Airport as follow: age, gender, education, frequency to airport, means of transport most frequently used, alternatives of transport that can be selected, time travel to airport, travel origin, travel destination, purpose of travel, number of dependents, and the one-time cost travel to airport.

From about 350 respondents, 56% of travel purpose was for work, 23% for social activities, 13% for business, and the rest was for others such as holiday and family matters. In addition to that, 51% of respondents who work were private employees, education level of passengers was dominated by under graduate level by 71%, and family income for taxi and bus passengers were 1 to 3 million Rupiahs per month while for private car passengers were 3 to 5 million Rupiahs per month.

Since the majority of passengers' purposes is for work, they choose air transportation because its punctuality. Since most of the passengers' purpose is for work, the frequency of passengers to airport 59% travel twice a month, 32% travel 4 times a month, and 9% travels more than 4 times a month. Only a very small fraction of the passengers are one time travellers.

b. Ability to pay (ATP)

There were four questions asked to measure the ATP for train service in this study: average income per month, percent of income allocated for transportation per month, percent of income allocated for transportation to airport per month and frequency to airport per month. Hence, respondents' ATP can be calculated.



Based on the calculation, the minimum ATP of respondents was US\$ 0.75 and maximum was US\$ 3.75 with an average of US\$ 2.6. The most ATP was in the range of < US\$ 1.5 (25%), then followed by US\$ 2.25 - 3 (16.67%), > US\$ 3 (16.67%) and US\$ 1.5 – 2.25 (15%). If the airport train fare are in the range of US\$ 0.75 – 2.25, the ATP of respondents are 60%. However, if the fare is increased to US\$ 2.25 – 3.75 the ATP of respondents decrease to 40%.

c. Willingness to pay (WTP)

The questions asked for this study consist of for questions as follow: appropriate airport train fare, highest priority of airport train service, willingness to pay more for improved safety, and added costs for the program. Hence, the respondents' WTP can be calculated.

Based on the calculation, minimum WTP of respondents was US\$ 0.75 and maximum was US\$ 4.5 with an average of US\$ 2.1. The most WTP of respondents was in the range of US\$ 1.5 – 1.9 (26.67%), then followed by US\$ 0.75 – 1.5 (20%) and US\$ 1.9 – 2.25 (20%). If the airport train fare are set in the range of US\$ 1.5 – 2.25, the WTP of respondents are 78,33%. However, if the fare is increased to US\$ 2.25 – 3 the WTP of respondents decrease to 50%.

The study results show that the average ATP was higher than the average WTP. This means that the respondents' ability to pay is greater than the desire to pay for the services. This condition is caused by:

- Low utility of public services often caused by users with relatively high income not willing to utilize it because the service are below their expectation. In this case, users are called choice riders since they have a choice on transportation modes. They tend to utilize transportation modes with a better service or using their own car even with a higher cost.
- Respondents' perception on airport train are is still influenced by the assumption that all public transportation have similar level of service, as a result they expected the fare would be similar.

d. Respondents' expectation

The questionnaire was designed to assess respondents expectations on service provided. The results can be he results can be used to determine the priority of service.

From about 350 respondents, 35% of taxi passengers and 37% of private car passengers were not willing to switch modes of transport to bus. On the other hand, the respondents were willing to switch from previous transportation to train because they expect the train will have shorter travel time/avoid congestion (49.3%), much cheaper (17.6%) and comfortable (10.3%).

Based on the survey on priority of services, respondents prioritize punctuality of service was 51%, comfort of service was 20%, convenience in obtaining service was 17% and others (responsibility, completeness, politeness and friendliness in providing services and other supporting attributes). In addition to this, 80% of respondents are willing to pay more than the original rate to increase safety.

3.2. Measuring sustainability of proposed railway – airport link

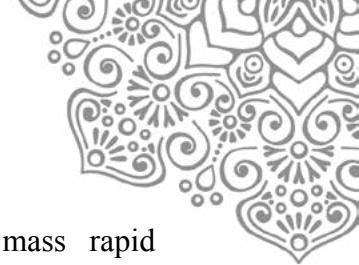
Opinion survey also carried out to gather key stakeholders preferences on the planning (physical and managerial interventions) to assess the sustainability of the planning. Stakeholders' opinion survey was carried out based on **Purposive Sampling Technique**. The sampling units or respondents in a *purposive sampling* method are selected based on certain consideration, characteristics or criteria. For this research, the selection of experts to serve as respondents were based the assumptions that someone was: (1) having sufficient



experience for the research field; (2) having position, reputation and credibility as stakeholders; and willing to be a respondent and can be met for an interview. The key stakeholders consisted of representatives from South Sumatra Region Railway Engineering Institution, Lampung Railway Development Office, Regional Division IV Tanjung Karang – Indonesia Railway Authority, the Province of Lampung Local Transport Authority, Radin Inten II Airport Office, Radin Inten II Railway Station Development Team, the Province of Lampung Local Planning Office, the Province of Lampung Office - National Road Planning and Supervision, the Province of Lampung Road Authority - the Department of Public Work, the Directorate General of Airport Transportation, the consultant companies of Radin Inten II Airport Development Planning (PT. Aria Graha and PT. Muara Consult) and the University of Lampung.

Table 2. The TBL Assessment on Proposed Interventions

Key Issue	Goal/objective	Criteria	TECHNICAL IMPROVEMENT									MANAGERIAL IMPROVEMENT								
			Install Automatic Machines for Ticketing and Gates			Construction of New Track (Double Track)			Construction of Airport Train Station			Increase Fare for Additional Services such as City Check-in			Diversifying Business by Opening Airport Link Service			Turnover Management of Airport Link Service to Private Sector		
			Score	Weight	Real score = score * weight	Score	Weight	Real score = score * weight	Score	Weight	Real score = score * weight	Score	Weight	Real score = score * weight	Score	Weight	Real score = score * weight	Score	Weight	Real score = score * weight
Technical and economic aspects	Technical viability	Reliability (punctuality)	3	1.2	3.6	3	4.8	14.4	2	1.7	3.4	2	1.6	3.2	3	2.7	8.0	1	1.1	1.1
		Efficiency	3	1.2	3.6	3	4.8	14.4	3	1.7	5.1	2	1.6	3.2	2	2.7	5.3	2	1.1	2.3
		Operation and maintenance	3	1.2	3.6	3	4.8	14.4	3	1.7	5.1	3	1.6	4.8	2	2.7	5.3	2	1.1	2.3
		Utilise existing infrastructure	1	1.2	1.2	2	4.8	9.6	1	1.7	1.7	2	1.6	3.2	2	2.7	5.3	2	1.1	2.3
		Upgradeability	3	1.2	3.6	3	4.8	14.4	3	1.7	5.1	2	1.6	3.2	3	2.7	8.0	2	1.1	2.3
	Technical sustainability	Future demand	3	1.2	3.6	3	4.8	14.4	3	1.7	5.1	3	1.6	4.8	3	2.7	8.0	2	1.1	2.3
		Flexibility	3	1.2	3.6	3	4.8	14.4	3	1.7	5.1	2	1.6	3.2	3	2.7	8.0	2	1.1	2.3
		Long-term operation and maintenance	3	1.2	3.6	3	4.8	14.4	3	1.7	5.1	3	1.6	4.8	3	2.7	8.0	2	1.1	2.3
	Economic viability	Investment cost*	3	1.2	3.6	2	4.8	9.6	1	1.7	1.7	2	1.6	3.2	1	2.7	2.7	2	1.1	2.3
		O&M cost efficiency	3	1.2	3.6	3	4.8	14.4	2	1.7	3.4	2	1.6	3.2	2	2.7	5.3	3	1.1	3.4
		Pricing users accurately	3	1.2	3.6	1	4.8	4.8	1	1.7	1.7	3	1.6	4.8	1	2.7	2.7	3	1.1	3.4
		Productivity	3	1.2	3.6	3	4.8	14.4	2	1.7	3.4	3	1.6	4.8	3	2.7	8.0	3	1.1	3.4
Economic sustainability	Financial sustainability	3	1.2	3.6	2	4.8	9.6	2	1.7	3.4	3	1.6	4.8	3	2.7	8.0	3	1.1	3.4	
Social, institutional, and legal aspects	Social viability	Complain/dissatisfaction*	2	1.2	2.4	2	4.8	9.6	2	1.7	3.4	1	1.6	1.6	3	2.7	8.0	2	1.1	2.3
		Acceptance	2	1.2	2.4	3	4.8	14.4	2	1.7	3.4	1	1.6	1.6	2	2.7	5.3	2	1.1	2.3
		Trust/confidence	2	1.2	2.4	3	4.8	14.4	2	1.7	3.4	2	1.6	3.2	2	2.7	5.3	2	1.1	2.3
	Institutional viability	Local capacity	3	1.2	3.6	2	4.8	9.6	2	1.7	3.4	2	1.6	3.2	2	2.7	5.3	2	1.1	2.3
		Acceptance	3	1.2	3.6	2	4.8	9.6	2	1.7	3.4	2	1.6	3.2	2	2.7	5.3	1	1.1	1.1
	Legal viability	Legislation/regulation	2	1.2	2.4	2	1.4	2.8	2	1.7	3.4	2	1.6	3.2	3	2.7	8.0	1	1.1	1.1
Environmental, and public health and safety aspects	Environmental viability	Pollution*	3	1.2	3.6	2	4.8	9.6	2	1.7	3.4	3	1.6	4.8	3	2.7	8.0	3	1.1	3.4
		Waste production*	3	1.2	3.6	2	4.8	9.6	2	1.7	3.4	3	1.6	4.8	3	2.7	8.0	3	1.1	3.4
		Resources efficiency	3	1.2	3.6	2	4.8	9.6	2	1.7	3.4	3	1.6	4.8	3	2.7	8.0	3	1.1	3.4
	Public health and safety	Comfort	2	1.2	2.4	3	4.8	14.4	3	1.7	5.1	2	1.6	3.2	3	2.7	8.0	2	1.1	2.3
		Health & safety	1	1.2	1.2	3	4.8	14.4	2	1.7	3.4	2	1.6	3.2	3	2.7	8.0	2	1.1	2.3
		Security	3	1.2	3.6	3	4.8	14.4	2	1.7	3.4	2	1.6	3.2	3	2.7	8.0	2	1.1	2.3
		Education/awareness	2	1.2	2.4	2	4.8	9.6	2	1.7	3.4	2	1.6	3.2	2	2.7	5.3	2	1.1	2.3
	Total score				82			305			96			94			174			64



As mentioned before that there some problems exist in developing a mass rapid transportation system from Tanjung Karang CBD to the airport via railway. The proposed alternatives of physical and managerial improvements to enable this link operated are shown on the Table 2. These proposed interventions then were tested against three key sustainability issues i.e., the goals to be achieved in implementing the alternatives. The three key sustainability issues were: technical and economic; social, institutional and legal issue; and environmental, public health and safety. These key issues were then developed further into several criteria of sustainability/viability that determined whether the goals were achievable. The key sustainability issue and its criteria were framed based on previous researches as summarized in Table 1.

Each criteria of the three key sustainability issues was measured through examining statements in which a score was imposed based on the ability to satisfy the statements. The scores were 1 for low, 2 for moderate and 3 for high. Weights were also allocated to each criteria based on the rank of the options obtained from the key stakeholders opinion survey analysis using the Pairwise Comparison Matrix and Analysis. The higher the value obtained by an action, the more viable. Further discussion on the TBL sustainability viability assessment of proposed intervention priorities is presented in the Table 2. From the table, it can be seen key stakeholders preferences were: constructing a double track, diversifying business by opening airport link service and constructing a new airport train station.

IV. CONCLUSIONS AND SUGGESTIONS

Based on the analysis on potential airport train users' responds, airport train station authority must provide transportation services with satisfactory level of service and appropriate fare, so the potential users are willing to utilize airport train services. In addition to these, to realize the plan to link railway and airport, there are physical and managerial alternatives that has to be taken by Indonesia Railway Authority. The following are conclusions and suggestions resulting from the study:

1. **Fare**

Appropriate fare (basic fare) for airport train service from Tanjung Karang Station to Branti Airport Station based on the study was about US\$ 2.6.

2. **Travel Time with Express Train and Special Track**

Average travel time for train services in Indonesia is 60 km/hour. With travel distance of 24.5 km (Tanjung Karang to Branti Airport Station), it is expected that the airport train travel time would be 30 minutes without stopping (express train). Since the travel time of private car for the same origin and destination is about one hour in normal condition, it is expected to attract users since it provides punctuality for passengers. Even with stopping at two places will not affect the travel time too much since it only needs to stop for 5 minutes each. This will greatly increase users' access to airport train. In addition to this, providing a special track for airport train also become an alternative to guarantee no delays.

3. **Travel Schedule (Frequency and Punctuality)**

Frequent and punctuality of departure as well as train schedule according to flight schedule will greatly affect the interest of airport users. It provides convenience and comfort to choose the time to go without fear of missing the train or the flight as well as reducing waiting time at station and airport.

4. **Supporting Facilities for Comfort**

Since it is a short distance travel, facilities such as toilet and free wifi are not crucial. However, air conditioner will greatly enhance travel comfort. In addition to this, some rules also needed to be enforced to maintain the cleanliness, health and comfort of



passengers. Smoking, eating (bottled water is permitted) and littering in the train are prohibited. Since it is a short distance train, there will be no restriction for the number of passengers and there is possibility of standing passengers.

5. **Safety and Security (Access In and Off Station)**

Rules regarding only people with ticket may enter the station must be upheld. In addition to this, security officers have always ready at the entrance and exit of the station. This will also remove hawkers from the station so that the station safer, cleaner and more comfortable. It is needed to consider to provide automated ticketing and automated entrance and exit gate.

6. **Additional Services**

City check-in enables airport passengers to check-in their flight and baggage at Tanjung Karang Station and arrive at the airport 30 minutes before departure time. This will also reduce queues and waiting time at the airport. This service is very helpful for visitors, so they have extra time to stroll, shop or do other activities without carrying heavy luggage.

7. **Priority of intervention alternatives**

In order the railway - airport link plan can be realized, several physical and managerial intervention alternative needs to be taken. Several phases are needed and the first three priorities are: constructing a double track, diversifying business by opening airport link service and constructing a new airport train station.

V. ACKNOWLEDGEMENT

The authors would like to thank for the support of the University of Lampung and the consultants PT. Aria Graha and PT. Muara Consult for providing some data for the study.

VI. REFERENCES

- Abernethy, C. L., Jinapala, K., and Makin, I. W., (2001), Assessing the opinions of users of water projects, *Irrigation and Drainage* 50(3): 173-193.
- Haghenas, H. and Vaziri, M., (2012), Urban sustainable transportation indicators for global comparison, *Ecological Indicators* 15: 115–121.
- Kusbimanto, I.W., (2013), Models of sustainable urban transport infrastructure development policies in Metropolitan Mamminasata Southern Sulawesi, Dissertation, Graduate School IPB Bogor.
- Litman, T. and Burwell, D., (2006), Issues in sustainable transportation, *International Journal of Global Environmental Issues* 6(4): 331-347.
- Sakthivadivel, R., Fraiture, C. D., Moden, D. J., Christopher, P. and Kloezen, W., (1999), Indicators of land and water productivity in irrigated agriculture, *International Journal of Water Resources Development* 15(1-2): 161-179.
- Sahely, H., Kennedy, C.A. and Adams, B.J., (2005), Developing sustainability criteria for urban infrastructure system, *Canadian Journal of Civil Engineering* 32(1): 72-85.
- Tamin, O.Z., (2007), Towards sustainable transportation system in Bandar Lampung City, *Proceeding of Sustainable Transportation Seminar*, Bandung Institute of Technology.
- Amirin, T.M., (2011), Research population and sample: Sampling from infinite and unspecific populations, Accessed 8 March 2017, <https://tatangmanguny.wordpress.com/2009/06/30/>.



CALCULATION THE EDGE OF SLAB DEFLECTION OF MODIFIED CAKAR AYAM SYSTEM BY APPLYING THE DISPLACEMENT FACTOR FROM PURI'S GRAPH

Anas Puri^{a,1*}, Rony Ardiansyah^{a,2}

^a*Civil Engineering Departement, Universitas Islam Riau, Pekanbaru*
¹anaspuri@eng.uir.ac.id, ²ronyardiansyah@eng.uir.ac.id

ABSTRACT

Simple method in Nailed-slab pavement system analysis was proposed by previous researcher. This method uses equivalent modulus of subgrade reaction (k'). This modulus consists of the modulus of sub grade reaction from plate load test (k) and additional modulus of sub grade reaction due to pile installing (Δk). The additional modulus of sub grade reaction has been also proposed by some authors. Displacement factor was used in determining the additional modulus of sub grade reaction. The curve of this factor was proposed by Puri (2017) for soft clay, and the curve of the invers one was proposed by Hardiyatmo (2011) for stiff clay. This paper will discuss the application of the curve of displacement factor from Puri's graph (2017) to calculate the deflections of Modified Cakar Ayam (MCA) pavement system. Calculated deflections based on this curve were compared to the observed deflection. The deflection was calculated by using Beam on Elastic Foundation method. Full scale test result from MCA pavement system was used. The concentric and edge loading points were considered. The calculated deflection based on single-row shell of MCA pavement system was compared to the observed deflection from three-row shell. Results show that the calculated deflection in good agreement with the observation, although it was very over-estimated about 390% to 665%. In this case, Over-estimated was caused by ignoring the end bearing resistance of shell in determining the additional modulus of subgrade reaction Δk . It could be also because of neglecting the lean concrete, shell connector, and vertical wall barrier. The Puri's graph can be used to determine Δk for MCA analysis, but in further research it should be considered the end bearing resistance of shell.

Keywords: rigid pavement; Modified Cakar Ayam System; slab deflection; subgrade modulus; displacement factor.



1. INTRODUCTION

Designing of road pavement on soft subgrade needs also about potential settlement that would be occur during and after construction and how to maintain the deformation. Hence, it is needed a such kind of system that can reduce the deflection of pavement. One of the system that can be used is *Sistem Cakar Ayam*. This system has two types; original type which uses cylindrical concrete shell and modified type which uses cylindrical steel shell (calls *Sistem Cakar Ayam Modifikasi*). In Modified *Cakar Ayam* System (MCA), the utilization of cylindrical steel shell was proposed by Ir. Maryadi Darmokumoro (Suhendro, 2006). Several analysis method of MCA were proposed such as Suhendro's Chart, Hardiyatmo method by using Beam on Elastic Foundation (BoEF), and Hardiyatmo's Chart (Hardiyatmo, 2010; Suhendro and Hardiyatmo, 2010). BoEF was used in MCA analysis such as Pempadi (2000), Muhu (2007), Afriliyani, et.al. (2017) and Agustin, et.al. 2017. MCA can be analyzed also by 3D finite element method (Suhendro, 1992; Romadhoni, 2008; Firdiansyah, 2009; Puri, 2015; Setiawan, 2015).

Hardiyatmo (2008) introduced a new method that was developed from the pavement of the MCA by changing the cylindrical foundation with short micro piles. This system is called the nailed-slab system. Hardiyatmo (2011a) proposed an analysis method for determining the additional modulus of subgrade reaction (Δk). The additional modulus of subgrade reaction is the additional modulus developed by a pile. Mean while, the modulus of subgrade reaction is the modulus considered from a slab. Puri et al. (2012) modified the Hardiyatmo method by considering the tolerable deflection or allowable deflection of a pavement slab (δ_a) as an approach to safety construction. This modified method has good validation (Puri et al., 2013). Puri (2017a) proposed curve of displacement factor ($\alpha = \delta_0/\delta_s$) for calculating the Δk .

This research is aimed to apply the analysis method of the additional modulus of subgrade reaction (Δk) by using Puri's graph (Puri, 2017a) to calculate the slab deflection of MCA system. Calculated deflection will be compared to observation results.

Hardiyatmo (2011a) used the displacement factor for determining the additional modulus of subgrade reaction. The displacement factor is the ratio of the relative displacement between piles and soils (δ_0) and the pile head settlement (δ_p). The pile head settlement is assumed to be similar to the slab deflection (δ_s). The inverse of the displacement factor is the ratio of δ/δ_0 . Hardiyatmo (2011b) developed the curve of the δ/δ_0 ratio based on the full-scale test of a single pile in stiff clay. The pile and slab were connected by bolts. In this paper, the curve of the δ/δ_0 ratio based on a full-scale test of a single-pile nailed slab in soft clay is developed. The pile and slab were connected monolithically. The curve of the δ/δ_0 ratio is also presented as the curve of the displacement factor. Validation based on the single-pile nailed slab will be explained.

The analytical approach in determining the equivalent modulus of subgrade reaction (k') is given as follows (Hardiyatmo, 2011a; Dewi, 2009; Puri et al., 2012):

$$k' = k + \Delta k \tag{1}$$

Where k : modulus of subgrade reaction from plate load test (kN/m^3) and Δk : additional modulus of subgrade reaction due to pile installation under slab (kN/m^3). The modulus of



subgrade reaction from a plate load test (k) is usually taken by using a circular plate, and it should be corrected to the slab shape of the nailed slab. The secant modulus is recommended. Hardiyatmo (2011a) proposed Eq. (2) in determining the additional modulus of subgrade reaction (Δk). The relative displacement between the pile and soil is considered.

$$\Delta k = \frac{\delta_0 A_s}{\delta_s^2 s^2} (a_d c_u + p_0 K_d \tan \phi_d) \quad (2)$$

Where δ_0 : relative displacement between pile and soil (m), δ_s : deflection of surface of slab (m), A_s : surface area of pile shaft (m²), s : pile spacing (m), a_d : adhesion factor (non-dimensional), c_u : undrained cohesion (kN/m²), p_0 : average effective overburden pressure along pile (kN/m²), K_d : coefficient of lateral earth pressure in pile surroundings (non-dimensional), and ϕ_d : soil internal friction angle (degree).

Hardiyatmo (2011b) re-published the relation between δ_0/δ_s and slab deflection for a full-scale model while the pile and slab were connected by bolts. The pile diameter was 20 cm, and the length of the pile varied between 1.0 m and 2.0 m. Puri (2017a) proposed curve of displacement factor ($\alpha = \delta_0/\delta_s$) as shown in Figure 1. This curve for soft clay which the Nailed-slab System was a full-scale model while the pile and slab were connected monolithically. Then, the Equation (2) can be rewritten as (Puri, 2017b)

$$\Delta k = \frac{\alpha A_s}{\delta_s^2 s^2} (a_d c_u + p_0 K_d \tan \phi_d) \quad (3)$$

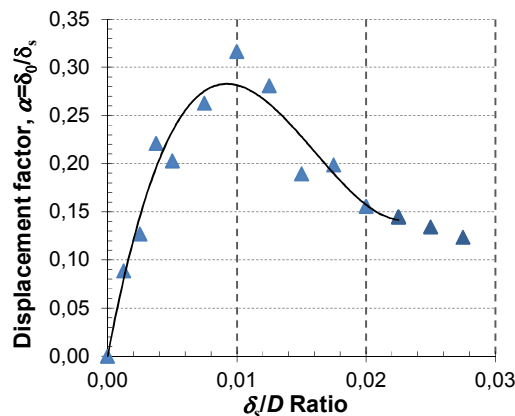


Figure 1. Curve of displacement factor α (Puri, 2017a).

Slab deflection can be calculated by BoEF while the input modulus is k' from Equation (1). Roark formula will be used for finite beam.

2. METHODOLOGY

2.1. Research object

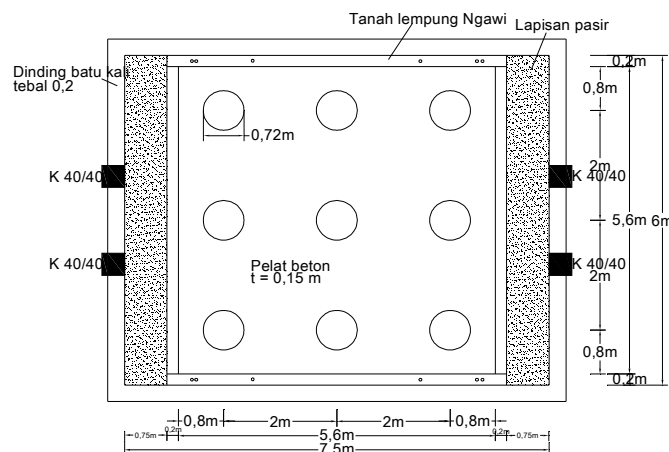
The research object was a full-scale model of MCA from Setiawan (2015). MCA consisted a slab with 6.00 m x 6.00 m in width and length and 0.15 m in thickness. The slab



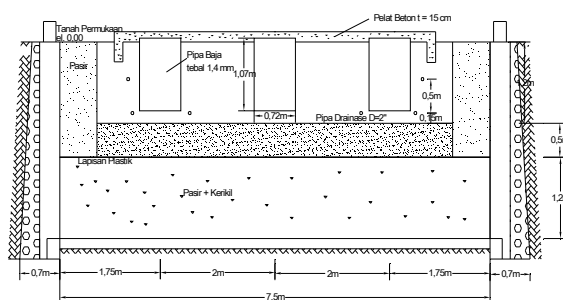
was constructed by reinforced concrete. Concrete compression strength characteristic, f_c' was 32.16 MPa. MCA was constructed in soft clay. Soft clay properties were presented in Table 1. Vertical modulus of subgrade reaction, k_v was taken from Plate Load Test by using 30 cm in plate diameter. Nine cylindrical steel shell were installed under the slab and connected monolithically. Shell spacing was 2.00 m. Shell had dimension 0.72 m in diameter, 1.015 m in length and 1.4 mm in thickness. Schematic diagram of MCA is presented in Figure 2. This sistem was loaded by vertical compression loading on point A (edge of slab) as shown in Figure 3. Load variations were 0 kN, 20 kN, 60 kN, 100 kN. Loads was transfer to slab surface by steel plate 30 cm in diameter.

Table 1. Properties of soft clay (Setiawan, 2015)

No.	Properties	Value	Unit
1	Undrained cohesion (c)	15	kN/m ²
2	Degree of soil field density	92	%
3	Vertical modulus of subgrade reaction, k_v	5,498.4	kN/m ³
4	Soil classifaction (USCS)	CH	-



a) Plan



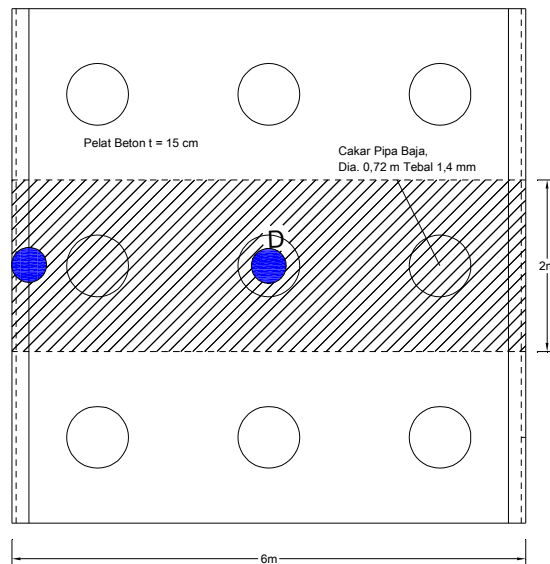
b) Cross section

Figure 2. Shcematic diagram of MCA (Setiawan, 2015).

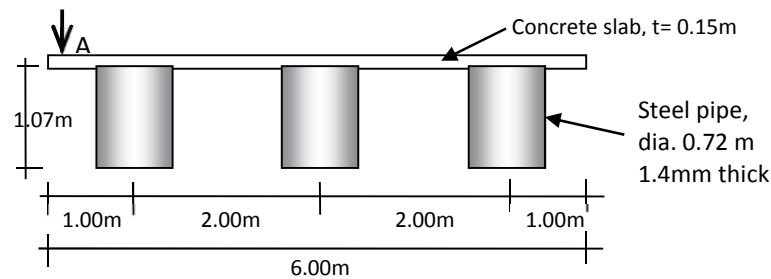


2.2. Method of analysis

Considered MCA in BoEF analysis was only one shell row as shown in Figure 3a. Simplification was done by neglecting the lean concrete, shell connector, and vertical wall barrier (Figure 3b). Ddeflection of surface of slab (δ_s) was taken from observation. From soil properties and MCA dimension, the k' was calculated. Slab deflection was calculated by input the k' , MCA dimension and properties to BoEF.



a) Plan of one shell row to be considered



b) Cross section

Figure 3. One shell row of MCA to be considered in analysis.

3. RESULTS AND DISCUSSION

3.1 Equivalent Modulus of Subgrade Reaction

Vertical modulus of subgrade reaction was corrected due to plate shape and dimension according to Das (2011). Hence, the k_v was 641.48 kN/m^3 . Considering the 2.00 m slab width, it was found $k = 1,282.96 \text{ kN/m}^3$. Based on soil cohesion $c_u = 15 \text{ kPa}$, the adhesion factor a_d was 1,0 according to Tomlinson's curve in McClelland graph (1974). Hence, unit



friction ratio f_s was 15 kPa. The surface area of shell shaft A_s was 2.30 m² and slab area which supported by one shell s^2 was 4.00 m². Slab deflection δ_s for 20 kN load was 0.558 mm. By 0.72 m in shell diameter D , we found the ratio of $\delta_s/D = 0.000775$. Then displacement factor α from Figure 1 was 0.05. By using Equation (3), the additional modulus of subgrade reaction Δk was 772.85 kN/m³. According to Equation (1), the equivalent modulus of subgrade reaction was 2,055.81 kN/m³. Since the edge of slab equipped by vertical wall barrier, the equivalent modulus should be considered the adjustment factor about 1.5 (Puri, dkk., 2013). So, the equivalent modulus of subgrade reaction k' beMCA e 3,083.72 kN/m³. Similar step of calculation also done to other load and the calculation results are presented in Table 2.

Table 2. Modulus of subgrade reaction for one shell row based on observed deflection

Load, Q (kN)	Load point A		
	δ_s (mm)	Δk (kN/m ³)	k' (kN/m ³)*
20	0,558	772.85	3,083.72
40	1,195	505.23	2,682.28
60	1,970	612.94	2,843.85
100	3,774	525.64	2,712.90

* Multiplied by adjustment factor 1.5.

3.2 Calculated Deflection

Table 3 presented the calculated deflection results. All calculated deflections were very over-estimated more than 260%, and higher than allowable deflection 5 mm (Puri, 2015). Over-estimated was caused by ignoring the end bearing resistance of shell in determining the additional modulus of subgrade reaction Δk as in Equation (2) and (3). It could be also because of neglecting the lean concrete, shell connector, and vertical wall barrier. It means that the Puri's graph (Figure 1) can be used to determind Δk . Figure 4 shows the P - δ relationship on loading point.

Table 3. Calculated deflection on loading point

Load, Q (kN)	Deflection (mm)		Defferentiation (%)
	Calculated	Observed	
20	4,273	0,631	665,77
40	8,284	1,347	593,22
60	11,204	2,215	468,71
100	18,525	4,222	390,86

The deflection along the slab is shown in Figure 5. Although claculated deflections were very over-estimated, it can be seen that the deflection shapes of calculated deflections were similar with the observed one.

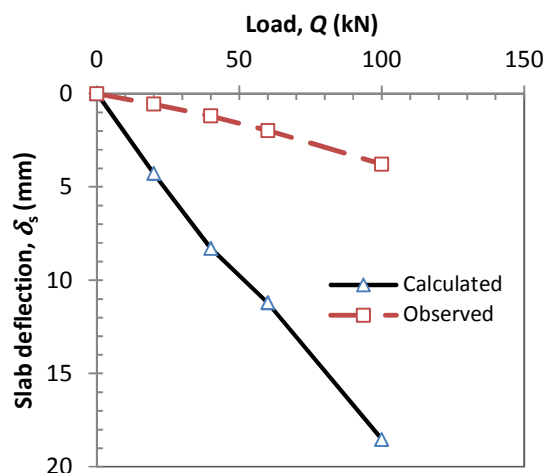


Figure 4. P - δ relationship for edge load.

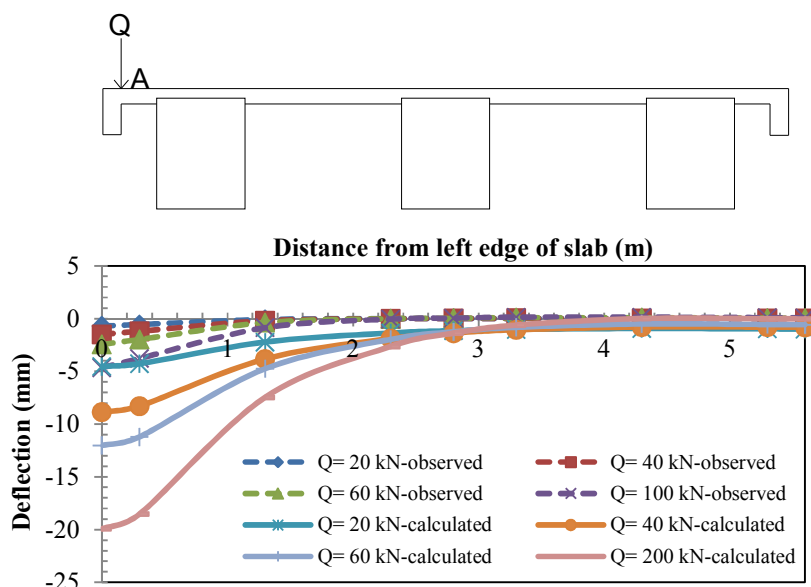
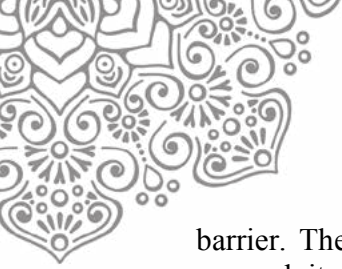


Figure 5. Deflection along the slab.

4. CONCLUSION

In this paper, the analysis method of the additional modulus of subgrade reaction (Δk) by using Puri's graph was applied to calculate the rigid pavement deflection of *Cakar Ayam Modifikasi* (MCA) system. Calculated deflections were also compared to observed deflections. All calculated deflections were very over-estimated around 390% to 665%, and higher than allowable deflection 5 mm. Over-estimated was caused by ignoring the end bearing resistance of shell in determining the additional modulus of subgrade reaction Δk . It could be also because of neglecting the lean concrete, shell connector, and vertical wall



barrier. The Puri's graph can be used to determine Δk for MCA analysis, but in further research it should be considered the end bearing resistance of shell.

5. ACKNOWLEDGEMENTS

The authors acknowledge the financial support from the Universitas Islam Riau, Pekanbaru and to Novia Afriliyani for her help in calculation.

6. REFERENCES

- Afriliyani, N., Puri, A., and R. Ardiansyah, (2017), Penerapan Modulus Reaksi *Subgrade* Ekuivalen Metode Puri, dkk (2012) dalam Perhitungan Lendutan Pelat pada Perkerasan Sistem Cakar Ayam Modifikasi, *In: Proceeding Konferensi Nasional Teknik Sipil dan Perencanaan (KN-TSP) 2017*, Program Studi Teknik Sipil, Universitas Islam Riau, Pekanbaru, 9 Februari 2017, pp. 29-35.
- Agustin, D.R., Puri, A., and R. Ardiansyah, (2017), Perhitungan Lendutan Perkerasan Jalan Sistem Cakar Ayam Modifikasi dengan Variasi Faktor Aman pada Tambahan Modulus Reaksi *Subgrade*, *In: Proceeding Konferensi Nasional Teknik Sipil dan Perencanaan (KN-TSP) 2017*, Program Studi Teknik Sipil, Universitas Islam Riau, Pekanbaru, 9 Februari 2017, pp. 76-84.
- Dewi, D.A., (2009), Study on Effect of Single Pile Due to the Value of Equivalent Modulus of Subgrade Reaction from Full-scale Loading Tests. Master's Thesis, Graduate Program Gadjah Mada University, Yogyakarta, Indonesia.
- Firdiansyah, A., (2009), Evaluasi Dimensi Sistem Cakar Ayam Akibat Pengaruh Variasi Letak Beban dan Kondisi Tanah, Thesis, Program Studi Teknik Sipil, Program Pascasarjana UGM, Yogyakarta, Indonesia.
- Hardiyatmo, H.C., (2008), Nailed-slab System for Reinforced Concrete Slab on Rigid Pavement. *In: Proceedings of the National Seminar on Appropriate Technology for Handling Infrastructures*, MPSP JTSL FT UGM, Yogyakarta, 12th April, Indonesia, pp. M1-M7
- Hardiyatmo, H.C., (2010), Perancangan Sistem Cakar Ayam Modifikasi untuk Perkerasan Jalan Raya, Gadjah Mada University Press, Yogyakarta
- Hardiyatmo, H.C., (2011a), Method to Analyze the Deflection of the Nailed-slab System, *International Journal of Civil and Environmental Engineering IJCEE-IJENS*, Volume 11 Number 4, pp.22-28.
- Hardiyatmo, C.H., (2011b), Designing of Pavement Roads and Soil Investigation: Flexible Pavement, Rigid Pavement, Modified Chicken Foot Foundations, Nailed-Slab System. Gadjah Mada University Press, Yogyakarta, Indonesia.
- Muhu, H.L.Y., (2007), Kajian Lendutan Pada Sistem Cakar Ayam Akibat Variasi Lebar Pelat (Model Sistem Cakar Ayam dari Pelat Baja), Diploma Thesis, Program Studi Teknik Sipil dan Lingkungan, UGM, Yogyakarta, Indonesia.
- Pempadi, I., (2000), Analisis Lendutan Pelat dengan Metode Beams on Elastic Foundation Aplikasi untuk Perancangan Fondasi Cakar Ayam dan Sumuran, Diploma Thesis, Jurusan Teknik Sipil & Lingkungan, Fakultas Teknik Universitas Gadjah Mada, Yogyakarta



- Puri, A., (2015), Studi Parametrik Jalan Beton Sistem Pelat Terpaku pada Tanah Dasar Lunak, *In: Proceeding The 1st Annual Civil Engineering Seminar (ACES)*, Fakultas Teknik Universitas Riau, 22 November, pp. 305-313.
- Puri, A., (2017a), Developing the Curve of Displacement Factor for Determination The Additional Modulus of Sub Grade Reaction on Nailed-slab Pavement System, *International Journal of Technology*, Vol. 1, pp. 122-131. ISSN 2086-9614.
- Puri, A., (2017b), Infrastruktur Jalan Beton Sistem Pelat Terpaku untuk Pembangunan Jalan Berkelanjutan pada Tanah Dasar Lunak dan Ekspansif, *In: Proceeding Konferensi Nasional Teknik Sipil dan Perencanaan (KN-TSP) 2017*, Program Studi Teknik Sipil, Universitas Islam Riau, Pekanbaru, 9 Februari 2017, pp. 1-17.
- Puri, A., Hardiyatmo, H.C., Suhendro, B., dan Rifa'i, A., (2012), Determining Additional Modulus of Subgrade Reaction Based on Tolerable Settlement for The Nailed-Slab System Resting on Soft Clay, *International Journal of Civil and Environmental Engineering IJCEE-IJENS*, Vol. 12 No. 03, pp 32-40
- Puri, A., Hardiyatmo, H.C., Suhendro, B., dan Rifa'i, A., (2013), Penerapan Metode Analisis Lendutan Pelat Terpaku Pada Model Skala Penuh dan Komprasi Dengan Uji Pembebanan, *In: Proceeding Konferensi Nasional Teknik Sipil 7 (KoNTekS7)*, Universitas Negeri Sebelas Maret, Surakarta, 24-26 October 2013, pp. G201-G211.
- Romadhoni, J., (2008), Perilaku Perkerasan Sistem Cakar Ayam Dengan Metode Elemen Hingga, Tugas Akhir S-1 Jurusan Teknik Sipil dan Lingkungan FT UGM, Yogyakarta.
- Setiawan, B., (2015), Perilaku Sistem Cakar Ayam Modifikasi pada Tanah Ekspansif, Disertasi, Program Studi Teknik Sipil, Program Pascasarjana UGM, Yogyakarta, Indonesia.
- Suhendro, B., (2006), Sistem Cakar Ayam Modifikasi Sebagai Alternatif Solusi Konstruksi Jalan di Atas Tanah Lunak, *In: buku 60 tahun Republik Indonesia*, Jakarta, Indonesia.
- Suhendro, B., and Hardiyatmo, H.C., (2010), Sistem Perkerasan Cakar Ayam Modifikasi (CAM) Sebagai Alternatif Solusi Konstruksi Jalan di Atas Tanah Lunak, Ekspansif, dan Timbunan, *In: Proceeding Seminar dan Pameran Sehari 2010 Inovasi Baru Teknologi Jalan dan Jembatan*, DPD HPJI Jatim, Surabaya, 31 Maret 2010.



PUBLIC PERCEPTION OF PUBLIC SERVICE ANNOUNCEMENT (PSA) ON TRANSPORTATION SAFETY AWARENESS THROUGH TELEVISION IN SURABAYA

Endang Widjajanti

*Civil Engineering Department, Faculty of Engineering and Planning, Institut Sains &
Teknologi Nasional (ISTN)
Jl. Moh Kahfi 2, Srengseng Jagakarsa
Jakarta 12640, Indonesia*

ABSTRACT

One form of transportation safety awareness carried out by the Ministry of Transportation of the Republic of Indonesia is the socialization through television known as Public Service Announcement (PSA) or in Indonesian known as “Iklan Layanan Masyarakat”. This study is part of the activities of Ministry of Transportation of the Republic of Indonesia in capturing responses and perceptions to the aired PSA in Surabaya. The survey method is an interview with a questionnaire. The results showed that only 5% -40% of respondents who noticed five PSA were aired. Approximately 57%-93% of respondents said PSA interesting. Factors of the less attractive PSA is the actors/actress are not interesting. Most respondents suggested in order to be understood and respected by the community, the PSA should be more attractive, the duration should be longer and its frequency should be increased and aired continuously.

Keywords: safety; transportation; public service announcement

1. INTRODUCTION

WHO data shows that, in the last two years, traffic accidents are the number three cause of death in Indonesia after heart disease and TBC. Global Status Report on Road Safety (2013) stated that “Rapid motorization in Indonesia over the past few decades has been accompanied by an increasing number of road traffic fatalities.”. Motorcyclists accounted for the biggest segment of fatalities, at 36 percent, followed by bus passengers at 35 percent. Pedestrians were the next most vulnerable at 21 percent, while car drivers and passengers accounted for just 1 percent of fatalities. It also noted that while motorcycle drivers wore a helmet in 80 percent of cases, their passengers only wore a helmet 52 percent of the time.

Moreover, passenger and air freight transportation growth have been increasingly significant. Referring to Indonesia National Air Carriers Association (INACA) data, there is a projected 15 percent growth in air transportation passengers in Indonesia in 2013. The association also reported there were over 51.5 million passengers flying from or arriving at Soekarno-Hatta International Airport in 2011, which far exceeds the 23 million passenger capacity of the airport. Unfortunately, Indonesia has been classified as a Category 2 country



by the Federal Aviation Administration (FAA), which is below international flight safety minimum requirements.

To increase the transportation safety in Indonesia, Ministry of Transportation of the Republic of Indonesia had produced and aired several PSAs in television during September 2013. This study is part of the Ministry of Transportation of the Republic of Indonesia survey in capturing feedback and the public perception of PSA which is presented on television.

The research's objective is to evaluate public perception and impression of five PSAs on transportation safety awareness that were aired through the medium of television in Surabaya, Indonesia.

2. LITERATURE REVIEW

2.1. Public Service Announcement (PSA)

The advertising messages can be in the form of text, pictures, films, or a combination of all these elements. Television announcement has unique advantages compared to advertising in printed media. The advantages of television announcement allow us to receive three kinds of power at once, such as narration, sound and visual. Those three powers then formed a labeling system that works to influence the audience. Of the three powers, the television announcement works effectively because it presents a message in the form of verbal and nonverbal as well.

A public service announcement (PSA) is an advertisement that a television or radio station airs for a cause or a charity. A PSA can tout the importance of medical check-ups for children or ask you to donate to the Salvation Army's bell ringers. (The Balance, 2016).

Public service advertising is designed to inform the public on issues that are frequently considered to be in the general best interests of the community at large. Typically, it is also commonly referred to as a public service announcement (PSA) or a community service announcement (CSA). The ads are usually broadcast on radio or television, but may also appear in newspapers or magazines. They are prevalent in industrialized countries throughout the world. PSAs are commonly aimed at altering public attitudes by raising consciousness about particular issues. Health, conservation and safety themes are prevalent in many PSAs. The public service advertising campaigns are often sponsored by trade associations, civic organizations, non-profit institutions or religious groups. (<http://www.wisegeek.com/what-is-public-service-advertising.htm>).

2.2. Content and Delivery of PSA

Elder R.W et al (2004) stated two aspects of mass media campaigns may influence their effectiveness. These can be categorized into variables related to message content and to message delivery.

- Message content. One important aspect of message content involves the themes used to motivate the desired behavior change.



- Message delivery. A mass media campaign cannot be effective unless the target audience is exposed to, attends to, and comprehends its message. Two important aspects of message delivery are control over message placement and production quality.

3. METHODOLOGY

The survey was conducted one week after the airing of several PSAs in television, which is on September 2013. The title of five public service announcements that are evaluated are as follows:

1. Do not Using Motorcycles for Long Distance Trip
2. Do not Using Motorcycles for “Mudik” (Mudik is the annual homecoming tradition that occurs ahead of major religious holidays, especially “Eid” holiday.)
3. Discipline in Driving
4. Be Alert and Obey the Rules at the Railroad Crossing
5. Air Transportation Safety.

The criteria of the respondents is as follows:

- The respondent selected are those who have never participated in the survey with the same purpose.
- Respondents have ages in the range of 17-50 years. The selection range so that there is no significant difference in expressing opinions.
- Respondents were not employees of the public transport operators or regulators, either Government or private
- The respondents have been watching PSA that aired on television

One of the respondent criteria the respondents have been watching PSA that aired on television.

The fact shows that it is difficult to get respondents to ever watch a PSA. Anticipation against these conditions, the surveyor is equipped with a PSA video that will be shown to the respondents. This step was taken because the majority of respondents watch a PSA only briefly and rarely watch the PSA.

The questions which were asked to the respondents include:

1. background of the respondents, namely: gender, age, education, experience of trauma when using public transportation in the last three years, the estimated average expenditure for transport in a month.
2. perceptions of the respondents against PSA, namely:
 - a. the PSA viewing experience;
 - b. the amount of PSA who has seen and understood its purpose by respondent
 - c. suggestions for the PSA that aired on television: concepts, actors/actresses, a message that has been delivered, the duration, frequency broadcast
 - d. Evaluation of the PSA: Impressions of the PSA, message delivered, the duration of the PSA, suggestion to PSA that had been broadcasted.



4. RESULTS AND DISCUSSION

4.1. Background of the Respondents

Respondents are 53% male and 47% female with daily mode of transportation as shown on Table 1. Most respondents use motorcycles for transportation (78.41%), while users of public transport (public transport-buses, public transport-car, and taxi) only 2.27% of total respondents. The age of respondents are 17-25 years old (55%) and has undergraduate level education (70%).

A great number of the respondents (82%) did not have transportation accident trauma. Respondents who have experienced the transportation accident trauma are around 18%, with the incidences especially on public transport modes, such as public transport-buses, public transport-car and motorcycles.

Most respondents have salary/month in the range of 2 million rupiah (43%) and 2.5 – 5 million rupiah (30%) per month and the biggest expenses for transportation is < 250.000 rupiah per month (47%) and 250,000 – 500,000 rupiah per month (32%). Based on the amount of revenue and transportation expenses per month, it is found that the average respondent in Surabaya has to expense 10% of their total revenue for transportation per month. Respondents' background is shown on Figure 1.

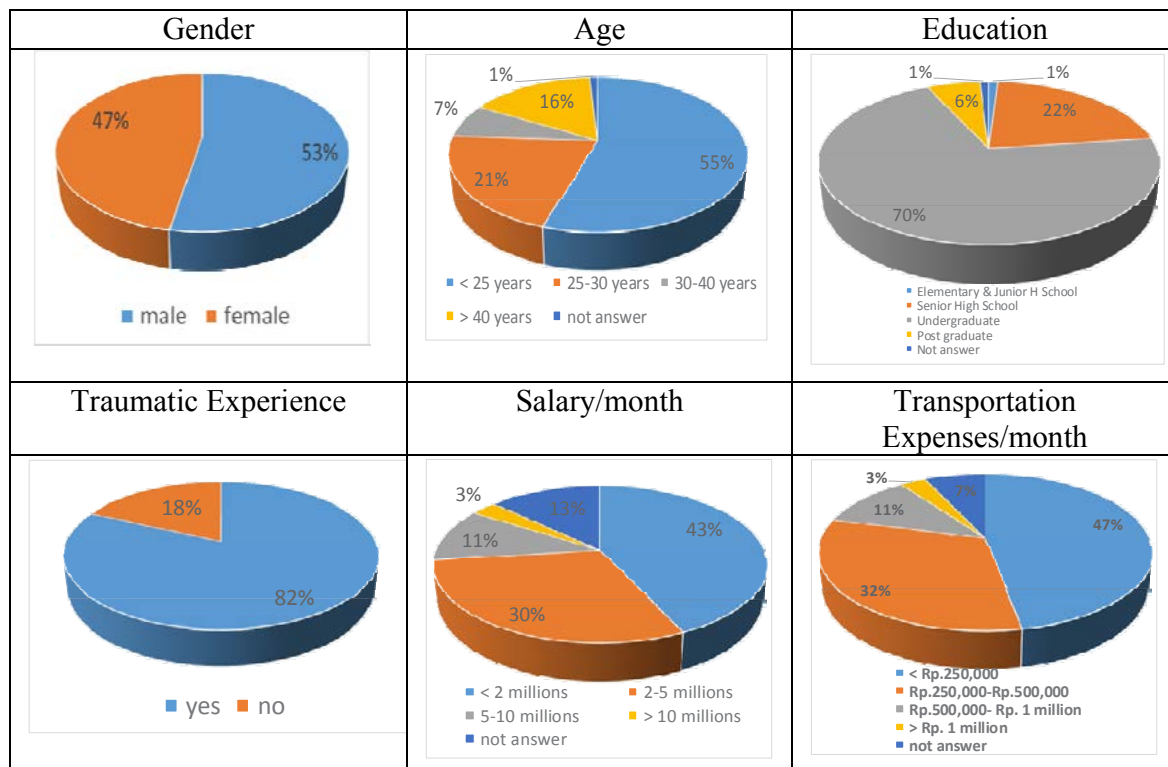


Figure 1. Background of the Respondents



Table 1. Mode of Transportation Used by Respondents

Transportation Mode	Frequency	%
Walking/cycling	20	7.58%
Motorcycle	207	78.41%
Private car	30	11.36%
Public transport	6	2.27%
Not answer	1	0.38%
Total	264	100%

4.2 Experience of Watching PSA on Television

From 264 respondents, 41 respondents said that they had watched PSA 1 (Do not Using Motorcycles for Long Distance Trip), 71 respondents had watched PSA 2 (Do not Using Motorcycles for “Mudik”), 106 respondents had watched PSA 3 (Discipline in Driving), 65 respondents had watched PSA 4 (Be Alert and Obey the Rules at the Railroad Crossing) and only 13 respondents had watched PSA 5 (Air Transportation Safety). Most watched ad is PSA 3 chosen by 40.15% of respondents.

Respondents who had the experience of watching the PSA, usually less attentive to the agencies that produce PSA. 40% chose not to answer the question, only 22% of respondents who viewed, while 38% of respondents not paying attention. Most of the respondents saw the PSAs only one time (44%), 25% have watched it twice, 14% watched it three to five times, 14% have watched it more than five times and 3% chose not to answer the question. Respondents’ attention to the agency and their watching frequency are shown on Figure 2.

Table 2. Experience of Watching PSA on Television

PSA	Audience	
	Number	%
1 Do not Using Motorcycles for Long Distance Trip	41	15.53%
2 Do not Using Motorcycles for “Mudik”	71	26.89%
3 Discipline in Driving	106	40.15%
4 Be Alert and Obey the Rules at the Railroad Crossing	65	24.62%
5 Air Transportation Safety	13	4.92%

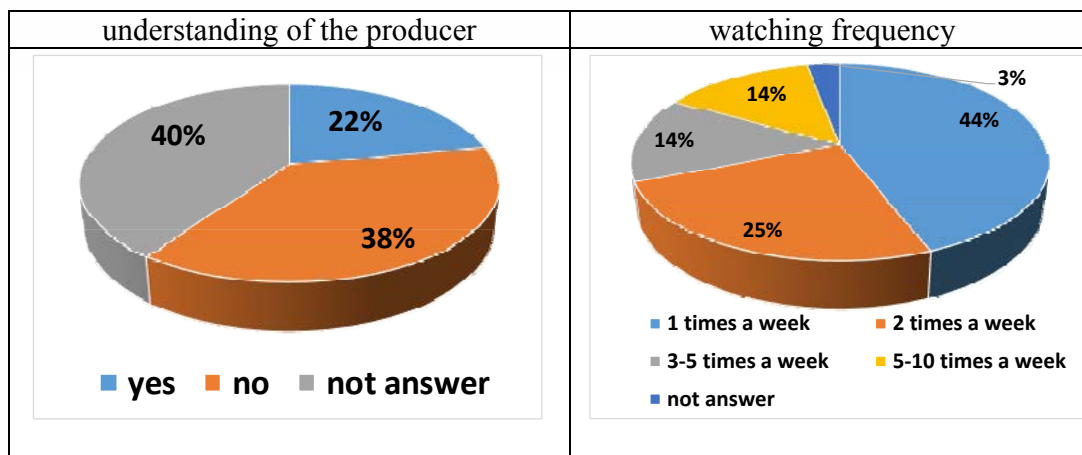


Figure 2. Attention to the Agencies and Frequency of Respondents Watch PSA

4.3 Respondents Impression

More than half of the respondents said that all PSA is interesting. Most respondents were interested in PSA 3 (“Discipline in Driving”) and 4 PSA (“Be Alert and Obey the Rules at Railway Crossing”) chosen by 90% and 93% of respondents. PSA 5 (“Air Transport Safety”) has the least number of respondents who are interested (selected by 57% of respondents). The reasons of respondents about why PSA unattractive shown on table 4.

Table 3. Respondents Impression

PSA	Respondents Impression (%)		
	interesting	Not interesting	Not answer
1	63	36	1
2	73	27	0
3	90	9	1
4	93	7	0
5	57	41	2

Table 4. The Reason about Why the PSA Unattractive

PSA	Reason
1	The actors/actress are not interesting, less expressive
2	Boring, the actors/actress are not interesting
3	Not special, monotonous, less expressive
4	Out of date, less attractive, not fun
5	Exaggerating, the message is not clear

The understanding on the message delivered by PSA is shown in the Table 5. Approximately 36%-75% of respondents in Surabaya captures the message that has been delivered by PSA. Messages that are captured by the respondents is the importance of



safety and discipline in driving. Constraints are often mentioned by the respondents to obey the message is because they “often break the rules”. This condition is extremely dangerous because it has become a culture that is bad for users of transportation in Surabaya.

Table 5. Understanding on the PSA’s Message

	PSA 1	PSA 2	PSA 3	PSA 4	PSA 5
capture the message clearly	54%	65%	68%	75%	36%
capture the message only a part	40%	30%	30%	23%	34%
cannot understand the message	5%	4%	2%	2%	28%
not answer	1%	1%	0%	0%	2%

Table 6 shows the overall evaluation that is marked with the percentage of respondents who gave a moderate and good value of all PSA which has aired on television in Surabaya as follows:

- Moderate to good concept: 76%
- Moderate to good actors/actress: 76%
- Moderate to good messages that were delivered in PSA: 82%
- Moderate to good duration: 71%
- Moderate to good frequency: 56%

Table 6. Respondents’ Evaluation which were aired on television in Surabaya

	concept	actors/ actress	message	duration	frequency
good	38%	22%	32%	8%	8%
moderate	38%	54%	50%	63%	48%
not good	24%	24%	18%	30%	44%

4.4. Reccomdaton for the PSA

Most respondents state that the PSA should 'more attractive' and “aired continuously”. They also expect that the PSA be aired to public continuously, not only during “Mudik” activities /Eid, but also aired throughout the year. According to some respondents advertisement made by the government is less attractive. Only 9%-26% respondents stated that the PSA are good enough. 46%-55% respondents want the PSA 'more attractive' and 15%-35% respondents state the PSA “be aired continuously”. The respondents’ recommendations to each PSA is shown on Table 7.

Table 7. Reccomdaton to the PSA

Recommendation for the PSA	PSA 1	PSA 2	PSA 3	PSA 4	PSA 5
good enough	10%	26%	23%	9%	17%
should be more attractive	55%	46%	47%	71%	68%
should be aired continuously	35%	29%	30%	19%	15%



5. CONCLUSION

- Most respondents are interested on PSA 3 (Discipline in Driving”) and PSA 4 (Be Alert and Obey the Rules at the Railroad Crossing) which has chosen by 90% and 93% of respondents.
- The reason why PSAs are unattractive predominantly because of the actors/actress are not interesting
- Around 36% - 75% of the respondents captures clearly the message that had delivered by each PSA. The most captured message is PSA 4 (captured by 75% of respondents). Obstacle often mentioned by respondents when not complying message delivered in PSA, is because they “often break the rules”. This condition is quite dangerous because it tends to be a bad culture of transportation users in Surabaya.
- The overall evaluation of the respondents is shown by percentage of respondents who give moderate and good value of all PSAs that had aired on television in Surabaya for the concept is 76%, for actors/actress is 76%, for messages that were delivered in PSA is 82%, for duration is 71% and for the airing frequency is 56%.
- Most respondents suggested in order to be understood and respected by the community, the PSA should be more attractive, the duration should be longer and its frequency should be increased and aired continuously.

6. REFERENCES

- Boyle Linda et al (2015), Effectiveness of Safety and Public Service Announcement (PSA) Messages on Dynamic Message Signs (DMS), FHWA, Washington DC
- Daniel, W. W. (1989). Statistika Non Parametrik Terapan. PT. Gramedia
- Elder R.W et al (2004), Effectiveness of Mass Media Campaigns for Reducing Drinking and Driving and Alcohol-Involved Crashes - A Systematic Review, Elsevier Inc, Am J Prev Med 2004;27(1):57–65 © 2004 American Journal of Preventive Medicine
- Györfi, La'szlo et al, (2002), A Distribution-Free Theory of Nonparametric Regression, Springer-Verlag New York, Inc
- Haskins JB (1985). The role of mass media in alcohol and highway safety campaigns. J Stud Alcohol Suppl 1985;10:184–91
- Kasali, Rhenald. (1992). Manajemen Periklanan. Bandung : PAU-Ekonomi-UI.
- Lastovicka JL (2004), Highway safety mass media youth project. Washington DC: U.S. Department of Transportation 1987 (contract DTNH22-85-C-15404).
- Roberts, Howard et al, (2015), Improving Safety Culture in Public Transportation, Transportation Research Board, Washington, D.C.
- <https://www.thebalance.com/public-service-announcements-are-a-vital-part-of-media-2315189>
- <http://www.wisegeek.com/what-is-public-service-advertising.htm>



IMPACT ON RIDERSHIP OF NEW RAILBASE TRANSIT DUE TO THE OPERATION OF EXTENSIVE BUS SEMIRAPID TRANSIT NETWORK (CASE STUDY: JABODETABEK PUBLIC TRANSPORT NETWORK)

Edy Hadian^a, Alvinsyah^b

^a*Transport Research Group, Civil Engineering Department, University Of Indonesia, Depok, Indonesia*

^b*Transport Research Group, Civil Engineering Department, University Of Indonesia, Depok, Indonesia*

ABSTRACT

The objective of this research is to observe the implication of an extensive bus semirapid transit network operation on the new railbase transit ridership. A transport demand model based on the four step modeling approach is utilized to analyze the change on the ridership. The model is developed from previous works and adjusted through a calibration and validation procedure with various data collected from the field. Model of the base year O-D matrix is calibrated by trip length frequency distribution through a matrix balancing process. While the passenger flow is validated through transit assignment procedure with passenger counting data on the existing bus routes. Based on the assumptions made and different operational characteristics and fare system scenarios, a simulation through the developed model on new railbase transit ridership is conducted. From the analysis, when operated individually, the new railbase transit ridership will reduce significantly due to the operation of bus semirapid transit network. Yet, if both transit modes are operated as an integrated system, the simulation result yield to a better ridership.

Keywords: Bus Semi Rapid Transit; Railbase Transit; Ridership; Transport Model

1. INTRODUCTION

In the near future Jabodetabek (Greater Jakarta) area will have a new railbase mass transit system which consists of Central Government Light Rail Train (CG-LRT) and Jakarta Local Government Light Rail Train (DKI-LRT). Currently, two CG-LRT corridors connecting Cibubur (Southeast of Jakarta) area and Bekasi (Eastern of Jakarta) area with City of Jakarta and DKI-LRT phase-1 of the first corridor connecting Kelapa Gading area with Velodrome at Pulo Mas area are under construction. Besides, the construction of Jakarta North-South MRT stage 1 connecting Southern part of Jakarta with Central part of Jakarta is also on progress. These new railbase mass transit shown in Figure 1, are expected to be in operation in the year of 2020. Meanwhile, in early 2016, the Central Government established a new agency under Ministry of Transportation called Badan Pengelola Transportasi Jabodetabek (BPTJ) which is responsible for all transportation issues in Jabodetabek (Greater Jakarta) Area.

Unfortunately, due to current prevailing regulation almost all public transport service are ruled and managed under different authority, and consequently this new established agency



cannot function optimally as it supposed to be. In the worst case, these all public transport include the new railbase mass transit could be potentially managed and operated independently. Hence, the sustainability of operation of such technology could be in hazard, if public money should be minimized in supporting this kind of public service. On the other hand, the most potential program of BPTJ that could be implemented in a very short period is the extensive high capacity bus network service as shown in Figure 2.

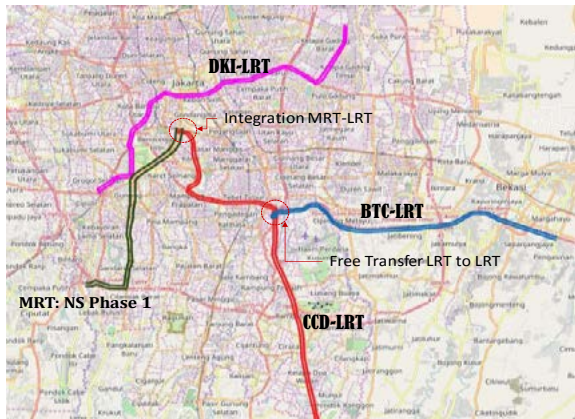


Figure 1. LRT & MRT Network in 2020



Figure 2. BST Network in 2020

Having reviewed to the Master Plan and the existing TransJakarta Busway system, and referring to Vuchic (2002), this kind of high capacity bus system can be categorized as Bus Semirapid Transit (BST). Referring to the Public Transport Master Plan (IUTRI, 2016), there are many BST services that share the route with the new railbase mass transit. Therefore, when all those mass transit are already in operation, number of ridership of each system could be a very potential issue if they are operated independently. Considering the flexibility and accessibility of BST service and its improved operational characteristics such as travel time, method of transaction, and directness of service (ITDP, 2007; Vuchic, 2002), the ridership of new railbase mass transit could possibly be affected in a very significant way.

Based on previous paragraphs, this research tries to analyze the implication of the proposed BST service to the new LRT ridership especially along the overlapping routes. The following sections describe the research framework, and model simulation, the result analysis and discussion and finally the research conclusion.

2. RESEARCH FRAMEWORK

The first step in this research is to prepare a transport model for the analysis. Generally, the preparation of public transport passenger demand forecasting model is based on network development on supply side and the projected socio-economic framework on demand side which involves network scenario development for mass transit system. The passenger traffic demand is forecasted by applying the four-step method. Diagrammatically, the research framework is summarized in Figure 3. A base year model both the network and demand model is adopted from previous work (Alvinsyah and Hadian, 2016; BSTP, 2009; BSTP, 2010; ; IUTRI, 2016; JICA, 2004; CTS, 2004) which has been calibrated and



modified several times (Alvinsyah and Hadian, 2016; IUTRI, 2016; JICA, 2012; KOICA, 2011).

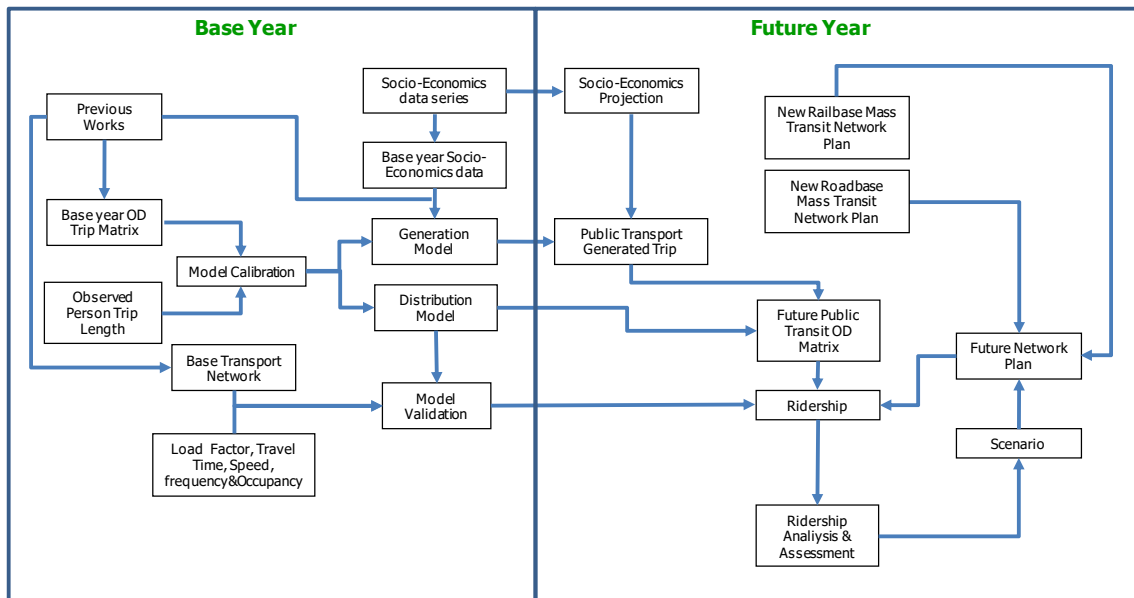


Figure 3. Research Framework

The modeling stage begins with defining a zone and network system based on the city base map and zoning system as well as the surrounding area. The traffic analysis zone (TAZ) system will be defined based on the administrative jurisdiction, namely kelurahan (district). Hence, it will ease in utilizing socio economic data based on the census data. Then, the distribution model is calibrated using trip length data from the field (Kemenhub, 2013; Kemenhub, 2014; Alvinsyah&Hadian, 2016). The distribution model used in this research adopts the gravity method as follows (Papacostas and Prevendeoros,2001);

$$T_{ij} = P_i \left[\frac{A_j \cdot F_{ij} \cdot K_{ij}}{\sum_x A_x \cdot F_{ix} \cdot K_{ix}} \right] \quad (1)$$

where:

- T_{ij} = Nuber of trip between zone i and zone j
- P_i = Total trip Production in zone i
- A_j = Total trip attraction Total in zona j
- F_{ij} = Friction factor or trip impedance between zone i and zone j
- K_{ij} = Socio-economics constant

While the *impedance* function in the gravity model is developed through the following basic formula (FHWA, 2010);

$$F_{ij} = A(d_{ij}^n) e^{(-\beta d_{ij})} \quad (2)$$



where,

- d_{ij} = friction factor (impedance/time) between zone i and zone j
- e = base natural of logarithms
- A, n, β = calibration constants

Utilizing the travel time and person trip data (Alvinyah and Hadian, 2016; Kemenhub, 2014; Kemenhub, 2013) a calibration procedure, an iterative process in curve fitting between trip length data and that of model is conducted to obtain an impedance function. Once the gap between data and model reaches convergency as shown in Figure 4, the impedance function parameters, A , n , and β are determined.

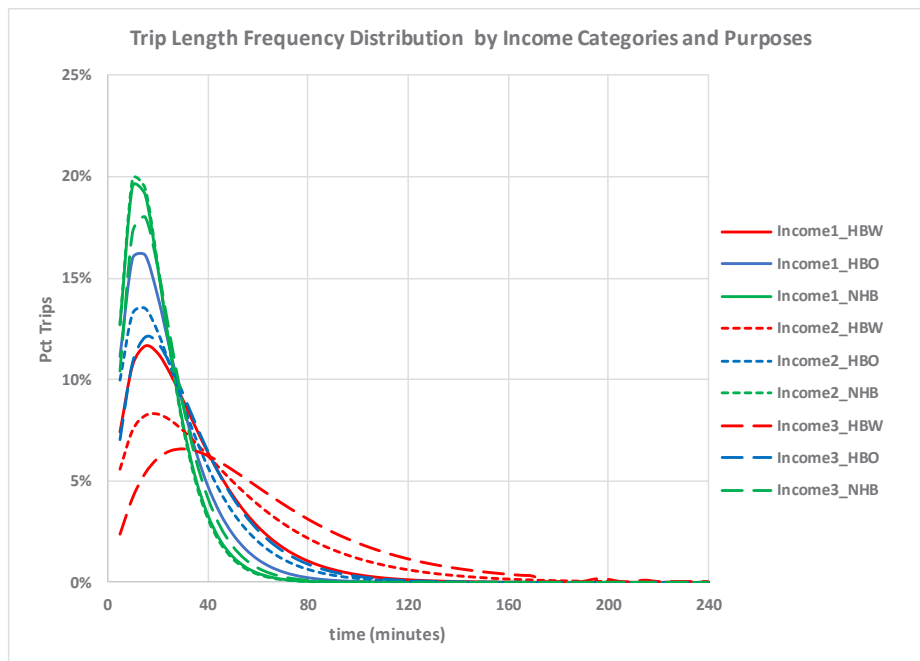


Figure 4. Transit User Trip Length Frequency Distribution

Having determined the impedance function for each transit user category, the base year synthesized O-D Matrix (i.e. Distribution Model) is developed by applying Furness Method (Ortuzar and Willumsen, 2011) for balancing trip between zone. The next step, based on the updated network, the synthesized O-D Matrix, passenger flow, and travel time data from the survey, is validate the model by applying transit assignment. The transit assignment includes links and section of the services running between two stops or stations. The concept of link capacity is associated to the capacity of each unit and its corresponding frequency. The travel time has an-in vehicle component and components for waiting at stops and access and egress time. The other component, the monetary cost (i.e. fare variable) for particular transit lines is converted to ‘time’, and is weight-combined with total travel time to represent “generalized costs” as shown in the following (INRO, 2015);

$$C_{ij} = a_1 t_{ij}^v + a_2 t_{ij}^w + a_3 t_{ij}^t + a_4 t_{ij}^n + a_5 \delta^n + a_5 F_{ij} \quad (3)$$



where,

- t_{ij}^v = In vehicle time from i to j
- t_{ij}^w = Walking time from station or to station
- t_{ij}^t = Waiting time at the station
- t_{ij}^n = Transfer Time at station
- δ^n = Penalty for transfer
- F_{ij} = Fare from i to j
- a_1 to a_3 = Coefficients.

In the validation process, the person trip from the O-D matrix is assigned to the transit network and adjustment to all parameter values in the generalised cost are made until the passenger flow from the assignment process is conformed with that of from field data. The macro planning software called EMME is used to execute the assignment process where the standard transit assignment model implemented in this software is based on the concept of optimal strategies which minimize transfer, waiting and in-vehicle time (INRO, 2015). The most general formulation of this model is described in Spiess (1989), where the cost of a strategy is the sum of link travel times, c_a , weighted by the probability of traveling on link a , and the waiting time at nodes i is weighted by the probability of traveling through node i . The assigning of the trips from all origins to destination r , according to the optimal strategy, corresponds to solving the following linear optimization problem:

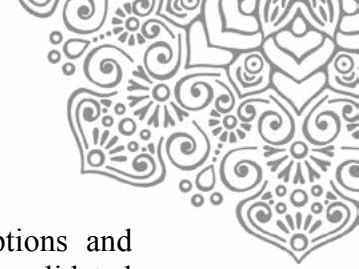
$$\text{Min } \sum_{a \in A} c_a v_a + \sum_{i \in I} \omega_i \tag{4}$$

Subject to

$$\sum_{a \in A_i^+} v_a - \sum_{a \in A_i^-} v_a = g_i \quad i \in I,$$

$$\begin{aligned} v_a &\leq f_a \omega_i & a \in A_i^+, \quad i \in I, \\ v_a &> 0 & a \in A \end{aligned}$$

Variables ω_i as in formula (4) represent the total waiting time (in person minutes) at node i . Further and detail explanation on the mathematical derivation of the above objective function can be found in Spiess (1989). Using this generalized formulation any transit network T can be represented, and the mechanics that are involved in constructing the links and the nodes of the generalized network depend very much on the particularities of the transit network and the degree of aggregation considered. The fundamental concept of this strategy is based on the assumption that a passenger arrived at a station select an optimum route from a group of route randomly to reach his or her destination and board the the first vehicle arrived. This mechanism is done repetitively until reaching the final destination. Prior to conducting a simulation, future O-D Matrix is developed by applying the gravity



model and the forecasted trip generation. Finally, based on several assumptions and scenarios set in this research, a simulation to ridership is conducted through the validated transit assignment procedure.

3. ASSUMPTIONS AND SCENARIOS

To obtain the ridership through model simulation, some basic assumptions and scenarios related with trip generation, public transport share, and operational parameter of the system need to be established first. Referring to previous work (IUTRI, 2016), the growth rate for Jabodetabek area from 1971 to 2005 is about of 4,7% per annum and that for DKI Jakarta is around 2,0% per annum. In 2020, the growth rate prediction is about 1,32% and 0,49% per annum for Bodetabek and Jakarta respectively. While in 2030, the predictionis about 1,03% and 0,19% per annum for Bodetabek and Jakarta respectively. Based on these growth rate prediction, the trip growth for each district (kelurahan) in Jabodetabek area is derived as shown in Table 1.

Table 1. Trip Growth for Jabodetabek Area (person/day)

Administrative Jurisdiction	2020	2025	2030
Kota Depok	1.58%	1.30%	1.12%
Jakarta Barat	0.82%	0.53%	0.40%
Jakarta Pusat	0.81%	0.52%	0.40%
Jakarta Selat	0.78%	0.50%	0.38%
Jakarta Timur	0.77%	0.50%	0.38%
Jakarta Utara	0.81%	0.52%	0.40%
Kab Bekasi	1.64%	1.39%	1.20%
Kab Bogor	1.67%	1.39%	1.21%
Kab Tangerang	1.99%	1.60%	1.43%
Kota Bekasi	1.45%	1.24%	1.08%
Kota Bogor	1.63%	1.35%	1.17%
Kota Tangerang	1.99%	1.58%	1.40%
Average	1.38%	1.10%	0.95%

The public transport share adopted for this research is taken from the survey conducted in the previous work (JICA, 2011), which is 24% from the total motorised person trip in Jabodetabek area. While, all each public transport mode parameter and and the tariff rate are adapted from the previous work (IUTRI, 2016). Basically there will be two basic scenarios that will be simulated in obtaining new LRT ridership, namely base case scenario and alternative case scenario, and these two basic scenario will be tested with three BST speed design, namely optimistic, moderate and pesimistic BST. The design speed are 40 km/hr, 25 km/hr and 17 km/hr respectively. The time horizon used for the ridership forecasting is only for year 2020 and, the predetermined scenarios are shown in Table 2.



Table 2. Scenario for Simulation

Scenario	Description	Remarks
Base Case (BC)	Consider no BST service, Fare integration applies for the same technology only , except for the existing bus system ^a , while for physical integration ^b applies for all type of public transport mode, excepts for the existing bus system.	
Alternative Case-1 (AC-1)	Similar with the BC , but considers BST service	
Alternative Case-2 (AC-2)	Similar with AC-1 , but fare integration applies between new railbase mass transit, but not with BST/ BRT and with KCJ.	Discount fare Rp 1,000,- between MRT and LRT
Alternative Case-3 (AC-3)	Similar with AC-2 , but fare integration applies for all new proposed mass transit, but not with KCJ	Discount fare Rp 1,000,- between BST/BRT, MRT and LRT
Alternative Case-4 (AC-4)	Similar with AC-3 , but fare integration applies for all new proposed mass transit and KCJ	Discount fare Rp 1,000,- between BST/BRT, MRT, LRT and LRT

^{a)} Fare integration is referred to IUTRI (2016)

^{b)} Physical integration means that passenger is able to transfer to all alternatives modes depend on his/her journey characteristics.

4. SIMULATION AND ANALYSIS

Based on the simulation result to the base case scenario, the potential demand (i.e. ridership) for new LRT system represented in total boarding passenger (in the peak hour) is shown in Table 3. While, simulation result to all alternative case is presented in Figure 5.

Table 3. Potential Demand of LRT System in 2020 (pax/hour in thousands)

DKI-LRT (Kelapa Gading-Kebayoran Lama)	CCD-LRT (Cibubur- Cawang-Dukuh Atas)	BTC-LRT (Bekasi Timur – Cawang)
23,761	50,556	50,017

Looking at Table 3, seems that the CG (i.e. CCD & BTC) LRT ridership in peak hour is very promising where this potential demand is considerably significantly high for such system. Taking into account the actual condition represented in the BC scenario, this simulation result is quite logic, because there are no reliable and good transit service that close to that of LRT in the origin area and mostly trip in the peak hour is dominated by commuting trip. In addition, the traffic performance reflected in travel speed along the existing toll and the arterial road where the LRT corridor lies are severely congested (IUTRI, 2016), while, on the other hand the LRT commercial speed is relatively high (40 km/hr). A bit different with the first corridor of DKI-LRT, the ridership is not as high as that of CG-LRT where it accounts only 47% of CG-LRT ridership. This is quite logic due to various public transport services in term of type of service and mode, includes



TransJakarta Busway, are available along and around this LRT corridor. Yet this figure is still within acceptable range for this kind of system (Deen and Pratt, 1992; Vuchic, 1992; Wright and Feljstorm, 2003).

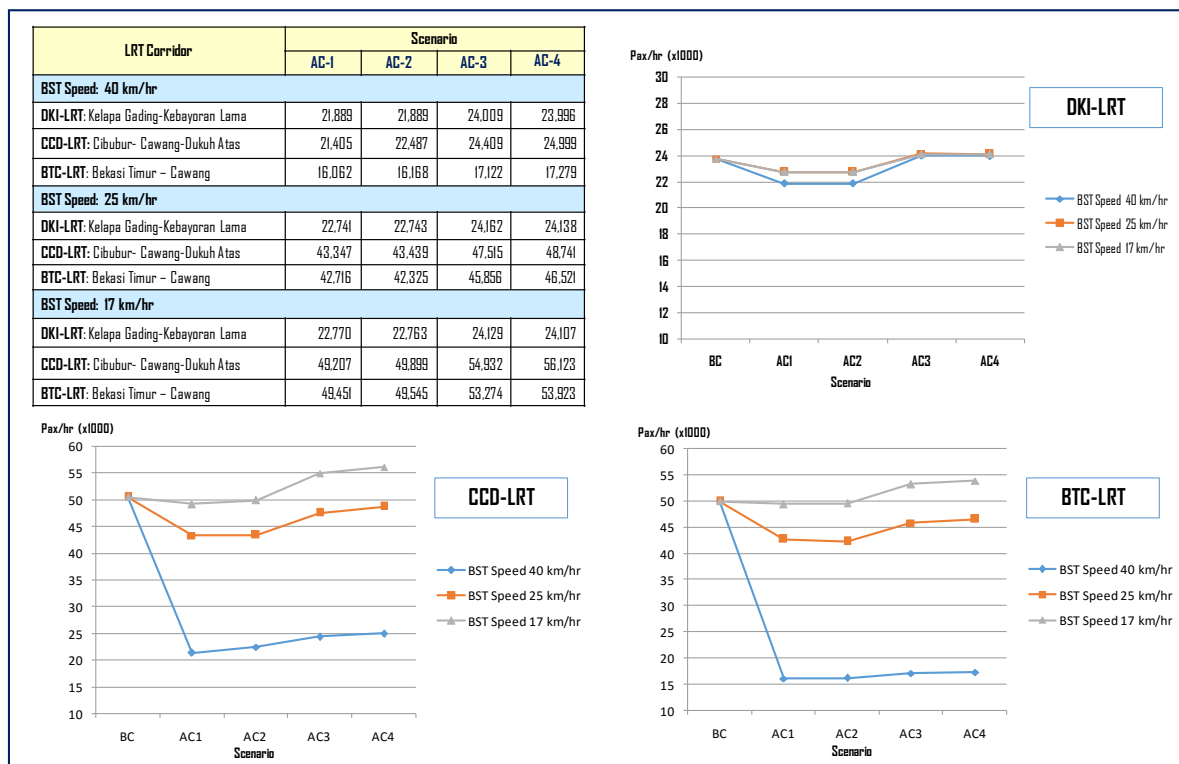


Figure 5. Simulation to all Alternative Scenarios

In contrary, when BST services with the same commercial speed as that of LRT are in operation reflected in AC-1 scenario, the CG-LRT ridership is significantly reduced, where the potential passenger is dropped around 57.66% for CCD-LRT and 67.89% for BTC-LRT compared with that of BC scenario. This significant change indicates that most of CG-LRT potential demand is shifted to the BST. There are several reasons that can be explained about this phenomenon, among others are; the BST routes have more accessibility to the passenger origin and destination compared with CG-LRT routes; its commercial speed is comparable with that of LRT due to the HOV lane provision along the tollroad; their services apply multiroute and direct service, so most passengers do not need to transfer several times to reach his or her destination. Furthermore, in Jakarta area, they are fully integrated with TransJakarta Busway in term of sharing the exclusive lane and stations, and also the transaction, so passengers get a high accessibility to fulfill his/her travel need without additional payment if they have to transfer to TransJakarta Busway and vice versa.

In contrary, this situation does not occur on DKI-LRT ridership, where the change is relatively small, around 7.89%. As explained previously, since DKI-LRT serves the area that becomes destination for the commuter from Bodetabek area, the existence of BST service does not have any significant influence to the DKI-LRT. If this situation is kept



going on without any intervention from the government to improve the CG-LRT ridership, as explained in previous section, in the long run it will endanger the sustainability of the CG-LRT operation due to revenue shortfalls.

One potential policy that can be implemented is to apply a full integration between all mass transit system in Jabodetabek by reinforcing the role and level of authority of BPTJ. Consequently, this kind of policy will reduced other related institution authority both at central government and local government level. To observe the impact of the above policy to the CCG-LRT ridership, three scenarios that mimic the policy as shown in Table 2 are introduced. But, since the fare system for BST is different with that of LRT, a discount method is applied to represent the fare integration between different system. Simulation result shows that there is an increase in ridership for LRT system. Although the increase is not significant, but at least this shows that such policy can help. In the other hand, if the HOV lane provision along the toll road is assumed cannot be realized, reflected by BST speed reduction to 17 km/hr, the simulation results show that the BST operation with low design speed does not significantly affect the LRT ridership where it decrease only 1.33% for CCD-LRT and 2.67% for BTC-LRT compared with BC scenario. While, if the fare is fully integrated as reflected by AC-4, the LRT gain additional ridership around 7.81% for BTC-LRT and 11.01% for CCD-LRT as shown in Figure 5. Now, assumming if BPTJ cannot provide HOV lane along the tollroad but still want to have an ideal BRT speed performance (ITDP, 2007), another scenario with the BST design speed set at 25 km/hr is tested. The simulation result indicates that with this design speed BST are able to attract the LRT ridership around 14.26% from CCD-LRT and 14.59% from BTC-LRT, and if fully integrated fare system is applied to all mass transit (AC-4) LRT ridership decrease only 3.59% for CCD-LRT and 6,69% for BTC-LRT. It is seen that if the proposed BST service is designed and operated in a very good way, and no fare or system integration policy is applied to manage these all mass transit, there will be a contra-productive situation will occur as indicates by significant reduction on LRT ridership.

5. CONCLUSION

An analysis has been conducted on the impact on the proposed LRT ridership due to the introduction of BST route network in Greater (Jabodetabek) area. The analysis is focused on the forecasted demand in term of total boarding passenger at peak hour for each LRT corridor by utilizing a transit model. Asumptions and scenarios which account for transit operational characteristics, fare setting, and trip growth rate are set for the analysis. Simulation results to the predetermined scenarios yield that the BST service will potentially attract a very significant number of passenger from the CG-LRT if this proposed BST is designed, operated and managed in a very porper and good method. In contrary, such situation does not occur for DKI-LRT in all alternative cases tested. When, a full system integration is applied to all mass transit, the simulation result shows that an increase in LRT ridership can be expected. This indicates that the government needs to enforce a strong and good policy to integrate all these proposed mass transit in all aspects when they are in operation in order to have a sustainable, reliable and satisfactory service for the Jabodetabek people.



REFERENCE

- Alvinsyah dan Hadian E. (2016), Analisis Dampak Aktifitas Kawasan Reklamasi Pantura terhadap Kinerja Jaringan Jalan di DKI Jakarta, *Jurnal MTI* Vol. 1 No. 1, hal. 43-58.
- BSTP (2010), Studi Pedoman Perencanaan Trayek Pengumpan (Feeder) untuk Angkutan Massal Berbasis Jalan, Direktorat Jendral Perhubungan Darat, Final Report
- BSTP (2009), Studi Penyusunan Master Plan Pola Transportasi Makro (PTM) Jabodetabek Tahap I, Direktorat Jendral Perhubungan Darat, Final Report
- CTS (2004), Pola Transportasi Makro Jakarta, Final Report, Dishub DKI - CTS UI.
- Deen, T.B. and Pratt, R.H. (1992), Evaluating Rapid Transit, in *Public Transportation* ed. Gray, G.G and Hoel, L.A., Prentice Hall, Inc., Englewood Cliffs New Jersey, pp. 293 - 331
- FHWA (2010), *Travel Model Validation and Reasonableness Checking Manual 2nd Ed.*, Federal Highway Administration, USA.
- INRO (2015), *User Manual, EMM Suite*, Montreal
- ITDP (2007), *Bus Rapid Transit Planning Guide*, Institute for Transport Development & Policy, New York.
- IUTRI (2016), *Capacity And Demand Analysis Of Jabodetabek Mass Transit Network*, Final Report, JICA.
- JICA (2011), *Study On Jabodetabek Urban Transportation Implementation Plan (Review On Sitramp-2004), 2nd Draft Final Report*
- JICA (2004), *Studi on an Integrated Transport Master Plan for Jabodetabek Area*, Final Report
- Kemhub (2014), *Survey Wawancara Rumah Tangga di Kota Bekasi, Depok dan Bogor*, Laporan Akhir, Badan Penelitian dan Pengembangan Kementerian Perhubungan.
- Kemhub (2013), *Survey Wawancara Rumah Tangga di Kota Tangerang dan Tangerang Selatan*, Laporan Akhir, Badan Penelitian dan Pengembangan Kementerian Perhubungan.
- KOICA (2012), *Master Plan for Jabodetabek Railway, PMC Service for Master Plan and Feasibility Study for Jabodetabek Railway in Indonesia*, Final Report.
- Ortuzar, J.D., and Willumsen, L.G. (2011), *Modelling Transport Fourth Edition*. Wiley Inc., West Sussex, UK
- Papacostas, C.S. and Prevenduros, P.D. (2001), *Transportation Engineering & Planning*, 3rd, Prentice Hall Inc., New Jersey, USA
- Spiess H., and Florian, M., (1989), *Optimal Strategies: A New Assignment Model for Transit Networks*, *Transportation Research Part B: Methodological*, Volume 23B No. 2, pp 83-102
- Vuchic V. R. (2002), *Bus Semirapid Transit Mode Development and Evaluation*, *Journal of Public Transportation*, Volume 5, Nomor 2.
- Wright, L. (2004), *Bus Rapid Transit*, Deutsche Gesellschaft für Technische Zusammenarbeit (GTZ) GmbH.
- Wright, L. And Fjellstrom, K. (2003), *Mass Transit Options*, Deutsche Gesellschaft für Technische Zusammenarbeit (GTZ) GmbH.



CAPACITY AND DUCTILITY ANALYSIS OF EXTERNALLY STRENGTHENED R/C COLUMNS USING STEEL PLATES

¹I Ketut Sudarsana*, ¹Putu Deskarta, ²Kadek Bangkit Tilem Sentosa

¹ Civil Engineering Department, Udayana University

² Alumni Civil Engineering Department, Udayana University

^{1,2}Jln Kampus Udayana, Jimbaran, Badung, Bali, Indonesia

Email : ksudarsana@unud.ac.id (*)

ABSTRACT

Strengthening of reinforced concrete (RC) members is usually done to increase the members' capacity and ductility. An external strengthening using steel plates is one of commonly used materials to strengthen columns. This paper presents analysis results of RC columns strengthened with steel plates. The main parameter on this study is the variation of steel plate arrangement on column sides of a controlled column section (KK) which having dimension of 300 x 300 mm and longitudinal reinforcement ratio of 1.8%. Four variations of strengthening sections (KPS, KPP, KPPP and KPSP) are analyzed to obtain their capacity and ductility. The average ratio of the steel plate area to that of RC sections in all sections is 4.7%. Sectional analysis was conducted to obtain axial force-moment interactions and moment-curvature diagrams to evaluate the capacity and ductility of the column sections for considering both confined and unconfined concrete. Three models of the stress-strain diagrams for concrete used in the analysis are Hognestad model (1951), Mander et.al model (1988) and Sakino and Sun model (1994), respectively, for unconfined concrete, confined concrete by hoops and confined concrete by steel plates or tube. Analysis results shows that using the steel strengthening ratio of 4.7% can improve the column capacity and ductility significantly regardless the arrangement of the steel plate. However, the highest improvement on the capacity is given by the section with steel plate concentrate at four corner sections (KPS) and then follows by KPSP, KPPP and KPP. Comparing to the control section (KK), the curvature ductility also increases by 12% to 22% for unconfined and 38% to 46% for confined sections.

Keywords: capacity, ductility, reinforced concrete, strengthening column section



1. INTRODUCTION

Column is one of the structural frame components to resist loads transferred from beams and slabs in the form of axial force, bending moment, shear force and torsion. Therefore, columns must have enough strength to resist and transfer the internal forces to foundations. However, in dealing with earthquake load, the columns must also have enough ductility to resist in-elastic reverse deformations without losing their strength significantly.

Indonesian seismic code (SNI 1726:2002) has been updated becomes SNI 1726:2012 which mostly refers to ASCE/SEI 7-10 and IBC 2009, therefore, 22 cities in Indonesia have changed the seismic design spectral (Afriadi, 2013). Due to changing in seismic loading, many buildings may need to be strengthened or retrofitted. The strengthening may only apply to some part of the structural elements such as columns, beams, and slabs or the whole structure. There are many ways to strengthen the columns, one of them is column jacketing using steel plate or combination of steel angles and plates.

Many researchers have done works on column steel jacketing such as Belal et al.(2014), Tarabia et al.(2104) and Abdel-Hay et al. (2015). It is found that the methods can increase load carrying capacities of column and improve the column behaviors. In practical applications, combinations of welded steel angles and plates are possibly used since most column sections are rectangular or square. Sudarsana (2017) studied the application of this method to retrofit SPS Building in Jimbaran-Bali, It is found that the strengthening system works very well to improve the capacity of the structural elements. However, the ductility of the strengthening section is not known, therefore, this research is done to investigate the effect of variation on steel angles and plates on the column's capacity and ductility. The column capacity and ductility are studied based on interaction P-M diagram and curvature ductility, respectively.

2. METHODOLOGY

Sectional analysis was conducted to obtain capacity and ductility of the strengthened column sections by considering the effect of confinement by hoops and steel plates on concrete. There are two confined concrete models were considered in the analysis such as Mander et.al.(1988) and Sakino and Sun (1994).

2.1. Concrete Materials

2.1.1. Unconfined concrete

The stress-strain unconfined concrete diagram commonly accepted for normal strength concrete is Hognestaad Model (1951). The curve consists of two parts such as ascending branch *OA* and descending branch *AB* as shown in Figure 1. The equations of these two parts are given in Equation 1 and 2.

For ascending branch *OA* ($0 \leq \varepsilon_c \leq \varepsilon_0$):

$$f_c = f'_c \left[\frac{2\varepsilon_c}{\varepsilon_0} - \left(\frac{\varepsilon_c}{\varepsilon_0} \right)^2 \right] \quad (1)$$

For descending branch *AB* ($\varepsilon_0 \leq \varepsilon_c \leq \varepsilon_{cu}$):



$$f_c = f'_c (1 - 100(\epsilon_c - \epsilon_0)) \quad (2)$$

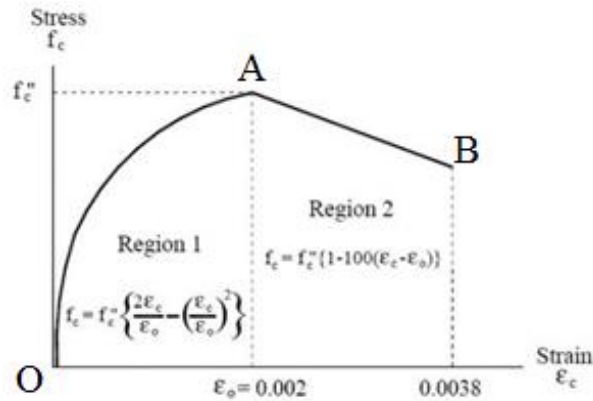


Figure 1. Stress-strain curve Hognestad Model (1951)

2.1.2. Confined concrete by hoops

Stress-strain concrete diagram proposed by Mander et al. (1988) has been accepted for confined concrete as shown in Figure 2 in which the confined concrete diagram is compared with unconfined concrete diagram. The curve is represented using a single Equation 3.

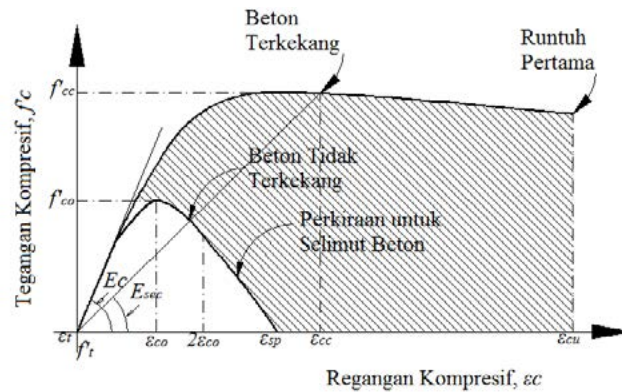


Figure 2. Stress-strain concrete diagram by Mander et al (1988)

$$f_c = \frac{f'_{cc} \cdot x \cdot r}{r - 1 + x^r} \quad (3)$$

where:

$$x = \frac{\epsilon_c}{\epsilon_{cc}} \quad (4)$$

$$\epsilon_{cc} = \epsilon_0 \left[1 + 5 \left(\frac{f'_{cc}}{f'_{co}} - 1 \right) \right] \quad (5)$$

$$r = \frac{E_c}{E_c - E_{sec}} \quad (6)$$

Definition of the parameters in Equation 3 to 6 and other details on the model can be found in Mander et al. (1988).



2.1.3. Confined concrete by steel plates or steel encase

Sakino and Sun (1994) proposed equations for stress-strain curve of concrete sections confined with steel plates on whole section surfaces as follows:

$$f_c = K \cdot f'_c \frac{ax + (b-1)x^2}{1 + (a-2)x + bx^2} \quad (7)$$

where:

$$K = \frac{f'_{cc}}{f'_c} = 1 + 11,5 \frac{f_y}{f'_c} \left(\frac{t}{B-2t} \right) \quad (8)$$

$$\rho_t = \left(\frac{B}{B-2t} \right)^2 - 1 \quad (9)$$

$$a = \frac{E_c}{E_{sec}} = \frac{E_c \cdot \varepsilon_{co}}{K \cdot f'_c} \quad (10)$$

$$\frac{\varepsilon_{co}}{\varepsilon_o} = \begin{cases} 1 + 4,7(K-1), & K \leq 1,5 \\ 3,35 + 20(K-15), & K > 1,5 \end{cases} \quad (11)$$

$$b = 1,5 - 0,017 f'_c + 2,4 \sqrt{\frac{(K-1)f'_c}{23}} \quad (12)$$

For more details on the model and definition of the parameters in Equation 7 to 12 can be found in Sakino and Sun (1994).

2.2. Model of strengthening column sections

The column section as a control specimen (KK) is chosen to meet the minimum requirements of special moment frame in SNI 2847:2013. The application of strengthening material such as steel angles and/or plates to the control section (KK) follows the steel requirements in SNI 1729:2015. Figure 3 and Table 1 show properties of the control section and strengthening sections (KPS, KPP, KPPP and KPSP).

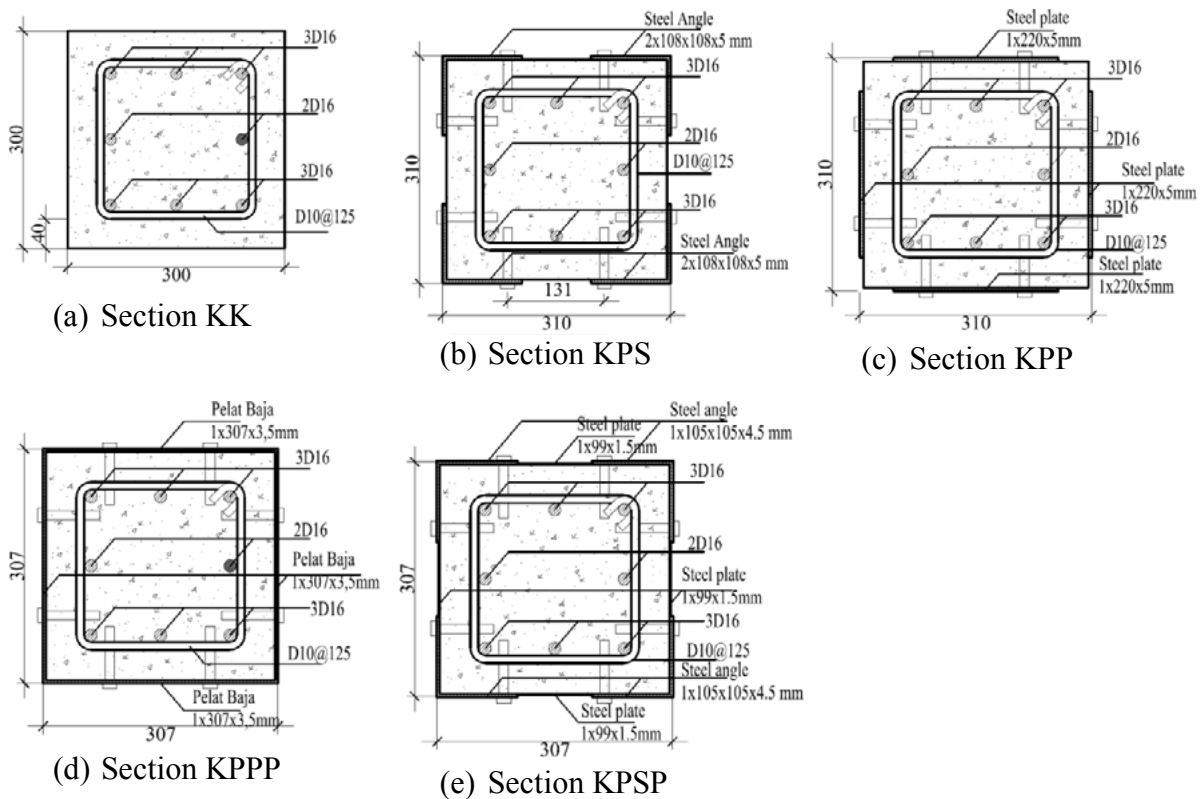




Figure 3. Control and strengthening column sections

All strengthening sections have similar area of steel angles and/or plates. The steel angles and plates are fixed using bolts and grout materials to fill empty spaces between existing concrete and steel. In the analysis, a perfect bound between concrete and steel angle or plates was assumed.

Table 1. Properties of strengthening column sections

Section ID	Dimension (mm)	Longitudinal rebars and Hoops	Steel Strengthening ratio (ρ_{steel})	Remarks
KK	300 x 300	8D16 D10@125	-	Control section
KPS	300 x 300	8D16 D10@125	4.49%	Column strengthening with steel angle (KPS)
KPP	300 x 300	8D16 D10@125	4.72%	Column strengthened with half steel plates (KPP)
KPPP	300 x 300	8D16 D10@125	4.72%	Column strengthening with full welded steel plates (KPPP)
KPSP	300 x 300	8D16 D10@125	4.77%	Column strengthening with welded steel angles and plates (KPSP)

2.3 Sectional analysis

Sectional analysis was conducted to develop P_n-M_n and $M_n-\phi$ diagram in order to evaluate capacity and ductility of strengthening column sections. The steel angles and plates on the section sides is divided into some elements to have more accurate moment lever arms, however, for the steels at end of the sections (tension or compression fibers) are considered as one resultant forces. Figure 4 shows internal strain and stress diagram of the strengthening sections (KPSP) as one of the example. The analysis procedures follow the reinforced concrete sectional analysis procedures where equilibrium and compatibility principles apply. The only difference is there is steel plate or angles outside of the sections.

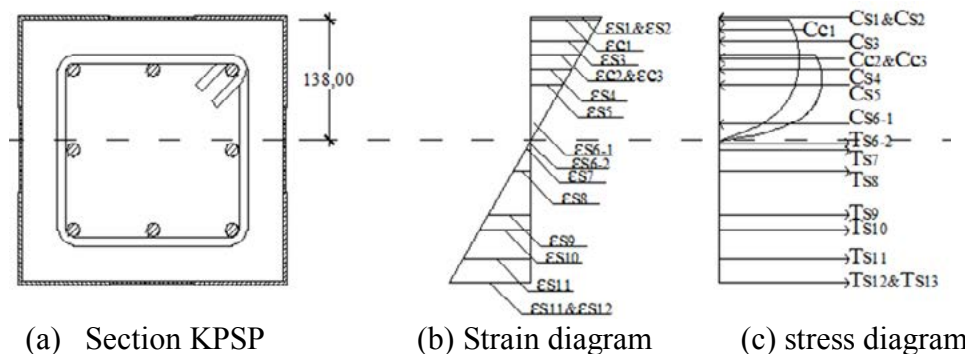


Figure 4. Section strain and stress of section KPSP



3. RESULTS AND DISCUSSION

3.1. Stress-Strain Concrete Diagram

Stress-strain curve for all concrete models considered in this study such as Hognestad (1951), Mander et al. (1988) and Sakino et al. (1994) as shown in Figure 5. All models are based on unconfined concrete strength of 20 MPa. The important point of the curve such as the stress and strain at peak and assumed failure points are given in Table 2 for all models. The models are developed base on an unconfined concrete strength of 20 MPa.

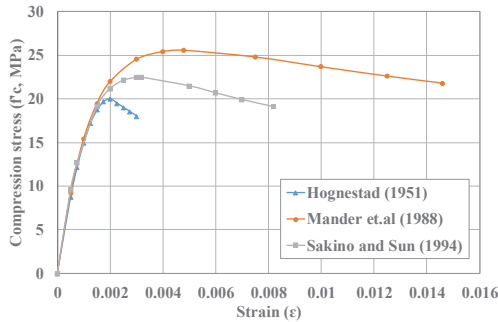


Figure 5. Stress-strain all concrete models

Table 2. Stress-strain value at peak and assumed concrete failure

Model	f'_c (MPa)	ϵ_0 (mm/mm)	$f'_{c,85}$ (MPa)	ϵ_{85} (mm/mm)
Hognestad (1951)	20.00	0.00200	18.00	0.0030
Mander et.al (1988)	25.60	0.00350	22.76	0.0146
Sakino and Sun (1994)	22.53	0.00320	19.15	0.0082

Table 2 and Figure 5 show that confinement can increase the concrete strength. Comparing the confined concrete models to Hognestad Model (1951), the concrete strength increases by 28% and 12.65% respectively for Mander Model (1988) and Sakino Model (1994). However, Sakino model (1994) gives lower concrete strength than Mander Model (1988) although a full confinement given by the steel plates to the concrete surface.

3.2. Interaction P_n - M_n of strengthening column sections

Sectional analysis was conducted to develop interaction diagram between axial force and bending moment for all column sections. Two concrete condition are considered such as without and with considering the effect of confinement.

3.2.1. Without considering concrete confinement

In this analysis, the concrete strength in all models follows stress-strain diagram of Hognestad model (1951). The only difference among the column sections is the ratio of strengthening steel as shown in Table 1. The results of the analysis are plotted in Figure 6 and the maximum value of section capacity is given in Table 3.

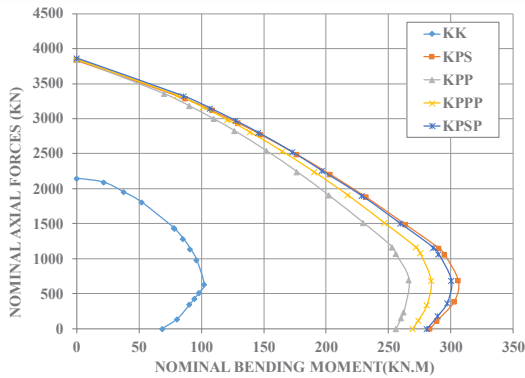
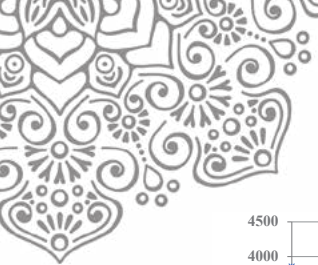


Figure 6. Interaction Diagram for all column sections

Figure 6 shows that the strengthening column using steel angle and/or steel plate by the ratio of 4.69-4.77% can significantly increase the column strength. Using steel angles at for column corners give greater nominal moment than using steel plate at middle sides of the section as shown by section KPS and KPP. This is due to longer distance of couple force for steel at corner. However, axial capacity of KPP a little bit higher than KPS due to having higher steel ratio (4.69% to 4.72%).

3.2.2. With considering concrete confinement

In the analysis of the column section KK, KPS and KPP, the concrete core bounded by the hoops follows Mander et al (1988) and the concrete cover outside the hoops follows Hognestad model (1951). For the column section KPPP and KPSP in which all concrete cover are confined by welded steel angle and/or plates, the concrete core and the concrete cover follow Mander et al (1988) and Sakino and Sun (1994) models. The analysis results are shown in Figure 7 and Table 4.

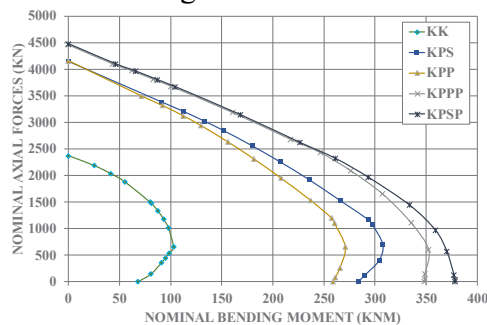


Figure 7. Interaction Diagram for all column sections

Table 3. Axial forces and bending moment at three conditions

Section ID	Condition			Pure Bending Mn (kNm)
	Axial Concentric	Balance		
	Pn (kN)	Pn (kN)	Mn (kNm)	
KK	2146.302	631.733	102.121	68.570
KPS	3834.302	1147.490	290.808	283.367
KPP	3846.302	1164.700	253.185	256.221
KPPP	3845.902	1163.473	272.156	269.636
KPSP	3863.502	1157.208	286.149	281.072

Table 4. Axial forces and bending moment for three conditions

Section ID	Conditions			Pure Bending Mn (kNm)
	Axial concentric	Balance		
	Pn (kN)	Pn (kN)	Mn (kNm)	
KK	2371.470	649.631	103.615	68.611
KPS	4148.418	1177.748	293.034	283.670
KPP	4160.418	1200.416	257.631	258.963
KPPP	4461.213	2428.279	246.869	348.255
KPSP	4478.813	1964.666	293.459	378.202

3.3. Ductility of column sections

The ductility of the column is measured base on curvature ductility. For comparison purposes, all column sections are assumed having ultimate axial force (P_u) of 20% $P_o = 343.41$ kN. Two concrete conditions are considered such as unconfined and confined concrete.

3.3.1. Without considering concrete confinement

Moment-Curvature diagrams for all column sections without considering the effect of confinement are shown in Figure 8.

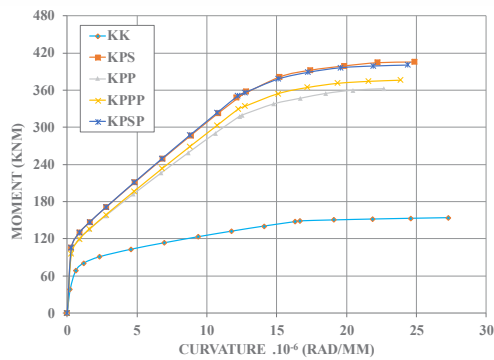


Figure 8. M-φ diagram for all column sections without confinement

All strengthening columns have higher bending capacity than the control section (KK). This is mainly due to additional of strengthening steel angle and/or plates. The column ductility does not differ significantly. By increasing the strengthening ratio of 4.69% to 4.77%, the column ductility increases about 12% to 22% as shown in Table 5. It is also shown in Table 5 that the addition of strengthening steel reduces yield and ultimate curvature of the strengthening sections.

3.3.2. With concrete confinement

The analysis moment-curvature (M-φ) for all section by considering confinement by hoops and steel plates is given in Figure 9. The curvature ductility is shown in Table 5. For Section KK, KPS and KPP, there is a drop in the section moment capacity due to reduction on the cover of column section after unconfined concrete reaches maximum concrete strain. For the section KPPP and KPSP, drop in the moment capacity occur after confined concrete cover according to Sakino and Sun (1994) reaches maximum strain.

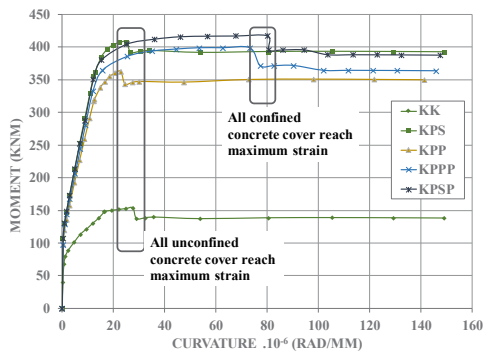


Figure 9. M-φ Diagram for all column sections with confinement

The curvature ductility increases due to steel strengthening about 37.35% to 47% when considering the effect of concrete confinement. Comparing the ductility of column sections for unconfined and confined concrete, the ductility of confined column section is about 5 to 6 times of that unconfined column sections.

Table 5. Curvature ductility without considering confinement concrete

Section ID	Yield Conditions		Ultimate Conditions		μ_ϕ
	M_y kNm	$\phi_y \cdot 10^{-6}$ rad/mm	M_u kNm	$\phi_u \cdot 10^{-6}$ rad/mm	
KK	148.60	16.67	153.74	27.30	1.63
KPS	357.79	12.82	405.56	24.88	1.94
KPP	317.46	12.34	361.95	22.67	1.83
KPPP	329.53	12.24	376.25	23.88	1.95
KPSP	350.91	12.20	400.75	24.40	1.99

Table 5. Curvature ductility with considering confinement concrete

Section ID	Yield conditions		Ultimate conditions		μ_ϕ
	M_y kNm	$\phi_y \cdot 10^{-6}$ rad/mm	M_u kNm	$\phi_u \cdot 10^{-6}$ rad/mm	
KK	148.61	16.60	139.78	138.2	8.3
KPS	354.77	12.18	392.74	149.0	12.2
KPP	317.37	12.31	349.97	141.4	11.4
KPPP	332.30	11.99	363.52	145.9	12.1
KPSP	350.74	12.15	387.79	147.5	12.1



4. CONCLUSION

Based on the analysis and discussions have been done, the following conclusions can be drawn:

- a. Confinement provided by hoops (Mander et.al, 1988) and full steel plates (Sakino and Sun, 1994) increases the concrete strength by 28% and 12.65% respectively.
- b. Strengthening of column sections using steel ratio of 4.69 to 4.77% significantly increases the column capacity both without and with considering confinement.
- c. Curvature ductility of the strengthening column sections using steel ratio of 4.69 to 4.77% increases in average of 18.25% and 31.5% for without and with considering concrete confinement, respectively.
- d. Curvature ductility of the strengthening column sections due to the effect of confined concrete is about 5 to 6 times higher.
- e. Strengthening of the concrete columns with steel jacketing can improve both column's capacity and ductility.

5. ACKNOWLEDGEMENT

This research has been possible with financial supports from Department of Civil Engineering at University of Udayana. Special thanks to colleagues at the department for their input and comments during various stages of the research program.

6. REFERENCES

- Abdel-Hay, A.S. and Fawzy Y.A.G., (2015), Behavior of Partially Defected R.C Columns Strengthened Using Steel Jackets, Journal of Housing and Building National Research Center (HBRC Journal). Vol 11, pp.194-200.
- Afriadi, Y. dan Satyarno, I. (2013). Perbandingan spektra desain beberapa kota besar di Indonesia dalam SNI gempa 2012 dan SNI gempa 2002, In Prosiding Konferensi Nasional Teknik Sipil 7, Surakarta, 24-25 Oktober.
- Badan Standarisasi Nasional, (2002), SNI 1726:2002 Standar Perencanaan Ketahanan Gempa untuk Bangunan Gedung, Jakarta.
- Badan Standarisasi Nasional, (2012), SNI 1726:2012 Standar Perencanaan Ketahanan Gempa untuk Bangunan Gedung, Jakarta.
- Badan Standarisasi Nasional, (2013), SNI 2847:2013 Persyaratan beton struktural untuk bangunan gedung, Jakarta.
- Badan Standarisasi Nasional, (2015), SNI 1729:2015 Spesifikasi untuk bangunan gedung baja struktural, Jakarta.
- Belal, M.F., Mohamed H.M. and Morad S.A., (2014), Behavior of Reinforced Concrete Columns strengthened by Steel Jacket, Journal of Housing and Building National Research Center (HBRC Journal).
- Hognestad, E., (1951), A study of combined bending and axial load in reinforced concrete members. Universitas of Illinois Engineering Experiment Station Bulletin Series No. 399 University of Illinois, Urbana.
- Mander, J. B., Priestley, M. J. N. and Park, R., (1988), Theoretical stress-strain model for confined concrete. Journal of the Structural Division, ASCE, Vol.114, No.STB, pp.1827-1849
- Sakino, K. and Sun, Y., (1994), Stress-Strain Curve of Concrete Confined by Rectilinear Reinforcement, Journal of Structural and Construction Engineering, Transactions of AIJ, No. 468, pp.94~103. (in Japanese)



Sudarsana, IK., (2017), Retrofitting of Low Rise Reinforced Concrete Building Using External Bolted Steel plates: Case Study SPS Building, Jimbaran-Bali, *Procedia Engineering* 171, pp. 1147-1156.

Tarabia, A.M. and Albakry, H.F., (2014), Strengthening of RC columns by steel angles and strips, *Alexandria Engineering Journal*. September, Vol 53, pp.615-626.



DEVELOPMENT OF INSTITUTIONAL FUNDING MODEL OF DEEP DISCOUNT BOND ON TOLL ROAD PROJECTS

Muhammad Haikal Syarief, Yusuf Latief, Ayomi Dita Rarasati*

Civil Engineering Department, Faculty of Engineering, Universitas Indonesia, Kampus UI Depok, Depok 16424, Indonesia

*corresponding author: ayomi@eng.ui.ac.id

ABSTRACT

The high investment in infrastructure projects including toll roads makes government seek new funding schemes without charging the entire construction budget on the State Budget. Therefore, an alternative funding scheme is necessary to attract investors to fund and develop toll roads in Indonesia especially at the Trans-Sumatera Toll Road (TSTR). The answer might be found with the Deep Discount Bond (DDB) funding scheme which is potentially positive for the development of toll roads in Indonesia. This answer can address new issues, but to ensure that it can be implemented, an institutional model is needed to regulate stakeholders' involvement. Realizing that interactions among stakeholders are very influential on the success of the project, the effective institutional model is aimed at avoiding possible conflicts. This institutional model cannot be properly designed without knowing the success factors required to effectively implement DDB funding scheme. This research has three objectives: firstly, to identify relevant stakeholders involved in providing DDB funding schemes; secondly, to identify DDB institutional model's success factors; and thirdly, to determine the appropriate DDB funding scheme institutional model for Trans Sumatera Toll Road. This research methodology included data collection, and three-phase in-depth interviews and Relative Importance Index and Multi Criteria Analysis. The results identified ten stakeholders with their roles, ten institutional success factors and an institutional funding model to implement DDB for TSTR.

Keywords: Deep Discount Bond; Institutional Model; Stakeholder; Toll Road

1. INTRODUCTION

Toll road development policies and strategies are aimed to increase and improve road availability, including their effective management systems like operation and maintenance (O&M), which can also support local communities' social and economic activities (Manarung, 2006). Referring to the Master Plan for the Acceleration and Expansion of Indonesia Economic Development (MP3EI), Sumatera is one of the economic corridors for local production and processing center of national energy resources. Therefore, it is crucial to develop connectivity between these economic corridors, one of which is by building a toll road across Sumatera (Trans-Sumatera Toll Road). However, this project ($\pm 2,713$ Km) requires 330 Trillion Rupiah worth of funding (Ministry of Public Works, 2011). Such high investment in toll road and the low rate of financial interest rate of return (FIRR) make it



difficult to attract investors to this project (Berawi, *et al.*, 2015). TSTR is also projected to be a part of the Asian Highway Network, and will serve as an artery network in the Southeast region, as described in the Master Plan on ASEAN Connectivity (MPAC) (Berawi, *et al.*, 2015).

The Indonesian Government (GoI) has already taken an initiative not to charge the above entire budget on its State Budget (APBN) (Manarung, 2006) hence in need of an alternative funding scheme to attract investors to the Trans-Sumatera Toll Road. The answer can probably be found in the DDB, which is potentially positive for the development of toll roads in Indonesia (Rarasati, *et al.*, 2016). The DDB model is funded by loans sourced from financial markets in the form of Zero Coupon Bond (Reilly & Brow, 2012). With the current lack of funding sources for infrastructure development, public investment with bonds has become an interesting alternative for the Government.

Bond is any interest-bearing, discounted government, or corporate security that obligates the issuer to pay bond-holders a specified sum of money, usually at specific intervals, and to repay the principal amount of the loan at maturity (Downes & Goodmand, 1998; Fitch, 2012). Although bond-holders have an IOU from the issuer, they do not have ownership privileges as stockholder. Raising fund from capital market has become an alternative source of financing and bond is one of the most popular debt instrument (Lam, *et al.*, 2011).

The DDB, also called pure discount bond, was first published by a US company in 1980's with only one time cash-in in the cash-flow until maturity. DDB does not provide a steady income; rather its appeal is in the low initial purchase price of its bonds (Elton, *et al.*, 2014). DDB is said to be similar to Zero Coupon Bond, with its primary definition "cheap prices traded bonds by the issuer because of discount" (Reilly & Brow, 2012). The investor's source of profit is the difference between the purchasing price when the (cheap) bond is issued at its par value and the value to be paid by bond-issuer at maturity (Faerber, 2009).

The use of bond funding scheme directly from project assets is driven by economic crisis in many countries around the world. As such, many infrastructure projects with great investment value currently use bonds as their source of funding (Latham & Watkins, 2009). Some of them are shown in Table 1.

Table 1 Projects Using Bond Funding Scheme

<i>Publisher / Project</i>	<i>Location</i>	<i>Publish Date</i>	<i>Nominal</i>	<i>Project Type</i>
<i>Dolphin Energy</i>	UAE	August 2009	\$ 1,25 billion	Natural Gas Pipes
<i>RasGas</i>	Qatar	July 2009	\$ 2,23 billion	Natural Gas Liquefaction Facility
<i>Maritimes & Northeast Pipeline</i>	US & Canada	May 2009	\$ 500 million	Gas Pipes Procurement
<i>Black Hills</i>	US	May 2009	\$ 250 million	Power Plants
<i>407 Highway</i>	Canada	April 2009	\$ 425 million	Highway
<i>Plenary Health Niagara</i>	Canada	March 2009	\$ 125 million	Health Infrastructure

Source: (Latham & Watkins, 2009)

DDB has a characteristic of longer maturity time (>10 years) compared to bank loans. This puts DDB in a good position to become a potential instrument for financing infrastructure projects because such projects take a long time and has the potential to generate considerable revenue, making bonds an alternative means of financing the much-needed infrastructure in Asia. The success of infrastructure bonds depends on the overall economic



environment and a few institutional factors; research on these the institutional success factor is therefore needed before implementing bond to finance infrastructure projects (Lam, *et al.* 2011) in Indonesia. In addition, stakeholders' interaction is very influential on the success of such projects and an effective institutional model can help avoid possible conflicts (Yudi, *et al.*, 2016; Yuttapongsontorn, *et al.*, 2008).

Institutional means an effort to plan, organize, steer, coordinate and monitor activities to achieve the desired goal effectively and efficiently (Reksohadiprodjo, 2000). An appropriate institutional model can overcome problems that arise due to the gap among stakeholders involved in the project (Grigg, 2005), one of which is by implementing Public-Private Partnership (PPP) scheme. PPP is an agreement or contract between public (government) and private parties in which the private sector holds some government functions in a certain period (Parente, 2006; Djunaedi, 2007).

The involvement of private parties in the concession is aimed at overcoming problems faced by the government while implementing the development and management of public facilities in urban areas, especially on funding issues (Grigg, 2005). In general, there are several stakeholders involved in Public Private Partnership, such as (1) Grantor/Government; (2) Project Company; (3) Shareholders; (4) Lenders; (5) Construction Contractor; (6) Operator and/or; and (7) Off taker/User (Sarmiento & Renneboog, 2016; Sari, 2014).

The institutional model cannot be designed properly without the success factors required to implement DDB. It is important to know which stakeholders bear the investment costs, provide facilities and infrastructure, and engage with third parties. Therefore, stakeholder identification is required. The success factor of private sector participation to finance toll road project depends on the responsive financial proposal proposed by special purpose vehicle (SPV) candidates. Private sector should have financial engineering techniques, resources, capital structure, as well as strong risk management capabilities and quality (Ashuri & Mostaan, 2015).

Considering the above background study, this paper has three aims: (1) to identify the stakeholders involved in providing DDB funding schemes; (2) to identify the success factors for the DDB institutional model; and (3) to determine appropriate institutional model for DDB funding scheme for Trans Sumatera Toll Road.

2. METHODOLOGY

A qualitative method is used in this research to find an effective institutional model to implement Deep Discount Bond (DDB) for a study object (Trans-Sumatera Toll Road). The variables were analyzed using Relative Importance Index (RII), ranked as institutional success factor and weighted with the Multi-Criteria Analysis. RII method is used to measure the importance of each variable as calculated using predefined parameters (Odusami, 2002).

Multi-Criteria Analysis (MCA) in this research is used to develop selected institutional funding models. MCA can determine the best institutional model analyzed based on



stakeholder and institutional success factors for DDB funding scheme. Current MCA offers much help for practical decision making (Mendoza, *et al.*, 1999).

In-depth interviews were conducted as instruments for data collection, and were divided into three phases to answer each research-question. The output of interview phase one is to identify related stakeholders and their roles, the second is to identify the success factor, and the third is to serve as input for the multi-criteria analysis. The aim of the in-depth interviews was to explore information or contents of the respondents' historical perspective, and to explore in detail as well as to get an understanding based on the respondents' experience (Seidman, 2005).

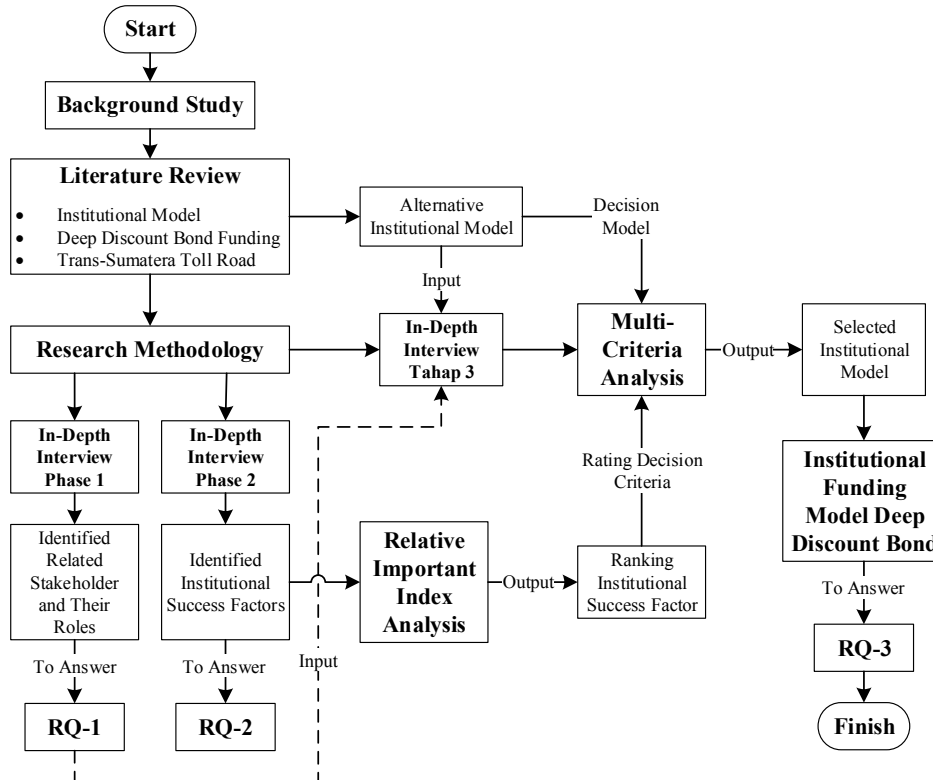


Figure 1 Flowchart of Research Methodology

The various literature studies found some key factors in a successful implementation of PPP institutional model, as shown in Table 2.

Table 2 Institutional Success Factor Variables

Institutional Success Factor	Reference
Government Effectiveness	Panayides, <i>et al.</i> (2015)
Quality of Regulation	Panayides, <i>et al.</i> (2015)
Openness of Market	Panayides, <i>et al.</i> (2015) & Romalis (2008)
Easy to Starting a Business	Panayides, <i>et al.</i> (2015) & Kaufman, <i>et al.</i> (2009)
Investor Protection	Panayides, <i>et al.</i> (2015) & Zhang (2005)
Duration of Concession	Panayides, <i>et al.</i> (2015)
Company Experience	Panayides, <i>et al.</i> (2015)
Financial Package	Gupta, <i>et al.</i> (2013) & Zhang (2005)
Readiness of Financial Proposal	Ashuri & Mostaan (2015) & Zhang (2005)
Effective Management	Liu, <i>et al.</i> (2015)



The 10 identified Success Factors used as the assessment criteria for DBD institutional funding model are a) Readiness of Financial Proposal; b) Effectiveness of Government; c) Company Experience; d) Ease of Starting a Business; e) Investor Protection; f) Effective Management; g) Openness of Market; h) Financial Package; i) Duration of Concession; and j) Quality of Regulations. These ten identified institutional success factors will be covered in an in-depth interview to discuss the success factors for Deep Discount Bond financing scheme.

3. RESULTS AND DISCUSSIONS

The selected respondents for the in-depth interviews in this research were nine experts on toll road infrastructure from government institutions, funding institutions, toll road companies and private individuals. The interviews were conducted at the locations specified by the interviewees themselves, all of which occurring between January 27, 2017 and April 11, 2017. The details of these respondents are shown in Table 3.

Table 3 Respondents' Background and Participation

No	Code	Experience (years)	Education	Institution	In-Depth Interview Phase 1	In-Depth Interview Phase 2	In-Depth Interview Phase 3
1	R1	22	Doctoral	Ministry of Public Work	√	√	
2	R2	20	Doctoral	Toll Road Regulatory Agency	√	√	√
3	R3	35	Doctoral	Government Coordination Committee	√		√
4	R4	24	Master	Infrastructure Financing	√		√
5	R5	30	Doctoral	Toll Road Company	√	√	
6	R6	21	Master	Infrastructure Financing	√	√	√
7	R7	32	Doctoral	Coordinating Ministry for Economic Affairs		√	√
8	R8	16	Master	Ministry of Finance		√	√
9	R9	25	Master	Toll Road Company		√	√

Related Stakeholders in a Deep Discount Bond Funding Scheme

The identified stakeholders involved in the Deep Discount Bond funding scheme are a) Special Purpose Vehicle; b) Credit Rating Agency; c) Bond-Holder; d) Financial Services Authority; e) Ministry of Finance; f) Infrastructure Guarantee Fund; g) Trustee; h) Mandated Lead Arranger; i) Securities Depository; and j) Stock Exchange Market.

Table 4 Stakeholders and Their Roles in Deep Discount Bond Funding Scheme

No	Stakeholder	Role
1	Special Purpose Vehicle	Issuers (DDB Publisher) and/or Design, Build, Finance, Operate & Maintain (DBFOM)
2	Credit Rating Agency	Bond Rating Issuer
3	Bond-Holder / Investor	Bond Buyer
4	Financial Services Authority	Bond Publishing Regulator
5	Stock Exchange Market	Capital Markets & Bond Securities Code Issuer
6	Ministry of Finance	Bond Guarantee as "Full / Government Guarantee"
7	Infrastructure Guarantee Fund	Guarantor of Loans and Political Risk
8	Mandated Lead Arranger	Facilitating and Steering Bond Investors Associations / Selling Agencies
9	Trustee	3 rd Parties Represented Bond-Holder
10	Securities Depository	Payment Agency / Custodian Services

Institutional Success Factors for Deep Discount Bond Scheme

In the second phase of data collection using in-depth interview, the respondents were asked to explain about institutional success factors. Based on the calculation of Relative



Important Index (RII) analysis as shown in Table 5, these factors then became the criteria applied in Multi-Criteria Analysis.

Table 5 Scores and Ranks Obtained from RII Analysis

No	Criteria	Score RII	Rank RII
K-1	Government Effectiveness	0.8857	2
K-2	Quality of Regulation	0.6000	10
K-3	Openness of Market	0.7143	7
K-4	Easy to Starting a Business	0.8000	4
K-5	Investor Protection	0.7429	6
K-6	Duration of Concession	0.6571	9
K-7	Company Experience	0.8571	3
K-8	Financial Package	0.6857	8
K-9	Readiness of Financial Proposal	0.9429	1
K-10	Effective Management	0.7714	5

The highest rank factor at RII analysis was the “Readiness of Financial Proposal” but all of the 10 identified Success Factors became the assessment criteria for institutional funding model DDB: a) Readiness of Financial Proposal; b) Effectiveness of Government; c) Company Experience; d) Ease of Starting a Business; e) Investor Protection; f) Effective Management; g) Openness of Market; h) Financial Package; i) Duration of Concession; and j) Quality of Regulation.

Deep Discount Bond Institutional Funding Model for Trans-Sumatera Toll Road

Based on the results of the literature study and in-depth interviews, three alternative institutional models of Deep Discount Bond (DDB) funding were identified. The fundamental differences between the three models are (M.1) Bond is issued under a corporate bond scheme using Mandated Lead Arranger as Selling Agency; (M.2) Bond is issued under a project bond scheme without a mandated selling agent; (M.3) Bond is issued under a project bond scheme using Mandated Lead Arranger as Selling Agency. Table 6 shows the calculation results of the combined weight from the multi-criteria analysis.

Table 6 Multi-Criteria Analysis Results

Code	Rank	Rating	Alternative Score			Combined Weight		
			M.1	M.2	M.3	M.1	M.2	M.3
K-1	2	16.36%	0.2500	0.1250	0.6250	0.0409	0.0205	0.1023
K-2	10	1.82%	0.3750	0.5000	0.1250	0.0068	0.0091	0.0023
K-3	7	7.27%	0.7500	0.0000	0.2500	0.0545	0.0000	0.0182
K-4	4	12.73%	0.2500	0.7500	0.0000	0.0318	0.0955	0.0000
K-5	6	9.09%	0.2500	0.0000	0.7500	0.0227	0.0000	0.0682
K-6	9	3.64%	0.3750	0.3750	0.2500	0.0136	0.0136	0.0091
K-7	3	14.55%	0.5000	0.5000	0.0000	0.0727	0.0727	0.0000
K-8	8	5.45%	0.2500	0.1250	0.6250	0.0136	0.0068	0.0341
K-9	1	18.18%	0.5000	0.0000	0.5000	0.0909	0.0000	0.0909
K-10	5	10.91%	0.3750	0.1250	0.5000	0.0409	0.0136	0.0545
Sum-Combined Weight						0.3886	0.2318	0.3795

After the calculation based on the relative important index ranking, the value of the combined weight is obtained from ratings equal to alternative scores, while the sum-combined weight resulted in the decision of which institutional model will be selected. Table 6 shows that alternative institutional model one (M.1) was selected with the highest (0.3886) multi-criteria analysis weight. To obtain the institutional model that can be implemented at the study object, the selected model was validated and corrected based on



current regulations. Afterwards, the effective institutional model obtained from this process can be implemented as the DDB financing scheme for Trans Sumatera Toll Road.

Based on the in-depth interview process with the respondents, this research obtained a valid and correct institutional model for Hutama Karya as the Direct Appointed Company to run Trans-Sumatera Toll Road Project (TSTR). Deep Discount Bond (DDB) scheme was issued in the form of Corporate Bond, because the use of project bond with TSTR will render the credit risk too high due to several conditions required, namely (1) High FIRR condition; (2) Mature land acquisition; (3) Bond guaranteed from Government or Guarantor (Full Guarantee); and (4) New regulation governing the issuance of project bond.

Hutama Karya (HK), appointed as the executor of Trans-Sumatera Toll Road (TSTR) project, received a Bond Guarantee from the Ministry of Finance to raise investors' interests. As can be seen after the guarantee was issued, HK bond rating which started as A became Triple A (idAAA) (PT Hutama Karya (Persero), 2016). According to respondents, HK bond has the lowest interest rate at AAA in their rating system. Bond Guarantee (full guarantee/government guarantee) is required because the existing TSTR project has a low level financial feasibility (FIRR). Therefore, the project's ability to leverage by applying loans or debt becomes low without guarantee. Figure 2 below illustrates the relationships among stakeholders in a DDB scheme.

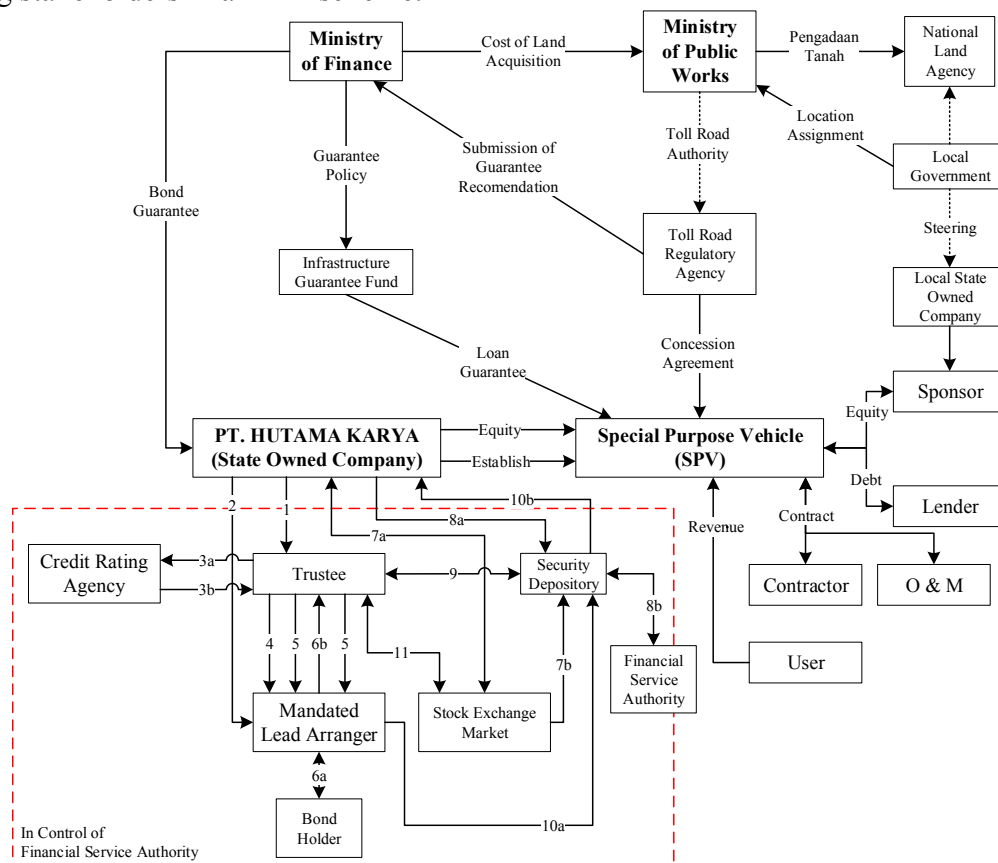


Figure 2 Deep Discount Bond Institutional Funding Model for Trans-Sumatera Toll Road



Hutama Karya issues Deep Discount Bond (DDB) with a corporate bond scheme because the existing regulations and project conditions make DDB issuance with project bond scheme highly risky. The institutional model also invites Local Government to support the project by involving Local State Owned Company (BUMD) to be sponsors. The above relationships in DDB institutional model are listed below:

- **[1]** Issuer appoints Trustee in a Trustee Agreement Letter. **[2]** Issuer appoints Mandated Lead Arranger (MLA) as Investment Bank (Selling Agency) in Agreement Appointment of MLA.
- **[3a]** Trustee provides Documents Credit Rating Assessment conducted by Credit Rating Agency (CRA). **[3b]** CRA provides Independent Rating regarding Rating Bond, in this process Rating Bond will be issued.
- **[4]** Trustee conducts Preparation of Bond Prospectus with MLA **[5]** Issuance of Prospectus & Underwrites Bond by Trustee to MLA as Investor Representative.
- **[6a]** MLA takes Preliminary to Investor & Conduct Market Condition to Investor. Facilitated by MLA, bond investors express an interest in purchasing DDB to be delivered to Trustee **[6b]** MLA submits bond interested from bond-holder candidates. In this process MLA delivers the bond marketing result and determines the Allocation and Distribution of DDB by MLA.
- **[7a]** Issuer submits a Listed to Issue the Bonds by filling in the Securities Registration Form (Bond) for Stock Exchange Market (SEM), SEM will then issue the Bond Code in accordance with the Number of Bond Series issued by Issuer, which is subsequently granted to Securities Depository **[7b]**
- **[8a]** Issuer conducts Bond Registration Agreement and Payment Agent Agreement with Securities Depository as Custodian Bank, which is subsequently given to Financial Service Authority to obtain Registration Statement on Bond Issuance **[8b]**
- **[9]** Distribution of DDB Allocation to Securities Depository for data recording with List of Allocation/Marketing DDB and Making Ownership List according to MLA distribution.
- **[10a]** After obtaining Proof of Listing of DDB Issuance, MLA transfers the proceeds of DDB allocation to Securities Depository. It is then transferred through Securities Depository to Issuer Account **[10b]**
- **[11]** SPV is facilitated by Trustee to issue DDB at Stock Exchange Market in accordance with the applicable Stock Exchange Mechanism.

DDB is influenced by bond rating and the rating can be improved by a guarantee. Thus, as illustrated in Figure 2, the Ministry of Finance issues a bond guarantee (with full guarantee/government guarantee characteristic) and guarantee policy, through infrastructure guarantee fund institution, in order to have lower bond interest rate and to be easily able accepted in the capital market. In addition, the appointment of Mandated Lead Arranger will be able to facilitate and to create a capital market more attractive. Therefore, it is expected that DDB can improve the toll road projects feasibility. Additionally, in order to complete this research, financial calculation is needed to identify the incremental feasibility level in toll road projects.



4. CONCLUSION

In conclusion, based on research data that has passed the analysis phase and shown in results and discussions, the following have been identified: ten stakeholders in Deep Discount Bond (DDB) funding scheme along with their roles, ten institutional success factors, and an institutional funding model with Bond issued under a corporate bond scheme using Mandated Lead Arranger as Selling Agency to implement DDB for Trans-Sumatera Toll Road.

5. ACKNOWLEDGEMENTS

The authors would like to express gratitude to the University of Indonesia for granting its support through PITTA scheme No. 742/UN2.R3.1/HKP.05.00/2017 in completing this research, and also to all participants in this research for their openness and excellent cooperation.

6. REFERENCE

- Ashuri, B. & Mostaan, K., 2015. State of Private Financing in Development of Highway Projects in the United States. *Journal of Management in Engineering*, 31(6), p. 04015002.
- Aziz, A. M. A., 2007. Successful Delivery of Public-Private Partnerships for Infrastructure Development. *Journal of Construction Engineering and Management*, 133(12), p. 918–931.
- Berawi, M. A., Zagloel, T. Y. M., Berawi, A. R. B. & Abdurachman, Y., 2015. Feasibility Analysis of Trans-Sumatera Toll Road using Value Engineering Method. *International Journal of Technology*, 29 July, 6(3), pp. 388-399.
- Djunaedi, P., 2007. *Public-Private Partnership Implementation and It's Impact to The State Budget*, Jakarta: Ministry of Finance Republic of Indonesia. [In Bahasa]
- Downes, J. & Goodman, J. E., 1998. *Dictionary of Finance & Investment Terms*. 5th ed. New York: Barron's Educational Series.
- Elton, E. J., Gruber, M. J., Brown, S. J. & Goetzmann, W. N., 2014. *Modern Portfolio Theory and Investment Analysis*. 8 ed. Hoboken NJ: John Wiley & Son's.
- Faerber, E., 2009. *All About Bonds, Bond Mutual Funds, and Bond ETFs*. 3 ed. New York: McGraw Hill Professional.
- Fitch, T., 2012. *Dictionary of Banking Terms*. 6th ed. London: Barron's Educational Series.
- Grigg, N. S., 2005. Institutional Analysis of Infrastructure Problems: Case Study of Water Quality in Distribution Systems. *Journal of Management in Engineering*, Volume 21, pp. 152-158.
- Gupta, A., Agrawal, R. & Gupta, M. C., 2013. Identification and Ranking of Critical Success Factors for BOT Projects in India. *Management Research Review*, Volume 36, pp. 1040-1060.
- Kaufmann, D., Kraay, A. & Mastruzzi, M., 2009. Governance Matters VIII: Aggregate and Individual Governance Indicators 1996-2008. *The World Bank Policy Research Working Paper No. 4978*.
- Lam, P. T. I., Chiang, Y. H. & Chan, S. H., 2011. Critical Success Factors for Bond Financing of Construction Projects in Asia. *Journal of Management in Engineering*, 27(4), pp. 190-199.
- Latham & Watkins, 2009. *Why Project Bond Now?*, Research Note, Bingley: Emerald Insight Publisher.
- Liu, J., Love, P. E. D., Smith, J., Regan, M. , 2015. Life Cycle Critical Success Factors for Public-Private Partnership Infrastructure Projects. *Journal of Management in Engineering*, 31(5), p. 04014073.



- Manarung, N., 2006. *Public-Private Partnership in Toll Road Development: Case Study Jogja-Solo-Kertosono*, Jakarta: Universitas Indonesia. [In Bahasa]
- Mendoza, G. A., Macoun, P., Prabhu, R., Sukadri D., Purnomo, H., Hartanto, H., 1999. *Guidelines for Applying Multi-Criteria Analysis to The Assessment of Criteria and Indicators*, Jakarta: Center for International Forestry Research.
- Ministry of Public Works, 2011. *Trans Sumatera Highway Development Plan Report*, Jakarta: Ministry of Transportation Indonesia.
- Oduami, K. T., 2002. Perceptions of Construction Professionals Concerning Important Skills of Effective Project Leaders. *Journal of Management in Engineering*, Volume 18, pp. 61-67.
- Panayides, P. M., Parola, F. & Lam, J. S. L., 2015. The Effect of Institutional Factors on Public-Private Partnership Success in Ports. *Transportation Research Part A: Policy and Practice*, Volume 71, pp. 110-127.
- Parente, W. J., 2006. *Public Private Partnerships - Fundamental Principles and Techniques for Effective Public Private Partnerships in Indonesia*, Jakarta: USAID Environmental Service Program.
- PT Hutama Karya (Persero), 2016. *Prospectus of Sustainable Public Offering Sustainable Bond I Hutama Karya Year 2016 with Target Funds Given 6.5 Trillion Rupiah*. [Online] Available at: http://www.idx.co.id/StaticData/NewsAndAnnouncement/ANNOUNCEMENTSTOCK/From_EREP/201701/2f91a94e5a_8c1539e7da.pdf
- Rarasati, A. D., Sihombing, L., Wibowo, A. & Latief, Y., 2016. *The New Toll Road Financing Model Determination*. Sarawak, Integrated Solutions for Infrastructure Development, pp. 1-6.
- Reilly, F. K. & Brow, K. C., 2012. *Investment Analysis and Portfolio Management*. 10 ed. Mason, OH: South-Western College Pub..
- Reksohadiprodjo, S., 2000. *Dasar-Dasar Manajemen*. Yogyakarta: BPFE-Yogyakarta.
- Romalis, J., 2007. *Market access, Openness and Growth*, Cambridge, MA: National Bureau of Economic Research.
- Sari, W., 2014. *Project Financing Agreements - The Role of Advisors in Project Finance Deals*, Depok: Faculty of Economic, Universitas Indonesia.
- Sarmiento, J. M. & Renneboog, L., 2016. Anatomy of Public-Private Partnerships: Their Creation, Financing, and Renegotiations. *International Journal of Managing Projects in Business*, Volume 9, pp. 94-122.
- Seidman, I., 2005. *Interviewing as Qualitative Research: A Guide for Researchers in Education and the Social Sciences*. 3 ed. New York: Teachers College Press.
- Yudi, K., Rarasati, A. D. & Adiwijaya, A. J. S., 2016. Stakeholder Management of Jakarta's LRT Using Stakeholder Analysis. *Symposium I University Network for Indonesia Infrastructure Development, 3 Agustus 2016, Surabaya, Indonesia* Surabaya, Universitas Airlangga.
- Yuttapongsonorn, N., Desouza, K. C. & Braganza, A., 2008. Complexities of Large Scale Technology Project Failure: A Forensic Analysis of the Seattle Popular Monorail Authority. *Public Performance & Management Review*, Volume 31, pp. 443-478.
- Zhang, X., 2005. Critical Success Factors for Public-Private Partnerships in Infrastructure Development. *Journal of Construction Engineering and Management*, Volume 131, pp. 3-14.



15th International Conference on Quality in Research (QIR 2017)

**PARTIAL PHASE I ENVIRONMENTAL SITE ASSESSMENT OF
PIYUNGAN LANDFILL AND ANAEROBIC FLUIDIZED BED REACTOR
(AFBR) PILOT STUDY FOR LEACHATE TREATMENT**

Christina Browning^{a,1}, Sholahudin Al Ayyubi^b, and Wiratni Budhijanto^{b,2}

^aEnvironment and Resource Management Department, Arizona State University, United State of America

^bChemical Engineering Department, Faculty of Engineering, Universitas Gadjah Mada, Jl. Grafika 2 Yogyakarta 55281 Indonesia

^bCenter for Energy Studies, Universitas Gadjah Mada, Sekip K-1A Yogyakarta 55281 Indonesia

Abstract

An abbreviated Phase I Environmental Site Assessment was performed to identify areas of potential contamination within the leachate management system at Piyungan landfill in Yogyakarta and to evaluate the mitigating effects of an Anaerobic Fluidized Bed Reactor (AFBR) pilot study on the recognized environmental conditions. The AFBR pilot system was found to reduce the quantity and hazardous components of the Piyungan leachate thus reducing the landfill's negative impact on surface waters and air emissions. The AFBR pilot system allows more quantities of high-organic content leachate to reach the methanogenic phase of decomposition in a shorter amount of time than in the naturally occurring process of untreated leachate, preventing the production of organic acids, alcohols, methane and nitrogen which can cause an adverse effect on vegetation, animal species and humans when exposed to unnatural levels of these compounds. The AFBR system is also effective in reducing methane emissions; a significant result due to the high global warming potential of this gas. However, these mitigation efforts are limited in the pilot system's current state. In order to have a more effectively alleviate the recognized environmental conditions (RECs) on site, the AFBR system would require scale up and calibration to reach maximum efficacy with additional treatment systems for hazardous non-organic contaminants.

Keywords: Phase I Environmental Site Assessment, Leachate Treatment, Anaerobic Treatment of Leachate, Anaerobic Fluidized Bed Reactor, Municipal Solid Waste Landfill Environmental Impact

1. INTRODUCTION

The Piyungan landfill (site) is located in the Bantul Regency, Special Region of Yogyakarta in Indonesia. The site was established in 1995 and utilizes an area of 12.50 hectares to

¹ Christina Browning is a graduate student in Environment and Resource Management Department, Arizona State University, USA, who took internship in CLEAN Project, Chemical Engineering Department under the support of USAID R&I Fellowship (May-August 2017)

² Corresponding email: wiratni@ugm.ac.id



landfill municipal solid waste (MSW) of the surrounding area. Approximately 595,000 m³ of MSW is disposed of annually while the waste already on site is estimated to be 2,700,000 tonnes with a depth of 20m. The majority of the MSW found at Piyungan is organic material with plant waste at 41.1% and food waste at 27.4 %. These organic wastes are ideal for decomposition and methanogenesis of leachate. The remaining waste is 11.19% glass, plastics and iron, 10.24% paper, 6.11% wood, and 3.94% textiles (Kristanty et al., 2016). The site is currently emitting a considerable amount of leachate, which is treated in seven leachate ponds. The flow of the treated leachate into a natural channel to the irrigation channels is illustrated in Fig. 1. The proximity of the leachate ponds to the aquifer system highlights the importance of the effort to improve the efficiency of leachate treatment for Piyungan Landfill Site.

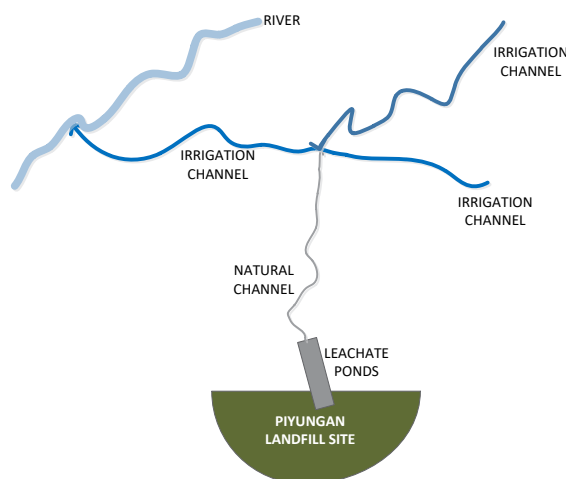


Fig. 1. Illustration of Piyungan Landfill leachate channel (Van Best, 2016)

Poor solid waste landfill management practices endanger public health and the environment. The purpose of this abbreviated Phase I Environmental Site Assessment is to identify areas of potential contamination within the leachate management system at Piyungan Landfill Site, as well as evaluate the impacts the AFBR pilot study would have on the recognized environmental conditions (RECs). RECs would include, but are not limited to, hazardous/toxic wastes spilled on the site; discharge of toxic leachate to surrounding bodies of water or soil; and identification of off-site communities potentially affected by the contamination of the subjected site. It is theorized that the AFBR pilot study would reduce the quantity and hazardous components of the Piyungan leachate thus reducing the landfill's negative impact on the environment.

An overhead view of the seven leachate ponds and an illustration of the AFBR pilot system is presented in Fig. 2. The pilot system diverts a portion of untreated landfill leachate to be treated through anaerobic digestion within a fluidized bed reactor. Untreated leachate from retention pond #1 is diverted to a holding section of pond #5. The isolated leachate in pond #5 is pumped to an equalization feed tank, referenced as feed tank in Fig. 2. The leachate is then mixed with chemical reagents to modify the pH and C/N ratio.

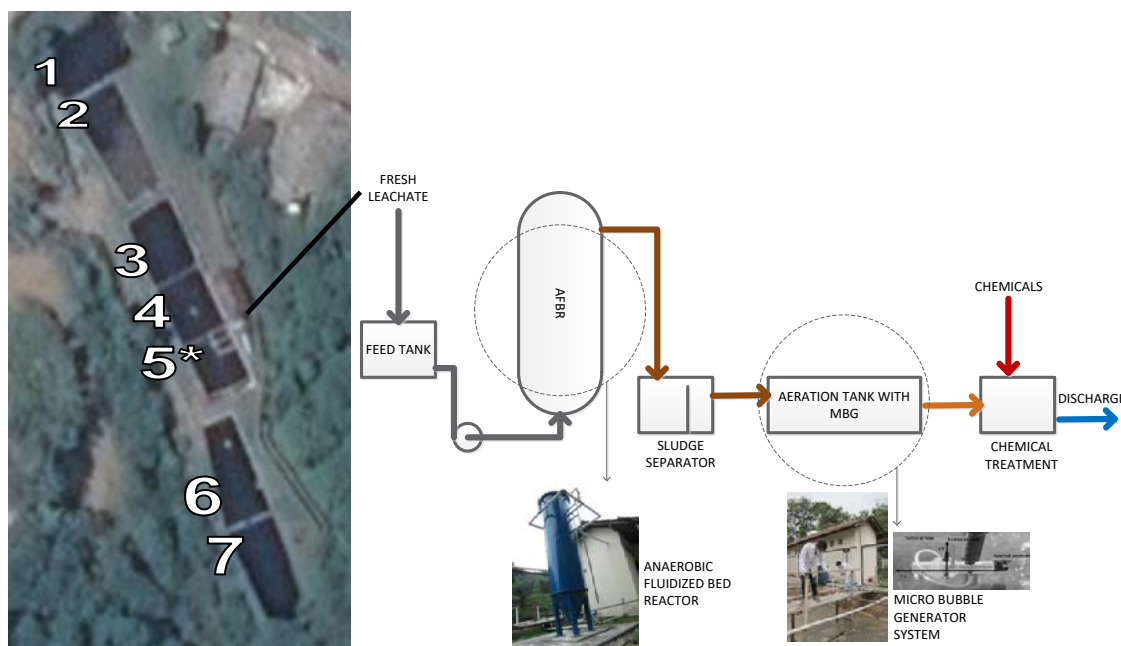


Fig. 2. The AFBR pilot system in Piyungan Landfill Site Yogyakarta

Once the proper parameters are achieved, the leachate is pumped to the fluidized bed reactor with zeolite as microbial immobilization medium seeded with naturally occurring microbes collected from bovine fecal matter. The immobilized microbes substantially reduce the dissolved organic content of the leachate. Nutrient imbalance can cause difficulties in maintaining an effective biological treatment, particularly in the start-up phase of system operations; If necessary, a small amount of fertilizer may be added during start-up to enhance the microbial population. Methane and other biogases are produced from the digestion of leachate which is then captured and measured through a gas meter. The effluent is pumped to a sludge separator and then an aeration tank for further decomposition of the organic matter, and then chemically treated, if necessary, before discharged to a nearby body of water.

2. METHODOLOGY

The ASTM Standard Practice E-1527-05 was intended to define a customary practice in the United States of America for conducting an Environmental Site Assessment of a parcel of commercial real estate with respect to the range of contaminants within the scope of Comprehensive Environmental Response, Compensation and Liability Act (CERCLA). The subject site is not for sale as commercial real estate, but an industrial property which may pose hazards to the surrounding environment and community. This report does not address all of the elements of the ASTM standard and is an abbreviated assessment of the site's leachate, surface waters and air emissions. This ESA may be used as an additional resource to GMU and the AFBR pilot system research project.



2.1 Assessment approach

The tasks of this report are in conformance with ASTM standard and are listed as followed:

1. A detailed walk-through inspection of the landfill site, or representative areas of the site, and the AFBR pilot system.
2. A review and detailed walk through inspection of the AFBR system design.
3. Identification of surrounding property use and human health exposures.
4. A review of historical maps and topographical maps and aerial photographs.
5. Review of sampling analysis.

Findings and conclusions are based on the careful consideration of the results of the above research. Any recommendations made are formulated with respect to maintaining or protecting the collateral value of the property and providing protection from environmental or human health hazards.

2.2. Measurement approach

At this early stage of environmental assessment, the target was limited to the identification of potential impacts and was not yet intended for verification with field data. However, to guide the theoretical assumptions, measurements were taken on samples from the leachate pond and AFBR outlet. The analysis of the samples was focused on the measurement of soluble Chemical Oxygen Demand (sCOD) and volatile fatty acids (VFA) following the APHA standard procedure (APHA, 1985).

3. SUMMARY OF FINDINGS

Based on the results of the research performed the Piyungan landfill leachate ponds and waste piles pose a significant risk to human health and the environment, and the AFBR pilot system has an effect of reducing the hazards of the RECs found within this report.

3.1 Leachate Assessment

The landfill site was designed to include a geo membrane liner and a drainage piping system to manage the discharge of landfill leachate. Leachate is the aqueous effluent generated from MSW accumulated by the decomposition of organic material, inherent waste moisture, and the percolation of rain water through the refuse. The leachate discharge is approximately 10-20 m³/day (based on field measurement during 2016). The drainage system directs the leachate into a series of leachate ponds for minor treatment. The liquid passes through seven leachate ponds (Fig.3) in total with five designed as a reservoir and used for chemical treatment, while the remaining two are for aeration. The leachate is then discharged to a nearby stream which ultimately leads to the Indian Ocean via the Kali Opak River. The surface area of each leachate pond is 96m² with a depth of 3m and a total volume of 2,016m³. Each pond is open to air and exposed to rainfall measured at 185.5cm annually (2016).



Fig. 3. Leachate ponds in Piyungan Landfill Site (Gadjah Mada University, 2015)

3.1.1 Leachate Environmental and Human Health Hazards

MSW leachate composition varies depending on a number of factors, but the pollutants can be categorized in four main groups; dissolved organic matter, inorganic matter, heavy metals and xenobiotic organic compounds (XOCs) (Kjeldsen et al, 2002). The contaminants vary and fluctuate depending on a variety of factors including waste composition, age of landfill, weather, temperature, moisture content and other deciding factors. The composition of leachate and their hazardous effects have been extensively researched and documented, providing a deeper understanding of the potential risks to human health and the environment.

The dissolved organic material found in leachate is derived from the decomposing and degradation of naturally occurring materials. Dissolved organic matter, Total Organic Carbon (TOC), Chemical Oxygen Demand and the Volatile Fatty Acids (VFAs), which accumulated during the acid phase of waste decomposition, reflect the organic contamination. (Slack, et al, 2005). The organic matter is further biodegraded naturally by certain microbial processes such as hydrolysis, fermentation, acidogenesis and methanogenesis. (Luo, et al., 2015). This produces organic acids, alcohols, methane and nitrogen which can cause an adverse effect on vegetation, animal species and humans when exposed to unnatural levels of these compounds. The organic matter within the leachate is reduced until these naturally occurring processes can no longer be sufficiently facilitated. The effects of organic matter on the environment are considered in later sections of this report.

Inorganic materials found in MSW leachate include calcium, magnesium, sodium, potassium, ammonia-nitrogen (ammonia), non-heavy metals such as iron and magnesium, and more. (Kjeldsen et al., 2002). Ammonia-nitrogen in particular is found in levels of great magnitude in MSW landfill leachate. Leachate samples collected from the Piyungan leachate ponds revealed an ammonia content of 1,056 mg/L, within the expected range of landfill leachate which may fall anywhere between 500 to 2000 mg/L (Kristanty et al.,



2016, Kjeldsen et al., 2002). The effects of inorganic material on the environment are considered in later sections of this report.

Heavy metals and XOC's will not be considered in depth in this report due to the lack of available data for review. Heavy metals include cadmium, chromium, copper, lead, nickel and zinc which may be present in the landfill leachate at the site. Leachate samples collected revealed cadmium content at 0.027 mg/L at its peak, well above the Indonesian environmental standard for surface waters of 0.01mg/L but almost an entire magnitude above the U.S. EPA standard of 0.005mg/L for surface waters (<https://www.epa.gov/regulatory-information-topic/regulatory-information-topic-water#>)

Due to the lack of analytical samples available for assessment, XOC's and their environmental effects are not included in this assessment. XOCs in municipal solid waste leachate include aromatic hydrocarbons, phenols, pesticides, plasticizers and other volatile organic compounds (VOCs) but are typically present in relatively low concentrations because of the initial low levels in household waste and volatilization to air. Monoaromatic hydrocarbons, such as benzene, toluene, and xylenes, as well as halogenated hydrocarbons, such as tetrachloroethylene and trichloroethylene, are consider some of the most hazardous compounds found in leachate (Christensen et al., 2001). The U.S. EPA has identified several of these compounds as priority pollutants due to their extremely harmful effects in the aquatic environment. There is insufficient data to make a site specific analysis, though estimates are made in this report for practical measures.

3.1.2 AFBR Pilot System Effect on Leachate

The AFBR pilot system primary aim is to control the natural microbial processes to reduce organic matter in leachate by containing and enhancing these reactions within the tank of a fluidized bed reactor using immobilized microbes. The chemical oxygen demand is reduced to prevent these biological processes from occurring in nature as it would if the leachate were released without treatment. Additionally, the AFBR would only be effective if the minimum nutrient requirements for methanogenesis were present to allow for the reaction to occur. Young leachate has high organic content which has not yet reacted is typically less than 5 years old and would viable for the treatment system. Older leachate will have naturally undergone the biological processes, losing the required COD and DO for AFBR treatment. This report recognizes this as a significant finding in regards to using the AFBR pilot system to reduce the hazardous components of leachate.

The AFBR pilot system must consider the influent characteristics such as COD and pH while also maintaining ideal operation conditions which affects both the microorganism growth and organic biodegradations by altering enzyme activity. These operational conditions include hydraulic retention times, temperature, volumetric flow, and organic loading rate. The pilot system began start up on 10 March 2017 and has experienced operational performance complications due to the fluctuating properties of the influent leachate. The biochemistry of anaerobic digestion begins with hydrolysis, converting complex organic molecules to the soluble organic molecules found in leachate. Then, the small organic molecules undergo acidogenesis to Volatile Fatty Acids. The Volatile fatty



acids are necessary for acetogenesis to produce the acetic acid required for methanogenesis, the final step to produce methane. Both Volatile Fatty Acids and COD efficiency will reveal the performance for the removal of dissolved organic matter.

Previous studies have shown the anaerobic processes within an AFBR to treat leachate could achieve 90% of COD removal efficiency with methane contents ranging from 60 – 90% (Luo et al., 2015). There has been difficulty meeting the nutrient requirements for the methanogens during the anaerobic digestion process as the leachate is inconsistent in its composition. The COD in the startup phase has not been consistent because the leachate collected from the landfill body is in various stages of decomposition. The system requires soluble organic molecules to undergo acidogenesis and produce volatile fatty acids for the next phase of the reaction. These VFAs are also naturally occurring in the leachate as the liquid naturally undergoes the digestions process. The effluent from the system maintains soluble organic material, COD, and VFAs necessary for the microbial processes to occur outside of the controlled AFBR environment, posing a risk to the environment.

The methanogens require acetic acid, which is referred as VFAs. The fluctuating VFA levels in the influent during the start up of the pilot AFBR, as shown in Fig. 4, reduces the efficacy of the system evident by the VFA in the effluent which had not been fully converted to methane. The immobilized microbes require a reliable steady feed to adequately convert all present VFAs to acetic acid. The VFA in the effluent shows a reduced potential for methanogenesis and the production of methane and carbon dioxide. An ideal reactor will have the same composition at all points at a given instant so the whole system is undergoing the same chemical reactions, and the biochemistry is the same throughout. This will facilitate efficient anaerobic digestion as there will be a lesser impact on a limiting reagent. As the system stabilizes, and the reactor becomes more homogenous VFA conversion may improve. The data shown in Fig 4. are promising but cannot be conclusive until system start-up is completed and the microbial population strengthened and stabilized. The nutrient requirements of the influent leachate feed and system parameters must be determined in start- up for optimization.

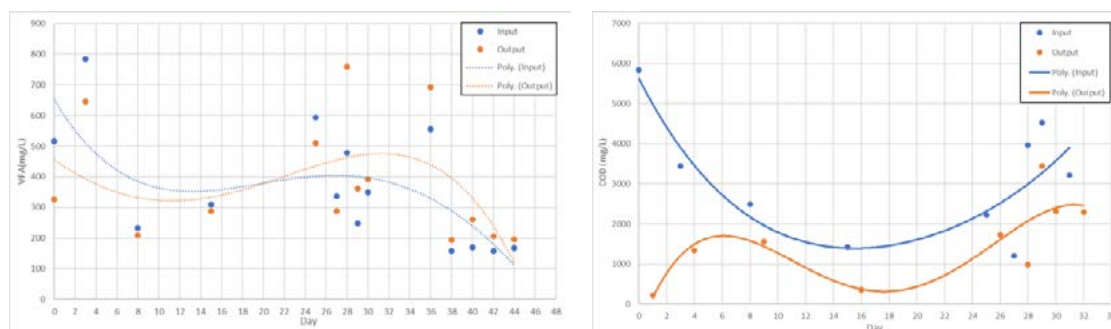


Fig. 4. Start-up data of the AFBR pilot



During the methanogenic phase, VFA are reduced. Calcium, magnesium, iron and manganese are lower due to the higher pH and lower DO. A higher pH enhances sorption and precipitation while the lower DO allows complex cations to form (Kjeldsen et al., 2002). Microbes reduce sulfate to sulfides in the methanogenic phase which lowers the overall concentrations of sulfates in the leachate. These sulfides may then lead to precipitation with miscellaneous metals present (2002). The AFBR pilot system allows more quantities of leachate to reach the methanogenic phase of decomposition in a shorter amount of time than in the naturally occurring process of untreated leachate.

3.2 Discharge to Surface Waters Assessment

The topography and geological conditions at the Piyungan landfill site prevent leachate penetration to the soil preventing contamination of surface water from the contaminated soil. However, the leachate ponds are inefficient to handle the quantity of leachate generated. It was observed that the landfill leachate exceeded the height of the reservoir ponds and overflowed. A steady stream of leachate from the leachate treatment ponds was discharged directly to a nearby river through a natural channel located near the leachate ponds. The necessary chemical treatment in the pond is subject to the fluctuating concentration of the fresh leachate. Should the treatment fail, there is significant risk for contamination of fresh surface waters surrounding the site.

Insufficient top cover and lack of vegetation has likely also led to leachate runoff and the volume of water that enters the site is uncontrolled. The waste is exposed to the region's heavy rainfall during the wet seasons and experiences 185.5cm annually. The mounded shape of the waste pile and resulting slope results in more infiltration of rainwater on the bottom edge. The waste piles at Piyungan are a recognized environmental condition due to the likelihood that leachate runoff may occur. Due to the historical and ongoing discharge at the site, the leachate drainage system represents a recognized environmental condition. It can be reasonably assumed that the overflowing retention ponds, and cracks found in the leachate retention dam is contaminated the surrounding the soil which will then impact surface waters which flow over the soil. Each of these findings represent a recognized environmental condition as the surface waters are expected to be impacted.

3.2.1 Discharge to Surface Waters Environmental and Human Health Hazards

As identified in the previous section, the surface waters surrounding the Piyungan landfill are likely contaminated with the pollutants of the linearly treated leachate in the leachate ponds. The organic material in the leachate may facilitate the acidogenesis and methanogenesis processes once released to the surface waters, further adding irregular compounds to the environment. The leachate's dissolved organic material will produce organic acids, alcohols, and nitrogen which may damage the flora and fauna who utilize the waters surrounding the site.

While Ammonia is not classified as a hazardous compound under the US. EPA or in Indonesia, there is the potential for the compound to act as a dominant environmental pollutant due to the magnitude of the contaminant levels which are at concentrations of greater magnitude than other pollutants found at the site (Kjeldsen et al., 2002). Discharge



of high ammonia content leachate to surface waters can cause ammonia toxicity by providing nutrients for eutrophication and facilitating in situ nitrification. The oxygen depletion of the surface waters would cause harm to plant and animal reliant on the surface water (2002). Ammonia has been frequently references as the most common groundwater pollutant stemming from MSW landfills (Christensen 2001).

The only heavy metal analytical data available for review is for cadmium. Cadmium exposure can result in renal system complications such as kidney stones, osteoporosis and osteomalacia, hypertension and further health complications. Cadmium is also a recognized carcinogen causing lung, kidney and prostate cancer. The same study which sampled the leachate on site, also analyzed surface water samples at three points; upstream from the leachate discharge, downstream, and a tributary intersection. Levels found at their peak were 0.014, 0.022, and 0.017 mg/L respectively (Kristanty et al., 2016). It is not clear if the surface waters are monitored or safeguarded by local authorities, so the potential for ingestion by human and animals is probable, therefore posing a serious risk. Other heavy metals may be present posing additional health risks from exposure of the contaminated surface waters. While the XOCs levels are likely low in the leachate at this landfill due to volatilization, there is a possibility for surface water contamination. The contamination of surface waters is a recognized environmental condition and mitigation efforts are needed to protect the environment and human health.

3.2.1 AFBR Pilot System Effect on Surface Waters

The AFBR pilot system technologies has been demonstrated to be effective for the treatment of high-strength organic waste waters, such as the leachate found at this site. (Luo et al., 2015). This pilot system promotes anaerobic degradation of the organic pollutants found in the waste water, therefore reducing the potential for contamination of organic pollutants in the surface waters surrounding the site. The performance of the reactor is measured in terms of COD removal, VFA production and methane production yield, which will be address in a later section.

Research on AFBR technology has not been found to effectively reduce ammonia in leachate (Renou et al., 2008, Luo et al., 2015). On the contrary, Ammonia is highly stable in anaerobic conditions like that of the AFBR and may accumulate within the system. Effects of high free ammonia concentrations can negatively impact the performances of anaerobic bioreactors. This inorganic compound inhibits methanogenesis so its presence may theoretically reduce the effectiveness of the pilot system (2015). The AFBR pilot study is not a reliable technology to treat Ammonia concentrations in leachate and the effluent from the system would need to undergo further treatment before discharged to surface waters. Heavy metals and XOCs are not targeted pollutants of the system there may be reduced concentration of heavy metals as compounds are reduced during the transition from the acid to methanogenic phase because of increased sorption and metal precipitation with the sulfates present in the leachate (Kjeldsen et al., 2002). XOCs exhibit different behaviors depending on the specific compounds and so it cannot be definitely determined if the AFBR pilot system would have a positive effect on all XOCs present in



the leachate (Slack et al., 2005). The effluent from the AFBR would need to undergo further treatment to address heavy metal and XOC contaminants.

3.3 Air Emission Assessment

Air emissions from landfill take the form of gaseous emissions of volatile organic compounds, airborne particulate matter, and greenhouse gases. The emissions may contain similar hazards to the liquid leachate as the degradation products produced because during in the methanogenic phase the degradation products in the acid anaerobic stage may volatilize (Christensen et al., 2001). The large percentage of organic material from the overall waste deposited will have an increased effect on the amount of emissions.

Landfill emissions typically contain 45 – 60% methane and 40 – 60% carbon dioxide (ATSDR, 2001). Other VOC emissions may also be present, but as the majority of the Piyungan waste composition is organic material (68.5%), the VOC's, including saturated and unsaturated hydrocarbons, acidic hydrocarbons and organic alcohols, aromatic hydrocarbons, halogenated compounds and sulphur compounds may be reasonably assumed to be low. Particulate matter (PM) emitted from landfills may also be contaminated with heavy metals (Christensen et al., 2001). The Piyungan site had a visible cloud of PM, as well as large debris picked up by the slight winds during the site inspection. Gases are produced under the landfill surface as the material under goes the stages of microbial decomposition.

The facility inspection performed and review of aerial photographs show no cover or cap on the waste piles. This will allow the methane and carbon dioxide produced to migrate up and out to the ambient air due to its density lower than air. The leachate ponds are also open to air, allowing for the migration of the contaminants. There were no gas collection and recovery systems present at Piyungan except the AFBR pilot study. Both the leachate ponds and waste piles themselves are considered a recognized environmental condition due to the potential for air emission releases.

3.3.1 Air Quality Environmental and Human Health Hazards

The landfill gases emitted to the ambient air tend to migrate from the landfill to the environment and communities surrounding Piyungan. The gases pose a series of environmental and human health risks which have been documented elsewhere. In the context of this report, the focus is on the gas emissions impact the environment. Both methane and carbon dioxide are greenhouse gases which contribute to global climate change. Greenhouse gas emissions have been categorized in their global warming potential (GWP) to compare the influence of the different GHG on the global climate. The GWP of carbon dioxide is equal to 1 while methane has a GWP of 25 for a time horizon of 100 years. Essentially, 1 kg of methane has the equivalent global warming effect as 25 kg of carbon dioxide (IPCC, 2007). Global warming threatens all life, not only in the local area surrounding Piyungan and the emissions from the site contributes to this global effect. There is the potential for other human health impacts due to the many minor constituents, such as heavy metals and VOCs, which are likely present at low concentrations. The



specific human health risks cannot be determined without air quality sampling and analysis.

3.3.2 AFBR Pilot System Effect on Air Quality

Over a start-up period of 75 days from 10 March 2017 to 24 May 2017, the AFBR pilot study captured 186 m³ of methane that would have otherwise been released to air. There are indicators that predict the AFBR pilot system may be able to produce more methane than has been measured during this start up face. Both VFAs and COD efficiency will reveal the systems potential for additional biogas production. The anaerobic fermentation of the biodegradable organic matter results in VFAs which are then converted to methane and carbon dioxide as the methanogenic phase occurs ((Christensen et al., 2001. Similarly COD removal efficacy will reveal the potential of further methane production as the COD available will be able to use in the microbial reaction. As reviewed in Fig. 4 of this report, there is the opportunity to increase the efficacy of the system to covert more organic material to methane for recovery.

The mitigating effect of the pilot system on the site's air emissions is minimal, particularly due to the volume of air releases predicted at many magnitude larger than the quantity produced by the system. However, the demonstrated yet slight reduction of 186m³ of methane is preferable to zero mitigation efforts. There is potential for increased optimization and ability to scale up this system to a more impactful size to further reduce air emissions. The AFBR pilot system is a proven mitigation technology to reduce the impact of methane (Luo et all, 2015). The carbon dioxide gas produced from the processes within the reactor are released to air, therefore this technology is not considered an effective mitigation tool for carbon dioxide emission release. The AFBR pilot system also does not address other minor constituents which may be present in the leachate. Ultimately, the AFBR pilot study has a positive impact on the environment by mitigating the air releases of methane to the atmosphere.

4. CONCLUSION

The Piyungan landfill presents a number of environmental and human health hazards due to the pollutant releases and recognized environmental conditions present on site. In assessing the landfill leachate, surface waters, and air emissions, the potential for environmental contamination is likely. The anaerobic treatment of leachate through an AFBR Pilot system installed on site was found to slightly reduce the hazards but these mitigation efforts are limited in its current state. The significant findings of this report are as follows:

- The targeted leachate pollutants of this treatment system are only organic pollutants, requiring further treatment for other hazardous constituents before release to the environment.
- The pilot study, while still in start-up phase, has shown effective in reducing dissolved organic material, but has not reached the peaked efficiency of 60 – 90% COD removal. Likewise, methane production levels may be similarly improved.



- The system may be inhibited by inorganic compounds which build up within the system (Table 1) and inconsistent influent leachate composition.
- The reduction of methane releases is a significant environmental mitigation effect because of the high GWP of this gas

This abbreviated Phase I Environmental Site Assessment requires further investigatory actions to meet the ASTM standards and determine the extent of the site's impact of human health and the environment. It is recommended that additional sampling and document review be performed to enhance this report.

5. ACKNOWLEDGEMENT

The report supports the USAID PEER-Science CLEAN Project. Both the pilot study and primary author are supported by the US Agency for International Development. The authors also expressed the highest appreciation to the Global Development Research Program at Arizona State University, as well as the Chemical Engineering Department of Gadjah Mada University. The previous research and data collected by authors referenced in this document have been invaluable to the completion of this report.

6. REFERENCES

- Agency for Toxic Substances and Disease Registry (ATSDR) (2001), Landfill Gas Emissions, website: <https://www.atsdr.cdc.gov/HAC/landfill/html/ch2.html>
- Annual Book of ASTM Standards (1976), "Phase I Environmental Site Assessment: Standard E-1527-05".
- APHA (1985) "Standard Method for the Examination of Water and Wastewater", 16th ed., American Public Health Association, Washington DC.
- Christensen T.H., Kjeldsen P., Bjerg P.L., Jensen D.L., Christensen J.B., A. Baun, *et al.* (2001), Biogeochemistry of landfill leachate plumes, *Appl. Geochem.*, 16, pp. 659–718
- Gadjah Mada University Chemical Engineering Department, (2015), Clean Project: Usaid Peer Science Grant Report, Yogyakarta, July 2015.
- Integrated Pollution Prevention and Control (IPPC). (2007), *Guidance for the Treatment of Landfill Leachate*, Integrated Pollution Prevention and Control (IPPC).
- Kjeldsen P., Barlaz M.A., Rooker A.P., Baun A., Ledin A. and Christensen T.H. (2002), Present and Long-Term Composition of MSW Landfill Leachate: A Review, *Critical Reviews in Environmental Science and Technology*, Volume 32, Issue 4, pp. 297 -336.
- Kristanty T., Sudibyho H., Mellayanawaty M., and Budhijanto W., (2016), Mathematical Modeling to Evaluate the Distribution of Leachate Discharge into the Water Streams Around Piyungan Landfill Site,
- Luo J., Qian G., Liu J., Xu Z.P., (2015), Anaerobic Methanogenesis of Fresh Leachate from Municipal Solid Waste: A Brief Review on Current Progress, *Renewable and Sustainable Energy Reviews*, Volume 49, pp. 21-28.
- Renou S., Givaudan J.G., Dirassouyan F., Moulin P., (2008), Landfill Leachate Treatment: Review and Opportunity, *Journal of Hazardous Materials*, Volume 150, Issue 3, pp. 468–493.

- Slack R.J., Gronow J.R. and Voulvoilis N. (2005), Household Hazardous Waste in Municipal Landfills: Contaminants in Leachate, *Science of the Total Environment*, Volume 337, Issue 1-3, pp. 119-137.
- Van Best S., (2016) Risk Assessment of Potential Hydrogeological Pollution of the on Site Ground and Surface Waters Located at the Piyungan Municipal Solid Waste Landfill in Yogyakarta, Indonesia, Avans University of Applied Science



QIR

*The Westin Resort
Nasa Dua, Bali*
24-27 July 2017

SYMPOSIUM B

**International Symposium on
Mechanical and Maritime
Engineering**





MODELLING AND SIMULATION CFD ANALYSIS FOR FLOW IN ECONOMIZER HOPPER

Gun Gun Ramdhan Gunadi^{1,2,*}, Ahmad Indra Siswantara^{1,†}, Budiarmo^{1,‡}, Asyari
Daryus^{1,3,§}, and Hariyotejo Pujowidodo^{1,**}

¹Department of Mechanical Engineering, Universitas Indonesia, Depok, Jawa Barat, Indonesia (16424)

²Department of Mechanical Engineering, Politeknik Negeri Jakarta, Indonesia (16424)

³Department of Mechanical Engineering, Universitas Darma Persada, Jl. Radin Inten II (Terusan Casablanca) Pondok Kelapa

Abstract

Increasing the mass of fly ash accumulation of coal ash in the electrostatic precipitator (ESP) and corrosion and erosion of the IDF, ESP, Air Pre Heater, because the system does not use an economizer hopper that can hold most of the fly ash. Therefore, the study of engineering design economizer hopper and ash distribution system becomes important. As an initial analysis, numerical simulation has more advantages in saving time and costs compared with experiments. Variations in flow conditions and geometry can be adjusted easily to get results. Modeling and Simulation CFD on economizer hopper aims to analyze the flow of particulate fly ash in the flue gas stream at the economizer hopper. Modeling and Simulation CFD process for flow analysis on economizer hopper is done by CFDSoft (r) software using the three-dimensional geometry model with turbulent flow model of the standard (STD) k-ε multiphase Eulerian. Economizer inlets, is Gas = 2.1 m / s and Particulate = 1 m / s. The results of modeling and simulation CFD calculations on economizer hopper indicate that the installation of economizer hopper significantly reduces the amount of particulate fly ash in the flue gas stream. At the time of inception, the particulate deposition rate highest 27%. Over time, the particulate deposition rate will drop due to the deposition of particulate matter on each hopper. The particulate deposition rate at 6 economizer hopper A began to stabilize in 11:25 - 25.00 hours, amounting to 6% to 5%.

Keywords: numerical simulation, CFD, particulate, fly ash, geometry, economizer hopper;

1. INTRODUCTION

Energy, especially electricity, has a very important role in supporting regional development, for it is the goal of energy development is to provide sufficient energy at affordable prices by purchasing power. Along with the growth of regional development and other sectors, then the demand for energy, especially electricity, will continue to increase.

Problems in the Steam Power Plant, which involves the accumulation of masses of fly ash coal in Electrostatic Precipitator (ESP) and corrosion and erosion of the Induced Draft Fan (IDF), ESP, Air Pre Heater, because the system does not use the economizer hopper can accommodate a portion of fly ash coal, therefore, study Engineering Design economizer Hopper and Distribution System of ashes becomes important.

As a preliminary analysis, numerical simulations have advantages in saving time and costs compared to the experiment. Simulations of turbulent flow by using a model, simply done simulations on the computer hardware. Flow phenomena can be quickly

* gun2rg@gmail.com; gungun.rg@mesin.pnj.ac.id

† a_indra@eng.ui.ac.id

‡ budiarso@ui.ac.id

§ asyari@yahoo.com

** hariyotejo.pujowidodo@gmail.com



obtained thus saving time and costs. The STD k-ε turbulence model, also called the k-ε turbulence model, is a simple model which only requires the input of boundary conditions, is mostly used for industry applications and is stable and widely validated. (Versteeg & Malalasekera 1995). Two different turbulence models, standard (STD) k-ε and renormalization group (RNG) k-ε, could be used to represent the combustion process phenomenon in micro gas turbine combustor without many significant differences. (Daryus et al. 2016). Standard (STD) k-ε, renormalization group (RNG) k-ε, and reynolds stress model (RSM) were applied for simulations of the turbulent flow in the wind tunnel. (Gunadi et al. 2016).

This paper will discuss the study Engineering Design Economizer Hopper and Distribution System of Ashes.

2. METHODS

Turbulence Model

The STD k-ε turbulence model has two additional transport equations for turbulent flow: the kinetic energy transport equation, k, and the dissipation transport equation, ε. Transport equation k is given by (Versteeg & Malalasekera 1995):

$$\frac{\partial(\rho k)}{\partial t} + \text{div}(\rho k \mathbf{U}) = \text{div} \left[\frac{\mu_t}{\sigma_k} \text{grad} k \right] + 2\mu_t E_{ij} \cdot E_{ij} - \rho \varepsilon \dots \dots \dots (1)$$

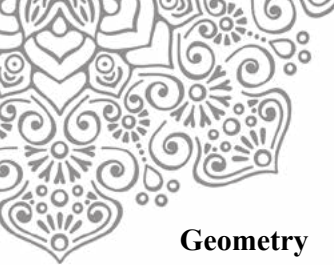
and transport equation ε is given by (Versteeg & Malalasekera 1995):

$$\frac{\partial(\rho \varepsilon)}{\partial t} + \text{div}(\rho \varepsilon \mathbf{U}) = \text{div} \left[\frac{\mu_t}{\sigma_\varepsilon} \text{grad} \varepsilon \right] + C_{1\varepsilon} \frac{\varepsilon}{k} 2\mu_t E_{ij} \cdot E_{ij} - C_{2\varepsilon} \rho \frac{\varepsilon^2}{k} \dots \dots \dots (2)$$

where:

$$\mu_t = \rho C_\mu \frac{k^2}{\varepsilon} \dots \dots \dots (3)$$

ρ is density, **U** is the velocity vector, μ_t is the viscosity eddy and E_{ij}. E_{ij} is the average speed of deformation. If i or j = 1, it relates to the x-direction; if i or j = 2, it relates to the y-direction; and if i or j = 3, it relates to the z-direction. C_μ, σ_k, σ_ε, C_{1ε} and C_{2ε} are constants.



Geometry

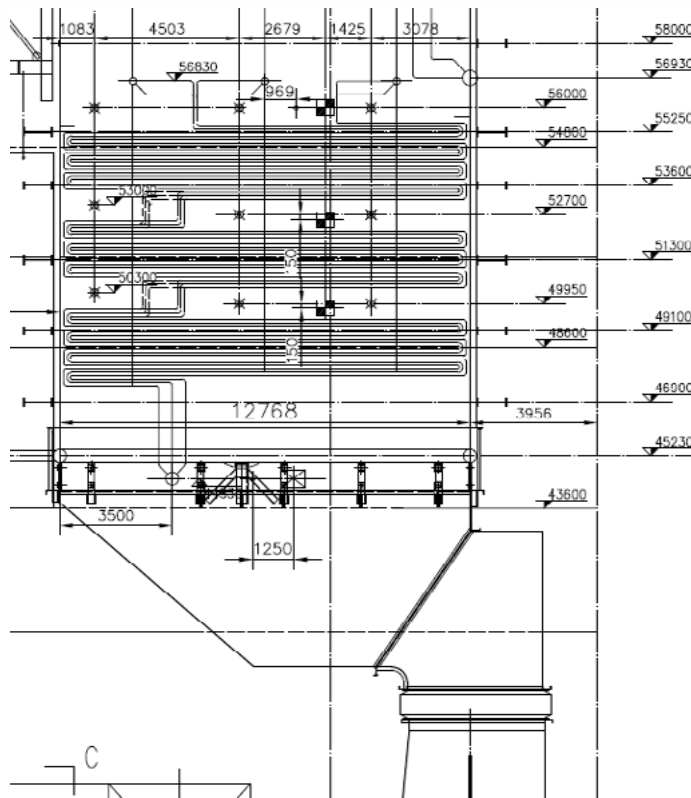


Figure 1. Geometry economizer flue gas tube ducting

Model geometry for economizer flue gas tube ducting can be seen in Figure 1.

Meshing

A 3-dimensional model was used for the simulation. The grid used was a type of structured cell with dimensions 49x22x49. Construction grid is shown in Figure 2 - Figure 6, for Economizer Without Hopper (Flat) (Figure 2), Economizer 3 Hopper (Figure 4), Economizer 6 Hopper A (Figure 5), Economizer 6 Hopper B (Figure 6), shows the construction of grid.

Dependence on the grid was tested on various dimensions of the grid, where the test results were consistent but not influenced by the size of the grid.

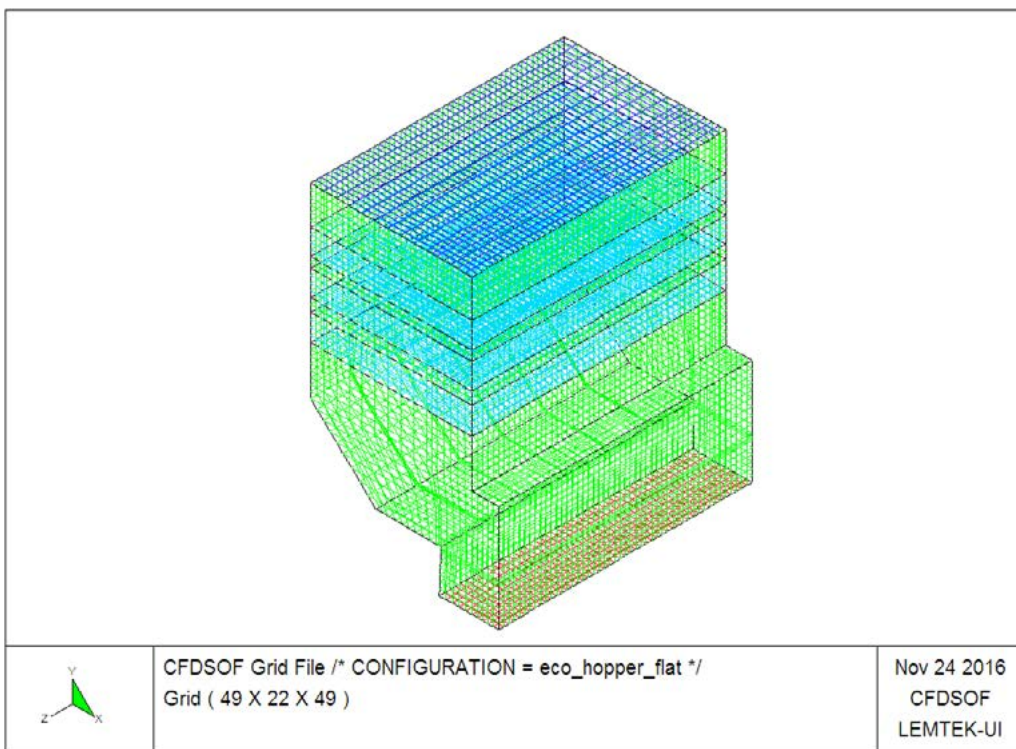


Figure 2. Meshing simulation model of economizer without hopper (Flat).

Economizer 1 to 3 is defined by Porous 1 to 3.

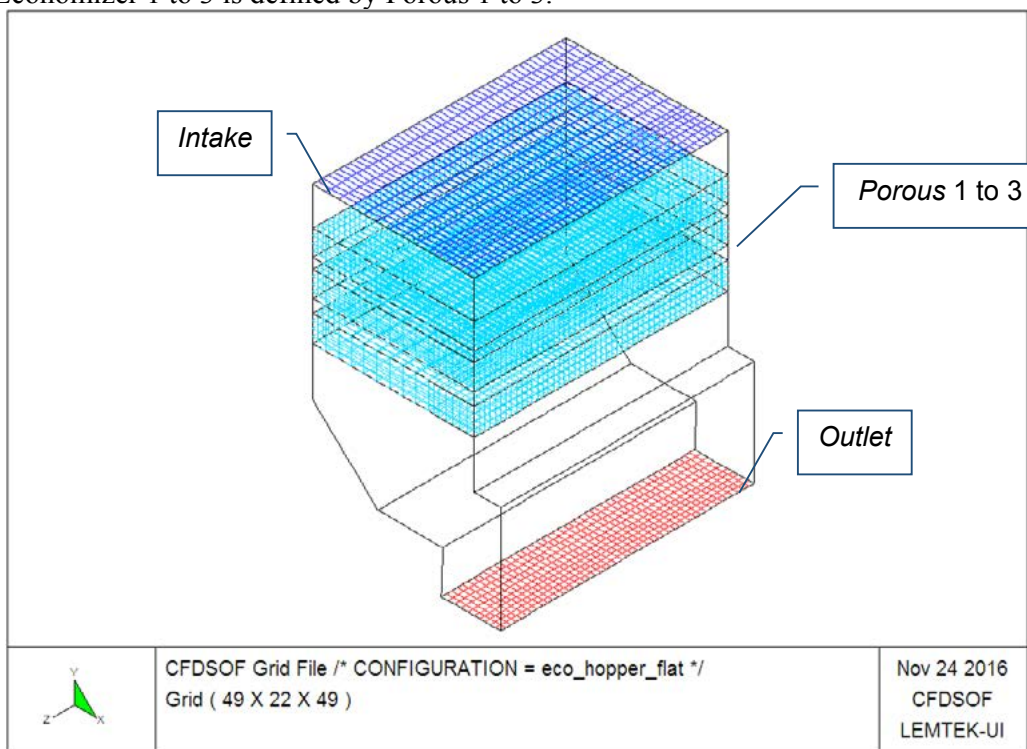


Figure 3. Meshing simulation model of porous.

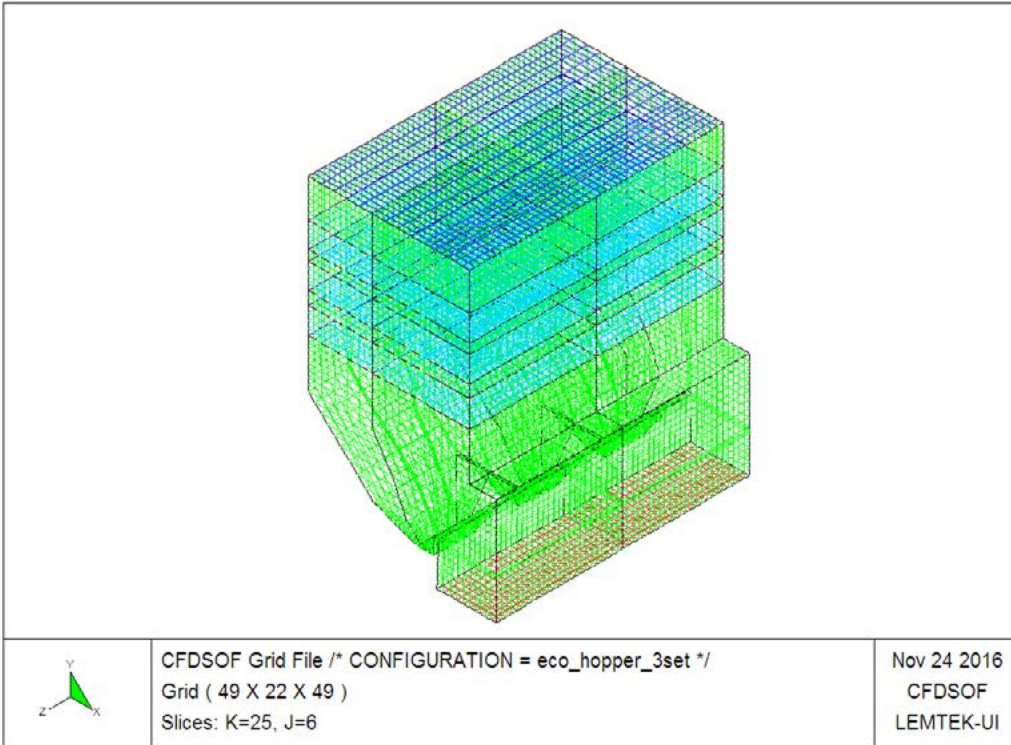


Figure 4. Meshing simulation model of economizer 3 hoppers.

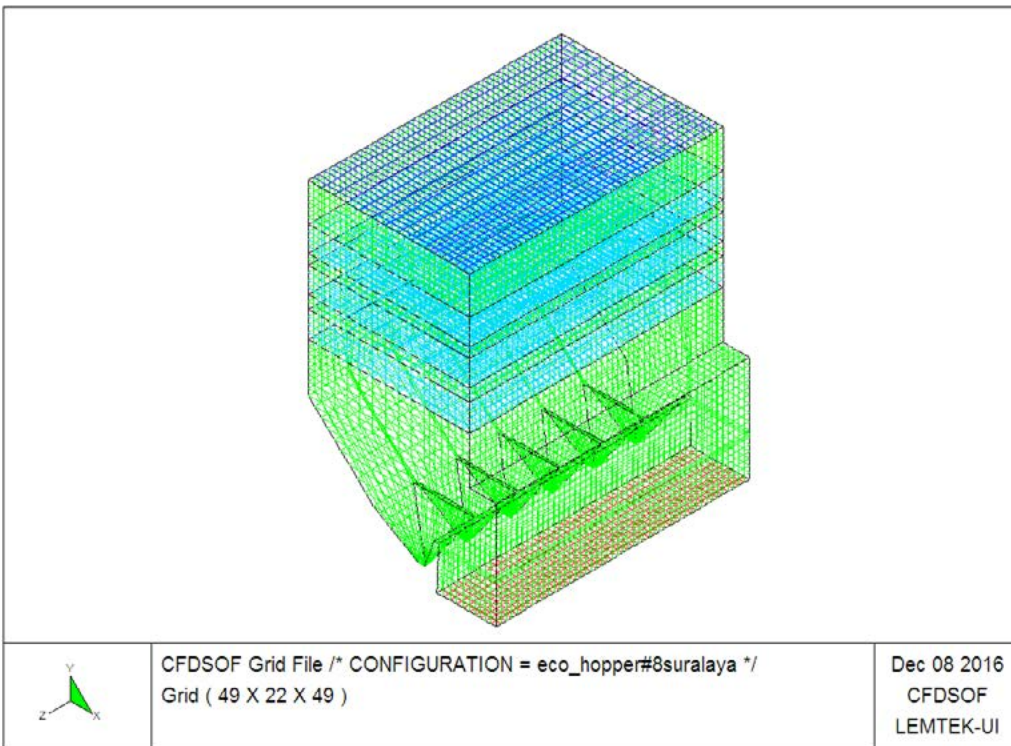


Figure 5. Meshing simulation model of economizer 6 hoppers A

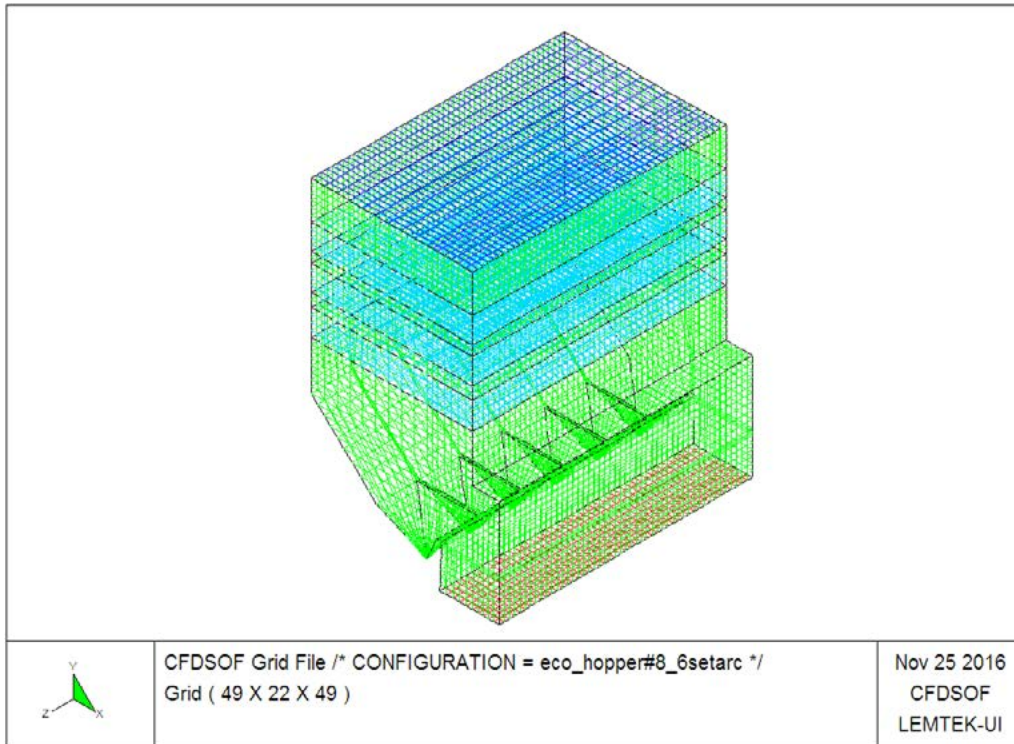
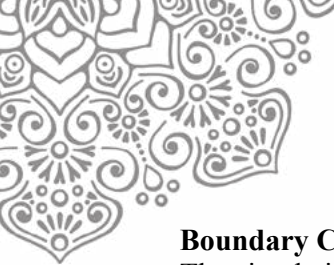


Figure 6. Meshing simulation model of economizer 6 hoppers B.



Boundary Conditions

The simulation model is a three-dimensional model with a total grid 52822. Movement direction intake gas and particulate matter in line with the y-axis. The flow consists of gas and particulate phase so that the condition of multiphase Eulerian models enabled. The movement of gases and particulate matter causing turbulence so that the k-ε turbulence model is enabled. The flow of gas and particulate matter is influenced by gravity, so the gravity (gaya badan) are activated. Parameter values that are intended to software are as follows:

- Gas velocity intake = 2.1 m / s, particulate velocity intake = 1 m / s, volume fraction = $3,5 \times 10^{-5}$
- Porosity porous = 1 m²
- Particulate density = 1,312x103 kg / m³
- Mean diameter of particulate = 1 x10⁻⁴ m

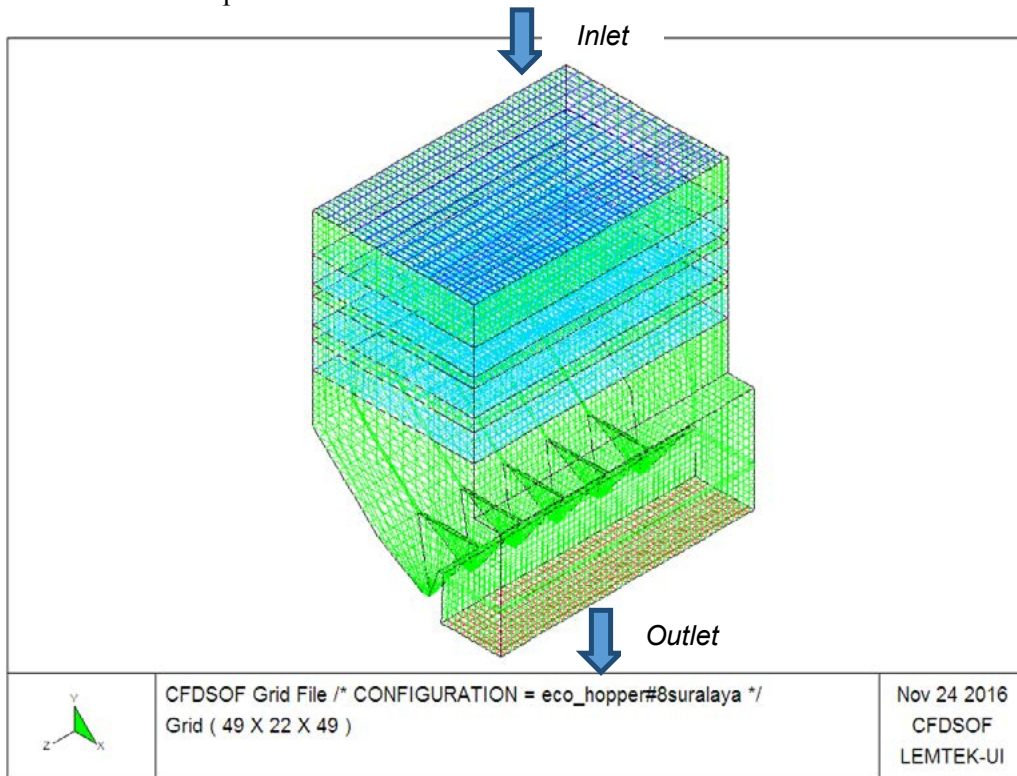


Figure 7. Computation parameter.

Verification

Verify to see how changing the time step on the simulation results, conducted three different time step; step 30 s, 45 s, and 60 s. The simulation results shown by gas magnitude velocity contours, as in Figure 8. The simulation results showed comparable contour better to steps 30, 45 and 60 s. Similarly, comparable conditions are shown in velocity vector graphics at i28, J8, K25 with a time step of 30 s, 45 s and 60 in Figure 9. Then, for the next simulation use time step of 60 s.

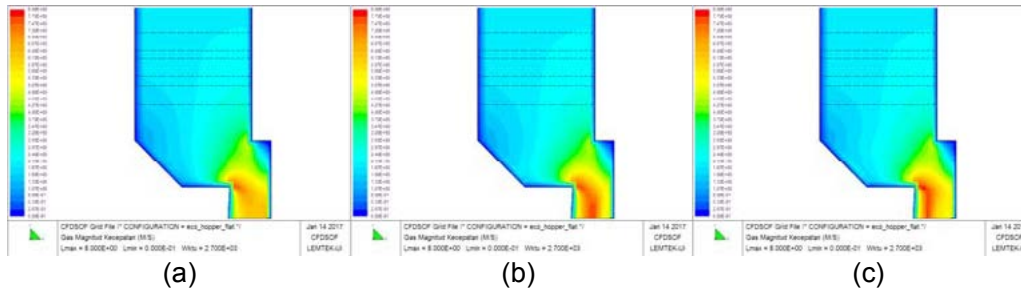


Figure 8. Gas magnitude velocity contour on economizer without hopper (flat) a) time step 30 s b) time step 45 s c) time step 60 s

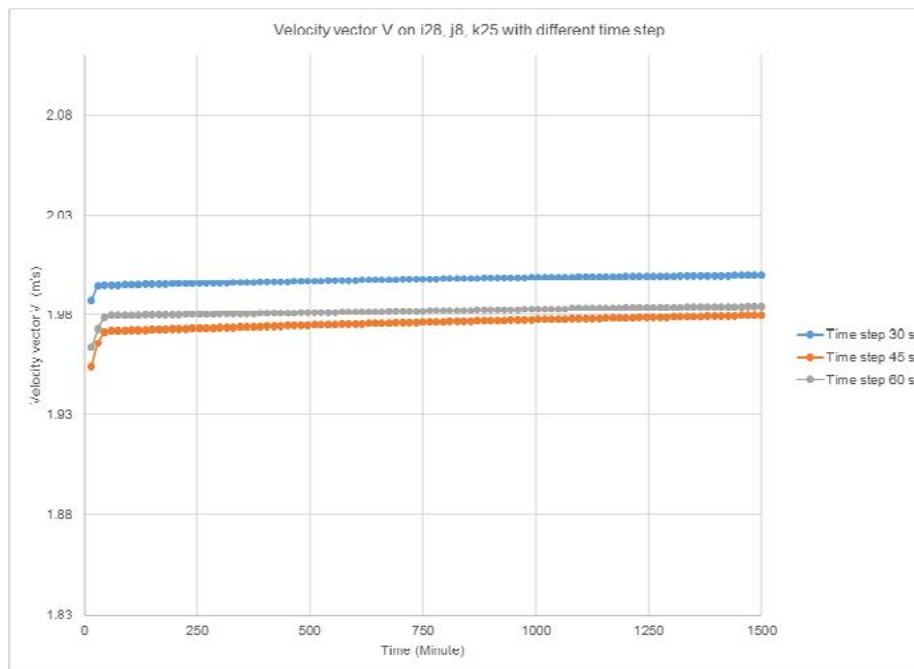


Figure 9. Velocity vector graphics at i28, J8, K25 with difference time step

Validation

Validation is comparing the simulation results with secondary/primary data. Validation is required to look at the suitability of the simulation results against actual data taken from surveys. The parameter is the volume fraction of particulate matter in comparison. The validation results can be seen in Figure 10, particulate volume fraction contours at the economizer without hopper (flat), showed in a corner of the flat area occurs high particulate concentrations, comparable with the ash build up data in the economizer bottom area indicated in Figure 11.

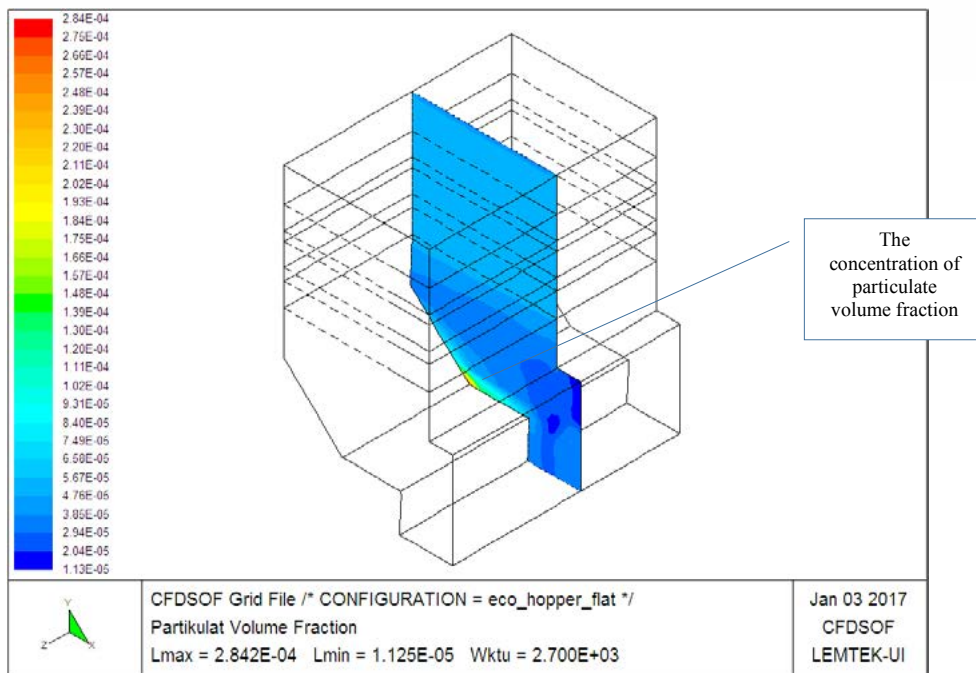


Figure 10. Particulate volume fraction contours on economizer without hopper (Flat).



Figure 11. Ash buildup in economizer bottom area.

3. RESULTS AND DISCUSSION

Figure 12 shows the particulate magnitude velocity contours on the economizer without hopper (flat), a portrait of flow along the wall, also in the flat area is quite low which allows particulates will be more concentrated on that area due to the force of gravity. Figure 13 shows that a flat area on the corner of formation of particulate concentration. In these areas, the accumulation of particulates, to stabilize at a certain time.

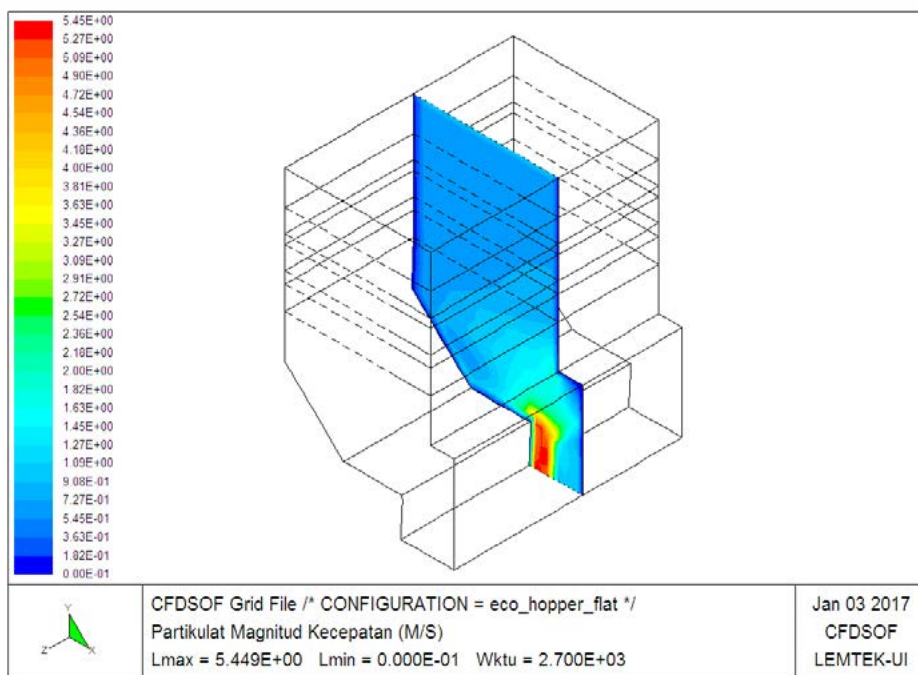


Figure 12. Particulate magnitude velocity contours on economizer without hopper (flat).

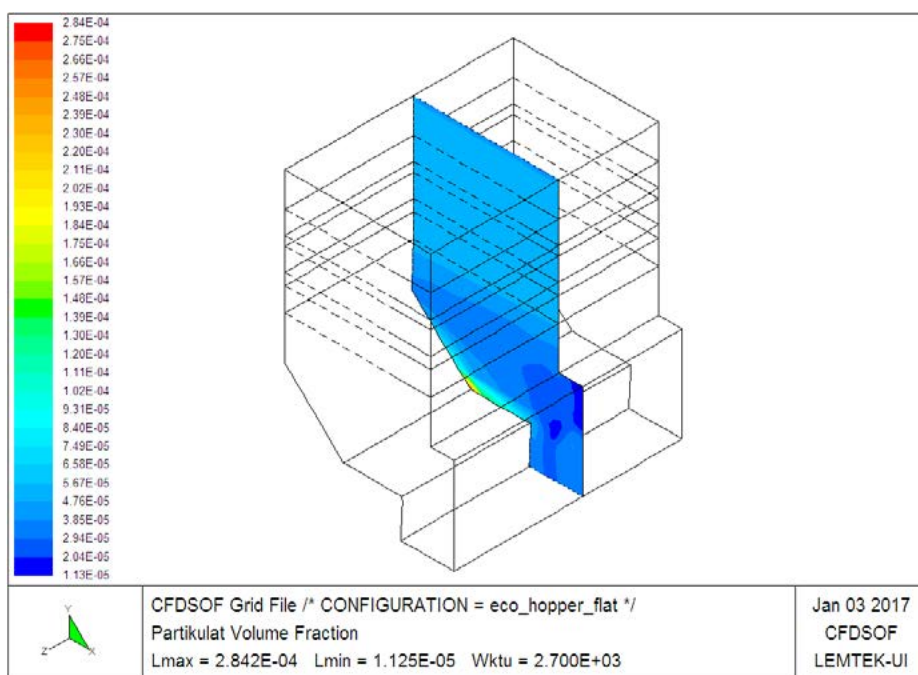


Figure 13. Particulate volume fraction contours on economizer without hopper (flat).

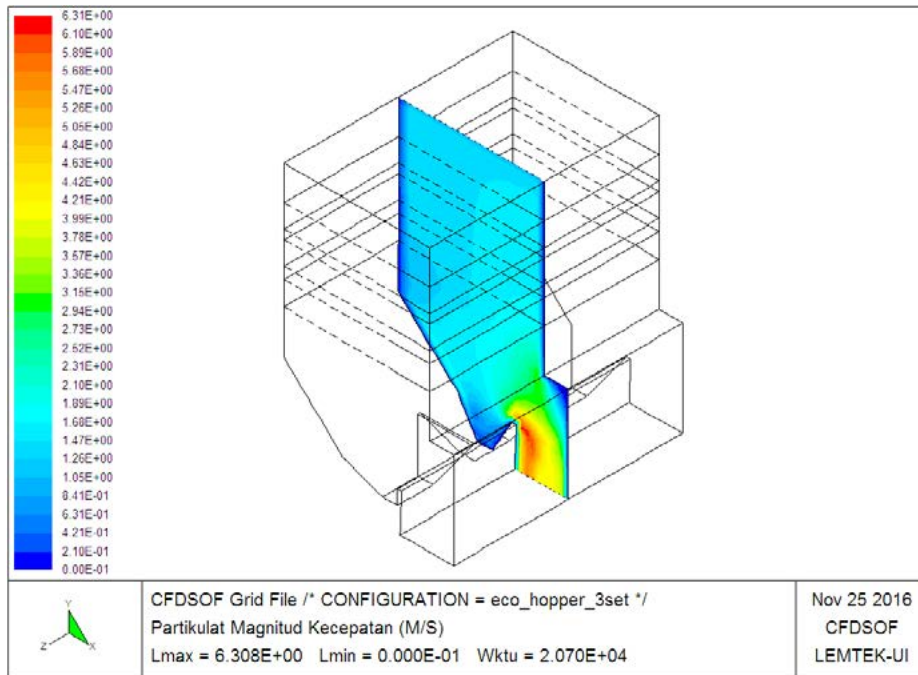


Figure 14 shows the particulate volume fraction contours on 3 economizer hopper, describe the flow in the hopper area, in addition to the low speed occurs also flow circulation, which will increase the higher particulate matter concentrated in these areas due to the force of gravity.

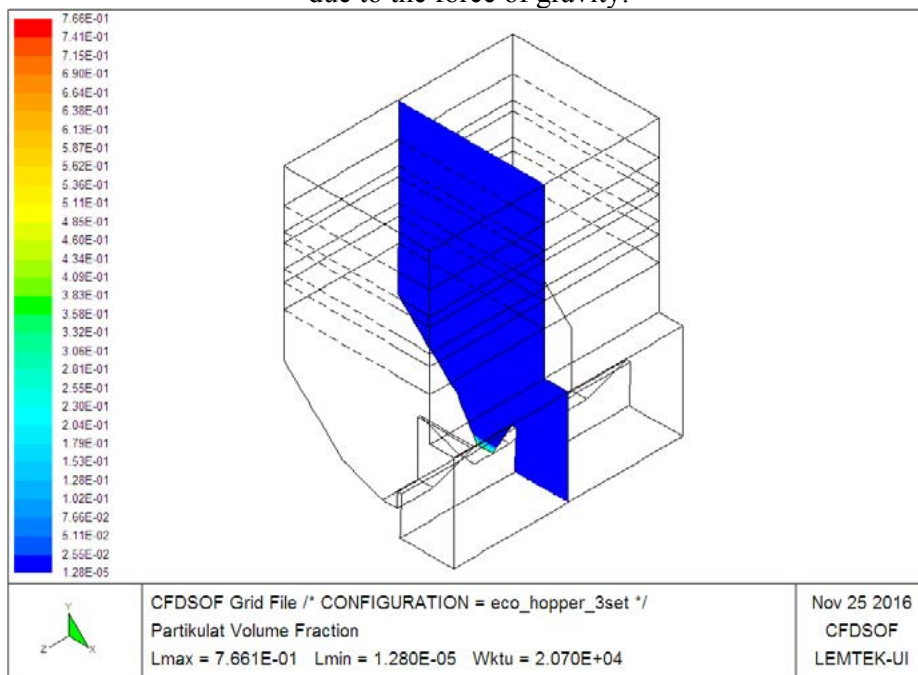


Figure 15 shows the particulate concentration is very high in the hopper area. In these areas, there will be an accumulation of particulates with a higher deposition rate.

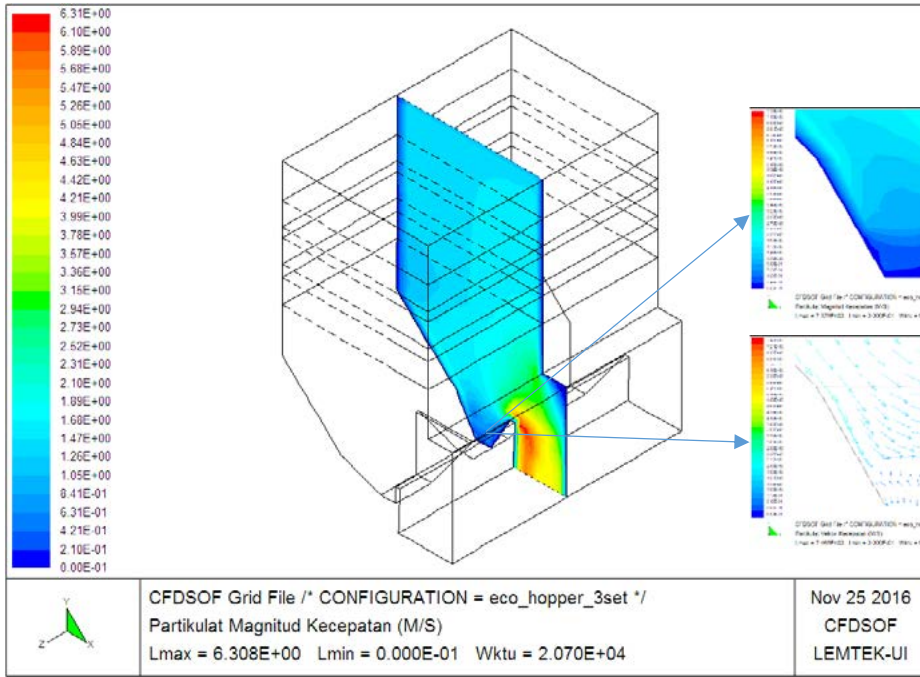


Figure 14. Particulate magnitude velocity contours on economizer 3 hopper.

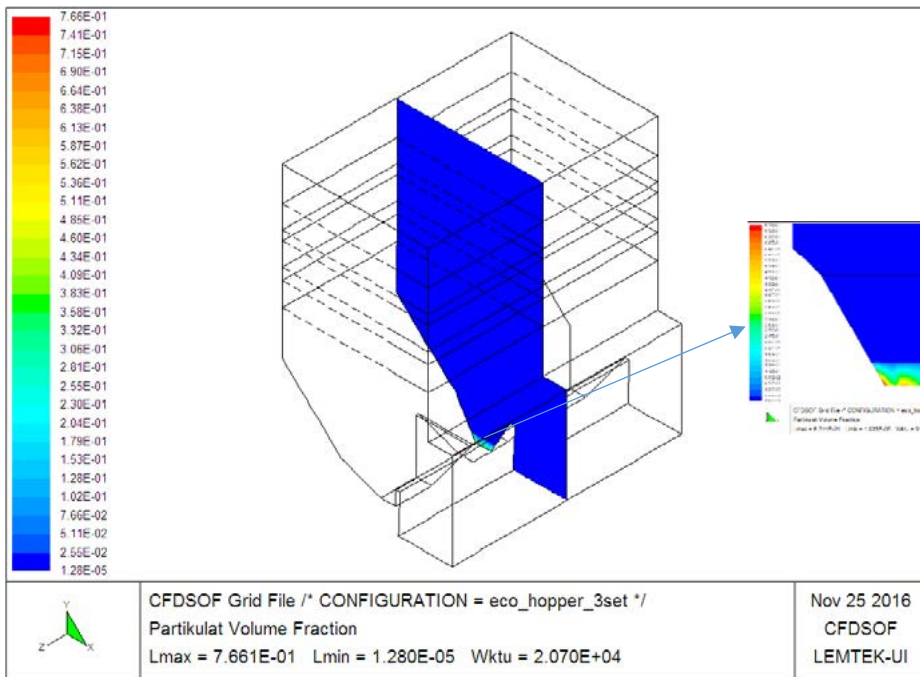


Figure 15. Particulate volume fraction contours on economizer 3 hopper.



Comparable conditions are shown in

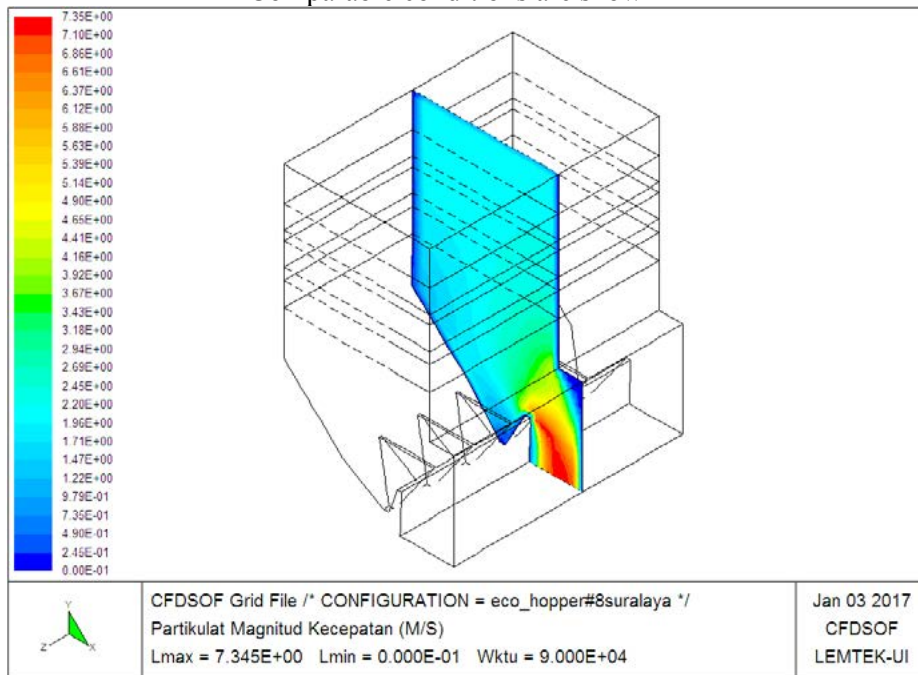


Figure 16 and

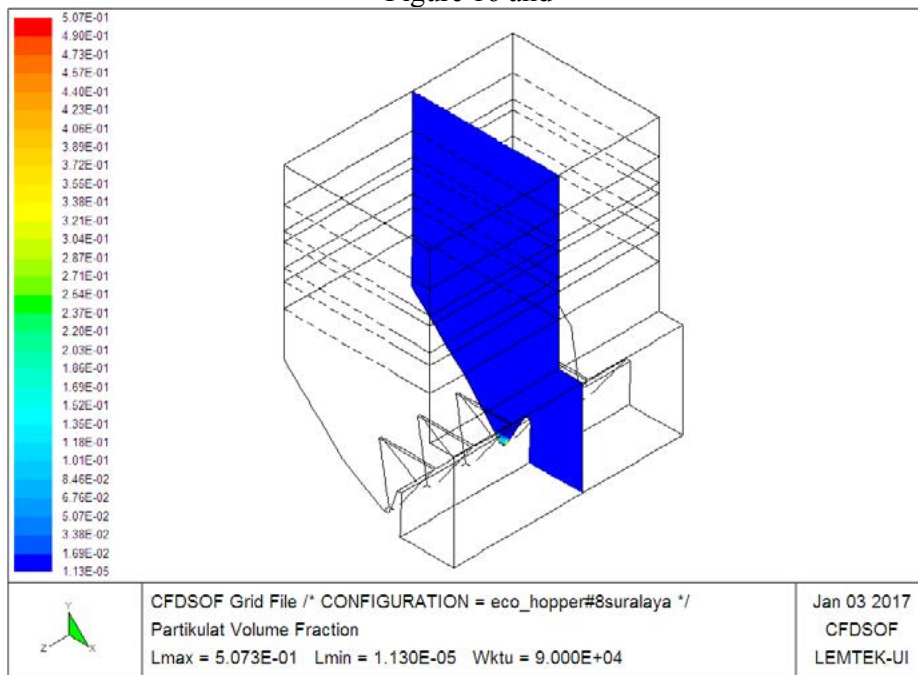


Figure 17, which shows the particulate magnitude velocity contours at 6 economizer hopper A, describe the flow at hopper area, low velocity and occurs the circulation flow, which will increase the higher particulate matter concentrated in these areas due to the force of gravity. Very high particulate concentrations in the hopper area. In these areas, there will be an accumulation of particulates with a higher deposition rate.

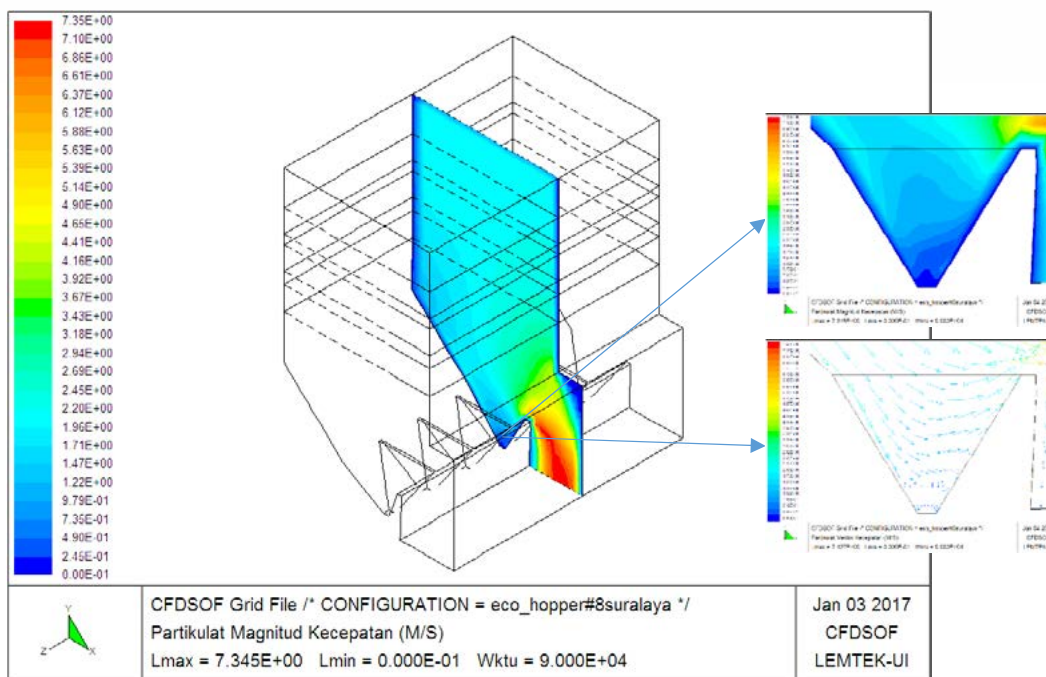


Figure 16. Particulate magnitude velocity contours on economizer 6 hopper A.

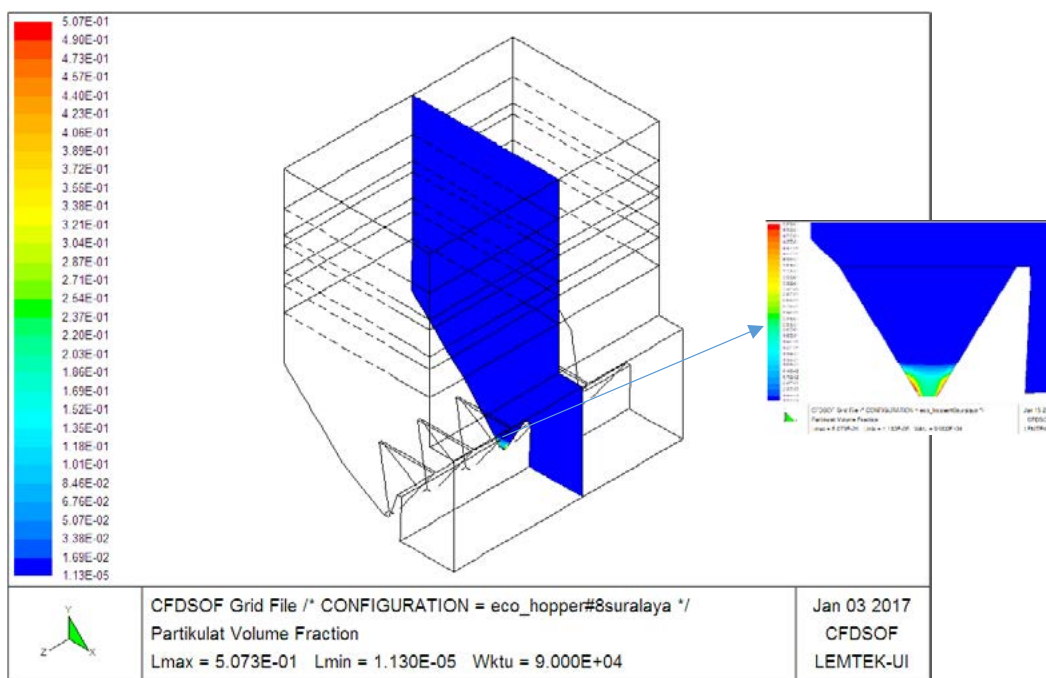
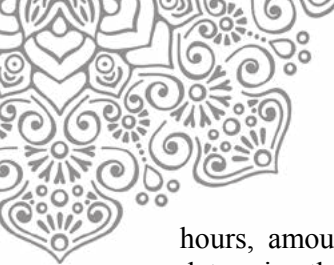


Figure 17. Particulate volume fraction contours on economizer 6 hopper A.

The graph on Figure 18 shows the particulate deposition rate matter over time. At the time of inception, the particulate deposition rate highest 27%. Over time, the particulate deposition rate will drop due to the deposition of particulate matter on each hopper. The particulate deposition rate at 6 economizer hopper A began to stabilize in 11:25 - 25.00



hours, amounting to 5% to 5%. Such conditions can be taken into consideration to determine the optimum time for issuing periodic particulate matter from the hopper.

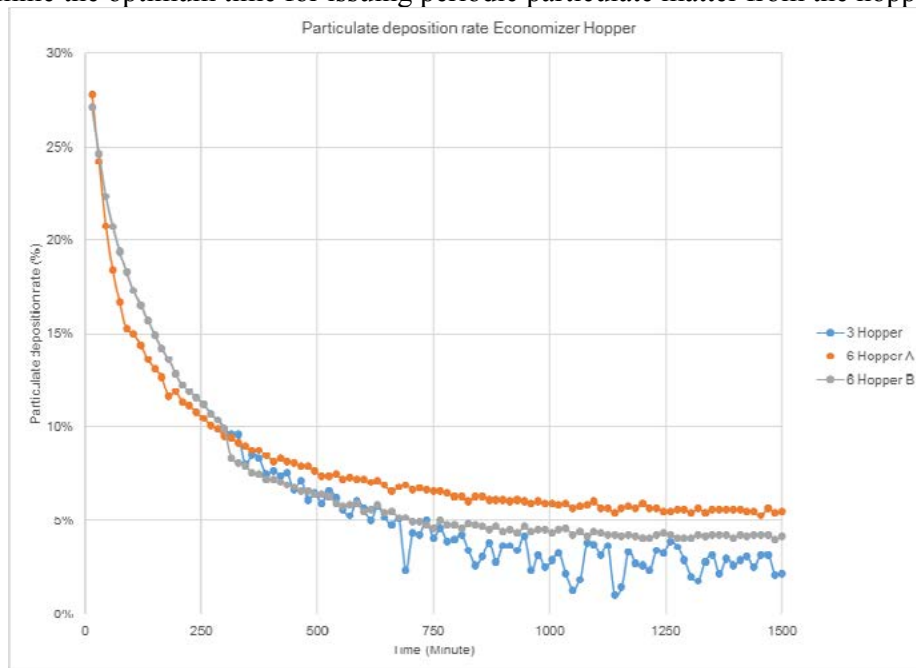


Figure 18. Particulate deposition rate economizer hopper.

4. CONCLUSION

The results of modeling and simulation CFD calculations on economizer hopper indicates that the installation economizer hopper will significantly help reduce the amount of particulate fly ash in the flue gas stream.

At the time of inception, the particulate deposition rate highest 27%. Over time, the particulate deposition rate will drop due to the deposition of particulate matter on each hopper. The particulate deposition rate at 6 economizer hopper A began to stabilize in 11:25 - 25.00 hours, amounting to 6% to 5%. Such conditions can be taken into consideration to determine the optimum time for issuing periodic particulate matter from the hopper.

5. ACKNOWLEDGEMENT

The authors would like to thanks, DRPM Universitas Indonesia for funding this research through “Hibah Publikasi Internasional Terindeks untuk Tugas Akhir Mahasiswa UI 2016” and to PT. CCIT Group Indonesia for CFDSOF® software license.

6. REFERENCES

- Daryus, A. et al., 2016. CFD simulation of turbulent flows in proto X-3 bioenergy micro gas turbine combustor using STD k- ϵ and RNG k- ϵ model for green building application. , pp.204–211.
- Gunadi, G.G.R. et al., 2016. Turbulence model and validation of air flow in wind tunnel. , pp.1362–1371.
- Versteeg, H.K. & Malalasekera, W., 1995. An Introduction to Computational Fluid Dynamics - The Finite Volume Method.



**15th INTERNATIONAL CONFERENCE ON QUALITY IN RESEARCH (QIR
2017)**

**OPEN FLUME PICO-HYDRO TURBINE BLADE DESIGN BY ANALYTICAL
AND NUMERICAL METHOD**

Budiarso, Ahmad Indra, Dendy Adanta, Hans Vohra, Reza Dianofitra*

Department Mechanical Engineering, Faculty of Engineering Universitas Indonesia,
Kampus Baru Depok 16242

ABSTRACT

Bengkulu is a province located in southwest coast of Sumatera, Indonesia. Bengkulu is quite underdeveloped when compared to other provinces in the country. The electrification ratio is as low as 51% in the region. The geographical condition of the region which includes mountains and hilly areas has contributed more to the difficulty in expanding the national grid. The lack of infrastructure such as roads have made the problem worse. As a result, the cost of expanding the national grid becomes high. Due to this condition, the only option left is to build off grid systems. Fortunately, there are many water sources in Bengkulu and the energy potential is high. With all these information, it can be concluded that a pico-hydro system is the right one to be developed. Selecting the right turbine for the right environmental conditions is therefore important as this will have a huge impact on the power output. Many studies have proved that the propeller type open flume turbine is the best choice for remote areas in Indonesia. The area that is focused on has a head of 2.7 m and flow rate of 0.041 m³/s. The right blade configuration is required to produce turbine with the best efficiency. This study compares turbine having different blade numbers i.e. 5 and 6 bladed turbines. In the design stage the blade number is kept as the free variable while the others are kept fixed. This ensures that the blade number is the only factor that influences the differences in the results that are obtained. Analysis was done with simulation using CFD. The turbulence parameter taken is STD k- ϵ . CFD simulation results showed that the greatest hydraulic efficiency is generated by the 6 bladed turbine and thus it is the right choice.

Keywords:

k- ϵ ; Open Flume; Pico-Hydro; Runner; Rural Area

1. INTRODUCTION

1.1 Background

Rural areas, by definition include all the areas outside major towns and cities. These areas often have mountainous terrains which are not suitable for development compared to plain fields and lands that are available in the city. (Ho-Yan, 2012) The question arises then as to how we can provide electricity to these areas. With the current state of the world where non- renewables are depleting, using renewable sources of energy would be a good option. Other than that, a power generation system for small rural areas should be cheap to manufacture, reliable and also efficient. (Prabu, 2012) Indonesia, is a country located in Asia, right under the equatorial line. It is now one of the fastest developing countries in the world and it has a population of 255 million people. Despite the growth, there are many areas in Indonesia that have little to no access of electricity. (BPS, 2015) One of it is Bengkulu, a province located in southwest coast of Sumatera, Indonesia. Bengkulu is quite underdeveloped when compared to other provinces in Indonesia. This province will



be the area that this research will be focused on as it has a huge water potential, it is a rural area and also a low electrification ratio. Bengkulu has mountainous terrains with many rivers and water streams with low flow rate and low head. This means that we can develop small hydro-power plants. The scale of this power plant is decided to be less than 5 KW or in other words, it will be of a pico-hydro level. The main component of a pico-hydro power plant is the turbine and thus selecting the right turbine for the job is a must. The turbine is designed based on the conditions of Salam Lake, inside the University of Indonesia area. To be precise, the head is 2.7 m and the flow rate is 0.041 m³/s. Based on Figure 1, it can also be concluded that the best turbine for the condition of Bengkulu is the propeller turbine. The propeller will be of open flume type as it is simpler as compared to other turbines and thus it would be easier to repair. Other than designing a turbine, this study also aims to find out the effect of the number of blades on turbine performance.

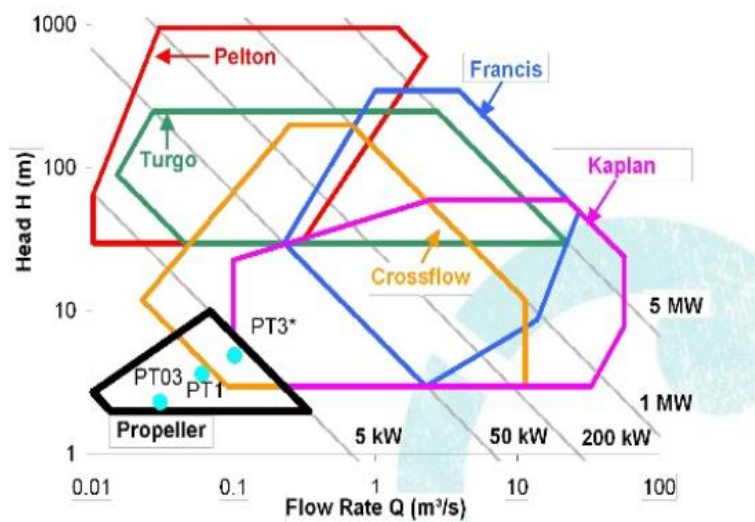


Figure 1 Flow rate vs Head (Sayeed, 2015)

1.2 Previous Research

Over the years students in University of Indonesia’s Fluid Mechanics Laboratory have designed several open flume turbines. This design is aimed at producing a turbine that is more efficient. The changes made in this turbine are:

- New overall turbine design
- Using different NACA airfoils

2. METHODOLOGY

2.1 Turbine Design

Available information:

- $H = 2.7\text{ m}$ $Q = 0.041\text{ m}^3/\text{s}$ $N = 1500\text{ RPM}$

2.1.1 Power

The first step is to calculate the power from the water. The formula used is:

$$P = \rho \times g \times Q \times H \tag{1}$$



2.1.2 Specific Speed

The next step is to find specific speed n_s and n_q . The specific speed n_s is based on the power developed of the turbine while the specific speed n_q comes from the flow rate of the turbine. Specific speed n_q is used in determining the hub to tip ratio as well as the diameter of the turbine.

$$n_s = n \frac{\sqrt{P}}{H^{\frac{5}{4}}} \quad (2)$$

$$n_q = n \frac{\sqrt{Q}}{H^{\frac{3}{4}}} \quad (3)$$

2.1.3 Hub to Tip Ratio, Diameter

Following the specific speed is the hub to tip ratio and diameter calculation. After finding the specific speed, we can use Figure 2 to find the variables needed. (Simpson, 2011) For this case, the resulting specific speed n_q is near the borderline of the 6 and 5 bladed turbine, thus there is a slight confusion on which configuration should be chosen and thus this study is dedicated to find the answer.

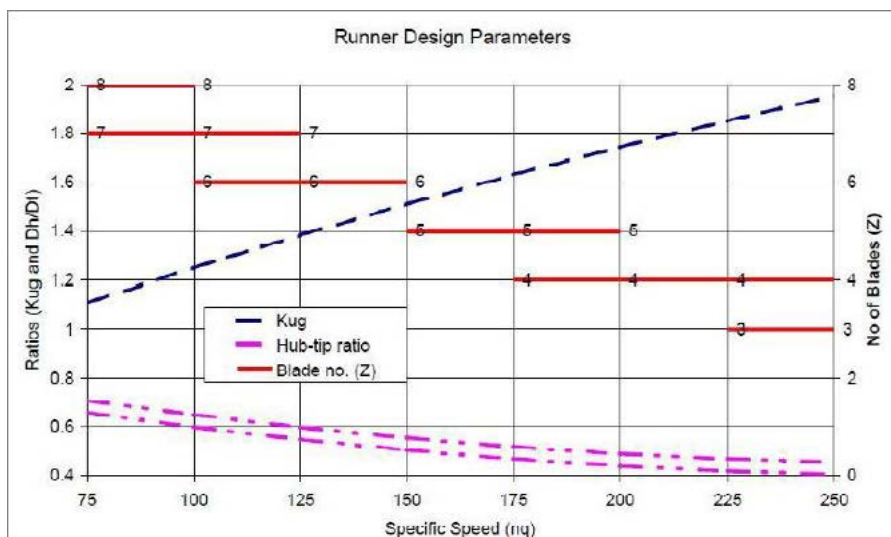


Figure 2 Runner Design Parameters (Simpson, 2011)

Insert the variables to the formula (Simpson, 2011):

$$K_{ug} = \frac{r_{tip} \times 2 \times \pi \times N}{\sqrt{2} \times g \times h \times 60} \quad (4)$$

2.1.4 Velocity Triangle

The velocity triangle helps in finding the velocity components of the turbine and in return the angle of attack of blades of the turbine. The blades used are NACA 4 series airfoil.

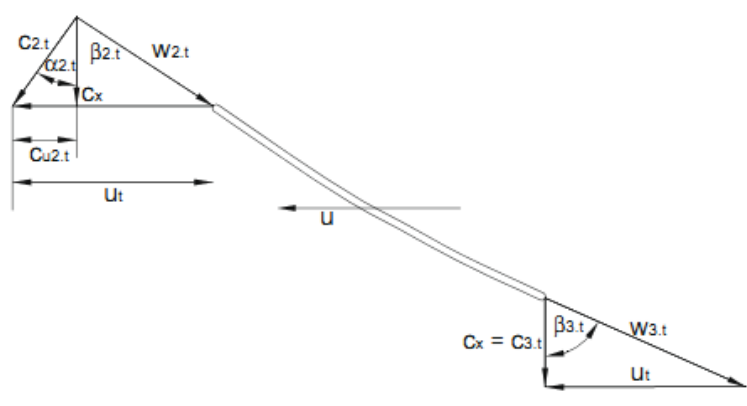


Figure 3 Velocity triangle at the tip (Punit Singh*, 2010)

The angle of attack and thus select the airfoil type for the blades.

$$\theta_i = \arctan\left(\frac{(u-cu_i)}{c_m}\right) \tag{5}$$

$$\beta_2 = 90^\circ - \theta_2 \tag{6}$$

$$\theta_i = \arctan\left(\frac{(u-cu_i)}{c_x}\right) \tag{7}$$

$$\beta_3 = 90^\circ - \theta_3 \tag{8}$$

$$\beta_{stagger} = \frac{\beta_2 + \beta_3}{2} \tag{9}$$

$$\alpha = \beta_{stagger} - \beta_2 \tag{10}$$

2.1.5 Design Summary

Table 1 shows the design summary as obtained from the calculations using the formula mentioned earlier. Table 1 shows the obtained angle of attack and selected NACA airfoil for the water turbine while Table 2 shows the design summary.

Table 1 Angle of attack and NACA airfoil at every hub to tip

dh/D_{tip}	α°	Airfoil (NACA)
0.5	10.51	4418
0.6	17.17	4415
0.7	20.36	4412
0.8	21.93	2412
0.9	22.65	2409
1.0	22.90	2406



Table 2 Design summary

Description	Value	Unit
Power	1.085	KW
N	1500	RPM
n_s	450	RPM
n_q	144	RPM
K_{ug}	1.5	-
D_{tip}	0.725	mm
D_{hub}	1.45	mm
Hup to tip ratio	0.5	-

2.2 Modelling

For this case, to make sure that the results of the study is due to the differences in blade number only, both the models are exactly the same with differences only in the blade number i.e. 5 and 6 blades. The modelling is done in Solidworks software.

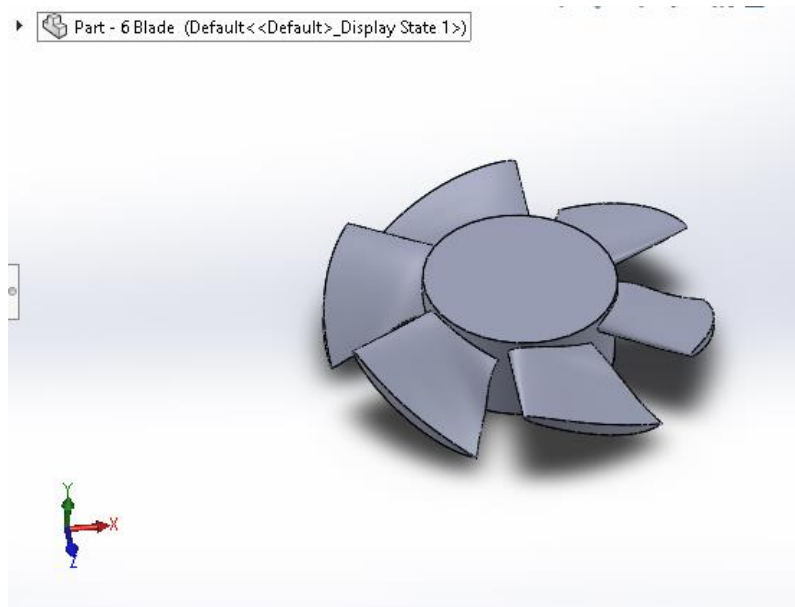


Figure 4 CAD of 6 bladed turbine

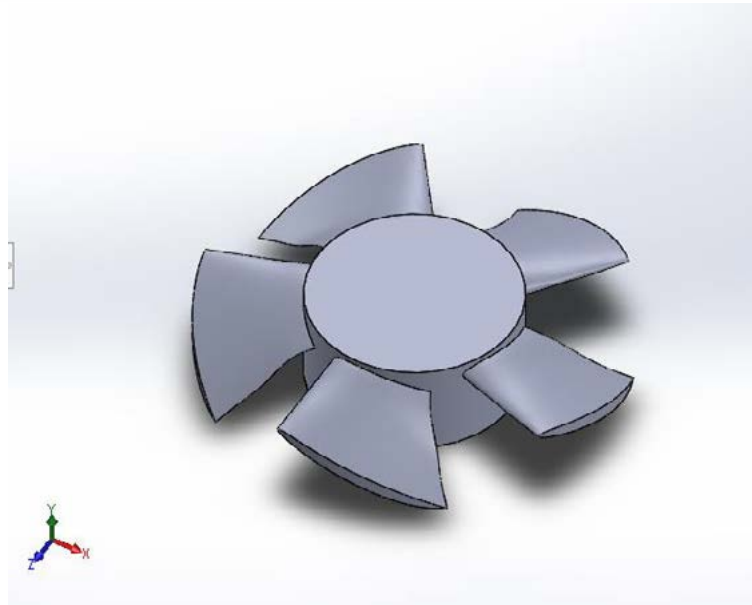


Figure 5 CAD of 5 bladed turbine

2.3 Simulation

Computational fluid dynamics software helps to increase our understanding of the interaction and movement of fluids. This is done by algorithms and numerical methods. CFD has 3 steps which is the pre-processing stage, solver and post processing stage. There are few turbulent models but for open flume propeller case, the k- ϵ turbulent model will be used. It is the most commonly used model and is suitable for general flow conditions. On top of that, the computing power required for this turbulence model is not as high compared to other models. (Launder B.E. , D. Spalding , 1974) For information such as a turbine characteristic curve for torque, power, flow rate and efficiency over the full speed range for a pico-hydro propeller turbine, the recommended turbulence model used for the simulations is the k- ϵ (k-epsilon) model. The simulation is done under a steady state condition. (R.G. Simpson, A.A. Williams, 2011)The main feature used here is the Turbo topology from which hydraulic efficiency of the turbine can be obtained. In Turbo topology, 1.6th and 1/5th of the turbine is inserted as the geometry. After iteration, whole turbine can be displayed through the animation tab. This feature in brief, enables the calculation to be done in the fraction of the component and times it by 6 and 5 respectively. This saves computing power and thus it is used. Figure 7 and Figure 8 show the flow visuals for both the 6 and 5 bladed turbine at 450 RPM.

2.3.1 Mesh Independency

Before carrying out with the simulation, a study which is called the Mesh Independency study should be conducted, the purpose of which is to find the best mesh setting that would provide the legitimate result without taking the most computing power. This would lead to a faster and more efficient CFD process. For this case, the Mesh Independency is performed by finding different velocities at $Y = 0.06$ m. Fig 8 shows the result. Based on the figure below, a medium setting is deemed to be the best for this case since the data obtained is not far off the fine setting.

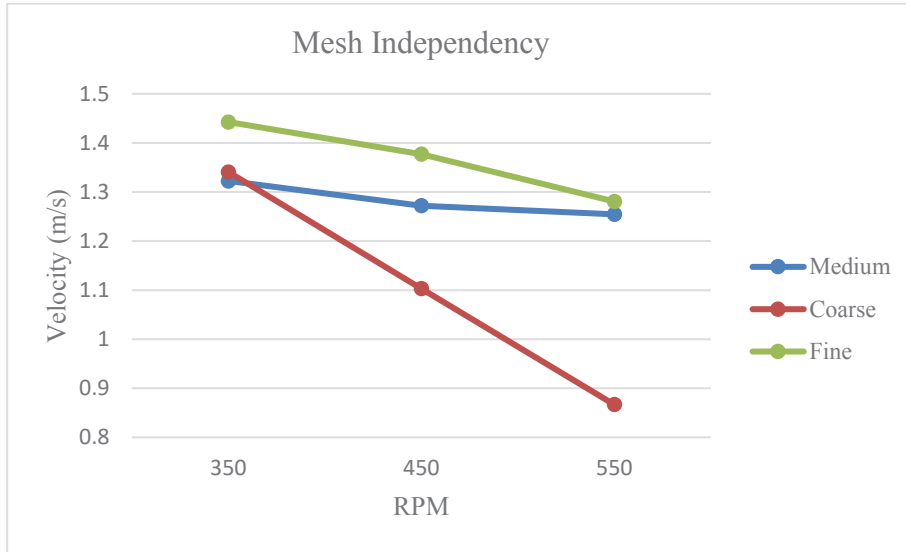


Figure 6 Mesh Independency result

3. RESULTS AND DISCUSSION

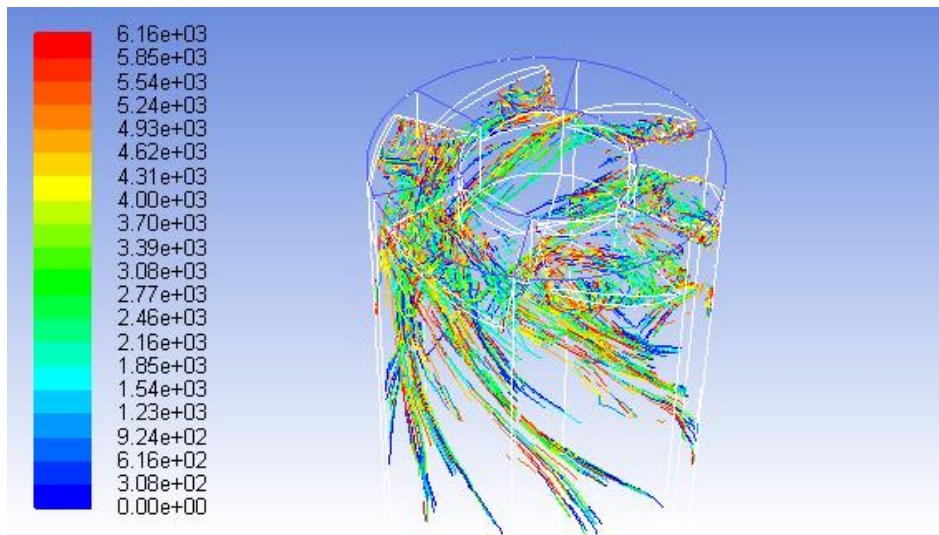


Figure 7 Pathlines of 6 bladed turbine at 450 RPM

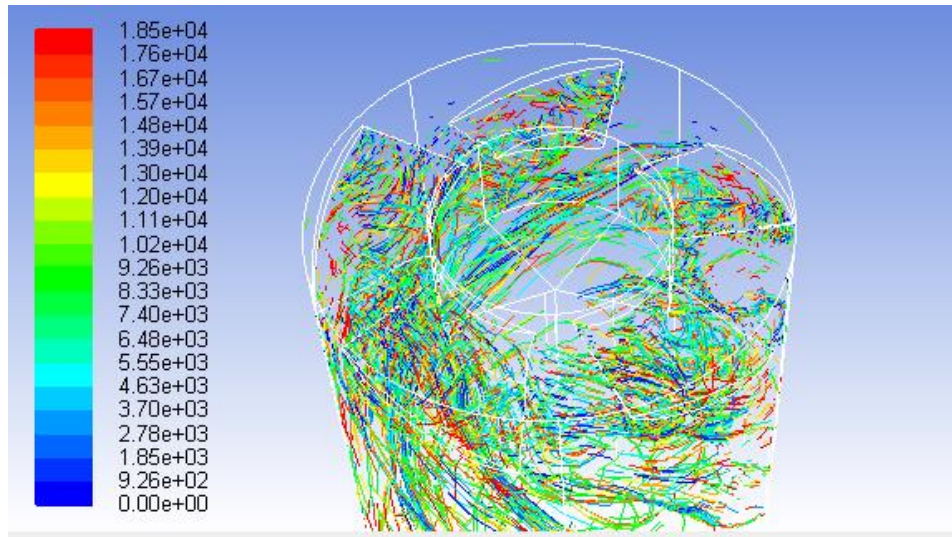


Figure 8 Pathlines of 5 bladed turbine at 450 RPM

From the 2 simulation at 450 RPM, it can be seen that the 6 bladed turbine has shown a more controlled flow with less losses visually as the distance between blades are less. The gaps in between the blades of the 5 bladed turbine has reduced the effective flow rate that come in contact with the turbine itself. The flow in the 5 bladed turbine seems to be less controlled which supports the result of it having a less efficiency. A less controlled flow means that there will be less energy transfer from the fluid in this case, water to the blade. The simulation at other turbine speed also showed similar pattern. After the simulation, hydraulic efficiency of the turbine can be obtained. Which can be otherwise calculated using this formula:

$$n_H = \frac{P_s + P_m}{P} \quad (11)$$

Since the purpose of this study is to compare the best turbine configuration for low head and low flow condition, the efficiency and power generated are the key variables that are presented. The results show that the efficiency of the 6 bladed turbine is higher at 3 different turbine speed.

Table 3 Result obtained from CFD

RPM	n_H 5 Blade	n_H 6 Blade
350	30.62%	38.26%
450	43.74%	52.46%
550	60.56%	67.37%

The total efficiency is inserted in equation (12):

$$P = n_H \times \rho \times g \times Q \times H \quad (12)$$



Table 4 Actual power generated based on simulation

RPM	Power 5 Blades	Power 6 Blades
350	332 W	415 W
450	475 W	569 W
550	657 W	731 W

From the results, the trend is as such that the higher the turbine speed, the higher is the efficiency of the turbines. The differences are high at around 10-15% per 100 rpm increase in turbine speed. From this result it is also worth noting that the optimum turbine speed of the turbine is around 550 rpm. The 6 bladed turbines have shown higher results in terms of power generated. This is because, the additional blade increases the surface area that comes in contact with the water, which leads to a higher torque. The torque is important as it is then multiplied with the angular velocity to obtain the power generated. Increased number of blades will also contribute to a higher friction which theoretically should reduce the power generated and the efficiency however, it is believed that for this case the losses due to friction in 6 bladed turbine is not as high as the losses due to the wider gaps in between the 5 bladed turbine.

4. CONCLUSION

From this study, it can be concluded that the 6 blade turbine configuration is the best for low flow and low head condition based on the head and flow rate at Salam Lake UI. However, much more study at different flow rate and head should also be conducted to find a conclusive answer. The author also believes that the analysis using CFD can be improved by using a more detailed methods which at the time of making this paper could not be done due to the unavailability of sophisticated computers. The results should also be validated with an experiment to make sure that it is accurate and thus can act as the guideline for further studies for the students in University of Indonesia's Fluid Mechanics Laboratory.

5. REFERENCES

- (BPS), S. O. o. I., 2015. *National Census*. [Online] Available at: www.bps.go.id/ [Accessed November 2016].
- Adhikari, P., n.d. A Study on Developing Pico Propeller Turbine for Low Head Micro. *Journal of the Institute of Engineering, Vol. 9*, p. pp. 36–53.
- ESDM, 2016. *Indonesia's Ministry of Energy and Mineral Resources*. [Online] Available at: esdm.go.id
- Ho-Yan, B. P., 2012. Design of a Low Head Pico Hydro Turbine for Rural Electrification in Cameroon.
- Hui, P., 2009. Analytical Solution of Hydraulics Calculation on Cross Sections of Different Spiral Cases.
- Lauder B.E. , D. Spalding , 1974. Computer methods in applied mechanics and engineering.



- Nechleba, M., 1957. *Hydraulic Turbines Their Design and Equipment*. Czechoslovakia: ARTIA Prague..
- PĂDUREAN, I., 2004. Study of Hydraulic Losses in Francis Turbines.
- Prabu, A., 2012. *Final Year Project - Propeller Turbine Design with 0.4 Hub to Tip Diameter Ratio*. Jakarta: University of Indonesia.
- Punit Singh*, F. N., 2010. Experimental investigation of the influence of blade height and blade number.
- R.G. Simpson, A.A. Williams, 2011. Application of computational fluid dynamics to the design of pico propeller turbines. Issue Nottingham Trent University.
- R., T., 1931. *Wasserturbinen und Turbinenpumpen Part 2*. Stuttgart: Wittwer.
- Rao, N. S. G., 1985. *Fluid Flow Machines*. New Delhi: Tata Mc Graw-Hill .
- S.J. Williamson, B. S. , J. B. b., 2012. Low head pico hydro turbine selection using a multi-criteria analysis. *Renewable Energy*.
- Sayed, M., 2015. *Promotion of appropriate green technologies for rural prosperity*. s.l.:s.n.
- Simpson, R., 2011. *Design of propeller turbines for pico hydro*. s.l.:s.n.



15th International Conference on Quality in Research (QIR 2017)

Blade Height Optimization of Undershot Banki Pico-Hydro Waterwheel by Analytical and Numerical Methods

Budiarso, A. I. Siswantara, D. Adanta, R. Pradito, R. Dianofitra*

Department Mechanical Engineering, Faculty of Engineering Universitas Indonesia,
Kampus Baru Depok 16242

ABSTRACT

Electricity is one of the primary needs in the daily life of a modern human. It is the main type of energy to power a modern human daily needs because it is easy to use, environmentally friendly, and can be easily converted to other forms of energy. However, electricity is not evenly distributed in Indonesia, especially the rural areas due to the lack of access to the power generation. Indonesia has an electrification ratio of 84.35% in the year 2015. This data shows that there are 49 million people who do not have access to electricity. Thus, an additional pico-hydro power generation (PLTPH) to minimize the use of fossil fuels and fulfill the electrification goals set by the ministry of energy and mineral resources. Pico-Hydro power generation becomes a solution because in Indonesia there are plenty of water sources and that can be utilized. This paper is mainly focused on banki undershot waterwheel, because of the simple construction, economical, and easy to move. In addition undershot banki waterwheel is suitable for water sources that have a low head like sources that found in Indonesia. The banki Undershot Pico Hydro Waterwheel is field tested in Salam Lake Located in University of Indonesia with the head set at 2.7 meter and channels 41 l/s of water. This waterwheel is to be applied in North Bengkulu at Palak Siring waterfall which is one of the remote areas located in Indonesia. In this study undershot waterwheel straight blade has an outer diameter of 0.81 m and an inner diameter of 0.54 m with 14 blades and 2 active blades. The blade has a height of 0.135 m and a width 0.13 m. Besides that the channel was reduced from 0.15 m (pipe) to 0.13 m to fill the height of blade so the blade can rotate. This analysis was done with simulation using CFD with STD k- ϵ turbulence modeling. The results of efficiency and power undershot is 32% and 348.8 watts.

Keywords: Banki Waterwheel, Electricity, Height of Blade, k- ϵ , Pico Hydro, Renewable Energy, Undershot

* Corresponding author.

E-mail address: riandhika.p@gmail.com

1. INTRODUCTION

Water energy is the energy that has been used widely in Indonesia on a large scale has been used as a power plants. In the decade, electricity needs in Indonesia show so large numbers in both rural and the city. To anticipate, then the presence of electricity very needed. But there are still many remote areas who do not get electrical service from the



Perusahaan Listrik Negara (PLN). While public needs about electricity more increasing. This happens because the limited existing power plants and the difficulty of transportation lines to the rural areas. In areas with topography mountainous encountered many streams the river has the potential to be developed as power plants. This potential mostly in rural areas, while many people in rural areas who have not enjoyed electricity, so it is appropriate to developing power plants with hydropower where the cost of the operation cheap, easily, and it is free pollution [1].

Indonesia has an electrification ratio of 84.35% in the year 2015. This data shows that there are 49 million people who do not have access to electricity. Thus, an additional source of energy is needed to power remote areas in Indonesia, one of the available methods is by using renewable energy that is pico-hydro power generation (PLTPH) to minimize the use of fossil fuels and fulfill the electrification goals set by the ministry of energy and mineral resources. Pico-Hydro power generation becomes a solution because in Indonesia there are plenty of water sources and that can be utilized [2]. One of it is Bengkulu, a province located in southwest coast of Sumatera, Indonesia. Bengkulu is quite underdeveloped when compared to other provinces in Indonesia. This province will be the area that this research will be focused on. The reasons are, Bengkulu has 51.46% electrification ratio, huge water potential (waterfall), and located at rural area [3].

Bengkulu has mountainous terrains with many rivers and water streams with low flow rate and low head. This means that we can develop small hydro-power plants. The scale of this power plant is decided to be less than 5 KW or in other words, it will be of a pico-hydro level. Based on the figure below, it can also be concluded that the best turbine for the condition of Bengkulu is the Undershot Waterwheel. Other than that the Undershot Waterwheel are simple construction, more economical, easy to be moved, and it would be easier to repair.

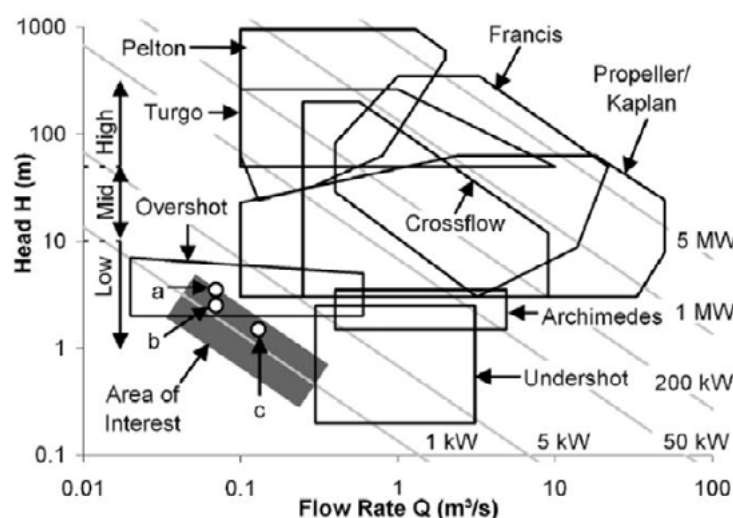


Figure 1. Flow rate vs Head [4]



The Banki Undershot Pico Hydro Waterwheel is field tested in Salam Lake Located in University of Indonesia with the head set at 2.7 meter and channels 41 l/s of water. This waterwheel is to be applied in North Bengkulu at Palak Siring waterfall which is one of the remote areas located in Indonesia.

2. METHODOLOGY

In this study used analytic numerical methods. Analytical methods are calculate for the dimensions of each design waterwheel that will be created. Whereas the numerical methods is to make sure and look up the pressure and the fraction of the flow of fluid hit the blades.

2.1 Undershot Waterwheel Design

Available information:

$$H = 2.7 \text{ m}$$

$$Q = 0.041 \text{ m}^3/\text{s}$$

$$D_{\text{Pipe}} = 0.15 \text{ m}$$

2.1.1 Power

The first step is to calculate the power of the water. The formula used is:

$$P = \rho \times g \times Q \times H \quad (\text{Watt}) \quad (1)$$

2.1.2 Water Velocity from Pipe (v_{pipe})

The formula for the water velocity from pipe is:

$$v_{\text{pipe}} = \frac{Q}{A_{\text{pipe}}} \quad (\text{m/s}) \quad (2)$$

2.1.3 Head Clear (Hc)

Head clear is a high fall of water from the pipe. The formula used is:

$$Hc = \frac{v_{\text{pipe}}^2}{2 \times g} \quad (\text{m}) \quad (3)$$

2.1.4 Waterwheel Diameter

To get the diameter of the waterwheel, first be known to the high fall of water (H). Waterwheel undershot with a straight blade types have the boundary conditions in the designing.

$$\text{Head } H < 2 \text{ m}$$

$$\text{Outter Waterwheel Diameter } D_1 = 3 \times Hc = 3 \times 0.27 = 0.81 \text{ m}$$

$$\text{The height of the blade } p = (1/3 D_1)/2 = (1/6 \times 0.81) = 0.135 \text{ m}$$

$$\text{Inner Waterwheel Diamoeter } D_2 = D_1 - 2p = 0.81 - 0.27 = 0.54 \text{ m}$$



2.1.5 Spacing of Blades (t)

Calculation to find the space between the blade required to rotate the wheel by wheel construction and design are:

$$K = \pi \times D \quad (m) \quad (4)$$

$$t_1 = \frac{K1}{Z} \quad (m) \quad (5)$$

$$t_2 = \frac{K2}{Z} \quad (m) \quad (6)$$

2.1.6 Number of Blades (z)

To determine the number of blades on the waterwheel with, the formula is [5]:

$$Z = \frac{\pi \cdot D_{kincir} \cdot \sin \theta}{(a \cdot p) + tr} \quad (7)$$

2.1.7 Blade width (b)

With the formula of the water capacity is $Q = A \times v$ and the height of blade is $1/6$ diameter of the waterwheel, then to determine the width of the blade are [6]:

$$b = \frac{Q}{P \times v_{pipa}} \quad (m) \quad (8)$$

2.1.8 Inter-blade angle (θ)

The last step from the blade is to known the blade angle. The formula is:

$$\theta = \frac{360}{z} \quad (^\circ) \quad (9)$$

2.1.9 Channel Undershot Waterwheel

The calculation for channel are from a pipe diameter of 6 inches (0.15 m) and then the flow is reduced to fit the width of waterwheel (b) for an unknown length of the channel.

$$P_{\text{Channel}} = P' \times \text{Bil. Pencegah Backward Facing} \quad (10)$$

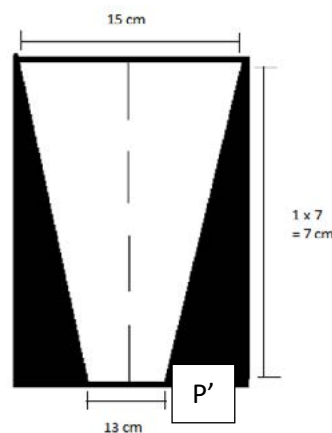


Figure 2. Pipe Channel



2.1.10 Design Summary

Table 1. Design Summary

Description	Symbol	Value	Unit
Head	H	2.71	m
Flow Rate	Q	0.041	m ³ /s
D Pipe	D	0.15	m
r Pipe	r	0.075	m
A Pipe	A	0.017671	m ²
Water Velocity	v	2.320125	m/s
Head Clear	Hc	0.27	m
Outter Diameter	D1	0.81	m
Height of Blade	p	0.135	m
Inner Diameter	D2	0.54	m
Outter Circumference	K1	2.54	m
Inner Circumference	K2	1.69	m
Thick Blade	t'	0.004	m
Number of Blade	z	14	blade
Space Between the Outter Blade	t1	0.18	m
Space Between the Inner Blade	t2	0.12	m
Blade Angle	θ	25.7	°
Width of Waterwheel	b	0.13	m

2.2 The Work of Undershot Waterwheel

2.2.1 Roving Speed of Waterwheel (U₁)

The amount of wheel peripheral speed can be calculated by the equation [7]:

$$U_1 = \frac{V_1 \times \cos \alpha_1}{2} \quad (\text{m/s}) \quad (11)$$

2.2.2 Rotation of Waterwheel (n)

$$n = \frac{60 \times U_1}{\pi D_1} \quad (\text{rpm}) \quad (12)$$



2.2.3 Energy on the Waterwheel ($P_{\text{Waterwheel}}$)

The calculations to determine the energy available in the waterwheel is:

$$P_{\text{waterwheel}} = T \times \omega \quad (\text{Watt}) \quad (13)$$

To determine the energy available waterwheel, first step is to known Torque. The formula is [8]:

$$\tau = F \times L \quad (\text{Nm}) \quad (14)$$

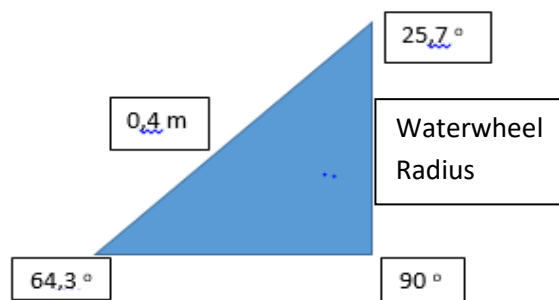


Figure 3. Undershot Waterwheel Active Blade

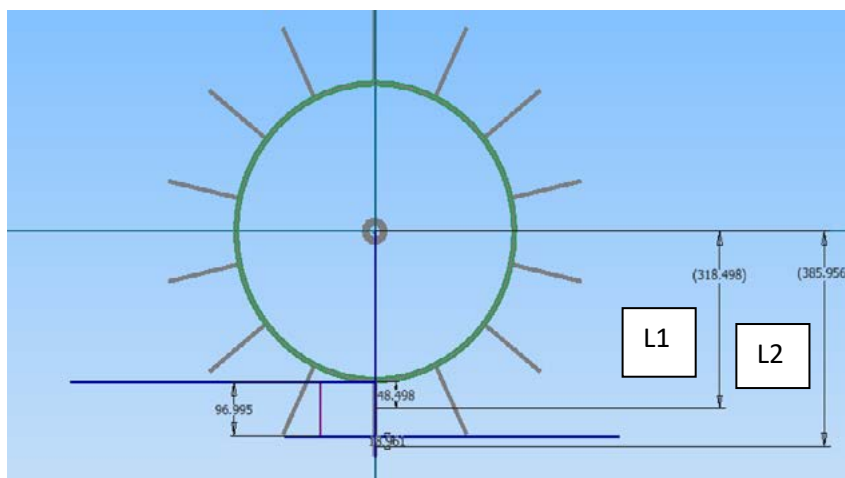


Figure 4. Water flow and Radius of Undershot Waterwheel

$$\text{Waterwheel Radius} = \sin 64.3 \times 0.4$$

$$L1 = \{(\text{Waterwheel Radius} - r_2)/2\} + r_2$$

$$L2 = \{(r_1 - \text{Waterwheel Radius})/2\} + \text{Waterwheel Radius}$$



Percentage of water discharge

$$L1_Q = (\text{Waterwheel Radius} - r_2) / \rho \times Q$$

$$L2_Q = (r_1 - \text{Waterwheel Radius}) / \rho \times Q$$

$$F1 = L1_Q \times \rho \times g$$

$$F2 = L2_Q \times \rho \times g$$

$$\tau_1 = L1 \times F1$$

$$\tau_2 = L2 \times F2$$

$$\tau_{\text{total}} = \tau_1 + \tau_2$$

Then after get torque, search the angular velocity (ω) with formula:

$$\omega = \frac{2 \times \pi \times n}{60} \quad (\text{rad/s}) \quad (15)$$

2.3 Modeling

For this case, to make sure that the undershot waterwheel design is correct, so the modelling is done made in Autodesk Inventor.

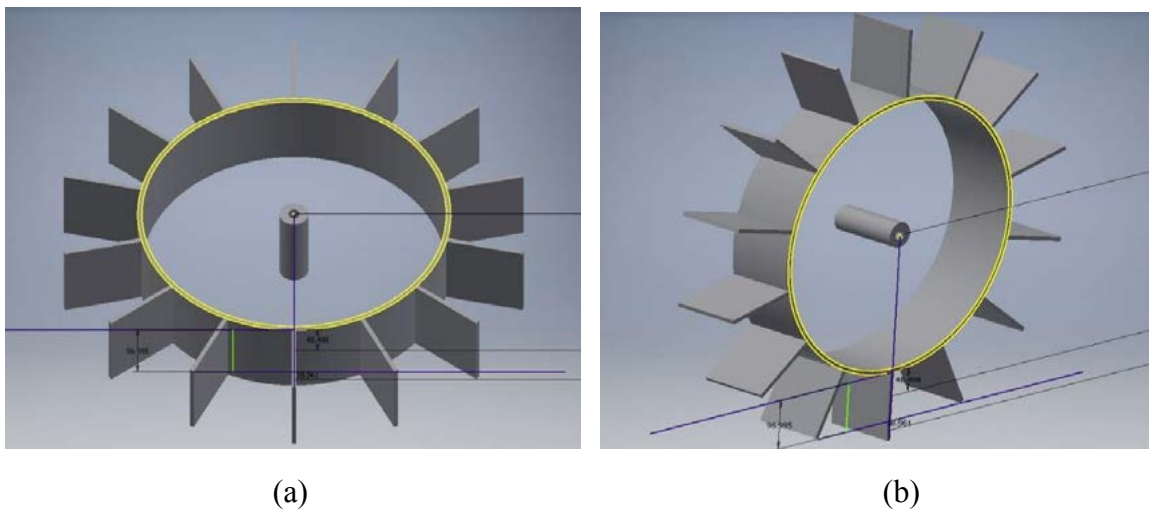


Figure 5. (a) Waterwheel Top View (b) Waterwheel Side View



2.4 Simulation

Computational fluid dynamics is a simulation for numerical method that helps our understanding to make calculation of power, torque, and efficiency of undershot waterwheel makes easier with an image of the flow fluid and the interaction that can be viewed directly on the computational fluid dynamics software. In Computational fluid dynamics there are various models of turbulent, but in this study k-epsilon ($k-\epsilon$) turbulent model will be used because is suitable for general flow conditions.

Computational fluid dynamics software used was ANSYS Fluent 15. The first step in using ANSYS Fluent 15 is import the geometry from Autodesk Inventor or Solid works into ANSYS fluent 15, the next step is to perform the naming in each field of the undershot waterwheel which is inlet, outlet, interface, and ambient. After that perform the meshing with fine mesh sizing. Then in setup activate phase multiphase for water and air, turn on energy and replacing viscous into k-epsilon. The boundary conditions on the inlet input water velocity values that 2.32 m/s, set wall.trg with 24.6 rpm value and mesh interfaces included angle that 25.7° of the undershot waterwheel blade, so when iterating the waterwheel can also rotate with the flow of the fluid. The last step is iterations that performed as many as 30 times each time step. Time step used period is 0.004 seconds, 600 time step. The focus of this study in numerical is to get the pressure and fraction of the undershot waterwheel.

After doing the steps and iterations, according to focus on the study in numerical is the pressure and fraction. So the pressure is obtained according to the figure 6, where the pressure is higher on the first two active blades that are hit by the speed of the water. While the fraction is where the water flow on the blades, so that the waterwheel can rotate as in figure 7. Therefore it can be proven the analytical methods because, as shown in Figure 6 and 7 that the blade is exposed to water are two active blade, and has been calculated on analytical methods by finding torque and force of active blades. So we can get the power and efficiency of the undershot waterwheel.

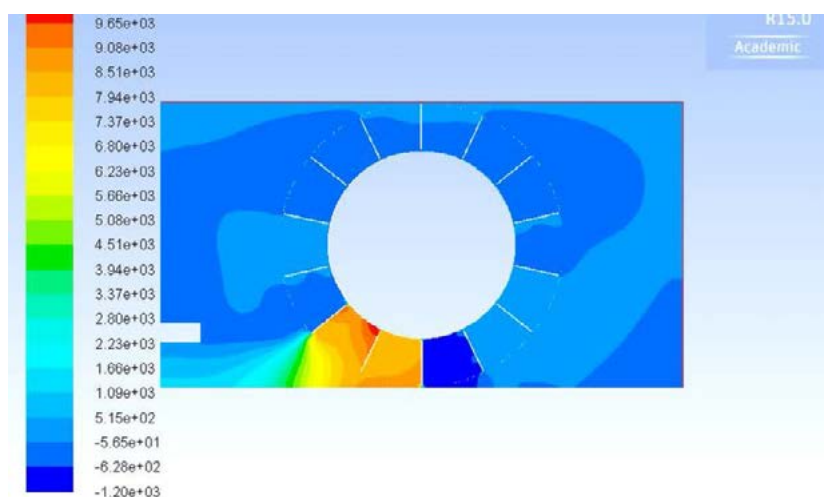


Figure 6. Static Pressure Undershot Waterwheel

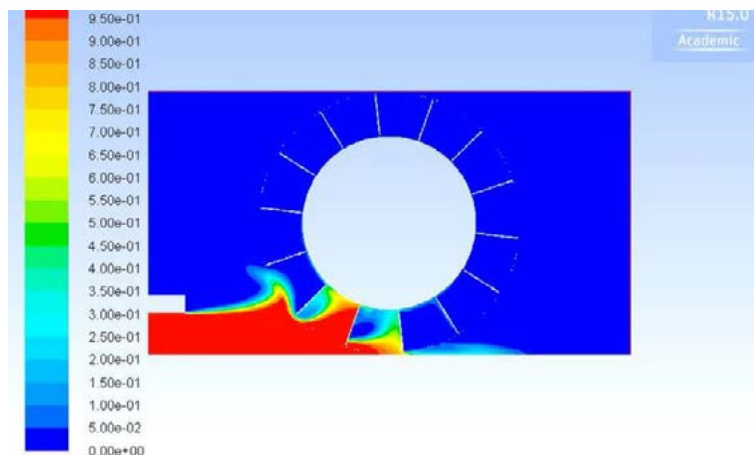


Figure 7. Fraction Undershot Waterwheel

3. RESULT AND DISCUSSION

From the analytical and numerical method, we get the result for force, torque, power and efficiency of undershot waterwheel.

Table 2. Variabels Needed to Obtain the Height of Blade

Description	Symbol	Value	Unit
Head clear	Hc	0.27	m
Outer Diameter	D1	0.81	m
Inner Diameter	D2	0.54	m
Height of Blade	p	0.135	m

Table 3. Result Summary for Torque and Force of Active Blade

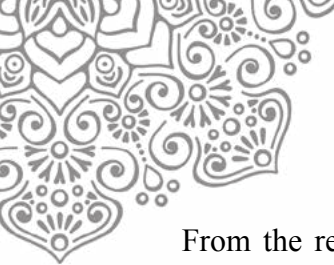
L1	L2	F1	F2	τ_1	τ_2	τ_{total}	ω
0.317 m	0.385 m	281.55 N	120.66 N	89.32 Nm	46.43 Nm	135.75 Nm	2,57

$$P_{waterwheel} = T \times \omega$$

$$P_{waterwheel} = 135.75 \times 2.57 \\ = 348.8 \text{ Watt}$$

$$P_{water} = 1090 \text{ Watt}$$

$$\eta_{Waterwheel} = 348.8/1090 \\ = 32 \%$$



From the results, we can see from 24.6 rpm rotation of undershot waterwheel with a height of blade of 0.135 m and a width 0.13 m obtained an efficiency of 32%. The efficiency is obtained from water power that has been known and waterwheel power that 348.8 watt derived from the torque and force existing in the radius of the waterwheel. In addition to the CFD can be concluded that the pressure and flow of water (fraction) focused on two active blades on a waterwheel where that could be calculated.

4. CONCLUSION

From this study, it can be concluded that undershot waterwheel is the best for low flow and low head condition based like in North Bengkulu at Palak Siring waterfall and also at Salam Lake University of Indonesia. Because undershot waterwheel with a straight blade, its design very easy and simple to be made in remote areas that will be applied. This undershot waterwheel with straight blade has an outer diameter of 0.81 m and an inner diameter of 0.54 m with 14 blades and 2 active blades. The blade has a height of 0.135 m and a width 0.13 m, so for pico-hydro and remote areas this waterwheel is very economical and easy to be moved. Especially this undershot waterwheel has the power and efficiency of 348.8 watts and 32%.

REFERENCES

1. Sipayung, S., *ENERGI AIR & ENERGI BENDA ANGKASA (SUMBER DAYA ENERGI)*. 2011.
2. Energi, S. *Pengawasan Keteknikan Untuk Mewujudkan Keselamatan Ketenagalistrikan*. 2015; Available from: <http://www.satuenergi.com/2015/10/pengawasan-keteknikan-untuk-mewujudkan.html>.
3. (BPS), S.O. *National Cencus 2015*; Available from: www.bps.go.id/.
4. Williamson, S., B. Stark, and J. Booker, *Low head pico hydro turbine selection using a multi-criteria analysis*. *Renewable Energy*, 2014. **61**: p. 43-50.
5. Ovens, W.G., *Design manual for water wheels; with details for applications to pumping water for village use and driving small machinery*, in *Design manual for water wheels; with details for applications to pumping water for village use and driving small machinery*. 1977, Vita.
6. Wibawa, U., H. Santoso, and I. Dharmayana, *PERANCANGAN KINCIR AIR PEMBANGKIT LISTRIK TENAGA MIKROHIDRO (PLTMH) DESA BENDOSARI KECAMATAN PUJON KABUPATEN MALANG*. *Jurnal Elektro Unika Atma Jaya*, 2014. **7**(1): p. 45-58.
7. Dietzel, F. and D. Sriyono, *Turbin pompa dan kompresor*. Jakarta: Erlangga, 1993.
8. Nuernbergk, D.M. and C. Rorres, *Analytical model for water inflow of an Archimedes screw used in hydropower generation*. *Journal of Hydraulic Engineering*, 2012. **139**(2): p. 213-220.



15th International Conference on Quality in Research (QiR 2017)
**Comparison between Airfoil Profiled Blade and Ordinary
Blade in Cross-flow Turbine Using Numerical Simulation**

Warjito, A.I. Siswantara, D. Adanta, A.P. Prakoso*, R. Dianofitra

*Department of Mechanical Engineering, Faculty of Engineering Universitas Indonesia,
Kampus baru, Depok, 16242*

Abstract

Isolated rural area makes on-grid electrification development becomes expensive and inefficient. For rural area with quite torrential river flow, it is recommended to build run-of-river pico-hydro power plant for their mini-grid power system to produce enough electricity for small village with low investment cost. Cross-flow Banki turbine is well known for its simplicity of shape, design, and construction. Thus, the construction cost of this type of turbine is very low rather than another turbine like propeller and Pelton. Moreover, it also makes cross-flow Banki turbine easier to maintain, moreover this turbine has self-cleaning ability. Furthermore, cross-flow Banki turbine is well known for its independent efficiency from fluctuation of water discharge. Beside of many advantage on this turbine, cross-flow Banki turbine efficiency is relatively lower than another turbine. The drag force usually present when water flowing around immerse body, like turbine blade because of eddy formation. This force usually reduces the turbine efficiency. Airfoil profiles are proven to reduce eddy formation in water flow around immerse body like turbine blade then increase some turbine efficiency. This study aim to investigate the effect of NACA airfoil in blade profile to the cross-flow turbine efficiency. NACA-6712 airfoil profile was chosen because it has bigger lift coefficient than others. In this study, the turbine with NACA-6712 airfoil profiled blade cross-flow turbine has been compared with ordinary one by using CFD simulation. This study use 2.7 m head and 0.04 m³/s of water discharge. ANSYS FLUENT 17 with k-epsilon turbulence model is used in this study. As a result, CFD simulation found that maximum efficiency of ordinary blades turbine is 77.6% with number of blades 45. While, the maximum efficiency of NACA turbine is 74.9% with 50 blades. From the results, it can be obtained that the ordinary turbine is better than NACA turbine.

Keywords: Rural Area, Power Plant, Pico-Hydro, Turbine, Cross-flow, Airfoil.

1. Introduction

Indonesia, especially Bengkulu consist of many hills and mountains, that's makes Bengkulu mountains land's topology. In the other hand, Bengkulu has heavy rainfall along the year (DLH, 2014). This topology make Indonesia especially Bengkulu has many geographically isolated area and create many of isolated rural area. Rare of household and difficult terrain caused by geographically isolation in isolated rural area makes transmission system development cost for on-grid electrification system become expensive (Kaunda, Kimambo, & Nielsen, 2014). That's make electricity difficult to be develop in isolated rural area in Indonesia and make Bengkulu's and Indonesia's electrification ratio low.

*ajipp13@gmail.com



Behind that faced adversity, mountains topology and heavy rainfall indicate great hydro energy potential for Bengkulu Province. For the isolated rural area, which has perennial river flow, pico-hydropower plant is recommended to electrify their village with their own mini-grid system. Pico hydropower and micro hydropower is small hydropower plant system which can utilize river stream with particular head (Kaunda et al., 2014). River stream utilization for electricity can be done by dam the river stream and channel it into the turbine at the lower place. The electrical power generated by pico-hydropower is lower than 5 kW electricity (Paish, 2002).

Cross-flow typed turbine is ideal for small hydropower plant which directly utilize river stream because the turbine's efficiency is independent from flow variation (Durgin & Fay, 1984). At this time, Michell-Banki turbines are often to use for small scaled hydropower plant especially because of their economic aspect (Kaniecki, 2002). Cross-flow turbine become good choice for efficiency, flexibility, and cost consideration, because this turbine is the cheap turbine with simple geometry, design, and easy construction (Sammartano, Morreale, Sinagra, & Tucciarelli, 2016).

The cross-flow typed turbine is firstly introduced by Australia's scientist and engineer named Antony Mitchell at 1903. Furthermore, the cross-flow turbine has been developed by a Hungarian scientist, Donàt Bànkì, this make the cross-flow turbine called as Mitchell-Banki turbine too. After that, study firstly conducted by Mockmore and Merryfield in 1949, they analytically explain the maximum efficiency for the Mitchell-Banki turbine as the equation below (Mockmore & Merryfield, 1949).

$$\mu \leq \cos^2 \alpha \quad (1)$$

Moreover, in that study, Mockmore and Merryfield also determine the optimum absolute angle of attack for this turbine is $\alpha = 16^\circ$, so, by using that equation, the maximum efficiency that can be attained by this turbine is 92.4%. That study has done with the 16 ft (4.88 m) head and 3 cfs (0.085 m³/s) discharge condition (Mockmore & Merryfield, 1949). Nowadays, many of study agree that the optimum angle of attack for this turbine is 22°. (Aziz & Desai, 1993; De Andrade et al., 2011; Durgin & Fay, 1984; Kaniecki & Steller; Sammartano, Aricò, Carravetta, Fecarotta, & Tucciarelli, 2013).

Sammartano conducted series of CFD simulation and experiment to determine the most optimum design of this turbine. One of parameter which is investigated is V_t/U variable. It is ratio between tangential speed of water and tangential turbine's tip speed. The optimum V_t/U value for this turbine design is 1.8 (Sammartano et al., 2013). In 2013, Budiarto conducted study to compare k- ϵ and RNG k- ϵ turbulence model for modelling cross-flow gas turbine, the result is RNG k- ϵ is better but more complicated (Darmawan, Indra Siswantara, & Budiarto, 2013). The most recent study about cross-flow turbine is conducted by Sammartano to determine the best turbulence model for modelling this turbine (Sammartano et al., 2016).

Beside studies above, Durgin has conducted some studies in 1984 with a cross-flow turbine which blades made from 3 mm tick plexiglass with standard cutting to investigate the 2nd stage energy transfer influence to the total turbine efficiency. As the result, the 2nd stage energy transfer contribute 17% of total 61% efficiency (Kaniecki, 2002). In 2002, Kaniecki conduct study with 3.6 mm tick blades cross-flow turbine. The turbine blade was sharpened and has been mashed with good machining. The efficiency accomplished



in this study was closely above 80% (Kaniecki, 2002). Sammartano, with some investigation explained before, the turbine can attain 85% efficiency. The turbine blade form is same like crescent moon. From studies above, it can be inferred that the blade profile of cross-flow turbine has some influences to its efficiency. This Study hypothesis thought that NACA-airfoil profiled cross-flow turbine blade has better efficiency than ordinary arc formed blade turbine.

2. Methodology

a. Analytical design of cross-flow turbine

The condition of this study is based on the survey result that held in North Bengkulu Regency, Bengkulu which has scaled 1:1 in Pico hydropower laboratories, Salam Lake, University of Indonesia. The available head of this site is 2.7 m with 0.04 m³/s discharge.

In Sammartano study, obtained not all of available potential head could be converted to be kinetical energy (velocity) in cross-flow turbine. The produced velocity from head is adhere the equation below (Sinagra, Sammartano, Aricò, Collura, & Tucciarelli, 2014).

$$V = C_T \sqrt{2gH} \quad (2)$$

With recommended C_T is 0.98, it can be calculated that the incoming water velocity to the turbine is 7.13 m/s with direction is 22° from turbine's tip speed. From discussion before, we know that the optimum V/U is 1.8. So, from that equation and mixed with velocity triangle analysis (Fig. 1), we can obtain the tangential tip speed is $U = 3.67$ m/s and the inlet angle of this cross-flow turbine is $\beta_1 = 42^\circ$.

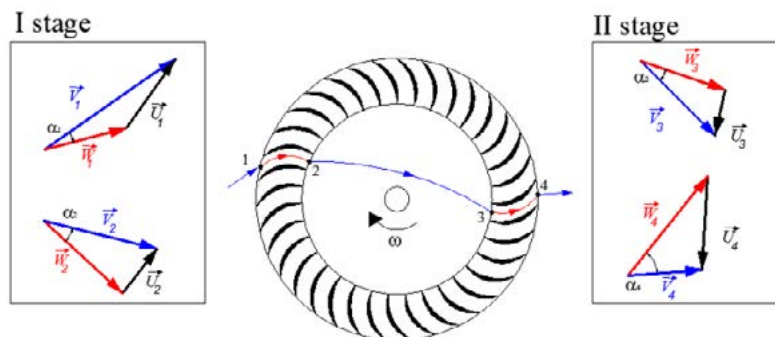


Fig. 1. Cross-flow turbine velocity triangle.(Sammartano et al., 2013)

For blade outlet, many of study agreed that the optimum angle is $\beta_2 = 90^\circ$. In the other hand, the 90° blade outlet angle, it would make the water exit the 1st stage angle below 90° , so the energy transfer in 1st stage not maximum. By using office computing software, particles path line has calculated to determine how water particles enter the 2nd stage. It can be obtained from figure 2, in $\beta_2 = 90^\circ$ condition, the water particles enter the 2nd stage by hitting the pod of turbine blades, so they push the turbine blades at the same direction with turbine's rotation. In $\alpha_2 = 90^\circ$ condition, water particles hit the back of turbine blades then makes negative power output in 2nd stage.

From the calculation discussed above also obtained the optimum way how the water enters the turbine. The inlet angle is optimum at $22^\circ \leq \theta \leq 112^\circ$. Then, to prevent turbulence inside the nozzle, it should be ascertained that the water has their own path to



flowing through the nozzle. Therefore, nozzle design should obey equation 3 and 4 (Sammartano et al., 2013).

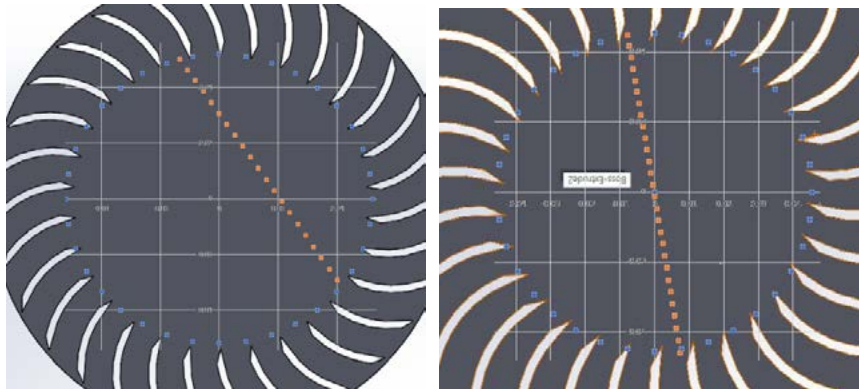


Fig. 2. Water particle path inside turbine at $90^\circ \beta_2$ and $90^\circ \alpha_2$ conditions

$$S_0 = \frac{q}{V} \tag{3}$$

$$B = \frac{Q}{q} \tag{4}$$

The q variable is flow per width unit of nozzle which calculated with equation below.

$$q = V \sin \alpha \lambda \pi D / 360 \tag{5}$$

To make the manufacture process easier, it's been decided to use PVC pipe as turbine blade. The PVC pipe is well known that has limited diameter choice, this make the turbine blade choosing become priority in this turbine design process. Some studies obtain some optimum ratio between outer and inner diameter. Sammartano, based on Aziz study use d/D ratio as 0.68, but after some optimization, the study obtained that best ratio d/D is 0.65 (Sammartano et al., 2013). Relations between that ratio and the turbine blade design were explained below.

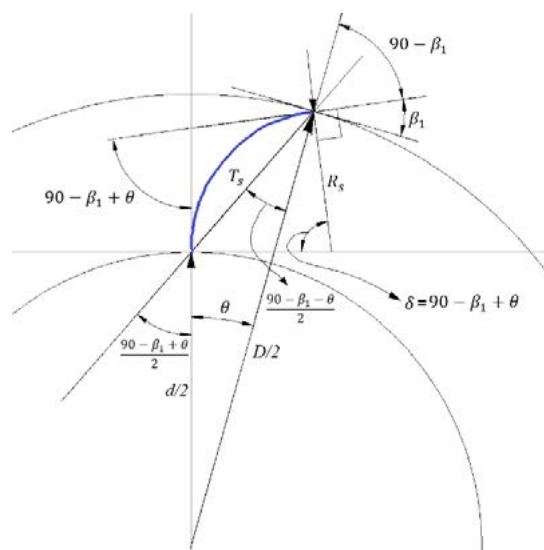


Fig. 3. Relation between turbine diameter and blade's design parameters.



At first, it's been known from studies before that the best blade outlet angle is $\beta_2 = 90^\circ$. From figure 4, it can be seen there is a triangle which edges are T_s , $d/2$, and $D/2$. It's also seen that two blade radius lines and their tangential line formed a kite shape which wing is orthogonal. This make the angle between both blade radius line or also named as blade curvature angle then obey this equation.

$$\delta = 90 - \beta_1 + \theta \quad (6)$$

From equation 6, it been obtained that the angle between T_s and $D/2$ is $(90 - \beta_1 - \theta)/2$, then the angle between $d/2$ and $D/2$ is θ , and then the angle between $d/2$ and T_s is $180 - (90 - \beta_1 + \theta)/2$. From triangle's low, we can generate these relations in the equation below.

$$\frac{T_s}{\sin(\theta)} = \frac{d/2}{\sin(\frac{90-\beta_1-\theta}{2})} = \frac{D/2}{\sin(180-\frac{90-\beta_1+\theta}{2})} \quad (7)$$

From equation above 7, relation between blade curvature chord (T_s) and the outer diameter (D) is $T_s = 0.19 D$. This chord can be used as the NACA profile chord. Next, relation between the cord and the curvature radius was explained by the equation 8.

$$\frac{T_s}{\sin(90-\beta_1+\theta)} = \frac{R_s}{\sin(\frac{90+\beta_1-\theta}{2})} \quad (8)$$

From equation 8, the blade curvature radius can be calculated as $R_s = 0.2 D$. Sammartano also make the equation between R_s , D and d as the equations below.

$$R_s = \frac{D}{4} \left[1 - \left(\frac{d}{D} \right)^2 \right] \cos(\beta_1)^{-1} \quad \left| \quad \tan(\delta/2) = \frac{\cos(\beta_1)}{\sin(\beta_1)} \quad (9)$$

But, the equations above are not valid with this case. By considering simplicity of the turbine manufacture and transmission design between the turbine and the generator, the chosen blade size is 36 mm radius using 2.5" PVC pipe.

b. Airfoil selection for blade profile

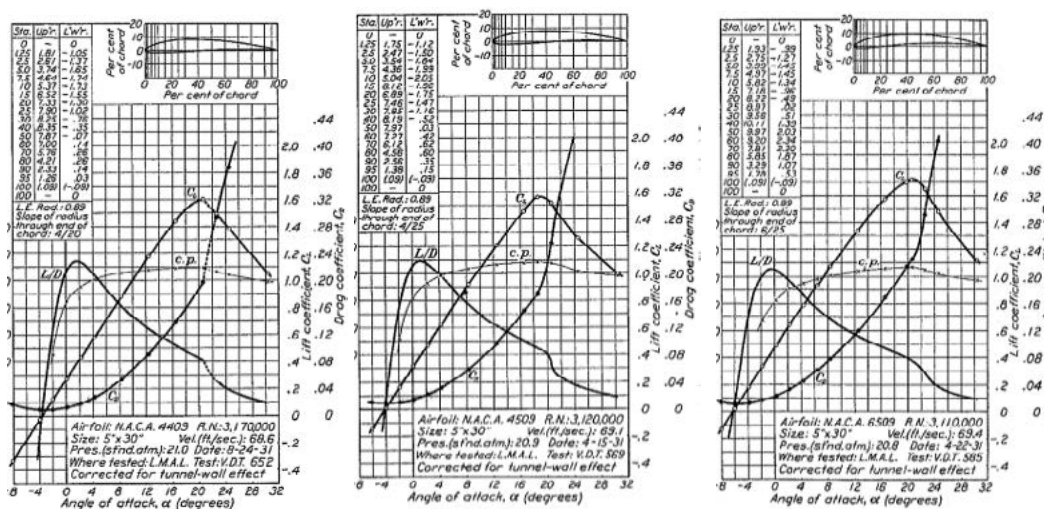


Fig. 4. Some airfoil testing results by NACA.



From some discussion above, it's been known that the turbine blades are have a curvature form. Then, in this study, the 4-digits series NACA profile was used for the turbine's blade profile. The choosing investigation is focused on 44XX, 45XX, 46XX, 47XX, 64XX, 65XX, 66XX or 67XX series which has big curvature camber. The chosen profile is considered as the bigger lift and drag coefficient because the angle between water flow and the turbine rotations is not perfectly orthogonal. Figure 4 shows some C_l , C_d , and C_p graphic in some airfoil testing by NACA (Jacobs; Ward & Pinkerton, 1933).

From some conducted analytical calculation, NACA-6712 has been decided as the best profile for the turbine blade with angle of attack 24° . The tested lift and drag coefficient at 24° AOA is 1.9 and 0.28. Table 1 show cross-flow turbine design parameter in this study. Figure 5 show NACA-6712 profiled blade position on turbine design.

Table 1. Some cross-flow turbine design parameters.

Design Parameter	Value	Design Parameter	Value
Outer Diameter (D)	180 mm	Blade Inlet Angle (β_1)	42°
Inner Diameter (d)	117 mm	Blade Outlet Angle	90°
Inlet Angle (α)	22°	Blade Curve Radius	36 mm
Nozzle Inlet Height (S_o)	53 mm	Blade Curve Angle	58°
Nozzle Width (B)	106 mm	Nozzle outlet angle (θ)	$22^\circ \leq \theta \leq 112^\circ$
Turbine Width (W)	159 mm	NACA airfoil	NACA-6712
Airfoil chord length	32 mm	Airfoil chord angle	18°
Airfoil AOA	24°		

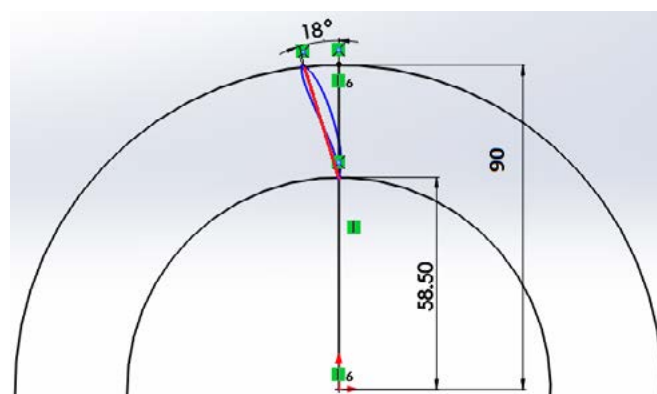


Fig. 5. NACA-6712 profiled blade location.

c. CFD Numerical Simulation Method

The CFD numerical simulation was conducted using ANSYS[®] FLUENT[®] 17 with 2D domain. The aims of this simulation are to obtain the detail of best design for cross-flow turbine using some optimizations and to find the best blades number for both NACA 6712 profiled blades turbine and the ordinary arc formed blades.

The turbulence model for this simulation is k- ϵ with realizable constants and scalable wall slip formula. The k- ϵ model is the simplest model for turbulence modelling so the computer can run faster in this complex case. Furthermore, the k- ϵ model is suitable for low pressure gradient case like this study (Sinagra et al., 2014). This simulation also use moving mesh mode with rotational speed of -40.8 rad/s. The multiphase equation used in



this simulation is volume of fluid equations, with implicit volume interaction equations and body force equations. This simulation also use an open channel mode equations. Figure 6 show CFD model of cross-flow turbine, white lines are walls, blue is inlet, red are pressure inlets, and yellow is interface.

After passing the mesh independency process, the most suitable grid size for the simulation of non NACA profiled blades cross-flow turbine in this study is smaller than 5×10^{-3} m, but not smaller than 1×10^{-5} m. While, for simulation of NACA profiled blades turbine is using grid size is smaller than 5.48×10^{-3} m and bigger than 5.48×10^{-5} m. Figure 6 shows the meshing size used in this study.

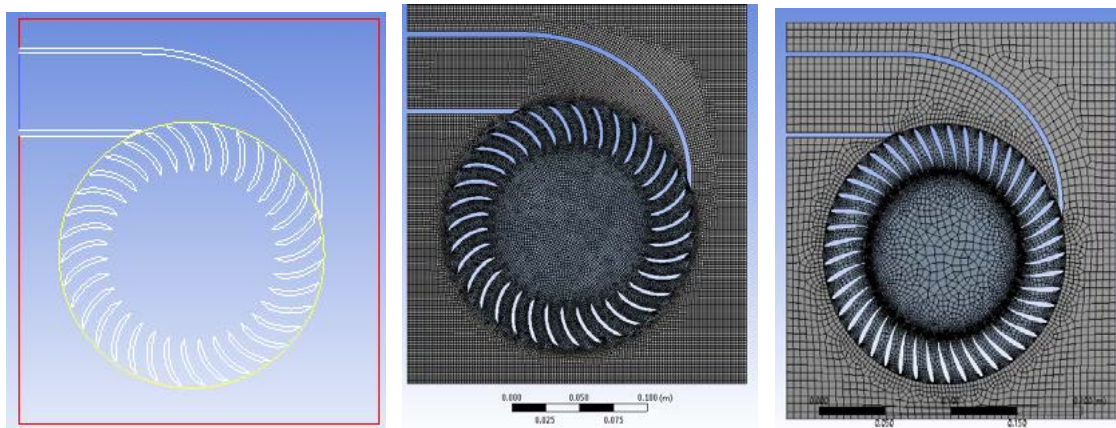


Fig. 6. Meshing size for non-NACA and NACA-profiled turbine.

3. Result and Discussion

a. Ordinary blades cross-flow turbine

From numerical simulation conducted, pressure distribution of the ordinary blade cross-flow turbine can be obtained in figure 7. From figure 7, it can be obtained that the pressure is concentrated at the pod of turbine blades. The maximum pressure at the blade's pod is about 16 kPa. That pressure then push the turbine and make the turbine rotating. The flow stagnancy can be obtained with the higher pressure at the top of second stage blade.

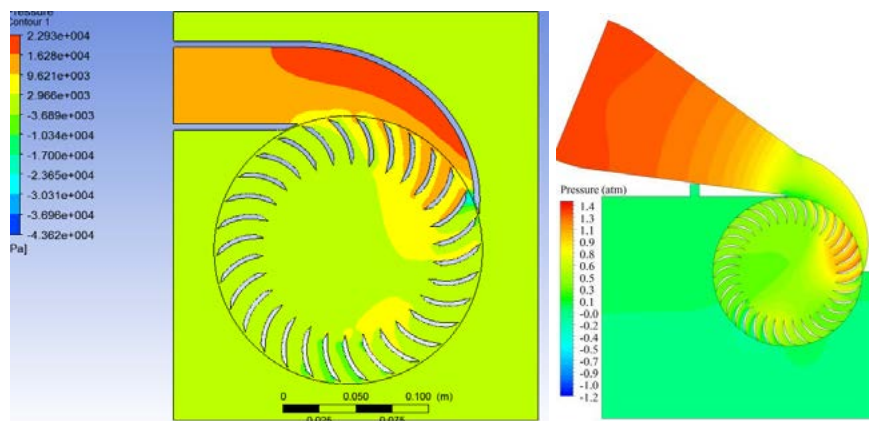


Fig. 7. Pressure contour results of ordinary blades cross-flow turbine. (a) this study, (b) Sammartano's study.



Figure 7 also show the pressure contour of numerical results on Sammartano cross-flow turbine design study (Sammartano et al., 2013). The similarities from the results above are the highest pressure at the turbine is on the pods of first stage's blades and the lowest is on the back of second stage's blades. The flow stagnancy also found at both results. Some differences could be found in the value of pressure like highest pressure at first stage's turbine blades in this result is 1.3 Atm (1.32×10^5 Pa), while in the results above 1.5×10^4 Pa. It is mainly caused by the difference of working head condition that this study has higher head condition (~ 10 m).

b. NACA profiled blades cross-flow turbine

The pressure distribution of the NACA-6712 profiled blades cross-flow turbine can be seen at the figure 8. It can be obtained from the figure8, in leading edge outside type of NACA-6712 profiled blades turbine the pressure concentration is located at the tip of turbine. That pressure concentration push the turbine blades not at the right direction. It also obtained that there is obstacle for the fluid flow inside the first stage. When the airfoil direction reversed, the pressure concentrations were moved to the pod of turbine blade like obtained in ordinary blade results. Figure 9 also show that after passing the first stage blade, the static pressure is increased in NACA-6712 profiled blades turbine. The figure also show there is some blades has pressure at the back of blade was higher than at the pod of blade, so it makes the negative power to the turbine.

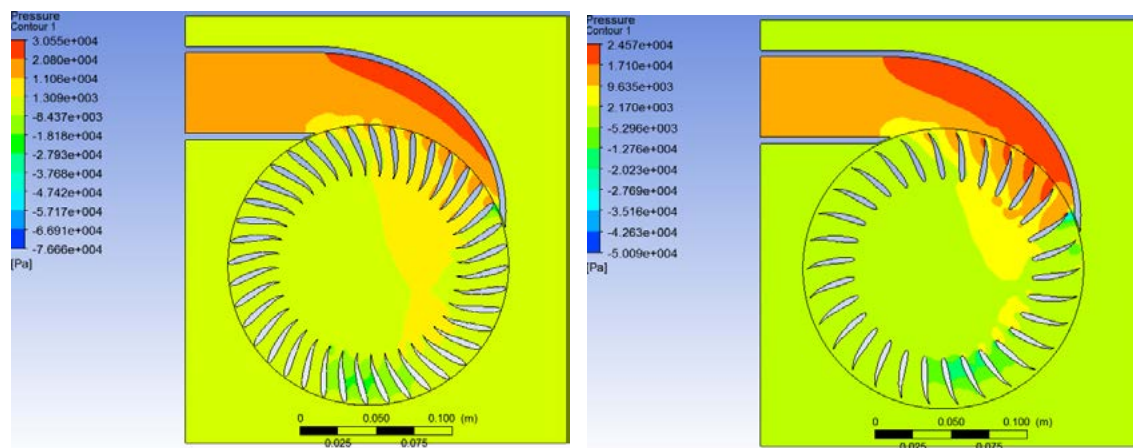


Fig. 8. Pressure contour on NACA-6712 profiled blades cross-flow turbines with different profile direction

c. Optimum blades number investigation

The next simulations are to obtain the best turbine blades number. Ordinary blades, airfoil blades, and reversed airfoil blades crossflow turbine had been simulated with some number of blades from 25 to 40 blades. Figure 9 summarize all the simulations conducted to obtain the number of blades which give best efficiency in each type of blades.

From figure 9, it can be obtained that the best efficiency of ordinary blades cross-flow turbine was 93.4% using 30 blades. It also obtained that airfoil and reversed airfoil profiled best efficiency was 90.5% and 93.4% using 25 blades. The results obtained that higher number of blade not always increase the efficiency of cross-flow turbine. If the blade spacing were too close, it can inhibit the water flow and decrease the cross-flow



turbine efficiency. Corresponding with results in figure 7 and 8, the efficiency of airfoil profiled cross-flow turbines were lower than ordinary one and reversed one.

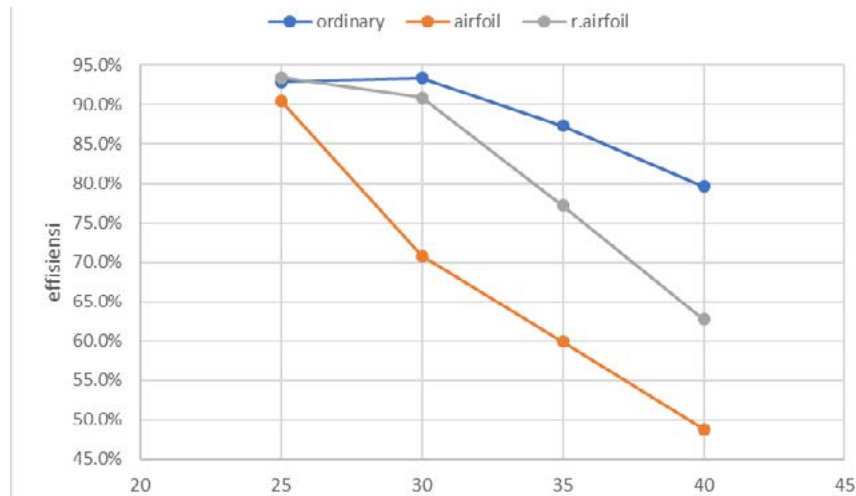


Fig. 9. Turbine efficiency in some numbers of blades

4. Conclusion

This study was resulting that the best blades number for cross-flow turbine is 30 blades which can have efficiency about 93.4% from the numerical results. From analytical calculations, the most suitable NACA profile for this turbine in this study is NACA 6712. The NACA 6712 profiled turbine can make 90.5% efficiency by using 25 blades. Then, when it reversed, it can make 93.4% efficiency by using 25 blades. This study concluded that the ordinary blades cross-flow turbine is better than the NACA-6712 profiled turbine. Another study can be conducted with different type of NACA airfoil profile to optimize the efficiency of the cross-flow turbine.

5. Reference

- Aziz, Nadim M, & Desai, Venkappayya R. (1993). A laboratory study to improve the efficiency of cross-flow turbines. *Engineering Report*.
- Darmawan, Steven, Indra Siswantara, Ahmad, & Budiarto, Budiarto. (2013). *COMPARISON OF TURBULENCE MODELS ON REYNOLDS NUMBERS OF A PROTO X-2 BIOENERGY MICRO GAS TURBINE'S COMPRESSOR DISCHARGE*. Paper presented at the Proceedings International Conference on Engineering of Tarumanagara.
- De Andrade, Jesús, Curiel, Christian, Kenyery, Frank, Aguillón, Orlando, Vásquez, Auristela, & Asuaje, Miguel. (2011). Numerical investigation of the internal flow in a Banki turbine. *International Journal of Rotating Machinery, 2011*.
- DLH. (2014). Laporan Status Lingkungan Hidup Daerah Provinsi Bengkulu. Kota Bengkulu: Dinas Lingkungan Hidup Provinsi Bengkulu.
- Durgin, WW, & Fay, WK. (1984). Some fluid flow characteristics of a cross-flow type hydraulic turbine. *Small Hydro Power Fluid Machinery*, p77-83.



- Jacobs, Pinkerton. Greenberg. *Tests of related forward camber airfoils in the variable density tunnel. NACA Report, 610.*
- Kaniecki, Maciej. (2002). Modernization of the outflow system of cross-flow turbines. *Task Quarterly, 6*, 601-608.
- Kaniecki, Maciej, & Steller, Janusz. *Flow Analysis through a Reaction Cross-Flow Turbine*. Paper presented at the Proceedings of Conference on modelling fluid flow CMFF.
- Kaunda, Chiyembekezo S, Kimambo, Cuthbert Z, & Nielsen, Torbjorn K. (2014). A technical discussion on microhydropower technology and its turbines. *Renewable and Sustainable Energy Reviews, 35*, 445-459.
- Mockmore, CA, & Merryfield, F. (1949). The Banki water turbine, bulletin series no. 25. *Oregon State College.*
- Paish, Oliver. (2002). Small hydro power: technology and current status. *Renewable and sustainable energy reviews, 6(6)*, 537-556.
- Sammartano, Vincenzo, Aricò, Costanza, Carravetta, Armando, Fecarotta, Oreste, & Tucciarelli, Tullio. (2013). Banki-michell optimal design by computational fluid dynamics testing and hydrodynamic analysis. *Energies, 6(5)*, 2362-2385.
- Sammartano, Vincenzo, Morreale, Gabriele, Sinagra, Marco, & Tucciarelli, Tullio. (2016). Numerical and experimental investigation of a cross-flow water turbine. *Journal of Hydraulic Research, 54(3)*, 321-331. doi: 10.1080/00221686.2016.1147500
- Sinagra, Marco, Sammartano, Vincenzo, Aricò, Costanza, Collura, Alfonso, & Tucciarelli, Tullio. (2014). Cross-Flow turbine design for variable operating conditions. *Procedia Engineering, 70*, 1539-1548.
- Ward, EN Jacobs KE, & Pinkerton, RM. (1933). NACA Report No. 460:" The Characteristics of 78 Related Airfoil Sections From test in the Variable-Density Wind Tunnel. *Langley Aeronautical Laboratory, NACA.*



15th International Conference on Quality in Research (QiR 2017)
**Comparison between Airfoil NACA-6712 Profiled and
Ordinary Blade in Cross-flow Turbine by Numerical
Simulation**

Warjito, A.I. Siswantara, D. Adanta, A.P. Prakoso*, R. Dianofitra

*Department of Mechanical Engineering, Faculty of Engineering Universitas Indonesia,
Kampus baru, Depok, 16242*

Abstract

Isolated rural area makes on-grid electrification development becomes expensive and inefficient. For rural area with quite torrential river flow, it is recommended to build run-of-river pico-hydro power plant for their mini-grid power system to produce enough electricity for small village with low investment cost. Cross-flow Banki turbine is well known for its simplicity of shape, design, and construction. Thus, the construction cost of this type of turbine is very low rather than another turbine like propeller and Pelton. Moreover, it also makes cross-flow Banki turbine easier to maintain, moreover this turbine has self-cleaning ability. Furthermore, cross-flow Banki turbine is well known for its independent efficiency from fluctuation of water discharge. Beside of many advantage on this turbine, cross-flow Banki turbine efficiency is relatively lower than another turbine. The drag force usually present when water flowing around immerse body, like turbine blade because of eddy formation. This force usually reduces the turbine efficiency. Airfoil profiles are proven to reduce eddy formation in water flow around immerse body like turbine blade then increase some turbine efficiency. This study aim to investigate the effect of NACA airfoil in blade profile to the cross-flow turbine efficiency. NACA-6712 airfoil profile was chosen because it has biggest lift coefficient than others. In this study, the turbine with NACA-6712 airfoil profiled blade cross-flow turbine has been compared with ordinary one by using CFD simulation. This study use 2.7 m head and 0.04 m³/s of water discharge. ANSYS FLUENT 17 with SST turbulence model is used in this study. As a result, CFD simulation found that maximum efficiency of ordinary blades turbine is 55.3% with number of blades 25. While, the maximum efficiency of NACA-6712 turbine is 54.7% with 25 blades. From the results, it can be obtained that the ordinary turbine is better than NACA-6712 turbine.

Keywords: Rural Area, Power Plant, Pico-Hydro, Turbine, Cross-flow, Airfoil.

1. Introduction

Indonesia, especially Bengkulu consist of many hills and mountains, that's makes Bengkulu mountains land's topology. In the other hand, Bengkulu has heavy rainfall along the year (DLH, 2014). This topology make Indonesia especially Bengkulu has many geographically isolated area and create many of isolated rural area. Rare of household and difficult terrain caused by geographically isolation in isolated rural area makes transmission system development cost for on-grid electrification system become expensive (Kaunda, Kimambo, & Nielsen, 2014). That's make electricity difficult to be

*ajipp13@gmail.com



develop in isolated rural area in Indonesia and make Bengkulu's and Indonesia's electrification ratio low.

Behind that faced adversity, mountains topology and heavy rainfall indicate great hydro energy potential for Bengkulu Province. For the isolated rural area, which has perennial river flow, pico-hydropower plant is recommended to electrify their village with their own mini-grid system. Pico hydropower and micro hydropower is small hydropower plant system which can utilize river stream with particular head (Kaunda et al., 2014). River stream utilization for electricity can be done by dam the river stream and channel it into the turbine at the lower place. The electrical power generated by pico-hydropower is lower than 5 kW electricity (Paish, 2002).

Cross-flow typed turbine is ideal for small hydropower plant which directly utilize river stream because the turbine's efficiency is independent from flow variation (Durgin & Fay, 1984). At this time, Michell-Banki turbines are often to use for small scaled hydropower plant especially because of their economic aspect (Kaniecki, 2002). Cross-flow turbine become good choice for efficiency, flexibility, and cost consideration, because this turbine is the cheap turbine with simple geometry, design, and easy construction (Sammartano, Morreale, Sinagra, & Tucciarelli, 2016).

The cross-flow typed turbine is firstly introduced by Australia's scientist and engineer named Antony Mitchell at 1903. Furthermore, the cross-flow turbine has been developed by a Hungarian scientist, Donàt Bànkì, this make the cross-flow turbine called as Mitchell-Banki turbine too. After that, study firstly conducted by Mockmore and Merryfield in 1949, they analytically explain the maximum efficiency for the Mitchell-Banki turbine as the equation below (Mockmore & Merryfield, 1949).

$$\mu \leq \cos^2 \alpha \quad (1)$$

Moreover, in that study, Mockmore and Merryfield also determine the optimum absolute angle of attack for this turbine is $\alpha = 16^\circ$, so, by using that equation, the maximum efficiency that can be attained by this turbine is 92.4%. That study has done with the 16 ft (4.88 m) head and 3 cfs (0.085 m³/s) discharge condition (Mockmore & Merryfield, 1949). Nowadays, many of study agree that the optimum angle of attack for this turbine is 22°. (Aziz & Desai, 1993; De Andrade et al., 2011; Durgin & Fay, 1984; Kaniecki & Steller; Sammartano, Aricò, Carravetta, Fecarotta, & Tucciarelli, 2013).

Sammartano conducted series of CFD simulation and experiment to determine the most optimum design of this turbine. One of parameter which is investigated is V_t/U variable. It is ratio between tangential speed of water and tangential turbine's tip speed. The optimum V_t/U value for this turbine design is 1.8 (Sammartano et al., 2013). In 2013, Budiarmo conducted study to compare k- ϵ and RNG k- ϵ turbulence model for modelling cross-flow gas turbine, the result is RNG k- ϵ is better but more complicated (Darmawan, Indra Siswantara, & Budiarmo, 2013). The most recent study about cross-flow turbine is conducted by Sammartano to determine the best turbulence model for modelling this turbine (Sammartano et al., 2016).

Beside studies above, Durgin has conducted some studies in 1984 with a cross-flow turbine which blades made from 3 mm tick plexiglass with standard cutting to investigate the 2nd stage energy transfer influence to the total turbine efficiency. As the result, the 2nd



stage energy transfer contribute 17% of total 61% efficiency (Kaniecki, 2002). In 2002, Kaniecki conduct study with 3.6 mm tick blades cross-flow turbine. The turbine blade was sharpened and has been mashed with good machining. The efficiency accomplished in this study was closely above 80% (Kaniecki, 2002). Sammartano, with some investigation explained before, the turbine can attain 85% efficiency. The turbine blade form is same like crescent moon. From studies above, it can be inferred that the blade profile of cross-flow turbine has some influences to its efficiency. This Study hypothesis thought that NACA-airfoil profiled cross-flow turbine blade has better efficiency than ordinary arc formed blade turbine.

2. Methodology

a. Analytical design of cross-flow turbine

The condition of this study is based on the survey result that held in North Bengkulu Regency, Bengkulu which has scaled 1:1 in Pico hydropower laboratories, Salam Lake, University of Indonesia. The available head of this site is 2.7 m with 0.04 m³/s discharge.

In Sammartano study, obtained not all of available potential head could be converted to be kinetical energy (velocity) in cross-flow turbine. The produced velocity from head is adhere the equation below (Sinagra, Sammartano, Aricò, Collura, & Tucciarelli, 2014).

$$V = C_T \sqrt{2gH} \quad (2)$$

With recommended C_T is 0.98, it can be calculated that the incoming water velocity to the turbine is 7.13 m/s with direction is 22° from turbine's tip speed. From discussion before, we know that the optimum V_t/U is 1.8. So, from that equation and mixed with velocity triangle analysis (Fig. 1), we can obtain the tangential tip speed is $U = 3.67$ m/s and the inlet angle of this cross-flow turbine is $\beta_1 = 42^\circ$.

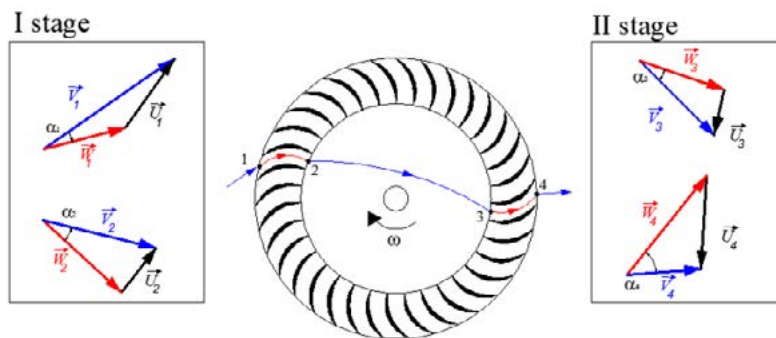
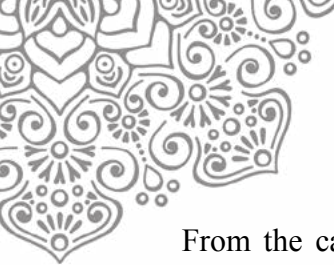


Fig. 1. Cross-flow turbine velocity triangle.(Sammartano et al., 2013)

For blade outlet, many of study agreed that the optimum angle is $\beta_2 = 90^\circ$. In the other hand, the 90° blade outlet angle, it would make the water exit the 1st stage angle below 90° , so the energy transfer in 1st stage not maximum. By using office computing software, particles path line has calculated to determine how water particles enter the 2nd stage. It can be obtained from figure 2, in $\beta_2 = 90^\circ$ condition, the water particles enter the 2nd stage by hitting the pod of turbine blades, so they push the turbine blades at the same direction with turbine's rotation. In $\alpha_2 = 90^\circ$ condition, water particles hit the back of turbine blades then makes negative power output in 2nd stage.



From the calculation discussed above also obtained the optimum way how the water enters the turbine. The inlet angle is optimum at $22^\circ \leq \theta \leq 112^\circ$. Then, to prevent turbulence inside the nozzle, it should be ascertained that the water has their own path to flowing through the nozzle. Therefore, nozzle design should obey equation 3 and 4 (Sammartano et al., 2013).

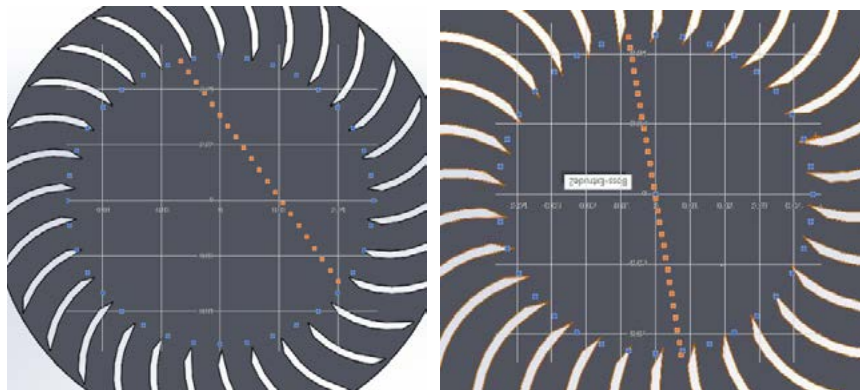


Fig. 2. Water particle path inside turbine at $90^\circ \beta_2$ and $90^\circ \alpha_2$ conditions

$$S_0 = \frac{q}{V} \tag{3}$$

$$B = \frac{Q}{q} \tag{4}$$

The q variable is flow per width unit of nozzle which calculated with equation below.

$$q = V \sin \alpha \lambda \pi D / 360 \tag{5}$$

To make the manufacture process easier, it's been decided to use PVC pipe as turbine blade. The PVC pipe is well known that has limited diameter choice, this make the turbine blade choosing become priority in this turbine design process. Some studies obtain some optimum ratio between outer and inner diameter. Sammartano, based on Aziz study use d/D ratio as 0.68, but after some optimization, the study obtained that best ratio d/D is 0.65 (Sammartano et al., 2013). Relations between that ratio and the blade design were explained below.

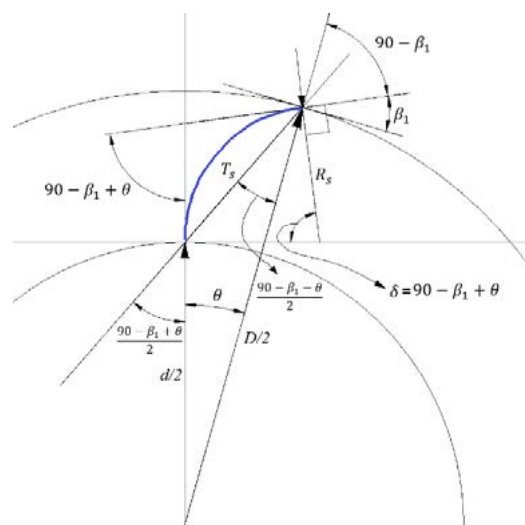


Fig. 3. Relation between turbine diameter and blade's design parameters.



At first, it's been known from studies before that the best blade outlet angle is $\beta_2 = 90^\circ$. From figure 4, it can be seen there is a triangle which edges are T_s , $d/2$, and $D/2$. It's also seen that two blade radius lines and their tangential line formed a kite shape which wing is orthogonal. This make the angle between both blade radius line or also named as blade curvature angle then obey this equation.

$$\delta = 90 - \beta_1 + \theta \quad (6)$$

From equation 6, it been obtained that the angle between T_s and $D/2$ is $(90 - \beta_1 - \theta)/2$, then the angle between $d/2$ and $D/2$ is θ , and then the angle between $d/2$ and T_s is $180 - (90 - \beta_1 + \theta)/2$. From triangle's low, we can generate these relations in the equation below.

$$\frac{T_s}{\sin(\theta)} = \frac{d/2}{\sin(\frac{90 - \beta_1 - \theta}{2})} = \frac{D/2}{\sin(180 - \frac{90 - \beta_1 + \theta}{2})} \quad (7)$$

From equation above 7, relation between blade curvature chord (T_s) and the outer diameter (D) is $T_s = 0.19 D$. This chord can be used as the NACA profile chord. Next, relation between the cord and the curvature radius was explained by the equation 8.

$$\frac{T_s}{\sin(90 - \beta_1 + \theta)} = \frac{R_s}{\sin(\frac{90 + \beta_1 - \theta}{2})} \quad (8)$$

From equation 8, the blade curvature radius can be calculated as $R_s = 0.2 D$. Sammartano also make the equation between R_s , D and d as the equations below.

$$R_s = \frac{D}{4} \left[1 - \left(\frac{d}{D} \right)^2 \right] \cos(\beta_1)^{-1} \quad \left| \quad \tan(\delta/2) = \frac{\cos(\beta_1)}{\sin(\beta_1)} \quad (9)$$

But, the equations above are not valid with this case. By considering simplicity of the turbine manufacture and transmission design between the turbine and the generator, the chosen blade size is 36 mm radius using 2.5" PVC pipe.

b. Airfoil selection for blade profile

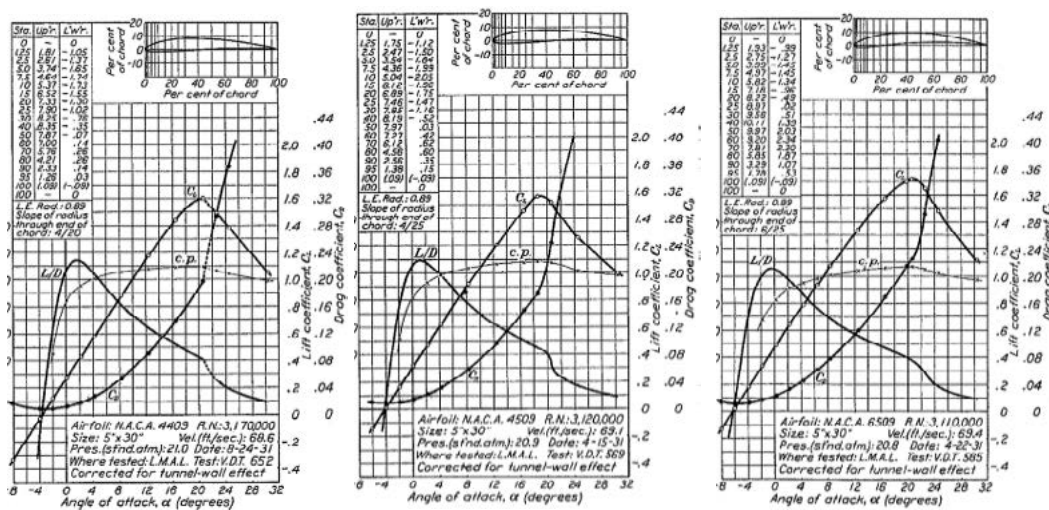


Fig. 4. Some airfoil testing results by NACA.



From some discussion above, it's been known that the turbine blades are have a curvature form. Then, in this study, the 4-digits series NACA profile was used for the turbine's blade profile. The choosing investigation is focused on 44XX, 45XX, 46XX, 47XX, 64XX, 65XX, 66XX or 67XX series which has big curvature camber. The chosen profile is considered as the bigger lift and drag coefficient because the angle between water flow and the turbine rotations is not perfectly orthogonal. Figure 4 shows some c_l , c_d , and c_p graphic in some airfoil testing by NACA (Jacobs; Ward & Pinkerton, 1933).

From some conducted analytical calculation, NACA-6712 has been decided as the best profile for the turbine blade with angle of attack 24° . The tested lift and drag coefficient at 24° AOA is 1.9 and 0.28. Table 1 show cross-flow turbine design parameter in this study. Figure 5 show NACA-6712 profiled blade position on turbine design.

Table 1. Some cross-flow turbine design parameters.

Design Parameter	Value	Design Parameter	Value
Outer Diameter (D)	180 mm	Blade Inlet Angle (β_1)	42°
Inner Diameter (d)	117 mm	Blade Outlet Angle	90°
Inlet Angle (α)	22°	Blade Curve Radius	36 mm
Nozzle Inlet Height (S_o)	53 mm	Blade Curve Angle	58°
Nozzle Width (B)	106 mm	Nozzle outlet angle (θ)	$22^\circ \leq \theta \leq 112^\circ$
Turbine Width (W)	159 mm	NACA airfoil	NACA-6712
Airfoil chord length	32 mm	Airfoil chord angle	18°
Airfoil AOA	24°		

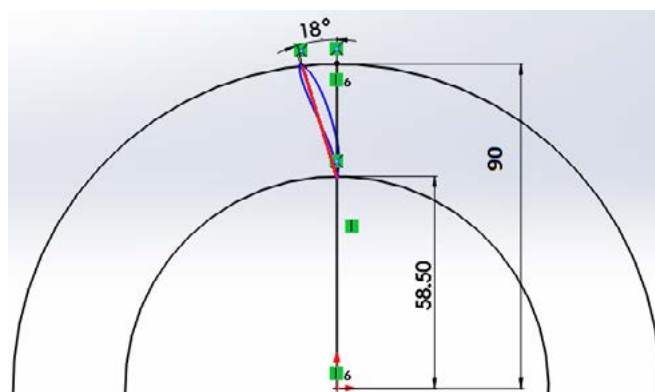


Fig. 5. NACA-6712 profiled blade location.

c. CFD Numerical Simulation Method

The CFD numerical simulation was conducted using ANSYS® FLUENT® 17 with 2D domain. The aims of this simulation are to obtain the detail of best design for cross-flow turbine using some optimizations and to find the best blades number for both NACA 6712 profiled blades turbine and the ordinary arc formed blades.

The turbulence model for this simulation is k- ϵ with realizable constants and scalable wall slip formula. The k- ϵ model is the simplest model for turbulence modelling so the computer can run faster in this complex case. Furthermore, the k- ϵ model is suitable for low pressure gradient case like this study (Sinagra et al., 2014). This simulation also use moving mesh mode with rotational speed of -40.8 rad/s. The multiphase equation used in



this simulation is volume of fluid equations, with implicit volume interaction equations and body force equations. This simulation also use an open channel mode equations. Figure 6 show CFD model of cross-flow turbine, white lines are walls, blue is inlet, red are pressure inlets, and yellow is interface.

After passing the mesh independency process, the most suitable grid size for the simulation of non NACA profiled blades cross-flow turbine in this study is smaller than 5×10^{-3} m, but not smaller than 1×10^{-5} m. While, for simulation of NACA profiled blades turbine is using grid size is smaller than 5.48×10^{-3} m and bigger than 5.48×10^{-5} m. Figure 6 shows the meshing size used in this study.

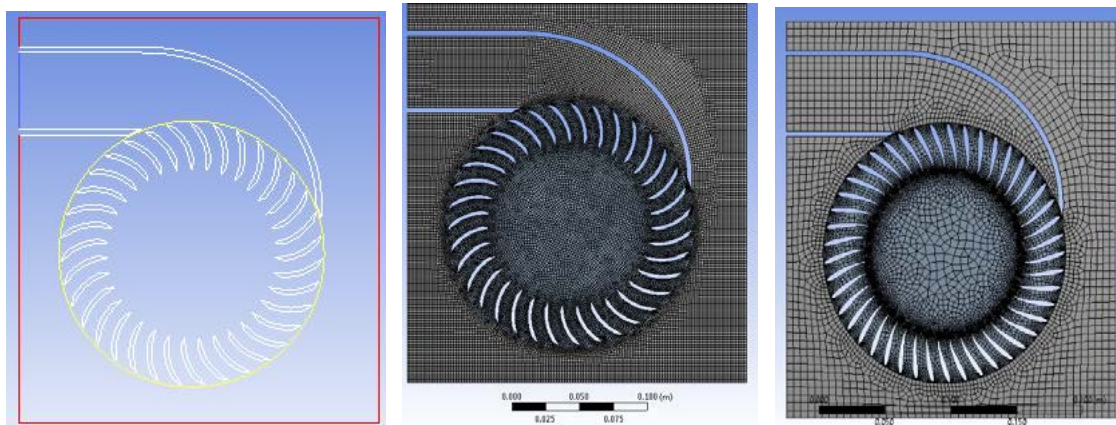


Fig. 6. Meshing size for non-NACA and NACA-profiled turbine.

3. Result and Discussion

a. Ordinary blades cross-flow turbine

From numerical simulation conducted, pressure distribution of the ordinary blade cross-flow turbine can be obtained in figure 7. From figure 7, it can be obtained that the pressure is concentrated at the pod of turbine blades. The maximum pressure at the blade's pod is about 16 kPa. That pressure then push the turbine and make the turbine rotating. The flow stagnancy can be obtained with the higher pressure at the top of second stage blade.

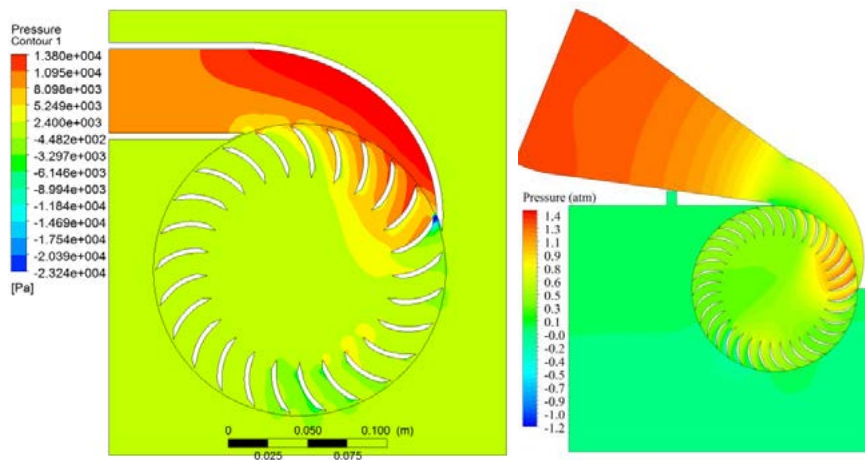


Fig. 7. Pressure contour results of ordinary blades cross-flow turbine. (a) this study, (b) Sammartano's study.



Figure 7 also show the pressure contour of numerical results on Sammartano cross-flow turbine design study (Sammartano et al., 2013). The similarities from the results above are the highest pressure at the turbine is on the pods of first stage's blades and the lowest is on the back of second stage's blades. The flow stagnancy also found at both results. Some differences could be found in the value of pressure like highest pressure at first stage's turbine blades in this result is 1.3 Atm (1.32×10^5 Pa), while in the results above 1.5×10^4 Pa. It is mainly caused by the difference of working head condition that this study has higher head condition (~ 10 m).

b. NACA profiled blades cross-flow turbine

The pressure distribution of the NACA-6712 profiled blades cross-flow turbine can be seen at the figure 8. It can be obtained from the figure8, in leading edge outside type of NACA-6712 profiled blades turbine the pressure concentration is located at the tip of turbine. That pressure concentration push the turbine blades not at the right direction. It also obtained that there is obstacle for the fluid flow inside the first stage. When the airfoil direction reversed, the pressure concentrations were moved to the pod of turbine blade like obtained in ordinary blade results. Figure 9 also show that after passing the first stage blade, the static pressure is increased in NACA-6712 profiled blades turbine. The figure also show there is some blades has pressure at the back of blade was higher than at the pod of blade, so it makes the negative power to the turbine.

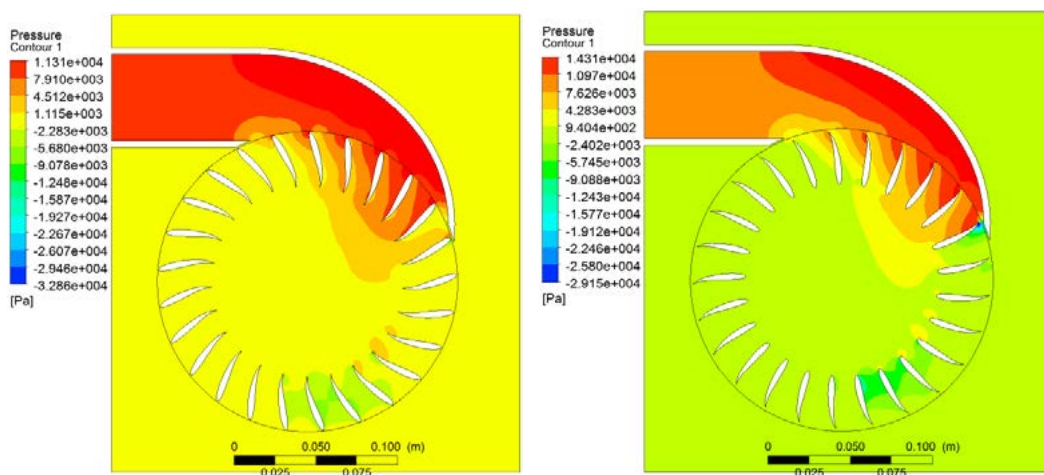


Fig. 8. Pressure contour on NACA-6712 profiled blades cross-flow turbines with different profile direction

c. Optimum blades number investigation

The next simulations are to obtain the best turbine blades number. Ordinary blades, airfoil blades, and reversed airfoil blades crossflow turbine had been simulated with some number of blades from 20 to 35 blades. Figure 9 summarize all the simulations conducted to obtain the number of blades which give best efficiency in each type of blades.

From figure 9, it can be obtained that the best efficiency of ordinary blades cross-flow turbine was 55.3% using 25 blades. It also obtained that airfoil and reversed airfoil profiled best efficiency was 43.6% and 54.7% using 25 blades. The results obtained that higher number of blade not always increase the efficiency of cross-flow turbine. If the blade spacing were too close, it can inhibit the water flow and decrease the cross-flow



turbine efficiency. Corresponding with results in figure 7 and 8, the efficiency of airfoil profiled cross-flow turbines were lower than ordinary one and reversed one.

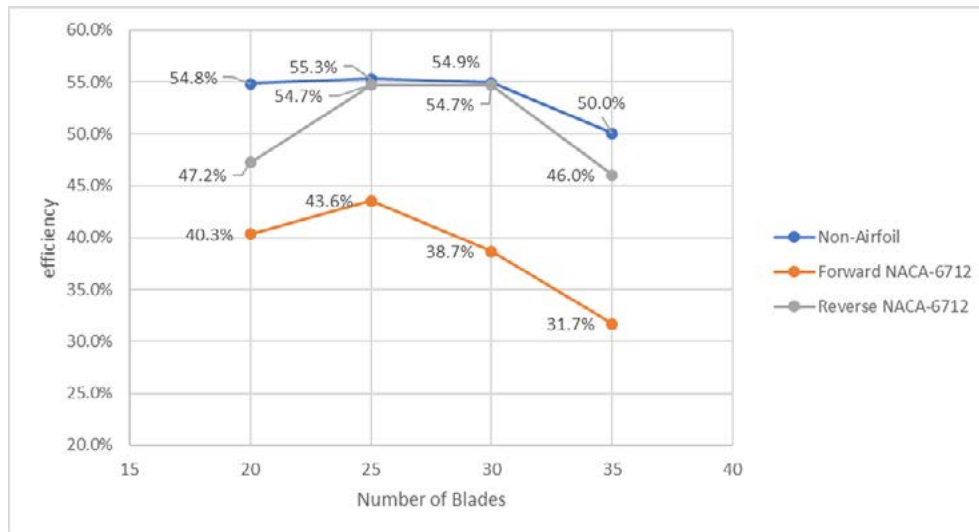


Fig. 9. Turbine efficiency in some numbers of blades

4. Conclusion

This study was resulting that the best blades number for cross-flow turbine is 25 blades which can have efficiency about 55.3% from the numerical results. From analytical calculations, the most suitable NACA profile for this turbine in this study is NACA 6712. The NACA 6712 profiled turbine can make 43.6% efficiency by using 25 blades. Then, when it reversed, it can make 54.7% efficiency by using 25 blades. This study concluded that the ordinary blades cross-flow turbine is better than the NACA-6712 profiled turbine. Another study can be conducted with different type of NACA airfoil profile to optimize the efficiency of the cross-flow turbine.

5. Reference

- Aziz, Nadim M, & Desai, Venkappayya R. (1993). A laboratory study to improve the efficiency of cross-flow turbines. *Engineering Report*.
- Darmawan, Steven, Indra Siswantara, Ahmad, & Budiarto, Budiarto. (2013). *COMPARISON OF TURBULENCE MODELS ON REYNOLDS NUMBERS OF A PROTO X-2 BIOENERGY MICRO GAS TURBINE'S COMPRESSOR DISCHARGE*. Paper presented at the Proceedings International Conference on Engineering of Tarumanagara.
- De Andrade, Jesús, Curiel, Christian, Kenyery, Frank, Aguillón, Orlando, Vásquez, Auristela, & Asuaje, Miguel. (2011). Numerical investigation of the internal flow in a Banki turbine. *International Journal of Rotating Machinery, 2011*.
- DLH. (2014). Laporan Status Lingkungan Hidup Daerah Provinsi Bengkulu. Kota Bengkulu: Dinas Lingkungan Hidup Provinsi Bengkulu.
- Durgin, WW, & Fay, WK. (1984). Some fluid flow characteristics of a cross-flow type hydraulic turbine. *Small Hydro Power Fluid Machinery*, p77-83.



- Jacobs, Pinkerton. Greenberg. *Tests of related forward camber airfoils in the variable density tunnel. NACA Report, 610.*
- Kaniecki, Maciej. (2002). Modernization of the outflow system of cross-flow turbines. *Task Quarterly, 6*, 601-608.
- Kaniecki, Maciej, & Steller, Janusz. *Flow Analysis through a Reaction Cross-Flow Turbine*. Paper presented at the Proceedings of Conference on modelling fluid flow CMFF.
- Kaunda, Chiyembekezo S, Kimambo, Cuthbert Z, & Nielsen, Torbjorn K. (2014). A technical discussion on microhydropower technology and its turbines. *Renewable and Sustainable Energy Reviews, 35*, 445-459.
- Mockmore, CA, & Merryfield, F. (1949). The Banki water turbine, bulletin series no. 25. *Oregon State College.*
- Paish, Oliver. (2002). Small hydro power: technology and current status. *Renewable and sustainable energy reviews, 6(6)*, 537-556.
- Sammartano, Vincenzo, Aricò, Costanza, Carravetta, Armando, Fecarotta, Oreste, & Tucciarelli, Tullio. (2013). Banki-michell optimal design by computational fluid dynamics testing and hydrodynamic analysis. *Energies, 6(5)*, 2362-2385.
- Sammartano, Vincenzo, Morreale, Gabriele, Sinagra, Marco, & Tucciarelli, Tullio. (2016). Numerical and experimental investigation of a cross-flow water turbine. *Journal of Hydraulic Research, 54(3)*, 321-331. doi: 10.1080/00221686.2016.1147500
- Sinagra, Marco, Sammartano, Vincenzo, Aricò, Costanza, Collura, Alfonso, & Tucciarelli, Tullio. (2014). Cross-Flow turbine design for variable operating conditions. *Procedia Engineering, 70*, 1539-1548.
- Ward, EN Jacobs KE, & Pinkerton, RM. (1933). NACA Report No. 460:" The Characteristics of 78 Related Airfoil Sections From test in the Variable-Density Wind Tunnel. *Langley Aeronautical Laboratory, NACA.*



15th International Conference on Quality in Research (QIR 2017)

NUMERICAL ANALYSIS OF PLUNGING AND PITCHING TANDEM FLAPPING FOIL POWER GENERATION

Michael Joevian^a, Christopher Susanto^a, Sheila Tobing^a, Harjadi Gunawan^a

^a*Atma Jaya Catholic University of Indonesia*, Jl. Jend. Sudirman No.51, RT.5/RW.4, Karet Semanggi, Setia Budi, Kota Jakarta Selatan, Daerah Khusus Ibukota Jakarta 12930, Indonesia

ABSTRACT

In the past two decades, numerous studies on flapping wing motion have been conducted. These studies were inspired by the flapping motion of natural flyers: birds and insects. The flapping wing motion of natural flyers utilizes unsteady aerodynamic mechanisms such as leading-edge vortices (LEVs), spanwise flow and rapid rotation at end-of-stroke to generate lift and thrust at low Reynolds number regime. The study of flapping wing motion was mainly driven by the potential applications in the design and development of micro air vehicles (MAVs).

In the more recent years, the application of flapping wing motion for power generation has been gaining more attention due to the need in replacing fossil fuel with renewable energy. In a conventional system of power generator, a rotary turbine drives a generator to produce power/electricity. The same mechanism is applicable for turbine blades that flap under a combined pitching and plunging motion, also known as flapping foil generator/turbine. Flapping foil generators were studied for their potential in extracting tidal/sea wave energy. The objective of this study is to study the effects of pitching frequency on the propulsion of flapping foil generator.

The numerical analysis shows that the highest lift coefficient is produced by the airfoil with 35° pitch amplitude. Although the highest pitch amplitude of 60° gives the highest power coefficient in tandem configuration, but the drag is substantially higher and the lift drops significantly even lower than the lowest pitch amplitude case of 10°. The lowest pitch amplitude does not produce much power and lift, therefore future research can be directed towards the higher pitch amplitude range.

1. INTRODUCTION

The need for energy is gradually becoming even more greater compared with several decades ago. And nowadays most of the energy sources are provided by fossil fuel which we already know is not a part of the renewable energy sources and need to be replaced immediately.

In the past two decades there have been numerous studies on flapping wing motion. These studies were inspired by the flapping motion of natural flyers of animals such as birds and insects. The results of the studies conducted had been applied in a wide variety of fields especially in aerospace engineering and also in design and development of Micro Air Vehicles (MAVs). MAVs is basically defined as an unmanned aircraft with dimension in between 15-20 centimeters and flies with cruising speed of 10 to 15 m/s operating in low Reynolds Number regime. MAVs are classified as four different categories which are fixed-wing, rotary-wing, ducted-propeller, and flapping-wing MAVs. According to Shyy *et al.* (2010), micro air vehicles (MAVs) have the potential to revolutionize our sensing and information gathering capabilities in areas such as environmental monitoring and homeland security. Flapping wings with suitable wing kinematics, wing shapes, and flexible structures can enhance lift as well as thrust by exploiting large-scale vortical flow structures under various conditions.



Studies on flapping-wing MAVs have revealed important results such as unsteady aerodynamics mechanism which enables natural flyers to generate lift and thrust. Some of the unsteady aerodynamics mechanism are leading edge vortices (LEVs), spanwise flow, and wake capture (rapid rotation at end of stroke).

Considering the current availability of fossil fuel, it has been the right time to start moving to the cleaner and more efficient energy sources. And to answer our ever-growing need for energy while restraining adverse effects on the environment, new renewable energy sources must be exploited (Kinsey, 2012). The corresponding energy sources in this study is an oscillating foil flapping in a sinusoidal motion to generate electricity from a power generation system. Especially, tandem airfoil in this case. Flapping foil is used as an alternative to rotating turbine blades and applied under shallow water or seawater.

The main objective of this study is to perform the numerical analysis of two-dimensional (2D) NACA 0012 tandem airfoils which flap under a combined plunging and pitching motion. Hopefully to achieve the optimized combination of plunging and pitching motion in order to be applied in seawater environment or tidal power generation system. The continuation purpose of this study is essentially to create a fully renewable energy sources by replacing the conventional rotary turbine with a possibly more energy efficient flapping foil turbine in a power generation system.

2. METHODOLOGY/EXPERIMENTAL

The numerical simulation was done by using Computational Fluid Dynamics (CFD) program named ANSYS FLUENT v.17 with student version free license. The license will expire at the 31st of October 2017. Student version of FLUENT limits the total grid elements to 512000.

In this paper, research was done by performing numerical analysis to simulate two-dimensional (2D) NACA 0012 tandem airfoils flapping under pitching motion in order to find the optimization suitable for a power generation system. The system is intended to be applied at the offshore water using the property of seawater at 20° C as shown in Table 1.

Table 1. Property of seawater at 20° C

Property of Seawater			
Fluid	Temp. (°C)	Density (kg/m ³)	Dynamic Viscosity (kg/ms)
Seawater	20	1030	0.00107

2.1. Validation

In this study, the validation stage takes several trials to achieve the maximum error below 10% or as low as possible. Validation is essentially comparing CFD results against data in an effort to establish a model's ability to reproduce physics (NASA, 1988). We used the turbulence modelling validation from the numerical simulation comparing time average thrust coefficient data, C_{Tmean} , against three variations of reduced frequency k utilizing a plunging NACA0012 airfoil at non-dimensional plunging amplitude $h = 0.4$, and at Reynolds number $Re = 3 \times 10^6$ (Ashraf, Young, Lai, 2010). Figure 1. shows the variation of C_{Tmean} against k graph obtained from Tuncer and Platzer numerical simulation.

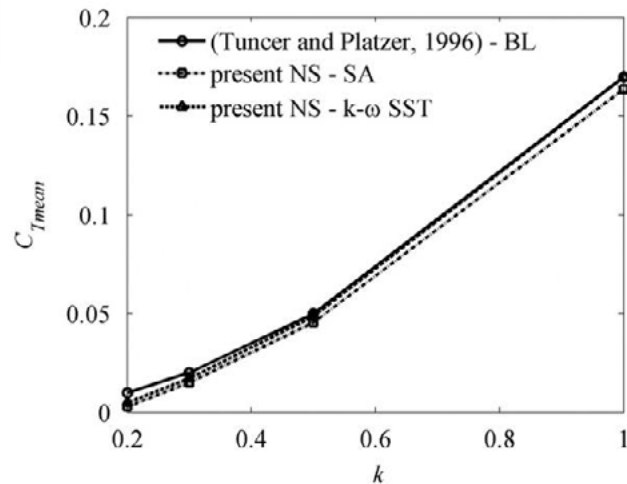


Figure 1. Variations of C_{Tmean} against k for plunging NACA0012. (Ashraf, Young, Lai, 2010)

Figure 1. shows the Tuncer and Platzer numerical simulation result presented in a graph of time average thrust coefficient values or C_{Tmean} against the variation of reduced frequency, k . We need at least three cases of C_{Tmean} vs k data to make sure the data is valid. In this case, we utilized k values of $k = 0.3$; $k = 0.5$; and $k = 1$ as shown in Table 2. The tested model duplicated the experimental model used by Ladson which is a single NACA 0012 airfoil with chord length of 60,01 cm (Ladson, 1988). Assuming the system is incompressible mode (pressure based) and the turbulent model chosen is $k-\omega$ SST to achieve the residual set in FLUENT at 1×10^{-4} .

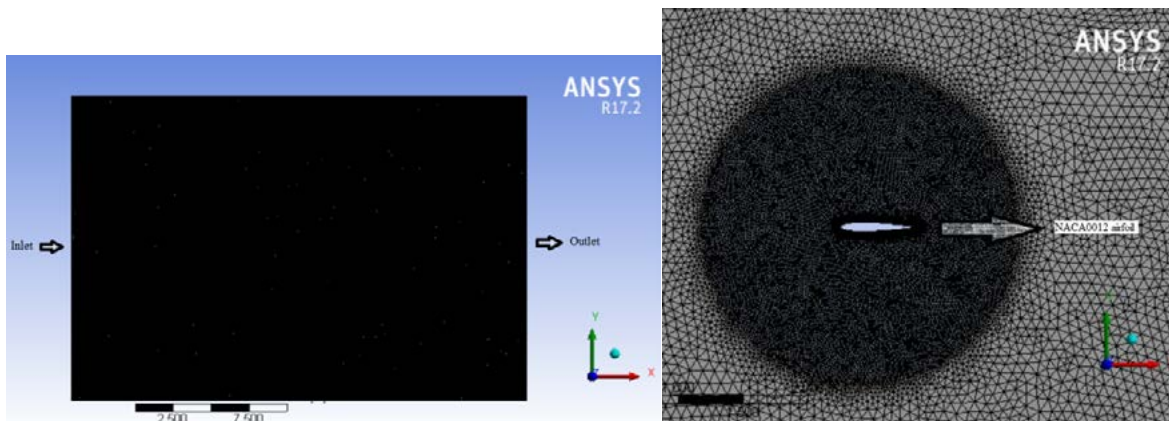


Figure 2. Left: full domain mesh, right: zoom-in to mesh around the airfoil.

Table 2. Validation C_{Tmean} data for plunging NACA0012 at $h=0.4$ and $Re=3 \times 10^6$

k	Tuncer and Platzer	Fluent	Error (%)
	C_{Tmean}	C_{Tmean}	
0.3	0.01629	0.016	1.78
0.5	0.04772	0.0494	3.52
1	0.1703	0.167	1.94



Table 2. above represents the comparison of values from the numerical simulation result and the literature as the validation data. The time average thrust coefficient C_{Tmean} results of three cases with three different variations of reduced frequency along with the error percentage are shown in Table 2. The C_{Tmean} differences between the literature (Tuncer and Platzer), which the values obtained by digitizer program, and the numerical simulation results were quite small. Therefore, the result of the study researched in this paper can be trusted and can be mentioned as valid. Proven from the percentage of error values are below 10%.

2.2. Parametric Study

After the validation stage has been completed, then the tandem airfoils is modeled as the main purpose of this study. The airfoils are in a configuration as shown in Figure 3., The tandem configuration is basically had the front and the rear airfoil. The airfoils chord length, c , are set to be 0.1 m in order to be operated underwater. The property of the fluid moving through the airfoils used the density and dynamic viscosity of seawater shown in Table 1.

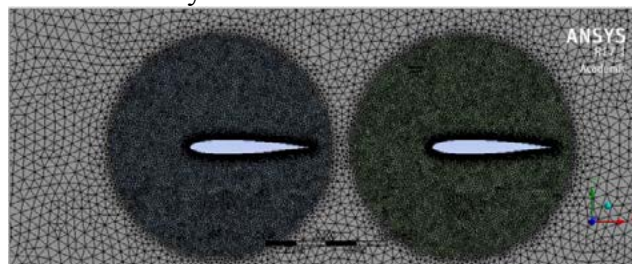


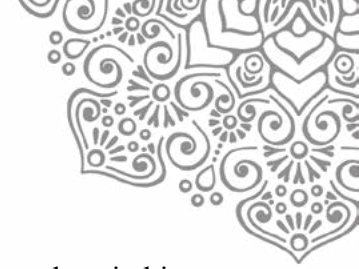
Figure 3. 2D mesh details on the airfoils in tandem configuration.

The airfoils are separated by 0.2 m stagger distance starting from a point at $0.25c$ (a quarter of a chord length) which is at 0.025 m from the front airfoil's leading edge until the $0.25c$ of the rear airfoil. The initial condition of the airfoils did not have pitching angle or at zero AoA. The stagger distance of 0.2 m is selected because any stagger distance above a certain value is considered does not give any benefit to the tandem configuration. It's basically simulating two different airfoils in two different cases. The flow affecting the front hydrofoil will not give any effect on the rear one. The point at the quarter of the chord length of each airfoil is intended to be the pivot point in which the location of the pitching moment takes place.

Three parameters chosen in this study are reduced frequency f^* , pitch amplitude α , and phase difference ϕ . For the details of the parameters tested is in Table. The pitching frequency is obtained from the equation below

Table 3. Pitch amplitude parameter tested.

Case	f^*	α	ϕ	f (Hz)
1	0.14	10°	0°	3.6008
1	0.14	35°	0°	3.6008
1	0.14	60°	0°	3.6008



3. RESULTS AND DISCUSSION

In this numerical study, we are analyzing the influence of pitch amplitude under pitching motion on the aerodynamics (drag, lift, moment, and power required) of 2D tandem airfoils. With the current high Re number regime (247.585), the flow is assumed to be transitioning from laminar to turbulence, therefore $k-\omega$ SST turbulence model is selected. Moreover, the convergence criterion of 10^{-4} is set for both continuity and momentum equations.

3.1. Pressure Contour

The figures below are basically the pressure contour of each case with the variation of pitch amplitude. It obviously shows that the red legend of the image has the highest pressure area and the blue represents the lowest pressure.

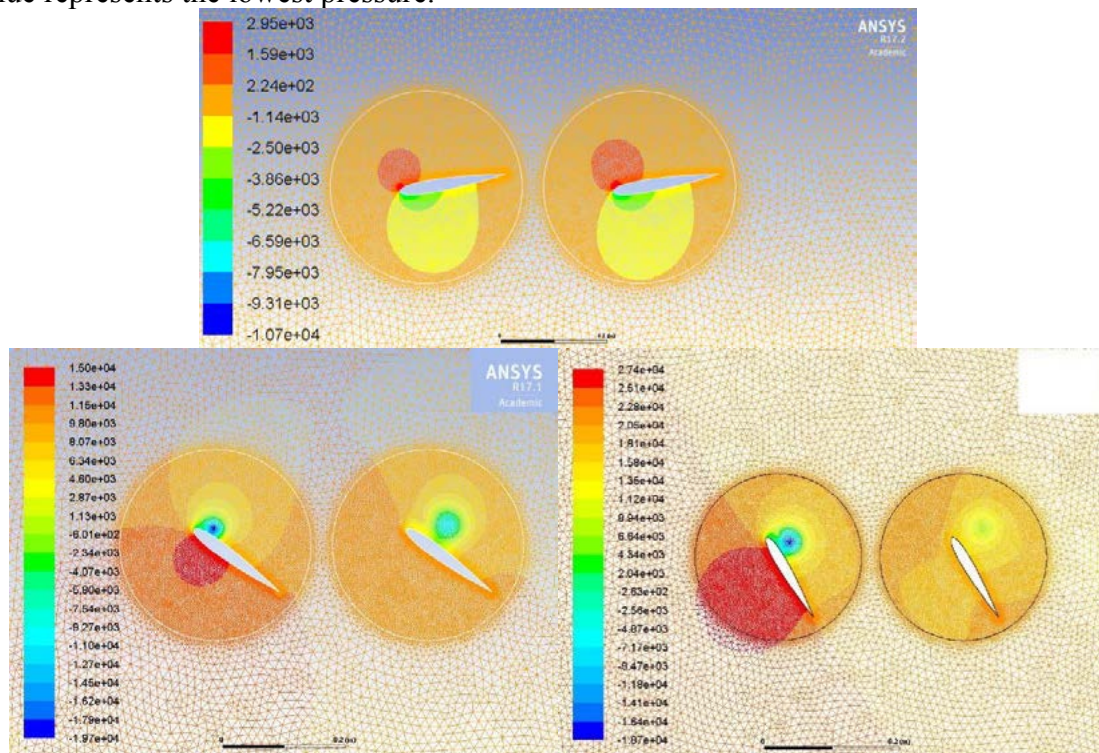


Figure 4. Pressure contour of three different pitch amplitude.

From Figure 4, it can be seen that when the hydrofoil is pitching in a down stroke motion, the highest pressure is located around the upper surface of the hydrofoil, and vice versa. So the up stroke of the hydrofoils' pitch motion are resulting higher pressure on the bottom surface than on the upper surface of the hydrofoils. These mechanisms induce the creation of LEV's (leading edge vortices). The blue region represents the vortices attached to the upper surface which is about the shed from the hydrofoil surface. It basically creates lower pressure area at the point near the leading edge so that the higher pressure on the bottom surface leads to enhance lift generation the hydrofoil tandem configuration.

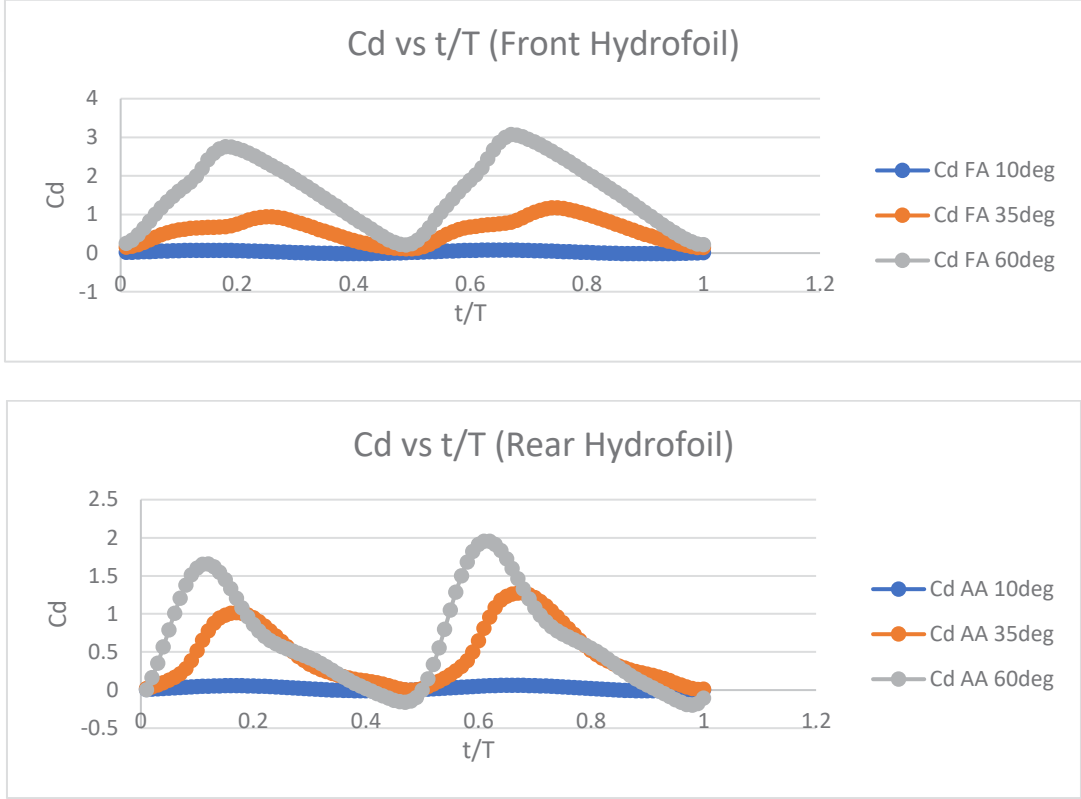


Figure 5. Drag coefficient vs dimensionless time.

Figure 5. shows the relation between drag coefficient and dimensionless time operating in the same reduced frequency ($f^*=0.14$) and in three different pitch amplitude. Obviously along with inclination of pitch amplitude, the drag of the front and rear hydrofoil increases significantly. And the highest drag is produced by the case with the highest pitch amplitude. The curves also show that the drag coefficient reaches the peak value in a faster period or faster dimensionless time for both hydrofoils, and reaches the lowest point at roughly the same time period. The peak values for the front hydrofoil are at around $0.2T$ and $0.7T$, the lowest values are at the beginning ($0T$), at the middle ($0.5T$) and at the end of the time period (T). The same thing occurred for the rear hydrofoil which the lowest values of the drag are at the beginning, the middle, and at the end of the time period. However, the rear hydrofoil reached the peak value at a faster time period, around $0.15T$ and $0.6T$. The positive values of the drag coefficient indicates the tandem configuration does not generate thrust because positive drag is in the direction of the moving fluid.

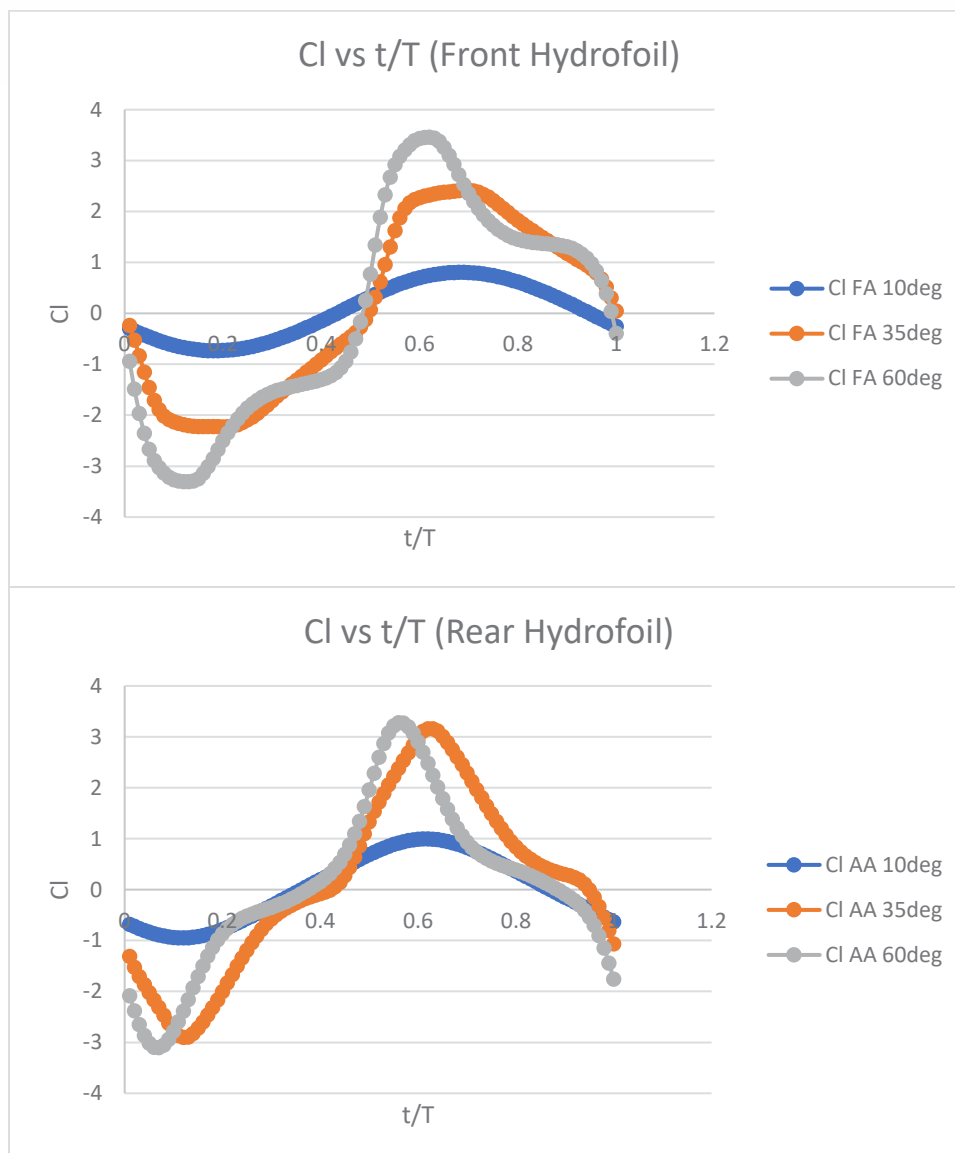


Figure 6. Lift coefficient vs dimensionless time.

Figure 6. shows the relation between lift coefficient vs dimensionless time of hydrofoils in tandem configuration, front and rear. For the front hydrofoil the curves show the higher the pitch amplitude, the bigger the lift creation. And the peak value of the lift is basically reached at around time period $0.1T$ and $0.6T$. On the other hand, the lift generation of the rear hydrofoil is not necessarily enhanced with the increase of pitch amplitude but the curves show that the lowest pitch amplitude produces the lowest lift. And then the comparison between the mid and the highest pitch amplitude does not show any significant difference in terms of the peak lift coefficient value. One thing that noticeable is that the higher pitch amplitude reaches peak lift coefficient value at an earlier time period.

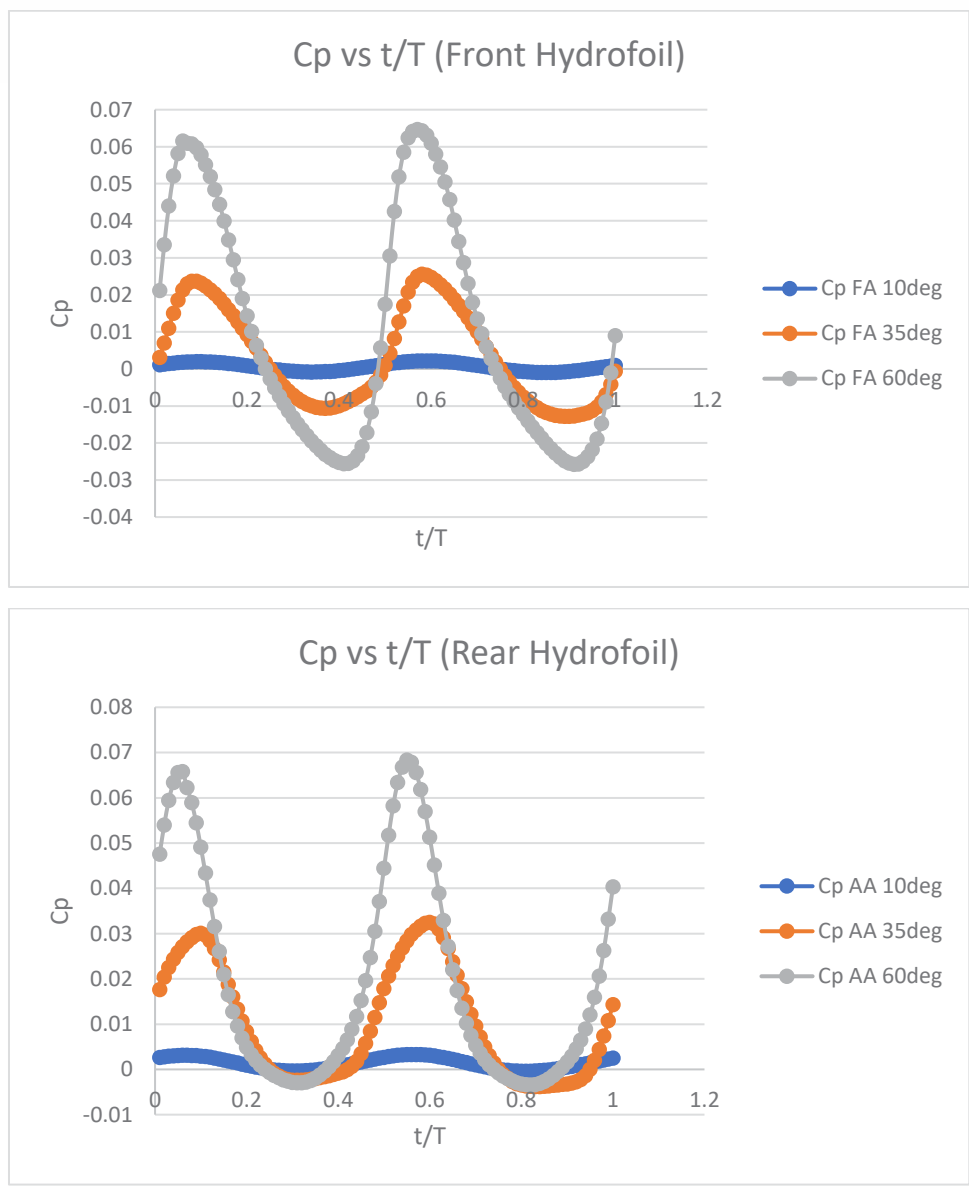


Figure 7. Power coefficient vs dimensionless time.

Figure 7. is essentially showing the relation between power coefficient and the dimensionless time. The power defined in this study is the power required for the tandem configuration of the hydrofoil. The curves show that the highest value of the C_p is possessed by the highest amplitude and it applies to both of the hydrofoil. The effect of the pitch amplitude in the curves above is obvious that the higher the pitch amplitude, the more the power required is produced.



3.2. Time Average Lift, Drag, and Moment

Table 3.2.1. Time average drag, lift, and moment of front and rear hydrofoil of all three different pitch amplitude.

θ	10°	35°	60°
Cd FA	0.029105834	0.599909885	1.59955584
Cd AA	0.025166567	0.437816916	0.715606828

θ	10°	35°	60°
Cl FA	0.019518838	0.059469632	0.022962247
Cl AA	0.012787285	0.059690923	0.023747292

θ	10°	35°	60°
Cm FA	0.000915697	0.002253957	0.000582583
Cm AA	0.00059448	0.00315806	0.001277427

Table 3.2.1. represent each time average output parameter by calculating the average values obtained from FLUENT calculation which are drag, lift, and moment of the front and rear hydrofoil in three different pitch amplitude as the tested parameter. The value of the time average drag obviously shows that drag increases with the higher pitch amplitude so the highest pitch amplitude 60° generates the biggest drag coefficient in terms of the average value. Especially the 60° case, the front hydrofoil has the most significant increase in generating drag compared with the lower pitch amplitude cases. Considering the positive values of the drag produced, it means thrust is not generated because the positive value of Cd is defined as in the same direction as the moving fluid through the hydrofoil.

While the drag increases as the pitch amplitude gets higher, the lift coefficient is not necessarily proportional to the inclination of the pitch amplitude. As shown in table 3.1., the second table shows the increase of lift from the 10° case to the 35° case for the front hydrofoil but experiencing lift drop from the 35° case to the 60° case. The value of Cl for the 60° case is even lower than the 10° case. The same goes with the rear one which is also experiencing drop in lift. The increment value of the rear hydrofoil lift coefficient is noticeably higher than the front one. It means that the tandem configuration is more beneficial to the rear hydrofoil rather than the front one.

3.3. Time-Averaged Power Coefficient

Table 3.3.1. Time-averaged drag, lift, and moment of front and rear hydrofoil of all three different pitch amplitude.

Case	f^*	α (degree)	\overline{Cp}_{FA}	\overline{Cp}_{AA}
1	0.14	10	0.000532833	0.001302235
2	0.14	35	0.002947891	0.009959437
3	0.14	60	0.010257814	0.018989065

And then the table above is basically showing the effect of pitching amplitude against the non-dimensional power coefficient. All three cases are distinguished by their pitching amplitude. We found that the non-dimensional power coefficient increases with the increasing pitch



amplitude. The 10° case is resulting a very small $\overline{C_p}$ value approaching zero for both hydrofoil while the 60° case is resulting a more significant increase of $\overline{C_p}$ value. So the effect of pitching amplitude in relation to the application of power

4. CONCLUSION

The data obtained and analyzed from this study shows that not necessarily higher pitch amplitude is more beneficial to the propulsion of wings in tandem configuration. Although the highest pitch amplitude case gives the highest instantaneous value of lift, the time-averaged lift coefficient is the lowest among the three cases.

For power, the highest time-averaged power is observed on the case with the highest pitch amplitude of 60°, but it is accompanied by low lift generation. So among three cases, we found that the 35° pitch amplitude gives the optimum results for lift and power generation.

In other words the propulsion of tandem airfoil, or in this case hydrofoils, under the influence of pitch amplitude needs to be further studied in order to find the suitable combination of pitch amplitude and reduced frequency and to be applied as an alternative power generation system. The phase difference and the horizontal distance (stagger) between airfoils, as well as plunging motion will be studied in the next stage of this study.

5. REFERENCES

- Ashraf, M.A., Young, J. and Lai, J.C.S., 2011. Reynolds number, thickness and camber effects on flapping airfoil propulsion. *Journal of Fluids and structures*, 27(2), pp.145-160.
- Kinsey, T., Dumas, G., 2012b. Optimal tandem configuration for oscillating-foils hydrokinetic turbine. *Journal of Fluids Engineering* 134 (3), 031103.
- Ladson, C.L., 1988. Effects of independent variation of Mach and Reynolds numbers on the low-speed aerodynamic characteristics of the NACA 0012 airfoil section.
- Shyy, W., Aono, H., Chimakurthi, S.K., Trizila, P., Kang, C.K., Cesnik, C.E. and Liu, H., 2010. Recent progress in flapping wing aerodynamics and aeroelasticity. *Progress in Aerospace Sciences*, 46(7), pp.284-327.d
- Young, J., Lai, J.C. and Platzer, M.F., 2014. A review of progress and challenges in flapping foil power generation. *Progress in Aerospace Sciences*, 67, pp.2-28.



15th International Conference on Quality in Research (QIR 2017)

A NUMERICAL ANALYSIS ON THE EFFECTS OF ANGLE-OF-ATTACK AND STAGGER ON THE PROPULSION OF TANDEM AIRFOIL AT HIGH AND LOW SPEED FLIGHT

Anthony Christian, Sheila Tobing, Riccy Kurniawan

Atma Jaya Catholic University of Indonesia, Jl. Jend. Sudirman No.51, RT.5/RW.4, Karet Semanggi, Setia Budi, Kota Jakarta Selatan, Daerah Khusus Ibukota Jakarta 12930, Indonesia

Abstract — Since its commercialization as a mean of mass transportation, the design and development process of an aircraft mainly focus on increasing its speed and/or size. The shape of aircraft wing, which is the primary device for lift generation, has remained generally unchanged. A variety of wing configuration, tandem wing configuration, has been utilized on a number of aircraft, yet there is limited research published on the subject. This research aims to analyze the effects of stagger, which is the stream-wise distance between the forewing and the rear wing, in tandem wing configuration on the aerodynamic forces generated by the wings.

The analysis is conducted numerically using ANSYS Fluent version 17.1 on two-dimensional (2D) NACA 0012 tandem airfoils at three variations of stagger, 1.5 chord, 2 chord, and 3 chord in laminar ($Re = 2 \times 10^3$) and turbulent flow ($Re = 6 \times 10^6$). As a first step, a 2D model of NACA 0012 airfoil is created using Autodesk Inventor and then uploaded to ANSYS. Subsequently, the solver is validated against the published results of wind tunnel tests on NACA 0012 airfoil. The results of current numerical analysis are in a good agreement with the experimental data.

The result of this study is that the tandem wing configurations flying in a turbulent flow regime experience a maximum increase in total lift (the total lift of fore- and rear wing) of 37% and a maximum decrease in total drag (the total drag of fore- and rear wing) of 3% in cases where the angle of attack of the rear wing is greater than that of the forewing. However, this increase in lift diminishes by a maximum of 11% and 10% as the stagger increases from 1.5 chord to 2 chord and from 2 chord to 3 chord, respectively. The effect of tandem wing configuration on laminar flow is that for several combinations of angles-of-attack, a maximum increase in lift of 241% and a maximum drop in drag of 23% were observed. This is caused by the flow separation on the airfoil that occurs early in laminar flow. Further study is necessary to gain a better insight on the effects of angle-of-attack on the propulsion of tandem wing airfoils in low Re regime.

Keywords — plunging airfoil, propulsion, tandem wing flight, unsteady aerodynamics.

INTRODUCTION

The utilization of jet engine on an aircraft marked its commercialization as a mean of public transportation. Jet engine offers a quieter, smoother, and faster flight. Due to these extra conveniences, the number of passengers has been increasing ever since. Despite the increasing usage of aircraft, its design has remained generally unchanged.

The design of aircrafts in use today resembles that from the early days. More research is needed to develop aircraft design as to increase its safety, comfort, and efficiency. Aircraft developments over the last few decades mainly focus on its size.

Modern day aircrafts are bigger in dimension. The extra space is needed to accommodate more passengers. Meanwhile, wing design has remained unchanged even though wings are the primary generators of aerodynamic forces on an aircraft. Therefore, more efforts must be put into the research and development of aircraft wings.

Since the first successful flight of heavier-than-air aircraft, many wing configurations have been developed and utilized. One of which is tandem wing configuration. Tandem wing configuration is an aircraft's wings configuration with two wings on each side of the aircraft.

Despite having been utilized on aircrafts, researches on this configuration are not widely available, unlike those on single wing configuration. Therefore, more researches have to be conducted in order to better understand the air flow characteristics around tandem wings.

Tandem Wing Configuration

Tandem wing configuration on an airplane is a wing configuration consisting of two lift-generating wings with an identical aspect ratio. Aspect ratio is the ratio of wing span to mean chord length. Both of the wings might be located on two different planes, horizontally or vertically.



There are three terms used to define a tandem wing configuration:

- **Stagger (St)**
Stagger is the horizontal distance between the fore- and aft-wing, measured from 0.25c position of each wing.
- **Gap (G)**
Gap is the vertical distance between the fore- and aft-wing, measured from 0.25c position of each wing.
- **Decalage (δ)**
Decalage is the relative angle-of-attack between the fore wing and aft-wing; the angle-of-attack of the fore- and aft-wing is measured relative to the direction of the air flow. A positive decalage indicates that the angle-of-attack of the fore wing (α_w) is greater than the angle-of-attack of the aft wing (α_p). A negative decalage indicates that the angle-of-attack of the aft wing (α_p) is greater than that of the fore wing (α_w).

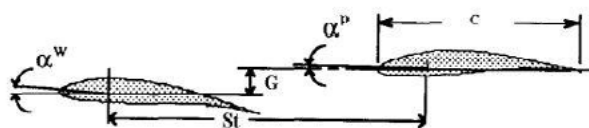


Fig 1. Tandem wing configuration [10]

Numerical Simulation

This experiment is conducted numerically using ANSYS Fluent 17.1 Student Version with a maximum element of 512,000. The mesh used in this experiment is c-mesh (Fig 2.)

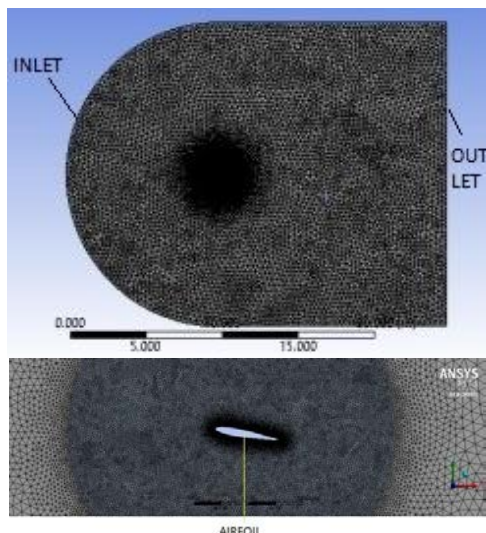


Fig 2. C-mesh

Numerical Validation

Before numerical data can be acquired, numerical simulation must be validated to ensure that the simulation is run correctly. This is accomplished by running simulations of single wing on turbulent flow, the result is then compared to

the experimental data. The experimental data used as a comparison is taken from Ladson's research.

The numerical simulation is conducted at $Re= 6 \times 10^6$ using Spalart-Allmaras viscous model. The simulation parameters are provided in Table 1.

Table 1. Numerical simulation parameters

Air density (ρ)	3.633 kg/m ³
Specific heat (C_p)	1,004.9 J/kg K
Dynamic viscosity (μ)	1.846 x 10 ⁻⁵ kg/m s
Air speed	50 m/s

Table 2. Numerical validation

Angle-of-attack (°)	Numerical Result		Experimental Data		Difference (%)	
	C _L	C _D	C _L	C _D	C _L	C _D
0	0.0001	0.0082	-0.006	0.0081		1.09
5	0.5507	0.0095	0.5304	0.0085	3.82	10.97
10	1.0758	0.0139	1.0674	0.0117	0.79	19.22
: percentage cannot be displayed since the denominator is close to 0						

Table 3. Drag coefficient validation

Angle of Attack (°)	Numerical C _D Result	Eleni's Numerical C _D Result	Difference (%)
0	0.0082	0.0090	9.02
5	0.0095	0.0104	8.81
10	0.0139	0.0150	7.01

Data from Table 2 shows that the maximum difference in lift coefficient is 4%, whereas the difference in drag coefficient is 19% compared to experimental data. Even though the drag coefficient acquired from the numerical simulation has a huge difference compared to Ladson's experiment, it differs less than 10% compared to the data from Eleni's research (Table 3). Therefore, the numerical simulation conducted is valid.

Analysis on The Effect of Angle of attack Variation on Aerodynamic Forces

To obtain an understanding on the effect of angle of attack variation to the aerodynamic forces generated by NACA 0012 airfoil, numerical simulations are conducted in turbulent flow ($Re= 6 \times 10^6$) using Spalart-Allmaras viscous model under parameters provided below:

Air density (ρ)	3.633 kg/m ³
Specific heat (C_p)	1,004.9 J/kg K
Dynamic viscosity (μ)	1.846 x 10 ⁻⁵ kg/m s
Air speed	50 m/s



Numerical simulations for tandem wing configuration in this research are conducted for stagger 1.5-, 2-, and 3-c, in several combinations of angle of attack of the fore wing and aft wing starting from 0° to 10°. Examples of the model used in the numerical simulation for stagger 1.5-, 2-, and 3-c are available in Figure 3, Figure 4, and Figure 5 respectively.



Fig 3. Example of numerical model for stagger 1.5-c



Fig 4. Example of numerical model for stagger 2-c



Fig 5. Example of numerical model for stagger 3-c

Numerical results for each stagger are provided in Table 4, Table 5, and Table 6 respectively.

Table 4. Numerical result for stagger 1.5-c in turbulent flow

Angle of Attack FA (°)	Angle of Attack AA (°)	CL _{FA}	CL _{AA}	CD _{FA}	CD _{AA}
0	0	-0.0006	-0.0013	0.0057	0.0099
0	5	0.2529	0.4574	-0.0006	0.0180
0	10	0.5100	0.9278	-0.0201	0.0417
5	0	0.4601	-0.1127	0.0099	0.0070
5	5	0.7139	0.3695	-0.0064	0.0257
5	10	0.9365	0.8139	-0.0326	0.0570
10	0	0.8981	-0.2235	0.0252	-0.0018
10	5	1.1132	0.2630	0.0017	0.0265

Table 5. Numerical result for stagger 2-c in turbulent flow

Angle of Attack FA (°)	Angle of Attack AA (°)	CL _{FA}	CL _{AA}	CD _{FA}	CD _{AA}
0	0	0.0001	0.0003	0.0073	0.0087
0	5	0.1726	0.4968	0.0040	0.0135
0	10	0.3459	0.9952	-0.0061	0.0278
5	0	0.5068	-0.0985	0.0105	0.0067
5	5	0.6795	0.4144	-0.0019	0.0213
5	10	0.8315	0.8743	-0.0188	0.0431
10	0	0.9825	-0.1969	0.0234	0.0010
10	5	1.1335	0.3184	0.0040	0.0245

Table 6. Numerical result for stagger 3-c in turbulent flow

Angle of Attack FA (°)	Angle of Attack AA (°)	CL _{FA}	CL _{AA}	CD _{FA}	CD _{AA}
0	0	-0.0005	-0.0010	0.0079	0.0082
0	5	0.1044	0.5225	0.0066	0.0110
0	10	0.2073	1.0391	0.0026	0.0192
5	0	0.5339	-0.0725	0.0102	0.0073
5	5	0.6365	0.4574	0.0022	0.0171
5	10	0.7302	0.9416	-0.0075	0.0317
10	0	1.0275	-0.1456	0.0206	0.0047
10	5	1.1212	0.3885	0.0072	0.0214

Analyzing the results of the angle of attack combination FA-AA 0°-0°, 0°-5° and 0°-10°, lift generated by the fore wing keeps on increasing, whereas the drag keeps on decreasing as the angle of attack of the aft wing increases. From the combination FA-AA 0°-0°, 5°-0°, and 10°-0°, it can be seen that the lift and drag of the aft wing keeps on decreasing as the angle of attack of the fore wing increases.

Case Analyses

The percentages displayed in these case analyses are calculated in reference to the numerical results of single airfoil displayed in Table 2.

Case I: FA = 0° and 0° ≤ AA ≤ 10°; 5° interval

Lift produced by the front airfoil in tandem wing configuration with 0° front airfoil angle of attack increases as the angle of attack of the aft airfoil increases whereas drag decreases, reaching negative value in FA-AA angle of attack combination of 0°-5° and 0°-10°. Negative drag means that the front airfoil produces thrust. The greatest thrust is produced by combination of FA-AA angle of attack 0°-10° at stagger 1.5-c.



Case II: FA = 5 and 0° ≤ AA ≤ 10°; 5° interval

Lift produced by the front airfoil in tandem wing configuration with 5° front airfoil angle of attack increases as the angle of attack of the aft airfoil increases whereas drag decreases, reaching negative value (producing thrust) in certain combinations of angle of attack (FA-AA 5°-5° and 5°-10°). FA-AA combination of 5°-10° at stagger 1.5-c produces an increase of 70% in lift while producing the greatest thrust, CTFA = 0.0326 (-CD_{FA} = CT_{FA}).

Case III: AA = 0° and 0° ≤ FA ≤ 10°; 5° interval

Lift and drag produced by the aft airfoil in tandem wing configuration with 0° aft airfoil angle of attack decreases as the angle of attack of the front airfoil increases. The combination of FA-AA 10°-0° at stagger 1.5-c produces thrust in the aft airfoil due to the decrease in drag of 120%.

Case IV: AA = 5° and 0° ≤ FA ≤ 10°; 5° interval

Lift produced by the aft airfoil in tandem wing configuration with 5° aft airfoil angle of attack decreases as the angle of attack of the front airfoil increases whereas drag increases. The greatest decrease in lift and the greatest increase in drag on aft airfoil occur in the combination FA-AA of 10°-5° at stagger 1.5-c. In this combination, lift decreases up to 50% and drag increases up to 180%.

The advantage of tandem wing configuration on aerodynamic forces in turbulent flow is seen more clearly if the sum of the aerodynamic forces is compared to the sum of the aerodynamic forces of two single airfoils at an identical angle of attack. This comparison is displayed on Table 7, Table 8, and Table 9

Table 7. Numerical and literature comparison of stagger 1.5-c in turbulent flow

Angle of Attack FA (°)	Angle of Attack AA (°)	Numerical Result		Numerical Literature (Sum of 2 Single Airfoils)		Difference in C _L (%)	Difference in C _D (%)
		C _L total	C _D total	C _L total	C _D total		
0	0	-0.002	0.016	0.000	0.016		-4.41
0	5	0.710	0.017	0.551	0.018	28.97	-1.17
0	10	1.438	0.022	1.076	0.022	33.64	-2.28
5	0	0.347	0.017	0.551	0.018	-36.92	-4.04
5	5	1.083	0.019	1.101	0.019	-1.63	1.68
5	10	1.751	0.024	1.627	0.023	7.62	4.31
10	0	0.675	0.023	1.076	0.022	-37.30	5.47
10	5	1.376	0.028	1.627	0.023	-15.38	20.39
: percentage is not displayed (denominator close to 0)							

Table 8. Numerical and literature comparison of stagger 2-c in turbulent flow

Angle of Attack FA (°)	Angle of Attack AA (°)	Numerical Result		Numerical Literature (Sum of 2 Single Airfoils)		Difference in C _L (%)	Difference in C _D (%)
		C _L total	C _D total	C _L total	C _D total		
0	0	4E-04	0.016	0.000	0.016		-2.40
0	5	0.669	0.018	0.551	0.018	21.53	-0.84
0	10	1.341	0.022	1.076	0.022	24.65	-1.76
5	0	0.408	0.017	0.551	0.018	-25.88	-2.19
5	5	1.094	0.019	1.101	0.019	-0.67	2.20
5	10	1.706	0.024	1.627	0.023	4.87	3.72
10	0	0.786	0.024	1.076	0.022	-26.98	10.12
10	5	1.452	0.029	1.627	0.023	-10.73	21.53
: percentage is not displayed (denominator close to 0)							

Table 9. Numerical and literature comparison of stagger 3-c in turbulent flow

Angle of Attack FA (°)	Angle of Attack AA (°)	Numerical Result		Numerical Literature (Sum of 2 Single Airfoils)		Difference in C _L (%)	Difference in C _D (%)
		C _L total	C _D total	C _L total	C _D total		
0	0	-0.002	0.016	0.000	0.016		-1.18
0	5	0.627	0.018	0.551	0.018	13.82	-0.60
0	10	1.246	0.022	1.076	0.022	15.84	-1.59
5	0	0.461	0.018	0.551	0.018	-16.23	-0.83
5	5	1.094	0.019	1.101	0.019	-0.68	1.88
5	10	1.672	0.024	1.627	0.023	2.79	3.67
10	0	0.882	0.025	1.076	0.022	-18.03	14.28
10	5	1.510	0.029	1.627	0.023	-7.18	21.96
: percentage is not displayed (denominator close to 0)							

From the tables above, it can be seen that FA-AA combination of 0°-5° and 0°-10° give off positive effects of increase in lift and decrease in drag. This is due to the shifting of the stagnation point on the front airfoil in downward direction influenced by the air flowing to the aft airfoil. This shift is displayed in Figure 6 and Figure 7. Figure 6 shows the stagnation point of a single airfoil at 0° angle of attack. Figure 7 shows the stagnation point of the front airfoil in tandem configuration at 0° angle of attack, whereas the angle of attack of the aft airfoil is 10°.

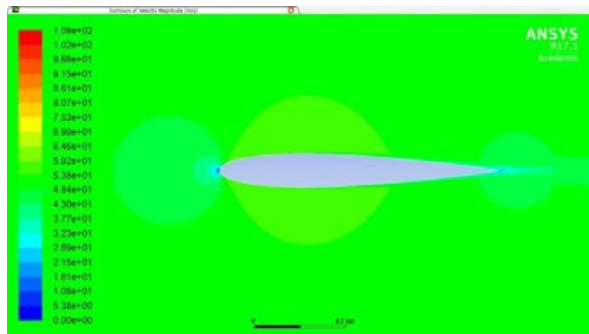


Fig 6. Stagnation point of a single airfoil at 0° angle of attack

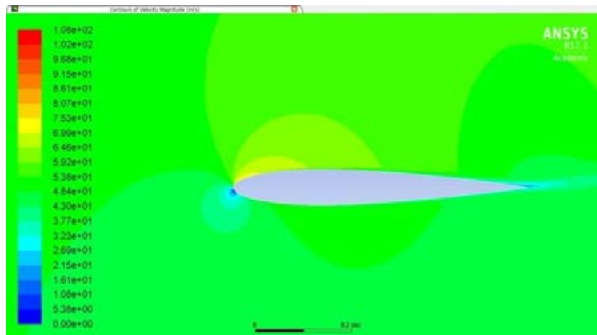


Fig 7. Stagnation point of front airfoil in tandem configuration at 0° angle of attack

Figure 6 shows that the stagnation point is right at the leading edge of the airfoil. This causes the air flowing over the upper and lower surface of the airfoil to be at the same speed. Consequently, no lift is generated due to the absence of pressure difference between the upper and lower surface of the airfoil.

In Figure 7, the stagnation point shifts below the leading edge of the airfoil. This causes the air particle about to flow through the upper surface of the airfoil to turn following the curvature of the leading edge before reaching the upper surface of the airfoil. Consequently, constriction occurs on the streamline around the leading edge and the front portion of the upper surface of the airfoil. Based on continuity equation, a constriction in streamline is followed by an increase in the velocity of the air. In reference to Bernoulli's principle, this increase in velocity causes the pressure on the upper surface of the airfoil to be lesser than the pressure on the lower surface of the airfoil. Therefore, lift is generated.

In conclusion, tandem wing configuration gives advantages of an increase in total lift and a decrease in total drag due to the shift of the stagnation point on the front airfoil if the angle of attack of the aft airfoil is greater than the angle of attack of the front airfoil.

Analysis on the Effect of Stagger on Aerodynamic Forces

Numerical results of three staggers show that the advantages that tandem wing configuration offer decrease as the stagger increases. Table 7, Table 8, and Table 9 show that tandem wing configuration with the front airfoil angle of

attack smaller than the angle of attack of the aft airfoil tends to generate a total lift greater than the sum of the lift of two single airfoils at an identical angle of attack, whereas the total drag tends to be lesser than the sum of the drag of two single airfoils at an identical angle of attack. But, these advantages of increased lift and decreased drag diminish as the stagger increases. This results from the greater distance between the front and aft airfoil, reducing the influence of the aft airfoil on the shift of the stagnation point of the front airfoil. This is demonstrated in Figure 8, Figure 9, and Figure 10.

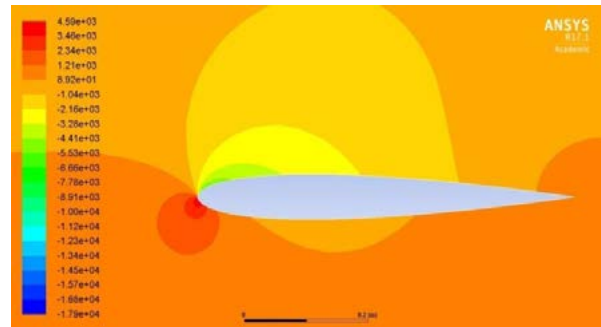


Fig 8. Stagnation point of the front airfoil at stagger 1.5-c

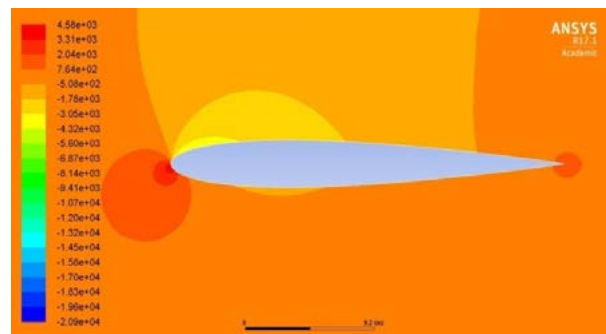


Fig 9. Stagnation point of the front airfoil at stagger 2-c

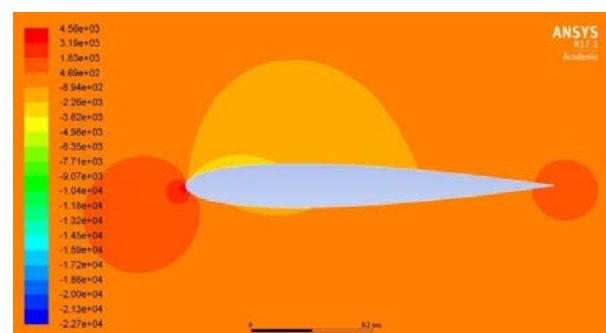


Fig 10. Stagnation point of the front airfoil at stagger 3-c

In Fig. 8, the stagnation point is not located on the leading edge, but more below the leading edge of the airfoil. Therefore, the air flows faster through the upper surface than through the lower surface, resulting in pressure difference between the lower surface of the airfoil and the upper surface of the airfoil. This generates lift. It can be seen in Fig. 8 that the front part of the upper surface of the airfoil is covered in green color, indicating a negative gauge pressure in that



region. This shift of stagnation point also causes the drag component of the aerodynamic forces to be smaller, causing the drag generated to decrease compared to the drag generated by a single airfoil at an identical angle of attack.

In Fig. 9, the stagnation point shifts closer to the leading edge. As a result, the velocity of air flowing over the upper surface of the airfoil decreases. Therefore, the pressure on the upper surface of the airfoil becomes greater. In Fig. 8, the front part of the upper surface of the airfoil is covered by green color, but in Fig. 9, the exact part is covered by dark yellow color. This dark yellow color indicates a negative gauge pressure, even though the pressure is greater than the pressure on the same area at stagger 1.5-c. The shift of the stagnation point closer to the leading edge also causes the drag component of the aerodynamic forces to be greater, resulting in an increased drag compared to the drag generated by the airfoil at stagger 1.5-c.

In Fig. 10, the stagnation point shifts even closer to the leading edge. The air flowing over the upper part of the airfoil experience a further decrease in velocity, causing the gauge pressure on the front upper part of the airfoil to increase. This is demonstrated by the change of color covering the front upper surface of the airfoil from dark yellow in Fig. 9 to soft yellow. The lift generated decreases compared to the lift generated at stagger 2-c. This shift of stagnation point closer to the leading edge causes the drag component of the aerodynamic forces to increase, resulting in an increased drag compared to the drag generated at stagger 2-c.

In conclusion, an increase in stagger in tandem wing configuration diminishes the advantages offered by the configuration, i.e. an increase in lift and a decrease in drag, especially on the front airfoil. The cause of this is the stagnation point shifting closer to the leading edge, reducing the total lift and increasing the total drag as the stagger increases.

Analysis on the Effect of Reynolds Number on Aerodynamic Forces

Besides running numerical simulations in turbulent flow, it is also necessary to run simulations in laminar flow to gain further information as to whether the characteristics observed in turbulent flow are also demonstrated in laminar flow. Before numerical simulations of tandem wing in laminar flow can be conducted, it is necessary to run simulations of single airfoil in laminar flow so as to have a reference. The data collected will be used as comparisons to understand the effects of tandem wing configuration in laminar flow.

Numerical simulations are conducted at angle of attack 0° to 10° in $Re = 2 \times 10^3$ using laminar viscous model under the parameters mentioned below:

Air density (ρ)	3.633 kg/m ³
Specific heat (C_p)	1,004.9 J/kg K
Dynamic viscosity (μ)	1.846 x 10 ⁻⁵ kg/m s
Air velocity	0.0167 m/s

The results are displayed in Table 10.

Table 10. Numerical simulations result of single airfoil in laminar flow

Angle of Attack (°)	C _L	C _D
0	0.0004	0.0846
5	0.2152	0.092
10	0.3061	0.1234

After the data of the numerical simulations conducted on single airfoil are gathered, numerical simulations of tandem wing in laminar flow can be run. The simulations are conducted at stagger 1.5- and 2-c for several combinations of angle of attack from 0° to 10°. The results of these numerical simulations are displayed in Table 4.8 and Table 4.9.

Table 11. Numerical results of tandem wing at stagger 1.5-c in laminar flow

Angle of Attack FA (°)	Angle of Attack AA (°)	CL _{FA}	CL _{AA}	CD _{FA}	CD _{AA}
0	0	-0.0003	-0.0003	0.0764	0.0432
0	5	0.0131	0.1131	0.0756	0.0536
0	10	0.0249	0.2517	0.0734	0.0843
5	0	0.1484	0.0093	0.0830	0.0404
5	5	0.1529	0.1081	0.0829	0.0404
5	10	0.1469	0.2268	0.0812	0.0647
10	0	0.3161	0.0032	0.1245	0.0262
10	5	0.3450	0.1208	0.1292	0.0225

Table 12. Numerical results of tandem wing at stagger 2-c in laminar flow

Angle of Attack FA (°)	Angle of Attack AA (°)	CL _{FA}	CL _{AA}	CD _{FA}	CD _{AA}
0	0	-0.0003	-0.0005	0.0801	0.0494
0	5	0.0123	0.1084	0.0796	0.0589
0	10	0.0278	0.2547	0.0784	0.0917
5	0	0.1728	0.0254	0.0859	0.0485
5	5	0.1750	0.1136	0.0856	0.0489
5	10	0.1679	0.2252	0.0839	0.0732
10	0	0.3108	0.0160	0.1242	0.0577
10	5	0.3201	0.1102	0.1242	0.0564

Case Analyses

The percentages displayed in these case analyses are calculated in reference to the numerical results of single airfoil in laminar flow displayed in Table 10.



Case I: FA = 0° and 0° ≤ AA ≤ 10°; 5° interval

Lift produced by the front airfoil in tandem wing configuration with 0° front airfoil angle of attack increases as the angle of attack of the aft airfoil increases. The greatest increase in lift occurs in combination FA-AA 0°-10° at stagger 2-c. Besides the increasing lift, the drag produced by the front airfoil decreases as the angle of attack of the aft airfoil increases. The greatest decrease in drag of 15% occurs in combination FA-AA 0°-10° at stagger 1.5-c.

Case II: FA = 5° and 0° ≤ AA ≤ 10°; 5° interval

Lift produced by the front airfoil in tandem wing configuration with 5° front airfoil angle of attack increases when the angle of attack of the aft airfoil increases from 0° to 5°, but decreases when the angle of attack of the aft airfoil increases from 5° to 10°. The drag generated by the front airfoil decreases as the angle of attack of the aft airfoil increases. The greatest decrease in lift and drag occurs in combination FA-AA 5°-10° at stagger 1.5-c. In this combination the lift decreases 30% and the drag decreases 10%.

Case III: AA = 0° and 0° ≤ FA ≤ 10°; 5° interval

Lift produced by the aft airfoil in tandem wing configuration at 0° aft airfoil angle of attack increases when the angle of attack of the front airfoil increases from 0° to 5°, but decreases when then angle of attack of the front airfoil increases from 5° to 10°. Lift produced by aft airfoil reach a maximum in combination FA-AA 5°-0° at stagger 2-c. The drag generated by aft airfoil at stagger 1.5-c decreases as the angle of attack of the front airfoil increases. At stagger 2-c, the drag generated by the aft airfoil decreases when the angle of attack of the front airfoil increases from 0° to 5°, but increases when the angle of attack of the front airfoil increases from 5° to 10°. Greatest drag decrease of 70% is experienced in combination FA-AA 10°-0° at stagger 1.5-c.

Case IV: AA = 5° and 0° ≤ FA ≤ 10°; 5° interval

Lift generated by the aft airfoil in tandem wing configuration at 5° aft airfoil angle of attack decreases when the angle of attack of the front airfoil increases from 0° to 5°, but increases when the angle of attack of the front airfoil increases from 5° to 10° at stagger 1.5-c. At stagger 2-c, lift generated by the aft airfoil increases when the angle of attack of the front airfoil increases from 0° to 5°, but decreases when the angle of attack of the front airfoil increases from 5° to 10°. Drag reaches a minimum in combination FA-AA 10°-5° at stagger 1.5-c. In this combination, a decrease of 75% in drag is observed.

To fully understand the effects of tandem wing configuration in laminar flow, the total aerodynamic forces generated in tandem wing configuration is compared with the

sum of aerodynamic forces of two single airfoils at an identical angle of attack. The comparisons are displayed at Table 13 and Table 14.

Table 13. Comparison of numerical result and literature of tandem wing configuration at stagger 1.5-c in laminar flow

Angle of Attack FA (°)	Angle of Attack AA (°)	Numerical Result		Literature (Sum of 2 Single Airfoils)		Difference in C _L (%)	Difference in C _D (%)
		C _L total	C _D total	C _L total	C _D total		
0	0	0.0006	0.1196	0.0009	0.1692		-29.32
0	5	0.1262	0.1292	0.2157	0.1767	-41.50	-26.88
0	10	0.2766	0.1577	0.3066	0.2081	-9.78	-24.18
5	0	0.1577	0.1235	0.2157	0.1767	-26.89	-30.11
5	5	0.2610	0.1233	0.4305	0.1841	-39.38	-33.06
5	10	0.3737	0.1459	0.5214	0.2155	-28.32	-32.31
10	0	0.3194	0.1507	0.3066	0.2081	4.17	-27.57
10	5	0.4658	0.1517	0.5214	0.2155	-10.66	-29.62
: percentage is not displayed (denominator close to 0)							

Table 14. Comparison of numerical result and literature of tandem wing configuration at stagger 2-c in laminar flow

Angle of Attack FA (°)	Angle of Attack AA (°)	Numerical Result		Literature (Sum of 2 Single Airfoils)		Difference in C _L (%)	Difference in C _D (%)
		C _L total	C _D total	C _L total	C _D total		
0	0	0.0008	0.1295	0.0009	0.1692		-23.46
0	5	0.1207	0.1384	0.2157	0.1767	-44.06	-21.66
0	10	0.2825	0.1701	0.3066	0.2081	-7.86	-18.26
5	0	0.1982	0.1344	0.2157	0.1767	-8.13	-23.91
5	5	0.2886	0.1345	0.4305	0.1841	-32.96	-26.96
5	10	0.3931	0.1571	0.5214	0.2155	-24.61	-27.12
10	0	0.3267	0.1819	0.3066	0.2081	6.57	-12.59
10	5	0.4303	0.1806	0.5214	0.2155	-17.48	-16.19
: percentage is not displayed (denominator close to 0)							

Comparison Analyses

The percentages displayed in these comparison analyses are calculated in reference to the sum of two single airfoils.

Case I: FA = 0° and 0° ≤ AA ≤ 10°; 5° interval

In tandem wing configuration with the front airfoil angle of attack at 0°, total lift decreases, but total drag also decreases as the angle of attack of the aft airfoil increases. The combination with the greatest advantages in this case is the combination FA-AA 0°-10° at stagger 1.5-c because even though the total lift generated decreases 9%, the total drag generated decreases



24%. The decrease in drag is almost 3x the decrease in lift. Therefore, this combination still gives off a positive effect.

Case II: FA = 5 and $0^\circ \leq AA \leq 10^\circ$; 5° interval

In tandem wing configuration with the front airfoil angle of attack at 5° , the total lift and the total drag decrease, but the decrease is about the same percentage. In the combination FA-AA 5° - 0° and 5° - 10° , the decrease in total drag are greater than the decrease in total lift. In combination FA-AA 5° - 5° the decrease in total lift is greater than the decrease in total drag. In this case, the most advantageous combination is the combination FA-AA 5° - 0° at stagger 2-c because the decrease in drag is almost 3x the decrease in lift.

Case III: AA = 0° and $0^\circ \leq FA \leq 10^\circ$; 5° interval

In tandem wing configuration with the aft airfoil angle of attack at 0° , the most advantageous combination is the combination FA-AA 10° - 0° at stagger 1.5-c. In this combination the increase in lift is 4% and the decrease in drag is 27%. This same advantages are also observed at stagger 2-c, the combination FA-AA 10° - 0° causes an increase in lift of 6% and a decrease in drag of 12%. In combination FA-AA 5° - 0° there is a decrease in lift, but the drag also decreases. The decrease in drag in this combination is still greater than the decrease in lift. Therefore this combination is still advantageous.

Case IV: AA = 5° and $0^\circ \leq FA \leq 10^\circ$; 5° interval

In tandem wing configuration with the aft airfoil angle of attack at 5° , the most advantageous combination FA-AA is the combination of 10° - 5° at stagger 1.5-c. In this combination, the decrease in drag is 3x the decrease in lift. In this case, there is an indication that tandem wing configuration in laminar flow has a certain optimum angle of attack and stagger because at the combination FA-AA of 0° - 5° and 10° - 5° , the lift decrease at stagger 1.5-c is greater than the decrease at stagger 2-c. This shows that an increase in stagger does not guarantee the reduction of tandem wing effects in laminar flow.

It can be inferred from the case analyses that the changes in lift do not have a certain pattern. Tandem wing configuration in laminar flow gives different advantages at each combination of angle of attack and at each stagger. This can be seen in Case II and Case IV. In Case II, the FA-AA combination of 5° - 0° is more advantageous at stagger 2-c than at stagger 1.5-c. In Case IV, the combination FA-AA 10° - 5° is more advantageous at stagger 1.5-c than at stagger 2-c. Therefore, it can be concluded that tandem wing configuration in laminar flow has optimum combinations of angle of attack and stagger to give off advantages. This is a result of flow separation and reattachment phenomenon.

Flow separation is the detachment of flow from the surface of the airfoil. This detachment is caused by the decreasing air velocity near the trailing edge (adverse pressure gradient). This detached flow can reattach to the surface of the airfoil, depending on the conditions of the flow. Flow separation and reattachment in laminar flow in this research is displayed in Fig. 11.

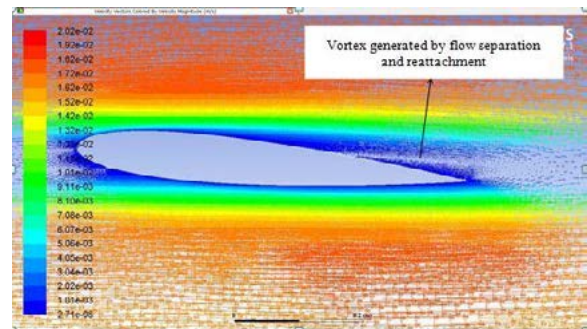


Fig 11. Flow separation and reattachment

REFERENCES

- [1] Anderson, J.D., 2011. Fundamentals of Aerodynamics. 5th ed. Singapore: McGraw-Hill Higher Education
- [2] Anderson Jr., J. D., 2012. Introduction to Flight. 7th ed. Singapore: McGraw-Hill.
- [3] Bertin, J.J, Cummings, R.M., 2014. Aerodynamics for Engineers. 6th ed. USA: Pearson Education International.
- [4] Boeing. 2017. Historical Snapshot. [Online]. Available at: <http://www.boeing.com/history/products/707.page>. [Accessed 18th January 2017].
- [5] Deck, S., Duveau, P., d'Espiney, P. and Guillen, P. (2002) Development and Application of Spalart-Allmaras One Equation Turbulence Model to Three-Dimensional Supersonic Complex Configurations, Aerospace Science and Technology, 6, pp. 171–183.
- [6] Eleni, D.C., Athanasios, T.I. and Dionissios, M.P. (2012) Evaluation of the turbulence models for the simulation of the flow over a National Advisory Committee for Aeronautics (NACA) 0012 airfoil, Journal of Mechanical Engineering Research, 4(3), pp. 100–111.
- [7] Frank M. White, 2003. Fluid Mechanics. 5th Edition. McGraw Hill Higher Education.
- [8] Hepperle, M. (2003). Laminar Separation Bubbles. [Online]. Available at: <http://www.mh-aerotoools.de/airfoils/bubbles.htm> [Accessed 18th January 2017].
- [9] Ladson, C. L., 1988. Effects of Independent Variation of Mach and Reynolds Numbers on the Low-Speed Aerodynamic Characteristics of the NACA 0012 Airfoil Section. United States of America: NASA.
- [10] Minardo, A, 2013. The Tandem Wing: Theory, Experiments, and Practical Realisations. Italy: Politecnico di Milano.
- [11] Nancy Hall. 2015. Airplane Cruise. [Online]. Available at: <https://www.grc.nasa.gov/www/k-12/airplane/cruise.html>. [Accessed 18th January 2017].
- [12] Nancy Hall. 2015. Lift to Drag Ratio. [Online]. Available at: <https://www.grc.nasa.gov/www/k-12/airplane/ldrat.html>. [Accessed 18th January 2017].
- [13] Photobucket. 2016. flyK1W1's Bucket. [Online]. Available at: <http://s2.photobucket.com/user/flyK1W1/media/GP09.jpg.html>. [Accessed 18th January 2017].
- [14] Ray Whitford. 2004. Chapter 3: Aerodynamics and Airfoils. [Online]. Available at: <http://www.globalspec.com/reference/30044/203279/chapter-3-aerodynamics-and-airfoils>. [Accessed 18th January 2017].
- [15] Rutan Long EZ. 2012. Rutan Aircraft Factory. [Online]. Available at: <http://rutan.co.uk/burt>. [Accessed 18th January 2017].
- [16] Smithsonian National Air and Space Museum. 2017. Pan Am Boeing 707 and 747 Jets. [Online]. Available at: <https://airandspace.si.edu/multimedia-gallery/7254hjpp>. [Accessed 18th January 2017].



THE 15TH INTERNATIONAL CONFERENCE QUALITY IN RESEARCH (QIR) 2017

STUDY OF TURBULENCE MODELLING ON PICO-HYDRO TURBINE

D. Adanta*, Budiarmo, Warjito, A.I. Siswantara

*Department of Mechanical Engineering, Faculty of Engineering, Universitas Indonesia,
Kampus Baru, Depok 16242*

Abstract

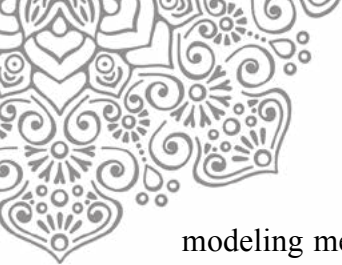
This study has a purpose to find the right turbulent model to be applied in pico-hydro simulation. Method used is literature study, the first step is to characterize the flow in open channels and pipes which is turbulent using the Reynolds number. The next step is to verify whether the flow is turbulent which is done by finding out whether the flow is uniform or non-uniform. Result shows that for open channel flow and pipes having 40 l/s flow rate, the flow is turbulent. Through visual inspection it can be concluded that the flow is non uniform. From characterization of flow, it can also be concluded the flow is turbulent and thus it needs to be simulated in the form of a turbine simulation. Using the right turbulent model is necessary and this is done by comparing CFD results with experiment that has been done by several researchers. The aspect that is compared is the power. The difference between the simulation and the experiment is taken as errors. The result showed that out of the 4 turbulent models namely k- ϵ , RSM k- ϵ , SST k- ω and RNG k- ϵ . RSM k- ϵ shown the minimal errors but this model requires a lot of computational power and time because it has the transport equation that needs to be solved in which one of it is the convection equation. The model that is deemed to be an all-rounder is the SST k- ω , the difference in simulation and experiment can be categorized as the same as the error is only between 1 to 4 %. The time and power saved by using this model is due to the fact that it has only 4 equations that is specific dissipation rate, kinetic eddy viscosity, turbulence kinetic energy and closure coefficients and auxiliary relations.

Key words: CFD; Pico hydro; SST k- ω ; Simulation; Turbulence modelling.

1. INTRODUCTION

Pico hydro system produces electrical energy which is less than 5 Kilo Watt (Porter 2006). Several studies have shown that pico-hydro systems are best adapted for remote areas that have water potential (Ho-Yan 2012; Adhikari et al. 2014; Chica et al. 2013; Shantika & Ridwan n.d.; Williams & Simpson 2009). Since the function of pico-hydro systems are mainly for rural electrification, it would be beneficial if the cost of building such systems can be reduced. One key area is in the manufacturing process, reducing the cost can be done by a good and accurate design. To increase the accuracy in design, a good analysis using CFD should be performed.

In computation, the degree of success depends hugely on the user and thus, the type of modeling used by the user (Versteeg & Malalasekera 2007). [8]. In determining the correct



modeling method that will be used, a knowledge of the flow should be kept in mind. The flow is assumed by the user (Aeschlimann et al. 2013).

This study can be used as a reference in choosing the modeling type that is suitable for the propeller type turbine in pico-hydro system. To minimize the error, a turbulent modeling is used with actual conditions (Darmawan 2015). This is due to the fact that there are several ways to approach it numerically these are: DNS (Direct Numerical Simulation), LES (Large-Eddy Simulation) and RANS (Reynolds Stress Navier-Stoke).

Every approach that is done numerically has its own advantages and disadvantages. RANS model doesn't need much computational power as it scales down the turbulence (Revell n.d.). However the DNS model even though having high accuracy but it is rarely used as it uses Navier-stroke without any modelling so it uses high computational power. LES is also a numerical approach that requires a lot of computing power as it scales down the model where there is dissipation. (Revell n.d.).

Keeping in mind the computational power, time and tools that are available in CFD software the RANS model is deemed to be the right one for the pico-hydro turbine.

2. METHODOLOGY RESEARCH

There are three methods used in this research, namely: Asymptotic Invariance, Local Invariance Analysis and literature study. Asymptotic Invariance will be used as it is the method that characterizes the flow from the Reynolds number (Tennekes & Lumley 1972). The local invariance analysis method is also used as it characterizes the flow from the time and distance perspective. Local invariance is used more often and more reliable because it characterizes the flow by visualizing the flow directly numerically or in real time (Tennekes & Lumley 1972).

The next step is the literature study, literature study was used to assess the turbulent models deemed suitable to be applied to the pico hydro turbine. The literature study discusses about performing CFD and compare it with experiment. Differences are taken as errors and the model with the least error and the one that does not over predict the results will be used for the pico-hydro application

3. RESULTS AND DISCUSSION

3.1. Characterization fluid flow in pipe and open channel

Generally pico-hydro turbine has to piping systems that are the pipe and open channel flow. To find out the turbulent level on each, we need to find out the characteristic of the flow first. Pico-hydro turbine has a max output of 5 kW. For that power range and with a head of 2.7 meters the flow rate are estimated to have a value of: 40 liter/s, 80 liter/s, 120 liter/s, 160 liter/s and 200 liter/s. If the flow rate is related to the Reynolds number then the range is Reynolds 50,000-250,000.

As explained before the Reynolds number determines whether flow is laminar or turbulent. From the analysis it can be concluded that the turbulent model is an important factor. In the open channel flow at the laboratory of fluid mechanics it can be seen that the flow is steady



and non-uniform. The flow is steady because at the wall there is no change with respect to time. Non uniform flow occurred because there is a change in properties from time to time as the bottom layer of the flow is too slow due to the shape at the end which is like a snail, so there is a decrease in area which leads to the turbine's draft tube. Uniform flow can be seen in Figure 1:



Figure 1 Non-uniform flow (Shawl n.d.)

Simulation result using DNS (Direct Numerical Solution) in an open channel flow shows the contour which is not uniform, the assumption for now is due to the reason that the turbulent flow is dependent on the roughness of the wall (Jin LEE n.d.). From simulation at the center ($\delta/y = 0.5$) there is a drop in viscosity due to the surface of the wall. This also reduces the speed at the wall as compared to the speed at the center.

The same explanation is also given by Townsend, that the roughness of the surface will affect the resulting boundary layer (Townsend 1976). Theory that is presented that the roughness can cause instability at the boundary layer of flow indicates the formation of disturbances at the flow, the phenomenon is called the turbulent flow. (Townsend 1976). The explanation is the representation of the viscosity and friction velocity equation 1 that is:

$$z_0 = z_r F_r \left(\frac{\tau_0^{1/2} z_r}{\nu} \right) \quad (1)$$

Where z_0 length of rough surface, $\tau_0^{1/2}$ is friction velocity or slip velocity between the wall and a standard location in the constant-stress layer.

3.2. Analysis dissipation rate (K) and energy kinetic turbulence (E) in open channel and pipe

In the turbulent flow known as mix length (l_m), mix length (l_m) is a random displacement of fluid particles through a certain distance (Munson et al. 2005). From the mix length (l_m) can be determined turbulence shear flow (τ_{turb}). Aspect of the appropriate election turbulence modelling relies too heavily accurate knowledge of τ_{turb} (Munson et al. 2005). The equation τ_{turb} can use equation 2:

$$\tau_{turb} = \rho l_m^2 \left(\frac{d\bar{u}}{dy} \right)^2 \quad (2)$$



To simplify the analysis, the result of the analysis assumed an average velocity of the flow in open channel is 0.15 m/s, so that from the equation 2 τ_{turb} value is 0.000055 Newton.

In determining energy kinetic turbulence (ϵ), variables that must be known is the coefficient drag (C_d) and dissipation rate (K) (Saad 2011). The equation ϵ can be seen equation 3:

$$\epsilon = C_d \frac{K^{3/2}}{l_m} \quad (3)$$

To determine the C_d must first find out the value of lost momentum due to turbulence flow is usually defined by D (Tennekes & Lumley 1972). Assumed the value of D in relation to the velocity rate (U), turbulent rotational speed (u) and the turbulent boundary layer thickness (δ) are considered the same (Tennekes & Lumley 1972). The analysis result Tennekes, compared δ/X with u/U is comparable (Tennekes & Lumley 1972), so the analysis the amount of u can be assumed is 0.000234 m/s.

Dissipation rate (K) is determined from the velocity of the three-axis vector (x y z). Vector velocity on three axes (x y z), the software Ansys or CFX, RANS models used isotropic assumption that the value of velocity the three axes being the same, so the equation K becomes:

$$K = \frac{3}{2} (\bar{u}'^2) \quad (4)$$

From the analysis of the energy loss due to the turbulence flow in channel is 0.000019 m²/s³. It is proved theoretically in pico hydro turbine turbulence flow occurs. The theoretical result are considered turbulent kinetic energy (ϵ) is small, RANS models are considered to represent real condition.

The next step is to compare analysis and experiment results. This is done to find the best turbulent model that us viewed to be the best for pico-hydro turbine based on the flow characteristics of the turbine itself.

3.3. Turbulence modelling in pico-hydro turbines

To get the turbulent model that is right, this study tries to compare previous researches where the focus is done on CFD analysis and experimental results comparison. The focus is only on the ANSYS software as it is the commonly used software where the simulation is accurate as compared to other software tools especially for water turbines (Židonis et al. 2015). This issue comes into consideration to correct the error value from simulation, after that the error value will be compared to the other error value. The table shows the researches, there at least 4 researches done these are:

Table 1 Turbulent models for pico-hydro turbine

Year	Author	Type Turbine	Turbulence Model
2009	Simpson and Williams	Propeller	k- ϵ
2012	Ramos, et.al	Propeller	k- ϵ



2009	Prasad et.al	Propeller	RSM k- ϵ
2013	Helena M. et.al	Propeller	SST k- ω
2016	Gupta. et.al	Pelton	SST k- ω
2007	Perrig	Pelton	SST k- ω
2002	Kaniecki	Banki	RNG k- ϵ

From Table 1 there are (4) turbulent models that are commonly used these are k- ϵ , RSM (Reynolds Stress Model) k- ϵ , SST (Sheer Stress Transport) k- ω and RNG (Re-Normalization Group) k- ϵ . Every modelling has its own advantages and disadvantages. It is compiled in table 2 which is already explained by Darmawan (Darmawan 2015):

Table 2 Advantages and Disadvantages of turbulent modeling (Darmawan 2015)

Model	Advantages	Disadvantages
k- ϵ	<ul style="list-style-type: none"> ▪ Simple ▪ Good for general simulation ▪ Most commonly used ▪ Computational power required is not too big 	<ul style="list-style-type: none"> ▪ Not suitable for closed flows with rotation ▪ Over estimation of the dissipation level
RSM k- ϵ	<ul style="list-style-type: none"> ▪ Good accuracy for simple and complex flow ▪ Very good for flow with minute pressure gradient, opposing pressure boundaries, jet flows and flow with no shear. ▪ Better than RNG k-ϵ for backward-facing step 	<ul style="list-style-type: none"> ▪ High computational power required ▪ Not as sophisticated as STD k-ϵ ▪ For open flow the result is similar to STD k-ϵ
SST k- ω	<ul style="list-style-type: none"> ▪ Suitable for high Reynold number ▪ Mesh number is related to the accuracy of the result ▪ Can be used for forced fluids with free shear forces. ▪ Can be used for transitional flow 	<ul style="list-style-type: none"> ▪ Meant for 2 phase simulation ▪ Over prediction for separated flows ▪ High computational power required.
RNG k- ϵ	<ul style="list-style-type: none"> ▪ General computing power ▪ Good for flow with more flexibility, expansion in area and back ward facing step flow. ▪ Calculation for small scale turbulence is better than k-ϵ 	<ul style="list-style-type: none"> ▪ Result not as good as k-ϵ where there is a reduction in area

3.3.1. k- ϵ model

Simpson and Williams (2006) performed CFD which is then compared with experimental results using k- ϵ model [15]. Research is done with flow rate of 180-220 l/s and head 4 meter and speed of 100-1650 rpm. The result from Simpson and Williamson can be seen in Figure 3.

From the data obtained by Simpson and Williams (2006) it can be seen that the efficiency of the turbine is over-predicted by 10% at the best point (Simpson & Williams 2006), Figure 2 shows that there is not much difference in the simulation and experimental result.

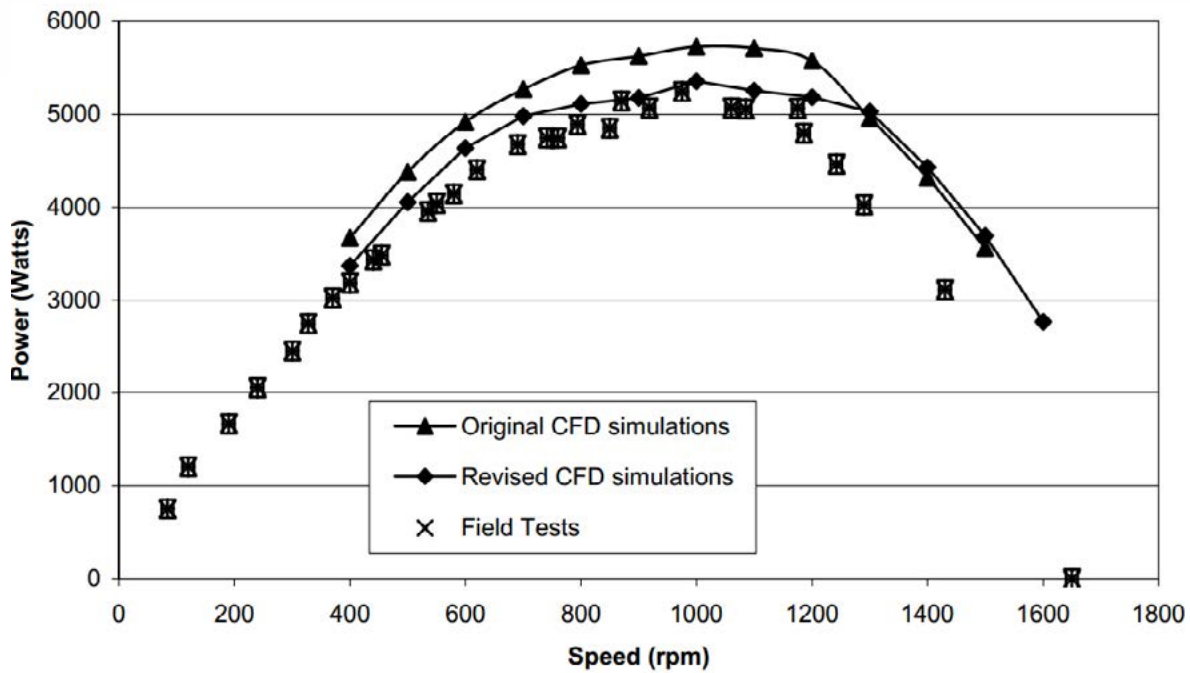
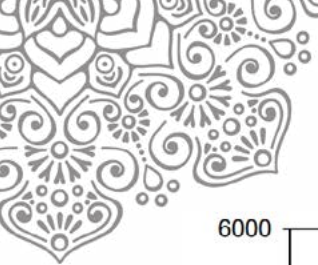


Figure 2 comparison of power output (Simpson & Williams 2006)

Ramos, et.al (2012) did a CFD analysis which is then validated with experiment using the same model as Simpson and William that is turbulent k-ε (H M Ramos et al. 2012). The parameter that is used for the 4 blade turbine simulation with 4 l/s flow rate and specific speed (Ns), 91 rpm. (m.m³/s), for 5 blades the flow rate is 3,4 l/s and specific speed (Ns), 80 91 rpm. (m.m³/s), the turbine speed is set at 300 rpm. The results are presented at table 3:

Table 3 Comparison of CFD and experimental results (H M Ramos et al. 2012)

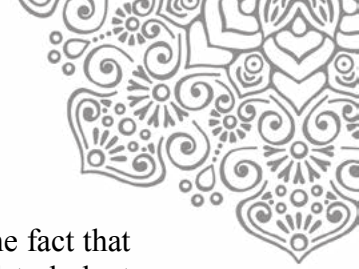
Turbine	D	H	Q	N	η	P	Range of application		
	mm	m	l/s	rpm	%	W	Q (l/s)	H (m)	N (rpm)
Propeller with 5 blades	1001	0,13	3,4	300	98	4	2,5-5	0,08-0,3	200-300
Propeller with 4 blades	1002	0,13	4,9	200	35	2	2,5-5	0,04-0,17	70-200
Propeller with 5 blades	1001	0,12	4	300	95	4	03-5	0,05-0,25	200-300
Propeller with 4 blades	1002	0,07	3,3	200	70	2	2,3-5,2	0,07-0,25	70-300

¹CFD analysis for lab condition, ²experiment results

Table 3 shows the result obtained from Ramos, et.al. This results show that differences in the results are twice as much. From this research, it can be concluded that the results obtained are not accurate so k-ε is not deemed to be the best.

3.3.2. RSM k-ε model

Helena M. et.al performed a study in 2013 using RSM k-ε. In the research the mac flow rate is 5.2 l/s, impeller diameter used is 100 mm and 200 mm and rotation ranges from 100-1650 rpm.



RSM k- ϵ modelling is used because the reliability of the model and also due to the fact that 2 equations are used where all the calculations are focused on convection and turbulent diffusion (Helena M Ramos et al. 2012). The conditions are $\rho = 998.2 \text{ kg/m}^3$ and $\mu = 1.01 \times 10^{-6} \text{ m}^2/\text{s}$. Comparison of experiment and CFD can be seen at Figure 4

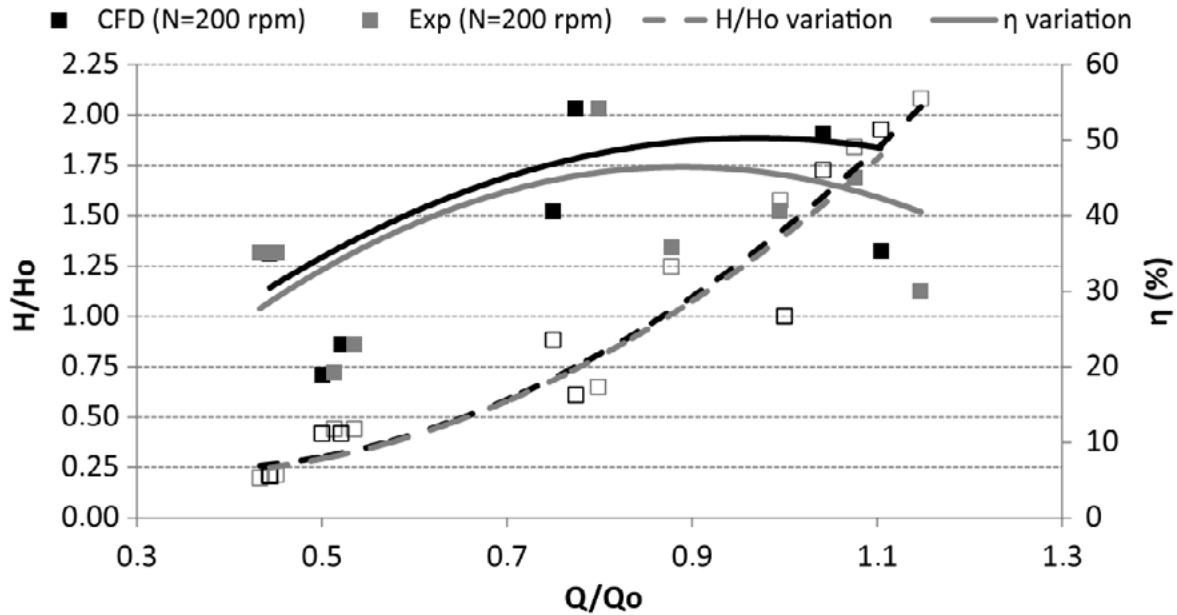


Figure 3 Comparison of CFD and experiment (Helena M Ramos et al. 2012)

From the curve Helena M. et.al claims that the error that from the CFD analysis and experiment is in between $0.00 < e < 0.02$.

3.3.3. SST k- ω model

SST k- ω model was done by Prasad et.al in 2009 (Prasad et al. 2009). The study 12 stay vanes, guide vane and 4 blades. The parameter variations are flow rate and speed. The simulation result will be used to determine non dimensional parameter such as Pressure coefficient, velocity coefficient, flow deflection, degree of reaction, circulation coefficient, lift coefficient, runner energy coefficient, and total energy coefficient.

The simulation and experimental results from Prasad, et.al. can be seen in table 4:

Table 4 comparison of computed and experimental result (Prasad et al. 2009)

Topic	Guide vane angle		
	50 ⁰	40 ⁰	35 ⁰
Numerically computed efficiency (%)	90.19	92.24	89.97
Experimental efficiency (%)	90.86	92.06	91.59

From the research by Prasad, the results obtained from both methods are similar and the differences are assumed to be obtained from the discretization of the governing equation and flow domain, secondly it can be caused by instrument or human error during inspection.



The SST $k-\omega$ that was done by Gupta, et.al. in a Pelton turbine. Gupta, et.al. used this model because the object had curvatures which can present more complex flow for an object like this as the main goal is also to find the flow near the walls (Gupta et al. 2016). The boundary condition are jet velocity that reached 30.7 m/s, relative pressure 0 atmospheric and other pressure is taken as 1 atm. Since the buckets were symmetrical the modeling also used a symmetrical concept.

Gupta, et.al tried two models SST $k-\omega$ and $k-\epsilon$, but from the results he felt that SST $k-\omega$ has shown a better result even though it took 8 hours more to complete the simulation since the equation that needs to be solved in SST $k-\omega$ is 4 (Gupta et al. 2016).

To increase the accuracy of the simulation the mesh number also plays an important role. For that reason Gupta, et.al. did a mesh independency study and from that the number of nodes obtained are 1,415,878 nodes meanwhile the element numbers are 7,098,630 (Gupta et al. 2016). From the study, the error obtained (differences between experiment and simulation) is 3.5%.

Modelling using SST $k-\omega$ were also done by Perrig (2007), Perrig performed testing on Pelton turbine to study the effect of the buckets. From his study the SST $k-\omega$ showed the best results for flow that is near the wall (Perrig 2007). The result of the study shows that there are several effects and forces that work in a bucket which are the Coanda and cavitation effect. The result obtained from multiplying the mesh at the bucket is done so that the result will be similar to the real condition. The result shows that SST $k-\omega$ is recommended for Pelton turbines (Perrig 2007).

3.3.4. RNG $k-\epsilon$ model

RNG $k-\epsilon$ model was studied by Kaniecky (Kaniecki 2002), due to the similar geometry of the crossflow turbine that the study was done using 2 dimensional analysis and the boundary condition used as input is the constant pressure at inlet. (Kaniecki 2002). RNG $k-\epsilon$ model was used because it will diminish the effect of a small scale turbulence by mathematical equations. This method will also save time and power while still giving accurate condition of the simulation. (Kaniecki 2002). The error is at 4%, which is caused by several geometry that is not used as an input in the simulation (Kaniecki 2002).

3.4. Result

The summary of 3.2 sub chapter is shown at the table below to ease the selection of the turbulence model that can be used for pico-hydro turbine.

Table 5 Comparison of simulation and experiment of Pico Hydro

Year	Author	Model Turbulence	Computing Power	Error
2009	Simpson and Williams	$k-\epsilon$	Low	10%
2012	Ramos, et.al	$k-\epsilon$	Low	50%
2009	Prasad et.al	RSM $k-\epsilon$	High	0.2%-2%
2013	Helena M. et.al	SST $k-\omega$	Medium	1%
2016	Gupta. et.al	SST $k-\omega$	Medium	3,5%
2007	Perrig	SST $k-\omega$	Medium	1%



From table above it can be seen that RSM k- ϵ the turbulence model that provided the most accurate result with a less error value but then the number of equations that need to be solved here is 7 and one of it is the convection evaluation. Remembering that pico-hydro turbine the convection is not significant and thus it can be ignored. From that we can say that this model is wastes time and also power for pico-hydro application.

From table 5 the turbulent model that does not take a lot of computing time and power while still keeping the result accurate is the SST k- ω , other than the low error value according to Menter this turbulent model is right if we want to analyze the area near the wall and k- ϵ is used for area that is further away from the wall or after there is a separation in flow (Menter 1992; Menter 1993).

4. CONCLUSION

The flow characteristics in pico-hydro turbine can be categorized as turbulent. Turbulent flow can be seen from Reynolds number that the fluid flow has. The characteristic of flow in open channel and pipes with flow rate of 40 l/s is steady and non-uniform. Steady flow is caused by the geometry of the wall that did not have any change while non-uniform is caused by the properties of the flow changing from one form of flow to another from time to time. From literature study it can be concluded that the RSM k- ϵ turbulence model provided the most accurate result with a less error value that is below 1%. However, after considering the power required and time to perform the simulation, SST k- ω can be a better solution.

5. ACKNOWLEDGEMENT

The authors would like to thanks to KEMENRISTEK DIKTI, which has funded research with no grant is No. SP. DIPA-042.06.1.401516/2016.

6. REFERENCES

- Adhikari, P. et al., 2014. A Study on Developing Pico Propeller Turbine for Low Head Micro Hydropower Plants in Nepal. *Journal of the Institute of Engineering*, 9(1), pp.36–53.
- Aeschlimann, V. et al., 2013. Inter-blade flow analysis of a propeller turbine runner using stereoscopic PIV. *European Journal of Mechanics-B/Fluids*, 42, pp.121–128.
- Chica, E., Agudelo, S. & Sierra, N., 2013. Lost wax casting process of the runner of a propeller turbine for small hydroelectric power plants. *Renewable energy*, 60, pp.739–745.
- Darmawan, S., 2015. *Pengembangan model turbulen RNG k- ϵ untuk aplikasi CFD pada runner cross-flow dalam komponen turbin gas mikro bioenergy proto x-2a*. Depok: Universitas Indonesia.
- Gupta, V., Prasad, V. & Khare, R., 2016. Numerical simulation of six jet Pelton turbine model. *Energy*, 104, pp.24–32.
- Ho-Yan, B., 2012. *Design of a low head pico hydro turbine for rural electrification in Cameroon*.
- Jin LEE, H.J.S., *Visualization of streamwise velocity in turbulent channel flow*, Proceedings



- of 8th International Symposium on Turbulence and Shear Flow Phenomena. Available at: www.youtube.com.
- Kaniecki, M., 2002. Modernization of the outflow system of cross-flow turbines. *Task Quarterly*, 6(4), pp.601–608.
- Menter, F., 1993. Zonal two equation kw turbulence models for aerodynamic flows. In *23rd fluid dynamics, plasmadynamics, and lasers conference*. p. 2906.
- Menter, F.R., 1992. Improved two-equation k-omega turbulence models for aerodynamic flows.
- Munson, B.R., Young, D.F. & Okiishi, T.H., 2005. *Mekanika Fluida Jilid 2*. Jakarta: Erlangga.
- Perrig, A., 2007. Hydrodynamics of the free surface flow in Pelton turbine buckets.
- Porter, A.W. & S., 2006. Comparison of Hydropower Options for Developing Countries with Regard to the Environmental, Social and Economic Aspects. In *International Conference on Renewable Energy for Developing Countries*. Washington DC, USA.
- Prasad, V., Gahlot, V.K. & Krishnamachar, P., 2009. CFD approach for design optimization and validation for axial flow hydraulic turbine. *Indian Journal of Engineering and Materials Sciences*, 16(4), p.229.
- Ramos, H.M., Simão, M. & Borga, A., 2012. CFD and experimental study in the optimization of an energy converter for low heads. *Energy Science and Technology*, 4(2), pp.69–84.
- Ramos, H.M., Simão, M. & Borga, A., 2012. Experiments and CFD analyses for a new reaction microhydro propeller with five blades. *Journal of Energy Engineering*, 139(2), pp.109–117.
- Revell, A., *Advanced Aerodynamics Part 2: Turbulence Modelling & Simulation (L2: Viscous flow and turbulence)*.
- Saad, T., 2011. Turbulence modeling for beginners. *University of Tennessee space institute*.
- Shantika, T. & Ridwan, M., *Perancangan Prototipe Picohydro Portable 200 Watt*.
- Shawl, J., *Open Channel Flow Concepts*, U.S. Available at: <https://www.youtube.com/watch?v=8vmTYmt0Y8Q>.
- Simpson, R.G. & Williams, A.A., 2006. Application of computational fluid dynamics to the design of pico propeller turbines. *ICREDC-06, School of Engineering and Applied Sciences, University of the District of Columbia, Washington DC, USA*.
- Tennekes, H. & Lumley, J.L., 1972. *A first course in turbulence*, MIT press.
- Townsend, A.A., 1976. *The structure of turbulent shear flow* Second Edi., Cambridge: Press Syndicate of the University of Cambridge.
- Versteeg, H.K. & Malalasekera, W., 2007. *An introduction to computational fluid dynamics: the finite volume method*, Pearson Education.
- Williams, A.A. & Simpson, R., 2009. Pico hydro—Reducing technical risks for rural electrification. *Renewable Energy*, 34(8), pp.1986–1991.
- Židonis, A., Benzon, D.S. & Aggidis, G.A., 2015. Development of hydro impulse turbines and new opportunities. *Renewable and Sustainable Energy Reviews*, 51, pp.1624–1635.



A REVIEW ON CURRENT STATUS AND POTENTIAL BIOMASS GASIFICATION TECHNOLOGIES IN INDONESIA

Priyambodo Nur Ardi Nugroho ^{1,2}, and Shuichi Torii ¹

¹*Department of Advanced Mechanical System Engineering, Kumamoto University, Kurokami, 2-39-1, Kumamoto 860-8555, Japan.*

²*Politeknik Perkapalan Negeri Surabaya, Jl. Teknik Kimia, Kampus ITS Sukolilo, Surabaya 60111, Indonesia.*

ABSTRACT

Energy security has become an important interest for many countries recently. For developing country like Indonesia, social and economic activities need the constant supply of energy. Establishing new and renewable energy has become the priority in regards to the economy and environmental issue. Biomass is considered as one of the potential sources of energy to prevent energy shortage and achieving energy conservation as well as emission reduction. Biomass gasification is one of the favorable technologies to convert biomass to fuel for power generation. However, challenges remain in the biomass gasification upstream and downstream process for practical applications. The purpose of this review is to list barriers and solutions for biomass gasification technology to encourage policy makers and industries in Indonesia to use biomass more. A review of the present condition of biomass gasification technologies in Indonesia was conducted in order to determine future strategic solutions for promoting biomass as an alternative source of energy.

Keywords: *Biomass gasification; Energy security; Renewable energy.*

1. INTRODUCTION

Energy had become the vital element to develop and maintain the world's economic. Initiated by the industrial revolution in the 18th century, economic growth had rapidly increased, mainly by the use of fossil source fuel like oil, coal and natural gas. Energy supply in the near future will become a serious issue and draw consideration of the world because human activities and economic prosperity is associated with the quantity and the quality of energy usage. Results showed that global energy demand increase rapidly in parallel with human population growth (Asif & Muneer, 2007), (Gonzales, 2007), (Ahmad, et al., 2011).

Only the past few years the world become aware of the consequence of economic growth that needs to be paid. Fossil fuel combustion release gas including carbon dioxide that has pushed the concentration of one of the most important greenhouse gasses into the highest level that never been reached before. Despite the fact that considered as controversial, shreds of evidence of global warming and climate change as a result of higher green house gasses in the atmosphere were shown (Letcher, 2008). Not only environment issues caused by the use of fossil fuel to the world, but also it has another negative effect on the competition of energy source. The exploration of fossil fuel substitute, the requirement to reduce the environment impact and the need to safely and economically dispose of waste produce by the society have stimulated the advancement of an alternative source of energy (Omer, 2008).

As one of the developing countries in the world, energy security is a substantial element for advancing economic growth in Indonesia. Together with the rise of economic particularly in industrial, electricity and transportation sector, demand for energy in quality and quantity aspect continues to accelerate inevitably (Hasan, et al., 2012). Indonesia currently uses fossil

* Corresponding author.

E-mail address : pr1y4mb0d0@gmail.com



source of energy like coal, oil, and gas as its major source of energy, primary energy supply share could be seen in table 1 (Ministry of Energy and Mineral Resources, 2016).

Indonesia is sufficiently supplied with a low and medium quality of coal (IEA, 2016). In 2009 Indonesia was the second world's top coal exporter to Japan, China, and India. However at the current rates of production, we still only have 80 years until coal stock no longer in existence. Oil used to be one of the most dominant sectors in Indonesia, particularly in the 1980s, when Indonesia was listed among the oil exporting countries. Yet started in the 2000s, oil production has been decreasing while consumption has continued to grow. As a result, Indonesia has begun to import a significant amount of oil from other countries. It is expected that oil in Indonesia will last only 23 years (Ministry of Energy and Mineral Resources, 2016). Gas has been developed well in Indonesia due to its promising potential, however with current production, only 52 years before natural gas run out from Indonesia unless there are additional natural gas fields found (Azwar, 2013).

Table 1 Indonesia Primary Energy Supply Share

Primary energy supply	Amount (mboe)		Share (%)	
	2010	2015	2010	2015
Oil	518	545	36	33
Gas	269	279	19	17
Coal	281	364	20	22
Hydro Power	43	35	3	2
Geothermal	15	16	1	1
Biomass	273	309	19	19
Biofuel	28	90	2	6

Because of the accelerated depletion of fossil fuel in Indonesia, alternative source of energy for sustainable economic growth is urgently required (Salim, 2000). In addition to that, following economic recession back in 1998, Indonesia economic growth steadily in 4-6% (ADB, 2016). Energy consumption rate also rise with annual growth rate of 7%, yet it didn't follow by adequate energy supply because the fossil fuel reserves are restricted, the reliance is remarkably high. Industrial and transportation sectors are anticipated to use the source of energy more than any other sectors, including household sector (Abdullah, 2002).

Sustainability issues of the energy are one of the most critical challenges in Indonesia. Indonesia should support and promote the implementation of new and renewable energy in order to improve energy security. By ensuring energy security, Indonesia will be less dependent on other country and create energy self-determination. Indonesia require energy policy and management both in generation and distribution part of energy chain (Ibrahim, et al., 2010). This review provides a study of the Indonesia current status and the potential for future development of biomass gasification technologies as an option for achieving energy autonomy.

2. BIOMASS IN INDONESIA

Biomass is defined as a natural source of energy, as a product of waste and residues from a farm, forest, and municipal area. Biomass is composed of living species like animals and plants, similarly with fossil fuel, but it does not need millions of years to form. Sunlight energy is used by plants through photosynthesis absorbing carbon dioxide and water to grow. Animals eat plants and the energy is transferred. Biomass is considered as renewable energy because biomass could reproduce in a relatively short time compare to fossil fuel. This is one of the most attractive points of biomass as an alternative source of energy. Biomass is



comparable cleaner than coal, and among other renewable carbon resource is able to directly converted into fuel exclusively (Tchapda & Pisupati, 2014). Biomass could be partly responsible for the world's energy demand if controlled continuously.

Plants absorb the carbon dioxide from the atmosphere through photosynthesis process. When burnt, they release the carbon dioxide that previously absorbed from the atmosphere. In this way, the burning of biomass does not add any net addition to the atmosphere level of carbon dioxide. In other words, as a source of energy, biomass is carbon neutral or no addition of carbon dioxide to the atmosphere (Basu, 2013). Biomass is unique because it is the only renewable energy that could form in all three states: solid, liquid and gas. Solid fuels from biomass could be formed as charcoal, torrefied biomass, biocoke, and biochar. While liquid fuels of biomass are ethanol, biodiesel, methanol, vegetable oil, and pyrolysis oil product. And gaseous fuels are including biogas (CH_4 and CO_2), producer gas (CO , H_2 , CH_4 , CO_2 and H_2), syngas (CO and H_2), and also substitute natural gas (CH_4).

Previous researches on biomass as an energy conversion in Indonesia were performed. Based on the fossil record, biomass already used by people in Indonesia and Papua New Guinea from very long time ago (Haberle, et al., 2001). Productivity research on using the typical plant as biomass in the plantation has been conducted (Sukardjo & Yamada, 1992). Bio-methanol potential from forest biomass already done (Suntana, et al., 2009). Investigation of the impact of biomass cogeneration to the environment (Duval, 2001), and energy analysis demand and supply for some of the Asian countries (Koopmans, 2005).

People in Indonesia are very familiar with the use of biomass. Approximately half of the total Indonesia population (about 105 million) mainly depend on traditional biomass for daily cooking, with wood as a primary source (REN21, 2015). This fact, however, has the negative findings that low-income people in rural areas need to collect wood from the forest, or moreover cut the tree down in order to get a source of energy for cooking. In total, annual biomass production in Indonesia was almost 150 million tons, proportional to nearly 500 GJ/year. Most of this was used by rural area and small industry to obtain energy for cooking, heating and electricity (Hasan, et al., 2012).

Biomass in Indonesia mainly derive from rice residues, any leftover of rice harvesting like husk, bran, stalk and straw possess energy about 150 GJ per year (ZREU, 2000). Java, Sumatra, Sulawesi, Kalimantan, Bali and Nusa Tenggara are the most contributing region for this. Stalk and straw usually generated at the field and burnt, or used for feeding animals, or as a raw material for paper industry, while farmer sometimes uncontrollably burnt husk. Rubber woods from Sumatra and Kalimantan own 120 GJ of energy annually, leftover part of rubber wood are being used as firewood in small brick and roof tile industry. Sugar residues, like bagasse, cane tops and cane leaf technically have 78 GJ per year. Sugar factories often used bagasse, while cane leaf and can tops need further investigation. Palm oil residues, such as empty fruit bunches, fibers, and palm shells in total have 67 GJ per year and already used as a common source of fuel. Other biomass sources like logging excess, coconut residues, sawn timber leftover, plywood and veneer production are potentially about 20 GJ per year.

Due to its characteristics, like low bulk density, and high ash content, rice husk is classified as one of the most challenging sources of biomass to gasify. However, despite its technical issues, rice husk gasification for the gas generation to power about 60-200 hp engines was proven successfully started from the 20th century in several countries (Kaupp, 1984). Apart from China, Thailand and India, Indonesia has already developed open core rice husk gasifier, including simple design variation of gasifiers (Salam, 2006). While gasification of rice husk already developed for electrical generation below 500 kW (Widodo & Rahmarestia, 2008).

Rice hull has been used as a source of power generation in Riau Province, and able to produce 18 kW electricity from 25 KAV unit, and sold at US\$ 0.03/kWh (Abdullah, 2002).



However, this still above-targeted purchasing price under the newly enacted Small Distribution Power Generation Program held by the Ministry of Energy and Mineral Resources. Production cost could be decreased with the installation of a higher capacity gasifier, for example up to 100 kVA with cogeneration system. Still, the production cost of the proposed unit remains higher than the basic selling price of electricity from the national grid, it is advisable that the improved import duty and taxation scheme of some important component could be adjusted accordingly by the government.

3. BIOMASS GASIFICATION TECHNOLOGY

Biomass conversion to energy encounter several issues due to its characteristics like bulkiness, low energy density, and inconvenient form of biomass, as a result, rapid transition of biomass is yet to happen. Compared to gas and liquid fuel, biomass is not easy to handled, stored and transported. As a consequence, scientists attempt to convert biomass into liquid or gaseous fuels, that are denser and handled or stored less complicatedly. There are two ways of biomass conversion, first is biochemical with digestion either anaerobic or aerobic through composting, or fermentation. In this conversion, biomass molecules are cracked down into smaller molecules with the assistance of bacteria or enzymes. Biochemical is much slower but does not need much external energy. Figure 1 explain about different options for biomass conversion into fuel gasses or chemicals (Basu, 2013).

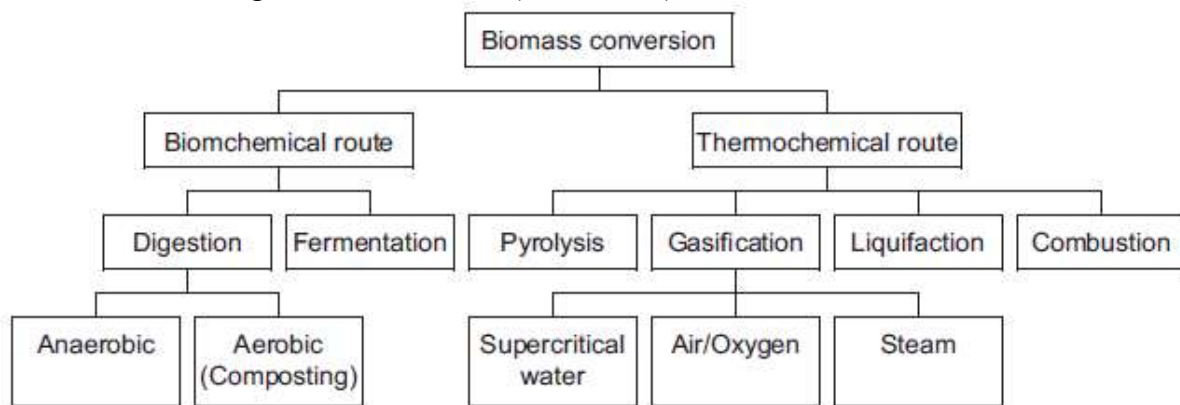
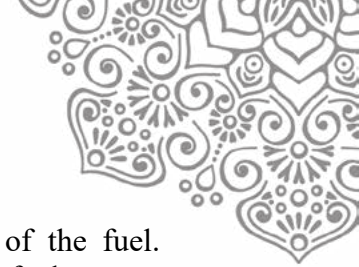


Figure.1 Biomass conversion into fuel gasses or chemical.

Another biomass conversion process is thermochemical through carbonization, torrefaction, pyrolysis, gasification, liquefaction, or combustion. In this process, biomass is converted into gas completely, which will then synthesized to usable chemical or being used as a gas. Combustion requires high-temperature exothermic oxidation in oxygen rich ambiance to hot flue gas. Carbonization including the process in which the carbon content of organic materials is increased through thermochemical decomposition. When biomass is heated to 200-300 °C without or very little contact with oxygen, its is called torrefaction. Different with combustion, gasification associated with chemical reactions in an inadequate level of oxygen environment producing syngas with heating values. While pyrolysis engages with very fast heating in a nonoxygen environment, and liquefaction decompose large molecules of solid into smaller molecules of liquids in an appearance of catalyst and a low temperature (Demirbas, 2009).

Basically, gasification converts fuel from one form to another form. Currently, gasification process is ordinary practice in fossil fuels, compared to nonfossil fuels like biomass for production of syngas. There are several reasons for transforming fuel through gasification like increasing the heating value of the fuel by dismissing noncombustible components like nitrogen and H₂O, removing the fuel gas of sulfur which is not released into



the atmosphere when burnt and increasing the hydrogen content mass ratio of the fuel. Gasification also reducing the oxygen content of the fuel, thus increasing its fuel energy density. Gasification of biomass resulting CO and H₂ gas that support a favorable base for liquid fuel and chemical, another gas product is methane that could be burned straightly for energy or heat production (Basu, 2013).

There were 50 gasifiers installed in Indonesia until 1990 (Knoef, 1991). Out of them, 37 were field units, 10 were commercial units (Manurung, 1995). Power gasifier size ranging from 10 to 120 kW_e, while the heat gasifiers were 600 to 900 kW_{th}. Nearly all of the heat gasifiers were commercial and operational. Interestingly, only one of the power gasifier was completely commercial and operational and the entire number of gasifiers were facing technical issues without exception, especially due to tar contaminant. Technical problems and cheap price of fossil fuels made the development of biomass gasifiers virtually halted, especially for some countries like Philippines and Thailand around the 1990s. other developing countries, particularly China and India continue sustained attempt to develop gasifier designs through research and development to popularize field applications. As a consequence in these countries, biomass gasification technologies is utterly well established recently.

Tar contaminant has been the main technical barrier for large-scale biomass gasification application and accountable for the major setback in the development. In order to reduce or remove tar from the syngas, several attempts have been done thoroughly. The development of wood gasifier system up to 200 kg/hr capacity show that the recycle of the syngas mixture produced in the pyrolysis zone, and combined with the incoming gasification air was the main design of gasifier. the syngas produced was essentially the product of charcoal gasification and possess low tar content (Gaudemard & Becker, 1989) .

Multistage gasification has been implemented at the Technical University of Denmark, (Nikolaisen, et al., 1992). The process separates volatile syngas during pyrolysis from the charcoal. The volatile matter was partially burnt and the product was used for charcoal gasification. Tar contaminant was claimed to be very low and could be used for running of an engine after cooling and removing the particulate matter (Henriksen, 1995). The design of vertical packed bed and partial oxidation pyrolysis reactor. This basic design was introduced and developed by Georgia Institute of Technology, and already successfully tested in several countries like Thailand, Philippines, and Indonesia (Tatom, et al., 1980).

By 2000, about 388 downdraft gasification systems using agricultural waste, like corn stalk, sorghum, cotton, soybean and wood waste, has been developed for domestic cooking in China. Prior to use, the syngas was cleaned in order to remove tar and other particulates, and then stored in a gas chamber, afterward it will be distributed to household though gas pipe networks (Yisheng, et al., 2005). Up to 1000 households could be served from this technology. However, many of these systems already stopped due to some technical problems, mainly tar accumulations, poor management and operational skills, and payment scheme dispute between users and government (Jingjing & DeLaquil., 2006).

Asian countries like China, India, Philippines and Thailand have developed gasifier stove as an alternative to overcome the smoking problem with conventional biomass stoves. Asian Institute of Technology's gasifier stove with the wood chip as fuel generate almost 30% of overall efficiency, with three capacity of 3.2 kg/hr, 5.5 kg/hr and 15 kg/hr. While in the Philippines, Central Philippines University have developed single and multiple burners forced draft rice husk gas stove. Rice husk is gasified and the gas is burned in stove near the gasifier and could perform a luminous blue flame. Even tough the manufacturing cost is one-fourth times higher than ordinary LPG stove, the operational cost is cheaper by about three-fourth (Belonia, 2005).



4. BIOMASS SUPPLY CHAIN

Naturally, biomass in any kind available plentifully almost everywhere, from farm to forest and municipal zone, but it is broadly scattered in a very wide area. Consequently, the supply chain of biomass from collecting in the site, handling, storage, to delivery to the power plant is expensive and will alter the advantages and further development of biomass. Another issue in collecting biomass as part of the supply chain system was caused by the unsteady market of biomass generated by the absence of sophisticated biomass energy conversion technology. Transportation of biomass from the source of origin to the power plant also leads to another problem, since typically biomass contain very high moisture content and very low bulk density (excluding wood). These components will boost the transportation cost, and biomass energy conversion as an entire process (Asadullah, 2014).

Scientists had already build comprehensive method to decrease the supply chain expense by optimization of a collection, handling, storage and delivery process, together with appropriate power plant point. Furthermore, development of transportation network and means of transportation mode as an integral part of the supply chain could guarantee the constant reserve of biomass from origin to the power plant, and as a result, lower the transportation cost.

Biomass densifying could be one of the solutions to overcome the problems in the supply chain. Densification clears the internal space within the biomass and raises the bulk density (Mupondwa, et al., 2012). Figure 2 shows two of the most common densifying techniques, briquetting and pelletizing.



Figure. 2 Briquette and Pellet.

Briquetting and pelletizing are the most frequent technique in densifying the biomass (Eriksson & Prior, 1990). Briquette technology already developed in Indonesia, and it is said that the briquette or sometimes called green charcoal is easily flare up and burn with clean fame. Combined or unmixed agricultural materials available in Indonesia could be used to produce biomass pellets to convert into syngas (H_2) to produce heat energy. The finest unmixed material derived from palm shell, while combined materials pellets composed of sugarcane bagasse and palm shell, with gasification time about 85 min/kg biomass pellets (Alamsyah, et al., 2015).

Moisture content in biomass play a critical part in biomass gasification, since more water will reduce the thermal efficiency of the gasification system. Performance of the thermal power increase with the decrease of the moisture content. Natural drying are still suitable for



most users in biomass pretreatment, however for better efficiency, forced drying techniques should need to be considered (Basha & Torii, 2014).

5. CONCLUSION

As a one of the largest source of energy in the world, biomass is anticipated to take the part in greenhouse gas reduction while improving the sustainability of energy supply in Indonesia. However, there are many issues in biomass application, like high investment cost, low conversion efficiency, supply chain barrier, and the high dependency on seasonal production. Another major problem is high moisture content that requires pretreatment and suitable technology. High-tech systems and transfer of knowledge to operators also need to be examined. In a larger scale, supporting law from the policy maker and familiarization of biomass usage need to be taken care seriously. In other words, extensive biomass exploitation still against some obstructions that need to be solved.

6. ACKNOWLEDGMENT

The first author acknowledges support from the Indonesia Endowment Fund for Education (LPDP).

7. REFERENCES

- Abdullah, K., (2002), Biomass Energy Potential and Utilization in Indonesia, Laboratory of Energy and Agricultural Electrification, Department of Agricultural Engineering, IPB and Indonesian Renewable Energy Society [IRES], Bogor, Indonesia.
- ADB., (2016), Asian Development Bank, website : <https://www.adb.org/countries/indonesia>.
- Ahmad, A.L., Mat Yasin, N.H., Derek, C.J.C., Lim, J.K., (2011), Microalgae as a Sustainable Energy Source for Biodiesel Production : A Review, *Renewable and Sustainable Energy Reviews*, Volume 15, pp. 584-593.
- Alamsyah, R., Loebis, E.H., Susanto, E., Junaidi, L., Siregar, N.C., (2015), An Experimental Study on Synthetic Gas Production Through Gasification of Indonesian Biomass Pellet, *Energy Procedia*, Volume 65, pp. 292-299.
- Asadullah, M., (2014), Barriers of Commercial Power Generation Using Biomass Gasification Gas: A Review, *Renewable and Sustainable Energy Reviews*, Volume 29, pp. 201-215.
- Asif, M. and Muneer, T., (2007), Energy Supply, its Demand and Security Issues for Developing and Emerging Economies, *Renewable and Sustainable Energy Reviews*, Volume 11, pp.1388-1413.
- Azwar, (2013), Energy: RI to Focus on Gas Potential with New Projects This Year, *The Jakarta Post*, Jakarta.
- Basha and Torii, S., (2014), A Numerical Study on Thermal Performance of Biomass and Its Impact Due to Moisture for Direct Combustion Based Electricity Generation, *International Journal of Energy Engineering*, Volume 4, pp. 159-163.
- Basu, P., (2013), Biomass Gasification, Pyrolysis and Torrefaction, 2nd ed., Elsevier, San Diego, USA.
- Belonia, (2005), Rice Husk Gas Stove Handbook, Appropriate technology Center Department of Agricultural Engineering and Environmental Management, College of Agriculture, Central Philippine University, Iloilo City, Philippines.
- Demirbas, A., (2009), Bio refineries : Current Activities and Future Development, *Energy Conversion and Management*, Volume 50, pp. 2782-2801.
- Duval, Y., (2001), Environmental Impact of Modern Biomass Co generation in Southeast Asia, *Biomass and Bio energy*, Volume 20, pp.287-295.
- Eriksson, S. and Prior, M., (1990), Briquetting of Agricultural Wastes for Fuel, Food and



- Agriculture Organization, Rome.
- Gaudemard, S. and Becker, J.J., (1989), Fixed Bed Gasification of Lignocellulosic Biomass: the CEMAGREF process. In *Pyrolysis and Gasification*, Elsevier Applied Science.
- Gonzales, P., (2007), How Do Energy and Environmental Policy Goals and Instruments Affect Electricity Demand? A Framework for the Analysis, *Renewable and Sustainability Reviews*, Volume 11, pp. 2006-2031.
- Haberle, S.G., Hope, G.S., van der Kaars, S., (2001), Biomass Burning in Indonesia and Papua New Guinea : Natural and Human Induced Fire Events in the Fossil Record, *Palaeoecology*, Volume 171, pp. 259-268.
- Hasan, M.H., Mahlia, T.M.I., Nur, H., (2012), A Review of Energy Scenario and Sustainable Energy in Indonesia, *Renewable and Sustainable Energy Reviews*, Volume 16, pp. 2316-2328.
- Henriksen, U., and Christensen, O., (1995), Gasification of Straw in a Two Stage 50 kW Gasifier. *Proceedings of the 8th EC Conference, Biomass for Energy, Environment, Agriculture and Industry*, Volume 2.
- Ibrahim, H.D., Thaib, N.M., Wahid, L.M., (2010), *Indonesia Energy Scenario to 2050; Projection of Consumption, Supply Option and Primary Energy Mix Scenarios*, Jakarta, Indonesia.
- IEA., (2016), International Energy Agency, website: <http://www.iea.org/>.
- Jingjing and DeLaquil, (2006), Biomass Energy in China and its Potential, *Energy for Sustainable Development*, Volume 5, pp. 66-80.
- Kaupp, A., (1984), A. 1984. Gasification of Rice Hulls. GTZ, Eschborn, Germany.
- Knoef, H.A.M., (1991), UNDP / World Bank Monitoring Program on Biomass Gasifier in Indonesia, 6th Conference on Biomass for Energy, Industry and Environment, Elsevier Applied Science.
- Koopmans A., (2005), Biomass Energy Demand and Supply for South and South East Asia - Assessing the Resource Base, *Biomass and Bio Energy*, Volume 28, pp.133-150.
- Letcher, T.M., (2008), *Future Energy, Improved Sustainable and Clean Options for Our Planet*, 1st ed., Elsevier Ltd., Oxford, UK.
- Manurung, R., (1995), Overview of the Biomass Energy Development in Indonesia: Problems with Dissemination of New Biomass Energy Technology, *Inter-regional Workshop on the Use of Coconut Industry Waste for Energy*, Bali, Indonesia.
- Ministry of Energy and Mineral Resources (2016), *Handbook of Energy and Economic Statistic of Indonesia*. Jakarta, Indonesia.
- Mupondwa E., Tabil, L., Phani, A., Sokhansanj, S., Stumborg, M., (2012), Techno-Economic Analysis of Wheat Straw Densification in the Canadian Prairie Province of Manitoba, *Bioresource Technology*, Volume 110, pp. 355-363.
- Nikolaisen, L.C., (1992), *Straw for Energy Production*, Centre for Biomass Technology, Danish Energy Agency, Copenhagen.
- Omer, A.M., (2008), Energy, Environment and Sustainable Development, *Renewable and Sustainable Energy Reviews*, Volume 12, pp. 2265-2300.
- REN21., (2015), *Renewables Global Status Report*, pp. 164.
- Salam, P.A., (2006), A Review of Selected Biomass Energy Technologies: Gasification, Combustion, Carbonization and Densification, *Regional Energy Resources Information Center*, Asian Institute of Technology, Thailand.
- Salim, (2000), Energy Reserve, Energy Demand and Future Technology, *Workshop on Environmentally Friendly Technology for the Future*, Jakarta.
- Sukardjo, S. and Yamada, I., (1992), Biomass and Productivity of *Rhizophora Mucronata* Lamarck Plantation in Tritih, Central Java, Indonesia, *Forest Ecology and Management*, Volume 49, pp. 195-209.



- Suntana, A.S., Vogt, K.A., Turnblom, E.C., Upadhye, R., (2009), Bio Ethanol Potential in Indonesia, Forest Biomass as a Source of Bio Energy that Reduces Carbon Emissions, Applied Energy, Volume 86, pp. 215-221.
- Tatom, J.W., Wellborn, H.W., Sasmojo, S., Harahap, F., (1980), Pyrolysis of Rice Husks in Indonesia, Pusat Teknologi Pembangunan, Institut Teknologi Bandung.
- Tchapda, A.H., and Pisupati, S.V., (2014), A Review of Thermal Co-Conversion of Coal and Biomass Waste, Energies, Volume7, pp. 1098-1148.
- Widodo, T.W., and Rahmarestia, E., (2008), Current Status of Bioenergy Development in Indonesia, Regional Forum on Bioenergy Sector Development: Challenges, Opportunity and Way Forward, pp. 49-66.
- Yisheng, Z., Minying, Y., Zhen, S., (2005), Rural Energy Policy in China, Research Group of Energy Policy Institute of Quantitative and Technical Economics, Chinese Academy of Social Sciences, Beijing.
- ZREU., (2000), Zentrum fur Rationell Energieanwendung und Umwelt GmbH, Biomass in Indonesia-Business Guide, German Energy Saving Project.



COMPARATIVE RESISTANCE TEST BETWEEN TWO TOWING TANKS (A CASE STUDY AT ITS AND IHL)

Dian Purnamasari^a, I Ketut Aria Pria Utama^a, and I Ketut Suastika^a

^a *Departement of Naval Architec and Shipbuilding Engineering, Sepuluh Nopember
Institute of Technology (ITS) Surabaya*

ABSTRACT

A complete comparative tests of ITTC procedures that exist among the towing tank facilities at Sepuluh Nopember Institute of Technology (ITS) and Indonesian Hydrodynamic Laboratory-BPPT was carried out. In the resistance tests at all laboratories, the ship model is connected to the towing carriage so that it is free to trim and heave and were restrained in surge, sway, roll and yaw. Each facility uses its own instrumentation, calibration procedure and test methodology. Regarding data acquisition and signal conditioning techniques, the data sampling rate, filtering of the analog signal from the force measuring device, and the actual length of record over which the ship resistance was averaged were the responsibility of each facility. Each institution has tested the model in 4 different sessions, in order to change the test conditions and some errors were detected in the uncertainties analysis for some particular Froude numbers and in those cases the data was withdrawn and not used in the analysis. From the test results of total resistance provided by each facility, the resistance was calculated as the component of the total, for any regression analysis of experimental data to yield reasonably reliable results, the data set should be large enough and more than one test should have been made for the same experimental conditions to check the repeatability of the data. The measurements included speed (V_m) and total resistance (R_{Tm}). There is good agreement overall between the test results obtained at the two facilities. The differences that do remain should be attributed to differences in experimental techniques and types of model used at the participating laboratories.

Keywords: Resistance tests; Froude numbers; Repeatability; Speed; Total Resistance

1. INTRODUCTION

The experimental fluid dynamics (EFD) community is expected to design and execute experiments that consider more real-world flow conditions and address a variety of physics of interest with advanced measurement techniques. The resistance of ships is a priority factor at the preliminary design stage, some of the factors associated with crushing failures are systematically considered in order to correctly estimate resistance, therefore, the performance of ships must be accurately calculated and evaluated through the use of model tests in model basin before construction starts. The best way to select a proper hull form and evaluate propulsive power (and resistance) is to have a good reference ship with model test results, full-scale predictions based on tests and sea-trial data. If the hull is found within a systematic series, that data is used and gives a reliable prediction of the resistance. Systematic study on the resistance of a ship by the starting point is a reference model with good properties regarding the resistance, and the



resistance of this reference model is measured with several velocities in a towing tank. Several similar models, which have the same main geometrical features and systematic variation in some parameters, are manufactured and tested.

Regarding the resistance performance of a ship, the Cooperative Experimental Program of the Resistance Committees of the 17-19 International Towing Tank Conferences [ITTC, 1987&1999] compare results from towing tank tests at 22 institutes. Comparisons are made of global (resistance, sinkage and trim, wave profile, wave cut, wake survey, form factor, and blockage) and local (surface pressure and boundary layer traverses) data for a standard geometry (Series 60) of different sizes (1.2-9.6 m). The cooperative uncertainty assessment example for resistance test of the Resistance Committee of the 22nd ITTC [ITTC,2002] compare results from towing tank tests at 7 institutes of resistance test bias and precision limits and total uncertainties following standard uncertainty assessment procedures, but for different model geometries and sizes (Series 60, container ships, and 5415). Gooden, et.al (1997) compares results from wind tunnel tests for same geometry and conditions at two different institutes, model scales, and using a number of different measurement techniques and extensive error-analysis.

In addition, routine test data more likely utilized in house, whereas detailed test data is more likely utilized internationally, which additionally requires use of standard procedures and uncertainty analysis and establishment of benchmark intervals of uncertainties. Detailed testing offers new opportunities for research institutes, as the amount and complexity of testing is increased.

This study is intended to conduct for evaluation of facilities; measurement systems; test procedures; uncertainty assessments; model size, offsets, and turbulence stimulation; and facility/model geometry and scale effect biases that contribute to the improvement of the techniques for resistance prediction ships. The facilities were a towing tank of Sepuluh Nopember Institute of Technology (ITS) and Indonesian Hydrodynamic Laboratory (LHI-BPPT). The model geometry is surface combatant. Between all two facilities, many conditions and physics are under investigation. The objective of this model test program was to generate a calm water resistance versus speed relationships.

This paper is organized as follows. The next section explains the experimental model, facility, measurement system, and conditions. The following section details the experimental results and discussion, wherein covers the resistance test results in calm water for the bare hull. The last section summarizes the conclusions and future work of this study.

2. METHODOLOGY/ EXPERIMENTAL

2.1 Coordinate System

The right-handed Cartesian coordinate system has been adopted with origin at the intersection of the forward perpendicular and design waterplane. The direction of the principal axes of this system is defined in Table 1. The model reference datum is located longitudinally at Station 0 (transom), transversely on the centreline and vertically on the baseline.



Axis	Direction
X	Positive Forward
Y	Positive Starboard
Z	Positive Down

2.2. Model Geometry

Ship model was conceived as a preliminary design for a surface combatant. The design test speeds at full-scale were 13 and 18 knots. The model, whose lines and main characteristics are respectively shown in Figure 1 and Table 1

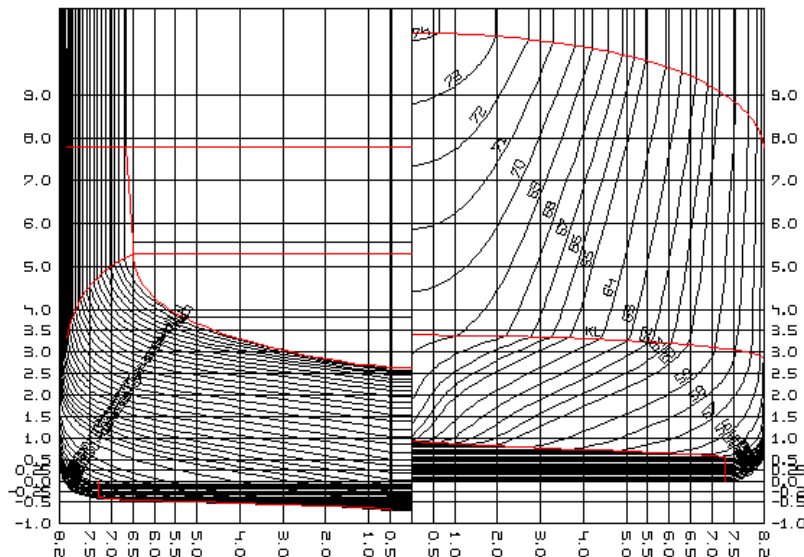


Figure 1. Body Plan of model test

Table 1. Geometry parameter of model test

Parameter	Units	ITS	LHI	Fullscale
Linear scale ratio λ		48.74	33.43	
Length L	m	2.302	3.357	112.212
Beam B	m	0.336	0.491	16.400
Draft T	m	0.061	0.090	3.000
Wetted Surface area S	m ²	0.916	1.947	2176.180
Displacement Volume	m ³	0.039	0.122	4573.360

Two identically shaped models were tested. The first one, namely LHI-187 model have been built at the Indonesian Hydrodynamic Laboratory (LHI-BPPT) models workshop. The second one, namely ITS-4115301001 model, model have been built at Sepuluh Nopember Institute of Technology. Both of model was constructed of wood. In order to stimulate turbulent flow, turbulence stimulators are present at the bow of the ship model to stimulate transition from a laminar into a turbulent boundary layer, both models adopted sand strips used for turbulence stimulation will typically comprise backing strips/adhesive of 10 mm width covered with sharp edged sand with grain size around 0.50 mm, with its leading edge situated about 5% LPP aft of the FP. The station and waterline markings shown on the hull are labelled according to ITTC



recommended procedures uses a 10 section numbering system starting from aft with station 0 at the Aft Perpendicular. The wetted surface area is an important parameter in resistance data reduction, the wetted surface area of a hull model at rest, is usually adopted and theoretically computed from the hull form lines. For model installation according ITTC Recommended Procedure 7.5-01-01-01, Ship Models. The geometry of the hull model is checked at a model workshop before ballasting.

The Reynolds number, based on the nominal velocity and length between the perpendiculars, is 5.84×10^6 for the LHI-187 models, while for the ITS-4115301001 model, that is shorter, the Reynolds number is 3.18×10^6

2.3. Test Design, Conditions and Procedures

The most typical towing-tank tests selected for the resistance, each institute followed their usual procedures, the experimental process as recommended by the ITTC standards. In the resistance test the ship model is towed by the carriage and the total longitudinal force acting on the model is measured for various speeds. Speed is kept constant for at least 10 seconds, average values of the measurements for the period of constant speed is calculated. During the measuring run the ship model is free to heave and pitch. The dependency of the density and kinematic viscosity on temperature T was accounted for by measurement of the towing-tank water temperature T using fresh water values as recommended by ITTC Fresh Water and Seawater Properties Procedure 7.5-02 -01-03. The individual measurement system for T was daily thermometer readings at mid draft of the model. The range of values of (T, ρ , ν) was (27.0-28.5°C, 996.51-995.94 kg/m³, $0.85-0.81 \times 10^{-6}$ m²/s).

The load cell, signal conditioner, and carriage PC AD card are statically calibrated to determine its voltage-mass relationship. A weight tray with standard weights is suspended plumb to the load cell and the output recorded. Starting and ending from zero mass, weights of known increments are placed on the tray in ascending then descending order. The voltage-mass relationship is linear. A first-order polynomial linear regression curve fit is used to determine the slope/intercept, which are then used to convert voltage to mass. The repeatability of the calibration between data procurement cycles is monitored.

The tests of ITS-4115301001 model have been conducted at Sepuluh Nopember Institute of Technology towing tank with particulars: length (L) of 50m, Breadth (B) of 3m, depth (H) of 2m, maximum draft (T) of 1.8m and maximum speed of carriage is 4.0 m/s and the tests of LHI-187 model have been conducted tested at the Indonesian Hydrodynamic Laboratory with particulars: Length of 234.5 m, Breadth of 11 m and Water Depth of 5.5 m. Other differences in the experimental setup between laboratories are the exact location of the towing point, for example, near the bow, in the vicinity of the center of gravity, and whether or not the location of the center of gravity or the gyradii in roll and pitch are duplicated in the model by correct ballast distribution.

Resistance measurement of model were made with dynamometer. The model attached to the measuring head of the resistance dynamometer by a connection which can transmit and measure only a horizontal tow force, even though raked the model should be run at the correct calculated displacement. The resistance dynamometers were



attached at the LCB of the model as close to the shaft line as possible. The electrical signal from dynamometer are transmitted through overhead cables on trolley wires to the signal conditioning equipment and ultimately to the computer. Data were sampled for resistance and speed in the longitudinal direction F_x . The forces are measured in mass (kg) and converted to N by multiplication by g.

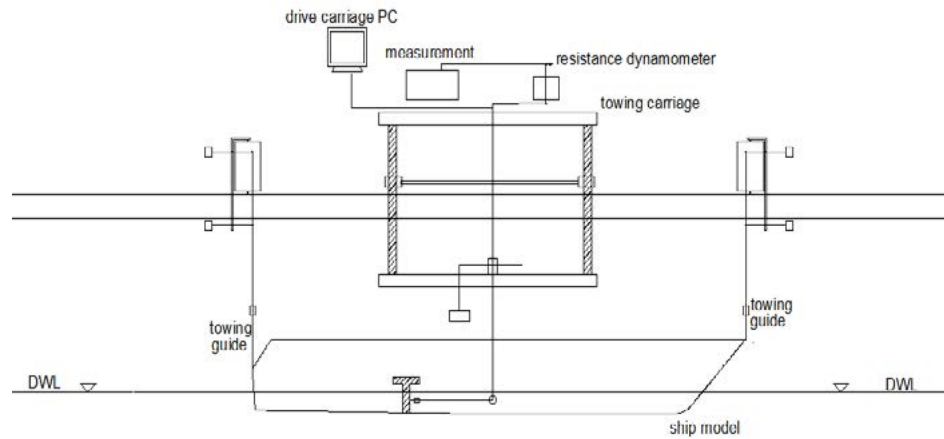


Figure 2. Experimental set up

2.4 Data Processing

The calculation of the total resistance coefficient was achieved by using the procedure as outlined in the ITTC recommended procedures [ITTC, 2011]. The total resistance coefficient was calculated using:

Total hull resistance is a function of hull form, ship speed, and water properties, the coefficient of total hull resistance is also a function of hull form, ship speed, and water properties. The coefficient of total hull resistance is found from the following equation

$$C_T = \frac{R_T}{0.5\rho SV^2} \quad (1)$$

Where:

- C_T = total resistance coefficient
- R_T = total hull resistance (N)
- ρ = water density (kg/m³)
- V = velocity (m/s)
- S = wetted surface area of the underwater hull (m²)

The equation for the Froude number is

$$Fr = V \sqrt{gL} \quad (2)$$

The frictional resistance coefficient (C_F) is calculated using the ITTC-1957 ship friction correlation line,

$$C_F = \frac{0,075}{(\log Re - 2)^2} \quad (3)$$

The residual resistance coefficient (C_R) of the model is calculated,

$$C_R = C_T - C_F \quad (4)$$



The test system consists of several uncertainty sources. The uncertainty analysis must be applied to the results for classification of uncertainties and to estimate it as quantitative. For the uncertainty analysis, new method has been published a more simplified fashion in the last 27th ITTC Conference in Copenhagen (ITTC, 2014). In ITTC 2014 Method, uncertainties was examined under a total of 5 main subject. These titles are Model Geometry, Test Setup, Calibration and Data Reduction.

The relative standard uncertainty components of resistance related to the hull geometry can be estimated as:

$$u'_1(R_T) = u'(S) = \frac{2}{3}u'(\Delta) \quad (5)$$

The uncertainty of carriage speed is obtained as quantitatively by the following equations,

$$u'_2(R_T) = 2u'(V) \quad (6)$$

The relative uncertainty of water viscosity resulted from temperature can be estimated

$$u'_3(R_T) = \frac{C_F}{C_T} \frac{0.87}{(\log_{10} Re - 2)} u'(v) \quad (7)$$

The uncertainty component of resistance resulted from calibration of dynamometer is estimated by standard error estimation (SEE)

$$u_4(R_T) = SEE \quad (8)$$

The standard uncertainty component from single test can be estimated by the following equations,

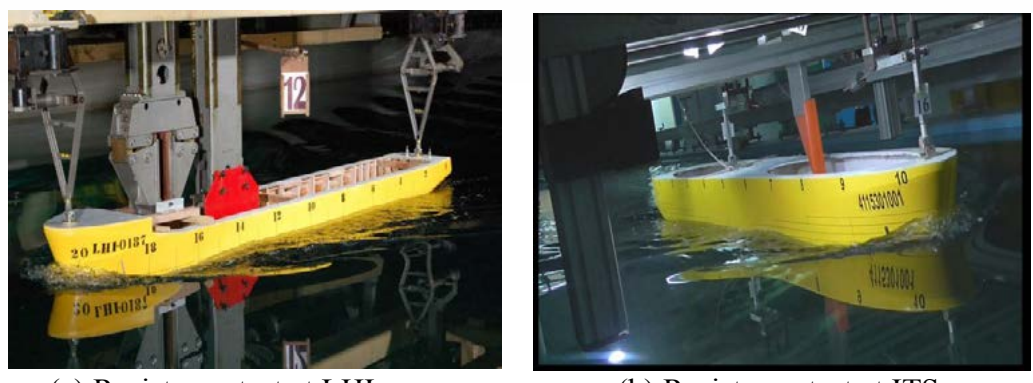
$$u'_A(R_T) = \frac{S_{dev}}{\bar{R}_T} \quad (9)$$

Analysis of all significant uncertainty components related to the total resistance are combined to obtain the overall standard uncertainty by RSS methods:

$$u'_c = \sqrt{(u'_1)^2 + (u'_2)^2 + (u'_3)^2 + (u'_4)^2 + (u'_A)^2} \quad (10)$$

3. RESULTS AND DISCUSSION

The resistance performance of a two identically shaped models were assessed through a series of model tests. The experiments on surface combatant model in order to investigate the scale effect of ship resistance using geosim models of 3,5m length in Indonesian Hydrodynamic Laboratory, and 2.5m of length in Sepuluh Nopember Institute of Technology. The experiments were separately performed on the following items and cooperatively analyzed.



(a) Resistance test at LHI (b) Resistance test at ITS
Figure 3. Resistance test at the individual facility

Results from towing tank experiments regarding resistance of the surface combatant model are presented. The resistance tests are for Froude numbers between $Fr = 0.20 - 0.28$ and free model conditions. The Resistance test has been performed following the ITTC standards, the measurement of the total model resistance having a maximum load of 20.047 N for the LHI-187 models, while for the ITS-4115301001 model having a maximum load of 6.090 N. Trends for all two facilities are similar.

Table 2. Resistance test result

Fr	LHI				ITS			
	$R_T(N)$	C_T	C_F	C_R	$R_T(N)$	C_T	C_F	C_R
0.20	7.074	$5.464 \cdot 10^{-3}$	$3.430 \cdot 10^{-3}$	$2.034 \cdot 10^{-3}$	2.108	$5.045 \cdot 10^{-3}$	$3.853 \cdot 10^{-3}$	$1.925 \cdot 10^{-3}$
0.22	8.562	$5.704 \cdot 10^{-3}$	$3.383 \cdot 10^{-3}$	$2.321 \cdot 10^{-3}$	2.599	$5.362 \cdot 10^{-3}$	$3.797 \cdot 10^{-3}$	$1.565 \cdot 10^{-3}$
0.23	10.651	$6.182 \cdot 10^{-3}$	$3.340 \cdot 10^{-3}$	$2.842 \cdot 10^{-3}$	3.177	$5.711 \cdot 10^{-3}$	$3.746 \cdot 10^{-3}$	$1.964 \cdot 10^{-3}$
0.25	13.738	$7.005 \cdot 10^{-3}$	$3.302 \cdot 10^{-3}$	$3.704 \cdot 10^{-3}$	4.236	$6.692 \cdot 10^{-3}$	$3.700 \cdot 10^{-3}$	$2.992 \cdot 10^{-3}$
0.26	16.925	$7.652 \cdot 10^{-3}$	$3.265 \cdot 10^{-3}$	$4.386 \cdot 10^{-3}$	5.139	$7.190 \cdot 10^{-3}$	$3.657 \cdot 10^{-3}$	$3.533 \cdot 10^{-3}$
0.28	20.047	$8.078 \cdot 10^{-3}$	$3.232 \cdot 10^{-3}$	$4.847 \cdot 10^{-3}$	6.090	$7.601 \cdot 10^{-3}$	$3.617 \cdot 10^{-3}$	$3.983 \cdot 10^{-3}$

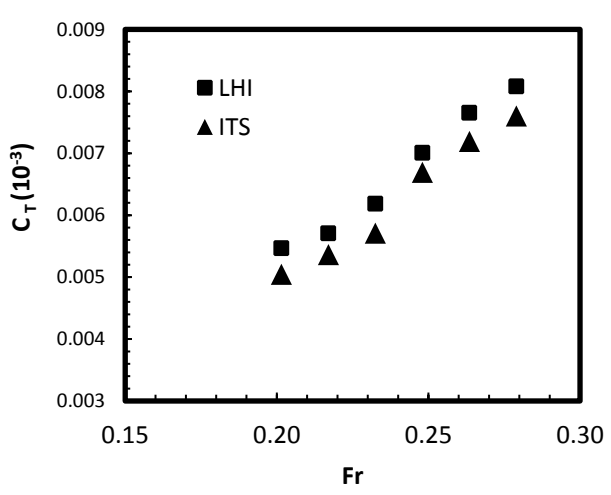


Figure 4. Comparison C_T results for range of Fr.

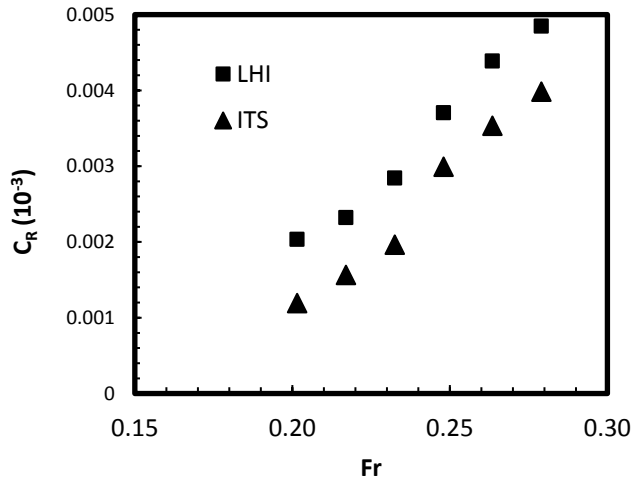


Figure 5. Comparison C_R results for range of Fr .

Figure 4-5 shows a comparison of C_T and C_R from two models over a Froude number range of 0.20 to 0.28. In general, the agreement between the model resistance data from the two facilities is fair.

All the uncertainty components in resistance measurement can be evaluated in detail as in Table 3 as expressed by Equations 5-10.

Table 3. The uncertainty analysis of resistance

R_T ($Fr=0.25$)	Type	Uncertainty	
		LHI	ITS
Wetted area	B	0.158 %	0.495 %
Speed	B	0.067 %	0.067 %
Water Temperature	B	0.030 %	0.033 %
Dynamometer	A	0.063 %	0.205 %
Repeat test, Deviation	A	0.230 %	0.371 %
Combined for single test		0.296%	0.656 %

The systematic uncertainty components from larger values to smaller values are resistance, wetted surface area, speed, dynamometer and temperature, respectively for LHI model, otherwise for ITS model the systematic uncertainty components from larger values to smaller values are wetted surface area, resistance, dynamometer, speed and temperature, respectively. The differences that do remain should be attributed to differences in experimental techniques between all two facilities, many conditions and physics are under investigation.

The blockage correction of two model is shown in Figures 6-7 for the Schuster and Tamura methods of ITTC (2011). The results are quite different. The corrections decrease with the measured velocity for the Tamura equations. The correction by the Schuster equation is about 0.07% for LHI model and 0.55% for ITS model, while it is about 0.41 % for LHI model and 3.14% for ITS model by the Tamura equation.

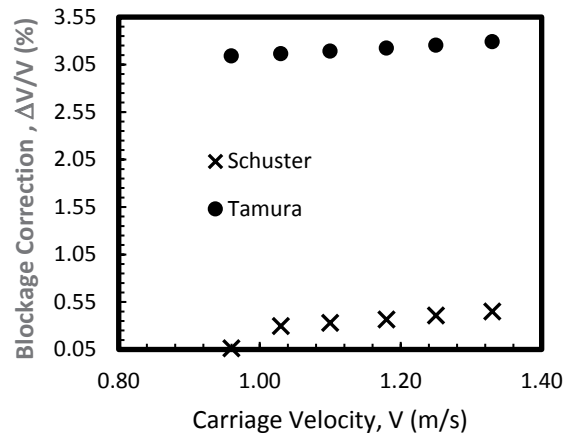


Figure 6. Blockage corrections for ITS model

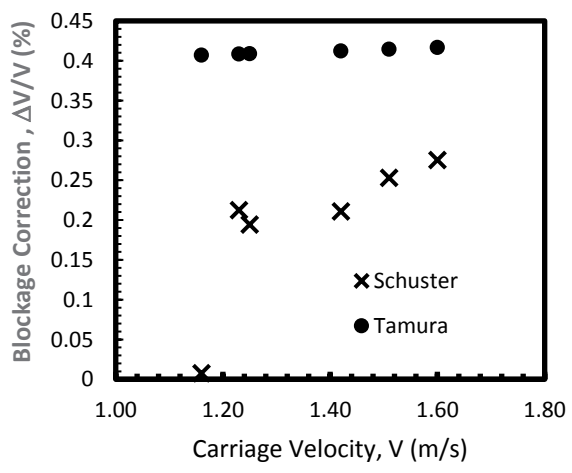


Figure 7. Blockage corrections for LHI model

4. CONCLUSION

Results from towing-tank experiments for model ship combatant were presented for resistance, the test design, measurement systems, and facility were described. The results were discussed with regard to the data trends. Between two institutions many conditions and physics are under investigation. The data contributes to the surface-ship resistance model-scale database for CFD validation.

In a test series of this nature, it is important that an appropriate procedure is adopted in order to preserve the confidentiality of the data, and to avoid the possibility that the evaluation of the data could be affected by a knowledge of the facility from which it originated.

In this study, the performed model tests focused on the resistance performance of the hull. research of the seakeeping of such hulls is needed to be pursued in the future study.



5. ACKNOWLEDGEMENT

The first author, in particular, expressed her gratitude to The Ministry of Research and Technology (Ristekdikti) which funding her PhD program at ITS under contract number 07/S3/D/PTB/XI/2015

The authors would like to thank members of staff at Indonesian Hydrodynamic Laboratory and Institute of Technology Sepuluh Nopember for their sincere support during the experiment and manufacture of the ship model.

6. REFERENCES

- ASME, 2005. Test uncertainty, The American society of mechanical engineers performance test code, No. 19.1-2005. American Society of Mechanical Engineers, New York, NY.
- ISO, (1995), *Guide to the Expression of Uncertainty in Measurement (GUM)*, International Organization for Standardization, Genève, Switzerland.
- ITTC, (1987), Report of the Resistance and Flow Committee, 18th International Towing Tank Conference, Kobe, Japan.
- ITTC, (1999), Report of the Resistance and Flow Committee, 22nd International Towing Tank Conference, Seoul, Korea/Beijing, China
- ITTC, (2008), Model Manufacture Ship Models, ITTC Procedure 7.5-01-01-01.
- ITTC, (2008b), Uncertainty Analysis Instruments Calibration, ITTC Procedure 7.5-01-03-01.
- ITTC, (2011), Resistance Test, ITTC Procedure 7.5-02-02-01.
- ITTC, (2011), Fresh Water and Seawater Properties, ITTC Procedure 7.5-02-01-03
- ITTC, (2014a), General Guidelines for Uncertainty Analysis in Resistance Tests, ITTC Procedure 7.5-02-02-02.
- ITTC, (2014c), *Resistance Committee Report*, Proceedings of 27th International Towing Tank Conference.
- Jamaluddin A, Utama I.K.A.P, Molland A.F, (2010), Experimental Investigation into Drag Characteristic of Symmetrical and Asymmetrical Staggered Catamaran, *International Conference on Ship & Offshore Technology (ICSOT)- Indonesia, RINA International Serie Conference*, Surabaya.
- J.H.M. Gooden, C. Gleyzes and Y Maciel (1997), Experimental study of the flow around two scaled 3D swept wings, *28th AIAA Fluid Dynamics Conference* held at Snowmass, CO, USA, June 29 - July 2.
- Joel T. Park, Toby J. Ratcliffe, Lisa M. Minnick, and Lauren E. Russell, (2010), *Test Results and Uncertainty Estimates for CEHIPAR Model 2716*, The 29th American Towing Tank Conference Annapolis, Maryland.
- Larsson L and Raven H.C. (2010). *Ship resistance and Flow*. In particular, Chapters 5 and 6, Sections 11.5-6. SNAME. (Knoval)
- Metcalf, B.J., Faul, L., Bumiller, E., Slutsky, J., (2005), Resistance Tests of a Systematic Series of U.S. Coast Guard Planing Hulls. *Report of Naval Surface Warfare Center Carderock Division, No. NSWCCD-50-TR-2005/063*. Naval Surface Warfare Center Carderock Division, Bethesda, MD.
- Molland, A.F., Turnock, S.R., dan Hudson, D.A. (2011), *Ship Resistance and Propulsion: Practical Estimation of Ship Propulsive Power*, Cambridge University Press, New York, USA.



THE 15TH INTERNATIONAL CONFERENCE QUALITY IN RESEARCH (QIR) 2017 TEMPLATE

OPTIMIZATION OF OPEN CHANNEL WATER TUNNEL DESIGN

Ismail^a, Erlanda Augupta Pane^{a*}, Damora Rhakasywi, Eko Prasetyo and Pekik Bayu Asmoro^a

^aDepartment of Mechanical Engineering, Faculty of Engineering, Universitas Pancasila Srengseng Sawah, Jagakarsa – Jakarta 12640, Indonesia

ABSTRACT

This research was conducted to develop an open channel water tunnel and analysis of the flow distribution in the test section, where geometry of the water tunnel, discharge of water flow and turbulence intensity are being basic parameters which influence Reynolds number to reach the best condition, so that the hydrodynamic found to be optimal. The previous researches of water tunnel explained that if the Reynolds number is the same fluid, the hydrodynamic on a similar model. The methods of research used numeric analysis and Computational Fluid Dynamics (CFD) simulations. The step of water tunnel design is used to determine the Area Ratio (AR) between the contraction and the test section. Area Ratio value is 5, which take it to calculate water tunnel design. Test section geometry has length is 0.6 m, width is 0.3 m, and height is 0.3 m. Pump PMP010 type is used to pass of water with various capacities. It has capacity about 900 L/min, 1000 L/min, and 1100 L/min, respectively. The optimum result is geometry water tunnel design has length inlet plenum is 0.76 m, contraction is 1.1 m included honeycombs is 0.2 m, test section is 0.6 m and outlet module is 0.51 m, So that, the total length of water tunnel design is 2.97 m. The design of water tunnel using discharge is 900 L/min; water speed is 0.167 m/s, turbulence intensity 0.044 and Froud number 0.097.

Keywords: Froud numbers; Hydrodynamic; Reynolds number; Turbulence intensity; Water tunnel

1. INTRODUCTION

Water tunnel are used for a variety of reasons such as testing a structure under flowing fluid, which affect the forces on the submerged body (Dol 2015). The benefit of water tunnel is the Reynolds number in water flow will be about fifteen times and dynamic head (H_d) in water flow is about 800 times the corresponding than the air flow, So that the water can be a much simpler task to measurement of turbulent pressure fluctuations than in the air (Arakeri & Govinda 1988). Water tunnel has three types are High Speed Water Tunnel, Low Speed Water Tunnel, and Open Channel Flow Water Tunnel (Ahmad Zulfadhli 2008). The previous researches of water tunnel explained that if the Reynolds number is the same

* Corresponding author.

E-mail address : pane_erlanda@yahoo.com



fluid, the hydrodynamic on a similar model. The previous researches of water tunnel design can be showed in Table 1.

Table 1. The previous of design of Water Tunnel

No.	Model Type	Testing Type		Researches
		Design	Experiment	
1	IISC-HSWT water tunnel	✓		(Arakeri & Govinda 1988)
2	DSTO water tunnel		✓	(Erm 1836)
3	NTU water tunnel	✓		(Lee et al. 2005)
4	Close circuit wind/water tunnel design	✓		(Gordon & Imbabi 2016)
5	Hills Research Corporation 1520	✓		(Dol 2015)
6	J.B Herbich water tunnel	✓		(Ko 1971)
7	K15 cavitation water tunnel of SSSRI		✓	(Yao et al. 2015)
8	DTMB high speed water tunnel	✓		(Nedyalkov 2012)
9	Oscillating water tunnel (OWT)		✓	(Yuan & Madsen 2014)
10	K15 cavitation water tunnel of SSSRI		✓	(Chuan-jing & Ting 2011)

This research was conducted to develop an open channel water tunnel. Open channel water tunnel have the six main components are inlet plenum, baffle, setting chamber, inlet module, test section, and outlet module. The six main components of open channel water tunnel can be showed in Figure 1.

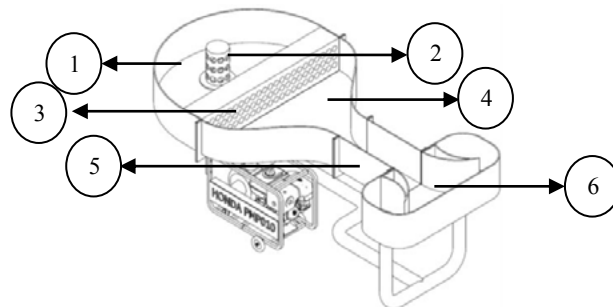
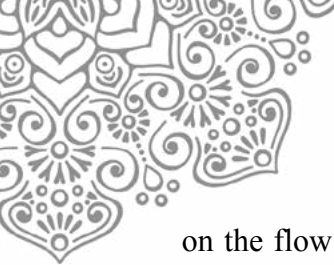


Figure 1 Open channel tunnel design. 1) Inlet Plenum; 2) Baffle Design; 3) Settling Chamber; 4) Inlet Module; 5) Test Section; 6) Outlet Module

The smooth surface of water tunnel can reduce friction of water flow and increase flow effectiveness (Dol 2015). This is being indicated by the flow speed changes with time, where the small different of flow speed along the length of the channel, it suggests the characteristic of this flow is nearly similar with the characteristic of uniform flow (Cengel & Cimbala 2006). Uniform flow has connection with Contraction Ratio (CR) shape, which it has a well design between 5 and 10; it is worthy to note that increasing the contraction ratio increases the maximum width of the contraction while a higher contraction ratio will damp flow perturbations (Kalyankar et al. 2015), can decrease of turbulence intensity (Nedyalkov 2012). The high Contraction Ratio (CR) definitely has a favourable influence



on the flow quality in test section to become uniform flow (Arakeri & Govinda 1988). So that, the test section is an important part to determine of water flow characteristic through of inlet module. The settling chamber take the honeycombs model also as an important part to determine of water flow, which reduces the lateral turbulence and straighten the flow (Kalyankar et al. 2015).

The lateral turbulence and straighten the flow, could defined characteristic of water flow was the laminar flow. The characteristic of water flow can be recognized by Reynolds number (Pritchard & Leylegian 2011). The flow will change from laminar to turbulent as the value of Reynolds number increase, which the flow can be considered to be laminar below the value 3×10^5 , and turbulent above the value 3×10^6 (Chuan-jing & Ting 2011). The Reynolds number can influence material drag coefficient, which the increase Reynolds number can make the drag coefficient effect decreases gradually (Yao et al. 2015). This research was conducted to develop an open channel water tunnel and analysis of the flow distribution in the test section, where geometry of the water tunnel, discharge of water flow and turbulence intensity are being basic parameters which influence Reynolds number to reach the best condition, so that the hydrodynamic found to be optimal.

2. METHOD

The design of open channel water tunnel used two approaches that the calculation of mathematics models and analysis simulation use Computational Fluid Dynamics (CFD). The calculation of mathematics models has designed the six components open channel water are the inlet plenum, baffle, settling chamber (honeycombs model), test section, inlet module, and outlet module. The calculation of mathematics model uses the basic parameters that discharge capacity and the dimension of test section which have determined by researcher use the Area Ratio (AR). The results of design have simulated in CFD to see the results of water speed, Reynolds number, turbulence intensity, and Froud Number.

II.1. Project and Planning Definition

The project definition of open channel flow water tunnel use the Pump PMP010 type, which it have the discharge capacity various such as 900 l/min, 1000 l/min, and 1100 l/min. Area Ratio (AR) which definition of contraction ratio in inlet module, and dimension of test section. The assumption value of Area Ratio (AR) is 5 and contraction length is 0.9 m, where the both of them can determine of discharge capacity. The test section dimension would be design by the water speed maximum and the lowest of turbulence intensity. The dimension of test section open channel flow water tunnel has length 0.6 m, width 0.3 m and height 0.3 m. The Reynolds number; turbulence intensity and Froud number of water flow must be known. The equations to calculate the three components of open channel water tunnel can be described in Table 2 below that.

Table 2 Calculate of three components open channel water tunnel and basic parameters

No	Parameters	Equations
1	Reynolds number	$Re = (\rho \cdot V \cdot R_h) / \mu$
2	Turbulence Intensity	$I = 0.16 \cdot Re^{-1/8}$
3	Froud Number	$Fr = V / (g \cdot Y)^{1/2}$



The design of three components open channel water tunnel

No	Components	Equations
1	Test Section	$AR = A_2 / A_1$
2	Inlet Module	$Y_c = Y_{C1} - (Y_{C1} - Y_{C0}) [6(X_c/L_c)^5 - 15(X_c/L_c)^4 - 10(X_c/L_c)^3]$
3	Settling Chamber	$V_{HC} = V_2 / CR ; V_2 = (A_1 \cdot V_1) / A_2 ; V_1 = Q/A$

M = The width of inlet module / The number of honeycombs hole

The other section of inlet plenum, baffle, and outlet module can be explained by the assumption value, which the dimension of inlet plenum, baffle, and outlet module is the development the previous open channel water tunnel design.

II.2. CFD Simulations

The CFD simulations can be done after calculate of open channel water tunnel design use mathematics model. The basic parameters to CFD simulation are discharge capacity and the calculate result of open channel water tunnel design. The results of CFD can show the water speed, Reynolds number, turbulence intensity, and Froud number.

3. RESULTS AND DISCUSSION

The design calculation have concept the six parts of open channel water tunnel such as inlet plenum design, baffle design, settling chamber which use the honeycombs model, test section design with Area Ratio (AR) optimum between 5 and 10, inlet module design and outlet module. Moreover, the calculate design have been determined the water speed, Reynolds number and turbulence intensity. The six parts of open channel water tunnel can be showed in Figure 1.

The graph in Figure 2 has given the information about the curvatures of geometry inlet module. The smooth curvatures can make the water tunnel distribution are quietly and uniform in Figure 2 (a). The X_c is the distance of contraction between the entrance inlet module and the middle section of inlet module (Y_c) give the effect to water speed, whereas if the length of contraction very high, can make the decrease of water speed because friction between water and inlet module surface area. The Y_c is the start of curvatures in the middle section of inlet module, which the small width of Y_c influences to increase water speed. The water speed in inlet module can be showed in Figure 2 (b).

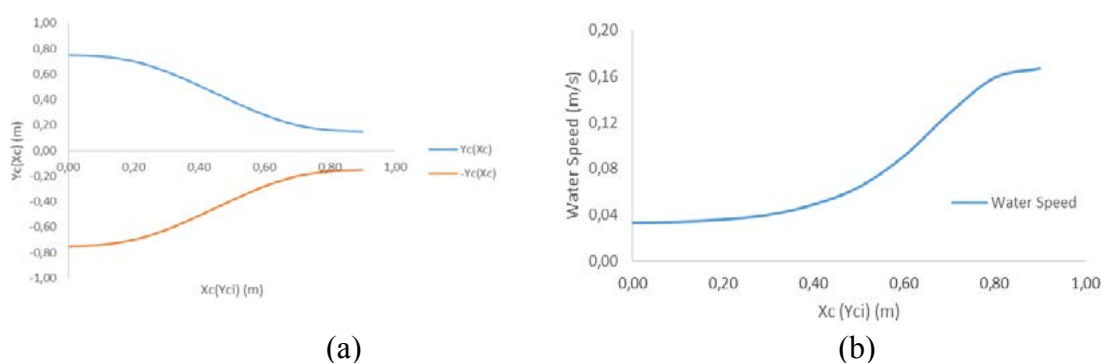


Figure 2 The curvatures of inlet module geometry a); The water speed b)



III.4. Design and Validation

The calculation of open channel water tunnel will produce the optimum design with the best result of the basic parameter. The discharge capacity is the ones of basic parameter to determine the optimum open channel water tunnel design. The dimension and parameter design can be showed that in Table 3.

The optimum of open channel water tunnel can influence of Reynolds number, which given the effect to hydrodynamic test. The best of Reynolds number determines the flow characteristic, which it can produce the laminar or turbulent flow. The improvement of kinematic viscosity gives the effect to increase water flow. Based on that condition, the hydrodynamic test on the open channel water tunnel can be optimal.

Table 3 Table of dimension and parameter design

No.	Section	Note
1	Area Ratio (R)	5
2	Discharge (Q) Water Speed (V _s)	900 l/min; 0.033 m/s (load speed)
	Discharge (Q) Water Speed (V _s)	1000 l/min; 0.037 m/s (load speed)
	Discharge (Q) Water Speed (V _s)	1100 l/min; 0.041 m/s (load speed)
3	High of water	300 mm
4	Material	Acrylic with the roughness of 3.92 nm

The CFD simulation, open channel water tunnel design have been seen the water speed, and turbulence intensity in the test section with the discharge capacity and position in the test section become basic parameter. The discharge capacity use the three variant that 900 l/min, 1000 l/min, and 1100 l/min. The simulated position in the test section use five positions that position A (0 m), B (0.15 m), C (0.30 m), D (0.45 m), and the end of test section E (0.60 m) based on the entrance of test section. The positions in the test section can be showed that in Figure 3.

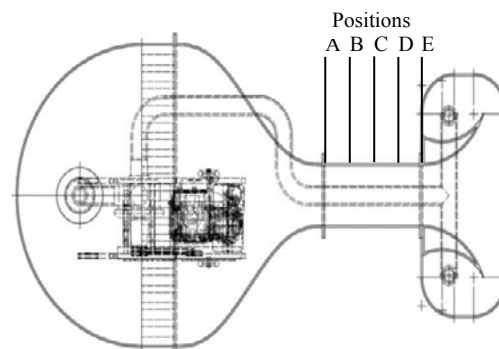


Figure 3 The position test in the test section

The result of CFD simulation with the parameter that position and discharge capacity can be determines the water speed and turbulence intensity. The result simulation can be showed that in the Figure 4.

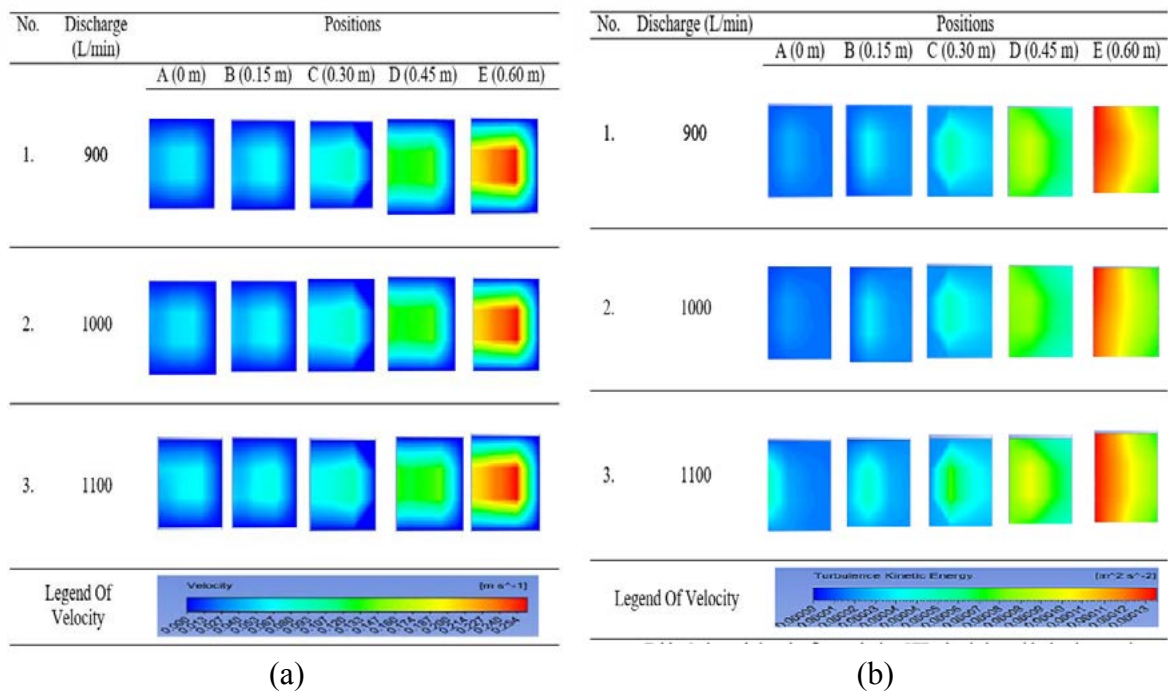


Figure 4 water speed a) and turbulence intensity b) in Test Section

Figure 4 a) showed that the water speed CFD simulation with the three several of discharge capacity in the five positions. The trend of the water speed value between the three variant of discharge capacity have been improved. This is can be indicated by the change of colour when the calculation of water speed is being tested by CFD simulation. Improvement of water speed influenced by discharge capacity and the area of surface test section. The two factors have been relations with the water speed; this is can be showed in the discharge equations. If the discharge capacity increases, the water speed can be increased when the surface area constant. Figure 4 b) showed that the turbulence intensity CFD simulation in the five positions with the three variant of discharge capacity. The trend of turbulence intensity has been similarity with the water speed. The turbulence intensity has been increased in the three variant of discharge capacity. The turbulence intensity between 900 l/min, 100 l/min, and 1100 l/min has the different value.

III.5. The result of validate calculation

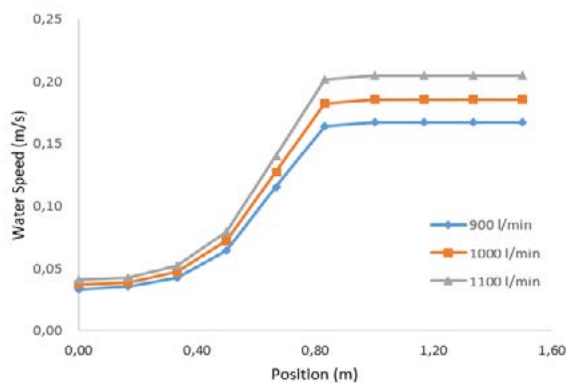
The result of validate calculation and the calculate of open channel water tunnel design simulated by Computational Fluid Dynamics (CFD) on the three various discharge capacity to determine water speed in Figure 5, Reynolds number in Figure 6 and turbulence intensity in Figure 7. This simulation have the aims to consideration result from the calculate design and the simulations, moreover this simulation can be managed of the operational cost to build the open channel water tunnel.

The graph of water speed showed in Figure 5(a) the different water speed between the three several of discharge capacity. The discharge capacity 900 l/min has the lowest water speed than the other. This is have the relation with the surface of area test section. The constant of surface area with the change of discharge capacity can give the effect to water

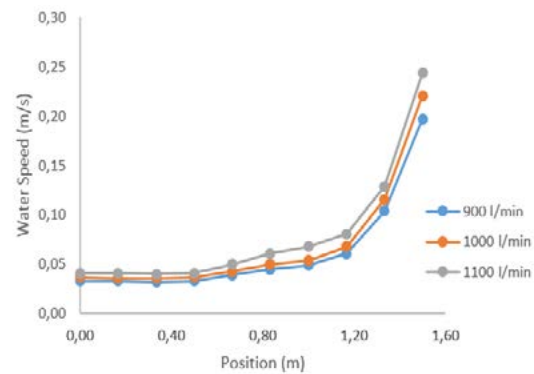


speed. This condition can be concluded that the increasing discharge capacity can make the increase of water speed. The trend of water speed CFD simulation in Figure 5(b) similarity with the calculate design, but the different of graph water speed both of them on the path line. The parameter that makes the different is external parameter such as roughness material parameter, when it's become the entrance data simulations.

The water speed influence the Reynolds number in Figure 6 (a). The Reynolds number can determine the flow characteristic that laminar or turbulent flow. The graph of Reynolds number open channel water tunnel design showed that the discharge capacity 900 l/min has the lowest of Reynolds number. The trend of Reynolds number has been similarity with the water speed. Graph of Reynolds number CFD simulation in Figure 6 (b). The graph of Reynolds number CFD simulation different than the graph of Reynolds number validates calculation, because the entrance data of water speed in CFD simulations. The highest of Reynolds number makes the flow characteristic become as a turbulent flow.

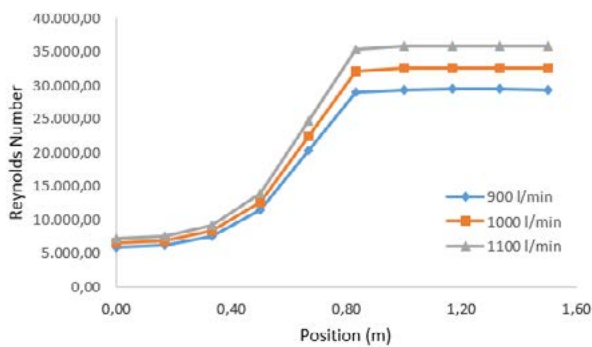


(a)

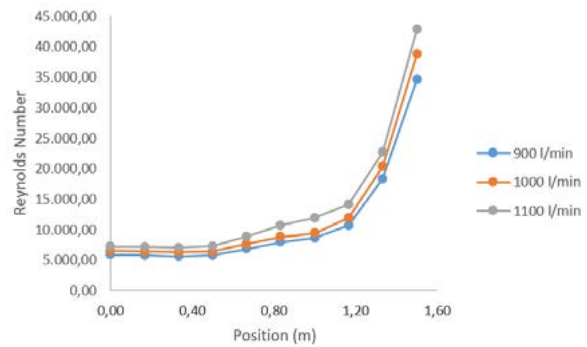


(b)

Figure 5 Water speed a); Validate Calculation b); CFD simulations



(a)



(b)

Figure 6 Reynolds number a); Validate Calculation b); CFD simulation

Besides of water speed and Reynolds number, the turbulence intensity can influence the open channel water tunnel design. The graph of turbulence intensity in Figure 7 (a) has



been different than the graph of water speed and Reynolds number. The graph of turbulent intensity indicated that the discharge capacity 900 l/min have the highest value than the other discharge capacity. This can conclude that the highest of turbulent intensity needed to the lowest of Reynolds number and makes the increase of water speed. The turbulence intensity of CFD simulation in Figure 7(b) and calculate design have been different. Graph of turbulence intensity CFD simulation when the water flow through the position E will be fall down to the lowest point. The lowest point caused by Reynolds number influence the turbulence intensity parameter.

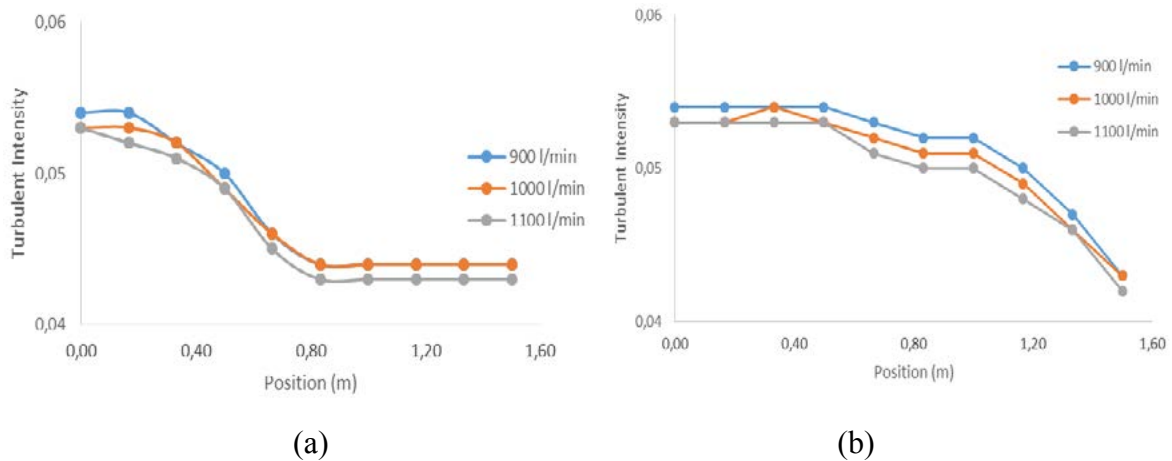


Figure 7 Turbulent Intensity a); Validate Calculation b); CFD simulation

III.6. Optimal Design

The design of open channel water tunnel has been optimized by the discharge capacity 900 l/min. The characteristic of optimal design open channel water tunnel have the length of contraction in 0.9 m, and the dimension of test section with the length 0.6 m, width 0.3 m, and the height 0.3 m. The figures of water speed in test section can be coughed from 0 m/s until 0.3048 m/s. The test visualization of open channel water tunnel uses the colour spray on the surface model. The best of water speed from the test visualization is 0.09144 m/s until 0.1524 m/s. The optimum of open channel water tunnel design can be showed that in Figure 1. The optimized of open channel water tunnel with the discharge capacity 900 l/min have been selected. The parameters of open channel water tunnel design such as water speed, Reynolds number, and turbulence intensity between calculation and CFD simulation can be considerate ones to each other, and can be showed that in Figure 8.

From the graph, it seems the different result between the calculate design and CFD simulations. The graph of water speed can be showed in Figure 8(a). The graph of water speed in the calculate design have the extreme increase when the water flow through the position C and position D, and the constant water speed in position E. The different result caused by the added external parameter, such as the roughness material test section when the open channel water tunnel design simulated by CFD simulations. The graph of Reynolds number between calculates design and CFD simulations have different result in



Figure 8 (b). The different caused by the constant value of material characteristic, when material characteristic data in CFD simulations different than in calculate of design. The graph of turbulence intensity between calculate design and CFD simulations have been different in Figure 8 (c), but the value in the entrance of test section, both of them have the similarity value. The value of turbulence intensity calculate design have been extreme decreased path line than the smoothly path line of turbulence intensity CFD simulations. The graph of Froud number between calculates design and CFD simulation in Figure 8(d). Froud number of water flow in CFD simulations have the decreasing path, but in the position of 0.8 m Froud number in CFD simulations increase, the increase of Froud number because the water flow through test section, the function of test section to make the water flow quickly and smoothly.

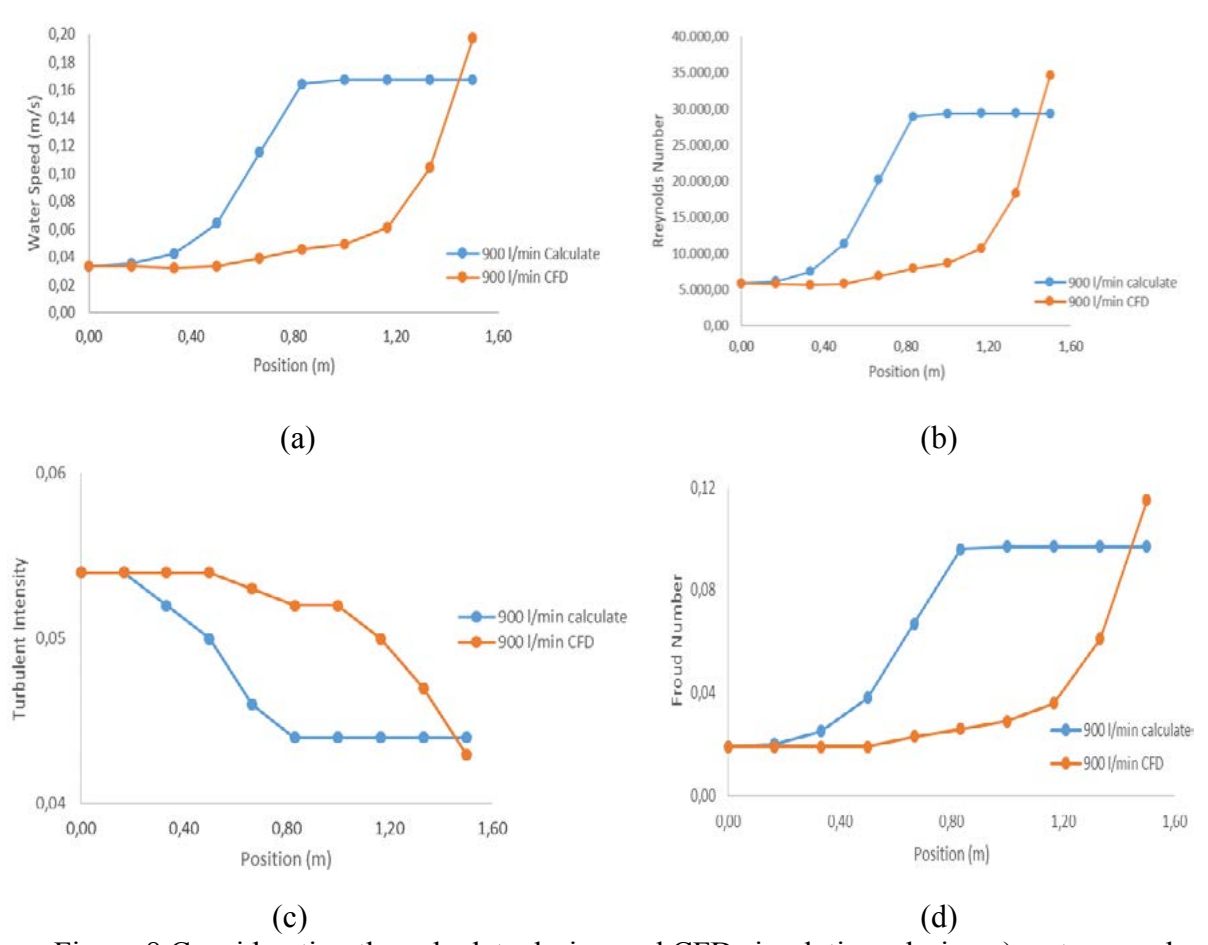


Figure 8 Consideration the calculate design and CFD simulations design a) water speed b) Reynolds number; c) Turbulent Intensity; d) Froud Number

4. CONCLUSION

The research of open channel flow water tunnel can be concluded that the optimum of open channel flow water tunnel model with the discharge capacity 900 l/min. This model has the total length 2.97 m. The length of contraction is 0.9 m included the honeycombs with the dimension of length 0.2 m and the diameter of cell 0.05 m. The test section has the



dimension with the length 0.6 m, width 0.3 m, and height 0.3 m. The optimum of open channel water tunnel have the optimum water speed with the value is 0.167 m/s, the lowest Reynolds number 29368, and turbulence intensity is 0.044 or with the percentage is 4.4 %, which have the means is intermediate turbulence intensity and Froude number 0.097. If the water flow rate increase, its produce the Reynolds Number high and the Reynolds Number will be constant when the water flow entrance to test section, this is being caused by the constant test section geometry. If the flow discharge increases, its produce turbulence intensity low and the turbulence intensity will be constant when the water flow entrance to test section, this is being also caused by constant test section geometry.

5. ACKNOWLEDGEMENT

The authors are grateful to the support simulation team in laboratories (Mr. Kismono, and Mr. Eko Prasetyo).

6. REFERENCES

- Ahmad Zulfadhli, 2008. *Design, Analysis, and Fabricate of Low Speed Water Tunnel*. Universiti Malaysia Pahang.
- Arakeri, V.H. & Govinda, H.S., 1988. The High Speed Water Tunnel Facility at The Indian Institute of Science. *Sadhana*, 13(December), pp.223–235.
- Cengel, Y. & Cimbala, J., 2006. *Fluid Mechanics Fundamentals and Applications*, New York: McGraw-Hill.
- Chuan-jing, L.U. & Ting, S.I., 2011. Water Tunnel Experimental Investigation on The Drag Reduction Characteristics of The Traveling Wavy Wall *. *Journal of Hydrodynamics*, 23(1), pp.65–70.
- Dol, M.Z. and S.S., 2015. Design and Development of Low-Cost Water Tunnel for Educational Purpose. *Material Science and Engineering*, 78, pp.1–8.
- Erm, L.P., 1836. *Development and Use of a Dynamic-Testing Capability for the DSTO Water Tunnel*, Australia.
- Gordon, R. & Imbabi, M.S., 2016. CFD Simulation and Experimental Validation of a New Closed Circuit Wind / Water Tunnel Design. *Fluids Engineering*, 120, pp.311–318.
- Kalyankar, H. et al., 2015. Design and Analysis of Low Speed Water Tunnel for Flow Visualization of Bluff Body. In *2nd International Conference on Advances in Mechanical Engineering and Its Interdisciplinary Areas*. Kolaghat, India: Academia.edu, pp. 49–57.
- Ko, S.C., 1971. *Design and Construction of a water tunnel*, Pennsylvania.
- Lee, C.S. et al., 2005. Development of 3-Component Force-Moment Balance for Low Speed Water Tunnel. *Modern Physics Letters B*, 19, pp.1575–1578.
- Nedyalkov, I., 2012. *Design of Contraction, Test Section, and Diffuser for a High-Speed Water Tunnel*. Chalmers University of Technology.
- Pritchard, P.J. & Leylegian, J.C., 2011. *Introduction to Fluid Mechanics* Eighth Edi., Manhattan: John Wiley & Sons, INC.
- Yao, Y. et al., 2015. Water tunnel experimental investigation on drag reduction of coating surface wall. *Procedia Engineering*, 126, pp.247–253.
- Yuan, J. & Madsen, O.S., 2014. Experimental study of turbulent oscillatory boundary layers in an oscillating water tunnel. *Coastal Engineering*, 89, pp.63–84.



PIPES OUTLET DIRECTIONS AND DIAMETER OF DOUBLE U PIPES CONFIGURATION ON CENTRIFUGAL REACTION PUMP

Budi Setyahandana^a, Y.B. Lukiyanto^{a,1}, Rines^a

^a*Mechanical Engineering, Sanata Dharma University; Paingan, Maguwoharjo, Depok, Sleman, Yogyakarta 55282; Indonesia*

¹*email : lukiyanto@usd.ac.id*

ABSTRACT

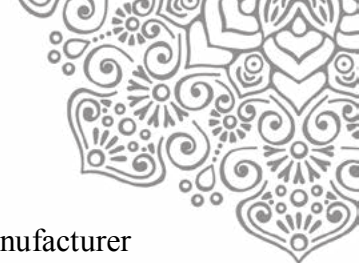
Centrifugal reaction pump is simple centrifugal pump, easy to built, highly local components and operate at very low shaft speed. Experiment study of double U configurations pipes with three outlet directions and pipes diameter of outer arms effects were carried out for centrifugal reaction pump at very low shaft speed. The outlet directions of double U configurations were 90 deg., 0 deg. and -90 deg. from horizontally straight arm pipes. T-junction fitting, a vertical inlet pipe and two horizontally straight arm pipes as main components of the pump were 18.5 mm diameter. The horizontally straight arm pipes are similar with pump impeller function. The arm pipes are replaceable with 22.5 and 28.0 mm. The pump was rotated with vertical pipes as an axis by adjustable speed electric motor at the top of T-junction. The shaft speeds were 70 rpm up to 150 rpm. Total head and diameter of the pump were 665 mm and 1000 mm. The experiment showed that double U configurations with various outlet directions could be used to replace orifices and springs as moving components of centrifugal reaction pump. The experiment resulted performance of the three configurations and backward-inclined-blades-like as the best configuration and is followed by forward-inclined-blades-like and straight-blades-like configurations respectively. Increasing pipes diameter of the arm increase the pump capacity and does not tend to increase the efficiency.

Keywords: centrifugal reaction pump, low shaft speed, double U pipes configuration, outlet direction, arm pipes diameters

1. INTRODUCTION

Wind power and solar photo voltaic power are dependable and renewable energy resources for the electric generation and water pumping for remote area. The hybrid of them ensures the continuity of energy suitable for the area (Dillon, et al, 2014). Wind energy water pumping system (WEWPS) is used for salt pans, drainage, irrigation, cattle watering, and domestic and community water supply with very low head (up to 3m) up to deep head (more than 10 m). Mechanical WEWPS with 1 up to 7 m rotor diameter pumps water 20 m³ up to 2500 m³ per day. Electric WEWPS having higher flexible placement can pump water continuously and larger capacity than the mechanical (Smulders, 1996).

WEWPS must be reliable to run unattended for most of the time, need minimum maintenance and attention. A WEWPS should run for over 20 years with maintenance only once every year without any major replacements. WEWPS used for irrigation seasonally tend to be indigenous designs that are improvized or built by the farmer to reduce the cost (Wind Power, 2013). Therefore, WEWPS for irrigation has low cost and this requirement tends to override other considerations. WEWPS can supply water at competitive cost



especially if manufactured locally (Smulders, 1996). The key actor is the manufacturer who is responsible for choosing and designing, production, marketing and also after sales service.

The main advantages of electric WEWPS are flexibility over other mechanical systems and have more components (Gopal, et al, 2013). The efficiency of electric WEWPS depends on performance of the electric components. It is reported that wind mill could convert 35% wind power to shaft power. For 51% can be lost by all of the electrical components, as a maximum only 17% of the wind energy can be available for water pumping operations. Since a large amount of energy dissipation in converting process, new configuration should be analyzed to avoid such losses (Lara, et al, 2011).

Among of pumps for WEWPS is centrifugal reaction pump. The pump consists of a vertical pipe with a T-joint at the top, from which extend two pipes whose length is dependent upon the rate of rotation of the assembly in operation. An orifice at the end of each pipe arm points, 90° away from the arm. The pump is well adapted to variable low shaft speed and construction is simple. One of these pumps connected to a 3 m diameter wind mill and pumped 30 m³ per hour at a head of 4.5 m in a 29 km/h wind speed (Rubinski & Rubinsky, 1955). Modification to the pump is done by replacing orifices to reduce moving components. Double U pipe configuration with outlet direction in-line with pipe impeller was successfully replace all of moving parts (Lukiyanto & Wahisbullah, 2014).

This present study aims to experimentally investigate effects of outlet flow directions and pipes diameter of outer arms of centrifugal reaction pump. The centrifugal reaction-pump with double-U pipe channels at each of both arms can be adjusted at three outlet directions. The outlet directions to the inlet are backward-inclined blades-like, straight blades-like and forward-inclined blades-like. The names refer to the three main types of centrifugal pump blades (Cengel & Cimbala, 2006). Each of them effects to the pump performances. The pipes of outer arm are modified and replaceable with various diameters of the pipes. The nominal diameters of pipes are 18.5, 22.5 and 28.0 mm (0.5, 0.75 and 1.0 inches).

2. METHODOLOGY/ EXPERIMENTAL

The pump consisted of a vertical pipe with a T-junction (5) at the top, from which extend two horizontally pipes (2) as straight impeller blades (Fig.1). At the end of horizontally pipes were attached double U pipe configurations (3). The upper U pipes were designed movable to adjust outlet direction of fluids. The pipes were arranged from pipes and elbow fittings with nominal diameter of 18.5 mm (0.5 inch). A foot valve (8) was attached at the bottom of the vertical pipe. The T-junction was attached to the shaft motor (1) as drivers. The motor shaft was in line with vertical pipe and foot valve. The assembly was attached to the rigid structure by two bearings (4).

A housing (6) was attached to receive, collect and measure the fluid flow rate that comes from the pumps outlets. Fluid from main pond (10) was delivered to feeder (9) excessively by a submersible pump (11). Excessive fluid at feeder was a mechanism to maintain water level input, thus the head always constant.

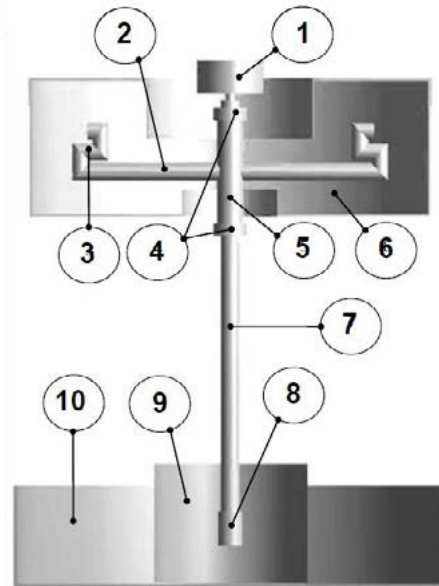


Figure 1. Schematic of centrifugal reaction pump.

The pump outlet directions were adjusted in three positions (Fig.2). The upper U pipes were adjusted 90 degrees (Fig.2a), -90 degrees (Fig.2b) and 0 degree (Fig.2c) away from the straight pipe impeller and were symbolized BB, DD and SS respectively. Based on inlet and outlet impellers geometry, Fig.2a–2c were called backward-inclined blades-like (backward-like blades, BB), forward-inclined blades like (forward-like blades, DD) and straight-like blades (SS) respectively.

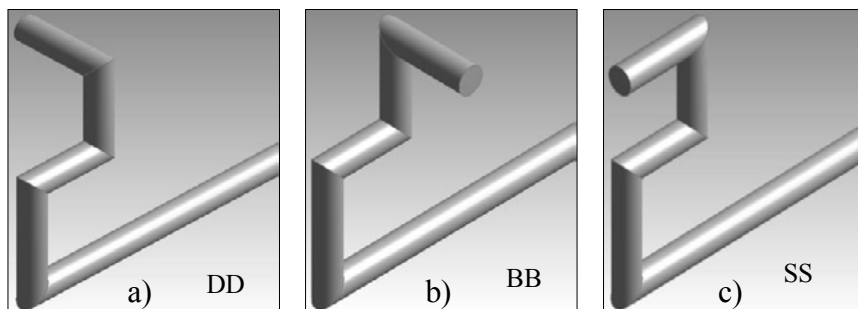


Figure 2. Outlet directions of impeller and symbols, a) backward-inclined blades-like (backward-like blades, BB), b) forward-inclined blades like (forward-like blades, DD) and c) straight-like blades (SS)

T-junction is cross fitting with nominal diameter 0.5 inch. At the ends of T-junction channels are for attaching the mountings (Fig.1). The horizontally channels are for impeller pipes mountings and vertical channels are for shaft mounting and input pipe mounting. The pipes of outer arm in various diameters are modified, replaceable and mountable at the horizontally T-junction mountings. The nominal diameters of outer arm pipes are 18.5, 22.5 and 28.0 mm (0.5, 0.75 and 1.0 inches). (Fig.3). The T-junction with various diameters of outer arm pipes is 1000 mm. The ends of double U pipe configuration as outlets are rotatable thus the outlet directions are adjustable.

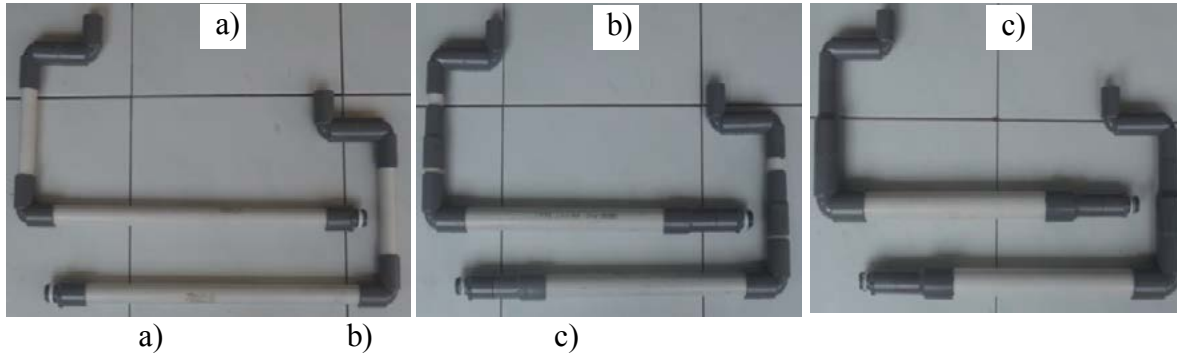


Figure 3. Diameters of arm pipes, a) 18.5 mm, b) 22.5 mm and c) 28.0 mm

The shaft driver was a brush DC (BDC) electric motor 48 volt, 250 watt, maximum speed 540 rpm. The motor speed controller was serial of electric transformer and adjustable voltage regulator. The pump was converted shaft power as power input into hydraulic power as power output. The measurement parameters of power input and power output were based on shaft power (Eq.1) and hydraulic power equations (Eq.2)

Shaft power:

$$P_{in} = 2 \pi \dot{n} T \quad (1)$$

Hydraulic power :

$$P_{out} = \dot{m} g h \quad (2)$$

Pump efficiency :

$$\eta_P = P_{out} / P_{in} \quad (3)$$

Where \dot{n} = shaft speed (rpm), T = shaft torque (N m), \dot{m} = mass flow rate (kg/s), g = standard acceleration of gravity (9.80665 m/s²) and h = total head (665 mm).

Based on the Eq.1 to Eq.3, the measured parameter were shaft speed (rpm), shaft torque (N m), flow rate (m³/s), and constant suction head (665 mm). The shaft speed was measured by tachometer. The shaft torque was measured by multiplying the length of torque-arm (345 mm) and the force reading on weight-scale. The Portable Electronic weight-scale (maximum 40 kg/5 g) was installed at the end of torque-arm. Mass flow rate was the result of multiplying fluid flow rate with standard of fluid density. The fluid was standard water ($\rho = 998.0 \text{ kg/m}^3$). Water flow rate was measured by using measuring glass and stopwatch. Total head parameter in this experiment was adjusted to be constant at 665 mm.

The measurement of the shaft torque was calculated based on the shaft torque of motor. Shaft power input was the difference between shaft motor power and the mechanical losses caused by the bearing friction. The mechanical losses were calculated by measuring torque and shaft speed without pumping load by deactivated foot valve.

3. RESULTS AND DISCUSSION

3.1. Various outlet directions

Mechanical power losses (P_{loss}) were found by measurement of motor shaft torque and speed without pumping load measurement. On the no-load measurement, foot valve was in off mode. The foot valve channel was blocked with removable sealer. The shaft speed



measurement was in the range of 70 up to 150 rpm (Fig.4). Pump shaft power input (P_{in}) was calculated by reducing motor shaft power (P_{motor}) with the P_{loss} .

On the experiment measurements, shaft speeds were started at 145 rpm and down to 75 rpm. The system was start pumping (cut-on) about 95 rpm and stopped pumping (cut-off) at about 84 rpm. The maximum speed and flow rate were 143.8 rpm and 0.244 dm³/seconds respectively. The total head was maintained constant at 665 mm. The main arm diameter was 1000 mm. Based on equation (2), hydraulic power was dependent on flow rate and total head. The study show that hydraulic power was only depended to single parameter flow rate linearly due to total head maintained constant. Due to flow rate dependency on shaft speed, the hydraulic power was only dependent on shaft speed. The results showed that hydraulic power of the three double-U pipe configurations tends to linear to the shaft speed (Fig.5). Each of the three double-U pipe configurations were also coincide.

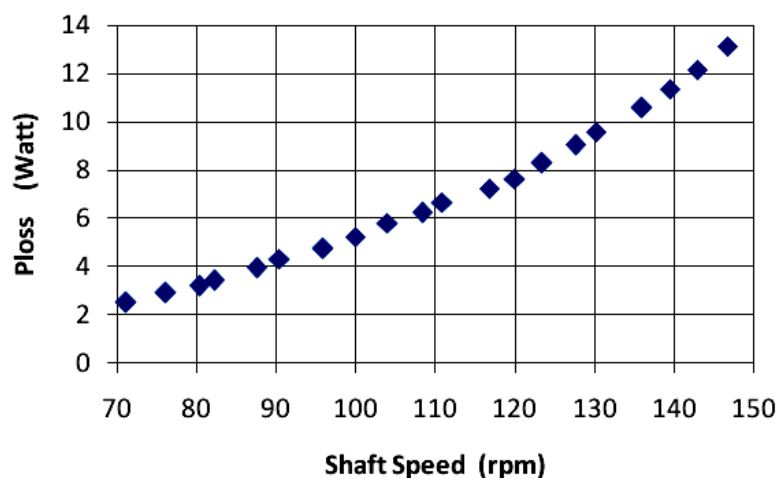


Figure 4. Mechanical power losses and shaft speed

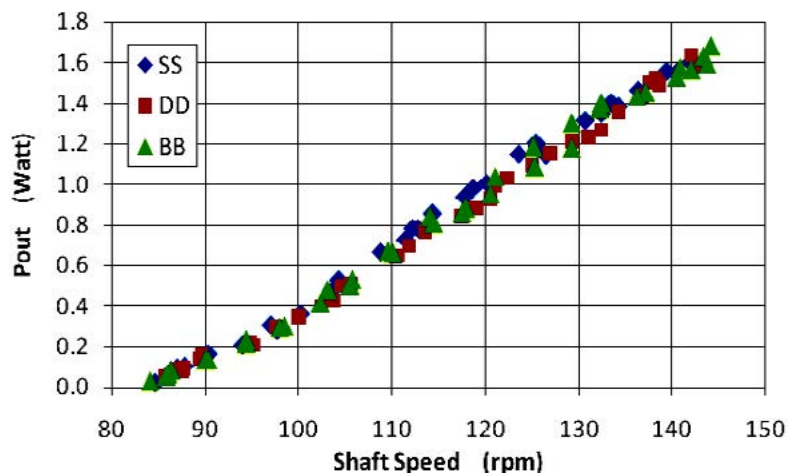


Figure 5. Pumping power outputs and shaft speed

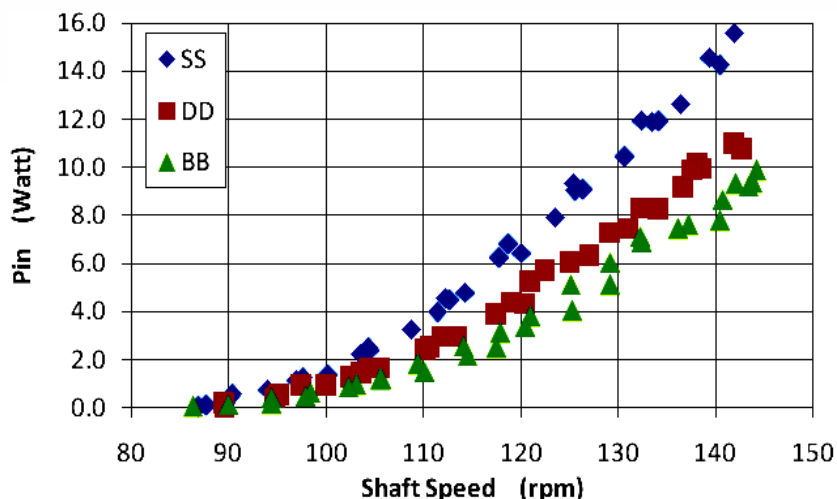


Figure 6. Shaft power inputs and shaft speed

Double-U pipe configurations were affected to the shaft power input (Pin) as Fig.6. The Pin was not coincide and linear for all of the configurations as hydraulic power. The SS and BB configurations were higher and lower Pin than the DD configuration.

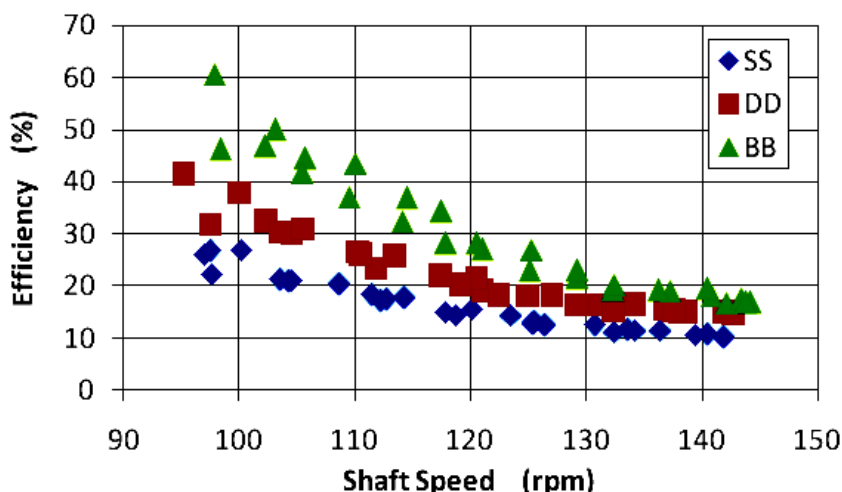


Figure 7. Pumps efficiencies and shaft speed

Shaft power inputs and hydraulic power outputs were resulted efficiencies of reaction centrifugal pumps with the three double U pipe configurations as Fig.7. The efficiencies of each configuration were not linier to the shaft speed. The efficiencies and its deviation tended to lower value for higher shaft speed. The BB configuration was the best configuration for the highest efficiency for all shaft speed evaluated. The DD configuration was better than SS configuration for the higher efficiency for all shaft speed evaluated.

For shaft speed 100 rpm down 84 rpm when the system was stopped pumping (cut-off), deviation data was higher due to foot valve was not fully opened. The uncontrolled opening foot valve was only depended on differential pressure of fluids in upper and below of foot valve.



3.2. Various outlet diameters

Based on result of the previous experiment, outlet direction for performance of centrifugal reaction pump with various diameters experiment is adjusted on BB configuration. Outlet directions of the upper U pipes were adjusted 90 deg. away from the straight pipe impeller and were also called backward-inclined blades-like.

Based on Fig.8, increasing diameter of the arm pipes could increase capacity of centrifugal reaction pump. Increase diameter of pipes to nominal diameter 0.75 increased capacity of the pump for shaft speed 130 rpm and up, compared to nominal diameter 0.5 inch. Increase diameter of pipes to nominal diameter 1.0 increased capacity of the pump significantly for all speed range of experiment, compare to nominal diameter 0.5 and 0.75 inch. The pump characteristics were similar with Eq. 2. The fluid mass and mass flow rate in channel were larger for larger pipe diameter.

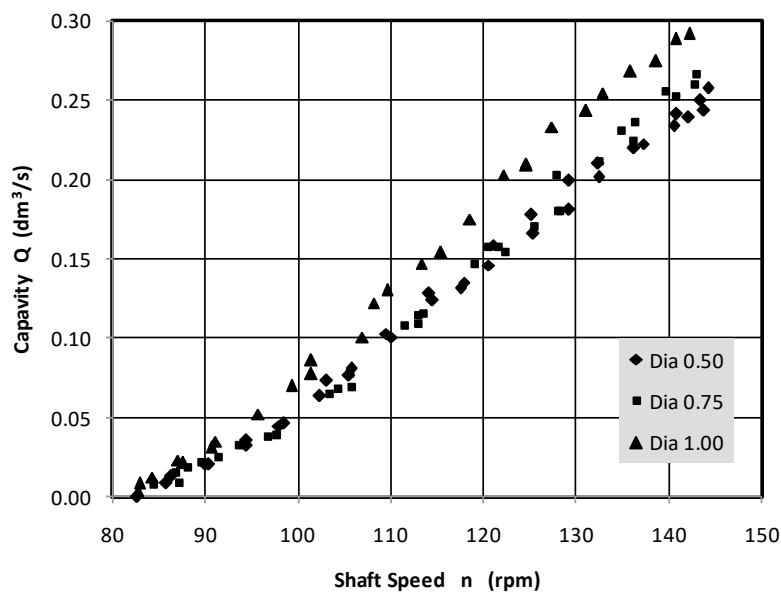


Figure 8. Pumps capacity and shaft speed

Experiments of the pumps showed that the efficiencies tends similar for various arm pipes diameters, especially for shaft speed range 120 up to 145 rpm (Fig.9). For various arm pipes diameters, the pump efficiency deviation was higher in shaft speed below 120 rpm as foot valve was not opened fully and the opening of the valve could not be controlled. Increase nominal diameter of arm pipes, although increase the pump capacity, was not increase the efficiency. It meant that the increasing of shaft power as power input to the pump was followed by the increasing of hydraulic power as power output of the pump and its power losses. The power losses came from T-junction, vertically inlet pipe, double U pipes and foot-valve as fixed parts on whole experiment. One of the losses comes from secondary flow in channels. Compare to non-rotating channels flow, effect of rotation is significant to the secondary flow (Colleti, et al, 2014; Roy, et al, 2013).

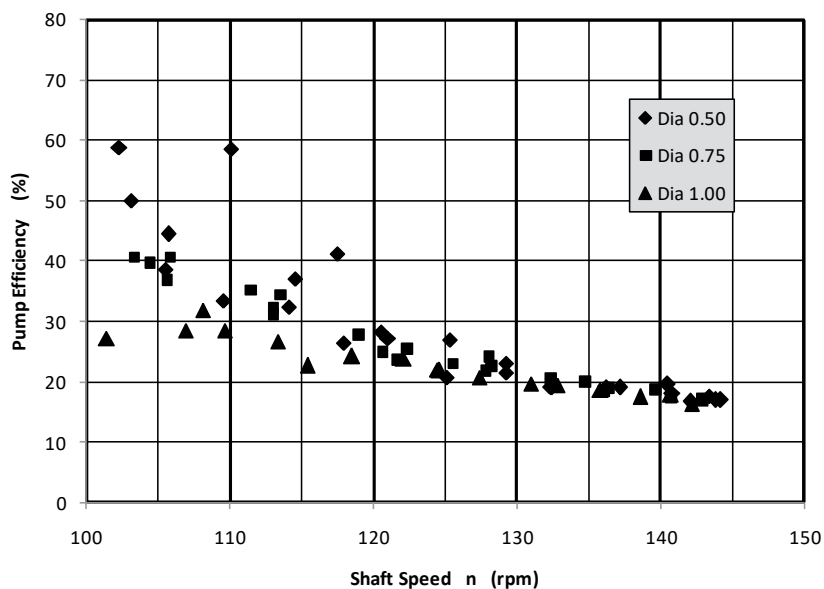


Figure 9. Pumps efficiency and shaft speed

4. CONCLUSION

The experiment study show that double U configuration with 90 deg, 0 deg and 90 deg outlet directions to the straight impeller blades and with 18.5, 22.5 and 28.0 mm (0.5, 0.75 and 1.0 inches) pipes nominal diameter of outer arms were successfully applied to the centrifugal reaction pump. The configurations can be used to replace a pair of fixed and sliding orifice as water gate restricts the air to flow into pipe impeller channel.

The result shows that the configuration has higher effects to the hydraulic power output than the shaft power output. The best efficiency is backward-inclined-blades-like, forward-inclined-blades-like and straight-blades-like respectively. Increasing nominal diameter of arm pipes significantly affect to increase of the pump capacity but has no significant effect to the pumps efficiency.

ACKNOWLEDGEMENT

The research was sponsored by LPPM – Sanata Dharma University, Yogyakarta, Indonesia and RISTEK DIKTI, Indonesia.

REFERENCES

- Cengel, Y.A. and Cimbala, J.M., (2006), Fluid Mechanics: Fundamentals and Applications, McGraw-Hill Education (Asia), New York), pp. 754-757.
- Colletty, F., Lo Jacono, D., Cresci, I. and Arts, T., (2014), Turbulent flow in rib-roughened channel under the effect of Coriolis and rotational buoyancy forces, Physics of Fluids, Volume 26
- Dhillon, J., Kumar, A. and Singal, S.K., (2014), Optimization methods applied for Wind-PSP operation and scheduling under deregulated market: A review, Renewable and Sustainable Energy Reviews, Volume 30, pp. 682–700



- Gopal, C., Mohanraj, M., Chandramohan, P., and Chandrasekar, P., (2013), Renewable energy source water pumping systems—A literature review, *Renewable and Sustainable Energy Reviews*, Volume 25, pp. 351–370
- Lara, D.D., Merino, G.G., Pavez, B.J. and Tapia, J.A., (2011), Efficiency assessment of a wind pumping system, *Energy Conversion and Management*, Volume 52, pp. 795–803
- Lukiyanto, Y.B. and Wahisbullah, E., (2014), A Simple Double U Pipe Configuration to Improve Performance of a Large-Diameter Slow-Speed Centrifugal Impeller; *Proceedings of the 3rd Applied Science for Technology Application, ASTECHNOVA 2014 International Energy Conference Yogyakarta, Indonesia, 13-14 August 2014*
- Roy, P., Anand, N.K., Banerjee, D., (2013), A review of flow and heat transfer in rotating microchannels, *Procedia Engineering*, Volume 56, pp. 7-17
- Rubinski, I.A. and Rubinsky, A.I., (1955), A low specific speed pump for small discharge, *Civil Engineering and Public Works Review*, Volume 591, pp. 987-990
- Smulders, P.T., (1996), Wind water pumping: the forgotten option, *Energy for Sustainable Development*, Volume 5, pp. 8-13
- Wind Power, <http://www.fao.org/docrep/010/ah810e/ah810e10.htm> downloaded 27/08/2013 13:54



OPTIMIZATION OF IMPACT ENERGY ABSORBER PARAMETERS FOR AUTOMOBILE CRUSH BOX USING RESPONSE SURFACE METHOD

Mohammad Malawat^{1,a*}, Danardono Agus Sumarsono^{1,c}.

Department of Mechanical Engineering, Faculty of Engineering, Universitas Indonesia¹

Kampus Baru UI Depok 16424 Indonesia¹

Phone: +62-21-7270032, Fax: +62-21-7270033

E-mail: ^cdanardon@eng.ui.ac.id, ^{a*}mohammad.malawat@ui.ac.id

ABSTRACT

*The Impact Energy Absorber (IEA) of an automobile provide the crush box to crumple when the collision is happening. The IEA is located on front end or rear end of automobile. Exactly, the IEA is located behind the bumper. The main functions of The IEA are to absorb any kind of energy due to collision and to protect the main structure of automobile from destruction that effects to prevent occupant fatality, distortion on battery or exploitation on fuel tank. The IEA is made from thin wall square tube where located holes as crush initiators. Three square tubes having thickness about 0.6 mm (specimen code A), 0.8 mm (specimen B) and 1 mm (specimen Code C) were tested under dynamic load. The crushing initiator is designed around the shape of the tube wall and has eight holes with a fixed diameter of 6.5 mm. For optimization, the result of experiment of the crushing initiator was determined at 3 different locations on the specimen wall. These locations are 10 mm, 30 mm, and 50 mm measured from the initial collision position of the specimen tested. There is the experiment result is going to optimized. The main aim of the research is to optimize the IEA parameter for automobile crush box. Wall thickness and crush initiators position on thin wall square tube are considered as input parameters. Sets of parameter for impact energy absorber are designed by employing *Response Surface Method (RSM)* in statistical software *Mat lab 2016*. The regression equation for impact energy absorber is developed using the experimental drop test result of different variant of wall thickness and crush initiators position of square tube as an IEA. The optimization result that the thin-walled square tube cross section 60.42; $h = 0.6$ mm almost complied to all optimal prediction on IEA design and crush initiators position 10 mm of from the edge of thin-walled square tube had the optimal prediction on IEA design.*

Keywords: Crush initiators position; Wall thickness; Impact energy absorber; Response surface method.

1. INTRODUCTION

The chassis elements that absorb the kinetic energy at the moment of a vehicle of crash approximately 40% are front rail columns. The possible impact of the occupants with the windshield of the car because of persistent rigidity during a short fraction of time and delay in initial folding this causes large negative accelerations if these columns are too rigid (I. Eren et al., 2009).

Cho et al. (2006) on I. Eren et al., (2009) studied front frame optimizations with a no



uniform closed-hat section using dent-type and hole-type crush initiators under an axial loading condition of frontal crash. They compared the results of the same size of design analysis of hole-type crush initiators with those of dent-type crush initiators (I. Eren et al., 2009).

By applying the response surface methodology (RSM) in which all factors are varied simultaneously over a set of experimental runs, these limitations of the classical method of experimentation can be avoided that involves statistical design of experiments (DoE) (Khayet et al., 2016). In fact, RSM is a collection of mathematical and statistical techniques can be used to evaluate the relative significance of several affecting factors and useful for developing, improving and optimizing processes, even using a minimum number of experiments in the presence of complex interactions between them (Khayet et al., 2010; Montgomery, 2001; Montgomery and Myers, 1995 on Khayet et al., 2016).

The objective of the method in adsorption is to achieve the best adsorption performance to simultaneously optimize the levels of these variables (M. Roosta et al., 2014 on M. Dastkhoo et al., 2017).

The main objective of this study is to optimize of IEA parameters for automobile crush box which wall thickness and crush initiators position on thin-walled square tube are considered as input parameters against to the reduction of peak force and to the increasing not only energy absorption, crush force efficiency, but also specific energy absorption.

2. METHODOLOGY/EXPERIMENTAL

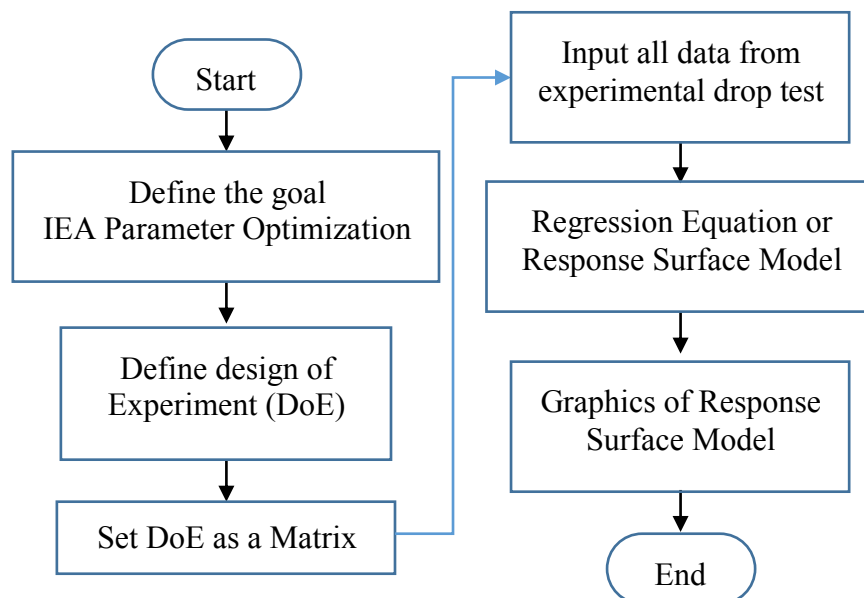


Figure 1. Flow chart of study

RSM is the most widely used mathematical modelling and statistical evaluation method for optimization of input parameters (independent variable) of any system. In addition, the method can easily be used in explanation and prediction of the existing relationship



between the input parameters with the responses (dependent variables) (A. Aloufi et al., 2011 on Tushar M. Patel et al., 2016).

Figure 1 shows the flow chart of study. Study begin with define the goal of IEA parameter optimization where wall thickness and crush initiators position on thin wall square tube are considered as input parameters (Table 2). After that, define design of experimental (DoE) by setting the level of parameter. Sets of parameter for IEA are designed by employing response surface method (RSM) in statistical software *Mat lab 2016*. The linear regression equation for impact energy absorber is developed using the experimental drop test result of different variant of wall thickness and crush initiators position of square tube as an IEA. The linear regression model produce optimization graphics.

Table 2. Parameter and level of IEA

Parameters	Level		
	(-1)	(0)	(+1)
Wall Thickness (X_1)	0.6 (0)	0.8 (1)	1.0 (2)
Crush Initiators Position (X_2)	10 (0.5)	30 (1)	50 (1.5)

The relationship between input parameters and their respective reactions in problems solved with RSM is generally expressed with the following second-degree polynomial equation (Montgomery and Myers, 1995; Khayet et al., 2007, 2010b on Khayet et al., 2016).

$$\hat{Y} = \beta_0 + \sum_{i=1}^k \beta_i x_i + \sum_{i=1}^k \beta_{ii} x_i^2 + \sum_{i \neq j}^k \beta_{ij} x_i x_j + \varepsilon \quad (1)$$

Where \hat{Y} is the predicted response, x_i and x_j ($j = k + 1, i < j$) are the coded independent variables (factors), $\beta_0, \beta_1, \dots, \beta_k, \beta_{ij}$ are the regression coefficients and ε is the statistical error.

RSM is a collection mathematical and statistical technique for empirical model building. By careful design of experiments, the objective is to optimize IEA parameters which is influenced by several function (independent variables). Response surface method is use to examine the relationship between a response and a set of quantitative experimental variables or factors.

The selected process variables were varied up to three levels and drop test was adopted to experimental. The two parameters considered for this study are wall thickness (mm) and crush initiators position (mm). The parameters are set at three levels each. The summary of the parameters is shown in Table 2 (Danardono A. S. et al., 2015; M. Malawat et al., 2016).

The value of IEA for all variants are measured using experimental drop test for finding out the optimum wall thickness and crush initiators position. Series of analysis is conduct to obtain the data sets for RSM model.



3. RESULTS AND DISCUSSION

Experiment was designed according to the test conditions. The analysis was conducted for all data sets, with the process parameter levels set as given in Table 2. Experimental result of drop test is given in Table 3. There are two parameters on three levels data set with three times data taken ($3^2 \times 3$) were conducted to prepare data set as a function for response surface model. Twenty-seven dynamics test having three different cross sections were crushed axially on the drop loading rig. The first parameter is wall thickness of square tube with three set up levels are cross section $c/h = 60.42$; $h = 0.6$ mm, $c/h = 45.69$; $h = 0.8$ mm, and $c/h = 36.80$; $h = 1.00$ mm. The second parameter is crush initiators position with three set up levels are 10 mm, 30 mm, and 50 mm.

Table 3. Experimental drop test data

Run	Parameters		Function			
	X ₁	X ₂	PF (kN)	EA (kJ)	CFE (%)	SEA (kJ/kg)
1	0.6	10	33.2	0.62	15.06	4.05
2	0.6	30	20.3	0.92	39.90	6.03
3	0.6	50	19.2	0.86	36.46	5.63
4	0.6	10	24	1.01	40.42	6.63
5	0.6	30	22.9	0.68	28.82	4.45
6	0.6	50	24.2	0.97	39.26	6.37
7	0.6	10	26.3	1.25	52.09	8.25
8	0.6	30	29.6	1.01	43.58	6.61
9	0.6	50	27.5	0.87	37.09	5.73
10	0.8	10	25.6	0.60	45.31	3.16
11	0.8	30	45.7	0.50	21.01	2.62
12	0.8	50	28	0.71	42.86	3.72
13	0.8	10	36.6	0.75	37.98	3.95
14	0.8	30	44.4	0.75	31.31	3.94
15	0.8	50	42	0.84	30.00	4.42
16	0.8	10	36.5	0.98	38.63	5.15
17	0.8	30	41.6	0.90	46.88	4.73
18	0.8	50	45	0.86	33.56	4.50
19	0.8	10	61.1	0.69	40.59	3.10
20	1.0	30	50.5	0.73	55.64	3.29
21	1.0	50	55	0.70	53.09	3.14
22	1.0	10	52.1	0.60	36.28	2.71
23	1.0	30	62	0.71	44.19	3.18
24	1.0	50	78	0.84	40.13	3.77
25	1.0	10	72.7	0.67	29.71	3.00
26	1.0	30	55.2	0.73	42.93	3.27
27	1.0	50	58	0.69	42.93	3.11



All data set as a matrix run by *Mat lab 2016* and produce the regression coefficients. The regression coefficients are going to insert into the linear regression equation. Those are linear regression equation or response surface model. The model shows the optimal condition of IEA as a crush box for peak force, energy absorption, crush force efficiency, and specific energy absorption value. The optimal IEA design of linear regression model shown on equation (2), (3), (4), and (5).

$$Y_{ts} = 37.4936 + 18.2334X_1 + 3.0415X_2 - 0.9306X_1X_2 + 1.1262X_1^2 - 0.9803X_2^2 \quad (2)$$

$$Y_{ts} = 0.7618 - 0.0973X_1 + 0.0931X_2 - 0.0053X_1X_2 - 0.0600X_1^2 - 0.0120X_2^2 \quad (3)$$

$$Y_{ts} = 0.7618 - 0.0973X_1 + 0.0931X_2 - 0.0053X_1X_2 - 0.0600X_1^2 - 0.0120X_2^2 \quad (4)$$

$$Y_{ts} = 3.9336 - 1.3612X_1 + 0.5630X_2 - 0.0294X_1X_2 - 0.3800X_1^2 - 0.0905X_2^2 \quad (5)$$

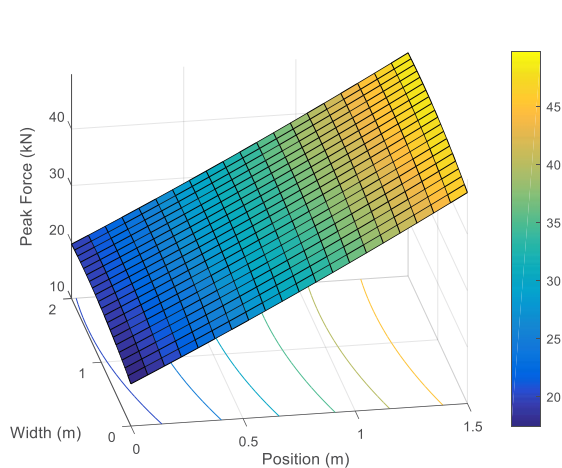


Figure 2 Optimization Graphic of Peak Force

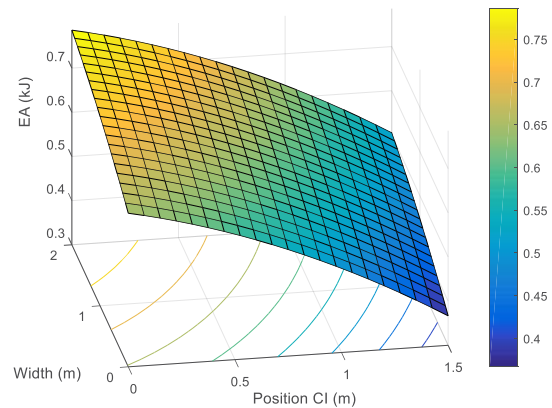
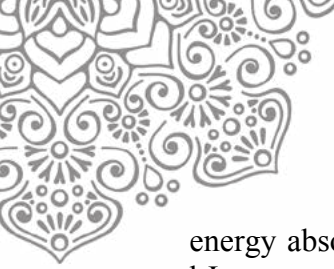


Figure 3. Optimization Graphic of Energy Absorption

Figure 2 shows the optimization graphic for peak force experimental result data. On IEA design, the lowest peak force value is the optimal IEA design. So, the optimal prediction surface of peak force from IEA design shown on the dark blue to dark blue area. The area shown around 0.6 mm of wall thickness or thin-walled square tube cross section 60.42 and 10 mm of crush initiators position. The prediction value of the peak force IEA design according to the response surface about 20 kN until 25 kN.

Figure 3 shows the optimization graphic for energy absorption experimental result data. The optimal prediction surface of energy absorption from IEA design shown on the orange to yellow area. The area shown around 0.8 mm of wall thickness or thin-walled square tube cross section 45.69 and 10 mm of crush initiators position. The prediction value of the



energy absorption IEA design according to the response surface about 0.70 kJ until 0.75 kJ.

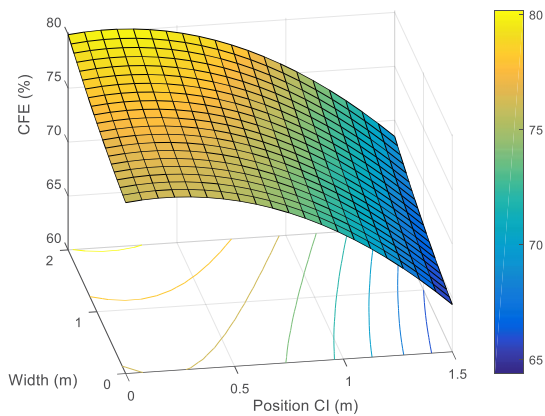


Figure 4 Optimization Graphic of Crush Force Efficiency

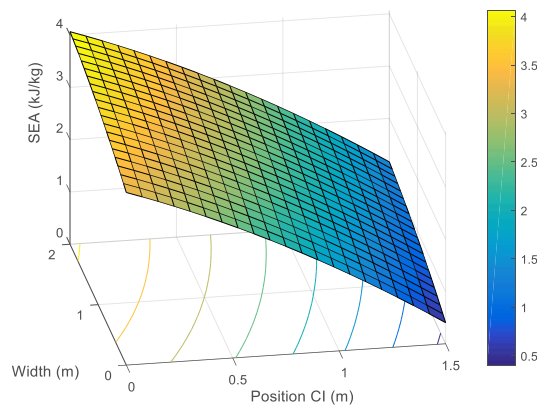


Figure 5 Optimization Graphic of specific energy absorption

Figure 4 shows the optimization graphic for crush force efficiency experimental result data. The optimal prediction surface of crush force efficiency from IEA design shown on the orange to yellow area. The area shown around 1.0 mm of wall thickness or thin-walled square tube cross section 36.80 and 10 mm of crush initiators position. The prediction value of the crush force efficiency IEA design according to the response surface about 70 % until 80%.

Figure 5 shows the optimization graphic for specific energy absorption experimental result data. The optimal prediction surface of specific energy absorption from IEA design shown on the orange to yellow area. The area shown around 0.6 mm of wall thickness or thin-walled square tube cross section 60.42 and 10 mm of crush initiators position. The prediction value of the specific energy absorption IEA design according to the response surface about 3.0 kJ/kg until 3.5 kJ.

4.CONCLUSION

The main conclusion of this study are:

1. RSM design was used to prepare prediction model to determine not only peak force, energy absorption, crush force efficiency, but also specific energy absorption generated for the given set of design IEA parameter.
2. It is found that the thin-walled square tube cross section 60.42; $h = 0.6$ mm almost complied to all optimal prediction on IEA design and crush initiators position 10 mm of from the edge of thin-walled square tube had the optimal prediction on IEA design.



5. ACKNOWLEDGEMENT

The Authors would like to thank the “Departemen Riset dan Pengabdian Masyarakat” Universitas Indonesia for funding this research by Hibah Riset Pascasarjana 2015.

6. REFERENCES

- Danardono Agus Sumarsono, Mohammad Malawat, Jos Istiyanto, (2015), Pengembangan Impact Energy Absorber dengan Pengaturan Jarak Crush initiators, Proceeding on Seminar Nasional Tahunan Teknik Mesin XIV 2015.
- Hazren A. Hamid, Youla Jenidi, Wim Thielemans, Christopher Somerfield, Rachel L. Gomes, (2016), Predicting the capability of carboxylated cellulose nanowhiskers for the remediation of copper from water using response surface methodology (RSM) and artificial neuro network (ANN) models, *Industrial Crops and Products* 96 108-120.
- Ilham Asilturk, Suleyman Neseli, Mehmet Alper Ince, (2016), Optimisation of parameters affecting surface roughness of Co28Cr6Mo medical material during CNC lathe machining by using the Taguchi and RSM methods, *Measurement* 78 120–128.
- I. Eren, Y. Gur, Z. Aksoy, (2009), Finite Element Analysis of Collapse of Front Side Rails with New Types of Crush Initiators, *International Journal of Automotive Technology*, Vol. 10, No. 4, pp. 451-457.
- Mehdi Dastkhon, Mehrorang Ghaedi, Arash Asfaram, Alireza Goudarzi, Seyyedeh Maryam Mohammadi, Shaobin Wang, Improved adsorption performance of nanostructured composite by ultrasonic wave: Optimization through response surface methodology, isotherm and kinetic studies, *Ultrasonics Sonochemistry*, 37 (2017) 94-105.
- M. Khayet, J.A. Sanmartino, M. Essalhi, M.C. Garcia-Payo, N. Hilal, Modeling and Optimization of a Solar Forward Osmosis Pilot Plant by Response Surface Methodology, *Solar Energy*, 137 (2016) 290-302.
- Mohammad Malawat, Jos Istiyanto, Danardono Agus Sumarsono, (2016) Effects of Wall Thickness and Crush Initiators Position Under Experimental Drop Test on Square Tubes, 3rd International Conference on Advanced Engineering Technology ICAET 2016.
- Tushar M. Patel, N. B. Bhatt, (2016), Development of a Mathematical Model of VMS for Automotive Structural Member using FEA-RSM Hybrid Modeling, 3rd International Conference on Innovations in Automation and Mechatronics Engineering, ICIAME 2016, *Procedia Technology* 23 98-105.



15th International Conference on Quality in Research (QIR 2017)

Optimization of Container Terminal Operational Performance through Suppressing its Idle Time

Fenti Suryadi¹, Sunaryo^{2*}, Komarudin³

¹ Mechanical Engineering Department, Universitas Indonesia,

² Mechanical Engineering Department, Universitas Indonesia,

³ Industrial Engineering Department, Universitas Indonesia,

ABSTRACT

The paper is aimed on the attempt of reducing the idle time of container loading-unloading operations at the port terminal, and specifically at Tanjung Priok Port Container Terminal, as a complementary to the one being newly built just off the existing harbor complex. In the last 5 years, container shipment traffic in Indonesia has been increasing significantly. It is predicted that in 2020 container loading operational activities at Tanjung Priok Port will reach more than 10 million TEUs. Idle time is ineffective time included in the daily operation caused by several factors, such as waiting for the containers to be lifted, machines break down, changing of operators, flow of head trucks etc. By suppressing the amount of idle time in container loading-unloading operation, operational performance of terminal will be higher thus creating a better, more efficient, and faster traffic of container entering or exiting the terminal.

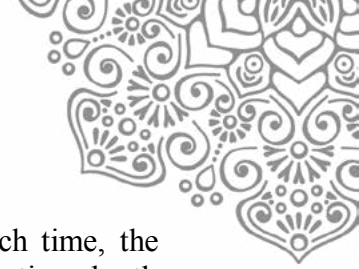
Keywords: Box Crane Hour, Container, Idle Time, Port, Terminal Performance.

1. INTRODUCTION

Indonesia is a country with more than 17,000 islands, 2/3 of its territory is covered by sea. Indonesia has abundant of natural wealth in its islands that makes Indonesia has the advantage of diverse natural products to meet the needs of each region. Marine transports are mostly used to distribute large amount of natural products and goods. To support marine transport adequate ports are needed, for ships to loading and unloading of their cargoes.

In the last 5 years, container shipment traffic in Indonesia has been increasing significantly. It is predicted that in 2020 container loading operational activities at Tanjung Priok Port only will reach more than 10 million TEUs. [1]. Furthermore, in anticipation for the growth Indonesia Port Corporation is building a new port with large capacity off the existing harbor complex, and upgrading the existing port system, infrastructure and human resources. Indonesia Port Corporation has 3 ports i.e.: PT. Port of Tanjung Priok, Port of Koja and Jakarta International Container Terminal. Port of Tanjung Priok has the highest throughput in the last 5 years, it operates 3 terminals: Terminal 1, Terminal 2, and Terminal 3. Terminal 2 is dedicated for handling domestic containers, while the other two are for international cargoes. For the purpose of this research case study was conducted at Terminal 2 Port of Tanjung Priok.

The goal of this research is to improve the operational performance of the existing domestic container terminal in order to act as a complementary to the one being newly built, by suppressing the amount of idle time in container loading-unloading operation. It is assumed that when the terminal has a proper strategy to minimize idle time in wharf operations it will also increase the box crane hour from each equipment, and increase the production throughput of the terminal.



The operational performance of the terminal can be seen from: ship's approach time, the effective time, idle time, not operation time, berthing time, turn around, postpone time, berth working time, and for the measurement of terminal operation of we can see from its production throughput, box crane hour, etc. In order to improve the performance of container terminal one of the approaches is to minimize idle time of loading and unloading of containers on berth. Based on the recorded performance reports, causes of the idle time among other things are: waiting for incoming container, slow flowing of head trucks, waiting for operators during changing of shift, and in-trouble equipment. It is also reported that the yard plan has very much influence on the idle time. Liang Ping Me et al [2] had done an optimization framework for yard plan at container terminal using strategic simulation, and their approach was adopted in this research.

There are two types of port terminals, transshipment terminal and import-export terminal. But in fact according to Sanen and Romert [3] there is no terminal that is absolutely 100% transshipment, as in the port of Tanjung Pelepas, Singapore, Salasah, Port Said, etc. they have an average transshipment of more than 90% and most other port transshipment have averaged less than 15%. Both at transshipment and import-export terminals loading and unloading of containers play very important role in determining the production throughput of the terminals. According to Ceghun and Deniz [4] there are 3 important aspects in determining the efficiency of a container terminal i.e. the container yard, cranes being used, and the vessels that are berthing at the terminal.

2. METHODOLOGY

The research was conducted based on the primary information and secondary information. The primary information is gathered mostly from on the spot observations at Terminal 2, PT. Port of Tanjung Priok in Jakarta, through interview with people in charge of the terminal operations, direct observation of the tasks being conducted, and informal discussions with the management of the terminal, while the secondary information is obtained from literature review, and discussions with experts. The gathered information is then analyzed using "fish bone" cause and effect analysis, results of the analysis are used further to propose the strategy for increasing the efficiency of the container terminal.

2.1. Identification of the causes of idle time

Terwiesch [5] defines idle time as cycle time minus processing time; it is for how long a source cannot do anything because he has to wait for another source. In fact it is an ineffective time included in the daily operation of a certain tasks. Based on the study carried out by Wibowo [6] indicated that idle time included in the operation of container terminal are: waiting for containers to be lifted to or from the ship, which comprised of about 35%; waiting for the head truck to carry or to bring the containers from or to the berth, which comprised of around 29%; waiting for the operator of Quay Container Crane during the changing of working shift, which comprised of 24%; due to repairing of break down equipment, which comprised of 12%, as shown in figure 1.

2.2 Container yard capacity and facility

Beside the efficiency of the activities carried out at the wharf, its container throughput is also determined by the productivity at the container yard, because both the incoming and outgoing containers have to be stacked at the container yard before being transported to the owners (for the incoming containers) or to be loaded to the ships (for outgoing containers), therefore capacity and the availability of the faculties play important role.



Container yard capacity in terminal 2 PT Tanjung Priok Port is shown in table 1, maximum capacity in this area is 7349.5 TEU's, divided in 10 blocks, each block is served by two rail mounted gantry crane, and one reach stacker.

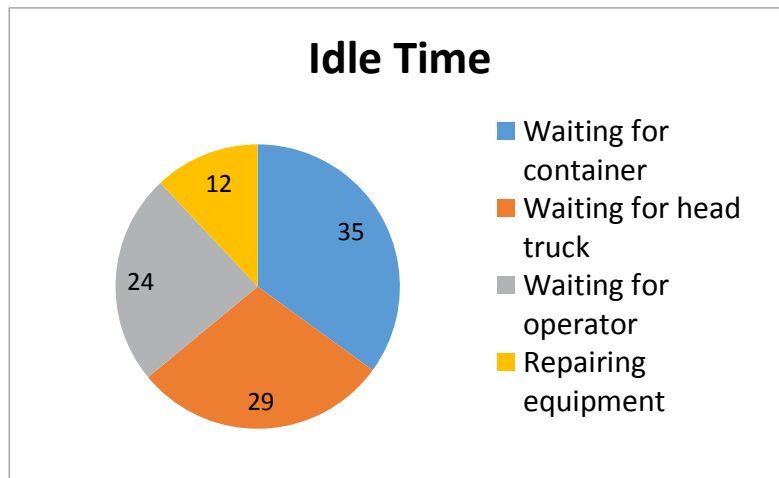


Figure 1. Causes percentage of the idle time in container terminal.

Table 1. Capacity of container yard at terminal 2

BLOCK	SLOT	ROW	TIER	GROUND SLOT	CAPACITY (Teus)
a	b	c	d	e = b*c	f = b*c*d
1	22	6	5	132	660
2	20	6	5,5	120	660
3	15	6	5,5	90	495
4	23	10	5,5	230	1265
5	22	10	5,5	220	1210
6	18	7	5,5	126	693
7	18	7	5,5	126	693
8	18	7	5,5	126	693
9	13	7	5,5	91	500,5
10	12	8	5	96	480
Total	181			1357	7349,5

2.3. Analysis for the cause of idle time

As has been identified that the main causes of the idle time are: waiting for the containers, waiting for the head truck, changing of operators, and repairing equipment. In order to investigate the sources of those causes “Fish Bone” cause and effect analysis was used, which is shown in figure 2.

It was discovered that the sources of idle time caused by waiting for containers are:

- Port navigation system for the ships to enter the port and berth at the terminal, this includes the congestion of the port entrance; the depth of the port basin; the wave and current in the port entrance.
- Container yard facilities, which would determine the speed of containers flowing from the container yard to the wharf.



- Queuing strategy implemented by the terminal.
- Container stacking both in the ship's cargo holds as well as at the container yard.

Caused by waiting for the head trucks are:

- Container yard facilities, which would determine the speed of putting the containers on the trucks.
- Number of trucks available in the terminal to transport the container from and to the wharf.
- Cargo handling policy implemented by the terminal whether sub-contracted to shipping companies or handled by itself.

Caused by changing of operator are:

- Human resources management implemented by the terminal, which includes recruitment policy, training and development of the operators, and welfare of the human resources.
- Cargo handling policy implemented by the terminal whether sub-contracted to shipping companies or handled by itself.
- Shifting plan of the operators that sometimes does not run smoothly such as due to bad weather.

Caused by repairing of equipment are:

- Maintenance system of the equipment implemented by the terminal.
- Number of equipment deployed at the wharf namely the quay container cranes.

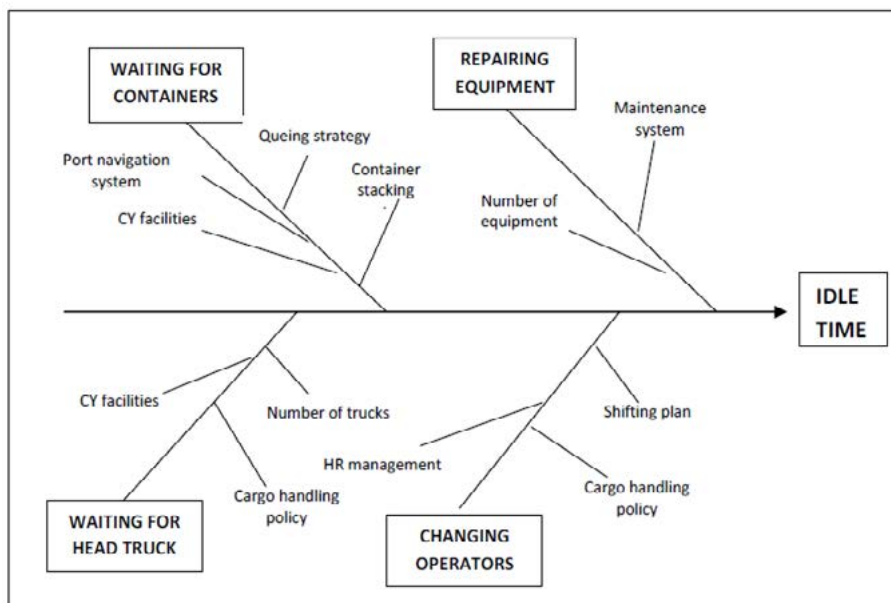


Figure 2. Fishbone analysis of idle time

3. RESULT AND DISCUSSION

Based on the analysis of the sources that cause the idle time, the solutions being proposed to minimize the idle time of each cause among other things are:

- Waiting for containers
 Improve port navigation access system, including the pilotage system; monitor the depth of port basin regularly; increase the efficiency in the container yard including the reliability and availability of the facilities utilized in it; increase the efficiency of the queuing strategy implemented both at the wharf as well as at the container yard, which include containers stacking plan system.
- Waiting for head truck



Increase the efficiency in the container yard, so that head trucks can flow smoothly; optimize the number of head truck deployed in the terminal, and maintain their condition for the tasks; improve cargo handling management in accordance with the development of latest technology, including information system for instructing the flow of the head trucks.

- Changing of operators

The terminal works 24/7; therefore the equipment operators who serve in loading and unloading of containers are divided into three groups, 8 hours for every shift. Since the tasks are not carried out directly by the port operator, but sub-contracted to the cargo handling companies or to the privilege shipping companies. This scheme sometimes creates delays during the changing of operators between the shifts. It is proposed that the terminal should have full control for the deployment of the operators and their working schedules. Welfare, training system and safety of the operator should also put into considerations, in order that loading and un-loading tasks could be carried out efficiently.

- Repairing equipment

The works are usually terminated if main equipment does not perform properly, and some repairs are required to make it functioning well again. In order to ensure that the tasks could be carried out as planned without any interruption, proper maintenance system should be applied by the terminal management, which includes proper inventory system of the spare parts needed for replacing the worn out parts.

4. CONCLUSION

Efficiency of the cargo handling in container terminal could be increased by reducing the idle time in loading and unloading of containers to and from the ships at the terminal wharf. Identified main causes of the idle time are: waiting for the containers; waiting for the head trucks; changing of operators; and repairing the equipment. There are some sources that create the causes of the idle time.

In order to reduce the idle time sources that create the causes of idle time manage properly in accordance to their individual characteristics and using appropriate approaches, mainly management approaches such as human resources management, inventory management, safety and traffic management, and maintenance management.

5. ACKNOWLEDGEMENT

The authors would like to express their appreciations and thanks to the Directorate of Research and Community Engagement (DRPM) Universitas Indonesia for providing PITTA funding, so that the results of students' final projects could be disseminated in various means such as this one. We also like to express our thanks to the management and staffs at PT Indonesia Port Corporation for giving us opportunity to collect information for supporting this research.

6. REFERENCES

- Chen, Chuanyu; Hsu, Wen-Jing; Huang, Shell-Ying. () Simulation and Optimization of Container Yard Operations: A survey, Port Journal, <http://www.simplus.sg/papers/SgMaritime>.
- Government Regulation No. 69/2001, (2001), Port Regulation, Directorate General of Sea Transport Republic of Indonesia.
- Hermanto, Andy Wahyu. (2008), Analysis on The Consumer Satisfaction To The Service Of The Port Semarang Container Terminal (in Indonesian), University of Diponegoro. Pp 11-18.
- Indonesia Port Corporation (IPC). (2015), Modernizing Pelabuhan Tanjung Priok, PT. Pelabuhan Tanjung Priok.



- Indonesia Port Corporation (IPC). (2015), Ship Planning Concept, Port Maritim Logistics, IPC Corporate University.
- Indonesia Port Corporation (IPC). (2015), Yard Planning Concept, Port Maritim Logistics, IPC Corporate University.
- Lasse, D.A.(2012). Cargo Management; Supply Chain Activity in Port Area (in Indonesian), PT.Grafindo Persada, Jakarta.
- Liang, Ping Ku et al. (2010), An Optimization Framework For Yard Plan In a Container Terminal: Case Automated Rail-Mounted Gantry Crane . OR Spectrum 32: pp 519–541.
- Obata, Kanji et al. (2001), Development of Automatic Container Yard Crane. Mitsubishi Heavy Industries, Ltd. Technical Review Vol.38 No.2.
- Suryadi,Fenti.(2016). Operation of Terminal 2 Port of Tanjung Priok, Vocational training report, Universitas Indonesia.
- Triatmodjo, Bambang. (1996), Harbor (in Indonesian), Beta Offset, Yogyakarta.
- Terwiesch, Christian. (2013) , An Introduction to Operation management, lecture note week one, University of Pennsylvania.
- Wibowo, Harmani. (2010). Analysis on factors that affecting the ships waiting time at Tanjung Mas Port Semarang, Postgraduate thesis, University of Diponegoro.
- Wiwoho, Soedjono. (1983). Suportin Facilities for Sea Transportation (in Indonesian), PT Bina Aksara, Jakarta.

*) Corresponding author.

E-mail address: naryo@eng.ui.ac.id



CONTAINER SHIP ACCIDENT ANALYSIS DUE TO CONTAINER STACKED ON DECK AS AN ATTEMPT TO IMPROVE MARITIME LOGISTIC SYSTEM

Gafero Priapalla Rahim¹, Sunaryo^{2*}

¹Department of Mechanical Engineering, Universitas Indonesia.

² Department of Mechanical Engineering, Universitas Indonesia.

Abstract

This paper analyses factors that might cause accidents to the container ships due to loading conditions of containers stacked on deck, and propose applicable actions on how to minimize these factors. Container ships play important role in the domestic and international maritime logistic system as one of the most efficient ways of transporting general cargo in a bulk quantity. The number, capacity, and speed of hatch-coverless container ships worldwide have increased significantly since the latest decade. There is also trend of stacking more containers on deck in order to increase the capacity of the ships and reduce the transport costs. This phenomenon makes the number of container ship accidents also increasing continuously; especially accidents that caused ship capsized or sink. Even though every merchant ship has to comply with the applicable classification and statutory rules and regulations for the safety of the ship and its cargo, but based on the accident data have been recorded, the number of accidents still significantly high. The accidents usually cause great losses to the cargo being transported and damage the overall logistic system. The sources of container ship accidents can be categorized into: the ship itself, the environment, human factor, and management. In this study accidents data and related information were gathered through literature study, on the spot observation, and direct interviews with relevant parties. Causes of accidents were then identified by analyzing every possible source that might trigger the accident using cause and effect analysis or known also as *Fish Bone* Diagram Analysis. Based on the findings from the analysis, options for overcoming them were simulated to obtain the most applicable solutions that would minimize the accidents and improve maritime logistic system.

Key word: accident sources, container ship accident, maritime logistic system, on deck stacking,

¹ gaferopr@gmail.com

² naryo@eng.ui.ac.id



1. INTRODUCTION

Indonesia is the largest archipelago in the world, comprising more than 17,000 islands, with the second longest coastline after Canada and vast ocean of nearly 6 million km² which includes the archipelagic waters, territorial sea and exclusive economic zone [1]. Indonesia makes the sea as access links between the islands. For Indonesia as a maritime country, the export-import of goods through sea is very important to promote the country's economy. Most of the cargo shipping is using containers, due to the international practices and their many benefits. Following the trend of containerization, so as the container ships are also developing in size; capacity; and stowage system.

The hallmark of the container ship is standardized so that the optimal placement of containers could be arranged. According to data published by the Maritime Journal, the carrying amount of the active container ships that sail around the world in 2016 approximately 6086 vessels. The container ship has become common too in Indonesia, as especially in conjunction with the government's policy in implementing "Sea Highway" program. It shows that the container vessel has an important role in the world's logistic system.

However, in line with the presence of many container ships, there are also many accidents occurred to container ships. According to the data recorded by the European Maritime Safety Agency, there were 1101 cases of container ship accidents worldwide in the range of 2011-2015. These accidents usually occur due to natural factors, incorrect stowage plan, overloaded containers, bad lashing system, hatch cover condition, the placement of dangerous goods containers, unsafe plugging of reefer container, human error, etc.

The focus of this research is to investigate the sources of accident caused by containers that were stacked on deck, so that attempts to minimize them could be proposed.

2. METHODOLOGY

In this study, statistical data related to container ships accidents were collected from many sources worldwide, as a basis for supporting the significance of the study. Only data related to accidents occurred due containers stacked on deck were used in the analyses. "Fish bone" cause and effect diagram analysis was carried out to investigate the core sources of the accidents, and based on the results of the analyses solutions were proposed to minimize the accident from its roots.

According data from the European Maritime Safety Agency, from 2011 to 2015 there were 6403 cargo ship involved in 5942 case of ship accidents, the number was increasing every year. For container ships, there are more than 1101 cases in the period of 2011-2015. Distribution of number of accidents every year and the type of ship involved is presented in figure 1.

From 4956 of specific cases, the most commonly occurring cases or around 25% of total cases were due to factors that were happened in the engine room. In addition, for the cases that were due to crash on deck are about 10% of the total cases. They occurred on cargo hold 5% and freeboard deck 5%. Although it has small percentage, but the cost of cargo lost and their effect to environment are worth considered. Main places where accident are usually occurred are shown in figure 2., while the type of accidents are presented in figure 3.

Based on the data published by the European Maritime Safety Agency in the range of 2011-2015, accidents that are often experienced by the container ship are collision; fire/explosion; grounding; and wear out equipment. There are more than 200 cases of collisions. Accidents happened to containers stored on deck are caused by reefer containers and dangerous goods containers due to wrong placement; leaks; and improper plugging. Example of a fire that occurred on a container ship "Norasia" on July 16, 2005 was caused by fire in cargo containers is shown in figure 4.



Accidents as result of wear out equipment include: bad lashing system and corroded hatch cover. Lashing system on the container is very important for the safety of containers. Lashing system should be checked regularly and replaced when they have already not met the standards. Especially those are stored on decks, because they have potential to fall due to the force from the wind and rolling of the ship. Furthermore, in the case of wear out hatch cover, even though this is rare, but may potentially lead to an accident. Similar to lashing system, the hatch cover must always be checked for its strength and shape, so as to spare from cracking. The strength of a hatch cover determines the balance and safety of cargo containers is on deck.

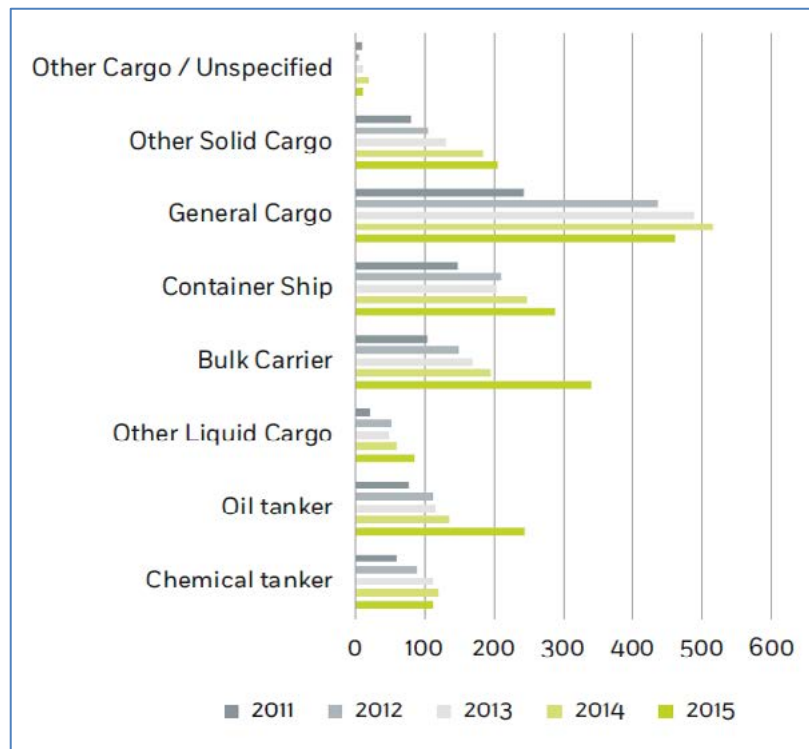


Figure 1. Distribution of cargo ships involved

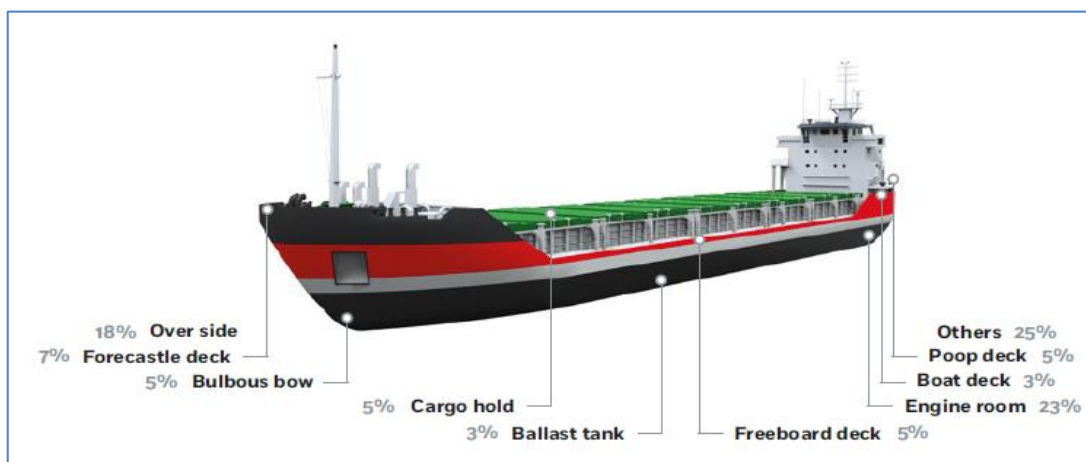


Figure 2. Main places of accidents in cargo ships

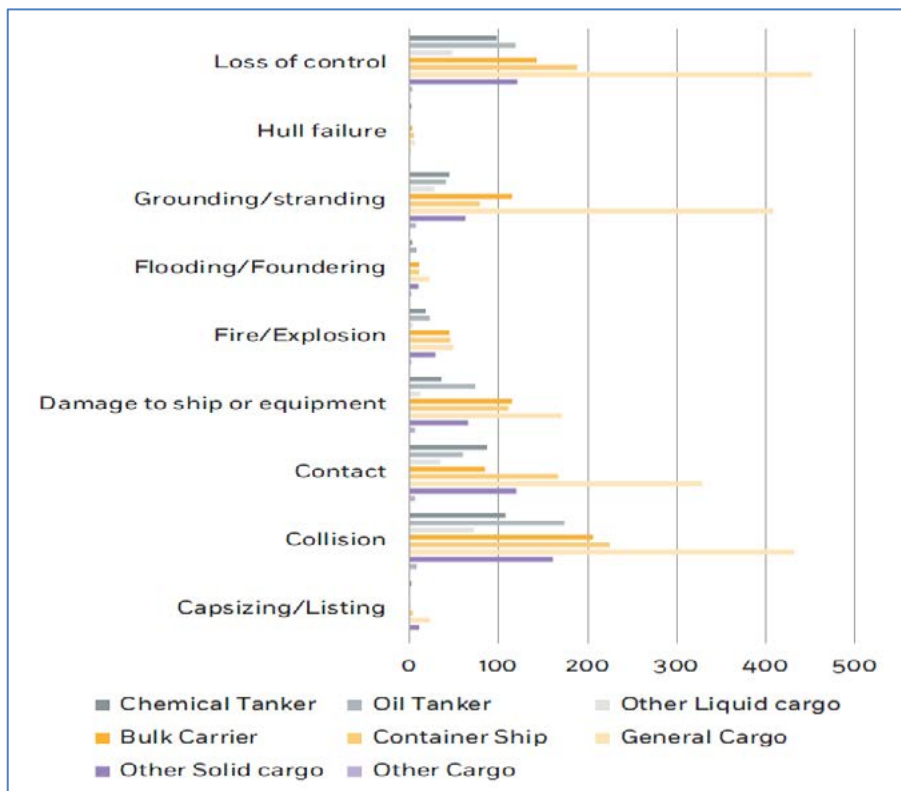


Figure 3. Types of accidents



Figure 4. Fires on container ship

3. RESULTS AND DISCUSSION

In order to identify the main sources of accidents occurred to containers stacked on deck, cause and effect or “fish bone” analysis was used. The causes are classified into four categories, including: ship system, the environment, human factors, and management as shown in figure 5.

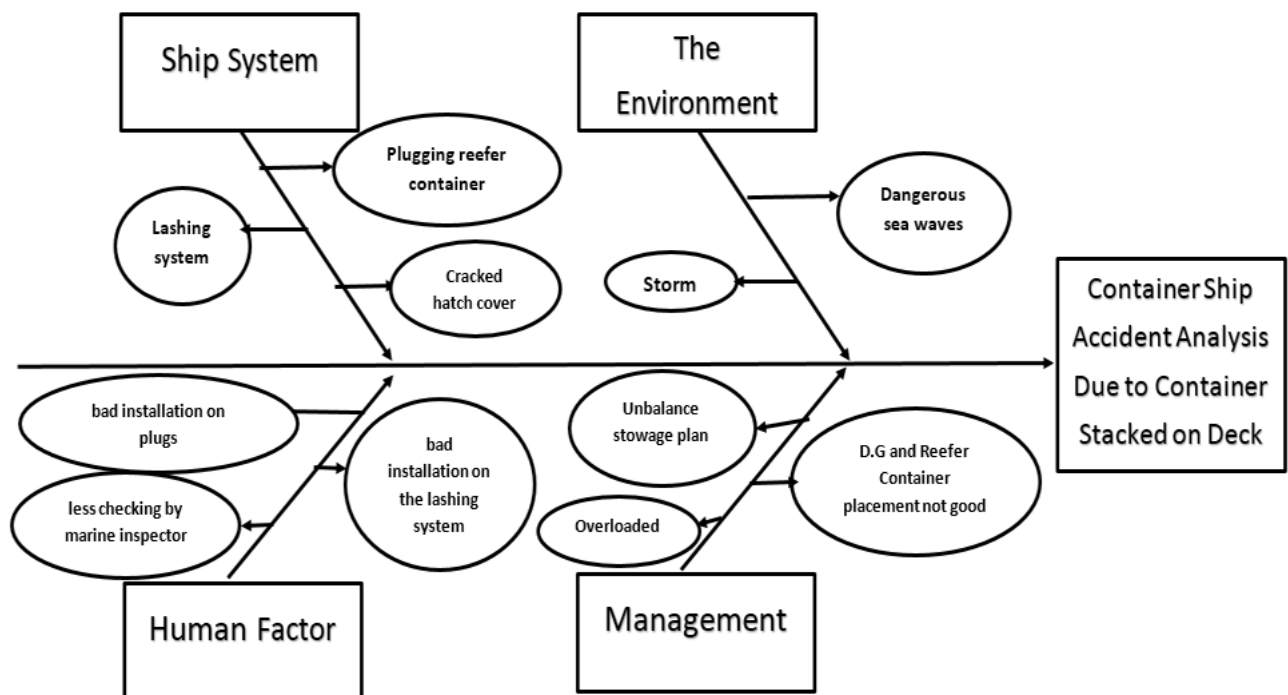


Figure 5. Fishbone diagram analysis

In the ship's systems, the sources of the accident are: bad deck lashing system; improper plugging of reefer container; and wear out Hatch cover.

In environmental aspect is the sources are: sea condition such as storm, and wave. This aspect has great influence in ship accident if it is not anticipated well.

In the human factor aspect the sources of accident are: bad plugging of reefer containers on the system, lack of checking the cargo, and improper installation of the lashing system.

The management aspect would include: the arrangement of stowage plan; bad arrangement of dangerous goods, as well as the arrangement of reefer containers.

To overcome the sources of identified accidents it is proposed that for ship's system, planned maintenance system should be implemented, so that all the equipment related to the stowing of the container are in a very good condition. For environmental aspect, prevention and anticipation procedures to face the bad weather should be prepared and informed to the ship's crews. For the aspect of human factor, proper training, and availability of clear standard operating procedures should be ensured. For the management aspect, commitment from all parties to the safety of the ship operation should be enforced well.

4. CONCLUSION

Based on the results of the analyses it could be concluded that the main causes of accident occurred to containers stacked on the deck of ship are: the ship's systems, the environmental aspect, human factor aspect, and management aspect. The sources of these causes category identified through fish bone diagram analysis are used to find the solution for preventing them to occur.

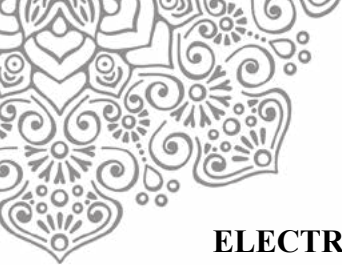
5. ACKNOWLEDGEMENT

The authors would like to express their appreciations to PITTA project initiated by Directorate of Research and Community Engagement Universitas Indonesia for funding the project.



6. REFERENCES

- American Institute of Marine Underwriters and Technical Services. (2012). Committee On Deck Stowage of Containers. New York: AIMU.
- European Maritime Safety Agency. (2016). Annual Overview of Marine Casualties and Accidents 2016., Lisbon: EMSA.
- Eyres, D, J. (2001). Ship Construction. Oxford: Butterworth-Heinemann.
- Kim, D. J. and S. Y. Kwak (2016), Risk Analysis of Container Ship Accidents and Risk Mitigation Measures, Journal of the Korean Society of Marine Environment & Safety, Vol. 22, No. 3, pp. 259-267.
- Komite Nasional Keselamatan Transportasi. (2009). Laporan Analisis Trend Kecelakaan Laut 2003-2008., Jakarta: KNKT.
- Liu, F. et al. (2010), Stowage Planning of Large Containership with Tradeoff between Crane Workload Balance and Ship Stability, International Multi Conference of Engineers and Computer Scientists, Vol. III.
- Maritime Journal. (2005, October 01). *SMIT Deals with Fire and Groundings*. Retrieved from <http://www.maritimejournal.com/news101/>
- Nakamura, T., Ota, S. and Nakajima, Y., (2001, Evaluation of Expected Maximum Values of Forces Acting on Containers and Lashing Rods on a Container Ship, Journal of Marine Science and Technology, No. 6, pp. 3–12.
- Ships Business. (2015). *Lashing requirements on board container ship*. Retrieved from <http://shipsbusiness.com/securing.html>
- Suzdayan. (2012). Container Ships and Cargo Securing Training. Jakarta: PT.Samudera Indonesia.



ELECTRIC CAR CONVERSION COMPONENTS LAYOUT ARRANGEMENT AND THEIR EFFECTS ON CENTER OF GRAVITY LOCATION

Mohammad Adhitya¹, Muchamad Aditya Rachmanto¹, Sudirja¹, Danardono Agus Sumarsono¹

¹ *Mechanical Engineering Department, Universitas Indonesia*

ABSTRACT

This study discusses design of layout arrangement of electric car conversion. This study consists of literature, method and the results. This study focused on the arrangement of the layout of components and change in center of gravity (CG) position that affected the vehicle handling performance. Change in CG position happened as an effect of replacing the components with certain masses affected vehicle's mass distribution. The new layout was designed to accommodate batteries, electric motor, and other complementary components resulting in CG position of the vehicle that is closer to its reference point in vertical axis and to its reference point in longitudinal axis compared to the car's original CG in standard condition.

Keywords: vehicle's component layout, electric vehicle conversion, vehicle's center of gravity.

1. INTRODUCTION

Electrical energy, in its energy generation effort, depends not only on nonrenewable energy sources. Renewable alternative energy sources can be exploited as generators, such as water, air, and geothermal. Electrical energy is an alternative energy source that is expected to meet the Indonesian people's need for energy. By utilizing electricity as the primary energy of vehicles, we can meet the challenges of Indonesia, as well as globally, in fulfilling the people's need for energy.

The application of electric motors in vehicles can be used as an alternative way in the future to replace motor fuel that is still commonly used. In electric vehicles, fuel oil as an energy source is replaced by a rechargeable battery when the energy is used up. If the electrical energy is generated by a generator derived from renewable energy, the electric vehicle produces zero emissions, either directly or indirectly. Further, it claims the position of electric vehicles in lieu of conventional vehicles in the future. Additional reason is the regulation in some developed countries that restrict the quality of emissions from vehicles.

In our project, one type of car developed is a type of city car that dominates Indonesian automotive market segment. Development is done by converting from a conventional motor fuel into an electric car. The conversion must mind the placement of new components that will replace the essential components of the combustion engine. It is expected to maintain the performance of the car, especially the stability and safety of driving.

2. METHODOLOGY/ EXPERIMENTAL

The following flowchart showed the steps of the study.

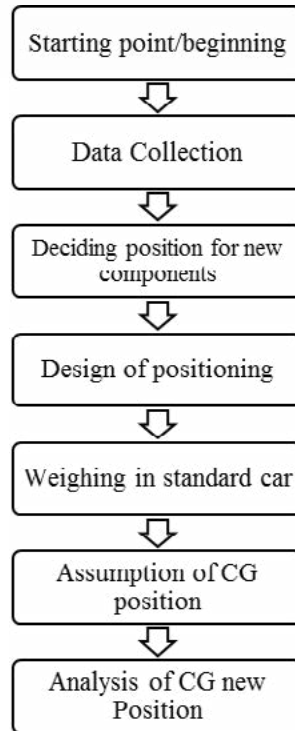


Figure 1 The Flowchart of Research

2.2. Selection of Components

New components used in this prototype car were battery, inverter, AC-DC converter, DC-DC converter, electric motor, and BMS (Battery Monitoring System). These new components would replace some of the essential components of combustion engines that are no longer used in electric cars, namely combustion engines, exhaust systems, and gasoline tanks.

In accordance with the procurement plan that has been used, components other than batteries already set on the vehicle blueprint. Whereas previously planned batteries for use have dimensions that do not match the space available on the car used as the basis for this study.

On the market, there are various types of rechargeable batteries that can be used on electric cars. Common used battery in electric cars is lithium-ion type battery. Lithium-iron-phosphate (LFP) battery was used in this study because LFP battery could provide longer cycles than lead-acid batteries, nickel-metal hybrid, and other lithium-ion batteries. LFP type battery is also commonly used in the conversion of electric cars so that various types and specifications on the market are available.

To keep the cabin and space utilities, the battery was moved on the floor of the car chassis. It takes single-cell battery of small dimensions to be placed according to the plan. The battery was assembled in a module in which the modules were assembled according to the needs of the car. Here's a comparison of some similar batteries available on the market:



Tabel 1 Comparison of Battery Types

Battery	Voltage (V)	Capacity(mAh)	Weight (kg)
AA LFP 26650	3,2	3300	0.09
AA LFP 32600	3,2	3000	0,11
Panasonic NCR18650	3,6	2750	0,05

From the battery specifications obtained, AA LFP 26650 battery was used. It is based on the need of the car to a large battery capacity so battery with the largest capacity is selected.

2.3. Data Collection

New components used in this prototype car are battery, inverter, AC-DC converter, DC-DC converter, electric motor, and BMS (Battery Monitoring System). These new components replaced some essential components of combustion engines that were no longer used in electric cars, namely combustion engines, exhaust systems, and gasoline tanks.

As the first step to design, the specifications of these components should be found first. The dimensions and weight of new components can be found in available data sheets such as brochures and manuals of each component.

Tabel 2 Data of New Component Used

Components	Weight (kg)	Total	Total of Weight (kg)
Battery	0,09	1260	113,4
<i>Battery Monitoring System</i>	2,43	1	2,43
<i>AC-DC Converter</i>	13,8	1	13,8
<i>DC-DC Converter</i>	3	1	3
Motor Listrik	52	1	52
Inverter	5,45	1	5,45

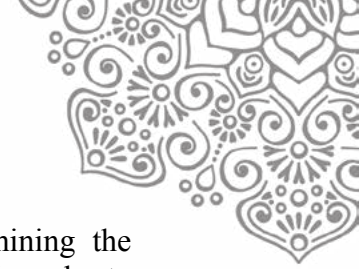
In addition, data on the weight of the old components were not used anymore. The data were obtained by weighing.

Tabel 3 Data of Replaced Components

Components	Weight (kg)	Total	Weight Total (kg)
Combustion Engine	100	1	100
Fuel Tank (full)	42,5	1	42,5
Exhaust	10	1	10

2.4. Positioning of New Components

In order to convert the original car using a motor fuel to become an electric car, replacement for several components was done. The essential components of unused motor fuel were removed and replaced by new components that support electric cars. The role of motor fuel was replaced with an electric motor, and the fuel tank was replaced with a battery.



Good layout planning was required in the process of replacing and determining the location of the components to be installed on the prototype of this electric car in order to retrofitting to get the optimal performance of the car. The appropriate architectural layout of the drive train components directly affected the distribution of the lifetime so greatly affected the CG position of the car. First thing to consider was removing the combustion engine and its supporting components such as the exhaust system and the gas tank, which was a major weight contributor to the conventional car (motor fuel). Then, the second consideration was the placement of new components namely electric motors, control systems, and batteries and accessories. As a primary consideration, the emphasis of retrofitting was to consider the replacement of combustion engines and gasoline tanks with electric motors and batteries because these components have heavy weight and large dimensions.

Placement of forward-leaning batteries, with 60% of the total mass on the front, the car tended to over steer when cornering. When the front of the car carries greater weight, the rear tire had larger slip angle than the front tire. For battery placement in the center, with 50% of the total mass on the front, the car tended to cornering in a neutral position so that the car maneuvered to follow the steering angle well. It was because the front and rear tires received the same load on static conditions. In dynamic condition, the front tires received larger load than the rear tires, resulting in a slight over steer that did not exceed the size of the car with the distribution of a forward-leaning mass. In the condition of placing the battery tended to the back, with 40% of the total mass on the front, the vehicle tended to understeer when cornering. It was because the rear tires received the largest load so that the slip angle experienced by the front tire was larger than the rear tire. From this, it could be seen how the effects of longitudinal CG positions affected the vehicle's performance, in this case an electric car.

Battery placement was major concern due to its heavy weight and large dimensions. Therefore, the placement of other components such as BMS, Inverter, AC-DC Converter, and DC-DC Converter was second priority so that it followed available place due to its relatively in small dimensions and light weight. As the consideration, these components were placed in an easily accessed position to make it easier for maintenance and monitoring. In addition, some heat-prone components were positioned as much as possible to accommodate heat exchange so that the components could work optimally.

Generally, the results of this conversion should not change the functionality of the passenger cabin, not to reduce the space accommodation for passengers that impact to the comfort and interior aesthetics. After making a placement plan, measurements were made on the planned places on the previous prototype car to validate the space capability to accommodate the components to be placed.

2.5. Design

The design stage was done using Autodesk Inventor software.



2.5.1 Design of Battery Module

The battery used was a single cell battery type LFP 26650-3300 by AA Portable Power Corp. The battery has a nominal voltage of 3.2 V and a nominal capacity of 3300 mAh.

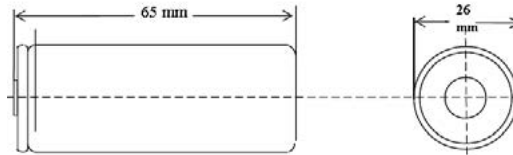


Figure 2 Battery LFP 26650-3300 single cell

In order to fit the needs of the motor, the battery was arranged into several modules. Each module contained 30 series of batteries arranged in series so that the voltage obtained for 96 V.

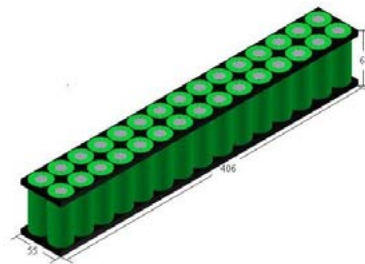


Figure 3 Battery Module

After that, the modules were arranged in parallel to increase the total capacity.

2.5.2. Layout Frame

Placement of the battery components affected the distribution of weight and loading on the frame. To keep the car's performance by maintaining the CG position, on this frame design the battery was placed in the center. Other electric drive components that must be considered was a motor that weighed up to 43.5 kg, to adjust to the drivetrain used on the front.

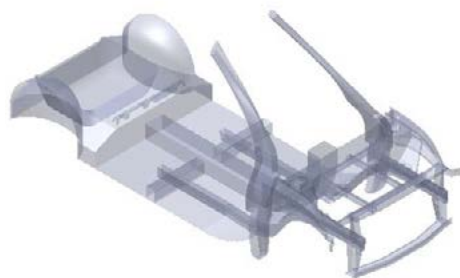


Figure 4 Car Frame Layout



The prototype powertrain layout is known as the Front Transverse engine-Four wheel drive configuration. Powertrain components in this configuration are the motor and transmission were placed on the front. The advantage is the availability of more roomy space for the placement of the battery in the middle because there is no transaxle distributed round to the rear axle.

2.6. Weighing and Estimating Position of Standard Car CG

Weighing tool used was portable scale Dini Argeo type WWSDRF Wireless Platform - 3590 EKR.

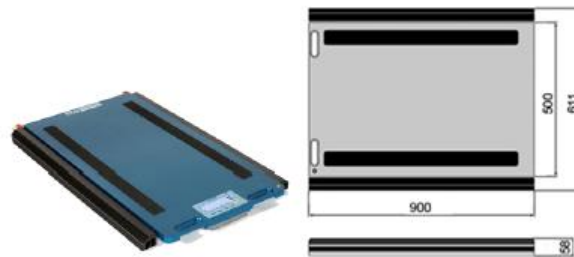


Figure 5 Dini Argeo WWSDRF Wireless Platform-3590 EKR

A set of scales consists of two platform units and one display unit. Each platform was placed on each wheel so that weighing a car takes twice the weighing, i.e. on both front wheels and continued by weighing the two rear wheels. Each platform would weigh the load which was received and displayed on the display unit connected to the wireless connection. The accuracy of this tool weighs 10 kg. Parameter used as analysis was CG obtained from the weighing on the car. CG of car in standard state would be compared with the design results.

Two conditions of weighing were conducted. They are weighing the car in flat state and tilt state. The first condition was performed to see the mass distribution of the car on both axles so that the longitudinal position of the car can be determined. While the second condition was done to see the change in the mass distribution of the car caused by the change of the angle, so that CG position in car can be seen vertically.

To determine the longitudinal position of the CG, the load received by both car axles represented the mass distribution in the front-rear direction.

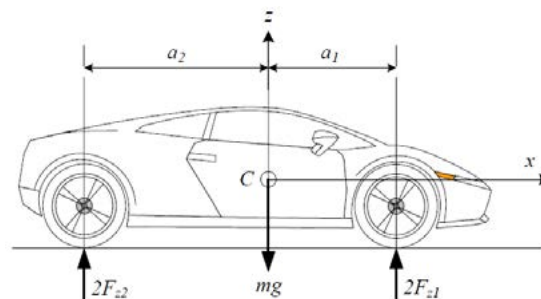
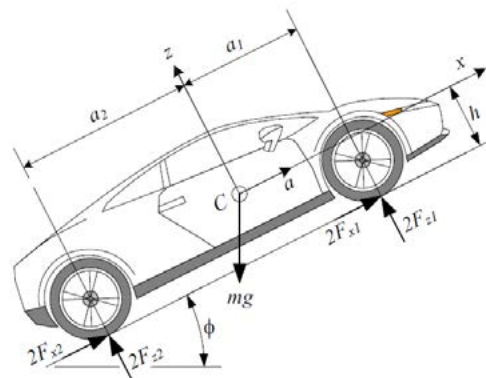


Figure 6 Determining longitudinal CG positions



Furthermore, weighing the car with a condition of tilt (pitch) was done. When weighing, the car was tilted up by jacking up the front or rear with the help of the jack so that the car has a certain angle.



Gambar 7 Determining the vertical CG position

2.7. Estimated Changes of CG Position on Prototype Car

After knowing the CG position of the standard car, CG changes after the conversion process can be estimated by referring to (2.2) by using the reference point on the front axle of the car for longitudinal position, and on the surface for vertical position. In the calculations, the new components were assumed to give positive force, while the old components replaced give negative force. With these calculations, it can be seen how big the change in CG positions that occur in the prototype.

3. RESULTS AND DISCUSSION

3.1. Design

As a first step, the placement of the car powertrain included an electric motor and the arrangement of battery modules designed with the following layouts:

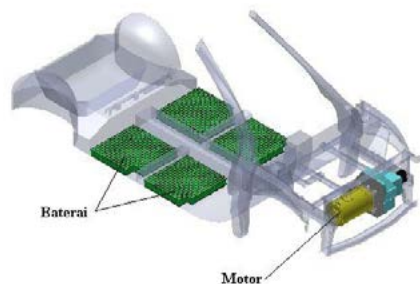


Figure 8 Layout powertrain on the prototype

After determining above configuration, other design of placement of the components was done as the following layout:

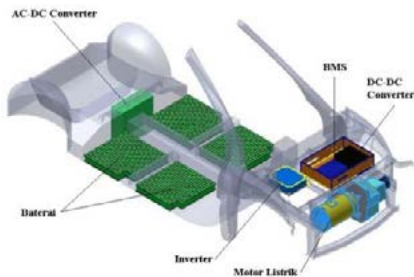


Figure 9 Layout of new prototype components

3.1.1 Weighing and Positioning of Standard Car CG

Weighing was done on a standard Nissan March car. It was done with a flat car position.



Figure 10 Weighing the car in a flat position

After weighing on above position, the following results were obtained:

Table 4 Weighing the car in a flat position result

Weighing	Front Axle (kg)	Rear Axle (kg)	Total (kg)
1	570	350	920
2	580	360	940
3	580	360	940
Average	576,6666667	356,6666667	933,3333333

From the weighing result by using equation (2.4), longitudinal CG car position can be estimated as:

$$a_1 = 936,25 \text{ mm}$$

Furthermore, weighing in a sloping position. The car was weighed with a jack-up condition of 190 mm so as to form a downward pitch angle of 3,44°.



Figure 11 Weighing the car in a sloping position



Weighing is done on the front wheel so that the force on the rear axle was calculated by reducing the total mass obtained in the previous weighing with force on the front axle read on the scales. The results are as follows:

Tabel 5 Result of Weighing in Sloping Position

Degree	Front Axle (kg)	Rear Axle (kg)	Total (kg)
3,44	570	393,333333	933,333333

The resulting weigh represented the gravity of the car. By knowing the angle of the slope, the normal force can be determined according to equation (3.1) as follows:

$$Fz1 = 196,311 \text{ N}$$

$$Fz1 = 269,514 \text{ N}$$

From the weighing result, with reference to (2.5) the vertical position of the car may be predicted:

$$h = 946,6404 \text{ mm}$$

The results of the weighing done are summarized in the following table:

Tabel 6 Summary of Weighing result

Curb Weight (kg)	Distance of the CG to front axle (mm)	Distance of CG to ground surface (mm)
933,333333	936,25	946,6404

From the result above, position of CG on the car can be visualized the as follows:



Figure 12 Approximate position of CG on car

3.1.2. Changes position of CG in Prototype

CG position influenced the moment of each component in the car. Here is an analytical calculation to find out the new CG positions on the prototype, either longitudinally or vertically.

3.1.2.1. CG Position After Removing Old Components

Combustion engine, gas tank, and exhaust that have been not used were released from the car. The momentary changes occurring from the discharge of the components below with the component spacing from the reference point as the moment arm were calculated. The reference point for the longitudinal CG was the front axle while for the vertical was the ground surface. The following weight and distance of each component of the reference points are as follows:



Tabel 7 Weight and Position of Released Components

Components	Weight (kg)	Longitudinal distance (mm)	Vertical distance (mm)
Combustion Engine	100	60	700
Fuel Tank (full)	42,5	2362	566
Exhaust	10	1602	380

By releasing the components, the mass of the car was reduced to 780,83 kg. By performing calculations according to the equations of moments in equation (2.2), here are the longitudinal CG positions:

$$\bar{x} = \frac{\int xdw}{W}$$

$$\bar{x} = \frac{(933,33 \times 936,25) + (100 \times 60) - (42,5 \times 2362) - (10 \times 1602)}{780,83}$$

$$\bar{x} = 1092,66 \text{ mm}$$

While CG in vertical way is as follow:

$$\bar{y} = \frac{\int ydw}{W}$$

$$\bar{y} = \frac{(933,33 \times 946,64) - (100 \times 700) - (42,5 \times 566) - (10 \times 380)}{780,83}$$

$$\bar{y} = 1006,2 \text{ mm}$$

From the calculation of the moments above, it can be known that after the motor fuel, gas tank, and exhaust were released, there were CG changes in the car. Longitudinal CG became 1092, 66 mm from the front axle, while the vertical CG was 1006.2 mm from the ground surface.

3.1.2.2. CG Position After Installing New Components

Installation of new components on the car was done. The moment changes that occur from the installation of the below components with variations on the three available types of batteries were calculated. The reference point for the longitudinal CG is the front axle while for the vertical is the ground surface.

3.1.2.3. Using The LFP-26650 Battery

The battery used had voltage 3.2 V and capacity of 3300 mAh with weight of 0.09 kg per cell. The followings are weight and distance of each component of the reference point:

Tabel 8 Weight and Position of New Components

Battery	113,4	1871	223,25
<i>Battery Monitoring System</i>	2,43	90	630
<i>AC-DC Converter</i>	13,8	2362	600
<i>DC-DC Converter</i>	3	90	630
Motor Listrik	52	60	300
Inverter	5,45	190	630



By installing the components above, the mass of the car increased to 970.91 kg. By performing calculations according to the equations of moments as in equation (2.2), here are the longitudinal CG positions:

$$\bar{x} = \frac{\int xdw}{W}$$

$$\bar{x} = \frac{(780,83 \times 1092,66) + (113,4 \times 1871) + (2,43 \times 90) + (13,8 \times 2362) + (3 \times 90) - (52 \times 60) + (5,45 \times 190)}{970,91}$$

$$\bar{x} = 1129,2 \text{ mm}$$

While CG in vertical way is as follow:

$$\bar{y} = \frac{\int ydw}{W}$$

$$\bar{y} = \frac{(780,83 \times 1006,2) + (113,4 \times 223,25) + (2,43 \times 630) + (13,8 \times 600) + (3 \times 630) + (52 \times 300) + (5,45 \times 630)}{970,91}$$

$$\bar{y} = 845,01 \text{ mm}$$

From the calculation of the moments above, it was obtained that the new components installed is a change of CG on the car. Longitudinal CG became 1129.2 mm from the front axle, while vertical CG was 845.01 mm from the ground surface.

3.1.2.4. Using The LFP 32600 Battery

As an alternative, LFP 32600 battery with 3.2 V voltage, 3000 mAh capacity, and weight of 0.11 was used, so the total weight of the battery to be used is 138.6 kg. With reference to the placement of other components as above, the longitudinal CG position is as follows:

$$\bar{x} = \frac{\int xdw}{W}$$

$$\bar{x} = \frac{(780,83 \times 1092,66) + (138,6 \times 1871) + (2,43 \times 90) + (13,8 \times 2362) + (3 \times 90) - (52 \times 60) + (5,45 \times 190)}{996,11}$$

$$\bar{x} = 1147,96 \text{ mm}$$

While CG in vertical way is as follow:

$$\bar{y} = \frac{\int ydw}{W}$$

$$\bar{y} = \frac{(780,83 \times 1006,2) + (138,6 \times 223,25) + (2,43 \times 630) + (13,8 \times 600) + (3 \times 630) + (52 \times 300) + (5,45 \times 630)}{996,11}$$

$$\bar{y} = 850,01 \text{ mm}$$

From the calculation of the moments above, it is known that there is a change of CG on the car after the new components were installed. The longitudinal CG became 1147.96 mm from the front axle, while the vertical CG was 850.01 mm from the ground.

3.1.2.5. Using Panasonic NCR 18650 Battery

As second alternative, NCR 18650 battery with 3.6 V voltage, 2750 mAh capacity, and weight of 0.05 each cell, can be used, so the total weight of the battery used is 63 kg. With reference to the placement of other components as above, the longitudinal CG position is as follows:

$$\bar{x} = \frac{\int xdw}{W}$$

$$\bar{x} = \frac{(780,83 \times 1092,66) + (63 \times 1871) + (2,43 \times 90) + (13,8 \times 2362) + (3 \times 90) - (52 \times 60) + (5,45 \times 190)}{945,71}$$

$$\bar{x} = 1059,58 \text{ mm}$$

While CG in vertical way is as follow:



$$\bar{y} = \frac{\int ydw}{W}$$

$$\bar{y} = \frac{(180,88 \times 1006,2) + (89 \times 223,35) + (2,43 \times 690) + (13,6 \times 600) + (3 \times 690) + (52 \times 300) + (5,45 \times 690)}{945,71}$$

$$\bar{y} = 833,71 \text{ mm}$$

From the calculation of the moments above, it can be known that there is a change of CG on the car after the new components were installed. Longitudinal CG became 1059.58 mm from the front axle, while the vertical CG was 833.71 mm from the ground.

3.2. Discussion

From the calculations done, the changes of position of CG both longitudinal and vertical can be clearly seen. The changes caused the load distribution between the front axle and the rear axle with previous ratio 38:62 become 47:53 so that the position of CG backward and tended to be more in than before. In line, the vertical CG position was also changed, which is previous position 60% of the total height of the car become 63% of the total height of the car.

4. CONCLUSION

Based on study conducted, it can be concluded that longitudinal CG position changed as far as 158.41 mm. The change is expected to improve the car's response during cornering because it reduces the over steer effect. Vertical CG position changed as far as 43.06 mm closer to the surface. The change is expected to improve the stability of the car. The comparison of mass distribution between the front and rear on the prototype is 47:53. Overall, the conversion was done to improve the position of CG so it will get a more optimal performance without sacrificing space capacity in the cabin. However, the car load increased by 37.58 kg after the conversion.

From the results of this study, many things need to be improved to get better results. More research is needed on the selection and range of batteries in order to increase the total capacity of the battery used. Conversions added more burden of the car so that further research need to find out the supporting components of the electric car. Due to the objective of this study on the layout of placement of components, further research is needed on the strength of the frame structure to obtain optimal design.

From this research, several things are suggested to the further research to get better results. Researches on issue of battery selection and sequencing, selection of electric car support components, structural strength and manufacturing processes, and adjustment of rider position are needed. In addition, weighing tool used has the smallest scale of 10 kg, so it is recommended in the next research to use a more accurate weigher with higher level of accuracy.

6. REFERENCES

Jazar, R.N., (2008), *Vehicle Dynamics: Theory and Applications*, Riverdale: Springer Science+Business Media.

Macey, S., (2009), *H-Point: The Fundamentals of car Designing and Packaging*. Design Studio Press.



- Gillespie, T.D., (1992), *Fundamental of Vehicle Dynamics*. Warrendale: Society of Automotive Engineering.
- Mazumder, H., (2011), *Performance analysis of EV for different mass distributions to ensure safe handling*.
- Smith, J.H., (2002), *An Introduction to Modern Vehicle Design*. Warrendale: Society of Automotive Engineering.
- Sperling, D., (1995), *Future Drive: Electric Vehicle and Sustainable Transportation*, Washington DC: Island Press.
- Allen, R.W. et al., (1991), "Characteristics influencing ground vehicle lateral/directional dynamic stability".
- Adhitya, Mohammad, (2013), *A New Control Strategy of Wet Dual Clutch Transmission (DCT) Clutch and Synchronizer for Seamless Gear Preselect*, SAE International.
- ISO 10392 (2011), *Road Vehicles - Determination of center of gravity.*: International Standard Organization.



THE VEHICLE LONGITUDINAL DYNAMIC SIMULATION TO SELECT THE OPTIMUM GEAR RATIO COMBINATION OF ELECTRIC VEHICLE CONVERSION

Mohammad Adhitya¹, Mohammad Ikhsan¹, Danardono Agus Sumarsono¹
¹ *Mechanical Engineering Department, Universitas Indonesia*

ABSTRACT

University of Indonesia, made the electric conversion of University of Indonesia's Multi-Purpose Vehicle. The vehicle used combustion engine at first, the conversion of electric motor as a power source affects the vehicle's performance such as torque, RPM even the total weight. Refer to the performance differences, the selection of gear ratio combination will be major concern in this thesis. Using Simulation Software, the performance of the vehicle is tested in Worldwide Harmonized Light Vehicles Test Procedure driving cycle. The conclusion of the simulation stated that the gear ratio combination that is proven to be the most optimum is the combination of first gear and third gear.

Keywords: Electric Vehicle Conversion, Gear ratio combination; MATLAB simulation.

1. INTRODUCTION

Nowadays almost every car manufacturers stated that electric cars will be the future of automotive industry, due to the increasing fuel price and global warming effect. Electric cars will produce zero emission thanks to the absence of conventional engine in their system. Using electric motor as a power source brings us a great advantage, such as higher torque, lower noise pollution, and lower operation cost. Car manufacturer such as European, Japanese, and American car manufacturers already produce road ready electric vehicles in their lineup. To response the conditions, Indonesia's Ministry of Research and Technology through Faculty of Engineering - University of Indonesia assigns a research team to study and design an electric vehicle, which leads the conversion of three conventional vehicles into a full electric vehicle.

Furthermore, the research will cover three specific areas which are Optimum Gear Ratio, Optimum Horse Power, and Optimum Battery Capacity. The research will be done specifically on UI's electric-converted vehicles project, which are Electric City Car, Electric Multi-Purpose Vehicle and an Electric Bus.

This research will focuses on how to obtain Optimum Gear Ratio Combination of Electric-Converted Multi-Purpose Vehicle using mathematical simulation in order to achieve its maximum efficiency and performance of its operation in Worldwide Harmonized Light Vehicles Test Procedure's class 2 driving cycle.



2. RESEARCH METHODOLOGY

2.1. Work Flowchart

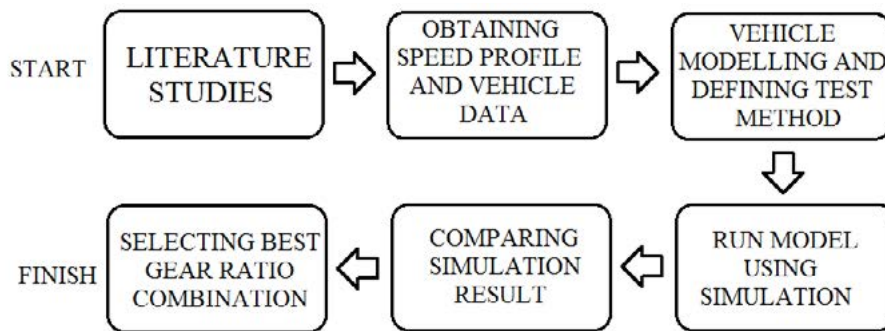


Figure 1 Work flowcharts

2.2. Obtaining Data

To run the simulation, there are some data that must be collected in order to simulate the real condition of the vehicle.

2.2.1. Speed Reference data

Speed reference for this simulation is based on the driving cycle of Worldwide Harmonized Light Vehicles Test Procedure (WLTP). WLTP is a global standard to determine the performance of light vehicle, especially in the levels of pollutants and CO₂ emissions, fuel or energy consumption, and electric range from light-duty vehicles (passenger cars and light commercial vans

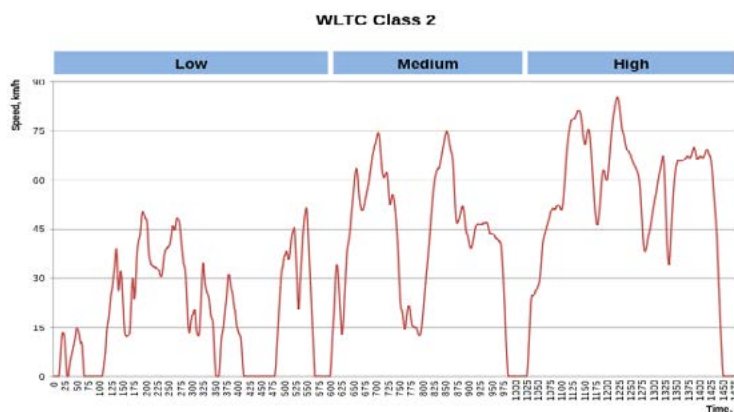


Figure 2 WLTC class 2 speed driving cycle

2.2.2. Vehicle data

Below is the specification of standard UI's Multi-Purpose Electric Vehicle.



Table 1 UI's Multi-Purpose Electric Vehicle

Parameter (unit)	Value
Dimension (mm)	4425 x 1620 x 1880
Curb Weight (kg)	1470
Engine Weight (kg)	210
Passenger Capacity	7
Tire size	185/70 R14
1 st Gear	4.925
2 nd Gear	2.643
3 rd Gear	.1.519
4 th Gear	1.000
Final Drive Ratio	4.778
Drag Coefficient	0.4

Table 2 Total Weight of UI's Multi-Purpose Electric Vehicle

Parameter (unit)	value
Curb weight minus engine (kg)	1260
Motor Weight (kg)	52
Total battery weight (kg)	108
Average weight of 5 passengers (kg)	400
Total weight (kg)	1820

2.2.3 Electric Motor data

Electric Motor that will be used in this simulation is based on HPEVS AC50 electric motor. AC50 motor has maximum torque of 163.4 Nm, maximum power of 53.47 Kw, and maximum rpm of 8000.

Table 3 HPEVS AC50 Motor Data

Parameter (unit)	Value
Type of Motor	AC induction
Mass (kg)	52 kg
Maximum voltage	130 VAC
<i>Rated torque</i> (Nm)	163,4
<i>Rated Power</i> (kW)	53,47
Max. Angular velocity (RPM)	8000
Continuous angular velocity (RPM)	5000



Below is the torque and power curve of HPEVS AC50 data.

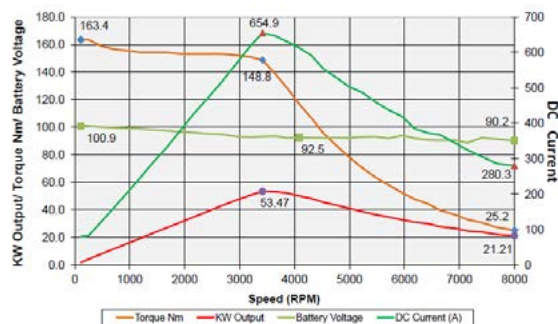


Figure 3 Specification Graph of HPEVS AC50 Electric Motor

Below are the supporting data of HPEVS AC50 electric motor, based on chapter 2.2.1, an Induction Motor should not exceed 80% of its capabilities,

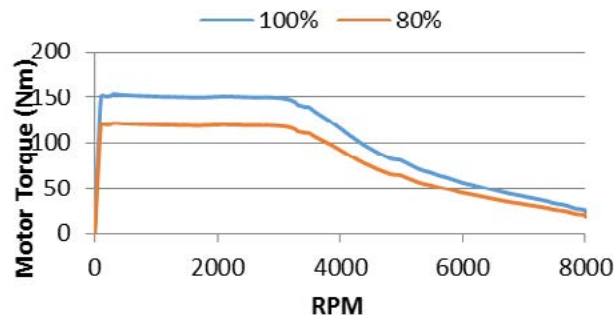


Figure 4 Supporting data of HPEVS AC50

2.3. Electric Vehicle Performance Simulation Using Simulink

The output of simulation is to know the proper transmission gear selection by knowing the vehicle performance in each gear as well as how much power it will cost along the track. To determine Optimum gear ratio combination for Multi-Purpose Electric Vehicle, the simulation result of the vehicle's performance in each gear ratio will be compared.

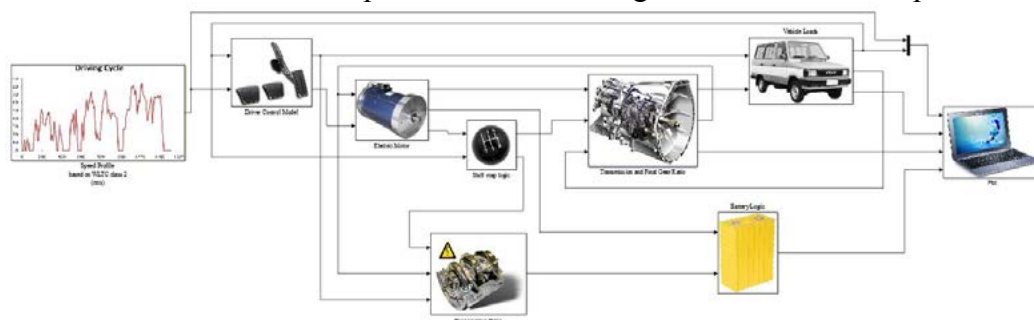


Figure 5 Schematic simulation models for Electric UI MPV

The Model input will be consists Speed Profile which will be transformed into Driver's Throttle Position Model. The Throttle Model, then it is connected into Electric Motor's



Performance graph (torque-RPM) and Electric Motor Efficiency Map model. From there, they will be connected to transmission model where the torque is multiplied by the gear ratio. The result from the transmission model is connected into Vehicle Model which consists of final drive ratio and various loads that will affect the vehicle at certain road profile and acceleration. Finally, the torque and RPM output will be connected into Battery Logic Model where the amount of electricity used by the car is shown.

3. RESULTS AND DISCUSSION

3.1. Vehicle Testing Result

Vehicle testing result is based on the methods in chapter 3.3. In this chapter, the results of the test will be plotted in tables and graphs. The output of this test is to determine on which gear ratio should be used as first gear and which gear ratio should be used to achieve high speed based on the driving cycle. Gear ratios that passed the tests will be inserted into the full simulation.

3.1.1 Speed Testing Result

In this section, the results of speed testing from 1st gear to 4th gear will be shown. Each gear will have achieved their own maximum speed based on speed table 3.2, and because of the loads acted on the vehicle as discussed on chapter 2.4, the vehicle's acceleration will be known.

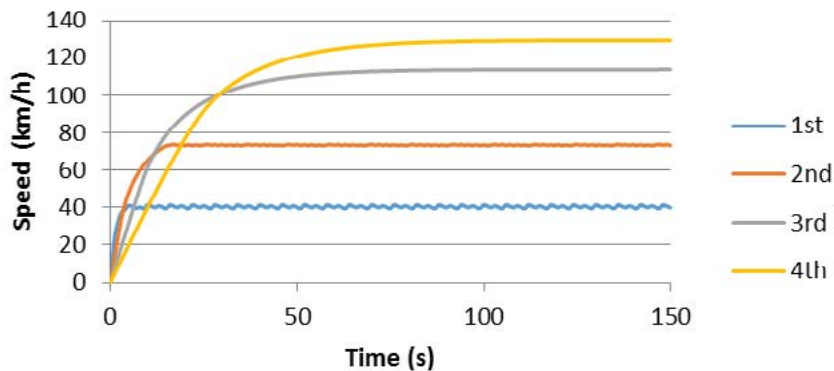


Figure 6 Speed comparison between each gear

From the graph, maximum speed of each gear could be seen. To be able to achieve Worldwide Harmonized Light Vehicles Test Procedure driving cycle class 2 maximum speed of 83 km/h, the vehicle must use at least 3rd gear.

3.1.2 Hill Climbing Test Result

In this section the result of each gear in hill climbing condition will be shown. If a gear is proven unable to climb, the test will be stopped and the next gear ratio will not be tested.



A. 1st gear

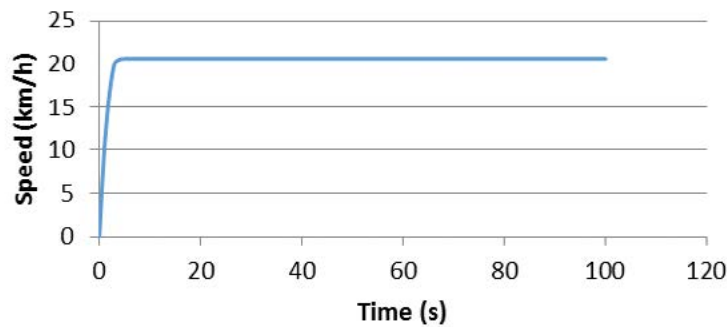


Figure 7 1st gear speed graph of hill climbing test result

B. 2nd Gear

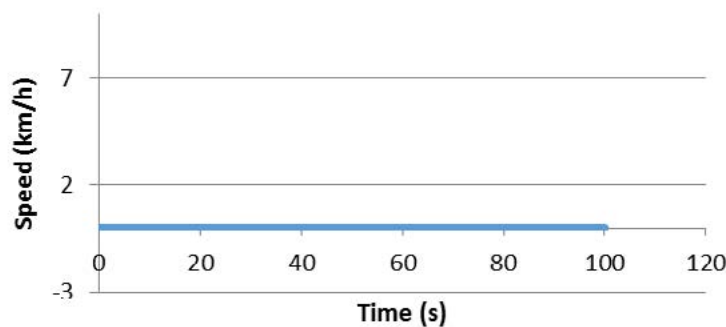


Figure 8 2nd gear speed graph of hill climbing test result

From the graphs above, the only gear that passed the hill climbing test is 1st gear, while 2nd gear is proven to be unable to move in the hill climb test.

3.1.3 Analysis on Both Tests

Based on the result of Speed Test and Hill Climbing test, which gears should be used in the simulation could be determined. First, based on Worldwide Harmonized Light Vehicles Test Procedure class 2, tested vehicle must be able to achieved the speed of 83 km/h which in this case that speed could be achieved by at least third gear. From the Hill Climb test, we can conclude that the only gear capable to across angle constant of 50% is the first gear. It is not recommended using the other gears on the fact that 2nd gear cannot capable to use in a hill terrain road. Even though Worldwide Harmonized Light Vehicles Test Procedure is done on a flat surface but, in real application where the road is unpredictable, the application of 1st gear is a must, in terms of safety.

In refer to the statements above, the combination of gears that will be used on the simulation are 1st gear until 3rd gear. In this simulation, 3rd gear is a must to put in the combination because 2nd gear could not have achieved the desired top speed of 83 km/h. The choices of gear ratio combination are either the combination three speed of 1,2, and 3 or two speed of 1 and 3.



3.2. Simulation Result

The simulation has 4 result parameters. They are Actual speed, Angular velocity of Electric motor, Efficiency of electric motor, and State of Charge. Based on the analysis on chapter 4.1.3, gear ratio combinations that will be tested in the simulation are Gear ratio combination 1, 2 & 3 and 1 & 3. Gear ratio combination 1 & 2 is excluded from the selection due to maximum speed problem.

3.2.1. Gear Ratio 1, 2, and 3 combination result

This section will show the simulation result of Gear Ratio combination 1, 2 and 3.

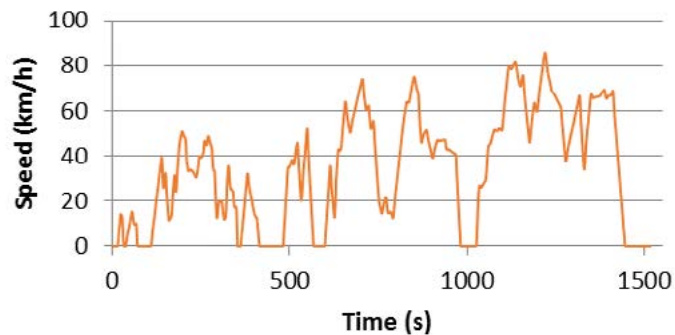


Figure 9 1, 2 & 3 Speed vs Time result

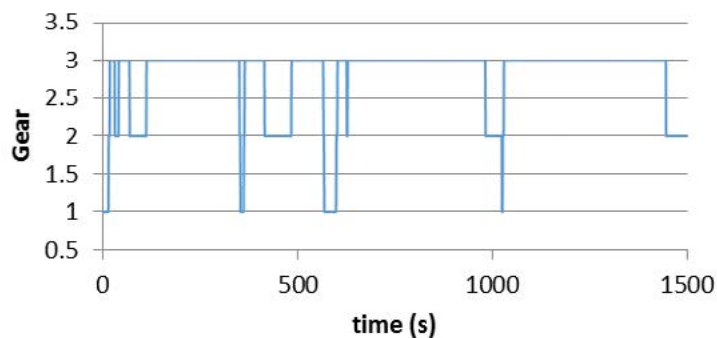


Figure 10 1, 2 & 3 Shifting Interval

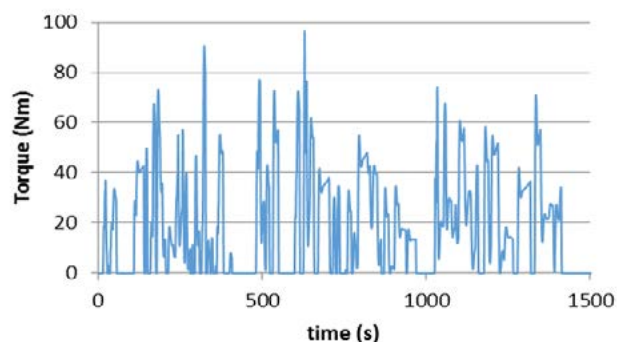


Figure 11 1, 2 & 3 Torque of Electric Motor



3.2.2. Gear Ratio 1 and 3 combination result

This section will show the simulation result of Gear Ratio combination 1 and 3.

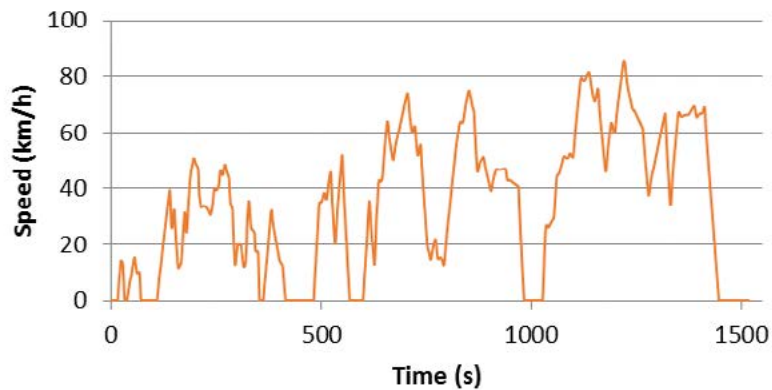


Figure 12 1 & 3 Speed vs Time result

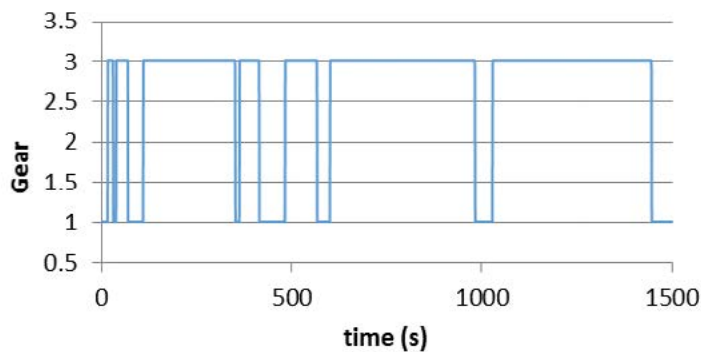


Figure 13 1 & 3 Shifting Interval

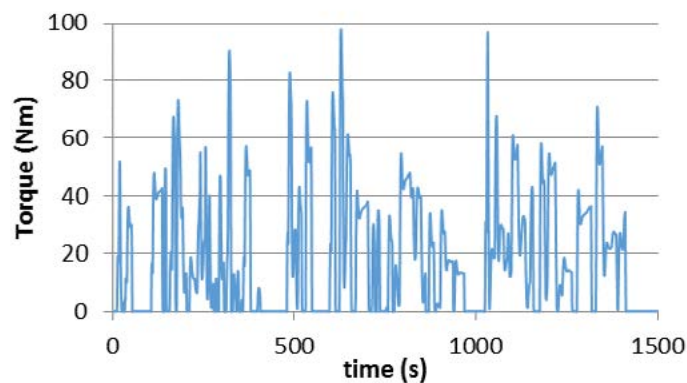


Figure 14 1 & 3 Torque of Electric Motor

3.2.3. Analysis on Simulation Result

The analysis is done based on figure 9 to figure 14. The parameters will be compared between each combination of gears.



Table 4 Summary of simulation result

	Gear Ratio 1,2,3	Gear Ratio 1&3
Avg. Motor Efficiency (%)	80,04	80,12
Max Motor eff. (%)	95,4	95,2
Min Motor eff. (%)	75,16	72,85
Highest RPM	5394	5394
SOC left (%)	70,60	70,61
SOC left w/ reg.brake (%)	71,72	71.73
Highest Torque Produced (Nm)	95,96	97,78
Shifting Action	23 times	14 times

3.2.3.1. Speed vs Time Analysis

All of the speed combinations manage to follow the speed reference of Worldwide Harmonized Light Vehicles Test Procedure class 2 perfectly, thanks to PID tuning that controls the throttle and brake on the simulation. Based on table 3.2, it is impossible if the vehicle only uses 1st gear to complete the class 2 driving cycle, because the maximum speed that 1st gear could provide is only 45 km/h, that is why the vehicle must use at least 1st gear and 3rd gear to achieve all of the speed range.

3.2.3.2. Efficiency Map analysis

In gear ratio combination 1 and 3, the absence of 2nd gear in that combination resulted in lowest minimum efficiency value of 72,85%, while the minimum efficiency value between combination 1,2 and 3 has value of 3% higher. Even though gear ratio 1 and 3 combination has the lowest minimum efficiency value, it has better average efficiency than gear ratio 1,2 and 3 combination, with the value of 80,12%. Standard deviation of 1 &3 is 2.19 while for 1,2&3 is 2.10.

3.2.3.3. Motor RPM analysis

As stated in chapter 4.1.3, the consideration of putting 3rd gear in the simulation resulting in Gear combination 1,2&3 and 1&3. Both speed combinations have motor usage below 8000 RPM. Their maximum RPM in this simulation are 5394. Their results are acceptable, because of electric motor's RPM used only 67%, which still below 80%.

3.2.3.4. State of Charge analysis

State of charge states how much battery % left on the vehicle after the operation. From state of charge value, we could determine how much distance the vehicle could actually manage. From the table 4.8, all of the SOC values does not have much difference, all of the speed combinations used barely the same amount of battery. Battery % left on the vehicle after its operation is 70.6 %. So, to complete Worldwide Harmonized Light Vehicles Test Procedure class 2 driving cycle, the Multi-Purpose Electric Vehicle uses 29.4% of battery.



With formula below, we could compare total distance that could be achieved by each speed combination.

$$X = \frac{80\% \text{ battery capacity}}{\text{battery consumed}} \times \text{WLTC distance}$$

Worldwide Harmonized Light Vehicles Test Procedure class 2 driving cycle distance is 23.16385 km. With the formula above, gear ratio combination 1, 2 & 3 and 1 & 3 have the same result of maximum distance of 63 km.

3.2.3.5. Shifting Action Analysis

From table 4.8, the shifting interval of gear ratio combination 1&3 is 14 times. While gear combination of 1,2, and 3 has shifting interval of 23 times. So, ergonomically the less the transmission needs to be shifted, in the case of manual transmission, the vehicle is more comfortable to drive.

3.2.3.6. Torque Analysis

From table 4.1, highest torque produced by each speed combinations are different. For gear ratio combination 1,2, and 3 highest torque produced by the electric motor are 95.9 Nm, while for gear ratio 1 and 3 combination the highest torque produced by the motor is 97 Nm. Both combinations almost have the same value, and their values are acceptable, because it is still below 80% of electric motor capabilities.

3.3. Speed Combination Comparison

Below is the comparison table, based on analysis from chapter 3.1 to 3.2.3.6. Each parameter is ranked from 3 (best) to 1 (least).

Table 5 Comparison table between gear ratio combination

	Gear Ratio 1,2,3	Gear Ratio 1&3
Avg. Motor Efficiency (%)	1	2
Highest RPM	3	3
SOC left (%)	2	2
Highest Torque Produced (Nm)	2	2
Shifting Action	2	3
Total	10	12

From the comparison table above, the combination that has the highest score is gear ratio combination 1 & 3.



4. CONCLUSION

4.1. Conclusion

Based on chapter 4, the conclusion of simulation results could be determined. From this conclusion, the best speed combination of UI's Multi-Purpose Electric Vehicle in Worldwide Harmonized Light Vehicles Test Procedure class 2 driving cycle will be known. Below are the conclusions:

- Based on Speed Testing and Hill Climbing Test result, 1st gear and 3rd gear must be applied on the combination due to the ability of 1st to handle steep angled road and the ability of 3rd gear to handle desired maximum speed.
- From the comparison result in table 4.9, gear ratio 1 and 3 combination is the best in choice in this case. This combination basically has the same result with combination 1, 2 and 3, with fewer shifting actions and better motor efficiency.

4.2. Suggestions

Below are write's suggestion for this thesis and upcoming research's

- The existence of Indonesia's driving cycle would be very useful for setting a standard for vehicle testing in Indonesia.
- Various parameters in this bachelor thesis such as AC50 electric motor efficiency map, and Battery's state of charge must be further tested and validated.

6. REFERENCES

- Jazar, R.N., (2008), *Vehicle Dynamics: Theory and Applications*, Riverdale: Springer Science+Business Media.
- Macey, S., (2009), *H-Point: The Fundamentals of car Designing and Packaging*. Design Studio Press.
- Gillespie, T.D., (1992), *Fundamental of Vehicle Dynamics*. Warrendale: Society of Automotive Engineering.
- Smith, J.H., (2002), *An Introduction to Modern Vehicle Design*. Warrendale: Society of Automotive Engineering.
- Sperling, D., (1995), *Future Drive: Electric Vehicle and Sustainable Transportation*, Washington DC: Island Press.
- Adhitya, Mohammad, (2013), *A New Control Strategy of Wet Dual Clutch Transmission (DCT) Clutch and Synchronizer for Seamless Gear Preselect*, SAE International.
- Larminie J., Lowry J. (2003), *Electric Vehicle Technology Explained*. West Sussex: John Wiley & Sons, Ltd
- Bradley, Allen, (1996), *Application Basics of Operation of three phase Induction Motor*



Influence of Number of Mold Cavity Vents on Wire Sweep in PBGA Encapsulation: FSI-MpCCI Simulation

Dadan Ramdan, Darianto
Mechanical Engineering Department
Engineering Faculty, Medan Area University
Medan, Indonesia
dadan@uma.ac.id

ChuYee Khor, Mohd. Zulkifli Abdillah
School of Mechanical Engineering
Universiti Sains Malaysia
Penang, Malaysia
mezul@eng.usm.my

Abstract— This paper presents three-dimensional (3D) fluid structure interaction (FSI) technique; using Mesh based Parallel Code Coupling Interface (MpCCI), for the visualization of wire sweep during encapsulation of plastic ball grid array (PBGA) package. The effect of number of mold cavity vents on the melt flow behavior, wire sweep, and pressure and stress distributions, are mainly studied. The 3D model of mold and wires are created using GAMBIT, and the fluid flow and structure are simulated using FLUENT and ABAQUS, integrated with MpCCI. The Castro-Macosko model is used to incorporate the polymer rheology and Volume of Fluid (VOF) technique is applied for melt front tracking. User-defined functions (UDFs) are incorporated to allow for curing kinetics. Wire sweep profiles and pressure distribution around wires region within the mold are presented. The numerical results of melt front patterns and filled volume are compared with the previous experimental results and found in good agreement. It is observed that the number of vents significantly influence the pressure force developed inside the mold cavity and the eventual wire sweep; as the number of vents increases, wire sweep decreases.

Keywords— fluid structure interaction; mesh based parallel code coupling interface; Castro-Macosko model; Epoxy molding compound; Volume of fluid; Wire sweep.

I. INTRODUCTION

The continuous reduction of chip size in the modern electronic industry has a significant impact on circuit design and assembly process of IC packages. Reduced chip size with increased I/O counts result in serious wire deflection during transfer molding process. If the deformation of wire is too large, it can cause a short circuit due to touching of adjacent wires or open circuit due to wire breakage [1]. Wire sweep has been recognized as one of the major defects in the encapsulation of microelectronic chips by the transfer molding process [2], [3]. The prediction of wire sweep during encapsulation involves coupled solution of mold flow and structural deformation of wires, making it a typical fluid-structure interaction (FSI) problem [4], [5]. Many researchers have focused on this issue using various computational Computer-aided engineering (CAE) techniques.

In all the previous works on wire sweep prediction, the fluid and structural solvers were run separately and coupled

manually. As a promising breakthrough in the FSI analysis, the Mesh based parallel Code Coupling Interface (MpCCI) technique has recently been introduced for the simultaneous real time coupling of fluid and structural solvers. The use of a finite volume flow solver and a finite element structural solver, coupled through MpCCI was reported for variety of engineering problems [6] – [8]. However, as far as the authors are aware, the use of MpCCI for wire sweep analysis and the study on the effect of number of vents on wire deformation during the encapsulation of plastic ball grid array (PBGA) package have not been reported so far. To address this problem, the finite-volume flow solver FLUENT and the finite-element structural solver ABAQUS are interfaced by MpCCI. Polymer rheology model with curing effect (Castro-Macosko model) is used in the fluid flow model and VOF technique is applied for melt front tracking of the EMC. The numerical analysis uses User-defined functions (UDFs) to account for curing kinetics. Keeping one gate, three configurations of mold cavity with 2, 4 and 6 vents are simulated. Melt front profiles, wire sweep, pressure field, and stress distribution on wires, are analyzed for each case. The proposed model is well validated by the published experimental results of Yang *et al.*, (2000) [9].

II. MATHEMATICAL MODEL

A. Fluid Flow Analysis

In the simulation model, the encapsulation process material and air are assumed incompressible and the governing equations describing the fluid flow are conservation of mass, conservation of momentum, and conservation of energy [10]. FLUENT normally solves the governing equations using Cartesian spatial coordinates and velocity components.

The conservation of mass or continuity equation is:

$$\frac{\partial \rho}{\partial t} + \frac{\partial}{\partial x_i}(\rho u_i) = 0 \quad (1)$$

Eq. (1) is the general form of the mass conservation equation and is valid for incompressible and compressible flows. Conservation of momentum in i^{th} direction in an inertial (non accelerating) reference frame is described by:



$$\frac{\partial}{\partial t}(\rho u_i) + \frac{\partial}{\partial x_i}(\rho u_i u_j) = -\frac{\partial P}{\partial x_i} + \frac{\partial \tau_{ij}}{\partial x_j} + \rho g_i + F_i \quad (2)$$

where, P is the static pressure, τ_{ij} is the viscous stress tensor and g_i and F_i are the gravitational acceleration and external body force in the i direction, respectively.

The energy equation cast in terms of h (static enthalpy) can be written as,

$$\frac{\partial}{\partial t}(\rho h) + \frac{\partial}{\partial x_i}(\rho u_i h) = \frac{\partial}{\partial x_i}(k \frac{\partial T}{\partial x_i}) + \eta \dot{\gamma} \quad (3)$$

where T is the temperature, k is the thermal conductivity, η is the viscosity and $\dot{\gamma}$ is the shear rate. The molding compound was assumed to be a generalized Newtonian fluid (GNF).

Several models have been used to predict the relationship between viscosity and the degree of polymerization. The Castro–Macosko model has been applied in encapsulation process [8] and is selected to use in this simulation. It can be described as follows:

$$\mu(T, \dot{\gamma}) = \frac{\mu_0(T)}{1 + (\frac{\mu_0(T)\dot{\gamma}}{\tau^*})^{1-n}} (\frac{\alpha_g}{\alpha_g - \alpha})^{C_1 + C_2 \alpha} \quad (4)$$

where n is the power law index, μ_0 the zero shear rate viscosity, τ^* is the parameter that describes the transition region between zero shear rates and the power law region of the viscosity curve, $\dot{\gamma}$ is the shear rate, α is the conversion, α_g is the conversion at the gel point and C_1 and C_2 are fitting constants.

$$\mu_0(T) = B \exp\left(\frac{T_b}{T}\right) \quad (5)$$

B is an exponential-fitted constant and T_b is a temperature fitted-constant. In addition, Kamal curing kinetics is coupled together with Castro–Macosko model. This model predicts the rate of chemical conversion of the compound as follows:

$$\frac{d\alpha}{dt} = (k_1 + k_2 \alpha^{m_1})(1 - \alpha)^{m_2} \quad (6)$$

$$k_1 = A_1 \exp\left(-\frac{E_1}{T}\right) \quad (7)$$

and

$$k_2 = A_2 \exp\left(-\frac{E_2}{T}\right) \quad (8)$$

where α is the conversion, A_1 and A_2 are the Arrhenius pre-exponential factors, E_1 and E_2 are the activation energies, m_1 and m_2 are the reaction orders and T is the absolute temperature. TABLE I summarized the material properties of the EMC considered in the current study.

The basic idea of the VOF scheme is to locate and evolve the distribution of, say, the liquid phase by assigning for each cell in the computational grid a scalar, f , which specifies the fraction of the cell's volume occupied by liquid. Thus, f takes

the value of 1 ($f = 1$) in cell which contains only resin, the value 0 ($f = 0$) in cells which are void of resin, and a value between 0 and 1 ($0 < f < 1$) in “interface” cells or referred as the resin melt front. The equation of melt front over time is governed by the following transport equation:

$$\frac{\partial f}{\partial t} = \frac{\partial f}{\partial t} + \nabla \cdot (uf) = 0 \quad (9)$$

TABLE I. EMC MATERIAL PROPERTIES [11].

	Parameter	Value	Unit
Castro Macosko Model	α_g	0.17	-
	B	0.000381	Kg/m/s
	T_b	5230	K
	n	0.7773	-
	τ	0.0001	N/m ²
	C_1	1.03	-
	C_2	1.50	-
Curing Kinetics	m_1	1.21	-
	m_2	1.57	-
	A_1	33530	1/s
	A_2	30540000	1/s
	E_1	7161	K
	E_2	8589	K
	α	0.05	-
Density	ρ	2000	Kg/m ³
Specific Heat	C_p	1079	J/Kg-K
Thermal Conductivity	-	0.97	W/m-K
Reference Temperature	T	298	K

B. Wire Sweep Analysis

To calculate the drag force exerted on the wires by the resin flow, the value of velocities and viscosities have to be determined from the mold filling simulation. The effect of wire density on the resin flow is considered according to their occupied volume in the three dimensional filling simulation. Then, the Lamb's model is utilized to calculate the drag force as follows [1]:

$$D = \frac{C_D \rho U^2 d}{2} \quad (10)$$

where D is the drag force per unit length, ρ is the fluid density, U is the undistributed upstream velocity, d is the wire diameter and C_D is the drag coefficient, which can be written as:

$$C_D = \frac{8\pi}{Re[2.002 - \ln(Re)]} \quad (11)$$

where Re is the Reynold number, which can be defined as:

$$Re = \frac{\rho u d}{\eta} \quad (12)$$

where η is the fluid viscosity.

Wire sweep deflection δ can be written as [12]:



$$\delta_{max} = S * D \left(f_B \left(\frac{H}{L} \right) \frac{H^3}{EI} + f_T \left(\frac{H}{L} \right) \frac{L^3}{GI_p} \right) \quad (13)$$

where S is the length of the wire bond, f_B is the bending geometry factor for the bending moment, f_T is the twisting geometry factor for the twisting moment, H is the height of wire, L is the length of wire span, G is the shear modulus of wire, E is the elastic modulus of wire, I is the momentum of inertia of the wire, I_p is the polar momentum of inertia of the wire.

III. SIMULATION MODEL

A. Simulation Model and Boundary Conditions in FLUENT

The volume of fluid (VOF) model in FLUENT 6.3.26 is utilized to simulate the process [13] – [15]. In the VOF model, a single set of momentum equations is shared by the fluids, and the volume fraction of each of the fluids in each computational cell is tracked throughout the domain [15]. Air and EMC are defined as the phases in the analysis. Implicit solution and time dependent formulation are applied for the volume fraction in every time step. The volume fraction of the encapsulation material is defined as one and zero value for air phase.

The Castro-Macosko viscosity model with curing effect was written into C language using Microsoft VISUAL Studio 2005 and compiled as UDF in FLUENT. The mold cavity package models with different number of vents, and its boundary conditions are shown in Fig. 1. The dimension of mold cavity is 100 mm × 100 mm × 5 mm, die is 30 mm × 30 mm × 1mm and inlet is 8 mm × 8 mm [16]. The flow direction is diagonal of x and z direction to the un-deformed wire axis and the properties are approximately the same as those used in ref. [16]. The model is created by using GAMBIT software and average 395,000 tetrahedral elements are generated for simulation (Fig. 2) in terms of accuracy and computational cost. Besides, time step size is also tested and 0.001 s is found to be the optimum. The governing equations are discretized by the first order upwind scheme, and solved by SIMPLE algorithm.

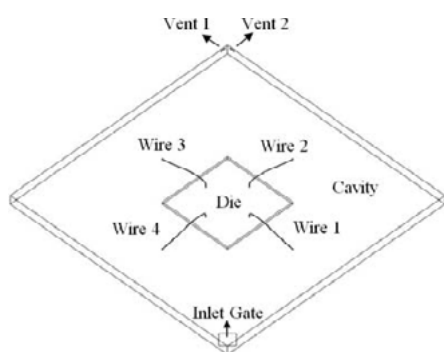


Fig. 1 (a)

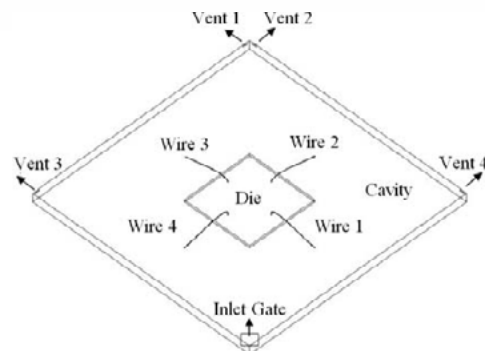


Fig. 1 (b)

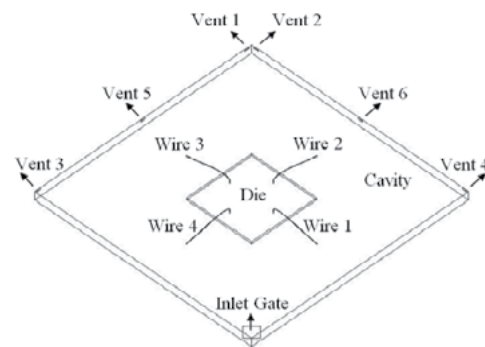


Fig. 1 (c)

Fig. 1. Mold cavity models with: (a) 2 vents (b) 4 vents and (c) 6 vents.

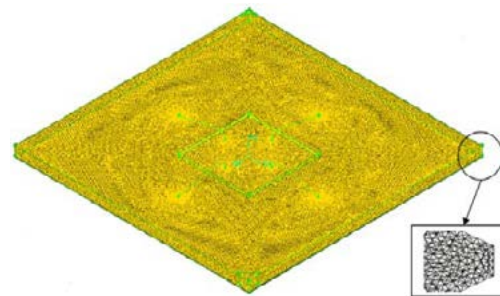


Fig. 2. Meshed model with 2 vents for FLUENT analysis.

The boundary and initial conditions used in the calculation are as follows [15]:

- (a) On wall : $u = v = w = 0$; $T = T_w$, $\frac{\partial p}{\partial n} = 0$
- (b) On centre line : $\frac{\partial u}{\partial y} = \frac{\partial v}{\partial y} = \frac{\partial w}{\partial y} = \frac{\partial T}{\partial y} = 0$
- (c) On melt front : $p = 0$
- (d) At inlet : $u = u_{in}(x,y,z)$; $T = T_{in}$



The mold temperature was considered as 175°C and the package inlet velocity was 0.6 m/s. The simulation is performed on an Intel Core 2 Duo processor E7500, 2.93 GHz with 2 GB of RAM; it took around 74 hours for each case to complete 15,000 iterations in time steps of 0.001s.

B. The computational domain and boundary conditions in ABAQUS

Commercial FEM based software; ABAQUS is used in this study to calculate the wire deformation. The structures of the wires are imported from GAMBIT in ACIS '.sat' format. The dimensions of the gold wire used in this study are chosen according to the model of Yang *et al.*, (2000). The wire (Fig. 3) has a span, $L = 20$ mm, height $H = 3.5$ mm and diameter $d = 0.14$ mm. The wire is divided into 10,191 tetrahedral elements as shown in Fig. 4. The shape of the wire is also classified as typical Q-auto loop wire [17]. The ball bond boundary conditions of wire are set as fixed in ABAQUS and shown in Fig. 5. The wire mechanical properties are as follows: elastic modulus, $E=50$ GPa [18], density, $\rho=1800$ kg/m³, Poisson's ratio, $\nu = 0.42$ and reference temperature, $T=175^\circ\text{C}$.

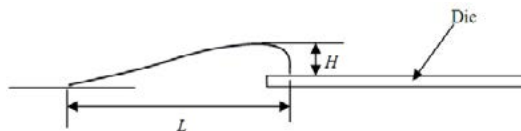


Fig. 3. Wire specifications.

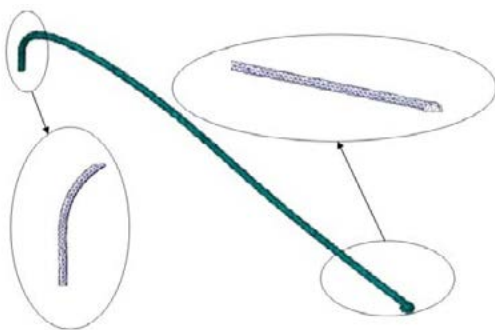


Fig. 4. Meshed wire for ABAQUS analysis.

C. Mesh based Parallel Coupling Code Interface (MpCCI)

MpCCI is a software library which enables the exchange of data defined on meshes of two or more simulation codes in the coupling region. Since the meshes need not match point by point, MpCCI performs an interpolation and, in case of parallel codes, keeps track of the distribution of the domains onto different processes [7]. In this way, the intricate details of the data exchange are hidden behind the concise interface of MpCCI. As a consequence, the simulation codes themselves

are changed only moderately when they are prepared for coupling via MpCCI (Fig. 6).

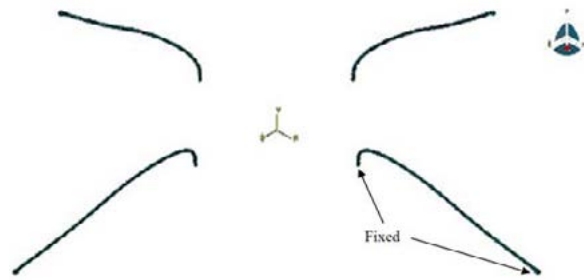


Fig. 5. Boundary condition of wires in ABAQUS [19].

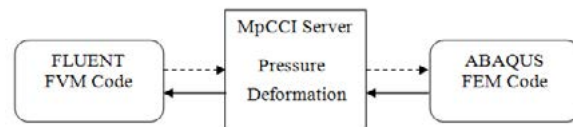


Fig. 6. FLUENT and ABAQUS coupling simulation process [20].

IV. RESULT AND DISCUSSION

A. Model Validation

The present simulation results of fluid flow (for 2 vents case) are validated with the experimental results of Yang *et al.*, (2000) [9] who investigated the flow behavior of epoxy resin (D.E.R.331, Dow Chemical). Fig. 6 shows the comparison of predicted and experimental flow profiles of the PBGA encapsulation process from 4 to 10 s of filling. The simulation results show separate profiles for wire sweep and EMC filling, at various stages of filling. The predicted EMC flow profiles show good agreement with the experimental results, at all time steps. Wire displacement phenomenon is observed when the EMC flow around the wire region. The EMC volume versus filling time for the simulation and the experiment is also plotted and compared as in Fig. 7; the maximum discrepancy is found about 6.7%.

Further, the wire deformation is validated with analytical method proposed by Kung *et al.* (2006) [21]. The comparison of simulation and analytical results [21] of wire deformation for wire 4 in x-direction is shown in Fig. 8. The analytical calculation refers to eq. (13) with $f_b = 0.165$, $f_r = 0.00165$ and $H/L = 0.175$. The average deviation at maximum displacement (after 9 s) is found to be 6.5%. The results demonstrate good quantitative agreement.

B. Melt Front Profile

First of all the effect of number of vents on the melt front profile is visualized for various stages of filling, as presented



in Fig. 9. It is observed that the melt flow pattern follows almost similar trend in all the cases; this indicates that the melt front advancement is not significantly influenced by the number of vents.

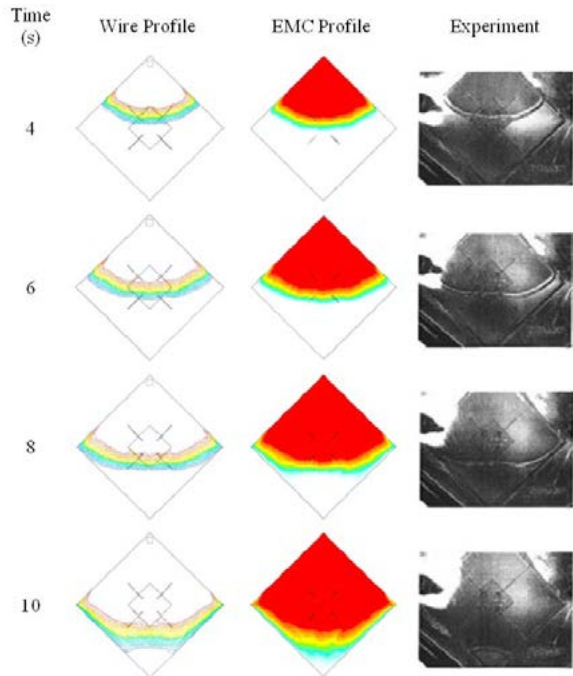


Fig. 6. Comparison of simulation and experiment [9] for wire deformation and EMC flow profiles (2 vents case).

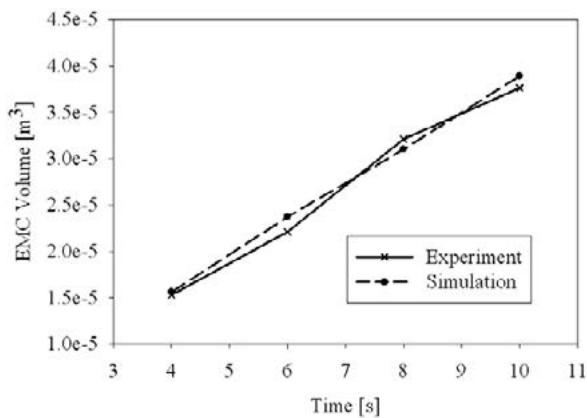


Fig. 7. Comparison of EMC filled volume for experiment [9] and simulation (2 vents case).

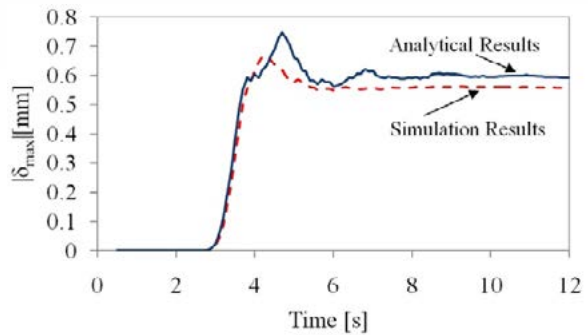


Fig. 8: Comparison simulation and analytical results [21] of wire deformation for wire 4 in x-direction (2 vents case).

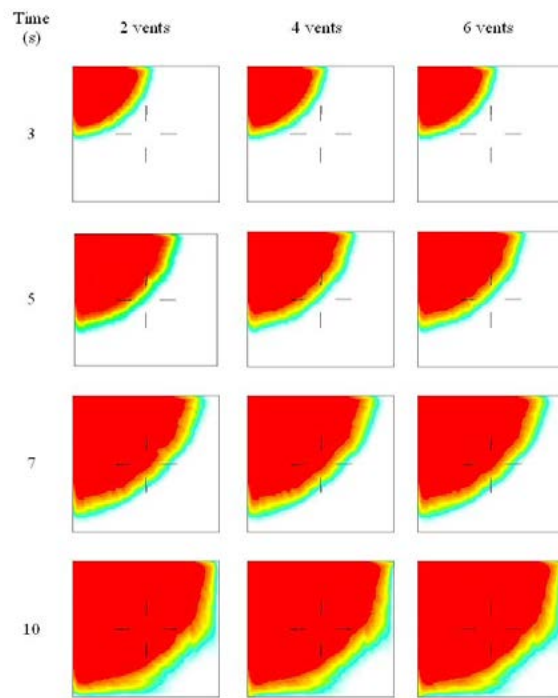


Fig. 9. Melt front profiles of three cases at various filling stages.

C. Wire sweep

Fig. 10 illustrates the phenomenon of wire deformation, predicted by ABAQUS. The magnitude of wire deformation for each wire is also estimated and plotted as shown in Fig. 11. It is clear that the wires 1 and 4 are significantly deformed compared to wires 2 and 3, in all the cases. At the same time, it is worth noting that, as the number of vents increases, the sweep tendency decreases, presumably due the reduced pressure force inside the cavity.

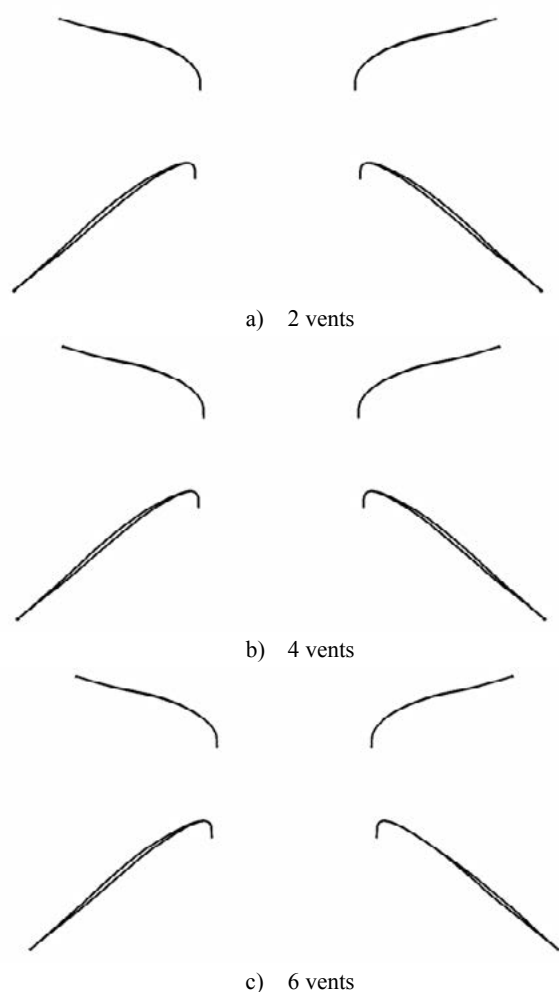


Fig. 10: Illustration of wire sweep predicted by ABAQUS.

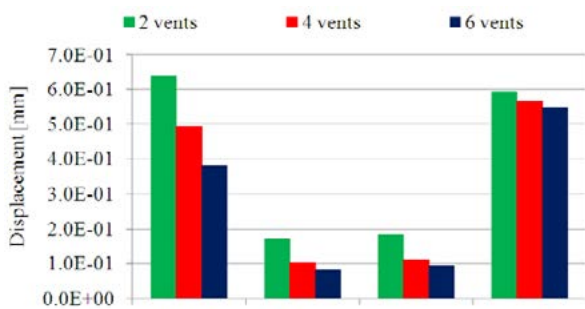


Fig. 11. Comparison of deformation of wires 1-4 for all the cases.

D. Void occurrence

It has been shown in the previous sections that increasing the number of vents could reduce the wire sweep. However, it would be interesting to study the limiting factors of increasing the vents for a given mold cavity and number of gate. Thus in the present study, an attempt is also made to observe how the number of vents influence the development of voids during the encapsulation process. Fig. 12 shows the melt front profiles showing the void locations for various cases, and Fig. 17 shows the graphical comparison of the respective percentages of voids. It is observed that, as the number of vents increases, the void formation increases significantly; this apparently imposes restriction on the number of vents. However, as is clear from Fig. 16, since the voids are situated near the walls, and the wire zone is not affected, the increased number of vents does not presumably pose significant threat on the quality of mold filling.

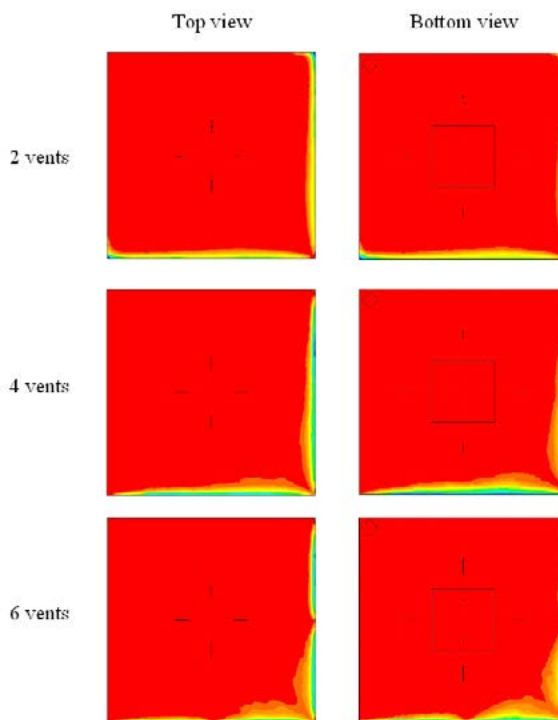
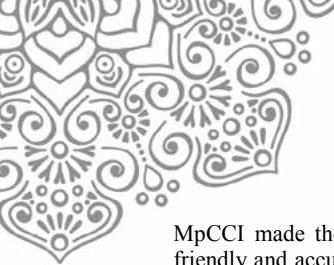


Fig. 12: Mold filling contours for various cases after 15s, showing voids.

V. CONCLUSION

The coupled three dimensional FLUENT-ABAQUS-MpCCI facility was successfully employed to study the effect of number of vents on wire sweep during the encapsulation of a typical PBGA package. The major contributions in this work are the use of MpCCI, and the investigation of the effect of number of vents on wire sweep. Unlike the conventional manual coupling of flow and structural simulations, the



MpCCI made the present FSI analysis more effective, user-friendly and accurate. The wire sweep and melt front profiles were compared with the previous experimental results and found in good agreement. It was observed that the number of vents had crucial influence on wire sweep which decreased with increase of vents. Further, the analysis of Von-Mises stress showed that the potential fracture of wires due to excessive stresses could be eliminated by the increase of number of vents. This study may be improved by considering the optimization of number of gates and vents, and their locations. Precise experiment on realistic packaging environment is also recommended to substantiate the present predictions.

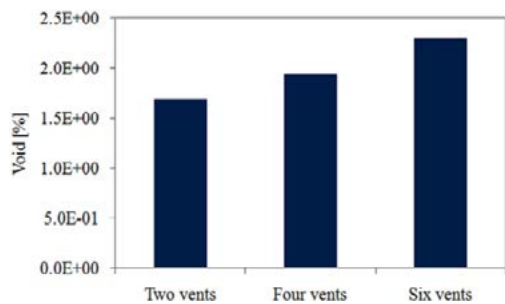


Fig. 17: Voids percentage in various cases after 15s.

ACKNOWLEDGMENT

The authors gratefully acknowledged the Intel Tech. Sdn. Bhd., Penang for the financial support of this research work. The author would also like to thank DGHE National Education and Culture Department of Republic of Indonesia for Research Found of PHB skim in 2016 FY. Lastly, the author would also like to thank C.Y. Khor for the technical software advices in the present study.

REFERENCES

[1] J. Su, S. J Hwang, F. Su, S. K. Chen, "An Efficient Solution for Wire Sweep Analysis in IC Packaging," *J. Electron. Packag.*, ASME, vol. 125, pp. 139-143, March 2003

[2] W. R. Jong, Y. R. Chen, T. H. Kuo, "Wire Density in CAE analysis of high pin-count IC packages: Simulation and verification," *Int. Commun. Heat and Mass Transfer*, vol. 2, pp. 1350-1359, 2005

[3] M. S. Rusdi, M. Z. Abdullah, A. S. Mahmud, C. Y. Khor, M. S. Abdul Aziz, Z. M. Ariff, M. K. Abdullah, 2016, Numerical Investigation on the Effect of Pressure and Temperature on the Melt Filling During Injection Molding Process, *Arab J Sci Eng* (2016) 41:1907-1919, DOI 10.1007/s13369-016-2039-0.

[4] C.Y. Khor, M.Z. Abdullah, Chun-Sean Lau, I.A. Azid, 2014, Recent fluid-structure interaction modeling challenges in IC encapsulation – A review, *Microelectronics Reliability* 54 (2014) 1511-1526.

[5] C.Y. Khor, Muhammad Ikman Ishak, M.U. Rosli, Mohd Riduan Jamalludin, M.S Zakaria, A.F.M. Yamin, M.S. Abdul Aziz, and M.Z. Abdullah, 2017, Influence of Material Properties on the Fluid Structure Interaction aspects during Molded Underfill Process, *MATEC Web of Conferences* 97, 01059 (2017) *ETIC 2016*, DOI: 10.1051/mateconf/20179701059.

[6] S. Yigit, M. Schafer, M. Heck, "Grid movement techniques and their influence on laminar fluid-structure interaction computations," *J. Fluids and structures*, Vol. 24, pp. 819-832, 2008.

[7] F. Thirifay and P. Geuzaine, "Numerical simulations of fluid-structure interaction problem using MpCCI," address: <http://citeseerx.ist.psu.edu/viewdoc/download>, 2008.

[8] B. Gatzhammer, M. Mehl, T. Neckel, "A coupling environment for portioned multiphysics simulations applied to fluid-structure interaction scenarios," *Procedia Comput. Science*, Vol. 1, pp.681-689, 2010.

[9] Yang S-Y., Jiang S-C., and Lu W-S. (2000), "Ribbed package geometry for reducing thermal warpage and wire sweep during PBGA encapsulation", *IEEE Transactions on Components and Packaging Technologies*, Vol. 23, No.4, pp. 700-706.

[10] D. Ramdan, M. Z. Abdullah, C. Y. Khor, "Plastic Ball Grid Array Encapsulation Process Simulation on Rheology Effect," *TELKOMNIKA*, vol. 9, no. 1, pp. 27 – 36, April 2011.

[11] L. Nguyen, C. Quentin, W. Lee, S. Bayyuk, S. A. Bidstrup-Allen, S. T. Wang, "Computational Modeling and Validation of the Encapsulation of Plastic Packages by Transfer Molding," *Trans. of the ASME*, vol. 122, pp. 138-146. 2000.

[12] H. K. Kung, J. N. Lee, C. Y. Wang, "The Wire Sweep Analysis Based on the Evaluation of the Bending and Twisting Moments for Semiconductor Packaging," *Microelectron. Eng.* 83, pp. 1931-1939, 2006.

[13] Khor C.Y., Abdullah M.Z., Abdullah M.K., Mujeebu M.A., Ramdan D., Majid M.F.M.A., Ariff Z.M., Abdul Rahman M.R. (2011), "Numerical analysis on the effects of different inlet gates and gap heights in TQFP encapsulation process", *Int. J.of Heat and Mass Transfer*, Vol. 54, pp. 1861-1870.

[14] Khor C.Y., Abdullah M.K., Abdullah M.Z., Abdul Mujeebu M., Ramdan D., Majid M.F.M.A., Ariff Z.M. (2010)-(a), "Effect of vertical stacking dies on flow behavior of epoxy molding compound during encapsulation of stacked-chip scale packages", *Heat and Mass Transfer*, Vol. 46, pp. 1315-1325.

[15] Khor C.Y., Abdul Mujeebu M., Abdullah M.Z., Che Ani F. (2010)-(b), "Finite volume based CFD simulation of pressurized flip-chip underfill encapsulation process", *J.of Microelectronics Reliability*, pp. 98-105.

[16] Han S-J. and Huh Y-J. (2000), "A study of wire sweep during encapsulation of semiconductor chips", *J. of the Microelectronics and Packaging Society*, Vol. 7, No. 4, pp. 17-22.

[17] J. M. Brand, S. A. Ruggero, A. J. Shah, "Wire sweep Reduction via Direct Cavity Injection During Encapsulation of Stacked Chip-Scale Packages," *J. Electron. Packag.*, Vol. 130, pp. 011011-1 – 011011-6, March 2008.

[18] Yang W-H., Hsu D.C., Yang V., Chang R-Y, Su F., Huang S-J. (2004), *Three dimensional CAE of wire-sweep in microchip encapsulation*, Technical Conference-ANTEC, Conference Proceeding, Vol.2, pp. 1679-1683.

[19] D. Ramdan, U. Harahap, A. Rubiantara, C. Y. Khor (2016), Fluid Structure Interaction Numerical Simulation of Wiresweep in Electronics Packaging, *TELKOMNIKA*, vol. 14, no. 1, pp. 262 – 272, March 2016.

[20] MpCCI 3.1.0-1 Documentation part I overview, Fraunhofer Institute for Algorithms and Scientific Computing SCIA, Germany, January 2009.

[21] Kung H-K., Lee J-N., Wang C-Y. (2006), "The wire sweep analysis based on the evaluation of the bending and twisting moments for semiconductor Packaging", *Microelectronic Engineering*, Vol. 83, pp. 1931-1939.



DRYING KINETICS OF PAPUA PEAT

Pither Palamba^a, Mohamad Lutfi Ramadhan^a, Engkos Achmad Kosasih^a, Yulianto Sulistyono
Nugroho^{a,*}

^a*Department of Mechanical Engineering, Faculty of Engineering University of Indonesia, Depok
16424, Indonesia*

ABSTRACT

Indonesia has the largest peatland in the tropical region that are scattered mainly in Sumatera, Kalimantan, and Papua. Peat is an organic substance which is highly combustible in dry conditions. Dried peat could easily burnt and spread vertically and laterally along peat layers. In Indonesia, peat fires often occur in recent decades. Besides influenced by the amount of the organic content, smoldering fires of peat is also effected by the drying rate, pyrolysis, and heterogeneous oxidation in the peat surfaces. Peatland fires is one of the biggest wildfire which has damaged the ecosystem and produce hazardous combustion products into the atmosphere. In contrast to flaming fire that has been widely studied, the smoldering fires of peat are still lack of understanding. The contribution of drying kinetics of peat on the peat fires phenomenon, are important mechanisms to be studied, so these could provide a complete understanding for the process of peat fires. So far, major works on peat fire related publications concern on the pyrolysis and combustion stages. The objectives of this paper are to study the isothermal and thermogravimetric drying kinetics analysis of peat. Peat sample used was taken from Papua, Indonesia. The isothermal test was conducted using Shimadzu MOC63u Moisture Balance Analyzer with 0.001 mg accuracy. At a certain time interval the weight of the specimen was measured until it reached a constant weight of less than 0.05% changes of moisture content. Isothermal analysis was conducted by moisture analyzer of each peat at setting temperatures of 60,70, 80, 90, 100, and 110°C. The results showed that the activation energy from the isothermal measurement and thermogravimetric test were 32.83 kJ/mole with the constant of reaction rate, $k = 0,0137 \text{ sec}^{-1}$.

Keywords: Peat; drying phenomena; effect of temperature; mass loss; moisture content; activation energy

1. INTRODUCTION

1.1 Distribution of Indonesian peat

Peatlands are ecosystems that have a very important role in maintaining the balance of carbon, water and climate. Indonesia is a tropical country with the largest peat lands approximately 20.6 million ha which are mainly distributed in three large islands of Sumatera (35%), Kalimantan (32%), Papua (30%) ([Ritung & Wahyunto, 2012](#)). Most of the peat land is still covered by forest and a habitat for many species of animals and rare plants. Peatlands store carbon (C) in large quantities and have a high water retention to act as a hydrological buffer for surrounding area. Equilibrium moisture content of the peat layer becomes difficult to maintain if the forests have

* Corresponding author.

E-mail address: yulianto@eng.ui.ac.id



been converted for plantations, agricultural or other uses because this process is usually irreversible.

In the long dry season, the depth of the water table fall and the surface layer of peat easily dry and hollow so as to allow air get into the bottom layer. If it has become dry the peat that was originally hydrophilic (water-loving, have an affinity for water because of the formation of hydrogen bonds) turned into a hydrophobic (water-repellent, not easily penetrated by water) (Valat et al., 1991, Doerr et al., 2000, Dekker et al., 2001, Murtlaksono et al., 2016). In these conditions, peat is highly flammable and if burning, embers can propagate laterally and vertical in-depth, consuming mass of peat and produce smoke with a number of toxic substances. During the dry season when wetland dry out, large scale wildland/forest fires may occur on dry land and also on wetland such as peatland or peat-forest (Nugroho, 2017). Wildland fires, especially when involving peat land fires can be viewed as a regional and global disaster. Smoldering combustion of peatland fires produces thick haze that directly impact the life of the local peoples and can spread to other region and neighboring countries. Peat fires that occurred in various locations is one of the major problem because periodically occur in a large scale in recent years. In Indonesia, forest and peatland fires occur almost every year in the last two decades and resulted in economic losses, health and environmental impact is enormous. When active, smoldering combustion in the peat and biomass layer can sustain for long periods of time and difficult to extinguish and even by propagating below the surface, smoldering fires offer the means for flaming combustion to reestablish during wildfires in unexpected locations and at unexpected times (e.g. long after burn out of the flaming front) (Rein, 2009). Nevertheless, research on Smoldering peat lands are still poorly studied compared to flaming fires.

In the solid fuel combustion, there are three stage of the process i.e. evaporation, pyrolysis and combustion. In certain cases, where the combustion takes place quickly (particularly influenced by the speed of the air supply), the process takes place with the phases: evaporation, where the water vapor evaporating through the pores; fuel oxidation, in which combustion occurs leaving charcoal; and char oxidation, where combustion takes place by consuming some flammable substances and leaves ash as a product.

Events peat fires started from peatland conditions are becoming dry, with moisture content maximum that can burn 250% (dry base) (Rein et al., 2008) or 150% (Prat-Guitart et al., 2016). A number of studies on the phenomenon of smoldering peat fire mostly concerned on the reaction of its pyrolysis and combustion. As the drying process, in general, the drying kinetics of peat should be studied to understand both the drying rate, moisture content and its activation energy. Some studies relating to the drying of peat among others in experimental study of thermophysical and thermokinetic characteristics of peat (Grishin et al., 2006) which finds the values of activation energy of 47.376 kJ/mole, and, in investigation of thermal analysis and decomposition kinetics of Chinese forest peat (Chen et al., 2011) which finds the value of activation energy of 68.510 kJ/mole.

Each type of material has a specific drying curve, which is dependent on the physical and chemical characteristics of the substance. This research aims to study the isothermal drying kinetics of peat taken from Papua, Indonesia, to determine the moisture content, drying rate and activation energy as the initial stage of the whole phase of peat smoldering fire.



1.2 Moisture content and water retention

Peat is an organic soil with a very high moisture content because it has a high water retention. However, if the water content is decreased excessively, it will lead to irreversible dry conditions (hydrophobic). Peat in such conditions is hard to absorb water, very light weight and easily washed away by rainwater, its structure became unravel such as sand, flammable, and hard to be replanted. In general, water in peat can be broadly classified as mechanically entrapped water, capillary water and chemically bound water. Investigations by Rebinder, quoted by Volarovich and Churaev ([Volarovich & Churaev, 1968](#)) indicate that water in peat can be divided into three categories: physically and chemically bound water; capillary and film water; and immobilized water. Physically and chemically bound water is water absorbed at the solid-liquid interface, contents range from 40-70 percent of the total water in raw peat of which 10-15 percent is very tightly bound. Capillary and film water is water retained by forces of negative and wedge pressure at the air-water interface. If there is no air in the soil, capillary and film water becomes free water without a surplus bond energy. Immobilized water is water held in peat by purely mechanical forces and its bond energy is negligible. It comprises intracellular water, entrained on cell structures and the water in closed pores. Dispersion, compression, or destruction of the structure may result in conversion of this water to free water. The bound water in peat consists mainly of capillary and immobilized water.

Investigations into drying indicate that the first drying stage is characterized by the removal of free water and of water from large pores. On further drying, the forces of capillary contraction increase and weakly bound intracellular and immobilized water is squeezed out. After removal of the mechanically bound water, the rate of drying is reduced still further. This is followed by the removal of physico-chemically bound water. The removal of moisture appears to follow a strict sequence determined by the bond energies. With further dehydration, irreversible changes in high molecular compounds take place and the peat becomes more fragile. This explains the coffee grounds and powdery peat structure formed in surface layers of reclaimed peat soils as a result of drying in the sun.

The outcomes experimental will provide scientific background on integrating fire risk considerations in national and local development strategies in Indonesia ([Nugroho, 2017](#))

1.3 Drying kinetics and activation energy

Drying is a complex process involving mass transfer, heat and momentum simultaneously. Chemically bound water, which is not removed in drying, possesses the highest binding energy ([Grishin et al., 2003](#)). Adsorptionally and osmotically bound moisture is assigned to physicochemically bound water. Evaporation of bound moisture is a complex multistage process which involves, except for desorption and adsorption of water, motion of water and vapor along the pores of a dried body and vapor flow in the boundary layer in the vicinity of the body.

Irreversible drying occurs after periods of intensive drying and is typical of many peat soils. Surface layers of organic materials in many reclaimed and drained peat swamps exhibit this behavior. After exposure to the sun, the materials become rather like coffee grounds, and are very difficult to re-wet. This may cause severe drought stress in shallow rooting crops. There are several explanations of the cause of the property. Coulter ([Coulter, 1957](#)) attributes the hydrophobic nature of dried peat to the presence of a resinous coating which presumably forms upon drying. He suggests this coating prevents the reabsorption of water. There is some doubt about this. For example, Driessen and Rochimah ([Driessen & Rochimah, 1977](#)) did not find such coatings in



Indonesian peats and the author has never seen them. Re-wetting resistance explained as due to adsorbed air films and iron coating around the organic particles. Resistance to re-wetting also appears to be related to bulk density. Thus, irreversible drying is marked in organic soils with low bulk density but those with high bulk densities are comparatively easy to re-wet.

Some research on drying kinetics of peat such as Filkov ([Filkov et al., 2012](#)) using three different kinds of boreal peat from two regions (Edinburgh, Scotland and Tomsk, Russia) by TGA for micro scale (thermogravimetry analysis) and isoconvensional method, KAS (Kissinger – Akahira – Sunose), based on the modeling of the mass loss with Arrhenius's Law, obtained the thermokinetic constants for the Drying Process of the peats, while Nugroho ([Nugroho, 2002](#)), used tropical peat material (Kalimantan, Indonesia) with the methods of differential form of Arrhenius equation. He stated that the activation energy of peat sample is lower than other materials such as palm fiber, and woods. This indicated that peat material is easier to react with the oxygen.

2. METHODOLOGY

Sample in current research is a part of the sample used in the other previous studies ([Palamba et al., 2017](#)) which was extracted from Kampung Bagaiserwar, Kabupaten Sarmi, Papua, Indonesia in coordinate S: 01° 55'14.11"; E: 138°6'17.35" at 50 – 110 cm deep using PVC pipe, 6 inch-diameter and 60 cm length. Sampling method used was undisturbed to retain sample characters and prevent contamination from microbes activity and other chemical reactions until test are conducted.

Tests were carried out using MOC63u Shimadzu Moisture Analyzer, an equipped with a high output halogen heater capable of rapid heating with power of 400W and temperature range of 50-200°C. Shimadzu MOC63u Moisture Content Analyzer is a test equipment with an accuracy of 0.001 mg at each time interval until the specimen reaches a constant weight with an accuracy of 0.05% Moisture Content. The tool connected to the computer to record the mass and moisture content evolution during the drying process. In contrast to the conventional moisture measurement generally associated with environmental conditions, this model operates in a closed state so it is not affected by humidity and other environmental conditions.

Measurements were performed with an isothermal drying respectively at 60, 70, 80, 90, 100 and 110 °C to the samples weighing 2 grams. The analysis was performed by using the Arrhenius equation, a formula for the temperature dependence of reaction rates. This equation has a vast and important application in determining rate of chemical reactions and for calculation of energy of activation. Arrhenius provided a physical justification and interpretation for the formula. Arrhenius' equation gives the dependence of the rate constant of a chemical reaction on the absolute temperature, a pre-exponential factor, an empirical relationship between temperature and rate coefficient. It is usually designated by A when determined from experiment. For a first-order reaction, it has units of s^{-1} . For that reason, it is often called frequency factor.

$$k = Ae^{-Ea/(RT)} \quad (1)$$

where

k is the rate constant (s^{-1})

T is the absolute temperature (K)



A is the pre-exponential factor, a constant for each chemical reaction that defines the rate due to frequency of collisions in the correct orientation

E_a is the activation energy for the reaction (kJ/mol)

R is the universal gas constant (8.314 J/K·mol)

Given the small temperature range kinetic studies occur in, it is reasonable to approximate the activation energy as being independent of the temperature. Similarly, under a wide range of practical conditions, the weak temperature dependence of the pre-exponential factor is negligible compared to the temperature dependence of the $e^{-E_a/(RT)}$ factor. Taking the natural logarithm of Arrhenius' equation yields:

$$\ln(k) = \ln(A) - \frac{E_a}{R} \frac{1}{T} \quad (2)$$

Rearranging yields:

$$\ln(k) = \frac{-E_a}{R} \left(\frac{1}{T}\right) + \ln(A) \quad (3)$$

This has the same form as an equation for a straight line:

$$y = mx + c \quad (4)$$

where x is the reciprocal of T .

So, when a reaction has a constant rate that obeys Arrhenius's equation, a plot of $\ln k$ versus T^{-1} gives a straight line, whose gradient and intercept can be used to determine E_a and A . Arrhenius argued that for reactants to transform into products, they must first acquire a minimum amount of energy, called the activation energy (E_a). Determining the amount of activation energy is done by graphical methods derived by a formula based on the Arrhenius equation. The formula used for the first-order reaction is as follows,

$$-\frac{dm}{dt} = km \quad (5)$$

w
h
e
w
h
e
m

$$-\frac{d(m-m_f)}{dt} = k(m - m_f) \quad (6)$$

$$-\ln\left(\frac{m-m_f}{m_0-m_f}\right) = kt \quad (7)$$

where m_0 is the initial mass of peat sample. Based on mass evolution data at each heating temperature, the relationship between $-\ln\left(\frac{m-m_f}{m_0-m_f}\right)$ and t (time) is a straight line with the slope of k . m_f is the mass of a sample at the end of the process. By arranging and integrating the equation the line represents the value of k (reaction rate constant), while the Arrhenius equation states,

$$k = k_0 \cdot e^{\left(\frac{-E}{RT}\right)} \quad (8)$$

R
E
w
h
e
m

$$\ln k = \ln k_0 - \frac{E}{RT} \quad (9)$$

A curve describes the relationship between $\ln k$ and $1/T$ will yield a straight line with a slope equal to E/R . By describing these relationships to all the appropriate temperature thereafter, the Arrhenius plot was used to determine the values of activation energies and frequency factors. A

4
0
8
4
8
6



curve describes the relationship between $\ln k$ and $1 / T$ will yield a straight line with a slope of equal to E/R . By describing these relationships to all the appropriate temperature thereafter, the Arrhenius plot was used to determine the values of activation energies and frequency factors.

3. RESULTS AND DISCUSSIONS

Figure 1 shows the mass evolution during evaporation at various temperature. Based on Figure 1, the characteristics of isothermal evaporation only depends on the heating temperature. On the heating with a low temperature, the curve will be much shallower than the heating with a higher temperature. Thus, the time to reach dry conditions (characterized by the absence of further loss up to 0.05% moisture) at low heating temperature will be longer. Similarly, as shown in Figure 2, the average evaporation rate tends to increase by the increasing of heating temperature. Measurement of moisture content with Shimadzu is accurate where of a number of measurements made by the temperature variation, it is known that the moisture content of the peat samples tested were $85.33 \pm 1.26\%$.

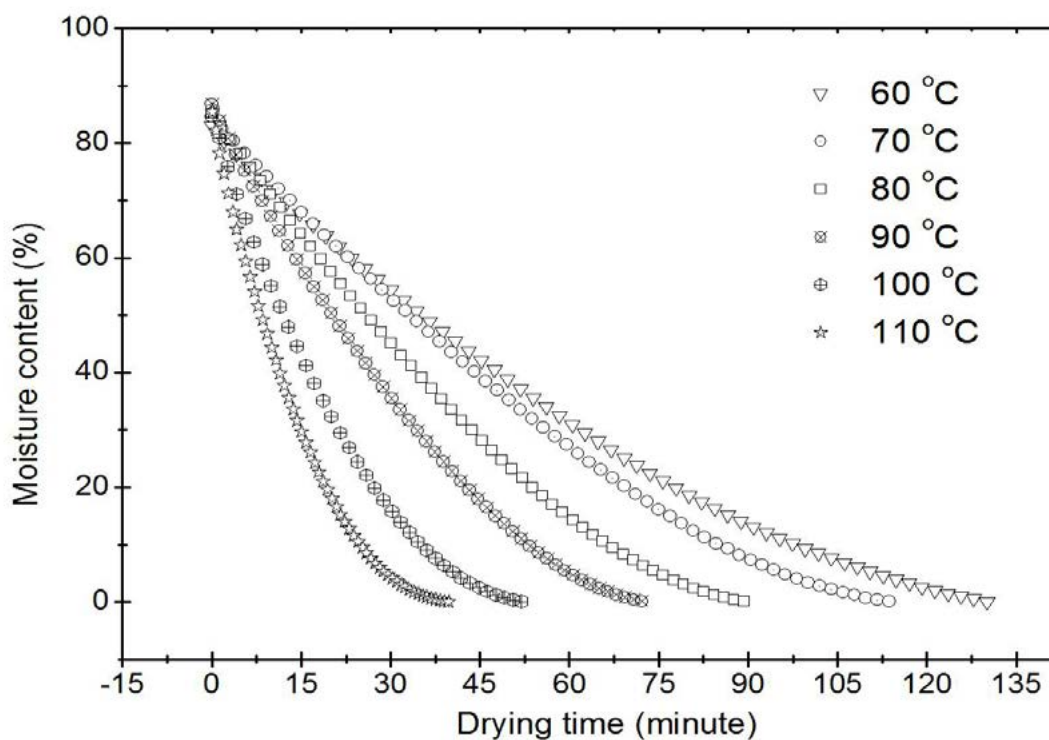
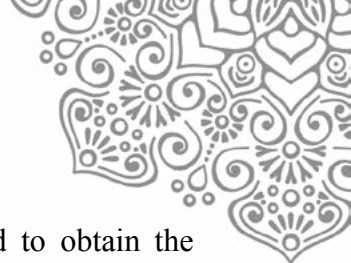


Figure 1. Drying curve of Papua peat

Drying curve illustrated in Figure 1 shows the moisture content (MC) change over time. As can be seen in the curve, the drying rate is not constant but changes over time. There are three different drying periods which will occur consecutively in time, i.e. **preheating period** (drying rate is almost 0), where all the heat provided is used to heat up the sample to the drying temperature; **constant-rate period** (drying rate is constant in time), wherein water starts to evaporate from the surface of the sample with constant rate; and **falling-rate period** (drying rate declines over time), is the phase during which migration of moisture (bounded water) from the inner interstices of each particle to the outer surface becomes the limiting factor that reduces the drying rate. Determination and calculation of evaporation rate (k) and activation energy (E_a) based on the data of the falling



period. By the drying curve (Figure 1) than the falling rate period determined to obtain the evaporation rate as shown in Figure 2.

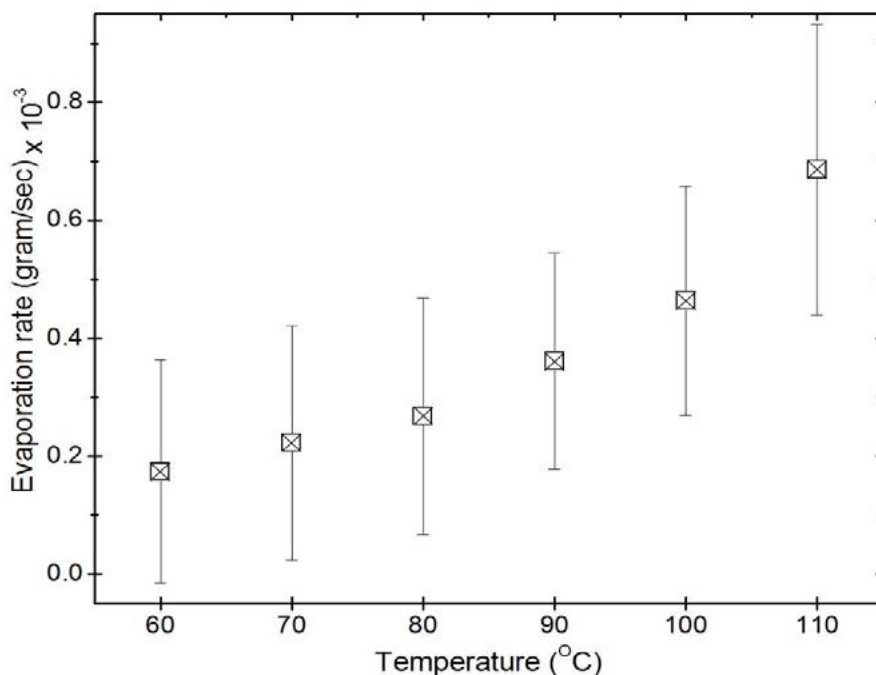


Figure 2. Average evaporation rate at falling period with standard deviation

Applying equation $-\ln\left(\frac{m-m_f}{m_0-m_f}\right) = kt$ (7) and plotting the relationship between mass evolution to t , obtained a polynomial curve for isothermal drying at each drying temperature. As example, polynomial curve for drying at 100 C is as shown in Figure 3.

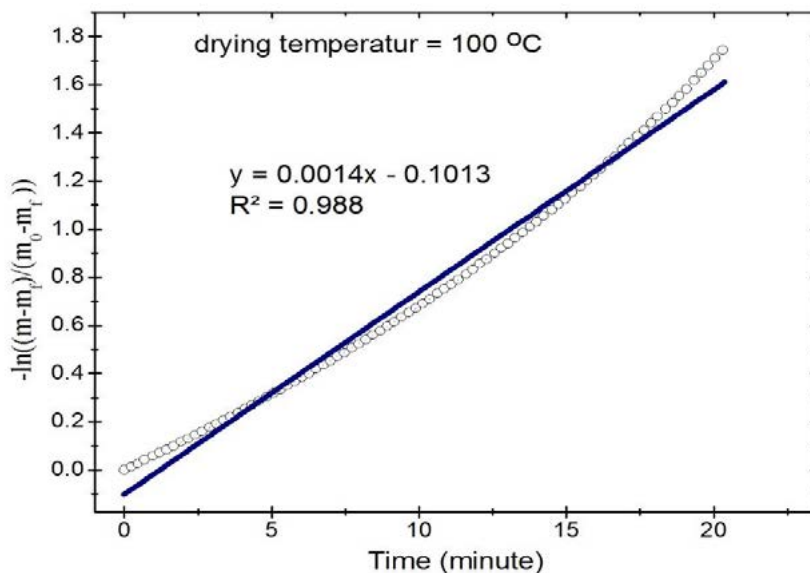


Figure 3. Natural logarithm of $(m - m_f)/(m_0 - m_f)$ versus time curves with a first order polynomial fit for isothermal evaporation at drying temperature 100°C.



Based on the equation of the straight line (Figure 3) it can be seen the reaction rate constants (k) at a drying temperature of 60 °C, 70 °C, 80 °C, 90 °C, 100 °C and 110 °C are 0.0006113, 0.000685, 0.000891, 0.001124, 0.001401 and 0.001726 s⁻¹ respectively. By taking logarithm of these constants and plotted against 1 / T then obtained equation of a line as Figure 4.

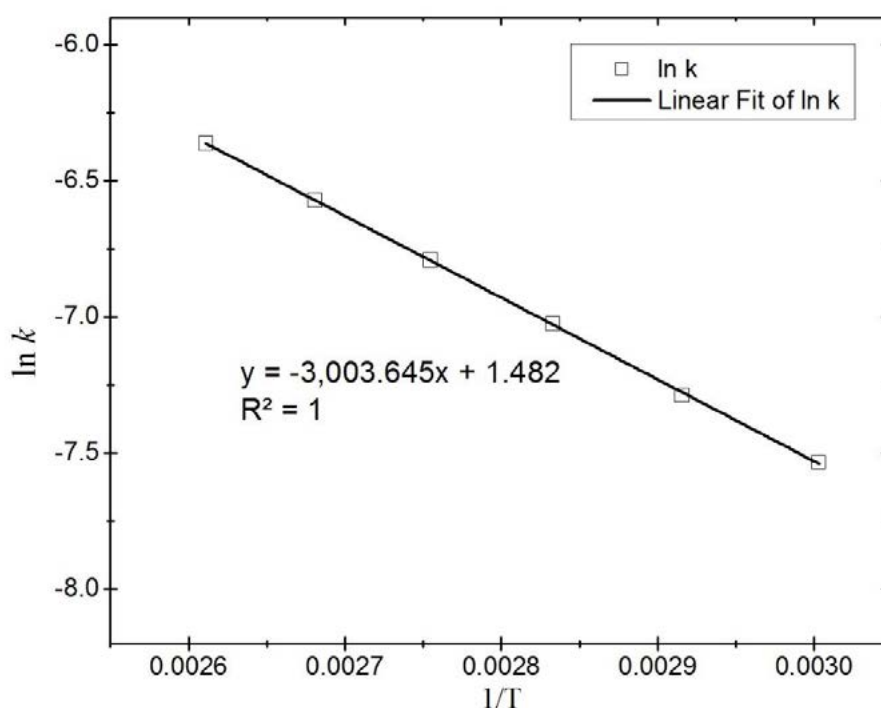


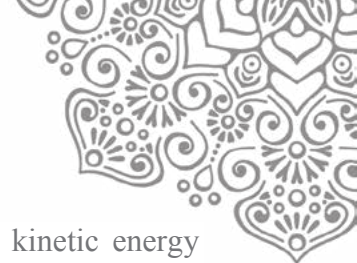
Figure 4. The trendline of ln k versus 1/T at various temperature

Figure 4 is obtained the equation of the line $y = -3003.645x + 1.482$ which is in correlation with the Arrhenius equation, it can be calculated that the activation energy of the test sample drying amounted to 24.97 kJ/mol. This value is relevant to the results of tests performed by Filkov (Filkov et al., 2012) to the boreal peat with the activation energy of 36.12 - 42.26 kJ/mol, as well as by Nugroho (Nugroho, 2002) who find value of 44 kJ/mol of Kalimantan peat, Grishin, 47 kJ/mol (Grishin et al., 2003) and Chen et al. (Chen et al., 2011) who find $E_a = 68.5$ kJ/mol for the Chinese peat. Likewise, the activation energy for soils from LTBF experiments situated at Askov (Denmark), Grignon (France), Ultuna (Sweden), and Versailles (France) ranged from 49 to 79 kJ/mol (Lefèvre et al., 2014) and on peat respiration at low temperatures considering O₂ uptake (Chapman & Thurlow, 1998), the activation energy varied between 58 and 148 kJ/mol.

Differences in the results obtained compared to the previous studies due to differences in physical and chemical properties of peat such as moisture content, bulk density and degree of decomposition. Determination of drying isothermal activation energy is strongly influenced by the accuracy of the equipment and the variant of temperature of the drying process because it will affect the slope of the trendline of the plots (because in this method, the value of activation energy depends on the slope of the line).

4. CONCLUSION

In general, an increasing the drying temperature will cause the reaction rate increases. Temperature is a measure of the average kinetic energy of the molecule; raise the temperature will increase the



existing kinetic energy to break molecular bonds when collide. The minimum kinetic energy possessed by the molecule must be equal to or greater than the activation energy for the reaction to take place. In other words, to initiate a chemical reaction, intermolecular collisions must have a minimum total kinetic energy equal to or more than the activation energy (E_a). As well as for peat drying, the minimum amount of drying activation energy required so that the evaporation process can take up the peat becomes dry. The activation energy for drying of Papua peat, Indonesia, was obtained amount to 33.05 kJ/mol. In this study, factors affected the drying process are temperature and moisture content. The given drying temperature determines reaction rate.

5. ACKNOWLEDGEMENT

The authors would like to thank the financial support provided by Universitas Indonesia through the PITTA 2017 program managed by Directorate for Research and Public Services (DRPM) Universitas Indonesia.

6. REFERENCES

- Chapman, S. J. and M. Thurlow (1998), Peat respiration at low temperatures, *Soil Biology and Biochemistry* **30**(8–9): 1013-1021 DOI: [http://dx.doi.org/10.1016/S0038-0717\(98\)00009-1](http://dx.doi.org/10.1016/S0038-0717(98)00009-1).
- Chen, H., W. Zhao and N. Liu (2011), Thermal Analysis and Decomposition Kinetics of Chinese Forest Peat under Nitrogen and Air Atmospheres, *Energy & Fuels* **25**(2): 797-803 DOI: 10.1021/ef101155n.
- Coulter, J. (1957), Development of the peat soils of Malaya, *Malayan Agricultural Journal* **40**: 188-199.
- Dekker, L. W., S. H. Doerr, K. Oostindie, A. K. Ziogas and C. J. Ritsema (2001), Water repellency and critical soil water content in a dune sand, *Soil Science Society of America Journal* **65**(6): 1667-1674.
- Doerr, S., R. Shakesby and R. Walsh (2000), Soil water repellency: its causes, characteristics and hydro-geomorphological significance, *Earth-Science Reviews* **51**(1): 33-65.
- Driessen, P. and L. Rochimah (1977). The Physical Properties of Lowland Peats from Kalimantan. Dalam: Peat and Podzolics Soils and Their Potential for Agriculture in Indonesia. Proceedings ATA 106 Midterm Seminar. Soil Research Institute, Bogor. Halaman.
- Filkov, A. I., A. Y. Kuzin, O. V. Sharypov, V. Leroy-Cancellieri, D. Cancellieri, E. Leoni, A. Simeoni, G. Rein, A. I. Filkov, A. Y. Kuzin, O. V. Sharypov, V. Leroy-Cancellieri, D. Cancellieri, E. Leoni, A. Simeoni and G. Rein (2012), Comparative Study To Evaluate the Drying Kinetics of Boreal Peats from Micro to Macro Scales, *Energy & Fuels* **26**(1): 349-356 DOI: 10.1021/ef201221y.
- Grishin, A., A. Golovanov and Y. V. Sukov (2006), Experimental determination of thermophysical, thermokinetic, and filtration characteristics of peat, *Journal of Engineering Physics and Thermophysics* **79**(3): 557-562.
- Grishin, A., A. Y. Kuzin and E. Alekseenko (2003), Determination of kinetic characteristics of the process of drying of forest combustibles, *Journal of Engineering Physics and Thermophysics* **76**(5): 1160-1165.
- Lefèvre, R., P. Barré, F. E. Moyano, B. T. Christensen, G. Bardoux, T. Eglin, C. Girardin, S. Houot, T. Kätterer and F. Oort (2014), Higher temperature sensitivity for stable than for



- labile soil organic carbon—Evidence from incubations of long-term bare fallow soils, *Global Change Biology* **20**(2): 633-640.
- Murti Laksono, K., S. Sabiham, A. Sutandi and E. S. Sutarta (2016), Hydrophobicity of Tropical Peat Soil from an Oil Palm Plantation in North Sumatra, *Journal of Agronomy* **15**(3): 114.
- Nugroho, Y. S. (2002), Sifat Self-Ignition pada Gambut, Sabut Kelapa Sawit dan Kayu, *J Makara Teknologi* **6**: 123-131.
- Nugroho, Y. S. (2017). Integrating Wildland and Urban Fire Risks in Local Development Strategies in Indonesia. *Fire Science and Technology 2015*, Springer: 31-43.
- Palamba, P., M. L. Ramadhan, F. A. Imran, E. A. Kosasih and Y. S. Nugroho (2017), Investigation of smoldering combustion propagation of dried peat, *AIP Conference Proceedings* **1826**(1): 020017 DOI: <http://dx.doi.org/10.1063/1.4979233>.
- Prat-Guitart, N., G. Rein, R. M. Hadden, C. M. Belcher and J. M. Yearsley (2016), Propagation probability and spread rate of self-sustained smouldering fires under controlled moisture content and bulk density conditions.
- Rein, G. (2009), Smouldering combustion phenomena in science and technology.
- Rein, G., J. Garcia, A. Simeoni, V. Tihay and L. Ferrat (2008), Smouldering natural fires: comparison of burning dynamics in boreal peat and Mediterranean humus, *WIT Transactions on Ecology and the Environment* **119**.
- Ritung, S. and N. K. Wahyunto (2012), Karakteristik dan Sebaran Lahan Gambut di Sumatera, Kalimantan dan Papua, *Pengelolaan Lahan Gambut Berkelanjutan*. Balai Besar Litbang SDLP, Bogor.
- Valat, B., C. Jouany and L. Riviere (1991), Characterization of the wetting properties of air dried peats and composts [surface tension, water retention capacity].
- Volarovich, M. and N. Churaev (1968). Application of the methods of physics and physical chemistry to the study of peat. *Proceedings of the Transactions of 2nd International Peat Congress*, Leningrad.



A PRELIMINARY CASE STUDY OF A ELECTRIC COMMUTER BUS IN UNIVERSITAS INDONESIA

Sonki Prasetya¹, Ghany Heryana¹, Yudan Whulanza¹, Mohammad Adhitya¹, Danardono
Agus Sumarsono¹

¹*Mechanical Engineering Department, Faculty of Engineering Universitas Indonesia,
Kampus
Baru UI Depok 16424, Jawa Barat, Indonesia*

ABSTRACT

A reliable mass transport system is one of the essential indicators for the development in a country. Unfortunately higher numbers of vehicle increase air pollution as well as the greenhouse gas emission. An electric bus commuter system is an alternative solution to overcome those problems. However, not only the electric bus but also infrastructures are required to be constructed to maintain the sustainability of the commuter system. This paper discusses a case study as a part of stages in order to implement a commuter bus system in a suburban area. Observations of passenger's quantity are conducted in every bus stations. Thus, this study successfully generates a pattern of the commuter passengers in the selected region. Among the monitored bus stations, the highest number of the average on-board and off-board passengers are 18.34 and 16.44 respectively. Furthermore, the result is utilized to obtain the needed power consumption of the electric bus during the trip. The total energy consumption of the electric bus during one trip is around 550 kWh during one trip operation with minimum electric motor rated power of 160 kW. And finally, the appropriate power management schedule system can be chosen to support this commuter system.

Keywords: Case Study, Commuter; Electric Bus; Greenhouse; Power Consumption

1. INTRODUCTION

The electric vehicles (EV) gaining back their popularity in 2000's. Triggered by the fuel sustainability as well as the climate change resulting research centers around the world competing to overcome those challenge (Chan, 2007). The statistic shows that the EV utilization increases rapidly. The EV possession has been risen to 200.000 in 2012 (Agency, 2013). Indonesia, a country with population of more than 250 million citizens requires a good viable transportation system. Particularly the capital city such as Jakarta which contains 5% of Indonesian population, decent mass transportation systems are inevitable. However, the commuter transport system focuses on two modes; railway and public four wheels vehicles such us buses and public mini vans. Those two latter modes still use oil fuels to operate.

Electric Buses (EB) have been deployed in several countries for instance in Seoul South Korea. A bus using 240kW electric motor was claimed to be the first commercial EB in



2010 (ksp, 2012). This bus covers a distance of 80 km with a single charging period along the way. Beijing China also developed EB with ultra-fast charging battery (Council). As an addition, inductive charging system for EB in Braunschweig Germany introduced in 2013. Covering 12km route, the battery will be charged when stop for only around 10 minutes (Eltis, 2013).

Utilizing electric engine vehicles into our daily activities require numerous steps of work. Countries around the world have been trying to overcome the problems through researches in this area for various aspects (Bjoernsson and Karlsson, 2016). Moreover, the adoption or optimization methods that are common to be used in automotive researches (Adhitya et al., 2013) can also be found in the EV areas (Li et al., 2016). Several companies, research foundations as well as universities in this country (including Universitas Indonesia) have been also involving to develop EVs since 2012 (Meryana, 2012). The electric bus for mass transportation purpose is one of the focuses of the research. However, considerations must be taken before applying this new technology. Infrastructures such as the maturity of the technology as well as the supporting equipment to ensure the operation of the system are the essential concerns. Hence, this study focuses on the early work of adopting this new technology to gradually replace the previous conventional system. For those reasons, a small scope of region is desired to be the case of study. Therefore, Universitas Indonesia campus bus system is selected to be the case for observation.

2. METHODOLOGY

Firstly, a bus size is predetermined according the needs before we calculate the power needs. Bus sizes can be categorized into three groups namely small, medium and large according to the regulation of transportation department (Darat, 2002). The average passenger capacity of the latter type is selected to be the bus dimension. Therefore, a typical bus of 14000kg with 60 passengers is chosen to be studied.

Secondly, the selected location of UI campus bus route is observed. One trip of journey (from start to the end point of the investigation site) requires a distance of around 5 kilometers. There are 10 monitored bus stops along the way for the bus to transit to pick-up and or drop-off passengers. Each bus stop has a range of around 0.5km. The trip duration requires 30 minutes with the average bus speed is 15km/h.

In order to get the quantity of passengers for simulating the power consumption along the journey, a survey to get the number of passenger is conducted in each bus stop. 50 data samples are collected during the office hour observation in a bus stop. The average numbers of passengers in each bus stop are then obtained. The average numbers of on-board bus passengers and also off-board passengers in every bus stops can be calculated by using mean value (\bar{x}_m) equation (1) (Harinaldi, 2005) .

$$\bar{x}_m = \frac{1}{n} \sum_{i=1}^n x_i \quad (1)$$

For 50 sampled data in 10 bus stops, we require information of mean value from $j = 1$ to 10 by equation (2).



$$x_{mj} = \frac{1}{50} \sum_{i=1}^{50} x_i \quad (2)$$

The result is presented in Table 1. At bus stop 1, there is no off-board passenger since it is the starting point of Bus. As an addition, bus stop 10 contradicts with the bus stop 1. No one will get on board since the bus has reached its destination of the trip.

Table 1. Number of passengers in each bus stop

Bus Station	On Board	Off Board	Difference	Passengers
Stop 1	29.5	-	29.5	30
Stop 2	18.34	2.9	15.44	45
Stop 3	6.76	5.48	1.28	47
Stop 4	15.06	3.52	11.54	58
Stop 5	0.12	3.12	-3	55
Stop 6	1.26	16.44	-15.18	40
Stop 7	0.24	6.8	-6.56	34
Stop 8	2.06	7.04	-4.98	29
Stop 9	1.54	5.82	-4.28	24
Stop 10	-	23.6	-23.6	0

Furthermore, the mass of the total passengers can be predicted by taking into account of an average ideal Asian weight (Sarah Catherine Walpole, 2012). Therefore, a constant value of 60kg is chosen. The prediction of weight of passengers in a journey route is shown in Figure 1. By the cumulative number of passengers in the bus, the weight integrated to the total load of the bus will also rises. First half of the journey, on-board passengers has the tendency to hike meanwhile it declines at the rest half.

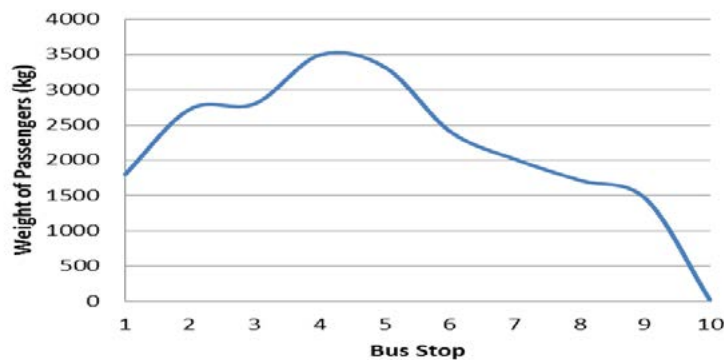
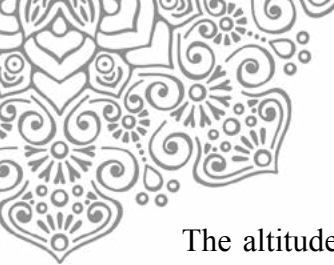


Figure 1. The weight of passengers in every bus stop during the trip



The altitude of the route as well as the vehicle speed are firstly collected using the GPS-software via smartphone namely Geo-Tracker. The average speed is 15 km/h. The contour of the path is plotted in Figure 2. The altitude fluctuation experienced by the bus during one trip gives information that the average is 81.61m and slope's deviation is between +2° to -2°.

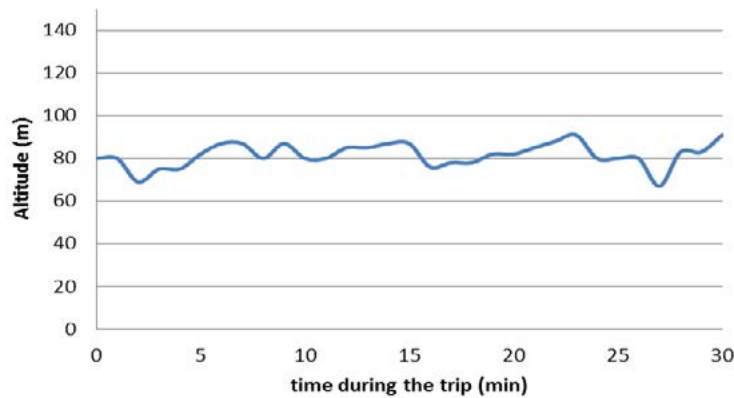


Figure 2. The contour of the road during the trip

Considering the terrain has a plane topography type since the slope is very small, forces acting on the moving bus can be described in equation (3) without the influence of gravitational forces (Gillespie, 1992, Michelin, 2003)

$$F_{mx} = F_r + F_d \tag{3}$$

The rolling force is represented by F_r meanwhile aerodynamic force is denoted by F_d . Those three forces are defined from equations (4)-(6).

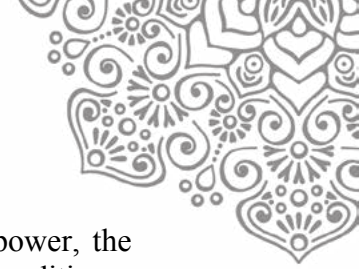
$$F_r = C_r G \tag{4}$$

$$F_d = \frac{\rho C_d A v^2}{2} \tag{5}$$

where C_r , G , ρ , C_d , A and v are the rolling coefficient (0.012), the total weight force, air density (1.3kg/m^3), the drag coefficient (0.6), frontal area (8 m^2) and the vehicle speed respectively.

Furthermore, the required energy for EB is generated by relating those forces into the energy formulas. As an addition, a typical air braking system that uses a compressor to trigger the brake-pad and an air conditioner are objects that require to be considered beside the main electric motor as the prime mover. Therefore, the hourly energy (Power) required to operate the electric bus is given by equation (6).

$$P_e = P_r + P_d + P_{aux} + P_{ac} + P_t \tag{6}$$



where P_r , P_d , P_{aux} , P_{ac} and P_l are the rolling power, the aerodynamic power, the auxiliary power (for braking compressor, steering and inverter etc.), the air conditioner power and the losses power (in the drive train) respectively. The energy required along the trip can be simulated as seen in Figure 3.

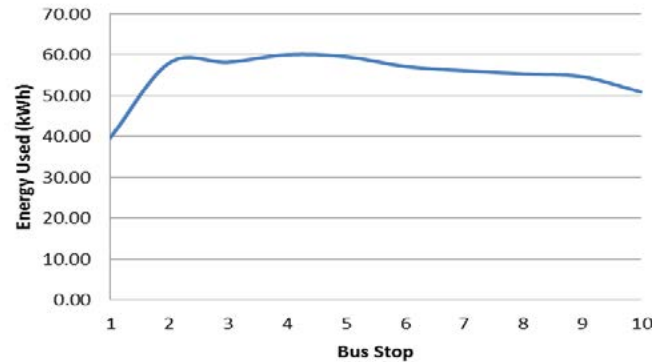


Figure 3. The energy usage in every bus stop during the trip

3. RESULT AND DISCUSSION

A 15 minutes running test data of the electric bus is collected. However, the journey takes a short distance path and it measures the electrical motor parameters only with no passengers on-board. The data shows that the average electrical power consumption is 7.84kW. It fluctuates with maximum power of 78.73kW and the electrical motor will consume 272kWh if it is utilized for half hours. Thus, with the increasing load and contingency, we can select the minimum electric motor rated power of 160 kW. Figure 3 shows a minor fluctuation with similar pattern as the passengers' load (as seen on Figure 1). Although number of passengers is different in each bus stop, the energy consumption changes slightly. This is due to the gravity force has less impact in the flat geographical contour.

During the 5 km trip of the studied case, the bus consumes energy nearly 550 kWh. This is higher than the obtained data since this value integrates the energy that occurs in the E-Bus system. The arguments of selecting the energy storage are not covered in this paper. However, if the chosen rated capacity of the energy storage is lower than that consumed energy value, it may require a battery replacement or charging station along the trip. This latter method has a consequence of extending the transit time along the way and perhaps the operation cost as well.

4. CONCLUSIONS

Implementing EB's require considerations particularly for the energy requirement. The calculation requires information of the bus size, the route, internal power losses and equipment used such as compressors as well as the air conditioner. The result shows that passenger's fluctuation gives insignificant influence related to the power consumed during the trip under the studied case. This is due to the route has very small graded position. The rated power can be sized from 160 kW or more. Furthermore, in order to reduce the energy storage capacity, the energy supply strategy under this track recommends the utilization of



either battery replacement system or charging station system along the trip since the trip consumes large amount of energy.

5. RECOMMENDATION

The calculations are particularly used for the flat contour route. Therefore, simulations with different cases such as for hilly terrains can be conducted when designing the E-Bus for a different location. Furthermore, the energy storage selection can be added by considering the optimum condition regarding the cost of the battery capacity with the chosen infrastructure (either charging stations or swap stations).

REFERENCES

- ADHITYA, M., MUSTAFA, R., PLOETNER, A. & KUECUEKAY, F. 2013. A New Control Strategy of Wet Dual Clutch Transmission (DCT) Clutch and Synchronizer for Seamless Gear Preselect. *SAE International Journal Passenger Cars*.
- AGENCY, I. E. 2013. Global EV Outlook: Understanding the Electric Vehicle Landscape to 2020.
- BJOERNSSON, L.-H. & KARLSSON, S. 2016. The potential for brake energy regeneration under Swedish conditions. *Applied Energy*, 168, 75-84.
- CHAN, C. C. Year. The State of the Art of Electric, Hybrid, and Fuel Cell Vehicles. In: *Proceeding of IEEE, 2007*. IEEE.
- COUNCIL, E. V. *Fully Charged Electric Bus in 10 Minutes* [Online]. Electric Vehicle Council. Available: <http://electricvehiclecouncil.com.au/fully-charged-electric-bus-in-10-minutes> [Accessed 30 December 2016].
- DARAT, D. J. P. 2002. Pedoman Teknis Penyelenggaraan Angkutan Penumpang Umum di Wilayah Perkotaan dalam Trayek Tetap dan Teratur. In: DEPARTMENT, I. T. (ed.). Jakarta.
- ELTIS. 2013. *Braunschweig Launches World's First Inductive Fast Charging Electric Bus* [Online]. Available: <http://www.eltis.org/discover/news/braunschweig-launches-worlds-first-inductive-fast-charging-electric-bus-germany-0> [Accessed 30 December 2016].
- GILLESPIE, T. D. 1992. *Fundamentals of Vehicle Dynamics*, Society of Automotive Engineers.
- HARINALDI 2005. *Prinsip-prinsip Statistik untuk Teknik dan Sains*, Erlangga.
- KSP, E. 2012. *Making Clean Future Seoul with Eco Friendly Vehicles : Seoul Bus Project* [Online]. [Accessed 30 December 2016].
- LI, G., ZHANG, J. & HE, H. 2016. Battery SOC constraint comparison for predictive energy management of plug-in hybrid electric bus. *Applied Energy*.
- MERYANA, E. 2012. *Kebijakan Mobil Nasional, Astra " Wait and See"* [Online]. Jakarta: Kompas. Available: <http://internasional.kompas.com/read/2012/08/09/19451838/Kebijakan.Mobil.Nasional.Astra.Wait.and.See>. [Accessed 09 August 2012].
- MICHELIN 2003. The Tyre : Rolling Resistance and Fuel Savings. Clermont-Ferrand
- SARAH CATHERINE WALPOLE, E. A. 2012. The Weight of Nations : an Estimation of Adult Human Biomass. *BMC Public Health*.



15th International Conference on Quality in Research (QIR 2017)

How Appropriate are Pyridinic Carbon Nitride Nanotubes for Hydrogen Storage? Molecular Thermodynamics Analysis

Supriyadi¹⁾, Nasruddin²⁾, Engkos A. Kosasih²⁾, I. A. Zulkarnain³⁾, Budhy Kurniawan⁴⁾,

¹ Department of Mechanical Engineering Faculty of Industrial Technology, Universitas Trisakti, Jakarta 11440 e-mail :
supriyadins@gmail.com, supriyadi.mesin@trisakti.ac.id

² Department of Mechanical Engineering Faculty of Engineering University of Indonesia, Depok 16424 e-mail :
nasruddin@eng.ui.ac.id, kosri@eng.ui.ac.id

³ Faculty of Engineering Presiden University, Cikarang, Indonesia 17550 e-mail : ihsan.a.zulkarnain@gmail.com

⁴ Department of Physics Faculty of Mathematics and Natural Sciences University of Indonesia, Depok 16424 e-mail :
bkuru07@gmail.com

Abstract

One of many efforts to enhance hydrogen adsorption capacity in a Single-Walled Carbon Nanotube (SWCNT) is through optimization and modification of the structure until material with new characteristic, or a brand new material is obtained. New material type that is attracting attention nowadays are Boron Carbide, Boron Nitride and Carbon Nitride. In this research, model of structure that will be discussed is Single-Walled Carbon Nitride Nanotube (SWC₃N₄NT) that is beginning to be discussed recently for hydrogen storage application. From semi-empiric study, optimum SWCNT diameter for storing hydrogen is on diameter below 5 Å or on diameter between 12 – 14 Å. From that result, hydrogen storage simulation is done next on (SWCNT) and SWC₃N₄NT on chirality (18, 0). This chirality is chosen to guarantee three dimensional symmetrical characteristic. The most important thermodynamical analysis to be done is calculating SSA value and in various material model, SSA value being obtained consecutively is 2600 and 2730 m²/g. Therefore, it can be alleged that structure modification with nitrogen substitution on carbon-based material will enhance hydrogen adsorption capacity. That modification also identifying enhancement of hydrogen adsorption energy significantly from 1.2 to 1.97 kcal/mole. Molecular dynamics (MD) simulation is resulting in adsorption capacity in temperature and pressure 120 atm consecutively 1.59 and 2.17 wt% in room temperature. In temperature 233 K, it increases to 2.26 and 2.96 wt% and also 6.1 and 6.84 wt % in temperature 77 K. To verify the simulation result, comparison is being done with semi-empiric calculation and isothermal model regression. MD result is also quite similar with isothermal adsorption model by Langmuir, Sips and Toth with determinant coefficient value above 0.99 in temperature 298 K, above 0.95 in temperature 233 K and above 0.85 in temperature 77 K.

Keywords: adsorption capacity, Hydrogen, molecular dynamics, SWCNT, SSA.



1. INTRODUCTION

Availability of fossil-based energy source is on a continuous decline, meanwhile energy needs is drastically increasing. Fossil-based energy usage also has a potential to release carbon monoxide/dioxide gas emission, and as the main contributor in environment pollution. Carbon gas emission being accumulated in our atmosphere can cause global warming and climate change [1]. All half of the increase of CO₂ gas concentration in the air predictably comes from the energy sector [2]. Therefore, if exploration and exploitation of fossil energy source continues, environment quality will continuously declining.

We need to search for new and renewable energy source that meet two criterias: clean and the continuity can be guaranteed. Hydrogen meets these two criterias for that means. The biggest potential of hydrogen for fuel-cell fuel is in ground vehicles technology. If we can implement vehicles technology with hydrogen fuel, energy and environmental problems can be solved simultaneously.

Hydrogen storage technique must be developed so that hydrogen usage as energy carrier can be applied massively. The most interesting choice between all is to store hydrogen in solid material with pores through adsorption. Adsorbant material that is often used in hydrogen adsorption system is carbon nano-structured. CNT research of hydrogen storage application began to be used after Iijima found the material in 1991 [3]. CNT has quite a few advantages, like pore characteristic, high surface area, high stability, and light material [4].

Many effort is continuously done to enhance CNT performance, such as: structure optimation [5] and substitution/doping metal element [6]. Another way to enhance adsorption capacity is with modification in CNT, so CNT with new characteristics or even with brand new material is obtained. New material type that steal attention nowadays are Boron Carbide [7], Boron Nitride [8] and Carbon Nitride [8, 9]. Many research found that nitrogen can be used as substitution element to replace carbon chain so that C_xN_y nanotube is created. In this research, material C₃N₄NT is chosen.

Research with MD simulation can be an alternative to complete experiment research which many of them have low repeatability. With molecule dynamics simulation, adsorbent and adsorbat adsorbant can be modeled through computer

program in real. Another advantage of MD simulation is many material characteristics can be obtained in various wanted conditions that experimentally hard to do [10]. Therefore, theoretical research about nanostructure carbon performance as hydrogen gas storing media can be a reference for effectively doing experimental research [11].

The purpose of this research are: i) do extensive study about carbon SWCNT and SWC₃N₄NT characteristics as hydrogen storage material empirically and through molecule dynamics simulation. Ii) estimating hydrogen gas molecule adsorption energy in SWCNT and SWC₃N₄NT.



2. RESEARCH METHODOLOGY

This research consists of two parts, that is: 1) material analysis and characterization and 2) hydrogen storage capacity optimization in SWCNT and SWC₃N₄NT. In the early step, structure optimization is studied with combining theoretical approach (mechanical quantum calculation) and semi-empiric study. According to the result of this step, next is diversification of adsorbent model through setting nitrogen position in SWCNT structure, so new structure is obtained, that is Triazine nanotube (SWC₃N₄NT). In this new structure, next is analysis of adsorption energy through mechanical quantum.

The next research is research about hydrogen gas adsorption process with molecular thermodynamics approach. This research covers specific surface area (SSA) analysis, monolayer and molecular dynamics simulation. Molecular dynamics simulation result is next being analyzed as pare of monolayer adsorption phenomena through molecular thermodynamics approach.

2. 1 Pemodelan Material Struktur Nano

In this research, CNT structure model will be focused on zig-zag type SWCNT with 33 Å length. The first material being investigated is SWCNT, that will be visually pictured in Figure 1

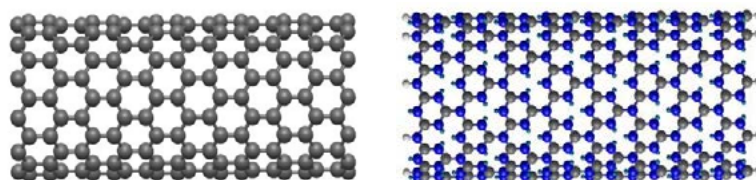


Figure 1 SWCNT modeling (left) and SWC₃N₄NT (right) zig-zag type with chirality (18, 0).

Next, development of carbon-based structure is done to obtain a better performing material. Experimentally, carbon and nitrogen element combination with various atom fraction is already synthesized in forms of sheets and tubes. The main consideration in structure modification is how to obtain material that is lighter, has more empty space, and has wider partial distribution. Hence, SWC₃N₄-NT model is seen as fulfilling those requirements listed above. Visually, that model can be seen in Figure 2.

Model as can be seen above is similar with micro structure of experiment made by Li (2007), but in this modeling, electron existence is added to every pyridine nitrogen. There are three advantages of this structure with SWCNT, i) lighter, it means the SSA value will be higher, ii) there are many empty space that is created by pyridine nitrogen bond, and iii) wider partial distribution that is caused by structure uniformity is made.



Inter-molecule interaction energy calculation is done with quantum mechanical theory approach and, in this research, PSI4 that is already trusted and used in few former researches is used [11, 12]. Hydrogen molecule is placed in perpendicular orientation above hexagonal structure center of CNT (hollow site), because that is the place where strong interaction configuration between hydrogen molecule and SWCNT happen. Next, a few one-dot energy calculation in various distance between nanotube wall and hydrogen molecule center is done using ab-initio

Potential energy between hydrogen molecule and between hydrogen molecule with adsorbent interaction calculation result is done while look at each adsorbent as one unity in which all compiling atom is involved. Hence, there is one other step needed to determine each compiling material interaction. To obtain an accurate potential model in this research, force-matching method is used. More simply, this method can depicted as curve fitting method with potential model that is generally used, and in this study, Lennard-Jones potential model is used.

Potential functioning model that is used in this research is Lennard-Jones potential model, that can simply be described with equation below [13],

$$\Delta E(r) = \begin{cases} 4\epsilon_{ab} \left[\left(\frac{\sigma_{ab}}{r_{ij}} \right)^{12} - \left(\frac{\sigma_{ab}}{r_{ij}} \right)^6 \right], & r_{ij} \leq r_c \\ 0, & r_{ij} \geq r_c \end{cases} \quad (1)$$

Where, $\Delta E(r)$ is potential interaction energy in r ; ϵ_{ab} , σ_{ab} distance, each are the lowest potential energy value and interaction distance where potential energy value is equal to zero; a and b is meant to identify two types of particle that is interacting and $r_{ij} = |r_i - r_j|$ is distance between particle ist particle and jst particle.

Force-matching method is done through adding all inter-particle interaction model and then match that with the amount of potential energy interaction of ab-initio calculation result. All the interaction sums in equation (1) resulting in total molecule potential interactin as written elow

$$\Delta E_{Total}(r) = 4\epsilon \sum_{j>i}^N \sum_{i=1}^{N-1} \left[\left(\frac{\sigma}{r_{ij}} \right)^{12} - \left(\frac{\sigma}{r_{ij}} \right)^6 \right] \quad (2)$$

In this paper, hydrogen molecule is simplified into united-atom model or often called isotropic model. This model is used by few former researchers, among them is Mahdizadeh et al (2014) [14]. Different from anisotropic model, in isotropic model, hydrogen molecule interaction orientation effect is ignored. This model is quite accurate even though it create different error in



different temperature simulation. This condition is next eliminated through searching for parameter value in every different conditions, and as a result time needed for simulation preparation takes longer.

3 Result and Discussion

3.1 Hydrogen molecule potential energy with SWCNT dan SWC₃N₄NT

Amount of researchers are doing analysis in exterior part more because experimentally, nanostructure material that can be synthesized is the closed-ended type. From ab-initio calculation result, hydrogen adsorption energy data in SWCNT is obtained, in the amount of 1.12 kcal/mole. Next, with force-matching method, potential parameter that will be used for estimating various thermodynamics sizes theoretically is obtained. This potential parameter is also used as one of input parameter in doing molecule dynamics simulation.

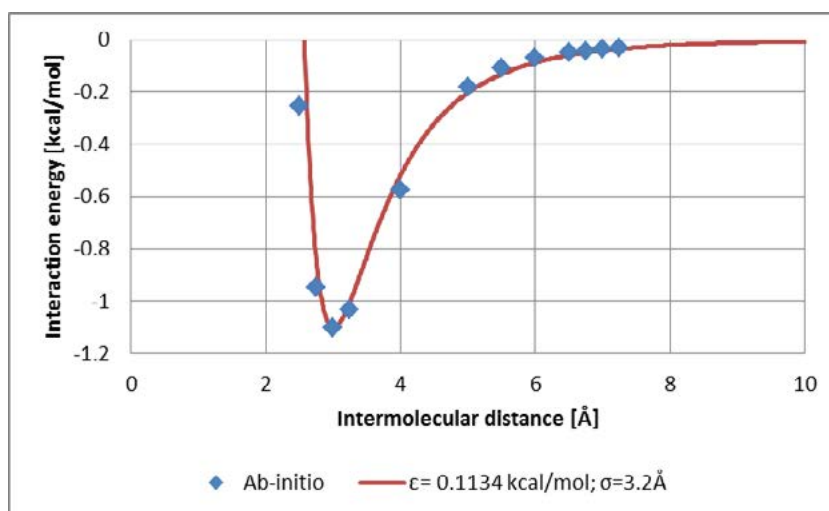


Figure 1 Theoretic Calculation Result of Hydrogen Interaction Potential Energy with SWCNT [11, 17]

Inter-molecule hydrogen gas interaction potential energy calculation with Triazine is done in various hydrogen positions in that structure. Monolayer adsorption potential energy value is calculated as hydrogen molecule distance function with Triazine walls in exohedral part. Result from force-matching to obtain potential parameter is done to two models of hydrogen molecule. The first model is an-isotropic model and the second model is isotropic model. Calculation result for these two models can be seen in Figure 3.

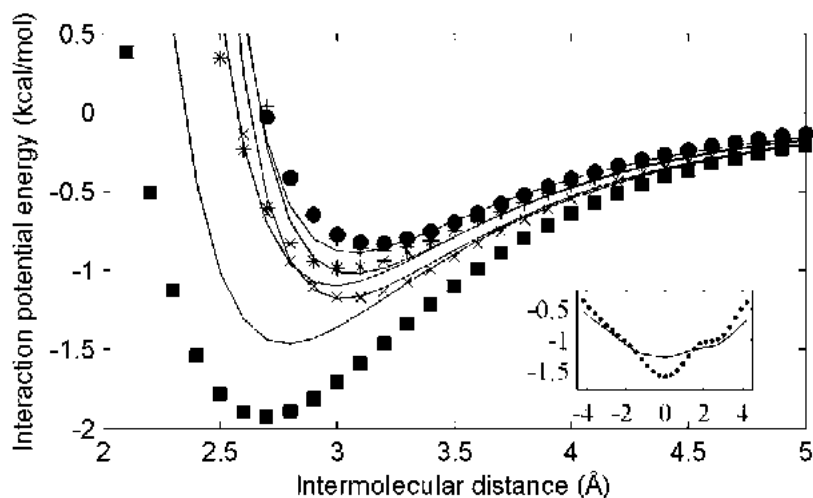


Figure 2 Hydrogen physics adsorption energy calculation in SWC₃N₄-NT using ab-initio method.

Adsorption energy in SWCNT is around 1,2 kcal/mole, meanwhile adsorption energy in SWC₃N₄NT is around 1.97 kcal/mole, which means it almost twice as big. Reviewed from the main adsorbent adsorption performance measure, that is SSA value, SWC₃N₄NT is also better than SWCNT. From those two factors, it can be alleged that adsorption through to SWC₃N₄NT hydrogen will also be better.

3. 2 Hydrogen adsorption capacity simulation result Hasil simulasi kapasitas adsorpsi hidrogen

Figure 4 is hydrogen adsorption capacity profile in three chiralities of SWCNT, in three temperatures, that are temperature 77, 233.15 and 298.15 K. MD simulation in this study using Lammps program developed by DoE of US [16]. Adsorption capacity in room temperature tend to be linear, which means adsorption capacity addition is equal to equilibrium pressure increase. Likewise in adsorption capacity in 233.15 K, that has almost the same characteristics with adsorption capacity in temperature 298.15 K.

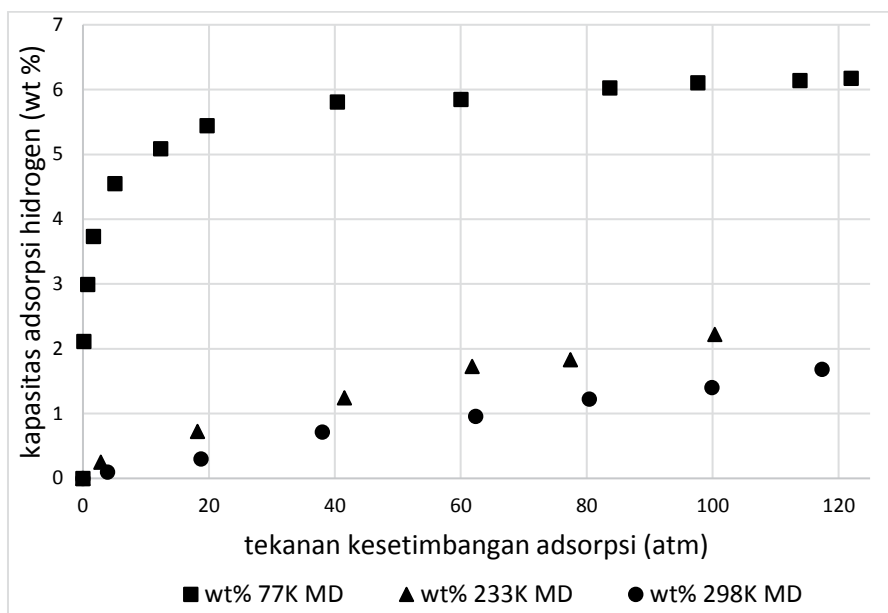


Figure 3 Hydrogen adsorption capacity in SWCNT in temperature 298,15 K, 233,15 K and 77 K in chirality(18,0).

From Figure 4, it can be seen that adsorption capacity of SWCNT (18, 0). In pressure to 120 atm, adsorption capacity that can be obtained is only 1,7 wt%, which means it is still far from target that is set by DoE. Similar with result that is reported by Shelvin, et. al in which SWCNT is hard to reach the set target without improvement [18]. Takagi (2006) has done investigation in various SWNT in temperature 303 K and pressure 30 atm with the result range from 0,13 – 0,24. Xu (2007) reported almost similar result, in temperature 303 K and in pressure until 100 atm ranging from 0-3 – 0,5 wt% [19]. With almost similar result too, Ritschel (2002) reported results ranging from 0,05 – 0,63 wt% in pressure 45 atm [20]. A few other researchers reported much smaller result, only ranging from 0,01 – 0,07 wt%. Researcher that reported a much higher result among other experimental research is Liu (1999), in temperature 298 K and pressure ranging from 100 – 120 atm, wt% value ranging from 2,4 – 4,2 is obtained [21].

As it is in room temperatur, in experiment research result that is reported in temperature 77, a very big disparity also happens. In pressure around 1 atm Anson (2004), it is reported that the result is under 1 wt%. Takagi (2006) reported result ranging from 0,8 – 1,7 wt% and with almost similar result with Kim (2007) the result reported is ranging from 0,6 – 1,76 wt% [22, 23]. Different from other experimental researches, Pradhan (2002) reported much higher result, in pressure 16 atm, result obtained is ranging from 6,4 wt% [24].



In this part, adsorption capacity simulation result in SWC₃N₄NT in various pressure and temperature will be presented. As it is in adsorption characteristic of SWCNT, hydrogen adsorption capacity in SWC₃N₄NT (18, 0). It can also be seen that pressure addition effect will only be effective in temperature 233 and 298 K. Meanwhile in temperature 77, pressure addition above 50 atm does not give significant effect.

In room temperature, SWC₃N₄NT (18, 0) has good adsorption capacity. In low temperature, pressure effect will only give adsorption capacity increase up to 50 atm, and temperature effect become more dominant. With bigger diameter, there will be more hydrogen that is absorbed in endohedral part. Meanwhile, in room temperature, hydrogen that can be absorbed is much less.

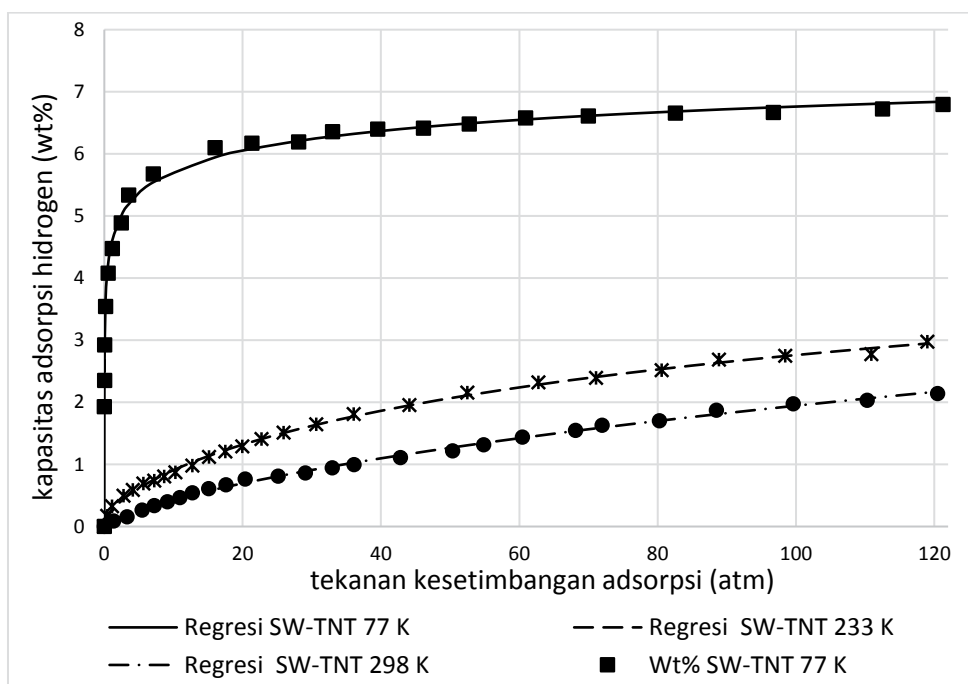


Figure 4 Hydrogen adsorption capacity function from equilibrium pressure on SWC₃N₄NT (18,0).

4. Conclusion and Discussion

SWC₃N₄NT has higher adsorption energy (1.97 kcal/mol) compared to SWCNT (1.1 – 1.2 kkal/mol). With theoretical calculation, SSA value obtained consecutively 2600 and 2730 2458 m²/g for SWCNT and SWC₃N₄NT. MD simulation result in pressure up to 120 atm, adsorption capacity obtained consecutively 1.59 and 2.17 wt% in room temperature. In temperature 233 increase to 2.26 and 2.96 wt% and also 6.1 and 6.84wt % in temperature 77 K. From various



thermodynamics measurement, it shows that SWCNT and SWC₃N₄NT can not reach the set target by DoE for hydrogen storage application without further modification.

5. REFERENCES

1. Martin, A., *Adsorpsi Isotermal Karbon Dioksida Dan Metana Pada Karbon Aktif Berbahan Dasar Batubara Sub Bituminus Indonesia Untuk Pemurnian Dan Penyimpanan Gas Alam*, in *Mechanical Engineering*. 2010, University of Indonesia: Depok.
2. Karekezi, S., *Renewables in Africa—meeting the energy needs of the poor*. *Energy Policy*, 2002. **30**(11): p. 1059-1069.
3. Iijima, S., *Helical microtubules of graphitic carbon*. *nature*, 1991. **354**(6348): p. 56-58.
4. Knippenberg, M.T., S.J. Stuart, and H. Cheng, *Molecular dynamics simulations on hydrogen adsorption in finite single walled carbon nanotube bundles*. *Journal of molecular modeling*, 2008. **14**(5): p. 343-351.
5. Zolfaghari, A., et al., *Molecular dynamics simulations on the effect of temperature and loading in H₂ exohedral adsorption on (3, 3) and (9, 9) SWCNTs*. *International Journal of Hydrogen Energy*, 2007. **32**(18): p. 4889-4893.
6. Zacharia, R., et al., *Enhancement of hydrogen storage capacity of carbon nanotubes via spill-over from vanadium and palladium nanoparticles*. *Chemical Physics Letters*, 2005. **412**(4): p. 369-375.
7. An, H., et al., *Li-doped B₂C graphene as potential hydrogen storage medium*. *Applied Physics Letters*, 2011. **98**(17): p. 173101-173101-3.
8. Umegaki, T., et al., *Boron- and nitrogen-based chemical hydrogen storage materials*. *International Journal of Hydrogen Energy*, 2009. **34**(5): p. 2303-2311.
9. Nair, A.A.S., R. Sundara, and N. Anitha, *Hydrogen storage performance of palladium nanoparticles decorated graphitic carbon nitride*. *International Journal of Hydrogen Energy*, 2015. **40**(8): p. 3259-3267.
10. Liu, Z., et al., *Hydrogen storage and release by bending carbon nanotubes*. *Computational Materials Science*, 2013. **68**(0): p. 121-126.
11. Zulkarnain, I.A., *Optimasi Struktur Material Adsorben Karbon Nanostruktur sebagai Media Penyimpanan Hidrogen: Studi Termodinamika Molekuler*, in *Mechanical Engineering*. 2014, University of Indonesia.
12. Turney, J., et al., *PSI4: an open source ab initio electronic structure program*. *WIREs Computational Molecular Science*, 2011. **2**(4): p. 556-565.
13. Yong, X., *Non-equilibrium molecular simulations of simple fluid transport at fluid-solid interfaces and fluidic behaviors at nanoscale*. 2012.
14. Mahdizadeh, S. and E. Goharshadi, *Hydrogen storage on silicon, carbon, and silicon carbide nanotubes: A combined quantum mechanics and grand canonical Monte Carlo simulation study*. *International Journal of Hydrogen Energy*, 2014. **39**(4): p. 1719-1731.
15. Nasruddin, S., I.A Zulkarnain, *Enhanced Hydrogen Storage Capacity on Metal Doping Carbon Nanotubes by Molecular Dynamics Simulation*, in *Osaka gas Foundation of International Cultural Exchange*. 2013, University of Indonesia: Depok.
16. Plimpton, S., *Fast parallel algorithms for short-range molecular dynamics*. *Journal of computational physics*, 1995. **117**(1): p. 1-19.



17. Shevlin, S.A. and Z.X. Guo, *Transition-metal-doping-enhanced hydrogen storage in boron nitride systems*. Applied Physics Letters, 2006. **89**(15).
18. Xu, W.-C., et al., *Investigation of hydrogen storage capacity of various carbon materials*. International Journal of Hydrogen Energy, 2007. **32**(13): p. 2504-2512.
19. Ritschel, M., et al., *Hydrogen storage in different carbon nanostructures*. Applied Physics Letters, 2002. **80**(16): p. 2985-2987.
20. Liu, C., et al., *Hydrogen storage in single-walled carbon nanotubes at room temperature*. Science, 1999. **286**(5442): p. 1127-1129.
21. Takagi, H., et al. *Hydrogen adsorption properties of single-walled carbon nanotubes treated with nitric acid*. in *Nanoscience and Nanotechnology, 2006. ICONN'06. International Conference on*. 2006. IEEE.
22. Kim, D.Y., et al., *Supercritical hydrogen adsorption of ultramicropore-enriched single-wall carbon nanotube sheet*. The Journal of Physical Chemistry C, 2007. **111**(46): p. 17448-17450.
23. Pradhan, B.K., et al., *Experimental probes of the molecular hydrogen-carbon nanotube interaction*. Physica B: Condensed Matter, 2002. **323**(1): p. 115-121.



Design a New Generation of Synchromesh Mechanism to Optimization Manual Transmission's Electric Vehicle

Rolan Siregar ^{*a}; Fuad Zainuri ^{**b} ; Muhammad Adhitya ^{**c}; Danardono .A. Sumarsono^{**d}

^{*}Department of Mechanical Engineering Universitas Darma Persada 13450,Indonesia;

^{**} Department of Mechanical Engineering Universitas Indonesia 16424,Indonesia;

^arolansiregar@ft.unsada.ac.id ; ^bfuad.zainuri@ui.ac.id ; ^cmadhitya@eng.ui.ac.id ;

^ddanardon@eng.ui.ac.id

ABSTRACT

Fuel consumption continues to rise will cause serious problems in the future due to the limited amount of fossil fuels on earth. In addition, emissions of carbon dioxide (CO₂) and carbon monoxide (CO), which is the burning of oil is very influential on global warming today. Therefore, the development of friendly technologies (green energy industry) has been started. One is the development of environmentally friendly vehicles (green vehicle) in which the battery is an energy source that pollution from vehicles is equal to zero. The design of optimal power train mechanism on electric vehicles is one of the best ways to save battery energy consumption. Transmission is one of the power trains is very influential on the performance of the vehicle. In this paper will discuss electric vehicle transmission system.

There are some major things that the reference design of the transmission that will be done is the first that the large wheel traction should have the same value as the traction conventional vehicles, and the second is the transmission model should be much simpler than the transmission of the motor fuel to meet the criteria for the use of the electric motor of the vehicle. Synchromesh is one of the constituent elements of the transmission which serves to smooth gearshift so that there is increased driving comfort. Further development synchromesh transmission is done to get a more simple construction, easily manufactured, and ease of use. Zero shift transmission is the latest development in transmission and then developed into an automatic manual transmission (AMT), where transmission has been used on racing vehicles to eliminate the current slowdown gear shift. Zero shift transmission is still relying on the clutch to change gear in which electromechanical be used to replace the clutch pedal. Therefore, the transmission is considered to be too complex for the transmission of electric vehicles, but its mechanism is considered very appropriate to increase the transmission efficiency. Starting from the transmission is then carried out new innovations transmission design for electric cars. The combination synchromesh with zero shift mechanism for manual transmission is a transmission which is ideal to increase the transmission efficiency. Installation synchromesh on zero shift mechanism is expected to replace the function of the clutch Manual Transmission (MT), and assisted with the motor torque setting when to change gear. This study displays a performance analysis of the electric vehicle transmissions.

Keywords: *zero shift; synchromesh; automatic manual transmission; electric vehicle*

1. INTRODUCTION

Electric vehicles do not have internal combustion engine so that the consumption of fuel is zero. Therefore, the production of electric vehicles is one of the best solutions to reduce fuel consumption of oil. Governments in many countries have a lot to apply rules to create an electric vehicle that is suitable to be used in each area. Indonesia is one country that has conducted research on electric vehicles. Broadly speaking the benefits of using electric vehicles compared to



conventional vehicles a fossil fuel is not required, zero emissions, and save energy costs (MING & CIN, 2010). Substitutes used vehicle combustion engine is an electric motor as the source of the power train movement. The electric motor can be switched on for their current source of battery used. To adjust the traction wheels to the road then made a transmission system that is the size of the box set of gear ratios. Source round of transmission is the rotational motion of the output shaft of the electric motor. Transmissions are designed to get more performance suitable for electric vehicles. The transmission system is one of the major components that affect power and fuel consumption of the vehicle. The transmission performance is also associated with gear efficiency, noise, and comfort during gearshift (Bedmar, 2013).

Transmission development has much to do to meet the needs of consumers ranging from the manual transmission models up to the automatic transmission. The development of this transmission is used for internal combustion engine vehicles that require fossil fuels as a source of mechanical power. By looking at the number of vehicles is increasing in society will require the fuel to increase as well. Availability of fuel tends to decline will lead to motivation for researchers to create more environmentally friendly vehicles such as vehicles with electric current as a source of drive power. This study aims to generate a new transmission design with development synchromesh mechanism to make it more efficient. The main thing that will be development is a transmission geometry, the concept of work, time shifting, gearshift quality, and will automatically increase the power efficiency of the electric motors in vehicles.

2. STATE OF THE ART DESIGN TRANSMISI EV

There are three types of vehicle transmissions are manual transmission (MT), automatic transmission (AT), and the continuous variable transmission (CVT). Manual transmission (MT) is the most efficient in fuel consumption, while AT and CVT are easier to use (Heath, 2007). MT efficiency level is 96.2 per cent, 86 per cent AT, CVT 84.6 percent, and AMT equivalent with MT (Kumbhar & Panchagade, 2014). Expertise driver was extremely influential in the use of manual transmission for improved fuel efficiency. In this paper will be more present manual transmission as well as its development since the transmission is considered to be more suitable for electric cars. The manual transmission is a component that serves to forward the torque from the engine to the drive wheels. There are several gear box in a box on the transmission system which is the option to set the speed of the vehicle. Election speed manually is done by the driver by utilizing the shifting lever (shift lever). There are several types of manual transmission that constant mesh and synchromesh. MT synchromesh transmission is widely used on the vehicle. The synchronizer is a key element which serves to align rotation between elements so that it can be done with a smooth change gear engaged. Some transmission systems, such as the manual transmission (MT), Dual Clutch Transmission (DCT), and Automatic Manual Transmission (AMT) their synchronizer (Back, 2013). In Figure 1 is shown Synchronizer manual transmission.

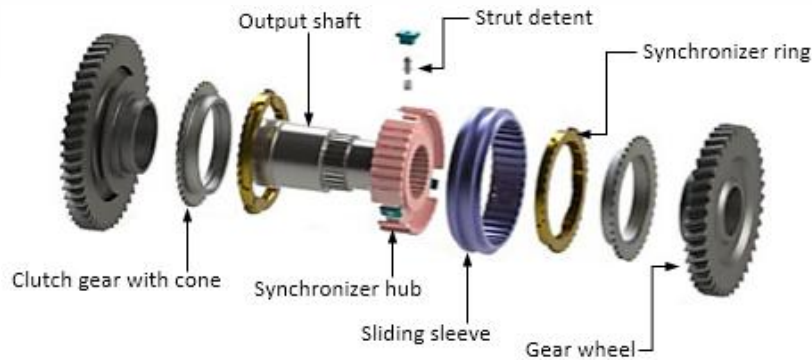


Figure 1. Exploded view synchromesh manual transmission (Bedmar, 2013).

Based on Figure 1 can be explained that the synchronizer ring is a harmonizing element rotational speed between the clutch gear cone, hub, and when the sliding sleeve gear set in motion to be paired. Synchronizer works by utilizing the friction in the cones. Therefore, engineering synchronizer should be considered to reduce the negative impact due to friction. Wear and tear that may occur will be selected on the components that better be the element that failure than any other element, in this case, is usually synchronizer been so elements are ductile than the surrounding elements.

The latest developments regarding the manual transmission is creating a manual transmission performance as if the auto is often called the automatic manual transmission (AMT). Broadly speaking AMT interpreted as a manual transmission without a clutch pedal clutch wherein movement is regulated by electronic sensors, processors, actuators (hydraulic or electromechanical), and change gear in accordance with the command of the driver. In figure 2 is shown schematically AMT.

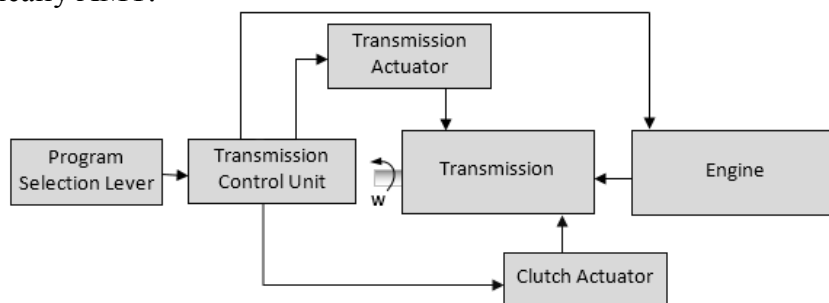


Figure 2. Schematic AMT

Furthermore, AMT has developed AMT zero shift transmission type. This transmission is a transmission that can shift gears without the need of the time (zero seconds) (Cheat & Child, 2007). This transmission offers easy to be manufactured, the price is cheaper than AT, fuel savings, there is no torque interrupt on one shaft when the change gear, change gear and finer (seamless). In Figure 3 is shown zero shift AMT.

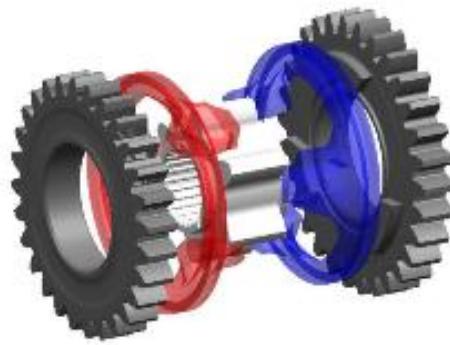


Figure 3. Zeroshift two gear (Cheat & Child, 2007).

The zero shift mechanism replaces the components synchromesh on manual transmission by using zero shift ring.

3. RESULT AND DISCUSSION

3.1. Design Transmission EV

Starting from the concept zero shift transmission which has advantages such as fuel economy, performance, shift quality, and easy to manufacture then created a draft new transmission for electric cars. The main concept is to eliminate the clutch to the transmission system then its function replaced by cone friction and torque setting of the motor. The simplicity of design and working mechanism that is simple is one of the considerations to obtain an effective transmission of the electric car. The following schematic working mechanism of transmission is made as shown in Figure 4.

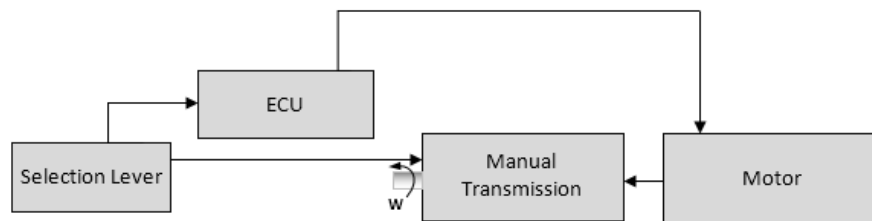


Figure 4. Schematic manual transmission EV

Selection lever is a lever operated by the driver to change gear. When the lever is moved, the sensor will send a signal to the ECU and signals to be transmitted to the motor to regulate the torque. Torque motor that has declined is the right time to change gear. Display electrical transmission vehicle can be seen in Figure 5.

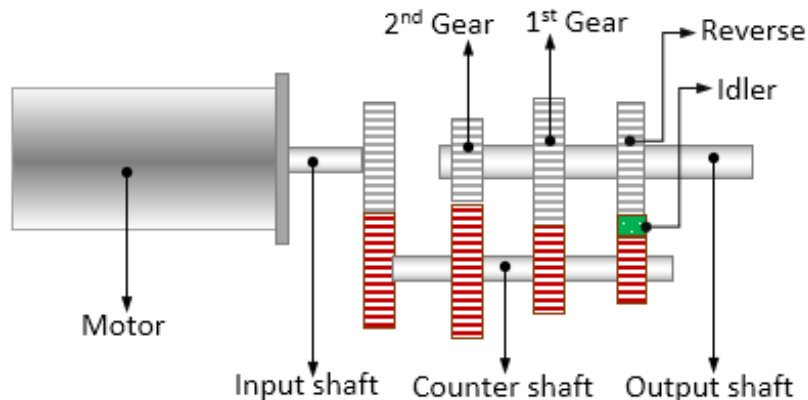




Figure 5. Manual transmission EV

Clutch manual transmission has been eliminated so that the working mechanism is simpler and easier to use. Such transmission will be lighter when compared with a conventional transmission. Gear ratios are such that they can be used for roads that need major traction as well as for high speed. To see more detail the concept of this transmission work, it can be shown describing elements to change gear as in Figure 6.

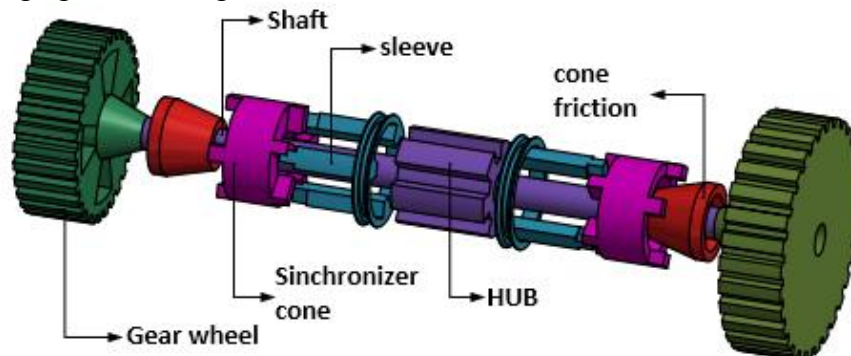


Figure 6. Element synchronomesh

Based on Figure 6 can be explained that the shaft merges with the main connecting hub so that the gear is a hub for the shaft rotation. The sleeve is an element that can be moved by the operator to change gear. When the sleeve has been shifted then the synchronizer cone will move simultaneously pressing the friction cone and the cone friction cone will hit the gears which aim to adjust the rotational speed, so that the synchronizer can be paired with the gears. For more details on how to change gear between two gears consists of several stages. The first stage is the sleeve is shifted by the driver via the gear shift lever so that the sleeve is pushed synchronizer cone and rotates together (Figure 7).

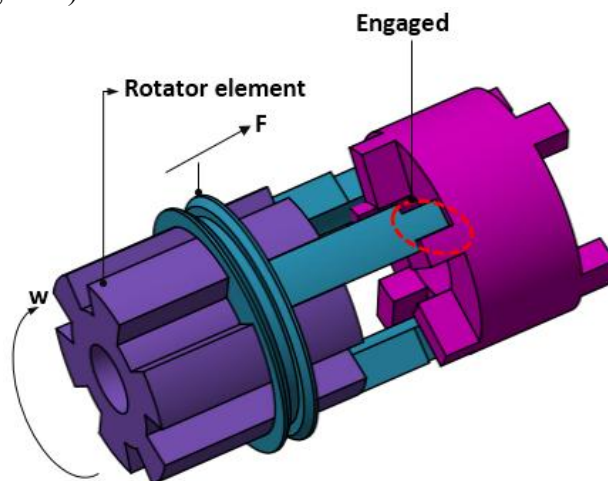


Figure 7. Synchronizer cone with sleeve is engaged

The next stage is adjustment round by utilizing the friction on the cone (Figure 8). Cone is the friction between elements of cone synchronizer friction cone made with different sizes according to the required large friction. Where things should be considered is how such friction does not cause serious problems such as lifetime due to wear, temperature and the other.

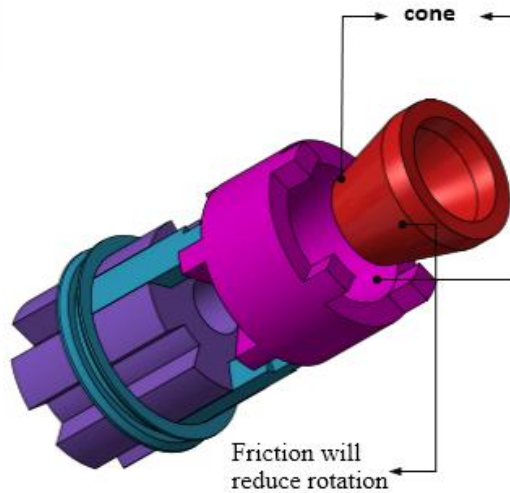


Figure 8. Element cone

Then the cone friction elements will rub against the gear cone element to add to the reduction of rotation between elements (Figure 9).

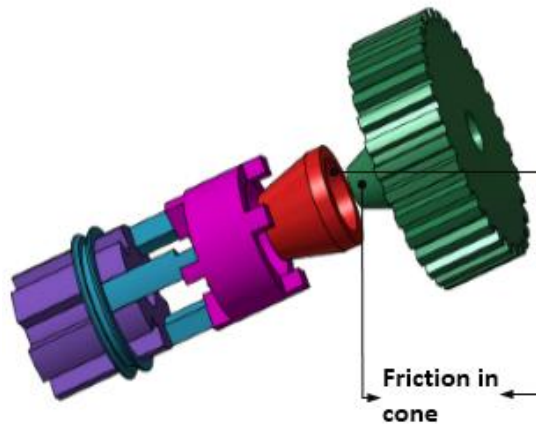


Figure 9. Gear cone friction

Cone on the gear elements is expected not easy to wear because it includes a vital category. After the rotation of the cone reduction gear then all elements will be paired to one level gear rotation (see Figure 10).

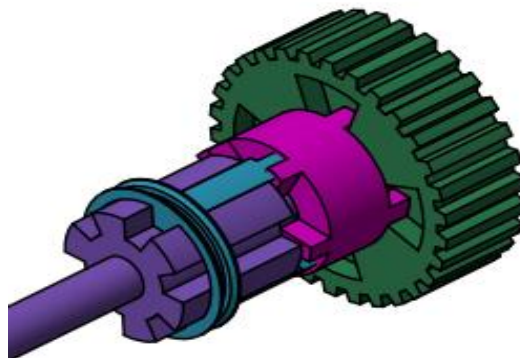


Figure 10. Engaged for one gear level

It can be concluded that the synchronization is done by utilizing some friction, it is to replace the function of a conventional clutch transmission that shifts gear can be carried out smoothly.



3.2. Calculation of synchronization

Source of the work force is the force exerted by the operator in the direction of the horizontal axis of the sleeve element of F . Large forces acting on the cone friction is the normal direction $F_1 \sin \theta$. Due to the friction at each cone, the rotational speed will be reduced from the first friction elements that experience to other elements. In Figure 11 displayed the forces acting on the system synchronizer.

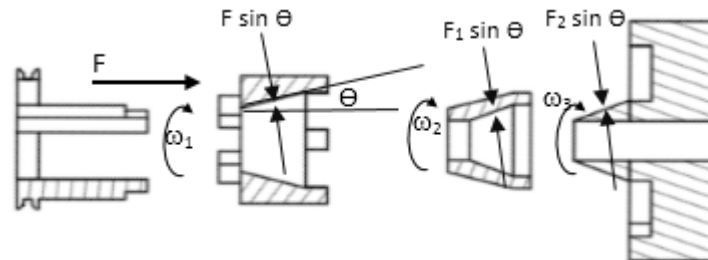


Figure 11. Forces acting on the synchronizer system

Based on Figure 11 it can be seen that the force that taste of the sleeve is F and F_2 will break down into $\sin \theta$ working on the x-axis gear. Rotational speed is also experiencing the same thing that will break down into ω_3 due to the friction that arises. Furthermore, torque and frictional forces acting on the gear can be shown in Figure 12.

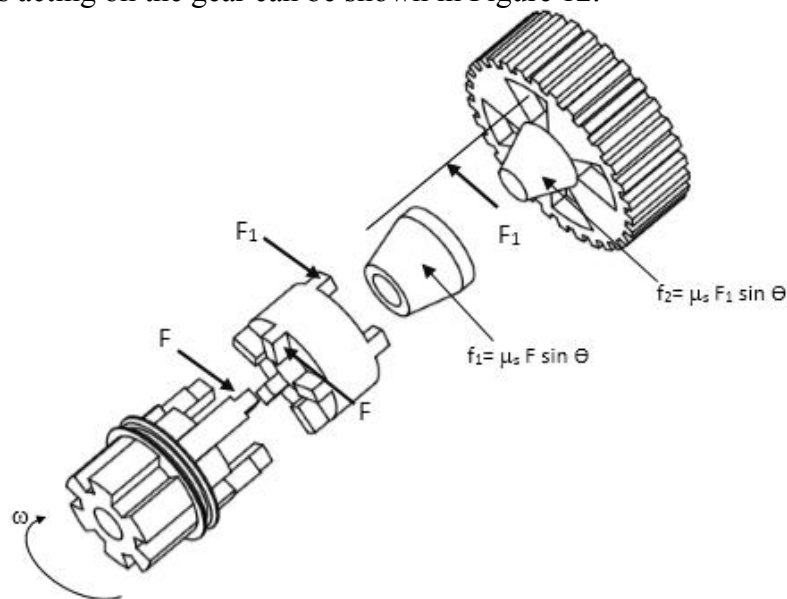


Figure 12. Torque and Friction

When calculating the torque acting on the paired element between the sleeve with synchronizer cone is the distance to the force multiplied by the horizontal axis of the workforce. Then the torque acting on the cone synchronizer with the gear is the distance to the horizontal axis force multiplied by that force.

3.3. Analysis Drive Performa EV

Performance analysis of vehicle motion is made to display the estimated motion acceleration and vehicle speed. It aims to determine the ability of the motor in accordance with the transmission design geometry. The following is shown Figure 13 Geometry transmission design.

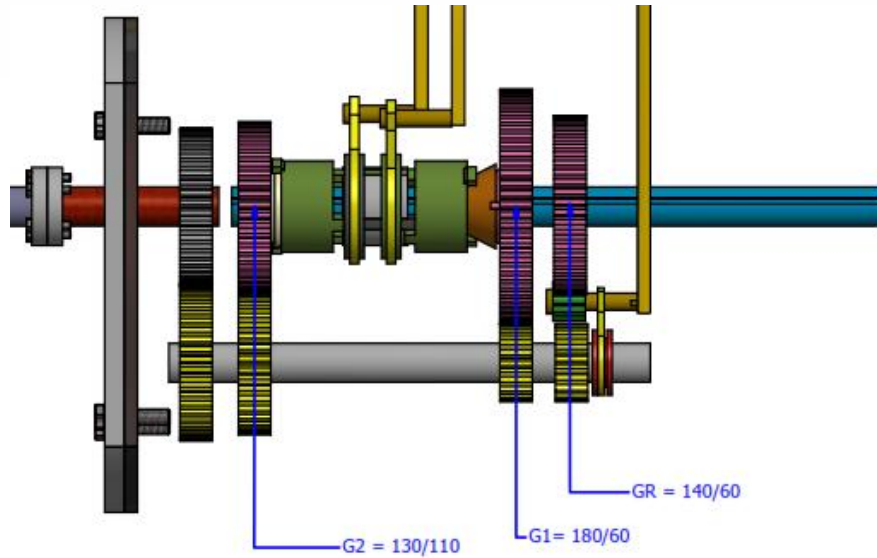


Figure 13. Gear ratio transmission EV

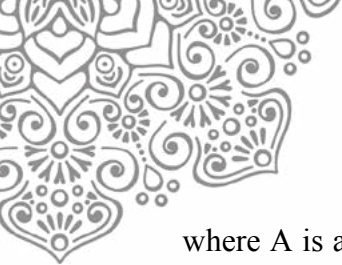
The gear ratio is the ratio between the diameter of the output gear to the input gear. Then the first gear ratio G1 is three, the second gear ratio G2 is 1.18 and reverse gear ratio GR is 2.33. For more details can be displayed in Table 1.

Table 1. Specification design transmission EV

Item	Value
Transmission	
Ratio 1 st Gear G1	3
Ratio 2 nd Gear G2	1.18
Ratio Reverse Gear GR	2.33
Application	
Rolling resistance coeff. μ	0.017
Weight transmission m_t (kg)	400
Gravitation g (m/s ²)	9.81
Tire Radius T_r (m)	0.31

Calculation of acceleration and speed of the vehicle was conducted to determine the performance of the vehicle motion. Furthermore, it is used as an evaluation of the selection of electric motors and other components of the main constituent. In Equation 1 is shown calculating vehicle acceleration with the influence of the transmission gear ratio.

$$A = \left(\frac{T \cdot G1 \cdot \eta_t}{T_r} - \mu \cdot m_t \cdot g \right) / m_t \quad (1)$$



where A is acceleration (m/s^2); T is Torsion motor (Nm); G1 is first gear ratio; η_t is efficiency transmission (90%); T_r is radius wheel (m); μ is Rolling resistance coefficient (0.017); m_t is weight transmission (kg); g is gravitation (m/s^2). Furthermore, the calculation of the vehicle speed can be calculated using Equation (2).

$$v = \frac{n_m \cdot T_r}{k \cdot G2} \quad (2)$$

where v is the speed of the vehicle (m / s); n_m is the rotation of the motor (rpm); k is a conversion coefficient of the motor vehicle speed (2.65). G2 is the second gear ratio.

4. CONCLUSION

Based on the results of the literature survey and design have made the design for the transmission of electric cars has been obtained. Additions for the synchromesh transmission mechanism zero shift a major topic as the development of new ideas for this research. The synchromesh serves to reduce the round elements will be partnered by utilizing the friction in some cone. The working mechanism of a manual transmission without using the clutch is the main aim is to utilize synchromesh and setting the motor torque as a replacement clutch MT. The design will be its own advantages as it will be very effective for the character of the electric motor. The number of gear changes made to two (2 speed) is useful for obtaining power efficiency has been considered from various factors. Transmission weight is one of the considerations to improve the performance of electric motors. In addition, ease of manufacturing, ease of installation of the electric motor, and ease of use by drivers is a thing to note is also to acquire new transmission system that is suitable for electric cars. Expected from searches conducted on the transmission of electric vehicles will help solve the problem of the availability of energy that specifically influences of transport.

5. ACKNOWLEDGEMENT

Thanks for organizers of a research grant from the University of Indonesia. All parties in the Jakarta State Polytechnic who have provided facilities, motivation, and opportunity to participate in education.

6. REFERENCES

- Cheat, R., & Child, A. (2007). A seamless automatic manual transmission (AMT) with no torque interrupt. *SAE International*.
- Back, O. (2013). *Basics of the synchronizer*. Germany: Hoerbiger.
- Bedmar, A. P. (2013). *Synchronization processes and synchronizer mechanisms*. Goteborg: Chalmers University of Technology.
- Heath, R. P. (2007). *Seamless AMT offers an efficient alternative to CVT*. 20075013.
- Kumbhar, M. S., & Panchagade, D. R. (2014). A Literature Review on Automated Manual Transmission (AMT). *IJSRD*, 1236.
- MING, C. C., & CIN, J. S. (2010). Performance Analysis of EV Powertrain system. *World Electric Vehicle Journal*.



SINGLE PHASE STEAM EJECTOR INVESTIGATION: EFFECT OF DIFFERENT AREA RATIO THROAT TO ENTRAINMENT RATIO

Stefan Mardikus and Gregorius Bryan H.R.

Mechanical Engineering Department, Faculty of Science and Technology, Sanata Dharma University, Indonesia

(E-mail: stefan@usd.ac.id, gregoriusbryan92@gmail.com.)

ABSTRACT

The utilization of waste and low-grade thermal energy has become an interest to researchers ever since this type of energy is available from sources, such as industrial processing waste, solar collectors, and emission from automobile. Steam ejector refrigeration system is an application, which is economically feasible and environment-friendly as it can operate with waste heat and a harmless refrigerant such as water. This refrigeration system has many advantages such as high reliability, structural simplicity, long life span, low cost, relatively flexible in terms of refrigerant use, easy to maintain and can be used with water which is the most environment friendly refrigerant. Ejector application in air-conditioning or refrigeration system is either to totally replace the compressor or is used for cycle optimization. The aim of this experiment is to investigate the entrainment behaviour and performance of steam ejector. Through enlarging the designed mixing chamber by replaceable throats, optimum area ratio throat of mixing chamber is studied experimentally. A small scale steam ejector refrigeration system was designed and manufactured. This ejector setup consist of an open loop configuration and the boiler operates in the pressure range of $P_b = 100$ to 400 kPa. The typical evaporator temperatures operates from $T_e = 50$ to 80 degree Celsius, while the condenser temperature fixed at $T_c = 27$ degree Celsius. The mixing chamber with 8 mm diameter and three length configurations (50 mm, 100 mm, 150 mm) are tested with 2 mm nozzle diameter. With variable area ratio throat of mixing chamber, this experiment shows that the optimum entrainment ratio is obtained by throat area ratio 18.75 at 100 kPa primary pressure and 80 degree Celsius secondary temperature at 1.00.

Keywords: Area Ratio Throat; Entrainment Ratio; Steam Ejector

1. INTRODUCTION

Waste heat is a type of energy that available from sources such as industrial process waste, solar collectors, and exhausts with temperature between 80°C - 200°C (Chandra & Ahmed, 2014). Based on U.S. Department of Energy, 20 – 50% energy losses on manufacture process were waste heat, where this type of energy is potentially can be reused again. Richard Law (2015) noted that utilization of waste heat on manufactures in U.S may produce 14 TWh, which is equal to £100 million per year. According to this potential advantage, waste heat can be utilized as main source of energy in absorption chiller, electrical heat pump, absorption heat pump, and non-mechanical refrigeration system (Meyer et al., 2008).



Steam ejector refrigeration system is one of non-mechanical refrigeration system that has been researched in decades. This refrigeration system is first discovered by Le Blanc and Parson on 1901 and has many advantages over the other type of systems such as high reliability, structural simplicity, long life span, low cost, relatively flexible in terms of refrigerant use, easy to maintain and can be used with water which is the most environment friendly refrigerant. Ejector application in air-conditioning or refrigeration system is either to totally replace the compressor or is used for cycle optimization. Ejectors are used in aerospace engineering for thrust augmentation, exhaust noise suppression and mixing of exhaust gases with fresh air to reduce the thermal effect. In process industries, ejectors are noted to be used widely for entraining and pumping corrosive liquids and other type of gasses which is difficult to handle (Chandra & Ahmed, 2014).

Figure 1 shows a schematic diagram of an ejector refrigeration system. This cycle is similar to the conventional vapor compression system except that the compressor is replaced by a liquid circulation pump, boiler and ejector. Briefly, as heat is added to the boiler, the evaporated refrigerant is evolved at high temperature and pressure (2). This high pressure refrigerant, which can be called either “primary fluid” or “motive fluid”, expands through the primary nozzle in an ejector and produces a very low pressure region at the primary nozzle exit plane (3). This low pressure allows a liquid refrigerant in the evaporator to vaporize at low temperature to create the refrigeration effect. Heat used to vaporize this refrigerant is the cooling load of the system. The evaporated “secondary fluid” will be entrained from the evaporator and mixed with the primary fluid in a mixing chamber of the ejector. The mixed stream is discharged via the diffuser to a condenser (4), where the vapor is condensed (5). The accumulated liquid refrigerant in the condenser is returned back to the boiler by the feed pump (1) whilst the remainder is expanded through the throttling valve to the evaporator (6), to complete the cycle (Sriveerakul et al., 2006).

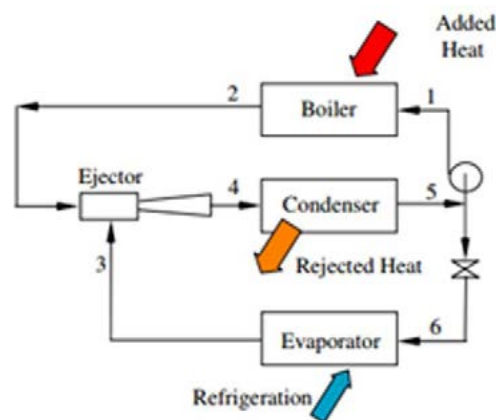


Figure 1 Schematic diagram of ejector refrigeration system

Figure 2 shows the schematic diagram of a typical steam ejector. According to Sriveerakul, a steam ejector consists of four principal parts, which are the primary nozzle, the mixing chamber, the ejector throat and the subsonic diffuser. Moreover, the diagram



describes the operating characteristic of an ejector. The high pressure primary steam (P) starts to accelerate as it enters a convergent section of the nozzle and reaches the sonic level at the nozzle throat (i). The speed of primary flow is further increased while expanding through a divergent section of the nozzle. At the exit plane, the primary fluid expands out with supersonic speed and results the low pressure region (ii). This expanded wave (jet core) of the motive steam entrains and draws the secondary fluid into the mixing chamber (S), where the secondary steam is accelerated and completely mixed with the primary steam (iii). A normal shock wave is then induced in the ejector throat (iv), creating a compression effect, and the flow speed suddenly drops to subsonic value. Further compression is achieved when the mixed stream passes through the subsonic diffuser (B).

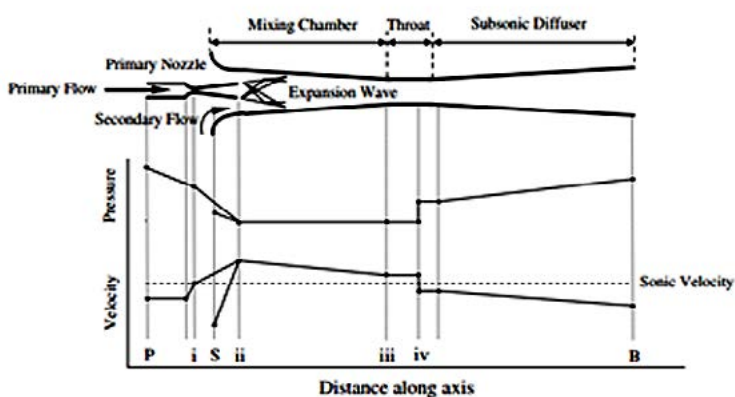


Figure 2 Schematic diagram of typical steam ejector and flow characteristic

2. METHODOLOGY

The schematic diagram and photograph of an experimental steam ejector refrigerator is shown in Figure 3. In this paper, the ejector was designed to operate with a boiler pressure of 100 – 400 kPa, while the temperature of evaporator operated at 50 – 80 °C with water as the refrigerant. The boiler was constructed using 8” diameter mild steel pipe with thickness 10 mm and used two 2 kW electric heaters which is attached the bottom plate. The evaporator also had same construction with boiler, but it equipped with 1 kW electric heater. The rubber gaskets and sealant were used to avoid any leakage. The condenser operates at constant temperature 27 °C and constructed from 150 mm diameter aluminum with maximum volume 20 L.

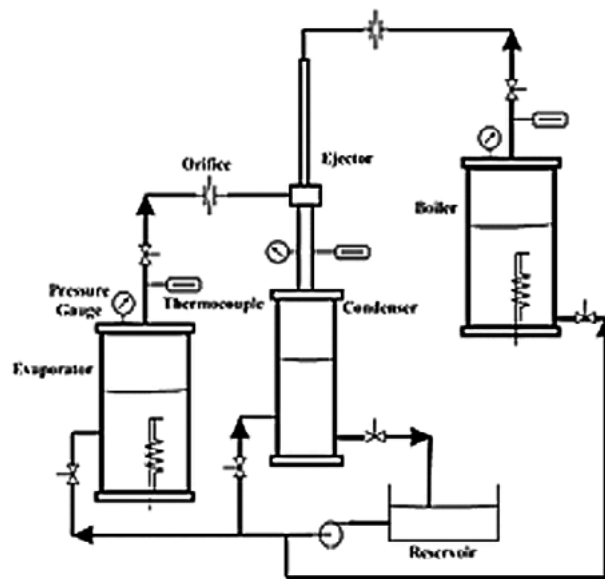


Figure 3 Experimental Steam Ejector Refrigeration System

The experimental are executed in batches. Before each test run the boiler and evaporator were filled with water up to 10 liter. The next step is switch the boiler and evaporator electric heaters on. While the boiler and evaporator heat up until designed operating condition, the condenser was filled with water up to 15 liter and remained at constant temperature 27 °C. After boiler and evaporator reached the designated pressure and temperature, both valves were opened for about 10 seconds at a time. The mass flow rate of boiler, evaporator, and outlet ejector were measured by orifice flow meter and recorded at the same time. Next, the boiler and evaporator valve remained open until all vapor removed from the system at atmospheric pressure in both vessels. Water in boiler, evaporator, and condenser then removed from vessel using a vacuum pump. The procedure was repeated again with different operating condition of boiler and evaporator, for 3 different replaceable throats that shown in Table 1.

Geometries of experimental ejector described in Figure 4. The ejector was designed based on the methods provided in literature (Sriveerakul et al., 2006). There were three throats constructed three different throat length, for the purpose of examining influence of mixing chamber throat on ejector performance. These throats had the same diameter 8 mm. The significant geometries of the experiment throat were listed in Table 1.

Table 1 Mixing Chamber's Throat Variable Geometries

Throat Diameter, x (mm)	Throat Length, y (mm)	Area Ratio Throat (L/D)
8	50	6.25
8	100	12.5
8	150	18.75

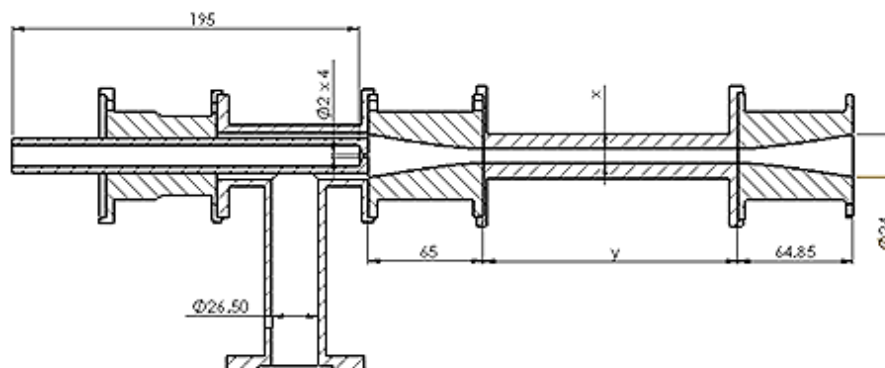


Figure 4 Experimental ejector geometries

3. RESULTS AND DISCUSSION

Based on measurements of ejector primary fluid and secondary fluid mass flow rates, the ejector entrainment ratio which is used to determine optimum throat area ratio can be defined as

$$\omega = m_s / m_p \quad (1)$$

where ω is the entrainment ratio of the ejector, is m_s the mass flow rate of the secondary fluid in kg/s, and m_p is the mass flow rate of the primary fluid in kg/s (Chandra & Ahmed, 2014).

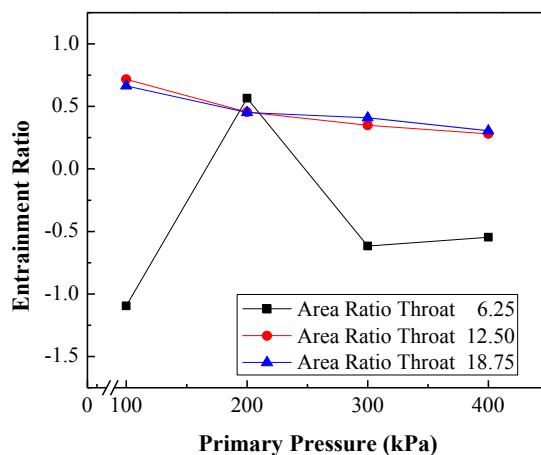
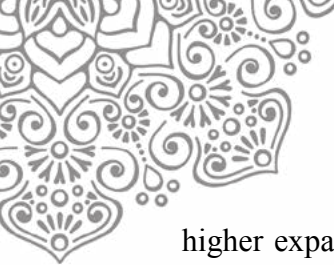


Figure 5 Variation of primary pressure with three area ratio throat ($T_e = 50^\circ\text{C}$).

Figure 5 shows the testing result for the three different area ratio throats (from 6.25 to 18.75) while the evaporator temperature fixed at 50°C . It was observed when the secondary temperature fixed at 50°C , the entrainment ratio decreased when the primary pressure increased. This phenomenon happened because higher primary pressure induced



higher expansion angle from primary fluid flow from outlet nozzle. High expansion angle caused entrainment region in suction chamber decreased (Chandra & Ahmed, 2014). Furthermore, higher primary pressure caused mass flow rate of primary fluid increased. This behavior agreed well with the experimental result was published by Yan Jia (2011). Area ratio throat 6.25 didn't make any significant effect on entrainment ratio, meanwhile showed negative value of entrainment ratio because momentum transfer didn't intensively occur or the primary and secondary flow got inadequately mixed, for such cases the pressure recovery region in pseudo-shock became shorter and thus the ejector efficiency decreased dramatically (Li, 2010). The optimum entrainment ratio reached at 100 kPa primary pressure with area ratio throat 12.5, $\omega = 0.71$. This phenomenon happened because the mixed flow in mixing chamber became fully developed due to adequate length of mixing chamber.

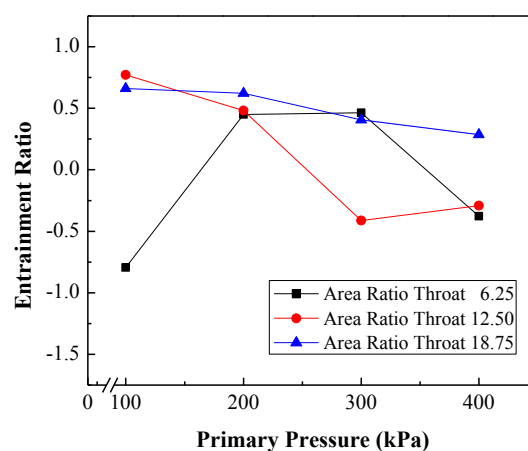


Figure 6 Variation of primary pressure with three area ratio throat ($T_e = 60^\circ\text{C}$).

Figure 6 showed the testing result for the three different area ratio throats at constant secondary temperature 60°C . The overall experiment result showed same phenomenon as previous evaporator temperature condition. The optimum entrainment ratio happened at 100 kPa with area ratio throat 12.5, $\omega = 0.77$. The entrainment ratio showed positive value for area ratio throat 18.75 in any operating primary pressure. This phenomenon occurred because mixed fluid that flow through constant area throat became fully developed. The fully developed flow produced smaller shock wave, therefore momentum transfer between primary and secondary fluids were better (Li, 2010).

Figure 7 and Figure 8 showed the testing result for the three different area ratio throats at constant secondary temperature 70°C and 80°C respectively. The experiment result showed same phenomenon with previous work, the entrainment ratio decreased as the primary pressure increased. Optimum entrainment ratio for secondary temperature 60°C reached at 100 kPa pressure with area ratio throat 12.5, with $\omega = 0.91$. Meanwhile, the maximum entrainment ratio of this experiment was 1.00 at operating condition of secondary temperature 80°C and 100 kPa primary pressure with area ratio throat 18.75. Based on four different secondary temperatures, the result showed entrainment increased as evaporator temperature increased. This phenomenon occurred because higher secondary



temperature caused back pressure increased (Li, 2010 and Jia, 2011). Moreover, higher secondary temperature caused density of secondary fluid decreased (Meyer et al., 2008).

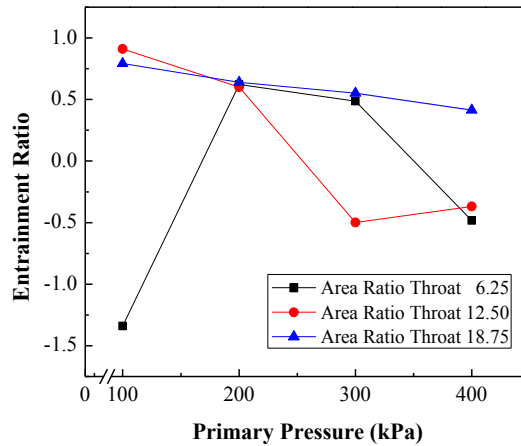


Figure 7 Variation of primary pressure with three area ratio throat ($T_e = 70^\circ\text{C}$).

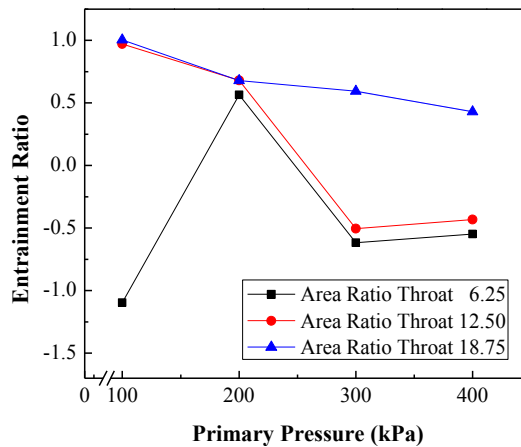


Figure 8 Variation of primary pressure with three area ratio throat ($T_e = 80^\circ\text{C}$).

4. CONCLUSION

Experimental investigation was performed on variable area ratio throat of mixing chamber in steam ejector refrigeration system. The experiment proved that the area ratio throat of mixing chamber was an important design parameter and can exert a remarkable influence on steam ejector performance. The area ratio throat optimum was 18.75. It caused the maximum entrainment ratio, which can be defined as the optimum length of throat that depends on the pseudo-shock. The operating conditions also had important influence due to back pressure value and formation of expansion angle in suction chamber. The maximum entrainment ratio for this experiment was 1.00 with area ratio throat 18.75, at 100 kPa primary pressure and 80 °C secondary temperature.



5. REFERENCES

- A.J. Meyer, T.M. Harms, and R.T. Dobson (2008), "Steam jet ejector cooling powered by waste or solar heat," *Renewable Energy*, vol. 34, pp. 297-306.
- C. Li and Y.Z. Li (2010), "Investigation of entrainment behavior and characteristics of gas-liquid ejectors based on CFD simulation," *Chemical Engineering Science*, vol. 66, pp. 405-416
- Richard Law, Adam Harvey, and David Reay (2015), "A Knowledge-Based System for Low-Grade Waste Heat Recovery in The Process Industries," *Applied Thermal Engineering*, vol. 94, pp. 590-599.
- T. Sriveerakul, S. Aphornatana, and K. Chunnanond (2006), "Performance prediction of steam ejector using computational fluid dynamics: Part 1. Validation of the CFD results," *International Journal of Thermal Science*, vol. 46, pp. 812-822.
- U.S. Department of Energy (2008), "Waste heat recovery: Technology and Opportunities in The U.S. Industry," *Industrial Technologies Program*.
- Vineet V. Chandra and M.R. Ahmed (2014), "Experimental and computational studies on a steam jet refrigeration system with constant area and variabel area ejectors," *Energy Conversion and Management*, vol. 79, pp. 377-386.
- Yan Jia and Cai Wenjian (2011), "Area ratio effects to the performance of air-cooled ejector refrigeration cycle with R134a refrigerant," *Energy Conversion and Management*, vol. 53, pp. 240-246.



DEVELOPMENT OF CONVERGING-DIVERGING (CD) NOZZLE GENE GUN TO INCREASE COMPRESSIBLE FLUID THRUST FORCE

Haris Setiawan^a, Gema Puspa Sari^b, Satria Putra Santoso^a,
Danardono A. Sumarsono^a, Fera Ibrahim^b

^a *Department of Mechanical Engineering, Faculty of Engineering, Universitas Indonesia, Depok, Indonesia*

^b *Virology and Cancer Pathobiology Research Center (VCPRC) FKUI-RSCM, Department of Microbiology, Faculty of Medicine, Universitas Indonesia, Jakarta, Indonesia*

Corresponding author: danardon@eng.ui.ac.id

ABSTRACT

This paper presents simulation investigation of the velocity contour with in a transonic converging-diverging (CD) nozzle prototype to produce higher pressure and momentum output. Carl de Laval invented two-pieces nozzles, converging and diverging. The discovery of this nozzle greatly facilitates the mass delivery process. A light mass particle is a mass that easily flows with air that can be compressed through the nozzle. It also can be applied in various ways, one of them is vaccination in health. Nozzle is an important part of the gene gun which used to accelerate DNA in particle form with a gas flow to reach adequate momentum to enter the epidermis of human skin and elicit immune response.

Keywords : Nozzle; Gene gun; DNA; Vaccination; Immune response

1. INTRODUCTION

This study focused on developing a converging-diverging (CD) nozzle as an essential part of gene gun that we developed in our lab. CD nozzle has supersonic flows where Mach number is higher than one. This type of nozzle consist of three parts which are convergent type of nozzle on the input, throat on the middle, and divergent type on the end of the nozzle. Our aim is to design a better system in construction than the device used in clinical application, such as HeliosTM Gene Gun, so that gene gun can deliver DNA vaccine effectively with economical cost. Key components of the gene gun prototype under development are shown schematically in Figure 1. We also developed a practical Gene gun which can be filled with pressurized gas fluid from gas cylinders, compressors or handheld air pumps.

Our objective was designing CD nozzle with enough speed and momentum on the outlet to give a good spread on light mass particle.

DNA (deoxyribonucleic acid) vaccination is a fairly novel technology which utilizes genetically engineered DNA to generate an immunologic response. The crucial strategy to achieve this purpose is to use DNA plasmids having antigens encoded on them. This antigen encoding DNA plasmid can elicit humoral and cellular immune response against pathogens including disease-producing viruses (Wen et al., 2014). Scientific community start to interested in DNA vaccines in the early 1990s, when it was reported that plasmid DNA, delivered into the skin or muscle, produced antibody responses to viral and nonviral antigens (Ulmer et al., 1993; Chow et al., 1998).



Gene gun offers simple yet effective means of DNA vaccine delivery on organisms. Tang (1992) utilized gene gun to deliver the gene encoding hGH (human growth hormone) to produce specific antibodies against hGH (Angel et al., 2008). Fynan (1993) reported the presence of antibodies against influenza antigen genes even if only used in small quantities by delivering the gene encoding influenza antigens using gene gun. Lodmell (1997) showed that the delivery of DNA with a gene gun Accell™ was able to induce protective antibodies produced against the rabies virus (Chong et al., 2007). Loehr (2000) showed that the DNA vaccine mediated by gene gun as its delivery system managed to protect cattle from infection of bovine herpesvirus 1 (BHV-1) (Tang et al., 1992). Leitner (2016) reported the delivery of DNA vaccines using tumor gene gun can improve protective immunity-dependent T cells in mice C57BL / 6.

The main advantage of gene gun technology is not dependent on the existence of binding ligand-receptor specific aspects, biochemical or structural components on the surface of target cells, therefore this technology can be applied to various biological systems such as bacteria (Fu et al., 1997), fungi (Kim and Sin, 2005), various intracellular organelles (Li et al, 2008; Uchijima 1998), and mammals (Pulsawat et al, 2010; Besse et al., 2008; Becker et al., 2008).

2. METHODOLOGY

2.1. CD Nozzle and Gene Gun Design

Nozzle is the most crucial part on our gene gun since nozzle will determine the efficiency of DNA vaccine delivery. Nozzle works to modify airflow at gene gun, to regulate the rate of flow, speed, direction, mass, shape, or pressure is exerted. CD nozzle, also known as de Laval Nozzle, is a device that allows supersonic flow to occur in the diverging portion of the nozzle. A supersonic flow allows a greater exit to inlet pressure ratio to be achieved.

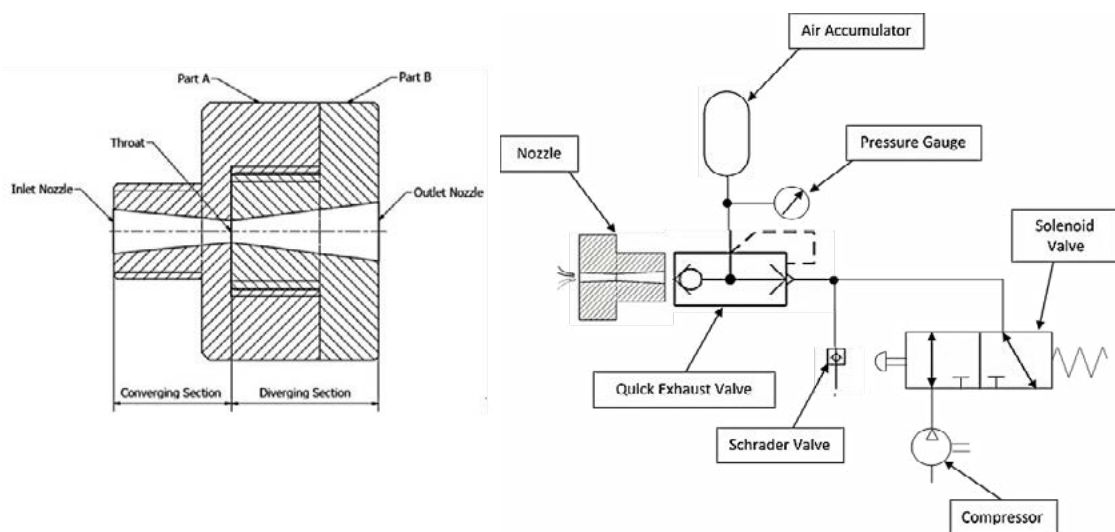


Figure 1. Schematic drawing of converging-diverging nozzle (a) and pneumatic diagram of Gene gun prototype for DNA vaccine delivery (b).

Nozzle that we used on this study is consisting two parts, the converging nozzle as Part A and the diverging nozzle as Part B as shown in Figure 1 (a). The converging part contain inlet nozzle as the gate for the particle when entering the nozzle through the



throat. Part A connected the quick exhaust valve (QEV) and the diverging nozzle on Part B. Throat is most important part of the nozzle because it will rise the velocity significantly and also the drop of the pressure which make the shockwave occur and the Mach number increase instantly. Three different diameter, 4 mm (type 1), 6 mm (type 2), and 8 mm (type 3) was used on the outlet of the divergent type.

2.2. Thrust force and spread of light mass particles

Thrust force from each nozzle was measured using scale which are recorded to know the exact measurement. Two shooting distance variation, 10 mm and 20 mm, was used on this experiment. Light mass particles was represent with flour as mock of DNA-microcarrier particle. 0,07 gr flour was shoot into black paper to observed its spreading of particles.

3. RESULTS AND DISCUSSION

3.1. Results

Fluid flow characteristic at 10 bars in the nozzle was simulated using CFD software ANSYS® as shown in Figure 2. The highest velocity which represent by red colour happened on nozzle throat for all pressure for all nozzles. Those nozzles will efficient enough to deliver the particles with low pressure since using higher pressure did not give any significant impact on the velocity.

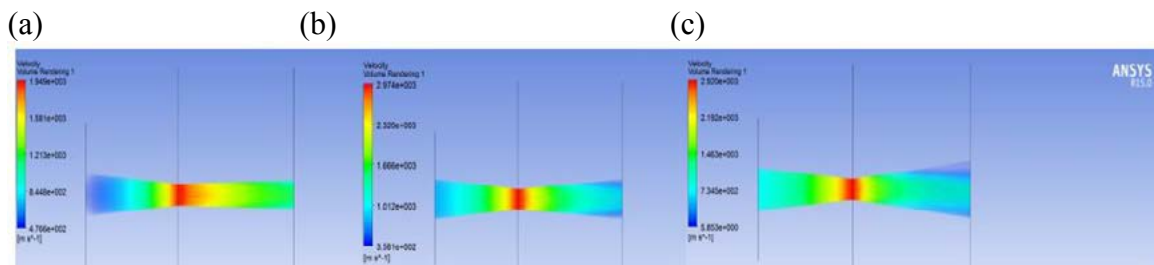


Figure 2. Flow velocity contour simulation inside of CD nozzle type 1 (a), type 2 (b), and type 3 (c) using 10 bars inlet gas pressure.

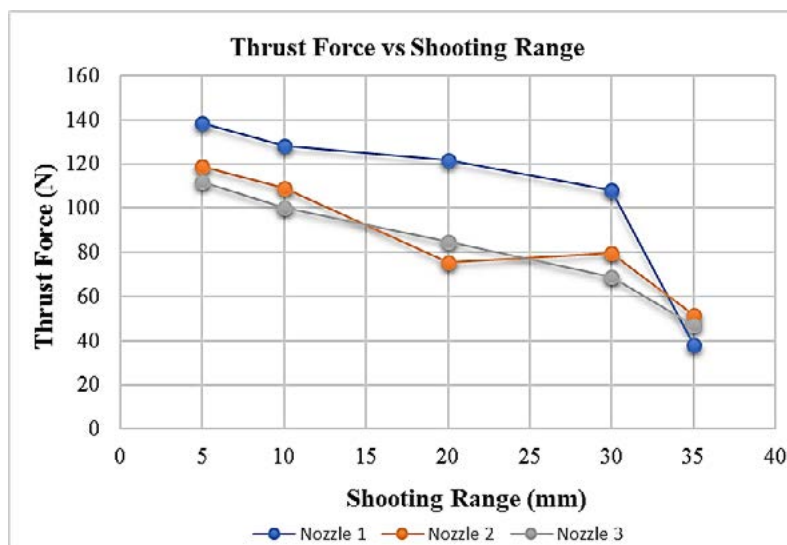


Figure 3. Graph of thrust force versus shooting range on pressure inlet 10 bar.



15th International Conference on Quality in Research 2017 (QiR 2017)
July, 24-27th 2017, Bali, Indonesia

The relation between thrust force and shooting range is shown in Figure 3. The smaller the thrust force, the shooting ranges were getting greater. Table 2 showed the particle spread on different shooting range on 10 mm and 20 mm and different gas pressure inlet on 6 bars, 8 bars, and 10 bars.

Table 2. The diameter of spreading of the light mass particle based on shooting range.

10 mm		Type 1	Type 2	Type 3	20 mm		Type 1	Type 2	Type 3
6 bar	∅ spread (mm)	4,2	8	10	6 bar	∅ spread (mm)	20	14	22
	∅ center (mm)	N/A	N/A	N/A		∅ center (mm)	4,6	8	N/A
8 bar	∅ spread (mm)	4	8	9	8 bar	∅ spread (mm)	16	12	12
	∅ center (mm)	3,4	7	N/A		∅ center (mm)	16	12	N/A
10 bar	∅ spread (mm)	3	7	8	10 bar	∅ spread (mm)	7	10	11
	∅ center (mm)	2,8	6,6	6		∅ center (mm)	4	7	N/A

3.2. Discussion

Our result shows that CD nozzle type 1 with 4 mm on diameter gave the best result to deliver DNA vaccine based on its particle spread, thrust force, and momentum. Based on light mass particle spreading, CD nozzle type 1 shows the best result on spread the particle where it had the widest spread are but the smallest center shooting area. The longer the shooting range, the particles will spread into wider area. However optimization on different range must be done because longer distance results in reduced particle speed and a decreased likelihood of target penetration, thereby decreasing the transfection efficiency (O'Brien and Lummis, 2006).

The flow in the throat is sonic which means the Mach number is equal to one in the throat. Downstream of the throat, the geometry diverges and the flow is isentropically expanded to a supersonic Mach number that depends on the area ratio of the exit to the throat. The expansion of a supersonic flow causes the static pressure and temperature to decrease from the throat to the exit, so the amount of the expansion also determines the exit pressure and temperature. The exit temperature determines the exit speed of sound, which determines the exit velocity.

Converging-diverging nozzle works based on isentropic flow (adiabatic phase) which means that total enthalpy and total pressure are constant, moreover the total temperature is also constant for a perfect gas. As a typical problem, the inlet thermodynamic state (pressure and temperature) is known as well as the inlet velocity (Mach number). Compressible fluid flowed suddenly from high pressure shall produce a shock wave phenomenon because of compressibility effects of the fluid itself.

The existence of shock waves provide vibration canal wall which makes the channel walls wheezes. Schrader valve also will replace the compressor, so that the gene gun can be used in remote areas that do not have a compressor. Quick Exhaust Valve (QEV) acts as regulator valve air release before being discharged into the nozzle and silencer functions as supporting components in the gene gun system, serves to muffle the sound when air is released freely.



In immunization using DNA vaccine, microparticle must be accelerated by a high speed flow began by a traveling shock wave, so that they can achieve a sufficient momentum to infiltrate in to the cells of interest (Liu et al., 2007; Corrie and Kendall, 2017). In DNA vaccination, powdered vaccines are directly delivered into the antigen presenting cells (APCs) within the epidermis/dermis (Liu et al., 2007).

Prompt innovations in many fields—including immunology and vaccines—have push the researchers to develop physical system for cell targeting in the successful DNA vaccination against major diseases. Currently, biolistic microparticle injection is the most established physical method of DNA vaccination, otherwise known as gene guns. In this needle-free procedure, pharmaceutical or immunomodulatory agents, formulated as particles, are accelerated in a high-speed gas jet to sufficient momentum to penetrate the skin (or mucosal) layer and to achieve a pharmacological effect. Biolistic DNA vaccination is achieved by the delivery of gold microspheres coated with plasmid DNA coding for specific antigens to epidermal dendritic cells (Lauterbach et al., 2006).

4. CONCLUSION

The transient gas inside the prototype of converging-diverging nozzle have been characterized by this experiment. Pressure contour was used to indicate the increase of Mach number on throat and shockwave on diverging section. Velocity contour was used to indicate that the velocity increased on the output, which is much higher than the input. In some applications of this form of needle-free pharmaceutical agent delivery to the skin, a tighter control of the particle impact momentum distribution may be required. In this case, inlet pressure need to be optimized to reach the best velocity and contact area target to spread the DNA vaccine effectively.

5. ACKNOWLEDGEMENT

The authors would like to thank to Universitas Indonesia, the Ministry of Health, and the Ministry of Research and Technology for funding support the development of DNA vaccines delivery system research.

6. REFERENCES

- Becker, P.D., Noerder, M. and Guzmán, C.A Genetic Immunization: Bacteria as DNA Vaccine Delivery Vehicle. *Human Vaccines*, 4. 2008. 189-202.
- Besse, F. and Ephrussi, A. Translational Control of Localized mRNAs: Restricting Protein Synthesis in Space and Time. *Nature Reviews Molecular Cell Biology*, 9, 2008, 971-980.
- Chong, S.Y., Egan, M.A., Kutzler, M.A., Megati, S., Masood, A., Roopchard, V., Garcia-Hand, D., Montefiori, D.C., Quiroz, J., Rosati, M., Schadeck, E.B., Boyer, J.D., Pavlakis, G.N., Weiner, D.B., Sidhu, M., Eldridge, J.H. and Israel, Z.R. Comparative Ability of Plasmid IL-12 and IL-15 to Enhance Cellular and Humoral Immune Responses Elicited by a SIV gag Plasmid DNA Vaccine and Alter Disease Progression Following SHIV(89.6P) Challenge in Rhesus Macaques. *Vaccine*, 25. 2007. 4967-4982.



15th International Conference on Quality in Research 2017 (QiR 2017)
July, 24-27th 2017, Bali, Indonesia

- Fu, T.M., Ulmer, J.B., Caulfield, M.J., et al. Priming of cytotoxic T lymphocytes by DNA vaccines: requirement for professional antigen presenting cells and evidence for antigen transfer from myocytes. *Mol Med*. 1997. 3(6):362-71
- Fynan, E.F., Webster, R.G., Fuller, D.H., Haynes, J.R., Santoro, J.C., Robinson, H.L. DNA vaccines: protective immunizations by parenteral, mucosal, and gene-gun inoculations. *Proc Natl Acad Sci U S A*. 1993. 90:11478–11482.
- Kim, M.S. and Sin, J.I. Both Antigen Optimization and Lysosomal Targeting Are Required for Enhanced Anti-Tumour Protective Immunity in a Human Papillomavirus E7-Expressing Animal Tumour Model. *Immunology*, 116. 2005. 255-266.
- Klein, T.M., Wolf, E.D., Wu, R., Sanford, J.C. High velocity microprojectiles for delivering nucleic acids into living cells. *Nature*. 327. 1987. 70-73.
- Lauterbach, H., Gruber, A., Ried C., Cheminay, C., Broker, T. Insufficient APC capacities on dendritic cells in gene gun-mediated DNA vaccination. *J Immunol*. 2006. 176(8):4600-7.
- Leitner WW, Baker MC, Berenber TL, Lu MC, Yannie PJ, Udey MC. Enhancement of DNA tumor vaccine efficacy by gene gun-mediated codelivery of threshold amounts of plasmid-encoded helper antigen. *Blood*, 113. 2009. 37-45.
- Li, K.B., Zhang, X.G., Ma, J., Jia, X.J., Wang, M., Dong, J., Zhang, X.M., Xu, H. and Shu, Y.L. Codon Optimization of the H5N1 Influenza Virus HA Gene Gets High Expression in Mammalian Cells. *Chinese Journal of Virology*, 24. 2008. 101-105.
- Lodmell, D.L., Ray, N.B., Ewalt, L.C. Gene gun particle-mediated vaccination with plasmid DNA confers protective immunity against rabies virus infection. *Vaccine*, 16. 1998. 115-118.
- Loehr BI, Willson P, Babiuk LA, van Drunen Littel- van den Hurk S. Gene Gun-Mediated DNA Immunization Primes Development of Mucosal Immunity Against Bovine Herpesvirus 1 in Cattle. *Journal of Virology*. 2000. 6077-6086.
- O'Brien, J.A. and Lummis, S.C.R. Biolistic Transfection of Neuronal Cultures Using a Hand-held Gene Gun. *Nat Protoc*. 2006 ; 1(2): 977–981
- Tang, D.C., DeVit, M., Johnston, S.A. Genetic immunization is a simple method for eliciting an immune response. *Nature*. vol. 356, 1992, 152-154.
- Wen, E.P., Ellis, R., Pujar, N.S. (2014) The Production of Plasmid DNA Vaccine in *Escherichia coli*: A Novel Bacterial-Based Vaccine Production Platform, in Vaccine Development and Manufacturing. Michael Chartrain (ed.). John Wiley & Sons, Inc., Hoboken, NJ, USA.
- Corrie, S.R., and Kendall, M.A.F. Transdermal Drug Delivery, in Drug Delivery: Fundamentals and Applications. 2nd ed. Hillery, A.M. and Park, K (eds). 2017. Taylor and Francis Group, LLC. NW, USA.
- Liu Y., Truong, N.K., Kendall, M.A.F., Bellhouse, B.J. Characteristic of A Microbiolistic System for Murine Immunological Studies. *Biomed Microdevices*. 2007. 9: 465-474.



ELECTRICAL SYSTEM DESIGN OF SOLAR-POWERED ELECTRIC WATER RECREATIONAL AND SPORT VESSEL

Sunaryo^a, Pradhana S Imfianto^b, Aldy Syahrihaddin Hanifa^c

^{a, b, c}Naval Architecture and Marine Engineering, Department of Mechanical Engineering, Universitas Indonesia, *E-Mail*:^a :*naryo@eng.ui.ac.id*,
^b:*pradhana.sadhu@ui.ac.id*, ^c:*aldy.syahrihaddin@ui.ac.id*

ABSTRACT

Indonesia is the world's largest archipelago with more than 17,000 islands, and the best marine tourism destination due to its beautiful beaches and underwater scenery, but Indonesia is also the most vulnerable country to be affected by climate change which is triggered by greenhouse effect in term of its geographical location along the equator. Beside industry, transportation sector is the highest contributor to the global greenhouse effect. In order to reduce the resource of greenhouse effect Indonesian Government has a strategic plan through Presidential Regulation no. 61/2011, and emphasized by the Ministry of Energy and Mineral Resources, and the Ministry of Transport in their 2015 – 2019 strategic plans for using new and renewable energy as alternative to fossil based fuel. In attempt to contribute to the Government's efforts and in advancing the national marine tourism sector, the research is aimed to design a water recreational and sport vessel that powered by solar generated electric engine. This is a further development of the solar boat created by the Universitas Indonesia team that participated in International Solar-boat Challenge competition in the Netherlands. The research is focused on the effective use of solar energy as the main source of powering the vessel's engine, and therefore the vessel is designed to the most efficient shape and dimensions obtained from various design aspects analyses. Information regarding the arrangement of the vessel, solar electric generation processes, and vessel powering system are obtained from literature study, discussion with experts, and on the spot surveys of various recreational locations. Collected data are then used as input for the calculation and simulation of the vessel being designed. The research is expected could be developed further for other usages such as fish farming, coastal fishing rig, floating restaurant etc.

Keywords: Design; Electric Propulsion; Solar-Electric Boat; Solar Energy; Water transportation

1. INTRODUCTION

In recent years, Indonesia has emerged as one of the most favorite tourist destination. With this positive growth from tourism aspect, the potential development of a water transportation vehicle that works on clean energy also emerged. This demand arises as the awareness of protecting environment of tourism spot become major issues in certain area of the world, especially Indonesia. The possibility of using solar energy as sole power source to a vessel is a perfect solution to solve this issue. In order to respond to that condition, this paper proposes a base design of a personal solar electric boat that is projected to replace small watercraft vehicle such as jet-ski or motorized kayak. We believe that this proposed design will be a proper reference in designing a solar electric boat which its application range would vary from personal watercraft up to big passenger vessel.



2. METHODOLOGY

2.1. The boat

For the purpose of the project the boat being proposed is shown in figure 1, and has the following main particulars:

- Mono Semi-Trimaran hull
- Single pilot
- Maximum speed: 20-25 km/h (~11 knots)
- Maximum Cruising time: 4-5 hours continuous operation and depends on sunlight. With optimum cruising time: 2-3 hours.
- Length over all: 5.8 m
- Width: 1.8 m
- Draft at full load: 0.124 m
- The boat is equipped with one 4.3 kW pod propulsion system permanent magnet asynchronous motors;
- cruising speeds equal to 15-20 km/h (~10knots);
- Average electrical power required during the cruise 4 kW
- Maximum cruising range : 60 km

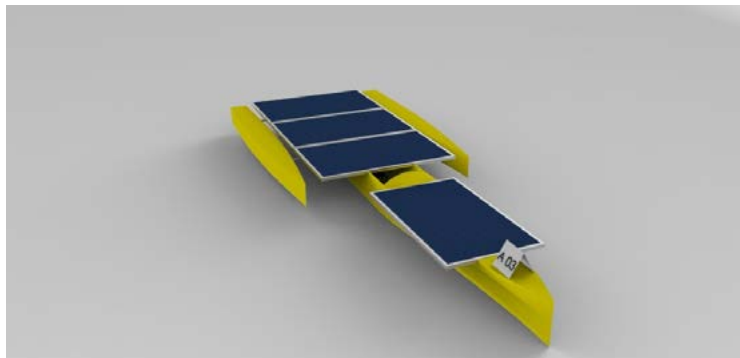


Figure 1 Semi-trimaran mono hull boat

Mono-hull semi-trimaran is selected in order to get best power to weight ratio, and to ensure proper stability and space availability for PV panels along with its electrical equipment's. Therefore, it is necessary to arrange optimum quantities of PV Panel.

2.2. Electrical System

2.2.1. Batteries

It is assumed that the average electrical power needed during the cruise is 3 kW and the maximum peak power is up to 5 kW with most of the power will be used for propulsion system. Since this boat is designed to take place of normal Jet Ski or other personal small watercraft, its daily operational will be around 2-3 hours per day with assumption that the boat propulsion system is always running. Also its maximum weight should be



as minimum as possible, as most electric vehicle has a problem with its weight due to battery pack weight, in this project the use of available area for the PV Panel and construct small but powerful enough battery pack is maximized.

To minimize the vessel weight, the battery package should be as simple as possible. Therefore, types of battery that will be used are essential to determine the weight of the package. In this project battery package was custom-made our using 144 cells of Lithium-ion Battery and this battery pack will be monitored with aftermarket BMS (Battery Management System).

Table 1 Battery Specification

Voltage nominal (V_n)	44.4 V	V_{max}	50.4 V
Normal Capacity	33 Ah	V_{min}	33 V
Weight	10.2 kg	Max Discharge Current/Solar Charging voltage	150A/50.4 V
Dimension	420 × 180 × 280 mm		

These cells of battery will be put in one battery box that will be lined up into 12 Series and 11 Parallel sets of batteries. Therefore, this custom made battery will resulted in this the specifications shown in table 2 and expressed in figure 2.

Table 2 Specifications of Custom Made Battery Pack LG

LG newest 18650 Battery LG HG2 INR18650 3000mAh (20A) LG 18650 Chocolate Battery E-cig battery 18650 high drain LG INR18650 HG2 Specifications:

Item	Condition / Note	Specification
Capacity	Std. charge / discharge	3000mAh
Nominal Voltage	Average of Std. Discharge	3.60V
Continuous Discharge Current		20A
Standard Charge	Constant current	1500mA
	Constant voltage	4.20V
	End current(Cut off)	50mA
Fast Charge	Constant current	4000mA
	Constant voltage	4.20V
	End current(Cut off)	100mA
Max. Charge Voltage		4.20V±0.05V
Max. Charge Current		4000mA
Standard Discharge	Constant current	600mA
	End voltage(Cut off)	2.5V
Fast Discharge	Constant current	10000mA, 20000mA
	End voltage(Cut off)	2.5V
Max. Discharge Current	For continuous discharge	20000mA
Weight	Approx.	Max. 47.0G
Operating Temperature	Charge	0 ~ 50°C
	Discharge	-20~ 75°C
Storage Temperature	1 month	-20 ~ 60°C
	3 months	-20 ~45°C
	1 year	-20 ~ 20°C



Figure 2 Custom Made Battery Pack

In order to guarantee the battery being well protected, this battery pack will be put inside a battery box that also has cooling system to ensure battery temperature stay under control. In conclusion we have built a storage system made by 144 Cells of batteries into one battery pack, with these features:

- Total weight: 10 kg (Battery box Included)
- Equipped with Cooling system and monitoring system, also safety features that prevent it from electrical failure.
- Volume: $0.420 \times 0.180 \times 0.280 \approx 0.024 \text{ m}^3$
- Maximum electrical energy storage $\approx 1.5\text{kWh}$.

With this compact design of Battery pack, the overall weight of its electrical storage system does not exceed 15 kg. Which means this boat will be handy and very light on the water. In addition, this electrical system minimizes needs of other mechanical equipment that may require additional weight. To activate it simply connects every electrical devices with the cable to battery terminals, such condition also occurs on motor propulsion which only to connect its power distribution system from motor controller to battery terminal, which creates less noise, better efficiency and reliability.

2.2.2. Photovoltaic Generating System and Solar Charge Controller

The area available in the boat for laying photovoltaic array is about 15 m². On this area, it is possible to install 4 Canadian Solar Polycrystalline 260 Wp solar module; this type of panel has a dimensions of 1.280 mm \times 928 mm \times 55 mm, each of the panel weighs 20 Kg; Maximum Power Voltage (V_{mp}) 50.4 V, Maximum Power Current (I_{mp}) 5.15 A, which leads to a Maximum Output Power (WP_{max}) 260 W in Standard Test Conditions. This 4 PV Panel will be connected in separated 2 series arrangement, then into parallel arrangement that will be connected into one solar charge controller. MPPT control technology is widely used in the application of solar power generation. As shown in Figure 2, the output voltage of photovoltaic array can be determined in such way that the corresponding power is the maximum out-power. If the working point is on the left of the maximum power point: $dP/dV > 0$; and if the working point is on the right of the maximum power point: $dP/dV < 0$. Such arrangement is designed to accommodate the usage of single



solar charge controller, MPPT Victron 150 A, which its function is to adsorbing all the energy from every single panel. In conclusion, this PV Panel will produce power up to 1.2 kWh, since this boat electrical system works in 48 Volts system, therefore maximum capacity produce by the PV is:

$$W_{pmax}(\text{Total})/\text{working voltage} = 1040\text{Wh}/48 \text{ V} = 21.667 \text{ A} \quad (1)$$

This amount of energy will be transferred in to battery pack, or when the main propulsion system works in a condition that not exceed maximum charging current from PV Panel then all the energy from PV will be directly use for the propulsion without taking energy from battery. However, there is another way to improve the amount of energy adsorbed, by installing every single panel with its own MPPT Solar charge controller. This arrangement will lead into better efficiency, because if power drop occurs to a panel it will not disturb whole system charging activity, so that power drop only occur at that drooping panel.



Figure 3 260 Wp Polycrystalline PV Panel

3. RESULTS AND DISCUSSION

In order to determine boat service speed and amount of energy used during sailing, it is necessary to recognized how energy flows in a solar boat. As seen on **figure 4**, it shows few components that works related to energy flows and things required to calculate boat service speed. Therefore, providing data of ship resistance is essential to determine boat service speed. In this research, such data will be provided by conducting software simulation using *maxsurf resistance software*. Then, this data will be use in energy consumption and constant speed calculation

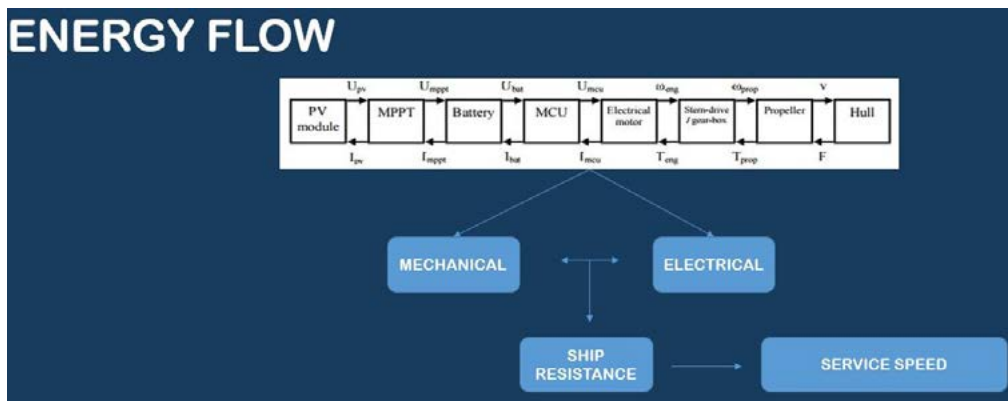


Figure 4 Solar Boat Energy Flow Diagram

3.1. Hull Resistance

To determine the amount of power required by the ship to be able to sail at a certain speed, then the simulation of ship resistance using *maxsurf resistance software* should be performed by using slender body method as a method of analysis of ship resistance. Parameter included in the simulation is 60% efficiency of hull resistance, where the results of this analysis will appear in the form of figure "Power vs. Speed" and the table results of software analysis, which will then be used for data processing of energy consumption analysis and determination of ship speed. The result of *maxsurf resistance software* analysis is shown in Figure 5.

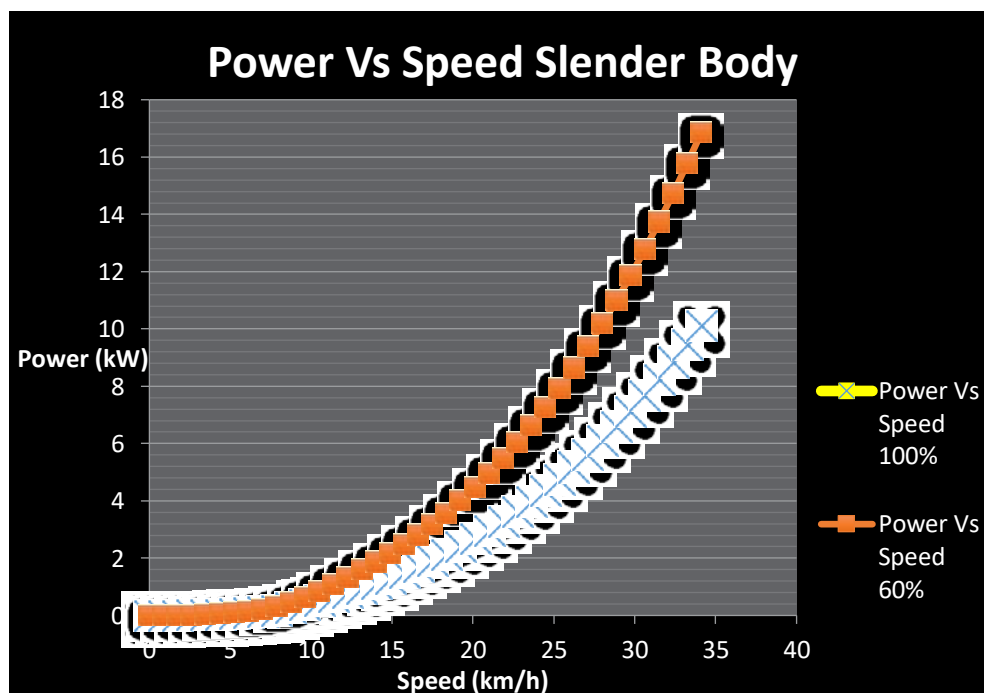


Figure 5 Power vs Speed Maxsurf Resistance Using Slender Body Method



3.2 Electrical Load From Variated Throttle Opening

Using hull resistance data, we could determine amount of power needed by each percentage used in throttle variations of the ship propulsion system in order to match with the ship's operating characteristics. This calculation will follow to the procedure of determining electrical current needed for motor by selected output power divided by electrical system voltage., then obtained the results of data processing as in **Figure 6** and **Table 3**.

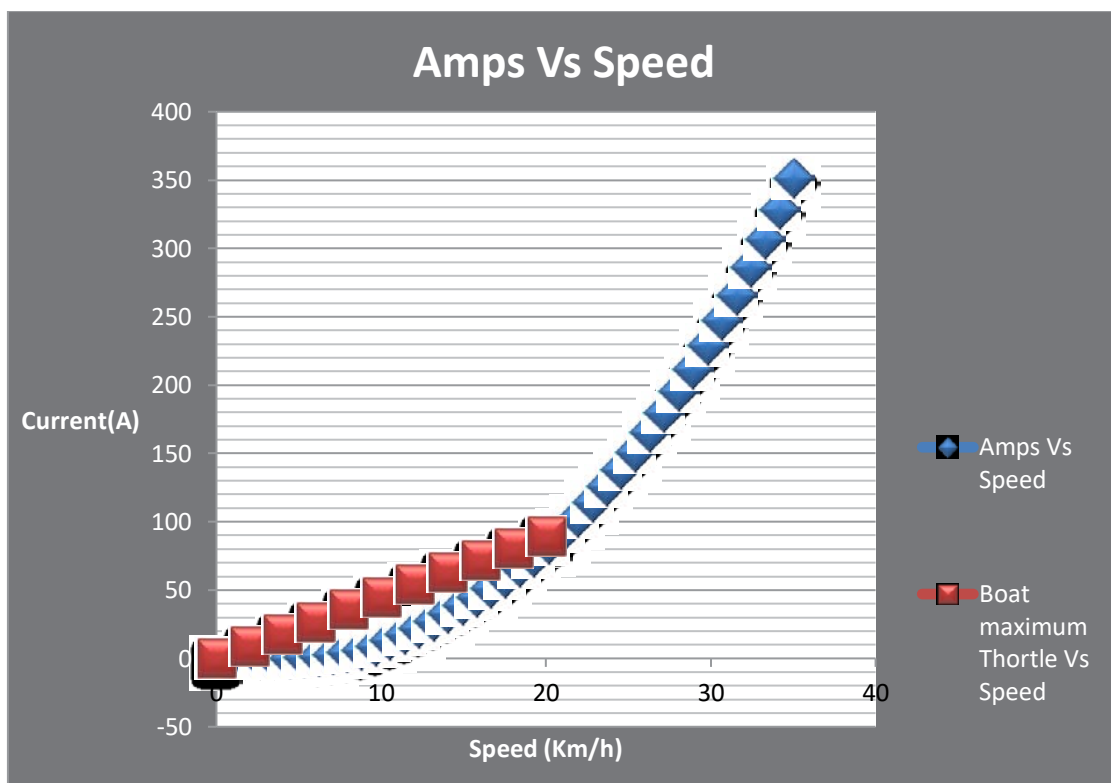


Figure 6 Amps Vs Speed



Table 3 Throttle Variation

Throttle Percentage (%)	Current (A)	Power (kW)	Speed (km/h)
100	89.58	4300	20.67
90	80.63	3870	19.83
80	71.67	3440	18.93
75	67.19	3225	18.44
70	62.71	3010	17.96
60	53.75	2580	16.88
50	44.79	2150	15.71
40	35.83	1720	14.39
30	26.87	1290	12.96
25	22.39	1075	12.18
20	17.92	860	11.42
10	8.96	430	9.58

3.3 Energy Consumption Calculation

After determining the magnitude of the power, the required current of the motor, and the speed of the vessel of each variation of the throttle. Furthermore, the data is processed in accordance with energy consumption procedure, using 60 km sailing range as targeted distance and maximum PV charging current as assumption of daylight condition. With data from sub-chapter 3.1 and 3.2 we will proceed to determine which speed to be used to fulfill 60 km sailing range, in constant speed mode, as shown in **Table 4** and **Table 5**.



Tabel 4. Energy Consumption

Speed (Km/h)	Input Current	Battery Capacity	Output Current (to motor) (A)	Throttle Percentage (%)	Battery Discharge Load(A)
	PV Panel (A)	Battery (80%) (Ah)			
20.67	21.67	26.4	89.58	100	67.92
19.83	21.67	26.4	80.63	90	58.96
18.93	21.67	26.4	71.67	80	49.99
18.44	21.67	26.4	67.19	75	45.52
17.96	21.67	26.4	62.71	70	41.04
16.88	21.67	26.4	53.75	60	32.08
15.71	21.67	26.4	44.79	50	23.13
14.39	21.67	26.4	35.83	40	14.17
12.96	21.67	26.4	26.88	30	5.21
12.18	21.67	26.4	22.395	25	0.73
11.42	21.67	26.4	17.92	20	-3.75
9.58	21.67	26.4	8.96	10	-12.71

Tabel 1. Energy Consumption

Battery Draining Time Until 20%		Sailed Distance (S= Vxt) (Km)	Distance to Travel
Hours	Minutes		
0.39	23 minutes 32 seconds	8.03	51.97
0.45	27 minutes 26 seconds	8.88	51.12
0.53	32 minutes 8 seconds	10.00	50.00
0.58	35 minutes 19 seconds	10.69	49.31
0.64	38 minutes 59 seconds	11.55	48.45
0.82	49 minutes 37 seconds	13.89	46.11
1.14	1 Hour 8 minutes 27 seconds	17.93	42.07
1.86	1 Hour 51 minutes 12 seconds	26.82	33.18
5.07	5 Hours 4 minutes 2 seconds	65.69	-5.69
36.21	36 Hours 12 minutes	> 60 km	> 60 km
Battery Charging	Battery Charging	More than 60 km	>60 km
Battery Charging	Battery Charging	More than 60 km	>60 km



4. CONCLUSIONS

The design of a Solar-Electric Boat for personal use as tourist's recreational vessel along the coast, in the rivers, in the lakes has been presented in detail. With this system, it is possible to replace common type of personal water recreational vehicle. In advance, this design can be a preference for fuel engine to electrical propulsion conversion of passenger vessel, by realizing a loss in power, and without changing the weight and the dimension of the boat. In aspect of new construction, the construction of the boat should be able to handle the boat load design. By optimizing the use of material in accordance with the boat load design, will provide a significant weight reduction and making it more efficient.

This particular boat will able to travel 60 km in constant speed at **30% throttle opening**, which provide the boat with **12.96 km/h** sailing speed and sailing time up to **5 hours 4 Minutes and 2 seconds**. With this performance, this boat will be a perfect candidate to replace common type of water recreational vehicle.

5. ACKNOWLEDGEMENT

This research is funded by PITTA from Universitas Indonesia. Thank you are delivered to Department of Mechanical Engineering - Universitas Indonesia, Naval Architect program study, also Solar Boat Team Universitas Indonesia 2016 who had race in the Netherland that provide us with significant data and experienced to work on this research, and for every party that support the development of this research.

6. REFERENCES

- [1] G.S. Spagnolo, D. P. (2012). Eco Friendly Electric Propulsion Boat. *Journal of Transportation Technologies*, 1-4.
- [2] Kurniawan, A. (2016). A Review of Solar-Powered Boat Development. *Journal for Technology and Science*, 1-8.
- [3] Mahmud, K. (2014). Design and Fabrication of an Automated Solar Boat. 1-4.
- [4] Salem, A. (2016). TECHNO-ECONOMIC APPROACH TO SOLAR ENERGY SYSTEMS ONBOARD MARINE VEHICLE. *Polish Maritime Research*, 64-71.
- [5] Spagnolo, G. S. (2012). Solar-Electric Boat. *Journal of Transportation Technologies*, 1-6.
- [6] Tukaram, S. (2016). Design and Fabrication of a Solar Boat. *International Journal of Innovation in Engineering Research and Technology*, 1-4.



VISUALIZATION OF WATER FLOW PHENOMENON IN HYDRAULIC RAM PUMP WORKING CYCLE BY DIFFERENT COLORS DYES INJECTION

Made Suarda^{1,5}, I Gusti Bagus Wijaya Kusuma^{2,6}, Made Sucipta³, and Ainul Ghurri⁴
^{1,3,4,6}*Department of Mechanical Engineering, Udayana University, Kampus Bukit Jimbaran
Badung-Bali 80362, Indonesia*

⁵*Doctoral Student of Engineering Science, Udayana University, Denpasar, Bali 80225,
Indonesia*

ABSTRACT

Hydrum (hydraulic ram) pump structure is simple. It consists of two moving parts. They are waste or impulse valve and delivery valve. However, interaction of all elements of hydrum pump system influence each other. This causes a comprehensive understanding of its operation becomes complex. Moreover, a detailed description of this hydrum pump has not been well understood. Hence, numerical analysis or simulations of hydrum pump model that has been done has not been able to describe accurately its phenomena. Therefore, a precise design and mathematical calculations of the hydrum pump has not been establish until now, thus making it still depends on the assumption based on preciding experiences. In order to get the hydrum pump designs, it needs to recognize comprehensively the water flow phenomenon that take place in the hydrum pump working cycles. Therefore, visualization of the water flow characteristic in the hydrum pump is done by constructing a hydrum pump model using a transparent material that is acrylic. In this study, the water flow phenomenon in hydrum pump system is visualized experimentally by three different color dyes injection method. Then, video and pictures recorded for investigating the water flow phenomena in hydrum pump working cycle which includes acceleration, compression, delivery and recoil steps. This work was introduced for the first time and used to investigate water flow phenomenon in the along flow line of the pump. The results show that the water flow characteristic at every step of the hydrum pump working cycle have been investigated. These results are very useful in well understanding of the working principle of hydrum pump, and in developing further analysis and simulation works.

Keywords: Dyes injection; Flow phenomenon; Hydraulic ram; Visualization

1. INTRODUCTION

Hydrum pump (hydraulic ram) is a mechanical pump that works automatically without the use of electrical energy, but use momentum of the driving water flow to pump some of the water into the reservoir (Jenning, 1996). Hydrum pump had been discovered by John Whitehurst in 1771 (Sheikh et al., 2013). The hydraulic ram represents a good alternative to conventional pumping devices with lower initial financial effort (Inthachot et al., 2015). This pump system is a very simple device, consisting of two pipes (drive pipe and delivery pipe), pump body, two valves (waste valves and delivery valve), and an air vessel (Diwan et al., 2016). Therefore, ideally, different combinations of the supply and delivery heads and flows, stroke length and weight of the impulse valve, length to diameter ratio of the drive pipe, volume of the air chamber and size of the snifter valve are parameters design of hydrum pump (Pathak et al., 2016). The design of waste valve is very much

² Corresponding Author. Tel.:+62-83872045869; fax:+62-361773021; E-mail address: wijaya.kusuma@unud.ac.id



15th International Conference on Quality in Research (QiR 2017)

importance aspect in hydram performance (Deo et al., 2016). Moreover, the waste valve is a key component of the hydram, requiring focus and further optimization to improve the overall efficiency of the mechanism (Nambiar et al., 2015). In addition, Yang et al. (2014) proposed a cambered diffuser rather than conical diffuser that connected to the hydram body in order to enhancing it efficiency. In general, a methodology that can be used for the primary design considerations and applications in various ways were proposed by Balguda (2015).

Although its construction is simple, but the flow phenomena actually happened has not been well understood. The first theoretical explanation of the concept of water hammer is used in hydram pump work presented by Zhukovsky in 1898 (Filipan et al., 2003). A rational theoretical analysis of the hydram pump characteristics was first presented by O'Brien and Gosline (1933). By using experimental data of pressure versus time was success to explain the working principle of the hydram pump. The analysis assumed hydram pump cycle in four steps, they are acceleration, compression, delivery and recoil periods, as described by Chi and Diemer (2002) as well. Lansford and Dugan (1941) conducted a similar approach with some improvements, and assume the six-phase of hydram pump cycle. They modify Gosline and O'Brien theory by performing an experiment with. Furthermore, Krol (1951) uses the rigid column theory for the entire of the hydram pump working cycle and uses the static characteristics that measured from valves and pipes in the mathematical models, as well as assumes seven phases in the hydram pump cycle. Krol has proved that it is possible to predict the characteristics of the hydram pump by giving properties of the hydram pump installation that are specified separately. Furthermore, an equation proposed by Alkouhi *et al* (2015) for determining efficiency of hydram pump by using non-linear regression. After comparing proposed equation with the artificial neural network, the proposed equation was validated with numerical model based on Lansford and Dugan's theory and experimental results of Lansford and Dugan tests.

Detailed mechanism of hydram pump operations are not well understood yet. Therefore, Taye (1998) conducted a laboratory test of a hydram pump to determine some parameters associated to hydram pump operation. A draft waste valve designed such that the weight and its stroke can be varied depending on the head of driving water supply. Furthermore, Filipan et al. (2003) create a mathematical model of hydram pump system and explain the simplified working cycle of hydram pump. Because of the flow of water in the hydram pump system is unsteady, then the equation of unsteady flow in a pipe and method of characteristic (MOC) is used.

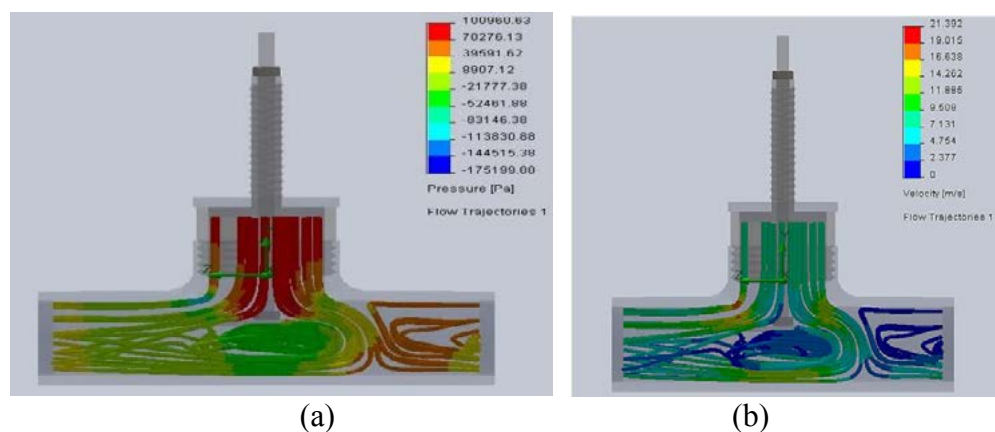


Figure 1 Pressure (a) and velocity (b) variation in waste valve



15th International Conference on Quality in Research (QiR 2017)

In the latest of this decade, CFD (Computational Fluid Dynamics) simulation methods tends to be used, as was done by Maw and Hte (2014). They created hydam pump design then simulated the phenomenon of water flow through a waste valve with commercial CFD software that is Solid Work software. However, this paper only show the pressure distribution and velocity on the waste valve, as shown in Figure 1, and did not identify any waste valve design influence on the hydam pump performance. Furthermore, analysis of the hydam pump performance using CFD was conducted by Shende and Choudary (2015). Analysis of the hydam pump performance was done by using one of the commercial CFD software ie. Fluent. The simulation results show that the mass flow rate of water through the new design of the waste valve is smaller than the old model, and provide a better performance of hydam pump system. The analytical calculations can be made further simple by writing a computer programme which will help to determine the optimum solution. Modelling and analysis can be carried out using Ansys Fluent software which determines the various design parameters (Sampath et al., 2015).

There is limited information in the literature about experimental flow characterization studies of hydraulic ram pump system. Flow visualization methods are very useful for identifying these deviations from the ideal conditions. Particle Image Velocimetry (PIV), Particle Tracking Velocimetry (PTV), Laser Doppler Anemometry (LDA) and smoke or dye injection are experimental flow visualization methods that have been used for this purpose (Karadeniz et al., 2013). One of the most important contributions was the use of aniline dye to produce colored water in the Osborne Reynolds experiment conducted in 1883.

In a very recent study, Goshayeshi and Chaer (2016) experimentally investigated the flow visualization in a closed-loop OHP which is constructed using a Pyrex glass with kerosene as the working fluid. The phase change phenomena and bubble generation in the heating section were recorded using a high-speed video camera (Panasonic VX87) with frame rate of 100 frames per second. The internal flow pattern in pipe or tube could be studied using flow visualization.

Hitherto, an analysis of the flow in the pump hydam has been done through simulation of hydam pump models using commercial CFD software. Some approaches and assumptions in determining the boundary conditions are often taken. This of course affects the accuracy of the simulation results. Up to this decade, no one work has presented a real condition of flow pattern that actually occur in the hydam pump system. Therefore in this study, the water flow phenomenon in hydam pump system is visualized experimentally by three different color dyes injection method. In addition, the components of the hydam pump system are constructed using clear tube material (acrylic). This visualization work was introduced for the first time for investigating the water flow patterns in the hydam pump system.

2. METHODOLOGY

In this study, an experimental work was carried out on the installation of hydam pump system as shown in Figure 2. All hydam pump components are created using the clear acrylic material. Flow visualization is carried out in water flow throughout the hydam pump model. The water is injected with dyes of three different color liquids through small orifices in the drive pipe of the hydam model so as to act as streamline tracers. The water flow phenomena in the hydam pump was recorded using a high-speed video camera (Sony) with frame rate 120 frames per second. Body



and air vessel of the hydam pump have 50 mm of diameter, and its drive pipe diameter is 25 mm with length of 2270 mm. The tests carried out on the drive head of 980 mm and 1425 mm delivery head. Mass of waste valve mass and delivery valve are 90 gram and 25 gram, respectively.

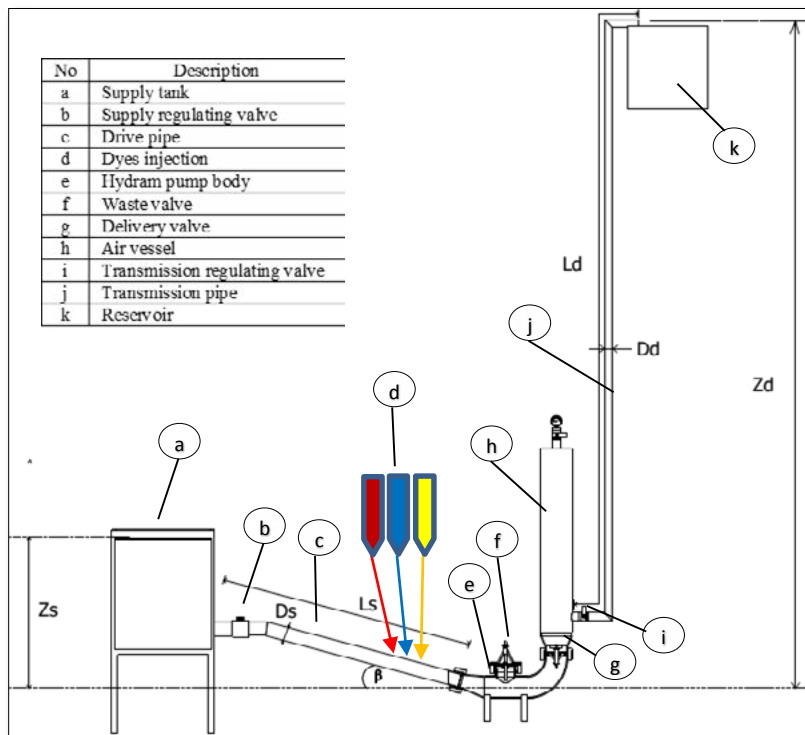


Figure 2 Scheme of the experimental set-up of the hydraulic ram system

3. RESULTS AND DISCUSSION

Based on test results of the hydraulic ram on the drive head of 0.98 m and 1.425 m of delivery head, capacity of waste and pumping water measured is 0.41 liter/second and 0.085 liter/second, respectively. It means that the total efficiency of hydam pump at this operation is about 25%. This is too low. It caused by this pump was just operated at too low head, considering on the material of the pump is constructed using a low strength material that is acrylic. In addition, the low head operation makes low pressure at the valves, hence the valves cannot be closed tightly.

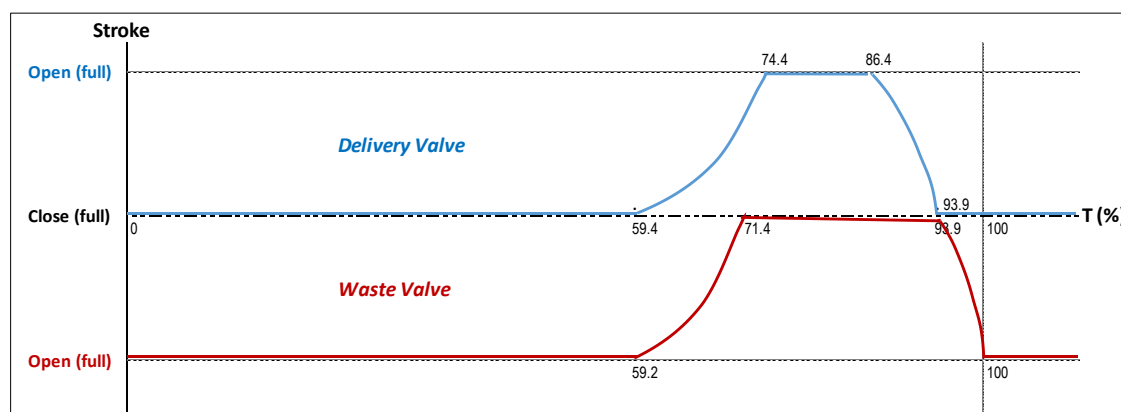


Figure 3 The waste and delivery valves movement in hydam pump cycle



15th International Conference on Quality in Research (QIR 2017)

By extracting video to frames, they show that the hydram pump operates at period of 1.11 seconds per cycle and at frequency of 54 pulses per minute. Furthermore, the period of time (T) of the waste and delivery valves movement can be illustrated as in Figure 3. In addition, the hydram pump operation can be described in four steps. They are acceleration, compression, delivery and recoil.

Acceleration step takes place when waste valve is open and delivery valve is close. The water from the drive tank begins to flow through the drive pipe and out through the waste valve, as shown in Figure 4. The flow of water is accelerated as a result of head of driving water through a drive pipe into the pump body and out through the open waste valve, up to a certain speed is reached in the drive pipeline. At a certain critical speed where momentum of the water flow capable to moving the waste valve, then this valve closes suddenly as a result of hydrodynamic force which overcomes the gravity force of the waste valve that tends to stay in open state. Acceleration step takes place around 0.74 seconds or 0.66 of period of the cycle. In addition, the water flow in drive pipe is turbulent but steady at average Reynolds number about 25,000. Furthermore, the picture shows that the water flow direction from the drive pipe to the tee of hydram pump body is turned at an angle $(180^\circ - \theta)$, where θ is the slope of the drive pipe. Moreover, suction side takes place at upper side of upstream hydram pump body.

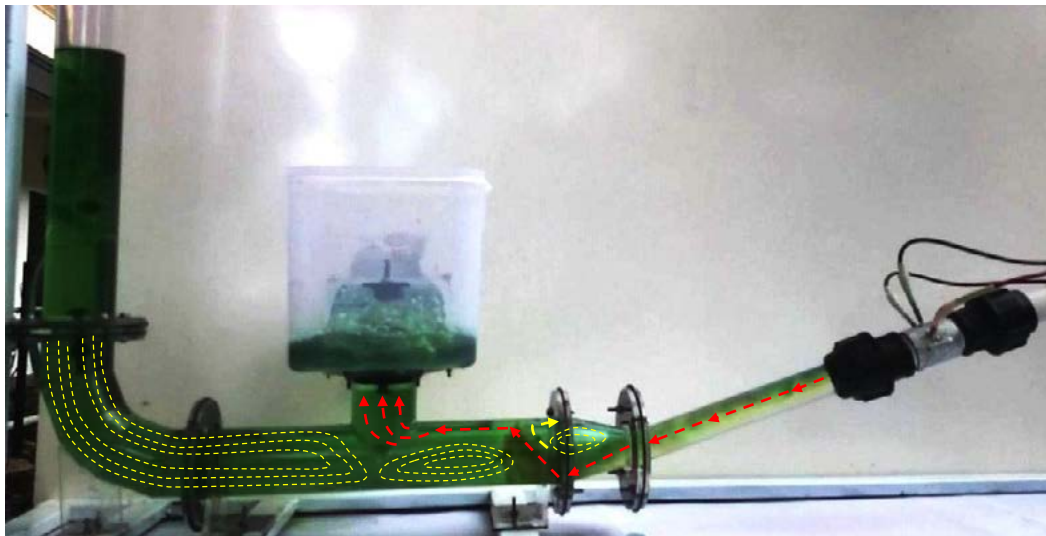


Figure 4 Acceleration step in the hydram pump cycle

The second step is compression, which occurs when a water hammer occurs due to the waste valve to close suddenly while the delivery valve is closed as well, as shown in Figure 5. The high pressure will occur in the pump body. The water can only come out through the delivery valve into the air vessel, then it compresses the air contained within the vessel until the water flow rate to be zero. When the waste valve is close, this causes in the cessation of the water flow and be causing a pressure wave. The water in the drive pipe will generate a great momentum and move in any direction. The water pressure wave will be partially enter the drive pipe and partly compressed in the pump body. Based on the frames of the video, the compression step takes place in very short time, around 0:03 seconds or 0.027 of period of the cycle.

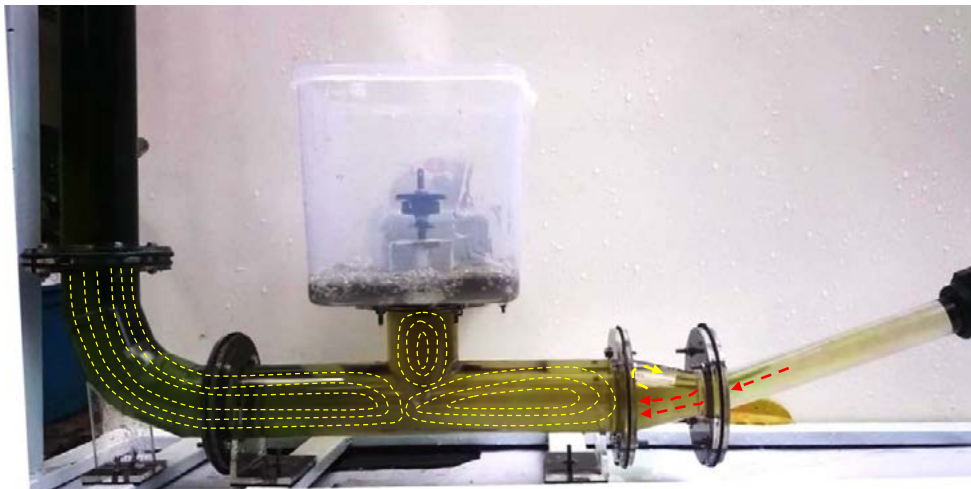


Figure 5 Compression step in the hydam pump cycle

The following step is delivery. This step takes place when the waste valve is closed and the delivery valve is open. The compressed air in the air vessel will press the water in the tank into the delivery pipe and then flows into the reservoir, as shown in Figure 6. The high increase in the pressure enter into the air vessel through the open delivery valve until the water in the drive pipe are in balance condition and the pressure in the pump body decreases. The delivery valve will be closed and stop the flow of water to the pump body, therefore, causing water flow towards the delivery pipe. Moreover, the frames of the video show that the suction side takes place at the upper side of the downstream hydam pump body. Furthermore, the delivery step takes place around 0:15 seconds or 0.135 of period of the cycle.

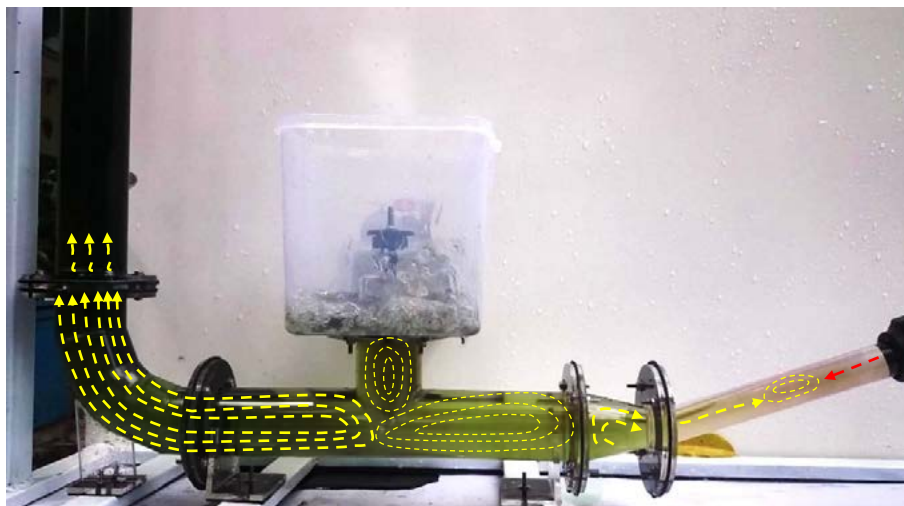


Figure 6 Delivery step in the hydam pump cycle

The final step is recoil. After the pressure of water above the delivery valve is higher than the static pressure of water in the pump body, the valve will close and the water flow into the air vessel will stop and then move back into the drive pipe. The water flow backs from the pump body into the drive pipe is clearly appear in the frames of the video. This will result in the pressure in the pump body will be low and the waste valve due to load the waste valve opens automatically and water will flow again through the waste valve. Hydam pump cycle will be repeated again.



15th International Conference on Quality in Research (QiR 2017)

Furthermore, based on the frames that are extracted from the high-speed video, the water flow phenomena in hydram pump system such as the shape and direction of flow, separation region, a back flow, and period time of every parameter of flow phenomena can be identified. The data will be very useful as a consideration in developing a CFD simulation.

4. CONCLUSION

The visualization of water flow phenomena in hydraulic ram pump using a transparent material of the pump construction and equipped with different color dyes injection has been shown the water flow characteristic at every step in over whole the cycle. Furthermore, the period of time of the waste and delivery valves stroke can be illustrated. These results are very useful in well understanding of the working principle of hydram pump, and in developing further analysis and simulation works.

5. REFERENCES

- Alkouhi, R., Ara, B.L., dan Keramat, A. 2015. Determine the Efficiency of Hydraulic Ram Pumps. E-Proceedings of the 36th IAHR World Congress. 28 June – 3 July. Netherland.
- Balguda, R.D., *et al.* 2015. Designing of Hydraulic Ram Pump. International Journal of Engineering and Computer Science. Vol 4 No 5, pp. 11966-11971
- Chi M., dan Diemer, P. 2002. Hydraulic Ram Handbook. Bremen Overseas Research and Development Association, Bremen
- Deo, A., Pathak, A., Khune, S. and Pawar, M.M. 2016. Design Methodology for Hydraulic Ram Pump. *IJIRST - International Journal for Innovative Research in Science & Technology*, Vol 5, No. 4, pp. 4737- 4745.
- Diwan, P., Patel, A. and Sahu L. 2016. Design and Fabrication of Hydraulic Ram with Methods of Improving Efficiency. International Journal of Current Engineering and Scientific Research (IJCESR), Vol. 3, No. 4, pp. 5-13.
- Filipan, V., Vireg, Z., dan Bergant, A. 2003. Mathematical Modelling of a Hydraulic Ram Pump System. Journal of Mechanical Engineering. In *Strojniski Vestnik*. Vol 49 No. 3, pp 137-149.
- Goshayeshi, H.R. and Chaer, I. 2013. Experimental Study and Flow Visualization of Fe₂O₃/Kerosene in Glass Oscillating Heat Pipes. *Applied Thermal Engineering*, Elsevier Inc. Vol. 103, pp. 1213–1218.
- Jennings, G.D. 1996. Hydraulic Ram Pumps. North Carolina Cooperative Extension Service. Publication Number: EBAE 161-92. North Carolina.
- Inthachot, M., Saehaeng, S., Max, J.F.J., Müllerc, J. and Spreer, W. 2015. Hydraulic Ram Pumps for Irrigation in Northern Thailand. *Elsevier B.V. Agriculture and Agricultural Science Procedia* Vol. 5 (2015), pp.107-114.
- Karadeniz, H.K., Kumlutas, D. and Ozer, O. 2013. Experimental Visualization of the Flow Characteristics of the Outflow of a Split Air Conditioner Indoor Unit by Meshed Infrared Thermography and Stereo Particle Image Velocimetry. *Experimental Thermal and Fluid Science*, Elsevier Inc. Vol. 44, pp. 334–344.
- Krol, J. 1951. The Automatic Hydraulic Ram. *Proceedings of the Institution of Mechanical Engineers*. Vol. 165, pp 53-73
- Lansford, W. M. and Dugan W. G. 1941. An Analytical and Experimental Study of the Hydraulic Ram. *University of Illinois Bulletin*. Vol 38 No. 22.



15th International Conference on Quality in Research (QiR 2017)

- Maw, Y.Y. dan Hte, Z.M. 2014. Design of 15 meter Head Hydraulic Ram Pump. International Journal of Scientific Engineering and Technology Research. Vol 03 No. 10, pp 2177-2181.
- Nambiar, P., Shetty, A., Thatte, A., Lonkar, S., and Jokhi, V. 2015. Hydraulic Ram Pump Maximizing efficiency. International Conference on Technologies for Sustainable Development (ICTSD), 4-6 Feb. 2015, Mumbai – India. Published by IEEE.
- O'Brien, M.P. dan Gosline, J.E. 1933. The Hydraulic Ram. University of California Press.
- Pathak, A., Deo, A., Khune, S., Mehroliya, S. and Pawar, M.M. 2016. Design of Hydraulic Ram Pump. IJIRST - International Journal for Innovative Research in Science & Technology, Vol 2, No. 10, pp. 290-293.
- Sampath, S.S., *et al.* 2015. Estimation of Power and Efficiency of Hydraulic Ram Pump with Re-circulation System. International Journal of Computer-aided Mechanical Design and Implementation. Vol 1 No. 1, pp 7-18.
- Sheikh, A., Handa, C.C., dan Ninawe, A.P. 2013. A Generalised Design Approach for Hydraulic Ram Pump: A Review. International Journal of Engineering & Science Research. Vol 3 No. 10, pp. 551-554.
- Shende, P.B., Choudhary, S.K. dan Ninawe, A.P. 2015. Analysis and Enhancement of Hydraulic Ram Pump Using Computational Fluid Dynamics (CFD). International Journal for Innovative Research in Science & Technology. Vol 2 No. 3, pp 109-133
- Taye, T. 1998. Hydraulic Ram Pump. Journal of the ESME. Vol. 2 No. 1, Addis Ababa, Ethiopia.
- Yang, K.L., *et al.* 2014. Design and Hydraulic Performance of a Novel Hydram. 11th International Conference on Hydroinformatics. New York, 8 January 2014. Paper no 108.



SIMULATION STUDY ON THE ESTIMATION OF ENERGY CONSUMPTION OF REFRIGERATED CONTAINER

Muhammad Arif Budiyanto ^{a*}, Nasruddin ^a, Fariz Zhafari ^b

^a *Department of Mechanical Engineering, Universitas Indonesia, Indonesia*

^b *Undergraduate Student at Department of Mechanical Engineering, Universitas Indonesia*

**Corresponding author arif@eng.ui.ac.id*

ABSTRACT

Refrigerated containers account for half of the total electricity consumption by storage yards and that this is expected to increase continuously each year. A refrigerated container is a special cargo container equipped with an integral refrigeration unit. The amount of power consumption of the refrigerated container will change depending on many external variables. Environmental factors mainly solar radiation received on the container walls caused surface temperatures increase will then affect the power consumption. This paper provides a simulation study on the estimation of energy consumption of refrigerated container. The simulation model performed on the building-design energy analysis used Integrated Environmental Solution (IES) software packages. The geometry of simulation model considers the actual dimension of refrigerated container consists of insulation walls in the three-dimensional analysis. Physical properties of the insulation walls and environmental factors used weather data are applied to the simulation model as parameter inputs. Estimation of energy consumption of the model based on the calculation of cooling load from the object considers the thermal effect from the sun energy. The measurement data from the experimentation was conducted by Shinoda and Budiyanto (2016) used as validation of simulation model. The comparison of energy consumption from simulation and measurement shows in shows in good agreement.

Keywords: Refrigerated container; Energy simulation; Energy consumption; Energy analysis; Environmental factors

1. INTRODUCTION

The growth of container traffic pushes container port to develop port infrastructure towards performance improvement. Nowadays reduction of energy consumption has been become trending issue in container port sector to cut greenhouse gas effect. Reduction of energy consumption has direct impacts on emissions, minimizing the environment effect and reducing operational costs. A greenhouse gas emitted from ships and cargo handling operations during at port for loading and unloading cargo. Some methods for greenhouse gas reduction has been implemented, such as electric power supplied system to rubber tired gantry crane, hybrid model straddle carriers instead of conventional straddle carriers and a trial system of roof shade for refrigerated container to reduce a load of solar insolation (Shinoda & Budiyanto, 2016).

Related to electricity consumption, refrigerated container facility has contributed the highest energy consumption in container terminal (Greencranes 2013). A refrigerated



container is a special cargo container equipped with an integral refrigeration unit. Electricity is used to run refrigeration system and to remove heat from the internal environment of the container. The amount of energy consumed by refrigerated will change depending on many external variables. These include the ambient air temperature and humidity, location of the refrigerated container, the age of the container, the refrigerant used and refrigeration technologies used (Wilmsmeier 2012). Electric power consumption by refrigerated container is key parameter to measure the energy consumption of this equipment will then become benchmarking value for development of energy saving in this area.

Several studies has been performed to measure energy consumption of refrigerated containers under given conditions for a fixed time (Jolly et al. 2000), Wild (2009) and Shinoda & Budiyanto (2016). Jolly et al. (2000) measured the energy consumption of refrigerated containers has values between 4.42 kW and 8.63 kW depend on the inside temperature setting. Wild (2009) was performed measurement experience of 20 feet and 40 feet refrigerated containers estimated the energy consumption was around 3.6 kW per TEU. Shinoda & Budiyanto (2016) was measured the high cube refrigerated container under the exposed of solar radiation consumed energy about 7.2 kW/h. Looking from these various values of energy consumption by refrigerated container, the estimation study by simulation will take benefit for further energy analysis in container terminal operation.

In order to predict energy consumption of refrigeration container, numerical analysis using building-design energy simulation will provide an overview of the thermal performance of the circumstances object therefore calculation of energy consumption in various condition can be estimate.

This paper aims to estimate the energy consumption of refrigerated container in the fixed condition by simulation model. The simulation model based on finite difference approach to the solution of the heat diffusion equation. A simulation model of high cube refrigerated container carried out to evaluate heat load on the refrigerated container. Physical properties of the insulation walls and environmental factors used weather data applied to the simulation model as parameter inputs. Furthermore, the validation of simulation result uses measurement data from the experimentation was conducted by Shinoda and Budiyanto (2016).

2. SIMULATION MODEL

The estimation of energy consumption was performed by means of a building energy modeling using Integrated Environmental Solution – Virtual Environment (IES-VE) software packages. IES-VE simulation is a dynamic thermal simulation program based on first principles mathematical modelling of the heat transfer processes occurring within and around a building. The simulation results provides an environment for the detailed evaluation of building and system designs, allowing them to be optimized with regard to comfort criteria and energy use. The calculation process of this simulation study shown in the Figure 1.

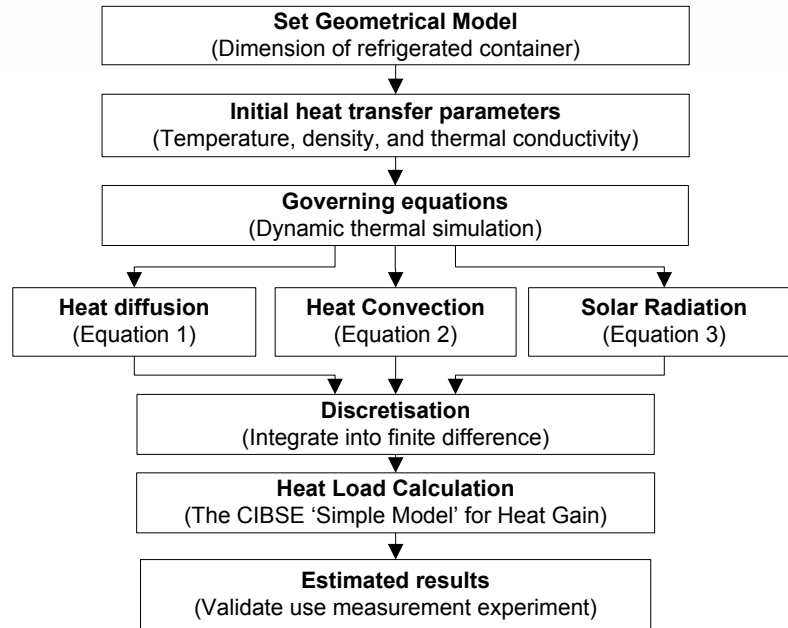


Figure 1 Calculation process of the simulation study

2.1. Governing equations

The heat transfer processes such as conduction, convection and radiation for each element of the building fabric are individually modelled and integrated with models of container heat load. The set of governing equations of the simulation models describes as follows:

- a. The heat diffusion

$$\nabla \cdot (\lambda \nabla T) = \rho c \frac{\partial T}{\partial t} \quad (1)$$

- b. Heat Convection

$$W = h_c (T_a - T_s) \quad (2)$$

- c. Solar Radiation

$$I_g = I_{df} + I_b \sin \alpha \quad (3)$$

Where in Equation 1, T is the temperature ($^{\circ}\text{C}$) in the solid at position and time t , λ is the conductivity of the solid ($\text{W}/\text{m}^2\text{K}$), ρ is the density of the solid (kg/m^3), c is the specific heat capacity of the solid (J/kgK). In Equation 2, W is the heat flux (W/m^2) from the air to the surface, T_a is the bulk air temperature ($^{\circ}\text{C}$), T_s is the mean surface temperature ($^{\circ}\text{C}$), and h_c is the convective heat transfer coefficient. Thus in Equation 3, I_g is the total solar flux (W/m^2) on the horizontal plane, I_{df} is the diffuse sky solar flux (W/m^2) on the horizontal plane, I_b is the solar flux (W/m^2) measured perpendicular to the beam and α is the solar altitude. In this study the simulation model is driven by real weather data measurement. For these purposes, the value of diffuse sky solar flux and beam solar flux was deliberately taken from experimental measurement on the certain time.



2.2. Geometrical model and parameter inputs

The geometry of simulation model considers the actual dimension of high cube refrigerated container consists of insulation walls in the three-dimensional analysis. The dimension of high cube refrigerated container is 12.1 meter length, 2.4 meter width and 2.8 meter height. The structures is consisted ceiling wall, side walls, floor, and corner metal casting foundation. Inside space of refrigerated container mainly serves as the cargo hold, with the floor is equipped with T-grating functioned as air circulation from the refrigeration system which attached at the end of the spaces. Figure 2 shows the illustration of the simulation model.

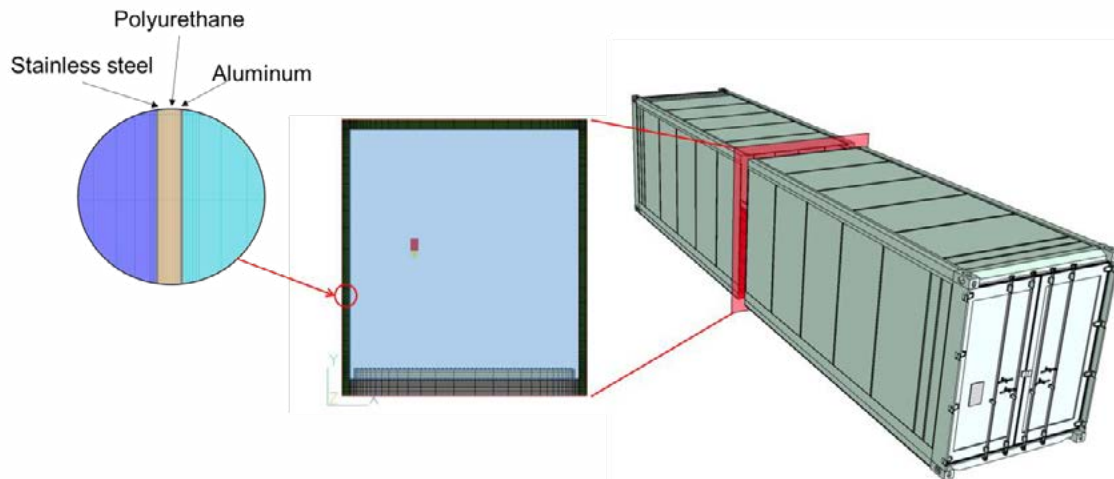


Figure 2 Geometrical model of the simulation study

For the instance of physical parameter inputs uses the design specification obtained from manufactured catalogs. Refrigerated container are constructed from the container walls are composed from three material layers that are aluminium, polyurethane and stainless steel with the thickness is 0.8 mm, 90 mm and 0.9 mm, respectively. The thermal conductivity of these material are 204 W/mK, 0.03 W/mK and 16 W/mK, respectively. Container design data available from the manufacturer is minimum inside temperature of -0°F (-18°C) and maximum outside temperature of 100°F (38°C). The overall heat transfer rate is 7,556 BTU/hour (1,904 kcal/hour) with a U-Factor is 75.0 BTU/hour $^{\circ}\text{F}$ (34 kcal/hour $^{\circ}\text{C}$). The exterior surface is composed from aluminium panel with flat surface, and all surfaces is painted with white color. Table 1 shows the physical parameter inputs of the simulation model in this study.

Table 1 Parameter inputs for the material properties of the simulation model

Material	Thickness	Thermal Conductivity
Aluminium	0.8 mm	204 W/mK
Polyurethane	90.0 mm	0.003 W/mK
Stainless steel	0.9 mm	16 W/mK



3. RESULTS AND DISCUSSION

The results of simulation model are presented here. Simulation results are provide the estimated value of energy consumption in one day and one year operation for a high cube refrigerated container. The estimated result of energy consumption in one day operation was compared with the measurement experiment data by Shinoda & Budiyo (2016). The measurement data on 15th August 2015 has been chosen as comparison since the weather condition on this day has clear sky condition which mean the global solar radiation emitted in the peak intensity.

Validation of simulation result and measurement data carried out to produce an accurate and credible model for further estimation of energy consumption. The simulation result was validated by measurement data at specific hours during the day's operations. The validation of the simulation was assessed by determining mean absolute error (E_{MAE}). The equation for E_{MAE} determination can be expressed as:

$$E_{MAE} = \frac{1}{n} \sum_{i=1}^n |P_m - P_e| \quad (4)$$

Where P_e is estimated energy consumption and P_m is measured energy consumption, n is the number of population. In order to ascertain the simulation result appertain in the confidence level, 99% confidence interval was predetermined for each validation to ascertain the validity of the simulation model. From the validation result using the Equation 4 obtained the mean absolute error of the simulation model is 0.47 kW. This value described that the difference value between simulation result and measurement data is around 0.47 kW for each ascertain time, therefore with the 99% confidence interval shows it difference values cover for almost estimation point range.

3.1. Estimated energy consumption in one day operation

Energy consumption of a reefer container particular define as the electricity consumption in one day operation. Design of energy consumption of refrigerated container in one day operation prepare inside cargo hold in the empty condition with set temperature into zero degree Celsius. The standard for energy consumption of refrigerated container following the rules of ISO 1496-2:2008 Series 1 freight containers - Specification and testing, Part 2: Thermal containers (ISO, 2008). According this standard, both simulation model and measurement experiment set inside temperature into zero degree Celsius with empty cargo hold. The simulation model performed in the transient time during one day operation provided the estimation of energy consumption each one hour time step.

In this study, the energy analysis for one day operation will use time range between 08:30 AM until 17:30 PM since the solar radiation take an effect to the heat load of the container during this time. Figure 3 shows the comparison value of energy consumption of a high cube refrigerated container between IES-VE result and measurement data. Simulation results estimated the maximum energy consumption around 3.1 kW at 08:30 AM and minimum energy consumption is 2.7 kW at 17:30 PM. The value of energy consumption indicate the amount of energy to remove heat load from the inside cargo effect from the heat penetration due to solar radiation.

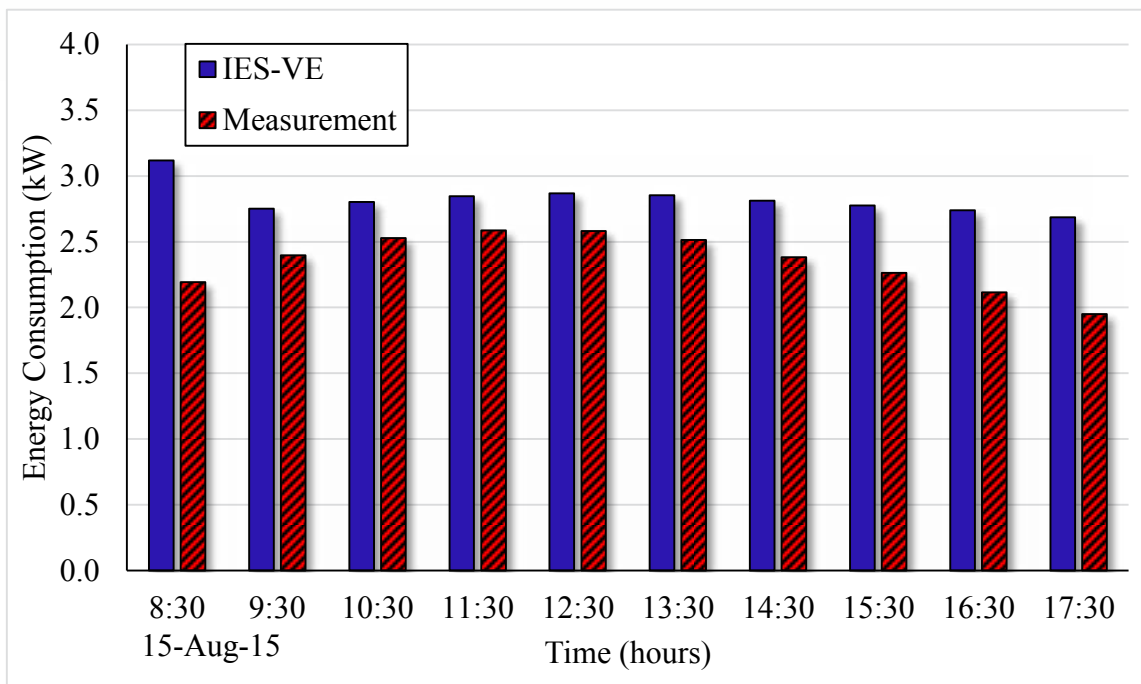


Figure 3 Energy consumption of a high cube refrigerated container in one day operation

The average energy consumption by simulation during one day operation is 2.8 kW, this result consistent with the result conducted by Fitzgerald et al. (2011). The comparison of energy consumption per hour shows that the energy consumption by simulation model has various difference values with measurement data. The highest difference value found at the initial time at 08:30, this circumstances due to simulation model assumed the refrigerated container object prepared as container without pre-conditioning, therefore the heat to be remove in the first calculation higher than other time step. The lowest difference value of energy consumption found in the noonday 11:30 AM, this result give direction of suitable time for the further analysis in the estimation of energy consumption.

3.2. Estimated energy consumption in one year operation

In field of energy analysis in container terminal, the overview of energy consumption in one year operation will provide a direction for the further development of opportunity on energy saving in this area. Concerning this circumstances, in this paper provide the estimation energy consumption of a refrigerated container in one year operation. Figure 4 shows estimated value of total energy consumption of a high cube refrigerated container in one year operation by IES-VE. The maximum of energy consumption of a refrigerated container in one year operation estimated around 0.57 MWh in August, thus the minimum of energy consumption estimated around 0.32 MWh in March. The profile of energy consumption in one year operation following the normal distribution of solar radiation. The trend of energy consumption following the trend of solar radiation which uses in the simulation model as shown in Figure 5. The trend of solar radiation imported from the weather data very influence to the calculation result as heat load from the environment, this result consistent with the result by Budiyanto and Shinoda (2017).

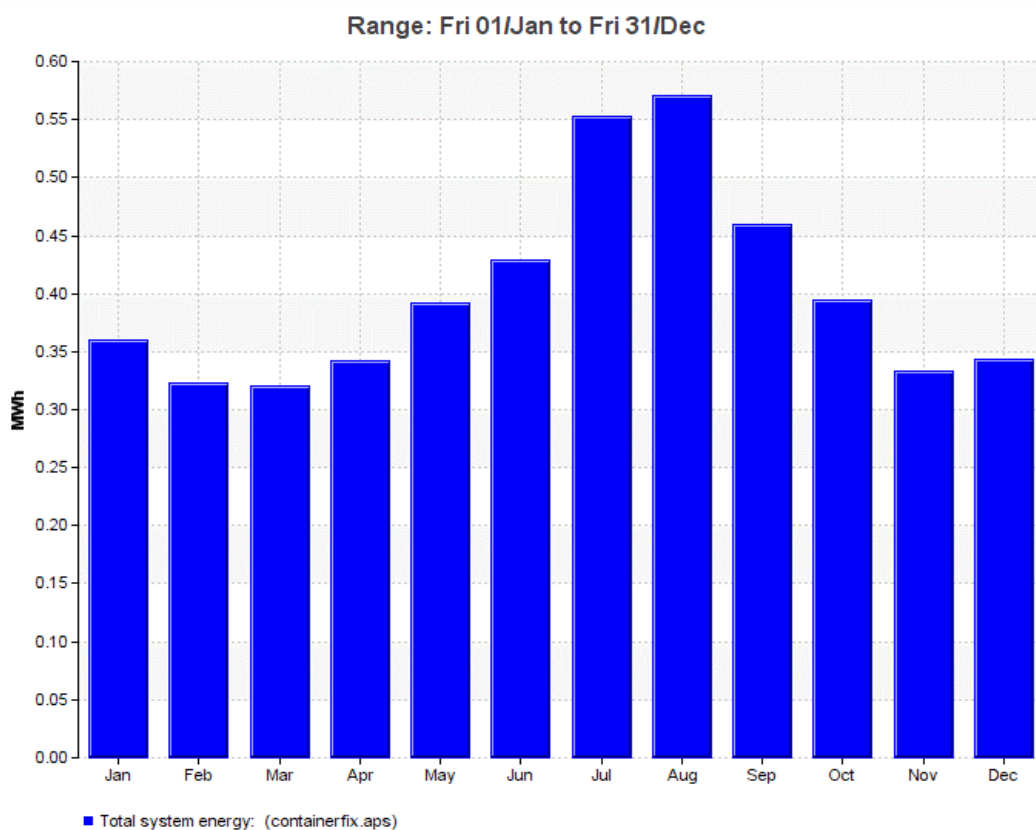


Figure 4 Estimated value of total energy consumption of a high cube refrigerated container in one year operation

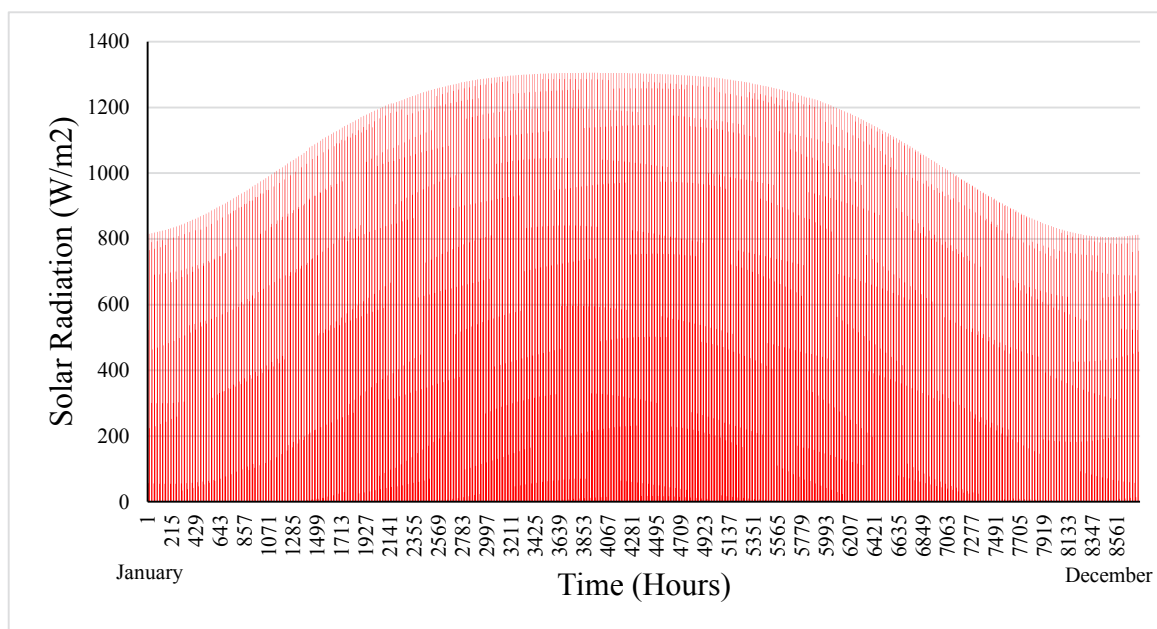


Figure 4 The intensity of solar radiation which uses in the simulation model



4. CONCLUSION

The estimation of energy consumption from a high cube refrigerated container was done performed use IES-VE software packages. The simulation result for one day operation has been validate using measurement data carried out by Budiyanto (2016). From the comparison result shows the simulation results has good agreement with the measurement data with the mean absolute error about 0.47 kW. From the estimation result obtained the average amount of energy to remove heat load inside cargo from the effect of heat penetration due to solar radiation during one day operation is 2.8 kW. Thus, the estimation of energy consumption in one year operation for a cube refrigerated container predicted about 4.81 MWh. Furthermore, this result give a direction for estimation of energy consumption in a container terminal for whole capacity of refrigerated container

5. ACKNOWLEDGEMENT

Authors would like to express our gratitude to Directorate Research and Community Engagement (DRPM) Universitas Indonesia in the providing of publication funding by PITTA 2017. Author also would like to thanks Department of Marine System Engineering, Kyushu University and Hakata Port Terminal Corporation for providing required data on this study. Author also would like to thanks to Department of Mechanical Engineering, Universitas Indonesia for providing the IES-VE software packages.

6. REFERENCES

- Budiyanto, M.A., Shinoda, T, (2017), The Effect of Solar Radiation on The Energy Consumption of Refrigerated Container, *Jurnal Teknologi*, UTM Malaysia.
- Fitzgerald, Warren B., Howitt, Oliver J. A., Smith, Inga J., Hume, A., (2011), Energy Use of Integral Refrigerated Containers in Maritime Transportation, *Energy Policy*, 39(4): 1885–96.
- Greencranes, (2013), Report on Port Container Terminals Energy Profile: Mapping of Port Container Terminals Energy Profile, Valencia.
- ISO, (2008), International Standard: Series 1 freight containers — Classification, dimensions and ratings.
- Jolly, P.G., Tso, Y.W., Wong, S.M. Ng., (2000), Simulation and Measurement on the Full-Load Performance of a Refrigeration System in a Shipping Container, *International Journal of Refrigeration* 23(2): 112–26.
- Shinoda, T., Budiyanto, M.A., (2016), Energy Saving Effect of Roof Shade for Refrigerated Container in Marine Container Terminal, *The Journal of Japan Institute of Navigation*, 134: 103-113.
- Tadeu, A. et al. (2014), Thermal Delay Provided by Floors Containing Layers That Incorporate Expanded Cork Granule Waste, *Energy and Buildings* 68: 611–19.
- Wild, Yves., (2009), Refrigerated Containers and CA Technology. *Container Handbook*, The German Insurance Association, Berlin, Germany.
- Wilmsmeier, Gordon., (2012), Energy Consumption and Efficiency : Emerging Challenges from Refrigerated Trade in South American Container Terminals, *FAL* (329): 1–9.



EFFECTS OF THE AIR MASS FLOW RATE ON THE DISTRIBUTION OF SOLIDS IN THE CIRCULATING FLUIDIZED BED BOILER USING CFD SIMULATIONS

Asyari Daryus^{a,b}, Ahmad Indra Siswantara^{a,*}, Budiarmo^a, Gun Gun R. Gunadi^{a,c}, Hariyotejo Pujowidodo^{a,d}, Candra Damis Widiawaty^c

^aDepartment of Mechanical Engineering, Universitas Indonesia, Depok, Indonesia

^bDepartment of Mechanical Engineering, Universitas Darma Persada, Jakarta, Indonesia

^cDepartment of Mechanical Engineering, Politeknik Negeri Jakarta, Depok, Indonesia

^dBadan Pengkajian dan Penerapan Teknologi (BPPT), Indonesia

ABSTRACT

The purpose of the study is to investigate the effects of air mass flow rate on the optimum distribution of solid phase. The CFD simulations used the Eulerian (granular) model to calculate the motion of particles and the standard $k-\varepsilon$ turbulence model to simulate the fluid flows. The simulations were carried out using six different air mass flow rates based on the excess air of the reactions. The air mass flow rate influenced the distribution and the velocity of solid phase, and also the pressure difference of gas inside the boiler. The results showed that the excess air between 10% - 20% gave the optimum results.

Keywords: Circulating fluidized bed boiler; excess air; distribution of solid; CFD simulations.



1. INTRODUCTION

Circulating Fluidized Bed boiler (CFB boiler) is a boiler that uses solid particles to enhanced the combustion process. Because of its superior heat and mass transfer, this type of boilers are used for wide range of applications, such as steam turbine system, oxyfuel combustion, gasification and combustion of biomass, drying of solids, etc. (Adamczyk, Weceł, Klajny, & Kozolub, 2014; Bakshi, Altanantzis, Glicksman, & Ghoniem, 2017; Ngoh & Lim, 2016). Design and performance optimization of this type of boiler is still challenging because there is still limitation for diagnostic tools and technique in the harsh condition where the boiler installed (Bakshi et al., 2017). Recently, many researches have been conducted in multiphase, multiscale modeling using Computational Fluid Dynamics (CFD), which can accurately calculate and simulate thermodynamics and fluid properties.

Using CFD to simulate the combustion processes and fluid flow has many advantages, such as low cost and save time, because it does not require expensive, and complex experiments to collect data, but rather a set of equipment that used to compute the numerical calculations (Daryus, Siswantara, Darmawan, Gunadi, & Camalia, 2016; Siswantara, Daryus, Darmawan, Gunadi, & Camalia, 2016). It also can calculate and provide data faster because there is no time to be spent to build the complex experiments apparatus.

Zhao et.al. has investigated the effect of exit geometry of high-density CFB risers using CFD. He concluded that the type of exit had the significant effects on the bed hydrodynamics while the cavity height of abrupt exit, the curvature-diameter of smooth exit and horizontal tube connecting the exit and the primary cyclone did not. The decrease of the diameter of abrupt exit tube increased the solids holdup significantly (Zhao, Zhou, Wang, & Li, 2015). Adamczyk et.al. has investigated the measured and numerical results of air-fuel combustion process with large scale industrial CFB boiler. The results showed that the comparison of the pressure and temperature distributions gave comparable trends in contrary to measured data (Adamczyk et al., 2015). Zi et.al. has conducted the CFD simulation of solid oscillation in two-dimension CFB. Their results showed that the solid oscillation circulation was influenced by the formation of the slugging in the downner and resulted the pressure drop in the downner and sharp increase of the riser bypass gas velocity. It also showed that the lateral solids volume distributions were uniform in the riser and in the downner (Zi et al., 2017).

This aim of this research is to find the optimum of air mass flow rate or excess air in the CFB boiler by investigating their effects on solid particle using CFD simulations.

2. COMPUTATIONAL MODEL

2.1. Combustion Model

The Westbrook-Dryer one-step model is used for combustion. It gives a good estimation of indicator of the expected temperature levels. The Finite Rate and Eddy Dissipation model is used to model the process of the turbulent non-premixed combustion. In this model, the reaction rates are assumed to be controlled by the turbulence, avoid the complex Arrhenius chemical kinetic calculations.



Coal is used in this CFB boiler. The chemical reaction of combustion is:



2.2. Turbulence Model

To simplify the complexity of the Navier Stokes equations for fluid flows, the Reynolds Average Navier Stokes (RANS) principle is developed and results 6 additional stresses to the Navier Stokes equations called Reynolds stresses. Some models are then developed for RANS equations to obtain the simpler calculations.

One of the RANS turbulence models is k - ϵ ., where it is simple (only needs the input of boundary condition only), stable, widely validated, and suitable for industrial problems solutions. This model uses the Boussinesq formula to find the Reynolds stresses, i.e. (Versteeg & Malalasekara, 2007):

$$\tau_{ij} = -\rho \overline{u_i' u_j'} = \mu_t \left(\frac{\partial U_i}{\partial x_j} + \frac{\partial U_j}{\partial x_i} \right) \quad (2)$$

where ρ is the density, u' and U is the fluctuating and mean velocity vector respectively, and μ_t is the turbulent or eddy viscosity. The turbulent viscosity can be calculated by:

$$\mu_t = \rho C_\mu \frac{k^2}{\epsilon} \quad (3)$$

Where C_μ is constant, k is the transport of kinetic energy, and ϵ is the transport of dissipation. The transport equation of kinetic energy is formulated as (Versteeg & Malalasekara, 2007):

$$\frac{\partial(\rho k)}{\partial t} + \text{div}(\rho k \mathbf{U}) = \text{div} \left[\frac{\mu_t}{\sigma_k} \text{grad } k \right] + 2\mu_t E_{ij} \cdot E_{ij} - \rho \epsilon \quad (4)$$

While the transport equation of dissipation is:

$$\frac{\partial(\rho \epsilon)}{\partial t} + \text{div}(\rho \epsilon \mathbf{U}) = \text{div} \left[\frac{\mu_t}{\sigma_\epsilon} \text{grad } \epsilon \right] + C_{1\epsilon} \frac{\epsilon}{k} 2\mu_t E_{ij} \cdot E_{ij} - C_{2\epsilon} \rho \frac{\epsilon^2}{k} \quad (5)$$

Where \mathbf{U} is the velocity vector, E_{ij} is the mean rate of deformation, if i or $j = 1$ corresponds to the x -direction, i or $j = 2$ the y -direction and i or $j = 3$ the z -direction, C_μ , σ_k , σ_ϵ , $C_{1\epsilon}$, and $C_{2\epsilon}$ are constants. Constants used in the numerical calculations are $C_\mu = 0,09$; $\sigma_k = 1,00$; $\sigma_\epsilon = 1,30$; $C_{1\epsilon} = 1,44$ dan $C_{2\epsilon} = 1,92$.

2.3. Geometry and Meshing

The geometry of CFB boiler is shown on Figure 1. While Figure 2 shows the 2D structured mesh model. The mesh consists of 42x162 cell.



2.4. Boundary Conditions

In this geometry model, the primary air (inlet 1) is located on the bottom of the boiler, while the secondary air (inlet 2 and 3) are located in the left and the right of boiler. The rate of coal assumed to be 14.4 ton/h, equivalent to 25 MW power output of generator, driven by the steam produced by the boiler. Based on the stoichiometry calculations, the air mass flow needed for the combustion is 20.10 kg/s. The velocity of air for the inlets for various value of excess air can be seen on Table 1.

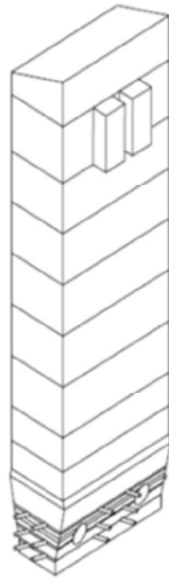


Figure 1 CFB Boiler geometry

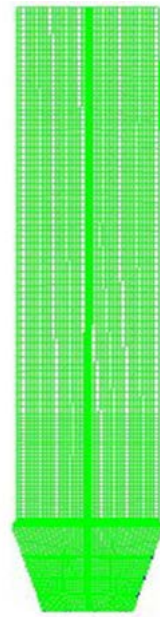


Figure 2. 2D mesh model of CFB Boiler.

Table 1 The value of inlet velocities

<i>Excess Air (%)</i>	<i>Air Flow (kg/s)</i>	<i>Inlet 1 (m/s)</i>		<i>Inlet 2 (m/s)</i>		<i>Inlet 3 (m/s)</i>	
		v	u	v	u	v	
0	20,10	12,7	-12,4	-12,4	13,1	-13,1	
10	22,22	12.7	-14,5	-14,5	15,2	-15,2	
15	23,14	12.7	-15,5	-15,5	16,2	-16,2	
20	24,05	12.7	-16,5	-16,5	17,2	-17,2	
25	25,03	12.7	-17,5	-17,5	18,3	-18,3	
30	26,03	12.7	18,6	18,6	19,4	-19,4	



3. RESULTS AND DISCUSSION

It has been conducted the fluid flow simulations in various excess air value, i.e. 0% (air mass flow 20.1 kg/s), 10% (air mass flow 22.22 kg/s), 15% (air mass flow 23.14 kg/s), 20% (air mass flow 24.05 kg/s), 25% (air mass flow 25.03 kg/s), and 30% (air mass flow 26.03 kg/s). The results of simulations presented here are taken on 35 second of operation, because it is assumed that the flow of fluid at this time has reached the stable condition.

The contour of solid volume fraction for various excess air values is shown on Figure 3. It can be seen that for the low value of excess air (0% of excess air), the solid particles are existing around the bottom of boiler, and for the higher value of excess air, the solid particles move upward, proportional with the value of excess air. This upward movement was driven by kinetic energy of air. For the value of excess air between 0% - 15%, the height of solid movement does not exceed the height of fire brick (sloping wall or elbow on the figure), but above of 20% of excess air, its height exceed it. When the solid particle height exceeds the firebrick, it will hit the boiler tube and will cause abrasion. This situation is not preferable. So, the optimum results of solid particle height is between 0% - 20% of excess air.

Figure 4 shows the contour of solid velocity in various values of excess air. For the excess air below 20%, the situations are safe, because the solid particle exists in the firebrick area. But for the excess air of 20% and above, the situations began to worry because the solid particles exist on the wall tube area and their velocity is more than 5 m/s; this conditions can cause the abrasion on the wall tubes. It is also shown that the flow of particles are deflected to the left side, resulting in the left wall tube will experience more abrasion than the right one. The optimum results are achieved by excess air below 20%.

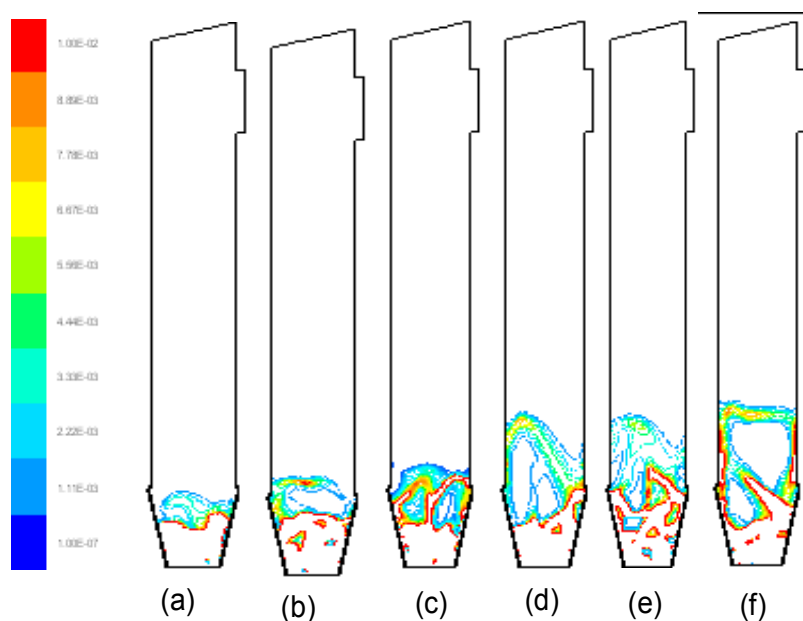


Figure 3. Contour of volume fraction at $t=35$ s for various excess air. (a) 0%; (b) 10%; (c) 15%; (d) 20%; (e) 25%; and (f) 30%.

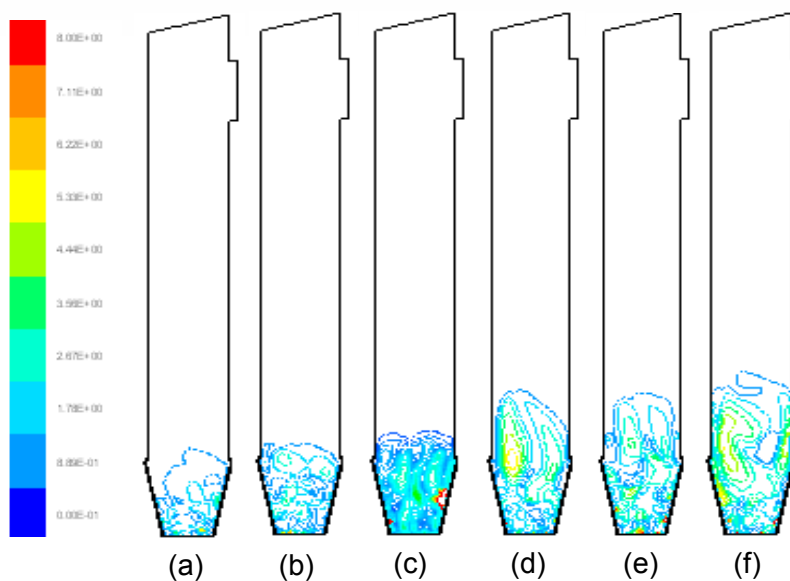


Figure 4. Contour of velocity of particle (m/s) at $t=35$ s for various excess air. (a) 0%; (b) 10%; (c) 15%; (d) 20%; (e) 25%; dan (f) 30%.

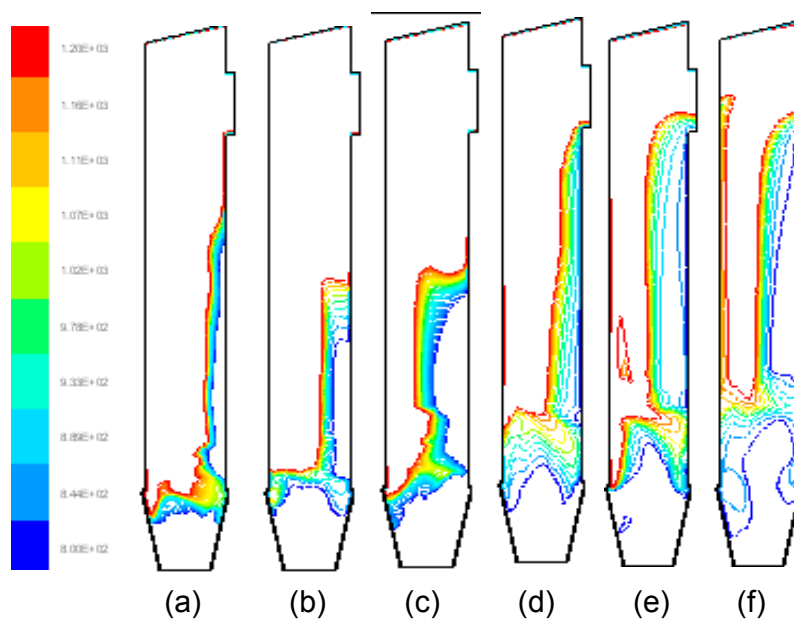


Figure 5. Contour of temperature of particle (K) at $t=35$ s for various excess air. (a) 0%; (b) 10%; (c) 15%; (d) 20%; (e) 25%; dan (f) 30%.

Figure 5 shows the contour of solid particle temperature for various values of excess air. For small value of excess air, the distribution of high temperature concentrated on left wall and extended to the near of right wall. The right wall has lower temperature than that of left wall. When the value of excess air increased, the high temperature area moves from the



right to the left and from the bottom to the top. But, as shown on Figure 4 and 5 that the most of the solid particles exist on the bottom area for all the value of excess air, resulting in the coal will be burnt efficiently (the white color in the bottom area is the high speed solid particle zone, the contour or color can not be seen because its value exceed the limit of velocity scale).

The simulation results for pressure difference between inlet (bottom) and outlet (top) is shown on Figure 6. These values are the average values of pressure difference for 30 seconds and 35 seconds. The pressure is constant for the value of excess air of 0% - 10% but then decrease and minimum on the value of excess air of 15%. Above 15%, its values are increase and maximum on the value of excess air of 20% and then decrease slowly afterwards. The best values of the pressure differences exist between the value of excess air of 0% - 17%.

Meanwhile, the wall tube heat absorbing efficiency is shown on Figure 7. It can be seen that the efficiency is decrease when the value of excess air is increase, except for the value of excess air below 10%. But this decrement is negligible because so small, less than 1%.

We come to the conclusion. From the contour of the volume fraction, and the velocity of solid particles, the optimum value of excess air is 0% - 20%; while from the contour of the temperature is 0% - 30%. From the pressure difference in the boiler, the best results of excess air is found to be 10% - 17%, but from wall tube heat absorbing efficiency the results are negligible. The conclusion, the recommended value of excess air for this boiler is 10% - 20%.

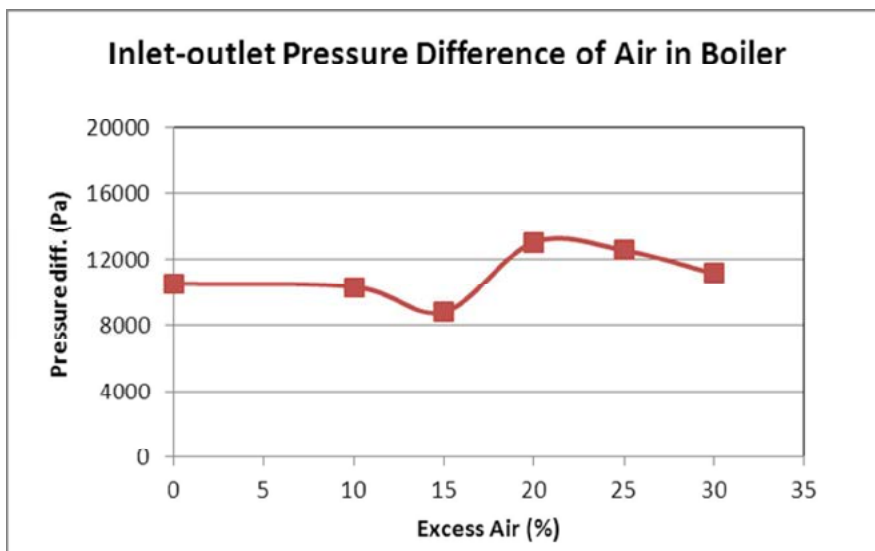


Figure 6. Pressure difference curve in the boiler from simulation results.

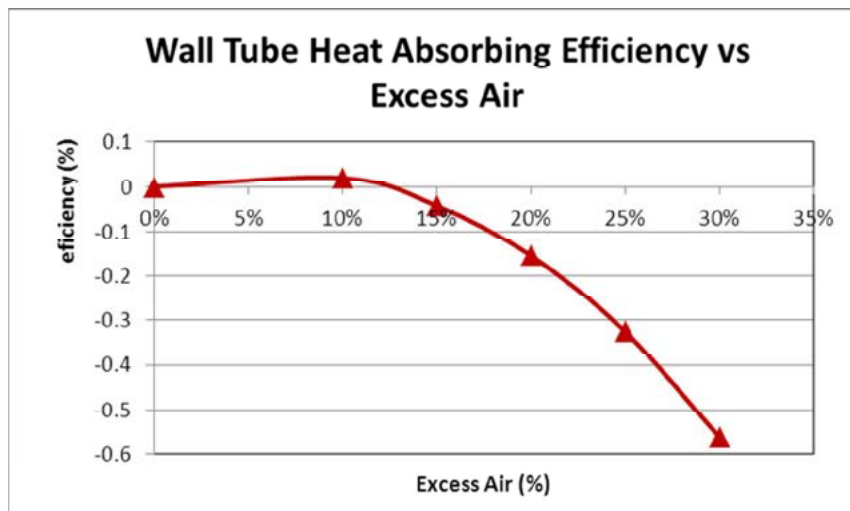


Figure 7. Wall tube heat absorbing efficiency.

4. CONCLUSION

The simulations of combustion and fluid flow in 25 MW Circulating Fluidized Bed (CFB) Boiler have been done to find the optimum value of excess air using CFD. The simulations were done using 2D geometry. The turbulence model used for fluid flow was $k-\varepsilon$, while for the combustion model was Eulerian. From the contour of the volume fraction and the velocity of solid particles, the contour of the temperature of air, the pressure difference of the air in the boiler and from the wall tube heat absorbing efficiency found that the optimum value of excess air was 10% - 20%.

5. ACKNOWLEDGEMENT

The authors would like to thanks DRPM Universitas Indonesia for funding this research through “Hibah Publikasi Internasional Terindeks Untuk Tugas Akhir Mahasiswa UI 2017” and to PT. CCIT Group Indonesia for CFDSOF® software license.

6. REFERENCES

- Adamczyk, Wojciech P., Kozolub, Pawel, Klimanek, Adam, Bialecki, Ryszard A., Andrzejczyk, Marek, & Klajny, Marcin. (2015). Numerical Simulations of the Industrial Circulating Fluidized Bed Boiler Under Air- and Oxy-fuel Combustion. *Applied Thermal Engineering*, Volume 87, pp. 127-136(2015).
- Adamczyk, Wojciech P., Weceł, Gabriel, Klajny, Marcin, & Kozolub, Pawel. (2014). Modeling of Particle Transport and Combustion Phenomena in a Large-scale Circulating Bed Boiler Using a Hybrid Euler-Lagrange Approach. *Journal of Particuology*, Volume 16, pp. 29-40(2014).
- Bakshi, A., Altantzis, C., Glicksman, L.R., & Ghoniem, A.F. (2017). Gas-flow Distribution in Bubbling Fluidized Beds: CFD-based Analysis and Impact of Operating Conditions. *Powder Technology*, (2017).
- Daryus, Asyari, Siswantara, Ahmad Indra, Darmawan, Steven, Gunadi, Gun Gun R, & Camalia, Rovida. (2016). CFD Simulation of Turbulent Flows in Proto X-3 Bioenergy Micro Gas Turbine Combustor Using STD $k-\varepsilon$ and RNG $k-\varepsilon$ Model for



- Green Building Application. *International Journal of Technology*, Volume 7, pp. 204-211(2).
- Ngoh, Jenson, & Lim, Eldin Wee Chuan. (2016). Effects of Particle Size and Bubbling Behaviour on Heat Transfer in Gas Fluidized Beds. *Journal of Applied Thermal Engineering*, Volume 105, pp. 225-242(2016).
- Siswantara, Ahmad Indra, Daryus, Asyari, Darmawan, Steven, Gunadi, Gun Gun R, & Camalia, Rovida. (2016). CFD Analysis of Slurry Flow in an Anaerobic Digester. *International Journal of Technology*, Volume 7, pp. 197-203(2).
- Versteeg, H, & Malalasekara, W. (2007). *An Introduction to Computational Fluid Dynamics, the Finite Volume Method*, 2nd ed. Essex, London: Pearson Educational Ltd.
- Zhao, Bidan, Zhou, Quan, Wang, Junwu, & Li, Jinghai. (2015). CFD Study of Exit Effect of High-density CFB Risers with EMMS-based two-fluid Model. *Chemical Engineering Science*, Volume 134, pp. 477-488(2015).
- Zi, Can, Sun, Jingyuan, Yang, Yao, Huang, Zhengliang, Liao, Zuwei, Wang, Jingdai, . . . Han, Guodong. (2017). CFD Simulation and Hydrodynamics Characterization of Solids Oscillation Behavior in a Circulating Fluidized Bed with Sweeping Bend Return. *Chemical Engineering Journal*, Volume 307, pp. 604-620(2017).



15th International Conference on Quality in Research (QIR 2017)

The Comparison of Performance Of Dimethyl Ether and Diesel Fuel B-20 Dual Fuel System On Diesel Engine Direct Injection System

Cahyo Setyo Wibowo, Maymuchar, Dimitri Rulianto, Faqih S

Researcher, Fuels and Aviation Groups, Research and Development Centre For Oil and Gas Technology, "LEMIGAS" Indonesia,
cahyoswibowo@gmail.com, cahyoswibowo@yahoo.com

Abstract

DME application can include multiple sectors, among others: the transport sector, domestic/household, power generation, but when used as a fuel substitution for diesel engine, modification will be required to the fuel line system. The purpose of this research was to compare the performance of DME as a fuel substitution for diesel oil by applying dual fuel system with B-20 (diesel fuel 80% mix biodiesel 20%) in a diesel engine direct injection system with the B-20 performance. Methodology used is testing the characteristics of DME fuel, diesel fuel (B-0) and B-20. Preparation was done by installing the fuel channel of DME with dual fuel system on the 4-cylinder diesel engine direct injection system. The performance test was done on electricity generator set with load bank and subsequent analysis was done on all assay results.

This research shows that DME fuel on the type of diesel engine with dual fuel system can be used directly if the modification made to the fuel line system. The dual fuel system of diesel fuel and DME on approximately 80% - 20% were able to generate power equal with a diesel engine that use B-20. Utilization of DME as a fuel for diesel engines can reduce emissions in term of opacity in a range of 10% - 20%, thus improving environmental concern.

Keywords: DME, diesel fuel, B-20, diesel engine, dual fuel system

1. INTRODUCTION

Dimethyl ether (DME) is alternative fuel for substitution of diesel fuel from fossil. DME can be produced from natural gas, biomass and coal. The purpose of this research is to compare performance of DME as a fuel substitution for diesel fuel by applying dual fuel system with B-20 (diesel fuel 80% mix biodiesel 20%) in a diesel engine direct injection system.

The most important properties of DME are the presence of oxygen in the fuel molecule, lower ignition temperature, and high cetane number. The kinematic viscosity of DME is significantly lower than that of diesel. However, low lower heating value (LHV), low viscosity, and low lubricity are some of the major disadvantages of DME (Hyun Gu Roh et.al 2017). DME engines can achieve high thermal efficiency and ultra low emissions, and will



play a significant role in meeting the energy demand while minimizing environmental impact (Zhen Huang et.al 2009).

The effective thermal efficiency is decreased, especially for temperature above 40 °C. Before beginning an experiment, the fuel properties of DME, including the density,(Gao Guangxin, et. al 2013).

Dimethyl ether (DME) is regarded as one of the promising alternative fuels or oxygen additives for diesel engines, with its advantages of a high cetane number and oxygen content. Over the past ten years, researchers have begun to consider the use of DME as a fuel. Because its cetane number and ignition temperature are close to that of diesel fuel (Prabhakaran, et.al 2015).

This research shows that the use of DME fuel on the type of diesel engine with dual fuel system can be used directly if modification is made to the fuel line system. A dual fuel of diesel fuel with DME at approximately 80% - 20% were able to generate power equal to a diesel engine that use B-20 with measurement on engine performance , fuel consumption, exhaust emissions (opacity), the stability of the engine operation, and easibility on starting .

2. METHODOLOGY/ EXPERIMENTAL

2.1. Preparation of testing equipment

At first we perform the testing for characteristics of physical and chemical properties of the tested fuel (dimethyl ether and B-20). Preparation of the diesel generator set were done by modification of fuel line system to support with dual fuel, continuing with checking engine all system follow the OEM standard for generator and load bank. Checking also conducted for the test equipment for fuel consumption and emission test. Preparation of the tested fuels including test for gas cylinder used for temporary storage and other supporting equipment. DME sample obtained from a company produce DME for industrial purpose. The diesel fuel used is diesel oil which has a cetane number of 48.



Figure 1. Dimetyl Ether in Cylinder Storage



The generator diesel engine that will be used in the performance test is: a compression ignition engine designed to use diesel fuel with four cylinders and four stroke and has direct fuel injection system. This propulsion electric generator diesel engine capable to generate power capacity of 10 kVA to 1500 rpm

Table 1. Generator Diesel Engine Specifications V1505-BG

Model		V1305-BG	V1505-BG	D1403-BG	
Tipe		Mesin Diesel pendingin air 4-langkah vertikal			
Jumlah Silinder		4		3	
Diameter x Langkah		76.0 x 73.6 (2.99 x 2.90)	78.0 x 78.4 (3.07 x 3.09)	80.0 x 92.4 (3.15 x 3.64)	
Kapasitas Total		1.335 (81.47)	1.498 (91.41)	1.393 (85.01)	
Dimensi (P x L x T)		634.3 x 405.2 x 609.7 (25.00 x 15.95 x 24.00)		607.5 x 502.6 x 645.0 (23.92 x 19.79 x 25.39)	
Berat Bersih		110.0 (242.5)		148.0 (326.3)	
Tetapan yang Dihasilkan	Stand-by	60Hz (1800 rpm)	13.1 (17.5)	15.1 (20.2)	14.2 (19.1)
		50Hz (1500 rpm)	10.9 (14.6)	12.5 (16.8)	12.1 (16.2)
	Bekerja	60Hz (1800 rpm)	11.6 (15.5)	13.4 (17.9)	12.6 (16.9)
		50Hz (1500 rpm)	9.6 (12.9)	11.1 (14.9)	10.7 (14.3)

2.2. Performance Testing of Propulsion Generator Diesel Engine

Tests conducted on these activities at the Performance Test generator engine using diesel fuel (B20) and fuel DME. To determine the effect and the response of engine power on the change in used fuel, then the engine should be tested its performance. This type of testing is done by giving the electrical load on the generator. Preparation of the test was conducted on the technical and non-technical preparation. Type of engine power used in these activities is a type of engine with compression ignition (compressed ignition engine) diesel. Fuel conversion systems on this machine if using fuel DME is dual fuel, which means that this machine can operate with two fuels simultaneously by a certain percentage.

Tests carried out on plants that use diesel fuel (B20) and diesel fuel mixture with DME. The test results are evaluated by comparing the performance of the generated electrical fueled with diesel fuel as fuel The reference / benchmark, using the converter tool kit that has been designed / modified. Performance test results data on power plant engines include:

- Fuel consumption
- Exhaust emissions (opacity)
- The stability of the engine operation
- Easibility on starting

3. RESULTS AND DISCUSSION

3.1 Characteristics Testing of Chemical Physics Dimethyl Ether

Testing the characteristics of DME includes 6 parameters such as gas composition, specific gravity, vapor pressure, water content, weathering test, and copper corrosion. The tested fuel



meet the specification in Indonesia.

Table 2. Properties of DME

No	Karakteristik	Satuan	Percontoh	Batasan		Metode Uji	
			DME	Min.	Max.	ASTM	Lain
1	Specific Gravity 60/60°F	-	0,76	To be reported		D-1657	
2	Vapour Pressure @100°F	P sig	115	-	120	D-1267	
3	Weathering Test @36°F	% vol.	99,95	95	-	D-1837	
4	Copper Corrosion 1 hour		1a	-	1a	D-1838	
5	Total Sulphur	grain/	1,13	-	15	D-2784	
		100cuft					
6	Water Content		No free	No free			
			water	water		-	Visual
7	Composition : DME	% vol	99,96	-	-	D-2163	

3.2. Test Engine Performance

The testing activities can result from the generator engine performance testing. Consumption measurements carried out starting from a position where the engine is operating at no load electricity and continued to provide load 20%, 40%, 60% and 80%.

a. Specific Fuel Consumption

Consumption measurements carried out starting from a position where the engine is operating at no load electricity and continued to provide load 20%, 40%, 60% and 80%. Fuel consumption is expressed in weight of the fuel needed for the required per unit load and per unit time. The results of the measurement of fuel consumption can be seen in Table 3. From table 3 shows that the higher the loading given on the larger engine fuel needed. Fuel is used in the diesel fuel is greater than the Dual Fuel System Dimethyl Ether.

Table 3. Fuel Consumption of Diesel Engine

Load (%)	Fuel consumption (Kg/h)	
	Diesel fuel(B20)	Diesel fuel + DME
20	1.17	0.93
40	1.31	1.16
60	1.43	1.25
80	1.71	1.66



Consumption of fuel required from application loading machines have a tendency to rise if given the increase in the load on the engine From the table above shows that with the same load, the consumption of the diesel-fueled generators + DME is less than the diesel-fueled generators. This is because DME has a high cetane number and a high cetane number will be very good when used for the diesel engine

b. Exhaust Emission Testing (opacity) Engine Generator

The chemical reaction of fuel combustion will produce exhaust emissions. Measurements of emissions in diesel engine emission opacity only. Opacity is a measure of the concentration of exhaust gases of diesel engines. Based opacity measurement unit density percentage. The greater the percentage figures deepened emission opacity emissions.

Table 4. Exhaust Emission Test (opacity) Diesel Engine

Load %	Opacity (%)	
	Diesel fuel (B20)	Diesel fuel + DME
20	1.98	1.15
40	2.74	1.93
60	3.14	2.43
80	4.45	3.17

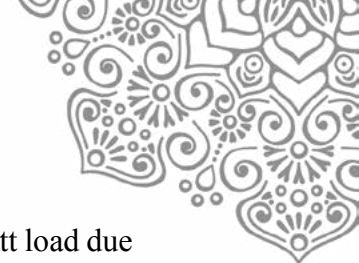
Exhaust emissions (opacity) diesel engine generator sets diesel + DME in several variations load conditions have lower smoke opacity compared with the engine diesel.

c. Stability Operations Engine

The observation of the stability of the engine operation either due to additions or changes to the fuel load. From the table it can be said that in general the engine is operating stably with the diesel fuel. As for the diesel engine with a fuel mixture of diesel and DME experienced an increase in cooling water temperature, although the converter kit already made arrangements DME gas channel.

Table 5. Stability Operations Diesel Engine

Load %	Opacity (%)	
	Diesel fuel (B20)	Diesel fuel + DME
20	Stabil	Stabil- temperature coolant sytem normal
40	Stabil	Stabil- temperature coolant sytem normal
60	Stabil	Stabil- temperature coolant sytem increase
80	Stabil	Stabil- temperature coolant sytem increase



The composition of 50% DME engine can not operate stably in 4000 and 4500 watt load due to engine operating temperature is high enough

d. Easibility of Starting

From the measurement of time required to start the engine seem that there is no significant difference between the engine that use diesel fuel or a mixture of diesel and DME, because the start-up all these machines can only be done with diesel fuel (B20) in advance and after it's done the addition of DME, so the converter kit that is used there is no constraint on the converter kit, from the measurement time required to turn on the diesel engine together with the results obtained in a diesel engine generator that is no significant difference between the engine that use diesel fuel or a mixture of diesel and DME, because the start-up all these engine can only be done with diesel fuel first and then the addition of DME

4. CONCLUSION

In this research aims to produce a system conversion apparatus that can apply the DME as an alternative fuel in the generator set power plant in the commercial sector. From the test results and the observation of a number of conclusions.

1. Fuel DME can be used in diesel engine which applying in a dual-fuel system with diesel fuel and with the addition of engine cooling systems;
2. The system conversion equipment that has been designed/modified can be applied to the conversion of DME to the engine generator
3. Consumption of Dual Fuel System Dimethyl Ether and Diesel Fuel engine is less than in the use of diesel fuel;
4. Opacity diesel engine generator Dual Fuel System Dimethyl Ether and Diesel Fuel is better compared with the opacity of diesel fuel (B20)

5. ACKNOWLEDGEMENT

We are so grateful for the work of our team of Fuel and Aviation Group (Kelompok Bahan Bakar dan Aviasi), Application Product Research Division of LEMIGAS.

6. REFERENCES

- Gao Guangxin, Yuan Zhulin, Zhou Apeng, Liu Shenghua, and Wei Yanju1 (2013) : Effects of Fuel Temperature on Injection Process and Combustion of Dimethyl Ether Engine, *J Energy Resour Technol.* 2013 Dec; 135(4): 0422021–0422025. Published online 2013 May 31.
- Hyun GuRoh, Chang SikLee (2017) :Fuel Properties and Emission Characteristics of Dimethyl Ether in a Diesel Engine, *SPRINGER LINK*, Date: 11 February 2017
- Prabhakaran, Thennarasu, Karthick (2015) : Performance and Characteristics of a CI



Engine Using DME (Dimethyl Ether), International Journal of Innovative Research in Science, Engineering and Technology, An ISO 3297: 2007 Certified Organization Volume 4, Special Issue 2, February 2015

Zhen Huang, Xinqi Qiao, Wugao Zhang, Junhua Wu, Junjun Zhang (2013) : Dimethyl ether as alternative fuel for CI engine and vehicle, J Energy Resour Technol. 2013 Dec; 135(4): 0422021–0422025. Published online 2013 May 31. doi: 10.1115/1.4023549

Z Wang, X Qiao*, J Hou, W Liu, Z Huang (2011) : Combustion and emission characteristics of a diesel engine fuelled with biodiesel/dimethyl ether blends, SAGE JOURNALS First Published July 7, 2011.

Zhi Wang, Haoye Liu, Jianxin Wang, Shijin Shuai (2015) : Performance, Combustion and Emission Characteristics of a Diesel Engine Fueled with Polyoxymethylene Dimethyl Ethers (PODE3-4)/ Diesel Blends, ENERGY PROCEDIA VOLUME 75, 2015, 2337-2344



THE 15TH INTERNATIONAL CONFERENCE QUALITY IN RESEARCH (QIR) 2017

INVESTIGATION ON THE HULL MATERIAL FOR SOLAR POWERED ELECTRICAL SPORT BOAT

Sunaryo^a, Pradhana S Imfianto^b, Aldy Syahrihaddin Hanifa^c

^{a, b, c} Naval Architecture and Marine Engineering Study Program, Department of
Mechanical Engineering, Universitas Indonesia, *E-Mail*:^a :naryo@eng.ui.ac.id,
^b:pradhana.sadhu@ui.ac.id, ^c:aldy.syahrihaddin@ui.ac.id

ABSTRACT

Analyses of sandwich materials that used in design of a water recreational and sport vessel that powered by solar generated electric engine are required to fully compatible to the hull strength of the boat. The work is a further development of the solar boat created by the Universitas Indonesia team that participated in International Solar-boat Challenge competition in the Netherlands. The aim of the work is investigate the strength of the modified hull material, and its manufacturing processes based on the calculation formulas provided in Bureau Veritas': Rules for Hull in Composite Materials and Plywood, Material Approval, Design Principles, Construction and Survey (NR 546 DT R00 E). The analyses are applied to the panel under global loads (laminare buckling, maximum stress in each layer, and combined stress) in order to determine the strength of the boat hull. In this study, the mechanical properties (tensile and flexural) of facing laminate and sandwich material were made using VARTM (Vacuum Assisted Resin Transfer Molding) or known as Vacuum Infusion. The Panel is made of two different materials (High Strength Carbon Fiber 240 gr/m² and Lantor Soric XF 5 mm) infused with Ripoxy R-802 EX-1 (vinyl ester resin).

Keywords: Hull Strength, Sandwich Material; Solar Powered Boat; VARTM-Vacuum Infusion.

1. INTRODUCTION

The work is a further development of the solar boat created by the Universitas Indonesia team that participated in International Solar-boat Challenge competition in the Netherlands. The using of materials for construction of the boat is important in order to meet optimum weight and strength. The boat hull is made of sandwich materials that consisted of High Strength Carbon Fiber 240 gr/m² and Lantor Soric XF 5 mm. The aim of the study is to investigate the weight and strength of the proposed materials based on the way they are manufactured and the composition of the sandwich layers, to ensure that the materials to be used are compatible to all requirements of the boat being designed for the next competition, and for other purposes such as for recreational and sport.

2. METHODOLOGY

To investigate the weight and strength of the proposed materials two approaches were conducted i.e. theoretical approach using available formulas, and experimental approach using samples. Samples are made in the form of panels. The shape, size, and dimensions of the panels were made in accordance with the standards provided by American Standards for



Testing of Materials (ASTM), and the results of the experiments were compared to the requirements stated in the rules of Bureau Veritas.

2.1. The Boat

The boat has the structural specifications as presented in table 1, and the distribution of weight of the overall boat components are shown in table 2. Based on these data the proposed hull materials were investigated.

Table 1 Boat Structural Specification

Length overall	5,8 m
Breadth	1,8 m
Draft	0,124 m
Height	0,35 m
Cb	0,532
Cp	0,568
Cm	0,939
Frame Spacing (Longitudinal)	0,5 m
Frame Spacing (Transversal)	0,26 m

Table 2 Boat Component Weight List

Item	Quantity	Kg	Item	Quantity	Kg
Hull Weight	1	86	MC	1	5
Solar Panel 1	1	20	Panel Box	1	10
Solar Panel 2	1	20	Box Fuse	1	5
Solar Panel 3	1	20	Battery Box	1	15
Solar Panel 4	1	20	Cabin	1	75
			Electric Motor	1	40
<i>Total (Kg)</i>	166		<i>Total (Kg)</i>	150	
<i>Total (Kg)</i>				316	

2.2. Hull Strength Analysis

In order to investigate the weight and strength of the proposed material for the boat hull, two approaches were carried out in the study i.e. theoretical and experimental approaches. The analyses of the panels are based on the assumption that the panels are under global loads, in a still water, and in a certain wave condition. There are three criteria selected for the strength analysis: Laminate buckling; Maximum stress in each layer; and combined stress in each layer.

Laminate buckling must fulfilled the following conditions:

$$\sigma_a \leq \sigma_c / SF_B ; \tau_a \leq \tau_c / SF_B \tag{1}$$

σ_a, τ_a = *compression* stress and shear stress applied to the panel

σ_c, τ_c = *critical* buckling stresses of the panel

SF_B = *minimum* buckling rule safety coefficient



Maximum stress in each layer must fulfilled this condition:

$$\sigma_i \leq \sigma_{br}/SF ; \tau_i \leq \tau_{br}/SF \quad (2)$$

$\sigma_i, \tau_i =$ *local* stress in individual layers induced by in-plane global loads

$\sigma_{br}, \tau_{br} =$ *theoretical breaking stress of layers*

SF = *minimum* rule safety coefficient

Combined stress in each layer must fulfilled this condition:

$$SF_{CS} \geq C_V \cdot C_F \cdot C_{CS} \cdot C_I \quad (3)$$

$C_V =$ *rule* partial safety coefficient taking into account the ageing effect on the laminates

$C_F =$ *rule* partial safety coefficient taking into account the fabrication process

$C_{CS} =$ *rule* partial safety coefficient for combined stresses in the individual layers of the laminates

$C_I =$ *rule* partial safety coefficient taking into account the type of the loads

$$SF_{CS} = \frac{-b \pm \sqrt{b^2 + 4a}}{2a} \quad (4)$$

$$a = \frac{\sigma_1^2}{|\sigma_{brc1} \sigma_{brt1}|} + \frac{\sigma_2^2}{|\sigma_{brc2} \sigma_{brt2}|} - \frac{\sigma_1 \sigma_2}{|\sigma_{brc1} \sigma_{brt1}|} + \frac{\tau_{12}^2}{\tau_{br12}^2} \quad (5)$$

$$b = \frac{\sigma_1 (|\sigma_{brc1}| - |\sigma_{brt1}|)}{|\sigma_{brc1} \sigma_{brt1}|} + \frac{\sigma_2 (|\sigma_{brc2}| - |\sigma_{brt2}|)}{|\sigma_{brc2} \sigma_{brt2}|} \quad (6)$$

$\sigma_i, \tau_{12} =$ *actual stresses, in the considered* ply axis induce by the loading case (N/mm²)

$\sigma_{br1}, \tau_{br12} =$ *ply* theoretical breaking stresses in the local ply axis(N/mm²)

To find the strength of panel under global loads “Rules for Hull in Composite Materials and Plywood, Material Approval, Design Principles, Construction and Survey (NR 546 DT R00 E)” of Bureau Veritas classification were used. Before performing a calculation of the hull strength, the mechanical properties of the material (sandwich material) must be first calculated. The standard under ASTM D3039 for tensile modulus of facing laminate and ASTM C393 for flexural modulus of sandwich material was used for these materials. The values of the mechanical property are used for comparison with results of the calculations through macro-mechanical analysis.

2.2.1. Theoretical Breaking Stress Layer 1,2,4, and 5

Analyses of *breaking stress* for layer 1,2,4 and 5 (figure 1) where four of them uses Fiber Carbon HDC-524-3K 240 gr/m² are using theoretical breaking stress calculation from BV classification rules. In table 3 there are break strain values of HS type carbon.

$$\sigma_{brt1} = \varepsilon_{brt1} \cdot E_1 \cdot Coef_{res} \quad (7)$$

$$\sigma_{brc1} = \varepsilon_{brc1} \cdot E_1 \cdot Coef_{res} \quad (8)$$

$$\sigma_{brt2} = \varepsilon_{brt2} \cdot E_2 \cdot Coef_{res} \quad (9)$$

$$\sigma_{brc2} = \varepsilon_{brc2} \cdot E_2 \cdot Coef_{res} \quad (10)$$

$$\tau_{br12} = \gamma_{br12} \cdot G_{12} \cdot Coef_{res} \quad (11)$$



$$\tau_{brIL1} = \gamma_{bril23} \cdot G_{23} \cdot Coef_{res} \tag{12}$$

$$\tau_{brIL2} = \gamma_{bril13} \cdot G_{13} \cdot Coef_{res} \tag{13}$$

- $\sigma_{brt1,2}$ = Tensile Break Stress 1 & 2 Direction (N/mm²)
- $\sigma_{brc1,2}$ = Compression Break Stress 1 & 2 Direction (N/mm²)
- τ_{br12} = Shear Break Stress 12 Direction (N/mm²)
- $\tau_{brIL1,2}$ = Inter Laminar Shear Break Stress 1 & 2 Direction (N/mm²)
- Coef_{res} = Vinyl Ester (0,9)

Table 3 Break Strain

Carbon	HS	Carbon	HS
ϵ_{brt1}	1%	ϵ_{brc2}	0,85%
ϵ_{brt2}	1%	γ_{br12}	1,55%
ϵ_{brc1}	0,85%	$\gamma_{br13}, \gamma_{brIL2}$	1,55%

(Marine Division Bureau Veritas, 2012)

2.2.2 Theoretical Breaking Stress Layer 3

The theoretical breaking stress for layer 3 is done by using micro-mechanical analyses on equation (14).

$$E_1 = E_f V_f + E_m V_m \tag{14}$$

E_1 = Young modulus for laminate

$V_{f,m}$ = Volume fraction fibre (lantor); matrix

$E_{f,m}$ = Young modulus from fibre (lantor); matrix

Young modulus value from lantor soric XF can be neglected. So, the mechanical properties of the core material infused with resin is only affected by the volume fraction of the resin type (matrix) that used for VARTM-vacuum infusion process.

2.3. Material

For sandwich material Fiber Carbon HDC-524-3K with 240 gr/m² as facing laminate (layer 1,2,4, and 5) was used. For core material Lantor Soric XF with thickness of 5mm (layer 3) was used as shown in figure 1. The matrix being used is Ripoxy R-802 EX-1 (vinyl ester) with catalyst MEKPO (Methyl Ethyl Ketone Peroxide) and promoter P-EX. The specimens that will be used for the analysis are the same with the material used for the boat hull which is produced using VARTM (Vacuum Assisted Resin Transfer Molding) Vacuum infusion method.



Figure 1 Sandwich Material



2.4. Experimental Test of Tensile Modulus & Flexural Modulus

Experimental method was used to investigate the tensile modulus and flexural modulus of the material. Several samples were prepared for the purpose of testing. To find the value of tensile modulus from facing laminate ASTM D3039 standard was used. The specimens with total length of 250 mm, width 25 mm, and gauge length 150 mm

To get the flexural modulus value of the sandwich material three point bending test specimens were prepared in accordance with ASTM C393 standard. The specimens have total length of 200 mm, width 75 mm, and support span 150 mm with load span at the middle of the specimens as seen in figure 2.

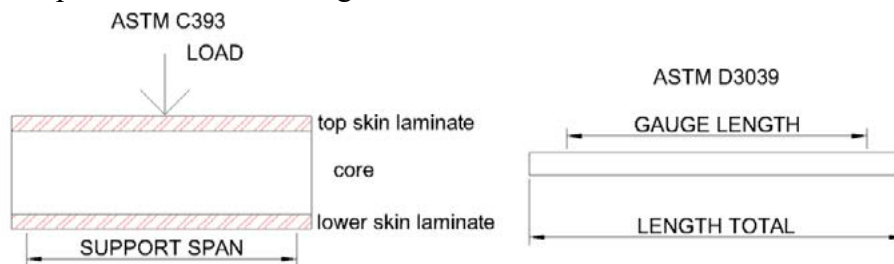


Figure 2 ASTM C393 & ASTM D3039

3. RESULTS AND DISCUSSION

3.1. Analyses of Sandwich Material

3.1.1. Tensile Test

This experiment used five specimens of facing laminate. Figure 3 shows the graph between stress vs strain obtained during the experiment progress. Tests were conducted at temperature 21,7°C and constant speed 2 mm/min. It can be seen through the graph that a linear line is formed between stress vs strain in all the five specimens. From the experiment an average tensile modulus 15,21 GPa with standard deviation ± 1 GPa. From the analysis calculation the tensile modulus value is 54,9905 GPa.

3.1.2. Flexural Test

Three point bending test was carried out to investigate the flexural modulus of the sandwich material. The experiment used five specimens of sandwich material. Figure 4 shows the graphs of stress vs. strain obtained during the experimental progress. Tests were conducted at the temperature at 23,1°C and a constant speed of 6 mm/min. It can be seen through the graph that a linear line is formed between stress vs. strain in all the five specimens before the failure occur. From the specimens obtained an average flexural modulus 21261,8 N/mm² (21,2618 GPa) with standard deviation $\pm 2301,17$ N/mm² ($\pm 2,30117$ GPa). From the analysis calculation the flexural modulus value is 26833,5 N/mm² (26,8335 GPa).

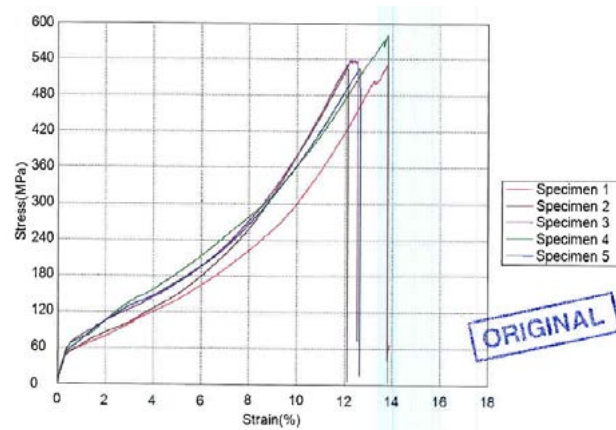


Figure 3 Stress vs Strain of Tensile Test Graph

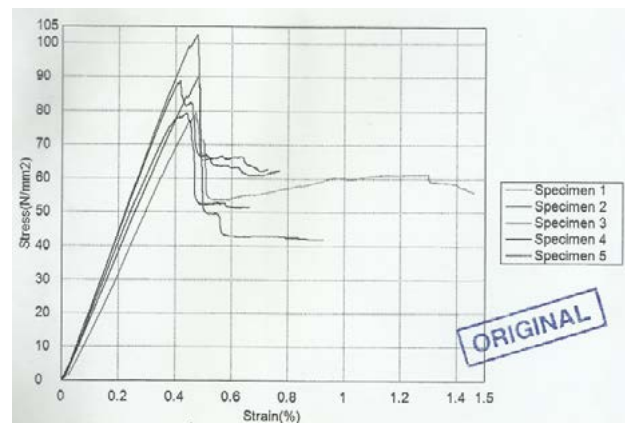


Figure 4 Stress vs Strain of Flexural Test Graph

3.2. Hull Strength

By comparing the experimental results and the analysis calculation of the panel under global loads based on regulation issued by Bureau Veritas’ “Rules for Hull in Composite Materials and Plywood, Material Approval, Design Principles, Construction and Survey (NR 546 DT R00 E)”, the values of the hull strength of the boat are obtained as follows:

- Laminate buckling (table 4)

Table 4 Laminate Buckling

Condition	Hogging	Sagging	Pass/not pass
$\sigma_a \leq \sigma_c / SF_B$ (N/mm ²)	$0,86 \leq 460,975$	$0,25 \leq 460,975$	pass
$\tau_a \leq \tau_c / SF_B$ (N/mm ²)	$0,062 \leq 129,139$	$0,0135 \leq 129,139$	pass



- Maximum stress in each layer (table 5 and table 6)

Table 5 Maximum Stress in Each Layer

Bottom				Side				Deck			
Layer 1		$\sigma \leq \sigma_{brk}/Sf$		Layer 1		$\sigma \leq \sigma_{brk}/Sf$		Layer 1		$\sigma \leq \sigma_{brk}/Sf$	
σ_1 (MPa)	0,183	122,02	pass	σ_1 (MPa)	5,62465E-06	122,02	pass	σ_1 (MPa)	0,1035	122,02	pass
σ_2 (MPa)	0,612	122,02	pass	σ_2 (MPa)	5,4304E-06	122,02	pass	σ_2 (MPa)	0,332	122,02	pass
Layer 2		$\sigma \leq \sigma_{brk}/Sf$		Layer 2		$\sigma \leq \sigma_{brk}/Sf$		Layer 2		$\sigma \leq \sigma_{brk}/Sf$	
σ_1 (MPa)	0,183	122,02	pass	σ_1 (MPa)	5,05597E-06	122,02	pass	σ_1 (MPa)	0,103	122,02	pass
σ_2 (MPa)	0,612	122,02	pass	σ_2 (MPa)	4,88136E-06	122,02	pass	σ_2 (MPa)	0,3312	122,02	pass
Layer 3		$\sigma \leq \sigma_{brk}/Sf$		Layer 3		$\sigma \leq \sigma_{brk}/Sf$		Layer 3		$\sigma \leq \sigma_{brk}/Sf$	
σ_1 (MPa)	0,00697	15	pass	σ_1 (MPa)	1,45971E-23	15	pass	σ_1 (MPa)	0,003715	15	pass
σ_2 (MPa)	0,0175	15	pass	σ_2 (MPa)	1,41848E-23	15	pass	σ_2 (MPa)	0,00933	15	pass
Layer 4		$\sigma \leq \sigma_{brk}/Sf$		Layer 4		$\sigma \leq \sigma_{brk}/Sf$		Layer 4		$\sigma \leq \sigma_{brk}/Sf$	
σ_1 (MPa)	0,183	122,02	pass	σ_1 (MPa)	-5,05597E-06	-103,7172	pass	σ_1 (MPa)	0,093	122,02	pass
σ_2 (MPa)	0,612	122,02	pass	σ_2 (MPa)	-4,88136E-06	-103,7172	pass	σ_2 (MPa)	0,321	122,02	pass
Layer 5		$\sigma \leq \sigma_{brk}/Sf$		Layer 5		$\sigma \leq \sigma_{brk}/Sf$		Layer 5		$\sigma \leq \sigma_{brk}/Sf$	
σ_1 (MPa)	0,183	122,02	pass	σ_1 (MPa)	-5,62465E-06	-103,7172	pass	σ_1 (MPa)	0,0922	122,02	pass
σ_2 (MPa)	0,612	122,02	pass	σ_2 (MPa)	-5,4304E-06	-103,7172	pass	σ_2 (MPa)	0,321	122,02	pass

Table 6 Maximum Stress between Layers

Between Layer 1 and 2				Between Layer 2 and 3			
Maximum Value from bottom, side, and deck (MPa)		τ_{brk}/SF (MPa)	$\tau_i \leq \tau_{brk}/SF$	Maximum Value from bottom, side, and deck (MPa)		τ_{brk}/SF (MPa)	$\tau_i \leq \tau_{brk}/SF$
τ_{yz}	0,009	12,58	pass	τ_{yz}	0,01707	1,273	pass
τ_{xz}	0,064	12,58	pass	τ_{xz}	0,12141	1,273	pass
Between Layer 3 and 4				Between Layer 4 and 5			
Maximum Value from bottom, side, and deck (MPa)		τ_{brk}/SF (MPa)	$\tau_i \leq \tau_{brk}/SF$	Maximum Value from bottom, side, and deck (MPa)		τ_{brk}/SF (MPa)	$\tau_i \leq \tau_{brk}/SF$
τ_{yz}	-0,014	-1,273	pass	τ_{yz}	-0,0222	-12,58	pass
τ_{xz}	-0,0999	-1,273	pass	τ_{xz}	-0,1577	-12,58	pass

- Combined stress in each layer (table 7 and table 8)

Table 7 Combined Stress for Layer 1, 2, 4, and 5

Position	Maximum (SFcs ₁ or SFcs ₂)	$C_p \cdot C_F \cdot C_{cs} \cdot C_i$	$SF_{cs} \geq C_p \cdot C_F \cdot C_{cs} \cdot C_i$
Bottom	844,55	2,808	pass
Side	88599160,55	2,808	pass
Deck	1563,366	2,808	pass



Table 8 Combined Stress for Layer 3

Position	Maximum (SFcs ₁ or SFcs ₂)	$C_p \cdot C_F \cdot C_{CS} \cdot C_i$	$SF_{CS} \geq C_p \cdot C_F \cdot C_{CS} \cdot C_i$
Bottom	2162,445	2,808	pass
Side	2,2924E+24	2,808	pass
Deck	4054,585	2,808	pass

4. CONCLUSIONS

Based on the boat design load, and calculation using BV regulations it was proved that the proposed sandwich material can be used effectively for the boat being designed. From the calculation, we can see the difference with analysis calculation and experiment value. This is can happen because three main reasons: Resin vinyl ester Ripoxy R-802 EX-1 that used in this study is more suitable with glass rather than carbon, unsuitable room temperature on curing process, and catalyst of MEPOXE M (*Methyl Ethyl Ketone Peroxide type M*) has less compatibility with resin vinyl ester Ripoxy R-802 EX-1. It is recommended to use CHP (*Chumene Hydroperoxide*) as the catalyst for the vacuum infusion process.

The final result of the hull strength analysis for laminate buckling, maximum stress in each layer, and combined stress are all passed the requirements of the proposed boat design loads.

5. ACKNOWLEDGE

The authors would like to express their appreciations to PITTA project initiated by Directorate of Research and Community Engagement Universitas Indonesia for funding the project. We also express our thanks to PT Justus Kimiaraya for supporting us in providing the materials and manufacturing process of the sandwich material together with STP (Sentra Teknologi Polimer) BPPT Serpong, and Solar Boat Team Universitas Indonesia 2016 who inspired the research.

6. REFERENCES

- Adalberto, S. R., Henrique, C. Z., Varella, R. d., & Fernando, F. D. (2007). Flexural Strength and Modulus of Elasticity of Different Types of Resin-based Composites. *Braz Oral Res*, 16-21.
- Alberth, M. T. (2014). *Prinsip Merancang Kapal*. Depok: Departemen Teknik Mesin, Fakultas Teknik Universitas Indonesia.
- ASTM. (2002). *ASTM D3039 Standard Test Method for Tensile Properties of Polymer Matrix Composite Materials*. West Conshohocken, PA: ASTM.
- ASTM. (2012). *ASTM C393 Standard Test Method for Core Shear Properties of Sandwich Constructions by Beam Flexure*. West Conshohocken, PA: ASTM.
- Bai, J., Xiong, J., & Liu, M. Z. (2016). Analytical Solutions for Predicting Tensile and Shear Moduli of TriaxialWeave Fabric Composites. *Acta Mechanica Solida Sinica*, 29.
- Biro Klasifikasi Indonesia. (2016). *Volume V Rules For Fiberglass Reinforced Plastic Ships 2016 Edition*. Jakarta: BKI.
- Dayyani, I., Ziaei-Rad, S., & Salehi, H. (2011). Numerical and Experimental Investigations on Mechanical Behavior of Composite Corrugated Core. *Applied Composite Materials*.



- Erdemli, S. G., Abdulhalim, K., & Emin, M. Ö. (2014). Properties of FRP Materials for Strengthening. *International Journal of Innovative Science*.
- Fotsing, E., Leclerc, C., Sola, M., Ross, A., & Ruiz, E. (2016). Mechanical properties of composite sandwich structures with core or face sheet discontinuities. *Composites Part B*, 229-239.
- Kaw, A. K. (2006). *Mechanics of Composite Materials*. Broken Sound Parkway NW: CRC Press.
- Lantor B.V. (2012). *Application Manual*. Veenendaal: Lantor B.V.
- Leksa, R. M. (2015). *Analisa Teknis dan Ekonomis Penggunaan Material Komposit Sandwich dengan Metode Vacuum Infusion Sebagai Material Kapal*. Semarang: Universitas Diponegoro.
- Liston, G. P. (2013). *Analisa Sifat Mekanik Komposit Serat E-glass Tipe Multiaxial dengan Matriks Vinyl Ester dengan Metode VARTM untuk Aplikasi pada Lambung Kapal Cepat*. Depok: Universitas Indonesia.
- Marine Division Bureau Veritas. (2012). *Hull in Composite Materials and Plywood, Material Approval, Design Principles*. Neuilly sur Seine Cedex: Bureau Veritas.
- Marine Division Bureau Veritas. (2012). *Rules for the Classification and the Certification of Yachts*. Neuilly sur Seine Cedex: Bureau Veritas.
- PT. Justus Sakti Raya. (2009). *Technical Information of Corrosion Guide and Others*. Jakarta.
- Uddin, N., Vaidya, U., & Ramos, L. (2013). *Development of Cost-Effective Vartm Technology for Repair and Hardening Design Method and Specifications for Aldot Contractor Phase 3*. Alabama: Alabama Department of Transportation.
- Umer, R., Waggy, E., Haq, M., & Loos, A. (2011). Experimental and Numerical Characterizations of Flexural Behavior of VARTM-Infused Composite Sandwich Structures. *Reinforced Plastics & Composites*, 67-76.



The Compensation Method for Tool Orientation Change to Avoid Collision in 5-axis Roughing of Faceted Models

Gandjar Kiswanto¹, Himawan Hadi Sutrisno¹, Jos Istiyanto¹

¹Department of Mechanical Engineering, Universitas Indonesia, Depok, Indonesia

ABSTRACT

Adding CC points during the rough machining process on a closed-bounded volume (CBV) may result in an interference between the tool and the workpiece in each initial tool orientation. Since the ultimate goal is to add the volume of the machining during the roughing process, the added CC points as well as the initial tool orientation must be positioned accordingly so that they are not affected by the collision between the tool and the workpiece. This paper discusses the method to avoid the collision for each CC point in CBV areas which is the numeric interpolation method and the method to detect collision faceted model-based method. The process of detection and avoidance may be conducted multiple times to obtain CC points with tool orientations which are free from interference. The result of the calculation is used as the basis for the creation of additional tool path in the rough machining process, especially for models with closed-bounded areas, in order to increase the effectiveness of the rough machining process.

Keywords: CBV area, gouging elimination, roughing, faceted models. tool orientation

1. INTRODUCTION

In the manufacturing industry, especially the mold and dies manufacture, the machining cost may be reduced by increasing the efficiency in the machining process. The higher efficiency can be achieved by using the 5-axis milling machine which allows a single-step process to create products. Generally, the machining process is divided into 3 processes: roughing, semi finishing, and finishing machining (Ali Lasemi, 2010). Unlike the other two stages, a large proportion of the rough machining process is spent on removing the bulk of the waste material and this process results in the coarsest feature of the workpiece (M. Balasubramaniam, 2000).

Faceted model is widely used in the research on the development of machining method until now (Yuan and Shao, 2012, Lin et al., 2013, Kruth, 2003). However, there are some using point cloud as the basis for data (Mohanad Makki, 2010, Masood et al., 2015)

In reality, due to the large variation of the complex volume model, there might be some parts that are difficult to reach by the tool during the machining process. These areas are commonly referred to as the CBV (Closed-Bounded Volume) area (Kiswanto. and Panuju, 2010). CBV area is generally a sign that there are obstacles present in the area and therefore, a special strategy shown below in Figure 1 as the illustration of the rough machining process for the complex model is required.

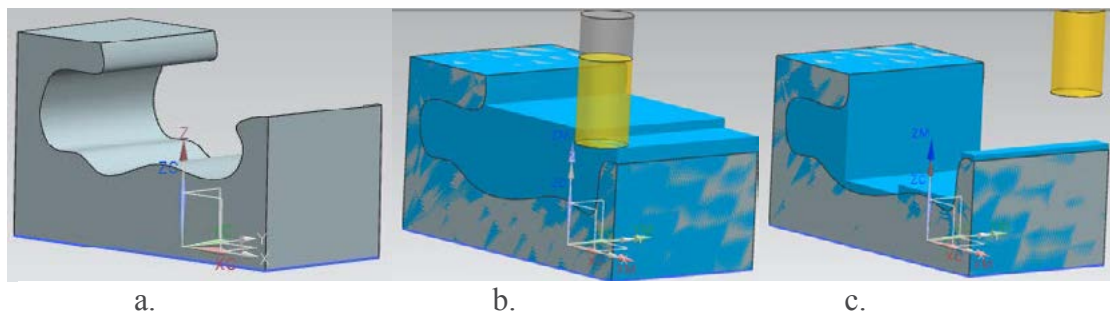


Figure 1. a) Complex models; b) The simulation of the rough machining; c). The remaining waste material in the model.

In increasing the effectiveness of the machining process, especially during roughing process, efforts are made to work on the models which contain CBV area in the machining process in order to reduce the total machining time for creating dies and molds and to add the machining volume in this area. The CC points and the initial tool orientation are determined based on the position of pre-determined point clouds. When determining the CC points and the initial tool orientation in this area, interference between the tool and the workpiece is prone to occur. Since this interference may damage the workpiece and/or the tool, a collision avoidance method needs to be done to allow a more effective determination of CC points in the rough machining process.

Chapter 3 of this paper further discusses the determination of CC points and initial tool orientation. Chapter 4 explains the interference detection method and explains on how to prevent the occurrence of interference.

2. SEPARATION OF THE CLOSED-BOUNDED AREA (CBV) AND THE OPEN-BOUNDED AREA (OBV) DURING THE ROUGH MACHINING PROCESS

The rough machining process generally adopts the 3-axis milling method. However, since this method has a lot of limitations, it takes much longer time to finish the product until the finishing process. Based on the features in the complex models, workpiece models can be categorized into 3 following models:

1. Figure 2a shows a model with a CBV model
2. Figure 2b shows a model with a CBV+OBV model
3. Figure 2c shows a model with a OBV model

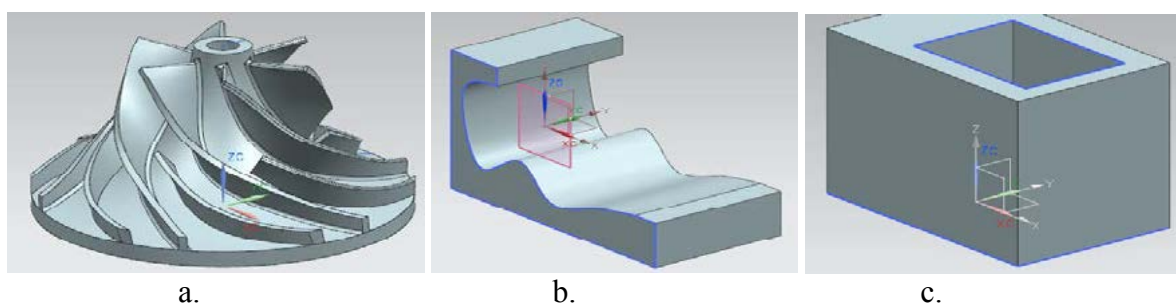
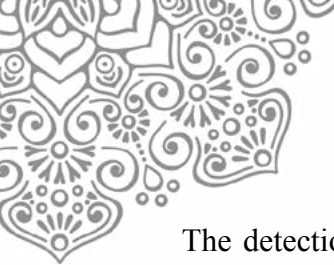


Figure 2. a) CBV models; b) CBV+OBV models; c)OBV/pocket models



The detection of the CBV area has been introduced by (Kiswanto. and Panuju, 2010) and updated by (Sutrisno et al., 2017b). The method for CBV area determination will later be used as the method to increase the effectiveness of the rough machining process for complex model. In the previous paper, it is explained that the CBV area is detected with an algorithm that the CBV area positions are always between 2 solid models with one visibility point parallel to the normal vector. Meanwhile in another form, what can directly be seen by the visibility point parallel with normal vector is commonly referred to as Open Bounded Volume or OBV. Figure 2 above shows that the model can be only CBV or only OBV, or CBV + OBV combined.

The previous paper also discusses that to assist calculation, the CBV dan OBV is grouped by creating point clouds in the machining area (Sutrisno et al., 2017a, Kiswanto et al., 2017). The separation between CBV area and OBV area based on the slicing process placed on each point cloud formed in $(x, y, 0)$. By slicing line method (Park, 2004) and fast minimum storage ray triangle intersection method (Moller and Trumbore, 1997), the slicing line is the form of perpendicular line cut against the model which is parallel to the normal z axis. In the machining area, the determination of point clouds resembles the determination of the point clouds at the base of the model, but with an addition of a certain z value. The z value added is the implementation of the depth of the cut from the rough machining process. Point clouds which are in the CBV area will be detected as the point clouds located among 4 slicing lines against the faceted model while the point clouds which are outside the 2 slicing lines are the point clouds in the OBV area.

3. INITIAL TOOL ORIENTATION IN CBV AND OBV AREA

After the point clouds are separated into position in the CBV area and OBV area, the point clouds formed are then used as CC points. The initial tool orientation is used as the references for the tool orientation in the local coordinate system. Figure 3 below shows the direction of the local coordinate which will be formed in CBV area.

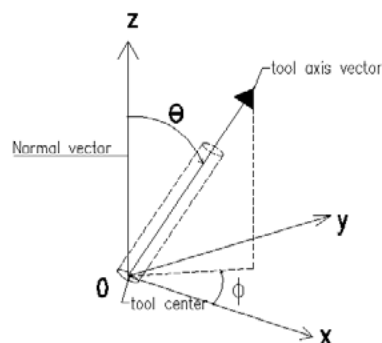


Figure 3. Local coordinate system.

The grouping of the point clouds in CBV area and OBV area will help the grouping of the tool orientation. In the OBV area, the tool orientation has the same direction with the normal vector of workpiece whereas in the CBV area, the determination of the tool orientation is based on the vector position reference formed between the CC points under the CBV area and the highest CC points outside the CBV area. The determination of the tool orientation in CBV area can be explained in the Figure 4 below.

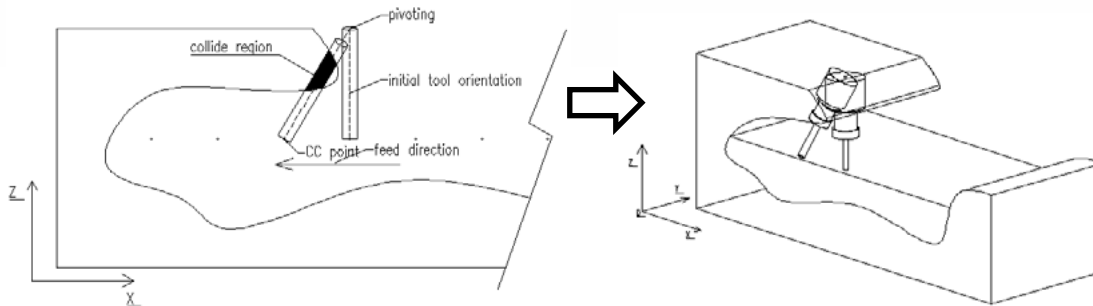


Figure 4. The determination of the tool orientation in CBV area

The CC points under the CBV area are in the (x, y, z) position. The closest point outside the CBV area selected is the closest points with the direction parallel to the feed direction. The reference points of the tool orientation are formed by the closest CC points outside CBV $(x1, y1, z1)$, with the highest z value so the position of the reference point becomes $(x1, y1, zmax)$. The following equation is then made for the determination of the tool orientation:

$$\vec{AB} = \begin{pmatrix} x1 \\ y1 \\ zmax \end{pmatrix} - \begin{pmatrix} x \\ y \\ z \end{pmatrix} \begin{pmatrix} i \\ j \\ k \end{pmatrix} \quad (2)$$

The model workpiece can be illustrated in the Figure 5 below:

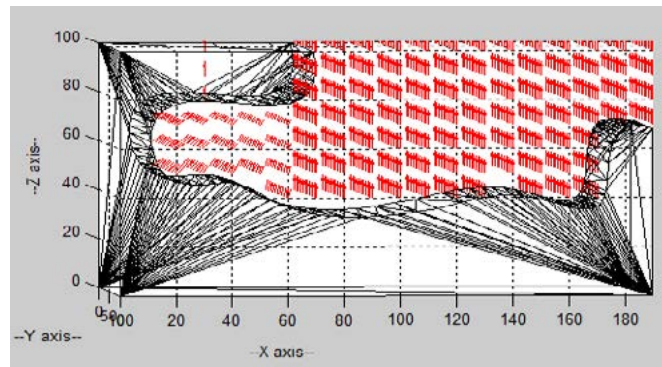


Figure 5. The determination of the tool orientation in the CBV and OBV area.

The above Figure shows that the orientation of each CC points on the OBV area is parallel to the normal vector of the workpiece while CC points under CBV area form the tool orientation to the closest highest point outside the CBV area. The machining process is illustrated in Figure 6 below:

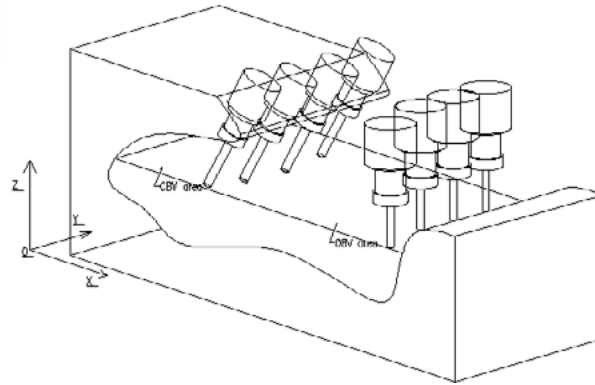


Figure 6. The illustration of the tool orientation in the machining process

When this action is performed, the positions of the tool in each CC point in CBV area are not instantaneously free from damaging interference while the formation of the tool path in each machining method is the accumulation of the tool orientation which is free from interference.

4. THE CONSEQUENCES OF THE CHANGES IN THE INITIAL TOOL ORIENTATION IN CBV AREA

Since in the tool orientation interference is still likely to occur, the next step is to detect in which CC points interference are likely to occur. The step for detecting, is done by first forming a tool posture. The tool posture used is the end-mill while the diameter and the length of the roughing are determined during the triangulation period.

a. Collision detection

There are 3 types of gouging occurred in the workpiece surface that might cause imperfection in the result of the machining(D.C.H.Yang, 1999):

1. *Type a* is a gouging caused by the presence of workpiece curvature which exceeds the minimum limit of the tool.
2. *Type b* or a rear gouging is when interference outside the pre-determined CC points occurs on the base of the tool.
3. *Type c* or a collision is when interference occurs in the tool outside the cut area (there is a feed on the uncontrolled side).

Figure 7 below illustrates the three types of gouging

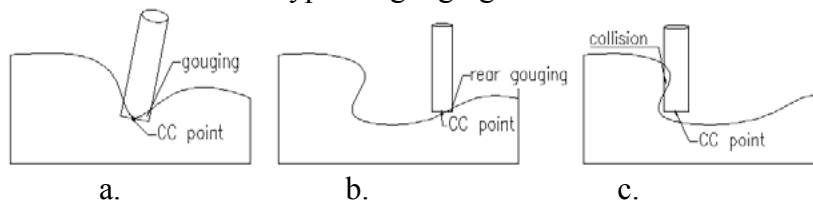


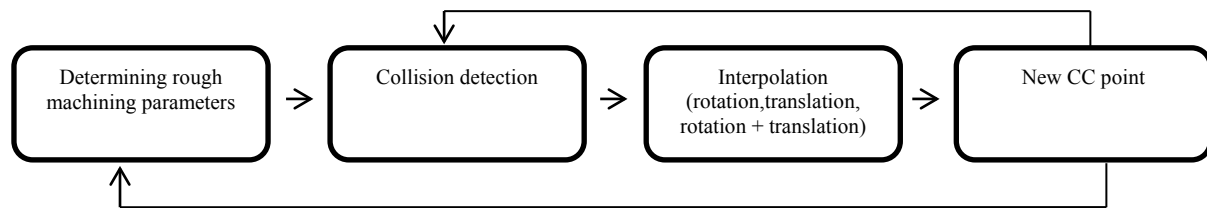
Figure 7. Types of gouging

To detect the parts which experience a collision, there are a many methods that can be used. Bounding volume based method by(Balasubramaniam et al., 2002, MAnnan, 2004),



accessability based method by(Lee, 1997). One of which is by projecting a triangle from the faceted model and the tool against the area which will be reached by the tool(Kruth, 2003, Kiswanto et al., 2007). The area which is covered by the shadow of the tool will be detected by moving the local coordinate system in the workpiece.

Meanwhile, based on the grouping of CC points in the machining area, a collision might occur in the CBV area while in OBV area and on certain layers, a rear gouging as shown in Figure 7b above is likely to occur. The process of collision detection and avoidance is done heuristically as shown in the following flowchart:



In this study, the collision detection uses the library from AABB (align axis bounding box). This method uses a virtual box as the basis of the detection. Each overlapping occurred in the workpiece model and the tool in the pre-determined axis means that CC points will experience an interference.

b. Collision avoidance

Aside from causing damage to the workpiece during the machining process, the collision may also cause a material loss due to the damage in the tool and other machinery components(Tang, 2014)

Similar to the method to detect collision, the method to avoid collision until now is still an interesting topic to discuss. There have been a few discussions on how to avoid collision in the workpiece and one of which is the method of tool rotating and tool lifting on the volume which experiences interference. In the previous paper, (Kiswanto et al., 2007)used the re-tool orientation in the detected area by determining the minimum change of orientation while the roughing gouging was avoided by having a constant orientation by lifting the tool in a constant orientation. The pattern of tool lifting is also done when the re-orientation reaches a maximum angle.

On the other hand, used sampling points and interpolation(Ziwei et al., 2012). The sampling points were taken from the volume and the calculation of the roughing posture was done on each point. This was done with the assumption that the area which could be reached by the tool would change. This area was then interpolated using *B-surface*. The other method, visibility and accessibility based method by(Balasubramaniam et al., 2002, Balasubramaniam et al., 2003)

Meanwhile, to find the CC points or the tool orientation which is free from interferences, the numeric pattern is done with θ angle determined with a certain increment. This pattern is applied to each CC point in CBV area. To ensure that each CC point in the local coordinate system is free from collision, the following steps are taken:

1. Check the determined CC point and the tool posture whether they are free from interference
2. If interference occurs, rotate $\leq 60^\circ$.



3. On each new tool orientation, re-check to see if interference still occurs
4. If the rotation has reached the maximum degree of change with $\theta \leq 60^\circ$, translation is performed with ΔL parallel to the feed direction
5. Each ΔL change can be used as the CC point and the same procedure can be repeated from Step 1.

From the grouping of the CBV and OBV area, the difference in the tool orientation indicates different interference avoidance pattern on each CC point. Generally, the interference avoidance can be done by changing the angle of the tool orientation and can also be done by avoidance movement away from the interference area or commonly referred to as translation. The limitation of rotation and translation will be further explained in the next sub-chapter.

c. Rotation

Rotation by an angle (Θ) about the origin the function is

$$\begin{aligned}
 x^l &= x \cos\Theta - y \sin\Theta \\
 \text{and } y^l &= x \sin\Theta + y \cos\Theta
 \end{aligned}
 \tag{2}$$

$$\begin{bmatrix} x1 \\ y1 \\ 1 \end{bmatrix} = \begin{bmatrix} \cos \Theta & -\sin \Theta & 0 \\ \sin \Theta & \cos \Theta & 0 \\ 0 & 0 & 1 \end{bmatrix} \begin{bmatrix} x \\ y \\ 1 \end{bmatrix}
 \tag{3}$$

The tool orientation on each CC point below the CBV is formed based on position vector formed by CC points under the CBV area and the closest points outside the CBV with a maximum z value as illustrated in Figure 8 below. The position of the tool orientation for this area which is different than the position for the tool orientation in OBV area will be further explained in the translation sub-chapter.

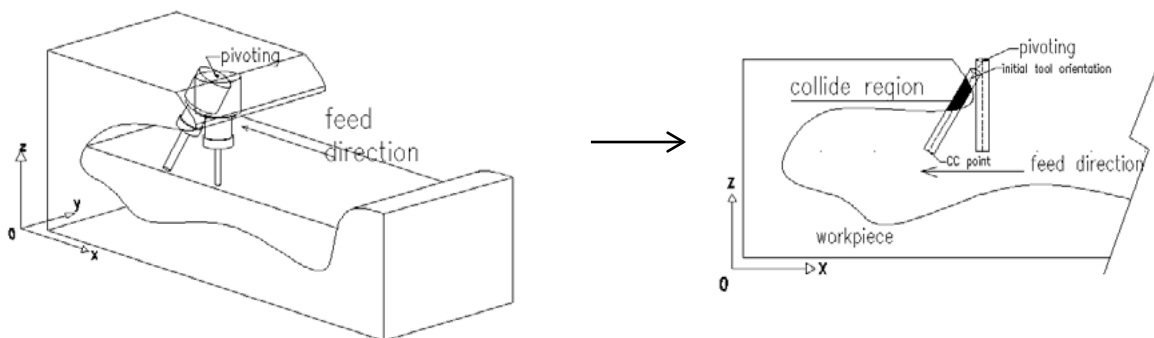


Figure 8. Initial tool orientation in CC points in CBV area

On the example above, after the CC points are obtained with the position (x, y, z) on the local coordinate system, the collision avoidance pattern can be performed. The procedure for the avoidance uses the numeric method with a fixed angle interpolation starting from the initial tool orientation position with the CC point as the pivoting point of the rotation with direction $(i, j, k) = \theta^0$ and for $(i^l, j^l, k^l) = (i, j, k) + \text{increment } \theta$. This process perform until the n increment with a maximum $\theta = 60^\circ$. In each new position (i^n, j^n, k^n) is reach. This procedure is illustrated in Figure 9 below. When the maximum change in the tool



orientation reaches $\theta = \theta_{max}$, the procedure of the rotation is then stopped and the collision avoidance is performed by moving the CC points to the interference-free points.

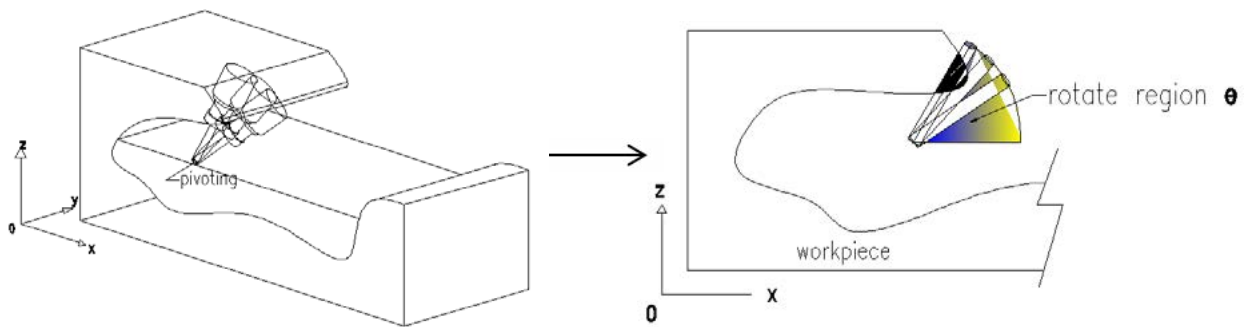


Figure 9. Re-orientation of tools

d. Translation

The translation method to avoid interference is used when:

1. The positions of the tool orientation on one machining method are uniform (Kiswanto et al., 2007)
2. The pattern for avoidance by using rotation has reached the pre-determined maximum angle.

Translation from the initial CC point to the new CC point are illustrated as equations below:

$$P^I = T.P \quad (4)$$

(Tx, Ty, Tz) = transformation distance (ΔL) so in matrix transformation

$$\begin{bmatrix} x1 \\ y1 \\ z1 \\ 1 \end{bmatrix} = \begin{bmatrix} 1 & 0 & 0 & tx \\ 0 & 1 & 0 & ty \\ 0 & 0 & 0 & tz \\ 0 & 0 & 0 & 1 \end{bmatrix} \cdot \begin{bmatrix} x \\ y \\ z \\ 1 \end{bmatrix} \quad (5)$$

In this paper, the uniformity of the tool orientation direction is gained during the rough machining process in OBV area. The tool orientation in this area is parallel to the normal vector of the workpiece so that the tool orientation can be done by adopting the 3-axis machining. The uniformity of tool orientation in OBV area is illustrated in Figure 10 below.

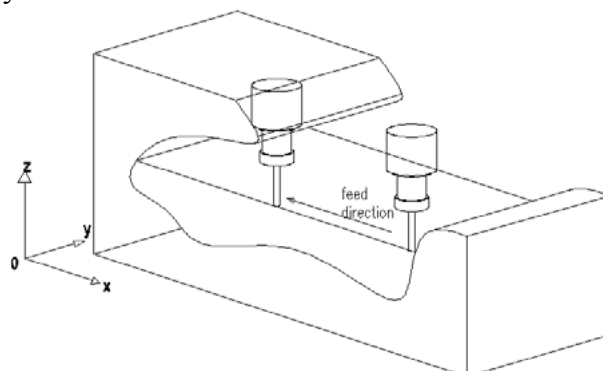
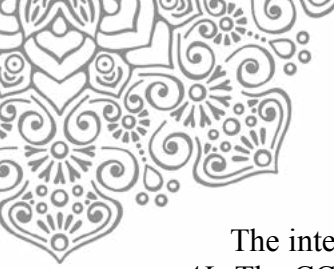


Figure 10. Direction of tool orientation in OBV area.



The interference avoidance pattern in Figure 11 uses the linear interpolation with a fixed ΔL . The CC points which experience interference (rear gouging) become the initial position (x^0, y^0, z^0) to obtain new CC points (x^1, y^1, z^1) . In each new CC point as the result of interpolation that become the initial position, an interference check is performed. This process is done until $n \times \Delta L$.

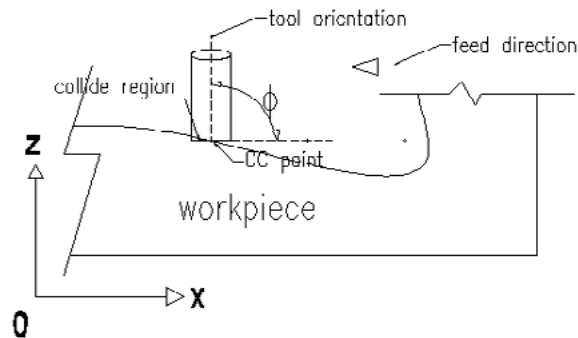


Figure 11. Translation in CC points which experience interference

Meanwhile, the second translation pattern is done when the re-orientation of tool in CBV area has reached the maximum θ angle. Figure 12 below illustrates how the rotation is conducted when the tool experiences interference with the model. However, if the change in the orientation angle has reached a maximum and an interference still occurs, the avoidance is performed by moving the tool with ΔL distance (Figure 13). Interference check is then performed in the result of the translation, which is the new CC points. If there is a collision, the rotation in the CC points is done again until there is no more collision occurred. This procedure is illustrated in Figure 14 below.

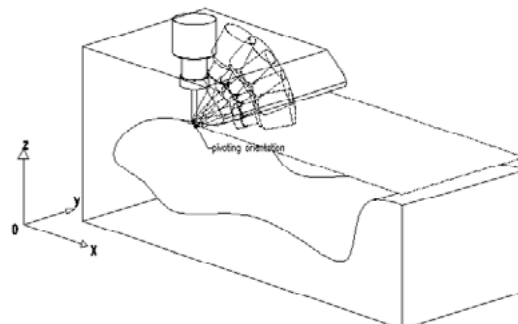


Figure 12. Tool rotation until a maximum angle

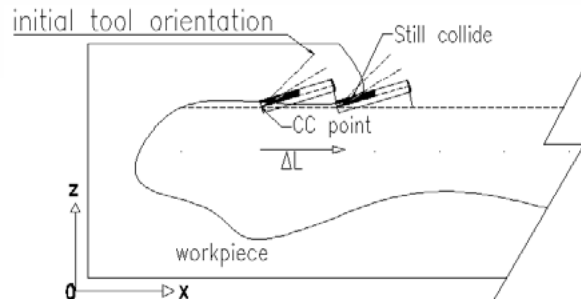


Figure 13. Translation after the tool rotation reaches a maximum angle

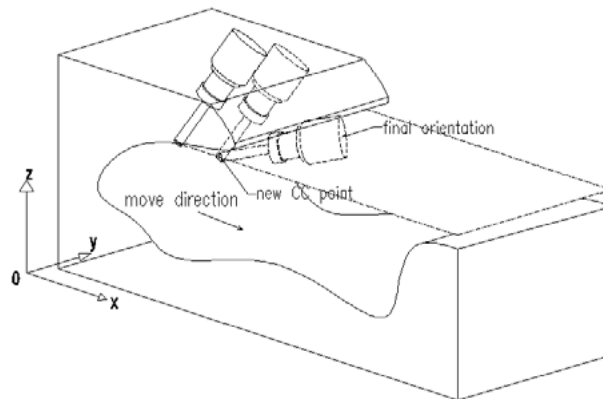


Figure 14. Translation and rotation until CC points are free from interference.

5. RESULTS AND DISCUSSION

The interference avoidance method uses the change in the rotation angle numeric and the length of the translation can be used as the compensation for the change in tool orientation during the rough machining process in CBV area. Adding CC points using initial tool orientation which is free of interference will significantly affect the effectiveness of the rough machining process, especially for models with CBV area. The compensation of the change in tool orientation has been tested in a few models as seen below in table1 (4 CC point at first layer), Figure 15 and Figure 17.

Table 1. The compensation of the change in tool orientation CBV area 1st layer model A

CC Point(x, y, z, i, j, k) At CBV area	Rotation (rot) θ^0	Translation (trx) ΔL	iteration (Σ)	Cutter location (I/O)*
(45, 10, 65, 15, 0, 35)	3	0	3	0
(40, 10, 65, 20, 0, 35)	9	3	7	1
(35, 10, 65, 25, 0, 35)	24	8	11	1
(30, 10, 65, 30, 0, 35)	21	7	8	1

*(1 = new CC point)

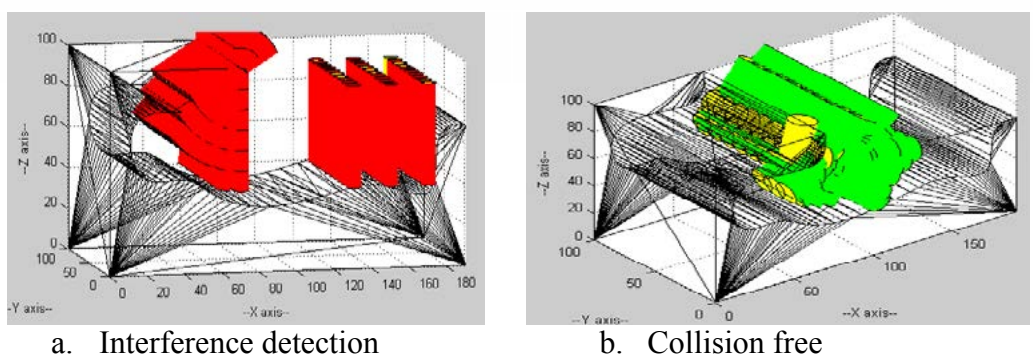


Figure 15. Model A

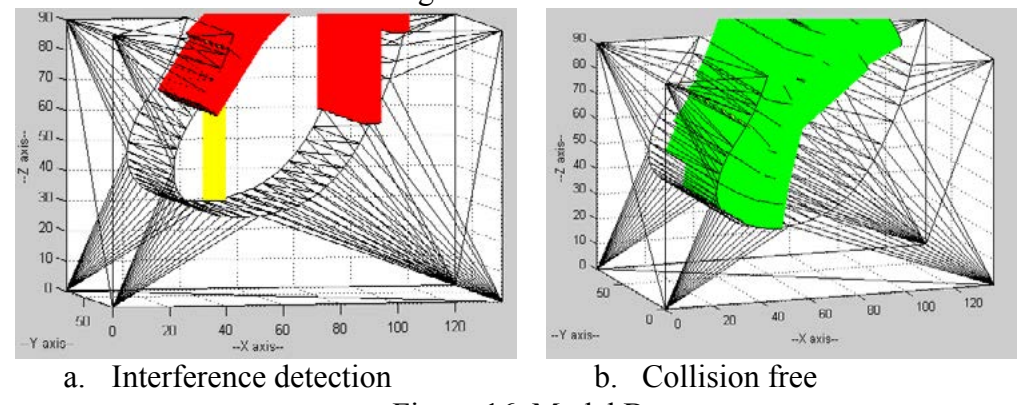


Figure 16. Model B

6. CONCLUSION

This paper presents a method of re-orientation of the tools on CC point at CBV area. This accomplished by interpolating fixed angles to the maximum limitation of 60° according machine capability. If the interference still occurs, translation to getting new CC point as used. Finally, new CC point and new tools orientation used as CC point tool trajectory at rough machining.

7. REFERENCES

ALI LASEMI, D. X., PEIHUA GU 2010. Recent development in CNC machining of freeform surfaces: A state-of-the-art review. *Computer aided design*, 42, 14.

BALASUBRAMANIAM, M., HO, S., SARMA, S. & ADACHI, Y. 2002. Generation of collision-free 5-axis tool paths using a haptic surface. *Computer-Aided Design*, 34, 13.

BALASUBRAMANIAM, M., SARMA, S. E. & MARCINIAK, K. 2003. Collision-free finishing toolpath from visibility data. *Computer-Aided Design*, 35, 16.

D.C.H.YANG, Z. H. 1999. Interference detection and optimal tool selection in 3-axis NC machining of free form surface. *computer aided design*, 31.

KISWANTO, G., LAUWERS, B. & KRUTH, J.-P. 2007. Gouging elimination through tool lifting in tool path generation for five-axis milling based on faceted models. *Int. J Adv Manuf Technol*, 32, 21.



- KISWANTO, G., SUTRISNO, H. H. & ISTIYANTO, J. 2017. Non Machinable Volume Calculation Method For 5-Axis Roughing Based On Faceted Models Through Closed Bounded Area Evaluation. *Int. Conf. Mechanical, Aeronautical and Automotive Engineering 2017*, 5.
- KISWANTO., G. & PANUJU, A. Y. T. 2010. Development of closed bounded volume(CBV) grouping method of komplek faceted model through CBV Boundaries identification. *IEEE*, 3, 5.
- KRUTH, B. L. G. K. J. P. 2003. Development of a Five axis Milling Tool Path Generation Algorithm based on faceted model.
- LEE, Y.-S. 1997. Admissible tool orientation control of gouging avoidance for 5 axis complex surfce machining. *computer aided design*, 29.
- LIN, Z., FU, J., SHEN, H. & GAN, W. 2013. Efficient cutting area detection in roughing process for meshed surfaces. *The International Journal of Advanced Manufacturing Technology*, 69, 525-530.
- M. BALASUBRAMANIAM, P., LAXMIPRASAP 2000. Generating 5-axis NC roughing path directly from a tessellated representation. *Computer aided design*, 32.
- MANNAN, S. D. M. A. 2004. Oriented bounding box and octree based global interference detection in 5-axis machining of free form surface.
- MASOOD, A., SIDDIQUI, R., PINTO, M., REHMAN, H. & KHAN, D. M. A. 2015. Tool path generation, for complex surface machining, using point cloud data. *conference on suitable manufacturing*, 26, 6.
- MOHANAD MAKKI, C. T., FRNACOIS THIEBAUT, CLAIRE LARTIGUE, CHARYAR SOZANI 2010. 5-axis Direct Machining of Rough Clouds of Points. *computer aided design*, 10.
- MOLLER, T. & TRUMBORE, B. 1997. Fast MinimumStorage RayTriangle Intersection.
- PARK, S. C. 2004. Sculptured surface machining using triangular mesh slicing. *Computer-Aided Design*, 36.
- SUTRISNO, H. H., KISWANTO, G. & ISTIYANTO, J. 2017a. Development of Initial Tool Orientation Method At Close Bounded Area for 5-Axis Roughing Based On Faceted Models. *ICMM*, 3.
- SUTRISNO, H. H., KISWANTO, G. & ISTIYANTO, J. 2017b. The Improvement of the Closed Bounded Volume (CBV) Evaluation Methods to Compute a Feasible Rough Machining Area Based on Faceted Models *int. Conf. on Manufacturing, Optimization, Industrial and Material Engineering 2017*, 5.
- TANG, T. D. 2014. Algorithms for collision detection and avoidance for five-axis NC machining: A state of the art review. *Computer-Aided Design*, 39.
- YUAN, E.-T. & SHAO, B. 2012. Tool-path Generation of Multi-axis Machining for Subdivision Surface. *AASRI Procedia*, 3, 6.
- ZIWEI, L., HONGYAO, S., WENFENG, G. & JIANZONG, F. 2012. Approximate tool posture collision-free area generation for five-axis CNC finishing process using admissible area interpolation. *Int. J Adv Manuf Technol*, 62, 13.



QIR

*The Westin Resort
Nasa Dua, Bali*
24-27 July 2017

SYMPOSIUM C

**International Symposium
on Electrical and Computer
Engineering**





COMPRESSED NATURAL GAS (CNG) TECHNOLOGY AT GRATI POWER PLANT

Retno Aita Diantari
Electrical Engineering Department
College of Engineering – PLN (Foundation for Education & Welfare PT. PLN (Persero))
Jakarta, Indonesia
retno_aita@yahoo.co.id

Isworo Pujotomo
Electrical Engineering Department
College of Engineering – PLN (Foundation for Education & Welfare PT. PLN (Persero))
Jakarta, Indonesia
isworop@yahoo.com

Abstract—Gas has great potential to be converted into electrical energy. Indonesia has natural gas reserves up to 50 years in the future, but the optimization of the gas to be converted into electricity is low and unable to compete with coal. Gas is converted into electricity has low electrical efficiency (25%), and the raw materials are more expensive than coal. Steam from a lot of wasted gas turbine, thus the need for utilizing exhaust gas results from gas turbine units. Combined cycle technology (Gas and Steam Power Plant) be a solution to improve the efficiency of electricity. Among other Thermal Units, Steam Power Plant (Combined Cycle Power Plant) has a high electrical efficiency (45%). Weakness of the current Gas and Steam Power Plant peak burden still using fuel oil. Compressed Natural Gas (CNG) Technology may be used to accommodate the gas with little land use. CNG gas stored in the circumstances of great pressure up to 250 bar, in contrast to gas directly converted into electricity in a power plant only 27 bar pressure. Stored in CNG gas used as a fuel to replace loadbearing peak. Lawyer System on CNG conversion as well as the power plant is generally only used compressed gas with greater pressure and a bit of land.

Keywords : Fuel; Compressed Natural Gas; power plants; efficiency of electricity

I. INTRODUCTION

Electricity consumption per capita is an index of living standard of a country. In Indonesia, with the increasing industrial activity and population, the need for electrical power also increased. Due to the increase in fuel prices today's world, PT. PLN (Persero) as one of the state electricity company should think businesses operating cost savings, of which 75% are in fuel costs. One effort that can be taken by PT. PLN (Persero) is the main power plant fuel switching from fuel oil (HSD and MFO) into natural gas.

Basically PLN operate Power Gas and Steam (Power Plant) as peaker plants (peak load) because operating costs are more expensive than base load generation (base load). Oil energy crisis that resulted in soaring oil prices caused the gas to be used as an alternative PLN for plant outside of peak load. During this time, when the load is low (outside of peak load), the supply of gas for the power plant is not absorbed optimally, as appropriate loading pattern in the Java-Bali

system more filled by many ordinary coal plant production is cheaper. Nevertheless, the unabsorbed gas must still be paid, the gas supply contract is a take or pay. While at peak load gas supply is insufficient, so that some plants have to be operated using the fuel.

Presence technology Compressed Natural Gas (CNG) is expected to be a solution to the problem mentioned above. Gas supply flow rate remain while outside of peak load, partially compressed into CNG tube pressurized to 250 bar for 10 hours. CNG use of technology for the generation of a rock thing, not in other countries. Much of the world uses Liquid Natural Gas (LNG) technology.

II. GAS POWER PLANT AND STEAM

Power Plant is a combination of the working principle of the power plant by gas and steam power plant or so-called combined cycle. Power plant using a gas turbine unit driving the generator, so that the working principle of the power plant following the working principle of the gas turbine. The gas turbine is designed and made for converting heat energy from burning fuel into mechanical energy. The system uses the principle of the Brayton cycle gas power plant. While the working principle of the power plant is converting the chemical energy in the fuel is converted into thermal energy in the form of vapor pressure and high temperature, the steam then changed to mechanical energy to drive generator. The system uses the principle of the Rankine cycle power plant. Figure 1 is a Grati power plant in East Java with a capacity of 526.850 MW which use the principle of combined cycle.



Figure 1. Grati Power Plant in East Java (Pasuruan)



Grati Power Plant in East Java (Pasuruan) consists of:
Gas Turbine: 112.450 MW x 3; Steam turbine: 189.500 MW;
Block output 526.850 MW.

a. Combined cycle;

In improving the efficiency of gas turbines do combined cycle gas turbine with a steam turbine cycle in order to obtain the combined cycle which is commonly referred to as "co-generation". Meanwhile, to improve the thermal efficiency of the gas turbine is used combined cycle, forming a so-called "Combined Cycle" or Steam Gas Power Plant (Power Plant). Cycle power plant applying the Brayton cycle, whereas the ideal cycle Rankine cycle power plant apply.

b. Brayton cycle;

Brayton cycle (Brayton Cycle) shown in Figure 2 consists of isentropic compression process that ended with the release of heat at constant pressure. In Bryton cycle of each state processes can be analyzed as follows:

1-2 (isentropic Compression).

Work required by the compressor:

2-3: Entry of the fuel at a constant pressure.

3-4: isentropic expansion in the turbine.

4-1: Discharge heat at constant pressure into the air.

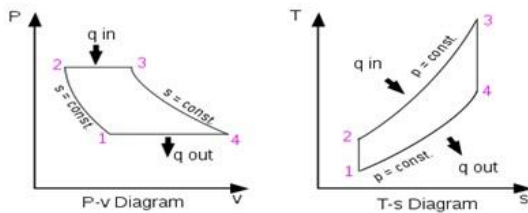


Figure 2. *p-v and t-s Brayton Syklus Diagram*

From Figure 2 on p-v diagram and t-s, it can be seen that the inclusion of heat takes place at a constant pressure:

$$Q_{in} = m \cdot c_p \cdot (T_3 - T_2) \quad (1)$$

- Spending too hot at constant pressure:

$$Q_{out} = m \cdot c_p \cdot (T_4 - T_1) \quad (2)$$

- Thus, useful work can be formulated as follows:

$$W_u = Q_{in} - Q_{out} \quad (3)$$

c. Rankine cycle;

Rankine cycle in Figure 3 is used in the steam turbine power plant system. The sequence steps as follows:

a - b: Water is pumped from the pressure p2 be p1. This step is a compression step isentropis, and this process occurs at the water pump filler.

b - c: Air pressure is increased the temperature until it reaches boiling point. Occurred in the Low Pressure heater, High Pressure heater and Economiser.

c - d: Water transformed into saturated steam. This step is called evaporation with isobars isothermis process, occurred in the boiler is in the wall tube (riser) and the steam drum.

d - e: Steam is heated further until the vapor reaches a temperature further work into hot steam (superheated vapor). The move occurred in the boiler superheater with the isobars.

e - f: Steam does work so that the pressure and the temperature dropped. This step is a step isentropis expansion, and occur within the turbine.

f - a: Disposal of latent heat of the steam that turns into condensate water. This step is isothermis isobars, and occurs in the condenser.

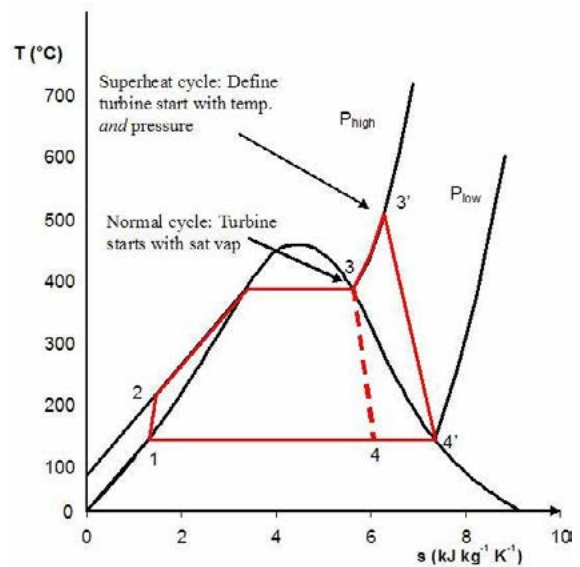
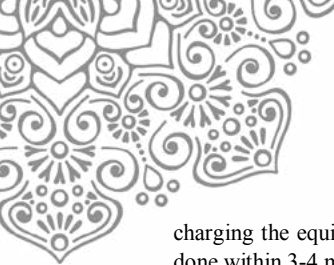


Figure 3 Diagram T - s Rankine Cycle
Source : Indian Institute of Technology Madras

III. COMPRESSED NATURAL GAS

Compressed Natural Gas (CNG) is a fluid gas that has been processed into a high-pressure natural gas compression in a tube. In general, the major components containing CNG methane (CH₃) and ethane (C₂H₈) with fraction of about 90%. CNG is made by compressing methane (CH₄), which is extracted from natural gas. CNG is stored and distributed through the packaging in the tank (pressure vessel or pressure vessel). Ideally, the pressure on the gas pipeline is 11 bar, while the CNG requires a pressure of 200 bar, or 197 atm, 197 times normal air pressure. With a pressure of 200 bar,



charging the equivalent of 130 liters of premium gas can be done within 3-4 minutes. Figure 4 shows an example of CNG tubes.

Calorific value is the amount of heat generated by the combustion of materials or fuels. Measured in units of energy per amount of material, for example kJ / kg. Calorific value of the fuel is divided into two kinds, namely: a calorific value above (HHV) and lower calorific value (LHV).



Figure 4. pressure of 200 bar CNG Tubes

Higher Heating Value (HHV) or above is the calorific value derived from the combustion of 1 kg of fuel, taking into account the vapor condensation heat (water resulting from combustion are in liquid form). HHV gas = 1089 Btu / ft³ = 52.225 MJ / kg.

Lower Heating Value (LHV) or lower calorific value is obtained calorific value of combustion heat regardless vapor condensation (water produced from burning was on gas / steam). LHV gas = 983 Btu / ft³ = 47.141 MJ / kg.

A fuel flash point is the lowest temperature at which the fuel can be heated so that steam output flame briefly when passed a flame. Flash point -187.80C CNG temperature. Burning point is the lowest temperature at which sufficient oxygen conditions, spontaneous combustion can occur. Burning point unit is degrees (°) or degrees Celsius (°) Fahrenheit. CNG point at a temperature of 540°C. Octane number is a number that shows the number as a percentage (%) volume of isooctane in a mixture that consists of n-heptane isooctane and that does not cause outbreaks in the fuels being tested in a compression chamber of a combustion chamber.

According to the science of thermodynamics, the higher the ratio / percentage of compression used, the higher the efficiency of combustion in the combustion chamber. CNG octane value of the percentage of 130%.

Tube specifications for CNG fuel is as follows:

Capacity	= 50-100 (m ³)
Dimensions	= 11657 x 2428 x 3028
Massa Netto	= 10760 kg
Nominal Diameter	= DN80
Material	= 16 MNR

The selected specification is commercial fleet refuel CNG compressor station, with a pressure of 1.4-250 bar and a capacity of 1.3 m³ / h.

CNG has both pluses and minuses. One advantage is it is a lot cleaner than gasoline and diesel fuel. CNG-powered vehicles emit a lot less carbon monoxide, nitrogen oxides—a primary component of smog—and particulates, which can trigger a range of health problems. But CNG has much lower energy density than liquid fuels. A gallon of CNG has only a quarter as much energy as a gallon of gasoline. The low energy density and the pressure of the highly compressed gas requires CNG vehicles to have big, bulky fuel tanks, which means that CNG is practical mainly for bus and truck fleets that refuel in central locations. And that, in turn, means that CNG use for transportation is still rare. In 2014, only 0.12 percent of the natural gas consumed in the United States was used to power vehicles, according to the Energy Information Administration.

LNG is a way of transporting natural gas long distances when pipelines aren't an option—across oceans, for example. Producing LNG involves compressing and cooling natural gas to around minus 260 degrees Fahrenheit. That process converts the gas to a liquid and cuts its volume to 1/600th of the original, making it possible to ship the LNG in special tankers. Once it gets to its destination, the LNG can be unloaded at a receiving terminal and regasified—turned back into a gas. It can then be delivered through local pipelines to customers.

The infrastructure for LNG—for cooling and compressing, shipping and regasifying—can be extensive and expensive. Producing and transporting LNG is also very energy intensive. These factors make it difficult for LNG to compete with U.S. domestic natural gas supplies given the recent dramatic increase in shale gas production. U.S. imports of LNG, which grew steadily in the late 1990s, peaked in 2007, and are now at their lowest level since 1987. They represent just 0.2 percent of U.S. natural gas consumption.

Still, LNG has continued to play an important role in providing gas in some regions in specific times of the year—in New England during the winter, for example. And, as a new paper from the Conservation Law Foundation shows, more strategic use of existing LNG infrastructure can help avoid the need for expensive new natural gas pipelines.

More broadly, natural gas has played an important role in the electric utility sector by lowering electricity costs, reducing carbon pollution, and helping the country move to more renewable energy. Natural gas provided more than 27 percent of U.S. electricity in 2014, up from 22 percent in 2007, while coal-fired generation fell from about half to 39 percent over that same period.



For the transportation sector, natural gas can address needs more effectively—with lower carbon emissions—through electrification than through CNG. While a natural gas-powered Honda Civic emits about 15 percent less global warming pollution than a conventional Civic, for example, using natural gas to generate electricity for a plug-in vehicle can deliver carbon emissions savings of as much as 40 percent.

But overly relying on natural gas in the electric sector—for electric vehicles or many other uses—could be a problem. A UCS analysis from earlier this year showed how dramatically expanding the use of natural gas for electricity generation would threaten the economy, public health and the climate. And our just-released analysis of state reliance on natural gas for power plants found that two-thirds of U.S. states may be putting electric ratepayers at risk by failing to diversify their electricity mixes.

Investing more in such clean energy resources as solar, wind and energy efficiency will be critical for managing overreliance on natural gas, even as utilities move away from coal. Many aspects of the Environmental Protection Agency's new Clean Power Plan will help make that happen, creating incentives for states to prioritize clean energy over natural gas as they look to clean up their fuel mixes.

IV. OUTPUT POWER CNG CAPACITY ANALYSIS

1. Technical Analysis

Grati power plant that has the capacity of 3.5 MMSCF CNG with gas turbine efficiency of 45% and CF = 0.8 / year in operation for 6 hours output power can be determined as follows:

$$\begin{aligned}
 \text{Production MWh} &= (\text{SCF} \times 922 \times \eta) / 3413 \\
 &= (3.5 \times 1,000,000 \times 922 \times 0.45) / 3413 \\
 &= 425.476 \text{ MWh} \\
 \text{Output power} &= (\text{Production MWh}) / (\text{operating time}) \\
 &= (425.476 \text{ MWh}) / (6 \text{ h}) \\
 &= 70.91 \text{ MW}
 \end{aligned}$$

Fuel is needed to generate power output of 70.91 MW are as follows:

$$\begin{aligned}
 \text{BBG} &= (3413 \times \text{Power Output}) / \eta \\
 &= (3413 \times 70.91) / 0.45 \\
 &= 538 \text{ MMBTU} \\
 &= 512,380.9524 \text{ ft}^3 \\
 &= 14,508,579.05 \text{ lt}
 \end{aligned}$$

with:

$$\begin{aligned}
 1 \text{ ft}^3 &= 1050 \text{ btu} \\
 1 \text{ ft}^3 &= 28.316 \text{ lt} = 28.316 \text{ dm}^3
 \end{aligned}$$

2. Economical Analysis

a) Fixed costs

According to the above matter at Grati power plant installed two units of CNG with a capacity of 2 x 70.91 MW. If the interest rate i of 12% by age 25 years plants can be seen:

$$\text{CRF} = (i(1+i)^n) / ((1+i)^n - 1) = (0.12(1+0.12)^{25}) / ((1+0.12)^{25} - 1) = 0.127$$

Development costs PLT-CNG = 5.94864 \$ / kWh

CF = 80%

$$\begin{aligned}
 \text{CC} &= (\text{cost of construction of generating capacity} \times \text{CRF}) / \text{W} \\
 &= (5.94864 \times 400 \times 10^3 \times 0.127) / (400 \times 10^3 \times 0.8 \times 6 \times 365) \\
 &= 4.4 \times 10^{-4} \text{ $ / kWh}
 \end{aligned}$$

b) operating and maintenance costs

$$\begin{aligned}
 \text{O \& M} &= (\text{total cost of O \& M}) / (\text{CF} \times \text{time} \times \text{cap}) = \\
 &= (20347106.98 \text{ ($)}) / (0.8 \times 6 \times 365 \times 400 \times 10^3 \text{ (kWh)}) = 0.03 \text{ $ / kWh}
 \end{aligned}$$

c) the cost of fuel

$$\text{Fc} = (\text{Ui} \times 860) / 0.45 = (860 \times 7.313 \times 10^{-7}) / 0.45 = 1.4 \times 10^{-3} \text{ $ / kWh}$$

d) Total cost

$$\text{Tc} = \text{CC} + \text{O \& M} + \text{Fc} = 4.4 \times 10^{-4} + 1.4 \times 10^{-3} + 0.03 = 0.03184 \text{ $ / kWh}$$

V. CONCLUSION

From the analysis of the utilization of CNG fuel at Grati power plant can be concluded that:

- The use of CNG is useful to reduce system losses on gas purchases at gas power plant (power plant) in take or pay that lead to wasted unused gas.
- Costs required by CNG stations is equal to 0.03184 \$ / kWh with details:
 - Construction of 4.4×10^{-4} Cost \$ / kWh
 - Operation and Maintenance Costs \$ 0.03 / kWh
 - Cost of Fuel 1.4×10^{-3} \$ / kWh

REFERENCES

- Kundur, P, (1994), Power System Stability and Control, EPRI, Mc.Graw Hill, Inc, New York.
- Saadat, H, (1999), Power System Analysis, Mc. Graw Hill Book Co, Singapore.
- "Liquefied Petroleum Gas (LPG), Liquefied Natural Gas (LNG) and Compressed Natural Gas (CNG)".
- "Gas South: Compressed Natural Gas". www.gas-south.com.
- "ISO 14469-2:2007 - Road vehicles -- Compressed natural gas (CNG) refuelling connector -- Part 2: 20 MPa (200 bar) connector, size 2". Iso.org.
- "ISO 15500-9:2012 - Road vehicles -- Compressed natural gas (CNG) fuel system components -- Part 9: Pressure regulator". Iso.org.



Analysis Study Level Total Harmonic Distortion (THD) at Substation - Customer Distribution Substation Industry, Business and Household

¹Albert Gifson

Lecturer, College of Engineering – PLN (Foundation for Education & Welfare PT. PLN (Persero)). PLN tower. Jl. Outer West Lingkar, Duri Kosambi, Cengkareng, Indonesia 11750

albertdoang@yahoo.co.id

²Juara Mangapul

Lecturer, College of Engineering – PLN (Foundation for Education & Welfare PT. PLN (Persero)). PLN tower. Jl. Outer West Lingkar, Duri Kosambi, Cengkareng, Indonesia 11750

juaramagapult_stmsi@yahoo.com

³Heri Suyanto

Lecturer, College of Engineering – PLN (Foundation for Education & Welfare PT. PLN (Persero)). PLN tower. Jl. Outer West Lingkar, Duri Kosambi, Cengkareng, Indonesia 11750

heri.suyanto@yahoo.co.com

Abstract - Harmonics is a symptom caused by his disability sinusoidal waveform of voltage or current permanent basis, with the occurrence of defects in the sinusoidal wave is then mathematically flawed sinusoidal wave can be decomposed into many pure sinusoidal wave with a frequency of integer multiples of the fundamental frequency. Symptoms harmonics are now often found in the distribution system in connection with many types of equipment especially those containing electronic components. Symptoms of harmonics that occur in the distribution system will cause some adverse impact on the operation of the distribution system including increased loss of power losses, increasing the temperature of operation of the equipment, and distort the gauge (cause inaccuracies in measuring tools).

In the course of this research will be studied, researched and analyzed the levels of harmonics in various types of distribution substations Jakarta area, especially for congested areas such as load industrial areas, business centers, dense residential area. And is expected to make reference to the design of the filter with the capacitor value calculation formula used in the method for reducing the influence of the harmonic distortion.

Keywords: *harmonics, filters, and capacitors*

1. Introduction

Power quality is a reference to ideals electric power system is indicated by the deviation value of frequency, voltage stability and continuity of distribution to the consumer, where all these parameters should be strictly in accordance with the standards and criteria, especially in the industrial world. The decline in power quality due to, among other :

1. The use of electronic equipment is increasingly widespread as information technology equipment, Adjustable Speed Drive (ASD), Programmable Logic Controllers (PLC), energy saving lamps resulted in a change in the nature of the electrical load.

2. Expenses for non-linear causes disturbance to the voltage waveform.

Lately a lot of electrical equipment, especially equipment that contains switching components in electronic equipment either used in homes, on the street lights and billboards as well as in industrial areas such as the control equipment and automation equipment industry will cause symptoms harmonics the distribution system. This is detrimental to both the power company and the customer. The content is quite high harmonics would distort equipment, such as measuring instruments, protective equipment and cause power losses and generate heat on some equipment such as transformers and others.

To reduce the level of harmonics (THD value) of the power system, should be known prior notice harmonic wave beberapa most dominant, it can be known from measurements of the frequency spectrum. Wave with a specific frequency which has the largest amplitude (dominant) are to be suppressed by installing in parallel a filter that "only" miss the wave with a specific frequency of the.

2. Objective

The main objective of this study was to analyze the level of harmonics at several distribution substations in Cengkareng Area Services, Distribution PT. PLN Jakarta and Tangerang. The contributor also to determine the contribution of its THD value from the source to the contribution of each order of the harmonics of the value of THD total. The other objectives of this study are:

1. With this study, is expected to make a reference to the design of the device with a passive filter capacitor value calculation formula to use in



methods for reducing the influence of harmonic distortion.

- Expected hasill this author can be used by various parties as a source of knowledge about harmonics.

3. Review of Literature

The literature review is taken reference is :

- IEEE *Recommended Practice For Monitoring Electric Power Quality*, IEEE Standard. 519 – 1992
- IEEE 2000 “*A Draft Standard Glossary Of Power Quality Terminology*” (7 Juli 1999).
- Mc. Graw – Hill, Roger C, buku *Electrical Power System Quality second Edition*.

4. Overview of Theoretical Basic Principles Harmonics

Harmonics is a disorder that occurs in the electricity distribution system caused by the current and voltage waveform distortion periodically. In the electric power system there are two types of loads, ie load linear and non-linear loads. Linear load is a load which provides a linear output waveform within the meaning of the current flowing is directly proportional to the impedance and voltage changes. While the non-linear load is a load which provides waveform output is not proportional to the voltage in each half cycle, so that the current waveform and the output voltage is not the same as the waves enter it (distorted). Harmonics are caused by a weight that is called non-linear loads.

Table 1. As a result of the polarity of the harmonic components

Order	The effect on the motor	The effect on the distribution system
Positive	Rotating magnetic fields cause the forward direction (forward)	<ul style="list-style-type: none"> Heat
Negative	Give rise to a magnetic field rotating backwards (reverse)	<ul style="list-style-type: none"> Heat Direction of rotation of the motor change
Zero	There is no	<ul style="list-style-type: none"> Heat Create / add to current on the neutral wire

Source : IEEE Standard 519-1992 : *Recommended Practices and Requirements for Harmonic Control in Electrical Power Systems*.

The formula for voltage THD:
a. THD of the fundamental RMS prices

$$THD_F = \frac{V_{HRMS}}{V_F} \times 100\%$$

Formula for current THD:
a. THD of the fundamental RMS prices

$$THD_F = \frac{I_{HRMS}}{I_F} \times 100\%$$

b. THD against RMS total price

$$THD_F = \frac{V_{HRMS}}{V_{RMS}} \times 100\%$$

b. THD against RMS total price

$$THD_F = \frac{I_{HRMS}}{I_{RMS}} \times 100\%$$

The total price of a wave based RMS Harmonic component expressed as:

$$I_{HRMS} = \sum_{n=2}^{\infty} I_n$$

$$I_{HRMS} = \sqrt{I_2^2 + I_3^2 + I_4^2 + I_5^2 + I_6^2 + I_7^2 + \dots}$$

Contributions total RMS wave Harmonic distortion is expressed as :

$$I_{HRMS} = \sqrt{I_2^2 + I_3^2 + I_4^2 + I_5^2 + I_6^2 + I_7^2 + \dots I_N^2}$$

RMS fundamental contribution to the waveform distortion is expressed as :

$$I_{RMS} = \sqrt{I_1^2} = I_1$$

Harmonic filter

The objective of the harmonic filter is to reduce the amplitude of frequency - a specific frequency of a voltage or current. With the addition of harmonic filter, then the flow of harmonic currents to the entire network can be minimized. Filter other methods for suppression of harmonics is :

1. Installation Parallel Passive Filter

Passive filter installed on the system with the primary objective to dampen harmonics and other purposes, namely to improve the power factor, a component of the L, C which can be tuned to one or two frequencies.

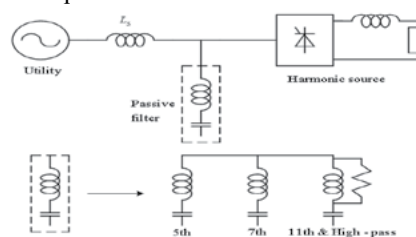


Figure 1. Parallel Filter Passive

2. Installation Parallel Active Filter

Active filter is a harmonic filter consisting of components - the active components, such as inverters are controlled specifically and actively detects harmonic current components in the network. Active Filter can also compensate for the power factor or the other function.

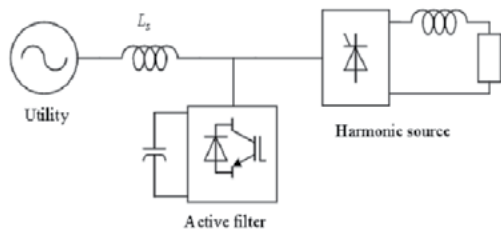


Figure 2. Parallel Active Filter

3. Installation Hybrid Filter

In a conventional hybrid active filter, active filter connected to a passive shunt filter through a transformer. For a filter configuration like this requires an active filter which is small for filter capacitor voltage lowers great on the fundamental component. Active filters are connected in series to the shunt passive filter through a transformer.

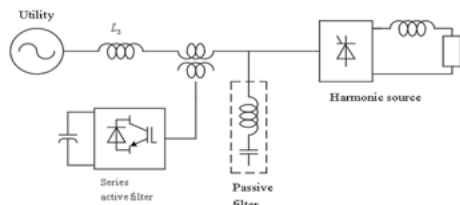
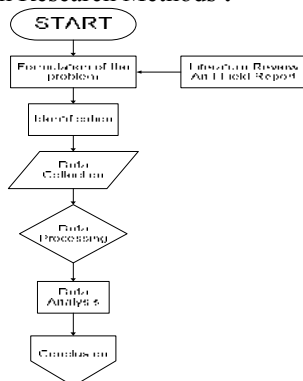


Figure 3. Parallel Hybrid Active Filter

5. Research methods

The method used in this study there are several stages as follows :

Flow Diagram Research Methods :



6. Research result

6.1 Technical Data Measurement

Measuring instrument used for data collection of this research is the Power Quality Analyzer DM III MultiTest. Here are the specifications of the instruments used to measure the amount :

1. The content level Voltage harmonics THD and THD Flow
2. Rated Voltage, Current, Power Factor (PF), Flow Neutral
3. Power terpakai value on load.



Figure 4. Figure Measuring Instrument Power Quality Analyzer DM III MultiTest

6.2 Implementation Measurement

Accurate data acquisition time is actually the time of peak load and off-peak hours, but due to limited access to the distribution substation at peak load measurements were mostly carried out during peak load. The following image measurement circuit implemented :

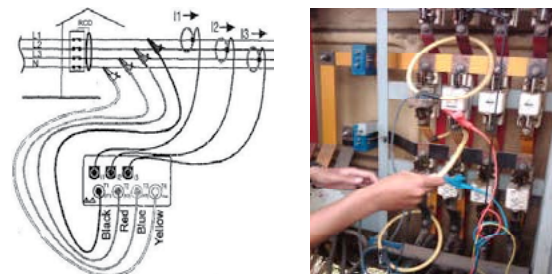


Figure 5. Network Performance Measurement Distribution Substation PT. PLN

6.3 Measurement and Data Acquisition

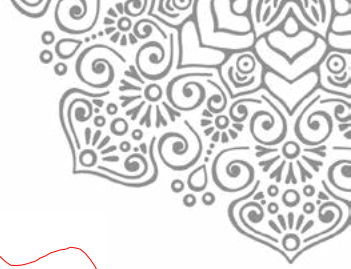
From the results of measurements in the field, especially in some of the 32 Distribution Substation total number of 123 all measurement data distribution substations Industrial Customers, Businesses and Households obtained as follows :

THD Observation Data Flow Distribution Substation Industrial Customers

From the measured data rate industrial customers current THD value of 36 field measurement data. THD current that exceeds the value of 15% there are 5 data from 36 data, and harmonics that occur in the harmonic 3 and 5.

Table 2. Maximum Flow THD At Industrial Customers

No. Data	Code Substation	THD current		
		THD IR (%)	THD IS (%)	THD IT (%)
3	TG 475	12.85	22.02	11.5
4	TG 475	12.392	23.12	12.4
11	MK 173	16.318	16.55	18.5
30	TG 105	19.191	14.39	13.9
32	DK 223 P	16.694	13.27	9.6

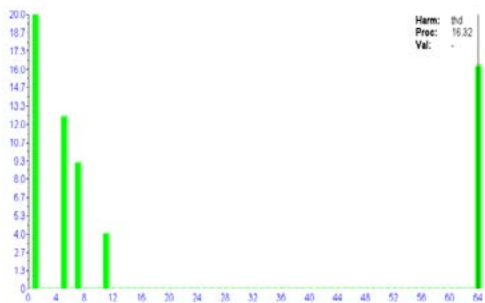


The distribution substations that current THD values that exceed the value of 15% as follows :

1. TG 475 substations to supply the industrial area daan mogot.
2. DK 223 P substation to supply special area of metal cutting and steel industry.
3. TG 105 substations to supply special area PT. Altus Nusa independent industrial towels and cloths.
4. MK 173 substations to supply special area PT. Light Prime Plastics (Lionstar) plastic and glass Industry.

Distribution substations highest levels of THD Maximum current Andes substation located on distribution feeders MK 173 Feeder 1 from the number 4 feeder, Here are the results overview Scope Spectrum harmonics and THD measurements of maximum current :

Fasa R (THD IR 16.32 %)



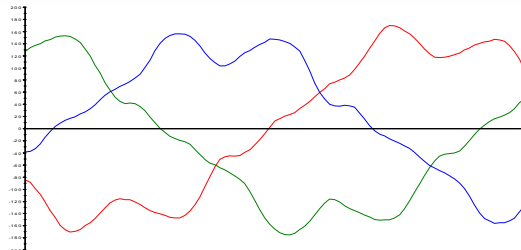
Fasa S (THD IR 16.55 %)



Fasa T (THD IT 18.53 %)



Figure Scope



Voltage THD of all data on industrial customers none exceeds the standard IEEE 159 - 2002 where the maximum voltage THD is 5%. This is because the harmonic voltage measurements performed source side THD Observation Data Flow Distribution Substation Business Customers

From the measured data rate of the value of THD business customers of 32 field measurement data. THD current that exceeds the value of 15%, there are 4 data from 32 data, and harmonics that occur in the harmonic 3 and 5.

Table 3. THD Maximum Flow In Business Customers

No. Data	Code Substation	THD current		
		THD IR (%)	THD IS (%)	THD IT (%)
41	RB 05	16.29	17.18	17.50
42	RB 05	19.52	17.67	20.24
43	RB 05	21.11	22.94	22.41
62	DK 86	20.01	7.04	5.58

Distribution substations that current THD values that exceeded the value of 15% as follows:

1. RB 05 substations to supply the shop area and buildings - office buildings.
2. DK 86 substations to supply special area of metal cutting and steel industry.

Distribution Substation THD Maximum Flow rate is highest in Eong substation feeder RB 05 Feeder 3 KML 9. Here are the results overview harmonic spectrum and THD measurements The maximum current scope :

Fasa R (THD IR 21.11 %)



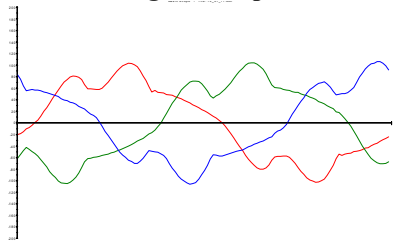
Fasa S (THD IS 22.94 %)



Fasa T (THD IT 22.41 %)

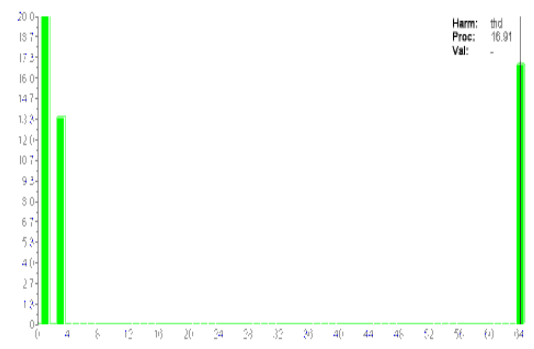


Figure Scope

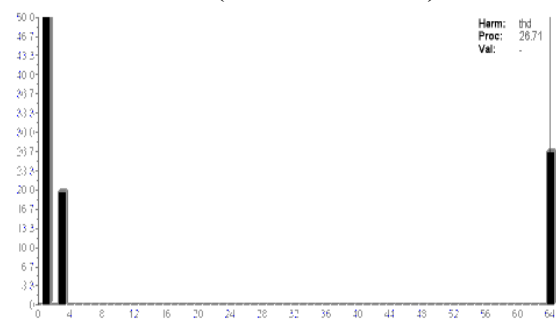


Distribution Substation highest levels of THD Flow On Domestic Customers are on a substation feeder Panca DK 163 Feeder 3 QTY 4, Here are the results overview of the scope and spectrum of harmonic measurement maximum current THD :

Fasa R (THD IR 16.91 %)



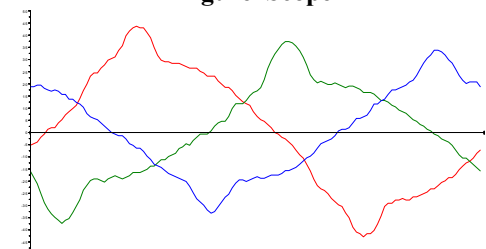
Fasa S (THD IS 26.71 %)



Fasa T (THD IT 16.91%)



Figure Scope



Voltage THD of all data on customers no business that exceeds the standard IEEE 159 - 2002 where the maximum voltage THD is 5%. This is because the harmonic voltage measurements performed source side. Observation Data Distribution Substation Domestic Customers.

From the measured data rate of the value of THD household customers of 55 field measurement data. THD current that exceeds the value of 15% are 8 data from the data 55 (14%) and the harmonics that occur in the harmonic 3 and 5.

Table 4. Maximum Flow THD At Home Customers

No. Data	Code Substation	THD Current		
		THD IR (%)	THD IS (%)	THD IT (%)
69	DK 125	9.903	9.364	16.655
81	MK 159	11.108	15.273	15.049
84	MK 159	8.644	10.086	15.562
86	MK 159	10.021	15.354	9.846
94	TG 388	17.671	7.877	7.817
107	DK 205	15.558	13.484	12.41
110	DK 58	17.84	7.441	10.97
119	DK 163	16.908	26.707	16.908

Distribution substations that current THD values that exceed the value of 15% as follows:

1. DK 125 substations to supply residential complexes Semanan beautiful region. The average housing area - average capacity of 2200 VA.
2. MK 159 substations to supply residential areas pakuan Block AA Daan Mogot.
3. TG 388 substations to supply residential areas motorways Durikosambi with the area are market - the market for the general public.
4. DK 205 substations to supply randu cottage area contained a mixed area settlements and residential complexes.
5. DK 163 substations to supply industrial area households prokopti (factory tempe and tofu).

Voltage THD of all data on household customers nothing that exceeds the standard IEEE 159 - 2002 where the maximum voltage THD is 5%. This is because the harmonic voltage measurements performed source side. Here the percentage rate of the value of THD voltage household customers.

7. Observation and Data Analysis Methods How to Overcome Observation Data Analysis



IEEE Standard 519-1992 is the standard used to control harmonics in electric power systems. This standard is described in Harmonic wave limit for use with a voltage of 120 V samapai pool with 69000 V. The range is typically used for housing, offices and other public facilities. Limits for harmonic current distortion allowed can be seen in the table.

Table 5. Limit Maximum Flow Distortion

Isc/IL	h < 11	11 ≤ h < 17	17 ≤ h < 23
< 20	4.0	2.0	1.5
20 < 50	7.0	3.5	2.5
50 < 100	10.0	4.5	4.0
100 < 1000	12.0	5.5	5.0
> 1000	15.0	7.0	6.0

Isc/IL	23 ≤ h < 35	35 < h	THD(%)
< 20	0.6	0.3	5.0
20 < 50	1.0	0.5	8.0
50 < 100	1.5	0.7	12.0
100 < 1000	2.0	1.0	15.0
> 1000	2.5	1.4	20.0

Sumber : IEEE Standard 519-1992 : *Recommended Practices and Requirements for Harmonic Control in Electrical Power Systems.*

Note:

* All the equipment that generated electricity is limited to the value of this harmonic distortion

I_{sc} : The maximum short circuit current at the PCC (Point of Common Coupling)

I_L : The maximum load current short circuit at the PCC (Point of Common Coupling)

h : Harmonics - n

THD : Total Harmonic Distortion

Table 6. Limitation Maximum Voltage Distortion

% Total Harmonic Distortion Voltage			
Voltage	< 69 kV	69 kV s/d 161 kV	> 161 kV
THD (%)	5	2.5	1.5

Source: IEEE Standard 519-1992 : *Recommended Practices and Requirements for Harmonic Control in Electrical Power Systems.*

- Calculation of short circuit current in the transformer

$$I_{sc} = \frac{kVA_T \times 100}{\% Z \times \sqrt{3} \text{ KV}}$$

Information :

I_{sc} = Short-circuit current (amperes)

KVA_T = Transformer Power (KVA)

% Z = Percentase Impedance

KV = Voltage phase - phase at the low voltage side (Volt)

- Calculation of short circuit current in the transformer

$$I_L = \frac{S}{\sqrt{3} \times V}$$

Information :

I_L = Full load current (Amper)

S = load capacity (VA)

V = Voltage phase - phase at the low voltage side (Volt)

Table 7. Calculation of the value of Isc / IL distribution substation industrial customers

No. Data	Code Substation	Load Capacity (kVA)	Transformer Capacity (kVA)	Isc / IL
3	TG 475	27.98	630	375.3
4	TG 475	31.26	630	335.9
11	MK 173	72.95	400	548.3
30	TG 105	22.41	1000	743.7
32	DK 223 P	76.47	400	523.1

Table 8. Perhitungan nilai Isc / I_L gardu distribusi pelanggan bisnis to XFMR Impedance 6 %

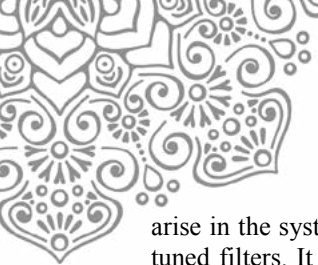
No. Data	Code Substation	Load Capacity (kVA)	Transformer Capacity (kVA)	Isc / IL
41	RB 05	45.02	400	129
41	RB 05	56.09	400	103.5
43	RB 05	41.73	400	139.2
62	DK 86	22.96	400	252.9

Table 9. The calculation of the value of Isc / IL distribution substations household customers XFMR Impedance 6 %

No. Data	Code Substation	Load Capacity (kVA)	Transformer Capacity (kVA)	Isc / IL
69	DK 125	24.67	1000	675.6
81	MK 159	34.91	400	191
84	MK 159	57.32	400	116.3
86	MK 159	87.41	1000	190.7
94	TG 388	50.09	630	209.6
107	DK 205	33.15	400	201.1
110	DK 58	46.58	1000	357.8
119	DK 163	14.03	400	475.2

Passive Filter Design Method For Suppressing Harmonics

To suppress harmonic current that occurs, then the selected filter passive harmonic filter types. Passive filters can be used to minimize harmonic currents that



arise in the system. Mode passive filter used is a single tuned filters. It is adapted to the load power factor that is below standard. This single capacitive tuned frequency below the set, to provide reactive power compensation. To design a harmonic filter, there are several stages, namely:

1. Select a frequency that would be set by the filter.

The frequencies will be set on the filter selected based on the characteristics of the load harmonics.

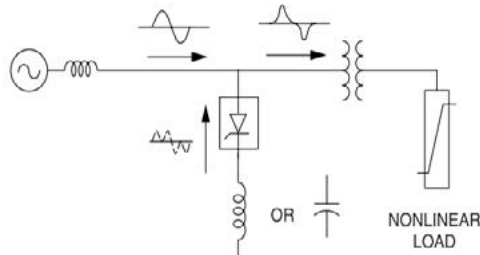


Figure 6. Application Design passive filter on the load

Examples of case studies to design a passive filter applications:

Is known :

Measurement data from distribution substation feeders DK 51 century type of service industries:

System Voltage (kV)	= 0.22 kV
Loads Capacity (kVA)	= 76.34 kVA
System PF (Lag)	= 0.99
System Frequency (Hz)	= 50 Hz
Loads THDi (%)	= 4.334 %
Harmonic orde (th) = 3	
Tranformer capacity (kVA)	= 400 kVA
XFMR Impedance (%)	= 6%
Utility VTHD (%)	= 0.881 %
Desired PF (Lag)	= 0.995
Tuned Frequency	= 2.7

Problems :

what value capacitor filter used for suppression of harmonics to 3 ?

Solving Problems

2. Calculate the size of the capacitor and large resonance

Generally, measure from the filter based on the amount of compensation required reactive power to improve power factor on the system so first done in the calculation of the harmonic filter component is seeking capacity than the capacitors first, and then determine the size of the reactor to determine the resonance to be suppressed.

Capacitors and Value Size Frequency
Reactive power at a power factor 0.99

$$\text{Existing reactive power (kVAR)} = \text{Load Capacity} \times \sin[\arccos(\text{System PF})]$$

$$= 76.34 \times \sin(\arccos 0.99) = 10.77 \text{ kVAR}$$

Reactive power in the power factor in Rev be 0.995

$$\text{Desired reactive power (kVAR)} = \text{Load Capacity} \times \sin[\arccos(\text{Desired PF})]$$

$$= 76.34 \times \sin(\arccos 0.995) = 7.62 \text{ kVAR}$$

Compensation of reactive power from Filter

$$\text{Required Compensation (kVAR)} = \text{Existing reactive power} - \text{Desired reactive power}$$

$$= 10.77 \text{ kVAR} - 7.62 \text{ kVAR} = 3.14 \text{ kVAR}$$

For a system voltage of 220 V, required XFilter filter reactance (capacitive) with:

$$X_{\text{FILT}} (\text{Filter Impedance}) (\Omega) = \frac{\text{System Voltage (KV)}^2 1000}{\text{Required Compensation (kVAR)}}$$

$$X_{\text{Filt}} = \frac{0.22^2 (1000)}{3.14} = 15.39 \Omega$$

$$X_{\text{CAP}} (\text{Capacitive Reactance}) (\Omega) = \frac{X_{\text{FILT}} (\text{Tuned Frequency})^2}{(\text{Tuned Frequency})^2 - 1}$$

$$X_{\text{cap}} = \frac{15.39 (2.7^2)}{2.7^2 - 1} = 17.84 \Omega$$

Filter Rated Voltage (kV) = New Sytem Voltage

Filter rated voltage (kV) = 0.22 kV new sytem Voltage

$$\text{Capasitor Size}_{(\text{Calculation})} (\text{kVAR}) = \frac{\text{New System Voltage (KV)}^2 1000}{X_{\text{CAP}} (\text{Capacitive Reactance})}$$

$$\text{Capasitor Size}_{\text{Calculation}} = \frac{0.22^2 1000}{17.84} = 2.71 \text{ kVAR}$$

Capasitor Size (Selection) (kVAR) = New Capasitor Size
New Capasitor Size = 400 kVAR

$$X_{\text{CAP (New)}} (\Omega) = \frac{\text{New System Voltage (KV)}^2 1000}{\text{Capasitor Size (Selection) (kVAR)}}$$

$$X_{\text{CAP (New)}} = \frac{0.22^2 1000}{400} = 0.121 \Omega$$

3. Calculate the reactance filter large

$$X_{\text{L (fund)}} (\Omega) = \frac{X_{\text{CAP (New)}} (\Omega)}{(\text{Tuned Frequency})^2}$$

$$L (\text{mH}) = \frac{X_{\text{L (fund)}}}{2\pi \times 60}$$

$$f_h (\text{Hz}) = \frac{1}{2\pi \sqrt{LC_{\text{New}}}}$$

$$X_{\text{L (fund)}} = \frac{0.121}{2.7^2} = 0.0166 \Omega$$

4. Evaluation of the results of measurement filter

The results of calculation of data for the pairs of active filter capacitor must be according to standard IEEE 18-1992, Standard for Shunt Power Capacitor,

5. Calculation fundamental measurement data

a. Reactance of the fundamental frequency of the combination of the capacitor and the reactance:

$$X_{\text{fund}} (\Omega) = |X_{\text{L}} - X_{\text{CAP (New)}}|$$

$$X_{\text{fund}} = |0.0166 - 0.121| = 0.1044 \Omega$$

b. Currents filter the fundamental frequency

$$I_{\text{fund}} (\text{Amper}) = \frac{\text{System Voltage (kV actual)} / \sqrt{3}}{X_{\text{fund}}}$$



$$I_{fund} = \frac{220/\sqrt{3}}{0.1044} = 1216.62 \text{ Amper}$$

c. Fundamental frequency voltage between the capacitor bank

$$V_{L-L, Cap (fund)} (\text{Volt}) = \sqrt{3} \times I_{fund} \times X_{Cap (new)}$$

$$V_{L-L, Cap (fund)} = \sqrt{3} \times 1216.62 \times 0.121 = 254.98 \text{ Volt}$$

6. Calculation of harmonics

a. Harmonics of the burden of non - linear.

$$I_h (\text{Amper}) = \text{Load THD } I_h (\%) \frac{\text{load Capacity (kVA)}}{\sqrt{3} \times \text{System Voltage (kV}_{actual})}$$

$$I_h = 4.334\% \frac{76.34}{\sqrt{3} \times 0.22} = 8.68 \text{ Amper}$$

b. Harmonics in in pairs filter

$$X_{T(fund)} (\Omega) = \text{XFMR Impedance } Z_T (\%) \frac{\text{System Voltage (kV}_{actual})}{\text{Transformer Capacity MVA}_{XFR}}$$

$$X_{T(fund)} = 0.06 \frac{0.22^2}{0.4} = 0.0073 \Omega$$

$$X_{T(harm)} (\Omega) = \text{harmonik orde (th)} \times X_{T(fund)}$$

$$X_{T(harm)} = 3 \times 0.0073 = 0.022 \Omega$$

$$X_{Cap(New),harm} (\Omega) = \frac{X_{Cap (new)}}{\text{harmonik orde (th)}}$$

$$X_{Cap(New),harm} = \frac{0.121}{3} = 0.04 \Omega$$

$$X_{L(harm)} (\Omega) = \text{harmonik orde (th)} \times X_{L(fund)}$$

$$X_{L(harm)} = 3 \times 0.0166 = 0.05 \Omega$$

$$I_{h(utility)} (\text{Amper}) = \frac{\text{Utility VTHD } V_h (\%) \times \text{System Voltage (kV}_{actual})}{\sqrt{3} \times (X_{T(harm)} - X_{Cap(New),harm} + X_{L(harm)})}$$

$$I_{h(utility)} = \frac{0.881\% \times 220}{\sqrt{3} \times (0.22 - 0.04 + 0.05)} = 35.8 \text{ Amper}$$

$$I_{h(total)} (\text{Amper}) = I_h (\text{amper}) + I_{h(utility)} (\text{amper})$$

$$I_{h(total)} (\text{amper}) = 8.68 + 35.8 = 44.5 \text{ Amper}$$

$$V_{Cap(L-Lrms-harm)} (\text{Volt}) = \sqrt{3} \times I_{h(total)} \times \frac{X_{Cap(max)}}{\text{harmonik orde (th)}}$$

$$V_{Cap(L-Lrms-harm)} = \sqrt{3} \times 44.5 \times \frac{0.121}{3} = 3.11 \text{ Volt}$$

7. Evaluation of total I rms and the V peak

a. The total current rms onFilter

$$I_{rms, total} = \sqrt{I_{fund}^2 + I_{h(utility)}^2}$$

$$I_{rms, total} = \sqrt{1216.62^2 + 35.8^2} = 1217.1 \text{ Amper}$$

b. The maximum voltage on the capacitor

$$V_{L-L, Cap (max, peak)} = V_{L-L, Cap (fund)} + V_{Cap (L-Lrms-harm)}$$

$$V_{L-L, Cap (max, peak)} = 254.98 + 3.11 = 258.09 \text{ Volt}$$

c. Total rms voltage

$$V_{L-L, Cap (max, total)} = \sqrt{V_{L-L, Cap (fund)}^2 + V_{Cap (L-Lrms-harm)}^2}$$

$$V_{L-L, Cap (max, total)} = \sqrt{254.98^2 + 3.11^2} = 255 \text{ Amper}$$

d. Total kVAR capacitor

$$\text{kVAR}_{Cap (wye, total)} = \sqrt{3} \times I_{rms, total} \times \text{kV}_{L-L, Cap (rms, total)}$$

$$\text{kvar}_{cap(wye), total} = \sqrt{3} \times 1217.1 \times 255 = 537.6 \text{ kVAR}$$

8. Evaluation of the value of the capacitor in the standard

$$\text{Peak voltage} = \frac{V_{L-L, Cap (max, peak)}}{\text{Filter Rated Voltage (kV)}} \dots \text{Limit } 120\%$$

$$\text{peak voltage} = \frac{258.09}{220} = 1.17 \sim 117.3\%$$

$$\text{RMS voltage} = \frac{V_{L-L, Cap (max, total)}}{\text{Filter Rated Voltage (kV)}} \dots \text{Limit } 110\%$$

$$\text{RMS voltage} = \frac{255}{220} = 1.159 \sim 115.9\%$$

$$\text{RMS Current} = \frac{I_{rms, total}}{I_{Cap (rated)}} \dots \text{Limit } 180\%$$

$$\text{RMS Current} = \frac{1217.1}{1049.73} = 1.1595 \sim 115.95\%$$

$$I_{Cap (rated)} = \frac{\text{Capasitor Size (Selection) (kVAR)}}{\sqrt{3} \times \text{Filter Rated Voltage (kV)}}$$

$$I_{Cap (rated)} = \frac{400 \times 1000}{\sqrt{3} \times 220} = 1049.73 \text{ Amper}$$

$$\text{kVAR} = \frac{\text{kVAR}_{Cap (wye, total)}}{\text{Capasitor Size (Selection) (kVAR)}} \dots \text{Limit } 135\%$$

$$\text{kvar} = \frac{537.6}{400} = 1.344 \sim 134.4\%$$

9. Evaluation frequency filter

$$h_o = \sqrt{\frac{X_{Cap (new)}}{X_{T (fund)} + X_{L (fund)}}$$

$$h_o = \sqrt{\frac{0.121}{0.0073 + 0.0166}} = 2.24$$

10. Evaluation of the effect of the filter parameters of a variety of different specifications

$$Q = \frac{n X_L}{R}$$

Where :

R = The series resistance of the filter element

n = harmonic resonance value

X_L = Reactance filter at the fundamental frequency



$R = 0.068 \Omega$

$Q = \frac{2.7 \times 0.0166}{0.068} = 0.66$

Before the tide Filter Loads THD I (%) = 4.3334 % = 4.3 %

After the tide Filter Loads TDD I (%) into : 2.94 %

$TDD = \frac{\sqrt{\sum_{h=2}^{\infty} I_h^2}}{I_L} \times 100\%$

I_h = magnitude of individual harmonic compents (rms amps)

h = harmonic orde

I_L = maximum demand load current (rms amps) defined above

$TDD = \frac{I_h (utility)}{I_{rms-total}} \times 100\% = \frac{35.8}{1217.1} \times 100\% = 2.94\%$

The design of the filter to suppress the harmonics at industrial customers

The calculation of the value of the capacitor filter for suppression design using the same formula as in the case study is written in the previous section.

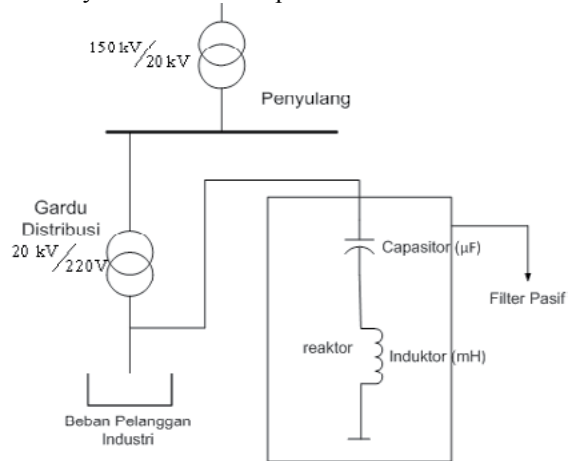


Figure 7. Installation Diagram passive filter on Industrial Distribution Substation

Here the value of the capacitor are mounted for harmonic suppression to 3 and 5 of the maximum current THD industrial customers.

Table 10. Harmonics filter THD current maximum total industrial customers

No. Data	Code Substation	Before Install Filter Loads THD i (%)	Harmonic Filter to 3	
			Capasitor size (selection) kVar	Install Filter Loads After TDD i (%)
11	MK 173	15.5	100	9.7
4	TG 475	16.0	100	9.7
30	TG 105	17.1	400	9.5
3	TG 475	15.8	400	8.4
32	DK 223 P	13.2	800	8.4

No. Data	Code Substation	Before Install Filter Loads THD i (%)	Harmonic Filter to 5	
			Capasitor size (selection) kVar	Install Filter Loads After TDD i (%)
11	MK 173	15.5	200	9.4
4	TG 475	16.0	200	9.4
30	TG 105	17.1	800	9.0
3	TG 475	15.8	400	9.6
32	DK 223 P	13.2	1000	8.5

To Suppress Harmonics Filter Design In Business Customers

Table 11. harmonics filter THD maximum total flow of business customers

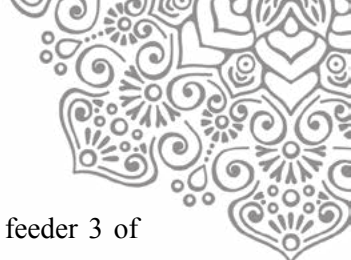
No. Data	Code Substation	Before Install Filter Loads THD i (%)	Harmonic Filter to 3	
			Capasitor size (selection) kVar	Install Filter Loads After TDD i (%)
41	RB 05	17	100	8.03
42	RB 05	19.15	100	6.43
43	RB 05	22.15	100	6.53
62	DK 86	10.88	200	10.33

No. Data	Code Substation	Before Install Filter Loads THD i (%)	Harmonic Filter to 5	
			Capasitor size (selection) kVar	Install Filter Loads After TDD i (%)
41	RB 05	17	400	9.95
42	RB 05	19.15	400	7.98
43	RB 05	22.15	400	8.10
62	DK 86	10.88	800	8.43

To Suppress Harmonics Filter Design In Domestic Customers

Table 12 Total current harmonic filter THD maximum household customers

No. Data	Code Substation	Before Install Filter Loads THD i (%)	Harmonic Filter to 3	
			Capasitor size (selection) kVar	Install Filter Loads After TDD i (%)
69	DK 125	12.0	400	8.2
81	MK 159	13.8	100	8.5
84	MK 159	11.4	100	8.5
86	MK 159	11.7	200	9.3
94	TG 388	11.1	100	8.1
107	DK 205	13.8	100	8.9
110	DK 58	12.1	400	7.0
119	DK 163	20.2	100	6.2



No. Data	Code Substation	Before Install Filter Loads THD i (%)	Harmonic Filter to 5	
			Capasitor size (selection) kVar	Install Filter Loads After TDD i (%)
69	DK 125	12.0	400	9.3
81	MK 159	13.8	200	6.6
84	MK 159	11.4	200	6.6
86	MK 159	11.7	400	8.0
94	TG 388	11.1	200	7.9
107	DK 205	13.8	200	6.9
110	DK 58	12.1	400	8.0
119	DK 163	20.2	100	8.4

Analysis of the results of the calculation of the harmonic filter is affected:

- The level of reactive power compensation value depends on the value of the total power of the two factors with the provisions of PF < DPF. So the total power factor will affect the size of kW and kVA capacity.
- Rated frequency and size of the capacitors to be mounted on harmonic filter.

8. Conclusion

The conclusion that can be obtained from the results of this study are as follows :

1. From the measured data 123 data and 32 distribution substations service areas cengkareng PT. PLN Jakarta and Tangerang, which exceeds the standard value of the maximum current THD 15% ie distribution substations 5 industrial customers, 2 business customer distribution substations and distribution substations 6 subscriber households.
2. From the measurement order harmonics common is the harmonic order 3rd and 5th. While the value of current THD highest level and most occur in distribution substations household customers. With the current THD value of 26.707% on the S-phase current THD region in DK 163 distribution

substations of the five feeder feeder feeder 3 of the number of household customers 4.

3. The method used for the suppression of harmonics is mounted passive filters, of calculations obtained capacitor value is chosen between 100 and 400 kVAR kVAR. harmonic filter influenced the level of reactive power compensation value depends on the value of the two factors with the provisions of kW and kVA. And the harmonic filter is influenced from the value of the frequency and size of the capacitors to be installed.
4. As for the value THD The voltage that exceeds the standard IEEE, 159-2002 which is the maximum voltage THD 5% is nothing beyond the standard this is due to the harmonic voltage measurements performed on the source side.

9. Bibliography

- Arrillaga, J., Bradley D.A, Bodger P.S, *Power System Harmonics*, (New York : John Willey dan Sons,1985).
- Abdul Kadir, Transformator, Jakarta: PT. Elex Media Komputindo, 1989.
- C. Sankaran, *Power Quality*, USA : CRC Press LLC, 2002.
- Cristof Naek Haloman Tobing, Effect of Harmonics On Distribution Transformer. Depok: Departemen Elektro Fakultas teknik Universitas Indonesia, 2008.
- Daut , H.S. Syafruddin, dkk, *The Effects Of Harmonic Components On Transformer Losses Of Sinusoidal Source Supplying Non-Linear Loads*, Malaysia : Science Publication, 2006.
- Hyat dan Kemmerly, et al., *Rangkaian Listrik Jilid 2*, Erlangga.
- Rashid, M.H., *Electrical Power Jilid 1*, Jakarta, P.T. Prehallindo, 1999.
- Roger C. Dugan, Mark F. McGranaghan, H. Wayne Beaty, *Electrical Power System Quality*, New York : McGraw-Hill, 1996.
- Schneider Electric, *Analyzing Neutral Conductor and transformer overload*, Power System Engineering solution, Nort American : 2000



TECHNICAL ANALYSIS FEASIBILITY STUDY ON SMART MICROGRID SYSTEM IN SEKOLAH TINGGI TEKNIK PLN

¹Heri Suyanto

Lecturer, College of Engineering - PLN
(Foundation for Education & Welfare PT. PLN (Persero)).
PLN tower. Jl. Outer West Lingkar, Duri Kosambi,
Cengkareng, Indonesia 11750

heri.suyanto@yahoo.com

²Rina Irawati

¹Research & Development Center for Electricity
New, Renewable Energy and Energy Conservation
Technology, Research & Development Agency of Ministry
of Energy & Mineral Resources Republic of Indonesia
Jl. Ciledug Raya Kav.109, Jakarta Selatan Indonesia 12230

rina.irawati@esdm.go.id

Abstract - Nowadays application of new and renewable energy as main resource of power plant has greatly increased. High penetration of renewable energy into the grid will influence the quality and reliability of the electricity system, due to the intermittent characteristic of new and renewable energy resources. Smart grid or microgrid technology has the ability to deal with this intermittent characteristic especially if these renewable energy resources integrated to grid in large scale, so it can improve the reliability and efficiency of the grid. We plan to implement smart microgrid system at Sekolah Tinggi Teknik PLN as a pilot project. Before the pilot project start, the feasibility study must be conducted. In this feasibility study, the renewable energy resources and load characteristic at the site will be measured. Then the technical aspect of this feasibility study will be analyze. This paper explains that analysis of this feasibility study.

Keywords : Smart Microgrid , New and Renewable Energy

1. INTRODUCTION

The conditions of electricity in Indonesia is still inadequate, which the ratio of electrification is still low at 87% as of October 2015 (PT. PLN Persero). ¹This shows that people access the energy is still limited. And also with the development of energy infrastructure in Energy for rural / remote and island - the outermost islands in general do not get adequate energy access. ⁴Dependence on electricity industry is more limited. ³Utilization of new and renewable energy and implementation of energy conservation are also not set optimal.

As the one of the way fulfol local needs for electricity, and in accordance with the policies of Indonesian

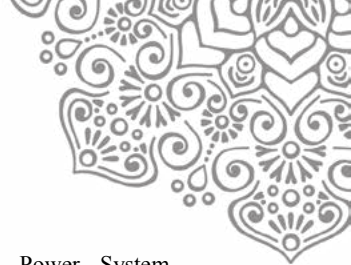
government, in the past few years has been started the development of power systems of new and renewable energy (EBT). ²Due to the nature Intermittent characteristic of new and renewable energy, we need a system to resolve the issue. Smart microgrid system or smart grid is one technology that can effectively and efficiently address the integration of new and renewable Energy in the electrical system for a large scale⁵.

Since 2015 STT PLN has been conducting some research of smart microgrid, with stage: study potentials stats with (2015) and design of the smart microgrid labotarioium scala model (2016), As the development of smart microgrid model and for application in the field, so as a first step of the implementation to start to establish the pilot project of smart microgrid system with in at the laboratory scale in STT PLN start in 2017

2. TECHNICAL REVIEW

Research and development of renewable energy especially for Solar Power Generation based on smart-grid technology has been listed on RIP STT PLN 2013 - 2018. One of strategies to fulfill the electric energy needs is to utilize the potential of new and renewable energy (EBT) at the local site, In order to reduce transmission and distribution costs. Potential of Renewable Energy (ET) in local area is used to meet the needs of electrical energy in the area. This will lead high concentration of renewable energy in into the grid. ⁵High concentrations of renewable energy sources can cause problems in stability, reliability and power quality on the main grid. Smart microgrid is the key of the future grids where high concentration of renewable energy does not affect or disrupt with the quality of the grid⁶.

A smart microgrid system can be interpreted as an electrical system consists of several Distributed Generations (DG) where the source is usually from EBT, such as



photovoltaic panels, wind turbines, microturbons, with the addition of a storage system, load control, and an energy regulation system (Energy Management System - EMS). EMS allows smart microgrid systems to make its own free adjustment regardless grid positive in standalone mode (islanding). ⁷This microgrid smart system can operate in two modes, On-Grid / Grid-connected and Off-Grid / Standalone / Islanding. Off-Grid / Standalone / Islanding operation mode is when circuit breaker isolates the system from the main grid (PLN), so power generator equipment, storage, load regulator, power quality controller and other system operation regulator are applied only to smart microgrid system. ¹¹In Off-Grid mode the load is supplied applied by DG, ⁹Diesel Generator (it backup) and Battery. In an on-grid / grid connected mode, the microgrid smart system is also a controllable load, or the power generated from the grid is a backup / supplemental energy source. ⁸In On-Grid / Grid Connected mode this load is supplied by DG, grid (as backup) and Battery.

3. RESEARCH METHODS

The expected outcome of this research program is the synergies which mutually beneficial and supportive synergies between university (STT PLN) and industrial partners to produce hybrid power plant products designed and manufactured in a micro-distributed (micro-gid structure), and Supported by high technology, so it can be operated inlocal/ remote island to fulfill needs of housing and also support the operation of NKRI territorial integrity.

Methodology and research stages to be used follow:

- Measure New and Renewable Energy potential, the wind and solar energy at Sekolah Tinggi Teknik PLN.
- Analysis of irradiation data on selected area (local / remote island), refers to data from BMKG and Lapan and other agencies.
- Measure the load characteristics at the smart micro grid site.
- Conducted an analysis of data on potential and characteristics of the load.
- Conduct the analysis of feasibility for smart micro grid system as the technical specifications of solar cells, and determining the electrical power control system based on "power electronics" based on the study of literature¹⁰.

4. RESULTS AND DISCUSSION

Sekolah Tinggi Teknik PLN is located at Lingkar Barat, Duri Kosambi, Cengkareng, Jakarta Barat, Jakarta 11750. Applied load in the Campus main building of 100KW, and the load in the Laboratory of STT PLN is 15 KW.

After the discussions among collengues and professors of Sekolah Tinggi Teknik PLN and by direct observation at the location it was determined that the project smart microgrid system will be built right at Laboratory at Research and

Training Center For Renewable Energy Power System. Presence of solar Laboratory will save the electricity bill from PT. PLN

Blueprint New and Renewable Energy STT PLN as follows according to Figure 1 among others as follows:

- Solar Power Plant (PLTS) capacity 14.5 kWp
- Bayu / wind power plant (PLTB) capacity of 20 kW
- Biomass Power Plant 16 kVA consisting of:
 - Waste Power Plants T gasifer 14 kVA
 - Waste Power Plants digester of 2 kVA
- With KWH Export and Import KWH meter system (Exim) from PT. PLN (Persero) and Battery

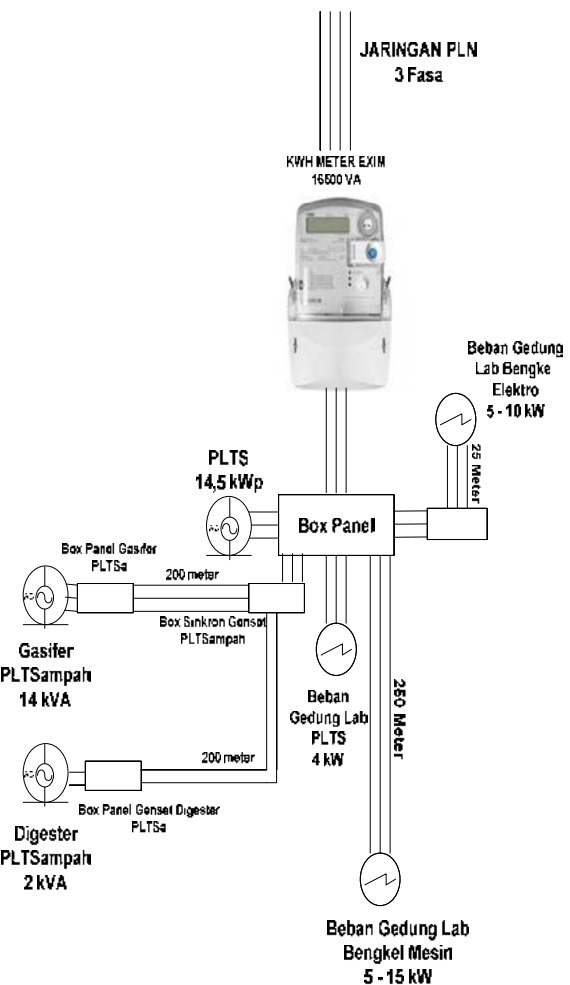


Figure 1. Blueprint STT PLN Smart microgrid System.

This Installation that has been installed with a capacity of 14.5 kW with microgrid smart system On Grid and Off Grid

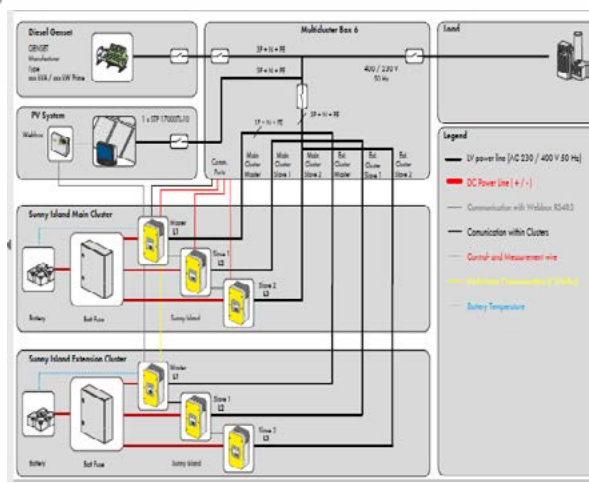
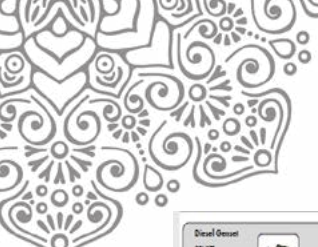


Figure 2. Smart grid system design of Microgrid system for off grid at STT PLN

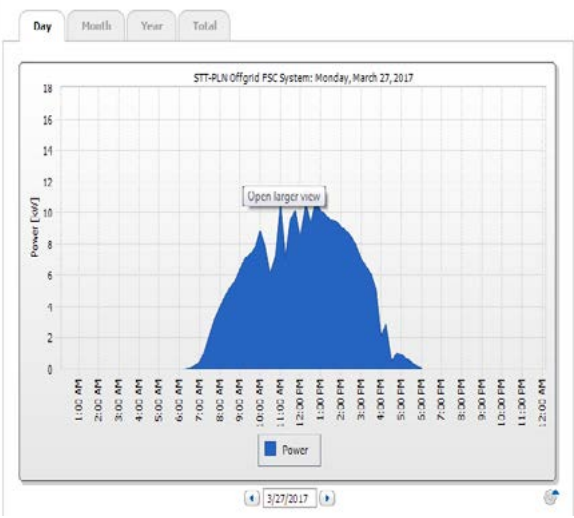


Figure 4. Daily electricity curve of PLTS

It shows the maximum peak at 11:00 to 14:00 hours to reach 10 kW so that one can reach 70 kW in the position of maximum results Daily and Daily Average reaches 40 kW.

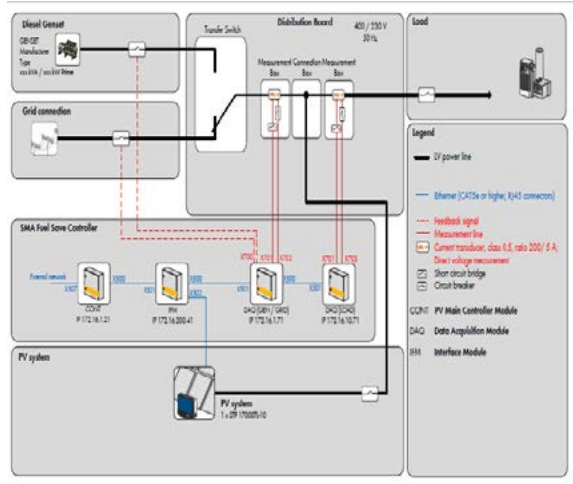


Figure 3 Smart System Design of Microgrid system on grid at STT PLN

Our Solar Power Plants Capacity of 17 kW / peak has already Integrated KWH Meter Exim Export and Import and has installed with advanced technology monitoring system. This design is made as a Research by knowing new and renewable energy technologies especially Solar Power Generation and as a saver of electricity usage from PT. PLN (Persero) and the electricity cost down. Figure of generated electricity from PLTS monitoring system.

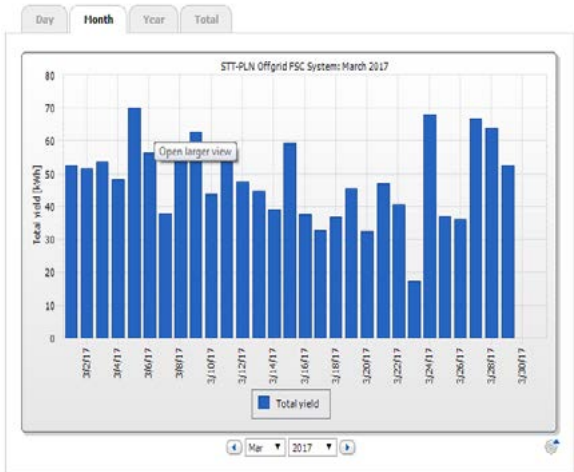


Figure 5. Monthly Electricity Curve of PLTS

From the curve above, electricity generated from Solar Power Generation can reach 1.4 MWh. and Biomass Power Plant is in the design stage For Bayu / Wind Power Generation and Biomass Power Plant is still under consumer.



This Microgrid Project Smart will be applied as Research and Learning on New and Renewable Energy at the Research and Training Center Laboratory for Renewable Energy Power System STT PLN.

5. CONCLUSION

1. From the analysis conducted on the technical aspects of the feasibility study of the application of Smart Microgrid System Project in Sekolah Tinggi Teknik PLN is feasible with high potential availability and installation area of equipment as we expected.
2. Microgrid Smart System Project in Sekolah Tinggi Teknik PLN Research and Training Center Laboratory for Renewable Energy Power system STT PLN as New and Renewable Energy Technology Research and as a saver of electricity usage from PT. PLN.
3. Blueprint of smartmicrogrid system for New and Renewable Energy STT PLN consists of PLTS capacity 14.5 kWp, PLTB capacity 20 kW, PLTbiomass with 14 kVA Gasifer PLTS garbage and 2 kVA of waste PLTS Digester) and Battery.

6. REFERENCES

- [1] J. B. (Secretary of U. S. D. of C. P. D.G. (Director of N. I. of S. and Technology), *NIST Framework and Roadmap for Smart Grid Interoperability Standards*, NIST Special Publication 1108R2 *NIST Framework and Roadmap for Smart Grid Interoperability Standards*, NIST Speci. Energy Independence and Security Act of 2007, 2012.
- [2.] “The Smart Grid: Coming Of Age”, Electric Power Research Institute Journal, EPRI, Inc. 2009.
- [3.] Jay Stuller, “An Electric Revolution”, Galvin Electricity Initiative
- [4.] CERTS Microgrid Symposium, Northern Power Systems
- [5.] Clarke, S., “Electricity Generation Using Small Wind Turbines At Your Home Or Farm”, Fact Sheet, September 2003
- [6.] Kurt Yeager, “The Microgrid Revolution”, Oktober 2010
- [7.] IEC Smart Grid Standardization Roadmap, Prepared by SMB Smart Grid Strategic Group (SG3) June 2010; Edition 1.0
- [8.] Smart Houses interacting with Smart Grids to achieve next generation efficiency and sustainability, Dr. Anke Weidlich, SAP Research 11.02.2009
- [9.] R. Ramakumar, “Integrated Renewable Energy System – Micro Grid (IRES-MG) For Sustainable Development”, ICSUNIDO, Trieste, Italy, April 2012
- [10.] T. Nakata, K. Kubo and A. Lamont, “Design For Renewable Energy System With Application To Rural Area In Japan”, white paper.
- [11.] C.W. Gellings, “The Smart Grid – Enabling Energy Efficiency and Demand Response”, CRC Press, 2009



DETEKSI APNEA TIDUR MELALUI SINYAL ELEKTROKARDIOGRAM MENGGUNAKAN METODE *DISCRETE WAVELET TRANSFORM*, PRINCIPAL COMPONENT ANALYSIS, DAN LINEAR DISCRIMINANT ANALYSIS

DETECTION OF SLEEP APNEA USING ELECTROCARDIOGRAM SIGNAL WITH DISCRETE WAVELET TRANSFORM, PRINCIPAL COMPONENT ANALYSIS AND LINEAR DISCRIMINANT ANALYSIS METHODS

Meidiana Ajeng Lestari¹, Unang Suryana, ST., MT.²,
¹meidiana.ajeng@gmail.com, ²unsur@telkomuniversity.ac.id

Abstrak

Sleep Apnea merupakan gangguan tidur yang langka, pendeteksiannya pun perlu dilakukan secara tepat salah satunya melalui sinyal elektrokardiogram yang dapat mendeteksi *Sleep Apnea* lebih mudah dan tepat.

Penelitian ini dilakukan untuk mendeteksi penyakit *Sleep Apnea* menggunakan perbandingan dua buah metode, yaitu *Discrete Wavelet Transform* (DWT) dan *Principal Component Analysis* (PCA) serta diklasifikasikan menggunakan *Linear Discriminant Analysis* (LDA).

Sistem yang dibuat dengan metode PCA mendapatkan akurasi yang cukup baik, yaitu 79.16%, sensitivitas 73.3% dan spesifitas 88.8% dengan pengambilan 1-60 PC. Waktu komputasi untuk metode PCA didapatkan 9.2 s. Sedangkan sistem dengan metode DWT mendapatkan hasil akurasi 75%, sensitivitas 68.75% dan spesifitas 87.5% dengan dilakukan proses *windowing* menggunakan *overlapping* 25%, menggunakan jenis wavelet Discrete Meyer, dan melakukan dekomposisi di level ke-5. Waktu komputasi metode DWT didapatkan 34 s.

Kata kunci : *Sleep Apnea*, DWT, PCA, LDA

Abstract

Sleep Apnea is a rare sleep disorder, so that the detection needs to be done correctly. Through electrocardiogram signal, the detection of sleep apnea can be easier and correct.

This type is to detection of *Sleep Apnea* using two comparison methods, those are *Discrete Wavelet Transform* (DWT) and *Principal Component Analysis* (PCA), and classified by *Linear Discriminant Analysis* (LDA).

System with PCA method produces a good accuration, which is 79.16%, sensitivity 73.3% and specificity 88.8% with taking 1-60 PC. Computation time with PCA method takes 9.2 s. System with DWT methods produces accuration 75%, sensitivity 68.75%, and specificity 87.5% by using some additional pre-processing which is *windowing* with *overlapping* 25%, using *Discrete Wavelet mother wavelet*, and decomposition in the fifth level. DWT method has 34 s computation time, and it is take a longer time than PCA methods.

Keywords: *Sleep Apnea*, DWT, PCA, LDA

1. Pendahuluan

Jantung merupakan organ terpenting dalam tubuh manusia dan juga berperan untuk menunjang keadaan organ tubuh lainnya. Melalui aktivitas kelistrikan jantung yang dikenal sebagai Elektrokardiogram, dapat dideteksi berbagai macam penyakit atau gangguan pada organ tubuh manusia, salah satunya gangguan pada tidur, yaitu *Sleep Apnea*. *Sleep Apnea* adalah gangguan tidur yang serius dan kronis yang ditandai dengan henti nafas sementara yang terjadi berulang kali ketika sedang tidur hingga menyebabkan kematian.

Perkembangan ilmu pengolahan sinyal dengan bantuan komputer pada saat ini memungkinkan untuk mendeteksi gangguan tidur, *Sleep Apnea*. Elektrokardiografi (EKG) merupakan salah satu tekniknya. Penggunaan Elektrokardiograf telah lama dikenal sebagai suatu alat dalam bidang kedokteran yang membantu menemukan gangguan elektrolit dan berguna untuk mendeteksi penyakit bukan jantung (*The Clinical Value of the ECG in non cardiac condition*, 2004). Teknik ini dapat membantu dokter syaraf dalam menganalisa gangguan tidur pada pasien namun tetap tidak dapat menghilangkan dugaan (*suspect*). Penentuan jenis penyakit melalui sinyal EKG bergantung pada pengetahuan dan pengalaman dokter syaraf serta hasil analisis spesialis jantung.

Tugas akhir ini dilakukan pengidentifikasi gangguan tidur *Sleep Apnea* melalui sinyal EKG dengan menggunakan metode *Discrete Wavelet Transform* untuk menganalisis sinyal berdasarkan frekuensi dan waktu, dan *Principal Component Analysis* untuk mencari ciri yang paling membedakan satu sama lain. Dari metode-metode tersebut terdapat beberapa parameter yang akan dibandingkan hasilnya. Parameter tersebut ialah Akurasi (*Accurate*), Sensitivitas (*Sensitivity*), dan Spesifitas (*Specifity*). Masukan (*Input*) yang digunakan adalah sinyal EKG yang diperoleh dari PhysioNet.org dengan format *.mat, berdurasi satu jam, dan memiliki spesifikasi masing-masing (seperti berat badan, tinggi badan, jenis kelamin dan umur pasien).



2. Tinjauan Pustaka

2.1 Sleep Apnea

Sleep Apnea (*Apnoea* dieja dalam bahasa Inggris) adalah gangguan tidur yang berpotensi mengancam jiwa yang ditandai dengan jeda yang abnormal dalam bernapas selama tidur. Terdapat dua jenis utama dari *sleep apnea*, yaitu apnea tidur sentral (*Central Sleep Apnea*), bentuk yang relatif jarang, yang terjadi ketika otak gagal untuk mengirim sinyal ke otot untuk mengambil napas dan terdapat periode dimana tidak ada usaha otot untuk bernapas. Dan apnea tidur obstruktif (*Obstructive Sleep Apnea*), bentuk yang lebih umum, dimana otak mengirimkan sinyal ke otot-otot dan otot-otot yang melakukan upaya untuk mengambil nafas tetapi mereka tidak dapat melakukannya secara efektif dikarenakan jalan nafas terhambat sehingga mencegah aliran udara yang masuk.

Episode Apnea dapat berlangsung dalam beberapa detik hingga menit (± 10 detik, baik untuk pbstruktif ataupun apnea tidur sentral) dan itu semua dapat terjadi dimana saja dari 5 hingga 30 kali atau lebih per jam. Karna hilangnya kemampuan otot yang terkait dengan *REM-Sleep*, yaitu waktu yang paling umum penderita mengalami apnea^[1].

2.2 Elektrokardiogram

Elektrokardiogram (EKG) adalah salah satu sinyal biopotensial yang digunakan untuk menganalisis kondisi kesehatan jantung.

2.3 Discrete Wavelet Transform (DWT)

Transformasi *wavelet* adalah dekomposisi dari suatu sinyal dengan suatu fungsi $\psi_{a,b}$ yang telah dilatasi dan ditranslasi. Pada *wavelet*, sinyal direpresentasikan sebagai jumlah dari kumpulan dilatasi dan translasi fungsi *mother wavelet*. Kumpulan fungsi tersebut didefinisikan pada persamaan berikut:

$$\psi_{a,b}(x) = \frac{1}{\sqrt{a}} \psi\left(\frac{x-b}{a}\right) > 0, b \in \mathbb{R} \dots \dots \dots (1)$$

2.4 Principal Component Analysis (PCA)^[4]

Principal Components Analysis (PCA) merupakan teknik linier untuk memproyeksikan data vektor yang berdimensi tinggi ke vektor yang mempunyai dimensi lebih rendah^[9].

Prinsip PCA pada dasarnya merupakan observasi sekelompok data yang memiliki kemungkinan saling berelasi, kemudian data tersebut dikonversi sedemikian rupa sehingga yang tidak ada lagi data yang tidak saling berelasi satu sama lain. Selanjutnya data akan diurutkan dari data yang dianggap paling penting sampai data yang kurang penting. Data pada baris pertama hasil konversi adalah *principal component* pertama dan yang paling berpengaruh terhadap variasi data asli.

2.5 Linear Discriminant Analysis (LDA)^[5]

Linear Discriminant Analysis (LDA) termasuk dalam klasifikasi yang digunakan untuk meningkatkan informasi diskriminatif kelas dengan transformasi linear. Metode LDA bekerja dengan mencari cara yang efisien untuk merepresentasikan ruang vektor dengan memanfaatkan informasi tiap kelas. Tujuan dari LDA adalah untuk mencari proyeksi linear untuk memaksimalkan matriks kovarian antar objek dan meminimumkan matriks kovarian di dalam objek itu sendiri.

Pengukuran kemiripan dilakukan antara representasi citra latih dan citra uji. Representasi di dalam metode ini, dianggap sebuah tranformasi linier dari vektor citra asal ke dalam sebuah ruang proyeksi (vektor-vektor basis). Persamaannya sebagai berikut:

$$Y = W^T X \dots \dots \dots (2)$$

3. Pembahasan

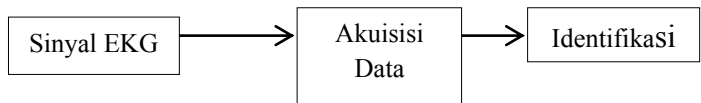
3.1 Proses Pengolahan Citra

Pengambilan *sample* sinyal EKG yang masing-masing berdurasi satu jam. Sinyal EKG tersebut memiliki ciri apneatasi. Dari ciri tersebut dapat disegmentasikan kapan terjadinya sleep apnea, waktu terjadi tersebut dapat dilihat dari sepanjang *sample* sinyal EKG. Data *sample* sinyal EKG diperoleh dari database *PhysioBank*, yaitu di *physionet.org* yang telah terjamin hasilnya dan banyak digunakan untuk referensi jurnal internasional. Dari sinyal





EKG tersebut dapat dibuat program untuk mendeteksi *sleep apnea*. Perancangan sistem deteksi *sleep apnea* ini dilakukan dalam satu tahap umum, yaitu tahap identifikasi yang digambarkan dalam diagram blok sebagai berikut:



Gambar 1. Diagram Model Sistem

3.2 Pre-Processing

3.2.1 Cropping

Cropping dilakukan setiap satu menit dengan mengambil 5 sample ciri *apnea* dan 5 sample ciri normal dari sinyal EKG pasien. Hasil *cropping* tersebut akan dijadikan *database* ciri latihan.

3.2.2 Filtering

FIR (*Finite Impulse Response*) Filter merupakan filter digital yang tidak memiliki *feedback* dan bersifat non-rekursif. Fungsi transfer pada FIR melakukan pendekatan ideal agar kualitas filter meningkat. Sehingga kompleksitas dan jumlah waktu yang dibutuhkan untuk memasukan *samples* sinyal untuk difilter juga meningkat.

3.2.3 DC Removal

DC Removal bertujuan untuk menghitung rata-rata dari data sampel sinyal EKG dan mengurangi nilai setiap sampel sinyal dengan nilai rata-rata tersebut sehingga didapat normalisasi dari data sinyal suara *input*.

3.2.4 Normalisasi

Proses normalisasi dilakukan untuk mencari nilai maksimum dari data hasil *filtering*. Keseluruhan nilai data *filtering* kemudian dibagi dengan nilai maksimum data yang telah ditemukan. Hal ini bertujuan agar amplitude sinyal memasuki rentang -1 sampai 1.

3.3 Ekstraksi Ciri dengan PCA

Hasil akhir dari ekstraksi ciri ini merupakan koefisien pembawa matriks ciri yang disebut dengan *principle component* [3].

3.4 Ekstraksi Ciri dengan DWT

Sebelum memasuki ekstraksi ciri DWT, dilakukan kembali beberapa proses untuk meningkatkan kualitas sinyal yang akan diproses. Berikut adalah proses yang dilakukan :

1. *Framming*, dilakukan setelah data di *load* dan bertujuan untuk menjadikan *frame-frame* lebih kecil. Proses ini menggunakan dua parameter yaitu lebar *frame* dan *overlap*.
2. *Windowing* [7]
Tahap ini dilakukan untuk mengurangi efek diskontinuitas dengan mengalikan *frame* dengan frekuensi *Window Hamming*. Persamaan *Window Hamming* adalah sebagai berikut :

$$w(n) = 0,54 - 0,46 \cos\left(\frac{2n\pi}{N-1}\right) \dots \dots \dots (3)$$

dimana $w(n)$ = fungsi *window*
 N = *frame size*, merupakan kelipatan 2
 n = 0,1,2,3,...,N-1.

3. *Fast Fourier Transform*
Koefisien-koefisien sinyal hasil *windowing* dianalisa dengan menggunakan *Fourier Transform*. Dalam analisa sepektrum dari sinyal yang diinputkan, digunakan *Fast Fourier Transform*. Sampel data diproses dengan mengambil *frame-frame* sebanyak lebar *frame*.

Teknik DWT ini menggunakan *low pass filter* (LPF) dan *high pas filter* (HPF). Sinyal akan diproses secara baris untuk semua baris dan dilanjutkan secara kolom untuk semua kolom. Hasilnya akan didapatkan koefisien *wavelet* level 1. Proses ini diulang sampai dekomposisi ke lima. Setelah proses dekomposisi selesai, maka akan dihitung energi setiap *sub-band* pada setiap levelnya sebagai hasil akhir dari ekstraksi ciri

3.5 Klasifikasi

Hasil dari ekstraksi ciri menjadi data dengan sinyal EKG normal dan sinyal EKG yang terdeteksi *Apnea*. Dalam proses klasifikasi ini, data latihan yang sudah di ekstraksi ciri akan disimpan untuk nanti dilihat kedekatan *eigenvalue* terbersarnya dengan *eigenvalue* terbesar pada citra uji yang sudah di ekstraksi juga. Proses klasifikasi menggunakan metode LDA. Tujuan dari LDA adalah untuk mencari proyeksi linear untuk memaksimalkan matriks kovarian antar objek dan meminimumkan matriks kovarian di dalam objek itu sendiri.

3.6 Evaluasi Hasil Klasifikasi

Adapun parameter yang diambil untuk mengevaluasi hasil klasifikasi adalah sebagai berikut:

1. *Accuracy* merupakan ketepatan klasifikasi yang diperoleh [9].

$$Accuracy (\%) = \frac{TP+TN}{TP+FN+FP+TN} \dots \dots \dots (4)$$



2. *Sensitivity* merupakan persentase probabilitas tidak adanya penyakit bila hasil tes dinyatakan negative.

$$Sensitivity (\%) = \frac{TN}{TN+FP} \dots\dots\dots(5)$$

3. *Specifity* merupakan persentase probabilitas adanya suatu penyakit bila hasil tes dinyatakan positif.

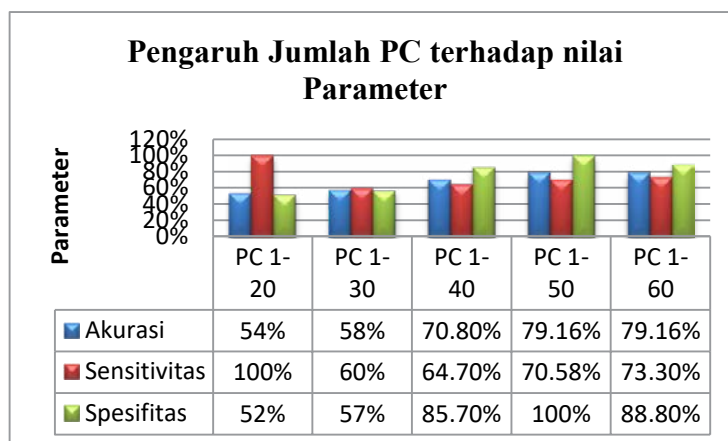
$$Specifity (\%) = \frac{TP}{TP+FN} \dots\dots\dots(6)$$

Keterangan :

- TP: *True Positive* (merupakan kondisi dimana *apnea* dideteksi sebagai *apnea*)
- TN : *True Negative* (kondisi dimana normal dideteksi sebagai normal)
- FP : *False Positive* (menyatakan kondisi *apnea* yang dideteksi sebagai normal)
- FN : *False Negative* (menyatakan kondisi normal yang dideteksi sebagai *apnea*)

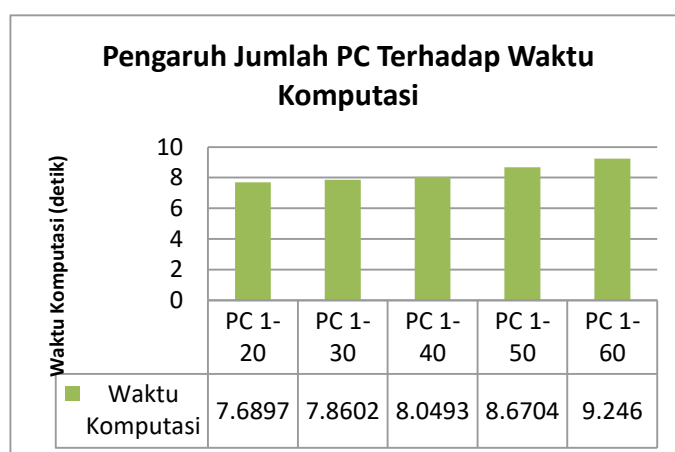
3.7 Hasil Pengujian dan Analisis

3.7.1 Hasil Perbandingan Parameter berdasarkan pengambilan Principal Component (PC) Menggunakan PCA



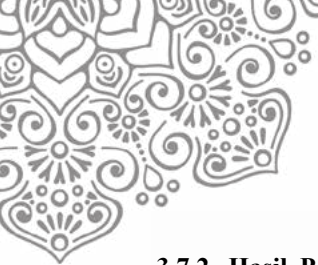
Gambar 2. Grafik Perubahan Nilai Parameter PC

Pada Gambar 2 dapat dilihat nilai akurasi maksimal terdapat pada pengambilan PC 1-50 dan 1-60 yaitu 79.16%. Hal tersebut terjadi karena semakin banyak PC yang diambil, semakin banyak pula ciri latih yang digunakan sebagai ciri untuk mendeteksi *apnea*. Nilai Sensitivitas tertinggi berada pada pengambilan PC 1-20 yaitu 100% karena pada PC 1-20 dari 12 kondisi tidak sakit, dideteksi sebagai tidak sakit dan Spesifitas tertinggi berada pada PC 1-50 yaitu 100%, karena pada PC 1-50 dari 12 kondisi *apnea*, yang terdeteksi sebagai *apnea* ada 12, maka dari itu menghasilkan spesifitas sebesar 100%.



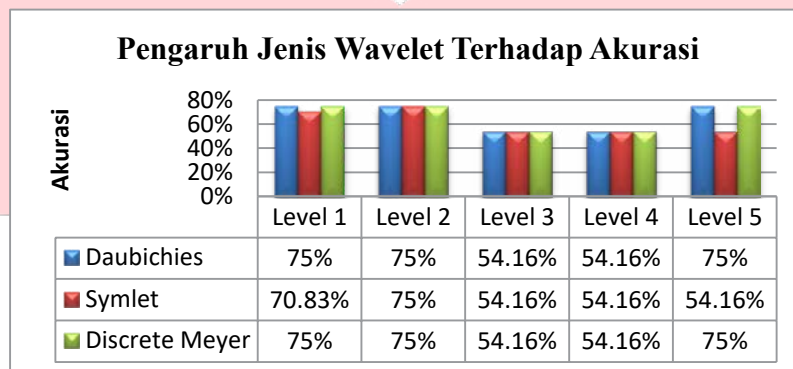
Gambar 3. Grafik Waktu Komputasi Terhadap Perubahan Jumlah PC .

Waktu komputasi tercepat diperoleh pada PC 1-20 dan yang terlama terdapat pada PC 1-60. Hal tersebut dikarenakan, semakin banyak data yang diproses maka semakin lama pula waktu yang dibutuhkan untuk memproses data.



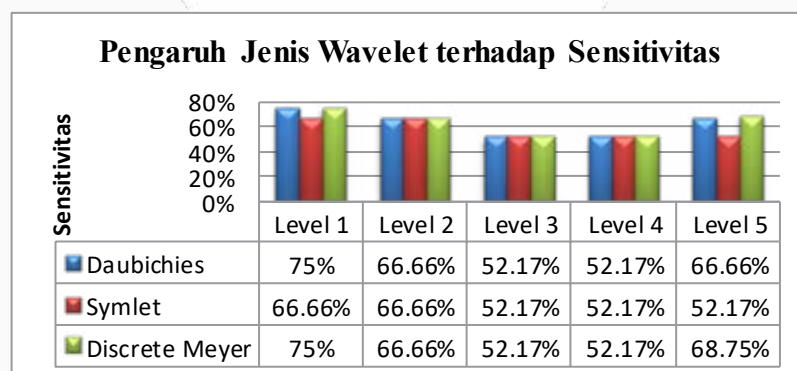
3.7.2 Hasil Perbandingan Akurasi, Sensitivitas, Spesivitas, Waktu Komputasi Berdasarkan Jenis *Wavelet* dan Level Dekomposisi.

Pengujian sistem dilakukan dengan melihat pengaruh perbedaan 3 jenis *wavelet* yaitu *Daubichies*, *Symlet*, dan *Discrete Meyer* terhadap nilai parameter sistem. Ketiga *wavelet* dilakukan sebanyak lima kali level dekomposisi dan masing-masing memiliki orde yang berbeda dalam proses pengambilan ciri. Data latih dan Data uji yang digunakan ada ekstraksi ciri DWT telah melewati proses *windowing* menggunakan *window hamming* dan FFT (*Fast Fourier Transform*).



Gambar 4. Grafik Tingkat Akurasi Terhadap Perubahan Jenis *Wavelet* dan Level Dekomposisi.

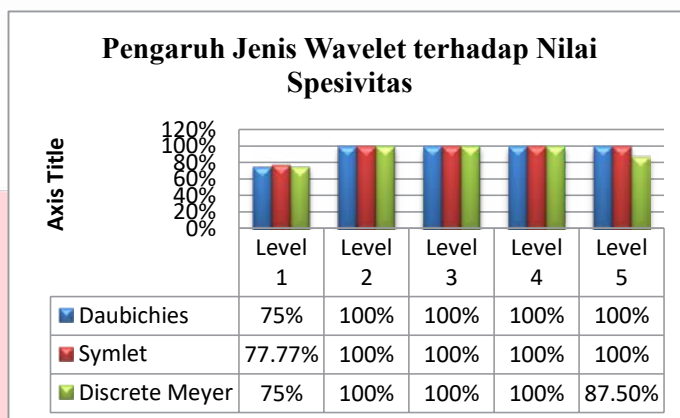
Hasil dekomposisi pada level 2, didapatkan nilai yang sama, yaitu sebesar 75%. Pada level 3 dan 4, didapatkan nilai sebesar 54.16%. Dari hasil tersebut dapat dianalisis bahwa ketiga *wavelet* mengambil atau memproses sinyal EKG secara acak yang dikarenakan pola (*trend*) sinyal tersebut sama, sehingga sulit untuk diamati secara visual dan melalui sistem



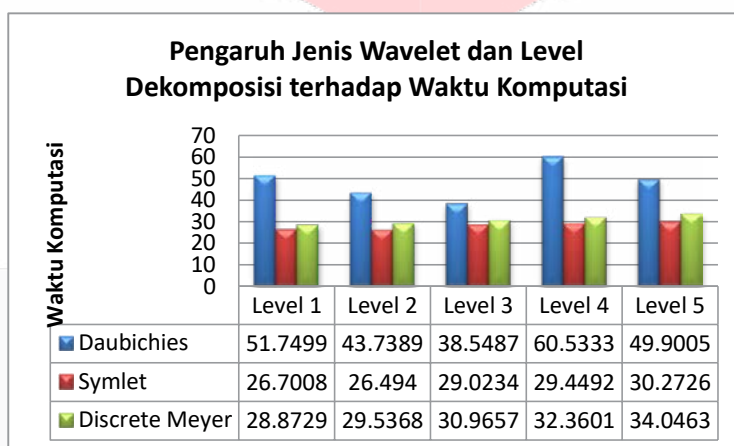
Gambar 5. Grafik Tingkat Sensitivitas Terhadap Perubahan Jenis *Wavelet* dan Level Dekomposisi

Nilai sensitivitas digunakan untuk mengetahui berapa banyak pasien yang berada pada kondisi normal, yaitu pasien normal yang dikenali system sebagai normal. Nilai sensitivitas tertinggi didapatkan dari *wavelet Daubechies* and *Discrete Meyer* pada level 1, yaitu 75%. Angka 75% ini menyatakan bahwa dari 12 pasien yang normal, terdapat 9 pasien yang benar dideteksi sebagai tidak sakit (normal). Sedangkan sensitivitas terendah berada pada level 3 dan 4 dengan menggunakan 3 *wavelet* yang berbeda. Selain itu juga pada *wavelet symlet* di level dekomposisi ke 5, dengan nilai sensitivitas 54.17%. Nilai tersebut menyatakan bahwa dari 12 kondisi normal hanya 1 yang benar dideteksi sebagai normal.

Pada Gambar 6 dapat dilihat nilai spesifitas terendah terdapat pada *wavelet daubechies* dan *discrete meyer* di level ke 1, yaitu 75%. Nilai 75% menyatakan bahwa dari 12 pasien sakit terdapat 3 pasien yang dideteksi sebagai kondisi normal.



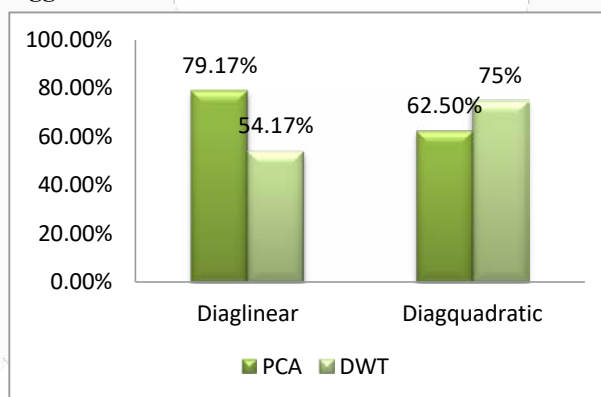
Gambar 6. Grafik Tingkat Spesivitas Terhadap Perubahan Jenis *Wavelet* dan Level Dekomposisi.



Gambar 7. Grafik Waktu Komputasi Terhadap Jenis *Wavelet* dan Level Dekomposisi.

Pada *mother wavelet symlet* dan *discrete meyer* bahwa semakin tinggi level dekomposisi maka semakin lama pula waktu yang dibutuhkan system untuk bekerja. Namun pada *mother wavelet daubechies*, kenaikan level dekomposisi tidak selalu mempengaruhi lamanya waktu komputasi, hal tersebut terjadi karena daubechies memiliki banyak orde dan panjang filter yang berbeda-beda.

3.7.3 Hasil Pengujian Menggunakan Klasifikasi LDA



Gambar 8. Grafik Nilai Akurasi Terhadap Perubahan Jenis *Discriminat Analysis*.

Pemakaian jenis diaglinear memberikan akurasi yang paling bagus, yaitu 79.16% untuk PCA dan jenis diagquadratic memberikan akurasi yang paling bagus sebesar 75% untuk DWT. Hal ini berarti jenis diaglinear



berhasil memaksimalkan jarak antar kelas dan meminimalkan jarak dalam kelas sehingga didapat hasil klasifikasi yang optimal.

4. Kesimpulan

Berdasarkan hasil pengujian yang dilakukan pada simulasi pendeteksian *Sleep Apnea* melalui sinyal elektrokardiogram ini, didapatkan kesimpulan sebagai berikut:

1. Sistem ini sudah mampu mendeteksi dan mengidentifikasi adanya *Sleep Apnea* melalui sinyal EKG menggunakan metode DWT dan PCA.
2. Identifikasi *Sleep Apnea* dilakukan dengan tahapan pre-processing berupa filter FIR, DC Removal, dan Normalisasi Amplitudo. Ekstraksi ciri dengan PCA dan pengambilan 60 PC, serta untuk masuk ke ekstraksi ciri DWT terlebih dahulu dilakukan proses *windowing* menggunakan *window hamming* dan FFT (*Fast Fourier Transform*) dengan menggunakan *wavelet discrete meyer* dan level dekomposisi 5.
3. Proses ekstraksi ciri dengan pengambilan jumlah PC yang banyak pada PCA tidak selalu memperbaiki atau menambah akurasi, PC dengan ciri terbaik yang memberikan akurasi maksimal. Waktu komputasi metode PCA menunjukkan bahwa semakin banyak PC yang diproses maka semakin lama pula waktu komputasinya.
4. Metode PCA cocok dipasangkan dengan metode klasifikasi LDA karena menghasilkan klasifikasi yang baik untuk sinyal EKG dengan akurasi sebesar 79.1667% dan waktu komputasi sebesar 8.6s. Metode DWT juga cukup cocok dipasangkan dengan LDA karena akurasi yang dihasilkan juga cukup bagus yaitu 75% dan waktu komputasi 51s.
5. Pada metode DWT jumlah orde dari suatu *wavelet* dan makin tingginya level dekomposisi tidak berarti bahwa nilai akurasi akan bertambah juga. Dikarenakan sinyal EKG yang digunakan sebagai masukan memiliki karakteristik yang pola nya hampir sama dan cukup sulit diamati baik secara visual maupun oleh system.
6. Semakin tinggi level dekomposisi pada DWT maka semakin lama pula nilai waktu komputasi system.
7. Jenis *discriminant analysis* diaglinear berhasil memaksimalkan jarak antar kelas dan meminimalkan jarak dalam kelas sehingga didapat hasil klasifikasi yang paling optimal.

Referensi:

- [1] Website <http://howsleepworks.com/sources.html> Mastin, Luk. 2013. (Terakhir diakses pada 28 November 2014)
- [2] Rizal, Achmad. 2014. *Instrumentasi Biomedis*. Yogyakarta : Graha Ilmu
- [3] Sutarno. 2010. *Analisis Perbandingan Transformasi Wavelet pada Pengenalan Citra Wajah*. Vol.5 No.2 (Juli 2010).
- [4] Smith, Lindsay I. 2002. *A Tutorial on Principal Component Analysis*. University of Otago. Vol. 1. (26 Februari 2002).
- [5] Adnan, Fajrian Nur, Pratnya Satria Saelindri, dan Binti Mamluatul Karomah. 2012. *Investigasi Hubungan antara Jumlah Dimensi Parameter Ekstraksi Terhadap Keakurasian Pengenalan Tanda Tangan Secara Offline*. Seminar Nasional Teknologi Informasi & Komunikasi Terapan 2012 (Semantik 2012).
- [6] V Urganlawar, Isha and Harshal Chowhan. 2014. *Pre-processing of ECG Signals Using Filter*. Nagpur : International Journal of Computer Trends and Technology (IJCTT)
- [7] Afifah, Nur. 2014. *KLASIFIKASI SUARA BATUK MELALUI SINYAL DATA SUARA MENGGUNAKAN EKSTRAKSI CIRI FOURIER TRANSFORM DAN POWER SPECTRAL DENSITY SERTA METODE JARINGAN SARAF TIRUAN PROPAGASI BALKI*. Bandung : Telkom University
- [8] Ayu Lestari, Fina. 2014. *DETEKSI KISTA PERIAPIKAL MELALUI CITRA RADIOGRAF PERIAPIKAL MENGGUNAKAN METODE DISCRETE WAVELET TRANSFORM, PRINCIPAL COMPONENT ANALYSIS, DAN LINEAR DISCRIMINANT ANALYSIS*. Bandung : Telkom University
- [9] Putri Handayani, Vivi. 2013. *KLASIFIKASI PENYAKIT KANKER PROSTAT MENGGUNAKAN PRINCIPAL COMPONENT ANALYSIS DAN LEAST-SQUARES SUPPORT VECTOR MACHINE (LS-SVM)*. Bandung : Telkom University
- [10] http://physionet.org/cgi-bin/atm/ATM?database=apneaecg&tool=plot_waveforms (diakses terakhir pada tanggal 3 Desember 2014)
- [11] Aditya, Rezza. 2012. *PROTOTYPE PENGENALAN SUARA SEBAGAI PENGGERAK DINAMO STARTER PADA MOBIL*. Depok : Universitas Gunadarma



A High Accuracy FPGA Vernier Time-to-Digital Converter Based on PLL Delay Matrix

Poki Chen, Member, IEEE, Yi-Su Chung, Wei Yang Tai

Abstract—A previous FPGA two-dimensional Vernier stochastic time-to-digital converter (TDC) was proposed to achieve 2.5 ps bin size and -2.98~3.23 LSB integral nonlinearity (INL). However, the delay lines cannot be compensated for PVT variations and thus the TDC performance is strongly dependent on the stochastic distribution of the cell delays. Moreover, the input range is limited to be less than 20ns. In this paper, a high accuracy FPGA Vernier TDC is realized with PLL delay matrix instead to provide a rather PVT-insensitive solution with both high resolution and wide measurement range. The cell delays are mainly under the control of major and minor PLLs to make all clock phases as evenly distributed over the reference period as possible to achieve an extremely fine resolution. Experimental results achieve a PVT-insensitive TDC resolution of 15.6 ps. The long-term DNL and INL are measured as -0.14~0.12 LSB and -0.14~0.11 LSB over a measurement range as wide as 1μs. A new milestone in the performance of FPGA TDC is thus established.

Index Terms—2D Vernier, field-programmable gate array (FPGA), Phase-Locked Loop(PLL), PLL Delay Matrix, stochastic, time-to-digital converter (TDC), PVT-insensitive.

I. INTRODUCTION

Time-to-digital converter (TDC) is an essential core that is required in many science and engineering applications nowadays. It is responsible for keeping track of time intervals between different sets of signals. Devices such as the laser range finder, time-of flight PET, on-chip jitter measurement tools, and positron emission tomography (PET) scanner are developed upon the concept of TDC [1] - [7]. As the need for obtaining accurate results increases, high resolution TDC becomes a necessity. Having complete control over the full characteristics of TDC is also a crucial challenge. Designers need to carefully prevent inaccuracies caused by process, voltage, and temperature (PVT) variations [7]. Mainstream TDC implementations must encompass the following factors: low manufacturing cost, wide measurement range [12], high resolution [13], and minimal process [14], voltage, and temperature (PVT) sensitivity [15]. Previously, most TDCs were realized in application-specific integrated circuits (ASIC). Although being able to achieve a resolution up to 10ps [8], both the implementation and manufacturing are expensive which clearly make them not suitable for small scale production. Field-programmable gate array (FPGA) provides a rewritable platform which is cost-effective, and lesser entry requirements for chip development in comparison to ASIC.

Field-programmable gate array has been a popular platform for engineers to develop both prototypes and **small volume** products. There is a growing interest in time measuring circuits implemented with FPGA. The vast advantages of FPGA are its flexibility and configurability. It requires less time-to-market and is relatively cheap compared to other system-on-chip solutions. FPGA also provide the benefit that new architectures and systems can be quickly

realized through its reconfigurable framework [9]. Conventional methods of achieving sub-nanosecond resolution TDC includes ECL logic, however it is both power-inefficient and area consuming [9], [10]. Such designs are not suitable for portable systems or integrated chips. Conversely, various techniques such as time-to-amplitude conversion, Vernier principle, time stretching, and time interpolation have been established to achieve a high resolution and a wide measurement range. The simplest TDC architecture is a high-frequency counter that increments every clock cycle [11]. Using time-consuming statistical method and lookup table (LUT), a 3-ps incremental resolution is achieved. Multistage interpolation [8] is able to maintain a high resolution, as well as obtaining a wide measurement range.

II. OPERATION PRINCIPLE

The simplest timing diagram of TDC is shown in Fig. 1. The input interval is counted by a stable reference clock with the output representing the digitization of the test time interval T_{in} . However, it is impossible to synchronize the input time to the reference clock and there are usually some measurement errors to the both ends of the input. To solve the problem, a two-stage time interpolation technique based on the classic Nutt method can be utilized as depicted in Fig. 2 [16]. The input interval T_{in} is segmented into T_1 , T_{12} and T_2 . T_{12} is synchronous with the reference clock CLK and can be digitized by a counter readily. On the other hand, T_1 and T_2 are less than one clock period T_{CLK} and need to be processed by interpolators or fine TDCs with resolutions much smaller than T_{CLK} . It can be seen from Fig. 2 that T_{in} is measured as

$$T_{in} = T_{12} + T_1 - T_2. \quad (1)$$

It can be theorized by increasing the frequency of the reference clock to at least 100GHz, the effective TDC resolution will be improved to less than 10ps. Rather than the nonrealistic idea of high frequency clocks, a practical solution to increase the TDC resolution in FPGA is still being investigated.

The most commonly used interpolation methods are tapped delay line [17], pulse stretcher (dual-slope conversion), pulse shrinking [18], and Vernier delay line (differential delay line) [19], these methods are able to achieve sub-gate delay resolution. A 9 b, a 1.25-ps bin size TDC based upon

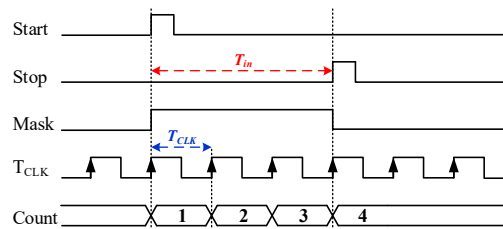


Fig. 1. Timing diagram of the counter-based TDC.

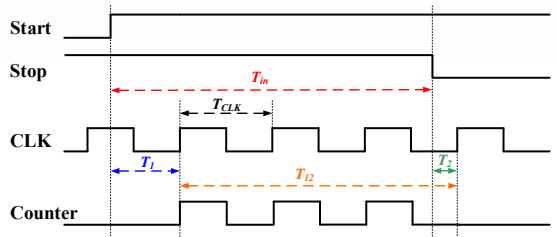
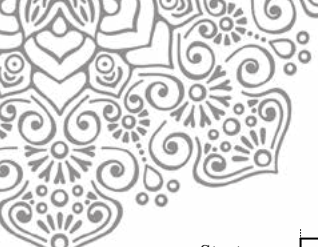


Fig. 2. Timing diagram of TDC based on Nutt interpolation method.

the amplification of time residue achieved an output standard deviation of <1 LSB, 0.8 LSB differential nonlinearity and 3 LSB integral nonlinearity (INL), the dynamic range was reported to be limited [20]. Secondary method consisted of cyclic time-domain successive approximation [21], achieving 1.2-ps resolution and a 327- μ s dynamic range. The RMS single-shot precision is 3.2ps obtained using an external INL-LUT for interpolation. Another implementation using Vernier ring [22] is created to generate an 8ps LSB width with an output standard deviation of <1 LSB. Further improvements were reported by using a gated Vernier ring structure [23] to realize a resolution of 3.2ps with an oversampling ratio of 16. Furthermore, an 8-b cyclic TDC [24] is proposed to achieve a 1.25ps LSB width, a ± 0.7 LSB DNL, and a -3 to +1 LSB INL. To enhance dynamic accuracy for applications with periodic TDC input, time-domain modulation for noise shaping is adopted [25], [26], overall producing an effective resolution of approximately 6ps.

With FPGA, traditional methods of realizing TDC is no longer applicable. The delay caused by the logic elements varies a lot due to different routing and placement on the chip. It is essential to realize a stable but flexible structure to fulfill the function of TDC in FPGA. The tapped delay line seems to be a good and easy to implement solution. Fig. 3 displays a typical tapped delay line made up of multiple D-type flip-flops in conjunction with non-inverting buffers. The START signal is delayed by time τ_m ($1 < m < n$) for each non-inverting buffer. Afterward, a STOP signal is issued to latch the states of all delay cells to generate an output in thermometer code which is fed into a priority encoder to get the equivalent binary output. However, the accuracy relies heavily on a consistent and stable delay time. Uneven delays ($\tau_0 \neq \tau_1 \neq \tau_2 \dots$) must be avoided because it disrupts the interpolation accuracy. FPGA design tool does not provide full control of the cell delay of the logic elements. The logic blocks are hardwired during its manufacture and the inter-block delay is much larger than intra-block one. Even with customized block layouts, every signal path still produces different delays. The uneven delays will affect the interpolation so that the INL and

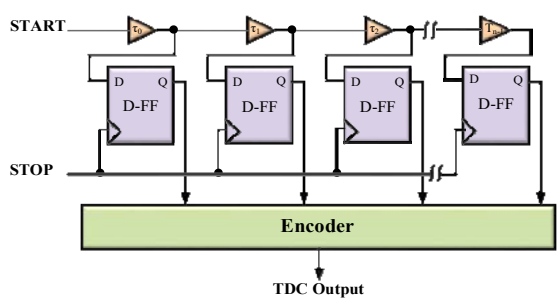


Fig. 3. Schematic of TDC based on tapped delay line.

DNL will become unacceptable for high accuracy applications.

One possible way out of the problem is to adopt delay wrapping [13] to achieve deep sub-gate-delay phase difference (resolution) for delayed clocks as illustrated in Fig. 4(a). The problem is it is really difficult to control the homogeneity of the cell delays and is even harder to make the wrapped delays uniformly distributed over the reference period. Consequently, the TDC linearity will be hampered as shown in Fig. 4(b). To gain more control on cell delay against PVT variations, the embedded PLL will be utilized in this paper.

III. PROPOSED STRUCTURE & CIRCUIT IMPLEMENTATION

The proposed TDC structure composes time-to-pulse generator, counter-based coarse TDC, two interpolators based on two-dimensional Vernier PLL delay matrices, and an offset canceller as revealed in Fig. 5. The time-to-pulse generator is employed to accommodate both high resolution and wide measurement range. It generates T_1 and T_2 for fine TDCs and T_{12} for coarse TDC from the input signal. The ALU is programmed to sum up all counters according to (1) with proper weightings between coarse and fine resolutions. The cancellation circuit is responsible for the reduction of measurement offset caused by PVT variations. The effective resolution of the TDC is decided by the fine TDCs which is composed of two-dimensional PLL delay matrix. In contrast to conventional delay wrapping [13], all cell delays are well controlled by PLL and have better PVT variation immunity. Fig. 6 (a) displays the conceptual structure of the delay matrix. The delays τ_M and τ_N are set to multiples of the reference clock period T_{CLK} , achieved by the PLL output phase division as

$$\tau_M = \frac{T_{CLK}}{M}, \tau_N = \frac{T_{CLK}}{N} \quad (2)$$

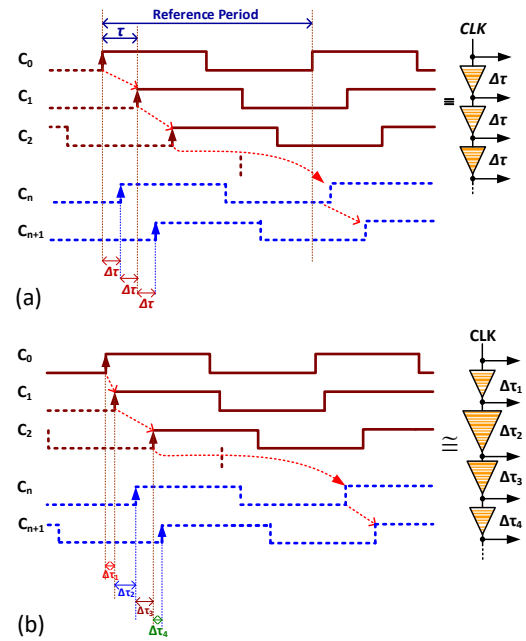


Fig. 4. (a) Ideal and (b) practical timing diagram of clock wrapping based from delay lines.

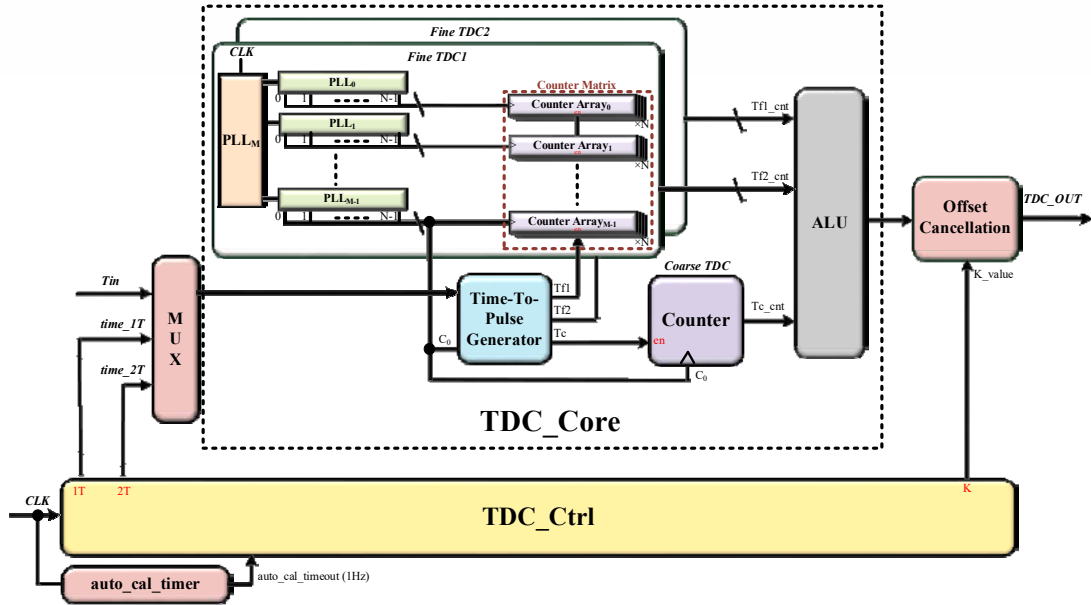


Fig. 5. Schematic of TDCs based on coarse counter and PLL.

where M, N are coprime to make the effective resolution becoming [33]:

$$\Delta\tau = \frac{1}{f \times M \times N} \quad (3)$$

where f is the reference clock frequency of the delay matrix. A good example is shown in Fig. 6 (b) with $M=3, N=4, 1.67$ GHz to accomplish 50ps effective TDC resolution.

IV. MEASUREMENT RESULTS

To demonstrate the excellence of the proposed structure, Altera Striatix IV platform was used for circuit implementation. In order to achieve the maximum number of clocks, the major PLL_M is designed to generate 4 phase-shifted outputs while each minor PLL generates 10 output phases. This is the largest PLL matrix allowed by the Altera Quartus II software. Major PLL_M operates at while the minor PLLs oscillates at 1600MHz. With overall 40 uniformly

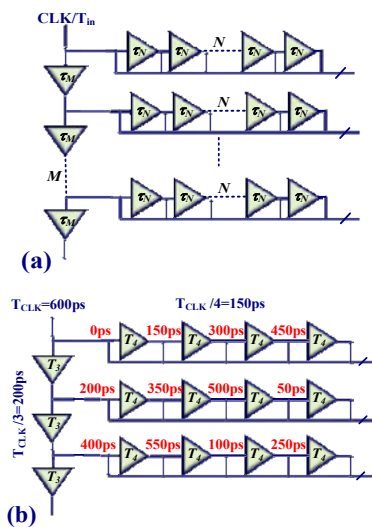


Fig. 6. (a) Two-dimensional Vernier time delay line (b) with delay time values.

distributed phases generated by the PLL matrix, the effective resolution is calculated to be 624ps/40=15.6ps.

Agilent 81134A pulse pattern generator and Tektronix DPO70404 oscilloscope are utilized for clock / input pulse generation and the pulse width measurement. For the long term measurement over 10ns~1μs in 10ns step size, the DNL and INL are measured to be -0.14~0.12 LSB and -0.14~0.11 LSB as revealed in Fig. 7. Not only the absolute offset is halved but also a μs-level measurement range is reached. The proposed TDC achieves not only 15.6 ps such a fine resolution but also μs-order wide measurement range which are among the best compared to the state-of-the-art TDCs in performance.

V. CONCLUSION

Only a few analog applications can be realized by pure standard cell-based design with performance comparable to the full-custom one's. Even fewer of them can be successfully implemented with FPGA chips due to the lack of aspect ratio tuning or bias adjustment. Nevertheless, a PVT insensitive FPGA TDC is proposed in this paper to accomplish 15.6 ps

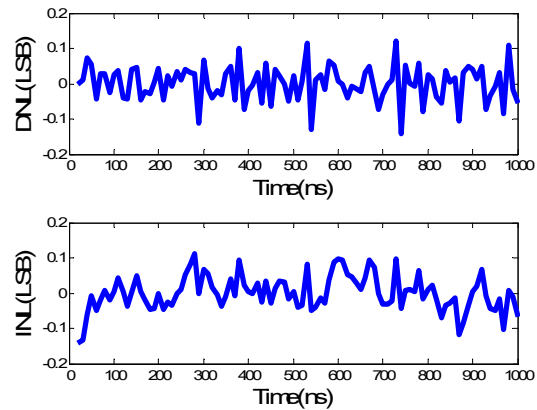
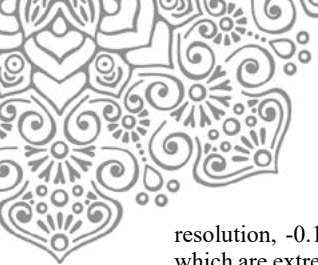


Fig. 7. (a) Differential and (b) integral nonlinearity of long term measurement



resolution, $-0.14 \text{ LSB} \sim 0.11 \text{ LSB INL}$ and μs input range which are extremely hard to achieve even for TDCs with full-custom design nowadays. The innovation and superiority of the proposed TDC is thus proved. It makes the circuit suitable for many high-end time-domain applications. The future research will further enhance the resolution to ps order.

VI. ACKNOWLEDGMENT

The authors appreciate National Chip Implementation Center (CIC) very much for the support of design and simulation tools.

REFERENCES

- [1] Chan and G. Roberts, "A jitter characterization system using a component-invariant Vernier delay line", *IEEE Transactions on Very Large Scale Integration (VLSI) Systems*, vol. 12, no. 1, pp. 79-95, 2004.
- [2] E. Kim, H. Lim, T. Lee, D. Choi, and J. Park, "Time of flight (TOF) measurement of adjacent pulses," in *Proc. IEEE Nucl. Sci. Symp. Conf. Rec.*, vol. 1, Nov. 2001, pp. 609–612.
- [3] K. Määttä and J. Kostamovaara, "A high-precision time-to-digital converter for pulsed time-of-flight laser radar applications," *IEEE Trans. Instrum. Meas.*, vol. 47, no. 2, pp. 521–536, Apr. 1998.
- [4] N. Paschalidis et al., "A time-of-flight system on a chip suitable for space instrumentation," in *Proc. IEEE Nucl. Sci. Symp. Conf. Rec.*, vol. 2, Nov. 2001, pp. 750–754.
- [5] P. Palojärvi, K. Määttä, and J. Kostamovaara, "Integrated time-of-flight laser radar," *IEEE Trans. Instrum. Meas.*, vol. 46, no. 4, pp. 996–999, Aug. 1997.
- [6] H. Brockhaus and A. Glasmachers, "Single particle detector system for high resolution time measurements," *IEEE Trans. Nucl. Sci.*, vol. 39, no. 4, pp. 707–711, Aug. 1992.
- [7] S. Yousif and J. W. Haslett, "A fine resolution TDC architecture for next generation PET imaging," *IEEE Trans. Nucl. Sci.*, vol. 54, no. 5, pp. 1574–1582, Oct. 2007.
- [8] J.-P. Jansson, A. Mäntyniemi, and J. Kostamovaara, "A CMOS time-to-digital converter with better than 10 ps single-shot precision," *IEEE J. Solid-State Circuits*, vol. 41, no. 6, pp. 1286–1296, Jun. 2006.
- [9] T. Dorta, J. Jiménez, J. L. Martín, U. Bidarte, and A. Astarloa, "Overview of FPGA-Based Multiprocessor Systems," 2009 International Conference on Reconfigurable Computing and FPGAs, pp. 273–274, Sep. 2009.
- [10] T.-I. Otsuji, "A picosecond-accuracy, 700-MHz range, Si bipolar time interval counter LSI," *IEEE J. Solid-State Circuits*, vol. 28, no. 9, pp. 941–947, Sep. 1993.
- [11] J. Kalisz, R. Pelka, and A. Poniecki, "Precision time counter for laser ranging to satellites," *Rev. Sci. Instrum.*, vol. 65, pp. 736–741, Mar. 1994.
- [12] W. W. Moses, S. Buckley, C. Vu, Q. Peng, N. Pavlov, W. Choong, J. Wu, and C. Jackson, "OpenPET: A flexible electronics system for radiotracer imaging," *IEEE Trans. Nucl. Sci.*, vol. 57, no. 5, pp. 2532–2537, Oct. 2010.
- [13] Poki Chen, Ya-Yun Hsiao, Yi-Su Chung, Wei Xiang Tsai and Jhih-Min Lin, "A 2.5 ps Bin Size and 6.7 ps Resolution FPGA Time-to-Digital Converter Based on Delay Wrapping and Averaging," *IEEE Transactions on Very Large Scale Integration Systems*, Vol. 25, pp. 114-124, Jan 2017.
- [14] G. Sportelli, N. Belcari, P. Guerra, F. Spinella, G. Franchi, F. Attanasi, S. Moehrs, V. Rosso, A. Santos, and A. Del Guerra, "Reprogrammable acquisition architecture for dedicated positron emission tomography," *IEEE Trans. Nucl. Sci.*, vol. 58, no. 3, pp. 695–702, Jun. 2011
- [15] T. Otsuji, "A picosecond-accuracy, 700-MHz range si-bipolar time interval counter LSI," *IEEE J. Solid-State Circuit*, vol. 28, pp. 941-947, Sept. 1993.
- [16] R. Nutt, "Digital time intervalometer," *Rev. Sci. Instrum.*, vol. 39, no. 9, pp. 1342–1345, Sep. 1968.
- [17] R. B. Staszewski, S. Vemulapalli, P. Vallur, J. Wallberg, and P. T. Balsara, "1.3 V 20 ps time-to-digital converter for frequency synthesis in 90-nm CMOS," *IEEE Trans. Circuits Syst. II, Exp. Briefs*, vol. 53, no. 3, pp. 220–224, Mar. 2006.
- [18] S. Tisa, A. Lotito, A. Giudice, and F. Zappa, "Monolithic time-to-digital converter with 20 ps resolution," in *Proc. 29th Eur. Solid-State Circuits Conf. (ESSCIRC)*, Sep. 2003, pp. 465–468.
- [19] P. Dudek, S. Szczepanski, and J. V. Hatfield, "A high-resolution CMOS time-to-digital converter utilizing a Vernier delay line," *IEEE J. Solid-State Circuits*, vol. 35, no. 2, pp. 240–247, Feb. 2000.
- [20] Minjae. Lee and A. A. Abidi, "A 9b, 1.25 ps resolution coarse-fine time-to-digital converter in 90 nm CMOS that amplifies a time residue," *IEEE J. Solid-State Circuits*, vol. 43, no. 4, pp. 769–777, Apr. 2008.
- [21] A. Mäntyniemi, T. E. Rahkonen, and J. Kostamovaara, "A CMOS time-to-digital converter (TDC) based on a cyclic time domain successive approximation interpolation method," *IEEE J. Solid-State Circuits*, vol. 44, no. 11, pp. 3067–3078, Nov. 2009.
- [22] Jianjun. Yu, Fa Foster Dai, R.C. Jaeger, "A 12-Bit Vernier Ring Time-to-Digital Converter in 0.13 μm CMOS Technology," *IEEE J. Solid-State Circuits*, vol. 45, no. 4, pp.830 - 842, Apr. 2010.
- [23] P. Lu, A. Liscidini, and P. Andreani, "A 3.6 mW, 90 nm CMOS gated-Vernier time-to-digital converter with an equivalent resolution of 3.2 ps," *IEEE J. Solid-State Circuits*, vol. 47, no. 7, pp. 1626–1635, Jul. 2012.
- [24] Y.-H. Seo, J.-S. Kim, H.-J. Park, and J.-Y. Sim, "A 1.25 ps resolution 8b cyclic TDC in 0.13 μm CMOS," *IEEE J. Solid-State Circuits*, vol. 47, no. 3, pp. 736–743, Mar. 2012.
- [25] Y. Cao, W. De Cock, M. Steyaert, and P. Leroux, "1-1-1 MASH time-to-digital converters with 6 ps resolution and third-order noise-shaping," *IEEE J. Solid-State Circuits*, vol. 47, no. 9, pp. 2093–2106, Sep. 2012.
- [26] Y. Cao, W. De Cock, M. Steyaert, and P. Leroux, "Design and assessment of a 6 ps-resolution time-to-digital converter with 5 MGy gamma-dose tolerance for LIDAR application," *IEEE Trans. Nucl. Sci.*, vol. 59, no. 4, pp. 1382–1389, Aug. 2012.
- [27] S. J. Kim, W. Kim, M. Song, J. Kim, T. Kim and H. Park, "A 0.6V 1.17ps PVT-tolerant and synthesizable time-to-digital converter using stochastic phase interpolation with 16 \times spatial redundancy in 14nm FinFET technology," *Solid-State Circuits Conference - (ISSCC)*, 2015 IEEE International, San Francisco, CA, 2015, pp. 1-3.
- [28] W. Pan, G. Gong, J. Li, "A 20-ps Time-to-Digital Converter (TDC) Implemented in Field-Programmable Gate Array (FPGA) with Automatic Temperature Correction," *IEEE Trans. Nucl. Sci.*, vol. 61, no. 3, pp. 1468–1473, Jun. 2014.
- [29] M. W. Fishburn, L. H. Menninga, C. Favi, and E. Charbon, "A 19.6 ps, FPGA-Based TDC With Multiple Channels for Open Source. Applications," *IEEE Trans. Nucl. Sci.*, vol. 60, no. 3, pp. 2203–2208, Jun. 2013.
- [30] L. Zhao, X. Hu, and S. Liu, J. Wang, Q. Shen, H. Fan, and Q. An, "The Design of a 16-Channel 15 ps TDC Implemented in a 65 nm FPGA," *IEEE Trans. Nucl. Sci.*, vol. 60, no. 5, pp. 3532–3536, Oct. 2013.
- [31] J. Wu, Z. Wang, C. Chen, C. Huang, and M. Zhang, "A 2.4-GHz all-digital PLL with a 1-ps resolution 0.9-mW edge-interchanging-based stochastic TDC," *IEEE Trans. Circuits Syst. II, Exp. Briefs*, vol. 62, no. 10, pp. 917–921, Oct. 2015.
- [32] A. Samarah and A. C. Carusone, "A digital phase-locked loop with calibrated coarse and stochastic fine TDC," *IEEE J. Solid-State Circuits*, vol. 48, no. 8, pp. 1829–1841, Aug. 2013.
- [33] J. Christiansen, "An Integrated high resolution CMOS timing generator based on an array of delay locked loops," *IEEE Journal of Solid-State Circuits*, Vol.31, pp. 952-957, July 1996.



Entropy-based Analysis on Dynamic Video Dimming Algorithm for Energy Efficient OLED Displays

Peter Chondro*, Shanq-Jang Ruan[†] and Chang-Chia Hua[‡]

Department of Electronic and Computer Engineering, National Taiwan University of Science and Technology
Taipei City 106, Republic of China (Taiwan)

Email: * peterchondro.ee@gmail.com, [†]sjruan@mail.ntust.edu.tw, [‡]luck89712@gmail.com,

Abstract—The active matrix light-emitting diode (AMOLED) display is a prospective technology that delivers high color gamut and contrast with low power consumption. Nevertheless, the power drawn by an OLED pixel increases non-linearly with respect to the corresponding intensity that results in high power consumption on bright pixel emission. This study examines this trade-off and proposes a pixel-based intensity dimmer that suppresses any color alteration, while reducing the power consumption on AMOLED displays. The entropy-based analysis reduces the complexity by detecting significant scene change that triggers the subtractive parameter update. According to the experimental result, the proposed method converses more than 48% of power consumption on AMOLED displays with high perceptual quality and faster frame rate compared with other representative method.

Keywords—pixel transformation; power law; active matrix organic light-emitting diode (AMOLED); perceptual entropy; dynamic subtractive.

I. INTRODUCTION

In the past decade, the demand for the consumer electronic products including mobile phones, personal computers (PCs), and tablet PCs have increased dramatically. Although these devices have specific telecommunication purposes, most of these devices are utilized as multimedia playback, which relies mainly on the display technology [1]. However, among the other components, the display panel consumes a substantial portion of power in devices [2]. Compared with the thin film transistor-liquid crystal display (TFT-LCD), the active matrix OLED (AMOLED) displays provide a better contrast ratio, smaller response time and lower energy demand. Yet, the AMOLED displays endure power disparity in high luminance level [3], [4]. Because the consumed power of AMOLED displays depends entirely on the displayed content, video playback on AMOLED displays may consume large energy portion [2], which opens for further optimization.

To optimize the power efficiency on AMOLED displays, different approaches that include the hardware optimization [5] to software-based developments [6]–[11] have been proposed. In the software-based developments, Lee et al. [6] proposed a tunable histogram-based modification technique, which is improved with an adaptive suppression rate in [7]. Although these methods may maintain the image quality, the power saving rates are inferior. Chang et al. [8] proposed a perceptually adjustable pixel dimming to reduce the pixel values

using a subtractive factor, which is further improved in [9] by suppressing the overexposed region and blue spectra. Although the trade-off between power-saving rate and image quality is minimized, the high complexity decimates applicability [9].

Another approach utilizes the scene classification based dynamic tone mapping scheme for video playbacks [10]. Despite the optimized power consumption, the video classifier fails in certain scenes. Furthermore, Park et al. [11] proposed an alpha blending method to reduce the power consumption while limiting the human perception on the video. This method achieves low computational complexity for video processing; however, certain parameters need to be initialized for different videos, which decimates the practicality of the method.

This paper proposes a low complexity pixel dimmer that adaptively shifts the image chrominance within subpixel level with hue-preserving transformation, dims the image luminance using a non-linear pixel transformation, and detects significant scene transition based on the entropy. This study contributes in providing a low complexity algorithm that converses the power consumption of OLED-based displays with inferior dynamic region distortions and no image flickers.

II. OLED POWER MODELING

Color image is constructed by three layers of pixel values including the red, green, and blue subpixels. Each pixel on the corresponding coordinate is emitted on an OLED with similar pixel configuration, i.e. red-, green-, and blue-emitting subpixels, of which intensity correlate accordingly with the drawn current. To characterize the power-demand of an OLED pixel with N bit depth, a power model is proposed in [12] as:

$$P = W_s + \sum_{i=0}^{N-1} (p_r(i) + p_g(i) + p_b(i)), \quad (1)$$

where p_r , p_g , and p_b are the function of power-demand on a single OLED pixel at i -th intensity level. The W_s represents the normalized auxiliary power-demand, which is bestowed by the embedded system to drive the displaying module per pixel. Based on the observations in [8], [9], [12], the p_r , p_g , and p_b are best-fitted with the polynomials. Using this model, the energy-dissipating character of each OLED pixel is reviewed to provide the ground knowledge of study.

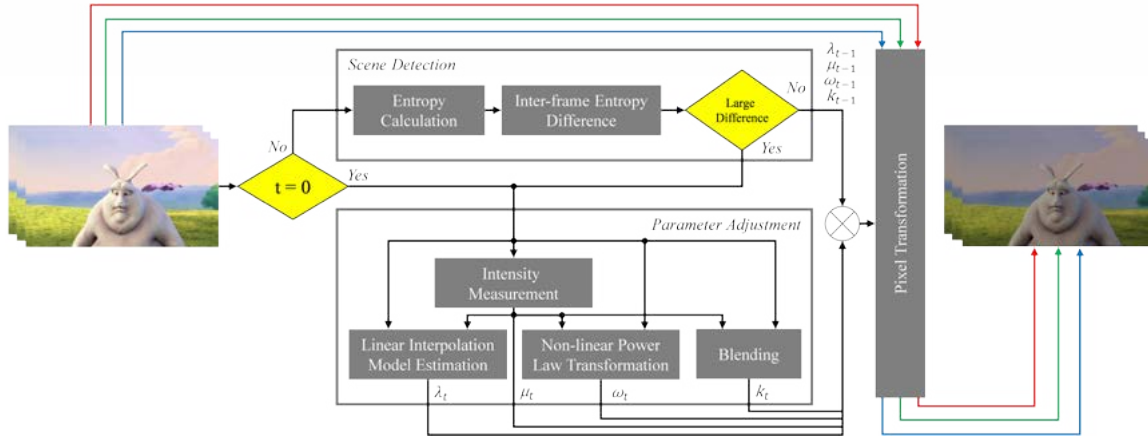


Fig. 1. Flow diagram of the proposed pixel transformation technique to conserve power on AMOLED displays.

III. PROPOSED METHOD

In this study, a novel power-saving scheme designed for video sequences on AMOLED displays is proposed. Figure 1 illustrates the flow diagram of the proposed method, which is detailed as a temporal-based technique that suppresses the RGB values of each pixel with four subtractive parameters, which have significances in conserving the power efficiency.

A. Intensity Measurement

The proposed power-saving technique is developed based on the perceptual properties, which are modeled in the statistical measures. Because image luminance yields direct influence on power consumption for AMOLED displays, a normalized luminance map (Y) is observed from the weighted color channels of the input frame (I) that is formulated as:

$$Y(j) = 0.299 \cdot R(j) + 0.587 \cdot G(j) + 0.114 \cdot B(j). \quad (2)$$

B. Linear Interpolation Model Estimation

According to [3], [4], [9], the power demand for each OLED pixel is proportional to the intensity of the corresponding pixel that comprises of three subpixels within the RGB color space. To reduce the power consumption on AMOLED displays, pixel transformation is a straightforward technique that subtracts pixel information by decreasing the intensity (ΔV), modifying the saturation (ΔS), and altering the hue (ΔH) towards the primary spectra of RGB space as:

$$\begin{cases} R_O(j) = R_I(j) - \Delta_\epsilon; \\ G_O(j) = G_I(j) - \Delta_\epsilon; \\ B_O(j) = B_I(j) - \Delta_\epsilon; \end{cases} \quad (3)$$

where R , G , and B are the sub-pixel intensities of the j -th pixel on either input (I) and output (O) frames. The Δ_ϵ is the subtractive coefficient that is expressed as:

$$\Delta_\epsilon = \frac{((\epsilon - 1) + \sqrt{(1 - \epsilon^2)}) \cdot \mu}{\epsilon} = \lambda \cdot \mu, \quad (4)$$

with μ is the average intensity of Y .

The λ in (4) is an eminent parameter that determines the saving ratio based on the ϵ , of which value should not be uniform for different frames (i.e. dynamic coefficient) due to the possibility of having distinct luminance distributions across frames. To ensure this character, this study proposes a linear interpolation model to seek an acceptable λ in (4). In certain scenes, lighting exposures from either natural or artificial exposures (A) are common to interfere with other pixels [13]. These lighting exposures can be modeled as:

$$I(j) = O(j) \cdot \tau + A \cdot (1 - \tau), \quad (5)$$

where $I(j)$ and $O(j)$ denote the j -th pixel at the input frame and the intensity-suppressed output frame, respectively.

The atmospheric-based coefficient (A) in (5) represents the estimated highest intensity of a pixel within the frames. Despite its complexity straightforwardness, the A coefficient does not discriminate or classify the high intensities whether sourcing from the exposures or the bright objects. To improve the interpolation model in (5), the A coefficient is estimated within the bright-representing class, which is expressed as:

$$A = \frac{L_{over} + (2^b - 1)}{2}, \quad (6)$$

where b denotes the bit depth that is commonly defined at 8 bit or higher. The L_{over} is formulated as:

$$L_{over} = \mu + \frac{\sqrt{\sum_{j=0}^{W \cdot H} (I(j) - \mu)^2}}{2 \times \sqrt{W \times H}} - \beta, \quad (7)$$

where W and H represent the width and the height of I .

The β constant in (7) is utilized as an adjusting parameter that normalizes the value of L_{over} by deducting the prior statistic measures that incorporates the summation of the average intensity and the bisected deviation of intensity on I image. In this study, β is defined as $\beta = 2^b/10.2$. The μ measures the overall intensity level of I as the prominent observation data that affects the dimming ratio. The μ for (7) are calculated as the total average intensity of Y map, which is similar to the μ in (4).

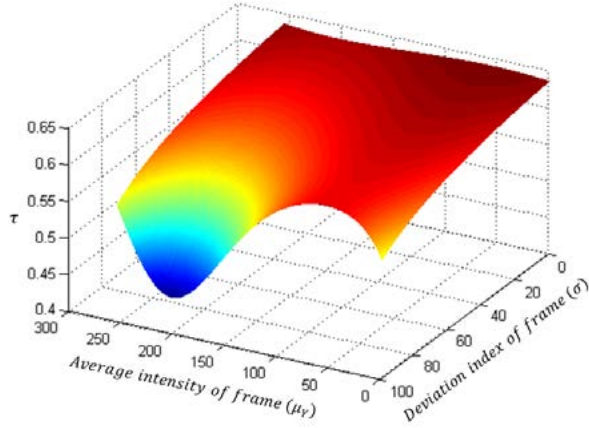


Fig. 2. The relationship between τ and the pixel distributions (μ and σ)

The ratio τ in (5) denotes the ratio of lightness of the frame to that of the atmospheric light. The τ is highly dependable with the perceptual content of each frame, of which value range from $0 \leq \tau \leq 1$. According to (5), reducing the τ to a certain value shall reduce the overall frame intensities and vice versa. In this study, τ is tuned

$$\tau = \tau_0 - \left(\frac{5}{\rho\sqrt{2\pi}} e^{-\left(1 - \frac{(\mu - 2^{b-1}) \cdot S}{2\rho^2}\right)} \right), \quad (8)$$

where τ_0 is the initial τ that is determined based on the Gaussian distribution. The S and ρ are auxiliary coefficients that observe the distribution of intensities on each frame.

In addition, the S coefficient in (8) observes the average intensities of each frame with the following expression:

$$S = \left(1 - \left(\frac{\mu - 2^{b-1}}{2^{b-1}} \right) \right)^2, \quad (9)$$

and similarly, the ρ coefficient observes the standard deviation of intensities on each frame as:

$$\rho = \frac{2^b \cdot 0.68 - \sigma}{10}. \quad (10)$$

Figure 2 illustrates the relationship of μ and σ against the τ .

Based on the pixel transformation in (3), the output O map in (5) is replaced with the subtractive coefficient (Δ_e) as:

$$I(j) = (I(j) - \lambda(j) \cdot \mu) \cdot \tau + A \cdot (1 - \tau), \quad (11)$$

which can be reformulated with the following expression:

$$\lambda(j) = \frac{(A - I(j)) \cdot (1 - \tau)}{\tau \cdot \mu}. \quad (12)$$

According to the pixel transformation in (12), the λ factor will exceed the range ($\lambda > 1$) when $I(j) > A$. Therefore, the power consumption of displays shall increase since the input value at I is larger than the output value at O . To avoid this condition, the $I(j)$ in (12) is replaced with the μ , as:

$$\lambda = \frac{(A - \mu) \cdot (1 - \tau)}{\tau \cdot \mu}. \quad (13)$$

C. Non-linear Power Law Transformation

The power consumption on OLED pixels depends entirely on the displayed content with incremental increase according to the pixel intensities. Although pixel transformation in (3) suppresses the overall intensity, few details in the lower histogram range may be lost. The high-frequency spectra (e.g. blue and violet colors) are also contributing in the inferiority of the power efficiency, unlike the lower frequency spectra [9].

To alleviate the undesired loss of image details and further increase the energy efficiency by suppressing high-frequency spectra on the higher histogram range, the non-linear is proposed by associating a weighting factor (w) in (3) that is:

$$O(j) = I(j) - (w(j) \cdot \lambda \cdot \mu), \quad (14)$$

where the $w(j)$ factor is calculated pixel-wisely on two normalized luminosity-based clusters:

$$\begin{cases} \eta_L \cdot \left(\left(\frac{Y(j)}{255} \right)^{\frac{255}{\mu}} + \frac{\mu}{255} \right), & Y(j) \leq \mu; \\ \eta_H \cdot \left(\left(\frac{\mu}{255} \right)^{\frac{255}{\mu}} + \frac{\mu}{255} + \eta_H \right), & \text{else.} \end{cases} \quad (15)$$

The η_L and η_H in (15) denote the non-linear power law-based transformation coefficients for the lower and higher histogram ranges, respectively, which are expressed as:

$$\eta_L = e^{\frac{\mu - \sigma}{255} - 0.5}, \quad (16)$$

and

$$\eta_H = 2 \cdot e^{\frac{\sigma}{100} - 0.5} \cdot \left(\left(\frac{Y(j)}{255} \right)^{\frac{\mu}{255}} - \frac{\mu}{255} \right)^{\frac{\mu}{255}}. \quad (17)$$

D. Hue Blending

Shifting hues toward the RGB primaries reduces the overall intensity and increases the power efficiency. However, color shifting may result in false hue reproduction; thus decimating the performance of the proposed method to preserve the chromatic information accurately. To minimize the trade-off between power conservation and image quality on AMOLED displays through color modification, hue blending is proposed by involving a scaling coefficient (k) in (14) as:

$$O(j) = k \cdot (I(j) - (w(j) \cdot \lambda \cdot \mu)). \quad (18)$$

The k coefficient is designed based on the ratio between the luminance and the lightness values of I as follows:

$$k = \frac{\mu^L}{(\mu + 1) \times N}, \quad (19)$$

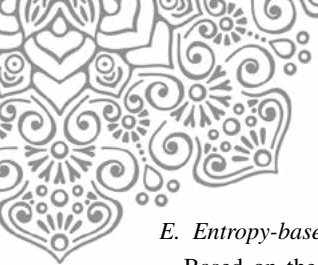
where μ^L denotes the overall lightness value of I :

$$\mu^L = 116 \times \sqrt[3]{\frac{\mu + 1}{256}} - 16. \quad (20)$$

The N in (19) is utilized to control the value of k to be smaller than one. Therefore, the N factor is set as follows:

$$N = C_1 - \left(C_2 \times \frac{\mu^L - \mu^{\bar{L}}}{100 - \mu^{\bar{L}}} \right), \quad (21)$$

where C_1 and C_2 are predefined constants that were empirically set at 2.3 and 1.5, respectively. The $\mu^{\bar{L}}$ is derived from (20) when $\mu = 0$ that helps to normalize the k factor.



E. Entropy-based Scene Detection

Based on the proposed pixel transformation in (18), the I image can be modified to generate the dimmed output O that is expected to reduce the power demand on AMOLED displays. To maximize the applicability of the proposed method based on the functionality of the AMOLED displays particularly for video playback, the proposed method can be applied to process each frame inside the video stream as follows:

$$O_t(j) = k_t \cdot (I_t(j) - (w_t(j) \cdot \lambda_t \cdot \mu_t)), \quad (22)$$

where t denotes the frame number (i.e. timestamp). Although updating the subtractive parameters (e.g. k_t , w_t , λ_t , and μ_t) on each frame provides the optimum performance for the proposed method, the computational complexity shall shoot up to a steep level depending on the input dimensions.

According to the proposed pixel transformation in (22), the subtractive dimming parameters are adjusted dynamically based on the perceptual information on each frame. Therefore the parameter updates are unnecessary for analogous frames. The entropy-based scene detection is proposed to identify any frame, of which information change dramatically from the prior iteration. The identified frame informs the proposed method to update the subtractive parameters.

To approximate the perceptual information of I , the entropy calculation is implemented:

$$E_t = - \sum_{l=0}^{l_{max}} pdf_t(l) \log(pdf_t(l)), \quad (23)$$

where $pdf_t(l)$ denotes the probability density function of I image at t -th frame. To detect any steep change in the perceptual information, the entropy at t -th frame is compared with the entropy at $(t-1)$ -th frame, which is expressed as:

$$\begin{pmatrix} \mu_t & = & \mu_{t-1} \\ \lambda_t & = & \lambda_{t-1} \\ w_t(j) & = & w_{t-1}(j) \\ k_t & = & k_{t-1} \end{pmatrix} \text{ if } |E_t - E_{t-1}| < \Theta; \quad (24)$$

otherwise, all parameters are updated using the corresponding equations that have been elaborated in prior subsections. In this study, the threshold (Θ) for (24) is empirically set to 0.05.

IV. EXPERIMENTAL RESULTS

The visual saliency-induced index (VSI) is implemented to primarily assess the image quality by comparing the perceptual similarities between the input I and the output O streams [14] with the following mathematical formulation:

$$VSI_t = \frac{\sum_{j=1}^{W \cdot H} V_t^m(j) \cdot S_t^V(j) \cdot S_t^G(j)^{\gamma_1} \cdot S_t^C(j)^{\gamma_2}}{\sum_{j=1}^{W \cdot H} V_t^m(j)}, \quad (25)$$

where S_t^V , S_t^G , and S_t^C represent the saliency similarities between visual saliency-induced maps, gradient maps, and chrominance of the I and the O streams at t -th frame, respectively. The S_t^V is expressed as:

$$S_t^V(j) = \frac{2S_t^{V1}(j) \cdot S_t^{V2}(j) + K_1}{(S_t^{V1}(j))^2 + (S_t^{V2}(j))^2 + K_1}. \quad (26)$$

The $S_t^{V1}(j)$ and $S_t^{V2}(j)$ denote the visual saliency-induced maps of I and O frames at the t -th iteration that are obtained from graph-based visual saliency [14]. Analogously, the $S_t^G(j)$ is mathematically expressed as:

$$S_t^G(j) = \frac{2G_t^1(j) \cdot G_t^2(j) + K_2}{(G_t^1(j))^2 + (G_t^2(j))^2 + K_2}, \quad (27)$$

where $G_t^1(j)$ and $G_t^2(j)$ are the gradient modulus maps of I and O frames at the t -th iteration generated from Scharr operator. Lastly, the $S_t^C(j)$ is defined as:

$$S_t^C(j) = \frac{2U_t^1(j) \cdot U_t^2(j) + K_3}{(U_t^1(j))^2 + (U_t^2(j))^2 + K_3} \cdot \frac{2V_t^1(j) \cdot V_t^2(j) + K_3}{(V_t^1(j))^2 + (V_t^2(j))^2 + K_3}, \quad (28)$$

where $U_t^1(j)$ and $V_t^1(j)$ as well as $U_t^2(j)$ and $V_t^2(j)$ are two chromatic components of I and O , which are generated from opponent color conversion.

Constant K_1 , K_2 , and K_3 are required to increase the stability of similarity metrics that are set based on the previous work as 1.27, 386, and 130, respectively [14]. Similarly, the significance of (27) and (28) are tuned by setting λ_1 and λ_2 to 0.4 and 0.02. To avoid imbalance human vision system caused by steep VS values, $V_t^m(j)$ weights the importance of the overall VSI metrics as

$$V_t^m(j) = \max(S_t^{V1}(j), S_t^{V2}(j)). \quad (29)$$

As the final stage, the overall VSI score is taken by measuring the average of VSI_t on the given time range.

In addition to the VSI metric, the CIEDE2000 (Δ_{00}) are implemented to further assess the perceptual similarity by generating a quality map from I and O streams [15] and measuring the Euclidean distance of chrominance channel between I and O [16]. To fairly assess the performance of the observed method in terms of minimizing the trade-off between the image quality and the power-saving rate, the average intensities of the I (μ_t^I) and O (μ_t^O) streams are measured to calculate the intensity-suppression ratio (%W):

$$\%W = \frac{\sum_t (\mu_t^I - \mu_t^O)}{\sum_t (\mu_t^I)} \times 100\%. \quad (30)$$

To assess the performance of the power-saving, a series of electrical current measurement was conducted on a 5.5 inch AMOLED display with 1080×1920 resolutions using a power monitor. A 20 seconds of resting time was defined before the power monitor measures and calculates the averages of 5 samples periodically. The measured current and the rated voltage are multiplied and then subtracted with the W_0 , which is defined as the measured power of the AMOLED display while displaying the black image. To understand the amount of saved power, the power-saving rate is calculated as:

$$\%P = \frac{P_{original} - P_{resultant}}{P_{original}} \times 100\%, \quad (31)$$

where $P_{original}$ and $P_{resultant}$ are the measured display power while displaying the input and the resultant frame, respectively.



TABLE I
PERFORMANCE COMPARISON OF THE EXISTING AND THE PROPOSED POWER-SAVING SCHEMES FOR AMOLED DISPLAYS

Video	Methodology	VSI	Δ_{00}	%W	%P
1	Chang et al. [8]	0.967	5.076	38.60	57.28
	Chondro et al. [9]	0.944	3.175	39.15	66.53
	Proposed Method	0.956	5.416	40.00	72.97
2	Chang et al. [8]	0.987	3.002	41.90	51.85
	Chondro et al. [9]	0.948	2.514	42.65	48.27
	Proposed Method	0.974	3.391	47.50	55.86
3	Chang et al. [8]	0.960	4.918	36.90	53.27
	Chondro et al. [9]	0.927	4.306	38.90	58.63
	Proposed Method	0.928	5.731	41.20	65.70
4	Chang et al. [8]	0.949	3.578	39.50	52.50
	Chondro et al. [9]	0.957	4.158	40.05	56.69
	Proposed Method	0.952	5.172	41.60	64.73

A. Objective Visual Quality Evaluation

Table I provides comprehensive performance benchmarks between the proposed method and the existing power-saving techniques [8], [9]. Although the proposed method obtains the lower perceptual scores compared with [8]; the perceptual degradations are considered minor since the average decline in VSI is 0.013. However, contrary to the [8], the proposed power-saving method achieves inferiorly 0.009 higher average VSI score compared with [9]. The chromatic reproduction of the proposed method is similar compared with [8], [9] as shown with slight differences in the Δ_{00} indexes on all input data. These observations indicate that all implemented methods (including the proposed method) provide analogous perceptual quality in the resultant videos.

According to luminance ratio in Table I, the proposed method outperformed [8], [9] with higher %W scores on most tested video sequences. In average, the proposed method is able to preserve the perceptual lightness at roughly 42.58% of the original intensities or 3.36% higher than [8] and 2.39% higher than [9]. This finding suggests that the proposed method is able to preserve the image lightness; thus minimizing the trade-off between the dimming ratio and the power-saving rate.

In terms of the power saving rate, Table I also elaborates the performance comparisons in terms of the power-saving capabilities. Although [8], [9] provide better perceptual quality of the resultant frames, these prior techniques achieve more inferior power saving rate as indicated by lower %P scores with averages of 53.73% and 57.53%, respectively. In contrast, the proposed method provides higher power-saving rate with average %P of 64.82%. provides higher power-saving rate with average %P of 64.82%.

The pixel transformation techniques modify the OLED pixel values by dimming the intensities to the lower level of energy consumption. For video sequences, the fluctuating dimming factors on consecutive frames using the pixel transformation technique will result in flickering effects that decimate the quality of the video. To assess the flickering effect of the resultant videos from all methods, the standard deviations of the power-saving rate on each frame are computed.

TABLE II

PERFORMANCE COMPARISON IN TERMS OF THE FLICKERING ARTIFACTS

Video	Chang et al. [8]	Chondro et al. [9]	Proposed Method
1	45.40	49.30	29.10
2	34.93	38.25	27.84
3	13.57	22.30	6.20
4	5.50	14.90	7.40

The units are in the scale of 10^{-3} .

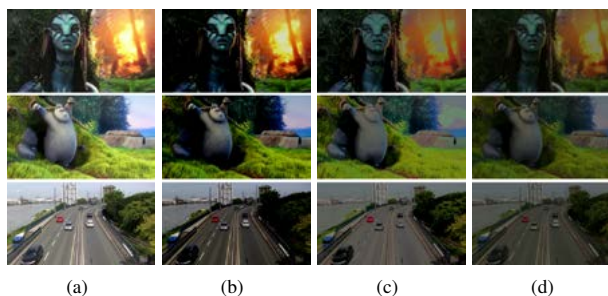


Fig. 3. Comparison of the resultant frames from (a) 2nd to 4th tested videos (top-bottom) generated by (b) [8], (c) [9], and (d) the proposed method.

Table II compares the implemented methods in terms of observing the flicker artifacts on distinct video data. Based on Table II, the proposed method achieves in averages 18.99% and 47.68% lower deviations of the power saving rates against [8], [9], respectively. By achieving lower deviations of power-saving rates, the proposed method has higher perceived quality of the resultant video playback with fewer occurrence of flicker artifacts than [8], [9] that decimate the total quality.

Figure 3 illustrates the sampled results from the proposed and the prior techniques on the 2nd, 3rd, and 4th test sequences with the corresponding original sampled frames are shown in Fig. 3(a). According to Fig. 3(b), the pixel transformation in [8] was able to produce high contrast frames with crisp details for the originally bright pixels. However, most details that have originally lied on the dark pixels were lost; thus removing textures through excessing dimming. For instance, details on the neck region at the 2nd footage as well as details on the bushes at the 4th footage were not produced properly. Differ from [8], the weighted pixel transformation in [9] was able to provide more details than [8]. However, obvious color distortions occur in the resultant frames. For instance, the color information at few regions shown in Fig. 3(c) including the bright sky at the 3rd footage and the red car at the 4th footage are altered, which result in poorly perceived quality.

Compared with the other implemented methods, the proposed power-saving technique is able to preserve image details in both bright and dark pixels with high chromatic reproducibility. According to the illustration of the sampled resultant frames from the proposed method in Fig. 3(d), image details in the neck region at the 2nd footage and the bushes at the 4th footage were completely preserved; color for the bright sky at the 3rd footage is accurately produced.



TABLE III
COMPARISON OF THE COMPUTATIONAL COMPLEXITY (SECONDS)

Video	Chang et al. [8]	Chondro et al. [9]	Proposed Method
1	0.165	0.856	0.210
2	0.351	1.970	0.435
3	0.339	2.007	0.434
4	0.750	4.474	0.919

B. Computational Complexity

In this work, the experiments were performed on a personal computer with a 3.40GHz Intel i7-3770 CPU and an 8GB of RAM. The implementations were developed on the Microsoft Visual Studio 2010. According to Table III, the proposed method was executed with marginally slower computational time than [8] and significantly faster computational time compared with [9].

V. CONCLUSION

This paper proposes a novel scheme to specifically reduce the power consumption of AMOLED displays by adjusting the pixel values. Using the dimming technique mixed with hue preserving, the transformation method dims the pixel contents and preserves the colors. A weighted transformation scheme based on power-law technique is presented to further suppress high-frequency spectra that are known to demand higher displaying power while preserving the details in the dark region. To reduce complexity on video sequences, parameter updates are performed when the high entropy difference is detected. Experimental results showed that the proposed method provides acceptable resultant images with an average visual saliency index of 0.962 and achieves on average 64.3% and up to 73% rate of power-saving, which is higher than other previous methods.

REFERENCES

[1] Google Inc. and IPSOS OTX MediaCT, "The Mobile Movement: Understanding Smartphone Users," 2011. [Online]. Available: https://ssl.gstatic.com/think/docs/the-mobile-movement_research-studies.pdf. [Accessed: 24-Jul-2016].

[2] D. Shin, Y. Kim, N. Chang, and M. Pedram, "Dynamic Driver Supply Voltage Scaling for Organic Light Emitting Diode Displays," *IEEE Trans. Comput.-Aided Des. Integr. Circuits Syst.*, vol. 32, no. 7, pp. 1017-1030, Jul. 2013.

[3] M. Dong and L. Zhong, "Chameleon: A Color-Adaptive Web Browser for Mobile OLED Displays," *IEEE Trans. Mobile Comput.*, vol. 11, no. 5, pp. 724738, May 2012.

[4] C.-K. Kang, C.-H. Lin, and P.-C. Hsiu, "A Win-Win Camera: Quality-Enhanced Power-Saving Images on Mobile OLED Displays," in *2015 IEEE/ACM Int. Symp. Low Power Electronics and Design, Rome*, 2015, pp. 267272.

[5] C.-S. Chae, H.-P. Le, K.-C. Lee, G.-H. Cho, and G.-H. Cho, "A Single-Inductor Step-Up DC-DC Switching Converter With Bipolar Outputs for Active Matrix OLED Mobile Display Panels," *IEEE J. Solid-State Circuits.*, vol. 44, no. 2, pp. 509524, Feb. 2009.

[6] C. Lee and C. Lee and Y.-Y. Lee and C.-S. Kim, "Power-Constrained Contrast Enhancement for Emissive Displays Based on Histogram Equalization," *IEEE Trans. Image Process.*, vol. 21, no. 1, pp. 8093, Jan. 2012.

[7] L.-M. Jan, F.-C. Cheng, C.-H. Chang, S.-J. Ruan, and C.-A. Shen, "A Power-Saving Histogram Adjustment Algorithm for OLED-Oriented Contrast Enhancement," *IEEE/OSA J. Display Technology.*, vol. 12, no. 4, pp. 368375, Apr. 2016.

[8] T.-C. Chang, S.S.-D. Xu, and S.-F. Su, "SSIM-based Quality-on-Demand Energy-Saving Schemes for OLED Displays," *IEEE Trans. Syst. Man Cybern. A, Syst. Humans*, vol. 46, no. 5, pp. 623635, May. 2016.

[9] P. Chondro, S.-J. Ruan, "Perceptually Hue-Oriented Power-Saving Scheme with Overexposure Corrector for AMOLED Displays," *IEEE/OSA J. Display Technology.*, vol. 12, no. 8, pp. 791-800, Mar. 2016.

[10] X. Chen, Yiran Chen, and Chun Jason Xue, "DaTuM: Dynamic Tone Mapping Technique for OLED Display Power Saving Based on Video Classification," in *Proc. of IEEE/ACM DAC*, pp. 16, 2015.

[11] M. Park and M. Song, "Saving Power in Video Playback on OLED Displays by Acceptable Changes to Perceived Brightness," *IEEE/OSA J. Display Technology.*, vol. 12, no. 5, pp. 483490, May. 2016.

[12] B. Geffroy, P. L. Roy, and C. Prat, "Organic light-emitting diode (OLED) technology: Materials, devices and display technologies," *Polym. Int.*, vol. 55, no. 6, pp. 572582, Jun. 2006.

[13] K. He, J. Sun, and X. Tang, "Single Image Haze Removal using Dark Channel Prior," *IEEE Trans. Pattern Anal. Machine Intell.*, vol. 33, no. 12, pp. 2341-2353, 2011.

[14] L. Zhang, Y. Shen, and H. Li, "VSI: A Visual Saliency-Induced Index for Perceptual Image Quality Assessment," *IEEE Trans. Image Process.*, vol. 23, no. 10, pp. 4270-4281, 2014.

[15] L. Zhang and H. Li, "SR-SIM: A Fast and High Performance IQA Index Based on Spectral Residual," in *19th IEEE Int. Conf. Image Process.*, Orlando, 2012, pp. 1473-1476.

[16] M. R. Luo, G. Cui, and B. Rigg, "The Development of the CIE 2000 Colour-Difference Formula: CIEDE2000," *Color Res. Applicat.*, vol.26, no. 5, pp. 340-350, 2001.



Improved Structure of Ground Terminals for Crosstalk Reduction in SAS-3 Storage Connector Design

Ding-Bing Lin^{#1}, Chung-Ke Yu^{*2}, Chih-Kang Lai^{*3}, Ko-Ying Huang^{*4}

[#]Department of Electronic and Computer Engineering, National Taiwan University of Science and Technology, Taipei, Taiwan,

^{*}Department of Electronic Engineering, National Taipei University of Technology, Taipei, Taiwan

¹dmlin@mail.ntust.edu.tw, ²jonk.yu56@gmail.com,

³dact8842412@gmail.com, ⁴mo060928@gmail.com

Abstract—In this paper, we proposed a board to board connector design for high-speed storage devices. The proposed design utilizes a terminal structure with ground clipper and ground blade to reduce the near-end crosstalk (NEXT) and far-end crosstalk (FEXT) such that the connector performance satisfies SAS-3 connector specification. Three improved designs of connector model are studied and compared with the legacy SAS-2 connector design. Also, the capacitive and inductive parameter of the transmission lines of proposed designs have been extracted in order to determine the contribution of crosstalk noise caused by capacitive and inductive coupling. Furthermore, the S-parameter results have been validated by full-wave simulation tool HFSS in the frequency domain analysis. For the NEXT and FEXT all proposed design shows significant improvement with 10–40dB than the legacy design and the strength under -40dB from DC to 6GHz. In addition, the proposed connector design can meet the crosstalk requirement of SAS-3 connector specification.

I. INTRODUCTION

Today's solid-state storage devices (SSDs) for servers are capable of data rates up to 10Gbps, the new SAS-3 12Gbps protocol standard has been promoted to accommodate the rapid growing data rate of SSDs. In addition, the operating frequency of the interconnection elements used to connect the storage devices, including the electrical connectors and cables must be increased as well. In legacy SAS-2 6Gbps storage connector, its terminal mating area was lack of a proper grounding terminal design, when the high frequency signals propagated through the interconnection of the mating area, a high frequency interference has been coupled between inter/intra-pair differential transmission lines and named near-end crosstalk (NEXT) and far-end crosstalk (FEXT). In order to improve storage connector's imperfection electromagnetic properties at higher operating frequency due to increased capacitive and inductive coupling, we proposed an improved structure of ground terminal for crosstalk reduction.

II. DESIGN METHOD

We proposed three 3D connector models with three different types of grounding terminals, and then the L-C

equivalent parameters of the legacy design and these three proposed designs were extracted by Q3D simulation tool. The L-C parametric analysis was studied to determine the interaction between the NEXT/FEXT and capacitive/inductive coupling. Finally, the NEXT and FEXT performances of all proposed models were simulated by HFSS for final validation.

III. 3D SIMULATION MODEL OF THE SAS CONNECTOR

A. A Brief Introduction

For the inter compatibility consideration, the mechanical configurations and the exterior of proposed SAS connector was based on the EIA SFF-8482 industrial standard model [1]. Because of the mechanical restriction its differential transmission line is not a well reference plane structure design as well as the stripline on the PCB or the coaxial cable, thus when the high frequency signal propagates through the mating area of the interconnected connector, it is liable to cause coupling effect and degrades the signal integrity and the reliability of the computer system.

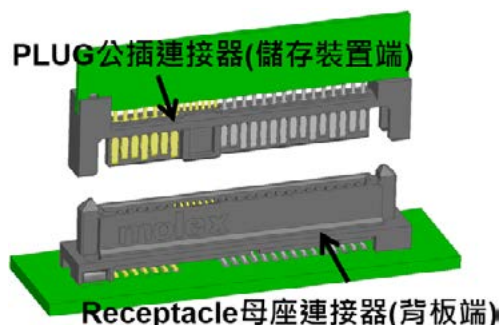
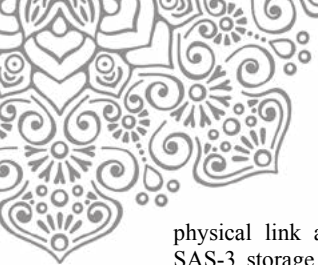


Fig. 1 The exterior of the mating SAS plug and receptacle connector.

First, the approximated multi-pairs differential line model should be illustrated to interpret the L-C equivalent parameters analysis. The T10/BSR INCITS 519 [2] is the technical committee of accredited standard committee who formulated the SAS-3 electrical specification, including the

This work was supported by the Ministry of Science and Technology of Taiwan under Grant MOST 104-2221-E-011-178 -MY2.



physical link and the signal integrity (SI) performance of SAS-3 storage connector. According to the standard, a real physical link of SAS storage connector has four differential pairs (i.e two lanes) transmission lines and six ground terminals, so the total of terminals in one plug or receptacle connector is fourteen. Fig.2 shows the simplified diagram of SAS interconnections.

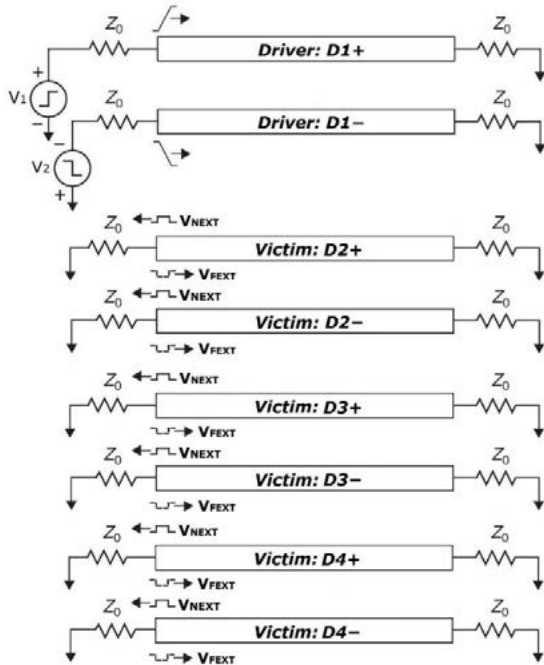


Fig. 2 The four pairs (two lanes) differential transmission lines configuration in one SAS storage interconnection.

Next, the approximated effective inductance and capacitance of every differential pair conductors could be derived and calculated by the single line equivalent model (SLEM) [3]. Though the SLEM can help to estimate the L-C equivalent parameters, characteristic impedance, and propagation velocity, in case of multi-conductor transmission lines as the SAS connector, it is an approximation for quick evaluation.

B. The Improved Structure of Ground Terminal

According to the SAS specification, the terminal's pinout configuration is GSSG, consists of four differential pairs in parallel, including clock signals, sharing a single common ground return terminal. When ground terminals are assigned throughout the entire length of the mating connector for best SI performance, we must make its ground loop areas as minimum as possible to avoid the energy of high frequency signals from being coupled to other differential pairs. Two improved structures of ground terminal for crosstalk reduction by using ground blade and ground clipper as shown in Fig. 3.

The ground clipper is an additional bended metal sheet to contact other three separated ground terminals of the legacy connector design, the ground blade is a redesign single piece of metal conductor instead of that three separated ground terminals in legacy connector design.

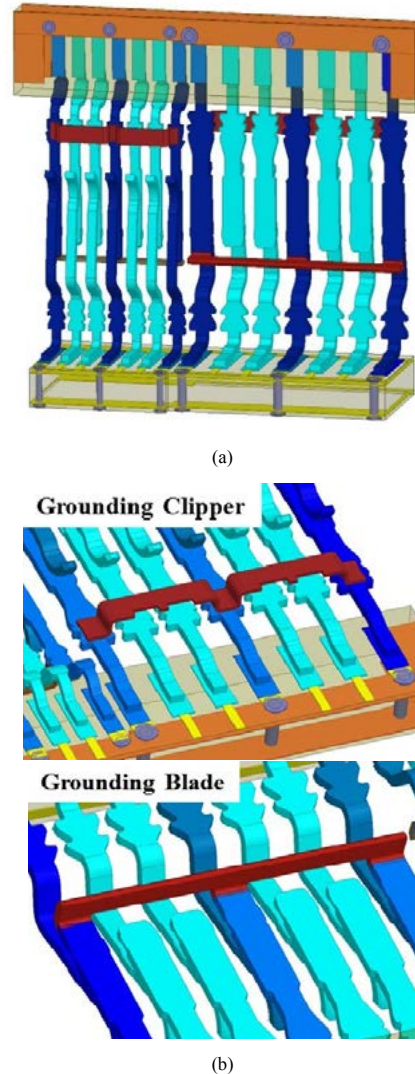
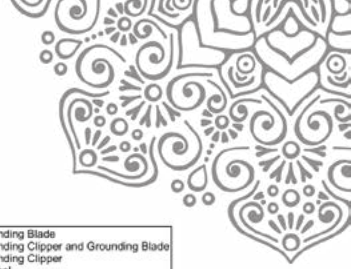


Fig. 3 (a) A SAS storage connector (housing removed) with ground blade and ground clipper structure terminal design. (b) The close-up of ground blade ground clipper.

C. Modelling for the Simulation

The plug and receptacle connector assembly have been soldered up on a printed circuit board, the board material is TU-872 with 3.8 of relative permittivity (ϵ_r) and 0.009 of



dielectric loss tangent, and then all metal terminals are brass, material of housing is Liquid Crystal Polymer (LCP) E471i with 3.5 of relative permittivity (ϵ_r) and 0.032 of dielectric loss tangent, the total volume of the model about 15x15x8 mm³. The SAS-3 spec. has defined the transmitter and receiver ends to the port settings of all differential pairs for Q3D and HFSS simulations.

IV. EXPERIMENT RESULTS

For NEXT analysis, the coupling between all adjacent differential pairs is worthy of notice. We noticed the ground clipper has good coupling reduction to capacitive but useless to inductive, and then the ground blade is very effective for both coupling. By the way, the result shows the lowest NEXT when using both two structure because the accumulation of capacitive coupling reduction. In FEXT analysis, we focus on the non-adjacent pairs. Because the distance between the non-adjacent pairs is farther than the condition of adjacent pairs, the inductive coupling is the factor who dominates the FEXT but not capacitive coupling. Based on the reasons we know the ground blade is more effective than the ground clipper to the FEXT. Obviously, the lowest FEXT is got by using both two proposed designs owing to the accumulation of inductive coupling reduction. Table.1 shows the comparison with the legacy design.

In frequency domain, the crosstalk performance has been validated through HFSS full-wave simulation, the result shows that two proposed designs can eliminate the peak resonance through DC to 6GHz of the NEXT/FEXT, but remain the insertion loss, return loss and the impedance to meet the SAS-3 compliance.

TABLE I
COMPARISONS OF NEAR-END AND FAR-END CROSSTALK COEFFICIENT BETWEEN THE ORIGINAL AND THREE PROPOSED DESIGNS

Type of Grounding terminals	K_b			K_f	
	D1 - D2	D2 - D3	D3 - D4	D1 - D3	D2 - D4
Clipper	-9.7 %	+0.3%	+1.7 %	-10.5%	+3.6%
Blade	-12.6 %	-14.8%	-11.4 %	-14.9%	-11.7%
Clipper and Blade	-19.6 %	-15.2%	-11.8 %	-23%	-13.9%

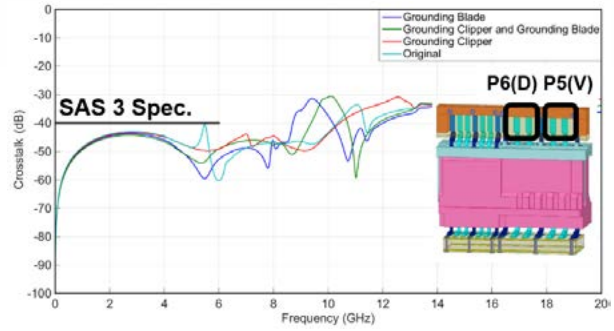


Fig. 4 The comparison of NEXT by using different grounding terminal structures. (D1 to D2)

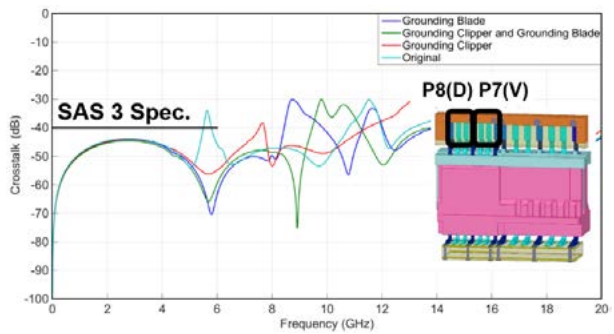


Fig. 5 The comparison of NEXT by using different grounding terminal structures. (D3 to D4)

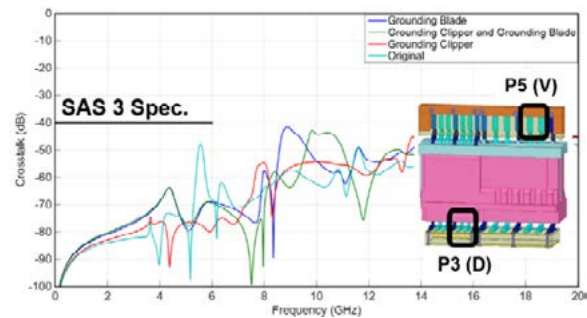


Fig. 6 The comparison of FEXT by using different grounding terminal structures. (D1 to D3)

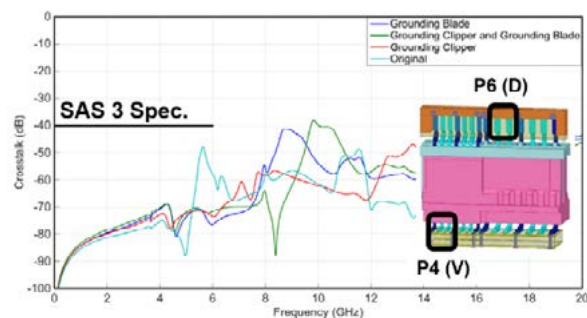


Fig. 7 The comparison of FEXT by using different grounding terminal structures. (D2 to D4)



V. CONCLUSIONS

In SAS-3 storage connector design, the crosstalk interference between its multi-pair differential transmission lines is an important consideration to avoid the SI issue. The additional clipper and blade structure of ground terminal that we proposed had a significant benefit to coupling reduction. After the L-C parametric analysis from the extracted connector models, the ground blade has a lower near-end and far-end crosstalk coefficient than the legacy design. Furthermore, because the ground clipper can gain the reduction of capacitive coupling, thus the near-end crosstalk coefficient has much more lower value by using both ground blade and ground clipper. In addition, the full-wave simulation result shows a similar trend as the L-C parametric analysis in

frequency domain. The peak value through DC to 6GHz of the near-end and far-end crosstalk has been reduced over 6~20dB by using ground blade and / or ground clipper. For this reason, the ground blade and ground clipper are feasible solutions for storage connector design to meet the SAS-3 compliance.

REFERENCES

- [1] *SFF-8482 Rev 2.4 Specification for Serial Attachment 2X Unshielded Connector (EIA-966)*, Electronic Industries Alliance, May 2015.
- [2] *Information Technology – Serial Attached SCSI – 3 (SAS-3), Working Draft Revision 06*, American National Standard, T10/BSR INCITS 519, Nov. 2013.
- [3] S. H. Hall, H. L. Heck, *Advanced Signal Integrity for High-Speed Digital Designs*, Hoboken, NJ, Wiley-IEEE Press, 2009.



Evolution from a Door Bell into an IP Door Phone

Daniel Hofman^{1,2}, Jenq-Shiou Leu¹, Pavel Troller²

¹National Taiwan University of Science and Technology

²Czech Technical University in Prague

hofmadan@fel.cvut.cz, jsleu@mail.ntust.edu.tw, patrol@sinus.cz

Abstract - This work introduces a general view on an evolution of door communication systems. The work evaluates a current market of IP-based systems which currently consists mainly of more expensive devices targeted on business customers. The goal is to design a doorphone prototype based on an IP protocol with suitable functions and easy control for a less demanding user. The Raspberry Pi computer was chosen for development together with other suitable hardware to accomplish desired functions. The Linphone open-source project was used to implement phone functionality. The low price or open-source solutions were preferred when selecting ideal hardware and software to use. The conclusion evaluates how successful the implementation was while keeping the device affordable.

Key Words - Internet Protocol, Session Initiation Protocol, Raspberry Pi, Linphone, Doorphone

I. INTRODUCTION

The history of intercom systems started a long time ago. Already several hundred years ago people wanted to be noticed of a guest arrival to their house. It all started with doorbells and the invention of electricity.[1] Until around middle of twentieth century the doorbell system included a button, transformer and a wiring which allowed us to place the bell to some remote location, where it was better heard. But especially after the World War Two, the development of doorbell systems accelerated.

New functions were added and at some point the system became even wireless. The most important was to allow the communication with the guest without actually going there to talk in person. It all began with utilization some first analog communication system. The development went fast forward and nowadays we call the new systems doorphones or intercoms instead of doorbells.

This paper is organized as follows: Section II describes the goal for implementing an IP-based doorphone prototype. Section III lists suitable functions. Section IV is about the advantages of IP solution. Section V introduces the hardware and section VI the software used in the project. Section VII summarizes the final device and its functions. Finally, a conclusion is offered in section VIII.

II. GOAL

My goal for this project is to explore the possibility of creating an IP-based doorphone system with appropriate functionality while keeping the price reasonable. The doorphone system should provide basic functions expected from a doorbell. Moreover it should add some additional functions which make the use of an intelligent doorphone more attractive.

III. DOORPHONE FUNCTIONS

I listed several functions which could be worthy to implement in the IP Door Phone prototype.

- **Bell/Notification Sound** - The doorphone notifies you of a guest arrival after a button is pressed.
- **Audio Call** - A doorphone should allow bidirectional communication.
- **Video Call** - To see who is standing outside.
- **Remote Control** - To remotely open the door without going there.
- **History** - To store a history of past visitors with timestamp.
- **Call Redirecting** - To redirect a call to your mobile phone, fixed line or even some VoIP applications like skype when nobody home.
- **Email Notification** - To receive a system status notifications.
- **Anti-Vandal Design** - The station might be exposed to a public area. The outlet should be made vandal resistant.

IV. IP SOLUTION

Several years back it was common to have a special cabling for TV, CCTV, telephone, computer network and intercoms and these systems were often closed. However now with the wide-spread of IP technology you can deploy only twisted pair cabling and push the building communication system to one platform and it is mainly Ethernet. This solution reduces the cost for developers and makes the construction faster and easier.

Another advantage is the possibility of advanced features like a quality calls even to fixed telephone networks, video calls and possibility to access the device over the network.

The last advantage is an easy way to add new functionality into an IP-based system and interconnection with other systems e.g. home automation systems.



V. HARDWARE

I would like to introduce now all the hardware used in this project.

- **Raspberry Pi 2** - This low-cost single board computer itself has everything you need to run a standalone computer machine. It has many additional interfaces and is powerful enough to run a SIP client application. A suitable Linux distribution will be running from a Micro SD card. The presence of GPIO pins makes it easy to receive some inputs or send outputs. The device itself has a low power consumption. Only one necessary connector is missing and it is an Audio In.
- **Micro SD Card** - The operating system is installed there and all the application data will be stored there. 2 or 4 GB SD card is sufficient when using the Raspbian Jessie Lite system. The card should be class 10 to ensure as high write speeds as possible.
- **Sound Card** - I need to use an USB sound card because RPi2 lacks an audio input. I chose a generic universal Channel USB External Sound Card Adapter because it is cheap, small, supported by Linux (C-Media 108 audio chipset supported by ALSA Project) and does not need much power.
- **Microphone** - I used one cheap office microphone (AY 0126). I disassembled it to fit into my device.
- **Speaker** - I used one 8 ohm 2W VECO speaker (78G 444-2-VL). I had to use an amplifier to amplify the audio signal from RPi2. I chose a 3 W Class-D Stereo Audio Amplifier (PAM8403) which can be powered from RPi2 +5V pin.
- **Camera** - I use a camera module developed for RPi. There is a good integration into Linux and the Python Picamera library is available for development. The camera low light conditions when an IR light is turned on.
- **GPIO** - These bi-directional I/O pins can control LED lights, spin motors or read button presses. Some current draw and voltage limitations have to be kept in mind while using 3.3 V GPIO ports. Never be connected to a source of a greater voltage than 3.3 V. Source or sink no more than 16 mA per pin and the maximum current sourced simultaneously from all pins is 50 mA. [2]. I use GPIO pins to read button presses, turning on LEDs and control a relay.
- **Button** - I use only one button. Usually at a family house you need to ring the whole house or maybe two separate rings because of two floors. I chose a monetary button which is actuated only when it is pressed.
- **IR LED Light** - I created a small board with 10 IR diodes to illuminate the scene during low light conditions. The 850 nm diodes have forward voltage (V_f) 1.4 V and maximal current (I) 20 mA. I have connected always two diodes in series with one 100 Ω resistor (R). The resistor value was calculated with the equation below.

$$R = \frac{(V_{in} - V_f)}{I}; V_{in} = 5V; V_f = 2 * (1.4V); I = 20mA$$

I added a NPN (2N3904) transistor to control the diodes and allow them to draw more current from +5 V pin than it would be able from other GPIO pins. The transistor base is

connected to a GPIO pin and the circuit is controlled by it. There is also one 5.1 k Ω resistor between the transistor base and GPIO pin to limit the current draw from the GPIO pin.

- **Relay Board** - I am using a 2-channel relay module with all the required electronic needed to be directly operated by RPi2's GPIO pins without the danger of damaging it. The module relays (SRD-05VDC-SL-C) are both able to switch up to 10A. It would not be possible to operate the relay itself from RPi2 pin because according to a datasheet the switching current is around 90 mA which is too much for RPi2 GPIO pins.

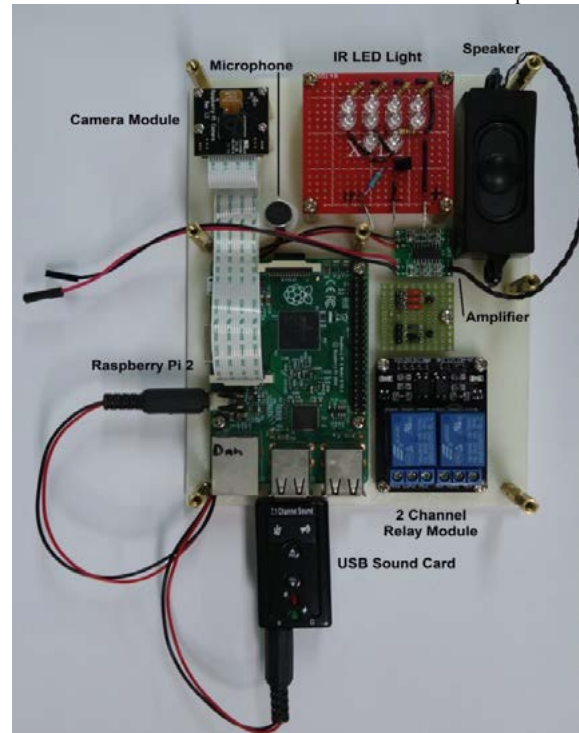


Figure 1 Final assembly of the IP Door Bell System

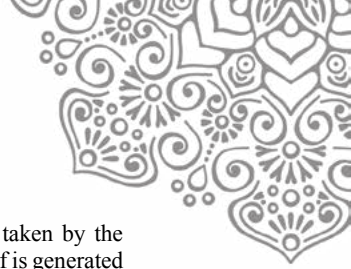
The device which actually opens a door is called an electric strike or a door release. It is attached in a door frame and when the relay turns ON the applied electric current will cause it to unlock. Electric strikes usually operate on 12 AC and the current draw might differ from 200 mA to 2 A. It is obvious that you cannot operate it directly.

Power - I am powering the RPi2 with a micro-USB power adapter (HNP10I-Micro, 5V/2A). Usually RPi2 needs around 700-1000 mA but for a stable run with some USB peripherals or powering anything through GPIO pins is input current of 2 A recommended.

VI. SOFTWARE

I would like to introduce all the software used in this project. I tried to choose only an open-source software for this project.

- **Operating System** - I used a Linux distribution called Raspbian Jessie Lite specially designed for RPi2 and it is



an official supported operating system by Raspberry Pi Foundation. Raspbian Lite version is missing graphical desktop environment packages and thus much smaller than the normal image. The size of extracted executables is 1.3 GB for Lite in comparison with 4 GB of normal full image. This means that even 2 GB SD cards should be sufficient. It comes with many preinstalled packages. e.g. Python, Java or GPIO control.

- Linphone** - Linphone is an open source VoIP phone library. The group standing behind this library creates also SIP client for Android, Windows and iOS. I will use a linphone library optimized for use with RPi. This library offers all SIP functions in one package. The audio codecs are PCMU (G711u) or PCMA (G711μ) which brings good audio quality. There is a difference between them how PCM is implemented. One uses μ-Law (used in North America) and the second A-Law (used in Europe). The video codec is VP8. It was developed by Google and it is free to use in comparison with codec H264. Using VP8 brings also some troubles because it is not supported by all SIP clients nor servers. On the other hand H264 is more spread over more applications but there are troubles with RPi2 which lacks a usable encoder.
- Photos and Videos** - I used the RPi NoIR camera module to take photos of visitors and use it as a video device during a call. When a button is pressed one photo is taken. This photo is stored into RPi2 storage and is possible to see the photo when opening the webserver address ({RPi2 IP address}:8800). The photos are taken in resolution of 1024x768 pixels to improve the speed and save some storage. All photos are timestamped in this format: %Y%M%D-%H%M%S. Y – year, M – month, D – day, H – hour, M – minute, S – second. The camera module is also used during video calls to see in real time who is outside. Either during taking a photo or a video call the IR LED light is turned on to illuminate the scene during low light conditions.
- Relay Control** – I control the relay with one GPIO output. When the pin is LOW the relay is on. When the pin is HIGH the relay is off. If number 1 is pressed during a call the relay turns on for 3 seconds.
- Main Cycle** - The main cycle waits until a button is pressed and when the button is pressed a photo is taken and a call to a predefined extension is initiated.
- Web GUI** - The web GUI allows quick changes of some settings and it is not dependent on any kind of platform. User just need a web browser. {RPi2 IP address}:8888. I choose a library called Tornado to implement it. Tornado is a Python web server and application framework. The library is distributed under open-source license. I chose it because the library comes with all functions I need and it is easy to use for my application. I created two pages. The first one is an IP Door Bell Setting page. A user can change some basic setting of the system like SIP Username, Password or Server Address. Before user can enter this setting page an authentication page pops up. First a correct password has to be entered otherwise the access is denied.

The second page is a photo gallery. Photos taken by the camera can be browsed there. The gallery itself is generated by an open-source tool called Sigal.

- Cron Job** – I created a Cron job to periodically check if the IP Door Bell services are running. The device would be useless without these services running and therefore when they are down this script turns them back on.

VII. EVALUATION

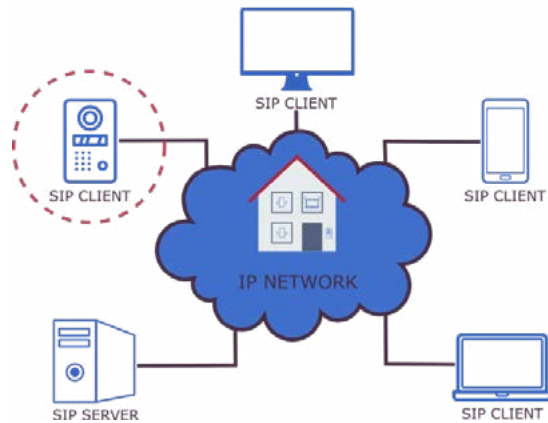


Figure 2 IP Door Bell (red circle) connected to an IP network

The Figure 2 IP Door Bell (red circle) connected to an IP network shows my IP Door Bell device inside an IP network. My IP Door Bell is another SIP client connected to IP network and has to be connected to a SIP server, which handles the setup of SIP calls with authentication and authorization of users for services. The IP Door Bell system works quite well without any big troubles but it is still in a development stage.

User can open the web GUI and change the most important setting like SIP username, password and server address or where to call when a button is pressed. Press **Save and Restart** the device to save the configuration and restart the service. After successful registration the status changes to **Registered**. I have to admit that the application does not check the input value anyhow. I just suppose that the user sets proper values e.g. standard IP address. The settings GUI has five sections: Status, SIP Server, Extension, Devices, Web Server. Most of them are working and ready to use except section Devices. This section is more like a preparation for a future development. Past visitors can be seen in the photo gallery. It takes some time when opening the gallery and it is caused by generating the library with new photos. With many new photos it can take even 5 to 10 seconds. The goal for next development would be to try to lower this delay.

The last thing that a user can do is to call the IP Door Bell. This way I can talk to anybody standing outside even before the person presses the ring. In fact it takes around 2 to 3 seconds before the call is established. This delay is caused by taking the photo for around 0.4 s and then by the network and



SIP clients delays. When somebody comes and press the button it takes around 2 to 4 seconds until a calling party (extension inside the building) starts to ring. The delay here might be a bit longer maybe because there is no automatic answer and the client in a smartphone or computer have to start signaling the incoming call.

The sound quality during a call is reasonably good and speech is always understandable but quality is based on the quality of speaker, audio output and network. The quality of a video call is quite good but it depends on the quality of a network, too. The IR light turns on when taking photos or using the camera for a video call and during low light.

The system is usually stable during a call but I experienced some troubles over a longer time span. The program gets sometimes into a SEGV error at unpredictable times. I did some debugging but I still have not found the problem. I created a Cron job which test if the service is running and restart it when necessary. It is not the best solution but it is working for now. I looked in a log file from one day of operation and the scripts gets into an error in average every 70 minutes. The condition when the IP Door Bell is malfunction took in average 38 seconds until it is active and running again. It means that it happens 20.6 times per day that the system is down. Together it makes 782 seconds (13 minutes) of down time during one day. It means that the system is down for 0.9 % of a day. To get better results of uptime I will have to find out a solution of this problem with a SEGV error.

I connected the IP Door Bell system to a power meter and ran into several possible situations. When the system is idle the power consumption is only 1.7 W. The power consumption gets higher when more parts of the system starts to work. In general I can say that my system is quite good in terms of consumption. Most of the time the system will reside in an idle state and the consumption will be around 1.7 W. It makes 14.9 kWh per.

Table 1 System power consumption

IP Door Bell Activity	Consumption [W]	Cons./year [kWh]
Idle	1.7	14.9
Call	2.4	21
Video Call	3.2	28
Video Call and Relay ON	3.6	31.5

The last concern during my project was the price of the whole project. The most expensive was the RPi2 computer and the camera module. Except that the rest of the items were quite cheap. The overall price of the project is below 100 USD. The price is several times lower than market solutions but does not reflect my work etc. Moreover for a mass-production should be done some analysis of more platforms to find the best platform in terms of functionality, price and consumption

Table II List of the Hardware with prices

Part	Info	Price [S]
------	------	-----------

Microcomputer	Raspberry Pi 2 (Model B)	35
Camera Module	Raspberry Pi NoIR Camera Module	25
Power Adapter	5V 2A Micro USB Power Adapter (HNP10I-microUSB)	9
Micro SD Card	Kingston Digital 8 GB microSDHC Class 10 UHS-1 (SDC10/8GB)	6
Speaker	8 ohm 2W VECO (78G 444-2-VL), price for a common speaker with similar spec.	5
IR LEDs (10x)	IR LED 850 nm 1.4 V 20 mA	4
Microphone	AY 0126	4
Relay Module	2 Channel 5V Relay Module	2
USB Sound Card	7.1 Channel USB External Sound Card	1.5
Amplifier	PAM8403	1
Jack Connector (2x)	3.5 mm Stereo Male	1
Proto Board	25x25 mm	1
Proto Board	50x50 mm	1
Resistor (5x)	100 Ω	0.5
Button	Monetary Push Button	0.4
Transistor	NPN, 2N3904	0.2
Resistor	5.1 kΩ	0.1

Total Price		96.7
--------------------	--	-------------

VIII. CONCLUSION

Figure 2 IP Door Bell (red circle) connected to an IP network shows the view and the whole IP system with a SIP server and many SIP clients. I have created a doorphone prototype which is one of the SIP clients in the system. The offers basic doorphone functionality. A guest can ring the house and alert the people inside. Voice and video call is possible and even some remote control of other devices during a call. The device is only a development prototype and is far from a mass-production. More work would have to be done before that and try also different platforms which might be more efficient, cheaper or suitable. The future plan is to remove the SEGV error and implement more functions. The web GUI should be also improved and allowed more settings and user customization.

REFERENCES

1. **Warren, Jason.** The History of the Doorbell. *1800 Doorbell*. [Online] LHE, Inc., November 18, 2015. [Cited: March 4, 2016.] <http://www.1800doorbell.com/resources/who-invented-the-doorbell-history.htm>.
2. **Mosaic Industries, Inc.** GPIO Electrical Specification. *Mosaic Documentation Web*. [Online] Mosaic Industries, Inc. [Cited: 03 17, 2016.] <http://www.mosaic-industries.com/embedded-systems/microcontroller-projects/raspberry-pi/gpio-pin-electrical-specifications>.



Naïve Bayes Algorithm Applied on Breast Cancer Expert System

Rayung Wulan, Mei Lestari, Ni Wayan Parwati

Information Technology
Indraprasta University
Jakarta, Indonesia

Utha2578@gmail.com, mei.lestari6@gmail.com, wayan.parwati@gmail.com

Abstract— Data mining is a process to obtain useful information from a large data warehouse, it can also be interpreted as the extraction of new information from a large chunk of data to make a decision. Naïve bayes classifier is one of data mining classification method and a statistical classification that can be used to predict the probability of class label. Breast cancer is a fast growing tumor that comes from breast tissue. There are two types of tumor malignant (cancerous) and benign (non cancerous). Obvious sign of breast cancer is ulcers that occurs in breast and growth gradually greater and deeper and will destroy the entire breast. Hence, it is important to detect a breast cancer at the early phase. This paper aims to calculate and classify breast cells and to design an expert system to detect breast cancer disease using naïve bayes algorithm. System are implemented using java programming language. The proposed system can help doctor and patients in making a decision or an expert advice.

Keywords—breast cancer; naïve bayes; expert system; classification; data mining

I. INTRODUCTION

Data mining is a process to gain information from a big data set to make a decision. Data mining also known as data discovery. These days there is huge amount of data being collected and stored in databases across the world, and this tendency is increasing. Methods are used for extracting the data aims to make it possible to mine the data. Data mining also defined as a process of discovering patterns of data. The process must be automatic or semiautomatic. The pattern must be meaningful and allow us to make non trivial prediction on new data [5]. Data mining is the analysis of large observational data sets to find unsuspected relationship to summarize the data in novel ways that are both understandable and useful to the owner of data set[3][4]. Data mining models and methods continues the coverage of data mining as a process. Particular standard process used is the Cross Industry Standard Process for Data Mining (CRISP-DM). It demands that data mining be seen as the entire process, from communication of business problem, through data collection and management, data processing, model building, model evaluation and finally model deployment [2]. Xiaoxin Yin and Jiawei Han [7] proposed a regression based method to predict the usefulness of inter database links that serve as bridges for information transfer. High cost of inter database communications, MDBM employs a new strategy for cross-

database classification that performs actions with high benefit to cost ratios. It shows that MDBM (Multi Database Miner) achieves high accuracy in cross database classification.

Classification methods are predicting a certain output based on a given input. The algorithm process a training set containing a set of attributes and the respective output. The algorithm tries to discover the relationship between the attributes that could make it possible to predict the output.

Naïve bayes is a method to established a classifier by making a probabilistic model of data within each class. It is based on bayes' theorem with independence assumption between predictors.

The Bayesian rule formula is

$$P(C|X) = \frac{P(X|C)P(C)}{P(X)} \quad (1)$$

Where:

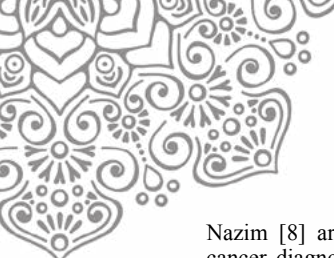
P(C|X) is the posterior probability of class given predictor (attribute), P(C) is the prior probability of class, P(X|C) is the likelihood which is probability of predictor given class, P(X) is the prior probability of predictor

Breast cancer is a fast growing tumor that comes from breast tissue. There are two types of tumor malignant (cancerous) and benign (non cancerous). Obvious sign of breast cancer is ulcers that occurs in breast and growth gradually greater and deeper and will destroy the entire breast. Hence, it is important to detect a breast cancer at the early phase. Naïve bayes can be used to predict breast cancer by using nine variables on breast cancer dataset from UCI data set. There are Uniformity of cell size, Uniformity of cell shape, Marginal Adhesion, Single Epthelial Cell Size, Bare Nuclei, Bland Chromatin, Normal Nucleoli, Mitoses.

II. LITERATURE REVIEW

A. Related Work

Nowdays expert system using classification data mining methods become an interesting research work. Ambica, Gandi and Kothalanka [1] optimized the dataset and applied the naïve bayes classifier to provides an efficient expert system for diabetes. Yousuf Qawqzeh and Khalid



Nazim [8] are work on a prototype websites of breast cancer diagnostic expert system. The system provides all collaborative information that are provisioned by the community member, online organization and expert in that field. Murat Karabatak [6] use Association Rules (AR) and Neural Network (NN) to diagnose breast cancer, their research shows that AR can be used for reducing the dimension of feature vector.

III. COMPUTATION METHODS

Classification process on this proposed expert system we used naïve bayes classifier. The following are steps to classify a new data as malignant (cancerous) or benign (non cancerous).

First step is to construct a frequency table of each attribute against the target.

TABLE I. PRIOR PROBABILITY

ATTRIBUTES	CASES	MALIGNANT	BENIGN	P(x c)		
				MALIGNANT	BENIGN	
TOTAL	536	204	332	0.38	0.62	
CLUMP THICKNESS	1	110	3	107	0.027273	0.972727
	2	40	3	37	0.075	0.925
	3	76	11	65	0.144737	0.855263
	4	57	7	50	0.122807	0.877193
	5	89	33	56	0.370787	0.629213
	6	30	17	13	0.566667	0.433333
	7	20	20	0	1	0
	8	39	35	4	0.897436	0.102564
	9	13	13	0	1	0
	10	62	62	0	1	0
UNIFORMITY OF CELL SIZE	1	276	4	272	0.014493	0.985507
	2	36	8	28	0.222222	0.777778
	3	46	23	23	0.5	0.5
	4	33	27	6	0.818182	0.181818
	5	28	28	0	1	0
	6	23	23	0	1	0
	7	15	15	0	1	0
	8	23	22	1	0.956522	0.043478
	9	5	4	1	0.8	0.2
	10	51	51	0	1	0
UNIFORMITY OF CELL SHAPE	1	259	2	257	0.007722	0.992278
	2	44	6	38	0.136364	0.863636
	3	45	22	23	0.488889	0.511111
	4	34	26	8	0.764706	0.235294
	5	30	29	1	0.966667	0.033333
	6	25	23	2	0.92	0.08
	7	26	24	2	0.923077	0.076923
	8	22	21	1	0.954545	0.045455
	9	7	7	0	1	0
	10	44	44	0	1	0
MARGINAL ADHESION	1	297	28	269	0.094276	0.905724
	2	51	21	30	0.411765	0.588235
	3	44	23	21	0.522727	0.477273
	4	30	25	5	0.833333	0.166667
	5	16	12	4	0.75	0.25
	6	18	16	2	0.888889	0.111111
	7	12	12	0	1	0
	8	20	20	0	1	0
	9	3	3	0	1	0
	10	45	44	1	0.977778	0.022222
S - I - Z	1	39	1	38	0.025641	0.974359

	2	276	21	255	0.076087	0.923913
	3	60	38	22	0.633333	0.366667
	4	39	32	7	0.820513	0.179487
	5	30	25	5	0.833333	0.166667
	6	34	33	1	0.970588	0.029412
	7	8	6	2	0.75	0.25
	8	19	18	1	0.947368	0.052632
	9	2	2	0	1	0
	10	29	28	1	0.965517	0.034483
	BARE NUCLEI	1	294	11	283	0.037415
2		24	6	18	0.25	0.75
3		24	11	13	0.458333	0.541667
4		16	12	4	0.75	0.25
5		24	16	8	0.666667	0.333333
6		3	3	0	1	0
7		8	7	1	0.875	0.125
8		19	17	2	0.894737	0.105263
9		9	9	0	1	0
10		115	112	3	0.973913	0.026087
BLAND CHROMATIN	1	104	2	102	0.019231	0.980769
	2	112	6	106	0.053571	0.946429
	3	145	36	109	0.248276	0.751724
	4	34	29	5	0.852941	0.147059
	5	32	28	4	0.875	0.125
	6	7	7	0	1	0
	7	60	54	6	0.9	0.1
	8	23	23	0	1	0
	9	10	10	0	1	0
	10	9	9	0	1	0
NORMAL NUCLEOLI	1	321	34	287	0.105919	0.894081
	2	29	4	25	0.137931	0.862069
	3	40	30	10	0.75	0.25
	4	15	15	0	1	0
	5	16	14	2	0.875	0.125
	6	18	15	3	0.833333	0.166667
	7	14	12	2	0.857143	0.142857
	8	21	19	2	0.904762	0.095238
	9	15	15	0	1	0
	10	47	47	0	1	0
MITOSES	1	434	111	323	0.25576	0.74424
	2	27	22	5	0.814815	0.185185
	3	27	25	2	0.925926	0.074074
	4	12	12	0	1	0
	5	6	5	1	0.833333	0.166667
	6	3	3	0	1	0
	7	8	7	1	0.875	0.125
	8	7	7	0	1	0
	9	0	0	0	0	0
	10	12	12	0	1	0

Second, is to calculate the probability of each class for data test 1:

TABLE II. POSTERIOR PROBABILITY DATA TEST-1

DATA TEST-1	VALUE	P(X _i C)	
		MALIGNANT	BENIGN
CLUMP THICKNESS	2	0.075	0.925
UNIFORMITY OF CELL SIZE	4	0.818182	0.181818
UNIFORMITY OF CELL SHAPE	4	0.764706	0.235294
MARGINAL ADHESION	1	0.094276	0.905724
SINGLE EPITHELIAL CELL SIZE	2	0.076087	0.923913
BARE NUCLEI	5	0.666667	0.333333
BLAND CHROMATIN	2	0.053571	0.946429
NORMAL NUCLEOLI	1	0.105919	0.894081
MITOSES	2	0.814815	0.185185



TABLE I shows the probability of malignant ($P|\text{malignant}$) is 0.38 and probability of benign ($P|\text{benign}$) is 0.62. Where on TABLE II shows probability of each class for data test-1. Total probability can be computed using equation (1) as follow:

$$\begin{aligned}
 &P(x|\text{malignant}) \\
 &= P(\text{clump thickness} = 2|\text{malignant}) \\
 &\times P(\text{uniformity of cell size} = 4|\text{malignant}) \\
 &\times P(\text{uniformity of cell shape} = 4|\text{malignant}) \\
 &\times P(\text{marginal adhesion} = 1|\text{malignant}) \\
 &\times P(\text{single epithelial cell size} = 2|\text{malignant}) \\
 &\times P(\text{bare nuclei} = 5|\text{malignant}) \\
 &\times P(\text{bland chromatin} = 2|\text{malignant}) \\
 &\times P(\text{normal nucleoli} = 1|\text{malignant}) \\
 &\times P(\text{mitoses} = 2|\text{malignant}) \\
 &= 0.075 \times 0.818182 \times 0.764706 \times 0.094276 \times 0.076087 \\
 &\times 0.666667 \times 0.053571 \times 0.105919 \times 0.814815 \\
 &= 3.9487E - 07
 \end{aligned}$$

$$\begin{aligned}
 &P(x|\text{benign}) \\
 &= P(\text{clump thickness} = 2|\text{benign}) \\
 &\times P(\text{uniformity of cell size} = 4|\text{benign}) \\
 &\times P(\text{uniformity of cell shape} = 4|\text{benign}) \\
 &\times P(\text{marginal adhesion} = 1|\text{benign}) \\
 &\times P(\text{single epithelial cell size} = 2|\text{benign}) \\
 &\times P(\text{bare nuclei} = 5|\text{benign}) \\
 &\times P(\text{bland chromatin} = 2|\text{benign}) \\
 &\times P(\text{normal nucleoli} = 1|\text{benign}) \\
 &\times P(\text{mitoses} = 2|\text{benign}) \\
 &= 0.925 \times 0.181818 \times 0.235294 \times 0.905724 \times 0.923913 \\
 &\times 0.333333 \times 0.946429 \times 0.894081 \times 0.185185 \\
 &= 0.001071
 \end{aligned}$$

$$P(\text{malignant}|x) = 0,38 \times 3,9487E - 07 = 1,50286E - 07$$

$$P(\text{benign}|x) = 0,62 \times 0,001071 = 0,000664$$

Since $0.000664 > 1.50286E-07$. data set-1 classified as benign

IV. PROPOSED SYSTEM

The proposed system is a knowledge expert system using naïve bayes classifier. System are implemented using java programming language. The proposed flowchart of an expert system using naïve bayes as follows:

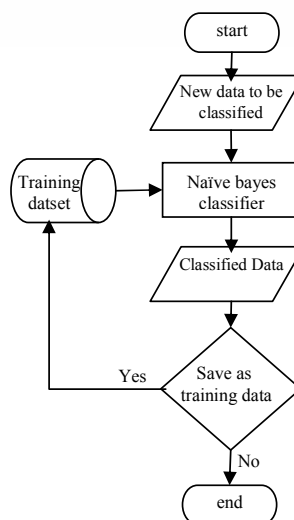


Fig. 1. Flowchart of breast cancer expert system using naïve bayes classifier

The following figure shows the implementation of naïve bayes on breast cancer expert system.

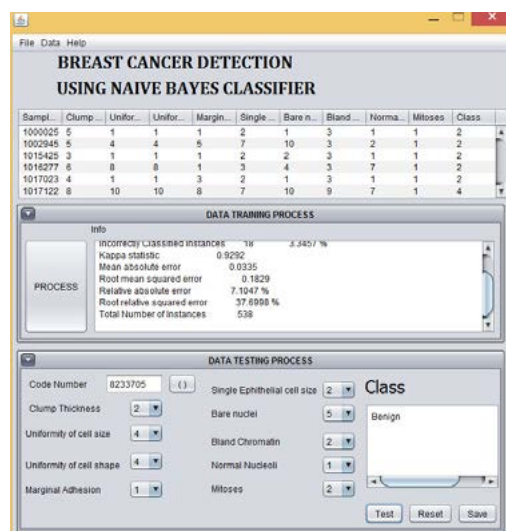


Fig. 2. Breast cancer expert system using naïve bayes classifier

On this expert system new data can be classified then classified data can be saved into training data set. "DATA TRAINING PROCESS" shows information as follows:

1. Correctly classified instances, numbers of how often the classifier predicted correctly
2. Incorrectly classified instances, numbers of hoe often the classifier predicted incorrectly



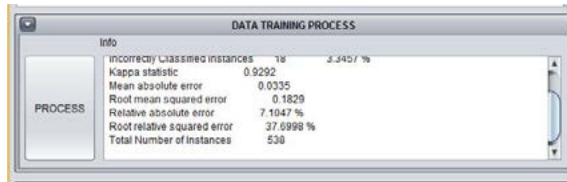
3. Kappa statistic, statistic that measures inter rater agreement for qualitative (categorical) items.
4. Mean absolute error, measure of diggerence between two continuous variables.

$$MAE = \frac{\sum_{i=1}^n |y_i - x_i|}{n} = \frac{\sum_{i=1}^n |e|}{n}$$

5. Root mean squared error, is a frequently used measure of the differences between values (sample and population values) predicted by a model or an estimator and the values actually observed.
6. Relative absolute error, the magnitude of the difference between the exact value and the approximation.
7. Root relative squared error, is relative to what it would have been if a simple predictor had been used.

$$E_i = \sqrt{\frac{\sum_{j=1}^n (P_{(ij)} - T_j)^2}{\sum_{j=1}^n (T_j - T)^2}}$$

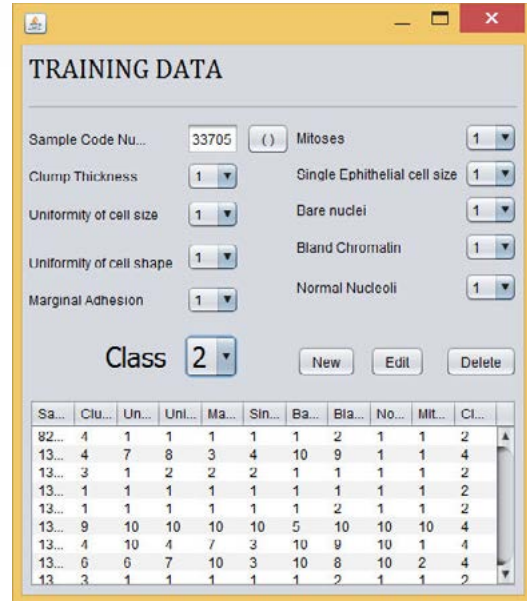
8. Total number of instances.



Info	Value	%
Incorrectly Classified Instances	18	5.3427 %
Kappa statistic	0.9292	
Mean absolute error	0.0335	
Root mean squared error	0.1829	
Relative absolute error	7.1047 %	
Root relative squared error	37.6998 %	
Total Number of Instances	538	

Fig. 3. Data training process

New data training also can be added into the system using “INPUT DATA TRAINING” menu as the following figure:



Sample Code Nu...: 33705 () Mitoses: 1
 Clump Thickness: 1 Single Epithelial cell size: 1
 Uniformity of cell size: 1 Bare nuclei: 1
 Uniformity of cell shape: 1 Bland Chromialin: 1
 Marginal Adhesion: 1 Normal Nucleoli: 1
 Class: 2 [New] [Edit] [Delete]

Sa...	Clu...	Un...	Unl...	Ma...	Sin...	Ba...	Bla...	No...	Mit...	Cl...
82...	4	1	1	1	1	1	2	1	1	2
13...	4	7	8	3	4	10	9	1	1	4
13...	3	1	2	2	2	1	1	1	1	2
13...	1	1	1	1	1	1	1	1	1	2
13...	1	1	1	1	1	1	2	1	1	2
13...	9	10	10	10	10	5	10	10	10	4
13...	4	10	4	7	3	10	9	10	1	4
13...	6	6	7	10	3	10	8	10	2	4
13...	3	1	1	1	1	1	2	1	1	2

Fig. 4. Input data training

V. CONCLUSION

This paper present breast cancer detection expert system using naïve bayes classifier to help doctor and patients in making a decision or an expert choice. Furthermore, it can also be contributed in biomedical science. The development of expert system using 536 cases, consist of 204 cases of malignant (cancerous) and 332 cases of benign (non cancerous). The proposed expert system implemented using java programming language.

REFERENCES

- [1] A. Ambica, Satyanarayana Gandhi and Amerandra Kothalanka. “An Efficient Expert System For Diabetes By Naïve Bayesian Classifier” in International Journal of Engineering Trends and Technology (IJETT). vol. 4 issue 10-oct 2013. pp. 4634-4639
- [2] Daniel Larose. “Data Mining Methods and Models”. wiley 2005
- [3] Daniel Larose. Discovering Knowledge in Data: An Introduction to Data Mining. Wiley, Hoboken, NJ. 2005
- [4] David Hand, Heikki Mannila and Padharic Smyth. “Principles of Data Mining. MIT Press. 2001
- [5] I.H. Witten, E. Frank Morgan Kaufmann. “Data mining: Practical Mechine Learning Tools and Techniques with Java Implementations”. Morgan Kauffman. 2000
- [6] Murat Karabatak. “An Expert System for Detection of Breast Cancer Based on Association Rules and Neural Network” Journal Expert System with Application an International Journal. 2009. pp.3465-3469
- [7] Yin X., Han J. (2005) Efficient Classification from Multiple Heterogeneous Databases. In: Jorge A.M., Torgo L., Brazdil P., Camacho R., Gama J. (eds) Knowledge Discovery in Databases: PKDD 2005. PKDD 2005. Lecture Notes in Computer Science. vol 3721. Springer, Berlin, Heidelberg
- [8] Yosouf Qawqzeh and Khalid Nazim. “O. online Diagnstic Expert System for Detection of Breast Cancer in Saudi Arabia” in International Journal of Computer Applications. vol. 113- no. 6. 2015. pp.40-47



Feature Extraction of Epilepsy Signal Using Sampling Technique

Hindarto Hindarto
Informatics Engineering
Universitas Muhammadiyah Sidoarjo
Sidoarjo, Indonesia
hindarto@umsida.ac.id

Sumarno Sumarno
Informatics Engineering
Universitas Muhammadiyah Sidoarjo
Sidoarjo, Indonesia
sumarno@umsida.ac.id

Abstract— Epilepsy is the brain disorder human, epilepsy Occurs Due Someone experiencing Excess to Electrical signals released by cells of the brain. Someone disturbed Due epilepsy resulted effect the convulsions and abnormal movements. Electroencephalogram (EEG) is a electrode sensor to detect electrical activity that exist in the human brain. EEG signal is a signal that is very complex and become a primary source of information for the study of brain function and neurological disorders. EEG signals the moment epileptic seizures have a characteristic pattern that enables healthcare professionals to distinguish from normal conditions. However, in visual analysis can not be done routinely, because the EEG signal generated from EEG monitoring system is very large and quite time consuming. Another problem that arises is the lack of clear differences in EEG signals between epileptic seizures and non epilepsi. Various methods have been done many researchers to classify someone who has epilepsy and who do not have epilepsy. Therefore in this study, researchers tried to classify someone who had epilepsy disorders and who do not have epilepsy disorders. Epilepsy signal data taken from public data that consists of data sets A, data sets B, data sets C, data sets D and data sets E. The data set consists of data on non epileptic ie data sets A and data sets B while data on epilepsy are data sets C, data sets D and data sets E. Signal data from Data sets A, data sets B, Data sets C, data sets D, and data sets E that have been taken, then performed the process of feature extraction. In this study, the sampling technique is a method for feature extracting of epilepsy signal. The sampling technique for feature extraction of the epilepsy signal that use is an average value, standard deviation value, maximum value and minimum value. After the feature extraction process, the next process is the classification of epilepsy signal and non-epilepsy signal. Epilepsy classification process signals using Backpropagation Neural Network. The results of the classification process of Backpropagation method of epilepsy signal with 20-10-15-1 obtained accuracy rate 87.5%.

Keywords—Epilepsy; EEG ; Sampling technique; Backpropagation; Classification;

I. INTRODUCTION

Epilepsy is a brain disorder with a different etiology, symptoms with a typical single thing, ie Periodic attacks and reversible, epilepsy is Characterized with Excess of Electricity From the cells of the brain, the which can lead to seizures and abnormal movements. Epilepsy is a disease of disorder neurological. epilepsy is a neurological disorder the second most common in people after stroke. Around 40 or 50 million people worldwide suffer from epilepsy [1]. Electroencephalogram (EEG) is a tool used as a test to detect abnormalities in the brain signal activity [2]. According to dr.

Darmo Sugondo there is a difference between electroencephalogram with Electroencephalografi. Electroencephalografi is the procedure for recording electrical activity in the brain that is the tool that can display in the form of a graph called electroencephalogram. So the brain activity that generates the electrical signal waveform, which can be recorded on the scalp called Electro-Encephalografi (EEG). EEG signal is a signal that is very complex and become a primary source of information for the study of brain function and neurological disorders. EEG signals for disease of disorder epileptic seizures have a characteristic pattern that enables healthcare professionals to distinguish from normal conditions (nonseizure). However, a visual analysis can not be done routinely, because the EEG signal generated from EEG monitoring system is very large and quite time consuming. Another problem that arises is the lack of clear differences in EEG signals between epileptic seizures and non epilepsi.

Transition of EEG signal is a model, which is a very good way and effective in helping to classify the EEG signals, identifies and quantifies the EEG signal spectrum. There waveforms on EEG signals, known as alpha waves (8-13 Hz), beta (14-30 Hz), theta (4-7 Hz), and delta (0.5-3 Hz), so the transformation of EEG signals into area -area frequency is very useful, especially in the identification of waves in the brain. The algorithm for the detection of epilepsy using a multistage nonlinear signal preprocessing filter combined with artificial neural network (ANN) for the automatic detection of epileptic seizures in the EEG signal [3]. The algorithm by using recurrent neural networks (RNNs) and feature extraction Lyapunov who trained with the Levenberg-Marquardt algorithm [4]. k-means and multilayer perceptron neural network (MLPNN) [5]. The algorithm using Least Square Support Vector Machine (LSSVM) and coefficient Autoregressive (AR) [6].

With a wide range of problems in finding methods to look for traits, characteristics and classification of EEG signals from multiple studies, then in the study present researchers used a method of Sampling technique to capture the characteristics, the characteristics of the EEG signal. As well as how to apply the Backpropagation method to do clasification and EEG signal identification against epilepsy and non epilepsy.

II. MATERIALS AND METHODS

Data of EEG signal Obtained from the University of Bonn dataset consists of five classes: A, B, C, D, and E. Each dataset



contains 100 segments single channel of EEG with a duration of 23.6 seconds. Each segment is selected and cut from a continuous multichannel EEG recordings after visual inspection of artifacts, such as eye movement or muscle activity. Set A and B are both signals are taken from EEG recordings were taken from five healthy volunteers with a standard electrode placement (International 10-20 system). At the time of trial the volunteers relaxed and awake with eyes open (for set A) and eyes closed (for set B). Set C-E derived from EEG records presurgical diagnosis. EEG signals from five patients were selected, and all have achieved complete seizure control, after the reaction of one of the hippocampal formation, so it diagnosed correctly entered epileptogenic zone. Signals of set D are recorded when epileptogenic zone, in the interval without seizures. set C is derived from the hippocampal formation in the opposite hemisphere of the brain. While the sets C and D contains activities that only measured during the interval without a seizure, while the set E only contains seizure activity. In this study, the data used is the data set A and set E. In accordance with the existing references, all recorded with signal amplifier system of EEG with 128 channels of data with a frequency of 173.61 Digitizing samples per second using the A / D converter 12 bit. Band pass filter 40 is set at 0.53 Hz (12 dB / oct). Each digital EEG signal data consists of 4097 discrete data. Plot pieces EEG signal set A and set E used in this study in the form of time series.

A. Method of Feature Extraction using Sampling Techniques

In this study, the data is taken from the data file 100 epilepsy signals for each of the data sets. One file has a 4097 point signal data. This study divides the signal into five sub signal. So that each sub signal has a 819 point data. Of the sub signal then sought the minimum value, maximum value, average value and standard deviation value to be used for the extraction characteristics for classification process as shown in Figure 1. The results for the minimum value, maximum value, average value and standard deviation value in Table 1 is an example of the process of finding each feature each signal. So in this study, each signal have 20 feature extraction characteristics.

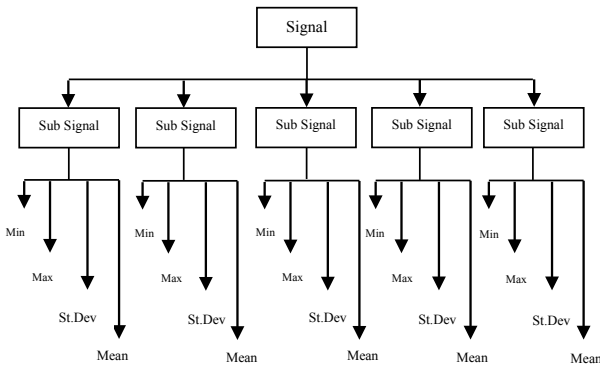


Fig 1. Sampling Techniques method (a) Signal, (b) Sub Sinyal and (c) Feature Extraction

In Figure 1 each value of max, min, mean and standard deviation are the value of each sub signal Epilepsy. So in

Figure 1 were obtained 4 x 5 sub signal = 20 points of data extraction features. 20 points of data extraction features can be used input to classification backpropagation neural network.

B. Backpropagation neural network

At the end of processing, classification of epileptic signals are processed using backpropagation neural network as shown in Figure 2. The final processing is done after the initial process is the search of feature by sampling techniques. Ekstrac characteristics used for input to the neural network. This study uses backpropagation (20-10-15-1) with 20 input derived from the signal characteristic of epilepsy and two hidden layers, each of which contained 10 units and 15 units as well as the targets (epilepsy and non-epileptic). In the process of identification with the process of neural network, first we need to do is implementing the training process with finding the best weight value with the acquisition value of the smallest error from the desired output targets. In the process of mapping done signal classification of epilepsy and non-epileptic epilepsy based on the weight values that have been obtained in the training process.

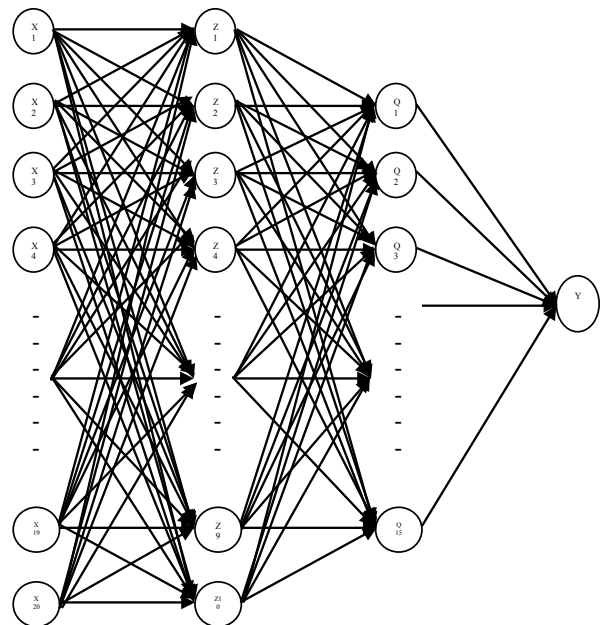
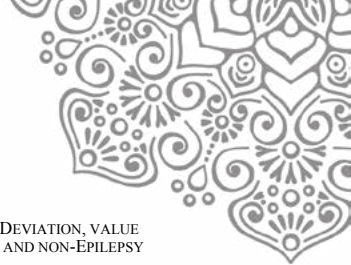


Fig 2. Backpropagation neural network architecture with 2 hidden layer.

III. RESULTS AND DISCUSSION

Feature extraction Epilepsy signal Obtained from the results of sampling techniques, as many as 20 point data. Epilepsy data signal that has been processed using a method of sampling technique consists of a set of the data sets A and E. The results of the sampling technique for the Signal Epilepsy is divided into 5 sub a data signals can be seen in Figure 3 and Figure 4. Each sub of signal epilepsy sought mean value, standard deviation, maximum and minimum, so that each sub



of signal epilepsy has four components values. Each value from the mean, standard deviation, maximum and minimum of epilepsy sub signals will be combined into one, the resulting signal in a epilepsy has 4×5 sub of signal = 20 component value. 20 komponen value is characteristic of each signal epilepsy.

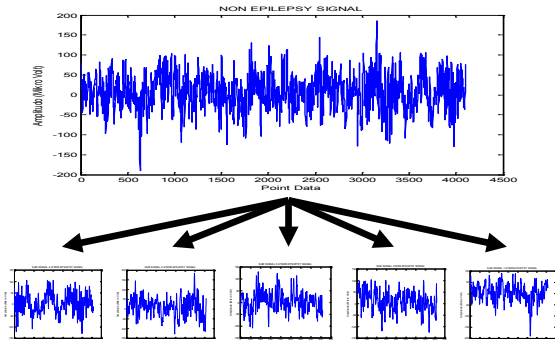


Fig 3. Process Technique Sampling for data set A

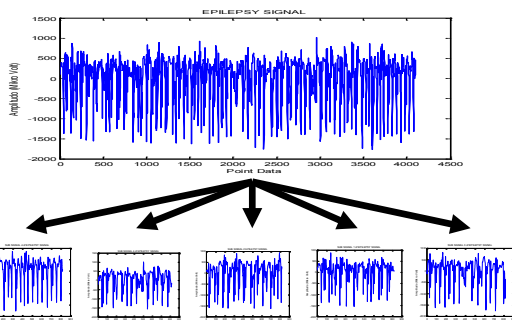


Fig 4. Process Technique Sampling for data set E

In Table 1 and table 2 are example of the value of the signal epilepsy that has been processed with sampling techniques. Each sub signal sought mean value, standard deviation, maximum and minimum.

TABLE I. VALUE OF MEAN, VALUE OF STANDARD DEVIATION, VALUE OF MAXIMUM AND VALUE OF MINIMUM SIGNAL EPILEPSY AND NON-EPILEPSY

Signal Epilepsy (Data Set E)	Mean Value	Standart Deviasion	Maximum Value	Minimum Value
Sub signal 1	60,06	424,42	885	-1585
Sub signal 2	30,76	529,15	1140	-1816
Sub signal 3	37,52	397,67	1435	-1232
Sub signal 4	5,64	158,06	324	-297
Sub signal 5	13,77	316,62	990	-1119

TABLE II. VALUE OF MEAN, VALUE OF STANDARD DEVIATION, VALUE OF MAXIMUM AND VALUE OF MINIMUM SIGNAL EPILEPSY AND NON-EPILEPSY

Signal non-Epilepsy (Data Set A)	Mean Value	Standart Deviasion	Maximum Value	Minimum Value
Sub signal 1	3,21	40,05	91	-190
Sub signal 2	-57,76	49,27	106	-195
Sub signal 3	11,11	44,81	153	-102
Sub signal 4	-6,03	44,96	162	-125
Sub signal 5	-19,54	42,70	144	-129

For data set A is the non epilepsy and for data set E is data Epilepsy, so that the classification process in the process of training for the data set A has a target of 0 (zero) and for the data set E has a target of 1 (one). In classification process for signals epilepsy, network architecture used is Backpropagation with 2 hidden layers using (20-10-15-1) and the error value of 0.0001. Results output on Backpropagation training process can be seen in Figure 5 and Figure 6.

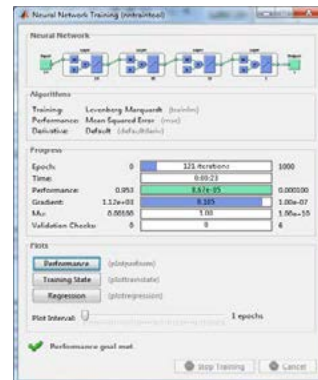


Fig 5. Results of Backpropagation training process 20-10-15-1

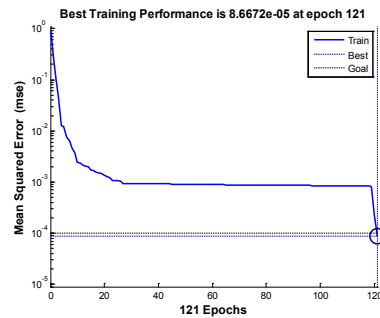


Fig 6. Results of the performance of the identification performance Backpropagion 20-10-15-1

Performance results on back propagation neural network 20-10-15-1 in Figure 5 and Figure 6 shows that the error desired targets of 0.0001 has been reached. In the process of training this network, generating error of $8,67 \times 10^{-5}$ so that



classification on epilepsy signal can reach 100% accuracy for the training process.

TABLE III. THE PERFORMANCE OF THE NEURAL NETWORK TO THE NUMBER OF DIFFERENT HIDDEN LAYER

	MSE (1 Hidden Layer)	MSE (2 Hidden Layer)
Time	35 Second	23 Second
Iteration	256	121
MSE	0,0007	8,67x10 ⁻⁵
Accuracy	80 %	87,5 %

From table 2 shows that the level of accuracy of the nicest is by using two hidden layers, namely accuracy of 87.5%.

IV. CONCLUSION

To classify someone who has epilepsy and non epilepsy using brain signals (EEG signals) as the source to be studied, this study introduces methods of Sampling Techniques by taking the average value, standard deviation, minimum and maximum from signal of epilepsy that produces 20 point data. This research uses Backpropagation neural network for signal classification process Epilepsy. The data used in this study were 160 data of epilepsy signal and non-epilepsy in the training process. As for classification process of testing, data is used is 200 Epilepsy signal data, ie all data signals epilepsy and non-epileptic, classification accuracy of neural network backpropagation reached 87.5% by using 2 hidden layer.

References

- [1] Eric R. Kandel, Larry R.Squire, 200, Neuroscience Breaking Down Scientific Barries to the study of brain and mind, Journal *Science* 10 Nov 2000, Vol. 290, Issue 5494, pp. 1113-1120 DOI: 10.1126/science.290.5494.1113.
- [2] Campellone, JV (2006). Eeg Brain Wave Test, date accessed 1 October 2016 From <http://www.nlm.nih.gov/medlineplus/ency/article/003931.htm>.
- [3] V Nigam and Daniel Graupe, 2004. Automated epilepsy detection via multistage nonlinear EEG filtering and a LAMSTAR Neural Network, *Neurological Research*, 26, pp.55-60,2004.
- [4] Nihal Fatma Gu'ler dkk, 2005. "Recurrent neural networks employing Lyapunov exponents for EEG signals classification". Elsevier, *Expert Systems with Applications* 29 (2005) 506–514.
- [5] Umut Orhan, dkki, 2011. "EEG signals classification using the K-means clustering and a multilayer perceptron neural network model". Elsevier, *Expert Systems with Applications* 38 (2011) 13475–13481.
- [6] Übeyli, E. D dkk, 2010. " Analysis of sleep EEG activity during hypopnoea episodes by least squares support vector machine employing AR coefficients", *Expert Systems with Applications* 37, 4463–4467.



Numerical Analysis of The Bandwidth Enhancement of an Inverted F Antenna for UHF Channel at 639 MHz

Erfan Rohadi^a, Amalia^{b*}, Indrazno Siradjuddin^c

Graduate School of Electronics Engineering Department

The State Polytechnic of Malang, Jl. Soekarno Hatta No. 9, Malang 65141, Indonesia

Email: ^aerfan@polinema.ac.id, ^bamalia@polinema.ac.id, ^cindrazno@polinema.ac.id

Abstract—Bandwidth characteristic enhancement of the antenna is interesting and challenging problems for antenna engineers. The low profile inverted F antenna (IFA) on a finite conducting plane with the designed frequency 639 MHz is proposed and its characteristics are analyzed numerically. The IFA is typically a narrowband antenna, due to the bandwidth enhancement the antenna parameters are considered. In this work, the antenna height (h), short stub (L_s) and size of conducting plane ($p_x \times p_y$) are adjusted. However, the lengths of the horizontal element (L and LI) are optimized so that the input impedance matches at the designed frequency. The IFA consists of a semi-rigid coaxial cable with the radii of inner and outer are 0.255 mm and 1.095 mm, respectively. The antenna heights (h) are investigated at 23 mm, 30.7 mm and 38.3 mm. The lengths of short stubs (L_s) are adjusted at 15.3 mm, 21.5 mm, 26.1 mm and 30.7 mm. The size of conducting planes ($p_x \times p_y$) has been investigated at 53.6 mm to 68.9 mm by 230 mm to 268 mm. The feed point is located between the end of the edge of the outer conductor and the front end of the inner conductors of the horizontal element. When the size of conducting plane is 115 mm by 230 mm, the return loss bandwidth (-10 dB) becomes 2.4 % and the gain becomes 6.58 dB. It is found that the return loss bandwidth becomes narrower when the height of the antenna is reduced. However, by extending the length of the short stub, the return loss bandwidth can be improved. The gains of IFA in all the calculation conditions are more than 6.5 dB. This means that the variation of the short stub lengths, the antenna heights and the size of conducting plane do not significantly affect the gain characteristics. In the numerical analysis, the electromagnetic simulator WIPL-D based on Method of Moment is used. The results show that the bandwidth enhancement of IFA is performed by extending the height of the antenna and enlarge the size of conducting plate. The proposed inverted F antenna is promising for the UHF channel receiver.

Keywords—bandwidth enhancement; inverted F antenna; method of moment; short stub; WIPL-D)

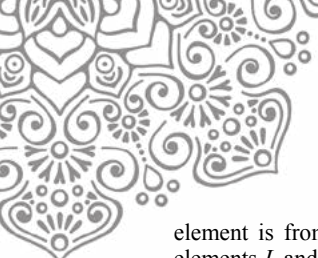
I. INTRODUCTION

A simple and compact antenna design with good performance nowadays still becomes the object of interest for antenna engineers, especially in bandwidth characteristic enhancement. As long as the dimensions of the antenna have no apparent way to install, therefore the light and small antenna are needed. One of possible design that met with those requirements is a low profile inverted F antenna. The Inverted-F Antenna (IFA) is a variation on the transmission line antenna, or bent monopole antenna (inverted L antenna), with

an offset feed that provides for adjustment of the input impedance. The resulting antenna geometry resembles the letter F, rotated to face the ground plane [1-4]. The element of inverted F antennas was originally evolved from the folded L antenna with the additional short stub [5-7]. The L-antenna (or inverted-L antenna) can be viewed as a bent monopole. The bending of the monopole results in a reduced size and low profile [8]. The monopole is the most widely used antennas for wireless mobile communication systems. An array of monopole perhaps the most common antenna element for portable equipment, such as cellular telephones, cordless telephones, automobiles, trains, etc. [9-11]. Both the inverted-L and the inverted-F antennas can be analyzed using equivalent transmission line models. Their radiation patterns in both principal planes are not much different from monopole [8]. One of the authors has investigated the ultra-low profile, unbalanced fed inverted F antenna for 2.45 GHz Wireless Communication System and the results show as the base station antenna with return loss bandwidth less than -10 dB becomes 3.67% and gain is 4.15 dB [12]. And also the ultra-low profile, conventional base fed inverted F antenna is analyzed numerically and its characteristics are compared with those of the unbalanced fed, ultra-low profile inverted L antenna. The results show as the antenna with return loss bandwidth less than -10 dB becomes 15.92% besides the gain is 3.94 dB [13]. In this work, the proposed inverted F antenna on a finite conducting plane is designed and analyzed numerically. The bandwidth enhancement of IFA is analyzed by extending the height of antenna while adjusting the size of conducting plane. In the numerical analysis, the electromagnetic simulator WIPL-D based on Method of Moment is used. The lengths of the horizontal element due to the antenna characteristic improvement such as radiation pattern, input impedance, return loss bandwidth and gain are optimized [14-16].

II. ANTENNA STRUCTURE

Figure 1 shows the structure of the proposed IFA mounted on conducting plane. The size of conducting plane is $p_x p + p_x m$ by $p_y p + p_y m$. The radius of the outer conductor is 1.095 mm and that of the inner conductor is 0.255 mm. The inner conductor of the semi-rigid coaxial cable is extended from the end of the outer conductor, this antenna is excited at the end of the outer conductor (feed point). The height h of the antenna is from 23 mm to 62 mm, and the length L_s of shorted antenna



element is from 15 mm to 31 mm. The length of horizontal elements L and $L1$ are optimized. The size of conducting plane is considered as 70~115 mm by 170~270 mm. Numerical analysis of the simulation results of the designed antenna to optimize all critical parameters such as return loss bandwidth with -10 dB at the design frequency of 639 MHz. The input impedance matching 50Ω at the center frequency is obtained by adjusting the length of horizontal elements L & $L1$. The radiation pattern characteristics, both components E_θ and E_ϕ are analyzed in order to determine the directive gain with its pattern. Moreover, antenna parameters, its size, length, height are optimized to obtain the best design. The wavelength λ at 639 MHz is 469.48 mm.

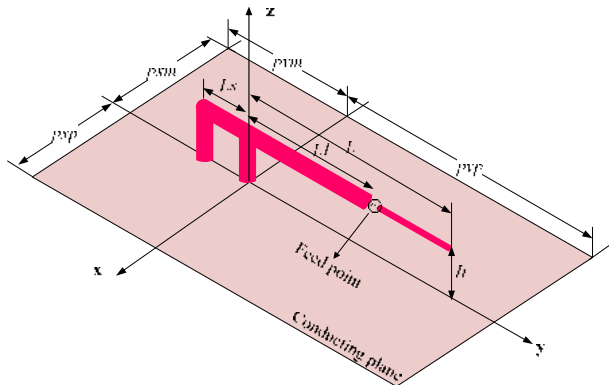


Figure 1. Structure of the proposed IFA

The effective length of IFA is $L_s + L + h$ where, h is the height of IFA. The resonance condition then is expressed by Eq. 1.

$$L_s + L + h = \frac{\lambda}{4} \quad (1)$$

Where λ is desired wavelength. As $\lambda = \frac{c}{f}$, where f is desired frequency of IFA and c is the speed of light [17]. Thus,

$$f = \frac{c}{4(L_s + L + h)} \quad (2)$$

III. RESULT AND DISCUSSION

The IFA performance was analyzed by adjusting the antenna parameters such as heights (h), short stub (L_s), horizontal element (L and $L1$) and size of conducting plane (px x py). The antenna heights (h) are investigated at 23 mm, 30.7 mm, 38.3 mm, 46 mm, 53.7 mm and 61.3 mm. The lengths of the horizontal element (L and $L1$) are optimized so that the input impedance matches at the designed frequency.

Table 1 shows the results of calculated return loss bandwidth -10 dB and the directive gain of IFA with the different size of conducting plane with $pxp = pxm = 57.5$ mm at 639 MHz. The return loss bandwidth becomes narrower when the height of the antenna is reduced. While the gain characteristics do not significantly affect with the changes of the height, the length of short stub and the size of conducting plane. The calculation result indicates that the height affects

total length of the horizontal element, the antenna bandwidth, and size of conducting plane associated with the current distribution of the conducting plane.

TABLE I.
RETURN LOSS BANDWIDTH AND DIRECTIVE GAIN OF IFA FOR DIFFERENT SIZE OF CONDUCTING PLANE AT 639 MHz

L_s	L	$L1$	pxm	pyy	Return Loss Bandwidth			Directive Gain at 639 MHz
					f-low (MHz)	f-high (MHz)	%	
$h=23$ mm								
15.3	186.7	155.0	53.6	200	635.18	641.84	1.0	6.66
21.5	180.8	149.2	59.8	200	635.6	642.4	1.1	6.61
26.1	177.0	144.9	64.4	200	635.5	642.5	1.1	6.58
30.7	173.2	140.9	69.0	200	635.5	642.6	1.1	6.56
$h=30.7$ mm								
15.3	177.2	136.4	53.6	186.4	633.6	644.7	1.7	6.62
21.5	171.8	130.1	59.8	186.4	633.3	645.0	1.8	6.55
26.1	168.0	126.4	64.4	186.4	633.1	644.9	1.8	6.55
30.7	164.5	122.8	69.0	186.4	633.1	645.1	1.9	6.49
$h=38.3$ mm								
15.3	168.8	120.8	53.6	176.4	631.4	647.1	2.5	6.54
21.5	163.6	115.0	59.8	170.2	631.5	647.4	2.5	6.54
26.1	160.1	112.0	64.4	165.6	631.3	646.9	2.4	6.55
30.7	156.6	108.9	69.0	161.0	631.5	647.0	2.4	6.58
$h=46$ mm								
15.3	161.7	106.5	50.0	168.0	629.2	649.5	3.2	6.48
21.5	156.2	103.5	52.0	162.0	630.0	649.0	3.0	6.52
26.1	152.8	99.8	56.0	160.0	629.6	649.0	3.0	6.52
30.7	149.3	96.5	58	158	630.1	649.3	3.0	6.54
$h=53.7$ mm								
15.3	153.2	90.4	50.0	168.0	632.2	660.2	4.4	6.38
21.5	150.2	88.5	52.0	162.0	626.9	652.8	4.1	6.4
26.1	144.8	82.3	56.0	160.0	632.8	660.5	4.3	6.42
30.7	141.5	79	58	158	632.8	660.4	4.3	6.44
$h=61.3$								
15.3	146.4	75.6	50.0	168.0	632.2	668.1	5.6	6.21
21.5	141.6	72.2	52.0	162.0	632.5	667.3	5.4	6.26
26.1	138.5	69.2	56.0	160.0	638.1	675.5	5.9	6.26
30.7	135	66	58	158	637.6	674.4	5.8	6.28

Table 2 shows the results of calculated return loss bandwidth -10 dB and gain of IFA with the same size of conducting plane with $pxp = pxm = 57.5$ mm at 639 MHz. The antenna heights (h) are investigated at 23 mm, 38.3 mm and 53.7 mm. The L_s adjustments do not significantly affect the bandwidth enhancement. Extending the height and the length of L_s will reduce the gain. The calculation results indicate that the bandwidth enhancement of IFA is performed by extending the height of the antenna and enlarge the size of conducting plane.



TABLE II.
RETURN LOSS BANDWIDTH AND DIRECTIVE GAIN OF IFA FOR THE SAME SIZE OF CONDUCTING PLANE AT 639 MHz.

L_s	L	$L1$	pym	pyp	Return Loss Bandwidth			Directive Gain at 639 MHz
					f-low (MHz)	f-high (MHz)	%	
[mm]								
$h=23\text{mm}$								
15.3	186.7	155.0	53.6	200	635.18	641.84	1.0	6.66
21.5	180.8	149.2	59.8	200	635.6	642.4	1.1	6.61
26.1	177.0	144.9	64.4	200	635.5	642.5	1.1	6.58
30.7	173.2	140.9	69.0	200	635.5	642.6	1.1	6.56
$h=38.3\text{mm}$								
15.3	169.5	116.8	53.6	200	630.1	648.9	2.9	6.27
21.5	164.4	111.0	59.8	200	629.7	648.9	3.0	6.22
26.1	160.8	107.6	64.4	200	629.8	649.1	3.0	6.2
30.7	157.4	103.8	69.0	200	629.9	649.4	3.1	6.19
$h=53.7\text{mm}$								
15.3	153.4	84.4	53.6	200	631.9	665.7	5.3	6.03
21.5	148.6	79.0	59.8	200	631.8	666.2	5.4	6
26.1	145.2	75.0	64.4	200	632.2	667.0	5.4	5.99
30.7	142	72	69.0	200	632.1	666.7	5.4	5.99

Figure 2a and Figure 2b show comparison return loss bandwidth and gain with different height at 639 MHz by investigating on the length of short stub (L_s). The L_s adjustments do not significantly affect the bandwidth enhancement and the gain characteristic. The results show that the bandwidth enhancement of IFA is performed by extending the height of the antenna, while the gain reduced.

Figure 3 show comparison return loss bandwidth with different length of short stub (L_s) at 639 MHz by investigates on the height of the antenna. The graph shows that the antenna bandwidth has significant achievement by increase the antenna height.

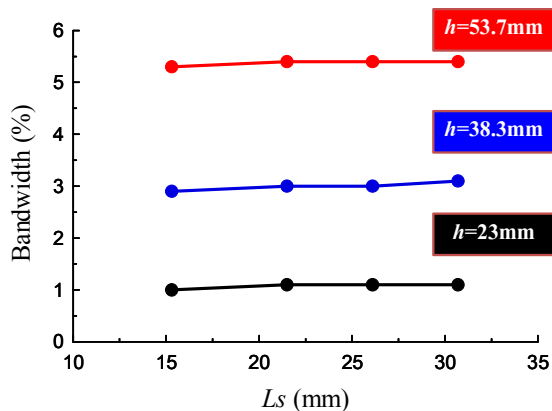


Figure 2a. Comparison the return loss bandwidth of IFA with different L_s at 639 MHz.

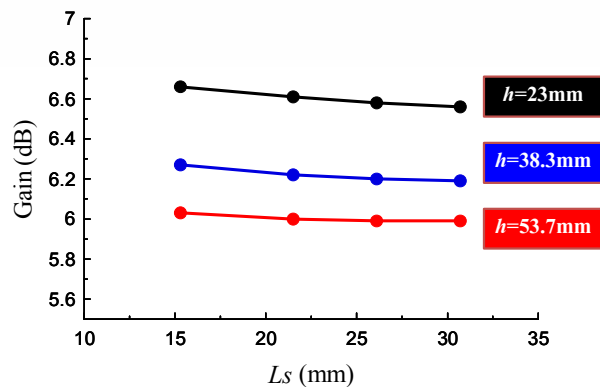


Figure 2b. Comparison the gain of IFA with different L_s at 639 MHz.

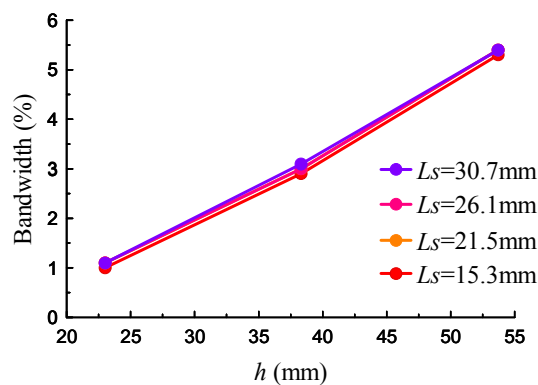


Figure 3. Comparison the return loss bandwidth of IFA with different h at 639 MHz.

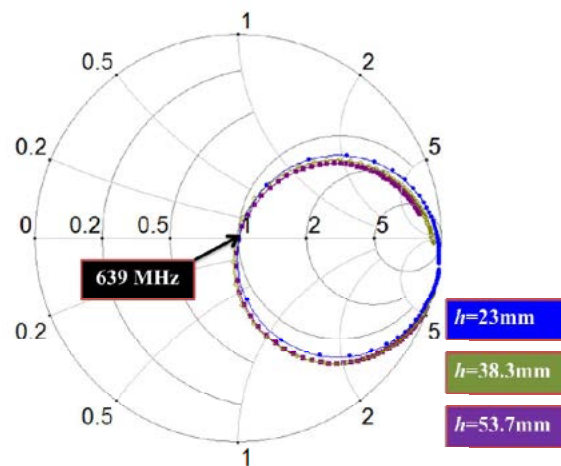


Figure 4a. Input impedance characteristic

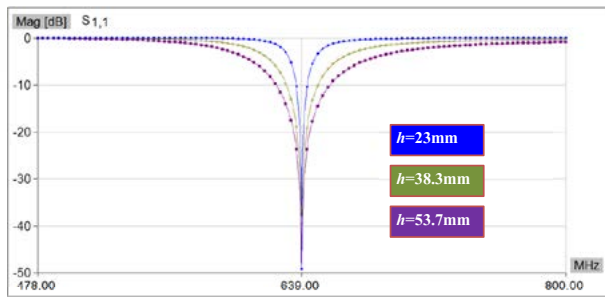
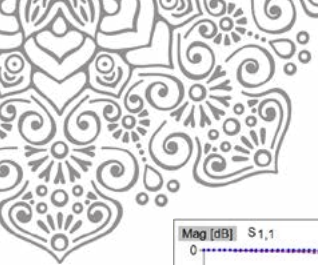


Figure 4b. S-Parameter

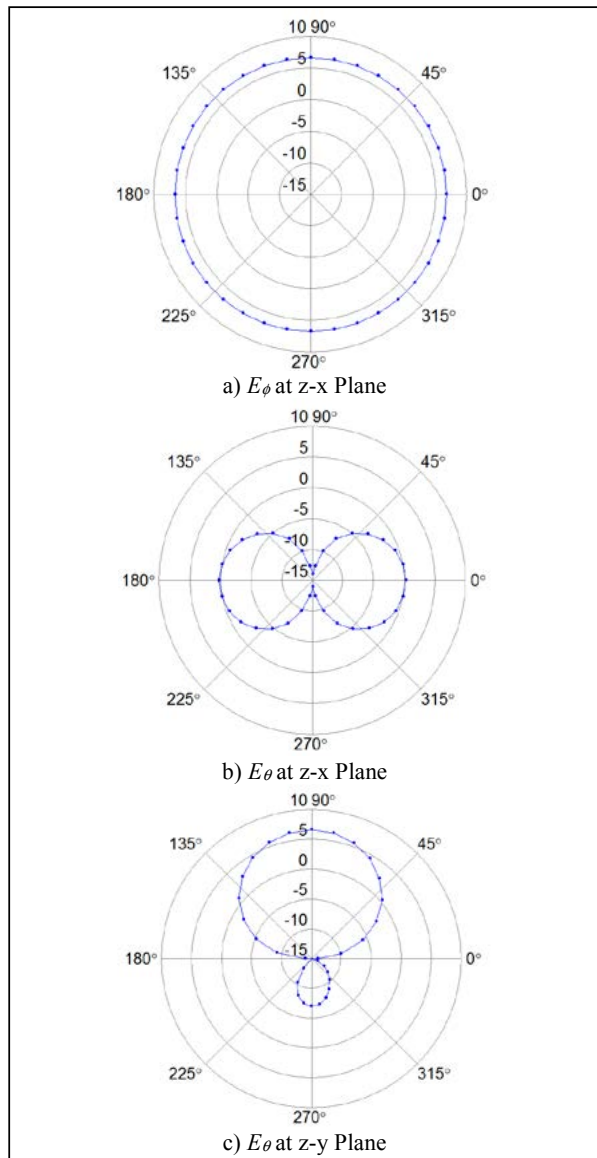


Figure 5. Electric field radiation pattern characteristic

Figure 4a shows the input impedance characteristic. The impedance matching at the center frequency is obtained by optimizing the length of horizontal elements L & $L1$. While Figure 4b show the calculation results indicate that the bandwidth enhancement of IFA is performed by extending the height of the antenna. The input impedance and S-parameter results of IFA are investigated between various heights and the same length of short stub, $h = 23$ mm and $L_s = 21.5$ mm, $h = 38.3$ mm and $L_s = 21.5$ mm, $h = 53.7$ mm and $L_s = 21.5$ mm.

Figure 5 shows the computed electric field radiation pattern of IFA (E_θ and E_ϕ) with height $h = 23$ mm and the length of short stub $L_s = 21.5$ mm. The directive gain of 6.61 dBi is achieved.

IV. CONCLUSION

The proposed IFA for UHF channel has been presented. The total length of the vertical and horizontal element of the proposed antenna is longer than a quarter wavelengths. The bandwidth enhancement is achieved by increasing the height of the antenna and extending the conducting plane size. The short stub adjustment does not affect the gain significantly. In the case of the height of antenna 38.3 mm, while the length of the short stub 30.7 mm and the size of conducting plane is 115 mm by 230 mm, the return loss bandwidth (-10 dB) becomes 2.4 % and the gain becomes 6.58 dB, respectively. When the height of the antenna become two times, the return loss bandwidth becomes almost three times. The proposed IFA is promising as antenna receiver for UHF channel application.

ACKNOWLEDGMENT

The Authors would like to thank The State Polytechnic of Malang for the support to attend this conference.

REFERENCES

- [1] Gobien, A. T., "Investigation of Low Profile Antenna Designs for Use in Hand-Held Radios", Department of Electrical Engineering, Virginia Tech, pp. 98-103, 1997.
- [2] H. Kuboyama, Y. Tanaka, K. Sato, K. Fujimoto and K. Kirasawa, "Experimental Results with Mobile Antennas Having Cross-Polarization Components in Urban and Rural Areas," *IEEE Transactions on Vehicular Technology*, Vol. VT-39, May 1990.
- [3] K., Fujimoto, A. Henderson, K. Hirasawa, and J.R. James, *Small Antennas*, England: Research Studies Press, 1987.
- [4] K. Ogawa and T. Uwano, "A Diversity Antenna for Very Small 800-MHz Band Portable Telephones," *IEEE Transactions on Antennas Propagation*, Vol. 42, September 1994.
- [5] Fujimoto T. and Taguri J., "Wideband Printed Inverted-F Antenna with Unidirectional Radiation Pattern", in *Proc. Of 2016 IEEE-APS Topical Conference on Antennas and Propagation in Wireless Communication (APWC)*, pp. 181-182, 2016.
- [6] Fujimoto T. and Yoshida T., "A printed inverted-F antenna for circular polarization", in *Proc. Of 2016 IEEE International Symposium on Antennas and Propagation (APSURSI)*, pp. 2171-2172, 2016.
- [7] Saita Y. et. al., "Low-Frequency Inverted F Antenna on Hemispherical Ground Plane", in *Proc. Of 2014 International Symposium on Antennas and Propagation*, pp. 183-184, 2014.
- [8] Nikolova, N.K., "Practical Dipole/Monopole Geometries. Matching Techniques for Dipole/Monopole Feeds", Department of Electrical and Computer Engineering, ITB/A308 McMaster University, pp. 15-16, 2016.
- [9] Balanis, C.A., "Antenna Theory: Analysis and Design", John Wiley & Sons, Fourth Edition, pp. 151-184, 2016.
- [10] Stutzman, W.L. and Thiele, G.A., "Antenna Theory and Design", John Wiley & Sons, Third Edition, pp. 229-235, 2012.
- [11] Sinnema, W., "Electronic Transmission Technology: Lines, Waves and Antennas", Prentice-Hall Inc., pp. 112-118, 1988.
- [12] Rohadi E. and Taguchi M., "Ultra-Low Profile, Unbalanced Fed Inverted F Antenna for 2.45 GHz Wireless Communication System", in *Proc. of 2013 URSI International Symposium on Electromagnetic Theory (EMTS)*, pp. 585-588, 2013.
- [13] Rohadi E. and Taguchi M., "Ultra Low Profile Antenna for 2.45 GHz Wireless Communication", in *Proc. of 2012 IEEE International Conference on Communication, Network and Satellite (ComNetSat)*, pp. 103-107, 2012.
- [14] Milligan, T.A., "Modern Antenna Design", John Wiley & Sons, Second Edition, pp. 67-72, 2005.
- [15] Shao Jun, "Mathematical Statistics, Springer, Second Edition", pp. 207-212, 2007.
- [16] WIPL-D d.o.o.: <http://www.wipl-d.com/>, 2016.
- [17] Khan N., "Design of Planar Inverted-F Antenna", in *Proc. Of 2014 International Journal of Advanced Technology in Engineering and Science*, vol. 2, no. 5, pp. 20-31, 2014.



State of the Art of Joint Torque Sensor for Human Robot Interaction

Indrazno Siradjuddin, Rendi Pambudi Wicaksono, Anggit Murdani, Zakiyah Amalia, Denda Dewatama
Malang State Polytechnic
Electrical Engineering Department
Mechanical Engineering Department
Malang, Indonesia
indrazno@polinema.ac.id

Abstract—Observations from biological systems make an impression that robots should have the same level of abilities that are embedded in biological systems to perform safe and successful interaction with human. The primary challenge in safe physical human robot interaction is to attach human like compliance behaviour into robots such that robot will not cause harm or injury to the human or robot themselves under any operating conditions. For instance, a robot surgery should comply with the movement command from the surgeon, a manipulator robot should follow the operators hand movement during the learning process for pick and place application. This review discussion is focused on the technical innovation of compliant robot manipulators which have the most range of industrial applications. To achieve such human like behaviour, a robot manipulator should have some degrees of flexibility of its movement in order to respond given external forces or torques. This behaviour and characteristic can be controlled and developed by using active, passive and semi active compliant actuator devices, which will be functioned as robot joints. The key part of the compliant actuator technology is the torque sensor. Many torque sensor technologies have been proposed and developed for industrial application such as industrial machineries. However a comprehensive review of torque sensor which can be applied for compliant joint development cannot be found. The review is urgently needed for robotics advancing the development of compliant robot in the near future. Therefore, this paper provides a review of torque sensor over a two last decade. The review classifies the torque sensors by their sensing methods. Thus, the torque sensors sensing methods can be discussed in detail. This review also determines the possible application in the development of a compliant robot manipulator. In addition, the shortcomings and the advantages of the torque sensors existing are discussed. The future research direction and technology trend are identified.

Keywords: Robot manipulator; Compliant joint; Torque sensor; Safe human robot interaction;

I. INTRODUCTION

Recently, most of robot available have been built to work in controlled environment and restricted working space to minimize robot related accident possibilities. However, robot applications today require a closer physical human robot interaction. In general, sensing of torque and force is useful in many applications, including the following:

- 1) In robotic tactile (distributed touch) and manufacturing applications such as gripping, surface gaging, and ma-

terial forming, where exerting an adequate load on an object is a primary purpose of the task.

- 2) In the control of fine motions (e.g., fine manipulation and micromanipulation) and in assembly tasks, where a small motion error can cause large damaging forces or performance degradation.
- 3) In control systems that are not fast enough when motion feedback alone is employed, where force feedback and feedforward force control can be used to improve accuracy and bandwidth.
- 4) In process testing, monitoring, and diagnostic applications, where torque sensing can detect, predict, and identify abnormal operation, malfunction, component failure, or excessive wear (e.g., in monitoring of machine tools such as milling machines and drills)
- 5) In the measurement of power transmitted through a rotating device, where power is given by the product of torque and angular velocity in the same direction.
- 6) In controlling complex nonlinear mechanical systems, where measurement of force and acceleration can be used to estimate unknown nonlinear terms. Non-linear feedback of the estimated terms will linearize or simplify the system (nonlinear feedback control or linearizing feedback technique or LFT).

Related with physical human robot interaction, robot applications such as: surgery robot, an assistant robot that helping human domestic works, those are robots that mostly required a safe closer physical human robot interaction. The primary challenge in safe physical human robot interaction is to attach human like compliance behaviour into robots such that robot will not cause harm or injury to the human or robot themselves under any operating conditions. The torque sensor is the most desirable to make a compliant joint[1]. Using torque sensor is to sense external forces presented on robot. Those forces can be caused by undesired contact between robot and its environment.

At this time there are various types of torque sensors are available and certainly each torque sensor has different purpose. The diversity of types of torque sensors is influenced by the differences in its sensing method of each torque sensor, such as strain gauge based torque sensor that detect



the resistance change of deformed body as a torque change, magnetic based that detect differential magnetic field as a torque change, etc.

In this context, the objective of this paper is to review the sensing method of existing torque sensor in this last two decades. The rest of this review paper is organised as follows: the principle method of the torque sensor is discussed in Section II. A detail discussion about the various techniques used in sensor development is presented in Section III followed by the presentation of identified recent patents is presented in Section IV. The conclusion of this review is expressed in Section V

II. THE TORQUE SENSOR PRINCIPLE

Figure 1 shows the basic diagram of a torque sensor principle.

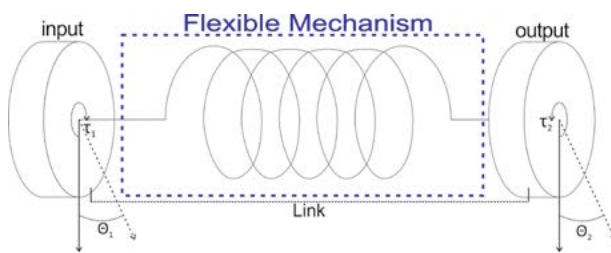


Fig. 1: Basic design of torque sensor

As it is shown in the Fig. 1, there is an input which linked to the end of the flexible mechanism and then from the other end of flexible mechanism, the output is linked. The vast majority of conventional systems used to measure torque operate by measuring the torsional deflection induced by the applied torque. It can be deduced that the angle deflection between the input and the output is proportional to the torque difference between the input and the output shafts. This condition can be expressed as

$$\Delta\theta = \theta_2 - \theta_1 \simeq \tau_2 - \tau_1 \quad (1)$$

where θ_1 is the angle change on input, θ_2 denotes the angle change on output, τ_1 represents the given torque on input and τ_2 is the given torque on output

From (1), if the torque applied at the input and the output are the same ($\tau_1 = \tau_2$) the deflection between the input angle or output angle does not occur, $\Delta\theta = 0$. It means there is no torque given at the output side. If the torque applied at the output is greater than the input ($\tau_1 < \tau_2$) it will make $\theta_1 < \theta_2$, hence $\Delta\theta \neq 0$. The difference of angle position between the input and output implies that there is a different torque that applied at the input and output, because $\Delta\theta$ are equivalent to $\Delta\tau$. So from the difference of angle position can be used to indicate the presented torque at the output.

III. SENSING METHOD

In most applications, sensing is done by detecting an effect of torque or the cause of torque. As well, there are methods for

measuring torque directly. Common methods of torque sensing include the following:

- 1) Measuring strain in a sensing member between the drive element and the driven load, using a strain-gage bridge [2][3][4][5][6]
- 2) Measuring displacement in a sensing member (as in the first method)?either directly, using a displacement sensor [7][8][9], or indirectly, by measuring a variable such as magnetic inductance or capacitance that varies with displacement [10][11][12][13][14][15]
- 3) In electric motors, measuring the field current or armature current, which produces motor torque; in hydraulic or pneumatic actuators, measuring the actuator pressure [16], [17]

A. Strain Gauge

Strain gauge is an instrument used to measuring the tension of an object. The strain gauge consists from a flexible insulating board which becomes a mainstay a pattern of metal foil. This metal foil can be stretched. When an object is deformed, the metal foil also deforms, which causes a change in electrical resistance. Resistance change is related to the amount of strain. resistance change is typically measured using a Wheatstone bridge as shown in Fig.2.

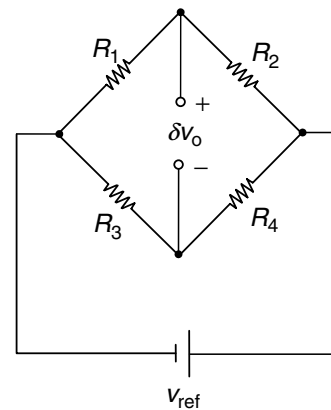


Fig. 2: Wheatstone bridge circuit

The torque sensor uses strain gauge as its sensing method, generally utilizing the flexible body of a sensor that deforms when given a torque to be measured using a strain gauge. From the the value of the strain generated by a strain gauge, be further translated as the magnitude of the torque value given.

Yu-Xiang Sun [2] develops a torque sensor based on the redundancy of each segment. Elastic body of this sensor forms a circular with 8 radial spokes. These sensors use a combination of semiconductor strain gauge and foil strain gauge for detecting deformation of elastic body. They stated that the sensor is capable of detecting up to 400Nm torque. In the other development of strain gauge-based torque sensor, there is Aghili torque sensor [3] that develop the strain gauge



based-torque sensor which have the hollow hexaform body. They claim that they have developed a sensor that has a high sensitivity to a direct drive torque, so the sensor is suitable to be used as a joint on a direct drive actuator.

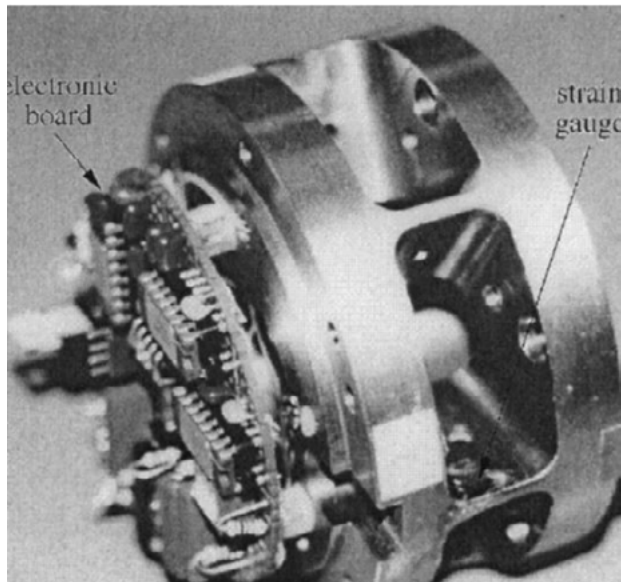


Fig. 3: This is the Prototype from Aghili [3] strain gauge based-Torque Sensor

Yoshihiro Kuroki [4] also developed the strain gauge based-torque sensor using Cr-N alloy. This sensor can be applied as a joint torque on a servo, that can enable human robot which can perform physical interaction safely. They make some type of torque sensor sizes, each size has a difference in the capacity of sensing and its resolution. Here some type and specification of this sensor

	Type A	Type B	Type C	Type D
Joint Torque Sensor (SUS630)				
Size (mm)	∅ 37 x 3t	∅ 43 x 4t	∅ 47 x 6t	∅ 56 x 7t
Weight (g)	19	35	63	105
Rated Torque (Nm)	7.5	30	75	105
Allowable Torque (Nm)	15	60	150	210
Allowable Peak Torque (Nm)	22.5	90	225	315
Resolution (Nm)	0.01	0.03	0.07	0.1

Fig. 4: Type and specification from each design of Yoshihiro Kuroki [4] strain gauge based-Torque Sensor

Not only the last few years, in fact torque sensors have been developed since decades ago. Lawrence E. Pfeffer and their colleagues [5] have developed a torque sensor for the joint of

robot manipulator PUMA 500. They stated that these sensors show a sensitivity 159 mV / N m with the level of non-linearity that is still within reasonable limits and acceptable (8 percent), and provide protection against excessive loads.

One more development of strain gauge based torque sensors, this is torque sensors developed by Hong-Xia Zhang and their colleagues [6]. They developed a torque sensor which is claimed to have a high sensitivity level. This is can affected by the placement of strain gauge that detects the deformation of flexible body. They put a strain gauge on the most sensitive section to deformation caused by the given torque, so the slightest torque given, this section will deform and will be read by the strain gauge and interpreted as change of of torque. Can be seen in the picture below is the design of their torque sensor

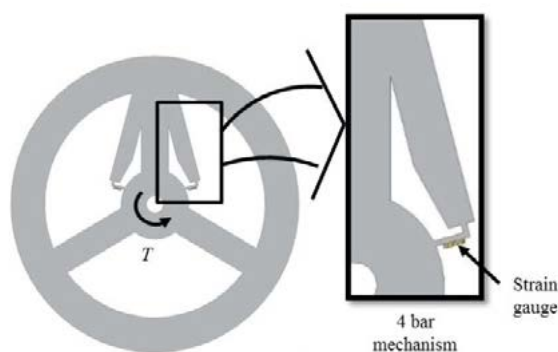
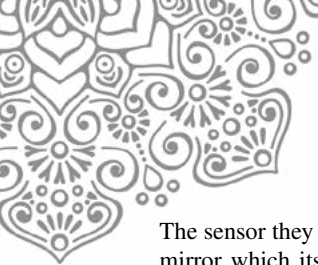


Fig. 5: Design of Strain gauge based Torque sensor by Hong-Xia Zhang [6]

B. Optical Sensor

Another sensing method of torque sensor is using optical sensors. Basically the principle of optical sensor are turn light into an electronic signal. It measuring the intensity of light and then translated into a form that can be easily read by the controller. The optical sensor is generally part of a larger system that combines light sources, measuring instruments and optical sensors.

In the application of optical sensor as the torque sensor sensing method is also different from each existing model. As the torque sensor from [7], they apply the principle of a reflective photoelasticity to detect the spin resulting from the a given torque. They stated that this torque sensor is suitable for measuring the torque from the a small to medium range. Installation of optoelectronic components, ambient light interference, the rotational speed and the effect from the additional arch photoelastic tubes must be considered due to measurement accuracy. In [8] also applying photoelastic concept on their torque sensors. Their developed torque sensor, used to detect the motor starting torque. Yohan Noh [9] Develop a torque sensorbased on optical sensor, for the medical world. This sensor is a torque sensor with multiple axis, which means it can detect change of torque from various directions.



The sensor they have developed work by reflecting light onto a mirror which its reflection will be caught by the photodiode. When affected by a torque, the position of this mirror will change even be able to move away which causes change of the intensity of light received by the photodiode. This is be further translated as torque changes.

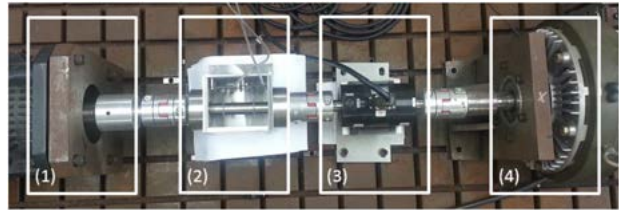


Fig. 7: The design from Kyungshik Chongdu Lee[13] magnetic based-Torque Sensor

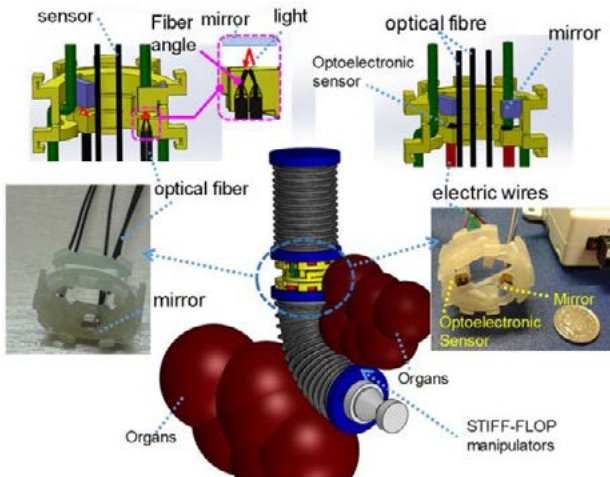


Fig. 6: The design and principle from Yohan Noh [9] optical based-Torque Sensor

C. Magnetic Type

Another sensing method of torque sensor is using magnetic sensor. This Sensor detect changes in the magnetic field generated by the displacement that occurs in the body sensors that are the result of a given torque. This method has the design of a flexible mechanism that is relatively similar to the type of other sensing methods.

This sensing method has been used since decades ago, for example, in 1989 by William J. Fleming and his research team[10], and then in 1990 by Kunio Miyashita and his research team[11], also in 1995 by V.Lemarquand and G. Lemarquand[12]. Not only that, these days there is still a torque sensor is developing with this type of sensing method is by Kyungshik Chongdu Lee and Cho in 2015[13].

Kunio Miyashita[11] developed a non-contact torque sensor magnetic. This sensor uses the principle of magnetic rotary encoder to detect the twisting angle changes caused by the deformation of rotate due to the torque given.

Kyungshik Chongdu Lee[13] developing a non-contact torque sensors by applying Magnetic Sensor Band, which they claim does not require calibration in its use. These sensors can be applied to a rotating shaft. They stated that this sensor has an error of less than 1 percent in detecting torque at a specified speed.

D. Capacitive Type

This Capacitive type sensing method uses the basic principle of capacitive displacement sensor that can be used to detect changes or capacitive displacement of the object. There are two types of capacitive displacement sensor. One type that is used to measure the thickness of the conductive material and the type of the other measures the thickness of non conductive material, such as measuring the water level.

Yong Bum Kim [14] has developed a capacitive type torque sensor that can be applied to the joint robot. The sensor consists of two cells capacitive sensors that detect changes in position caused by the deformation. Both cells are located on opposite sides of each other, which compensates for cross coupling of torque when the external load Force / Torque applied. Figure 8 are the design and sensing principle of these sensor.

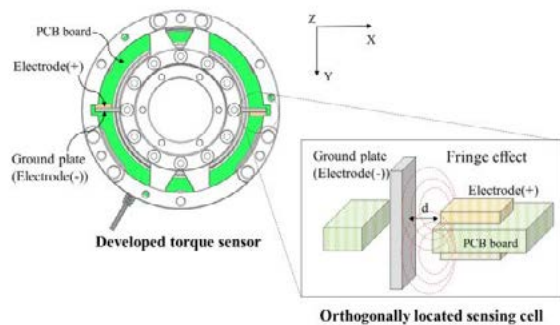


Fig. 8: The design and sensing principle of Yong Bum Kim [14] capacitive type Torque Sensor

Development of another one with a capacitive-type torque sensor is in the torque sensor belongs to Asad M. Madni and his colleagues [15]. They also developed a capacitive-type torque sensor is based on differential capacitive technology to measure the angle of twist and torque applied by steering effort. They stated that the test results showed that the kinematic very high linearity can be achieved by this sensor.

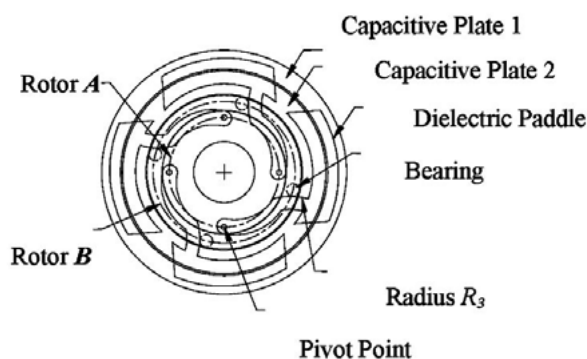
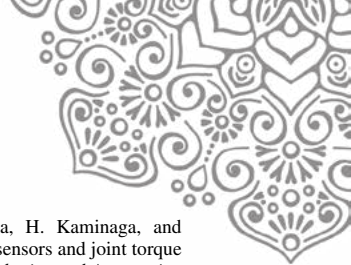


Fig. 9: The design of Asad M. Madni [15] capacitive type Torque Sensor

IV. RECENT PATENT

From some sensing methods that have been applied to the torque sensor by several researchers, also has made the patent. In the following table is a list of the torque sensor patent that applied the sensing method. This patent data we get from google patent.

V. CONCLUSION

Various examples torque sensor that can be applied as a robot joint has been shown in this review. From various examples of the torque sensor has been classified by the sensing method that is: Strain gauge based, Optical Based, Based Magnetic and Capacitive based. Additionally, examples of existing patents is also featured in this review.

From a variety of sensing methods that exist and each of its instances, it can be seen that the outline design of a flexible mechanism that is relatively similar. Only way to detect changes in the deformation of its flexible mechanism different. Moreover to making a more sensitive torque sensor can be done by making the design of flexible mechanism as thin as possible so that it can be easily deformed when given a torque. But you must remember, the thinner a flexible mechanism, the smaller the maximum torque that can be given.

ACKNOWLEDGMENT

The authors would like to thank to Kemenristek Dikti and Malang State Polytechnic for their support, and also to Mr. Erfan Rohadi for his invaluable advise on scientific writing.

REFERENCES

[1] J. Xia, Z. Xie, H. Fang, T. Lan, J. Huang, and H. Liu, "Collision detection of flexible joint manipulator by using joint torque sensors," in *2009 IEEE/ASME International Conference on Advanced Intelligent Mechatronics*, July 2009, pp. 1816–1821.

[2] Y. X. Sun, H. B. Cao, M. Li, R. H. Lin, H. Q. Pan, F. Shuang, L. F. Gao, and Y. J. Ge, "Design and calibration of a torque sensor based on sectional redundant measurements," in *2015 IEEE International Conference on Information and Automation*, Aug 2015, pp. 262–267.

[3] F. Aghili, M. Buehler, and J. M. Hollerbach, "Design of a hollow hexaform torque sensor for robot joints," *The International Journal of Robotics Research*, vol. 20, no. 12, pp. 967–976, 2001. [Online]. Available: <http://dx.doi.org/10.1177/02783640122068227>

[4] Y. Kuroki, Y. Kosaka, T. Takahashi, E. Niwa, H. Kaminaga, and Y. Nakamura, "Cr-n alloy thin-film based torque sensors and joint torque servo systems for compliant robot control," in *Robotics and Automation (ICRA), 2013 IEEE International Conference on*. IEEE, 2013, pp. 4954–4959.

[5] L. E. Pfeffer, O. Khatib, and J. Hake, "Joint torque sensory feedback in the control of a puma manipulator," *IEEE Transactions on Robotics and Automation*, vol. 5, no. 4, pp. 418–425, 1989.

[6] H.-X. Zhang, Y.-J. Ryoo, and K.-S. Byun, "Development of torque sensor with high sensitivity for joint of robot manipulator using 4-bar linkage shape," *Sensors*, vol. 16, no. 7, p. 991, 2016.

[7] P. Horvath and A. Nagy, "Optical torque sensor development," in *Recent Advances in Mechatronics*. Springer, 2010, pp. 91–96.

[8] A. Bojtos and N. Szakály, "Photoelastic torque sensor development for measurement of starting torque of a dc micromotor," *Procedia Engineering*, vol. 168, pp. 1358–1361, 2016.

[9] Y. Noh, A. Shiva, E. Hamid, H. Liu, K. Althoefer, and K. Rhode, "Light intensity based optical force/torque sensor for robotic manipulators," 2016.

[10] W. J. Fleming, "Magnetostrictive torque sensor performance-nonlinear analysis," *IEEE Transactions on Vehicular Technology*, vol. 38, no. 3, pp. 159–167, Aug 1989.

[11] K. Miyashita, T. Takahashi, S. Kawamata, S. Morinaga, and Y. Hoshi, "Noncontact magnetic torque sensor," *IEEE Transactions on Magnetics*, vol. 26, no. 5, pp. 1560–1562, Sep 1990.

[12] V. Lemarquand and G. Lemarquand, "Magnetic differential torque sensor," *IEEE Transactions on Magnetics*, vol. 31, no. 6, pp. 3188–3190, Nov 1995.

[13] K. Lee and C. Cho, "Study of noncontact torque measurement method with magnetic sensor band," *Journal of Mechanical Science and Technology*, vol. 29, no. 9, pp. 3897–3903, 2015.

[14] Y. B. Kim, U. Kim, D. Y. Seok, J. So, and H. R. Choi, "A novel capacitive type torque sensor for robotic applications," in *2016 IEEE International Conference on Advanced Intelligent Mechatronics (AIM)*, July 2016, pp. 993–998.

[15] A. M. Madni, J. B. Vuong, D. C. H. Yang, and B. Huang, "A differential capacitive torque sensor with optimal kinematic linearity," *IEEE Sensors Journal*, vol. 7, no. 5, pp. 800–807, May 2007.

[16] A. H. Z. Farnaz, H. S. Sajith, P. J. Binduhewa, M. P. B. Ekanayake, and B. G. L. T. Samaranyake, "Low cost torque estimator for dc servo motors," in *2015 IEEE 10th International Conference on Industrial and Information Systems (ICIS)*, Dec 2015, pp. 187–192.

[17] S. H., K. S.F., and S. B., "Improvements in direct torque control of induction motor for wide range of speed operation using fuzzy logic," *Journal of Electrical Systems and Information Technology*, pp. –, 2017. [Online]. Available: <http://www.sciencedirect.com/science/article/pii/S2314717217300107>

[18] S.-m. Kwom, H. Jung, and H. Lee, "Strain gauge type force-torque sensor and method for manufacturing the same," Mar. 18 2014, uS Patent 8,671,780.

[19] P. Krippner, P. Szasz, M. Wetzko, and T. Brogardh, "Set of multiaxial force and torque sensor and assembling method," May 20 2014, uS Patent 8,726,741.

[20] J. Dietrich and J. Schott, "Force-torque sensor," Aug. 16 1988, uS Patent 4,763,531.

[21] R. J. Hazelden, "Optical torque sensor incorporating sensor failure diagnostics," Jun. 3 1997, uS Patent 5,636,137.

[22] F. M. Discenzo, "Photoelastic neural torque sensor," Mar. 3 1998, uS Patent 5,723,794.

[23] D. W. Cripe, "Magnetoelastic torque sensor," Mar. 2 2004, uS Patent 6,698,299.

[24] T. Ueno, N. Wako, and T. Yoshida, "Capacitive torque sensor and method of detecting torque," Aug. 5 2003, uS Patent 6,601,462.



TABLE I: Patent from each sensing method

Sensing Method	Patent Title	Claim
Strain Gauge	Strain gauge type force-torque sensor and method for manufacturing the same[18]	The present invention provides torque strain gauge sensor and method for manufacturing torque sensor, and save on production costs, and can overcome the difficulties in attaching gauge and sensor deficiencies and errors are generated when installing gauges.
	Set of multiaxial force and torque sensor and assembling method[19]	A sensor assembly force / torque multiaxial and method for assembling like a sensor assembly is disclosed. Assembling sensor includes a series of at least two sensors each made of strain gauges, which are each arranged at an angle and the exact distance relative to one another and are each fixed to the body of the transducer, which is a mechanical contact with the printed circuit board
	Force-torque sensor[20]	A force-torque sensor is provided to measure the force of the sixth possibility and torque components in the Cartesian coordinate system by using a strain gauge. The sensor has two integral spoke wheels are designed identically where each cylindrical on the outer circle, and connected with four fingers on the inside of the circle.
Optical	Optical torque sensor incorporating sensor failure diagnostics[21]	Improved torque sensor, or the sensor relative to the movement of angular, consisting of input, output, the LED light source, a pair of the unit photodetector is intended to receive light from the LED light source, and a means of signal processing, in which said signal processing means adapted to receive the signal output from the photodetector unit, the output signal from the photodetector unit depends on the intensity of the light received, and signal processing adapted to process the output signals from the photodetector unit that produces an output signal that is translated as an indication of the angular displacement, or torque provided, between input and output.
	Photoelastic neural torque sensor[22]	A single device opto-mechanical torque sensor that is suitable for use on a spinning machine, combine polymer photoelastic detector, a light source, the image sensor photoelastic intelligence and neural networks and algorithms. Photoelastic polymer is then shaped into a hollow cylinder and bonded metal collars located at each end of the cylinder. Collar serves to easily place the detector cylinder on the engine shaft and affixed to the shaft using a peg, setscrew, or pin spring.
Magnetic type	Magnetoelastic torque sensor[23]	The present invention relates to magnetic sensors are applied to the active magnetic shaft structure, and more particularly, to non-contact magnetoelastic torque transducers to measure the torque applied to the a rotating shaft.
Capacitive type	Capacitive torque sensor and method of detecting torque[24]	In this patent, provided the torque sensor capacitive cross-section circular dielectric layer is placed on the edge of the surface of the outermost which is variable in dielectric constant that depends on strain, and a pair of electrodes interdigital facing into the dielectric layer and forming a single capacitor, electrode interdigital comprising of a number of linear electrodes tilting at a predetermined angle with respect to the central axis of the bar.



A Garbage Collection Management Method for Reliable Non-Volatile Memory Systems

Chin-Hsien Wu

Department of Electronic and Computer Engineering of
National Taiwan University of Science and Technology
Taipei, Taiwan.
chwu@mail.ntust.edu.tw

Ting-Wei Wang

Department of and Computer Electronic Engineering of
National Taiwan University of Science and Technology
Taipei, Taiwan
M10102127@mail.ntust.edu.tw

Abstract—NAND flash memory is a popular non-volatile memory device and has been used for the data storage of mobile devices, Laptops, and various embedded systems. However, NAND flash memory requires a garbage collection mechanism due to its erase-before-write characteristic. Garbage collection consists of a series of activities (such as read, write, and erase operations) that usually degrade the lifetime and the performance of NAND-based storage systems. In this paper, we survey a garbage collection management method for reliable non-volatile memory (i.e., NAND flash memory) in embedded systems. Furthermore, we also propose the concept to cache a small part of appropriate information about garbage collection in RAM-limited embedded systems. We hope the concept can reduce the RAM space requirements and only cause a little increase in the amount of the original workloads such that the response time of the original workloads is not much affected.

Index Terms—NAND Flash Memory, Garbage Collection, Storage Systems, Embedded Systems

I. INTRODUCTION

NAND flash memory [1] is a popular non-volatile memory device that has many advantages such as high-density, lightweight, shock-resistance, non-volatile, and low-power features. Because of the advantages, NAND flash memory is widely used in various storage devices and portable embedded systems. Nowadays, because of the technology breakthrough, the cost per gigabyte of NAND flash memory has been reduced every year, and its capacity is growing rapidly [2]. Although NAND flash memory has many attractive features, it still has several limitations due to its architectural characteristics. Unlike traditional hard-disk drives, NAND flash memory cannot support in-place updates. Once a page is written, the page is no longer available until the residing block is erased first. Data must be written to free pages, and the old version of pages will become invalid. For managing the distinct characteristics of NAND flash memory, a flash translation layer (FTL) (such as [3], [4], [5], [6], [7], [8], [9]) has been proposed to maintain a mapping table to locate the up-to-date pages and appropriately trigger the activities of garbage collection to recycle the invalid pages. In order to reduce the overhead of garbage collection and extend the lifetime of flash memory, a victim block should be selected with more invalid pages and less erase count due to the expensive copy and erase operations. In recent years, the technology of NAND flash memory continues to

progress dramatically such that the capacity of NAND-based storage systems (i.e., embedded systems or mobile devices) is increasing quickly.

Different from the traditional hard-disk drives, the management of NAND flash memory needs additional resources (i.e., computing power and RAM space) to perform the flash translation layer and maintain its related information (e.g., information of the mapping table, garbage collection, and the wear-leveling policy). In particular, the size of RAM usage should be considerable [10]. Recently, a specific flash translation layer (i.e., DFTL [3]) is trying to solve the RAM issue by putting a small (frequently used) part of the mapping information into the RAM space and the rest is storing in the flash memory. However, an intuitive approach is to put the frequently used information of garbage collection into small RAM space and could cause problems. This is because the frequently used information of garbage collection could not denote the suitable victim blocks because some suitable victim blocks may have not been used for some time. In this paper, we survey a garbage collection management method for reliable non-volatile memory (i.e., NAND flash memory). Furthermore, we also propose the concept to cache a small part of appropriate information about garbage collection in RAM-limited embedded systems. We hope the concept can reduce the RAM space requirements and still reduce the overhead of garbage collection and extend the lifetime of flash memory. Note that NAND flash memory and flash memory are used interchangeably in the paper.

II. CHARACTERISTICS OF NAND FLASH MEMORY

A NAND flash memory chip consists of many blocks, and each block has a fixed number of pages. A block is the smallest unit for erase operations, while reads and writes are done in a page unit. A page contains user area and spare area, where the user area is for the storage of actual data, and the spare area stores ECC and other housekeeping information (i.e., page status). Flash memory has three kinds of operations: page read, page write, and block erase. An erase operation needs more time and energy than a read or a write operation. Unlike hard-disk drives, every pages in flash memory need to be erased before they are rewritten. We can't overwrite data into a page which has been already written. We call the "erase-before-

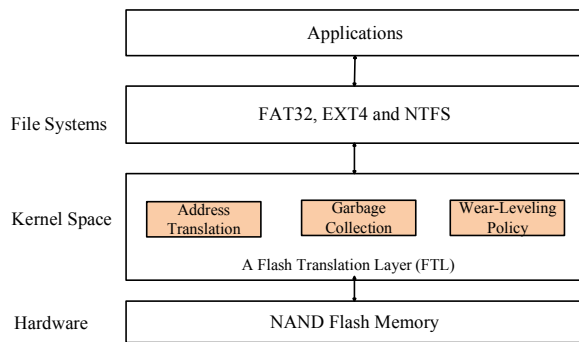


Fig. 1: A Flash Translation Layer (FTL)

write” characteristic. When new data of an LBA (logical block address) is written to a free page, the old version of the LBA becomes an invalid page. The update strategy is called ”out-of-place” update. Note that pages that store valid and invalid data are called valid pages and invalid pages, respectively.

After a certain number of page writes, free space in flash memory would become insufficient. Then, the activities of garbage collection (that consists of a series of read, write, and erase operations) will be performed to generate free space. The objective of the garbage collection is trying to recycle invalid pages scattered over blocks so that they could become free pages for reuse. Because an erase operation needs more time and energy, the activities of garbage collection usually degrade the performance of NAND-based storage systems. Therefore, how to intelligently choose victim blocks for recycling becomes an important topic. Another issue of flash memory is that the erase count allowed to each block is limited. If a block’s erase count exceeds the limit, the block could be worn out and suffer from access errors. Thus, the wear-leveling policy should consider the erase count of each block and try to control the erase count of each block as evenly as possible.

A flash translation layer (FTL) is proposed to emulate as a block-device emulation (e.g., hard-disk drives) for NAND flash memory by hiding the out-of-place update and the erase-before-write characteristic. With the flash translation layer (FTL), many existing file systems (e.g., FAT32, EXT4 and NTFS) could be built on it without any modifications. As shown in Fig. 1, an FTL consists of three main functions: address translation, garbage collection, and the wear-leveling policy. Address translation is trying to solve the out-of-place update by maintaining a mapping table to record the mapping information from an LBA (logical block address) to an PBA (physical block address).

III. OBSERVATION

For the NAND-based storage systems, the activities of garbage collection with a wear-leveling policy are required to manage the free space of flash memory. In order to reduce the overhead of garbage collection and extend the lifetime of flash

memory, a victim block should be selected with more invalid pages and less erase count due to the expensive copy and erase operations. Different from the traditional hard-disk drives, the management of NAND flash needs additional resources (i.e., computing power and RAM space) to perform the flash translation layer and maintain its related information (e.g. information of the mapping table, garbage collection, and the wear-leveling policy). In particular, the size of RAM usage is considerable [10]. In the near future, assume that we have a 1TB NAND-based storage device in an embedded system, where each page is 4KB and each block contains 64 pages (i.e., 256KB). Therefore, the 1TB NAND-based storage device consists of 268,435,456 pages (i.e., 4,194,304 blocks). If a page-level flash translation layer is used to handle the address mapping of the 1TB NAND-based storage device, it could require 2,048 MB (i.e., 268,435,456*8 bytes) RAM space to record the information of the mapping information, where 8 bytes are used for the address mapping from a logical address to a physical page address. Furthermore, assume that each block requires 16 bytes RAM space to record the information of garbage collection (e.g., number of invalid pages, erase count, weighting value, and recency), the page-level flash translation layer will require 64MB (i.e., 4,194,304*16 bytes) RAM space to record the information of garbage collection. Recently, a specific flash translation layer (i.e., DFTL [3]) is trying to solve the RAM issue by putting a small (frequently used) part of the mapping information into the RAM space and the rest is storing in the flash memory. Even DFTL can reduce the required RAM space by 90% to record the mapping information, DFTL still requires 204.8MB (i.e., 2,048*10%) RAM space for the mapping information. Therefore, the ratio of the information of garbage collection to the mapping information will be 31.25% (i.e., 64MB/204.8MB) and is considerable. However, an intuitive approach is to put the frequently used information of garbage collection into small RAM space and could cause problems. This is because the frequently used information of garbage collection could not denote the suitable victim blocks because some suitable victim blocks may have not been used for some time. Although the garbage collection algorithms (e.g., Greedy, CB, or CAT) have been proposed, they mainly focus on how to reduce the recycling cost and extend the lifetime of flash memory. Based on the above observations, we should investigate the relationship between the information of garbage collection and the performance of flash memory, especially when the capacity of NAND-based storage systems grow rapidly. Therefore, we survey a garbage collection management method for reliable non-volatile memory systems. We also propose the concept to reduce the RAM space requirements and still reduce the overhead of garbage collection and extend the lifetime of flash memory.



IV. A GARBAGE COLLECTION MANAGEMENT METHOD FOR RELIABLE NON-VOLATILE MEMORY SYSTEMS

A. Garbage Collection Algorithms

When there are not enough free blocks, the activities of garbage collection are performed to find appropriate victim blocks based on a specific policy for recycling. For example, the intuitive choice is to find a block without any valid pages. However, if there are no such blocks, the victim block may contain some valid pages. If we want to recycle a block with some valid pages, the valid pages should be copied out to other free space before it is erased. Hence, the activities of garbage collection can be summarized by the following steps:

- Step 1: To select an appropriate victim block based on a specific policy for recycling.
- Step 2: If the victim block has some valid pages, the valid pages are copied out to other free space.
- Step 3: After the victim block is erased and becomes a free block, the related information of the FTL should be updated accordingly.
- Step 4: If the free space is still not enough, go to Step 1.

To make sufficient free space, the activities of garbage collection could perform many times and need a lot of read, write and erase operations. Furthermore, if the victim block has many valid pages, the recycling cost would be very high and degrade the whole flash memory performance. Therefore, how to intelligently select an appropriate victim block is very important. In the following, we will introduce some famous garbage collection algorithms.

1) *The Greedy Algorithm:* The greedy (Greedy) algorithm [11] selects a victim block with the minimum valid pages. The selection can minimize the overhead of valid pages copied during the garbage collection. However, the greedy algorithm does not consider the wear-leveling effect of flash memory, because it does not consider the erase count of the selected blocks and could select an over-erased block with the minimum valid pages.

2) *The Cost Benefit Algorithm:* The cost-benefit (CB) algorithm [12] evaluates the weighting value of each block and selects a victim block with the largest weighting value. The weighting value is defined by a formula ($age * \frac{1-u}{2u}$), where age means the time since the most recent modification per block and u means the utilization of valid pages in the block. Therefore, CB could reduce the overhead of valid pages copied by $\frac{1-u}{2u}$ and consider the wear-leveling effect by age . Therefore, if a block haven't been erased for a long time, CB could select the block due to its age and force it to be erased. CB could eventually improve the wear-leveling effect of flash memory and also consider the overhead of valid pages copied.

3) *The Cost Age Time Algorithm:* The cost-age-time (CAT) algorithm [13] evaluates the weighting value of each block and selects a victim block with the smallest weighting value. The weighting value is defined by a formula ($\frac{u}{(1-u)} * \frac{1}{age} * CT$), where CT denotes the erase count of a block, and the definitions of u and age are similar to CB. CAT tries to improve the wear-leveling effect of flash memory by considering not

only age but also the erase count (i.e., CT). Furthermore, CAT also performs data redistribution to classify hot and cold data. Hot and cold data are separately written into different blocks to reduce the recycling cost and improve the wear-leveling effect.

4) *The Turn-Based Selection Algorithm:* The turn-based selection (TB) algorithm [14], [15] consists of two turns: X and Y turns. In X turn (e.g., the probability of 99 percents), TB selects a victim block with the minimum valid pages (e.g., the greedy algorithm) to reduce the overhead of valid pages copied. In Y turn (e.g., the probability of 1 percents), TB selects a victim block by other algorithms (e.g., CB or CAT) that considers the wear-leveling effect to extend the lifetime of flash memory.

5) *The Hot-Cold Swapping Algorithm:* The hot-cold swapping (HC) algorithm [16] selects a victim block with the smallest weighting value by a formula $(1-\lambda)u_i + \lambda(\frac{\epsilon_i}{\epsilon_{max}+1})$, where u_i denotes the utilization of valid pages of block i , ϵ_i denotes the erase count of block i , ϵ_{max} denotes the maximum erase count of block max , λ is the wear-leveling weighting ratio that is between zero and one. Thus, HC considers both the overhead of valid pages copied and the erase count of each block. Moreover, HC can swap hot and cold data between two blocks with the minimum and maximum erase count, respectively. Assume that H_{min} and H_{max} denote two blocks with the minimum and maximum erase count, respectively. If the difference between H_{min} and H_{max} is larger than a threshold, HC would start the garbage collection and swap two blocks' data for the wear-leveling effect.

B. Cache Concept for Garbage Collection in RAM-limited Embedded Systems

The garbage collection algorithms need to select appropriate victim blocks to reduce the recycling cost and balance the erase count of each block for improving the lifetime of flash memory. Most of them use a weighting function to determine each block's weighting value and select an appropriate victim block for recycling. Therefore, a good garbage collection algorithm certainly need enough RAM space to record the related information (such as the weighting value and the erase count for each block), especially when the capacity of flash memory has grown rapidly. Therefore, the cache concept is to reduce the RAM space requirements and still can help the garbage collection algorithms to reduce the overhead and extend the lifetime of flash memory. In fact, we need some data structures to cooperate with the activities of garbage collection and maintain the appropriate victim blocks as candidates in the RAM space during the garbage collection. We also need the selection of victim blocks to select a suitable victim block for recycling with the limited RAM space. The selection must consider both the recycling cost and the wear-leveling effect to reach good performance and extend the lifetime of flash memory. However, because we only records partial information about garbage collection and could be out-of-date, we need to update the information in data structures in RAM space by synchronizing with the complete information



in flash memory. We think the synchronizing process could cause additional overhead by reading all blocks' information (e.g., weighting values) from flash memory.

When a flash-memory storage system is initialized, we need to construct some data structures in RAM space for the garbage collection mechanism. The intuitive process is to scan all flash memory and record the appropriate victim blocks' information based on the comparison of all blocks' weighting values. The overhead is to read the entire flash memory. Because the occupied RAM space of data structures for the garbage collection mechanism could not be large and can be controlled, the overhead to store them in flash memory is not significant before the system shuts down. When the flash-memory storage system is initialized again, we can quickly construct them without scanning the entire flash memory. However, when the system crashes, the latest information of data structures for the garbage collection mechanism in RAM space could be lost. Note that logging and recovery are important technologies for database systems and file processing in the past decades. In fact, we can adopt the write-ahead logging method to ensure the integrity of data structures and the checkpointing mechanism to facilitate the system recovery. However, it will cause additional overhead for the crash recovery. We refer interested readers to the previous work [17]. Based on the previous work [17], a similar method can be used to efficiently reconstruct the required data structures for the garbage collection mechanism after a crash.

V. CONCLUSION

In the paper, we survey a garbage collection management method for reliable non-volatile memory systems. We also propose the concept to reduce the RAM space requirements and still maintain the effectiveness of the garbage collection. The activities of garbage collection could cause significant overhead (due to a series of read, write, and erase operations) and require more RAM space to maintain the entire information of garbage collection, especially when the capacity of flash memory has grown rapidly. Therefore, we need some RAM-limited data structures to reduce the RAM space requirements as much as possible and can cooperate with the weighting functions of the garbage collection algorithms (e.g., Greedy, CB, or CAT) in the future. Furthermore, we should extend the garbage collection management method by including the multi-controller architecture. Because the current architecture of SSDs is using multiple controllers to maintain and handle a lot of NAND flash memory chips, the power of the multiple controllers should be utilized to increase the execution parallelism.

VI. ACKNOWLEDGMENT

The manuscript is supported in part by a research grant from the National Science Council under Grant NSC 105-2628-E-011-007-MY3.

REFERENCES

- [1] R. Bez, E. Camerlenghi, A. Modelli, and A. Visconti, "Introduction to flash memory," in *Proceedings of the IEEE*, vol. 91, pp. 489–502, April 2003.
- [2] A. Leventhal, "Flash storage memory," *Commun. ACM*, vol. 51, pp. 47–51, July 2008.
- [3] A. Gupta, Y. Kim, and B. Urgaonkar, "DFTL: A flash translation layer employing demand-based selective caching of page-level address mappings," in *Proceedings of the 14th International Conference on Architectural Support for Programming Languages and Operating Systems, ASPLOS XIV*, (New York, NY, USA), pp. 229–240, ACM, 2009.
- [4] J. Kim, J. M. Kim, S. Noh, S. L. Min, and Y. Cho, "A space-efficient flash translation layer for compactflash systems," *Consumer Electronics, IEEE Transactions on*, vol. 48, pp. 366–375, May 2002.
- [5] C.-H. Wu and T.-W. Kuo, "An adaptive two-level management for the flash translation layer in embedded systems," in *Proceedings of the 2006 IEEE/ACM International Conference on Computer-aided Design, ICCAD '06*, (New York, NY, USA), pp. 601–606, ACM, 2006.
- [6] S.-Y. Kim and S.-I. Jung, "A log-based flash translation layer for large NAND flash memory," in *Advanced Communication Technology, 2006. ICACT 2006. The 8th International Conference*, vol. 3, pp. 1641–1644, Feb 2006.
- [7] S.-W. Lee, D.-J. Park, T.-S. Chung, D.-H. Lee, S. Park, and H.-J. Song, "A log buffer-based flash translation layer using fully-associative sector translation," *ACM Transactions on Embedded Computing Systems*, vol. 6, July 2007.
- [8] H. Cho, D. Shin, and Y. I. Eom, "Kast: K-associative sector translation for nand flash memory in real-time systems," in *Proceedings of the Conference on Design, Automation and Test in Europe, DATE '09*, (3001 Leuven, Belgium, Belgium), pp. 507–512, European Design and Automation Association, 2009.
- [9] S. Lee, D. Shin, Y.-J. Kim, and J. Kim, "Last: Locality-aware sector translation for nand flash memory-based storage systems," *ACM SIGOPS Operating Systems Review*, vol. 42, pp. 36–42, Oct. 2008.
- [10] R. Lucchesi, "SSD flash drives enter the enterprise." http://www.silvertonconsulting.com/newsletter/SSDf_drives.pdf, 2008. Silverton Consulting.
- [11] M. Rosenblum and J. K. Ousterhout, "The design and implementation of a log-structured file system," *ACM SIGOPS Operating Systems Review*, vol. 25, no. 5, pp. 1–15, 1991.
- [12] A. Kawaguchi, S. Nishioka, and H. Motoda, "A flash-memory based file system," in *Proceedings of the USENIX 1995 Technical Conference Proceedings*, pp. 13–13, 1995.
- [13] M.-L. Chiang and R.-C. Chang, "Cleaning policies in mobile computers using flash memory," *Journal of Systems and Software*, vol. 48, no. 3, pp. 213 – 231, 1999.
- [14] D. Woodhouse, "JFFS : The jouralling flash file system." <https://sourceware.org/jffs2/jffs2.pdf>, 2001. Proceedings of Ottawa Linux Symposium.
- [15] C. Manning and Wokey, "YAFFS specification," 2012. Aleph One Limited.
- [16] S.-g. L. Han-joon Kim, "An effective flash memory manager for reliable flash memory space management," *IEICE Transactions on Information and System*, vol. 85, pp. 950–964, 2002.
- [17] C.-H. Wu, T.-W. Kuo, and L.-P. Chang, "The design of efficient initialization and crash recovery for log-based file systems over flash memory," *ACM Transactions on Storage*, vol. 2, no. 4, pp. 449–467, 2006.



Implementation Of Fuzzy Mamdani In The Diagnosis Of Diabetes Mellitus In Puskesmas Pasar Rebo And Puskesmas Makasar

Za'imatun Niswati
Technical Information
Indraprasta PGRI University
Jakarta, Indonesia
zaimatunnis@gmail.com

Fanisya Alva Mustika, Aulia Paramita
Technical Information
Indraprasta PGRI University
Jakarta, Indonesia
alva.mustika@gmail.com, aulia.pps@gmail.com

Abstract— Diabetes mellitus is a chronic disease characterized by glucose levels blood (blood sugar) exceeds the normal value. According to the World Health Organization (WHO), Indonesia now ranks 4th in the world after India, China and the United States in the number of diabetics. Number of patients with Diabetes Mellitus increases from year to year. This is due to late diagnosis of the disease and also because of an unhealthy lifestyle. Many people initially did not know that they suffer from Diabetes Mellitus. Therefore we need a device or system that has the ability like a doctor in diagnosing the disease. This research aims to implement Mamdani method for diagnosing the disease Diabetes Mellitus in Puskesmas Pasar Rebo and Puskesmas Makasar. Variable support disease diagnosis is used in the formation of fuzzy set. Fuzzy set will be processed by Mamdani method to produce a decision. The results of trials involving the medical records of doctor's diagnosis, and the resulting decision of this application has a value of 97.5% accuracy. While the test results FGD (Focus Group Discussion) is all the functions contained in the Expert System has been able to operate properly and are in accordance with the needs of the Puskesmas. In general, this application can be used as an aid in the diagnosis of Diabetes Mellitus.

Keywords—Mamdani; Diabetes Mellitus; Expert System ; Fuzzy Inference System (FIS); Focus Group Discussion (FGD).

I. INTRODUCTION

Diabetes Mellitus is a chronic disease characterized by blood glucose (blood sugar) that exceeds the normal value. According to the World Health Organization (WHO), Indonesia now ranks 4th largest in the world after India, China and the United States in the amount diabetics.

Many people initially did not know that they suffer from Diabetes Mellitus, it is caused by the lack of information about diabetes, symptoms and the lack of specialist doctors at Puskesmas Pasar Rebo and Puskesmas Makasar. Therefore, a system is needed as a tool to assist in determining Diabetes Mellitus disease. With this system, made someone become more familiar about Diabetes Mellitus. Expert systems are created only on certain knowledge domains for a particular skill that approach human capabilities in one field.

Etiologic Classification of Diabetes Mellitus is Type 1 Diabetes Mellitus, Type 2 Diabetes Mellitus, other type Diabetes Mellitus and Pregnancy Diabetes (Gestational). In Indonesia, the total number of cases of Type 1 Diabetes Mellitus is not known for certain, this type is rarely encountered. It is because Indonesia is located on the equator or genetic factors that do not support. Another case in Type 2 Diabetes Mellitus, which covers more than 90% of the total population of diabetics - hereinafter called diabetes, environmental factors are very important [1]. If we did not concern about, it would lead to serious health problems.

The increase in the number of diabetics is due to delays in diagnosis and also because of unhealthy lifestyles. Fuzzy logic concept is very flexible and has tolerance to data that is not appropriate and based on natural language. Therefore required a system as a tool in determining whether the patient was suffering from Diabetes Mellitus or not with the concept of Fuzzy logic.

In this study, a method will be applied to help diagnose Diabetes Mellitus that is FIS Mamdani. The purpose of this application is to implement FIS Mamdani method in diagnosing Diabetes Mellitus disease at Puskesmas Pasar Rebo and Puskesmas Makasar. The Mamdani method is also known as the Max-Min Method. This method was introduced by Ebrahim Mamdani in 1975. To get the output, it takes 4 stages :

1. Formation of fuzzy set. In the fuzzification process, the first step is to define the Fuzzy Variables and the fuzzy set. Then specify the degree of membership between the fuzzy input data and the defined fuzzy set for each input variable of each fuzzy rule. In the mamdani method, both input and output variables are divided into one or more fuzzy sets.
2. Application function implication on mamdani method. The implication function used is min. The results of the fuzzy implications of each rule are then combined to produce fuzzy inference output.



3. Composition of Rules. Unlike monotonous reasoning, if the system consists of several rules, then the inference is derived from the set and correlation between rules. There are 3 methods used in fuzzy system inference, namely: max, additive and probabilistic OR.
4. Defuzzy. The input of the defuzzification process is a fuzzy set obtained from the composition of fuzzy rules, while the output is a number in the fuzzy set domain [2].

With this software, it is expected to help Puskesmas in improving its service to the patient and can be used by doctors and medical personnel to help diagnose Diabetes Mellitus. Ease of accessing the software through a computer or notebook is expected to speed up the diagnosis process appropriately.

II. LITERATURE REVIEW

A. Expert System

In general, the expert system is a system that seeks to adopt human knowledge into the computer, so that the computer can solve problems as usually done by experts. A good expert system is designed to solve a particular problem by imitating the work of the experts. Expert system structure consists of two principal that is [3] The development environment and the consultation environment. The developer environment is used as the development of expert systems both in terms of component development and knowledge base. The consultation environment is used by someone not an expert to consult.

To build a good expert system required several components, that is:

1. User Interface (UI)
2. Knowledge Base
3. Inference Engine
4. Working Memory

User Interface: The expert system replaces an expert in a given situation, then it must provide the support required by the user who does not understand the technical problem. Expert system also provide communication between systems and users which are called the interface. An effective and user-friendly interface is especially important for users who are not expert in the field applied to expert system.

Knowledge base is a collection of knowledge of a particular field at an expert level in a certain format. This knowledge is derived from the accumulation of expert knowledge and other sources of knowledge. In this expert system, the knowledge base is separate from the inference engine. This separation is useful for the development of expert systems freely adjusted to the knowledge development.

Inference engine, the brain of an expert system in the form of software that performs an inference task of expert system reasoning, commonly referred as a thinking machine. Principally, this engine that will find a solution of a problem.

The inference engine is actually a computer program that provides a methodology for reasoning about information on the knowledge base and working memory as well as for

formulating conclusions. This component presents directives on how to use the knowledge of the system by building an agenda that manages and controls the steps taken to solve problems when consulted.

Working memory, is part of the expert system that stores the facts obtained during the consultation process. These facts will then be processed by inference machines based on knowledge to determine a problem-solving decision.

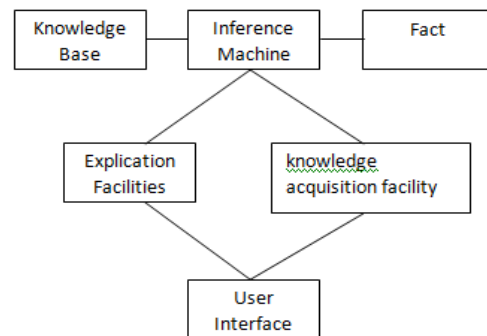


Fig 1. Structure of expert systems [4]

Explication facilities, this section provides an explanation to the user about the system. It is very useful for the user to know how the system can decide a conclusion.

Knowledge acquisition is the process of transfer and transformation of knowledge source from an expert (domain expert) into the program. This process is done with the help of Knowledge Engineer who acts as a mediator between the expert system with experts.

B. Diabetes Mellitus

Diabetes Mellitus is a disease caused by chronic disorder primarily on system metabolism of carbohydrates, fats, and proteins in the body. The World Health Organization (WHO) recognizes three forms of diabetes mellitus :

1. Type I Diabetes Mellitus
Type I Diabetes Mellitus is a condition of the body where the body is unable to produce its own insulin so that the required injection of insulin from the outside. Type I Diabetes Mellitus much influenced by heredity, although the contribution of hereditary factors on the risk of diabetes represents only 5%.
2. Type II Diabetes Mellitus
Type II Diabetes Mellitus, or often called the Non Insuline Dependent. Diabetes Mellitus (NIDDM) is a disease caused by the body's resistance to the effects of insulin produced by the beta cells pancreas. Most cases are type II Diabetes Mellitus were found in people who are obese or overweight due to lifestyle she lived.
3. Gestational Diabetes Mellitus
Gestational Diabetes Mellitus is a disorder of various levels of glucose tolerance that is known first time



during pregnancy without distinguishing whether the patient needs to get insulin or not.

There are several complications of Type I Diabetes Mellitus, Type II Diabetes Mellitus and Gestational Diabetes, that are:

1. Diabetic Neuropathy
Diabetic neuropathy is a common complication of diabetes. Diabetic Neuropathy is damage to a set of nerves caused by high blood sugar levels (hyperglycemia).
2. Diabetic Retinopathy
Diabetic retinopathy is a retinal disorders (retinopathy) were found in patients with diabetes mellitus.
3. Diabetic Nephropathy
Diabetic nephropathy is a disorder of renal function due to leakage of blood film membrane.
4. Diabetes Ketoacidosis
Diabetic ketoacidosis is an acute condition of type I Diabetes Mellitus. Diabetes Ketoacidosis occurs because the acidity of the ketone body is increased due to insulin deficiency.

C. Fuzzy Inference System

Fuzzy inference system is a computational framework that is based on fuzzy set theory, fuzzy rules in the form of IF-THEN, and fuzzy reasoning. Fuzzy inference system receives input crisp. Then this input is sent to the knowledge base containing n fuzzy rules in the form of IF-THEN. Fire strength will be searched on every rule. If the number of rules more than one, then will be aggregated from all rules. Furthermore, on aggregation result will be done defuzzy to get crisp value as system output.

The application of fuzzy logic can improve the performance of the control system by suppressing the appearance of wild functions at the output caused by fluctuations in input variables. Fuzzy logic implementation phase :

1. Fuzzification is the mapping of the firm input to the fuzzy set.
2. Inference phase is the generation of fuzzy rules
3. Defuzzification is the transformation of the output from a fuzzy value to a crisp value.

III. METHOD

A. Data analysis technique

Data will be processed using the approach of Fuzzy Inference System (FIS) Mamdani with supported by matlab toolbox.

Table 1. Fuzzy Variable Sets

<i>Function</i>	<i>Variable</i>	<i>Range</i>
<i>Input</i>	<i>Plasma Glucose Concentration a 2 hours</i>	<i>[0 – 10]</i>
	<i>Diastolic Blood Pressure (mm Hg)</i>	<i>[0 – 10]</i>
	<i>Body Mass Index</i>	<i>[0 – 10]</i>
	<i>Diabetes Pedigree Function</i>	<i>[0 – 10]</i>
<i>Output</i>	<i>Pregnant</i>	<i>[0 – 10]</i>
	<i>Laboratory test score</i>	<i>[0 – 10]</i>

This research was conducted to produce the necessary data and information and to connect with the things that will be written. The collection of data and information conducted using the method of collecting primary and secondary data from the Puskesmas Pasar Rebo and Puskesmas Makasar.

Research Instrument

1. This research uses primary and secondary data of diabetes mellitus which used as instrumentation to obtain data in process of disease diagnosis.
2. Data is presented in the form of tablatore models and variables each of the 100 diabetes patients and 100 non diabetes mellitus patients.
3. To analyze data, this research uses Fuzzy Inference System (FIS) Mamdani with matlab Toolbox and Graphical User Interface (GUI).

Data analysis use quantitative with the rules of mathematics to the data numbers or numerical. Fuzzy set in the input and output variables are divided into one or more fuzzy sets. Application function implications are used for each rule is a function min. Defuzzification use the facilities on the matlab toolbox with fuzzy mamdani method.

B. Design Knowledge Base

The success of the expert system lies in the knowledge and how to process the knowledge in order to be drawn a conclusion. Knowledge gained from the interviews and analysis of the book is converted into a table of types of illnesses and symptoms to facilitate the process of finding solutions. This table is used as an information matching pattern entered by the user and the knowledge base.

C. Rule

Rule is a knowledge structure that links some known information to other information to get a conclusion. Rule is a



form of procedural knowledge. Rule-based expert system is a computer program for processing problems from specific information contained in active memory with a set of rules in a knowledge base, using an inference engine to generate new information.

D. Testing

Researchers conducted tests to analyze the output system. This test is performed to determine the performance of the expert system to provide a diagnosis of positive or negative conclusions of Diabetes Mellitus.

1. Validation Testing

Validation testing is testing to ensure expert system that has been made in accordance with the needs. Testing validation is also to test whether the requirements specification is in accordance with the expected. The method used in this validation testing is Focus Group Discussion (FGD).

FGD conducted at Indraprasta University with 8 participants who are lecturer of Indraprasta PGRI University. To begin the FGD, the researcher presents a presentation and demo of Expert System Diagnosis of Diabetes Mellitus which has been developed and explains every function that exist based on the prepared variables. Furthermore, the FGD participants provide information, responses and approvals. Then the researchers made a conclusion based on FGD results.

System testing is done by distributing questionnaires to respondents. At the time of trial all respondents tried to operate Diagnose Diabetes Mellitus Diagnostic System directly. This test is conducted to determine whether all the functions contained in this Expert System can already be operated properly and is in accordance with the needs of Puskesmas.

2. Application Testing.

Testing the application is done by input data from the laboratory results of Puskesmas Pasar Rebo and Makasar. The data tested were 40 samples from Pasar Rebo Puskesmas and Makasar. Then performed expert analysis and system analysis of the data.

$$\text{Accuracy} = \frac{\text{the number of accurate data}}{\text{total number of data}} \times 100\%$$

IV. RESULT

A. System Implementation

The diagnostic form contains the patient's laboratory test results to determine Diabetes Mellitus or not. After the data input process is complete, then will be process of diagnosis of diabetes mellitus disease that will produce the output of positive diabetes mellitus or negative diabetes mellitus.

Fig 2. Diagnosis Form

The user interface is the interface between the admin system and the user. In this section there will be communication between the two. The program is in the form of choice where users can easily enter the value of each variable in the diagnosis of Diabetes Mellitus disease then the system will count to produce a decision. User friendly interface to facilitate users in using fuzzy inference system for Diabetes Mellitus disease diagnosis.

B. Analysis Of Output

The test is performed to determine the performance of the expert system to provide the diagnosis of positive DM or negative DM conclusions.

The results obtained from the calculation recommendation in expert systems, matched with the results of the expert analysis. The test results of 40 samples were tested, resulting in 39 samples corresponding to the expert diagnosis.

$$\begin{aligned} \text{Accuracy} &= \frac{\text{the number of accurate data}}{\text{total number of data}} \times 100\% \\ &= 39/40 \times 100\% = 97.5\% \end{aligned}$$

Thus, it can be concluded that the accuracy of the expert system based on 40 tested data is 97.5% indicating that this expert system can function well according to the expert diagnosis. The inaccuracy of the expert system is 4% due to several possibilities such as errors in assigning a variable trust value for diagnostics, miscalculation of applying method calculations or incorrect input variable information in the



application. Test results are then evaluated to determine the performance of expert systems generated, so it is expected to improve the quality of Puskesmas services.

V. CONCLUSION

It can be concluded that the expert system implementation Puskesmas Pasar Rebo and Puskesmas Makasar generate 97.5% accuracy value where diabetes mellitus diagnosis expert system can function properly in accordance with expert diagnosis.

Results of testing the FGD is all functionality in the Expert System can be operated properly and are in accordance with the needs of the Puskesmas.

References

- [1] Soegondo. S., 2004. *Stylists Implementing Integrated Diabetes Melitus*. Jakarta: Balai Penerbit Fakultas Kedokteran Universitas Indonesia.
- [2] Marimin dan Nurul Maghfiroh, "Applications Decision Making in Supply Chain Management ", IPB Press, Bogor, 2010
- [3] Kusumadewi, S. dan Purnomo, H., 2010. *Application of Fuzzy logic for Decision Support*. Yogyakarta : Graha Ilmu.
- [4] Giarrattano, J. and Riley, G., 1994. *Expert System Principles and programming*. Boston: PWS Publishing Company



The Development and Analysis of a Decision Systems for Student Tuition Fee at Malang State Polytechnic Using Multi-Objective Optimization by Ratio Analysis (MOORA) Method

Rudy Ariyanto^{*a}, Erfan Rohadi^b, Rosa Andrie Asmara^c, Imam Fahrur Rozi^d,

^{a,b,c,d}, Department of Information Technology, The State Polytechnic of Malang, Jl. Soekarno Hatta No. 9, Malang 65141, Indonesia

Nugroho Suharto^e

Department of Electronics Engineering, The State Polytechnic of Malang, Jl. Soekarno Hatta No. 9, Malang 65141, Indonesia

Abstract—This Policy for student tuition fee for higher degree institutions has been changed since year 2015. This policy is stated in Ministerial Decree of research, technology and higher education of Indonesia Republic No. 22 year 2015 (Permeristekdikti). The main objective of this decree is for broadening access to society to pursue their degree in higher degree institutions, focusing for those who have economical limitations. Student tuition fee regulation as stated in the decree is named student single tuition fee policy (Indonesian: UKT, Uang Kuliah Tunggal). In UKT scheme, the regulated student tuition fee will cover all cost components, such as: fee for courses, laboratory, exams and graduations. In contrast, in previous years before the decree of Ministry of research, technology and higher education of Indonesia Republic No. 22 year 2015 was implemented, the tuition fees were varying significantly between one and the other institution of higher education. In present, by the decree No. 22 year 2015, the tuition fees nominal is varying between categorized student. The student categorization is based on the student or the family income. This means that the student who has more capable financially will support to those who has less financial support, in some extent, to support the total operational costs of the higher education institution. Indeed, the Indonesian government involvement is financially needed to support the operational costs such that the regulated tuition fee is equitable concerning the local economic situation. The main issue for the implementation of the decree No. 22 year 2015 is to have a proper reasoning for the institution to decide the categorization scheme. The policy made has to be justified and reasonable. In addition to the current problem, the prospectus students come from so many different backgrounds: economically and demographically. This work proposes a decision support system that can filter and classify students based on variables that describe economic capability. The Multi-Objective Optimization by Ratio Analysis (MOORA) method is used to filter and classify the prospectus student data. The detail MOORA implementation and Web application development are presented in this work. The proposed application has been examined and presented to the institution committee board. The results can be used to decision support for tuition fees policy applied in the State Polytechnic of Malang.

Keywords: UKT, MOORA, Decision Support System

I. INTRODUCTION

Single Tuition (UKT) is applied in the financing system that has to be borne by the State University student which is under the Ministry of Research, Technology and Higher Education (Kemenristek Dikti). In this case, the financing of lectures unlike in the previous times where students tuition are comprised of several kinds of separate components, eg 'SPP', Lab Fee, Parent Contribution '(IOM)', Thesis Exam Fee, Graduation Fee, Donation for Education Improvement (SPKP), and others. Through the application of UKT of Single Tuition means that there is only one type of tuition fees will be charged to students. The latest regulatory which cover UKT implementation is Regulation of Ministry of Research, Technology and Higher Education of the Republic of Indonesia Number 22 The year 2015 Concerning the Single Tuition Fee and Single Tuition On State Universities in the Environment of Ministry of Research, Technology and Higher Education. UKT is part of the Single Tuition Fee (BKT) which impose on each student based on their economic capabilities. BKT is the total of operational costs of education per student per semester on a specific course. UKT is determined based on BKT deducted by cost which has to be borne by the Government

One of the important aspects referred to in the implementation of UKT is that the imposition of tuition fees adjusted to the economic capability of each student. Therefore, in the application or implementation of UKT in state Universities has been generated UKT categories charges, so in addition to accommodate community members who can not afford economically to higher education, Universities revenue targets for the implementation of education operational costs can also be achieved.

In determining the students into groups of UKT that are based on the economic capacity of the students, several things need to be done is to develop the details of the criteria that are intended to filter (filter) and categorize (classify) a student into categories of UKT aforementioned based on economy capability and most importantly, involving the information technology excellence in developing a Decision Support System Application in the Determination of Students UKT.



II. MATERIAL AND METHOD

In this chapter describes the research methods used and the concept of creating the system, so that every stage of the research can be done properly.

A. Multi-Objective Optimization by Ratio Analysis

This Multi-Objective Optimization by Ratio Analysis (Moora) Methods is a method introduced by W.K.M. Brauers et.al. [1]. This relatively new method was first used by the Brauers in a multi-criteria decision. Moora method has a degree of flexibility and convenience to be understood in separating the subjective part of a process of evaluation criteria into decision weights with multiple attributes of decision making Mandal and Sarkar [2]. This method has a good level of selectivity because it can determine the purpose of the conflicting criteria. Where the criteria can be worth the benefit (benefit) or unfavorable (cost).

Moora methods are widely applied in areas such as management, construction, contractor, road design, and economics. This method has a good level of selectivity in determining an alternative. The approach taken by Moora is defined as a process simultaneously to optimize two or more conflicting matter on some constraints Attri and Grover [3].

In the application method of Moora in solving the problem of supplier selection of chemicals, and biotechnology by applying fuzzy and Moora. The resulting decision-making model is able to carry out a continuous evaluation in problem-solving of supplier selection and evaluation issues Seema et. al. [4].

Moora method consists of five main steps ([1], [5–8]) as follows method consists of five main steps as follows:

- Step 1: The first step is to determine the purpose and identify the attributes of the respective evaluation.
- Step 2: The next step displays all the information available to the attributes in the form of a decision matrix. x is the value of each criterion that is represented as a matrix x shown in Eq. (1).

$$x = \begin{bmatrix} x_{11} & x_{12} & \dots & x_{1n} \\ x_{21} & x_{22} & \dots & x_{2n} \\ \dots & \dots & \dots & \dots \\ x_{m1} & x_{m2} & \dots & x_{mn} \end{bmatrix} \quad (1)$$

- Step 3: [1] concluded that the denominator, the best choice of the square root of the sum of the squares of each alternative per attribute. This ratio can be expressed as follows.

$$X_{ij}^* = \frac{x_{ij}}{\sqrt{\sum_{j=1}^m x_{ij}^2}} \quad (2)$$

where x_{ij} is a response of alternative j on objective i ; $j = 1, 2, \dots, m$; m is the number of alternatives; $i = 1, 2, \dots, n$; n is the number of objectives; X_{ij}^* is a dimensionless number representing the normalized response of alternative j on objective i .

- Step 4: for multi-objective optimization, the results of normalized is the addition in term of maximizing result

(from favorable attribute/benefits) and a reduction in terms of minimizing (from attributes which unfavorable/cost). Furthermore, the optimization becomes:

$$y_i = \sum_{j=1}^g x_{ij} - \sum_{j=g+1}^n x_{ij} \quad (3)$$

Now where g is the value of the criteria to be maximized, $(n - g)$ is the value from criterion that is minimized, and y_i is the value from the alternative normalization assessment in relation to all attribute. In some cases, it is often observed some other more important criteria. ordered to give a more important attribute, it is done with the corresponding weights (significant coefficient). When the weight of this criteria is taken into consideration, the y_i equation can be described as following:

$$y_i = \sum_{j=1}^g w_j x_{ij} - \sum_{j=g+1}^n w_j x_{ij} \quad (4)$$

Where w_j is the weight from attribute j .

- Step 5: The value of Y_i can be positive or negative depending on the maximum number of (criteria benefits) and minimal (criteria unfavorable) in the decision matrix.

B. Business Process

Process depicted in Figure 2.1 is admin of academic uploads the new students data to the Information Systems determination of UKT, students can log in using the test number and password in accordance with the time they enroll to fill the student's economic capabilities data, within the limits of the allotted time, furthermore, decisions makers team by accessing the system determines the range of scores of each UKT, the determination of the range of scores is used to display the UKT information of each group of students. The data is used by a team of decision-makers to determine the UKT group of each student.

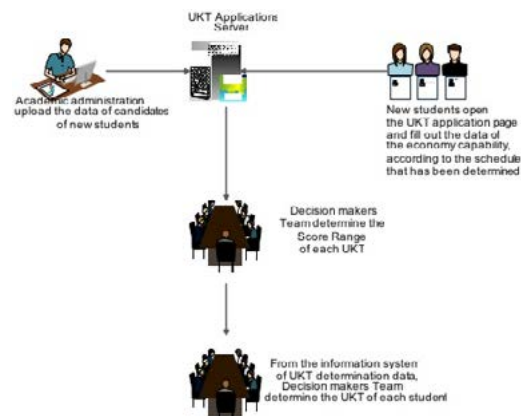


Figure 2.1. The Process of UKT Determination

C. Flow Chart of Design System

In this study the weighting of criteria, sub-criteria and data value of economic capacity all the students whose UKT will be



determined is a unit of data to be processed in the determination of the Decision Support System of Students UKT determination using the MOORA method. The decision maker team only able to determine the value range of each UKT group after all the data of economic capability of students per period and the line entrance has been filled during the specified time limit.

In Figure 2.2 below is an overview of the system flowcharts, Decision Support System of Students UKT determination using MOORA method.

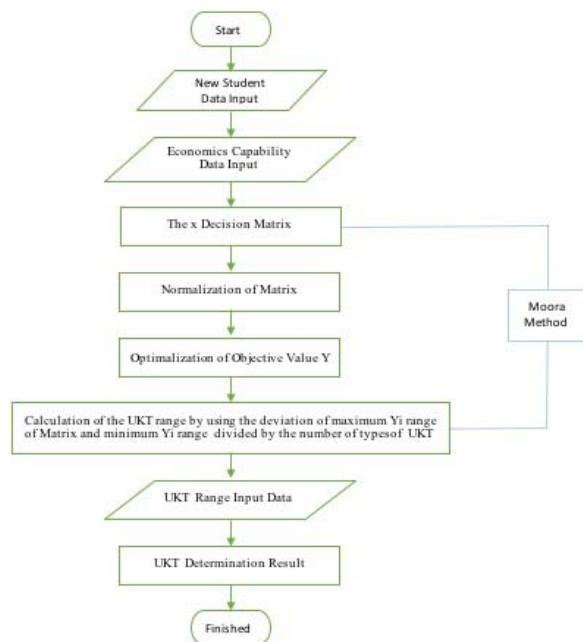


Figure 2.2 Overview of the Flow Chart System

III. RESULTS AND DISCUSSION

A. Implementation

Implementation is the process of changing a system that has been designed in use case form and then implemented in the program code. In Figure 3.1 Academic administrators have access rights to log in, CRUD (Create Read Update Delete) Line entrance data, new student data, the program studies data and log out.

Finance Admin have access rights to log in, CRUD (Create Read Update Delete) UKT type data, the tuition data and log out.

The team of Decision Makers has access rights to log in, CRUD (Create Read Update Delete) Sub Criteria data, Criteria weighting of data, Range Score of UKT., Viewing results on Ranking. RU (Read Update) students economic capability data and logout.

Super Users have access rights to log in, CRUD (Create Read Update Delete) the period data, Permissions, Application Menu, User, Group Menu, Menu Permissions and logout.

Students have access rights to log in, add and view the document of economic capabilities data of the student respectively, logout.

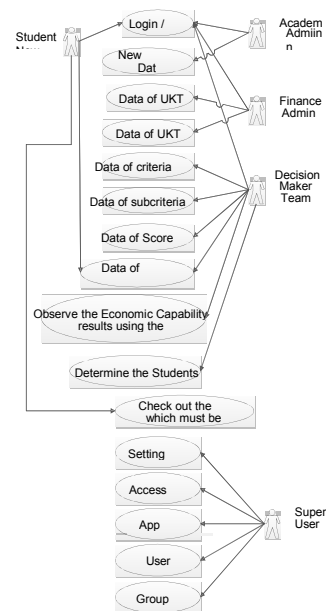


Figure 3.1 Use case Design of Decision Support System of student's UKT Determination

B. Test/ Trial

After the process of implementing the system design, the next stage is the process of testing and analysis of the results of implementation. The testing process conducted in three ways, namely functional test, manual calculation test, system calculation test. Tests conducted aims to ensure that the system constructed has been running as expected.

C. Functional Test

Functional tests are used to determine whether the system is built in accordance with the needs of the user. The test is done by using a black-box. A functional test is considered successful if the function of the existing decision support systems of student's UKT determination is in accordance with the user's expectation.

D. Manual Calculation Test

Manual calculation using the MOORA method, using 30 sample data of economic capabilities of students, which is obtained from the academic department of Polytechnic of Malang. In addition has been entered 2 default data, with 1 data of maximal value, and 1 data of minimum value. Below is a flowchart of the Moora Method calculation as displayed in Figure 3.2.

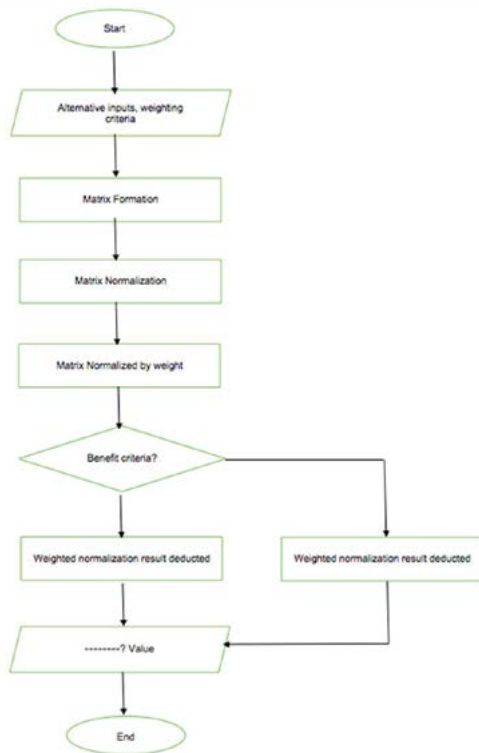


Figure 3.2 Flowchart of MOORA Calculation Method

IV. CONCLUSION

Based on research conducted by the author on The Decision Support System of Single Tuition Determination of Polytechnic Student Malang using the MOORA method, it can be deduced the following matters; by using the method of MOORA, the level of precision in calculating the ranges value between groups UKT is better than using the previous calculation method (as the range of each UKT is equal) and the MOORA method which can be implemented in the determination of this student Single tuition can be demonstrated in Table 6.10 The Comparison of Ranking Results, by using this method The Single Tuition revenue could be bigger compared by using the previous calculation method. However, to improve the accuracy of Single Tuition Determination System Development of Malang Polytechnic Students, moving forward, is expected to consider matters following; there should be other additional

methods used to compare the ranking and determination on Single Tuition based on the economic ability of students and it is necessary to perform 'the weighting' of each criterion.

VII. ACKNOWLEDGMENT

The author would like to thank to Kemenristekdikti and Polinema for their support.

REFERENCES

- [1] W.K.M. Brauers, E.K. Zavadskas, F. Peldschus, Z. Turskis., (2008), Multi-Objective Decision-Making for Road Design, Transport, Volume 23, Number 3, pp. 183-193, Taylor and Francis.
- [2] U.K. Mandal, B. Sarkar, (2012), Selection of Best Intelligent Manufacturing System (IMS) Under Fuzzy Moora Conflicting MCDM Environment, International Journal of Emerging Technology and Advanced Engineering, Volume 2, Number 9, pp. 301-310, IJETAE.
- [3] R. Attri, S. Grover, (2014), Multi-Objective Decision-Making for Road Design, International Journal of System Assurance Engineering and Management, Volume 5, Number 3, pp. 320-328, Springer.
- [4] Seema, R. Kaur, D. Kumar, (2014), Designing A Mathematical Model Using Fuzzy Based Moora Method for Supplier Selection, International Journal of Advanced Engineering Technology, Volume V, Number 1, pp. 16-24.
- [5] S. Chakraborty, (2011), Applications of the MOORA method for decision making in manufacturing environment, International Journal of Advanced Engineering Technology, Volume 54, Number 9, pp. 1155-1166, Springer.
- [6] V.S. Gadakh, (2011), Application of MOORA method for parametric optimization of milling process, International Journal of Applied Engineering Research, Volume 1, Number 4, pp. 743-758, Integrated Publishing Association.
- [7] B. Singaravel, T. Selvaraj, S. Vinodh, (2016), Multi-Objective Optimization of Turning Parameters Using the Combined Moora And Entropy Method, Transactions of the Canadian Society for Mechanical Engineering, Volume 40, Number 1, pp. 183-193.
- [8] D. Kalibatas, Z. Turskis, (2008), Multicriteria Evaluation of Inner Climate by Using Moora Method, Information Technology and Control, Volume 37, Number 1, pp.79-83.



LiFi As An Emerging Technology To Be Utilized in Indonesia

Lesti Setianingrum

Centre of Technology for Electronics
 Agency of The Assessment and Application of Technology
 (BPPT)
 Jakarta, Indonesia
 lesti.setianingrum@bppt.go.id

Sasono Rahardjo

Centre of Technology for Electronics
 Agency of The Assessment and Application of Technology
 (BPPT)
 Jakarta, Indonesia
 sasono.r@bppt.go.id

Abstract— The needs of internet connection for supporting internet connectivity and social media access become much more important. Many places, nowadays, are connected with Wireless Fidelity (WiFi) services to answer these needs. The WiFi which uses radio waves has limitation on capacity spectrum and bandwidth. So that, it may cause trouble related to spectrum crunch and over bandwidth. Meanwhile, recently Light Fidelity (LiFi) technology has been developed in some countries, where data is transmitted via LED's light while it is illuminating. LiFi becomes an emerging technology to answer bandwidth problem in the near future where telecommunication are expected grow highly. Since, LiFi provides the possibility of the real wireless broadband services. Furthermore, it gives no harmful effect to human body, since light spectrum has no electromagnetic interference. This paper shows literature study of the possibility of LiFi technology application for Indonesia. This technology will be one of the best solution to balance telecommunication technologies available to get maximum access, secure transmission and much wider bandwidth for the coming 5G technology demands.

Keywords— Light Fidelity (LiFi); telecommunication; spectrum crunch; wireless broadband; 5G technology

I. INTRODUCTION

Social media becomes a huge and an effective tool for any purpose to achieve a goal. Since now on, almost everyone has account to at least one of social media. Then it is used for any campaign, business, entertainment and also government uses it for official page to give information to all citizen. A survey result concludes that Facebook has been being a king of social media with 1.590 Million active users all around the world [2]. On the other hand, another survey says that traffic for internet video has been increasing 48% per year which is supported with video services such as Netflix and Youtube, and now they share 50% of internet traffic [1]. It shows that data traffic and video traffic will continue increasing in line with people lifestyle who spend their time to internet contents.

Indonesia almost has the same condition which ranks 6th on most internet users in the world [3]. In fact, survey conducted in 2016 says that there are 132.7 Million of internet users in Indonesia and 65% of them come from Java island as shown

in Fig.1 [4]. This is quite a huge number of internet users for Indonesia as a developing country, unfortunately it is not in line with internet connectivity in some areas such as basement, lift or room and rural areas as well which still cannot be established. Average speed of internet connectivity data in 2016 says that Indonesia ranked 80th in the world with the speed are around 6.7Mbps [5], whereas Asian countries such as South Korea, Japan and Singapore are ranked among the tops in the world in the speed of internet connectivity. In South East Asia level, Indonesia is left behind by Thailand, Malaysia and Vietnam. This is very contrast condition between internet user population and internet connectivity in Indonesia.



Figure 1. Internet users penetration in Indonesia [4]

Internet infrastructure is one of the main parts of whole system which can bring good internet connectivity, and it should be concerned along with the very fast growth of internet users demand. Almost 50% internet users in Indonesia is using mobile access for their connection [4]. It means that wherever they are, they need to be connected to the internet. That is why nowadays Wireless Fidelity (WiFi) is utilized in many, both paid and free, hot spot areas, whereas the number of internet users increases then it affects the traffic much heavier and consecutively reliability will be decreased.

The rapidly dwindling RF spectrum along with increasing wireless network traffic has substantiated the need for greater bandwidth and spectral relief. Take a look at these condition, Indonesia government tries to increase capability of internet connectivity and spreads its penetration by deploying a broadband infrastructure program called Palapa Ring which will connect several islands in Indonesia using fiber optic as



backbone of telecommunication. Some telecommunication industries has deployed fiber optic as backhaul and spreading Fiber to The Home (FTTH). Thus in the near future, all of these can support the Visible Light Communication (VLC), it is an emerging field in Optical Wireless Communication (OWC) which utilizes the superior modulation bandwidth of Light Emitting Diodes (LEDs) to transmit data

II. LiFi

A. LiFi and WiFi

WiFi and mobile communication operated on radio frequency which has limitation on capacity, in the near future will be burdened much heavier traffic density of data transmission then eventually going to be overwhelmed in providing it services. If no one concerns about this problem, spectrum crunch will happen in line with emerging Internet of Things (IoT) which needs big connection. Dr. Harald Haas, who has idea of LiFi said that LED-based Li-Fi could reach data rates of 10 Gb/s^[6]. It uses light wave spectrum which not yet utilized, with narrow spectrum it has no limitation for bandwidth. The main reason to choose light is because of harmless biological and environmental effect and widely available as an infrastructure globally. If we compare to Wireless Fidelity which uses radio wave spectrum, Light Fidelity (LiFi) has much higher speed and broader spectrum. Beside it is more secure than WiFi because we can see the network territory and difficult for hijacking.

Table 1. Comparison WiFi and LiFi^[7]

Parameter	LiFi	WiFi
Speed	High	High
Spectrum	10,000 times broader than WiFi	Narrow spectrum
Data Density	High	Low
Security	High security due to non penetration of light through walls	Less secure due to transparency
Reliability	Medium	Medium
Bandwidth	High due to broad spectrum	Low
Transmit/Receive Power	High	Medium
Ecological Impact	Low	Medium
Device to Device Connectivity	High	High
Obstacle Interference	High	Low
Bill of Material	High	Medium
Market Maturity	Low	High
Latency	In the order of microseconds	In the order of milliseconds

B. Working of LiFi

LED as light source has a very potential opportunity to be developed since it can be flickered faster than human eye can detect. This means also optical wireless communication technology may grow faster. The invisible on-off activity enables data transmission using binary codes. Modulation is so rapid that humans cannot notice it. A light sensitive device

(photo detector) then receives the signal and converts it back into original data.

Visible Light Communication (VLC) uses light visible light between 400 THz (780 nm) and 800 THz (375 nm) as the optical carrier for data transmission and for illumination. It becomes LiFi's reference for using rapid pulse of light to transmit information.

A server is responsible for managing traffic and sending information service. Overhead lamp is fitted with LED (Fig.2) streams data to the photo detector. Device will receive information using photo detector which converted back to the original data.

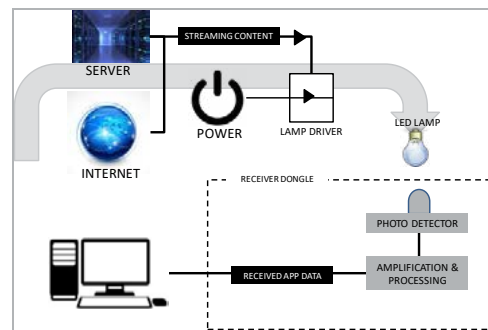


Figure 2. Working of LiFi

C. Application of LiFi^[8]

•Healthcare Field

Using radio waves for wireless technology in hospital can make harmful in operating rooms and interference with medical equipment in hospital. Thus LiFi may become a solution because it harmless and larger spectrum.

•Aviation Industry

When we use airplane, we must turn on flight mode to reduce interference of radio waves, but by utilizing lamp on airplane we can use LiFi for communication.

•Chemical Industry

Chemical or petrochemical industries is sensitive to frequencies harmful. LiFi based on visible light communication can utilize lamp on industry for transmission.

•Office and Institute Use

We are presently using Wi-Fi in office and education institute for data transmission and internet access, which is limited in bandwidth. Thus, we can adopt LiFi to existing lightening system to communicate at the speed of light without worrying about bandwidth.

III. POTENTIAL LiFi APPLICATION IN INDONESIA

A. Hospital

In many countries, over half of the population uses mobile phones and the market is growing rapidly. Mobile phones emit electromagnetic radiation in the microwave range, and the exposure of these electromagnetic (EM) fields emitted by mobile phones has greater possibility of causing adverse health effects.



In hospitals, emergency situation occurs very frequently and this may threaten patient's life. It is very time-sensitive for a responsible personnel to react to the emergency calls. Many hospitals are using WiFi to assist the activities of data transmission connections. WiFi which uses radio waves is actually contrary to the conditions in the hospitals filled with medical equipments which cause interference with radio waves. Using LiFi, wave interference and harmful body can be avoided, furthermore data transmission for the purpose of patient information as well as hospital management information sharing can be conducted with much higher speed than WiFi.

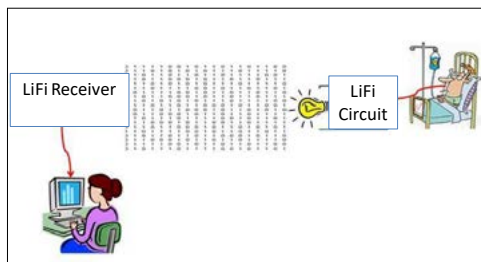


Figure 3. Working model LiFi in hospital^[9]

B. Indoor Communication

Global 2014 Ericsson ConsumerLab study of 23 countries established that consumers spend 77 percent of their day indoors^[11]. It means that many people who connect to internet and enjoying internet activity mostly conducted indoor. For more, many hot spot are deployed in building area to cover internet connectivity and supporting fixed broadband which has not yet cover wider area. With many hot spot, wave interference is easy to happen, bandwidth limitation will also happen in line with heavy traffic. And all of these connectivities mostly are just supported by Base Transceiver System which means power loss to cover both indoor and outdoor communication will increase sharply.



Figure 3. Percentage of Location Experience for Internet Activity^[11]

By the fact of indoor activity, all buildings and offices have well equipped with lighting system and it always on even in daylight. With the incoming of LiFi technology, the light does not just have a function as lighting but can also be functioned as a data transmission. With this technology we can create indoor optical wireless network by using existing lighting system which already set up on buildings. Bring LiFi for indoor communication, not only reducing waves

interference in a room but also reducing power loss of BTS. So, BTS can be focused to cover outdoor communication for power efficiency. Beside, it can be an opportunity to make new business for Power Line Communication Hybrid with Fiber Optic Communication, electricity company has possibility to be a telecommunication provider as LiFi using light electricity in buildings.

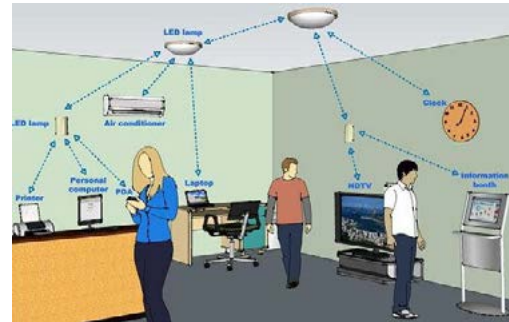


Figure 4. LiFi application in building (illustration)^[12]

C. Transportation

Traffic congestion problem is a phenomena which contributed huge impact to the transportation system in a country. This causes many problems especially when there are emergency cases at traffic light intersections which are always busy with many vehicles. The traffic control system in Indonesia has not been equipped with appropriate method when emergency case occurs. Most traffic lights in big city of Indonesia have used LED lamp. This can be used for vehicle-to-vehicle and vehicle-to-roadside communications. This can be applied for road safety and traffic management purposes.

Public transportation in Indonesia somehow has no stability of internet connectivity. Communication on public transportation such as train or bus come from handover processed by nearest Base Transceiver Station (BTS) while moving. The unstable of handover process causes latency and/or missing signal in some area or sometimes blank spot. On the other hand, this process needs high power to back up transmission data inside the vehicle. So, LiFi can be one of solution for transmission inside the vehicle by using lamp and radio waves covered transmission outside the vehicle. By balancing several technology it can reduce power consumption for BTS and make better connection to achieve customer satisfaction for internet connection service.

IV. CONCLUSION

As many other countries are trying to develop LiFi for any sector, Indonesia has chance to develop LiFi as this technology brings much wider spectrum and bandwidth, more secure, more cost efficient, more environmental friendly. Hospital, indoor communication and transportation sectors can become the right fields for the development of LiFi system, as hospital is critical place which needs more secure condition to avoid harmful and medical equipment interference. Building, where lighting system is utilized, can reduce wave interference



and spectral relief. Furthermore in the transportation field, the LiFi implementation may be developed as vehicle to road side communication or communication inside the public transportations by utilizing the lighting system inside.

All sectors have their own impact to each field. But the most important thing is, visible light wave spectrum is much wider than radio wave, it offers much more bandwidth capacity and it is not yet utilized as a communication media. This excess can answer a variety of problems that arise about the spectrum crunch, wave interference, etc. The emerging technology LiFi which uses VLC utilizing LED lamp as media transmission becomes an opportunity for human history to create many innovation on several sectors. LiFi is one of the best solution candidates which brings green technology even green networking.

REFERENCE

- [1] <http://www.smartinsights.com/social-media-marketing/social-media-strategy/new-global-social-media-research/>, April 2016
- [2] Sandvine report, "Global Internet Phenomena (Latin America & North America)", September 2015
- [3] https://www.kominfo.go.id/content/detail/4286/pengguna-internet-indonesia-nomor-enam-dunia/0/sorotan_media, 2014
- [4] APJII report, "Infografis Penetrasi & Perilaku Pengguna Internet Indonesia", Asosiasi Penyelenggara jasa Internet Indonesia, 2016
- [5] <https://www.harianaceh.co.id/2017/03/13/kecepatan-internet-indonesia-naik-72-dan-kini-pepet-singapura/>, 2017
- [6] <http://spectrum.ieee.org/tech-talk/semiconductors/optoelectronics/laser-lifi-could-blast-100-gigabits-per-second>
- [7] Anurag Sarkar, Prof. Shalabh Argawal, Dr. Asoke nath, "Li-Fi Technology: Data Transmission through Visible Light", International Journal of Advance Research in Computer Science and Management Studies ISSN 2321-7782 Vol 3, Issue 6, June 2015.
- [8] Gurbinder Singh, "Li-Fi – An Overview to Future Wireless Technology in Field of Data Communication", Journal of Network Communication and Emerging Technologies Vol 5, Issue 1, November 2015.
- [9] Dr. S. Shuda, Ms. Indumathy D, "Patient Monitoring in The Hospital management Using LiFi", IEEE International Conference on Technological Innovations in ICT For Agriculture and Rural Development, 2016
- [10] Hyung Jae Chang, "Framework for Data Communication in the Hospital using Li-Fi Technology", International Journal of Scientific & Engineering Research, Volume 7, Issue 8, August 2016.
- [11] <https://www.ericsson.com/res/docs/2015/consumerlab/ericsson-consumerlab-the-indoor-influence-europe.pdf>, 2015
- [12] <http://www.centralvozip.com/wp-content/uploads/2013/10/VoZip-News-Li-Fi-D-Light-Visible-Light-Communication-VLC-Technology-Harald-Haas-Inventor-C3%B3moFunciona.jpg>



QIR

*The Westin Resort
Nasa Dua, Bali*
24-27 July 2017

SYMPOSIUM D

**International Symposium on
Materials and Metallurgy**





THE IMPLEMENTATION OF THE TRACK LINK TANK MANUFACTURING FOR A LIGHT TYPE ARMY TANK AS A SUBSTITUTION IMPORTED

Hafid^a dan Sri Bimo P.^b

^{a,b}Metal Industries Development Centre (MIDC) - Ministry of Industry Indonesia
Jl. Sangkuriang No. 12 Bandung 40135
E-mail : hafidochan@yahoo.com

ABSTRACT

The Indonesia dependency level of track link tank component import are still very high, expensive, and long time procurement, therefore disturb the operational readiness of army tank when needed (Hafid & Sri B.P., 2016). In order to reduce import dependency of track link tank, the implementation of the track link tank manufacturing for a light type army tank as a substitution imported has been done (MIDC, 2015). The purpose of research is to produce the track link tank prototype which required by the user, a good quality and added value with high price competitive. Materials technique that used is steel bainite (Sri B.P, et al, 2015) with the superiority hardness and high tensile strength but still strong (ductile). The implementation methods was taken, which cover: (1) design casting, (2) pattern making, (3) molding sand (4) melting and pouring, (5) heat treatment, (6) testing of mechanical properties before and after heat treatment, namely: tensile strength, hardness test, chemical composition, microstructure analysis by SEM/EDS, ductility test, wear resistance, and (Sri B.P, et al, 2015) (7) application field test a prototype in army tank (Hafid,et al., 2016; 2014). Level 9 of Technology Readiness Levels (TRL) is obtained based on the result of the techno-meter measurement. Based on the economical analysis obtained by the benefit cost ratio (BCR) = 1,67% > 1 (good) (MIDC, 2015). By mastering the technology of the track link tank manufacturing for a light type, we can develop any other the track link tank manufacturing, such as medium tank type of track link tank.

Key words: track link tank, benefit cost ratio (BCR), technology readiness levels (TRL)

1. INTRODUCTION

Foundry Industry is an industry that became the foundation of capital goods which is widely used in various sectors (Hafid, 2014). Casting components are widely used in various industrial sectors, such as: industrial machinery and factory equipment, agricultural industry, textile industry, transportation industry, mining industry, armament industry, medical equipment industry, chemical industry, petroleum, steam power plants, military equipment (Alutsista) etc that is very needed in Indonesia (Hafid,et al.,2016; 2015). Foundry industry also accomodate a lot of employment and increase incomes, reduce dependence on imported components so it would be save foreign exchange, increase non-oil and gas exports, and strengthen the industrial structure and equitable development (Hafid & Eddy Herjanto, 2015).

Casting process technology is one of the metal working techniques capable of producing products with high complexity (Tatang, Roslina & Hafid, 2005). The development of casting technology is needed very much to produce high quality casting



products with specified characteristics, namely, high mechanic and physical properties, minimum content of flaws in casting products, good appearance of casting products, smooth surfaces of casting products, accurate measurement of casting products, high rate of production, and low cost production (Hafid & Sri B.P, 2013; Hafid, Sri B.P & Sony H., 2014; Rochim S., (2015). The improvement of mechanical and physical properties of a metal in a solid state can be performed by a heat treatment, i.e., a combination of solid heating and cooling processes for a certain time period (Hafid & Sri B.P, 2013; Hafid, Sri B.P & Sony H., 2014; Rochim S., (2015).

As we know that the track link tank is a battle vehicles that serves to tread on and drive the tank battle vehicles. Due the function, the materials for these components must have certain mechanical properties, which have a high hardness and tensile strength, but still toughness (ductility) (Hafid & Sri B.P 2013; Hafid, Sri B. P.& Sony H., 2014).

Currently the track link tank for army tank using manganese steel and tempered martensite steel. Both the steel and heat treatment process requires a complex process with long processing times.

Bainite is a material that has a hardness and high tensile strength but still have the toughness. This because it has a hard carbide phase which will take the form of particles evenly dispersed in the ferrite phase ductility.

This invention is the obtaining of new materials for the track link tank for light type army tank, namely steel bainite, which has the required mechanical properties, the heat treatment process is easier than the process of heat treatment of the track link tank previously materials.

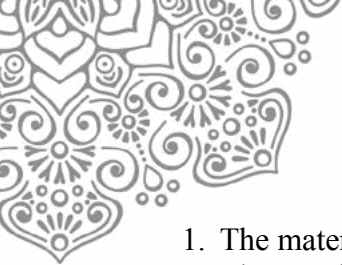
The main purpose of this invention is to produce a materials the track link tank for a light type army tank to replace the material commonly used are manganese steel and tempered martensite steel. Bainite steel used as a new material for the track link for a light type army tank these mechanical properties with the required standard without a complicated process of heat treatment.

Based on the description above, then as an effort to reduce import dependency Indonesia of main defense system equipment and to improve the self-sufficiency of Indonesian National Armed Forces (TNI) armament, a research and development has been conducted to enhance the material properties in producing track link tank adapted to the casting technology in Indonesia so as to produce track link components of high quality and value added at competitive prices.

2. METHODOLOGY

Based on the nature of the problem, this applied research method begins with an analysis of products and materials imported track link tank. Development shape (dimensions) were performed in accordance with the expert judgment of users, namely the TNI-AD. This research was conducted at the workshop foundry and heat treatment MIDC, the Ministry of Industry of Indonesia. Disposable test prototype track link tank, both static and dynamic tests conducted at Cavalry Army Education Center Padalarang.

The research methodology applied was by the following steps of activities (Hafid & Sri B.P, 2013; MIDC, 2015; Hafid, Sri B.P & Sony H., 2014):



1. The materials used: (a) pattern material, (b) sand molding material, (c) melting material.
2. The machines and equipments used: (a) wood cutting machine and pattern creating equipment, (b) sand molding machine, (c) *continue mixer* (capacity 1 tons), (d) induction furnace (capacity 200 kg), (e) Thermocouple, (f) spectrometer, CMM (coordinate measurement machine) gauge, (h) heat treatment machines and tools, (i) machines and equipments for chemical composition test, hardness test, wear resistance and ductilities tests, dye penetrant, SEM and EDS tests.
3. Working stages:
 - a. Working preparation, involving: field survey and discussion with experts of materials, development of an implementation schedule, determination of materials and workforces required, order of working processes, and determination of workshop and productive facilities needed.
 - b. Implementation of works, involving: an analysis of imported track link tank material. Next, a research and development of material for producing a track link prototype was conducted by the stages of processes as follows: casting design, pattern making, molding making, melting and pouring processes, finishing, after casting testing, before and after heat treatment process testing, pin and rubber installation on track link, and track link using test on army tank.

3. RESULTS AND DISCUSSIONS

3.1. Technology

1. The results of prototype production.

This invention relates to new materials (steel bainite) for the track link tank for a light type army tank. The manufacture is using of the casting process, followed by heat treatment process. Stage of the casting process started from making casting design, pattern making from wood, sand mold making, melting and pouring, fettling, testing and quality control after casting. The casting process temperature is was approximately 1.680°C (Hafid & Sri B.P., 2016; MIDC, 2015). The casting process of manufacturing track link tank can be seen figure 1.



Figure 1. The casting process of manufacturing track link tank



The heat treatment process is a process to obtain the mechanical properties of the casting product desired. The heat treatment process (Figure 2) which is used for the material of the present invention is a heat treatment process of normalizing with cooling fan. The track link tank product is heated in the furnace heat treatment at a temperature was approximately 920°C, holding time for 30 minutes, taken out of the furnace, and then cooled with a fan (blower) with a distance of 1 meter up to room temperature.



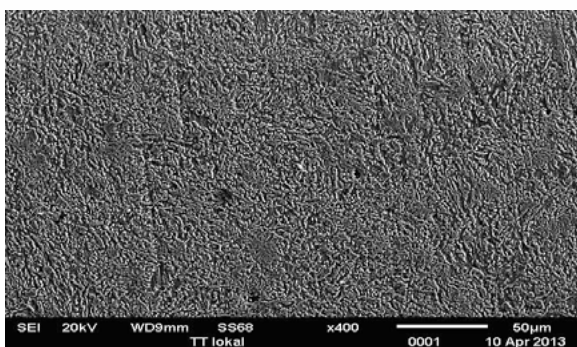
Figure 2. The heat treatment process of manufacturing track link tank

Table 1 below shows the chemical composition of the tread bainite steel the track link tank for a light type army result from this invention.

Table 1 The chemical composition of bainite steel for the track link tank for a light type army tank (wt%)

Carbon (C)	Silicon (Si)	Mangan (Mn)	Posphorus (P)	Sulfur (S)	Chrom (Cr)	Molibden (Mo)	Iron (Fe)	Total
0,25-0,35	0,25-0,35	1,15-1,25	0,008 Maximum	0,010 Maximum	0,85-0,95	0,25-0,35	The balance	100

The combination of Mn, Cr and Mo elements in the variations of quantity, as well as normalizing heat treatment with cooling fan will be able to produce compacted vermicular bainite. From the microstructure material picture of the present invention (Figure 3). Visible bainite formed has a compacted vermicular morphology evenly distributed. The bainite forms of violence and produce a high tensile strength with toughness that is still awake. Expenses incurred on material to be disseminated in all directions so that the value of tensile strength and good toughness. Compacted vermicular phase containing a higher amount of Cr causes the aggregate ferrite (austenite) will be harder than the matrix. The increase in hardness is due to the mechanism of strengthening substitution atoms. Cr atoms replace carbon atoms in the fcc crystal ferrite (austenite) that an increase in hardness.



Magnification 400X

Figure 3. The microstructure material invention

Faster cooling rates experienced by the material imported products as a result of the cooling fan, causing chromium contained in solid solution austenite could not segregated, so aggregate ferrite phase (austenite) containing chromium formed more that will form the compacted vermicular morphology of bainite.

Value of hardness, tensile strength and reduction area of material for each invention is 31 HRC, 96 (kgf/mm²), and 21%. Values of tensile strength and a vast reduction of material of this invention has already exceeded the highest value of the minimum standard of JIS G5111 High Tensile Strength Carbon Steel Casting and Low alloying Steel Casting for Structural Purposes, which is 88 kgf/mm² and 20%, which has a composition similar to the material of invention this.

Disposable test or dynamic function test is done by placing the 2nd prototype track link tank on tank combat vehicles are coupled together with another track link tank. Fighting vehicle tank run with a variety of difficult maneuvers in accordance with the desired operating conditions of the field. Wear test conducted at Kaveleri Army Education Center Padalarang. More details are shown in Figure 4 and Figure 5.



Figure 4. Dynamic function test



Figure 5. Prototype track link



After the function test of the 2nd prototype track link tank is successfully implemented and passed well. 2015 has been mass production ± 7,500 pieces of track link tank in foundry industry. In the exercise of this mass production of researchers served as supervisor to keep track link tank products are made according to the SOP that has been determined.

Technology Readiness Levels (TRL) is a measure of the technology readiness level which interpreted as an indicator that shows how ready or mature a technology can be applied or adopted by users or potential users (Arwanto, et al, 2011; 2013). In technometer there is 9 scale of technology readiness levels. 1-3 scale is the level of basic research technology, a 4-6 scale applied research group, and a 7-9 scale development research (Figure 6) (Arwanto, 2013). The measurement results of R & D technometer of the track link tank manufacturing for a light type obtained levels technology readiness reached level 9 (Figure 7).

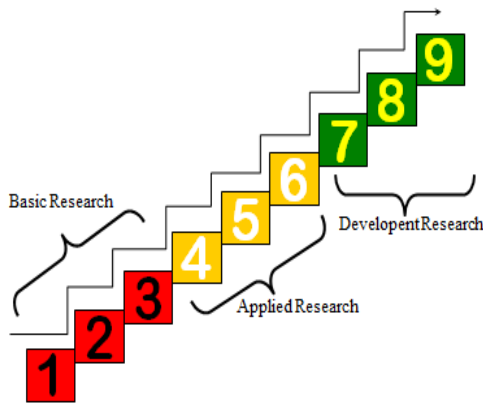


Figure 6. TRL the results R & D

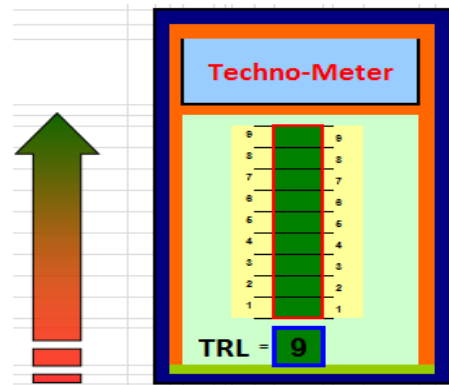


Figure 7. TRL implementation of the track link tank manufacturing for a light type army tank

3.2. Economics

To make a business unit needed capital/investment amount depends on the desired production capacity. Machinery and equipment used is a furnace facilities, equipment and core pattern making, mold manufacturing equipment, testing equipment and quality control, equipment finishing and heat treatment[1]. Operational costs (cost of good sold/CGS) (Hafid, 2016; MIDC, 2015; Horngren, 2008; Baldric S., et al. 2013) of making the track link, include: (1) the cost of materials, (2) labor costs, (3) the cost of machine hours, (4) the indirect costs (over head), (5) the cost of testing, (6) the cost of heat treatment. The results of the calculation of benefit cost ratio (BCR) of the track link tank manufacturing for a light type army tank as follows:

$$\begin{aligned}
 &= \frac{1.875.000.000 \text{ (benefit)}}{1.162.500.000 \text{ (cost)}} \times 100\% \quad (1) \\
 &= 1,61\% \text{ (BCR > 1) (Good)}
 \end{aligned}$$



Based on the calculations results obtained the value of project ($BCR > 1$) so it could be said that the R & D project of the track link tank for the light type is very feasible because it has economically profitable.

4. CONCLUSIONS

The research and development of the track link tank prototype manufacturing for a light type army has been done, made of steel bainite, with the following chemical composition (wt%): C = 0.25 - 0.35; Si = 0.25 - 0.35; Mn = 1.15 to 1.25; P = 0.008 max; S = 0.010 max; Cr = 0.85 - 0.95; Mo = 0.25- 0.35; Fe = Time; with a total overall amount of the chemical composition is 100.

The process for making the track link tank material as mentioned in point 1, where is manufacture of the bainite steel material by using a heat treatment process of normalizing with fan cooling to room temperature.

The process for making the track link tank material as mentioned in items 1 and 2 produce compacted vermicular microstructure of bainite.

The track link tank material for a light type army, made of steel bainite mechanical properties with 31 HRC hardness, tensile strength of 96 kgf/mm^2 , and the value of reduction area of 21%.

It need further research and development any other of the track link tank manufacturing, such as medium tank type of the track link tank.

5. ACKNOWLEDGEMENT

The author would like to thank: (1) the Ministry of Research and Technology of the Republic of Indonesia that has funded research grants Research Incentive SINas 2012,2013, 2015 (2) Director of MIDC (3) technical team and technicians Research Incentive activities 2012,2013,2015, Mr. Abdul Malik, Mr. Edy Suyanto and Mr. Rohendy for them advice and suggestions and all those who have contributed usefull ideas and useful discussion that may not be written one by one.

6. REFERENCES

- Hafid and Sri Bimo Pratomo., (2016), Analysis of Cost of Good Sold the track link tank manufacturing as substitution import, Proceedings of the National Seminar on Industrial Technology, 2016. ISSN: 2355-925X, FTI-USAKTI, Jakarta. pp. 39.
- _____. (2013), Manufacturing track link tank scorpion from CrMo alloy steel casting through the casting process, Journal of Metal Indonesia, Vol.35 No.1, June 2013. ISSN: 0126-3463, Metal industries Development Center (MIDC), Bandung. pp 1.
- Hafid., (2014), Analysis of production facilities on ferrous foundry industry as an effort for competitiveness advantage of companies, Proceedings of the National Seminar on Industrial Technology, 2014. ISSN: 2355-925X, FTI-USAKTI, Jakarta. pp 019-1.
- _____. (2015), Analysis of the workplace culture for continuous improvement on foundry Industries in Indonesia, Proceedings of the 14 th International Conference on QIR. ISSN: 1411-1284. Faculty of Engineering University of Indonesia, Jakarta, pp 1225.



- Hafid and Eddy Herjanto., (2014), Analysis of growth obstacles in national machinery industries and factory equipment, *Journal of Industrial Research*, Vol.9 No.1, ISSN: 1978-5852, Ministry of Industry Indonesia, Jakarta. pp 50.
- MIDC., (2015). The Continuation 3rd year the implementation of the track link tank manufacturing substitution imported to support the self sufficiency of national defense and security system, Final Report of Research Incentive SINas 2015, The Ministry of Research, Technology and Higher Education, Metal industries Development Center (MIDC), Bandung. pp I-4.
- Sri Bimo Pratomo, Hafid, Husen Taufiq, et al, (2015), Morphology the structure and mechanical properties and wear of normalizing bainitic steel with various manganese for track link of combat vehicle, *Journal of Metallurgy*, Vol. 30 No.2, August 2015. ISSN: 0126-3188, Metallurgy and Materials Research Center LIPI, Serpong, Tangerang. pp 55.
- Tatang Taryaman, Roslina and Hafid, 2005. Casting defect of fly wheel product as the results of casting process by sand moulding, *Journal of Metal Indonesian*, Vol.027 / 2005. ISSN: 0126-3463, Metal industries Development Center (MIDC), Bandung. pp 44.
- Hafid, Sri Bimo Pratomo and Sony H., (2014), The development of process technology of track link tank scorpion to countermeasure defects at casting product , *Journal of Industrial Research*, Vol.8 No.1, April 2014 ISSN: 1978-5852, Ministry of Industry Indonesia, Jakarta. pp 2,3.
- Suratman, Rochim., (2015), Competency of Human Resources Deevlopment (HRD) foundry industries, Workshop the Development of Foundry Industry for Advanced Materials, Date. October 2nd, 2005 in Bandung, MIDC Ministry of Industry Indonesia, Bandung. pp V-8-V-14.
- Ahmad T.J and Waspodo., (2010), Improvement of mechanical properties of nodular cast iron by of alloy and heat treatment austempering, *Journal of Metal Indonesian*, Vol. 32 No. 2, December 2010, ISSN: 0126-3463, Metal Industries Development Centre (MIDC), Bandung. pp 21.
- Arwanto, et al, (2011), Handbook: measurement of the Technology Readiness Levels (TRL), BPPT, Serpong, Tangerang, pp 8.
- Arwanto, Kuncoro Budy Prayitno., (2013). Techno-Meter measurement of the technology Readiness Levels (TRL), <http://www.gin.web.id/index.php>. pp.3.
- Horngren, Charles T. (2008), *Cost accounting a managerial emphasis*, fourth edition, Prentice Hall International Inc. London, pp. 20.
- Baldric Siregar, Bambang Suropto, Dody Hapsoro, et al. (2013), *Cost accounting*, 2nd Edition, Publisher by Salemba Four, Jakarta, pp. 28-31.



ENHANCEMENT OF CUI INSPECTION ON INSULATED DEAD-LEG PIPING IN LNG PLANT BONTANG

I Wayan Yuda S.^{a,1}

^aTechnical Department, PT Badak NGL
Bontang 75324, Kalimantan Timur, Indonesia

¹semaradipta@badaklng.co.id

ABSTRACT

Maintaining plant integrity becomes a significant issue to sustain LNG plant operation. A proper decision in developing inspection program and strategy is highly required regarding the issue. In such LNG plant, piping system facilities act as one of important roles in transporting fluid where temperature varies widely from -160°C up to 450°C. On piping system, corrosion under insulation (CUI) is considered as one of the frequent damage mechanism, which may lead to losses of plant integrity. Combination of CUI survey and risk based inspection (RBI) have been implemented effectively to manage this risk. CUI survey was conducted on the line operated under the range of susceptible temperature. However, on the stream operated outside the susceptible CUI temperature range, CUI may still occur such as on dead-leg line. A stagnant flow on dead-leg line generates a thermal gradient compared to its main stream and this condition shifts the temperature into susceptible CUI range, especially in carbon steel pipe. This issue, together with selection on critical point to be inspected will be discussed in the paper. They will govern the success of inspection and improvement program.

Keywords: CUI; Dead-leg; Corrosion; Inspection; Piping System

1. INTRODUCTION

One of the most common issues being faced by gas and oil processing plant is material/metal damage or properties change due to reaction/contact with its environment called corrosion. Various mechanism are defined in regard to corrosion, brought to detrimental effect of economy and environment and a challenge on maintaining plant integrity. Insulation used to serve heat conservation on piping system provides a hidden problem when it leads to CUI. CUI tends to remain undetected until the insulation is removed or when leaks occur. Moreover, when the handled range of fluid temperature is relatively wide as on LNG plant and where numerous dead-leg lines existed, the probability of CUI occurrence will be higher.

This study aimed to classify the critical point to give more detailed area to be inspected on the insulated carbon steel line containing multi-component refrigerant (MCR) fluid in regard with CUI and dead-leg by using Solid Work simulation method.

2. LITERATURE REVIEW

Referring to API 571 [1], CUI is described as corrosion on piping, pressure vessels and structural component resulting from water trapped under insulation or fireproofing. It affects externally insulated piping and equipment and those that are intermittent service or operated between -12°C and 175°C for carbon and low alloy steels.



Dead-leg is a component of piping system that normally has a little or no significant flow. Some examples include blanked (blinded) branches, lines with normally closed block valve, stagnant control valve bypass piping or pressure relieving device inlet, high vents, and drains [2]. Dead-leg and attachment that protrude from insulated piping and operate at a different temperature than the operating temperature of active line are susceptible to CUI [3].

3. DISCUSSION AND RESULT

3.1. Inspection Finding & Suspected Root Cause

Pipe leaking occurred on an online insulated carbon steel pipe SA 333 Gr. 6 containing multi-component refrigerant (MCR) fluid, as shown by Figure 1a. Leakage point was located on upstream block valve of pressure safety valve (PSV), as shown by Figure 1b. The line was then isolated for repair and further investigation. After removing the insulation, it was revealed that the pipe experienced severe corrosion, which leads to metal thinning. Figure 1c visualizes the condition of the pipe.

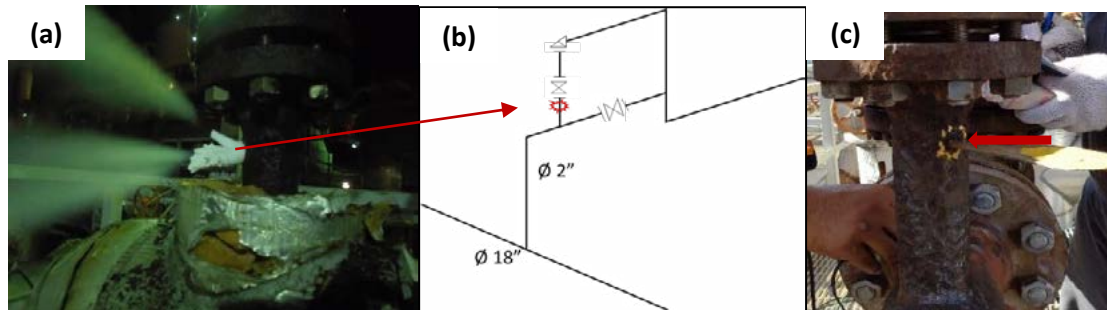


Figure 1 Photograph of leaking pipe; (a) initial pipe condition with insulation and online condition; (b) simplified diagram of leakage location; (c) pipe condition after removing the insulation

The leakage is suspected due to CUI promoted by dead-leg location. Actually, the fluid (MCR) which is transported by the mainstream line has an operating temperature of -34°C . However, increasing temperature on stagnant flow of dead-leg section pipe on the upstream of PSV occurred and generated an undetected active corrosion beneath the insulation. Measurement of actual temperature by using thermo gun on other identical line showed that the actual line temperature reaches 15.9°C .

3.2. Basic Data of Simulation

Table 1 shows the properties of MCR (containing C_1 , C_2 , C_3 , iC_4 , nC_4 , & N_2) in liquid state. The data was taken from actual operating parameters in LNG Plant Bontang. The fluid is flown in a carbon steel pipe (SA 333) totally insulated by 2-inch in thickness of poly-isocyanurate insulation material. By considering the gradient temperature of the environment (33°C) and the fluid temperature (-34°C), continuous heat transferred through insulation and pipe material is calculated to be 9.98 watt/m.

Two different header pipes, 18 and 24-inch in diameter, are combined with 1 and 2-inch in diameter branches in a certain length, as shown by Figure 2. Fluid is continuously flown in the header line. While the end of branch line was isolated by PSV. Then, the behavior of fluid velocity, density, and temperature on the branch line are observed to give the indication of the critical distance where CUI might take place.



Table 1 Properties of MCR in liquid state

Properties		Unit
Density	151.4	kg/m ³
Temperature	-34	°C
Pressure	42	kg/cm ²
Flow rate	15.34 x 10 ³	m ³ /h

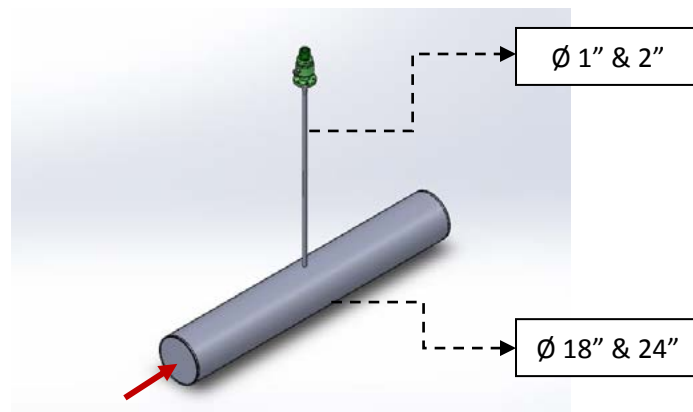


Figure 2 Header and branch pipe modeling by using Solid Works

3.3. Solid Work Simulation Result

As shown by Figure 3a, the flow condition inside the branch line, dead end, is different compared to its header line. The velocity on the branch will decrease as the distance from the header increases. However, the fluid will always be circulated even in a very low velocity (close to 0 m/s). The fluid will be continuously heated up due to heat in leak from the environment, which is transferred through insulation and pipe surface. The fluid density also decreases as distance to the header line increases. This indicates that the fluid tends to change from liquid to gaseous state.

Figure 3b shows the correlation between those fluid parameters with the change in pipe metal temperature. The temperature gradient in the pipe can obviously be seen. Greater the distance from the header line, the higher the pipe temperature as a result of heat absorption from the environment by the fluid inside the pipe, which has a lesser velocity. In a certain point on the surface of the pipe, the temperature reaches -12°C. This point is considered as a critical distance as the temperature is already within the susceptible temperature of CUI occurrence.

Table 2 shows the comparison of critical distance on various sizes of header and branch lines. The critical distance is affected by the size of header and branch. The larger the header size, the higher the critical distance on branch. Moreover, the larger the branch size, the higher the critical distance. It means that a lesser header and branch size will have higher possibility for CUI occurrence. This is caused by the higher the pipe size, amount of fluid which absorb the heat will also be greater.

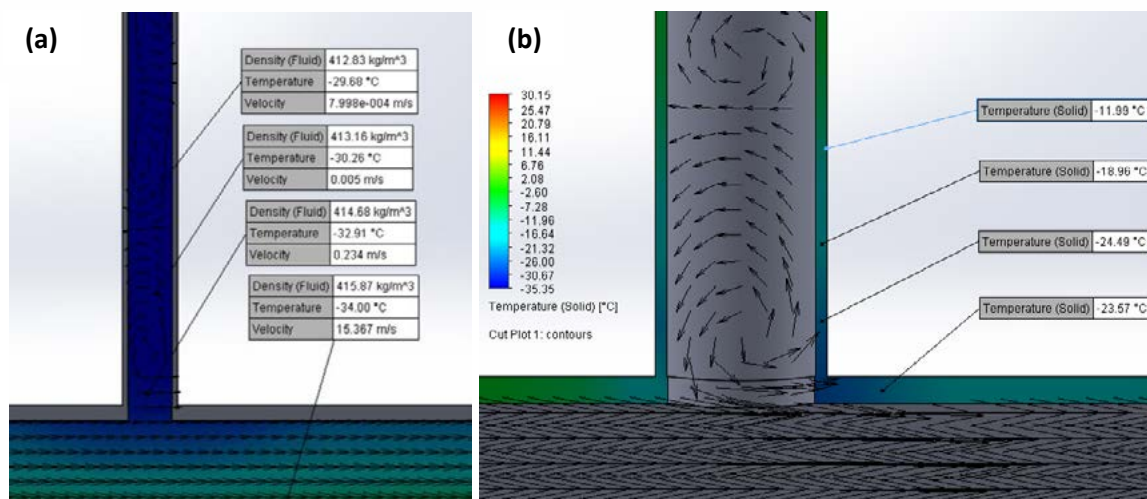


Figure 3 (a) Fluid condition in three parameters (density, temperature, and velocity) inside the branch line; (b) profile of surface temperature on the branch line

Table 2 The comparison of critical distance for different header and branch pipe sizes

Header Line OD (inch)	Branch Line OD (inch)	Critical Distance* (cm)
18	1	5.20
	2	8.03
24	1	6.63
	2	8.12

*Header line contains MCR liquid with temperature of -34°C

4. CONCLUSION

The fluid behavior on an isolated branch line is totally different from its header line. Velocity, temperature, and density of the fluid gradually changes as the distance from header line increases. Header and branch sizes affect the critical distance, which indicates the tendency of CUI occurrence on the branch line.

5. REFERENCES

- API Recommended Practice 571 (2011), Damage Mechanism Affecting Fixed Equipment in the Refining Industry
- API 570 (2016), Piping Inspection Code: Inspection, Repair, Alteration, and Rerating of In-service Piping Systems
- API Recommended Practice 574 (2009), Inspection Practices for Piping System Components



THE CHARACTERIZATION OF PORE STRUCTURE AND CAPILLARY SINTERED BASALT FOR WICK HEAT PIPE DEVELOPED

Luh Putu Ike Midiani^{a,c1}, Wayan Nata Septiadi^{b2}, I Nyoman Suprapta Winaya^b

^a*Program Doktor Ilmu Teknik, Pascasarjana Universitas Udayana, Denpasar-Bali*

^b*Teknik Mesin Universitas Udayana, Kampus Bukit Jimbaran, Badung-Bali*

^c*Teknik Mesin Politeknik Negeri Bali, Kampus Bukit Jimbaran, Badung-Bali*

ABSTRACT

Heat pipe is one of heat transfer device is a passive cooling system. The device uses a certain size which contains a certain fluid functioning as a heat conductor from heat to cold side. Heat pipe contribution to engineering field is as electronic cooling, solar heater, air conditioning and HVAC system. Heat pipe basically consists of three components; they are container, working fluid and wick. A lot of research had been undertaken to develop components of heat pipe. One of components which will be developed in this research is wick structures. It is a component functioning to generate capillary pressure to flow working fluid from condenser to evaporator. Currently, wick is made of metal which is easily oxidized and often caused corrosion problems. This condition will affect the heat pipe thermal performance, force capillarity and working fluid boiling process. An alternative direct method to improve the wick structure of heat pipe is using basalt. Basalt is one of non metal materials, from volcanic lava, having potential as wick material since it does not react with water and inflammable. In addition, it also has hardness and good thermal feature. The purposes of this experimental study are to examine and analyze basalt as a wick structure. This study was undertaken by making basalt powder of 100 mesh. The particle size and shape of basalt powder was measured with SEM. Its chemical composition was tested with EDS. Furthermore samples were prepared in cylinder form with varying of compaction pressure. Samples tested to know the pore structure and capillary pumping amount of basalt. The test result showed that wick pore structure using basalt has a structure which can be used as wick heat pipe with sufficient capillarity force.

Keywords: heat pipe, wick, pore structure, capillary, basalt.

* Corresponding author.

E-mail address: ike.midiani@gmail.com, wayan.nata@gmail.com



1. INTRODUCTION

Heat pipe heat exchanger technology is a highly flexible, capable of transporting large amounts of energy during the heat pipe with a small drop in temperature, so that the equipment with very high thermal conductivity. In the implementation as thermal control, heat pipes have been used in heat pumps, refrigeration, cooling of electronic components and systems other two-phase thermal control (Vasiliev, 2005). Heat pipes can harness solar energy, the heat recovery process (waste heat) or heating fuels as an energy source.

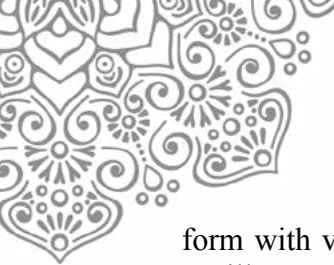
Heat pipe basically consists of three components; they are container, working fluid and wick. A lot of research had been undertaken to develop components of heat pipe. One of components which will be developed in this research is wick structures. It is a component functioning to generate capillary pressure to flow working fluid from condenser to evaporator (Yang, et al., 2016; Deng, et al., 2017; Nishikawara, et al., 2017). Currently, wick is made of metal which is easily oxidized and often caused corrosion problems. This condition will affect the heat pipe thermal performance, force capillarity and working fluid boiling process (Putra et al, 2014).

The wick material other than metal that has been widely researched with the use of biomaterials. Use of the biomaterial is inspired by research on the basic behavior biomimetic at a flow rate of water in the vessels xylem at two plants, *Musa X Paradisiaca* and *Salix Flamingo* (Wang, et al (2014), and has been conducted by the behavior base biomimetic inspire directly or indirectly on wick heat pipe, and biomimetic can be applied to heat pipe modern technology. Research the use of biomaterials as a base material for the wick capillaries have also been carried out by and generate total thermal resistance pipe heat is lower when using the wick capillary with a basis of *Collaria* biomaterial (Putra, et al., 2014). Application of biomaterials tabulate as a wick can reduce thermal resistance by 56.3% compared to the sintered copper wick. However, the use of biomaterials tabulate is feared will disturbed to the survival of corals.

Other natural ingredients that could potentially be used as a wick is basalt which is a natural rock. Basalt is one of non metal materials, from volcanic lava, having potential as wick material since it does not react with water and inflammable. In addition, it also has hardness and good thermal feature (Singha, 2012). Basalt does not react with air or water, when in contact with chemicals, will not form a chemical reaction that is harmful to health or the environment.

As the wick materials, basalt must have several requirements such as permeability, capillarity and good pore structure, because the wick is a component that flow back the working fluid from the condenser to the evaporator by utilizing capillary force (Vasiliev, 2005). Need to do the initial testing and the formation of a good structure that basalt suitable as a wick. Wick performance is strongly influenced by the pore structure for generating capillary pressure in order to flow the working fluid. The speed of flow distribution in the pore structure is strongly influenced pore size distribution (Yang, 2016). Although basalt is a porous media with various dimension, still expected basalt will have a high permeability, porosity and capillary force.

Several tests are performed to see the effect of pore structure to basalt capillary and permeability. The particle size and shape of basalt powder was measured with SEM. Its chemical composition was tested with EDS. Furthermore samples were prepared in cylinder



form with varying of compaction pressure. Samples tested to know the pore structure and capillary pumping amount of basalt.

2. EXPERIMENTAL

2.1. Preparasi Basalt Powder

One of the most important parameters of a porous wick is called capillary pumping amount. That stated the maximum amount of working fluid can be pumped into a porous wick. Must be tested basalt to know the ability of capillary pumping amount of basalt. For this test, basalt samples prepared formed from basalt powder. Preparation of basalt powder made by crushing basalt to obtain a smaller granules. Basalt has been destroyed subsequently sieved to obtain a grain size of 200 μm . Basalt powder with a grain size of 200 μm still have the irregular form. Pictures of basalt and basalt powder shown in Fig. 1.



Figure 1 Basalt and basalt powder

The shape and grain size testing of basalt that has not been uniform is tested by SEM (Scanning Electron Microscopic). It is seen that the form of granules have an irregular shape with a rough surface, as shown in Fig. 2.

Testing with EDS was conducted to determine the chemical composition of basalt. The composition are Si, Al, K, Ca, Fe, Mg, Na, C, Ti where the results are shown in Fig. 3. below.

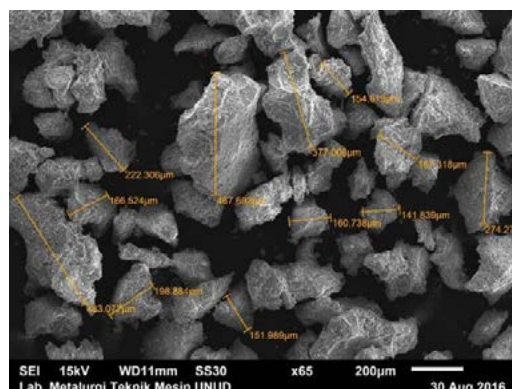


Figure 2 Shape and grain size of basalt powder

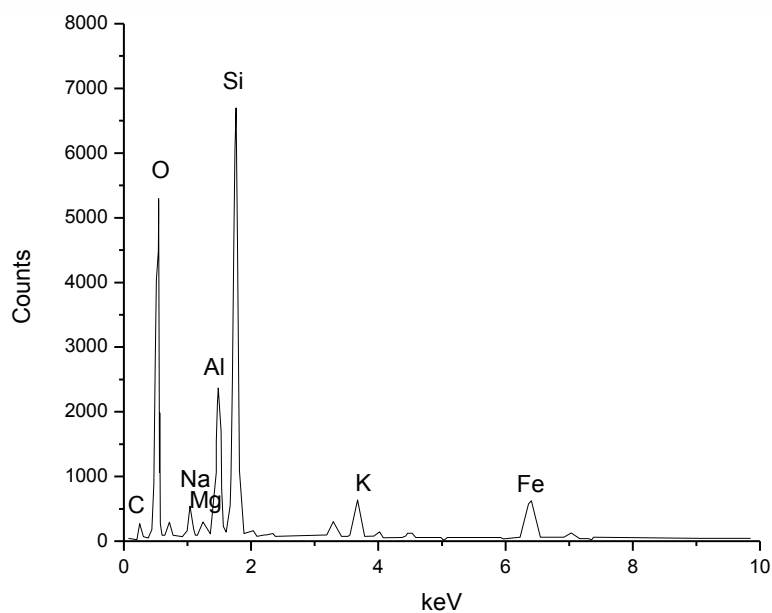


Figure 3 Chemical composition of basalt

2.2. Preparasi Sintered Powder Wick

Sintered basalt samples were made from a 200 μm basalt powder, formed into a cylindrical shape with a diameter of 25 mm and a length of 31 mm. Basalt powder compacted using a compacting machine Prestopress-3 with some variations in pressure of 300, 400 and 500 MPa, compacting temperatures between 140-180°C. Basalt sample need starch as the adhesive, and the composition not exceeding the basalt composition. Basalt samples that have been compacted further tested by SEM to see the pore size distribution of the sample, and further tested the capillary pumping amount. Basalt samples are shown in Figure 4. After got the SEM result, the pore distribution can count by the ImageJ programme. The figure 5 below show the pore distribution of basalt samples.



Figure 4 Basalt samples

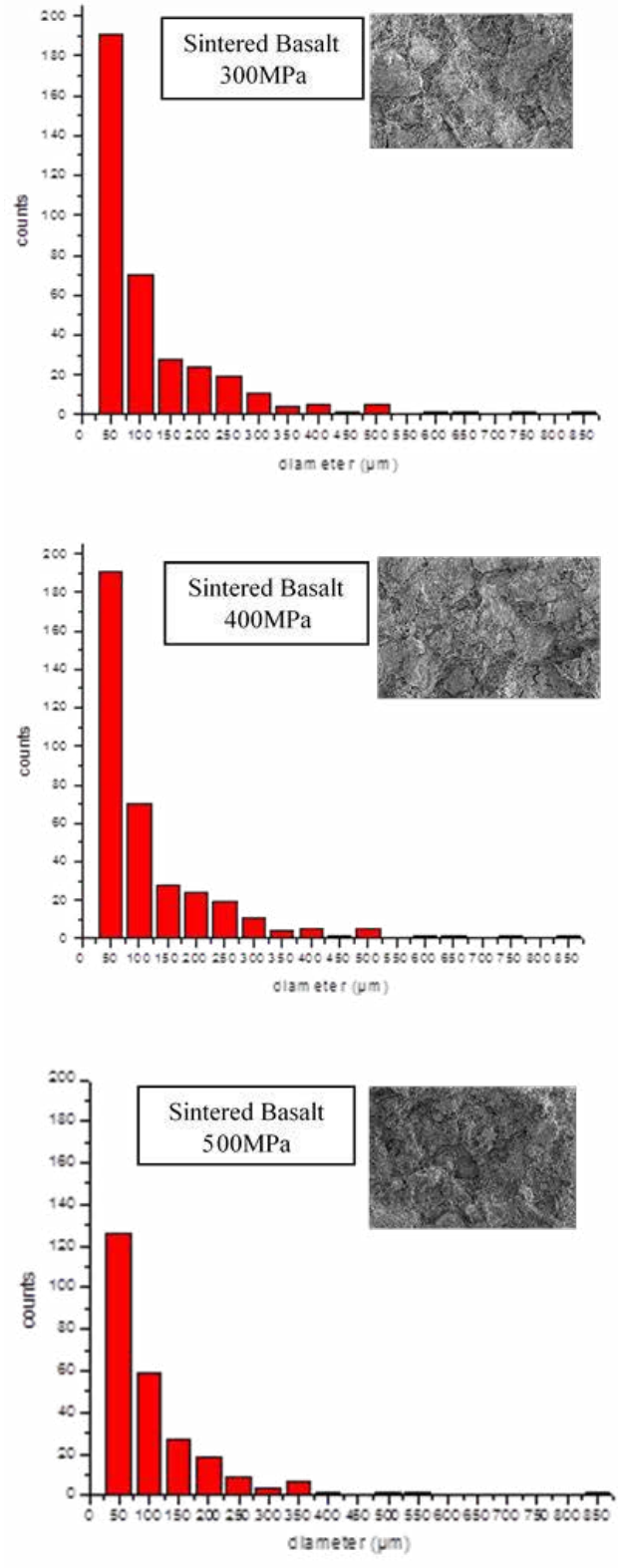


Figure 5 SEM photograph and pore diameter distribution of sintered basalt



2.3. Set Up Eksperimen

Capillary pumping testing methods in basalt samples is based on the testing that was done (Putra, et al., 2014), which measures the amount of fluid that is able to be transported by basalt samples for a time specified. The testing can be seen as in Fig. 6.

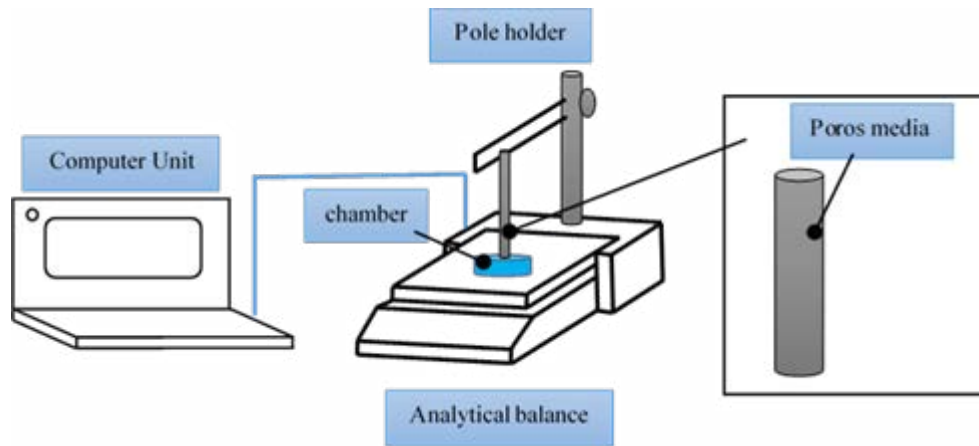


Figure 6 The method of capillary test

Capillary pumping amount testing performed by Archimedes law which states that the weight of the wick weighed when dry and when saturated with water. Basalt samples that have been compacted weighed when dry and after saturated with water. To perform this test prepared a beaker, and electronic scales that connected to the computer. The beaker filled with water placed on electronic scales to determine the weight of the water early. Further samples of basalt dipped into the beaker and begins measuring the weight reduction of water in the beaker. Measurement of weight reduction of water carried to the sample of basalt saturated or can no longer absorb water in the beaker. The amount of water that can be absorbed by a sample of basalt indicated by the electronic scales with the reduced weight of water in the beaker.

For the calculation of the porosity (ϵ) basalt sample is based on the following formula (Putra, et al., 2014)

$$\text{Porosity}(\epsilon) = \frac{\text{volume of pore wick}}{\text{volume of porous media}} \quad (1)$$

The results of porosity calculation of basalt samples shown in Table 1 below:

Table 1 Porosity of Basalt sintered powder

No.	Wick material	Porosity (ϵ) %
1	Sintered basalt 300MPa	36.2
2	Sintered basalt 400MPa	33.3
3	Sintered basalt 500MPa	26.2



3. RESULTS AND DISCUSSION

3.1. Effect of compaction on porosity

The varying pressure compaction during manufacture basalt samples will affect the porosity of the basalt samples. Influence of compacting pressure on the porosity shown in Table 1 and Fig. 7. Fig. 7 shows that the increase in compacting pressure will reduce the porosity of the samples of basalt. A high compacting pressure will form the grains density increase, so the fewer gaps between grains will happen.

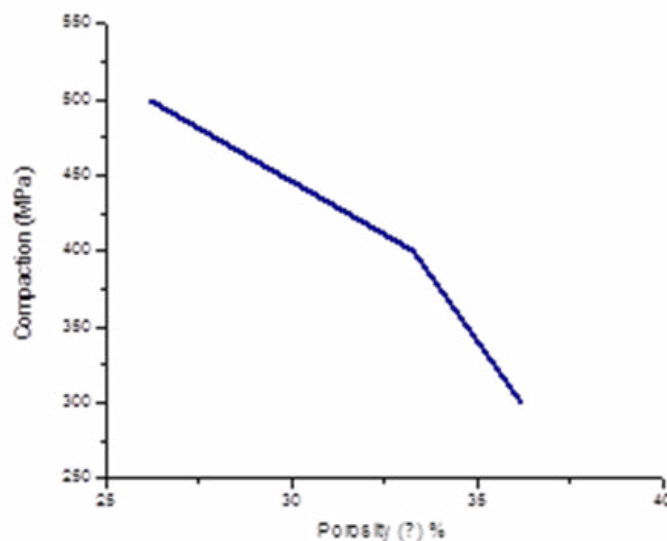


Figure 7 Porosity by varying of compaction pressure

3.2 Effect of compaction on capillary pumping amount

Capillary pumping amount shown in graphical form between the weight of water to the capillary pumping time. From fig. 8 seen within 800 seconds, the sample of basalt with compacting pressure of 300 MPa is able to absorb water as much as 5.5 grams, samples of basalt with compacting pressure of 400 MPa is able to absorb water as much as 5.5 grams and basalt samples with compacting pressure of 500 MPa is able to absorb water as much as 4.5 grams.

The ability of capillary pumping amount of basalt sampel is depends on porosity. Capillary pumping amount meningkat dengan meningkatnya porositas. Fig. 8 shows the capillary pumping amount of basalt sampel.

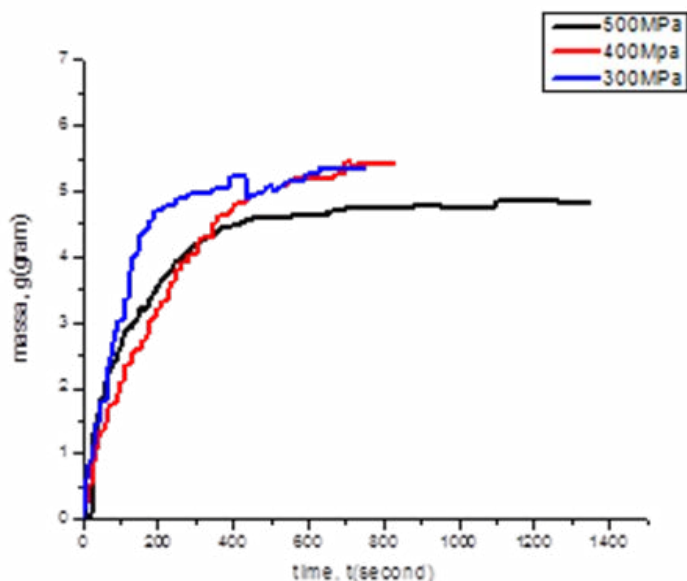


Figure 7 Capillary based on mass amount transported

4. CONCLUSION

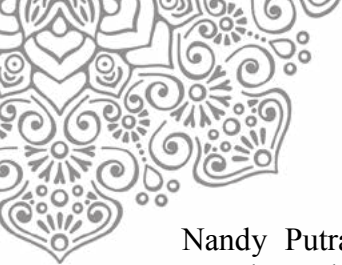
This study was performed basalt as an alternative wick. The ability of the basalt to use as a wick indicated by the test results that basalt can absorb water to a specific period. This basalt capability need to be improved by improving the granular form, or in the process of formation as a wick later.

5. ACKNOWLEDGEMENT

The authors would like to thank the Udayana University. This work is supported by Udayana University's Laboratory and the authors greatly appreciate their support and helpful suggestions.

6. REFERENCES

- Leonard L. Vasiliev, (2005), Heat Pipes in Modern Heat Exchangers, Applied Thermal Engineering, Volume 25, pp. 1-19.
- Peipei Yang, Zhi Wen, Ruifeng Dou, XunLiang Liu, (2016), Permeability in multi-sized structures of random packed porous media using three-dimensional lattice Boltzman metod, International Journal of Heat and Mass Transfer xxx xxx-xxx
- Daxiang Deng, Yong Tang, Guanghan Huang, Longseng Lu, Dong Yuan, (2013), Characterization of capillary performance of composite wicks for two-phase heat transfer devices, International Journal of Heat Mass Transfer, Volume 56, pp. 283-293.
- M. Nishikawara, H. Nagano, (2017), Optimization of wick shape in a loop heat pipe for high heat transfer, International Journal of Heat Mass Transfer, Volume 104, pp. 1083-1089.



- Nandy Putra, Rosari Saleh, Wayan Nata Septiadi, Ashar Okta, Zein Hamid, (2014), Thermal performance of biomaterial wick loop heat pipes with water-base Al₂O₃ nanofluids, *International Journal of Thermal Sciences*, Volume 76, pp. 128-136.
- Kunal Singha, (2012), A Short Review on Basalt Fiber, *International Journal of Textile Science*, 1(4): pp. 19-28.
- Jinwang Li, Yong Zou, Lin Cheng, (2010), Experimental study on capillary pumping performance of porous wicks for loop heat pipe, *Experimental Thermal and Fluid Science*, Volume 34, pp. 1403-1408.
- Jian Zeng, Can Chen, Yong Tang, Xingang Wang, Li Zhang, Shiwei Zhang, Wei Yuan, Jieling Chen, (2016), Effect of powder size on capillary and two-phase heat transfer performance for porous interconnected microchannel nets as enhanced wick for two-phase heat transfer devices, *Accepted Manuscript Applied Thermal Engineering*.
- Y. Qu, K. Zhou, K.F. Zhang, Y. Tian, (2010), Effect of multiple sintering parameters on the thermal performance of bi-porous nickel wicks in Loop Heat Pipes, *International Journal of Heat and Mass Transfer*, Volume 99, pp. 638-646.
- Jeehoon Choi, Wataru Sano, Weijie Zhang, Yuan Yuan, Yunkeun Lee, Diana-Andra Borca-Tasciuc, (2013), Experimental investigation on sintered porous wicks for miniature loop heat pipe applications, *Experimental Thermal and Fluid Science*, Volume 51, pp. 271-278.
- Hamid Ghayour, Majid Abdellahi, Maryam Bahmanpour, (2015), Optimization of the high energy ball-milling : Modelling and parametric study, *Accepted Manuscript Powder Technology*.
- Jian Zeng, Lang Lin, Yong Tang, Yalong Sun, Wei Yuan, (2017), Fabrication and capillary characterization of micro-grooved wicks with reentrant cavity array, *International Journal of Heat and Mass Transfer*, Volume 104, pp. 918-929.
- Mettam, G.R., Adams, L.B. in: Jones, B.S., Smith, R.Z. (Eds.), (1994), *Introduction to the Electronic Age*, E-Publishing, Inc. New York, pp. 281-304.
- Mamat, M., Kusrini, E., Yahaya, A., Hussein, M.Z., Zainal, Z., (2009), Synthesis and characterization of Zn-Al-Anthranilate nanocomposites. *In: Proceedings of the 25th Regional Conference on Solid State Science and Technology 2009*, Perlis, 2 December, Malaysia.



REMAINING LIFE ASSESSMENT OF FIBER REINFORCED PLASTIC (FRP) PIPE IN LNG PLANT AFTER 20 YEARS IN OPERATION

Luthfi Ardiansyah¹

*¹Inspection Engineer, Technical Department, PT Badak NGL
Bontang 75324, Indonesia
luthfi@badaklng.co.id*

ABSTRACT

Fiber Reinforced Plastic (FRP) pipe has been utilized as one of the important part in Oil and Gas Industry including in LNG Production Facilities. Its ability to withstand corrosive fluids and good mechanical properties make the FRP pipe become an option in LNG Plant as cooling water distribution facilities. However, delamination and aging degradation has become big issue in FRP Pipe utilization. Proper method should be applied to assess the reliability and integrity of FRP Pipe facilities especially after reaching lifetime design in operation. One of promising method for this assessment is the Remaining Life Assessment method. This method was applied to one of PT Badak NGL's Process Train (Train G) which has already reached its 20 years' design life. A sample of FRP pipe was taken from 16 inch cooling water outlet of Propane Desuperheater Heat Exchanger, considered as the most critical location with the highest vibration level and minimum remaining thickness. Several analysis methods were carried out to ascertain the actual condition, such as visual analysis, size dimension measurement, and NDT analysis. Pipe characterizations were assessed by using flexural test, tensile test, and hardness test. Creep test has also been conducted to determine the remaining lifetime which is based on time-temperatures superposition principle. Those comprehensive observations are used to determine the estimation whether the FRP Pipe can be used properly for another 20 years. Moreover, there are some inspection programs already obtained after the assessment. Those programs were addressed as the strategic plan to sustain LNG plant operation.

Keywords: Remaining Life Assessment, Fiber Reinforced Plastics, LNG Plant, Process Train.

1. INTRODUCTION

PT Badak NGL operates eight Process Trains (A~H) to produce LNG with maximum annual capacity of 22.5 Millions Tons Per Annum (MTPA). Supporting LNG production, FRP material pipings are utilized to distribute sea water as cooling media for heat exchanger equipment. Since the FRP pipe material is potentially degrade by service condition, evaluation of its reliability after reaching design life becoming mandatory strategy. Remaining life assessment is one of method to determine reliability of equipment to continue in service after reaching its design life. PT Badak NGL already use this method to assess the reliability of Process Trains A until Process Train F, including the FRP piping facilities. So far, these Process Trains are provenly reliable to continue its service for another 20 years. In 2017, one of Process Trains, Train G, will reach its 20 year's design life and its reliability need to be evaluated. This paper will explain the detail study to determine the remaining life of FRP pipe facilities in Process Train G of PT Badak NGL after operating around 20 years. Besides estimating the remaining life, this study were performing several tests and



evaluations considering several damage phenomena like delamination, aging, weathering, and loss of mechanical properties to give a general condition assessment of existing FRP pipes.

2. METHODOLOGY

Actual site assessment such as stress analysis, ultrasonic test and vibration measurement were conducted to determine the most critical location of FRP pipe that can be selected as a sample. Stress analysis was used to calculate stress on all FRP piping to ensure the applied stress is still under the maximum allowable stress of the material and define the critical location. Ultrasonic and vibration measurement were conducted to determine the deterioration level of FRP pipe based on de-lamination, actual thickness and level of vibration. The result from the above assessment was evaluated to determine the most critical location of FRP pipe in plant and used as samples for laboratory assessment.

Laboratory assessment was conducted on FRP pipe sample with several examinations. Flexural strength test [1], tensile strength test [4], hoop strength test [2], hardness test [8] and fiberglass content test [3] were conducted and the results were compared with technical specification of FRP material from manufacturer. Fatigue test was performed to determine fatigue properties of FRP pipe by using six specimens, three pieces of specimens by 70% tensile load and the rest by 50% tensile load. After broken cycles of each variable was obtained, then residual strength was evaluated. The evaluation performed by applying up to 500 cycles (70% tensile load) for the first specimen and 25,000 cycles (50% tensile load) to the others. Each specimens then subjected to tensile test and the result is being compared with original properties. Creep test was used to determine the remaining life of material by using time-temperature superposition principle method [7, 9]. It was conducted by temperature variation at 23°C, 40°C, and 60°C, with level of load at 70% of yield strength.

3. RESULT AND DISCUSSION

3.1. Site Assessment

For ultrasonic test on site, selection of examination locations was based on piping stress analysis results with value of stress greater than 25% allowable stress. As shown in Table 1, it was found that there are three locations with delaminating indication occurred on FRP pipes installed. All delamination were found in the level 1 which means that size of lamination is less than 25x 25 mm²[5]. Decreasing thickness up to 15% from nominal wall thickness was also obtained on outlet cooling water FRP pipe of G4-E-1B during thickness measurement while two other locations were still above minimum nominal wall thickness. From vibration test result, the vibration in radial direction has higher value than axial direction. All vibration levels are obtained in micrometer scale, hence vibration parameter has low possibility to damage FRP pipe during operation. Even though, the highest amplitude (movement) level of FRP piping in Train G is at the 16-inch cooling water outlet pipe of G4-E-1B (Propane Desuperheater Heat Exchanger) with resultant amplitude up to 818.473 μm. By considering decreasing of thickness and level of amplitude (movement) from vibration test, the 16-inch cooling water outlet pipe of G4-E-1B was selected as the most critical location and decided to be the sample pipe for laboratory assessment. Summary of site assessment results are shown on Table 1.



Table 1. Summary of Site Assessment Results

No	Location*	Outside Diameter of Pipe (Inch)	Ultrasonic Test			Vibration Test Result	
			De-lamination Size (mm ²)	Nominal Wall Thickness (mm)	Actual Thickness (mm)	Freq. (Hz)	Resultant Amplitude (μm)
1	G4-E-1B	16	< 100	7.49	6.4	0.750	818.473
2	G4-E-2F	30	< 100	10.7	11.6	1.125	68.824
3	G4-E-2D	30	< 100	10.7	11.6	5.500	106.617

* Equipment numbering system in PT Badak NGL

G4-E-1B : Propane Desuperheater Heat Exchanger

G4-E-2F/D : Propane Condenser Heat Exchanger

3.2. Laboratory Assessment

Visual inspection on internal sample of FRP pipe showed that the internal layer of the pipe has largely disappeared which is indicated by lighter glass fiber pattern as shown in Figure 1. However, the resin as fiberglass binder still existed completely and did not exposed to outside surface. Internal liner layer was used to provide chemical and abrasion resistance characteristics of FRP pipe to service fluids. If this component disappeared during service due to abrasion of service fluids, intrusion mechanism of fluids to FRP structure will take place and lead to delamination process, potentially decrease the reliability of FRP Pipe [9].



Figure 1. Internal Condition of FRP Pipe Sample

Ultrasonic test has resulted in varying actual thickness with maximum thickness at 6.16 mm and minimum thickness at 5.19 mm. These actual thicknesses have decreasing about 18% until 30% from nominal thickness but still above the required minimum thickness (0.356 mm) as calculated with Eq. 1. Table 2 summarize the thickness result by considering operating pressure of cooling water system at 3.5 kg/cm² and Hoop Strength of FRP piping material at 197.14 MPa. The decreasing of wall thickness during service may happen due to many factors. The effects of erosion from internal flow of carrying fluids, in this case is seawater, is one of factors that should be considered. Fluid velocity, percent solids and system



configuration are some of the variables that affect erosion rates. Other than that, aging damage may affect to thickness reduction since the FRP pipe has already been operated for about 20 years.

Table 2. Thickness Measurement Result by Ultrasonic Test

Minimum Actual Thickness (mm)	Initial. Thickness (mm)	Thickness Required (@ P= 3.5 kg/cm ²) (mm)
5.19	7.49	0.356

$$t_{req} = PD / (2s + P) \tag{1}$$

Physical and mechanical properties of the FRP samples that obtained from laboratory tests are summarized in Table 3. By flexural test [1], sample has average flexural strength of 93.758 N/mm². From tensile test [4] and hoop tensile test [2] results, the samples have value of tensile strength and hoop strength about 52.02 N/mm² and 197.14 N/mm² respectively. These values have decreased by 35% from initial tensile strength (80 N/mm²) and 11% from initial hoop strength (220 N/mm²). The appearances of FRP responds to subjected load during those tests are shown in Figure 2. The decreasing of tensile properties and hoop properties may indicate aging phenomena [6]. There are several factors can lead to degradation or aging damage of FRP material such as weathering, moisture, temperature, fluids and stress during in service environmental conditions. Weathering referred to the chemical and physical changes that occurred when radiation is absorbed by a polymer. This condition initiated by solar radiation, which results in the absorption of UV radiation by chromospheres and in the activation of excited states in macromolecules. However, other climatic quantities such as heat, moisture and air born pollution have influenced the mechanisms of degradation and the subsequent results of aging [6]. Other factors that may decrease mechanical properties especially tensile properties are effect of moisture and water. Potentially damaging amounts of moisture from the surrounding environments with the degree of degradation linked directly to the amount of moisture absorbed. The absorbed water may adversely affect the material in a number of ways as many as reduction in the glass transition temperature of resin, swelling and reduction in mechanical and physical properties (i.e. stiffness, strength and hardness) [6].

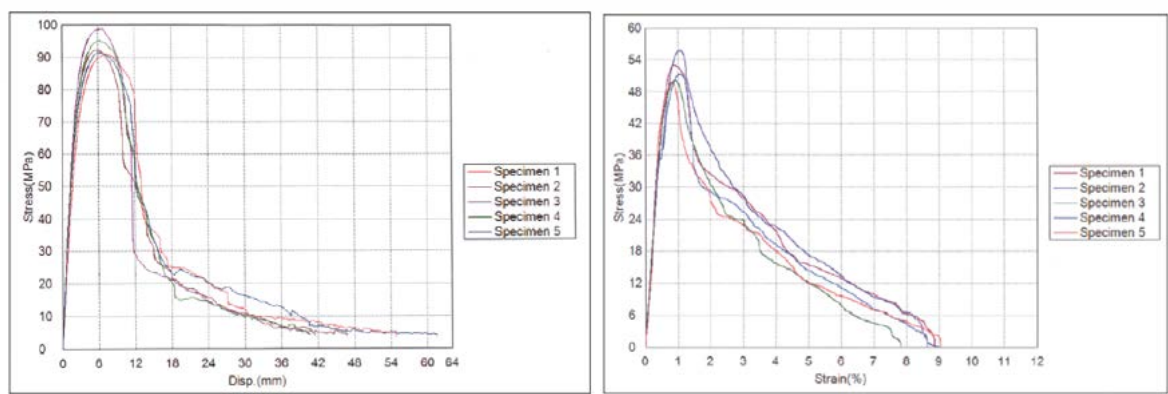
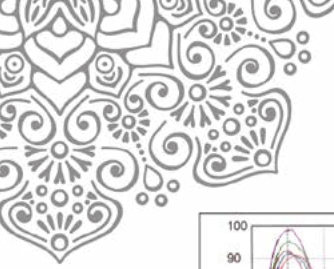
By using ball indentation method for plastic [8], hardness level of sample on the inside wall was 240 N/mm² while on the outside wall was 209 N/mm². As stated in technical specification of FRP from manufacturer, this type of FRP product have a value of hardness 40 - 65 Barcol hardness number. Since there is no conversion chart/method between Barcol hardness and Ball Indentation hardness as per ISO 2039-1, comprehensive evaluation related to hardness properties could not be conducted including whether there is decreasing in hardness value or nor. However, in general, the hardness range of polymer reinforced by fiberglass by ball indentation method is between 180 – 316 N/mm², which the sample hardness value is still between that ranges [8, 10].



Table 3. Materials Characterization Result Summary

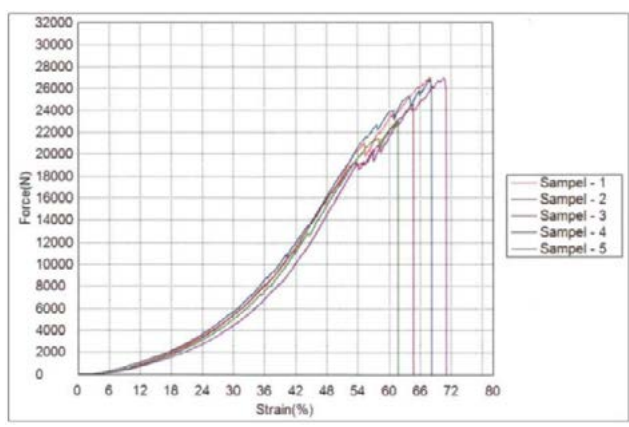
No	Standard	Average Thickness (mm)	Parameter	Result	Product Specification	Unit
Flexural Test						
1	ASTM D790	5.73	Max. Load	234.11		N
			Max. strength	93.76	85	MPa
			Modulus Elasticity	9.685		GPa
Tensile Test						
2	ASTM D638	5.86	Max. Load	3,883		N
			Max. Strength	52.02	80	MPa
			Strain at ultimate	0.93		
			Modulus Elasticity	9.62		GPa
Hoop Tensile Test						
3	ASTM D2290	6.36	Max. Load	25,754.8		N
			Max. Strength	197.14	220	MPa
Hardness Test						
4	ISO 2039-1	6.70	Inside wall	240		N/mm ²
			Outside wall	209		
Fiber Glass Content Test						
5	ASTM D3171	-	-	79.02		%

The hardness of an FRP composite is a direct result of the resin matrix and curing process. The more rigid the resin, the higher the level of hardness, whereas the more flexible laminate will have lower hardness level. Beside it, reinforcement component has a duty attaining mechanical properties of composite, in this case, reinforcement component is fiberglass. From glass content test [3] result, FRP sample has glass fiber composition about 79% and categorized as Glass Fiber Dominant FRP Pipe [7]. Delamination degradation is not big issue to glass fiber dominant type except when piping was subjected to compression stress that led to buckling [7].



(a).

(b).



(c).

Figure 2. (a). Flexural Test Curve Result. (b). Tensile Test Curve Result. (c). Hoop Tensile Test Curve Result.

Table 4 summarizes the result of fatigue test with several specimens and variables. Fatigue test was conducted by using two basic condition. The first condition, applying 70% tensile load by load Ratio, R, 0.1 (load maximum at 5.432 kN & minimum load 0.5432 kN) and frequency 8 Hz to the three pieces of specimens. The second conditions, test was conducted by applying 50% tensile load with load ratio, R, 0.1 (load maximum at 3.880 kN & minimum load 0.388 kN) and frequency 3 Hz. For the first condition, it resulting that the lifetime of the three specimens are 1,111 cycles, 949 cycles and 720 cycles respectively. Others conditions, lifetime of the three pieces of specimens are 68,988 cycles, 48,420 cycles and 88,044 cycles respectively. Furthermore, average lifetime on each condition are 926 cycles and 68,484 cycles.



Table 4. Summary of Fatigue Test Results

No	Specimen	F _{maks} (kN)	F _{min} (kN)	R	Freq. (Hz)	Life Time (Cycles)	Average Life Time (cycles)	Results
1	70.1	5.432	0.5432	0.1	8	1,111	927	Broken
2	70.2	5.432	0.5432	0.1	8	949		Broken
3	70.3	5.432	0.5432	0.1	8	720		Broken
4	50.1	3.880	0.3880	0.1	3	68,988	68,484	Broken
5	50.2	3.880	0.3880	0.1	3	48,420		Broken
6	50.3	3.880	0.3880	0.1	3	88,044		Broken

After broken cycles limit of each variable was obtained, evaluation was continued to obtain the residual strength properties. The evaluation performed by applying up to 500 cycles (with 70% tensile load) for the first specimen and 25,000 cycles (with 50% tensile load) to the others. Each specimens then subjected to tensile test and being compared to the original tensile strength. As the result summarized on Table 5, tensile strength decreased by only 9% (48.39 MPa) and 7% (47.09 MPa) from original tensile strength (52.02 MPa). This show that fatigue stress did not have any significant effect on FRP mechanical properties. As glass fiber dominant type, performance of FRP pipe during service lifetime was affected by creep stress rather than fatigue stress [7].

Table 5. Summary of Residual Strength Result

No	Sample	Condition			Tensile strength , MPa	
		Load Max (kN)	Load Min (kN)	Life Time (Cyclic)	Original	Residual
1	70.R	5.432	0.5432	500	52.02	48.39
2	50.R	3.880	0.388	25,000		47.09

Estimating the remaining life by creep load required long time of test/examination. However, by using Time-Temperature Superpositioning method, it can be accelerated especially for plastic/polymer material specimen. Polymer, because of their viscoelastic nature, exhibit behavior during deformation which is both temperature and time (frequency) dependent. Time Temperature Superpositioning method principle is based upon the premise that the processes involved in molecular relaxation or rearrangements occur at greater rates at higher temperatures. The time over which these processes occur can be reduced by conducting the measurement at elevated temperatures and transposing the data to lower temperatures. In this study, FRP Specimens constantly loaded by 70% of yield strength at three temperatures (23°C, 40°C & 60°C). Superposition was conducted by 23°C as reference temperature and resulting Curve Strain-Time graph as shown in Figure 3. It concludes that the estimation remaining life is 157,447 hours or 17.94 years (red dot line). The absence of inflection point in the curve is indicating that the specimen still not broken yet and has longer remaining



lifetime than 17.94 years. From the estimation result and the condition during test, the FRP pipe sample is estimated to have the remaining life for another 20 years.

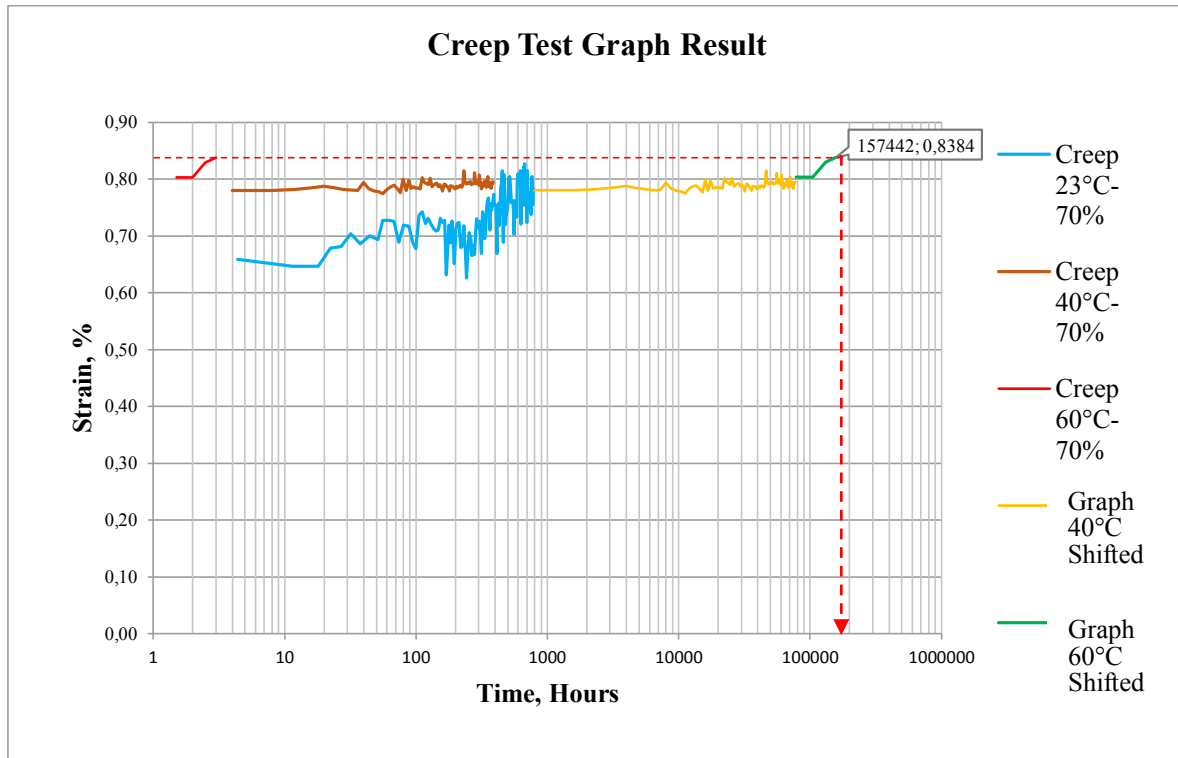


Figure 3. Summary of creep test by 70% yield strength of constant load at variation temperature

In the end, by concluding all the evaluation result above, the FRP sample is still reliable to service under normal condition even though aging indication is discovered. Since the sample is considered as the most critical location in Process Train G, it can reflect condition of all FRP piping in Train G. So that, FRP piping facilities in Process Train G, owned by PT Badak NGL, is considered safe for operating in another 20 years just as other Process Trains.

4. CONCLUSION

FRP Pipe in PT Badak NGL's Process Train G, was assessed to determine its remaining useful life and the following conclusions were obtained:

1. De-lamination of above ground FRP pipes were found on several locations but still within acceptable level (L-1) and the size of lamination is less than 25x 25 mm².
2. All vibration levels obtained in micrometer scale, hence vibration parameter has low possibility to damage FRP pipe during operational.
3. From characterization results, the FRP pipe experienced aging phenomena indicated from the decreasing of mechanical properties (hoop strength & tensile strength) even though flexural strength still above minimum technical specification of FRP product.



4. Fatigue test showed that the remaining lifetime of FRP sample is about 926 cycles (at load 70% of tensile strength) and 68,484 cycles (at load 50% of tensile strength).
5. Fatigue stress did not have any significant effect on tensile strength properties of FRP since the residual strength difference to initial the tensile strength only 7%-9%.
6. Based on creep test, curve condition during creep test still in linear position and ended before reaching inflection point was achieved (sample not yet broken), showed that the remaining life of FRP Pipe is still more than 20 years.

5. REFERENCES

- [1] American Standard Testing & Material (ASTM) D790. (2015). Standard Test Methods for Flexural Properties of Unreinforced and Reinforced Plastics and Electrical Insulating Materials.
- [2] American Standard Testing & Material (ASTM) D2290. (2016). Standard Test Method for Apparent Hoop Tensile Strength of Plastic or Reinforced Plastic Pipe.
- [3] American Standard Testing & Material (ASTM) D3171. (2015). Standard Test Methods for Constituent Content of Composite Materials.
- [4] American Standard Testing & Material (ASTM) D638. (2014). Standard Test Method for Tensile Properties of Plastics.
- [5] American Standard Testing & Material (ASTM) E114. (2015). Standard Practice for Ultrasonic Pulse-Echo Straight-Beam Contact Testing.
- [6] Bagherpour, Salar. (2012). Fiber Reinforced Polyester Composites, Chapter 6, pp. 150-154.
- [7] Det Norske Veritas (DNV). (2010). Offshore Standard DNV-OS-C501: Composite Components.
- [8] International Organization for Standardization (ISO) 2039-1. (2001). Plastics - Determination of hardness - Part 1: Ball indentation method.
- [9] Miyano, Y., M., Ichimaru, J., Hayakawa, E., (2008), Accelerated Testing for Long Term Strength of Innovative CFRP Laminates for Marine Use, Composites Part B, 39, pp. 5 - 12.
- [10] Quadrant. Product & Application Guide. (2007). General and Advanced Engineering Plastic.



15th International Conference on Quality in Research (QIR 2017)
**RISK-BASED APPROACH FOR REMAINING USEFUL LIFE (RUL)
ASSESSMENT OF LNG/LPG TANKS AT BADAK LNG**

Vicky Indrafusa

Corrosion and Material Engineer
Technical Department, PT Badak NGL
Bontang 75324, Kalimantan Timur, Indonesia
Email: indrafusa@badaklng.co.id

ABSTRACT

In 2016, Badak LNG operates 5 LNG Tanks and 4 LPG Tanks to maintain LNG/LPG inventory in Badak LNG Plant. Those tanks have reached 30 years service life. Therefore comprehensive remaining useful life (RUL) assessment of LNG/LPG Tanks is required to estimate equipment's life period within a safe integrity operating window. Direct assessment of internal LNG/LPG Tank will give useful information regarding the actual condition, but this activity is hardly performed due to operational limitation. Therefore RUL assessment of LNG/LPG tanks was performed using Risk Based Inspection (RBI) approach by reviewing design and operating conditions as well as inspection and maintenance history. Besides the risk and RUL, inspection and maintenance strategies for life extension purposes will be recommended from this assessment. Based on the assessment result, LNG/LPG tanks at Badak LNG are within medium risk category at the time of assessment (in 2016) and for further 10 years (in 2026). The risk level of the tank can be reduced by 48.06% for LNG tank and 70.97% for LPG tank in 2026 by performing recommended inspection. All subjected LNG/LPG Tanks have remaining useful life over 20 years.

Keywords: Tank; Remaining useful life (RUL); Inspection; Risk-based inspection (RBI)

1. INTRODUCTION

Badak LNG operates eight Process Trains to produce LNG with a maximum capacity of 22.5 million tons per annum (MTPA) and Liquid Petroleum Gas (LPG) with a capacity of 1.02 million ton per annum (MTPA). At the time of assessment (in 2016), Badak LNG operates 5 LNG Tank and 4 LPG Tank, while the remaining 1 LNG Tank and 1 LPG Tank are in offline condition.

The LNG and LPG storage tanks in Badak LNG are the single containment type with double steel walls designed and constructed according to API Standard 620 Appendix Q and R. In order to sustain the cryogenic operation, the inner tank of the LNG is made of 9% nickel steel and the outer tank is made of carbon steel. To minimize heat leak and boil off, insulation perlite is placed around the inner tank bottom, side wall and top of the suspended deck which is supported from the carbon steel outer tank. The general view and the general specification of the tank are shown in Figure 1 and Table 1 respectively.

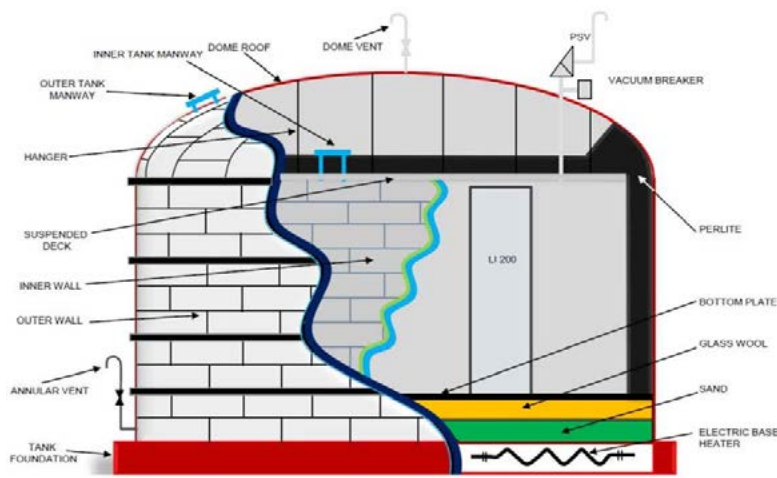


Figure 1. Tank general view.



Table 1. General tank specification.

Tank Design Specification				
Description	LPG Inner Tank	LPG Outer Tank	LNG Inner Tank	LNG Outer Tank
Content	Liquefied petroleum gas	Natural gas vapor	Liquefied natural gas	Natural gas vapor
Nominal Capacity	40000 m ³	-	95000 m ³ to 127500 m ³	-
Tank Type	Suspended Ceiling Type	Dome Roof Type	Suspended Ceiling Type	Dome Roof Type
Design Pressure	2.0 psig	2.0 psig	Liquid at 29.3 PCF	2.0 psig
Design Temperature	-45°C	Ambient (25°C)	-161°C	Ambient (25°C)
Material				
Shell	Carbon Steel A537	Carbon Steel A537	9% Ni Steel A553 Grade A	Carbon Steel A283 C
Bottom	Carbon Steel A537	Carbon Steel A537	9% Ni Steel A553 Grade A	Carbon Steel A283 C
Roof	Carbon Steel A537	Carbon Steel A537	Carbon Steel A283 C	Carbon Steel A283 C
Corrosion Allowance	None	None	None	None
Plate Thickness				
Shell	8 mm to 25 mm	9 mm to 28 mm	7 mm to 25 mm	11 mm to 18 mm
Bottom	5 mm	5 mm	5 mm	5 mm
Roof	-	6 mm	-	8 mm

All tanks in Badak LNG Plant have been operated for more than the design life (20 years) as shown in Table 2. Therefore, these assets are required to be evaluated for the risk and respective remaining useful life (RUL) to ensure that they are operated within a safe integrity operating windows (IOW).

Ideally, direct assessment of internal LNG or LPG Tank will give the actual condition for risk and remaining life evaluation. Nonetheless, direct assessment cannot be performed due operational constraint. As an alternative, a technical approach using Risk Based Inspection (RBI) was conducted to assess the RUL of the tank. The evaluation is performed by reviewing design and operating conditions as well as inspection and maintenance histories.

Table 2. General data of LNG & LPG Tank Badak LNG.

No	Equipment No.	Construction Year	Service Start	Age (years)	Fluid	Capacity (m ³)
1	LPG Tank 1	1988	Dec 1988	28	LPG (Propane)	40,000
2	LPG Tank 2	1988	Dec 1988	28	LPG (Propane)	40,000
3	LPG Tank 3	1988	Dec 1988	28	LPG (Butane)	40,000
4	LPG Tank 4	1988	Dec 1988	28	LPG (Butane)	40,000
5	LPG Tank 5 *	1988	Dec 1988	28	LPG (Propane)	40,000
6	LNG Tank 1	1976	July 1977	39	LNG (Methane)	95,000
7	LNG Tank 2	1976	July 1977	39	LNG (Methane)	95,000
8	LNG Tank 3	1976	July 1977	39	LNG (Methane)	95,000
9	LNG Tank 4	1976	July 1977	39	LNG (Methane)	95,000
10	LNG Tank 5	1982	July 1983	32	LNG (Methane)	128,150
11	LNG Tank 6 *	1998	Nov 1999	18	LNG (Methane)	127,200

*The tank is excluded from the assessment

2. METHODOLOGY AND TECHNICAL APPROACH

The remaining life assessment has a goal to determine which tanks components are likely to have a limited remaining life, and assess the current and future risks. The assessment is conducted by combining risk and reliability concepts. RUL assessment is performed with 2 (two) general steps as shown in Figure 2.

2.1. DATA GATHERING AND SITE SURVEY

Data is gathered to provide an overview that may be necessary to develop the RBI plan. For the probability of failure assessment, inspection results, previous failure reports (if any), repair reports and process



information are examples of mandatory data required. While for the consequence of failure assessment, data such as the population density, cost of injury, cost of business interruption and cost of equipment repair/replacement were gathered.

Site visual inspection was also conducted for all tanks in conformance with API 653, API RP575 and EEMUA 159. The visual survey was conducted to provide a good current condition of the tanks.

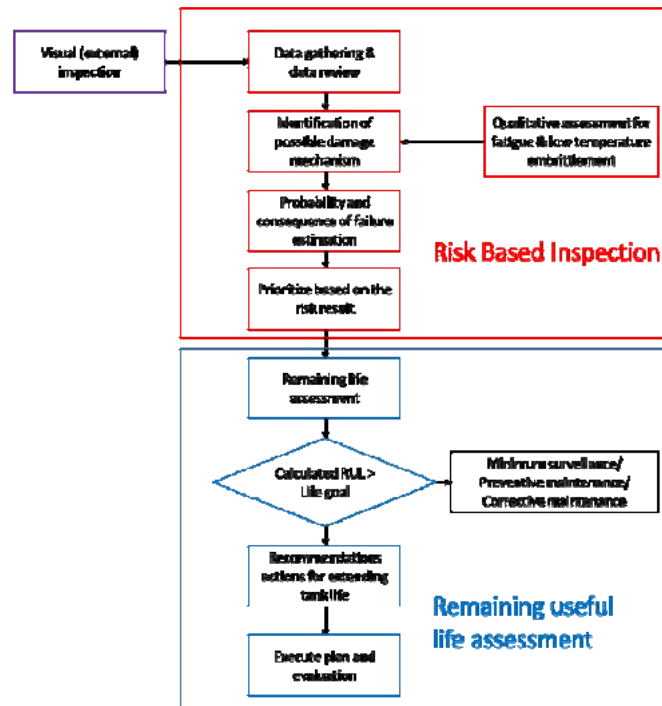


Figure 2. RUL assessment methodology integrated with RBI approach.

2.2.RBI ASSESSMENT

RBI assessment is performed to focus inspection activities on high risk equipment with the aim to reduce its risk to As Low As Reasonably Practical (ALARP) with the following steps.

Table 3. Possible damage mechanism of LNG/LPG tank component.

Damage Mechanism	Expression
Internal thinning	PoF internal thinning General thinning Localized thinning Erosion
External thinning	PoF external thinning General thinning Localized thinning
Brittle fracture	PoF brittle fracture Cryogenic embrittlement
Fatigue	PoF fatigue Thermal Vibration Corrosion fatigue

*PoF: Probability of Failure which depends on DF, GFF, Fi, and MF as shown in Figure 3.

- a. Define asset hierarchy
Asset hierarchy was down from the highest equipment level to the lowest component level. In this analysis, each tank is broken down into component levels which are inner shell course, inner floor, outer shell course, outer floor, and outer roof.
- b. Define risk acceptance criteria (safety and economic)
Inspection target is based on potential loss life (PLL) and total cost. The criteria for the PLL is 0.001/year and for the total cost is USD 50,000/year.



c. RBI assessment

At this step, risk of each component is calculated using the equation in Figure 3 and then plotted in a 5x5 risk matrix as shown in Figure 4. In this study, RBI assessment is performed by Synergi RBI Onshore (AST) software version 5.3.2. Possible damage mechanism commonly encountered in LNG/LPG tank is shown in Table 3. A quantitative analysis is provided for potential corrosion damage due to internal or external thinning. While a qualitative analysis is provided for brittle fracture, fatigue, and cracking susceptibility. Apart from identifying damage mechanism & susceptibility, the consequence of the failure of each component is categorized into personnel injury and total cost as shown in Table 4.

Table 4. The consequence of failure category based on personnel injury and total cost.

No	Personnel injury	Total cost	Category
1	No injuries to workers possible	Maintenance costs only, standard repair of common part	A
2	Low possibility of minor injury from failure	Maintenance costs only, more costly repair. Expensive/labour intensive	B
3	Significant possibility for minor injury from failure	Profit loss up to 2 days business loss plus maintenance costs	C
4	Worker lost time injury or low possibility of public minor injury	3 to 5 days profit loss plus maintenance costs	D
5	Any fatality or significantly public minor injury possible	More than 5 days profit loss plus maintenance costs	E

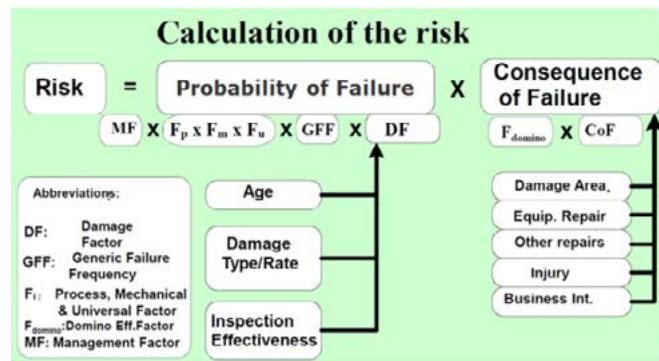


Figure 3. Risk calculation elements.

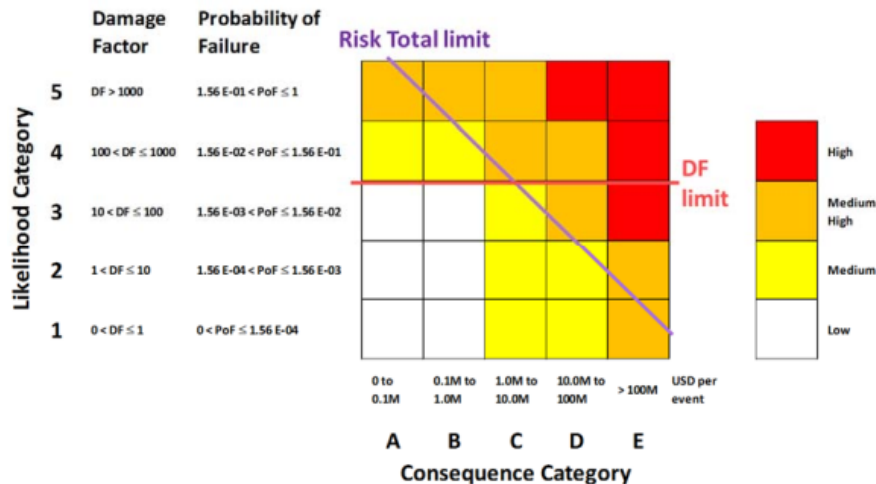


Figure 4. Representation of 5x5 risk matrix.

2.3.RUL ASSESSMENT

Remaining life assessments in this study use the actual operating conditions and inspection data (if available) along with nominal material properties to make remaining life projections. When possible, the current condition is assessed based on the inspection record. From the current condition of the material,



obtained by measurements or calculated estimates, the remaining life is predicted. The simplest approach is to assume that future operations will be the same as those of the past and to make a linear extrapolation. The RUL of tank component is categorized by criticality category as shown in Table 5.

Table 5. Categorization of RUL Tank

	Criticality 0	Criticality 1	Criticality 2	Criticality 3	Criticality 4
RUL	≤ 0 year	> 0 year to ≤ 5 years	> 5 years to ≤ 10 years	> 10 years to < 20 years	≥ 20 years
Action	Immediate inspection detailed inspection	Immediate inspection detailed inspection	Immediate inspection or next shutdown, whichever is shorter detailed inspection	RBI planning	RBI planning

Remaining life of the tank component is determined by comparing nominal thickness and minimum required thickness (t_{min}). Over years, the wall thickness may be consumed due to corrosion or another damage mechanism until a critical value (t_{min}) below which the tank is deemed unsafe for continued operation under the original design conditions.

The minimum required thickness (t_{min}) for cylindrical tank is calculated using equation (1).

$$t_{min} = \frac{T_2}{S_{ts}E} = \frac{PR_c}{S_{ts}E} \tag{1}$$

where,

T_2 = latitudinal unit force, PR_c

P = total pressure acting at a given tank under a particular condition of loading

R_c = inside radius of the centreline of shell course under consideration

S_{ts} = maximum allowable stress for simple tension, Table 5-1 in API 620

E = joint efficiency

The RUL is calculated using equation (2) as shown below. If the current thickness is not available, the corrosion rate is based on literature and experience.

$$Remaining\ Useful\ Life,\ RUL = \frac{t_{current} - t_{min}}{Corrosion\ rate} \tag{2}$$

$$Corrosion\ rate = \frac{t_{previous} - t_{actual}}{time(years)between\ t_{previous}\ and\ t_{actual}}$$

where,

CR = corrosion rate input from personnel expertise or literature/ measured rate

$t_{current}$ = current thickness

$t_{previous}$ = previous year of thickness measurement taken

t_{min} = minimum required thickness as per design code

2.4.INSPECTION PLANNING

For each component, the driving damage mechanism is identified for inspection. Based on the inspection planning target, the Damage Factor for the relevant driving damage mechanism is reduced by assigning an effectiveness of inspection (as shown in Figure 5). Synergi RBI Onshore will attempt to reduce the risk (via the Damage Factor) by performing first Fairly Effective inspection. Unless the recalculated risk falls below the target value, the software will continue to perform with Highly Effective inspection.

3. RESULT & DISCUSSION

A number of tank components analysed for the respective remaining useful life and risk profile are shown in Table 6 below.

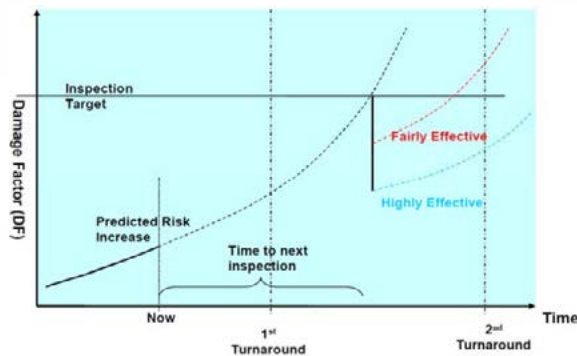


Figure 5. Risk can be reduced with inspection of different effectiveness.

Table 6. List of equipment (equip) or component (comp) of the tank.

Tank	Inner Shell (Equip)	Inner Shell Course (Comp)	Inner Floor (Equip)	Outer Shell (Equip)	Outer Shell Course (Comp)	Outer Floor (Equip)	Outer Roof (Equip)*
LPG Tank 1	1	10	1	1	11	1	1
LPG Tank 2	1	10	1	1	11	1	1
LPG Tank 3	1	10	1	1	11	1	1
LPG Tank 4	1	10	1	1	11	1	1
Total	4	40	4	4	44	4	4
LNG Tank 1	1	14	1	1	14	1	1
LNG Tank 2	1	14	1	1	14	1	1
LNG Tank 3	1	14	1	1	14	1	1
LNG Tank 4	1	14	1	1	14	1	1
LNG Tank 5	1	14	1	1	15	1	1
Total	5	70	5	5	71	5	5

* Outer roof risk is not calculated in the risk matrix since it is calculated semi-quantitatively.

A. LPG TANK

The LPG tank risk is calculated for the tank shell and tank floor. Outer roof tank risk is calculated separately and the result shows all outer roofs are assessed to be in low risk rating using a semi quantitative method. The risk of each tank component was analyzed for total risk in USD per year, potential loss life in PLL per year (only for tank shell) and it is ranked comparatively through a risk matrix representative of the risk profile of those assets.

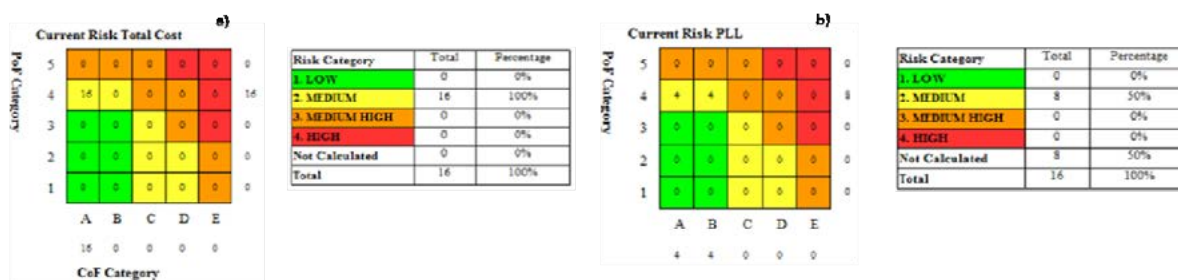


Figure 6. The risk profile of LPG tank component at the time of assessment, a) total cost, b) PLL.

Figure 6 shows the risk profile for LPG tank component at the time of assessment (2016). All tank components fall into medium risk ranking at the time of assessment. The future risk has been projected for 10 years in order to determine the high risks before any failure occur. This will help to plan for the future inspection. Figure 7 and Figure 8 are the future risks without and with inspection in 2026 in term of total



cost and PLL category respectively. If the suggested inspection is carried out, the damage factor will be decreased so the risk (total cost) can be reduced by 70.97 % as shown in Figure 9.



Figure 7. Future risk profile (Total Cost) of the LPG Tank before and after an inspection in 2026.

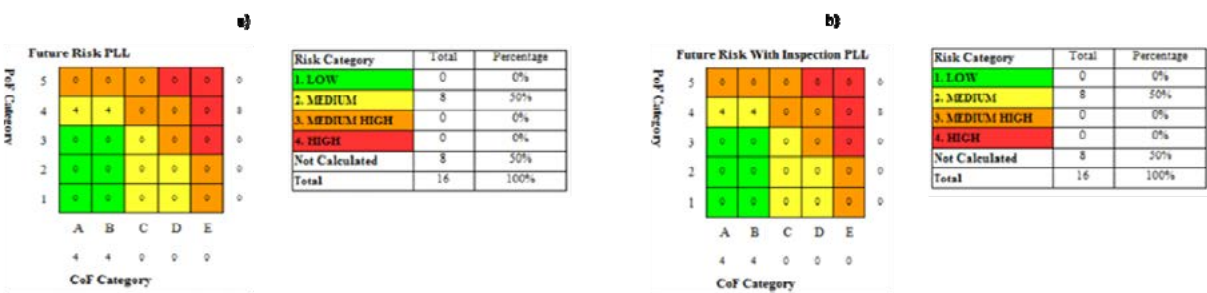


Figure 8. Future risk profile (PLL) of the LPG Tank before and after an inspection in 2026.

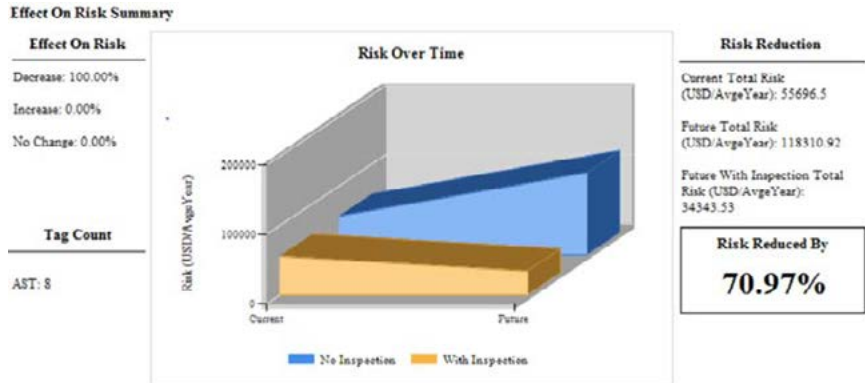


Figure 9. Future risk of LPG tank with inspection and without inspection in 2026.

All LPG tank components subject to the assessment were found to have a remaining useful life more than 20 years. The lowest remaining life for the LPG tank component is 21.68 years (Outer shell course 6 of LPG Tank 1 tank) as shown in Table 7.

B. LNG Tank

Figure 10 shows the risk profile for LNG tank component. Based on the result, the entire tank component is calculated to be in medium risk in term of total cost and PLL category.

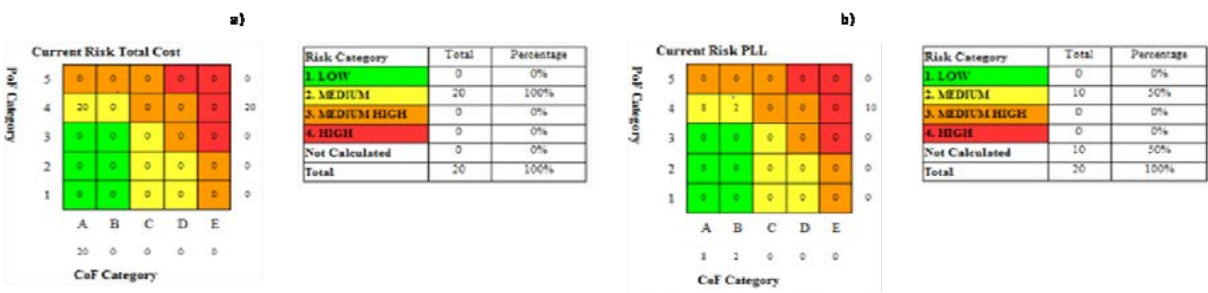
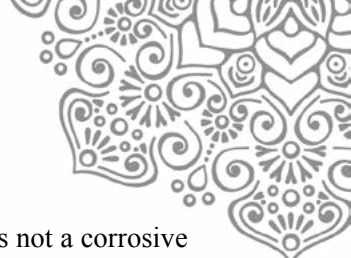


Figure 10. The risk profile of LNG tank component at the time of assessment, a) total cost, b) PLL.



The damage mechanism affecting the storage tank is expected to be minimal. The methane is not a corrosive service but inspection has not been done to verify that no thinning of the storage tank inner wall/floor has taken place for all tanks subjected to this assessment. In October 2016, internal inspection of tank inner shell and floor is performed in the identical LNG tank (LNG Tank 6) which happens to be in off-service condition. Based on this finding, the corrosion rate was found to be very minimal (near 0 mm/year). Therefore, the expert rate of 0.0001 mm/year was applied to all the tanks inner shell and inner floor in this study.

The future risk has been projected for 10 years in order to determine the high risks before any failure occur. Figure 11 and 12 are the future risks without inspection and with inspection in term of total cost and PLL category respectively. Figure 13 shows the risk (total cost) that can be reduced by 48.06 % due to decreasing damage factor if the suggested inspection is carried out.

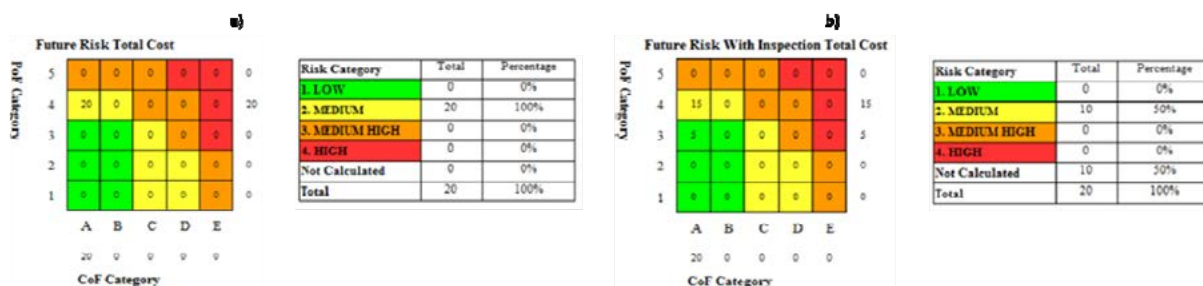


Figure 11. Future risk profile (Total Cost) of the LNG Tank before and after an inspection in 2026.

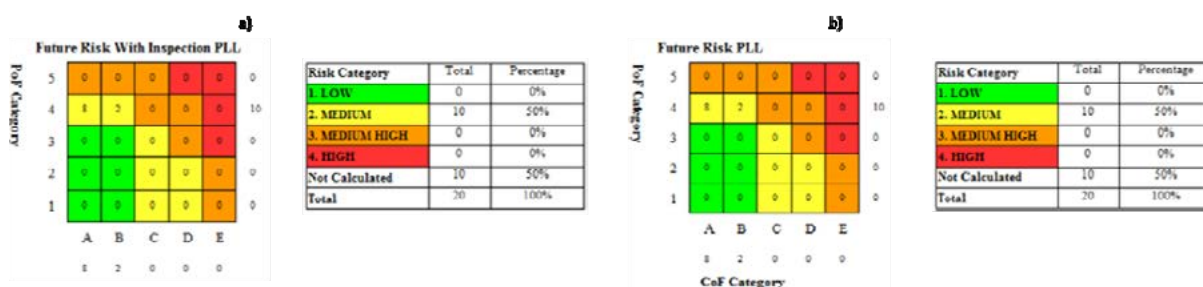


Figure 12. Future risk profile (PLL) of the LNG Tank before and after an inspection in 2026.

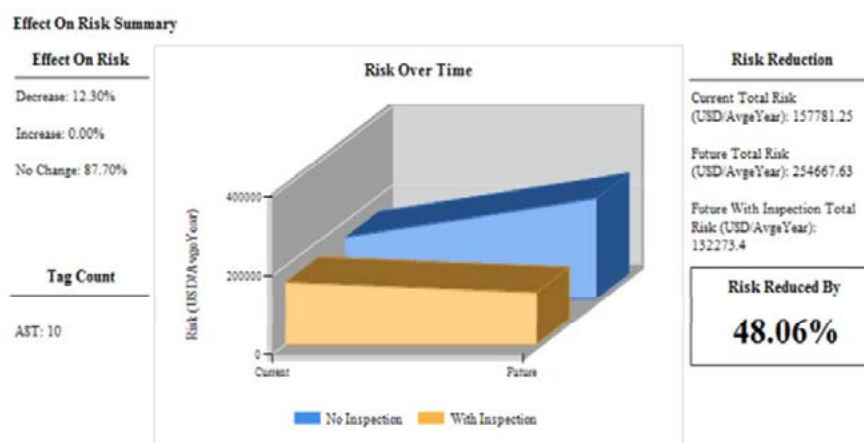


Figure 13. Future risk of LNG tank with inspection and without inspection in 2026.

All LNG tank components were found to have a remaining useful life more than 20 years. The lowest remaining life for the LNG tank component is 21.58 years (Outer shell course 1 of LNG Tank 2). Table 7 below shows the percentage of distribution based on remaining useful life.



Table 7. RUL distribution of LPG and LNG Tank component.

Criticality	Remaining Useful Life (RUL)	LPG Tank Component	LNG Tank Component
Criticality 0	RUL less than 0 year	0	0
Criticality 1	RUL between 0 to 5 years	0	0
Criticality 2	RUL between 5 to 10 years	0	0
Criticality 3	RUL between 10 to 20 years	0	0
Criticality 4	RUL more than 20 years	96	156
Total		96	156

4. CONCLUSIONS

Based on the RUL assessment of LNG and LPG tank, some conclusions can be summarized as follow.

- 1) All LNG/LPG tanks in Badak LNG are within medium risk category in 2016 and for further 10 years services (in 2026) if without inspection activities.
- 2) It is recommended to perform a minimal UT inspection (fairly effective) in 2026 to assess the condition and to reduce the risk level of the tank.
- 3) The risk level can be reduced by 48.06% for LNG tank and 70.97% for LPG tank in 2026 if inspection is performed as per RBI suggestion.
- 4) All components of LNG or LPG tank have a remaining useful life more than 20 years (Criticality 4). Therefore the LNG and LPG tanks can be put in service for further 20 years.

5. REFERENCE

API RP 580: Risk-Based Inspection, 3rd edition, 2016, American Petroleum Institute.
API RP 581: Risk-Based Inspection Technology, 2nd Edition, 2008, American Petroleum Institute.
API RP 653: Tank Inspection, Repair, Alteration, and Reconstruction, 5th Edition, 2014, American Petroleum Institute
API RP 571: Damage Mechanisms Affecting Fixed Equipment in the Refining Industry, 2nd Edition, 2011
API RP 620: Design and Construction of Large, Welded, Low-Pressure Storage Tanks, 12th Edition, 2013
EEMUA Publication 159 Above ground flat bottomed storage tanks - a guide to inspection, maintenance and repair, 4th Edition, 2014
DNV/AOR20030012 Rev 1, Risk Based Inspection Planning Methodology-Aboveground Storage Tank, 2005
NACE Corrosion Data Survey, Metal Section 6th Edition, 1985
Corrosion Consideration for Aboveground Storage Tanks (NACE paper 02487), Vincent A. Carucci et al, 2002
Evaluation of LNG facilities for Aging, Richard A.Hoffmann et al, 2007
Advanced Risk Assessment of LNG Storage Tanks Based on Risk Based Maintenance Planning Evaluation, Hajimi Anzai, Masayuki Kobayashi et al.



MOLECULAR AND IONIC MOBILITY OF CHITOSAN BASED SOLID POLYMER ELECTROLYTE FOR LITHIUM-ION BATTERY

Sudaryanto^a, Evi Yulianti^a, Nur Shofiana Khaironi^b

^aCenter for Science and Technology of Advanced Materials, BATAN, Kawasan Puspiptek, Serpong, Tangerang Selatan, Banten, 15314, Indonesia

^bDepartment of Physics, Mataram University, Jl. Majapahit 62, Mataram, NTB, 83125, Indonesia

ABSTRACT

Ionic conductivity, the most vital electrolytes properties of chitosan based solid polymer electrolytes (SPE) was increased by several methods. In this study, the relation between polymer molecular mobilities and conductivity have been studied. The SPE were prepared simply by mixing lithium salt into chitosan solution, followed by casting method. The SPE micro-structure and segmental mobilities were studied by using X-ray diffractometer and mechanical test measurement, respectively. The conductivities were studied using electrochemical impedance spectrometer. Ionic mobility was studied based on ion transference number measurement. The results showed that the addition of nanoparticle, e.g. ZrO₂ decreased the chitosan crystallinity so that increased the molecular motion flexibility, but did not change the conductivity significantly. However, addition of lithium perchlorate (LiClO₄) as lithium salt clearly increased the the chitosan conductivity up to 3 order (from 10⁻⁷ to 10⁻⁴ S/cm). A higher salt concentration leads to a higher segmental motion and cationic mobility.

Keywords: Chitosan; Ionic Conductivity; Lithium-Ion Battery; Lithium Salt; SPE.

1. INTRODUCTION

Lithium ion secondary batteries, having a high voltage and a high energy density, are widely used in various mobile devices such as smart phone and tablet PC. However, due to using a flammable liquid electrolyte, there is a risk of explosion or fire accidents. To reduce the risk, a protection circuit may be embedded to the battery system. On the other hand, in very cold climates, the liquid electrolyte may be frozen so that the battery capacity will be significantly reduced or the battery become unworkable. To overcome this inconvenience, the liquid electrolytes are substituted by solid ones, making all-solid-state lithium batteries are proposed as the best solution (Ogawa et.al., 2012).

Solid polymer electrolytes (SPE) show a lower ionic conductivity than the liquid electrolyte; however, they can increase the safety of battery due to less reactive with lithium, The SPE can play as both electrolyte and separator. Moreover, they exhibit a high compliance, good mechanical stability up to its melting point, and excellent process ability for making films (Polo Fonseca et.al., 2007). SPE are formed by the incorporation of inorganic such as lithium salt into polymer matrices. The polymer more studied is the poly (ethylene oxide) (PEO) with inorganic salts dissolved in its matrix. However, the high



degree of crystalline of PEO restricts its use in battery, and it can be used only at temperatures above the melting point of the crystalline phase, which is approximately 60°C (Manuel Stephan, 2006; Gray 1991). Thus, it is necessary to find others alternative polymer instead of PEO.

Utilization of biodegradable polymer such as Chitosan as the SPE will not only make an environmental friendly but also gives an excellent processing ability for making films, thus it can be freely designed such as multiple cell battery system. Lithium based biodegradable polymer battery system may be one of the promising candidates of next generation due to high performance lithium battery system and cost-effective due to the abundant resources, and of course environmental friendly. Therefore, we did several effort to obtain chitosan based SPE (Yulianti et.al., 2012; Yulianti and Sudaryanto, 2015; Sudaryanto et.al., 2015; Sudaryanto et.al., 2016).

Chitosan based SPE show a lower ionic conductivity, however it can be increased by several methods. Previously we have done a preliminary study on the utilization of ion implantation method to prepare a solid-state electrolyte based on natural polymer (Yulianti et.al., 2012). Various ion salts (Li^+ , Cu^{++} , Ag^+) was involved into the polymer matrix. The result show that after implanted with Li^+ , Cu^{++} or Ag^+ ion, the conductivity of polymer film increased but still in low level. We have also studied the effect of lithium salt addition into the chitosan film (Yulianti and Sudaryanto, 2015; Sudaryanto et.al., 2015). However, it was found that the addition of salt affected not only to the properties but also the structure of the chitosan matrix. Furthermore, we studied the structure and properties of chitosan based SPE. It was found that the decrease in sampel crytallinity increased the molecular mobility result in the increasing sampel conductivity and cationic transfer number (Sudaryanto et.al., 2016). Therefore, it is of interest to explore furthermore about the molecular and ionic mobility of chitosan based SPE.

Principally, the solid electrolyte plays as the medium for the transference of ions, between the anode and cathode. Therefore, the ion transference number is of important properties of SPE. An increase in ion transference number, is generally observed with the addition of nanofillers (Sudaryanto et.al., 2016; Xiong et.al., 2006; Croce et.al. 1999; Xi et.al., 2006). For examples, an increase in cationic transfer number (t^+) was obtained in PEO– lithium perchlorate (LiClO_4) electrolytes with the addition of TiO_2 (Croce et.al. 1999) and mesoporous SiO_2 (Xi et.al., 2006). We also found an increase in ionic transference number with increasing Zirconia (ZrO_2) nanoparticle addition into Chitosan- LiClO_4 electrolyte system (Sudaryanto et.al., 2016).

The aim of this study is to investigate the effect of molecular mobility onto the conductivity of chitosan based SPE. In order to understand the effects of nanoparticle additions onto molecular mobility and SPE conductivity, in this study, firstly ZrO_2 nanoparticle was added in a chitosan solution without lithium salt. After studying their structure and properties, LiClO_4 as lithium salt was added in the system and the conductivity as well as ionic mobility were studied. Some results of this study have been presented previously (Khoironi et.al., 2015), in this paper further discussion with additional data will be presented.

2. METHODOLOGY



2.1. Materials

Similar with previous study (Sudaryanto et.al., 2016), the chitosan used was national product from crab shells and purchased from Bogor Agricultural Institute Laboratory (low molecular weight, 86% deacetylated degree). Acetic acid as solvents was analytical grade purchased from Merck and used without further purification. Deionized water was used to make 1 wt.% acetic acid solution. Lithium perchlorate (LiClO_4) and Zirconia (ZrO_2) nanoparticle were purchased form Sigma-Aldrich and used as-received.

2.2. Sample preparation

The chitosan powder was dissolved into 1 wt.% acetic acid to make a polymer solution. A certain amount of ZrO_2 was added into the solution as shown in Table 1. The ZrO_2 were varied from 2 to 8 wt.% of chitosan weight. A certain amount of the solution was put into a cast mold and kept for several days to evaporate the solvent. The obtained film was then stored under vacuum condition at room temperature to complete the solvent evaporation. Similar method was done when a certain amount of LiClO_4 , as in Table 1, was added in a selected chitosan- ZrO_2 system. The wt.% indicates the weight (g) of LiClO_4 and/or ZrO_2 when dissolved in 100 g solution of 4 wt.% chitosan solution.

Table 1. The composition of chitosan based solid polymer electrolyte

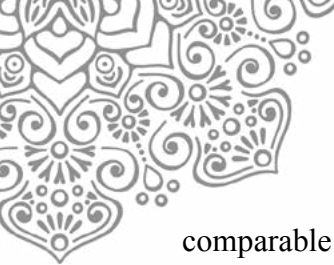
Sample No.	Composition (g)		
	[Chitosan]	[ZrO_2]	[LiClO_4]
1	100	0	0
2	100	2	0
3	100	4	0
4	100	6	0
5	100	4	10
6	100	4	20
7	100	4	30
8	100	4	40

2.3 Sample characterization

XRD was carried out using PANalytical that employs Cu- $\text{K}\alpha$ X-radiation of wavelength $\lambda=1.5418 \text{ \AA}$ between a 2θ angle of 5° until 45° . A mechanical property of films was tested using TOYOSEIKI VGS 5-Estrogaph. The values of tensile strength and elongation at break were taken from the average of three samples which were stretched in 10 mm/min. Electric conductivity measurement was performed with a computer controlled impedance analyzer (HIOKI LCR Hi-Tester Model 3532, Japan) in the frequency range of 42 Hz to 1 MHz. The films were sandwiched between two electrodes with 0.99 cm in diameter under spring pressure. The DC conductivity (σ_{dc}) was defined as the frequency independent plateau in the low frequency region. The ionic transference number was measured by a polarization technique as describe by Morni and Arof (Morni and Arof, 1999).

3. RESULTS AND DISCUSSION

Figure 1 shows an XRD pattern of chitosan with various concentration of ZrO_2 . The chitosan without ZrO_2 addition exhibits slightly widening peaks at 11.5° , and 18.5° ,



comparable with previous studies (Yulianti and Sudaryanto, 2015; Islam et.al., 2011). It indicated the sample was a semi crystalline or has a partly amorphous. This is typical of polymer (Rosli et.al., 2012). The peaks decreased when the addition of ZrO₂ increased. This may suggest that with increasing ZrO₂ the crystallinity of chitosan has changed to be more amorphous. The peaks disappear when the addition of 4 wt% of ZrO₂, showing an optimum concentration to have the most amorphous part (Figure 1 (c)). Further addition of ZrO₂ beyond the optimum concentration the chitosan film became more crystalline again that proved by the appearance of the peaks as shown on Figure 1(d-e). In addition, the peaks of ZrO₂ typically appear at 28° and 31° which increased with ZrO₂ concentration.

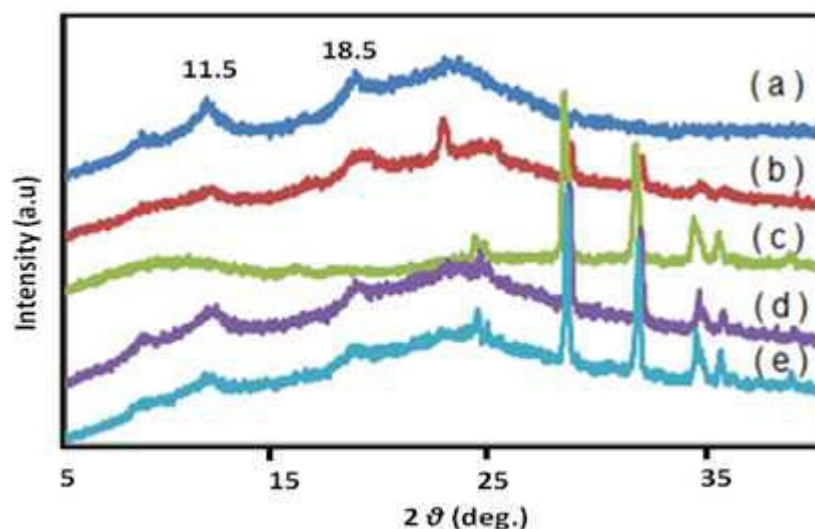


Figure 1. XRD spectra of chitosan containing ZrO₂ (a) 0 wt.% (b) 2 wt.% (c) 4 wt.%, (d) 6 wt.%, and (e) 8 wt.%.

Figure 2 demonstrated the tensile strength of chitosan film with increasing ZrO₂ concentration. The mechanical properties of chitosan slightly changed with the ZrO₂ addition. The tensile strength of chitosan decreased from 48.5 to 40.3MPa with 8 wt.% of ZrO₂ addition. It will be due to the decreasing in chitosan crystallinity as discussed in Figure 1. The decrease in the tensile strength may also be due to an increasing in polymer segmental mobility with decreasing the crystallite (Yulianti and Sudaryanto, 2016; Nada et.al. 2004). The decrease in crystallites can be considered to increase the free volume, hence increase the segmental mobility. Tensile measurements are usually performed in conjunction with elongation break measurement. Elongation break percentage determines the elasticity of the samples. The higher the value of the elongation break, the more elastic the samples. Elasticity of a material can also be interpreted as the material flexibility.

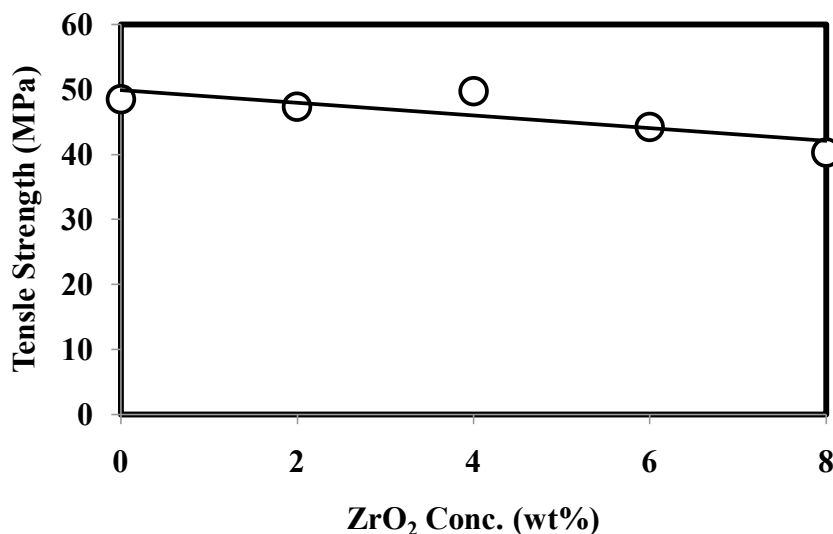


Figure 2. The tensile test of chitosan as function of added ZrO₂ concentration.

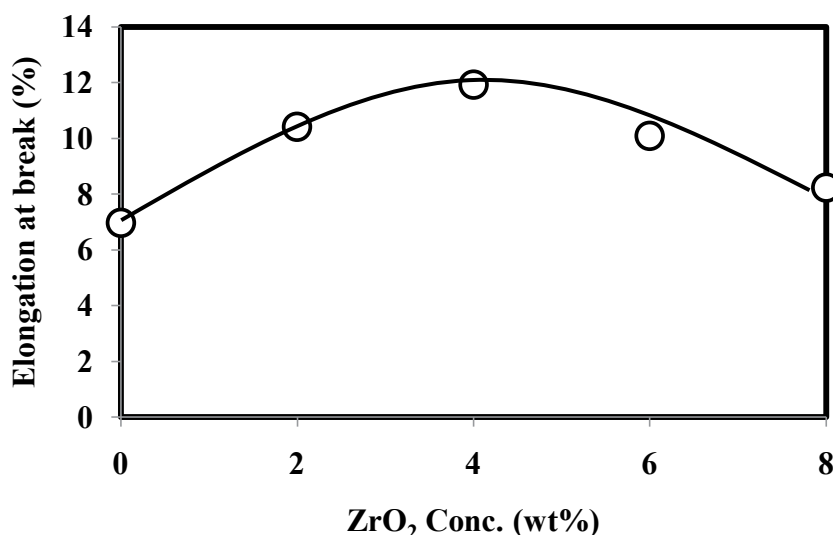


Figure 3. The elongation at break of chitosan as function of added ZrO₂ concentration.

Figure 3 shows the percentage of elongation at break for chitosan as function of added ZrO₂ concentration. The figure exhibits the existence of maximum value of elongation at ZrO₂ concentration of 4 wt.%. It is in accordance with the crystallinity change as mention above, in which the addition of 4 wt% of ZrO₂, showing an optimum concentration to have the most amorphous part (Figure 1 (c)). The addition of ZrO₂ over the optimum concentration (4 wt%) shows the formation of ZrO₂ particle agglomeration. This explains that the more concentration of ZrO₂ particles in the chitosan film causes the



cohesive force between ZrO_2 particles stronger than the adhesive force between ZrO_2 particles with chitosan polymer. This caused the polymer matrix of chitosan crammed by ZrO_2 and ease to endure particle agglomeration. This progress also made the sample harder but the elasticity was reduced then the sample became cracked easily. This was indicated that agglomeration was disrupted the mechanical properties of chitosan films.

The segmental motion was also depicted by $\tan \delta$ profile of chitosan as shown in Figure 4. The $\tan \delta$ peak shifted the higher frequency, indicated smaller relaxation time or faster segmental motion, with addition of ZrO_2 nanoparticle up to 4 wt.%.

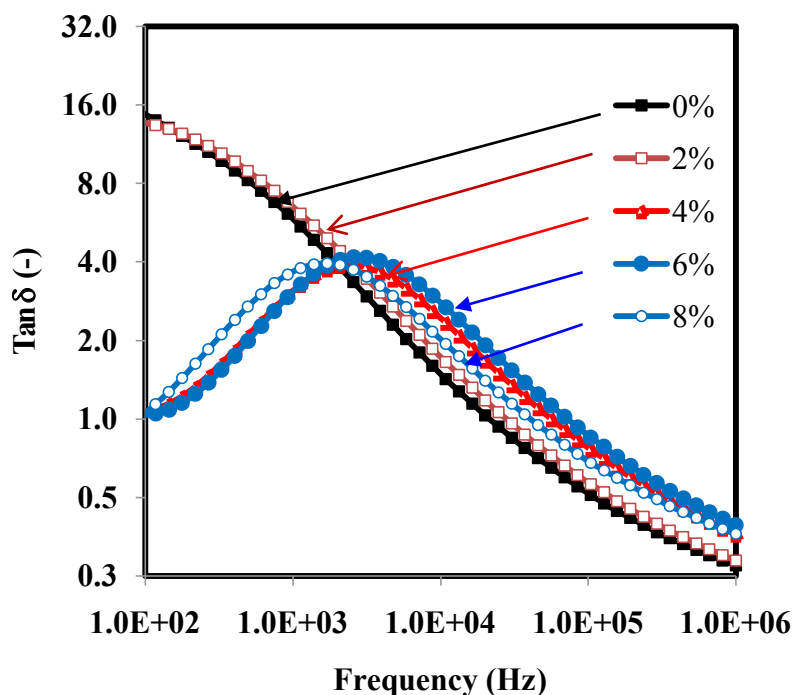
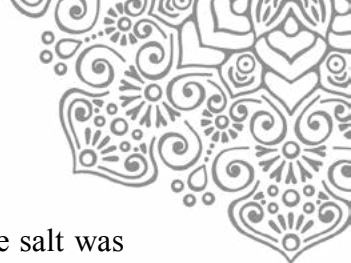


Figure 4. $\tan \delta$ profile of chitosan film with various ZrO_2 concentration as frequency function at room temperature.

The conductivities at room temperature of chitosan film with various ZrO_2 concentrations are presented at Figure 5. The figure shows that even if at the same order, the conductivity slightly increased with the increasing ZrO_2 concentration. The maximum conductivity reached at 4% w/w of ZrO_2 concentration, it was about 6.57×10^{-7} S/cm and only little bit higher than conductivity of chitosan without addition of filler. It has mentioned above that the addition of 4% ZrO_2 made the film more amorphous and caused the increase in segmental motion of polymer. Since there is no ion source in the sample, the conductivity changes were not so significant or still on the same order.

A significant change, however, was obtained when a lithium salt was added into the system as shown in Figure 6. $LiClO_4$, as the lithium salt, was added to chitosan solution with 4 wt.% ZrO_2 . It is clear that the addition of lithium salt significantly increased the chitosan conductivity up to order (from 10^{-7} to 10^{-4} S/cm), linear with the salt



concentration. The chitosan in this system can play as solid solution in which the salt was dissolved and provide ion in the system, result in the increasing chitosan film conductivity.

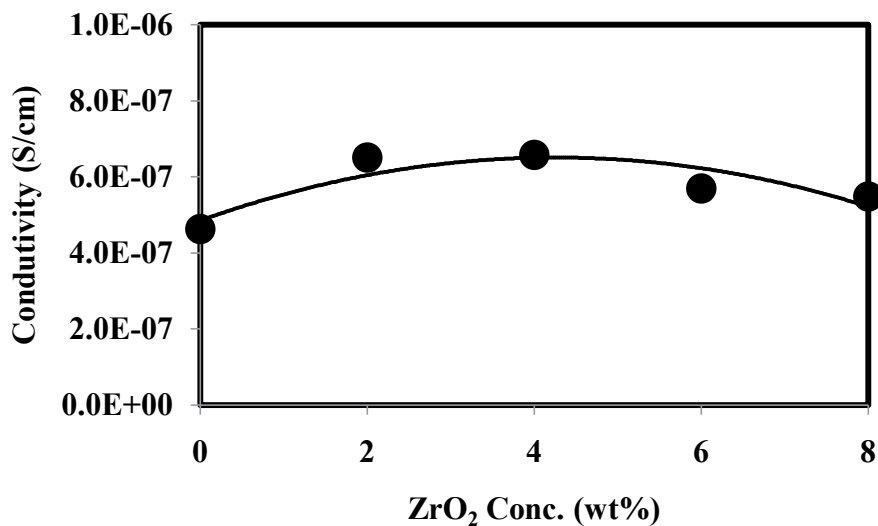


Figure 5. The conductivity of chitosan film as function of added ZrO₂ concentration.

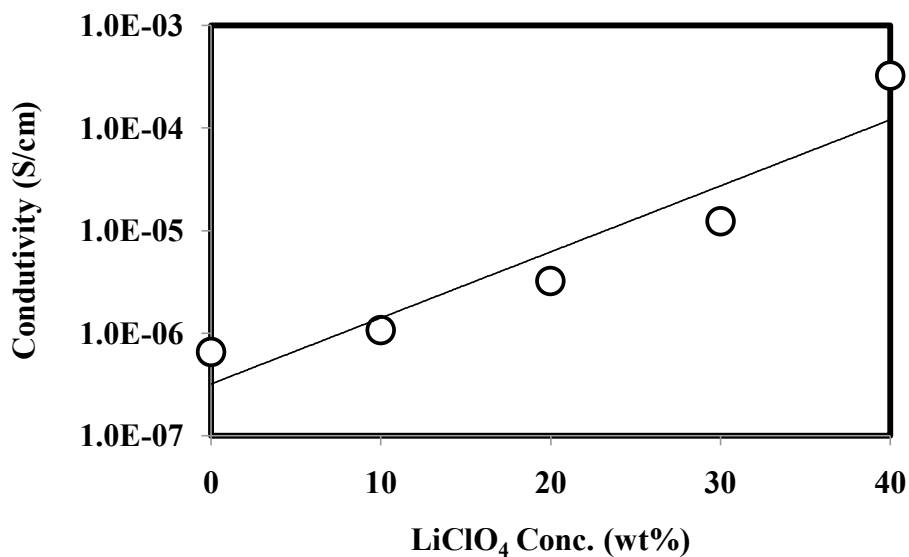


Figure 6. The conductivity of chitosan-ZrO₂ films with various LiClO₄ salt concentrations.

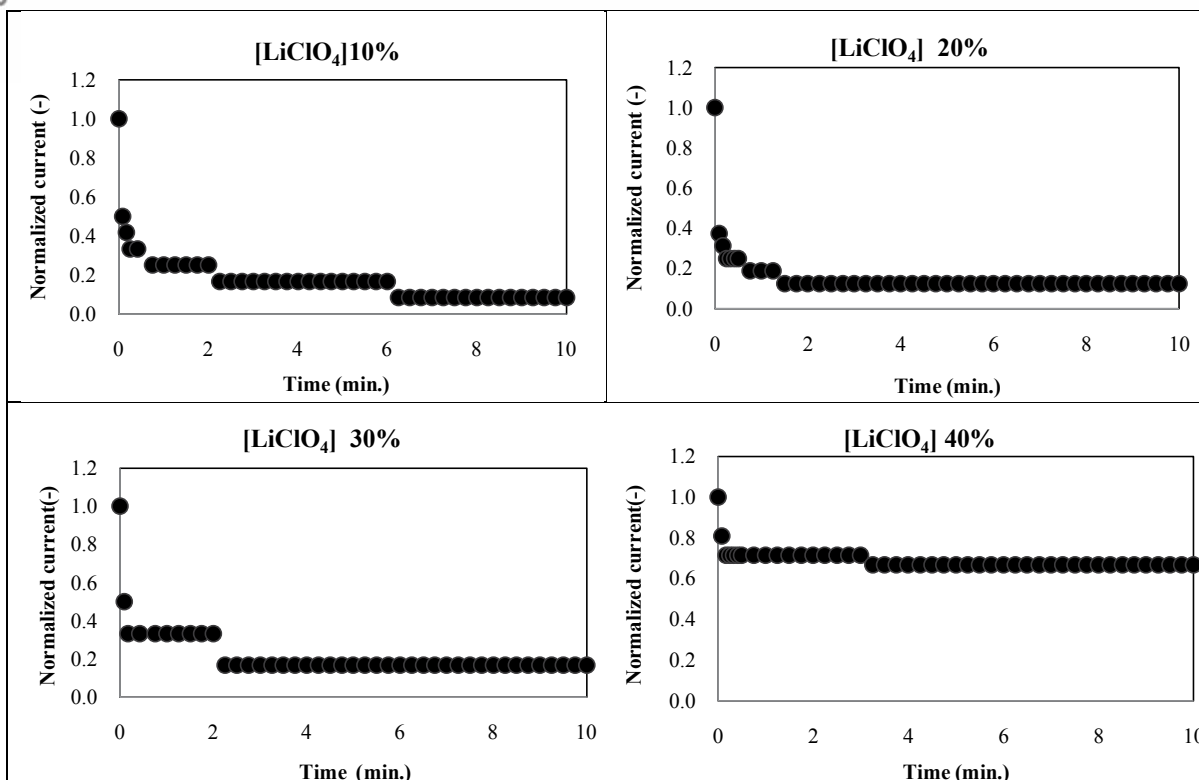


Figure 7. Normalized current as function of monitoring time for the chitosan SPE with various salt contents.

As mentioned above, the increase in conductivity can be due to the ability of ion motion in the SPE system. Therefore, the ion mobility may be studied from polarization phenomena which will occur when a polymer film was sandwiched between two electrodes in a circuit. The ions in the polymer film will travel to the electrode connected to the terminal which has an opposite charge to that of their own. Hence, polarization occurred and current in the circuit decreased which can be monitored every several minutes until a constant current attributable to cations will be obtained. Figure 7 shows the normalized polarization current as function of monitoring time for the chitosan SPE with various salt concentrations. The current could not pass the film of chitosan without LiClO₄ salt, since there was no ion in the system, hence no polarization happened. The cationic transference number was under 0.2 for sample salt concentration less than 40%, showing the conduction role mainly played by the ClO₄ anion. However, a dramatic increase of cationic transference number up to 0.6 obtained when the salt concentration was 40 wt. %. Other studies have obtained a lithium ion transference number of about 0.31 for chitosan with LiCF₃SO₃ (Morni and Arof, 1999) and 0.55 for chitosan with LiClO₄ (Sudaryanto et.al. 2016). However, it is of interest when comparing with our previous study. Chitosan with 40 wt. % LiClO₄ showed low cationic transference number (0.09) when no ZrO₂ added into the system. However, the value was increase dramatically up to 0.50 and 0.55 by adding 2 wt.% and 4 wt.% of ZrO₂, respectively (Sudaryanto et.al. 2016). In this study a higher transference number can be reached only when a sufficient concentration (40 wt.%)



of LiClO_4 salt was added. It means that the cationic transference number is function of ion concentration and segmental mobility.

4. CONCLUSION

The relation between polymer molecular mobilities and conductivity of chitosan based Solid Polymer electrolyte (SPE) have been studied. The SPE were prepared simply by mixing lithium salt into chitosan solution, followed by a casting method. The SPE micro-structure and segmental mobilities has been studied by using X-ray diffractometer and mechanical test measurement, respectively. The conductivities were studied using electrochemical impedance spectrometer. While the ionic mobility was studied based on ion transference number measurement. The results showed that the addition of zirconia (ZrO_2) nanoparticle decreased the chitosan crystallinity, thus increased the molecular motion flexibility, however the conductivity did not change significantly. Meanwhile, addition of lithium perchlorate (LiClO_4) as lithium salt clearly increased the chitosan conductivity up to 3 order (from 10^{-7} to 10^{-4} S/cm). The higher salt concentration the lower matrix crystallinity, and result in the higher segmental motion and cationic mobility. The cationic transference number was under 0.2 for sample with salt concentration less than 40%, showing the conduction role mainly played by the ClO_4^- anion. However, a dramatically increase of cationic transference number up to 0.6 obtained when the salt concentration was 40 wt.%

5. ACKNOWLEDGEMENT

This study was conducted using 2014 and 2015 Budget Implementation List (DIPA) of Center for Sains and Technology Advanced Materials – BATAN. Nur Shofiana Khaironi from Department of Physics Mataram University, as one of authors would like to thank to BATAN for giving chance to join in this work.

6. REFERENCES

- Croce, F., Curini, R., Martinelli, A., Ppersi, L., Ronci, F., Scrosati, B., Caminiti, R. , (1999), Physical and chemical properties of nanocomposite polymer electrolytes, *J. Phys. Chem. B*, Volume **103**, pp. 10632-10638.
- Gray, F.M., (1991), *Solid polymer electrolytes-fundamentals and technological applications*, VCH, New York, USA.
- Islam, M. M., Masum, S. M., Molla, M. A. I., Rahman, M. M. Shaikh, A. A. , Roy, S. K., (2011), Preparation of chitosan from shrimp shell and investigation of its properties, *Intenational Journal of Basic & Applied Sciences* , Volume **11**, No. 1, pp. 116-130.
- Khoironi, N. S., Yulianti, E., Sudaryanto, (2015), Study of Structural and Electrical Properties of chitsan- ZrO_2 Composites Material, in *Proceedings of The International Conference on Materials Science and Technology ICMST 2014*, pp. 239-244.



- Manuel Stephan, A., (2006), Review on gel polymer electrolytes for lithium batteries , European Polymer Journal, Volume 42, pp. 21-42.
- Morni, N.M., Arof, A.K., (1999), Chitosan–lithium triflate electrolyte in secondary lithium cells, Journal of Power Sources, Volume 77, pp. 42–48.
- Nada, A.M.A. , Dawy, M. , Salama, A.H. , (2004), Dielectric properties and ac-conductivity of cellulose polyethylene glycol blends, Materials Chem. and Phys., Volume 84, pp. 205-215.
- Ogawa, M. , Yoshida, K., and Harada, K., (2012) , All-solid-state lithium batteries with wide operating temperature range, SEI Technical Review, Number 74, pp. 88-90.
- Polo Fonseca, C., Cavalcante, Jr., F., Amaral, F.A., Zani Souza, C.A., Neves, S.,(2007) Thermal and conduction properties of a PCL-biodegradable gel polymer electrolyte with LiClO₄, LiF₃CSO₃, and LiBF₄ salts. Int. J.Electrochem. Sci., Volume 2, pp. 52–63.
- Rosli, N.H.A., Chan, C.H. , Subban, R.H.Y., Tan Winie, (2012), Studies on the Structural and Electrical Properties of Hexanoyl Chitosan/Polystyrene-based Polymer Electrolytes , Physics Procedia, Volume 25, pp. 215 – 220.
- Sudaryanto, Yulianti, E., and Jodi, H., (2015), Studies of dielectric properties and conductivity of chitosan-lithium triflate electrolyte, Polymer-Plastics Technology and Engineering, Volume 54, pp. 290–295.
- Sudaryanto, Yulianti, E. and Patimatuzzohrah, (2016), Structure and properties of solid polymer electrolyte based on chitosan and ZrO₂ nanoparticle for lithium ion battery, *in*; AIP Conference Proceedings 1710, 020003 (2016); doi: 10.1063/1.4941464.
- Xi, J., Qiu, X., Zhu, W., Tang, X. , (2006), Enhanced electrochemical properties of poly(ethylene oxide)-based composite polymer electrolyte with ordered mesoporous materials for lithium polymer battery, Micropor. Mesopor. Mater., Volume 88, pp. 1-7.
- Xiong, H-M., Wang, Z-D., Xie, D-P., Cheng, L. Xia, Y-Y., (2006), Stable polymer electrolytes based on polyether-grafted ZnO nanoparticles for all-solid-state lithium batteries , J. Mater. Chem., Volume 16, pp. 1345-1349.
- Yulianti, E., Karo Karo, A., Susita, L., Sudaryanto, (2012), Synthesis of electrolyte polymer based on natural polymer chitosan by ion implantation technique, Procedia Chemistry, Volume 4, pp. 202 – 207.
- Yulianti, E. and Sudaryanto, (2015), The effect of plasticizer addition to solid polymer electrolyte based on chitosan monmorillonite nanocomposite, *in*; Proceedings of the 14th Asian Conference on Solid State Ionics (ACSSI 2014), S. Adams and J. Kawamura (Eds.), (Research Publishing, Singapore, 2015), pp. 606-615.



SYNTHESIS AND CHARACTERIZATION CHITOSAN/ ALGINATE/GEOTHERMAL SILICA SCAFFOLD

Fiska Yohana Purwaningtyas^a, Yuni Kusumastuti^{a,b*}, Himawan Tri Bayu Murti Petrus^{a,b},
Budhijanto^a

^a*Department of Chemical Engineering Universitas Gadjah Mada, Yogyakarta 55281, Indonesia*

^b*Center for Advanced Material and Mineral Processing CAMMP, Department of Chemical Engineering Universitas Gadjah Mada, Yogyakarta 55281, Indonesia*

ABSTRACT

Scaffold has an essential role to facilitate the repair of bone injury or disease. Chitosan and alginate are the two most commonly used natural polymers for scaffold material. Despite its recognizable role in tissue engineering, chitosan/alginate scaffold was known to possess low mechanical properties. Hence, an effort was taken to improve the mechanical properties of chitosan-alginate scaffold by silica addition. Geothermal silica refers to silica with 50% amorphous silica content that obtained as the solid waste of Geothermal Power Plant. Geothermal silica was purified using sol-gel methods to obtain silica with 97.23% purity prior to use. In this study, the lyophilized technique had been used to fabricate chitosan/alginate and chitosan/alginate/geothermal silica scaffold. Swelling ratio, mechanical strength, and pore size of scaffolds were investigated in order to observe the effect of geothermal silica addition. Furthermore, SEM analysis was conducted on the prepared scaffolds to characterize their morphology. From the experiment results, addition of geothermal silica was found to increase mechanical strength of scaffold and control its swelling ability. The highest mechanical strength value was achieved by chitosan/alginate/geothermal silica scaffold with raw materials ratio of 1:1:1. In addition, chitosan/alginate scaffold exhibits higher swelling ratio than chitosan/alginate/geothermal silica scaffold. This correlation could be explained by the presence of interconnected pores in scaffold with silica addition shown by SEM results. The interconnected pores have the essential role to increase cell infiltration and nutrients absorption for cell growth. In conclusion, geothermal silica exhibited great potential as scaffold material for biomaterial application.

Keywords : Scaffold; Chitosan; Alginate; Geothermal Silica

1. INTRODUCTION

Tissue engineering has been established as one of the several methods for disease or injury treatment using molecular and cells biological technology to induce tissue regeneration. This field combines engineering with other disciplines such as material, chemistry, cell biology, and molecular science. Bone graft serves as one of the existing solutions to repair bone defect. The common types of bone graft are autograft, allograft, and xenograft. While, those commonly used bone graft have some drawbacks, such as, the limited amount of substitute tissue, body's immune rejection, the possibility of infection, and the necessity of secondary surgery area.



Many efforts have already been initiated to provide an alternative solution, including scaffold (Karp, et al., 2003). Scaffold is a composite fabricated from biomaterial that has to possess the ability to support cell and tissue growth physically, chemically, and mechanically. In addition, the scaffold is required to possess high porosity in order to be used as the supporting matrix for cell infiltration and nutrient transfer for cell growth. Raw materials in scaffold fabrication are biomaterials, such as polymer and ceramics. On the other hand, chitosan exhibits a great potential to be used as raw material for scaffold fabrication as it can be converted into porous sponge or hydrogel as 3D scaffold (Kusumastuti, et al, 2015). Chitin, an abundant polysaccharide in Indonesia, can be synthesized from shells of crustaceans such as crabs and shrimps. Partial deacetylation of chitin (*1,4-linked 2-acetamido-2-deoxy- β -D-glucan*) will generate chitosan product. However, the mechanical properties of the chitosan-based scaffold have to be improved (Levengood and Zhang, 2014).

Chitosan is a polycation that consists the amino group, hence a polyanion polysaccharide (such as alginate) could be added to increase its mechanical strength. Alginate is an anionic polymer produced by brown algae (Phaeophyceae) extraction. It is a linear polymer composed of mannuronic acid (*β -D-mannuronic acid (M)*) and guluronic acid (*α -L-guluronic acid (G)*). Alginate is also biocompatible, hydrophilic, and biodegradable in the natural environment (Becker, 2001). Chitosan/alginate composite will generate polyionic complexes that increase the mechanical properties of scaffold and form stable bonds with chitosan (Ramay, et al., 2005). The pKa value of amino group in chitosan is 6.5, while the pKa value of alginate carboxyl group is 3.5. On the other hand, the pH interval from 4 until 6 incurs strong ionic interaction between positively charged chitosan and negatively charged alginate (Khong, et al., 2013).

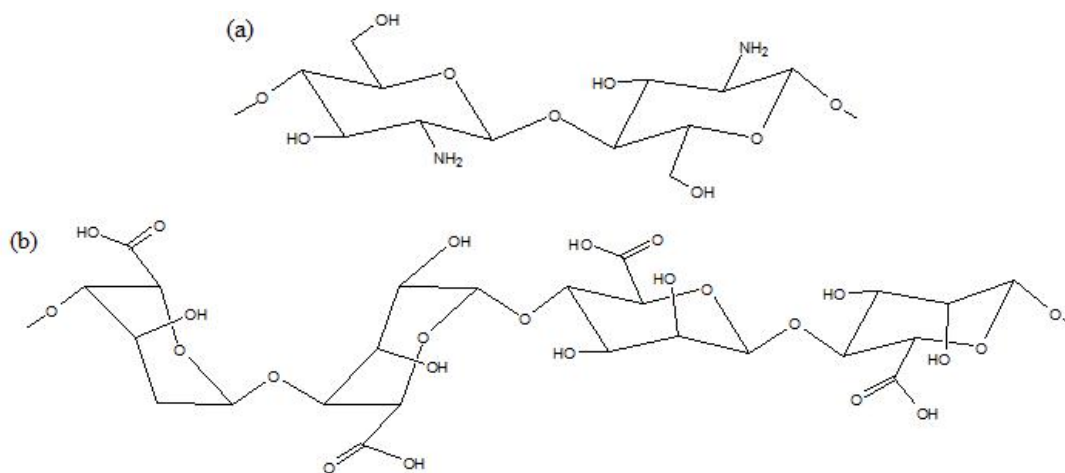
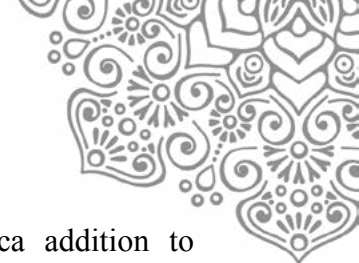


Figure 1. Chemical structure of (a) chitosan, and (b) alginate

In order to increase the mechanical strength of chitosan and alginate composite, collected silica from the geothermal waste (sludge) of PT. Geo Dipa Energi Dieng was added. Geothermal sludge has become an attractive source of silica due to its abundance and high amorphous silica content (>50%). Amorphous silica has bioactive characteristic and abilities to assist bones forming process and also to stimulate cell mineralization (Velvet-Regi and Balas, 2008). In order to fully employ their outstanding properties, silica purification is performed by sol-gel methods consisting two steps: geothermal silica dissolution using alkali and acid



precipitation. This study aimed to determine the effect of geothermal silica addition to mechanical properties of obtained chitosan/alginate scaffold.

2. MATERIALS & METHODS

2.1. Materials

Medical grade chitosan with deacetylation degree more than 90% was obtained from PT. Biotek Surindo, Cirebon, West Java. Geothermal sludge was obtained from PT. Geo Dipa Energi, Dieng, Central Java. Sodium alginate, acetic acid (CH₃COOH) 98%, hydrochloric acid (HCl) 37%, and sodium hydroxide (NaOH) pellet were purchased from Merck. The prepared PBS (pH 7.4) was prepared and stored at room temperature.

2.2. Methods

2.2.1. Purification of geothermal silica

Geothermal sludge was sieved with a 60-mesh sieve, washed with demineralized water and dried afterwards. As much as 20 grams of dried geothermal sludge were dissolved in 800 mL of 1.5 N NaOH solution at 90°C for 1 hour with the stirring velocity of 400 rpm. The solution was then cooled and filtered through a filter paper. After that, sodium silicate solution was titrated with 2 N HCl until the gel was formed at pH of 6.5. The formed gel was subsequently stored for 18 hours. It was filtered and washed until it reached pH of 7 afterwards, then dried in an oven.

2.2.2. Synthesis of scaffold

Chitosan (1% w/v) was dissolved in 30 mL of 1% acetic acid solution. While, sodium alginate (1% w/v) was dissolved in 30 mL of demineralized water. Chitosan solution was added into alginate solution until the gel was formed. The silica powder (1% w/v) was added to the solution and stirred for 2 hours at ambient temperature. This mixture was poured into a petri dish and froze overnight at -20°C. It was lyophilized for 24 hours to obtain dry scaffold.

Table 1. Various Composition Ratio of Scaffold

Sample	Chitosan : Alginate : Geothermal Silica
A1	1 : 1 : 0
A2	1 : 1 : 0.5
A3	1 : 1 : 1
A4	1 : 1 : 1.5
A5	1 : 1 : 2

2.3. Characterization

2.3.1. Energy dispersive x-ray spectroscopy (EDX)

The components in geothermal silica were analyzed by using EDX 8000 (Shimadzu Co., Japan) through the x-ray emitted from the material as a response to collision among charged particles with area of analysis 3 cm².



2.3.2. Swelling study

The dry weight of scaffold was measured and noted as (W_d). Scaffold samples were immersed in PBS solution with pH of 7.4 at 37°C for 1 hour. After that, the scaffold was taken out and any excess liquid on the surface of scaffold was blotted onto filter paper and the wet weight was recorded as (W_w). Swelling ratio could be calculated by using the following formula:

$$\text{Swelling ratio} = \frac{W_w - W_d}{W_d} \quad (1)$$

2.3.3. Mechanical testing

The tensile strength of scaffold was investigated with the mechanical testing machine (Pearson Panke Equipment Ltd., UK) by following the ASTM D638 standard. The Young's modulus value (E) could be calculated by using the formula:

$$E = \frac{F}{A} \quad (2)$$

2.3.4. Fourier transform infrared spectroscopy (FTIR)

The molecular interaction between components in scaffold was analyzed with FTIR (Shimadzu Co., Japan) by using KBr pellet. The recorded spectra were ranging from 4500 to 400 cm^{-1} .

2.3.5. Scanning electron microscopy (SEM)

The morphology and porosity of gold coated lyophilized scaffold was observed by Scanning Electron Microscopy (SEM) (Model S-4800, Hitachi, Tokyo, Japan) at an acceleration of 15 kV.

3. RESULTS AND DISCUSSION

3.1. Silica purification

Geothermal silica purification processes with sol-gel method consisted of two steps, which were silica dissolution using NaOH solution and acid precipitation to form the gel. During the dissolution step, geothermal silica would react to form sodium silicate. The stirring speed was faster than the previous study (Kusumastuti, et al. 2017), from 300 rpm to 400 rpm. Faster stirring speed was meant to increase sodium silicate forming. Subsequently, sodium silicate reacted with HCl solution to form silica gel (SiO_2) in the acid precipitation step. In this step, HCl solution was added until pH of 6.5 due to the increasing of silica solubility at pH more than 8. The purity of obtained silica could be analyzed by using EDX. The results were shown in Table 2. The EDX result indicated that the purity of silica was quite high (97.78%), therefore exhibited a great potential to be utilized as the bioactive material for scaffold.

Table 2. Results of EDX Analysis

Component	% Mass	% Oxide Mass
Si	97.78	97.26
Al	1.18	2.07
S	0.67	0.31
Fe	0.18	0.24
Ca	0.16	0.11
Cu	0.03	0.02



3.2. Swelling study

Swelling analysis was performed for 1 hour to observe the ability of scaffold to absorb PBS as a body fluid model. The effect of geothermal silica addition to swelling ratio of scaffold were shown in Figure 2. The results indicated that silica addition could reduce swelling ratio. This results was consistent with the effect of geothermal silica addition to chitosan/pectin and chitosan/gelatine scaffold (Kusumastuti, et al, 2017). Swelling ratio reduction could be ascribed by silica addition which contributed to reduce the affinity of chitosan/alginate to interact with water molecules, consequently the absorbed PBS in scaffold was low.

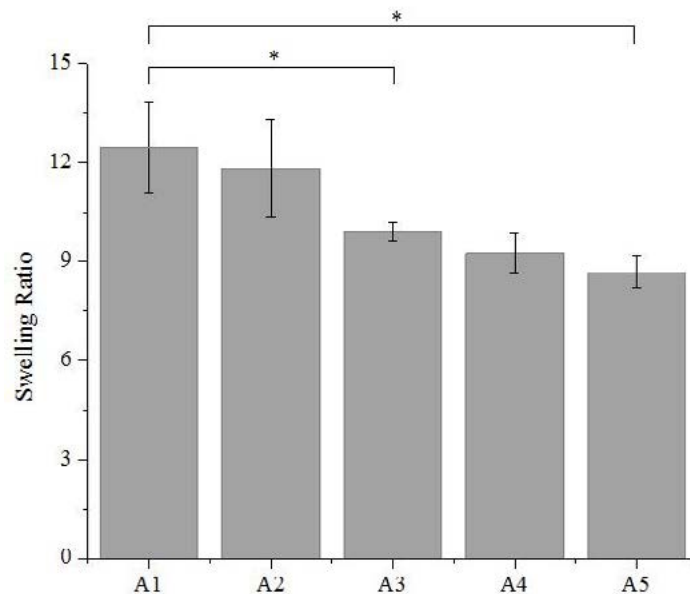


Figure 2. Swelling behavior of chitosan/alginate/geothermal silica scaffold. * $p < 0.05$

3.3. Mechanical Testing

Mechanical testing results are represented by Young's Modulus value. Furthermore, the results of tensile strength analysis indicated that the scaffold with chitosan/alginate/geothermal silica ratio = 1:1:1 had the highest Young's Modulus value. Theoretically, alginate would form a stable ionic bond with chitosan, thus alginate and chitosan mixture had favorable mechanical properties. Figure 3 showed that silica addition will improve mechanical properties of the scaffold. It showed similar results where the existing of geothermal silica increased Young's Modulus value at ratio of 1:1 of chitosan/gelatin scaffold and 1:2 of chitosan/pectin scaffold (Kusumastuti, et al. 2017). However, the higher silica content would make chitosan/alginate scaffold increasingly fragile due to the lower polymer matrix which binds with silica and the fragile properties of silica itself. The decreasing of Young's Modulus value was started at sample A4 with composition ratio of 1:1:1.5.

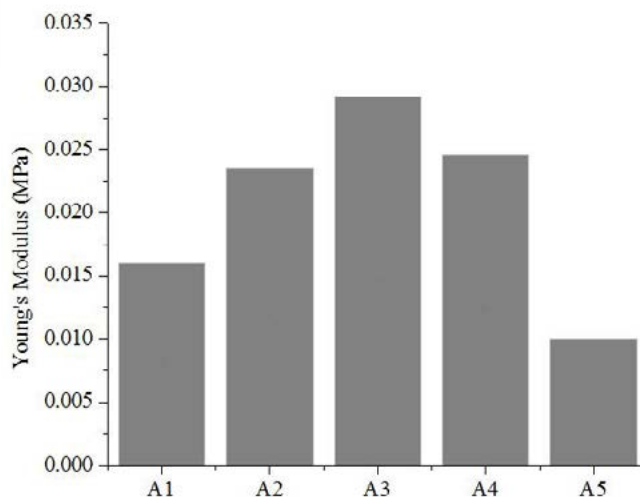


Figure 3. Mechanical testing of chitosan/alginate/geothermal silica scaffold

3.4. FTIR

FTIR was performed to study the molecular interaction between scaffold's components. As seen in Figure 4, chitosan was shown at the wavelength of 1647 cm^{-1} for amide I and 1600 cm^{-1} or amide II. Double peaks in the amide were caused by partial deacetylation of chitin. Amine group (N-H) in chitosan and carboxyl group (C=O) in alginate were shown at the peak of 3315 cm^{-1} and 1621 cm^{-1} , respectively, meanwhile carboxylic acid (-OH) was shown at a wavelength of $\pm 3000\text{ cm}^{-1}$. The peak of 1097 cm^{-1} indicated any silica Si-O-Si content. On the other hand, the peak of 3446 cm^{-1} showed any -OH group on the surface of $n\text{SiO}_2$. The interaction between chitosan and alginate led to friction at the amine group of chitosan. Peak shifts from 1647 cm^{-1} to 1632 cm^{-1} and from 1600 cm^{-1} to 1561 cm^{-1} were caused by interaction between Si-OH group in silica and chitosan.

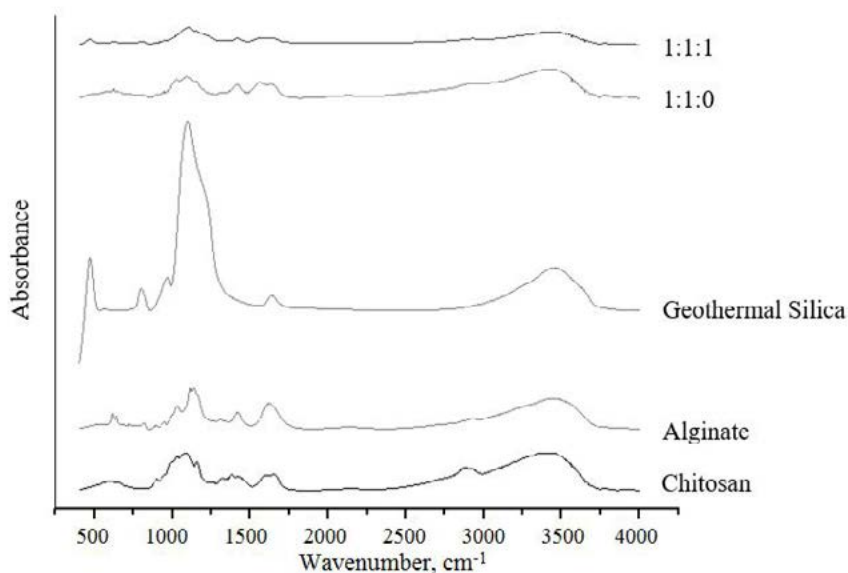


Figure 4. FTIR spectra of each components, scaffold without silica addition, and scaffold with silica addition



3.5. SEM

The SEM analysis was performed to observe the surface morphology of chitosan/alginate and chitosan/alginate/silica scaffold. Figure 5 showed the porous scaffold with pore sizes ranging from 10 to 30 μm , and 15 to 50 μm for chitosan/alginate (A1) and chitosan/alginate/geothermal silica scaffold (A3). The SEM results showed that silica-added scaffold had interconnected pore, compared to scaffold without silica content. This comparison can be observed from Figure 5 (A1) and (A3). From Figure 5 (A5), chitosan/alginate/geothermal silica scaffold with composition ratio of 1:1:2 was more fragile due to lower silica binding polymer, for the same value of total mass. These SEM images may support the reason of the excess addition of silica content which resulted lower its mechanical properties.

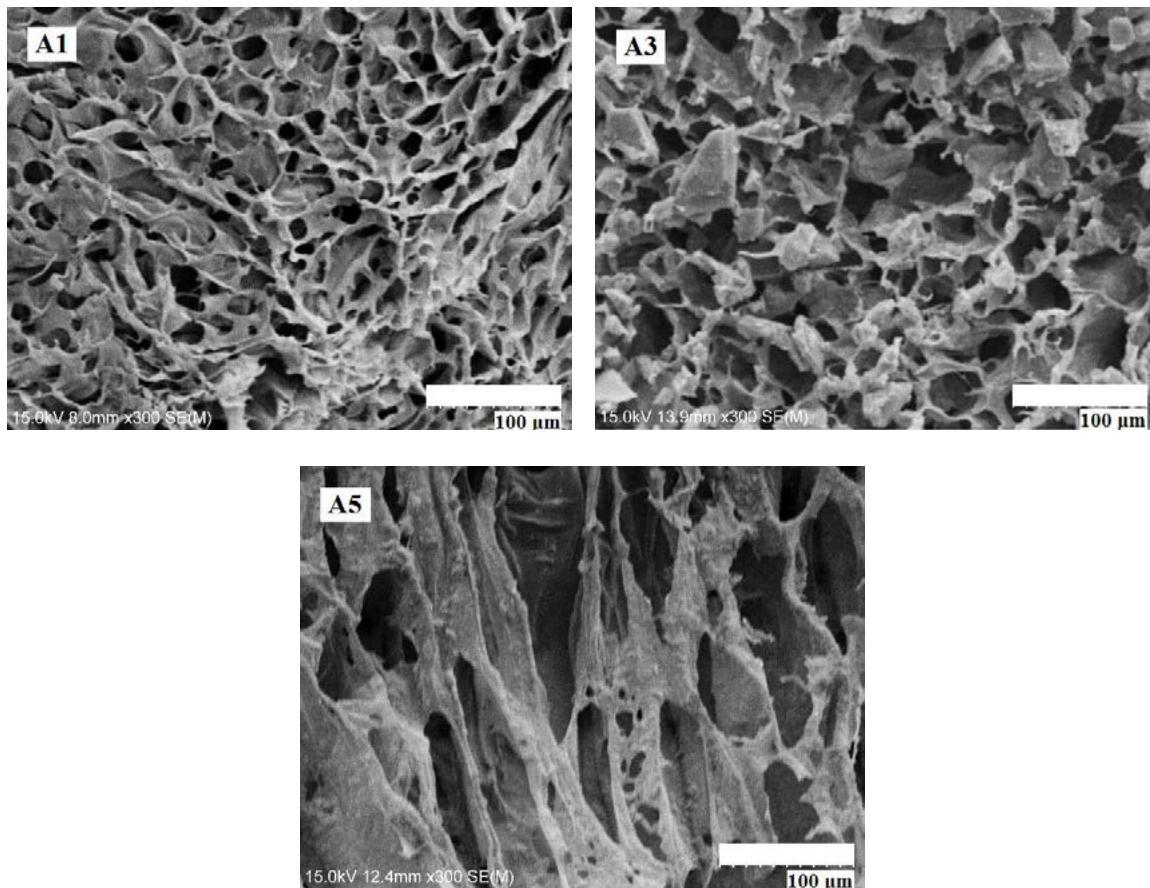


Figure 5. SEM images of chitosan/alginate/geothermal silica scaffold with ratio 1:1:0 (A1); 1:1:1 (A3); and 1:1:2 (A5)

4. CONCLUSION

The effects of geothermal silica addition to the mechanical properties of chitosan/alginate scaffold were successfully investigated. Silica addition improved the mechanical strength of scaffold, wherein the highest Young's Modulus value was achieved by composition ratio of 1:1:1. While, geothermal silica addition reduced the swelling ratio of the scaffold.



5. ACKNOWLEDGEMENTS

The authors gratefully acknowledge for the financial support provided by The Global Collaboration Program of Nara Institute of Science and Technology sponsored by MEXT, Japan.

6. REFERENCES

- Becker, T. A., Kipke, D. R., Brandon, T., 2001, Calcium Alginate Gel: a Biocompatible and Mechanically Stable Polymer for Endovascular Embolization, *J. Biomed. Mater. Res.* 54, pp.76.
- Karp, J. M., Dalton, P. D., Shoichet, M. S., 2003, Scaffolds for Tissue Engineering, *MRS Bull* 28, pp.301.
- Khong, T. T., Aarstad, O. A., Skjåk-Bræk, G., Draget, K. I., Vårum, K. M., 2013, Gelling Concept Combining Chitosan and Alginate-Proof of Principle, *Biomacromolecules*, 2765-2771.
- Kusumastuti, Y., Petrus, H. T. B. M., Yohana, F., Buwono, A. T., and Zaqina, R. B., 2017, March, Synthesis and Characterization of Biocomposites Based on Chitosan and Geothermal Silica. *In: AIP Conference Proceedings*, Vol. 1823, No. 1, p. 020127. AIP Publishing
- Kusumastuti, Y., Shibasaki, Y., Hirohara, S., Kobayashi, M., Terada, K., Ando, T., and Tanihara, M., 2015, Encapsulation of rat bone marrow stromal cells using a poly-ion complex gel of chitosan and succinylated poly (Pro-Hyp-Gly). *Journal of tissue engineering and regenerative medicine*.
- Levengood, S. L., Zhang, M., 2014, Chitosan-Based Scaffold for Bone Tissue Engineering, *J Mater Chem B Mater Biol Med*, pp.3161-3184.
- Ramay, H.R., Li, Z., Hauch, K.D., Xiaou, D., Zhang, M., 2005, Chitosan-Alginate Hybrid Scaffold for Bone Tissue Engineering, *Biomaterials* 26, pp.3919.
- Vallet-Regi, M., Balas, F., 2008, *Silica Materials for Medical Application*, *The Open Biomedical Engineering Journal*, pp.1-9



Flux Coating Effect of SMAW 308L Electrode on Its Mechanical Properties and Corrosion Resistance for Cryogenic Application

Andi Rustandi^{a*}, Suganta Handaru^b

^aDepartment of Metallurgy and Material Engineering, Faculty of Engineering, Universitas Indonesia, Depok 16424, Indonesia

^bPT. Voestalpine Bohler Welding Asia Pacific, Cikarang Sel. 17530, Bekasi, Indonesia

Abstract

Flux coating type of stick electrode of shielded metal arc welding (SMAW) could influence the properties of weld metal. This work described a study of mechanical and corrosion behavior of austenitic stainless steel weld metal grade 308L which deposited by using different type electrodes, namely rutile electrode, lower nitrogen content and basic electrode. Both electrodes were designed to produce the same ferrite content namely 4FN. Several tests such as tensile at room temperature, Charpy impact V-notch and lateral expansion at cryogenic temperature -196°C were conducted to observe the mechanical behavior. Electrochemical testing such as cyclic polarization method was also performed. The used of basic electrode significantly increased charpy impact by 16%, lateral expansion by 51% and slightly increases tensile strength by 6%. Pitting corrosion resistance value was shown by lower properties for weld metal 308L which had lower nitrogen content while rutile and basic type electrode had better its resistance.

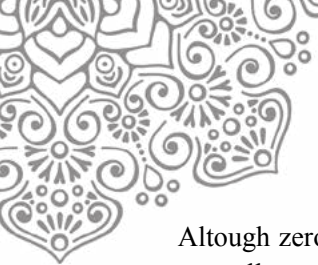
Keywords: Austenitic stainless steel 308L; Weld electrode; Cryogenic; Flux basicity; SMAW

Introduction

Austenitic stainless steel is well known as excellent engineering material due to its good atmospheric corrosion resistance, formability, weldability and superior mechanical properties in cryogenic temperature [1]. Good metal toughness up to temperature below -269°C make austenitic stainless steel widely used in cryogenic application such as in LNG facilities [2]. In LNG production process, after non-methane component are removed, natural gas which manly consists of methane will be cooled to -161°C in atmospheric pressure for liquefaction. Volume of the liquefied gas is 1/620 of the natural gas and makes it more economic for transport. [2,3]. This condition requires material that able to withstand in cryogenic temperature such as austenitic stainless steel grade 304L (18%Cr, 8% Ni) which has charpy impact at -196°C > 100 Joule [4]. 304L parent metal can be welded using GTAW (Gas Tungsten Arc Welding) with filler grade ER308L. This process can produce excellent cryogenic toughness with Charpy impact > 50 J at -196°C [4,5]. However GTAW process has slow productivity and expensive operation cost. In general, SMAW (shielded metal arc welding) is still popular and attractive at this present due to its simplicity, flexibility and relatively low operational cost [6]. However weld metal cryogenic toughness deposited by SMAW is not as good as GTAW where lateral expansion is not consistently achieve ≥ 0.38 mm at -196°C as minimum requirement at many LNG specification that refer to ASME SEC VIII. This is caused by high non-metallic inclusion and high oxygen content at flux shielded processes [7]. Previous intensive researches have been conducted to understand metallurgical factor that influence cryogenic toughness at austenitic stainless steel. Szumachiwski, et all [7] investigated cryogenic toughness at varies austenitic stainless steel weld metal grade with chemical composition not confined with AWS A5.4 chemistry range. The maximum cryogenic toughness (-196°C) were achieved by low carbon, low ferrite and the used of lime-covered electrode. Further research conducted by Szumachowski, et all [8] revealed that low nitrogen content at weld metal (<0.05%) promoted good cryogenic toughness.

* Corresponding author.

E-mail address: rustandia@gmail.com



Although zero ferrite or low ferrite content provided beneficial effect for cryogenic toughness, it is needed as well to prevent hot cracking during welding of austenitic stainless steel [9]. Basic/lime covered electrode has better toughness compare to rutile electrode however weldability of basic electrode is not as good as rutile electrode where the slag detachability is poor and it can lead to welding defect such as slag inclusion [8]. Special desain of SMA 308L weld metal need to be controlled in order to get optimum properties which cover good cryogenic toughness, good hot cracking resistance and good weldability. The objective of this study was to determine the effect of nitrogen content and flux basicity in shielded metal-arc austenitic stainless steel weld metal grade E308L-16 on mechanical properties.

Experimental Method

Several series of 308L covered electrode were specially produced in order to get weld metal chemistry with variation in ferrite number, nitrogen content and flux basicity as described in Table 1. Sample F series consist of four electrodes E308L-17 with typical nitrogen $0.055 \pm 0.03\%$ w.t and ferrite content i.e 2, 4, 6, and 10 FN were varied by modifying recovery of nickel and chromium via addition of chromium and nickel powder in the flux. One electrode E308L-17 was produced with lower nitrogen content i.e 0.037% w.t and ferrite 4 FN. The last electrode E308L-15 has ferrite 4 FN and produced using more basic flux by adding more carbonate and fluorite bearing minerals in the flux. All electrodes were produced using 308L core wire 4.0 mm sizes and with the same heat except sample N4(3-5) that used low nitrogen in the wire. All specimens were welded by the same welder and welding machine. Welding parameter were maintained in the same level i.e. heat input between 0.93 -1.33 KJ / mm and interpass temperature 130°C max. Chemical analysis was measured using optical emission spectroscopy. Ferrite contents were calculated using WRC-92 diagram and measured by using fisher ferritscope as comparison. Impact specimen were tested at cryogenic temperature (-196°C). All weld metal tension tests were carried out at room temperature according to standard AWS B.4.0. Further another test was performed to evaluate corrosion behavior of the weld metal samples by using cyclic polarization method as per ASTM G61-86.

Table 1. Weld Metal Chemistry of Samples

Identity	F2(7-10)	F3(5-7)	F4(3-5)	F5(0-3)	N4 (3-5)	B4(3-5)
Flux Type	Rutile	Rutile	Rutile	Rutile	Low N	Basic
% C	0.022	0.020	0.019	0.017	0.018	0.027
% Si	0.820	0.780	0.770	0.980	0.980	0.340
% Mn	0.590	0.570	0.570	1.530	0.650	1.290
% P	0.025	0.027	0.022	0.024	0.037	0.024
% S	0.022	0.022	0.021	0.018	0.014	0.019
% Cr	19.75	19.04	19.08	18.48	18.30	19.22
% Ni	9.730	9.850	10.53	10.71	10.37	10.64
% Mo	0.001	0.001	0.055	0.001	0.002	0.001
% Nb	0.004	0.004	0.004	0.009	0.008	0.004
% Cu	0.019	0.014	0.153	0.011	0.296	0.013
% N	0.052	0.055	0.058	0.053	0.037	0.044
Ferrite Content						
WRC92	10	6	4	2	4	4
Ferritescope	10	6.1	3.4	2.2	4.0	3.9

Individual groove weld assemblies were prepared and welded by each electrode according to AWS.A5.4 as shown in Fig.1(a). Charpy impact V-notch specimens were prepared according to ASTM E23 with specimen sizes 10 x 10 x 55 mm taken from cross section of welded specimen and notch location was perpendicular to welding direction as shown in Fig.1 (b).

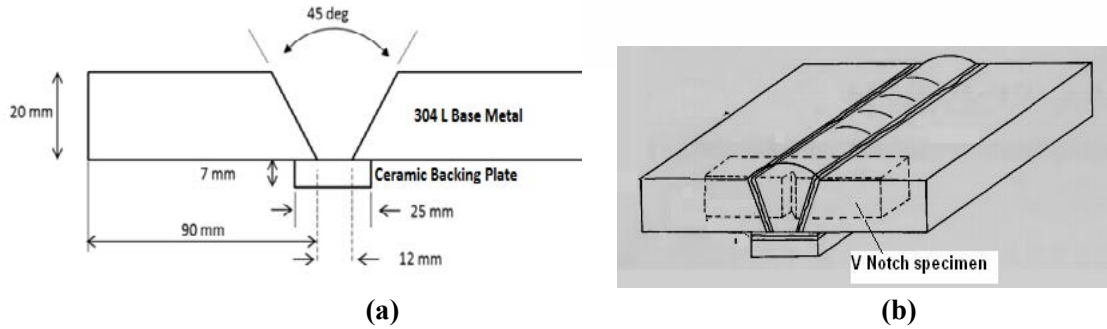


Figure. 1 Groove weld test assembly (a). Charpy V-notch specimen (b).

Results and Discussion

Hot Cracking Resistance Prediction. Hot cracking resistance of stainless steel weld metal can be predicted using Suutala diagram by plotting value of impurities elements sulfur and phosphorus versus ratio of Cr_{eq}/Ni_{eq} [10]. According to the calculation shown in Table 2, the ratio of Cr_{eq}/Ni_{eq} for all 308L samples are between 1.5 – 1.7 which indicating less cracking susceptible.

Table 2. Calculation of Suutala and WRC-92 Ratios

Sample Code	Suutala Ratio	WRC-92					Ferrite Scope
		Cr_{Eq}	Ni_{Eq}	Cr_{eq}/Ni_{eq}	FN	Solidification	
F2(7-10)	1.88	19.8	11.5	1.7	10	FA	10
F3(5-7)	1.81	19.0	11.7	1.6	6	FA	6.1
F4(3-5)	1.68	19.1	12.4	1.5	4	FA	3.4
F5(0-3)	1.62	18.5	12.4	1.5	2	FA	2.2
N2 (3-5)	1.72	18.5	11.8	1.6	4	FA	4
B2(3-5)	1.61	19.2	12.5	1.5	4	FA	3.9

Fig. 2 shows all weld metal samples 308L presents in the region that had good resistance with hot cracking. This result is supported by other methodology described in Fig 2(b) which shows cracking susceptibility according to WRC 92. Based on this method, the weld metal with Cr_{eq}/Ni_{eq} – WRC92 more than 1.5 has less cracking susceptibility [10,11].

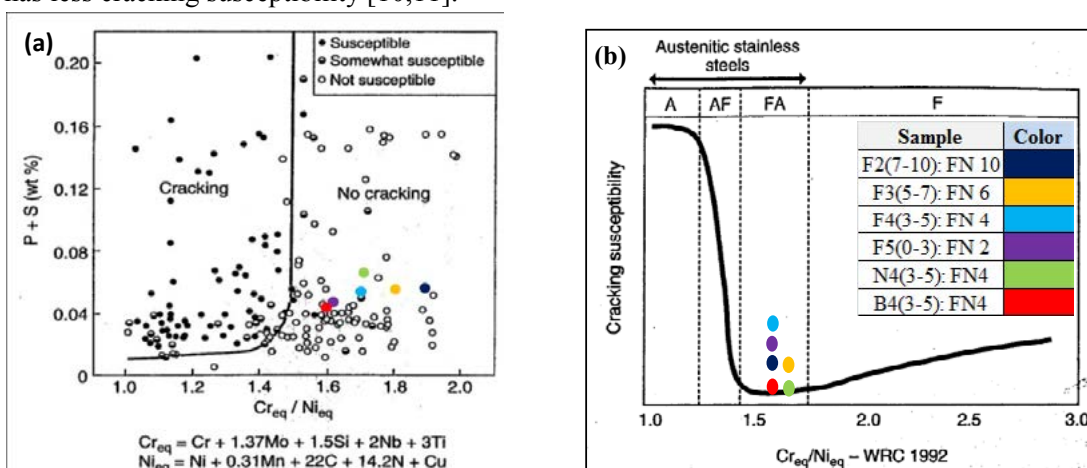


Figure. 2 Weld Solidification Cracking Susceptibility based on (a) Plot Sutalla Diagram. (b) WRC 92



Hot cracking resistance of weld metal is affected by several factors such as :

a. Low level of impurities sulphur and phosphor (< 0.051%w.t.).

Sulphur and phosphor are well known as harmful elements that led to hot cracking [10] where these elements according to J.C. Lippold et all [11] will segregate along fusion zone grain boundaries and promoted present of low melting eutectic phase. Effect of low level of sulphur and phosphor will prevent formation of low melting intermetallic phase and reduce potential of hot cracking.

b. Microstructure with ferrite content 2-10 FN.

The presence of ferrite effect was reported by Hull, and Brook [13,14] which could prevent hot cracking in many austenitic stainless steel weld metal. Ferrite had higher solubility of sulphur and phosphor compared with austenitic, so it could reduce formation of low melting intermetallic phase by restricting segregation of sulphur out from interdendritic region during solidification of primary ferrite.

c. Solidification mode FA.

Most austenitic stainless steel weld metals are designed to solidify to give primary ferrite and secondary austenite to minimize the occurrence of hot cracks. This solidification mode is known as the ferritic-austenitic solidification mode (FA mode). Hot cracking resistance are strong function of solidification mode with FA mode offer the greatest resistance [11]. Kujanpaa,et all [15] mentioned that primary ferrite solidification inhibited crack initiation and propagation and promote backfilling. FA mode had also solidification grain boundary which involved a mixture of ferrite and austenite that prevented liquid film wetting. In addition, this boundary had very non-polar crack path where crack would be very difficult to propagate once initiated [9].

Effect of Nitrogen and Flux Basicity. Fig. 3 shows the effect of nitrogen and flux basicity on tension properties of 308L weld metal at room temperature. Mechanical properties of weld metal with low nitrogen (0.037%w.t) is lower which compared to weld metal with 0.058% w.t nitrogen at the same ferrite content 4 FN in the weld metal. The significant decrease of yield strength results in 6% from 419 MPa to 394 MPa. Besides that, the elongation of weld metal with lower nitrogen content is 7.5% higher. McCowan et. all [19] described that addition of nitrogen between 0.05%-0.25%w.t increased linearly yield strength from 600 – 1300 MPa which is an interstitial solid solution strengthening, thus lowering nitrogen content will reduce weld metal strength.

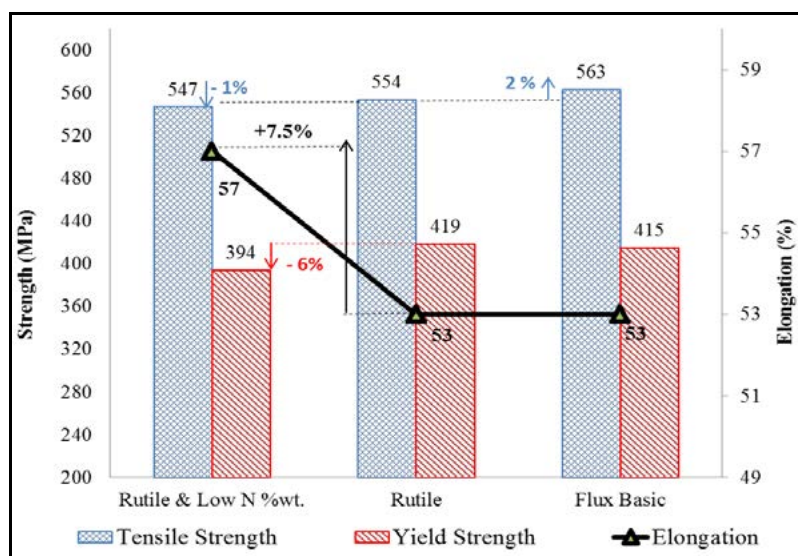


Figure. 3 Effect of Nitrogen Content and Flux Basicity on Mechanical Strength



Weld metal deposited with basic electrode has marginally higher tensile strength compared with weld metal deposited by rutile type at the same ferrite content (4FN). Better CO₂ shielding gas protection produced by basic type electrode [20] results in higher recovery of manganese i.e. 1.29% w.t vs 0.57%w.t rutile type. In addition better CO₂ protection also leads to low dissolution of nitrogen content during reaction at interface liquid weld metal – gas phase [20]. Lower nitrogen content is observed at basic type deposited with nitrogen content 0.044% w.t vs 0.058%w.t rutile type which produced using same heat core wire. This composition causes yield strength of basic type weld i.e. 415 MPa which is 1% lower than rutile type i.e. 419 MPa. The elongation of basic type is the same as rutile type which is 53%. Fig. 4 shows the effect of nitrogen and flux basicity on cryogenic toughness of 308L weld metal. Reducing nitrogen content from 0.053% to 0.037%w.t at the same ferrite content increases the impact strength from 29 Joule to 32 Joule, which is 10 % higher. The same behavior is also observed at lateral expansion where the weld metal with 0.037% w.t nitrogen has 37% higher than 0.053% w.t nitrogen with increment of lateral expansion from 0.36 mm to 0.49 mm.

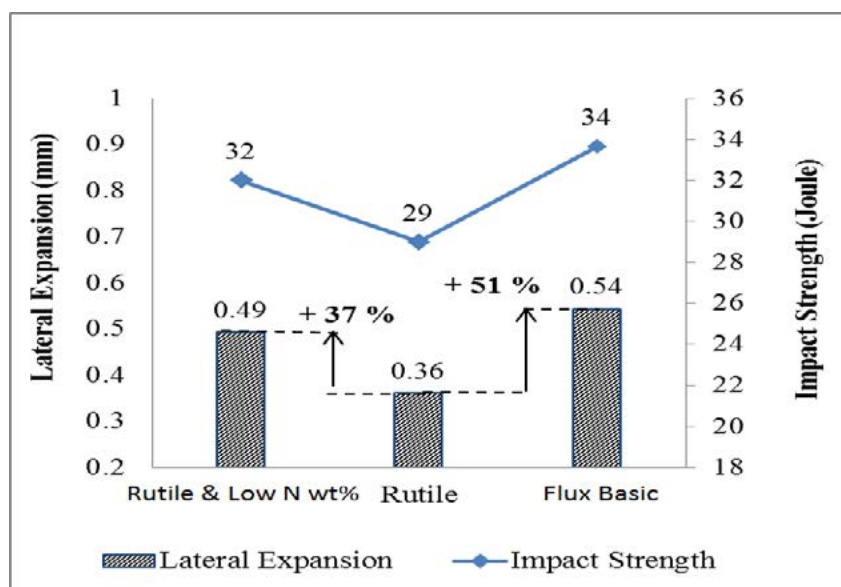
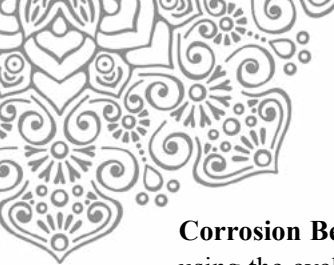


Figure. 4 Effect of Nitrogen Content and Flux Basicity on Cryogenic Toughness

This results confirm with previous research that involved E308-15 weld metal with FN 3 which conducted by Szumachiwski et all [7,8]. They found that nitrogen reduction from 0.55% to 0.035%w.t increase lateral expansion by 25% from 0.39 mm to 0.49 mm. which concluded that optimum cryogenic toughness of austenitic stainless steel weld metal was achieved by controlling nitrogen content as low as possible or less than 0.05% w.t. Deposited weld metal from electrode type basic, remarkably improved lateral expansion by 51% from 0.36mm to 0.56 mm. Impact strength of basic type electrode also 17% higher compared with rutile type electrode at the same ferrite content level. Impact strength was increased from 29 Joule to 34 Joule for basic type electrode. This result was also supported by Szumachowski et all. which revealed that deposited weld metal from basic type electrode provided better cryogenic toughness at all ferrite content [7,8,9]. Superior cryogenic toughness at basic type electrode resulted from less oxygen content due to better weld pool protection by shielding gas from decomposition of carbonate mineral. Kotecki [21] reported that weld metal oxygen content at basic type was around 500 ppm while rutile type was between 600 – 900 ppm. The higher oxygen content could increase non-metallic inclusion density.



Corrosion Behavior. The corrosion behavior of three different weld metal samples can be represented by using the cyclic polarization testing results to evaluate pitting corrosion resistance respectively as shown in figure 5.

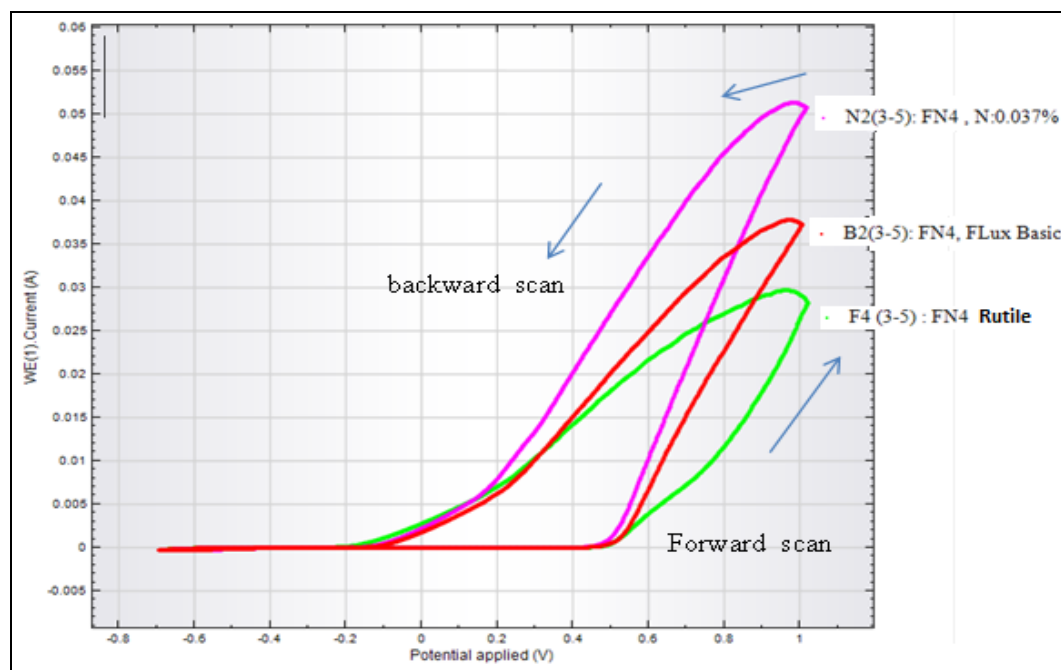


Figure 5. Cyclic Polarization Curves for Pitting Corrosion Resistance Evaluation

It shows the cyclic polarization curves for weld samples which are slightly different from each other but the weld metal sample with lower nitrogen content has the lowest pitting corrosion resistance compared to the others. In other words, the lower the nitrogen content then the weld metal has lower “pitting resistance equivalent number” (PREN) which indicates the pitting resistance parameter that affected by its nitrogen content.

Conclusions

The effect of nitrogen content and flux basicity on mechanical properties of different types of weld metals SMA 308L are concluded as the following :

- A reduce in nitrogen content from 0.058% w.t to 0.037%w.t at the same ferrite level reduces yield strength by 6% and increases elongation by 7.5%. Lower nitrogen significant improves cryogenic toughness which provides 37% higher lateral expansion and 10% higher impact strength.
- The used of basic electrode slightly increase weld metal strength 308L. It also significantly improves cryogenic toughness which has 51% higher lateral expansion and 17% higher impact strength.
- Based on its corrosion behavior, lowering nitrogen content in weld metal can reduce pitting corrosion resistance.

Acknowledgements

The authors are greatly thankful to DRPM-Universitas Indonesia and PT. Voestalpine Bohler Welding Asia Pacific for supporting this research.



References

- [1] Micheal McGuire. *Stainless Steel for Design Engineer*. ASM International.2008
- [2] Swales,G.L. *Role of Nickel Steels in LNG Tankers*.Metal Progress.1975
- [3] Lide. *CRC Handbook of Chemistry & Physics*.Edition 76. 1995
- [4] Liane Smith, Bruce Craig.*Properties of Metallic Materials for LNG Service*.Presented at 9th MECC, Bahrain,2001.
- [5] Welding Solutions for the LNG Industry. Voestalpine Bohler Welding.2014
- [6] Linnert.G.E Welding Metallurgy Volume 1.AWS.1994
- [7] E.R. Szumachowski, H.F.Reid. Cryogenic Toughness of SMA Austenitic Stainless Steel Weld Metals: Part I-Role of Ferrite. Welding Journal,November 1978.
- [8] E.R. Szumachowski, H.F.Reid. *Cryogenic Toughness of SMA Austenitic Stainless Steel Weld Metals: Part II-Role of Nitrogen*. Welding Journal,February 1979.
- [9] John C. Lippold, Damian Kotecki. *Welding Metallurgy and Weldability of Stainless Steel*.Wiley.2005
- [10]Kujunpaa, Suutala. *Correlation between Solidification Cracking and Microstructure in Austenitic and Austenitic-Ferritic Stainless Steel Welds*.Welding Research International.9:55 (1979).
- [11]Lippold.J, Savage.W.F.*Solidification of Austenitic Stainless Steel. Part III: The Effect of Solidification Behavior on Hot Cracking Suceptibility*. Welding Journal:388s-396s.(1982).
- [12]J.Wu.Fu. Formation of a Blocky Ferrite in Fe-Cr-Ni Alloy during Directional Solidification. Journal of Crystal Growth 311: 3661-3666.(2009)
- [13]Hull.F.C.*Effect of Delta Ferrite on the Hot Cracking of Stainless Steel*.Welding Journal 46:339s-409s.(1967).
- [14]Brook,J.A. *A Fundamental Study of the Beneficial Effects of Delta Ferrite in Reducing Weld Cracking*. Welding Journal, 63(3):71s-83s.(1984).
- [15]Kujunpaa, S.A David, C.L.White. Formation of Hot Crack in Austenitic Stainless Steel Welds-Solidification Cracking. Welding Journal :203s-212s.(1986).
- [16]Lippold.J, Savage.W.F.*Solidification of Austenitic Stainless Steel. Part I: Proposed Mechanism*. Welding Journal:362s-372s.(1979).
- [17]David.S.A. Ferrite Morphology and Variation in Ferrite Content in Austenitic Stainless Steel Welds. Welding Journal:63s-70s.(1981)
- [18]Hauser,D et all. Effect of Ferrite Content is austenitic Stainless Steel Welds. Welding Journal,61(2).37s-44s.(1982)
- [19]McCowan.C.N, Siewert.T.A,et all. *Manganese and Nitrogen in Stainless Steel SMA Welds for Cryogenic Service*.Welding Journal: 84s-92s.(1987).
- [20]Sindo Kou. *Welding Metallurgy* 2nd Edition. A Willey Interscience Publication.(2002).
- [21] Kotecki. *Stainless Q&A*. Welding Journal, 82(11):80-81.(2003).



PREDICTING MODELS OF CO₂ MATERIALS PIPING/PIPELINE FOR INITIATION STEP-PERTAMINA'S CO₂ EOR PROGRAMS: FIELD DATA, SOFTWARE SIMULATION AND LABORATORY

Harris Prabowo^{1,2}, Johny W Soedarsono², Badrul Munir², Andi Rustandi², Yudha Pratesa²

¹ *Pertamina UTC (h_prabowo@pertamina.com)*

² *Departemen Teknik Metalurgi & Material Faculty of Engineering Universitas Indonesia (harrisprabowo90@gmail.com)*

ABSTRACT

As Indonesia's national energy company fully owned by the Government of Indonesia, Pertamina is faced to oil production enhancement on brown fields, relatively low cost oil, government policy to reduce gas prices and reduction of CO₂ gasses emission. Field development issues and production operation tend to set course to a condition of which the oil/gas wells have the tendency to carry relatively high impurities components (CO₂, H₂S, chloride ions) that results in early corrosion occurrence, creating damages that can start from underground equipment (casing, tubing, and packer) then leads to production facilitation on ground, which are well head, flowline, header manifold and also into gas processing plant.

Pertamina CO₂ EOR program is part of a program planned increasing production based on data from the Ministry of Energy & Mineral Resources of the Republic of Indonesia that the potential pilot project is Jatibarang Field in West Java with 0.09 TSCF potential gas reserves, oil is 49.3 MMSTB and $\pm 23\%$ CO₂ content. Given the impact caused by the CO₂ component and the possibility of other components such as H₂S and chloride ions (Cl⁻), therefore, this paper will lead to the possibility of material damage and the risk of corrosion of the material selection options in the PERTAMINA program plan.

Predicting model of material method is for initiation phase proposal by the evaluation of closest field data/literature review, simulation software, material and fluid analysis test and corrosion resistance test on the test sample and Materials Duplex 22Cr-15 Cr. The output of predictive models is to forecast corrosion allowance for new design and predict will be able to extend the life of the operating performance of production equipment, the requirements of HSSE (Health Safety Security and Environment) and to optimize the investment costs (Capex) and operating costs (Opex) on the next selection phase.

Keywords: Predicting Models, CO₂ Corrosion, CO₂ Materials, CO₂ EOR

1. INTRODUCTION

Oil and gas currently still become the source of income in The Indonesian Budget (APBN), hence the relatively low oil price and Government's policy plan to reduce gas selling price along with global charges on carbon gas emissions reduction. Therefore, oil and gas production eventually still be one of the most strategic incomes and naturally the production decline rate should be resisted and developed. On the other side, oil and gas potential that are yet to be discovered and unable to be produced/lifted commonly found in challenging locations.

As Indonesia's national Energy Company fully owned by the Government of Indonesia, PERTAMINA operates not only onshore/offshore upstream production facilities (oil and gas field and geothermal) but also gas plants, refinery, fuel product, fuel distribution on Indonesia area, petrochemical product and lubricants.

It has to be admitted that Indonesia's oil production is experiencing production deflation down to around 800 thousand barrels per day and based on data from Indonesia's Ministry of



Energy and Mineral Resources, it is mentioned that unrecoverable resources substitution potential have reached 46.42 billion STB, of which are EOR (Enhanced Oil Recovery) method in the amount of 4.3 billion STB and potential pilot project CO₂ Flooding EOR Project is Jatibarang Field in West Java with 0.09 TSCF potential gas reserves, oil is 29.3 MMSTB and \pm 23% CO₂ content¹. One of the oil lifting methods with EOR is injecting CO₂ into future production's formation candidate and CO₂ gas source can be extracted from its vicinity. Few of Indonesia's gas fields which are owned by PERTAMINA contain CO₂ components that can be used for oil lifting using CO₂ EOR method².

Currently, oil and gas prices are relatively low around US\$ 50 per barrel but in Indonesia, gas prices are still considered to be high to industries and expecting the Government's discourse to lower the natural gas selling prices, so that local industrial activities can be more encouraged. Based on this, oil and gas companies are facing a special challenge, which are optimizing on capital price/investment and operational cost, encountering problems that are initially based on oil and gas with slight impurities during exploration/production, but also activities that lead to formation rock zone with high impurities.

H₂S, CO₂ and Chloride ions are less favoured impurity contents. The existence of these impurities, other than causing more special processes on separation process, conditioning process, and specified material choosing, will also face high risks on corrosion and material degradation.

Lifting activities and transporting oil and gas will transport impurities (H₂S, CO₂ and Chloride ions) which impact on corrosive/material degradation on metal-based material surfaces that eventually will stop the production activity, loss of income and opportunities costs, and also HSSE (Health, Safety, Security, Environment) impact and equipment's reliability problems. Material degradation or commonly mentioned as corrosion, which is 60% material failure³ in oil and gas fields, is caused by CO₂ corrosion. The impression that occur from corrosion on oil and gas industries is the expenses of annual capital expenditure, estimated as much as US\$ 1.372 billion, consists of US\$ 589 million piping cost and surface production facilities, US\$ 463 on annual well tubing pipes and miscellaneous costs connected to corrosion claimed as US\$ 320 million⁴.

The process of discovery oil and gas is initially started by oil and gas exploration activity, i.e. seismic survey, prospect evaluation, exploration risks analysis, volumetric magnitude reserve, and extreme environmental conditions occurrence along with the environment regulation and other commercial requirements that has to be fulfilled, which nevertheless are considered as economical values and final investment decisions (FID).

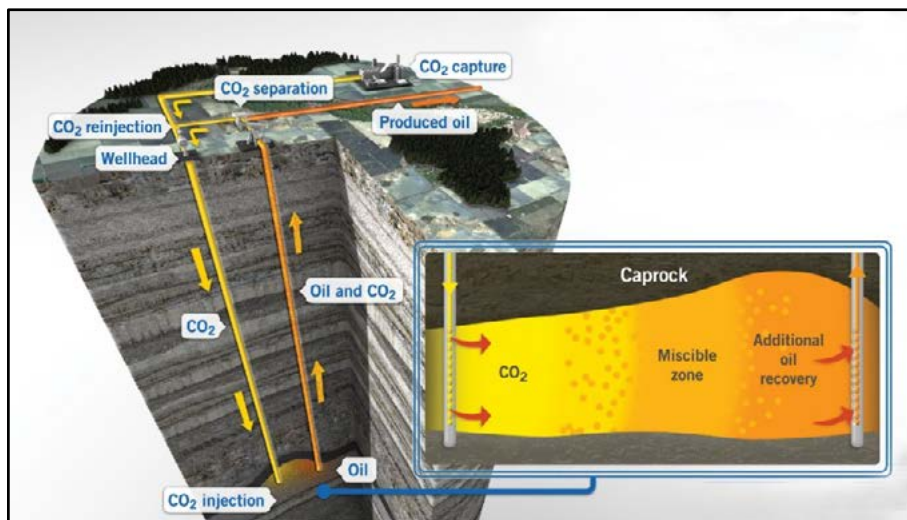
Prospect evaluation results, volumetric magnitude reserve, and the result of well tests on pressure, volume, temperature and fluid compositions are effect on variable techno economic assessment, material selection and corrosion control.

In oil and gas production's environment, there are few components in oil and gas fluids that are corrosive in nature, which are oxygen-O₂ (Oxygen Attack), Carbon Dioxide-CO₂ (Sweet Corrosion), hydrogen sulphide - H₂S (Sour Corrosion), fluid temperature, water salinity, water cut, fluid dynamics, and pH⁵. The effect of carbon steel alloy base damages due to the exposal of corrosive fluid components has piqued interests from researchers, mainly because of the existence of CO₂ and other impurities that are commonly present in oil and gas fluids, which cause not only general corrosion but also localised corrosion. Adjacent to that, CO₂ components and other impurities existence are potential to the decrease of material's thickness which leads to weight loss, pitting, and sulphide/chloride stress cracking. It eventually depends on how much CO₂ and other impurities existence and the possibility of other water phase and hydrocarbon occurrence.



Oil lifting method using EOR by injecting CO₂ is an opportunity and challenge in oil and gas industries that usually applies few steps in its final investment decision (**Initiation Step**, **Selection Step**, **Advanced Study Step**, and **Execution Step**).

The main focus in EOR CO₂ injection (**Figure 1**) is downhole injection system and flowline production toward header manifold before undergoes the separation process, condition process, capturing CO₂ process and back to reinjection process system. Downhole injection system itself consists of casing pipe, tubing pipe, and wellhead with appurtenances, whilst the operational condition is injection pressures that are relatively high and CO₂ condition is in supercritical state.



Source: <http://www.powermag.com/is-eor-a-dead-end-for-carbon-capture/>

Figure 1 Schematic Flow Diagram CO₂ Injection.

This paper will explain how the writer is assigned to make suggestions on materials for oil and gas development scenario using EOR CO₂ injection method in **Initiation Step** by using field data evaluation, software simulation and laboratory test data. The collected data are the field data from exploration/production drilling, material degradation study in oil and gas field that contains CO₂ impurities up to 25 %mol and H₂S up to 1 %mol, and also software simulation and laboratory tests.

Nowadays, oil and gas fields that contain fluid impurities, the use of CRA (Corrosion-Resistant Alloys) materials, has become the main deliberation in designing production facility equipment's and piping system, of which in development of oil and gas field is generally high cost and high risk.

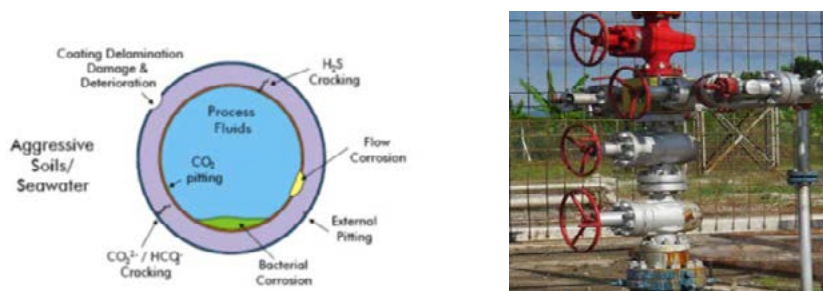


Figure 2 Area of predicting corrosion



The objective of material prediction model within initiation-step of the scope of the development of oil and gas wells (Figure-4 and Figure-5) using CO₂ EOR injection methods in the **initiation phase** is to acquire different options on appropriate material for fluid flow line having a content of impurities and under conditions of high pressure and supercritical state.

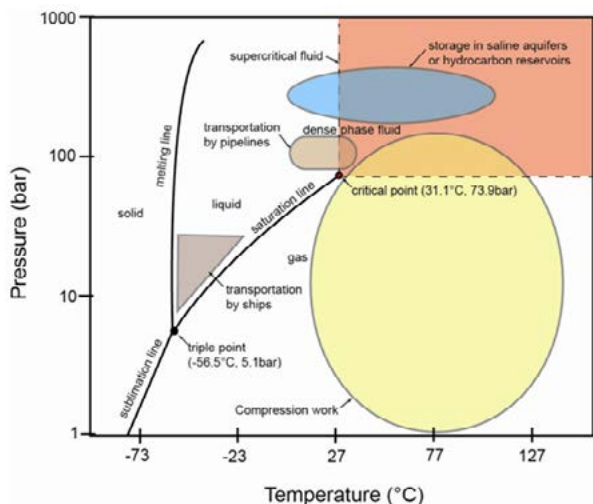


Table 1 The design required for the injection of CO₂ (Data Field)

Operating Condition		Max.Flow	Ave.Flow	Min.Flow
CO ₂ Injection Pressure	psia	1.150	1.250	1.270
CO ₂ Injection Temperature	°C	32	32	32

Figure 3 Various Operations on the CO₂ phase diagram⁹

2. METHODOLOGY/EXPERIMENTAL

Considering the complexity of instruments that will be used on production development of an oil and gas field (Figure 4) and stages of Scope of Business Process on Oil and Gas Company (Figure 5), along with the variety of impurities, accordingly this paper will be limited into initiation step and its material select options are based on provided data which have actual condition of relatively high on oil and gas field (CO₂ 25 %mol, H₂S 1-1.2 %mol and the presence possibilities of Chloride ions), and hence will be selected 2 (two) material types as early prediction material, which are material with 15% chromes and 22% chromes that are widely known for CRAs.

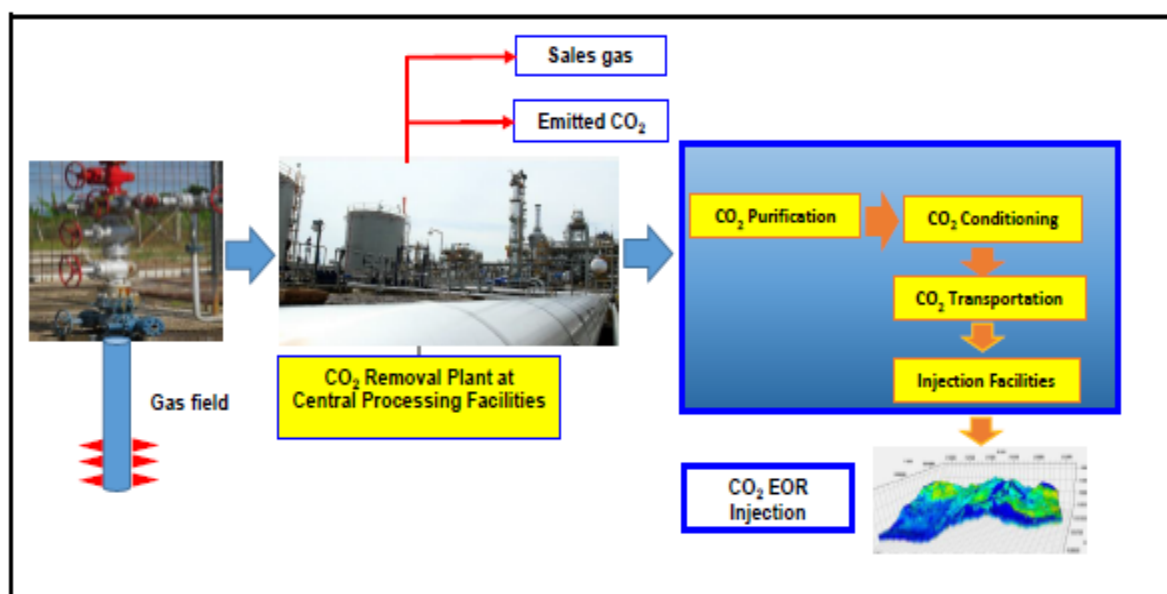


Figure 4 Typical Scope of Work Surface Process and Facilities on Oil and Gas

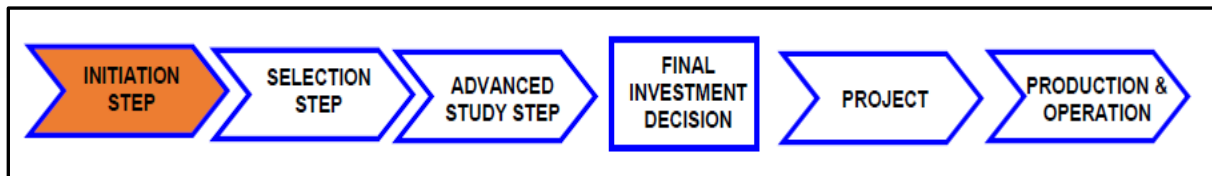


Figure 5 Typical Evaluation Stages Scope of Business Process on Oil and Gas Company

Model predictions of the corrosion rate can utilize common operational parameters available, laboratory data / field existing and theoretical models to get the realistic prediction of corrosion rate⁶ (B. Khajotia, 2007).

There has been a plenty of CO₂ prediction model development in oil and gas production system using different assumptions/methods/references/studies. Prediction toward a few prediction model⁷ (Nyborg, 2010) that are applied on oil and gas industries, is using field data (DeWaard Model, Norsok M-506 Model, Hydrocor, Corpor, Casandra, KSC Model, Multicorp, ECE Model, Predict, Tulsa Model, ULL Model, CorPos, OLI Model, and SweetCor) and factors from the effect of protective corrosion films and the effect of oil wetting on CO₂ corrosion. The application of predicting model method is also applied on oil and gas production operation problems in top of line corrosion (TLC) on seabed pipelines, specifically the cold spot where detected leaks are estimated in conjunction to water condensation rate and corrosion rate⁸ (Y. Gunaltun et/ al, 2010), based on modelling using field data.

2.1 Research Method and Process Flow Diagram

In order to conform the mentioned business process steps (Figure 5), as new material option predicting evaluation, recent suggestion on suitable material model predicting based on oil and gas field developing investment scenario will be using EOR CO₂ injection method is based on literature study, evaluating field data including production estimation scenario on field that becomes fitting development candidates and then the first step data will be evaluated using oil and gas production facility concept simulation, of which are needed to field development using *Questor IHS software* to obtain *unclassified (conceptual)* estimation of capital expenditure (CAPEX) and operating expenditure (OPEX) also Decommissioning Cost.

The data that are needed for the simulations are Recoverable Reserve, Condensate gas ratio, Reservoir Depth, Reservoir Pressure, Reservoir Length, Reservoir Width, field terrain contours, and estimated contents of CO₂ and H₂S (fluid test laboratory data from drilling results). Pipeline material options in *Questor IHS software* are Carbon Steel X-60, X-65, X-70, X-80, Clad 316 Stainless Steel, Clad 825 Alloy, Duplex and CRA. Therefore, material selection of the predicting model is chosen based on assumed material, software simulation and laboratory test to choose materials and estimated appropriately and economically, also based on field development scenario and company's policy management.

2.2 Experimental/Materials Database (Internal Data)

Laboratory simulation is established to acquire corrosion rate of the materials for flowlines, both for the selected and predicted flowline, that will run into material degradation upon field application. Laboratory simulation that is done by using potentiometer and CMS 100. Kinetic reaction that occurs on sample test dipped in a soluble inside polarization flask will be measured by potentiometer and CMS 100 into polarization chart. This polarization chart then will be analysed further using CMS 100 software, which then will acquire the parameter values of kinetic corrosion that consists of corrosion potential, current density, tafel constants and corrosion rate.

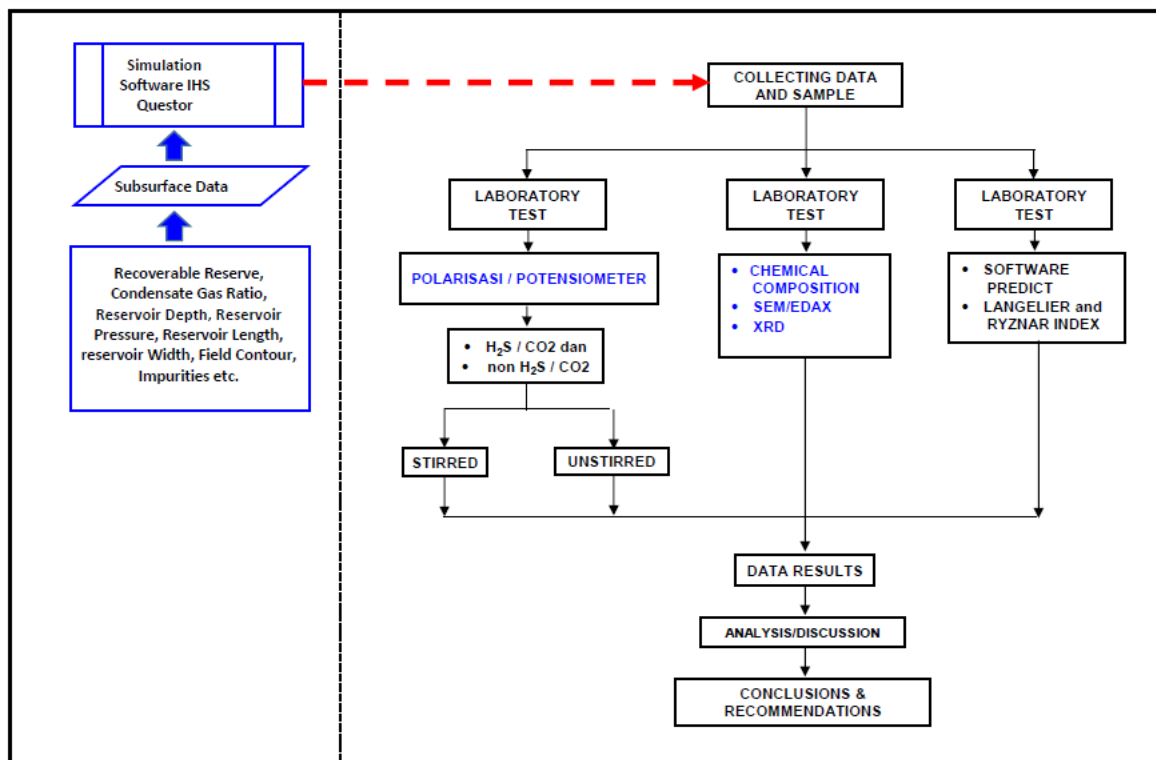


Figure 6 Flow Diagram Research Methods

Composition test is done to understand the accuracy of material compositions. By doing so, the acquired compositions then compared to the existed standard composition. Chemical composition test is done by using Optical Emission Spectrometer. This optical emission spectrometer is a way to analyze based on principle of physics, which is electromagnetic radiation characteristics, where chemical composition test is obtained based on observing the radiation energy interaction spectrum with the substance. To understand how high the percentage of the contents and composition, the specimens are cut according to the required sizes, then placed in the spectrometer. The next step is to emit the contents and tested material's percentage.

Material test is also done by using Philips' Scanning Electron Microscope 515 (SEM 515) which includes disperse energy X-ray PV 9900 model (EDAX PV 9900). The specification of SEM has the resolution of 12.5 Ampere, magnification is between 15 to 240,000 times, and depth of field is ranged between 0.5 μm on 80 times. SEM-EDAX is used to observe the microstructures of carbide chrome materials by detecting the amount of intensities toward the accounted energies. The mentioned compounds distribution is approached by the wavelength value. The obtained results are analyzed by mapping method. This method can precisely perceive the elements of a sample. Mapping is done by firstly set the detector position to match the utilized element.

3. LABORATORIUM TEST: ANALYSIS AND RESULT (THE COMPANY'S INTERNAL DATA)

3.1 Composition of Materials Test

Material composition test using spectrometer on 2 CRA materials (15-Cr and 22-Cr) shows each mixed compositions as follows on Table 2.



Table 2 Composition of Materials Sample Test SS 15Cr

	Fe	C	Si	Mn	P	S	Cr	Mo
1	75.6	0.0844	0.198	0.305	< 0.0030	< 0.0050	14.9	2.05
2	75.6	0.0564	0.193	0.294	< 0.0030	< 0.0050	15.2	1.98
3	75.4	0.0611	0.213	0.291	< 0.0030	< 0.0050	15.2	2.02
Ave	75.6	0.0673	0.201	0.297	< 0.0030	< 0.0050	15.1	2.02
	Ni	Al	Co	Cu	Nb	Ti	V	W
1	5.48	0.0535	0.0946	0.941	0.0665	0.0074	0.0426	< 0.0200
2	5.36	0.0460	0.0931	0.898	0.0637	0.0076	0.0439	< 0.0200
3	5.48	0.0490	0.0928	0.884	0.0654	0.0084	0.0422	< 0.0200
Ave	5.44	0.0495	0.0935	0.908	0.0652	0.0078	0.0429	< 0.0200

Table 3 Composition of Materials Sample Test SS 22Cr

	Fe	C	Si	Mn	P	S	Cr	Mo
1	66.6	0.0471	0.533	1.47	0.0083	< 0.0050	22.8	3.31
2	66.1	0.0558	0.531	1.47	0.0097	< 0.0050	23.2	3.25
3	66.3	0.0463	0.508	1.46	0.0075	< 0.0050	23.0	3.47
Ave	66.3	0.0497	0.524	1.47	0.0085	< 0.0050	23.0	3.34
	Ni	Al	Co	Cu	Nb	Ti	V	W
1	4.67	0.0167	0.0892	0.236	0.0112	0.0061	0.0708	0.0247
2	4.74	0.0173	0.0899	0.240	0.0114	0.0050	0.0746	0.0200
3	4.66	0.0135	0.0904	0.232	0.0116	0.0055	0.0704	0.0249
Ave	4.69	0.0159	0.0898	0.236	0.0114	0.0055	0.0719	0.0212

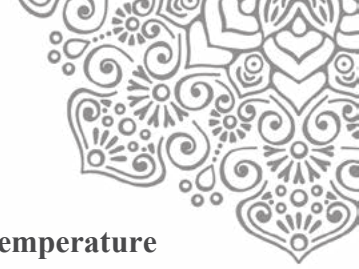
For sample test 15-Cr is acquired using PREN by 21.8 and 36.9 on sample test 22-Cr.

3.2 Porization Test

Porization test using cyclic method on 2 CRA materials (15-Cr and 22-Cr) shows the result comparison of potential value differences in varied condition as follows:

Table 4 CRA Corrosion Potential and Corrosion Rate base on the Calculations of the Carbon Steel

TEMPERATURE		ROOM (27°C)			MEDIUM (50°C)			HIGH (80°C)		
Cl ⁻ (ppm)	Condition	E _{pit} - E _{corr} (mV)		mpy	E _{pit} - E _{corr} (mV)		mpy	E _{pit} - E _{corr} (mV)		mpy
		15-Cr	Duplex	CS	15-Cr	Duplex	CS	15-Cr	Duplex	CS
5,000	Natural	768	1325	0.01	600	1400	0.002	700	1000	0.06
	CO ₂	996	1455	40.24	575	1365	86.32	480	656	88.8
	H ₂ S	650	1230	24.86	600	1110	31.56	250	520	62.6
	CO ₂ + H ₂ S	700	1335	29.43	600	1157	29.5	550	680	51.64
18,000	Natural	618	1374	0.01	650	1025	0.02	425	575	0.07
	CO ₂	598	1350	45.32	525	975	97.12	550	475	100.1
	H ₂ S	624	990	27.99	475	1150	35.54	350	400	70.5
	CO ₂ + H ₂ S	644	910	32.71	425	1200	33.23	450	550	58.16
25,000	Natural	604	1432	0.01	275	1000	0.02	325	350	0.07
	CO ₂	858	1482	48.05	400	1250	102.98	350	500	106.04
	H ₂ S	802	1300	29.68	325	1150	37.68	150	400	74.76
	CO ₂ + H ₂ S	375	1225	34.69	375	775	35.23	350	425	61.67



3.3 Interpretation of test polarization 5,000 ppm Cl⁻ 1 atm CO₂ with room temperature at 27 °C

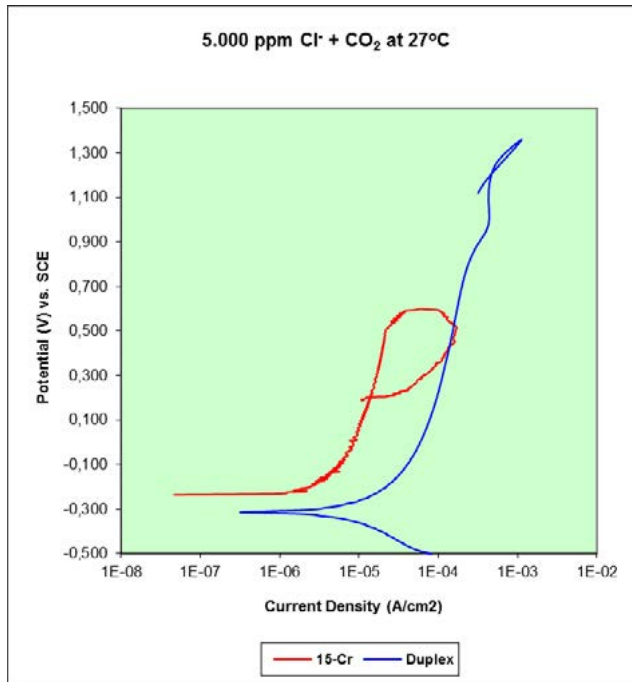


Figure 7 Polarization Curve at 5,000 ppm Cl⁻, 1 atm CO₂ at Room temperature (27 °C)

In polarization curve (Figure 4.2) the tendency of pitting occurrence is displayed on material sample test of 15% Cr and Duplex, which is illustrated as looping line or hystericist. On material sample test 15% Cr will experience higher chance of pitting compared to duplex material sample test, that is shown by the relatively small area of duplex. On material sample test of 15% Cr component, critical pitting potential occur on potential value of +0.700 V SCE and its protection potential approximately +0.300 V SCE.

On the other hand, the critical pitting potential of Duplex occur on +1.400 V SCE and its protection potential is +1.200 V SCE, in which this condition will not develop the well activation and the existing hole will remain passive.

3.4 Recommended Materials for CO₂ Injection Wells

As a depiction, the material needed for CO₂ well injection in downhole equipment which are casing and tubing, cement and casing heads, packer (completion work material), tubing and wellhead, along with its completeness are different from conventional well, where the materials should be corrosion resistance and in some cases, should be able to resist high pressure and temperature.

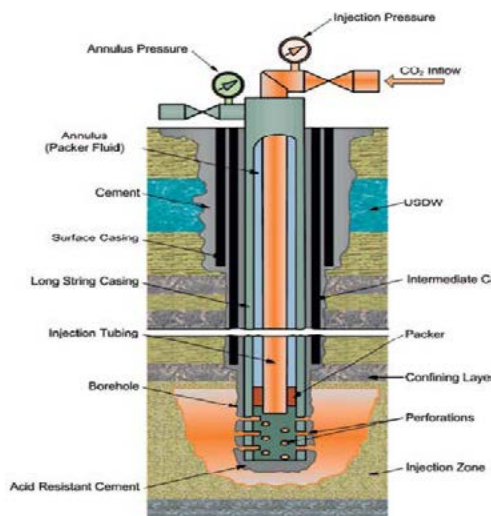


Figure 8 Schematic of a CO₂ Injection Well¹¹



Figure 9 Picture of Surface Production Facilities



The recommended materials for CO₂ Injection Wells^{9,10,11,12} are shown in Table 5.

Table 5 Recommended Materials for CO₂ Injection Wells^{10,11,12,13}

Components	Materials
Christmas Tree (Trim)	316SS, Nickel, Monel
Valve Packing and Seals	Teflon, Nylon
Tubing Hanger	316 SS, Incoloy
Tubing	GRE Lined Carbon Steel, IPC Carbon Steel, CRA
Tubing Joint Seals	Seal Ring (GRE), Coated Threads and Collars (IPC)
On/Off Tool, Profile Nipple	Nickel plated wetted parts, 316 SS
Packers	Internally coated hardened rubber of 80-90 durometer strength (Buna-N), Nickel plated wetted parts

4. CONCLUSION

1. The result of chrome 15 %Cr material polarization test has the tendency of pitting occurrence, which has happened on Chloride ion 5,000 ppm in room temperature 27°C.
2. The result of chrome 22 %Cr material polarization test in room temperature (27°C) and medium (50°C), the pitting tendency occur in Chloride ion 25,000 ppm, while the pitting in high temperature (80°C) in Chloride ion 5,000 ppm has occurred.
3. The objective of material prediction model within **initiation-step** of the scope of the development of oil and gas wells (Figure-4 and Figure-5) using CO₂ EOR injection methods in the **initiation phase** is to determine base case material for preliminary unclassified cost estimate.
4. Other material types can be put into consider while initiating Front End Engineering Design step, meanwhile for 15Cr and Duplex are recommended as basic references in investment proposal steps from Initiation Step to Final Investment Decision Step.

ACKNOWLEDGMENT

I would like to express my special thanks to Management of Upstream Technology Center (UTC)-PT PERTAMINA (Persero) which has given the opportunity to play an active role in the research of CO₂ EOR at Pertamina, also thanks to LEMTEK FTUI who has assisted in various research material within UTC PT PERTAMINA (Persero).

REFERENCES

1. D. Siswanto, (2016), Way Forward For Oil and Gas Development in Indonesia, presentation JOGMEC Technoforum-Tokyo.
2. I.G.S Sidemen, (2016), CCS/CCUS Program and Activities in Indonesia, presentation Deep Dive Workshop CCS Way Forward in Asia-Manila.
3. T.E Perez, (2013), Corrosion in the Oil and gas Industry: An Increasing Challenge for Materials, Vol. 65, No.8., JOM



4. M.R. Simmons, (2008), Report of Offshore Technology Conference (OTC) presentation (Houston, TX: NACE International Oil and Gas Production.
5. R. Heidersbach, (2011), Metallurgy and Corrosion Control in Oil and Gas Production, John Willey & Sons, Inc.
6. B. Khajotia, D. Sormaz, S. Nestic, (2007), Case-based Reasoning Model of CO₂ Corrosion Based on Field Data, NACE Corrosion 2007 Conference & Expo,.
7. R. Nyborg, (2010), CO₂ Corrosion Models for Oil and Gas Production Systems, NACE Corrosion 2010 Conference and Expo.
8. Y. Gunaltun, U. Kaewpradap, M. Singer, S. Nestic, S. Punpruk, M. Thammachart (2010), Progress in the Prediction of Top of the Line corrosion and Challenges to Predict Corrosion rates Measured in Gas Pipelines, NACE Corrosion 2010 Conference and Expo.
9. Shiladitya Paul, Richard Sheperd, Paul Woolin, (2012), Selection of materials for high pressure CO₂ transport, presented at Third International Forum on the Transportation of CO₂ by Pipeline, Newcastle.
10. American Petroleum Institute, Background Report (2007), “Summary of Carbon Dioxide Enhanced Oil Recovery (CO₂ EOR) Injection Well Technology”, 120 L Street NW, Washington DC.
11. M.E. Parker, J.P Meyer, S.R. Meadows (2009), Carbon Dioxide Enhanced Oil Recovery Injection Operations Technologies.
12. N. Gaurina, B. Pasic (2011), Design and Mechanical Integrity of CO₂ Injection Wells, Rudarsko-geološko-naftni zbornik, Vol 23.
13. L. Smith, M.A. Billingham, C.H. Lee, D. Milanovic (2011), Establishing and Maintaining the Integrity of Wells used for Sequestration of CO₂, Elsevier.



UTILIZATION OF FLY ASH AND NICKEL SLAG PT. ANTAM AS MATERIAL
SUBSTITUTION FOR CONCRETE

Musnajam, Vita Astini , Fachryano

Science and Technology Faculty, University of Sembilanbelas November Kolaka

Abstract

The use of concrete for road and bridge work has long been used, and nearly 80% of the bridge elements made of concrete. In concrete, aggregates it self-occupies 70% to 75% of the volume of concrete, so the quality of aggregates influence on the properties of concrete. High demand for concrete also increases demand for aggregates. As a result of the increased demand for aggregates, exploration of natural materials would potentially harm the environment. In addition, as fuel prices increase, resulting in increasing prices of construction materials and other basic commodities. Because of that, many industries switched to using coal as an alternative fuel. PT. Antam as one of the nickel mining industry also used coal as an alternative fuel. The result of using coal as fuel is the production of residual waste coal that is fly ash. The nickel production also produces nickel slag as residual waste that contains very small amount of nickel and not economically to recovered. To reduce by-product of nickel mining industry, a research use of fly ash and nickel slag as a substitution material for concrete rigid pavement was investigated. The purpose of this research, to characterized the chemical and physical fly ash and nickel slag properties. The last step of this research is the analysis of the effects of the use fly ash and nickel slag on the compressive strength of concrete as the main indicator of the strength of concrete.

Keywords: Mine Waste, Fly ash, Nickel Slag, Concrete Compressive Strength.

1. INTRODUCTION

The use of concrete for road and bridge work has long been used, and nearly 80% of the bridge elements made of concrete. Even today many pavement using concrete materials. In concrete, aggregates it self occupies 70% to 75% of the volume of concrete, so quality of aggregates influence on the properties of concrete (Nugraha and Antoni, 2007).

Today, due to rising fuel prices for the industry, many companies are turning to coal as fuel. Waste products of combustion of coal produces ash called fly ash and bottom ash. The percentage of ash produced is 80-90% fly ash and 10-20% bottom ash (PJB Paiton). Fly ash as a waste ash from coal-burning process has mineralogy that arranged in an amorphous phase, crystalline and have adhesion (pozzolan) with the chemical composition of primary SiO₂, Al₂O₃, MgO, and the secondary composition are CaO, NaO and Fe₂O₃ (American Electric Power 2004). Meanwhile, nickel slag is a nickel processing wastes consisting of dense and porous slag. The chemical composition of the nickel slag of highest to smallest consisting of Fe₂O₃, Fused Silica, MgO, Al₂O₃, CaO, Cr₂O₃, and SiO₂Ni (optaminerals.com, 2015).



Research by Adibrot F. and Yelvi (2008) suggests that the fly ash use can improve the nature of workmanship and reduces the amount of water use for mortar, thus reducing the amount of heat hydration that occurs. Fly ash can be used as a cement substitution material with optimum of 50% substitution. While slag substitution as a partial substitution of coarse aggregates concrete cause decreased flexural strength and density of normal concrete obtained on a 80% slag substitution (Susilowati D. et al, 2013). According to Ganti A. (2008), the use of low nickel slag as a substitute coarse aggregates, can improve the compressive strength of 12.32%, reduces abrasion 24.17%, and reduces shrinkage 11.6% compared to normal concrete. Based on composition of the constituent structure, Bukit Asam Tarahan Lampung fly ash eligible to be used as a ceramic material (Karo-karo and Sembiring, 2008). But however, according to Eisenring, M.P. (2013) explained that utilization of fly ash in Indonesia less than 10% in the last five years.

The aims of this research are to characterize the chemical and physical fly ash and nickel slag properties, analyze the strength of concrete using fly ash as a cement substitute, and analyze the compressive strength of concrete using nickel slag as coarse aggregates substitute.

2. METHODOLOGY/ EXPERIMENTAL

This research designed to manufacture rigid concrete by adding by-product materials of PT. Antam that are nickel slag as a coarse aggregate substitute and fly ash as a cement substitute in concrete mixing. The experiment done as follows:

a. Making the specimen test in the form of concrete cylinders

Specimen test made based on the variation composition in Table 1. The specimen test is cylinder specimen with diameter 15 cm and height 30 cm. Fly ash used as cement substitution and nickel slag used as coarse aggregates substitution. Cement that used to make specimen using Portland Composite Cement (PCC) (SNI 15-700-2004). Three specimen test made for each variant composition for compressive strength test. The samples made were immersion in 4 variances those are 1, 3, 7 and 28 days.

b. Physical and chemical test for concrete material

Physical tests for concrete material is a compressive strength test. The goal of a compression test is to determine the behavior or response of a material while it experiences a compressive load by measuring fundamental variables, such as, strain, stress, and deformation. By testing a material in compression the compressive strength may be determined. With the understanding of compressive strength it determined whether or not the material is suited for specific applications or if it will fail under the specified stresses. Chemical test conducted to figure the



constituent material elements and compounds. The type testing and testing methods for each variable shown in Table 1 to Table 3 following:

Table 1. Compressive Strength Testing for cylinder specimen (15 cm x 30 cm) and the number of specimen test

Type Concrete	Total Objects Test For Immersion			
	1 Day	3Days	7Days	28 Days
Normal Concrete	3	3	3	3
Concrete with 10% Fly ash as cement substitution	3	3	3	3
Concrete with 20% Fly ash as cement substitution	3	3	3	3
Concrete with 30% Fly ash as cement substitution	3	3	3	3
Concrete with 40% Fly ash as cement substitution	3	3	3	3
Concrete with 50% Fly ash as cement substitution	3	3	3	3
Concrete with 10% nickel slag as coarse aggregate substitution	3	3	3	3
Concrete with 25% nickel slag as coarse aggregate substitution	3	3	3	3
Concrete with 50% nickel slag as coarse aggregate substitution	3	3	3	3
Concrete with 100% nickel slag as coarse aggregate substitution	3	3	3	3

Table 2. Testing methods

No.	Testing	Methods
1.	Compressive Strength	SNI 1974-2011

Table 3. Chemical Composition Test

No.	Testing	Equipment
1.	Chemical Molecule	<i>X-Ray Diffraction</i>
2.	Chemical element	<i>Scan Electron Microscopy (EDAX)</i>
		<i>X-Ray Flourescence</i>



3. RESULTS AND DISCUSSION

Aggregates are one of the filler material in the concrete, which reached 70% -75% of the volume of concrete. So, the properties of aggregates influence on the properties of concrete. With a good aggregates, concrete workable (workable), strong, long-lasting (durable) and economical (Nugraha and Antoni, 2007). Prior to using fly ash and nickel slag for the substitution of concrete materials, preliminary research was undertaken to analyze the chemical composition of elements and compounds contained in the samples using X-Ray Diffraction (XRD) and X-Ray Fluorescence (XRF). Nickel slag composition test by XRF carried out for 2 months in July and September 2016 in PT. Antam. Distribution composition of nickel slag described in Figure 1 and Figure 2. From the composition test results, showed that PT Antam's nickel slag contains an average of 0.06% Ni, 9.25% Fe, 52.66% SiO₂, 31.79% MgO, 1.25% CaO, 0.94% Cr, and 2.72% Al₂O₃.

Based on Figure 1 and Figure 2 show that nickel slag processing results PT. Antam has a composition which is relatively stable from day-to-day. This composition is close to the chemical composition according to the literature (Sugiri, 2005) slag chemical composition consisting of 41.47% Silica, 30.44% Ferric Oxide, 2.58% Alumina, and 22.75% Magnesia (MgO).

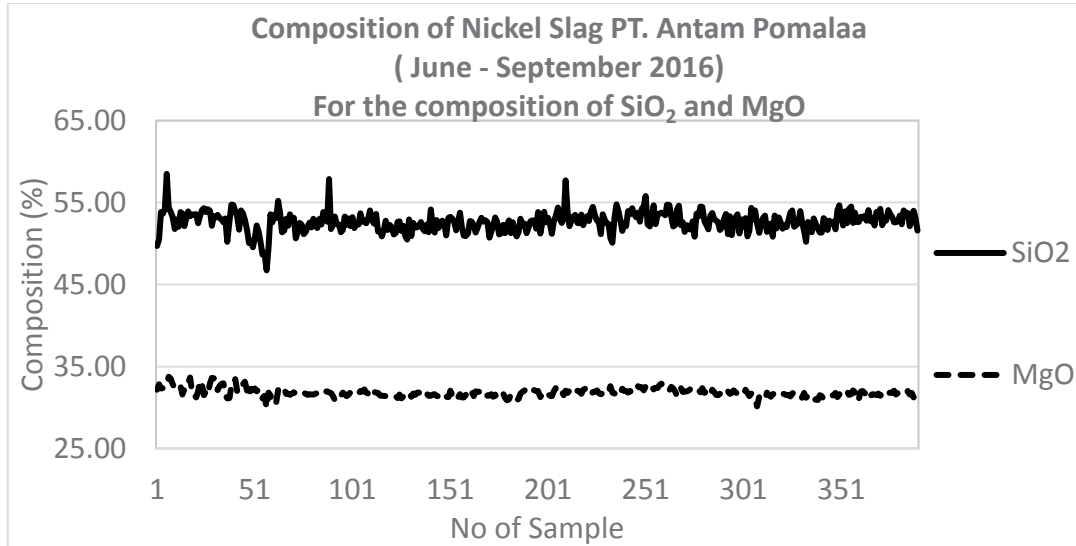


Figure 1. Composition of Nickel Slag PT. Antam Pomalaa (July-September 2016) For the composition of SiO₂ and MgO

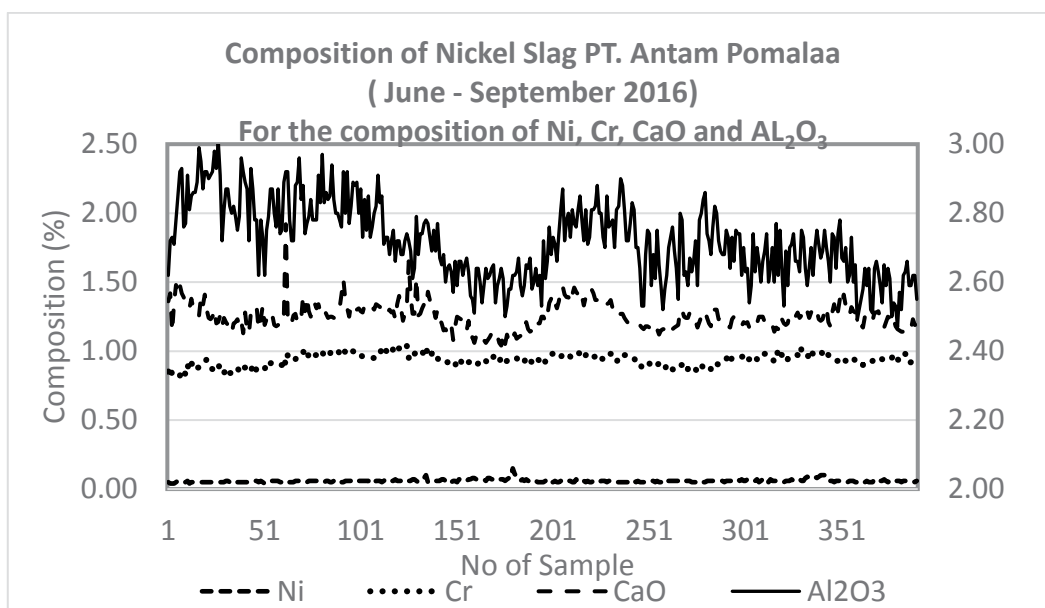


Figure 2. Composition of Nickel Slag PT. Antam (July-September 2016) For the composition of Ni, CaO, Cr and Al₂O₃

The test results of XRD on fly ash shown in Figure 3, obtained estimate quantity of the chemical compound that are consist of quartz or silica (Quartz, syn) SiO₂ 57%, Particle Iron (Magnetite, syn) Fe₃O₄ 21%, Magnesium silicate (Magnesium Silicon Oxide) MgSiO₃ 17,5%, Titanium dioxide (rutile) TiO₂ 3,9%, Calcium silicate (calcium silicon oxide) Ca(SiO₃) 1%. XRD testing on the river sand (Figure 4) obtained quantity of chemical compounds as follows: Felspar or Anorthoclase (Na_{0.85} K_{0.14}) (AlSi₃O₈) 77%, Potassium feldspar (microcline) KAlSi₃O₈ 12.8%, Magnetite iron particles Fe₃O₄ 3.9%, quartz or silica (quartz) SiO₂ 0.64%, iron oxide or ferric oxide (hematite HP, iron (III) oxide) Fe₂O₃ 0.1%, Titanium Dioxide (Rutile, syn) 1.34% TiO₂, Clinoenstatite, syn (Ca_{0.15}Mg_{0.85})Si₂O₆ 4.7%. The results of XRD observations on the nickel slag (Figure 5) obtained chemical composition these are : Forsterite, ferroan (Mg_{1.8}Fe_{0.2}SiO₄) 78%, Mg₂(Si₂O₆) 21.4% and Nickel Iron Oxide (Ni_{0.6}Fe_{2.4}O₄) 0.5%. The different color in Figure 3, 4 and 5 shows Miller indices (hkl) used to identify different planes of atoms. Observed diffraction peaks can be related to planes of atoms to assist in analyzing the atomic structure and microstructure of a sample.

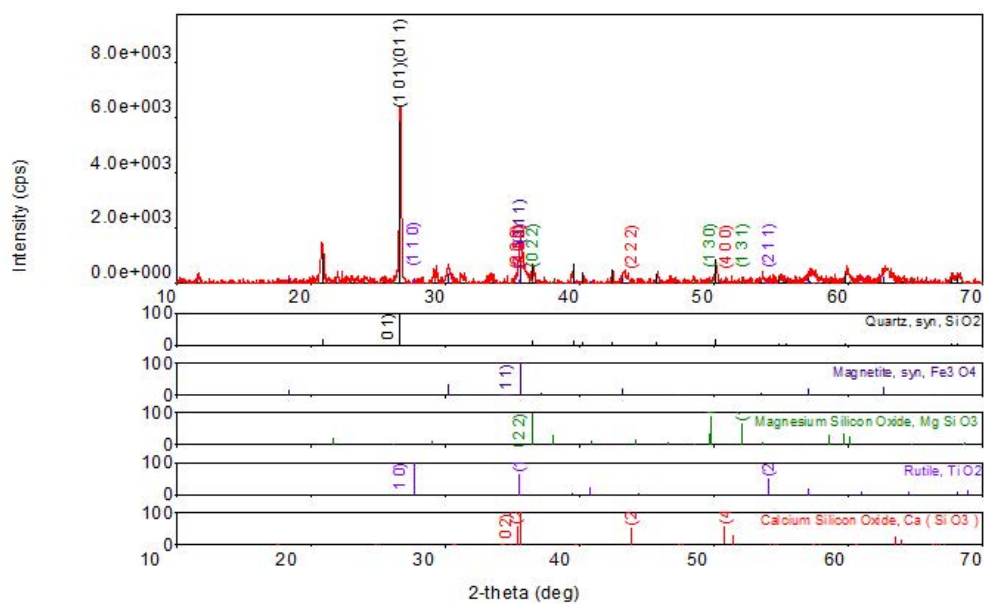


Figure 3. The results of the characterization of XRD Fly ash

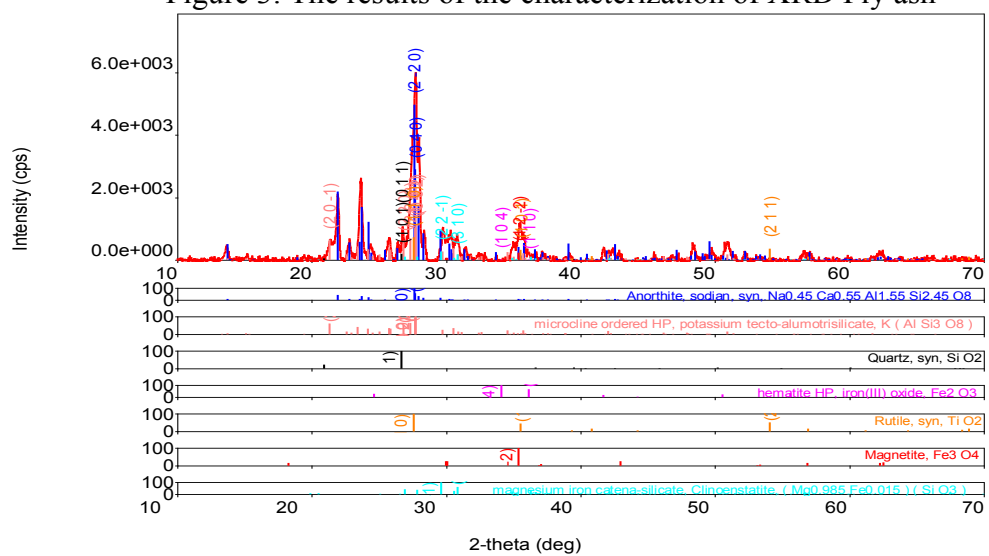


Figure 4. The results of the characterization of XRD Sand River

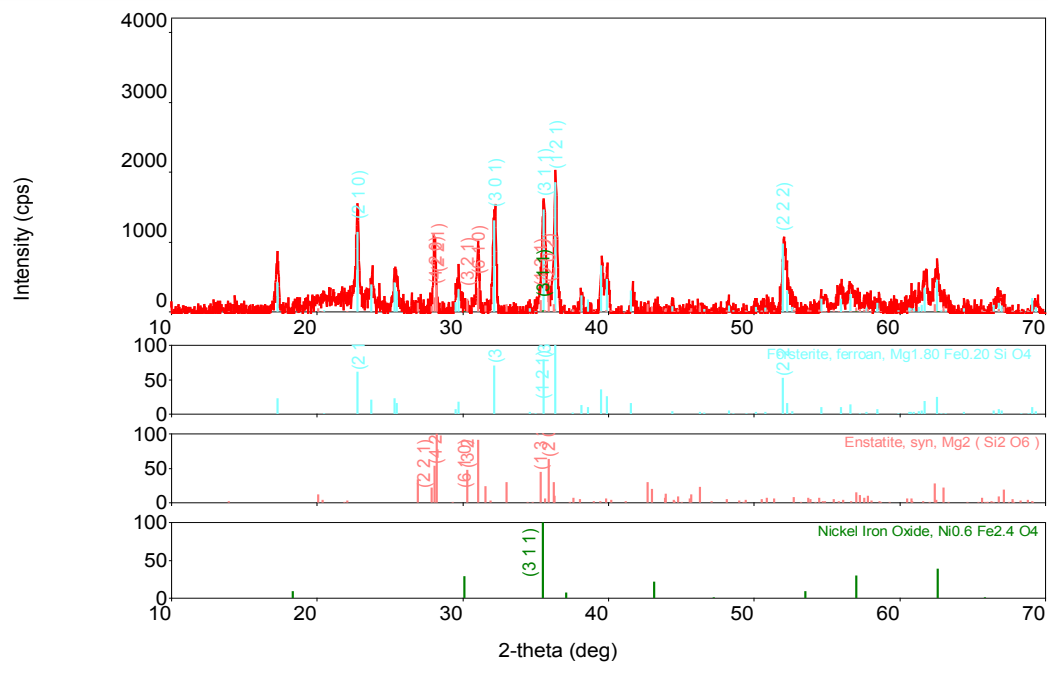


Figure 5. The results of the characterization of XRD Nickel Slag

From Figure 6 shows that the decline in hard concrete density on average, in line with the increase percentage of fly ash as a cement substitute. Based on Dorf Richard, (1996), the density of normal concrete is 2400 kg/m³ and the density of lightweight concrete is 1750 kg/m³. A normal concrete, from the experiment, has density 2.320 kg/m³. Using 50 % fly ash as cement substitution decrease the density of concrete to 2.249 kg/m³. From the Figure 7. shows that the concrete density increase with nickel slag substitution as coarse aggregates. Using 100 % nickel slag as coarse aggregates substitution increase the density of concrete to 2.498 kg/m³.

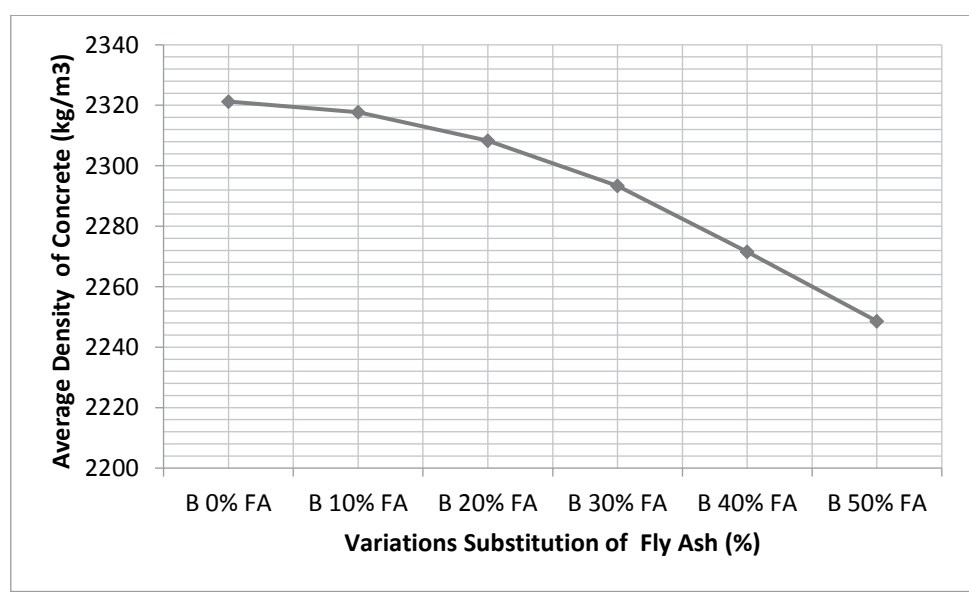


Figure 6. The average Density of the concrete for each cylinder specimen (15 cm x 30 cm) on every variation of fly ash

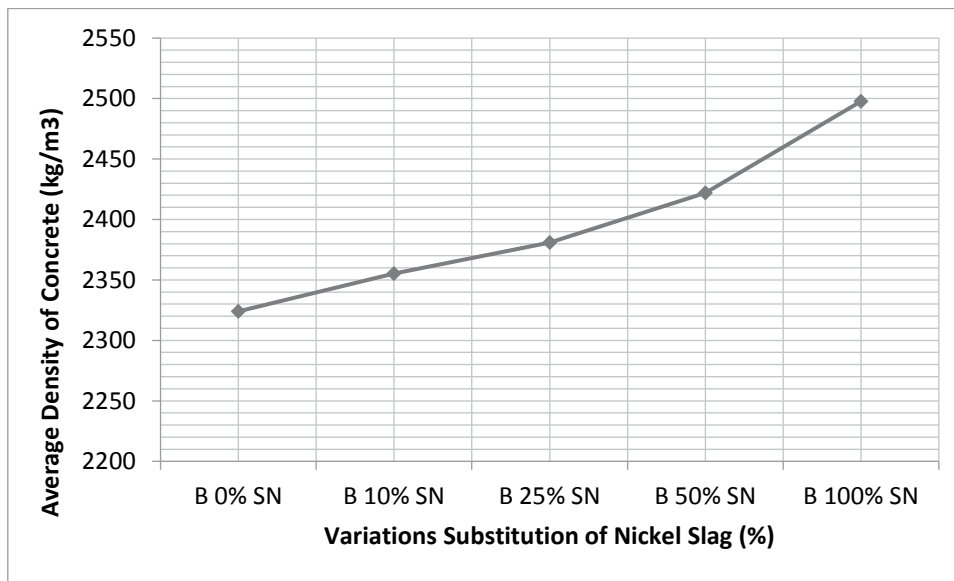


Figure 7. The average Density of the concrete for each cylinder specimen (15 cm x 30 cm) on every variation of nickel slag

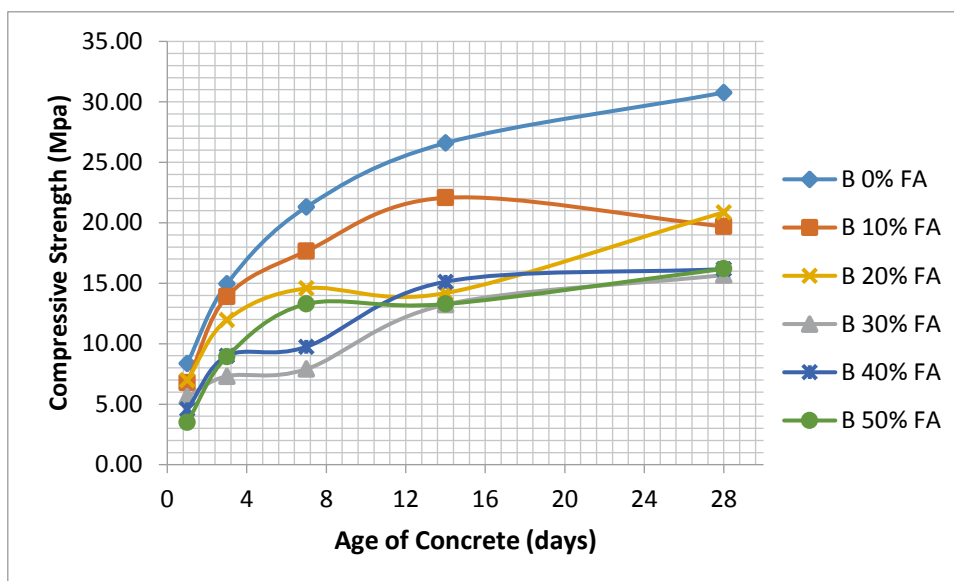


Figure 8. Graph increase concrete compressive strength of fly ash every age

Figure 8 shows that the concrete made by using basic component of cement, river sand, and crushed stone obtained the compressive strength 30 MPa. While the use fly ash as a cement substitution, from the lowest percentage of 10% until the percentage of 50%, is only able to achieve the highest compressive strength of 20.86 MPa, far below the planned compressive strength. Each variant has increased compressive strength at early ages 1 day to 3 days, but then stagnant or not increasing compressive strength in subsequent ages 7 days to 28 days.

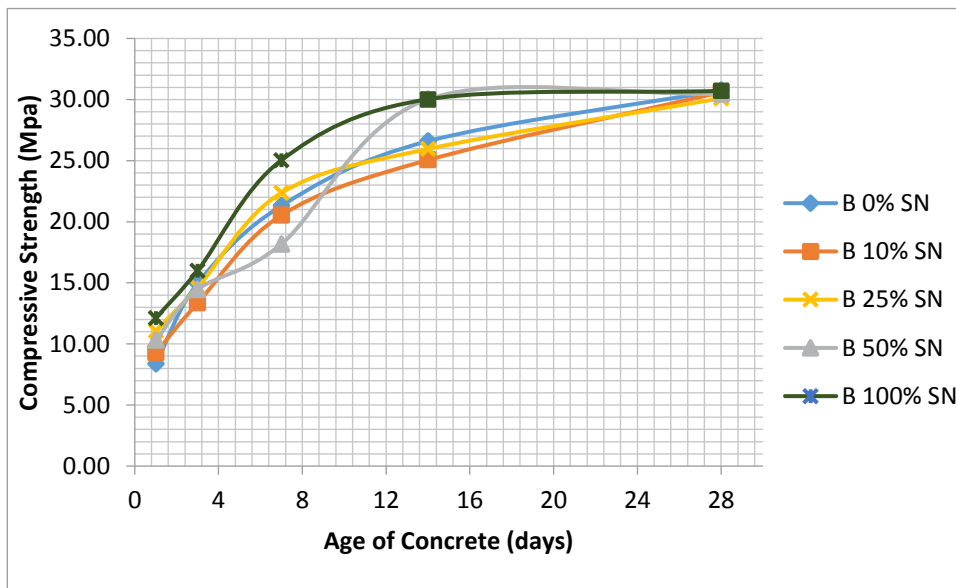


Figure 9. Graph increase nickel slag concrete compressive strength every age

In figure 9 shows that using nickel slag as a coarse aggregate substitution tends to increase the compressive strength of concrete at an early age. According to the compression strength data, there is a tendency of obtaining a better compressive strength at every added percentage of nickel slag as well as the use of the overall nickel slag (slag nickel 100% variation) in 1, 3, 7, and 14 days, but at 28 days the compressive strength are similar to normal concrete that is around 30.71 MPa.

4. CONCLUSION

1. Based on the XRF test results, nickel slag composition of PT. Antam contain an average 0.06% Ni, 9.25% Fe, 52.66% SiO₂, 31.79% MgO, CaO 1.25%, Cr 0.94%, and 2.72% Al₂O₃.
2. Based on the characterization using XRD, indicating that Fly ash samples consist of quartz or silica (Quartz, syn) SiO₂ 57%, iron particles (Magnetite, syn) Fe₃O₄ 21%, Magnesium silicate (Magnesium Oxide Silicon) MgSiO₃ 17.5%, Titanium dioxide (rutile) TiO₂ 3.9%, Calcium silicate (calcium silicon oxide) Ca(SiO₃) 1%. Fly ash composition has some similarities with Portland cement composition.
3. The higher percentage of nickel slag in concrete resulted in the higher density of the concrete. It is closely related to nickel slag specific gravity (3.01) which is greater than crushed stone specific gravity (2.75). The average density of normal concrete is 2.320 kg/m³. While the average density is highest in concrete with 100% nickel slag substitution of coarse aggregates that is 2.498 kg/m³.
4. The concrete made by using basic component of cement, river sand, and crushed stone obtained the compressive strength 30 MPa. While the use fly ash as a cement substitution, from the lowest percentage of 10% until the percentage of 50%, is only able to achieve the highest compressive strength of 20.86 MPa, far below the planned compressive strength. Every added 10% of fly ash as a cement substitution, the compressive strength decreased by an average of 2.02 MPa.
5. The using of nickel slag as a coarse aggregate substitution tends to increase the compressive strength of concrete at an early age. At 7 days, the normal concrete obtains compressive strength 21.30 MPa, but the concrete with 100% nickel slag



substitution obtain 25.03 MPa. At 28 days the compressive strength 100% nickel slag substitution concrete are similar to normal concrete that is around 30.71 MPa.

5. ACKNOWLEDGEMENT

This work supported by Ministry of Research, Technology and Higher Education of the Republic of Indonesia grant competition and PT Antam Tbk. Southeast Sulawesi Nickel Mining Business Unit.

6. REFERENCES

- Adibroto, Fauna and -, Yelv (2008) Pemanfaatan Limbah Abu Batu Bara Sebagai Bahan Pengganti Sebagian Semen Dan Agregat Untuk Pembuatan Paving Block. *Rekayasa Sipil*, 4 (1). pp. 20-30. ISSN 1858-3695
- Antoni dan Nugraha, P, (2007), *Teknologi Beton*, C.V Andi Offset, Yogyakarta
- ASTM, (1985). *American Standart Test Material* Vol. E, New York.
- ASTM, (1995). *Concrete and Agregat*, Philadelphia: Annual Book of ASTM Standard Vol.04.02.1995.
- Bouguerra, A., Ledhem, A., de Barquin, F., Dhilly, R.M., Queneudec, M. (1998), *Effect of Microstructure on the Mechanical and thermal Properties of Lightweight Concrete Prepared from Clay, Cement and wood Aggregates*, *Cement and Concrete Research*, 28, p1179-1190.
- Departemen Pekerjaan Umum R.I., (2005), *Pedoman Pelaksanaan Pekerjaan Beton untuk Jalan dan Jembatan*. Pd. T-07-2005-B.
- Departemen Pekerjaan Umum R.I., (2004), *Pelaksanaan Perkerasan Jalan Beton Semen*. Pd T-05-2004-B
- Eisenrig, M.P., (2013), *Abu Batubara Sebuah Konsep Inovatif Bagi Produksi Bata Abu-abu untuk Memperoleh Kekuatan Tinggi dan Aman Terhadap Lingkungan (Studi Literatur)*. Majalah Ilmiah Mektek.
- Ferriera, C., Ribeoro, A., and Ottesen, L., (2003), *Possible Application for Minicipal Solid Waste Fly ash*, *Journal of Hazardous Material B* 96, p 201-216.
- Ganti A., (2008), *Potensi Pemanfaatan Low Nickel Slag Dalam Beton Sebagai Pengganti Semen dan Agregat Kasar*. Library. Universitas Kristen Petra. Surabaya.
- Saptahari Sugiri, (2005), "Penggunaan Terak Nikel sebagai Agregat dan Campuran Semen untuk Beton Mutu Tinggi", *Jurnal Infrastruktur dan Lingkungan Binaan*, Edisi Volume I No. 1
- Karo-karo, P., Sembiring., (2008), *Karakteristik Abu Hasil Pembakaran Batubara Bukit Asam Sebagai Bahan Keramik.*, *Jurnal Ilmu Dasar*. Jurusan Fisika. Universitas Lampung.
- Mulyono, T., (2004), *Teknologi Beton*, Andi Yogyakarta
- Susilowati D., Saputra I.N., Nurhidayati N., (2013), *Pengaruh Penggunaan Terak Sebagai Pengganti Agregat Kasar Terhadap Kuat Lentur dan Berat Jenis Beton Normal dengan Metode Mix Design*. Pendidikan Teknik Bangunan. UNS.



Comparison of Pitting Corrosion Resistance of Austenitic Stainless Steel 304L and 316L Exposed to Aqueous Sodium Chloride Solution

Andi Rustandi^{a*}, Nuradityatama^a, M. Faisal Rendi^a, Suganta Setiawan^b

^a*Metallurgy and Material Engineering, Universitas Indonesia, Depok- Indonesia*

^b*PT. Voestalpine Bohler Welding Asia Pacific, Cikarang, Bekasi- Indonesia*

Abstract

Corrosion behavior of austenitic stainless steels 304L and 316L types in various concentrations of aqueous sodium chloride solutions were investigated related to its pitting corrosion resistance. Experimental testing was carried out by using cyclic polarization method at room temperature (27°C) to evaluate its corrosion mechanism. Aqueous sodium chloride solutions were prepared with various concentrations, namely 1%, 2%, 3.5%, 4% and 5% NaCl. Testing results were represented by cyclic potentiodynamic polarization curves for both alloys which showed potentials that indicated the onset of breakdown potential E_b and protection potential E_p respectively. The results were influenced by sodium chloride concentrations and the chemical composition of alloys. Rank of the values of E_b and E_p for 304L and 316L at various sodium chloride concentrations from the highest to the lowest were 1%, 2%, 5%, 4%, 3.5% NaCl consecutively. It was observed that the lowest corrosion resistance of both alloys was at 3.5% NaCl which was similar to typical seawater environment with maximum dissolved oxygen solubility. It was shown that 316L had more positive potentials for both E_b and E_p as well as its difference values compared to 304L at all concentrations of aqueous sodium chloride solutions.

Keywords: Austenitic Stainless Steel, Corrosion Behavior, Pitting Corrosion Resistance, NaCl Aqueous Solution, Cyclic Polarization

1. INTRODUCTION

Stainless steels are widely used in various industries and environments due to its better corrosion resistance which compared to carbon steels. Stainless steels can be classified as: austenitic, ferritic, martensitic and duplex stainless steels. Suitable material depends on the material selection technique and the needs of application requirements such as mechanical properties and corrosion resistance. This study will focus on austenitic stainless steels related to its corrosion behavior. In austenitic grades of stainless steel, carbon content is usually held to a maximum of 0.08%, chromium content ranges from 16 to 28%, and nickel content ranges from 3.5 to 32%. In some types of austenitic stainless steel, 2 – 4% molybdenum was added to improve the stability of passive layer by reducing the intensity of the oxidizing effect. Among the types of austenitic stainless steels, 304L and 316L are the most commonly used in various industries. “L” is designated as low carbon stainless steel. SS 304L is the most widely used stainless steels and described as standard 18Cr 8Ni steel. The corrosion resistance of SS 304L is classified as fair to good in various environments. Type 304L is mostly used in food and beverages industry, automotive, chemical containers, construction, and heat exchangers. SS 316L is the second most used austenitic stainless steels in various industries. The corrosion resistance of SS 316L is also classified as fair to good in various environments[1]. SS316L is used mostly in more severe corrosion environment containing chloride solution especially in marine application and well known corrosion resistant due to its Mo content.

*Corresponding author

E-mail address: rustandia@gmail.com



Austenitic stainless steels have a wide spectrum of resistance to corrosion by chemical environment due to the formation of protective passive film on its surface[2]. However, such passive film is susceptible to breakdown in the presence of chloride ions resulting in pitting attack as localized form of corrosion[3]. Corrosion has been a major problem in various industry, especially oil and gas industry. Corrosion failure has caused a major damage commonly found in oil and gas production facilities. The reduction of dissolved oxygen reaction is very common because of the fact that aqueous solutions in contact with air will contain significant amounts of dissolved oxygen[4]. The corrosion rate of a metal in aqueous environments tend to be determined by the rate at which dissolved oxygen can be delivered to the metal surface[5]. For stainless steels, numerous interrelated metallurgical, geometrical, and environmental affect both corrosion initiation and propagation[6]. Although the passivity of the exposed surfaces of stainless steels are maintained by dissolved oxygen, the release of metal ions particularly chromium produces an acidic condition as a result of a series of hydrolysis reactions which can initiate corrosion process[7]. Because of acidic condition in environment, chloride ions migrate and concentrate from the bulk environment and the initiation of corrosion will occur if the concentration becomes sufficient to cause breakdown of the passive film. And after the breakdown of passive film, dissolved oxygen will further propagate corrosion process so the corrosion process will be faster and more aggressive[8]. Material selection is one of the well-known methods that can be used to mitigate corrosion[9]. Material selection is a method that control the corrosion rate by choosing the suitable material based on its application or working environment. Pitting corrosion is a localized form of corrosion that produces small holes and propagate deep inside the material[10]. Pitting corrosion is considered to be more severe impact than uniform corrosion due to its unanticipated occurrence and unpredictable propagation rate[11]. Once pits are initiated, it may continue to grow by a self-sustaining or autocatalytic process that produce conditions that are both stimulating and necessary for the continuing activity of the pit. The corrosion rate of pitting corrosion is extremely faster than general corrosion[12]. Its aggressiveness is due to the very small size and high penetration ability of chloride ion through passive layer[13]. Marine corrosion is deterioration of structures, machinery and piping systems that use seawater for cooling and other industrial purposes immersed in seawater the corrosion of and also corrosion in marine atmospheres[14]. Although salt water is generally known as a corrosive environment, it is not widely understood how much the aggressiveness of its corrosive behavior. Because of those factors, seawater is not easily simulated in the laboratory for corrosion testing purposes. Stored seawater is notorious for exhibiting behavior as a corrosive medium that is different from the condition before it was taken[15]. Researcher often put one or two factors to approach the real condition of seawater such as chloride concentration and dissolved oxygen concentration. The aims of this study are to compare and determine the corrosion resistance of SS 304L and SS 316L in various aqueous sodium chloride solutions. Aqueous solutions were prepared in 1%,2%,3.5%,4%,and 5%, expected to be similar to marine environment. Corrosion resistance of both alloys are represented by the evaluation of the cyclic potentiodynamic polarization curves.

2. METHODOLOGY/EXPERIMENTAL

2.1. Materials Specification

Materials used in this study were commercial grade SS 316L and SS 304L. SS 316L and SS 304L both were machined and well prepared prior to polarization testing. The chemical compositions of both alloys were evaluated using an optical emission spectrometer machine according to ASTM E415 and E1086. The results are shown in Table I.

Table 1. Chemical Composition of SS 304L and SS 316L

Metal	C	Si	Mn	P	S	Cr	Mo	Ni	Cu	Fe
SS 304L	0.039	0.418	1.14	0.0313	<0.005	18.89	0.001	8.16	0.027	70.98
SS 316L	0.039	0.438	1.65	0.023	<0.005	16.5	2.38	9.89	0.076	68.7



2.2. NaCl Solutions

Aqueous sodium chloride solutions containing 1%, 2%, 3.5%, 4% and 5% of sodium chloride were prepared by dissolving 10 gr, 20 gr, 35 gr, 40 gr and 50 gr NaCl in 1 liter of water and stirred with magnetic stirrer to produce homogeneous solution. Solutions were made at room temperature 27^o C.

2.3. Samples Preparation

Both stainless steels were cut into 4cm x 4cm x 0,5cm plates from their original plates form. Samples then were ground by grinding machine with 40, 60, 100, 180, 400, 500, 600, and 800 grades abrasive papers followed by polishing, cleaning and drying.

2.4. Dissolved Oxygen Solubility Measurement

The purpose of this experiment is to find out the relation between dissolved oxygen solubility and its effect to corrosion resistance to material especially stainless steel in this study.

2.5. Polarization Cell

Electrochemical measurement by using cyclic polarization method was conducted in a cell chamber with three electrodes which composed of carbon counter electrode, stainless steel as working electrode and saturated Ag/AgCl electrode as reference electrode. The connection of the three electrodes is shown by Fig 1.

2.6. Cyclic Polarization Experiment

Cyclic polarization experiment was carried out by AUTOLAB potentiostat and NOVA AUTOLAB 1.10 software. The measured potentials were referred to Ag/AgCl electrode. The illustrative connection between potentiostat and polarization cell is shown by Fig 1.

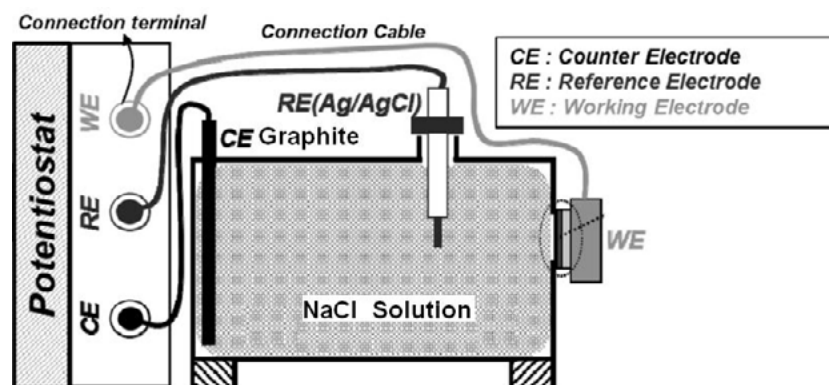


Figure 1. Scheme of cyclic polarization testing apparatus[16]

3. RESULTS AND DISCUSSION

3.1. Dissolved Oxygen Solubility Measurement

Table 2 and Fig. 2 below are the results of dissolved oxygen solubility measurement by using the dissolved oxygen meter.

Tabel 2. Oxygen concentration values at various aqueous sodium chloride concentration

NaCl (%)	1.0	2.0	3.5	4.0	5.0
Oxygen (ppm)	2.6	3.9	4.5	4.4	4.0

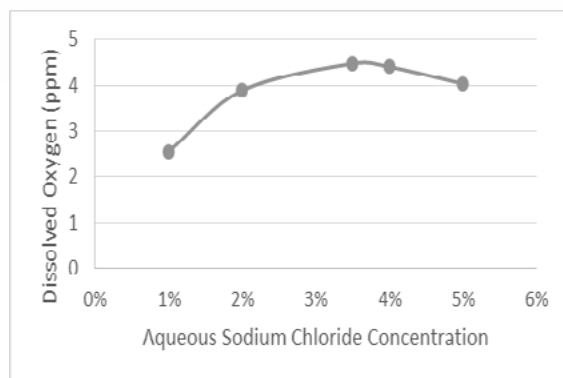


Figure 2. Dissolved oxygen concentration at various aqueous sodium chloride concentration.

Based on the dissolved oxygen solubility measurement results, it is shown that dissolved oxygen solubilities increase with increasing aqueous sodium chloride concentration until reaching its maximum point at 3.5% aqueous sodium chloride concentration and decrease with further increasing aqueous sodium chloride. Therefore, higher solubility of dissolved oxygen in a solution will increase the corrosion rate of the material. But after it reached the maximum point, corrosion rate will drop following the depletion of dissolved oxygen in the solution. The rank of dissolved oxygen concentrations in aqueous sodium chloride from lowest to highest are 1%, 2%, 5%, 4%, 3.5%.

3.2.Cyclic Polarization Experiment

Cyclic polarization experiment is a combination of anodic and cathodic polarization that form a cyclic process. Cyclic polarization methods were conducted in order to investigate the tendency of pitting occurrence for a specimen in any environment. The tendency of pitting were evaluated by considering its breakdown potential (E_b) and protection potential (E_p). And also, size of the loop curve indicated the propagation process of pitting occurrence. The results of the experiments were cyclic polarization curves for both alloy at various aqueous sodium chloride concentrations. Interpretation E_b and E_p from this method was done by using qualitative analysis. E_b or breakdown potential is the potential that indicates the onset of pitting and E_p or protection potential is the potential that halted pitting propagation. The higher values of breakdown potential and protection potential, the specimen will exhibit better corrosion resistance.

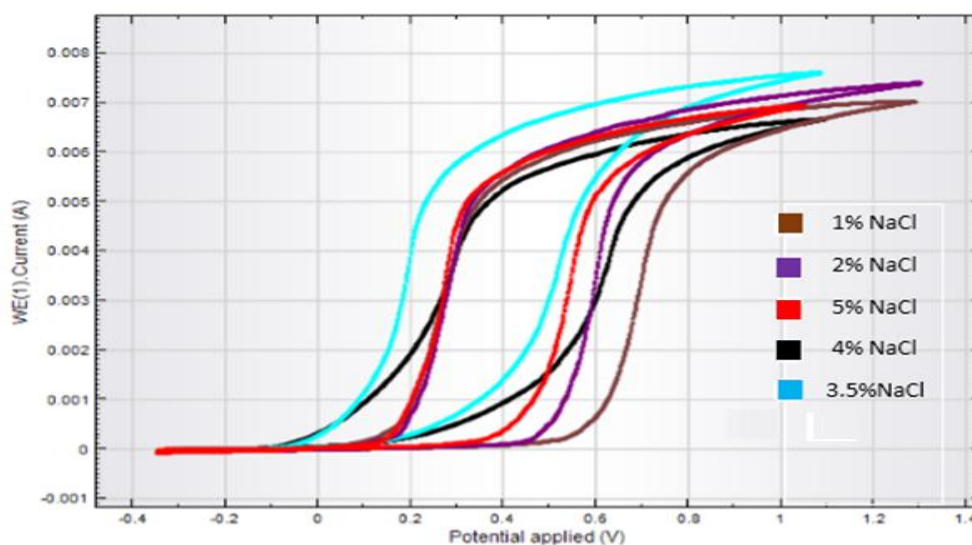


Figure 2. Cyclic polarization curves of SS 316L in various sodium chloride concentration.



Table 3. Eb and Ep values for SS 316L

NaCl (%)	1	2	3.5	4	5
Eb (V)	0.58	0.47	0.31	0.37	0.46
Ep (V)	0.02	-0.09	-0.10	-0.09	0.11

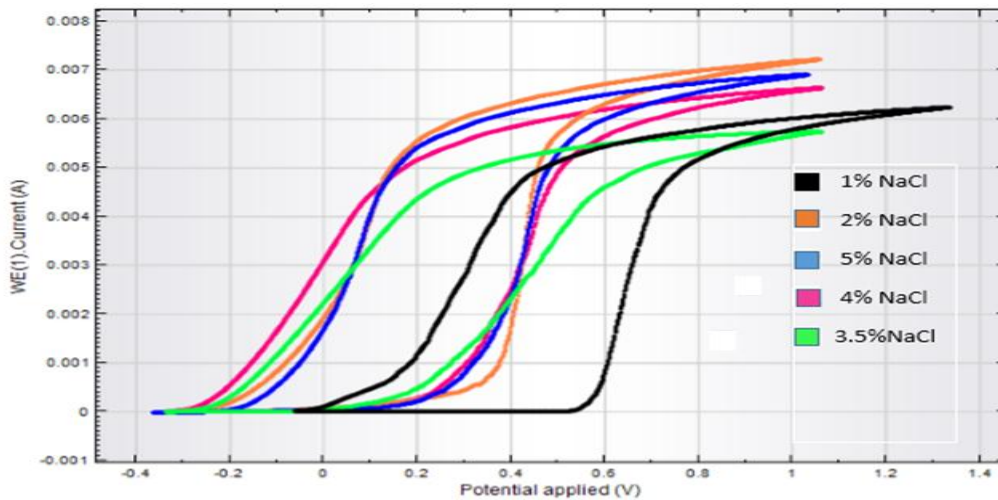


Figure 3. Cyclic polarization curves of SS 304L in various sodium chloride concentration.

Table 4. Eb and Ep values for SS 304L

NaCl (%)	1	2	3.5	4	5
Eb (V)	0.54	0.37	0.20	0.22	0.27
Ep (V)	-0.05	-0.15	-0.28	-0.27	-0.21

Fig. 3 and Fig. 4 shows the cyclic polarization curves for both alloys at various aqueous sodium chloride concentration. The values of Eb and Ep for both alloys are shown by Table 3 for SS 316L and Table 4 for SS 304L. The variety of curves revealed corrosion behavior of both alloys depending on sodium chloride concentration. With qualitative analysis based on the figures, it can be interpreted that the higher the values of breakdown potential and protection potential in cyclic polarization curve, the higher its corrosion resistance. The corrosion resistance from the highest to the lowest were 1%, 2%, 5%, 4%, 3.5% NaCl consecutively. It is shown that dissolved oxygen solubility is also a considerable factor affecting corrosion resistance of an alloy. Both figures shows that corrosion resistance of both alloys will drop at 3.5% NaCl concentration which is similar of typical seawater with maximum dissolved oxygen solubility. It was proven by the value of Eb and Ep of both alloys at 3.5% are 0.31V and -0.1V for SS 316L and 0.20V and -0.28V respectively which was the lowest value from both alloys.

3.3. Comparison of cyclic polarization curves between SS 316L and SS 304L

Fig. 4 – 8 and Table 5 – 9 below are the data comparison between alloy SS 316L and SS 304L at various aqueous sodium chloride concentration.

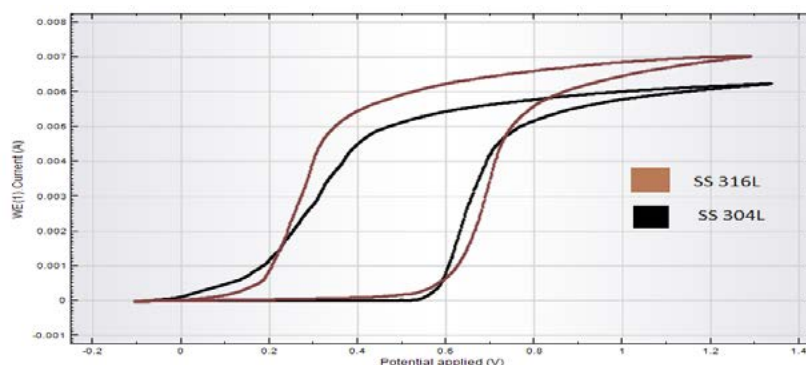


Figure 4. Cyclic polarization curves of SS 316L and SS 304L in 1% sodium chloride.



Tabel 5. Eb and Ep Values in 1% Sodium Chloride Concentration

Material	Eb (V)	Ep (V)
SS 316L	0.58	0.02
SS 304 L	0.54	-0.05

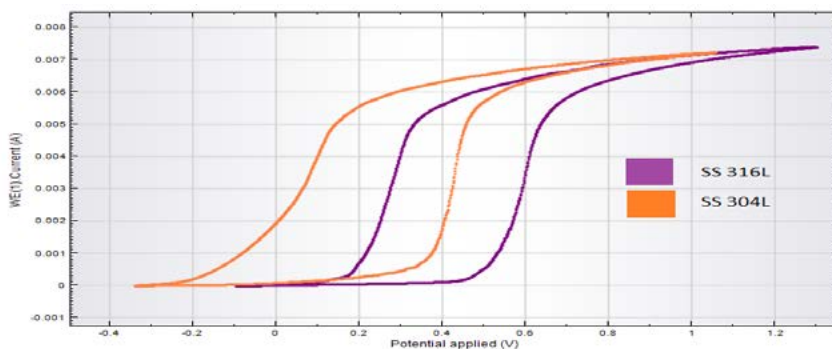


Figure 5. Cyclic polarization curves of SS 316L and SS 304L in 2% sodium chloride.

Tabel 6. Eb and Ep Values in 2 % Sodium Chloride Concentration

Material	Eb(V)	Ep(V)
SS 316L	0.47	-0.09
SS 304L	0.37	-0.15

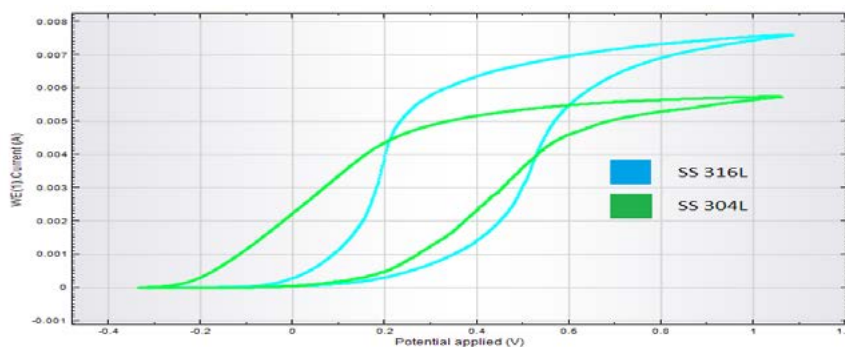


Figure 6. Cyclic polarization curves of SS 316L and SS 304L in 3.5% sodium chloride.

Tabel 7. Eb and Ep Values in 3.5 % Sodium Chloride Concentration

Material	Eb(V)	Ep(V)
SS 316L	0.31	-0.10
SS 304L	0.20	-0.28

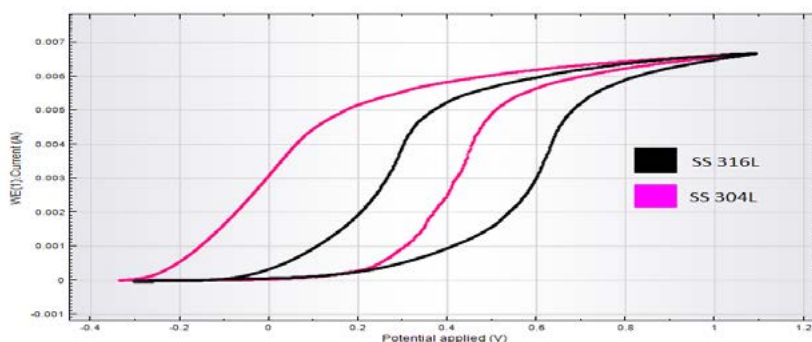


Figure 7. Cyclic polarization curves of SS 316L and SS 304L in 4% sodium chloride.



Tabel 8. Eb and Ep Values in 4 % Sodium Chloride Concentration

Material	Eb (V)	Ep (V)
SS 316L	0.37	-0.09
SS 304L	0.22	-0.27

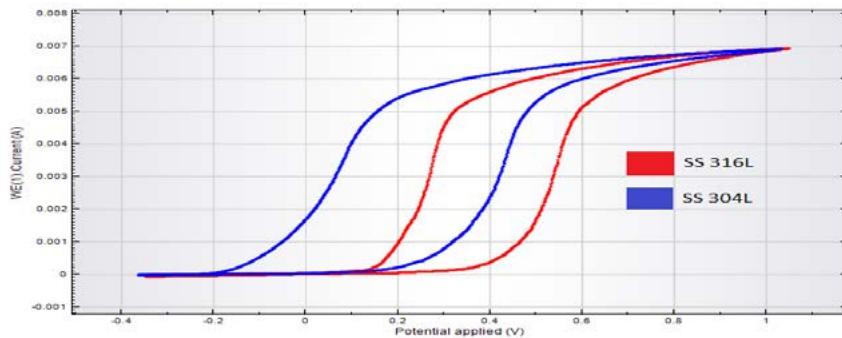


Figure 8. Cyclic polarization curves of 316L and 304L in 5% sodium chloride.

Tabel 9. Eb and Ep Values in 5 % Sodium Chloride Concentration

Material	Eb(V)	Ep(V)
SS 316L	0.46	0.11
SS 304L	0.27	-0.21

Fig. 4-8 and Table 5-9 shows the comparison of corrosion behavior of both alloys at various aqueous sodium chloride concentration. Based on Fig. 4-8, SS 316L tend to has higher corrosion resistance at various aqueous sodium chloride concentration. By looking at the cyclic polarization curve's width on Fig. 3-7, it is known that pitting corrosion propagates more aggressively in SS 304L because it has larger width than SS 316L. As shown in Table 5-9 SS 316L also has better corrosion resistance by looking at its breakdown (Eb) and protection (Ep) potential which is higher than SS 304L at various aqueous sodium chloride concentration. The difference in corrosion behavior of both alloys was because of the addition of 2% molybdenum in SS 316L which influenced stainless steel to form better and more stable passive layer and more resistant to pitting corrosion.

4. CONCLUSIONS

The rank of corrosion behavior according to cyclic polarization curve results for SS 316L and 304L at various chloride concentrations from the highest to the lowest are 1%, 2%, 5%, 4%, 3,5% NaCl consecutively. The results show that both alloys have the lowest corrosion resistance at 3.5 % NaCl. It is due to dissolved oxygen solubility reaches its maximum at 3.5% NaCl which is similiar to typical seawater condition. It is recommended that SS 316L is preferred for material design compared to SS 304L in highly corrosive chloride containing environment because it has better corrosion resistance due to the higher molybdenum content in its composition.

5. ACKNOWLEDGMENT

The authors wish to thank PT. Voestalpine Bohler Welding Asia Pacific for the supplied materials and also Direktorat Riset dan Pengabdian Masyarakat Universitas Indonesia (DRPM UI) for the research support.



6. REFERENCES

- [1] The International Nickel Company, INCO, *Corrosion resistance of the austenitic chromium-nickel stainless steels in chemical environment*. (1967) 1-20
- [2] M. G. Fontana, N. D. Greene, *Corrosion Engineering 2nd Ed.* McGraw –Hill Int. Book Co. (1978) pp. 194.
- [3] M. D. Asaduzzaman, C. M. Mustafa, M. Islam, *Effects of concentration of sodium chloride solution on the pitting corrosion behavior of AISI-304L austenitic stainless steel*, Chemical Industry & Chemical Engineering Quarterly, 17 (4) (2011) 477-483
- [4] R. L. Martin, R. R. Annand, D. Wilson, and W. E. Abrahamson, *Inhibitor Control of Oxygen Corrosion: Application to a Sour Gas Gathering System*, Mater. Prot. Perform., Vol 10 (No. 12), Dec 1971, p 33
- [5] S. Wang, D. Liu, N. Du, Q. Zhao, S. Liu, and J. Xiao, *Relationship between dissolved oxygen and corrosion characterization of X80 steel in acidic soil simulated solution*, Int. J. Electrochem. Sci., vol. 10, no. 5, pp. 4393–4404, 2014.
- [6] ASM, Vol 13., *Corrosion*, ASM Handbook., p. 244, 1992.
- [7] A. Ismail and N. H. Adan, *Effect of Oxygen Concentration on Corrosion Rate of Carbon Steel in Seawater,* Am. J. Eng. Res., vol. 3, no. 1, pp. 64–67, 2014.
- [8] K. Hashimoto, M. Naka, J. Noguchi, K. Asami, and T. Masumoto, *Proceedings of the Fourth International Conference on Passivity*, R.P. Frankenthal and J. Kruger, Ed., The Electrochemical Society, 1978, p 156-169
- [9] *External Corrosion of Oil and Natural Gas Pipeline*, ASM Handbook Vol 13C. Corrosion.
- [10] H. L. Bilhartz, *High Pressure Sweet Oil Well Corrosion*, Corrosion, Vol 7 (No. 8), Aug 1951, p 256-264
- [11] H. L. Bilhartz, *How to Predict and Control Sweet Oil Well Corrosion*, Oil Gas Journal., Vol 50 (No. 50), April 1952, p 116-118, 151, 153.
- [12] K. Darowicki., *Evaluation of Pitting Corrosion by means of Dynamic Electrochemical Impedance Spectroscopy*, Science Direct , Electrochimica Acta, 49 (2004) 2909-2918
- [13] *Standard Guide G48-92*, Annual Book of ASTM Standards, Philadelphia PA, ASTM-1994.
- [14] El Hassan J, P. Bressolette, A. Chateauneuf, El Tawil K., *Reliability-based Assessment of the Effect of Climatic Conditions on the Corrosion of RC Structures Subject to Chloride Ingress*, Eng Struct. 2010;32(10):3279–87.
- [15] S. Paul., *Model to Study the Effect of Composition of Seawater on the Corrosion rate of Mild Steel and Stainless Steel*, Journal of Materials Engineering and Performance 2011;20:325–34.
- [16] Han-Seung Lee, et.all, *Protection of Reinforced Concrete Structures of Waste Water Treatment Reservoirs with Stainless Steel Coating Using Arc Thermal Spraying Technique in Acidified Water*. Materials 2016, 9(9), 753.



QIR

*The Westin Resort
Nusa Dua, Bali*
24-27 July 2017

IDWELL

**International Conference on
Dwelling Form**





COMMUNITY ENGAGEMENT AND CHILDREN SPATIAL NEEDS IN RUSUN KEMAYORAN

Nevine Rafa Kusuma^{a*}, Rossa Turpuk Gabe^{b**}, Triatno Yudo Harjoko^{c**}

^{abc}Departement of Architecture, Faculty of Engineering, Universitas Indonesia 16424,
Depok

ABSTRACT

Human life-cycle space includes the necessary space, especially for the playing age stage. Playing is necessary in terms of human development in this stage. This will enhance both physical and psychological development of a child. We may argue that the lack of this in human being dwells will make them deprive of both physical and psychological development.

Children spatial needs such as a play space in multi-stories housing (*rumah susun - Rusun*) in many cases is usually neglected due to its limited space. In fact, playing is an essential aspect for children to develop their social competence and emotional maturity. Moreover, the cultural context in Kemayoran Multi-storey housing showed that parents' supervision has influence on the chosen site. In this regard, suitable space for playing in the vicinity of their home is necessary.

The objective of dwelling issue that raised by team of community engagement project of the department of architecture Universitas Indonesia is the possibility for children to have a decent and proper playing ground in their vicinity of the *rusun*. The site chosen for this project is Kemayoran multi-storeys housing (*Rumah Susun Kemayoran*). The program is focused on setting up an Educational Play Area or *Ruang Bermain Edukatif (RBE)*. This program has been implemented with the involvement of local community. The project has succeeded to develop community participation for engaging and setting up an educational playing area immediate to their residence in *rusun*, in the ground floor area.

Keywords: Rusun or Multi-storey housing; children spatial needs; community engagement;



1. INTRODUCTION

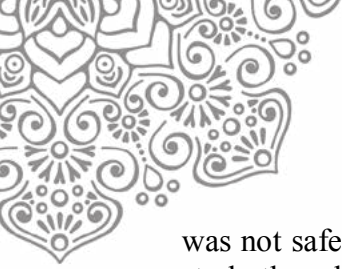
Dwelling is a concept that seems to have a simple meaning, yet it actually consists of a wide range of definitions. The concept of dwelling, other than a physical place, includes the whole residence along with all necessary facilities and services for family's well-being and also working, education and health-care programs for people (Shidfar, 2013). Furthermore, Dwelling should not be merely perceived on basis of the activities that it shelters; it also provides space for man's everyday 'habitual' activity experiences that associated with peace, residence, care, and integration in the Fourfold (Heidegger, 1958, p.174). Thus, considering 'dwell' definition as someone's peacefulness in a place, this forced people to take care of its place.

As regards with this matter, dwelling in multi-stories housing is usually facing difficulties to fulfill every residents' needs, such as adults and children, due to its spatial limitation. For instance, multi-stories housing providers often forget that children's basic need is including their need to play. As regards to dwelling comprehension, many children expressed their appreciation of the peacefulness and privacy of their play areas (Wheway, R and Millward, A.,1997).

During children physical and psychological growing process, they need playing space as part of their basic needs (labouring body and mind). Research showed that children's education that based on playing activities could affect children's development (*Article 31 of the UN Convention on the Rights of the Child in Children's need for time and space to play*). Children's abilities could be stimulated through different ways. Some children's abilities that even could be improved through playing are linguistic intelligence, logic-mathematical intelligence, visual-spatial intelligence, and interpersonal intelligence (Christianti, M., 2007). Moreover, in terms of Indonesia's circumstance, people lives in surrounding that practice the importance of being *rukun* (maintaining harmonious relationship) and *tepaslira* (helping, sharing, and emphathizing with others) as human virtues and children are taught early to approximate these ideals (Jo Ann & Wimbari, 1995). Consequently, those cultural phenomena created the kind of games that are widely played by the children, such as congklak, bekel, etc.

Furthermore, considering that children could learn about themselves through various plays and their surroundings, therefore play area environment should offer rich opportunities, allowing each child to explore and grow safely at their own rate (Wheway, R and Millward, A.,1997). In relation to this matter, the common problem in multi-stories housing are often in the form of struggles between procurement of play area and limited space to meet the ever-demanding housing needs. The difficulty to decide where to locate play areas is widespread, and often results in play areas being placed away from the housing unit, in secluded area, which would otherwise afford a level of informal community supervision. In addition, the quality of the environment for playing is extremely important as well, in order to satisfy children's needs for active, quiet, imaginative, creative and social play.

Based on our discussion with the community in Kemayoran Multi-stories housing, most children choose to play outdoors that taken place near their unit and by moving around the outdoor environment for which they have access to, although the environment in question



was not safe enough for playing. Moreover, most of the parents that are interviewed in this study thought there were not enough play facilities in their areas, even on the block where such play areas were provided. This is due to the cultural context in the vicinity, which also supported this matter. Derived from Jo Ann & Wimbari (1995) who stated that Indonesian children grow up in extended family households with many adults and siblings who give them much attention. It shows that parents and community's supervision in children's daily life is essential.

Regarding to community's role, Norberg-Schulz stated that dwelling is according to space and time, related to how it uses, the meaning of it and its role in community (King, 2004). In his opinion, dwelling has three meanings. Firstly, dwelling involved an interaction between people and also related to ideas exchange. Secondly, dwelling means accepting and sharing. And the last, dwelling means how to be ourselves, where we have our little world, our privacy. These three meanings are related to each other, where human's life consists of interaction with others, exchanging, sharing, and running those things as habituation. In dwelling process, people tend to reach those three meanings with their society (family and community). Furthermore, active participation from the community will determine the quality of their dwelling.

Conyers (1994, p.26) explained that there were three main reasons in the urgency of community participation. Foremost, community as the tool to gain information regarding their needs, condition and views. Furthermore, achieving trust and support from the community due to their existence involvement is crucial as well. Finally, the community could control the development based on 'man-centred development'. Therefore, referring to the substantial impact on participatory design, an utmost community involvement is expected to gain a strong sense of ownership towards the design.

Based on the explanation above, community's role in multi-stories housing could not be ignored to fulfil children's basic need, for instance, community's supervision and facilities procurement for children by community empowerment. Therefore, in multi-stories housing condition where spatial limitation was the main issue, community participation becomes main potency to create peacefulness dwelling for all residents, including children.

2. CASE STUDY

2.1. The Program

Regarding the issue related to the dwelling that is unacceptable to be occupied yet required playing ground, the program proposed in UI Community Engagement, was Educational play area. This program was developed in regards to escalate children's intelligence and potency when they were trying to learn about their world. The targets were children (6 to 12 years old) and their parents, it is due to their psychological condition in their age.

Educative games that we developed was including education values that stimulates children's social, emotional and cognitive skill development. It was accommodated through architectural aspects in play-space, included vertical and horizontal area in the limited space. Our aim was not only to fulfil children's needs of playing, but also to



develop their potencies and skills through playing.

The location was in the area around Apron 8, Kemayoran Multi-stories housing, specifically in informal multifunction space in ground floor that is always used by the residents to gather, from children to adulthood. This location was chosen due to its setting that was easy to access and parents' consideration regarding their needs of supervision (Figure 1).



Figure 1. the location for Educational play area

Source: Personal illustration

2.2. The Community and The Process

In the development process of this program, community's role was the main factor in achieving its success. The residents, parents and their kids were involved through participatory design. In its implementation, the residents' contribution was on giving suggestion and building design process. The purpose was that after the program, residents' sense of ownership could last, so that they will take care of it in the future. Eventually, it became a strong foundation due to program sustainability and advancement.

In terms of program sustainability, this program was granted for the community. Within the community involvement and knowledge which had given on the workshop, we hope that this community could manage and develop this program further.

This program was proposed in 2 stages, 1) Community participation in discussion and workshop, 2) Design development and built along with the community based on the discussion.

Stage 1 - Community participation in discussion and workshop

In this stage, it started by dealing with the community to establish an Educational play area in their settlement and focus on the feedback from the community regarding the play-space. In terms of this, we held a workshop for parents and children about types of games that are save and educative, conducted by a child psychologist.



Figure 2. Discussion with the community (parents and children)

Stage 2 - Design development and built along with the community based on the discussion.

During this stage, the program was developed in selected location based on discussion and feedback with the community. The design was built through application of spatial elements (vertical and horizontal partition, materials, etc.) to facilitate playing needs and encourage children's creativity. The development of this idea should be flexible in terms of accommodating other activities, such as informal meeting or extracurricular. Finally, our team had renovated and redecorated this multifunction space based on on the design plan.

This Educational play area was equipped with simple games that used recycle materials with the intention of enforcing children to think creatively in creating their own games. Although it was simple, these games were chosen due to the development children's linguistic intelligence, logic-mathematical intelligence, visual-spatial intelligence and interpersonal intelligence. The chosen games were scrabble wall and geo-board.

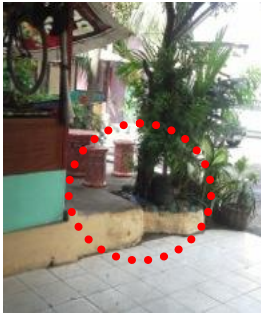






Figure 3. Workshop with children in Apron 8 Multi-storeys housing
Source: Personal Documentation



3. DISCUSSION


Planning and design participation with the community: Various alterations are experienced in the design, location and management of play areas and play areas:

No.	Before Program	Activities	After Program
1	<p>The gazebo's position is too high to be reach by children</p> 	<p>Make steps with proper dimension that provide user's comfort.</p>	<p>A safe and comfortable circulation for children.</p>  
2	<p>The gazebo's base is uncomfortable because the material which easy dirty.</p> 	<p>Replace the gazebo's base material with HPL (High Pressure Laminate)</p>	<p>A comfortable gazebo for children activities and easy for maintenance.</p>
3	<ul style="list-style-type: none"> • The temporary gazebo's partition that only for prevent mice • An unorganized storage. 	<p>Replace the gazebo's partition.</p>	<p>The gazebo's partition became a playing and learning media that also as an organized storage</p>  



No.	Before Program	Activities	After Program
4	<ul style="list-style-type: none"> • Wall area is underutilized • An unorganized storage. 	<ul style="list-style-type: none"> • Redesign wall area • Make a mini stage 	<ul style="list-style-type: none"> • Projector screen • <i>Mini stage</i> provides an additional space for playing and learning and also as an organized storage 
5	Wall for projector screen. 	Added scrabble wall for children	An additional function of wall area. Children can play scrabble wall in that area. 
6	<ul style="list-style-type: none"> • Parking space as a play space for children. • Types of game that is only for children's motoric development. 	Educative playing workshop that can applied in RBE	Children can play in RBE and create some game tools used recycle materials. 



No.	Before Program	Activities	After Program
7	<ul style="list-style-type: none"> Communal space but doesn't consider children's needs for playing and learning. 	Discussion with community, accommodate their aspirations and develop educative playing space in selected location.	Educative playing space which also facilitate other needs for community. 

The direct impact of this program is that around 60 children (of elementary-level education) in the selected location can use Educational Play area for them to play and foster their creativity in limited space. In addition, a direct impact that parents can feel is in the development of their child's cognitive social skill and easy supervision of the children. Given this condition, the occupants of *Rusun* Apron 8 acknowledged the improvement in their quality of life. In an effort to meet the needs of the children and parents living in it, it is safe to say that this *Rusun* falls under the category of "possible dwelling".

The indirect impact felt by the partners is that the occupants are able to resolve their own issues (duplicating design) with regard to the need for children play area in the *Rusun*. Therefore, the role of the occupants can directly support *Kota Layak Anak*, a program run by the government, in particular in giving a practical solution for providing play area needed for children development within their housing complex. Having this Educational Play area installed can add to the *Rusun's* positive image as a *Rusun* looking after of children's need for space.

This Educational Play area serves as a drive for the public with regard to providing space needed by every child. In other words, every child is entitled to have a decent life according to his/her need for development, which is the need to play. The response shown by the public regarding the importance and usefulness of this program for the community in particular those living in *Rusun*, is illustrated in figure 6. It is therefore expected that this program will receive special attention from the government and for it to serve as a model in designing *Rusun* in the future.

Based on the response received both during the implementation of the program and afterwards, the dedicated team sees a relatively high potential for this program to continue developing. Moreover, the program running now is aimed at producing an initial model for



Educational Play area expected to be further developed in relation to Kota Layak Anak program.

Several positive responds to the Educational Play Area from the society:



Figure 6. Positive respond to our project
Source: Personal documentation

4. CONCLUSION

Space for play in limited area, such as in multi-stories housing, is as crucial as children’s basic needs. However, due to the limitation of its space, space for play does not need to be in outdoor area. In terms of this, communal space in each tower for instance, could work for children’s play-space. The use of vertical and horizontal surface that applied the games on each part.

Through Educational play area for children in multi-stories housing, it changed the paradigm about multi-stories housing that are usually looked utilitarian or impossible to possible dwelling (child friendly) due to the children’s life-cycle. Furthermore, the built educative children play-space is adding value to children’s games. Based on the interview with some parents who live there, this educative games are valuable for their daily life. Although the proposed games (scrabble wall and geo board) originated from different culture, children adopted easily with the games, because it consists of same cultural values, such as *rukun* and *tepaselira*, and also the same logic in terms of strategic thinking. Therefore, children could learn varying values of the games, not only playing but also improving their social, emotional and cognitive skills.

The role of the community in providing play area for children living in *rusun* is not only limited to providing the space itself but also giving comfort for children to play safely since they are already familiar with the surroundings. It is related to cultural context in the Rusun, that Indonesian people are naturally living in peer. In addition, a play area located near their unit is likely to give the parents sense of security for being able to supervise their children while playing. This condition is in line with the study on providing play area in housing complex and Indonesian culture, in terms of parents-children relationship, to ease



the worry of parents regarding the location of the play area which is often out of parents' reach of supervision due to limited housing space.

The key to this program is the involvement of the local community from the planning stage to its development, from determining the location to the procurement of space and toys. This involvement is likely to suit the program to the children's need and to ensure its sustainability.

Based on these findings, we expect this program to be able to produce an alternative Educational Play area that can accommodate types of games requiring active or passive participation in all *rusun* in Indonesia, in particular in Jakarta. The Government, (Deputy of Child Growth and Development of the Ministry of Woman Empowerment and Child Protection, the Ministry of Public Housing) and academicians need to see the potential of the program in order for the public to be able to facilitate the space needed for life cycle in its place of living especially in places where play area is limited such as in this case.

6. REFERENCES

Christianti, M. (2007). Jurnal Club Program Studi Pendidikan Guru Taman Kanak-kanak . *Anak dan Bermain*. Yogyakarta: Universitas Negeri Yogyakarta.

Heidegger, M. (1951). *Building, Dwelling, Thinking*. London: Routledge.
stitute Of Housing And The Joseph Rowntree Foundation.

Jo Ann M. Farver, & Wimbari, S. (1995). Indonesian Children's Play with Their Mothers and Older Siblings. *Child Development*, 66(5), 1493-1503. doi:10.2307/1131659

Shidfar, S. (2013). The Difference Between Dwelling and Home in Architecture. *International Journal of Computer Science Issues*, Vol. 10, Issue 4, No 2: 240.

Wheway , R and Millward , A. (1997). *Child's Play: Facilitating Play On Housing Estates. A Report For The Chartered In*

Article 31 of the UN Convention on the Rights of the Child dalam Children's need for time and space to play, http://www.sagepub.com/upm-data/15553_CASEY_C01.PDF

Space for active play dalam Developing child-inspired play space for older children, <http://www.heartfoundation.org.au/SiteCollectionDocuments/Space-for-active-play.pdf>



TRANSLATION OF *RUMAH* ULU OF SOUTH SUMATRA INTO A MODERN HOUSE

ABSTRACT

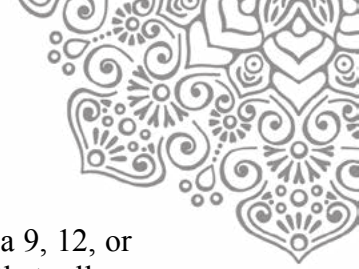
For people who moved from their village to a city, it is not easy to build a house following vernacular building like their house in the village. Vernacular buildings are built to support the needs and values of their inhabitants and provide instructive examples of sustainable solutions to building problems. Yet, these solutions are sometimes assumed to be inapplicable to modern buildings. If the design of a modern house is adapted from a vernacular house, there should be a translation of vernacular ideas. The translation makes the concept of modern house is not exactly the same as a traditional house, even though both of the houses have similar forms. This study investigates the use of vernacular ideas of *rumah* Ulu in South Sumatra into modern houses. The house forms of *rumah* Ulu, with tropically-suited roofs, elevated interior, and harmonious proportions are considered by some people to still have relevance. This study focuses on the translation of *rumah* Ulu including how the house forms and rooms such as *serambi* (verandah), living room, and bedrooms are changed by inhabitants. Some aspects of house forms and building designs of both the traditional and modern houses are explored through a qualitative method and field research in order to discuss the suitability of *rumah* Ulu to its inhabitants' needs.

Keywords: Rumah Ulu, Translation in Architecture, Vernacular House

1. INTRODUCTION

Vernacular houses are built to meet the specific needs of their inhabitants, including to cope with values, culture and way of life of the inhabitants. Amos Rapoport (1969) says that a house expresses the ideal environment and the social system of people who live in that area. Socio-cultural factors affect mostly the house form of vernacular houses and terms modifying factors to specify aspects that determine the architectural form of the vernacular houses. The modifying factors, such as climate, material, religion, and site, are some factors that influence the house form to fit people's need, their culture, and the environment. It is not easy for traditional people who move to a city to build a house, especially because often their reference of a good house is the vernacular house from the area where they belong. A house is a living quarter of people or a family that accommodate the needs of the inhabitants and are built in accordance with the environment and the culture. In addition, when designing a place to dwell, interactions among people, culture and environment are important. Different groups are affected differently by the same aspects of environments and sometimes those different aspects of environments become salient to those groups since their preferences vary on the basis of their values, ideals and evaluations. People also express themselves through built environments differently. If a house in a city is adapted from a vernacular house, then there is a process of translating or transferring ideas.

Rumah Ulu or Ulu house is a traditional house located in several villages in South Sumatra, one of them in Ogan Ilir where the case study is conducted. Ulu house is a Malay



a house with some typical features such as a plan reducible to modules based on a 9, 12, or 16 post set, and post and lintel construction with wedged mortise joints that allow dismantling, posts standing on plinths (Hilton, 1992). Ulu house also has a raised main floor with additional floor at lower level, access via a ladder or flight of steps of odd number of treads the roof ridged supported over the summits of the posts, and decoration by carving rather than painting.

This paper will explore the translation of Ulu house into modern houses by investigating changes and adaptation in the form of the dwelling and the how the modern house functions in comparison to Ulu house. The paper will discuss the house form, plan and functions of rooms in Ulu house and how the inhabitant translates this house for a modern house.

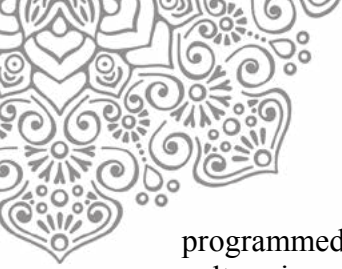
2. TRANSLATING VERNACULAR ARCHITECTURE

Amos Rapoport (1969) defines a new thinking about the origin of a house form as a symbol created by a complex interaction between of socio cultural factors. There are two factors that influence house form for traditional communities: socio-cultural and modifying factors. In relation of house, man, culture and environment, a house becomes an expression of conceptualized model of interaction between culture and behavior that happend for a long time. House form is a result of the need of climatic shelter but the interaction among many factors related to cultre and society. Socio-cultural factors combine some values and basic needs of the family, sucha as privacy, position of woman, the relation of house and settlement, the site, and constancy and change. Socio-cultural factors are not independent but related to other factors. The modifying factors that affect the house physically are climate, technology, material, construction, site, defense, economics, and religion. Both socio-cultural and modifying factors relate to each other. In short, Rapoport shows a vernacular house as an expressions of the value of culture.

The concept of translation in architecture is good to complement the future of architecture (Akcan, 2012). The translation, as described in her book *Architecture in Translation*, is a state where there is a cultural flow from one place to another. Translation in architecture can be discussed in relation to the conversion of images to buildings, from diagrams to projects, from one place to another, passing different distinctions to architecture, and from text to visual image.

Translation definitions include change actions from one place, position, condition, media, or language. Translation in architecture not only can raise the possibility of cultural exchange, but also cause tension for instance the loss of authenticity of a vernacular building so that sometimes there is a gap when receiving the translation. Translation in architecture involves two things, linguistic and visual (Akcan, 2012). Linguistic literature is related to concepts and theories in a region while concepts and theories can be found from the form, meaning, and function of the building. The translation on the visual thing related to the principle of making space and representation that can be found from the form, the idea of space, technology, and building Function. The translation used in this study is mainly conceptual and visual displacements from one form or place to another.

People develop a correspondence between how they live and their houses through choices that express their cultural values and traditions (Rapoport, 1989). At first, culture is



programmed in a house's form through a functional specification of ways of living. Second, culture is embedded as choice – through a capacity that enables residents to choose how to dwell. The first limits resident choices by assuming culture to be static while the second increases choice by recognizing culture as constantly defined and renewed. One important expression of culture comes through the ways in which people dwell. In relation how people uses spaces, there are three aspects of house design that architects can use to enable choices in using the house namely access, dimension, and control over space (Chow, 1998).

In the case of people who move to a new area, one should adapt to new conditions by choosing the right values to be reflected in the house. The variety of ways in which people live can be addressed simply by translation or “reprogramming” such as by defining room composition and matching activities, spaces and life-style (Chow, 1998).

There are two main characteristics that describe the approach to choice embedded in building a house with vernacular house as its precedence. First, it is related to normative life-styles, with differences in ways of living taken as adaptations to the different situation. Second, it is program driven that tries to relate life-styles with houses. The second characteristic engages a process of matching activities and spaces and personalize spaces. It seems that inhabitants of the house will most likely correspond activities and spaces inside the house through reprogramming access, dimension and control over space. Access is useful to provide a way to move from one room to another so that it can be said that access connects between the “container” of activity and the “contain” or the activity itself. Dimension of spaces can change the capacity of a room or a house which is required to create a perfect space for each and accommodate different spatial requirements and privacy. The capacity of a room can be changed to fit the activity of the inhabitants through configuration and adjustment of dimensions.

Translation or reprogramming are important in the process of transferring an architectural idea to be adapted in different areas and conditions. When designing a house, the designer or the inhabitants may use the concept, depending on the way the inhabitant live. The house may be built exactly like its precedence, including the arrangement of space, materials, and construction. However, if the new house is built through translation, the culture of the inhabitants probably will be adapted in varying degree. In the concept of reprogramming, the house is not exactly the same as the original house because there are several things that are adapted to the living ways of the inhabitant and the house environment. The possibility that will happen to the house using the concept of reprogramming is the house will have a culture that intercepts the house precedent culture and the house environment culture.

3. RUMAH ULU IN SOUTH SUMATRA

Ulu houses are associated with a Malay house type that is modular, transportable, and adapted to the Ulu people way of life. The form of *rumah* Ulu is the result of Ulu's culture and how Ulu people respond to their environments. The modular post (a 9, a 16 or a 12 post plans) and lintel construction with a main floor raised sufficiently to permit activities beneath it. The Ulu is commonly called *rumah panggung* for having a raised floor and is usually located close to the river. The raised floor can protect the inhabitants from wild animals as well as flood. There is a subsidiary floor at a lower level determined by the



mortising of its supports while the posts stand on masonry foundation blocks or stilts. They are rigidly held upright by mortised cross members at their upper parts and at floor level. A ridged roof covers the whole house on a framework built over the uprights. The houses are to be moveable by dismantling at the mortises.

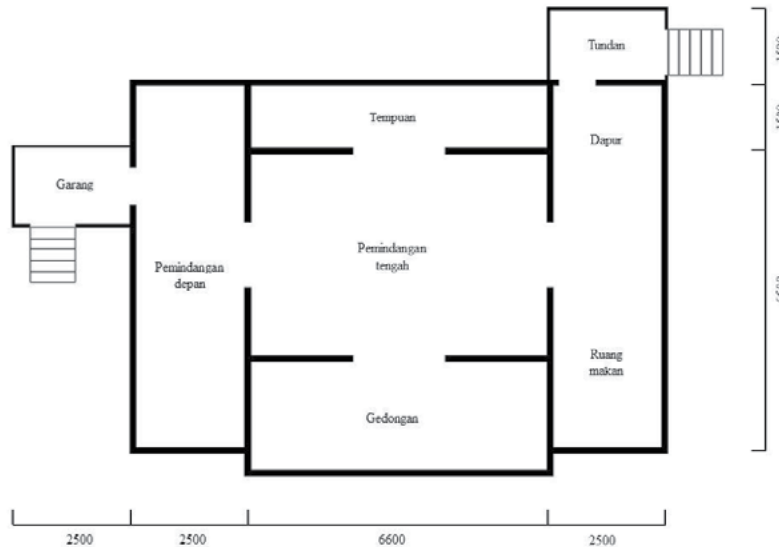
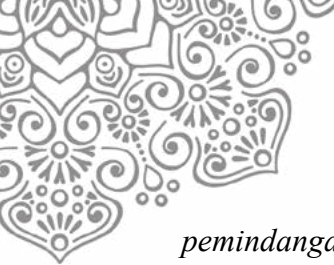


Fig. 1 Plan of Rumah Ulu

Depicted in Figure 1 is the plan of Ulu house. The main door of *Rumah Ulu* is predominantly located at the left side when facing the interior. Ulu house is basically divided into three parts; front, center and back. The front part of the house consists of a floor terrace *garang* and *pemindahan depan*. *Garang* is the first room after one climbs the stairs and enter the house. *Garang* functions as a living room for guests who are still single (*bujang*) and for guest categorized as unfamiliar. Some people still travel on foot in Ogan Ilir and a family may allow those traveling people to be their guest and rest for a while or even spend a night in *garang*. This room is also a multi-functioned room usually for a bedroom for *bujang* when the owner of the house holds a wedding ceremony, a circumcision celebration, or as a place for children when the whole house is used for ceremonies. The room located next to *garang* is called *pemindahan depan*. The family members usually sit on this room and sometimes they look out the window to see who is coming or check their surroundings. The owners of the house may also call their neighbor to come to their house. In addition, *pemindahan depan* also functions as a living room for relatives, a place for girls to weave in the evening, as well as a place where religious and cultural ceremonies take place. When one of the family members dies, the family will place place for dead body in this area.

The center part of the house is in the form of a big space located next to *pemindahan depan* and called *pemindahan tengah* that function as a family room. The family usually gather in the *pemindahan tengah* after Maghrib prayer. Moreover, the center part is also usually well decorated and becomes a place to show the guests how prosper the owner of the house is. Beside as a gathering place, this room is a place for the family to do their daily activities. It is possible for female to weave in this room if the



pemandangan depan is used as a bedroom for guests. Next to *pemandangan tengah* is *ruang tempuan*; this room is reserved when the family need more space for their activities or when both *pemandangan* are used for cultural and religious ceremonies. *Gedongan* is a family bedroom in a form of a big hall. All members of the family except *bujangan* can sleep in *gedongan*. When the family need several cubicals, they usually use cloth or *kain tebar* to create divisions cubicals. *Gedongan* also serves as a place of small children to play and do their activities.

The back of the house is reserved for a dining room and a kitchen. There is a door and a stair to go out of the house to *tundan* - a room for washing and cleaning. *Tundan* is usually located outside the house in an open area or near a river. The bottom of the house is also functional and regularly used for various activities such pounding rice and a playground for children. This place is also reserved for storing equipments such as for paddy plantation, stoves and households.



Fig. 2 Typical Ulu House

The whole house uses wood as building materials based on the strength or other character of the woods. The exterior of *rumah Ulu* typically responds to the possibility of flood and protecting the house from rainwater by using waterproof wood. For structural parts, the house has strong *gehunggang* and *merbau* wood and for the walls *seluha* and *merawan* woods. In addition, some parts of the house also use bamboo such as for the floor. Wood and bamboo are commonly taken from the surrounding areas. The roof of the house is covered with *enau* leaves with *rangkai-tumpuk* or overlapping techniques. The construction of the *Ulu* house does not use nails or iron hinges, but the house uses mortises and tenons called *meruang, jalu, jalin, tumpu, jepit, dan sambung kait* techniques.

In the form of decoration, there is a particular symbolic meaning according to what applies conventionally in the community (Toekio M, 1987). Based on the history of the *Kesultanan* in South Sumatra, the art of carving is one of the art of decoration as a symbol of culture and belief. There are various motifs in traditional houses of South Sumatra such as geometric (lines, rectangular, square, spiral, *tumpal*, etc.) and non geometric (plants). A typical carving motif is a motif that depicts plants, because plants symbolized life and humans also lived from plants (Susanto, 1993). Geometric ornamental shapes have their own meanings, for example curved or bending lines mean rest and silence while diagonal lines mean war and confusion. Non-geometric motifs that are often the depiction of leaves, flowers and trees is commonly based on a sense of admiration, or other impressions and



feelings towards nature. The motifs are usually place on the door, posts and *garang* fence. Due to the strong influence of Islam in South Sumatra, animal motifs are rarely found.

4. DISCUSSIONS

The study case of modern Ulu house, which was built in 2010, is located in Desa Buluelok, Kecamatan Muara Kuang, Ogan Ilir, South Sumatra. Although this house is in Ogan Ilir, this house has some characterisitics of the original of *rumah Ulu*. The stair at the front of the house is the only stair to reach the upper floor. After climbing the stairs, one can find *garang* as the first room. The space organization and the house form in this modern house is similar to a typical *rumah Ulu*, which is easily recognized as a stage house made mostly from wood and having a front terrace.

After choosing the land to build a house, the inhabitant will consider how the house is related to how the environment, which is in a city. The inhabitants take *rumah Ulu* as the precedence since this kind of house is very suitable to their culture and needs. In Ulu vernacular house, culture is programmed in a house's form through a functional specification of ways of living. Culture in Ulu house in Ogan Ilir is embedded as choice, which is through a capacity that allows inhabitants to choose how to dwell. Unlike in the vernacular house, in which culture seems to be static, the second increases choice by recognizing culture as continously renewed and defined.



Fig. 2 Plan of modern house in Ogan Ilir

In general, *garang* functions like the one in *rumah Ulu*, as a terrace and the connection between inside and outside of the house that has the least privacy comparing to



other rooms within the house. In addition, *garang* not only has a door that becomes access between the *garang* and the front rooms of the house, but there is a door that connects *garang* and the back of the house. The inhabitants often use both of the doors.

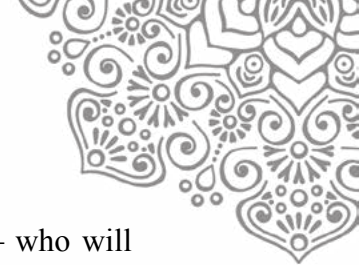
Both *pemandangan depan* and *pemandangan tengah* are translated into one big common room. However, in this translation of *pemandangan* areas, the owner of the house put a sofa facing the window so that the family are still able to look out the window. Moreover, some part of this room functions like *pemandangan tengah*, which becomes a family room. In this big room, the family spend sometimes together although there is no different level of privacy. This room is a place for family meetings and ceremonies. This room is connected to three bedrooms or *gedongan*; one of them can be a guest room when necessary.

At the back of the house, there are some translation of *rumah Ulu*'s organization that consists of a dining room, a kitchen, and a *tundan*. The house has two bathrooms since the family members do not feel comfortable if they should take a bath in a river. The lower part of the house is not for doing daily activities but just to park motorcycles. Even children do not play below the house anymore but the front yard.

The house mostly uses woods and bricks as its materials. Woods are mainly used for the front part of the house such as living room and bedrooms, and bricks are used particularly for the back of the house such as dining room and kitchen. The use of wood for the front part create a continuation with the surroundings as well as protecting the façade to be similar to *rumah Ulu*. Although there are many parts of the house that are still made of woods, the house has no ornaments. The use of bricks for the back part of the house shows consideration that the owner is actually want to avoid fire and stronger structure from concrete column. Moreover, there is fences to protect the house.

In the process of transferring an architectural idea of *rumah Ulu*, there are some translation and reprogramming activities as a way to adapt to new environment. The house may be built exactly like vernacular house in Ulu, including the arrangement of space, and the materials. However, the inhabitants has done some adaptation to modern condition such as using bathroom instead of going to the river for cleaning and washing. Through the idea of reprogramming, the house is not exactly the same as *rumah Ulu* because it is adapted to the living ways of the inhabitant and the environment. There may be a loss of harmony between the house and its environment such as indicated by the use of fences.

The front area or *garang* of the two houses can be understood in relation to access. This terrace offers choices for the owner of the house to allow the guest to have more closeness to the core of the house or to exclude the guest from the rest of the house parts. *Garang* in the house located in Ogan Ilir also gives a choice not only to exclude the guest from the rest of the house but also to enter the back areas such as kitchen when the common living room is occupied. Dimensions in vernacular houses are usually laid out according to the body of the owner or a common cultural practice while in the house in Ogan Ilir it seems that dimensions are selected from a standard range of spatial and furniture configurations. In Ogan Ilir, the dimensions are generated to fulfill a house's program or the owner's needs so that the owner has a greater capacity of choices. The open plan of the living and dining areas includes private activities although individual spaces are separated from the rest of the house to provide privacy. In Ulu vernacular house, there is a strong public-to-private gradient based on the position of a space either toward front or back areas.



In Ogan Ilir house, the open plan of the common living room excludes guest – who will probably stay in the terrace – through the use wall and door.

People develop a correspondence between how they live and their houses through choices that express their cultural values and traditions. At first, culture in a vernacular house is programmed in a house's form through a functional specification of ways of living. Then, in modern house culture is embedded as a choice – through a capacity that enables residents to choose how to dwell. The first limits resident choices by assuming culture to be static while the second increases choice by recognizing culture as constantly defined and renewed.

5. CONCLUSION

From the discussions of Ulu vernacular house and a modern Ulu house in Ogan Ilir, the two houses serve as a living place that follow characteristic of *rumah Ulu*. For the modern house in Ogan Ilir, although the house form still represents Ulu vernacular house, there is a translation or a reprogramming of the original one. The idea of Ulu house with *garang* and *pamandangan* constitutes, either consciously or unconsciously a constant in the design of modern Ulu house and serves to promote the continuity inherent in traditional Ulu architecture. Other contextual elements of tradition, i.e. the use of material, decoration, detail and so on, are employed as secondary variables. The built pattern of the house has not become a fixed remnant of the past, but has been restated by new designs and means. It can be maintained that, contemporary Ulu house resonates with spatial features that link modern life either practically or symbolically to traditional aspects of Ulu people and culture through the intermediary of the *panggung* house idea. The analysis of the case studies shows that while the formal attributes of Ulu vernacular house may be deterministic, the form of the house has the potential to inspire a translation between house and inhabitant who move to a city.

4. REFERENCES

- Hilton, R. (1992) Defining the Malay House, *Journal of the Malaysian Branch of the Royal Asiatic Society*, Vol. 65, No. 1 (262), pp. 39-70
- Rapoport, A. (1969). *House form and culture*. Englewood Cliffs, N.J., Prentice-Hall.
- Akcan, E. (2012). *Architecture in Translation: German, Turkish, and Modern House*. Duke University Press.
- Chow, R. (1998). House Form and Choice, *Traditional Dwellings and Settlements Review*, Vol. 9, No. 2 (SPRING), pp. 51- 61
- Lozar, C. (1970). Review: House Form and Culture by Amos Rapoport, *Journal of Aesthetic Education*, 4(4), 142-143.
- Wigley, M. (1989). The Translation of Architecture, the Production of Babel. *Assemblage*, (8), 7-21.
- Rapoport, A. (1989) in “Forward,” in S. Low and E. Chambers, eds., *Housing, Culture and Design: A Comparative Perspective*, Philadelphia: University of Pennsylvania Press



I Dwell in *[Im]possibility*: Utopian Planning & Design in Indonesia as bias toward a city of one-dimensional society

Abstract. The dominant paradigm and the practice of urban planning and design in Indonesia has been overwhelmed with foreign idea, Western urbanism. Planners and designers deny the persistence of dual existence of society, that is of modern/traditional, capitalist/bazaar. This paper will discourse the ambiguity of the *[im]possibility* of *dwelling* in the light of the duality of the society.

The research is based on theoretical discourse related to the idea of dwelling. The analysis of the study will focus on a single case study of private development of Kota Wisata that is planned as un-integrated the large development of housing area in the suburban Jakarta. The rest occupying densely urban *kampung* represent those of traditional or non-modern one. In many cases, new modern development may exist mutually exclusive as separate entities against the *kampung* settlement that has no connection with one to the other.

Findings have shown that Kota Wisata is an exemplary model of the city of one-dimensional community. It denies the *possibility* of the low income, let alone the poor, to dwell and share urban facilities within.

Keywords: dwelling; dual society; mono-dimensional society

Introduction

This paper deals with discourse analysis in the context of the conference theme. It analyzes sign language and written sources. *I dwell in [im]possibility* is a sign language in this regard related to physical planning and design issues. The objective is i) to raise a critical understanding on how urbanism is conceived by certain ideology of planning and design that stays aloof in providing just living space for everyone; ii) to understand architecture in particular as a physical object to be hermeneutically understood out of its existence.

The poem of Emily Dickinson (1830-1886) *I Dwell in Possibility* which was first published in 1929 has fascinated many scholars, especially those associated with its syntactic ambiguity.¹ Therefore, it can be assumed and is reasonable to state, “*I Dwell in [im]possibility*,” where the phenomena observed may exist in ambiguity within which it enfolds the reality of presence and absence. *I Dwell* refers to and can be conceived as the individual ‘*I*’ live among (plural) humans (group of individuals, community, or society) and *I* live in a material and immaterial world. The word *dwell* originates from Old English *dwellan*,

¹ A situation where a sentence may be interpreted in more than one way due to ambiguous sentence structure.



to wander, to linger, to tarry. (Partridge, 1983:172) *I Dwell* means I wander, linger in the *world (being-in-the-world)*. It portrays the human existence in the world. The act of dwelling together justifies the co-existence of human beings and their urban environment. Here, in this paper, *I dwell* particularly implies ‘we’ that particularly refer to those who engage in the informal economy. ‘*I dwell* in [im]possibility’ illustrates an ambiguity of the condition of “[il]legitimacy” whether or not we are recognized and accepted by the *community* or the public at large. I distinguish the terms between *dwell* and *settle*; the latter means *to seat*, to stay permanently over space. This paper will uncover how urban planning and design practices remain stay aloof overlook the constitution of society that consist in dual form – *two-in-one*.

For the purpose of clarifying the concept of *dwelling*, I need to discuss the conceptual difference between world thinkers, such as Heidegger and Norberg-Schultz. Heidegger asserts that dwelling metaphysically justifies that humans live on earth. It also describes how humans live and condition themselves in the world. Heidegger (1971:144) claims that dwelling refers to,

“... [the] way in which you are and I am, the manner in which we humans *are* on the earth, is *Buan*, dwelling. To be human being means to be on the earth as a mortal. It means to dwell.”

Further, in this concept of humans as being mortals, Heidegger gives further details on the idea of dwelling – Four-fold. Humans as being weak mortals believe or have faith in divinity. To some humans, they believe that there is a connection between heaven and earth (axis mundi). Humans who live in the world accordingly have to be grateful to the sky that gives light, air and water. Humans also should be grateful to the earth that gives water, rivers, plants, woods as well as animals in it. In such a set of beliefs, such as in the Balinese culture, humans should live side-by-side with the environment and destroy neither the earth nor nature. In this regard, Heidegger (1971:147) further emphasizes,

“To dwell, to be set at peace, means to remain at peace within the free, the preserve, the free sphere that safeguards each thing in its nature. *The fundamental character of dwelling is this sparing and preserving*. It pervades dwelling in its whole range. That range reveals itself to us as soon as we reflect that human being consists in dwelling and, indeed, dwelling in the sense of the stay of mortals on the earth.”



While many have misunderstood the metaphysics of Heideggerian dwelling, to my understanding, he illuminates the very basic, as well as a simple idea of human and nature's ecology.

In a rather different conception, as put forward by Norberg-Schultz (1985), dwelling implies both staying and wandering. He expands the philosophic idea of Heidegger and explains the idea of dwelling in a much more pragmatic way. He refers to three aspects of the human condition related to dwelling (Norberg-Schultz, 1985:7). First, dwelling is a “means to meet others for exchange of products, ideas and feelings, that is, to experience life as a multitude of possibilities.” Second, dwelling is a “means to come to an agreement with others”, that is, to accept a set of common values, and third, dwelling is being “oneself, in the sense of having a small chosen world of our own.” Within the framework of thinking in architecture, Norberg-Schultz argues that modes of dwelling in architecture encompass private, public and collective spheres. Norberg-Schultz takes dwelling as a guiding concept for architectural practice. Heidegger and Norberg-Schultz are great scholars and noteworthy in their respective views. Heidegger and Norberg-Schultz are incomparable in thinking to have better understanding of urban dwellers than that most of ‘them’ as being poor migrants. ‘They’ are the other side of the duality of the society in general. In the logic of understanding ‘them’, we cannot simply *see* ‘them’ as an objective concept, which is external to our mindset. ‘They’ are far beyond any empirical understanding that we could capture. Possibility or impossibility of dwelling associated with the activity of informal economy will be assumed to refer to a [dual] structure in the constitution of the society.

One Dimensional Man or Society. Herbert Marcuse, in his famous book *One-Dimensional Man*, offers a wide-ranging critique of both contemporary capitalism and the then Communist society of the Soviet Union, documenting the parallel rise of new forms of social repression in both these societies, as well as the decline of revolutionary potential in the West. According to Douglas Kellner, (in Marcuse, H., 1964: xii) Marcuse puts forward a social theory

“... a theory of ‘advanced industrial society’ that describes how changes in production, consumption, culture, and thought have produced an advanced state of conformity in which the production of needs and aspirations by the prevailing societal apparatus integrates individuals into the established societies.”



“Advanced industrial society”, he argues, created false needs, which integrated individuals into the existing system of production and consumption via mass media, advertising, industrial management, and contemporary modes of thought.

This results in a “one-dimensional” universe of thought and behavior, in which aptitude and ability for critical thought and oppositional behavior wither away. Against this prevailing climate, Marcuse promotes the “great refusal” as the only adequate opposition to all-encompassing methods of control.



Figure 1
One-dimensional Man

(Source: Trappen, S., *Marcuse's One-Dimensional Man*, <http://sandratrappen.com/2016/03/11/one-dimensional-man/>, 31.03.17)

Rose (1990:56) further emphasizes that,

“... advanced industrial society has perfected new, deceptively insidious, and immeasurably effective forms of social control. Through the successful expansion of systems of mass production and distribution, the implementation of a “totalitarian” economic/technical coordination, and the manipulation of the deepest and innermost human needs by “vested interests,” advanced industrial society has successfully implemented a technological rationality that simultaneously obliterates the possibility of radical critique, as it creates an extensive regime of manipulated and unauthentic “needs””.

Planning and Design Ideology.

While it is important to see the city as a site of individual and collective emancipation, a tradition that incorporates Marx and Engels as well as Nozick and Milton Friedmann, it is just as important to remember that the city is an imposition and adherence to a series of master narratives. From Rameses II to Frank Gehry, through Baron Haussmann and Le Corbusier the city has been inherently authoritarian, sometimes totalitarian and occasionally fascistic. (J.R. Short: 18)

Planning is derived from the Latin adjective *planus*, flat, level, hence straight forward.

Becomes the English *plane*, a level surface, and a tool. Early Modern English – French *plan*,



in the 16th century, acquires the sense ‘a design’ (Partridge, 1983: 500). In this regard, ontologically, the concept of planning and design is essentially the same, namely, about decision of progress. However, as a process they are different in the sense that planning deals primarily with strategies that manifest in policies, programs and implementations, or *plan-do-check-act*. Urban planning is a technical and political process concerned with the development and use of land, planning permission, protection and use of the environment, public welfare, and the design of the urban environment, including air, water, and the infrastructure passing into and out of urban areas, such as transportation, communications, and distribution networks. Design, on the other, primarily deals with *creating* things. In a narrow definition, *designing* has an ultimate end of 3-D object, such as, urban design.

Faludi (1973: 76-79) put forward propositions related to the ideology of planning:

- i) *Town planning's main task is to reconcile competing claims for the use of limited land so as to provide a consistent, balanced and orderly arrangement of land uses;*
- ii) *Town planning's central function is to provide a good (or better) physical environment; a physical environment of such good quality is essential for the promotion of a healthy and civilized life;*
- iii) *Town planning, as part of a broader social programme, is responsible for providing the physical basis for better urban community life; the main ideals toward which town planning is to strive are (a) the provision of low-density residential areas (b) the fostering of local community life and (c) the control of conurban growth.*

Ideology iii seems to shift dominant paradigm of planning ideology up to the early seventies. Urban planning puts more emphasize on socio-political issues. Ideally, urban planning as a public undertaking and initiatives *should* embody the aspiration as well as the need of the people in the city. Despite criticisms especially from socio-political point of views such as Jane Jacobs in the sixties and Ruth Glass in the seventies, planning practices remain positive, technical in nature rather than normative. For as R. Glass puts it (Glass, 1973),

“ . . . it is undoubtedly the ideology of planning, far more than techniques of design and administration, which needs to be considered and developed. Planning without social policy does not make sense, and social policy without social theory and research is liable to become meaningless and eventually unacceptable.”[Glass, 1973:66-67]

Since then, society has become more complex, and the prospect of social change far more ambiguous, and yet the old ideas have been maintained and have become fixed prejudices. Though several movements contributed to town planning, and traces of the old divisions still remain, it is the ideology of the Utopians which has become predominant. [Glass, 1973:55-56]

In Indonesia, politics of the state since independence has changed dramatically with regard to



the socio-political freedom of the society. Reformation era in the late 1990s have laid a basic principle of democracy in the society. With the increasing role of the technology in media communication, *public sphere*² as once inspired by Jürgen Habermas (1987), people nowadays are bestowed a liberation and “free-talk” in the social media people. However, this political blessing as yet has not been effected in the urban planning and design practices. The local government that desperately attracts investments has exercised “less controls” against big and large area development. *Erratic* planning and development take place. Without proper spatial structure that especially provides framework for settlement patterns vis-à-vis transport system, the city becomes simply a calculus or mosaic of new town developments. They are congregating and crisscrossing along the spinal highways. (Fig. 2)

Urban planning and design that covers very large areas in Jakarta remains foreign to public scrutiny. They are resulted from technical exercises of the planning and design practices. They are market-based physical planning and design as a consequence they discount the poor or the people who live on the tradition of informality. They are deprived from proper and healthy urban dwellings.

Capitalist Tradition & Hyper-reality. In the history of capitalism, a cultural transformation in the meaning and measurement of time related to control and working methods can be observed. It economizes time and space at one moment.³ It assumes organized economic activities in the time-space dimension encompassing production, distribution, and marketing. Modernity that corresponds to the rise of capitalism is characterized by the development in science and technology, and especially where it concerns mass production and consumption. Economic activity deals with the mechanics of the aggregate of production and consumption. When the society like Indonesian is not prepared to participate in this mechanic, people are simply not ready and at worst they are merely spectator.

² The public sphere in Habermas's sense is also conceptually distinct from the official economy; it is not an arena of market relations but rather one of discursive relations, a theater for debating and deliberating rather than for buying and selling. Thus this concept of the public sphere permits us to keep in view the distinctions among state apparatuses, economic markets, and democratic associations, distinctions that are essential to democratic theory. Fraser, N., ‘Rethinking the Public Sphere: A Contribution to the Critique of Actually Existing Democracy’, in Craig Calhoun (ed.). *Habermas and Public Sphere*. Cambridge: Massachusetts, London: England, 1996, p. 111.

³ Friedland, R. and D. Boden, ‘NowHere: An Introduction to Space, Time and Modernity’, in Friedland, R. and D. Boden (eds.), *NowHere: Space, Time and Modernity*, Berkeley, Los Angeles, and London: University of California Press, 1994: 1-60, p. 8.

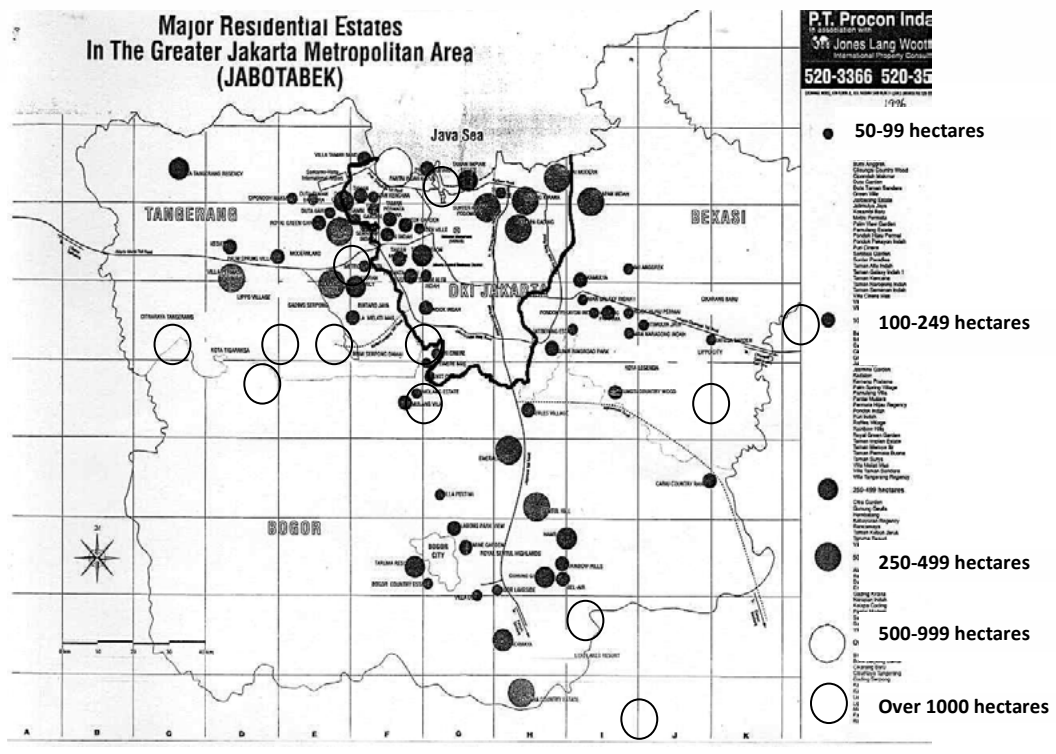
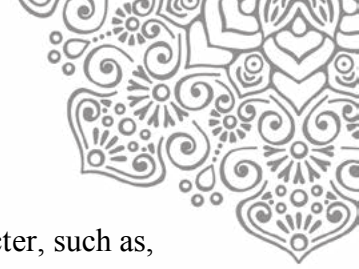


Figure 2
Development as it goes
The private development patterns relative to their sizes that range from 50 to over 1000 hectares.
(Source: Harjoko, T.Y. (2009), *Urban Kampung: Its Genesis and Transformation into Metropolis with particular reference to Penggilingan in Jakarta*, VDM Verlag Dr. Müller)

During the New Order, ‘modernization’ was taking place through the ideology of ‘economic growth’ and through authoritarian government (Harjoko, 2008). The signification of *pembangunan* or ‘development’ conveys meanings intended to economically increase the GNP. This was done by letting resources be developed by advanced countries, and physically by building a ‘modern’ beautiful city to promote *pembangunan*. Jakarta as a Capital City was especially supposed to provide services to achieve *pembangunan*. The services and infrastructure was to conform to an international standard characteristic of best cities in the advanced world. In short, Jakarta should simulate the ‘modern’ city of the world. This simulation inevitably depresses the ‘real’ map of the *kampung*'s social, economic, and political existence.

Following the establishment of Real Estat Indonesia (REI) in the 1970s, property development gained its momentum. Ever since, private housing and commercial centers grew rapidly like mushrooms in and around Jakarta or within the area of Greater Jakarta (JABODETABEK – Jakarta, Bogor, Depok, Tangerang, and Bekasi). They vary in size from simply small of hundred hectares up to large ones of thousand. Initially housing projects



began and adopted names quite simply and familiar to the people and local character, such as, *Pondok Indah* (Beautiful Home), *Kelapa Gading* (literally Ivory Coconut), and *Bumi Serpong Damai* (Peaceful Serpong Land – the name after the area).

Globalization further paves the way that capitalism has turned into its real ‘being’ – as G. Deleuze and F. Guattari term it a body without organ⁴. Empire of capital needs no fixed country or state like it used to be in the past. They manifest as ‘market state’ that incomprehensibly controls nation-states across the globe through global market.⁵ Capital no longer corresponds to the order of political economy; it uses political economy as a simulation model – simulacra, hyperreal.^{6 7}

Kota Wisata. Kota Wisata is one of the real estate development under the company of Duta Pertiwi, which is part of the Sinar Mas Group Real Estate Division (SMGRED). SMGRED started its business in 1988 and focuses its main business in housing, such as Kota Legenda and Kota Wisata in Cibubur, and Delta Mas in Tangerang, retailing, mall, super block project (World Trade Center and International Trade Center) and industrial estate in Jakarta. *Kota Wisata* or literally Tourism City. It is located in the southeast Jakarta. The estate covers an area of about 90 hectares.

Kota Wisata was designed initially by Australian architect. It is located in the Cibubur, Bogor Regency in the south of Jakarta. The site stretches across the north-south of Cibubur. It is ingeniously planned mainly for high-income residential areas. The designer designed housing in various cluster across the site (Figure 3). These are given with their unique Western names across the site. Each cluster has an entrance-gate that makes it a gated-community.

Competition in property development and globalized information, media has inspired large corporation to utilize media to expand their market. Residential design and development has turned into schism, as Deleuze and Guattari state

⁴ Deleuze, G. and F. Guattari, *Anti-Oedipus: Capitalism and Schizophrenia*. Minneapolis: University of Minnesota Press, 1983.

⁵ Wood, E. M., *Empire of Capital*. London, Newyork: Verso, 2003.

⁶ According to Baudrillard, “Simulation is no longer that of territory [i.e., abstraction of the map], a referential being or a substance. It is the generation by models of a real without origin or reality: a hyperreal.” M. Poster (ed.), *Jean Baudrillard: Selected Writings*. Polity Press, 2001, p.169.

⁷ “We live a world where there is more and more information, and less and less meaning.” J. Baudrillard. *Simulacra and Simulation*. Translated by F. Glaser, Ann Arbor: The Michigan University Press, 1981, p. 79.



“... everywhere capitalism sets in motion schizo-flows that animate ‘our’ arts and ‘our’ sciences, just as they congeal into the production of ‘our own’ sick, the schizophrenics.”⁸

It no longer connects local culture, values.

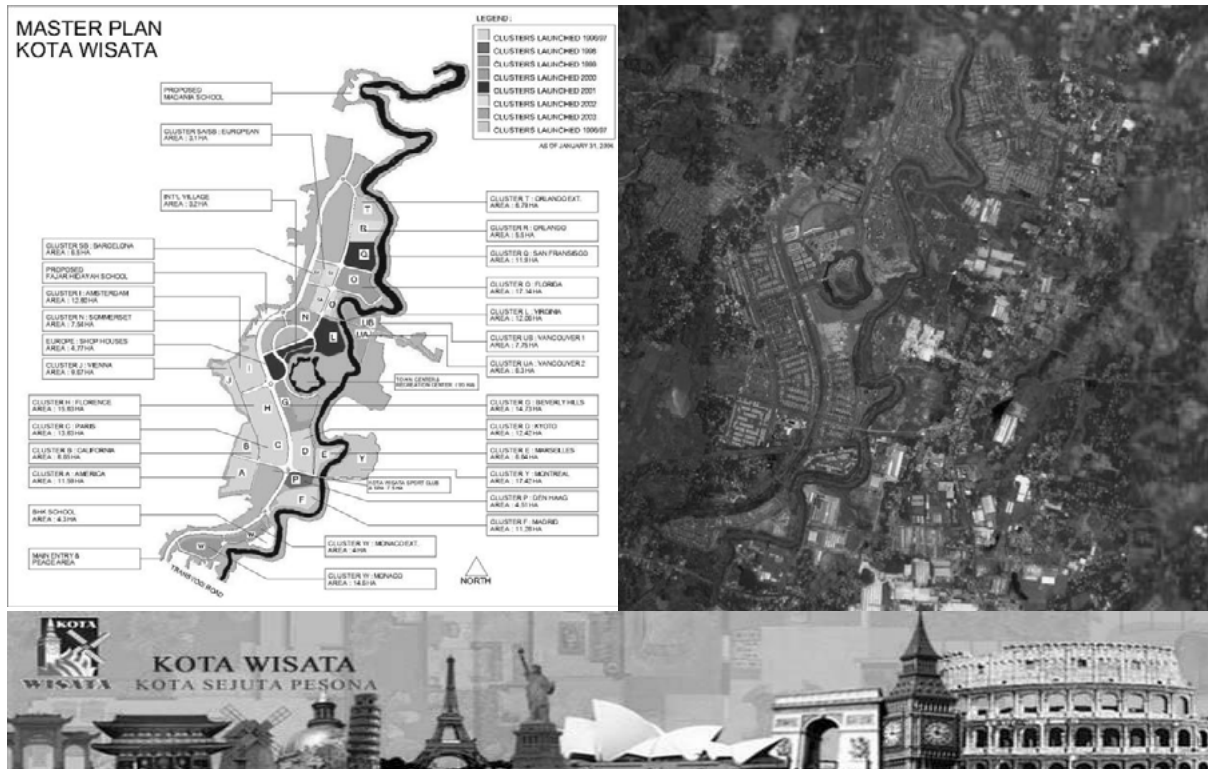


Figure 3

Plan of Kota Wisata Residence

Source: Harjoko, T.Y., ‘HYPER- versus INVOLUTED-TRADITION: Urbanism in Indonesia’, *ISVS IV: Pace Or Speed?, 4th International Seminar on Vernacular Settlement*, Ahmedabad, India, February 14-17, 2008 : Proceedings.

⁸ Deleuze, G. and F. Guattari (1983), *Anti-odipus: Capitalism and Schizophrenia*. Translated by Robert Hurley, Mark Steem, and Helen R. Lane, Minneapolis: University of Minnesota Press, p. 245



Figure 4
Utopian Dwelling: Kota Wisata Residence and its some of the Cluster Names and Gates

A Case of an Un-appreciated Urban Planning for a Dual-society

Integrated development has become an empty concept when it is related to *kampung*. There has no single urban development in Jakarta that has integrated the *kampung* within it. An attempt was once made by a private consultant, who proposed a development that integrated the *kampung* as part of a coherent urban development strategy. In 1989, PT. Triarco Development Consultants⁹ had a model of integrated *kampung* development, or Guided Land Development, in Klender, which is next to Penggilingan (see Figure 7.12). The project proposed to integrate the government program, that is, the *Kampung* Improvement Project (KIP), with Private Housing Development. The model was called an infill land consolidation as an alternative to land acquisition, or land compensation, for private development usually practiced by developers in Jakarta dealing with *kampung* settlement. In this model, infrastructure development was devised to guide new development in conjunction with the

⁹ This consultant has been involved in other different realised projects of integrating low-income housing and commercial development into private development. For example, Citra Niaga Project in Samarinda, Kalimantan, which won the Aga Khan Awards in 1989. See Ismael, A., ' Guided Land Development: Klender, Jakarta', *Integrated Urban Development through 'Co-Development'*, Triarco Development Consultants, Jakarta, Paper presented for International Workshop on Housing ' Urban Coherence and Housing Strategies', Bandung, 1990, Case 3.



KIP, so that high, middle, and low-income people can supposedly live in an integrated planned settlement. The project developed an innovative and alternative land use approach, applied to pedestrian as well as road circulation systems. It was experimenting with housing development in such a situation through 'Land Pooling and Readjustment'. By this it was intended that unorganized, inefficient, and idle land with no infrastructure was to be efficiently 'pooled', re-planned and integrated. The construction of the buildings by the low-income people on the 'serviced area' was conceived as three different avenues. It could be done either through a third party either by using 'build contract', or 'sharing contract', or through mutual aid, self-help, or through a formation of a Cooperative as a developer. The basic idea of this approach was that the *kampung* people could remain and benefit mutually from the guided land development. The proposed project was never realized.

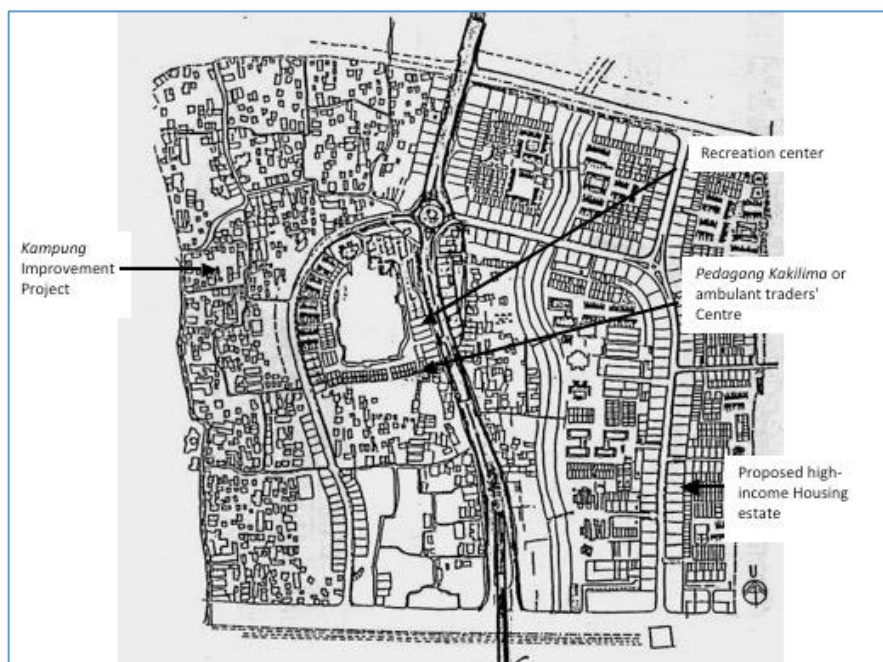


Figure 5
A Proposal of Guided Land Development in Buaran, Klender, Jakarta:
A Development Consultant's Unrealized Project

This is a good example of the guided land development in Klender which incorporates *kampung* and new housing estate as a *dual-society* or two-dimensional society of housing. Unfortunately, such a scheme was left on the selves. The scheme that has been granted for development is a 'segregate community' for the high-income settlements.

Source: Ismael, A., ' Guided Land Development: Klender, Jakarta', *Integrated Urban Development through 'Co-Development'*, Triarco Development Consultants, Jakarta, Paper presented for International Workshop on Housing ' Urban Coherence and Housing Strategies', Bandung, 1990, Case 3. In Harjoko, T.Y., *Urban Kampung: Its Genesis and Transformation into Metropolis with particular reference to Penggilingan Jakarta*. VDM Verlag Dr. Muller, 2009, p.146.



Figure 6
Segregated Housing Estate in Buaran Klender as it is now
 (Source: Google Earth, 18th May 2017)

Concluding Remarks

Dual society constitutes urban population. This does not seem to be appreciated by urban planners and designers. This is exacerbated by policy makers who are dreaming their city as modern and beautiful as those in West. They deny their own society that is not mono-dimensional.

Urbanizing poor rural migrants are denied by planners and designers to have access to the descent living in the city. Impossibility to dwell in the city has been justified both by politicians, urban planners as well as designers. They are dominated by the image of society that is alien to society as a whole. physical planning system and practices.

The epistemological problem of the concept of formal/informal arises when they are conceived as separate, unconnected entities. Informality, as a noun, is then conceived strictly as a state of exception from the formal order of social formation in certain settings, such as urbanization. The formal/informal economy has not been constructed in a state of opposition or dichotomy. This is why the dual-image of modernism/traditionalism perseveres in the city.



Urban economy means management of the possibility/impossibility of urban dwellings that result in a dual-image of human existence. The dwellings will be impossible, if norms are fixed to the particular group of people and are denied to others. In a capitalist society the structure is fixed, formal and simply is based on capitalism, while society which is based on tradition take the informal form of urbanism.

Domination of particular group, namely the modern and formal one, in the planning and design practices inevitably envisions and engenders a city plan of one-dimensional society. Liberalization of property development by private business coupled with un-coordinated urban planning and control has generated a *wild* urban generation. The city becomes a calculus of isolated private housing development and especially commercial centers such as malls everywhere across the city. Utopian Dwellings emerge here and there. Design *metaphors*, such as *Georgia Residence* in Kota Wisata, are just a commercial gimmick to fascinate the haves.

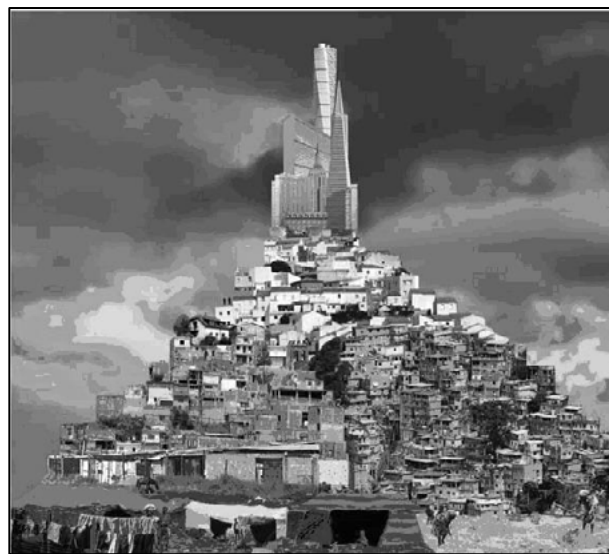


Figure 7
The Challenge of Inequality
(Source: International Poverty Center, *Poverty in Focus*,
June 2007)



References

- Baudrillard, J. (1981), *Simulacra and Simulation*. Translated by F. Glaser, Ann Arbor: The Michigan University Press, 1981
- Calhoun, C., (1996). *Habermas and the Public Sphere*. Cambridge: Massachusetts, London: England.
- Deleuze, G. and F. Guattari (1983), *Anti-odipus: Capitalism and Schizophrenia*. Translated by Robert Hurley, Mark Steem, and Helen R. Lane, Minneapolis: University of Minnesota Press.
- Friedland, R. and D. Boden (1994), ' NowHere: An Introduction to Space, Time and Modernity', in Friedland, R. and D. Boden (eds.), *NowHere: Space, Time and Modernity*, Berkeley, Los Angeles, and London: University of California Press.
- Giddens, A., *The Constitution of Society*. Berkeley and Los Angeles: University of California Press, 1984
- Glass, R.(1973) , 'Some Sociological Considerations', in Andreas Faludi (ed.), *Reader in Planning Theory*, Pergamon Press.
- Habermas, J. (1987), *The Theory of Communicative Action*. Boston.
- Harjoko, T.Y. (2008), 'HYPER- versus INVOLUTED-TRADITION: Urbanism in Indonesia', *ISVS IV: Pace Or Speed?, 4th International Seminar on Vernacular Settlement*, Ahmedabad, India, February 14-17, 2008 : Proceedings.
- Harjoko, T.Y. (2009), *Urban Kampung: Its Genesis and Transformation into Metropolis with particular reference to Penggilingan in Jakarta*, VDM Verlag Dr. Müller.
- Heidegger, M. (1971), *Poetry, Language, Thought*. Trans. Albert Hofstadter, New York: Harper & Row.
- Ismael, A., ' Guided Land Development: Klender, Jakarta', *Integrated Urban Development through 'Co-Development'*, Triarco Development Consultants, Jakarta, Paper presented for International Workshop on Housing ' Urban Coherence and Housing Strategies', Bandung, 1990, Case 3.
- Kellner, D. (1964), 'Introduction to the Second Edition', in Marcuse, H., *One-Dimensional Man: Studies in the Ideology of Advanced Industrial Society*. Boston: Beacon Press, p. xii.
- Marcuse, H. (1964), *One-Dimensional Man: Studies in the Ideology of Advanced Industrial Society*. Boston: Beacon Press.
- Norberg-Schulz, C.(1985) *The Concept of Dwelling: On the way to figurative architecture*. NewYork: Rizzoli International Publications, Inc.
- Partridge, E. (1983), *Origins: A Short Etymological Dictionary of Modern English*. New York: Greenwich House.
- Rose, B. (1990), 'The Triumph of Social Control? A Look at Herbert Marcuse's "One Dimensional Man", 25 Years Later.' *Berkeley Journal of Sociology*, Vol. 35, 1990.
- Short, J. R. (2000), 'Three Urban Discourses,' in Bridge, G. and Watson, S. (eds.). *A Companion to the City*, Blackwell Publishing, Ch.3.
- Wood, E. M. (2003), *Empire of Capital*. London, Newyork: Verso.



I DWELL IN FLUID SPACE: READING SMOOTH AND STRIATED SPACE ON PASAR CIPUTAT TANGERANG

Eka Permanasari, PhD^a, Bonardo Tobing^b

^aUniversity of Pembangunan Jaya, Bintaro, 15413, Indonesia, eka.permanasari02@gmail.com

^bUniversity of Pembangunan Jaya, Bintaro, 15413, Indonesia, bonardo17@gmail.com

ABSTRACT

Deleuze (1987) introduced the term striated and smooth space in several metaphoric ways. Both terms intermingle, “smooth space allows itself to be striated, and striated space re-imparts as a smooth space” (Deleuze, 1987: 486). Striated is seen as a fixed space, closed at one side and assigns breaks. It carries a sense of border. On the other hand, smooth space is seen as continuous and open interval. However, both terms are always intermingling, at one point smooth can be striated and vice versa. A city can be seen as a striated space and an ocean is a smooth space. However, at the same time the city can also be seen as smooth (urban sprawl, shanty town) and the ocean can be seen as striated as we see it on the map and lines of latitude and longitude (Deleuze, 1987: 476).

This research looks at the way in which people dwell in a fluid space. Space is a highly fluid in terms of its uses and occupation depending on its users. Looking at a strip near Pasar Ciputat, Tangerang Selatan, this paper investigates how the space changes function and identity overtime. The strip on the road of Pasar Ciputat becomes a good example of analyzing the smooth and striated space practiced in everyday life. This strip is heavily populated by street vendors who has ‘occupying schedule’ and continuously changes the patterns of occupation. They prefer to sell the goods on the road instead of in the provided building. By midnight, the strip is not accessible as the vendors closed off and sell their goods on the road. In the morning, some vendors disappear and their former space has been used by other vendors to sell different goods. The road is becoming accessible again. By noon, different vendors take over the space and sell different stuffs. Space becomes highly fluid where uses and meaning collapse together. Through observation, urban morphological mapping and photographic analysis, this paper will uncover the everyday uses of space and how the spaces become fluid following the different ways of its users.

Keywords: Fluid space; Pasar Ciputat, smooth and striated space.

1. INTRODUCTION

A city constitutes layers of history as it houses human events, buildings and stories. Perception is associated through the uses and symbolism of the space. Rossi sees the city as an archaeological artefact and an autonomous structure (Rossi, 1986). The city is influenced by the way architecture works as remnant of history and thus influences back the users. Rossi argues that a city should not be seen as functional only as it collects memory, attachment and history which connect the users and the place. A city is place where people congregate together, making layers of meanings and history by the way they inhabit the city. The city is a *locus* where possibilities of events can be accommodated and constituted.

The image of the city depends on the perception of individuals through their interaction and association within the city. However, this individual image is often being imposed by the public image associated with it. As city image is constituted through paths, edges, districts, nodes and landmarks, this research looks at specifically to path, edge and landmarks as they influence the imageability of the city. Path is easily recognized as people observe the city while they are moving through it (Lynch, 1959). An edge is seen as boundaries which assign breaks in continuity (Lynch, 1959). Edge can be barriers with more or less penetrable. On the other hand, Landmark is something which people can easily associate the image of a city with. Through the experience people have gone through, they associate a certain sign, prominent building or activities as the landmark for the site. Some of the landmarks are innumerable and are associated once the



traveler are becoming more familiar with the sign. Some of these elements may occasionally shift from one to another. For driver, a road is a path which enable them to move swiftly from one place to another. However, for a sidewalker, a road is the edge for them not to cross. The differentiation, the classification is somehow blur at some point. What if a path is no longer seen as an edge for the sidewalker but mereley an extension of its walkway? What if a path is becoming an edge for the driver when they cannot get through the road? What if the path has become an edge with less penetrable for people to go through? These ambiguities and shifting roles between a path and an edge which in turns resulting in shifting the landmark for the city. The “continues assigned break” is relevant to Deleuze and Guattari’s notion of smooth and striated space.

Smooth and striated spaces are twofold binary concepts where the definition of one is so dynamic and intermingling. Smooth space is seen as continues, travels though times, infinite and unlimited in every direction (Deleuze, 1987: 476). Striated space assigns breaks, closed at least on one side, limited and fixed. However, as these two terms are twofold binary concepts, smooth space is constantly reversed into a striated space and vice versa (Deleuze, 1987). The story of quilt made out of a stitched patchwork might be useful in understanding the smooth and striated space. The patchwork (either made out of embroidery or leftover fabric) are stitched together shaped as a continues form (the quilt). The patch can be seen as striated while the process of stitching it together and shaping a continues fabric can be seen as smooth. In this case, smooth sprang from a striated space. However, the smooth space as much as it looks continues, it is limited in size. The smooth has become a striated space again and vice versa. The space becomes very fluid in terms of it uses, meaning and trajectory. However, the aim is not to erase one side of the concepts, but rather to see which concept that appears first and how it was folded (Dovey, 2010). As in Deleuze’s term, “the two spaces in fact only exist in mixture” (Deleuze, 1987:474). This fluidity concept occurs where the twofold coexist together and change the use and meaning of space. The looseness occurs when the different uses and meaning of space coexist with negotiable government rule. The concept of smooth and striated space is used as framework to analyze the use and meaning of urban space in Pasar Ciputat, Tangerang Selatan.

Perusahaan Daerah Pasar Niaga Kerta Raharja famously known as Pasar Ciputat is one of the markets built by the Provincial Government of Tangerang Regency in 1992. Located in between South of Tangerang and South of Jakarta, Pasar Ciputat became a strategic place for people to gather and do business. The building is 3 storey in height where each floor was to house certain activities. The ground floor caters commodities such as rice, flour, meat, fish and vegetables. The first and second floor house clothing, shoes, bags and accessories (Tangsel, July 2010). Like many other market building built and managed by the government, Pasar Ciputat Building were mismanaged and poorly maintained. From its early development, the first and second floor were empty from customers. The sellers start to sell their stuff on the ground floor hoping they could attract customers to the first and second floor. The more they go down, the more customers never reach the first and second floor.

In late 1992, the Provincial Government of Tangerang District made a deal with a private company PT Betania Multi sarana to integrate the market and terminal in order to invite more visitor and generate more income (Tangsel, Perjanjian Kerjasama Bersyarat No. 551.22/1755-Um/1992). As the terminal and the market collide, the traffic and the sellers start occupying the street and cause traffic jams. In 2004, there was a change in the regulation where the market can open during the day and the night (District, 2004). Here, the number of sellers increase by the numbers of hours the market can operate. If previously they could only sell stuff during the day, with this new regulation, they can do business 24 hours.

The biggest shift occurred in 2008 when the area in Regency of Tangerang was divided. The Ciputat area including pasar Ciputat became under the Municipality of South Tangerang (Mendagri, 2009). The problem arised when the regency of Tangerang delaying to hand over the land to the municipality. Furthermore, the deal with PT Betania multi Sarana aso faced another obstacle. The Regency required certain amount of money to be paid as part of the retribution from parking and lease from sellers inside the market. These conditions made the ambiguity as to who is in charge managing the pasar Ciputat. Through its heyday, the management of Pasar Ciputat is now under the Tangerang Selatan municipality. Hence, the mismanagement has made the number of unregistered sellers rise. Most of sellers have left the market building and prefer to sell their goods on H. Usman road leading to the market building. This informality has its own structures.



Although the sellers are not formally registered they have patterns in selling stuffs, schedule as when to sell, and location as where to display their goods. The roads is no longer accessible for cars and pedestrian. In certain times the road may be totally closed down due to the market activity, while some other times the road may still be penetrable.

Due to the high level activity on this road, poor sanitation and management, Pasar Ciputat is notorious for being dirty, filthy and unhygienic. Since the activity are mostly carried out outside of the building, the image of the market shifted from being in the building into being on the road. The H Usman road has become a fluid space where striated and smooth spaces are performed.

2. METHODOLOGY

In order to understand the variety of uses and fluid meaning of space, we use qualitative research methodology with data gathering methods as followed:

a. Observation

Observation was used to determine the use of places in everyday life. This method was aimed to understand the meaning and use of the case study by observing the way in which people appropriated the spaces. Observation was carried out on Haji Usman road using photographic survey techniques. These techniques were conducted unobtrusively within the bounds of normal procedures for observation in public spaces (Nachimias, 1976). The sellers are classified based on the items that they sell and pattern of occupying the space.

The observation is conducted within two different time frames during the weekend and weekday: during the day and during the night. This approach is aimed to capture the different uses and spatial practices within the space.

b. Morphological Mapping and analysis

Morphological mapping and analysis included decoding the various uses on, within, and around the Haji Usman road. This method includes tracing the movement of sellers activities; and highlighting certain sellers which play a role in understanding the fluidity uses and spatial practices.

c. Traces analysis

Traces analysis gathers evidences which relate to the traces use of the four case study sites. I particularly looked at the remnants that were left by sellers as clues of understanding how space was used, appropriated and anticipated.

d. Photographic analysis

Photographing survey analysis was conducted to record both the behavioural observation and traces analysis. To record possible variety of uses, photographic survey was carried out on two different period of times during the weekday and weekend (during the day and during the night). Photographic survey analysis became primary means of generating detailed database for morphological analysis, the transformation of the use of the space, verbal presentation, and particularly evidences to support argument.

3. RESULTS AND DISCUSSION

Pasar Ciputat Building is located in the corner of Aria Putra road and H Usman road. The position is prominent as it is accessible from Aria Putra, Haji Usman and Dewi Sartika roads (Figure 1). As the policy in 2010 changed, the intended planning to integrate the market and the terminal was uncertain. Yet the area in front of market on Aria Putra road has been used informally for terminal. Interestingly, although the market is located in Aria Putra road, the market never really take place in the building. The building is always empty and abandoned (Figure 2). The provided stalls are left behind and no longer in use. The market informally takes place along Haji Usman road instead (Figure 3). The constant use of this road for informal market is interesting where the sellers may change, the stall may disappear adjusting the needs of sellers. The smooth and striated spaces are performed within this road.

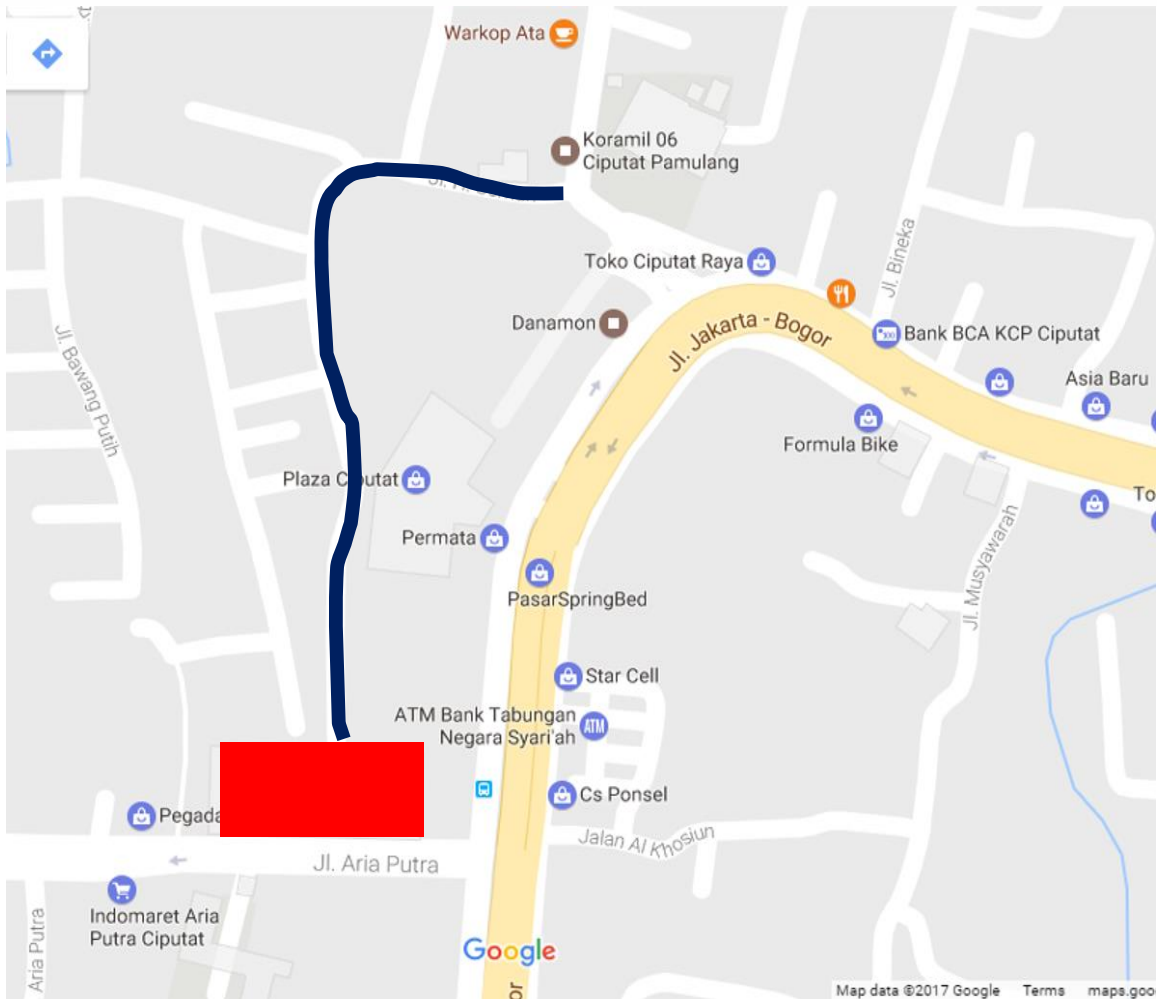


Figure 1: Location of Pasar Ciputat and Haji Usman road

Source: google map modified by the author



Figure 2: Empty formal stall inside of Pasar Ciputat Building

Source: author



Figure 3: Sellers take place on the road and outside of the intended building

Source: author

Although Haji Usman road is notorious for its traffic due to the informal market activities, the road is the only access which links Ki Hajar Dewantara road to Aria Putra road. The road is consistently being used as ‘road Ciputat market’ and displaces the function of the intended market located in the corner of Haji Usman and Aria Putra road. Regardless its bad traffic due to the road market activities, Haji Usman road is always full of vehicles trying to go through, passerby, visitors and sellers. In fact, due to its very bad traffic, the



google street view currently cannot access Haji Usman road fully. The road intended to be on one way direction has been used in two ways. The road is crammed with stalls taking place on the road, by shoppers parking their motorbikes in front of the stalls whenever they need to buy anything, and by the large vehicles trying to get through. Haji Usman road functions as a market, a parking space, a path, and at the same time as a node where people meet (Figure 4). Regardless the chaotic scene, the crammed road does not prevent the cars and passerby to go through.



Figure 4: stalls and visitors' vehicles are taking place on the road.

Source: author

In order to access this Haji Usman road, visitor can enter from Aria Putra road or from Ki Hajar Dewantara road. On this road, lay some public buildings such as Office of Religious Affair (KUA), post office, mosque and military office (Koramil) (Figure 5). Although it seems that the entire road has become more like a market, but as a matter of fact, some public buildings are still in operation. To access these buildings, most visitors came from Ki Hajar Dewantara road, slowly entering the road in competition with parked vehicles as well as the food stalls and visitors. To allow access, the gate of these buildings are kept clear while other area are mostly covered by sellers and shoppers

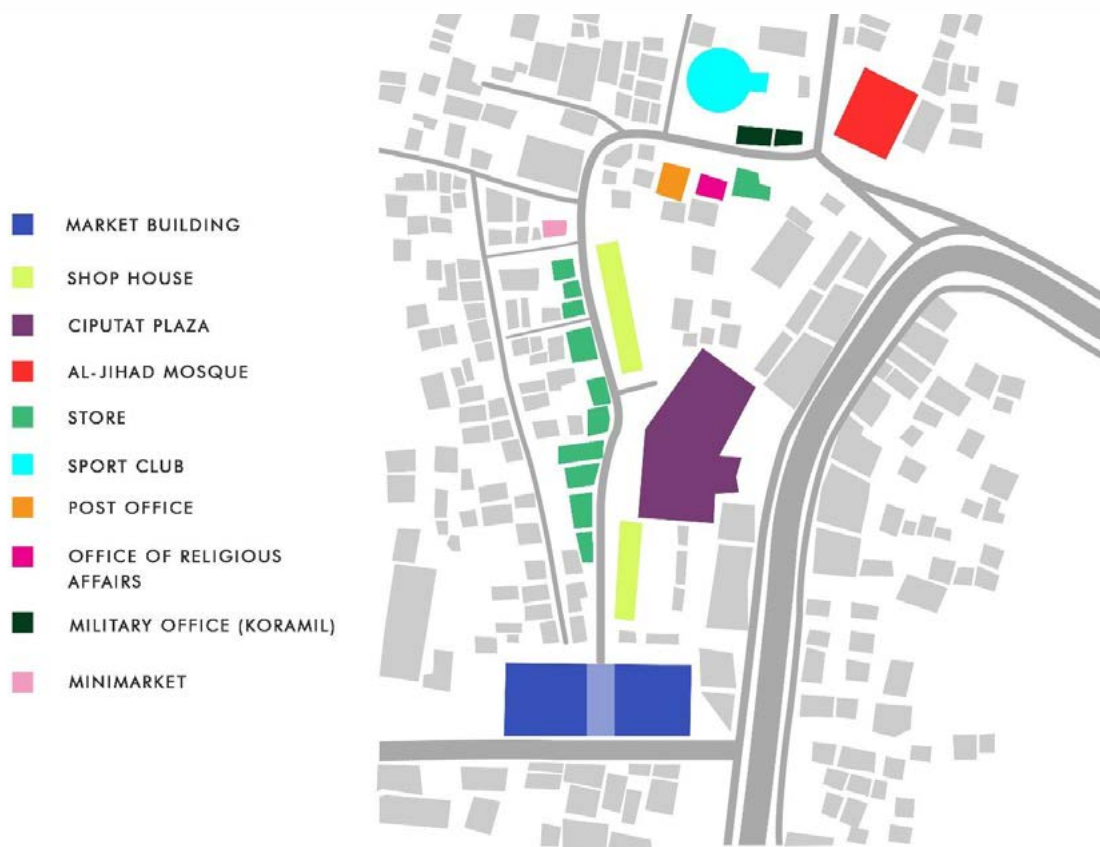


Figure 5: Public building surrounding Haji Usman road
source: Author

Smooth and striated spaces are displayed on this Haji Usman road. The sellers constantly change and occupy the space in certain time. There is no hierarchy and clear boundary as which section sells particular items. Vegetable sellers can be next to the meat, fish or other products. The pattern of occupation varies according to the shift. For instance, in the morning certain sellers take position on certain spot. In the afternoon, the earlier spot may have been taken over by other sellers. In other occasion, the spot is left empty by the sellers, but in some cases the stall and the spot remain but the sellers are not in duty. Constant changes in occupying the space has created layers of space patterns. The pattern in the evening would be different from the day pattern.

In order to understand the fluid use and meaning of the space, the observation was carried out with within two different times: morning, afternoon and night. The observation, urban morphological mapping and photographic analysis starts from the corner of Ki Hajar Dewantara road to Haji Usman road and ends on Aria Putra road. The analysis will be presented in the following morphological mappings:

The first mapping is conducted during the day to capture the users and stalls and kind of product being sold (Figure 6). Based on this mapping, majority vendors sell fruits, vegetables and fish. Their stalls occupy most of the road with little access for the vehicles to get through. The pattern of occupying space is also different during the day. If in the morning people tend to occupy more of the roadside, in the afternoon the occupation shifts little bit backwards. The permanent stall stay while the temporary tents seems to disappear.



MAPPING PASAR CIPUTAT JL.H.USMAN 02.30 PM

- VEGETABLES
- CHICKEN
- TOFU & TEMPE
- INGREDIENTS HERBS
- LIVE FISH
- COCONUT
- FRUIT
- MEAT
- CASSAVA & SWEET POTATO
- SMOKED FISH
- PLASTIC SHOP
- FOOD STALL
- CLOTHES SHOP
- WARONG
- DVD STORE
- KITCHEN TOOLS
- FIREWORKS
- ONION & CHILLI



Figure 6: Morphological mapping during the day

Source: Author

In the morning the vegetable sellers are more compare to the afternoon. The traffic is worse in the morning and gets better by later of the day. But by afternoon, different sellers starts occupying the road again and the numbers increases during the night. Therefore, the morpohological mapping during the night is different from the morning (Figure 7). Based on this mapping, the informal market on Haji Usman road is majorly filled by the fruits sellers, vegetables and chicken. The pattern of occupying changes drastically. At night, sellers tend to occupy the road more freely since the numbers of vehicles that pass through this road are low.



**MAPPING
 PASAR CIPUTAT
 JL.H.USMAN
 03.00 AM**

- VEGETABLES
- CHICKEN
- TOFU & TEMPE
- INGREDIENTS HERBS
- LIVE FISH
- COCONUT
- FRUITS
- MEAT
- CASSAVA & SWEET POTATO
- SMOKED FISH
- PLASTIC SHOP
- FOOD STALL
- FRIED SNACK
- WARONG
- DVD STORE
- KITCHEN TOOLS



Figure 7: Morphological mapping in the evening

Source: author

Apart from different patterns of occupying space during the day and the night, the fluid use and meaning is also demonstrated through the morphological mapping and traces analysis on certain spots on this Haji Usman road. The first spot is an area where sellers of mix vegetable, water spinach, live fish, chicken and banana can be found in the morning. By afternoon the urban players change. The live fish, water spinach and chicken disappear, leaving the space only for the mix vegetable and banana. Even though the seller of live fish is not working, yet his stall is still there. The stalls for chicken and water spinach are gone. The space is little bit empty compare to the morning scene. In fact, the space which previously used as a stall for chicken and water spinach has been transformed as a parking space for motorbikes (Figure 8). By evening, the urban players change again where sellers of mixed vegetables, water spinach, banana and live fish exist. From this analysis, fixed sellers are banana and mixed vegetable sellers, whereas fluid sellers are chicken, water spinach and live fish sellers.

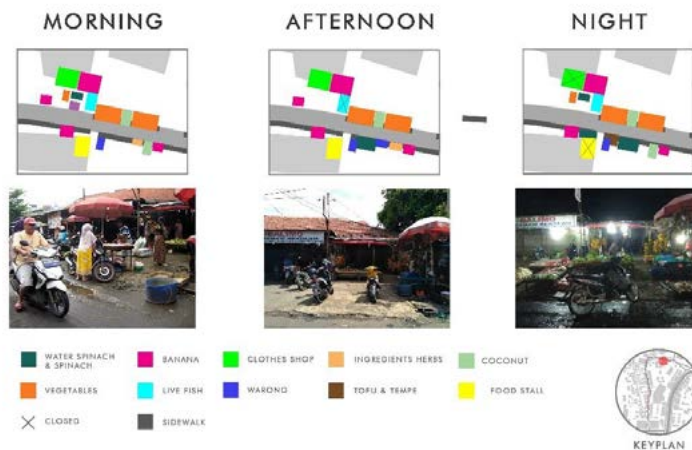


Figure 8: Striated and smooth space on spot 1

Source: author

The fluid use and meaning of Ciputat market can also be seen from the second case study. Located right in the middle of the road, the area is filled with stall for selling smoke fish. Although the stall and the stock remain the same, the person selling the smoke fish changes in the morning, afternoon and evening. Yet, these three different people are not sharing one source of income. They simply informally rent the same stall selling the same product (Figure 9). The ‘fixed’ is represented through the stall and the selling product, whereas the ‘fluid’ is represented by the different sellers. The smooth and striated spaces are performed continuously. The use and meaning of the space is forever challenged

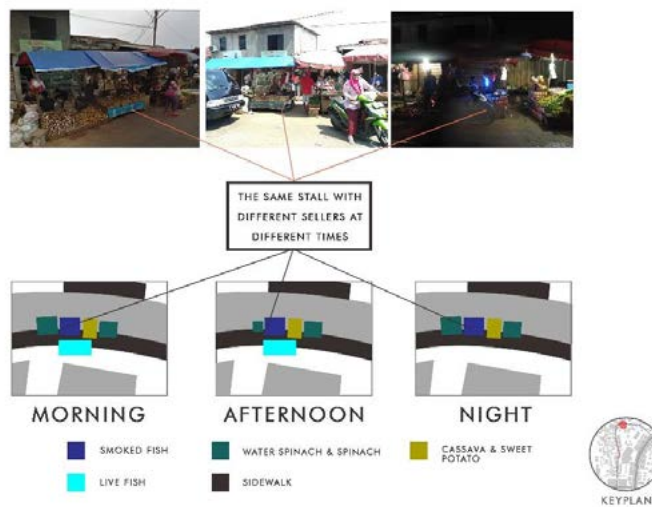


Figure 9: Smooth and Striated space on spot 2

Source: author

The constant use of Haji Usman road as an informal market has created an urban collective memory. The road which was supposed to be a path has changed its meaning to become a node and at the same time a landmark. Never does occur for resident or visitor that Ciputat market should be in the building located at the corner of haji Usman and Aria Putra roads. Public image of Ciputat market is on haji Usman road.

The fluidity also not only from the everyday uses of space, but also from the blur and inconsistent system which somehow finds its own models. These sellers pay certain amount of money periodically to the ‘fee



collector'. Although the amount is only around US 50 cent per collection, yet the sellers have to pay it several times to different fee collector at different times. No one knows exactly where the money goes and ends up. Yet, since the sellers pay the fee, they have 'informal right' to be on the road selling their product without fear being evicted. Should there be formal eviction from the local authority, they are already well informed way before the eviction day. This informality which infiltrates the formal system is rhizomatic, well structured without formal structure; just like the body without organ (Deleuze, 1987). The analysis of smooth and striated space has shown a new perspective of understanding informal dwelling. Through the analysis of fluid market settlements on Jalan Haji Usman road, the image of the city may shift from once to be known as a regular road, and now it has become a market. The way people understand and remember the dwelling is through this trajectory continues interplay uses and meaning.

4. CONCLUSION

The uses, meaning and trajectory of the space has become very fluid. The smooth and striated space coexist together as one unfolds the other. The stalls are striated patch, yet the whole patch of stalls are smooth space. The road may seem impermeable, but somehow people and vehicles can constantly go through it. There seems to be no clear system, but amid the informal system the market continues to exist and be alive. The informal economy co-exists with the informal ways of [im]possibility of dwelling. The looseness (smooth) and the fixation (striated) occur when the different uses and meaning of space juxtapose with negotiable government rules as well as informality. Haji Usman road has become an arena where the binary oppositions is being displayed, played and contested which in turns changes people's perception about the market, the road and the city landmark.

5. REFERENCES

- Adkins, B. (2015). *Deleuze and Guattari's Thousand Plateaus: A Critical Introduction and Guide*. Edinburgh: Edinburgh University Press.
- Alsayyad, N. (. (1992). *Forms of Dominance: On the Architecture and Urbanism of the Colonial Enterprise*. Avebury: Aldershot.
- Cowen, M., & Shenton, R. (1996). *Doctrines of Development*. London: Routledge.
- Deleuze, G. &. (1987). *A Thousand Plateaus: Capitalism and Schrizophrenia*. London: University of Minesota Press.
- District, T. (2004). *Surat Keputusan Bupati Tangerang No 511.2/Kep 249-Huk/2004*. Tangerang Regency: Bupati Tangerang.
- Dovey, K. (2010). *Becoming Places*. New York: london.
- Jacobs, J. (1992). *The death and life of great American Cities*. New York: Vintage Books.
- Jones, P., Petrescu, D., & Till, J. (2012). *Architecture and Participation*. London and New York: Routledge.
- Kusno, A. (2000). *Architecture, Urban Space, and Political Cultures in Indonesia*. London and New York: Routledge.
- Lefebvre, H. (1996). *Writing on Cities*. Oxford: Blackwell Publisher.
- Lynch, K. (1959). *The Image of the City*. Cambridge: The MIT Press.
- Macleod, M. (1997). Henri Lefebvre's Critique of Everyday Life. In S. Harris, & D. Berke, *Architecture of the Everyday*. New York: Princeton Architectural Press.
- Mendagri. (2009). *Surat Keputusan Menteri Dalam Negeri No 131.36-833. 2009*.
- Nachimias, D. &. (1976). *Research Methods in the Social Science*. United Kingdom: Edward Arnold.
- Rossi, A. (1986). *The Architecture of the City*. US: The MIT Press.
- Sanders, Elizabeth B-N; SonicRim. (2002). From User-Centered to Partisipatory Design Approach. In J. Frascara, *Design and Social Sciences: Making Connections*. London And New York: taylor and Francis.
- Tangsel, P. K. (July 2010). *Executive Summary: Kajian dan Evaluasi Pasar Ciputat*. Tangerang selatan.
- Tangsel, P. K. (n.d.). *Perjanjian Kerjasama Bersyarat No. 551.22/1755-Um/1992*. 1992.
- Vale, L. (1992). *Architecture, Power and National Identity*. London: Yale University Press.



THE 15TH INTERNATIONAL CONFERENCE QUALITY IN RESEARCH (QIR) 2017

BUMI AWI KABULA KABALE: A PROPOSAL TO ALTER THE FATE OF MANKIND THROUGH ADAPTIVE BAMBOO STRUCTURE

Anastasia Maurina^{a1}, Budianastas Prastyatama^a, Carissa^a,
Altho Sagara^a, Sisi Nova Rizkiani^a, Buen Sian^a, Jung Eun Shin^b

^a*Faculty of Engineering, Universitas Katolik Parahyangan,
Ciumbuleuit 94, Bandung 40141, Indonesia*

^b*JUBIT International, Jalan Hegarbudi, No. 2, Bandung 40141, Indonesia*

ABSTRACT

The urban expansion effects on the physical-spatial density of “new urban” areas, called urbanizing rural, which in its constructions mostly used the “urban” conventional materials. These materials usually have to be delivered from far distance, which can be immensely costly - economical, time, social cost, and also environmental cost. The building itself, as a dwelling physical space, is always limited to a certain size through a certain time-space context and have no tendency for adaptation. In fact, people will ceaselessly expand their lives through time, which bring about the complaint about the rigidity of their building, which become inadaptable to their evolving needs through time. At a certain time or the end of the intended time, that built object should constructively have altered, received subtraction, given addition, or demolished to allow the new object extended or new needs. The alteration will consume numerous building materials, which leads to even more cost. The exploitation of the massive building material, particularly the supporting structure of buildings (which stash approximately 60% of the environmental load of building materials) will be excessively impacted on the fate or sustainability of a built environment itself. The statement above allows us to set forth a question of [im] possibility: can man reverse, alter, and modify the path towards the demise of mankind through the very act of consumption itself? Can dwelling as the act to exist and as the constructed object provides the material means for the alteration? Creating an adaptive structure with a local resources, is an important point to alter the fate of mankind. This paper reports the experiment with the constructed object that allows dwelling to provide options for alteration of dwelling itself, through an adaptive bamboo structure, named ‘*Bumi Awi Kabula Kabale*’. This structure has been proven to enable the dwelling’s adaptation: available, extendible, flexible, refit-able, movable and recyclable and enable to reduce material’s consumption at the time of building’s alteration. Ultimately, it could alter the fate of mankind and create human’s dwelling, that is more harmonious balance between man and nature.

Keywords: dwelling; adaptive structure; adaptability; bamboo

¹ Corresponding author:
Email address: maurin@unpar.ac.id / anastasia.maurina@gmail.com



1. INTRODUCTION

The urban expansion effects on the altering characteristics of rural areas into “new urban” areas, called urbanizing rural. The tangible characteristic’s change in this area is an enhancement of physical-spatial density, which in its constructions mostly used the “urban” conventional materials. These materials usually have to be delivered from far distance, which can be immensely costly. Besides incurring economical, time and social cost, there are intangible environmental cost of the procurement process of building materials. The building itself, as a dwelling physical space, is always limited to a certain size through a certain time-space context. Gibb, et al., (2007) stated that the buildings as bespoke creations are designed in accordance with the particular use at a certain time, with little thought for the future or sustainability. Subsequently, that the buildings have no tendency for adaptation, notably in aspect in on coming function.

In fact, people are ceaselessly changing. In today’s contemporary urban culture, where human atomization through consumption of things and services, replaced the previous cultural tradition of the common good, there is more to ‘dwelling’ as an object than just a building in which the act of dwelling takes place. Arguably, it dictates that the only possible way of human existence is through the expansion of the level of one’s consumption of things as the manifestation of progress. People will ceaselessly expand their lives through time, which bring about the complaint about the rigidity of their building, which become inadaptable to their evolving needs through time (Nakib, 2010). The people’s expansion will ultimately insist the substantial adjustment to the built object, physically and spatially. At a certain time or the end of the intended time, that built object should constructively have altered, received subtraction, given addition, or demolished to allow the new object extended or new needs.

The alteration will consume many building materials, which leads to even more cost - economical, time, social and also environmental cost. As is well-known, “The building industry, directly or indirectly causing a considerable part of the annual environmental damage, can take up the responsibility to contribute to sustainable development by finding more environmentally benign ways of construction and building” (Lugt, et al., 2006). The exploitation of the massive building material, particularly the supporting structure of buildings (which stash approximately 60% of the environmental load of building materials) (Dobbelsteen, et al. (2002), will be excessively impacted on the fate or sustainability of a built environment itself.

The statement above allows us to set forth a question of [im] possibility: can man reverse, alter, and modify the path towards the demise of mankind through the very act of consumption itself? Can dwelling as the act to exist and as the constructed object provides the material means for the alteration? Responding to this questions, Mehaffy and Salingaros (2015) stated that “We need to create durable structures that are fitted into our lives, and that can be customized, repaired and adapted to our needs. They need to be thought about throughout their life cycle, as they interact with local conditions and local resource cycles”, which confirmed Nakib’s statement: adaptability allows reducing resources and energy consumption and ensures a minimum environment perturbation (2009), thus adaptability plays a major role to improve the sustainable attributes of the building in order to keep harmony with the natural environment and lie within the new imperatives of sustainable



development (2010). Creating an adaptive structure with a local resources, is an important point to alter the fate of mankind. Through this structure, the built object's alteration can be done without consuming numerous materials. Therefore, minimizing the material's consumption will decrease the cost, especially environmental cost, thus the evansive of demise man's fate and the creation of human's dwelling, that is more harmonious balance between man and nature, are possible to do.

This study explored the possibilities of spatial and geometric adaptability of the building structure with local materials. Bamboo is selected for the reason that bamboo's availability refers to local aspects that is beneficial, especially in West Java (Sunda). In addition, bamboo is a prime example of sustainability, with respect to both the plant itself and its use as a building material." (Liwei, 2012). This paper reports the experiment with the constructed object that allows dwelling to provide options for alteration of dwelling itself, through an adaptive bamboo structure, named '*Bumi Awi Kabula Kabale*'. '*Bumi Awi*' is Sudanese's word, which means a house or shelter ('*bumi*') made from bamboo ('*awi*'). Whereas the '*kabula kabale*' is derived from Sundanese's Proverbs "*Kudu Bisa Kabula Kabale*", which represent that people ought to adapt or adjust themselves wherever they are. Thus, '*Bumi Awi Kabula Kabale*' (hereafter referred to as BAKK) transforms that cultural value into a technical value through a bamboo structure that can be adapted and adjusted with limited land, various functions, and also various people's needs and wants.



Figure 1 Bumi Awi Kabula Kabale

2. METHODOLOGY

The research through design was applied in three phases to explore the possibility of adaptive bamboo structure. Firstly, framing the criteria and the concept of adaptive structure were obtained through literature studies. Secondly, creating the principle prototype, as a hypothesis, was carried out through the design's process of adaptive bamboo structure using a scaled model and computational modelling. The aims of this phase are to test the design's performance of adaptability and also to ensure the strength of the structure in every possible structural configuration. Thirdly, proofing the principle prototype, through constructing full scale modelling, which demonstrated its feasibility and potential for real-world application.

3. RESULTS AND DISCUSSION

At the time when encountering the issue about the fate of mankind, sustainability is becoming more influential in building design and construction. Beadle et al (2008) denoted that there are few examples where its key principles have been successfully combined with



adaptability. Once the building has the ability to adapt, it will be more sustainable, wherein the building’s life can be longer and material consumption will decrease.

According to Kronenburg (2001), adaptability is the built-in ability to adapt and adjust to change by meeting different uses, allowing various spatial and functional configurations, and updating technologies without requiring significant disruption of the building, the ongoing activities and the environment. The building structure, which is the most fixed element compared with other building elements, limited the building’s adaptability.

3.1. Bamboo as Sustainable Building Structure Material

As stated above, bamboo is selected because of its availability and its sustainability. Bamboos have a wide natural distribution, occurring from approximately 46° N latitudes to approximately 47° S latitude and from sea level to as much as 4,300 meters (ca. 14,000 feet) in elevation in equatorial highlands (Clark, 2006). Bamboos are abundant in Indonesia, especially in West Java, thus making it accessible from any given place in Indonesia. Such accessibility reduces the time and cost required for transporting the materials. In addition, bamboo has exemplary “green” credentials. It is adaptable to most climatic conditions and soil types, acts as an effective carbon sink and helps counter the greenhouse effect. It is being used increasingly in land stabilization to check erosion and conserve soil. It can be grown quickly and easily, even on degraded land, and harvested sustainably in three- to five-year rotation. (Jayanetti, et al., 2003). Lugt, et al. (2006) has done the environmental assessment by environmental life cycle analysis (LCA) method and concluded the relatively small environmental load of bamboo with respect to other materials more commonly used, i.e., steel, timber, and concrete.

3.2. The Criteria of Adaptive Structure

According to Wagg, adaptive structures have the ability to adapt, evolve or change their properties or behavior in response to the environment around them (Wagg, et al., 2007). Beadle, et al., (2008) has defined six criteria of adaptive building, such as availability, extendibility, flexibility, refit-ability, movability, and recyclability.

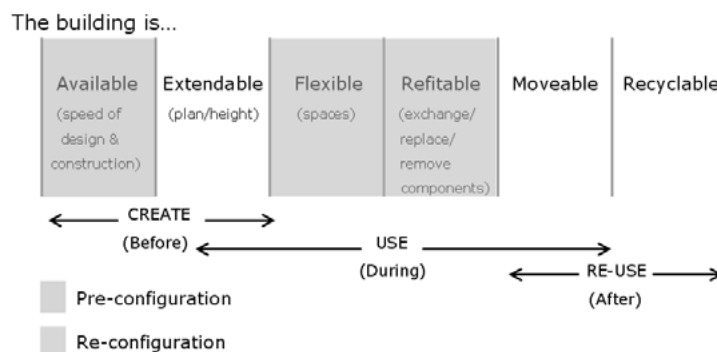


Figure 2 Adaptable Building (Beadle, et al., 2008)

3.3. The Concept of Adaptive Structure: BAKK

However, on this research, the adaptive structure - named BAKK was designed to meet the criteria of adaptability that has stated above.



3.3.1 Availability

The means of intended availability has considered about the speed of design and construction. Therefore, this research adopted the deployable structure, which can be transformed from a closed compact configuration to a predetermined expanded form (Gantes, 2001). Deploy-ability of a structure is potentially stored in a compact form, transported, and easily erected and also dismantled. Creating a sole deployable structural module is highly beneficial, this module will be easily duplicated during the production and erection, thus speeding up the construction process. The preferred structural system is an adjustable portal truss, reimagining the bending moment diagram as its optimum structural module form (Figure 3). This structural form can withstand the bending moment of a simple cantilever beam and column with fixed joint and will transfer the axial loads despite all the members. In order that this module structure can be deployed, there has to be one adjustable bar, which is noteworthy.

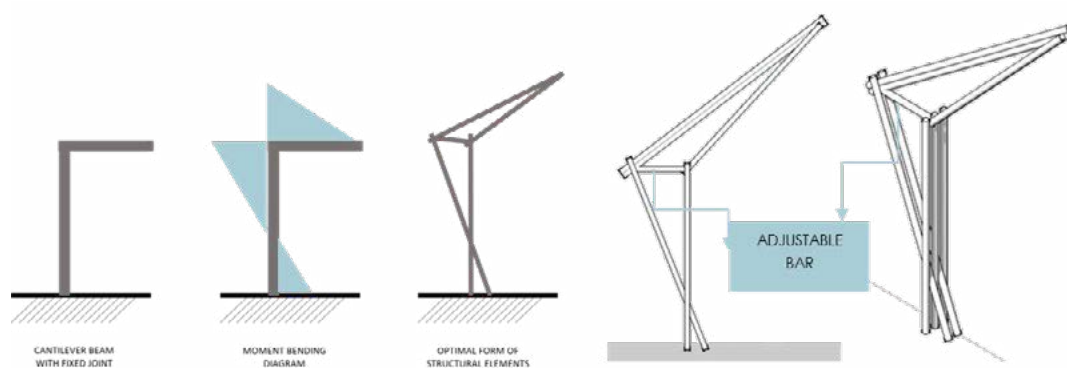
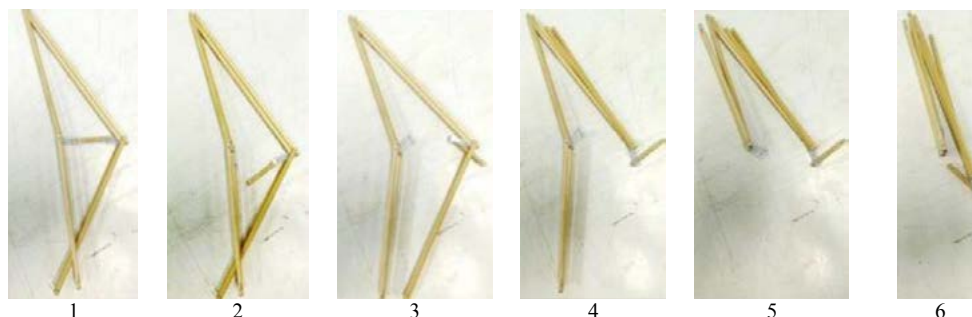


Figure 3 Sole Module: An Adjustable Portal Truss



Foldable Structural Module



closed compact configuration



predetermined expanded form

Figure 4 Deployable Structural Module



3.3.2 Extendibility and Flexibility

An adaptable building should provide a space plan able to be arranged in several scenarios to meet different needs, life styles and uses. Functional and spatial adaptability can be achieved by include multifunctional spaces, allowing for a large variety of functions, as well as trans-functional spaces leading to the creation of new undetermined and unpredictable activities according to the users’ personal experiences and their consumption of space (Nakib, 2010). BAKK have spatial and functional adaptability, though adjustable modular design approach. Simply having a sole structural module, BAKK proof to be configured with various building’s spans and form so BAKK can re-adjust to the land’s size, building function and also user’s needs-and-wants. The BAKK structural module has only one adjustable bar to adjust building span, which varies between 3m and 7,3m. Some such variation may also be attached to mezzanine floor (Figure 5). In addition, this module can be duplicated horizontally, thus creating the various building’s form (Figure 6).

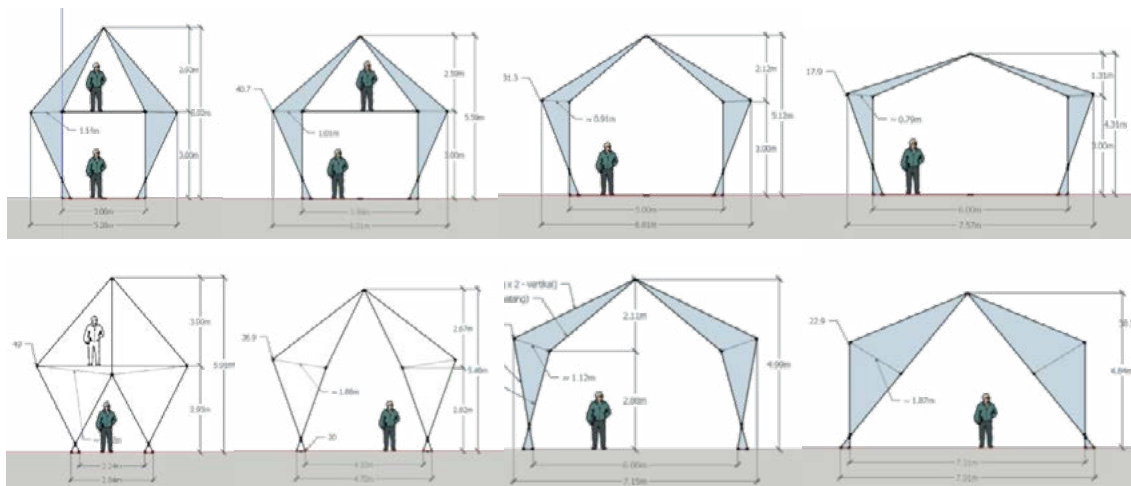


Figure 5 Various Building’s Span

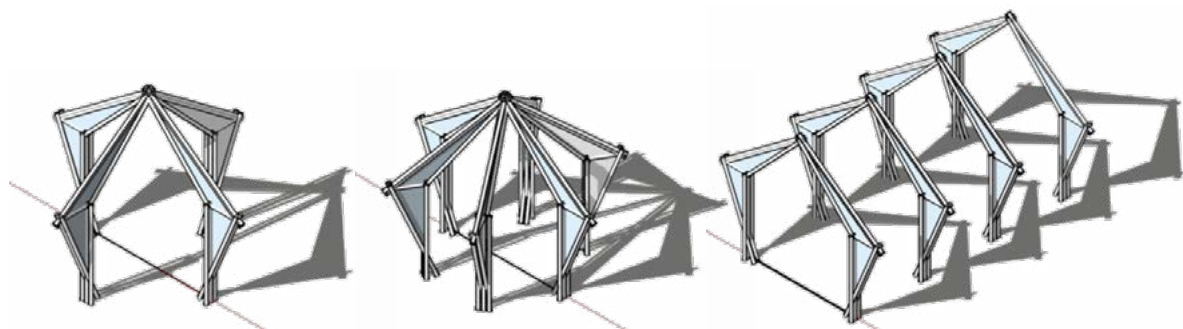
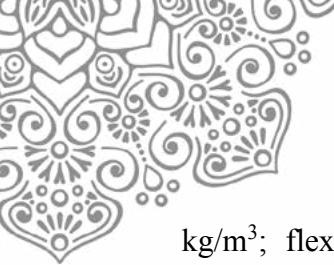


Figure 6 Various Building’s Form

Computational structural modeling by SAP program has been conducted to ensure the strength of the structure in any possible structural configuration. The proposed species of bamboo is ‘*Gigantochloa Apus*’ whose diameter around 80mm and wall thickness around 10mm, while the material properties take advantage of Kaminski et al., (2016) research, that are modulus of elasticity 10.000 MPa with moisture content 19%; dry density 500-800



kg/m³; flexure 30 N/mm²; shear 2 N/mm²; tension parallel to fibre 40 N/mm²; and compression parallel to fibre 20 N/mm². Variants of building's span have a safety factor 2.5 (compression limit) and 6 (tensile limit). It can be concluded that the proved is extremely safe. In this structure, the element's bending will determine the limit of the structure.

Table 1 Structural Analysis

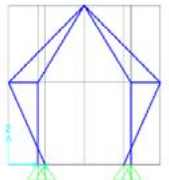
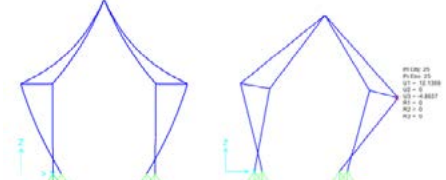
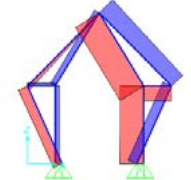
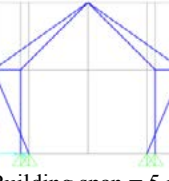
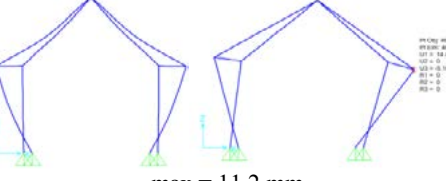

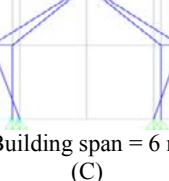
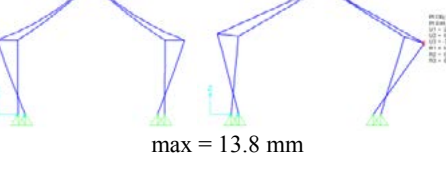
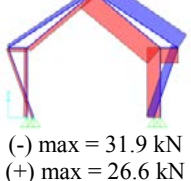
Model	Deformation due to a combination of serviceability	Axial force due to an ultimate combination
 Building span = 4 m (A)	 max = 10.5 mm	 (-) max = 22.1 kN (+) max = 14.6 kN
 Building span = 5 m (B)	 max = 11.2 mm	 (-) max = 24.3 kN (+) max = 19 kN
 Building span = 6 m (C)	 max = 13.8 mm	 (-) max = 31.9 kN (+) max = 26.6 kN

Table 2 Stress and Deflection

	Model A	Model B	Model C	Stress Limit
Building Span (m)	4	5	6	
Compression Force Maximum (kN)	22.1	24.3	31.9	
Tension Force Maximum (kN)	14.6	19	26.6	
Compression Stress Max (MPa)	5.03	5.53	7.25	40
Tension Stress Max (MPa)	3.32	4.32	6.05	20
Deflection Max (mm)	10.5	11.2	13.8	L/300 = 14

3.3.3 Refit-ability

Refit-ability means that the structural components can be possibly and easily exchange or replaces. BAKK fulfilled this ability through interlocking multi-layer bamboo system and also bolts-and-nuts joinery system. The use of interlocking multi-layers' bamboo system (Figure 7) makes the excessive of the structure, but it has another advantage in the possibility of exchanging or replacing the bamboo without destroying the entire building. The bolts-and-nuts joinery are the most commonly connection, used in modern bamboo



construction even in other construction. Thus the procurement of this material will be easier, both at the beginning of construction and at the time of replacement. In addition, using such connection will be easily disassembled and re-installed, allowing the bamboo's replacement without defecting the connection itself. With this consideration, the connection between bamboo and foundation uses a steel plate as a connector.



Figure 7 interlocking multi-layers bamboo system



Figure 8 steel plate: the connector between bamboo and foundation

3.3.5 *Movability and Recyclability*

The fold-ability of BAKK allows for this structural element to be moved and re-used in other location. The dimensions and weight of each module is a very important consideration in the design. The length of each module structure in the closed compact configuration is 4.2 meters, which can be transported using an ankle truck. While the weight of this module is about 30 kilograms, which can be transported by two people.



Figure 9 Moveability



4. CONCLUSION

The main principle of a proposed adaptive bamboo structure, BAKK, has been introduced through a sole structural module of the adjustable truss frame portal. Using bamboo as local-and-sustainable material of the adaptive structure' design of *Bumi Awi Kabula Kabale*, are highly potential to attain adaptable building. BAKK has been proven to enable the dwelling's adaptation: available, extendible, flexible, refit-able, movable and recyclable. This structure's ability enables to reduce material's consumption at the time of building's alteration. Ultimately it could alter the fate of mankind and create human's dwelling, that is more harmonious balance between man and nature. This research can be a nifty commencement for further research, such as post occupancy evaluation of this structure, impact using this structure to the dwelling itself, and also the technical aspect of this structure.

5. ACKNOWLEDGEMENT

This research was awarded grant by JUBIT International and also supported by Research and Community Service Institute of Universitas Katolik Parahyangan, Bandung, Indonesia. We thank our colleagues from Sustainable Building Material and Technology Research Center (SuBMiT), who provided insight and expertise that greatly assisted the research.

6. REFERENCES

- Clark , L., (2006). *Bamboo Biodiversity*. [Online]
Available at: www.eeob.iastate.edu/research/bamboo/index.html
[Accessed 31 March 2017].
- Dobbelsteen, A. v. d., Linden, A. v. d. & Klaase, D., (2002). *Sustainability Needs More Than Just Smart Technology*. Oxford, UK, Elsevier Science, pp. 1501-1508.
- Gantes, C., (2001). *Deployable Structures: Analysis and Design*. Boston: WIT Press.
- Gibb, A. G., et al., (2007). *An Integrated Project Proposals to the IMCRC (Innovative Manufacturing and Construction Research Center): Adaptable Futures, Developing adaptable building products, processes and people..* Loughborough: Department of Civil and Building Engineering, Loughborough University.
- Jayanetti, L., Follett, P. & Wycombe, H., (2003). Bamboo in Construction: Status and Potential. *UNEP Industry and Environment*, April - September, pp. 64-65.
- Kaminski, S. et al., (2016). Structural use of bamboo Part 3: Design Value. *The Structural Engineer*, December, pp. 42-45.
- Beadle, Katty., et al., (2008). *Adaptable Futures: Sustainable Aspects of Adaptable Buildings*. Cardiff,UK, Association of Researchers in Construction Management, pp. 1125-1134.
- Kronenburg, R., (2001). *Flexible: Architecture that Responds to Change*. Great Britain: Laurence King.
- Liwei, L., (2012). *Bamboo as a Low Impact Construction Material: A Research on Bamboo Architecture in Yunnan, China*, s.l.: s.n.
- Lugt, P. v. d., Dobbelsteen, A. v. d. & Janssen, J., (2006). An environmental, economic and practical assessment of bamboo as a building material for supporting structures. *Construction and Building Materials*, November , 20(9), pp. 648-656 .



- Mehaffy, M. F. & Salingaros, N. A., (2015). *Design for a Living Planet: Settlement, Science, & the Human Future*. Portland: Sustasis Foundation.
- Nakib, F., (2009). *Theoretical ad Practical Approaches to Adaptability and Sustainable Architecture*. Cairo, Ain Shams University.
- Nakib, F., (2010). *Toward an Adaptable Architecture Guidelines to integrate Adaptability in the Building*. Salford Quays , United Kingdom, s.n., pp. 276-286.
- Wagg, D., Bond, I., Weaver, P. & Friswell, M. eds., (2007). *Adaptive Structures: Engineering Application*. West Sussex: Wiley.



SPATIAL TRANSFORMATION PATTERN DUE TO COMMERCIAL ACTIVITY IN KAMPONG HOUSE

ABSTRACT

Kampung houses are houses in kampung area of the city. Kampung House oftenly transformed into others use as urban dynamics. One of the transformation is related to the commercial activities addition by the house owner. It make house with full private space become into mixused house with more public spaces or completely changed into full public commercial building.

This study investigate the spatial transformation pattern of the kampung houses due to their commercial activities addition. Site observations, interviews and questionnaires were performed to study the spatial transformation. This study found that in kampung houses, the spatial transformation pattern was depend on type of commercial activities and owner perceptions, and there are several steps of the spatial transformation related the commercial activity addition.

Keywords: spatial transformation pattern; commercial activity; owner perception, kampung house; adaptability

1. INTRODUCTION

Urban developments were influenced by it's society changes and the dynamic causality is a natural process which cant be separated from architecture principles (Zahnd,1999). Koztof (1991) also emphased the urban developments were triggered by design (planned city) and natuaraly (organic city). The physical embryo of the cities always accumulated from the urban life activities each period of time

Housing as part of urban landuse area always been transformed from time to time along with urban dynamics. The transformation in housing oftenly occurs in their functions, such as : private house into mixuse house (not only private function but also commercial function) and if the transformation continues it will become entirely commercial building (no longer become a house). In other words, the private house has changed into public space. According to Scrutton (1980) The Public space due to commercial activity determined as a space which can be accessed and functioned by all people with no boundary. This public spaces are having some pattern and it influenced by the owner perception about consumer interaction space (emic).

This study investigate the spatial transformation pattern of the kampung houses due to their commercial activities addition. This study based on my master thesis "The Relations Between Inhibitant's Perception With Public Spaces Pattern of Housing Units Interlaced It's Commercial Activity" which aimed to find out the relation between inhibitant perception's with public space pattern of housing unit interlaced commercial activities. The spatial transformation were studied by literature review, site observations, interviews and questionnaires. This study found that in kampung houses, the spatial transformation pattern was depend on type of commercial activities and owner perceptions, and there are several steps of the spatial transformation related the commercial activity addition



2. METHODOLOGY

This study was performed in :

1. Literature review

This method was performed to summarize basic knowledge and theory about spatial transformation, housing and commercial activities to discuss findings in the later stages

2. site observation

This method applied to gather primary data of spatial transformation directly from kampong houses at kampung Pendrikan Kidul in Semarang, Central Java). This method has found that the spatial transformations were concentrated in a street named Jl.Nakula I.

Related to the findings this study was focused on this area and investigate the 23 houses which all of them are using their house as mixuse building.

3. interview

The depth interview in aim to collect the owner perception about their activities, perceptions, kampong developments and business prospect

4. purposive sampling questionnaire

The questionnaires were constructed based on interview, observation and literature review to validate and measure the owner perception.

Later on Qualitative descriptive analyst were applied to explain the meanings of site observation, interview, questionaire result related to the literatures review.

3. RESULTS AND DISCUSSION

Commercial activities regarding their commodity were devided into : goods and service commercial. The good selling merchants are dominating in the study area with 50% followed by mix-commodity 27% and service with 22% (see the figure 1). The commercial activities has been triggered by new activity generator on the kampong. It resulted the spatial transformation of the housing, from full private space into shared public space to support the commercial activities. Most of the spatial transformation are concentrated on Nakula I street as the main road to the new generator activity.

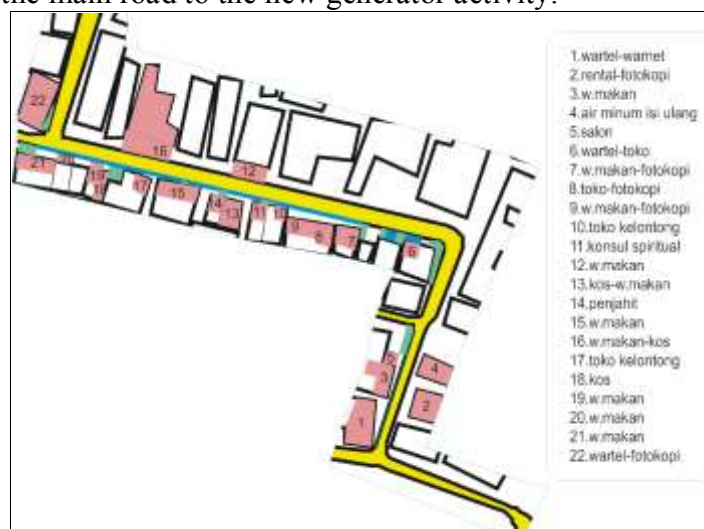


Figure 1 the study area



Residential used for business activities and the room function accommodates human activities. The occurrence of a change or transformation use of space within the residence, so it needs identification into several categories (Lang, 1994):

- a. Fixed-feature space , a space that is limited to the elements and is not easily changed.
- b. Semifixed-feature space, there is a space furnishings and wall dividers are easily relocated as needed.
- c. Informal space , there is a change to the fixed and semi fixed feature space, involve more man inside of a function space has been determined.

There are certain type of spatial transformation pattern in the study object. The transformation of private space into shared public commercial space, terrace, until the local street in front of their house (see figure 2). The small house (<60m²) only subtract their private space inside the house without change their terrace. The medium houses are having more type in transforming their private house with 4 types. The big houses has 5 type of spatial transformation due to their commercial activities.

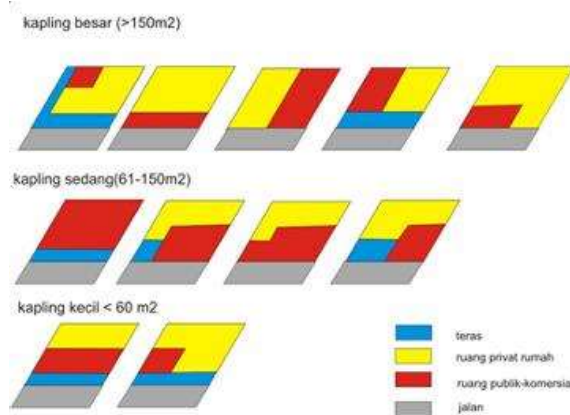


Figure 2 Commercial Space Pattern

Related to the findings, there are several type of spatial transformation pattern which put the public commercial space at the space between the street to private house and their terrace to private house (see figure 3). The changes in the pattern of space in a home showed reduced the private spaces (accessible only by the owner) and the entire space has been used as commercial space (Kurniati, 2016). Changes of space for commercial activity also appears in the pattern of space inside the house, eventhough commercial activity only changed the pattern of space outside the house at the beginning. However, with the increasing needs of the changing function of the building have an impact on the occurrence of a change in the shape of the building. Some pattern in kapling sedang shown that the fixed features space can be informal space in needs.

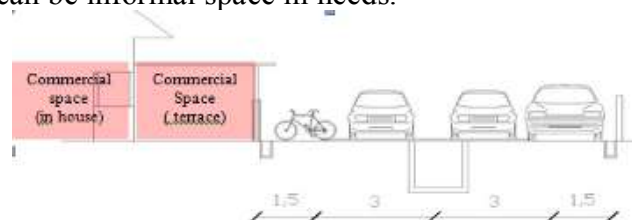
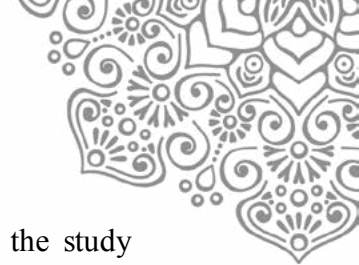


Figure 3 Section of Commercial Space



Both of commercial and private need parking spaces as vehicle ownership. In the study object, most of the houses use the street side as parking area (see figure 3) because the streets are having 9m width. Refer to Shirvani (1985) the parking space in this area are “on street parking”. That condition explained that commercial activities are demanding more space rather than previous residential since the client or buyer’s vehicles addition. The Commercial activities with goods commodity (See figure 4) showed the high demands of on street parking may result problems, such : parking space limitations and local traffic jam are appearing in this area (Tamin, 1999)

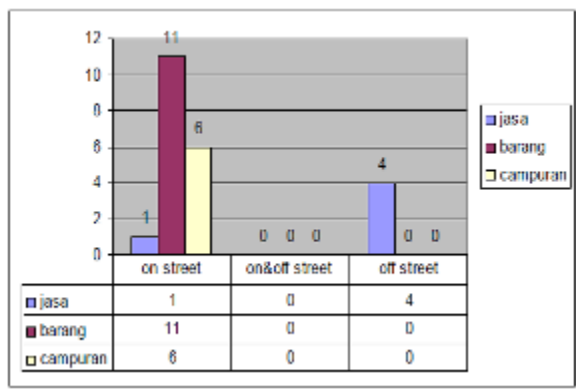


Figure 4 Parking spaces for the commercial

Entering the private house area, there are patterns of entrance for commercial space and residential space in the study findings (see figure 5). The first is using same entrance for commercial and residential which resulted the owner and guest for residential purpose must go through the commercial space. This informal space showed that the owner was not ready to perform commercial activities in their house. The second is using separation between commercial and residential activities (see figure 5 right side). Some houses have transformed their house’s entrance or changed their side entrance area (carport) into commercial space as the adaptation effort of semi fix featured space.

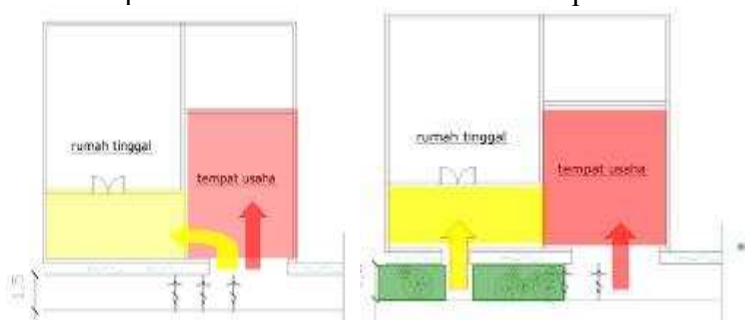


Figure 5 Plan of Commercial Space

The further spatial transformation of commercial activities were expanding into the house through the next room to the commercial space as shown in figure 6. This situations showed that the owner get more benefits in making their house parts as commercial space and continue to expand that space. In further development, the secondary space will become primary space or respectively depend on space owner perception (Harsritanto,



2008). According to the owner perception the commercial developments will continued inside their house rather than outside the house (see figure 7). Regarding to their perception , author noticed that the transformation will continued until their house become totally commercial building. However some dwellers also decided not to develop their house into commercial building.

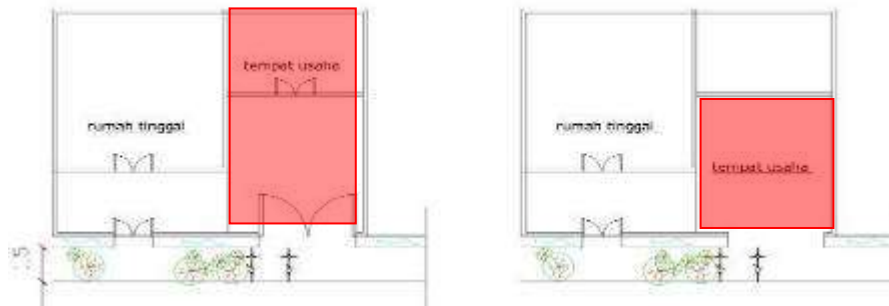


Figure 6 Development of Commercial Space

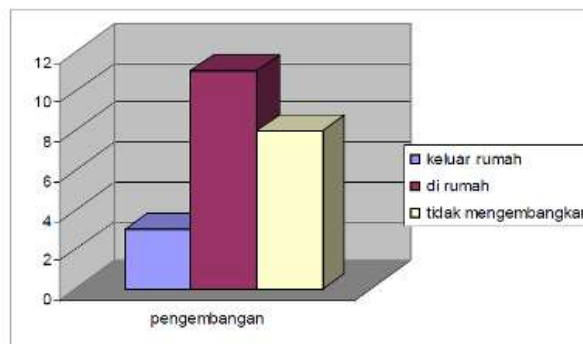


Figure 7 Owner Development Plan

The spatial transformations are more than fixed featured space occupation expressed above. Some adaptability artifacts are also found in the area which showing that space can be manipulated according to the demands (Harsritanto, 2008). The figure 5 show the fix adaptation and the figure 8 shown that carports were manipulated into commercial space during the day. The owners do on street parking to accommodate their commercial activities and park inside the house after the commercial activity stopped. Furthermore the figure 9 shown the terraces were modified into semi fixed features like shop/resto and most of the commercial related tools will be relocated on the warehouse.

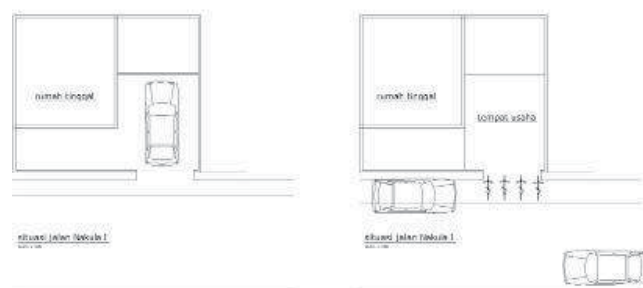


Figure 8 Adaptation in owner parking (left: during night, right : during day)



Figure 9 Space adaptability using semi fix fixtures

Spatial Transformation Pattern Due to Service Providing Commercial Activity

The owner perform all commercial activities inside the house because they thought the commercial activities need privacy. That condition was contrassed, since space for commercial activities on the house has started from the parking space, terrace until the first accessed room unexpectedly become public since everyone can enter. The pattern resulted residential activities must be located behind the commercial spaces which may bring unconvinience to the owners and guests. This misconception about privacy of public-private space may bring unconvinience situations for both. Some adjustments were operated to minimize the situation, such as : entrance separation and transform the terrace into lobby, deploy semi fix features space, etc.

Spatial Transformation Pattern Due to Goods Providing Commercial Activity

The goods providing owners do their commercial almost in all part of their houses. This type of commercial activities are more expansive and adaptive in using their house rather than the service provider. They are using their house area as parking space, display unit, trade rooms, until storehouse. Refer to the type of commercial activities on figure 8, they are dominant and made major transformation either to the house and kampong area (especially in changing fixed features space into informal space and respectively). The changes start from their parking area which located on the street side may reduce the corridor function as public acces to the rooms inside their house (see figure 5) and according to the owner development plan on figure 6, most of them will change their house into full shop/resto if there opportunity arise.

Some adjustment to separate commercial and residential were found, such : entrance splits, special passages (I shape), pavilion style, un-permanent setting, etc. Those showed that adaptability concept applications are much evolving in this type of houses.

Since the progress of commercial space occupation will be varied as displayed on figure 2 regardless the size of the house (kapling), this the limit of spatial transformation for this goods provider commercial activity is just the owner perception as mentioned on figure 8.

Spatial Transformation Pattern Due to Goods+service Providing Commercial Activity

The similarities in spatial transform between this type and goods providing one are the expansive transformation and the separation between commercial-residential. In



adaptability concepts in serving customer's privacy which mentioned as misconception between owner (as private) and customer (as public) above, a special passage/door connect this two type of spaces. In this case, the customer privacy must not be interfered by residential activities which can be named as client oriented space.

4. CONCLUSION

Some conclusion were resumed in this spatial transformation pattern due to commercial activity in kampong houses as follows :

1. There some spatial transformation pattern in kampong houses due to the type of commercial (goods, service, mix providing) activities which performed by the owner.
2. The transformations were performed from the spaces on street side to all space inside the house
3. The transformations conduct permanently or partialy with some adaptation tools/habit
4. The owner perceptions have strong influence in the further spatial transformation

5. REFERENCES

- Atkinson, Rita L., 1983, Pengantar Psikologi Dalam Arsitektur Lansekap, Bumi Arta, Jakarta
- Bell, Paul A. dkk, 2001, Environmental Psychology Fifth Edition, Hartcourt College Publisher, Orlando Florida
- Dewangga, Viko Trah, 2006, Hubungan Atribut Persepsi Pedagang Kaki Lima pada Malam hari Terhadap Setting Trotoar di Lapangan Pancasila Simpang Lima Semarang, Program Pasca Sarjana, Universitas Diponegoro, Semarang
- Dewantoro, Dwi Agung, 2007, Morfologi Perubahan Ruang Privat menjadi Ruang Publik dikaitkan dengan Kegiatan Komersial di Jalan Prof.H. Soedarto, SH. Semarang, Program Pasca Sarjana, Universitas Diponegoro, Semarang
- Gita Dianing S, 2005, Hubungan Perubahan Setting Ruang Privat Terhadap Persepsi Pengguna Unit Bangunan Dikaitkan dengan Kegiatan Komersial (studi kasus Jl.Utama Lingkungan Permukiman Tlogosari, Semarang) Magister Teknik Arsitektur, Program Pasca Sarjana, Universitas Diponegoro, Semarang
- Harsritanto, Bangun IR, 2008, Hubungan Persepsi Penghuni Dengan Pola Ruang Publik Unit Rumah Tinggal Terkait Kegiatan Komersial, Magister Teknik Arsitektur, Program Pasca Sarjana, Universitas Diponegoro, Semarang
- Koztoff, Spiro (1991) The city shaped, Thames Hudson, London
- Kurniati, R., & Erlambang, F. R. (2015). SPACE IN CHINATOWN SEMARANG. *Procedia Environmental Sciences*, 23(Ictcred 2014), 307–314. <https://doi.org/10.1016/j.proenv.2015.01.045>
- Scrutton, Roger (1980) The Meaning of Conservatism, Augustine Press
- Shirvani, Hamid (1985) The Urban Design Process, Van Nostrand Reinhold Co. Newyork
- Tamin, OZ; Soedirjo, TL; Kusumawati, H.A, 1999, Pengaruh Kegiatan Perparkiran di Badan Jalan Terhadap Kinerja Ruas Jalan, Proceeding Forum Studi Transportasi Antar Perguruan Tinggi,
- Lang, John. Urban Design : The American Experience, Van Nostrand Reinhold, New York, 1994
- Williams, C. C., & Martinez-perez, A. (2014). Why do consumers purchase goods and services in the informal economy? . *Journal of Business Research*, 67(5), 802–806. <https://doi.org/10.1016/j.jbusres.2013.11.048>
- Zahnd, Markus, 1999, Perancangan Kota secara Terpadu, Kanisius, Yogyakarta



15th International Conference on Quality in Research (QIR 2017)

CO-RESIDENCY AMONG MIGRANTS IN BALIKPAPAN EAST KALIMANTAN INDONESIA

Wendy I. Hakim^{a*}

^aUniversitas Indonesia, Depok, Indonesia

ABSTRACT

The background of this study is urban housing problem in Indonesia, which is still viewed solely from its physical aspect and the demand of it is mostly calculated quantitatively only. This view considers a house as physical entity only, excluding the variety of aspirations of its occupants. This is becoming a gap in the housing supply in Indonesia, in the terms of diversity in social, economy, and culture. This context has shaped various aspects of the society, including housing.

This research highlights co-residency phenomenon among migrants in Balikpapan, East Kalimantan, Indonesia. The idea of co-residency is a part of internal migration issue in Indonesia, in which the migrants will co-reside with their relatives at their city of destination. The aim of this study is to identify housing strategy of migrants in urban area and discover their housing aspiration in terms of affordability in economics and socio-cultural aspect in this kind of housing. Grounded Research method is used due to the fact that co-residency is an existence reality – not an empirical object of architecture itself. Co-residency phenomenon contains the ideas of living in other people's house; hence this study focuses on the aspect of the presence of house occupants.

The co-residency of migrants can be seen as dwelling issue on a micro level – in a house – as well as on a macro level, that is city as a human settlement. For migrants, in one hand, co-residency with relatives at their city of destination is one of the available choices for housing besides renting and buying, which relating to what young-adult migrants can afford while still looking for a job and not yet earning any income. On the other hand, co-residing with relatives in a foreign city is an acceptable idea and way of living, which is practiced as a cultural matter that carries out certain values and traditions. Both sides of the co-residency phenomenon can be discussed as to how a dwelling process is becoming possible for migrants in their city of destination.

Keywords: Co-residency; Dwelling; Housing; Migration



1. INTRODUCTION

Housing Needs and Diversities of Occupants

By examining the concept through a case study of Indonesia, different sources report a deficit of between 3 and 14 million dwelling units estimated. The wide range of estimates of the housing deficit in Indonesia makes it an ideal case to discuss the common lack of clarity not only in the methods used to estimate the housing need, but also in the meaning of the concept itself. The focus is on the quantitative component of the deficit as it turns out that the qualitative component is actually less problematic a concept. Once the decision about minimum housing quality is established, it is only a matter of estimating how many houses are below this standard. The quantitative housing deficit is more difficult to calculate because it depends on either a normative decision about how many should live in one household or, more commonly, on assumptions about the relationship between rates of past and present household formation (Monkkonen, 2013).

In Indonesia, two major institutions i.e. Kementerian Perumahan Rakyat (Kemenpera) and Badan Pusat Statistik (BPS), define housing deficit or commonly called housing backlog, differently. As mentioned by the secretary of Kementerian Perumahan Rakyat, Iskandar Saleh, "In BPS's standard, backlog is estimated based on house ownership while in Kemenpera's standard, backlog is estimated based on whether or not a house is physically proper enough to live in"

Housing problem in Peru was framed as a letdown when the government and also the NGO perceived a house as 'what it is' which lead to failure in delivering the precise outcome of housing need. The 'what it is' paradigm was lack of specific and detail context(s) of who the house ought to be catered. Instead of 'what it is', the problem of housing was alternately perceived as 'what it does'. This view offered a focus on how the complexities and variation of context(s) of the occupants carried some different needs in housing (Turner, 1976).

Migration, Housing Needs Among Migrants, and Co-residency

Housing in the context of migration is one of cases that could be discussed as a further challenge that tend to be a concern for Indonesia in its rapidly urbanization. The issue on migration in this study is focused on city of Balikpapan, East Kalimantan, Indonesia. East Kalimantan Province is considered as one of the main destination area on mid-eastern Indonesia.

In early 1990s, the majority of internal migrants migrate from outer islands to the inner island of Indonesia. But, this pattern began to turn oppositely in 1997-1998 when monetary crisis happened; migrating out Jawa Island is increasing while migrating to Jawa Islands is decreasing (Groppo and Mendola, 2014).

Some provinces that have potential natural resources, such as Irian Jaya (Papua) and East Kalimantan tend to pull the internal migrants in; while the less potential ones, such as Central Kalimantan and Nusa Tenggara Timur (NTT) veer to push the migrants out (Perwira, 2001)

The Island of Java is a highly urbanized region, but many provinces in the outer islands also experienced a significant increase in the proportion of urban population over



the 2000–2010 period, most notably Riau Islands (Kepulauan Riau), East Kalimantan, Bali, Bangka Belitung, North Sumatera and North Sulawesi. The Provinces of East Kalimantan and North Sumatera are rich in resources, especially palm-oil plantation, forestry, oil and gas (Firman, 2016)

Recent migrants who just migrated to their new cities of destination face vary housing options as well as its constrain. Buying a house could be one of them. Renting a house or a room is also possible. Other than buying and/or renting, migrants in Indonesia also have housing option by staying and living with their families or/and relatives.

Migrant's tendentious behaviors in Indonesia are (1) in the time they arrived in the cities of destination, they tend to stay among their families and relatives and (2) the previously arrived migrants will be the main helper of the recently arrived one by providing some information relating to job seeking and also providing place to stay (Mantra, 1985).

This study explores the phenomena of co-residency –the recent migrants that stay in their families/relatives' house in Balikpapan as the city of migration's destination. The co-residency could be simply explained as living together in others' people or/and household.

Co-residency can be defined as multigenerational living arrangement that includes other member(s) than the family affiliates. Both of parties live and stay in one household with various intentions, such as health issues, economy matters, and/or cultural factors (Keri, 2008).

Based on some family and household historiographies in some cities in England, there was a rather specific term to a person or/and a group of people who was a stranger or outsider that in the official record of demographic survey named as inmate(s) (Laslett (1972). In West Africa, there were some households that include their extended families member(s) to live with them (Verdon, 1983). Study on family and household in England showed evident of non-members who live with non-nuclear family household that was mentioned as co-resident relatives (Tadmor, 2004).

Research Purposes

This study concerns the modus of co-residency as housing and furthermore as dwelling option for the migrants in Balikpapan, East Kalimantan, Indonesia. The aims of this study are (1) to identify the housing strategy among migrants to dwell in the city of destination and (2) to reveal the dwelling and housing aspiration of the migrants relating to financial affordability as well as its socio-cultural aspects.

2. METHODOLOGY

The co-residency as dwelling phenomena and the dwellers of architectural object are realities of existence –instead of merely an empirical object of the architecture itself. Thus, this study focused on revealing the architectural object by observing the existence of the people that are categorized as the dwellers of co-residency. The apt method to accomplish is Grounded Research.

Grounded Theory refers to a theory that is developed and analyzed systematically from the data as the result of a research. By applying this method, the researcher begins the study without any preconceived theory, unless the researcher aims to assembly two or



more theories and aims to develop the existing theory. Grounded Theory is utilized to develop theory –instead of testing –and helps the researcher to find alternative meaning of a phenomenon (Strauss and Corbin, 1990).

11 households that practice co-residency are interviewed and observed to gather the data. The data gathering are focused on the meaning of co-residency, experiences during the practice of co-residency, and also the description of everyday routines in the household. The data gathering involved the household members as well as the tenants who co-reside in the households. The data is analyzed qualitatively, particularly under the scrutiny of coding method (Glaser and Strauss, 1967; Strauss and Corbin, 1990; Ryan and Bernard, 2003; Saldana, 2009).

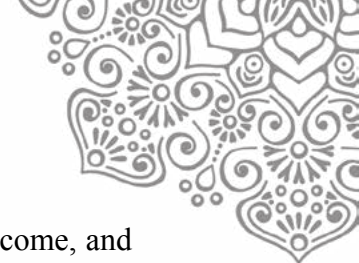
3. RESULTS AND DISCUSSION

The Tradition of Communal Living, “Merantau”, and Co-residency

There are correlations among the tradition of communal living, merantau –refer to migration, and co-residency. The actors of the co-residency, both the householder and the tenant, have tradition of communal living. This term of communal living can be understood by the actors’ explanations of both prior experiences of living with extended family in one household, living locally near them in the past, maintaining personal relationship despite of migration and resettlement, prior involvement in co-residency, involvement in “paguyuban” (association of migrants who came from the same hometown), and also the preference to preserve such way of living that past through generations to generations. Living with extended family and relatives is considered to be custom as well as keeping the good quality of their relationship. Beyond their comprehension of their status of kin and non-kin, the actors see the each other as “semua itu saudara” (all are our family).

This tradition of communal living is being related in the context of migration. When the first comers migrated and settled, they intended to encourage their extended family members and some relatives from their hometown to migrate and then offering supports by inviting their families and relatives to live with them in their house in the city of destination. The actors, especially the first comer migrants, see this matter as some kind a way to maintain “persaudaraan” (brotherhood and sisterhood) in the time of “sudah pencarpencar” (loosen because of the members already migrated). The actors continually keep contact with their families and relatives and at least once or twice a year, they visit their hometown. The small talks between two members of the families or relatives include the tales of ‘merantau’. They discuss the possibility of migration as well as co-residency. By planning it and then inviting and accepting their family members and relatives as soon to be living with them, the actors believed that in this way they would be able to even fastened the bond within their families and relatives that already migrated and left behind in their hometown.

Living with families and relatives in the city of destination is considered as the even more idyllic way of live in the context of migration. Both of the actors argue that there’s no easy way to establish a new life in rather unfamiliar city without any help from their families and/or relatives. Thus, the presence of their families/relatives member in the city of destination becomes one of the considerations before they migrate. They consider the



obstacles on housing, job seeking, living cost while they not yet have job and income, and administrative matter regarding the status in demographic matter that could be supported by the families/relatives in the city of destination.

This matter of communal living and migration can be discussed as polarization between communal living as country way of life and individual living as urban way of life. This issue was previously discussed by some researchers related to rural-urban, country-city, and etc.

In the time of Industrial Revolution in England, there was a contrast between country and city. The country way of life included some activities such as hunting, poultry, farming; and there were tribal and feudal organizations. Meanwhile, the city was framed as the center of administration, market places, and the center of industry (Williams, 1973). Urbanism as way of life has a heterogenic population, specialization of function, impersonal, and there's standardized behavior (Wirth, 1938). Those arguments tend to differentiate and contrast the characters of country and city and/or rural and urban. Meanwhile, the issue of communal living that renders the phenomena of co-residency is happening in the context of migration. Communal living that was framed as country or rural way of living, takes place in the city of destination that is urban.

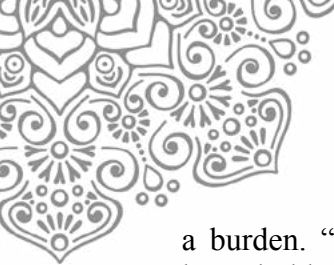
Urbanization refers to the system of urban relation that the origin of tribal (tribe, hometown, and ethnicity) of the population is seen as secondary aspect after the urban itself. In the rural area, becoming the tribesman is a part of a particular social and political system while in the urban area, the tribe is merely an identification of migrant workers. However, since many tribes occupy the city, therefore the roles of tribal affiliations are significant (Gluckman, 1961).

In Zambia, there's "abakumwesu" that supports the network of migrants in the city. "Abakumwesu" literally means "anyone who has the same hometown as me" and refers to relatives, extended family members, neighbors, and clans. "Abakumwesu" operates voluntarily to support the everyday life of tribal relation in urban context in many aspects, including financial supports, linkage between the city of destination and the hometown, and also political backing (Harries-Jones, 1969).

Gluckman's and Harries-Jones' arguments of the tribal affiliations of the migrants in the city is essential to apprehend the existence of co-residency due to the presence of tradition of communal living in the context of migration.

Incorporation from Non Member to Member in Co-residency Household

Actors who involve in co-residency –the householder and the tenant –are tied as families and/or relatives but not all of them have personal attachment yet. For example, the tenants of co-residency know their householders as their uncle and/or aunt (the siblings or/and the cousins of their parents), but they do not personally know them due many reasons. The soon to be their householders are their uncle and/or aunt who migrated long ago when they were still a child and they only meet them once a year. Some tenants and their householders are also total strangers because they are in-laws, never meet before, and/or only know them by telephone. They are linked by third person that has closer or tighter relationship personally with one of the actor. The third person mediates the soon to be co-residency. The everyday life of the actors in the setting of co-residency is veiled by "kesungkahan". "Kesungkahan" refer to the awkwardness, uneasiness, and worry of being



a burden. “Kesungkanan” in co-residency exists on the both sides, the tenants and the householder, in the matter of many aspects in everyday activities as well as personal one.

In this case of co-residency, more than shelter, the tenants also depend on their co-reside household in basic needs especially daily consumptions of foods. The householders provide daily meals for their co-reside tenants just like providing the entire members of the family. The householders aware of “kesungkanan” in eating so they constantly inform the tenants to eat freely anything, whenever, and anywhere they want to, without any invitation from the householder. As the tenants, they try to consume less, adapt to the eating habits of their co-reside households, and also expect the invitation from the householder before eating.

Other than the issues of eating habits, the matter of household chores also becomes the subject of “kesungkanan”. As the tenants, they argue that doing household chores is just a routine that people has to deal with anywhere they live. Thus, in the context of co-residency, they feel oblige to contribute. Some of them feel uncomfortable because the householders never ask for any assistance despite of the demanding situation and when they mean to help, the householders often refuse. Meanwhile, the tenants who already have job and feel tired after working at the office, constantly feel conflicted if they didn’t help although the householders understand their situation and suggest them to unwind.

As the householders, they do not expect their tenants to do household chores, especially the hard and time-consuming one. One reason is because the householders expect the tenants to only focus and allocate their time on the job seeking and their careers. Many householders in this case, were former tenants of co-residency in their youth. They experienced a kind of hard time when it came to obligation to do household chores for their householders while struggling with their personal objectives back then. As they are becoming the householders in present co-residency, they have intention to diminish that kind of hardship. However, the householders may appreciate tenants’ good deeds to assist and the householders give the tenants similar-level tasks as their children. The householders find it helpful to make the tenants feel at home by given the same tasks as other household member. Also, the assistance from the tenants is practical and helps them greatly sometimes when the household chores are too much to handle.

As time goes by, personal relationship among the tenants and the rest of the family members in the co-residency household grows. Both parties are synchronizing each other in the situation of “kesungkanan”. The householders grant the tenants the similar right and obligations as the children in the household. There are also personal relationships between the tenants with specific members of the household. Some tenants have closer relationship with the children of the household. Some tenants much closer with the wife/mother in the household than the husband/father. In the practices of this living arrangement that involve the householders and the tenants who are personally stranger to each other despite of their families and relatives status, there is a kind of incorporation from non-member to become member.

There are characteristics of what Arnold van Gennep (1909) has called the "liminal phase" of rites de passage. Van Gennep has shown that all rites of passage or "transition" are marked by three phases: separation, margin (or limen, signifying "threshold" in Latin), and aggregation. The first phase (of separation), includes symbolic behavior indicating the detachment of the individual or group either from an earlier fixed point in the social



structure, from a set of cultural conditions or from both. During the intervening "liminal" period, the characteristics of the ritual subject (the "passenger") are ambiguous; he passes through a cultural realm that has few or none of the attributes of the past or coming state. The third phase is reaggregation or reincorporation (Turner, 1966).

Turner's argument that was based on van Gennep's notion can capture the everyday practice of co-residency between the tenants and the householder in the process of incorporation of relatively stranger parties in becoming members of the households. However, the further findings indicate that there is limitation on the incorporation as household members. There is expression among them, "bagaimanapun juga mereka tetap orang lain" that literally mean "after all, they are still outsiders". This expression means that despite the fact of gradual personal relationship and acceptance as member of the household in everyday routine, both parties are essentially strangers. Some householders concern about the sex and gender differences between the tenants and their children. Some of them also concern about the age gap between the tenants and the children. The householders attempt to set the clear boundary of the tenants' and the children's domain for the sake of both parties' nature of sex and age.

On the other hand, there is a status of the tenants as "anak titipan", refers to children that are entrusted under the foster care of the householders by their families/relatives during the co-residency. As the householders, their main objective is to succeed the aims of migration of the tenants, i. e. to become an adult with job and financial independency. This aim ought to be accomplishing without any distraction of the burden of household chores and other obstacles. In this case of co-residency, the householders are not only providing shelter and daily basic needs of their tenants, but also providing advices and counsels –just like the elders to their younger relatives –concerning professional career and also personal issues.

Co-residency as Possibility of Dwelling Among Young Adults Migrants

Co-residency can be seen as first step of the tenants as recent migrants' housing career in the city of destination. The tenants as recent migrants in this case of co-residency are young adults who migrate from their hometown to the city of destination. They are high school or diploma or bachelor fresh graduate who are willing to find job, earn income, and start their life as adult. They will live and stay with their co-reside households until they are able to maintain their independent livelihood. Some of them go back to their hometown without getting any job or/and migrate to another city, while some of them still co-residing until they get married and move out to establish their own household.

Almost everyone has the same housing progression or 'career'. Young people with income move out their parents' house to rent and experience the single life. After getting married, husband and wife work and economize on rent thus they can deposit to buy a house in which they will take care of their children. While some of them move to bigger houses before their children grow up or to a flat after children leave home. It is commonly expected that most households remain in their first home until old age (Kendig, 1984).

In the issue of housing transition among young adults in Australia, there are some theories and previous findings about housing career that are included some indications of the relation between housing problem and life cycle of an individual or/and household (Beer and Faulkner, 2013). In the keyword of life cycle, I expand the discussion of housing



career with the leverage of the findings about life cycle of the tenants as young adult migrants.

Housing problem among young adults is a matter of transition from the dependency to independency towards the parents (Forrest and Yip, 2013). Young adults have three choices of housing, i. e. living with the parents, becoming renter, or becoming house owner (Yu and Myers, 2010; Yu and Haan, 2012). The argument about housing choices is limited regarding the relationship between the young adult with the parents only. Meanwhile, in this case of co-residency, as migrants, the young adults have extensive relationship with their extended families and/or relatives so the other option of housing is enabled and the dwelling is possible in the city of destination.

In their housing careers, young adults tend to have higher residential mobility than the older adults, relating to the young adults' activities in job seeking. Furthermore, in the matter of house ownership, their housing careers are identical with the choice to rent. There is a relation between the mobility of young adults with their status of renter before they become house owner (Clark and Huang, 2003).

The phenomena of co-residency can expand the discussion of housing options in the housing career of young adult other than renting and owning. The tenants' status as young adults and recent migrants situates them in the state of insecurity. Not only in the matter of financial dependency, but also the uncertainty of transition in becoming adult. To compare, while to rent and own a house in the city of destination are the options that require specific assurance –in financial affordability –and the objective to settle down, co-residency accommodates the term of transitory in fitting to adulthood and to dwell as recent migrants in the city of destination.

4. CONCLUSION

The housing strategy among migrants to dwell in the city of destination and the dwelling aspiration of the migrants relating to financial affordability as well as its socio-cultural aspects are revealed through some findings, that are (1) co-reside with families/relatives as housing option among migrants in the city of destination is reinforced by the spirit of communal living with extended families and relatives while contextualizing it in the time of migration, (2) there is an incorporation of tenants as non member to become member of the co-reside households, but there are some restraints due to the relationship between the householders and the tenants as inevitably strangers and also the nature of the co-residency that aims to succeed the adjective of tenants' migration, and (3) co-residency provides other housing option rather than renting and owning a house for the tenants who recently migrate in the city of destination without affordability in housing and are currently in their transition to adulthood.

5. REFERENCES

Clark, W. and Huang, Y., (2003), The life course and residential mobility in British housing markets, *Environment and Planning A* 2003, Vol. 35.



- Faulkner, D. and Beer, A., (2011), *Housing transitions through the life course: aspirations, needs and policy*, The Policy Press.
- Firman, T., (2016), *Demographic Patterns of Indonesia's Urbanization, 2000–2010: Continuity and Change at the Macro Level* in C.Z. Guilmoto, G.W. Jones (eds.), *Contemporary Demographic Transformations in China, India and Indonesia, Demographic Transformation and Socio-Economic Development*, Springer International Publishing Switzerland.
- Forrest, R. and Yip, N.M., (2013), *Young People and Housing: Transitions, Trajectories, and Generational Fractures*, Routledge.
- Glaser, B. and Strauss, A., (1967), *The Discovery of Grounded Theory: Strategies for Qualitative Research*, Aldine Publishing Company.
- Gluckman, M., (1961), *Anthropological Problems Arising From The African Industrial Revolution* in Southall, A., (eds) *Social Change in Modern Africa*, Oxford University Press.
- Grosso, V. and Mendola, M., (2014), *The Short-Run Costs of Moving: Internal Migration and Consumption Growth In Indonesia*, Editorial Express.
- Harries-Jones, P., *Home-boy Ties and Political Organization in a Copperbelt Township* in Mitchell, J. C., *Social Network in Urban Situation*, Manchester University Press.
- Household And Family In Past Time: Comparative Studies In The Size And Structure Of The Domestic Group Over The Last Three Centuries In England, France, Serbia, Japan And Colonial North America, With Further Materials From Western Europe*, Cambridge University Press.
- Kendig, H., (1984), *Housing Careers, Life Cycle and Residential Mobility, Implications for the Housing Market*, *Urban Studies*, Vol. 21 No. 3.
- Keri, J., (2008), *Coresidence*, *Encyclopedia of Aging and Public Health*. Springer US.
- Laslett, P., (1972), *Introduction: The History of The Family* in Laslett, P. and Wall, R. (eds)
- Mantra, I. B., (1985), *Pengantar Studi Demografi*. Pustaka Pelajar, Yogyakarta.
- Monkkonen, P., (2013), *Housing Deficits as a Frame For Housing Policy: Demographic Change, Economic Crisis And Household Formation in Indonesia*, *International Journal of Housing Policy*.
- Perwira, S. M., (2001), *International and Internal Migration in Indonesia*, Paper prepared for Ad Hoc Expert Group Meeting on the Theme "Migration and Development Opportunities and Challenges for Poverty Reduction in the ESCAP Region" held by ESCAP Bangkok.
- Ryan, G. and Bernard, H., (2003), *Techniques to Identify Themes*, *Field Methods*, Vol. 15 No. 1, Sage Publication.
- Saldana, J., (2009), *The Coding Manual for Qualitative Researchers*, Sage Publication.
- Strauss, A. and Corbin, J., (1990), *Basics of Qualitative Research: Techniques and Procedures for Developing Grounded Theory*, Sage Publication.
- Tadmor, N., (2004), *Family and Friends in Eighteenth-Century England Household, Kinship, and Patronage*, Cambridge University Press.
- Turner, J., (1976), *Housing by People: Toward Autonomy in Building Environments*, Pantheon Books.
- Turner, V., (1966), *The Ritual Process: Structure and Anti-Structure*, Cornell University Press.

- Verdon, M., (1983), *The Abutia Ewe of West Africa a Chiefdom That Never Was*, Mouton Publisher.
- Williams, R., (1973), *The Country and The City*, Oxford University Press.
- Wirth, L., (1938), *Urbanism as Way of Life*, *The American Journal of Sociology*, Vol. 44, The University of Chicago Press.
- Yu, Z. and Haan, M., (2012), *Cohort Progress Toward Household Formation and Homeownership: Young Immigrant Cohorts in Los Angeles and Toronto Compared*, *Ethnic and Racial Studies*.
- Yu, Z. and Myers, D., (2010), *Misleading Comparisons of Homeownership Rates When The Variable Effect of Household Formation is Ignored: Explaining Rising Homeownership and The Homeownership Gap Between Blacks and Asians in The US*, *Urban Studies*.



QIR

*The Westin Resort
Nasa Dua, Bali*
24-27 July 2017

SYMPOSIUM E

International Symposium
on Chemical Engineering





PHOTO-BASED ADVANCED OXIDATION PROCESSES FOR REMOVAL OF PHARMACEUTICAL COMPOUND IN WATER

Sandyanto Adityosulindro ^{a,b}, Laurie Barthe ^b, Henri Delmas ^b, Carine Julcour ^b

^a Civil Engineering Department, Faculty of Engineering, Universitas Indonesia, Kampus UI Depok 16424, Indonesia

^b Laboratoire de Génie Chimique, Université de Toulouse, CNRS, INPT, UPS, Toulouse, France

ABSTRACT

As a consequence of huge consumption, pharmaceutical compounds have been detected in various water compartments, such as wastewater treatment plant effluents or even drinking water. This fact indicates that conventional processes used in water treatment plants (e.g. chemical precipitation and activated sludge) cannot completely eliminate them. In this study, different photo-based advanced oxidation processes (*i.e.* direct photolysis, UV-Vis/hydrogen peroxide and photo-Fenton oxidation) were evaluated for the removal of a non-steroidal anti-inflammatory drug, ibuprofen. It was chosen as model pollutant due to its high consumption worldwide. Its degradation was evaluated by HPLC/UV for pollutant conversion and total organic carbon analyzer for mineralization yield. Low pressure (254 nm) and high pressure (200-600 nm) mercury lamps, as well as xenon lamp (360-740 nm) were used to determine the effect of light irradiation wavelength on photo-oxidation processes. Irradiation with high pressure mercury lamp completely converted ibuprofen in 20 mg/L solution within 60 min and yielded up to 45% TOC removal after 3 hours, while pollutant photolysis was only partial at 254 nm and ineffective under visible irradiation. Addition of H₂O₂ considerably improved ibuprofen degradation rate at 254 nm (due to peroxide photolysis leading to OH[•] radical, while visible light was shown as an efficient activation technique for Fenton oxidation due to photo-regeneration of ferrous ions. In the latter case, final mineralization yield reached 60% in the following conditions: [H₂O₂]₀ = 6.4 mM and [Fe²⁺]₀ = 0.134 mM. Evaluation of electrical energy and oxidant consumptions showed that LP Hg lamps are the most cost-effective for photo-based AOPs. Considering the similarity in light spectrum between xenon lamp and sunlight, solar photo-Fenton oxidation also appears as a promising wastewater treatment process for the remediation of pharmaceuticals, especially in tropical countries such as Indonesia.

Keywords: Water treatment; Light irradiation; Photolysis; Peroxide photo-oxidation; Photo-Fenton; Ibuprofen

1. INTRODUCTION

Water shortage indeed is the main challenge in this millennium. Unfortunately, the availability of clean water is actually dwindling due to rapid population growth and increase of consumption of water per capita. This is exacerbated by development of agriculture and industry. Pharmaceutical industries are the most developed one with more



than 4000 compounds and hundreds of tons of pharmaceutical are commercially produced worldwide each year (Rehman *et al.*, 2015). For instance, in France, more than 3 milliards drug boxes are sold annually (ANSM, 2013) with pharmaceutical market about \$46.2 billion in 2014 (PharmExec, 2017). In Indonesia, pharmaceutical sector will be boosted by the establishment of a national healthcare program, known as the *Jaminan Kesehatan Nasional* with the objective of providing health insurance to 250 million Indonesian citizens by 2019, which would make it the world's largest social health insurance (DDDMAG, 2016). Nevertheless, this program may increase drugs consumption and probably rejection of pharmaceutical active compounds into environment.

Actually, complete elimination of pharmaceuticals by conventional wastewater treatment plants is still a challenge. Physical process such as adsorption and membrane filtration are rather selective and not efficient for hydrophilic pharmaceuticals (Vona *et al.*, 2015; Wang and Wang, 2016). This process is also only pollutant-transfer methods that require a post-destructive process. Chemical oxidation with chlorine and chlorine dioxide are also selective and only effective for pharmaceuticals containing amines functional group (Rivera-Utrilla *et al.*, 2013). Chlorine can also react with other organic compounds and form toxic organochlorinated compounds (Mao *et al.*, 2016). Biological treatments are usually cost-effective but it may be not adequate since some pharmaceutical compounds could be toxic to microorganism (Klavarioti, Mantzavinos and Kassinos, 2009). For instance, anti-inflammatory and analgesic drugs were only partially removed (30 – 75%) by combined settling-activated sludge process (Deblonde, Cossu-Leguille and Hartemann, 2011; Ziylan and Ince, 2011; Rivera-Utrilla *et al.*, 2013). In addition, removal efficiency during this process may be only physical separation process because hydrophobic pharmaceuticals tends to adsorb onto (bio-)suspended solids and accumulated in settling tank (Bouissou-Schurtz *et al.*, 2014). In all cases, partial degradation of pharmaceuticals can be dangerous considering the degradation/transformation products could be more toxic than the parent compounds (Quero-Pastor *et al.*, 2014).

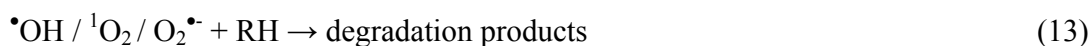
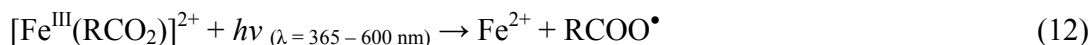
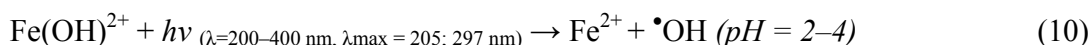
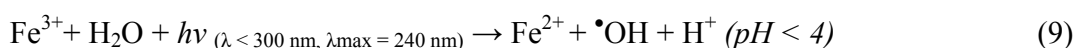
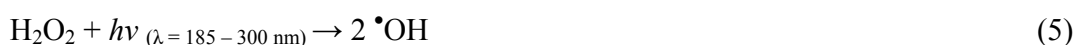
Indeed, various pharmaceutical molecules have been detected in rivers or even drinking waters around the Europe from some ng/L to hundreds µg/L (Ziylan and Ince, 2011; Ortiz de García *et al.*, 2013; Bouissou-Schurtz *et al.*, 2014), indicating the incapability of conventional water treatment plant to remove these compounds. Moreover, the presence of pharmaceuticals in aquatic environment also indicates that direct photo-degradation of pharmaceuticals by sunlight is not effective.

Despite the fact that pharmaceuticals are currently non-regulated and have unclear effect to human health, low concentration-chronic exposure of pharmaceutical compounds can cause ecological impacts *e.g.* toxicity, endocrine disrupting effects and development of microbial resistance, etc. (Bouissou-Schurtz *et al.*, 2014). These facts lead pharmaceutical compounds to become emerging pollutants.

One of the most promising destructive techniques to remove pharmaceutical compounds (PhCs) is advanced oxidation processes (AOPs). AOPs are based on the generation of hydroxyl radical ($\bullet\text{OH}$), a powerful and non-selective oxidant that are capable to degrade and mineralize the organic compounds into water (H_2O) and carbon dioxide (CO_2) as final products. Among AOPs, photo-degradation (reaction (1)–(4) and (13)), photolysis of hydrogen peroxide ($\text{UV}/\text{H}_2\text{O}_2$) (reaction (5) and (13)), Fenton and photo-



Fenton reactions (reaction (6)–(13)) were reported as efficient processes for pharmaceuticals removal (Méndez-Arriaga, Esplugas and Giménez, 2010; Shu *et al.*, 2013).



The aim of this study was to investigate the application of photolysis, photo-H₂O₂ and photo-Fenton oxidation processes for removal of pharmaceutical compounds in water. Ibuprofen (IBP) was chosen as the model pharmaceutical contaminant, considering its high consumption France and Indonesia (ANSM, 2013; McGettigan and Henry, 2013). Various types of lamp as the source of light irradiation were compared including LP Hg lamp, MP Hg lamp and Xenon lamp.

2. METHODOLOGY/ EXPERIMENTAL

2.1. Reagents

Ibuprofen (C₁₃H₁₈O₂; purity 99.99%) was purchased from BASF Corporation and used as received. Hydrogen peroxide (H₂O₂) solution 30% w/w, sodium hydroxide (NaOH) solution 1 M, sulfuric acid (H₂SO₄) solution 1 M, monopotassium phosphate (KH₂PO₄), sodium phosphate dibasic dehydrate (Na₂HPO₄·2H₂O), potassium iodide (KI), titanium



tetrachloride (TiCl_4) solution 0.09 M in 20% HCl, sodium sulfite (Na_2SO_3) and iron sulfate heptahydrate ($\text{FeSO}_4 \cdot 7\text{H}_2\text{O}$) were obtained from Sigma-Aldrich.

2.2. Experimental setup

Experiments were carried out in 1.5 L batch reactor consist of photo-reactor (0.5 L) and auxiliary-reactor (1 L). Circulation of ibuprofen solution between photo and auxiliary reactor was carried out by peristaltic pump (loop system, flow rate of 150 mL/min), giving only 33% of solution irradiated. To maintain a constant temperature (25°C), both reactors were connected to a thermostatic bath. A lamp as a light source was placed into a cylindrical quartz tube installed inside the photo-reactor. The main characteristics of the lamps are given in table 1. It should be mentioned that experiments without light irradiation were conducted only in auxiliary-reactor.

Table 1. Characteristics of UV-Vis lamps

Characteristics	Lamp 1 (L1)	Lamp 2 (L2)	Lamp 3 (L3)	Lamp 4 (L4)
Supplier	Heraeus	Heraeus	Peschl Ultraviolet	Peschl Ultraviolet
Model	GPH150T5L	GPH212T5L/4	TQ150	TXE150
Type	LP Hg	LP Hg	MP Hg	Xenon
λ (nm)	254	254	200 – 600	360 – 740
Electric power (W)	6	10	150	150

2.3. Experimental procedure

Synthetic ibuprofen solution at 20 mg/L (~ 15.12 mg/L TOC) was prepared by dissolving 40 mg of ibuprofen powder in 2 L distilled water and stirred for 14 hours using a magnetic stirrer (600 rpm) at 25°C to ensure complete powder dissolution. This relatively high concentration (compared to that observed in aquatic environment) was chosen considering that application of AOPs is more economical for high contaminant loadings and small volumes (Miralles-Cuevas *et al.*, 2013). A first sample was taken once the desired temperature was reached (referred to as zero time of the reaction) and oxidation was starting by the addition of H_2O_2 . In case of experiment using light irradiation, lamp was turned on 2 min before in order to attain a constant irradiation prior to the oxidation. In case of Fenton reaction, ibuprofen solution was previously mixed with iron salt ($\text{FeSO}_4 \cdot 7\text{H}_2\text{O}$) and the pH was adjusted to 2.6 with 1 M H_2SO_4 and 1 M NaOH. Aliquots samples were withdrawn throughout the reaction ($t = 5, 10, 30, 60, 120, 180$ min). In order to stop the reaction, samples were immediately treated by phosphate buffer (mixture of KH_2PO_4 0.05 M and $\text{Na}_2\text{HPO}_4 \cdot 2\text{H}_2\text{O}$ 0.05 M) before HPLC analysis or quenching solution (mixture of phosphate buffer, KI 0.1 M and Na_2SO_3 0.1 M) before TOC analysis and filtered through $0.45 \mu\text{m}$ RC syringe filter prior to analyses.



2.4. Analytical technique

Ibuprofen concentration during experiments was determined by liquid phase chromatography with UV detection at $\lambda = 222$ nm (PDA detector, Thermo Finnigan). Separation was performed on a C18 reverse phase column (ProntoSIL C18 AQ 5 μ m, 250 x 4 mm) at 40°C. The mobile phase consisted in a mixture of acetonitrile and water (acidified with phosphoric acid at 0.1% v/v) fed in isocratic mode (60/40) at 1 mL/min.

Total organic carbon (TOC) concentration was obtained from the difference between total carbon (TC) and inorganic carbon (IC) measured by a TOC analyzer (TOC-L, Shimadzu Corp.). In this case, samples were diluted by twofold with ultrapure water after addition of the quenching solution and filtrated.

Residual concentration of hydrogen peroxide was determined by titanium tetrachloride method. A 5 mL sample was diluted to 25 mL then mixed with 1 mL TiCl₄ and 1 mL H₂SO₄ solution. After the formation of pertitanic acid (yellow color), hydrogen peroxide concentration was measured spectrophotometrically at 410 nm.

3. RESULTS AND DISCUSSION

3.1. Degradation of ibuprofen under light irradiations

Degradation of ibuprofen was firstly evaluated under different light sources, namely L1, L2, L3 and L4 (see table 1). As shown in figure 1, photo-degradation of IBP was observed under ultraviolet (L1, L2, L3) but very stable under visible light irradiation (L4). These results can be explained by high spectral absorption of IBP in UV-C region ($\lambda = 200 - 280$ nm). An improvement in IBP degradation (40% vs. 73% after 180 min) was observed when higher power lamp was used (L1: LP Hg lamp 6 W vs. L2: LP Hg lamp 10 W). In case of lamp L3, complete removal of IBP can be achieved in 1 hour. It can be attributed to both high lamp power and wide emission spectrum in UV-C region ($\lambda = 200 - 280$ nm). On the contrary, IBP degradation under visible light (L4) was found to be negligible, proving that photo-degradation of IBP by sunlight should be very limited in the natural environment.

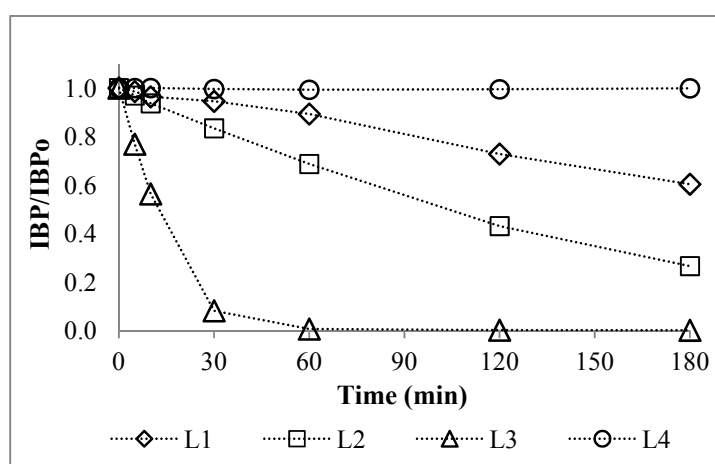


Figure 1. Effect of lamp type on IBP photolysis



Regarding the mineralization yield, 45% of TOC was removed after 3 h of irradiation with L3 lamp, compared to only 19% for L1 and L2 lamp. These findings are in agreement with previous studies reporting TOC conversion less than 50% (Szabó *et al.*, 2011; da Silva *et al.*, 2014).

3.2. Degradation of ibuprofen under light/H₂O₂ processes

Addition of H₂O₂ as radical promoters was also evaluated. According to reaction (5), ultraviolet light can decompose H₂O₂ into $\cdot\text{OH}$. As expected, an enhancement in term of IBP was observed in light/H₂O₂ processes (figure 2) compared to sole light irradiation (figure 1). For instance, first order removal rate constant of IBP under L1 was improved from 0.0028 min⁻¹ to 0.0664 min⁻¹ (24- fold increase). An improvement in degradation rate constant was also observed with L3 lamp resulting in a 5-fold increase of the rate constant (from 0.0567 to 0.261 min⁻¹). Improvement in L1 and L2 was more remarkable compared to L3 because photolysis of IBP was already very effective with L3, and thus H₂O₂ decomposition contributed to a lesser extent to IBP degradation. Regarding mineralization yield, L3/H₂O₂ was the most effective for TOC removal as almost complete mineralization (97%) was achieved after 3 h vs. only 30 and 46% by L1/H₂O₂ and L2/H₂O₂, respectively.

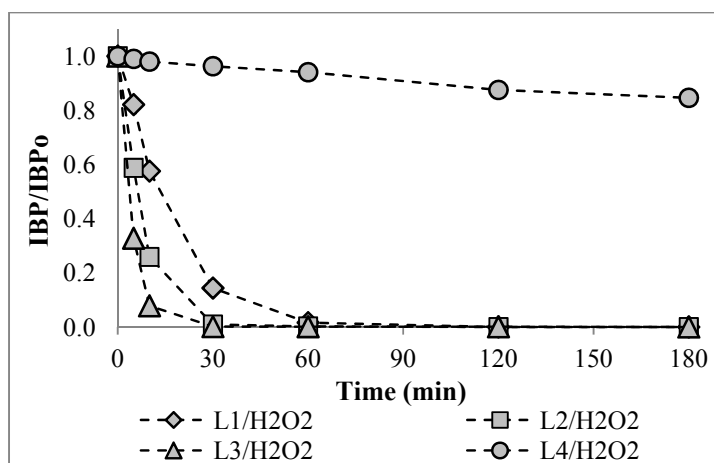


Figure 2. Effect of H₂O₂ addition on IBP photolysis

On the other hand, degradation of IBP under L4/H₂O₂ was not expected due to the negligible absorbance of IBP and H₂O₂ above 280 and 300 nm, respectively. However, according to the manufacturer of the xenon lamp, if 97% of its emission is in the 400-740 nm range, it also exhibits a small portion (3%) at lower wavelength range that might be responsible for 15% of IBP conversion after 3 h. Indeed, H₂O₂ consumption was observed in all cases, from only 5% in L4/H₂O₂ process, up to 99% in L3/H₂O₂ process.

3.3. Degradation of ibuprofen under photo-Fenton processes

In this part, L1 and L4 were selected for photo-Fenton oxidation experiments. L1 (LP Hg lamp 6 W) is interesting considering its low capital cost and low electrical energy consumption, while L4 (Xenon lamp 150 W) spectrum mimics sunlight. Concentration of



Fenton's reagent was set as follows: 0.134 mM of Fe and 6.4 mM of H₂O₂. In addition, Fenton experiment (without light irradiation) was also carried out for comparison purpose. As seen from figure 3, a clear positive effect of ultraviolet light (L1) and visible light (L4) on Fenton reaction was observed. In photo-Fenton processes, more than 95% of IBP removal was observed in 30 min, while 180 min reaction was necessary to achieve similar conversion. Likewise, appreciable TOC conversion was also observed in photo-Fenton giving 82% and 59% for L1/Fenton and L4/Fenton processes, respectively. Indeed, higher H₂O₂ consumption was also observed in photo-Fenton processes (L1/Fenton = 99%; L4/Fenton = 80%) compared to light/H₂O₂ processes (L1/H₂O₂ = 14%; L4/Fenton = 5%) and Fenton (13%) indicating the contribution of reaction of photo-regeneration ferric ion and ferric complexes (reaction (9)–(12)).

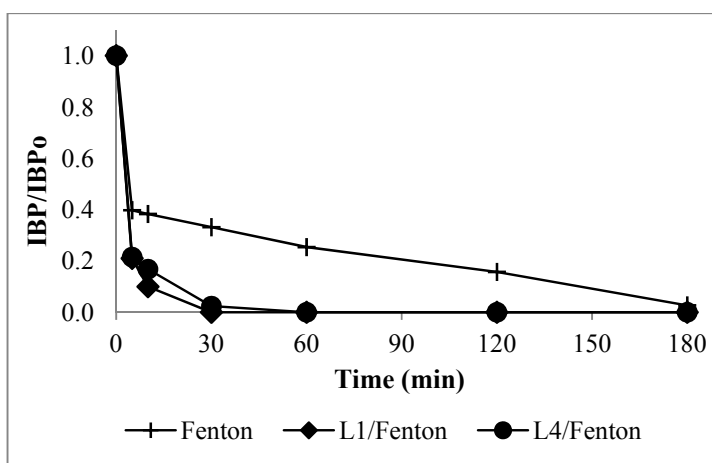


Figure 3. Fenton and photo-Fenton oxidation of IBP

3.4. Evaluation of electric energy and oxidant consumption

Despite the potent oxidation performance, AOPs are also known as more consumptive processes compared to biological process due to the utilization of expensive reagent H₂O₂ and high electric energy consumption. Therefore, a simple economical assessment of the different applied processes was carried out by calculating the electrical energy per order of pollutant removal (EEO) (Bolton *et al.*, 2001). Electric energy per order (EEO) is the electric energy in kilowatt hours (kWh) required to degrade a contaminant C by one order of magnitude in a unit volume, thus smaller value indicates lower energy consumption (high energy efficiency) as shown in following equations:

$$EEO = [P \times t \times 1000] / [V \times 60 \times \log(C_i/C_t)] \quad (14)$$

where *EEO* is the electrical energy per order of pollutant removal (kWh/m³/order), *P* is the power input (kW), *t* is the irradiation time (min), *V* is the volume (L) of the water in the reactor, *C_i* is the initial pollutant concentration (20 mg/L) and *C_t* is concentration of pollutant at reaction time *t*.



In addition, oxidant consumption index (OCI) (Shahbazi *et al.*, 2014) was also calculated in order to taking into account the amount of H₂O₂ consumed for pollutant mineralization. Smaller value of OCI indicates lower oxidant consumption (high oxidant efficiency) as shown in following equations:

$$OCI = \Delta[H_2O_2] / \Delta[TOC] \quad (15)$$

where $\Delta[H_2O_2]$ and $\Delta[TOC]$ are the amount of H₂O₂ consumed and TOC removed during 180 min reaction, respectively.

The EEO and OCI values under different processes are presented in table 2. LP Hg lamps (L1 and L2) were found to be the most cost-effective in photo-based AOPs. It was also clear that the addition of H₂O₂ and Fenton reagent can significantly reduce the energy consumption, while high energy consumption needed in case of L4 can be replaced by sunlight.

Table 2. Electric energy and oxidant consumption

Processes	t _{TOC} (min)	[TOC] _t (mg/L)	EEO _{TOC}	Δ[H ₂ O ₂] (mg/L)	Δ[TOC] (mg/L)	OCI
L1	180	12.2	131	N/A	2.9	N/A
L2	180	12.2	219	N/A	2.9	N/A
L3	180	8.3	1151	N/A	6.8	N/A
L4	180	15.1	N/A	N/A	0	N/A
L1/H ₂ O ₂	180	10.6	77	30.5	4.5	6.7
L2/H ₂ O ₂	180	9.1	90	106.6	7.0	15.2
L3/H ₂ O ₂	180	0.5	197	215.4	14.7	14.6
L4/H ₂ O ₂	180	14.4	13467	10.9	0.8	14.4
L1/Fenton	180	2.7	16	215.4	12.4	17.4
L4/Fenton	180	6.2	775	174.1	9.0	19.4

4. CONCLUSION

The objective of this work was to study ibuprofen degradation in water under photo-based advanced oxidation processes. Four types of lamps as light source were compared including two LP Hg lamps, a MP Hg lamp and a Xenon lamp. Ibuprofen was very stable under visible light irradiation proving its persistency in aquatic environment. On the other hand, ultraviolet irradiation was effective for IBP removal. Addition of H₂O₂ and Fenton reagent significantly enhances not only ibuprofen but also TOC conversion, wherein almost complete mineralization can be achieved in 3 hours (59 – 97%). Evaluation of electrical energy and oxidant consumptions showed that LP Hg lamps are the most cost-effective for photo-based AOPs. Considering the similarity in light spectrum between xenon lamp and sunlight, solar photo-Fenton oxidation also appears as a promising wastewater treatment process for the remediation of pharmaceuticals, especially in tropical countries such as Indonesia.



5. ACKNOWLEDGEMENT

The authors are grateful to ANR (French National Research Agency) for research funding through ANR project “SOFENcoMEM” (ANR-14-CE04-0006) and RISTEKDIKTI (Ministry of Research, Technology and Higher Education of Indonesia) for the scholarship of S. Adityosulindro (Ref. 2017/E4.4/K/2013).

6. REFERENCES

- ANSM (2013) *Analyse des ventes de médicaments en France en 2012*. Available at: http://ansm.sante.fr/var/ansm_site/storage/original/application/796352eff0e9119cca0ea5bbd898353a.pdf (Accessed: 30 January 2017).
- Bolton, J. R., Bircher, K. G., Tumas, W. and Tolman, C. A. (2001) ‘Figures-of-merit for the technical development and application of advanced oxidation technologies for both electric- and solar-driven systems (IUPAC Technical Report)’, *Pure Appl. Chem.*, 73(4), pp. 627–637.
- Bouissou-Schurtz, C., Houeto, P., Guerbet, M., Bachelot, M., Casellas, C., Mauclaire, A.-C., Panetier, P., Delval, C. and Masset, D. (2014) ‘Ecological risk assessment of the presence of pharmaceutical residues in a French national water survey’, *Regulatory Toxicology and Pharmacology*, 69(3), pp. 296–303. doi: 10.1016/j.yrtph.2014.04.006.
- DDDMAG (2016) *Indonesia’s pharmaceutical market to see rapid five year growth*. Available at: <https://www.dddmag.com/article/2016/02/indonesias-pharmaceutical-market-see-rapid-five-year-growth> (Accessed: 7 March 2017).
- Deblonde, T., Cossu-Leguille, C. and Hartemann, P. (2011) ‘Emerging pollutants in wastewater: a review of the literature.’, *International journal of hygiene and environmental health*. Elsevier GmbH., 214(6), pp. 442–8. doi: 10.1016/j.ijheh.2011.08.002.
- Klavarioti, M., Mantzavinos, D. and Kassinos, D. (2009) ‘Removal of residual pharmaceuticals from aqueous systems by advanced oxidation processes.’, *Environment international*. Elsevier Ltd, 35(2), pp. 402–17. doi: 10.1016/j.envint.2008.07.009.
- Mao, Y., Wang, X., Guo, X., Yang, H. and Xie, Y. F. (2016) ‘Characterization of haloacetaldehyde and trihalomethane formation potentials during drinking water treatment’, *Chemosphere*, 159, pp. 378–384. doi: 10.1016/j.chemosphere.2016.05.088.
- McGettigan, P. and Henry, D. (2013) ‘Use of non-steroidal anti-inflammatory drugs that elevate cardiovascular risk: an examination of sales and essential medicines lists in low-, middle-, and high- income countries’, *PLOS Medicine*, 10(2).
- Méndez-Arriaga, F., Esplugas, S. and Giménez, J. (2010) ‘Degradation of the emerging contaminant ibuprofen in water by photo-Fenton.’, *Water research*, 44(2), pp. 589–95.
- Miralles-Cuevas, S., Arqués, A., Maldonado, M. I., Sánchez-Pérez, J. a. and Malato Rodríguez, S. (2013) ‘Combined nanofiltration and photo-Fenton treatment of water containing micropollutants’, *Chemical Engineering Journal*. Elsevier B.V., 224, pp. 89–95. doi: 10.1016/j.cej.2012.09.068.
- Ortiz de García, S., Pinto Pinto, G., García Encina, P. and Irusta Mata, R. (2013) ‘Consumption and occurrence of pharmaceutical and personal care products in the



- aquatic environment in Spain.’, *The Science of the total environment*. Elsevier B.V., 444, pp. 451–65. doi: 10.1016/j.scitotenv.2012.11.057.
- PharmExec (2017) *Slow growth to 2020 for France’s pharma market*. Available at: <http://www.pharmexec.com/slow-growth-2020-frances-pharma-market> (Accessed: 6 March 2017).
- Quero-Pastor, M. J., Garrido-Perez, M. C., Acevedo, A. and Quiroga, J. M. (2014) ‘Ozonation of ibuprofen: a degradation and toxicity study.’, *The Science of the total environment*, 466–467, pp. 957–64. doi: 10.1016/j.scitotenv.2013.07.067.
- Rehman, M. S. U., Rashid, N., Ashfaq, M., Saif, A., Ahmad, N. and Han, J.-I. (2015) ‘Global risk of pharmaceutical contamination from highly populated developing countries’, *Chemosphere*. Elsevier Ltd, 138, pp. 1045–1055. doi: 10.1016/j.chemosphere.2013.02.036.
- Rivera-Utrilla, J., Sánchez-Polo, M., Ferro-García, M. Á., Prados-Joya, G. and Ocampo-Pérez, R. (2013) ‘Pharmaceuticals as emerging contaminants and their removal from water. A review’, *Chemosphere*. Elsevier Ltd, 93(7), pp. 1268–1287.
- Shahbazi, A., Gonzalez-Olmos, R., Kopinke, F.-D., Zarabadi-Poor, P. and Georgi, A. (2014) ‘Natural and synthetic zeolites in adsorption/oxidation processes to remove surfactant molecules from water’, *Separation and Purification Technology*, 127, pp. 1–9. doi: 10.1016/j.seppur.2014.02.021.
- Shu, Z., Bolton, J. R., Belosevic, M. and El Din, M. G. (2013) ‘Photodegradation of emerging micropollutants using the medium-pressure UV/H₂O₂ Advanced Oxidation Process.’, *Water research*, 47(8), pp. 2881–9. doi: 10.1016/j.watres.2013.02.045.
- da Silva, J. C. C., Teodoro, J. A. R., Afonso, R. J. de C. F., Aquino, S. F. and Augusti, R. (2014) ‘Photolysis and photocatalysis of ibuprofen in aqueous medium: characterization of by-products via liquid chromatography coupled to high-resolution mass spectrometry and assessment of their toxicities against *Artemia salina*.’, *Journal of mass spectrometry: JMS*, 49(2), pp. 145–53. doi: 10.1002/jms.3320.
- Szabó, R. K., Megyeri, C., Illés, E., Gajda-Schranz, K., Mazellier, P. and Dombi, A. (2011) ‘Phototransformation of ibuprofen and ketoprofen in aqueous solutions.’, *Chemosphere*, 84(11), pp. 1658–63. doi: 10.1016/j.chemosphere.2011.05.012.
- Vona, A., di Martino, F., Garcia-Ivars, J., Picó, Y., Mendoza-Roca, J.-A. and Iborra-Clar, M.-I. (2015) ‘Comparison of different removal techniques for selected pharmaceuticals’, *Journal of Water Process Engineering*, 5, pp. 48–57. doi: 10.1016/j.jwpe.2014.12.011.
- Wang, J. and Wang, S. (2016) ‘Removal of pharmaceuticals and personal care products (PPCPs) from wastewater: A review’, *Journal of Environmental Management*, 182, pp. 620–640. doi: 10.1016/j.jenvman.2016.07.049.
- Ziylan, A. and Ince, N. H. (2011) ‘The occurrence and fate of anti-inflammatory and analgesic pharmaceuticals in sewage and fresh water: Treatability by conventional and non-conventional processes’, *Journal of Hazardous Materials*, 187(1), pp. 24–36.



15TH INTERNATIONAL CONFERENCE ON QUALITY IN RESEARCH (QIR 2017)

EVALUATION OF TRAY BIOREACTOR TO UPSCALE XYLANASE PRODUCTION USING SOLID STATE FERMENTATION OF OIL PALM EMPTY FRUIT BUNCHES (OPEFB) BY ASPERGILLUS FUMIGATUS

Briantono Djakaria, Tjandra Setiadi*, M.T.A.P. Kresnowati

*Microbiology and Bioprocess Technology Laboratory,
Chemical Engineering Department, Institut Teknologi Bandung*

ABSTRACT

The potential of xylanase production by *Aspergillus fumigatus* using solid state fermentation of oil palm empty fruit bunches (OPEFB) as a low-cost lignocellulosic material has been convincing. Not only have xylanases been prevalently used in pulp and paper industry, but also in food and agricultural industries. In order to upscale the production of xylanase, multiple tray bioreactors (8 cm x 5 cm x 4 cm) have been arranged in an incubator (65 cm x 50 cm x 50 cm), maintained at 32°C and high relative humidity. OPEFB were then mixed aseptically with Prado's media along with *A.fumigatus* spores in tray bioreactors. Since keeping a high level of water activity is one of the main challenges in larger scale enzyme production using tray bioreactors, two factors were explicitly evaluated in this study: solid loading to media ratio as well as different particle sizes of OPEFB. The significance of these factors was assessed so that optimum xylanase activity could be achieved while scaling up enzyme production using tray bioreactor. An optimum xylanase activity of 6.59 U/g OPEFB was obtained at substrate length of 1 – 2 cm and solid loading ratio of 25%.

Keywords: empty fruit bunches; tray bioreactor; solid loading ratio; solid state fermentation; xylanase; xylose

1. INTRODUCTION

Xylanase (EC 3.2.1.8) is the enzyme that hydrolyze the 1,4 – β – D – xylosidic linkages in xylan, i.e. the backbone of hemicellulose. Commonly found in saprophytes, this enzyme is responsible for the degradation of hemicellulosic material. As scientific discovery and technology advances, humans can produce and utilize this enzyme for industrial purposes. In food and agricultural sectors such as bread industry, xylanase is found to improve crumb structure and bread volume. Not only does it improve the quality of the product, it also helps to reduce the stickiness of the bread dough. This ultimately reduces the case where dough gets stuck to the machinery parts, thus improving the lifetime of the machineries (Butt, et al., 2007). On the other hand, xylanase is also utilized in wine and juice industries to clarify wine and juices. The

* Corresponding author.
E-mail address: tjandra@che.itb.ac.id



same enzyme has also been used prevalently in pulp and paper industry, where it helps to enhance the bleachability of the paper, thus reducing the consumption of chlorine chemicals in bleaching process (Buchert, et al., 1994).

This enzyme is commonly produced using Submerged Fermentation (SmF), where the substrate xylan is dissolved in liquid media along with the suspension of microorganism. However, this conventional method requires more expensive pure substrate as well as strict aseptic condition. On the other hand, an alternative method to produce xylanase is using Solid State Fermentation (SSF). SSF is a mean to grow microorganism on moist solid particles; where the desired substrate (xylans in hemicellulose) to produce xylanase is abundant (Mitchell, et al., 2006). The microorganisms of choice, commonly saprophytes such as filamentous fungi, naturally live on this condition. When decomposing solid substrates as carbon source, the desired enzyme is released to the surroundings of the fungi as an extracellular product. Many scholars and industries are starting to look at SSF as a viable alternative to produce meaningful microbial products due to the cheap raw material as substrates for SSF (Jou & Lo, 2011). To produce high concentration of xylanase, one should choose lignocellulosic material with high hemicellulose content such as corn cobs (Pointner, et al., 2014), rice bran (Mohseni, et al., 2012), palm fiber (Sounders & Walker, JR, 1968), and oil palm empty fruit bunches (Mardawati, 2015). These materials are often considered waste to many industries and therefore could be obtained with low to no cost at all. Moreover, it has been reported that SSF could also yield the same product with significantly higher productivity compared to SmF (Motta, et al., 2013).

To produce xylanase with SSF, it is important to decide upon which solid substrate to work with. One of the potential solid substrate is Oil Palm Empty Fruit Bunches (OPEFB) due to its high hemicellulose content. The composition of OPEFB is 43.39% cellulose, 23.3% hemicellulose, 21.69% lignin, and 11.62% other components (Mardawati, 2015). The second important reason is due to the availability of OPEFB in Indonesia. Being the largest producer of palm oil in the world, Indonesia supplied nearly 32.5 million tons of palm oil in 2015 (Indonesia Investments, 2016). However, in the process of separating the fruit from bunches called threshing, almost 7 million tonne of OPEFB is incinerated annually. Instead of incineration, utilization of OPEFB as solid substrate for potential large scale enzyme production is promising.

In 2015, Mardawati reported optimizations of xylanases production in Erlenmeyer scale and investigated the factors thoroughly. The study investigated xylanase production using different species of fungi, optimum cultivation period, as well as temperature (Mardawati, 2015). Another similar investigation by Lashkmi reported their study on the optimization of xylanase production by *Aspergillus fumigatus* and *Aspergillus terreus* using different parameters such as pH, particle size, moisture content and fermentation period. They successfully achieved an improvement of xylanase enzyme productivity to 2.8 folds (Lakshmi & Shetty, 2011). These investigations, however, were done in an Erlenmeyer scale.

In order to increase the production capacity of xylanase production, the study of scaling up the xylanase production must be done. However, scaling up of SSF comes with different sets of problems, with low water activity being one of the crucial factors (Mitchell, et al., 2006). Even though microorganisms live on the surface of the solid



substrate, water is still crucial to support the metabolism of the microorganism. It acts as a solvent for nutrient and metabolic products even in SSF. Low water activity will negatively affect the activity of enzyme and biomass production since all of the metabolic activity happens in water (Mitchell, et al., 2006).

In this study, the bioreactor of choice is the tray bioreactor, where different aspects contributing to maintain water activity were assessed. Xylanase production by *Aspergillus fumigatus* were conducted in multiple tray bioreactors (8 cm x 5 cm x 4 cm). They were arranged in an incubator (65 cm x 50 cm x 50 cm) at high relative humidity (80 – 90%). The effects of solid loading ratios (SLRs) and OPEFB sizes were evaluated in this study via the activity of xylanase and growth of the microorganism.

2. MATERIALS AND METHODS

2.1 Microorganism

Aspergillus fumigatus was isolated in our laboratory from Oil Palm Empty Fruit Bunches (OPEFB), which was identified and deposited as *A.fumigatus* at Microbiology and Bioprocess Technology Laboratory, Chemical Engineering Department, Institut Teknologi Bandung, Indonesia. Immobilized *A.fumigatus* spores on rice were used as inoculum for the solid state cultivation experiments in the study.

2.2 Solid Substrate and Tray Preparation

OPEFB were washed and dried at 105°C in the oven overnight. The fibres were cut into different length: 1–2 cm and 3–5 cm. To achieve such sizes, waring blender was used as necessary. 10 g of the cut OPEFB were placed in the aluminum food trays (8 x 5 x 4cm). A total of 6 holes with a diameter of 3mm (2 on each of the 8cm side and 1 on each of the 4cm side) were then made using a nail on the top part of the tray. The trays were then closed with aluminum foil and sterilized using an autoclave at 121°C for 15 minutes.

2.3 Fermentation and Extraction Media Preparation

The fermentation medium was made according to Prado by mixing 1.5g of NH₄SO₄, 2g of KH₂PO₄, 0.3g of urea, 0.03g of CaCl₂, 0.2g of MgSO₄.H₂O and H₂O to 1L (Prado, et al., 2010). The extraction medium used in the experiment was 50mM citrate buffer at pH 5. Both media were sterilized using an autoclave at 121°C for 15 minutes.

2.4 Solid State Fermentation

The solid state fermentation was conducted in a temperature controlled incubator at 32°C. The humidity of the incubator was kept by placing containers filled with sterile water near a fan. The solid-state fermentation setup is shown in Table 1.



Table 1 – Solid State Fermentation Setup

Trials	1 – 2 cm		mixed		3 – 5 cm	
OPEFB	10 g of 1 – 2 cm OPEFB		5 g of 1 – 2 cm and 5 g of 3 – 5 cm OPEFB		10 g of 3 – 5 cm OPEFB	
Fermentation Media in mL (SLR in %)	20 mL (50%)	40 mL (25%)	20 mL (50%)	40 mL (25%)	20 mL (50%)	40 mL (25%)
Spores	10 ⁶ viable spores / gram OPEFB					

The sterilized OPEFB trays were cultivated aseptically with the mixture of dried *A. fumigatus* 10⁶ viable spores/ g OPEFB and fermentation medium as shown in the Table 1. The serene wrap was used to close the tray without closing the 3 mm openings in each tray. The trays were then incubated for 7 days.

2.5 Sampling

Samples were collected at the end of the fermentation period. Aseptically, 80mL of extraction medium was mixed in each tray and shaken for 2 hours using laboratory shakers to ensure complete extraction of the desired enzyme. Thereafter, the fermented OPEFB were squeezed through cheesecloth to collect residual extract. The extract was then collected and centrifuged at 6000 rpm for 15 minutes at 4°C. The supernatant was collected as a extracellular protein solution, used as crude enzyme.

2.6 Protein Analysis

Protein analysis was done using Bradford assay (Bradford, 1976). The extract before centrifugation was analyzed as the total protein content, while the supernatant after centrifugation was quantified as extracellular protein content. The supernatant was used as the crude enzyme solution. The difference between the two was considered as the cell protein content (ISU Protein Facility, 2017).

2.7 Xylanase Activity Analysis

The xylanase activity was analyzed by DNS method specified in NREL 42628 (Adney & Baker, 2008) by using xylan from corncob (CAS 9014-63-5). The enzyme was incubated with 0.1% xylan at 50°C for 15 minutes. The absorbance was measured at 540nm.

3. RESULTS AND DISCUSSIONS

3.1 Influence of Different OPEFB Particle Sizes and Solid Loading Ratios on Cellular Growth

Due to the nature of the fungus growth on solid substrate, direct cell quantification is impossible. Therefore, protein determination was utilized to indirectly quantify growth after the fermentation period ends. Figure 1 summarizes the average cell protein after 7 days of fermentation period. The highest cell content was shown by mixed OPEFB with



25% SLR at 1.13 mg protein/g EFB; while the lowest was shown by mixed OPEFB with 50% SLR at 0.37 mg protein/g EFB.

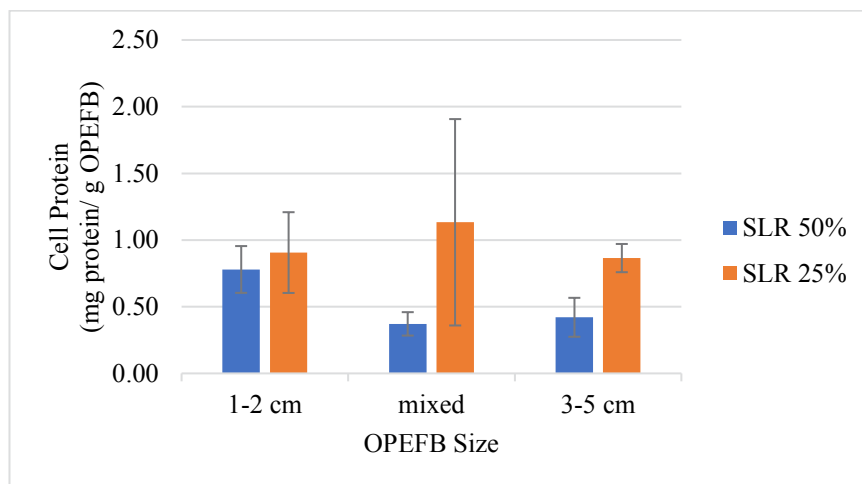


Figure 1 - Average Cell Protein with Different Substrate Sizes and SLRs

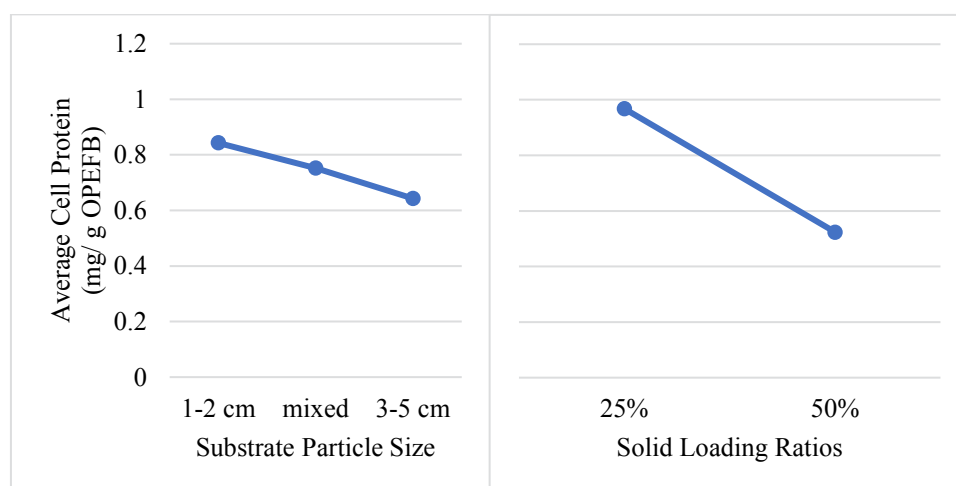


Figure 2 - Effects of Different Substrate Sizes and SLRs on Cell Protein

Figure 2 summarizes the effects of different OPEFB sizes on cell growth. The optimum substrate size for cell growth was 1 – 2 cm. On the other hand, 3 – 5 cm OPEFB size resulted in the poorest cell content among the three. It was predicted that the shorter OPEFB length affected the moisture content in each tray. Shorter length retained the fermentation media better, providing sufficient water activity to support cell growth. Larger OPEFB length were expected to not only have higher O₂ and heat transfer capability, but also low moisture holding capacity. Consequently, the mixed OPEFB size produced higher concentration of cell than large sized OPEFB (3 – 5cm) because the smaller OPEFB in the mixture helped to maintain the moisture needed for growth, as well as the 3-5cm OPEFB provided higher O₂ and heat transfer capability. Nevertheless, whether the mixture of OPEFB sizes could help to maintain moisture was heavily dependent to the homogeneity of the mixture in the tray bioreactor. Homogeneity itself is already a known issue, as it is already hard enough to minimize substrate gradient in SFF. The large error bar in the tray with mixed OPEFB with 25%



SLR addresses the issue even further; as the combination of mixed sizes of OPEFB and lower SLR created problems in both uneven substrate distribution as well as significant moisture gradient.

Figures 1 and 2 clearly shows the correlation between the growth of the fungi and solid loading ratio (SLR): higher solid loading ratio shows less growth compared to its pair. Tray with 1-2 cm OPEFB (50%) and 3-5 cm OPEFB (25% and 50% SLR) had their fermentation media mostly evaporated due to the heat generated by fungal metabolism. At the end of the fermentation period, the solid substrates were rather dry on these trays. On the other hand, the rest of the trials had higher amount of fermentation media at the end of the fermentation period. Higher amount of fermentation media indicated that the solid substrate was kept moist in the trays even after 7 days of fermentation. This phenomenon was seen in trays with 1-2 cm OPEFB at 25% SLR and mixed OPEFB at both SLRs which therefore were reflected in the higher amount of the cells quantified. It was concluded that the maximum solid loading ratio to support cellular growth is 25%.

3.2 Influence of Particle Sizes and Solid Loading Ratios on Xylanase Activity

Similar trend could be observed in the extracellular protein content. Figure 3 shows that the lowest extracellular protein content is found in 3-5 cm OPEFB tray with 50% SLR at 0.185 mg protein/g OPEFB; while the highest is found in mixed OPEFB tray with 50% SLR at 0.396 mg protein/g OPEFB.

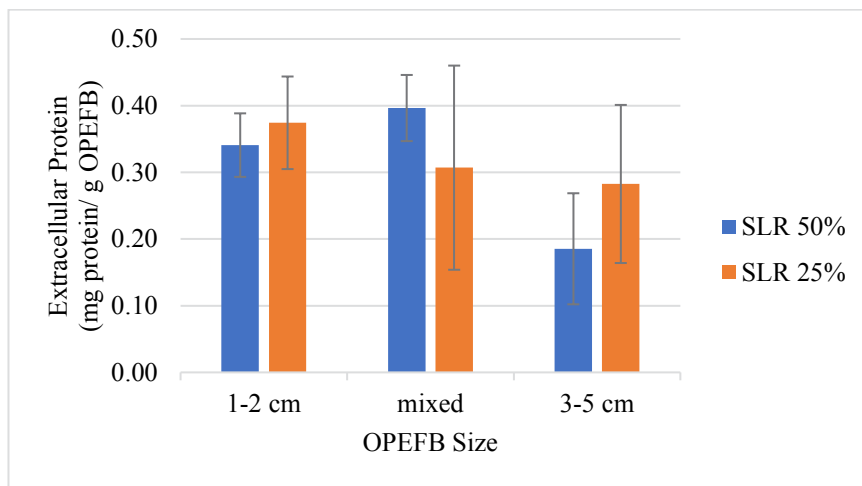


Figure 3 - Average Extracellular Protein Content with Different Substrate Sizes and SLRs

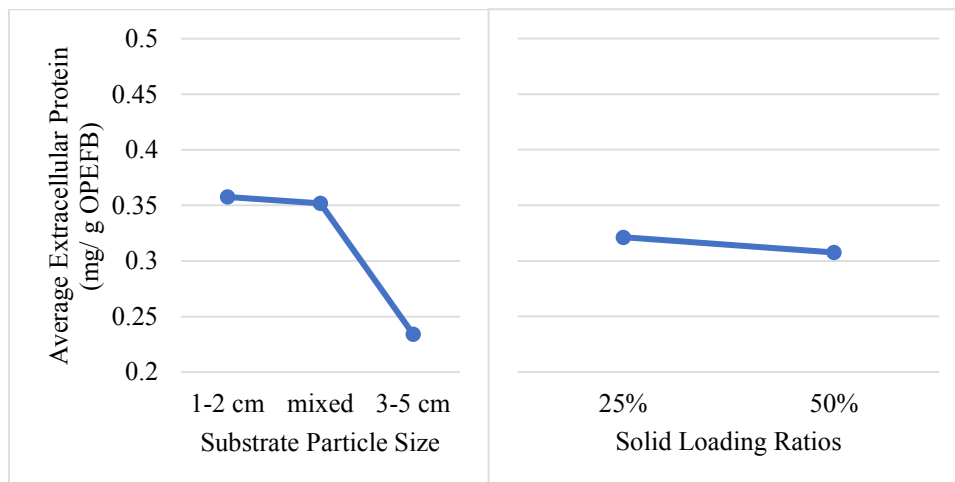


Figure 4 - Effects of Different Substrate Sizes and SLRs on Enzyme Protein

According to figure 4, however, the OPEFB length is the more significant factor in the amount of extracellular protein produced. However, microbes in trays with mixed OPEFB sizes produced nearly identical concentration of extracellular protein compared to trays with 1 – 2 cm OPEFB. There was no significant difference in extracellular protein production between 1 – 2 cm and mixed substrate size.

It was expected that lower the SLR would produce higher concentration of extracellular protein. While trays containing 1 – 2cm OPEFB and 3-5cm OPEFB followed this SLR trend, tray containing mixed EFB size with 50%SLR contained more protein that its pair (tray containing mixed EFB size with 25% SLR). This phenomenon might be caused by inconsistent substrate mixture as mentioned previously.

Although high content of enzyme protein looks promising, the aim of this study is to produce high concentration of xylanase. Some of the extracts might have high extracellular protein content but have low xylanase activity. On the other hand, other extracts may show lower protein content but higher xylanase activity. The specific activity of the produced xylanase was measured and summarized in figure 5.

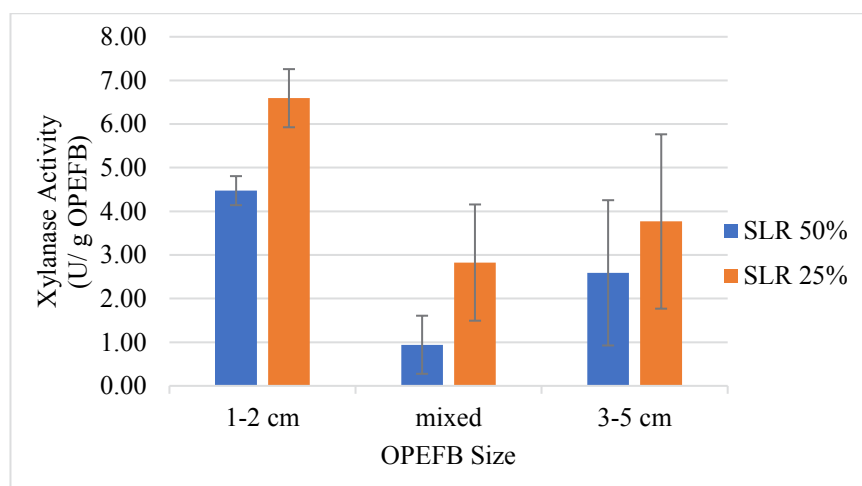


Figure 5 - Average Xylanase Activity with Different OPEFB Substrate Sizes and SLRs



The average highest xylanase activity was shown in tray containing 1-2cm EFB size with 25% SLR at 6.59 U/g EFB, while the lowest was found in tray containing mixed EFB sizes with 50% SLR at 0.94 U/g EFB. Although tray containing mixed size EFB with 50% SLR produced the highest extracellular protein as shown in figure 4, the extracellular protein produced was not the desired enzyme.

All trays clearly demonstrated that lower SLR produced higher xylanase activity. Solid loading ratio affected xylanase production significantly; similar to how it affected cell growth and extracellular protein content. This was due to the fact that xylanase is one of the growth associated enzyme. Furthermore, different substrate sizes also affected xylanase activity distinctively. The shorter length (1 – 2cm) produced a higher xylanase activity (tray A and B) compared to the other treatments as shown in figure 6.

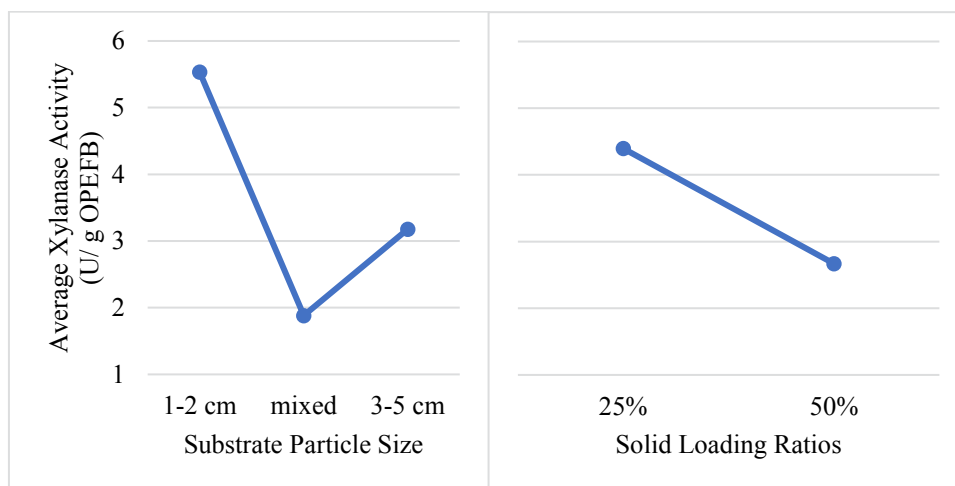


Figure 6 - Effects of Different Substrate Sizes and SLRs on Enzymatic Activity

Figure 6 summarizes the effects of different OPEFB sizes and SLRs on xylanase activity. The shorter substrate length (1 – 2 cm) produced the highest concentration of xylanase. Even though the extracellular protein content of mixed substrate fermentation was almost as high as the 1 – 2 cm substrate (Figure 4), the xylanase activity of the mixed substrate fermentation was the lowest. One of the possible reason was that most of the enzymes produced by the mixed substrate fermentation was other enzymes that hydrolyze cellulose in the substrate.

4. CONCLUSIONS

Solid loading ratio was shown to be the factor that affected cell growth as well as xylanase production in solid state fermentation of Oil Palm Empty Fruit Bunches. This study concludes that optimum cell growth of *A. fumigatus* and xylanase production were achieved at 25% solid loading ratio. Secondly, the size of OPEFB affected the cell growth as well as xylanase activity. The optimum substrate size is 1 – 2 cm because it helps to keep the moisture in the tray, as well as maintaining high water activity needed for the metabolism of *A. fumigatus*.

Unfortunately, some of the data points in figure 1, 3, and 5 contain large error bars. In addition to the limitation of homogeneity when working with solid substrates as mentioned before, other source of error such as inconsistency of solid spore cultivation



as well as extraction methods could affect the consistency of the data. Even though the methods were kept consistent, human errors were most likely responsible for these phenomena.

At the optimum conditions conducted, the xylanase activity achieved was 6.59 U/g OPEFB. Future studies should investigate and optimize the tray bioreactor size and configuration in order to support the growth of the microorganism better.

5. REFERENCES

- Adney, B. & Baker, J., 2008. *Measurement of Cellulase Activities*, s.l.: National Renewable Energy Laboratory.
- Bradford, M. M., 1976. *A Rapid and Sensitive Method for the Quantitation of Microgram Quantities of Protein Utilizing the Principle of Protein-Dye Binding*, Athens: Analytical Biochemistry.
- Buchert, J., Tenkanen, M., Kantelinen, A. & Viikari, L., 1994. Application of Xylanases in the Pulp and Paper Industry. *Bioresource Technology*, pp. 65-72.
- Butt, M. S., Tahir-Nadeem, M., Ahmad, Z. & Sultan, M. T., 2007. Xylanases and Their Applications in Baking Industry. *Food Technology and Biotechnology*, pp. 22-31.
- Chen, H., 2014. *Biotechnology of Lignocellulose*. Dordrecht: Springer.
- Indonesia Investments, 2016. *Minyak Kelapa Sawit*. [Online]
Available at: <http://www.indonesia-investments.com/id/bisnis/komoditas/minyak-sawit/item166>
- ISU Protein Facility, 2017. *Introduction to Protein Techniques*, s.l.: s.n.
- Jou, R. Y. & Lo, C. T., 2011. Heat and Mass Transfer Measurements for Tray-Fermented Fungal Products. *International Journal of Thermophysics*, pp. 523-536.
- Koba, Y. & Ishizaki, A., 1990. Chemical Composition of Palm Fiber and Its Feasibility as Cellulosic Raw Material for Sugar Production. *Agricultural and Biological Chemistry*, pp. 1183 - 1187.
- Lakshmi, G. S. & Shetty, P. R., 2011. Sustainable bioprocess evaluation for xylanase production by isolated *Aspergillus terreus* and *Aspergillus fumigatus*. *Current Trends in Biotechnology and Pharmacy*, October, Volume 5, pp. 1433-1444.
- LookChem, 2008. *A General introduction to Xylitol*. [Online]
Available at: <http://www.lookchem.com/Chempedia/Health-and-Chemical/15625.html>
[Accessed 17 April 2016].
- Mardawati, E., 2015. *Produksi Xilitol dari Tandan Kosong Sawit melalui Proses Hidrolisis Enzimatis dan Fermentasi*. Bandung(West Java): s.n.



Mitchell, D. A., Krieger, N. & Berovic, M., 2006. *Solid-State Fermentation Bioreactors*. Berlin: Springer.

Mohseni, S., Najafpour, G. D., Vaseghi, Z. & Mahjoub, S., 2012. Solid State Fermentation of Agricultural Residues for Lipase Production in a Tray - Bioreactor. *World Applied Sciences Journal*, pp. 1034-1039.

Motta, F. L., Andrade, C. C. P. & Santana, M. H., 2013. A Review of Xylanase Production by the Fermentation of Xylan: Classification, Characterization, and Applications.

Natural Habitats, 2013. *Red Palm Oil Extraction Process*. [Online]
Available at: http://www.natural-habitats.com/en/blog/red_palm_oil_extraction_process/

Pointner, M. et al., 2014. Composition of Corncobs as a Substrate for Fermentation of Biofuels. *Agronomy Research*, pp. 391-396.

Prado, H. et al., 2010. Screening and Production Study of Microbial Xylanase Producers from Brazilian Cerrado. *Applied Biochemistry and Biotechnology*, Volume 161, pp. 333-346.

Sekretariat Panitia Teknis Sumber Energi, 2006. *Blueprint Pengelolaan Energi Nasional 2006 - 2025*, Jakarta: s.n.

Sounders, R. M. & Walker, JR, H. G., 1968. *The Sugars of Wheat Bran*, Albany: Western Regional Research Laboratory.



FORMULATION OPTIMIZATION AND CHARACTERIZATION OF COPOLYMER ACRYLAMIDE-(2-ACRYLAMIDO-2-METHYLPROPANESULFONIC ACID) FOR ENHANCED OIL RECOVERY (EOR)

A. Z. Abidin¹, I. A. Suryawijaya¹, A. Indiarni¹, D. A. Trirahayu¹

¹Department of Chemical Engineering, Faculty of Industrial Technology, Institut Teknologi Bandung, Jl. Ganesa 10 Bandung, Indonesia 40132

ABSTRACT

Copolymers have been synthesized from acrylamide (AM) and 2-Acrylamido-2-methyl propane sulfonic acid (AMPS) that will be used for Enhanced Oil Recovery application. The polymerization had been performed for 6 hours at ambient pressure and temperature, using nitrogen as purging gas, with variation of AM:AMPS mass ratio 60:40, 65:35, 70:30, and 75:25. The initiator used in this experiment was a mixture of ammonium persulfate and sodium thiosulfate with a total weight of 0.35% from the monomers total weight. The product of the polymerisation is a gel material that will be dissolved in water and characterized. There are three analysis that performed to characterize the polymerization product: IR spectrum analysis (testing with FTIR), thermal degradation analysis (testing with TGA-DSC), and viscosity analysis. The results of this study indicate that the best mass ratio formula of AM:AMPS that produces the best viscosity for EOR is 65:35. The synthesized AM-AMPS copolymer solution has good resistance to salt and high temperature but has pseudo plastic properties. Viscosity of the solution decreased every day during storage and stopped declining after 30 days of storage. This characteristic shows suitability of the synthesized AM-AMPS copolymer for EOR applications.

Keywords: Acrylamide, AMPS, EOR, Salinity, High temperature

1. INTRODUCTION

The world consumption of petroleum keeps increasing. As predicted by the International Energy Agency (IEA), the consumption will increase by 54% in the first 25 years of the 21st century in line with the amount of oil production is predicted to decline by 3% each year. Petroleum needs will no longer be met by conventional exploration methods. One promising method to anticipate this is the Enhanced Oil Recovery (EOR) that allows the oil recovery increased by around 20% [1]. The basic principle of EOR is the injection of a substance into the reservoir to push the oil out. EOR consists of several ways such as water flooding, chemical injection, gas injection, and heat injection [1]. In the process of chemicals injection, the common material used is a polymer. EOR methods that use polymer called polymer flooding, a method in which a water-soluble and high molecular mass polymer added to the injection water to increase the viscosity and decrease the mobility ratio of injection water to oil that transferred [2]. This technology causes the water in the reservoir thickened so that the amount of water that is carried out together with the oil decreases. But, EOR still has not provide optimum results due to problems related with the viscosity decreasing at high temperature and salinity.

A study of acrylamide (AM) polymerization with some monomers such as sodium 2-Acrylamido-2 methyl propane sulfonate (Na-AMPS), N-vinylpyrrolidone (N-VP), sodium 3-acrylamide 3-methyl butyrate (Na -AMB), and N-vinyl amide (N-VAM), showed that AM-AMPS copolymer has the highest viscosity compared to three other polymers. However, the viscosity of the polymer is not stable at high temperature and salinity so that more research is needed to improve the viscosity stability by copolymerization of acrylamide (AM) with the AMPS [2]. Abidin and Elsadik [3] studied the AM-AMPS copolymerization by variations of AM:AMPS monomer ratio, 90:10, 80:20, and 70:30. The last composition produce copolymer with high viscosity and fairly stable at high temperature and high salinity. Copolymer solution viscosity has tendency to increase along with copolymer ratio AM: AMPS 90:10, then 80:20, to the highest is 70:30. However, the study did not go further in optimization of AM-



AMPS copolymer formulations. Moreover, the characterization performed on the study still limited to the temperature, salinity, IR, and TGA-DSC test. Therefore, further research is needed to optimized AM-AMPS copolymer formulation and characterization of copolymers more, like a test of shear rate and aging.

This study aims to synthesize polymers for EOR applications that are water soluble, have good viscosifying ability, and resistance to salinity and high temperature. In particular, this study aims to synthesize AM-AMPS polymers using ammonium persulfate and sodium thiosulfate as initiator, perform the optimization of the formulation and conduct characterization of synthesized copolymers.

2. EXPERIMENT

The experiments consist of two stages: the polymer synthesis and analysis. Before the analysis stage, all samples are sorted to obtain polymer formulations of AM and AMPS that produces the best viscosity for EOR. The analysis stage consisted of IR spectrum, thermal degradation, and the viscosity analysis. The viscosity analysis of polymer solution is done by looking at the effects of time, shear rate, temperature, salinity, and concentration against the viscosity of polymer solution.

2.1. Polymer Synthesis Stage

Polymer synthesis stage: assembling experiment tool for polymerization, dissolving monomer AM and AMPS in water, dissolving the initiator in water, the reactor purging with nitrogen, mixing and reaction stages. The experiment tool as in Figure 1. Polymerization was carried out for 6 hours at room temperature with a variation of the AM:AMPS mass ratio 60:40, 65:35, 70:30, and 75:25. The initiator used was a mixture of ammonium persulfate and sodium thiosulfate with a total weight 0.35% of the monomers total weight.

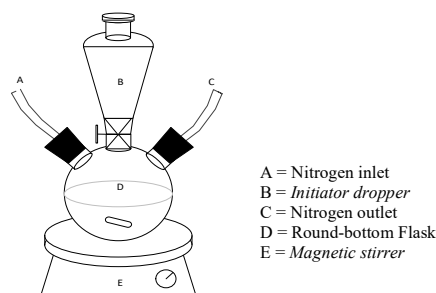


Figure 1 Polymerization experiment tool

2.2. Analysis Stage

There are three analysis that performed: IR spectrum analysis (test with FTIR), thermal degradation analysis (testing with TGA-DSC), and viscosity analysis (see the effects of time, shear rate, temperature, salinity, and concentration on the viscosity polymer solution).

2.2.1. IR Spectrum Analysis

FTIR testing is done on AM-AMPS copolymer to identify the occurrence of the polymerization reaction. The peaks of the FTIR results are compared with peaks in the constituent monomers (AM and AMPS).

2.2.2. Thermal Degradation Analysis

Analyses were performed by Thermogravimetry Analysis (TGA) integrated with Differential Scanning Calorimetry (DSC). Polymers tested in the temperature range 25°C to 550°C with temperature increased by 10 °C / min.

2.2.3. Viscosity Analysis

The viscosity analysis of the polymer solution is done by observing the effect of five factors: time, shear rate, temperature, salinity, and concentration on the viscosity of the polymer solution.



2.2.3.1. Time Effect

Viscosity of the copolymers AM-AMPS solution is measured using a Brookfield viscometer every day for 50 days. To avoid the impact of specific spindle value on the results, the angular velocity test was done by varying the angular velocity of the spindle at range 6 rpm to 60 rpm.

2.2.3.2. Shear Rate Effect

Viscosity of the AM-AMPS copolymers solution is measured using a Brookfield viscometer with varying spindle speeds: 2, 6, 20, 30, 50, and 60 rpm). To avoid its impact of the particular concentration value of the solution on the result, the test was done at a concentration of 1000 ppm solution of the copolymer and 3000 ppm.

2.2.3.3. Temperature and Salinity Effect

Viscosity of the AM-AMPS copolymers solution is measured using a Brookfield viscometer at various temperatures and salinity variations. Variations in temperature used was 25 °C, 45 °C and 75 °C while the variation of salt levels are 0%; 0.05%; 0.15%; and 0.25%-weight. Tests were also conducted on commercial polymer 1130 and 1130 W and later will be compared with AM-AMPS.

2.2.3.4. Concentration Effect

Viscosity of the AM-AMPS copolymers solution is measured using a Brookfield viscometer with varying concentrations of copolymer solution: 1000, 2000, 3000, and 5000 ppm. To avoid the impact of specific spindle value on the results, angular velocity test was done by varying the angular velocity of the spindle at range 6 rpm to 60 rpm.

3. RESULT AND DISCUSSION

3.1. AM:AMPS Composition Ratio Effect

From the four of AM-AMPS copolymers created, we want to know which ones has highest viscosity and be selected to test further. The four polymers were tested at concentrations 13333.33 ppm using spindle 5 at 6 rpm and 50 rpm. Tests carried out on more than one value of rpm to prove the consistency of the test results. The test results are shown in Figure 2.

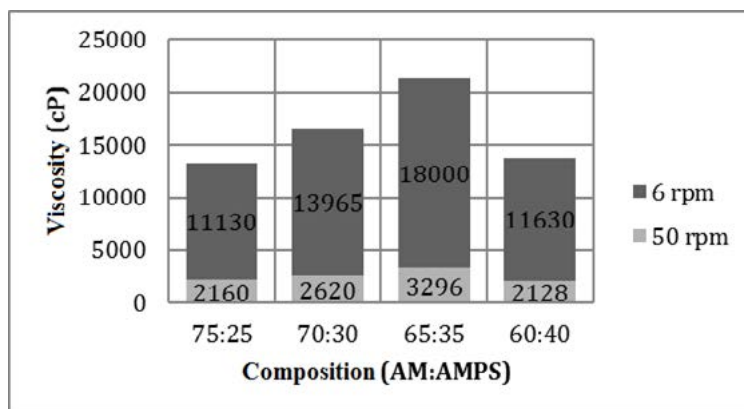


Figure 2 AM:AMPS composition effect

From result, it can be seen that along with increasing of AMPS concentration, initially viscosity is increasing. However, after passing through the AMPS composition of 35%, increasing the number of AMPS resulted in decreased viscosity. This shows that there is a value of composition ratio of AM:AMPS that produce optimum viscosity. From this research, the optimum ratio is AM:AMPS with composition 65:35.

In the AM-AMPS copolymer, AMPS contribute to increase the solubility of the polymer in water and the viscosity of the polymer solution. Nonionic acrylamide-based polymer has a low solubility in water so that when copolymerized with anionic AMPS will produce copolymers with higher solubility in water



[4]. Meanwhile, the viscosity of a polymer solution can be increased by the addition of AMPS caused by four main reasons: the extension of molecular chains, SO_3^- group contained in AMPS (anionic polymer), and the association of hydrophobic groups. Extension of the molecular chain will increase the molecular mass of the solution and result in an increase in viscosity. The negative charge (SO_3^-) chains AMPS side suffered electric Repulsion one another that causes hydrodynamic volume increase (expansion of molecular chains), which later resulted in increased of viscosity. In addition, SO_3^- group also increase steric hindrance which significantly reduces hydrolysis. Meanwhile, there is also the association of hydrophobic groups AMPS either intramolecular hydrophobic associations or intermolecular hydrophobic associations that contribute significantly to the increased of viscosity.

However, there is an optimum number of AMPS used. When used exceeds the optimum, will lead to overloading that causes the polymer charge Repulsion is too large and hydrophobic associations weaken, causing the viscosity decreases [4]. In addition, the repulsion charge is too big and steric hindrance inhibits radical polymer collision molecular chain so the elongation reaction does not occur [5]. This resulted in molecular mass decreases causing viscosity also decreased.

3.2. IR Spectrum Analysis

The analysis is done by identifying the bonds according to the structure of acrylamide. Wave numbers 626.87 s^{-1} and 987.55 s^{-1} indicates the group $\text{C}=\text{C}$ double bond. While the amide groups (NH_2) is shown in wave numbers peak at 657.73 s^{-1} and 1610.56 s^{-1} . $\text{C}=\text{O}$ group in which carbon atoms are also bound to the amide groups (NH_2) is shown in the wave number 3190.26 s^{-1} . The same analysis was performed on the IR spectrum of 2-Acrylamido-2-methylepropanesulfonic acid (AMPS). The analysis showed functional groups corresponding to the AMPS structure theoretically. Sulfonate group ($-\text{SO}_3^-$) that binds with H atoms are shown in wave numbers 1043.49 s^{-1} ; 1128.36 s^{-1} ; and 1159.22 s^{-1} . While the $\text{C}=\text{C}$ double bonds are in wave numbers 626.87 s^{-1} . Group $\text{R}-\text{CH}_2-\text{S}$ shown in wave numbers 2947.23 s^{-1} and secondary amide bond group ($-\text{NH}-$) are shown in the wave number 3427.51 s^{-1} .

The IR spectrum analysis of synthesized AM-AMPS copolymer (Figure 3) results show the groups in the AM-AMPS copolymer and the monomers constituent are Acrylamide and AMPS. Sulfonate group ($-\text{SO}_3^-$) at wave number 1039.63 s^{-1} and secondary amide groups ($-\text{NH}-$) at wave number 3466.08 s^{-1} are clusters of AMPS monomer. While the amide groups (NH_2) at wave number 1633.71 s^{-1} is a group of Acrylamide monomer. This indicates that these polymers composed of constituent monomers are Acrylamide and AMPS. Another analysis is done by comparing the group of unsaturated $\text{C}=\text{C}$ from IR spectrum results of Acrylamide and AMPS with the IR spectrum results of the polymer synthesized (AM: AMPS). In the IR spectrum of AM-AMPS copolymer synthesis result, there are no peak from the group of unsaturated $\text{C}=\text{C}$. This shows that the polymerization between Acrylamide and AMPS has occurred as indicated by the termination of the $\text{C}=\text{C}$ double bond.

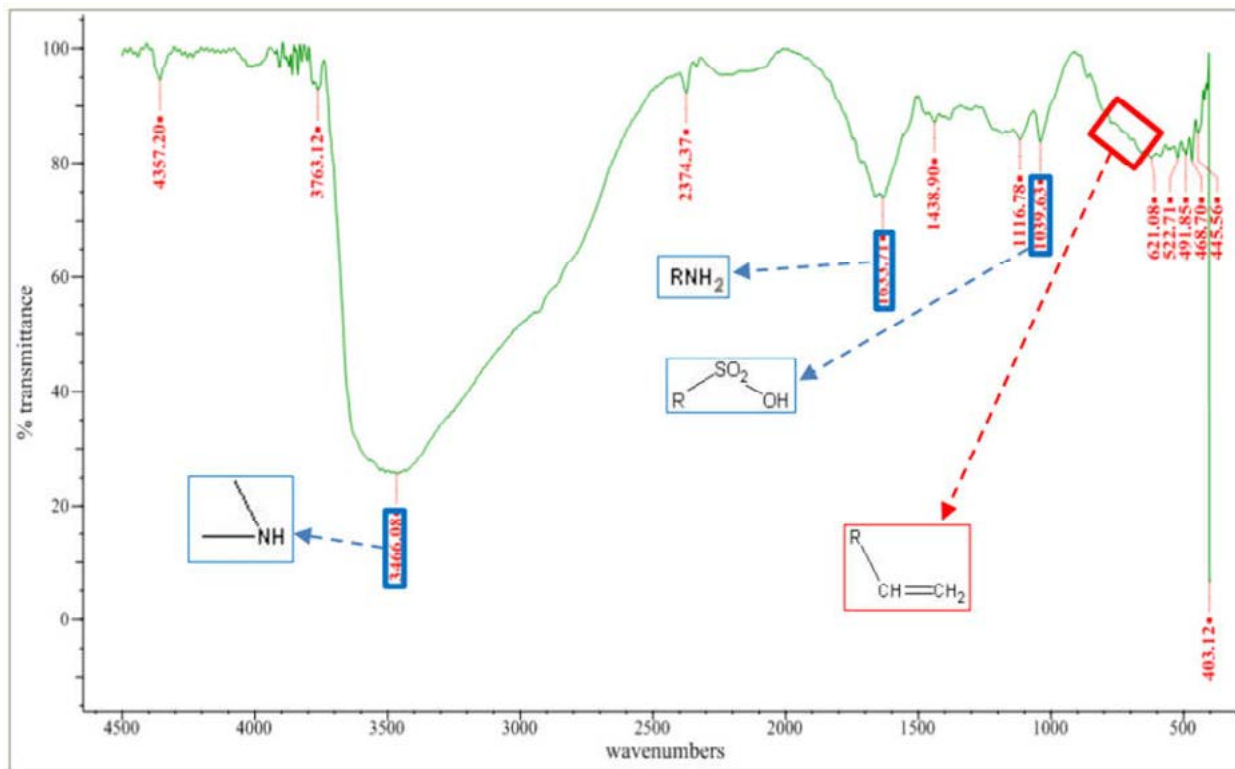


Figure 3 IR spectrum analysis of AM-AMPS copolymer

3.3. Thermal Degradation Analysis

TGA analysis results in Figure 4 shows decreasing of relative mass as indicated by changes in the gradient of the curve of relative the mass to the temperature. Mass reduction indicates decomposition of AM-AMPS copolymer which occurred at a temperature of 220.82 °C. Figure 4 also shows no decrease in the relative mass were detected before the temperature 220.82 °C which indicates good thermal resistance of AM-AMPS copolymer material until that temperature. DSC analysis results are shown in Figure 5 can be used to determine the character of the AM-AMPS copolymer i.e. glass transition temperature (Tg). Tg point in Figure 4 is shown by onset point at the first peak that is 217.7 °C.

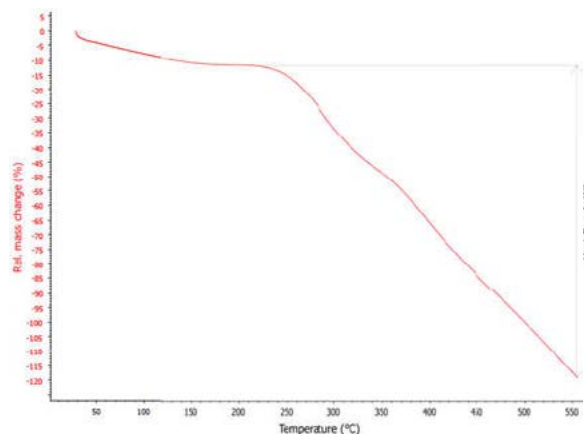


Figure 4 TGA analysis result

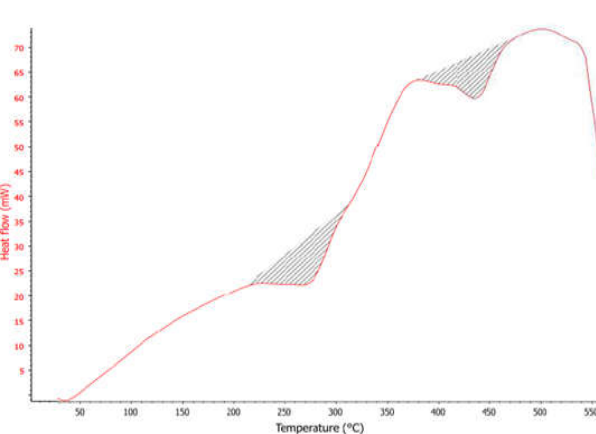


Figure 5 DSC analysis result



3.4. Polymer Solution Viscosity Analysis

The viscosity analysis of the polymer solution is done by looking at the effect of five factors: time, shear rate, temperature, salinity, and concentration on viscosity of the polymer solution.

3.4.1. Time Effect

It can be seen from Figure 6 that the viscosity of the synthesized AM-AMPS copolymers solution continued to decrease from day to day. Polymer solution viscosity at all rpm decreased with the constant gradient on the first 30 days. After the first 30 days passed, the gradient of viscosity getting smaller until finally the viscosity is constant (no longer decreasing). Generally, the factors that can decrease the viscosity of the AM-AMPS copolymers solution as time goes by are as follows [6]:

- *Thermal - static heat ageing, sub-zero exposure or thermal cycling*
- *Complete immersion in water at ambient and elevated temperatures*
- *Continuous or intermittent saltwater immersion or spray*
- *Combined load (i.e. stress) and environmental exposures*
- *Chemical (including water, fuel, acids, alkalis, solvents and oxygen)*
- *Micro-organisms (e.g. fungi)*

Among all of these factors, the factor which significantly lead to a decrease in viscosity of the synthesized AM-AMPS copolymers solution is a result of complete immersion in water that causes the chemical attack in the form of an advanced hydrolysis by water, acid, or alkali. Ester, amide, imide, and carbonates are the groups susceptible to chemical attack until break and result in a decrease in viscosity. Although the amide groups on AM-AMPS copolymer lies in the side chain (instead of the main chain), the hydrolysis of these groups still cause a decrease in viscosity is significant because the cut recurring at the side chains of the copolymer. Another possibility that causing a decrease in viscosity with time is a microorganism, which is mushroom. High air humidity caused quite humid conditions of storage cabinets and allow the emergence of fungi. It was observed that the polymer solution in jars began contaminated by the fungus after it has stored more than a week even in the closed jar.

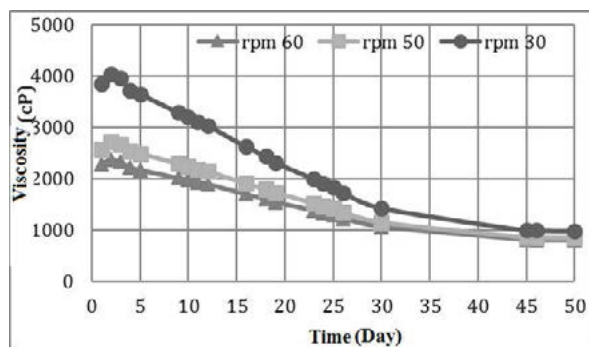


Figure 6 Time effect toward viscosity of AM-AMPS copolymer solution

3.4.2. Shear Rate Effect

Based on Figure 7 and Figure 8 at low shear rate, the viscosity gradient of the polymer decreases significantly. The order based on the gradient of polymer viscosity are commercial 1130, synthesized AM-AMPS copolymer, then Commercial 1130 W. However, after reaching 20 rpm, the gradient getting smaller (ramp) for all of three polymers. It can be concluded that the viscosity of the three polymers were not differ significantly when tested at above 20 rpm.

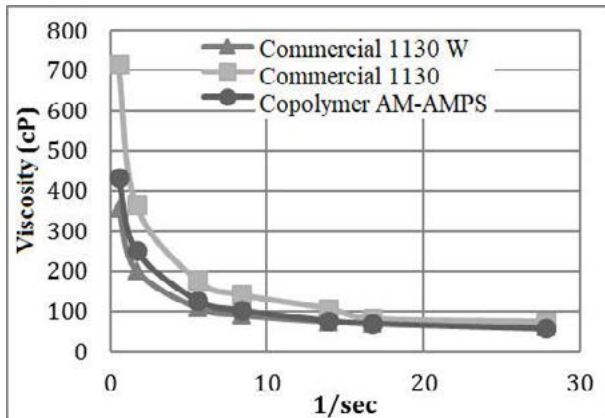
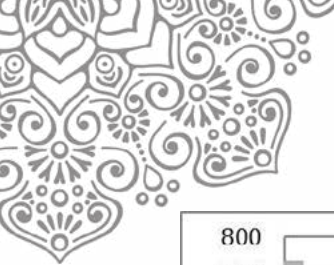


Figure 7 shear rate effect toward viscosity of 1000 ppm AM-AMPS copolymer solution

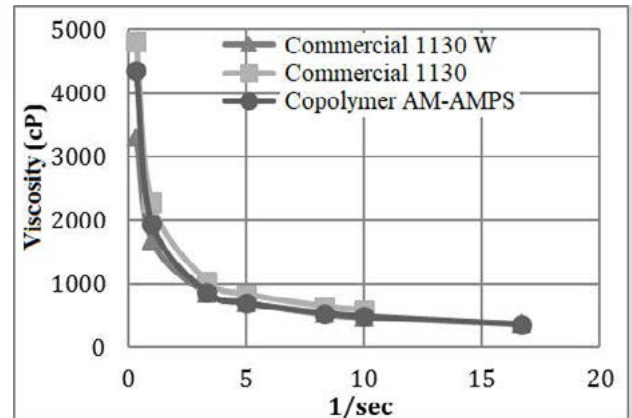


Figure 8 shear rate effect toward viscosity of 3000 ppm AM-AMPS copolymer solution

From these results, can be concluded that the synthesized AM-AMPS copolymer is a non-Newtonian fluid due to viscosity changes at different shear rate. If categorized further, synthesized AM-AMPS copolymer includes in non-Newtonian fluid whose viscosity is not dependent on time (time-independent viscosity) and a shear thinning (pseudo plastic) polymer due to viscosity decreased with increasing of shear rate. A decrease in viscosity as the shear rate increase is an indication that the electrostatic interaction between the particles is defeated by the viscous force (in this case is the shear force) in the solution. Shear force causes disruption of the equilibrium structure and lead. To a decrease in flow resistance (in this case is the viscosity) on the polymer solution.

AM-AMPS copolymers belong to the non-Newtonian fluid so it is follow the Power-Law equation (Equations 1 and 2). Plotting chart of $\log \gamma$ to $\log \mu$ is shown in Figure 9.

$$\mu = K\gamma^{(n-1)} \quad (1)$$

$$\log \mu = \log K + (n - 1)\log \gamma \quad (2)$$

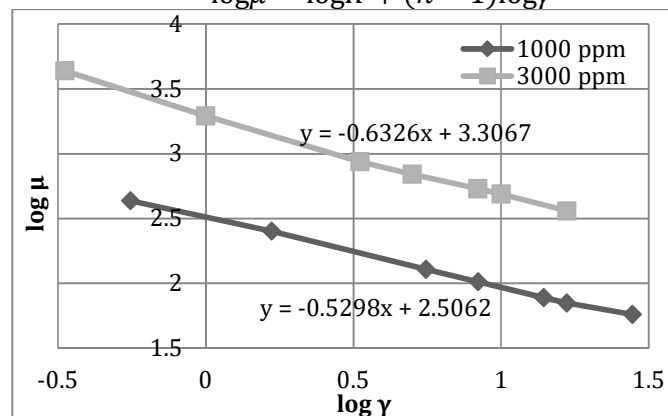


Figure 9 Power-Law constant and exponent of AM-AMPS copolymer solution determination

From Figure 9, the AM-AMPS copolymer solution with concentration 1000 ppm has a Power-Law constants (K) 320.8 and exponent Power-Law (n) 12:47. While the AM-AMPS copolymer solution with concentration 3000 ppm has a Power-Law constants (K) 2026.3 and Power-Law exponent (n) 12:37. It can be concluded that the difference in the concentration of the copolymer in the solution causes significant difference of constants K and n (especially on the constant K).

3.4.3. Temperature Effect

Temperature effect on the viscosity of the hydrophobically modified polymer is essential to observe. synthesis AM-AMPS copolymer showed a decrease in viscosity with increasing shear rate. This is caused by the declining strength of intermolecular hydrophobic associations along with the increase in temperature. This then leads to increased solubility, increased mobility, as well as the viscosity



decreases. In addition, a decrease in viscosity of a polymer solution can also be caused by coiling events that tend to occur when the temperature increases.

The synthesis polymer is compared with commercial polymers 1130 and commercial polymer 1130 W, the comparison is shown in Figure 10 and Figure 11. It can be seen that the synthesis copolymer AM-AMPS solution has a lower viscosity compared with the polymer commercial polymers 1130 solution but higher than the commercial polymer 1130 W solution. For polymer concentration 3000 ppm, the viscosity gradient decrease of AM-synthesis AMPS polymer solution is not much different from the viscosity gradient decrease of the commercial polymer solution. But for 1000 ppm polymer concentration gradient decrease in viscosity of the solution copolymers AM-AMPS gradients steeper than the decrease of viscosity in commercial polymer solution. This indicates that the AM-AMPS copolymer has a temperature sufficient good stability for concentration 1000 ppm but much better for the concentration 3000 ppm. At a concentration 3000 ppm, temperature stability of copolymer solution as good as temperature stability for both Chinese commercial polymer.

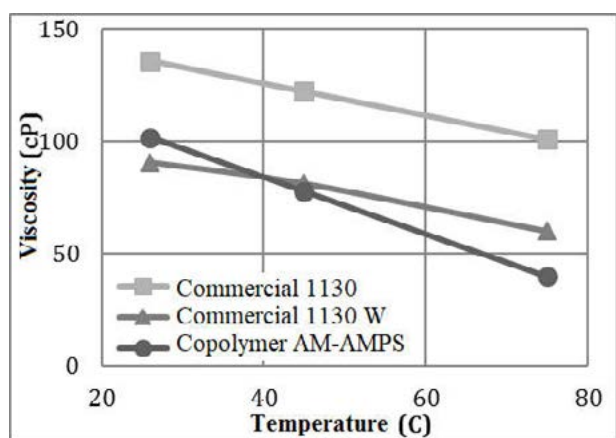


Figure 10 Temperature effect on 1000 ppm polymer solution

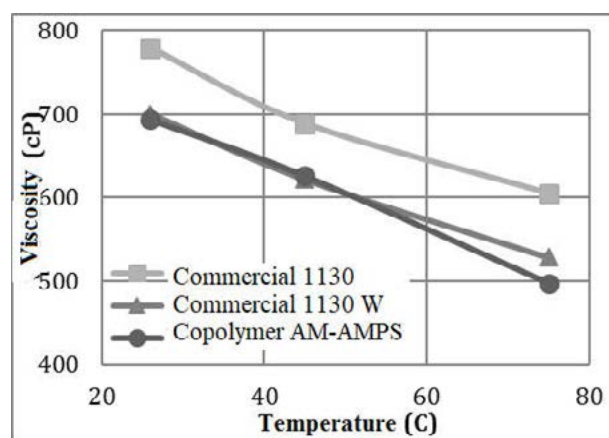


Figure 11 Temperature effect on 3000 ppm polymer solution

3.4.4. Salinity Effect

The test results of AM-AMPS copolymer in Figure 12 and Figure 13 shows that the higher the levels of salt will cause a decrease of the viscosity of polymer solution. The commercial polymer solution 1130 and 1130 W also showed a similar thing. This phenomenon shows the influence of Na^+ ions to the viscosity of the polymer. NaCl in water is ionized into ions Na^+ and Cl^- that will be bond with copolymer. AM-AMPS. Copolymer AM-AMPS is an anionic polymer that has a negative charge. The charge comes from the ionization of H^+ which is the major components AMPS. The negative charge on each polymer chain will lead to increased hydrodynamic volume so that the viscosity of the polymer solution will increase. The presence of Na^+ ions in the polymer solution causes the negative charge on the AM-AMPS copolymer into neutral because the ionic bonds between the negative charges of the polymer with Na^+ ions. The less negative charge residing on the polymer chain will cause a reduction in the hydrodynamic volume of the AM-AMPS copolymer and cause a decrease in viscosity of a polymer solution [7].

There is a difference between the viscosity of a polymer solution concentration of 1000 ppm with 3000 ppm concentration. The polymer solution with a concentration of 1000 ppm was not able to maintain its viscosity and imply a significant decrease when NaCl is added to the solution. While on a solution with a concentration of 3000 ppm have stability or resistance to salinity better. Figure 13 shows that the viscosity decreases with small gradient. This indicates a polymer solution with a concentration of 3000 ppm has better resistance to salinity in specific NaCl concentration. This phenomenon may indicate that the higher the concentration of the dissolved polymer would provide resistance to salinity better with slighter decrease in viscosity.

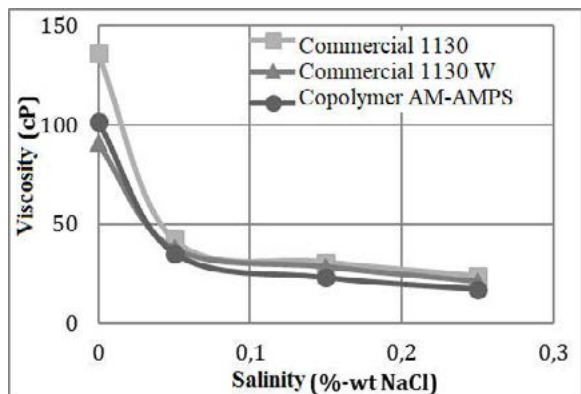
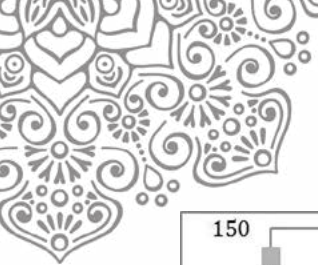


Figure 12 Salinity effect on 1000 ppm polymer solution

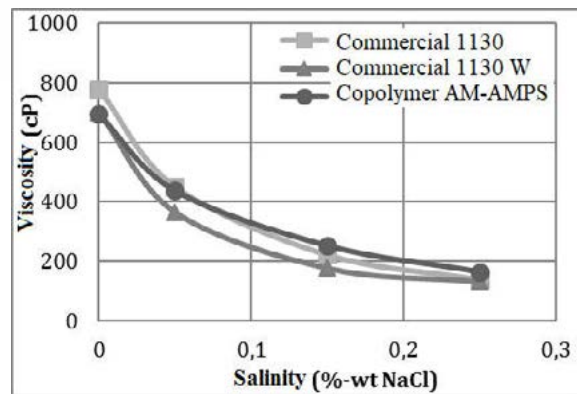


Figure 13 Salinity effect on 3000 ppm polymer solution

Figure 12 and Figure 13 shows a very significant reduction in viscosity when initially added to a solution of NaCl. However, elevated levels of salt afterwards showed no significant reduction and is relatively constant. This shows the effect of polyelectrolyte polymer due to the presence of Na^+ ions that bind to negatively charged as described previously in the early addition of NaCl. At salinity with a certain concentration, there is no binding between Na^+ ions to the negative charges on the polymer chain as a whole chain of the polymer has been neutral so that the polymer chains no longer be anionic or polyelectrolyte. Therefore, at a certain salinity, salinity will not have much effect on the viscosity of the polymer solution [8].

A test is conducted for the commercial polymer solution 1130 and 1130 W to compare the performance of AM-AMPS copolymer solution with commercial polymer solution. Figure 12 and Figure 13 shows the slight differences between AM-AMPS copolymer with the commercial polymer solution. AM-AMPS copolymer at a higher salinity show highest viscosity compared with commercial polymer solution, although at first polymer having a viscosity similar to commercial polymer solution. This indicates that the AM-AMPS copolymer has a stability and resistance to salinity slightly better when compared with commercial polymer solution 1130 and 1130 W.

3.4.5. Polymer Solution Concentration Effect

The viscosity of the polymer injected into the reservoir varied and adapted to the viscosity of petroleum that are driven out of the reservoir. The higher the viscosity of the oil, the viscosity of the polymer solution needed will be higher to be able to push the oil out of the reservoir. High-viscosity polymer solution can be generated by increasing the concentration of the polymer that dissolved into water to make water flooding. The effect of concentration on viscosity of the polymer solution is shown in Figure 14.

From figure 14 viscosity of the polymer solution increases linearly with the increasing of the polymer concentration. This shows the concentration effect against the viscosity of polymer solution. This influence shows that the more polymer is dissolved will lead to more and more groups in the hydrophilic polymer chains that bind with water molecules. When many molecules are bound to the polymer chains, the viscosity of the polymer solution will increase. Another influence is the association of hydrophobic groups due to the effect of thickening phenomenon that occurs because the increased amount of polymer in solution. Association hydrophobic groups will form a three-dimensional network which can increase the viscosity of the polymer solution.

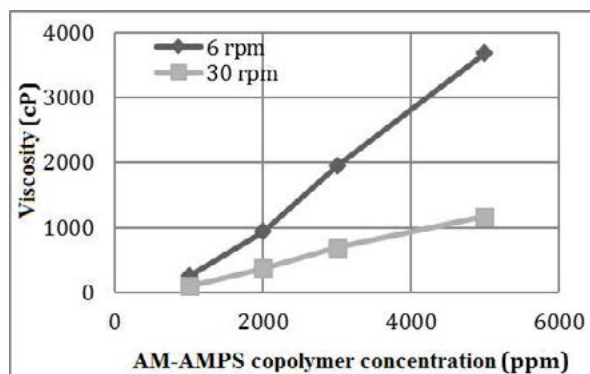


Figure 14 AM-AMPS copolymer concentration effect

4. CONCLUSION

This study showed that AM-AMPS copolymer could be synthesized at room temperature as indicated by the FTIR test results and produced the best viscosity for EOR at mass ratio of AM: AMPS equal to 65:35. The copolymer has high solubility in water, good viscofying ability, good resistance to salt and high temperature. AM-AMPS copolymer is a pseudo plastic material which showed a decrease in viscosity with increasing shear rate. The viscosity of the AM-AMPS copolymers solution decreased every day in storage and stopped after 30 days of storage. The copolymer solution with concentration of 3000 ppm has better resistance to salt and high temperature than the concentration of 1000 ppm. Additionally the TGA-DSC test results show that synthesized AM-AMPS copolymer has good thermal stability.

5. ACKNOWLEDGMENT

The donation of acrylamide by Zekindo Chemicals (PT Zeus Kimiatama Indonesia) is gratefully acknowledged.

6. REFERENCES

- [1] Abidin, A.Z.; Puspasari, T.; Nugroho, W.A., (2012) Polymers for Enhanced Oil Recovery Technology”, *Procedia Chemistry* **4**, p 11-16.
- [2] Wu, Y.; Mahmoudkhani, A.; Watson, P.; Fenderson, T.; Nair, M.; Kemira, (2012) “Development and Performance of New Polymers with Better Performance under Conditions of High Temperature and High Salinity”, SPE EOR Conference at Oil and Gas West Asia, Muscat-Oman.
- [3] Abidin, A.Z. and M.A.A. Elsadik, (2016) “Synthesis of Water Soluble Copolymers of Acrylamide-(2-Acrylamido-2-methylpropanesulfonic Acid) for Enhanced Oil Recovery (EOR)”, International Seminar on Chemical Engineering in conjunction with Seminar Soehadi Reksowardojo, Bandung, Indonesia.
- [4] Zhong, C.; Wang, W.; Yang, M., (2012) “Synthesis and solution properties of an associative polymer with excellent salt-thickening”, *Journal of Applied Polymer Science* **125**, p 4049-4059.
- [5] Xu, J.; Wu, Y.; Wang, C.; Wang, Y., (2009) “Dispersion polymerization of acrylamide with 2-acrylamide-2-methyl-1-propane sulfonate in aqueous solution of sodium sulfate”, *Journal of Polymer Research* **16**, p 569-575.
- [6] Maxwell, A.S.; Broughton, W.R.; Dean, G.; Sims, G.D., (2005) “Review of accelerated ageing methods and lifetime prediction techniques for polymeric materials”, National Physical Laboratory, Teddington,
- [7] Samantha, A.; Bera, A.; Ojha, K.; Ajay, M., (2010) “Effects of Alkali, Salts, and Surfactant on Rheological Behavior of Partially Hydrolyzed Polyacrylamide Solutions”, *Chemical Engineering Journal* **55**, p 4315-4322.
- [8] Ye, Z.; Gou, G.; Gou, S.; Jiang, W.; Liu, T., (2012) “Synthesis and Characterization of a Water-Soluble Sulfonates Copolymer of Acrylamide and *N*-Allylbenzamide as Enhanced Oil Recovery Chemical”, *Journal of Applied Polymer Science* **128**, p 2003-2011.



15th International Conference on Quality in Research (QIR 2017)

THE EFFECT OF ANIONIC AND NONIONIC CO-SURFACTANT FOR IMPROVING SOLUBILITY OF POLYOXY-BASED SURFACTANT FOR CHEMICAL FLOODING

Yani F. Alli^{a*}, Dadan Damayandri^a, and Yan Irawan^b

^aResearch and Development Centre for Oil and Gas Technology "LEMIGAS"
Jl. Ciledug Raya Kav.109, Cipulir, Kebayoran Lama, P.O. Box 1089/JKT, Jakarta Selatan 12230
Tromol Pos: 6022/KBYB-Jakarta 12120, Telephone: 62-21-7394422, Fax: 62-21-7246150

^bResearch Centre of Chemistry, Indonesian Institute of Sciences
Kawasan PUSPIPEK Serpong, Tangerang – Banten, 15314
Telephone: 021 – 7560929, Fax: 021 – 7560549
Email: faozani@lemigas.esdm.go.id

ABSTRACT

Surfactant is one of the crucial components for chemical flooding to recover oil production in the tertiary stage owing to the inefficiency of the conventional primary and secondary recovery that yields only 20-40% of the OOIP (original oil in place) as incremental oil. The mechanism includes decreasing interfacial tension (IFT), increasing capillary number, as well as enhancing microscopic displacement efficiency. The present study showed the effect of commercial nonionic and anionic co-surfactant Tergitol, Teepol, Mergol and SDS on the solubility of POS through compatibility analysis, filtration ratio analysis, and IFT measurement. Whereas the presence of Teepol and Mergol did not change the original compatibility of polyoxy based-surfactant (POS) in all concentrations, the addition of co-surfactant Tergitol and SDS were able to alter the solubility of POS into a clear transparent solution. However, the most important characteristic of surfactant for reducing the IFT of oil-water was affected by the addition of co-surfactant which does not have sufficient IFT to release the trapped oil in the reservoir. Thus, exposing the mixture of surfactant and co-surfactant for a few days at the reservoir temperature has changed the visual appearance of solution from a clear transparent solution into a milky suspension, indicating the occurrence of thermal hydrolysis. These results suggest that the addition of anionic and nonionic co-surfactant improved the solubility of POS, but increased the IFT. It can be concluded that the compatibility of POS in the brine can then be achieved by mixing it with suitable co-surfactant. However, screening the other co-surfactant is required to obtain the one that enhances the compatibility as well as maintaining the ultralow IFT of POS.

Keywords: polyoxy-based surfactant; enhanced oil recovery; chemical flooding; solubility; co-surfactant.

1. INTRODUCTION

The use of surfactant for chemical flooding has been recognized to be effective to increase the displacement efficiency of oil in a mature oilfield by decreasing interfacial tension (IFT), increasing the capillary number, as well as enhancing the microscopic displacement efficiency (Ahmadi et al., 2014; Bera et al., 2014). As one of the best methods in enhanced



oil recovery (EOR) technologies, chemical flooding is then expected to recover the remaining oil that cannot be produced by primary and secondary recovery which yield only 20-40% of the OOIP (original oil in place). Along with surfactant, the other substances with different roles, such as polymer as well as alkaline, were used as injected materials into the reservoir (Olajire, 2014; Fletcher et al., 2015). While polymer was used for increasing the mobility control (Pingping et al., 2009; Crespo et al., 2014), alkaline was injected as a sacrificing agent to minimize the adsorption effect of surfactant into the core (Seng et al., 2011; Hirasaki et al., 2011).

Surfactant for chemical flooding application has unique and tailor-made properties associated with different reservoir fluid characteristics (Babu et al., 2016). The chemical is required to be salinity resistant and hardness resistant due to the high saline and high cationic divalent of formation water (Guo et al., 2015; Yuan et al., 2015; Song et al., 2016). Thus, in order to reduce the IFT between oil and water, the surfactant has to be optimized to adjust to the targeted crude oil properties. Usually, two or three kinds of surfactant consisting of main surfactant and co-surfactant were formulated for generating the sufficient surfactant for chemical flooding (Li et al., 2017). However, both chemicals have the characteristic as surfactant by the presence of hydrophilic and hydrophobic at the end of the molecule. Four types of surfactant were classified based on the ionic charge of the molecule, cationic, anionic, nonionic and zwitterionic surfactant. Commercially surfactant that is available in the market includes teepol, merpol, and tergitol which are identified as nonionic surfactant, and sodium dodecyl benzene sulfate (SDS) which is identified as an anionic surfactant.

Teepol, merpol, tergitol, and SDS are market brand surfactant that usually is used for household applications, such as detergent, personal care, cleanings and food processing (Adeniyi et al., 2015). The study of utilizing brand market surfactant for surfactant flooding has been reported on recently. Taiwo et al. (2016) investigated the use of Teepol for recovering light oil, the addition of Tergitol and SDS for lowering the adsorption (Bera et al., 2013) and wettability alteration (Bera et al., 2015).

Previously, we investigated the effect of polyoxy groups of sulfonated natural oil-based surfactant for chemical flooding application. It showed that the presence of polyoxy groups are able to reduce the IFT of oil and water in a targeted oilfield to the level of 10^{-3} dyne/cm as required for chemical injection. However, sulfonated surfactant consisting of polyoxy groups formed a whitish solution with precipitation indication. This phenomenon is not expected due to the possibilities of chemicals to plug in the reservoir pore throat. In the present study, the effect of the addition of Teepol, Merpol, Tergitol and SDS was analyzed as co-surfactant to improve the aqueous stability of POS for chemical flooding.

2. METHODOLOGY

POS as the main surfactant was synthesized and developed in the Research Centre of Chemistry, Tangerang, Indonesia. Nonionic surfactant Teepol, Merpol, and Tergitol as well as anionic surfactant SDS were used as co-surfactant. Crude oil was collected from "X" Oil Field (South of Sumatera) with a viscosity of 3.16 cP at reservoir temperature (60°C), and oil gravity of 34.39°API. Brine was synthetically formulated based on



formation water composition from “X” Oil Field to ensure the similar component of water during the experiments. The synthetic water formulation is shown in Table 1. POS at various concentrations was mixed with synthetic water in the presence of various co-surfactants at different concentrations. The effect of the addition of co-surfactant was investigated on the presence and absence of co-surfactant through the EOR analysis.

2.1. Compatibility Observation

The effect of co-surfactant on the compatibility of surfactant was analyzed by visual observation of surfactant solubilization in the absence and presence of co-surfactant at different concentrations. Compatibility of surfactant was performed at room temperature as well as at the reservoir temperature to study the effect of elevated temperature on the aqueous stability of surfactant formulation, the mixture of surfactant and co-surfactant.

Table – 1. Synthetic water formulation of “X” Oil Field

Chemicals	Mass (g/4 L)
CaCl ₂	2.654
MgCl ₂ .6H ₂ O	8.133
NaHCO ₃	14.445
Na ₂ SO ₄ .10H ₂ O	0.094
Na ₂ CO ₃ .10H ₂ O	1.775
NaCl	56.800

2.2. IFT Measurement

In order to investigate the effect of co-surfactant on the IFT of the main surfactant, various concentrations of single POS and co-surfactant in the synthetic brine were measured and compared with the mixture of surfactant and co-surfactant. The IFT measurement was conducted by Spinning Drop Tensiometer TX500 C/D. The capillary tube filled with surfactant solution was injected with 2 µl of crude oil “X”, and put into the IFT unit. The tube was spun at 6000 rpm and 60 °C to adjust to the reservoir temperature of “X” Oil Field. Thermal stability of surfactant was also observed by putting the surfactant solution in the air bath for one month. The IFT was then measured and compared with the initial condition to identify its thermal stability characteristics.

2.3. Filtration Ratio Analysis

The addition of nonionic or anionic surfactant was believed to alter the solubility of POS. To quantify the precipitation indication, filtration ratio analysis was carried out on the absence and presence of various co-surfactant. The mixture of surfactant and co-surfactant was diluted in the synthetic brine and allowed to flow into the 0.45 µm filter paper under pressurized air 30 psi. The filtration ratio was then calculated by $F_R = (T_{500}-T_{400})/(T_{200}-T_{100})$, where T_x is the time to collect x ml of surfactant mixture.



3. RESULTS AND DISCUSSION

3.1. The effect of co-surfactant on the solubility of POS

Compatibility of surfactant as an injected chemical is the most crucial parameter for chemical flooding. A homogeneous solution is required for the effectiveness of chemical performances in the targeted fluid reservoir. Previously, we found that POS from palm oil was able to reduce the IFT to the ultralow level. However, it formed a milky/whitish solution with the precipitation indication as the concentration was increased. The addition of co-surfactant is then expected to improve the solubility of POS for chemical flooding. The compatibility of surfactant on the presence of various co-surfactant at different concentrations of surfactant and co-surfactant is presented in Table-2.

Table – 2. Compatibility of POS on the addition of various non-ionic and anionic co-surfactant at different concentrations of surfactant and co-surfactant

Conc. (%)	0.3% POS				1.0% POS	
	SDS	Tergitol	Merpol	Teepol	SDS	Tergitol
(-)	++	++	++	++	++	++
0.3	++	++	+++	+++	++	++
0.5	++	+	+++	+++	++	++
1.0	+	+	+++	+++	++	++
2.0	+	+	+++	+++	+	+
3.0	+	++	+++	+++	+	+

+ : clear; ++ : light milky; +++ : milky

As can be seen in Table-2, the addition of co-surfactant affects the solubility of POS. While the mixture of surfactant with non-ionic surfactant (either Merpol or Teepol) formed more whitish solution, the presence of nonionic co-surfactant Tergitol and anionic co-surfactant SDS improved the solubility of the targeted surfactant at the different concentrations. Clear mixture solution occurred with the addition of SDS in the range of 1.0 – 3.0%, whereas the addition of Tergitol produced a clear solution in the range of 0.5 – 2.0% and forming suspension again as the concentrations of the co-surfactant were increased. To analyze the solubility as a ratio POS function, the solubility of POS at 1.0% with the addition SDS and Tergitol was also observed, and indicated that higher concentrations of POS required more co-surfactant to dissolve POS to become a clear solution.

Identification of solubilization ability of the surfactant mixture with the synthetic formation water was performed by filtration analysis and the filtration ratio was calculated. The results showed that 0.5% POS in the presence of 1% Tergitol which produced a clear solution were having lower F_R at 1.00 than single surfactant 0.5% POS which generated F_R at 1.80 (Fig. 1), indicating the ability of Tergitol to dissolve the suspension of POS.

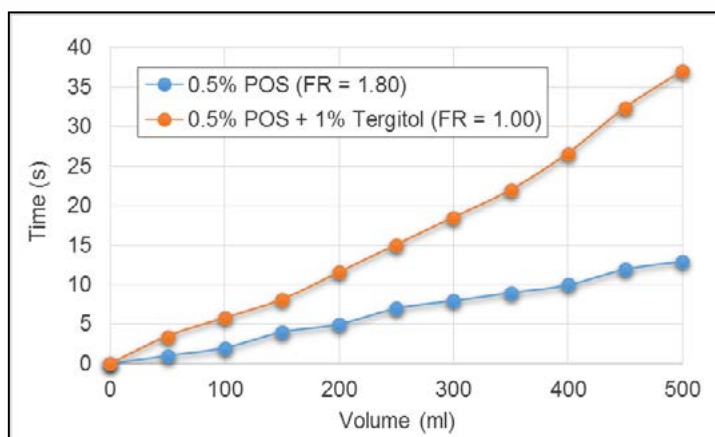
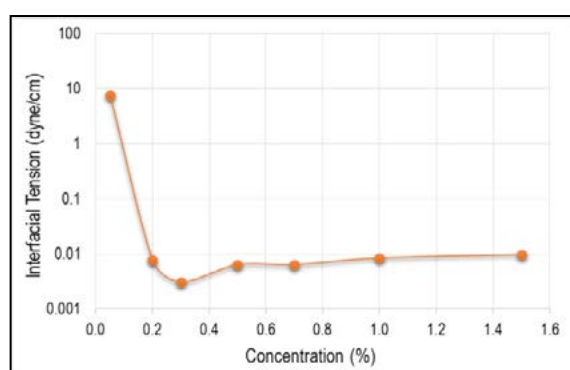


Figure – 1. Filtration analysis of single surfactant 0.5% POS compared with the mixture of 0.5% POS and 1.0% Tergitol.

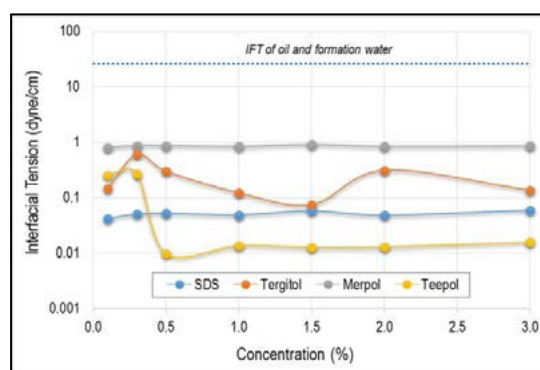
3.2. The effect of co-surfactant on the IFT of POS

Aside from the effect of co-surfactant on the compatibility of surfactant, the influence of the second surfactant on the IFT of the main surfactant was also investigated to ensure the critical performance of surfactant as a displacing agent was not affected. IFT measurement was performed on the single POS and each co-surfactant as well as the mixture of surfactant and the co-surfactant solution. It was found that POS successfully reduced the IFT of oil and water to the level of 10^{-3} dyne/cm at 0.3 and 0.5% surfactant, as required (Fig. 2a), whereas the addition of single co-surfactant SDS, Tergitol, Merspol, and Teepol can only decrease IFT from original oil-water 39 dyne/cm, to the range of 10^{-1} - 10^{-2} dyne/cm (Fig. 2b). The IFT of surfactant solution in the presence of co-surfactant was also measured and presented in Figure 2c. As shown in the figure, the addition of various co-surfactant increased the IFT of POS, suggesting the higher influences of co-surfactant IFT's rather than POS itself.

a)



b)





c)

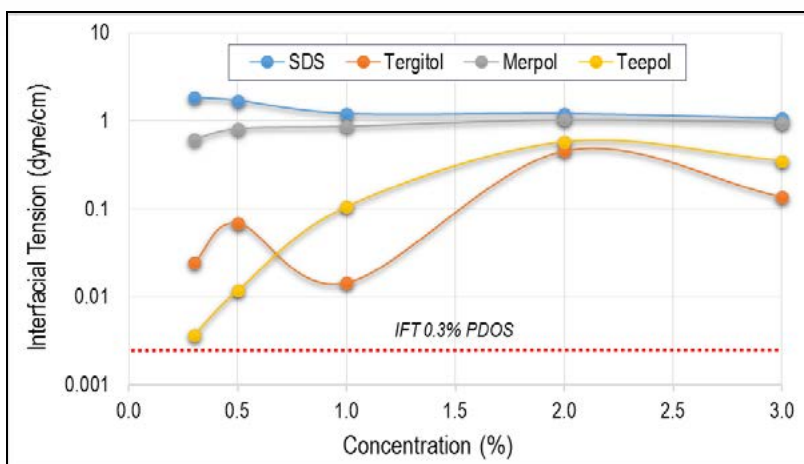


Figure – 2. Results of IFT measurement of a) single POS; b) single anionic and nonionic co-surfactant; c) mixture of 0.3% POS and various concentrations of each co-surfactant.

3.3. Aqueous stability of the mixture of POS and co-surfactant at elevated temperature

To simulate the aqueous stability of POS at the reservoir temperature, the solubility of surfactant was observed after being exposed to heating for several days. The mixture of surfactant in the presence of SDS and Tergitol which generated a clear solution were put in the oven for days. It was found that the mixture of 0.5% POS and 1% of SDS as well as 0.5% POS and 0.5% Tergitol formed a whitish/milky solution after being stored in the oven after 3 days (Table 2), which suggested that co-surfactant SDS and Tergitol were sensitive to being heated, and were not likely to be used as chemicals for chemical injection.

Table – 3. Compatibility of POS on the addition of various non-ionic and anionic co-surfactants at different concentrations of surfactant and co-surfactant

Time (days)	0.3% POS		1.0% POS	
	SDS	Tergitol	SDS	Tergitol
0	+	+	+	+
1	+	+	++	++
3	++	++	++	++
7	++	++	++	++
14	++	++	++	++
30	++	++	++	++



4. CONCLUSION

The presence of non-ionic surfactant Mergol and Teepol in the POS solution has been shown as not having a great impact on the solubility of POS, but they did lead to an increasing IFT of the POS solution. Whereas the addition of SDS and Tergitol were identified as improving the appearance of the POS solution from milky suspension to transparent and clear. These results were confirmed by the filtration analysis that produced lower F_R than a single POS. On the other hand, the addition of SDS and Tergitol affected the IFT of POS as the main characteristic of surfactant to be higher and generated a hazy solution at the reservoir temperature. It can be concluded that the use of co-surfactant has the potential to improve the solubility of the main surfactant. However, a study to screen the other co-surfactant which improves the solubility of POS at room temperature as well as at reservoir temperature without an increase in the IFT is required.

5. ACKNOWLEDGEMENTS

This paper is the result of collaboration between the Research Centre for Oil and Gas Technology "LEMIGAS" and the Indonesian Institute of Sciences, Research Center for Chemistry. Special thanks to Ika Juliana and Indri Badria from the Research Centre of Chemistry for their contributions to this work. The financial support from DIPA Research Center for Oil and Gas Technology "LEMIGAS" is fully acknowledged.

6. REFERENCES

- Adeniyi A.T., Onyekonwu M., Olafuvi O.A., Sonibare L.O., (2015), Development of cost effective surfactants from local materials for enhanced oil recovery, In: SPE Nigeria Annual Conference and Exhibition, Nigeria, SPE-178403-MS.
- Ahmadi M.A., Arabsehi Y., Shadizadeh S.R., and Behbahani, (2014), Preliminary evaluation of mulberry leaf-derived surfactant on interfacial tension in oil-aqueous system: EOR application, *Fuel*, Volume 117, Part A, pp. 749-755.
- Babu K., Pal N., Saxena V.K., and Mandal A., (2016), Synthesis and characterization of a new polymeric surfactant for chemical enhanced oil recovery, *Korean J of Chem Eng*, Volume 33(2), pp. 711-719.
- Bera A., Kumar T., and Mandal A., (2014) Screening of microemulsion properties for application in enhanced oil recovery, *Fuel*, Volume 121, pp. 198-207.
- Bera A., Kumar T., Oih K., and Mandal A., (2013), Adsorption of surfactants on sand surface in enhanced oil recovery: Isotherm, kinetics and thermodynamic studies, *Applied Surface Science*, Volume 284, pp. 87-89.
- Bera A., Mandal A., and Kumar T., (2015), The effect of rock-crude oil-fluid interactions on wettability alteration of oil-wet sandstone in the presence of surfactants, *Petroleum Science and Technology*, Volume 33(5), pp. 542-549.
- Crespo F., Reddy B.R., Eoff C.L., and Pascarella N., (2014), Development of polymer gel system for improved sweep efficiency and injection profile modification of IOR/EOR treatments, In *International Petroleum Technology and Conference (IPTC)*.



- Fletcher P.D.I., Savory L.D., and Woods F., (2015), Model study of enhanced oil recovery byflooding with aqueous surfactant solution and comparison with theory, *Langmuir*, Volume 31, pp. 3076–3085.
- Guo S., Wang J., Shi J., Pan B., and Cheng Y., (2015), Synthesis and properties of a novel alkyl-hydroxyl-sulfobetaine zwitterionic surfactant for enhanced oil recovery, *J of Pet Exploration and Prod Tech*, Volume 5(3), pp. 321-326.
- Hirasaki G.J., Miller C.A., and Puerto M., (2011), Recent advances in surfactant EOR. *Soc Pet Eng J*, Volume 6, pp. 889-907.
- Li Y., Puerto M., Bao X., Zhang W., Jin J., Su Z., Shen S., Hirasaki G., and Miller C., (2017), Synergism and Performance for systems containing binary mixtures of anionic/cationic for enhanced oil recovery, *J of Surf and Detergents*, Volume 20(1), pp. 21-34.
- Olaire A.A., (2014), Review of ASP EOR (Alkaline surfactant polymer enhanced oil recovery) technology in the petroleum industry: prospects and challenges, *Energy*, Volume 77, pp. 963–982.
- Pingping S., Jialu W., Taixian Z., and Xu J. (2009), Study of enhanced oil recovery mechanism of alkali/surfactant/polymer flooding in porous media from experiment. *Soc Pet Eng J*, Volume 14(2), pp. 237–244.
- Sheng J.J., (2011), *Modern chemical enhanced oil recovery: Theory and Practice*, Elsevier, Amsterdam.
- Song B., Hu X., Shui X., Cui Z., and Wang Z., (2016), A new type of renewable surfactants for enhanced oil recovery: Dialkylpolyoxyethylene ether methyl carboxyl betaines, *Colloids And Surfaces A: Physicochem Eng Aspects*, Volume 489, pp. 433-440.
- Taiwo O.A., Uzezi O., Mamudu A., Onuoha S., Adijat O., and Olafuvi O., (2016), Fractional wettability effects on surfactant flooding for recovering light oil using Teepol, In: *SPE Nigeria Annual Conference and Exhibition, Nigeria*, SPE-184298-MS.
- Yuan C.D., Pu W.F., Wang X.C., Sun L., Zhang Y.C., and Cheng S., (2015), Effects of interfacial tension, emulsification, and surfactant concentration on oil recovery in surfactant flooding process for high temperature and high salinity reservoirs, *Energy Fuels*, Volume 29(10), pp. 6165-6176.



Synthesis and Characterization of Cellulose Acetate from Natural Fiber As Substitute Microbeads Polyethylene that more environmental friendly

Abstract

Cellulose acetate made by acetylation between cellulose and acetic acid anhydrous. Cellulose extracted from empty palm oil bunches (EPB) and leaves dry jackfruit leaves (DJL) through delignification process with NaOH 8, 10, 12, and 14 % then continued with bleaching using H₂O₂ 10%. Reaction acetylation use special variable the ratio between a reactant cellulose and acetic acid anhydrous of 1/5, 1/10, 1/15, and 1/20 (v/v) and obtained the highest yields 16,2% to EPB and 42,72% DJL. The success of making cellulose acetate analyzed acetyl group with Fourier Transform Infra Red (FTIR) and morphology with scanning electron microscopy (SEM). As an alternative to substitute *microbeads* environmentally friendly, then cellulose acetate and *microbeads* measured of weight relegated with the burial. Degradation cellulose acetate reached 69 % to EPB and 63,2 % to DJL to 20th day.

Keywords : Acetylation, jackfruit, microbeads, cellulose, cellulose acetate, EPB

Introduction

Some research on the negative consequences of microbeads highly developed recent years. This is what caused some country is banned the use of microbeads in products containing scrub and find alternative his successor. Formulator cosmetics and personal care had certain criteria to replace microbeads polyethylene with nature scrub and can relegated naturally (Morice *et al.*, 2015). Several criteria these include visual particles must have the same effect, the abrasion and should like skin taste, particles must have the same capacity of suspension, stability color must be equal to polyethylene, must meet the needs of the world number of scrub.

Based on several criteria to substitute microbeads above, cellulose acetate appropriate. Cellulose acetate also has other excellence that is made of material to be renewed and could relegated naturally. Cellulose acetate is one of the oldest

macromolecules a man made widely used in textiles and polymer (Barkalow *et al.*, 1989). Cellulose acetate is derived from cellulose with the quality of being extraordinary of transparency good, hard, heat resistant, water which low, and degradable naturally (Bahmid *et al.*, 2013).

Cellulose on empty bunches of oil palm is 38,76 % (Bahmid *et al.*, 2013). According to Akmad (2012), capacity of empty bunches oil palm in Indonesia about 20-23 % of total palm oil production in Indonesia (Wardani&Widiawati, 2012). Based on BPS data in 2014 total production of Indonesian palm oil is 18.661 million tons. Dry jackfruits leaves has high cellulose like empty bunches of oil palm about 21,45 % (Sasongko *et al.*, 2010).

Cellulose acetate can be made by the acetylation between cellulose and acetic acid. Cellulose acetate highly influenced by acetyl content and degrees of substitution as it would affect on the outcome of the production and solubility



cellulose acetate in a solvent (Bahmid *et al.*, 2013). According to Susanti (2003) acetyl content in cellulose acetate influenced by several factors among others the ratio between cellulose and acetic acid anhydrous, acetylation time, and the interaction of treatment factor (Bahmid *et al.*, 2013). The optimal time to get cellulose acetate with the acetyl 40,108 % is 30 minutes (Bahmid *et al.*, 2013).

Success of cellulose modification into cellulose acetate can be characterized using Fourier Transform Infra Red (FTIR) (Muliawati, 2012) and Scanning Electron Microscopy (SEM) (Sasongko *et al.*, 2010). If the analysis is groups C=O viewed by wavelength 1759 cm^{-1} is this shows acetylation of acetic acid anhydrous (Sasongko *et al.*, 2010). With scale of SEM 2000x can be seen fibers morphology of cellulose acetate on the micron size. Fibers morphology of cellulose acetate shaped fiber cylindrical and a hollow (Sasongko *et al.*, 2010).

Cellulose acetate is common material recommended as biodegradable polymers. Research showing that biodegradation of cellulose acetate occurs in various the type of environment including ground, compost, and facilities wastewater treatment (Morice *et al.*, 2015). Cellulose acetate sheets can relegated within 2-3 weeks with heavy reduction of 67 % (Morice *et al.*, 2015). According to Zenjian & Hamano (2003) cellulose acetate made of the cotton degradable well by the reduction of heavy sample 60 -70 % three weeks (Morice *et al.*, 2015). Cellulose acetate faster relegated compared with polyethylene that takes time to 1000 years to relegated naturally in the environment (Sangale *et al.*, 2012).

Methodology

The synthesis process of cellulose acetate started by extraction cellulose of empty bunches of oil palm and dry jacfruits leaves by heating in NaOH solution 12 % on the temperature $90\text{-}100^{\circ}\text{C}$ by comparison raw materials and NaOH solution of 1 : 30 (b/v) for 3 hours to deprive lignin. Then it be washed and heated back in H_2O_2 solution 10 % to bleaching on the temperature $80\text{ - }90^{\circ}\text{C}$ for 1.5 hours by comparison materials and solution H_2O_2 of 1 : 20 (b/v). Then cellulose obtained washed clean and dried in the oven on the temperature 105°C for 6 hours to remove the water. Cellulose obtained weighed to know heavy cellulose produced. The moisture content of cellulose obtained by extending warm up the temperature 105°C to gain weight constant. Making cellulose acetate begins with the activation cellulose with 1 gram cellulose heated and stirred in 15 ml acetic acid glacial for 1 hour. The process continued with the addition of acetic acid and acetate anhydrous with comparison 2 : 3 (v/v) and H_2SO_4 catalyst pekat as many as 0.1 ml warming and continued for 30 minutes with a temperature that guarded less than 50°C .

Variable at this research is the comparison between cellulose and acetic anhydrous by 1/5, 1/10, 1/15, 1/20 (b/v). The process of acetylation was stopped by adding a mixture of aquades and acetic acid glacial by comparison 1 : 2 (v/v) and heating continued for 30 minutes in temperature no more than 50°C . After hydrolysis, separation of cellulose acetate done with centrifugal at speeds 1500 rpm for 15 minutes. Cellulose acetate washed until clean that nothing smell acetic and



evaporate on the temperature 50 °C to remove the water. Characterization cellulose acetate done by FTIR and SEM. Cellulose acetate as many as 50 mg wrapped in plastic breathable and buried in soil from sewer household wastes by adding a mixture of water, detergents 10 %, and ammonia of 2 % at about 1 min/ml continuously with variable of time 5, 10, 15 and 20 days. Cellulose acetate the relegation dried in an oven and weighed to determine how mg that lost.

Result and Discuss

Cellulose Extraction

Cellulose fibers in this research is extracted using variations NaOH solution which serves to delignifikasi, the omission of hemiselulosa fiber and other components. Variation NaOH used is NaOH 8, 10, 12, and 14 % (b/v). Concentration NaOH chosen not exceed 17 % because the use of concentration below on concentration was not undermine or cause to degradation on cellulose (Hutomo, 2012). Empty bunches of oil palm and dry jacfruits leaves each heated in solution NaOH for 3 hours. Of heating this was obtained cellulose fibers with a solution that is colored brown to blackish formerly light-brown. Change color was caused by browning namely the process of oxidation reaction phenolic compounds by air. A reaction which occurs at process delignifikasi is as follows (Riama *et al.*, 2012).

Fiber + NaOH → cellulose + Alkohol + acid + residu

In this research, cellulose extracted from empty bunches of oil palm reach a maximum of 36,383 % (figure 1) with

NaOH 12 % (b/v) and dry jacfruits leaves 7.523 % with NaOH 10 % (b/v). The extraction cellulose of empty bunches of oil palm approaching the maximum cellulose in literature namely 38,76 % (Bahmid *et al.*, 2013). On dry jacfruits leaves, yield of cellulose is still below the cellulose dry jacfruits leaves from literature 21,45 % (Sasongko *et al.*, 2010).

The state of structure dry jacfruits leaves cellulose that tends to amorphous causing the molecules bound weaker than crystal structures in empty bunches of oil palm so that more the cellulose dissolved in NaOH. So, NaOH concentration advocated for cellulose extraction is 10 %.

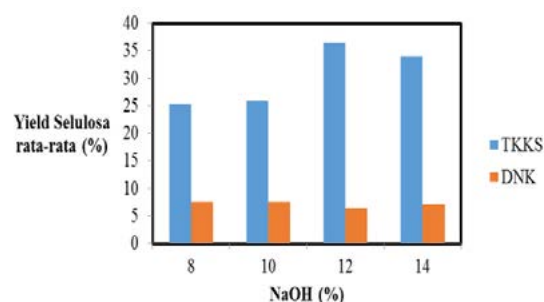
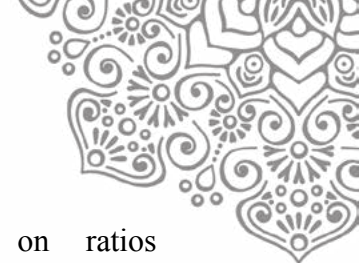


Figure 1. Corelation NaOH concentration with yield of cellulose

Synthesis of Cellulose Acetate

Production of cellulose acetate done with the acetylation. Acetylation begins with the activation 1 gr of cellulose added 15 ml acetic acid glacial and stirred by stirrer aimed at inflating cellulose fibers to make broad the surface increased and reduce hydrogen bonds intermolecular (Bahmid *et al.*, 2013) so that the tying acetyl group be maximum. Stirring made over 60 minutes. The process of followed by acetylation the additional a mixture of glacial acetic and acetic acid anhydrous by comparison 2: 3 and 0,1 ml H₂SO₄ as a catalyst. It is based on previous studies that addition acetic



acid about 5-20 % heavy cellulose will help in speed up for acetylation (Bahmid *et al.*, 2013). When acetylation, acetic acid anhydrous will protonized with the sulphuric acid forms carbonium ion. Carbonium ion will react with cellulose forms cellulose acetate (Nurhayati *et al.*, 2014).

The acetylation process lasted for 30 minutes. The amount of acetic acid anhydrous added according to research variable the 5, 10, 15, and 20 ml (based on b/v). The acetylation process it does not require heating but fairly by stirring as heat reaction produced enough to process. The yield of cellulose acetate to research can be seen in figure 2. Yields a comparison between weights cellulose acetate obtained by weights cellulose used in the acetylation process (Bahmid *et al.*, 2013).

The increasing number of a reactant will upping the odds of the collision between a reactant that accelerates speed reaction thus produced yield larger. But if the number is too greater and will speed reaction faster and having no the product will cause some products degraded and reduce yield total. In this study yield of empty bunches of oil palm cellulose acetate small enough to the ratio cellulose/acetate anhydrous 1 / 5 of 7.36 % and went to the ratio of 1/ 0 16.2%. On ratios 1/15 yield empty bunches of oil palm cellulose acetate declining to 15.02% and fall on ratios 1/20 be 9,59%. So steady empty bunches of oil palm yield to get to the ratio 1/10. On dry jacfruits leaves yield get to the ratio of 1/5 42,72% and decreased on larger ratios. In previous studies (Bahmid *et al.*, 2013) yield of

cellulose steady obtained on ratios cellulose/acetate anhydrous on 1/10.

Cellulose solid forming a structure microcrystal with regional order amorphous on that low (Suryanto, 2016). Dry jacfruits leaves cellulose more amorphous tend to be more reactive than empty bunches of oil palm more crystalline. So that, more dry jacfruits cellulose molecules that react with a reactant (acetic acid anhydrous) produce cellulose acetate compared empty bunches of oil palm.

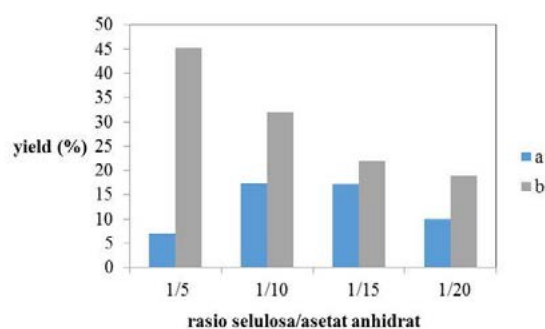


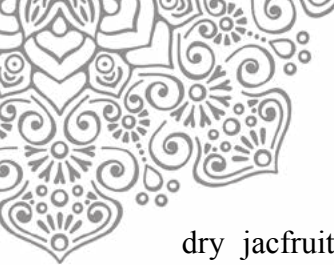
Figure 2. Correlation ratio of cellulose/acetic anhydrous with yield of cellulose acetate (a). empty bunches of oil palm, (b). dry jacfruits leaves

Characterization of Cellulose Acetate

FTIR (Fourier Transform Infra Red)

Cellulose

Cellulose composed by three the functions C-O, O-H, and C-H. The analysis of FTIR against cellulose empty bunches of oil palm and dry jacfruits leaves is presented in figure 4.7. Of pictures 3 shows that cellulose empty bunches of oil palm indicated by absorption at the numbers 3334,06 cm^{-1} to group O-H, 2895,93 cm^{-1} to C-H, 1029,63 cm^{-1} to group C-O and



dry jackfruits leaves on $3334,86\text{ cm}^{-1}$ to group O-H, $2911,27\text{ cm}^{-1}$ to C-H, $1027,34\text{ cm}^{-1}$ to group C-O. In this study cellulose of empty bunches of oil palm and dry jackfruits leaves having absorption at panjag waves similar. Research conducted by Bahmid *et al.* in 2014 against cellulose extracted from empty bunches of oil palm there are infiltration to the O-H at the 3348 cm^{-1} , C-H on 2901 cm^{-1} and C-O on 1065 cm^{-1} .

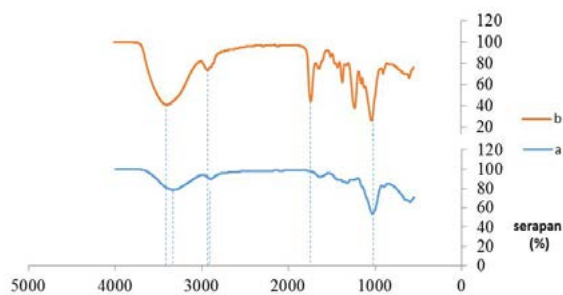


Figure 3. FTIR spectrum on empty bunches of oil palm (a) cellulose (b) cellulose acetate

Cellulose acetate

Based on the graphic in figure 3 and 4, the success of acetylation seen from before and after the acetylation process (Kannamba, 2015). Cellulose acetate composed of four the functions C-O, O-H, C-H, and C=O.

From picture 3 seen change the function in a spectrum cellulose and cellulose acetate empty bunches of oil palm. These differences is the forming of a the group C=O (the carbonyl group) at wavelengths $1732,93\text{ cm}^{-1}$ on cellulose acetate and not on cellulose. At length $1732,93\text{ cm}^{-1}$ was seen the depth peak are high as well as at wavelengths $3394,97\text{ cm}^{-1}$. This shows that the majority of the O-H on cellulose subtited by acetyl group (Bahmid *et al.*,

2013). Something similar happened to research conducted by Nurhayati *et al.* in 2014 producing cellulose acetate of sewage treatment where happened to the absorption sharp at the carbonyl group C=O showed the acetylation. Cellulose acetate from the study showed the same approach with cellulose commercial infiltration demonstrated by an absence of sharp at the O-H and C=O and sharp happened infiltration also in acetyl group C-O at wavelengths $1227,73\text{ cm}^{-1}$. Change the function in a spectrum cellulose and cellulose acetate dry jackfruit leaves. These differences is the forming of a the group C=O (the carbonyl group) at wavelengths $1728,82\text{ cm}^{-1}$. FTIR spectrum can be proven that the process acetylation cellulose dry jackfruit leaves have managed to be done.

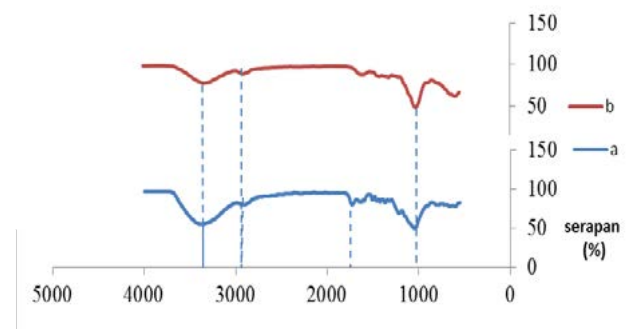
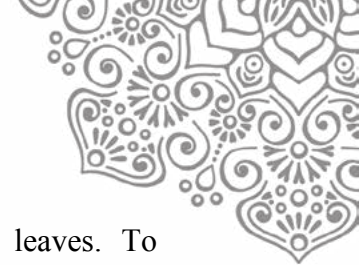


Figure 4. FTIR spectrum on dry jackfruit leaves (a) cellulose (b) cellulose acetate

SEM Analysis

In figure (a), the surface cellulose acetate empty bunches of oil palm looked crowded with pores who disappeared. Cellulose acetate of dry jackfruit leaves looks more solid with color quite equally and a little shiny. From the description morphology cellulose acetate empty bunches of oil palm and dry jackfruit leaves it appears that cellulose acetate dry



jackfruit leaves harder than empty bunches of oil palm. The result of this research have a difference with research conducted Bahmid *et al.*(2013) that cellulose acetate empty bunches of oil palm yielding fibers perforated. According to Rachmawaty *et al.*(2013) morphology membrane obtained from cellulose acetate plant hyacinth showed pores in diameter 1-10 μm . cellulose acetate morphology of empty bunches of oil palm and dry jackfruit leaves was different as different types of crops selulosanya sources. According to Vallejos *et al.*(2012) no change form or morphology cellulose acetate because in reaction of acetylation would only acetyl group to the molecule polymer cellulose and not change morphology. So, cellulose acetate empty bunches of oil palm and dry jackfruit leaves having specific morphology.

Cellulose acetate empty bunches of oil palm on ratios this 1/10 showed fiber denser and the surface wavy with pores wider. It is like research conducted by Natalia *et al.*(2015) where by comparison cellulose/acetate anhydrous = 1/16 produce cellulose acetate with pores greater than 1/32. While cellulose acetate dry jackfruit leaves show results that the same will and yet seemingly fiber shaped ring so clearly lined up lined. The horizontal looking of the is cellulose acetate with acetyl group while fiber ring shaped is a compound chromophore aromatic seems clearly when almost all cellulose react with acetic acid anhydrous. A compound chromophore aromatic dye cellulose was still carried away after the bleaching. A compound chromophore aromatic was allegedly is a compound phenol form lignin leaves and still brought

in cellulose of dry jackfruit leaves. To know exactly the compound were necessary an analysis of the composition cellulose the extraction before acetylation and analysis composition cellulose acetate with SEM-EDX or XRD.

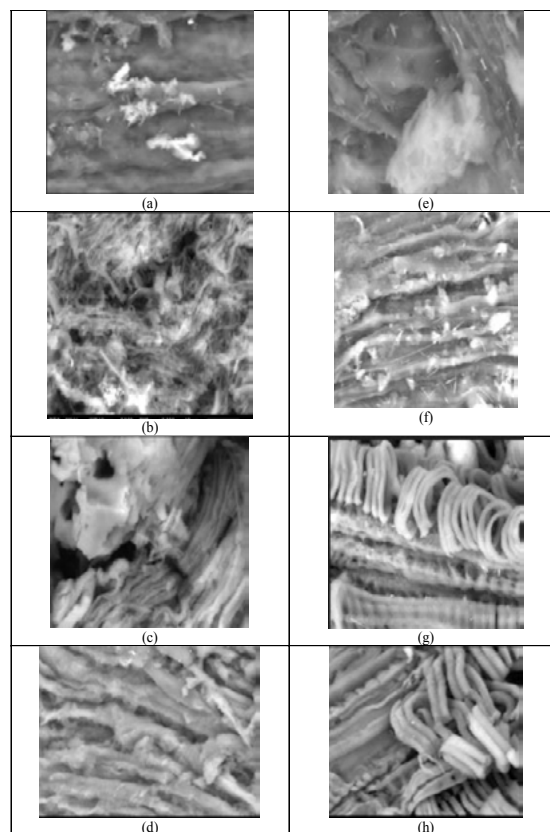
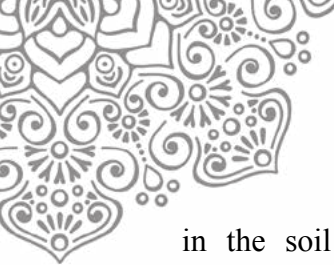


Figure 5. Cellulose acetat SEM result of empty bunches of oil palm (a,b,c,d) dan dry jackfruit leaves (e,f,g,h) : (a)/(e). rasio selulosa/asetat anhidrat = 1/5; (b)/(f). 1/10; (c)/(g). 1/15; (d)/(h). 1/20

The degradation cellulose acetate

As an alternative on substitute for microbeads polyethylene, cellulose acetate must have the trait of being readily described by environment naturally by microorganisms. So, testing done to burial



in the soil that taken of a drain from household a number of one liter of in a glass container. 50 mg cellulose acetate wrapped in breathable plastics and was buried in the land.

The land was drained a mixture of water, detergent, and slightly ammoniac continuously. Sample buried for 5, 10, 15, and 20 days to acknowledge the number of cellulose acetate that is decomposed by microorganisms in a media the ground. Samples have been buried in accordance variable day in washing clean and dioven at a temperature less than 50°C, then weighed heavy the rest of cellulose acetate that is not yet decomposes. From these results can be calculated how cellulose acetate that is decomposed by the environment. The number of cellulose acetate that is degraded can be seen on a figure 6. Cellulose acetate suffered degradation until 69 % and 63.2 % to 20th day.

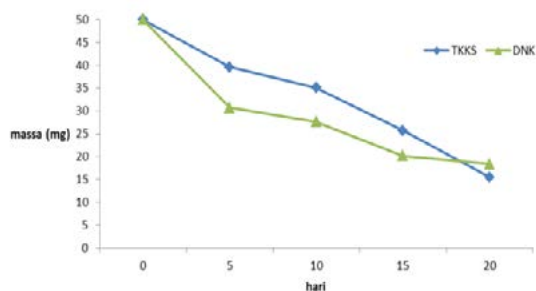


Figure 6. Corelation day with cellulose acetate mass lost

Conclusions

Cellulose acetate resulting from bunches empty palm oil and dry jackfruit leaves having percent acetyl around 39,8 % and in accordance with SNI 39-40 %. Making yield largest cellulose acetate empty bunches of oil palm is on the ratio cellulose/acetate anhydride 1/10, and

leaves nangka dry equal to 1/5. Cellulose acetate is an ingredient bioplastic capable of relegated to 69 % that bunches of oil palm and 63,2 % that dry jackfruit leaves based on the day 20th.

References

- Bahmid, N.A. 2014. Pengembangan Nanofiber Selulosa Asetat dari Selulosa Tandan Kosong Kelapa Sawit untuk Pembuatan Bioplastik. Bogor : IPB. Pp. 15-18.
- Gaol, M.R., Sitorus, R., Yanthi. 2013. Pembuatan Selulosa Asetat dari α -selulosa Tandan Kosong Kelapa Sawit. Departemen Teknik Kimia. Medan : Universitas Sumatera Utara. pp. 33-38.
- Nazir, M.S. 2013. Eco-friendly Extraction and Characterization of Celullose from Oil Palm Empty Fruit Bunches. *BioResources*8(2). pp. 2161-2172.
- Ngadi, N. dan Lani, N.S. 2014. Extraction and Characterization of Cellulose from Empty Fruit Bunch (EFB) Fiber. *Jurnal Teknologi*. pp.35-39.
- Morice C.H., Radigue B. & Winckler C. (2015). Cellulose Acetate Technology to Replace Banned PE beads. p. 1-4.
- Sasongko W.T., Yusiati. 2010. Optimalisasi Peningkatan Tanin Daun Nangka dengan Protein Bovine Serum Albumin Protein. Yogyakarta : UGM. p. 156.
- Istiqhlah, A. 2006. Biodegradasi Membran Selulosa Asetat Berpori dari Limbah Kulit Nanas



- Menggunakan *Bacillus subtilis*.
Bogor : IPB. pp. 1-12.
- Puls, J. 2011. Degradation of cellulose acetat –based material : A review. *J polum Environ.* pp. 152-154.
- Putera, R.D. 2012. Ekstraksi serat selulosa dari tanaman eceng gondok (*Eichornia Crassipes*) dengan variasi pelarut. Depok : FTI-DTK. pp.29-35.
- Bahmid, N.A., Maddu, A., Syamsu, K. 2013. Production of cellulose acetate from oil palm empty bunch fruit bunches cellulose. pp. 12-18.
- Pinnata, R. dan Damayanti, A. 2012. Pemanfaatan Selulosa Asetat Eceng Gondok sebagai Bahan Baku Pembuatan Membrane untuk Desalinasi. Jurusan Teknik Lingkungan. Surabaya : ITS. pp. 7-8.
- Sakai, K. 1996. Biodegradation of Cellulose Asetat by *Neisseria sicca*. *Bioscience, biotechnology, and biochemistry.* Taylor & Francis. pp. 6-9.
- Barkalow, D.G., Rowel, R.M., dan Young, R.A. (1989). A new Approach for the Production of Cellulose Acetate : Acetylation of Mechanical Pulp with Subsequent isolation of Cellulose Acetate by Differential Solubility. *Journal of Applied Polymer Science, Vol. 37*, p.1009.
- Sasongko, W.T., Yusiati, L.M., Bachruddin, Z., dan Mugiono. (2010). Optimalisasi Peningkatan Tanin Daun Nangka dengan Protein Bovin Serum Albumin. *Buletin Peternakan Vol.34 (3).* p.156.
- Wardani, A.P., dan Widiawati, D. (2014). Pemanfaatan Tandan Kosong Kelapa Sawit sebagai Material Tekstil dengan Pewarna Alam untuk Produk Kriya. *Jurnal Tingkat Sarjana bidang Senirupa dan Desain.* p.1.
- Tresnawati, A. (2006). Kajian Spektroskopi Inframerah Transformasi Fourier dan Mikroskop Susunan Elektron Membran Selulosa Asetat dari Limbah Nanas. p. 20.
- Mohan S.K., dan Srivastava T. (2010). Microbial deterioration dan degradation of polymeric materials. *J Biochem tech.* p.3.
- Mulawati E,C. (2012). Pembuatan dan Karakterisasi Membran Nanofiltrasi untuk Pengolahan Air. p. 5.
- Widyaningsih, S. dan Radiman, C.L. (2007). Pembuatan Selulosa Asetat dari Pulp Kenaf (*Hibiscus cannabinus*). p.10.
- Gaol M.R., Sitorus, R., Surya, Y.S., dan Manurung, R. (2013). Pembuatan selulosa asetat dari α -selulosa tandan kosong kelapa sawit. p. 2.
- Syamsu, K. dan Kuryani, T. (2014). Pembuatan biofilm selulosa asetat dari selulosa microbial nata de cassava. p. 6.



THE 15TH INTERNATIONAL CONFERENCE QUALITY IN RESEARCH (QIR) 2017

DEVELOPMENT METHOD OF MAKING DYE SENSITIZED SOLAR CELL (DSSC) USING CARBON AS COUNTER ELECTRODE

Wisnu Ananda^a, Anies Mutiari^a, Pramujo Widiatmoko^b

^a*Center for Material and Technical Product, Ministry of Industry of Indonesia, Jl Sangkuriang 14 Bandung West Java, Indonesia*

^b*Department of Chemical Engineering, Institute Technology Bandung, Jl. Ganesha 10 Bandung West Java, Indonesia*

ABSTRACT

Dye Sensitized Solar Cell (DSSC) is known as one of the promising third generation types of solar cell which is being developed nowadays. The main challenge on the development of DSSC is to increase solar-electricity conversion efficiency. To reduce cost of cell, Pt-based counter electrode needs to be substituted with carbon. It is identified that structure of electrode affects to DSSC performance. Hence, electrode deposition method is important. Our study therefore identifies effect of electrode preparation method on the performance of DSSC. The method will be important for scaling-up the cell size. Working and counter electrode were prepared from TiO₂ and activated carbon, respectively. Both TiO₂ and activated carbon were coated on transparent conductive glass using two methods, i.e. bar coating and doctor blade coating. Eosin yellowish and iodide-triiodide redox couple were used as dye and electrolyte, respectively. Crystalline structure of TiO₂, surface area of carbon particles, and electrochemical properties were examined using X-ray diffractometer, surface area analyzer, and electrochemical impedance spectroscopy. We found that doctor blade coating method provide higher performance of DSSC compared with bar coating. The efficiency of prepared DSSC reached 2.76%.

Keywords: Solar Cell; Dye Sensitized Solar Cell; Carbon; Counter Electrode; Bar Coating; Doctor Blading



1. INTRODUCTION

Increasing global demand for energy security is facing depletion of fossil-based energy reserve (i.e. oil, coal and natural gas). This condition drives the increasing demand on renewable, low-cost and omnipresent energy sources. One of the most anticipated ways to secure the future world energy supply is utilization of solar energy. Photovoltaic device is attractive approach for the solar utilization as it can directly convert solar energy into electricity. Globally, the photovoltaic production growth reaches 47% per year (Platzer, 2015). The growth is expected to increase to meet the challenge of solar cells installation worldwide of 200 gigawatts in 2020 and two terawatts in 2050 (Abermann, 2013).

There are two types of commercially available photovoltaic cell. The first is silicon wafer-based photovoltaic cells i.e. single-crystal and polycrystalline silicon wafers. The cells already have high efficiency, 20% -21.5% (Abermann 2013). High energy for processing the cells and waste issue however become constraint for producing silicon wafer-based photovoltaic. The second type of commercial photovoltaic is made using thin film technology. This technology has been demonstrating the use of less than 1% of silicon compared with the requirement of raw material for silicon wafer type (Nathan S. Lewis 2005). The key feature of second generation photovoltaic is the utilization of certain materials with high optical absorption coefficient as solar absorber. Materials such as amorphous silicon (a-Si) (laboratory record efficiency of 12 %), Cadmium Telluride (CdTe) (efficiency of 17%) and group chalcopyrite such as Cu(In,Ga)Se₂ (CIGS) (efficiency 22.3%) (Kamada et al. 2016) have been explored. Compared with the silicon wafer based-photovoltaic, thin film photovoltaic has obvious drawback of lower efficiency.

To reduce the production cost meanwhile maintains high solar-electricity conversion efficiency, third generation solar cells are being developed. One of them is Dye-Sensitized Solar Cells (DSSC). The DSSC was first developed in 1970s using oxide semiconductors, dye-based sensitizer, and electrolyte (Bose et al. 2015). A publicly noticed breakthroughs has occurred in 1991, when Michael Grätzel and Brian O'Regan showed improved conversion efficiency of 7.12% (Ye et al. 2015). DSSC are expected to be used for future clean energy. Its performance is primarily depend on the material and quality of the semiconductor electrode, the sensitizer dye used, and fabrication. In DSSC, the dye sensitizer plays a keyrole in absorbing sunlight and transforms solar energy into electrical energy. Numerous metal complexes and organic dyes have been synthesized and utilized as sensitizers. Up to now, the highest efficiencies for DSSC have been obtained using Ru-containing sensitizer compounds absorbed onto Nano crystalline TiO₂, reached efficiency of 11–12 % (Kalaivani et al. 2016).

DSSC is different to conventional PV cells, with the semiconductor accomodated both functions as absorber layer and charge transfer. DSSCs required different component for the photoreceptor and charge carrier. This separation of functions leads to lower purity demands on raw materials and consequently makes DSSCs a low-cost alternative. Because of the low cost, relatively easy preparation, good performance, and environmental benignity compared with traditional photovoltaic devices, DSSCs have aroused intense interest and



been regarded as one of the most prospective solar cells among the third-generation PV technologies (Wu et al. 2015).

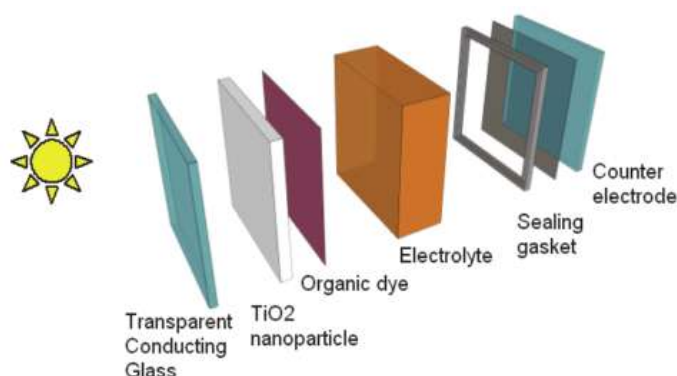


Figure 1 Typical configuration of a DSSC (Kosyachenko 2011)

The current DSSC design involves a set of different layers of components stacked in serial, including glass substrate, transparent conducting layer, TiO₂ nanoparticles, dyes, electrolyte, and counter electrode covered with sealing gasket (Kosyachenko 2011). The typical configuration is shown in Fig. 1. In the front of the DSSC, there is a layer of glass substrate which covers a thin layer of Transparent Conductive Oxide (TCO). It allows sunlight penetrates into the cell while conducts electron to outer circuit. The commercial TCOs are prepared from Fluor-doped Tin Oxide (FTO), Indium-doped Tin Oxide (ITO), and Aluminum-doped Zinc Oxide (AZO) (Hofstetter & Morkoc 2010). The ITO has the best performance among all TCOs substrates (Bright 2007). However, Indium in ITO is regarded as rare metal, toxic and expensive metal. Therefore some research groups prefers FTO rather than ITO (Kosyachenko, 2011).

For semiconductor material, nanocrystalline-TiO₂ has been commonly chosen to provide high light capture efficiency. It has been fabricated by hydrothermal autoclaving and screen-printing deposition (Daniyan et al. 2013). Screen-printing of TiO₂ is a widespread industrially-applied method because of the fast-printing technique and of the coating facility with fine controlling of the position and thickness (Ito et al. 2007).

Dye molecules are the key component of a DSSC. It can increase cell efficiency with their abilities to absorb visible light photons. Early DSSC designs involved transition metal coordinated compounds (e.g., ruthenium polypyridyl complexes) as sensitizers. The compounds have strong visible absorption, long excitation lifetime and efficient metal-to-ligand charge transfer (O'Regan & Grätzel, 1991; Grätzel, 2005; Ito et al., 2008). However, high cost of Ru dyes (>\$1,000/g) is one significant factor hindering the large-scale implementation of DSSC (Dileep & Reddy 2015). Eosin Yellow can be an alternative since it's cheaper and showed a good performance as a photoanoda (Arote et al. 2014).

Redox couple of I⁻/I₃⁻ in organic solvents is commonly used as electrolyte. The electrolyte has good ion diffusion and infiltrate well with TiO₂ film which is important to keep highest



efficiency. Limited long-term stability due to volatilization of liquid however may hinder wider application (Konno et al., 2007).

In other side of DSSC, glass-covered thin layer platinum (Pt) is commonly used as a catalyst to regenerate I⁻ and as the cathode material (Thomas et al. 2014). Recently, the Pt is considered as the best material to gain efficient devices, despite of its high price. Conducting polymers can also be applied as counter electrode. Polyaniline film on stainless steel by electrochemical polymerization has been reported as a counter electrode of DSSC (Qin et al., 2010). Meanwhile, carbon has been proposed as ideal substitute for the cathode material. Carbon black, carbon nanotubes and other types of carbon have been explored (Imoto et al. 2003). In 2006, Grätzel's group employs carbon black as the material of counter electrode, and reaches an efficiency of 9.1%, which is 83% of efficiency using Pt (Yu et al., 2009). To our knowledge, the information on the effect of carbon electrode preparation on the performance of DSSC is less available.

2. METHODOLOGY/ EXPERIMENTAL

Working and counter electrodes, dye solution, and electrolyte solution have been prepared. Identification of TiO₂ and characterization of DSSC have been conducted using X-ray diffraction, surface area analyzer, and electrochemical measurement.

2.1 Preparation of working electrode and counter electrode

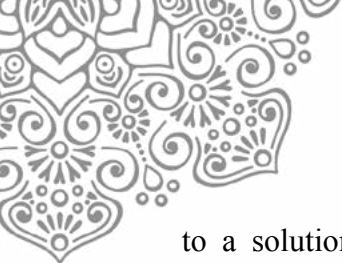
Working and counter electrodes were prepared from particles of TiO₂ and commercial activated carbon, respectively. Before being deposited, the FTO glass resistance is tested by using multimeter to determine the conductive side. Counter electrode was prepared from 0.25 g carbon powder and 15 mL dimethylformamide. The carbon-coated counter electrode was heated in electric furnace at 160 °C for 40 minutes. Working electrode was prepared from paste of 1 g of TiO₂ powder and 30 ml of acetic acid deposited onto conductive glass surface. Sintering of the working electrode was conducted at temperature of 450 °C for 30 minutes. Preparation of electrodes made using two methods i.e. bar coating and doctor-blade coating. Both working and counter electrodes were prepared on conductive glass with dimension of 2.5 cm x 2.5 cm and 10 cm x 7 cm. Schematic diagram of particle coated TCO is presented in Figure 2.

2.2 Preparation of dye sensitized

Eosin Yellowish solution was prepared by dissolving the dye into ethanol. The solution composition is 0.138 g Eosin Yellowish in 20 mL ethanol.

2.3 Preparation of electrolyte solution

Electrolyte solution is consisting of redox couple of iodine and Iodide (I⁻ / I₃⁻). First, 6 g potassium iodide and 3 g of iodine was mixed and stirred for 1 hour. KI solution was added



to a solution of iodine-acetonitrile with iodine concentration of 0.05 M. The prepared solution then was stored in sealed bottles to prevent evaporation.

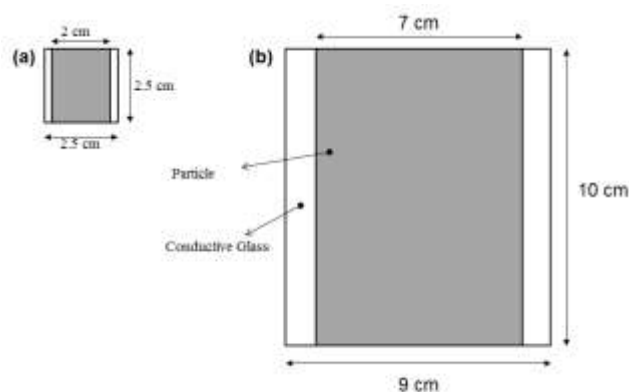


Figure 2 Scale-up scheme particle layer on a conductive glass size (a) small (b) big. Comparison of the size of the image represents the actual size comparison.

2.4 Immersion of working electrode with dye solution

The TiO₂ deposited working electrode was immersed in the dye solution to allow dye attachment. The dye was allowed to permeate and dry on the TiO₂ layer for 24 hours, and the dye-coated working electrode was ready for the next stage.

2.5 Assembling of DSSC

The working and counter electrodes were stacked to form a solar cell. The DSSC was assembled to be sandwich-like structure by placing the Dye-TiO₂-coated working electrode and carbon-coated counter electrode. Both electrodes were then clamped using a paper clip. Electrolyte solution was pipette dropped between the electrodes.

3. RESULTS AND DISCUSSION

We prepare the electrodes using bar coating and doctor blade techniques. The activated carbon can be coated successfully on the surface of counter electrode with both techniques. A layer of carbon that formed relatively stable and does not exfoliate after exposed to heating process at 160 °C for 40 minutes. The carbon layer also relatively stable, even after exposed to electrolyte.

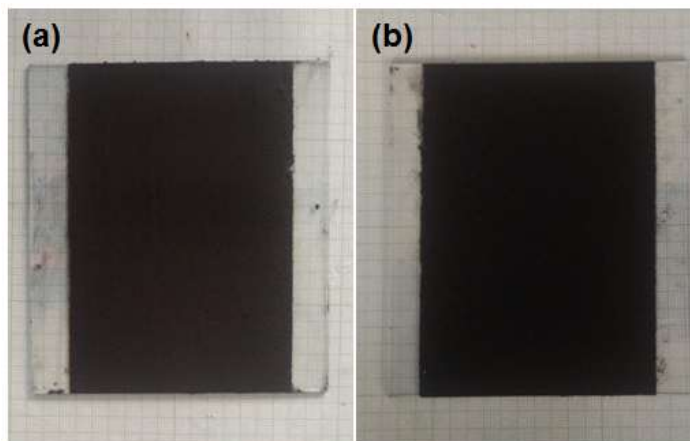


Figure 3 Working Electrode Layer of Carbon to the Method (a) Bar Coating (b) Doctor Blading Coating

TiO₂ coating for working electrode are more difficult than carbon coating. The main problem to be solved is cracking that occurred after the heating process at 500 °C. Based on qualitative observations, the conductive glass deformed after heating, caused breakage of TiO₂ layer (see Figure 4). Statistically, the successful deposition with the 500 °C heating process is one to four. To overcome this problem, the heating temperature was then lowered to 450 °C. Decreasing heating temperature managed to eliminate the effects of deformation of the conductive glass, as well as the cracking.

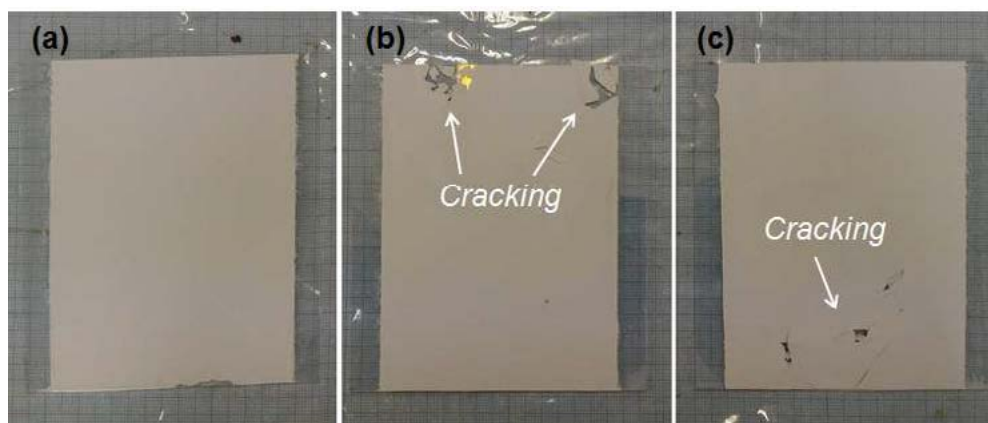
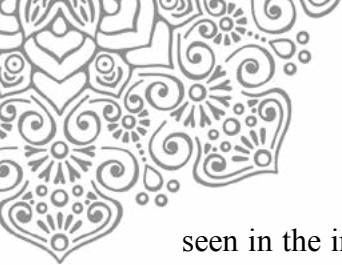


Figure 4 Duplication TiO₂ depositions after Heating Process at 500 °C for 30 minutes with the Doctor Blade Coating Method

Cracking the TiO₂ layer is supposed also affected by the evaporation of acetic acid solvent. The solvent evaporates leaving behind pores under a layer of TiO₂. Rapid heating and the distributed particle size aggravate the condition. Further effects of these conditions can be



seen in the immersion process TiO_2 layer in the dye solution. These layers are not strongly attached to the conductive glass and exfoliate after immersion for 12 hours (see Figure 5). To overcome these obstacles, the coating method is modified to provide slight pressure on the pasta particles which stick better on conductive glass. A simple modification has increased the chances of successful coating to 100% (in four experimentals). The examples of working electrode prepared with the modified TiO_2 coating technique are presented in Figure 6.

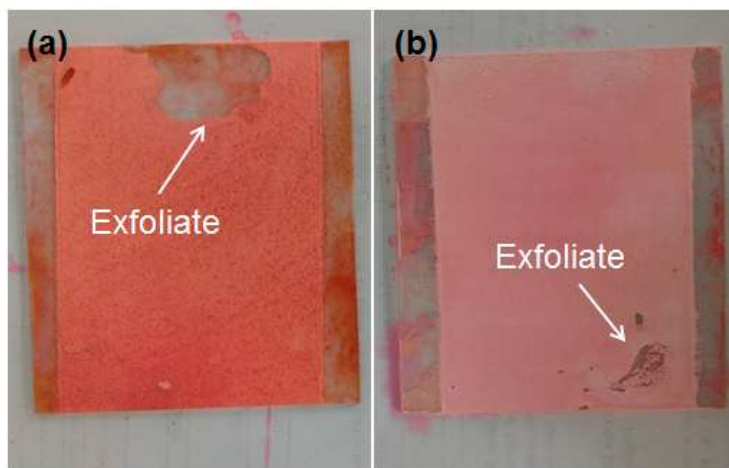


Figure 5 Results TiO_2 Immersion in the Dye Method (a) Doctor Blading Coating (b) Bar Coating

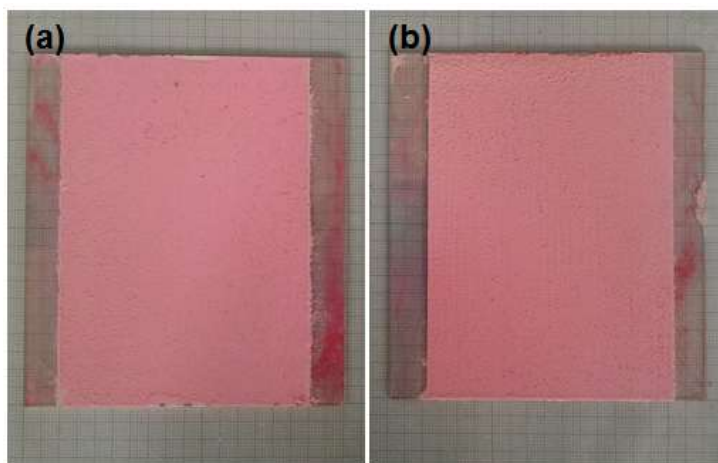


Figure 6 Results duplication TiO_2 immersion in the dye with a modified method of Bar Coating (a) Experiment 1 and (b) Experiment 2



The next experiment was testing the performance of the DSSC. Current-Voltage curve (I-V curve), including Open circuit voltage (V_{oc}) and short circuit current (I_{sc}), was measured using digital multimeter over a given load under 100W halogen lamp. The load was varied to the circuit by using a variable resistor.

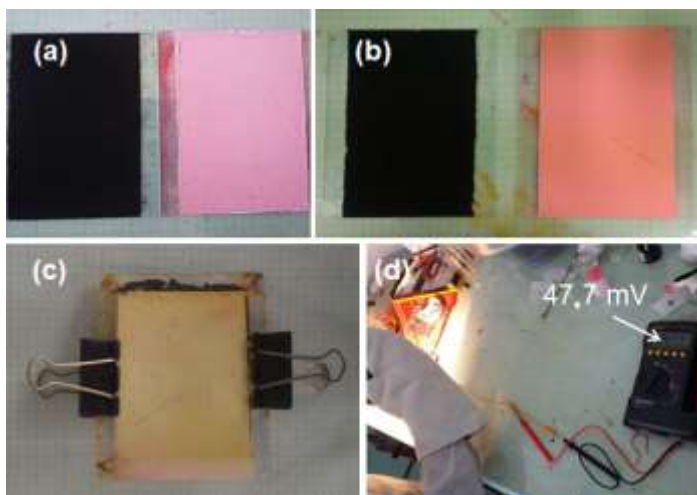


Figure 7 Pair of electrodes with the method (a) Bar Coating, (b) Doctor Blade Coating, (c) the typical range of DSSC and (d) an example of the open circuit voltage measurements

We test the big size DSSC cells prepared using bar coating and doctor blade coating (Figure 7). The first experiment with cell method produces Open Circuit Voltage (V_{oc}) in the range of 10-20 mV. This result is much smaller when compared to V_{oc} of small size cell which reaches 400 mV. Modification was carried out on the second experiment by adjusting the distance between the electrodes and improved circuit contacts. This adjustment successfully increased the V_{oc} to 47.7 mV. However, the cell voltage dropped to 8 mV when tested for I-V curve. Repair cell coupling method is currently the focus of an experiment to improve V_{oc} . Meanwhile, the DSSC prepared using doctor blading coating method does not give any voltage. It is supposed that the dye does not adsorb well on a smooth surface of doctor blade coating results. After adjustment of immersion time to 48 hours, the prepared DSSC produced V_{oc} of 34 and 63 mV for bar coating and doctor blade technique, respectively. Small I_{sc} (30 – 125 μ m) indicated that the system is still facing high resistance problem.

Comparing with small size DSSC, the big size DSSC performance is significantly low. The efficiency of small size DSSC with commercial activated carbon-based reached 2.76%, with I_{sc} of 0.423 mA and V_{oc} of 400 mV. Figure 8 shows the I-V curve generated using commercial carbon with mesh size of 170.

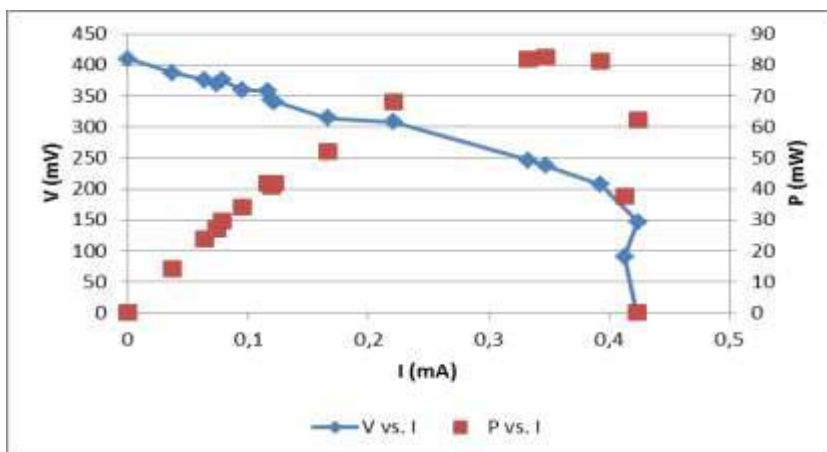


Figure 8 shows the I-V curve generated from small size DSSC using commercial carbon with mesh size of 170.

3.1 Result of BET

Qualitatively, curve adsorption-desorption isotherms of nitrogen to commercial activated carbon samples shown in Figure 9 shows that the sample follows the curve of type I isotherm (Langmuir type). In the early stages of an increase in the volume of nitrogen adsorption quite sharply due to increased gas pressure. This indicates that the pore size of particles mainly consist of micro pores. With this size, interaction between electrolyte and electrodes surface is hindered. Hence, the performance of DSSC becomes low. We need to increase the pore size into mesopore by chemical or physical treatment to improve diffusion and interaction on the surface of electrode.

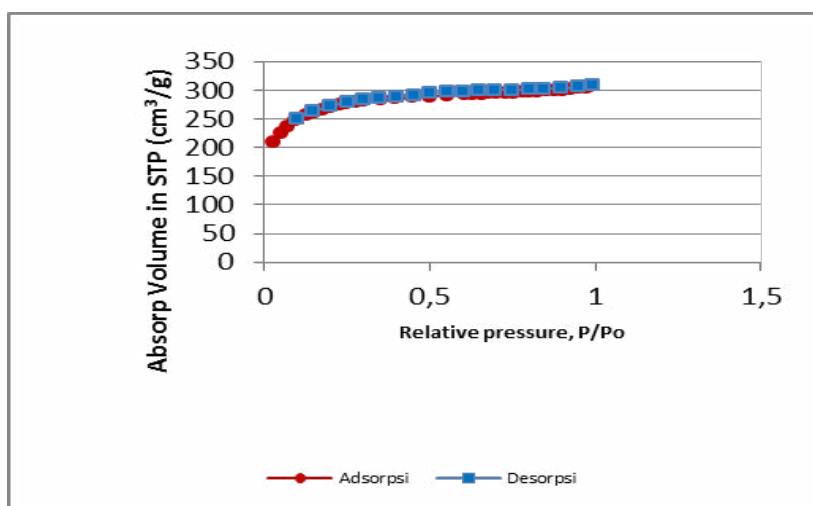


Figure 9. Isotherm curve adsorption-desorption sample of commercial active carbon



3.2 Result of EIS

Typical graph EIS of DSSC has three peaks. The first peak indicates the electron transfer process in counter electrode/electrolyte interface, the second peak showed diffusion isotherm on the TiO_2 layer and the reverse reaction isotherm with the result of oxidation at the interface of TiO_2 /electrolyte, and a third peak I_3^- describe diffusion in electrolyte solution. A systematic approach was also performed to characterize the test results of the EIS. Based on the results in Figure 10, we indicate the three semi-circles. While the peak one and three are much smaller than the second one, it can be said that the charge diffusion occurred at the interface of carbon / electrolyte and FTO / electrolyte and electrolyte diffusion I_3^- significantly affect the performance of DSSC. This EIS result seems in agreement with the BET result.

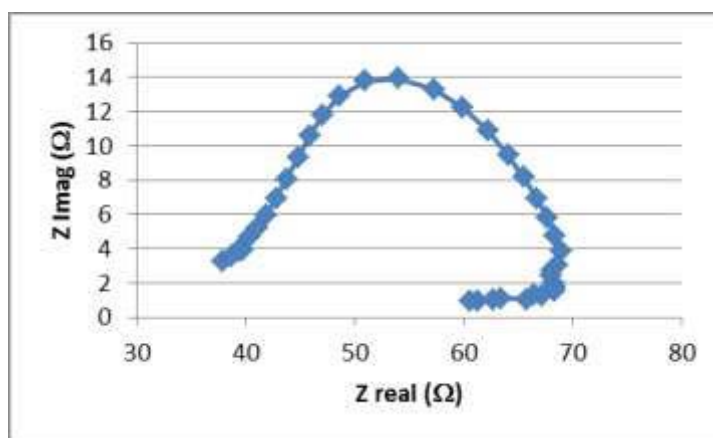


Figure 10. Results of EIS of DSSC with commercial activated carbon counter electrode

Figure 11 shows the results of XRD analysis of TiO_2 powder, which is used for coating the working electrode. The structure of TiO_2 powder is dominated by anatase. The use of TiO_2 nanoparticles in the anatase phase of DSSC potentially increases efficiency of solar-electricity conversion due to its high absorption capability (Kosyachenko 2011). The TiO_2 anatase phase has higher photocatalytic activity than the rutile and brookite phases (Kavan et al. 2014). TiO_2 with nanopore structure will increase the performance of the DSSC system because higher surface area. Therefore, it will increase the amount of absorbed dye as well as solar light.

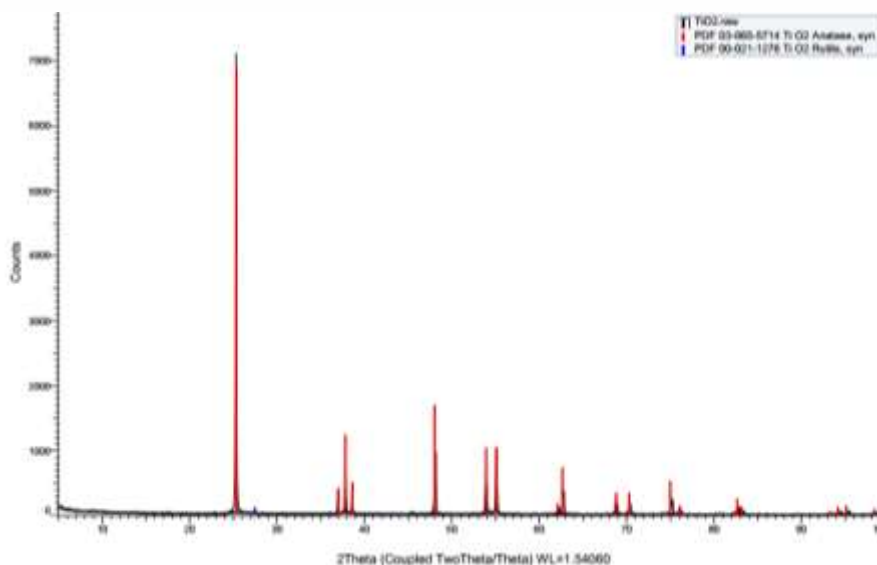


Figure 11 The results of XRD analysis of TiO₂

4. CONCLUSION

We successfully prepared DSSC with carbon based-electrode. The result of scale up DSSC is still lower than small size DSSC. Based on the experiment result, the charge diffusion transfer from electrolyte to electrode surface is the main challenge during the DSSC scale-up process. We also found that deposition method significantly affects performance of DSSC. Therefore we will explore the deposition technique further to achieve higher conversion efficiency.

5. ACKNOWLEDGEMENT

This research was supported by 2016 State Budget of Center for Material and Technical Product, Indonesia Ministry of Industry. We thank our colleagues from Electrochemical Laboratory, Institute Technology of Bandung (assisted by Mhd Ridho Utomo and Hilham Zamriko Koto) who provided insight and expertise that greatly assisted the research. We thank Jumail Soba, Elmi Cahyaningsih and Sanny Febriany for assistance with particular technique and methodology.



6. REFERENCES

- Abermann, S., 2013. Non-vacuum Processed Next Generation Thin Film Photovoltaics : Towards Marketable Efficiency and Production of CZTS Based Solar Cells. *Solar Energy*, 94, pp.37–70. Available at: <http://dx.doi.org/10.1016/j.solener.2013.04.017>.
- Arote, S. et al., 2014. Eosin-Y sensitized tin oxide photoelectrode for dye sensitized solar cell application: Effect of dye adsorption time. *Journal of Renewable and Sustainable Energy*, 6(1).
- Bose, S., Soni, V. & Genwa, K.R., 2015. Recent Advances and Future Prospects for Dye Sensitized Solar Cells: A Review. *International Journal of Scientific and Research Publications*, 5(1), pp.2250–3153. Available at: www.ijsrp.org.
- Bright, C.I., 2007. Review of Transparent Conductive Oxides (TCO).
- Daniyan, A.A., Umoru, L.E. & Olunlade, B., 2013. Preparation of Nano-TiO₂ Thin Film Using Spin Coating Method. , 2013(July), pp.138–144.
- Dileep, A. & Reddy, M.D., 2015. Dye Sensitized Solar Cell (Dyssc). , 5(11), pp.43–48.
- Hofstetter, D. & Morkoc, H., 2010. ZnO Devices and Applications : A Review of Current Status and Future Prospects. , (7), pp.1255–1268.
- Imoto, K. et al., 2003. High-performance carbon counter electrode for dye-sensitized solar cells. *Solar Energy Materials and Solar Cells*, 79(4), pp.459–469.
- Ito, S. et al., 2007. Fabrication of Screen-Printing Pastes From TiO₂ Powders for Dye-Sensitized Solar Cells.
- Kalaivani, J. et al., 2016. TiO₂ based dyesensitized solar cell using natural dyes. *Nanosystems: Physics, Chemistry, Mathematics*, 7(4), pp.633–636. Available at: <http://nanojournal.ifmo.ru/en/articles-2/volume7/7-4/paper12/>.
- Kamada, R. et al., 2016. New World Record Cu(In, Ga)(Se, S)₂ Thin Film Solar Cell Efficiency Beyond 22%. In *Photovoltaic Specialists Conference (PVSC) IEEE 43rd*.
- Kavan, L. et al., 2014. Electrochemical Characterization of TiO₂ Blocking Layers for Dye-Sensitized Solar Cells. *The Journal of Physical Chemistry C*, p.140114142307002. Available at: <http://dx.doi.org/10.1021/jp4103614>.
- Kosyachenko, L.A., 2011. *Solar Cells – Dye-Sensitized Devices*,
- Nathan S. Lewis, 2005. *Basic Research Needs for Solar Energy Utilization “Report of the Basic Energy Sciences Workshop on Solar Energy Utilization,”*
- Platzer, M.D., 2015. US Solar Photovoltaic Manufacturing: Industry Trends, Global Competition, Federal Support.
- Thomas, S. et al., 2014. A review on counter electrode materials in dye-sensitized solar cells. *Journal of Materials Chemistry A: Materials for Energy and Sustainability*, 2(13), pp.4474–4490.
- Wu, J. et al., 2015. Electrolytes in dye-sensitized solar cells. *Chemical Reviews*, 115(5), pp.2136–2173.
- Ye, M. et al., 2015. Recent advances in dye-sensitized solar cells: From photoanodes, sensitizers and electrolytes to counter electrodes. *Materials Today*, 18(3), pp.155–162. Available at: <http://dx.doi.org/10.1016/j.mattod.2014.09.001>.



EMULSION STABILITY OF FUNGICIDE FROM EUGENOL AND CITRONELLA OIL IN 350 EC FORMULATION

Yenny Meliana^a, Savitri^a, Melati Septiyanti^a, Feni Amriani^a, Syahrul Aiman^a, Veny Luvita^b

^aResearch Center for Chemistry, Indonesian Institute of Sciences

^bResearch Center for Metrology, Indonesian Institute of Sciences

ABSTRACT

The emulsion stability of fungicide formula from eugenol and citronella oil had been studied. Eugenol and citronella are well known as active ingredients from clove and lemongrass oil, respectively. Their ability for fungus removal had been well recognized. Eugenol and citronella dissolved imperfectly in pegasol and ethanol, thus emulsifier surfactants are required to form an emulsion system of fungicide formula. Polyethylene glycol mono oleate (PMO) as non-ionic surfactants and methyl ester sulfonate (MES) as an-ionic surfactants are employed in present study. The emulsion system has the optimum stability in addition of surfactants ratio, PMO and MES, at 9:1 respectively. Moreover, the dispersion phase of these compounds (in 350 EC) is stable in emulsion system for 180 minutes. Further study, as the application, the performance and residues in plants, waters, and soil of pesticide's current formulation will be evaluated to acquire more valuable data which support the pesticide potential application.

Keywords: emulsion stability; fungicide formula; eugenol; citronella; emulsifer surfactants.

1. INTRODUCTION

Fungicide is a pesticide group which inhibits fungal growth by damaging the fungal cell or preventing its life cycle. The use of synthetic or chemical fungicides is a common use in these past years. It is already used for fungal control in world wide to protect crops and other agriculture products (Martínez 2012). Chemical fungicide causes environmental and human health issues due to residue trace on the crops for human consumption. Moreover, the resistency of fungal towards the synthetic fungicides is even more increasing (Zabka et al. 2014). Thereby, botanical extract based fungicides show negligible toxicity and less impact for human, other organisms and environmental. The new alternative is highly encouraged by using natural and ecofriendly products, like essential oil. Essential oils are volatile secondary metabolites produced in plants which can protect plants from pathogens, insects and solar radiation (Juárez et al. 2015).

Essential oil contain citronella from thyme, peppermint and lemongrass has antifungal activity against *Colletotrichum gloeosporioides*, *Lasiodiplodia theobromae*, *Monilinia fruticola*, *Rhizopus stolonifer* and *Penicillium* in avocado and peach plant (Sellamuthu et al. 2013). Citronella based essential oil also has strong antifungal effects against *Aspergillus niger* ATCC 16404 by destroying cell wall of *A. Niger* hyphae and working on main organelles to eliminate the hypae cell (Li et al. 2012). Another natural compound that has antifungal activity is eugenol which is main component of clove oil, cinnamon, basil and nutmeg. Eugenol has been reported to restrain the growth of *Escherchia coli*, *Listeria monocytogenes*, *Lactobacillus sakei*, wood decay fungi and *Botrytis cinerea* (Wang et al. 2010).

The limitation of active agent from essential oil is its properties that hardly dissolved in water. It is very important to develop stable formulation to increase the antimicrobial or antifungal efficacy. Formulating water insolubled active agent is an essential factor in the process of developing effective fungicide (Hu et al. 2016). Emulsion concentrate is



considered as economic fungicide formulation, since it can be spontaneously diluted in water and practically applied (Allawzi et al. 2016). Emulsion is a system which contains oil, water and surfactant. Surfactant role is to decrease the interfacial tension between oil and water to create smaller droplets and it is able to stabilize the emulsion system (Gupta et al. 2016). Stability is one of significant component in emulsion system because it is tend to breakdown overtime due to physicochemical mechanism (Restu et al. 2015). Many researches investigate the efficacy of eugenol and citronella oil (Koul et al. 2008; Barbas et al. 2017; Licciardello et al. 2013), however it is apparent that there is a knowledge gap regarding the role of surfactant agent addition to particular essential oils like eugenol and citronella oil which affected to emulsion stability of pesticide formula and simplifies its further application.

This study aimed to investigate the stability of emulsion concentrate system of eugenol and citronella oil based fungicide in 350 EC formulation with polyethylene glycol mono oleate (PMO) as non-ionic surfactants and methyl ester sulfonate (MES) as an-ionic surfactants.

2. EXPERIMENTAL

2.1 Material

The material used in this study are eugenol USP and citronella oil as the active agent was purchased from local essential oil industry. Polyethylene glycol mono oleate (PMO) and methyl ester sulfonate (MES) as surfactant was given by polymer chemistry research group, research center for chemistry LIPI, and ethanol (Merck, Indonesia, 96% wt/v), water and pegasol were used as the solvent. The composition of respective material is shown on Table 1 and Table 2 below.

Table 1 Composition Variation of Fungicide with Ethanol (%w/w)

	I	II	III	IV	V
Eugenol	25	25	25	25	25
Citronella oil	10	10	10	10	10
Pegasol	15	15	15	15	15
Ethanol	40	40	40	40	40
MES	5	4	3	2	1
PMO	5	6	7	8	9

Table 2 Composition Variation of Fungicide without Ethanol (%w/w)

	I	II	III	IV	V
Eugenol	25	25	25	25	25
Citronella oil	10	10	10	10	10
Pegasol	55	55	55	55	55
MES	5	4	3	2	1
PMO	5	6	7	8	9

2.2 Procedure

2.2.1. Formulation of Fungicide 350 EC

Formulation of fungicide consist of two solution. For first solution, eugenol and citronella oil were mixed with pegasol and MES in beaker glass and homogenized with speed 8000 rpm for 15 minutes. For second solution, ethanol 96% and PMO were mixed by magnetic stirrer for 15 minutes. Both solution were mixed and homogenized for 30 minutes. For the second formulation, the procedure was repeated but without ethanol 96% addition.



2.2.2 Stability Test of Fungicide 350 EC

Ten test tube were prepared for the stability test for all formulation. Each test tube was added by 10 ml water and 1 ml fungicide. The test tube was mixed manually by shaking the test tube until spontaneous emulsion formed. The creaming formation is recorded every 10 minutes for 3 hours. The best formulation from Formulation I and Formulation II was measured by micro particle size analyzer (Coulter LS 100 Q) to investigate the droplet size stability every 10 minutes for 180 minutes, zeta potential and conductivity measured by nano particle size analyzer (Horiba Nano Partica SZ-100).

3. RESULTS AND DISCUSSION

The stability result of fungicide formulation with several ratio of MES and PMO with ethanol is shown in figure 1 and the fungicide formulation without ethanol is shown in figure 2. The stability was investigated by recording the occurrence of creaming phenomena every 10 minutes for 180 minutes.

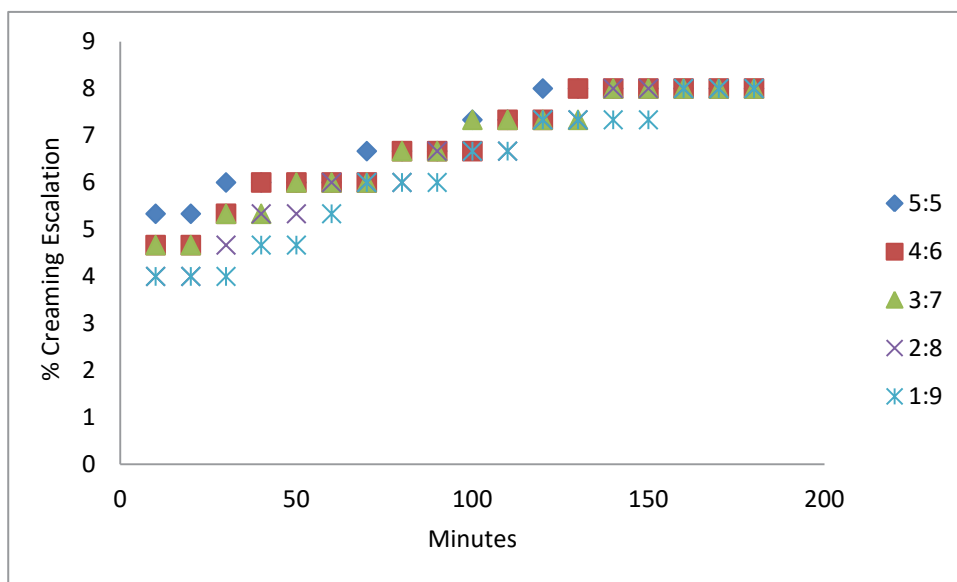


Figure 1. Creaming Escalation of Fungicide 350 EC with Ethanol

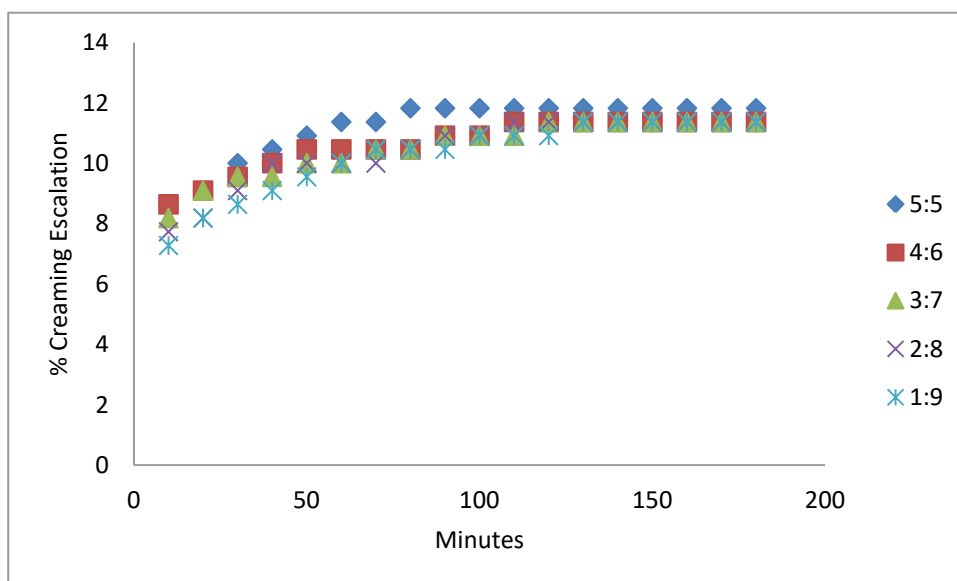


Figure 2. Creaming Escalation of Fungicide 350 EC without Ethanol



In Formulation I (shown in Figure 1), it is seen that creaming phenomena occurred in all formulation at minutes 10. Creaming percentage increase until 150 minutes and remain stable in 8% until 180 minutes. As for the ratio 1:9 the escalation of creaming slower than the remaining ratio where this formulation withstand the creaming escalation until 160 minutes. The similar result trend occurred in Formulation II (shown in Figure 2). Creaming percentage increase until 120 minutes and remain stable in 11.36% until 180 minutes in which these are the significant difference showing in figure 1 and 2 with the formulation with and without ethanol. Formulation with surfactant ratio 1:9 has slower creaming formation where it can maintain lower creaming percentage until 130 minutes.

Formulation with high nonionic surfactant concentration is able to withstand the cream much longer. This phenomena occurred because nonionic surfactant has higher concentration than anionic surfactant. Surfactant has important role in droplets' deformation and break-up. It is enable the presence of interfacial tension gradient, which is a key for formation of stable droplet. The existence of nonionic surfactant could lower the interfacial tension which could reduce the size and create a more stable emulsion system (Tadros et al. 2004). PMO as non-ionic surfactant is amphiphilic and the structure of the hydrophilic head group is necessary to improve the stability and also enhance binding the water molecule in the emulsion (Ibrahim et al. 2015).

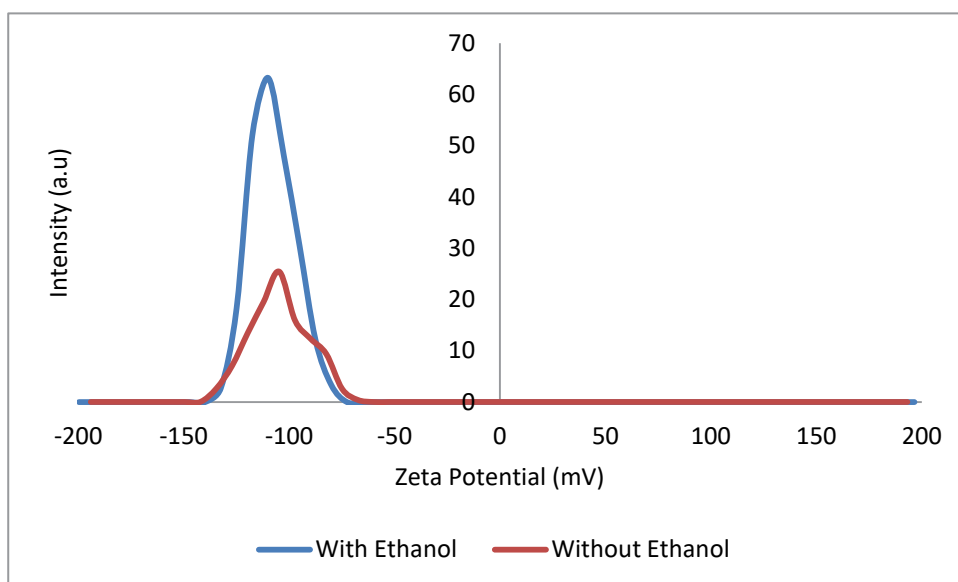


Figure 3. Zeta Potential Chart of Fungicide with MES : PMO (1:9)

Table 3 Zeta Potential and Conductivity of Fungicide with MES : PMO (1:9)

Formulation	Zeta Potential (mV)	Conductivity (mS/cm)
Fungicide with Ethanol	-109.3	0.116
Fungicide without Ethanol	-105.4	0.101

MES as anionic surfactant posses conductivity properties and the addition of non-ionic surfactant doesn't affect the conductivity in emulsion system (Danov et al. 2015). The formation of micelle is necessary to reduce surface tension and increase emulsion stability (Azizinezhad & Aghchehrood 2014). The tendency of creaming in emulsion indicate micelle is



not formed significantly due to low conductivity, as seen on table 3 where the conductivity of fungicide formulation with ethanol is 0.116 mS/cm and without ethanol 0.101 mS/cm. This can be concluded that non-ionic surfactant played dominant role in this system, yet MES as anionic surfactant doesn't compatible as co-surfactant in this system. Zeta potential commonly used to estimate the stability of emulsion. Theoretically, a high negative zeta potential indicate a stable system due to electrostatic repulsion (Achouri et al. 2012). The zeta potential result for fungicide formulation with ethanol is -109.3 mV and without ethanol is -105.4 mV. However, the emulsion formed in this study is unstable where the creaming phenomena occurred as shown in Figure 1 and Figure 2. Having a high value of zeta potential is no guarantee that the system will be stable in all condition. It is because zeta potential measurement is made on idle system. During the formulation the system is often subjected to shear such as stirring and other treatment that caused destabilization (Fairhurst 2013). In this case, the formulation due to time lapse where creaming occurred which is one of destabilization phenomena.

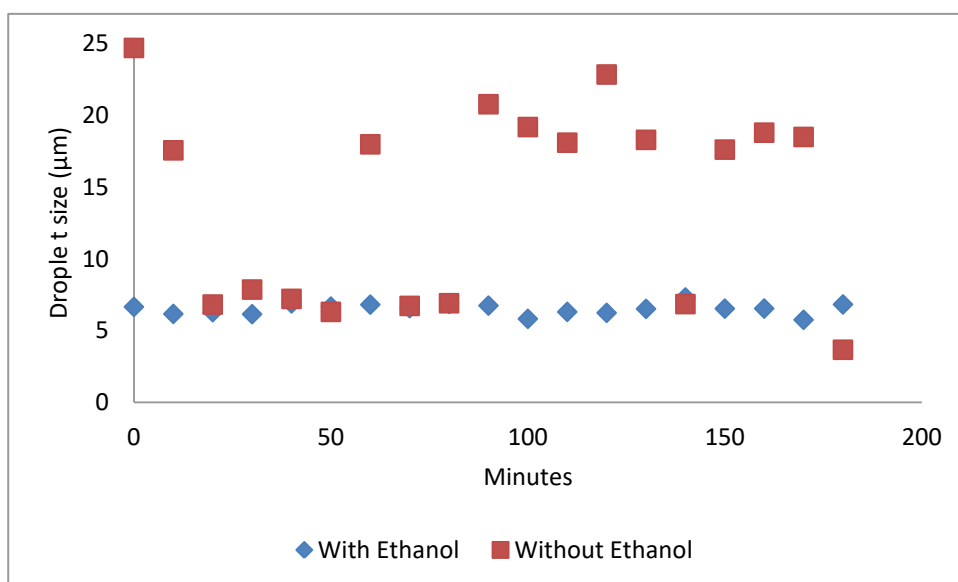


Figure 4. Average Droplet Size of Fungicide with MES : PMO (1:9)

The droplet size stability also investigated in this study. Figure 4 shown that the droplet size of fungicide formulation with ethanol is table compared than formulation without ethanol. The range droplet size range for Formula I is 5.756-7.313 µm, while the Formula II has wider range droplet size which is 3.672-24.69 µm. This shown that Formulation I is more stable and homogeneous droplet size than Formulation II. Due to bigger droplet size, Formula II tend to cream faster than Formula I. The creaming velocity in emulsion increased as increasing droplet size (Chanamai & McClements 2000).

It is also seen in Figure 1 and Figure 2 that the formulation with ethanol has lower creaming percentage which is 8% compared with the formulation without ethanol that is 11.36%. It showed that ethanol could enhance the solubility and the stability of this system compared with pegasol due to its water solubility properties. Pegasol is a petroleum based oil which is insoluble in water (Milne 2005). Ethanol is used as solvent because it is a polar solvent and miscible in water. The addition of ethanol into PMO in this research was aimed to alter interfacial impromptu flection and elasticity film of hydrophilic surfactant (PMO) that will improve emulsion stability system when they were mixed with the oil based solution (Garti N



et al. 2001). Thus, the solubility and stability in a formulation with ethanol were more significant than the formulation without ethanol. Moreover, it is also considered environmentally safe because ethanol less hazardous compared with aromatic solvent which is common used in pesticides formulation (Allawzi et al. 2016). Emulsion in application on antifungi is composed of oil and water, stabilized by surfactant and alcohol (Rajalakshmi et al. 2011).

The emulsion process mechanism is shown in Figure 5. There was no chemical reaction involved in emulsification process. Anionic surfactant MES will formed invisible layer for a droplet surrounded by aqueous phase and PMO as nonionic polymeric surfactant will be formed a protect shell as the steric stabilization effect (Raffa et al. 2015).

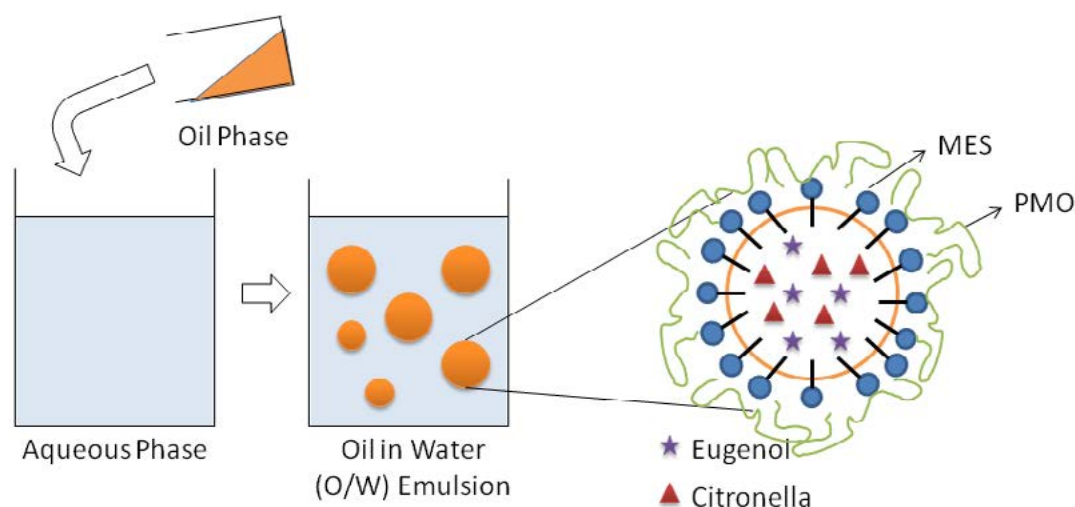


Figure 5. Emulsion Process Mechanism

4. CONCLUSION

The optimum stability of fungicide formulation with citronella oil and eugenol as active agent is the following condition, surfactant ratio MES and PMO is 1:9 using ethanol as solvent with creaming escalation 8% and droplet size range 5.756-7.313 μm for 180 minutes.

5. ACKNOWLEDGEMENT

Research Center for Chemistry and Research Center for Metrology, Indonesian Institute of Sciences supported by Kegiatan Unggulan LIPI 2016.

6. REFERENCES

- Achouri, A., Zamani, Y. & Boye, J.I., 2012. Stability and Physical Properties of Emulsions Prepared with and without Soy Proteins. *Journal of Food Research*, 1(1), pp.254–267.
- Allawzi, M.A., Allaboun, H. & Qazaq, A.S., 2016. Formulation , Emulsion , and Thermal Stability of Emulsifiable Malathion Concentrate using Ethanol as a Solvent. *International Journal of Applied Engineering Research*, 11(11), pp.7385–7390. Available at: <http://www.ripublication.com>.
- Azizinezhad, F. & Aghchehrood, M.T., 2014. Conductometric Investigation of the Interaction of Chitosan- Dioctyl Sulfo-Succinate Surfactant in Water-Toluene Solution. *Bulletin of Environment, Pharmacology and Life Sciences*, 3(January), pp.39–44. Available at: <http://www.bepls.com>.
- Barbas, L.A.L. et al., 2017. Essential oil of citronella modulates electrophysiological



- responses in tambaqui *Colossoma macropomum*: A new anaesthetic for use in fish. *Aquaculture*, 1, pp.1–29.
- Chanamai, R. & McClements, D.J., 2000. Creaming Stability of Flocculated Monodisperse Oil-in-Water Emulsions. *Journal of Colloid and Interface Science*, 225, pp.214–218. Available at: <http://www.idealibrary.com>.
- Danov, K.D. et al., 2015. Journal of Colloid and Interface Science Sulfonated methyl esters of fatty acids in aqueous solutions: Interfacial and micellar properties. *Journal of Colloid and Interface Science*, 457, pp.307–318. Available at: <http://dx.doi.org/10.1016/j.jcis.2015.07.020>.
- Fairhurst, D., 2013. An Overview of the Zeta Potential Part 3 : Uses and Applications The Relation of ZP to Suspension Behavior. *American Pharmaceutical Review*, pp.1–11. Available at: <http://www.americanpharmaceuticalreview.com>.
- Gupta, A. et al., 2016. Nanoemulsions : formation, properties and applications. *Royal Society of Chemistry*. Available at: <http://dx.doi.org/10.1039/C5SM02958A>.
- Hu, J., Akula, N. & Wang, N., 2016. Development of a Microemulsion Formulation for Antimicrobial SecA Inhibitors. *PLoS ONE*, 11(3), pp.1–15.
- Ibrahim, N., Raman, I.A. & Yusop, M.R., 2015. Effects Of Functional Group Of Non-Ionic Surfactants On The Stability Of Emulsion. *The Malaysian Journal of Analytical Sciences*, 19(1), pp.261–267.
- Juárez, Z.N. et al., 2015. Antifungal activity of essential oils extracted from *Agastache mexicana* ssp . *xolocotziana* and *Porophyllum linaria* against post-harvest pathogens. *Industrial Crops & Products*, 74, pp.178–182. Available at: <http://dx.doi.org/10.1016/j.indcrop.2015.04.058>.
- Koul, O., Walia, S. & Dhaliwal, G.S., 2008. Essential Oils as Green Pesticides : Potential and Constraints. *Biopesticides International*, 4(1), pp.63–84.
- Li, W., Shi, Q. & Ouyang, Y., 2012. Antifungal effects of citronella oil against *Aspergillus niger*. *Appl Microbiol Biotechnol*, pp.1–10.
- Licciardello, F. et al., 2013. Effectiveness of a novel insect-repellent food packaging incorporating essential oils against the red fl our beetle (*Tribolium castaneum*). *Innovative Food Science and Emerging Technologies*, 19, pp.173–180. Available at: <http://dx.doi.org/10.1016/j.ifset.2013.05.002>.
- Martínez, J.A., 2012. *Natural Fungicides Obtained from Plants* D. Dhanasekaran, ed., Croatia: In Tech. Available at: <http://www.intechopen.com/books/fungicides-for-plant-and-animal-diseases/natural-fungicides-obtained-fromplants>.
- Milne, G.W.A., 2005. *Gardner's Commercially Important Chemicals : Synonyms, Trade Names, and Properties* 11th ed. G. W. A. Milne, ed., Hoboken, NJ, USA: John Wiley & Sons, Inc.
- Raffa, P. et al., 2015. Polymeric Surfactants : Synthesis , Properties , and Links to Applications. *Chemical Reviews*, 115(16).
- Rajalakshmi, R., Mahesh, K. & Ashok Kumar, C., 2011. A Critical Review On Nano Emulsions. *International Journal of Innovative Drug Discovery*, 1(1), pp.1–8.
- Restu, W.K. et al., 2015. Effect of Accelerated Stability Test on Characteristics of Emulsion Systems with Chitosan as a Stabilizer. *Procedia Chemistry*, 16, pp.171–176.
- Sellamuthu, P.S., Sivakumar, D. & Soundy, P., 2013. Antifungal Activity And Chemical Composition Of Thyme , Peppermint And Citronella Oils In Vapor Phase Against Avocado And Peach Postharvest Pathogens. *Journal of Food Safety*, 33, pp.86–93.
- Tadros, T. et al., 2004. Formation and stability of nano-emulsions. *Advances in Colloid and Interface Science*, 109, pp.303–318.
- Wang, C. et al., 2010. Antifungal activity of eugenol against *Botrytis cinerea*. *Tropical Plant Pathology*, 35(3), pp.137–143.



Zabka, M., Pavela, R. & Prokinova, E., 2014. Chemosphere Antifungal activity and chemical composition of twenty essential oils against significant indoor and outdoor toxigenic and aeroallergenic fungi. *Chemosphere*, 112, pp.443–448. Available at: <http://dx.doi.org/10.1016/j.chemosphere.2014.05.014>.



15th International Conference on Quality in Research (QIR 2017)

HAZARD IDENTIFICATION OF PRIMARY COOLING SYSTEM G.A SIWABESSY REACTOR

Ratih Luhuring Tyas, Geni Rina Sunaryo, Heri Hermansyah*

National Nuclear Energy Agency, University of Indonesia

*Corresponding author:

heri.hermansyah@ui.ac.id

ABSTRACT

The research reactor has lower hazard potential than the power reactor. However, most research reactor was built a few decades ago, when the design requirement was not completely fulfilled the safety requirement as well as the Reaktor Serba Guna G. A Siwabessy (RSG – GAS) that has been operating for 28 years and located close to the housing resident. Learning from Fukushima accident, it is necessary to assess the safety analysis of RSG – GAS. The safety analysis including the identification of potential hazard, characterization of the postulated initiating event, determination of failure probability, and measuring the frequency. This paper will be focused on hazard identification of the primary cooling system. The worst effect, as a result of the failure of primary system, because of the fuel of the reactor melts. Based on identification and hazard analysis of the primary cooling system using HAZID (Hazard Identification) and HAZOP (Hazard and Operability Analysis) method, there are five initiating events : loss of coolant accident (LOCA) because the leakage of the primary coolant boundary beyond the isolation valves, LOCA because the rupture of a pump casing due to impeller failure, LOCA because heat exchanger leakage, loss of flow accident (LOFA) because the loss of primary pump, and LOFA because the inadvertent closure of the primary isolation valves.

Keywords: Accident; Hazard; Primary cooling system; Safety

1. INTRODUCTION

Fukushima Daiichi nuclear reactor accident on March 11, 2011 is a lesson to perform safety analysis, as an effort to prevent accidents release radioactive material, in the world of nuclear installations, including research reactors. The potential hazard of research reactor is lower than power reactors. But most of research reactor was built several decades ago, where the design requirements not fulfilled the safety requirements. In addition several research reactors located close to the housing resident, and the site characteristics may have changed since the reactor was built.

As an input from the Fukushima accident, it is necessary to review the safety analysis of RSG-GAS (IAEA, 2014). Safety analysis covering the stages of hazard identification, characterization of postulated events, determines and measures the consequences of failure frequency (BAPETEN, 2011). The safety analysis carried out throughout the lifetime of the installation, from the design, commissioning, operation to decommissioning (Jeong K.S., 2008).



Hazard identification is an early stage in the safety analysis. Potential hazards can be identified include the hazard of physics, chemistry, biology, ergonomics, physiology (BATAN, 2008). Hazard can also classified be toxic, explosive and flammable (V. Rao Kolluru). Identification of existing hazards includes internal hazard (material, product, equipment/machinery, processes, working methods) and external hazard (environmental, human) (NRC, 1981). Reactor design affects the internal hazard, while the site / location influences the external hazard. Based on the potential hazard, hazard analysis using HAZOP (Hazard and Operability Analysis) (Hashemi-Tilehnoee, 2010). The resulting nodes, selected based on a list of Postulated Initiating Event (PIE) in nuclear safety standards (IAEA, 2005).

Overview RSG-GAS and Primary Cooling System

(PRSG 2011) RSG-GAS is one of three research reactors owned by Indonesia. RSG-GAS is a reactor pool with specifications can be seen in Table 1.

Table 1. Specifications of RSG-GAS

Reactor Power	30 MW
Neutron Flux	10^{12} n/cm ² .s
Type	Pool, Muti Purpose
Type of Fuel Element	U ₃ Si ₂ Al, MTR LEU (19,75 %)
Configuration of Fuel Element	Plat 1,30x70,75x625 mm
Material Cladding	AlMg
Reactor Coolant	H ₂ O
Flow Rate	800 kg/s

The main reactor cooling systems consisting of the primary cooling system, the secondary cooling system, the pool cooling system, the warm water layer system and the purification system. These systems are integrated to keep the reactor operating conditions are within limits.

The primary cooling system serve to assure safe temperatures in the core and the reflector during normal operation up to the design thermal power. During power operation of the reactor, the heat released in the core and surrounding reflector is removed by the primary cooling system flowing downwards through the core and the reflector. The primary water is cooled in the heat exchangers, through which heat is transferred to the secondary cooling system and then dissipated to the atmosphere through mechanical draft cooling towers.

The primary cooling system is designed to withstand the SSE in such a way that the safe flow cost down and the integrity of the system are assured. Components of the primary cooling system consists of primary pumps, heat exchangers, valves and piping that connect the components with a pool and the reactor core to form a closed circuit.



2. METHODOLOGY

2.1 Hazard Identification

Hazard identification of the primary cooling system RSG-GAS is done by description the source of the hazard that exists; determining the potential hazard and trigger factor. This identification process lasts until all sources hazard included in the identification.

2.2 Hazard Analysis

The method used in hazard analysis is HAZOP (Hazard and Operability Study). Each node parameters is specified the deviation. Then analyze the deviation to get the possible consequences and protection system available. Not a whole Node is used in this study, because node selection based on PIE in nuclear safety standards.

3. RESULTS AND DISCUSSION

3.1 Hazard Identification

Identification of the primary cooling system RSG-GAS conducted using Hazard Identification (HAZID). Hazards that exist in the primary cooling system consist of pumps, heat exchangers, piping, and valves. The primary cooling system has three pumps. Hazards that exist on the primary pump are a pump failure and rupture of the pump casing. The primary cooling system has two heat exchangers that work in parallel. The Hazards from the heat exchanger is leaking water pipe, where the water primer can contaminating radioactive the secondary water.

The worst possible cause of the leak pipe is a pipe with a smaller size. Each inlet and outlet channels of the primary coolant are equipped with two isolation valves. Inadvertent closure of primary isolation valves may reduce the amount of coolant flow. Based on the identification result there are 5 events that can be seen in Table 2.

Table 2. Hazard Identification Results

No	Description	Potential Hazard	Cause
1.	Leakage of the primary coolant boundary beyond the isolation valves	Loss of coolant	Corrosion, fatigue, fracture, aging
2	Rupture of a pump casing due to impeller failure	Loss of coolant	Corrosion, fatigue, fracture, aging
3.	Heat Exchanger Leakage	Loss of coolant	Corrosion, fatigue, fracture, aging
4.	Loss of Primary pump	Loss of flow	Maintenance and Inspection are not good
5.	Inadvertent closure of the primary isolation valves	Loss of flow	Maintenance and Inspection are not good

3.2 Hazard Analysis

The primary cooling system consists of 1 Node and 3 Parameter. Determination parameters of the node based on parameters connected with the Reactor Protection System (RPS). The flow rate past the primary cooling system is 860 kg/s, if the flow rate times $\leq 90\% \pm 5\%$, RPS will trip the reactor, and causes the reactor power off, which in controls by the flow rate JE-01 CF 811/821/ 831. Control of pool water levels JAA-01 CL 811/821/831 activate the RPS on the condition if water level drops bellow 12.25 m \pm 0.05 m. The Inadvertent closure of



primary isolation valves will cause a reduction in the flow of coolant. Position control JE-01 CG 811/821/831 and JE-01 CG 812/822/832 will activate RPS at the limit of 3° rounds.

When the heat exchanger leakage, radioactive water would leak into the secondary system because the pressure in the primary circuit is higher than that in the secondary. Radioactivity is continuously monitored in the secondary system by measurement instrumentation γ activity of PA-01 / PA-02 CR 001. If the alarm limit value of 5×10^{-5} Ci/m³ is exceeded, the operator shuts down the reactor and isolates the heat exchanger with secondary isolation valves PA-01 AA-14 / AA-16, PA-02 AA-14 / AA-16. Because of the isolation valves closes, the heat cannot be released into the environment. When the condition of the primary outlet temperatures greater than 44 °C that controled by temperature control JE-01 CT 811/821/831, the reactor then trip automatically. Hazard analysis results obtained 5 events that can be seen in Table 3.

Tabel 3. Hazard Analysis Results

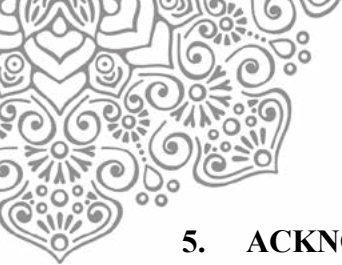
Deviation	Cause	Consequence	Protection System
Node : 1. Primary Cooling Systems			
1.1 No/ less flow of core inlet	Rupture of pump casing Leakge of pipe Loss of primary pump	Loss of coolant Loss of coolant Loss of flow	JE-01 CF 811/821/831 JAA-01 CL 811/821/831 JE-01 CF 811/821/831
1.2 Less flow of core outlet	closure of the primary isolation valves	Loss of flow	JE-01 CG 811/821/831 JE-01 CG 812/822/832
1.3 High temperature outlet of Primary Heat Exchanger	Heat Exchanger Leakage	Loss of coolant	JE-01 CT 811/821/831

4. CONCLUSION

There are five postulated initiating events can be identified of primary cooling system RSG–GAS which can be seen in Table 4.

Table 4 Postulated Initiating Events of Primary Cooling System RSG-GAS

No.	Event Group	Postulated Initiating Event
1.	Loss of Coolant Accident (LOCA)	1. LOCA because the leakage of the primary coolant boundary beyond the isolation valves; 2. LOCA because the rupture of a pump casing due to impeller failure; 3. LOCA because heat exchanger leakage;
2.	Loss of Flow Accident (LOFA)	1. LOFA because the loss of primary pump, and 2. LOFA because the inadvertent closure of the primary isolation valves.



5. ACKNOWLEDGEMENT

I would like to thank to BATAN, University of Indonesia and USAID SHERA.

6. REFERENCES

- BAPETEN. (2011). Ketentuan Keselamatan Desain Reaktor Non Daya. Indonesia
- Hashemi-Tilehnoee, M., Pazirandeh, A., Tashakor, S. (2010). HAZOP-study on heavy water research reactor primary cooling system. *Annals of Nuclear Energy*, 37(3), 428-433. doi: 10.1016/j.anucene.2009.12.006
- IAEA. (2005). Safety of Research Reactor NS-R-4. Vienna.
- IAEA. (2014). Safety Reassessment for Research Reactors in the Light of the Accident at the Fukushima Daiichi Nuclear Power Plant No. 80.
- Jeong K.S., Lee D.S., Lee K.W., Lim H.K.,. (2008). A Qualitative Identification And Analysis Of Hazards, Risks And Operating Procedures For A Decommissioning Safety Assessment Of A Nuclear Research Reactor. *Annals of Nuclear Energy* 35, 1954–1962.
- PRSG. (2011). Laporan Analisis Keselamatan (LAK) RSG-GAS Rev 10.1: PRSG.
- Rao V. Kolluru, Steven M. Bartell, Robin M. Pitblado, R. Scott Stricoff. Risk Assessment and Management Handbook For Environmental, Health and Safety Professionals.: McGraw-Hill, Inc.
- NRC, US. (1981). Fault Tree Handbook.



Extraction of Nickel from Laterite Using Phytic Acid and Salicylaldoxime

Agustino Zulys*, Fajar Prihatno, Afip Jaya Saputra

Department of Chemistry University of Indonesia
Kampus Baru FMIPA UI Depok 16424 Depok

Abstract

Laterite mineral from west Sulawesi contain chlorite, pyroxene, talc, quartz, olivine and amphibole and it has low grade nickel contain up to 0.93%. In this research, we develop a method for extraction of nickel laterite using phytic acid and salicylaldoxime. The analytical methods to measure nickel contain and ratios of metal to ligand are used by mean of FTIR, UV-vis spectrophotometer. The heap leaching process was done using 25 g of laterite in variation of sulfuric acid and hydrochloric acid concentration. Results heap leaching has yellowish green color indicate the contamination of iron ion. The existence of Fe^{3+} interfere the extraction of Ni^{2+} by salicylaldoxime. The use of phytic acid will lead to iron precipitation, minimizing the iron content. It turned out that optimum concentration of sulfuric acid is 0.5 M yielded 56.01% of nickel extraction, whereas the optimum concentration of hydrochloric acid is 5 M yielded 14,63% of nickel extraction. Then liquid-liquid extraction of Ni^{2+} was carried out using salicylaldoxime in toluene, and yielded 18.88 % of Ni^{2+} . It concluded that the use phytic acid increase the yield of nickel content and the use of sulfuric acid is more efficient than hydrochloric acid.

Keywords : Extraction, Laterite, Heap Leaching, Phytic Acid, Salicylaldoxime

INTRODUCTION

Nickel consumption and reduction rate of nickel sulfide ore which is fast, making a nickel oxide lateritic ore to be a major source of nickel in the world potentially. The complexity of minerals and low content of nickel in laterite make extraction is difficult and expensive. Heap Leaching be an alternative method for the extraction of nickel from laterite at a low cost.

Heap Leaching is the process of extraction of metal ions by sprinkling minerals with chemical reagents so that metal ions are released from the minerals and dissolve. Heap Leaching Method is done by flushing laterite using acid solution with a certain concentration so that the ion nickel (II) dissolved in acid that has been contact and flows to bottom of laterite due to gravity (Oxley, Smith, & Cacere, 2015). The result of Heap Leaching or PLS (Pregnant Leach Solution) in the form of a solution containing metal ions will be separated and purified. This method can be used for low quality laterite nickel to reduce production costs. In this study, we appeal between sulfuric acid and chloride acid then determined the optimum concentration of acid using a measurement method standard calibration curve. Measurement methods have been due in 2016 by Çetintas and Bingol that compared the method of measuring ion Ni^{2+} on matrix leaching sulfuric acid. This study shows there is no real difference between the standard addition method with a calibration curve in the measurement method of Ni^{2+} ions.

Potential uses for extracting nickel salisilaldoksim emerged in 2001 by Smith, et al., that successfully determined the structure of Ni^{2+} ion complexes with salisilaldoksim. This study proves the existence of pseudo-macrocycle hydrogen bond in the complex by the addition of tetramethyl ethylenediamine.

METHODS

Laterite was characterized using XRD to know the inner minerals. Then laterite was deconstructed using aqua regia and nickel content is measured using FAAS. Heap Leaching is done with a sample of 25 grams laterite for each variation. Variation of sulfuric acid used 0.01



M; 0.1 M; 0.5 M; 1 M; And 2.5 M. Variation of chloride acid used 1 M; 2M; 3M; 4M; And 5 M. Job method between phytic acid and iron to know the effectiveness of phytic acid in precipitation. The method of action is carried out between the salicylaldehyde and nickel nitrate in neutral pH. The acid type and the best concentration are added phytic acid to form maximum precipitate amount. The solution is neutralized using NaOH. Then solution was added by salicylaldehyde in the toluene solvent.

RESULT AND DISCUSSION

Laterite Characterization

Seemed like Figure 1, laterite appears to be brown with small bit of silica fragment. Laterite has a moisture content of 0.52%. Physically the laterite mineral does not differ with the soil generally. To determine the nickel content in laterite is done by wet destruction. The decomposition was carried out using a concentrated HCl mixture and concentrated HNO₃ with a ratio of 3:1. laterite decomposition performed leaving a white silica. Solution result from wet destruction was yellow. This is due to the presence of excessive chloride ions. Ni²⁺ concentration was measured using FAAS. So the total nickel content in the laterite is 0.93%.

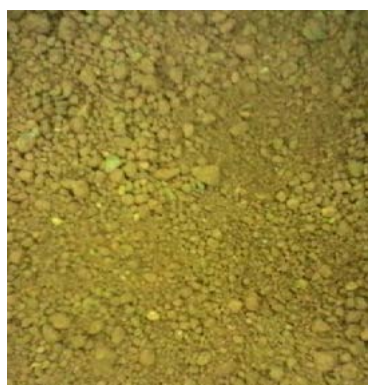


Figure 1. Laterite

XRD spectroscopy results show that laterite is composed by chlorite, pyroxene and talc as the main mineral. Other minor minerals present in laterite samples are quartz, olivine and amphibole. Ni²⁺ ions inside the laterite are present in an olivine mineral containing iron oxide and silica. From the XRD spectra calculation shows that the nickel content in the sample is 1.2%.

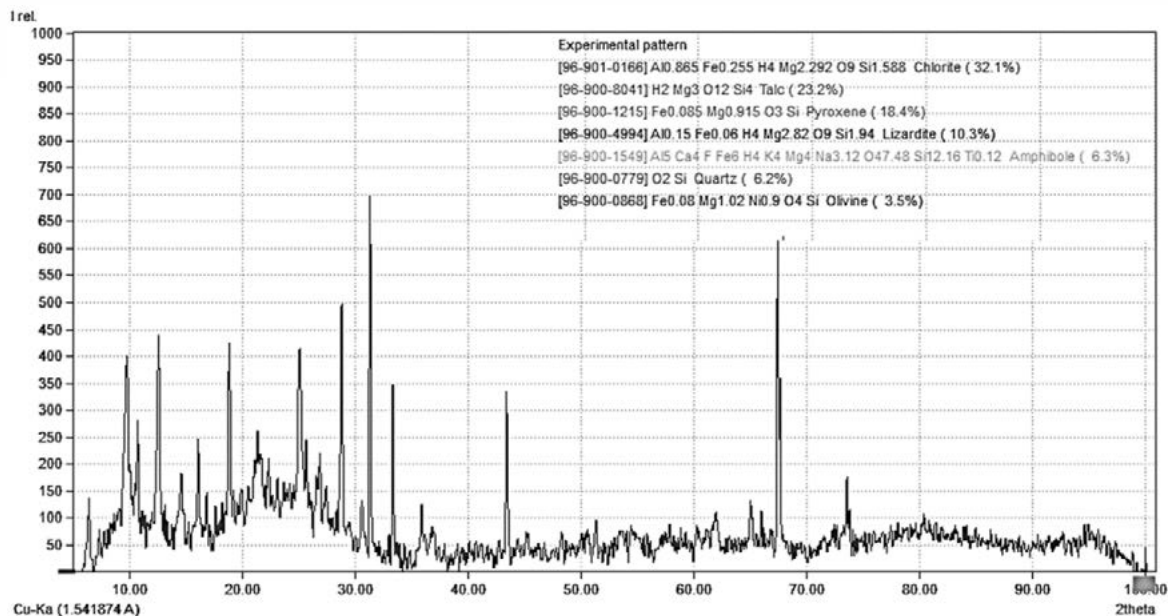
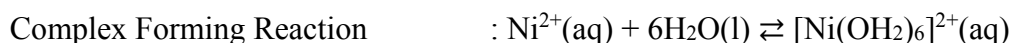
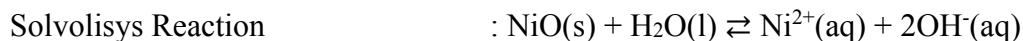


Figure 2. XRD Characterization of Laterite

Heap Leaching

Ni^{2+} solubility in heap leaching method was done by Le-Chatelier principle. Laterite is a lithophylic mineral. Ni^{2+} are form in solid nickel (II) oxide in laterite. Theoretically, addition of acid solution into the laterite will increase the solubility of Ni^{2+} by shift the equilibrium. Furthermore, Ni^{2+} form a complex ion. The result solution after Heap Leaching process has of yellowish green color and directly proportional to the concentration of sulfuric acid used. Green color possibilities provided by $[Ni(OH_2)_6]^{2+}$. Whereas, the yellow color is given by ion $[Fe_x(OH_2)_yCl_z]^{3-y}$ or $[Fe(OH_2)_6]^{3+}$.



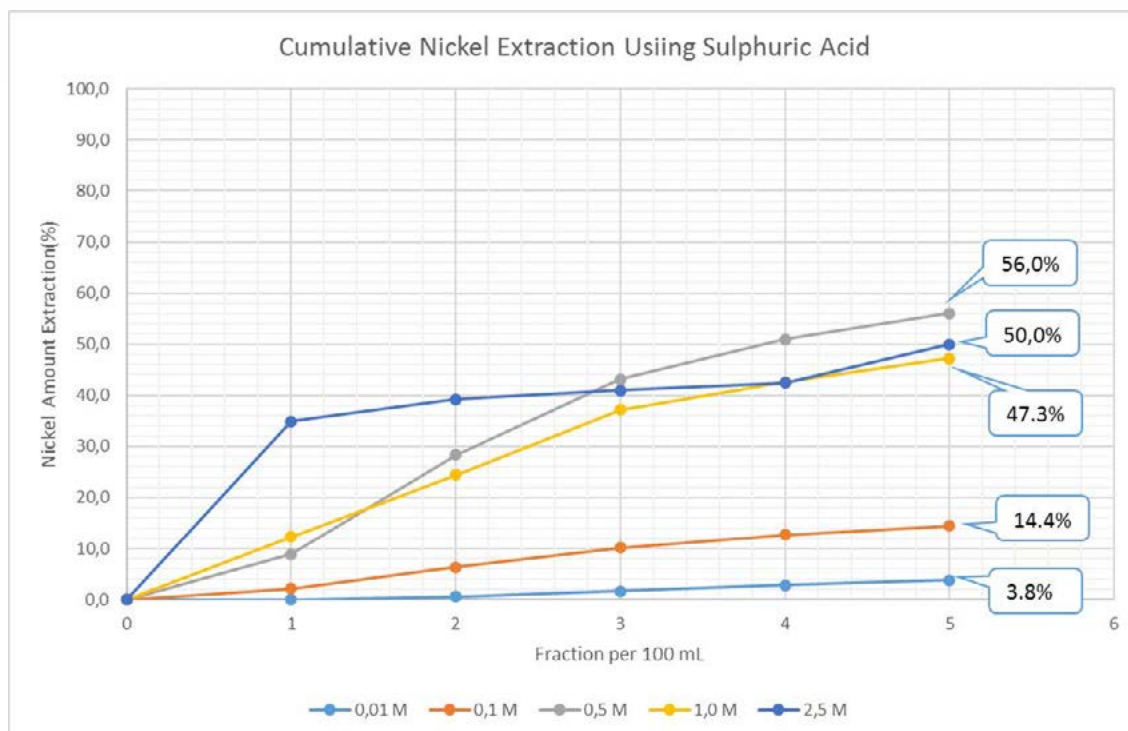


Figure 3. Cumulative Nickel Extraction using Sulphuric acid

Measurements of Ni^{2+} in every PLS fraction with sulfuric acid concentration variation was done using FAAS with a wavelength of 341.5 nm. Ni^{2+} which is at PLS accumulated. Sulfuric acid with a concentration of 0.5 M can extract Ni^{2+} more than others at the end of Heap Leaching process. Sulphuric acid with concentration of 0.5 M, 1 M and 2.5 M contain 56.01%, 50.03% and 47.26% of Ni^{2+} . That number has only a low margin of less than 10%. But the number of Ni^{2+} that can be extracted with sulfuric acid with concentration of 0.1 M and 0.01 M is very bit than others. This is caused by the low concentration of acid that is not a lot of Ni^{2+} ion dissolved in the laterite is ultramafic minerals.

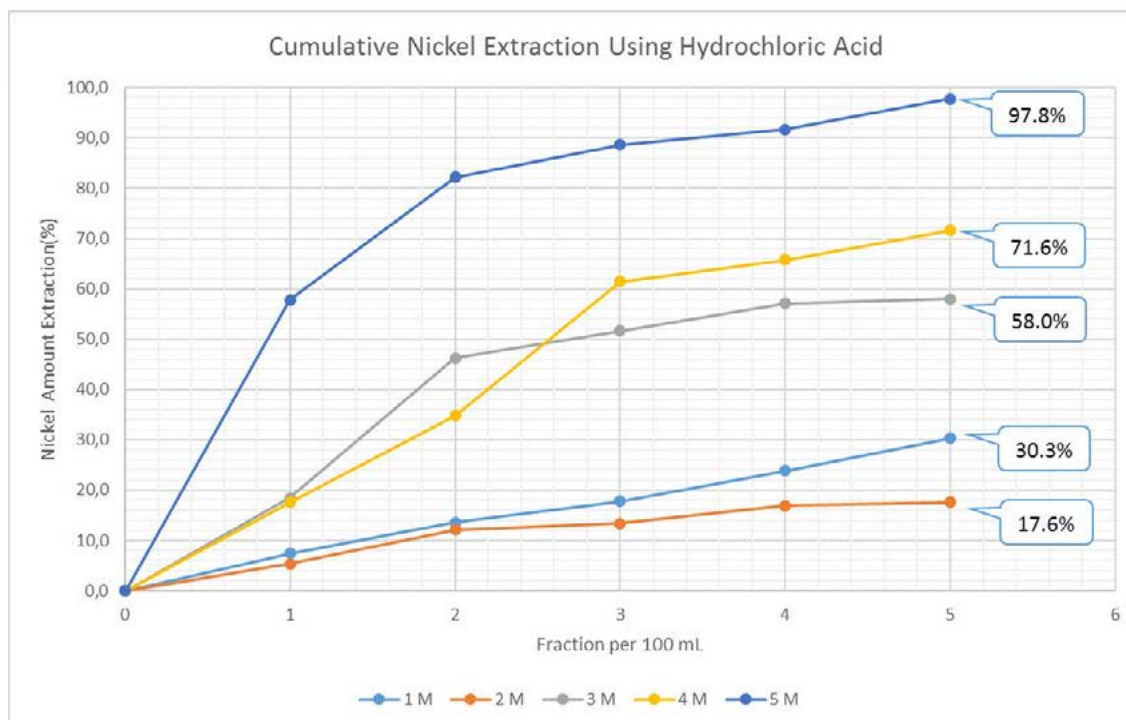


Figure 4. Cumulative Nickel Extraction using Hydrochloric acid

Extraction using hydrochloric acid was done by different variations. The higher hydrochloric acid concentration was used, the more Ni^{2+} can be extracted. The use of 3 M, 4 M and 5 M hydrochloric acid extracted a higher amount of Ni^{2+} than using 0.5 M sulfuric acid. But the use of high concentration of hydrochloric acid makes the laterite was yellow. This indicates the presence of very high chlorides that damage laterite and result soil pollution. So 0.5 M sulphuric acid will be used for next process.

Pregnant Leach Solution

PLS contains various dissolved metal ions. Ni^{2+} and Fe^{3+} are ions which are thought to give the dominant color in the solution. The resulting color of the solution is due to Fe^{3+} that forming complex ion with certain ligands. Ligands that may be bound to Fe^{3+} are H_2O and Cl^- . The presence of Cl^- comes from dissolved laterite minerals in PLS.

To know what is complex ion in PLS, we compare UV-VIS graph of PLS, $[\text{Fe}(\text{OH})_x(\text{OH})_y\text{Cl}_z]^{3-y-z}$ and $[\text{Fe}(\text{H}_2\text{O})_6]^{3+}$. Fe^{3+} complex with Cl^- was prepared by dissolving $\text{FeCl}_3 \cdot 6\text{H}_2\text{O}$ using a neutral condition of aquades. Fe^{3+} Complex with H_2O was prepared by dissolving $\text{FeCl}_3 \cdot 6\text{H}_2\text{O}$ using H_2SO_4 concentration of 0.5 M. Both solutions were measured by UV-Vis spectrophotometry from 600 nm to 200 nm. Then compared with diluted PLS solution.

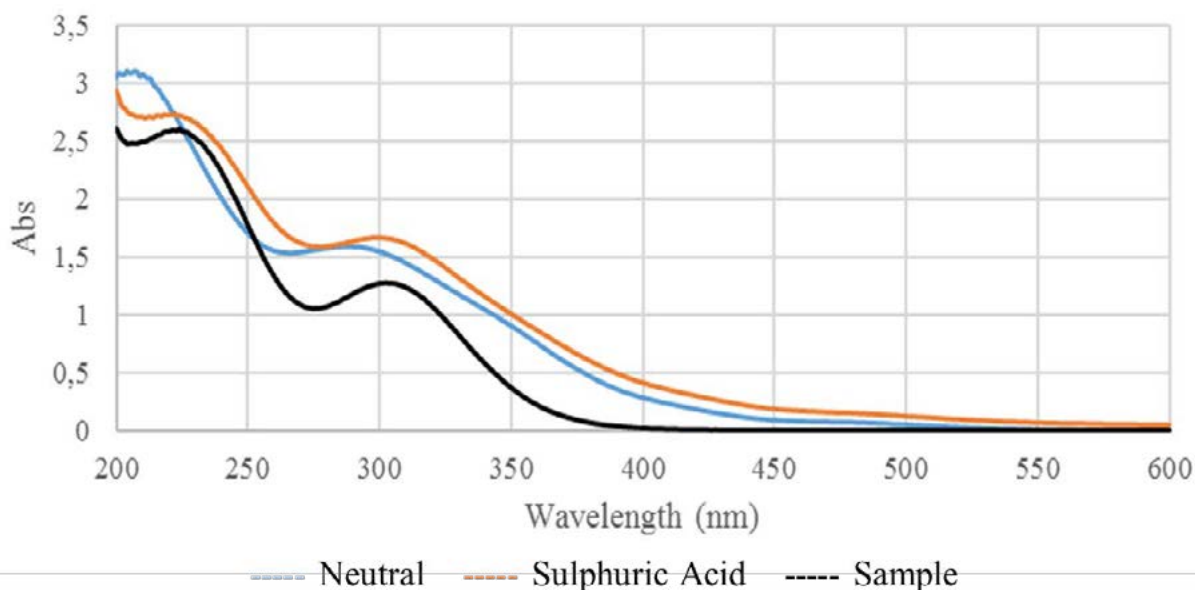
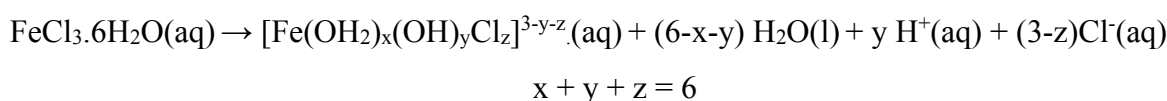
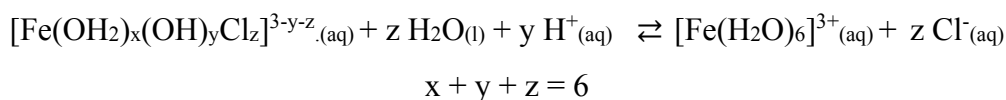


Figure 5. Fe³⁺ Complex Characterization using UV-VIS Spectrophotometer

Figure 4.7 shows different graph between Fe³⁺ complex dissolved in neutral conditions with H₂SO₄ 0.5 M. Fe³⁺ complex formed in neutral conditions is [Fe(OH₂)_x(OH)_yCl_z]^{3-y-z}. This complex ion is generally formed by hydrolysis of FeCl₃.6H₂O salt under neutral conditions.



The image also shows graph of Fe³⁺ complex in PLS. It mean Fe³⁺ complex has an absorption peak at the same wavelength as FeCl₃.6H₂O dissolved to H₂SO₄ 0.5 M. The Fe³⁺ complex is [Fe(H₂O)₆]³⁺. This complex was formed by increased solvation of chloride anion by H⁺ and shift the equilibrium of the following reaction to [Fe(H₂O)₆]³⁺.



The Fe³⁺ complex graphs in neutral conditions and acid condition show the absorption peaks at different wavelengths. It was not caused by solvatochromic condition. Both graphs were formed by different complex ions that can be proved by Tanabe-Sugano Diagram. [Fe(H₂O)₆]³⁺ has an absorption peak at 218 nm and 300 nm whereas [Fe(OH₂)_x(OH)_yCl_z]^{3-y-z} has absorbance at 201 nm and 289 nm. By changing the wavelength of the UV-Vis spectra into electron volt, we can know the energy ratio for each of peak wavelengths. [Fe(H₂O)₆]³⁺ has an absorption peak at 4.133 eV and 5.687 eV so it has an energy ratio of 1:1.376. While [Fe(OH₂)_x(OH)_yCl_z]^{3-y-z} has an absorption peak at 4,290 eV and 6,168 eV so it has an energy ratio of 1:1.437. Using the Tanabe Sugano chart, we can see that the value of the comparison between the two peaks that will show different Δo values. [Fe(OH₂)_x(OH)_yCl_z]^{3-y-z} has a lower Δo value because Cl⁻ ligand is σ-donor and π-donor ligands that can decrease splitting energy Δo.

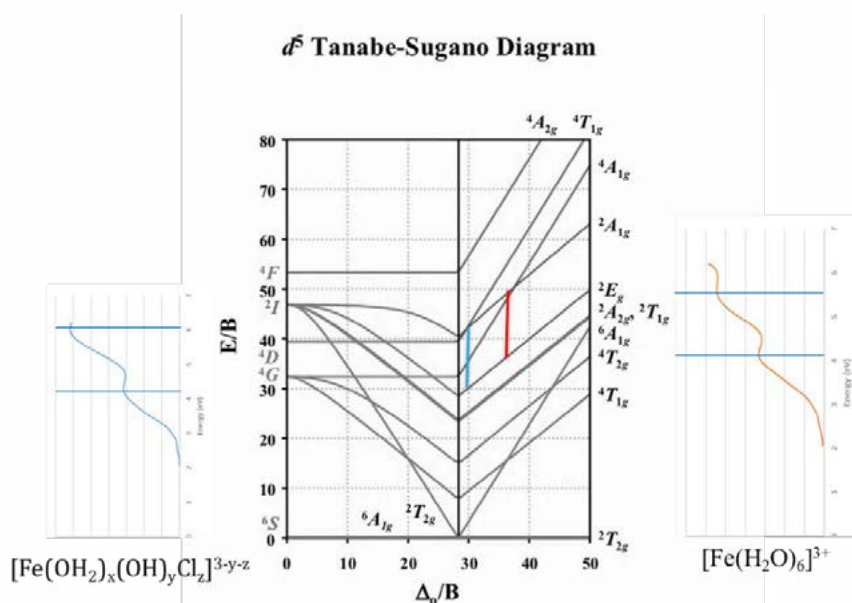


Figure 6. d^5 Tanabe Sugano Diagram

$[\text{Fe}(\text{H}_2\text{O})_6]^{3+}$ concentration in PLS were determined using UV-Vis spectrophotometer. Scanning of the standard solution of $[\text{Fe}(\text{H}_2\text{O})_6]^{3+}$ $1.2 \cdot 10^{-4}$ M to $6.0 \cdot 10^{-4}$ M was prepared by dissolving $\text{FeCl}_3 \cdot 6\text{H}_2\text{O}$ into 0.5 M H_2SO_4 solution. Then the sample was diluted to 40 times using H_2SO_4 0.5 M to obtain the graph below.

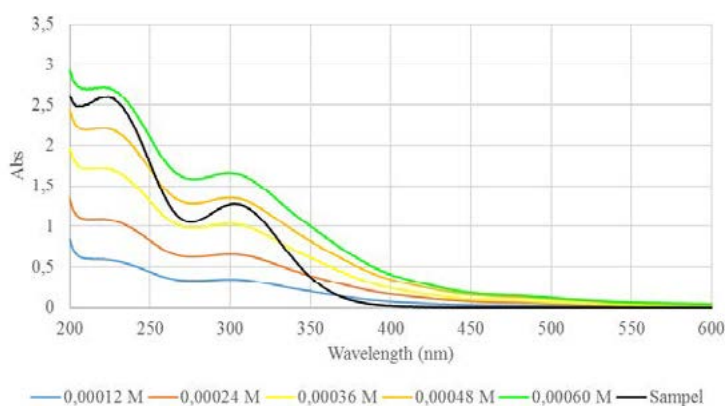


Figure 7. Standard Spectra Array of $[\text{Fe}(\text{H}_2\text{O})_6]^{3+}$

Figure 4.9 shows that there are 2 peaks of different wavelengths. At a wavelength of 218 nm sample absorbance was between standard $[\text{Fe}(\text{H}_2\text{O})_6]^{3+}$ solutions that has concentration of $4.8 \cdot 10^{-4}$ M and $6.0 \cdot 10^{-4}$ M but wavelength of 300 nm the sample absorbance was between standard $[\text{Fe}(\text{H}_2\text{O})_6]^{3+}$ solutions that has concentration $3.6 \cdot 10^{-4}$ M and $4.8 \cdot 10^{-4}$ M. This difference is due to the presence of $[\text{Ni}(\text{OH}_2)_6]^{2+}$ in the sample solution. The graph shows the results of scanning the UV-Vis Spectrophotometer $[\text{Ni}(\text{OH}_2)_6]^{2+}$ with concentration of 0.01 M up to 0.05 M.

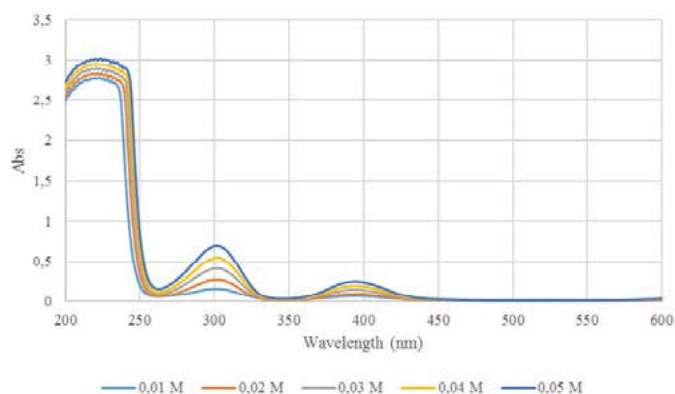


Figure 8. Standard Spectra Array of $[\text{Ni}(\text{OH}_2)_6]^{2+}$

The standard spectra array of $[\text{Ni}(\text{OH}_2)_6]^{2+}$ indicates that there is a high absorbance at wavelengths of 200 nm to 250 nm. The absorbance of $[\text{Ni}(\text{OH}_2)_6]^{2+}$ at these wavelengths will influence measurement of Fe^{3+} concentration at 218 nm. At wavelengths of 300 nm and 394 nm, the standard spectral series $[\text{Ni}(\text{OH}_2)_6]^{2+}$ shows a lower absorption peak with ϵ_0 of $13.39 \text{ cm}^{-1}\text{M}^{-1}$ and $4.74 \text{ cm}^{-1}\text{M}^{-1}$. But ϵ_0 values of $[\text{Fe}(\text{H}_2\text{O})_6]^{3+}$ at 300 nm was $2775.5 \text{ cm}^{-1}\text{M}^{-1}$. The low ϵ_0 values at 300 nm of $[\text{Ni}(\text{OH}_2)_6]^{2+}$ was too lower than $[\text{Fe}(\text{H}_2\text{O})_6]^{3+}$ cause the measurement noise at and 300 nm by $[\text{Ni}(\text{OH}_2)_6]^{2+}$ negligible. So the measurement of $[\text{Fe}(\text{H}_2\text{O})_6]^{3+}$ concentration was done by using absorbance at 300 nm and got $[\text{Fe}(\text{H}_2\text{O})_6]^{3+}$ concentration on PLS equal to 0,182 M.

Phytic Acid Precipitation

Fe^{3+} is an ion that interferes Ni^{2+} extraction process using salicylaldoxim. This is because Fe^{3+} can bind to phenolic groups of salicylaldoxim strongly and form red complex ions that soluble in water. The presence of Fe^{3+} must be eliminated. Phytic acid can react with Fe^{3+} to produce white precipitate. But the stoichiometric reaction should be known using the Job method to minimalizing the amount of phytic acid used to separate Fe^{3+} from PLS. The precipitate that was produced by Fe^{3+} and phytic acid reaction is subtle and light. This causes the measurement of job methods with gravimetry difficult to do. In addition to gravimetry, the measurement of job methods can be performed by measuring the dissolved Fe^{3+} concentration after the precipitate is separated. Below shows the result graph of job method by measuring Fe^{3+} concentration using UV-Vis Spectrophotometer at 300 nm.

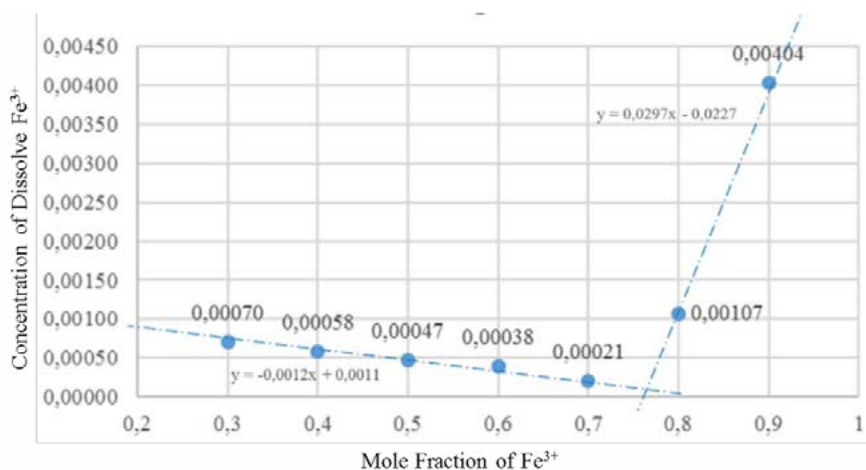


Figure 9. job method of Fe^{3+} with Phytic Acid

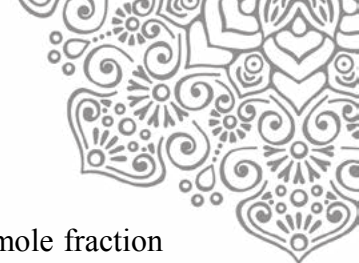
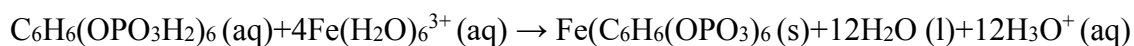


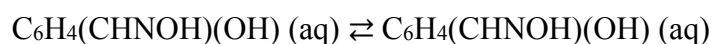
Figure shows the point of intersection lines on x-axis at 0.7702. It means mole fraction ratio between Fe^{3+} and Phytic acid is 0.77 : 0.23. This comparison in accordance with the amount of acid that can be produced phytic acid after precipitate reaction. So it can be concluded that the phytic acid can used in acidic condition effectively without hydrolysis of the phosphate ester group.



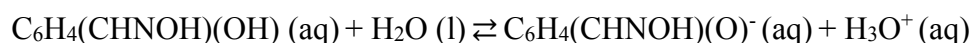
In PLS, 5% excess phytic acid was added to anticipate the presence of other metal ions which may interfere with Fe^{3+} precipitation. After the separation of the precipitate was done, the measurement of Fe^{3+} concentration using UV-Vis Spectrophotometer. This precipitation process has eliminated the amount of Fe^{3+} in the solution about 98.88%.

Nickel-Salicylaldoxime Extraction

Ni^{2+} extraction using salicylaldoxim is a liquid-liquid extraction with a 2 phase of solvent in form of water and toluene. Salicylaldoxim is a perfectly soluble organic compound in toluene and partially dissolved in water. Salicylaldoxime is soluble in toluene because it has a phenolic group as the main carbon chain. While its solubility in water is due to the acidity of the phenolic group causing salicylaldoxime ionized and has negatively charged. The solubility of salicylaldoxime in water is an equilibrium reaction that is strongly influenced by the pH of the water solvent.

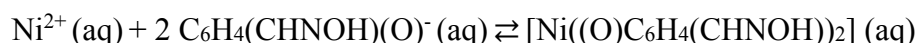


Organic Phase Water Phase

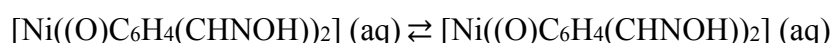


Water Phase

Ni^{2+} ion has a positive charge and is soluble in water. To make Ni^{2+} switch to the organic phase, the positive charge is neutralized by the anion of salicylaldoxim that is soluble in water. To counteract a Ni^{2+} need 2 anion of salicylaldoxim. Before extraction, the water phase is green because of their complex ion $[\text{Ni}(\text{OH}_2)_6]^{2+}$ and organic phase will look clear. After extraction, the aqueous phase containing Ni^{2+} would seem clear and loss of Ni^{2+} whereas organic phase will appear green because it has formed a complex between Ni^{2+} ion and salicylaldoxim. Colors in the organic phase and the aqueous phase can be an indicator in this extraction process.



Water Phase



Water Phase Organic Phase

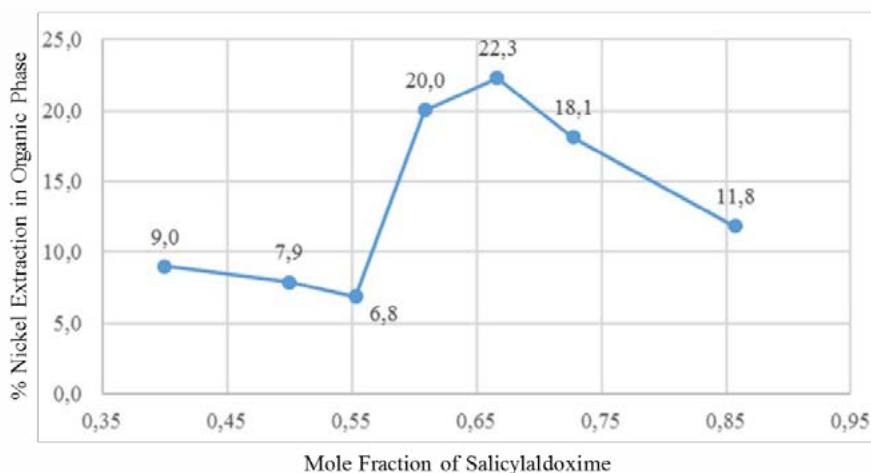


Figure 10. Job Method of Nickel Extraction Organic Phase

Job method in Figure gives 2 cut points. This is because the formation of some types complex compound formed. The first cut point has low percentage of extraction because the complex is soluble in water with a ratio between Ni^{2+} and salicylaldoxim about 1:1. The complex have positive charge that $[\text{Ni}(\text{OH}_2)_4(\text{OC}_6\text{H}_4\text{CHNOH})]^+$. While the second cut point has a high percent extraction value because the complex is formed soluble in the organic phase with a ratio of Ni^{2+} ions with salicylaldoxim of 1:2. Complexes that was formed and have no charge is $[\text{Ni}((\text{O})\text{C}_6\text{H}_4(\text{CHNOH}))_2]$. Then for the greater amount of salicylaldoxime, Ni^{2+} amount decreased into the organic phase. This is because the formed complex is likely to have negative charge and dissolve in water $[\text{Ni}(\text{OC}_6\text{H}_4\text{CHNOH})_3]^-$. Job method is done in neutral condition. The best mole ratio between Ni^{2+} with salicylaldoxim was 1: 2. The amount of Ni^{2+} that can be extracted is very low. This indicates salicylaldoxim and Ni^{2+} complex ions was formed partially and switch to the organic phase.

After extraction, the organic phase and PLS are separated. Organic phase containing Ni^{2+} was added by 1 M nitric acid. This causes Ni^{2+} in the organic phase move to water phase. Then Ni^{2+} concentration was measured using FAAS. From the measurement, obtained that the extractable Ni^{2+} is 18.875%. To ensure the complex structure of Ni^{2+} ions located in the organic phase, an FT-IR measurement was performed.

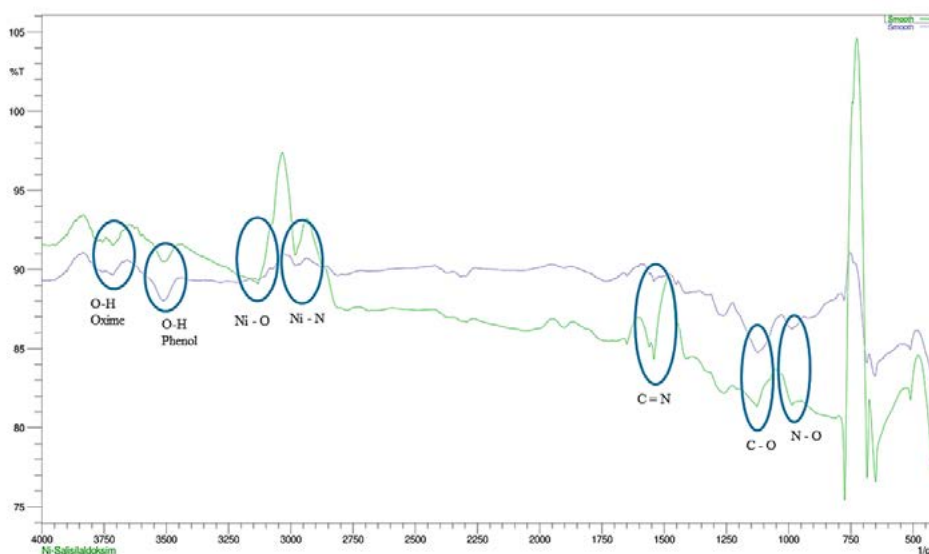


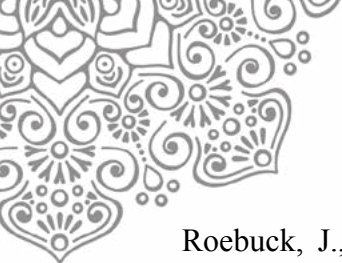
Figure 11. FTIR Salicylaldoxime (green) dan nickel(II) ion - Salicylaldoxime complex (blue)



FTIR measurements in Figure 2 shows the different absorption at 2900 cm⁻¹ and 3050 cm⁻¹. That absorbance occur because there are Ni-O and Ni-N bonds in complex [Ni((O)C₆H₄(CHNOH))₂]. Then O-H absorption of oxime and phenol still have similar absorbance. This indicates that the bond is formed then the complex compound [Ni((O)C₆H₄(CHNOH))₂]. Ni²⁺ will generally form a quadrilateral complex macrocycle with a pseudo-hydrogen bond (Smith, Tasker, & White, 2001).

DAFTAR PUSTAKA

- Çetintas, S., & Bingol, D. (2016). Response surface methodology approach to leaching of nickel laterite and evaluation of different analytical techniques used for the analysis of leached solutions. RSC.
- Dalvi, A., Bacon, G., & Rober. (2004). The Past and the Future of Nickel Laterites. PDAC 2004 International Convention, 2.
- E. Housecroft , C., & G. Sharpe, A. (2008). Inorganic Chemistry. London: Pearson Education.
- Forgan, R., Davidson, J., Fabbiano, F., Galbraith, S., & Henderson , D. (2010). Cation and Anion Selectivity of Zwitterionic Salicylaldoxime Metal Salt Extractants. Dalton Transactions.
- Glascok, M. D. (2016, 6 5). Overview of Neutron Activation Analysis. Retrieved from Archaeometry Laboratory: http://archaeometry.missouri.edu/naa_overview.html
- Harvey, D. (2000). Modern Analytical Chemistry. New York: Mc Graw Hill.
- Jacobsen, T., & Ellingsen, D. S. (1983). Phytic Acid and Metal Availability: A Study of Ca and Cu Binding. Cereal Chem 60(5).
- Latt, M. M., Rice, D., & Sin, D. (1997). Copper, Streamlined Atomic Absorption Procedures for Exploration and Mining. The Analyst.
- Leonardou, S. A., & Zafiratos, I. G. (2004). Beneficiation of a Greek serpentinic nickeliferous ore Part II. Sulphuric acid heap and agitation leaching. Elsevier.
- McDonald, R., & Whittington, B. (2007). Atmospheric acid leaching of nickel laterites review. Elsevier.
- McKenzie, D., Denys, L., & Buchana, A. (1987). The Solubilization of Nickel, Cobalt and Iron from Laterites by Means of Organic Chelating Acids at Low pH. International Journal of Mineral Processing.
- Oxley , A., Smith , M. E., & Cacere, O. (2015). Why heap leach nickel laterites? Elsevier.
- Petersen, J. (2015). Heap leaching as a key technology for recovery of values from low-grade ores - A brief overview. Elsevier.



- Roebuck, J., Turkington, J., Rogers, D., Pelsler, M., & Griffin, V. (2016). Preorganized Tridentate Analogues of Mixed Hydroxyoxime/Carboxylate Nickel Extractants. *Dalton Transaction*.
- Rosenqvist, T. (1983). Hydrometallurgy. In T. Rosenqvist, *Principles of Extractive Metallurgy* (pp. 398 - 419). Singapura: McGraw-Hill Book Company.
- Smith, A. G., Tasker, P. A., & White, D. J. (2001). The structures of phenolic oximes and their complexes. Elsevier.
- Sufriadin, Idrus, A., Pramumijoyo, S., I Wayan, W., & Imai, A. (2011). Study On Mineralogy And Chemistry Of The Saprolitic Nickel Ores From Soroako, Sulawesi, Indonesia: Implication For The Lateritic Ore Processing. *J. SE Asian Appl. Geol.*, 23-33.
- Wilson, M., Bailey, P., Tasker, P., Turkington, J., Grant, R., & Love, J. (2013). Solvent Extraction: The Coordination Chemistry Behind Extractive Metallurgy. *Chem Soc Rev*.



DIURETIC EFFECT OF JAMU ANTIATHEROSCLEROSIS BY IN VIVO TESTING ON MALE RATS

Dewi Tristantini^{a*}, Clarissa Ancella^b

^aChemical Engineering Department, Universitas Indonesia, Kampus Baru UI Depok, Depok 16424, Indonesia

^bChemical Engineering Department, Universitas Indonesia, Kampus Baru UI Depok, Depok 16424, Indonesia

ABSTRACT

Hypertension has become the worldwide's focus because mortality rate due hypertension is increasing every year. One of the antihypertensive drug is diuretic which cause a decrease in blood pressure. Active substances provide a diuretic effect is a flavonoid. Flavonoid in combination of bullet wood leaves, curcuma and starfruit leaves empirically proven, research and published in decrease blood sugar levels, decrease cholesterol and improve blood circulation. The combination of bullet wood leaves, curcuma and starfruit leaves become jamu antiatherosclerosis. Jamu antiatherosclerosis extracted using reflux so particle size affects the flavonoid produced. Particle size jamu antiatherosclerosis is smaller than 60 mesh so jamu antiatherosclerosis which has the highest apigenin and catechin is particle size smaller than 60 mesh. The method used is testing *in vivo* to male rats (*Rattus norvegicus*). The study used 6 group of rats are normal control (without treatment), negative control (induced NaCl and standard feed), positive control (captopril 0.72 mg), dose I (13.2 mg herb), dose II (26.4 mg herb) and dose III (52.8 mg herb). Data retrieval urine volume and blood pressure of the rats were taken within 21 days. The data showed that diuretic activity jamu antiatherosclerosis dose I was 0.724, dose II was 0.792 and dose III was 0.843. The results showed that caused an increase in urine volume in which higher diuresis effect is achieved by increasing the amount of extract. This research conclude that jamu antiatherosclerosis can use as an inexpensive diuretic herbs in lowering blood pressure and the results can be used to improve public welfare.

Keywords: Diuretic; Antihypertensive; Tanjung leaves (*Mimusops elengi L.*); Starfruit leaves (*Averrhoa carambola L.*); Curcuma (*Curcuma xanthorrhiza L.*); Particle size.

1. INTRODUCTION

Complications due to hypertension cause 9.4 million people die each year in the world (Lim et al, 2012). Hypertension cause 45% deaths due to heart disease and 55% deaths due to stroke (WHO, 2008). Hypertension become worldwide focus because mortality due to hypertension increase from 1999 to 2009 which is 17,1% (Go et al, 2014). Several causes of hypertension are unhealthy lifestyle, high stress level and genetic factor (WHO, 2013). Treatment of hypertension divided into 2 are the therapeutic use of pharmaceutical drugs and herbal medicine.

One of the antihypertensive drug is diuretic which cause a decrease in blood pressure. Diuretics are substances that can increase urinary expenditure (diuresis) through direct action on the kidneys. Diuresis causes a decrease in plasma volume in the veins, increased release of renin, decreased cardiac output and decreased blood pressure (Conway,



et al, 1960). Synthetic diuretic drugs have side effects that are contraindicated in hypersensitivity to sulfonyleureas, hypokalemia, hypercalcemia, liver disorders, renal impairment and pregnancy (NFKDOQI, 2004; Lacy et al, 2006; BPOM RI, 2008; WHO, 2009). Active substances provide a diuretic effect is a flavonoid (Anna, 2011). Flavonoid's mechanism as diuretic is inhibit reabsorption Na^+ , K^+ dan Cl^- , so it increase electrolytes in the tubules then diuresis occurs (Khabibah, 2011).

The development of diuretics from herbal ingredients have benefit such as decrease blood pressure and minimize side effects of synthetic diuretics drug. Indonesia is rich in herbal plants that contain flavonoids that are Tanjung, starfruit and curcuma. Tanjung is used as an antiulcer, anti-inflammatory, antianxiety, antihyperlipidemic, anticonvulsant, analgesic, antipretic, antioxidant, cytotoxic, antidiabetic, diuretic and antihypertensive (Gami et al, 2012 and Manjeshwas et al, 2011). Curcuma is used as an antitumor (Vimala et al, 1999) and antiinflammation (Ozaki, 1990). Starfruit is used as antidiabetes, blood pressure-lowering, and believed to be an appetite enhancer and antidiarrhea (Soncini, 2010).

Empirically, the combination of these three herbs has been proven and studied to have properties as herbs that can break blood clots, blood circulation, lower cholesterol levels and lower blood sugar so it can be called herbal antiatherosclerosis. Herbs can be consumed in powder form dissolved in a solvent. The size of herbs particles circulating differently that is greater than 20 mesh is a rough herb, 40-60 mesh is a fine herb and smaller than 60 mesh is a herb packed in capsules. One of the factors affecting solid-liquid extraction is particle size (Richardson, 2001). The particle size of the herb influences the optimization of the active substance content when the extraction is performed.

Testing of ingredients for treatment or general medicine is done in vivo to the test animals to determine the pharmacological effects before human consumption. Rats include mammals, and therefore their impact on a treatment may not be much different from that of other mammals (Smith and Mangkoewidjojo, 1988). Test results in animal tests will provide an overview of the results of drug use in humans. This research is feasible because it will improve and develop herbal as low cost treatment as antihypertension.

2. METHODOLOGY/ EXPERIMENTAL

Methods applied in this study was started by simplicia preparation and extraction procedure, animals treatment then diuretic test.

2.1. Simplicia preparation and extraction procedure

The fresh leaves of *Mimusops elengi* Linn, *Averrhoa carambola* L. and *Curcuma xanthorrhiza* Roxb were collected. The leaves and rhizomes were air-dried for 7 days using indirect sunlight. The leaves and rhizomes were mashed become powder. The particle size of leaves and rhizomes is >60 mesh. The leaves and rhizomes powder have to weighed and mixed. It name is jamu antiatherosclerosis. Jamu antiatherosclerosis 24 g were extracted using a soxhlet apparatus with aqueous at 85°C for 45 minutes. Jamu solution was filtered and dried in vacuum rotary evaporation at 65°C .



2.2. Animals

Adult male Sprague-Dawley rats, each in the weight range of 180-200 g, were used for this research. The rats obtained from Pharmacological laboratory, faculty of Pharmacy University of Indonesia. The rats were randomly grouped to six treatment groups of 4 rats each and kept in cages and housed under standard conditions of temperature, humidity and dark light cycle.

2.3. Experimental protocol

Diuretic test was used rats. Diuretic effect procedures were consists of various steps. acclimatization animals and treatment. First, the rats were randomly grouped to six treatment groups of 4 rats each as shown in Table 1. On the day-1 until day-20 the process named acclimatized which was the rats were given hypertension induction to raise their blood pressure. On the day-21 until day-42, the rats got treatment accorded to their group. All the rats fed with pellets and water.

Table 1. Each group treatment for diuretic test

Group	N	Treatment (days)					
		1	7	14	21	35	42
Normal	4		Water			Water	
Negative	4		NaCl			NaCl	
Positive	4		NaCl			NaCl	
Dose I	4					NaCl and Jamu antiatherosclerosis (13.2 mg/ 200 g weight)	
Dose II	4		NaCl			NaCl and Jamu antiatherosclerosis (26.4 mg/ 200 g weight)	
Dose III	4		NaCl			NaCl and Jamu antiatherosclerosis (52.8 mg/ 200 g weight)	

The each of rats was placed in metabolism cages. Urine was collected in a graduated cylinder and its volume was measured each hour intervals for 4 hours. The urine volume will be calculated to show diuretic action and diuretic effect of each group. The equation of diuretic action and diuretic activity shown in equation 1 and 2.

$$\text{Diuretic action} = \frac{\text{Urine volume treatment group}}{\text{Urine volume control group}} \quad (1)$$

$$\text{Diuretic activity} = \frac{\text{Diuretic action treatment group}}{\text{Diuretic action standard drug group}} \quad (2)$$



3. RESULTS AND DISCUSSION

The aqueous extract of the jamu antiatherosclerosis produced diuresis. A results of this research was an total volume urine for 4 hours. Measurement the diuretic effectiveness of treatment will be shown in diuretic action and diuretic activity. Table 2 shows total urine volume diuretic action and diuretic activity. Figure 1 shows changes in urine volume of each group

Table 2. Effect of oral administration on urine volume for 4 hours

Group	Total urine volume (mL)			Diuretic action	Diuretic activity
	Day-21	Day-35	Day-42		
Normal	1,675±0,287	1,925±1,556	1,425±1,161	-	-
Negative	6,275±1,730	7,8±1,756	7,925±1,330	1	-
Positive	8,25±2,422	10,035±1,042	11,275±2,513	1,461	1
Dose I	7,125±0,250	7,95±0,858	8,1±1,626	1,058	0,724
Dose II	7,775±1,438	8,625±0,170	8,9675±0,731	1,158	0,792
Dosis III	8,1±1,626	9,300±0,581	9,6450±0,762	1,233	0,843

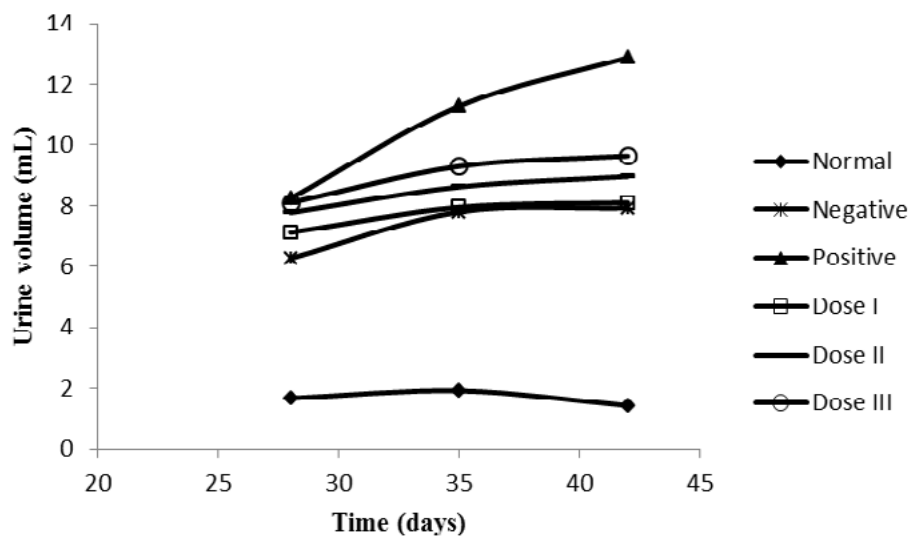


Figure 1. Effect of oral administration on urine volume for 4 hours

Normal group represent rats without hypertension induction, drug and jamu extract so their urine volume shows normal urine volume. Urine volume normal group can use as reference healthy urine volume. Rats negative group were given hypertension induction and their urine volume as reference hypertensives urine volume without treatment. Average urine volume's negative group is greater than normal group, because a body have homeostatis function. This function is maintain fluid balance in the body by a way



decrease antidiuretic hormone secretion, reduce the permeability of the distal tubule and the duct collingentes to water thereby decreasing the reabsorption of water which will ultimately increase urinary excretion (Guyton, 2006). On the 28th day, 35th day and 42th day positive group, dose I, dose II and dose III group were given captopril and jamu extract. The urine volume each group were recorded and the results showed an increase urine volume compared with normal and negative group. It means captopril and jamu antiatherosclerosis extract have diuretic effect. Diuretic effect indicated by value of diuretic action and diuretic activity. Diuretic action is a comparison treatment group with the control group which is negative group and diuretic activity is a comparison of diuretic action with the group that has been given standard drugs, in this study is positive group with the administration of drug captopril. Diuretic activity value shows the diuretic strength and it is shown in Table 3.

Table 3. Relation between diuretic activity and diuretic strength

Diuretic activity value	Diuretic strength
1,5	Strong
1-1,5	Moderate
0,72-1	Week
< 0,72	Null

Urine volume positive group is the highest and has the highest diuretic activity compared with other groups. It means that captopril has the highest diuretic effect than jamu antiatherosclerosis extract. Successfull material test parameter if a result of jamu antiatherosclerosis extract approaching positive group's result (Pradana, 2016). Jamu antiatherosclerosis extract were varied and given to group dose I, dose II and dose III. Table 2 showed that the urine production and diuretic activity of dose I is less than dose II and urine volume's dose II is less than dose III. Dose I is the least and dose III is the most jamu extract dosage. Based on the classification diuretic strength, the three groups of dosage variation jamu antiatherosclerosis are weak diuretic with the range of diuretic activity are 0,72-0,84. It means dosage affect the diuretic activity and the greater dosage produced more urine than lower dosage. The effect of dosage of herbal extract on rats urine indicates that the larger the dose given the flavonoid content of catechin and apigenin increased so stimulate regional blood flow or vasodilatation, or by producing inhibition of tubular reabsorption of water and anions, with the result in both cases being diuresis (Martín et al, 2008). The urine volume excreted by rats are directly proportional to the time of giving jamu extracts. Provision of drugs or herbal extract on a regular basis will increase urinary excretion to the normal level of urine of mice. The normal limit of urinary white rat excretion (*Rattus novergicus*) is 5.5 mL / 100 g body weight / day (Carpenter, 2012). Aqueous extract of *Ajuga remota* Benth (Lamiaceae) leaves has proven produced a better diuretic effect than methanol as solvent (Hailu et al, 2014), so water choosen as solvent of jamu. The aqueous extract of jamu antiatherosclerosis produced weak diuretic effect. It is therefore possible to suggest that the ingridients of jamu antiaterosclerosis material responsible for increasing urine output could probably be polar and hence better extracted in water.



4. CONCLUSION

These observations provide evidence for the ethnomedical use of jamu antiatherosclerosis as diuretic for treatment of hypertension. The results showed that jamu antiatherosclerosis is weak diuretic. A dosage and a period time for taken medicine affect the diuretic activity. The larger doses of jamu antiatherosclerosis particularly of the aqueous extract produced the highest urine excretion was comparable to the other dosage variation of jamu antiatherosclerosis. The longer time to take the drug or jamu antiatherosclerosis, the greater the urine excretion but not significant and it have a limit.

5. ACKNOWLEDGEMENT

Authors would like to thank all parties that have supported this study, especially University Of Indonesia via Grant of International Publication Indexed for Thesis of UI's Students or known as PITTA 2017.

6. REFERENCES

- Carpenter, J.W., (2012), *Exotic animal formulary*, 4th ed, Philadelphia, Saunders.
- Conway J., Lauwers P., (1960), Hemodynamic and hypotensive effects of long-term therapy with chlorothiazide, *Circulation*, Volume 21, pp. 21-27.
- Gami B., Pathak S., Porabia M., (2012), Ethnobotanical phytochemical and pharmacological review of *Mimusops elengi* Linn, *Asian Pacific J Tropical Biomed*, Volume 2, Number 9, pp. 743-748.
- Go, A.S., (2014), *Heart Disease and Stroke Statistics 2014*, Update: A Report From the American Heart Association, *Circulation*, Volume 129, pp. 28-292.
- Guyton, A.C. and Hall, J.E., (2006), *Textbook of Medical Physiology*. 11th ed. Philadelphia, PA, USA: Elsevier Saunders.
- Hailu W. and Engidawork W., (2014), Evaluation of the diuretic activity of the aqueous and 80% methanol extracts of *Ajuga remota* Benth (Lamiaceae) leaves in mice. *BMC Complementary and Alternative Medicine*. Volume 14, pp 135.
- Khabibah, N., (2011), Uji Efek Diuretik Ekstrak Buncis (*Phaseolus Vulgaris* L.) Pada Tikus Putih Jantan Galur Wistar, STIKES Ngudi Waluyo. Ungaran. pp. 2.
- Lacy, C.F., Armstrong, L.L., Goldman, M. P., Lance, L.L., (2006), *Drug Information Handbook*, 14th ed. Lexi Comp, North American.
- Lim S.S., Vos T., Flaxman A.D., Danaei G., (2012), A comparative risk assessment of burden of disease and injury attributable to 67 risk factors and risk factor clusters in 21 regions, 1990-2010 : a systematic analysis for the Global Burden of Disease Study 2010, *Lancet*. 380 (9859), pp. 2224-60.
- Manjeshwar S.B., Ramakrishna J.P., Harshit P.B., Princy L.P., Rekha B., Chemistry and medicinal properties of Bakul (*Mimusops elengi* Linn). (2011), *Rev Food Res Int*. Volume 44, pp. 1823-1829.
- NKF-K/DOQI. (2004), *Clinical Practice Guidelines for Cronic Kidney Disease: Evaluation, Clasification, and stratification*, *American Journal Kidney Disease*, Volume 45, Number 1, pp. 1-268.



- Ozaki, Yukihiro., (1990), Antiinflammatory effect of Curcuma xanthorrhiza ROXB and its active principles, Chemical Pharmaceutical Billetin, Volume 38, Number 4, pp. 1045-1048.
- Pradana, Bhayangkara., (2016), Pengujian Aktivitas Antikolesterol Dari Ekstrak Daun Tanjung (*Mimusops elengi L.*) Dalam Pelarut Air Dengan Metode In Vivo Pada Mencit (*Mus musculus L.*) Galur DDY, Universitas Indonesia. Depok.
- Richardson, J.F., (2001), Chemical Engineering Particle Technology and 38 Separation Processes, Oxford: Butterworth-Heinemann.
- Smith, J.B., Mangkoewidjojo, S., (1988), Pemeliharaan, Pembiakan dan Penggunaan Hewan Percobaan di Daerah Tropis. Tikus Laboratorium (*Rattus norvegicus*), Universitas Indonesia, pp. 37-57.
- Vimala, S., Norhanum, A.W., Yadav M., (1999), Antitumor promoter activity in Malaysian ginger rhizobia used in traditional medicine, Br J Cancer, Volume 80, pp. 110-116.
- WHO., *Global Health Observatory Data Repository [online database]*. Geneva, World Health Organization, (2008), Available from: <http://apps.who.int/gho/data/view.main> [Accessed 7th September 2013].
- WHO., *Media Centre. Nocommunicable diseases*. (2013) Updated March 2013. Available from: <http://www.who.int/mediacentre/factsheets/fs355/en/> [Accessed 7th September 2013].
- WHO., (2009), *WHO Model Formulary 2008*, World Health Organization Press, Geneva. pp. 262-293, 326-334.



OPTIMIZATION OF LNG REGASIFICATION PLANT USING MODEL PREDICTIVE CONTROL

Abdul Wahid¹ and Ferdi Fajrian Adicandra²

^{1,2}*Sustainable Energy Research Group, Department of Chemical Engineering, Faculty of Engineering, Universitas Indonesia, Depok 16424, Indonesia*
Corresponding Author: ¹wahid@che.ui.ac.id; ²ferdi.fajrian@ui.ac.id

ABSTRACT

Optimization of liquefied natural gas (LNG) regasification plant is important to minimize costs, especially operational costs. Therefore, it is important to select the LNG regasification plant design and obtain optimum operating conditions while maintaining the optimum operating conditions through the implementation of model predictive control (MPC). The optimal criterion is the minimum amount of energy used and or the integral of square error (ISE). As a result, the optimum design is to use scheme 2 with an energy savings of 40%. While the optimum operating conditions occur if the vaporizer output temperature is 6°C. In order to maintain the optimum conditions, MPC is required with parameter setting P (prediction horizon), M (control horizon) and T (sampling time) as follows: tank storage pressure controller: 90, 2, 1; product pressure: 95, 2, 1; temperature vaporizer: 65, 2, 2; and temperature heater: 35, 6, 5, with ISE value at set point tracking respectively 0.99, 1792.78, 34.89 and 7.54, or improvement of control performance respectively 4.6%, 63.5%, 3.1% and 58.2% compared to PI controller performance. The energy savings that MPC controllers can make when there is a disturbance in sea temperature rise of 1°C is 0.02 MW and MPC controller also reduces error to product quality by 34.25% compared to the PI controller.

Keywords: Control, optimization, predictive, regasification, re-identification

1. INTRODUCTION

Fuel subsidy for 14 years (2001-2014) ranks the top with an average share of 61.6% compared to subsidies for other sectors (Ministry of Finance, 2014). The use of natural gas in addition to saving fuel subsidies can also improve the quality of the environment because natural gas is more environmentally friendly than fuel. However, the important issue of using natural gas is related to its transport. It is therefore sought by the best way to transport it more safely and efficiently. Several ways have been done to transport gas, one of which is by building gas pipes or liquefying natural gas into LNG, to reduce its volume and make the gas in liquid phase so that transportation is easier. Gas pipe is very limited utilization. Because the installation of gas pipelines has a high difficulty, as well as very expensive costs, especially for long distances and through the oceans. For LNG itself, in West Java has been built units FSRU (Floating Storage and Regasification Unit). This unit is useful for returning LNG back into gas phase to be utilized as industrial fuel.

The LNG regasification plant used must be optimally designed, both the design of the equipment and the control design in order to minimize the energy used. Therefore, in this research we will select the optimal LNG regasification plant design, look for optimum operating conditions, and set the control parameters used in order to maintain optimum operating conditions in case of process disturbances. The controller used is



MPC because MPC is one of the advanced process control that implements the optimization method in its control and has been proven to have better control performance compared to conventional controller (Wahid and Adha, 2016).

2. METHODOLOGY

2.1 FOPDT Model

Figure 1 shows the research flow diagram. The research begins by creating a steady state model developed by Wahid and Tanuwijaya (2015) and Devold (2013). Then for the selection of models based on energy use and optimization of operating conditions. After that, change the simulation to dynamic mode and install the control system on each equipment according to the control objectives. After that, the test model is performed on each controller. This model test is performed to obtain the PRC curve as shown in Figure 2 to obtain an empirical model.

Empirical model used is first order plus dead-time model (FOPDT) with equation:

$$G_p(s) = \frac{K_p e^{-\theta s}}{\tau s + 1} \quad (1)$$

with $K_p = \Delta/\delta$ (Δ = magnitude of change of output variable and δ = amount of input variable change affecting output variable), $\tau = 1,5 (t_{63\%} - t_{28\%})$ with $t_{63\%}$ dan $t_{28\%}$ respectively are output response times when it reaches 63% and 28% of the final value of the output variable, and $\theta = t_{63\%} - \tau$ (Marlin, 2000).

2.2 Controller Tuning

Based on the parameters of this FOPDT empirical model, the PI controller is adjusted using the Ziegler-Nichols method (Smith and Corripio, 1997). The transfer function PI controller is used equation:

$$G_c(s) = K_c \left(1 + \frac{1}{T_i s} \right) \quad (2)$$

where K_c is the controlling gain and T_i is the integral time. For Ziegler-Nichols method used equation:

$$K_c = \frac{0.9}{K_p} \left(\frac{\theta}{\tau} \right)^{-1} \text{ dan } T_i = 3.33 \theta \quad (3)$$

For the MPC controller, the empirical model parameters obtained from PRC can be directly used on UniSim software R390.1 as a process model. Then re-identified the system, by retesting the model with the close loop method using the default MPC adjustment constants and then the results are compared with the MPC performance by using the previous PRC. The re-identification process is completed if the MPC performance using the previous PRC is better than the performance of MPC with the PRC used. The performance parameter used is ISE (Altman, 2005). The system identification is performed to obtain the optimum empirical model. After that done, setting parameters MPC Prediction Horizon (P), Control Horizon (M), and Sampling Time (T) by using the fine-tuning method. MPC fine-tuning adjustment is done by trial error and then view system behavior to change adjustment parameters (P, M, T) to obtain stable settings.

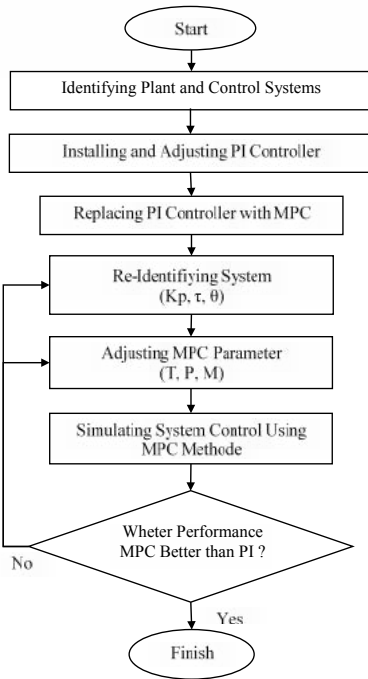


Figure 1. Research Flow Diagram

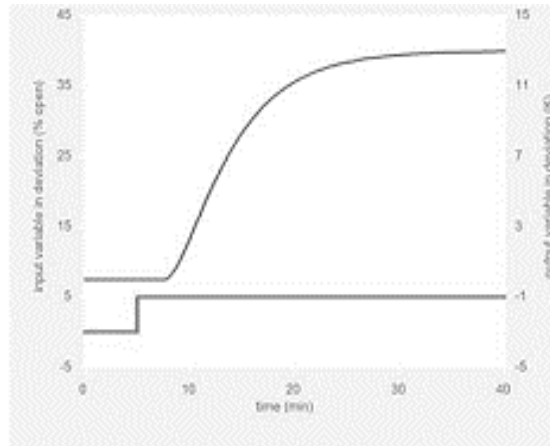


Figure 2. Process Reaction Curve

3. RESULTS AND DISCUSSION

3.1 Optimization of LNG Regasification Scheme

To determine the most optimum regasification process scheme between the two schemes in Figure 3, a simulation is performed that can calculate the energy requirements for each process scheme. From the simulation results in Table 1 and Figure 4, it can be seen that the energy in scheme 1 is very large for the compressor process equipment, and small enough for the LNG pump energy needs compared to scheme 2. In scheme 2, the amount of energy required is in the heater unit that functions to increase the gas temperature to achieve the gas pipe specification. In scheme 2, there is no compressor to increase pressure but is replaced by a high pressure LNG pump which requires considerable magnitude compared to scheme 1. If viewed as a whole, scheme 2 requires less energy than scheme 1. Energy savings can be done by replacing the process in order to increase in pressure from the compressor unit to the high pressure LNG pump unit reaches 40%.

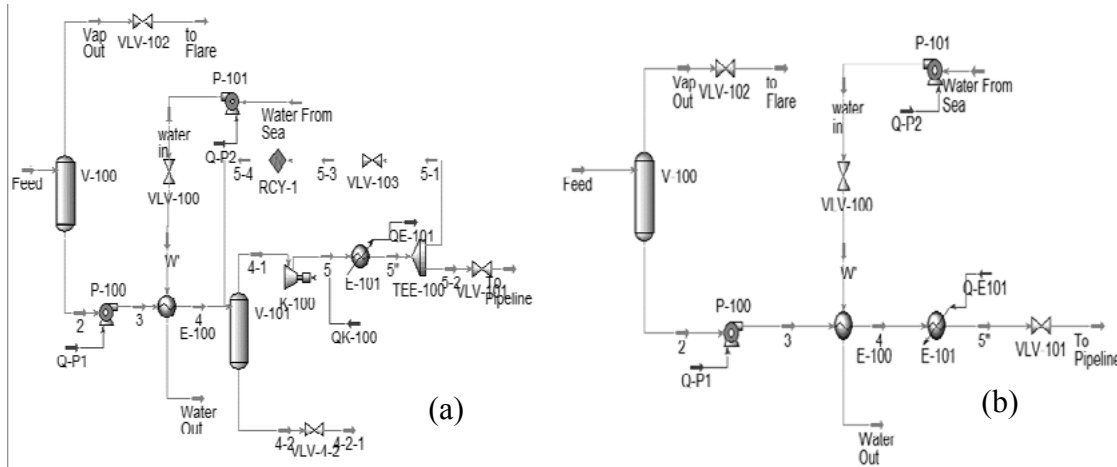


Figure 3. Regasification Process: (a) scheme 1, (b) scheme 2



Table 1 Use of Energy at Regasification Plant (MW)

Process Equipment	Scheme 1	Scheme 2
LNG Pump	1.04	2.37
Water Pump	0.79	0.81
Compressor	21.15	-
Cooler	8.87	-
Heater	-	15.97
Total	31.85	19.15

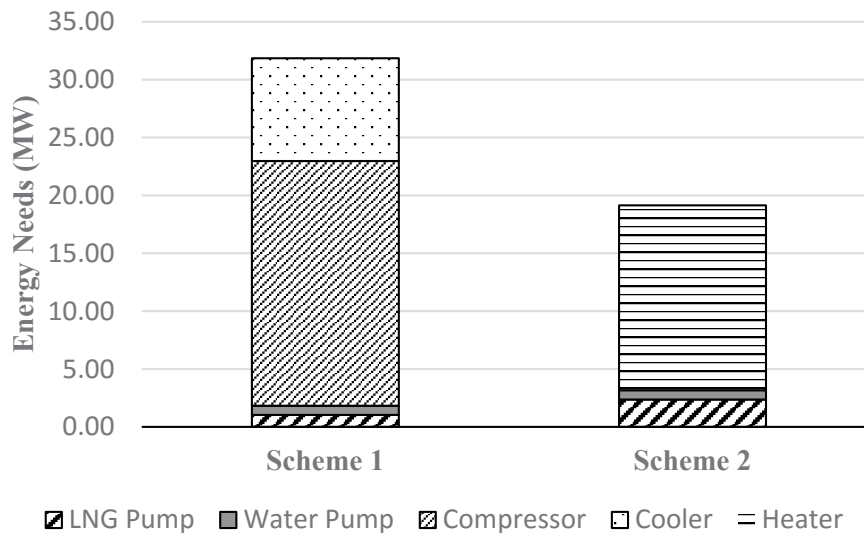
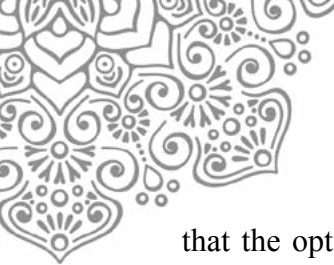


Figure 4. Proportion of Energy Requirement of LNG Regasification Plant

3.2 Optimization of LNG Regasification Operating Conditions

At the LNG regasification plant the unit that has an important role is the vaporizer unit. In this unit, there is a phase change from liquid LNG to gas which is the main objective of the regasification process. Therefore, an optimum operating condition is required for this unit to make the plant run efficiently. To obtain optimum condition simulations are performed using Unisim R390.1, to see the effect of vaporizer output temperature with required seawater pump power and duty of heater needed to achieve gas pipe specification.

In Figure 5, the relationship between the vaporizer output temperature and the required duty heater is inversely proportional, the larger the vaporizer output temperature the duty heater required will be less. Different relationship is shown by graph between vaporizer output temperature with sea water pump power, the higher temperature of vaporizer output will increase the required sea water pump power. This is because it will require more sea water that acts as a hot fluid in the vaporizer if the desired vaporizer output temperature is greater. From the Figure 5 of the simulation results, it was found



that the optimum conditions for the vaporizer output temperature were at the point of intersection between the two graphs at 6 °C.

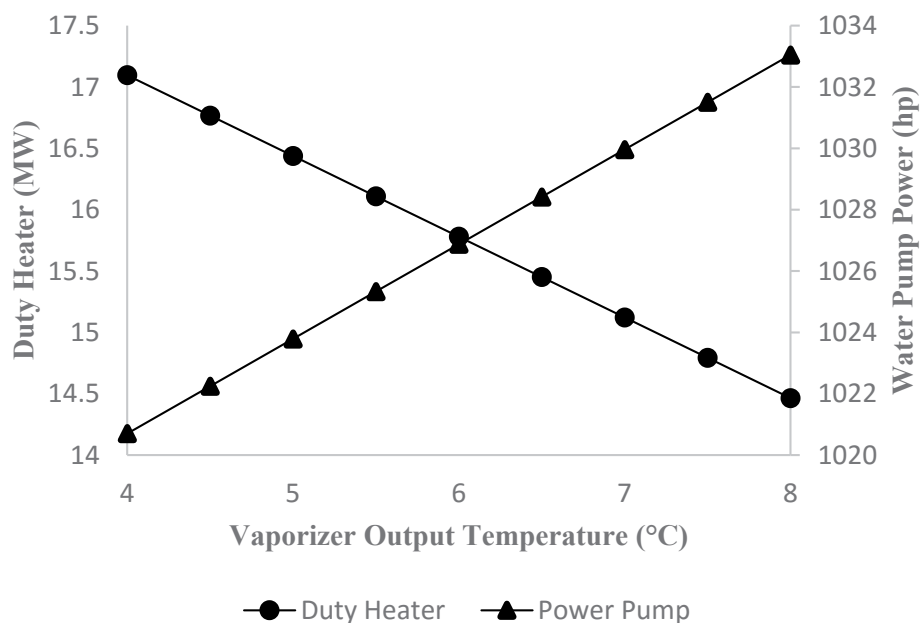


Figure 5. Relation of Vaporizer Output Temperature with Duty Heater and Water Pump Power

3.3 Empirical Model and Adjustment of Control

The empirical model is obtained from PRC (process reaction curve) resulting from system identification for each controller. From the PRC, FOPDT empirical models were developed as shown in Table 2, which is computed by equation (1).

Table 2. Process Model of Regasification LNG Plant

Controller	FOPDT
Pressure Control V-100	$\frac{0.069 e^{-0.0108s}}{0.103s + 1}$
Pressure Control Stream 4	$\frac{0.121 e^{-0.003s}}{0.017s + 1}$
Temperature Control E-100	$\frac{0.045 e^{-0.0182s}}{0.642s + 1}$
Temperature Control E-101	$\frac{0.381 e^{-0.0088s}}{0.0438s + 1}$

3.4 Performance of Control

The way to find out the performance of each controller, set point tracking and disturbance rejection are performed and evaluated with the value of ISE. Here are the results of both methods:

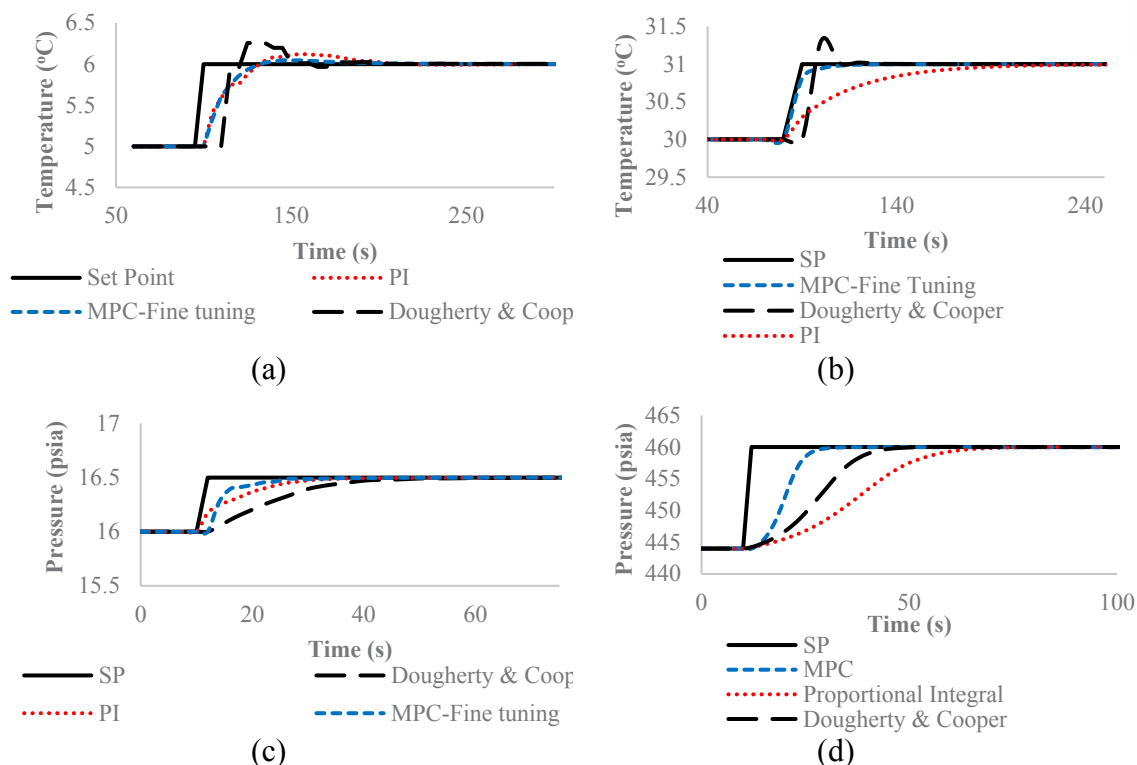


Figure 6. Comparison of Three Controller (Set Point Tracking): (a) Vaporizer (b) Heater (c) Storage Tank (d) Stream 4

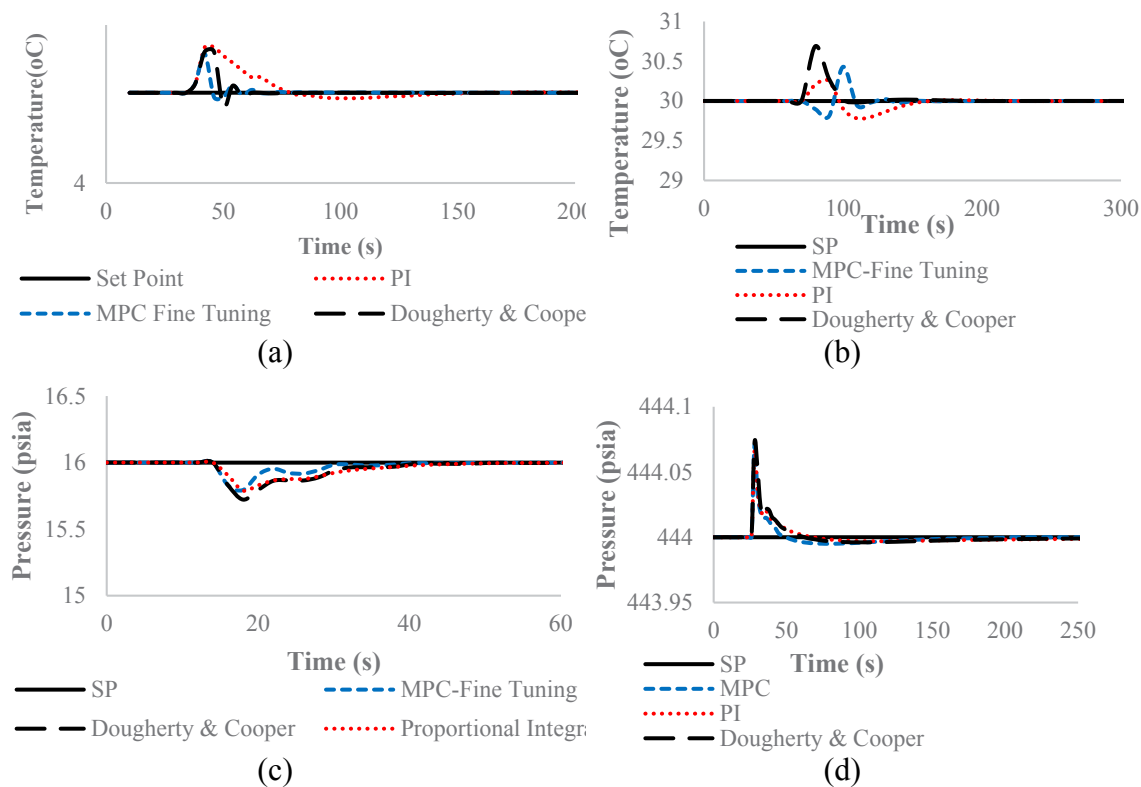


Figure 7. Comparison of Three Controller (Disturbance Rejection): (a) Vaporizer (b) Heater (c) Storage Tank (d) Stream 4



3.4.1 Set Point Tracking. In this method, a set point change is made to see how the controller response to achieve process stability. The controller that has the lowest ISE value is the best controller. The result for the set point tracking can be represented by Figure 6. From Figure 6, the tuning with MPC-Fine tuning method produces the best performing control with the total ISE scores in sequence for the vaporizer, heater, storage tank, and stream 4 controllers are 34.88, 7.54, 0.98 and 1792.78.

3.4.2 Disturbance Rejection. In this method, disturbance is given to the system to see the controller response in overcoming the disturbance on the system. The results of the test for disturbance rejection can be seen in Figure 8. From Figure 7, the tuning with MPC-Fine tuning method produces the best performing control with the total ISE scores in sequence for the vaporizer, heater, storage tank, and stream 4 controllers are 7.4, 7.54, 0.35 and 0.016.

3.5 Energy Efficiency

To determine the effect of errors on both controllers on energy to be used can be seen in Figure 8 and Figure 9. Based on the calculation of energy deviation, the use of control with the MPC-fine tuning method has fewer errors than the proportional-integral method controller. The use of MPC-fine tuning controller can reduce 0.02 MW and MPC controller also reduces error to product quality by 34.25% compared to the PI controller.

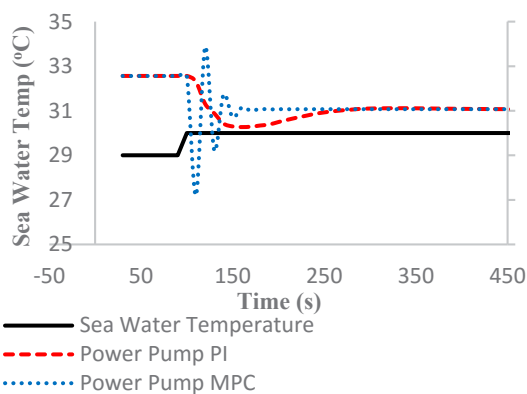


Figure 8. Relationship needs of pump power to disturbance on Sea water temperature

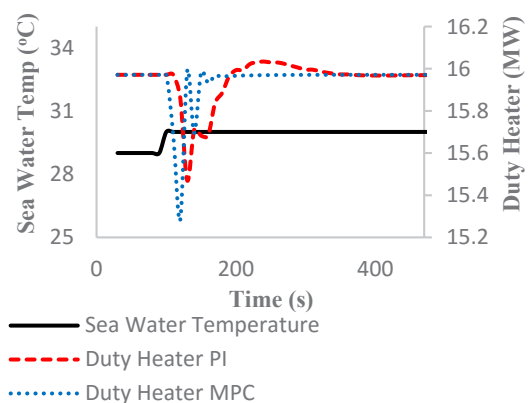


Figure 9. Relationship needs of Duty Heater to disturbance on Sea water temperature

4. CONCLUSION

Scheme 2 LNG regasification plant requires less energy than scheme 1, with energy savings reaching 40% from scheme 1, so scheme 2 is chosen. The optimum condition of vaporizer output temperature is 6°C, while MPC (P, M and T) parameter settings are as follows: pressure tank control (90, 2, 1), pressure on stream 4 (95, 2, 1), vaporizer temperature (65, 2, 2) and heater temperature: (35, 6, 5) with ISE value in set point tracking respectively 0.99, 1792.78, 34.89 and 7.54, or improved control performance respectively 4.6%, 63.5%, 3.1% and 58.2%, compared to PI controller performance. The energy savings that MPC controllers can perform when a disturbance



in sea temperature rise of 1°C is 0.02 MW and MPC controller also reduces error to product quality by 34.25% compared to the PI controller.

5. ACKNOWLEDGMENTS

We express our gratitude to the Universitas Indonesia which has funded this research through the scheme of Hibah Publikasi Internasional Terindeks untuk Tugas Akhir Mahasiswa (PITTA) No.2068/UN2.R3.1/PPM.00/2017.

6. REFERENCES

- Altman, W. 2005. *Practical Process Control for Engineers and Technicians*. IDC Technologies
- Devold, H. 2013. *Oil and Gas Production Handbook: An Introduction to Oil and Gas Production, Transport, Refining and Petrochemical Industry*. Oslo : ABB Oil and Gas.
- Marlin, T. 2000. *Process Control: Designing Processes and Control Systems for Dynamic Performance*. United States: McGraw-Hill Higher Education.
- Ministry of Finance. 2014. *Dasar-dasar Praktek Penyusunan Anggaran di Indonesia*.
- Smith, C. and Corripio, A. 1997. *Principles and Practice of Automatic Process Control*. United States: John Wiley & Sons Inc.
- Wahid, A. and Tanuwijaya, R. 2015. Pemilihan Metode Penyetelan Pengendali PI pada Pengendalian Pabrik Regasifikasi LNG Menggunakan Metode Skor. *Proceeding of Seminar Nasional Teknik Kimia UNPAR*. Bandung, 19 November 2015.
- Wahid, A. and Adha, Afdal. 2016. Model predictive control based on system re-identification for methanol and dymethyl ether synthesis control. *Proceeding of Seminar Nasional Teknik Kimia "Kejuangan"*. Yogyakarta, 17 March 2016




QIR

*The Westin Resort
Nusa Dua, Bali*
24-27 July 2017

ICSEERA

**International Conference
on Saving Energy in
Refridgeration and
Air Conditioning**





EXPERIMENTAL STUDY ON THERMAL PERFORMANCE OF REFRIGERANTS IN MICROCHANNEL HEAT EXCHANGER FOR AIR-CONDITIONING APPLICATION

Ardiyansyah Yatim^{1*}, Muhammad Idrus Alhamid¹, Budihardjo¹, Dicky Alamsyah¹, Hotdian Sinambela¹

¹*Department of Mechanical Engineering, Faculty of Engineering, Universitas Indonesia, Kampus UI Depok, Depok 16424, Indonesia*

ABSTRACT

This paper describes: experimental comparison in thermal performance (COP) as the effect of the use of high ODP refrigerants and zero ODP and GWP refrigerants; and pressure drop of the microchannel heat exchanger, in air-conditioning applications. It is found that the maximum COP of 1.88 achieved when charged with R22 of 300 g with cooling capacity of 1.1 kW. The maximum COP of 1.92 achieved when charged with R290 of 300g with cooling capacity of 1.5 kW. When apply with any refrigerant, the refrigerant pressure drop in the microchannel heat exchanger remains at around 5.0 bars.

Keywords: COP; GWP; Microchannel heat exchanger; ODP

1. INTRODUCTION

Microchannel heat exchangers are widely used due to its compactness in dimension without significantly reducing thermal performance (Shah, R.K., 2006). Microchannel heat exchangers are sufficient to use in energy efficient systems (Roth, K.W. et. al., 2002). The potential for this technology to grow is convincingly evolving, marked with number of research and development on it (Kandlikar, S.G., 2006). In the discipline of air conditioning, the use of different types of HCFC-based refrigerants is phased out, replaced with HC, HFO, and CO₂-based refrigerants that possess zero ODP and GWP, make those use is promising in the future (Babu, P.S., 2015). Most of cooling units for residential are still earmarked for HCFC-based refrigerants (Wan, T., et. al., 2011). For the sake of knowing how the thermal performance of cooling systems with miniaturized heat exchange devices, paired to HCFC-based cooling systems, charged with drop-in environmentally friendly refrigerants, further study is needed.

2. METHODOLOGY

2.1. Experimental setup

The P&ID of the testing facility is shown in Fig. 1, comprising the main components of the vapor-compression refrigeration system, namely: compressor; condenser; expansion device; and evaporator. The main components were adopted from S09LFG-2 split air-conditioning system by LG, with capacity of 9,000 Btu/hr, and scroll compressor with power of 1 hp with maximum voltage and current of 220 V and 4.3 A, compatible to R22. Evaporator of fin and tube type from LG was included in parallel with the microchannel heat exchanger as the test section. During testing, the ball valve was left closed, so as not



to allow refrigerants to flow into the evaporator of fin and tube from LG. The needle valve was left to fully opened, not to give an effect of expansion.

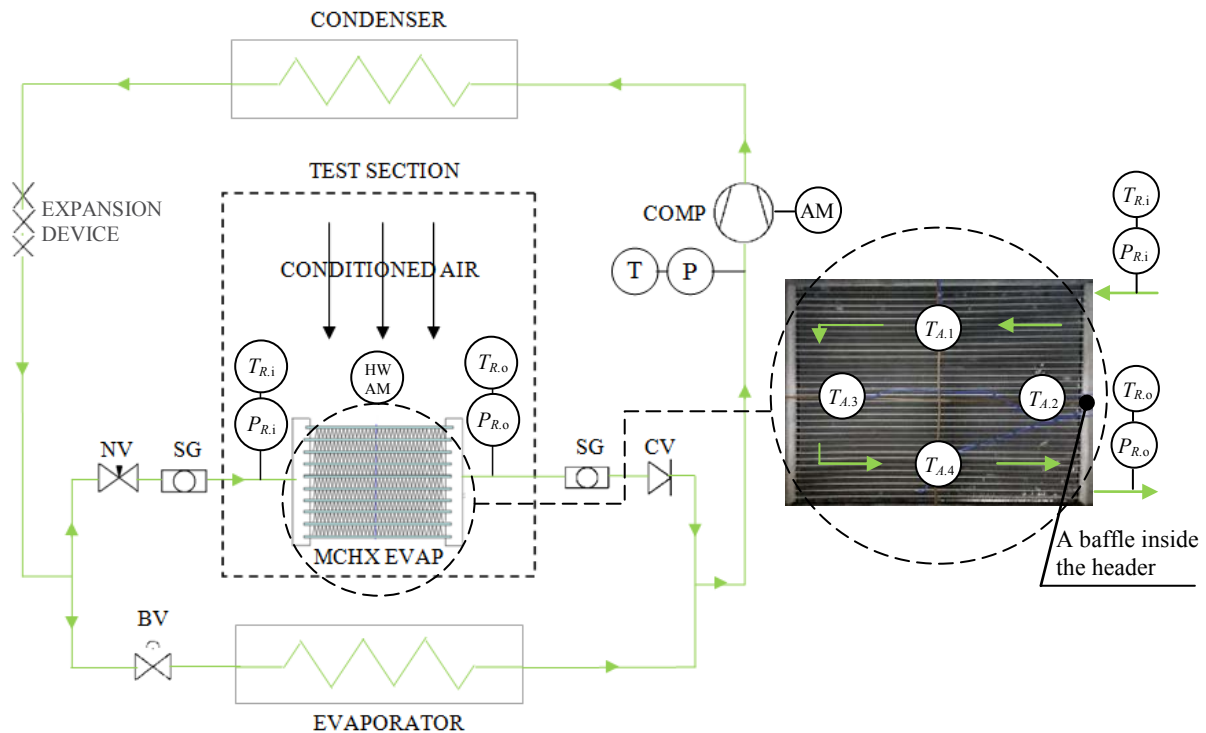


Figure 1 P&ID of thermal performance and pressure drop on microchannel heat exchangers testing facility, consisted of: COMP or compressor; MCHX EVAP or the microchannel heat exchanger as evaporator; NV or needle valve; CV or check valve; BV or ball valve; SG or sight glass; expansion device; T or thermocouple; P or pressure gauge; HWAM or hot wire anemometer; and AM or ampere meters

Table 1 Detailed specification of the microchannel heat exchanger

Parameter	Specification
Material	Aluminium
Fin type	Louvered
Number of tube	98
Height	320 mm (12.6 in)
Width	450 mm (17.7 in)
Number of slab/passes	2
Hydraulic diameter of one entire tube	1.46 mm(0.057 in)
Microchannel tube thickness	0.35 mm (0.014 in)
Fin Pitch	0.79 fin/mm (20 fpi)
Fin Height	7.44 mm (0.29 in)
Louver length	6 mm (0.236 in)
Louver pitch	0.89 n.louv./mm (22.6 n.louv./in)
Louver angle measured from fin plane	30 deg.



Header diameter (measured as envelope diameter)	31.75 mm (1.25 in)
Internal volume of the microchannel evaporators	1.90 L (115 in ³)

The sensors used for data retrieval were: 10 points of thermocouple at the inlet and outlet of the microchannel heat exchanger for air and refrigerant sides; pressure gauge at the inlet and outlet of refrigerant side in regards to the microchannel heat; a hot wire anemometer at the air side; and ampere meter clamped on the cable right after the compressor's capacitor.

2.2. Data reduction

Data retrieval conducted for 3 minutes and 30 seconds. The independent variables defined in the test were the mass of refrigerant of R22 and R290. Each charging went up every 50 g, and stopped at 300 g. The dependent variables defined in the test were: the refrigerant pressure and temperature at the input and output of the microchannel heat exchanger; the output of air temperature at the external flow of the microchannel heat exchanger; and operating current to supply energy to the compressor. The control variables defined were: the expansion capacity by the needle valve at about to negligible; the average air temperature entering the microchannel heat exchanger of 28.0 °C, evenly distributed; operating voltage at the compressor of 220 V; and the average air velocity and temperature at the inlet on the external flow of the microchannel heat exchangers of 0.9 m/s, evenly distributed. The data recorded were partitioned into categories of: air side; refrigerant side; and compressor, reduced with Eq. 1 to Eq. 4 as follow:

$$\bar{T}_{A,o} = \frac{1}{1,050} \sum_{i=1}^{210} (T_{A,1}^i + T_{A,2}^i + T_{A,3}^i + T_{A,4}^i) \quad (1)$$

$$\dot{Q}_A = (\rho v c_p) (L_{MCHX} \times W_{MCHX}) (\bar{T}_{A,i} - \bar{T}_{A,o}) \quad (2)$$

$$W = VI \quad (3)$$

$$COP = \frac{Q_A}{W} \quad (4)$$

Where ρ and c_p were taken at the mean air temperature of $\bar{T}_{A,i}$ (28.0 °C) and $\bar{T}_{A,o}$ based on database from Keenan, J. H. and Kaye, J, 1945.

3. RESULTS AND DISCUSSION

3.1. Profile of output air temperature

Fig. 2 shows the profile of air temperature at the outlet of the microchannel heat exchanger when ran with R290 of 300 g. Temperatures $T_{A,2}$ and $T_{A,4}$ show consistency to exchange the least and the most heat yield the average outlet temperature of 13.0 °C and 25.6 °C. This condition illustrates the distribution of flow of refrigerant inside the microchannel heat exchanger. After passing the inlet nozzle of the heat exchanger, the refrigerant flows to the headers and the channels, see Fig. 1. Lower output temperatures illustrate heat exchange occurs more effectively due to the refrigerant is not yet escalates its temperature, yield in high heat transfer. Headers closer to the nozzle tend to cause the air outlet temperature in the external flow of the microchannel lower heat exchanger compared to the farther header, this indicates the refrigerant flows to the header closer to the nozzle first. This may also apply to channels. High pressure drop inside the channels, which discussed in Chapter 3.5, does not allow refrigerant to flow into the channels if the



baffle in the header is eliminated. The use of baffle in the header forces the refrigerant to flow into the canal first before leaving the heat exchanger.

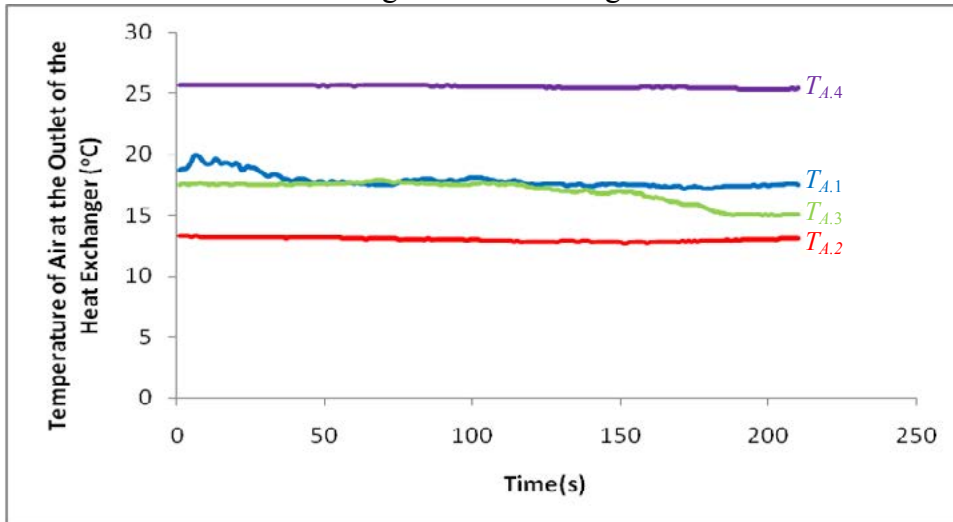


Figure 2 Profile of air temperature at the outlet of the microchannel heat exchanger against time at R290 of 250 g

3.2. Cooling capacity

Fig. 3 shows the correlation between the cooling capacity of the air system against mass charge of the refrigerants. The more the mass charge of refrigerant, representing the greater the mass flow rate or the refrigerant mass flux. If the mass flux increases, more heat is absorbed to evaporate the refrigerant. This reveals the reason why the higher the mass charge of the refrigerant will result in maximum heat transfer. It applies until the optimum condition is passed. The least heat that is able to carry, limits the heat transfer which can occur as it is dependent to mass flow rate and specific heat capacity of the refrigerant and the air. In the test, the maximum cooling capacity of 1.5 kW achieved at R290 of 300 g.

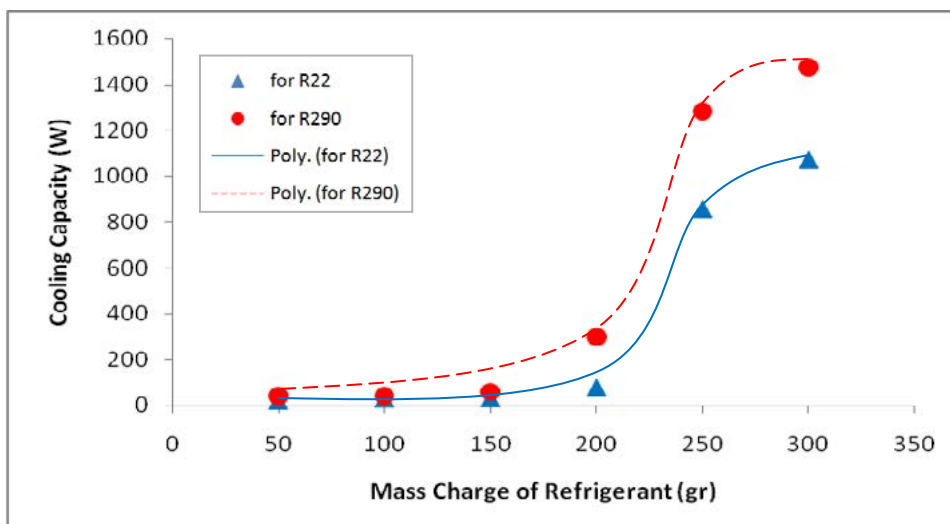




Figure 3 The cooling capacity of the air system against mass charge of refrigerant with microchannel heat exchanger as evaporator

3.3. Energy consumption

Fig. 4 shows the correlation between the energy consumption by the compressor and mass charge of the refrigerants. The more mass charge of the refrigerants, the more the compressor consumes energy. The energy consumption by the compressor is a response to the type of refrigerant and the operating conditions of the system. Under the same mass charge, the energy required by the compressor to compress R290 is relatively greater. At the same pressure and temperature as R290, R22 has a greater density. As the mass of refrigerant to compress increases, the energy required by the compressor will escalate.

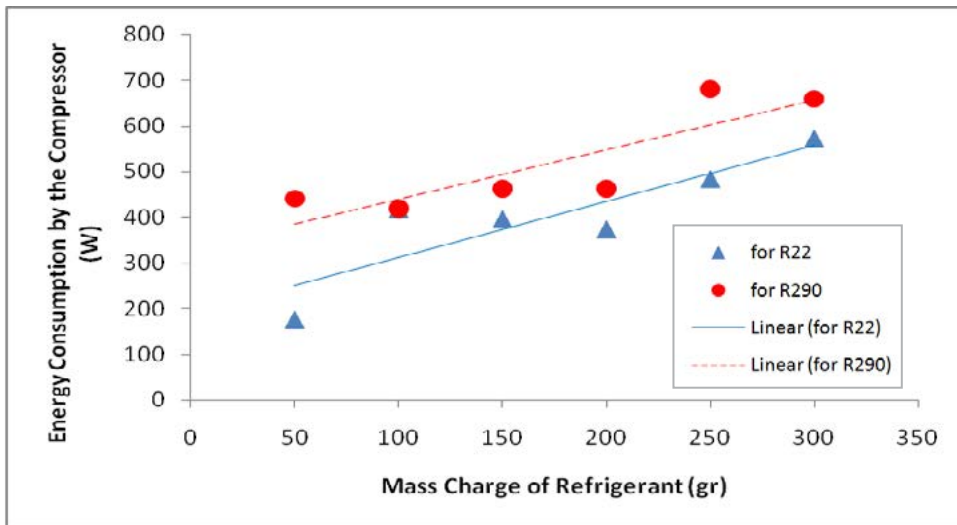


Figure 4 Energy consumption by the compressor against the mass charge of refrigerant

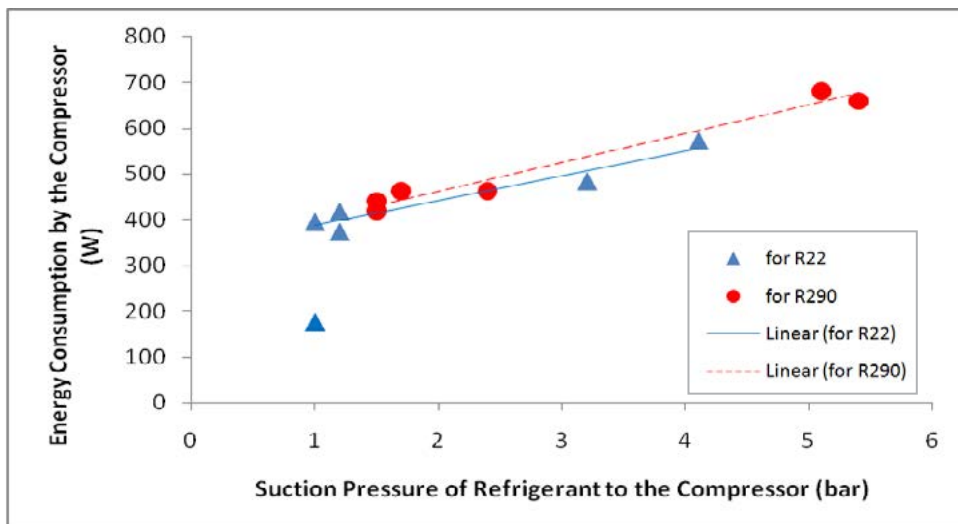




Figure 6 Energy consumption by the compressor against the suction pressure of refrigerant enters the compressor

Fig. 6 shows the energy required to perform compression increases as the input pressure of the refrigerant into the compressor increases. Input pressures to compress are a time higher to produce output pressures, as compressors always have a fixed compression ratio. In the test, the scroll compressor used is compatible to R22 instead of R290. The role of refrigerant oil is considered too. This can be considered as one of the factors why for lower pressure of R290, energy consumption by the compressor tends to be higher than to compress R22.

3.4. COP

Fig. 7 shows no significance in COP difference regarding to variation of refrigerant type of R22 and R290. The optimum COP of 1.88 achieved with R22 of 300 g, and the optimum COP of 1.92 with R290 of 300 g. There are two sides, the left side and the right side of the optimum COP. If the COP is at the left of the optimum point, then the heat transfer is limited to the refrigerant side. When the COP is at the right of the optimum point, the compressor finds more difficult to compress the refrigerant, with unequal proportionality to the resulting cooling capacity, resulting in a decreased COP.

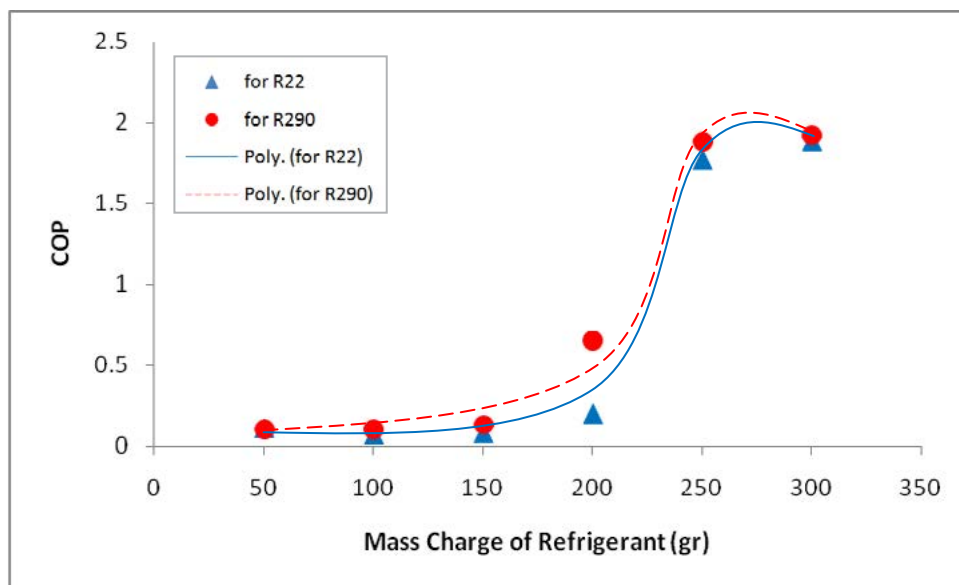
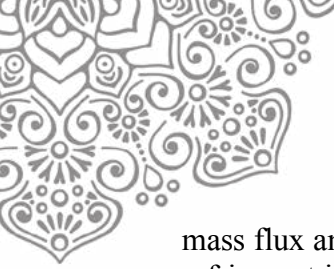


Figure 7 COP against mass charge of refrigerant

3.5. Pressure drop

The pressure drop characteristics at refrigerant side are shown in Fig. 8. R22 at mass charge of 200 g and R290 at mass charge of 150 g are not capable to overcome pressure drop in the microchannel heat exchanger. The test shows, the more mass charge of refrigerant, the less pressure drops will be generated. The mass charge of refrigerant, represents the greater the mass flow rate or the refrigerant mass flux. When the mass flux increases, more heat is required to evaporate the refrigerant. Correlation between refrigerant



mass flux and the amount of heat transferred from the air affects the phase conditions of the refrigerant in the test section. When maximum refrigerant mass flux and minimum input air temperature apply, the existence of liquid phase of refrigerant becomes more and more, and vice versa for minimum refrigerant mass and maximum input air temperature. The liquid phase of the refrigerant has a higher density than the vapor phase, which affects the pressure drop of the friction factor.

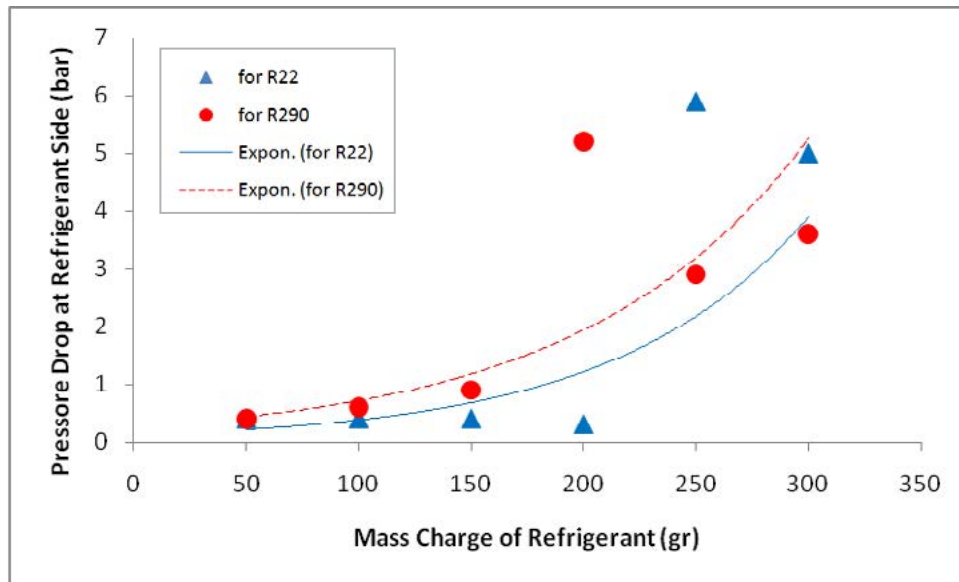


Figure 8 Pressure drop at refrigerant side against mass charge of refrigerant

4. CONCLUSION

The conclusions that can be drawn from the results of microchannel canal exchanger testing are as follows:

1. Temperatures $T_{A,2}$ and $T_{A,4}$ show consistency to exchange the least and the most heat;
2. The highest cooling capacity of 1.1 kW achieved in the test with R22 is at a mass charge of 300 g, and the highest cooling capacity of 1.5 kW achieved in the test with R290 is at a mass of 300 g;
3. Energy consumption by the compressor rises linearly with the increase of mass charge of refrigerant and refrigerant pressure input to the compressor;
4. Differences in COP are not significant between R22 and R290. The highest COP of 1.88 achieved with R22 is at a mass charge of 300 g, and the highest COP of 1.92 with R290 also at a mass charge of 300 g; and
5. Pressure drop increases exponentially. When apply with any refrigerant, the pressure drop remains at around 5.0 bars.

5. NOMENCLATURES

- $\bar{T}_{A,i}$ average temperature of air at the inlet of the heat exchanger ($^{\circ}\text{C}$)
 $\bar{T}_{A,o}$ average temperature of air at the outlet of the heat exchanger ($^{\circ}\text{C}$)
 $T_{A,1}$ average temperature of sensor 1 of air at the outlet of the heat exchanger ($^{\circ}\text{C}$)



$T_{A,2}$	average temperature of sensor 2 of air at the outlet of the heat exchanger ($^{\circ}\text{C}$)
$T_{A,3}$	average temperature of sensor 3 of air at the outlet of the heat exchanger ($^{\circ}\text{C}$)
$T_{A,4}$	average temperature of sensor 4 of air at the outlet of the heat exchanger ($^{\circ}\text{C}$)
\dot{Q}_A	cooling capacity (W)
L_{MCHX}	bulk length of the microchannel heat exchanger (m)
W_{MCHX}	bulk width of the microchannel heat exchanger (m)
ρ	density of air (kg/m^3)
v	velocity of air (m/s)
c_p	energy consumption by the compressor (W)
W	energy consumption by the compressor (W)
V	compressor voltage (V)
I	compressor current (A)
COP	thermal performance

6. ACKNOWLEDGEMENT

The research is funded through 2016 International Collaboration and Publication Research Grant from the Ministry of Research and Higher Education, Republic of Indonesia.

7. REFERENCES

- Babu, P. S. (2015). Hydrocarbon Refrigerants, Promising Substitutes in Low Capacity Refrigeration Systems – A Review. *International Journal of Research in Engineering & Technology* 2321-8843.
- Department of Mechanical Engineering Section of Energy Engineering at the Technical University of Denmark. (1995). CoolPack (1.50 Version) [Computer Program].
- Kandiklar, S.G., Garimella, S. V., Colin, S., Peles, Y., Pease, R. F. W., & Brandner J. J. (2013). Heat Transfer in Microchannels-2012 Status and Research Needs. *Journal of Heat Transfer* 53:175-93.
- Kavanaugh, S. P. (2006) HVAC Simplified. American Society of Heating Refrigerating and Air-Conditioning Engineers.
- Keenan, J. H. & Kaye, J. (1945). Gas Tables. The U.S.A.: John Wiley & Sons, Inc.
- Roth, K. W., Westphalen, D. Dieckmann, J. Hamilton, S. D., & Goetzler, W. (2002). Energy Consumption Characteristics of Commercial Building HVAC Systems Volume III: Energy Savings Potential. TIAX LCC, Ref. No. 68370-00 for Building Technologies Program, Contact no. DE-AC01-96CE23798, Cambridge.
- Shah, R. K. (2006). Advances in Science and Technology of Compact Heat Exchangers. *Heat Transfer Engineering* 27:3-22.
- Wan, T., Dou, Y., Wang, L., Yang, L., Zhou, X., Wan, D., & Hu, J. (2011). Environmental Benefits for Phase-Out HCFC-22 in the Residential Air-Conditioner Sector in China. *Advances in Climate Change Research*.



Investigation of Flow Boiling Heat Transfer Coefficient of R410A in Various Minichannel Multiport Tubes

Nguyen-Ba Chien^{1,a}, Pham Quang Vu^{1,b}, Kwang-Il Choi^{2,c}, Jong-Taek Oh^{2,d*} and Honggi Cho^{3,e},

¹Graduate School, Chonnam National University, 50 Daehak-ro, Yeosu, Chonnam 59626, South Korea

²Department of Refrigeration and Air Conditioning Engineering, Chonnam National University, 50 Daehak-ro, Yeosu, Chonnam 59626, South Korea

³Advanced R&D Team, Digital Appliances, Samsung Electronics, 129 Samsung-ro, Yeongtong-gu, Suwon, 16677, South Korea

bachien@ejnu.net , ohjt@chonnam.ac.kr

Keywords: Heat Transfer Coefficient; R-410A; Multiport Minichannel; Correlation.

Abstract. This study demonstrates the two-phase heat transfer coefficient of R410A during evaporation in the aluminum multiport minichannels with the hydraulic diameter of 1.16 mm (7 parallel channels – Type A), 1.14 mm (11 parallel channels – Type B) and 1.07 mm (16 parallel channels – Type D). The experimental data were measured in the following conditions: the mass fluxes ranged from 50-150 kg/m²s, the heat fluxes of 3-6 kW/m² and the saturation temperature of 6°C. The effect of mass flux and heat flux on heat transfer coefficient were analyzed. The experimental data were also compared with some well-known heat transfer coefficient correlations.

Introduction

Minichannel multiport tube has being used in various advanced heat exchanger systems including electronics cooling, automotive and modern domestic devices due to its effectiveness and compactness. Even though two-phase flow boiling in minichannel have performed through various studies in literature, the extensive reviews [1–3] have pointed out some remaining fundamental issues of this topic. The wide range of tube size has been reported, but a well-established classification is still lack of. Some transition criteria recommended by Kandlikar and Kew and Cornwell [1,4] need further physical proof. Moreover, the heat transfer behaviour in small channel acts differently than that in conventional channel [1,2,5]. The general accepted heat transfer coefficient form for conventional tubes proposed by Chen [6] that combine two important mechanisms: nucleate boiling and forced convective boiling should be should be reevaluated. In fact, most of well-known heat transfer coefficient correlations developed until present are based on the empirical or semi-empirical method rather than basing on the physical approach. Hence, more experimental data of two-phase flow boiling in small channel is necessary to improve the prediction as well as to expand the knowledge of the inside mechanism.

In addition, to date, report on two-phase flow boiling heat transfer and pressure drop of R410A, and, even, other refrigerants in minichannel multiport tube is still limited.

Kaew-On and Wongwises [4] performed the evaporation heat transfer coefficient and pressure drop of R410A flowing through aluminium multiport minichannel. The experimental data was collected in 3.48mm hydraulic diameter tube type, the mass flux of 200 – 400 kg/m²s, the heat fluxes of 5 - 14.25 kW/m², and the saturation temperature of 10 - 30°C. The authors concluded that the average heat transfer coefficient of R-410A during evaporation tended to increase with increasing average quality, mass flux, and heat flux, but tended to decrease with increasing saturation temperature while the pressure drop increased with increasing the mass flux, but decreased with increasing the saturation temperature, and the heat flux has no significant effect.



Vakili-Farahani et al. [7] reported the flow boiling heat transfer of R245fa and R1234ze in multiport tubes with 7 channels of 1.4 mm inner diameter. They proposed a new approach to account the non-uniform distribution of heat flux. The heat transfer coefficient was found to increase with the increase of mass flux, heat flux and saturated temperature. On the other hand, the study proposed the flow pattern based approach to predict the heat transfer coefficient.

Li et al. [8] showed the flow boiling of R-1234yf in vertical aluminum multiport tube with 16 and 40 parallel channels. The results were measured with the fixed saturated temperature of 15°C, the mass flux ranged from 60 – 240 kg/m²s, and the heat flux ranged from 3 – 16 kW/m². As reported in this study, the experimental heat flux decreased linearly with the increase of vapor quality. More importance, the geometry, especially aspect ratio, strongly affects to the heat transfer performance. Three existing pressure drop correlations used in this study [9–11] fail to predict the experimental data.

Hence, the aim of this study is to experimental investigate the two-phase flow boiling heat transfer characteristics and pressure drop of R410A in three types of minichannel multiport tubes. The analysis is carried out by varying the mass flux, heat flux and the comparison between different tube types. In addition, the data was also compared with various heat transfer coefficient correlations in literature.

Experimental procedure

The schematic diagram of the experimental apparatus was shown in Figure 1. The model mainly consists the refrigerant loop, three water loops and the data acquisition system. The refrigerant loop included a magnetic gear pump, a sub-cooler, a mass flow meter, an evaporator, a test section, a condenser and a receiver. When the test facility was operated for evaporation, the refrigerant was delivered into the test section by the gear pump. The mass flow rate of refrigerant was measured by a Coriolis mass flow meter and can be adjusted by changing the pump speed. The quality of the refrigerant at the inlet test section was controlled by pre-heater. The test section was heated by a water loop as shown in the figure. The heat capacity could be varied by mastering the mass flow rate and working temperature of water. The vapor at the outlet of test section was condensed by a condenser unit then accumulating in the receiver for a new testing cycle. The experimental apparatus was well insulated with foam to minimize heat transfer between the system and

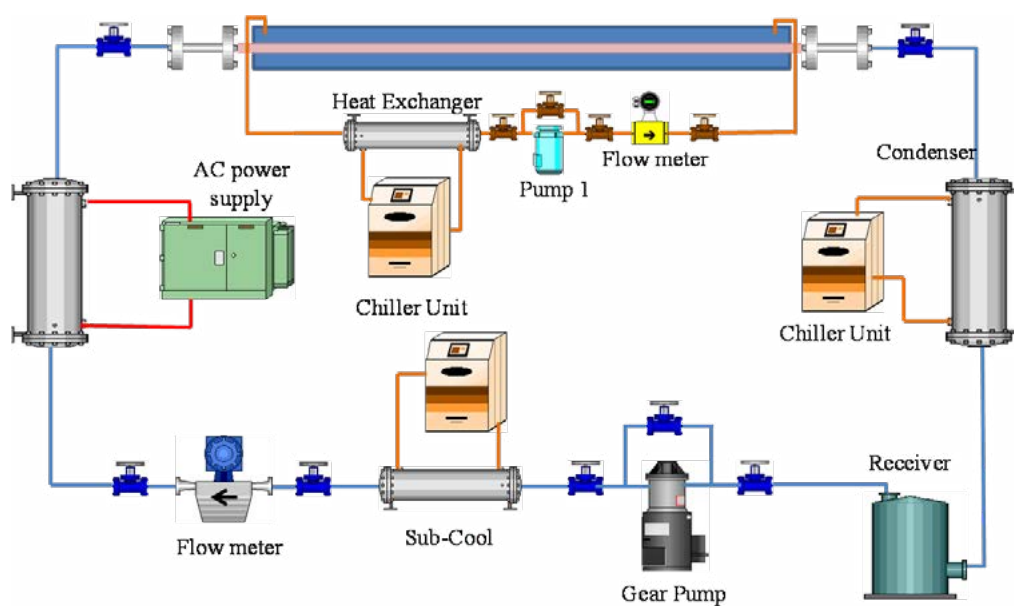


Figure 1. Experimental apparatus

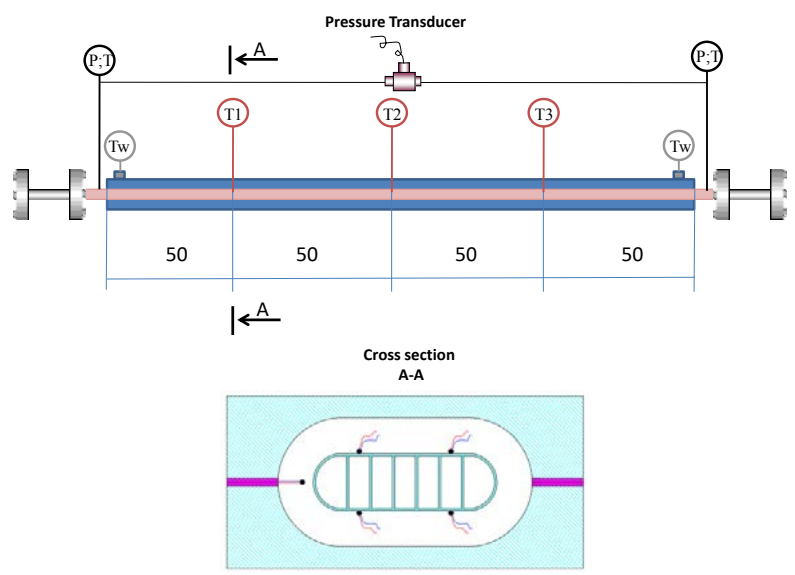


Figure 2. schematic of test section

environment.

The detail of test sections was depicted in Figure 2. The test tubes made of aluminum tube with hydraulic diameters of 1.14mm 1.16mm and 1.04 mms. The effective length was 200mm. As shown in the figure, the heat flux applied on test sections by a water loop. The T-type thermocouples were attached at top and bottom points every 50mm along the test section. Thermocouples and pressure transducers were also set up at the adiabatic pipes between the inlet and outlet. To visualize the flow pattern, two sight glasses were installed at the beginning and the end of test tubes.

The data were collected using a data acquisition and analyzed in real time by the data reduction program. All the information about test conditions and data during the operation were displayed on the monitor.

The heat flux of each subsection Q_n , is calculated from mass flow rate and rising enthalpy of cooling water flowing inside the water tubes as follows:

$$Q_n = W_n c_p (T_{nout} - T_{nin}) + Q_{loss} \tag{1}$$

where W_n , c_p , T_n are the mass rate of flow, specific heat and temperature of heating water loop. Q_{loss} is the heat loss on the test section which was determined by calibrating system. The vapor quality, x , at the measurement locations, z , were determined based on the thermodynamic properties:

$$x = \frac{i - i_f}{i_{fg}} \tag{2}$$

The local heat transfer coefficient inside the channel can be evaluated as the ratio of the heat flux

Table 1. Summary of the estimated uncertainty

Parameter	Uncertainty
Temperature	±0.15 °C
Absolute pressure	±0.2 %
Different pressure	±2.5 kPa
G refrigerant	±0.2 %
G water	±0.2 %
q	±3 %
x	±5 %
h	±10 %



to saturation minus the inside wall temperature:

$$h = \frac{Q}{A(T_{wi} - T_{sat})} \quad (3)$$

The physical properties of the refrigerant were obtained from REFPROP 8. The temperature and mass flow rate data were recorded using data acquisition and flow meter, respectively. Table 1 presented a summary of the estimated uncertainty associated with all the parameters at a 95% confidence interval.

Results and discussions

The effect of mass flux on the heat transfer coefficient of R410A in multiport minichannel is illustrated in Fig. 3. As shown in the figure, the heat flux was fixed at 6 kW/m² while the mass flux was varied from 50 to 150 kg/m²s for the experiment with tube A. The heat transfer coefficient of R410A increases with the increase of mass flux.

Figure 4 show the dependence of heat flux on the heat transfer coefficient of R410A in minichannel. Mass flux was fixed at 100 kg/m²s while two heat fluxes of 3 and 6kW/m² were applied on tube B. The effect of heat flux on the heat transfer coefficient can be clearly seen in the trends. Higher heat flux causes the higher heat transfer coefficient.

In this study, the experimental heat transfer coefficient was compared with some well-known correlations [5,12–16]. Table 2 shows the overall deviation of three tube types. Two best prediction are correlations of Bertsch et al. [5] and Sun and Mishima [15] with the overall mean deviations of about 28%. However, five among six heat transfer coefficient correlations are under predicted,

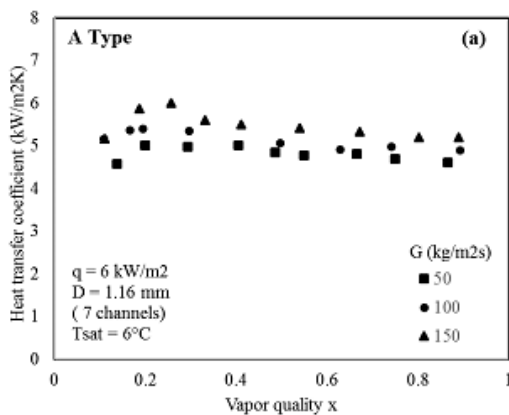


Figure 3. Effect of mass flux

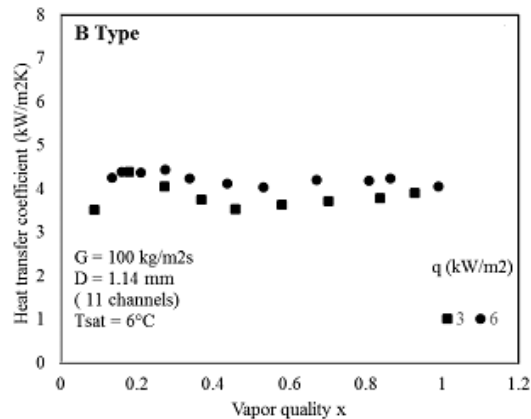


Figure 4. Effect of heat flux

Table 2. Summary of correlation comparison

Correlation	MD (%)	AD (%)
Lazarek & Black[12]	61.71	-61.71
M.Shah [13]	47.66	-45.41
Liu and Winterton[14]	58.62	-57.24
Bertsch et al. [5]	27.53	-19.90
Sun and Mishima [15]	28.75	-28.62
Li and Wu [16]	46.26	39.72



exception is the one proposed by Li and Wu [16], which is over predicted.

Conclusions

This study demonstrated the two-phase heat transfer coefficient of R410A in side multiport minichannels. The results show that the heat transfer coefficient increase with the increase of mass flux and heat flux. The experimental data was also compared with several well-known correlations. Among them, the correlation proposed by Sun and Mishima [15] and Bertsch et al. [5] show the best prediction with the overall mean deviation for 3 tubes about 28%.

Acknowledgement

This research was supported by Basic Science Research Program through the National Research Foundation of Korea (NRF) funded by Ministry of Education, Science, and Technology (NRF-2016R1D1A1A09919697) and Samsung Electronics Company

References

- [1] S.G. Kandlikar, Fundamental issues related to flow boiling in minichannels and microchannels, *Exp. Therm. Fluid Sci.* 26 (2002) 389–407.
- [2] J.R. Thome, Boiling in microchannels: A review of experiment and theory, *Int. J. Heat Fluid Flow.* 25 (2004) 128–139.
- [3] L. Cheng, Flow Boiling Heat Transfer with Models in Microchannels, in: *Microchannel Phase Chang. Transp. Phenom.*, Elsevier, 2016: pp. 141–191.
- [4] P. Kew, K. Cornwell, Correlations for the prediction of boiling heat transfer in small-diameter channels, *Appl. Therm. Eng.* 17 (1997) 705–715.
- [5] S.S. Bertsch, E. a. Groll, S. V. Garimella, A composite heat transfer correlation for saturated flow boiling in small channels, *Int. J. Heat Mass Transf.* 52 (2009) 2110–2118.
- [6] J.C. Chen, Correlation for boiling heat transfer to saturated fluids in convective flow, *Ind. Eng. Chem. Process Des. Dev.* 5 (1966) 322–329.
- [7] F. Vakili-Farahani, B. Agostini, J.R. Thome, Experimental study on flow boiling heat transfer of multiport tubes with R245fa and R1234ze(E), *Int. J. Refrig.* 36 (2013) 335–352.
- [8] E. Li, Jiyang; Dang, Chaobin; and Hihara, Experimental investigation on up-flow boiling of R1234yf in aluminum multi-port extruded tubes, in: *Int. Refrig. Air Cond. Conf.*, 2016: p. 8.
- [9] H.J. Lee, S.Y. Lee, Heat transfer correlation for boiling flows in small rectangular horizontal channels with low aspect ratios, *Int. J. Multiph. Flow.* 27 (2001) 2043–2062.
- [10] R.W. Lockhart, R. c. Martinelli, Proposed correlation of data for isothermal two-phase, two-component flow in pipes, *Chemical Eng. Prog.* 45 (1949) 39–48.
- [11] K. Mishima, T. Hibiki, Some characteristics of air-water two-phase flow in small diameter vertical tubes, *Int. J. Multiph. Flow.* 22 (1996) 703–712.
- [12] G. Lazarek, S. Black, Evaporative heat transfer, pressure drop and critical heat flux in a small vertical tube with R-113, *Int. J. Heat Mass Transf.* 25 (1982).
- [13] M.M. Shah, Chart correlation for saturated boiling heat transfer: equations and further study, *ASHRAE Trans.:(United States).* 88 (1982) 185–196.
- [14] Z. Liu, R. Winterton, A general correlation for saturated and subcooled flow boiling in tubes and annuli, based on a nucleate pool boiling equation, *Int. J. Heat Mass Transf.* 34 (1991) 2759–2766.
- [15] L. Sun, K. Mishima, An evaluation of prediction methods for saturated flow boiling heat transfer in mini-channels, *Int. J. Heat Mass Transf.* 52 (2009) 5323–5329.
- [16] W. Li, Z. Wu, A general correlation for evaporative heat transfer in micro/mini-channels, *Int. J. Heat Mass Transf.* 53 (2010) 1778–1787.



MASS FLOW CHARACTERISTICS ANALYSIS OF R245FA IN EEV

Ting Chen^a, Kyungjin Bae^b, Dongan Cha^b, Ohkyung kwon^{a,b*}

^a*Advanced Energy and Technology, Korea Institute of Industrial Technology Campus,
Korea University of Science and Technology, Cheonan 31056, Republic of Korea*

^b*Korea Institute of Industrial Technology, 89 Yangdaegiro-gil Ipjang-myeonl, Cheonan-si
31056, Republic of Korea*

ABSTRACT

In this paper, mass flow characteristics of R245fa through EEV are investigated. By keeping temperature at EEV outlet at constant, the experiments were conducted under varying EEV inlet temperature, subcooling temperature and EEV opening. According to the experimental results, the mass flow rate of R245fa is found to increase with increasing condensing temperature and EEV opening. And subcooling temperature has some but little impact on the mass flow rate.

Keywords: R245fa; Flow characteristics; EEV

**Corresponding author. Email adress: kwonok@kitech.re.kr*

1. INTRODUCTION

As an expansion device that can control the refrigerant flow and balance the system pressure (Park, C., 2007), electronic expansion valve, which is always abbreviated as EEV, has attracted more and more attentions from researchers all over the world. EEV has a wide flow adjustment range, it is widely used in all aspects of the refrigeration industry, and it can make quick response to variations in operational conditions (Saleh and Ayman 2016). Therefore, EEVs have been more and more widely applied in refrigeration&air conditioners (R&AC), vehicle air-conditioning system and heat pumps. Many experimental researches on flow characteristics of R22, R410A and R407C in EEVs have been done. Park et al.(2007) and Zhang(2006) measured the mass flow rate of R22, R410A and R407C through the EEVs with different operating conditions respectively, as a result, empirical correlations were proposed to predict mass flow rate for corresponding refrigerant. Hou et al. (2014) find that the flow characteristics of refrigerant would be not affected by EEV outlet temperature when the flow is choking flow. Besides, many analytical studies have been done by using ANN model and other models (Tian et al., 2015; Chen et al., 2009).

However, most of the existing researches are related to high or medium temperature refrigerant, studies on high temperature refrigerant flow characteristics through EEV are still limited. The purpose of this study is to investigate the mass flow rate variation of R245fa refrigerant in EEV.

2. EXPERIMENTAL SET-UP AND CONDITIONS

2.1. Experimental setup

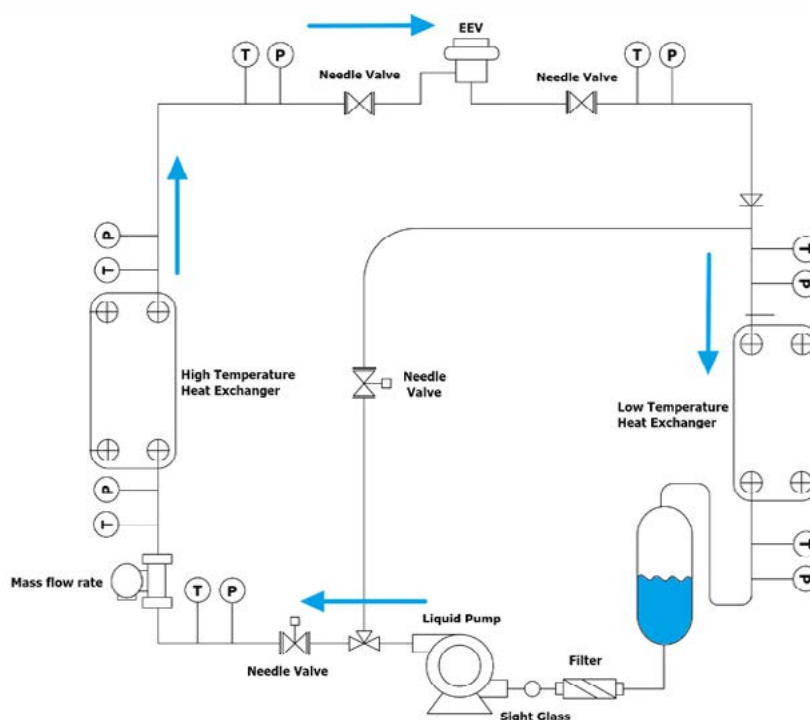


Figure 1 Schematic diagram and Photo of experimental setup.

The schematic of the experimental set-up is shown in Fig. 1. The set-up is mainly consist of an EEV (test subject), high temperature heat exchanger, low temperature heat exchanger and liquid pump. The temperature at the inlet and outlet of the EEV is controlled by adjusting the temperature of high temperature heat exchanger and low temperature heat exchanger respectively. For the sensors used in the experimental set-up, the errors of temperature sensor RTD, pressure sensor and mass flow meter is $\pm 0.1^\circ\text{C}$, $\pm 0.25\%$ and $\pm 0.5\%$, respectively.

2.2. Conditions

The parameters of EEV and test conditions were listed in Table 1. EEV has orifice diameter of 1mm. By changing the operating conditions, the variation of mass flow rate flowing through the EEV is measured and recorded. Since the temperature at outlet of EEV can hardly influence mass flow rate, it is kept constant at 35°C , and the temperature at EEV inlet ranges from 60°C to 70°C , subcooling temperature varies from 5°C to 15°C . All data were obtained when the system was under steady state.

3. RESULTS AND DISCUSSION

Fig. 2 shows the mass flow rate variation of R245fa flow with EEV opening when condensing temperature is 60°C . As shown in this figure, the mass flow rate of R245fa increases with EEV opening, when EEV opening increases from 20% to 100%, the mass flow rate increases by about 30 kg/h, and mass flow rate increases with increasing subcooling temperature slightly under the same EEV opening.



Table 1 Operating conditions

Parameter	Value
EEV orifice diameter (mm)	1
Pressure at EEV inlet (kPa)	463.4, 609.8, 788.7
Condensing temperature (°C)	60, 70, 80
Temperature at EEV outlet (°C)	35
Subcooling temperature (°C)	5, 10, 15
EEV opening (%)	0~100

Fig. 3 shows the mass flow rate variation with opening degree when condensing temperature is 70 °C. Similar to what we observed in Fig. 2, mass flow rate increases with EEV opening significantly and subcooling temperature slightly. Fig. 4 shows the mass flow rate variation with opening degree when condensing temperature is 80 °C. The same tendency can be observed in this figure, mass flow rate increases with EEV opening significantly and subcooling temperature slightly. By comparing the three figures, we can find that, with the increasing condensing temperature, the mass flow rate increases for every certain EEV opening.

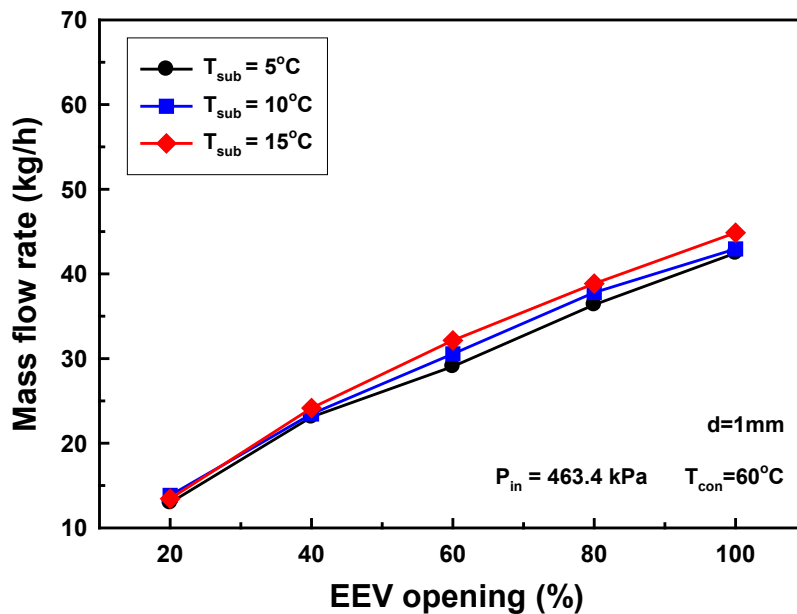


Figure 2 The variation of mass flow rate with EEV opening under 60°C condensing temperature.

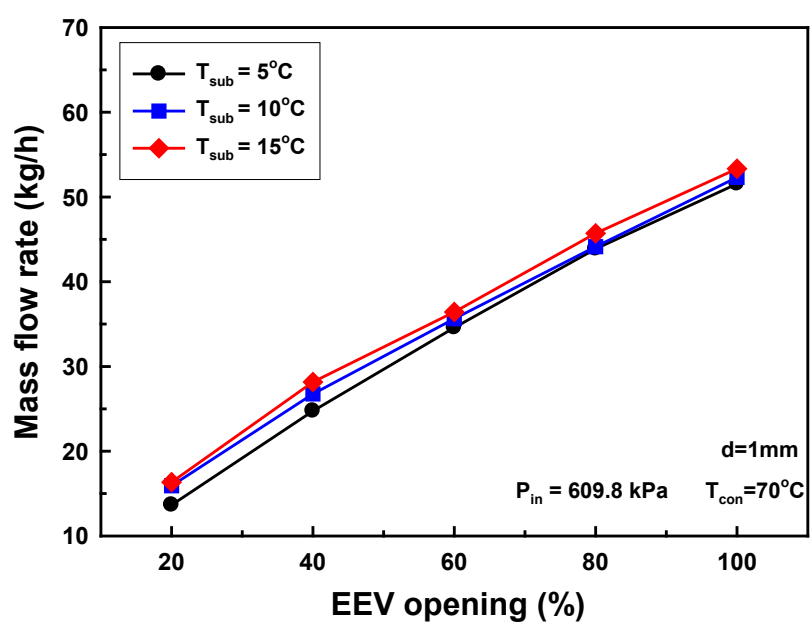


Figure 3 The variation of mass flow rate with EEV opening under 70°C condensing temperature.

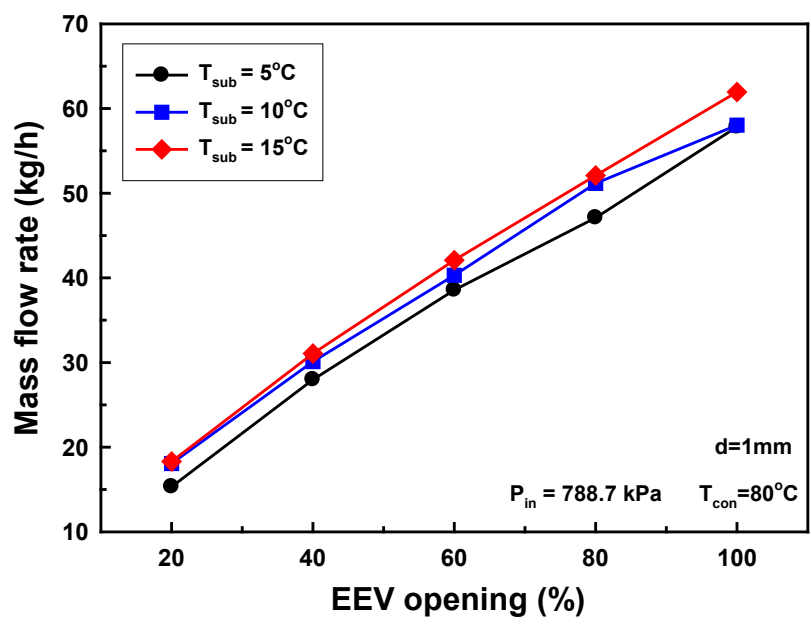


Figure 4 The variation of mass flow rate with EEV opening under 80°C condensing temperature.



4. CONCLUSION

According to the experimental results, we can find that, the mass flow rate increases with increasing EEV opening. subcooling temperature has little impact on the mass flow rate. With the increasing condensing temperature, mass flow rate increases a lot.

5. ACKNOWLEDGEMENT

This work was supported by the platform program of KITECH(Korea Institute of Industrial Technology). The authors gratefully acknowledge this support.

6. REFERENCES

- Park, C., Cho, H., Lee, Y., Kim, Y., (2007), Mass flow characteristics and empirical modeling of R22 and R410A flowing through electronic expansion valve, *International Journal of Refrigeration* 30, 1401-1407.
- Saleh, B., Aly, A.A., (2016), Artificial neural network models for depicting mass flow rate of R22, R407C and R410A through electronic expansion valves. *Int. J. Refrigeration* 63, 113-124.
- Zhang, C., Ma, S., Chen, J., Chen, Z., (2006), Experimental analysis of R22 and R407C flow through electronic expansion valve, *Energy Conversion and Management* 47, 529-544.
- Hou, Y., Liu, C., Ma, J., Cao, J., Chen, S., (2014), Mass flow rate characteristics of supercritical CO₂ flowing through an electronic expansion valve. *Int. J. Refrigeration* 47, 134-140.
- Chen, L., Liu, J., Chen, J., Chen, Z., (2009), A new model of mass flow characteristics in electronic expansion valves considering metastability, *International Journal of Thermal Sciences* 48, 1235-1242.
- Tian, Z., Gu, B., Qian, C., Yang, L., Liu, F., (2015), Electronic expansion valve mass flow rate prediction based on dimensionless correlation and ANN model, *International Journal of Refrigerant* 57, 1-10.



EXPERIMENTAL INVESTIGATION ON THE HEAT TRANSFER CHARACTERISTICS OF ZEOLITE ADSORBENT COATED FIN-TUBE HEAT EXCHANGER

Kyungjin Bae^a, Ting Chen^b, Dongan Cha^a, Ohkyung kwon^{a, b, *}

^a*Korea Institute of Industrial Technology, 89 Yangdaegiro-gil Ipjang-myeonl, Cheonan-si 31056, Republic of Korea*

^b*Advanced Energy and Technology, Korea Institute of Industrial Technology Campus, Korea University of Science and Technology, Cheonan 31056, Republic of Korea*

ABSTRACT

In this paper, adsorbent coating thickness of heat exchangers; 0.1 mm, 0.15 mm, 0.2 mm are experimented. The adsorbent used for the present adsorption experiment is a powder zeolite(FAPO). The performance of adsorbent coating heat exchanger was analysed by heat transfer rate and adsorption rate with adsorption time. In the basic conditions, the maximum overall heat transfer coefficient of 2 mm coating thickness is 189.1 W/m²°C, which is 18%, 50% higher than that of 0.15 mm and 0.1 mm, respectively.

Keywords: Adsorption; Heat exchanger; Overall heat transfer coefficient; Zeollite.

*Corresponding author. Email adress: kwonok@kitech.re.kr.

1. INTRODUCTION

In the conventional vapor compression refrigeration is powered by electricity and uses CFC refrigerations. Thus, the use of vapor compression refrigeration causes large energy consumption and ozone depletion. Despite the development of less ozone damaging alternatives such as the HCFCs and HFCs, they still contribute to the undesirable effect of global warming. Adsorption refrigeration can be driven by low temperature heat sources such as waste heat and solar energy, and employs natural refrigerants with no ozone depletion such as water and methanol.

Adsorption chillers employs silica gel/water as an adsorbent-refrigerant pair. The adsorption bed is one of the most critical components in the adsorption system. In order to design a more effective adsorption system, many researchers have focused on how to improve the performance of the adsorption bed. In the conventional adsorption chillers(Saha, et al., 2003; Loh, et al., 2009), silical gel is packed in between heat exchanger fins by wire meshes. Poor contact between adsorbent and metal fins deteriorates heat transfer efficiency and performance of adsorption system.

In this study, to improve the heat transfer of an adsorbent embedded heat exchanger, a fin-tube heat exchanger was coated with zeolite adsorbent. Adsorbent coating thickness of heat exchanger ; 0.1mm, 0.15mm, 0.2 mm are experimented. The performance of adsorbent coated heat exchanger was analysed by heat transfer rate and overall heat transfer coefficient with coating thickness

2. EXPERIMENTAL SETUP AND PROCEDURE



2.1. Experimental setup

The adsorbent coated heat exchanger was manufactured in order to evaluate performance characteristics of adsorption bed with adsorbent coating thickness. Adsorption bed of the fin-tube type was designed that the inlet and outlet pipes of cooling water branched from header. The tube and fins are made of copper and aluminium, respectively. The dimensions of heat exchanger were designed as 420×274×116 mm, fin pitch 0.2 mm. The heat exchangers used in the present experiment are shown in Figure 1(a) and Table 1. An adsorbent used for the adsorption experiment is a powder zeolite(FAPO). In order to investigate the heat transfer characteristics of adsorbent coated fin-tube heat exchanger, the heat exchanger is coated by adsorbent with coating thickness of 0.1 mm, 0.15 mm and 0.2 mm. The tested samples are shown in Figure 1.

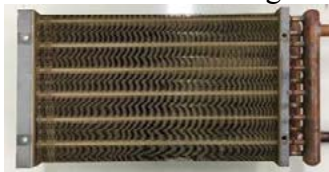
The schematic diagram and photo of experimental setup are shown in Figure 2. The experimental setup comprises an adsorption chamber, an evaporator, condenser, connecting pipes and refrigerant valves. Also, auxiliary facilities include the vacuum pump to maintain the vacuum inside system and constant temperature water baths to simulate the adsorption and desorption conditions. Three constant temperature water baths were used to control the temperatures of chilled, cooling, hot water for adsorption, desorption, evaporating, condensation load.



(a) Fin-tube heat exchanger



(b) Coating thickness 0.1 mm



(c) Coating thickness 0.15 mm



(d) Coating thickness 0.2 mm

Figure 1 Photo of fin-tube heat exchanger with adsorbent coating.

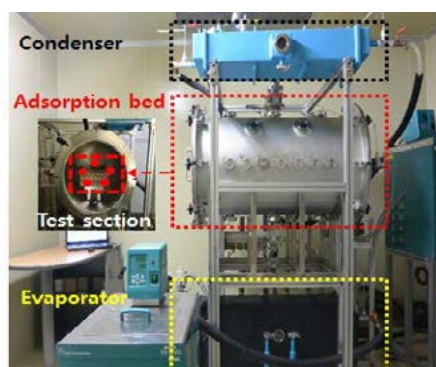
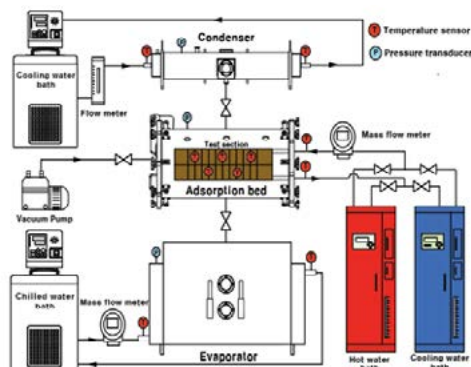


Figure 2 Schematic diagram and photo of experimental setup.



Table 1 Coating specifications

		Unit	Value
Heat exchanger size(L,W,H)		mm	420, 274, 116
Tube	Row	-	12
	Step	-	4
	Pt	mm	21.65
	Pl	mm	25
	Out diameter	mm	9.53
	Thickness	mm	0.36
	Material	-	Copper
Fin	Pitch	mm	0.8
	Thickness	mm	0.115
	Material	-	Aluminum

The uncertainties of RTD (PT 100 Ω) and temperature sensors (T type) used in this study are ±0.1 and ±0.3 °C, pressure transducer and mass flow meter have uncertainties of ±0.25%, ±0.2%, and the data are obtained by a data acquisition.

2.2. Data analysis procedure and operational conditions

The heat transfer rate of adsorption bed is expressed by equation (1). Also, the overall heat transfer coefficient is given by equation (2). The LMTD was proposed by Saha et al.(Saha, et al., 2010)

$$Q_{ads} = \dot{m}_{cw} C_{p,cw} (T_{cw,out} - T_{cw,in}) \quad (1)$$

$$U_{overall} = \frac{Q_{ads}}{A_{bed} LMTD} \quad (2)$$

$$LMTD = \frac{(T_{cw,in} - T_{ads}) - (T_{cw,out} - T_{ads})}{\ln \left(\frac{T_{cw,in} - T_{ads}}{T_{cw,out} - T_{ads}} \right)} \quad (3)$$

Table 2 Coating specifications

	Unit	Value
Adsorbent	-	FAPO
Binder	-	Organic
Binder ratio	wt%	10
Adsorbent weight	g	400
Coating thickness	mm	0.1



Table 3 Experimental conditions

Conditions		Unit	Value
Chilled water temperature		°C	12
Cooling water	Temperature	°C	30
	Flow rate	m ³ /h	1.316
Adsorption time		s	420

Where, T_{ads} is adsorbent temperature inside adsorption bed. And fin-tube heat exchanger surface area is 10.077 m².

The experiment was conducted by setting the cooling water inlet temperature at 30°C, cooling water flow rate 1.316 m³/h. The Evaporating temperature was 12°C. At this time, the adsorption time was set equally 7 minutes. The experimental conditions are shown in Table 2.

The temperatures of inside adsorption bed were measured at three places(bottom, center, top side) by T-type thermocouples. The temperatures of evaporator and the inlet and outlet temperatures of cooling/hot water were measured by the RTD sensors. Pressures of the adsorption bed and evaporator were measured by absolute pressure transducers.

3. RESULTS AND DISCUSSION

Figure 3 shows the variation of bed temperature with adsorption time when cooling water and chilled water are 30°C and 12°C, respectively. The temperature at absorbent surface increases rapidly during the first 50s and then decreases. Like the results from Gao et al. (Gao, et al., 2016), due to the hydrophilicity of the adsorbent itself, a lot of water vapor can be absorbed in the beginning accompanied by a lot of heat release, this leads to the increase in surface temperature of the adsorbent. After that, with the flowing of the cooling water, the heat released in the process of adsorption is absorbed slowly and surface temperature decreases. The highest surface temperature is detected to be 32.3°C when coating thickness is 0.2 mm, while highest surface temperatures for coating thickness of 0.1 mm and 0.15 mm are 32 °C and 31.8°C, respectively.

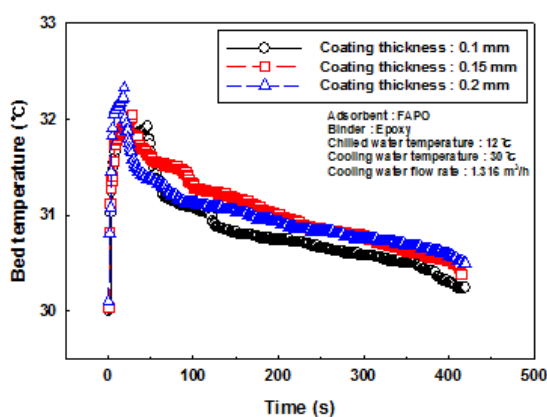


Figure 3 The variation of bed temperature with adsorption time.

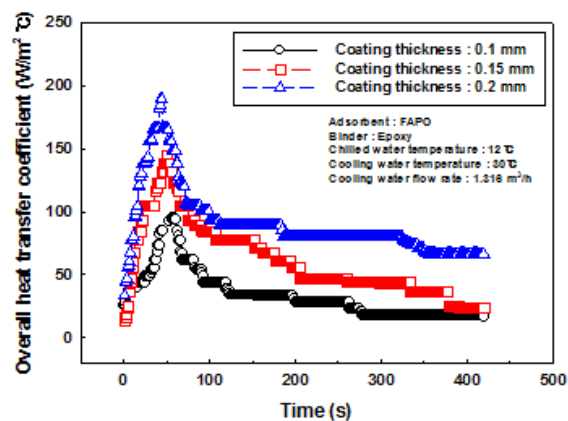


Figure 4 The variation of overall heat transfer coefficient with adsorption time.



Figure 4 shows the variation of overall heat transfer coefficient with adsorption time when cooling water and chilled water are 30°C and 12°C, respectively. The variation of overall heat transfer coefficient shows a similar tendency with surfaces temperature as shown in Figure 3. And the peak point appears when adsorption time is about 100s. This is because that it need some time to transfer the released heat during adsorption to cooling water. In this result, the overall heat transfer coefficient increases with increasing coating thickness and more time is needed to reach maximum overall heat transfer coefficient. The maximum overall heat transfer coefficient of 2 mm coating thickness is 189.1 W/m²°C, which is 18%, 50% higher than that of 0.15 mm and 0.1 mm, respectively.

4. CONCLUSION

In order to increase heat transfer characteristics of fin-tube heat exchanger with adsorbent coated, experiments are conducted on fin-tube heat exchangers with different coating thickness. And conclusion can be draw as follows: The highest surface temperature is detected to be 32.3°C when coating thickness is 0.2 mm, while highest surface temperatures for coating thickness of 0.1 mm and 0.15 mm are 32 °C and 31.8°C, respectively. The maximum overall heat transfer coefficient of 2 mm coating thickness is 189.1 W/m²°C, which is 18%, 50% higher than that of 0.15 mm and 0.1 mm, respectively.

5. ACKNOWLEDGEMENT

This work was supported by the Energy Efficiency & Resources of the Korea Institute of Energy Technology Evaluation and Planning(KETEP) grant funded by the Korea government Ministry of Trade, Industry and Energy(No. 20172010105570)

6. REFERENCES

- Saha, B.B., Koyama, S., Kashiwagi, T., Akiswa, A., Ng, K.C., Chua, H.T.,(2003) Waste heat driven dual mode, multi-stage, multi-bed regenerative adsorption system, *International Journal of Refrigeration*, Vol. 26, pp. 749-757.
- Loh, W., El-Sharkawy, I., Ng, K.C., Saha, B.B., (2009), Adsorption cooling cycles for alternative adsorbent/adsorbate pairs working at partial vacuum and pressurized conditions, *Applied Thermal Engineering*, Vol. 29, pp. 793-798.
- Kyaw, Thu., Ng, K.C., Saha, B.B., Chakraborty, A., (2010), Overall of heat transfer analyses of a heat-driven adsorption chiller, *International Symposium on Next-generation Air Conditioning and Refrigeration Technology*, Tokyo, Japan.
- Gao, W., Li, C., Wang, D., Wu, D., (2016), An experimental investigation of salt-water separation in the vacuum flashing assisted with heat pipes and solid adsorption, *Desalination*, Vol. 399, pp. 116-123.



A NEW METHOD USING EFFECT THERMAL CONDUCTIVITY FOR A FULL THERMAL STORAGE TANK

*Jae Dong Chung, Min Ho Kim, Yong Tae Lee
Sejong University, 209 Neungdong-ro, Gwangjin-gu, Seoul 05006, Korea*

ABSTRACT

This study numerically carried out a research on a latent heat thermal energy storage system (LTES) filled with phase change material (PCM). In the previous works, one capsule which was arbitrarily positioned in the tank, was selected and this capsule was usually assumed to represent the performance of the whole LTES. A few of researches have been conducted for a whole domain of LTES because a tremendous computer memory and CPU time are required. This study introduces an effective thermal conductivity method to overcome the difficulties involved with phase changing problem. A previous method using the effective thermal conductivity ignored timewise variation of the strength of the natural convection in molten PCM. Conversely, the present method increases the accuracy of the model by including the effect of temporal variation of the natural convection in molten PCM.

Keywords: Latent thermal energy storage; Phase change material (PCM); Effective thermal conductivity.



1. INTRODUCTION

The latent heat thermal energy storage system (LHTESS) is an effective and widely used solution for dealing with electrical peak loads during the daytime. It operates chiller to flow cool refrigerant and stores cool thermal energy in a storage tank during midnight, at relatively cheap operating cost to operate. By shifting the cooling electric load to night hours, LHTESS can reduce the energy needed for cooling during daytime hours, when electrical peak load is higher and more expensive. Among the various types of LHTESS in use today, one typical approach uses an encapsulated type storage tank system, which contains a number of capsules installed in a suitable arrangement inside a storage tank. A phase change material (PCM) is charged inside each capsule. A heat transfer fluid (HTF) flows outside the capsules and transfers thermal energy to the PCM, to melt or solidify the material.

This study numerically carried out a research on a latent heat thermal energy storage system (LTES) filled with phase change material (PCM). Considering that each capsule will experience different melting behavior due to the different HTF temperature passing the capsule, a whole domain of LTES should be modeled at a time. Due to the required computer memory and CPU time, effective thermal conductivity model is applied, which is superior to the earlier one, in the view point of including timewise variation of the strength of the natural convection in molten PCM.

2. NUMERICAL ANALYSIS

2.1. Effective thermal conductivity model

The effective thermal conductivity model for phase change problem has already been used. Figure 1 shows the schematics of the previous effective thermal conductivity model and the present model. Note that the value of effective thermal conductivity in the previous model in Eq. (1) is constant, which is apparently oppose to the motivation of applying effective thermal conductivity. Effective thermal conductivity includes the effect of the enhanced melting due to the convection by using higher value of thermal conductivity. The strength of convection in the molten PCM is changing as melting proceeds, thus the value of effective thermal conductivity should be a function of time. That is the motivation of this model. In Eq. (2), present model chooses the characteristic length as $L_c(t) = (D_o - D_i(t)) / 2$, and the change of the convection strength in time is properly implemented.

$$\frac{k_{eff}}{k_{liq}} = CRa^m = C \left(\frac{g\beta(T_{ref} - T_m)D_o^3}{\alpha\nu} \right)^m \quad (1)$$

$$\frac{k_{eff}}{k_{liq}} = CRa^m \left(1 - \frac{D_i(t)}{D_o} \right)^m = C \left(\frac{g\beta(T_{ref} - T_m)L_c(t)^3}{\alpha\nu} \right)^m \left(1 - \frac{D_i(t)}{D_o} \right)^m \quad (2)$$

where $L_c(t) = (D_o - D_i(t)) / 2$

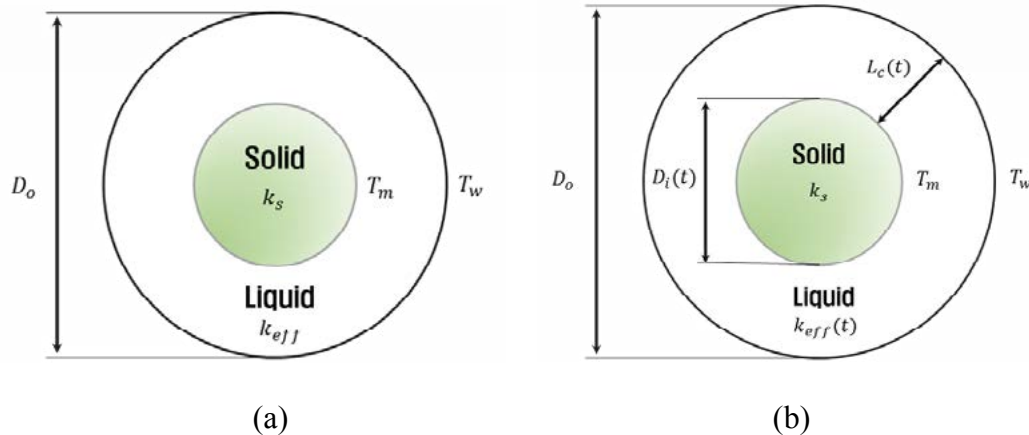


Figure 1 Schematics of effective thermal conductivity: (a) previous model and (b) present model.

2.2. Governing equation

The governing equations for a two-dimensional model utilizing the enthalpy–porosity formulation, which were introduced by Brent et al. (1988), can be derived as follows

$$\rho \frac{DH}{Dt} = k \nabla^2 T \quad (3)$$

The enthalpy is combined sensible enthalpy $h = h_{ref} + \int_{T_{ref}}^T c_p dT$ and latent enthalpy $\Delta H = \gamma L$ in the energy equation. In contrast to the constrained melting model, the unconstrained melting model incorporates the movement of solid PCM by considering the density difference between the solid and liquid PCM. The γ means liquid fraction and is expressed in Eq. (4).

$$\gamma = \begin{cases} 1 & (T > T_l) \\ \frac{T - T_s}{T_l - T_s} & (T_s < T < T_l) \\ 0 & (T < T_s) \end{cases} \quad (4)$$

2.3. Model validation

The present model is validated with experimental result of one capsule ($D=101.66\text{mm}$) (Tan, 2008). The initial, wall and melting temperatures are 27.2°C , 40.0°C and 28.2°C , respectively. Figure 2 shows the molten fraction for 4 different models. Experimental data, numerical method of including natural convection in the present model and the previous model are examined. We have conducted a close examination of the model by extending the range of Stefan number, and also for different capsule diameters. The result shows good agreement for large range of each parameter.

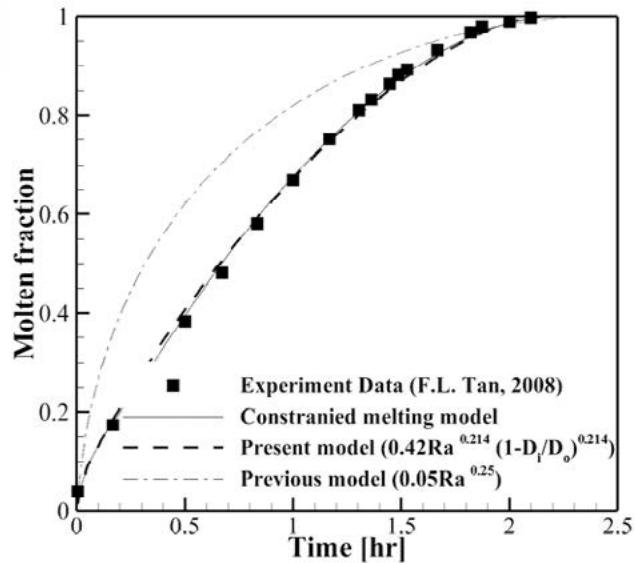


Figure 2 Comparison of the molten fraction for each model with experiment.

3. RESULTS AND DISCUSSION

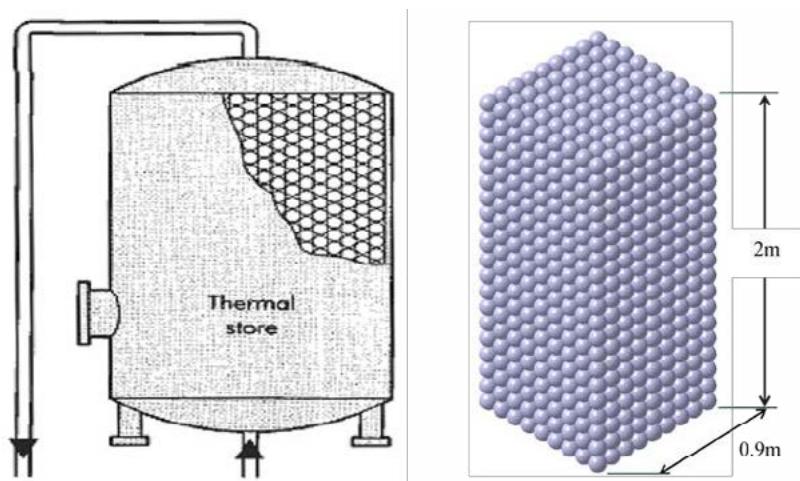


Figure 3 Schematic of computational domain.

Figure 3 shows the schematic of the present model. Charging and discharging of a thermal storage tank, which is composed of 9x9x20 capsules, i.e., total 1620 capsules, are calculated. Capsule structure is assumed to be simple cube type. To examine the superior of the present model, we have compared the results from the previous effective thermal conductivity model and present model. Clear advantage can be found in the present model.

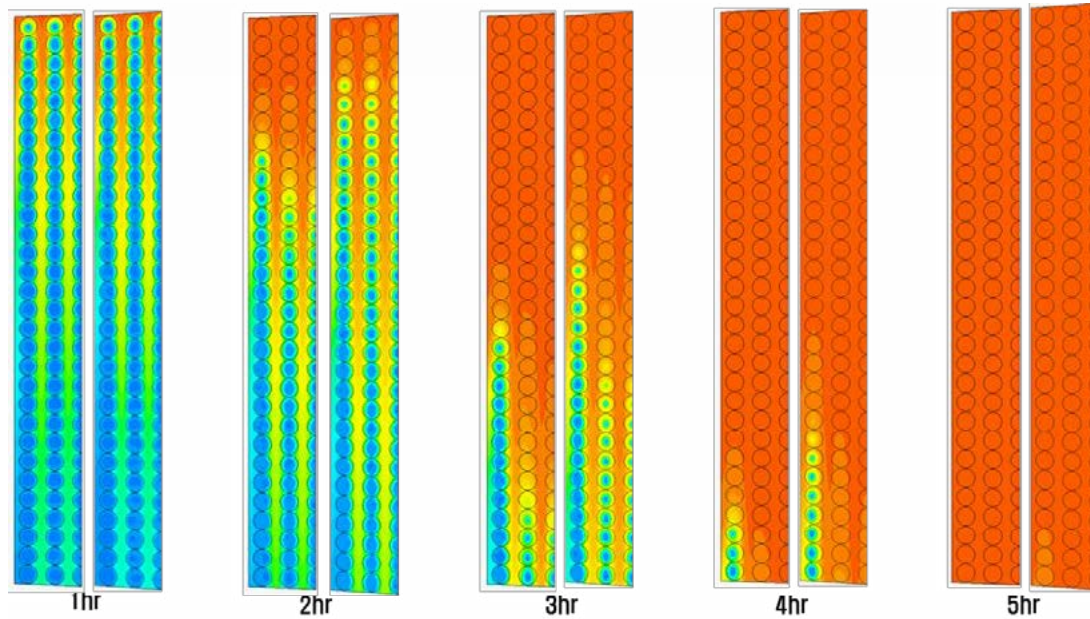


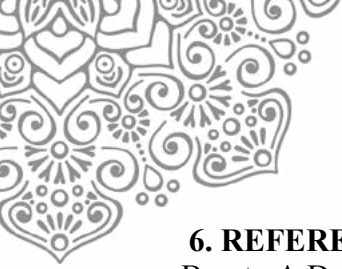
Figure 4 Temperature profiles for (left) present model and (right) previous model.

4. CONCLUSION

This study numerically carried out a research on a latent heat thermal energy storage system (LTES) filled with phase change material (PCM). The LTES has been utilized for air conditioning because of a high thermal storage density. However, a few of researches have been conducted for a whole domain of LTES because a tremendous computer memory and CPU time are required. Usually, a capsule is selected and assumed to represent the performance of the whole LTES, which is composed of hundreds of capsules. This study introduces an effective thermal conductivity method to overcome the difficulties involved with phase changing problem. A previous method using the effective thermal conductivity ignored timewise variation of the strength of the natural convection in molten PCM. Conversely, the present method increases the accuracy of the model by including the effect of temporal variation of the natural convection in molten PCM. The present method has been compared with experimental result and shown no significant difference. This method is also valid for a wide range of Stefan number, capsule sizes, and initial temperature. The developed method can be applied to the systems for both purpose of heating and cooling in a thermal storage tank. The volume ratios of cooling PCM to heating PCM in a thermal storage tank can be obtained to satisfy the desired cooling and heating loads.

5. ACKNOWLEDGEMENT

This research is supported by Korea Institute of Energy Technology Evaluation and Planning (KETEP) granted financial resource from the Ministry of Trade, Industry & Energy of Korea. (No. 20132010101780)



6. REFERENCES

- Brent, A.D., Voller, V.R., and Reid, K.J, (1988), The enthalpy-porosity technique for modeling convection-diffusion phase change: application to the melting of a pure metal, *Numerical Heat Transfer, Volume 13*, pp. 297-318.
- Tan, F.L., (2008), Constrained and unconstrained melting inside a sphere, *International Communications in Heat and Mass Transfer, Volume 35*, pp. 466-475.



Investigation of Optimal Design of Flow Header in Heat Exchangers

Nguyen-Ba Chien^{1,a}, Jong-Taek Oh^{2,b*}

¹Graduate School, Chonnam National University, 50 Daehak-ro, Yeosu, Chonnam 59626, South Korea

²Department of Refrigeration and Air Conditioning Engineering, Chonnam National University, 50 Daehak-ro, Yeosu, Chonnam 59626, South Korea

bachien@ejnu.net , ohjt@chonnam.ac.kr

Keywords: CFD, Genetic Algorithm, Maldistribution, Header, Optimization, Open FOAM.

Abstract. In this study, we investigate an automated procedure to optimization the distribution of flow in manifolds by coupling the computational fluid dynamics (CFD) simulation and a genetic algorithm (GA). The design point is performed by balancing the liquid phase flow rate at each outlet, and the controlled parameter is the high of baffle between each channel. The simulation of flow distribution of R134a in manifolds has been demonstrated by using a VOF model. The flow pattern of R134a with various flow rates and inlet qualities are well observed. The objective of this study is to overcome the difficulty of experimental test at high quality due to the unstable of the flow. In addition, using this methodology, a set of results which would improve the distribution of flow is finally proposed.

Introduction

One of the most common issues in designing air-cooled heat exchanger is the maldistribution of flow in manifolds. The performance and efficiency of the heat exchanger could be significantly affected by the non-uniformity of flow. Therefore, exploring the behavior of flow in manifolds or header is necessary to improve the design.

In practical design, flow maldistribution in manifolds can be induced by the geometry and operating conditions [1-4]. Beside of using experiment, various studies used modelling approaches to analyse the flow distribution. Tonomura et al. [5] demonstrated a CFD approach to discover the effect of design header to the uniform of flow. The results of this study showed that the shape of manifolds, length and location of inside fins, and inlet flow rate strongly affect to the flow uniformity. The authors also proposed a CFD-based optimization method to find the optimal design of plate-fine microdevices. Wang et al. [6] suggested a different computational approach. The authors presented a Lattice Boltzmann method for shape optimization of the distributor. Recently, Facao [7] developed a correlation model to improve the uniformity of flow in a solar collector. The model was then validated by the CFD simulation.

In this study, beside of demonstrating the simulation of flow, we also investigate another approach to optimize the flow distribution by coupling the CFD simulation and a genetic algorithm. It comes from the fact that the uniformity of flow could depend on various parameters and has no general form for specific applications. Hence, the combination of GA and CFD would be a solution that could save time and design cost.

Numerical model

The dimensions of the manifold are referred from a report of Fei and Hrnjak [8]. In the first phase, we set up a model to validate the experiment. A three-dimensional model was then created in Catia. The grid was manually generated with hexahedral meshes to reduce the computational cost as well as enhanced the accuracy and stability of simulation. In addition, to validate the independence of grid, three types of mesh with the total elements of 377540, 415644 and 453748 were also made, and the



last mesh was chosen for the simulation in this study. The detail dimension of manifold is illustrated in Table. 1. The sample of a grid is shown in Fig. 1.

In the second phase, we propose a new geometry with the baffles between each outlet channel. Since the baffles divide the header to subsections, the solution now can be reduced to 2D problem. The geometry and grid are then generated using C code. The schematic of proposed is shown in Fig. 2.

In this study, two-phase flow of refrigerant is simulated using the Open FOAM software. The working fluid is R-134a. Since the experimental test was taken under the adiabatic condition, the simulation will only solve the continuity and momentum equations. VOF method, therefore, has been implemented. VOF solver in Open FOAM calculates one momentum and one continuity equation for both liquid and gas phases of R134a. The physical properties of one phase are determined based on the volume fraction, α , of two phases in a cell. The continuity equation is defined as follow:

$$\nabla \cdot U = 0 \tag{1}$$

The momentum equation is determined as follow:

$$\frac{\partial \rho U}{\partial t} + \nabla \cdot (\rho U U) - \nabla \cdot (\mu \nabla U) - \rho g = -\nabla p - F_s \tag{2}$$

where F_s is the surface tension force at free surfaces and is defined as:

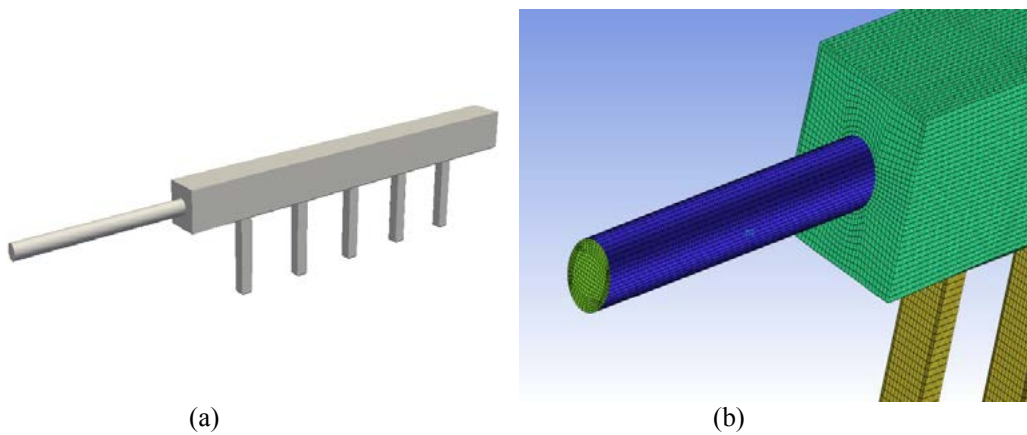


Fig. 1 3D model: (a) Geometry; (b) Sample of grid



Fig. 2 Schematic of proposed model



Table 1 Dimension of genetic manifold

Inlet length (mm)	Inlet diameter (mm)	Body length (mm)	Body height (mm)	Outlet dimension (mm)
120	9.5	305	25.4	8.8

Table 2 Properties of R134a

Saturation Temp. (°C)	Pressure (kPa)	Density of liquid (kg/m ³)	Density of vapor (kg/m ³)	Viscosity of liquid (Pa.s)	Viscosity of vapor (Pa.s)
24.473	665	1208.7	31.841	1.96E-4	1.17E-5

$$F_s = \sigma \kappa(x) n \quad (3)$$

where κ is the curvature of the interface and n is a unit vector normal to the interface. κ and n are calculated as follow:

$$\kappa(x) = \nabla \cdot n \quad (4)$$

and

$$n = \frac{\nabla \alpha}{|\nabla \alpha|} \quad (5)$$

Volume fraction, α , in a cell is 0 if it is completely filled by vapor phase and, on the contrary, volume fraction equals 1 if cell is completely filled by liquid phase. Volume fraction is calculated by a transport equation as following:

$$\frac{\partial \alpha}{\partial t} + \nabla \cdot (\alpha U) = 0 \quad (6)$$

The compression of the surface in Open FOAM is defined as follow:

$$\frac{\partial \alpha}{\partial t} + \nabla \cdot (\alpha U) + \nabla \cdot (\alpha (1 - \alpha) U_r) = 0 \quad (7)$$

where U_r is a suitable velocity field to compress the interface.

The properties of two-phase flow of R134a are obtained in REFPROP 8 and are listed in Table 2.

In present study, a single objective genetic algorithm (SOGA) was implemented. The purpose of the algorithm is to minimize the mean difference between the flow rate in each outlet and the average mass flow rate of the liquid phase. The fitness type was set as domination count. The cross over is 80%, the mutation scale is 10%, and the number of evaluation in this study was set as 60. SOGA script automatically generates baffle dimension, updates the boundary conditions. In addition, script drives the CFD code run and export the results for next evaluation in SOGA.

Results and discussions

A flow pattern is shown in Fig. 3. At second zero, there is no flow in manifold. At 5th second, the flow mostly enters the first outlet and the fifth outlet. The flow bounces back from the end wall is prevented by the forward flow from inlet. As a result, a pool of liquid is accumulated in the last space. It turns out that, optimizing the last distance could improve this waste area.

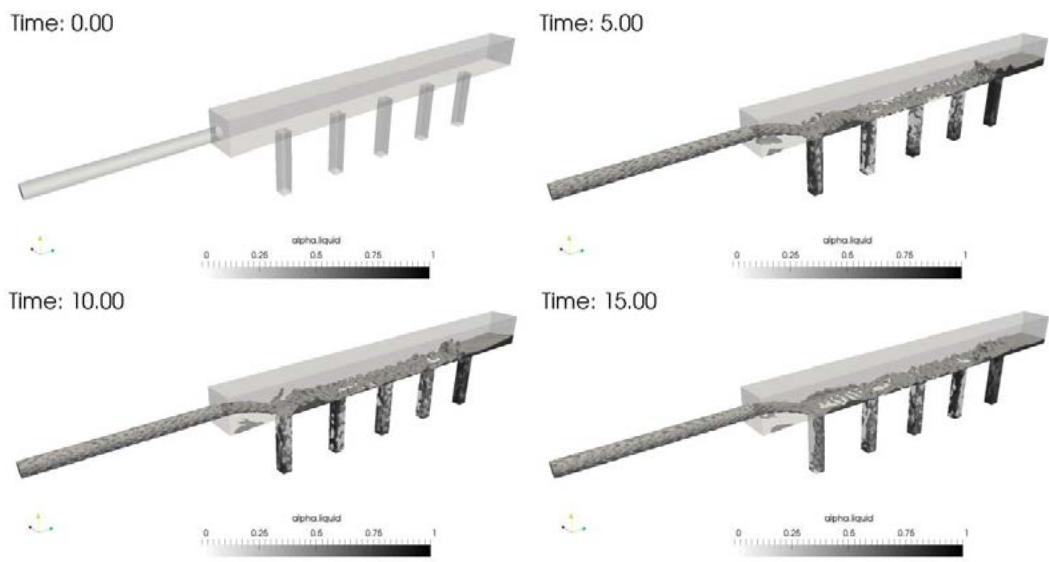


Fig. 3 Distribution of flow by time with the inlet mass flow rate and volume fraction are 25 g/s and 0.7, respectively

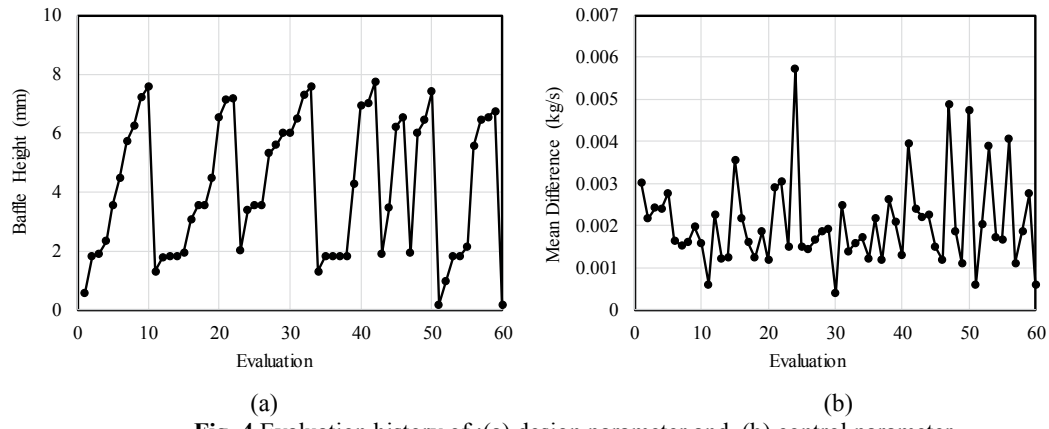


Fig. 4 Evaluation history of : (a) design parameter and, (b) control parameter

Fig. 4(a) shows the variation of baffle height during evaluation. In this cases, vapor quality is set as 0.5, the mass flow rate is 25 g/s and the diameter of inlet is 5 mm. The baffle high is ranged from 0.1 to 7.9 mm and 9 populations was created.

Fig. 4(b) illustrates the mean difference of flow rate at outlets. The optimal point is found at evaluation 30 with the baffle height of 6.012 mm.

Conclusions

The simulation and optimization of two-phase flow distribution of R134a in a manifold have been performed in this study. A procedure that combines the CFD model and GA has been developed. This result could be used as the brief step in optimizing the shape of manifolds, and further, could be expanded its application to other assignments like optimizing flow conditions in current equipment.

Acknowledgement

This research was supported by Basic Science Research Program through the National Research



Foundation of Korea (NRF) funded by Ministry of Education, Science, and Technology (NRF-2016R1D1A1A09919697).

References

- [1] S. RK, D. Sekulić, *Fundamentals of heat exchanger design*, 2003.
- [2] A. Jiao, R. Zhang, S. Jeong, Experimental investigation of header configuration on flow maldistribution in plate-fin heat exchanger, *Appl. Therm. Eng.* 23 (2003) 1235–1246.
- [3] J. Wen, Y. Li, Study of flow distribution and its improvement on the header of plate-fin heat exchanger, *Cryogenics (Guildf)*. 44 (2004) 823–831.
- [4] C.C. Wang, K.S. Yang, J.S. Tsai, I.Y. Chen, Characteristics of flow distribution in compact parallel flow heat exchangers, part II: Modified inlet header, *Appl. Therm. Eng.* 31 (2011) 3235–3242.
- [5] O. Tonomura, S. Tanaka, M. Noda, M. Kano, S. Hasebe, I. Hashimoto, CFD-based optimal design of manifold in plate-fin microdevices, *Chem. Eng. J.* 101 (2004) 397–402.
- [6] L. Wang, Y. Fan, L. Luo, Lattice Boltzmann method for shape optimization of fluid distributor, *Comput. Fluids*. 94 (2014) 49–57.
- [7] J. Facão, Optimization of flow distribution in flat plate solar thermal collectors with riser and header arrangements, *Sol. Energy*. 120 (2016) 104–112.
- [8] P. Fei, P.S. Hrnjak, *Adiabatic developing two-phase refrigerant flow in manifolds of heat exchangers*, 2004.



Pressure drop during condensation of R410A inside horizontal multiport mini-channels rectangular tubes

PHAM Quang Vu^{1,a}, Kwang-II CHOI², Jongg-Taek OH^{2,b*}, Honggi CHO³

¹Graduate School, Chonnam National University, San 96-1, Duduk-Dong, Yeosu, Chonnam 550-749, Republic of Korea

²Department of Refrigeration and Air Conditioning Engineering, Chonnam National University, San 96-1, Dunduk-Dong, Yeosu, Chonnam 550-749, Republic of Korea

³ Advanced R&D Team, Digital Appliances, Samsung Electronics, Suwon, 16677, Korea,

^aphamquangvu911273@gmail.com, ^bohjt@chonnam.ac.kr

Keywords: Condensation, Pressure drop, R410A, Correlation, Multiport mini-channel

Abstract. In this research work, a new developing two-phase frictional pressure drop correlation during condensation processing based on experimental data has been presented. The frictional pressure drop of R410A experimental data points of two types multiport mini-channels, having 8 channels with a 1.16 mm hydraulic diameter and 11 channels with 1.14 mm hydraulic diameter. The test sections were designed as a counter-flow tube in a tube exchanger. The experiment is performed with mass fluxes of 50-400 kg/m²s and 3-12kW/m² of heat fluxes, and saturation temperature of 48^oC. The frictional pressure gradient increased with increasing of mass flux and vapor quality but insignificant effect on with heat flux. The results showed that the new model can predict the two-phase pressure drop during condensation and comparison between experimental data with some well-known correlations-

Introduction

The use of mini and microchannels multiport tubes in the heat exchangers have been widely using in automotive air-conditioning systems. There are many advantages of the using mini channels, such as the compact size of heat exchangers, reduced air-side pressure drop, and low refrigerant charge. Understanding the frictional pressure drop behavior of condensation flow in micro and mini channels is important to improve the design of thermal systems. Several researchers have investigated experimentally and theoretically the pressure drop characteristics in mini channels. Yang and Webb [1] measured the pressure drop of single phase, adiabatic, and two-phase flow for R12 flowing in both micro fine and rectangular plain tubes. For two-phase flow, the authors concluded that the Lockhart-Martinelli two-phase multiplier correlation is not predicted well the experimental data. However, the equivalent mass velocity concept proposed by Akers, Deans, and Crosser [2] provided a very good correlation of the experimental data. Zhang and Webb [3] measured single phase and adiabatic two-phase flow pressure drop of R134A, R22 and R404A flowing through the 2.13mm hydraulic diameter of multiport extruded tubes and two copper tubes having 6.25 and 3.25mm inside diameter, respectively. For single phase flow, the Blasius correlation reasonably predicted the frictional factor within $\pm 10\%$ error rate. Koyama et al. [4] conducted experiments of the condensation flow of R134A in multiport tubes whose hydraulic diameters ranged from 0.81 to 1.06mm. They found that the frictional pressure drop agrees with the correlation of Mishima and Hibiki [5]. Cavallini et al. [6] investigated the pressure drop characteristics of R236ea, R134a and R410A inside 1.4mm hydraulic diameter multiport mini channels. The result showed that the R410A has a lower pressure drop in comparison with R134a and R236ea. Cavallini et al. [7] proposed an update of frictional pressure drop model in mini channels of with different cross section geometries and hydraulic diameter range from 0.4 to 3mm. (Ramírez-Rivera et al. 2015) performed an experiment to measure two-phase pressure drop in 0.715 and 1.16mm hydraulic diameters multiport mini channels tubes using R134a and R32.



In this study, the condensation pressure drop characteristics of R410A inside 1.16 and 1.14mm hydraulic diameters rectangular mini-channel tubes were investigated experimentally. Effects of mass flux, vapor quality, heat flux and hydraulic diameter of rectangular channels on the frictional pressure drop are examined. In addition, the experimental data are compared with some previous pressure drop correlations in the literature.

Experimental apparatus and method

The experimental facility as shown in Fig.1 consists of liquid receiver tank, gear pump, sub-cooler, Coriolis mass flow meter, DC pre-heater, test section, and condenser. The test section tubes have 8 and 11 rectangular channels with the test section length of 0.2 and 0.5m. The mass flow rate of refrigerant was measured using a Coriolis mass flow meter with flow pressure generated by the variable speed gear pump. The saturation temperature, pressure and vapor quality of refrigerant before entering the test section were controlled by the heat applied in pre-heat by adjusting the DC power supply. After condensing in the test section, the two-phase refrigerant condenses to the liquid in the plated heat exchanger. All of the temperature and pressure sensors are collected by a data acquisition system. The experimental apparatus was well insulated with foam to reduce the heat loss to surrounding

Fig.2a shows the schematic diagram of the test sections using in this study. Two types of aluminum multiport mini channels having 8 and 11 channels, with 1.16 and 1.14mm hydraulic diameters, respectively. The test sections were designed as a counter-flow tube in a tube exchanger with 200 and 500mm of effect length. The cooling water side was made of acrylic and designed as the same geometric shape the test tube with 1mm of gap size. Four high accuracy RTDs sensors were set up at the inlet and outlet of both fluids to measure the temperature of the refrigerant and cooling

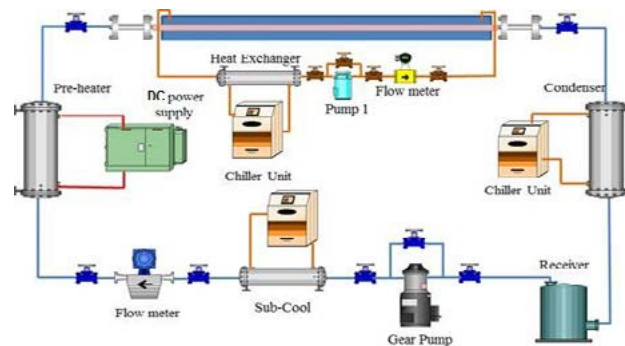


Figure 1. Schematic diagram of experimental apparatus facilities

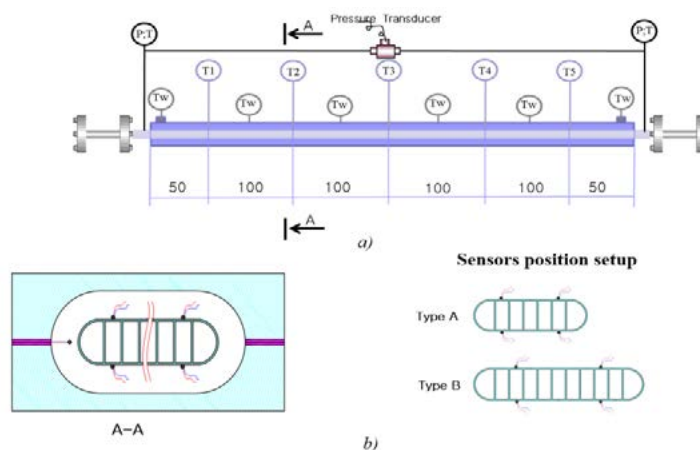


Figure 2. a) Detail of test section; b) Cross section of test tubes



water. A differential pressure transducer was installed between the inlet and outlet of the test section for measuring the pressure drop in the test section, the length between the pressure taps is 600mm and the accuracy of the differential pressure drop is $\pm 0.25\%$ of full scale or $\pm 0.5\text{kPa}$. Fig.2b shows the detail of a cross section of the test tubes.

The heat flow rate transferred in the test section was derived from a thermal balance on the cooling water side along with measured data of the refrigerant flow rate, the wall heat flux, and the pressure. The vapor quality at the inlet of test section was controlled by a DC power supply and can be determined as follows:

$$x_{inlet} = \frac{1}{h_{fg}} \left[\frac{Q_{pre}}{m_{ref}} - C_p (T_{sat} - T_{p,inlet}) \right] \quad (1)$$

The total pressure gradient can be calculated as combined of the two-phase frictional gradient, the gravitational frictional gradient, and the acceleration pressure gradient.

$$-\left(\frac{dp}{dz}\right)_{tp} = -\left(\frac{dp}{dz}\right)_F - \left(\frac{dp}{dz}\right)_g - \left(\frac{dp}{dz}\right)_{acc} \quad (2)$$

The test sections were set up is horizontally oriented, thus the gravitational pressure gradient is neglected. And the acceleration pressure gradient can be determined from

$$-\left(\frac{dp}{dz}\right)_{acc} = G^2 \frac{d}{dz} \left[\frac{x^2}{\alpha \rho_v} + \frac{(1-x)^2}{(1-\alpha) \rho_l} \right] \quad (3)$$

Where the void fraction α can be determined by the Steiner (1993) model.

The experiments of R410A condensing flow in test sections were carried out at the condensation temperature of 48°C , $50\text{-}500\text{kg/m}^2\text{s}$ of mass fluxes and $3\text{-}15\text{kW/m}^2$ of the heat fluxes. The physical properties in data reduction of each experiment was calculated by using the REFPROP Version 8.0.

Results and discussions

Fig.3 shows the effect of mass fluxes and vapor qualities on the frictional pressure gradient. The two-phase frictional pressure gradient increases with increasing values of mass flux and vapor quality. The increasing of vapor quality result in the increasing of the differential velocity of liquid and vapor phases. As a result, interfacial shear stress causing higher two-phase frictional pressure gradients increase. The velocity of vapor and liquid phases increase with increasing of mass velocity. The two-phase interfacial shear stress and the shear stress between the liquid film and wall both increase causing higher friction pressure gradients.

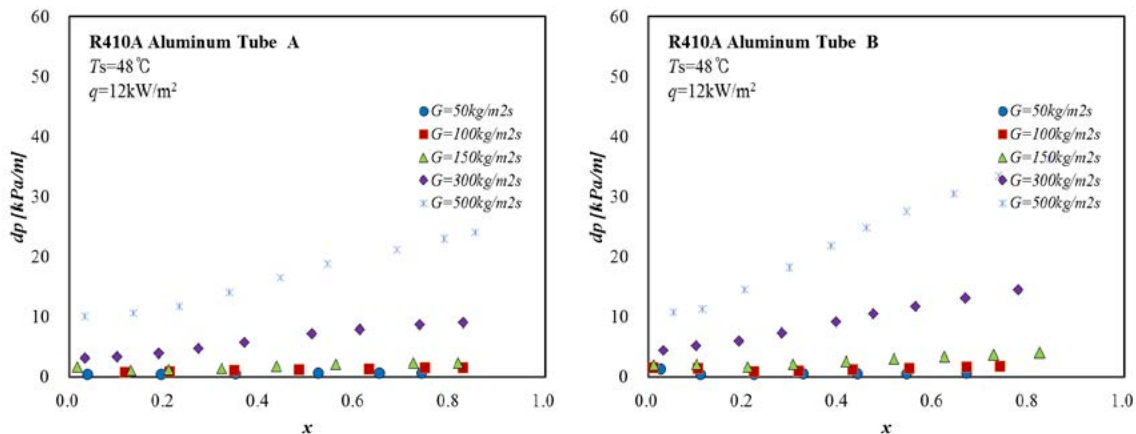


Fig. 3 The effect of mass flux on the frictional pressure drop

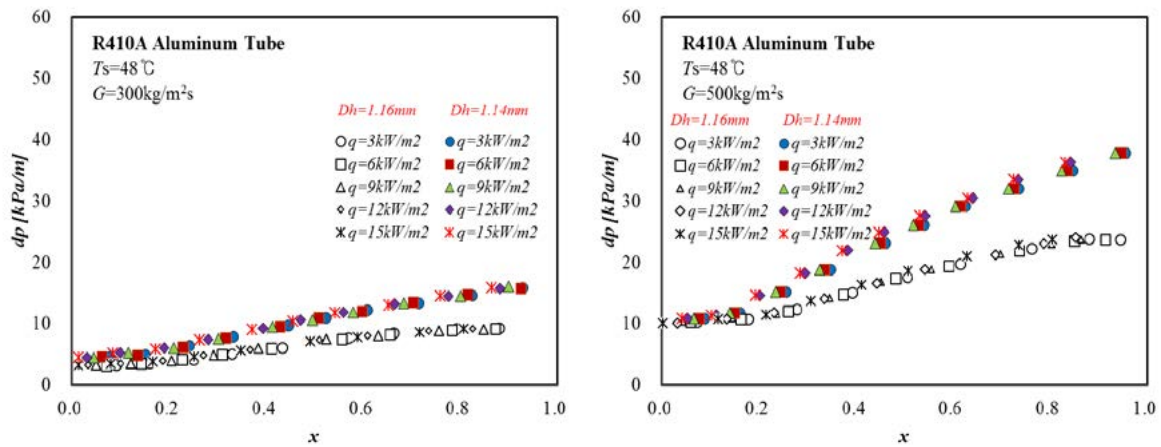


Fig. 4 The effect of heat flux and hydraulic diameter on the frictional pressure gradient

The effect of heat flux on the frictional pressure gradient is shown in Fig.4. The average of heat flux is calculated on the effect length of the test section. The heat flux is controlled by adjusting the cooling water at the inlet of cooling water side, and the cooling water mass flow rate is 1kg/min was fixed. It can be clearly seen that the heat flux had an insignificant effect on the frictional pressure gradient. At the high qualities ($x>0.8$) the effect of vapor quality becomes ambiguously and pressure drop appears constant with vapor quality. At the high vapor qualities, the flow pattern might transform to mist flow, so the liquid droplet included in the vapor, hence, resulting in the lower increasing of velocity at those regions. Also, the comparisons of the measured frictional pressure gradient between the 2 types multiport mini-channel tube in all similar test condition are shown in the Fig.4. The frictional pressure drops for $dh=1.11\text{ mm}$ are 1.07-1.4 times higher than those for $dh=1.14\text{ mm}$ at the same mass flux and vapor quality, this means frictional pressure drop increases with decreasing of hydraulic diameter.

The condensation frictional pressure drop of refrigerant in mini/micro horizontal channels has been studied for many years and many correlations have been proposed in the past decade. Therefore, the experimental data for R410A in two multiport rectangular mini-channel tubes were compared with the prediction values of the homogeneous model, Friedel [8], Bankoff [9], Mishima and Hibiki [5], Zhang and Webb [3], Chen et al. [11]. The experimental data can be acceptable with the predicted

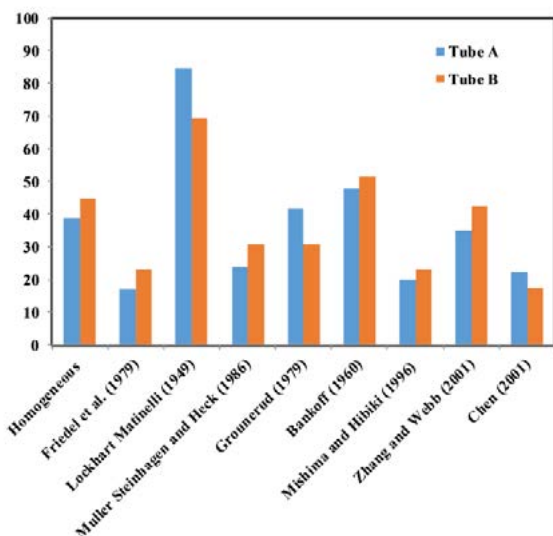


Fig. 5 Correlations comparison

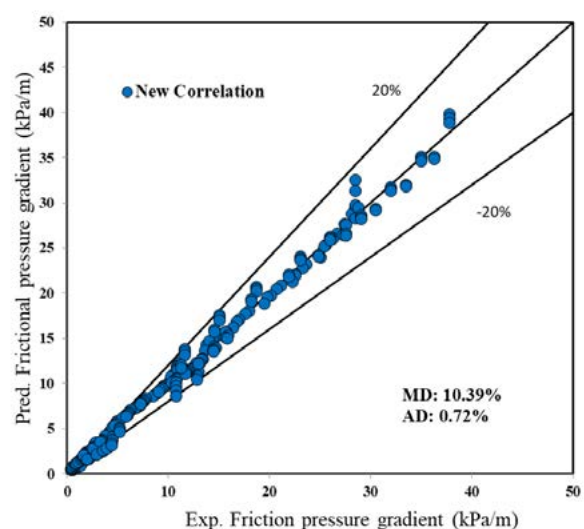


Fig. 6 New correlation comparison



values from some of the frictional pressure gradient correlations such as Mishima and Hibiki [5], Chen et al. [11] and Friedel [8] with the mean deviation about $\pm 20\%$.

In order to improve the predicted heat transfer coefficient, a new heat transfer coefficient correlation was developed from all the experimental data. The new correlation is as follows:

$$\left(\frac{dp}{dz}\right)_f = 12.65x^{0.509}(1-x)^{-0.059}Bo^{-4.15}\left(\frac{dp}{dz}\right)_{fLo} \quad (4)$$

The comparison of condensation heat transfer between the experimental data and the prediction value using new correlation is shown in Fig. 6, and the proposed heat transfer correlation shows good agreement with the mean deviation of 10.4%.

Conclusion

The condensation pressure drops of R410A in the multiport mini channel were performed in this study. The results were summarized as flowing:

1. The frictional pressure gradient increases with increasing of mass flux and vapor quality, but insignificant effect with heat flux
2. The frictional pressure gradient increase with decreasing of hydraulic diameter of channel
3. The Chen et al.(2001) and Friedel (1979) correlations are in agreement with measurement data. A new correlation is proposed that give a mean deviation of 10.39%.

Acknowledgements

This research was supported by Samsung Electronic Company.

References

- [1] Yang CY, Webb RL. Friction pressure drop of R-12 in small hydraulic diameter extruded aluminum tubes with and without micro-fins. *Int J Heat Mass Transf* 1996;39:801–9. doi:10.1016/0017-9310(95)00151-4.
- [2] Akers WW, Deans HA, Crosser OK. Condensation Heat Transfer within Horizontal Tubes. *Chem Eng Prog Symp Ser* 1959;55:171–6.
- [3] Zhang M, Webb RL. Correlation of two-phase friction for refrigerants in small-diameter tubes. *Exp Therm Fluid Sci* 2001;25:131–9. doi:10.1016/S0894-1777(01)00066-8.
- [4] Koyama S, Kuwahara K, Nakashita K, Yamamoto K. An experimental study on condensation of refrigerant R134a in multi-port extruded tube. *Int J Refrig* 2003;26:425–32. doi:10.1016/S0140-7007(02)00155-X.
- [5] Mishima K, Hibiki T. Effect of inner diameter on some characteristics of air-water two-phase flows in capillary tubes. *Nippon Kikai Gakkai Ronbunshu* 1995;61:3197–204. doi:10.1299/kikaib.61.3197.
- [6] Cavallini A, Del Col D, Doretti L, Longo GA, Rossetto L. Heat transfer and pressure drop during condensation of refrigerants inside horizontal enhanced tubes. *Int J Refrig* 2000;23:4–25. doi:10.1016/S0140-7007(99)00032-8.
- [7] Cavallini A, Col D Del, Doretti L, Matkovic M, Rossetto L, Zilio C, et al. Condensation in Horizontal Smooth Tubes: A New Heat Transfer Model for Heat Exchanger Design. *Heat Transf Eng* 2006;27:31–8. doi:10.1080/01457630600793970.
- [8] Friedel L. Improved friction pressure drop correlations for horizontal and vertical two-phase pipe flow. *Eur Two-Phase Flow Gr Meet Pap E* 1979;18:485–91.
- [9] Bankoff SG. A Variable Density Single-Fluid Model for Two-Phase Flow With Particular Reference to Steam-Water Flow. *J Heat Transfer* 1960;82:265. doi:10.1115/1.3679930.
- [10] Mishima K, Hibiki T. Some characteristics of air-water two-phase flow in small diameter vertical tubes. *Int J Multiph Flow* 1996;22:703–12. doi:10.1016/0301-9322(96)00010-9.
- [11] Chen IY, Yang KS, Chang YJ, Wang CC. Two-phase pressure drop of air-water and R-410A in small horizontal tubes. *Int J Multiph Flow* 2001;27:1293–9. doi:10.1016/S0301-9322(01)00004-0.



Experimental study of condensation heat transfer of R410A, R32 and R22 inside a micro-fin copper tube

PHAM Quang Vu^{1,a}, Kwang-II CHOI², Jonng-Taek OH^{2,b*}, Honggi CHO³

¹Graduate School, Chonnam National University, San 96-1, Duduk-Dong, Yeosu, Chonnam 550-749, Republic of Korea

²Department of Refrigeration and Air Conditioning Engineering, Chonnam National University, San 96-1, Dunduk-Dong, Yeosu, Chonnam 550-749, Republic of Korea

³ Advanced R&D Team, Digital Appliances, Samsung Electronics, Suwon, 16677, Korea,

^aphamquangvu911273@gmail.com, ^bohjt@chonnam.ac.kr

Keywords: Condensation, Heat transfer coefficient, Micro-fin, Correlation, R410A, R32, R22

Abstract. Two-phase flow condensation heat transfer characteristics of R410A, R32, and R22 inside a straight micro-fin tube with the outside diameter of 7mm were investigated experimentally. This study was especially focused on the influence of heat transfer area on the condensation heat transfer coefficient. The test section was a double tube of counter-flow type; the refrigerant was flowed condensation inside the test tube by heat exchange with cooling water flowing in the annular side. The temperature and pressure of refrigerant were measured at the inlet and outlet of the test section, and the surface temperature of tubes was measured. The pressure drop in the test section was directly measured by a differential pressure transducer. The heat transfer coefficient and frictional pressure gradient were calculated using the experimental data. The heat transfer coefficient was measured at the saturation temperature of 48°C within mass fluxes of 50-380 kg/(m²s) and heat fluxes of 3-12 kW/m². The experiment results were compared with the existing heat transfer coefficient correlations, and a new correlation was developed with good prediction.

Introduction

The enhancement of the condensation heat transfer in micro-fin tubes is due to the increased wetted area, the thinning of the condensate liquid film because of helical flow and surface tension forces, increased turbulence and mixing of vapor and liquid phase, and faster bubble coalescence and breakup [1]. A great number of experimental studies have been done on condensation heat transfer in the micro-fin tubes. Among these are Chamra and Webb [2] performed experiments on the condensation of R22 inner of 15.88mm outside diameter of both single-helix and cross-grooved surface tubes. They reported that the heat transfer coefficient increases with the helix angle and the cross grooved tubes provided higher condensation effect than the single-helix geometries. Jung et al. [3][4] studied the condensation heat transfer of R22, R407C and R401A on a horizontal plain, low fin and turbo-C tubes and showed that the condensation heat transfer of R410A was similar to those of R22. Cavallini et al. [5] proposed new heat transfer model to compute the heat transfer coefficient during condensation inside the horizontal smooth tube from an extensive analysis of 425 experimental heat transfer points. The model includes a simple and objective criterion for the definition of the transition between two different flow categories, depending on whether the heat transfer coefficient is dependent or independent on the temperature difference ΔT . Kim et al. [6] performed the condensation heat transfer of R22 and R410A in 9.52mm O.D. horizontal tubes. The data were measured for the mass flow rate of 40-80kg/h, the constant heat flux of 11kW/m² and the saturation temperature at 45°C. They concluded that the average condensation coefficient of R22 and R410A for micro-fin tubes were 1.7-3.19 and 1.7-2.94 times larger those in smooth tubes, respectively. Dobson and Chato [7] performed an experimental study on the condensation of R12, R134a, R410A and R32/125 (60/40%) in horizontal smooth tubes with various ID of 3.14, 4.57, and 7.04 mm. They proposed two correlations to predict the heat transfer coefficient in the stratification and annular flow



regime, respectively. Liebenberg and Meyer [8] studied the experiments performed with R22, R134, and R407C at a saturation temperature of 40°C and at mass fluxes ranging from 300 to 800 kg/m²s. They concluded that the transition from annular flow to intermittent flow occurred at an average vapor quality of 0.49 for the smooth tube, 0.29 for the herringbone micro-fin tubes. Miyara et al. [9] measured the experiment condensation and pressure drop of R22 and R410A in the herringbone-type micro-fin tube and compared to those of a helical micro-fin tube and a smooth tube. They conclude that the heat transfer coefficient of herringbone micro-fin tube is higher than that of the helical micro-fin tube in the high mass velocity region, while is has slightly lower value in the low mass velocity region.

The purpose of this study is condensation heat transfer characteristics in condensing of R410A, R32, and R22 inside 7mm OD helical micro-fin copper tube at the saturation temperature of 48°C. The experimental results are performed and discussed, also in present study developed a new correlation of condensation heat transfer coefficient.

Experimental apparatus and method

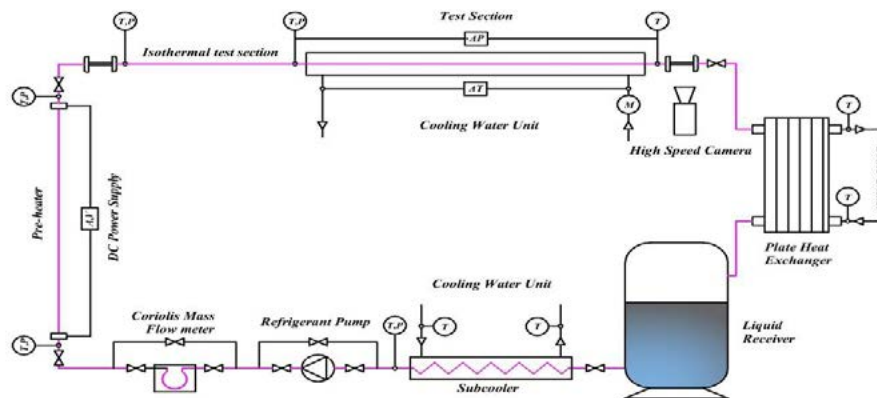


Fig. 1 Schematic diagram of experimental apparatus

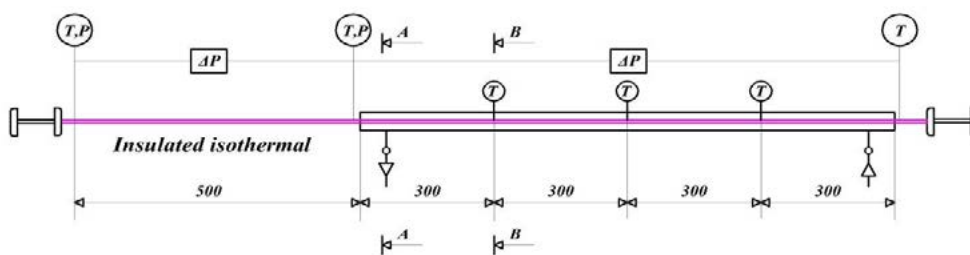


Fig. 2 Schematic diagram of test section

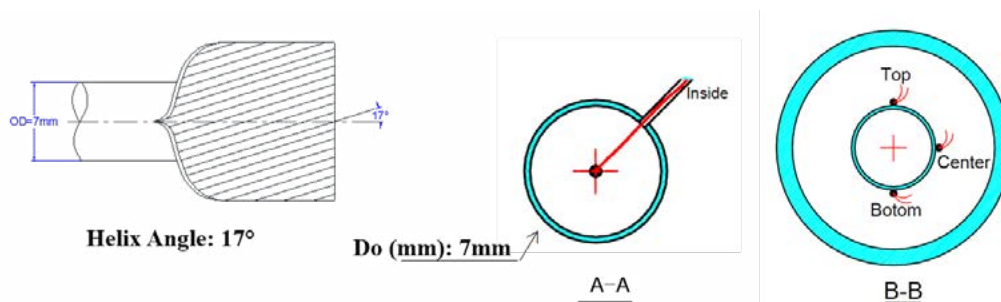


Fig. 3 T-Type thermocouples attachment

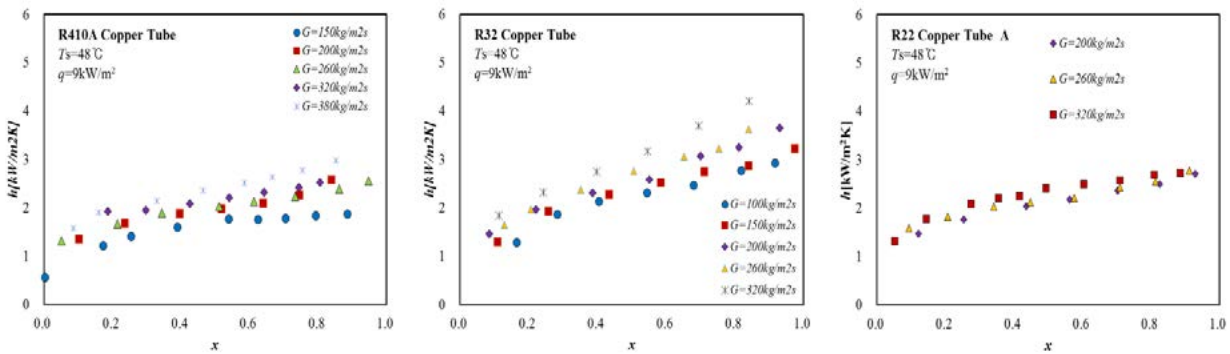


Fig. 4 The effect of mass flux on the heat transfer coefficient

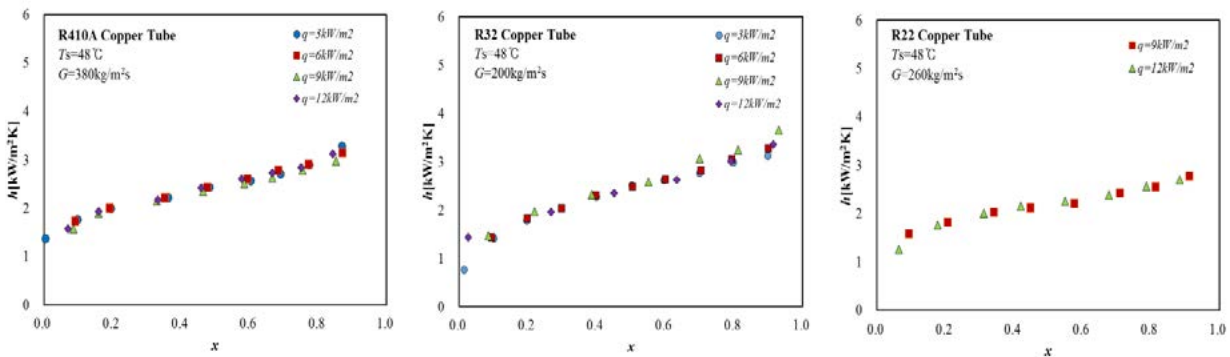


Fig. 5 The effect of heat flux on the heat transfer coefficient

The experimental apparatus is schematically shown in the Fig.1. The refrigerant loop is designed to measure the heat transfer of refrigerant. It is mainly composed of a receiver, a magnetic gear pump, a sub-cooler, a Coriolis flow meter, a pre-heater, a test section and a condenser. The refrigerant flow rate can be controlled by a magnetic gear pump and the vapor quality of refrigerant was controlled by a pre-heater before it entered the test section. Fig.2 shows the details of the test section. The test section was designed as a straight and horizontal counter flow tube in tube heat exchanger with a total length of 1.7m. The test section tube consisted of 2 sub-sections: 0.5m of the isothermal section and 1.2m of condensation section. The insulated isothermal test section was stabilizing the flow pattern of refrigerant inside a test tube. Three absolute pressure transmitters and two differential pressure transducers were connected to three pressure taps located along of the test section to measure the static pressure and pressure drop, respectively. The temperature of the tube wall was measured using twelve T-type thermocouples that were welded at points at the top, middle and bottom of the measurement test section. All of the thermocouples using in the experimental model were calibrated before installation, the uncertainty of the thermocouple measurement was estimated conservatively of ± 0.1 K.

The data reduction process for measuring the results was done using the methods outlined below. The physical properties of the refrigerant were obtained from the measured temperature and pressure of the refrigerant. The condensation heat transfer coefficients are obtained as Eq (1):

$$h = \frac{\dot{Q}}{A_{in} (T_{sat} - T_{w,i})} \quad (1)$$

The inside tube wall temperature obtained from the one-dimensional heat conduction in the tube wall was calculated as:

$$T_{w,i} = T_{w,o} + \frac{q}{2k} d_o \ln \left(\frac{d_o}{d_i} \right) \quad (2)$$

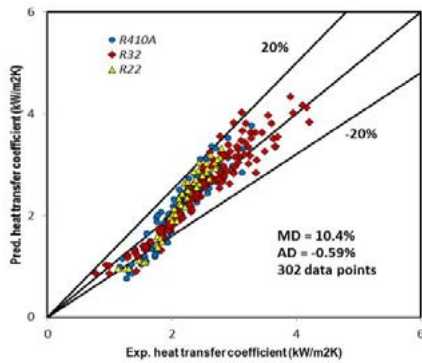


Fig. 6 Comparison of experimental data with proposed heat transfer coefficient correlation

Table 3: Summary of HTC's comparison

Correlation	Refrigerant					
	R410A		R32		R22	
	MD (%)	AD (%)	MD (%)	AD (%)	MD (%)	AD (%)
Aker (1959)	16.4	-8.12	23.44	-19.67	27.25	-26.39
Shah (1979)	55.24	54.10	33.52	30.28	23.87	21.11
Bivens and Yokozeki	38.39	37.27	34.28	34.18	14.51	6.86
Tang	18.73	8.30	19.39	1.89	20.43	10.99
Kedzierski	12.22	0.65	16.51	15.40	12.49	-0.21
Kaushik and Azer	53.47	53.47	44.50	44.39	46.03	46.03
Dobson and Chato	55.62	54.15	38.21	36.46	30.87	27.63

Where k is the thermal conductivity of the copper tube, in the present experiment, the different temperature between inside and outside tube was less than 0.025K. The vapor quality of refrigerant at the inlet of test section was controlled by controlling the power of DC power supply and was defined by Eq. (3):

$$x_{in} = \frac{1}{h_{fg}} \left(\frac{\dot{Q}_p}{\dot{m}_r} - C_{pr} (T_{sat} - T_{p,in}) \right) \quad (3)$$

Where \dot{Q}_p is the heat supplied to the pre-heater and $T_{p,in}$ is the refrigerant temperature entered the preheater.

Results and discussion

The effects of mass flux, heat flux and vapor quality on the condensation heat transfer coefficient of R410A, R32, and R22 were examined and discussed in the present study. Figure 4 shows the effect of mass flux on the heat transfer coefficient of R410A, R32, and R22 inside 7mm OD micro-fin tube. The saturation temperature was fixed at 48°C, the mass flux was varied from 100 to 380kg/m²s, and the heat flux was 9kW/m². The trend illustrates that the mass flux has a significant effect on the heat transfer coefficient of three refrigerants. The condensation heat transfer coefficient increase with increasing mass velocity and vapor quality, the results for which were effect by forced convection.

At high mass fluxes and high vapor qualities, the forced convection contribution is dominate. Moreover, the flow takes on the annular flow regime, as the vapor quality increase the liquid film thickness between the wall and vapor core become thinner, which results in the reduction of thermal resistance and the increase of heat transfer coefficient. Jung et al. [10] found the same results and they explained that due to a reduction of thermal conduction resistance in the liquid film caused by thinning of the of the liquid layer as well as an increase in momentum exchange as the mass flux and vapor quality increase. At the lower mass flux, the entrance region annular flow is formed but this quickly transforms to intermittent flow or stratified flow with its characteristic large amplitude waves washing the top of the tube or to stratified wavy flow with smaller amplitude waves, respectively.

The heat flux was determined by keeping constant the mass flow rate of cooling water is 1kg/min and controlled the inlet temperature. The effect of heat flux on the condensation heat transfer coefficient while the heat flux was varied from 3 to 12kW/m² is depicted in Figure 5. It is clearly seen that the heat flux has an insignificant effect on the variable of heat flux of three refrigerant.

Several correlations of heat transfer coefficient were developed for smooth and micro-fin tube have been published in the literature, such as [11],[7],[12],[13], [14], [15], [16]. Table 3 show the summary comparison of experimental condensation heat transfer with the existing correlations. The Aker [11], Tang [15], Kedzierski and Goncalves [16] correlations give the acceptable prediction with



measurement data. However, in order to improve the predicted heat transfer coefficient, a new heat transfer coefficient correlation in the form proposed by Kedzierski and Goncalves [16] was developed from all the experimental data. The new correlation is as follows:

$$h = \frac{k_f}{D_h} 0.002818 \text{Re}^{0.294} \text{Ja}^{(-0.232x)} \text{Pr}^{-2.002} (P_r)^{(-0.578x^2)} (-\log(P_r))^{(-0.474x^2)} \text{Sv}^{(2.531x)} \quad (4)$$

Where the Reynold number (Re), the Jacob number (Ja), the Prandtl number (Pr), the reduced pressure (Pr), the dimensionless specific volume (Sv) and the vapor quality (x).

The comparison of the experimental heat transfer coefficient with the prediction value calculated from newly proposed correlation is presented in Fig. 6. The proposed correlation shows a good prediction with the mean deviation of 10.4%.

Conclusion

The condensation heat transfer of R410A, R32, and R22 in a micro-fin tube was performed in this study. The results were summarized as follows:

1. The heat transfer coefficient of three refrigerants increase with increasing of vapor quality, mass flux but have insignificant effect with a variation of heat flux.
2. The Aker [11], Tang [15], Kedzierski and Goncalves [16] correlations give the acceptable prediction with measurement data.
3. The proposed heat transfer coefficient correlation was also developed based on the measurement data and the prediction values were in good agreement with the measurement data within the mean deviation of 10.4%.

Acknowledgements

This research was supported by Basic Science Research Program through the National Research Foundation of Korea (NRF) funded by Ministry of Education, Science, and Technology (NRF-2016R1D1A1A09919697) and Samsung Electronic Company.

References

- [1] Liebenberg L, Meyer JP. The characterization of flow regimes with power spectral density distributions of pressure fluctuations during condensation in smooth and micro-fin tubes. *Exp Therm Fluid Sci* 2006;31:127–40. doi:10.1016/j.expthermflusci.2006.03.023.
- [2] Heat IJ, Transfer M, Chamra LM, Webb RL. Advanced micro-fin tubes for condensation. *Int J Heat Mass Transf* 1996;39:1839–46. doi:10.1016/0017-9310(95)00275-8.
- [3] Jung D, Kim CB, Hwang SM, Kim KK. Condensation heat transfer coefficients of R22, R407C, and R410A on a horizontal plain, low fin, and turbo-C tubes. *Int J Refrig* 2003;26:485–91. doi:10.1016/S0140-7007(02)00161-5.
- [4] Jung D, Cho Y, Park K. Flow condensation heat transfer coefficients of R22, R134a, R407C, and R410A inside plain and micro fine tubes. *Int J Refrig* 2004;27:25–32. doi:10.1016/S0140-7007(03)00122-1.
- [5] Cavallini A, Col D Del, Doretti L, Matkovic M, Rossetto L, Zilio C, et al. Condensation in Horizontal Smooth Tubes: A New Heat Transfer Model for Heat Exchanger Design. *Heat Transf Eng* 2006;27:31–8. doi:10.1080/01457630600793970.
- [6] Kim MH, Shin JS. Condensation heat transfer of R22 and R410A in horizontal smooth and micro fine tubes. *Int J Refrig* 2005;28:949–57. doi:10.1016/j.ijrefrig.2005.01.017.
- [7] Dobson MK, Chato JC. Condensation in Smooth Horizontal Tubes. *J Heat Transfer* 1998;120:193–213. doi:10.1115/1.2830043.
- [8] El Hajal J, Thome JR, Cavallini A. Condensation in horizontal tubes, part 1: Two-phase flow pattern map. *Int J Heat Mass Transf* 2003;46:3349–63. doi:10.1016/S0017-9310(03)00139-X.
- [9] Miyara A, Nonaka K, Taniguchi M. Condensation heat transfer and flow pattern inside a herringbone-type micro-fin tube. *Int J Refrig* 2000;23:141–52. doi:10.1016/S0140-7007(99)00037-7.



- [10] Jung D, Song KH, Cho Y, Kim SJ. Flow condensation heat transfer coefficients of pure refrigerants. *Int J Refrig* 2003;26:4–11. doi:10.1016/S0140-7007(02)00082-8.
- [11] Akers WW, Deans HA, Crosser OK. Condensation Heat Transfer within Horizontal Tubes. *Chem Eng Prog Symp Ser* 1959;55:171–6.
- [12] Shah MM. A general correlation for heat transfer during film condensation inside pipes. *Int J Heat Mass Transf* 1979;22:547–56. doi:10.1016/0017-9310(79)90058-9.
- [13] Bivens DB, Yokozeki A. Heat transfer coefficients and transport properties for alternative refrigerants 1994.
- [14] Tang L, Ohadi M, Johnson AT. Flow Condensation in Smooth and Micro-fin Tubes with HCFC-22, HFC-134a and HFC-410A Refrigerants. Part I: Experimental Results. *J Enhanc Heat Transf* 2000;7:289–310. doi:10.1615/JEnhHeatTransf.v7.i5.10.
- [15] Kaushik N, Azer NZ. A general pressure drop correlation for condensation inside internally finned tubes. *ASHRAE Trans* 1990;96:242–8.
- [16] Kedzierski MA, Goncalves JM. Horizontal convective condensation of alternative refrigerants within a micro-fin tube. *J Enhanc Heat Transf* 1999;6:161–78. doi:10.1615/JEnhHeatTransf.v6.i2-4.90.



QIR

*The Westin Resort
Nasa Dua, Bali*
24-27 July 2017

SYMPOSIUM F

International Symposium
on Architecture





FROM NEGOTIATING IDENTITY TO CLAIMING SPACE: AN OUTLOOK ON SOCIO-POLITICAL DYNAMICS OF COMMUNITY MOSQUES IN MALANG, EAST JAVA

Yulia Eka Putrie^{1,3}, Widjaja Martokusumo²

¹ Student of Doctoral Program, School of Architecture, Planning, and Policy Development, Institut Teknologi Bandung (ITB), Indonesia, e-mail: ekaputrie.yulia@gmail.com

² Department of Architecture, School of Architecture, Planning, and Policy Development, Institut Teknologi Bandung (ITB), Indonesia

³ Department of Architecture, Faculty of Science and Technology, UIN Maulana Malik Ibrahim Malang, Indonesia

ABSTRACT

Mosque architecture in Indonesia is inseparable from the socio-political context of various Islamic groups or organizations, such as Nahdlatul Ulama, Muhammadiyah, PERSIS, Al-Irsyad, etc. Mosque is considered as an important institution in developing and educating the majority of Indonesian Muslim society. Many mosques were built by Muslim communities which had culturally been affiliated to one of the groups or organizations. Therefore, their mosque architecture can be considered as one means of expression of their specific identity or their particular perspective on the ideal picture of a mosque. However, there is also another condition where mosques were built by heterogeneous Muslim community. In this context, the image of an ideal mosque brought by the community members of each Islamic group then became the object of negotiation, where each element related to the mosque was negotiated by the members of various Islamic groups. This paper discusses to what extent these negotiations were resulted in the architecture of the negotiated mosques. The research is located in Malang, East Java, where the dynamic interactions among various Islamic groups take place. This study reveals that the negotiation process can lead to space claim with the negotiated elements of identity, as the result of the domination on the activity system or the physical control over the mosque.

Keywords: Community mosque; Identity; Islamic groups; Malang; Negotiation

1. INTRODUCTION

Indonesian Islamic groups and organizations have an important role in shaping the development of mosque in Indonesia. According to Barliana (2010: 4), the basis of communities in many mosques can be identified as the proponents of certain Islamic school of thoughts, such as Nahdlatul Ulama and Muhammadiyah. In fact, many mosques were built by affiliated Muslim communities. These affiliated mosques are popularly known as Nahdliyin mosques, Muhammadiyah mosques, etc. Some of these mosques' management are structurally related to the organizations, while some others are culturally related with the affiliated communities. One of the biggest Indonesian Islamic organizations, Nahdlatul Ulama (NU), even established *Lembaga Takmir Masjid Nahdlatul Ulama* (LTMNU) in order to organize a large number of Nahdliyin mosques all over the country.

The deep concern towards mosque development was due to the importance of mosque institution for the Muslim society. Mosque is a religiously meaningful place where Muslim



people gather together for various ritual and non-ritual Islamic activities. Together with *pesantren* as an institution for the specific and formal Islamic education of a limited number of Muslim students, mosque becomes an institution for a more informal Islamic basic education of the majority of Muslim society.

Moreover, socio-politically mosque is also important as the physical representation of the ideals, values, perspectives, and traditions of its Muslim community. As the physical representation, mosque can be used as a means of expression of the more specific identity other than the commonly shared-identity of Islam. Eric Roose in his dissertation stated that a specific religious view of a Muslim group expresses a specific construction of Islam through some cultural elements of their mosque (Roose, 2009: 34). Different Islamic groups with different values and perspectives tend to have different ideal pictures on their mosque architecture. However, these groups' respect on their own values, and the differences between the perspectives of Islamic groups have not considered properly in many contemporary studies about mosques. Roose stated, "More often than not, studies of modern mosques in the West seem to regard patrons as a force to be countered or educated, driven by a lack of taste or historical knowledge and by the need for cheap, populist recognizability," (Roose, 2009: 22).

In Indonesian context, the specific construction of Islam is represented by community affiliation to a specific Islamic group, such as Nahdlatul Ulama, Muhammadiyah, etc. The Traditionalist Muslims (represented by Nahdlatul Ulama) and the Modernist Muslims (represented by Muhammadiyah) with their own specific values and perspectives, conceive mosque in quite different pictures. For example, the existence of *bedug* and *kentongan* according to van Dijk (2009: 64), were viewed as heresy and the remnant of Hindu tradition by the Modernist Muslims. In other cases, graves which are frequently preserved in the sites or inside the mosque buildings by the Traditionalist Muslims had also led to some rejection from other Muslim groups (van Dijk, 2009: 78). Moreover, interior spatial division between men and women is another subject of disagreement. Women area which is frequently situated at the left or right side of men area in the Traditionalist mosques, is not considered as an ideal arrangement by the Modernist Muslims who tend to place women area symmetrically behind men area. In line with this, Roose found that the differences in some meaningful choices of architectural elements are based on the light of the construction of Islam required to be represented in their own mosques (Roose, 2009: 34).

However, there is also another condition where mosques were built by a heterogeneous Muslim community. These mosques of heterogeneous Muslim community have become the object of negotiations where the existence of each element of the mosques was negotiated by the members of the community. In this context, the images of an ideal mosque were brought by the community members of various Islamic groups. Each of them could take different actions on the existing mosque. In a more assertive statement, Abidin Kusno argued that architecture, particularly mosque, "became the site of negotiation between the global pan-Islamic Islam and the Javanese world" (Kusno, 2003: 57).

In a broader context of built environment, Amos Rapoport in his book "Culture, Architecture, and Design", showed that various actions towards built environment were taken after people evaluated their built environment based on their own ideals, images, values, norms, etc. These actions include designing new environment, modifying existing environment, moving, or even giving up (Rapoport, 2005: 53). Therefore, this paper will mainly discuss how these negotiations were resulted in mosque architecture of heterogeneous Muslim communities. Related to this conference theme on dwelling, this paper will discuss how identity negotiation in the settlement occurs not only in the private area but also in the more public area such as mosque.



This paper is an initial part of a qualitative research on the identity representation in Nahdliyin mosque architecture related to the local socio-political context in Malang, Jawa Timur. Malang is one region in East Java where the dynamic interactions between various Islamic groups and organizations take place. On the other hand, Malang is also known as a great basis of Nahdliyin people maintaining Nahdlatul Ulama's *Aswaja* traditions in their daily lives. An idiographic analysis of the dynamics between Nahdliyin and non-Nahdliyin communities related to their mosques as the center of their neighborhoods were resulted in two different categories of neighborhoods (Figure 1). One is the neighborhood with "multi-centered Muslim communities", where two (or more) differently affiliated mosques were built in a neighborhood, relatively near to each other, but with different ideals one another. Another category is the neighborhood with a "negotiated single-centered Muslim communities", where a mosque were built together in a neighborhood. The dynamics between the majority and the minority, the dominant and the less-dominant parties of its heterogeneous Muslim community in the second category of mosque is the main focus of this paper. However, this paper will also discuss the case of two mosques in the first category to give a clear description about the ideal picture of mosque of each Islamic group.

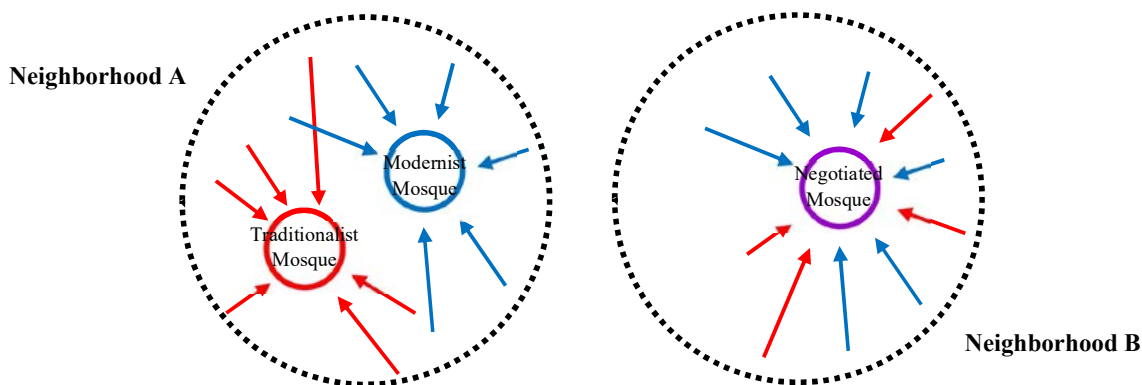


Figure 1. Neighborhood with Multi-Centered Muslim Communities (A) and Neighborhood with Negotiated Single-Centered Muslim Communities (B)

2. RESULTS AND DISCUSSION

2.1 Neighborhood with Multi-Centered Muslim Communities

One interesting case in this category is the case of two adjacent mosques in a neighborhood known as Pasar Kidul, Malang: Masjid Noor and Masjid Ar-Rahmat (Figure 2). Masjid Noor represents Nahdliyin community, while Masjid Ar-Rahmat represents Muhammadiyah community. Nahdliyin community is the majority in the region, which can be observed from the size of the mosque building. Both mosques serve the local community as well as people from the surrounding business area.



Figure 2. Masjid Noor (left) and Masjid Ar-Rahmat (right) in Kidul Pasar, Malang
(Source: Googlemap, 2016 (center); Documentation of Putrie, 2016 (left & right))

Besides a shared-identity of mosque architecture in general, both mosques also showed differences in some architectural aspects. The different choices of those aspects are related to the different ways to view several rules in Islam (*Fiqh*), local tradition, beauty and aesthetics, etc. These meaningful choices of architectural elements are more than mere pragmatic choices. The Table 1 below shows some pictures of both mosques' physical aspects.

Table 1. The Physical Aspects of Two Mosques: Masjid Noor and Masjid Ar-Rahmat

Mosque's Name	Building's Exterior	Interior and Spatial Division	Furniture	Ornamentation	Ablution Facility
Masjid Noor (the Traditionalist)					
Masjid Ar-Rahmat (the Modernist)					

Source: Documentation of Putrie, 2016

From the visual data above, a comparison were made on physical aspects of both mosques. The Table 2 below is a comparative analysis based on the visual and interview data from each mosque.



Table 2 Comparative Analysis on Architectural Aspects of Two Mosques in a Neighborhood: Masjid Noor and Masjid Ar-Rahmat

Architectural Aspects	Masjid Noor (the Traditionalist)	Masjid Ar-Rahmat (the Modernist)
Physical Aspects:		
Building's exterior and interior	Eclectic, elaborated, excessive ornamentation, with a huge dome and a minaret. Reason(s): "Allah is beautiful and loves beauty." Calligraphy is thought as one way to spread Islamic teaching.	Simple, "clean", less ornamented, dome or minaret are permitted but not a must-have one. Reason(s): Calligraphy is thought as unnecessary. "We prefer the mosque looks clean, therefore calligraphy is not necessary".
Spatial division	Women area is placed at the right corner of men area, with non-transparent and above-eye-level partitions. Reason(s): The Shafi'i <i>Fiqh</i> rule shows flexibility in certain condition. The important thing is men and women are well separated, with less contact physically and visually.	Women area is placed symmetrically behind men area, with transparent and below-eye-level partitions. Reason(s): The hadith stated that women are placed behind men in congregational prayers. "According to the Sharia, women are behind men, not beside them..."
Furniture	Throne-shaped <i>minbar</i> with three-step ladder and a <i>khotib</i> stick. No <i>bedug</i> were found. Reason(s): Maintaining tradition of the Prophet (pbuh) as well as the <i>Walisanga</i> tradition. "The <i>minbar</i> is the characteristics of NU. The <i>khotib</i> stick, the three-step ladder... The <i>khutbah</i> is different from the regular speech... <i>Bedug</i> is the request of the elders. It actually must exist, we already planned it."	Podium-shaped <i>minbar</i> with no stair and no <i>khutbah</i> stick. No <i>bedug</i> were found because it was thought as unnecessary. Reason(s): Nowadays, Muslim people are not in a state of war like the Prophet times, so the <i>khotib</i> stick is not necessarily used.
Ornamentation	The representation of NU tradition, such as <i>Asmaul Husna</i> and some quotations from Sufi tradition. Iconographic ornaments: The logo of NU on the door and the minaret's wall, the massive use of star shapes in the <i>mihrab</i> area. Reason(s): "Allah is beautiful and loves beauty." Calligraphy is one way to spread Islamic teaching.	The only ornament in the building exterior is the iconographic ornament calligraphy of "Muhammadiyah" and a small logo of Muhammadiyah on the glass doors. Reason(s): Calligraphy is thought as unnecessary. "We prefer the mosque looks clean, therefore calligraphy is not necessary".
Colors	Iconographic colors such as green, white, and gold. Green is widely used by Nahdliyin people and the organization of Nahdlatul Ulama in their official flag, logo, etc.	Dominated by grey and light blue, with red as an accent. Blue is known as the color of the logo of Muhammadiyah organization.
Ablution Facility	<i>Kullah</i> or shallow pools with minimum 216 liters of water to wash feet before <i>wudhu</i> . Reason(s): The Shafi'i <i>fiqh</i> rule of <i>thaharah</i> . "The <i>kullah</i> is one of the characteristics of NU. We prevent <i>najis</i> (dirt) from contaminating the floor by making people go through the shallow pool with min. 216 liters of water."	<i>Kullah</i> was thought as unnecessary. Reason(s): Muhammadiyah does not adopt the rule of minimum 216 liter of water as the precondition for <i>thaharah</i> from Imam Shafi'i.
Site & Setting	No preserved grave in the site, because the founder of the mosque was exiled by the Dutch and he died in Bandung. Setting: Main street, unplanned settlement (<i>kampung kota</i>), business area. Reason(s): "The mosque was just a small prayer area (<i>langgar</i>) behind the market. After some times, we decided to make a bigger mosque at the main street."	No preserved grave. Its existence was feared to be something sacred. Setting: Narrow street (<i>gang</i>), unplanned settlement (<i>kampung kota</i>), business area. Reason(s): "Because the crowd street were felt annoying and disturbing for the ritual activity of the mosque."
Non-Physical Aspects:		
Ritual	Maintains NU's tradition in 23 <i>rakaat</i> tarawih prayer, <i>Shalawat Diba</i> , <i>Tadarusan</i> , <i>Yasinan</i> , etc. Reason(s): "This mosque is already known with <i>Aswaja</i> tradition of Nahdlatul Ulama. We maintain our tradition in Friday Prayer, Tarawih prayer..."	Maintains 8 <i>rakaat</i> tarawih prayers. Strictly follow only the tradition of the Prophet (pbuh). Reason(s): "We realized that many things are different. It's quite clear."
Audial	Two times Friday <i>adhan</i> , collectively recite the <i>doa</i> with the loud voice after the congregational prayers, <i>shalawat tahrir</i> before <i>adhan</i> . Reason(s): "The difference is we perform two times Friday <i>adhan</i> , but they only perform one time Friday <i>adhan</i> . After Tarawih, <i>tadarus</i> is one characteristics of the mosque. We begin to lower the voice about 10.00 pm in order not to disturb the others."	One time Friday <i>adhan</i> . No loud voice from the mosque except regular <i>adhan</i> , because it was thought as possibly disturbing people. Reason(s): "In the mosque of NU, they held <i>shalawatan diba'an</i> every Friday night with loud voice heard outside the mosque. We don't have that kind of activity. We only recite al-Qur'an with low voice inside our mosque."
Historical Background	Built in 1929 as <i>waqf</i> from one of the Nahdliyin. The mosque has a historical background as the learning and training center for Indonesian fighters against the Dutch. At that time, the role of the <i>Kyai</i> is very important. The mosque also served as the place to hold the Mukhtar NU in 1933.	Built in 1968 by the Pemuda Muhammadiyah Sukoharjo. The community thought that they need to have their own mosque. "Before having a mosque, we held Tarawih prayers from house to house. We need a mosque for ritual and non-ritual activities such as studying Islam and training the young generation."

Source: Analysis on the visual and interview data of Putrie, 2015-2016



From the Table 2, we can trace the differences in both physical and non-physical aspects of the mosques of the Traditionalist and the Modernist. The differences in the physical aspects were found in the overall building's exterior and interior image, spatial division, furniture selection, the use of ornamentation, aesthetic preferences, the use of *kullah* on ablution facility, etc. Meanwhile, the difference in the non-physical aspects were found in ritual and audial aspects of both mosques. Their historical backgrounds were another non-physical aspect which strengthen the sense of specific identity in each mosque.

The physical and non-physical differences are based on different views and ideals of each Islamic group. Even on those aspects that physically showed similarities, the view behind the decision-making could be different. For example, physically the *bedug* does not exist in both mosques. However, how they view the absence of *bedug* in their mosques are pretty much different. The absence of the *bedug* in the Traditionalist mosque is due to some pragmatic reasons. Ideologically and politically, the Nahdliyin thought that the existence of the *bedug* is very important as a part of the ritual, as well as an attempt to show the identity of the NU's. On the other hand, the absence of the *bedug* in the Modernist mosque mainly due to ideological reasons.

The different ideals of each group can also be observed from the mosques' interior spatial division between men and women. The position of women area towards *mihrab* and men area, the height, and the transparency of the partitions indicate the different ideals in each mosque. In the Traditionalist mosque, the spatial division between men and women are more flexible. Women area can be placed at the right or left side of men area, or at the back corner of the mosque (Figure 3, left side). The important rule is that in the congregational prayers, the first row (*shaf*) of women is one row behind the men's row. On the other hand, the spatial division in the Modernist mosque is more rigid, because the women area should as much as possible be placed symmetrically behind the men area (Figure 3, right side). Meanwhile, the height and the transparency of the partition between men and women area is another important aspect of the spatial division in the Traditionalist mosque. There should be less visual and physical contact between men and women in the mosque, so the height of partition should be above the eye level and the materials are not transparent. In contrary, the height of partition in Modernist mosque is frequently below the eye level and the materials are quite transparent. The visual contact from the *makmum* (followers) area to the *mihrab* or to the *imam* (the leader of congregational prayer) is thought to be important for the Modernist.

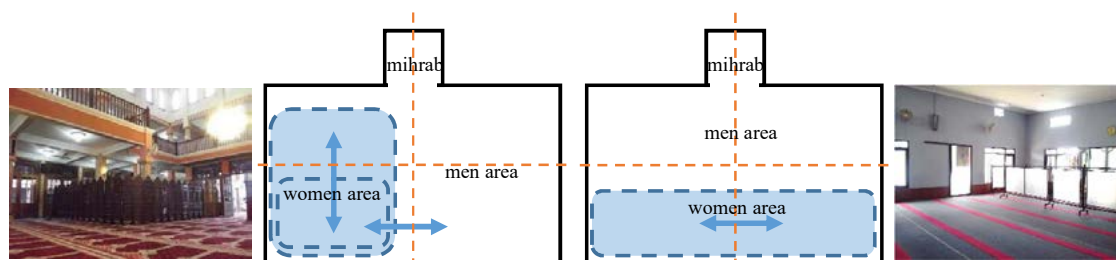


Figure 3. Possibilities and tendencies of the position of women area towards *mihrab* and men area in Traditionalist Mosques (left) and in Modernist Mosques (left)

The Table 2 shows that these meaningful choices of each Islamic group were obtained from their own specific ideals towards mosque and its activities. However, those ideals are easier to be put into the realization in a clearly affiliated mosque of specific Muslim community. In many neighborhoods of heterogeneous Muslim communities with only one mosque as the center of various Islamic groups, more complex socio-cultural phenomena occur frequently.



2.2 Neighborhoods with Single-Centered Muslim Communities: From Negotiating Identity to Claiming Space

The next discussion is the three cases of mosques in three different neighborhoods which are culturally multi-affiliated. In these multi-affiliated mosques, the mosque's ideals of each Islamic group experienced the process of negotiation among the members of each Muslim community. Because of the heterogeneity in the community, there are the majority and the minority, as well as the dominant and the less-dominant, although the majority is not always the dominant party. The Modernist could be the dominant, even if they are minority, vice versa. The dominant affiliation can be observed by its non-physical aspects, such as ritual and audial aspects of the mosques, because these aspects are the most un-negotiated aspects in the negotiated mosques. The Table 3 shows some pictures of these mosques' physical aspects.

Table 3. The Physical Aspects of Mosques of Heterogeneous Muslim Communities

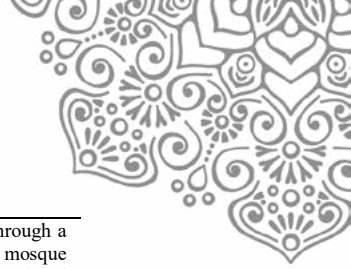
Mosque's Name and Dominant Affiliation	Building's Exterior	Interior and Spatial Division	Furniture	Ornamentation	Abution Facility
Masjid Al-Falah, Polehan Blimbing (The Modernist, Non-Nahdliyin)					
Masjid Muhajirin, Sumpansari (The Modernist, Non-Nahdliyin)					
Masjid Nurul Falakh, Klojen (The Traditionalist, Nahdliyin)					

Source: Documentation of Putrie, 2016

The Table 4 below is a brief description about the socio-cultural setting of the mosques based on the interview data from each of the mosque.

Table 4. The Socio-Cultural Setting of Five Mosques in the Neighborhoods with Heterogeneous Muslim Communities

Mosque's Name and Dominant Affiliation	The Socio-Cultural Setting
Masjid Al-Falah, Polehan Blimbing (The Modernist, Non-Nahdliyin)	The <i>takmir</i> of this mosque are people from various Islamic groups, dominated by the Modernists. However, they have a strong willingness to embrace all elements of Muslim people in the mosque. Therefore, some negotiation process took place on several aspects of the mosque, such as <i>bedug</i> , <i>minbar</i> , <i>kullah</i> , and ornamentation. One of the Nahdliyin in the neighborhood donated a <i>bedug</i> and a throne-shaped <i>minbar</i> . At first, the <i>takmir</i> tended to reject the donation. However, the donor insisted to give them away, eventhough those will not be used in the ritual. After the negotiation process, the <i>takmir</i> finally accept the <i>bedug</i> and the throne-shaped <i>minbar</i> . The <i>bedug</i> is situated on the 2 nd floor, while the throne-shaped <i>minbar</i> is modified into the podium-shaped <i>minbar</i> . Other negotiation also occurred about the <i>kullah</i> in the abution area. The <i>takmir</i> finally planned to renovate the <i>kullah</i> and change it into regular floor with the water flow. Another negotiation is about the placement of ornamentation. The decision is to place the rich ornamentation on the interior side of the dome and temporarily left the <i>mihrab</i> walls unornamented. Moreover, non-physical aspect such as the ritual and non-ritual activities also became the object of negotiation. Some people once asked the <i>takmir</i> to hold the Traditionalist's activities as they thought that the mosque belongs to the Traditionalist when they saw the <i>bedug</i> on the second floor. After a discussion, the <i>takmir</i> decided to reject the request.
Masjid Muhajirin, Sumpansari	Masjid Muhajirin was initially related with one university in Malang which is located adjacent to this mosque. However, since it is located separately from the campus, this mosque became a public mosque for a more



(The Modernist, Non-Nahdliyin)	<p>heterogeneous community. The mosque is opened for 24/7 for Muslim people. Therefore, it has been through a dynamic history related to some changes in the group dominance over the mosque. For several years the mosque was under the domination of the Salafist groups in the management of mosque and the organization of ritual and non-ritual activities. At that time, the throne-shaped <i>minbar</i> was replaced by a podium-shaped <i>minbar</i>. However, the throne-shaped <i>minbar</i> was not removed from its place. It was modified into a place for the <i>imam</i> by removing the three-step ladder, the seat, and the <i>khotib</i> stick. The podium-shaped <i>minbar</i> was placed on the left side, while the modified throne-shaped <i>minbar</i> was still on the right side. This pattern is different from the general pattern of the <i>minbar</i> placement in other mosques. Other fixed elements, such as fences with the inscription of Walisanga names and the <i>gunungan</i> decorations with the inscription of <i>Quranic</i> verses remain unchanged. Around the year 2013, the mosque was taken over by the local community. The management of the mosque was replaced, and the activities of the Salafist Muslim in the mosque were stopped. Today, the mosque is managed by the Yayasan Integritas Malang. Although it is dominated by the Modernist Muslim, the mosque management is eager to include other Islamic groups in this mosque. They want to eliminate the impression of a mosque belonging to a single group. They also call this mosque an "independent mosque". The <i>takmir</i> then arranged the participatory roles for various Islamic groups, such as Muhammadiyah and Nahdlatul Ulama. In order to promote tolerance in all of their activities, they considered not to perform any <i>wiridan</i> after congregational prayers or <i>shalawatan</i> before <i>adhan</i>. It is because both of these activities are considered as the characteristic of one Islamic group only. Moreover, elements considered as the identity of the particular group were also excluded from this mosque, such as <i>bedug</i> and <i>kentongan</i>. However, these policies actually indicated the representation of the Modernist religious identity itself. From an early form of the mosque which is retained, it appears that this mosque is designed with the feel of a mixture between the modernity and traditionality. The mosque's ornamentation utilized local carvings with the inscriptions of Walisanga's names. A great <i>gunungan</i> ornament that contains the calligraphy of Quranic verses is permanently installed above the <i>mihrab</i>. There is also a three-dimensional shape of a lotus bud at the top of the guardrail. Although being modified, the initial throne-shaped <i>minbar</i> is maintained as the <i>imam</i> area. The roof of the mosque is the two-stacked of pyramidal roof, while the <i>façade</i> of the mosque is made geometrically simple.</p>
<p>Masjid Nurul Falakh, Klojen (The Traditionalist, Nahdliyin)</p>	<p>Masjid Nurul Falakh is the Nahdliyin mosque with heterogeneous Muslim communities in the neighborhood. The <i>takmir</i> of this mosque are people from more than one Islamic groups, dominated by the Nahdliyin. They seek to respect the heterogeneity although the others are minority. Therefore, the <i>takmir</i> thought that it is not necessarily to put the logo of NU on their mosque <i>façade</i> or interior wall. They said that the <i>bedug</i> on the porch is an adequate symbol to state that this mosque is actually the Nahdliyin mosque. Some tolerance consideration towards the others occurred on the spatial division, the use of ornamentation, the design of the <i>minbar</i> and the <i>kullah</i>. The first row of women area has been moved three rows behind the first row of men area, however the overall position of women area remains on the side of men area. The height of the partition remains above the eye-level and the material is not transparent. The design of <i>minbar</i> has also been modified smaller than the regular throne-shaped <i>minbar</i>, but the seat, the three-step ladder, and the <i>khotib</i> stick are still maintained. Other than that, the design of the <i>kullah</i> is made smaller and people can choose whether they want to step on the shallow pool or not. Moreover, the selection of the ornamentation also considered the heterogeneity of the community members. They chose the calligraphy of the name of four Imams in Aswaja's <i>Fiqh</i> tradition: Imam Syafi'i, Imam Maliki, Imam Hanbali, and Imam Hanafi in order to keep the unity and harmony among the members of heterogeneous Muslim community. However, they made a clear restrictions on the role of strangers who aim to occupy the mosque. They also try to keep the Nahdliyin tradition in the form of the ritual and non-ritual activities, such as <i>shalawat nariyah</i>.</p>

Source: Analysis on the observation and interview data of Putrie, 2013-2016

From the Table 4, we can comprehend the fact that socio-cultural setting of the mosques have influenced the decision making process of their architectural elements. The Table 5 below is the brief coding of the Table 4.

Table 5. Types of Negotiation and Negotiated Elements of Three Negotiated Mosques

Mosque's Name and Dominant Affiliation	Types of Negotiation	Negotiated Elements	Un-negotiated Elements
Masjid Al-Falah, Polehan Blimbing (The Modernist, Non-Nahdliyin)	Negotiating identity elements; Considering tolerance; Restricting roles	Physical: the absence of the affiliation logo, <i>bedug</i> , <i>minbar</i> , <i>kullah</i> , ornamentation Non-physical: -	Physical: spatial division Non-physical: ritual and non-ritual activities, audial
Masjid Muhajirin, Summersari (The Modernist, Non-Nahdliyin)	Negotiating identity elements; Claiming space; Managing participatory roles	Physical: the absence of the affiliation logo, ornamentation, <i>minbar</i> placement and design Non-physical: -	Physical: spatial division, the height and transparency of the partition, <i>minbar</i> design Non-physical: ritual and non-ritual activities, audial
Masjid Nurul Falakh, Klojen (The Traditionalist, Nahdliyin)	Negotiating identity elements; Considering tolerance; Restricting roles	Physical: the absence of the affiliation logo, the selection of ornament, spatial division, <i>minbar</i> design, <i>kullah</i> design Non-physical: -	Physical: the height and transparency of the partition, <i>bedug</i> , the three-step ladder and the <i>khotib</i> stick, the volume of the <i>kullah</i> Non-physical: ritual and non-ritual activities, audial

Source: Analysis on the observation and interview data of Putrie, 2013-2016

The result of this research shows that negotiations do happen in the mosques of heterogeneous Muslim community. The negotiation process were resulted in the negotiated elements of identity as well as the claimed space. It happened through the domination of activity system,



role restriction, or physical control over the mosque. The mixture of negotiated and un-negotiated elements in these mosques of heterogeneous Muslim communities have made these mosques showed some kind of eclectic and obscure identity.

In this matter, Roose urged that in order to understand the reasons why certain building elements were chosen, “especially when combinations seem mixed up, confusing, cheap, fantasy, or fake,” the researcher should study “the patrons and their rational constructions of their own realities,” (Roose, 2009: 32). His study about the architectural varieties within mosque design in the Netherland showed that the design represents, ‘we are Muslims with such-and-such a religious view’ instead of ‘we are Muslim with such-and-such a culture,’ (Roose, 2009: 34). According to him, “The design expresses a specific construction of Islam in direct contestation of specific other constructions of Islam,” (Roose, 2009: 34). Following that, in Indonesian context we can also conclude that mosques represent various religious views, where the different views towards culture were inherent in the religious views as a whole. Some cultural elements, such as *bedug* and *minbar* become the object of negotiation because of the different religious views towards some cultural aspects related to religious ritual activities.

However, in the Table 5, we can see that some elements considered ideals in a single-affiliated mosque turned out to be opened for negotiations in the multi-affiliated mosques. Among the negotiated elements are mostly physical, such as the interior spatial division, the *bedug*, the *minbar*, the *kullah*, and the use of ornaments. Meanwhile, the un-negotiated elements are mostly non-physical such as the ritual and non-ritual activities. These negotiated elements in the multi-affiliated mosques are mostly the characteristics or the identity representation of specific single-affiliated mosques, such as the *minbar* and the *bedug* for Nahdliyin or the Traditionalist mosques. Therefore, negotiating these elements can be the representation of negotiating mosque’s identity as a whole. The combination of negotiated and un-negotiated elements form some kind of new eclectic identity in the sense of its heterogeneity. As Woodward (2002: xi) stated, “Identity gives us a sense of who we are and to some extent satisfies a demand for some degree of stability and of security.” Therefore, the new eclectic identity might give the community a sense of togetherness, engagement, and in turn, a sense of stability and security in its heterogeneity.

Moreover, even though some elements were negotiated, they are not completely changed. The important aspects of the elements, some conceptual aspects, such as the height and the transparency of the partitions, are hardly being negotiated, while the placement of the partition to form the women area can easily be negotiated. The existence of three-step ladder and the *khotib* stick in the *minbar* of the Traditionalist mosque is another example of the un-negotiated aspects of negotiated elements. As described in the Table 4, the size and the shape of *minbar* in Masjid Nurul Falakh were negotiated, however the three-step ladder and the *khotib* stick in the *minbar* is remain un-negotiated. These un-negotiated aspects of mosque’s architectural elements indicate that these aspects of elements are ideologically or politically important as specific identity of certain Islamic groups. As one of the mosques dominated by the Traditionalists, Masjid Nurul Falakh was willing to negotiate some aspects of its *minbar* in order to seek harmony by making people from other Islamic groups feel more accommodated and welcomed. Therefore, the negotiated and un-negotiated aspects of mosque elements can also be seen as an effort to seek mutual understanding between the various Islamic groups.

Besides intended to strive for the ideals of each group, the complex process of negotiation among the various groups in the mosques is also intended as the effort to prevent conflict and crisis, to seek tolerance, and to keep the community from the possibility of disintegration. The strong relationship between the negotiation of identity in mosques and the possibility of conflict and crisis is also mentioned by Woodward in her book, “Understanding Identity”. She cited



Kobena Mercer's statement that identity becomes an issue when it is in crises (Mercer in Woodward, 2002: xi). She also stated that crises occur when an identity position is challenged or becomes insecure (Woodward, 2002: xi). In this context, insecurity arises when more than one groups present and strive for their own ideals in the mosque. Following this perspective, Yasser Tabaa as cited by Roose in his dissertation stated that, "Art, like cultures and religions, defines itself against its opponents, and the more intense the conflict, the sharper this self-image," (Tabaa in Roose, 2009: 25). However, in this research, it is found that people handled the possibility of conflict in quite diverse ways. In the single-affiliated mosques as described in the first part of this article, affirming or representing identity is one way to prevent conflict with other groups. On the other hand, in the multi-affiliated mosques as described in the second part, concealing identity is another way to prevent the possibility of conflict.

Furthermore, the negotiation process should be viewed as an on-going process. It is inseparable from the dynamics of the community, shaped and re-shaped by the socio-cultural context of the neighborhood. Roose even stated, "Religious architecture in the Islamic world never simply 'adapted itself' to 'its time' or 'its region' but instead dynamically followed politico-religious alliances," (Roose, 2009: 25). The example of the on-going process happens in community mosques is the phenomena of space claim, where one heterogeneous community mosque could be dominated by one group at one time, and then claimed by another group at different times, and so on. In this research, the space claim phenomena was found in Masjid Muhajirin. For several years the mosque was under the domination of the Salafist Muslims. Around the year 2013, the management of the mosque was replaced, and the activities of the Salafist Muslim in the mosque were stopped. Today, the mosque is managed by the Yayasan Integritas Malang which is apparently dominated by the Modernist Muslims. However, the mosque management manages the participatory roles to welcome the participation of other Islamic groups such as the Traditionalist Muslims in this mosque activities.

The space claim as one of the temporary results of the negotiation process is an interesting topic to be researched further. In unplanned settlements, the space claim could happen spontaneously because of the regeneration of the *takmir*. In other cases, the space claim happens because of the dominance of one party over the others. In planned settlements built by the developers, space claim in mosques could occur because the site and the building were provided by the developers, not by individuals with a clear affiliation. Therefore, mosques of this kind of neighborhood do not possess an adequate historical justification to prevent the space claim by one or more groups. This kind of mosques will be explored deeper in the next steps of this research.

3. CONCLUSIONS

Socio-political context of the surrounding community have a great impact on mosque architecture. In Indonesia, the existence of various Islamic groups with their own ideals on mosque architecture has influenced the specific identity of mosques, where mosques can be seen as a single-affiliated mosque or a multi-affiliated mosque. Each category of mosque offers different ways to handle the possibility of conflict and crisis, from negotiating identity to claiming space, from affirming identity to concealing identity. It is important to study Indonesian mosque architecture in their socio-political context, not only because it raises our understanding in the various ideals and perspectives of Indonesian Muslim communities in developing their mosques, but also because it offers a proper perspective to view and to promote tolerance in the middle of the plurality of Indonesian religious lives.



4. REFERENCES

- Barliana, S., (2010), Tradisionalitas dan Modernitas Tipologi Arsitektur Masjid, Metatekstur, Bandung.
- Kusno, A., (2003), “The Reality of One-Which-Is-Two” – Mosque Battles and Other Stories: Notes on Architecture, Religion, and Politics in the Javanese World, *Journal of Architectural Education*, 2003, pp. 57-67
- Rapoport, A., (2005), *Culture, Architecture, and Design*, Locke Science Publishing Company, Inc., Chicago.
- Roose, E., (2009), *The Architectural Representation of Islam; Muslim-Commissioned Mosque Design in the Netherlands*, ISIM/Amsterdam University Press, Amsterdam.
- Van Dijk, K., (2009), ‘Perubahan Kontur Masjid’, in Nas, PJM & de Vletter, M (eds.), *Masa Lalu dalam Masa Kini: Arsitektur di Indonesia*, PT Gramedia Pustaka Utama, Jakarta.
- Woodward, K., (2002), *Understanding Identity*, Oxford University Press Inc., London



15th International Conference on Quality in Research (QiR 2017)

The Visual Aesthetic of Landscape in Semarang

Prof. Ir. Edy Darmawan, M.Eng.^a; Dr. Ir. Suzanna Ratih Sari, MM., MA.^b; Adhisti Samsinar Enis, A.Md.^c

^{a,b,s} *Architecture Department, Engineering Faculty, Diponegoro University, Semarang, Central Java, Indonesia*

Abstract

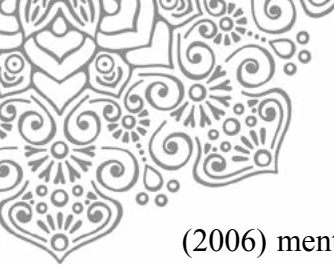
The visual aesthetic of landscape in Semarang is determined by the lively of the landscape, the category of the park: active and passive, aesthetic hardware and software the landscape. In addition, the visual aesthetic can be identified from the landscape of street and square. The researchers use qualitative identification method. The researchers determine the qualification of landscape in Semarang. Based on the analysis of the elements of the parks, it can be concluded that the aesthetic of landscape in Semarang has high visual value. Finally, the result of this study can be used as the reference in making the map of aesthetic landscape in Semarang. The landscape would be developed to become aesthetic visual.

Keywords: Visual Aesthetic; Landscape; Semarang City.

A. Introduction

City is a combination of natural ecosystems and artificial ecosystems. Wirasonjaya in Sasongko (2002) says that one of the characteristics of the artificial ecosystem is the existence of relatively small natural ecosystems and its quality which will affect the quality of urban ecosystems. To maintain the ecosystem in urban areas, it is necessary to develop the green open spaces in the city. Green open space, according to Regulation of the Minister of Home Affairs Number 1 Year 2007 on Green Open Space Arrangement Urban Area, is a longitudinal/ path and/ or grouped area which is accessible to the public, and it is covered by plants, trees, or other vegetation. Landscape is part of the green open space and one of the elements of urban space which is needed by the community. Rob (1979) defines the landscape as a comprehensive system in which there is a connection between the biotic and abiotic components, including the components of human influence. However, the landscape is constantly changing due to the influence of human's activities. Thus, the right landscape governance is needed so that the components in it can be preserved. Danier (2015) says that landscape arrangements and landscape governance can contribute to a unique landscape character. Landscape design principles should be applied in designing a visually-appealing landscape. According to Judge (2003) landscape design principles consist of balance, rhythm and repetition, emphasis and accentuation, simplicity, contrast, proportion, and unity.

One of the most common typologies of urban landscape is the city park. Urban parks considerably important in urban landscapes as it can shape the city's character and provide the visual beauty of urban environments to create unity between spaces (Simonds, 1983). Frick

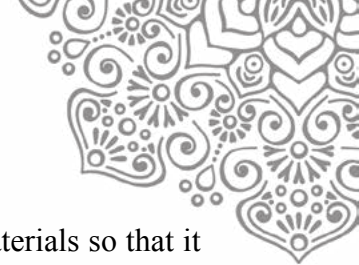


(2006) mentions that city parks function as urban lungs (improving air quality), as living spaces of local flora and fauna, and as human resting places. Today, the city park is not simply a physical part of a city, but also part of the citizen's lives. According to Nassar (1988), the aesthetic quality of a landscape can provide individual satisfaction to the individuals and indirectly affect human behavior. The existence of urban parks and elements that are in it is strongly influenced by human activity. The city park reflects the state of society, so the city park is designed not only as an important attribute for orientation, but also to meet human needs in relaxation, identification or stimulation (Jessel, 2006). Darmawan (2015) said that the arrangement of city parks should be able to create the interaction between the elements in it and the community as its users, so that the park will become lively. City park should be able to provide comfort and prosperity for the citizens, and it should have aesthetic value to maintain and enhance the beauty of the city. Therefore, according to Susiloarifin (1994), city park should be arranged in such a way as to provide beauty, comfort, and security in its use.

Semarang, as one of the big cities in Indonesia, experienced a very rapid development. The development and growth of the city has resulted in reduced green open space in Semarang and has affected the quality of urban environment. Many green areas have been converted into establishments. This situation leads to many problems, such as rising air temperature, air pollution, noise, congestion, and dense settlements. Many buildings are constructed without taking the surrounded environment condition into considerations, resulting in a less good scenery. This condition for certain cause discomfort and turns the city into such a dull place. This condition can be stressful for the community. For that reason, the city government of Semarang has developed and managed the city park in the last few years. This activity is not only to meet the green open space needs of Semarang City which is still far from the existing provisions, but also to improve the aesthetic visual of the city and to restore the comfort of urban environment. City park in the center of Semarang consists of an active garden and a passive garden, where each park has its own potential and uniqueness in creating aesthetic visuals of the city. Based on the situation described above, the researcher are interested to study the aesthetic visuals of the existing park in Semarang City and arrange the research result into a recommendation that can be used as input in arrangement of city park.

B. Methodology

Methodology in a study is related to data collection, compilation, and analysis. The purpose of this study is to determine the aesthetic visuals of existing parks in the city of Semarang. Aesthetics, according to Simonds (1983), is defined as a harmonious relationship of all elements or components perceived. The method used is descriptive qualitative. According Arikunto (2006), the aim of descriptive qualitative research is gathering actual and detailed information, identifying problems, making comparisons or evaluations, and determining what others are doing in the face of similar problems and learn from their experiences to organize decision in the future. By taking samples at the parks in the center of Semarang City, we will describe the physical conditions and elements of the parks, as well as the landscape design principles. The data are obtained from direct observation and documentation. Direct observation activities is an activity of recording an object or event in a systematic way to obtain information about the observed phenomenon (Moelong, 2002). Documentation can be photographs or images, rules, history of the object being observed. Sugiyono (2014) said that document study is a complement of the use of observation and interview methods in qualitative research. Once the data are collected, the researcher proceed to the data analysis. Data analysis is a process of



searching and compiling data obtained from interviews, field notes, and other materials so that it can be understood easily and the findings can be informed to others (Bogdan in Sugiyono, 2014). The process of data analysis is carried out as soon as the data collection process begins, and it will be continued after all the data are obtained.

C. Results and Discussion


The results and discussion in this article include descriptions of the physical condition of the park, the analysis of the elements of landscape design, the analysis of landscape design principles, and aesthetic visual analysis of the park located in the center of Semarang.

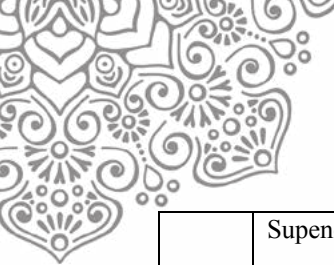
1. Physical Condition of Parks in the Center of Semarang

Semarang has several urban parks located around the district. The parks are categorized as active parks and passive parks. Active park is a park open for public. It can be used for public events and functions as center of social interaction. Meanwhile, the passive park is an aesthetic park which is designed for aesthetic purpose. People can only see the park without being able to go inside to do activities because the park is usually surrounded by a fence (Darmawan, 2015). This research focuses on both active parks and passive parks located in the center of Semarang. The parks include Taman Pandanaran, Taman Menteri Supeno, Lapangan Pancasila Simpang Lima, Taman Tugu Muda, Taman Jalan Imam Barjo, and Bundaran Taman Jalan Pemuda. The parks have their own unique characteristics based on location, area, facility, service area, and local people need of open public space. Despite the fact that number of open in Semarang is still far from the ideal number, but the number of the current parks still adequately support the public needs of public open spaces.

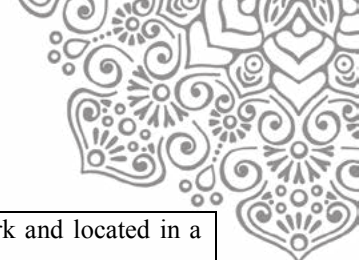
Based on the observation of the selected parks, the physical condition of the parks are described as follows:



Table 1
Physical Condition of Parks Located in the Center of Semarang

No.	Name	Physical Condition	
1.		Location	Located between Jalan Pandanaran and Jalan MH. Thamrin.
		Types	The park, that covers an area of ± 6,000 m ² , is an active garden that can be accessed freely by citizens, but not many people visit this park due to lack of trees.
		Facilities	Park benches, garden lights, parking lots, fountain, plazas, drinking water taps, public toilets, garbage cans, several stalls and minimarkets around the park, Warak Ngendok statue as one of the icons of Semarang. The statue itself symbolizes the idea of different ethnicities that can co-exist and get along.
		Activities	Play and relax. Not many people do exercise due to the lack of shade and crowded street close to the park.
		Function	(A) To lower air temperatures and reduce pollution, but it does not really helpful. (B) Adorn the city with an attractive garden design and furnished with sculpture as a marker. (C) As a public place for citizens to socialize, although the park has not be used for this purpose optimally.
		Maintenance	The park is not well taken care of as some facilities are in bad condition due to irresponsible action by visitors.
		Access	It can be accessed easily because there is no fence surrounding it.
		Types of vegetation	Shade trees, grasses, cover crops, and ornamental plants varied in sizes and colors.
2.	Taman Menteri	Location	In Kelurahan Mugasari, South Semarang District.



	Supeno  	Types	This 5,000 m ² park is an active park that people can be easily accessed by people.
		Facilities	Parking lot, playing area, pool and fountain, sculpture, park bench, garden lights, skateboarding area, pedestrian path, PKL area, vegetation.
		Activities	Sports, play, recreation, stroll around, culinary tour.
		Function	(A) To lower air temperature and reduce pollution, which works well because of the trees surrounding this park. (B) Adorn the city and cool the surrounding area off. (C) Place of socialization for the citizens and as an alternative tourist attractions. (D) Culinary destination because there are street vendors who sell various types of food and beverages around the park.
		Maintenance	The park is in good condition, well maintained, and quite clean.
		Access	Easy to reach by any means of transportation, both public and private.
		Types of vegetation	The trees provide shade for the visitors and cool the area off. In addition, there are also grass and plants covering the area, and ornamental plants varied in sizes and colors.
3.	Lapangan Pancasila Simpang Lima  	Location	Located in the center of city (Simpang Lima area).
		Types	An active park that can be visited by public.
		Facilities	Sports area, park bench, garbage can, parking lot, lights, pedestrian ways, public toilets, playing area, and plants.
		Activities	Exercise, playing, recreation, ceremony, led prayer, stroll around.
		Function	To lower air temperature and reduce air pollution, but the park does not serve this function optimally yet. In addition, the park adorns the city and functions as place for citizens to socialize.
		Maintenance	The park is in good condition and well maintained, but there are still parts filled with garbage due to lack of awareness of the citizens.
		Access	Easy to reach by using any means of transportation, but the access to this place is quite difficult due to the heavy traffic.
Types of vegetation	There are trees, grass, and plants covering the ground, and ornamental plants varied in sizes and colors.		
4.	Taman Tugu Muda  	Location	Located in Tugu Muda area
		Types	The circular garden, covering an area of ± 1.700 m ² , is a passive garden.
		Facilities	Fountains, garden lights, sculpture, pedestrian ways, guardrail, plants.
		Activities	Because it is a passive park, there is not many activities spotted in this area. Sometimes people come to this place to relax or take pictures.
		Function	The main function is to reduce air temperature and reduce air pollution, but the park has not functioned optimally. In addition, the park is a beautiful view in the middle of crowded traffic.
		Maintenance	The park is well maintained and clean.
		Access	Easy to reach by any means of transportation, but access to this place is quite difficult due to the heavy traffic.
Types of vegetation	The are trees, grass, plants covering the ground, and ornamental plants varied in sizes and colors.		
5.	Bundaran Taman Jalan Pemuda 	Location	Located in the center of Jalan Pemuda, Jalan Depok, and Jalan Tanjung.
		Types	Categorized as a passive park.
		Facilities	Fountains, plants, pavements such as pedestrian ways, garden lights, bulletin boards/ information, traffic lights.



	Activities	No activity spotted because it is a passive park and located in a crowded street.	
	Function	The park is expected to lower the air temperature and absorbs the air pollution, yet it has not functioned optimally. It also provides aesthetic visual in the middle of traffic.	
	Maintenance	The condition is quite good and well maintained, but sometimes there are flags of parties or organizations that disrupt the park's visual.	
	Access	Easy to reach because it is on the main street, but access is quite difficult because of heavy traffic.	
	Types of vegetation	There are trees, shrubs, grass covering the ground, ornamental plants of different sizes.	
6.	Taman Jalan Imam Barjo 	Location	Located on Jalan Imam Barjo, Pleburan.
		Types	It is a passive park as it is surrounded by offices and campus of Undip Pleburan
		Facilities	Pedestrian ways, garden lights, sculpture, plants.
		Activities	Not many activities spotted, but during the day the park is sometimes occupied by employees taking a break from work.
		Function	As the lungs of the city, it absorbs air pollution, lower the air temperature, adorn the surrounded environment.
		Maintenance	Good enough, because there are officers who clean up around the street and the park. Nevertheless, there is still some waste that is thrown away arbitrarily due to lack of public awareness.
		Access	The open garden space is easily accessed by public and private transportation.
Types of vegetation	Grass as ground cover, shrubs, shade trees, ornamental plants with varying sizes and colors.		

Source: Analysis Result, 2017.

2. Elements of Landscape Design at Parks in Central Semarang City

Elements of landscape design is one component in designing a landscape. The elements of landscape design of the parks in Semarang will be explained in the table below.

Table 2
Elements of Landscape Design at Parks in Central Semarang City

No.	Name	Elements of Landscape Design	
1.	Taman Pandanaran	Line	The lines are a combination of straight lines and curved lines.
		Field	The visible field element is a rectangular field.
		Space	The space emphasized in this garden is a circular transparent space.
		Form	The statue of Warak Ngendok is placed in the middle of the park and serve as a new icon for the city of Semarang.
		Texture	It is clearly visible on the composition of an attractively designed garden floor pavement.
2.	Taman Menteri Supeno	Line	The lines are dominated by curved lines.
		Field	Dominated by circle shape.
		Space	The space formed includes a circular transparent space.
		Form	Public restroom buildings and merchant.
		Texture	Texture can be seen from the pavement provided for pedestrians with some smooth or rough point.
3.	Lapangan Pancasila Simpang Lima	Line	The element of the line is dominated by a straight line.
		Field	The visible field element is a rectangular field.
		Space	The space formed includes a square transparent space.
		Form	The shape element can be clearly seen from the wall with the park's name on it.



4.	Taman Tugu Muda	Texture	The texture can be seen from the pedestrian ways pavement.
		Line	The element of the line is in the form of straight line elements and curved lines.
		Field	Applied in square shape.
		Space	The visible space is a transparent space with a circle shape.
		Form	The form of the park can be seen from the monument in the middle of the park which is a landmark of Semarang City and sculpture in the form of bamboo spears.
5.	Bundaran Taman Jalan Pemuda	Texture	Demonstrated on various vegetation arrangements and pavement of the pedestrian ways.
		Line	The line element is a straight line.
		Field	The element of the field is the square and rhombic plane.
		Space	The space element is created in the form of a square transparent space.
		Form	Form elements can be identified from the vegetation arrangement and the presence of sculpture.
6.	Taman Jalan Imam Barjo	Texture	The texture element can be seen from the pavement arrangement applied to the road.
		Line	The line element is dominated by curved lines.
		Field	The field element is applied in a circle.
		Space	The space element is created in the form of a square transparent space.
		Form	The shape element is visible on the fountain pool in the middle of the garden.
		Texture	The texture element can be seen from the pavement arrangement applied to the road so it looks attractive.

Source: Analysis Result, 2017.

3. The Analysis of Landscape Design Principle of Parks Semarang

The principles of landscape design are the basis for the realization of a design or form engineering. The principles of landscape design should connected one another to result the expected design. Therefore, the design of the parks in Semarang has applied the principles of landscape design as described in table below:

Table 3
Principles of Landscape Design At Park in Semarang City

No.	Name	Principles of Landscape Design	
1.	Taman Pandanaran	Balance	The design of the garden is made symmetrical between the two sides of the garden footprint.
		Rhythm and Repetition	The repetition of colors and shapes on the pedestrian ways provides good visual.
		Emphasis and Accentuation	Warak Ngendok statue in the middle of the park applies the principle of emphasis in Taman Pandanaran.
		Simplicity	Every part is designed to maximize the function of the park.
		Contrast	Various plants in different colors.
		Proportion	The siteplan is ideal and well-balanced.
		Unity	This park has a good unity design principles as it fulfills all landscape design principles.
2.	Taman Menteri Supeno	Balance	A well-balanced design of triangle-shaped park.
		Rhythm and Repetition	The repetition of the line design to the path and the circular-shape space.
		Emphasis and Accentuation	The fountain placed in the middle of the park.
		Simplicity	Every part of the park is designed to maximize the function of the park itself.
		Contrast	The arrangement of the garden floor pavement which enhance the aesthetic visual of the garden gives a contrast look of the park.



		Proportion	A well-balance ratio of the size and the number of every part of the park.
		Unity	This park has a good unity design principles as it fulfills all landscape design principles.
3.	Lapangan Pancasila Simpang Lima	Balance	The balance of the square form of the park and the plants planted surrounding the park.
		Rhythm and Repetition	The trees, park benches, and dumpster are placed one after the other in a certain distance.
		Emphasis and Accentuation	This element can be seen clearly from a wall with the park name written on it.
		Simplicity	Every part of the park is designed to maximize the function of the park itself.
		Contrast	The pedestrian ways are paved in different colors to create a contrast visual.
		Proportion	A well-balance ratio of the size and the number of every part of the park.
		Unity	This park has a good unity design principle as it fulfills all landscape design principles.
4.	Taman Tugu Muda	Balance	The park is designed symmetrically between two pedestrian ways.
		Rhythm and Repetition	The repetition of colors and shapes on pedestrian ways and vegetation placement gives an interesting visual.
		Emphasis and Accentuation	The monument of Tugu Muda and fountain in the middle of the park.
		Simplicity	Every part of the park is designed to maximize the function of the park itself.
		Contrast	The use of plant colors and paving on the pedestrian ways.
		Proportion	Well-balance ratio of the size and the number of every part of the park.
		Unity	This park has a good unity design principle as it fulfills all landscape design principles.
5.	Bundaran Taman Jalan Pemuda	Balance	The park is designed symmetrically between two paths.
		Rhythm and Repetition	It can be seen from the settling of the plants and the pavement of the pedestrian ways. It can also be seen from the colors used on pedestrian paving paths.
		Emphasis and Accentuation	A fountains is placed in the middle of the park that attracts the attention of people.
		Simplicity	Every part of the park is designed to maximize the function of the park itself.
		Contrast	The plants are varied in types and size. Contrasting colors are applied the pavements.
		Proportion	Well-balance ratio of the size and the number of every part of the park.
		Unity	This park has a good unity design principles as it fulfills all landscape design principles.
6.	Taman Jalan Imam Barjo	Balance	The park designed symmetrically between the two sides paths.
		Rhythm and Repetition	Repeated plants settling.
		Emphasis and Accentuation	A statue that resembles a temple with several platforms.
		Simplicity	Every part of the park is designed to maximize the function of the park itself.
		Contrast	Plants in different size.
		Proportion	Well-balance ratio of the size and the number of every part of the park.
		Unity	This park has a good unity design principles as it fulfills all landscape design principles.

Source: Analysis Result, 2017.



4. The Analysis of Visual Aesthetic of Landscape of Parks in Semarang

Simonds (1983) mentions that aesthetics is a harmonious relationship of all elements or components perceived. The aesthetic quality of the landscape can be identified by comparing the physical conditions, landscape design elements, and landscape design principles of the parks in Semarang. The comparison is conducted by assessing the parks in the center of Semarang using the nominal data scale. The categories used in the assessment are 0 = poor; 1 = good; 2 = very good. The assessment of the parks can be seen as follows:

Tabel 4
Visual Aesthetic Analysis of Landscape At Parks in Central Semarang City

No.	Indicators	Variables	Park A	Park B	Park C	Park D	Park E	Park F	
1.	Principles of Landscape Design	Balance	2	2	2	2	2	2	
		Rhythm and Repetition	2	2	1	1	1	1	
		Emphasis and Accentuation	2	2	2	2	1	1	
		Simplicity	2	2	2	2	2	2	
		Contrast	2	2	1	2	1	1	
		Proportion	2	2	2	2	2	2	
		Unity	2	2	2	2	2	2	
2.	Landscape Function	Ecological	0	2	0	0	0	0	
		Social	0	2	2	1	0	0	
		Aesthetic	2	2	1	2	1	1	
3.	Quality of Parks	Hard Material	2	2	1	2	1	1	
		Soft Material	2	2	1	2	1	1	
		Facilities Completeness	1	2	2	0	0	0	
		Design of Park	2	2	1	2	1	0	
		View	2	2	1	2	2	0	
		Physical Condition	Access	2	2	2	0	0	2
		Maintenance	0	2	2	2	1	1	
Total Assessment			27	34	25	26	18	17	

Source: Analysis Result, 2017.

Information:

- A = Taman Pandanaran
- B = Taman Menteri Supeno
- C = Lapangan Pancasila Simpang Lima
- D = Taman Tugu Muda
- E = Bundaran Taman Jalan Pemuda
- F = Taman Imam Barjo

From assessment above, it can be seen that Taman Pandanaran has the highest value, while the lowest value is Taman Jalan Imam Barjo. Distinguished by its function as an active park and a passive park, then Taman Menteri Supeno is regarded as an active park with a high aesthetic



visuals, followed by Taman Pandanaran and Lapangan Pancasila Simpang Lima. Meanwhile, Taman Tugu Muda is identified as passive park with high aesthetic visual, followed by Bundaran Taman Jalan Pemuda and Taman Jalan Imam Barjo. All in all, parks with aesthetic visuals should be maintained properly so that it can be one of tourism destinations in Semarang.

D. Conclusion

City parks around Semarang is classified into two types parks; they are active parks and passive park. In the center of Semarang, there are Lapangan Pancasila Simpang Lima, Taman Menteri Supeno, Taman Pandanaran as an active park and Taman Tugu Muda, Bundaran Taman Jalan Pemuda, Taman Jalan Imam Barjo. The parks are attractively designed to meet the needs of Semarang's residents. Of the six parks, Taman Menteri Supeno has the highest aesthetic visuals because it is equipped with various elements of interesting garden, such as complete facilities, and various plants to cool the area off. In addition, there is a statue of KB as icon for this area.

Overall, the condition of the park is relatively good, adequately maintained, and well grown plants. However, there is a need for further attention to the maintenance of the park because there are still some damaged park facilities. The park has not serve its functions of absorbing pollution can be more optimal. The selection of elements of park also need to be considered so that the value of aesthetic quality of the park can be higher and it can be used by citizens.

Reference

- Arikunto, 2006. *Prosedur Penelitian: Suatu Pendekatan Praktik*. Jakarta: PT Rineka Cipta.
- Danier, L. 2015. *The Little Sustainable Landscape Book*. Oxford: Global Canopy Programme.
- Darmawan, Edy dan Andy Wijaya Nugraha. 2015. *Visual Estetika Taman Arsitektur Kota*. Semarang: Badan Penerbit Universitas Diponegoro.
- Frick, Heinz dan Tri Hesti Mulyani. 2006. *Arsitektur Ekologis*. Yogyakarta: Kanisius.
- Hakim, Rustam, dan Hardi Utomo. 2003. *Komponen Perancangan Arsitektur Lanskap (Prinsip-Unsur dan Aplikasi Desain)*. Jakarta : Penerbit Bumi Aksara.
- Jessel, B. 2006. *Elements, Characteristics, and Character Information Functions of Landscapes in Terms of Indicators*. Ecological Indicators 6: 153-167.
- Moleong, Lexy. 2002. *Metodologi Penelitian Kualitatif*. Bandung: PT. remaja Rosdakarya.
- Nassar JL. 1988. *Environmental Aesthetic*. New York (US): Cambridge University.
- Peraturan Menteri Dalam Negeri Nomor 1 Tahun 2007 tentang Penataan Ruang Terbuka Hijau Kawasan Perkotaan.
- Rob, Krier. 1979. *Urban Space*. London: Academy Editions.
- Sasongko, Purnomo Dwi. 2002. *Kajian Perubahan Fungsi Taman Kota di Kota Semarang*. Program Pasca Sarjana Magister Teknik Pembangunan Kota Universitas Diponegoro Semarang.
- Simonds JO. 1983. *Landscape Architecture*. New York: Mc Graw - Hill Book.
- Sugiyono. 2014. *Memahami Penelitian Kualitatif*. Bandung: Penerbit Alfabeta.
- Susiloarifin, Hadi dan Nurhayati. 1994. *Pemeliharaan Taman*. Jakarta: Penebar Swadaya.



A LUXURIOUS PREFABRICATED HOUSE: A DIFFERENT WAY OF UNDERSTANDING PREFABRICATION HOUSING

Rossa Turpuk Gabe^{a*}, Gregorius A Gegana A^{b**}, Ima Rachima^{c**}

^a*Departement of Architecture, Faculty of Engineering, Universitas Indonesia 16424, Depok*

^b*Departement of Architecture, School of Design, Universitas Pelita Harapan 15810, Tangerang*

^c*Departement of Architecture, Faculty of Engineering, Institut Sains dan Teknologi Nasional 12630, Jakarta*

ABSTRACT

In this modern age, prefabricated buildings have various benefits such as, faster, more sustainable, and more affordable. The prefabricated buildings have been mass produced for various purposes such as, temporary housing after disaster, low-income housing and temporary worker housing. A prefabricated house is believed eco-friendlier than a conventional house, because it produces lesser waste than conventional house. However, as common dwelling use, prefabricated construction for housing is not as popular as conventional brick-and-mortar house. A quick survey to companies that practice prefabrication reveals that prefab house is not popular as common housing for many people in Indonesia because an assumption of its non-permanent construction and its limited design preferences. In spite of these reasons, prefabricated house still can be made luxurious and well designed for upper class segment people. This paper presents examples of deluxe prefab houses and analyze the systems and methods. Furthermore, we compare the examples on their prefab systems and methods to common prefab houses which have been built in Indonesia. Finally, the investigation attempts to formulate how systems and methods of prefabrication can be made to enable prefab houses compete with traditional brick-and-mortar houses in providing luxurious and well-accepted dwelling.

Keywords: prefabricated house, a luxurious prefabricated house, prefab systems and methods



1. INTRODUCTION

Since the industrial revolution, prefabrication concepts and methods have been explored. Prefabrication originally took the basic form of developing systems, either conceptual or actual, that led to the production of parts that could be used in a variety of ways (Hilgeman, 2004). Modular prefab housing is faster, more sustainable and more affordable to build. (Nadim & Goulding, 2011)

Because of its fast and cheap characteristics, prefab house gains popularity for mass production as an ideal solution to provide low-cost housing or post-disaster housing. In western countries, prefab house became popular choice for mass development and housing rehabilitation after World War II. In developing countries, the growing concentration of people is obvious. A mass house project is one of the most established projects of the construction industry to provide affordable and high quality houses (Mostafa & Dumrak, 2014). This situation is also true for Indonesia. In addition of rapid people growth and urbanization, Indonesia's position in earth ring of fire makes the country vulnerable to various natural disasters. Aceh Tsunami in 2004 forced the Ministry of Housing to provide fast and mass produced emergency housing and rehabilitation. The solution is now developed and well known as RISHA (Rumah Instan Sederhana Sehat) to fulfill mass demand of low-cost housing as well as earthquake resistant.

Nowadays, in developed countries prefabricated housing is becoming increasingly popular because of its potential as sustainable building. Prefabricated housing has rapidly become more popular over the last few years as an affordable, eco-friendly and modern alternative housing. A unique benefit of using prefab systems is the ability to consider open-systems thinking, where a house may be flexible and re-configurable post-occupation (Luo, Riley, & Horman, 2005). These definitions help us to understand the potential of prefabrication housing, more than just providing fast and cheap housing demand.

However, housing choice and preference usually conforms to the society perspective about house itself. There is a lot of emotion involved in buying house (Koklic & Vida, 2011). Negative consumer perceptions are a significant barrier to develop a large market for prefabricated housing, even if some of these perceptions are not representative of the emerging industry (Dale, Karen, & Wendy, 2013). Prefabricated housing in Indonesia carries a stigma of cheap, low quality and temporary. This paper intends to examine prefabricated housing from its design innovation to gain a greater understanding of luxurious and well-accepted dwelling.



2. METHODOLOGY/ EXPERIMENTS

We conducted this research with the following questions: 1) How is the application of prefab house in Indonesia nowadays? and 2) How can the use of prefab house in Indonesia be developed further to provide sustainable and modern living? To answer those research questions, we conducted literature studies about various prefab house systems. Afterwards, we conducted 2 further literature studies about examples of prefab houses.

The first study is about examples of prefab houses that have been developed in Indonesia to understand how is the development of prefab house in Indonesia nowadays. The second study is about the application of prefab house overseas to compare with the development in Indonesia and to understand how is the development of prefab house can be pushed further. We limited the study on single family housing, therefore we omitted the prefab house for mass and industrial housing. We analyze the examples based on their specifications and prefab systems or prefab constructions. In the end, we compare the development of prefab house in Indonesia and overseas. We discussed all factors that can refine the application of prefab house to fulfill modern house lifestyle.

3. PREFABRICATED HOUSE

The term modular prefab system is a construction methods ranging from completely off-site and completely on-site (Nadim & Goulding, 2011). These methods promise an innovation which more environmentally friendly building practices. As we can see on Table 1, there are six different types of prefabricated housing systems: fully modular, sectional, panelized, precut, components, and chassis & infill (Huang & Krawczyk, 2006)

Table 1 Prefab House Types

Type	Description
Fully Modular	All components are assembled in factory as single complete 3D modules Module size is limited by transport (road and ship) constraints Requires only simple connection to foundation and MEP service connector
Sectional	Components are assembled as incomplete 3D modules for easy transport Requires additional components and treatments on site
Panelized	Only modular panels are made in factory Modular panels are usually for walls (structural/ infill), floor, roof, ceiling Structure is still constructed on site (cast in place) Requires panel assembly on site
Precut (wood)	Components are made in various shapes/ dimensions for various function The wood/ lumber components are numbered/ identified Requires on-site construction to assemble the woods as in a kit
Components/ Kits of Parts	Components are made in various shapes/ dimensions for various function The components are numbered/ identified Requires on-site construction to assemble the components
Chassis and Infills	The components are divided into 2 parts Chassis: prefab structural (posts and beams) 3D frame module Infills: Interchangeable panels for customization and adaptability Requires assembly on site or off site



4. THE USE OF PREFAB HOUSE TODAY

We take examples from 6 prefab house provider in Indonesia: RISHA, Mulya Bahtera Marina Industri, Sanwa Prefab Technology, Indocont, Domus, and J Steel.

Table 2 Prefab House in Indonesia

House Specification	Picture
<p>RUMAH INSTAN SEDERHANA SEHAT (RISHA) (Pusat Litbang Perumahan dan Permukiman Balitbang Kementerian PUPR Republik Indonesia, 2017) <u>Function:</u> Temporary Mass Housing Emergency/ Post-Disaster Housing Low-cost Permanent Single Family Housing <u>Unit Area:</u> 21-45 m2, 1-2 floor(s) <u>Features:</u> 2 bedrooms(s), 1 bathroom(s), living room <u>Prefab Systems:</u> Panelized: Precast Concrete</p>	<p>Figure 1 Rumah Instan Sederhana Sehat</p>
<p>MULYA BAHTERA MARINA INDUSTRI (PT Mulya Bahtera Marina Industri, 2015) <u>Function:</u> Permanent Single Family Housing <u>Unit Area:</u> 36-60m2, 1floor(s) <u>Features:</u> 2 bedrooms(s), 1 bathroom(s), living room, kitchen <u>Prefab Systems:</u> Light Steel frame, Fiber Cement, Paint finish, Metal roof</p>	<p>Figure 2 Mulya Bahtera Prefab House</p>
<p>SANWA PREFAB TECHNOLOGY (Sanwa Prefab, 2017) <u>Function:</u> Permanent Single Family Housing <u>Unit Area:</u> 60-96 m2, 1 floor(s) <u>Features:</u> 2 bedrooms(s), 1 bathroom(s), living room <u>Prefab Systems:</u> Panelized: Metal Panel</p>	<p>Figure 3 Sanwa Prefab House</p>



House Specification

Picture

INDOCONT

(Indocont Prefab, 2017)

Function:

Low-cost Permanent Single Family Housing

Unit Area: 36 m², 1 floor(s)

Features: 2 bedrooms(s), 1 bathroom(s), living room, kitchen

Prefab Systems:

Panelized: Composite styrofoam panel



Figure 4 Indocont Prefab House

DOMUS

(PT Tatalogam Lestari, 2017)

Function:

Low-cost Permanent Single Family Housing

Unit Area: 21-45 m², 1 floor(s),

Features: 2 bedrooms(s), 1 bathroom(s), living room, kitchen

Prefab Systems:

Chasis and Infills: Steel structure frame, Lightweight concrete blocks



Figure 5 Domus Prefab House

J STEEL

(PT Jaindo Metal Industries, 2013)

Function:

Low-cost Permanent Single Family Housing

Emergency/ Post-Disaster Housing

Unit Area: 36-65 m², 1 floor(s),

Features: 2 bedrooms(s), 1 bathroom(s), living room, kitchen, maid & storage, laundry & service, terrace

Prefab Systems:

Panelized: Steel frame, Calci-board composite panel



Figure 6 J Steel Prefab House



From all 6 prefab house providers in Indonesia, we can see that prefab house development in Indonesia is mainly used for low-cost housing or emergency/ post-disaster housing with total floor area less than 100 m², and typically only has 1 floor. Some of the providers claim that the cost to build 1 unit of house is less than IDR 100.000.000¹.

From prefab construction system, most of the house has Panelized prefab system with steel frame structure and wall panels. The foundation is casted in place concrete. The steel structure components are made in factory and assembled on site. Other components, such as wall, comes to the site in panels and assembled after the steel structures is constructed. As in ordinary 1-story house, the MEP systems are lined up on site and there is no special connection or treatment correlated with prefabricated panels or structure.

We observed 5 providers of prefab housing from various regions overseas: SCG Heim (joint with Sekisui Japan) in Thailand, Prebuilt Residential in Australia, BLU Homes in California, Karoleena in Canada, and NOEM in Spain. All of them are luxurious prefab house and price range around USD 100.000-1.000.000. Typically, it has 1-2 floors with total floor area around 100-500 m².

An interesting finding from this study is: all luxurious prefab houses use Fully Modular prefab construction system. The on-site works are the foundation, concrete floor bed, and base for MEP systems. The main structure, infill structure, wall panels, floor, ceiling, roof, and finishing are assembled as house modules (usually as big as one room) in manufacture plant. The MEP system is prepared inside the panels and ready to connect with the installation on-site. By doing the assembly in factory, the design details and craftsmanship can be done and measured more accurate. Moreover, this detail refining and design innovations can be enabled by recent technology in Architecture Engineering and Construction (AEC) industry such as Building Information Modeling (BIM) and CAM. It allows designers and engineers to do simulation and experiments to the space module arrangement and detail solution before actual construction on site. As a result, the house design can have more sophisticated appearance. Moreover, it can reduce a lot of on-site working which also reduce manual errors, construction cost, and pollution during the construction processes.

Although it can result accurate and sophisticated design, Fully Modular prefab system has a weakness on delivery to the site. It needs big containers and heavy machineries to assemble the module on site. Therefore, the restriction would be site accessibility. The site should be located in area that can be accessed by good road infrastructures for heavy and big vehicles.

¹ Based on articles at Kompas.com Properti:

- PT Kompas Cyber Media. (2015, September 22). Rumah Instan Buatan Indocement Hanya Rp 35 Juta Per Unit. Retrieved from Kompas.com Properti: <http://properti.kompas.com/read/2015/09/22/225930621/Rumah.Instan.Buatan.Indocement.Hanya.Rp.35.Juta.Per.Unit>
- PT Kompas Cyber Media. (2016, Mei 26). Biaya Bangun Rumah Permanen Domus Rp 19 Juta Saja... Retrieved from Kompas.com Properti: <http://properti.kompas.com/read/2016/05/26/114005521/biaya.bangun.rumah.permanen.domus.rp.19.juta.saja>.



Table 3 Luxury Prefab House

House Specification	Picture
<p>SCG HEIM, THAILAND (SCG-Sekisui Sales Co.,Ltd , 2015)</p> <p><u>Function:</u> Permanent Singe Family Housing <u>Unit Area:</u> 150-400 m2, 2 floors <u>Features:</u> 2-3 bedrooms(s), 3 bathroom(s), living room, dining room, garage for 2 cars, terrace & balcony</p> <p><u>Function:</u> House for Disability Care <u>Unit Area:</u> 100-200 m2, 1 floor <u>Features:</u> 1 bedroom(s), 2 bathroom(s), Caretaker room, Living & dining room</p> <p><u>Prefab Systems:</u> Fully Modular: Steel frame, Lightweight concrete panel, Ceramic finish</p>	
<p>PREBUILT RESIDENTIAL, AUSTRALIA (Prebuilt, 2016)</p> <p><u>Function:</u> Permanent Single Family housing <u>Unit Area:</u> 150-200 m2, 1-2 floor(s) <u>Features:</u> 3-4 bedrooms(s), 1-2 bathroom(s), 1-2 living room(s), dining room</p> <p><u>Prefab Systems:</u> Fully Modular: Steel & wood frame, Wood/ metal panel, Wood finish</p>	

Figure 7 SCG Heim Prefab House

Figure 8 Prebuilt Prefab House




House Specification	Picture
<p>BLUHOMES, CALIFORNIA (BLU Homes, 2017)</p> <p><u>Function:</u> Permanent Single Family housing</p> <p><u>Unit Area:</u> 60-570 m² 1-2 floor(s)</p> <p><u>Features:</u> 1-6 bedroom(s), 1-6 bathroom(s), living room, dining room, kitchen, garage add-on, cabin add-on</p> <p><u>Prefab Systems:</u> Fully Modular: Steel frame, Wood/ metal panel, Tile and Wood finish</p>	

Figure 9 BLU Homes Prefab House


<p>KAROLEENA, CANADA (Karoleena, Inc., 2016)</p> <p><u>Function:</u> Permanent Single Family housing</p> <p><u>Unit Area:</u> 70-276 m² 1-2 floor(s)</p> <p><u>Features:</u> 1-4 bedroom(s), 1-3 bathroom(s), living room, dining room, kitchen</p> <p><u>Prefab Systems:</u> Fully Modular: Steel frame, dry-wall/ metal panel, Tile and Wood finish</p>	
---	---

Figure 10 Karoleena Prefab House



House Specification	Picture
<p>NOEM, SPAIN (NOEM, 2014)</p> <p><u>Function:</u> Permanent Single Family housing</p> <p><u>Unit Area:</u> 95-200 m² 1-2 floor(s)</p> <p><u>Features:</u> 1-4 bedroom(s), 1-3 bathroom(s), living room, dining room, kitchen</p> <p><u>Function:</u> Vacation Cabin</p> <p><u>Unit Area:</u> 25-30 m² 1 floor(s)</p> <p><u>Features:</u> 1 studio unit, 1 bathroom</p> <p><u>Prefab Systems:</u> Fully Modular: Wood frame, Wood panel, Laminate and Wood finish</p>	

Figure 11 NOEM Prefab House

5. A COMPARISON: RETHINKING PREFABRICATED HOUSE

Compared to prefab house application overseas, prefab house definition in Indonesia is still limited to prefabricated materials, especially steel structure and wall panels, and also still requires a lot of manual works on site by labor. Moreover, the design and on-site construction solution are still the same as how to build a conventional house, which could lose its accuracy during on-site processes and have lack of innovation in design and details. As a result, the house made from prefabricated components looks dull and frail. In the end, this gives a stigma that prefab houses are cheap, low quality, and temporary houses.

Nevertheless, the prefabricated components need to be treated accurately. Due to their limitation in module size and requirements for precision in the joints, prefabricated components should enable innovation in design and detailing processes. However, the design innovation and detailing processes need to be in conjunction with the expanding skills of designers, engineers, and construction workers in handling prefabricated components. Designers and engineers have to be equipped with skills of utilizing recent technology in AEC industry, such as BIM, in order to enhance design innovation and detail refinement. Construction workers need to understand how to work with prefabricated parts and maintain its accuracy control.



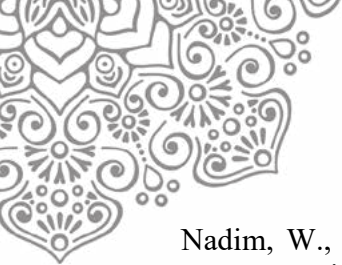
6. CONCLUSION

This paper has presented the recent application of prefabricated house in Indonesia compared with prefabricated house overseas. In addition, the paper also has been prepared in order to examine prefabricated housing from its design innovation to gain a greater understanding of luxurious and well-accepted dwelling. This study has revealed that limited design innovation is the central to understand why prefabricated house in Indonesia not popular for a luxurious modern house. The findings of this study indicate that prefabricated house in Indonesia has crucial problems, especially inability on transforming each component to innovation system for greater use of prefabrication. There is limited design innovation between connection of the prefabricated panels or structure with its systems and details. The findings also suggest that prefabricated house as an open-system thinking has enabled wide opportunities for designers and engineers to create ideas and innovation for a luxurious design.

However, this study does not review effects of regulations and government policies which potentially influence in encouraging greater use of prefabrication house in Indonesia. More detailed aspects are needed to generate more comprehensive analysis for further study of the potential of prefabricated house in Indonesia, especially to provide a sustainable and a modern living.

7. REFERENCES

- BLU Homes. (2017). *Homes*. Retrieved from BLU Homes: <https://www.bluhomes.com/homes-landing>
- Dale, S., Karen, M., & Wendy, M. (2013). *Reshaping Housing - The Role of Prefabricated Systems*. Queensland: Queensland University of Technology.
- Hilgeman, J. (2004). *A Prefabricated Framing and Enclosure System: Economy, Flexibility, and Applications*. Washington: University of Washington.
- Huang, J. C., & Krawczyk, R. J. (2006). Integrating Mass Customization with Prefabricated Housing. *Re-Thinking the Disclosure: The Second International Conference of the Arab Society for Computer Aided Architectural Design*, (pp. 124-136).
- Indocont Prefab. (2017). *Rumah Prefab*. Retrieved from Indocont: Supply & Aplikator Kontraktor: <http://www.indocont.com/page11.php>
- Karoleena, Inc. (2016). *Designer Prefab Homes. Ready in 6 months, delivered anywhere*. Retrieved from Karoleena: <http://karoleena.com/>
- Koklic, M., & Vida, I. (2011). Consumer Strategic Decision Making and Choice Process: Prefabricated House Purchase. *International Journal of Consumer Studies*, 634-643.
- Luo, Y., Riley, D. R., & Horman, M. J. (2005). Lean Principles for Prefabrication in Green Design-Build (GDB) Projects. *The 13th International Group for Lean Construction Conference*, (pp. 539-548).
- Mostafa, S., & Dumrak, J. (2014). Synergistic Supply Chain for Prefabricated House Building in Developing Countries. *International Journal of Advanced Research in Engineering and Technology*, 100-111.



- Nadim, W., & Goulding, J. S. (2011). Offsite Production: A Model for Building Down Barriers: A European Construction Industry Perspective. *Engineering, Construction, and Architectural Management*, 81-101.
- NOEM. (2014). *Home*. Retrieved from NOEM: <http://www.noem.com/en/>
- Prebuilt. (2016). *Prebuilt Residential*. Retrieved from Prebuilt Residential: <http://www.prebuilt.com.au/>
- PT Jaindo Metal Industries. (2013). *Products*. Retrieved from J Steel: <http://www.jsteel.co.id/products>
- PT Kompas Cyber Media. (2015, September 22). *Rumah Instan Buatan Indocement Hanya Rp 35 Juta Per Unit*. Retrieved from Kompas.com Properti: <http://properti.kompas.com/read/2015/09/22/225930621/Rumah.Instan.Buatan.Indocement.Hanya.Rp.35.Juta.Per.Unit>
- PT Kompas Cyber Media. (2016, Mei 26). *Biaya Bangun Rumah Permanen Domus Rp 19 Juta Saja...* Retrieved from Kompas.com Properti: <http://properti.kompas.com/read/2016/05/26/114005521/biaya.bangun.rumah.permanen.domus.rp.19.juta.saja>.
- PT Mulya Bahtera Marina Industri. (2015). *Rumah Baja*. Retrieved from PT Mulya Bahtera Marina Industri: www.besibesi.com/page/rumah-baja
- PT Tatalogam Lestari. (2017). *Domus: Rumah Permanen Instant*. Retrieved from PT Tatalogam Lestari: <http://tatalogam.com/portfolio/domus/>
- Pusat Litbang Perumahan dan Permukiman Balitbang Kementerian PUPR Republik Indonesia. (2017). *RISHA (Rumah Instan Sederhana Sehat)*. Retrieved from Pusat Litbang Perumahan dan Permukiman: Badan Penelitian dan Pengembangan Kementerian Pekerjaan Umum dan Perumahan Rakyat: <http://puskim.pu.go.id/risharumah-instan-sederhana-sehat/>
- Sanwa Prefab. (2017). *Our Product*. Retrieved from Sanwa Prefab Technology: <http://sanwaprefab.co.id/>
- SCG-Sekisui Sales Co.,Ltd . (2015). *รู้จักกับเอสซีจี โฮม*. Retrieved from SCG Heim: The Ultimate of Living: <http://www.scgheim.com/home/>



CHOREOGRAPHING FLOW AND PAUSE: INHABITING TRANSITIONAL SPACE

Enira Arvanda^a, Amy K. Marku^{b*}

^aUniversitas Indonesia, Depok 16424, Indonesia

^bUniversitas Indonesia, Depok 16424, Indonesia

1. Abstract

Pedestrian underpass is a transit space commonly found in urban space. As the name suggests, it is a structure that enables the act of passing through underground tunnel. Architecturally, this type of space is typically utilitarian, straightforward and only serves the act of walking from one point to another within the city. For its users, underpass is just a vessel that contain and direct their movements, a space without further meaning that no one could really related to. Thus, it fits perfectly with Marc Auge's description of '*non place*'. Furthermore, user's detachment from this space and its spatial characteristics could trigger anxieties.

This paper suggests that pedestrian underpass has more potentials rather than just being a channel for mobility. As walking is an embodied act, if one's body could engage with its environment, in result, meaningful relationship between the body and the space could be formed. Bodies could temporarily inhabit space through events produced in-between/while moving from one destination to another. Thus, the idea of stasis in space of movements need to be explored, it is to find balance between act of walking (flow) and act of momentary stopping (pause). The dynamics of flow and pause within the pedestrian underpass will enable users to engage with the space, hence, changing it from non-place to place.

Case study for this paper is an underpass in Kota Tua, Jakarta, which applied cross-programming, mixing utilitarian with commercial use. In result, the writer found that flow and pause in transitional space need to be choreographed carefully and accordingly. Various public uses can be integrated within its spatial program, along with careful planning of interior architectural elements, which consider behavioral, ergonomic and psychological aspects of its users. This will result underground passage as a 'habitable' place.

Keywords: movements; transit space; pedestrian underpass; interior architecture

2. Introduction

This paper begins with the authors' fascination with underground transit spaces. Being practically in juxtaposition with the ground space, yet everything in the space below is so contradictory. Being underground feels otherworldly and gives off strong negative atmosphere to human. Along with gained interest in utilization of underground spaces in Jakarta (especially due to its ongoing MRT project) the authors feel the urgency to study its impact on people, spatial design aspects that alleviates its negative presence, well-being of people while being underground and especially in exploring possibilities of spatial engagement within this space. Underground transit space will be dissected from the perspective of interiority, which is quite a rare topic in the field of Interior Architecture.

3. Methodology

Objective of this paper is to discuss about the possibility of inhabiting pedestrian underground passages through movements and other gestures that could encourage engagement and connections. Thus, the authors explored some theoretical idea connected with mobility and urban context, particularly from scholar Ole B. Jensen, that explores

* Corresponding author.

E-mail address: enira.arvanda28@gmail.com, amymarku@gmail.com



mobility as 'pleasurable movement' within the city' (Jensen 2009). Along with other references about walking as an embodied practice (Lorimer 2011; Livesey 2004; Urry 2000; Edensor 2010), potentials of underground space and tunnels (Lanng 2016; Hasse 2016; Spencer 2010; Hunt et al. 2016), transit space as public realm (Livesey 2004; Worrell 2011) also on behavior and gestures at transit space (Bissell 2010; Bissell 2009; Löfgren 2008; Hagen et al. 2009).

Synthesis from literature studies became foundation to analyse the case study, a pedestrian underpass in Kota Tua Jakarta, which according to authors is an interesting example of how temporary inhabitation in transit space were enabled by events and practiced by pedestrians movements and occupations through cross-programming and atmospheric interior. Data collection were done by direct observations, while photographs, videos and architectural drawings were used as tools for analysis. The study was part of an Interior Architecture Studio Project in Universitas Indonesia, thus some observational photographs and diagrams belong to students. But further study and analysis were done by authors.

4. Literature Studies

Definition Of Pedestrian Underpass

Underpass is a passage that runs under something. According to Meriam-Webster Dictionary, Passage is the "the action or process of passing from one place, condition, or stage to another; a way of exit or entrance : a road, path, channel, or course by which something passes; a continuous movement or flow; a specific act of traveling or passing especially by sea or air" (Meriam-Webster Dictionary 2017). The word passage unites movement with the constructed entity, it is the defined linear space through which people, products and information may pass (Livesey 2004).

According to Design Guideline for Pedestrian Network in Urban Area issued by the Indonesian Ministry of Public Works (Kementrian Pekerjaan Umum 2014) pedestrian underpass is a street crossing facility for pedestrian which is located below ground. Pedestrian underpass can also act as building connector, so people can travel between blocks of buildings without having to go outside of it. Or, it can perform as an annex from transit station or interchange to the surrounding areas. Access to the underpass has to be connected with the pedestrian system above. Other than functional and safety aspects, the guidelines has actually recognised the need for comfort, aesthetic, and possibility for connections and interactions (Kementrian Pekerjaan Umum 2014), but there's no further explanation about the indicators for those aspects.

Potentials and Challenges Of Underground Passage

Albeit studies of underground space that clearly state its benefit and potentials (Hunt et al. 2016; Belanger 2007; Labbé 2016), it suffers from people's negative impression. Studies found that it's being labelled so because of its aseptic and claustrophobic atmosphere (Carmody & Sterling 1987; Hasse 2016). Other concerns that might also lead to underutilization of underground space are of technical difficulties and high initial costs and operating costs (Hunt et al. 2016)

Negative psychological effect occur in underground spaces are resulting from its physical properties which are fully enclosed, detached to the aboveground, no visual connection to its surrounding, often bare and sterile. These spatial qualities often triggered misconduct behavior or even crime to happen (Carmody & Sterling 1987). For some people, especially women (Loukaitou-Sideris et al. 2009; Loukaitou-sideris 2012; Valentine 1990), fear of crime, or the feeling of being victimized or powerless, vulnerable and anxious, could be triggered because of the unknown nature of underground space.



In result, to alleviate fear and other negative perceptions, people tend to behave defensively, by reducing proximity to others, avoiding visual contact with strangers, speed-walking and protecting belongings closer to their bodies. Negative affection with space will result minimum engagement with space, discouraging other possibilities than just movement through space.

Passage as Living Space

In many cities, streets are extension of dwellings, thus a living space. The intertwine of building and streets enabled people to engage with the space, hence traditional streets are also vital public space, they function as corridors or even front yard, where people informally meet, gather and connect with each other (Livesey 2004). Since underground pedestrian system is also a part of the city's street network, it's necessary for the underpass to have the same livable qualities as its above counterpart.

On Walking

For Certeau, there's no space without movements, space is a performed place, which activated by ensemble of movements (Certeau 1988). Inside the underground passage, movements, primarily by walking, construct its interiority. According to Ingold, the walk is an event, the walker is the human subject and walking is an embodied act (Ingold 2011). A walk can be understood as a cultural activity that is made distinctive and meaningful by the physical features and material textures of place (Lorimer 2011). Thus, it can also be said that there's an affective relationship between the walker and place, activated by spatial elements and atmosphere, responded with emotion, activities and gestures by the walker (Bissell 2010). In result, 'dwelling-in- motion' emerges (Sheller and Urry 2006).

Moving inside the passage

There are different modes of walking (strolling, wandering, marching..to name a few). Walking produces time-space and the experience of a place (Certeau 1988). The ensemble of place-time-human movements create rhythm, which are specific from one time-location to another (Edensor 2010). Walking rhythms are adaptive to circumstances and qualities of space, which are responded by altering pace, ways of walking, pausing, and other gestures (Edensor 2010).

Bisell (Bissell 2007) argued that, in everyday mobility, immobility is also part of the journey, or what he rather call 'inactivity'. Hence, waiting or pausing for a while, is an event which experienced affectively by the body. For that reason, experience inside a passage should be understood more than just the act of getting from point A to B through series of movements. We should also consider about the senses and emotions involved while someone walks or stops, also the qualities of space which affect the overall experience. For example, being inside a passage full of strangers is not always perceived as negative experience, there can be tactile pleasures from walking in a crowd, from an embodied participation as one co-ordinates one's body with that of the moving mass of other bodies (Shields 1997a: 25). Walking requires a tactic to maintain one's flow, he must be aware of the surroundings and events that occurs expectedly or unexpectedly. In one's overall journey through a passage, ensemble of movements and stillness produce rhythm, thus create sense of place.

Flow and Pause: Choreographing Movements & Engagements

Space is activated when there are events that encourage people's interaction, connection and occupation. Temporary occupation in transit space will encourage inhabitation hence will cultivate public life. Hinkel argued that, design insertions into public space could possibly



support the development of new relationships, between people and people, between people and places, even people and things. (Hinkel 2009).

So, the new paradigm of transportation architecture should not only excel at functional level, but also at aesthetic level and atmospherically could regulate society's emotional relationship with mobility (Hasse 2016). Ditte Bendix Lanng (2016) explored the feeling of travelling through a tunnel and sought the potential atmospheric qualities of transit space design. She proposed a design which invited people to engage with the materiality of the tunnel, and providing possibilities for different kind of gestures and activities. As stated by Lanng, architecture of the passage and its materiality might allow various affordance to pedestrians, hence allowing self-programming and become self-organising public space (Lanng 2016). Rather than pre-programmed events (like the passage in Kota Tua), the self-programmed architecture offer pedestrian to experience their journey through the underpass, regarding to their own version of interiority.



Fig.1 Tunnel architecture that invites people to interact through its form and materiality (source: Lanng 2016)

5. Case study

1. Site and Context

The case study taken for this paper is a pedestrian underpass located in Kota Tua area which connects Jakarta Kota Railway Station with Trans Jakarta Station and Mandiri Museum (see fig.2).



Fig. 2: Kota Tua Underpass Before Renovation. monofunctional and stark atmosphere (Source: Arvanda 2015)



The underpass mainly accessed by people coming to and from Jakarta Kota Railway Station and Trans Jakarta Station, both are important nodes in the area. Thus, the underpass also serves a major role as connectors between these two nodes. According to the design guidelines issued by the Ministry of Public Works (2014), Kota underpass has to fit requirements for "D" standard. This means that the underpass can be accessed in normal speed by pedestrians, but altering positions by changing lines might also happen due to conflicting flows and crowding. To achieve the required condition with minimum possibility of frictions between pedestrians, the minimum width of 1,2-2,1m²/person and pedestrian flow of 33-49 person per minute/meter have to be regarded.

The Kota underpass was built in 2005 And it became the first public pedestrian underpass facility in Jakarta which design feature was prominent. Seemingly, the municipal was well aware of its importance and prime location, therefore it was carefully designed to meet the requirements of good public facility. Entrance heading downward to the underpass was noticeable because of its contrast of form and materiality from the surroundings. Although the interior was mainly stark and monofunctional, in the middle of the tunnel lies a pleasant surprise, an open area with water fountain at its center which gives a nice break after being enclosed underground.

2. Cross-programming the Tunnel

After roundabout 10 years of operation, the Kota underpass started to dilapidate. Based on our previous study of the underpass in 2015, many pedestrians were feeling anxious when accessing this underpass (Arvanda 2015), especially women and mostly at night. The anxieties were caused by internal factors (decaying interior-architectural elements, bare atmosphere, lack of surveillance, etc) and external factors (lack of maintenance, occupation by the homeless and certain community, illegal conduct). Causes of anxiety and fear of crime were all relevant to findings from theories and research references (Valentine 1990; Carro et al. 2008; Loukaitou-Sideris et al. 2009).

In 2016, the underpass interior had gotten renovated, which seemingly address primarily on the safety aspects of the underpass. As preventive attempt for illegal occupation and misconduct activities, cross-programming was introduced to the passage. Commercial activities were injected within the existing spatial program.



Fig.3 Kota Tua Underpass After Renovation: pedestrians occupied the space
(Source: <http://poskotanews.com> ; <http://assets.kompas.com>)

3. Spatial Analysis – Flow And Pause

Apparently, the presence of commercial activities help to enliven the underpass' atmosphere. The previously stark tunnel interior is now enlightened by colorful goods from the sellers' booths. Inside the tunnel, presence of sellers give pedestrians a chance and reason to momentary stop in between their transit journey. The sellers produce events in which



responded by pedestrians through their movements and gestures. The once loosely populated corridors are now crowded with people of various purposes : those who use the passage as it is, those who stroll around leisurely, those who watch others, those who sit and relax, those who wait, etc. The new program has successfully altered people's movements, activities and gestures.

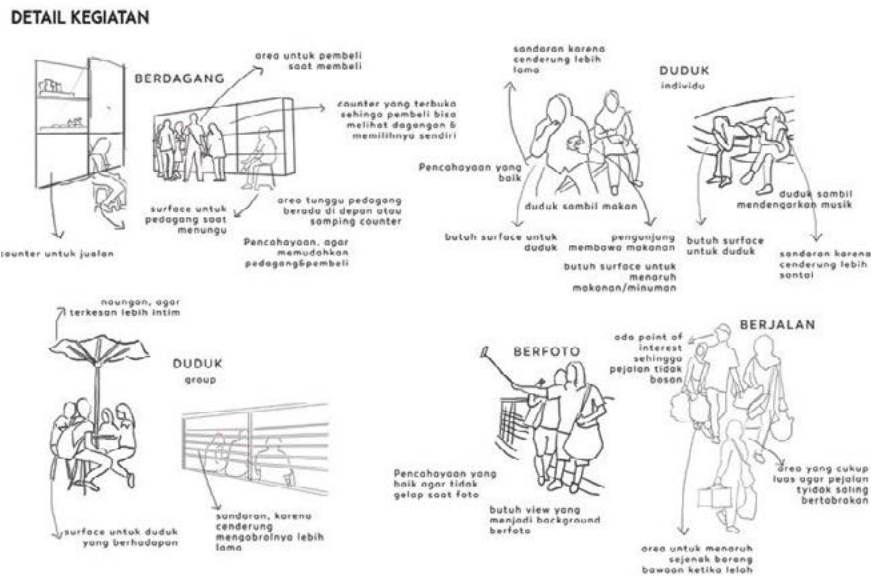


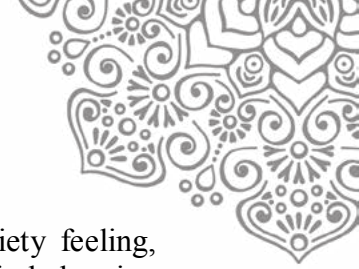
Fig. 4 various activities and gestures inside the underpass (Source: Intan Astari 2016)

Alteration of the underpass also has impact on the fountain area. Before the renovation, fountain area was perceived as negative space and avoided because it was oftenly occupied by group of homeless people and punk community. Now, it becomes the center of attraction. Decorative objects (fake plants, seasonal decorations, etc) which are placed around the fountain and the ramp also have its share to uplift the atmosphere. Around the edges of the fountain now has become a preferred space for momentary pause: meeting and gathering location, as well as a favourite photo spot. People's gestures around this area seemed to change a little bit, they become less alert and their rhythm slowed down. Some people even walked leisurely while going up to the ramp that leads to the exit/entrance gate.



Fig.5 Crowding inside the underpass (Source: beritajakarta.com)

The downside of the new spatial arrangement is placement of sellers take up too much space that it ends up interrupting pedestrian flows. Although the design of seller's booth is quite compact, the planner seemingly didn't consider how much space will be used when crowds



accumulate around the sellers. The presence of crowds are the source of anxiety feeling, which are reflected through people's gestures, they walk faster and keep their belonging closely attached to their bodies to maintain their social distance and proximity to others. Wayfinding in the tunnel also becomes more difficult because people can hardly see where and what happen at the end of the tunnel. The flow inside the tunnel becomes unpredictable because there are too many elements and crowds that interfere. Oftentimes, pedestrians are pausing not because they want to engage with the space, but because something or someone is blocking their way.

4. Choreographing Flow And Pause

For any transit space, flow of movements is the main objective for its existence, thus it becomes the focus of architecture of the passage. However, from literature studies and field observation, authors realized that in everyday mobility, there are actually various movements (flow) and non-movement (pause) in the overall journey of a pedestrian inside the underground passage. Those variety of flows and pauses are gestures in response to spatial qualities and behavior of others/strangers, or in Certeau's word, the pedestrians bodies are performing spatial tactics.

Momentary pause is a gesture that come from pedestrians in respond to certain situations and their surroundings which is consciously done and resulting positive feedbacks and experience for their overall journey. Momentary pauses can be abrupt and short (taking pictures,checking on spatial features, etc) but it can also be thoughtful and longer (sitting,resting,waiting for others,etc). Motives for those gestures are various, but certainly physical and atmospherical attributes of space play a big role in affording those pauses.

In contrary, unwanted pauses are gestures that performed consciously or unconsciously in respond to situations and surroundings, that result negative emotion. Unwanted pause is an obstacle to flow, which produced by crowding (bumping into strangers,unwanted physical contact with others,long queue,etc) or spatial attributes that might interrupt flow.

Coreographing movements inside the passage doesn't mean to shift the primacy of flow, rather to afford pedestrians with various gestures,that in the end will help them to create spatial engagements. There are no exact formula in composing flow and pause, rather than sensibilities from architects as planners who has to be well aware of the physiological and psychological aspects of walking inside the underpass, in the end it will also depends on the kind of scenario architects are planning for pedestrians.

Conclusion

From the case study we learned that the pedestrian underpass as non-place could potentially be transformed into public realm when complimentary programs were allowed to coexist within its utilitarian function. Although, the injected programs have to be carefully chosen, not to interrupt its initial function as a channel for mobilities. As various events were produced, spatial occupation will occur, thus new interiority of the underpass will emerge. A sense of place could be formed by its spatial quality through the role of interior elements that produce atmospheric and sensorial effects.

From the case study we also learned that spatial elements could act as choreographer of movements. Objects such as seatings or vending machines might suggest a pause, smooth walking surfaces might trigger continous flow, while advertisings on the wall might cause flow to slow down.

Different kind of movements would also trigger different emotions, monotonous flow would exude boredom, while chaotic pattern of flow would trigger anxiety and disorientation. These choreographed movements, in return will produce sense of engagements with space, resulting positive or negative affect from users or pedestrians. In result, spatial engagement would



trigger temporary inhabitation (or dwelling-in motion, a term suggested by Sheller&Urry), users would alternate their walking rhythm and change their behavior and gestures to a more relax and flexible state, allowing connections and interactions with the space and other people.

Acknowledgement

The authors would like to show gratitude to students from Interior Architecture Design Studio 5 at Interior Architecture study program, Universitas Indonesia. Some materials (photographs and diagrams) shown in the paper are part of their initial observations for the studio project. All materials are respective to their owners and authors have been granted permission to use them with credit.

References

- Belanger, P., 2007. Underground landscape : The urbanism and infrastructure of Toronto ' s downtown pedestrian network. *Tunnelling and Underground Space Technology*, 22, pp.272–292.
- Bissell, D., 2007. Animating Suspension: Waiting for Mobilities. *Mobilities*, 2(2), pp.277–298. Available at: <http://www.tandfonline.com/doi/abs/10.1080/17450100701381581>.
- Bissell, D., 2009. Conceptualising differently-mobile passengers: geographies of everyday encumbrance in the railway station. *Social & Cultural Geography*, 10(2), pp.173–195. Available at: <http://www.tandfonline.com/doi/abs/10.1080/14649360802652137>.
- Bissell, D., 2010. Passenger mobilities: Affective atmospheres and the sociality of public transport. *Environment and Planning D: Society and Space*, 28(2), pp.270–289.
- Carmody, J.C. & Sterling, R.L., 1987. Design Strategies to Alleviate Negative Psychological and Physiological Effects in Underground Space. , 2(1), pp.59–67.
- Carro, D., Valera, S. & Vidal, T., 2008. Perceived insecurity in the public space: personal, social and environmental variables. *Quality & Quantity*, 44(2), pp.303–314. Available at: <http://link.springer.com/10.1007/s11135-008-9200-0> [Accessed June 19, 2014].
- Certeau, M. de, 1988. *The Practice of Everyday Life*, London: University of California Press.
- Edensor, T., 2010. Walking in rhythms: place, regulation, style and the flow of experience. *Visual Studies*, 25(1), pp.69–79. Available at: <http://www.tandfonline.com/doi/abs/10.1080/14725861003606902>.
- Hagen, M. Van, Pruyn, A. & Kramer, J., 2009. Waiting Is Becoming Fun ! the Influence of Advertising and Infotainment on the Waiting Experience. *Transport*, (October), pp.6–8.
- Hasse, J., 2016. Traffic Architecture: Hidden Affections. In M. Bille & T. F. Sørensen, eds. *Elements of Architecture: Assembling Archaeology, Atmosphere and The Performance of Building Spaces*. New York: Routledge, p. 177.
- Hinkel, R., 2009. Occupation within Urban Conditions. In *Occupation: Negotiations with Constructed Space*. pp. 1–8.
- Hunt, D.V.L. et al., 2016. Liveable cities and urban underground space. *Tunnelling and Underground Space Technology*, 55, pp.8–20.
- Ingold, T., 2011. *Being Alive: Essays on Movement, Knowledge and Description*, New York: Routledge.
- Jensen, O.B., 2009. Flows of Meaning, Cultures of Movements – Urban Mobility as Meaningful Everyday Life Practice. *Mobilities*, 4(1), pp.139–158. Available at: <http://www.tandfonline.com/doi/abs/10.1080/17450100802658002> [Accessed June 5, 2014].
- Kementrian Pekerjaan Umum, 2014. *Pedoman Perencanaan. Penyediaan, dan Pemanfaatn Prasarana dan Sarana Jaringan Pejalan Kaki di Kawasan Perkotaan*, Indonesia: Kementrian Pekerjaan Umum.



- Labbé, M., 2016. Architecture of underground spaces : From isolated innovations to connected urbanism. *Tunnelling and Underground Space Technology*, pp.1–23.
- Lanng, D.B., 2016. How does it feel to travel through a. *Ambiances*, (October 2014). Available at: <http://ambiances.revues.org>.
- Livesey, G., 2004. *Passages: Explorations of the Contemporary City*, Calgary: University of Calgary Press.
- Löfgren, O., 2008. Motion and Emotion: Learning to be a Railway Traveller. *Mobilities*, 3(3), pp.331–351. Available at: <http://www.tandfonline.com/doi/abs/10.1080/17450100802376696>.
- Lorimer, H., 2011. Walking: New Forms and Spaces for studies of pedestrianism. In T. Cresswell & P. Merriman, eds. *Geographies of Mobilities: practices, spaces, subjects*. Ashgate.
- Loukaitou-sideris, A., 2012. Safe on the Move: The Importance of the Built Environment. In V. Ceccato, ed. *The Urban Fabric of Crime and Fear*. Springer.
- Loukaitou-Sideris, A. et al., 2009. *How to Ease Women ' s Fear of Transportation Environments: Case Studies and Best Practices*, San José, CA.
- Spencer, K., 2010. *Flow and Pause: Exploring human movement within a transit interchange*. University of Manitoba.
- Urry, J., 2000. *Sociology Beyond Societies. Mobilities for the Twenty-First Century* J. Urry, ed., New York: Routledge.
- Valentine, G., 1990. Women ' s and the Design Fear of Public Space. *Built Environment*, 16(4), pp.288–303.
- Worrell, V., 2011. *Inhabiting the Transitional*. Carleton University. Available at: http://www.openpsychodynamic.com/?page_id=32.



QIR

*The Westin Resort
Nusa Dua, Bali*
24-27 July 2017

**The 3rd Biannual Meeting
on Bioprocess engineering**





BATCH STUDIES OF CADMIUM (II) BIOSORPTION BY DRIED *Aphanothece sp* BIOMASS FROM CARBON DIOXIDE FED PHOTOBIOREACTOR SYSTEM

Awalina ^{a,b}, Eka Oktariani ^a, Ardiyan Harimawan ^a, and Tjandra Setiadi ^a

^a Department of Chemical Engineering-The Faculty of Industrial Technology, Institut Teknologi Bandung, Jln. Ganessa No.10, Bandung 40132

^b Research Center for Limnology-The Indonesian Institute of Sciences, LIPI Cibinong Science Center, Cibinong-Bogor 16911

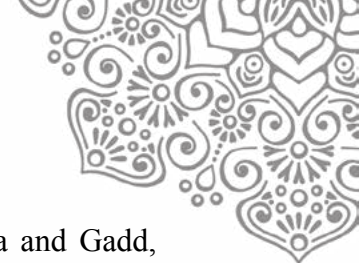
ABSTRACT

Dried biomass of *Aphanothece sp* (Cyanobacter) was produced from a photobioreactor system fed with 15% (v/v) carbon dioxide gas and employed as a biosorbent in batch biosorption test of cadmium (Cd) (II) ions from aqueous phase. It was conducted as function of pH, biomass concentration, and solution temperature as well as contact time. The optimum operational condition was achieved at pH, biomass concentration, temperature and contact time of 8 ± 0.1 , 0.1 g/L, 30°C and 60 minutes respectively. The equilibrium isotherm data was most fitted well with Langmuir model and Dubinin-Radushkevich (D-R) isotherm models. Hence, it means the biosorption process proceed in monolayer with maximum uptake capacity of 60.24 mg/g (at initial Cd concentration range of 0.29 to 7.13 mg/L or low concentration range) and 526.23 mg/g (at initial Cd concentration range of 5.41 to 83.07 mg/L or high concentration range). The mean of the free energy derived from D-R isotherm model, resulted 12.91 kJ/mol both at those two range of initial Cd concentrations suggested that chemisorption was occurred. The calculated thermodynamic parameter ($\Delta G = -8.39$ to -10.88 kJ/mol, $\Delta H = -49.78$ kJ/mol and $\Delta S = -0.13$ kJ/mol) indicated that biosorption process was feasible, spontaneous and exothermic under observed condition. Experimental data followed better to pseudo second order kinetics with $k_2 = 1.06E-01$ to $1.68E-01$ g/mg.minute at low concentration range and $1.52E-03$ to $5.2E-03$ g/mg.minute). Further, the repetitive reusability of dried *Aphanothece sp* biosorbent can be done for three cycles with HCl 1 M as eluent. In comparison with biosorbent produced from atmospheric carbon dioxide fed photobioreactor, the biosorbent used in this study gave five higher in magnitude of maximum biosorption capacity. It indicated a prospective usage of this biosorbent not only as cadmium biosorbent but also a carbon dioxide bio fixer.

Keywords: Biosorption, *Aphanothece sp*, Cadmium, Isotherm equilibrium, Kinetics, Thermodynamics

1. INTRODUCTION

Industrial activities have led to mobilize heavy metals in aquatic system. This problem must be regarded as serious concern since these element have severe toxic impacts on human's health and other organisms. Aquatic environment is frequently received improper treated metal borne waste water streams. It will cause a significant environmental problem since heavy metals are non- bio degradable and prone to bio-accumulated through aquatic food chain. Cadmium (Cd) is one of those toxic metals that posed great potential hazard to human and the aquatic ecosystem. Due to some of its deleterious effects on organisms, including humans, it is considered as a priority pollutant. It also known that Cd has wide range of usages in industrial processes such as electroplating, batteries, paints, and plasticizers, etc. which discharged into water bodies. Consequently, in recent decades, there is a need to explore the proper technology



for Cd removing from industrial discharge effluents (Chojnacka, 2010, Fomina and Gadd, 2014).

The existing conventional methods for removing metal ions, such as physical/chemical precipitation, ion exchange, electrochemical deposition, evaporation, adsorption, reverse osmosis, etc., are expensive and less efficient when applied to treat low metal content in the range of 1 to 100 mg/L. Mostly, these methods require high quantity of reagents as well as energy. Therefore, new affordable technologies are needed to overcome those problems. And with that purpose, Biosorption based technology is immensely intriguing to be implemented. This implementation of biomaterials as metals biosorbents, compared to other methods, is more effective and inexpensive. Not to mention, this method also offers an eco-friendly approach for remediation of metal contaminated waters (Kaur and Bhatnagar, 2002, Volesky, 2001). However, there are still few studies regarding of microalgae to its ability to remove Cd, particularly on kinetic, isotherm, and thermodynamics of this process along with information on its repetitive use. In this study, an indigenous cyanobacter named *Aphanothece sp* was isolated from a polluted urban lake Situ Rawa Kalong-Depok. Situ Rawa Kalong, located on an area surrounded by a least five chemical/metal processing based industries, were reported by Awalina et al. (2014) that it has been polluted with Cd. Yet it thrives there and so it has been decided to use these microalgae for its high resistant and capability of accumulating huge amount of Cd. These microalgae were then isolated and cultivated in the laboratory for most probable removal efficiency. The biosorbent made of these dried biomass of cultivated algae were then utilized for batch aqueous solution of Cd (II) ions biosorption test. The effect of some operational condition on biosorption efficiency have been investigated. Study on equilibrium isotherm, kinetics, and thermodynamics of biosorption process as well as reusability of spent biosorbent were conducted in detail.

2. METHODOLOGY/ EXPERIMENTAL

2.1. Biosorbent preparation

Microalgae isolated from Situ Rawa Kalong, then cultivated for 14 days in laboratory of Bioprocess Engineering-Dept. of Chemical engineering-ITB in a photobioreactor system fed with 15% (v/v) carbon dioxide gas under illumination of ~5700 lux. Dewatering process was conducted by centrifugation at 6000 rpm for 15 minutes. Continued by drying process in oven 60°C for 7x24 hours. Dried biomass was grounded with mortar and sieved with 354µm particle size to produce the biosorbent powder. The biosorbent powder then kept in air tight bottle for further experiments in required amount.

2.2. Cadmium solution

A stock solution (1000 mg/L) of Cd (II) was prepared using CdCl₂.2.5H₂O in demineralized water added with 20 mL of 1:1 HCl solution. Working solution was prepared by diluting stock solution with distilled water.

2.3. Effect studies

The effect of pH, biosorbent concentration, contact time, initial Cd concentration and temperature on Cd biosorption efficiency were studied. Effect of pH were conducted in total volume 25 mL with biomass concentration 0.1g/L and pH ranged 3 to 11 for 1 hour at 30°C. Effect of contact time was done in 25mL solution with biomass concentration 0.1 g/L at pH 8, initial Cd concentration of 1.29; 9.58 and 83.07 mg/L, temperature of 30°C, for 120 minutes. Biosorbent concentration effect was studied in total volume of solution 25 mL resulted biosorbent concentration of 0.1; 0,2; 0.4; 1,0; and 2,0 g/L at pH 8, temperature 30°C, initial Cd concentration of 8 mg/L. Operational temperature effect was observed at 27, 30, 32, 37,42, 47 and 50 °C with biosorbent concentration of 0.1 g/L, pH8 and contact time of 60 minute. All of these effects studies were done by continuous agitation at 120 rpm.



2.4. Desorption studies

Desorption of adsorbed Cd from exhausted biosorbent were conducted with 1 M HCl solution. Pre adsorbed biosorbent was taken in 1 M HCl and shaken at 120 rpm for 60 minutes. The eluted biosorbent was washed repeatedly with demineralized water to remove any residual desorbing solution and placed into Cd solution for the next biosorption cycle.

2.5. Equilibrium studies

Equilibrium experiments for biosorption were carried out at different initial concentrations. There were two concentration ranges, low range (0.29 to 7.13 mg/L) and high range (5.41 to 83.07 mg/L). All were done at pH 8, 30°C and biomass concentration of 0.1g/L. Agitation rate was at 120 rpm, total volume of 25 mL and contact time of 60 minutes. The reaction mixtures then filtered and analyzed with Flame Atomic Absorption Spectrophotometer Shimadzu AA-7000 series for Cd determination. All experiments were carried out in duplicate. Biosorption and desorption capacities (q_e) at specified time (t) were calculated as

$$q_e = \frac{V(C_0 - C_e)}{m} \quad (1)$$

Where q_e is equilibrium biosorption or desorption capacity (mg/g); C_0 and C_e are the initial and equilibrium Cd concentration in solution (mg/L); V is volume of used solution (L); m is the mass of biosorbent (g).

2.6. Kinetic studies

Kinetics experiments for biosorption was performed in total volume of 25 mL at 120 rpm and 30°C. Biomass concentration of 0.1g/L was thoroughly mixed with each initial Cd concentration according to concentration in two concentration ranges, which were low range (0.29 to 7.13 mg/L) and high range (5.41 to 83.07 mg/L). All of those samples were filtered before analyzed with Flame Atomic Absorption Spectrophotometer Shimadzu AA-7000 series for Cd determination. The Cd concentration retained in the biosorbent phase (q_t , mg/g) was calculated by following expression

$$q_t = \frac{(C_0 - C_t)V}{m} \quad (2)$$

where C_0 and C_t are the initial and concentration of Cd at t time in solution (mg/L), V is solution volume (L) and m is mass of biosorbent (g).

2.7. Thermodynamic studies

Measurement of thermodynamic parameters were conducted with experiments at temperature range of 303 to 323 K for Cd biosorption. Those parameter are ΔG° (standard Gibb's free energy change), ΔH° (enthalpy change) and ΔS° (entropy change) were estimated to evaluate the feasibility and nature of biosorption process using standard equation at constant temperature according to van't Hoff as follow

$$\ln K_d = \frac{\Delta S^\circ}{R} - \frac{\Delta H^\circ}{RT} \quad (3)$$

Where K_d is thermodynamic equilibrium constant of biosorption, which defined as ratio of mg Cd adsorbed per gram of biosorbent and C_e (the equilibrium of Cd concentration in solution, mg/L). The values of ΔH° and ΔS° were calculated from the slope and intercept of the plot of $\ln K_d$ versus $1/T$.

3. RESULTS AND DISCUSSION

3.1. Characteristic of biosorbent

The surface properties of biosorbent named AB was measured and tabulated in Table 1. The BET surface area is close to adsorbents made from banana peel (in normal grounded form) which shown 2.0 m²/g and compost that gave 1.36 m²/g. It was 8 magnitudes higher compared to normal grounded form of macroalgae that result 0.22 m²/g as mentioned by other researchers (Castro et al., 2011, Ulmanu et al., 2003, Cochrane et al., 2006). Pore area and pore volume



are comparable with garden grass which shown 40.18 Å and 0.03 cc/g as reported by Hossain et al. (2012).

Table 1. Physical and chemical characters of biosorbent AB of dried *Aphanothece sp*

Parameter of Biosorbent	Methods	Values
1. Surface area	BET surface area	1.735 m ² /g
2. Pore diameter	BJH adsorption	30.74 Å
3. Pore volume	BJH adsorption	5.0E-03 cc/g
4. Carbon	Elemental analysis	43.80%
5. Hydrogen	Elemental analysis	6.66%
6. Nitrogen	Elemental analysis	6.43%
7. Sulfur	Elemental analysis	0.53%
8. Moisture	Gravimetric	90.97 to 99.46 %

3.2. Effect of operational conditions

Biosorption efficiency of Cd increased as with its increasing concentration of 1.29 to 83.07 mg/L in solution test (Figure 1). As Cd concentration was increased, biosorption efficiency increased from 82.31% to 97.64%. Maximum biosorption efficiency was achieved within 60 minutes (1 hours) along with its equilibrium (Figure 2).

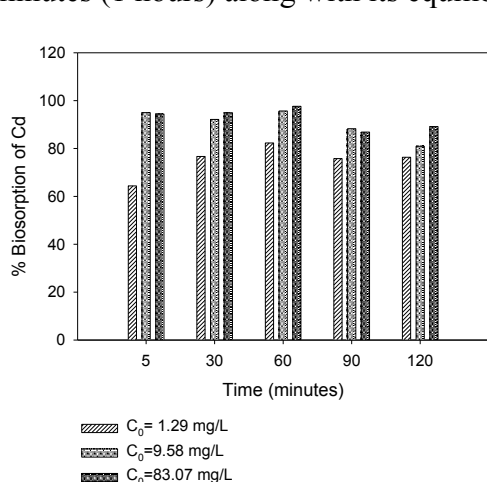


Figure 1. Effect of contact time on biosorption efficiency of various initial Cd concentration

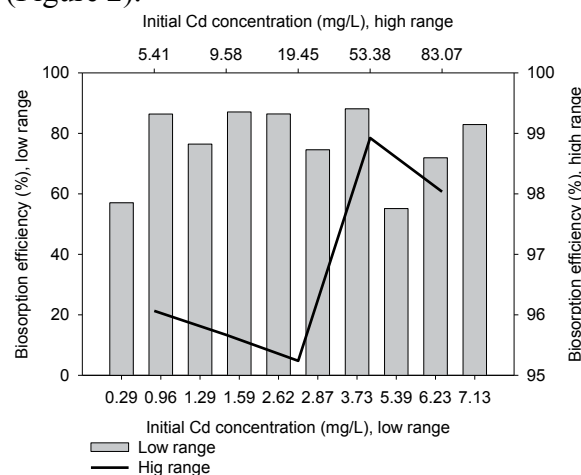


Fig 2. Effect of initial Cd concentration on biosorption efficiency both of two initial concentration range

Biosorbent surface charge, ionization degree and Cd speciation are strongly affected by pH of solution. Therefore pH are observed in this experiments as well. As present in Figure 3, in the range of pH 3-11, highest biosorption efficiency was achieved at pH of 8. It suggested that at pH 8, mainly Cd ions were formed as free Cd (II) ions which involved in biosorption process. Beyond pH 8, the biosorption process was obstructed due to immediate precipitation of cadmium hydroxide. Hence, in the next biosorption tests, pH adjustment fixed at pH 8 has been conducted. Biosorbent dose were varied 0.1 g/L; 0.2 g/L; 0.4 g/L; 1.0 g/L and 2.0 g/L for biosorption test at initial Cd concentration in tested solution of 7.99 mg/L, pH8 and 30°C . The results showed that the percent removal of Cd rapidly decreased with the increased of biosorbent dose (Figure 4). The decreasing biosorption efficiency was due to massive agglomeration which hampered further Cd biosorption as the increasing biomass concentration. The maximum biosorption efficiency was found at biosorbent dose at 0.1 g/L. The highest biosorption efficiency (91.10%) was observed at temperature of 30°C (Figure 3).

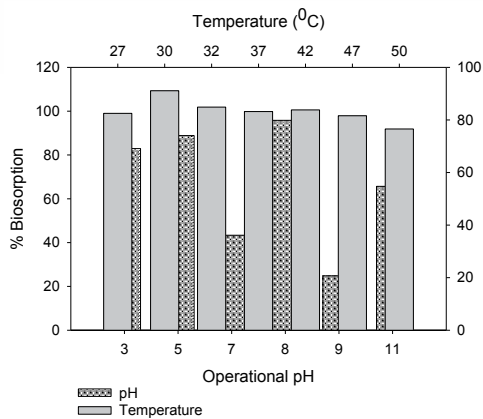


Figure 3. Effect of operational pH and Temperature on Cd biosorption efficiency

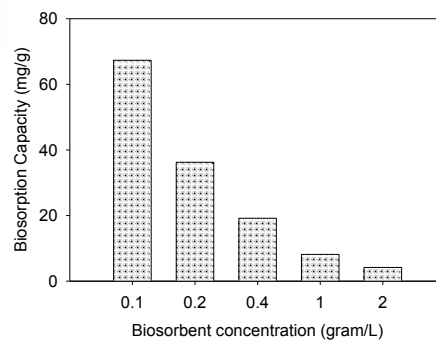


Fig 4. Effect of biosorbent concentration on biosorption efficiency

In chemical design, knowing distribution of Cd ions between solution and biosorbent are important. To describe the Cd distribution on both compartment, the fitting of experimental results on equilibrium isotherms mathematical model is needed to be determined. In this study, the three equilibrium isotherm models (Langmuir, Freundlich and Dubinin-Radushkevich) were used (Sari and Tuzen, 2008b). The Langmuir model supposes that biosorption process occurs at a specific sorption surface and describe single coating layer on sorption surface. This model can be written as linearized equation form

$$\frac{C_e}{Q_e} = \frac{C_e}{Q_m} + \frac{1}{K_L Q_m} \quad (3)$$

where q_e is the equilibrium metal ion concentration on the biosorbent (mg/g), C_e is the equilibrium metal ion concentration in the solution (mg/L), q_m is the monolayer biosorption capacity on biosorbent (mg/g), and K_L is the Langmuir biosorption constant (L/mg) relating to free energy of biosorption. The plots of C_e/q_e versus C_e were drawn as shown in Figure 5 for two initial concentration range of Cd to calculate these constants. The maximum biosorption capacity (q_{max}) was 60.24 mg/g at low initial concentration range and 526.32 mg/g at high range. These value were five magnitudes higher compared to q_{max} of *Aphanothece sp* produced from atmospheric fed photobioreactor system, reported by Awalina et al. (2016), which is only 17.27 mg/g at low concentration range and 119.05 mg/g at high concentration range. Meanwhile Freundlich isotherm model is used for modelling biosorption on heterogenous surface. The linearized Freundlich model is represented by the equation:

$$\ln q_e = \ln K_F + \frac{1}{n} \ln C_e \quad (4)$$

where K_F and n are constants related to the sorption capacity and intensity. The plots of $\ln q_e$ versus $\ln C_e$ to calculate the values of K_F and $1/n$ are given in Table 1. It was found that the plots exhibit deviation from linearity and the correlations coefficients indicates that the data are not well correlated to Freundlich correlation coefficients, compared to Langmuir correlation coefficients. Same result are also reported by Sari and Tuzen (Sari and Tuzen, 2008a) who applied dried biomass of marine macroalgae *Ulva lactuta* in eliminating aqueous solution of Cd (II). The equilibrium data were also subjected to D-R isotherm model to determine the nature of biosorption processes as physio-sorption or chemo-sorption. The linear presentation of the D-R isotherm model is expressed by equation (5) to equation (7)

$$\ln q_e = \ln q_m - \beta \varepsilon^2 \quad (5)$$

$$\varepsilon = RT \ln \left(1 + \frac{1}{C_e} \right) \quad (6)$$

$$E = \frac{1}{\sqrt{-2\beta}} \quad (7)$$



where q_e is the amount of metal ions adsorbed on per unit weight biomass (mol/L), q_{max} is the maximum biosorption capacity (mol/g), β is the activity coefficients related to biosorption mean free energy (mol²/J²) and ϵ is the Polanyi potential. C_e is equilibrium concentration (mol/L). The q_{max} value was found using the intercept plotting of $\ln q_e$ against ϵ^2 (Figure 6), while E is the mean free energy (kJ/mol). The E value give information about sorption mechanism, as physiosorption or chemisorption. Chemisorption takes place between 8 and 16 kJ/mol while physiosorption proceeds in E less than 8kJ/mol. Table 1 presents calculation results for determining parameter of those three isotherms modelling. As seen on the Table 1, very high correlation coefficient (>0.990) were found at both of Langmuir and Dubinin-Radushkevich isotherms modelling. Therefore, biosorption Cd (II) by *Aphanothece sp* dried biomass was very suitable described with both of Langmuir and Dubinin-Radushkevich isotherm models. It means that biosorption process in this study proceeded in monolayer biosorption which took place at the functional groups/binding sites on the cell surface. This biosorption process also carried out via chemisorption, since calculated E of both at initial concentration were 12.91 kJ/mol. This biosorption process involving valence forces through sharing or exchange of electron between biosorbent and ion Cd (II) in aqueous phase. The value of q_{max} were prone to increase as the increase of initial Cd (II) concentration.

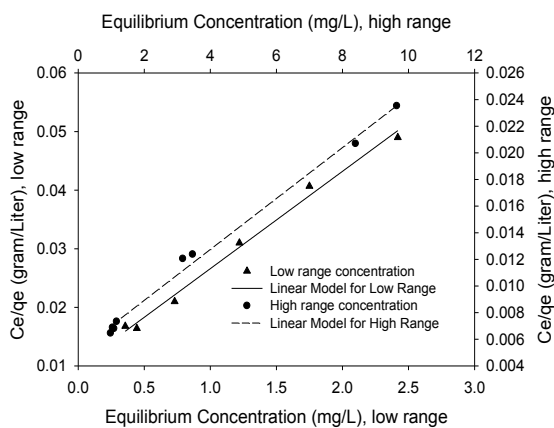


Fig 5. Linear modelling of Langmuir Isotherm applied on two concentration range

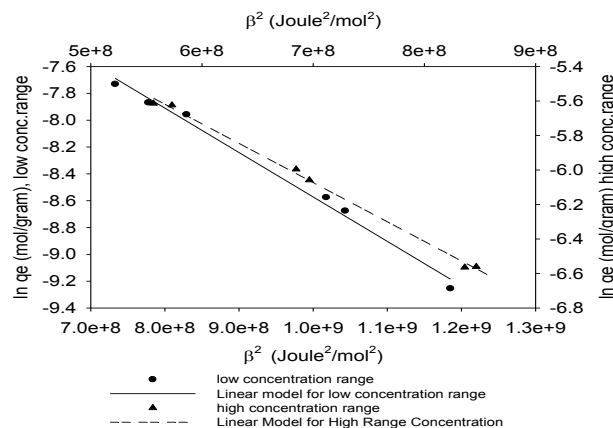


Fig 6. Linear modelling of Dubinin-Radushkevich Isotherm applied on two concentration range

Information on biosorption rate prediction is needed to design batch biosorption. In other words, information on pollutant's uptake kinetics is required to select optimum operating conditions for full scale batch proses. In order to clarify the biosorption kinetics of Cd (II) by dried biomass of *Aphanothece sp*, the two kinetic models which are Lagergren's pseudo-first order and pseudo second order (Ho and McKay, 2000) were applied to the experimental data. Linear form of those kinetic models are given as follows

$$\ln(q_e - q_t) = \ln q_e - k_1 t \quad (11)$$

where q_t and q_e (mg/g) are the amounts of adsorbed ion at equilibrium (mg/g) and t (minute), k_1 is the rate constant of the biosorption (min⁻¹). Plotting of $\ln (q_e - q_t)$ versus t must be done to find k_1 . Experimental data were also tested by the PSO-2 which given in the following linearized form:

$$\frac{t}{q_t} = \frac{1}{k_2 q_e^2} + \left(\frac{1}{q_e}\right) t \quad (12)$$

where k_2 (g/mg.min) is the rate constant of PSO-2, q_t (mg/g) is the amount of biosorption at time t (minute) and q_e is amount of biosorption equilibrium (mg/g). The rate constants (k_1 and k_2), coefficients determination (R^2) and q_e values are given in Table 2. As seen from the R^2 and



$q_{e,(exp)}$ values in Table 3, the pseudo second order model more suitable for modelling the biosorption of Cd (II) ions onto dried biomass of *Aphanothece sp.* than pseudo first order model.

Table 1. Three isotherms parameter of Cd biosorption using dried biosorbent of carbon dioxide treated *Aphanothece sp*

Range of Initial Cd conc. (mg/L)	Langmuir constants			
	q_{max} (mg/g)	K_L (L/mg)	R^2	
A. $C_0=0.29-7.13$	60.24	1.66	0.992	
B. $C_0=5.41$ to 83.07	526.32	0.35	0.995	
Range of Initial Cd conc. (mg/L)	Freundlich constants			
	K_F (mg/g(L/g) ^{1/n})	n	R^2	
A. $C_0=0.29-7.13$	34.79	1.810	0.9561	
B. $C_0=5.41$ to 83.07	113.60	1.567	0.943	
Range of Initial Cd conc. (mg/L)	Dubinin-Radushkevich constants			
	q_{max} (mol/g)	β (mol ² /J ²)	E (kJ/mol)	R^2
A. $C_0=0.29-7.13$	5.19E-03	3.00E-09	12.91	0.993
B. $C_0=5.41$ to 83.07	2.50E-02	3.00E-09	12.91	0.997

Table 2. Kinetics parameter of Pseudo First Order model and Pseudo Second Order model applied on two of initial Cd concentration range

Initial conc (mg/L)	$q_{e,(exp)}$ (mg/g)	Pseudo First Order rate constants			Pseudo Second Order rate constants		
		k_1 (min ⁻¹)	$q_{e(cal)}$ (mg/g)	R^2	k_2 (g/mg.min)	$q_{e(cal)}$ mg/g)	R^2
A. Low range concentration							
1.29	9.92	1.24E-01	8.60	0.941	1.68E-01	9.43	0.999
7.13	55.38	1.63E-01	40.54	0.811	1.06E-01	55.25	0.999
B. High range Concentration							
5.4	45.83	2.91E-01	42.84	0.962	5.20E-03	45.45	0.994
83.2	482.40	1.95E-02	467.83	0.930	1.52E-03	476.19	0.999

Thermodynamic behavior of biosorption Cd (II) into dried biomass of *Aphanothece sp* was described by using the free energy change (ΔG^0), enthalpy change (ΔH^0), and entropy change (ΔS^0). The value of ΔH^0 (kJ/mol) and ΔS^0 (kJ/mol K) parameter can be calculated the from slope and intercept of the plot $\ln K_d$ versus $1/T$ yields (Sari and Tuzen, 2008b), respectively as seen on Figure 7. The results of calculation on ΔG^0 , ΔH^0 , and ΔS^0 are given in Table 3. The negative ΔG^0 values indicated that the nature of biosorption of Cd (II) onto dried biomass of *Aphanothece sp* thermodynamically feasible and spontaneous. The decrease in negative ΔG^0 values with increase in temperature shows an increase in feasibility of biosorption at higher temperature. Negative ΔH^0 indicates exothermic nature of biosorption process at 303-323K. Furthermore, the negative value of ΔS^0 reveals the decreased randomness at solid-solution interface during cadmium (II) ions binding on the active sites of the biosorbents.

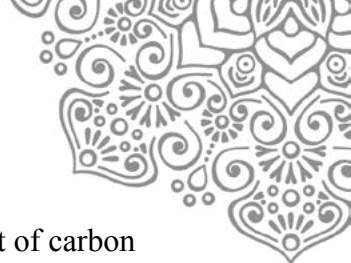


Table 3. Thermodynamic parameter of biosorption process using dried biosorbent of carbon dioxide treated *Aphanothece sp*

T (K)	ln (qe/Ce), (L/g)	ΔG (kJ/mol)	ΔH (kJ/mol)	ΔS(kJ/mol.K)
303	4.32	-10.88	-49.78	-0.128
305	4.20	-10.65		
310	3.88	-10.00		
315	3.50	-9.17		
323	3.13	-8.39		

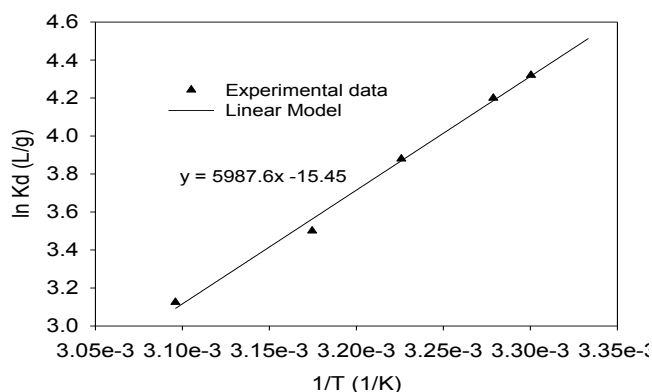


Fig 7. Plotting of ln Kd versus 1/T for obtaining enthalpy and entropy of biosorption process

Cadmium biosorbent reusability in this study was conducted using HCl 1 M as de-sorbent solution. As shown in Figure 8 the equilibrium capacity observed in biosorption are relatively unchanged over three cycles. However, due to the equilibrium capacity of desorption, it was dropped at third cycle, as represented by ratio of desorption to biosorption. It suggested that there was occurred a damaged on the surface of biosorbent caused by HCl 1 M which lead to decreasing of binding capacity of the biosorbent.

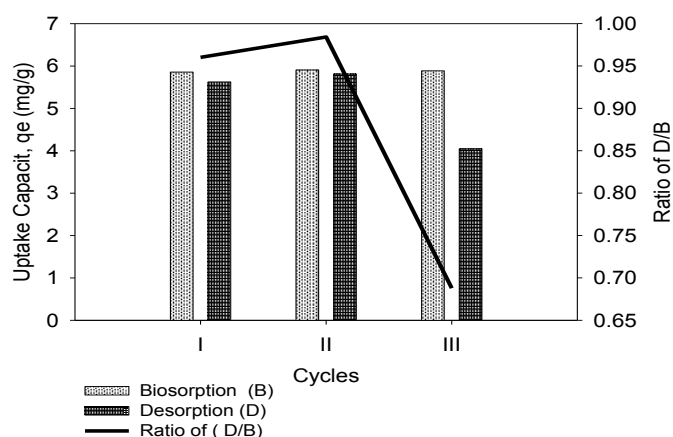
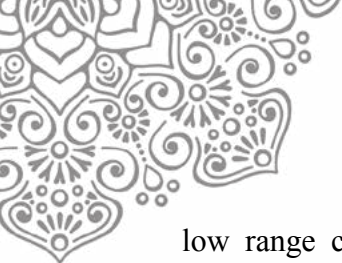


Fig 8. Effect of reusability cycles on biosorption process using dried biosorbent of carbon dioxide treated *Aphanothece sp*

4.CONCLUSION

The dried biomass of *Aphanothece sp* has been successfully used as the biosorbent of cadmium (II) ions from aqueous solution which show maximum biosorption capacity of 60.24 mg/g at



low range concentration and 526.32 mg/g at high range concentration. The biosorption mechanism and kinetics depend on experimental condition particularly pH of solution, initial Cd concentration and biosorbent concentration. The equilibrium was best described by Langmuir isotherm and Dubinin Radushkevich isotherm, while due to reaction kinetic was obeyed the pseudo second order reaction. It suggested that the biosorption process was occurred in monolayer coverage and proceeded in chemisorption with mean of free biosorption energy of 12.91 kJ/mol. In term of thermodynamic aspect, this biosorption process was feasible, spontaneous, and exothermic. Biosorbent also tend to be more ordered after Cd was adsorbed. The *Aphanothece sp* dried biosorbent could be regenerated using 1 M HCl and repeatedly used successive biosorption/desorption cycle for three cycles.

5. ACKNOWLEDGEMENT

The authors would like to acknowledge the financial and technical supports of Dept. of Chemical Engineering-ITB, Research Center for Limnology-The Indonesian Institute of Sciences, and Research Center for Geo technology-The Indonesian Institute of Sciences.

6. REFERENCES

- AWALINA, HARIMAWAN, A. & SETIADI, T. Biosorption of Cadmium Ion from Aqueous Solution by *Aphanothece sp*: Equilibrium, Kinetic and Thermodynamic Studies. Current Trends in Biotechnological Research for Environmental Sustainability, 3rd International Postgraduate Conference on Biotechnology (IPCB) 2016, 2016 24-26 August 2016 in Surabaya City, Indonesia. IPCB Organizing Committee Dept. of Environmental Engineering-Institut Teknologi Sepuluh Nopember, Dept. of Environmental Engineering for Symbiosis-Soka University, Institute of Marine Biotechnology-Universiti Malaysia Terengganu.
- AWALINA, SULAWESTY, F., OKTARIANI, E., CHRISMADHA, T., SATYA, I., NAIDIDA, E. & SETIADI, T. Freshwater Phytoplankton as Potential Heavy Metal Biosorbent and its Natural Aquatic Physico-Chemical Characteristics s: A Study case on Situ Rawa Kalong-Depok. ChemPro2014 Mineral and Material Processing. International Seminar on Chemical Engineering in Conjunction with Seminar Teknik Kimia Soehadi Reksowardojo (STKSR) 2014. "Minerals and Material Processing Toward Sustainable Development" 30-31 October 2014 2014 Bandung.
- CASTRO, R. S. D., CAETANO, L. R., FERREIRA, G., PADILHA, P. M., SAEKI, M. J., ZARA, L. F., MARTINES, M. A. U. & CASTRO, G. R. 2011. Banana peel applied to the solid phase extraction of copper and lead from river water: preconcentration of metal ions with a fruit waste. *Industrial and Engineering Chemistry Research*, 50, 3446-3451.
- CHOJNACKA, K. 2010. Biosorption and bioaccumulation – the prospects for practical applications. *Environment International*, 36, 299-307.
- COCHRANE, E. L., LU, S., GIBB, S. W. & VILLAESCUSA, I. 2006. A comparison of low-cost biosorbents and commercial sorbents for the removal of copper from aqueous media. *Journal of Hazardous Materials*, 137 (1), 198-206.
- FOMINA, M. & GADD, G. M. 2014. Biosorption: current perspectives on concept, definition and application. *Bioresource Technology*, 160, 3-14.
- HO, Y. S. & MCKAY, G. 2000. The Kinetics of Sorption of Divalent Metals onto *Sphagnum Moss Peat*. *Water Res.*, 34, 735-742.
- HOSSAIN, M., NGOA, H. H., GUOA, W. & SETIADI, T. 2012. Adsorption and desorption of copper(II) ions onto garden grass. *Bioresource Technology*, 121, 383-395.



- KAUR, I. & BHATNAGAR, A. K. 2002. Algae-dependent bioremediation of hazardous wastes. In: SINGH VED, P. & STAPLETON RAYMOND, D. (eds.) *Progress in Industrial Microbiology*. Elsevier.
- SARI, A. & TUZEN, M. 2008a. Biosorption of cadmium (II) from aqueous solution by red algae *Ceramium virgatum*: Equilibrium, kinetic and thermodynamic studies. *Journal of Hazardous Materials*, 157, 448-454.
- SARI, A. & TUZEN, M. 2008b. Biosorption of Pb(II) and Cd(II) from Aqueous Solution using Green Alga (*Ulva Lactuta*) Biomass. *Journal of Hazardous Materials*, 152, 302-308.
- ULMANU, M., MARANON, E., FERNANDEZ, Y., CASTRILLON, L., ANGER, I. & DUMITRIU, D. 2003. Removal of copper and cadmium ions from diluted aqueous solutions by low cost and waste water material adsorbents. *Water, Air and Soil Pollution*, 142, 357-373.
- VOLESKY, B. 2001. Detoxification of metal-bearing effluents: biosorption for the next century. *Hydrometallurgy*, 59, 203-216.



15th International Conference on Quality in Research (QIR 2017)

IDENTIFICATION AND CLASSIFICATION OF HONEY'S AUTHENTICITY BY ATR-FTIR SPECTROSCOPY AND CHEMOMETRIC METHOD

Seffiani¹, Heri Hermansyah¹, Anondho Wijanarko¹, Etin Rohmatin², Muhamad Sahlan^{1,3*}

¹Departement of Chemical Engineering, University of Indonesia, Depok, 16424, Indonesia

²Midwifery Department of Health Polytechnic Republic of Indonesia's Health Ministry, Tasikmalaya, Indonesia

³Research Center of Biomedical Engineering, University of Indonesia, Depok, 16424, Indonesia

Corresponding Author: Muhamad Sahlan, Email: sahlan@che.ui.ac.id

ABSTRACT

Honey is a natural product produced by honeybees from various secretions of plants, and it has many benefits, especially for human's healthiness. Authentication of honey has importance for both industries and consumers because until now; there is no guarantee of honey's authenticity especially in Indonesia. As for the classification of honey bees, is based on the fact that the content of honey produced between *Apis sp.* and stingless bees (most widely harvested honey bees in Indonesia) have differences. Honey from stingless bees is much more expensive than *Apis sp.* because the yield of honey per colony is never very high. Current rapid detection methods like a raw fish test, turbidity test, foam test, test with ants usually either have challenges for the accuracy. In this experiment, there is an alternative testing to identify the authenticity of honey by using Attenuated Total Reflectance Fourier Transmission Infrared Spectrometer (ATR-FTIR) with the range of wavelengths between 550 - 4000 cm^{-1} . By using ATR-FTIR, the spectrum of each sample for real and fake honey were obtained and plotted using the chemometric discriminant method. Real honey's samples have been achieved from the local honey bees breeder from all around Indonesia while the fake honey were made from the mixture of water, sugar, NaHCO_3 , and real honey. Data were collected using OMNIC software and processed using TQ Analyst software. This method was able to differentiate the authenticity and classification of honey based on the honey's spectrum. For identification of authenticity purpose, there were 2 classes formed, real and fake honey, the best region which can differentiate them are 4 regions: 1700 -1600 cm^{-1} , 1540 - 1175 cm^{-1} , 1175 - 940 cm^{-1} and 940 - 700 cm^{-1} . For classification purpose, there were 2 classes formed based on the type of honey bees, *Apis sp.* and stingless bees, the best region specifically is 1700 -1600 cm^{-1} . This study aimed to obtain a method that can detect the authenticity and classification of honey which is fast, precise, and accurate.

Keywords: *Apis sp.*; ATR-FTIR; Discriminant; Distance Analysis; Spectrum; stingless bees

1. INTRODUCTION

Honey is a complex compound derived from the nectar synthesis where the nectar are collected by honey bees from various plants. Honey is very famous for its therapeutic potential. There are 3 types of honey bees in Indonesia, namely wild bees (*Apis dorsata*), farming bees (*Apis cerana* and *A. mellifera*) and stingless bees. Honey that are produced from *Apis sp.* and stingless bees have some differences. Honey produced by *Apis sp.* have a sugar content of 62 % -70 % and water content of 14.86 % -17.53 % (Moniruzzaman et al., 2013). Honey from



stingless bees has a moisture content between 30 % - 35 % and 44.08 % of reducing sugar content. Because of the small size of stingless bees, the yield of honey per colony is never very great, so the price for its honey is much higher than the other honey.

The benefit that comes from honey makes many people like to consumed honey as a health supplement. As a result, honey has been searched by many people as a natural supplement. Unfortunately, this request can not be fulfilled by the availability of honey in nature because it can not be harvested every time. Based on the data from Ministry of Forest, the demand for honey in Indonesia reached 7,500 ton/year whereas the supply only reached 5,000 ton/year. So, the opportunity is used by some persons who are not responsible for making fake honey.

Therefore, it is critical to developing a rapid, sensitive, accurate method to detect the authenticity of honey. However, current rapid detection methods usually either have challenges for the accuracy. Many of conventional method like raw fish test, turbidity test, foam test, test with ants still have low level of precision, that is 60% for the raw fish test, 52.5% for the turbidity test, 17.5% for the foam test and 0.8% for the test with ants (Rachmawaty, 2011).

Here we developed an innovative method based on the characteristics of honey's spectrum using ATR-FTIR and chemometric method which is Discriminant Analysis. The advantage of this approach builds on the fact that each compound has different and specific IR spectrum, so the sample's spectrum obtained is represent the characteristics of an organic sample as a whole. Fourier transform infrared (FTIR) spectroscopy can be used to achieve biochemical fingerprints of samples non-destructively and rapidly (Sivakesava, 2001). The crystal used in ATR cells are made from zinc selenide (ZnSe) that have low solubility in water and are a very high refractive index so it can be more precision (Stuart, 2004). Also, ATR-FTIR has several advantages such as cheap and fast in operation, does not damage the sample, does not require sample preparation and requires only a little amount of sample in the measurement. Through this research, we expect to produce an identification and classification methods to determine the authenticity of honey which are fast, precise and accurate.

2. METHODOLOGY/EXPERIMENTAL

2.1 Samples

A total of 85 samples consisting of 58 samples of real honey and 27 samples of fake (adulterated) honey. Real honey were collected from different geographical regions of Indonesia and various floral origin. Most of the samples were collected directly from the primary producers.

Samples of real honey produced by *Apis cerana* (n = 5), *Apis mellifera* (n = 19), *Apis dorsata* (n = 17), stingless bees (n = 10) and others (n = 7) were included in the study. As for fake honey, there are 27 samples in total and were made from the mixture of water, sucrose, NaHCO₃, and real honey. The sample amount of each group is indicated as "n." Honey samples were grouped as real and fake ones basically for identification purpose. For classification purpose, honey samples were a group as *Apis sp.* and stingless bees.

2.2 Instrumentation and sample analysis

Spectra from all samples were collected with Nicolet iS5 FT-IR Spectrometer (ThermoFisher Scientific Inc., USA) equipped with ATR accessory. The software OMNIC version 9 was used for spectral acquisition. Samples were placed on Diamond/ZnSe crystal plate (ThermoFisher Scientific Inc) and scanned from 4000 – 550 cm⁻¹ for 16 scan time with a resolution of 16 cm⁻¹ at room temperature. Each sample was replicated three times. Identical spectra were analyzed in each case. This process was done to see the absorbance value accuracy, which might be affected from the homogeneity of the sample. The diamond was cleaned between samples using propanol.



2.3 Chemometrics

Discriminant Analysis was applied to classify the samples based on spectral differences. Discriminant Analysis was performed with TQ Analyst software (ThermoFisher Scientific Inc) for determination of spectral differentiation. In this work, Discriminant Analysis was conducted on ATR-FTIR spectra with range of $3000 - 2800 \text{ cm}^{-1}$, $1700 - 1600 \text{ cm}^{-1}$, $1540 - 1175 \text{ cm}^{-1}$, $1175 - 940 \text{ cm}^{-1}$ and $940 - 700 \text{ cm}^{-1}$.

3. RESULTS AND DISCUSSION

In this study, ATR-FTIR spectroscopy has been used to compare honey samples based on their spectral differences in $4000 - 550 \text{ cm}^{-1}$ regions. The crystal used in ATR cells are made from materials that have low solubility in water and are a very high refractive index. A representative of ATR - FTIR spectrum of honey are given in Figure 1 and Figure 2. The explanation of band assignment with the corresponding modes of vibration is shown in table 1, based on literature (Gok, 2014)

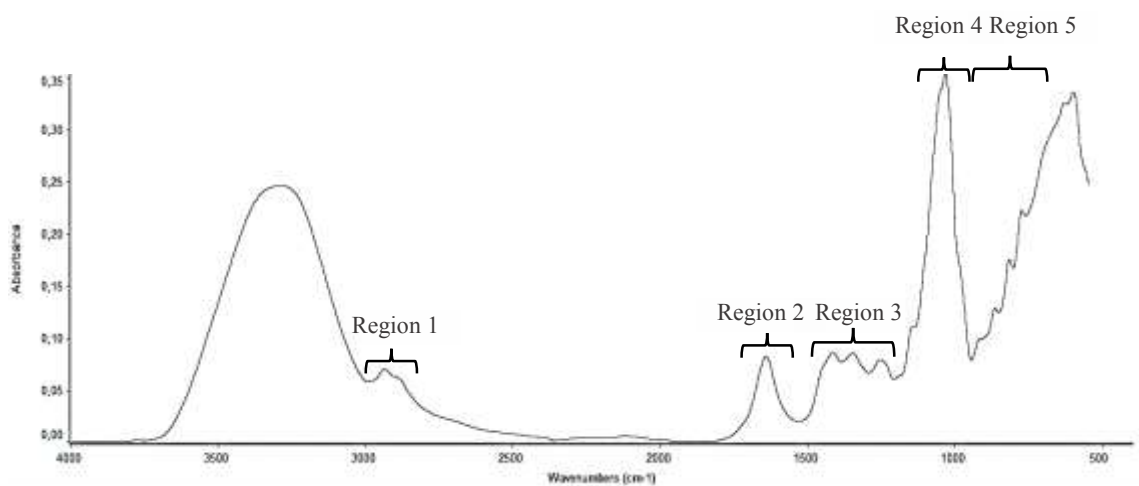


Figure 1. Representative of honey's spectrum in the $4000 - 550 \text{ cm}^{-1}$ spectral region using ATR-FTIR

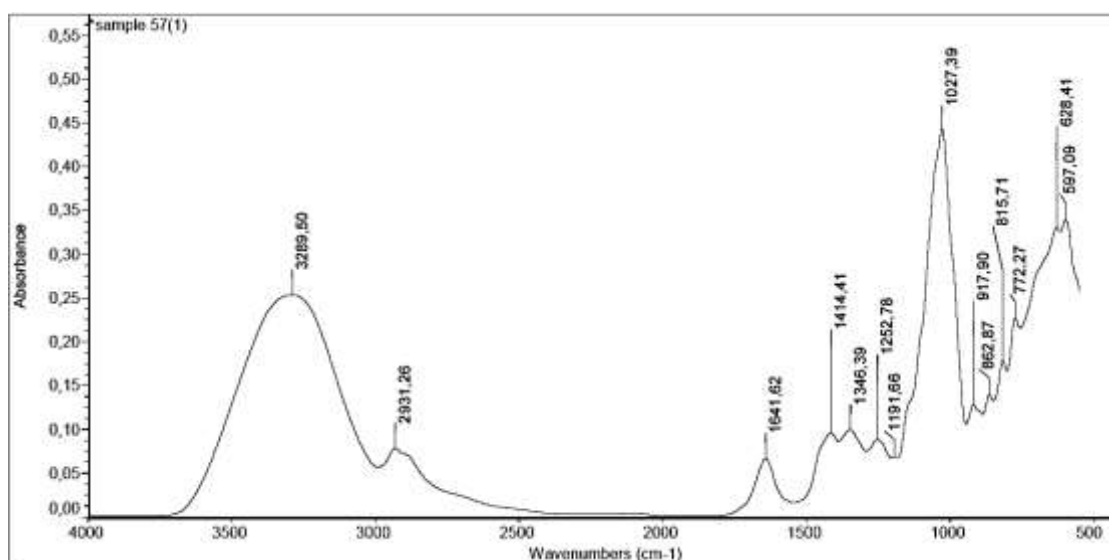


Figure 2. ATR-FTIR spectrum for real honey in the $4000 - 550 \text{ cm}^{-1}$ spectral region

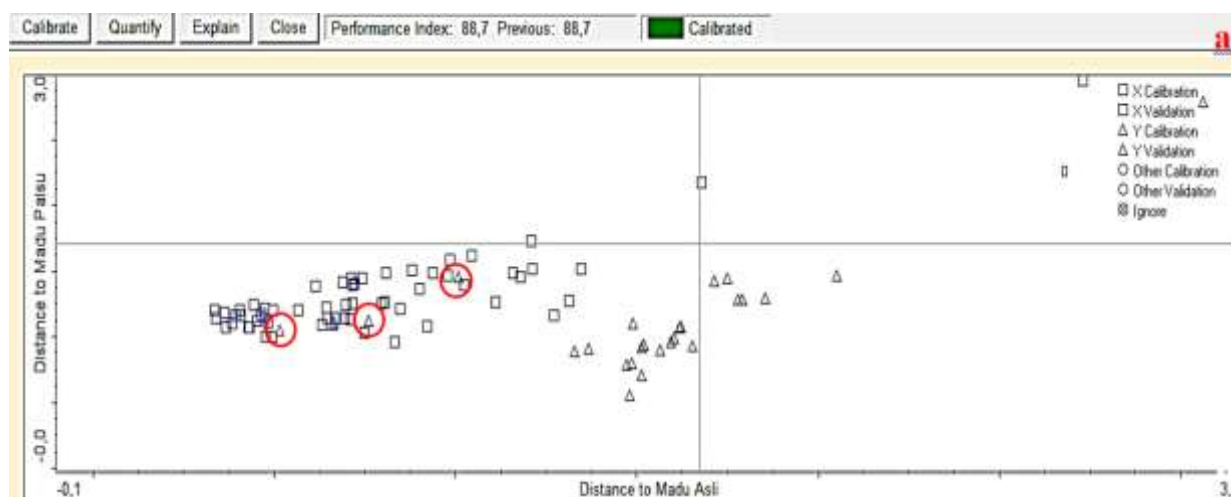


Table 1. General band assignment of ATR-FTIR spectrum of honey

Region 1	3000 - 2800 cm ⁻¹	C-H stretching (carbohydrates) O-H stretching (carboxylic acids) NH ₃ stretching (free amino acids)
Region 2	1700 -1600 cm ⁻¹	O-H stretching/bending (water) C=O stretching (mainly from carbohydrates) N-H bending of amide I (mainly proteins)
Region 3	1540 - 1175 cm ⁻¹	O-H stretching/bending C-O stretching (carbohydrates) C-H stretching (carbohydrates) C=O stretching of ketones
Region 4	1175 - 940 cm ⁻¹	C-O and C-C stretching (carbohydrates) Ring vibrations (mainly from carbohydrates)
Region 5	940 - 700 cm ⁻¹	Anomeric region of carbohydrates C-H bending (mainly from carbohydrates) Ring vibrations (mainly from carbohydrates)

Source: Gok, 2014

The different spectral region has been applied to Discriminant Analysis. The grouping classes for identification purpose divided into 2 groups, real and fake honey. Square symbols show the spectrum of real honey and the triangle symbols demonstrate the spectrum of fake honey. In Figure 3a, showed that the grouping was not good enough because there was still fake honey's spectrum within real honey's group. It is because the region of spectral was the whole area which is 4000 - 550 cm⁻¹ region. The performance index for Figure 3a was 88.7, and there were 7 samples which still misclassified. For Figure 3b, 2 regions separated between real honey (square symbols) and fake honey (triangle symbols). The results that shown in Figure 3b was the best result of many trials before, where the performance index is 91.8 and no misclassified class. The spectral differences used are 4 regions, there are 1700 -1600 cm⁻¹, 1540 - 1175 cm⁻¹, 1175 - 940 cm⁻¹, and 940 - 700 cm⁻¹. As we seen in Table 2, the best performance index based on the result is when we use region 2 to 5. While the trial for region 1 to 5 has the same score for the performance index, but region 1 can be ignored since it is a region of group frequency. Group frequency region of 3000 – 2800 cm⁻¹ shows the absorption of C-C and C-H compound so it can be ignored since it owned by all of the organic compound (Janori, 2016).



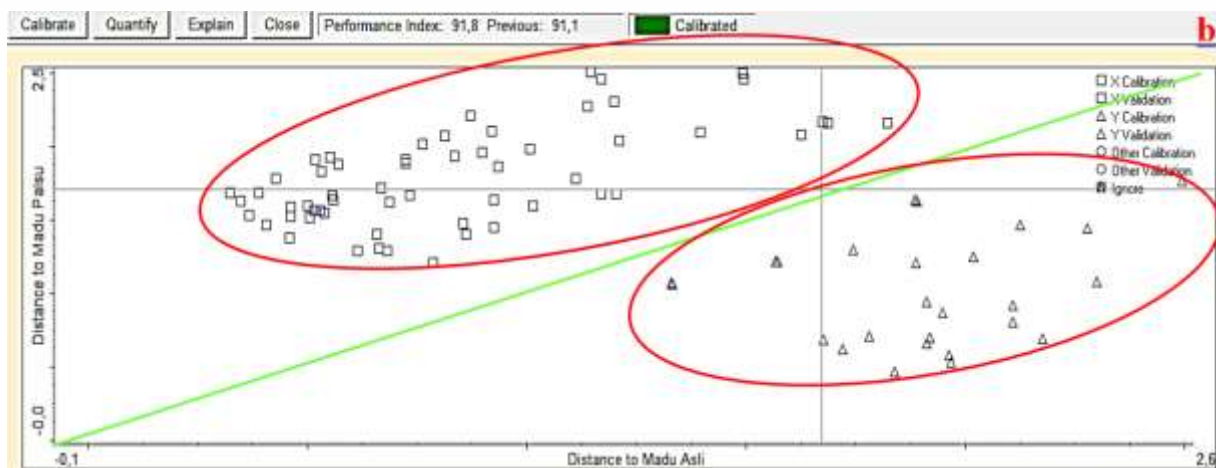


Figure 3. Discriminant Analysis scatter plots for all of the samples of honey’s authenticity identification (a) 4000-550 cm^{-1} (b) 1700 -1600 cm^{-1} , 1540 - 1175 cm^{-1} , 1175 - 940 cm^{-1} , 940 - 700 cm^{-1}

The region 800 to 1500 cm^{-1} corresponds to the absorption zones of the 3 major sugar constituents of honey: fructose, glucose, and sucrose. The 900 to 750 cm^{-1} region is the anomeric region and is characteristic of the saccharide configurations. The bands in the 904 to 1153 cm^{-1} region are assigned to C-O and C-C stretching modes, and those around 1474 to 1199 cm^{-1} are due to the bending modes of O-C-H, C-C-H, and C-O-H angles. Negative bands were observed around 1618 and 3635 cm^{-1} . These bands are due to lower water concentration in the honey sample compared with the reference employed and the fact that water presents an O-H stretching overtone at these wavelengths (Sakhamuri, 2001).

Table 2. Calculated result of selected region for identification purpose between real and fake honey

Region	Performance Index	Misclassified	Total Samples
All (4000 – 650 cm^{-1})	88.7	7	85
1 - 5	91.8	-	85
2-5	91.8	-	85
Only 1 (3000 – 2800 cm^{-1})	90.0	3	85
Only 2 (1700 – 1600 cm^{-1})	90.1	6	85
Only 3 (1540 – 1175 cm^{-1})	90.4	6	85
Only 4 (1175 – 940 cm^{-1})	90.5	1	85
Only 5 (940 – 700 cm^{-1})	92	2	85
700 – 550 cm^{-1}	87.7	7	85

As for classification, the grouping were divided into 2 classes; there are *Apis sp.* and stingless bees. Square symbols show the spectrum of honey from *Apis sp.*, and the triangle symbols indicate the spectrum of stingless bees. Figure 4a and 4b show the scatter plots of Discriminant Analysis when the performance index is 88.2 and 95.4, respectively. In Figure 4a, we can see that there was still spectrum misclassified whereas there was none in Figure 4b. The red circle in the figure shows the misclassified spectrum. The results that shown in Figure 4b was the best result of many trials before. The trial’s purpose is to find the precise grouping



between 2 classes where the spectral region is different each other. There are significant differences between honey which are produced by *Apis sp.* and stingless bees.



Figure 4. Discriminant Analysis scatter plots for all of the samples of honey's classification (a) 4000–550 cm^{-1} (b) 1700 -1600 cm^{-1}

Table 3. Calculated result of selected region for classification purpose between *Apis sp.* and stingless bees

Region	Performance Index	Misclassified	Total Samples
All (4000 – 650 cm^{-1})	88.2	1	50
1 - 5	93.0	-	50
2-5	93.1	-	50
Only 1 (3000 – 2800 cm^{-1})	92.9	1	50
Only 2 (1700 – 1600 cm^{-1})	95.4	-	50
Only 3 (1540 – 1175 cm^{-1})	93.2	-	50
Only 4 (1175 – 940 cm^{-1})	92.0	1	50
Only 5 (940 – 700 cm^{-1})	93.8	-	50
700 – 550 cm^{-1}	92.4	1	50

Based on the result of Table 3, the best performance index for the classification of honey is 95.4 and no misclassified samples when we use region 2 only. The bands in the region 1700–



1600 cm^{-1} had been previously assigned as amide I vibrations of the honey proteins. Protein is a minor honey component. However, they are used in detecting adulteration (Chalhoub, 2005). Studies revealed that pollen proteins could be utilized as a marker for taxonomic classification of honey. The bands at 1700-1600 cm^{-1} were originated to stretching band of carboxyl groups C=O and C \equiv C stretching, this region was found to be related to phenolic molecules (Tahir, 2017). Phenolic compound is linked to the biological origin of the nectar and pollen and the species of the honey-producing bees (Almeida, 2013). However, water molecules give strong absorption between 1640 and 1650 cm^{-1} (Gok, 2014) so the discrimination in this region can be explained by the difference in protein and moisture content, and also water-carbohydrate interactions between sample groups.

4. CONCLUSION

Results of this study showed the potential power of ATR-FTIR spectroscopy in automated and highly sensitive to differentiate between real and fake also *Apis sp.* and stingless bees estimation of honey. This Discriminant Analysis method was able and success to differentiate the authenticity and classification of honey based on the honey's spectrum. The best region which can divide between the real and fake honey are 4 regions; there are 1700 -1600 cm^{-1} , 1540 - 1175 cm^{-1} , 1175 - 940 cm^{-1} , 940 - 700 cm^{-1} and region 1700 -1600 cm^{-1} for classification of *Apis sp.* and stingless bees. The method is straightforward and suitable for large-scale industrial monitoring of honey samples.

5. ACKNOWLEDGEMENT

The author would like to thank the member of Indonesian Apiculture Association for supplying the real honey samples used in this study. Also, the author gratefully acknowledges the financial support from DRPM Grant of Indexed International Publication of Student Final Project (Publikasi Internasional Terindeks untuk Tugas Akhir Mahasiswa/PITTA) 2017.

6. REFERENCES

- Almeida da Silva, Isnandia Andréa; Sarmiento da Silva, Tania Maria. 2013. Phenolic Profile, Antioxidant Activity and Palynological Analysis of Stingless Bee Honey from Amazonas, Northern Brazil. Elsevier. Department of Food Engineering, Center of Technology, Brazil, 4.
- BPS Statistics Indonesia. 2014. Forest Production Statistic. Jakarta (ID) : BPS, page 6.
- Bunaciu, A.A., Aboul-Enein, H.Y. dan Fleschin, S. 2011. Recent applications of Fourier Transform Infrared Spectrophotometry in Herbal Medicines Analysis. *Applied Spectroscopy Reviews* 46, 251-260.
- Chalhoub, C; Gotsiou, P; 2005. Novel Quality Control Methods in Conjunction with Chemometrics (Multivariate Analysis) for Detecting Honey Authenticity. Taylor and Francis Inc. University of Thessaly, Hellas, Greece, 2.
- Ellis, D.I and Goodacre, R. (2006) Quantitative Detection and Identification Methods for Microbial Spoilage, In Food Spoilage Microorganisms (Ed. Blackburn, C), Woodhead Publishing, Cambridge, UK, 3-27
- Feronica, Inessya. 2012. Study of Purity Degree of Commercial Honey in Bogor Using Various Method Tests. Faculty of Animal Science. Bogor Agricultural University, 37 – 54.
- Gok, Seher; Severcan, Mete; Goormaghtigh, Erik; Kandemir, Irfan; Severcan, Feride. 2014. Differentiation of Anatolian Honey Samples from Different Botanical Origins by ATR-FTIR Spectroscopy using Multivariate Analysis. *Food Chemistry* 170, 2-7.



- Janori, Hamdani. 2016. Analytical Instrument Report : Qualitative Analysis of Solid and Liquid Phase Compound Using IR Spectroscopy. Chemical Major, Science and Mathematics Faculty, University of Mataram, 17.
- Jessica, Sherly. 2014. Chemical and Organoleptic Characteristics of Honey from *Apis mellifera*, *Apis cerana*, *Apis dorsata*, and *Trigona sp.* Faculty of Animal Science. Bogor Agricultural University, 20-24.
- Moniruzzaman M, Md Ibrahim Khalil, siti Amrah Sulaiman, Siew Hua Gan. 2013. Physicochemical and Antioxidant Properties of Malaysian honeys Produced by *Apis cerana*, *Apis dorsata*, and *Apis mellifera*, 13-43.
- Rachmawaty, Maya. 2011. The Effectiveness of Several Adulteration Tests Cotton Tree Honey. Faculty of Animal Science. Bogor Agricultural University, 26 – 27.
- Sivakesava, Sakhamuri; Irudayaraj, Joseph. 2001. Classification of simple and complex sugar adulterants in honey by mid-infrared spectroscopy. Department of Agricultural and Biological Engineering. The Pennsylvania State University, 2.
- Sivakesava, Sakhamuri; Irudayaraj, Joseph. 2001. Detection of Inverted Beet Sugar Adulteration of Honey by FTIR Spectroscopy. Department of Agricultural and Biological Engineering. The Pennsylvania State University, 1-8.
- Stuart, Barbara. 20014. Infrared Spectroscopy : Fundamentals and Applications. John Wiley & Sons, Ltd: Analytical Techniques in the Sciences, 33-34.
- Tahir, H; Xiaobo, Zou *et. al.* 2017. Rapid prediction of phenolic compounds and antioxidant activity of Sudanese honey using Raman and Fourier transform infrared (FT-IR) spectroscopy. Elsevier. Departement of Food and Technology of Sudan University, 5.
- Wang, L., & Mizaikoff, B. (2008). Application of Multivariate Data-Analysis Techniques to Biomedical Diagnostics Based on Mid-Infrared Spectroscopy. Analytical and Bioanalytical Chemistry, 391(5), 1641–1654.



MAKING HARD CANDY CONTAINING PURE HONEY AS A FUNCTIONAL FOOD PRODUCT

Atikah Ridhowati¹, Heri Hermansyah², Anondho Wijanarko³, Muhamad Sahlan^{4*}

¹²³⁴*Department of Chemical Engineering, University of Indonesia, Depok, 16425, Indonesia*

⁴*Research Center of Biomedical Engineering, University of Indonesia, Depok, 16425, Indonesia*

¹*atikah.ridhowati@ui.ac.id*

²*heri@eng.ui.ac.id*

³*anondho@eng.ui.ac.id*

⁴*sahlan@eng.ui.ac.id*

ABSTRACT

This study aims to test the potential of honey as an additional ingredient in candy. Candy to be used in the form of hard candy that has a hard and shiny texture. Research begins with finding the optimal composition of honey contained in candy, optimal honey levels in candy by 29%. Honey candy test data obtained from panelist assessment result in hedonic test consumer panel which includes color, aroma, taste and texture rating on four types of honey candy, honey from China, klanceng honey, randu honey and forest honey. Data analysis for the nutritional content of honey candy using descriptive analysis and for the hedonic test using ANOVA test. The results of the overall hedonic assessment of honey candy statistically there is a significant difference. Based on the research, the honey candy produced has moisture content (0.09 - 0.62%) and ash content (0.04 - 0.54%), it meets the requirements of SNI 3547.1: 2008. This is in line with the expectation that the honey candy being studied has potential as a functional food product.

Keywords: candy, hard candy, honey, functional, food product



1. INTRODUCTION

Food products is growing rapidly with the emergence of new creations. As the increasingly rapid development of the times in this era of globalization, changing society's views about a food product. In the past the food just to satisfy the stomach but it is different this time. In addition to filling the public now see from the nutritional value and benefits in the body. Therefore manufacturers to innovate by using a substance which can increase the nutritional value of the food product.

Efforts to use natural resources are diverse and have economic value in tropical countries such as Indonesia, became one of the alternative economic solutions Indonesian society. One of the diversity and availability of alternative utilization of biological resources is a bioactive biological utilization for high-value food and has economic value. Examples are the products produced by honeybees, one of which is honey.

Honey is a unique product of the insects, which contain a high percentage of carbohydrates, practically no protein or fat. The nutritional value of honey depends on the content of simple sugars are fructose and glucose. The sweet foodstuffs are thick with gold until dark, produced in the pocket of various types of bee honey and nectar from various flowers. The taste and scent is strongly influenced by the type of flower where the nectar is collected.

Codex Alimentarius Commission (1984) defines honey as a sweet substance produced by honeybees, derived from the nectar of flowers that develop or secreted plant collected by the bees, then changed form dann combined with special substances that exist in the body of the bee, then stored to cook on cells of honey. Natural bee Indonesia consists of three species, namely *Apis adrenoformis*, *Apis cerana* and *Apis dorsata*. Special substance on bees that function in the process of breaking down sugar is the bee salivary fluid containing hydrolase enzymes. The enzyme invertase, written by worker bees when drinking and brings back honey, serves to convert sucrose into dextrose (glucose) and levulose (fructose).

According to the Indonesian National Standard (SNI) 01-3545-1994, honey is a sweet fluid produced by honey bees from various sources of nectar. Nektar is a kind of liquid produced by the glands of nectar plants, rich in various forms of carbohydrate (3-87%), such as sucrose, fructose and glucose, containing little pengandung nitrogen compounds, such as amino acids, amides, organic acids, vitamins, compound aromatic and mineral. Honey that has been cooked contains 41% fructose, 35% glucose, sucrose 1.9%, dextrin 1.5%, 17% water and other substances such as amino acids as much as 3.5%.

Besides the high sugar content, honey also contains other components such as pollen and various digestive enzymes. In addition, honey also contains a variety of vitamins, namely vitamins A, B1, B2, and minerals such as calcium, sodium, potassium, magnesium, iron, iodine salt even radium. Honey also contains antibiotics and various organic acids such as malic, tartaric, citric, lactic and oxalic. Because honey is very high usefulness.

The role of honey for the growth of small children is very important because in the honey contained folic acid, which can improve blood composition, increasing the number of erythrocytes and also contains hemoglobin. Thus giving honey to children can increase levels of hemoglobin. From the results, comparison, children who were not given the hemoglobin content of the honey only rose 4% for 40 days. While the honey, the content of hemoglobin increased by 23% at the same time with the normal diet.

Based on these reasons the study of the content of honey should be developed to determine the potential utilization of one of them in food products such as candy. Chewing is one of the food products are easily enjoyed, fun and penchant for consumption of children. There are many types of candy one of which is a hard candy. Hard candy candy candy is kind of hard to have the texture and appearance of clear and sparkling (glossy), the main ingredient in the manufacture of hard candy in this study is the honey.



2. METHODOLOGY/ EXPERIMENTAL

2.1. Flowchart of Research

This research will be carried out in several stages, the first stage of making hard containing honey. Then the next step is to elucidate methods of extraction for each sample hard candy, and then identify the quality of honey hard candy.

2.2. Research Time and Location

This research was conducted in February - May 2017 in *Centre for Nanobiotechnology Laboratory, Integrated Laboratory and Research Center, Universitas Indonesia*.

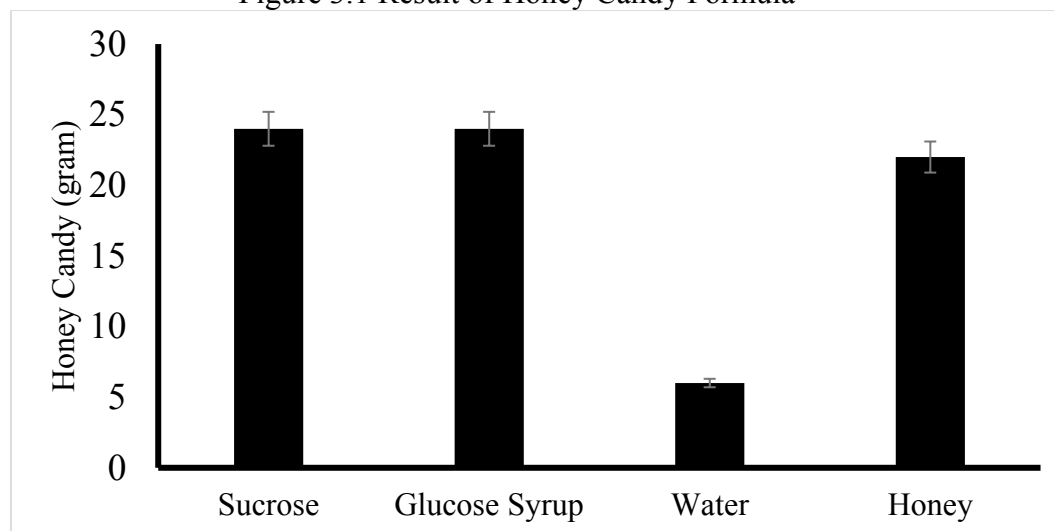
3. RESULTS AND DISCUSSION

3.1. Honey Hard Candy-Making

The research begins with making honey hard candy with varying concentrations of sucrose, glucose syrup, water and honey in order to get the optimum concentration of honey can be added to get a good and tasty honey hard candy.

Used rating scale ranging from (1) to (5). Figures (1) very not hard, (2) not hard, (3) little hard, (4) hard, (5) very hard.

Figure 3.1 Result of Honey Candy Formula



From the results (Figure 3.1) obtained that the best variation concentration to produce hard candy containing honey is 29%. Where in this combination harden properly.

3.2. Organoleptic Test

Organoleptic assessment honey hard candy products using hedonic test is done subjectively based on observations by the human senses. The parameters observed color, aroma, flavor, and texture. The purpose of the organoleptic test was to determine the extent of a commodity or product can be accepted or not by the consumer, so that in this test is required panelists who represent consumers' assessment of the product.

To determine the level of consumer acceptance of these products, tested by 20 panelists by performing 2 replicates. Technically panelists judging by filling out the organoleptic test format that has been provided in accordance with the level of individual favorite.

Organoleptic test conducted on honey hard candy is hedonic test and hedonic quality (level favorite) include color, aroma, flavor and texture. The hedonic rating scale used range from (1) to (9). Figures (1) showed extremely dislike, (2) very not like, (3) not like, (4) somewhat dislike, (5) normal or neutral, (6) little like, (7) like, (8) very like (9) extremely like.

How to data processing which is often used is by using analysis of variance / covariance analysis (Analysis of variance or ANOVA). If the price of the F count larger than F table,



means among the examples there is differences which affect significantly against consumer acceptance (panelists). If the calculated value is smaller than the value of F table means the opposite. Honey hard candy hedonic test results obtained majority of panelists liked the candy added forest honey. Then, from the ANOVA data obtained that the example of honey hard candy samples were significantly different. This is shown in Figure 3.2 to Figure 3.5.

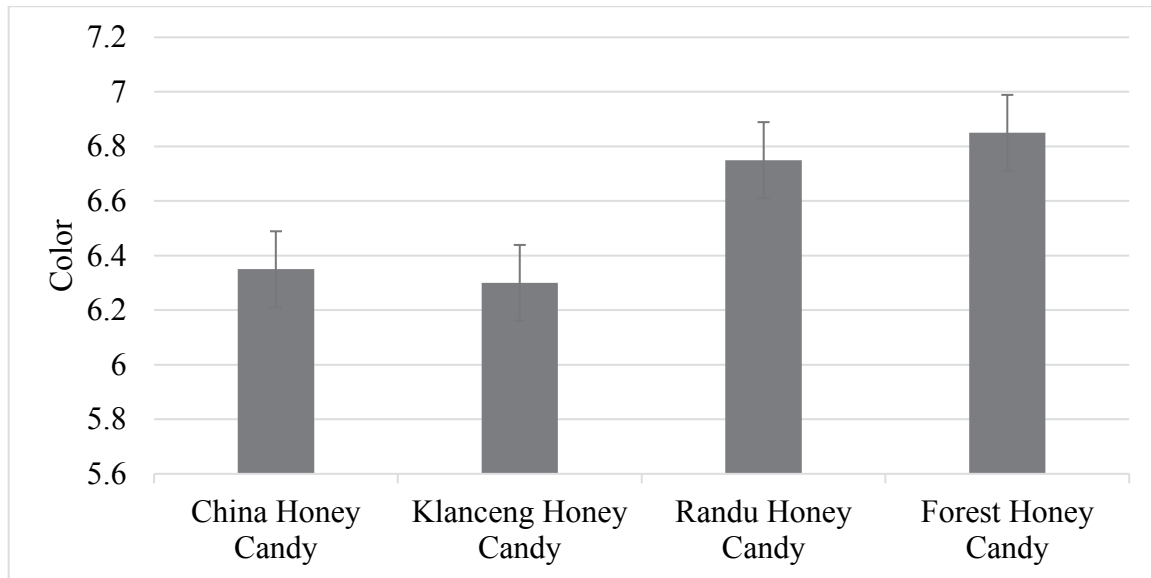


Figure 3.2 Test Graph Hedonic-Organoleptic Color of Honey Hard Candy

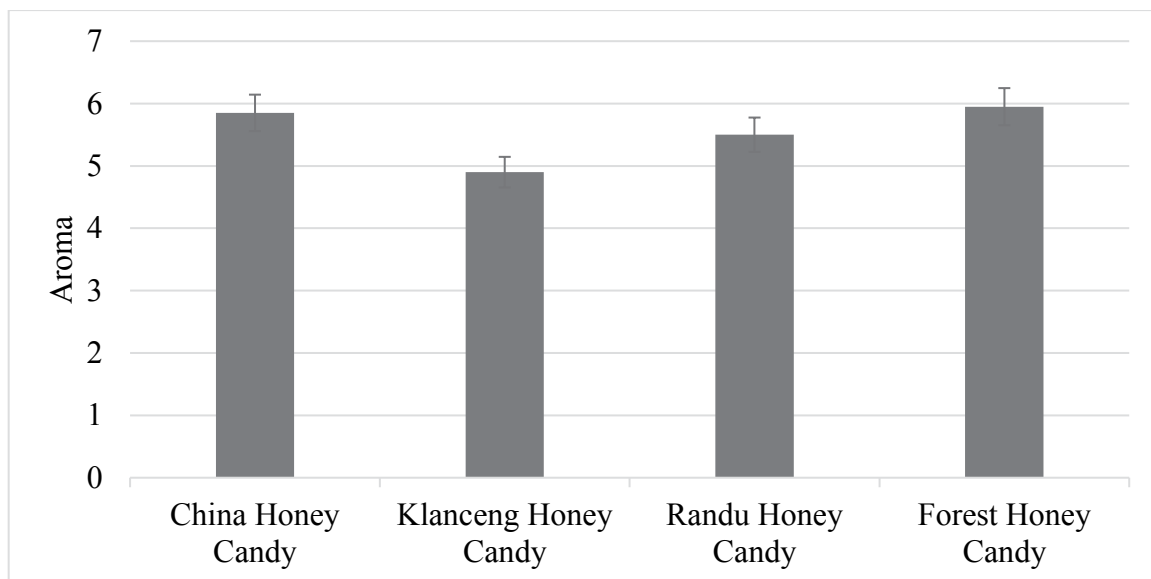


Figure 3.3 Test Graph Hedonic-Organoleptic Aroma of Honey Hard Candy

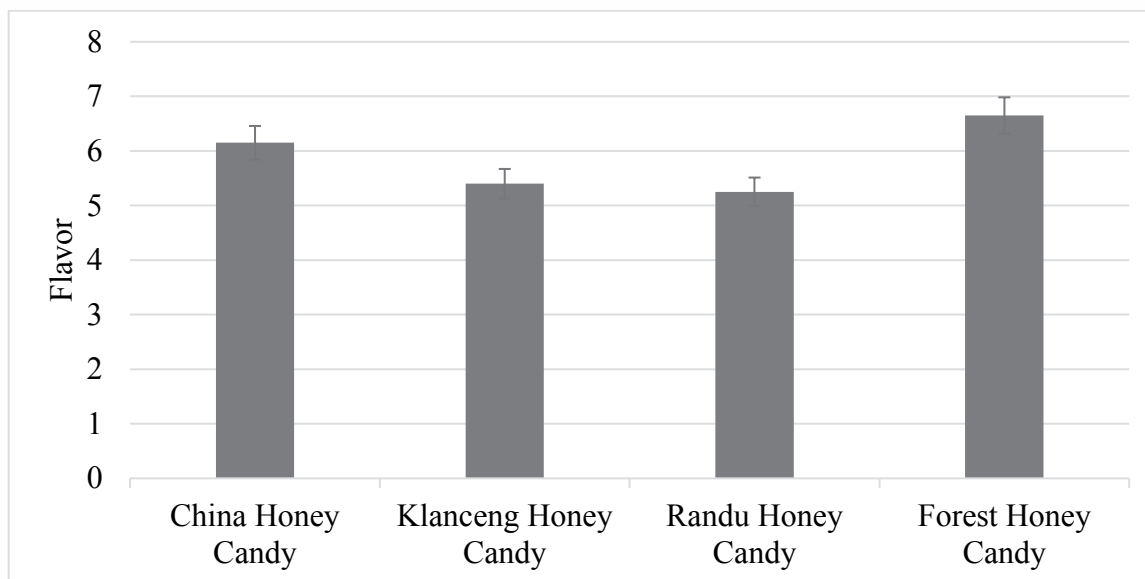


Figure 3.4 Test Graph Hedonic-Organoleptic Flavor of Honey Hard Candy

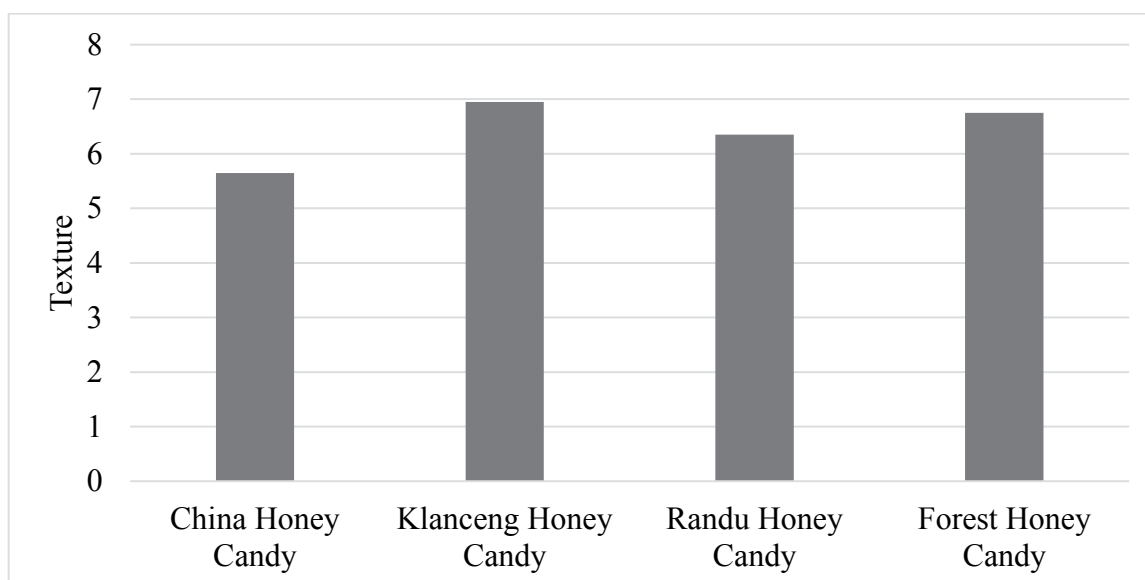


Figure 3.5 Test Graph Hedonic-Organoleptic Texture of Honey Hard Candy

3.3. Moisture Content Test

Determination of moisture content by oven method most widely used and very simple. This method can be used for all food product, unless the product contains components that easily evaporate.

The moisture content affects the appearance and texture of the hard candy. In addition, the amount of water contained in candy affect the structure of hard candy. If the moisture content in the hard candy is too high can cause hard candy not can be hardened so its not formed hard candy or formed hard candy is easy to melted. Then the high water levels will also cause humidity so easily contaminated by microorganisms as bacteria and fungi will be easy to grow, given that bacteria and fungus will grow on damp substrates. Meanwhile, if the result of low water levels below the limit specified requirements are expected to generate a maximum of hard candy. Results of testing the moisture content of honey hard candy are shown in Table 3.9.

Table 3.9 Data Result of Honey Hard Candy Moisture Content Test



Honey Concentration %	Honey Candy Moisture Content (%)			
	China Honey	Klanceng Honey	Randu Honey	Forest Honey
29	0.27	0.31	0.20	0.62
14	0.23	0.34	0.16	0.60
10	0.23	0.32	0.14	0.56
9	0.21	0.30	0.10	0.56
8	0.17	0.28	0.09	0.50

Based on test data that the moisture content of honey hard candy ranging from 0.20 to 0.62%. Based on these results it has met specifications of ISO 3547.1: 2008 is no more than 3.5% mass fraction.

3.4. Ash Content Test

Determination of ash content in candy shows the total content of organic material with mineral identics oxidized to form the oxide because in this process all organic material has been burned. The ash content determined by gravimetric method by finding the difference weight of sample before and after ashing. Ashing process occurs at a temperature of 525°C. The purpose of testing the ash content is to determine the amount of minerals in the sample.

Determination of ash content is very useful as parameters nutritional value of foodstuffs because it is a test to determine the ingredients mineral (inorganic) (Sudarmadji, et. Al, 1989). Too high mineral content in a foodstuff not be accepted by the human body. High mineral will also result in damage to the intestines and digestive disturbances. The ash content is correlated with the mineral content in general, the greater the mineral content of which have a high ash content. Results of testing the ash content of honey hard candy are shown in Table 3.10.

Table 3.10 Data Result of Honey Hard Candy Ash Content Test

Honey Concentration %	Honey Candy Ash Content (%)			
	China Honey	Klanceng Honey	Randu Honey	Forest Honey
29	0.54	0.34	0.13	0.06
14	0.53	0.31	0.10	0.06
10	0.52	0.26	0.10	0.05
9	0.52	0.26	0.09	0.05
8	0.50	0.24	0.09	0.04

Based on the data test on the ash content obtained that honey hard candy ranging from 0.06 to 0.54%. Based on these results it has met specifications of ISO 3547.1: 2008 is no more than 2.0% mass fraction.

4. CONCLUSION

In this study, honey candies meet the requirements set by ISO 3547.1: 2008, based on analysis of sample hard candy has a moisture content 0.09 - 0.62%, while the ash content 0.04 - 0.54%. Although the manufacture of hard candy candy heating process requires high temperatures but the stability of the nutrients of honey after it became hard candy confectionery products continue to function.

According to organoleptic hard candy is significantly different because of the different candy content, where trigona honey is more acidic than sweetened forest honey as of panelists prefer hard candy from forest honey. It can be concluded that honey hard candy products can be a



good variety of food for health but need a refinement in terms of taste, physical, and color to obtain the attractive candy.

5. ACKNOWLEDGEMENT

This research was supported by Directorate of Research and Community Service, Universitas Indonesia. I thank my colleagues from Chemical Engineering Departement Universitas Indonesia who provided insight and expertise that greatly assisted the research, although they may not agree with all of the interpretations/conclusions of this paper.

I thank Dr. Eng Muhamad Sahlan, S.Si, M. Eng. for assistance, Prof. Dr. Ir. Anondho Wijanarko, M.Eng. and Prof. Dr. Heri Hermansyah, S.T., M.Eng. for comments that greatly improved the manuscript. I would also like to show my gratitude to them for sharing their pearls of wisdom with me during the course of this research, and reviewers for their so-called insights. I are also immensely grateful for their comments on an earlier version of the manuscript, although any errors are our own and should not tarnish the reputations of these esteemed persons.

6. REFERENCES

- Badan Standardisasi Nasional, SNI 3547.1: 2008, *Kembang Gula – Bagian I: Keras*. Pusat Standardisasi Industri. Departemen Perindustrian. Jakarta.
- Buckle, K.A., Edward, R. A., Fleet, G.H., Wotton, M. 1987. *Ilmu Pangan*. Universitas Indonesia Press, Jakarta.
- De Man. 1997. *Kimia Makanan*. Institut Teknologi Bandung, Bandung.
- Izzi, Shalliya Eggy. (2016). *Kajian Keekonomian Pabrik Permen Propolis*. Depok: Universitas Indonesia.
- Nurwati. 2011. *Formulasi Hard Candy Dengan Penambahan Ekstrak Buah Pedada (Sonneratia caseolaris) Sebagai Flavor*. *Naskah Skripsi-S1*. Fakultas Perikanan dan Ilmu Kelautan. Institut Pertanian Bogor, Bogor.
- Prasetyowati. 2013. *Kualitas Permen Keras Dengan Variasi Konsentrasi Ekstrak Daun Sirih Hijau (Piper bettle L.) Naskah Skripsi- S1*. Fakultas Teknobiologi. Universitas Atma Jaya Yogyakarta, Yogyakarta.
- Pratiwi, Hestiawan, M.S., Hestiana., Bachtiar, A., dan Kusumaningrum. 2008. *Pengembangan Produk Permen Lolipop dari Ekstrak Daun Sirih (Piper bitle) sebagai Functional Confectionary*. Institut Pertanian Bogor, Bogor.
- Ramadhan. 2012. *Pembuatan permen hard candy yang mengandung propolis sebagai permen kesehatan gigi*. *Naskah skripsi-S1*. Fakultas Teknik. Universitas Indonesia, Depok.
- Winarno ,F.G. 2002. *Kimia Pangan dan Gizi*. PT. Gramedia Pustaka Utama, Jakarta.
- Winarno, F.G. 2004. *Kimia Pangan dan Gizi*. PT. Gramedia Pustaka Utama. Jakarta. 251 hal.



QIR

*The Westin Resort
Nasa Dua, Bali*
24-27 July 2017

SYMPOSIUM G

**International Symposium
on Industrial Engineering**





THE 15TH INTERNATIONAL CONFERENCE QUALITY IN RESEARCH (QIR) 2017

Developing and Implementing the Patient-centered Care Model for Hospital in Indonesia

Jonny^a, T. Yuri Zagloel^{b1}

^a*Department of Industrial Engineering, Faculty of Engineering, University of Indonesia and Department of Accounting, Faculty of Economic and Communication, Bina Nusantara University*

^b*Department of Industrial Engineering, Faculty of Engineering, University of Indonesia*

ABSTRACT

This paper is intended to present a health care model for Indonesian health care industry. Based on previous researches, a patient-centered care model is preferred due to its capability in reducing health care cost and improving its quality simultaneously. However, any model that integrates not only health care cost reduction and quality improvement but also patient satisfaction and hospital profitability is still questionable. Therefore, this research is conducted in order to fulfill the gap in order to integrate those performance goals such as hospital's profitability, patient satisfaction, quality of health care and health care cost. In doing so, a patient-centered care model for Indonesian hospital is being developed by deploying Kano's model, Quality Function Deployment (QFD) and Balanced Scorecard (BSC). From that research, it can be concluded that there are several elements that need to be considered such as leadership, context of the organization, planning, support process, operations, continual improvement, patient satisfaction and financial performance. After having the model developed, then a case study is to be considered in order to measure those elements by their sub elements' performances based on Indonesian Commission on Accreditation of Hospitals in order to study whether there is any improvement taken place after deploying the model. For the result of its self assessment as presented in percentage of compliance, it can be understood that all elements have improved such as Leadership from 50% to 90%, Planning from 50% to 93%, Continual Improvement from 50% to 85%, Operations from 48% to 86%, Support Process from 50% to 84%, Patient Satisfaction from 50% to 82%, Health care cost for in-patient from average IDR 1,000,000 to IDR 800,000 and Return on Equity of the hospital from 0.56 to 0.58. By having these good results, it can be concluded that the model is suitable for the hospital in order to achieve those integrated goals for the hospital's performance.

Keywords: Patient-centered care model; Kano's model; Quality Function Deployment; Balanced Scorecard; Hospital's profitability; Patient Satisfaction; Quality of Health care; Health Care Cost

1 * Corresponding author.
E-mail address: Jonny & Zagloel@ui.ac.id



1. INTRODUCTION

In general, hospital is a part of a holistic health-care system in a certain country including Indonesia. As in other countries, in Indonesia, hospital is regarded as the tertiary health-care institution in Indonesian health-care system. Besides this institution, they are also other institutions including general or family physicians as primary health-care institution and specialist physicians as secondary health-care institution.

As the tertiary institution, hospital is intended to deliver any maintenance and improvement of the society's prevention of any disease, accident or physical and mentally disability. In doing this role, it cooperates with any other related industries to provide healthcare services to the society including both out-patient and in-patient care services.

In Indonesia, there are about 2,506 hospitals established to give various medical services to the society making this industry more complex and attractive than ever before and this number is believed to grow annually due to its attractiveness and the huge Indonesian population (Hukormas, 2016). Unfortunately, Hukormas: 2016 reported that from this number, there are only 284 hospitals among that industry are accredited by *Komite Akreditasi Rumah Sakit* (KARS) or Indonesian Commission on Accreditation of Hospitals. This number is only 11.3% of total hospitals in Indonesia. Therefore, it is not surprisingly to learn that there were about 182 mall-practice cases during the year of 2012 (Wibisono, 2013) although the correlation was not researched yet. This, of course, has signified the importance of quality of care in this industry.

In hospital, there are generally two distinct models regarding to the issue of quality of care such as disease- and patient-centered care models. On the first model, it emphasizes on the physician as the person who decides any required medical treatment needed for his patients based on his clinical experiences and his patient's related medical results. Meanwhile, on the second model, it requires the participation of patient in his medical treatments based on his needs, preferences and his physician's medical advice (Stanton, 2002). Therefore, the patient is the central point of the medical care services not the physician as described in the previous model.

However, in their development, the second model, namely patient-care model, has been widely accepted and adopted especially after many hospitals (Stanton, 2002) have been benefited from its ability to reduce the failure risk both in quality improvement and healthcare cost as the impact of the improved relationship between physician and patient and the efficient utilization of diagnosis tests, prescriptions, hospitalizations and referral (Rickert, 2015).

Although this model has ensured the benefit of both quality improvement and health-care cost reduction, there was still no any integrated model to generate not only these two benefits but also on patient satisfaction and hospital profitability. Therefore, Jonny & Zagloel: 2016 has proposed an integrated Indonesian health care model. This model was developed by employing several TQM tools such as Kano's model, Quality Function



Deployment (QFD) and Balanced Scorecard (BSC) that resulted in several important elements of the model including leadership, context of the organization, planning, support process, operations, continual improvement, patient satisfaction and financial performance. These seven elements were furthermore named as TQM enablers by Jonny & Zagloel:2016.

Based on Jonny & Zagloel:2016, these seven TQM enablers are to be measured by their sub-elements such as 1) Leadership with Governance, Leadership, and Direction (TKP); 2) Context of the Organization; 3) Planning with Staff Qualifications and Education (KPS); 4) Support Process with Prevention and Control of Infections (PPI), Facility Management and Safety (MFK) and Management of Information (MKI); 5) Continual Improvement with Quality Improvement and Patient Safety (PMK); 6) Operations with Access to Care and Continuity of Care (AKP), Patient and Family Rights (HPK), Assessment of Patients (AP), Care of Patients (PP), Anesthesia and Surgical Care (PAB), Medication Management and Use (MPO), and Patient and Family Education (PPK); and 7) Performance Evaluation (Jonny & Zagloel, 2016).

From previous study, these seven-elements have been tested their correlation as the model's validity. However, it was not yet implemented. Therefore, this study was intended to implement whether the hospital can gain any simultaneous improvement in quality improvement, health care cost reduction, patient satisfaction and hospital profitability as intended in the model after implementing this model or not by using PDCA (Plan-Do-Check-Action) method.

2. METHODOLOGY/ EXPERIMENTAL

As mentioned in the previous section, an improvement methodology namely PDCA method was employed to implement the model in the hospital. Therefore, a hospital is selected as a case study to ensure the improvement after implying the model in the hospital. In doing so, there are several actions taken based on the phases on the PDCA method based on McCartry: 2005. This method consists of four phases such as Plan-Do-Check-Action and is widely used in any improvement project. The following sections give more detail on how this method is employed.

2.1 Plan

In this stage, several steps are taken such as 1) the management and staffs of the hospital were gathered in order to be socialized and trained related to this model, 2) After having the mutual understanding from the related parties, the management and staff were given time to prepare for the self assessment to give a clear picture on the quality condition of the hospital based on the Indonesian Accreditation Standard regulated by Indonesian Commission on Accreditation of Hospitals, 3) Then, an independent team was formed to do the self assessment and give recommendation and 4) the management and staffs were to be required to design improvement scenario plan based on the recommendation as the countermeasure on the gap.



2.2 Do

Based on the self-assessment result, the hospital was to implement the recommendation by conducting several quality improvement programs as the countermeasure for closing the gap.

2.3 Check

After the implementation of those recommendations, an independent team was to check the result of the compliance of the hospital on its Indonesian Commission on Accreditation of Hospitals. This stage is needed to ensure that the model was implemented properly or not. Furthermore, the results were also to be compared with the four performance measures a prior-mentioned such as: hospital's profitability, patient satisfaction, quality of health care and health care cost. If the result is not satisfactory then the team will back to the first phase to do the improvement until those prior-mentioned benefits were achieved.

2.4 Action

This is the final stage of the PDCA method. In this phase, the model which has been proved in its efforts to achieve the targeted level of achievement is to be standardized as effective model, therefore, it can be served as additional new knowledge as contribution to the greater knowledge on the knowledge of Total Quality Management in Health-care industry, especially for Indonesian Health-care industry.

Although this methodology is familiar with manufacturing fields, however through many researches and practical applications, it has been proved that this methodology is also suitable in service field. Therefore, this method can be also served as an appropriate methodology in improving the training program.

The company also found this methodology is simple than other available methodology. Therefore after having trained, the team starts using this methodology to improve the program.

3. RESULTS AND DISCUSSION

In this section, the result of the implementation of the Indonesian Health-care model as proposed by Jonny & Zagloel:2016 is elaborated and discussed rigorously based on PDCA cycle as proposed by McCarty: 2005. Therefore, there will be four stages to discuss it.

3.1 Plan

As elaborated in the previous section, in this stage, the management and staffs of the hospital were gathered in order to be socialized and trained related to two topics such as the Indonesian Health-care model as proposed by Jonny & Zagloel: 2016 and standard from Indonesian Commission on Accreditation of Hospitals as proposed by KARS:2012.

In the first topic, according to Jonny & Zagloel:2016, the model that is suitable for Indonesian health care industry consists of seven TQM enablers as depicted in the



following figure:

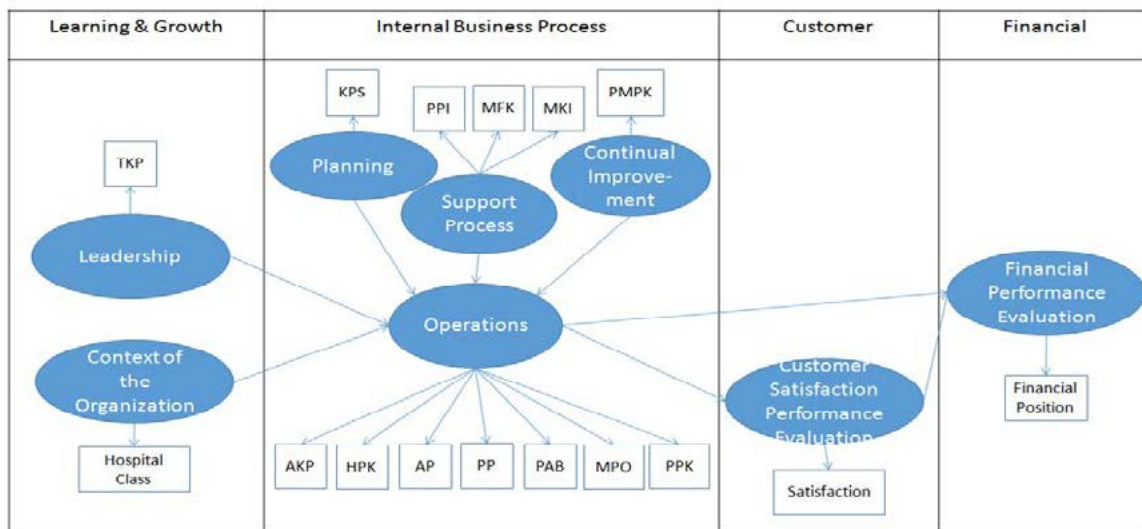


Figure 1. Integrated Indonesian Health-care Model as proposed by Jonny & Zagloel, 2016

From the above figure, Jonny & Zagloel: 2016 proposed that the proper health-care model for Indonesian health-care industry was consisted of seven TQM enablers such as 1) leadership, 2) context of the organization, 3) planning, 4) support process, 5) operations, 5) continual improvement, 6) patient satisfaction and 7) financial performance. This model was tested to randomly 30 patients of an accredited hospital in order to validate the model by administrating an adopted HospiSE questionnaires as proposed by Voon & Abdulah: 2014.

As proposed Voon & Abdulah: 2014, there are 21-items in the questionnaire which are grouped by its element and sub-elements such as 1) Leadership – TKP: hospital is committed in serving the patients, 2) AP – Operations: hospital serves patients based on good understanding of their needs, 3) HKP – Operations: hospital believes in delivering excellent service to the patients, 4) Satisfaction – Customer Satisfaction Performance Evaluation: hospital regularly measures patient satisfaction, 5) MPO, PP, PAB – Operations: hospital solves patients' problem as fast as possible, 6) TKP – Leadership: hospital knows its competitors well, 7) TKP – Leadership: hospital responds fast to the competitor's actions, 8) TKP – Leadership: Hospital targets for patients that it can serve better than its competitors, 9) TKP – Leadership: hospital always tries to be better than its competitors, 10) TKP – Leadership : the employees of the hospital can relate well, 11) TKP – Leadership: there are good co-ordinations among the hospital's staffs, 12) MKI – Support Process: there is good communication among different functions in the hospital, 13) AKP – Operations: necessary patient information is easily accessible from different departments in the hospital when needed, 14) MFK – Support Process: the hospital provides resources to enable the staff to provide excellent service, 15) PMPK – Continual improvement: the hospital is creative and innovative (new ideas and things) in serving the patients, 16) KPS –



Planning: employees of the hospital who serve the patients are very well trained, 17) TKP- Leadership: employees who interact with patients are always motivated or joyful, 18) KP – Planning: hires sufficient number of staff for delivering quality service, 19) KP- Planning: the hospital chooses the suitable staff to serve the patients, 20) TKP- Leadership: the employees are given the authority to decide and act accordingly, and 21) PPI – Support Process: hospital ensures excellent safety for employees and patients all the time.

As the result, this model signifies that in learning & growth perspective, there are two elements naming leadership and context of the organization that have impact on operations. Meanwhile, in internal business process, it signifies that the quality of operations is certainly influenced by three elements such as planning, support process and continual improvement. Furthermore, this operations element will have significant impact both on customer satisfaction evaluation on the customer perspective and financial performance evaluation on the financial perspective (Jonny & Zagloel, 2016).

Meanwhile, on the second topic, that was standards from Indonesian Commission on Accreditation of Hospitals as proposed by KARS:2012. These standards are grouped into four groups totaled 319 standards and 1226 assessment elements as shown in the following table:

Table 1. Standards form Indonesian Commission on Accreditation of Hospitals as proposed by KARS, 2012

Group	Chapter	Standard	Assessment Element
I. Patient-centered care Standards including APK, HPK, AP, PP, PAB, MPO, PPK	7	157	614
II. Hospital Management Standards including PMPK, PPI, TKP, MFK, KPS, and MKI	6	153	569
III. Hospital's Patient Safety Goals	1	6	24
IV. Millennium Development Goals	1	3	19
Total	15	319	1226

From the above table, it can be concluded that there were 13 standards regarding to patient centered care and hospital management while 2 standards with one regulating how the hospital to achieve its patient safety goals and the other regulating how it can achieve Millennium Development Goals. These 13 standards were used to be assessed by the tea



in order to evaluate on how the hospital has implemented the Indonesian Health-care Model as proposed by Jonny & Zagloel: 2016. Therefore there will be 310 standards with 1,183 assessment elements to be assessed by the team.

For assessment purpose, there is a guideline from Indonesian Commission on Accreditation for Hospitals as proposed by KARS: 2012. In this guideline, it will be 3 score criteria covering 3 if fulfilled (80-100%), 2 if partly fulfilled (20%-80%), and 1 if not fulfilled (0-20%). From these scores, there will be standard and chapter assessment by deploying the following formula such as:

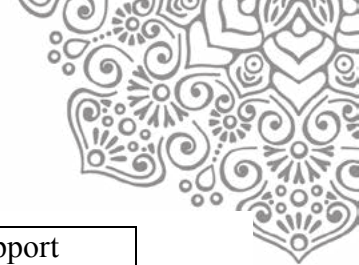
- 1) Standard assessment = $(\text{total score: total assessment} \times 10) \times 100\%$
- 2) Chapter assessment = $(\text{total assessment: total assessment} \times 10) \times 100\%$

In conclusion, it can be understood that these two topics are interrelated. Therefore, it can also be said that by implementing these standards it also implements the model. This mutual understanding was promoted and understood among the management and staffs from the hospital.

After having the mutual understanding from the related parties, the management and staff have done the self assessment using the Indonesian Accreditation Standard as regulated by Indonesian Commission on Accreditation of Hospitals. The following table elaborates more on detail related to its result:

Table 2. Self Assessment Result based on Indonesian Commission on Accreditation of Hospitals as proposed by KARS, 2012

Chapter	Total Score	Total Assessment x10	% fulfillment	Covered in
1. Access to Continuity of Care (APK)	525	105*10=1050	50,0%	Operations = 47.63% or 48%
2. Patient and Family Rights (HPK)	450	100*10=1000	45,0%	
3. Assessment of Patients (AP)	660	172*10=1720	38,4%	
4. Care of Patients (PP)	370	74*10=740	50,0%	
5. Anesthesia and Surgical Care (PAB)	255	51*10=510	50,0%	
6. Medication Management and Use (MPO)	420	84*10=840	50,0%	
7. Patient and Family Education (PPK)	140	28*10=280	50,0%	
8. Quality Improvement and Patient Safety (PMKP)	440	88*10=880	50,0%	Continual Improvement = 50%



9. Prevention and Control of Infections (PPI)	415	83*10=830	50,0%	Support Process = 50%
11. Facility Management and Safety (MFK)	460	92*10=920	50,0%	
13. Management of Information (MKI)	545	109*10=1090	50,0%	
12. Medical Professional Education (KPS)	495	99*10=990	50,0%	Planning = 50%
10. Governance, Leadership and Direction (TKP)	490	98*10=980	50,0%	Leadership = 50%

From the above table, it can be concluded that Leadership was 50%, Planning was 50% Continual Improvement was 50%, Operations was 48%, Support Process was 50%. All elements were below required at 80%. This result gives insight that operations of the hospital was the lowest and needed to be improved. That is why from questionnaire it can be concluded that the Patient Satisfaction was as low as 50%. On the other hand, the health-care cost for in-patient was reported at average of IDR 1,000,000.00. Meanwhile, the Return on Equity of the hospital was at 0.56.

The above results have been compiled and discussed with the management and staff. From that discussion, there were some recommendations generated as improvement programs for the team to design improvement scenario plan in order to close the gap.

3.2 Do

From the improvement scenario plan as described in the previous section, team was formed in order to implement the plan thoroughly to the plan with a tight time line of one year as its implementation period. A PDCA person-in-charge (PIC) was also appointed to make sure all needed action can be taken accordingly. Besides that, the high level of top management's commitment has also proven its effectiveness in making this happened. During the implementation period, several problem identification and corrective actions were also taken to ensure the plan was implemented as accordingly to the plan.



figure 1. Assessment situation in a hospital

3.3 Check

After the implementation of the plan, a team was formed to check the result of the compliance of the hospital on its Indonesian Commission on Accreditation of Hospitals. This result is presented in the following table:

Table 3. Self Assessment Result based on Indonesian Commission on Accreditation of Hospitals as proposed by KARS, 2012 after implementation of the scenario plan

Chapter	Total Score	Total Assessment x10	% fulfillment	Covered in
1. Access to Continuity of Care (APK)	525	105*10=1050	50,0%	Operations = 47.63% or 48%
2. Patient and Family Rights (HPK)	450	100*10=1000	45,0%	
3. Assessment of Patients (AP)	660	172*10=1720	38,4%	
4. Care of Patients (PP)	370	74*10=740	50,0%	
5. Anesthesia and Surgical Care (PAB)	255	51*10=510	50,0%	
6. Medication Management and Use (MPO)	420	84*10=840	50,0%	
7. Patient and Family Education (PPK)	140	28*10=280	50,0%	
8. Quality Improvement and Patient Safety (PMKP)	748	88*10=880	85,0%	Continual Improve-



				ment = 85%
9. Prevention and Control of Infections (PPI)	697	$83 \times 10 = 830$	84%	Support Process = 84%
11. Facility Management and Safety (MFK)	772	$92 \times 10 = 920$	84%	
13. Management of Information (MKI)	915	$109 \times 10 = 1090$	84%	
12. Medical Professional Education (KPS)	921	$99 \times 10 = 990$	93,0%	Planning = 93%
10. Governance, Leadership and Direction (TKP)	882	$98 \times 10 = 980$	90,0%	Leadership = 90%

The above table was then compared with table 2 to learn that there was improvement where Leadership was improved from 50% to 90%, Planning was improved from 50% to 93%, Continual Improvement was improved from 50% to 85%, Operations was improved from 48% to 86%, Support Process was improved from 50% to 84%. Meanwhile, from survey, it can be learnt that Patient Satisfaction was improved from 50% to 82%. Furthermore, from financial perspective, Health care cost for in-patient was reduced from average IDR 1,000,000 to IDR 800,000 and Return on Equity of the hospital was increased from 0.56 to 0.58. These results were satisfactory and it can be concluded that the model is effective in improving the hospital condition.

4. CONCLUSION

From the previous section, it can be concluded that the Indonesian healthcare model was able to integrate quality improvement, cost reduction, patient satisfaction and hospital profitability after its implementation in the selected hospital. However, the authors realize that this finding is insufficient to be claimed as a whole Indonesian hospital industry. Therefore, for future research, it can be taken into consideration on adding more hospitals as its sample to be claimed as a whole Indonesian hospital industry.

This finding may have several theoretical and managerial implications. As theoretical implication, by implementing this model, there are several principles that can be found. These principles cover seven TQM enablers such as 1) leadership, 2) context of the organization, 3) planning, 4) support process, 5) operations, 5) continual improvement, 6) patient satisfaction and 7) financial performance. Meanwhile, for managerial implications, this model may encourage the stakeholders of the hospital to implement this model in order to gain the same benefit in their hospital.

However, this research may have several limitations due to its limited sample and it should be extended to cover many types of hospital. Therefore, in order to cover these limitations, future research directions can be extended to other types of hospitals.

5. ACKNOWLEDGMENT



This paper was supported by RS Bina Husada Cibinong as the first and only accredited private hospital in Bogor Regency for administrating the survey needed to evaluate and validate the model.

6. REFERENCES

- Bina, Lorika. (2016). Transition ISO 9001: 2008 to ISO 9001:2015. Retrieved June 13th 2016 from <http://www.slideshare.net/PECBCERTIFICATION/pecb-webinar-49304033>
- Cekspot.(2016). RS Bina Husada Cibinong. Retrived June 29th 2016 from <http://m.cekspot.com/RumahSakitBinaHusadaCibinong>
- Chassin, Mark R and Robert W. Galvin (1998). The Urgent Need to Improve Health Care Quality. *Journal of the American Medical Association*, vol 280, no. 11, p.1000-1005
- D'Souza, Sunil C and A.H. Sequeira (2011). Application of MBNQA for Service Quality Management in Health Care Organizations. *International Journal of Engineering, Science and Technology*, vol. 3, No. 7, pp. 73-88
- Dhae, Arnoldus (2014). Tiap Tahun, 600 Ribu Orang Indonesia Berobat ke Luar Negeri. Diakses 16 Oktober 2015. <http://rona.metrotvnews.com/read/2014/10/21/308075/tiap-tahun-600-ribu-orang-Indonesia-berobat-ke-luar-negeri>.
- Duggirala, M., Rajendran, C., & Anantharaman, R. N. (2008). Patient-perceived Dimensions of Total Quality Service in Healthcare. *Benchmarking: An International Journal*, 15, 560–583
- Dunbar, Nicola (2013). The state we are in: A (new) National Approach to Health Literacy in Australia. Retrieved June 20th 2016 from <http://www.slideshare.net/CharlesPerkinsCentre/nicola-dunbar>
- Feigenbaum, A. V. (1991). *Total Quality Control*. 3rd ed. Singapore: McGraw Hill
- Gyrna, Frank M. (2001). *Quality Planning and Analysis from Product Development through Use*. 4th ed. New York: McGraw Hill
- Hazilah, A. M. N. (2009). Practice Follows Structure: QM in Malaysian Public Hospitals. *Measuring Business Excellence*, 13(1), 23–33.
- Hemme, David. 2015. *Customer Focused Process Innovation*. USA: McGraw Hill
- Hukormas. (2016, 19 Feb). Jumlah Surveior Akreditasi Rumah Sakit Terus Ditambah. Retrieved June 16th 2016 from <http://www.yankes.kemkes.go.id/read-jumlah-surveior-akreditasi-rumah-sakit-terus-ditambah-715.html>
- Joint Commission International. 2016. JCI-Accredited Organizations. Retrieved June 20th 2016 from <http://www.jointcommissioninternational.org/about-jci/jci-accredited-organizations/>
- Jonny, T. Yuri Zagloel, (2016), The Development of An Integrated Indonesian Health Care Model Using Kano's Model, Quality Function Deployment and Balanced Scorecard, Proceeding of 2016 Annual Conference on Industrial and System Engineering (ACISE), Yogyakarta, 6-7 October 2016, Indonesia.
- Kamaru, Society (2013). Model Kano. Diakses 25 November 2015. <http://societykamaru.blogspot.co.id/2013/11/model-kano.html>
- Komisi Akreditasi Rumah Sakit. (2011). *Standar Akreditasi Rumah Sakit*. Jakarta.



- Kaplan, Robert. 1996. *Balanced Scorecard: Translating Strategy into Action*. USA: HBS Press
- Kozak, M., Asunakutlu, T., & Safran, B. (2007). TQM Implementation at Public Hospitals: A Study in Turkey. *International Journal of Productivity and Quality Management*, 2(2), 193–207.
- Meyer, S. M., and Collier D. A. (2001). An Empirical Test of the Causal Relationships in the Baldrige Healthcare Pilot Criteria. *Journal of Operations Management*, 19, 403–425.
- Miller, W. J., Sumner, A. T., & Deane, R. H. (2009). Assessment of Quality Management Practices within the Healthcare Industry. *American Journal of Economics and Business Administration*, 1(2), 105–113.
- Pro, QFD (2015). Quality Function Deployment. Diakses 25 November 2015. http://www.hoshinkanripro.com/qfd_phase_1.html
- Rad, A. M. Mosadegh (2005). A Survey of Total Quality Management in Iran: Barriers to Successful Implementation in Health Care Organizations. *Leadership in Health Services*, 18(3), 12–34.
- Raja, M. P. N., Deshmukh, S. G., & Wadhwa, S. (2007). Quality Award Dimension: A Strategic Instrument for Measuring Health Service Quality. *International Journal of Health Care Quality Assurance*, 20, 363–378
- Rickert, James. (2012). Patient-Centered Care: What It Means and How to Get There. Diakses 01 Januari 2015. <http://healthaffairs.org/blog/2012/01/24/patient-centered-care-what-it-means-and-how-to-get-there/>
- Rao, Ashok et. al. (1996). *Total Quality Management: A Cross-Functional Perspective*. USA: John Wiley & Sons, Inc
- Lab, Cybermetrics. 2015. Ranking Web of World Hospitals. Retrieved June 20th 2016 from <http://hospitals.webometrics.info/en/node/17>
- Milner, Brigid M. 2007. *Implementing Hospital Accreditation: Individual Experiences of Process and Impacts* (Doctoral's thesis). Available from ProQuest Dissertation and Theses database.
- Salaheldin, S. I., & Mukhalalati, B. A. (2009). The implementation of TQM in the Qatari healthcare sector. *Journal of Accounting-Business and Management*, 16(2), 1–14.
- Schumacker, Randall E., Richard G. Lomax (2010). *A Beginner's Guide to Structural Equation Modelling*. 3rd Ed. New York: Taylor and Francis Group, LLC
- Stanton, Mark W. (2002, May). Expanding Patient-Centered Care to Empower Patients and Assist Providers. Agency for Healthcare Research and Quality: *Research in Action*, Issue No. 5, 1-5.
- Vallejo, Paula et al. (2006). A Proposed Adaptation of the EFQM Fundamental Concepts of Excellence to Health Care based on PATH Framework. *International Journal for Quality in Health Care* 2, vol. 18 No. 5, pp. 327-335
- Voon, Boo Ho and Firdaus Abdulah (2013). Developing a HospiSE Scale for Hospital Service Excellence. *International Journal of Quality & Reliability Management*, vol. 31 No. 3, 2014 pp. 261-280
- Wachter, Robert M. (2008). *Understanding Patient Study*. 1st edition. USA: McGraw Hill
- Wardhani, V., Utarini, A., van Dijk, J. P., & Post, D. (2009). Determinants of Quality Management Systems Implementation in Hospitals. *Health Policy*, 89, 239–251.
- Wibisono (2013). Sampai Akhir 2012, Terjadi 182 Kasus Malpraktek. Diakses 25 November 2015. <http://nasional.tempo.co/read/news/2013/03/25/058469172/sampai-akhir-2012-terjadi-182-kasus-malpraktek>



IMPROVING QUALITY AND PRODUCTIVITY ANALYSIS AS AN EFFORT TO DEVELOPMENT THE SUPPORTING INDUSTRIES IN INDONESIA

Hafid Abdullah^a dan Eddy Herjanto^b

^{a)} Metal Industries Development Centre (MIDC), Ministry of Industry Indonesia
Jl. Sangkuriang No. 12 Bandung 40135

Email: hafidochan@yahoo.com

^{b)} Ministry of Industry Indonesia, Jl. Jenderal Gatot Subroto Kav.52-53 Jakarta

ABSTRACT

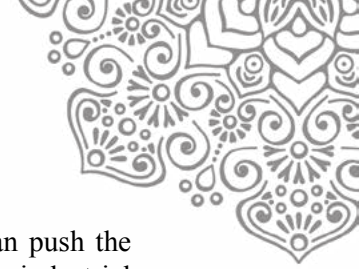
The quality and productivity on supporting industries in Indonesia was identified low. The target of this research is to improve quality and productivity products increased as an effort to development the supporting industries to be able to complete both in domestic market an in a free market. The research method was taken, consist of: analysis of the condition of supporting industries currently that seen from the reject ratios and quality control, SWOT analysis and improved way through the implementation of the Quality Control Circle (QCC) management for continuous improvement. The analysis showed that most of the rejected ratio can be decreased to be 2% approximated 45,65%, Indonesian National Standard is less used (23.91%), which are widely applied quality system is ISO 9000:2008 (30.43%) and work instructions (30,43%). Quality improvement methods that used are QCC approximated 45.65%, benchmark (34.78%), Failure Method and Effect Analysis (17.39%), Quality Function Deployment (8.7%) and others 15.22% did not use the method. The weakness of the SWOT analysis result is that the implementation of QCC quality management system has not been optimally implemented. For examples, the implementation QCC in PT. MTM. Result of the improvement the percentage of rejected ratios spacer component is 25% (before improvement) claimed by PT. Komatsu Indonesia as its consumer (partnership) can be decreased to be 0% (after improvement).

Key words :QCC, 5W1H, continuous improvement, supporting industries.

1 INTRODUCTION

National industrial development is a part of industrialized process challenges all industrial sectors to tightly compete, especially in facing globalization era. The external challenge that must be faced is Indonesia as a member of World Trade Organization (WTO), and therefore its domestic market is open to the ASEAN economic community (MEA) and China as stipulated by ASEAN-China Free Trade Agreement (ACFTA) and APEC in the year of 2020. It impacts on increasingly export opportunities as well as threats for supporting industries in the country from the emergence of much larger quantities of imported products at very competitive prices (Hafid, 2012).

Supporting industries based on GAIKINDO (Indonesian Automotive Industry Association) is (Achadiat Atmawinata, et al, 2008) component and parts industries to meet the needs of other industries to support the final manufacture or as a component/part after market.



Its important role in supporting the development of industry in Indonesia, can push the pace of regional economic development because it can provide stimulation for other industrial sectors either directly or indirectly related through multiplier effect (Hafid dan Eddy Herjanto, 2015). Its location is spreading in DKI Jakarta, West Java (Tangerang, Bekasi, Bogor, Karawang, Sukabumi, Bandung), Central Java (Tegal, Klaten, Juwana) and East Java (Sidoarjo, Pasuruan, Surabaya) and some in Medan (MIDC, 2012). Viewed from the scale of the industry is very diverse ranging from small and medium enterprises (SMEs) industry to large scale companies with network of capital and international marketing. Large-scale industry is generally a PMA company or a joint venture company while SMEs are generally local companies (PMDN).

In order to the quality, productivity and competitiveness of companies in the free markets (Klaus Schwab, 2016), especially supporting industries scale SMEs- in order to survive and win the competition. The key is to be able to improve productivity and maintain the quality of products to be marketed. This condition presupposes the optimal effort of an industrial system (James L. Riggs, 2008; Richard B. Chase, et al, 2004; RI Law No. 3 on Industry, 2014), namely the existence of quality control at every stage of the production process, from input of raw materials to be finished good output (ATQC, 2004; Sambas and Hartono, 2014), in order to satisfy consumer (*partnership*) and who do it.

According to Michael E. Porter (Yuyun, 2013) competitiveness is formed by the interaction of several factors, namely: (1) rivalry among the same business people, (2) new comer threats, (3) supplier threats, (4) substitute threats, (5) the buyer's threat. If the threats and rivalries inside are very high, the situation will affect profitability.

One of the method to improve the competitive advantage of a company is to implement a Total Quality Control (TQC) management system in which its implementation is carried out with its Quality Control Circle (QCC). To produce a continuous improvement recommendation (Jeffrey K. Liker and David Meier, 2007) is through the method of improving the quality and productivity of the products that can satisfy the consumers and able to improve competitiveness, both in the domestic and in global markets.

Total Quality Control (TQC) is a management system that includes all leaders and employees of all levels by applying the concept of quality control with statistical methods to improve customer satisfaction and who do it (ATQC, 2004).

Quality Control Circle (QCC) management is defined as an effort to control QCC activities so as to support the company's activity plan. While the QCC is a small group of employees/organizations (4-10 peoples) of similar work who voluntarily hold regular meetings outside of working hours to make improvements to work methods and product quality at work place (Kaoru Ishikawa, 2005).

Based on the problems above, the research objectives are: (1) to know the condition of supporting industries currently, that seen from the reject ratio and quality control, (2) what factors influence the internal and external environment supporting industries by using SWOT analysis method, (3) implementation of QCC management system containing example case decreasead rejected ratio of spacer component (Figure 5) in PT. MTM due to claims from PT. Komatsu Indonesia is a consumer (*partnership*).

We hope that the results of research can be used for founder or the owner (managers) of the company as an effort to develop domestic supporting industries and increase the national competitiveness.



2 METHODOLOGY

In this research method is used the analysis of historical data, descriptive and action. Primary data source obtained during the year of 2011 to 2016 through survey to supporting industries by doing observation and interview directly to management of selected company which become object of research besides hearing with technicians and expert judgements from practitioners, academics and industry agency related. Secondary data were obtained from literature studies from various publications, journals and institutional reports related to the discussion, etc.

To know the quality control in integrated to product quality at supporting industries done implementation of TQC/QCC management system with case example in PT. MTM. To maintain the confidentiality of the company name only mentioned initials.

Stages of TQC/QCC implementation activities in PT. MTM is as follows:

1. Preparation of the TQC / QCC committee, organizational structure and work program.
2. The kick of implementation of the TQC/QCC method.
3. Socialization of work programs of TQC/QCC committee activities: (a) establishment of TQC/QCC team, (b) preparation of TQC/QCC team meeting schedule (c) training/implementation guidance.
4. Industry survey and start TQC/QCC team activities at PT. MTM, which includes: (a) identification of the condition of the company before improvement, (b) observing the flow of the manufacturing process, (c) documenting the initial conditions before and after the improvement, (d) research the factors causing the rejected product from: materials, finished products, operators, machinery and equipment, working methods and work environment.
5. Consultation, evaluation and countermeasured plan.
6. Take picture after improvement.
7. Standardization and the countermeasured plan.
8. Conclusions and recommendations of research results.
9. Presentation of results of activities by TQC/QCC team in front of company leaders and employees.
10. Evaluation and reporting of research.

The stages of research conducted according to Moch. Nazir (2011) is as follows:

1. Identification and selection of problems.
2. Selection of conceptual frameworks for research problems and relationships with prior research.
3. Formulate research problems.
4. Build an investigation.
5. Provide definitions of variable measurements.
6. Selecting the sampling procedures and techniques used (Sugiono, 2012; Wibisono, 2004).
7. Collection and processing of data.
8. Analyze and interpret the data.
9. Conclusions and suggestions
10. Reporting of research results.



3. RESULT AND DISCUSSION

3.1. The Condition *Supporting Industries* at Present

Survey on supporting industries is to obtain data and information about the supporting industries at this time and the obstacles that is faced. Some aspects studied are the rejected ratio and quality control with the picture as follows (Ministry of Industry, 2011):

1. Rejected Ratios

From the survey results obtained (Figure 1) shows that most supporting industries are able to suppress the rejected ratio $\leq 2\%$ (45.65%). This condition indicates that most supporting industries already perform standardized workmanship procedures. For industries with rejected ratios greater than 10% need to be supported to reduce the rejected ratio by less than 5% by increasing the employee's capability (technician) and improving production process control in accordance with standard requirements.

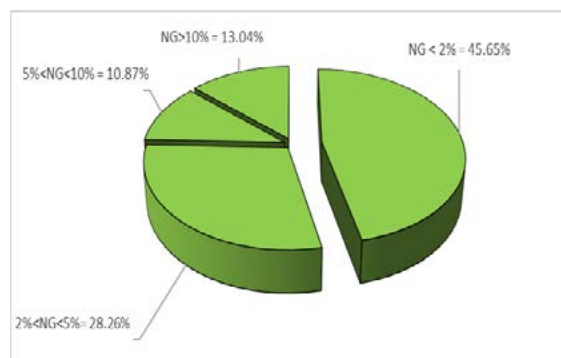


Figure 1. *Reject ratio*

2. Quality Control

From the survey data obtained (Figure 2) shows that the supporting industries do the quality control, that is apply international quality standard (36,96%), quality standard from buyer (36,96%) and company quality standard (36,96%). Quite interesting to note, it is less use the Indonesian National Standard (SNI) or quality standards of export destination countries While the method of quality improvement (Figure 3) used is dominated by Quality Control Circle (45.65%) and Benchmark (34.78%).

Quality system applied in the company, mainly quality system ISO-9000: 2008 (30.43%) and Work Instruction guide (30.43%) company. Implementation of ISO 9000: 2008 quality management system that has not been certified and apply other quality management system respectively 15,22%.

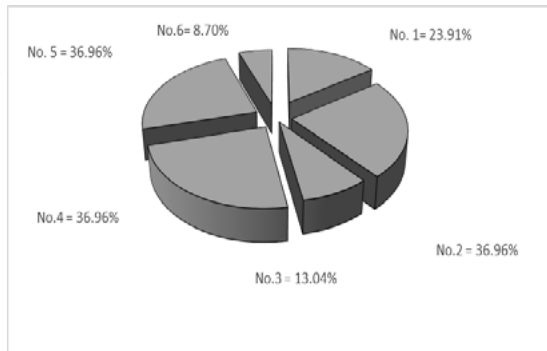


Figure 2. Quality standards used
Note: (1) SNI, (2) International quality standards, (3) Quality standards of export destination countries, (4) Quality standards of buyers, (5) Company quality standards, (6) None.

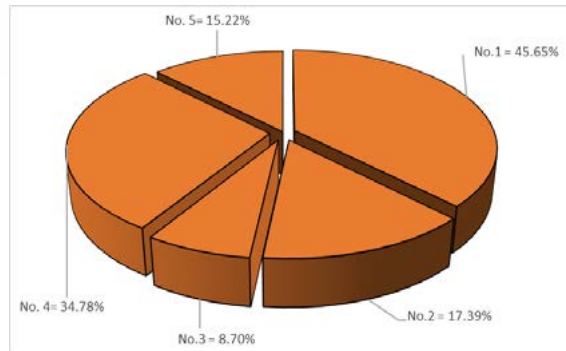


Figure 3. Quality improvement methods
Note: (1) QCC, (2) FMEA, (3) QFD, (4) Bench mark, (5) None

3.2. SWOT Analysis

The tools used to analyze the state of the internal environment and external supporting industries in this study are SWOT analysis (Che-Wei Chang, 2013, Rangkuti, 2005,2013), namely: (1) Strengths, (2) Weaknesses, (3) Opportunities, and (4) Threats.

Details of the SWOT analysis on the current supporting industries are as follows (Hafid, 2014):

1. Strengths:

- a. Various programs and support from the government, State-Owned Enterprises (BUMN), Private Enterprises (BUMS) and Universities (PT) and other institutions in an effort to improve ability and development are continuously improved.
- b. The absorptive capacity of human resources and the increase of people's incomes.
- c. The application of the product usage has a wide spectrum in the industrial field, namely: industrial machinery of factory equipment, agriculture, textile, health, weapon, electronics, electrical components, automotive and other much needed Indonesia.
- d. Assist the government in reducing dependence on imported components so as to save the country's foreign exchange, increase non-oil exports, strengthen industrial structure and even distribution of development.

2. Weakness:

- a. The resulting product has low added value.
- b. The machines and equipment used are still limited, most of them old enough for more than 10 years and have not followed the development of new technology.
- c. Production equipment technology is not up to date, especially SMEs.
- d. The quality of human resources is still relatively low, especially the SMEs scale.
- e. Not enough qualified human resources qualified and professional. SKKNI already exist but not yet socialized and well adopted.
- f. The investment capability for machinery and equipment procurement is still low due to limited capital.



- g. Low attention research and development for materials, products, product functions, processes and equipment.
 - h. Produce very diverse product types with small quantities.
 - i. Procurement of raw materials is still imported.
 - j. The efficiency of production costs are still likely to be improved.
 - k. Implementation of operations management, such as: kaizen method (TQC/QCC) is still not optimally implemented.
3. Opportunities:
- a. Market demand continues to increase in both automotive components, heavy equipment, oil and gas equipment, petrochemicals, cement, paper industry, electronics and others.
 - b. The domestic market opportunity is the import of components (spare parts) is still high with a high price.
 - c. Still a great opportunity to use raw materials originating from within the country.
 - d. There are still many competent and experienced human resources that have not been given the responsibility in accordance with his expertise.
 - e. The opening of assistance from various institutions of government, universities and private for the improvement of human resources, management and technology.
 - f. Still high idle capacity.
4. Threats:
- a. Competition from imported products will be sharper as a result of the opening of the global market.
 - b. To produce a quality product in accordance with the standards and technical specifications set need the mastery of adequate technology from the engineers and technicians.
 - c. Mass production capabilities, in which the production process flow and control system, as well as supporting equipment for quality assurance are essential.
 - d. The user industry (partnership) of the product requires quality assurance, timeliness of completion and continuity of supply as well as competitive and competitive prices

3.3 Improving Quality and Productivity Analysis

For example case of quality improvement and productivity done in part production of PT. MTM located in LIK Takaru Tegal Central Java. The company has a type fabrication of sheet metal working heavy equipment (Figure 4). Some of its customers are PT. Komatsu Indonesia (main customer), PT. Katsushiro and PT. Hanken.

The company's quality policy is (1) fulfilling the satisfaction of its partnership, (2) maintaining the quality and productivity targets, (3) providing the best quality.

Quality control measures are performed by the QCC method (Komatsu, 2015) are as follows:

1. Step I. Theme Selection

- a. Theme: "Improved quality of PC 130-F production"
- b. Title: "Reduced rejected ratio of component spacer 2075465260 in drilling process"
- c. Reasons for choosing a theme:
 - Based on the results of inspections conducted under the production of PT. MTM is still a lot of spacer components that claimed by PT. Komatsu.



- Improving the quality of PT. MTM as an effort for the satisfaction of PT. Komatsu who became consumers or partnership.

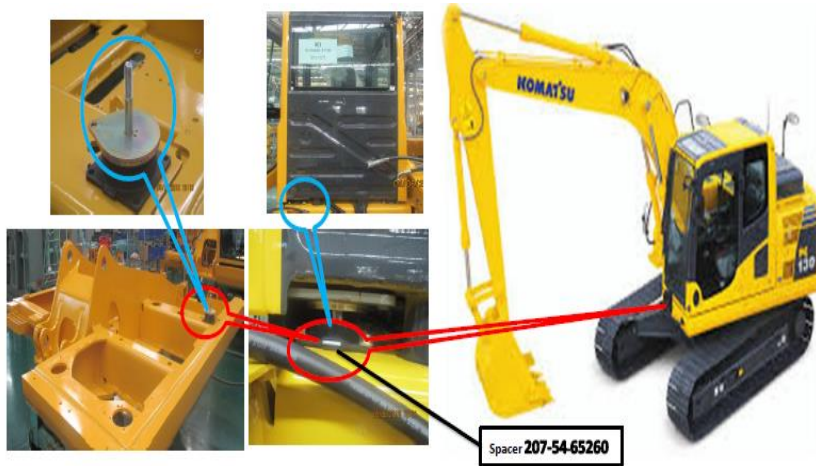


Figure 4. Hydraulic excavator PT. Komatsu Indonesia



Figure 5. Component spacer

2. Step II: Know the current condition and determine the target

Based on the examination of the spacer component type data of production in 2016 under the production of PT. MTM which is made for order PT. Komatsu, spacer component 2075465260 (Figure 5) has the highest reject ratio (25%) claimed by PT. Komatsu as shown in Figure 6 and Figure 7. This indicates that the component needs to be given top priority to be addressed. Next team QCC PT. MTM sets the target ratio of reject to 0% claimed.

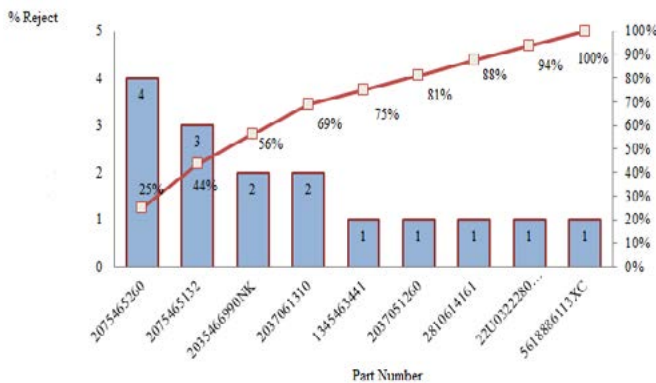


Figure 6. The spacer component production PT. MTM which is claimed

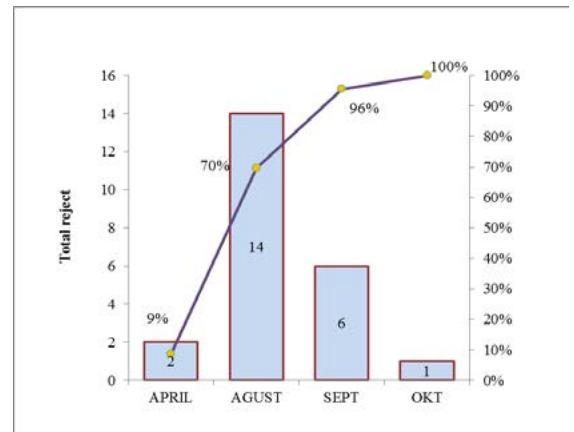


Figure 7. Rejected ratio component spacer the year of 2016 in PT. MTM

3. Step III: Activity plan

After forming a QCC team consisting of small group activities with 6 members, with group leaders, facilitators and advisors of 1 person each, then the program schedule (plan and actual) QCC method application as shown in Table 1.



Table 1. QCC team activity schedule at PT. MTM (November to December 2016)

Schedule of activity (Pland and actual)			Activity QCC 2016											
Step of improvement			Weeks											
			1	2	3	4	5	6	7	8	9	10		
Plan	1.	Selecting theme and title Pemilihan tema dan judul	x											
	2.	Recognizing current situation and setting the goals	x	x	x	x								
	3	Creating the action plan	x	x										
	4	Analysis of cause and effect			x	x	x	x						
Do	5	Implementation of countermeasure												
Check	6	Verifying the effects								x	x			
Action	7	Establishing Standard											x	
	8	Remaining problem and future plan												x

Note : x = plan according to actual

4. Step IV: Analysis of the cause of the problem

To find out the cause of product damage problem of the current conditions first made the production process of spacer production in PT. MTM, as shown in Figure 8. Figure 6 and Figure 7 show that the spacer component becomes the highest cause of damage so it's needs to be addressed immediately. The cause of the damage was re-analyzed using a fish bone covering 5M (materials, machinery and equipment, human, work methods and work environment), is described in Figure 9.

Through QCC team discussion the main cause of damage is due to technician PT. MTM uses a mall to mark the spacer that will be in the drilling process. After used some time and time, then the hole in the mall getting bigger, so that the process of the mall position is not center.

In a production process drilling (Figure 9) there can be a dispersion of product quality, therefore, to analyze the cause of causal problems affecting the quality of Spacer component, brainstorming method is used with QCC team members (Table 2).

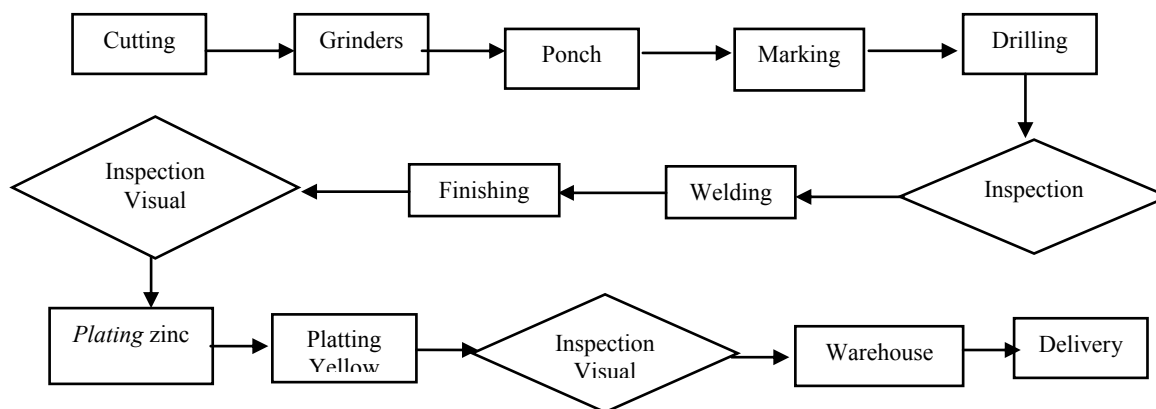


Figure 8. The process of making spacer components in PT. MTM



Table 2. Analysis of the cause of the problem

Faktor	Why 1	Why 2	Why 3	Why 4
Metode	There are already methods but not optimally implemented work instruction in the drilling machine.	Many components reject 2075465260	On the check sheet look various types of reject	The results of the work of new operators are different from those experienced
Operator	Dimensions between NG holes	When the process of marking with the mall is not center	Mall marking is not standard	The hole point on the marking mall is already enlarged



Figure 9. Drilling process using mall (before improvement)

5. Step V: Implement the repair

After knowing the root of the problem by using the method of causal analysis (Figure 9) then is determined the ways of countermeasures reject component spacer 2075465260 through discussion in the QCC group, attempted to eliminate or reduce the damage that occurred.

Improving product quality can be achieved one of them by using a tool (jig drill) to the production process (Figure 10). Inaccuracy caused by the position and size of the middle hole is not in the middle due to the use of manual drilling machine. This condition causes loose. One effort that can be done to fix it is by using a tool (jig drill) (Henro, et al, 2010). The use of jig drill helps the technician/operator position the position correctly, so that the quality and productivity of the spacer can increase. The next step is to implement improvements using the 5W1H method (Table 3) as follows:

Table 3. 5W1H

What	How	Why	Where	Who	When
Tool making mall replaced with jig drill	Create jig drill & inspection jig	<ul style="list-style-type: none"> Accelerate the production process and avoid non-standard marking. Accelerate the process of checking and replacing products 	Drilling area	1. Irfan 2. Joko 3. Eko S 4. Eko W.	November 1, 2016



Figure 10. Drilling process using jig (after improvement)

6. Step VI: Evaluate the results of the improvement

The evaluation of the improvement results can be compared with the conditions before and after the application of QCC which can be seen in Figure 11. From the figure it can be seen that the percentage of reject spacer component ratio is 25% (before improvement) so it needs to be improved. After quality control is done, the result is decreased and the reject ratio becomes 0% (after improvement).

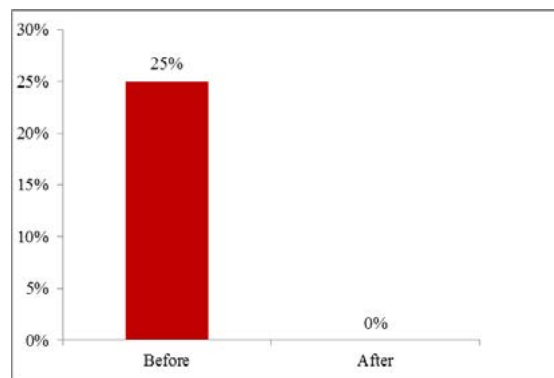


Figure 11. Result of improvement effort of quality and productivity

7. Step VII: Standardization

To demonstrate the success of the QCC group in decreasing the extent of damage to spacer components produced, then:

- a. Improving the knowledge and skills of machinery, supervisors (foremans).
- b. QC control uses check jig after drilling process.
- c. Implement preventive maintenance of machinery and equipment
- d. Implement continuous deviation prevention monitoring by following improvement steps and examine other factors that still arise, so that the product quality deviation factor can be optimally suppressed.

8 Step VIII: The next plan

Discusses the themes of process improvement, products or other components arising on a priority scale. The benefits gained by PT. MTM with the QCC is a manager and supervisor regardless of routine jobs that meet their schedule. Decisions that initially require management approval may be given to supervisors or foreman. Decisions made at lower levels are what should be made there.



QCC has managed to deliver success in improving the quality of spacer component production results in PT. MTM unit production. So the QCC team has brought profits as much as possible for both employees and companies.

4 CONCLUSIONS

Based on the results of improvements in quality and productivity that have been done, then obtained some conclusions and suggestions as follows: Improving quality and productivity analysis on supporting industries in Indonesia has been done. The research was taken analysis of the condition of supporting industries at present that seen from the rejected ratios and QC, SWOT analysis and implementation of the QCC management for continuous improvement. The result of implementation QCC in PT. MTM is component spacer 2075465260 has the highest rejected ratios claimed by PT. Komatsu Indonesi so that it is a priority to be overcome soon. Before improvement the production process drilling by using mall and after improvement change by using drilling jig, the result is rejected ratio component spacer decreased becomes zero percent claimed. The results achieved by PT. MTM can be used as example for founder or managers of any other companys for developing their domestic supporting industries.

5. ACKNOWLEDGEMENT

The author would like to thank: (1) Directors and management in the supporting industries which has given license to visits industry and discussion, (2) Mr. Sakri Widhianto and Mr. Achmad Sufiardi and Mr. M. Furqon from Ministry of Industry Indonesia, (3) Mr. Nishida as experts JICA on Project on Enhancement of Metal Working for Supporting Industries of Construction Machinery in Indonesia (2014-2016) (4) Mr. Dwiwanto as the Director PT. MTM and Staff who have provided ease of data needed and good cooperation in implementing QCC mehods, and all those who have contributed useful ideas and discussions that may not be written one by one.

6. REFERENCES

- Astra., (2010), Astra Guidlines for Total Quality Control (ATQC), Jakarta. Pp.11.
- Achadiat Atmawinata, et. Al, 2008. Depth Report of Industry Studies with Global Competitiveness, Ministry of Industry, Jakarta. Pp. 1-3.
- Cheng-Wei Chang and Chia Chun Liao, (2013), Applying SWOT analysis to explore Taiwan foundry industry management strategy, International Journal of Innovation Management and Technology, Vol. 4, No.1, February, Taiwan. Pp.114-115.
- Hedro Prasetyo, Harsono Taroepratjeka, Jonathan Felix, (2010), Jig & Fixture Design for Yamaha Motorcycle Rear Gear Production, Proceeding National Seminar IV Quality Management and Engineering 2010, ITENAS, Bandung, Pp. 211-212.
- Hafid Abdullah and Kuntari Adi Suhardjo., (2012), The Highest No Good (NG) Quality Control Problem in Battery Carbon Manufacturer Using QC Seven Tools Method, Journal of Technology for Material and Technical Product, ISSN:2089-4767, Vol.2 No.2 December 2012, B4T- Ministry of Industry Indonesia, Bandung. Pp. 63.



- _____ and Eddy Herjanto., (2015), Analysis of Growth Obstacles in National Machinery Industries and Factory Equipment, Journal of Industrial Research, Vol.9 No.1, ISSN 1978-5852, Ministry of Industry Indonesia, Jakarta. Pp 50.
- _____. (2014), Analysis of Production Facilities on Ferrous Foundry Industry as an Effort for Competitiveness Advantage of Companies, Proceedings of the National Seminar on Industrial Technology, 2014. ISSN: 2355-925X, FTI-USAKTI, Jakarta. Pp 019-4,5.
- Jeffrey K. Liker and David Meier., (2007), *The Toyota Way Fieldbook*. Translation Copyright, Publishing Erlangga. Jakarta. Pp. 5.
- Klaus Schwab., (2016), The Global competitiveness report 2016-2017, World Economic Forum (WEF), Geneva. Pp. 7.
- Komatsu, (2010), Casting Quality Improvement; in order to Make Quality Globally Accepted, PT. Komatsu Indonesia, Jakarta. Pp. 7-31.
- Kaoru Ishikawa, 2005, How to Operate QC Circle Activities, QC Circle Headquarters, Juse, Japan. Pp. 4.
- Ministry of Industry., (2011), A Study of Growth Obstacles in The Manufacturing Industries Bed on Metal, The Ministry of Industry Indonesia, Jakarta, Pp. 39-40.
- MIDC., (2012), Research Capabilities Technology Manufacturing in Metal and Machinery Industries for Development Product Substitution Imported, MIDC-Ministry of Industry Indonesia, Bandung.
- Nazir, Mochamad. (2011). Research Methods. Seventh Print. Bogor: Galia Indonesia.
- Riggs, James L. (2007), Production Systems: Planning, Analysis and Control, Singapura: John Wiley & Sons.
- Richard B. Chase, F. Robert Jacobs, Nicholas J. Aquilano. (2004), Operation Management. USA: Mc. Graw Hill/Irwin.
- Rangkuti, Freddy., (2005), Case dissecting SWOT analysis techniques, PT. Heritage Gramedia Utama, Jakarta. Pp. 24-25.
- _____. (2013). The Balanced Scorecard SWOT, Edition 4th, PT. Heritage Gramedia Utama, Jakarta. Pp.29, 64-65.
- RI Law No. 3 The Year of 2014 on Industry.
- Sugiyono. (2012). Business Research Methods. Alfabeta, Bandung, Pp. 121 and 132.
- Sambas and Hartono, (2014), Application of The Kaizen Concept as an effort to decreased the appearance rejected for Xenia-Avanza Painting Process in PT. Astra Daihatsu Motor, National Seminar on Science and Technology, FT Muhamadiyah University, November 12, 2014, Jakarta. Pp. 1.
- Wibiksono Darmawan, (2004). Business Research, Guide For Business and Academic, Alpha Beta, Bandung. P. 47.
- Law No. 3 Year of 2014 on Industry.



LEVERAGING MOTOR CYCLE DRIVING SATISFACTION USING VEHICLE OPERATION AND MAINTENANCE QUALITY IMPROVEMENT

Djoko Sihono Gabriel^{1, a}, Palito J. Endthen¹

¹Department of Industrial Engineering, Universitas Indonesia, Depok Campus, Indonesia 16424

^adsihono@gmail.com, gabriel@ie.ui.ac.id

ABSTRACT

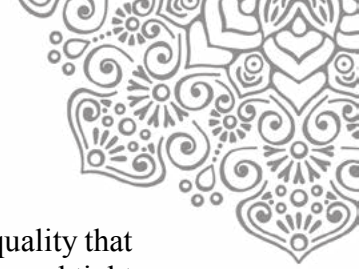
Vehicle quality usually considered as key variable in maintaining Customer Satisfaction. Good logistic and delivery of motorcycle, spare parts as well as post purchase service quality also enhance customer satisfaction. These variables are mostly depended to overall effort of motorcycle manufacturers and their value chain: from vehicle and spare parts design, materials choice, methods and quality of manufacturing processes, products and spare parts quality control as well as service quality of authorized service and maintenance workshop. No one doubt if motor cycle producers continually invest and operate their production and maintenance facilities to ensure their products quality. But who care with motor cycle owner role? When a motor cycle bought, its operation and maintenance quality were strongly depend on the owner of the vehicle that vary in their knowledge and awareness. This research proposed Vehicle Operation and Maintenance Quality as a variable that leverage Driving Satisfaction if the owner had good knowledge and good awareness in operating as well as maintaining the vehicle. Otherwise, dissatisfaction will occur to owners who had lower knowledge and awareness. A Structural Equation Modelling with Lisrel 8.8 software used as tool of analysis in proofing of those hypothesis by identifying experience of 247 motor cycle drivers in Jakarta, Bogor, Depok, Tangerang and Bekasi. The results indicated that most of the research hypothesis were accepted, especially that Vehicle Operation and Maintenance Quality variable intervened the relationship between one of independent variables with Driving Satisfaction variable. This research concluded that the proposed intervening variable will give valuable benefit if motor cycle producers and dealers develop and maintain the variable correctly. Operation and Maintenance Quality will enhance Driving Satisfaction and the better satisfaction will create better customer loyalty and brand loyalty. A new way of customer satisfaction improvement revealed by this research and strategic efforts of motor cycle producers can be developed with a new perspective that never known before.

Keywords: motorcycle; intervening variable; operation and maintenance quality; driving satisfaction; Structural Equation Modelling.

1. INTRODUCTION

1.1. Background

This study focused on motorcycle drivers who live in Jakarta, Bogor, Depok, Tangerang and Bekasi as sample respondents. The motor cycles drivers were selected as sample for two



basic reasons. First, they are need appropriate vehicle operation and maintenance quality that support driving quality. Second, motor cycle businesses with huge number of sales and tight competition need a break-through in satisfying their customers. Scooter motorcycle with automatic transmission selected in this research because this type of vehicle need better maintenance rather than the manual transmission one.

1.2. Objective

To deliver quantitative evident that vehicle operation and maintenance quality intervened positively to the relationship between certain independent variable and driving satisfaction of motorcycle.

2. METHODOLOGY

2.1. Sample and Research Instrument

With the research rationale, the sample includes 247 motor cyclists with automatic transmission who have responded to a set of questionnaire with tested answers before. Subjects were asked to report their reactions to instrument statements by considering their perceptions of vehicle quality, operation and maintenance quality and their driving satisfaction. A six-item Likert scale was used as a response scale, from strongly disagree to strongly agree. All of the 247 questionnaires were considered valid and reliable to be used in the data processing.

2.2. Measurement Model

Measurement model is a specification of the measurement theory that shows how constructs are operationalized by sets of measured items. Confirmatory Factor Analysis (CFA) is used to test the reliability of a measurement model. CFA allows the researcher to tell the SEM program which variable belongs to which factor before the analysis (Hair et al., 2007). Salisbury et al. (2001) mentioned that CFA allows the researcher to specify the actual relationship between the items and factors as well as linkages between them.

According to Hair et al. (2007) construct validity is the extent to which a set of measured items actually represents theoretical latent construct; those items are designed to measure. The reliability of variables' value scale was examined by specifying a model in CFA using Lisrel 8.8 software. Reliability of an instrument can also be calculated by Cronbach's alpha, but use of SEM technique makes such a practice unnecessary and redundant (Bagozzi and Yi, 2012). According to Hair et al. (2007) one incremental fit index (CFI), one goodness of fit index (GFI), one absolute fit index (GFI) and one badness of fit index, with chi-square statistic should be used to assess a model's goodness of fit.

2.3. Structural Model

After assessing the eligibility of scale for measuring different variables in the research, the next step is to test the hypothesized relationships in a structural model. Some variables affect to motor cycle customer satisfaction according to previous research, like quality of service, price, brand image, mileage of fuel, design (Yuvaraju & Rao, 2014) and vehicle quality (Shaharudin et al., 2010). Because of limited study of motorcycle customer satisfaction, this



case study evaluated variables affected to customer satisfaction in passenger car by previous researchers, because of car is categorized as motorized vehicle and have similarities that exist in motorcycle.

Some variables affect to passenger car satisfaction identified as vehicle quality (Stylidis, 2016), brand service quality, brand value, technology anxiety (Aziz, 2016), service quality (Al-Shammari & Kanina, 2014), economical to use (Srinivas, 2013), customer service quality, product quality (Jahanshahi, 2011), and maintenance cost, fuel efficiency, and comfort (Mahapatra, 2010). Independent variables were proposed as predictors for customer satisfaction, but no intervening variable proposed in previous research. Table 1 resumes proposed determinants of both motor cycle and automobile customer satisfaction by previous research.

Table 1. Determinant of Customer Satisfaction of Motorized Vehicle

Determinant of customer satisfaction	Researcher (year)
Motor cycle	
Quality category	Shaharudin et al. (2010)
Quality of service, price, brand image, mileage of fuel, design	Yuvaraju & Rao (2014)
Automobile	
Quality category	Stylidis (2016); Aziz (2016); Zhang & Zhang (2015); Hamza, (2014); Jahanshahi (2011); Chiu et al. (2011); Spreng et al. (1996)
Post sales service quality	Aziz (2016); Al-Shammari & Kanina (2014); Jahanshahi (2011);
Price and cost category	Zhang & Zhang (2015); Srinivas (2013); Mahapatra (2010);
Brand image and reputation	Aziz (2016); Zhang & Zhang (2015);

Vehicle quality proposed as key predictors to driving satisfaction in this research. Description of vehicle quality varies among researchers. Many of them suggest performance as common terminology of quality, but various attributes proposed as quality, including reliability, durability, serviceability, aesthetics, special feature, conformance to specification, technology, convenient, technicalities, speed, fuel efficiency, emission, ease of driving, space utilization, functions and customization. Watson et al. (2007) mentioned that vehicle quality strongly related to driving safety both in motorcycle and passenger car.

According to literature study of motor cycle and passenger car, three independent variables proposed in this study as follow:

1. Vehicle Reliability
2. Operational Quality
3. Functional Quality



With new insight in this study, a variable proposed as intervening or moderating variable was Operation and Maintenance Quality. If the three independent variables related and managed by vehicle manufacturers, the intervening variable managed by owner of vehicle. The intervening variable is new variable that have not been introduced before. Figure 1 was a preliminary model proposed for SEM with three independent variables, one intervening variable and one dependent variable.

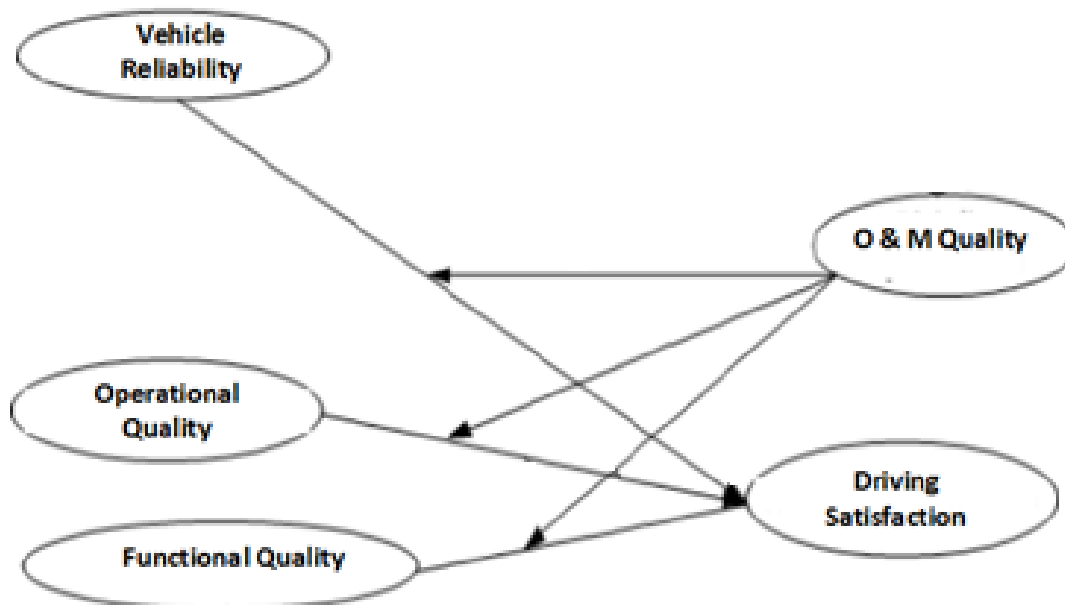


Figure 1. Preliminary Model Proposed for SEM

3. RESULTS AND DISCUSSION

A computer program prepared for Structural Equation Modelling with serial steps of model specification, model identification, model estimation, goodness fit tests, and then re-specification of structural models generated the following figures within the model. Table 2 show evaluation of structural model between three independent variables, one intervening variable and Driving Satisfaction as dependent variable.



Table 2.
Evaluation of the Structural Model

Relationship among variables	Coefficient	T-Value	Relationship
Vehicle Reliability to Driving Satisfaction	+0.08	1.33	Rejected
Operational Quality to Driving Satisfaction	+0.45	3.55	Accepted
Functional Quality to Driving Satisfaction	+0.43	3.51	Accepted
O & M Quality*Vehicle Reliability to Driving Satisfaction	-0.14	-2.01	Rejected
O & M Quality*Operational Quality to Driving Satisfaction	+0.29	3.31	Accepted
O & M Quality*Functional Quality to Driving Satisfaction	-1.44	-0.11	Rejected

Structural equation according to SEM indicated that t-statistic value of Vehicle Reliability to Driving Satisfaction was less than 1.96 and the other two relationship were greater than 1.96. Therefore Vehicle Reliability will not be considered in the next analysis, including the role of intervening variable on the relationship between Vehicle Reliability and Driving Satisfaction. The next analysis focused on the relationship between Operational Quality and Functional Quality with Driving Satisfaction and the role of Operation and Maintenance Quality as intervening variable. Since intervening role on the relationship between Functional Quality to Driving Satisfaction was also rejected, the only intervening role existed on the relationship between Operational Quality and Driving Satisfaction. Evaluation of the structural equation showed in Table 2 as followed by graphic representation in Figure 2.

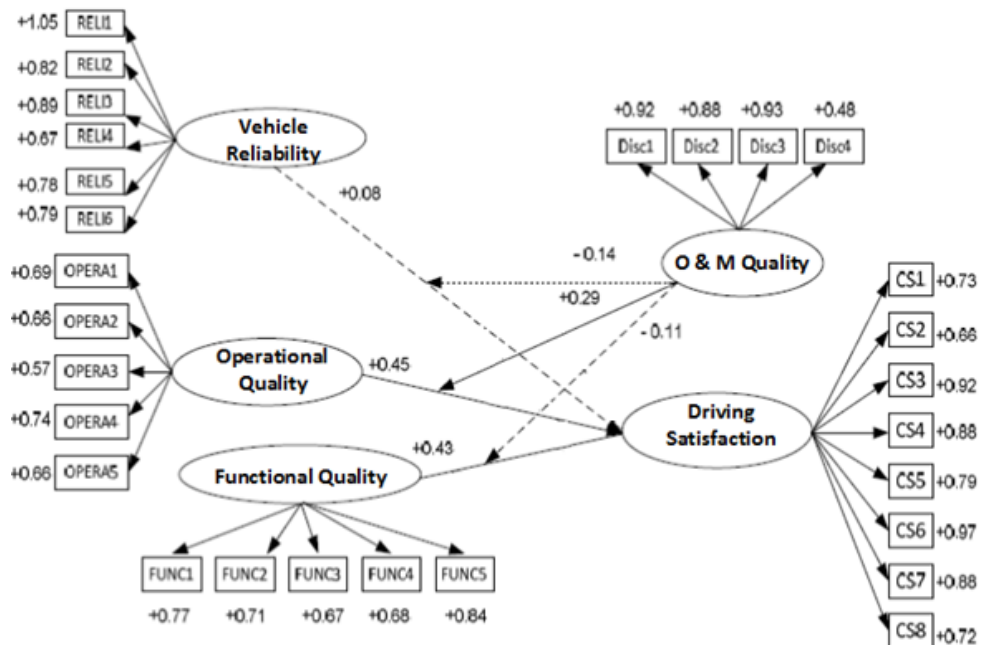


Figure 2.
Result of Structural Equation Modelling between Variables



The structural model evaluation indicated that Operation and Maintenance Quality accepted as intervening variable in the relationship between Operational Quality and Driving Satisfaction as shown in the Table 2 with good t-statistic value (3.31) and its significant coefficient (0.29). Otherwise, Vehicle Reliability became not accepted in this context of relationship.

In this case study, observed variables in Operational Quality exists in the vehicle itself and manufacturer and its supply chain efforts, included the following description:

1. Mileage per liter of fuel
2. Durability of vehicle and its spare parts
3. Easy in driving
4. Simple in daily maintenance
5. Easy in periodic maintenance, both technical and financial aspects

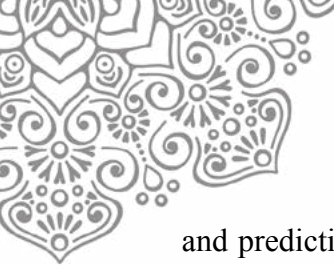
Otherwise, Operation and Maintenance Quality more depend on owner intention in operation and maintenance of vehicle as follow:

1. Ability to describe schedule and type of routine maintenance and repair of vehicle
2. Ability to pay all of vehicle maintenance and repair
3. Commitment for scheduled vehicle maintenance and repair implementation
4. Commitment for vehicle operation in its loading limit

According to the accepted structural model, Operation and Maintenance Quality strengthen causal relationship between Operational Quality and Driving Satisfaction. A vehicle with better Operation and Maintenance Quality tends to improve its driver satisfaction. Otherwise, lack of Operation & Maintenance Quality made no improvement in Driving Satisfaction. Finding in this research contributes a new perspective in customer satisfaction determinant. If in the past motorcycle manufacturer and their supply chain focused on vehicle quality and its post sales service, in the next era, motorcycle manufacturer who care and support vehicles users in improving their Operation & Maintenance Quality will take important advantage in their customer satisfaction that also will improve their loyalty and intention to buy the brand.

4. CONCLUSION

Leveraging driving satisfaction of motorcycle using Operation & Maintenance Quality improvement was well tested by structural equation modelling in this research. This finding also can be interpreted that bad Operation and Maintenance Quality would weaken the Driving Satisfaction, whether the quality of motorcycle was actually genuine. Lack of Operation and Maintenance Quality could reduce the user satisfaction. Owner role in Operation and Maintenance Quality improvement should be supported by motorcycle manufacturers and its supply chain in order to improve customer satisfaction and loyalty. The new finding suggests a new way of understanding about by whom and how customer satisfaction can be improved. Motorcycle owners with lack of operation and maintenance knowledge, and then used breakdown maintenance rule of thumb would have bad experience in driving satisfaction. Therefore manufacturers aiming to boost their customer satisfaction should thus consider this finding and recommend their vehicle buyers to use both preventive



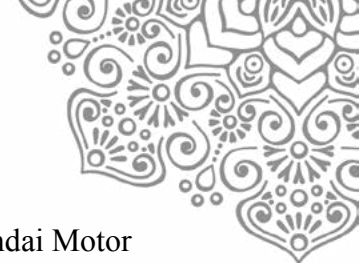
and predictive maintenance with good standard of maintenance practices. They might find that an appropriate brochure and good operation and maintenance manual as well as its direction, both in written and oral explanation, followed by regular and repetitive reminders to vehicle owners may become more efficient means in encouraging Operation and Maintenance Quality improvement, not only focused on improvement of vehicle quality and post sales services. Fair and competitive pricing by authorized maintenance workshop with good standardized maintenance practices also support the new finding implementation.

5. ACKNOWLEDGEMENT

This research would not have been possible without the kind support of Hibah PITTA 2017 scheme. We are grateful to Universitas Indonesia for funding the research that has been carried out.

6. REFERENCES

- Al-Shammari, M. & Kanina, A. S., (2014), Service Quality and its Relationship with Customer Satisfaction and Loyalty in a Saudi Arabian Automobile Company, *Global Journal of Management and Business Research: E Marketing*, Vol. 14 No. 8, pp. 13-21.
- Aziz, S. A., (2016), Does Fear of New Car Technologies Influence Brand Loyalty Relationship? *Journal of Marketing Management*, Vol. 4, No. 1, pp. 125-136.
- Bagozzi, R., & Yi, Y. (2012), Specification, evaluation, and interpretation of structural equation models, *Journal of the Academy of Marketing Science*, Vol. 40 No. 1, pp. 8–34.
- Chiu, S., et al. (2011), Preliminary research on customer satisfaction models in Taiwan: A case study from the automobile industry, *Expert Systems with Applications*, Vol. 38, pp. 9780-9787.
- Hair, J., Black, W., Babin, B., Anderson, R., & Tatham, R. (2007). *Multivariate data analysis* (6th ed.). New Delhi: Pearson Education India.
- Hamza, P.K., (2014). A Study on the Determinants and Impact on Overall Customer Satisfaction Evaluations with Special Reference to Automobile Industry, *Journal of Science, Technology and Management*, Vol. 7 No. 2, pp. 0974-8334.
- Jahanshahi, A. A., (2011), Study the Effects of Customer Service and Product Quality on Customer Satisfaction and Loyalty, *International Journal of Humanities and Social Science*, Vol. 1 No. 7, pp. 253-260.
- Mahapatra, S. N. et al., (2010), Consumer Satisfaction, Dissatisfaction and Post-Purchase Evaluation: An Empirical Study on Small Size Passenger Cars in India, *International Journal of Business and Society*, Vol. 11 No. 2, pp. 97-108.
- Salisbury, W.D., Pearson, R.A., Pearson, A.W., & Miller, D.W. (2001), Perceived security and World Wide Web purchase intention, *Industrial Management & Data Systems*, Vol. 101 No. 3/4, 165.
- Spreng, R. A. et al., (1996), A reexamination of the determinants of consumer satisfaction, *Journal of Marketing*, Vol. 60 No. 3, pp. 15-31.



- Srinivas, K. T., (2013), The Study on Customer Satisfaction with Respect to Hyundai Motor Cars i20 in Bangalore City, *International Journal of Management Research and Review*, Vol. 3 No. 9, pp. 3569-3579.
- Stylidis, K. et al., (2016), A Preliminary Study of Trends in Perceived Quality Design Attributes in the Automotive Luxury Market Segment, *International Design Conference – Design 2016*, Dubrovnik, Croatia, May 16-19, 2016.
- Watson, B. et al., (2007), *Psychological and social factors influencing motorcycle rider intentions and behaviour*, Centre for Accident Research and Road Safety (CARRS-Q) Queensland University of Technology, August 2007.
- Yuvaraju, D. & Durga Rao, S. D., (2014), Customer Satisfaction towards Honda Two Wheelers: A Case Study in Tirupati, *IOSR Journal of Business and Management*, Vol. 16 No. 5, pp. 65-74.
- Zhang, D. & Zhang, D. M., (2015), Determinants of Consumer's Automobile Purchase Decisions in China: Focus on Automobile Size, *Int. J. Mgmt Res. & Bus. Strat.*, Vol. 4 No. 4, p. 61-66.



MANAGING PORT CLUSTER DYNAMICS: DEVELOPMENT OF PORT POLICY MODEL

Armand Omar Moeis^{a1}, Himawan Pranamukti^{ac}, Akhmad Hidayatno^a, Mohammad Rizky Nur Iman^a, Naufa Muna^b

^a*Universitas Indonesia, Kampus Baru UI, Depok 16424, Indonesia*

^b*Trade Analysis and Development Agency, Ministry of Trade Republic of Indonesia*

^c*PT Sucofindo (persero), Jakarta, Indonesia*

ABSTRACT

A port is a hub of a trading network. Its role becomes even more strategic in an archipelago country such as Indonesia, as a driver of national economic growth. Tanjung Priok Port is the most important port in Indonesia, where Indonesia's economic growth is highly dependent on its capacity. The port's capacity development planning has been designed through 2030 and will dynamically affect the existing systems and its environment. This study will analyze the system, explore the policy area and synthesize result of system analysis and institutional analysis. The result of the synthesis is the port policy model itself and then simulated with system dynamic modelling to challenge the policy prior to its implementation.

Keywords : System Analysis, Actors Analysis, Port Capacity, Port Policy, System Dynamics

1. INTRODUCTION

Ports are hubs of the national trading and logistics network, even some for international trading and logistics. The role of ports has evolved over time. At first, orientation of logistic integration as well as the networking in maritime and port industry has redefined its functional role regarding the value chain and has moved a new pattern on the sailing distribution and new approach for the port hierarchy (Notteboom & Rodrigue 2005).

Up until 1980, the port activities is highly related to the economical process of its city (Ferrari et al. 2015). Port services heavily rely on human workforce and is under the control of the government and efficiency was not the main goal of port. The application of technology, especially technology related to the standardization of cargo and containers, encouraged privatization in port management. It aims for the enhancement of the overall port performance (Langen & Heij, 2013; Ferrari et al., 2015).

The shipping sector with the highest growth rate (8.2%) during 1990 until 2010 was the containered goods (Carlo, Vis, & Roodbergen, 2014 as quoted from UNCTAD, 2011). This growth goes in line with the increase of container availability, which now is capable of shipping 14.500 TEUs when earlier in 1955 could only ship hundreds. Therefore, the ports must adjust its capacity to the arrival of the ships with that particular size.

The need of the capacity enhancement is limited by the country's funding. One way to overcome this limited funding is by granting concession to private and foreign parties for commercially attractive ports. There are four known types of concession-granting combination: (a) state/public ownership and public participation of port operation; (b) state/public ownership and private role on port terminal construction; (c) public/state ownership and private participation in the superstructure construction of the port (e.g.: quay crane) and port operation; and (d) private ownership and its operations (Notteboom 2006).

¹ Corresponding Author
email address: armand.omar@ui.ac.id



The usage of public ownership and private operations (POPO) has been widely spread (Ng et al. 2014). In POPO concession model, the agreement is signed by the private terminal operators and the authority of port owner or any government institution whom is appointed as port authority. The concession can be a form of long term lease agreement or operational license for private party to operate certain terminals for a fixed period of time.

The enhancement of port capacity will increase the number of containers in the port. Moreover, there is a need to determine what kind of policy is needed to deal with the port capacity enhancement.

The container port policy model shall be designed to fulfill that particular need. The method used in designing the policy covers (1) Substantive diagnostic with system analysis approach; (2) exploration of the policy area; (3) Synthesis of the system analysis and policy exploration, measured with System Dynamics simulation.

2. SUBSTANTIVE DIAGNOSTIC WITH SYSTEM ANALYSIS APPROACH

2.1. Analysis of Objective and Criteria Specification

In the analysis of the objective and criteria specification, there are two diagrams that is used, which are the Means-ends diagram (figure1) and the Objective Tree (figure 2). Means-ends diagram is used to identify and communicate the basic goal. It is chosen at the beginning and is intentionally taken in accordance to the limitation of the problem so that it is considered as the starting point for further analysis. This diagram provides bigger range of solutions.

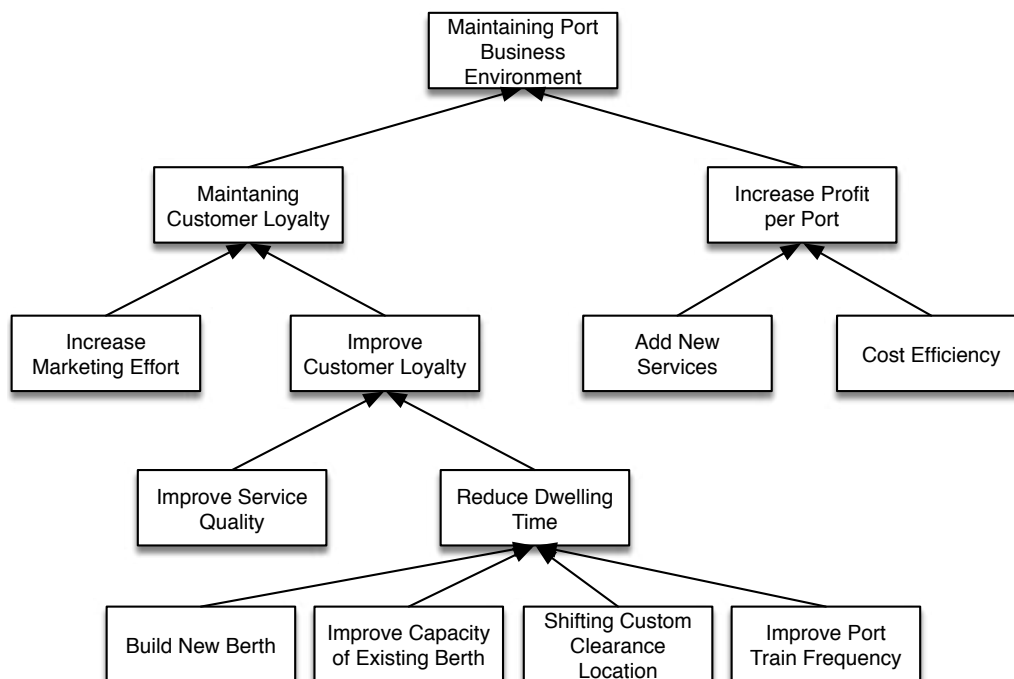


Figure 1 Means-Ends Diagram

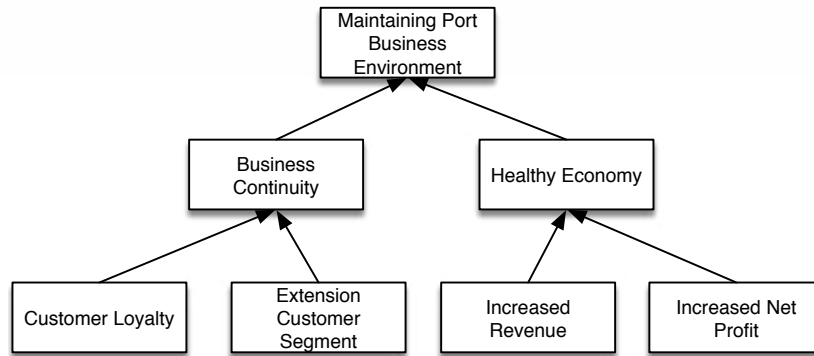


Figure 2 Objective Tree Diagram

2.2. Causal Analysis

The next phase is the exploration of the factors that affect the end result. Those factors and their impact is illustrated in a causal diagram. The differences between causal diagram and other, similar, tools such as means-ends and the objective tree are a). The causal diagram shows the causal relationship, not the aim or the direction of change, b). Factors that cannot be changed or controlled by actors but are impactful to the result is included.

2.3. Identification of Possible Solutions

The ideas for problem-solving actions can be defined in a different specification levels and combined in several ways. At this phase, we first determine the terms for specific policy solutions. The terms used are composed by Thissen and Walker (2013).

- Policy option is the individual examination which directly affects the system.
- The strategy is the combination of the policy option which aims to accomplish a specific goal.
- The policy is combination of strategies, which is possibly designed to help achieve multiple goals.

There are several additional approaches to shape the idea about possible policy options such as the causal diagram, means-end diagram, diagnostic thinking, etc.

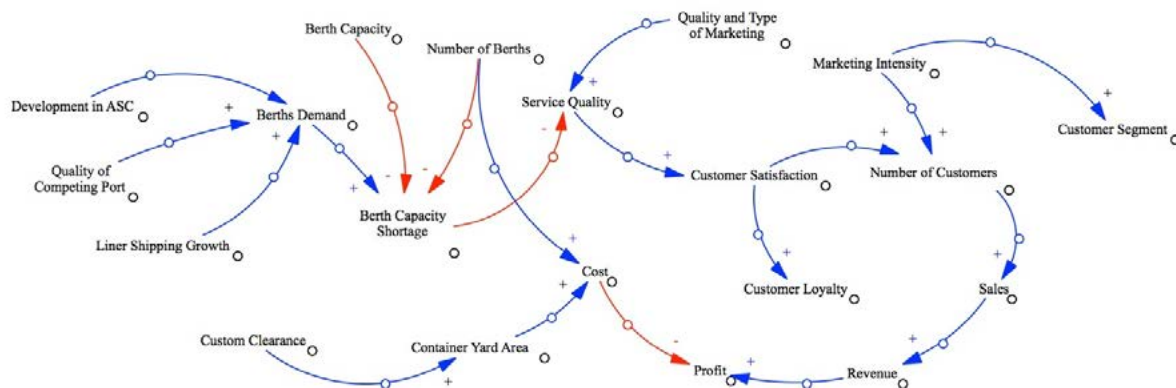


Figure 3 Causal Analysis Diagram

3. EXPLORATION OF POLICY AREA

3.1. Actors Analysis

In this part, the analysis of relevant actors is performed, after that the indication of basic information is elicited from those actors. The steps of actor analysis are: 1) identification of relevant actors, 2) needs, perception, and actors' position, 3) interdependent analysis between all actors and 4) the passage analysis.



The analysis of relevant actors includes the identification of the parties besides the issue owner who play part or have any interest in the port system. The identified actors for this system are the port operator, shipping company, and the bureaucracy involved, which are the Customs, Quarantine and Immigration, especially the ones in charge of dwelling time. Others are container trucks transport company, local government and citizens.

3.2. Institutional and Decisional Analysis

As the complement of the actors analysis, institutional and decisional situation analysis focuses on the formal and informal context where the policy issue occurs and possibly solved. There are also characteristics of the inter-actor relationship, such as the cultural factors and relation dynamics, the dominant habit of the actors' interaction, the networking characteristics like the communication pattern and the potential changes of the actors' position and relationship.

The informal interaction structure is not easy to identify but it is possibly relevant. Interviews with key actors or thorough research of secondary sources can be a resourceful way to find out more about informal interactions. A deeper discovery can be obtained by exploring the history of the issue: which actors play a part and alliance to which party as well as if there were any coalitions between the existing actors.

4. SYNTHESIS FROM THE SYSTEM ANALYSIS AND THE ACTORS ANALYSIS

Results of system analysis and actors analysis, subsequently synthesized to produce a model of port policy (Figure 4). This synthesis is usually called System Diagram.

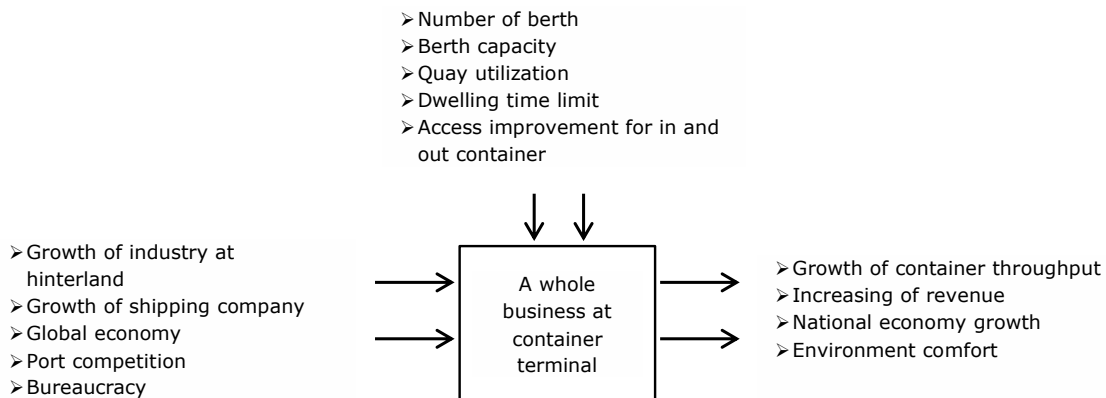


Figure 4 System Diagram of Port Policy Model

5. THE EXAMINATION OF POLICY MODEL WITH SYSTEM DYNAMICS

The policy model needs to be tested utilizing simulations to prevent fatal errors upon the policy before it is issued. The examination for this policy model is a simulation with System Dynamics. The influential factors in the system are displayed in a stock and flow diagram, and simulated using PowerSim software, as seen in figure 5 (Anon 2016). The dynamic model was inspired from a work by Soares et.al (2010). It was a model that illustrates predictive capacity of a container terminal state in Brazil. We based our model on that and conducted significant changes that reflects the requirements of our research.

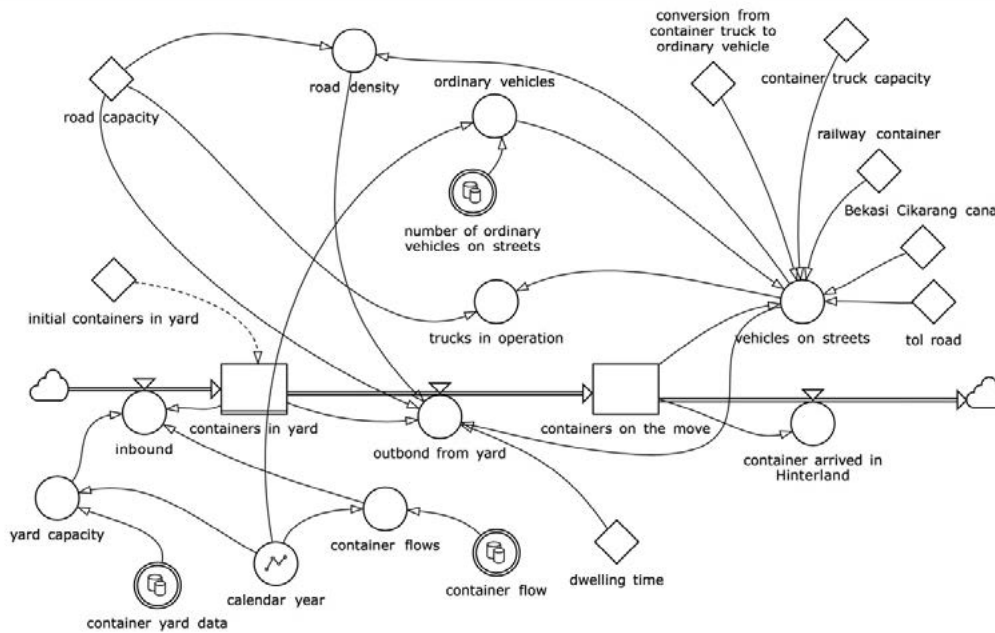


Figure 5 Stock and Flow Diagram of Container Terminal

6. RESULT AND DISCUSSIONS

In a dynamic simulation, there are several factors that were tested to determine their impact on the capacity of the port in the future. The factors include the condition of the road around the harbor at this time, the addition of toll ports, railways and canals. As the indicator is the number of containers moving out of the port. The proposed projection period is up to 2030. The result of simulation is shown in the figures below.

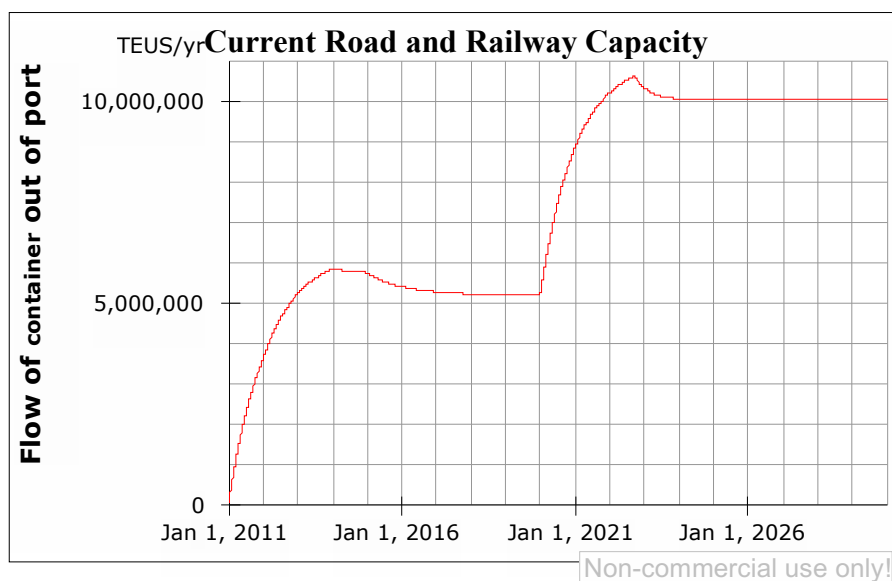


Figure 6 Flow of container moving out of the port for current road and railway capacity

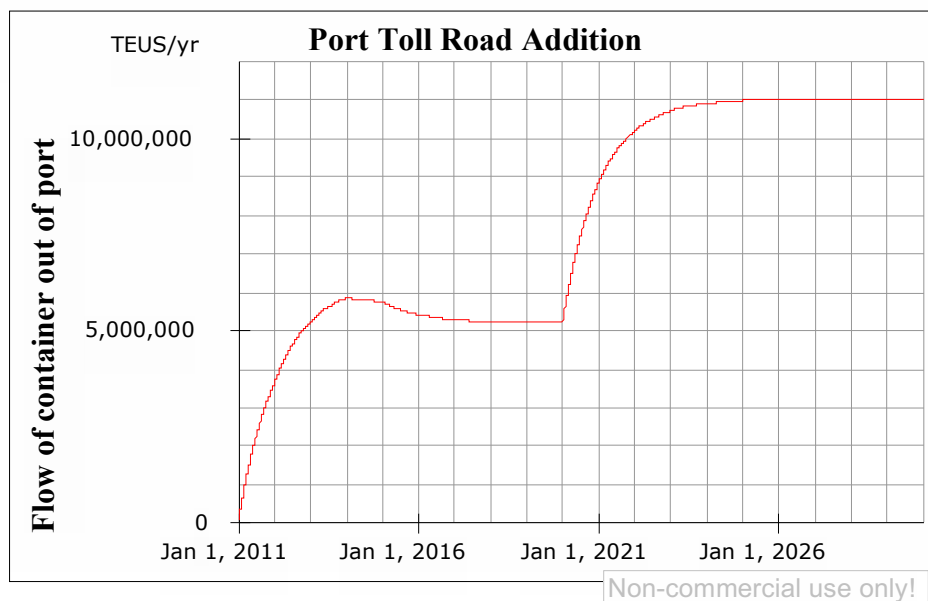


Figure 7 Flow of Container Moving Out of the Port with the Additional Port Toll Road

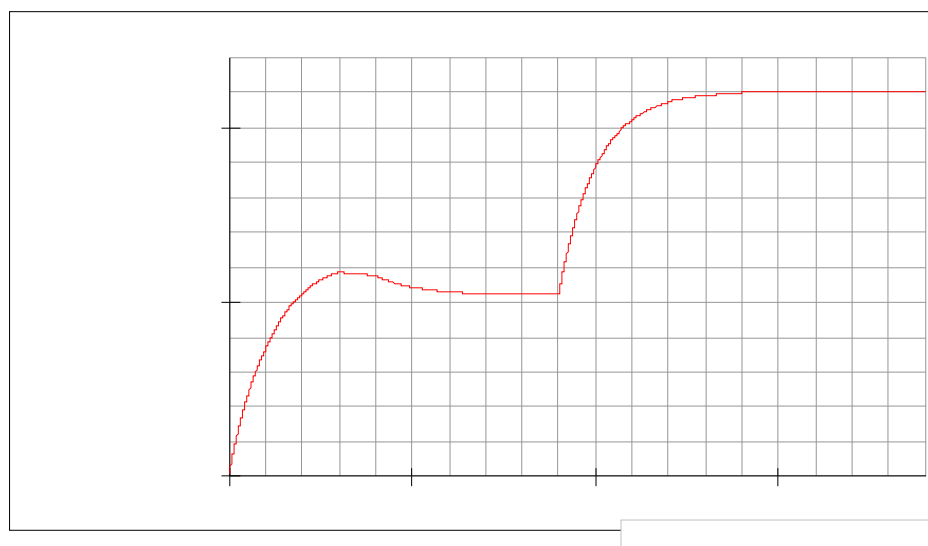


Figure 8 Flow of container moving out of the port with the additional waterway

The enhancement of the container port in Tanjung Priok can be implemented as long as it is followed by the increment of in-and-out container access from the Tanjung Priok Port. Based on the simulation performed by PowerSim software (Anon 2016), it can be inferred that:

- i. Provided that the enhancement of the container port is not followed by the increment of the terminal (in-and-out) access, the container will be held in the holding field (container yard).
- ii. The usage of trains from the port to hinterland does not affect much to the enhancement of the out flow of the container if the train frequency did not significantly increased. The hinder of the train frequency is that there is no dedicated railway for



- containers/goods service, yet (still hitched on the passenger railway). Therefore, an investment on a dedicated port railway is needed to the enhancement of port capacity.
- iii. The usage of the port highway can increase the in-and-out access of the containered goods to/from the port so that it does not interfere with the arrival of those from the ship.
 - iv. The canal construction from Bekasi Laut to Cikarang can increase the flows of goods, henceforth the terminal's throughput as well.
 - v. The usage of canal will affect the competition between different modes of transport providers (intermodal competition).
 - vi. Dwelling time does not have significant impact to the outflow of the port if the projection is done annually, however, it influences the decision of international shipping companies (in determining their liner services). The decision regarding the maximum duration is decided by the Ministry of Finance for the pre-clearance, clearance, and post-clearance processes, which must be juxtaposed with the providing appropriate holding field out of the port.
 - vii. Dwelling time is also influenced by container-using importers who prefer keeping their containered goods in the port, rather than to moving it elsewhere, due to lower cost. The new progressive tariff is determined by increasing the tariff after the fixed time limit. Hopefully this can lower the dwelling time.

7. CONCLUSION

The development of container ports involves many actors, each with different interest. The study was carried out by synthesizing System Analysis and Actors Analysis to produce a policy model. The policy model is then tested with System Dynamics simulation to obtain insights of the impacts (or effects) of that. The model has not explored factors that affect the container demands at the port, and still assumes the number of containers according to port capacity. Further studies are needed to develop this research in order to obtain a more comprehensive container port policy model.

References

- Anon, 2016. Powersim. Available at: <http://www.powersim.com>.
- Carlo, H.J., Vis, I.F.A. & Roodbergen, K.J., 2014. Transport operations in container terminals: Literature overview, trends, research directions and classification scheme. *European Journal of Operational Research*, 236(1), pp.1–13. Available at: <http://www.sciencedirect.com/science/article/pii/S0377221713009405> [Accessed October 5, 2015].
- Claudio J.M. Soares, H.X.R.N., 2010. A Model for Predictive Capacity of a Container Terminal State : a System Dynamics Approach. , pp.1–15.
- Ferrari, C., Parola, F. & Tei, A., 2015. Governance models and port concessions in Europe: Commonalities, critical issues and policy perspectives. *Transport Policy*, 41, pp.60–67.
- Langen, A.P. De & Heij, C., 2013. Performance effects of the corporatisation of Port of Rotterdam Authority.
- Ng, A.K.Y. et al., 2014. Port geography at the crossroads with human geography: Between



flows and spaces. *Journal of Transport Geography*, 41, pp.84–96. Available at:
<http://dx.doi.org/10.1016/j.jtrangeo.2014.08.012>.

Notteboom, T.E., 2006. The Time Factor in Liner Shipping Services. *Maritime Economics & Logistics*, 8(1), pp.19–39.

Notteboom, T.E. & Rodrigue, J.-P., 2005. Port regionalization: towards a new phase in port development. *Maritime Policy & Management*, 32(3), pp.297–313.

Thissen, W.A.H. & Walker, W.E. eds., 2013. *Public Policy Analysis: New Development*, Dordrecht: Springer.



15th International Conference on Quality in Research (QIR 2017)

Modeling and Simulation of Stacking Rules in Container Terminals with a Discrete Event Simulation Approach

Armand Omar Moeis^{*}, Muhammad Harisuddin

Universitas Indonesia, Kampus Baru UI, Depok 16424, Indonesia

ABSTRACT

The traffic flow enhancement of international containers increases every year along with continuous economic growth. Therefore, there is a need to improve container terminal operations. This study focuses on modeling a stacking yard. Good container stacking rules should reduce reshuffling, which is considered as waste in container terminal operations. This study provides a means to understand what stacking rules are and its impact on container terminal operations efficiency.

Keywords: Container Terminal, Stacking Yard, Stacking Rules, Discrete Event Simulation

1. INTRODUCTION

The traffic flow of containers increases every year, especially in the Port of Tanjung Priok as the biggest port in Indonesia. According to the study, the traffic flow of containers will increase to 10,84 million TEUs (twenty equivalent units) in 2020. Meanwhile until the end of year 2012 it has reached 5 million TEUs. To anticipate the enhancement of traffic flow containers through the Port of Tanjung Priok, the container terminal at the Port of Tanjung Priok should improve its productivity and efficiency in loading and unloading containers.

Several main factors that have significant impacts on the container terminal productivity are stowage planning, berth allocation, crane optimization, transportation optimization and container stacking (Stahlbock & Voß 2008). One of the main factors is the container stacking in stacking yard. The way the containers are being stacked is the key determinant to container terminal productivity and efficiency (Moeis & Goputra 2015; Carlo et al. 2014)

Therefore, the purpose of this research is to develop a container terminal model that represents loading and unloading activities inside it. The objective of this model to help evaluating the stacking rules that used in container terminal for stacking the containers. By developing this model, hopefully it will give some insights about how the container terminal works, especially in stacking yard.

The main objectives of the stacking rules are efficiency of ground usage, minimize transportation time and minimize reshuffling (Böse 2011; Meisel 2009). Reshuffling is classified as unproductive move in container terminal activities, especially during container off loading/on loading from a ship and in stacking yard. Moreover, another purpose of this

^{*} Corresponding author

email address: armand.omar@ui.ac.id



model is to give understanding and deep insight about container terminal operational activities. Therefore, we build this model using discrete event simulation approach supported with animations. The animated objects represent the activities in container terminal, such as: gantry cranes that lift the containers, terminal trucks that carry the containers etc. The use of animated objects in a model can aid the verification and validation process, facilitate the understanding of the model, provide the help to view the result of the model and achieving the credibility for the model (Trunfio 2011; Hou & Geerlings 2016; Van Houten & Verbraeck 2006).

2. METHODOLOGY

This study uses discrete event simulation in building a model of the container terminal. Model development begins with the conceptualization of making the model as the main basis for building a model. Conceptualization model provides a thorough understanding of the model. It is because it contains objective of the model, input and output model as indicator, the process flow model, alternative scenarios and concerned stakeholders of the model. The activity will then continue with construction, where the actual model is developed. Furthermore, it continues with verification (where we check whether all technicalities are correct) and validation (whether the model represents the real system or not), then ended with model use (see figure 1).

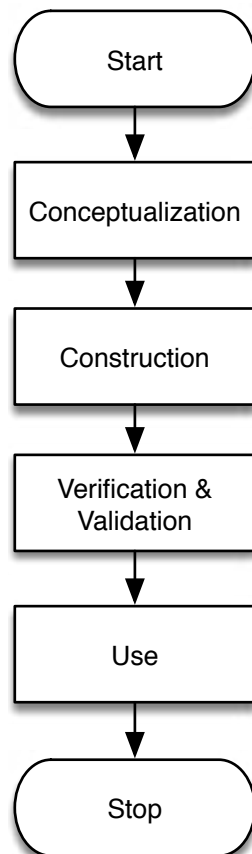


Figure 1 Basic Simulation Study Methodology



The purpose of this model is to evaluate two methods of stacking (stacking rules) in the conduct of container stacking. Input variables of the model are the vessel departure time, destination of the container, the arrival of containers at the container terminal, and the capacity of the stacking area. Vessel's departure time and destination of the container will be used as an attribute in the container as the container identification. The output of this model is the amount of reshuffling and it will be used as the main indicator of the model. This model will do some experiments with two methods of stacking, the stacking category based on destination and stacking category based on vessel. Problem owner of this model is the yard planner who responsible in planning the container stacking yard.

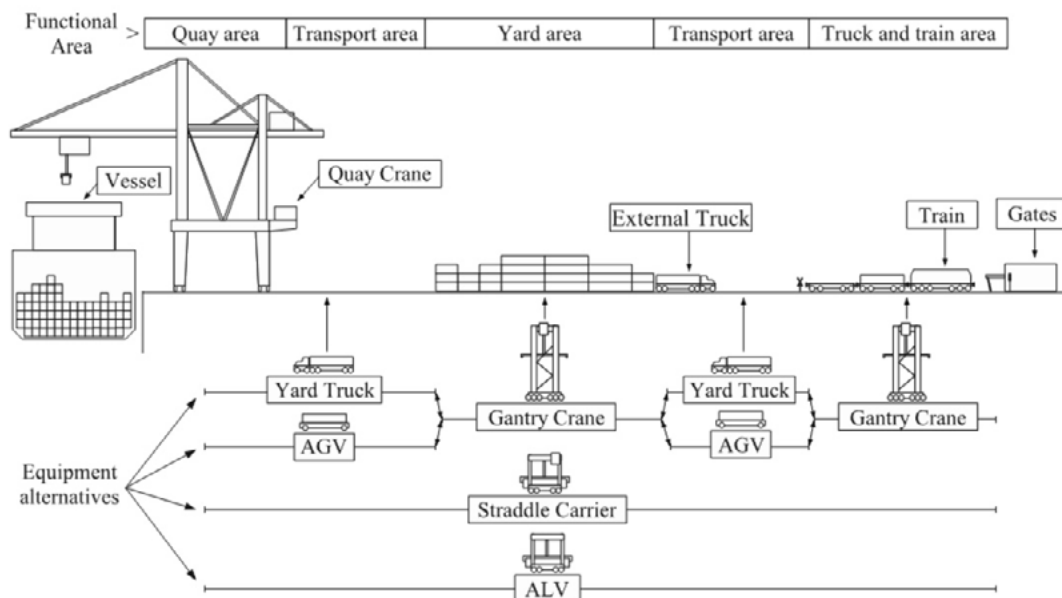
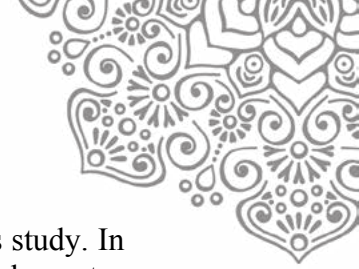


Figure 2 Conceptual Model (adapted from Meisel 2009)

2.1. Model Development

We choose to use Tecnomatix Plant Simulation 9.0 (Anon 2013) to build our model. This software is specialized to build discrete event model based on object oriented simulation. This model only represents the flow of containers export. This is because the implementation of the stacking rules is only give significant effect on the accumulation of containers that will be heading to the vessel. While the implementation of stacking rules on container imports that will come out of the container terminal by truck does not really have significant influence for the container terminal performance. It is because the container trucks arrive randomly in container terminal. Due to that situation, it is somewhat difficult to develop stacking rules based on the unpredicted arrival of container truck (Dekker et al. 2007).

The model represents an international container terminal in Jakarta, i.e. Jakarta International Container Terminal (JICT). JICT is owned by Hutchison Port Holding and Indonesia Port Corporation. JICT is mainly used as our learning experience. Knowledge and insights



derived from this JICT model will then be used in our further Maritime Logistics study. In this model, there are 11 blocks of the stacking yard. Each block is served by single gantry cranes. There are three berths for vessel, and each of them served by 3 quay cranes. The model simulates the arrival of 15,598 TEUs of containers in a container terminal. Simulation is run for 13 days including a 4-days-warm-up period to initialize the stacking yard. This phase is used to fill the yard with containers so that when the simulation starts stacking area is not empty.

There are two kinds of transporters are used in the model. The transporter built as trucks that transport containers in the container terminal. The first transporter is named external truck. It responsible to bring containers into the container terminal and heading to the stacking area. The second transporter named head truck. It is responsible for carrying container from the stacking yard to the berth area. While in the berth, quay crane will transport containers on board.

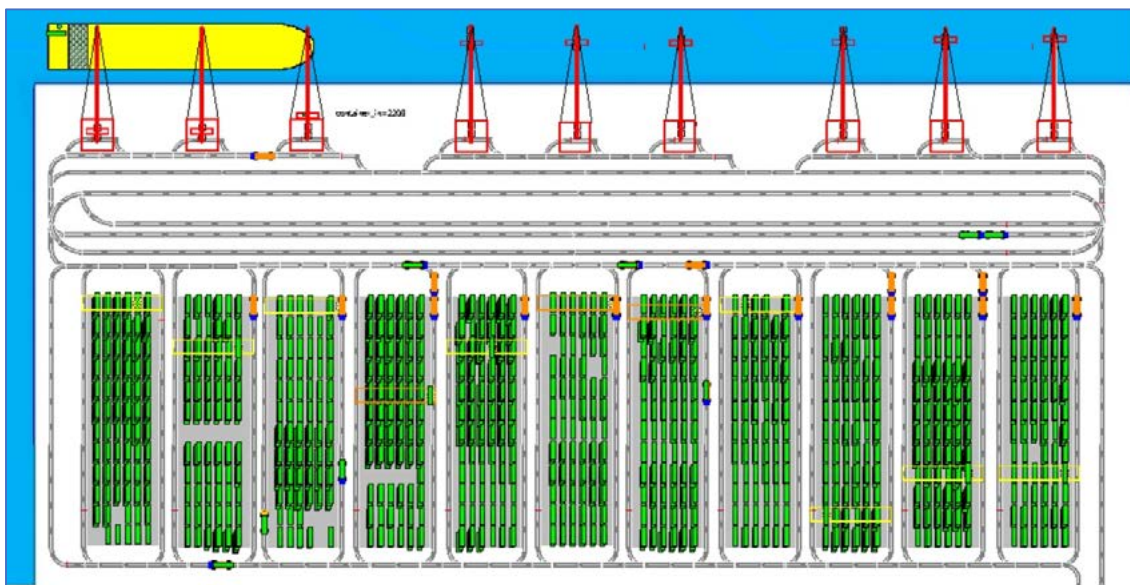


Figure 3 Layout of Container Terminal Model

Simulations were run with two kinds of stacking methods (stacking rules). The first method is based on vessel category. In this method, the containers will be stacked based on their vessel category that exist in each container. Therefore, the container with the same vessel will be on the same area and the same container piles. The second method is based on destination category. In this method, the container allocation is done based on the attributes of the destination in each of the containers. So that the container with the same destination attribute will be in the same piles.

2.2. Model Validation

Model validation is done to ensure that the model is valid and able to represent the system of container terminal in the real world. Basically, the model is not able to produce models with 100% accuracy, but the model is a simplification that is easy to understand and can explain the actual reality.

In this model validation is performed by measuring the occupancy rate at the yard by yard



occupancy rate models on the JICT. Based on the data obtained during the last 5 weeks, the average occupancy rate of JICT yard is equal to 88%. While the values obtained in model-yard occupancy rate at 11 pieces' block stacking area is at 89%.

The result shows that the difference between the numbers obtained in the model with the value of the container terminal performance JICT only differs by 1%. The difference is small enough that it can be stated that the design model of the container terminal operation with designs Jakarta International Container Terminal operations are similar. So, it can be stated that the model in this study are valid.

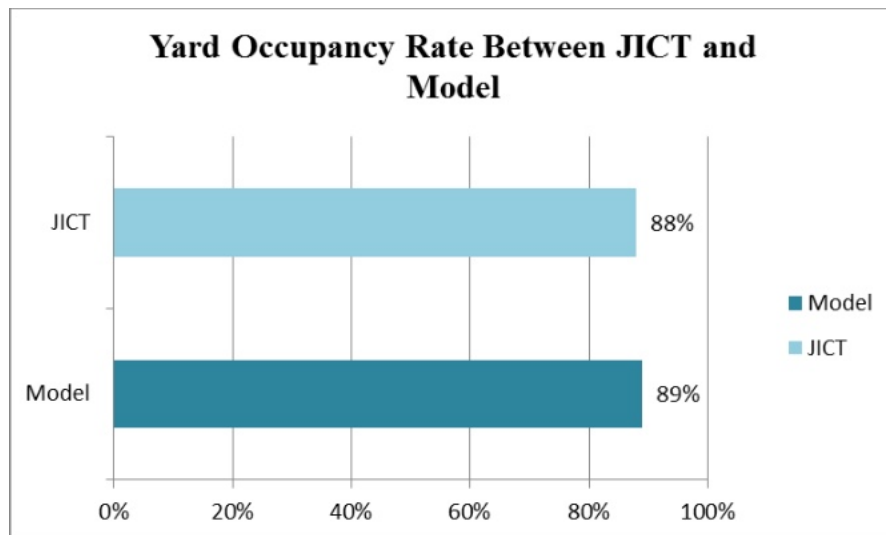


Figure 4 Model Validation

3. RESULT AND DISCUSSIONS

There are three simulation models compared in this study are: the basic model, the model with stacking rule based on destination and stacking rule based on vessel. The main indicator of the model we want to look in this research is the amount of reshuffling. The less reshuffling generated, it indicates the higher efficiency of operational performance in the stacking area. Because the reshuffling itself is a waste in container terminal operations. It makes the unloading operation take longer time than it should.

Figure 5 shows the results of simulations run on three models. The graph shows that the value of reshuffling on three kind of the model has significant difference. Each method has a responsibility to serve the same number of containers that 5,836 container boxes. At each model, there is a difference of the amount of movement of the gantry crane in handling 5,836 boxes. The greater the amount of movement required to serve 5,836 boxes, the more inefficient operational stacking yards. Because it indicates high amount of reshuffling in serving the stacking yards.

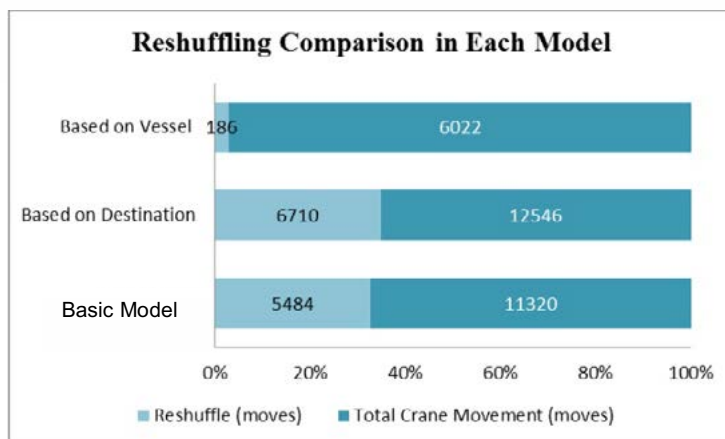


Figure 5 Simulation Results

Figure 5 also shows that container stacking rule based on vessel gives result as follows: 6,022 moves to unload 5,836 boxes, with 186 reshufflings. Container stacking rule based on destination requires 12,546 moves to unload 5,836 boxes of containers, with 6710 reshufflings.

The simulation results indicate that the stacking rule based on vessel show higher performance efficiency because it produces a smaller value of reshuffling. Performance efficiency of the model with category stacking based on vessel is higher because the main factor in determining the order of unloading containers is based on the arrival of the ship. So, grouping stacking containers by vessel/ship will be very significant effect on the efficiency of the container unloading activity in stacking yard. The opposite occurs in another model, where the containers are grouped with the same destination.

4. CONCLUSIONS

The use of simulation to model the activity of container terminal is one of the tools to evaluate and deliver improvement of the activities that occurred in the container terminal. The use of simulation to evaluate the stacking rules between category stacking based on vessel and category stacking based on destination shows that the efficiency of container terminal (i.e. JICT) is higher if the containers are grouped by vessel (stacking rule based on vessel). Although this model only applies to JICT, it might give researchers in Maritime Logistics/Container Terminal domain a base knowledge on how to model/improve such system.

5. ACKNOWLEDGEMENT

This research is one of our earliest work in Maritime Logistics/Container Terminal domain. Further researches have been done and more are on the go. We thank Universitas Indonesia and the Indonesian government that gave us financial support in doing research in this field.



6. REFERENCES

- Anon, 2013. Tecnomatix Plant Simulation. Available at:
https://www.plm.automation.siemens.com/en_us/products/tecnomatix/manufacturing-simulation/material-flow/plant-simulation.shtml.
- Böse, J.W., 2011. Handbook of terminal planning. *Operations Research/ Computer Science Interfaces Series*, 49(1).
- Carlo, H.J., Vis, I.F.A. & Roodbergen, K.J., 2014. Transport operations in container terminals: Literature overview, trends, research directions and classification scheme. *European Journal of Operational Research*, 236(1), pp.1–13. Available at:
<http://www.sciencedirect.com/science/article/pii/S0377221713009405> [Accessed October 5, 2015].
- Dekker, R., Voogd, P. & Van Asperen, E., 2007. Advanced methods for container stacking. *Container Terminals and Cargo Systems: Design, Operations Management, and Logistics Control Issues*, 586, pp.131–154.
- Hou, L. & Geerlings, H., 2016. Dynamics in sustainable port and hinterland operations: A conceptual framework and simulation of sustainability measures and their effectiveness, based on an application to the Port of Shanghai. *Journal of Cleaner Production*, 135, pp.449–456. Available at:
<http://dx.doi.org/10.1016/j.jclepro.2016.06.134>.
- Van Houten, S.P. & Verbraeck, A., 2006. Controlling simulation games through rule-based scenarios. In *Proceedings - Winter Simulation Conference*. pp. 2261–2269.
- Meisel, F., 2009. *Seaside Operations Planning in Container Terminals*, Available at:
<http://www.springerlink.com/content/v621985274355864/>.
- Moeis, A.O. & Goputra, A., 2015. Container Stacking Activity Modeling in Jakarta Container Terminal (JCT) with Three Different Stacking Rules Using Discrete Event Simulation Approach. In *International Conference on Logistics and Maritime Systems*. Hong Kong.
- Stahlbock, R. & Voß, S., 2008. Operations research at container terminals: A literature update. *OR Spectrum*, 30(1), pp.1–52.
- Trunfio, R., 2011. Modeling, simulation and optimization in logistics. *4or*, 9(4), pp.433–436.



**ANALYSIS OF SITUATION AND COMPETITIVE STRATEGY FORMULATION
FOR THE VISION AND MISSION TOWARD THE IN YEAR OF 2020
(Case: in MIDC Ministry of Industry Indonesia)**

Hafid Abdullah^a and Sony Harbintoro^b

^{a,b}Metal Industries Development Centre (MIDC) - Ministry of Industry Indonesia
Jl. Sangkuriang No. 12 Bandung 40135
E-mail : hafidochan@yahoo.com

ABSTRACT

Analysis of situation and competitive strategy formulation for the vision and mission towards in the year of 2020 (Case: in MIDC Ministry of Industry Indonesia) has been done. The aim of this research is to guide the direction for the company leaders and the entire employee of the MIDC in carrying out research and development (R & D) metal and machinery programs during the period year of 2014-2020. Also to sharpen R & D activities as an effort to increase the performance of MIDC value increase R & D results in an optimal benefit. This research method is using primary and secondary data. The primary data obtained through field surveys pick-test data collection through observation, directly interviews and discussions with the expert judgements. While secondary data obtained from the BPS, scientific journals, browsing internet and other sources. The analysis, include: (1) the vision, mission, strategic goals and objectives of the company, (2) current business analysis of the position, both internal and external, using EFAS and IFAS (TOWS) methods, (3) the corporate strategy of MIDC, (4) strategic policy direction of MIDC based on core competencies, core products, marketing strategies and work programs. Based on the results of the analysis the obtained value EFAS dan IFAS approximately 7.6 and 6.6. To shown the position of MIDC is winner in the growth. The results of this analysis are expected to MIDC can achieve this goal in accordance with the vision and mission.

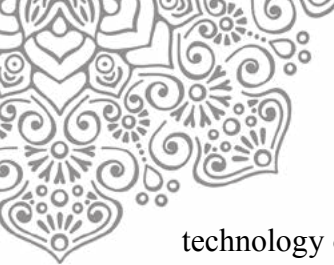
Key words : external strategic analysis (EFAS), internal strategic analysis (IFAS), Treath, Opportunity, Weakness and Strength (TOWS/SWOT)

1. INTRODUCTION

Free competition which is full of competition and consumer demand for products/services better with the delivery time, has spurred the company of any organization or institution, both private and government to improve its performance. To be successful, they are required to cost-saving efforts, optimize production capacity, increased efficiency and productivity and also improve services (Hafid,2013;2005).

Metal Industries Development Center (MIDC) is an institute of research and development (R & D) owned by the Ministry of Industry. MIDC have a duty and a strategic role in the effort to accelerate the development of metal and machinery industry and other industrial sectors of metal products and machine in Indonesia. In providing support services to the industry, MIDC accept a job (job orders) are done in the workshops (casting, machining and welding) as well as calibration and testing laboratories (Hafid, 2005).

As an R & D institutions, especially in the field of metal and machinery manufacturing technology, the MIDC rule are required, at least, must have a level of



technology one step ahead compared to the fostered metal industry. However MIDC seems too late in anticipating the needs of the technology in the industry so its presence needs to get new Recognition through a show of technological capability, so that the metal industry both SME and large-scale feeling homesick and need to get help from MIDC (Hafid, 2013; A. Wahid,2002;Kompas,2016).

Currently the technology advances metals and machinery manufacturing industry has been very rapid. Therefore MIDC need to have a human resources (HR) qualified with a sharp cleverness power so that they can see and solve problems. MIDC should be able to provide a rail or path for industry so that the industry train is capable of traveling at high speed. This can be realized when its human resources, education and experience sufficient to be able to follow the rhythm of the speed of progress of science and technology which is very fast. MIDC required to be able to translate and simplify the high level of technology so that small and medium enterprises were able to apply it.

An example of the weakness of the domestic industry where MIDC should more proactive role. According to the source: WEF and IMD survey of competitiveness ranking obtained Indonesia in 2016 on the ranking of 41 is under the Malaysia (ranked 25th) and Thailand (ranked 34th). Even very far behind when compared with Japan (ranked 9th) and Singapore (ranked 2th) (Klaus Schwab, 2016). According to Michael Porter competitiveness is productivity, defined as output produced by labor (1990).

Based on the above mentioned problems, it is known that various fundamental problems faced by MIDC currently include the following: (1) the condition of the quality and quantity of human resources not currently support, (2) the facility machinery and equipment that is not utilized optimally, (3) ability to understand and apply technology processes and products will no longer be support the industry because most of the metal and machinery industry is able to grow more rapidly, (4) the results of applied research and technical service is yet many are be used by the industry (users), etc.(Hafid,2013).

In order to enhance the role and ability of MIDC to face challenges in accordance with the development of metal and machinery industry in the future, it is necessary to analyze the situation and formulating strategies to compete for the Vision and Mission in the year of 2020. The vision and Mission can be used as a guide (reference) directions for the management and the staff of the MIDC in carrying out research and development activities during the period year of 2014-2020.

The purpose of analysis is (a) determine the competitive strategy of MIDC in the face of competition from metal and machinery industry players as well as other relevant institutions, (b) to formulate a follow-up strategy to compete in the business for the long term which is expected to boost MIDC business growth at the future in a sustainable manner in the face global competition. The benefit is expected to MIDC can know the strengths, weaknesses, threats and opportunities that can be exploited and take appropriate policy in competition with its stakeholders.

2. METHODOLOGY

In this study used survey methods : taking a sample of the population using a list of questions (questionnaires) and interviews directly to the company management selected the object of research as well as the technicians and experts (respondents). As for the secondary



data obtained from literature and from various publications, reports and activities of the relevant institutions and other sources.

The object of research is in MIDC the field of metals and machinery located in Bandung, West Java Indonesia during the period of 2013-2014. The stages are carried out in this research is the formulation of the problem, determining the purpose of research, literature, problem-solving model development, data collection, formulation of strategic alternatives and conclusions, namely:

1. Formulation of the problem: What will be discussed is the company's external environment changes with studying the strengths and weaknesses of the company and also the analysis of opportunities and threats that may be encountered in the future.
2. Determination of research objectives: The purpose of the analysis are: (a) determine the competitive strategy of MIDC in the face of competition from the metal and machinery industry competitor as well as other relevant institutions, (b) to formulate a follow-up strategy to compete in the business for the long term which is expected to boost MIDC business growth in a sustainable future in the face of global competition.
3. The study of literature: Learning theories that supporting this study include the concept of Strategic Management, Strategic Management Model Matrix, among others External Factor Evaluation (EFE), Internal Factor Evaluation (IFE) Matrix, Opportunities Threats (SWOT) Matrix (Hafid, 2013; Rangkuti, 2005, 2013).
4. Field study: Performed to clarify the problems faced.
5. Data collection: The data that is required in this study consisted of internal data and external environmental data. Internal data is data obtained from the company itself, where we can see and assess the strengths and weaknesses of the MIDC. External data collected from the environment outside the company, so it can see the threats and opportunities that are important to note as a reference and comparison to MIDC.
6. The formulation of strategic alternatives: This stage is the stage of solving the problem by formulating several alternative strategies. The formulation of strategic alternatives conducted using analytical models of Fred R. David (2004) that has been modified and adapted to the conditions of MIDC. This stage produces several alternative strategies that will be proposed to be implemented by MIDC based on the priority scale.
7. The proposed implementation of the strategy: Based on the strengths and weaknesses of the internal factors and the opportunities and threats in the external factors.
8. Clearly outlined and more detail of the data processing to see the strengths and weaknesses of the internal condition that is associated with the opportunities and threats from external conditions.
9. Conclusions and recommendations : At this stage the conclusions drawn from the data collection and processing in the form of analysis and the formulation of the proposed strategy. Furthermore, the conclusion can be suggested as several steps to MIDC for consideration to enhance and improve the performance of institution to face global competition.



3. RESULTS AND DISCUSSIONS

3.1. Profile MIDC

Institute of Research and Development for Metal and Machinery Industry (BBLM) was established in 1969, under the name Project of Metal Industries Development Centre or better known as the Metal Industries Development Centre (MIDC). Until now MIDC is under the auspices Ministry of Industry of the Republic of Indonesia (MIDC, 2014).

MIDC Vision as a leading R & D institutions in Indonesia and the world in the process engineering product in 2020. The Mission as following :

1. Perform the applied R & D on product design, materials, processes and quality assurance in the metals and machinery field.
2. Provide Technical services : consultancy and supervision, conformity assessment, competency development of human resources , product certification, personnel certification and quality management system for metal and machinery industries.
3. Dissemination and assist the application of technology in the metal and machinery field into industrial society.

3.2. Analysis of Business Position

Identification of the MIDC position effort done by using TOWS/SWOT (Hafid, 2014). It start with determining Threat, Opportunity, Weakness and Strength (strength and excellence) facing MIDC to day and the future.

Results of interviews and field observations, the study conducted to analysis of external strategic factors (External Strategic Analysis/EFAS) and analysis of the situation of strategic factors Internal (Internal Strategic Analysis/IFAS) is a major problem faced by MIDC. Then set MIDC current business position become a reference material for consideration for MIDC future development (Hafid, 2013;2014).

A. External Analysis

External strategic factor (External Strategic Analysis / EFAS), consist of :

1. Demand:
 - a. Applied research and development needs (government internal budget, national research incentives)
 - b. Process technology capability is still low (No good or NG casting > 30%, the amount of usage of imported products) need coaching and development
 - c. Technical services (guidance consultation, calibration and testing, training, etc.)
2. The technical cooperation at domestic and abroad:
Opportunities to improve the reputation of the organization (ITB, Belgium, Japan, Korea, etc.).
3. Protection of government:
Standardize their product requirements with the national standart (SNI) and use of domestic products
4. Competition:
 - a. Competition with another government institutions (B4T- PT. Pindad, PT. DI, etc.)
 - b. University (ITB, Polman, UI, etc.)
 - c. Competition with private companies (PT. WIKA, PT. Bakri, etc.)



5. Trend Import:

Increased imports of machinery equipment manufacturers, in year of 2010: Imported machines = US \$ 11.31 billion and Export machines = US \$ 6.03 billion. While Th 2013: Import of machinery = US \$. 34.227 billion and Export machinery = US \$ 5.561 billion (MOI, 2014).

B. Internal Analysis

Internal strategic factors (Internal Strategic Analysis/IFAS), includes:

1. Brand name MIDC: already known, their recognition and have a good relationship with metal and machinery industry.
2. Facilities: machinery and equipment is complete, have some new machines but optimalization still low.
3. Government support: government assistance (research and development, staff salaries and maintenance of the facility)
4. Human resources: many of experience employee has already retire and new employees are lacking of knowledge and inexperienced.
5. Knowledge Technology: Only 30% of all metal machinery technology competencies controlled by MIDC
6. Customer Service: technical services order completion time is often too late
7. Marketing: The marketing function (promotion) do not play a significant role

3.3. MIDC Corporate Strategy

From the figure of matrix external and internal environment (Figure 1) concluded that Section calibration and testing of MIDC currently on-1 cells (7.6; 6.6), then the position of MIDC rated Winner in the growth (Hafid, 2013).

In the mapping products/services, approached method through the analysis of industry attractiveness and business strength MIDC. Industry attractiveness is part of the external factors relating to the scope of the industry. While the strength of MIDC businesses reflect the internal strength of the products. The products being mapped, as shown in the figure below, that is:

1. Research and development of products
2. Technical services : casting, machining, heat treatment, welding, calibration and testing
3. Training and consulting services

From the results of the mapping position of business and product/service MIDC note that at this time in a state of survival, so MIDC should make efforts into the improvement to increase their competitiveness. MIDC set business direction is as follows:

1. MIDC should reach a stable condition in the period of 2013-2014 by:
 - a. Utilize as much as possible of existing resources, in order to maintain market share and products/services that have been mastered.
 - b. Improve performance by consolidating a fundamental way.
2. MIDC should be independent and going to the growing conditions in the next 5 years (2015-2020) by:
 - a. Improving product featured R & D results and the potential market selectively.
 - b. Cultivate metal and machinery industry in Indonesia, especially SMEs by providing training and technical guidance, consulting and continuous supervision.

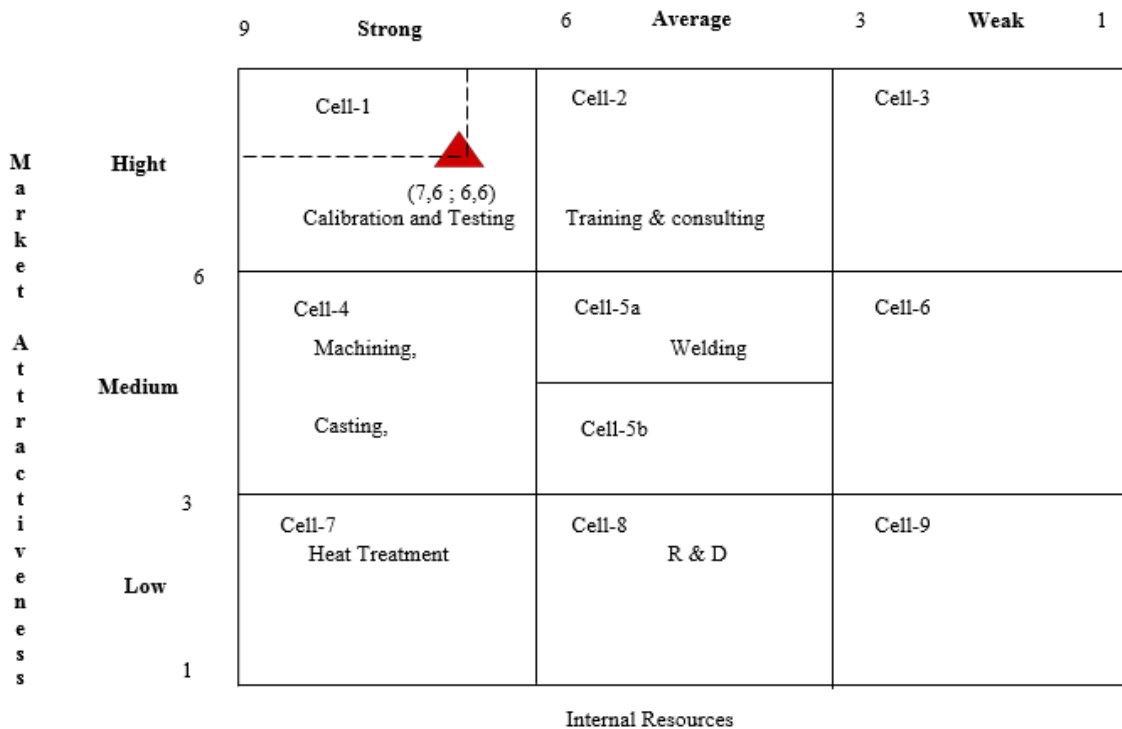


Figure 1. Position/services MIDC

3.4. Directions Policy and Strategy

In order to pursuit its business objectives, MIDC will implement a common strategy based on competence and products. General strategy to be implemented is cost leadership with an emphasis on the benefits of competitive prices while still maintaining the quality of the product.

This policy direction is applied for at the moment, because MIDC still get permanent funding from the government, and the absence of depreciation of existing equipment. With the implementation of this strategy, MIDC will perform segmentation and market the following products:

1. Product strategy and development

As an institution engaged in the development of the metal and machinery industry, MIDC should retain its core competence. To be able to still exist in the business. MIDC has set the reverse engineering and prototyping in metal working processes as a core competency (core competence), by reason of (Hafid, 2013):

- a. The market opportunity is still large metal castings
- b. Facilities of machinery and equipment owned by MIDC can be optimized to produce high value-added products.
- c. Improving human resource competencies MIDC

MIDC core product is the casting products, tools manufacturer, and product trials, while the final product provided to customers can be grouped into:



- a. Technical services: manufacture prototypes/products services of the equipment (calibration and testing)
 - b. Training services: technical training (casting, machining and welding), management training
 - c. Technical assistance and consulting services as well as supervision
2. Marketing Strategy
- a. Selected market segmentation: Large-scale industry, medium industry, small industry
 - b. Seeing the competition is very high both from domestic and abroad (imports), the business strategy that is made to enter the market segment that has been announced is to strengthen the business with cooperation between public and private institutions as follows: Development of the technology with academics/university, development of the industrial market, the development of policies by the government, development funds by financial institutions, the development of the information with the relevant institutions

4. CONCLUSIONS

1. Based on the analysis of strategic factors external situation (EFAS) and internal (IFAS), the obtained values 7.6 and 6.6. The figure shows that the calibration and testing section in the position as the winner (winners) in growth.
2. MIDC applied business strategy is cost leadership with an emphasis on competitively price advantage while still maintaining the quality of the product.
3. In the making a strategic plan requires a team from each of the areas concerned, it is very important to make a long-term plan that is integrated as a whole in order to achieve the vision and mission carried by MIDC.
4. Implementation of the formulated strategy must be executed consistently and continuously despite the replacement of the Director of MIDC.
5. Establish and implement the chosen strategy in this study that is market growth strategy in order to immediately address the issues at this the moment.

5. ACKNOWLEDGEMENT

In this moment the authors would like to thank: (1) The Director of MIDC which has opportunity to carry out this research (2) Directors and management in the metal and machinery industry which has given license to visits industry and discussion, (3) expert judgements and all those who have contributed usefull ideas and discussion that may not be written one by one.

6. REFERENCES

- Hafid., (2013), MIDC development Mapping: the Vision and Mission toward the year of 2020, Final Report Government Internal Budget MIDC, the Ministry of Industry, Bandung. pp 1-1.
- ____., (2005), Plant layout machine in MIDC machinery workshop in order to increase productivity, Journal of Metal Indonesian, Vol.27/2005, ISSN 0126-3463, Metal Industries Development Center, Ministry of Industry, Bandung. pp. 56.



- _____. (2005). Human Resource Development (HRD) patterned P3JJ for foundry technology competency enhancement, *Journal of Metal Indonesia*, ISSN 0126-3463, Vol.27/2005, Metal Industries Development Center, Ministry of Industry, Bandung. pp. 68.
- _____. (2014), Analysis of production facilities on ferrous foundry industry as an effort for competitiveness advantage of companies. *Proceedings of the National Seminar on Industrial Technology*, 2014. ISSN: 2355-925X, FTI-USAKTI, Jakarta, pp.019-5.
- Wahid, A., (2002), MIDC development plan : Papers in Internal Seminar MIDC, the Ministry of Industry, Bandung. pp. 1.
- Klaus Schwab., (2016), *The Global competitiveness report 2016-2017*, World Economic Forum (WEF), Geneva. pp. 7.
- David, Fred. R., (2004), *Strategic Management Concepts ninth edition Indonesian*, translation by Kresno Sasono. PT. The index, Jakarta. Pp. 5,14,52.
- Cheng-Wei Chang and Chia Chun Liao, (2013), Applying SWOT analysis to explore Taiwan foundry industry management strategy, *International Journal of Innovation Management and Technology*, Vol. 4, No.1, February, Taiwan. pp.114-115.
- MIDC., (2003), *Revitalization MIDC: Business Plan 2003-2007*, Metal Industries Development Center, Ministry of Industry, Bandung. pp. 14-30.
- _____. (2014), *MIDC Strategic Plan 2015-2019*, Metal Industries Development Centre (MIDC), Ministry of Industry, Bandung. pp.30-31.
- _____. (2014), *Company Profile*, Bandung. pp.3.
- Porter Michael E., (1990), *The Competitive Advantages of Nations*. New York: The Free Press. Pp.12.
- Rangkuti, Freddy., (2005). *Case dissecting SWOT analysis techniques*, PT. Heritage Gramedia Utama, Jakarta. pp. 24-25.
- Rangkuti, Freddy., (2013), *The Balanced Scorecard SWOT*, Edition 4th, PT. Heritage Gramedia Utama, Jakarta. pp.29, 64-65.
- Kompas., (2016), *Inovation : Main problem mindset* , Publisher Kompas, 1 Juli 2016, Jakarta. pp.14.
- Ministry of Industry (MOI)., (2014), *Ministry of Industry Indonesia*, Jakarta.



APPLICATION OF TECHNOLOGY ASSESMENT IN CARBON CAPTURE AND STORAGE TECHNOLOGY IMPLEMENTATION FOR CO₂ EMISSION IN INDONESIA

Akhmad Hidayatno, Arry Rahmawan Destyanto, Reinaldo Giovanni
*System Engineering, Modeling, and Simulation Laboratory, Industrial Engineering
Department
Faculty of Engineering, Universitas Indonesia*

ABSTRACT

Green house gases (GHG) emission is one of the environmental issues that hasn't been resolved and continued to increase annually. Carbon dioxide gas is known as the largest contributor for GHG emissions. This environmental issue also happens in Indonesia as a developing country which has focused on sustainable development. In 2020, the total emission of carbon dioxide gas in Indonesia is predicted around 960 million ton if there is no mitigation action. In developed countries, they have a bold step to mitigate their emission of CO₂ gas by using Carbon Capture and Storage (CCS) technology. This technology is effective to reduce the CO₂ emission in large-scale. The study and information about CCS, as a new technology to reduce emission, haven't well developed in Indonesia. Based on the situation, the author tries to find important criteria for conducting a research of CCS technology implementation in Indonesia using participatory technology assesment. The output from this research are giving understanding how CCS could be used by seeing what important criteria needed by stakeholder to develop, particularly in Indonesia. The rate of carbon capture of CO₂ emission and the cost of investment for carbon capture technology are the main subcriterias for each criteria of environment and economic if the carbon capture technology implemented in Indonesia.

Keywords: Technology assesment, carbon capture and storage technology, CO₂ emission, assesment criteria

1. INTRODUCTION

Green house gases emission (GHG emission) is one the environmental issues which has not yet settled on a completion until now in the whole world, and it keeps increasing from year-to-year. The escalation of the GHG emission is a major cause of climate change that has happened in the last few years (Vianello, Mocellin, & Maschio, 2014). Since 1997 to 2000 the GHG emission had increased about 1.3% per year, but in the next decade (2000-2010) the increase of green houses gases emission was 2.2% per year. This phenomenon has also happened in Indonesia, as a developing country focuses on sustainable development.

On the report written by Ministry of Environment Republic of Indonesia (2010) stated that GHG emissions are divided into four types of gas. There are carbon dioxide, methane, dinitrous oxide, and PFC. The largest contributor of GHG emissions is carbon dioxide emission, which is accounted more than 1.1 million Gg CO₂ (Ministry of Environment, Republic of Indonesia, 2010). In 2020, the emission of carbon dioxide gas in Indonesia is



predicted in total amount 960 million tons if there isn't any mitigation action (Kementerian Energi dan Sumber Daya Mineral, 2013).

The government has already thought on reducing CO₂ emission through various policies, so that it can be implemented in Indonesia. Bioletty, Syahrial, & Tobing (2007) wrote some of the policies that could be implemented in Indonesia: energy efficiency and material development, reforestation, increasing-use of renewable and nuclear energy, a decrease in the carbon intensity of fossil fuels, and the use of carbon capture and storage (CCS) technology.

Using carbon capture and storage technology, as well as in developed countries, considered as one of promising mitigation action. CCS is a highly effective technology to capture and store the GHG emissions generated from various sectors (Department of Energy & Climate Change, 2012). One of the oil and gas state-company has already had one CO₂ capture facility, but it has not been fully utilized. In addition, the source of carbon dioxide gas emission will increase because the government has plan to build more power plants using coal as their fuel.

Indonesia has an opportunity to implement CCS technology, however, there are still lacks of research and information about CCS technology implementation in Indonesia. Indonesia must initiate an active role in finding out more about this technology. Huisingh et al. (2015) did a fine research about the potential of carbon emission reduction in various sectors at different scale and how technology could reduce carbon emissions.

In this research, the authors consider to apply technology assessment method as preliminary study before implementing CCS technology. The output of this research are generating criteria and subcriteria needed if the CCS technology will be implemented in Indonesia. This method is expected to be a reference framework for the application of CCS technology in the future, particularly in Indonesia. Therefore, this study focuses on fostering technology assessment method in capturing carbon dioxide gas emission using CCS technology. The authors also see how the implementation of CCS technology could be a considerable action in Indonesia based on economy and environment aspects.

2. LITERATURE REVIEW

2.1 Carbon Capture and Storage (CCS)

From 1970 to 2010, GHG emissions continued to rise until reach 2.2% per year in the world (IPCC, 2014). Carbon dioxide emission becomes the largest contributor to the increase in green house gas emissions. In purpose to tackle the increase in these emissions, several countries have implemented carbon capture and storage (CCS) technology. The application of CCS technology in developed countries has been used in power plant and industry sector. It is because the largest contributor to GHG emissions, in general, are from power plants and industrial production activities especially those using coal and fossil fuel as their primary energy source.

Carbon capture is one of the processes in carbon capture, utilization, and storage (CCUS). The objective of this process is to prevent the carbon dioxide emissions resulted from human activity reaching the atmosphere. The process is started with the separation of carbon dioxide gas emissions with other gas components. After the separation, the emission



of carbon dioxide gas is compressed at high pressure to save carrying cost and storage before being delivered to the final storage (Indonesia CCS Study Working Group, 2009). Carbon dioxide gas that has been captured, typically, will be transported through the pipes to be stored. Storage of carbon dioxide gas can be placed in three different areas: geological sequestration, mineral carbonation, and storage in the ocean (Li, et al., 2013).

There are many variations on the evolution of CCS technology, which is divided into three main technologies: post-combustion capture, pre-combustion capture, and oxy-combustion capture (Folger, 2013). From capturing those carbon emissions, the CO₂ gas will be obtained which can be stored and/or reutilized. By storing the CO₂ emission, the carbon emission that comes out into the air can be reduced and the increasing of greenhouse gas emissions can be suppressed.

2.2 Technology Assessment

Developed countries, such as England, Japan, and Norway have applied CCS technology to reduce GHG emissions from their industrial activities (CCS Roadmap, 2012). Before implementing CCS technology, these countries conducted a preliminary study of CCS technology in their countries. One of the methods used is technology assessment (TA) method. TA is a method to investigate the conditions resulting from the implementation of new technology to meet future requirements and aspects of sustainability. The terminology of TA itself has been known since the 1970s. Formerly, the technology assessment term appeared due to the need of policy makers made and decided the appropriate policies to the public about new technology implementation (Grunwald & Achternbosch, 2013).

One example in application of technology assessment method is not only branched out in the energy sector, such as CCS technology, but also applied in other industrial sectors. Telecommunication service provider in China (Zhang, Daim, Choi, & Phan, 2008) used technology assessment method as a basis for selecting telecommunication technology in its country. Previous research conducted by Huisinigh et al. (2015) briefly discussed the potential of technology assessment to reduce carbon emissions not only for telecommunication service, but also in various industries and agriculture sectors.

Many studies on decreasing carbon dioxide emission using carbon capture technology is still being conducted. Several studies linked to the carbon capture technology on energy sector are being developed: technology assessment on capturing CO₂ emission in Natural Gas Combine Cycle (NGCC) power plant (Cormos, 2015), utilization of CO₂ using *monoethanolamine* (MEA) technology (Kang, Jo, Lee, & Park, 2016), and technology assessment based on performance-cost criteria on CCS technology in power plant (Davison, 2007).

2.3 The Integration Between Economy-Environment Aspects for Carbon Capture Technology

In this research, the authors foster the TA method based on economy and environment criteria. There are several previous studies on using technology assessment method based on economic criteria: carbon capture technology in NGCC power plant (Cormos, 2015), cost assessment on CCS in power plant (Davison, 2007), the estimate cost of capturing CO₂



from the flue gas with a pressure/vacuum swing adsorption (Susarla, et al., 2015). The assessment of carbon capture technology with the environmental criteria generally focused on energy sector, especially in power plant and exploration-production of oil-gas: the capture of CO₂ emission from the extraction oil-gas in Norway (Gavenas, Rosendahl, & Skjerpen, 2015), and case study of capturing CO₂ in Austria (Reiter & Lindorfer, 2015). By looking from the two aspects, the economy and environment aspect, play important role in the implementation of carbon capture storage technology using technology assessment method.

Indonesia, until now, has not discussed further about the technology assessment of carbon capture technology for carbon dioxide. There are lacks of informations and researches of capturing carbon dioxide emission in Indonesia. Based on those reasons, the authors do focus the study on integrating economy-environment aspects and other two aspects (performance and technology innovation) to know the assessment criteria needed if the CCS technology implemented in Indonesia.

3. RESEARCH METHODOLOGY

3.1 Data Gathering

This study involves two types of data: secondary data and primary data. Secondary data contain reference criteria from reputable and trusted literatures about actual conditions of energy and carbon dioxide emission in Indonesia. The primary data contain the result from focus group discussion (FGD – involving some stakeholders and expert) and the result from questionnaires. The questionnaires are filled by the experts which have deep understanding about the issue of carbon capture technology and carbon dioxide gas emission.

3.1.1 Data About Current Energy Situation and Carbon Emission in Indonesia

The GHG emissions are consisted of four main types of gas: carbon dioxide gas emission, methane emission, N₂O emission, and *perfluorocarbon* (PFC). From the four types of gas, carbon dioxide gas emission is the largest contributor to GHG emissions. This condition also happen in Indonesia.

Total emissions of carbon dioxide gas in the world reached 23.684 Mt/year (Davison, 2007). That number will continue to increase every year. Power generation sector is the largest contributor to the carbon dioxide gas emissions globally, which is about 35% of the total CO₂ emissions. It is because the power plant still uses fossil fuels such as coal as primary energy sources for the power plant. In 2011, the use of coal still counted 3.773 million TOE and it is predicted to increase by 44% in 2035 (DEN Republik Indonesia, 2014). This study will focus on carbon dioxide emissions obtained from the power plant sector in Indonesia.

The requirement of energy needed in power plant fueled with coal will increase significantly until 2050 in Indonesia. In 2011, the consumption of primary energy in Indonesia derived from fossil energy attained to 71% of total primary energy (Kementerian Energi dan Sumber Daya Mineral, 2013). In the BaU (Business as Usual) scenario, primary energy coal plays fairly large with a percentage up to 41% in 2050.

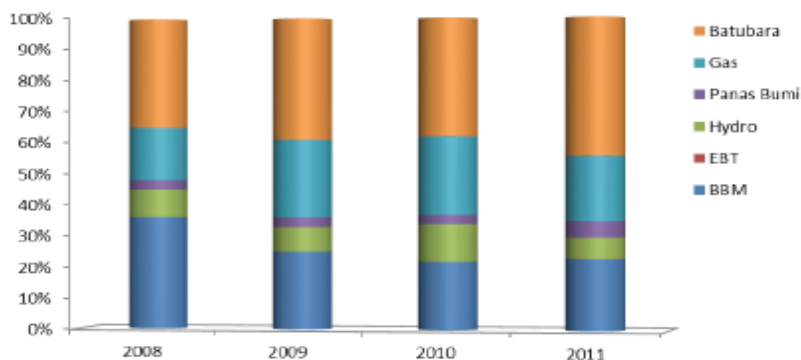


Figure 1 Comparison of energy source usage in power plant

Figure 1 above shows how the comparison of using coal and other energy sources in power plant. The use of fossil fuels such as coal in power plants (in Indonesia) produces the carbon dioxide gas emission in large amount and makes it as the largest contributor to GHG emissions.

The National Electricity Company (PT PLN) which is a state-owned company in Indonesia is still using coal as the dominant energy sources for generators. The emissions out are varied, but the greatest amount of emissions is the carbon dioxide gas emissions. Power plant sector accounts for a percentage of about 32% in 2012 (amount to 138,82 million tonnes of CO₂) followed by industry (29%), transportation (28%), households (7%), commercial (3%), and others (1%) (PT PLN Persero, 2014).

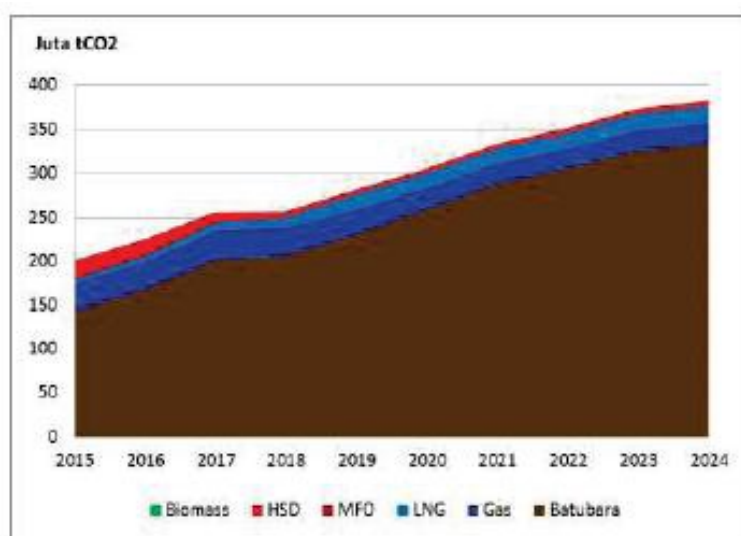


Figure 2 CO₂ emissions in Indonesia from power plant

Figure 2 shows the amount of CO₂ emissions that would be produced if the electricity production in Indonesia carried out with a fuel mix strategy (the composition of the electricity energy production by type of primary energy projected until 2024 in Indonesia).



3.1.2 *Data About Potential for Implementing Carbon Capture Technology for CO₂ Emissions in Indonesia*

Most industries that produce carbon dioxide gas emissions, generally, emit the gas directly into the atmosphere, either by burning or just releasing directly into the air through an air filter instantly. These technologies have not been able to reduce carbon dioxide emissions on a large scale.

Other technologies that are often used to reduce carbon dioxide gas emissions are: the gasification of coal, natural gas splitting, gasification of biomass, shift converter, methanol synthesis, methane synthesis, and water electrolysis. Syahrial, Pasarai, & Iskandar (2010) conducted a joint study with several government agencies and foreign companies regarding to the potential of CCS technology in Indonesia. Those three researchers explained where the origin of carbon dioxide emissions is, a general overview of CCS technology, and its potential for implementing it in Indonesia. Indonesia has large opportunity to apply CCS technology because Indonesia already have a great amount of CO₂ emissions as a source and enough storage capacity for CO₂ emissions.

3.1.3 *Data About Carbon Capture Technology from Main Stakeholders*

Data about carbon capture storage technology included as one of primary data which was gathered from focus group discussion (FGD) and questionnaire filled by the expert and stakeholder. The first step to do is doing the FGD. In FGD of this research, authors asked three persons (expert and stakeholders) from government and private institutions to get involve in FGD. FGD was more like a discussion that lasted one day concerned in finding out how energy conditions are, the emission's conditions are, and the criterias needed are if the carbon capture applied in Indonesia.

Stakeholders which representing Pertamina Hulu Energi Offshore North West Java said that Indonesia had already the potential sources of CO₂ emissions and the concentration of CO₂ is high enough. On the other hand, expert said that the biggest challenge in implementing the technology was how the technology, technically, is capable of capturing CO₂ emissions directly without any leaks because the slightest error would cause substantial financial losses.

Based on FGD, expert and stakeholders see the potential for implementing carbon capture technology for CO₂ emissions are feasible and realistic in the long term. Government should be involved in terms of financial support and policy so that the implementation can proceed smoothly without any interventions.



3.2 Conducting participatory technology assesment (pTA) for CCS implementation in Indonesia

Authors used TA activities because technology assesment is method which systematically involve various kinds of actors with may different backgrounds or different kinds of organizations. One of TA that authors pick is participatory TA (pTA). pTA usually invite many different actors which have influence and interest about technology that would be implemented. Person which can be invited as participant to join can be an individual stakeholders, citizens, technical scientist/experts. Standard pTA methods include consensus conferences, focus groups, or scenario workshops. Sometimes pTA is further divided into expert-stakeholder pTA and public pTA (including lay persons).

Expert-stakeholder which involved in this study consist of three representatives, first is representing academic, second is representing government, and others are representing professionals / practitioners. List of detailed experts whom involved are shown below.

Table 1 List of experts involved in participatory technology assesment

	Representative	Occupation
1 st Participant	Academics	<i>PhD Researcher</i>
2 nd Participant	Professionals	Board of Executive PT. Surya Esa Perkasa
3 rd Participant	Government	Deputy Minister of Maritime and Natural Resources
4 th Participant	Professionals	VP Drilling PHE ONWJ
5 th Participant	Professionals	Environmental Engineer PHE ONWJ

pTA is expected to provide an equal understanding to stakeholder and public on the proposed of new technology, how is technology affect the society and stakeholder, and what criteria should be considered if new technology will be applied to reduce CO₂ emission in Indonesia.

Authors conduct following steps to obtain level of importance in criteria and sub-criteria as final result of technology assesment,

1. Set the issue in the study;
2. Search some literatures related to researches that using technology assessment method and in what field of knowledge TA method has already applied;
3. Find the literatures related to TA method concern on energy sector, especially the reduction of carbon dioxide emissions in power plant;
4. Conduct focus group discussion (FGD) as an initial step to know the perspectives from expert and stakeholder about the conditions, potentials, and challenges in facing the new technology (carbon capture technology in Indonesia);
5. Select the criteria and subcriteria: economy, environment, performance, and technology innovation from the result of previous FGD and literatures



The subcriteria that have been obtained then inserted into the questionnaire to be filled by experts. The experts will determine level of importance and also discussing it from each subcriteria and criteria for the implementation of new carbon capture technology in Indonesia. Detailed list of criteria and sub-criteria used in participatory technology assesment is listed below,

Table 2 Criteria and sub-criteria considered for technology assesment

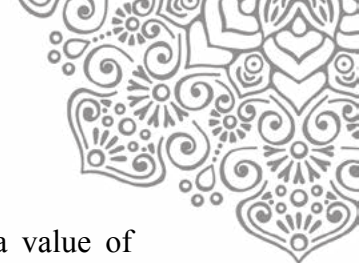
Main Criteria	Sub-criteria	Unit
Performance	Cleaner emission that would be produced because carbon capture technology implementation	MW or Kg/Kg _{output}
	Energy usage in carbon capture technology	KWh/t
Economy	Investment cost for CO ₂ removal	IDR/t
	CO ₂ capture penalty cost	IDR/t
	Profit percentage from carbon capture technology installation comparing to its energy output	%
Environment	Total amount of CO ₂ that can be reduced	KgCO ₂ per toe or t/h
	Capture level of CO ₂	%
Technology innovation	Technology reliability and risk of accidents	Point
	Carbon capture technology capacity to reduce gas emission	MW
	Technology resilience for a long term	year

After discussion session and all of questionnaire had been filled by experts would be treated with the help of Expert Choice software to display the results of the weight of each sub-criteria.

4. RESULTS AND DISCUSSION

Based on intensive discussion and questionnaire result, this research obtain that the highest weight value is reliability of technology subcriterion with a value 0,211 (out of total 1,0). All results that have been obtained is listed below (ordered from highest to lowest value),

- a. The reliability technology with a value of 0,211
- b. The resilience of technology with a value of 0,173
- c. The capacity of carbon capture technology with a value of 0,129
- d. The rate of capturing of CO₂ emissions with a value of 0,116
- e. The amount of CO₂ emissions reduced with a value of 0,111
- f. Investment cost of carbon capture with a value of 0,075
- g. Cost of CO₂ penalty with a value of 0,067
- h. The profit percentage on the installation cost of carbon capture technology per output energy with a value of 0,047



- i. Clean energy produced after the use of carbon capture technology with a value of 0,035
- j. Total use of energy (additional energy) for carbon capture technology with a value of 0,035

The final result of the final weights each subcriteria gives an information on what the criteria and subcriteria are more considered if there will be an implementation of new carbon capture storage technology for CO₂ emissions in Indonesia. Technology innovation criteria becomes main concern criterion with the greatest weight value, whereas this criterion is the first criteria considered for implementing carbon capture technology based on the completed questionnaires from participants. Environment and economy criteria are the next highest weight value obtained from the questionnaire.

Inconsistency value from this calculation is about 3% where the value is still below the maximum tolerance of 10%. This inconsistency value gives the sense that all the participants involved in filling out the questionnaire is an expert on climate change, especially carbon dioxide gas emissions and carbon capture technology. Their answers on the questionnaire is valid and reliable.

From the result of the questionnaire and the analysis both individual and general, overall shows that the potential application of carbon capture technology is already open and the novelty of this technology becomes a criteria with a more weight value than other criterias. It is necessary needed a support from the government and investors as an enabler (on economic aspect) to assist in the implementation of carbon capture technology for Indonesia's power plant.

5. CONCLUSION

Based on the results and analysis from this research, it could be concluded from result of the study suggests that technology assessment method could be developed in the energy sector. Technology assesment using participatory from expert-stakeholder can provide clear and appropriate most-concerned criteria and sub-criteria while implementing new technology by combining economy and environment, beside performance and technology innovation aspect.

The investment cost of carbon capture equipment (economic criterion) and the rate of capturing CO₂ emissions (environment criterion) become sub-criterion with the highest weight in their own respective criteria. Sub-criterion technology innovation gains more weight value because of the novelty value of carbon capture technology in Indonesia is really needed to reduce CO₂ emission more effectively in the future.

6. REFERENCES



- Badan Pengkajian dan Penerapan Teknologi. (2010, Januari 01). *BPPT Kembangkan Biological Carbon Capture and Storage (CCS)*. Dipetik Februari 12, 2016, dari bppt.go.id: www.bppt.go.id
- Bioletty, L., Syahrial, E., & Tobing, E. (2007). Peranan Teknologi Sekuestrasi CO₂ dalam Menciptakan Mekanisme Pembangunan Bersih di Indonesia. *Proceeding Simposium Nasional IATMI*.
- Black, J., Kabatek, P., & Zoelle, A. (2014). *Cost and Performance Metrics Used to Assess Carbon Utilization and Storage Technologies*. Energy Sector Planning and Analysis. US: DOE.
- Boot-Handford, M., Abanades, J., Anthony, E., Blunt, M., Brandani, S., Dowell, N. M., et al. (2013). Carbon capture and storage update. *Energy & Environmental Science*, 130-189.
- Cormos, C.-C. (2015). Assessment of chemical absorption/adsorption for post-combustion CO₂ capture from Natural Gas Combined Cycle (NGCC) power plants. *Applied Thermal Engineering* 82, 120-128.
- Davison, J. (2007). Performance and costs of power plants with capture and storage of CO₂. *Energy* 32, 1163-1176.
- DEN Republik Indonesia. (2014). *Outlook Energi Indonesia 2014*. Jakarta: Dewan Energi Nasional Republik Indonesia.
- Department of Energy & Climate Change. (2012). *CCS Roadmap: Supporting Deployment of Carbon Capture and Storage in The UK*. United Kingdom.
- Fleischer, T., & Grunwald, A. (2008). Making nanotechnology developments sustainable. A role for technology assessment? *Journal of Cleaner Production* 16, 889-898.
- Folger, P. (2013). *Carbon Capture: A Technology Assessment*. Congressional Research Service.
- Fujii, Y., & Yamaji, K. (1998). Assessment of technological options in the global energy system for limiting the atmospheric CO₂ concentration. *Environmental Economics and Policy Studies* 1, 113-139.
- Gavenas, E., Rosendahl, K. E., & Skjerpen, T. (2015). CO₂-emissions from Norwegian oil and gas extraction. *Energy* 90, 1956-1966.
- Grunwald, A., & Achternbosch, M. (2013). Technology Assessment and Approaches to Early Engagement. Dalam N. Doorn, D. Schuurbijs, I. van de Poel, & M. Gorman, *Early engagement and technologies: Opening up the laboratory* (hal. 15-34). Karlsruhe: Springer.
- Hidayatno, A., & Maulidiah, W. (2015). *Perancangan Model Pengembangan Strategi dalam Mendukung Penerapan FLNG di Indonesia Menggunakan Pendekatan Technology Roadmapping dan Hoshin Kanri*. Depok.
- Huang, B., & Mauerhofer, V. (2016). Low carbon technology assessment and planning-Case analysis of building sector in Chongming, Shanghai. *Renewable Energy* 86, 324-331.
- Huang, B., Yang, H., Mauerhofer, V., & Guo, R. (2012). Sustainability assessment of low carbon technologies-case study of the building sector in China. *Journal of Cleaner Production*, 244-250.



- Huisingsh, D., Zhang, Z., Moore, J. C., Qiao, Q., & Li, Q. (2015). Recent advances in carbon emission reduction: policies, technologies, monitoring, assessment and modeling. *Journal of Cleaner Production* 103 , 1-12.
- Indonesia CCS Study Working Group. (2009). *Understanding Carbon Capture and Storage Potential in Indonesia*.
- IPCC. (2014). *Climate Change 2014 Synthesis Report Summary for Policymakers*.
- Johansson, D., Franck, P.-A., Pettersson, K., & Berntsson, T. (2013). Comparative study of Fischer-Tropsch production and post-combustion CO₂ capture at an oil refinery: Economic evaluation and GHG balances. *Energy* 59 , 387-401.
- Kementerian Energi dan Sumber Daya Mineral. (2013). *Kajian Inventarisasi Emisi Gas Rumah Kaca Sektor Energi*. Jakarta: Pusat Data dan Teknologi Informasi ESDM.
- Kementerian Energi dan Sumber Daya Mineral. (2012). *Kajian Supply Demand Energy*. Pusat Data dan Informasi Energi dan Sumber Daya Mineral, Kementerian ESDM.
- Kementerian Lingkungan Hidup, Negara Indonesia. (2010). *Indonesia Second National Communication Under The United Nations Framework Convention on Climate Change (UNFCCC)*. Jakarta.
- Li, L., Zhao, N., Wei, W., & Sun, Y. (2013). A Review of Research Progress on CO₂ Capture, Storage, and Utilization in Chinese Academy of Sciences. *Fuel* 108 , 112-130.
- Martijn G. Rietbergen, K. B. (2013). Assessing the potential impact of the CO₂ performance ladder on the reduction of carbon dioxide emissions in the Netherlands.
- PT PLN Persero. (2014). *Rencana Usaha Penyediaan Tenaga Listrik (RUPTL) 2015-2024*.
- Saaty, T. L. (2008). Decision making with the analytic hierarchy process. *Int. J. Services Sciences* .
- Setiawan, A. D., & Cuppen, E. (2013). Stakeholder perspectives on carbon capture and storage in Indonesia. *Energy Policy* 61 , 1188-1199.
- Simpson, J., McConnell, C., & Matsuda, Y. (2011). *Economic Assessment of Carbon Capture and Storage Technologies*. Canberra: Global CCS Institute.
- Sliogeriene, J., Turskis, Z., & Streimikiene, D. (2013). Analysis and choice of energy generation technologies: the multiple criteria assessment on the case study of Lithuania. *Energy Procedia* 32 , 11-20.
- Susarla, N., Haghpanah, R., Karimi, I., Farooq, S., Rajendran, A., Tan, L. S., et al. (2015). Energy and cost estimates for capturing CO₂ from a dry flue gas using pressure/vacuum swing adsorption. *Chemical Engineering Research and Design* 102 , 354-367.
- Syahrial, E., Pasarai, U., & Iskandar, U. P. (2010). Understanding Carbon Capture and Storage (CCS) Potential In Indonesia. *Lemigas Scientific Contributions Vol. 33 No. 2* , 129-134.
- Theeyattuparampil, V. V., Zarzour, O. A., Koukourzas, N., Vidican, G., Al-Saleh, Y., & Katsimpardi, I. (2013). Carbon capture and storage: State of play, challenges and opportunities for the GCC countries. *International Journal of Energy Sector Management Vol. 7 No. 2* , 223-242.
- Tokushige, K., Akimoto, K., & Tomoda, T. (2007). Public acceptance and risk-benefit perception of CO₂ geological storage for global warming mitigation in Japan. *Mitig Adapt Strat Glob Change* , 1237-1251.



SHIPPING ROUTE MODEL DEVELOPMENT FOR THE INDONESIAN PENDULUM PORTS

Zulkarnain, Komarudin, Armand Omar Moeis, Seto Banuwijoyo

*Department of Industrial Engineering, Universitas Indonesia, Depok Campus, 16424,
Indonesia*

ABSTRACT

Maritime logistics sector has a very important role in Indonesia for almost all domestic commodities shipped by sea. Indonesian state has a program to balance the economy by balancing the levels of domestic cargo shipments between the western region and the eastern region. Due to the nature of this non-commercial program, a design of marine transport with the aim of minimizing costs is needed. The study aims to develop a shipping route model by considering several factors: the type of Landing Craft Tank (LCT) used, the route passed, and the amount of cargo shipped. The method used in this research is known as the Mixed Integer Programming with the design of the shipping route called Butterfly Route, simulated using the Gurobi software. Several factors that affect the results of the design is the availability of LCT, the distance between the ports and the planned amount of cargo.

Keywords: Maritime Logistics; Cargo; Landing Craft Tank; Port; Mixed Integer Programming; Butterfly Route; Gurobi software

1. INTRODUCTION

There is domestic cargo shipments imbalance between the western and the eastern region of Indonesia (Kalem, 2015). Majority of the Indonesian population is situated in Java and Sumatera island (western region of Indonesia), which contribute to 80.14% of the total population. Java is the most developed region hence become the centre of the trading activity, especially for the importers (Kalem, 2015).

National Logistics System Development blueprint stated that Indonesia as a maritime country, hence the marine transportation infrastructure had a significant role to facilitate logistics transport effectively and efficiently. It becomes a huge challenge, where the trend of Indonesia logistics costs has tremendously increased every year from 2004 to 2011 by an average of 23% annually. (World Bank, 2013).

Some research with various cost-efficiency solution on the maritime logistics problem have been conducted. This research focused on maritime logistic network design, which is different with onshore logistics network design. Maritime logistic network design uses different payload in each fleet meanwhile onshore logistic use the same payload in each fleet (Ronen, 1983). In addition, a port cannot handle all vessels type, while onshore terminal supply can serve all type of vessel (Ronen, 1983).



Selection of a vessel or fleet is one particular focus, where the type and size of the fleet must be determined and minimized (Danzig and Fulkerson, 1954). Fleet type and routes should be combined in the form of a model (Cho and Perakis, 1996). Hence there should be a sensitivity relationship between determining the type of fleet and the sequencing route.

Rana and Vickson (1988) discussed the optimal route for container shipping fleet to maximize profit. Operating costs determination is calculated by scheduling each fleet sailing (rental cost) as well as the recommended cruising speed (consummable goods) (Fagerholt and Christiansen, 2000).

Meijer (2015) stated that, there are three stages of decision-making to determine the type and route of the fleet. Firstly, customize the type of fleet available, determine the route randomly and the last is to test the feasibility of the route by including a combination of fleet and route into the Cargo Model Routing with Generic Algorithmic implementation to determine the route sequencing.

Line Blender (2011) resolve a problem in determining the fleet, ships and cargo flow using full exact methods. Somewhat different from the Mulder and Dekker method (2013) adopted by Van Rijn and Meijer (2015) in the Indonesia pendulum route optimization.

The differences in Line Blender's mathematical models and solution methods (2011) with other researchers is on LCT service, where Line Blender (2011) refers to the Agarwal and Ergun's "Butterfly Route" design of Relaxing Outbound-Inbound fleet principle (2008). Meanwhile Van Rijn (2015) and Meijer (2015) refers to Vickson Rana (1991)'s Inbound-Outbound Principle. Rana and Vickson (1991) presented the state of the North Atlantis sea trade route Liner Shipping art models using outbound-inbound principle where LCT docked at the port that has been defined prior to shipping and each port only docked once before returning to first "Butterfly route" port. Rana and Vickson (1991) used a better route, the relaxing outbound-inbound principle, in Mediterranean, Baltic and the Black Sea intercontinental trading shipment design where LCT docked at the predefined port before sailing more than once on each port before returning to the first port.

According to previously mentioned background discrepancy, a further study is required to draw together the research about the application of *Relaxing Outbound-Inbound Principle route* that is *butterfly route* using a *Mixed Integer Programming* method as a recommendation for Indonesia Pendulum route planning.

2. METHODOLOGY

Linear programming is a general model that can provide best solution of limited resources problem, which are required to determine any carried-out activity, each activity requires the same resources but with a limited amount (Handy Taha, 1987). Integer Programming is a model that has restrictions and objective functions which are identical to linear programming, however it has integer value of decision variables (Render, Stair Jr., and Hanna, 2012).



Assignment problems is a matter of limited resource allocation to certain limit with the goal in profit maximization or cost minimization (Markland, 1983). Transportation is a logistics series activity that play a role in the overall movement of the product from upstream to downstream processes (Bowersox and Closs, 1996). The network model affect performance of supply series through infrastructure development method, in which the operating related scheduling and routing decisions is taken (Chopra, 2010).

Transportation costs take one-third to two-thirds of logistics total cost (Ballou, 1999). Therefore the best way to maximize profits is to make an efficient transportation costs. Vessel is suitable transportation method for a low-mass or low volume products and used for sturdy products (Ballou, 1999).

Shipment planning stage is divided in three stages (Meng In, 2014):

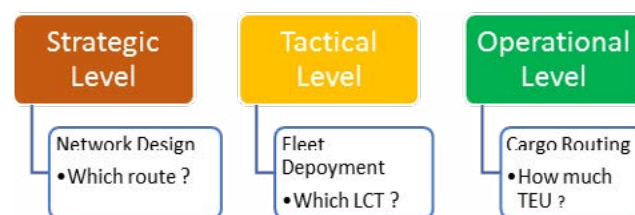


Figure 1 Liner Shipping Stage Planning (Meng In, 2014)

Shipment route planning stage is divided into three steps (Meijer, 2015):

- Feeder Network

Feeder network shipment route use a centralized port (sub port), which in charge to accommodate relatively small volume cargo from other ports.

- Port to port Route

Port to port route shipment route visit all ports in a single cycle

- Butterfly Route

Butterfly route shipment route is free visit for each cyclic but have centerpoint for each route cycle.

2.2. Data Collection

This research aims to provide a Landing Craft Tank (LCT) vessel route recommendation and cargo quantity (LTE) to be transported or unloaded at the port. In order to make an optimum route recommendation, related data such as port location, the distance across ports, port cargo demand, the type of vessel based on the capacity used, the used resources cost and cargo shipping income.

Ports

There are six main ports that must be travelled in Pendulum Nusantara route (Figure 2), i.e. as follows:

- Belawan (Sumatera)
- Tanjung Priok (Java)



- Tanjung Perak (Java)
- Banjarmasin (Kalimantan)
- Makassar (Sulawesi)
- Sorong (Papua)

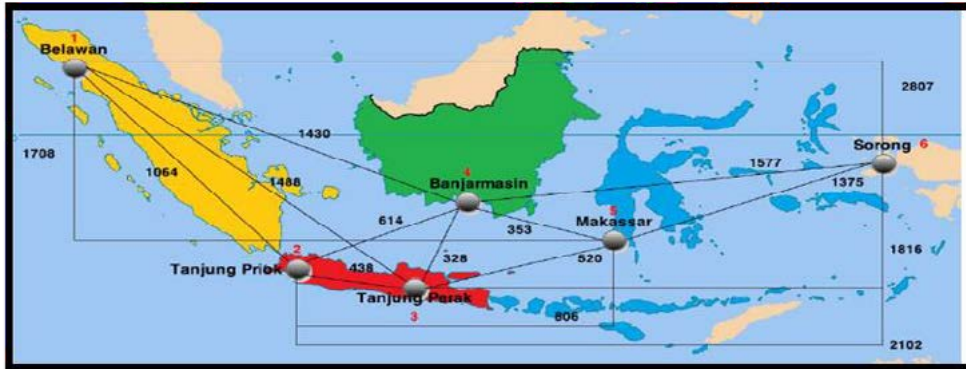


Figure 2. Pendulum Nusantara Ports

Distance across ports

The following matrix distance across ports in Nautical Miles units:

Table 1: Distance across Ports

Matrix Distance	Belawan	tj. Priok	Tj.Perak	Banjarmasin	Makasar	Sorong
Belawan	-	1.064	1.488	1.430	1.708	2.807
tj. Priok	1.064	-	438	614	806	2.102
Tj.Perak	1.488	438	-	328	520	1.816
Banjarmasin	1.430	614	328	-	353	1.577
Makasar	1.708	806	520	353	-	1.375
Sorong	2.807	2.102	1.816	1.577	1.375	-

Demand across Ports

The following matrix across ports demand in TEU units (Wardana, 2014):

Table 2: Demand across Ports

Matrix Weekly Demand	Belawan	tj. Priok	Tj.Perak	Banjarmasin	Makasar	Sorong
Belawan	-	6.693	1.058	87	81	27
tj. Priok	6.740	-	1.916	4.092	2.798	464
Tj.Perak	1.036	2.437	-	3.795	4.820	2.174
Banjarmasin	90	3.637	3.498	-	13	-
Makasar	91	3.501	4.109	73	-	-
Sorong	39	661	2.174	-	-	-



LCT Type

LCT capacity type used in Indonesia shipping (Wardana, 2014):

Tabel 3: LCT type in Pendulum Route

Vessel	Cap (FFE)	Cost	Design Sped	Bunker Cons	Idle Cons
		Rate/ day	Knots	ton/ day	ton/ day
1	450	\$ 5.000	12	18,8	2,4
2	800	\$ 8.000	14	23,7	2,5
3	1200	\$ 11.000	18	52,5	4
4	1750	\$ 15.000	18	55	4,5
5	2400	\$ 21.000	16	57,4	5,3

Cost and Earnings Assumptions

Estimated handling fee of 34 USD per TEU, 215 USD income per TEU per port charges, docking ports 625 USD per port (Kalem, 2015). To estimate the fuel consumption cost (Brouer et al., 2014) with fuel consumption function (27) as follows:

$$f_s(v) = 600 \times \left(\frac{v}{v_s}\right)^3 \times f_s \times \text{number of days sailing} + f_{idle} \times \text{number of day dock in port} \quad (27)$$

- $f_s(v)$: Fuel consumption for each distance (s) speed (v) speed.
- 600 : Fuel prices USD per liter.
- v : Cruising speed (Nautical miles per Hour).
- v_s : Cruising speed (Nautical miles per Hour).
- f_s : Cruising vessel fuel consumption s.
- f_{idle} : Idle vessel port Fuel consumption.

3. RESULTS AND DISCUSSION

3.1. Model Development

The research aims to develop an exact shipping route model using Mixed Integer Butterfly Route Programming on Pendulum Route Indonesia to provide more effective route recommendations.

The main referral of this study was the results of Rana and Vickson (1991), the state of the art models of Liner Shipping for the sea trade in Atlantis North using outbound-inbound principle where LCT docked at the port that has been defined prior to sailing and just docked one each port before returning to the first butterfly route port. Rana and Vickson (1991) used to the relaxing outbound-inbound principle in designing intercontinental



trading shipment in the Mediterranean, Baltic and the Black Sea where LCT docked at the predefined port before sailing more than once on each port before returning to the first port.

The main outcome expected is the Butterfly Route for the Pendulum Ports in Indonesia. The advantage of incorporation between exact method and butterfly shipping route models is an ability to cover up the weaknesses of non-exact methods and the selection of these types Inbound Outbound-Principle used in previous studies.

The first step taken was to design the butterfly route models. The model refers to the Line Blender (2011)'s research which resolved some problem; determining the fleet, shipment route, cargo flow; using the full method to minimize the cost.

The following notation, parameters, and variables are used in this research:

Notation

- I : The Initial set of anchorage point with index i
- j : The Destination set of anchorage point with index j
- v : The set type of LCT with index v
- m : The set amount of TEU cargo index m

Parameter

- C^v : Individual LCT capacity v
- t_{ij}^v : Cycle time t, LCT v from port i-j
- t_{max} : Simulation time unit
- t_j : Time docked at the port j
- b_i^m : b cargo demand, m positive if i origin
- b_i^m : b cargo demand b, m negative if i destination

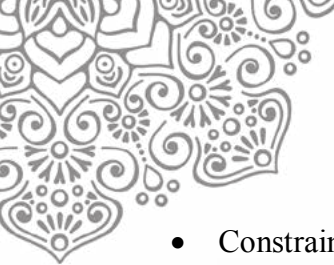
Variable

- X_{ij}^{mv} : Number of request m, transported using LCT v from port i to port j
- u_{ij}^v : Binary variabel value 1 if network (i, j) is the first or last network LCT v with two cycle, otherwise is 0.
- e_{ij}^v : The order of the LCT, Positive integer variable.
- y_{ij}^v : Binary variable, equal to 1 if the network (i, j) is LCT v s, otherwise is 0.
- f_j^{mv} : Demand variable LCT v m being transported for transit in the port j.
- s_i^v : Binary variable, equal to 1 if the port i connect two LCT cycle v, denotated as a centerpoint.
- f_{ijk}^{mv} : Demand v m at LCT, enter the port i to port j, does not pass through the network (i, h).
- toh_v : The cycle time LCT v.
- h^v : binary variable, equal to 1 if the LCT v selected, otherwise value is 0.

Constraints

- Constraint (1): ensure the cargo shipment flow meet all demand of each port.

$$\sum_{v \in V} \sum_{j: (i,j) \in A} x_{ij}^{mv} - \sum_{v \in V} \sum_{j: (i,j) \in A} x_{ji}^{mv} = b_i^m \quad i \in N, m \in M \quad (1)$$



- Constraint (2): ensure the cargo flow deliver all transshipping cargo.

$$f_i^{mn} \geq \sum_{j:(i,j) \in A} x_{ij}^{mn} - \sum_{j:(i,j) \in A} x_{ij}^{mn} \quad i \in N, m \in M, v \in V \quad (2)$$

- In Van Rijn (2015) and Meijer (2015) Pendulum model refers to the Inbound-Outbound Principle. Constraint (3) to constraint (13) are identified to make sure the cargo left at the port transported with the same type of LCT in one lane vertex (Butterfly Route) with the amount of ports more than once visited centerpoint.

$$f_i^{mn} \geq \sum_{j,h \in N, v \in V} f_{jh}^{mn} - M_1 (1 - s_i^v) \quad i \in N, m \in M, v \in V \quad (3)$$

$$f_{jh}^{mn} \geq x_{ji}^{mn} - x_{ih}^{mn} - M_1 (2 - y_{ji}^v - y_{ih}^v + u_{ji}^v + u_{ih}^v) \quad j, i, h \in N, m \in M, v \in V \quad (4)$$

$$f_{jh}^{mn} \geq x_{ji}^{mn} - x_{ih}^{mn} - M_2 (4 - u_{ji}^v - u_{ih}^v - y_{ji}^v - y_{ih}^v) \quad j, i, h \in N, m \in M, v \in V \quad (5)$$

$$\sum_{i \in V} s_i^v = 1 \quad v \in V \quad (6)$$

$$\sum_{(i,j) \in A} u_{ij}^v = 2 \quad v \in V \quad (7)$$

$$s_i^v - \sum_{j:(i,j) \in A} u_{ij}^v \leq 0 \quad i \in N, v \in V \quad (8)$$

$$s_i^v - \sum_{j:(i,j) \in A} u_{ji}^v \leq 0 \quad i \in N, v \in V \quad (9)$$

$$\sum_{j:(i,j) \in A} y_{ij}^v - \sum_{j:(i,j) \in A} y_{ji}^v = 0 \quad i \in N, v \in V \quad (10)$$

$$\sum_{j:(i,j) \in A} y_{ij}^v - s_i^v \leq 1 \quad i \in N, v \in V \quad (11)$$

$$e_{ji}^v - e_{ih}^v + M_4 (y_{ji}^v + y_{ih}^v - 2 - u_{ji}^v - u_{ih}^v) \leq -1 \quad j, i, h \in N, v \in V \quad (13)$$

- Constraint (14): Ensure the LCT rent cost calculated

$$y_{ji}^v - h^v \leq 0 \quad (j, i) \in A, v \in V \quad (14)$$

- Constraint (15): Ensure ship cycle time value equal to the cruising time and docking time.

$$toh_v = \sum_{j:(i,j) \in A} y_{ij}^v (t_{ij}^v + t_j) \quad v \in V \quad (15)$$

- Constraint (16) – (21): Ensure the variable value is greater than or zero.

$$f_{jh}^{mn} \geq 0 \quad j, i, h \in N, m \in M, v \in V \quad (16)$$

$$f_j^{mn} \geq 0 \quad j \in N, m \in M, v \in V \quad (17)$$

$$x_{ij}^{mn} \geq 0 \quad (i, j) \in A, m \in M, v \in V \quad (18)$$

$$toh_v \geq 0 \quad v \in V \quad (19)$$

$$q^v \geq 0 \quad v \in V \quad (20)$$

$$r_{gh}^v \geq 0 \quad g, h \in A, v \in V \quad (21)$$

- Constraint (22): Ensure every demand is delivered in each ship's route.

$$\sum_{m \in M} x_{ij}^{mn} \leq y_{ij}^v M \quad j, i \in A, v \in V \quad (22)$$



- Constraint (23): Ensure if the capacity is already loaded, consider cruising time and docking time.

$$r_{gk}^v + M(1 - y_{gk}^v) - q^v (t_{gk}^v - t_k) \geq 0 \quad g, h \in A, v \in V \quad (23)$$

- Constraint (24): Ensure there is not route that exceeds maximum period which is 30 days.

$$t_{max} - \sum_{(g,h) \in A} r_{gk}^v \geq 0 \quad v \in V \quad (24)$$

- Constraint (25): Ensure total cargo transported not exceed the LCT capacity in 30-day period.

$$q^v C^v + M(1 - y_{ij}^v) \geq \sum_{m \in M} x_{ij}^{mv} \quad i, j \in A, v \in V \quad (25)$$

Objective function: to minimize the delivery cost, the transshipping cost, and the LCT rental cost.

$$\text{Min } \sum_{m \in M} \sum_{(i,j) \in A} c_{ij}^m \sum_{v \in V} x_{ij}^{mv} + \sum_{m \in M} \sum_{j \in N} c_j^m \sum_{v \in V} f_j^{mv} + \sum_{v \in V} c^v h^v \quad (26)$$

3.2. Simulation Results

Table 4 resumes cargo volume in each route and individual type of LCT generated from the simulation process.

- Demand: planned TEU volume.
- Volume TEU 1,2,3: Spread volume transported each LCT.
- These 1,2,3 TEU: Sequence routes that pass each LCT.
- Vessel TEU 1,2,3: LCT used for each route and volume

The total cargo volume to be shipped in Pendulum Indonesia are as much as 56.104 TEU in one week. The volume is the total volume of 6 ports in Indonesia refers to the weekly demand as follows:



Table 4: *Butterfly* Route and Shipment Planning

Demand	Volume 1 (TEU)	Vessel 1	Route 1	Volume 2 (TEU)	Vessel 2	Route 2	Total Vol
0	6.693	3	0-1				6.693
1	1.058	3	0-1-2				1.058
2	87	3	0-1-2-3				87
3	81	3	0-1-2-3-4				81
4	27	3	0-1-2-1-4-5				27
5	6.740	3	1-0				6.740
6	417	3	1-2	1.499	4	1-2	1.916
7	366	2	1-3	3.726	3	1-2-3	4.092
8	222	3	1-2-3-4	2.576	4	1-4	2.798
9	464	4	1-4-5				464
10	1.036	3 & 4	2-1-4-1-0				1.036
11	2.437	4	2-1				2.437
12	3.795	2	2-1-3				3.795
13	4.820	4	2-1-4				4.820
14	2.174	4	2-1-4-5				2.174
15	90	3 & 4	3-1-4-1-0				90
16	3.637	4	3-1				3.637
17	3.498	4	3-1-2				3.498
18	13	4	3-1-4				13
19	91	3	4-1-0				91
20	3.501	3	4-1				3.501
21	4.109	3	4-1-2				4.109
22	73	3	4-1-2-3				73
23	39	2 & 3	5-1-3-4-1-0				39
24	661	2	5-1				661
25	2.174	2	5-1-2				2.174

4. CONCLUSION

It can be concluded that the mathematical model developed by using the Mixed Integer Programming method produces a Butterfly Route scheme. Total cargo volume of 56.103 TEU is successfully transported in the one week period, hence the proposed mathematical model has met the actual operational needs.

The three schemes did not use the 400 TEU LCT at all, hence the LCT used can be replaced with a larger capacity of LCT. For the future research, the utilization of time window and forecasting demand are strongly recommended so that the sailing day and the use of LCT type based on the tidal conditions can be considered.



5. REFERENCES

- Bradley, Hax & Magnanti. (1977). *Applied Mathematical Programming*. Massachutes: MIT.
- D. Ronen. (1983). *Cargo Ship Routing and Scheduling : Surveys of model and problems*. Our Journal of Operational Research, 12: 119-126.
- K. Rana, & R. Vickson (1991). *Routing Container Ships using Lagrangean Relaxation and Decomposition*. Trans Sci, 25: 201-214.
- R. Presenti. (1995). *Hierarchical Resource Planning for Shipping Companies*. European Journal of Operational Research, 86: 91-102.
- Ballou, R.H. (1999). *Business Logistics Management*. New Jersey : Prentice-Hall.
- Fagerhoul, K. (1999). *Optimal Fleet Design ina Shipping Routing Problem*. New Jersey : International operation Resesarch.
- Christiansen & Fagerhoul, K. (2002). *Robust Ship Scheduling with Multiple Tuime Window*. New Jersey : Naval Research logistic.
- Li, Ling . (2007). *Supply chain Management :concep, techniquest and practice*. London : World Sceintefic Publishing Co.Pte.Ltd..
- R. Agarwal & O.Ergun . (2008). *Supply Ship Scheduling and Network Design for Cargo Routing in Liner Shipping*. Transportation Science, 42(2): 175-196.
- Chopra, Sunnil & Meindl. (2010). *Supply chain Management:strategy, planning and operation*. New Jersey : Pearson.
- L. Blander Reindhart & D. Pisinger. (2010). *A Branch and Cut Alghorithm for Container Shipping Network Design problem*. Danish: Springer Science and Bussines Media.
- Q. Meng & S. Wang. (2011). *Liner Shipping Network design with Empty Container Repositioning*. Transp Res Part E, 47: 695 - 708.
- J. Mulder & R.Dekker . (2013). *Methods for Strategic Liner Shipping Network Design*. European Journal of Operation Research.
- Wardana, W. (2014). *Centre gravity Model and Network Design to Determine Route of Liner Shipping: The Case of East-West Container Shipping Coridor in . Rotterdam : Erasmus*.
- Meijer, J. (2015). *Creating Liner Shipping Network Design*. Rotterdam : Erasmus.
- Van Rijn, L. (2015). *Service Network Design for Liner Shipping in Indonesia*. Rotterdam : Erasmus.
- Kalem, H. (2015). *Container Liner Shipping Network Design Using a Path Formulation Model in Indonesia*. Rotterdam : Erasmus.



WHY DID NOT ALL HIGH QUALITY PRODUCTS ALWAYS SATISFY THEIR USERS? A CASE STUDY OF PASSENGER CARS AND ITS DRIVERS

Muhammad Habiburrahman^{1, a}, Djoko Sihono Gabriel^{1, b}, Rahmat Nurcahyo^{1, c}

¹Department of Industrial Engineering, Universitas Indonesia, Depok Campus, Indonesia 16424

m.habib.st@gmail.com, dsihono@gmail.com, rahmat@eng.ui.ac.id

ABSTRACT

Quality improvement of a product becomes an important program at most of manufacturers and needs various resources to make the programs work properly. But if the products quality achieved at highest level of criteria, will the customers always satisfy with it? Previous research and experience proved that statement but need deeper elaboration why not all of users satisfied by genuine quality of products. A case study of multi purposes van (MPV) automobile and its user using Structural Equation Modelling with Partial Least Square (PLS-SEM) and SmartPLS software supported the analysis prepared for this work. In depth data collecting with questionnaires from 516 car drivers in Jakarta, Bogor, Depok, Tangerang and Bekasi conducted to reveal the role of users related to their post purchase satisfaction. A computer program prepared for SEM with steps of analysis designed to clarify the relationship between the quality of MPV and driving satisfaction as well as the role of driving quality. This research concluded that driving quality of MPV drivers intervened the relationship between variables. Lower quality of driving will reduce driving satisfaction whether the quality of MPV was very good. Otherwise, high quality of driving will not only enhance the satisfaction, but also leverage the effect of other variable to driving satisfaction. The intervening variable role will give new approach in developing and maintaining driving satisfaction. A new approach of customer satisfaction improvement proposed and valuable programs of MPV producers with a new paradigm will improve manufacturer competitive advantage.

Keywords: multi purposes van; intervening variable; driving quality; driving satisfaction; PLS-SEM.

1. INTRODUCTION

1.1. Background

This study assessed MPV drivers experience while driving and conducting the operation of the vehicles. The MPV drivers were selected as respondents for two important consideration. They are need appropriate skills and good driving practice that support their driving quality. And the other one, MPV businesses in Indonesia, especially in low end quality MPV business, face tight competition that need a new approach to support customer satisfaction improvement.

1.2. Objective of the Study

To find out a quantitative approval that the higher a certain variable, the higher driving



satisfaction of MPV, but the effect to driving satisfaction reduced by the lower driving quality.

2. METHOD AND DATA ACQUISITION

As an alternative to the classical covariance-based approach, PLS-Path Modelling is claimed to seek for optimal linear predictive relationships rather than for causal mechanisms, therefore, this method also viewed as a very flexible approach to multi-block (or multiple table) analysis, that arise when a few sets of variables are available for the same set of samples (Vinzi et al, 2010). This approach is suitable to the problem in this case study that constructed by some latent variables with many number of manifest variables.

2.1. Driving Satisfaction and Its Predictors

Some variables affect to passenger car satisfaction identified as vehicle quality (Stylidis, 2016), brand service quality, brand value, technology anxiety (Aziz, 2016), service quality (Al-Shammari & Kanina, 2014), economical to use (Srinivas, 2013), customer service quality, product quality (Jahanshahi, 2011), and maintenance cost, fuel efficiency, comfort (Mahapatra, 2010). Independent variables were proposed as predictors for customer satisfaction, but no intervening variable proposed in previous research. According to Watson et al. (2007), vehicle quality strongly related to automobile driving safety.

Description of vehicle quality varies among researchers. Many of them suggest performance as common terminology of quality, but various attributes proposed as quality, including reliability, durability, serviceability, aesthetics, special feature, conformance to specification, technology, convenient, technicalities, speed, consumption of fuel, emission, stability, ease of driving, space utilization, functions and customization.

2.2. Data Collection

The research respondents were MPV drivers who have responded to a set of questionnaire according to a preliminary model and hypothesis. The low end of quality MPV used included the brand of Chevrolet (2%), Daihatsu (19%), Honda (11%), Mazda (1%), Nissan (8%), Suzuki (18%) and Toyota (40%). The drivers were asked to explain their experience according to instrument statements by chosen their perceive experience of vehicle quality, driving quality and their driving satisfaction. The data obtained by questionnaire represents driver perception with scores within Likert scale of 1 to 6. A number of 528 customers who drive their own MPV participated. Of the 528 questionnaires that had been obtained, 12 questionnaires collected were not considered valid because some of the answers were still empty, therefore only 516 questionnaires considered in the data processing. Latent variables with each number of manifest variables represented in the Table 1.

2.3. Blocks Building

Partition the manifest variables into homogenous blocks allocate each one manifest variable being explicitly associated with only one latent variable. After many trials and with the deep of assessment of their casual system, can be considered the division of the 28 manifest variables into 5 blocks of latent variable as seen in Table 1.



Table 1. Latent and Manifest Variables

Block	Latent Variable (5)	Manifest Variable (23)
1	Driving Quality	QDRIV1, QDRIV2, QDRIV3, QDRIV4
2	Functional Quality	QFUNC1, QFUCN2, QFUCN3, QFUCN4, QFUNC5
3	Operational Quality	QOPER1, QOPER2, QOPER3, QOPER4, QOPER5
4	Reliability	RELI1, RELI2, RELI3, RELI4, RELI5, RELIS6
5	Driving Satisfaction	DRISAT1, DRISAT2, DRISAT3, DRISAT4, DRISAT5, DRISAT6, DRISAT7, DRISAT8

2.4. Causality Scheme and Structural Model

As a result of literature study of passenger car, four independent variables proposed in this study as follow: driving quality, vehicle reliability, operational quality, and functional quality. But according to new insight in this study, Driving Quality variable proposed both as independent and intervening variable. If the other three of independent variables related and managed by vehicle manufacturers, the intervening variables managed by owners and drivers of vehicles. The intervening variable was a new variable that have not been introduced before. Supposing that the scheme reflect correctly the predictors of the driving satisfaction, it must then propose relations between these variables, to explain the latent variable relationship. In Table 2 the relationships proposed as a set of hypothesis.

Table 2. Hypothesis Proposed for PLS-SEM

Hypothesis	Relationship Description	Relationship Type
H1	The lower the Driving Quality, the lower the Driving Satisfaction	Causal
H2	The higher the Functional Quality, the higher the Driving Satisfaction	Causal
H3	The higher the Operational Quality, the higher Driving Satisfaction	Causal
H4	The higher the Reliability, the higher the Driving Satisfaction	Causal
H5	The lower the Driving Quality, the weaker the effect of the Functional Quality on the Driving Satisfaction	Intervening
H6	The lower the Driving Quality, the weaker the effect of the Operational Quality on the Driving Satisfaction	Intervening
H7	The lower the Driving Quality, the weaker the effect of the Reliability on the Driving Satisfaction	Intervening

2.5. Data Processing with SmartPLS Software

Before using SmartPLS Software in the PLS-SEM analysis, a preliminary test of 30 completed questionnaires conducted to ensure the appropriateness of questionnaires before conducting further data collection. Validity and reliability tests results suggested that the questionnaires were worth for further purpose, to test the hypothesized relationships in a structural model. Structural Equation Modelling Procedures with PLS conducted according to Hair et al. (2014) as following steps: specifying the structural model, specifying the measurement model, data collection and examination, PLS path model estimation, assessing



PLS-SEM results, analysis, interpretation and conclusion. Reliability test of the data indicated that the model was accepted according to its internal consistency reliability with Cronbach's Alpha and Composite Reliability more than 0.7, and Average Variance Extracted (AVE) more than 0.5. A structural model measurement with bootstrapping for all samples resulted as the following figures and tables.

3. RESULTS AND DISCUSSION

Structural equation according to SEM showed that T-Statistic Value of four variables to Driving Satisfaction were more than 1.96, therefore Driving Quality, Functional Quality, Operational Quality and Reliability strongly considered in the next analysis. The next analysis focused on the role of Driving Quality as intervening variable. Evaluation of the structural equation showed in Figure 1 and Table 3 concluded that the equation with four independent variables and one dependent variable was well accepted according to the good results of standard deviation, T-Statistic Value and P-Value. But the intervening variable role only accepted in Hypothesis 6: the Driving Quality intervened the relationship between Operational Quality and Driving Satisfaction only, as shown in Table 3, Figure 2 and more specific in Figure 3 with good T-Statistic Value, P-Value and path coefficient. The structural model evaluation indicated that the lower the Driving Quality, the weaker the effect of the Functional Quality to the Driving Satisfaction.

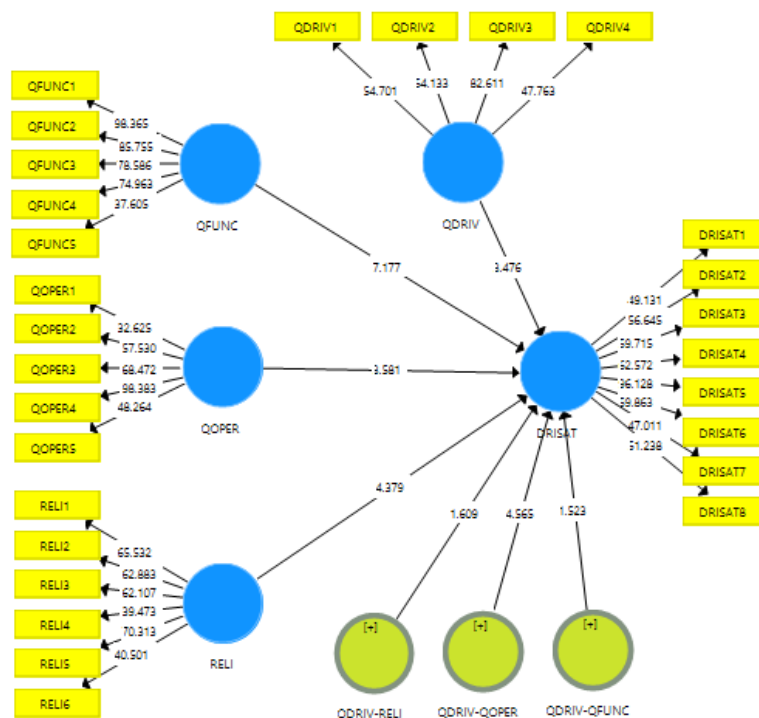


Figure 1.
T-Statistic Value of Structural Model between Variables

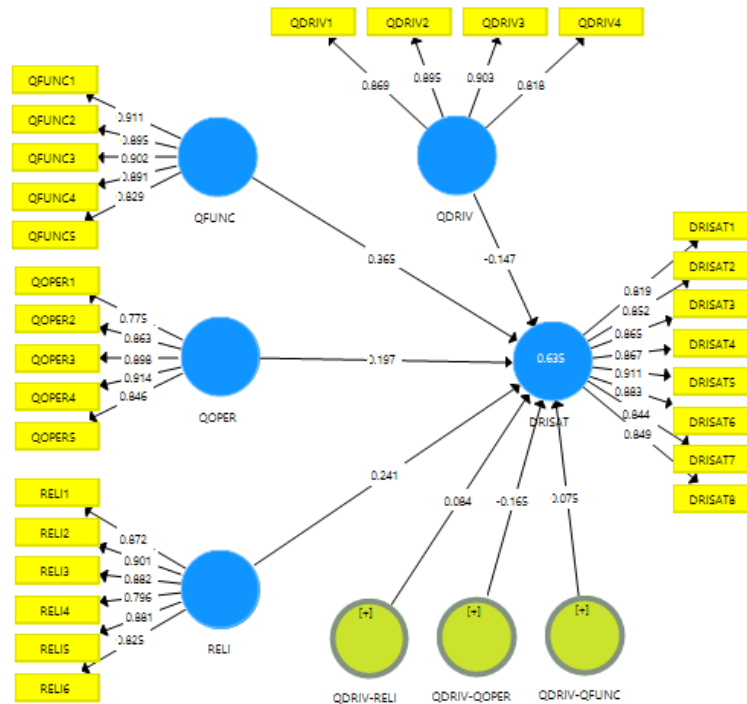


Figure 2.
Path Coefficient between Variables

Table 3.
Evaluation of Structural Model among Latent Variables

Relationship among variables	Path Coefficient	Std. Deviation	T Statistic	P Value	Decision
Driving Quality to Driving Satisfaction	-0.147	0.043	3.476	0.001	Accepted
Functional Quality to Driving Satisfaction	0.365	0.051	7.177	0.000	Accepted
Operational Quality to Driving Satisfaction	0.197	0.055	3.581	0.000	Accepted
Reliability to Driving Satisfaction	0.241	0.055	4.379	0.000	Accepted
Driving Quality-Functional Quality to Driving Satisfaction	0.075	0.048	1.523	0.119	Rejected
Driving Quality-Operational Quality to Driving Satisfaction	-0.165	0.036	4.565	0.000	Accepted
Driving Quality-Reliability to Driving Satisfaction	0.084	0.051	1.609	0.096	Rejected

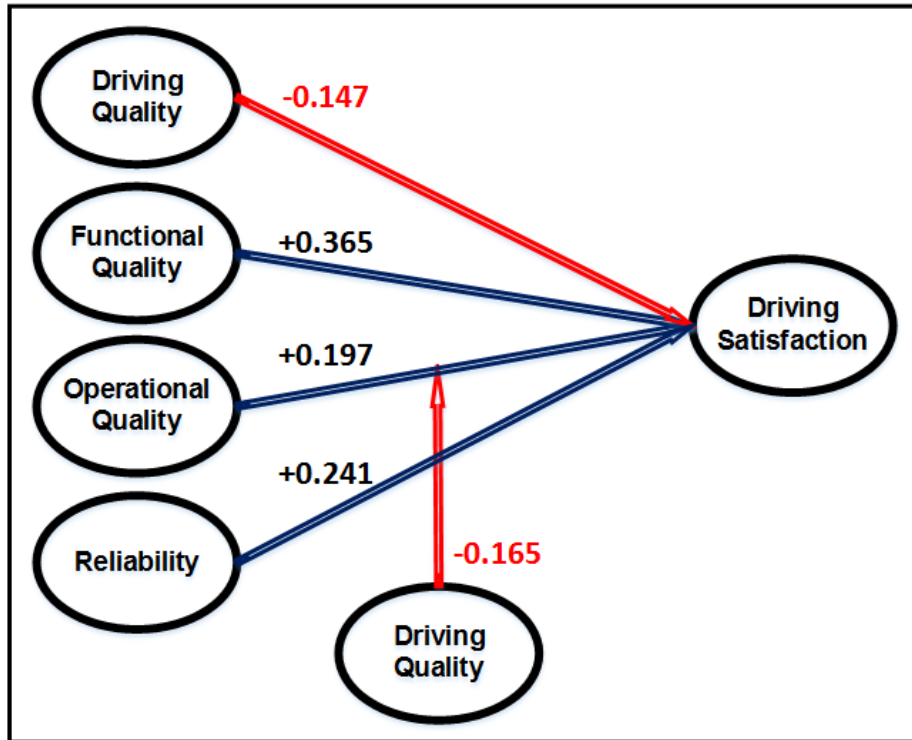


Figure 3.

Driving Quality as Independent and Intervening Variable in the Structural Model

Manifest or observed variables in Operational Quality exists in the vehicle itself and the vehicle manufacturer efforts, included the following description:

1. QOPER1: Mileage per liter of fuel
2. QOPER2: Durability of vehicle and its spare parts
3. QOPER3: Easy in driving
4. QOPER4: Simple in daily maintenance
5. QOPER5: Easy in periodic maintenance, both technical and financial aspects

Otherwise, Driving Quality depend on driver's knowledge, skill and driving commitment as the follow manifest variables:

1. QDRIV1: Ability to describe good conduct in vehicle driving
2. QDRIV2: Ability to describe driver skill requirements in vehicle driving
3. QDRIV3: Driving skills fulfilment when driving a car
4. QDRIV 4: Commitment for right, safe and good conduct in vehicle driving

In the accepted structural model, Driving Quality not only affected to Driving Satisfaction, but also intervened the causal relationship between Operational Quality and Driving Satisfaction. The causal relationship (Hypothesis 1): The lower the Driving Quality, the lower the Driving Satisfaction and the intervening role (Hypothesis 6): The lower the Driving Quality, the weaker the effect of the Operational Quality to the Driving Satisfaction were



supported by this study. Otherwise, better of Driving Quality not only improve Driving Satisfaction, but also strengthen the effect Operational Quality to Driving Satisfaction.

The new evident delivered precious information both to MPV manufacturers and MPV users. MPV manufacturer and their supply chains strategy that focused on vehicle quality only, would be less competitive when other manufacturers more care and deliver better support to vehicles drivers in improving their Driving Quality. The last manufacturers will take important advantage in their customer satisfaction and loyalty. A good brochure and a simple but effective driver manual distribution for automobile buyers will support driving quality improvement. Qualified driving instructors from the manufacturers comply with automobile purchase also become a strategic delivery in driving quality improvement as well as good promotional effect in increasing intention to buy and repeat order the brand.

4. CONCLUSION

The role of driving quality as intervening variable of operational quality to driving satisfaction of MPV was well approved by structural equation modelling with PLS. A genuine quality of MPV still need another factor that strengthen the driving satisfaction. Bad practice in driver license approval affected not only to unsafe driving, but also reduce safety awareness, driving quality and driving satisfaction. These results suggest a new way of understanding about who, whom and how customer satisfaction can be improved. MPV manufacturer aiming to boost their customer satisfaction should thus consider this finding. Good driving tutorials and practices may be effective and efficient means of encouraging driving quality improvement.

5. ACKNOWLEDGEMENT

This research would not have been possible without the kind support of Hibah PITTA 2017 scheme. We are grateful to Universitas Indonesia for funding the research that has been carried out.

6. REFERENCES

- Al-Shammari, M. & Kanina, A. S., (2014), Service Quality and its Relationship with Customer Satisfaction and Loyalty in a Saudi Arabian Automobile Company, *Global Journal of Management and Business Research: E Marketing*, Vol. 14 No. 8, pp. 13-21.
- Aziz, S. A., (2016), Does Fear of New Car Technologies Influence Brand Loyalty Relationship?, *Journal of Marketing Management*, Vol. 4, No. 1, pp. 125-136.
- Bagozzi, R., & Yi, Y. (2012), Specification, evaluation, and interpretation of structural equation models, *Journal of the Academy of Marketing Science*, Vol. 40 No. 1, pp. 8–34.
- Chiu, S., et al. (2011), Preliminary research on customer satisfaction models in Taiwan: A case study from the automobile industry, *Expert Systems with Applications*, Vol. 38, pp. 9780-9787.
- Hair, J. F., Hult, G. T., Ringle, C. M., & Sarstead, M. (2014). *A Primer on Partial Least Squares Structural Equation Modeling (PLS-SEM)*. Los Angeles: SAGE Publications.



- Hamza, P.K., (2014), A Study on the Determinants and Impact on Overall Customer Satisfaction Evaluations with Special Reference to Automobile Industry, *Journal of Science, Technology and Management*, Vol. 7 No. 2, pp. 0974-8334.
- Jahanshahi, A. A., (2011), Study the Effects of Customer Service and Product Quality on Customer Satisfaction and Loyalty, *International Journal of Humanities and Social Science*, Vol. 1 No. 7, pp. 253-260.
- Mahapatra, S. N. et al., (2010), Consumer Satisfaction, Dissatisfaction and Post-Purchase Evaluation: An Empirical Study on Small Size Passenger Cars in India, *International Journal of Business and Society*, Vol. 11 No. 2, pp. 97-108.
- Spreng, R. A. et al., (1996), A reexamination of the determinants of consumer satisfaction, *Journal of Marketing*, Vol. 60 No. 3, pp. 15-31.
- Srinivas, K. T., (2013), The Study on Customer Satisfaction with Respect to Hyundai Motor Cars i20 in Bangalore City, *International Journal of Management Research and Review*, Vol. 3 No. 9, pp. 3569-3579.
- Stylidis, K. et al., (2016), A Preliminary Study of Trends in Perceived Quality Design Attributes in the Automotive Luxury Market Segment, *International Design Conference – Design 2016*, Dubrovnik, Croatia, May 16-19, 2016.
- Vinzi, V.E., et al. (2010). Editorial: Perspectives on Partial Least Squares. In: *Handbook of Partial Least Squares. Concepts, Methods and Applications*. Editors: Vinzi, V.E., et al. Heidelberg: Springer.
- Watson, B. et al., (2007), *Psychological and social factors influencing motorcycle rider intentions and behaviour*, Centre for Accident Research and Road Safety (CARRS-Q) Queensland University of Technology, August 2007.
- Zhang, D. & Zhang, D. M., (2015), Determinants of Consumer's Automobile Purchase Decisions in China: Focus on Automobile Size, *Int. J. Mgmt Res. & Bus. Strat.*, Vol. 4 No. 4, p. 61-66.



OPTIMAL PHYSICAL ENVIRONMENT TO MAINTAIN CONCENTRATION ON OFFICE WORK IN TROPICAL CLIMATE IN INDONESIA

Lovely Lady^{a*}, Nisfaeni^b

^{a,b}Industrial Engineering Department, Faculty of Engineering-Untirta
Jl. Jend.Sudirman Km.3 Cilegon, Banten 42435 – Indonesia

ABSTARCT

Doing Office work or learning requires concentration. The people will design comfortable work space physical environment, including the temperature and lighting. Sometimes they set of music background so they can work comfortable. The purpose of this study is to determine the optimal temperature setting and sound background to maintain concentration when doing office work in tropical climate in Indonesia. Others indoor physical environment on this study is set fixed and at appropriate conditions for office work. Level of lighting is at the 250 lux, noise when there is no music at the level of 60 dB, and humidity at the level of 56%. Research was done by an experiment in the officeroom, independent variables are temperature and sound background, and the dependent variable is concentration levels. Temperature was set using the Air Conditioner at three levels 18°C, 23°C, and 28°C that represents the level of indoor temperatures in Indonesia. And two setting of sound background was background of prepered music, type of pop music with the tempo of 74 BPM and background without music. Respondent is students with a range of age between 19 to 22 years old. Concentration test was performed with a test of *psychophysics* based of *software* ' Design Tools ' version 3.00 of the Method, Standard and Work Design 11th Edition by Benjamin Niebel and Andris Freivalds-Mc Graw Hill in printed version. Model of the question of concentration test is choosing a longer line between two lines on the display. The length and position of two lines at each question is displayed randomly. According to analysis of variance, temperature and background music affect work concentration significantly, value of significancy = 0,000. According to post hoc test at temperature variabel, the level of work concentration at temperature of 18°C and 23°C did not differ significantly, $\alpha = 0.504$. But at room temperature of 28°C, there was a decrease in concentrations significantly by the value $\alpha = 0.000$. There was no difference in the level of concentration when working with the preferred music background or without music background on temperatures of 23°C and 28°C which respondents dominantly feel cool, warm, or heat on thermal sensation. But music background help improving concentration score in cold thermal sensation. Based on a subjective assessment against the convenience of room temperature using the *thermal sensation scale points 7*, dominant respondent stated they felt cool (60%) and felt sligtly cool (20%) on room temperature of 23°C, above number of respondent who felt cool on others level of room temperture. Based on this research the efficient temperature setting for work concentration and comfortable is 23°C either by music background or no music background.

Keywords: Concentration; physical environment; temperature; music background; efficient.

1. INTRODUCTION

Office work need of cognitive ability to do it. Cognitive concerned with the internal process involved in making sense of the environemnt and deciding what action might be appropriate (Eysenk, 2005). Cognitive process also known as mental activity include: Acquisition of – perception – memory, storage, retrieval – imagery, use of knowledge – reasoning, problem solving, decision making.



Mental activity needed a high concentration to achieve the desired results. There are three things that affect concentration, i.e. the power from the outside, various information and willingness. In order to be comfortable and concentration in doing the work, work place is designed ergonomically include the physical environment of room. Room temperature conditioned at the desired temperature using the Air Conditioner, even by giving the background music during work to improve comfort.

Unhealthy physical environment may result bad work. It's not just affect physical work but also mental work. The mental work require lower calories than physical activity. But morally and responsibility, mental activity has heavier workload than any physical activity because it involves more brain works than muscle. Creating a comfortable environment for human beings is crucial, so it will improve the attitude and performance of the individual work, even the safety of the work.

Based on the decision letter of the Minister of health of Indonesia number: 1405/Menkes/SK/XI/2002 about air room in offices, work room temperature is recommended in the range between 18°C – 28°C. Moreover, according to Lippsmeir (in Rilatupa, 2008) boundary condition for the comfort in the equator area are in the range of temperature 22.5°C- 29°C with an air humidity 20% – 50%. Excessive heat conditions will lead to a sense of fatigue and sleepiness, reduce stability and increase the number of error. Instead of excessive cold conditions will lead reducing a sense of alertness and reducing work concentration.

Performance increases with temperature up to 21-22°C, and decreases with temperature above 23-24 °C. The highest productivity is at temperature of around 22°C. (Seppanen, 2006). They also have developed a relation between performance and temperature in USA and showed a decrease in performance by 2% per°C increase of the temperature in the range of 25-32°C, and no effect on performance in temperature range of 21-25°C. Other similar research conducted by Haditia (2012) said that visual inspection capabilities decrease on temperature 29.4°C and 32.2°C. In general the level of visual ability decreases in accordance with the increase in the temperature of the environment and it also increased workload.

Thermal comfort is usually measured subjectively, but there is the influence of habit factors and the effect of the room contextual so that the assessment of the subject on thermal comfort can be different. The majority of researchers have assigned the differences between reported and predicted thermal sensation of occupants on two main factors: a) errors in measurements; and b) contextual effects (Beizaee, 2012). The study has shown that the Fanger's PMV model is not accurate enough in predicting people's thermal sensation in naturally ventilated homes and offices in the UK during the summer.

North and Hargreaves (in Arya, 2014) stated that listening to music and run tasks concurrently affect the cognitive burden of processing, where there are limited resources. Music stimulates the brain's emotional center, as it has the dimension of creative and have parts that are identical to the learning process in general. But often people use sound background music to enhance comfort in work. Workers relished working in presence of music, the felt motivated and fresh at work (Talwar, 2016). The value of music listening made positive mood change and quality-of-work were lowest with no music (Lesiuk, 2005). Extroverts performed significantly better during the completion of the test in presence of music, but poorer in silence, compared to the Introverts who performed better in silence than in the presence of music (Mistry, 2015).

Influence of indoor temperature against human performance has already examined, including its effects on productivity (Seppanen, 2006, Federspiel et al. 2004, Heschong, 2003), complex task (Chao et al. 2003, Heschong 2003), Vigilance task or manual tasks related to office work (Wyon et al. 1996). All the research is conduct on the respondent who live in subtropical areas. While the research of influence of music background against productivity is conducted separately without analyse the effect of combination of background music and indoor temperature. MC Nulty (2015), Padmasiri (2014), Lesiuk (2005) researched that the employee performance can be improved further



by using of background music. Previous studies generally have conducted on respondents who live in subtropical climates and no combination of physical environmental conditions.

While working, most office workers in Indonesia set indoor temperature below 20°C, and set up music background to improve comfort. Indonesia have environmental temperature is always warm because it has a tropical climate so Indonesia people would have a level of comfort for room temperature is different from people in subtropical climates. This research aims to determine the optimal temperature of office room in Indonesia to maintain high levels of concentration. The study also will look at how the effects of background music combined with room temperature towards concentration in the work.

2. METHODOLOGY

This research is a laboratory research using design of experiment. The level of concentration will be seen from the output of cognitive tests. Cognitive test was done in laboratory room in some combinations of temperature levels and background music. Research done in the Laboratory optimization of production systems the Faculty of Engineering, Department of Industrial Engineering University of Sultan Ageng Tirtayasa. Indoor physical environment on this study was set fixed and at appropriate conditions for office work. Level of lighting was at the 250 lux, noise when there was no music at the level of 60 dB, and humidity at the level of 60%. In each combination of physical environment, respondents were given five minutes to perform a set of test. After working on the concentration test, they filled the questionnaire about thermal comfort that they felt during the test. The questionnaire is based on the 7-Scale Fanger.

2.1 Respondent

Respondents in this research are Industrial Engineering students of UNTIRTA with a range of 19 to 22 years of age. The total number of respondents 45 people, with 30 of the women respondents and 15 male respondents. Respondents were divided into three groups based on the room temperature that is conditioned, so that each group contained 15 respondents. Each group respondent has done concentration test on two conditions : with background music and without background music conditions. Each group conducted simulations for 30 minutes. The first ten minutes was used for conditioning of the respondents against the temperature of the work room and filling out the form of the respondent identity. The next twenty minutes was used to perform tests of concentration and fill the thermal comfort questionnaire.

2.2 Variables

This study using two independent variables and one dependent variable. The dependent variable is the variable that is affected, due to the independent variable. In this research the dependent variable is the concentration during work. The independent variable is the variable that affect or be a cause of occurrence of changes to a dependent variable. In this research independent variable is room temperature and the presence of background music.

2.3 Physical environment setting

Based on the regulation of the Minister of health of the Republic of Indonesia work room recommended temperature ranges between 18°C – 28°C. Therefore, the levels of the temperatures that are conditioned on this research is at 18°C, 23°C, and 28°C. Temperature 18°C represent the lower limit, 23°C represent the mid, and 28°C represent the upper limit of the recommended range. Background music using music from player and loud speaker. Type of music is preferred by the respondent, a kind of pop music with the tempo of 74 BPM. On environmental factors with music



background, reference is used as the normal condition is the room environment without music background.

2.4 Concentration test

Concentration test is performed using a *psychophysics* test based of *software* ' Design Tools ' version 3.00 of the Method, Standard and Work Design 11th Edition by Benjamin Niebel and Andris Freivalds-Mc Graw Hill in printed version. Model of the question of concentration test is choosing a longer line between two lines on the display. The length and position of two lines at each question is displayed randomly. A set of concentration test consists of thirty questions. After completing a set of questions on the conditions with the background music, the respondents fill out questionnaires of thermal comfort. Thermal comfort is a subjective assessment against the convenience of room temperature using Fanger thermal sensation scale points 7. After filling out the questionnaire of thermal comfort, simulation continued on second condition of physical environment, without music background.

2.5 Measure of physical environment

On this research some tools are used for conditioning and measuring physical environment. Air Conditioner for conditioning the environment temperature. Thermo-Hygrometer is used to measure indoor temperature and humidity during simulation takes place. Psychophysics tests is used to find out the level of concentration of the respondent. Speakers and player is used to play music background during executing the cognitive test. And lux meter for measuring the level of lighting in the room.

3. RESULTS AND DISCUSSION

The data of cognitive test due to the effects of temperature and the presence of background music was processed using the Statistical software Package For Social Science (SPSS) 22. Output of concentration test have be carried out normality test prior to be used in analysis of variance. Analysis of the influence of the temperature level of the work environment and the presence of background music was analyzed by anova test. There was six combinations of the physical environment which was obtained from 3 levels room temperature and two conditions of music background. Table 1 presents the score of concentration test in six combinations of the physical environment.

Output of concentration test should be ensured have normal distribution prior to be used in analysis of variance. Kolmogorov smirnov and shapiro-wilk test was used in this research to check that data have normal distribution, because of the number of respondent per-simulation is less than thirty. Output of the normal distribution test on score of concentration test in every physical environment condition are presented in the table 2. According to the table, all of data have normal distribution in every combination of physical environment because it have significant value more than 0.05.



Tabel 1 Score of concentration test

Respondent	Background music			No music		
	18°C	23°C	28°C	18°C	23°C	28°C
1	27	28	23	27	26	23
2	28	30	20	26	29	25
3	27	27	25	25	25	21
4	29	29	19	23	27	24
5	27	30	23	26	28	20
6	26	28	20	24	25	20
7	27	26	24	28	28	24
8	28	30	23	26	29	24
9	28	22	23	26	24	26
10	26	28	22	25	27	23
11	25	29	20	24	28	22
12	28	23	24	25	29	24
13	27	25	25	28	28	19
14	26	27	28	27	25	20
15	26	24	27	23	22	21
Average	27,00	27,07	23,07	25,53	26,67	22,40

Table 2 Normal distribution test on score of concentration

Music Background	Temperature (oC)	<i>kolmogorov smirnov</i>			<i>shapiro-wilk</i>		
		Statistic	Df	Sig.	Statistic	Df	Sig.
Yes	18	,167	15	,200*	,934	15	,316
No	18	,148	15	,200*	,944	15	,431
Yes	23	,175	15	,200*	,915	15	,160
No	23	,205	15	,091	,904	15	,109
Yes	28	,156	15	,200	,950	15	,517
No	28	,174	15	,200	,937	15	,350

3.1 The effect of the temperature of the working room and the presence of background music towards concentration of work.

Based on Shapiro wilk test all output of concentration test have Gaussian distribution, so that all of data can be used to analyze the effect of temperature and the presence of background music towards work concentration levels. Anova test is used to analyze the effect of the physical environment conditions against concentration. The following table is the output of anova test between concentration score of respondent that worked in some combination temperature room and the presence of background music. The independent variables are room temperature and the presence of background music, and dependent variable is concentration score.



Table 3 Analysis of variance of influence of temperature and music background against score of concentration

Source	Type III Sum of Squares	df	Mean Square	F	Sig.
Corrected Model	323,365 ^a	5	64,673	15,043	,000
Intercept	57511,675	1	57511,675	13377,630	,000
Temperatur	301,442	2	150,721	35,059	,000
Background	21,270	1	21,270	4,948	,029
temperatur * background	2,794	2	1,397	,325	,724
Error	361,124	84	4,299		
Total	58242,000	90			
Corrected Total	684,489	89			

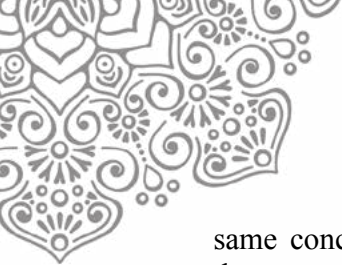
The influence of all independent variables (Temperature and music background) and interaction between the temperature and music background (Temperature * music background) are jointly against the dependent variable (the output of the concentration test) has the significance of less than 0.05 (see from corrected model significance) means the model is valid. Based on the table the value of significance for temperature factor is less than 0.05. So it can be inferred that the temperature has significant effects against concentration. The value of music background factor significance is also smaller than 0.05, mean music background effect concentration significantly. The results of the third, namely the interaction of temperature and music background, have significance 0.724. The value is greater than 0.05, meaning the interaction between temperature and background music has no significant effect against concentration.

Based on the Anova is known that there are significant effects of temperature and background music on concentration of work. To find out if these two factors generated a significant different of concentration level, post hoc test was done. Indicators are seen from the values of significance, if the value of significance < 0.05 mean concentration on both levels differ significantly.

Tabel 4 *Post Hoc Test* of temperature on respondent concentration

(I) Temperature	(J) Temperature	Mean Difference (I-J)	Std. Error	Sig.	95% Confidence Interval	
					Lower Bound	Upper Bound
18	23	-,6000	,53536	,504	-1,8773	,6773
	28	3,5333*	,53536	,000	2,2560	4,8107
23	18	,6000	,53536	,504	-,6773	1,8773
	28	4,1333*	,53536	,000	2,8560	5,4107
28	18	-3,5333*	,53536	,000	-4,8107	-2,2560
	23	-4,1333*	,53536	,000	-5,4107	-2,8560

Based on table 4 working at room temperature of 28°C had concentration score different significantly from working at temperature of 18°C and 23°C because it had value significance smaller than 0.05. While working at room temperature of 18°C and 23°C didn't have significant different of score of concentration. At temperature of 18°C and 23°C respondent had nearly the



same concentration score, but at higher temperatures of 28°C the score of concentration had decrease significantly.

The score of concentration when work in the environment with music background and without music background at the same temperature is analysed with t-test. Next table show result of t-test.

Table 5 t-test score of respondent concentration on environment with music background and without music background

No	Indoor temperature	t-test result (α)
1	18°C	0.006
2	23°C	0.758
3	28°C	0.451

The result showed there wasn't significant different of score of concentration when working in the room with music background and without music background at temperature of 23°C and also at temperature 28°C with value of significancy 0.451 and 0,758. And score of concentration when work in the room with music background and without music background at temperature of 18°C showed different significantly, with value of significancy 0,006. Music background helped increasing the concentration of working at temperature of 18°C, which on that temperature dominant respondent felt cold based on their opinion on Thermal comfort questionnaires. But the background music did not increase the concentration of the respondent at a temperature of 23°C because at that temperature they felt cool and comfort based on their opinions on Thermal comfort questionnaires, and background music also didn't increase the concentration of the respondent at temperature of 28°C because they felt warm and hot based on their opinions on Thermal comfort questionnaires. Music can help improving concentration in cold thermal sensation but not in cool, warm and hot thermal sensation.

3.2 Thermal Comfort

To find out the subjective assessment of the respondent against the room temperature, the respondent fill out Thermal comfort questionnaires. Based on the ISO 7730-1994, in stating a condition termis used index introduced by Fanger, a researcher who analyzed the Thermal comfort PMV (Predicted Mean Vote) and PPD (Predicted Percentage Dissatisfied). Value of PMV is revealed with a number between-3 (cold), up to + 3 (hot). Questionnaire was given to the respondents to refer to standards of comfort are commonly used. The respondents must select the range of comfort room which they felt. Next is the graph the results of the questionnaire of thermal comfort by PMV magnitudes at temperature of 18°C, 23°C, and 28°C.

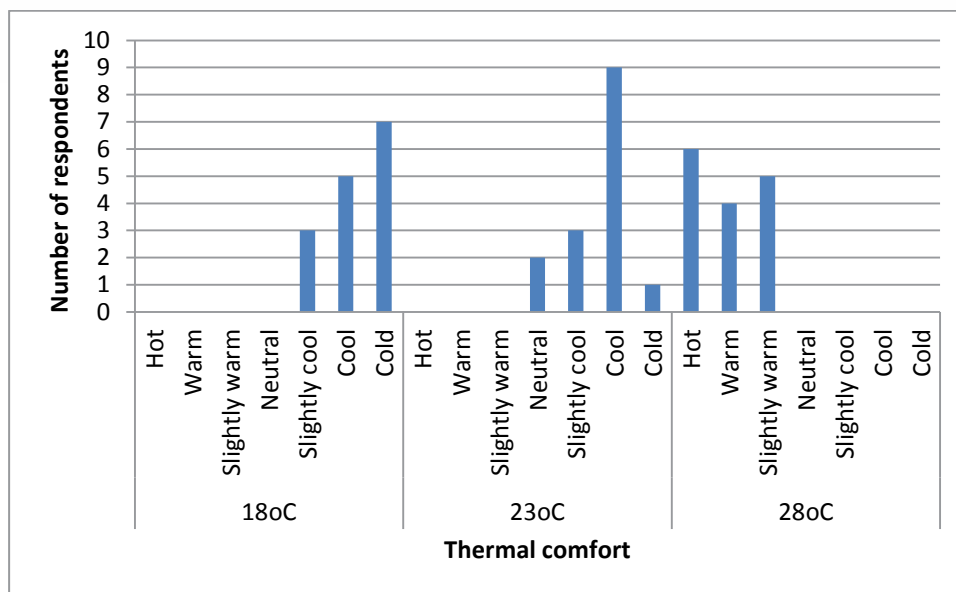


Figure 1 Graph of subjective thermal sensation

At room temperature of 18°C, dominant respondent as much as 47% stated that they felt cold, 33% felt cool, and 20% felt slightly cool. At a temperature of 23°C dominant respondent as much as 60% stated they felt cool, 13% of respondents stated a neutral temperature conditions, 20% felt slightly cool, and 7% felt cold. At a temperature of 28°C dominant respondent as much as 67% felt the heat, 20% of respondents felt warm, and 13% of respondents felt slightly warm.

Indonesia people assess thermal comfort questionnaires based on their viewpoint which live in tropical climate. The Indonesia people dominantly feel comfort at temperature of 23°C, because they stated the thermal sensation is cool or slightly cool. This selection is based on Indonesia climate which tends to be warm or hot, so Indonesia people more prefer the cool conditions than warm or slightly warm. This preference contrast to people who live in subtropical climate that more prefer warm condition. Indonesian appraisalment on neutral conditions is identical to the daily conditions in Indonesia. Based on the answers of the respondent, the condition that most comfortable for Indonesia is workroom temperature of 23°C because of number of respondent felt cool and slightly cool as much as 80%, the highest among others temperature. While presence of music background in that room temperature despite increased concentration of work but not significantly better than the concentration of work in the room without music background.

4. CONCLUSION

Analysis of variance on score of concentration, the level of work concentration at temperature of 18°C and 23°C did not differ significantly, $\alpha = 0.504$. But at room temperature of 28°C, there was a decrease in concentration significantly by the value of $\alpha = 0.000$. Music background will help improve work concentration at temperature of 18°C which have cold thermal sensation, but not at at temperatures of 23°C and 28°C which have cool, warm ant hot thermal sensation. Based on a subjective assessment against the convenience of room temperature using the *thermal sensation scale points 7*, dominant respondent (80%) stated felt comfort with sensation of cool dan slightly cool on room temperature of 23°C, above the number of respondent who felt comfort in others temperature level. Based on this research the efficient temperature setting for

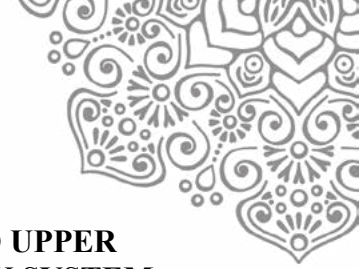


work concentration and comfort is 23°C because it gives the highest level of concentration and comfort either by music background or no music background.

5. REFERENCES

- Arya, Ayu W., Caecilia S.W., and Arie D.,(2014), Analisis Pengaruh Tempo dan Genre Musik Terhadap Kewaspadaan Pengendara Mobil Pribadi, *Jurnal Teknologi Industri*. ITENAS, Vol. 002 No. 03.
- Beizaee, A., Firth, S.K., Vadodaria, K., Loveday, D.,(2012), Assessing the ability of PMV model in predicting thermal sensation in naturally ventilated buildings in UK, Proceedings of 7th Windsor Conference: *The changing context of comfort in an unpredictable world* Cumberland Lodge, Windsor, UK, 12-15 April 2012. London.
- Chao HJ, Schwartz J, Milton DK, Muillenberg ML, Burge HA. (2003). Effects of Indoor Air Quality on Office Workers' Work Performance - a Preliminary Analysis. Proceedings of healthy Buildings, pp 237-243.
- Eysenck, M.W. Keane, M.T.,(2005), Cognitive Psychology: A Student's Handbook, 6th Edition, Psychology Press, New York.
- Federspiel CC, Fisk WJ, Price PN, Liu G, Faulkner D, Dibartolemeo DL, Sullivan DP, Lahiff M. (2004). Worker Performance and ventilation in a Call Center: Analyses of Work Performance Data for Registered Nurses. *Indoor Air Journal*, vol 14. Supplement 8: 41-50.
- Haditia, I.P.(2012). *Analisis Pengaruh Suhu Tinggi Lingkungan dan Beban Kerja Terhadap Konsentrasi Pekerja*, Skripsi Sarjana, Universitas Indonesia. Jakarta.
- Heschong Mahone Group. (2003). Windows and offices: A study of Office Workers Performance and the Indoor Environment. Prepared for California energy commission. Fair Oaks, California.
- Lesiuk, T. (2005).The Effect of Music Listening on Work Performance. *Psychology of Music*, vol 33; 173, Sage Publications.
- McNulty, N.J., (2015) . The Effects of Music on Employee Affect. Honors Program Thesis, University of Dayton.
- Mistry, H. (2015). Music While You Work: The Effects of Background Music on Test Performance amongst Extroverts and Introverts. *Journal of Applied Psychology and Social Sciences*, 1 (1), 1-14.
- Niebel, B., and Freivalds, A., (2001), Method, Standard and Work Design 11th Edition, Mc Graw Hill in printed version, Singapore.
- Padmasiri, M.K.D., Dhammika, K. A. S., (2014). The Effect Of Music Listening On Work Performance: A Case Study Of Sri Lanka. *International Journal of Scientific & Technology Research*, Vol 3, Issue 5.
- Rilatupa, J., (2008). Aspek Kenyamanan Termal Pada Pengkondisian Ruang Dalam. *Jurnal Sains dan Teknologi EMAS*, Vol. 18, No. 3.
- Seppänen, O., Fisk, W.J., Lei, Q.H.,(2006), Effect of Temperature on Task Performance in Office Environment, Lawrence Berkeley National Laboratory Environmental Energy Technologies Division Indoor Environment Department, Berkeley-USA.
- Talwar, M., Marwah, S., Narula, V., Sushant. (2016). Effect of Music on Productivity of Industrial Workers Engaged in Repetitive Work. *International Journal of Research in Aeronautical and Mechanical Engineering*, Vol.4 Issue 4, Pg: 11-19.
- Wyon D, Wyon I, Norin F. 1996. Effects of Moderate Heat Stress on Driver Vigilance in a Moving Vehicle. *Ergonomics* 39,1,61-75.

* Lovely Lady
E-mail address:lady@untirta.ac.id



THE RISK ASSESSMENT WORK OF OPERATOR BASED ON RAPID UPPER LIMB ASSESSMENT METHOD (RULA) TO IMPROVEMENT OF WORK SYSTEM

Ayu Bidiawati*¹, Lestari Setiawati

**¹Universitas Bung Hatta Padang, Fakultas Teknologi Industri, Jurusan Teknik Industri,
Jl. Gajah Mada 19, Olo Nanggalo, Padang(25143)
E-mail: ayubidiawati@bunghatta.ac.id
ayubidiawati@yahoo.com*

ABSTRACT

A good working system can't be separated from the workplace and operational procedures that need to be done in a job. Arranging the workplace, equipment, and body position while working will be very influential in creating integrated working system. Through good working environment, industry could be run effectively and efficiently. Less supportive working method or working system can lead to discomfort for workers during work. It could be due to unergonomic working environment. The process of making bread is divided into several activities, namely mixing dough, weighing, milling, printing, burning, cutting and packing. The process of making bread involves several workers. During production process, most of workers' activities are carried out in standing position and perform the same hand movements over and over again (repetitive). Repetitive and monotonous activities, unergonomic working attitude, bad temperature on some activities, are ergonomic problems that often occur in this bread-making factory. These adversely affected workers' physical state and raise the work risk in form of pain on the part of worker's body. Because of these conditions, work risk identification was performed by method called RULA (Rapid Upper Limb Assessment). RULA method can analyze the risks associated with disturbances in upper body. Analysis was performed to obtain risk level, so work system can be improved to reduce work risk that could endanger workers. The results of RULA method ; work stations that have high risk with action 7 category, are work station of stirring, milling, and printing. At the end of the research, we design working aid in form of buffer table, pallet, work support table, and stroller. We hope that the design of working aid can change how the workers work, so work risks can be minimized or even eliminated.

Keyword: RULA Method, Ergonomics, Occupational Risk Levels, Work Systems

1. INTRODUCTION

Inconvenience for workers occur due to less supportive working method or systems, such as uncomfortable and unsafe work atmosphere. Conditions like this will bring operational performance into optimal points and on the other hand, working situation will accelerate fatigue, complaints, lead to pain or injury to workers' body both in short and long term. The impact in short term will lead to work fault, loss of work, and increase workplace accidents. While on the long-term, it can cause pathological changes (shape) in muscle tissue (Chamela, 2006). In one of bread-making industry, the production process is divided into several activities, namely mixing dough, weighing, milling, printing, burning, cutting and packing. The process of making bread involves five workers. During production process, majority of workers work in standing position and perform the same hand movements over and over again (repetitive).



Factory's narrow space and close to the oven, can also cause hot temperatures and bad working attitude. These conditions will lead to decreased moisture and greater energy expenditure, fatigue, increase the workload, and muscle injuries. Based on results of the questionnaire, some workers had complaints for some activities of bread making process. Industrial workers are easier to feel discomfort and pain in the workplace (Mali and Vyavahare, 2015). The more work activity done by the workers, the greater the chances of suffering occupational health disorders (Bidiawati et.al, 2016).

Repetitive, monotonous work, unergonomic working attitude, bad temperature on some activities are ergonomic problems that arise in bread making factory. These activity conditions will automatically have negative impact on workers' physical condition, causing work risk in form of pains on the parts of worker's body. The pains felt by workers are in form of pain in spine, arms, neck and in some other parts of the body. The pain can also pose potential hazards that cause workplace accidents such as injury, disability, and joint disorders. The accident is commonly called WMSDs (Work Related Musculoskeletal Disorder) (Najarkola, 2006). WMSDs can reduce worker's health, thereby reducing worker's performance in completing the work. It will also reduce workers' productivity and product quality (Mali and Vyavahare, 2015; Bidiawati and Suryani, 2015; Rosnah and Suhada, 2016). Such circumstances should be solved as soon as possible, otherwise ergonomic work system will not be achieved.

To reduce unergonomic problems of some activities on bread production process, we perform work risk identification called RULA (Rapid Upper Limb Assessment) method. This method is used to analyze the risks associated with upper body disturbances. It was developed to identify muscular effort that related with work posture, exertion and repetitive work, which can cause muscle fatigue. Many researchers use RULA assessment methods to evaluate work risks in some work activity. The assessment results can lead to right working posture to reduce occupational risk level (Kaden et.al, 2015; Mali and Vyavahare, 2015; Sahebagowda et.al, 2016). By using this method, we can identify occupational risk that occur, and know the risk level in each activity of bread production process. Once the risk level is known, we can design work system to reduce work risk so it no longer endangering workers.

The study of human beings in work environment by utilizing information about nature, capabilities and limitations of human beings to design a system so people can live and work well is called Ergonomics (Sutalaksana, 1979; Santoso, 2004). Ergonomics have important role in improving occupational health and safety factors. It is to reduce visual discomfort and work posture. To design instruments and control systems in order to optimize information transfer process and generate quick response to minimize error, and to obtain optimization, work efficiency and eliminate health risks due to the lack of proper working methods. One type of ergonomic problems often encountered in the workplace, especially relating to human strength and endurance in doing their jobs or biomechanics, is musculoskeletal or flexes (Bidiawati and Suryani, 2015).

According to Kroemer (2001), skeletal muscles are striped muscles attached to the bones that generate motion power when needed to carry out decisive force. Musculoskeletal are injuries and diseases on muscles, nerves, tendons, ligaments, joints, cartilage and spinal cord. Musculoskeletal caused by work and fatigue have something in common. Both are caused by increasing intensity and duration of work (the higher work intensity and duration, the more cases of work-related musculoskeletal and fatigue), both cause pain and affect work performance. Therefore, when musculoskeletal occur; it will increase the cost due to waste of



time when employee can't work, increase cost of competence demanded by employees and others (Nurmianto, 2004; Dewayana, 2007).

RULA (Rapid Upper Limb Assessment) is a research method to investigate work-related disorders / pain in upper limbs. This method does not require special equipment. RULA method will observe the parts of upper body, neck, torso and legs (Lynn McAtamney and E Nigel Corlett, 1993). Each position of each part will have certain value. Factors that have been investigated are called external load factor, ie the number of movements, static muscle work, energy/power, work posture determination of work and equipment, and working time without a break. RULA was developed for :

- Quick screening method for working population, which relates to work risk causing disturbances in upper limbs,
- Identify muscular effort associated with work posture, exertion and repetitive activity, which can cause muscular fatigue.
- Provide results that can be combined with ergonomical assessment methods namely physical mental, mental, environmental and organizational factors.

Body parts were evaluated by RULA method which includes hand, wrist, elbow, shoulder, neck and lower back. The use of this approach is in ergonomic evaluation of different risk scores between 1-7, where higher score indicates greater degree of risk. RULA score is developed to detect work posture or risk factors that should receive more attention. (Qutubuddin et.al, 2013; Kaden et.al, 2015).

Many researchers use RULA assessment method to evaluate the work risk in some type of work (Mali and Vyavahare, 2015; Kaden et.al, 2015; Rosnah and Suhada, 2016; Sahebagowda et.al, 2016; Kale and Vyavahare, 2016). The assessment results can lead to solutions for right work posture that reduce work risk level.

2. METHODOLOGY

The study was conducted on bread-making industry. Steps being taken are: (a) system assessment. (b) work risk identification and assessment with RULA method (c) analysis and improvement recommendation.

2.1 Assessment System

Assessment system covers bread making production process. The production processes are through seven stages with 5 workers. They are ; (1) Stirring (worker A) (2) weighing (worker A) (3) milling (workers B) (4) printing (worker C) (5) combustion (workers D) (6) Cutting (worker E) (7) Packing (labor E). Bread production process is about 3 hours / dough, where workers were always doing repetitive work. These movements affect worker's body that will result in pain / complaints.

2.2 Work Risk Identification with RULA Method

Phases performed using RULA methods are;

- Identify work posture by entering data of full body posture, upper arms, forearms, hands, wrists, neck, back and legs.
- Calculating RULA scores.
- RULA Scores are obtained by inserting score C and D using table C. The result is in form of risk and action level.
- Scale of action level that provides a guideline on risk level and required to drive more detailed assessment related to analysis obtained.



2.3 Analysis and Proposed Work System Improvement

To analyze bread production process, labour activities are divided into 7 working ways (working conditions) with total labour movement of 33, where each working way is analysed with score assessment of RULA Method. Then perform the proposed work improvement system by taking into account the level of work categorized as high risk.

3. RESULT AND DISCUSSION

White bread production process lasted for about 3 hours / batter. During production process, workers were always doing repetitive work. Those movements will affect worker's body that will result in pain / complaints. Based on the questionnaire results, workers' complaints in bread production process are as follows:

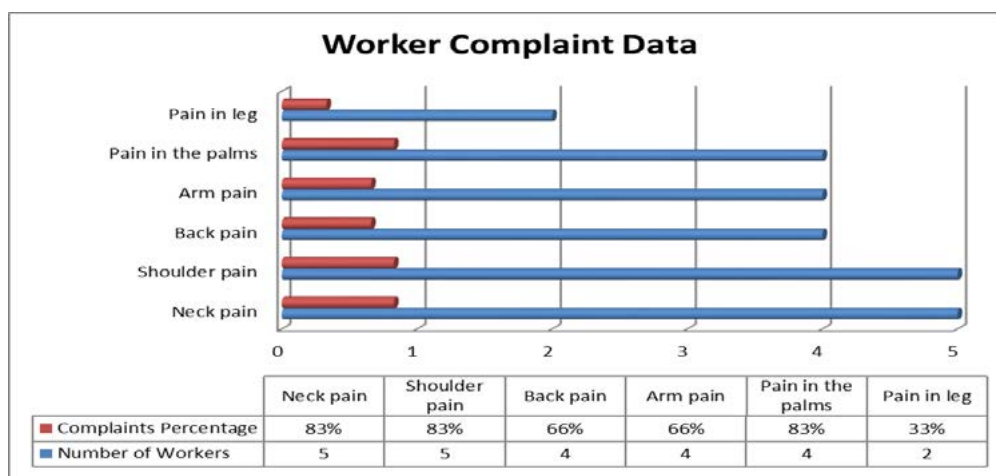


Figure 1 : Worker Complaints Percentage

Bread production process has seven stage and involving five workers. It can be seen in Figure 2 below;

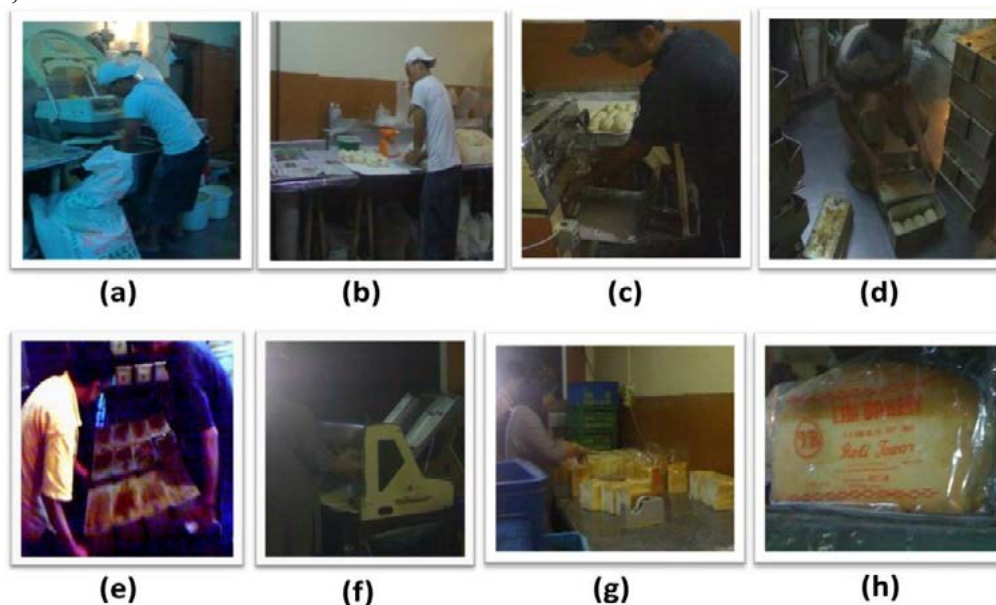


Figure 2 : (a) Stirring Process (Worker A) (b) Weighing Process (Worker A)
 (c) Milling Process (Worker B) (d) Printing Process (Worker C)
 (e) Combustion Process (Worker) (f) Cutting Process (Worker E)
 (g) Packing Process (Woker E) (h) Bread

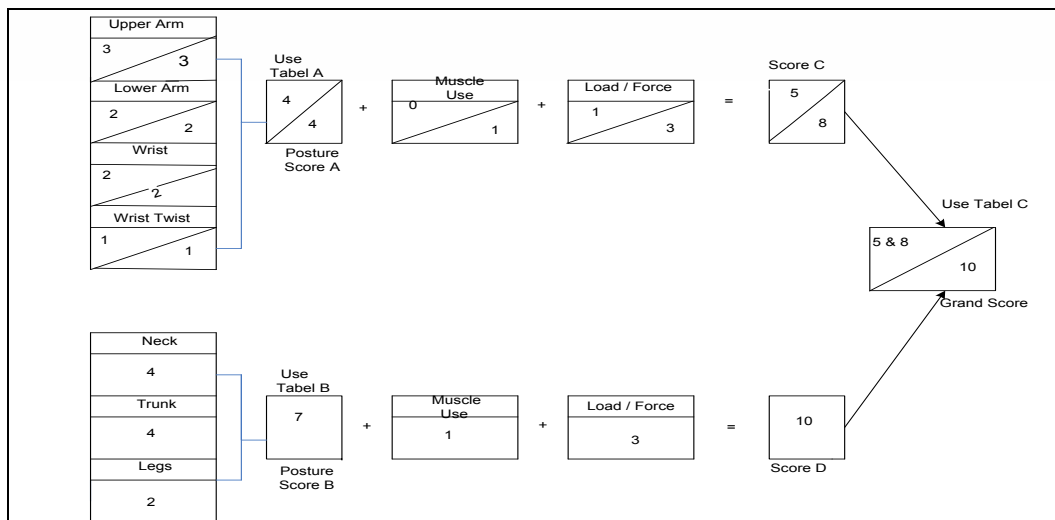
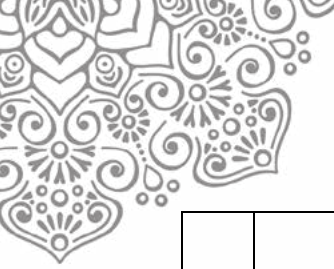


Figure 3. Score Sheet of RULA Method for Labour Movement 1

Table 1. Result of Calculation of RULA Method

No.	Working Condition	Worker Movement	Grand score	Action Category	Risk Level
1.	Stirring	1	5 dan 8, 10	7	high
		2	8,6	7	high
		3	4,3	4	low
2.	Weighing	4	4,5	5	low
		5	2 dan 3,4	4	low
		6	2 dan 3,4	4	low
3.	Milling	7	4,8	4	low
		8	4 dan 3,4	4	low
		9	5 dan 3,5	4	low
		10	4,8	4	low
		11	6,5	7	high
		12	4,5	4	low
		13	3,5	4	low
		14	5,4	4	low
4.	Printing	15	4,4	4	low
		16	6,9	7	high
		17	6,8	7	high
		18	5,7	7	high
		19	5,7	7	high
		20	5,7	7	high
		21	5,8	7	high
5.	Combustion	22	5,9	7	high
		23	5,9	7	high
		24	6,9	7	high
		25	6,9	7	high
		26	6,5	6	middle
		27	6,8	7	high
		28	6,9	7	high



		29	8,6	7	high
		30	3 dan 4,3	4	low
6.	Cutting	31	3.2	4	low
		32	3.3	4	low
7	Packing	33	4,3	4	low

Based on risk level that has been obtained using RULA methods, we analyze worker's position if it can cause injury or not. During production process, it turned out that most of their working positions are at level 7, which means that their position must be corrected immediately. Otherwise, the risk of injury to workers' upper body will be big. Therefore work system improvement by designing new work system in bread making process must be performed immediately. The design of work system is carried out at work station that has high-risk work including the design of work support tools, dough stir machine and stroller.

Ergonomics is achieved by evaluation and design of the workstation and by achieving a golden mean between task, operator and working area. In industries there is a continuous change regarding new employee, new adjustments, new processes etc. So every time new ergonomic solutions are required as per the situation. (Kale and Vyavahare, 2016). Ergonomic is a way of designing tools to accommodate the capabilities of workers. Good ergonomic design will reduce work risk factors which will give solutions for right posture level and also contribute to the ergonomic illness. Therefore, researcher applied designed work system for workers such as for stirring station, for milling work station, and for printing work station.

Work System Improvement For Workers

- **For Stirring station**

Stirring station is work station with high risk, because workers must bend while doing this stirring. Figure 4 shows stirring movement performed by workers, where the state of bending is reduced because the machine has buffer. Work movement in figure 4 shows bread dough flattening motion. The proposed work movement shows the change in the neck, torso and legs that initially at risk, but now it is minimized.

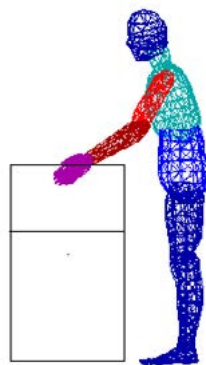


Figure 4. Worker Movement 1

- **For Milling Work Station**

In milling work stations, workers put pallet into shelves. Pallet is used without handle, so workers lift it to their shoulder. Figure 5 shows the design of worker's workings ways, after adding grip / handle to pallet. With this design, the position of arm and wrist to workers in bringing pallet will be more comfortable.

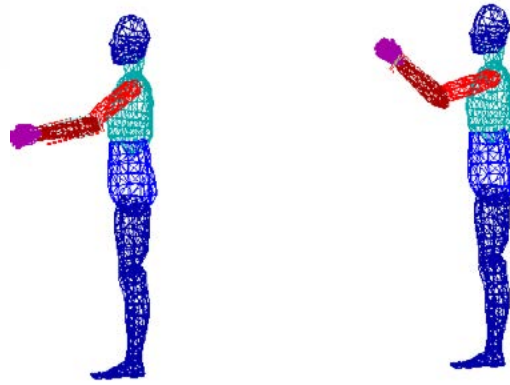


Figure 5. Worker Movement 13

- **For Printing Work Station**

Figure 6 shows the design of improved working way of preparing Kanso and deliver Kanso to burning place. Workers now use stroller, so working way is fixed and the risk is minimized.



Figure 6. Worker Movement 16, 17 Dan 21

In printing work station, we do not only design stroller, but also helping desk which serves to close Kanso so squatting position can be eliminated. Figure 7 shows the work covering Kanso in standing position.

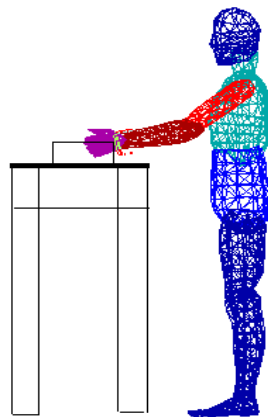


Figure 7. Worker Movement 19



4. CONCLUSION

- RULA method is able to analyze movement of upper body against muscle disorders that may occur.
- RULA methods identify work stations that have high risk is stirring, milling, and printing work stations.
- Work risk occurs because the body posture bent at work, unbalanced standing position, the use of big force when preparing Kanser, and operator's risky arm position while working and uncomfortable hand position when carrying Kanser to put on the shelf.
- Work system improvement by designing buffer of dough stirring machine, pallets, help desk and stroller so work risk arised can be minimized and even eliminated.

5. ACKNOWLEDGEMENT

The authors would like to acknowledge Kemenristek Dikti for the funding support of the research project [Penelitian Produk Terapan].

6. REFERENCES

- Bidiawati, Ayu and Eva Suryani, (2015), Improving The Work Position of Worker's Based on Quick Exposure Check Method to Reduce the Risk of Work Related Musculoskeletal Disorders, *Procedia Manufacturing* 4 (2015), pp 496 – 503, Elsevier.
- Bidiawati, Ayu, Wahyuni A. and Eva S., (2016), Ergonomic Design Tool For Brick Operator In : *Proceeding of 9th International Seminar on Industrial Engineering and Management*, Padang, September 21-23, 2016, Indonesia.
- Chamela, Yolly, (2006), Perancangan Sistem Kerja Pembuatan Galamai dengan Metoda RULA untuk Mendapatkan Sistem Kerja yang Ergonomis (Studi Kasus : Usaha Erina). Universitas Bung Hatta. Padang.
- Dewayana, Triwulandari (2007). Identifikasi Variabel yang Berpengaruh Terhadap Keluhan Musculoskeletal di PT.Sun Indo Adipersada, Universitas Trisakti : Prosiding.
- Kaden, Butree, Kritisada Wannapa and Preecha Khansri, (2015), Study of Ergonomic Risks in Wooden Furniture Production, *Australian Journal of Basic and Applied Sciences*, Volume 9, Issue 17, pp 64-70, AENSI Publisher.
- Kale, PN and Vyavahare, RT, (2016), Ergonomic Analysis Tools : A Review, *International Journal of Current Engineering and Technology*, Volume 6, Number 4, pp. 1271-1280, Inpressco.
- Kromer, K.H.E, (2001), *Ergonomics: How To Design For Ease And Efficiency*, New Jersey: Second Edition, by Prentice Hall.
- Mali, SC and Vyavahare, RT, (2015), RULA Analysis of Work-Related Disorders of Foundry Worker Using Digital Human Modelling (DHM), *International Research Journal of Engineering and Technology*, Volume 02, Issue 05, pp 1373-1378.
- McAtamney, Lynn. dan Corlett, E.Nigel., (1993), "RULA : A Survey Based Method for The Investigation of Work Related Upper Limb Disorders", *Applied Ergonomics*, 24(2) : 91-99.
- Najarkola, SA Mossavi, (2006), Assessment of Risk Factors of Upper Extrimity Musculoskeletal Disorders (UEMSDS) by OCRA Method in Repetitive Task". *Iranian J Publ Healt*, Vol 35, No.1, Hlm 68-74.
- Nurmianto, Eko, (2004), *Ergonomi : Konsep Dasar dan Aplikasinya*, Jakarta: Guna Widya.
- Qutubuddin S.M., S.S. Hebbal and A.C. S. Kuma, (2013), Ergonomic Evaluation of Tasks Performed by Workers in Manual Brick Kilns in Karnataka, India, *Global Journal of*



- Researches in Engineering Industrial Engineering, Volume 13, Issue 4 Version 1.0 Year 2013, pp 34-42, Publisher: Global Journals Inc. (USA).
- Rosnah, Mohd Yusuff and Suhada, Nor Abdullah, (2016), Ergonomics As a Lean Manufacturing Tool for Improvements in a Manufacturing Company *In* : Proceedings of the 2016 International Conference on Industrial Engineering and Operations Management, Kuala Lumpur, March 8-10, 2016, Malaysia, IEOM Society International.
- Sahebagowda, Vinayak K. and Chetan Kapali, (2016), Ergonomics Study for Injection Moulding Section Using RULA and REBA Techniques, International Journal of Engineering Trends and Technology, Volume 36, Number 6, pp 294-301.
- Santoso, Gempur, (2004), Ergonomi: Manusia, Peralatan dan Lingkungan, Jakarta : Prestasi Pustaka
- Sutalaksana ,I.Z,dkk, (1979), Teknik Tata Cara Kerja : Laboratorium Tata Cara Kerja dan Ergonomi, Dept.Teknik Industri-ITB.



JOB RISK ASSESMENT TOWARD LABOR FACILITIES USING JOB STRAIN INDEX METHOD

Dessi Mufti ^{a*}, Eva Suryani^b, Yusrizal Bakar^c, Tri Marta Putri^d
^{a,b,c} Bung Hatta University, Gajah Mada Street No 19, Gunung Pangilun, Padang, 25134, Indonesia

ABSTRACT

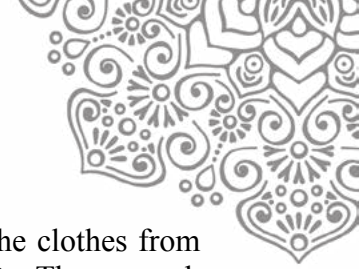
The effectiveness of tool aids is of vital importance in conducting a job. Employing inappropriate tool aids would cause inconvenience and yet risk potential or work injury to the worker. The purpose of this research is to assess the level of occupational risk toward the use of tool aids in the traditional food making process. The production process requires the strength of the hand muscles by utilizing coconut shell. It requires repetition as well. This may cause grievance of pain in both wrists and hands. There are ten respondents in this research. The data collection method is interview and filling out the Nordic Body Map (NBM) questionnaire toward the all ten respondents. NBM is used as a tool to identify the grievance experienced by the worker. Job Strain Index (JSI) is utilized to measure the level of occupational risk. NBM questionnaire result shows the existence of Musculoskeletal Disorders (MSDs) pain particularly on hand and feet. The calculation result of JSI consists of: first, intensity of exertion with a value of 6, second the duration of exertion with a value of 2, third efforts per minute with a value of 1,5, fourth hand/wrist posture with a value of 2, fifth speed of work with a value of 1,5, and the last one task duration per day with a value of 1. And thus, the result of occupational risk assessment is 54. The value of JSI > 7, which means the process of making food with attitude and working position at this time is very dangerous and resulted in MSDs toward the worker. One of the ways to reduce the occupational risk is to improve the facility of food printing and its tool aids. It is expected that these would reduce the occupational risk but improve the productivity.

Keywords: Distal Upper Extremity, Job Strain Index, Labor facility, Occupational Risk

1. INTRODUCTION

Raynauld's phenomenon is a disorder that is triggered by the use of hand tools repetitively which resulted in vibration effect. This condition can cause numbing sensation on the fingers (Wickens et al. 2004). Job strain index is a method that can be employed to assess the estimation of hand risk. Anwar, Syamsul (2015) in their research by using job strain index method toward the making of leather shoes found many risky working positions at certain jobs. Sulaiman, Surajo Kamalanathan (2015) in their research found that the risk factor of the MSDs occurrence involving the long working hours particularly for female worker. Next, Sartang, Ayuob Ghanbary 2015 also concluded that the use of the non-ergonomic tools with excessive force can cause the hand, wrist and neck to experience MSDs. Ulfah, Nur (2014) also investigated that the ergonomic problem is closely related with the repetitive work movement for all working days, odd or static working position, lift the heavy things, implementing extra force or affected by more frequent vibration or work in an extreme temperature.

One of the disease resulted from the inappropriate working position is MSDs. Moreover, Ulfah (2014) has conducted research toward the laundry worker, particularly washing division in



relation with MSDs. The laundry workers need to bend their back to dispense the clothes from washing machine. As the result, 60% of them are in high risk to experience MSDs. The research conducted by Tyas (2013) revealed that there occurs a significant relationship between lifting attitude and low back pain as part of MSDs. High repetitive work with longer time span would result in operator injury risk, although it has minor work load (Andriani, 2016). One of the methods to analyze work posture risk and to estimate hand injury risk is Job Strain Index (Chiasson, et al, 2012). Drinkaus, 2005 conducted a research to determine job risk of distal upper extremity at the automotive work through strain index. The most common methods with nearly accurate result and inexpensive cost are systematic observation method such as ROSA (Rapid Office Strain Assessment) and Job Strain Index (Wijaya, Caesar Danu, et al 2012).

The effectiveness of tool aids is of vital importance in conducting a job. Employing inappropriate tool aids would cause inconvenience and yet risk potential or work injury to the worker (Mufti 2014), productivity will be decreased (Samudra, Bambang Cipto 2002) and the like. The use of appropriate tool aids can accelerate and ease the burden of the work (W. Soebroto, Sritomo, 2003). The manual working activity which neglecting the convenience factor will influence effectiveness, efficiency and working productivity (Jovianto, 2005).

Initial survey of this research was implemented to home industry that produces traditional food at Cangkiang village, Agam District West Sumatera. Here, the workers conducting a great variety of task at production process by using non-ergonomic tool aids. The main characteristic of the task is the utilization of intensive hand muscle, repetitive working cycle and quite extreme hand posture. These indications are suspected to cause injury at distal upper extremity. Inappropriate body posture when lifting heavy load and inappropriate seated position would also cause the existence of MSDs (Hariyanto, 2016). The purpose of this research is to identify Musculoskeletal Disorder experienced by the worker when using food processor equipment through employing Nordic Body Map Questionnaire and to get to know the risk level as the effect of highly intensive and repetitive working intensity through Job Strain Index method. According to Chiasson, (2012) JSI method is more conservative compared to Hand Activity Level (HAL) to identify high risk at the workstation. This research would later focus more on traditional food printing workstation.

2. METHODOLOGY

This research was implemented to many same kind of small and middle enterprises that produce traditional food located at Cangkiang village, Agam district West Sumatera. The data was collected directly and recorded by using video. The recording shows motion and time needed by the worker to conduct the task of food processing since the very beginning to the end. The food processing can be classified into many stages, started from stirring the ingredients, shaping or printing, frying and caramelization. Direct interview with the workers can be implemented toward research related with injury risk of MSDs (Hariyanto, 2016). In order to obtain data of pain felt by the automotive and controlling workers, Drinkaus, 2005 observed it directly through video recording the types of job and divided the job into many elements.

The research procedure employing interview and worker observation through Nordic Body Map questionnaire. The Nordic Body Map questionnaire can identify the MSDs experienced by the worker. The questionnaire was distributed toward 10 workers of traditional food processing at



Cangkiang. Most of them have been working for seven years. The distributed questionnaire can be seen in figure 1:

The form consists of a central human figure with 27 numbered points. To the left and right are tables for scoring skeletal parts. Each table has columns for 'Otot Skeletal' and 'Skoring' (1-4). The left table lists parts 0-26, and the right table lists parts 1-27. At the bottom, there are fields for 'TOTAL SKOR KANAN', 'TOTAL SKOR KIRI', and a formula: 'TOTAL SKOR INDIVIDU MSOs = TOTAL SKOR KANAN + TOTAL SKOR KIRI'.

Figure 1: Nordic Body Map Questionnaire Form

In order to obtain information and to measure the risk level of body part that experience distal upper extremity, JSI was implemented. The result of JSI measurement will be used to analyze the level of working risk for every step in the food processing. The interpretation of JSI score is as follow: if the value of $JSI \leq 3$, the observed task is sufficiently safe, if the value of $JSI > 5$, the observed task suspected to have potency of upper limbs risk injury, and if $JSI \geq 7$, the observed task is highly risk.

Moore and VOS (2004) examined the implementation procedure of JSI as follow:

- (1) Data collection of the kind of task conducted by the worker in food processing
- (2) In Determining the rating values by using table 1, as follow:

Table 1. Rating values to assign for calculating The Strain Index.

Rating Values	Intensity of Exertion	Duration of Exertion	Efforts/Minute	Hand/Wrist Posture	Speed of Work	Duration/Day
1	Light	<10	<4	Very Good	Very Slow	hour
2	Somewhat Hard	10-29	4-8	Good	Slow	1-2
3	Hard	30-49	9-14	Fair	Fair	2-4
4	Very Hard	50-79	15-19	Bad	Fast	4-8
5	Near Maximal	> 80	>20	Very Bad	Very Fast	>8

- (3) Determining the value of multiplier of each task variable based on table 2, as follow:

Table 2. Determining multipliers to calculate The Strain Index.

Rating Values	Intensity of Exertion	Duration of Exertion	Efforts/Minute	Hand/Wrist Posture	Speed of Work	Duration/Day
1	1	0.5	0.5	1.0	1.0	0.25
2	3	1.0	1.0	1.0	1.0	0.50
3	6	1.5	1.5	1.5	1.0	0.75
4	9	2.0	2.0	2.0	1.5	1.0
5	13	3.0	3.0	3.0	2.0	1.5

- (4) Calculating the value of Strain Index which is obtained from the result of sixth multiplication



- (5) Determining the risk level, where the value of $SI \leq 3$ with low risk category or safe level, $3 < SI \leq 7$ moderate risk level, and the value of $SI > 7$ with high risk or dangerous.

In general, this traditional food processing can be divided into 4 kinds of task such as: stirring the ingredients, shaping or printing, frying and caramelization. Table 3 shows the details of the task.

Table 3. Steps and time required in the food processing

No	The steps of the work order	The equipment/ working tools	Time (Minute)
1.	Stirring the ingredients such as flour, egg, butter, and salt	Hand	24
2.	Shaping or printing sakura cake (traditional food)	Coconut shell as the printing or shaping equipment	342
3	Frying	Frying pan and stove	78
4.	Caramelization	Frying pan and stove	42

There are six variables that need to be collected for each task; each variable is assigned a rating and a multiplier. The abbreviations for the multipliers are in parentheses.

- Intensity of Exertion (IE) is a qualitative measure of the percent maximum voluntary contraction that a task requires to perform one time. This is a function of the force required and upper extremity posture. Guideline for assigning a rating criteria are presented in the following table 4:

Table 4 : Intensity of Exertion for IE

Rating Criteria	%MS ^A	Borg Scales	Perceived Effort
Light	< 10%	<=2	Barrely noticeable or relaxed effort
Somewhat Hard	10% – 29%	3	Noticeable or definted effort
Hard	30% – 49%	4 -5	Obvious effort, unchange facialexpression
Very Hard	50% – 79%	6- 7	Substantial effort, change facial expression
Near Maximal	>80%	>7	Uses shoulder or trunk to generate force

- Duration of Effort (DE) is determined by timing the duration of the exertion and is a measure of the physiological and biomechanical stress related to how long an exertion is maintained. DE of exertion is calculated b measuring the duration of all exertion period then dividing the measured duration of exertion by the total observation time and multiplying by 100%

$$\% \text{ Duration of Exertion} = 100 \% \times \frac{\text{duration of all exertion (sec)}}{\text{total observation time (sec)}} \dots\dots\dots(1)$$

- Efforts per Minute (EM) is synonymous with frequency of exertions per minute. EM are measured by counting the number of exertion that occur during an observation period then diving of exertion by the duration of the observation period measured in minutes.

$$\text{Effort per Minute} = \frac{\text{Number of exertion}}{\text{total observationtime (min)}} \dots\dots\dots(2)$$

- Hand/wrist posture (HWP) relates the anatomical posture of the hand. Hand/wrist posture is an estimate of the position of the hand or wrist relative to neutral position. Guideline for assigning a rating are presented in the following table 5:



Tabel 5: Hand/wrist posture guideline

Rating Criteria	Wrist Exertion	Wrist Flexion	Ulnar Deviation	Perceived Posture
Very Good	0 - 10 ⁰	0 - 5 ⁰	0 - 10 ⁰	Perfectly Neutral
Good	11 - 25 ⁰	6 - 15 ⁰	11 - 15 ⁰	Near Neutral
Fair	26 - 40 ⁰	16 - 30 ⁰	16 - 20 ⁰	Non neutral
Bad	41 - 55 ⁰	31 - 50 ⁰	21 - 25 ⁰	Marked deviation
Very Bad	>60 ⁰	>50 ⁰	>25 ⁰	Near extreme

5. Speed of Work (SW) estimates the perceived pace of the task and accounts for the additional stresses associated with dynamic work. Guideline for assigning a rating are presented in the following table

Tabel 6: Speed of Work guideline

Rating criteria	Compared to MTM 1 [^]	Perceived Speed
Very Slow	<=80%	Extremely relaxed pace
Slow	81 - 90%	Taking one's own time
Fair	91 - 100%	Normal speed motion
Fast	101 - 115%	Rushed, but able to keep up
Very Fast	>115%	Rushed and barely or unable to keep up

6. Duration of Task (DD) per day is a measure of how much of the workday is allocated to performing that task.

$$SI = IE \times DE \times EM \times HWP \times SW \times DD$$

The measurement through implementing job strain index method for shaping or printing task is as follow:

1. Intensity of exertion (IE), is at level of in need for more obvious effort, unchanged facial expression with the value of multiplier = 6
2. Duration of exertion (DE), the result of DE shows 4 seconds with 3510 cycles and the total amount of exertion time is 4 seconds x 3510 times = 14.040 seconds. The total amount of observation time of 3510 shaping/printing task cycle is 342 minutes (20.520 seconds), hence the value of DE = (14.040/20.520) = 0.68 =68%. This value is at rating 4 (50-79) with the multiplier value = 2
3. Effort per minute (EM), the amount of exertion is 3510 times and total observation time is 5.7 hour = 342 minutes = 20.520 seconds, so the value of EM = 3510/342 = 10.26 times. This value is at rating 3 (9-14 with the multiplier value = 1.5).
4. Hand/wrist posture (HWP), the result of observation and measurement shows posture at rating 3 (flexi = 50⁰) with category “non-neutral” / fair with the multiplier value = 2
5. Speed of work (SW), shows working speed in fast category but can still be controlled with the multiplier value = 1.5.
6. Duration of task per day (DD) is the duration of working time. Working time for 5.7 hours at rating 4 (4-8) hours with multiplier value = 1

After obtaining the multiplier value of each task of the food processing, particularly for shaping or printing section, the obtained value is as follow:

$$SI = 6 \times 2 \times 1,5 \times 2 \times 1,5 \times 1 = 54$$

It means that the SI value of 54 is at highly risk level.



3. RESULT AND DISCUSSION

a. The Data of MSDs Pain

The result of direct observation of the worker's posture in the traditional food processing is working in the static position and repetitiveness. As the effect, there occur the blockage of blood flow and resulted in lack of oxygen in that part. This will cause pain and influence MSDs. Below is the data of MSDs of 10 workers who process the traditional food:

b. The Measurement of Strain Index

The observation result shows that the biggest time proportion is at the shaping or printing the food as follow:

$$\% \text{ time for shaping/printing} = \frac{\text{printing time}}{\text{Total time}} \times 100\%$$

$$\% \text{ time for printing} = \frac{342 \text{ minutes}}{24 + 342 + 78 + 42} \times 100\%$$

$$\% \text{ time for printing} = 70,3\%$$

The measurement of strain index is based on one worker at the shaping/printing process which can represent the whole working system. The number of musculoskeletal complaints was recorded by using the Nordic Body Map Questionnaire filled in by the worker (fig.1)

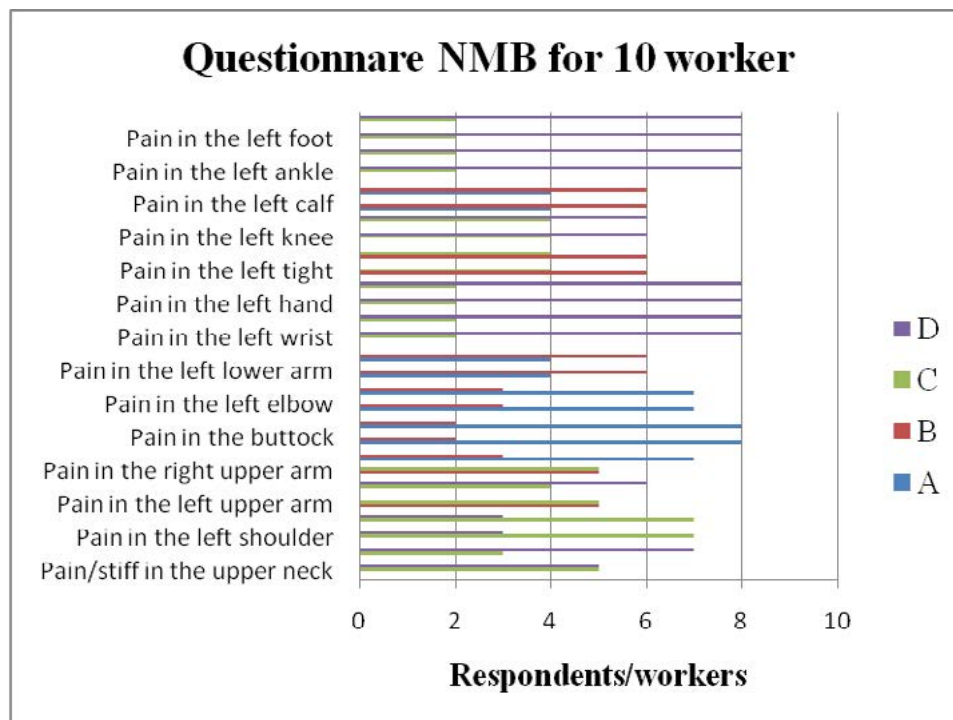


Figure 1: MSDs complaints

Most of the workers pain in the neck, pain in the left shoulder, pain in the right shoulder, pain in the left hand and pain in the right hand. This is particularly occurring during shaping or printing process. It happens since the shaping or printing process requires emphasis rests on the wrist with a static body posture. Finneran, Aoife (2013) in their study revealed that the effect of



strong gripping hand combination or holding hand position with a static body posture can cause MSDs.

This shaping or printing food process has to be conducted as soon as possible right after stirring the ingredients. Otherwise, the batter would be dry and complicate the shaping or printing process. The observation result of this task shows that the worker keep sitting with both legs folded.

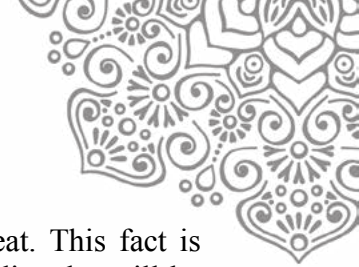
The measurement through employing the Job Strain Index method shows that $SI = 54 \geq 7$. It indicates that the observed task is highly risk. The static working position particularly on shaping or printing task process with body posture and back bend for 20° and both hands emphasis strongly toward the printing process can cause pain and numb at both wrists and both hands. The following pictures show the worker position during shaping or printing process.



Figure 2. Working position on shaping or printing task

One of the factors contributed to the injury risk of very high repetitive work is the inappropriate distribution of resting time. The research finding of Andriani, 2016 by implementing Occupational Repetitive Action (OCRA) method displayed injury risk of high repetitive work in a working cycle less than 30 seconds although the work load experienced by the operator is relatively small.

The pain in the right thigh, pain in the right knee and pain in the left and right calf sections is caused by working position with legs bent and do not touch the floor. This working attitude was performed due to the non-ergonomic working facility. The temporary effort the worker can do in order to reduce the pain is practicing stretching during the break of the working hours. The workers should not work under this circumstance. They should be enriched with knowledge of how to work in an appropriate body postures. They should also equipped with the ergonomic working facility. Moreover, it is necessary for the workers to know the impact of facility or tools utilization. Most of the MSDs grievance experienced by the workers involving both of shoulder, both of wrists, and both of hands, particularly the worker who conducted the task of shaping or printing in a repetitive manner. The research conducted by Mokhtar (2013) concluded that repetitive work is the main factor that has contribution in improving MSDs prevalence. In addition, during shaping or printing process, the worker employed a non-



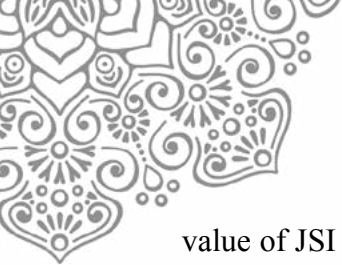
ergonomic seat. One of the ways to prevent MSDs is the use of ergonomic seat. This fact is supported with a study conducted by Kusri (2005) who revealed that muscle disorder will be compounded by certain situation, for example the incorrect seat position, the age of the worker and non-ergonomic seat. Instead of working attitude, the length of the working period also influence the working risk or MSDs. This is supported with a study investigated by Salminen (2016) who revealed that the risk of working accident influenced by the duration of the working period. The research was implemented toward workers who spend 12 hours for working. They were exposed to a higher working risk, 38% compared to the workers who spend 8 hours working per day. The workers of the traditional food processing has an uncertain working hours. It depends on the target of the amount of the food resulted. However, they used to work around 6-12 hours per day.

Ulfah (2014) in her research investigated the relationship between working attitude and MSDs. The current working position has caused the blood flow to the muscle become obstructed and automatically affecting the oxygen supply brought by the blood toward the muscle. It obstructs the carbohydrate metabolism and cause the lactic acid build up in the muscle. As the effect, the muscle was forced to experienced pain and grievance. Index Strain is a work analysis method used to determine whether the worker experienced the increasing distal upper extremity disorder and this is proven as valid for single-type job (Rucker, 2010). Most of the pain occurs at both wrists and both hands and sometimes it resulted in numbing sensation. It is caused by the use of non-ergonomic printing tools. The current equipment for shaping or printing task is the coconut shell with certain print motive on it. Both hands were located at both edges of coconut shell and should be pressed hard to shape or print the food.



Figure 3: The attitude of both hands at shaping or printing task

Overall, the problem related with ergonomic appear to be the incompatibility between the equipment and the worker. The ergonomic discipline examines the limitation of human capacity interaction with technology and its products. Ergonomic omit the man fits to the design, but the design fits to the man. In other words, it is man centered in which the whole working system design should be in line with the human need. The improvement of tool aids design, the reduction of lifted work load, the layout transformation and the establishment of standard operational procedure are to reduce the injury risk of Musculoskeletal Disorders (Hariyanto, 2016). Workplace Ergonomic Risk Assesment (WERA) is also one of the technique to obtain the worker injury risk which later would recommend improvement toward working tool aids in order to reduce pain and workplace design (Budiprasetya, 2016). The strength of Job Strain Index is more accurate result. However, the weakness is it requires longer time to determine the score



value of JSI as well as requires additional facility, so that the injury risk can be reduced (Wijaya, Caesar Danu, et al, 2012). Prior test by using JSI method shows accurate result to identify related work, however big scale research requires the latest validation and methodology (More, J Steve, 2010). Hand Activity Level (HAL) and Job Strain Index (JSI) methods are really useful to estimate the exposure of biomechanics pressure and to predict the Carpal Tanel Syndrome (CTS) risk (Garg, A, et al, 2012).

The corrective action relies heavily on the skeletal muscle risk which may experience obstruction or inconvenience. The main priority to be improved in this traditional food processing is to design an appropriate facility of shaping or printing the food or to substitute the coconut shell with an ergonomic facility. The next priority is to fix the facility used during seat with one leg folded and one leg touch the floor.

4. CONCLUSION

- The result of Nordic Body Map shows parts of the body that experience grievance as the result of tiredness in working are neck, both shoulders, both wrists and both hands.
- The result of the measurement by using job strain index method revealed that the risk of MSDs toward these traditional food processing workers is in dangerous category.
- The design of ergonomic working facility has to be executed as soon as possible, particularly facility that is being used to print or to shape the food as well as the seat facility employed by the workers.
- Strain Index method is appropriate in observing single-activity, particularly for repetitive activity on both hand and wrist in detail. This method also add observation time factor to determine the injury risk.
- Strain index is able to assess well for the occurrence of Musculoskeletal Disorders (MSDs) risk injury.

5. ACKNOWLEDGEMENT

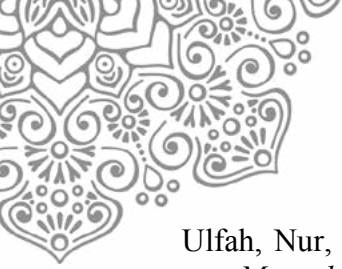
This research is supported by the Ministry of Research and Technology of Higher Education (Kemenristekdikti) in the scheme of research on applied products academic year I 2016/2017.

6. REFERENCES

- Andriani, Puspita Debrina., Sugiono, Penjadwalan Waktu Istirahat Optimal untuk Mengurangi Risiko Musculoskeletal Disorders berdasarkan OCRA Index, Jurnal Ilmiah Teknik Industri, Vol 15 (2), Des 2016, pp 157-167
- Anwar, Syamsul, Yuri Fandi Tanjung, Jasril., (2015), Penilaian Risiko *Distal Upper Extremity* pada Pekerjaan PembuatanSepatu Kulit dengan Metode *Strain Index*, Seminar Nasional Teknik Industri Universitas Gadjah Mada, pp. E-55-E-61.
- Bidiawati, Ayu, Eva Suryani., (2015), Improving The Work Position of Workers's Based on Quick Exposure Check Method to Reduce the Risk of Work Related Musculoskeletal Disorders, *Procedia Manufacturing* 4, Elsevier, pp. 496 -503
- Budiprasetya, Andhika Ramdhan. Sugiono, Remba Yanuar Efranto., (2016), Analysis Of Musculoskeletal Disorder On Wiring Harness Work Station With Wera(Workplace



- Ergonomic Risk Assessment)Method, *Jurnal Rekayasa Dan Manajemen Sistem Industri* Vol. 4 No. 10 Teknik Industri Universitas Brawijaya
- Chiasson, Marie-Ève, Daniel Imbeau , Karine Aubry , Alain Delisle., (2012), Comparing the Results of Eight Methods Used to Evaluate Risk Factors Associated with Musculoskeletal Disorders *International Journal of Industrial Ergonomics*, 42, pp. 478-488
- Drinkaus, Phillip., Donald S. Blawieck Richard,(2005), Job Level Risk Assessment Using Task Level Strain Index Scores: A Pilot Study, *International Journal of Occupational Safety and Ergonomics (JOSE)* 2005, Vol. 11, No. 2, 141–152
- Finneran, Aoife, Leonard O’Sullivan ., (2013), Effects of Grip Type and Wrist Posture on Forearm EMG Activity, Endurance Time and Movement Accuracy, *International Journal of Industrial Ergonomic*, pp. 91-99
- Garg A., J. Kapellusch, K. Hegmann, J. Wertsc, A. Merryweather, G. Deckow Schaefer, E.J. Malloy & The Wistah Hand Study Research Team, (2012), The Strain Index (SI) and Threshold Limit Value (TLV) for Hand Activity Level (HAL): risk of carpal tunnelsyndrome (CTS) in a prospective cohort, *Journal Ergonomics*, pp 396-414
- Hariyanto, Hendro., Sugiono, Dewi Hardiningtyas., (2016), Working Risk Analysis On Manual Transfer Activities Of Tile With Rivised Niosh Lifting Equation Methods (Case Study: UKM Genteng Talangsuko, Malang, East Java) *Jurnal Rekayasa Dan Manajemen Sistem Industri VOL.4 NO.8 Teknik Industri Universitas Brawijaya*.
- Kusrini I., (2005), Faktor-faktor yang Berhubungan dengan Keluhan Musculoskeletal Petugas Cleaning Service Rumah Sakit X Kota Semarang (skripsi). Semarang: Fakultas Kesehatan Masyarakat Universitas Diponegoro
- Mokhtar, Deros BM, Sukadarin., (2013), Evaluation of Musculoskeletal Disorders Prevalence During Oil Palms Fresh Fruit Bounces Harvesting using RULA, *Advanced Engineering Forum.*, 10: 110-15
- Moore, S.J and Vos G.A., (2004), The Strain Index, dalam Stanton N., Hedge A., Brookhuis K., Salas E., Hendrick, Editor, *Handbook of Human Factors and Ergonomis Methods*, CRC Press, Boca Raton.
- Moore, J.Steven., Arun Garg., (2010), The Strain Index: A Proposed Method to Analyze Jobs For Risk of Distal Upper Extremity Disorders, *American Industrial Hygiene Association Journal*, pp 443-458
- Mufti, Dessi., (2014), Aplikasi Analytical Hierarchy Process dalam Pemilihan Alternatif Rancangan Alat Tenun, *Indonesia Journal of Industrial Engineering*, Volume 4, No.1.
- Rucker, Nathan., J. Steven Moore., (2010), Predictive Validity of the Strain Index in Manufacturing Facilities, *Applied Occupational and Enviromental Hygiene*, pp 63-73
- Salminen, Simo., (2016), Long Working Hours and Shift Work as Risk Factors for Occupational Injury *The Ergonomics Open Journal*, Volume 9, pp. 15-26
- Sartang, Ayoub Ghanbary, Ehsanollah Habibi, Arezou Abbaspoor Darbandy., (2015), Evaluation of Musculoskeletal Disorders in Household Appliances Manufacturing Company, Volume 2, No.4, pp. 380-384
- Sulaiman, Surajo Kamilu, Kamalanathan P, Aminu Alhassan Ibrahim, Jibril M.Nuhu., (2015), Musculoskeletal Disorders and Associated Disabilities Among Bank Workers, *International Journal of Research in Medical Sciences*, Volume 3, Number 5, pp. 1153-1158
- Tiyas R., (2013), Hubungan Sikap Angkat dan Frekuensi Angkut dengan Keluhan Nyeri Punggung pada Tenaga Kerja Pengangkut Barang di Gudang Bulog 402 Sukaraja Kabupaten Banyumas. *Jurnal Kesehatan Masyarakat Indonesia*, Volume 8, No.2, pp. 63-71



- Ulfah, Nur, Siti Harwanti, Panuwun Joko Nurcahyo, Kesmas., (2014), Sikap Kerja dan Risiko *Musculoskeletal Disorders* pada Pekerja *Laundry Work Attitude and Musculoskeletal Disorders Risk in Laundry Worker*, *Jurnal Kesehatan Masyarakat Nasional Vol. 8, No. 7, pp.313-317*
- Wickens, Christopher. D, John Lee, Yili Liu, Sallie Gordon Becker., (2004), *An Introduction to Human Factor Engineering*, 2nd Edition, Prentice Hall
- Wignjosoebroto , Sritomo., (2003), *Ergonomi Studi Gerak dan Waktu : Teknik Guna Widya*, Surabaya
- Wijaya, Caesar Danu., Karimah, Yunita, (2012), *Analisis Pengukuran Risiko Kelelahan Pengguna Meja Notebook Dengan Metode Job Strain Index Dan Rapid Office Strain Index*, TI Working Paper, Teknik Industri, Fakultas Teknik, Universitas Bina Nusantara.



MANGUSADA HOSPITAL GO TO THE ERGONOMICS HOSPITAL

I Ketut Widana

Bali State Polytechnic, Kuta Selatan, Badung 80364, Indonesia

ABSTRACT

Mangusada Hospital is a regional public hospital of Badung Regency in Kapal City is a hospital which was designed with a modern architectural approach. Ready to become the modern tourism hospital by ergonomics approach. The shape of the building is mounted with concrete piles spread around, makes it always be susceptible to all kinds of threats, especially acts of God such as: earthquake, fire, and whirling wind. From those kinds of disaster mentioned above, the earthquake is the most serious threat. The capability to escape of the medical patients when the earthquake happens is on the lowest priority as they need assistances from their relatives. In such condition, the evacuation path, prepared rescuing facilities and volunteers are the factors that determine the success of human life saving effort, especially the medical patients who are staying in the hospital. Generally, tools and infrastructures of emergency response that are available at the site are very limited. Most of the hospital management staffs do not understand or less care about the possibilities of dangers. This research is aimed at studying the readiness of Mangusada Hospital management in planning emergency responses, especially in facing a threat of collapse of the physical construction of the hospital due to the earthquake. The analysis of emergency response capability is performed with methods of observation and interview. The data collection comprises a risk identification, a building lay out, an evacuation procedure, an accuracy of physical facility supports such as in placing fire hydrants, and emergency doors. The interview is done with a safety expert and management staffs of the hospital and also observers of construction problems, especially those of the regional assembly commissions and the contractor of the building. The result of analysis shows that the management's commitment that is not written yet makes the implementation of safety care is less maximal. As big potencies of danger at the hospital wards, such as a lot of easy burning materials, lack of volunteers, unavailable of emergency evacuation path, make it necessary to work on an emergency management through training, preparing tools and operators as well as the hospital management's commitment to be care about the disaster threats.

Keywords: commitment; management; hospital; disaster; analysis

1. INTRODUCTION

Some aspects of ergonomics are important and should be a concern stake-holders Hospitals, like the medical community, the management, the facility provider for hospitals and patients, among others: service bureaucracy, anthropometric, physiological work,

* Corresponding author.
E-mail address: widketut@yahoo.com



bio-mechanics, environmental design work, psychology work, ergonomics and design work systems, emergency response / disaster plan, potential hazards, occupational accidents, risk management and occupational diseases. Of the many problems existing ergonomics, the ability of hospitals to shorten the service bureaucracy, anticipating potential hazards and emergency response, including the use of floor space will be focused on the study.

Hospital to be ergonomic, management must begin to declare aspects of care that need improvement, such as patient admission procedure when first arriving at the hospital. As well as government hospitals in general, applied Hospital services Mangusada for new patients still need to be improved, as well as the ability to anticipate potential hazards and emergency response.

Regional Public Hospital of Badung Regency in Kapal is an hospital that grows well although its age is relatively young. The location of the hospital is about 8 kilometers from Denpasar city and it takes about 45 minutes from Ngurah Rai International Airport. A range of requirement to become a big hospital has been fulfilled, among those are the big buildings for hospitalization, polyclinic and some supporting buildings that are ready to welcome patients.

The development of the hospital is directed to become 'a world class hospital' with a service-based setting. The goal above becomes a challenge for the hospital management. Several efforts has been done, such as a guaranty of in safe hands and secure environment for the employees, medical staffs, patients and their family. Grandjean. 1988. Efforts to achieve security involve professional security staffs who are mostly from the locals. In the future, the management will give a thought to an emergency managing strategy in facing a variety of threats, such as threats from the nature and human beings.

The research is directed to identify factors that have been existing and should be existing to anticipate emergency situations, especially those of acts of God. The strategic design that will be made has to consider the key of making decision, mechanism of emergency respond system, evacuation paths, facilities, communications, infrastructures and the field implementers.

The act of God is a natural phenomenon that cannot be predicted when will happen. We often hear and read various theories and predictions of natural disasters, however none of them are indeed in accordance with the realities (Manuaba, 1992a). The seismograph is indeed able to measure the earth quake power, however, it cannot predict or even make sure when the disaster will occur. The location of Indonesia that is among three world main ground plates, namely Australian, Eurasian, Pacific ground plates as well as in the position of the ring of fire makes Indonesia frequently experiences earthquakes. The powerful earthquake has happened recently in Jogjakarta which has destroyed many big buildings. A lot of people were dead and countless were wounded. The emergency condition that occurs when an earthquake suddenly takes place was able to be recovered as the readiness of the rescue squads, especially those from the Indonesian Army and Police, and the aids from the Center and Regional Governments. The aids were delivered fast to those who needed since the transportation was good, supported with an emergency management system which was well planned.



The emergency condition is an extraordinary condition that cannot be predicted or planned before. A decision in anticipating an emergency condition truly affects the amount of victims and length of the emergency situation. The mistake in handling the emergency condition can result in the death of patients, a failure of service system, damages of physically and environmentally, malfunctions of filing and financing system and also a bad image for the hospital in general.

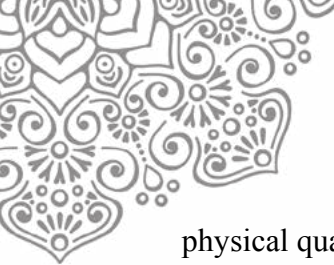
The hospital as a public service institution has to pay attention all the time to the risk management. The planning of emergency respond as a part of the risk management is directed to lessen the moral and material loss, to be responsive to the emergency and critical conditions. The plan can be forethought by simulations, trainings or socialization efforts. Trainings of emergency management can be carried out with theoretical and practical teaching systems (Manuaba, 1992b). The effort to involve the community surrounding as a supporting emergency management system, is a breakthrough that can be done. The success of emergency system needs a supporting management in the form of a good will of the top management and the stake holders, including the Regional Top Manager namely the Regent. Downward delegation of authority in anticipating the emergency situation, the designation of authority from the highest chairman to the lower level management is a supporting factor of the emergency management success.

The anticipation towards disasters or emergency respond management is carried out with a consideration of prosperity in a wider scope. The approach that can be used to determine the disaster position is : 5 W namely, the first one is What, what should be done?, the second one is When, when will it be done?, the third one is Why, why will it be done?, the fourth one is Which, which one is done first or the priority?, the fifth one is Who, who will implement it?

The emergency respond management emphasizes on the fluffiness of management responsibility towards the safety of patients, patients' family, employees and people surrounding the hospital. Identification of the hospital capability in general can be seen from the plans of evacuations, K3 implementation, environment policy, security procedure, supporting personnel, SOP, dangerous material handling, safety process judgment, informal consent, risk management planning, corporation with other parties, and closest communication (Suma'mur, 1995). In general, identification of human resources and internal capability of emergency responds, comprises of :

1. Physical matter of building: signposts, a main door and an emergency exit as paths of evacuation, an emergency operational center, a shelter area to gather in, and emergency sanitation facilities.
2. Equipments : K3 tools, communication tools (HT, intercom, Central Sound System, regular phones, mobile phones, and an alarm system as well as a back up generator).
3. Personnel : an emergency respond team, an evacuation team, a public relation, an emergency respond management team, medical supports, and security squads.
4. Back-up System.

A judgment of susceptibility — is an expression to describe a systemically failure of a facility towards a possibility and potential effect of any events (Sutalaksana, 2004). It needs to be considered about the kinds and levels of emergency conditions, policies, and technologies, technical mistakes or human errors, physical facilities (lay out, illumination,



physical quality of buildings, entrance and exit line, evacuation paths, and also the distance of shelter area to gather in).

2. METHODOLOGY/ EXPERIMENTAL

This research was conducted on December 2016 through a direct observation by taking photos of building lay – out and physical facilities of the hospital (Sutjana and Sutajaya, 2000). The identification of risks was conducted to analyze the susceptibility of the building. Interviews and discussions were conducted with the management of the hospital. This research is a descriptive study with a qualitative approach to the source of information in this study were 10 people plus 2 expert informants.

3. RESULTS AND DISCUSSION

Hospital Director or his representative has the legitimacy to make decisions in emergencies. Decision quality is closely related to the timeliness and speed of response to an emergency warning system. The decision making process begins and ends during the disaster known as an alternative to the decision taken. In an emergency when the alternative is not too much temptation a limited time, the range control officer decides should be made as short as possible, so that each section, such as treatment rooms, administrative space and other support units it is possible to decide on their own efforts to save by using standard operating procedure (SOP) is available (Usakti, 2008).

Mechanisms of emergency in response to the emergency system need to consider GeoMedic mapping, the integration of the concept of health services in disaster preparation to facilitate the mobilization of resources (Saain, 2002). (human resources, logistics medic and ambulance).

Every hospital needs to map out evacuation routes and determine the safe assembly (assembly point). Hepiman, et.al. 2010a. Map of evacuation hung in each room or section and plugged in rallying point signpost points specified. Simulation disasters and rescue measures need to be done regularly, especially for new employees. In the hospital emergency system update regional public hospital in Badung need to establish emergency events such as medical emergencies, fire, security threats, kidnapping babies, bomb threats, earthquakes and evacuation orders by using the code emergency order not to cause panic in the patient, family members, visitors and hospital employees. Emergency code that can be used there are 7 (seven) types, namely: blue, for a medical emergency; red, for fire; Grey, for safety; Pink, for kidnapping a baby; Green, for earthquakes; Black, for bomb threat; Purple, action for evacuation. Evacuation begins to walk, a wheelchair and a bed based on the evacuation plans of each building (Imarsan, 2011).

Communication is also vital. The use of communication tools such as radio communications using radio waves of certain frequencies that have been agreed upon, to the relationship between buildings and between spaces or parts (Anonim, 2010;. Putri, et al., 2004). Mobile phone infrastructure that integrates the web service with mobile communication network and voice of over internet protocol (VOIP) so the message short message service (SMS) can be quickly delivered to your room or another part of the hospital or related institution. As the field staff, the hospital needs to form a disaster



response team drawn from hospital security guards and employees trained in each section or unit care (Hepiman, et al., 2010b)

The Regional Public Hospital of Badung Regency in Kapal is situated on the main road of Denpasar-Gilimanuk, kilometer 8. The building for the emergency room service consists of a two storey building in which the first floor is used as the patient reception service, triage, roentgen, dispensary and waiting rooms. While, the second floor is used as the rooms for hospitalization, nurses and medical doctors. From the lay out perspective, the emergency room which is a center of hospital service, is situated in a very strategic position and reachable from all service units with a spacious access.

The building that is susceptible to the earthquake threats and need to have more attentions is the treatment building of Jepun which consists of four floors. The first floor is used as the pharmacy service while the second, third and fourth floors are used as hospitalization rooms. The estimation of the amount of patients and their family plus administration, cleaning service, paramedic staffs, and doctors day by day is more or less 200 people, in the building. The hazard potencies that we are worried about, besides the fire, stormy rain, thunder, chaos, bomb threats, hurricane, is the earthquake.



Pc. 1 Treatment Building seen from East

Capability to overcome threats

From the lay out viewpoint, concerning about the safety of building according to the law of *UU No. 28 tahun 2002*, the place and location as well as the path to the treatment building of Jepun makes quite easier in supporting the evacuation aid process for those from outside the hospital. However, as the design as well as the construction of the building, especially the treatment building of Jepun, are less supporting to the passive protection system when the shake occurs due to the earthquake, therefore it should be come into consideration of making an emergency exit. Generally, some items need to be prepared to anticipate the



earthquake disaster, namely a signpost to the evacuation path, emergency respond mechanism, preparation of AVAR (fire extinguisher), fire alarm, sprinkler and hydrant systems.

The vulnerability towards the electricity supply troubles influences the treatment services and so does the availability of inter-building communication system such as intercom, which is better prepared earlier. The Regional Public Hospital of Badung Regency at the moment does not have a written management commitment. It should be considered by all stakeholders: patients, patients' family, the surrounding community, supporting staffs, paramedics, and doctors from the very beginning, in order to pay more attention and care about the prevention and overcome the effects of earthquake. The forming of a rescue team is essential. Giving training and fixing on SOP (standard operating procedure) as references for the field executors.

4. CONCLUSION

1. Director of the hospital or their designated real authority to make decisions in emergencies.
2. Hospitals need to have GeoMedic mapping to facilitate the mobilization of resources.
3. Evacuation routes and rallying points needed to accelerate rescue efforts and minimize the number of casualties.
4. There are 7 types of emergencies that need to be anticipated to facilitate rescue efforts and avoid panic patients and their families.
5. Radio communication and mobile communication network devices and voice of over internet protocol (VOIP) is a facilities and infrastructure required to anticipate disaster.
6. Hospitals need to be equipped with a disaster response team.

The Regional Public Hospital of Badung Regency in Kapal is a new hospital that does not need to be merely judged. All parties, including the researchers, should give data and solutions that make possible the hospital management and the owner, namely the regional Government of Badung, are able to do things considered necessary for the establishment of comprehensive emergency respond plan to overcome various dangers and threats, including earthquake.

Some suggestions that can be recommended as considerations in making decision regarding the emergency respond are :

1. An emergency respond plan needs to be put into action, especially for the Regional Public Hospital of Badung Regency in Kapal.
2. The regional government is hoped to give a good will continuously until the emergency respond team formed which involves all elements in the Regional Public Hospital of Badung Regency in Kapal.

Supporting funds from the Regional Government of Badung should be included into the routine budget to maintain the existence of the Emergency Respond Team.

5. ACKNOWLEDGEMENT

Author would like to thank Ir. Made Mudhina, MT., director of Bali State Polytechnic and A.A.Bgs. Mulawarman, ST., M.T, The head of Mechanical Engineering Programme, for opportunity and facilities to follow the research.



6. REFERENCES

- Anonim, (2010). Bencana Kesehatan. (Cited 2016 May 7). Available from: <http://bencana-kesehatan.net>.
- Grandjean, E., (1988). *Fitting the Task to the Man : A Textbook of Occupational Ergonomics*. 4 th Edition. London: Taylor & Francis Ltd.,London.
- Hepiman, F., Januar, R.S., Hasyim, H. (2010a). Evakuasi dan assembly point. (Cited 2016 April 11). Available from: <http://webcache.googleusercontent.com/abstract+jalur+evakuasi+darurat+rumah+sakit>.
- Hepiman, F., Januar, R.S., Hasyim, H., (2010b). Kebakaran di Rumah Sakit. (Cited 2016 February 4). Available from: <http://eprints.unsri.ac.id/>.
- Imarsan, (2011). K3 di Rumah Sakit. (Cited 2016 May 9). Available from: <http://www.rscm.co.id>.
- Manuaba, A., (1992a), "*Makalah disampaikan pada Seminar Produktivitas Tenaga Kerja di Jakarta, 30 Januari 1992*". Pengaruh Ergonomi Terhadap Produktivitas" : Hal 14.
- Manuaba, A., (1992b). "*Makalah disampaikan pada Seminar Membudayakan Ergonomi di Pabrik Gula PTP XXI-XXII di Surabaya, 30 November 1992*". "Upaya membudayakan Ergonomi di PTP XXI-XXII. Hal. 26.
- Putri, GAA., Rhamani, PAS., (2004), Infrastruktur telepon seluler. (Cited 2014 March 5). Available from: <http://ojs.unud.ac.id/index.php/jTE/article>.
- Suma'mur, (1995), *Higiene Perusahaan dan Kesehatan Kerja*. Jakarta : PT.Toko Gunung Agung.
- Sutalaksana, I. Z., dalam Tarwaka, dkk., (2004), *Ergonomi Untuk Keselamatan, Kesehatan Kerja dan Produktivitas*. UNIBA PRESS, Surakarta-Indonesia.
- Sutjana dan Sutajaya, (2000), "Penuntun Tugas Lapangan Program Pasca sarjana Program Studi Ergonomi-Fisiologi Kerja UNUD Denpasar".
- Usakti, (2008). Ringkasan Modul Jurusan Ekonomi Manajemen. (Cited 2016 December 2). Available from: <http://sites.google.com/site/kuliahteoripengambilan/gery/SPGDT11.pdf>.
- UU. No. 28 Tahun 2002, (2002), "Bangunan Gedung".



THE ERGONOMIC *KUE BALOK* BAKING TOOL PRODUCTION WHICH FUELED BY CHARCOAL

Dwi Novirani^a, Gita Permata Liansari^b

^{a,b} **Industrial Technology, Institut Teknologi Nasional Jl. PKH. Mustapha No. 23, Bandung 40124, Indonesia**

Email: dwinovirani@gmail.com, gitapermata@itenas.ac.id

ABSTRACT

The traditional cake which is popular again in the area of western Java which have increasing demand is *Kue Balok*, but the baking tool of the cake does not currently take into consideration of the Ergonomic factors as ECSHE (Effective, Convenient, Safe, Healthy and Efficient), so that the cake operator always feel pain mainly on his back and waist because he always bends, and also the heat produced by the charcoal as the fuel hit directly to the operator, the grip of iron baking tool is hot and not convenient, etc. The output of this research is the ergonomic baking tool prototype which is charcoal-fueled by a functional test process. The choosing of the material for the manufacture of baking tool prototype is taken into consideration of the ECSHE factors and the prototype of the *Kue Balok* baking tool is also made to be portable.

Keywords: *Kue Balok*, Traditional Cake, Baking tool, Ergonomic, ECSHE, Portable



1. INTRODUCTION

Kue balok is the traditional cake increasingly popular in the Bandung city, but the existing baking tools do not provide favourable conditions for the operators who use it. From the sample of 30 operators that have the same baking tool, taken at various places in the Bandung city resulted in complaints such as operator always feel pain mainly on his back and waist because he always bends, and also the heat of charcoal as the fuel hits directly to the operator, the grip of iron baking tool is hot and not convenient, etc.

This issue will be risking the operator's safety, when more often interact with the *Kue Balok* baking tool, there will be higher problems perceived by the operator, thus an ergonomic baking tool is required. Ergonomics is the practice in designing equipment and details of the work in accordance with the capacity of workers. (OSHA, 2000).

In the previous research, prototype baking tool design using EFD (Ergonomic Function Deployment) has been done, so the product becomes ergonomic (Effective, Comfortable, Safe, Healthy and Efficient) (Liansari, 2016), but no function test and food grade determination, therefore further research is done that makes *Kue Balok* baking tool prototype which is charcoal fuel by a functional test process sees every part of component that must be perfected and the determination of food grade material that will be in use.

2. METHODOLOGY/ EXPERIMENTAL

Existing *Kue Balok* baking tool, like Figure-1 is very inefficient to operate it. Research attributes derived from ergonomic aspects ECSHE (Liansari, 2016) as shown in Table-1

Tabel-1. Research Attributes *Kue Balok* design baking tool

No	Ergonomi Aspect	Defines	Research Attributes
1	Effective	Goals and objectives achieved	Dimension precision molds
			Nonstick the mold
			Food grade grill tools
2	Convenient	Minimizing discomfort / anxiety operator in using the product	The heat from the baking tool, do not expose directly to the operator
			Table height can be adjusted
3	Safe	Minimizing the risk of operator, while interacting directly with product	Baking tool are safe to use
			Grip and the lid of the grill is not hot
			Sparks of charcoal is not to operator
4	Healthy	avoid health problems	Smoke does not expose directly to the operator
5	Efficient	Minimization of cost, effort and time in product use	Baking tool is easy to use
			Baking tool is not easily broken
			More number of hole in the mold
			Faster cooking time

Based on the derived attributes, produced three design alternatives of *Kue Balok* baking tool.



Figure-1. Existing *Kue Balok* baking tool

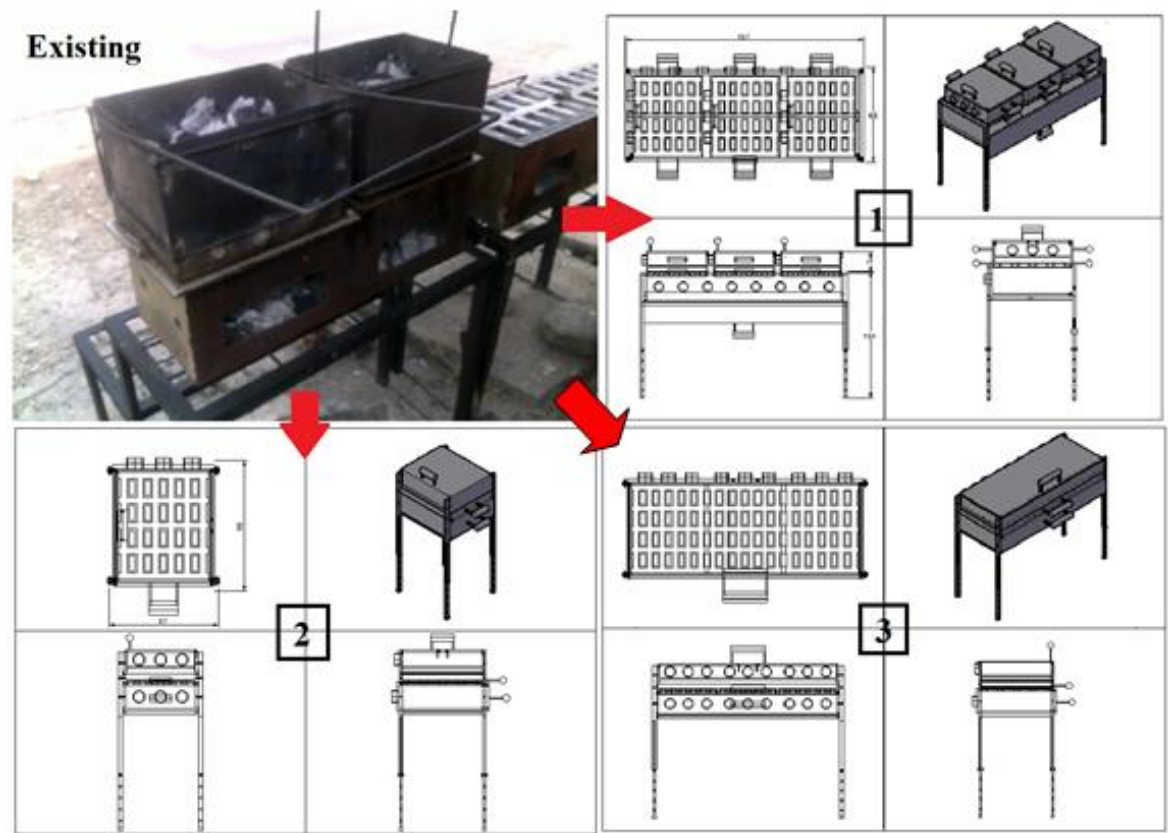


Figure-2. Existing *Kue Balok* baking tool and the three alternatives design

The first alternative, the dimension of the fuel container is 159 cm x 64 cm x 20 cm, three units of mold dimension 60 cm x 49 cm x 8 cm with the capacity of each 20 pieces. The handle of the mold is moved separately. There are three separate units of baking tool cover, which serve to cover the dough during baking process.



The second alternative, the dimensions of the fuel container is 53 cm x 64 cm x 20 cm, one piece of mold dimension 49 cm x 60 cm x 8 cm with a capacity of 20 pieces. There is a handle of the mold to insert the dough into the mold. There is one unit baking tool cover that can be used to cover the dough while baking process.

The third alternative, fuel container dimension 159 cm x 64 cm x 20 cm, three units mold of container dimension 60 cm x 49 cm x 8 cm with each capacity 20 pieces. The mold container can be pulled out to fill the dough into the mold and there is one cover of baking tool, which serves to cover the dough while baking process.

All these alternative baking tools, the molding material used is Teflon, the material used for the components of the fuel container, the desk, and the mold cover is aluminum mixture consisting of a mixture of aluminum, zinc, copper, manganese, and magnesium. In general, the mixture has been used in the manufacture of products that already exist at the moment.

The results of the three alternatives, selected the best by morphological process sequence, the concept of screening and concept selection. In the morphology chart, point out the development of product concepts from a number of alternatives for each section response. The concept of alternative products developed into a maximum of three alternative product concepts that can be combined.

The concept of screening is the stage of assessment of product concepts that may arise from a combination of graphical parts of the morphological response, followed by selecting concepts, alternative judgments and product concepts based on the weight of each of the attributes of the product research.

The concept of selecting the results is the highest total value of the results obtained, in this research the second alternative is selected for product design *Kue Balok* baking tool (Liansari, 2016). Here is the picture of the product that has been designed, which can be seen in Figure 3.

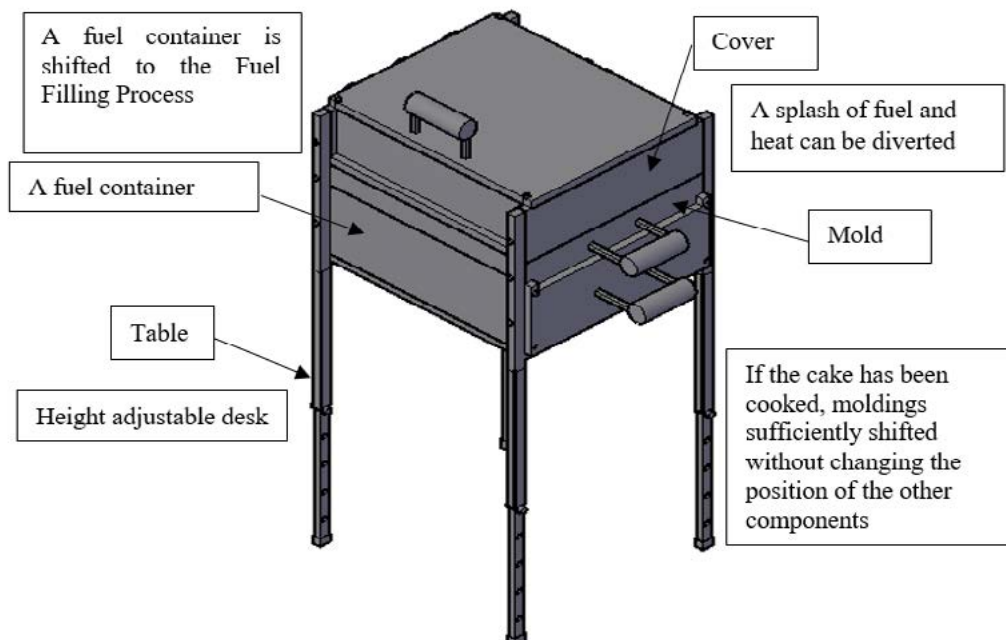
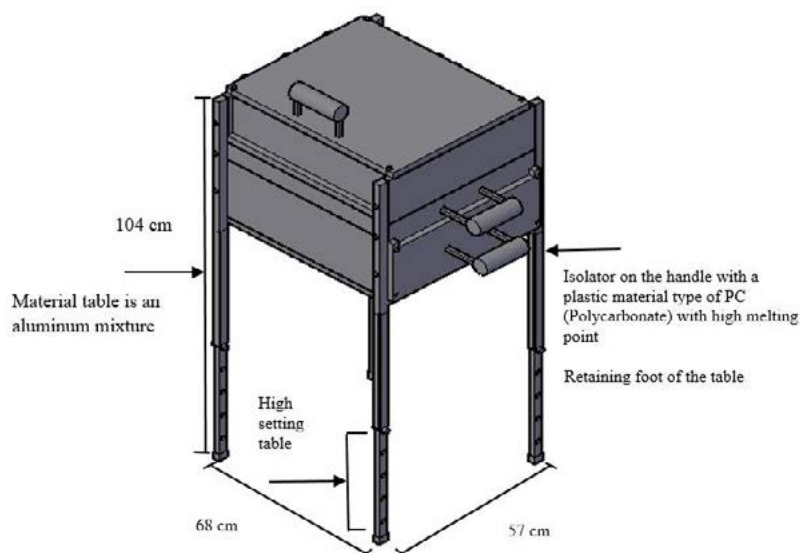


Figure-3. Blueprint *Kue Balok* baking tool (Liansari, 2016)



3. RESULTS AND DISCUSSION

After the design of the prototype is made, the collection of opinion from the users of the tool is later conducted. The result of the user response is useful as a functional testing process for the perfection of the tool. And later on it is useful to help create a prototype design part by part of the charcoal-fueled baking tool, and then the analysis can be made, resulting the blueprint design that can be seen in figure-4, AutoCAD software results (Omura, 2010)

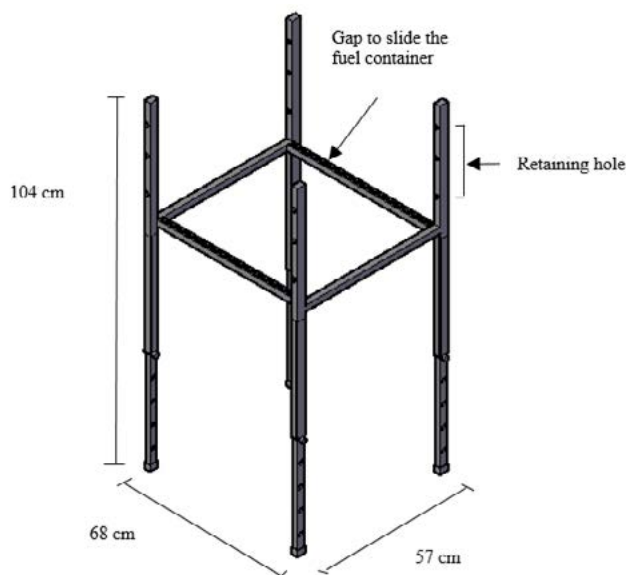


Effective Aspects (Precision)

In the previous product, the main component has a different size and not in accordance with the shape of the mold, while the results of the design, the mold is made of precision components having direct influence, so there are no gaps that can make the heat become

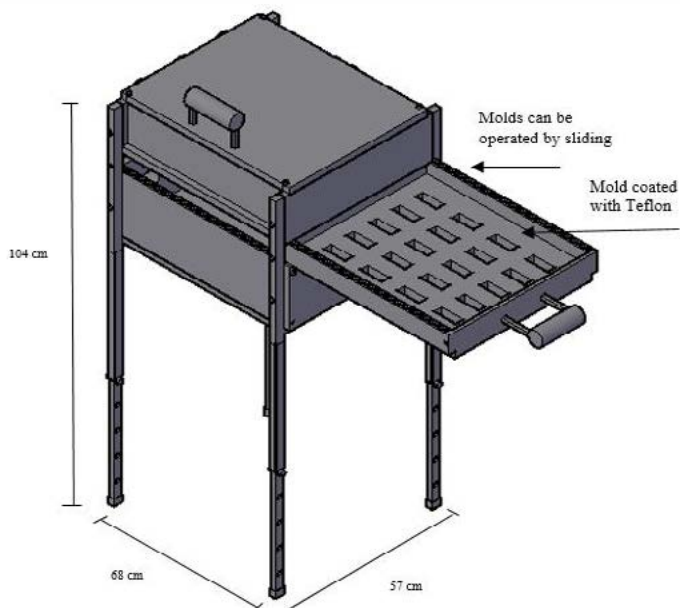
Safe aspect (Cookware safe)

The baking tool is less secure when used, because the heat generated spreads freely and there is no thermal insulation on the component in contact with the hand. The design results, baking tool safe to use, because there is a tool to withstand heat, heat can be transferred, so indirectly hit the operator body.



Aspects comfortable (Adjustable table)

In existing baking tool, operator cannot adjust the table, so that operators often adjust the table's height with additional tools. Results of the design, the table can be adjusted in accordance with the posture of the operator by adjusting the height of the table leg

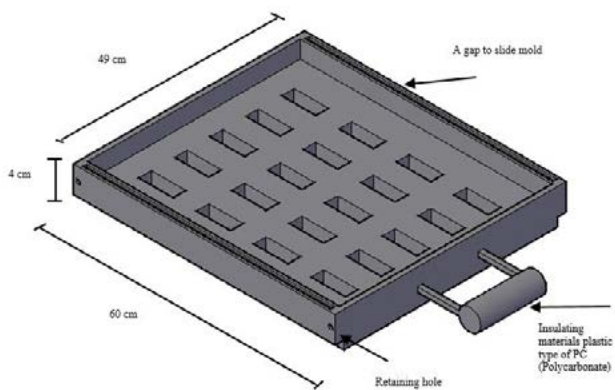


Efficient (cooking time)

The existing baking tool requires about 13 to 15 minutes to produce one batch of *Kue Balok*. The newly design baking tool will only need about 8 minutes to produce one batch of *Kue Balok* due to larger fuel volume used.

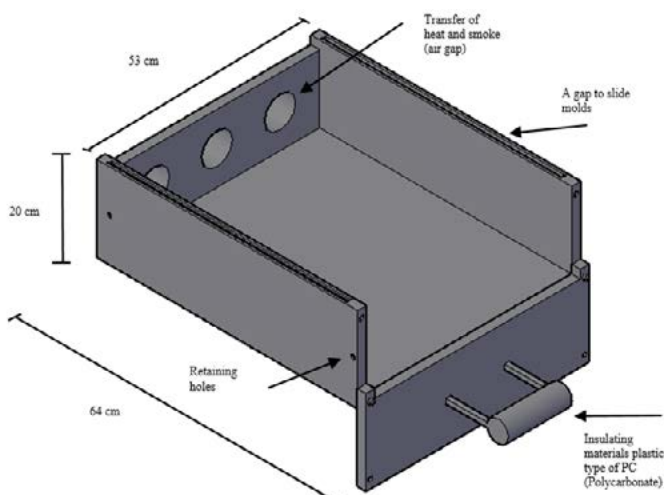
Efficient (Easy to carry)

In previous baking tool, each component is separated, making it difficult to carry and moved. The results of the design, compact baking tool or no component separated from one another and not difficult when carried and moved.



Convenient Aspects (Sticky)

In the previous product, when the *Kue Balok* cooked and then removed from the mold they are still attached to the mold. On the results of product design, when the *Kue Kalok* baked, nothing sticks in the mold, because the mold material used is Teflon (non-stick)



Healthy (Transfer of smoke)

The smoke produced is very disturbing for the operator, because there is no tool for transferring the smoke. Results of the draft, Smoke will be well transferred, because there is a transfer tool for the smoke, so the operator will not experience respiratory issues.

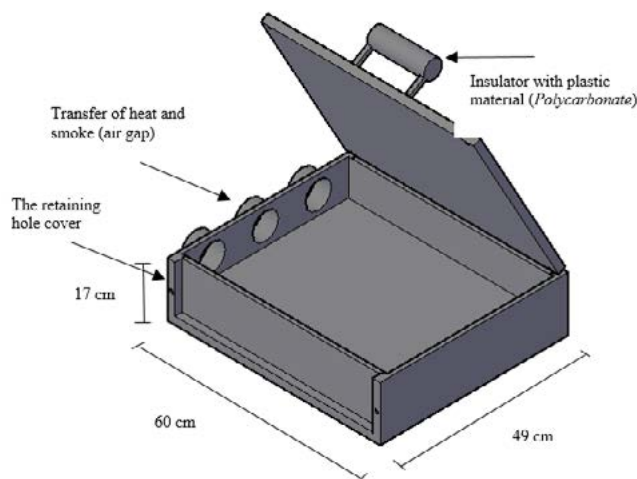
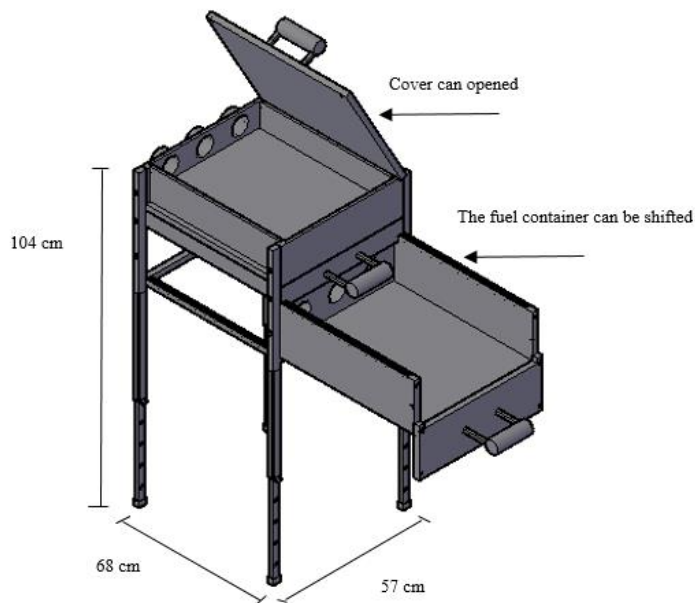


Figure-4. Break down Blueprint part of the charcoal-fueled baking tool and analyzed

By distributing additional questionnaires to users of the tool then get feedback from them about the specially made charcoal-fuel tray, which is useful for facilitating fast-burning charcoal. The prototype design of charcoal-fuel tray can be seen in Figure-5.

The additional input of the tool users is to pair four wheels at the foot of the baking tool table to facilitate the movement of the tool. The complete *Kue Balok* baking tool prototype can be seen in Figure-6 and the *Kue Balok* baking tool engineering drawing is shown in Figure-7.

Efficient (Movement)

In previous baking tool, a cover that weighs about 3 kg must be removed to pick up the bake *Kue Balok*. Results of the design, Molds will be just simply pulled, no cover will be required.

Convenient Aspects (The Heat)

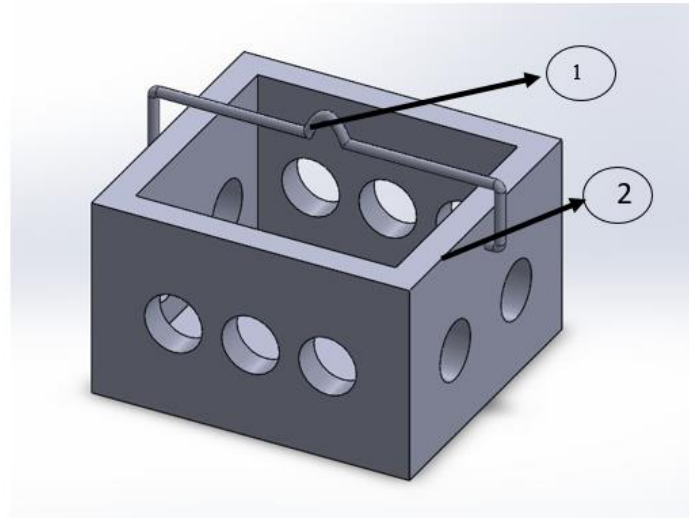
Previous product, the heat is freely dispersed in the air and direct to the operator's body, due to unavailability of cover in the fuel container and dough, the operator often feel the heat from the combustion process. The results of product design, the heat will be transferred properly due to a fuel container and cover tightly closed during the cooking process, because there is a switch component of the heat.

Safe (Handle not hot)

In previous baking tool, no heat retainer on the handle, so it takes the help of a wet cloth during use of the mold and cover. Results of design, there are tools for heat resistance, so that operator can operate it easily.

Safe (Operation tool)

Operators often hit by the splashes from the fuel at the time due to moving the cover. Results of the design, the operator's body will not hit by splashes, because there are spark of diversion of fuel in each component.



NO	Qty	Name	Material
1		Handle Tray	Stainless Steel
2		Main Tray	Stainless Steel

Figure-5. Prototype Charcoal-fuel tray

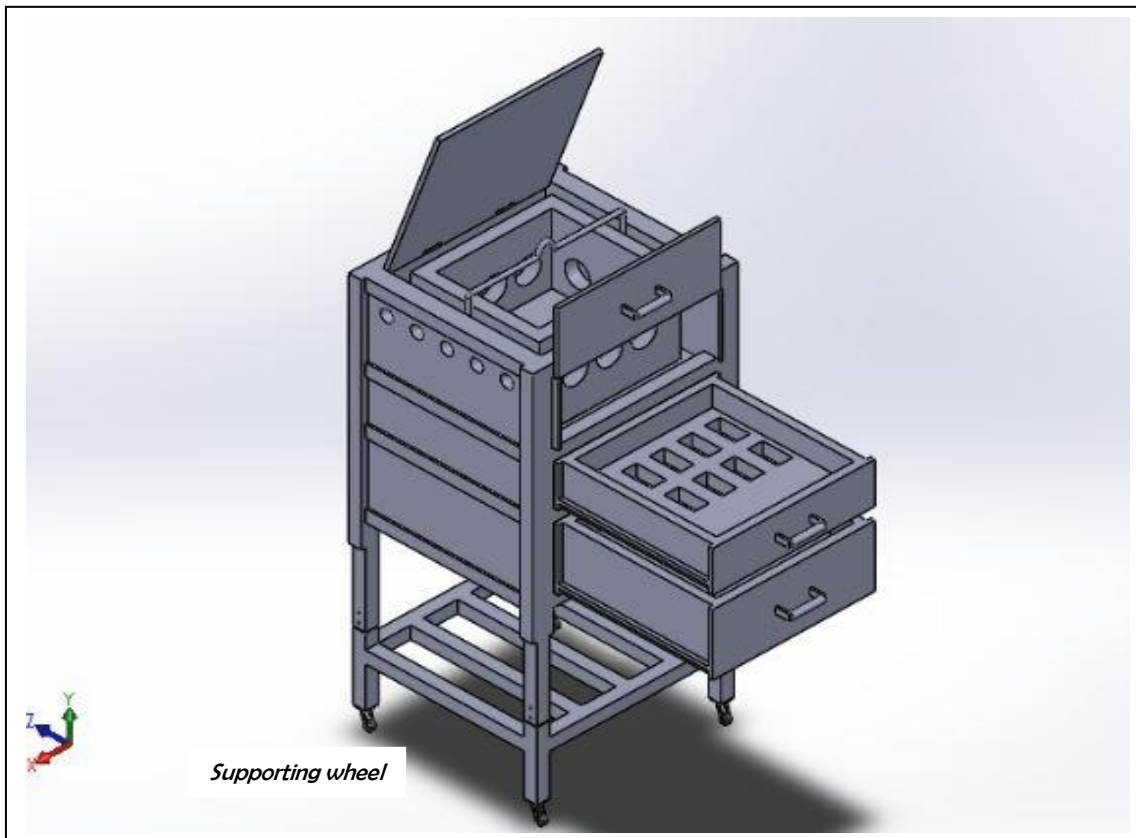
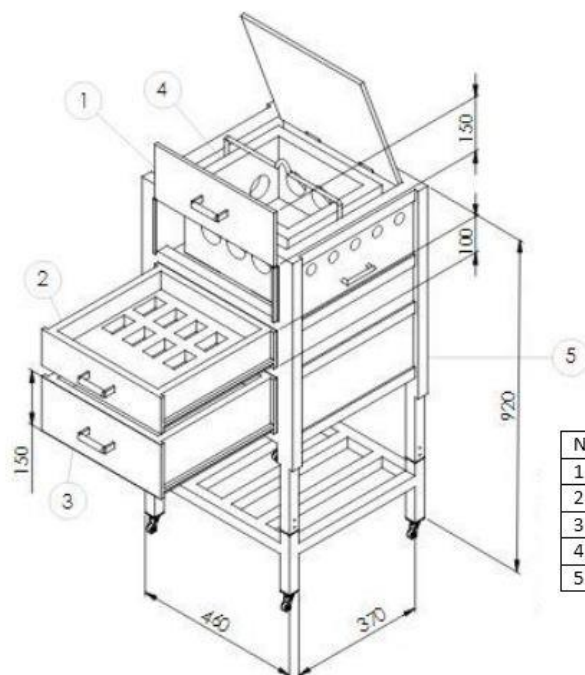


Figure-6 Prototype Kue Balok baking tool



No	Qty	Name	Material
1		Upper furnace	Stainless steel & Wood
2		Lower furnace	Stainless steel & Wood
3		Mold	Stainless steel
4		Tray	Stainless steel
5		Frame	Stainless steel

Figure-7 *Kue Balok* Baking tool engineering drawing

The making of tools for food should also include food grade material that is safe and healthy for food. The material chosen for the manufacture of portable baking prototype is stainless steel, because it is not corrosive, and the type of stainless steel used is S30400. Type 304 is a variation of base class 18-8, type302, with higher levels of chromium and lower carbon. Low carbon minimizes the precipitation of chromium carbide due to its welding and its susceptibility to granular corrosion (Askeland, 2010) and (Callister and Rethwisch, 2010). Thickness of 304 stainless steel between 0.025 to 6.35 mm and width up to 1219 mm. AMS 5513 design specifications; ASTM A240; ASTM A666.

4. CONCLUSION

Prototype *kue balok* baking tool is Ergonomic and ECSHE (effective, convenient, safe, healthy, and efficient) fueled by charcoal, portable, and easy to carry.

5. ACKNOWLEDGEMENT

The Author wish to acknowledge the support of LPPM Itenas Bandung in enabling the production of this research.

6. REFERENCES

- Ashby, M., Shercliff, H. and Cebon, D (2007), "*Materials, Engineering, Science, Processing and Design*", Published by Elsevier Ltd., UK, pp. 1-500.
- Askeland, D.R., Fulay, P.P., and Wright, W.J. (2010), "*The Science and Engineering of Mterials*", Cengage Learning, 200 First Stamford Place, Suite 400, Stamford, CT 06902, USA, Sixth Edition, pp 1-900.



- Budynas, R.G. And J Keith Nisbett, J.K, (2006), “*Shigley’s Mechanical Engineering Design*”, 8th Edition in SI Units, The Mc Graw-Hill Companies, Inc. pp. 71-118.
- CRAIG, JR, R.R (2011), “*MECHANICS OF MATERIAL*”, John Wiley & Sons, Inc., USA, Third Edition, pp.22-61
- Callister, Jr. W.D. and Rethwish, D.G.(2010), “Material Science and Engineering-An Introduction”, Eighth Edition, Jphn Willey &Son, Inc. River Street, Hoboken, NJ. Pp. 1-800
- Khurmi, R.S, and Gupta, J.K.(2005), “A Text Book of Machine Design”, Eurasia Publishing House, Ram Nagar, New Delhi, 14th Revised Edition, pp.281-676.
- Lawrence Gyansah, Design, Construction and Modeling of a Mechanical Portable Barbecue Machine, globaljournals.org/GJRE_Volume12/5 (2012)
- Liansari, G.P., Novirani, D., Rifqi Nanda S. 2016, “Design *Blueprint* Ergonomic Kue Balok Mold Tool Using *Ergonomic Function Deployment* (EFD)” in: Jurnal Rekayasa Sistem Industri Vol.5 no 2 Universitas Khatolik Parahyangan Bandung, Indonesia.
- Novirani, D., Liansari, G.P., 2016, “Design *Prototype* Ergonomic Kue Balok Mold Tool Using *Ergonomic Function Deployment* (EFD)” in: Proceeding of The role of engineering and design in the acceleration of national sustainable development, 2016 Bandung, 30 November, Indonesia.
- OSHA. 2000. Ergonomics: The Study of Work. U.S. Department of Labour.
- Omura, G (2010), “*Mastering AutoCAD 2011 and AutoCad LT 201*” Wiley Publishing, Inc., Indianapolis, Indiana, pp. 4-911
- Ullman, D.G. (2010), “The Mechanical Design Process”, Published by McGraw-Hill, A business unit of The McGraw-Hill Companies, Inc., 1221 Avenue of the Americas, New York, NY 10020, Four Edition, pp81-91



15th International Conference on Quality in Research (QIR 2017)

NEUROMARKETING EVALUATION OF ONLINE SHOP ADVERTISEMENT USING ELECTROENCEPHALOGRAM (EEG)

Danu Hadi Syaifullah^{a1}, Maya Arlini Puspasari^b, Timotius Alfin^c

^{a,b,c} *Department of Industrial Engineering
Faculty of Engineering – University of Indonesia, Depok 16424
Tel: (021) 78888805. Fax: (021) 78885656*

ABSTRACT

Indonesia has a very strong growth as an online shop market. Big market growth at Indonesia makes there are many online shops join and operate at Indonesia. To gain the market, online shop in Indonesia was doing so many marketing activities; one of them is through Youtube channel. Using Youtube channel as marketing channel means using video as the content. Before using video as marketing content, developer needs to know characteristics of online shop advertisement which can attract the viewer. In this research, writer evaluates online shop advertisement based on cognitive and emotional response of viewer. The methods of this research are Frontal Alpha Asymmetry Analysis (FAA) and Positive and Negative Affect Scale (PANAS) questionnaire. Frontal Alpha Asymmetry Analysis using data from electroencephalogram of response of respondent while watching advertising video. Based on result of this research, there are several characteristics of online shop advertising video that affect and did not attract viewers significantly.

Keywords: Frontal Alpha Asymmetry (FAA), Electroencephalogram (EEG), Neuromarketing, Positive and Negative Affect Scale (PANAS), Digital Marketing

* Corresponding author.
danu_syaifullah@yahoo.co.id



1. INTRODUCTION

Based on the survey from McKinsey, internet users in Indonesia who have ever shopped online was only about 7%. That opportunity makes many online shops join to Indonesian market. Data from Minister of Communication shows that online transaction in Indonesia at 2013 was up to 130 trillion Rupiah. Moreover, based on data from TBI 2016 (*Top Brand Index*), OLX, Lazada, and Tokopedia is the top three of *online shop* which well known by internet users. OLX is at the first place with 44.5 percent, followed by Lazada with 19.9 percent, and the third place is filled by Tokopedia with 12.1 percent.

To gain their users, online shops use variance of marketing strategies such as poster, promotion, and advertisement. Nowadays, advertising in Youtube channel has been widely used by online shop as their marketing strategies. By using Youtube channel, online shop needs to make their video advertisement. But, not every Youtube advertisement will be succeed to effectively gain viewers interest. Therefore, we need to evaluate characteristics of online shop advertisement that will gain viewers interest. One of the methods to evaluate advertisement is using neuromarketing.

For this research, we aim to know the characteristics of online shop advertisement that will be interesting to viewers based on cognitive and emotional aspects by using electroencephalogram (EEG).

2. METHODOLOGY/ EXPERIMENTAL

a) Participants

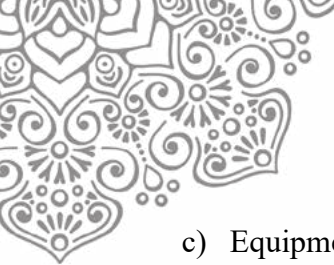
This research involves 30 participants (15 male and 15 female) with age 18-25 years old. Participant is right-handed and never seen the stimuli before.

b) Stimuli

A stimulus for this research is online shop advertisement with duration within 2.5 to 3 minutes. Video advertisement that been used is video from Lazada, Tokopedia, and OLX. Table 1 describes the object for more detail.

Table 1 Research Object

No.	Perusahaan	Part 1: Emotional Part	Part 2: Product Description	Part 3: Logo
1	Tokopedia	Sad	N/A	With Animation
2	Lazada	Happy	Implicit Description	N/A
3	OLX	Scared	Explicit Description	Without Animation



c) Equipment

Equipment that has been used is Electroencephalogram (EEG) Emotiv EPOC+, computer, earphone, software Emotiv EPOC Test Bench, software VLC video player, and PANAS (*Positive and Negative Affect Scale*) questionnaire.



Figure 1. Emotiv EPOC+

d) Variable

In this research, the variables are:

- Independent Variable is variable that had been changed to know the response at dependent variable. Independent variable in this research is combination of each part of video advertising for the stimuli.
- Dependent Variable is variable that has been measured as the response of changes of independent variables. In this research, dependent variable is measured by Relative Power Ratio (RPR) for frontal lobe of brain to represent viewers' interest in the stimuli.

e) Recording and Analysis

EEG recording was done during the video advertising for each online shop. Sequence of the play decided randomly by random number. For each video changeover, participant told to be relaxed and closed their eyes for 60 seconds. Before EEG recordings, EEG was applied to participant head until every marker show a green signal at Emotiv EPOC Test Bench software. Green signal means that brain wave for that channel has already recorded by EEG. In this research, recording focus on six points which are Fp1, F3, F7, Fp2, F4, and F8. This point is based on Frontal Alpha Asymmetry (FAA) which only measures the difference of alpha wave between frontal left lobe and frontal right lobe. Based on FAA model, left frontal lobe activities related to positive emotion which caused by interest while right frontal lobe activities related to negative emotion which caused by disinterest (Chai et al., 2014). The point of EEG can be seen at Figure 2.

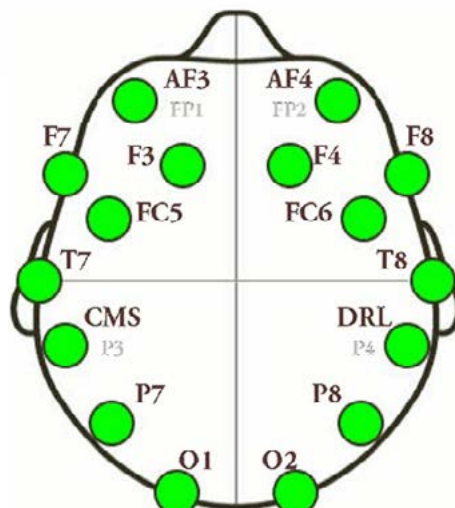


Figure 2. EEG Emotiv EPOC+ Channels

f) Data Processing

Steps of EEG data processing are:

1. Pre-Processing (Band Pass Filter)

First step of EEG data processing is Band Pass Filter to eliminate data outliers which have the frequencies outside human brain frequencies range. Human brain frequency is between 0 to 30 Hz. Therefore recorded data with frequency above 30 Hz was eliminated.

2. Signal Decomposition (Fast Fourier Transform)

Next step of process is signal decomposition which is to separate brain wave depend on the frequencies category. Based on the frequencies, brain wave can be categorized into four types which are, alpha (7.5-13 Hz), beta (14-30 Hz), delta (0-3 Hz), and theta (3,5-7,5 Hz). In this research, only the alpha will be used for analysis.

3. Power Spectral Density

Then, based on the frequencies, power of wave is measured and called Power Spectral Density.

4. Relative Power Ratio

Since we know the Power Spectral Density, the last step is to convert Power Spectral Density into Relative Power Ratio (RPR) value. The value will be a ratio and will be used for analysis.

Relative Power Ratio data that will be used is RPR data for AF3, AF4, F3, F4, F7, and F8. The six points that stated above is part of frontal lobe EEG.



3. RESULTS AND DISCUSSION

Here is the result of this research:

a) Comparison of Total RPR for each video

Based on ANOVA, between total RPR of the three video, there are significant difference ($p\text{-value} \leq 0.05 = 0.000$). The difference occurs between first video and third video and also second video and third video. From these result, we can know that overall, video advertising by Tokopedia and Lazada is more interesting to viewers than video of OLX.

b) Comparison of RPR for Video Part 1

Based on ANOVA, between RPR for video part 1, there is no significant difference ($p\text{-value} \geq 0.05 = 0.356$). It means that there is no difference between three video for part 1 with confidence interval 95%.

c) Comparison of RPR for Video Part 2

Based on ANOVA, between RPR for video part 2, there is significant difference ($p\text{-value} \leq 0.05 = 0.000$). The difference occurs between second video and third video. It shows that with confidence interval 95%, there are differences between part 2 of the second and the third video.

d) Comparison of RPR for Video Part 3

Based on ANOVA, between RPR for video part 3, there is no significant difference ($p\text{-value} \geq 0.05 = 0.272$). It means that there is no difference between part 3 of the first video and the third video.

e) RPR Plot for each Video

To know the trend of RPR value during the video advertisement, RPR plot of Video was made. The higher difference between left frontal RPR value than right frontal RPR value means that participant had interest in the stimuli, and vice versa. The RPR plots for all three video advertisements are given as follow:

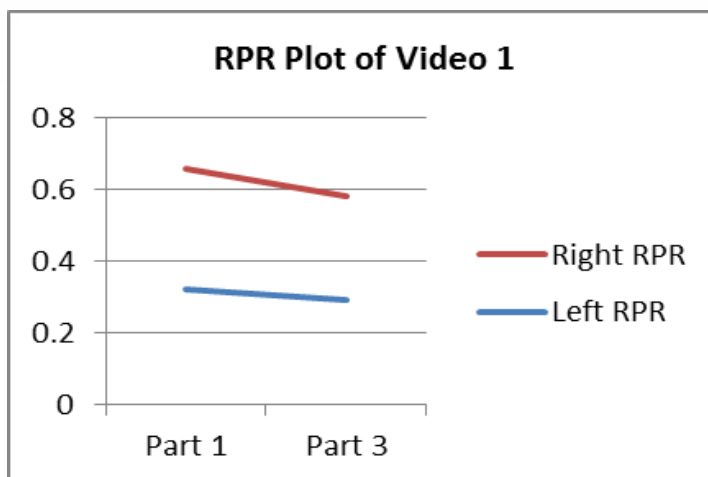


Figure 3. RPR Plot of Video 1

From Figure 3, RPR value for frontal right lobe always higher than for frontal left lobe. It happened for part 1 and part 3 of first video.

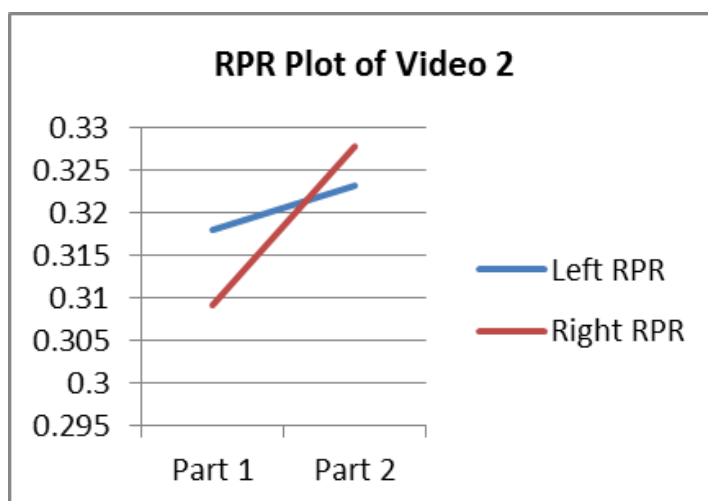


Figure 4. RPR Plot of Video 2

From Figure 4, RPR value for frontal left lobe is higher than for frontal right lobe for part 1 of second video. Otherwise, for part 2 of second video, RPR value for frontal right lobe is higher than for frontal left lobe.

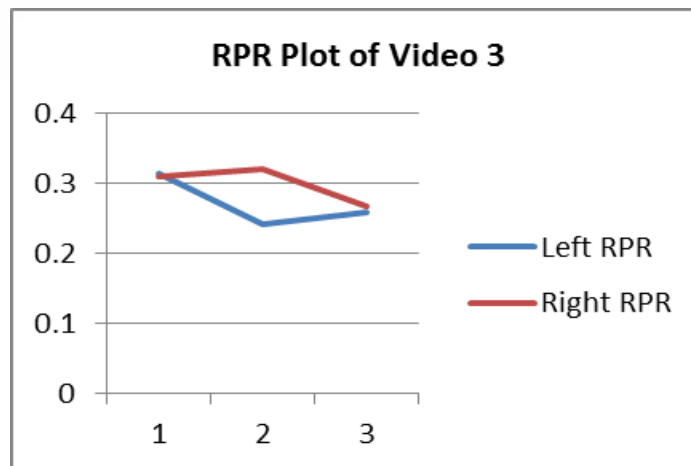


Figure 5. RPR Plot of Video 3

From Figure 5, RPR value for frontal left lobe is higher than for frontal right lobe for part 1 of third video. Otherwise, for part 2 and 3 of third video, RPR value for frontal right lobe is higher than for frontal left lobe.

f) Comparison of PANAS questionnaire

PANAS Questionnaire is counted by decreasing negative value from positive value of the questionnaire. Based on the result with Friedman test, there is significant difference between all video ($p\text{-value} \leq 0.05 = 0.000$). Difference occur between first video and third video, and also second vide and third video. Based on PANAS Questionnaire compared to RPR data with FAA method, it can be seen that both tests show the same results with earlier research (Ohme, Reykowska, Wiener, & Choromanska, 2010), so can be said that Frontal alpha asymmetry method can be used to measure customers interest toward some marketing activities.

4. CONCLUSION

Due to time limitation, video advertisement used for research object is only one for each emotion (sad, happy and scared). Nevertheless, based on the research, we can conclude that based on RPR value with FAA method, different approach in emotional part of advertising video (sad, happy, and scared) is not affect significantly to viewer's interest in Indonesia while watching the advertisement for the first time.

Then, based on RPR value with FAA method, different approach in product description part of advertising video (implicitly and explicitly) affect significantly. Implicit products description brings more interest for the viewers than explicit product description to viewer's interest in Indonesia while watching the advertisement for the first time.

For the next part, based on RPR value with FAA method, different approach in logo part of advertising video (with animation and without animation) is not affect significantly to viewer's interest in Indonesia while watching the advertisement for the first time.



Overall, based on RPR value with FAA method, online shop video advertisement from Lazada dan Tokopedia bring more interest than video advertisement from OLX.

Last, generally based on RPR Plot, interest of viewers tend to be declined when they saw product description and logo part of video advertisement.

6. REFERENCES

- Andrejevic, M. (2012). Brain Whisperers: Cutting through the Clutter with Neuromarketing. *Somatechnics*, 2(2), 198–215.
- Blakeslee, S. (2004). If you have a buy-button in your brain, what pushes it? *The New York Times*.
- Chai, J., Ge, Y., Liu, Y., Li, W., Zhou, L., Yao, L., & Sun, X. (2014). Application of Frontal EEG Asymmetry to User Experience Research Application of Frontal EEG Asymmetry to User Experience Research.
- Drewniany, B. L., Jewler, A. J., Bingham, L., Sandberg, K., & Perry, J. (2008). *Creative Strategy in Advertising*. Thomson Learning Academic Resource Center (9th ed.).
- Fugate, D. L. (2014). Neuromarketing: a layman's look at neuroscience and its potential application to marketing practice. *Journal of Consumer Marketing Iss Journal of Consumer Marketing Journal of Consumer Marketing Sons Canada Journal of Consumer Marketing*, 2499(4), 385–394.
- Maria, Z. M. (2009). Neuromarketing – Getting Inside The Customer's Mind, *Pop Ciprian-Marcel*, (1), 804–807.
- Ohme, R., Reykowska, D., Wiener, D., & Choromanska, A. (2010). Application of frontal EEG asymmetry to advertising research. *Journal of Economic Psychology*, 31(5), 785–793.
- Pamplona, C. I. O. A. (2014). Neuromarketing : insightful, but not mind reading, 93–112.



THE 15th INTERNATIONAL CONFERENCE ON QUALITY IN RESEARCH (QIR 2017)

RISK MANAGEMENT OF NEW PRODUCT DEVELOPMENT PROCESS ON FOOTWEAR INDUSTRY IN INDONESIA. CASE STUDY : PT BRODO GANESHA INDONESIA

Amalia Suzianti^a, Priandra Aditya Wattimena^b, Rheinanda Kaniawari^{a,b,*}

^{a,b}*Laboratorium Pengembangan Produk dan Inovasi Departemen Teknik Industri, Fakultas Teknik, Universitas Indonesia, Kampus Baru UI Depok 16424, Indonesia*

ABSTRACT

Footwear industry has been one of the Indonesian government's concern in order to enhance the nation's economy. Each year, the footwear industry's economic value is increasing and significantly contributing to the national non-mineral export. This indicates that Indonesia has a great opportunity to further enhance its footwear global market share. However, due to the significant growth of the global market demand, the number of competitors in the footwear global industry are also increasing with China as the market greatest influencer. Hence, to compete in the global footwear industry, Indonesian business owners have to increase their competitiveness level. This research is focused on the risk management that might arise during the developing process of a new product in the footwear industry, to increase the competitiveness level of Indonesian footwear industry. Using PT Brodo Ganesha Indonesia as a study case. The method used for the research is House of Risk, a new method adopted from the Failure Mode Effect Analysis and House of Quality methods. The method is not only showing the possibility of risks that might arise, but also focused on giving a proactive strategy to mitigate the identified risk. The outcome of this research is the list of risks that found in the developing process of a new product and the strategy to mitigate those risks involved. This research is designed for footwear industry's business owners as a benchmark for their product development process to make it more efficient.

Keywords: House of Risk; Risk Management; New Product Development; Footwear Industry; PT Brodo Ganesha Indonesia

1. INTRODUCTION

Footwear industry is one of the industrial sectors that has a considerable contribution to the Indonesia's exports level. Based on the report from Ministry of Industry of Republic Indonesia, in 2014, the footwear product's exports rate accounts for 2.9% and has a tendency to keep increasing. In addition, since 2010 until 2015 the trade value also increased with the average increasing rate of 37.3 trillion Rupiahs. Beside that, Ministry of Industry of Republic Indonesia also reveals



that the industry of footwear has a great contribution for the absorption of the labor. By 2015, it had reached the total number of 643,000,000 local labors.

Although the needs of the global market tend to increase towards footwear products, the competition between producing countries in this sector is also increasing. Based on the report of APICCAPS (Associação Portuguesa dos Industriais de Calçado, Componentes, Artigos de Pele e seus Sucedâneos), a footwear association based in Portugal, in 2012, China has the largest export market share with the number of 38%. While Indonesia only has 3% export market share, after China, Italy, Germany, Viet Nam, Hong Kong and Belgium.

Footwear industry is a part of fashion industry that identically has a short period of trend changing, which is opposite to the common product-based industrial market with a short product life cycle, high level of volatility, unpredictable and frequent purchases without planning (Bandinelli et al., 2011).

Study by Cornell University (2010) revealed that in general, fashion product has a relatively short product life cycle. The cycle starts during the product's launch, this graph will keep on rising due to an additional number of consumers adopting the current style or a trend, and when most customers leave, this cycle will end. The life cycle of fashion product has a steep degression slope after the product reaches the highest point of sale. Therefore, the producer of fashion products should continuously develop new products in order to keep up with the short life cycle of fashion product, which increases the risk of the development process.

In order to respond to the risks that might occur in the process and the activity of business, some models had been developed to perform risk assessment and designing several strategies to mitigate those risks. In 2002, Preston developed a risk management model for product development by using five steps of the risk handling, start from identification stage until monitor risk stage. Then, in 2008 Segismundo and Miguel developed a model of risk management of the development of new automotive products by using the FMEA (Failure Mode Effect Analysis) approach. This model aims to calculate the Risk Potential Number (RPN) which is the result of the multiplication of the level of Severity (S), Occurrence (O) and the level of ease of the Detectability of risk (D).

One of the latest models in risk management is the House of Risk (HOR). This model has a specialization in conducting preventive actions which combines the FMEA and the House of Quality method to quantify the risks (Pujawan and Geraldin, 2009). HOR model provides the company a risk priority that should be addressed and also strategy recommendation along with the effectiveness level of the strategy to mitigate the risk. HOR method is once applied in the supply chain risk management at the fertilizer company and also in the risk management of new product development at hijab product company in Indonesia.

This study will use the HOR method to quantify risks in the footwear industry in Indonesia. A study case on PT Brodo Ganesha Indonesia (PT BGI) will be used to show the pattern of footwear consumption in the Indonesian Market. Critical risk points and stages would be analysed with its impacts, priorities, and mitigation strategies.



2. METHODOLOGY/ EXPERIMENTAL

The risk of the developing process of new products can be distinguished into two categories, the internal risk and the external risk. The internal risk consists of operational, technology and organization risks. Operational risk is the risk that may occur in the inefficient process on business activity of company such as production activity, labor distribution, etcetera. Technology risk is the risk associated with internal technology capabilities such as the ability to use new technology, science acquisition capabilities in responding to the development of technology as well as the ability of facing the external technology. The Organization risk is the risk associated with the system as well as organizational management strategy such as the response to the changing of structure, changing between project team's member, etcetera. While the external risk consists of the market risk and the provider or supplier risk. Market risk is the risk associated with market dynamic such as the ability to respond to the demand changing and the knowledge of the competitor. Supplier risk is the risks that may occur associated with supplier capabilities such as the reliability of the supplier and also the production cost of the vendor (Park, 2010).

The HOR method is used to analyze the risk that might happen in the developing process of a new product at PT BGI and obtain the strategy needed to mitigate the risk, it consists of two models, namely HOR 1 and 2. HOR 1 is used to identify the risk that might occur in the process, while the HOR 2 is used to create mitigation strategy in order to overcome the risk. For HOR 1, the data taken for this research is the process data for a new product development, along with the steps adopted by PT BGI, risk event in each step, and the causes of the risk (risk agent), the rate of severity, the rate of incidence (occurrence) and the correlation. For HOR 2, the strategy will be obtained by assessing the difficulty level and also the total effectivity. This method is emphasizing the determination and the mitigation of risk agent as the cause of the risks that are identified.

On HOR1 quantification is done by calculating the Aggregate Risk Potential (ARP). The calculation of the ARP value considers the severity factor as the driving factor for the risk event and the level of occurrence as the driving factor of risk agent.

The first stage of the HOR1 is the risk identification with interview and brainstorming methods with several members of the internal management at PT BGI. The members are the Chairman of the Company, the head of Marketing Department, the head of Supply and Operation Department of, the head of Product Development Departement, and also the head of the Finance Department. The output that will be obtained from this step is a complete the elaboration about the developing process of new products at PT BGI and also the risk event as well as the risk agent.

The next stage is to determine the severity level, occurrence level and also the correlation of risk and event risk agents which had been identified earlier. The scale criteria for higher severity and occurrence level is adjusted to the actual condition of the company. Table 1 and Table 2 elaborate the scale used to measure the level of severity and occurrence



Tabel 1. PT BGI Severity Scale

Rank	Criteria	Financial (million Rupiahs)	Production Delay (days)	Company Image/ Negative Publicity Scope
1	Insignificant	< 15	< 7	Internal company
2	Minor	15 - 30	7 - 13	Internal and External
3	Moderate	45 - 60	14 - 29	Local media
4	Major	60 - 75	30 - 60	National media
5	Catastrophe	>75	> 60	National media with law suits

After the severity and occurrence level is identified the next stage is to calculate the ARP value for each risk agents. The succeeding is the calculation for the ARP:

$$ARP_j = O_j \sum_i S_i R_{ij}$$

Severity (S) multiplied with the degree of correlation between risk agent and risk event. In general, risk agent can cause more than one risk event, so the multiplication and the degree of severity of the correlation (R) should be summed up, then the sum will be multiplied with the level of occurrence (O) from risk agent. After the ARP is gained, sort the risk agents from the largest to smallest, based on the ARP value, the aim is to acknowledge the risk that has greatest impact. The risk agents should be sorted using the pareto principle or the 80:20.

Tabel 2. PT BGI Occurrence Scale

<i>Scale</i>	<i>Level of Occurrence</i>	<i>Description</i>
1	Never Occur	0
2	Very Minimum Occurrence	Happening Once
3	Rare Occurrence	Happening once in every 5 year
4	Minor	Happening once every 3 year
5	Moderate	Happening once in every year
6	Significant	Happening once in every 6 month
7	Major	Happening once in every 3 month
8	Extreme	Happening once in every month
9	Serious	Happening once in every week
10	Very Dangerous	Happening almost everyday

Risk agents are sorted so that the company can put their main focus on the potential risk agent, which has the biggest ARP value. Once ARP is calculated and the rule of 80:20 applied, 10 risk agents will be gained as shown in table 3.



After the risk agent is determined, the next step is to establish the mitigation strategy to confront the risk agent. The strategy is designed based on the study of literature and interview with those who expertise in specific area such as marketing, information system, etcetera.

The determination of strategy is the first step of HOR 2 process, and after that, the strategy will be quantified by looking at the difficulty level, the level of effectiveness and its impact on each risk agent.

Quantification of strategy is done by looking at the difficulty level by establishing the scale level of difficulty which can only be applied to a particular company due to the adjustment that made based on the actual condition of the company. The level of difficulty of HOR 2 are described in table 4, and for the scale level of effectiveness are described in table 5.

Tabel 3. PT BGI Difficulty Scale

Scale	Name	Financial	Labor Needed
1	Very Easy	Cost needed < 20.000.000	Labor workforce < 3 people
2	Easy	Cost needed > 20.000.000 and < 30.000.000	Labor workforce between > 3 people and < 6 people
3	Moderate	Cost needed > 30.000.000 and < 40.000.000	Labor workforce between > 6 people and < 9 people
4	Hard	Cost needed > 40.000.000 dan < 50.000.000	Labor workforce between > 9 people and < 12 people
5	Very Hard	Cost needed > 50.000.000	Labor workforce > 12 people

Tabel 4. PT BGI Effectivity Scale

Scale	Name	Description
0	Has no effect	Doesn't reduce the risk agent occurrence
1	Slightly impactful	Reduce the risk agent occurrence level to 3 level (1-3 level)
3	Impactful	Reduce the risk agent occurrence level to 6 level (4-6 level)



9	Have a big impact	Reduce the risk agent occurrence level to 9 level (7-9 level)
---	-------------------	---

Once difficulty level and the level of effectiveness are determined from the strategy, the next step is to calculate the rate of effectiveness in the risk handling (TE) by multiplying the ARP from the risk agent with their level of effectiveness (E) in the risk agent handling. The succeeding is the calculation for the level of effectiveness against the strategy:

$$TE_k = \sum_j ARP_j E_{jk}$$

After the level of effectiveness in the risk agent is determined, the ratio is then calculated with the difficulty level (Dk), the succeeding is the calculation for the rate of effectiveness ratio with the difficulty level (EtD):

$$ETD_k = \frac{TE_k}{Dk}$$

After the EtD is determined, the strategies are then sorted by using the biggest EtD value rule, the biggest one means having the highest effectivity rate. The result of this value will be a reference for the company to carry out the strategy in order to mitigate the risk agent that been identified.

3. RESULTS AND DISCUSSION

(The HOR method presents two different type of results that contain in HOR 1 and HOR 2)

HOR 1

HOR 1 produced the list of risk agent along with the ARP value that became the basis for the level of impact for the developing process of a new product. The ARP value and the list of risk priority are described in Table 6. While Table 7 describes risk agent that became a priority. On HOR 1, the data shows that the biggest risk is the risk of the organization and in the developing process of a new product, the biggest risk is located in the process of idea generation, prototyping and design.

Tabel 5. Identified Risk Agent With Its ERP Value

Rank	Risk Agents	Code	ARP
1	Poor Information System	A04	1848
2	Miscommunication	A16	1824
3	Poor working procedure	A07	1728
4	Poor designers' coordination	A05	1239



5	Dynamic market change	A01	1188
6	Wrong customer preferences prediction	A19	984
7	Human Error	A06	910
8	Technology Development	A10	724
9	Supplier doesn't fulfill the agreement	A08	690
10	Poor facility	A02	648
11	There is no brand guideline	A03	558
12	A lack of quality control	A15	441
13	No demand forecasting	A14	324
14	Delayed material delivery	A17	252
15	Supplier doesn't recognize the material specification	A22	216
16	Change of supplier	A13	198
17	Vendor has a minimum quantity policy	A20	189
18	High dependency towards one supplier	A09	72
19	The fluctuation of currency	A11	36
20	Supplier doesn't understand the design direction	A18	27
21	Supplier and vendor bankrupt	A21	12
22	There is no project manager	A12	10

Tabel 6. Risk Agent Priorities

Rank	Risk Agents	Code
1	Poor Information system	A04
2	Miscommunication within the internal environment of the company	A07
3	Poor working procedure	A07
4	Poor designers' coordination	A05
5	Dynamic market change	A01
6	Wrong customer preferences prediction	A19
7	Human Error	A06
8	Technology Development	A10
9	Supplier doesn't fulfill the agreement	A08
10	Poor facility	A02



HOR 2

The final result of the HOR 2 is the list of mitigation strategy along with their managing priority. Table 7 shows the list of mitigation strategy along with the list of priority and EtD Value. Table 8 describes the name of mitigation strategy.

Table 7. Value of EtD for Each Stratgy

Priority	Code	Tek	Dk	ETD
1	PA2	30019	1	30019
2	PA1	23823	3	7941
3	PA3	14592	4	7296
4	PA9	27450	4	6851
5	PA5	22647	4	5662
6	PA4	14368	3	4789
7	PA8	11919	3	3973
8	PA6	2070	1	2070
9	PA7	5832	5	1166

Tabel 8. Generated Strategy

Priority	Code	Strategy
1	PA2	Conduct a team building activity
2	PA3	Conduct a customer preference analysis
3	PA9	Using a specific project manager for each project
4	PA5	Develop an ERP system
5	PA4	Market Monitoring
6	PA8	External training
7	PA6	Develop a partnership with various vendor
8	PA7	Build a supporting facility
9	PA1	Conduct a job analysis

4. CONCLUSION

The results from this research are the risks obtained from the developing process of a new product at PT BGI along with the strategy to mitigate those risks. In the developing process of a new product at PT BGI, there are 23 risk events and



22 risk agents which can obstruct and causing a short term as well as long term financial loss. To identify the risk properly, an analysis of the risk and its risk agent is needed. Risk Agent is the main attribute in risk handling. There are 10 risks that assumed as the risk agents that must be dealt with. 12 other risk agents assumed don't give a significant impact so it is not considered in this study. The 10 risk agents are:

- a) Poor Information System
- b) Miscommunication within the internal environment of the company
- c) Poor working procedure
- d) Poor designer' coordination
- e) The dynamic market change
- f) Wrong customer preference prediction
- g) Human error
- h) Technology Development
- i) Suppliers who doesn't fulfill the agreement
- j) Poor facility

In the developing process of a new product at PT BGI, the most risky stage is at the stage of Idea Generation, Design and Prototyping with 10 risk agents for each one of the risk. While the low-risk process is the stage of production. Risk category that has most impact on the developing process of a new product at PT BGI is the category of organizational risk while the risk category that has the least impact is the category of operational risk. There are nine risk mitigation strategies in the developing process of a new product at PT BGI. Nine of these strategies are:

- a) Conduct team building activity
- b) Conduct job analysis
- c) Conduct customer preferences analysis
- d) Using a specific project manager for each project
- e) Develop an ERP system.
- f) Market monitoring
- g) External training
- h) Develop a partnership with various vendor
- i) Build a supporting facility

6. REFERENCES

- Agaugol, M., Yurtkoru, E. (2015). The effect of ERP implementation CSFs on business performance: an empirical study on users' perception. *Procedia Social and Behavioral Science* 210, 35 - 42.
- Bandinelli, R. Rinaldi, R. Rossi, M. Terzi, S. (2013). New product development in the fashion industry: an empirical investigation of italian firms. *Journal International of Engineering Business Management*. Vol.5, pp.1-9.
- Dyah, D. Bambang, S. Eka, N. (2015). Risk management in new product development process for fashion industry : Case study in hijab industry. *Procedia Manufacturing* 4, 383 – 391.



- Kim, J. Park, S. (2011). A risk management system framework for new product development (NPD). *International Conference on Economics and Finance Research*. Vol.4, pp.51-56.
- Kenneth, K. (2013). *The PDMA Handbook of Product Development*. John Wiley & Sons : New Jersey
- Kementrian Perindustrian RI (2015). Nilai Ekspor Indonesia
- Mohamed, B. Robert, K. Alison, O. Josef, O. (2014). Analysis of the effect of risk management practices on the performance of new product development programs. *Technovation* 34 441–453
- Park, Y.H. (2010). A study of risk management and performance measures on new product development. *Asian Journal on Quality*, Vol. 11 Iss 1 pp. 39 - 45
- Prein, P. Goodstein, L. Goodstein, L. Gamble, J. (2009). *A Practical Guide to Job Analysis*. Pfeiffer Publishing : San Fransisco.
- Pritchard, C. (2015). *Risk Management : Concept and Guidance*. CRC Press Taylor and Francis Group : New York.
- Pujawan, N. Geraldine, L. (2009). House of risk: A Model for Proactive Supply Chain Risk Management. *Business Process Management Journal* Vol. 15 No. 6, pp. 953-967
- Reed, J. Leavengood, S. (2002). Pareto Analysis and Check Sheet”, *Performance Excellence in Wood Products Industry Statistical Process Control*. EM 8771
- Segismundo, A. Paulo, M. (2008), "Failure mode and effects analysis (FMEA) in the context of risk management in new product development", *International Journal of Quality & Reliability Management*, Vol. 25 Iss 9 pp. 899 - 912
- Syvantek, J. Gard, J. Goodman, J. Benz, J. (1999). The Relationship Between Organizational Characteristic and Team Building Success. *Journal of Business and Psychology* Vol. 4 (265-283)



DESIGNING USER INTERFACE OF MOBILE APPLICATION FOR MONITORING CHILDREN'S HEALTH AND DEVELOPMENT FROM USER AND PEDIATRICIAN PERSPECTIVES

Amalia Suzianti, Shabila Anjani, Hatara Trirama, Tesar Dayansyah and Alviana Alicia Syafinal

*Laboratorium Product Development and Innovation, Departemen Teknik Industri, Fakultas Teknik, Universitas Indonesia
Depok 16424, Indonesia*

Abstract

The quality issues of infant's health in Indonesia are reflected in the number of infant's death that are still quite high compared to other countries in ASEAN. In order to solve this problem, creating a powerful information systems is an important component in improving the quality of health services. A strong and trusted information system can be built by making a mobile app which could be a source of health information and connecting parents with the pediatrician. Methods that are used in this research are analysis of persona, card sorting, conjoint analysis, and system usability scale. The research begins by identifying problems as well as the features and sub-features, obtained through questionnaires and interviews. Based on the questionnaire results, each persona will be identified by looking at the behavior and features needed by the pediatrician on the mobile app. Open-ended question was conducted to ensure the needs of the features and the results were used as the reference in generating the information architecture and application flow diagrams. Next step, conjoint analysis method is used to find the mobile app's main page design that suits the pediatrician. Last, usability testing using Retrospective Think Aloud method. The output of this research is a mobile app that is capable of improving health care services by connecting the parents to the pediatrician and help to ease the pediatrician work.

Keywords: Healthcare Mobile Application, Persona, Conjoint Analysis, Retrospective Think Aloud, System Usability Scale

1. Introduction

Indonesia's next generation, especially infants under three years old, still faces many problems on the health aspects. This is reflected on the number of deaths in Indonesia's infants, which is still relatively high. Based on the CIA The World Fact Book (2014), there are at least 25 infants die out of every 1000 infants in Indonesia. Obviously, this does not reflect the quality of the health of the future generation. Moreover, if we compare the number of infant's death in Indonesia with large numbers of infant's death in Singapore or Thailand, the number of infants' death in Singapore and Thailand is only 3 and 10 deaths out of 1000 infants respectively. Among other countries in ASEAN, Indonesia is still on the bottom of the list along with Laos, Cambodia, Myanmar and Timor Leste. Therefore, it is highly important for Indonesia to improve the quality of children's health. In 2012, The United Nations Children's Fund, or commonly known as UNICEF, published a study summary Maternal and Child Health Indonesia (2012), which contains five recommendations to improve the quality of maternal and child health in UNICEF:

1. The development and implementation of standards and guidelines for health services by the Central Government.
2. Private health services should also be included in the Government's health policies and frameworks.
3. Increase the number of health facilities that provide services PONEK (Services Comprehensive Emergency Obstetric Neonatal)
4. Increasing resources in developing and motivating health workers.
5. Creating a powerful information systems as one important component in improving the quality of health services.



From the industrial engineering's perspective, this study will focus on the fifth point which is creating a powerful information systems as one important component in improving the quality of health care. Related to this, referring to eMarketer (2014), there is a very significant increase in the number of smartphone users in Indonesia. Indonesia is one of the countries that have the largest growth, under China, India, and the United States. In addition, in 2018 Indonesia will have 103 million smartphone users and will be the fourth-largest country with smartphone users. Adobe's Inspire Magazine (Klein, 2012) did a comparative analysis of the mobile app and mobile web based on three aspects, namely:

- Business Consideration
- Development Consideration
- Performance Consideration

Based on business considerations, the user tends to download the mobile app to do activities very closely with their lives and routine. Users can have better user experience with mobile apps compared to the website. However, the development of the mobile app require larger funds compared to the website. Based on the consideration on the development, the mobile app has a more complicated process as well as the limitations due to the differences of the operating system and the size of the gadget. Therefore, the time required for the development of mobile app tends to be longer if compared to the mobile web. Based on consideration of the performance, the mobile web has a step of update and maintenance more simple and direct. mobile web is also easier to find using a search engine. Therefore, it is advisable to provide a link on the official website mobile app so that the mobile app can be found easier by the user. Despite of some weaknesses, mobile app can be used offline and thus, this study focuses on the development of mobile application for monitoring children's health and development.

2. Literature Study

There are 2 interfaces applied in this paper, 1 for pediatrician and the other for the user. It comes from different experiments, which is why there are different methods and flow process chart.

2.1 Persona Identification

When a mobile app developers want to design an application and want to identify what are the functions that can be done with a mobile app, then he had to learn like What is a user, how users think, and how they make decisions. This is necessary so that the mobile app is able to function properly in accordance with user needs. This phase is known for the manufacture of the user's persona. Cooper (1999) explains that the persona is a fictional character created to describe the types of users in the target demographic would use a site or product. Persona is the characteristics of which are assumed to be the basic behavior and needs of users that can be used as consideration when the developer will develop scenarios for conceptualizing a site (Wong et al., 2012). Persona is used to study the behavior, mindset, lifestyle, ambitions, motivations, aspirations, product usage, age, education, and much more. Persona serves to study the behavior, mindset, needs, lifestyle, ambitions, motivation, aspirations, product use, age, education, and much more. In the use of smartphones, the person's behavior can be examined from their motivation in using existing media on Smartphones. According to the Seyring, Dornberger (2009) there are 4 aspects which can motivate someone to use media:

- Surveillance i.e. for information retrieval.
- Personal Identity i.e. the search for reference and strengthening identity.
- Personal Relationship that is to communicate.
- Diversion to escape from the routine and problem.

2.2 Generating Information Architecture and Application Flow Diagram Using Card Sorting Method

In designing a mobile app, the navigation structure and organization is a factor that affects the convenience of mobile app to be able to understand how it is used by the user. Therefore, it is important to have a good information architecture, and it can be achieved through structural design of mobile app based methods that can understand the mindset of the user. Card sorting is a research method that uses input from users in helping to generate the navigation structure and effective organization. The advantage of this method is that this method can be used directly to mobile app users, which would make the output from this method better reflects the mindset and personality of the user.

2.3 Determining Mobile App's Home Page Design Using Conjoint Analysis Method

Homepage is the main page of an application on the home page where there is the whole main function of the mobile app. The design of a mobile app home page can affect the level of comfort in using the



mobile app. Elements - elements that need to be considered in designing the home page is a groundbreaking feature, the use of font type, coloring, type of icon used and graphics. However, to determine the type of home page design preferred by the user needs is passed to a study by the conjoint analysis method that is in addition to convenient mobile app can also be used to satisfy the user. Surjandari (2010) explains that the Conjoint Analysis is a multivariate analysis method is used to analyze how respondents build a preference for a product (both goods and services) under the terms of the attributes that make up the nature of the product. The main output of this method is a set scale interval "path-works" (utility) of each level for each attribute, which from the merger of these utilities will be obtained prediction preferences of each level for each attribute of the product.

2.4 Usability Testing Using System Usability Scale

In making a product or system required a usability test on a prototype before the product was launched into the market. It aims to find out how easy the product is used and whether the product is quite easy to use. However, if the results of usability testing did not reach the prescribed limit, then the usability test results will be used as a benchmark in redesigning the product. One method that is often used to measure the usability of a product or system is the System Usability Scale. This method was created by Brooke (1996) as one measure of the subjective perception of a product or system users. Question on SUS was developed to measure the usability of three criteria previously defined by ISO 9241-11 consisting of:

- The ability of users to finish tasks using the system and the quality of the results of these tasks.
- How many resources are used in a task.
- subjective reactions to the use of a system user.

3. Research Method



Figure 1. Flow Chart From The Pediatrician

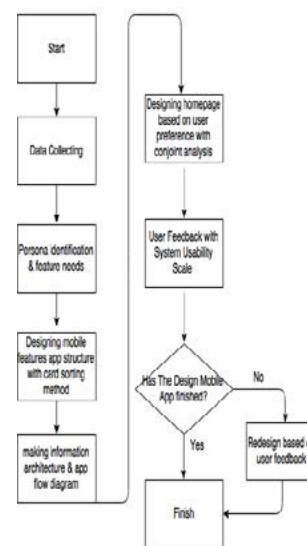


Figure 2. Flow Chart From The User

3.1 Persona Data Classification

The behavior of the parents in taking decisions related to the child's health problem is influenced by several factors: the work of parents, parental education and how big the family of the (Case, 2002). Therefore, the type of persona divided by 3 (three) factors and obtained nine kinds of combinations persona. The first persona (employees, bachelor&diploma degree, the first child) has 78,8% average needs, the second persona (employees, bachelor&diploma degree, not the first child) has 53% average needs the third persona (employees, magister &doctor degree, the first child) has 93% average needs, the fourth persona (entrepreneur, bachelor&diploma degree, the first child) has 84% average needs, the fifth persona (entrepreneur, magister &doctors degree, not the first child) has 80% of average needs, the sixth persona (students, the first child) has 82% of average needs, the seventh persona (students, bachelor & diploma degree, the first child) 56% of average needs, the eighth persona (students,bachelor &diploma degree, not the first child) has 65% of average needs and last,the ninth persona(students, magister &doctors degree, the first child) has 60% of average needs. Based on the results of each persona, it was found that all the features have exceeded the average requirement of 50%, which indicates that all of the features



required by the respondent.

3.2 Data collection Preferences Pediatrician Respenden

Of the respondents who participated in this research totalled 26 Pediatrician at Cipto Mangunkusumo Hospital (RSCM). The existing division in the RSCM consists of 14 divisions which include:

Table 1. Profile of Pediatrician Respondents

14 Divisions of RSCM	
1	Gastro-Hepatologist
2	ICU/PGD
3	Nutrition & Metabolic
4	Neurologist
5	Alergic Imunologist
6	Nefrologist
7	TK(Ped-Sos)
8	Ped Tropik Infection
9	Hemato-Onkologist
10	Imaging
11	Respirologist
12	Endokrinologist
13	Cardiologist
14	Perinatologist

The result of the data features and subfeatures mobile app are obtained using the tools the questionnaires and interviews from 26 respondents divided into the 14 divisions.

3.3 Data Collection of Design Mobile App Preferences Pediatrician

In this study, researcher undertook to take the data designer homepage preferences mobile app from Pediatrician to help researcher in obtaining the best homepage mobile app design based on calculation method of conjoint analysis. This data was taken based on the preference of the Pediatrician that consists of 3 attributes with each attribute consist of 2 levels.

Table 2. Attributes of Application Design Pediatrician Interface

Attribute	Level
Menu	Grid
	List
Icon	3D
	Flat
Color	One
	Many Colors

Attributes and this level of benchmarking with similar mobile app are:

1. Buku Saku Dokter
2. Epocrates

For the features and subfeatures of chatting, researcher conducting benchmarking with the mobile app Whatsapp. Then, researcher conducting studies of literature in terms of drafting features, background, colors and fonts in designing mobile app which consists of:

Table 3. Attributes of Application Design User Interface

Background	White
Color	Orange
	Yellow
	Red
	Tahoma



Font	Verdana
Plant Layout	Alphabet

3.4 Data Retrospective Think Aloud (RTA)

Retrospective think aloud data is done to find out the location of the existing problems of the usability of an interface that is seen from the point of view of the Pediatrician. The number of Pediatrician who will be the users or respondents i.e. totaling 9 people in accordance with the persona that has been obtained. With measurement techniques retrospective think aloud usability for the user interface on the display of the mobile app, the stage is done is as follows:

1. Before interviewing users, researcher must first perform a playback back video data when the user are performing their work. The user then briefed to be able to tell the clear details of what users think when performing the duties provided.
2. If the first phase is completed, the user is then given questions about the criticisms and suggestions about the display of the mobile app.

Here is a task given to the qualitative assessment of knowing the preferences of the Pediatrician that consists of:

1. Open Subfeatures blood.
2. Open the Subfeatures kidney and urinary tract
3. Open the Subfeatures Immunization Schedule IDAI

3.5 Data Processing Persona Pediatrician

Based on the features and subfeatures that have been obtained, the processing is done on the basis of the activity and needs of the Pediatrician to get persona from the Pediatrician. 9 persona are obtained from the Pediatrician. The first one is from division TK (PEDSOS) the activities are browsing children's health education and chatting and his needs are diagnoses and therapy, nutrition, growth, development, immunization and parents chat. The second one is from division neurologist with activities such as browsing children's health education and chatting and her needs are diagnoses and therapy, nutrition, growth, development, immunization, parents chat, and doctors chat. The third one is from division Gastro-hepatologist the activities are browsing children's health education and her needs are diagnoses and therapy, nutrition, growth, development and immunization. Then another from division Alergic Immunologist, with activities such as browsing children's health education, email, and chatting and needs diagnoses and therapy, nutrition, growth, development, immunization and doctors chat. The fifth one is from division nutrition metabolic with activities such as browsing children's health education, email and chatting her needs are diagnoses and therapy, nutrition, growth, development, immunization and parents chat. The sixth one his activity is browsing children's health education and needs such as diagnoses and therapy, nutrition, growth, development, immunization, parents chat and doctors chat. The next one from division cardiologist. The activities are browsing children's health education, email and needs parents and doctors chat. Next is from division ICU/PGD the activities are browsing children's health education, email and chatting. Her needs are nutrition, growth, development, immunization and parents chat. Last, from division respirologist, her activities are browsing children's health education, email, chatting and activities such as diagnoses and therapy, nutrition, growth, development, immunization, parents chat and doctors chat.

3.6 Make the Information Architecture

Preparation of information architecture based on the results of an open-ended question and decision researchers subjectively which are then arranged in the form of a flow which contains information or functionality of the mobile app. Arranged in the form of flow in order to be easy to understand function or what features on the mobile app.

3.7 Information Architecture and App Flow Diagram

Information Architecture and Flow Diagram App created based on the results of the calculation and processing of card sorting has been done. Here is the IA and Flow Diagram App.

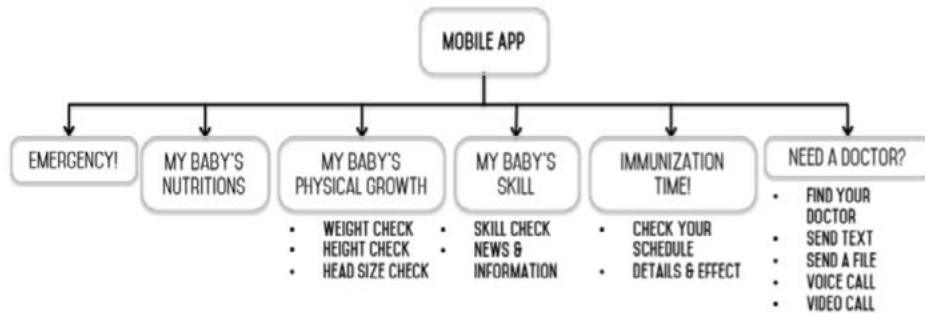


Figure 3. Information Architecture Diagram Pediatrician Interface

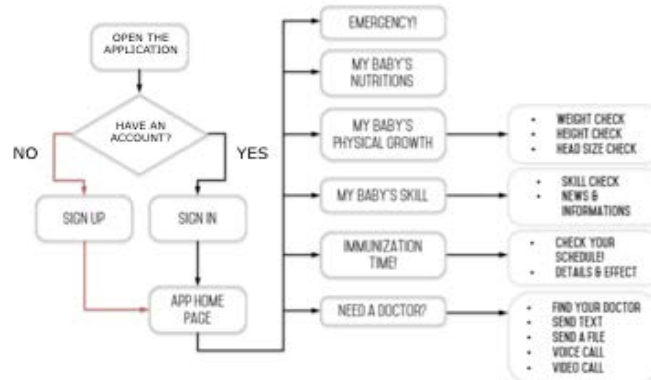


Figure 4. Application Flow Diagram User Interface

3.8 Create the Application Flow diagrams

Preparation of the application flow diagrams based on results from information architecture which are then arranged in the form of a flow which contains process flow when someone is accessing it from the start of opening the applications (sign up or login) to close the application (logout).

3.9 Make a Mobile App Wireframe

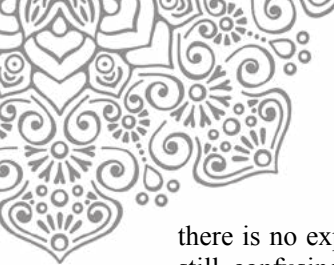
In the creation process, researcher can directly create the wireframe design mobile app of their own based on the literature and then compare with the mobile app wireframe model of the mobile app with the same or similar functions that already exist in the market. In this study, researcher combine both ways. First, the researcher compare the two mobile app design mockup that already exist in the market in terms of information and one mobile app design mockup that already exist in the market in terms of interaction (chat)

3.10 Usability Testing using Retrospective Think Aloud

In this section, the analysis of the data processing of engineering Retrospective Think Aloud (RTA) will be discussed. The purpose of the use of this technique is to find the cause of the problem in terms of the usability user experience when interacting with the display of the first mobile app to help respondents. researcher get the design preference data of the mobile app by Pediatrician which measured using a likert scale of 1-5. The next step is to calculate the level of attributes which have the most high value so that it creates a combination that is best. On this research obtained result of the conjoint analysis as follows: To help respondents assess the usability of the problems, there will be video footage screened when the respondent perform the tasks. The result of this data is in the form on points of perceived problems when interacting with mobile app. Analysis of this data will be discussed based on the results of task 1, 2, and 3. Analysis of each task as follows:

- Task 1

The first task given is to open subfeature blood. The most problem that is obtained is respondents are confused as there is no further designation on each subfeature. That subfeature just describe one blood disease, even though there are various blood diseases which should be drawn up more detailed or completed. The next issue is the data on the subfeature. On the subfeature data file or blood disease but



there is no explanation about categories of disease blood. The next problem was the subfeature the blood still confusing because the naming of features and subfeatures are not clear. Should be explained in advance features and functions on mobile app subfeatures. For other problems, the respondents feel confused when looking at such a mobile app design because the dividing line between the subfeatures is too small and the size of the font in every feature is still too small.

- Task 2

The second task is to open the kidney and the urinary tract subfeature. The most problem that is obtained is that there is no further designation on each subfeature. On the subfeature only described one kidney and urinary tract diseases, whereas there are an assortment of kidney and urinary tract diseases that should have drawn up more detailed or completes. The next issue is the data on the subfeature. On the subfeature data file or kidney disease and urinary tract but there is no explanation about categories of kidney disease and urinary tract. The next problem was the subfeature of the kidney and urinary tract that are still confusing because the naming of features and subfeatures are not clear. Should be explained in advance the usefulness of features and subfeatures on mobile app. For other problems, the respondents feel confused when looking at such a mobile app design because the dividing line between the subfeatures is too small and the size of the font in every feature is still too small.

- Task 3

The third task is to open Immunization Schedule IDAI subfeature. Most of this subfeature do not experience problems due to the subfeature is on immunization and easy to note. The existing data on the subfeature do not the assortment because it may explain its use. For other issues, respondents feel confused when looking at such a mobile app design because the dividing line between the subfeature is too small and the size of the font in every feature is still too small.

3.11 Conjoint Analysis

Conjoint analysis process begins by determining each attribute and level and then compiled into combinations as shown in Table 3. The next step is to take user preference data using a questionnaire with a scale of 1-5 for each combination of design. Once all the data obtained, the authors conducted a reliability test on the data which will then be processed by the method of conjoint analysis using SPSS 23. Based on the results of reliability test, the value of Cronbach's alpha of the data obtained is above the minimum value (0.70). amounting to 0.79. This indicates that the data obtained by the authors is reliable. Having in mind that the data used is reliable, the authors proceed to the stage of data processing calculation using conjoint analysis software SPSS 23. Based on the calculation shown in Figure 3.5 on the chart utilities, it can be seen that the grid has a value of 0.256 and the list has a value of - 0.256. Referring to the value of Pearson's R it can be seen that Pearson's R value of these calculations is above the value of 0.5, which is worth 0.959. Based on these values, it can be said that the results of calculations performed conjoint analysis is valid. layout, white as the color of the font and icon, and Tahoma as font that will be used on the mobile app.

3.12 System Usability Scale

To see the level of usability of each score, then there should be a scale that can be stated that a system is classified as having a low or high usability. SUS-scale research on this has been done by Bangor, Kortum, Miller in 2009. A product or system fit into a category based on the scale adjective usability. Based on the above assessment scale, the SUS score calculation results can be grouped into six (6) groups: "Worst Imaginable", "Poor", "OK", "Good", "Excellent", and "Best Imaginable". Results grouping scores and graphs distribution SUS results can be seen in Table 4 and Figure 3. The level of reusability mobile app can be assessed based on the calculation SUS, where it appears that there are only three (3) assessment of respondents who considered that this prototype "Not Acceptable", while six (6) the results of assessments of other states that this prototype "Acceptable" and quite unfit for use by the public.

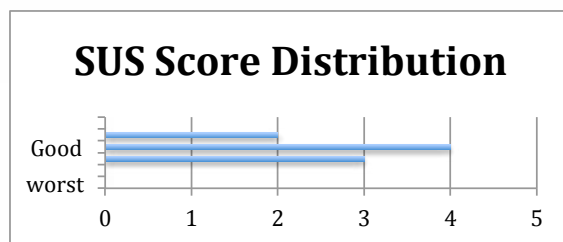


Figure 5. SUS Score Distribution

Table 4. SUS Score Calculation

Persona	Q1	Q2	Q3	Q4	Q5	Q6	Q7	Q8	Q9	Q10	SUS Score
1	3	4	4	2	3	3	4	2	4	2	62.5
2	2	5	5	1	2	3	4	1	5	1	67.5
3	4	3	3	4	3	3	4	3	2	4	47.5
4	4	2	3	4	5	3	4	4	4	2	62.5
5	2	1	3	2	4	4	2	1	4	2	62.5
6	2	3	3	1	3	4	2	3	4	4	47.5
7	5	2	5	1	5	1	3	3	3	4	75
8	2	4	2	4	2	1	3	1	2	3	45
9	5	1	5	1	5	2	2	3	5	2	82.5
Average SUS Score											61.4

4. Results

Based on the collection and processing of data above, researcher conducting the determination of design home mobile app by using the method of conjoint analysis. The results obtained are a combination of Grid + Flat + many colors.



Figure 6. The Results of The Combination Of Conjoint Analysis From The Pediatrician Perspective



Figure 7. The Result of The from The Combination Of Conjoint Analysis from The User

5. Conclusion

- Features and content of a mobile app must be made specifically according to user needs a mobile app so that it can work optimally and can be utilized by the user right to the purpose of the manufacture of the mobile app. Therefore, by analyzing the persona can be seen that the user requires 5 features relating to the health, growth, development, immunization and consultation on the mobile app later.
- Navigation and organizational structure of a mobile app will greatly affect the ease of the user in understanding the mobile app. Therefore, the navigation structure and organization of a mobile app must be made in accordance with the mindset and how users make decisions, one of them with a



card sorting method. In accordance with the calculation results obtained 5 card sorting initial feature group split into 6 groups, namely emergency feature, my baby's nutrition, my baby's physical growth, my baby's skills, immunization time, and need a doctor.

- To be able to produce a mobile app home page design in accordance with user preferences, conjoint analysis calculation required in order to obtainment of the best design of the home page. Results of calculation of conjoint analysis is obtained that the user prefers the grid as a type of layout, font color and white as Tahoma as font type used in the design of the home page.
- To find out how easy and convenient to use a mobile app prototype, usability test is required by methods such as system usability scale for assessing the subjective perception of the user as well as how easy and comfortable are the mobile app to use.
- The test results of reusability using the system usability scale was 6 of 9 respondents' assessment of the prototype is categorized as a prototype of "Acceptable". This indicates that this prototype mobile app is quite feasible for use by the general public
some conclusions and suggestions are obtained, among others:
 - Obtain a mobile app which functions in facilitating work activities Specialist Child and improve health services to the parents of the patient.
 - In addition to having to meet the needs of its users, a mobile app also should be able to make convenience for users in terms of speed of access.
 - Features and subfeatures in a mobile app can be designed on the basis of the questionnaire in the determination of the needs of the Pediatrician.
 - The results of the questionnaire in the determination of Pediatrician needs, will create persona based on work activities and needs
 - On ensuring the needs of features and subfeatures, open-ended question technique was taken by interviewing each persona.
 - The order of the functions or features, subfeatures, process flow and navigation in a mobile app can be designed in the form of application flow diagrams.
 - To generate a corresponding mobile app design with preference Pediatrician conjoint analysis methods, it is useful to get the mobile app design fit the desires of the Pediatrician.
 - To know the mobile app beta prototype in accordance with the wishes of the child, it takes a Specialist usability testing with Retrospective Think Aloud which is useful to know the problems of usability of the mobile app.

6. References

- Altuntac, P(2015). The Comparison of Concurrent and Retrospective Think Aloud Methods in Unmoderated Remote Usability Testing 1-26
- Banum, C.M (2011) *Usability Testing Essential: Ready, Set.. Test!* Morgan Kaufmann.
- Brown D.(2010) *Eight Principles of Information Architecture*, 30-34
- eMarketer (2014, Desember 11). Article : eMarketer, Maret 2015.
- Galitz, W.O. (2007) *The Essential Guide to User Interface Design 2nd Ed.* Nwq York : John Wiley&Sons, Inc
- Holzinger, A Errath, M.(2007) Mobile Computer Web-Application Design In Medicine : Some Research Baed Guidelines, 31-41
- Jaspers, M.W (2009) A comparison of usability methods for testing interactive health technologies : Methodological aspects and empirical evidence. *international journal of medical informatics* 78,340-353
- Kementrian Kesehatan RI (2015) Profil Kesehatan Indonesia
- Klein D (2012) *Inspire* : Adobe www.adobe.com
- Mayhew D.I (1992) Principles and guidelines in software and user interface design *Englewood Cliffs* : Prentice-Hall
- Andreas Holzinger M.E (2007) *Mobile Computer Web-application design in medicine : some research based guidelines.* Graz
- Anne Case C.P (2002) *Parental Behavior and Child Health.* New Jersey
- Bangour J (1996) SUS : A Restropective : *Journal of Usability Studies* Vol 8 Issue 3 29-40.
- Central Intelligence Agency (2014) CIA *The World Fact Book*
- eMarketer (2014 Desember 11) Retrieved Oktober 10,2015 from www.emarketer.com



- Kementrian Kesehatan RI (2015) Profil Kesehatan Indonesia
Orne B (2002) *Formulating Attributes and Levels in Conjoint Analysis*. Washington.
Princeton University (2008). *Guide to Creating Website Information Architecture and Content*
Righi, C (2013) *Card Sort Analysis : Konsep dan Aplikasi*, Universitas Trisakti.
UNICEF (2012) Ringkasan Kesehatan Ibu dan Anak Jakarta



SERVICE INNOVATION DESIGN FOR PLATINUM MEMBERS IN GARUDA INDONESIA SALES AND SERVICES OFFICE

Amalia Suzianti, Nadira Winaputri, and Serdi Akbar Maulana

Industrial Engineering, Faculty of Engineering, University of Indonesia
Kampus Baru UI Depok 16424

Email : suzianti@eng.ui.ac.id ; nadira_ti2011@yahoo.com ; serdiakma@gmail.com

Abstract

Garuda Indonesia as one of the best airlines in Indonesia offers a wide range of services, one of which is sales office service. Based on previous surveys indicates that the customer satisfaction rating for sales office service is relatively low compared to the other services. It is due to the service design for sales office service does not yet include the voice of customer comprehensively. Therefore, this study uses the Kano Model and Customer Journey Mapping to determine services attributes which in line with customers (Platinum Members) preferences. The Kano Model shows that there are several service attributes on Garuda Indonesia sales office included in “attractive” and “one dimensional” category. Customer Journey Mapping indicates that there are two disfavored activities, which is when waiting queue and waiting for service process. Therefore, this study followed by conducting the Focus Group Discussion to determine the problem’s causes as well as recommendations for improving current services. This study further followed by determining the priority recommendations using importance-performance analysis. The result shows that there are four recommendations need to be priorities, which are increasing the number of frontliners during peak hours, providing charging station, providing self city check-in machine and providing supporting facilities in the Platinum Lounge.

Keywords : Customer Journey Map; Garuda Indonesia; Importance-performance Analysis; Kano Model; Platinum Members; Sales Office

1. Introduction

The Indonesian airline industry will face tight competition along with increasing the number of new airlines. In order to compete and maintain a good relationship with customers, Garuda Indonesia has a Customer Loyalty Program which called GarudaMiles Program.

GarudaMiles Program memberships consist of several levels, from the highest level is Platinum, and then followed by Gold, Silver and Blue. These membership levels indicate the level of members’ loyalty and activity. However, these membership levels also show that not all

members have a major contribution to company’s revenue. Previous research also identified seven segments of members which are sorted based on their values to the company. The segmentation shows the difference between the average flight frequency, contribution per member to the company's revenue and the value of RFM (Recency, Frequency and Monetary) of each segment during a certain period of time (Kristiani et al, 2013). According to table 1 and figure , it can be concluded that Top Members segment, which is consists of Platinum Members, have the highest



RFM value and generate the most to company's revenue.

Table 1. Frequent Flyer Membership Segmentation

Segmentation	RFM Value	Membership Level	Frequency	Rev/Member (IDR Mio)
Top Members	48.3	Platinum	43	353.71
Next Best Members	45.3	Platinum, Gold	56	192.59
Active Members	32.1	Gold	43	98.99
Average Members	21.3	Gold, Silver	29	52.52
Base Members	12.7	Silver	17	25.77
Infrequent Members	7.3	Silver, Blue	8	10.08
Inactive members	2.32	Blue	2	1.51

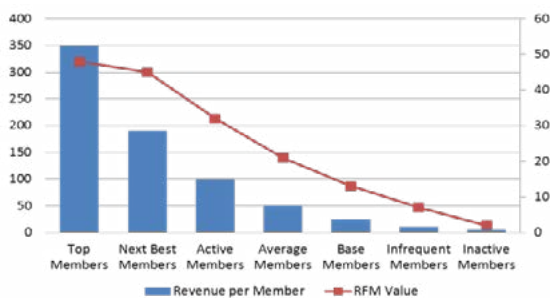


Figure 1. Comparison between RFM Value and Revenue per Member

In order to maintain the most valuable customers' loyalty, Garuda Indonesia offers service priorities to the Platinum Members. However, as the five starts airline, these service priorities focus only on flight services. Hence, other service areas also worth nothing the service's quality, especially Pre-Journey phase. There are 4 touch points in Pre-Journey phase, including Website, Call Center, Social Media and Sales Office.

However, based on previous surveys indicates that the customer satisfaction rating for sales office service is relatively low compared to the other services. It is due to the service design for sales office service does not yet include the

voice of customer comprehensively. This resulted in the customers' preferences and needs at Garuda Indonesia Sales Office clearly uncharted. Therefore, Garuda Indonesia needs a service design which in line with customers' preferences and needs, in order to provide more satisfaction levels for the customers.

2. Literature Review

2.1 Kano Model

Kano Model introduced by Professor Noriaki Kano in Tokyo Rika University with the aim to categorize the attributes of a product or service. The attribute categorization based on how well the product or service can satisfy the needs of customers. Kano Model is divided into three categories that affect customer satisfaction (Tan dan Pawitra, 2001):

1. *Must be or basic requirements*

If these requirements are not fulfilled, the customer will be extremely dissatisfied. On the other hand, as the customer takes these requirements for granted, their fulfillment will not increase his satisfaction.

2. *One dimensional or performance requirements*

With regard to these requirements, customer satisfaction is proportional to the level of fulfillment - the higher the



level of fulfillment, the higher the customer's satisfaction and vice versa.

3. *Attractive or excitement requirements*

Attractive requirements are neither explicitly expressed nor expected by the customer. Fulfilling these requirements leads to more than proportional satisfaction. If they are not met, however, there is no feeling of dissatisfaction.

Besides those categories, there are two other categories that can be identified :

4. *Indifferent requirements*

This category refers to things that are not good or bad. Performance of the attributes of a product or service that does not produce satisfaction or customer dissatisfaction.

5. *Reversal requirements*

In this category, the customer was not satisfied when the performance of an attribute of products or services increases.

Figure 2 below shows the relationship between customer satisfaction and performance attributes of a product or service.

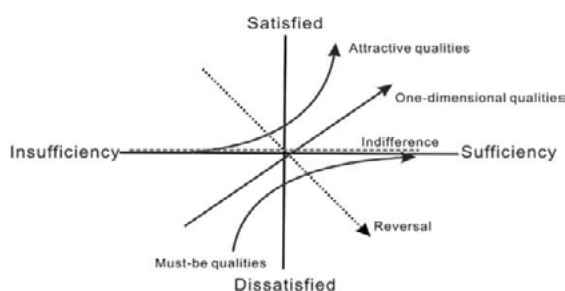


Figure 2. Kano Model

Determination of customers' needs by Kano's category can be classified in the form of Kano's questionnaire (Kano et al., 1984). The questionnaire contained a pair of questions for each of the attributes of products or services, which are the functional and dysfunctional question. For each product feature a pair of questions is formulated to which the customer can answer in one of five different ways. By combining the two answers in the following evaluation table, the product features can be classified into: A = *Attractive*, M = *Must-be*, O = *One-dimensional*, I = *Indifferent*, R = *Reverse*, dan Q = *Questinable* in accordance with Table 2.

Table 2. Kano Evaluation Table

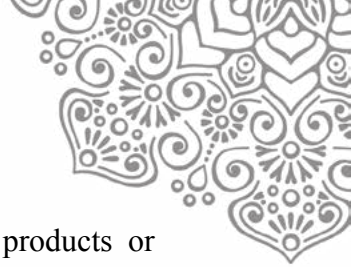
Customer Requirements	Disfunctional					
	1	2	3	4	5	
Functional	1	Q	A	A	A	O
	2	R	I	I	I	M
	3	R	I	I	I	M
	4	R	I	I	I	M
	5	R	R	R	R	Q

Description :

- 1 – I like it that way
- 2 – It must be that way
- 3 – I am neutral
- 4 – I can live with it that way
- 5 – I dislike it that way

2.2 Customer Journey Map

Customer Journey Map is a visual picture of the customer's experience with a company. It describes that experience from customer's perspective, describing the



activities the customer would undertake, in words the customer might use. By identifying the key moments of truth – those steps that are most important to customer satisfaction and renewal - Customer Journey Maps provide a resource allocation guide. They identify the places where investments in higher levels of service are more likely to attract or retain customers. The steps that need to be considered when designing a Customer Journey Map is as follows

- **Set-up The Mapping Context.**
The first thing to do is to know who they are and choose what customer groups that are going to be mapped.
- **Walk in the customer’s shoes**
To meet the needs of customers, the company needs to find out everything about the customers, tracking and describing customer experiences, what happens to them and how they feel.
- **Draw The Map**
After all the information collected, the company needs a tool that describes the overall information so that it can be concluded as well as identifying the corrective actions.
- **Analyze The Map and Identify Corrective Actions**
The next step is to analyze the things that need to be improved, as well as

improving the quality of products or services.

- **Take Action and Measure Success**
The next step is to implement the corrective actions at a certain time. Once applied, then corrective actions should be evaluated.

2.3 Importance-Performance Analysis

The aim of Importance-Performance Analysis (IPA) is to measure the relationship between customer perception with priority to improve the quality of products or services (Brandt, 2000). IPA method main function is to display information relating to the factors on the products or services based on the level of importance and the level of performance and shown in a two-dimensional graph to facilitate explanation of the data as well as get priority proposed improvements to be made. IPA chart consists of four quadrants based on the importance-performance measurement as shown in Figure 3.

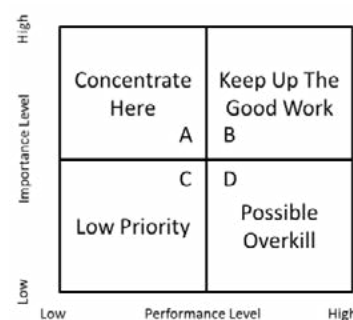


Figure 3. Importance Performance Analysis Quadrants



The following is an explanation of each quadrants (Brandt, 2000).

1. Concentrate Here (High Importance and Low Performance)

This sends a direct message that improvement efforts should be concentrated here

2. Keep Up The Good Work (High Importance and High Performance)

The organization seems to have exhibited high levels of performance in these areas.

3. Low Priority (Low Importance and Low Performance)

Customers do not think the product or service quality characteristic is important and the organization fails to perform too.

4. Possibly Overkill (Low Importance and High Performance)

Customers do not think the product or service quality characteristic is important, but the organization performs well.

3. Method

3.1 Population and Sample

The target population of this study is the Platinum Members of GarudaMiles program who visit the Garuda Indonesia sales office in Senayan City. The number of Platinum Member visitors is around 591 visitors per month. This study was conducted for 3 months, so the population

of this study is around 1773 visitors. This study used sampling method with 10% percentage of allowance, so total samples needed are 94,66 respondents. Thus the number of samples required in this study can be fulfilled with 100 respondents

3.2 Service Attributes and Customer's Activities

Table 3 shows the service attributes of Garuda Indonesia sales office, which grouped by SERVQUAL (*Service Quality*) dimensions. There are five SERVQUAL dimensions (Parasuraman et al., 1988) including tangible, reliability, responsiveness, assurance, and empathy.

Table 3. Service Attributes

Tangible	Platinum Lounge
	Convenience of Platinum Lounge
	Entertainment
	Beverages
Reliability	Frontliner's Appearance
	Guidance from Security
Responsiveness	Guidance from Frontliner
	Service Time
	Waiting Time
	Listen and Understand Customer Needs
Assurance	Answer and Give Recommendation
	Product Knowledge
	Kindness and Politeness
Empathy	Professional Services
	Welcoming from Security
	Welcoming from Frontliner
	Frontliner Introducing Themselves
	Farewell from Frontliner
	Farewell from Security

Moreover, the customer's activities in Garuda Indonesia sales office can be seen in Table 4.

Table 4. Customer's Activities



No	Activity
1	Entering Sales & Service Office
2	Declaring as Platinum Member
3	Entering Platinum Lounge
4	Waiting
5	Heading to Counter
6	Sitting in Counter's Seat
7	Giving Personal Information
8	Explaining The Purpose
9	Waiting The Process
10	Approving The Results
11	Finishing
12	Leaving Platinum Lounge
13	Leaving Sales & Service Office

3.3 Questionnaire Design

The questionnaire in this study is divided into four major sections, including the description of the respondent, the Kano question which consists of 19 service attributes and consists of functional and dysfunctional questions, suggestion form and customer journey mapping where respondents were asked to describe their emotions or feelings on each activity undertaken during in the Garuda Indonesia sales office.

4. Results

4.1 Kano Model Results

According to the results, those service attributes are dominated by “must-be” and “one dimensional” category. This indicated that customers believe that the service attributes should have been contained in the service process at Garuda Indonesia Sales Office.

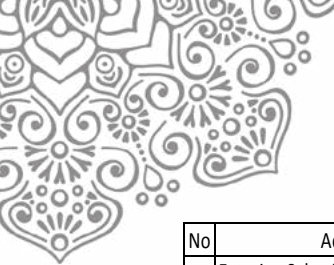
Table 5. Kano Category for Each Service Attribute

	A	O	M	I	R	Category
Platinum Lounge	30	56	14	0	0	O
Convenience of Platinum Lounge	18	50	30	2	0	O
Entertainment	29	38	16	17	0	O
Beverages	38	39	8	15	0	O
Frontliner's Appearance	16	36	43	5	0	M
Guidance from Security	33	7	7	53	0	I
Guidance from Frontliner	22	29	33	16	0	M
Service Time	25	46	17	12	0	O
Waiting Time	27	32	31	10	0	O
Listen and Understand Customer Needs	2	43	51	4	0	M
Answer and Give Recommendation	8	39	47	6	0	M
Product Knowledge	18	26	50	6	0	M
Kindness and Politeness	10	41	45	4	0	M
Professional Services	15	27	50	8	0	M
Welcoming from Security	33	7	7	53	0	I
Welcoming from Frontliner	45	25	7	23	0	A
Frontliner Introducing Themselves	35	15	12	38	0	A
Farewell from Frontliner	50	11	2	37	0	A
Farewell from Security	46	7	4	43	0	A

4.2 Customer Journey Mapping Results

Customers were asked to express their emotions while undergoing the activities in accordance with predetermined parameters. There are three parameters, first is "smile" which shows happy, relaxed and excited feeling. Second is “neutral” and the last is “frown” which shows bored, annoyed and anxious feeling. Table 6 shows the customer's emotion while in Garuda Indonesia sales office.

Table 6. Customer's Emotion



No	Activity	Smile	Neutral	Frown	Emotion
1	Entering Sales & Service Office	47	53	0	Neutral
2	Declaring as Platinum Member	62	38	0	Smile
3	Entering Platinum Lounge	82	18	0	Smile
4	Waiting	20	35	45	Frown
5	Heading to Counter	58	42	0	Smile
6	Sitting in Counter's Seat	63	37	0	Smile
7	Giving Personal Information	41	59	0	Neutral
8	Explaining The Purpose	45	55	0	Neutral
9	Waiting The Process	15	41	44	Frown
10	Approving The Results	61	39	0	Smile
11	Finishing	73	27	0	Smile
12	Leaving Platinum Lounge	48	52	0	Neutral
13	Leaving Sales & Service Office	48	52	0	Neutral

According to Customer Journey Mapping results, there are two disfavored activities, which is when waiting queue and waiting for service process. Once the data are collected, then proceed with the preparation of Customer Journey Map to evaluate the customer experience.

4.4 Importance Performance Analysis Questionnaires

This study further followed by importance-performance analysis (IPA) questionnaires deployment. This questionnaire is addressed to the frontliners who manage the service operations at Garuda Indonesia Sales Office Senayan City. The IPA questionnaire distributed to 35 frontliners consist of several positions.

4.5 Importance-Performance Analysis Results

This study followed by calculating the average value of the importance and performance level of each recommendation as shown in Table 8. Later the value is

used to determine the coordinates of the importance-performance analysis diagram.

Table 8. Average Value of Importance and Performance Level

Provide More Convenience While Waiting Queues	I	P
Provide Wifi ID and password for Platinum Lounge	4,29	3,49
Provide charging station facility for gadget charging	4,20	3,11
Provide an easy-operate coffe maker facility in Platinum Lounge	4,06	3,37
The allocation of additional human resources during peak hours	4,57	3,06
CSA regularly monitor the Platinum Lounge (every 10-15 minutes)	4,51	3,63
Improve Service Efficiency	I	P
Provide supporting facilities in Platinum Lounge	4,60	2,94
Provide <i>self city check-in machine</i>	4,54	2,63
Additional operating hours	2,51	3,14
Standard <i>handling time</i> for each customer purpose	3,23	3,31
Reservation and <i>mobile staff</i> to deliver <i>First Class</i> and <i>Business Class tickets</i>	3,69	3,66
Average	4,02	3,23

5. Discussion

According to questionnaire results, the importance-performance analysis (IPA) diagram for service innovation recommendations on Garuda Indonesia sales office shown in Figure 5 with the description of the IPA diagram is shown in Table 9.

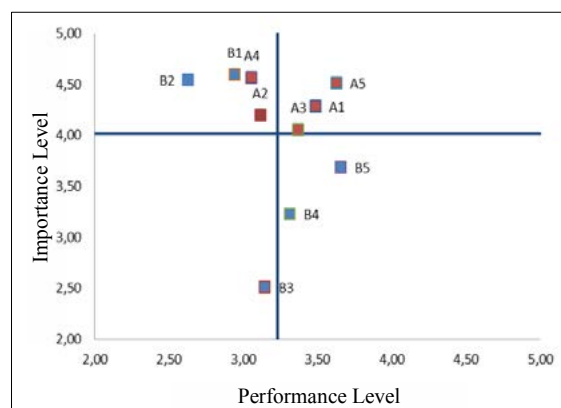


Figure 5. Importance-Performance Analysis Diagram



Table 9. Descriptions of Importance-Performance Analysis Diagram

Code	Provide More Convenience While Waiting Queues
A1	Provide Wifi ID and password for Platinum Lounge
A2	Provide charging station facility for gadget charging
A3	Provide an easy-operate coffe maker facility in Platinum Lounge
A4	The allocation of additional human resources during peak hours
A5	CSA regularly monitor the Platinum Lounge (every 10-15 minutes)
Improve Service Efficiency	
B1	Provide supporting facilities in Platinum Lounge
B2	Provide <i>self city check-in machine</i>
B3	Additional operating hours
B4	Standard <i>handling time</i> for each customer purpose
B5	Reservation and <i>mobile staff</i> to deliver <i>First Class and Business Class tickets</i>

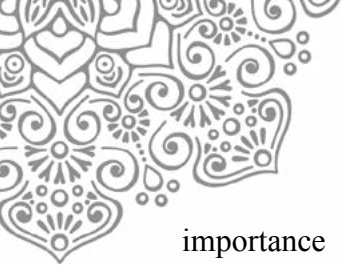
(X) axis shown the actual performance level which has been achieved so far based on the opinions of frontliners as the operational activities executor. (Y) axis shown the importance level of each service innovation recommendation to be implemented based on the opinions of frontliners. There are ten activities proposed as the recommendations to improve service at Garuda Indonesia Sales Office. Five activities to provide more convenience for customers while waiting queues and five activities to improve service efficiency.

In the first quadrant, there are four recommendations which have a high importance level and low performance level, so it needs to be the priority in improving existing services. First recommendation is allocation of additional human resources during peak hours,

especially on weekend. Currently, Platinum Lounge has been equipped with various facilities, but there is no charging station facility to recharge the gadget's batteries. Therefore, charging station facility is important in order to provide more convenience for customers. Next recommendation is the provision of self city check-in machine. The customers can process city check-in by themselves and no need to queue to the counter. Moreover, Garuda Indonesia needs to provide supporting facilities in Platinum Lounge so the frontliners do not need to go to back office and service processes can be completed quickly and efficiently.

In the second quadrant, there are three activities which have both high importance and performance level, so these activities is considered good enough in providing services to customers. First recommendation is provide Wifi ID and password in Platinum Lounge. It is expected to provide more convenience for customers. Next recommendation is to provide an easy-operate coffee maker in Platinum Lounge. Next recommendation is Customer Service Assistant as the floor director during the operatting hours, regularly monitor Platinum lounge (every 10-15 minutes) to ensure no customers have to wait too long.

In third quadrant, there is one recommendation which have both low



importance and performance level. That recommendation is additional operating hours. This is because at the moment the customer is not able to buy tickets at the airport, so they require an alternative way to purchase the tickets.

In the last quadrant, there are two activities which have a high performance level and low importance level. The first recommendation is standard handling time for each customer purpose, such as ticket reservation, ticket refund, redemption, etc. Next recommendation is ticket reservation and mobile staff to deliver First Class and Business Class tickets.

6. Conclusion

According to the results, there are two things to be concluded in accordance with the purpose of research. Service attributes corresponding customer preferences are the service attributes that has "attractive" and "one dimensional" category because both categories have an influence on customer satisfaction. Service attributes which have "attractive" category are farewell from security, welcoming from frontliners, frontliners introducing themselves and farewell from frontliners. Service attributes which have "one dimensional" category are the existence and the convenience Platinum Lounge, entertainment facilities, beverages in

Platinum Lounge, waiting time and service time.

According to importance-performance analysis results, there are four recommendations it needs to be the priority in improving existing services. Two recommendations to provide more convenience for customers while waiting queues and two recommendations to improve service efficiency. Those service innovation recommendations, including allocation of additional human resources during peak hours, providing charging station facility, providing self city check-in machine and providing supporting facilities in Platinum Lounge.

7. Future Research

This study used qualitative methods in determining the level of customer satisfaction and customer emotions, so further research is recommended to use quantitative methods. This study focuses only on pre-stage journey, especially in the sales office, therefore, further research is recommended to be focused on the other stage of Garuda Indonesia services, such as pre-flight, post-flight and post-journey or at other touchpoints such as websites, call centers or service at the airport. This study was specifically targeted for Platinum Members, therefore, further research can focus on other more general objects, so the



research results can be applied to a wider service.

8. References

Boger, Davis, et al. 1993. *Kano's Method for Understanding Customer defined Quality*. Center for Quality of management Journal. 2 (4).

Brandt, D.R. 2000. *An "Outside-In" Approach to Determining Customer Driven Priorities for Improvement and Innovation*. White Paper Series.

Centre for Asia Pacific Aviation. 2011. *Indonesia - a massive aviation opportunity*. Centre for Asia Pacific Aviation.

Garuda Indonesia. 2014. *Annual Report – Connecting Diversity*. Garuda Indonesia

Hagen, Mark van; Bron, Pauline. 2013. *Enhancing the experience of the train journey: changing the focus from satisfaction to emotional experience of customers*. Transportation Research Procedia 1 253 –263

Isaacson, Bruce. 2012. *Using Customer Journey Map To Improve Your Customer Experience*. MMR Strategy Group.

Kano, N, et al. 1984, *Attractive Quality and Must-be Quality*. Hinshitsu. Vol.14, pp.39-48.

Kristiani, Enny; Sumawarman, Ujang. 2013. *Customer Loyalty and Profitability: Empirical Evidence of Frequent Flyer Program*. International Journal of Marketing Studies; Vol. 5, No. 6.

Li, Mingzi. 2011. *Applying Kano Theory on Career Service in Library & Learning Resources of University of Boras*. International Journal of Business and Management. 6 (1).

Martinez, C.L. 2003. *Evaluation Report: Tools Cluster Networking Meeting*. Center Point Institute, Inc. Arizona.

Nenonen, Suvi; Rasila, Heidi. 2007. *Customer Journey – a method to investigate user experience*

Organisation for Economic Co-operation and Development. 2014. *Airline Competition – Note by Indonesia*. Directorate for Financial and Enterprise Affairs Competition Committee

Parasuraman, A., Zeithaml, V.A. and Berry, L.L. 1988. *SERVQUAL: a multiple-item scale for measuring consumer perceptions of service quality*. Journal of Retailing. Vol. 64, pp.12-37.

Sauerwein, Elmar, et al. 1996. *The Kano Model : How To Delight Your Customers*. International Working Seminar on Production Economics, pp. 313 -327.

Tan, K.C. and T.A. Pawitra. 2001. *Integrating Servqual and Kano's Model into QFD for Service Excellence Development*. Managing Service Quality. 11(6), pp.418-430.

Walden, D. 1993. *Special issue on Kano's Methods for Understanding Customer Defined Quality*. The Center for Quality of Management Journal. 2 (4), pp.3-35.



INTEGRATING IDEAS DIGITAL HUMAN MODELING IN ELECTRONIC INDUSTRY TO IMPROVE HUMAN-SYSTEM PERFORMANCE

Tegar Septyan Hidayat ^a

^aUniversitas Indonesia, Depok

Abstract

In Indonesia, most of companies don't consider Human factors as the important part in the workplace, so it affects occupational risk as well as performance of industrial workers especially in manufacturing sector. In this research, we explore the ergonomics aspect from electronics industry based in Indonesia using Digital Human Modeling (DHM) approach. DHM is ergonomics concept which usually refers to modelling physical aspect of human with main focus on anthropometry and physical strain. It is used as the part of ergonomics improvement initiative to avoid worker injuries and improve human performance in order to be more productive. Based on the previous researches, we found that there is a need to propose a step by step framework in DHM in order to make the work redesign more systematically. We propose IDEAS framework as a step by step approach for work redesign which includes 5 steps (Identify, Design, Evaluate, Adapt, and Synergize) from situation identification until it can be ready to be implemented. The analysis of working posture based on Rapid Upper Limb Assessment (RULA), Low Back Analysis (LBA), and NIOSH Lifting Equation using Jack Tecnometrix Siemens software to compare result of ergonomics postures and their interaction in current condition and simulated environment. After evaluating condition, we propose the solution based on ergonomics consideration and making pilot testing in order to implement it successfully in the real system. As the output of this research, we provide several alternative design which can reduce the musculoskeletal risk of operators as well as the service level in production line. Based on this research, using IDEAS framework is suitable for redesigning occupational task based on digital human modelling approach, because it can provide structured approach from identifying the task, designing virtual environment, evaluating ergonomics condition, adapting, and synergizing solutions. Furthermore, IDEAS framework is feasible to be adopted in managing work redesign in many areas for occupational ergonomics.

Keywords: IDEAS; Digital Human Modeling; Work Redesign; Electronic Company; Human Factors

1. INTRODUCTION

Ergonomics, as the science that concern about human factors in a system, can be applied on many areas including in electronics industry. However, in industrially developing countries, especially in Indonesia, ergonomics improvement still limited and relatively new. Several ergonomics studies that were carried out in electronic industry focused on health hazards of chemical exposure and musculoskeletal problems among fabrication and non-fabrication workers (Schenker MB et al.,1995; Pocekay P,1995). Other ergonomics studies have been conducted in developing countries to improve



occupation health and safety in electronics factory in Malaysia (Yeow,2004;Tan,1997), carpal tunnel syndrome in Egyptian electronics (Abbas, 2001), and wrist pain study among workers in Singapore (Ho et al.,1997).

As the novelty in this research, we use digital human modeling as the focus of the ergonomics improvement. We propose IDEAS framework as a step by step approach for work redesign using digital human modeling approach. IDEAS framework includes 5 steps (Identify, Design, Evaluate, Adapt, and Synergize) in order to make the work redesign more systematically from situation identification until it ready to be implemented. The electronics industry which have a very diverse range of production processes need ergonomics improvement as pathway to reduce ergonomics hazard in their workplace. In electronics industry, workers used to work in awkward postures, lift awkward load, repeat monotonous motion, and work at high pace and precision also, so it affects the ergonomics requirement of the workers which have to adapt the risk especially in upper extremity movement. In Digital human modeling can be used to analyze the work systematically and more cost-efficient than most of traditional approach. Until now, there is no study that has been conducted to integrate digital human modeling in developing countries electronics industry.

Therefore, this research attempts to fill the gap in comprehensive study in ergonomics improvement and give pilot study using digital human modeling framework. The study conducted in electronics industry, specifically in semiconductor factory producing integrated circuits.

1.1 Objective

The objective of this research is to adopt digital human modeling approach in work system redesign in semiconductor factory to make it systematically.

1.2 Advantage

The advantage of this research is to adopt IDEAS digital human modeling in semiconductor factory. By increasing the comfort, risk on injury could be minimized. It will also have a positive impact on health and performance of workers in order to improve service level of manufacturing sector in Indonesia.

1.3 Previous Research

The publication of research on digital human modeling that related to electronics industry is still limited. Most of the previous researches, mainly focused on musculoskeletal risk using traditional approach (Yeow, 2004 ; Tan, 1997 ; Ho et al., 1997). Several studies that used digital human modeling approach mostly not specified in electronics industry using fatigue index (T.Septyan., 2013) and posture evaluation index (T. Septyan & B. Nurtjahyo, 2013).

Based on the previous researches, we found that there is a need to propose a step by step framework in digital human modeling to be applied in electronics industry specifically in semiconductor factory. Furthermore, we expect that this research can give contribution to industrial workers and manufacturing sector in Indonesia.

2. METHODOLOGY

In this research, the main area is related to Digital Human Modelling (DHM). DHM is ergonomics concept which usually refers to modelling physical aspect of human with main focus on anthropometry and physical strain. A step by step DHM framework is proposed named as IDEAS. It contains 5 steps in the process, Identify, Design, Evaluate, Adapt, and Synergize.

In the identify phase, we focus on the defining scope, task process, and anthropometric data. For data, it can be divided into several types: work design dimension and anthropometry data workers for



designing the dimensions of an ergonomic workstation. We observe 29 male operators as the subject for this research. After gathering initial data, we focus on creating virtual environment and virtual human using the input data from previous phase. We position virtual human model in virtual environment in accordance with the real situation and providing assignments or work on a virtual human according to the desired working movement. After making virtual simulation, we evaluate the model using Task Analysis Toolkit using Jack Software. It is the software to model and simulate human interaction with the environment and working tools when analyzing the ergonomics aspects of the model that has been created (Siemens, 2008; Wilson, 1999). The analysis results will be used to see conditions of ergonomics postures and their interaction. In this methodology, we use RULA, LBA, and NIOSH Lifting Equation Index as ergonomics evaluation tools. After evaluating condition, we propose the solution based on ergonomics consideration and making pilot testing in order to implement it successfully in the real system.

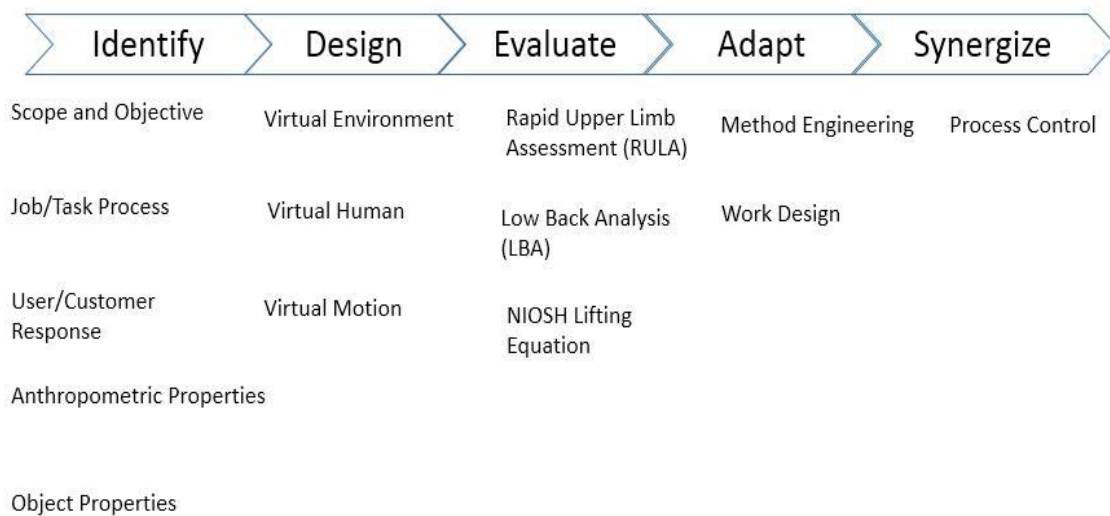


Figure 1. IDEAS Framework in DHM

2.1 Identify

In the identify phase, Firstly, we identify the process task using micromotion study. After defining the process task, we specify the anthropometry measurement of operators with total sample 29 operators. From measurement, we divide the data into 2 percentiles, they are 5th and 95th percentile as can be seen in **Table 1**.

Table 1. Percentile of Operators

Percentile	5 th	95 th
Height (cm)	149	178.4
Weight (kg)	44.3	78.4



2.2. Design Phase

In the design phase, we create virtual environment using 3D CAD model and virtual model in software Jack. We set the virtual human model in virtual environment in accordance with the real situation and provide assignments on a virtual human according to the desired working movement. Below the virtual environment based on 3D CAD and Virtual Human:

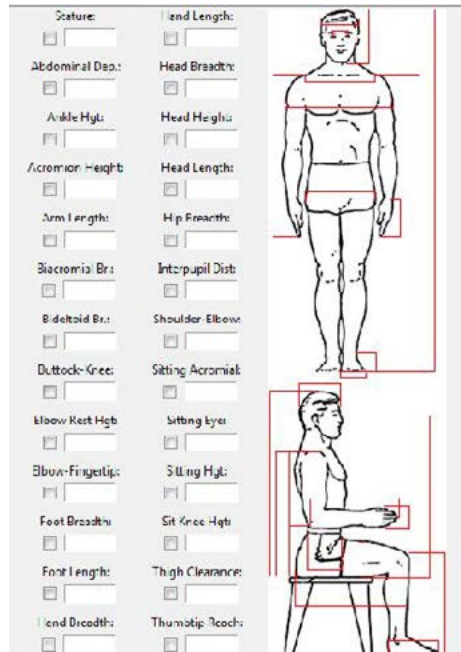


Figure 2. Body Dimension

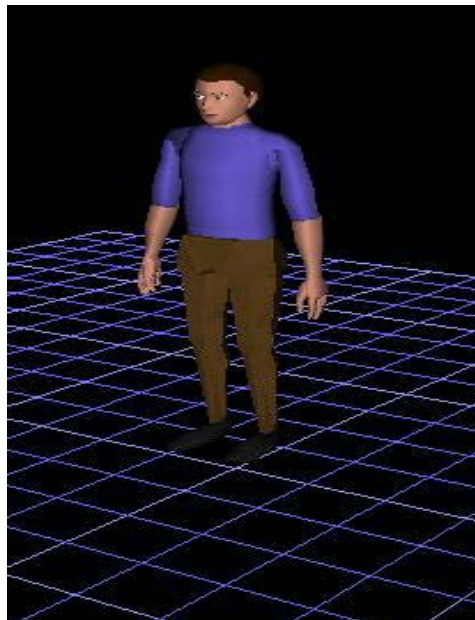




Figure 3. Body Dimension

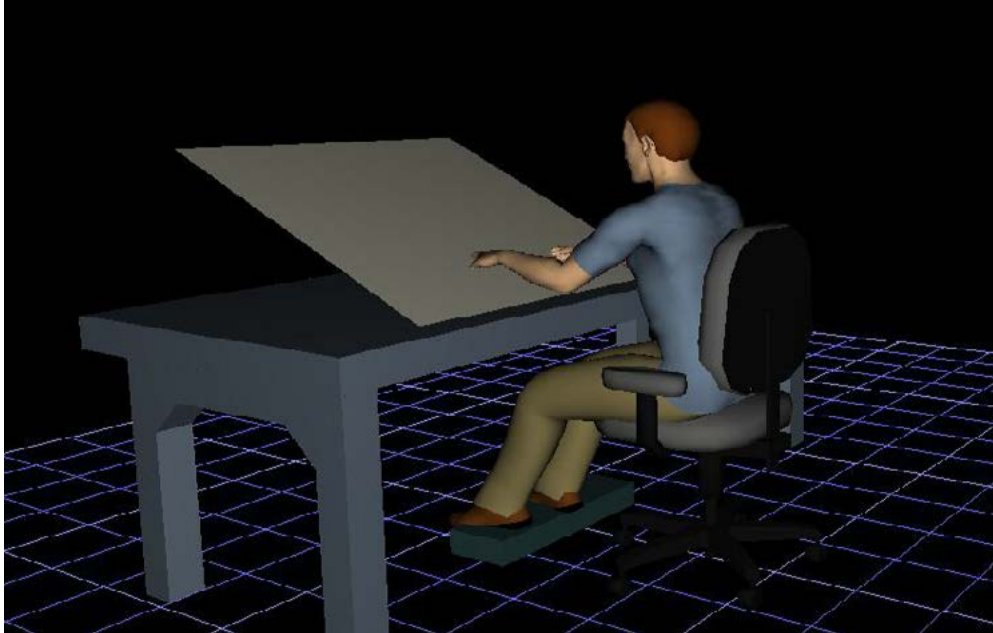


Figure 4. Virtual Human

2.3. Evaluate Phase

In this phase, we conduct evaluation based on Low Back Analysis (LBA), Rapid Upper Limb Assessment (RULA), and NIOSH Lifting Equation using Task Analysis Toolkit in Jack to assess ergonomics level of this task. For the first method, we use LBA, it is a method for evaluating the forces working in the human spine on certain load condition and posture. This analysis evaluates the load received by the spine of mannequin models when performing a given task in real time. Then pressure value is compared with the existing restrictions on the standard pressure NIOSH 3400 N. Using posture simulation, we found that the score is 3734 N which exceed standard of NIOSH standard.

RULA (Rapid Upper Limb Assessment) is the method to assess musculoskeletal posture risk for the activity. Posture assessment by using RULA will produce a score that has range of numbers from 1 to 7 which illustrates the risk posture of the musculoskeletal system of the worker.

Table 2. RULA Action Level

Action Level	RULA Score	Description
--------------	------------	-------------



Action level 1	1 or 2	The posture that examined or observed can be accepted if it's not done continuously in a long time.
Action level 2	3 or 4	The further investigation is needed and also the changes of working posture should be done.
Action level 3	5 or 6	The investigation is needed and also the changes of posture should be done soon.
Action level 4	7	The investigation is needed and also the changes of posture urgently must be done.

In this result from figure 5, we obtained the score 7 using current condition. Based on this value, we found that RULA score need to be reduced because exceed the ergonomics standard. So, we have to arrange the workstation in order to reduce ergonomics risk.

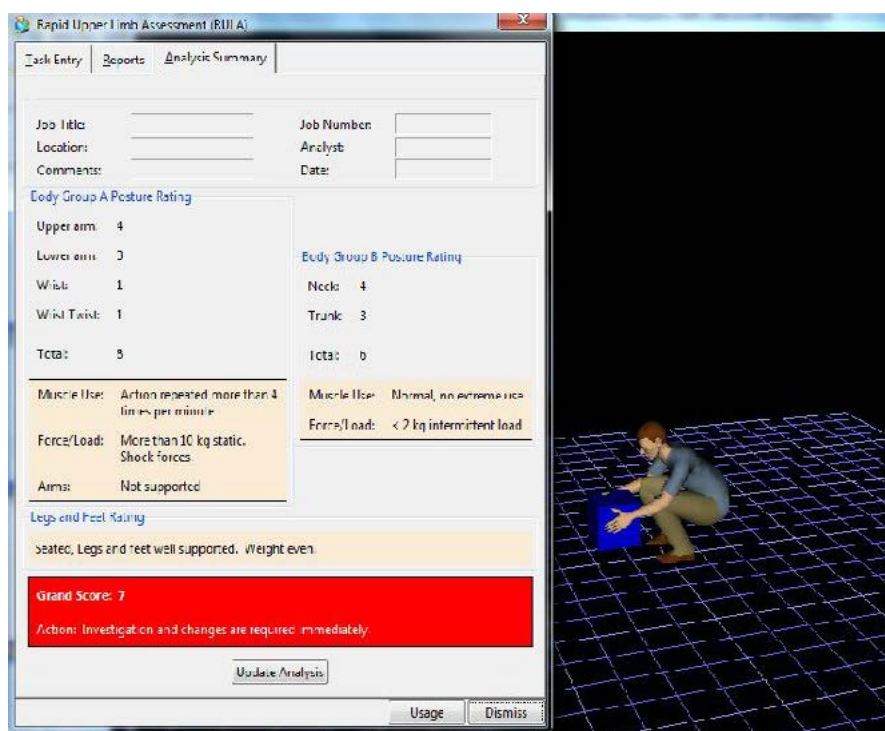


Figure 5. RULA Score

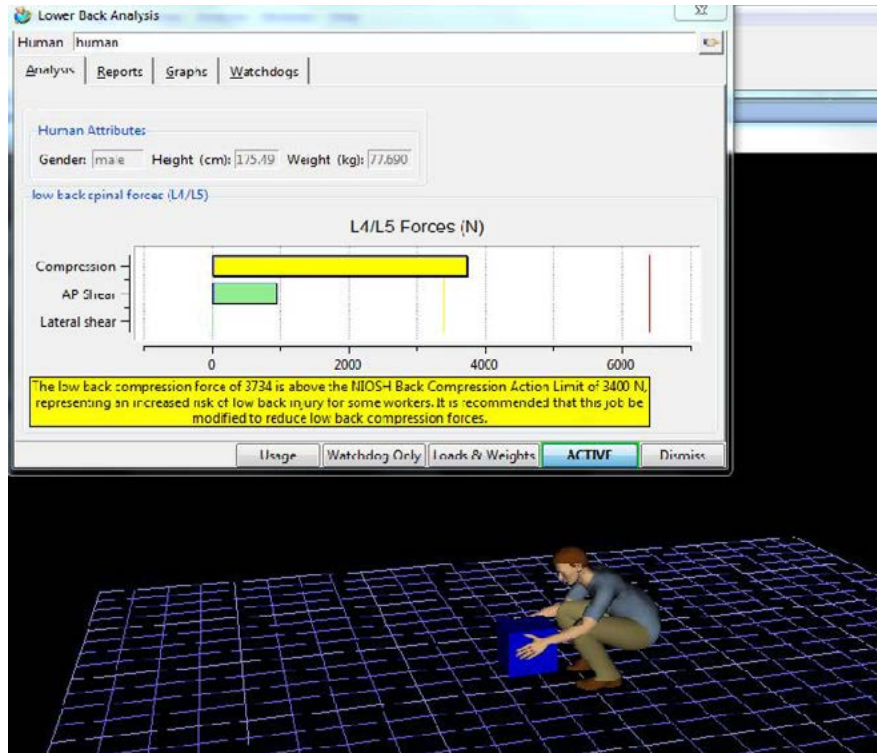


Figure 6. LBA Score

2.4. Adapt and Synergize Phase

In the adapt and synergize phase, we tried to rearrange the work station based on method engineering and work design. We propose 2 solutions here:

For the first solution, we change posture mechanism such as in lifting, sitting, and standing position . We also eliminate ineffective motion to reduce the waste in the process and adjust workload using NIOSH formula.

For the second solution, we change the specification of workstation with the adjustment regarding anthropometry of operators. We also add the armrest and footrest in the chair regarding to improve comfort of operators. We conducted testing for these solutions to compare the result before and after simulation.

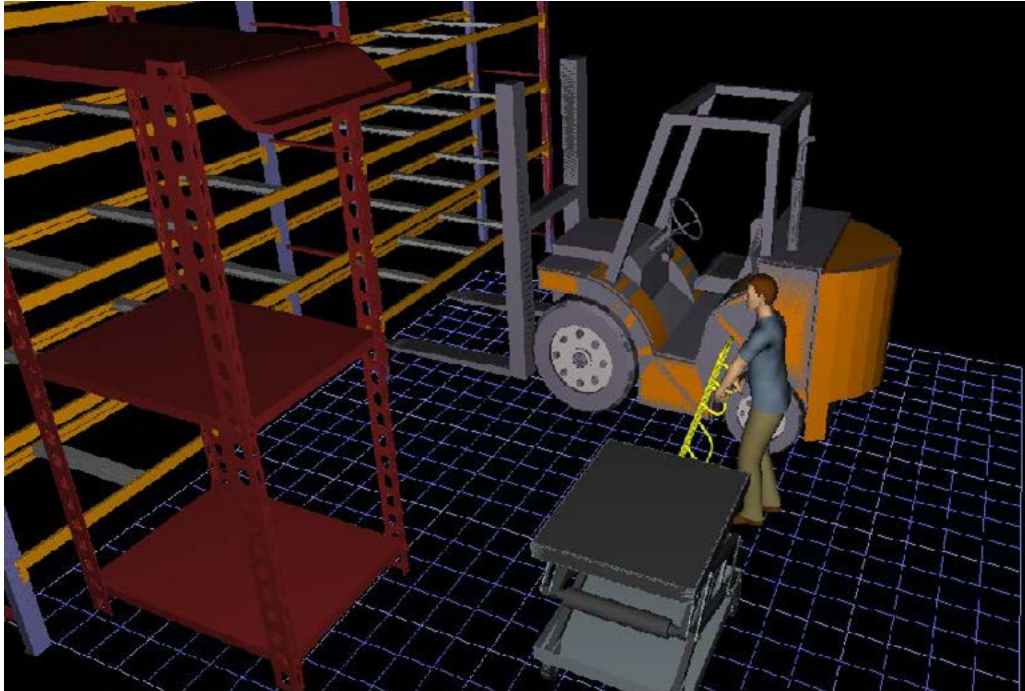


Figure 7. Workstation Redesign

3. RESULT AND DISCUSSION

Based on the simulation, we compare proposed design and actual design. After calculating RULA for proposed design we obtained score 2. From this result, we can conclude that the proposed design is better than actual design.

Table 3. LBA and RULA Score

Condition	LBA	RULA	NIOSH Lifting Index
Current	3734	7	1.42
Proposed	854	3	0.86

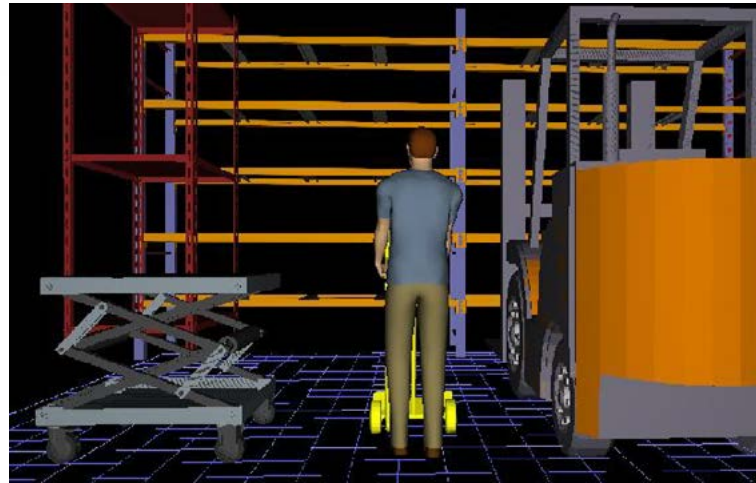


Figure 8. Method Mechanism and Workstation



Figure 9. Model Outputs in NIOSH Lifting Equation

From the **Figure 9** above, it can be seen that reconfiguration design can reduce ergonomics risk. In the first indicator, LBA, the solution has successfully decreased low back risk from 3734N in actual condition to 854N in proposed condition. In the second indicator, RULA, there is also decrease in the ergonomics risk from 7 to 3. In the last indicator, NIOSH Lifting index indicates that bigger the lifting index score, bigger the risk. The standard score for NIOSH is 1, which means that it needs adjustment if exceeding that standard. Based on calculation, there is decrease about 39.4% from 1.42 to 0.86. In the last phase, we form the guideline about the proposed method and work design as an initiative for sustaining solution in the synergize phase.



4. CONCLUSION

Based on this research, using IDEAS framework is suitable for redesigning occupational task based on digital human modelling approach, because it can provide structured approach from identifying the task, designing virtual environment, evaluating ergonomics condition, adapting and synergizing solution.

Furthermore, IDEAS framework is highly feasible to be adopted in managing work redesign in many areas for occupational ergonomics for the manufacturing and service sector.

5. ACKNOWLEDGEMENTS

Authors acknowledge Ergonomics Center Universitas Indonesia for support during the research.

6. REFERENCES

- Abbas MF, Faris RH, Harber PI, Mishriky AM, El- Shahaly HA, Waheeb YH, Kraus JF., (2001), Worksite and personal factors associated with carpal tunnel syndrome in an Egyptian electronics assembly factory, *Int J Occup Environ Health*, vol 7.
- Ho SF, Phoon., (1997), The significance of aches/pain among workers in an electronics factory, *Medical Journal Malaysia*, vol 52.
- Pocckay P, McCurdy SA, Samuels SJ, Hammond SK, Schenker MB., (1995), A cross-sectional study of musculoskeletal factors in semiconductor workers, *Journal of Ind Medical*, vol.28.
- Schenker MB, Gold EB, Beaumont JJ, Eskenazi B, Hammond SK., (1995), Association of spontaneous abortin and other reproductive effects with work in the semiconductor industry, *Journal of Ind Medical*, vol. 28.
- Siemens PLM Software Inc., (2008), Jack task analysis toolkit (TAT) training manual, California: Author
- Tan GLE., (1997), Ergonomics in manufacturing industries in Malaysia. Education and Training, Small Industries, Countries in Transition, Theories and Methodologies, Miscellaneous Topics In: *Proceedings of the Triennial Congress of the International Ergonomics Association*
- T.Septyan., (2013), Virtual Human Modeling and Biomechanics Fatigue Index Assessment for Toll Booth in Indonesia, *Technology, Education, and Science International Conference (TESIC) Proceeding*
- T. Septyan, B. Nurtjahyo., (2013), Virtual Human Modeling and Simulation for Toll Booth Design in Indonesia, *Advanced Engineering Forum*, vol. 10
- Wilson, J.R., (1999), Virtual Environments and Applied Ergonomics, *Applied Ergonomics* 30
- Yeow PHP, Sen RN.,(2004), Ergonomics improvements of the visual inspection process of a printed circuit assembly factory, *International Journal of Occupational Safety and Ergonomics (JOSE)*.



THE PROPOSAL OF FOOTWEAR PRODUCT IMPROVEMENTS BY USING THE METHODS OF SIX SIGMA AND QUALITY FUNCTION DEPLOYMENT IN PT. PRIMARINDO ASIA INFRASTRUCTURE TBK

Julian Robecca
*Universitas Komputer Bandung, Fakultas Teknik dan Ilmu Komputer,
Program Studi Teknik Industri
Jl. Dipati Ukur no.102-116, Bandung 40132, Indonesia*
julian.robbecca@email.unikom.ac.id
ivorobbecca@gmail.com

ABSTRACT

Six Sigma is a holistic approach to solve the problem and process improvement through a phase of DMAIC (Define, Measure, Analyze, Improve and Control). DMAIC is the heart of Six Sigma analysis that ensures voice of the customer to run in the overall process to produce products that satisfy customers. Quality Function Deployment (QFD) is a methodology in the process of designing and developing products or services that are able to integrate the 'voices of consumers' into the designing process. Producing the products that are 100% good is not easy. This is experienced by PT Primarindo Asia Infrastructure Tbk., as the casual shoes type production company in Bandung area. Until 2016, there are still many defects which are generated. Although sigma level of Tomkins shoe production has reached level 4, the company must continue to reduce the number of defects that occur in order to raise the sigma level. The results showed that the defect types are most widely produced from four shoes models; they are the defect types of slanted lasting. Although the sigma level which is resulted already exceeds level 4, it needs improvement so that the defects number is reduced. For junior shoe model variables, what must be corrected is the shoes durability, tears on shoes, easily broken shoe eyelets, the power of adhesive glue on shoes, and slippery footwear. The improvement on shoes durability is done at the assembly aspect. The selection of good glue raw materials and glue polishing on shoe components should also be improved because it will influence the adhesive power. The improvement on slippery footwear variable is the materials selection for good footwear so the shoes does not become slippery, and the pattern on the outsole also influences the shoe grip to the ground and it is not easily slip to the users. The Methods of Six Sigma and QFD are expected to reduce the number of defects with the improvements as proposed by each method.

Keywords: Defect, Six Sigma, Quality Function Deployment, House of Quality



1. INTRODUCTION

Shoes are one of present society primary needs. The demand of shoes continues to rise from time to time. PT. Primarindo Asia Infrastructure Tbk is a company that is engaged in the manufacture of casual shoes type of whose its production number continues to increase each year. The shoes which are manufactured based on two market areas are the areas of international market and domestic market. For the production of local/domestic market, Tomkins shoes brands have 4 shoes models; they are the shoes models for child, junior, women and man. The company has had its own method in producing shoes, but in the implementation, there remains to find defective product units. Total production from 2013 continues to increase until 2016. However, defective products are inevitable and there is still quite a lot defects number that occurs. The defects types in the shoes production are very diverse including slanted lasting, slanted velcro, wrinkles, upper defect, out sole, and etc. Based on the number of defective units which is still high, it needs the improving action in order to minimize the defects number annually. The use of proper methods in determining the improvement technique is very helpful, including the method of Six Sigma and Quality Function Deployment (QFD).

By applying Six Sigma methods approach, it is expected to improve the stability of capability process, to define, to measure, to analyze, to improve and to control the processes to reduce or even to eliminate defective products so that companies are able to compete in global market which is increasingly competitive and to increase productivity and profitability. While the application of QFD method in this case, House of Quality (HOQ), it is expected that the structure and process of improvement and development are obtained based on converting the voice of consumers (Costumers Need's) directly to the characteristics or the technical specifications of a product. PT. Primarindo Asia Infrastructure Tbk as one of the largest shoes manufacturers in Indonesia must be able to compete with other manufacturers by continuously maintaining and improving its product quality.

2. METHODOLOGY

Systematic research methodology can be seen in the figure below

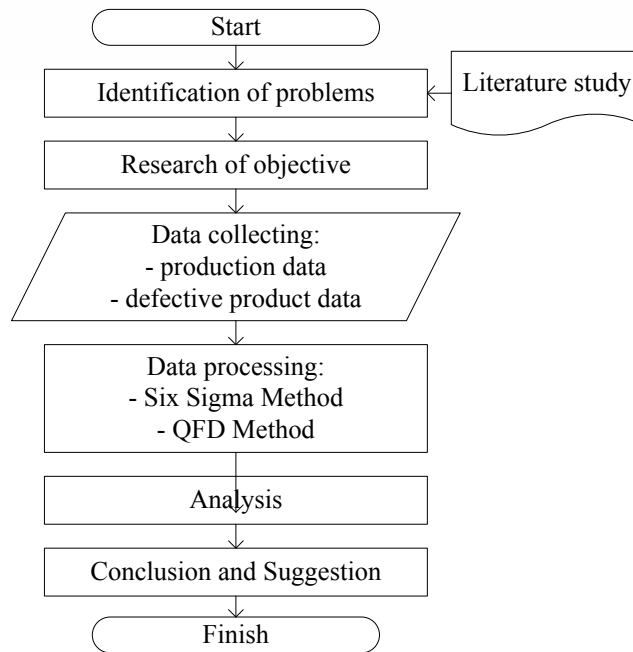


Figure 1 The Methodology of Troubleshooting

3. RESULTS AND DISCUSSION

3.1 The Method of Six Sigma

3.1.1 Define

In the define phase, it is conducted the determination of the products type that has the greatest number of defects. From the four types of Tomkins shoes, the greatest number of defects was found in junior shoes type of 927 units. The next step is to identify the variables of Critical to Quality (CTQ), of which CTQ variables on junior shoes type are slanted lasting, slanted eyelet/velcro, out sole, wrinkles, upper defect and etc (dirty, scratches).

3.1.2 Measure

In the measure phase, it is conducted the measurement of dominant defect and sigma level. The dominant defect types on junior shoes type is slanted *lasting* defect (the slanted uppers shoes component). The measurement results of sigma level on junior shoes type is at 4.4 level, which means that to get to six sigma level still needs improvement.

3.1.3 Analyze

Analyze phase is performed to find the defect cause occurs. The cause of slanted lasting defect is identified by using causal diagram (cause-effect diagram). The following is a causal diagram (cause-effect diagram) which describes the cause factors that slanted lasting occurs.

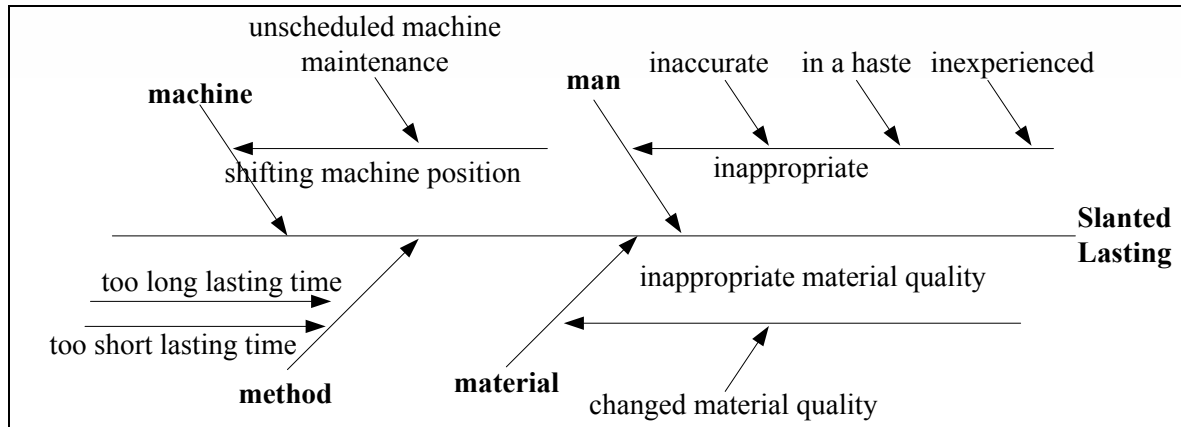


Figure 1 The Defect Cause Factors of Slanted Lasting

3.1.4 Improve

The method of 5W + 1H is used to make the technical improvement stages based on cause factors of the defect which are obtained from the analyze phase.

Table 1 The Stages of Slanted Lasting Improvement Using 5W + 1H Method

Improve ment Priority	Current Condition	What	Why	Where	When	Who	How
Operator's error in the lasting process (inappropriate lasting position)	Supervision of foreman/leader line	The placement of laste position must be appropriate to the instruction	To make lasting position not slanted and slanted can be detected prior to the next work processing	Assembling department, lasting section	During production process	Foreman, Lasting operator	Adding foreman and inspecting each completed lasting process
	The training is at start working				Not in production hours	Lasting operator	More intensive training
Inappropriate lasting time	Manually through operator monitoring	Lasting time must be fitted, should not be too long or too short	In order lasting to be fully formed	Assembling department, lasting section	During production process	Lasting operator	Using automatic mode or using sonant time reminder



The shifting machine position	Setting to start	The machine position should be fixed, according to the lasting form	In order lasting to be fully formed	Assembling department, lasting section	Not in production hours	Maintenance officers	Periodic machine condition monitoring
Last material quality is changed	Last replacement when it is broken	The last quality must be maintained	To make last appropriate to its specification	Assembling department, lasting section	Not in production hours	Maintenance officers	Periodic last condition monitoring

3.2 The Method of Quality Function Deployment (QFD)

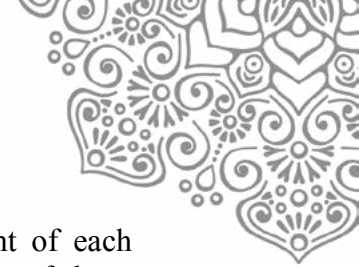
QFD method that is used is to create House of Quality (HoQ). The first stage is to collect the voice of consumers which is gained 8 variables through the questionnaires that were distributed.

The second stage is the measurement of consumers' interest level. It aims to determine the priority of consumers' interests and to be a reference for company to develop strategies in order to meet the desires and needs of the consumers. The consumers' interests level of Junior shoes type shows that consumers value 5 scores on the variables of shoes durability, shoes comfort, and non-slippery shoes outsole, value 4 scores on the variables of the power of adhesive glue on shoes, no tears on the shoes, shoe eyelets are not easily broken and neat shoes stitching, while for the variables of shoe accessories, consumers simply value 3 scores, which means consumers are not concerned with the aspects of shoe accessories variables.

The third stage is to calculate the value of junior shoes type quality. The variables of shoes durability, the power of adhesive glue, and non-slippery shoes outsole, junior shoes type have just got 3 scores. While in the variables of shoes comfort, shoes accessories, no tears on the shoes, neat shoes stitching, materials quality, shoes color, materials types, shoes size and shoes elasticity have got 3 scores. The company must make improvements in order to get better respondents' assessment.

The next stage is to determine the technical characteristics of the voice of consumers variable and the variables relation level with all the existing technical characteristics, which the relation level has 1 or 3 or 9 scores.

The next stage is the fifth stage. It is to identify the matrix of relation between the technical characteristics. The results showed that there were only 2 relations; they are strong positive and weak positive relations.



The last stage is the determining stage that should be taken for improvement of each variable. For junior shoes type, the variables that should be improved are variables of shoes durability, no tears on the shoes, not easily broken shoe eyelets, the power of adhesive glue on shoes, and non-slippery footwear. The improvement on shoes durability is done on the assembly aspect. Good selection of raw materials and glue polishing on shoe components should also be improved because it will influence the adhesive power. The improvement on non-slippery footwear variable is with the materials selection for good footwear so it does not become slippery; and the pattern on the outsole also influences the shoes grip to the ground and not easily slip to users.

4. CONCLUSION

Based on the results of data processing and analysis, it can be concluded as follows:

- a. The types of shoes which are made as the study object is Junior shoes type, with defect variables that occurs are slanted *lasting*, upper defect, outsole, slanted eyelet/velcro, wrinkled, and etc.
- b. The most dominant type of defect is slanted *lasting*
- c. Overall, sigma level which is achieved is 4.4
- d. The factors which make slanted *lasting* are:
 - Improper *lasting* position for the operator is in haste, inaccurate, and inexperienced
 - Inappropriate *lasting* time
 - The machine position is shifting for unscheduled maintenance
 - The quality of *laste* material is changed
- e. The corrective actions that must be taken are:
 - Adding foreman and inspecting each *lasting* process which is completed for the factor of improper *lasting* position for the operator is in haste, inaccurate, and inexperienced
 - More intensive training to the operators for the factor of inappropriate *lasting* time
 - Using automatic mode or sonant time reminder for the factor of inappropriate *lasting* time
 - Monitoring to the machine condition regularly for the factor of the machine position is shifting for unscheduled maintenance
 - Monitoring *laste* condition periodically for the factor of the quality of *laste* material is changed
- f. The variables based on the voice of consumers that should be improved are:
 - The shoes' durability
 - No tears on the shoes
 - Shoe eyelets are not easily broken
 - The power of adhesive glue on shoes
 - Non-slip footwear

6. REFERENCES

Cohen, Lou. (1995), *Quality Function Development: How to Make QFD Work for You*, Addison-Wesley Publishing Company, Massachusset.



- Heizer, J., & Render, B. (2009), *Manajemen Operasi (Operation Management)*, Salemba Empat, Jakarta.
- Syukron, A., & Kholil, M. (2013), *Six Sigma Quality for Business Improvement*, Graha Ilmu, Yogyakarta.



OPTIMIZATION OF INDUSTRIAL PRODUCTION PLANNING WITH UNCERTAIN RAW MATERIAL SUPPLY

Farizal, Sucipto, Amar Rachman

Department of Industrial Engineering, Faculty of Engineering, Universitas Indonesia
Kampus BaruUI Depok, Jawa Barat, 16424, Indonesia

Corresponding E-mail: farizal@eng.ui.ac.id

ABSTRACT

This study discusses the optimization model of industrial production planning in patchouli oil derivatives industry. Production planning always deals with uncertain demand. This industry, as addition, is also characterized with uncertain raw material supply. Taking those issues into consideration, the objective of this optimization model is to minimize the production cost, carrying, and backlogging costs. For the purpose the forecasting methods used is moving averages method through software Oracle Crystall Ball while the linear programming model was optimized by Lingo software. The result shows that the model can streamline 19.09% of the actual conditions in the absence of planning. In addition, further analysis of efficiency can also be done by raising the purchase price of raw materials less than 1,67% if supplying to be under certainty

Keywords: Optimization, production planning, production costs, forecasting, uncertain supply.

INTRODUCTION

Chemical industry is one of the largest industrial sectors of the world. With the highly competitive environment, companies are increasingly facing external pressure to improve customer response time, increasing product bargaining power, managing a wide range of demands as well as making competitive product prices.

Production planning is one tool that can be used to reduce operational costs, improve customer service and utilize resources optimally. Production planning will be more complicated if there exist uncertainties (Arellano-Garcia, 2009). One chemical industry facing such a problem is natural essential oil chemical company. The raw materials used, i.e. patchouli oil are among the highest price when compared with other essential oils. The aroma of patchouli oil known as 'heavy' and 'strong' and has been used for centuries as fragrances (perfume) and materials incense in eastern tradition. Indonesian patchouli oil contributes 80% of the total supply for the world patchouli essential oil.

Despite having high price, the availability of patchouli essential oil is also very uncertain. This condition leads the industry, for many cases, could not fulfill orders or when the unfulfilling demand is unavoidable, it leads to soaring production cost. Figure 1 shows patchouli price from 2010 to 2015.

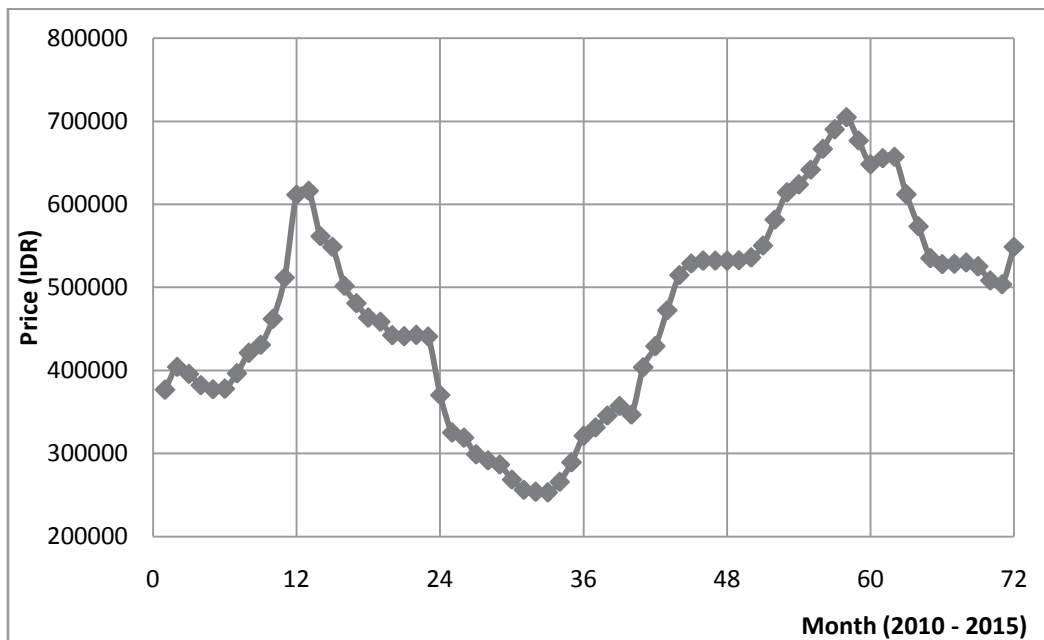


Figure 1. Patchouli Oil Prices at 2010 – 2015

Figure 2 shows patchouli oil availability and request for raw productl A and B. The figure clearly indicates that the supply is scarce and barely enough to fulfill the industrial need. This means the competition among the industries to satisfy their need is fierce.

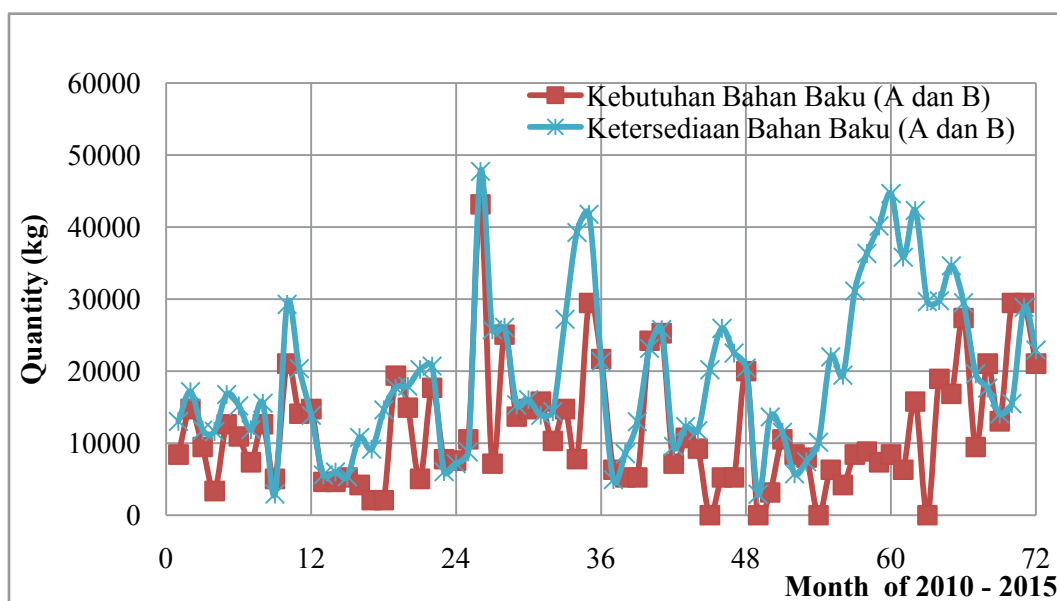


Figure 2. Patchouli Oil Availability vs Request of Raw Materials A and B

To cope with the problem, this study will demonstrate how forecasting and optimization will help the industry to be more competitive. For the purpose moving average forecasting method and linear programming model will be used.



LITERATURE REVIEW

Several studies on production planning using optimization have been done. Lin, et al (2004) studied a new approach to address the planning and scheduling of processing time uncertainty using model Mix Integer Linear Programming (MILP). Dileep (2007) discussed the multi-engine, multi-product lot size and planning problems. The model was developed considered not only the operational costs associated supplies, but also the cost of the machine is available. The solution to minimize inventory and costs associated resources. Adida and Joshi (2009) investigated the uncertainty in project management.

Javanmard and Kianehkandi (2011) proposed MILP models for optimal production planning with a single machine. The model takes into account all the standard constraints encountered in scheduling production (material balance, the limited supply, the capacity of the engine, shift of labor and labor restrictions). Chen and Cao (2015) presents a robust optimization models for problems integrated multi-product of planning and scheduling under uncertainty product prices. The approach used in the model uncertainty robust optimization is a box set, set ellipsoidal, polyhedral set, combined Boxes and ellipsoidal set, combined Boxes and polyhedral sets, combined Boxes, ellipsoidal and polyhedral sets.

METHODOLOGY

The production process of patchouli oil shows in Figure 3:

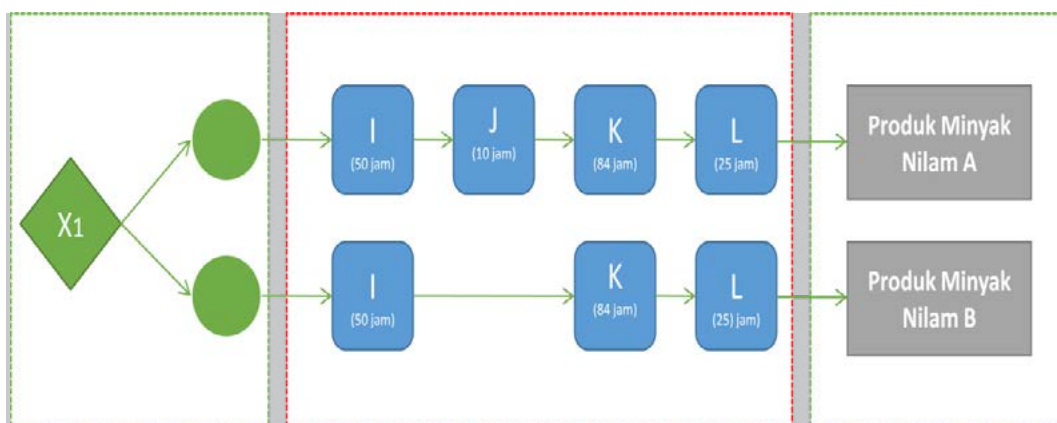


Figure 3. Flow Patchouli Oil Derivative Production Process Single Line

I = Reaction 1 in Utilities I, J = Reaction 2 in Utilities J, K = Fractionation in Utilities K
L = Mixing and Filling in Utilities L, X1 = Raw Material for Patchouli Oil Patchouli oil products A and B. Product A: a product of patchouli oil with 30% purity level specifications, the acid value is small, a small iron content and color clarity. A product is obtained with several stages like showed on Figure 3 above. Product B: a product of patchouli oil purity level of 30%, an acid value is small and rather dark color.

A mathematical model of how to optimize production quantities will be produced and how much will be saved and there backlog to limit the availability of raw materials (Taha, 2007). Complete mathematical model is presented as follow:

$$Min Z = \sum_{t=1}^{12} \sum_{i=1}^2 N_{i,t} \times B_{i,t} + \sum_{t=1}^{12} I_t \times H_t + \sum_{t=1}^{12} \sum_{i=1}^2 A_{i,t} \times L_t$$



Subject to

$$\sum_{i=1}^2 N_{i,t} \leq Q \quad \forall i = 1,2; t = 1, 2, \dots, 12$$

$$N_{i,t} \geq MQ \quad \forall i = 1,2; t = 1, 2, \dots, 12$$

$$0 \leq N_{i,t} \leq Q \quad \forall i = 1,2; t = 1, 2, \dots, 12$$

$$I_{t-1} + P_t \geq \frac{N_{i,t}}{0,95} + I_t \quad \forall i = 1,2; t = 1, 2, \dots, 12$$

$$N_{i,t} \geq O_{i,t} \quad \forall i = 1,2; t = 1, 2, \dots, 12$$

$$O_{i,t} - N_{i,t} = A_{i,t} \quad \forall i = 1,2; t = 1, 2, \dots, 12$$

$$N_{i,t} \geq 0 \quad \forall i = 1,2; t = 1, 2, \dots, 12$$

$$I_t \geq 0 \quad \forall t = 1, 2, \dots, 12$$

$$A_{i,t} \geq 0 \quad \forall i = 1,2; t = 1, 2, \dots, 12$$

$$P_t \geq 0 \quad \forall t = 1, 2, \dots, 12$$

Variable:

- $N_{i,t}$ = Total production kg of product i in month t where $i = A, B$ and $t = 1, 2, \dots, 12$
- I_t = Total kg stock of raw material in month t
- A_t = Total kg backlog in month t

Parameter: $B_{i,t}$ = Production cost per kg i in month t (in IDR), H_t = Holding cost per kg i in month t (in IDR), L_t = Backlog cost per kg i in month t (in IDR), Q = Kg equipment capacity per month (Kg), MQ = Minimal amount of production (Kg), P_t = Purchase of raw materials per kg i in month t , I_{t-1} = Saldo raw material stock in month $t-1$, and $O_{i,t}$ = Total order kg i in month t

RESULTS AND DISCUSSION

Before running the model, based on the available data, forecasting was run. Accuracy of the forecast is presented on Figure 4 and Table 1. Table 1 clearly shows that ARIMA (1,1,0) gives the best forecast.

Table 1. Forecasting method accuracy

Forecasting Method	MAPE	RMSE	MAD	Rank
ARIMA(1,1,0)	3.39%	23081	15970	Best
Damped Trend Non-Seasonal	3.42%	23201	16079	2nd
Double Exponential Smoothing	3.79%	25410	17880	3rd

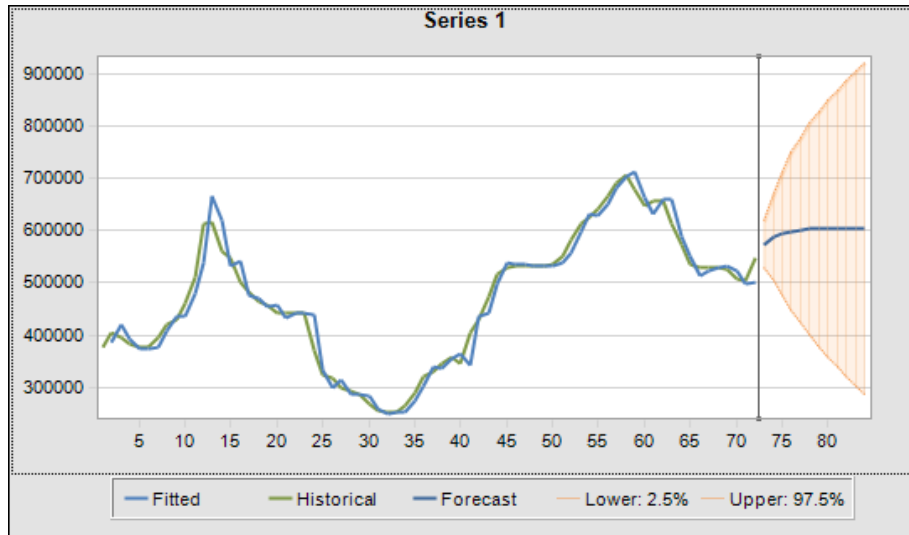
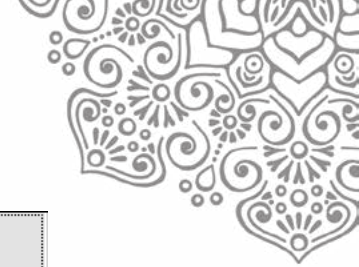


Figure 4. Fitted, Historical, and Forecast of Raw Material Price

Based on the data, the model is solved using LINGO. The results are summarized on Tables 2-4.

Table 2. Comparison of Actual Production Planning and Optimization

Month	Product A (kg)			Product B(kg)		
	Demand	Production		Demand	Production	
		Optimization	Actual		Optimization	Actual
1	6.000	6.000	7.000	0	0	0
2	10.000	10.000	9.600	5.000	5.000	4.400
3	0	0	0	0	0	2.400
4	18.000	18.000	16.000	0	0	0
5	0	0	0	16.000	16.000	16.400
6	18.000	18.000	19.400	8.000	8.000	8.000
7	9.000	9.000	10.000	0	0	0
8	16.000	16.000	16.600	4.000	4.000	4.000
9	8.000	8.000	8.800	4.400	4.400	4.400
10	8.000	8.000	7.500	20.000	20.000	10.000
11	4.000	4.000	9.000	24.000	24.000	22.800
12	10.000	10.000	11.400	10.000	10.000	9.000
Total	107.000	107.000	115.300	91.400	91.400	81.400

Table 2 shows a significant different results between production planning proposed by the optimization model and the actual planning for both products A and B. the optimization model results produce the amount of products exactly the same as the demand. While the actual planning ends up with either producing the products more than the demand (meaning over production) or less than the demand (unfulfilled demand).



Table 3. Comparison Unused Raw Materials and Over Stock Products in 2015

Month	Unused Raw Material (kg)		Over Stock Product A and B (kg)	
	Optimization	Actual	Optimization	Actual
1	0	28.447,06	0	0
2	0	27.577,22	0	600
3	0	27.103,91	0	3.000
4	0	12.936,8	0	2.400
5	0	17.351,64	0	2.800
6	0	220,73	0	4.600
7	0	10.152,75	0	4.600
8	0	0	0	2.800
9	0	142,86	0	2.800
10	0	0	0	0
11	0	0	0	400
12	0	0	0	0

Table 3 shows that under ideal conditions (using the model) the unused raw material and the stock at the end of the month is zero, so there is no storage costs for both raw material and finish product. While the actual planning provides some inventory for both raw material and finish product for almost each month. This results make sense since for the actual planning, the company compensate the uncertainty with buying raw material more than needed and set some level of safety stock for the finish product. But, unfortunately, this practice will make the inventory costs higher to the company.

Table 4. Comparison of Raw Material Purchasing and backlog for the model and Actual for 2015

Month	Raw Material Purchasing (kg)		Total Backlog (kg)	
	Optimization	Actual	Optimization	Actual
1	0	2.343,8	0	0
2	15.780	13.867	0	600
3	0	2.053	0	0
4	18.936	2.675	0	1.400
5	16.832	21.678	0	0
6	27.352	12.132,25	0	0
7	9.468	19.405,7	0	0
8	21.040	7.479,5	0	1.600
9	13.044,8	14.037,6	0	0
10	29.456	15.346,5	0	10.500
11	29.456	28.842	0	1.200
12	21.040	22.940,7	0	1.000



Table 4 shows planning for raw material purchased according to the optimization model and the actual practice. According to the model, raw material is not necessary purchased every month; contrary to the actual practice. By so doing the material will directly be used up for fulfillment the demand. For this scenario, the total cost incurred by the company for the production of product A and product B for one year is Rp. 1.254.877.000, whereas if no actual planning in Rp. 3.228.225.464. The difference is Rp. 1.973.328.960. This difference is the value of planning the production process, so there are 61.13% of potential costs can be reduced on the actual condition to the ideal conditions.

To allow the company to increase the probability from the availability of raw materials, it can buy more material when the purchase price is high to avoid backlog, it occurs at scarcity situation. This situation will be traded off with backlog cost. By shifting the value of Rp. 1.973.328.960 per year to raise the purchase price will obtain trade off value of 1,67%, about Rp 9.742 per kg. This means that if the availability of raw materials will be guaranteed, with a raise of 1,67% of the price of a standard, then the condition is still equal to the costs incurred in the actual process.

CONCLUSION

This research provides a production planning model to minimize the total cost of production, the production costs, storage costs, and the cost of the backlog. The ideal conditions on a model are characterized with the availability of raw materials, purchase only needed raw materials, no backlog occur, no any additional costs incurred. The proposed model offers 61.13% potential saving costs compare to the actual condition. There are two model approach performed in this study, the forecast and optimization. Raw material price forecast is using Autoregressive integrated moving average (1,1,0) model whereas raw material forecast is using double moving average models. This optimization model developed can streamline up to 19.09% of the actual conditions.

In the case when high raw material price occurs, the trade-off value is 1.67% to the actual condition. This condition is a result of balancing between minimizing the raw materials storage and minimizing the occurrence of backlog.

REFERENCE

- Adida, E. and Joshi, P. (2009). A Robust Optimization Approach to Project Scheduling and Resource Allocation. *Int. J. Services Operations and Informatics*, Vol. 4, No. 2.
- Arellano-Garcia, H. (2009). Chance constrained optimization of process systems under uncertainty. *Computers & Chemical Engineering*, Vol. 33, Issue 10, 14 October 2009, 1568–1583.
- Chen, M. and Cao, C. (2015). Robust Optimization for a Multi-Product Integrated Problem of Planning and Scheduling under Products Uncertainty. *Journal of Applied Mathematics and Physics*, Vol. 3, pp. 16-24.
- Dileep, D.G. (2007). Product Costing for Decision-Making in Certain Variable-Proportion Technologies. *Journal of Management Accounting Research*, Vol. 19, pp. 51-70.
- Javanmard and Kianehkandi. (2011). Optimal Scheduling in a Milk Production Line Based on Mixed Integer Linear Programming. *International Proceedings of Economics Development & Research*, Vol. 13.
- Lin, X., et al. (2004). A New Robust Optimization Approach for Scheduling Under Uncertainty: I. Bounded Uncertainty. *Computers & Chemical Engineering*, Vol. 28, 1069-1085.
- Taha, H. A. (2007). *Operations Research: An Introduction* (8th ed.). Singapore: Pearson Prentice Hall.



Maintenance Strategy on Boiler System Steam Power Plant Based on Reliability Centered Maintenance (RCM)

Rahmat Nurcahyo, Nanang Tri Wahyuna dan Yadrifil
Industrial Engineering Department, University of Indonesia
E-Mail: nanangntw1@gmail.com

ABSTRAK

This research discusses about Maintenance Strategy on Steam Power Plant. The steam power plant has Complex Systems and Equipment subsystems consists of Mechanical Equipment, Electrical equipment and Instrumentations equipment with types and characteristics of different damage. Based on the distribution system and according to the function, the power plant has 8 Main System. Failure History Data System grouped by damage and Pareto diagram visualize Top 20% Failure on whole system. By doing Failure Modes and Effects Analysis (FMEA) obtained by analysis of failure modes, failure causes and effects on the equipment failure to overcome the highest risk at a power plant. After analyzing the highest failure based on the evaluation the highest risk of failure, the failures eliminated by approach of Reliability Centered Maintenance (RCM). As a result study is a Maintenance Strategy with approach based on RCM. Logic Tree Analysis (LTA) is a deductive method of analysis used as a Maintenance Strategy for classifying some failure modes required in determining maintenance decisions (Maintenance Action).

Keywords: Steam Power Plants , Failure Modes and Effect Analysis (FMEA), Reliability Centered Maintenance (RCM), Equipment Failure, Logic Tree Analysis (LTA), Maintenance Strategy, Maintenance Action.

1. Introduction

Indonesia has the State-Owned Enterprises (BUMN) which is engaged in power generation that is called the State Electricity Company (PLN). In the last 6 years, 2009 until 2014, PLN's business continued to grow in line with economic growth and electricity consumption by the public. Electricity sales increased from 133.1 TWh in 2009 to 196.4 TWh in 2014, the number of subscribers increased from 39.8 million in 2009 to 57.1 million in 2014, and the electrification ratio increased from 63.5% in 2009 to 84.0% in 2014.

PT PJB is one of the subsidiary company PT PLN which responsible for supplying electricity in Java and Bali. PT PJB has a mission dedicated to producing electric power that reliable and competitive in order to support national development considering the needs of electricity consumption in Indonesia how many on the island of Java and Bali.

Based on statistical data of PT PJB years 2008 - 2012 it was noted that the installed power of the average largest in power plant PT PJB produced by Power Gas and Steam (Power Plant) by 41, 972%, Steam Power (power plant) amounted to 30.488%, Power hydroelectric of 19.844% and Gas Power plant amounted to 7.704%.

From the statistical data company of PT PJB required more effort to maintain the reliability of electricity supply for the community needs and the company's data required high availability for the plants to meet the electricity needs. To maintain the reliability of the power generation, PT PJB must perform maintenance on the engine generator. In the dicision operation, the steam power plant is the core unit to be active in generating electricity because the steam power plant to generate electricity requires a long time in preparation it is about 8 hours from heating steam to generate electricity.

Gas turbine power plant and hydroelectric power plant is a standby unit which generating units require less time to generate electricity which is about 30 minutes. Due the steam power plant is the core unit so the maintenance of the steam power plant must be optimized to support the performance of generating units. Steam power plant consists of a lot of different tools depending among other mechanical equipment, electrical and instruments for the operation damaged the diverse, so that the necessary maintenance according to the type and characteristics of each damages.



The power plant has a complex system and usually a lot of production machinery manufacturers little receive feedback from the operating history so the maintenance of the engine manufacturers are less suitable for production machines which have undergone aging (Carazas dan souza, 2009). In this study will discuss maintenance strategy that systematically into account the type kind of failure and failure characteristics that is different to improve performance of power systems effectively and efficiently.

2. Literature Review

Maintenance is an activity that is intended to prevent the occurrence of downtime (lost production hours) that are not planned by way of planned downtime, both when and how long time. This activity is known as the shutdown management (joshi, 2012). The main purpose the maintenance is to increase the availability of production machines. Availability (availability) is important in the production systems in industrial companies which is largely determined by the availability of the machines or systems and production equipment availability is a measure of the percentage of time where the machines / systems production equipment capable of producing at a certain level that is acceptable.

Availability is an important production system at industrial company which is largely determined by the availability of machines or production equipment system and availability is a measure of the percentage of time the machines / systems production equipment capable of producing at a certain level that is acceptable (Carazas and Souza, 2009).

RCM is the optimum mix of reactive, time or interval-based, condition-based and proactive maintenance. The principle of this maintenance strategy is to integrate the advantages of each power maintenance to maximize maximize reliability and minimize maintenance costs (Afehy, 2010). And RCM is a qualitative approach, risk-based systematic approach aimed at achieving optimal maintenance to ensure the functionality of a system. RCM also concluded a systematic analysis of the functions of the system and how the system can fail and priorities based on safety and economic considerations that identify preventive maintenance applicable and effective task (Besnard et. al. 2010)

The problem faced by the Power plant is the system of power plant has large capacity, complex and multilevel include levels of system and subsystem devices that separate and interrelated in producing electrical energy, And the maintenance requirements are also more complex. Besides, the power plant has varied the type of failure that requires maintenance treatment which different to be able to keep generating machine reliability at minimum cost.

3. Methodology

This study aims to obtain systematic maintenance strategies into account type of failure and failure characteristics that is different to improve system performance effectively and efficiently.

Strategies Maintenance based on Reliability Centered Maintenance made to address the failure of the type and characteristics are different depending where in making the strategy undertaken mapping of the entire power system, definition systems is analyzed with a Pareto chart to determine the subsystem selected for analysis based on the highest percentage of history of failure, Manufacture FMEA (failure modes and effects Analysis) to identify any equipment failure modes, failure causes of each failure mode and effect of any failure.

After FMEA next step is to identify critical equipment to sort the RPN value of the RPN RPN steeper to the lowest. Critical RPN is used as the Risk Assessment (Risk greatest and the effect on the system is indicated by the value of the highest RPN) and failure mode at critical RPN can be included as inputs in the Logic Tree to determine Maintenance Action obtained from maintenance strategy. Here are the steps RCM in this study:

- Step 1 :Selection of the system, identifying, and collecting a history of failure
- Step 2 :Defining the system boundary
- Step 3 :Describing the system and Functional Block
- Step 4 : Pareto Analysis
- Step 5 : Failure Modes and Effect Analysis



- Step 6 : Critical equipment analysis
- Step 7 : Maintenance Strategy

Steps in defining RCM approach implemented in the power plant to maintain the function of the system, identification of failure modes, failure prioritization is used to maintain the function of power plan and maintenance strategies to create a Maintenance Action of each failure mode.

3.1 Discussion

Total Productive Maintenance (TPM), Total Maintenance Assurance, Preventive Maintenance, Reliability Centered Maintenance (RCM) and many other innovative analytical approaches to overcome failure and all of them aim to make the machine work effectively and increase machine productivity (Shayeri, 2007). Components of the RCM program is shown in Figure 1. The figure shows the RCM program consists of Reactive Maintenance, Preventive Maintenance, Condition Based Maintenance dan Proactive maintenance.

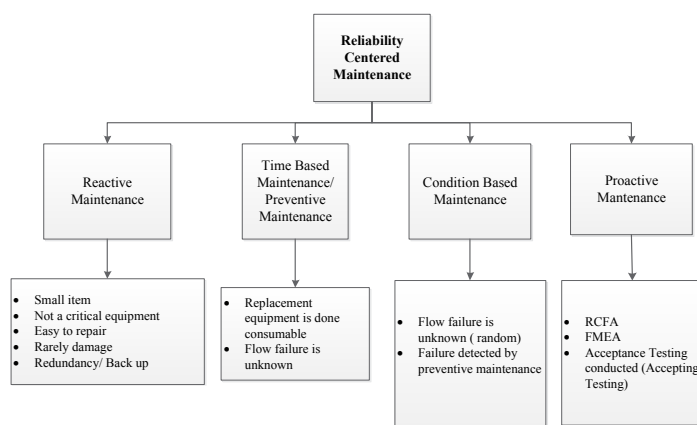


Figure 1. Components of the RCM program (Afehy, 2010)

4. Case Study

4.1 Functional Tree Steam Power Plant

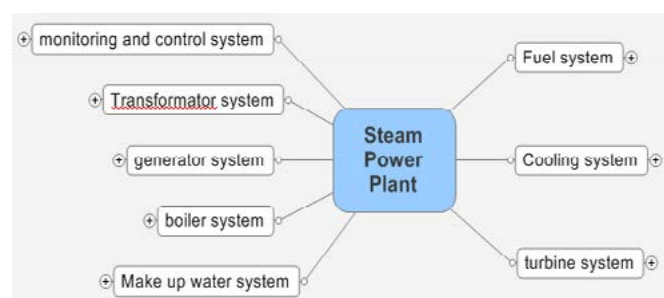


Figure 2 Steam Power Plant systems

Functional Tree map all plant systems aimed to identifying the entire system of the plant. Power plant is divided into eight main systems by function, Fuel System, Cooling System, Turbine System, MakeUp Water System, Boiler System, Generator System, Transformator System, Monitoring and Control System.



4.2 Power Plant Structure

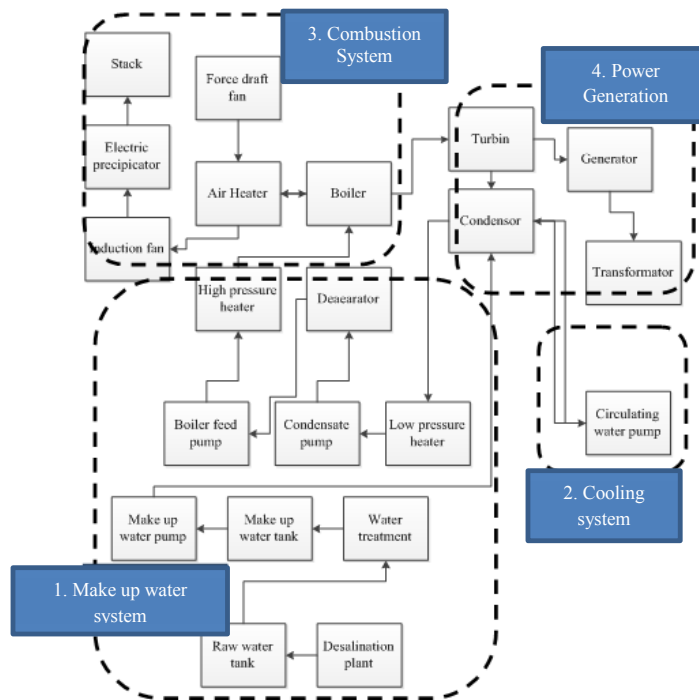


Figure 3 Power Plant structure

The structure shows that the power plant power plant consists of a lot of equipment that is different in produce Electricity, the equipment is broken down by operating system. Figure 3 is a structure of power plant equipment in the power plant structure. Figure 3 can be seen the power plant has 4 operational systems among others

1. Make up water system: This system is a system comprising water boiler which the water will be converted into superheated steam by the boiler. Water filler taken from sea water is then separated saline water into fresh water treatment plant. After that, in the freshwater was reduced mineral content in demin plant that aims to prevent corrosion in the engine plant. After the water has been slightly put condensor mineral content to add closedloop systems in steam cycle power plant. After that experience primary heating at low pressure heater and a secondary heating at high pressure to feed the heater before the boiler that is converted into steam
2. Cooling system: Cooling system is a system used to change the phase of the output steam turbine into liquid phase in the condenser. This system utilizes the temperature of the sea water to cool the residual heat in the engine plant.
3. Combustion system: Combustion system is a system that produces steam from the vapor phase into mixture of superheat which used to turn on turbines. The main fuel in the combustion is HSD oil, natural gas or coal.
4. Power Generation: The steam from the boiler is used to turn a turbine, the rotation of the turbine is used to turn generator that produces electricity. Electricity from the generator is transfer to voltage transformer to be raised before the entrance to the home network.

4.3 Power Plant Pareto Diagram

Pareto diagram is helpful in determining and identifying priority issues to be resolved. The problems most often happen is a top priority in determining maintenance planing. Pareto created from data processing history of failure. Pareto diagram can be seen from the subsystems of the most



influential in the major failure of the power plant. Pareto diagram of the power plant is shown in figure 4-10.

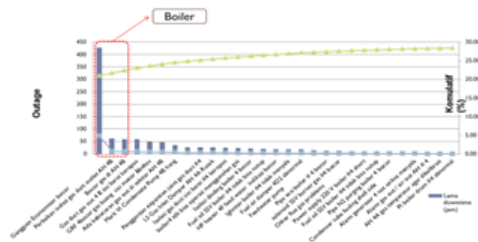


Figure 4 Power plant Pareto diagram, 2009

Figure 4 illustrate the whole problem of power that occurred in 2009 and breaking up the red dotted line is the problem caused by boiler system. The problem is leakage on economizer, improved insulation of gas duct outlet 4B Air Heater and leak on the water heater 4B.

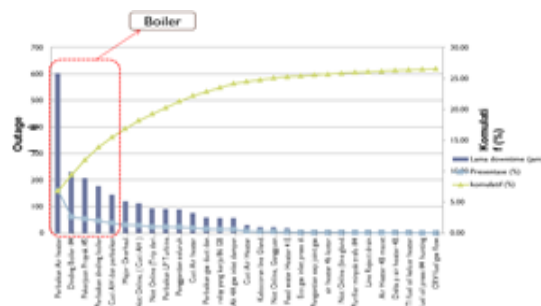


Figure 5 Power plant Pareto diagram, 2010

The problem in 2010 is repair air heater, Repair boiler Fire walls 4, project work 5, Air Heater cleaning and repair gas duct.

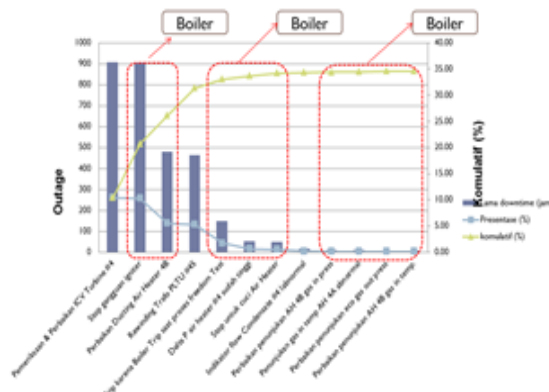


Figure 6 Power plant Pareto diagram, 2011

The problem in 2011 is stop igniter, repair ducting air heater, Boiler trip, repair pressure indicator air heater 4b, repair temperature indicator air heater 4b, repair economizer gas out pressure, repair air heater 4b.

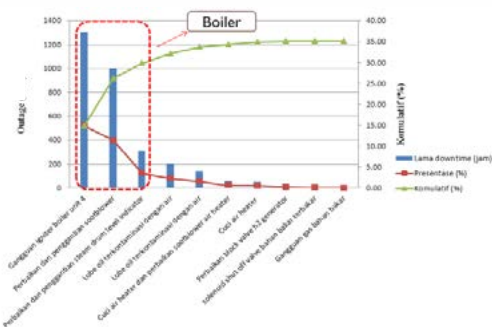


Figure 7 Power plant Pareto diagram, 2012

The problem in 2012 is igniter boiler unit 4 Stop, improvement and replacement sootblower, and improvement and replacement steam drum level.

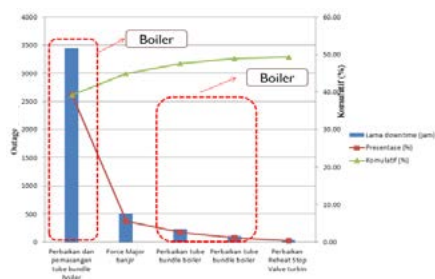


Figure 8 Power plant Pareto diagram, 2013

The problem in 2013 is improvement and replacement tube bundle (39, 3%) and Boiler System 87,53 %.

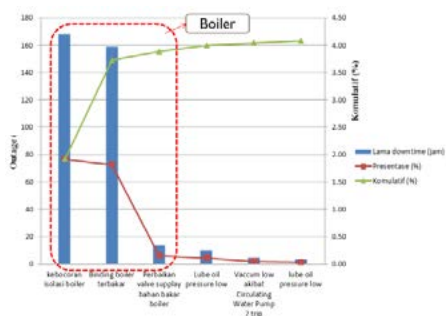


Figure 9 Power plant Pareto diagram, 2014

The problem in 2014 is broken boiler isolation, burn boiler wall, and Corrective supply valve boiler

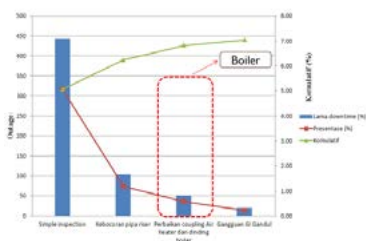


Figure 10 Power plant Pareto diagram, 2015



The problem in 2015 is incorrect air heater coupling and boiler wall, so it can be concluded from data 2009 - 2015 the most problems is on boiler system

4.4 Failure Modes and Effect Analysis (FMEA)

FMEA is used to identify any equipment failure modes, failure causes of each failure mode and effect of any failure.

Appendix 1 is the result of the main boiler FMEA. FMEA is done by analyzing failure modes, failure causes and effects of any equipment failure. To determine the priority of failure it must be defined first of severity, occurrence, and detection as well as the final outcome from FMEA form of Risk Priority Number. Ordinal scale to assess the severity, occurrence, and detection is shown in appendix 2, while the RPN is the multiplication of value Severity, occurrence, and detection.

4.5 Critical RPN

Next step is calculated the critical value of the main boiler subsystem with RPN rank from highest value to lowest value. Figure 11 shows the value of the RPN of the main boiler subsystem

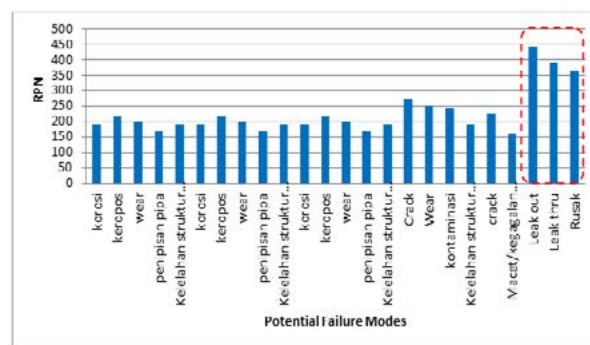


Figure 11 RPN value main boiler subsystem

From the entire value of the RPN in the main boiler selected third highest RPN as the critical value. 3 selected critical value because the value of the RPN differ much between grades 3 and 4, namely 360 and 270. Table 1 shows the critical value of the main boiler subsystem

Table 1 Critical RPN

System	Sub system	Equipment	Potensial failure modes	RPN	Nilai kritis
Boiler	Main Boiler	Control valve	Leak out	441	1
			Leak trough	392	2
		Insulation	Broken	360	3

From the table 1 can be seen that the highest value is the equipment control valve and pipe wall insulation main boiler. This failure is the benchmark in the maintenance and critical RPN is used as the Risk Assessment (Risk greatest and the effect on the system is indicated by the value of the highest RPN) and failure mode at critical RPN can be included as inputs in the Logic Tree to determine Maintenance Action. Table 2 is determine maintenance action to eliminate potential failure modes by condition based maintenance, preventive maintenance, back up or redundancy, emergency, run to overhaul and run to failure.



Table 2 Maintenance Action

Equipment	Potensial Failure Modes	Cbm	Preventive	Backup	Emergency	Run to overhaul	Run to failre
Control valve	leak out	monitoring failure	-	back up another valve to cover failure	shutdown unit and replace valve	replace valve until next inspection	run valve until unit down
	leak through	monitoring failure	-	back up another valve to cover failure	shutdown unit and replace valve	replace valve until next inspection	run broken insulation until unit down
Insulation	broken insulation	monitoring failure	-	-	shutdown unit and replace new insulation	replace insulation until next inspection	run valve until unit down

In determining Maintenance Action on failure mode by using Maintenance Strategy for things to do into the failure mode Failure input on Logic Tree (blue box in Figure 12) and then follow the decision yes and no to obtain the Maintenance Action.

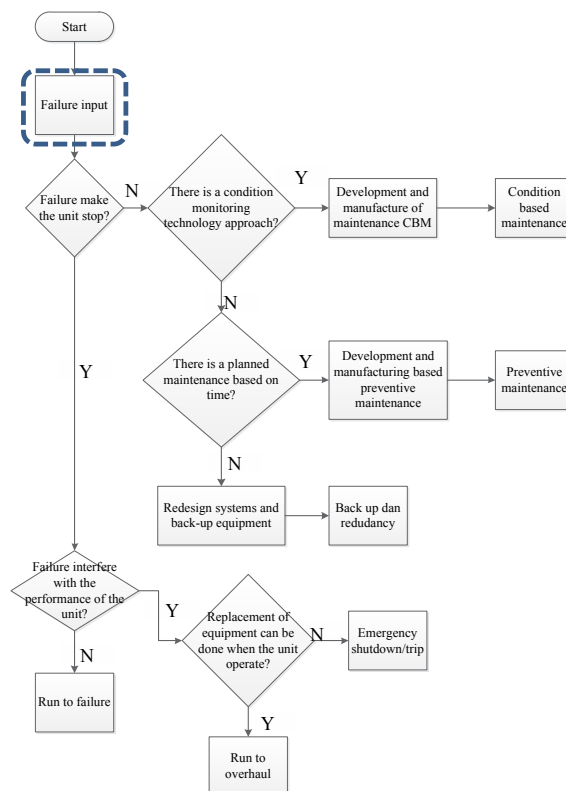


Figure 12 Maintenance Strategy

Damage leakout on valve inserted as the failure input then answer some questions as follows to get Maintenance Action:

1. Is the failure to make the unit stop?
If the answer is no,
2. Is there are condition monitoring technology? If the answer is no,



3. Is there a planned maintenance based on time? If the answer is no,
4. Redesign and manufacture system back up equipment, so the maintenance action is to do a back-up equipment and redundancy.

5. Conclusion

Based on the results of research conducted to conclude several things:

1. Maintenance Strategy has been obtained based on Reliability Centered Maintenance to overcome Flaws by classifying the type of failure and failure characteristics which differ to determine the type of maintenance in accordance with the characteristics of the failure to improve system performance effectively and efficiently.
2. Logic Tree Analysis is used to select the appropriate maintenance strategy with RCM approach in this study.

Bibliography

1. Afefy, Islam. 2010. Reliability-Centered Maintenance Methodology and Application. Engineering, Vol. 2 No.11 , 2010, pp. 863-873
2. Jozi, Ali seyed et. al. 2012. Environmental Risk Assesment of a Gas Power Plant Exploitation Unit Using Integrated TOP-EFMEA Method. Pol. Journal Environmental Study. Vol 21 , No. 1 (2012), 95-105
3. Igba, Joel et. al. 2013. A System Approach towards Reliability-Centered Maintenance (RCM) of Wind Turbine. Procedia Computer Science. 16 (2013) 814 -823
4. Carazas, Fernando & Souza, Gilberto. 2009. Availability Analysis of Gas Turbines Used in Power Plants. Int. J. of Thermodynamics. Vol 12 , No 1, pp. 28-37
5. Bangu, N. 2011. *Reliability Centered Maintenance* in a Thermal Power Plants: a Case Study. Int. J. Productivity and Quality Management, vol. 7, No 2, pp. 209-228
6. Feili et. Al. 2013. Risk analysis of geothermal power plants ushing Failure Modes and Effect Analysis (FMEA) technique. Energy Conversion and Management 72 (2013) 69-76
7. Carazas, Fernando & Souza, Gilberto. 2010. Availability analysis of heat recovery steam generators used in thermal power plants. Energy 36 (2011) 3855-3870
8. Eti, M. et. al. Reliability of the Afam electric power generation station, Nigeria. Applied Energy 77 (2014) 309-315
9. Garg, Amik & Deshmukh, S. 2006. Maintenance management: literature review and directions. Journal of Quality in Maintenance Engineering, Vol. 12, No 3, pp 205-238



Appendix 1.

Table 2 FMEA Boiler Subsystem

Equipment	Potential failure modes	Potential Cause of Failure Mode	Potential Effect of Failure Mode	S	O	D	RPN
Bundle tube superheater	Corroton	Steam contamination	Pipe leak	8	6	4	192
	Porous	FOD	Pipe leak	9	6	4	216
	Wear	FOD	Pipe leak	7	7	4	196
	Thinning of the pipe	Friction with steam	Pipe leak	7	6	4	168
	Fatigue material structure	operating at high temperatures	Pipe leak	8	6	4	192
Bundle tube economizer	Corroton	Steam contamination	Pipe leak	8	6	4	192
	Porous	FOD	Pipe leak	9	6	4	216
	Wear	FOD	Pipe leak	7	7	4	196
	Thinning of the pipe	Friction with steam	Pipe leak	7	6	4	168
	Fatigue material structure	operating at high temperatures	Pipe leak	8	6	4	192
Bundle tube downcomer	Corroton	Steam contamination	Pipe leak	8	6	4	192
	Porous	FOD	Pipe leak	9	6	4	216
	Wear	FOD	Pipe leak	7	7	4	196
	Thinning of the pipe	Friction with steam	Pipe leak	7	6	4	168
	Fatigue material structure	operating at high temperatures	Pipe leak	8	6	4	192



FMEA Table Main Boiler Subsystem (extension)

Equipment	Potential failure modes	Potential Cause of Failure Mode	Potential Effect of Failure Mode	S	O	D	RPN
Boiler burner	Crack	Fatigue material structure	trip	9	6	5	270
	Wear	Friction with fluida	crack	7	6	6	252
Steam drum	Contamination	Strainer make up water choke	erosion and abrasion	7	7	5	245
	Fatigue material structure	Operating at high temperatures	Crack	8	6	4	192
	crack	Pressure too high	leakage	8	4	7	224
Igniter	Jams / Ignition failure	Logic function failure	Boiler cannot operated	4	5	8	160
Control Valve	Leak out	body leakage	Burned out	9	7	7	441
	Leak thru	Disk leakage	Burned out	8	7	7	392
Pipe wall and Insulation	Broken	Burned out	Heat leak	8	5	9	360



Appendix 2.

Table 3 Severity rating scale

Severity Rank	Description
1 - 2	Small failure so that the operator may not detect the failure.
3 - 5	Failure will result in less damage to the part or system performance.
6 - 7	Failure would lead to dissatisfaction and damage to some systems operator performance.
8 - 9	Failure would lead to dissatisfaction and been cause non-functioning of the system.
10	Failure would lead to dissatisfaction very big for a big operator or damage.

Table 4 Occurrence rating scale

Occurrence Rank	Description
1	The probability of no occurrence: probability of occurrence $<0,001$
2 - 3	A remote probability of occurrence: $0,001 < \text{probability of occurrence} <0,01$
4 - 6	Probability occasional occurrence: $0.01 < \text{probability of occurrence} <0,10$
7 - 9	Probability occasional occurrence: $0.10 < \text{probability of occurrence} <0,20$
10	High probability of occurrence: probability of occurrence > 0.2



Table 5 Detection rating scale

Detection Rank	Description
1 - 2	Very high probability that defects will be detected
3 - 4	High probability that defects will be detected
5 - 7	Moderate probability that defects will be detected
8 - 9	low probability that defects will be detected
10	Very low (or zero) probability that the defect will be detected



FAILURE RISK ANALYSIS ON CORE NETWORK OF GPRS EQUIPMENT USING FMEA & FTA METHOD AND SCENARIO OF TREATMENT COST ALLOCATION

Yadrifil¹, Anisa Fithrasari², Annisa Marlin Masbar Rus³

^{1,2,3}*Industrial Engineering Department, Engineering Faculty, University of Indonesia, UI Depok 16424, Indonesia*

E-mail : yadrifil@ie.ui.ac.id, anisafithrasari@yahoo.com, annisamarlinmr@gmail.com

ABSTRACT

Due to the increasing of mobile communication development, GSM operators are motivated to provide more efficient data services with a high speed feature and also introduce new services. In order to do this, GPRS could be applied as a solution to address the challenge. However, as the GPRS becomes a key for GSM operators to compete in the market especially in internet service are, focus on GPRS potential risk failure should get more attention. Thus, the purpose of this research is to conduct a risk analysis on GPRS maintenance activity that lead to designing risk treatment action and scenario of treatment cost allocation. In this research, FMEA method is employed to obtain the critical risks which will be further analysed using FTA to identify the basic event of those critical risk. Moreover, OptQuest-Crystal Ball simulation is employed to find the optimal treatment cost allocation. As a result of this research, three main points could be concluded. First, 8 critical risks are successfully drawn from 28 identified risks. Furthermore, based on the research, it is suggested that every critical risk should have different treatment actions. Lastly, according to the result of cost allocation using OptQuest simulation, the higher the cost allocation that is given to treat critical risks, the higher the maximum total advantage.

Keywords: GPRS; risk analysis; FMEA; FTA; OptQuest-Crystal Ball simulation.

1. INTRODUCTION

Rapid development in mobile communication motivate GSM operators for developing more type of services to increase their profit while keep maintaining their customer's loyalty. In this case, GPRS can be a solution to provide efficient data services with a high speed feature and introduce new type of services to compensate the decreasing of communication cost per minute. GPRS is a technology that can be used by Global System for Mobile (GSM) operators to provide high speed data services with a low price, thus their services could be more competitive in the market. To be precise, GPRS enable the customer to create a faster relation phase, stay connected permanently and use faster data speed by only paying for every transferred bit. By employing GPRS, GSM provider could attract more customer because surely the market tendency is not moving towards increasing cost and subscription rate. For this reason, GPRS becomes a key for GSM operators to compete in the market especially in internet services area.



Today, GPRS have also been used as a corporate solution. For instance, GPRS has been used in banking system for cost efficiency. Instead of using the satellite technology, banking corporate currently use GPRS technology to provide link service for ATM machine by leasing bandwidth. Moreover, GPRS has also been employed on *Electronic Data Capture* (EDC) technology to facilitate customer to make a payment anywhere. This technology is usually used in hypermarket and taxi company.

As the GPRS has become important for GSM operators, they need to pay more attention to GPRS equipment in order to maintain the services. The principle is to get customer loyalty and also have more customer because of excellent service. Thus, maintenance for GPRS equipment becomes crucial to have a good performance. In this way, most of the potential failure can be avoided or eliminated to achieve the company goals.

One of solution which could be done for achieving excellent services is by determining *Key Performance Indicator* (KPI) for maintenance division should. In this research, there are 2 point of KPI, they are Attach Success Rate and PDP Context Success Rate. Attach Success Rate refer to success of having signal and PDP Context Success Rate refer to success of internet connection. These KPI are driven from the common problem which frequently faced, signalling and connection failure. These failures could lead to revenue loss and customer dissatisfaction. Beside these 2 factors of KPI, company should also focus on security attack because it enables fraud scheme in GPRS system.

As the GPRS is a key for GSM provider to deliver the service, maintaining the GPRS equipment becomes crucial. Consequently, in order to address the challenge of delivering excellent service, application of risk management for the GPRS maintenance activity is proposed in this research.

2. METHODOLOGY

As a limitation, this research will only review risks in operational and maintenance activity of GPRS equipment. Expert team which are involved in this research encompass Network Service O&M Center General Manager, VAS Cellular Team Leader, and VAS Cellular Engineer with more than 5 years of experience.

The research method of this paper will refer to standardization of FMEA step.

a. Identify the risk event

To identify risk, previously we need to collect data. Data collection is conducted by collecting historical data of GPRS system failure, searching for similar failure data from literature, and then making *Cause Failure Mode Effect* (CFME) diagram to identify and list the risk.

b. Determine occurrence, severity, and detection rating

Determination of occurrence, severity, and detection rating is conducted by brainstorming with expert which is supported by literature data.

c. Assess occurrence, severity, and detection of every risks

Assessment of occurrence, severity, and detection is conducted through questionnaire to calculate the *Risk Priority Number* (RPN) from each risk and determine critical risks.



d. Analyse risks and develop risk response planning for critical risk.

In this step, Fault Tree Analysis (FTA) is a tool that is used to get the root cause of the critical risk, so that the treatment action could be determined. As for the treatment cost for every critical risks, it will be simulated by *OptQuest* to get an optimal treatment cost allocation. In order to run the simulation, revenue loss and treatment cost data from historical data and expert judgment will be used.

3. RESULT AND DISCUSSION

3.1 Risk Identification

Risk identification is an important step in risk management before continuing to the next step. Risk identification involve risk determination which may influence the performance of GPRS equipment. The purpose of this step is to identify the probable risk to decrease or eliminate the impact.

After the failure and potential failure which are driven from the experts' discussion, historical problem, and literature are all identified, then Cause Failure Mode Effect (CFME) diagram is made. The result of the CFME then will help the creation of FMEA in term of impact identification, failure mode, and root cause. CFME diagram is shown in Figure 1.

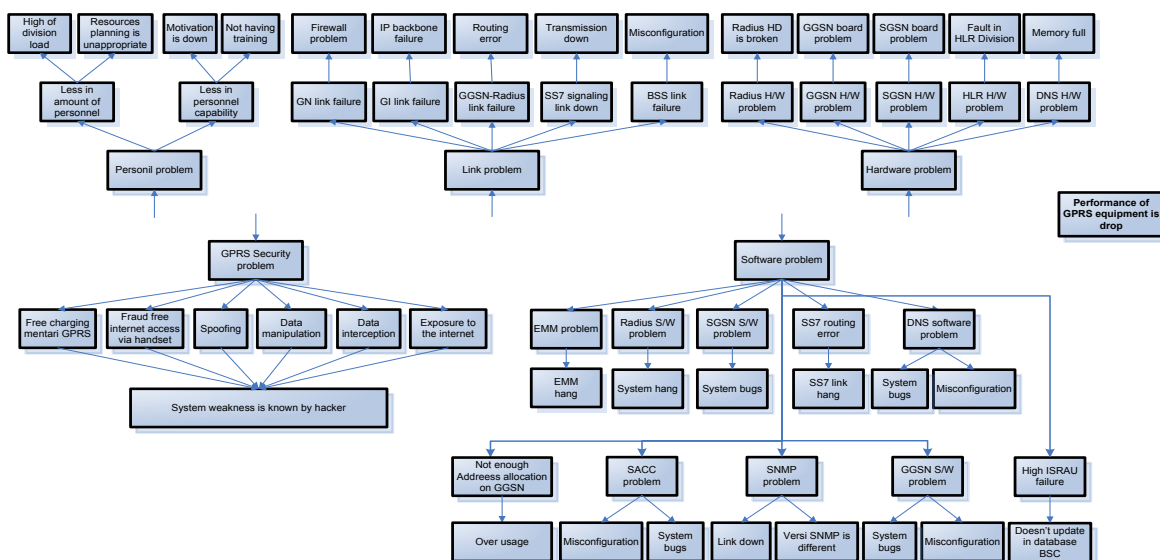


Figure 1 Cause Failure Mode Effect Analysis (CFME) Diagram

3.2 Determiation of Occurrence, Severity, and Detection Rating

In this step, rating is determined through brainstorming process with the expert in accordance with the company condition. The determination of occurrence, severity and detection rating then will influence the priority of the critical risk.

Occurrence rating is the quantification of the level of risk probability. The range of scale which is used is from 1 to 5, where 1 refers to the lowest probability while 5 refer to highest probability. The rating could be seen in Table 1.



Table 1 Occurrence Rating

Scale	Risk Probability	Note
5	Very high: cannot be avoid	Risk probability per year: 81 - 100
4	High: repetitive	Risk probability per year: 61 - 80
3	Moderate	Risk probability per year: 41 - 60
2	Low: seldom	Risk probability per year: 21 - 40
1	Very low	Risk probability per year: 0 - 20

Table 2 Severity Rating

Scale	Risk Impact	Note
5	Emergency	Fully system failure, it cause loss of charging data
4	Critical	System error, the risk give impact to revenue management system
3	Major	The risk give impact only on certain work area not on all of system
2	Minor	Have minor effect to product function, but not give impact to service and data traffic
1	Warning	Does not give impact neither to service nor system

Table 3 Detection Rating

Scale	Risk Detection	Note
5	Very low	Detection method / alert system is not available
4	Low	Current detection method is not effecti detect the risk on time
3	Moderate	Current detection method is less effective, so it needs more time to detect the risk
2	High	Current detection method is effective enough to detect the risk
1	Very high	Current detection method is very effective to detect the risk real time



Moreover, severity rating is the quantification of impact level of the risk. The scale ranging from 1 to 5, where the value of 1 refer to the condition where there is no effect from the risk and value 5 refer to the whole system failure as impact from the risk. This rating could be seen in Table 2.

Lastly, detection rating is a quantification of level of risk detection. Detection serves as an early warning to see whether the risk could be identified before the failure happened and whether there is control that could be done to minimize the risk. The scale for this rating ranging from 1 to 5 as well, where 1 refer to a condition with high level of control to detect the failure and 5 refer to a condition with a low level of control. The rating could be seen in Table 3.

3.3 Determining value of Occurrence, Severity, Detection for Every Risk and Calculation of Risk Priority Number (RPN)

After the risk has been identified, the next step is to determine the occurrence, severity, and detection value for every risks. This step is conducted by brainstorming with the expert to filling out questioner. The value of occurrence, severity, and detection for every risk could be seen in Table 4.

Calculation of RPN is an important step in FMEA because from this calculation the risk could be prioritized as critical or not. RPN can be calculated by the following formula:

$$RPN = Occurrence * Severity * Detection \quad (1)$$

After calculating RPN value for every risks, the critical risks can be determined. That critical risks will be further analysed as the first step of treatment action for maintaining the performance of GPRS equipment. Risk is categorized as critical risk if the RPN value is higher than the critical value. RPN critical value is determined by calculating the average of RPN value from all of risks.

$$\begin{aligned}
 RPN \text{ Critical Value} &= \frac{Total \ RPN}{Number \ of \ Risks} \quad (2) \\
 &= \frac{986}{31} = 31.81
 \end{aligned}$$

As a result of the expert discussion and considering the RPN critical value, 8 critical risks are obtained. These risks have RPN value with more than 31,81, which is the RPN critical value. Those critical risks are:

- EMM Problem, RPN = 125
- GGSN-Radius Link Failure, RPN = 100
- DNS Software Problem, RPN = 80
- GI Link Problem, RPN = 64
- GGSN Software Problem, RPN = 48
- Radius Software Problem, RPN = 40



- SS7 Signalling Link Down, RPN = 36
- SS7 Routing Error, RPN = 36

Table 4 Occurrence, Severity, Detection and RPN Value for Every Risks

Risk ID	Risk on Core Network of GPRS Equipment	O	S	D	RPN
1	SGSN Hardware Problem	1	4	3	12
2	HLR Hardware Problem	1	4	3	12
3	SGSN Software Problem	1	3	3	9
4	SS7 signaling link down	3	4	3	36
5	BSS link failure	3	3	3	27
6	SS7 routing error	3	3	4	36
7	GGSN Hardware Problem	1	4	4	16
8	Radius hardware problem	1	4	5	20
9	GGSN Software problem	3	4	4	48
10	Radius software problem	2	4	5	40
11	GGSN-radius link failure	4	5	5	100
12	High ISRAU failure	2	3	4	24
13	Not enough address allocation on GGSN	2	3	3	18
14	EMM problem	5	5	5	125
15	SACC problem	1	4	5	20
16	DNS hardware problem	2	4	3	24
17	DNS software problem	4	4	5	80
18	GN link failure	1	4	4	16
19	GI link problem	4	4	4	64
20	Free charging mentari GPRS	1	5	5	25
21	Fraud free internet access via handset	1	5	5	25
22	Spoofing	1	5	5	25
23	Data manipulation	1	5	5	25
24	Data interception/unauthorized access to confidential data	1	5	5	25
25	Exposure to the internet	1	5	5	25
26	SNMP problem	2	1	2	4
27	Lack number of personnel	2	3	5	30
28	Lack of personnel capability	2	3	5	30



3.4 Risk Analysis

At the beginning of the risk analysis process, fishbone diagram is constructed. Fishbone diagram is a tool for probing the root cause of a problem based on 5M & 1E (Man/Personnel, Method, Machine, Material, Measurement, and Environment) classification. According to the questioner result of this research, the root cause of the critical risk could be cut down into 3 classifications; method, personnel, and equipment. The result of this fishbone diagram then will be further narrowed down by employing Fault Tree Analysis (FTA) to obtain the cause of basic event of the top event (critical risk).

FTA is a graphical model which consists of many parallel and sequence of fault combinations as it shown in Figure 2 for EMM problem. Among these fault combinations, one of them may be the original cause of the failure event. In this research, critical risk is determined as the top event. Eventually, the basic event which is the root cause of the top event, or the critical risk, is obtained and right action could be executed for handling the critical risk. After discovering the root cause of the critical risk, then the right treatment actions could be determined and the treatment cost could also be calculated.

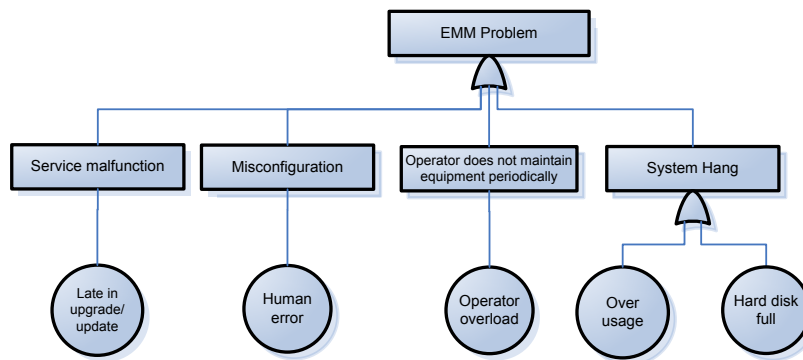


Figure 2 FTA of EMM Problem

After creating the FTA, then Cut Set of the FTA is determined to identify basic event of the critical risk as it shown in Figure 3. Cut set of the fault tree are $E1 \cup E2 \cup E3 \cup (E4 \cup E5)$. It means that if event 1 or 2 or 3 or 4 or 5 is happened simultaneously, then the top event will happen. For instance, in EMM problem, the cut set will be as below.

- Top Event : EMM Problem
- Basic event 1 : Late on update/upgrade software
- Basic event 2 : Human error
- Basic event 3 : Operator overload
- Basic event 4 : Over usage
- Basic event 5 : Hard disk full

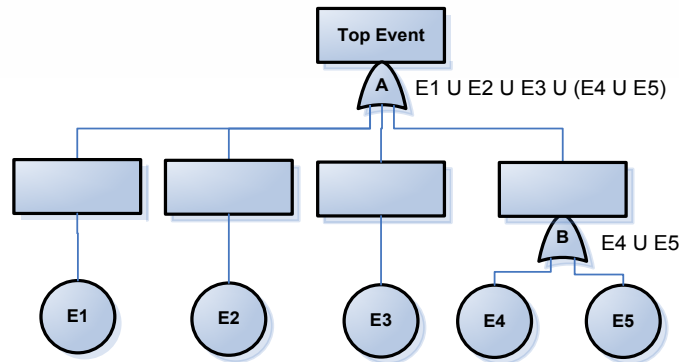


Figure 3 Cut Set of EMM Problem

Subsequently, after obtaining the basic event of every critical risks, then the treatment action is constructed. Treatment action is created by mitigating the risk in 2 ways, which are mitigate the risk probability and mitigate the impact of the risk. Risk impact mitigation is done by doing remedy action. Remedy action is the first action which is performed by the operator when the risk happened. In order to obtain effective remedy actions, the following suggestion is proposed based on data analysis and evaluation:

- a. Create automatic monitoring system for every equipment in GPRS infrastructure
- b. Create standardization of problem solving action
- c. Manage historical problem

After that, if the operator is still unable to solve the problem, then the risk could be transferred to the vendor (Risk Transfer). Moreover, to lessen the risk probability, the following suggestions are made based on the result of FTA:

- a. Provide more operator for handling operators' overload problem
- b. Provide training for every person in charge for solving the current problem
- c. Upgrade the hard disk
- d. Ask vendor commitment to decrease the tardiness in upgrading the equipment information
- e. Perform routine maintenance for hardware and change broken part immediately
- f. Coordinate with other division about IP routing, transmission, hardware HLR, and router internet gateway problem

3.5 Optimization of Treatment Cost Allocation using OptQuest Simulation

OptQuest is one of functions in Crystal Ball. It can be used to determine cost allocation which give optimal benefit. The following are the main terms which is used in OptQuest :

- a. *Risk cost/revenue loss*: cost / revenue loss incurred when the risk happened.
- b. *Risk coverage*: risk cost / revenue loss that can be covered with given treatment cost allocation.
- c. *Decision*: determinant variable of how much budget which is allocated for any risk. The value is 1 if the budget is allocated for the risk.
- d. *Advantage*: (risk coverage – treatment cost) * decision



To run the simulation, data of revenue loss and treatment cost is required. For the purpose of revenue loss determination, the critical risks are classified into 3 groups. The first one is EMM problem refer to revenue loss historical data which is captured on GGSN equipment-duration based; the second is DNS software problem, GI link failure, GGSN software problem, and radius software problem refer to revenue loss historical data which is captured on GGSN equipment-volume based; and the last one is SS7 signalling link down and SS7 routing error based on expert judgment. According to data collection, following are data of revenue loss for every critical risks.

- a. EMM problem (normal distribution):
 - Mean : Rp. 214,870,286
 - Standard deviation : 43856839
- b. DNS software problem, GI link failure, GGSN software problem, and radius software problem (normal distribution) :
 - Mean : Rp. 345,108,000
 - Standard deviation : 87460770
- c. SS7 signalling link down and SS7 routing error (uniform distribution) :
 - Maximum : Rp. 360,000,000
 - Minimum : Rp. 12,000,000

Treatment cost is collected from cost of treatment action which is driven from FTA. Total treatment cost for all of critical risks is Rp505.000.000, and the detail is shown as below :

- EMM Problem : Rp. 130,000,000
- DNS Software Problem : Rp. 20,000,000
- GI Link Failure : Rp. 20,000,000
- GGSN Software Problem : Rp. 130,000,000
- Radius Software Problem : Rp. 55,000,000
- SS7 Routing Error : Rp. 50,000,000
- SS7 Signalling Link Down : Rp. 100,000,000
- GGSN-Radius Link Failure : Fund allocation for GGSN-Radius link failure does not run in this simulation because that problem is connected with GGSN software problem and radius software problem are handled, which if those problems are handled then automatically GGSN-Radius link failure will solve.

Before running the simulation, variable of assumption, decision, and forecast is determined. Assumption variable is an uncertainty value which have certain distribution. In this model, risk cost/revenue loss is the assumption variable because the value is uncertain. Then, decision variable is budget allocation that is given for risk treatment. Lastly, the forecast variable is formula cell which connects the assumption cell and the decision cell. This variable is the total advantage which is wanted to be maximized.

Optimization's constraint in this simulation is treatment cost allocation need to be less than the budget (treatment cost allocation \leq budget). It is assumed that company provide 4 conditions of budgeting, they are $\leq 25\%$, $\leq 50\%$, $\leq 75\%$, and 100% from total treatment cost.



Table 5 The Result of Treatment Cost Allocation using OptQuest Simulation

Critical Risk	Condition of Budget Availability			
	≤ 25% from total treatment cost	≤ 50% from total treatment cost	≤ 75% from total treatment cost	100% from total treatment cost
EMM problem	Rp. 0	Rp. 0	Rp. 4,704,900	Rp. 130,000,000
DNS software problem	Rp. 20,000,000	Rp. 20,000,000	Rp. 20,000,000	Rp. 20,000,000
GI link problem	Rp. 20,000,000	Rp. 20,000,000	Rp. 20,000,000	Rp. 20,000,000
GGSN software problem	Rp. 0	Rp. 107,580,000	Rp. 130,000,000	Rp. 130,000,000
Radius software problem	Rp. 53,657,000	Rp. 55,000,000	Rp. 55,000,000	Rp. 55,000,000
SS7 signaling link down	Rp. 0	Rp. 0	Rp. 99,481,000	Rp. 100,000,000
SS7 routing error	Rp 32.593.000	Rp 49.727.000	Rp 50,000,000	Rp. 50,000,000
Sum of Cost (Σ)	Rp.126,250,000	Rp.252,307,000	Rp.378,749,900	Rp.505,000,000

The next step is running the OptQuest simulation. Simulation is conducted for every condition. Every simulation is run for 1000 trials. As the result, the simulation yield is different for every condition.

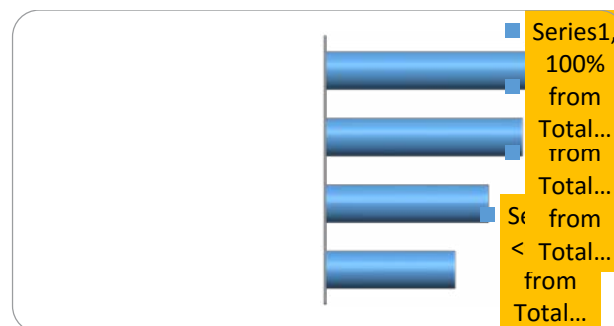
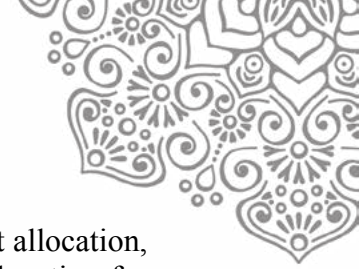


Figure 4 Total Advantage on Every Condition of Budget Availability



Based on the simulation result, it is shown in Figure 4 that the higher the budget allocation, the higher the total advantage. In detail, the following are the result of cost allocation for every condition using OptQuest simulation.

- For budget with $\leq 25\%$ from total treatment cost, GI link problem and DNS software problem will receive the full budget. Maximum total advantage is Rp. 1,135,316,690.
- For budget with $\leq 50\%$ from total treatment cost, GI link problem, DNS software problem, and radius software problem will receive the full budget. Maximum total advantage is Rp. 1,426,641,543.
- For budget with $\leq 75\%$ from total treatment cost, GI link problem, DNS software problem, GGSN software problem, radius software problem, and SS7 routing error will receive the full budget. Maximum total advantage is Rp. 1,726,020,586.
- For budget with 100% from total treatment cost, all of critical risks will receive the full budget. Total advantage is Rp. 1,810,302,286.

4. CONCLUSION

Based on the result of the above data analysis, it could be concluded that:

- a. There are 8 critical risks which is drawn from 28 identified risks. The critical risks are EMM problem, GGSN-Radius link problem, DNS software problem, GI link problem, GGSN software problem, Radius software problem, SS7 signalling link down, and SS7 routing error.
- b. Every critical risk will have different treatment action. Suggestions for treatment action are proposed based on 2 methods, which are risk mitigation and risk transfer.
- c. The result of cost allocation using OptQuest simulation can be seen in analysis data. In the nutshell, the higher cost allocation that is given to treat critical risks the higher the maximum total advantage.

5. REFERENCE

- Carbone, T & Tippett, D. (2004). Project Risk Management Using the Project Risk FMEA. *Engineering Management Journal*. Vol 16, No.4. hal 31.
- Crystal Ball® 7.2.2 User Manual.
- Harold Kerzner,(2006). *Project Management, A System Approach to Planning, Scheduling, and Controlling 9th ed.* John Wiley & Sons, Inc.
- Information Risk Management. *GPRS/3G Services : Security*. O2 White Paper.
- Project Management Institute. (2000) *A Guide to The Project Management Body of Knowledge : PMBOK Guide*. Pennsylvania : Project Management Institute, Inc.



SUPPLIER PERFORMANCE EVALUATION METHODS USING DATA ENVELOPMENT ANALYSIS BANKER, CHARNES, COOPER MODEL AND SUPER EFFICIENCY MODEL IN PUMPING UNIT PRODUCER

Yadrifil¹, Irmawati Ulfah², Annisa Marlin Masbar Rus³

*Department of Industrial Engineering, Faculty of Engineering, University of Indonesia
Kampus Baru UI Depok, 16424, Indonesia*

E-mail: ¹yadrifil@eng.ui.ac.id, ²irmawati_ulfah@yahoo.com,
³annisamarlinmr@gmail.com

ABSTRACT

Performance of raw materials suppliers affects the productivity of firms. Performance is the primary information for management decisions in managing a cooperative relationship to a supplier. So the term evaluation is needed to monitor the performance of suppliers. Commonly, evaluation conducted with limitation so that the result could not satisfy improvement targets. This study attempts to propose a supplier performance evaluation using the method of Data Envelopment Analysis (DEA) which is a relative efficiency measurement method based on linear programming. Supplier evaluation results then enhanced by ranking the suppliers using the Super Efficiency DEA model. This model can determine the ranking of suppliers even if the BCC model consider it as efficient. Supplier ranking aims to determine the most ideal supplier of the overall supplier as a benchmark for future evaluation assessment. As a result, four out of six suppliers are considered as efficient. Moreover, by applying the Super Efficiency DEA, rank orders of the suppliers are found as well.

Key Words: Data Envelopment Analysis; model of Banker, Charnes, Cooper; supplier evaluation; Super Efficiency DEA.

1 INTRODUCTION

Efficiency concept of Supply Chain Management (SCM) is consuming the attention of academics and practitioners in recent years. Developing from the transportation and physical distribution channels (Croom et al., 2000), SCM has such authority to purchase and managing inventory. Parts purchasing played a key role in cost reduction and supplier selection. This authority is a strategic role of SCM to reach a competitive advantage, especially for companies that spend inventories of materials and components in a high percentage (Saen, 2007).

The development of SCM concept is the concept of SRM (Supply Relationship Management) which is a process that defines how companies interact with suppliers. As the name suggests, this is the mirror image of customer relationship management (CRM). Just as companies need to develop relationships with customers, companies also need to foster relationships with suppliers. The desired result from this relationship is a win-win solution where both generate benefits for both parties.



As the condition of the ideal 100% efficiency is extremely difficult to obtain in industrial sector, this situation also occurred in Supply Chain Management (SCM). This ideal condition is very difficult to be achieved because there are factors that affect supply chain processes, they are the specification and the size of the material / raw materials used, time of booking, and the high price of materials/feedstocks. In the case of pumping unit companies, scarcity of raw material has implications for high prices. Moreover, late delivery of raw materials can lead to disruption of production processes such as the declining number of production and delays in production schedules. These events are more likely to disadvantage pumping unit industry because they work based on contract.

Therefore, since raw material plays an important role for the company to start their process, considerate decision need to be made to evaluate and choose a reliable supplier. In order to address this challenge which, in this particular research, is faced by the pumping unit company, this research attempt to recommend alternative for supplier performance evaluation. Due to the ideal efficiency is very difficult to achieve, then the efficiency is measured in relative terms. This means that an object is not compared to the 100% efficient, but compared with the efficiency of other objects. The method that accommodate this concept is known as Data Envelopment Analysis (DEA). This method is a relative efficiency measurement method based on linear programming techniques by using some of the objects of research that has the same characteristics.

2 METHODOLOGY

2.1 Data Envelopment Analysis (DEA)

Besides the previous three methods, Data Envelopment Analysis (DEA) was first introduced by Charnes, Cooper, Rhodes (1978). It is a development of the concept of "Technical Efficiency" which was introduced by Farrell (1957) (Tao Chun-hai, 2010). DEA is a linear programming techniques (nonparametric methods) used to measure the relative efficiency of a homogeneous Decision Making Unit (DMU) in the use of multiple inputs to produce multiple outputs (State Service Provision, 1997)

DEA measures the relative efficiency of each DMU compared with other DMU that is on efficient frontier. Efficient frontier is determined by the most efficient DMU among all DMUs based on the principle of Pareto optimal. This principle states that a particular DMU is efficient if there is no other DMU or combination of DMUs which is able to produce at least the same amount of output, using the same amount of inputs or fewer. On the contrary, a DMU is called Pareto inefficient if there are other DMU or combination of other DMUs that is able to produce at least the same amount of output, using the same amount of inputs or fewer.

In term of mathematical expression, assume that there are n decision making units (DMU), which will be evaluated, $j = 1, \dots, n$. There are s outputs ($r = 1, \dots, s$) and the input m ($i = 1, \dots, m$). DMU efficiency scores to evaluate the p can be obtained by:



$$\underset{u_r, v_i}{Max} \quad h_p = \frac{\sum_{r=1}^s u_r y_{rp}}{\sum_{i=1}^m v_i x_{ip}} \tag{1}$$

$$\text{Constrained to : } \frac{\sum_{r=1}^s u_r y_{rj}}{\sum_{i=1}^m v_i x_{ij}} \leq 1; j = 1, \dots, n$$

$$v_r, u_i \geq \varepsilon > 0$$

Where:

s = number of output

m = number of input

u_r = weight for r -th output

v_i = weight for i -th input

x_{ij} = value from input i -th using by j -th DMU

y_{rj} = value from output r -th using by j -th DMU

2.2 Banker, Charnes, Cooper Model

DEA model results that provide scalable return variable is called BCC model; Banker, Charnes and Cooper (1984). In this model, u_r and v_i should be positive. Mathematical model for this BCC model is shown as follows in Table 1.

Table 1. Model BCC

<i>Input Oriented</i>	<i>Output Oriented</i>
$\text{Max : } h_o = \sum_{r=1}^s u_r y_{io} + C_o$	$\text{Min : } h_o = \sum_{i=1}^m v_i x_{io}$
Constrained to : $\sum_{i=1}^m v_i x_{io} = 1$	Constrained to: $\sum_{r=1}^s u_r y_{io} + C_o = 1$
$\sum_{r=1}^s u_r y_{rj} - \sum_{i=1}^m v_i x_{ij} - C_o \leq 0$	$\sum_{r=1}^s u_r y_{rj} - \sum_{i=1}^m v_i x_{ij} - C_o \leq 0$
$u_r, v_i \geq \varepsilon$	$u_r, v_i \geq \varepsilon$

2.3 Super Efficiency Model

When the evaluated DMU is not included in the reference set of measurement models, the results of the DEA solution is called super-efficiency DEA model. The concept of super efficiency was first proposed by Andersen and Petersen and its use is supported because its simplicity and its benefits. Based on this concept, it becomes possible to rank all the units, even the efficient units. With this concept, it is possible to rank all the units, even the efficient units. The idea of super-efficiency concept is to let the DMU efficiency values were observed more than one or 100%.



Table 2 Super Efficiency Model

Input Oriented	Output Oriented
Min γ	Max ρ
Constrained to:	Constrained to:
$\sum_{j=1}^n \lambda_j x_j \leq \gamma x_o$ $\sum_{j=1}^n \lambda_j y_j \geq y_o$ $\sum_{j=1}^n \lambda_j = 1$ $\lambda_o = 0$ $\gamma, \lambda_j \geq 0, j \neq 0$	$\sum_{j=1}^n \lambda_j x_j \leq x_o$ $\sum_{j=1}^n \lambda_j y_j \geq \rho y_o$ $\sum_{j=1}^n \lambda_j = 1$ $\lambda_o = 0$ $\gamma, \lambda_j \geq 0, j \neq 0$

Zhu (1996) and Seiford and Zhu (1998) then developed a super-efficiency model above to determine the stability of efficiency that is useful for sensitivity analysis. Sensitivity analysis is designed to study the effect of the change (disruption) in the linear model parameters programming towards optimum solution. In other words, super-efficiency DEA model can also be used in detecting extreme efficient DMUs (Thrall, 1996).

Assume that there are n DMU. Each DMUj ($j = 1, 2, 3, \dots, n$) consumes the input vector x_j to produce output vector y_j . Based on the basic DEA model given in Seiford and Zhu (1999), super-efficiency DEA model can be expressed as it can be seen in Table 2 (Zhu, 2009).

In the super-efficiency model, the analyzed DMU were not included in the calculation of efficiency optimization ($\lambda_o = 0$). So, it is possible that the result of the analysis is infeasible which then cause the optimal solution becomes difficult to be found.

Table 3 Equation of One Super Efficiency Model

Orientation	Equation
Input	$S_o = w_\gamma \gamma_o + \frac{w_\tau}{\tau_o}$
Output	$\hat{S}_o = w_\gamma \frac{1}{\gamma_o} - w_\tau \tau_o$

As a solution to infeasibility which happened, Chen integrate γ_o (value of input oriented super efficiency) and τ_o (value of output oriented super efficiency) into one super-efficiency score (Shapiro, 2007). For example, we can determine the weight and the weight γ_o as w_γ dan the weight τ_o as w_τ where $w_\gamma + w_\tau = 1$ and calculate the one super-efficiency with formula in Table 3.



3 RESULTS AND DISCUSSION

3.1 Selection of Decision Making Units (DMU)

DMU to be analyzed is the suppliers who are registered to the Approved Supplier List (ASL) for the company which indicates that these suppliers are reliable supplier because they have had long cooperation relationship with the company. Following in Table 4 is the list of material suppliers for equal angle bar 50 x 50 x 5 mm which are suggested to be evaluated and included in the ASL.

Table 4 List of DMU analyzed

DMU _j	Name of Supplier
1	SAPTA ASIEN MID-EAST
2	KUALA ELOK
3	SINARINDO MEGAH PERKASA, PT
4	LESTARI ERA GEMILANG, CV
5	MENTARI PARAMITRA, PT
6	SURYA PERKASA MANDIRI, PT

3.2 Selection of Input and Output Variables

Input variable in the DEA are all supports that are used by suppliers as sources to produce output. While output variables are the output of resources which has gone through transformation process by the supplier.

Selection of input and output variables are generally not far from the standard criteria which has been set by the company in evaluating suppliers. In other words, after going through interviews with purchasing sub unit combined with some insight from literature, it was agreed that the input and output variables which will be analyzed include product quality, delivery, price, and service. Where the input variable includes price factor while the output variable encompasses service, product quality and delivery.

3.3 DEA Model Selection Used

The model used in this research oriented to model input or output maximization. This choice is based on the purchasing sub-unit consideration that gives higher priority to the criteria of quality, performance and service rather than the price criteria. In this study, it is assumed that increases in price do not always result in improved levels of quality, performance and service delivery in proportion. This assumption is called variable return-to-scale (VRS) because this assumption is better suited to applications in the real conditions.

3.4 Data Collection and Discussion

Data collected with requirement that all suppliers have the historical order record within the range of data collection time. Since the nature of the production that is applied is based on job order, then the production of pumping units can vary in numbers



depending on existing orders or tender within a year. Therefore, in this study, it is determined that order data which will be processed comes from a period of three years as it can be seen in Table 5 for all six suppliers.

Table 5. Data of Supplier Evaluation

Supplier	Price (%)	Quality (%)	Delivery Performance (%)	Services (%)
1	93,34	100	100	66,67
2	100	98,83	85,67	73,33
3	79,70	99,08	93,34	68,89
4	66,56	78,35	72,03	73,33
5	98,89	100	100	75,56
6	65,57	98,18	77,27	77,78

The next step is to process raw data from suppliers using the selected DEA model. DEA model combine weights that represent management's assessment of the relative importance towards input and output variables. The process of this DEA model is conducted using Microsoft Excel Solver software 2007.

As the result of the process, it can be seen from Table 6 that the efficiency scores for supplier 1, 3, 5 and 6 are considered efficient. Besides the efficiency, other results are also generated by the DEA is a benchmark for inefficient suppliers. This list contains information about efficient DMU as the benchmark and the appropriate intensity for each DMU. Benchmark results from DEA are presented in Table 7.

Table 6. Supplier's Efficiency Score

DMU	Efficiency Score	Benchmark
		DMU (Intensity)
1	1,0000	—
2	0,7551	1(0,328); 3(0,058); 6(0,613)
3	1,0000	—
4	0,9851	6 (1)
5	1,0000	—
6	1,0000	—

In addition to the benchmark, DEA also provides information about the value of slack for inefficient suppliers as shown in Table 7. This value represents the shortage of output variables or excessive use of variable inputs. In other words, since the used model in this study try to maximize output, this value can be interpreted as lack of output. The value of this slack then can be used as evidence-based reason for recommending improvement for targeted suppliers who are less efficient.



Table 7. Slack Value

DMU	Price {S}	Quality {S}	Deliver y {S}	Service s {S}
1	0,0000 0	0,0000 0	0,0000 0	0,0000 0
2	0,0000 0	0,0000 0	0, 00000	0,0028 3
3	0,0000 0	0,0000 0	0,0000 0	0,0000 0
4	0.0000 0	0,1983 0	0,0524 0	0,0445 0
5	0,0000 0	0,0000 0	0,0000 0	0,0000 0
6	0,0000 0	0,0000 0	0,0000 0	0,0000 0
7	0,0000 0	0,0000 0	0,0000 0	0,0000 0

In accordance with earlier decisions, the orientation which is used is the input orientation as it shown in Table 8. But the obtained result shows the occurrence of infeasible model for calculation of supplier the 5th and 6th. Infeasibility occurs when a collection of other suppliers that are observed do not achieve efficient condition because the observed DMU weights is not included into the set of references. If this happens, then it can be concluded that the observed DMU is an extreme point which means that the supplier has an extreme value of efficiency and do not have a reference input or output when measured using super-efficiency DEA model.

Table 8. Result of Input Oriented Super Efficiency Model

DMU	Input Oriented Super Efficiency (γ_0)
Sinarindo Megah Perkasa, PT	1,0595
Sapta Asien Mid-East	0,7551
Mentari Paramitra, PT	1,0779
Surya Perkasa Mandiri, PT	0,9851
Lestari Era Gemilang, CV	infeasible (1)
Kuala Elok	infeasible (1)



Infeasible happens cause problems in determining the ranking of suppliers. One solution that can be done in completing infeasibility is introduced by Yao Chen (2004). Chen developed a model where both model input and output-oriented VRS super-efficiency is used to rank the efficient DMUs. Table 9 shows the results of calculation of One Super Efficiency model and ranking suppliers.

Table 9. Supplier Rating Result

DMU	One Super Efficiency	Ranking
1	1,038707655	2
2	0,860084695	6
3	1,067547103	1
4	0,99255	5
5	1,038444971	3
6	1	4

4 CONCLUSION

Based on the results of supplier performance evaluation by using Data Envelopment Analysis, the basic model of Banker, Charnes, and Cooper (BCC), while ranking suppliers using Super Efficiency DEA model on manufacturing companies pumping unit, the authors can conclude a few important points as follows:

1. Supplier performance evaluation with DEA method that uses the price criteria as a input variable and service, product quality and delivery criteria as output variables. From six suppliers of iron elbow 50 x 50 x 50 mm component, it is obtained that four suppliers are considered as efficient. The four suppliers are suppliers 1, 3, 5 and 6, while the supplier 2 and 4 are classified as less efficient suppliers.
2. Continuing from the supplier evaluation, the rank order of overall supplier is determined using Super efficiency DEA model. These ratings can be used as a reference for managerial information in selecting the ideal supplier for future long-term cooperation.
3. Following is the obtained rank, descending from first to last rank:
 - 1) Sinarindo Megah Perkasa, PT
 - 2) Sapta Asien Mid-East
 - 3) Paramitra Mentari, PT
 - 4) Surya Perkasa Mandiri, PT
 - 5) Sustainable Era Gemilang, CV and
 - 6) Kuala Elegance



5. REFERENCES

- Chen, Y., Motiwalla, L. and Riaz Khan, M., 2004. Using super-efficiency DEA to evaluate financial performance of e-business initiative in the retail industry. *International Journal of Information Technology & Decision Making*, 3(02), pp.337-351.
- Croom, S.R., Romano, P. & Giannakis, M., 2000. Supply Chain Management: An analytical framework for critical literature review. *European Journal of Purchasing and Supply Management*, 6, 67-83.
- R. Nugroho Purwantoro, 2003. "Penerapan Data Envelopment Analysis (DEA) dalam Kasus Pemilihan Produk Inkjet Personal Printer", *Usahawan*, No. 10, Th. XXXII, p. 37.
- Robert M. Monczka, Robert B. Handfield, & Larry Giunipero., 2009. *Purchasing and Supply Chain Management*, South-Western : Mason, USA, p. 311-313
- Shapiro, J., (2007), *Modeling The Supply Chain*, Second ed. Thomson Brooks Cole.
- Steering Committee for the Review of Commonwealth/State Service Provision, 1997. *Data Envelopment Analysis: A technique for measuring the efficiency of government service deliver*, Canberra: AGPS.
- Tao Chun-hai, 2010. *Review on productivity measurement of medical services Based on data envelopment analysis*. *International Conference on Financial Theory and Engineering*, pp. 323
- Zhu, Joe, 2009. *Quantitative Models for Performance Evaluation and Benchmarking*. Springer Science+Business Media: Worcester, p. 206



QIR

*The Westin Resort
Nasa Dua, Bali*
24-27 July 2017

SYMPOSIUM H

**International Symposium
on Industrial Innovation
and Community Engagement**





ENGAGING COMMUNITY IN DEVELOPING ELECTRICAL WIND POWER IN REMBITAN VILLAGE, CENTRAL LOMBOK

Teti Zubaidah¹, Bulkis Kanata², Made Sutha Yadnya³

*Research Group on Applied Electromagnetic Technology
Electrical Engineering Department, University of Mataram, Jl. Majapahit 62 Mataram,
Lombok – INDONESIA
E-mail: ¹tetizubaidah@unram.ac.id, ²uqikanata@te.ftunram.ac.id,
³msyadnya@unram.ac.id*

ABSTRACT

The Rembitan village is located in the Central Lombok district, with topography of hills on elevations of 250 - 300 m. A grant for community service (Ipteks bagi Masyarakat - IbM) is focused on this village towards an energy independent village by means of electricity from wind energy. These activities are intended to strengthen the relationship between the University of Mataram and the village community, as well as to empower the local communities to supply their electricity needs. The activities are considered very appropriate, considering that Rembitan is close to the South coast of the Lombok island, with high wind energy potential that unexploited up today. Activities will also be in a close relevance to the needs of local communities, since the availability of electrical energy in the village is not yet fully equitable. The provision of an independent electrical energy from wind power is also expected to be a solution for social and economical problems. A wind turbine with capacity of 1 kWp has been installed successfully in Rembitan village. By using additional installation of batteries, inverter, and charger controller (MPPT), it can be used to supply lighting loads and water pump. In the meantime, the University of Mataram has operated the Lombok Geomagnetic Observatory since 2014 in Rembitan village, in cooperation with the Deutsches GeoForschungsZentrum (GFZ) Germany and the Government of Central Lombok District. Considering the importance of this observatory for the purpose of earthquake mitigation, it is indispensable for realizing mutualism relationship with the local communities to sustain its operations. Following some other previous community services in Rembitan village, the current activities through IbM 2016 should also be a part for strengthening the mutual relationship.

Keywords: Wind power; Electricity; IbM; Rembitan village; Lombok.

1. INTRODUCTION

Rembitan village is located in the southern part of Lombok island, 18 km from Praya (the capital city of Central Lombok District), around 10 km from the south coast of Lombok. Figure 1 shows the location of Rembitan village on the map of Indonesian territory. Topographic of this village consist of many hills with elevations of 250-300 m, covering area of 1475 hectare, inhabitant by 2146 families. Most of populations of this village are farmers, which are actually not familiar with electrical power generations and installation.



Figure 1 Location of Rembitan village in Central Lombok district, marked with a pin point on the map of Indonesian territory.

The wind energy potential of Lombok island in West Nusa Tenggara (NTB) province is middle, with average wind velocity of 4-5 m/s. The data are based on measurements in 110 locations over Indonesian regions, issued by the Indonesian Aviation and Aeronautical Agency (LAPAN), as shown in Table 1 and Figure 2. Among the locations that have been used as a pilot project of wind power plant is in the village of Selayar (East Lombok), with the installation of wind turbines with a capacity of 7 x 1 kW, which can be used for household electricity and public lighting.

Meanwhile, along the southern coast of the Lombok island, the wind energy potential are relatively high, as shown in Figure 3 (Zubaidah et al., 2012). Optimal wind velocities occur mainly in the afternoon, which can reach 6 m/s. If the wind potential is optimally used, it will generate enough energy to meet the needs of small household and public lighting. While for small-scale wind turbine, an annual average of wind velocity between 2.5 - 4.0 m/s is required (<http://www.library.ohiou.edu/indopubs/1994/10/19/0001.html>).

A community service through “Ipteks bagi Masyarakat” (IbM) grant at this time is focused on Rembitan village. The specific aim is community empowerment through self generating of electricity supply by means of wind energy. These activities are intended to fulfill small scale electricity needs of community, are considered very appropriate, since Rembitan village is in an area close to the South coast of the Lombok island, where the wind potential is quite high but has not been utilized up today. The activities have close relevance to the needs of local communities, since the availability of electricity in the village is not yet fully equitable. Only view peoples who live along the major roads that have access to electricity supplied by the National Electric Company (PLN), while poor peoples who are staying on top of the hills still have no access to electricity services. The electricity is also still very frequently outages, especially at night, which can last for more than eight hours. Meanwhile, the road over the hills at night is very dark, because there is no street lighting. These conditions lead to a lot of crime at night, such as the loss of livestock. The condition is also not conducive particularly for children's learning activities. Public facilities, such as mosques or prayer rooms, are optimally less at night, because of the lack of lighting. Therefore, providing electrical energy from wind power is expected to be a solution to the above problems and also be a way to solve other social and economical problems.



Table 1 Wind energy potential over Indonesian regions (Soeripno, 2007)

No	Province	Number of Measurement	Wind Velocity		
			Low	Middle	High
1	NTT	43	10	23	10
2	NTB & Bali	10	2	7	1
3	Maluku & Papua	6	4	2	-
4	Sulawesi	19	8	6	5
5	Java & Madura	12	1	4	7
6	Sumatera	5	2	3	-
7	Kalimantan	2	1	1	-
8	Others	9	-	-	9
Total		110			



Figure 2 Map of wind energy potential over Indonesian regions (Soeripno, 2007).

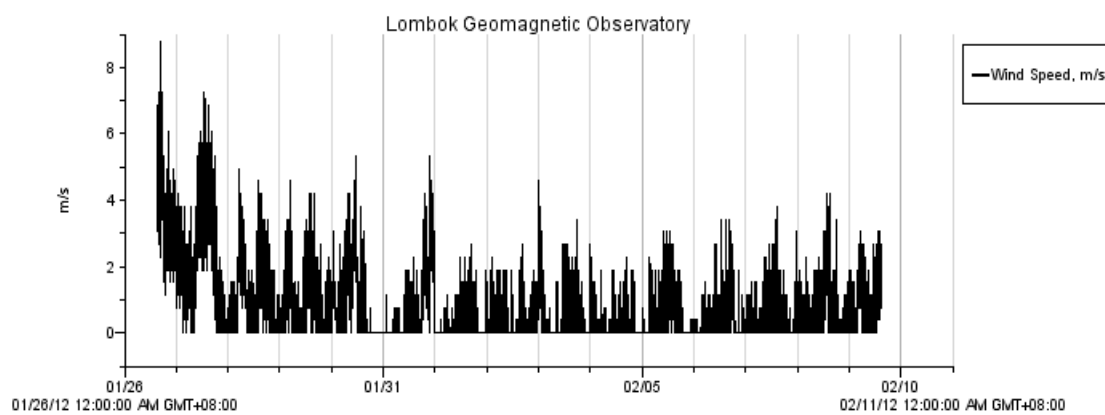


Figure 3 Measurements of wind velocity at Kidang village, in the southern coast of Lombok island (Zubaidah et al., 2012)



In the meantime, the University of Mataram has operated the Lombok Geomagnetic Observatory in Rembitan village since 2014, in cooperation with the Deutsches GeoForschungsZentrum (GFZ) Germany and the Government of Central Lombok district. Data from this observatory is integrated internationally and will be used for earthquake mitigation purposes. Given the importance of this observatory and its sustainable operation, it is indispensable to keep mutualism relationship with the local communities of Rembitan village. To maintain a good relationship between the University of Mataram and community of Rembitan village, several community service activities have been done previously, including sacrifice on Eid Adha, Greening the land, Social Charity, and Foster Children program. Besides socializations have been organized, to introduce the Lombok Geomagnetic Observatory and utilization of biogas energy (Zubaidah et al., 2013), and also to introduce wind energy potential (Zubaidah et al, 2015). The current activities through IBM 2016 should also be a part for strengthening the mutual relationship.

2. METHODOLOGY

Based on the above situations, the lists of some problems to be resolved are:

1. How to exploit the potential of wind energy to fulfil the electricity needs of households and public lighting in the Rembitan village.
2. How to do survey and mapping of wind potential, to select the most appropriate location in the Rembitan village for running a 1 kW wind turbine.
3. How to invite the local community of Rembitan village to play an active role in the implementation of wind potential survey and construction of wind turbine.
4. How to raise public awareness of Rembitan village to maintain public facilities, mainly the constructed wind turbine and the Lombok Geomagnetic Observatory.

To achieve the expected targets, it will be pursued through several phases of activity:

1. Survey on the field, such as measuring and recording wind velocity for a few days in some hilly areas that are physically demonstrated as potential locations for the placement of wind turbines. Data recording is not adequate if it is carried out only for a day, because the wind velocity varies with time and is not the same for each month (Musyafa et al., 2011; Soeripno and Murti, 2014)
2. Socialization of development plan of wind turbine to the local community.
3. Construction and installation of wind power plants, including the establishment of wind turbines, installation of battery and inverter, and other control equipment.
4. Maintenance training for local youth groups, relating to metering procedures and trouble shooting.
5. Evaluations on a regular basis (every month), with the involvement of the local youth groups who have been trained.
6. Reporting the results of activities to the Indonesian Ministry of Research and Higher Education, and produce a scientific publication on a seminar.



3. RESULTS AND DISCUSSION

3.1 Discussion for planning activities with the local community

Before we start field activities, we have organized discussions with local community who will be directly involved in the implementation of activities. Discussions were held with the aim to achieve mutual understanding and commitment, as well as to explain the purpose and objective of activities, in order to have a full support of local people. The head of Bontor sub-village be a mediator of the discussions, which were attended by the chairman and members of the local youth group. Discussions were held at the residence of the sub-village head on 10 August 2016, as the documentation in Figure 4.

3.2 Field survey for best placement of the wind turbine

Field surveys have been conducted to estimate the wind potential over some hilly areas that are physically demonstrated as potential locations for the placement of wind turbines. The head of Bontor sub-village and some representatives of local community were actively involved in the survey, since it was needed to determine the ownership status of the locations, as well as to give permission to use the location for IbM activities. The documentation of survey activities is in Figure 5. One among the surveyed locations will be chosen as the most suitable place, as qualified by criteria: elevation and flatness of the location, stable velocity and direction of winds, ease of access to transport for construction and installation, located close to population who need electricity, safe from potential irresponsible parties, absence of problems in land ownership and permit for its use.



Figure 4 Discussion with the local youth group of Rembitan village, mediated by the head of Bontor sub-village.



Figure 5 Survey for choosing the most suitable location.



3.3 Preparation of equipment and materials

Preparation of equipment and materials has been carried out in the New and Renewable Energy Laboratory of Engineering Faculty, University of Mataram, such as checking the wind turbine components, including details of their number and actual conditions. It was found that the steel frames are needed for repainting to avoid the possibility of rust (considering that the location which is quite close to the coastal area). Figure 6 and Figure 7 show the activities carried out. It was also noted that it is still necessary for procurement of some additional components, so that the electrical energy generated by the wind turbine can be used to serve the load of lighting and water pumps. The additional components needed are a 1-phase inverter to power 1000 VA, batteries for energy storage with a capacity of 2 x 100 Ah, a 24 volts charger controller MPPT to avoid over charging on the battery, power cable for connecting the wind turbine to the electrical panel and battery, as well as the terminal end of the electric socket that can be used to take the electrical power.

3.4 Installation of foundation

Upon completion of equipment and materials are prepared, we performed the installation of turbine foundation. The planning were done directly at the predetermined location, together with the local community who will be involved, to ensure that the foundation will be installed correctly. Figure 8 and Figure 9 show the activities carried out.



Figure 6 Preparation of equipment at the New and Renewable Energy Laboratory.



Figure 7 Re-painting of the steel frames at the Structural Laboratory.



Figure 8 Planning for turbine foundation together with the local community.



Figure 9 Turbine foundation which has been constructed perfectly by the local community.

3.5 Testing of Generator

The testing was carried out to ensure that the generator can actually produce electricity as expected. It was conducted at the New and Renewable Energy Laboratory of the Engineering Faculty, University of Mataram. The testing was done in the form of assembly of all components of the wind turbine, and voltage measurements on the generator output terminals when the turbine was rotated. Figure 10 shows the activities carried out.

3.6 Construction of wind turbine

Construction of wind turbine was done for three full days on 2 - 4 October 2016 by IBM team together with the local community of Rembitan village. The activity began with the raising of piles, consisting of three high steel iron frames with a total height of 11 (eleven) meter. It followed by the installation of a generator at the top of the pile, and installation of blades and wind turbine head. Figure 11 shows the construction activities carried out, and Figure 12 shows the results.



Figure 10 Testing of generator at the New and Renewable Energy Laboratory.



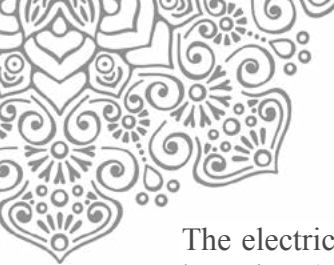
Figure 11 Construction of wind turbine which has been done by IbM team together with the local community of Rembitan village.



Figure 12 Results of wind turbine construction.

3.7 Electrical installation

After successful construction of the wind turbine and it has been in stable operation for a couple of days, the activities are continued with the installation of electrical panel on 5 October 2016. Figure 13 shows the activities carried out. The installation was done by IbM team, and the local people were involved to help for making simple installation. Activities began by pulling the power cord from the wind turbines to the electrical panel, which is placed in one of the local houses. The output of this electrical panel is still a direct current (DC), with its magnitude depends on the rotation speed of the turbine. Therefore, it needs to provide an additional electrical installation, so that the output can be used to supply the lighting load and water pump in the form of alternating current (AC) 220 volts (<https://nugrohoadi.wordpress.com/2008/05/03/pembangkit-listrik-tenaga-angin-di-indonesia/>).



The electricity from electrical panel that have been installed must be stored in advance on batteries (accumulators). This activity was resumed on 8 November 2016, with the installation of a charger controller (MPPT), batteries, and inverter. Local community were also involved in this activity, so that they understand the function of each part of the installation. After the electrical installation is complete, the generated wind energy has been used to run a bulb light. Figure 14 shows the activities carried out.



Figure 13 Installation of electrical panel on a house of local community.



Figure 14 Installation of additional equipment, and the bulb light is shining.

3.8 Impacts for the community

The above activities are intended to fulfill small scale electricity needs of community, particularly for poor peoples, which are still have no access to electricity services from the national electrical company. The availability of electricity at Rembitan village is also still very frequently outages, and especially at night the road over the hills is very dark, because there is no street lighting. By using electricity from the installed wind turbine, we do hope that the night situations at the village will be less of crimes and more conducive particularly for children's learning activities and for public facilities, such as mosques or prayer rooms. Figure 15 shows the condition of people who will receive the results of the activities.



Figure 15 Local community which will use the electrical power from the wind turbine.



4. CONCLUSION

The activities of IbM 2016 in Rembitan village has been well done, although not fully correspond to the expected target date. The activities got very good participations and much help from the local community, indicating that the engagement process is quite successful. The results of activities in the form of wind turbine construction must be followed by various activities to be undertaken at a later stage. It is very useful to involve students as much as possible in community service activities, for transferring of knowledge from one generation to the next.

5. ACKNOWLEDGEMENT

We thank to the Indonesian Ministry of Research and Higher Education, in providing funding for IbM 2016 entitled **“Pemberdayaan Masyarakat Desa Rembitan Menuju Desa Mandiri Energi Melalui Penyediaan Listrik Dari Energi Angin”**.

6. REFERENCES

- Musyafa, A., Negara, I.M.Y, Robandi, I., (2011), A Wind Turbine for Low Rated Wind Speed Region in East Java. *International Journal of Academic Research*, Volume 3, Number 5, pp. 353-358, II Part.
- Soeripno, M., (2007), Utilization of Wind Energy Conversion System in Indonesia. *Jurnal Ilmiah Teknologi Energi*, Volume 1, Number 5, pp. 59-68, ISSN 1858 – 3466.
- Soeripno, M., and Murti, N., (2014), Promoting Wind Hybrid Power Generation for Economic Development in Remote Islands. *Proceeding Renewable Energy World Asia Conference and Expo*.
- Zubaidah, T., Rosmaliati, Paniran, Sultan, (2012), Solar and Wind Hybrid Power Generation for the Lombok Geomagnetic Observatory. *Progres Report for CAPacity development and strengthening for energy policy formulation and implementation of Sustainable energy project in INDONESIA (CASINDO)*.
- Zubaidah, T., Kanata, B., Rosmaliati, Paniran, Nababan, S., (2013). Sosialisasi Pembangunan Observatorium Geomagnetik Lombok dan Energi Biogas di Desa Rembitan Kab. Lombok Tengah. Laporan Pengabdian Kepada Masyarakat, Fakultas Teknik Universitas Mataram (in Bahasa).
- Zubaidah, T., Kanata, B., Yadnya, M.S., Muvianto, C.M.O., Ramadhani. C., (2015), Sosialisasi Potensi dan Pemanfaatan Energi Angin di Desa Rembitan, Kec. Pujut, Kab. Lombok Tengah. Laporan Pengabdian Pada Masyarakat PNBPN, Fakultas Teknik Universitas Mataram (in Bahasa).
- <http://www.library.ohiou.edu/indopubs/1994/10/19/0001.html>.
- <https://nugrohoadi.wordpress.com/2008/05/03/pembangkit-listrik-tenaga-angin-di-indonesia/>



THE 15TH INTERNATIONAL CONFERENCE QUALITY IN RESEARCH (QIR) 2017

Identification and Characterization of Mangrove Forest in View of Sustainability Conservation and Management: Mangrove Identification of Southern Coast Malang Region, East Java, Indonesia

Erfan Rohadi^{a*}, Aida Sartimbul^b, Imam Fahrur Rozi^c

^{a,c}*The State Polytechnic of Malang, Jl. Soekarno Hatta No. 9, Malang 65141, Indonesia*

^b*University of Brawijaya, Faculty of Fisheries and Marine Science, Jl. Veteran No. 16, Malang 65145, Indonesia*

ABSTRACT

The characteristic of Southern of Java coast area is typically rocky beach (rocky shore). Its characteristics which are connected directly to the Indian Ocean may affect the ecosystem of flora and fauna therein. The mangrove performs diverse functions and service on an ecosystem and landscape scale. The important factors for sustainable coastal management are the both economical values and ecological management as the association functions. Furthermore, the typical of tropical marine ecology is a chain as a triangular pattern that means each associated with one another such as the coral reefs, the seagrass and mangrove. Those may have distinct characteristics in the ecosystem. The mangrove in the Southern coast region of Malang grows scattered with various kind of interesting to do data collection based on the characteristics of mangrove found in Southeast Asia. This work is a collaboration between The State Polytechnic of Malang with The Faculty of Fisheries and Marine Sciences of University of Brawijaya which attempt to provide helpful information and integrative condition of mangrove ecosystems in Southern coast of Malang Region. The information contains in the form of the identification of species, mangrove biodiversity of the 18 beaches. The research methods of this study based on data processing of satellite image ALOS (AVNIR-2) and Landsat 7. The software ENVI 4.4 and Arc GIS 9.3 are used for data processing. The identification of various mangrove species using methods of in situ and laboratory observations. However, the satellite datum must be processed with in situ data so that it provides the informative map with some density classification. The results show that the recent mangrove vegetation (forest) condition in Southern Malang Region is recommended as a prior conservation for sustainability coastal management system. This work also provides the mangrove iBook format and e-book. The hard copy is obliged to the library flora Malang Regency as a supporting information for Southern Malang Region management system and as the academic learning process reference for high school students and universities students.

Keywords: Mangrove, Coastal Management, Southern Malang, ALOS, Ecosystem, e-book.



1. INTRODUCTION

Indonesia is an archipelago country that has the largest mangrove forest in the world (Onrizal, A. et.al., 2009). Mangrove forests are generally found around the coast of Indonesia and live and grow in locations that have a relationship tidal influence (tidal) seeping in watersheds that are along the coast (Tarigan, M. S., 2008). The mangrove forest is an ecosystem with an important role in terms of the ecological and socio-economic aspects. The mangrove forest is overgrown with forest type mangrove trees (mangrove) which are typical along the beach or estuary and is influenced by the tide. The mangrove forest has a dual function and is a very important link in maintaining biological balance in a water cycle (Hogarth, P.J., 1999).

As an ecosystem and natural resources, utilization of mangrove directed to the welfare of mankind and to realize its utilization in order to be sustainable. the mangrove ecosystem need to be managed and maintained. Mangrove forest management framework, there are two main concepts. First, the protection of mangrove forest which is a safeguard against mangrove forests into mangrove forest conservation. Second, the rehabilitation of mangrove forests are greening activities performed on land that used to be one of the rehabilitation efforts that aim not only to restore the aesthetic value, but the main thing is to restore the ecological function of mangrove forest that has been logged and transferred its functions to the activity other.

Walters et al., stated that the mangrove forests along the coast and rivers generally provide habitat for many species of fish (Walters, BB., et.al., 2008). Mangrove forests as one of the wetlands in the tropics with easy access and usability of components of biodiversity and high land that has made these resources as tropical endangered resource (Valiela, I., J. L. et.al., 2001) and became one of the centers of global environmental issues. Increasing conversion of mangrove forests to agricultural land or fish/ shrimp ponds, causing a decrease in productivity of the ecosystem (Dave, R., 2006). One of the areas in Malang Region of East Java, which one of still has a fairly extensive mangrove forests is Sinjai. Management of mangrove forests in this area has been done by the people independently, given some time ago when they sail into various areas, then upon return they bring mangrove seedlings to then planted around the beach because they believe that mangroves have many functions, including can withstand strong winds, large waves, and so on. The increasing tendency of destruction of mangrove forest along with the increasing needs of local communities, such as felling of mangrove trees were used as firewood for household use and charcoal to be traded, regardless of the carrying capacity and recovery, as well as increased activity of search crab seeking mangrove crabs into the region also led to increased damage to mangrove forests.

2. MATERIAL AND METHODS

The Southern coast Malang Region is located at 8° 20' S 112° 21' E bordered with Blitar Region to 8° 21' S 112° 57' E bordered with Jember Region. The total area of Malang Region is 3.534,86 km² with the temperature of rainy season and hot season are 18-23 °C and 21-31 °C, respectively. Thus, the minimum rainfall and maximum rainfall are 201 mm and 400 mm, respectively.



2.1. The Malang Coastal Area

Figure 2.1 shows the objects of the coastal Malang Region. The mangrove vegetation are observed at 18 beaches for two years period.

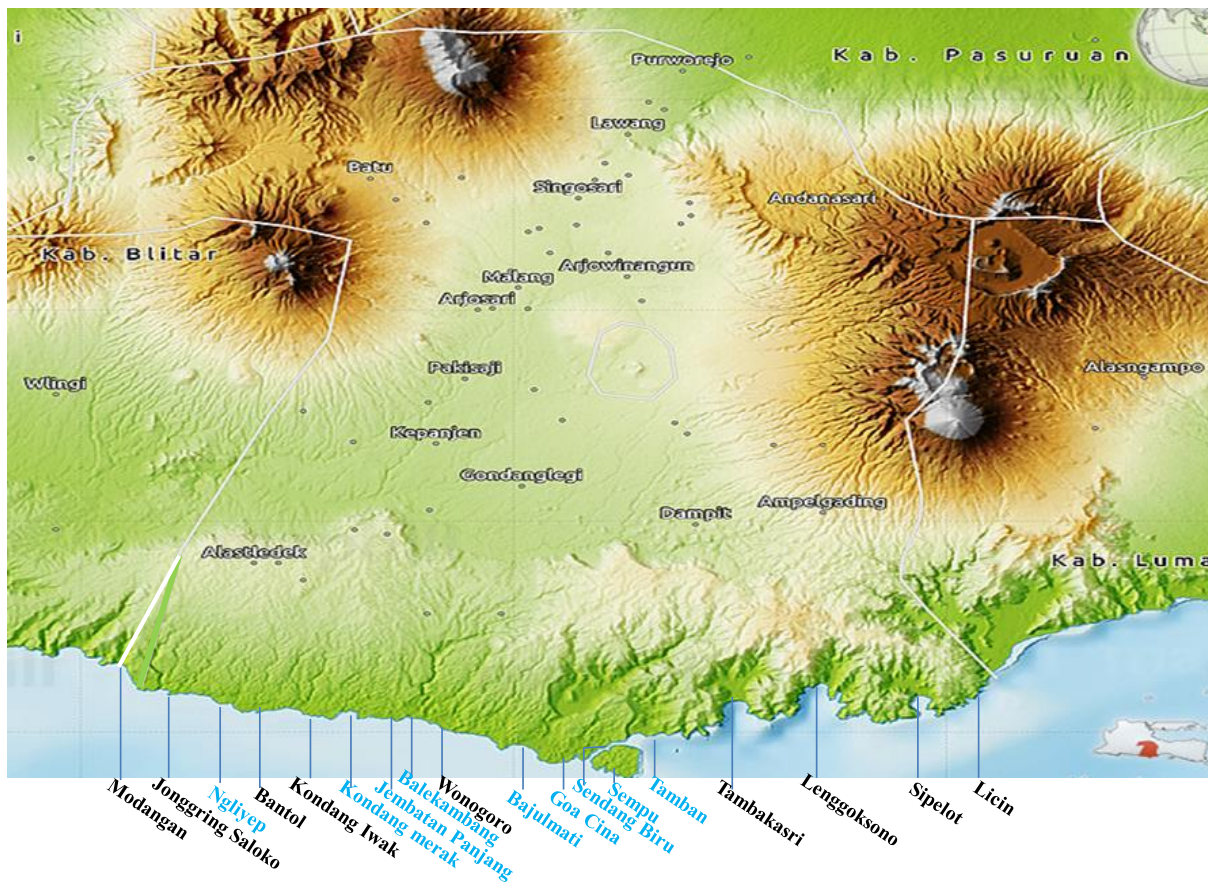


Figure 2.1 The Malang Coastal Region

2.2. Methods

In this work, the potential of mangrove forests and mangrove forest management strategies in the coastal of Malang Region are analyzed and mapped. The information contains in the form of the identification of species, mangrove biodiversity of the 18 beaches by two years scheme. The research methods of this study based on data processing of satellite image ALOS (AVNIR-2) and Landsat 7. The software ENVI 4.4 and Arc GIS 9.3 are used for data processing. The identification of various mangrove species using methods of in-situ and laboratory observations. In the first year, the in-situ data are collected. Then in the second year, the in-situ data will be processed the satellite data (Landsat Imagery, 2016, Santosa, P.B., 2005, Jensen, J.R., 1998).



3. RESULTS AND DISCUSSION

Figure 3.1 shows the satellite image of Malang Coastal Region. Since 2013 the South Route has been developed due to economic strategy management. Consequently, the new objects tourism has been developed while the communities are growing. However, the mangrove vegetation is becoming narrower for hundred hectares. Figure 3.2 shows the satellite image of associated mangrove vegetation domination in Sempu Island and Sendang Biru Area. The population of residences have been grown for recent years. However, the development of marine and fisheries sector at this time become one of the development priorities announced by the government Malang. The policy was adopted in view of Malang has 18 beaches with a coastline of 77 km and is located in the waters of the Indian Ocean is rich in resources large pelagic fish, such as yellow fin tuna (*Thunnus albacares*), bigeye tuna (*Thunnus obesus*), Albakora (*Thunnus allalunga*), southern bluefin tuna (*Thunnus macoyii*), and gray tuna (*Thunnus tonggol*) and skipjack (*Katsuwonus pelamis*). Based on the assessment of fish stocks in the Indian Ocean conducted by the National Commission on stock assessment of Marine fish Resources in 19 981, reported the potential of tuna resources in the South Java, is estimated at 22,000 tons / year with a production rate of 10,000 tons/ year, meaning the new utilization rate reached 45%. Thus, the prospects for development is still wide open, which amounted to 55%.

Changes in national development paradigm from land-based economic development into ocean-based economic development. Marine development platform used Malang Regency Government's economic development, particularly in South Malang. The Coastal areas of development priority due to the center of fisheries in Malang.

The consideration of the coastal areas development need to be planned well, because the coastal area is an area of transition between marine and terrestrial ecosystems with some important insights include: 1) Ecological, areas inland were still influenced by the processes of the marine, such as tide, intrusion sea water, etc. 2) Administrative, namely the outer limit upstream from the village beach or definitive arbitrary distance (2 km, 20 km, ff. Of shoreline and 3). Planning: depends on the problem or the substance that became the focus of the management of coastal areas. Similarly, the processing industry development planning, in order to be sustainable needs to be adjusted with the existing commodity good quantity.



Figure 3.1 The satellite image Malang Coastal Region



Figure 3.2 The satellite image of mangrove distribution at Sempu Island and Sendang Biru

Figure 3.3 and Figure 3.4 show the examples of mangrove vegetation Island and mangrove plantation at Sendang Biru, respectively.

Figure 3.5 shows flowchart of satellite image processing of mangrove vegetation at Tamban Beach (Sendang Biru area). The verified satellite image data of Landsat 7 ETM+ with field work data at Tamban Beach. The mangrove vegetation has been become narrower as 5.4 Ha is shown at Table 3.1.



Figure 3.3 Mangrove vegetation at Sendang Biru



Figure 3.4 Mangrove plantation at Sendang Biru

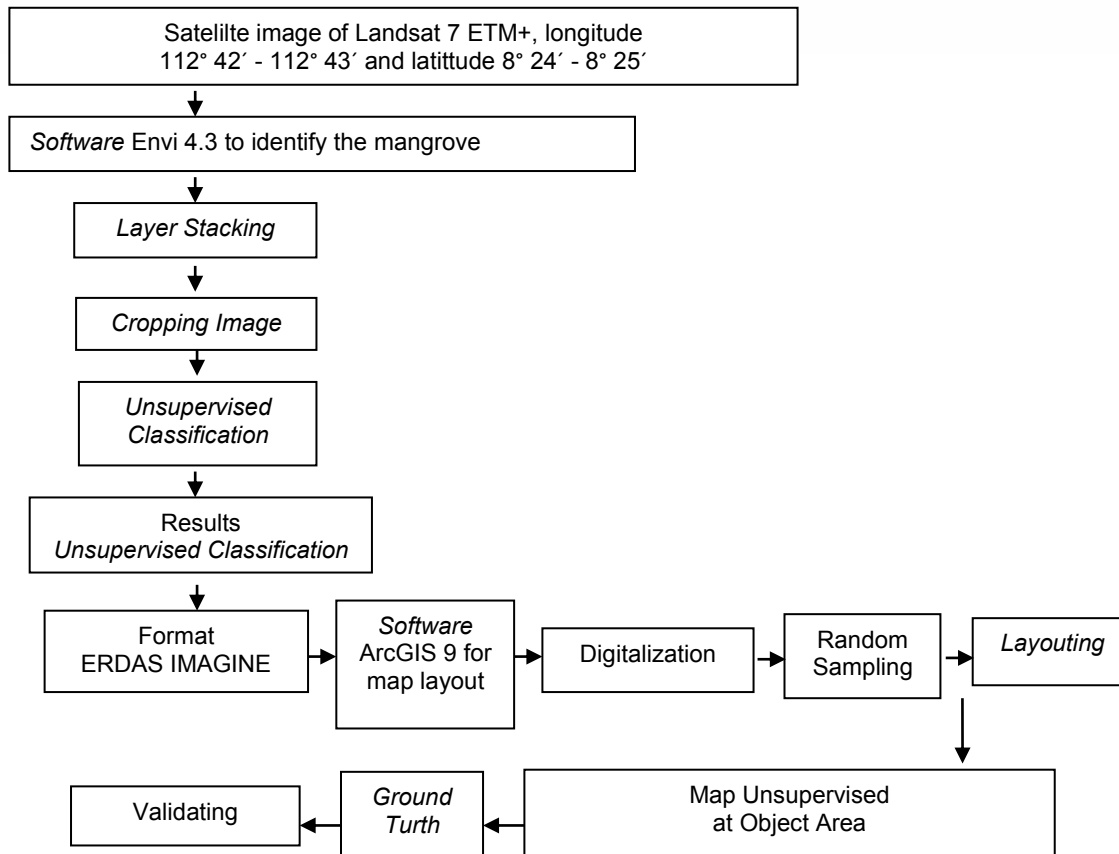


Figure 3.5. Flowchart of unsupervised mapping at Tamban Beach (Sendang Biru area)

Tabel 3.1. Verified satellite image data of Landsat 7 ETM+ with field work data

Class	Mangrove	Forest	Field	Agriculture field	Sallow water	Sand	Sea	Total
Mangrove	29	0	1	0	0	0	0	30
Forest	4	16	0	0	0	0	0	20
Field	0	1	18	1	0	0	0	20
Agriculture field	0	1	1	16	0	2	0	20
Sallow Water	12	0	0	0	6	2	0	20
Sand	0	0	0	0	3	17	0	20
Sea	0	0	0	0	0	0	20	20
Total	45	21	18	16	9	21	20	150

Figure 3.6 shows the map of validated Random Sampling of mangrove vegetation at Tamban Beach (Sendang Biru area).

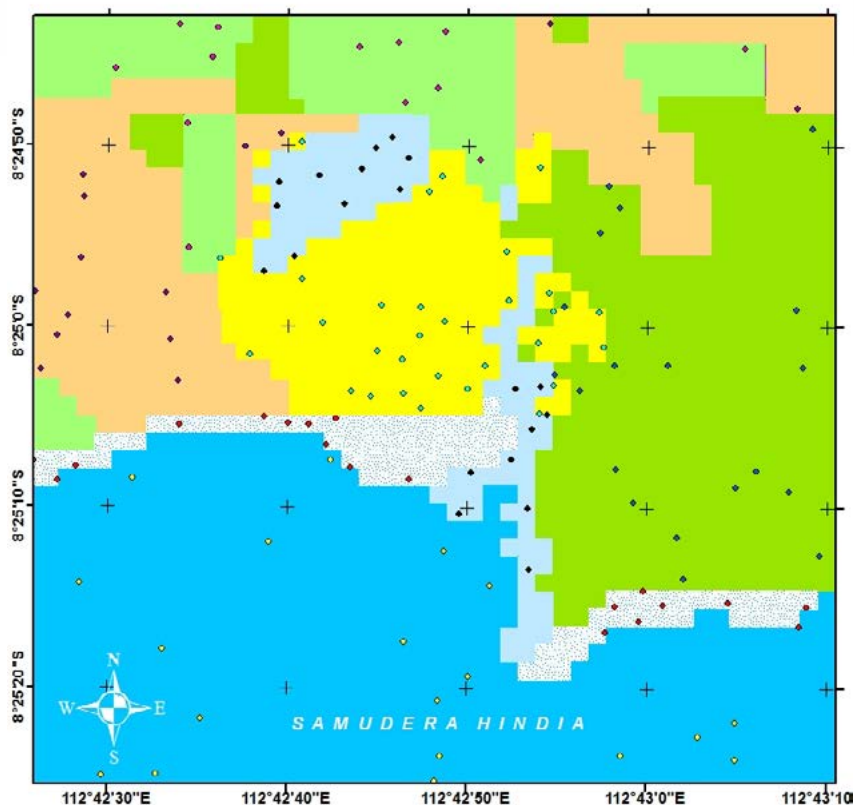


Figure 3.6. Map of validated *Random Sampling*

Table 3.2 shows the mangrove vegetation which identified in Malang Coastal Region. The mangrove vegetation is dominated by associated mangrove.

Table 3.2 Mangrove Vegetation Diversity in the South Malang
Index of mangrove vegetation and associated salt tolerant plant species identified from the South Malang

No.	Scientific name	Family
Mangrove Flora		
1.	<i>Acanthus ebracteatus, ilicifolius, volubilis</i>	Acanthaceae
2.	<i>Acrostichum aureum, speciosum</i>	Pteridaceae
3.	<i>Aegialitis rotundifolia</i>	Plumbaginaceae
4.	<i>Aegiceras corniculatum</i>	Myrsinaceae
5.	<i>Avicennia alba, marina, officinalis</i>	Avicenniaceae
6.	<i>Bruguiera cylindrica, gymnorrhiza, hainessi, parviflora, sexangula</i>	Rhizophoraceae
7.	<i>Ceriops decandra, tagal</i>	Rhizophoraceae
8.	<i>Excoecaria agallocha</i>	Euphorbiaceae
9.	<i>Heritiera fomes, littoralis</i>	Sterculiaceae
10.	<i>Lumnitzera littorea, racemosa</i>	Combretaceae
11.	<i>Kandelia kandel</i>	Rhizophoraceae



12. <i>Nypa fruiticans</i>	Arecaceae
13. <i>Rhizophora apiculate, mucronata</i>	Rhizophoraceae
14. <i>Scyphiphora hydrophyllacea</i>	Rubiaceae
15. <i>Sesuvium portulacastrum</i>	Aizoaceae
16. <i>Sonneratia alba, apetala, caseolaris, griffithii</i>	Sonneratiaceae
17. <i>Xylocarpus granatum, moluccensis</i>	Meliaceae
18. <i>Albizia procera</i>	Leguminosae
19. <i>Amyema mackayense</i>	Loranthaceae
20. <i>Bidens pilosa</i>	Asteraceae
21. <i>Brownlowia tersa</i>	Tiliaceae
22. <i>Canavalia maritima</i>	Leguminosae
23. <i>Clerodendum inerme</i>	Verbenaceae
24. <i>Cynodon dactylon</i>	Poaceae
25. <i>Cynometra ramiflora</i>	Leguminosae
26. <i>Dalbergia candenatensis</i>	Leguminosae
27. <i>Dalbergia spinosa</i>	Fabaceae
28. <i>Derris scandens, trifoliata</i>	Leguminosae
29. <i>Dolichandrone spathacea</i>	Bignoniaceae
30. <i>Drymoglossum piloselloides</i>	Polypodiaceae
31. <i>Eclipta alba,</i>	Asteraceae
32. <i>Eupatorium adoratum</i>	Asteraceae
33. <i>Fimbristylis ferruginea</i>	Cyperaceae
34. <i>Finlaysonia abovata</i>	Asclepiadaceae
35. <i>Flagellaria indicata</i>	Flagellariaceae
36. <i>Hibiscus tiliaceus</i>	Malvaceae
37. <i>Hoya carnaso</i>	Asclepiadaceae
38. <i>Ipomoea alba</i>	Convolvulaceae
39. <i>Ipomoeae pes-caprae</i>	Convolvulaceae
40. <i>Leucaena leucocephala</i>	Fabaceae
41. <i>Melastoma villosum</i>	Melastomataceae
42. <i>Merope angulata</i>	Rutaceae
43. <i>Paspalum sp</i>	Poaceae
44. <i>Phoenix paludosa</i>	Arecaceae
45. <i>Pluchea indica</i>	Asteraceae
46. <i>Pongamia pinnata</i>	Legununosae
47. <i>Sarcolobus globosus</i>	Asclepiadaceae
48. <i>Scaevola taccada</i>	Goodeniaceae
49. <i>Scirpus sp</i>	Cyperaceae
50. <i>Sesbania sp</i>	Fabaceae
51. <i>Tamarix troupii</i>	Tamaricaceae
52. <i>Vanda sp</i>	Orchidaceae



4. CONCLUSION

The results show that the recent mangrove vegetation (forest) condition in Southern Malang Region is recommended as a prior conservation for sustainability coastal management system. This work also provides the mangrove iBook format and e-book. The hard copy is obliged to the library flora Malang Regency as a supporting information for Southern Malang Region management system and as the academic learning process reference for high school students and universities students after two years' period observation. The strategic management of mangrove forests in Malang Region is people planted by the potential that exists, establish protected forest areas of mangrove that can not be bothered, further enhancing the role of community-based organizations and empower the community, dissemination to the public about the dangers of harvesting of mangroves, a touch of technology in the development of mangrove, the people involved in every decision-making on mangroves and increasing the role of government, elucidation of environmental and mangrove ecosystems, provide insight to the public about the use of mangrove, improving education/ training to the community, as well as consultation between the public and the government about the use and management of mangrove, socialization the application of government regulations on the environment, involving the community in the preparation of the planning and implementation of mangrove management, government and the community together to support the management of mangrove, the increase in planting mangroves around the coast. In principle, the position of mangrove forest management model in Malang Region in the category of growth and stability strategy is a strategy that is implemented without changing the direction of a predetermined strategy.

5. ACKNOWLEDGEMENT

The Authors would like to thank to Ministry of Research, Technology and Higher Education of Republic Indonesia for providing the funding decentralization scheme research program. Also, The State Polytechnic of Malang that supporting to attend this conference. One of the author would like to thank to Indrazno Sirahjuddin, Ph.D for supporting the scientific writing.

6. REFERENCES

- Dave, R. 2006. Mangrove ecosystem of south, west Madagascar: an ecological, human impact, and subsistence value assessment. *Tropical Resources Bulletin* 25: 7-13
- Hogarth, P.J. 1999. *The Biology of Mangroves*. Oxford University Press, Oxford.
- Jensen, J.R. 1998. *Introductory Digital Image Processing a Remote Sensing Perspective*. Prentice Hall. New Jersey. 361p.
- Landsat Imagery. 2016. An Overview the Global Land Cover Facility (GLCF). University of Maryland <http://www.glcg.umd.edu/data/landsat/>. Diakses tanggal 10 November 2010.
- Onrizal, A. Purwoko, dan M. Mansor. 2009. Impact of mangrove forests degradation on fisherman income and fish catch diversity in eastern coastal of North Sumatra,



- Indonesia. *International Conference on Natural and Environmental Sciences 2009 (ICONES'09)* at the Hermes Palace Hotel Banda Aceh on May 6-8, 2009.
- Santosa, P.B. 2005. Pemetaan Awal Hutan Mangrove Pantai Cairns Berdasarkan Data Landsat TM (*Preliminary Mapping Of Mangrove Forest Of The Cairns Coast Based On Landsat TM*). Disampaikan pada Pertemuan Ilmiah Tahunan MAPIN XIV "Pemanfaatan Efektif Penginderaan Jauh untuk Peningkatan Kesejahteraan Bangsa" pada tanggal 14-15 September 2005. Jurusan Teknik Geodesi UGM. Yogyakarta. <http://oc.its.ac.id/ambilfile.php>.
- Tarigan, M. S. 2008. Sebaran dan Luas Hutan Mangrove di Wilayah Pesisir Teluk Pising Utara Pulau Kabaena Provinsi Sulawesi Tenggara. *Bidang Dinamika Laut, Pusat Penelitian Oseanografi, LIPI, Jakarta 14430, Indonesia. Makara, Sains, Vol. 12, NO. 2, November 2008: 108-112.*
- Walters, BB., P. Ronnback, JM. Kovacs, B. Crona, S.A. Hussain, R. Badola, J.H. Primavera, E. Barbier, dan F. Dahdouh-Guebas. 2008. Ethnobiology, Socio-Economic and Management of Mangrove Forests: *a review. Aquatic Botany* 89: 220-236
- Valiela, I., J. L. Bowen, dan J. K. York. 2001. Mangrove Forest: One of the World's Threatened Major Tropical Environments. *Bioscience* 51(10): 807-815.

